U.S. Department
of Commerce

Volume 98
Number 1
January 2000

Fishery Bulletin

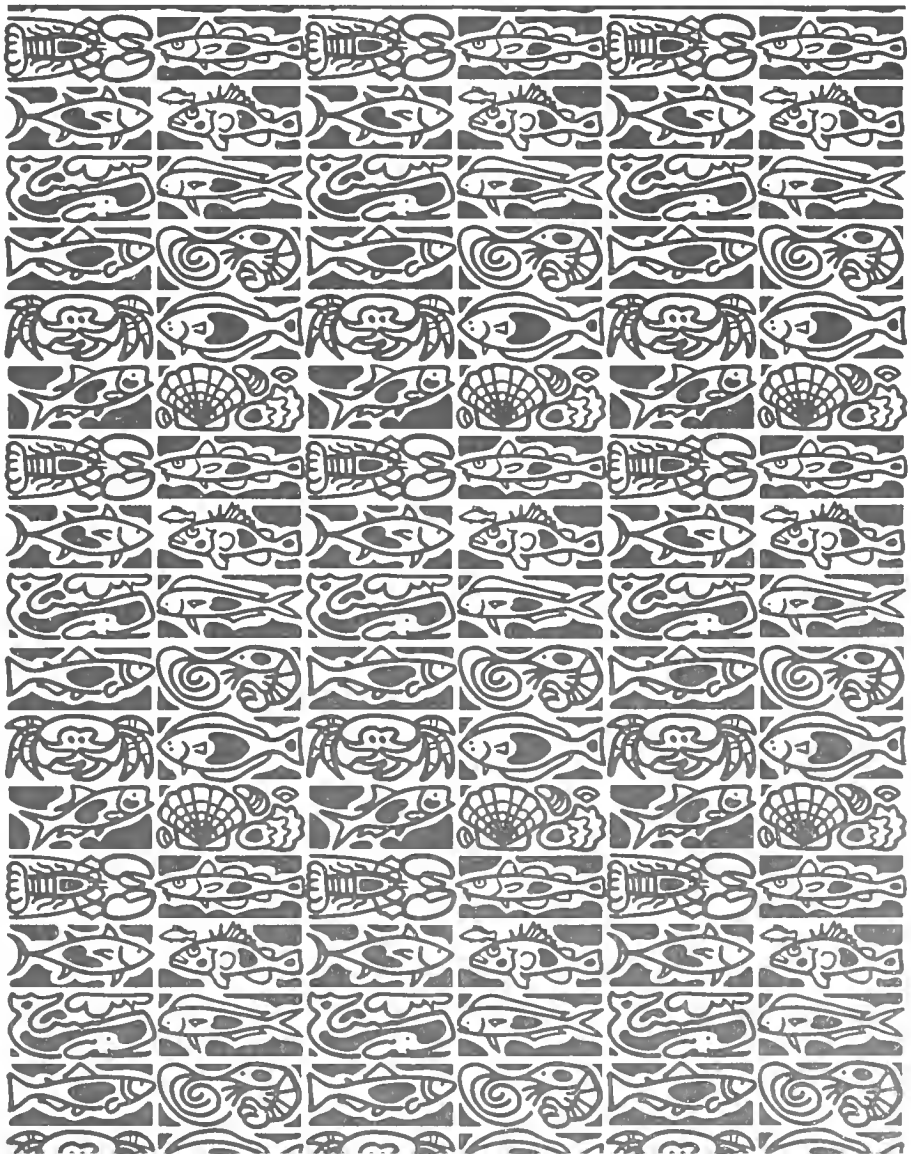

Fishery Bulletin

The *Fishery Bulletin* (ISSN 0090-0656) is published quarterly by the Scientific Publications Office, National Marine Fisheries Service, NOAA, 7600 Sand Point Way NE, BIN C15700, Seattle, WA 98115-0070. Periodicals postage is paid at Seattle, WA, and at additional mailing offices. POSTMASTER: Send address changes for subscriptions to Fishery Bulletin, Superintendent of Documents, Attn.: Chief, Mail List Branch, Mail Stop SSOM, Washington, DC 20402-9373.

The Secretary of Commerce has determined that the publication of this periodical is necessary according to law for the transaction of public business of this Department. Use of funds for printing of this periodical has been approved by the Director of the Office of Management and Budget.

For sale by the Superintendent of Documents, U.S. Government Printing Office, Washington, DC 20402. Subscription price per year: $50.00 domestic and $62.50 foreign. Cost per single issue: $19.00 domestic and $23.76 foreign. **See back for order form.**

The *Fishery Bulletin* carries original research reports and technical notes on investigations in fishery science, engineering, and economics. It began as the Bulletin of the United States Fish Commission in 1881; it became the Bulletin of the Bureau of Fisheries in 1904 and the Fishery Bulletin of the Fish and Wildlife Service in 1941. Separates were issued as documents through volume 46; the last document was No. 1103. Beginning with volume 47 in 1931 and continuing through volume 62 in 1963, each separate appeared as a numbered bulletin. A new system began in 1963 with volume 63 in which papers are bound together in a single issue of the bulletin. Beginning with volume 70, number 1, January 1972, the *Fishery Bulletin* became a periodical, issued quarterly. In this form, it is available by subscription from the Superintendent of Documents, U.S. Government Printing Office, Washington, DC 20402. It is also available free in limited numbers to libraries, research institutions, State and Federal agencies, and in exchange for other scientific publications.

U.S. Department of Commerce
Seattle, Washington

Volume 98
Number 1
January 2000

Fishery Bulletin

Contents

Intrapopulation structure of winter-spawned Argentine shortfin squid, *Illex argentinus* (Cephalopoda, Ommastrephidae), during its feeding period over the Patagonian Shelf

Alexander I. Arkhipkin

Atlantic Research Institute of Marine Fisheries and Oceanography (AtlantNIRO);
5 Dm. Donskoy street, Kaliningrad, 236000 Russia
Present address: Fisheries Department, Falkland Islands Government
PO Box 598, Stanley, Falkland Islands

E-mail address: fish.fig@horizon.co.fk

Abstract.—Stock structure dynamics of the important commercial squid *Illex argentinus* were studied by using biological data from about 25 thousand squid caught January–April 1991 by Russian trawlers in three fishery regions: 51–52°S; 47–49°S within the exclusive economic zone of Argentina (EEZA); and 45–47°S outside the EEZA. A total of 2664 statoliths were read to prepare age-length keys for each 10-day interval of the period studied. It was found that between January and April, the Patagonian shelf south of 45°S was a feeding ground of two intraspecific groups of winter-hatched *I. argentinus*: a shelf group that matured at medium sizes (ShG) and a slope group that matured at large sizes (SlG). After massive immigration of *I. argentinus* from the north in January–February into the two fishery regions within 45–49°S, the stock structure remained rather stable until April, composed predominantly of June- and July-hatched squid. Squid grow and mature rapidly, and males mature at younger ages (from one to two months) than do females. During feeding, some redistribution of the stock was observed: maturing and mature SlG squid (mainly females) tended to shift from the shelf (130–150 m depth) in a northeast direction and concentrate over the shelf edge (160–170 m depth). In April, mature SlG squid began to shift to the continental slope around 45–47°S and migrated to depths >600 m where they then mixed with schools of SlG squid that had fed in the region 51–52°S and that were already migrating northwards along the slope. ShG squid remained on the shelf and made their prespawning northward migrations along the shelf edge.

Manuscript accepted 13 July 1999.
Fish. Bull. 98:1–13 (2000).

The Argentine shortfin squid, *Illex argentinus* (de Castellanos, 1960), is a common neritic species occurring in waters off Brazil, Uruguay, Argentina, and the Falkland Islands in the Southwest Atlantic (Nesis, 1987). This squid is an important world fishery resource. According to the FAO (1997), since 1978, its total annual catch has varied from 180 to 250 thousand metric tons (t), achieving 300–330 thousand tons in 1993–95. However, actual total annual catch of *I. argentinus* could reach up to 700 thousand tons (Uozumi and Shiba, 1993). *Illex argentinus* is captured by the international fleet consisting of both jigging light vessels (mainly from Asian countries) and trawlers (mostly from European countries: Poland, Spain, and Russia (former USSR) in two fishery regions off the Argentine Exclusive Economic Zone (EEZA): at 42°S and 45–47°S. In the 1970s and 1990s, *I. argentinus* was also caught in considerable numbers within the EEZA and Falkland Islands Interim Conservation Zone (FICZ) (Csirke, 1987; FAO, 1997). Such an extensive fishery has induced detailed studies of different biological aspects of *I. argentinus* in order to monitor and forecast its stock structure dynamics.

Originally, *I. argentinus* was considered to be a single stock (Sato and Hatanaka, 1983; Csirke, 1987). Then it was found that the species consisted of two populations differing both by season and place of their spawning: an abundant winter-spawning population (more than 95% of the total stock) and a small summer-spawning population (Hatanaka et al., 1985; Hatanaka, 1988). Brunetti (1988) divided winter-spawning squid into two stocks: the bonaerensis north Patagonian stock (BNPS) and the south Patagonian stock (SPS), differing both by feeding grounds and size of adults (medium and large, respectively). On the basis of occurrence of mature females in different seasons, Nigmatullin (1989a) revealed that *I. argentinus* spawn throughout the year, and proposed to subdivide the total stock into four seasonal spawning groups. Although Tsygankov (1987) found qualitative differences in three loci of esterases extracted from the buccal muscles of various intrapopulational groups of *I. argentinus*, the taxonomic status of these groups, however, still remained unclear. Analysis of dynamics in length-frequency compositions showed that completion of the life cycle of *I. argentinus* populations took one year (Hatanaka et al., 1985; Hatanaka, 1986) and this length of time was then confirmed by statolith aging investigations (Arkhipkin, 1990; Rodhouse and Hatfield, 1990).

The life cycle of the most abundant winter-spawned group can be subdivided into five stages: a postlarval

period that takes place in waters off Brazil and Uruguay in August–September (Leta, 1987; Santos and Haimovici, 1997); a juvenile period that takes place in shelf and oceanic waters off Uruguay and Argentina in September–December (Brunetti, 1988; Parfeniuk et al., 1992); a feeding period that takes place on the Patagonian and Falkland Islands shelves in January–April (Brunetti, 1988; Hatanaka, 1988); a prespawning period that takes place on the shelf edge and slope off Argentina and Uruguay in May–July (Hatanaka, 1986, 1988; Arkhipkin, 1993); and a spawning period that takes place in shelf and slope waters off northern Argentina, Uruguay, and Brazil in July–August (Brunetti, 1988; Santos and Haimovici, 1997). Squid aggregate and are fished mainly during their feeding period on the shelf, as well as during their prespawning period on the shelf edge and slope (Nigmatullin, 1989b).

Stock structure dynamics of *I. argentinus* during their feeding period on the Patagonian Shelf were studied both in the fishery region of 45–47°S outside the EEZA and within the FICZ by using data obtained from Japanese jigging vessels (Rodhouse and Hatfield, 1990; Uozumi and Shiba, 1993). It was found that the age composition of *I. argentinus* catches changed between January and April owing to the gradual migrations of feeding schools of these squid. Earlier hatched squid immigrated to and emigrated from the fishery region earlier than later hatched groups (Uozumi and Shiba, 1993). Squid of the former group had slower growth rates than those of the latter group (Rodhouse and Hatfield, 1990). Data from trawling vessels showed that, during the prespawning period, winter-spawned *I. argentinus* made active northward migrations from the southern Patagonian Shelf along the continental slope of Argentina. Squid migrated in waves of abundance, consisting of 2–4 successive monthly generations. Males moved 2–3 weeks earlier than females of the same monthly group (Arkhipkin, 1993).

An analysis of length-frequency distributions of *I. argentinus* showed that the jigging fishery had a higher selectivity for squid than did the trawl fishery (Koronkiewicz, 1995), and therefore data from the trawl fishery reflected the natural population distribution far better than those from the jigging fishery. In the present report I examined the stock structure dynamics of *I. argentinus* during the January–April feeding period, using both data from two research vessels and two commercial trawlers (both fishing within the fishery) and statolith aging techniques, and comparing these stock structure data with those obtained by the Japanese jigging fishery both within and outside the EEZA. Together with the data obtained during the prespawning period (April–June) (Arkhipkin, 1993), the results of the present study make it possible to reconstruct the full picture of the stock structure dynamics of *I. argentinus* during the entire fishery period.

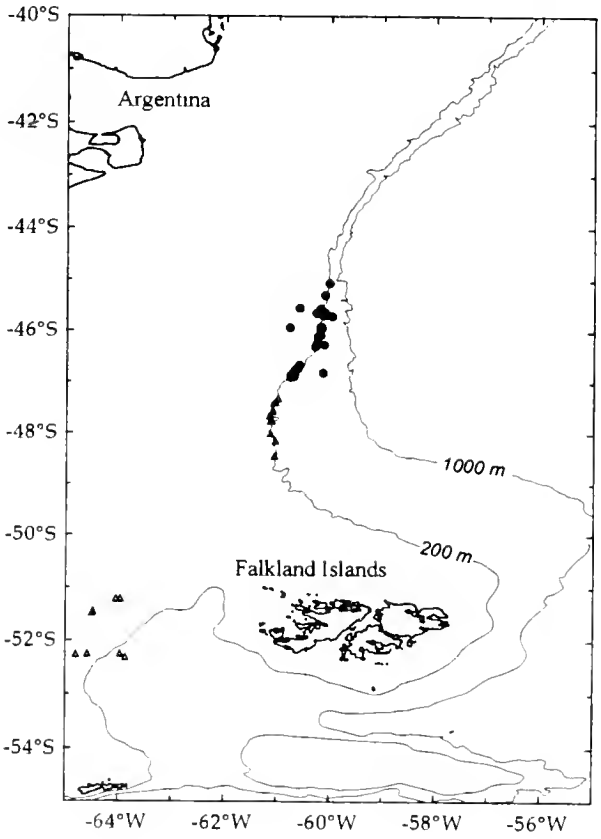

Figure 1

Sampling locations of *Illex argentinus* off (circles) and within (triangles) the Exclusive Economic Zone of Argentina (EEZA) in the southwest Atlantic in January–April 1991.

Materials and methods

Data on the Argentine shortfin squid, *Illex argentinus*, for the present study were collected during four experimental surveys carried out in the fishery region of 45–47°S outside the EEZA by the Soviet research vessels *Anchar* and *Volzhanin* (2700 GRT) and within the EEZA (in 47–49°S and 51–52°S) by the fishing trawlers *Petropavlovskaya krepost* and *Batiliman* (4000 gross registered tonnage [GRT]) between January and April 1991 (Fig. 1). Trawls were conducted with different types of rope trawls with a mean horizontal opening of 60–75 m and mean vertical opening of 40–50 m. Trawls were made in the superficial water layer at night and near bottom in the daytime at bottom depths ranging from 140 to 190 m in January–March

and from 190 to 660 m in April. The duration of trawls ranged from 4 to 8 hours, and the average towing speed was 6–8 km/h.

Every ten days, average daily catch per unit of effort (CPUE) was calculated as a mean of daily CPUEs of the Soviet fishing trawlers that caught squid in each fishery region. Mean CPUEs were calculated separately for the fishery region of 45–47°S outside the EEZA (where a majority of fishing vessels are 2700-GRT trawlers) and for the fishery regions within the EEZA (where all fishing vessels were 4000-GRT trawlers). To obtain an objective picture of the squid fishery, CPUEs of the 2700 GRT trawlers may be adjusted to those of 4000-GRT trawlers by a coefficient of 0.7 (Arkhipkin, 1993).

Length-frequency sampling

A random sample of one hundred squid was taken by scientific observers from each of two catches (at night and day) everyday on board each of the four vessels. Dorsal mantle length (ML) was measured to the nearest 1 mm, total body weight (BW) was weighed to the nearest 1 g. Sex and maturity stages were identified according to the maturity scale elaborated for *Illex argentinus* (Nigmatullin, 1989a). Sex ratio was determined. A total of 16,436 squid were analyzed in the fishery region of 45–47°S outside the EEZA and 9893 squid were analyzed within the EEZA. Every ten days, three length-frequency curves of males and females were constructed for three maturity periods: immature (maturity stages 1–2), maturing (maturity stages 3–5_1) and mature (maturity stages 5_2–5_3).

Age sampling and statolith processing

Every ten days, from January to April, statoliths were dissected from 100–150 individuals of *Illex argentinus* from two successful catches on board each of the four vessels. The length-frequency distribution of the 10-day age sample was proportional to the length-frequency distribution of squid caught during these ten days. Statoliths were washed in distilled water and stored in oil-paper envelopes in 96% ethanol. A total of 1700 statoliths were sampled in the fishery region of 45–47°S outside the EEZA, and 1150 statoliths were collected within the EEZA.

All statoliths sampled were processed by statolith aging techniques in the Laboratory of Commercial Invertebrates of AtlantNIRO (Arkhipkin, 1991). Statolith terminology follows Clarke (1978) and Lipinski et al. (1991). Statoliths were attached to the microscopic slides with Pro-texx mounting medium and were ground on both sides on a wet waterproof sandpaper of 1000-grit grade. During grinding, the statolith rostrum was completely removed, so that growth increments could be easily distinguished from the nucleus to the edge of the dorsal dome. Ground statoliths were embedded in Canada balsam and covered with glass covers. Ready preparations were placed in an oven at 90–100°C for one hour to dry the balsam and improve the readability of growth increments. Statoliths were read under a Biolam R1 light microscope at 450–500× magnification. To avoid possible counting errors, each statolith was counted twice by two observers using the gradation of an eye-piece micrometer. The total number of growth increments for each specimen was obtained as a mean of these replicate counts if the deviation between the two counts was less than 5%. If deviation exceeded 5%, the statolith was recounted by the two observers once more. If such deviation did not decrease after the recounting, the statolith was rejected from further analysis. From the whole sample, 1597 statoliths from the region outside the EEZA (93.9%) and 1067 statoliths from the region within the EEZA (92.7%) were prepared and read.

Length-at-age data analysis

Deposition of putative growth increments within *I. argentinus* statoliths has not yet been validated. However, incorporation of either tetracycline or strontium marks into statoliths of the congeneric species *I. illecebrosus* kept in captivity has shown that growth increments are formed daily (Dawe et al., 1985). Statolith microstructure in both species is similar; therefore growth increments within statoliths of *I. argentinus* are considered to form daily in the present paper. Hence, their total number was considered to represent squid age in days. Hatching dates were backcalculated. Month classes of hatching were defined by pooling squid into each month of hatching (Arkhipkin, 1990; Rodhouse and Hatfield, 1990). Length-at-age data were analyzed separately for both sexes. The 10-day age structure was determined by construction of age-length keys. Age-length keys were constructed by using numbers of squid for each month class separately for each sex and maturity period (Arkhipkin et al., 1996).

Results

CPUE dynamics

Region 45–47°S *Illex argentinus* were caught in all trawls of the research vessels (Fig. 2). In January, schools of squid aggregated mainly north of the region. Trawl catches were variable (from 1 to 20 t per vessel day, t/d), and mean January CPUEs were low (8–9 t/d).

During the first 10-day period of February, concentrations of *I. argentinus* were observed in all parts of the region. Squid concentrated near the bottom during the daytime and ascended to the upper water layers at night. The CPUE was twice as high as in January, and the squid fishery stabilized at 16–17 t/d. However, aggregations of *I. argentinus* quickly dispersed, and during the second 10-day period of February, the CPUE fell sharply to the January level (Fig. 2). Catches of squid were low but stable (around 10 t) until the second 10-day period in April, when fishing vessels shifted from the shelf edge (170–190 m depth) to the continental slope (440–660 m depth) and changed fishing tactics. The vessels performed near-bottom trawls at the shelf edge during the daytime, and on the continental slope at night. These tactics considerably increased CPUE (up to 15–18 t/d) for the third 10-day period of April and in the beginning of May because the fleet began to target not only shelf aggregations but also the slope aggregations of *I. argentinus* that were beginning to appear at that time.

Region 47–49°S Fishing trawlers operated in this region between February and the second 10-day period of March. The fishing tactics were the same as those used in the previous region. Abundance of *I. argentinus* was considerably greater than that in the region outside the EEZA (Fig. 2). The peak of CPUE was observed in the third 10-day period of February (51 t/d).

Region 51–52°S All fishing vessels that had operated in the 47–49°S region moved to the fishing region west of the Falkland Islands during the second 10-day period of March and fished there until the middle of May (Fig. 2). The fishing tactics were different from those used in the two previous regions. Trawlers fished for squid in midwater both at night and in the daytime. CPUE in March–April was high, similar to those in the 47–49°S region with a prominent peak (53 t) during the second 10-day period of April. At the beginning of May, CPUE decreased sharply and the fleet ceased fishing for squid in the region.

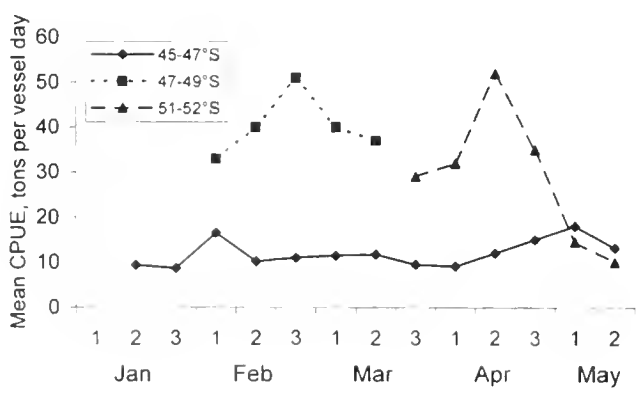

Figure 2

Mean CPUE (tons per vessel day) of the Russian trawlers in the *Illex argentinus* fishery in three fishery regions of the Southwest Atlantic in 1991: 45–47°S (bold solid line), 47–49°S (dotted line) and 51–52°S (dashed line).

Sex ratios

Region 45–47°S The proportion of females was the highest during the second 10-day period of January (ca 80% of the total sample). From the end of January through the beginning of February, the proportion of females decreased sharply (to 55–60%). Sex ratio was close to 1:1 between the second 10-day period of February and the first 10-day period of April, when the proportion of females occurring on the shelf edge decreased to 30%. However during the third 10-day period of April on the continental slope at depths of 480 m, the sex ratio was found to be close to 1:1, and females prevailed in catches (65%) at deeper depths (630 m) (Fig. 3).

Region 47–49°S Except the first 10-day period of February (when the sex ratio was close to 1:1), males always predominated in catches at a ratio of 2:1 (Fig. 3).

Region 51–52°S The sex ratio was close to 1:1, but the proportion of females tended to decrease from 55% to 45% (Fig. 3).

Length and hatching-month composition

Region 45–47°S During the second 10-day period of January, June-hatched maturing females (modal sizes 210 mm ML) and mature males (200 mm) predominated in catches. The proportion of mature May-hatched squid was low. Hatching-month composition changed considerably during the third 10-day period of January owing to an appearance of maturing and mature May-hatched squid (males of 200 mm and females of 220–250 mm ML) in the region (Fig. 4).

Massive appearances of dense schools of immigrating June and July-hatched immature and maturing females (200–220 mm ML) and mature males (200–210 mm ML) were observed in the first 10-day period of February which resulted in a double increase in CPUE of the fishing fleet (Fig. 2) and in corresponding changes in the hatching-month compositions of squid: June-hatched squid

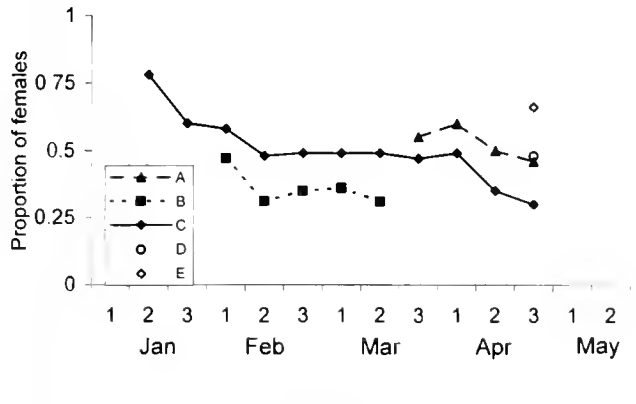

Figure 3

Proportion of females in sex ratio of *Illex argentinus* in three fishery regions of the Southwest Atlantic in 1991: (A) 51–52°S; (B) 47–49°S; and (C–E) 45–47°S. Depths for the last region were 160–190 m (C), 480 m (D), and 630 m (E).

became the most abundant in catches, as in the middle of January. During the second and third 10-day periods of February, hatching-month composition was the same as that of January, with June- and July-hatched squid predominating. However during the third 10-day period, the number of large mature females (280 mm ML) increased considerably (Fig. 4).

In March, the hatching-month composition of the *I. argentinus* catch was approximately similar to that of the second 10-day period of February; June- and July- hatched squid were the most abundant. The proportion of July-hatched squid increased by the end of March with a corresponding decrease in June-hatched squid. Modal sizes of males increased from 220–230 mm ML in the beginning to 230–240 mm ML at the end of the month. Length composition of females was bimodal (240–250 and 290–300 mm ML). The proportion of immature females decreased, whereas the proportion of mature females increased by the end of March (Fig. 5).

In April, hatching-month composition of *I. argentinus* caught over the shelf edge (170–190 m depths) remained almost similar to that of the second and third 10-day periods of March; July-hatched squid were predominant. Almost all males were mature. Immature females disappeared from catches in the first and second 10-day periods of April, but were caught in small numbers in the third 10-day period. At the beginning of the month, the length composition of both maturing and mature females was bimodal (260–270 and 300 mm ML). During the second 10-day period, large maturing and mature females (310 mm ML) began concentrating over the shelf edge, whereas medium-size females (270–280 mm ML) were still dispersed (Fig. 6). These concentrations caused another increase in CPUE for the fishing fleet (Fig. 2). During the third 10-day period of April, large mature squid (females of 310–320 mm ML and males of 270 mm ML) appeared in deeper waters over the continental slope, and they became most abundant at 480–630 m depths. Medium-size squid (maturing females of 280 mm ML and mature males of 250 mm ML) remained over the shelf edge (Fig. 6).

Region 47–49°S During the first 10-day period of February, the length composition of males was unimodal (230 mm ML) and most of these males were mature. Among females, two different modal groups occurred in the catches: immature June-hatched females (220 mm ML) and maturing and mature April- and May-hatched females (260 mm ML). Large catches of June- and July-hatched squid were evident between the second 10-day period of February and first 10-day period of March (Fig. 2). Hatching-month compositions did not change significantly in this period, June- and July-hatched squid were caught almost in equal proportions. Mature males increased slightly in length from 230 to 240 mm ML. The proportion of immature females decreased and that of maturing and mature females increased by the second 10-day period of March (Fig. 7).

Region 51–52°S Hatching-month composition was similar between the third 10-day period of March and second 10-day period of April; July-hatched males and females were predominant in catches. Length compositions were unimodal for both sexes. Except during the third 10-day period of March when about a third of males were maturing, most of the males were mature, and their sizes increased from 260 mm ML at the end of March to 280 mm ML at the end of April. Females grew more rapidly in length than did males (from 280 to 320 mm ML). They matured quickly; immature females prevailed at the end of March, whereas maturing females were predominant at the end of April. During the third 10-day period of April, age composition of *I. argentinus* changed owing to a high proportion of August-hatched squid (Fig. 8).

Comparative comments

Simultaneous sampling in the regions of 45–47°S and 47–49°S between February and March and in the regions of 45–47°S and 51–52°S between March and April enabled a comparison of both length and hatching-month compositions of *I. argentinus* in these regions.

Hatching-month compositions were almost similar in the regions of 45–47°S and 47–49°S during the same 10-day periods (Figs. 4, 5, and 7). Modal sizes

of mature males were about 10–20 mm greater in the southern region than those in the northern region. During the first 10-day period of February, the proportion of large mature females was much higher at 47–49°S (Fig. 7) than at 45–47°S (Fig. 4). After the second 10-day period of February, the opposite situa-

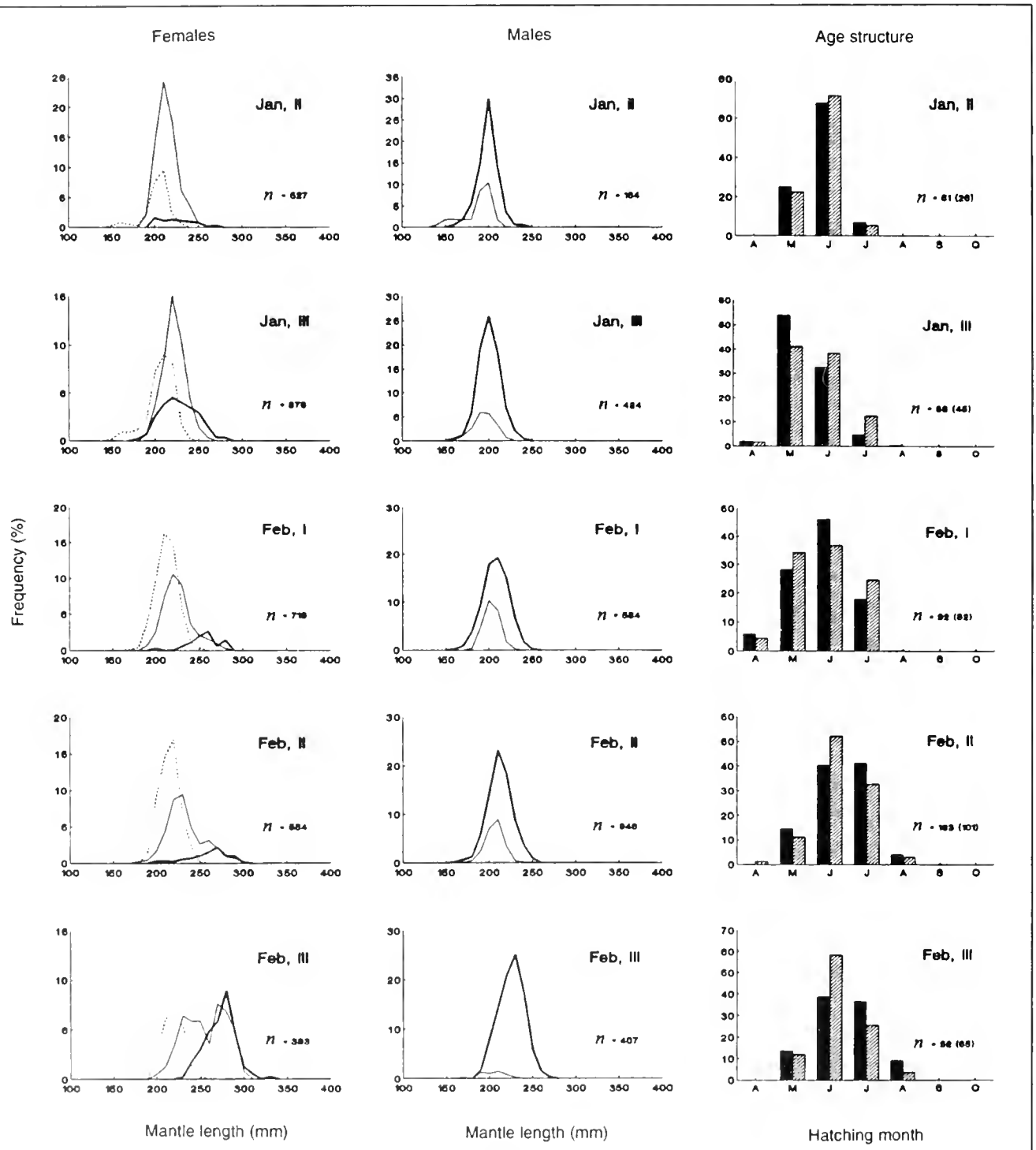

Figure 4

Length-frequency compositions of immature (dotted line), maturing (solid line) and mature (bold solid line) squid and hatching month compositions (age structures) of females (black bars) and males (dashed bars) of *Illex argentinus* in the fishery region of 45–47°S outside the EEZA in January–February 1991. Number of males in parentheses.

tion was observed; the proportion of mature females decreased at 47–49°S and increased at 45–47°S.

Both the length and hatching-month compositions of *I. argentinus* catches were different over the Patagonian Shelf at 45–47°S and 51–52°S. In the southern region, squid were 20–30 mm larger, about a month younger, and less mature than in the northern region, except during the third 10-day period of April when the

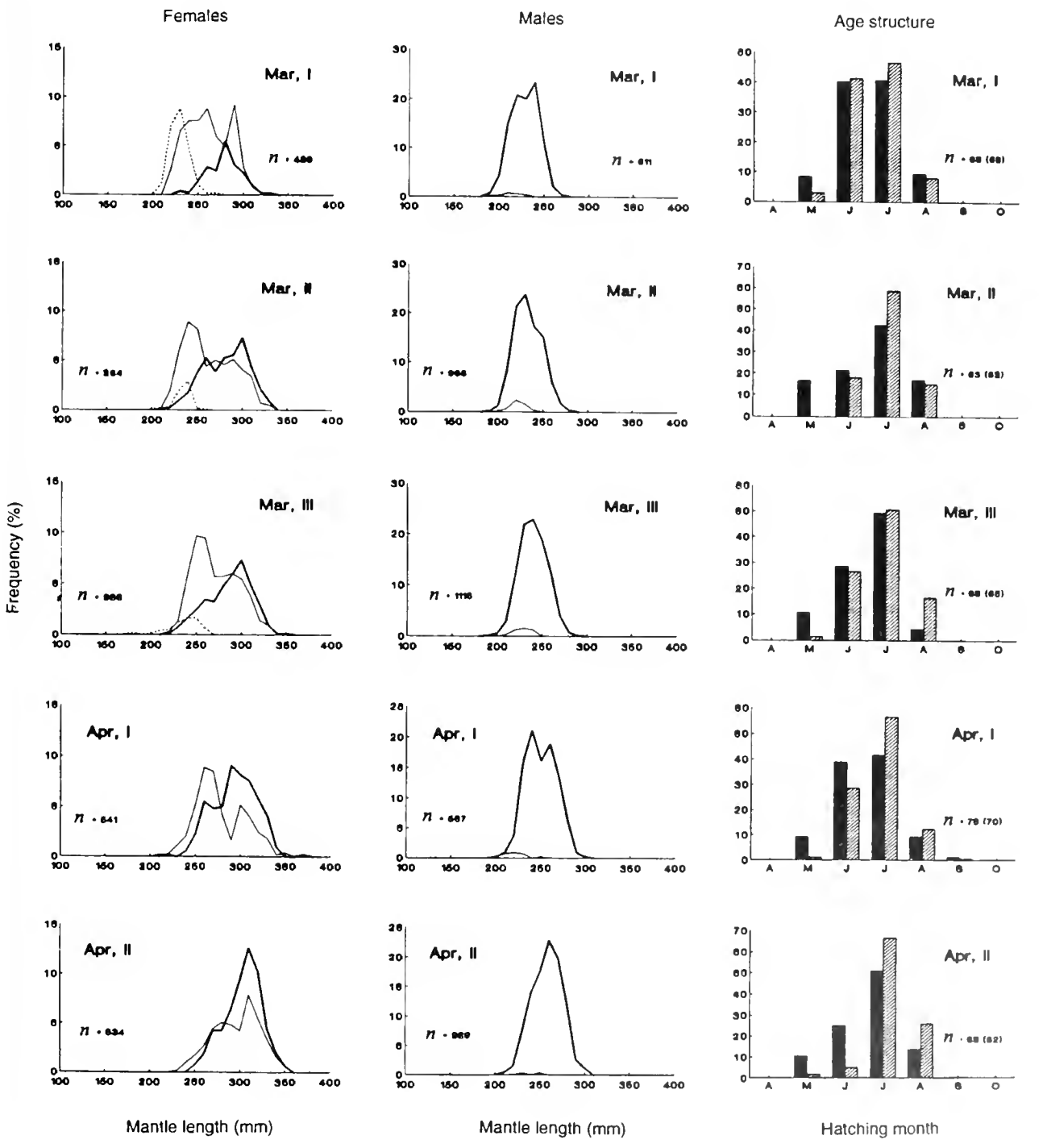

Figure 5

Length-frequency and hatching month compositions (age structures) of *Illex argentinus* in the fishery region of 45–47°S outside the EEZA in March–April 1991. Symbols are the same as in Figure 4.

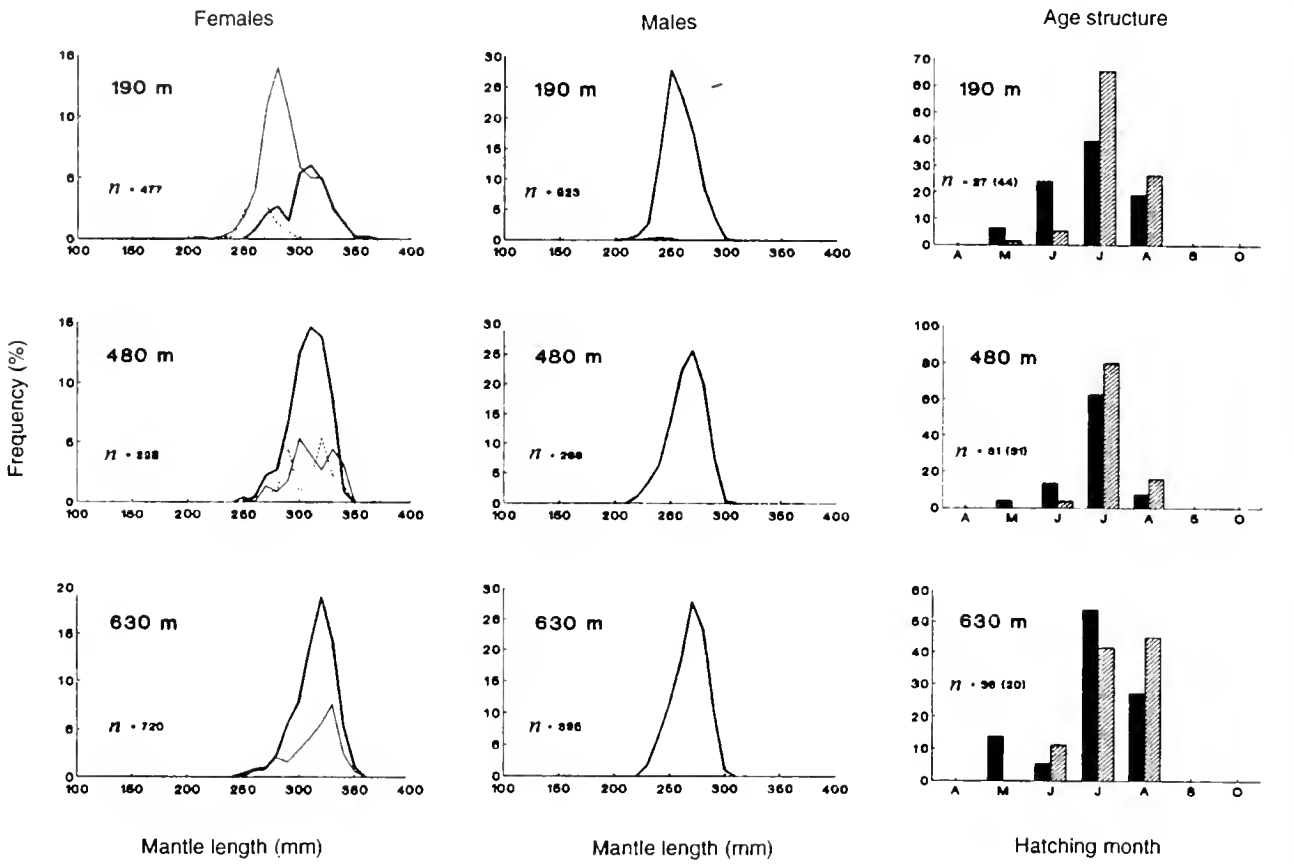

Figure 6

Length-frequency and hatching month compositions (age structures) of *Illex argentinus* at different depths of the fishery region of 45–47°S outside the EEZA between 21 and 30 April 1991. Symbols are the same as in Figure 4.

hatching-month compositions were practically similar to those for the continental slope (630 m) at 45–47°S and shelf (190–210 m) of 51–52°S. However, in spite of the similarity in modal length both in males and females in the last case, most of the females were mature in 45–47°S, whereas those at 51–52°S were still maturing (Figs. 5 and 8).

Discussion

Stock structure dynamics

Studies of the length-at-age structures for immature, maturing, and mature squid (separately) of both sexes, with a 10-day interval, revealed in detail the intrapopulation structure dynamics and migratory patterns of *I. argentinus* during the January–April feeding period on the Patagonian Shelf. Previous investigations, in which length-at-age data were pooled separately for each sex, revealed only general patterns in the age structure dynamics of *I. argentinus* (Rodhouse and Hatfield, 1990; Uozumi and Shiba, 1993).

Stock structure of winter-hatched *I. argentinus* was rather stable during the feeding period (January–April). After massive immigration of June- and July-hatched squid into the region 45–47°S from the end of January through the beginning of February, probably from an area farther north on the Patagonian Shelf (Hatanaka, 1988; Parfeniuk et al., 1992), the age structure of squid remained rather stable until the middle of April. During each 10-day period, from four to five month classes were observed, similar to the number obtained from the jigging fishery data (Uozumi and Shiba, 1993). Predominance of monthly classes changed gradually from June-hatched squid in February to July-hatched squid in March–April.

A considerable portion of the June and July-hatched squid continued their southward feeding migrations and reached 47–49°S by the end of February, which

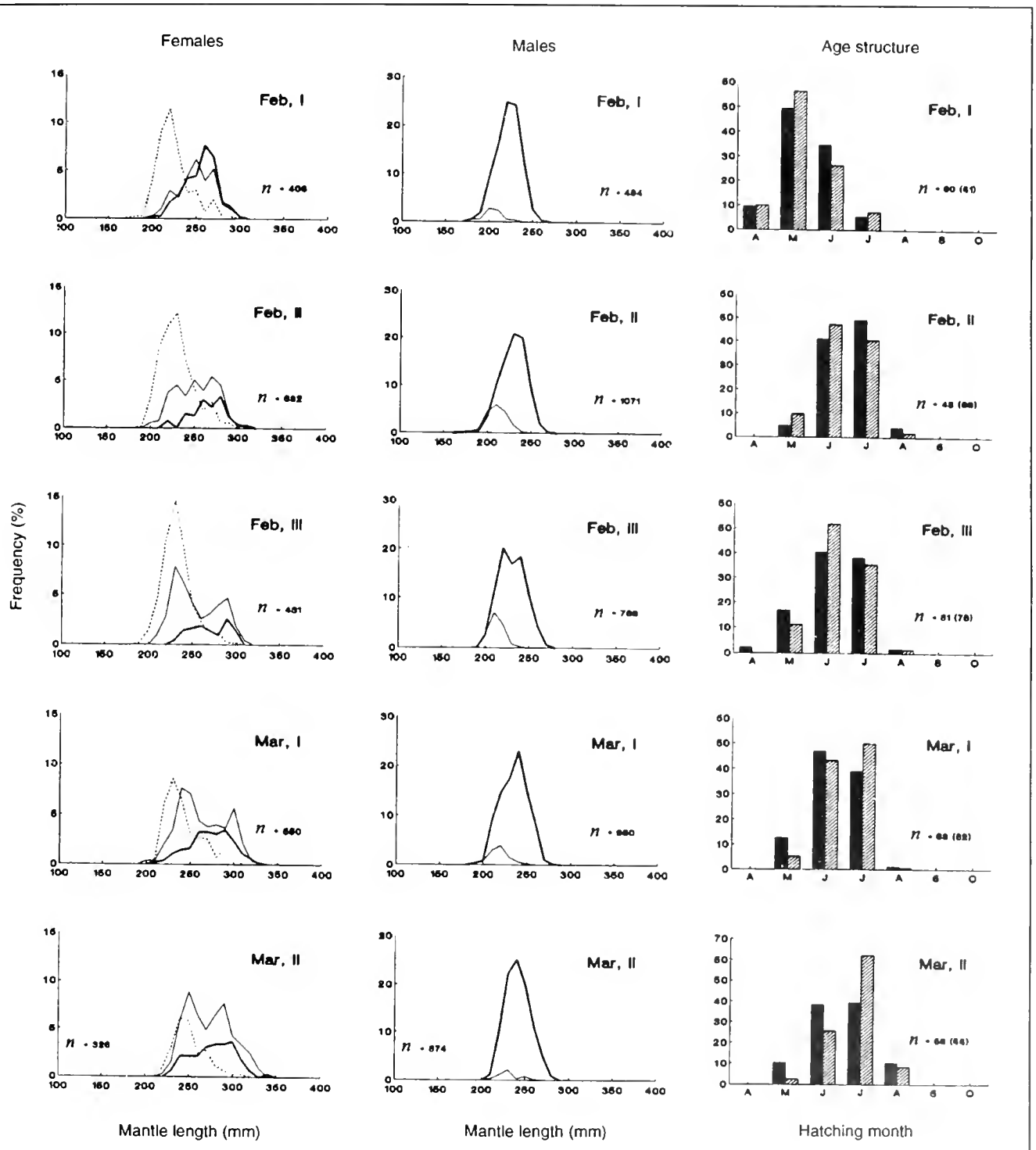

Figure 7

Length-frequency and hatching month compositions (age structures) of *Illex argentinus* of the fishery region of 47–49°S within the EEZA in February–March 1991. Symbols are the same as in Figure 4.

was confirmed both by similar hatching-month compositions and prominent peaks of the CPUE in both regions.

During the feeding period, winter-hatched *I. argentinus* grew rapidly and matured—males maturing at younger ages (from one to two months) than females

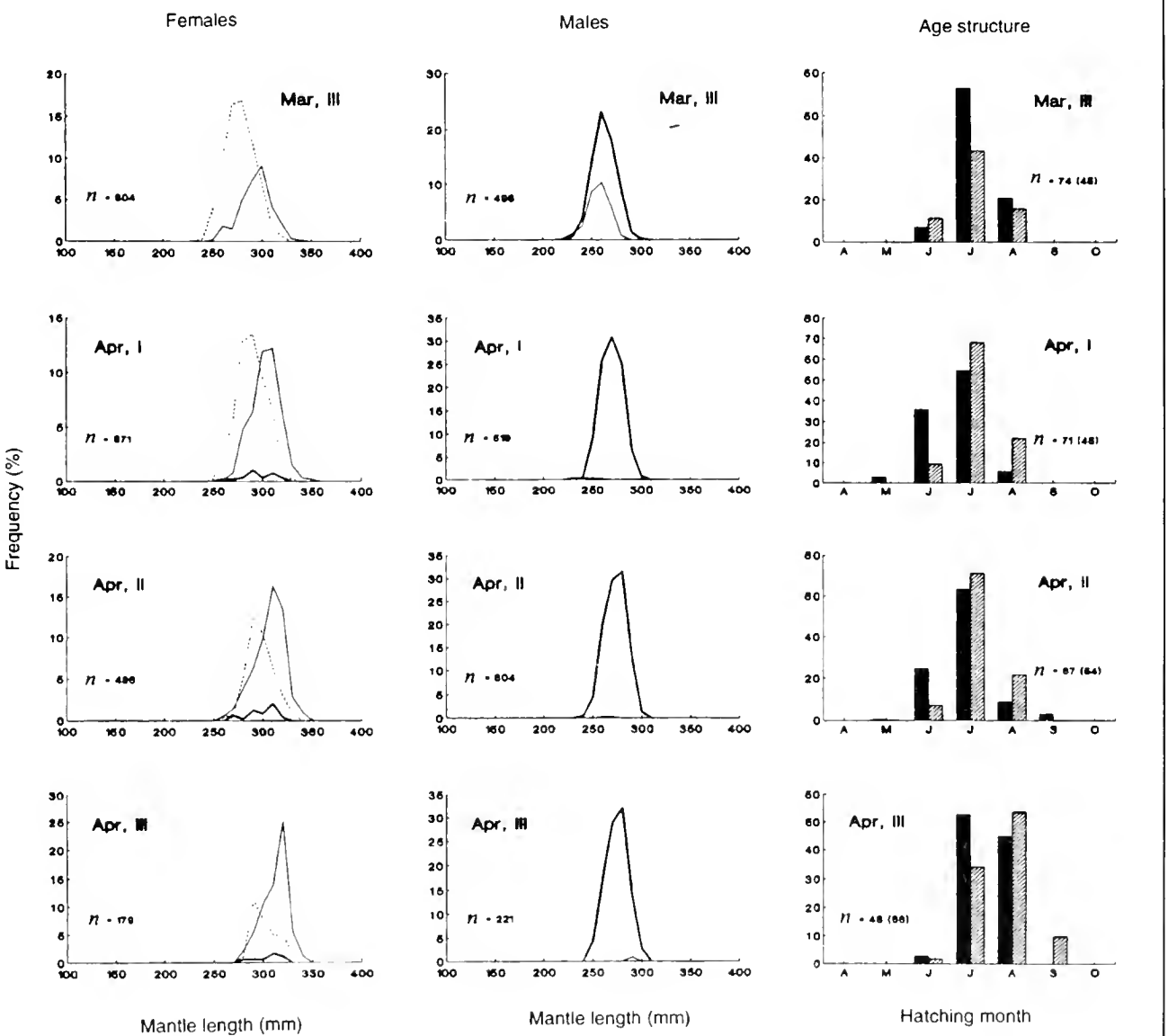

Figure 8

Length-frequency and hatching month compositions (age structures) of *Illex argentinus* of the fishery region of 51–52°S within the EEZA in March–April 1991. Symbols are the same as in Figure 4.

(Arkhipkin, 1990; Rodhouse and Hatfield, 1990). Taking into account the rather stable hatching month compositions during February–April, the squid were not performing any active spatial migrations after their arrival into the region of 45–49°S. Therefore, growth curves that were constructed on the basis of the increase in modal lengths of squid during February–April are valid, and growth rates calculated from these curves are probably close to actual growth rates (Koronkiewicz, 1986; Hatanaka, 1988). During feeding, some redistribution of the *I. argentinus* population was observed; large maturing and mature squid (mainly females) tended to shift from the shelf (130–150 m depth) in a northeast direction and to concentrate over the shelf edge (160–170 m depth). This shift resulted in an increase in their proportion in catches in the region outside the EEZA (45–47°S) and a simultaneous decrease in their proportion within the EEZA (47–49°S). A similar shift of maturing squid from the shelf to the shelf edge has been noted by Brunetti et al. (1998). Probably, this shift of maturing and mature females was also a reason for the consid-

erable predominance of males (2:1) in catches within the EEZA in February–March. Similar sex ratios have also been noted in the fishery region north of the Falkland Islands (Koronkiewicz, 1995). Another explanation for the predominance of males in shelf catches may be the earlier migrations of mature males (in contrast to females) from the southern part of their feeding area through the region of 47–49°S. This migratory pattern occurs during prespawning migrations of *I. argentinus* from the southern part of the Patagonian Shelf (Arkhipkin, 1993).

In April large mature males and females, which had been aggregated over the shelf edge, began to shift to the continental slope and migrate to great depths (>600 m), where they mixed with the already migrating schools of July- and August-hatched squid that had fed in the southern part of the Patagonian Shelf and around the Falkland Islands (Arkhipkin, 1993). Such a redistribution of *I. argentinus* aggregations caused a rather sharp decrease in the CPUE of jigging vessels on the shelf in April–May and a simultaneous regrouping of trawlers—a shift from the shelf to one over the continental slope (Hatanaka, 1988; Nigmatullin, 1989b). Medium-size squid remained on the shelf and probably made their prespawning migrations along the shelf edge.

Stock structure of winter-hatched *Illex argentinus*

From the complex of biological characteristics (statolith microstructure, modal length in different months, sizes at maturity, types of feeding, and prespawning migrations), it is possible to consider the Patagonian Shelf south of 45°S as a feeding ground for two intraspecific groups of winter-hatched *I. argentinus*: the "shelf group that matures at medium sizes" (ShG) and the "slope group that matures at large sizes" (SlG). These two groups correspond well with the bonaerensis north Patagonian stock (BNPS) and south Patagonian stock (SPS) distinguished by Brunetti (1988) by using length-frequency analysis. Later, Brunetti et al. (1998) postulated that the spawning of both groups takes place near the shelf edge and over the continental slope; the BNPS squid spawn north of 43°S in winter, whereas the SPS squid spawn south of 43°S in autumn. It was shown however that the SPS squid definitely migrated from the southern part of the Patagonian and Falkland shelves along the continental slope farther north at 41–42°S (Arkhipkin, 1993), but location of their spawning grounds is still unknown (Haimovici et al., 1998).

The shelf group also corresponds to the winter shelf group (WSG), and the slope group corresponds well to the winter oceanic group (WOG), both (WSG and WOG) of which were distinguished by different locations of juvenile feeding and by type of life cycle (Parfeniuk et al., 1992; Nigmatullin and Laptikhovsky, 1996).

The shelf group of *I. argentinus* has a neritic life cycle, characterized by the following features: spawning in warm waters of the northern part of the species range (27–36°S); southward feeding migrations of juveniles <100–150 mm ML over the Patagonian Shelf; a "shelf" type dark zone within the statolith microstructure (Arkhipkin, 1993); fast juvenile growth but rather slow growth of immature squid; medium sizes at maturation (males at 160–220 mm ML, females at 180–240 mm ML); medium maximum sizes for mature squid (males of 180–260 mm ML, females of 220–320 mm ML); and northward prespawning migrations over the shelf. The slope group of *I. argentinus* has an oceanic-slope life cycle characterized by the following features: slope spawning in the northern part of the species area (27–36°S); southward feeding migrations of juveniles <100–150 mm ML in the open part of the Argentine Basin; an "oceanic" type dark zone within the statolith microstructure (Arkhipkin, 1993); slow juvenile growth but rather fast growth of immature squid; large sizes at maturation (males at 180–240 mm ML, females at 240–340 mm ML); large maximum sizes for mature squid (240–340 mm ML, females up to 280–400 mm ML); and northward prespawning migrations over the continental slope. The taxonomic status of the two groups of winter-spawned *I. argentinus* remains unclear (Arkhipkin and Scherbich, 1991; Parfeniuk et al., 1992; Nigmatullin and Laptikhovsky, 1996; Santos and Haimovici, 1997).

Interannual changes in stock structure

It has been shown that growth rates of *I. argentinus* from the same hatching month vary to a lesser extent between different years from those of the different months of hatching within one year (Arkhipkin and Laptikhovsky, 1994). Thus it is possible to make comparisons of modal lengths of squid from the same month of hatching but in different years. The results of this study (based on data collected by the trawl fishery in 1991) are somewhat different from those obtained from the Japanese jigging fishery in 1989–1990 (Uozumi and Shiba, 1993). Generally, during the same month and in the same region of sampling, a majority of males and females caught by jigs in 1989 were about a month younger and correspondingly 20–30 mm smaller than those sampled by the trawl fishery in 1991 (Figs. 8 and 9 in Uozumi and Shiba, 1993; and Figs. 4 and 5 of the present study). Unfortunately, there are no data on the length-frequency composition of trawl-caught *I. argentinus* in 1989 (Arkhipkin and Laptikhovsky, 1994), and

thus it is difficult to explain the reasons for such a difference in length composition between the two years. It was found that *I. argentinus* caught by jigging gear were significantly larger and more mature (especially females) than trawl-caught squid fished in the same location and time (Koronkiewicz, 1995). Thus, differences in age and length compositions observed in 1989 and 1991 can be explained by interannual changes in population structure of *I. argentinus* rather than by various selectivity of the two different sampling gears.

The results of the present study show that in January–April, the international squid fishery in the southwest Atlantic catches aggregations of both groups of winter-spawned *I. argentinus*. Squid of the shelf group are captured by trawlers and jigging vessels over the depth range of 150–200 m mainly in the region of 45–49°S. Squid of the slope group are caught by trawlers and jigging vessels mainly in the southern part of the Patagonian Shelf within the EEZA (47–51°S) over the depth range of 150–250 m in February–March, and by trawlers over the continental slope (45–47°S) at depths of 600–700 m in April.

Acknowledgments

I gratefully acknowledge the generous help of scientific observers of the trawlers *Anchar, Volzhanin, Petropavlovskaya krepost* and *Batiliman* for data sampling. I would like to thank L. A. Vavilova and A. B. Mikheev for processing statoliths, Ch. M. Nigmatullin and A. Z. Sundakov for discussions and comments on an earlier version of the manuscript. The edtiorial work of Emma Hatfield (NOAA, Woods Hole) and Emma Jones (FIFD, Stanley, Falkland Islands), who helped with the text in English, is most appreciated.

Literature cited

Arkhipkin, A. I.
1990. Edad y crecimiento del calamar *Illex argentinus*. Frente Maritimo 6 (sec. A):25–35.
1991. Methods for cephalopod age and growth studies with emphasis on statolith ageing techniques. *In* P. Jereb, S. Ragonese, and S. von Boletzky (eds.), Squid age determination using statoliths, p. 11–17. Note Tecniche e Reprints dell'Istituto di Tecnologia della Pesca e del Pescato (N.T.R.-I.T.P.P.) Special Publ.
1993. Age, growth, stock structure and migratory rate of prespawning short-finned squid *Illex argentinus* based on statolith ageing investigations. Fish. Res. 16:313–338.

Arkhipkin, A.I., V. A. Bizikov, V. V. Krylov, and K. N. Nesis.
1996. Distribution, stock structure and growth of the squid *Berryteuthis magister* Berry, 1913 (Cephalopoda, Gonatidae) during summer and fall in the Western Bering Sea. Fish. Bull. 94(1):1–30.

Arkhipkin, A. I., and V. V. Laptikhovsky.
1994. Seasonal and interannual variability in growth and maturation of winter-spawning *Illex argentinus* (Teuthida, Ommastrephidae) in the Southwest Atlantic. Aquat. Living Resour. 7:221–232.

Arkhipkin, A. I., and Zh. N. Scherbich.
1991. Crecimiento y estructura intraespecifica del calamar *Illex argentinus* (Ommastrephidae) en imbierno y primavera en el Atlantico Sudoccidental. Scient. Mar. 55(4):619–627.

Brunetti, N.
1988. Contribucion al conocimiento biologico-pesquero del calamar argentino (Cephalopoda, Ommastrephidae, *Illex argentinus*). Trabajo de Tesis presentado para optar al grado de Doctor en Ciencias Naturales, Universidad de la Plata, Mar del Plata, Argentina, 135 p.

Brunetti, N., M. Ivanovic, G. Rossi, B. Elena, and S. Pineda.
1998. Fishery biology and life history of *Illex argentinus*. *In* T. Okutani (ed.), Contributed papers to international symposium on large pelagic squids (July 18–19, 1996), p. 217–232. JAMARC, Tokyo.

Clarke, M. R.
1978. The cephalopod statolith—an introduction to its form. J. Mar. Biol. Assoc. UK. 58:701–712.

Csirke, J.
1987. Los recursos pesqueros patagonicos y las pesquerias de altura en el Atlantico Sud-occidental. FAO Doc.Tec. Pesca 280, Rome, 78 p.

Dawe, E. G., R. K. O'Dor, P. H. O'Dense, and G. V. Hurley.
1985. Validation and application of an ageing technique for short-finned squid (*Illex illecebrosus*). J. Northwest Atl. Fish. Sci. 6:107–116.

FAO Yearbook.
1997. Fishery statistics. Catches and landings, 1995, vol. 80. FAO Fisheries Series 48, 714 p.

Haimovici, M., N. Brunetti, P. G. Rodhouse, J. Csirke, and H. R. Leta.
1998. *Illex argentinus*. *In* P. G. Rodhouse, E. G. Dawe, and R. K. O'Dor (eds.), Squid recruitment dynamics: the genus *Illex* as a model, the commercial *Illex* species and influences on variability, p. 27–58. FAO Fish. Tech. Pap. 376. FAO, Rome.

Hatanaka, H.
1986. Growth and life span of short-finned squid *Illex argentinus* in the waters off Argentina. Bull. Jap. Soc. Sci. Fish., 52:11–17.
1988. Feeding migration of short-finned squid *Illex argentinus* in the waters off Argentina. Nippon Suisan Gakkaishi 54(8):1343–1349.

Hatanaka, H., S. Kawahara, Y. Uozumi, and S. Kasahara.
1985. Comparison of life cycles of five ommastrephid squid fished by Japan: *Todarodes pacificus, Illex illecebrosus, Illex argentinus, Nototodarus sloani sloani* and *Nototodarus sloani gouldi*. NAFO Sci. Counc. Studies 9:59–65.

Koronkiewicz, A.
1986. Growth and life cycle of *Illex argentinus* from the Patagonian shelf and Polish squid fishery in the region, 1978–85. ICES C.M./K 27:1–25.
1995. Size and maturity differences between trawl and jigger caught short-finned squid *Illex argentinus* (Cephalopoda: Ommastrephidae). Acta Ichtyol. Pisc. 25 (1):97–112.

Leta, H. R.
1987. Descripcion de los huevos y juveniles de *Illex argentinus* (Ommastrephidae) y juveniles de *Loligo brasiliensis* (Loliginidae) en la Zona Comun de Pesca Argentino-Uruguaya. Publ. Cient. Instituto Nacional de Pesca (INAPE), Montevideo, Uruguay 1(1):1–8.

Lipinski, M. R., E. G. Dawe, and Y. Natsukari.
1991. Practical procedures of squid ageing using statoliths. A laboratory manual. Introduction. *In* P. Jereb, S. Ragonese, and S. von Boletzky (eds.), Squid age determination using statoliths, p. 77–81. Mazara del Vallo, N.T.R.-I.T.P.P. Special publication 1.

Nesis, K. N.
1987. Cephalopods of the world. T.F.H. Publications, Neptune City, NJ, 351 p.

Nigmatullin, Ch. M.
1989a. Las especies del calamar mas abundantes del Atlantico sudoeste y sinopsis sobre ecologia del calamar *Illex argentinus*. Frente Maritimo 5 (sect. A):7—81.
1989b. Squid of the world ocean. *In* V. V. Ivchenko (ed.), Development of the fishery in the open oceanic waters, p. 26–48. Kaliningrad Book Press, Kaliningrad. [In Russian].

Nigmatullin, Ch. M., and V. V. Laptikhovsky.
1996. Soviet/Russian fishery of the Argentine squid (*Illex argentinus*) in the Southwest Atlantic, its ecological fishing periodicity and probable reasons of anomalous fishery conditions in 1993–1995. *In* V.A. Sushin (ed.), Fishery and biological research carried out by AtlantNIRO in 1994–1995, p. 138–156. AtlantNIRO Press, Kaliningrad. [In Russian with English summary].

Parfeniuk, A. V., Yu. M. Froerman, and A. N. Golub.
1992. Particularidades de la distribucion de los juveniles de *Illex argentinus* en el area de la depresion argentina. Frente Maritimo 12 (sect. A):105–111.

Rodhouse, P. G., and E. M. C. Hatfield.
1990. Dynamics of growth and maturation in the cephalopod *Illex argentinus* de Castellanos, 1960 (Teuthoidea, Ommastrephidae). Phil. Trans. Roy. Soc. Lond. (ser. B) 329:229–241.

Santos, R. A., and M. Haimovici.
1997. Reproductive biology of winter-spring spawners of *Illex argentinus* (Cephalopoda: Ommastrephidae) off southern Brazil. Scient. Mar. 61(1):53–64.

Sato, T., and H. Hatanaka.
1983. A review of assessment of Japanese distant-water fisheries for cephalopods. *In* J. F. Caddy (ed.), Advances in assessment of world cephalopod resources, p. 14–180. FAO Fish. Tech. Pap. 231.

Tsygankov, V. Y.
1987. Squid polymorphous protein systems and an analysis of intraspecific differentiation of *Illex argentinus* (Castellanos). *In* Genetic investigations of marine hydrobionts, p. 243–251. Annals of the III All-Union symposium. Moscow, VNIRO. [In Russian].

Uozumi, Y., and C. Shiba.
1993. Growth and age composition of *Illex argentinus* (Cephalopoda: Oegopsida) based on daily increment counts in statoliths. *In* T. Okutani, R. K. O'Dor, and T. Kubodera (eds.), Recent advances in cephalopod fishery biology, p. 591–605. Tokai Univ. Press, Tokyo.

Microsatellite DNA variation and estimation of stock composition of sockeye salmon, *Oncorhynchus nerka*, in Barkley Sound, British Columbia

Terry D. Beacham
Khai D. Le
Monique R. Raap
Kim Hyatt
Wilf Luedke
Ruth E. Withler

Pacific Biological Station
Department of Fisheries and Oceans
Nanaimo, British Columbia
Canada V9R 5K6

E-mail address (for T.D. Beacham): beachamt@pac.dfo-mpo.gc.ca

Abstract.—Microsatellite DNA variation at six microsatellite loci (Omy77, Ots3, Ots100, Ots103, Ots107, and Ots108) was examined in approximately 900 sockeye salmon, *Oncorhynchus nerka*, collected between 1987 and 1995 from three stocks on the west coast of Vancouver Island, British Columbia, Canada. Variation in allele frequencies among stocks was, on average, about 12 times greater than temporal variation within stocks. Individual locus F_{ST} estimates ranged from 0.013 to 0.107 among stocks, with an overall value of 0.056. Analysis of simulated mixed-stock samples indicated that data from four to six of the microsatellite loci surveyed would enable relatively accurate and precise estimates of stock composition for mixtures composed of fish from the three stocks. Application of the mixture analysis to 1100 fish sampled in Barkley Sound and Alberni Inlet fisheries during 1997 indicated that sockeye salmon from Great Central Lake constituted about 70% of the commercial catch. The later time of return of sockeye salmon from Henderson Lake than of those from Great Central or Sproat Lake as previously indicated by analysis of parasite frequencies was confirmed in the 1997 fishery sampling. Stock composition of catches varied among gears, presumably owing to gear selectivity.

Manuscript accepted 27 April 1999.
Fish. Bull. 98:14–24 (2000).

In the sockeye salmon (*Oncorhynchus nerka*) fishery in Barkley Sound on the west coast of Vancouver Island, three stocks (Sproat Lake, Great Central Lake, and Henderson Lake) account for all of the catch in the mixed-stock fishery (Hyatt and Steer, 1987) (Fig. 1). These stocks have been exploited for over 100 years, but the area of the fishery has changed. The present fishery is conducted over a wide area in Barkley Sound. Lake fertilization has been used to increase production of Barkley Sound sockeye salmon (LeBrasseur et al., 1978; Hyatt and Stockner, 1985). Of the lakes sampled in our study, Great Central Lake has been fertilized most extensively, with annual applications of fertilizer between 1970 and 1973, and from 1977 to the present. Sproat Lake was fertilized between 1985 and 1987, and Henderson Lake has been fertilized from 1976 to the present.

Assessment of the effects of fertilization on the productivity of Great Central and Henderson lakes required accurate and reasonably precise estimates of stock composition in the Barkley Sound sockeye salmon catch. The frequency of occurrence of two myxosporean parasites, *Myxobolus arcticus* in the brain and *Henneguya salmonicola* in the muscle, differed substantially among sockeye salmon in the three lakes during 1977–84 (Quinn et al., 1987), and these differences in prevalence were used to provide estimates of stock composition in the fishery until 1984 (Steer et al., 1986, 1988). Sockeye salmon from Sproat Lake and Great Central Lake accounted for 95% of the catch from 1980 to 1984 (Hyatt and Steer, 1987). In the 1990s, it became apparent that the frequency of occurrence of the two parasites had changed in Great Central Lake sockeye salmon (Beacham et al., 1998), and fishery managers no longer considered estimates of stock composition derived from parasites to be reliable for management decisions. The timing of the change in parasite frequency of occurrence between 1984 and the 1990s was unknown, rendering post-1984 estimates of stock composition and associated estimates of individual lake productivity uncertain. It became imperative to develop a reliable alternative method of stock identification that could be applied to fishery samples for accurate estimation of both catch and productivity by stock.

A preliminary survey of DNA variation at microsatellite loci indicated that there was some differentiation among the Barkley Sound sockeye salmon stocks (Nelson et al., 1998). Evaluation of alternative methods of stock identification indicated that mixture analysis based on microsatellite allele frequencies would likely provide reliable estimates of stock composition (Beacham et al., 1998). In the present study, we expanded the analysis of variation at microsatellite loci of Barkley Sound sockeye salmon to six polymorphic loci, examined the differentiation among and within stocks at each locus, evaluated the precision of data and accuracy of stock composition estimates for a range of mixture sample sizes based on data from three to six loci, and finally used the microsatellite variation to estimate stock compositions from 1997 fishery samples.

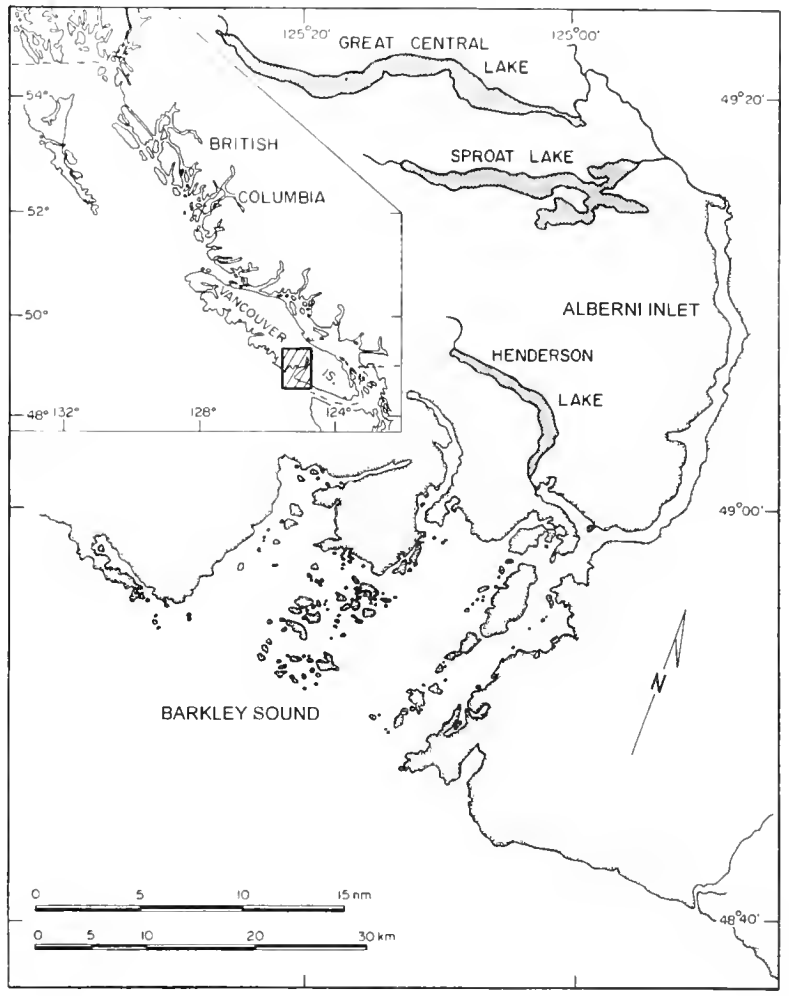

Figure 1

Location of Barkley Sound on Vancouver Island. Sockeye salmon are produced in Great Central Lake and Sproat Lake, both part of the Somass River drainage, as well in Henderson Lake.

Materials and methods

Collection of DNA samples and amplification by PCR

Scales were collected from sockeye salmon returning to spawn in the Sproat Lake and Great Central Lake drainages in 1987, 1990, and 1992. Scales were collected from Henderson Lake sockeye salmon in 1988 and 1993, and liver samples preserved in 95% ethanol were collected in 1995. Scales or operculum punches were collected from sockeye salmon sampled in fisheries in 1997. DNA was extracted from scales as outlined by Nelson et al. (1998). For the operculum or liver samples, approximately 0.3 g of tissue was placed in each well of a 96-well plate containing 0.2 mL of 5% chelex in TE buffer (10 mM Tris pH 7.4, 1 mM EDTA pH 8.0, 0.10 mg/mL proteinase K, and 0.1% SDS) and incubated for 15 min at 50°C, and then incubated for an additional 15 min at 95°C. The supernatant from each well was collected and placed in a fresh 96-well plate and stored at –20°C. About 1 mL of this extract was required for each amplification of the sample by the polymerase chain reaction (PCR).

Loci amplified by PCR were the dinucleotide repeats Omy77 and Ots3 and the tetranucleotide repeats Ots100, Ots103, Ots107, and Ots108 (Table 1). For all primer sets used in this study, PCR was conducted in 25-μL reactions containing 12 pmol (0.48 μM) of each primer, 80 μM of each nucleotide, 20 mM Tris-pH 8.8, 2 mM $MgSO_4$, 10 mM KCl, 0.1% Triton X-100, 10 mM $(NH_4)SO_4$, and 0.1 mg/mL of nuclease-free bovine serum albumin. Each PCR reaction was preceded by an initial denaturation step of three min at 94°C. All cycle extension (30 cycles for all loci except Ots108 which was 35 cycles) steps were for 60 sec at 72°C and all cycle denaturation steps were for 20 sec at 94°C. PCR of Omy77, Ots3, Ots100, Ots103, Ots107, and Ots108 was accomplished with annealing temperatures of 48°C, 50°C, 57°C, 55°C, 48°C, and 46°C, respectively. Annealing times were 30 sec for Omy77 and Ots100, and 60 sec for the other loci.

Gel electrophoresis and band analysis

PCR products were size fractionated on 16 cm × 17 cm nondenaturing polyacrylamide gels and visualized by

staining with 0.5 mg/mL ethidium bromide in water and ultraviolet light illumination. Nelson et al. (1998) provide a complete description of gel electrophoretic conditions. All gels were run for 14–18 h at 65–70 V, using 8% acrylamide for analysis of Ots100 and Ots103, and 10% acrylamide for analysis of Omy77, Ots3, Ots107 and Ots108. Twenty-nine lanes per gel were loaded. One outside lane contained a one-kb ladder (Gibco BRL), three lanes contained a 20-bp ladder (Gensura Labs Inc., Del Mar, CA) evenly spaced across the gel, one lane contained a standard fish to determine precision of estimation of allele size, and 24 lanes contained an individual fish for analysis.

Gels were scanned at a 1024 × 1024 pixel density with a Kodak charge coupled device (CCD) camera with low-light capability and a yellow filter. Images were analyzed by using BioImage Whole Band software (Genomic Solutions Inc., 1995), where the size of the amplified microsatellite alleles were reported to the nearest base pair (bp) based upon the molecular size grid created with the 20-bp markers.

Because some uncertainty occurred in estimation of allele size from the 20-bp grid, we identified alleles on the basis of a binning procedure (Gill et al., 1990). Peaks in the allele frequencies used to identify main alleles and bin widths generally corresponding to a repeat unit were set so that the main allele was located in the middle of the bin. Precision of estimation of allele size was evaluated with the standard fish analyzed for each locus.

Data analysis

Annual variation in allele frequencies within populations was tested with GENEPOP version 3.1 with the Markov-Chain approach by using χ^2 probability values (Raymond and Rousset, 1995). The dememorization number was set at 1000, and 50 batches were run for each test with 1000 iterations/batch (Raymond and Rousset, 1995). Each stock at each locus was tested for departure from Hardy-Weinberg equilibrium by using GENEPOP. Gametic linkage disequilibrium between loci in each population was also evaluated with GENEPOP. Tests of genetic differentiation with three pairwise comparisons among the populations were also conducted with GENEPOP with the Markov-Chain approach by using χ^2 probability values. Critical significance levels for simultaneous tests were evaluated by using sequential Bonferroni adjustment (Rice, 1989). F_{ST} estimates for each locus were calculated with GENEPOP, and the standard deviation of the estimate for an individual locus was determined with FSTAT (Goudet, 1995) by jackknifing over stocks and for all loci combined by bootstrapping over loci. Estimation of variance components of stock differences and annual variation within stocks was determined with BIOSYS (Swofford and Selander, 1981). Principal components of nine (three annual samples multiplied by three stocks) composite arrays of allele frequencies for six loci were calculated with the PRINCOMP procedure in SAS (SAS, 1989).

Estimation of stock composition

The effectiveness of using variation at microsatellite loci for the practical assessment of stock composition in mixed-stock fisheries of Barkley Sound was evaluated from the stand points of precision of stock composition data and accuracy of stock composition estimates in simulated fishery samples. Although only three stocks could contribute to the fishery samples, we wished to determine the sample size required to detect accurately the relatively small proportion of Henderson Lake sockeye salmon that were expected to be present in most fishery samples. In addition, we wished to examine the effect of the number of loci used in the estimation of stock composition. The simulated mixtures were composed of 30% Sproat Lake fish, 60% Great Central Lake fish, and 10% Henderson Lake fish because these proportions are the approximate long-term mean of the Barkley Sound fishery.

Allele frequencies were determined for each locus in each stock, and the model of Fournier et al. (1984) was used to estimate stock composition by the condi-

Table 1

Primer sequences for the microsatellite loci analyzed in the study.

Locus	Sequence (5'–3')	Source
Omy77	F: CGT TCT CTA CTG AGT CAT R: GGG TCT TTA AGG CTT CAC TGC A	Morris et al. (1996)
Ots3	F: CAC ACT CTT TCA GGA G R: AGA ATC ACA ATG GAA G	Banks et al. (1999)
Ots100	F: TGA ACA TGA GCT GTG TGA G R: ACG GAC GTG CCA GTG AG	Nelson et al. (1998)
Ots103	F: AGG CTC TGG GTC CGT G R: TGA TAT GGT GTG ATA GCT GG	Beacham et al. (1998)
Ots107	F: ACA GAC CAG ACC TCA ACA R: ATA GAG ACC TGA ATC GGT A	Nelson and Beacham (1999)
Ots108	F: TCT GTT TAT CTT TCT ATT A R: AAG GAG AGA CAG AGG G	Nelson and Beacham (1999)

tional maximum likelihood method. Baseline genotypic frequencies for each of the three stocks were calculated from the observed allele frequencies under the assumption of Hardy-Weinberg equilibrium. Each baseline stock was resampled with replacement in order to simulate random variation involved in the collection of the baseline samples during the estimation of stock composition of each mixture. Hypothetical fishery samples of 100–300 fish with fixed stock composition were generated by randomly resampling with replacement the baseline stocks, and adding the appropriate number of fish from each stock to the mixture. Estimated stock composition of the mixture was then determined, and the whole process was repeated 100 times to estimate the mean and standard deviation of the individual stock composition estimates.

Table 2

Precision of estimates of allele size (in basepairs) at each microsatellite locus for standard fish run only once per electrophoretic gel. *n* is the number of gels on which allele sizes for a standard fish were estimated. Standard deviation is given in parentheses.

Locus	*n*	Allele size	Range	Allele size	Range
Ots3	15	74.1 (0.35)	74–75	93.1 (0.35)	93–94
Omy77	28	94.9 (0.63)	94–96	110.3 (0.53)	109–111
	24	100.4 (0.53)	100–101	116.0 (0.62)	115–117
	8	104.0 (0.00)	104–104	116.1 (0.64)	115–117
Ots107	46	109.7 (0.55)	109–111	117.7 (0.48)	117–118
Ots108	12	112.1 (0.67)	111–113	184.6 (0.51)	184–185
Ots100	8	158.3 (0.71)	157–159	184.4 (1.30)	183–186
	26	164.5 (0.71)	163–166	181.6 (0.64)	180–183
	11	158.4 (0.50)	158–159	196.5 (0.52)	196–197
Ots103	33	175.1 (0.60)	174–176	213.4 (1.00)	211–215

Fishery samples

In 1997, samples were collected from three commercial gillnet fishery openings in Barkley Sound, a gillnet test fishery, a purse-seine test fishery, the recreational fishery, and an aboriginal fishery. The commercial gillnet fishery was conducted primarily in Barkley Sound, with gillnet mesh sizes ranging from 114 mm (4.5 inches) to 133 mm (5.25 inches). The gillnet test fishery was conducted farther inland at the head of Barkley Sound and at the mouth of Alberni Inlet with a gill net 110 m (60 fathoms) in length and 180 meshes deep, and having a mesh size of 114 mm. Samples from the purse-seine fishery, the recreational fishery, and the aboriginal fishery were derived entirely from Alberni Inlet. The recreational fishery was conducted near the head of Alberni Inlet and the aboriginal fishery, conducted at the head of Alberni Inlet and in the Somass River, was the most terminal fishery. Estimated stock contributions to each sample were determined as a point estimate from all the fish in the sample, and standard deviations of the estimates were derived from bootstrap resampling of both the baseline stocks and the mixture.

Results

Precision of estimation of allele size

Standard deviations of the estimated allele sizes for the heterozygous standard fish analyzed at each locus ranged from 0.00 to 1.30 and tended to increase with allele size (Table 2). For both alleles at Ots3, 100% of the estimated sizes for each allele spanned a 2-bp interval. For alleles <110 bp at Omy77, 93% (56/60) of the estimated sizes of the allele were in a 2-bp interval, as were 90% of the estimated sizes of alleles between 110 and 120 bp. Estimated sizes of alleles of the standard fish that were analyzed at the other loci were all estimated within a 4-bp interval for alleles <200 bp, with 85% of the estimated sizes of the larger allele (213 bp) at Ots103 within a 4-bp interval.

Variation within stocks

All six microsatellite loci examined were polymorphic for all three stocks. Observed heterozygosity of the loci examined over all stocks was as follows: Omy77 0.70 (stock range 0.61–0.80), Ots3 0.67 (0.64–0.70), Ots100 0.75 (0.69–0.79), Ots103 0.83 (0.81–0.86), Ots107 0.28 (0.17–0.40), and Ots108 0.85 (0.80–0.89). Significant departures (correction for three tests per locus, α=0.0167) from the expected Hardy-Weinberg distribution of genotypic frequencies were observed at the Omy77 locus in all stocks, owing, in the case of Sproat and Henderson lakes, to a deficiency of heterozygotes. A similar significant heterozygote deficiency was also detected at Ots108 in Sproat Lake sockeye salmon. Significant annual variation (correction for six tests per stock, α=0.0083) in allele frequencies was observed at Omy77 in Sproat Lake and Henderson Lake sockeye salmon, and at Ots108 in Henderson Lake sockeye salmon. No significant linkage disequilibrium between any pair of loci in any stock was observed.

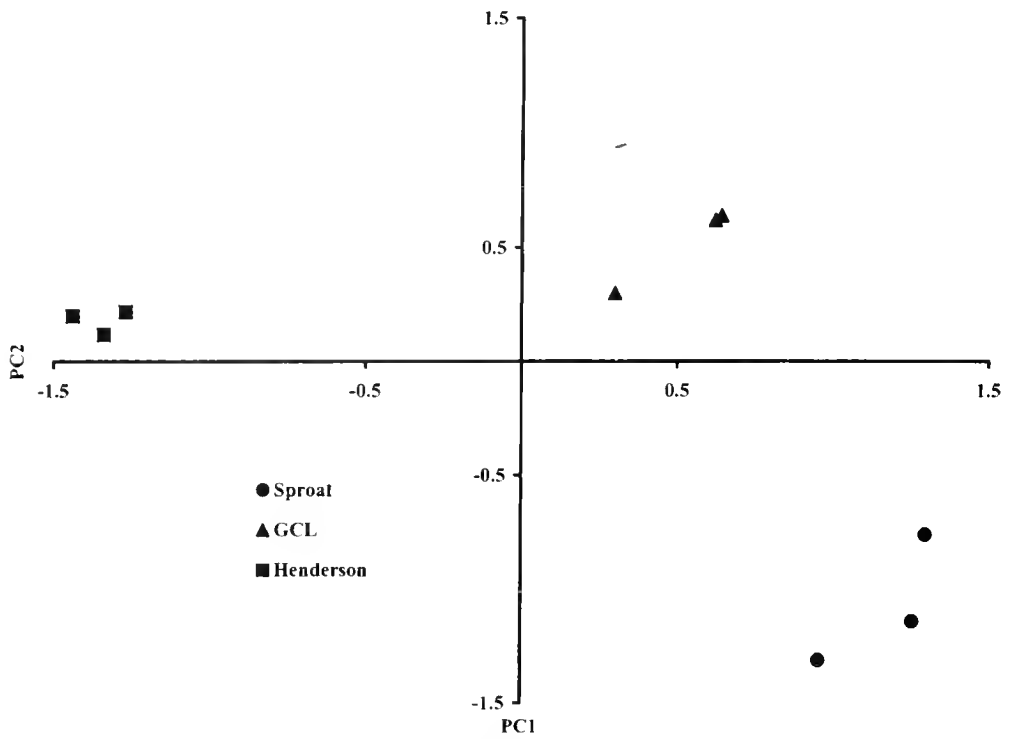

Figure 2

Plot of the first two principal components incorporating variation at microsatellite loci for Great Central Lake (GCL), Sproat Lake, and Henderson Lake sockeye salmon sampled in each of three years.

Variation among stocks

The three sockeye salmon stocks in Barkley Sound were genetically distinct at all six loci examined. All pairwise tests of allele frequencies among stocks were highly significant at all loci ($P<0.001$). At Omy77, the frequency of the Omy77^{94} allele ranged from 0.005 in Henderson Lake sockeye salmon to 0.449 in Sproat Lake fish, and the frequency of Omy77^{104} ranged from 0.216 in Sproat Lake fish to 0.546 in Henderson Lake fish (Table 3). Substantial differentiation in allelic frequencies among stocks was observed at Ots3. For example, the frequency of Ots3^{88} in Henderson Lake sockeye salmon was 0.114, whereas in Sproat Lake fish it was 0.543. Similarly, the frequency of Ots3^{99} was 0.059 in Sproat Lake fish and 0.243 in Henderson Lake fish. At Ots100, the frequency of Ots100^{158} ranged from 0.256 in Sproat Lake sockeye salmon to 0.504 in Henderson Lake fish (Table 3). Although the three stocks were distinct at Ots103, the allele frequency variation was less marked at that locus. At Ots107, the combined frequency of four alleles (81, 109, 113, 117) was greater than 0.95 in all stocks, but stock differentiation was nonetheless apparent. For example, the frequency of Ots107^{81} was 0.135 in Great Central Lake sockeye salmon, but < 0.010 in the other two stocks (Table 3). Variation in allelic frequencies at Ots108 was evident among stocks, with the frequency of Ots108^{122} ranging from 0.000 to 0.196. Strong genetic differentiation among these three stocks was evident at all six microsatellite loci.

Comparison of the relative magnitude of differentiation among stocks and among samples from the same stock collected in different years showed that differentiation among stocks always exceeded temporal variation within stocks and was on average 12 times greater (Fig. 2; Table 4). At Ots3, the differences among stocks were 235 times greater than the observed annual variability. With data combined over years, individual locus F_{ST} estimates ranged from 0.013 to 0.107, with an overall value of 0.056 (Table 4). The loci displaying the greatest differentiation among stocks were Ots3 and Omy77, whereas Ots103 displayed the least differentiation. Sproat Lake and Great Central Lake stocks, both in the same river drainage, were genetically the most similar (pairwise F_{ST} estimate over all loci: 0.032). The Great Central Lake and Henderson Lake stocks were more genetically distinct

Table 3

Observed allele frequencies at six microsatellite loci for three stocks of Barkley Sound sockeye salmon. Alleles have been designated by the lower size limit of the bin. *n* is the number of fish scored at each locus in each stock.

Allele	Sproat	Great Central	Henderson	Allele	Sproat	Great Central	Henderson
Omy7				Ots103			
n	264	303	305	*n*	221	304	308
90	0.000	0.000	0.002	144	0.007	0.021	0.000
92	0.011	0.003	0.002	152	0.043	0.026	0.000
94	0.449	0.172	0.005	156	0.027	0.002	0.002
96	0.042	0.020	0.000	160	0.009	0.018	0.003
98	0.006	0.007	0.000	164	0.034	0.008	0.013
100	0.125	0.231	0.277	168	0.016	0.015	0.006
102	0.011	0.015	0.030	172	0.038	0.033	0.019
104	0.216	0.361	0.546	176	0.020	0.025	0.034
106	0.002	0.002	0.020	180	0.029	0.064	0.080
108	0.040	0.005	0.000	184	0.032	0.076	0.057
110	0.051	0.054	0.100	188	0.050	0.178	0.073
112	0.002	0.003	0.002	192	0.305	0.268	0.312
114	0.004	0.086	0.008	196	0.269	0.151	0.185
116	0.038	0.040	0.010	200	0.075	0.079	0.130
118	0.004	0.002	0.000	204	0.043	0.028	0.071
Ots3				208	0.002	0.008	0.011
n	219	296	303	212	0.000	0.000	0.003
74	0.112	0.127	0.086	Ots107			
78	0.000	0.000	0.003	*n*	269	307	310
80	0.000	0.000	0.002	81	0.006	0.135	0.000
82	0.000	0.003	0.005	101	0.000	0.002	0.000
84	0.002	0.000	0.000	105	0.000	0.000	0.005
86	0.000	0.002	0.000	109	0.084	0.062	0.053
88	0.543	0.378	0.114	113	0.866	0.762	0.913
92	0.002	0.007	0.000	117	0.030	0.036	0.029
93	0.274	0.394	0.526	121	0.015	0.003	0.000
96	0.000	0.002	0.005	Ots108			
97	0.007	0.005	0.013	*n*	214	199	269
99	0.059	0.073	0.243	122	0.196	0.106	0.000
103	0.000	0.005	0.000	126	0.014	0.035	0.004
105	0.000	0.005	0.003	130	0.002	0.000	0.000
Ots100				133	0.002	0.000	0.000
n	242	321	282	137	0.000	0.128	0.002
130	0.010	0.003	0.000	141	0.002	0.008	0.002
134	0.039	0.006	0.000	145	0.007	0.010	0.000
138	0.000	0.002	0.000	149	0.121	0.038	0.035
142	0.006	0.000	0.002	153	0.056	0.098	0.007
150	0.008	0.002	0.004	156	0.136	0.095	0.178
154	0.025	0.037	0.025	160	0.086	0.146	0.229
158	0.256	0.364	0.504	164	0.189	0.163	0.158
162	0.169	0.064	0.133	168	0.042	0.070	0.048
166	0.052	0.047	0.064	172	0.035	0.038	0.043
170	0.002	0.003	0.007	177	0.068	0.050	0.216
174	0.002	0.006	0.004	182	0.016	0.010	0.039
179	0.324	0.202	0.193	187	0.019	0.005	0.035
184	0.085	0.115	0.050	192	0.005	0.000	0.004
190	0.008	0.107	0.007	197	0.002	0.000	0.000
195	0.012	0.039	0.009				
200	0.000	0.002	0.000				

(pairwise F_{ST} estimate: 0.042), and the Sproat Lake and Henderson Lake stocks showed the greatest differentiation (pairwise F_{ST} estimate: 0.091).

Estimation of stock composition

The three loci with the highest F_{ST} estimates (Omy77, Ots3, and Ots107) also possessed the highest ratio of spatial to temporal variation (Table 4) and were therefore selected to form the core database for the analysis of the simulated mixtures. The number of loci used in the determination of stock composition or mixture sample size had little effect upon the accuracy of the estimated stock compositions (Table 5). Precision of the estimated stock compositions increased as both the number of loci and mixture size used in the determination increased. However, different options were available to obtain estimates of a desired precision. For example, higher levels of precision were obtained with four loci (Omy77, Ots3, Ots107, Ots100) in conjunction with a 150-fish sample size (600 units of data) than with all six loci and a 100-fish sample (600 units of data) (Table 5). The coefficient of variation for the estimated proportion of the predominant Great Central Lake stock was always less than that for estimated proportions of the other two stocks in the mixture. For the 4 loci in 150-fish mixture analysis, the coefficient of variation for the estimated proportion of Great Central Lake fish was 12%, whereas it was 22% for Sproat Lake fish, and 38% for Henderson Lake fish. The simulations indicated that fewer than six microsatellite loci could be used to provide reasonably precise data and accurate estimates of sockeye salmon stock composition for Barkley Sound fishery samples.

Conditional maximum likelihood estimation can overestimate the relative abundance of rare stocks. For Barkley Sound, this would likely be the Henderson Lake stock. The precision of data and accuracy of stock compositions estimates were investigated for mixture samples of 100 fish composed of 2% Henderson Lake (38% Sproat Lake, 60% Great Central Lake) and 5% Henderson Lake (35% Sproat Lake, 60% Great Central), where stock compositions were estimated by using the four microsatellite loci (Omy77, Ots3, Ots100, and Ots107) generally used for estimation of stock compositions in the 1997 fishery samples. Estimated stock compositions of the simulated 100 mixtures for the 2% Henderson Lake composition were 2.5% (SD=3.1%) Henderson Lake, 34.3% (SD=9.3%) Sproat Lake, and 60.4% (SD=9.3%) Great Central Lake. For the 5% Hender-

Table 4

F_{ST} estimates and the ratio of the variance components attributable to among and within stock differentiation (over time) for six microsatellite loci of Barkley Sound sockeye salmon. Standard deviation of F_{ST} estimates is given in parentheses.

Locus	F_{ST}	Variance ratio
Omy77	0.107 (0.094)	20.3
Ots3	0.099 (0.089)	235.2
Ots100	0.027 (0.013)	5.8
Ots103	0.013 (0.007)	3.9
Ots107	0.043 (0.035)	6.3
Ots108	0.039 (0.018)	3.6
All	0.056 (0.032)	11.8

Table 5

Average estimated stock composition (%) of simulated mixtures of Barkley Sound sockeye salmon based on variation at three to six microsatellite loci. True mixture percentages were as follows: Sproat Lake 30%, Great Central Lake 60%, and Henderson Lake 10%. The three loci initially used to estimate the percentages of the mixtures were Omy77, Ots3, and Ots107, and Ots100, Ots108, and Ots103 were added sequentially. Each mixture was generated 100 times with replacement, and stock compositions of the mixtures were estimated by resampling each baseline stock with replacement to obtain a new distribution of allele frequencies, with the same sample size in the new distribution as in the original one. Standard deviation is given in parentheses.

Source and loci	Mixture size (no. of fish)			
	100	150	200	300
Sproat Lake				
3	30.7 (9.98)	31.1 (8.51)	30.8 (6.81)	30.7 (6.48)
4	30.7 (8.21)	30.8 (6.87)	30.8 (6.38)	30.2 (4.44)
5	30.1 (7.54)	30.6 (5.87)	30.0 (4.44)	29.4 (4.18)
6	31.2 (7.23)	29.0 (5.27)	29.8 (4.42)	29.8 (4.00)
Great Central Lake				
3	60.5 (11.74)	60.1 (9.27)	60.2 (7.40)	59.7 (7.74)
4	60.4 (9.41)	59.8 (7.40)	59.7 (6.88)	60.7 (5.21)
5	60.1 (8.26)	60.0 (6.63)	60.1 (5.11)	60.8 (4.50)
6	58.8 (8.03)	60.9 (5.96)	60.1 (5.09)	59.9 (4.31)
Henderson Lake				
3	8.8 (5.62)	8.8 (4.84)	9.0 (3.89)	9.6 (3.98)
4	8.8 (5.30)	9.3 (3.53)	9.6 (3.52)	9.1 (2.89)
5	9.8 (4.56)	9.5 (3.73)	9.9 (2.76)	9.8 (2.52)
6	10.0 (4.33)	10.1 (3.70)	10.0 (2.81)	10.3 (2.39)

son Lake composition, estimated stock compositions were 5.3% (SD=3.9%) Henderson Lake, 34.3% (SD=8.2%) Sproat Lake, and 60.4% (SD=8.9%) Great Central Lake. No significant bias was observed when Henderson Lake sockeye salmon composed 5% or less of the mixture.

Application of estimates to 1997 fisheries

Although estimated stock contributions varied according to sampling period, sockeye salmon from Great Central Lake tended to predominate in all fisheries at any week (Table 6). However, differences in stock composition estimates among fishing gears were evident. In the commercial gillnet fishery, Great Central Lake sockeye salmon constituted about 70% of the catch (Table 6). In the gillnet test fishery, the proportion of Great Central Lake sockeye generally varied between 55 and 75% prior to July 25th. In the purse-seine test fishery, they accounted for about 50–55% of the catch. Higher proportions of Great Central Lake sockeye salmon were observed in the selective gillnet gear than in the more nonselective purse-seine gear. For example, for the week ending 4 July, Great Central Lake sockeye were estimated to have represented 70–75% of the catch in the commercial gillnet fishery and in the gillnet test fishery, but only about 40% of the catch in the seine test fishery. Although the samples analyzed from the purse-seine fishery were derived from more inland locations than those from the commercial and test gillnet fisheries, the differences in proportions of Great Central sockeye salmon more likely resulted from differences in gear selectivity than from differences in stock distribution because fish from all three stocks are generally distributed throughout Barkley Sound and Alberni Inlet when present.

Sockeye salmon stock from Henderson Lake are the smallest salmon exploited in the fishery, and thus the most vulnerable to overfishing in the mixed-stock harvest that takes place. Henderson Lake fish, which do not have to travel through Alberni Inlet in their spawning migration, were apparently caught in fisheries throughout Alberni Inlet, although there was a high degree of uncertainty about whether they were caught in the aboriginal fishery at the extreme head of Alberni Inlet (Table 6). Henderson Lake sockeye salmon generally represent 10% or less of the catch, except for sockeye salmon sampled after 18 July in the gillnet test fishery, when the relative abundance of Henderson Lake sockeye salmon substantially increased. By late July, Henderson Lake sockeye salmon constituted nearly 30% of the gillnet test fishery sample.

Table 6

Estimated stock compositions (%) for sockeye salmon from three lakes sampled in gillnet test fisheries, seine test fisheries, commercial fishery openings, a native fishery, and recreational fishery in Barkley Sound during 1997. Four loci (Ots3, Ots100, Ots107, and Omy77) were used to estimate stock composition. *n* is the number of fish analyzed, and standard deviation of the estimates is given in parentheses.

Source	Week ending	*n*	Sproat	Great Central	Henderson
Commercial	4 Jul	118	25.8 (7.3)	73.9 (8.2)	0.3 (2.8)
Commercial[1]	11 Jul	95	22.3 (6.2)	71.1 (7.9)	6.2 (3.8)
Commercial[1]	18 Jul	95	29.7 (6.9)	63.0 (7.8)	7.3 (4.8)
Seine	27 Jun	120	35.9 (7.3)	56.6 (8.0)	7.5 (3.4)
Seine	4 Jul	111	48.4 (8.6)	42.2 (10.4)	9.0 (5.4)
Seine	18 Jul	117	37.3 (7.0)	59.6 (7.8)	3.1 (4.6)
Gillnet	20 Jun	50	34.4 (10.3)	65.6 (10.4)	0.0 (0.9)
Gillnet	27 Jun	50	36.2 (10.9)	51.0 (12.9)	12.9 (6.8)
Gillnet	4 Jul	50	21.2 (9.2)	71.9 (10.5)	6.7 (5.1)
Gillnet	11 Jul	50	33.1 (9.7)	54.1 (11.7)	12.8 (7.7)
Gillnet	18 Jul	50	24.5 (11.8)	72.2 (13.6)	3.4 (6.3)
Gillnet	25 Jul	50	19.9 (11.5)	60.0 (13.8)	20.2 (9.1)
Gillnet	1 Aug	50	28.2 (11.6)	42.7 (13.7)	29.1 (10.3)
Aboriginal	18 Jul	86	45.0 (8.4)	52.8 (8.5)	2.2 (2.3)
Recreational	18 Jul	33	33.5 (12.3)	54.8 (13.3)	11.7 (8.4)

[1] Additional loci, Ots103 and Ots108, were used in estimation of stock composition.

Discussion

DNA variation at microsatellite loci is becoming an increasingly important tool in fisheries research and management (see review by O'Connell and Wright [1997]). In salmonids, microsatellite loci are generally characterized by high levels of variability and differentiation among spawning populations (Angers et al., 1995; McConnell et al., 1997; Seeb et al., 1998), even in very localized areas (Beacham and Dempson, 1998). The feasibility of applying biological markers to salmon stock identification is enhanced when they display limited annual variation. With temporal stability of the discriminating characters, annual surveys of contributing populations are unncecssary once they have been adequately characterized. As for other neutral genetic markers (Wood et al., 1994; Beacham et al., 1996), temporal stability of allele frequencies at microsatellite loci has generally been observed in salmonid populations (Small et al., 1998). For popula-

tions in which annual variation has been detected, the magnitude of variation has been substantially less than that among populations (Nielsen et al., 1997; Beacham and Wood, 1999).

For sockeye salmon, in which the greatest geographic determinant of neutral genetic differentiation is the nursery lake (Wood, 1995), the task of identifying the contributions of three different lake systems to a mixed-stock sample should be relatively straightforward. Although significant genetic variation can occur among spawning sockeye salmon subpopulations isolated by time or space (or both) within a lake system, the extent of this variation is consistently much less than that observed among lakes—even those lakes within a single drainage system (Wood, 1995). Each of the three lakes is the confluence of multiple tributaries and may harbor genetically differentiated subpopulations of sockeye salmon. The spawning ground samples in our study were collected from locations within each lake system at which fish from more than one subpopulation may have been present, and different subpopulations may have been sampled among years. Thus, the departure of Omy77 (and Ots108 for Henderson Lake) genotypes from Hardy-Weinberg equilibrium and significant annual variation observed at these loci might both have reflected subpopulation differentiation in allele frequencies. It is unlikely that the heterozygote deficiency observed at Omy77 in Sproat Lake and Henderson Lake sockeye salmon would be a result of a null allele because genotypic frequencies of other sockeye salmon stocks surveyed at this locus have been in Hardy-Weinberg equilibrium (Beacham and Wood, 1999). Nevertheless, the level of differentiation at Omy77 was about 20 times greater among lakes than was the temporal variation observed within lakes. For all six microsatellite loci surveyed, differences among lakes were on average 12 times greater than variation within populations, confirming the relative stability of the microsatellite loci in Barkley Sound sockeye salmon populations over the 5–8 yr sampling period.

The six microsatellite loci used in the current study were also surveyed in nine sockeye salmon stocks of the Nass River drainage in northern British Columbia (Beacham and Wood, 1999). In the Nass River, the three loci displaying the greatest differentiation among stocks were Ots100 (F_{ST}=0.131), Ots3 (F_{ST}=0.111), and Ots108 (F_{ST}=0.084), whereas in the Barkley Sound stocks, the three most discriminating loci were Omy77 (F_{ST}=0.107), Ots3 (F_{ST}=0.099), and Ots107 (F_{ST}=0.043). The fact that loci differed in their relative levels of variation between the two areas is not surprising given the rapid evolution of microsatellite loci and the likelihood that the regions were founded postglacially by different sockeye salmon "races" (Wood, 1995). For stock identification applications, surveys of microsatellite variation in each geographic region of interest will generally be necessary to determine which loci are the most effective in differentiating local populations.

Effective assessment and management of sockeye salmon production in Barkley Sound is dependent upon determination of stock composition in fishery catches. Previous evaluation has indicated that the application of microsatellite technology to stock identification can provide the most reliable and cost-effective results (Beacham et al., 1998), but determination of the feasibility of such technology for Barkley Sound fisheries awaited examination of the relation between the number of loci used, the sample size of the stock mixture to be analyzed, and the precision of the estimated stock contributions. For any stock identification application, the optimal combination of number of loci surveyed and number of fish sampled from the catch is dependent on the genetic distance among stocks, the desired precision for an individual stock estimate, and the cost of the analysis for each locus.

The simulated mixtures evaluated for Barkley Sound sockeye salmon indicated that microsatellite variation could be used to provide accurate and reasonably precise estimates of individual stocks in the catch mixtures. They further indicated that although genotypic frequencies at Omy77 and Ots108 were not in Hardy-Weinberg equilibrium in some stocks, but assumed to be so in the stock composition estimation procedure, the violation of this assumption did not have a marked influence on the accuracy of the estimated stock compositions. The precision, but not accuracy, of the estimated contributions increased with both the number of loci (from 3 to 6) and the sample size of the mixture (from 100 to 300). For sample sizes of 150 fish and larger, a greater increase in precision for stock contribution estimates could always be achieved by increasing the number of loci surveyed to six than by increasing the sample size to 300. However, these simulations did not include estimation of the random error associated with sampling only a portion of the catch, and this error will always be reduced by increasing sample size. The level of precision of an estimated stock contribution increased with the contribution of the stock to the mixture. For estimation of the more abundant Great Central and Sproat sockeye salmon, the increase in precision afforded by additional data was approximately equivalent whether more fish (beyond 150) or more loci were analyzed (i.e. approximately equally precise stock contribution estimates were achieved by analyzing four loci in 300 fish and six loci in 200 fish). However, estimation of the small (10%) Henderson Lake contribution to the mixture was more sensitive to sample size and was more precise in the analysis of four loci in 200 fish than of six loci in 150 fish.

Successful application of microsatellite loci to estimation of stock composition in mixed-stock fisheries requires that loci be chosen that highlight differences among stocks to be separated and that adequate numbers of fish in the baseline stocks be surveyed to provide reliable estimates of allele frequencies, and thus genotypic frequencies used in the conditional maximum likelihood analysis. Microsatellite loci can contain a large number of alleles, and baseline sample sizes need to be of sufficient size to ensure that alleles present in fish from a stock in the mixture have also been observed in the baseline samples. Binning low-frequency similar-size alleles (Small et al., 1998) is also a strategy to consider in practical applications.

Although simulated mixtures can provide insights into the expected performance of the mixture analysis, the stock contribution estimates for actual fishery samples can only be evaluated by corroboration with data from other sources. Two supportive sources of independent information occur: time of return of the Henderson Lake stock and the typical catch composition for Barkley Sound that was previously derived from parasites. In Barkley Sound, the time of return of Henderson Lake sockeye salmon has been reported to be later than that of either Sproat Lake or Great Central Lake fish (Steer et al., 1988). For example, in 1984, Henderson Lake sockeye salmon were evident, on the basis of parasite analysis, in the commercial fishery prior to 27 June but increased in relative abundance after that time. The current analysis indicated that Henderson Lake sockeye salmon were absent from, or at low abundance in, the 1997 commercial fishery prior to the week of 4 July. Analysis of the gillnet test fishery and purse-seine samples indicated that the proportion of Henderson Lake sockeye salmon in those catches was low until mid-July but thereafter was substantial, consistent with a later time of arrival of the Henderson stock in Barkley Sound. In a typical return year, about 60% of the Barkley Sound sockeye salmon catch is derived from Great Central Lake, 30% from Sproat Lake, and 10% from Henderson Lake (Steer et al., 1988). Estimated stock compositions for the 1997 fishery catches are in reasonable agreement with the expected stock contributions. Results of the simulation analysis indicated that more precise, but not necessarily more accurate, estimates of the stock contributions (especially that from Henderson Lake) could have been obtained for the fishery catches if sample sizes had been larger than 50 (for the gillnet test fisheries) or approximately 100 (for the purse-seine test and commercial gillnet fisheries).

Differences in estimated stock composition were obtained for the purse-seine and gillnet test fisheries in July samples, where higher proportions of Great Central Lake sockeye salmon were observed in the gillnet fishery samples. Although the fishery samples came from different areas (the purse-seine samples were collected farther inland in Alberni Inlet than were the gillnet samples), the most likely explanation of the difference in estimated proportions of stock composition between the two gears is a difference in size selectivity. Sockeye salmon caught in purse seines in Barkley Sound are generally more variable in size and of smaller mean size than those caught in gill nets (Steer et al., 1986). Probably gill nets were more selective for Great Central Lake sockeye salmon than for Sproat Lake salmon. Thus, it is important to estimate stock contributions to a fishery catch based on samples collected with the type of gear employed in the fishery. Furthermore, the analysis of catch samples to estimate the stock composition of fish present in an area (as opposed to those caught in an area) will be biased to the degree that the sampling gear nonrandomly catches the fish that are present. The results of this study and other analyses (Beacham et al., unpubl. data) indicate that for salmonids, different gear types sample the various stocks in a stock mixture with very different efficiencies.

Differentiation among local spawning populations that are relatively stable over time provides the basis for applying biological markers to problems of salmonid fisheries management. This study confirmed our expectation that the level of differentiation observed at microsatellite loci among sockeye salmon of the three major lake systems draining into Barkley Sound is sufficient and stable to assess stock composition of the fishery catches. The abundance of highly polymorphic microsatellite loci in salmonid fish, the relative ease of nonlethal sample collection, and the moderate cost per fish for laboratory analysis combine to provide a technology that will become increasingly used in the assessment and management of salmonid fisheries.

Acknowledgments

We would like to acknowledge all those involved in sampling collections from sockeye salmon spawning grounds. The collection of test fishery samples was supervised by Bruce Patten and Jim Mitchell, and scale samples from the 1997 fisheries were provided to us by D. Gillespie of the Ageing Laboratory at the Pacific Biological Station. J. Candy assisted in some of the data analysis and figure preparation. Funding was provided by the Department of Fisheries and Oceans.

Literature cited

Angers, B., L. Bernatchez, A. Angers, and L. Desgroseillers.
1995. Specific microsatellite loci for brook charr reveal strong

population subdivision on a microgeographic scale. J. Fish. Biol. 47 (suppl. A):177–185.

Banks, M.A., M. S. Blouin, B. A. Baldwin, V. K. Rashbrook, H. A Fitzgerald, S. M. Blakenship, and D. Hedgecock.
1999. Isolation and inheritance of novel microsatellites in chinook salmon (*Oncorhynchus tshawytscha*). J. Heredity 90:281–288.

Beacham, T. D., and J. B. Dempson.
1998. Population structure of Atlantic salmon from the Conne River, Newfoundland as determined from microsatellite DNA. J. Fish Biol. 52:665–676.

Beacham, T. D., L. Margolis, and R. J. Nelson.
1998. A comparison of methods of stock identification for sockeye salmon (*Oncorhynchus nerka*) in Barkley Sound, British Columbia. North. Pac. Anad. Fish. Comm. Bull. 1:227–239.

Beacham, T. D., R. E. Withler, and T. A. Stevens.
1996. Stock identification of chinook salmon (*Oncorhynchus tshawytscha*) using minisatellite variation. Can. J. Fish. Aquat. Sci. 53:380–394.

Beacham, T. D., and C. C. Wood.
1999. Application of microsatellite variation to estimation of stock composition and escapement of Nass River sockeye salmon (*Oncorhynchus nerka*). Can. J. Fish. Aquat. Sci. 56:297–310.

Fournier, D. A, T. D. Beacham, B. E. Riddell, and C. A. Busack.
1984. Estimating stock composition in mixed stock fisheries using morphometric, meristic, and electrophoretic characteristics. Can. J. Fish. Aquat. Sci. 41:400–408.

Genomic Solutions Inc.
1995. Biolmage Whole Band analyzer. Genomic Solutions, Inc., Ann Arbor, MI, 68 p.

Gill, P., K. Sullivan, and D. J. Werrett.
1990. The analysis of hypervariable profiles: problems associated with the objective determination of the probability of a match. Hum. Genet. 85:75–79.

Goudet, J.
1995. FSTAT A program for IBM PC compatibles to calculate Weir and Cockerham's (1984) estimators of F-statistics (version 1.2). J. Heredity 86:485–486.

Hyatt, K. D., and G. J. Steer.
1987. Barkley Sound sockeye salmon, (*Oncorhynchus nerka*): evidence for over a century of successful stock development, fisheries management, research and enhancement efforts. *In* H. D. Smith, L. Margolis, and C. C. Wood (eds.) Sockeye salmon (*Oncorhynchus nerka*) population biology and future management, p. 435–457. Can. Spec. Publ. Fish. Aquat. Sci. 96.

Hyatt, K. D., and J. G. Stockner.
1985. Responses of sockeye salmon (*Oncorhynchus nerka*) to fertilization of British Columbia coastal lakes. Can. J. Fish. Aquat. Sci. 42:320–331.

LeBrasseur, R. J., C. D. McAllister, W. E. Barraclough, O. D. Kennedy, J. Manzer, D. Robinson, and K. Stephens.
1978. Enhancement of sockeye salmon (*Oncorhynchus nerka*) by lake fertilization in Great Central Lake: Summary Report. J. Fish. Res. Board Can. 35:1580–1596.

McConnell, S. K. J., D. E. Ruzzante, P. T. O'Reilly, L. Hamilton, and J. M. Wright.
1997. Microsatellite loci reveal highly significant genetic differentiation among Atlantic salmon (*Salmo salar* L.) stocks from the east coast of Canada. Mol. Ecol. 6:1075–1089.

Morris, D. B., K. R. Richard, and J. M. Wright.
1996. Microsatellites from rainbow trout (*Oncorhynchus mykiss*) and their use for genetic study of salmonids. Can. J. Fish. Aquat. Sci. 53:120–126.

Nelson, R. J., and T. D. Beacham
1999. Isolation and cross species amplification of microsatellite loci useful for study of Pacific salmon. Anim. Genet. 30:228–229.

Nelson, R. J., T. D. Beacham, and M. P. Small.
1998. Microsatellite analysis of the population structure of a Vancouver Island sockeye salmon (*Oncorhynchus nerka*) stock complex using non-denaturing gel electrophoresis. Mol. Mar. Biol. Biotech. 7:312–319.

Nielsen, E. E., M. M. Hansen, and V. Loeschcke.
1997. Analysis of microsatellite from old scale samples of Atlantic salmon *Salmo salar*: a comparison of genetic composition over 60 years. Mol. Ecol. 6:48–492.

O'Connell, M., and J. M. Wright.
1997. Microsatellite in fishes. Rev. Fish Biol. and Fisheries 7:331–363.

Quinn, T. P., C. C. Wood, L. Margolis, B. E. Riddell, and K. D. Hyatt.
1987. Homing in wild sockeye salmon (*Oncorhynchus nerka*) as inferred from differences in parasite prevalence and allo zyme allele frequencies. Can. J. Fish. Aquat. Sci. 44:196–1971.

Raymond, M., and F. Rousset.
1995. GENEPOP (vers. 1.2): population genetics software for exact tests and ecumenism. Heredity 86:248–249.

Rice, W. R.
1989. Analyzing tables of statistical tests. Evolution 43:223–225.

SAS Institute Inc.
1989. SAS/STAT users guide, version 6, 4th ed., vol. 1. SAS Institute, Cary, NC, 890 p.

Seeb, J. E., C. Habicht, J. B. Olsen, P. Bentzen, J. B. Shaklee, and L. W. Seeb.
1998. Allozyme, mtDNA, and microsatellite variants describe structure of populations of pink and sockeye salmon in Alaska. North Pac. Anad. Fish. Comm. Bull. 1:300–318.

Small, M. P., T. D. Beacham, R. E. Withler, and R. J. Nelson.
1998. Discriminating coho salmon (*Oncorhynchus kisutch*) populations within the Fraser River, British Columbia using microsatellite markers. Mol. Ecol. 7:141–155.

Steer, G. J., N. B. F. Cousens, H. W. Stiff, and K. D. Hyatt.
1986. An analysis of gear selectivity and sources of bias in estimates of age and stock composition of the 1980–1984 Barkley Sound sockeye salmon (*Oncorhynchus nerka*) catch. Can. Tech. Rep. Fish. Aquat. Sci. 1445, 77 p.

Steer, G. J., N. B. F. Cousens, H. W. Stiff, K. D. Hyatt, and D. W. Welch.
1988. A description of the 1984 fishery, stock composition, and biological characteristics of sockeye salmon (*Oncorhynchus nerka*) in the catch from Area 23, Barkley Sound. Can. Tech. Rep. Fish. Aquat. Sci. 1667, 78 p.

Swofford, D. L., and R. B. Selander.
1981. BIOSYS-1: a FORTRAN program for the comprehensive analysis of electrophoretic data in population genetics and systematics. J. Hered. 72:281–283.

Wood, C. C.
1995. Life history variation and population structure in sockeye salmon. Am. Fish. Soc. Symposium 17:195–216.

Wood, C. C., B. E. Riddell, D. T. Rutherford, and R. E. Withler.
1994. Biochemical genetic survey of sockeye salmon (*Oncorhynchus nerka*) in Canada. Can. J. Fish. Aquat. Sci. 51(suppl. 1): 114–131.

Direct validation of annual increments in the otoliths of juvenile southern bluefin tuna, *Thunnus maccoyii*, by means of a large-scale mark-recapture experiment with strontium chloride

Naomi P. Clear
John S. Gunn
Anthony J. Rees
CSIRO Marine Research
GPO Box 1538 Hobart, Tasmania, 7001, Australia
E-mail address (for N. P. Clear): Naomi.Clear@marine.csiro.au

Abstract.—From 1990 to 1996, during a large-scale tag-and-release program in the Great Australian Bight, 20,204 southern bluefin tuna (SBT), *Thunnus maccoyii*, were injected with strontium chloride ($SrCl_2$). The objectives of the marking experiment were to examine the efficacy of $SrCl_2$ as an otolith marker and to determine the periodicity of increment formation in SBT otoliths. Nine-hundred and sixty-one Sr-injected fish were recaptured and 616 otoliths were sampled from these; the high level of sampling success was attributable to a major liaison effort throughout the multinational SBT fishery. The same tag return rates for fish that were tagged and injected and for fish that were tagged only, indicated that the injection of strontium did not affect the survival rate of tagged fish. Strontium marks were detected with a Robinson detector or an energy dispersive spectrometer (EDS) (or with both) linked to a scanning electron microscope; 59 of the 67 otoliths from injected fish examined had discernible marks. The intensity of the strontium mark and the dosage rates were linked; a dosage of 100 mg Sr/kg fish weight is recommended to ensure easy identification of the strontium mark. Using the strontium marks, we established that in SBT with 1 to 6 increments in their otoliths, one increment is laid down per year at liberty. In the 59 marked fish that were examined, there was 100% agreement between the expected and observed number of increments after marking. These results, and the data from two supplementary tag returns from unmarked fish recaptured after long times at liberty, provide unambiguous evidence that increments on the otoliths of SBT are formed annually, to at least the age of 13 years. In addition, a recent study that used bomb-radiocarbon levels to estimate ages of older SBT has provided strong evidence that annual increments are deposited in the sagittal otoliths of SBT throughout life.

Manuscript accepted 11 January 1999.
Fish. Bull. 98:25–40 (2000).

Southern bluefin tuna (SBT), *Thunnus maccoyii* Castelnau, 1872, is a large, long-lived, migratory, pelagic fish with a circumglobal distribution between 30°S and 50°S (Caton, 1991). Its only known spawning ground is in the Indian Ocean south of Java, between 7°S and 20°S (Caton, 1991). Since it was first exploited in the 1950s the stock has declined dramatically to between 16% and 25% of its initial level (Sainsbury[1]). The fishery is currently managed by individual transferable quotas (ITQ) and the total allowable catch (TAC) is assessed each year.

Virtual population analysis (VPA) has been the main method of assessing the condition of SBT stock since 1980 (Murphy and Majkowski, 1981). The age structue of the population, a major input to VPA, has been estimated by converting lengths and weights to ages, using growth curves derived from tagging data (Hampton, 1991; Polacheck et al.[2]). To reduce the unmeasurable uncertainties that the estimates introduce into VPA assessments, a validated direct method for determining age was required.

In 1992 we began a study to develop reliable techniques for determining ages of SBT. Validation of assigned ages is critical in age estimation studies (Beamish and McFarlane, 1983; Smith, 1992; Secor et al., 1995); therefore a large-scale mark-recapture experiment was initiated to provide the basis for validating the age estimates. From the validation study we aimed to confirm the periodicity of the zones that were counted on the hard parts collected from SBT. The overall objective of these two studies was to develop a validated length-at-age key for the entire size range of the SBT population. We present details of the mark-recapture experiment and our evidence that increments in otoliths are formed annually.

[1] Sainsbury, K. 1993. What is happening to the southern bluefin stock? *In* W. Whitelaw and V. Mawson (eds.), Proceedings of the inaugural southern bluefish tuna science-industry-management workshop, Port Lincoln, Australia, p. 5–19. Commonwealth Scientific and Industrial Research Organization (CSIRO) Marine Research, GPO Box 1538 Hobart, 7001 Australia.

[2] Polacheck, T., K. Sainsbury, and N. Klaer. 1995. Assessment of the status of the southern bluefin tuna stock using virtual population analysis—1995. Paper SBFWS/95/17. First scientific meeting of the Commission for the Conservation of Southern Bluefin Tuna (CCSBT), Shimizu, Japan, 70 p. Commonwealth Scientific and Industrial Research Organization (CSIRO) Marine Research, GPO Box 1538, Hobart, Tasmania, 7001, Australia.

Previous attempts to estimate SBT ages directly, either did not attempt validation, or attempted it for only a few age classes. Hynd (1965) used scales to estimate ages of fish up to 80 cm fork length (FL) but did not attempt to validate his age estimates. Yukinawa (1970) counted up to eight rings on scales, using marginal increment analysis, to show that the rings form at the same time each year. Thorogood (1987) used otoliths to estimate age in fish from 42 to 167 cm FL and, using marginal increment analysis, was able to show seasonal band formation in what he called ages 2 to 4. Jenkins and Davis (1990) examined microincrements in the otoliths of SBT larvae between 3.5 and 12 mm standard length (SL) collected from the same cohort over consecutive days. From these microincrements, they validated daily increment formation and assigned approximate ages of 7 to 18 days to their samples.

In many age determination studies of other species of tuna, tetracycline has been used in marking experiments to validate daily increment formation in wild and captive tunas: e.g. yellowfin tuna, *Thunnus albacares* in the wild (Wild and Foreman, 1980; Wild et al., 1995) and in captivity (Yamanaka[3]); skipjack tuna, *Katsuwonus pelamis*, in the wild (Wild et al., 1995); black skipjack tuna, *Euthynnus lineatus*, in captivity (Wexler, 1993); and Atlantic bluefin tuna, *Thunnus thynnus*, in the wild (Inter-Am. Trop. Tuna Comm.[4]).

However, similar experiments using oxytetracycline (OTC) as a marker in SBT in the 1980s were less successful. In high proportion of OTC-injected fish, a mark failed to show up in the otoliths (Gunn[5]). Given this previous failure, and public health concerns over the use of tetracycline (in the USA, the Federal Drug Administration [US FDA] prohibits its use in wild fisheries), we selected strontium chloride ($SrCl_2$) as an alternative marker.

Strontium chloride is a nontoxic salt that occurs naturally in sea water. It is a component of some foods and is considered to be benign at the concentrations used as a marking agent (Sax and Lewis, 1987). Strontium is readily incorporated into the bloodstream of fish and, although not used previously on scombrids, it has been used successfully with other fish species to mark vertebrae (by introduction into food or in the surrounding water [Behrens et al., 1990]), and otoliths (by immersion and injection [Brothers, 1990]). Strontium is chemically and biologically similar to calcium. Because calcium and strontium ions have the same valency (2+) and a similar ionic radius (Ca, 0.099 nm; Sr, 0.113 nm), strontium readily substitutes for calcium during deposition of calcium carbonate.

The first two objectives of this study were 1) to evaluate whether intramuscular injection of strontium chloride resulted in effective and reliable marking of otoliths, and 2) to determine if strontium chloride injections increased mortality and, hence, affected recapture rates.

If successful and benign marking was demonstrated, we planned to use the strontium chloride marks to verify the accuracy of direct aging techniques by determining the periodicity of increment formation for as many year classes of SBT as possible.

Materials and methods

Tagging and marking

From 1990 to 1996, a total of 64,497 juvenile SBT in the Great Australian Bight were tagged and released. Of these, 20,204 tagged SBT were injected with $SrCl_2$ (Table 1). All fish were double-tagged (in case of "tag shedding") (Williams, 1992): strontium-injected fish were tagged with orange tags, fish that were not injected were tagged with yellow tags. When both orange and yellow tags were being deployed, an equal number of fish from targeted schools were chosen at random for injecting or not injecting. The smallest fish caught during the tagging program was 40 cm fork length (FL); we did not tag and inject fish smaller than this size because they were considered prerecruits, i.e. were not caught in the fishery. The lengths of orange-tagged fish ranged from 41 to 120 cm in FL. The return rates of yellow-tagged and orange-tagged fish were compared by using a chi-squared test to determine if they were significantly different.

The strontium chloride solution for injection was prepared in the laboratory. A stock solution of 1 g $SrCl_2.6H_2O$/mL was made up by dissolving 1 kg of analytical grade $SrCl_2.6H_2O$ crystals in 1 liter of distilled water, resulting in a 0.21 g/mL solution of Sr^{2+}. The solution was buffered to pH 7.0 with KOH and stored between 0°C and 4°C.

For rapid injections into large numbers of fish, a 5-mL automatic vaccinator fitted with a 0.2-mm needle was used. Flexible tubing connected the vaccinator to a plastic storage container that was either worn as a

[3] Yamanaka, K. L. 1990. Age, growth and spawning of yellowfin tuna in the southern Philippines. FAO, Indo-Pacif. Tuna Dev. Man. Prog. Working paper 90/WP/21, 87 p.

[4] Inter-Am. Trop. Tuna Comm. 1982. Annual Rep. for 1981, 303 p.

[5] Gunn, J. S. 1992. Progress report on strontium chloride marking of SBT during 1990–92 CSIRO–JAMARC tagging programs. Paper MWS4/WP–3. Fourth workshop of the southern bluefin tuna recruitment monitoring and tagging programs, Hobart, Australia, 9 p. Commonwealth Scientific and Industrial Research Organization (CSIRO) Marine Research, GPO Box 1538 Hobart, 7001, Australia.

Table 1

Numbers of southern bluefin tuna released with yellow tags and numbers of SBT injected with $SrCl_2$ and released with orange tags, and a summary of yellow and orange tag returns from 1990 to 1996. The number of returned yellow and orange tags released in each year of the tagging program, and the number of returned tags as a percentage of the total number released in the year (shown in parentheses) are shown. (The years of release and recapture are from October of one year to September of the next.) NS = not significant.

	1990–91		1991–92		1992–93		1993–94		1994–95		1995–96		1990–96 All release years	
	yellow tags *n*=6909	orange tags *n*=835	yellow tags *n*=4543	orange tags *n*=3595	yellow tags *n*=5907	orange tags *n*=5304	yellow tags *n*=8253	orange tags *n*=8251	yellow tags *n*=15,683	orange tags *n*=2219	yellow tags *n*=2998	orange tags *n*=0	yellow tags *n*=44,293	orange tags *n*=20,204
Fish recaptured														
1990–91	183 (2.65)	25 (2.99)	—	—	—	—	—	—	—	—	—	—	183	25
1991–92	180 (2.61)	19 (2.28)	84 (1.8)	55 (1.53)	—	—	—	—	—	—	—	—	264	74
1992–93	111 (1.61)	11 (1.32)	116 (2.6)	86 (2.39)	56 (0.95)	63 (1.19)	—	—	—	—	—	—	283	160
1993–94	62 (0.90)	6 (0.72)	102 (2.2)	76 (2.11)	130 (2.20)	90 (1.70)	50 (0.61)	47 (0.57)	—	—	—	—	344	219
1994–95	29 (0.42)	6 (0.72)	43 (0.95)	36 (1.00)	177 (3.00)	116 (2.19)	171 (2.07)	168 (2.04)	67 (0.43)	20 (0.90)	—	—	487	346
1995–96	2 (0.03)	0	6 (0.13)	6 (0.17)	29 (0.49)	17 (0.32)	86 (1.04)	89 (1.08)	94 0.60)	25 (1.13)	21 (0.70)	—	217	137
1990–96	567	67	351	259	392	286	307	304	161	45			1,779	961
All recapture years	(8.22)	(8.03)	(7.68)	(7.20)	(6.64)	(5.40)	(3.72)	(3.69)	(1.03)	(2.03)			(4.01)	(4.76)
Difference between yellow and orange tag returns	5.02 (0.83)		3.17 (0.94)		1.44 (0.61)		3.22 (0.40)		1.68 (0.39)				2.10 (0.56)	
(χ^2(*P*))	NS		NS		NS		NS		NS				NS	

back-pack or attached to the tagging cradle (Williams, 1992).

We injected the fish about 2 cm below the dorsal midline, in line with the center of the first dorsal fin. We occasionally observed a loss of the solution from the muscle, especially in larger fish. When this happened, we noted the loss and injected the fish a second time. To minimize loss of solution we carefully expelled all the air from the vaccinator so that air bubbles were not injected into the muscle.

To determine a suitable dosage rate for SBT, initial trials with strontium were made on three nontuna species in captivity: silver trevally, *Pseudocaranx dentex*, sand flathead, *Platycephalus bassensis*, and purple wrasse, *Pseudolabrus fucicola*, the largest fish weighing 500 g. The dosages were based on Brothers' (1990) immersion and injection trials with strontium on trout—100 mg/kg—and Wild and Foreman's (1980) tetracycline experiments on tuna—0.3 mL/kg or 27.5 mg/kg of fish. Dosages between 50 and 200 mg Sr/kg resulted in clear Sr marks on otolith sections and no mortalities (CSIRO, unpubl. data[6]). In the field, the length of the fish was measured to the nearest centimeter, but weight could only be estimated. We therefore chose the required $SrCl_2$ dose according to length (Table 2). These dosages were increased for fish longer than 90 cm when the marks on the first otoliths recovered from SBT of this size showed up faintly, indicating low strontium absorption. The dosages were adjusted so that at least 80 mg of Sr was injected per kilogram of fish.

Tag collection and otolith sampling

A critical factor in the experiment was the sustained effort, over many years, to recover otoliths from recaptured fish. An extensive campaign was conducted to explain the objectives of the marking experiment to the SBT fishing industry and to develop a protocol for

[6] CSIRO (Commonwealth Scientific and Industrial Research Organization) unpublished data. 1989. CSIRO Marine Research, GPO Box 1538, Hobart, Tasmania, 7001, Australia.

Table 2

Dosages for $SrCl_2$-injected fish, based on length and weight of fish. FL = fork length.

FL (cm)	Approx. wt (kg)	Dose 1990–92			Dose 1993–96		
		$SrCl_2$ (mL)	Sr (mg)	mg Sr/kg fish	$SrCl_2$ (mL)	Sr (mg)	mg Sr/kg fish
40–50	1.5–3.0	2	400	130–270	2	400	130–270
51–70	3.0–7.0	3	600	86–200	3	600	86–200
71–80	7.0–10	4	800	80-114	4	800	80–114
81–90	10–15	5	1000	67–100	5	1000	67–100
91–95	15–18	6	1200	67–80	7	1400	78–93
96–100	18–21	7	1400	67–78	9	1800	86–100
>100	>21	8	1600	76	12	2400	114

collecting the samples. Posters and information notes, in Japanese and English, were distributed throughout the fishery. Rewards were offered for the return of tags and a substantial bonus for allowing scientists to sample otoliths from orange-tagged fish. To aid in otolith recovery, kits containing large orange disks were distributed to the crew of Japanese vessels; when an orange-tagged fish was caught, the disks were attached to the fish to clearly identify it in the freezers.

Given the high value of SBT on the Japanese sashimi market, it was essential that otoliths could be sampled without affecting the external appearance of the fish. Using a modification of the technique described by Thorogood (1986), we removed from the skull 35–44 mm cores that contained the semicircular canals and sagittal otoliths with a holesaw attached to a drill. The points of entry for the cores were over the basioccipital plates, which are anterior to the first vertebra and immediately lateral to the junction of the skull and first vertebra; this area was exposed when the tuna were cleaned and dressed—a process which removes the gill-filaments and surrounding tissue and most of the opercular flaps. By drilling through each of the plates in the direction of the back of the opposite eye, the cores coalesced at a point beyond the sagittal otoliths and could be removed easily from the skull, leaving no external mark on the fish (Fig. 1) Sagittal otoliths were removed from the cores, cleaned in distilled water, and dried at 28°C.

Age estimates

An age estimate was made from the otoliths before we attempted to identify a Sr mark. Increments on the whole sagittal otoliths comprised two zones: an opaque (assumed to be fast growth) and a narrower translucent zone (assumed to be slow growth) that appeared dark under a dissecting microscope with reflected lighting and a black background. Following Thorogood's (1987) method, one of each pair of sagittae was burned on a 400°C hot plate until it turned golden brown. The color change was greater in the translucent zones, making them more visible (Fig. 2A). A digital image of the burnt otolith was taken (using the public domain "NIH Image" program[7] and a video camera mounted on a Wild M5A dissecting microscope) and measurements were made of the otolith length and of the distance between the primordium and the inside of the translucent zones along both the postrostral (PR) and transverse axes. We use terminology that is currently widely accepted (Secor et al. [1992]; Kalish et al. [1995]; Stequert et al. [1996]). For each specimen, the reader made three independent age estimates by counting the number of increments obvious on the distal surface of the sagitta. These were made without reference to either the length of the fish or the time that the fish was at liberty after tagging and injection.

Detection of strontium marks

Scanning electron microscope (SEM) with a Robinson backscatter detector In the early stages of the project we used a Robinson backscatter detector coupled to a Philips 515 SEM for detecting the strontium-rich band in the otoliths (which we refer to as "the strontium mark"). The Robinson detector visualizes differences in the total atomic weight (Z) across a specimen. Because a strontium mark within the calcium carbonate contains a higher concentration of Sr, and hence a higher Z than surrounding uncontaminated calcium carbonate, it appears as a weak to intense bright band across the growth axis of the section (Figs. 2B and 3). The

[7] Rasband, W. 1994 NIH Image, vers. 1.54. U.S. National Institutes of Health. [Available from the Internet by anonymous ftp from zippy.nimh.nih.gov or as a floppy disk from NTIS, 5285 Port Royal Rd., Springfield, VA 22161, part number PB93-504868.]

intensity of the band depends on the magnitude of the difference in Z between the two portions of the otolith.

This kind of analysis requires a flat, polished surface; therefore we sectioned the sagittal otoliths either along the postrostral axis to produce an oblique longitudinal section (LS), or along a transverse axis. The rostral axis often shows clear increments, but we did not find distinct Sr marks in this part of the otolith. The sections were ground and polished following Gunn et al.'s (1992) methods and an evaporated carbon coat (25–30 nm thick) was applied to the sections to minimize charging in the SEM. The position of the Sr mark along the axis was measured with the vernier attached to the SEM stage drives (Fig. 2B).

Energy-dispersive spectroscopy (EDS) In the later stages, an EDS x-ray microanalysis system became available and we used it to confirm the presence of Sr in the bright bands, and also to detect Sr marks in unsectioned otoliths (the use of unsectioned otoliths decreased the preparation time required for SEM analysis). The system consisted of a Link 133 eV Si(Li) detector with light element capability and a Thomson Scientific "WinEDS" PC-based analyzer attached to a Philips 515 SEM. Before x-ray analysis, whole (unsectioned) otoliths were acid-etched along the postrostral axis from the surface with 1 N and 3.5 N HCl, to expose the growth plane, then rinsed in bleach and distilled water, and dried. To minimize charging in the SEM, the otoliths were dipped in a dilute carbon DAG solution (approximately 1:50 with dichloroethane) immediately before analysis. Strontium marks were detected by operating the SEM in "spot" mode and searching for a point or zone where a significant Sr signal was detected on the x-ray microanalyzer (typically, a strong peak at 1.81 keV in the spectrum, corresponding to emission of Sr Lα x-rays). When a strontium mark was detected, its position along the PR axis was measured and the mark photographed either with conventional SEM photography (Fig. 4) or with a rapid, low-grade video print, which also showed the features of interest. To confirm that the suspected mark was strontium-rich, two plots of the x-ray spectra from the otolith were taken: one on the strontium mark and one just before the mark. Acceptable evidence of the correct identification of a strontium mark was considered to be the presence of an enhanced Sr level in the area analyzed, together with an absence of Sr (except for background levels) immediately before the area (Fig. 5).

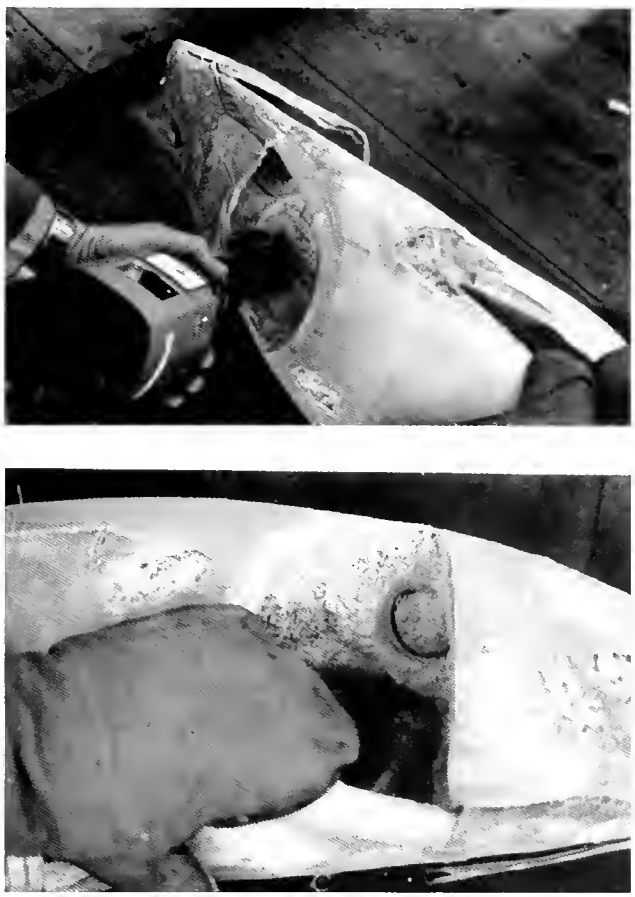

Figure 1
The drilling technique used to extract otoliths from southern bluefin tuna destined to be sold as "whole" fish.

The measurements of increments on the whole otoliths, and the strontium mark in sections or whole otoliths, were made along the same axes without reference to the other. This procedure enabled us to compare the number of increments observed after the strontium mark with the number expected, calculated from the known time at liberty after tagging.

Quantitative EDS analyses for linescans were carried out on carbon-coated polished sections in the Philips 515 SEM operated at an accelerating voltage of 20 kV, by using a focused electron beam of 0.15 µm diameter and analysis times of 60–200 seconds. The effective area analyzed by the beam was larger than the diameter of the beam itself because the beam spreads within the specimen after entry; examination of superficial beam damage to specimens after analysis suggested that the area analyzed by the beam is in the order of 2 µm diameter. Elemental concentrations were calculated by reference to appropriate standards

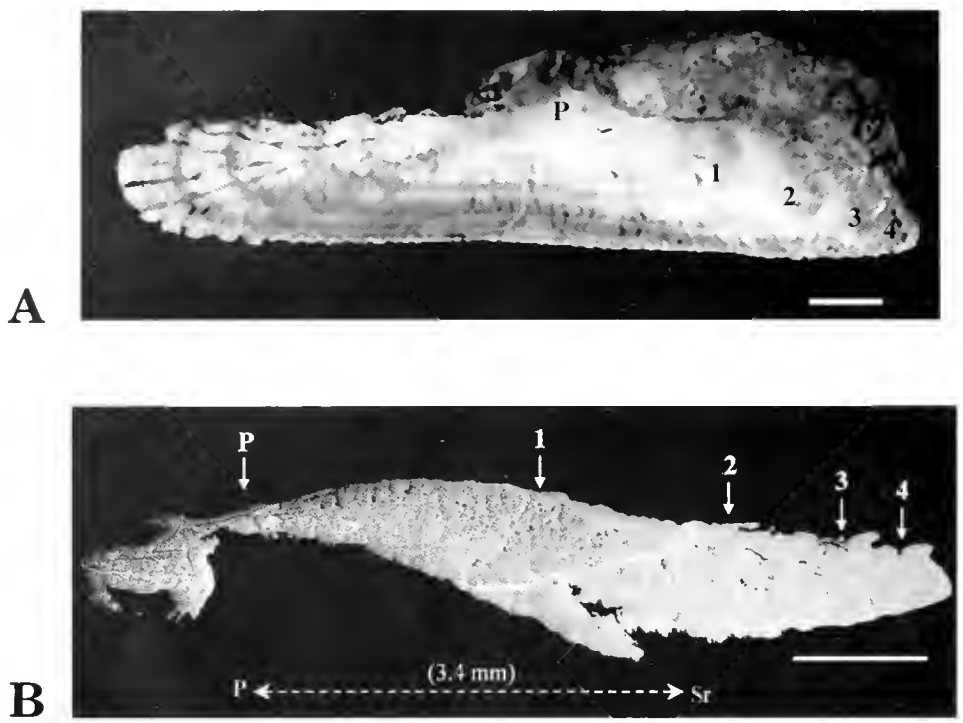

Figure 2

Sagitta (specimen OB 764) from a fish tagged and injected in March 1994 at 57 cm FL and recaptured in February 1997 at 111 cm FL. (**A**) Four increments were counted on the whole, burnt otolith and measured from the primordium (P) to the beginning of each translucent zone apparent on the distal surface along the postrostral axis at 2.2 mm, 3.6 mm, 4.4 mm, and 4.9 mm. (**B**) The sagitta was sectioned through the postrostral axis and viewed in the SEM: the micrograph shows the strontium mark which was located 3.4 mm from the primordium and the positions of the translucent zones measured on the otolith before it was sectioned. Scale bars: 1 mm

(calcite and celestite for Ca and Sr, respectively), with the "WinEDS" software.

Results

Of the 20,204 fish injected with $SrCl_2$ between 1990 and 1996, 9614 had been recaptured and 616 sets of sagittal otoliths were recovered from these by 1 January 1996. Seventy sets of otoliths were chosen for the validation study, selected from the range of size classes in the recaptures—fish of 45 to 102 cm FL at release and 57 to 133 cm FL at recapture—and from the range of times at liberty. Age estimates were made from 67 of the 70 otoliths; three sets of otoliths were excluded from the experiment because the increments on the whole otoliths were either ambiguous or uninterpretable and the reader could not give an age estimate with confidence.

Recapture rates of orange-tagged fish and recovery of otoliths

There were no statistically significant differences between the return rates of yellow tags (from fish not injected with $SrCl_2$) and orange tags (from fish injected with $SrCl_2$) released in all years of the program (χ^2=2.10, P=0.56) nor between the return rates of yellow tags and orange tags for any of the release years (Table 1). The number of otoliths recovered, as a percentage of orange tags recaptured, varied between 20%, in the first year of the tagging program, and 88% in the final year (Table 3); overall, otoliths were recovered from 65% of the orange-tagged fish that were recaptured.

Detection of Sr marks in the otoliths of orange-tagged fish

The otoliths removed from fish injected with strontium chloride typically showed a bright band in back-

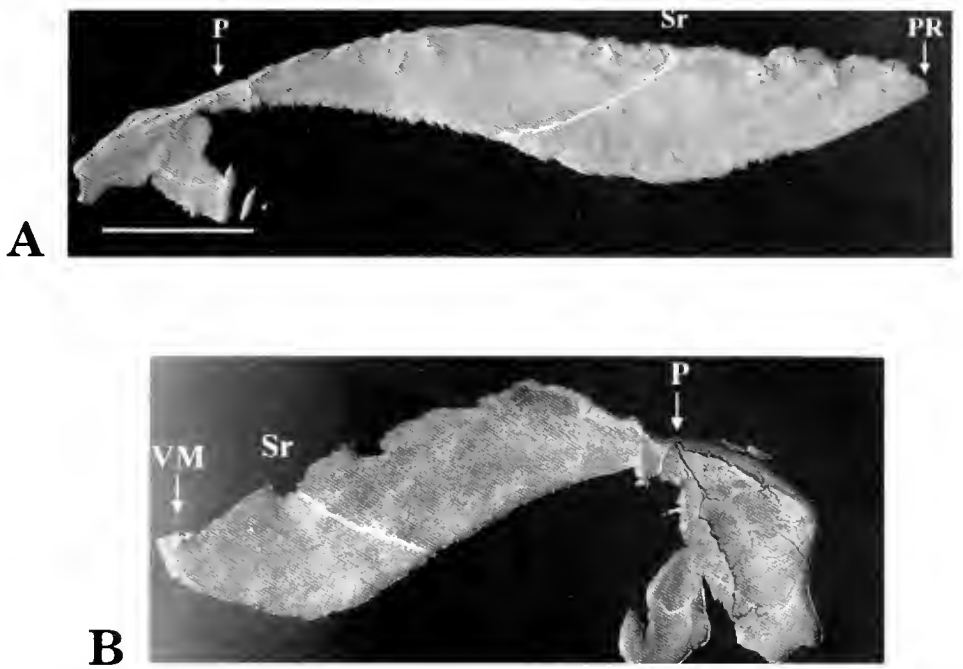

Figure 3

SEM micrographs showing strontium marks apparent as bright bands on sections taken from sister otoliths of specimen OB 102. (**A**) An oblique longitudinal section through the postrostral axis on which the primordium (P) and postrostrum (PR) are marked. (**B**) A transverse section on which the primordium and ventral margin (VM) are marked. Scale bars: 1 mm

Table 3

The number of tagged fish recaptured, and the number of otoliths recovered from orange-tagged fish during each year of the tagging program. (Data to 16 February 1996. The years of release and recapture are from October of one year to September of the next.)

Recapture year	Yellow-tagged fish recaptured	Orange-tagged fish recaptured	Otoliths recovered (otoliths recovered as a percentage of the orange-tagged fish recaptured)
1990–91	183	25	5 (20)
1991–92	264	74	49 (66)
1992–93	283	160	94 (59)
1993–94	344	219	107 (49)
1994–95	487	346	248 (72)
1995–96	238	137	120 (88)
Total	1799	961	623 (65)

scattered electron images of polished sections through appropriate growth planes (e.g. the oblique longitudinal section along the PR axis). The visibility of the Sr mark (brightness in the backscattered electron image) was highest in fish that had been relatively small at the time of injection (e.g. 50–55 cm FL). An example is specimen OB 102 (Fig. 3), which measured 49 cm at time of release and was injected with 2 mL $SrCl_2$ solution. This bright band was frequently associated with a local growth interruption immediately before the band, presumed to be a tagging check. This check was sometimes seen on the whole, etched otoliths (Fig. 4) but, although apparent in the SEM at high magnifications, it was not discernible from the other surface

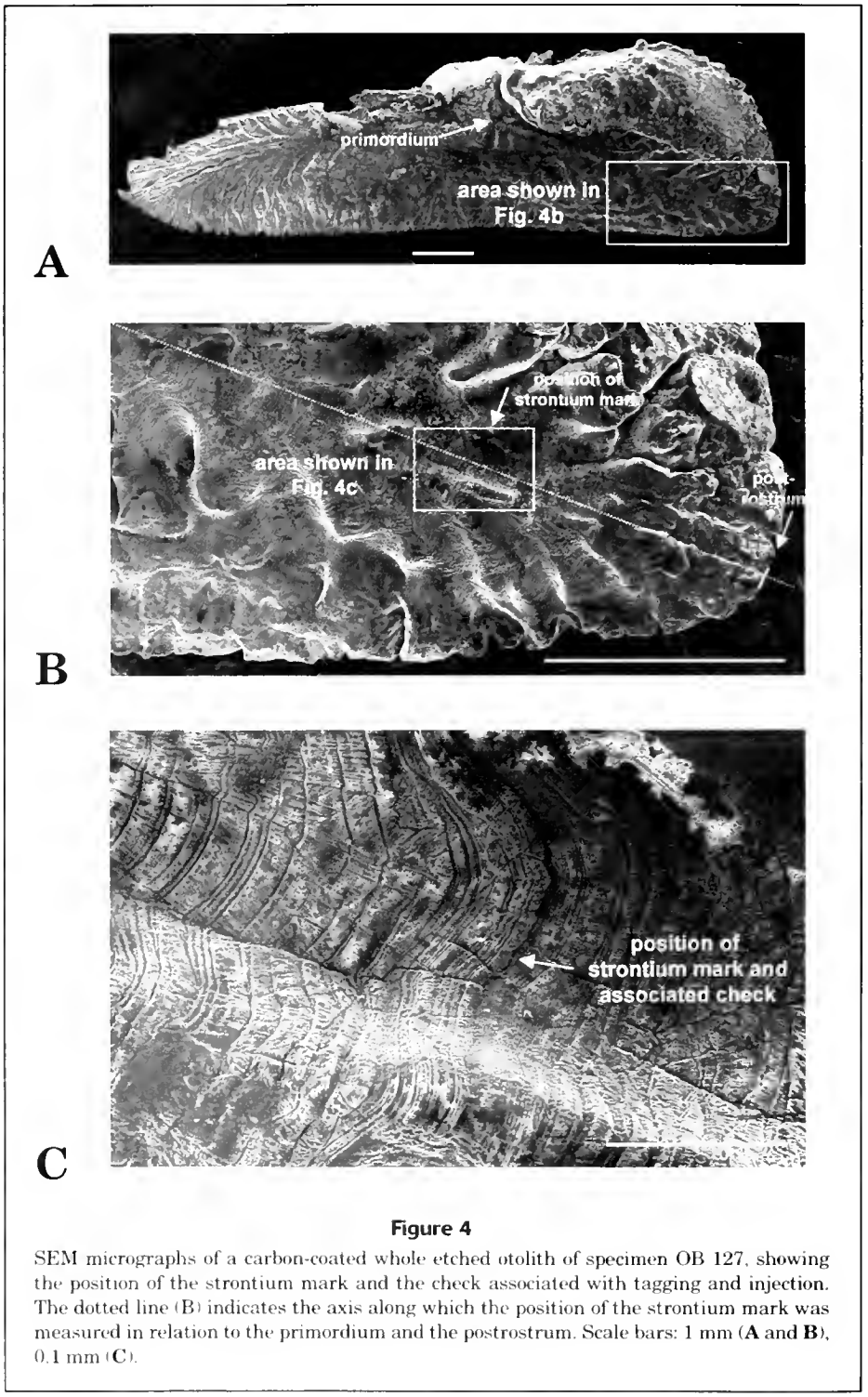

Figure 4

SEM micrographs of a carbon-coated whole etched otolith of specimen OB 127, showing the position of the strontium mark and the check associated with tagging and injection. The dotted line (B) indicates the axis along which the position of the strontium mark was measured in relation to the primordium and the postrostrum. Scale bars: 1 mm (**A** and **B**), 0.1 mm (**C**).

features on the whole otolith when increments were counted. We could not identify Sr marks on vertebral sections from fish injected with $SrCl_2$.

The presence of strontium in the bright bands was demonstrated by EDS spectra, which showed a strong peak of strontium Lα x-rays when the electron beam was directed to the Sr mark, in contrast with very low (background) levels in the regions of the otolith preceding the mark (Fig. 5). The relative levels of strontium and calcium in the bright band were further confirmed by inspection of the difference spectrum obtained by subtracting a spectrum acquired in the area

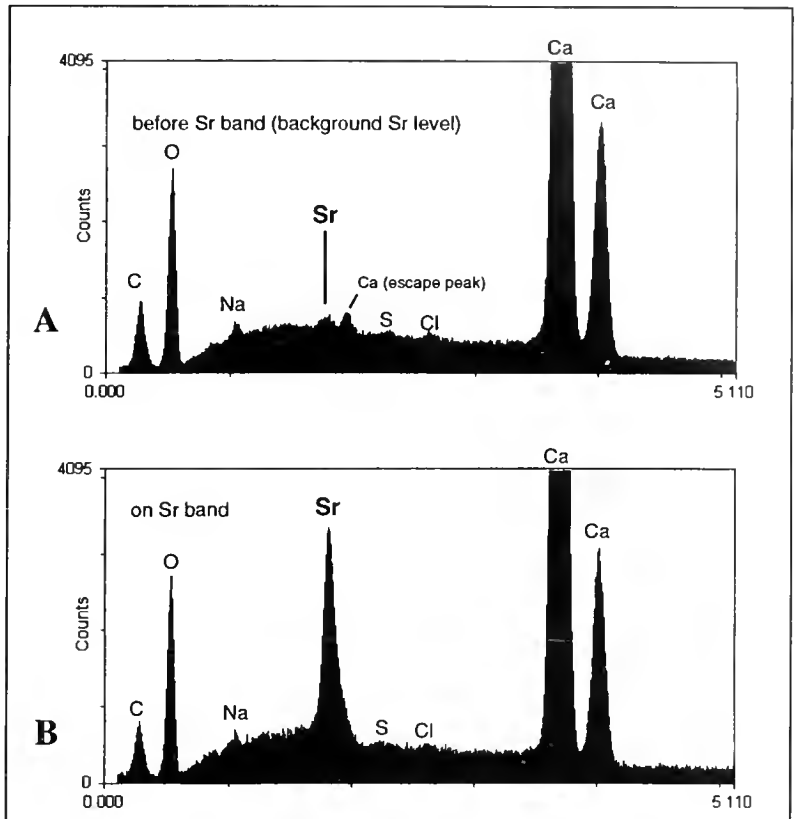

Figure 5

Examples of EDS spectra from a sectioned SBT otolith showing peaks due to background levels of Sr (**A**) and enhanced Sr levels associated with the strontium mark (**B**). Spectra similar to that shown in Figure 6B were used to positively identify the location of strontium marks in sections and etched whole otoliths (see text for further details).

preceding the mark (e.g. Fig. 5A) from one acquired on the bright band (Fig 5B), which demonstrated that strontium levels were enhanced and calcium was reduced in the bright band; however, no increase in chlorine was apparent. A quantitative EDS linescan across a bright band in one specimen, SBT OB 96, sectioned in oblique LS along the PR axis and analyzed along the direction of maximum observed growth, revealed "background" levels of 0.1% to 0.25% Sr by weight up to 5 microns before the band and a measured peak of 7.1% Sr on the band, falling to 3.5% (50% of peak level) 6 µm after the start of the band, and 0.7% (10% of peak level) approximately 15 µm after the start of the band. There is some indication of continuing slightly elevated Sr levels out to around 50 µm beyond the band, although visibility of these levels is at the limits of the EDS technique (Fig. 6).

Accompanying the measured maximum 7.1% increase in Sr level in the bright band is a fall in measured Ca concentration from 39% to 40% before the band to a minimum of 35.5% on the band—a decrease of 3.5–4.5% in absolute value or 10% relative value. Within the limits of accuracy of the EDS technique, this decrease in calcium concentration supports the theory that Ca atoms are being replaced by Sr atoms in the atomic structure on a 1:1 basis, each Sr atom being approximately twice as heavy as a Ca atom. Calculation of the increase in mean atomic number of the specimen resulting from a 7% increase in Sr and a 3.5% decrease in Ca gives a value of approximately 104 for the Sr-enriched zone. This value compares with 100 for the unaltered $CaCO_3$—a difference resolvable with backscattered electron imaging on the SEM on a suitably polished and coated specimen. The extent of the visible bright band in this specimen (OB 96) coincided with measured Sr levels in the range of 5–7%; thus it is possible that elevated Sr concentrations in the range of 0.5–5% may not be detectable by backscattered imaging although they should still be detectable by EDS. The EDS system is also essential for testing the identity of weak bright bands in sectioned specimens when it is not clear from

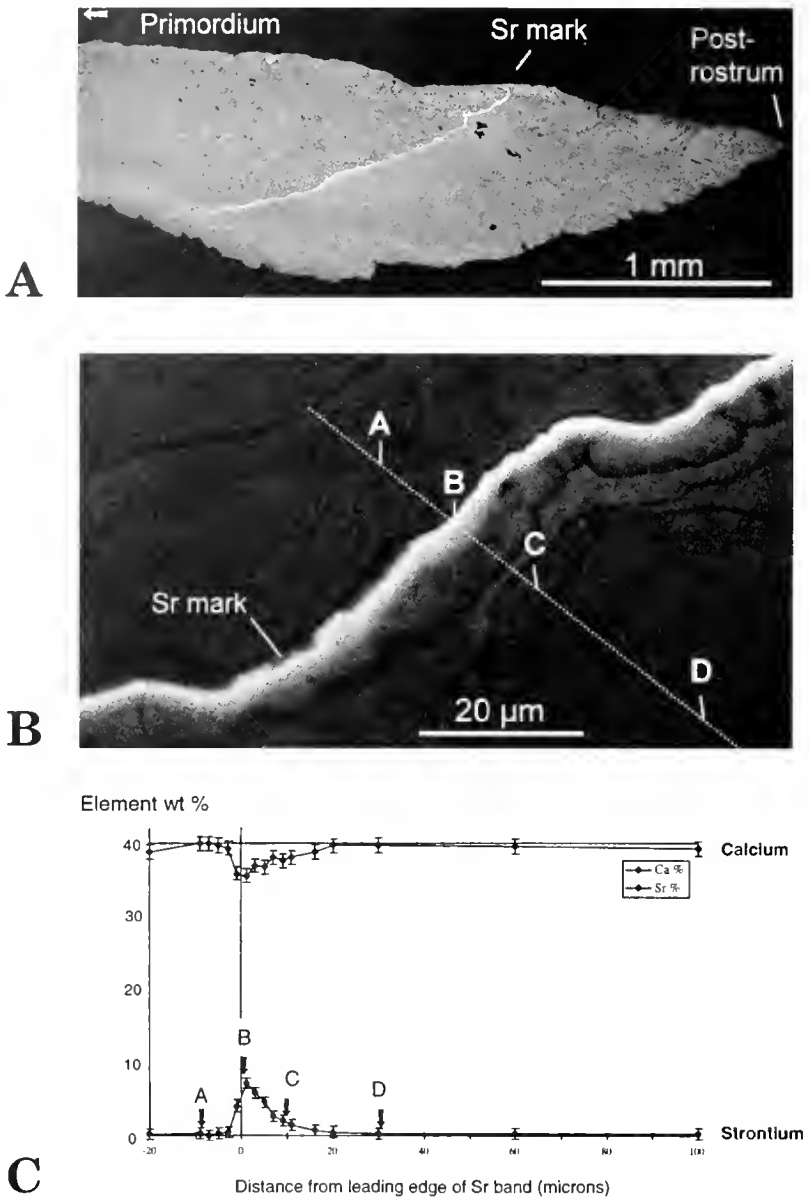

Figure 6

Details of the strontium mark on polished LS of specimen OB 96. Backscattered SEM images showing overall location of mark (**A**) and detail of region analyzed for Sr and Ca levels (**B**). Dashed line indicates transect followed for x-ray microanalysis (**C**): Measured variation in Sr and Ca levels along transect shown in B; points A–D indicate representative positions along the transect to enable comparison of sections B and C.

the backscattered imaging which band, if any, is a strontium mark.

Reliability of marking through injection of strontium

Of the 67 otoliths from which an age was estimated, strontium marks were detected with the Robinson detector in 19 of the 20 sectioned otoliths (95% detection rate) and with EDS in 40 out of 47 whole otoliths (85% detection rate). Strontium marks were as visible in the oblique longitudinal section (postrostral axis) as in the transverse section (Fig. 3). However, as increments are more widely spaced along the postrostral axis, we generally used the postrostral axis on the whole otolith for measuring the

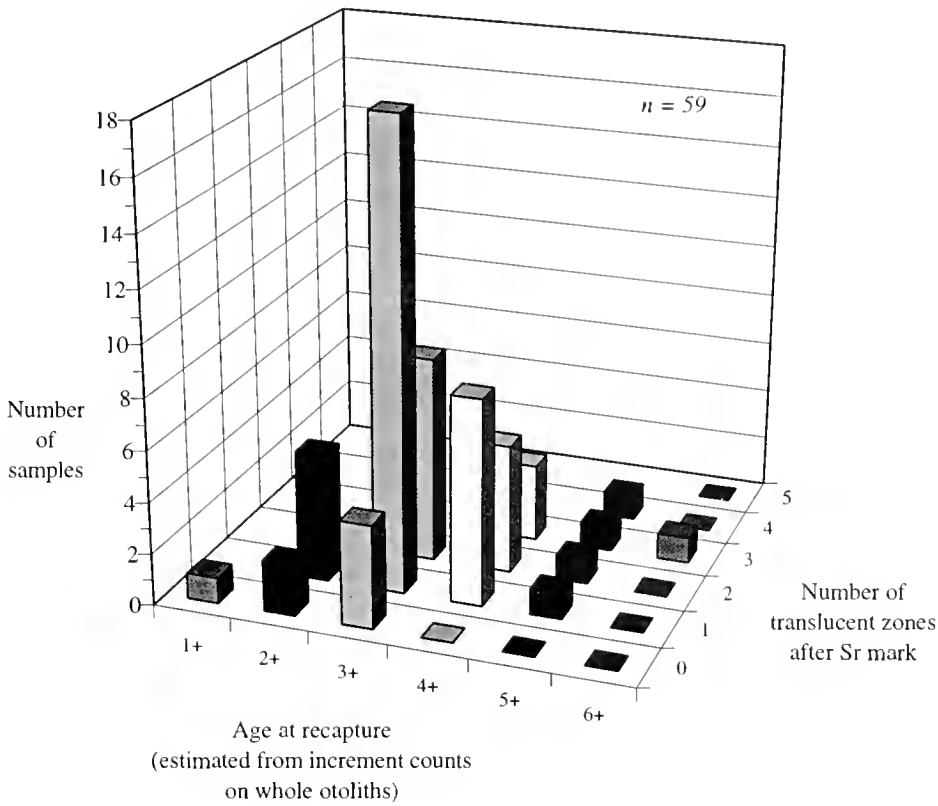

Figure 7

The number of strontium-marked otoliths used to validate age estimates that were made by counting increments on whole otoliths. The number of translucent zones observed after the strontium mark is shown for each age class. For all otoliths analyzed, the number of translucent zones counted after the Sr mark equalled the number that were expected from the period at liberty after fish were tagged and injected with $SrCl_2$.

position of translucent zones and for locating the strontium mark, either on a section (on the Robinson detector), or from the whole, etched otolith (with EDS).

Early in the experiment we found that the Sr marks in fish tagged and injected when they were 90 cm FL or larger were consistently fainter than in smaller fish. The concentration of Sr in the Sr marks of large fish was also significantly lower than in smaller fish caused, possibly, by loss of some of the solution during injection. To overcome this, dosages for large fish were increased in 1993 (Table 2), after which the bands were markedly more intense and easier to detect.

There was no apparent correlation between the time at liberty (i.e. time between Sr injection and recapture) and the intensity of the Sr marks; the longest time at liberty for a fish from which otoliths were analyzed for Sr was 1638 days. There was also no correlation between the intensity of the Sr marks and the delay between otolith recovery and analysis. Unlike tetracycline, which is photosensitive, the strontium mark did not fade after exposure to light.

Validation of annual increment formation from Sr marks

The 59 fish in which Sr marks were located ranged from 45 to 102 cm FL at the time of release, which corresponds to estimated ages of 1 to 4 (Gunn et al.[8]). Times at liberty ranged from 8 to 1638 days. The oldest recaptured fish was estimated to be 6+ years old; it had been at liberty for 1242 days (over 3 years).

[8] Gunn, J., N. Clear, T. Carter, A. Rees, C. Stanley, J. Kalish, and J. Johnstone. 1995. Age and growth of southern bluefin tuna. Paper SBFWS/95/8. First scientific meeting of the Commission for the Conservation of Southern Bluefin Tuna (CCSBT), Shimizu, Japan, 37 p. Commonwealth Scientific and Industrial Research Organization (CSIRO) Marine Research, GPO Box 1538 Hobart, 7001 Australia.

We counted six translucent zones on the otolith and the Sr mark occurred between the third and fourth zones (Fig. 7).

For all otoliths examined, there was agreement between the number of increments observed after the strontium mark and the number of increments expected, calculated from time at liberty. Thus, the annual periodicity in formation of increments 2 to 6 was validated for the otoliths analyzed. Because we were unable to tag young-of-the-year fish, in which the first translucent zone on the sagitta had yet to form, we could not determine when this translucent zone is laid down and when the formation of the first increment is completed. However, studies of daily microincrements (Itoh and Tsuji, 1996; Rees et al.[9]) have calculated that the approximate size at age 1 is 50 cm. We found otoliths of 50-cm fish had one increment.

Of the otolith increments counted, the first translucent zone was typically the most difficult to measure. The beginning of the first translucent zone occurred between 2.2 and 3.2 mm from the primordium along the postrostral axis, the most commonly used axis for analysis. Rees et al.[9] found microincrements in this region to be narrower than those deposited earlier, indicating a period of slow growth of the fish.

Additional validation of annual increment formation from tagged fish at liberty for extended periods

During the course of our experiment, two fish tagged by CSIRO in the 1980s were recaptured and their otoliths sampled. From lengths at first release of 45 cm and 82 cm FL, the fish had grown to 163 cm and 162 cm after being at liberty for 9 years, 7 months, and 10 years, 8 months, respectively. From the age-length key developed by Gunn et al.[8] we calculated that the 45-cm fish tagged in 1983 was one year old when tagged, whereas the 82-cm fish tagged in 1984 was two years old. The ages at recapture of these two fish were estimated from transverse sections through the primordium of the sagittal otoliths. Eleven increments (opaque and translucent zones) were counted on the otoliths from the fish released as a one-year-old and caught 9.58 years later; 13 increments were counted in the fish released as a two-year-old and recaptured 10.75 years later.

[9] Rees, A. J., J. S. Gunn, and N. P. Clear. 1996. Age determination of juvenile southern bluefin tuna, *Thunnus maccoyii*, based on scanning electron microscopy of otolith microincrements. *In* J. Gunn, N. Clear, T. Carter, J. Farley, A. Rees, and C. Stanley, Appendix 1: The direct estimation of age in southern bluefin tuna. Second scientific meeting of the Commissionfor Conservation of Southern Bluefin Tuna (CCSBT), Hobart, Australia. 26 August–5 September 1996, 22 p. Commonwealth Scientific and Industrial Research Organisation (CSIRO) Marine Research, GPO Box 1538, Hobart, Tasmania, 7001 Australia.

Discussion

Validation

This study demonstrated that, in the sagittae of SBT, the second through sixth increments, are deposited annually. This validation is independent of when the marked fish were tagged or recaptured. Because daily age estimates have been used to demonstrate that the first major increment in the sagitta forms in the first year of life (Rees et al.[9]), the annual formation of translucent zones appears to hold for the first six increments in SBT sagittae—corresponding to fish up to approximately 133 cm fork length.

The close agreement between increment counts on otoliths and the sum of age-at-tagging and time-at-liberty for two fish tagged in the 1980s and recaptured in the 1990s indicated that increment formation continues to be annual in fish up to at least 13 years old. Further evidence that increments in SBT sagittae are formed annually throughout life has been provided by a recent comparison of increment counts with age estimates derived from levels of bomb-radiocarbon in the early growth zones of sagittae (Kalish et al. 1996). This study reports close agreement between the two methods of estimating age for fish up to 34 years old.

Three sources of data—those from our marking experiment, the increment counts for two fish at liberty for over a decade, and the bomb radiocarbon data—provide strong evidence that seasonal changes in growth are expressed as clearly identifiable annual increments in the sagittal otoliths of SBT. These increments can be used to estimate the age of individual fish at any point in their lifespan.

Prior to our studies, Yukinawa (1970, using scales) and Thorogood (1987, using otoliths) used marginal increment analyses to demonstrate the annual check or translucent band deposition in fish they considered to be between 2 and 4 years old. Their results differ from ours only in the identity of year classes; their two- to four-year-olds correspond to our one- to three-year-olds. The difference in scale readings derives from Hynd's (1965) observation of two "checks" on the scales of new recruits (approximately 50 cm FL) to the Western Australian fishery. Interpretation of otolith microincrements (Itoh and Tsuji, 1996; Rees et al.[9]) indicates that these fish are only one year old. Unequivocal validation of these estimates is not possible at this stage because samples from prerecruits were not available to either Hynd or Yukinawa and we were not able to tag and mark prerecruit fish. In a number of other *Thunnus* species however, 50–60 cm fish were found to be around one year old (Uchiyama and Struhsaker, 1981; Wild, 1986; Foreman, 1996) and our counts of otolith microincrements and the data based on their inter-

pretation are consistent with this age. Therefore, we believe that the interpretation of Itoh and Tsuji (1996) and Rees et al.[9], that 50-cm-FL fish are one-year-olds, is most likely correct.

The identification of fish that we considered to be one-year-olds as two-year-olds was made by Thorogood in his 1987 study. However, we have found no evidence of two increments in the otoliths of new recruits. The early zones on all axes of otolith growth are difficult to read on some otoliths, and the increments in these areas are less distinct than those deposited later. In some fish a poorly defined "band" is also present very close to the primordium (within 2 mm along the postrostral axis). Although these two factors may confuse an inexperienced reader, Thorogood makes no mention of difficulty in reading the first increment. An alternative explanation for Thorogood's interpretations may be that his readings were influenced by the findings of Hynd (1965) and Yukinawa (1970) that were based on scales, because their estimates of age at recruitment were entrenched within the dogma of SBT population dynamics current in the 1970s and 1980s.

It has been hypothesized that more than one translucent zone forms per year in the otoliths of mature Atlantic bluefin tuna, *Thunnus thynnus* (Berry et al., 1977; Lee et al., 1983). In females, one translucent zone may correspond to a winter slow-growth period, the other to a spawning period (Lee et al., 1983). In the two large, tagged fish examined in our study, only one opaque and one translucent zone were deposited per year throughout life. The outer increments (i.e. those assumed to be deposited after sexual maturation) were consistent in both their width and optical density and were visually equivalent to the increments described by Lee et al. (1983), comprising a wide opaque region and a narrow translucent area that, on a black background, appears dark under reflected light. Occasionally, there appeared to be two translucent zones closer together than normal and, if these bands coalesced at the margin, they were counted as part of the same increment. These may be equivalent to the bands described by Berry et al. (1977) who hypothesized that a pair of these paired bands represented an annual increment. The close agreement between otolith increment counts and bomb-radiocarbon age estimates for mature SBT up to 34 years old (Kalish et al., 1996) supports our hypothesis that one increment, comprising one translucent and one opaque zone, continues to form per year, as does the consistency of the width and optical density of increments deposited after sexual maturation in the otoliths aged by Kalish et al. (1996). In summary, there is no significant evidence to suggest that mature female SBT deposit two translucent zones per year. In this regard our findings are similar to those of Hurley and Iles (1983) and Hurlbut and Clay (1988) for *T. thynnus*; they found, albeit in the absence of direct validation, that a single translucent zone is laid down per year in medium- and giant-size classes.

The use of strontium chloride to mark otoliths of large fish

This study has shown that intramuscular injection of strontium chloride leaves a distinct mark on the otoliths of SBT that is clearly visible as an SEM backscatter image in the Robinson detector. In the 20 otolith sections from Sr-injected fish that we examined, 95% had detectable marks. On this basis, we conclude that the compound is an efficient marker. Success of OTC as a marker at this rate of detection (95%) leads to high mortalities (McFarlane and Beamish, 1987). The high detection rates and lack of evidence of mortality for $SrCl_2$ are not surprising. This mineral occurs naturally in sea water, the mean concentration being 3.8–8.2 ppm (Carriker et al., 1991) or 0.09 mM/kg (Bruland, 1983), and both Sr and Cl are major constituents of the otoliths of SBT (Gunn[5]). When $SrCl_2$ is injected into the muscle it is taken up into the blood stream and incorporated in the endolymph and then the otolith, substituting for Ca within the $CaCO_3$ portion of the aragonite. The combined weight fraction of Ca and Sr (approximately 42%) within the otolith does not change as a result of the injection. However, the Ca:Sr ratio changes from 250:1 before injection to as low as 5:1 during the period over which the Sr spike induced by the injection is metabolized. At a distance of 6 μm beyond the injection mark, the Sr levels have dropped to about 50% and at 15 µm to 10% of peak values (Fig. 6). These distances correspond to time periods in the order of 2 and 5 days, respectively, based on median growth rates of around 3.0 µm/day estimated along this axis (Rees et al.[9]).

Detecting Sr marks on whole otoliths by using EDS was possible because the growth plane of tuna otoliths lies near the surface of the distal face. In otoliths of young fish, etching will expose the growth plane, so that sectioning is not required. Although this method of detection was slightly less successful (85%), it had two advantages. First, the preparation time was around half that required to prepare sections suitable for the Robinson detector. Second, the age estimate and measurements of increments were made along the postrostral axis on whole otoliths from the smaller fish (up to six years old), and the method of locating the strontium mark by EDS meant that the position of the strontium mark was measured along the axis in the same plane. With the Robinson detector, the same axis was measured but in cross section.

In fish older than about 6 years, the increments deposited on the margin can be unclear on whole oto-

liths; therefore transverse sections are used to determine ages of older fish (Gunn et al.[8]). In the future, as strontium-marked otoliths are returned from older fish that have been at liberty for longer periods, we will locate the strontium mark in transverse sections with the SEM and increase the number of increments that have been validated.

The recapture rates of orange-tagged and injected SBT were not significantly different from the recapture rates of yellow-tagged SBT; therefore the Sr injections apparently did not affect survival rate. Although the dosages of Sr varied between 65 and 250 mg/kg of fish, there is no evidence to suggest that higher doses increased mortality because Sr-injected fish with the highest doses were among those recaptured. A direct relation between the dosage and the intensity of the mark had been found in trials with three other species in 1990–91 (CSIRO, unpublished data[6]). The increased dose for large SBT resulted in much more distinct marks on their otoliths, which have a larger surface area than that in smaller fish. The less distinct marks could also be attributable in some large fish to a loss of strontium solution from the muscle after injection. Although more solution was injected if a loss was noticed, there may have been further loss of solution after the fish was returned to the water, resulting in a less effective dose. Thus, as a general guideline, we recommend a dose of 100 mg Sr/kg for marking otoliths in SBT. We note, however, that tissue area around the injection should be observed to ensure that there is no loss of injected solution from the muscle tissue.

The problem of detecting indistinct marks that result from low dosage levels are eliminated by using $SrCl_2$ as a marker. Unlike fluorescent marking, where it is very difficult to evaluate faint or ambiguous marks objectively (particularly if they are close to the outside edge of the otolith), it is possible to evaluate Sr marks objectively by x-ray analysis. Because the concentrations of the Ca and Sr on the Sr mark are high, very simple energy dispersive spectroscopy systems, which are available in many SEM facilities, can be used. Although not a trivial procedure, x-ray analysis requires preparation methods similar to those used for examining fluorescent markers and can usually be contracted to facilities at a low cost. Given the often substantial investment in tagging programs, and the common combination of low recapture rates and even lower otolith sampling rates, every sample is extremely valuable in a marking experiment. The safety net of chemical analysis is thus very advantageous.

Comparison of strontium and fluorescent markers

At the beginning of this project we chose strontium chloride over the more commonly used fluorescent markers because previous work on SBT with oxytetracycline had been unsuccessful. Although immersion in high concentrations of strontium or feeding with strontium-laced food (or both) had been used successfully for marking hard parts of larvae and juveniles of hatchery-reared salmon (Behrens Yamada and Mulligan, 1982; 1990), salmonids and a variety of tropical fish species (Brothers, 1990) and squid (Hurley et al., 1985), strontium had not previously been used to mark otoliths of large fish. On the basis of his experiments, Brothers (1990) concluded that, for mass marking of fish in captivity, detection of strontium marks was expensive and involved more difficult preparation than did fluorescent markers and other marking techniques such as thermal inducement (Volk et al., 1990).

Brothers' (1990) comment on expense is certainly pertinent but the expense of analyzing marked otoliths is often a small fraction of the cost of a marking experiment, particularly one where large numbers of fish have been tagged, injected, and released. Perhaps most important in the cost equation should be the rate of success of detecting marks in the otoliths of marked fish rather than the comparative cost of analysis. In otoliths from large tuna whose time at liberty has been long, the strontium marks are covered by a large amount of otolith material deposited after the time of injection. Sectioning is necessary for either marker; thus preparation times in these cases are much the same. For smaller tuna and those at liberty for short periods, fluorescent markers can be detected in the whole otolith, whereas detection of strontium without an EDS system would require sectioning, which would increase preparation time. The equipment for fluorescent markers is cheaper and comprises a light microscope equipped with an ultraviolet illumination source and filters to match the wave length of the fluorescence emitted from the marker when excited by the light source (see Wild and Foreman, 1980). For strontium, an SEM equipped with a Robinson detector is the minimum requirement; an EDS system is a useful extra. Although an SEM is a common apparatus in large research laboratories, hourly charges to the user can be high, although we have found that, with well prepared specimens, as many as four otoliths can be examined and analyzed per hour with an SEM.

Apart from preparation time and costs, strontium marking for age validation has clear advantages over fluorescent marking. One benefit of a technique that requires both a light microscope and an SEM is that measurements of increments and strontium marks are independent: the strontium cannot be detected in whole otoliths under the light microscope and the annual increments cannot be observed in the SEM. Allergic reactions by humans to compounds such as oxytetracycline have led the U.S. FDA to ban their use

in commercial fisheries. Strontium chloride, on the other hand, is regarded as safe for human consumption because it is a salt with a low order of toxicity (Sax and Lewis, 1987). It is even used in toothpaste by some manufacturers (e.g. "Sensodyne"). Strontium chloride, unlike fluorescent markers such as oxytetracycline, is not photosensitive. Neither the marking solution nor the marked otoliths need to be stored in the dark, and the mark does not fade with exposure to light or with time. In our study, strontium marks were as evident in fish that had been at liberty for long periods as in fish recaptured soon after release.

In summary, strontium chloride injection has proved to be a very successful way to mark the otoliths of southern bluefin tuna: 95% of those marked and recaptured in this study had detectable Sr marks in sectioned otoliths. This high "success rate," the harmless nature of $SrCl_2$ to both fish and humans, the capacity of EDS to positively identify the strontium mark, the insensitivity of the strontium mark to light, and the longevity of the strontium mark indicate that it should be seriously considered by those interested in large-scale marking experiments on commercial fishes.

Acknowledgments

The study was part of a tag-recapture project run by the Commonwealth Scientific and Industrial Research Organisation (CSIRO) and the Japan Marine Fishery Resource Research Centre (JAMARC). The efforts of K. Williams, D. Waddington, W. Whitelaw, T. Carter, and the Australian Fisheries Management Authority observers ensured the collection of adequate numbers of marked otoliths. We acknowledge the valuable contribution of W. Hearn, C. Proctor, and K. Williams, who initiated and implemented the 1990–91 study to assess the feasibility of injecting strontium chloride to mark juvenile SBT which was partly financed by an Environmental Research Grant from the Australian Government Department of Primary Industries and Energy. Our thanks also go to Sandy Morison, Craig Proctor, and other anonymous reviewers who gave their time to assess this manuscript and to Vivienne Mawson for her editorial comments.

Literature cited

Beamish, R. J., and G. A. McFarlane.
1983. The forgotten requirement for age validation in fisheries biology. Trans. Am. Fish. Soc. 112 (6):735–743.

Behrens Yamada, S., and T. J. Mulligan.
1982. Strontium marking of hatchery reared coho salmon, *Oncorhynchus kisutch* Walbaum, identification of adults. J. Fish Biol. 20:5–9.

1990. Screening of elements for the chemical marking of hatchery salmon. Am. Fish. Soc. Symposium 7:550–561.

Berry, F. H., D. W. Lee, and A. R. Bertolino.
1977. Progress in Atlantic bluefin tuna ageing attempts. Coll. Vol. Sci. Pap. Int. Comm. Conserv. Atlantic Tunas. 6(2):305–317.

Brothers, E. B.
1990. Otolith marking. Am. Fish. Soc. Symposium 7:183–202.

Bruland, K. W.
1983. Trace elements in sea-water. *In* J. P. Riley and R. Chester (eds), Chemical Oceanography, vol. 8. Academic Press, London.

Carriker, M. R., C. P. Swann, R. S. Prezant, and C. L. Counts, III.
1991. Chemical elements in the aragonitic and calcitic microstructural groups of shell of the oyster *Crassostrea virginica*: a proton probe study. Mar. Biol. 109:287–297.

Caton, A. E.
1991. Review of aspects of southern bluefin tuna biology, population and fisheries. *In* R. B. Deriso and W. H. Bayliff (eds.), World meeting on stock assessment of bluefin tunas: strengths and weaknesses. Inter-Am. Trop. Tuna Comm. Special Report 7:181–350.

Foreman, T.
1996. Estimates of age and growth, and an assessment of ageing techiques, for northern bluefin tuna, *Thunnus thynnus*, in the Pacific Ocean. Inter. Am. Trop. Tuna Comm., Bull. 21(2):75–123.

Gunn, J. S., I. R. Harrowfield, C. P. Proetor, and R. E. Thresher.
1992. Electron probe microanalysis of fish otoliths—evaluation of techniques for studying age and stock discrimination. J. Exp. Mar. Biol. Ecol. 158:1–36.

Hampton, J.
1991. Estimation of southern bluefin tuna *Thunnus maccoyii* growth parameters from tagging data, using von Bertalanffy models incorporating individual variation. Fish. Bull. 89(4):577–590.

Hurlbut, T., and D. Clay.
1988. A review of age and growth of Canadian giant bluefin as estimated from otoliths. Coll. Vol. Sci. Pap. Int. Comm. Conserv. Atlantic Tunas. 28:192–195.

Hurley, G. V., P. H. Odense, R. K. O'Dor, and E. G. Dawe.
1985. Strontium labelling for verifying daily growth increments in the statolith of the short-finned squid (*Illex illecebrosus*). Can. J. Fish. Aquat. Sci. 42:380–383.

Hurley, P. C. F., and T. D. Iles.
1983. Age and growth estimation of Atlantic bluefin tuna, *Thunnus thynnus*, using otoliths. *In* E. D. Prince and L. M. Pulos (eds.), Proceedings of the international workshop on age determination of oceanic pelagic fishes: tunas, billfishes and sharks, p. 71–75. U.S. Dep. Commer., NOAA Tech. Rep. NMFS 8.

Hynd, J. S.
1965. Southern bluefin tuna populations in south-west Australia. Aust. J. Mar. Freshwater Res. 16:25–32.

Itoh, T., and S. Tsuji.
1996. Age and growth of juvenile southern bluefin tuna *Thunnus maccoyii* based on otolith microstructure. Fish. Sci. 62(6):892–896.

Jenkins, G. P., and T. L. O. Davis.
1990. Age, growth rate, and growth trajectory determined from otolith microstructure of southern bluefin tuna *Thunnus maccoyii* larvae. Mar. Ecol. Prog. Ser. 63:93–104.

Kalish, J. M., R. J. Beamish , E. B. Brothers, J. M. Casselman, R. 1. C. C. Francis, H. Mosegaard, J. Panfili, E. D. Prince, R. E. Thresher, C. A. Wilson and P. J. Wright.
1995. Glossary. *In* D. H. Secor, J. M. Dean and S. E. Campana (eds.), Recent developments in fish otolith research, p. 723–729. Belle W. Baruch Library in Marine Science, No. 19, Univ. South Carolina Press, Columbia, SC.

Kalish, J. M., J. M. Johnston, J. S. Gunn, and N. P. Clear.
1996. Use of the bomb radiocarbon chronometer to determine age of southern bluefin tuna *Thunnus maccoyii*. Mar. Ecol. Prog. Ser. 143:1–8.

Lee, D. W., E. D. Prince, and M. E. Crow.
1983. Interpretation of growth bands on vertebrae and otoliths of Atlantic bluefin tuna, *Thunnus thynnus*. *In* E. D. Prince and L. M. Pulos (eds.), Proceedings of the international workshop on age determination of oceanic pelagic fishes: tunas, billfishes and sharks, p. 61–69. U.S. Dep. Commer., NOAA Tech. Rep. NMFS 8.

McFarlane, G. A., and R. J. Beamish.
1987. Selection of dosages of oxytetracycline for age validation studies. Can. J. Fish. Aquat. Sci. 44:905–909.

Murphy, G. M., and J. Majkowski.
1981. State of the southern bluefin tuna population: fully exploited. Australian Fisheries 40(11):20–29.

Sax, N. 1., and R. J. Lewis Sr.
1987. Hazardous chemicals desk reference. Van Nostrand Rienhold, New York, NY, 1084 p.

Secor, D. H., J. M. Dean, and E. H. Laban.
1992. Otolith removal and preparation for microstructural examination. *In* D. K. Stevenson and S. E. Campana (eds.), Otolith microstructure examination and analysis, p.19–57. Can. Spec. Publ. Fish. Aquat. Sci. 117.

Secor, D. H., J. M. Dean, and S. E. Campana.
1995. Fish otoliths: faithful biological and environmental chronometers? *In* D. H Secor, J. M. Dean and S. E. Campana (eds.), Recent developments in otolith research, p. xxv–xxvii. Belle W. Baruch Library in Marine Science 19, Univ. South Carolina Press, Columbia, SC.

Smith, D. C.
1992. Introduction. *In* D. C. Smith (ed.), Age determination and growth in fish and other aquatic animals. Aust. J. Mar. Freshwater Res. 43:vii–viii.

Steqert, B., J. Panfili and J. M. Dean.
1996. Age and growth of yellowfin tuna, *Thunnus albacares*, from the western Indian Ocean, based on otolith microstructure. Fish. Bull. 94:124–134.

Thorogood, J.
1986. New technique for sampling otoliths of sashimi-grade scombrid fishes. Trans. Am. Fish. Soc. 115:913–914.
1987. Age and growth rate determination of southern bluefin tuna, *Thunnus maccoyii*, using otolith banding. J. Fish Biol. 30:7–14.

Uchiyama, J. H., and P. Struhsaker.
1981. Age and growth of skipjack tuna, *Katsuwonus pelamis*, and yellowfin tuna, *Thunnus albacares*, as indicated by daily growth increments of sagittae. Fish Bull. 79(1):151–162.

Volk, E. C., S. L. Schroder, and K. L. Fresh.
1990. Inducement of unique otolith banding patterns as a practical means to mass–mark juvenile Pacific salmon. Am. Fish. Soc. Symposium 7:203–215.

Wexler, J. B.
1993. Validation of daily growth increments and estimation of growth rates of larval and early–juvenile black skipjack, *Euthynnus lineatus*, using otoliths. Inter–Am. Trop. Tuna Comm. Bull. 20(7):399–440.

Wild, A.
1986. Growth of yellowfin tuna, *Thunnus albacares*, in the eastern Pacific Ocean based on otolith increments. Inter. Am. Trop. Tuna Comm. Bull. 18(6):423–482.

Wild, A., and T. J. Foreman.
1980. The relationship between otolith increments and time for yellowfin and skipjack tuna marked with tetracycline. Inter–Am. Trop. Tuna Comm. Bull. 17(7):507–560.

Wild, A., J. B. Wexler, and T. J. Foreman.
1995. Extended studies of increment deposition rates in otoliths of yellowfin and skipjack tunas. Bull. Mar. Sci. 57(2): 555–562.

Williams, K.
1992. The tagging technique. Australian Fisheries 51(6): 15–17.

Yukinawa, M.
1970. Age and growth of southern bluefin tuna *Thunnus maccoyii* (Castelnau) by use of scale. Bull. Far Seas Fish. Res. Lab. 3:229–257.

Reproduction, embryonic development, and growth of the porbeagle shark, *Lamna nasus*, in the southwest Pacific Ocean

Malcolm P. Francis
National Institute of Water and Atmospheric Research
P.O. Box 14-901
Wellington, New Zealand
E-mail address: m.francis@niwa.cri.nz

John D. Stevens
CSIRO Marine Research
G. P.O. Box 1538
Hobart, Tasmania, Australia

Abstract.—Porbeagle sharks, *Lamna nasus*, are caught in large numbers as bycatch in tuna longline fisheries in the southwest Pacific Ocean. Information on reproduction, embryonic development, and size and sex composition was collected by scientific observers from New Zealand and Australian waters, and supplemented with data from other sources. Most sharks were juveniles less than 150 cm fork length (FL), and length-frequency distributions showed 3–5 modal peaks that we interpret as age classes. Juveniles grow linearly and rapidly (16–20 cm per year), reaching 110–125 cm FL in three years. Females mature at around 165–180 cm. Litter size is usually four embryos and parturition probably peaks in June–July (winter). This finding contrasts with data for North Atlantic porbeagles which give birth in spring–summer. Embryos grow about 7 cm per month, and are born at 58–67 cm FL. The gestation period appears to be about 8–9 months, but there is considerable variability in embryo length at any one time, suggesting an extended mating period. Embryos are nourished by oophagy, and develop a grossly distended abdomen as their "yolk stomach" fills with ova. Small embryos have fang-like functional teeth that tear open egg capsules to release the contained ova. The fangs are shed at 34–38 cm FL. The weight of yolk in the stomach peaks at 30–42 cm FL, and accounts for up to 81% of total body weight. Waste products of yolk digestion accumulate steadily in the spiral valve throughout gestation, and the liver reaches its maximum size in near-term embryos as excess energy from yolk digestion is stored for postnatal use.

Manuscript accepted 26 June 1999.
Fish. Bull. 98:41–63 (2000).

The porbeagle, *Lamna nasus* (Bonnaterre, 1788) is a pelagic mackerel shark (family Lamnidae) that inhabits cool, temperate oceans. It occurs in the North Atlantic Ocean and in a circumglobal band in the southern Pacific, Atlantic and Indian Oceans (Compagno, 1984; Last and Stevens, 1994; Yatsu, 1995). It is absent from the North Pacific, where it is replaced by its closest relative, the salmon shark (*Lamna ditropis*).

Lamnid sharks produce a small number of large, live young that are nourished by oophagy (Gilmore, 1993). In this unusual form of embryonic development, the pregnant female ovulates an enormous number of ova which are consumed by the embryos in the uteri. The embryos develop grossly swollen abdomens as they store large quantities of yolk for later growth. Oophagy was first described in porbeagles (Swenander, 1906, 1907; Shann, 1911, 1923) and salmon sharks (Lohberger, 1910), but has only recently been confirmed in shortfin and longfin makos (*Isurus oxyrinchus* and *I. paucus*) and white sharks (*Carcharodon carcharias*) (Gilmore, 1983; Stevens, 1983; Francis, 1996; Uchida et al., 1996).

The unusual bloated appearance of porbeagle embryos has led to a number of reports in the literature (Bigelow and Schroeder, 1948; Graham, 1956; Templeman, 1963), but the absence of a series of embryos at different stages of gestation has hampered attempts to understand their development. Litters usually consist of four embryos (Templeman, 1963; Gauld, 1989), which are thought to be born at about 60–80 cm total length (TL) (Shann, 1923; Compagno, 1984; Last and Stevens, 1994). Female size at maturity is often cited as 152 cm TL (Bigelow and Schroeder, 1948; Compagno, 1984; Last and Stevens, 1994), apparently based on two pregnant females reported to have been "about five feet long" (Shann, 1911). However, no other mature females under 2 m TL have been reported, leading some authors to regard the length at maturity as 2–2.5 m TL (Aasen, 1963; Pratt and Casey, 1990). The length of the gestation period is unknown; estimates, however, range from eight months to two years (Shann, 1923; Aasen, 1963; Gauld, 1989). The timing of parturition is variously stated as spring, summer, or autumn in the North Atlantic (Bige-

low and Schroeder, 1948; Aasen, 1963; Gauld, 1989). Thus, despite the early discovery of oophagy in porbeagles, little is known about their reproduction. Most parameter estimates are imprecise, and several are speculative or conflicting.

Few pregnant females have been reported from the Southern Hemisphere, and few details have been provided for any of them. Graham (1939, 1956) reported one caught at Otago Heads, New Zealand, in 1933. It had three embryos that were approaching full term and weighed 3.4–4.3 kg each. Graham (1956) also examined several other pregnant females but he reported few details. Duhamel and Ozouf-Costaz (1982) found four small embryos in a female caught in 1981 near Kerguelen Island in the southern Indian Ocean (51°S, 70°E).

Growth curves are available for northwest Atlantic porbeagles, based on modal analysis of length-frequency distributions, and back-calculation of length-at-age from bands on a vertebra (Aasen, 1963). They suggest that growth is relatively fast, at least in the first few years, and that longevity is 20–30 years. No growth information is available for the Southern Hemisphere.

Porbeagles have been exploited for their flesh for many decades, and have proven to be vulnerable to overfishing. A target longline fishery in the northwest Atlantic in the 1960s lasted only six years before collapsing (Anderson, 1990; Pratt and Casey, 1990). In the Southern Hemisphere, porbeagles have not been targeted, but they are frequently taken as bycatch in tuna fisheries, especially the pelagic driftnet fishery for albacore (*Thunnus alalunga*) during 1982–91 in the South Pacific (Murray, 1994; Yatsu, 1995), and the longline fishery for southern bluefin tuna (*Thunnus maccoyii*) and bigeye tuna (*Thunnus obesus*) in the southern Indian and Pacific Oceans (Stevens et al., 1983; Francis et al., 1999). In the New Zealand longline fishery, porbeagles are the second most commonly caught shark after the blue shark (*Prionace glauca*) (Francis et al., 1999).

The collapse of the northwest Atlantic fishery in the 1960s provides ample justification for a cautious approach to managing porbeagles. In view of recent increased landings in the North Atlantic (O'Boyle et al., 1996), and the size and scope of the tuna longline fishery in the southern oceans, there is an urgent need for improved information on reproduction, growth, and stock productivity as a basis for effective management. Much of the Southern Hemisphere longline fishery occurs in international waters, making monitoring and management difficult. Recently, the New Zealand and Australian governments implemented scientific observer programs to monitor catches of foreign and domestic longline vessels in their respective Exclusive Economic Zones (EEZs). These programs provided an opportunity to collect information on the reproduction and growth of porbeagles. In this paper, we describe the geographical distribution and length composition of sharks taken by longline vessels in the southwest Pacific, estimate the growth rate of embryos and juveniles, and describe embryonic development and oophagy. We also estimate the length of the gestation period, the timing of parturition, and the size at birth, and compare these with estimates for North Atlantic porbeagles.

Materials and methods

Data sources

Most of our data and specimens were collected by scientific observers aboard Japanese and domestic tuna longline vessels operating in the New Zealand and Australian EEZs. In New Zealand, fishing and observer effort was concentrated in two regions: 1) northeast New Zealand (north and east coasts of North Island and the Kermadec Islands), and 2) southwest New Zealand (east and west coasts of South Island) (Fig. 1). In Australia, most effort was around Tasmania (Fig. 2). New Zealand observers began recording the quantity of bycatch in 1987, measuring and sexing porbeagles in 1990, and examining females for embryos in 1992. In Australia, the respective years were 1988, 1990 and 1991. The primary task of observers was to monitor the target tuna species (mainly southern bluefin and bigeye tuna). Porbeagles were counted on most longline sets but were not always measured or examined for embryos. Therefore our data represent a subsample of the catch taken by observed longliners. The opportunistic nature of this collection process, and the low catch rate of pregnant females, necessitated the accumulation of specimens and data over a lengthy period.

Embryos collected by observers were supplemented by specimens and data from other sources, and the literature, including three litters from Heard and Kerguelen Islands in the southern Indian Ocean (Table 1). The four embryos from the Kerguelen female were deposited in the Museum National d'Histoire Naturelle (MNHN 1981-1432–1981-1435) (Duhamel and Ozouf-Costaz, 1982), and were photographed and remeasured for us by Duhamel.[1] A 185-cm-fork length (FL) female from Macquarie Island (Fig. 1) was the only intact pregnant female we examined.

[1] Duhamel, G. 1997. Museum National d'Histoire Naturelle (MNHN), 75231 Paris cedex 05, France. Personal commun.

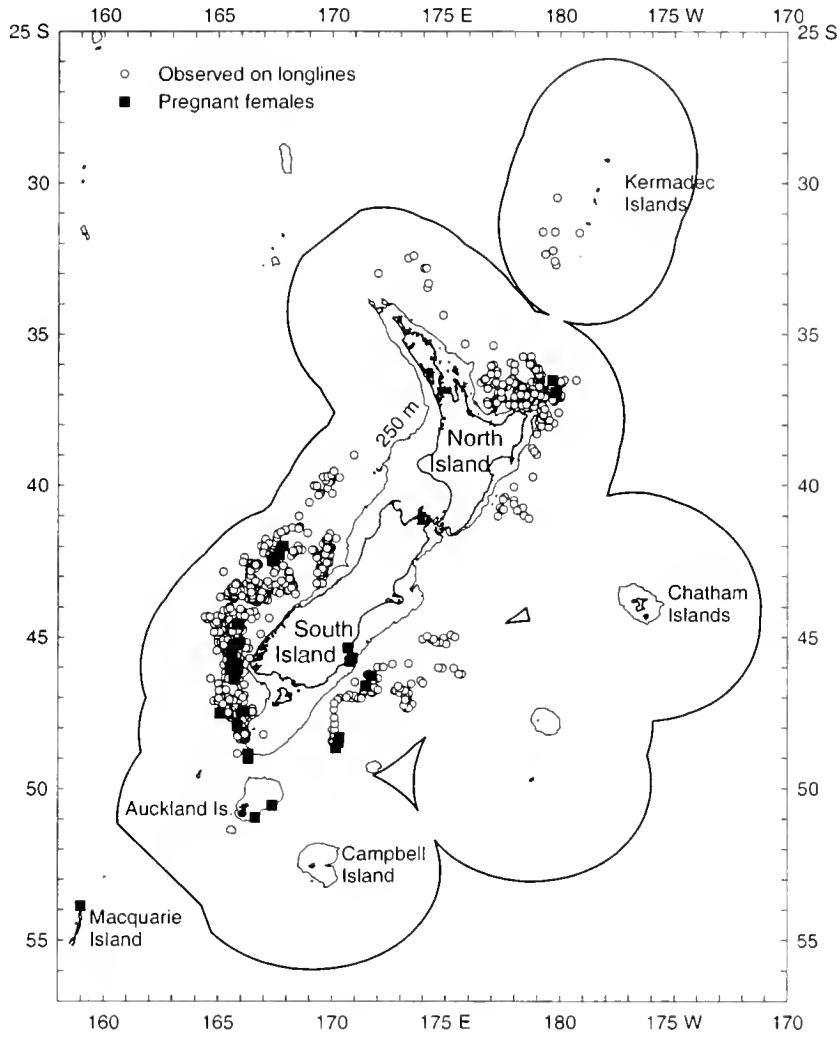

Figure 1

Map of the New Zealand region showing start positions of tuna longline sets from which porbeagles were recorded, and capture locations of pregnant females (n=35). The 250-m isobath and Exclusive Economic Zone are also shown.

Size and growth

Porbeagles were measured in one or more of three ways: precaudal length (PL; snout to the precaudal pit), FL (snout to the fork in the tail), and TL (snout to the tip of the tail). TL can be measured in two different ways—with the tail in the natural position (TL_{nat}) (Bigelow and Schroeder, 1948), or with the tail flexed down so that the upper caudal lobe lies parallel to the long axis of the body (TL_{flex}) (Compagno, 1984). Observers probably measured TL_{nat} on postnatal porbeagles because TL_{flex} is difficult to measure in species with a relatively rigid caudal fin. TL_{nat} measurements in embryos are not strictly comparable with TL_{nat} measurements in postnatal porbeagles because of the curved and folded nature of the caudal fin in embryos.

Most observers measured FL; therefore we adopted that as our standard. Regression equations relating FL to TL and PL are given in the "Results" section. Literature reports of TL were converted to FL before comparison with our data. Hereafter, FL is reported unless otherwise stated. Porbeagles were also sexed, weighed whole, and sometimes weighed after processing. Data were inspected for outliers on bivariate plots of PL, FL, TL, whole weight, and processed weight. Obvious errors were corrected if possible, and deleted if not. Before 1993, some New Zealand observers confused porbeagles and shortfin makos. We therefore restricted our New Zealand analyses of length, weight and location to data collected from 1993 onwards.

Initial inspection of the length-frequency data revealed modes that might correspond with juvenile age

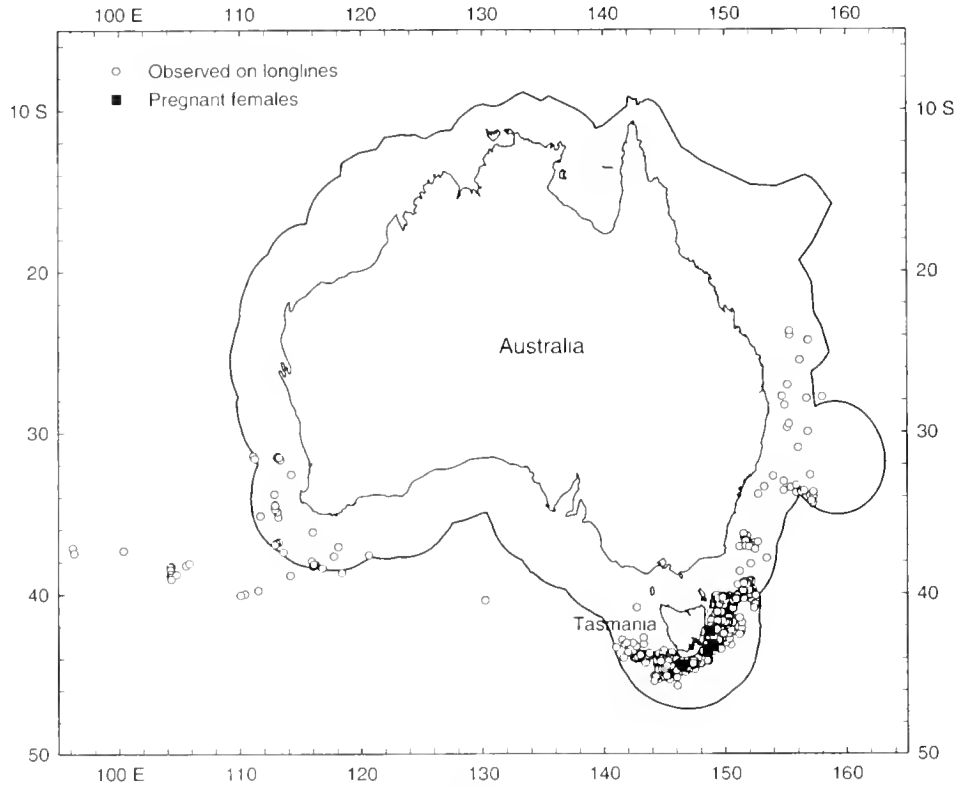

Figure 2

Map of the Australian region showing start positions of tuna longline sets from which porbeagles were recorded, and capture locations of pregnant females (n=5). The Exclusive Economic Zone is also shown.

classes. To assist modal discrimination, we limited our length-frequency analyses to the period April–July, during which 87% of New Zealand and 86% of Australian length measurements were taken. The MIX computer program (MacDonald and Pitcher, 1979; MacDonald, 1987; MacDonald and Green, 1988) was applied separately to the New Zealand and Australian length-frequency data for combined sexes to decompose the distributions into their component age classes. The program estimates the mean length, and the standard deviation of the lengths, for each age class, and the proportion of the sample in each age class. Length-frequency data were grouped into 3-cm class intervals, and truncated at 162 cm (New Zealand) and 150 cm (Australia) before analysis because large sharks were poorly represented in the samples. For each data set, we fitted a MIX model with three age classes and then progressively added extra age classes until there was no significant improvement in the χ^2 goodness of fit (MacDonald and Green, 1988). Occasionally, partially constrained fits (alternately fixing the standard deviations and proportions of one or two of the older age classes) were necessary for successful convergence (MacDonald and Green, 1988). This had no effect on the estimates of mean length, which were never constrained.

Embryos and ova

Embryos were placed in plastic bags and frozen; sometimes only partial litters were retained. Rarely, the uteri were removed intact and frozen with the embryos still inside. In the laboratory, embryos were thawed, sexed, and their jaws were examined for functional teeth. The embryos were then weighed, and measured (usually PL, FL, TL_{nat}, and TL_{flex}). FL was estimated from TL for three embryos without FL measurements (see "Results" section for regression equations). The liver and the contents of the stomach and intestine were weighed separately. Stomach contents were expressed as a percentage of total weight. Liver weight, and the weight of the intestinal contents were expressed as percentages of yolk-free embryonic weight to avoid distortions caused by the large variation in the stomach contents.

The uteri and right ovary[2] of the Macquarie Island female were examined. The diameters of a subsample of ovarian ova were measured using an image analysis system attached to a binocular microscope, and an

[2] The left ovary of lamnid sharks is vestigial (Pratt, 1988).

estimate was made of the total number present by counting ova in six weighed subsamples.

The four MNHN embryos from Kerguelen Island were measured for TL, FL, and weight in December 1997. Because there was a mean shrinkage of 4.4% from the original TL measurements (Duhamel and Ozouf-Costaz, 1982), we applied an equivalent shrinkage correction to the 1997 FL measurements. Fresh embryo weights were not reported by Duhamel and Ozouf-Costaz (1982), and we have not used the 1997 weights because they probably underestimate the original weights due to dissolution and leaching of lipids from the yolk in the stomach. Similarly, measurements from the Museum of New Zealand (NMNZ) embryos are not included here because of likely shrinkage and weight loss following preservation.

North Atlantic embryo lengths and dates of capture were obtained from the literature for comparison with Southern Hemisphere data (Swenander, 1906, 1907; Shann, 1911, 1923; Nordgård, 1926; Bigelow and Schroeder, 1948; Templeman, 1963; Gauld, 1989; Moss[3]; Newton[4]). For some litters, only one or two embryos were measured. Data were used only if they specified the month of capture, and some measurements that were known or thought to have been made on preserved specimens were corrected for shrinkage.

Results

Geographical distribution

Porbeagles have a wide latitudinal distribution. In the New Zealand region, they range from the Kermadec Islands (30°30'S) to Macquarie Island (53°52'S) (Fig. 1). In the Australian EEZ, they range from near the Tropic of Capricorn in southern Queensland (23°44'S) to south of Tasmania (45°44'S) (Fig. 2). The large number of capture records from northeast and southwest New Zealand, and around Tasmania, reflect concentration of fishing effort, and not necessarily high shark densities. Porbeagles also occur near Heard Island (51–52°S), and Kerguelen Island (51°S) in the southern Indian Ocean (Duhamel and Ozouf-Costaz, 1982).

Porbeagles were caught off southern Queensland (Fig. 2, north of 31°S) only in winter (June–September), when water temperatures were lowest. Sea surface temperature (SST) at the time of capture of six sharks off Queensland in July–August 1997 was 21.3–21.6°C, about 4°C lower than normal.

Sea surface temperature was recorded at about hourly intervals during hauling of each longline in New Zealand. The number of sharks caught per 1000 hooks (CPUE) was determined for each set and plotted against the mean of the hourly SSTs. There was no apparent trend in CPUE between 9.85°C (the minimum set temperature) and 19.5°C (mean CPUE=1.82, maximum=44.8, n=1292 sets). Between 19.5 and 23.0°C, mean CPUE was lower (mean=0.54, maximum = 5.0, n=105), and above 23.0°C no porbeagles were caught (n=23).

Most pregnant females were caught in the cooler southern waters of New Zealand and Australia (Figs. 1 and 2), and some were taken from the subantarctic Auckland, Macquarie, Heard, and Kerguelen Islands (50–54°S). However, two were also caught in northeast New Zealand. For longline-caught females, SST was 10.2–17.2°C (mean 12.9°C, n=32), and bottom depth at the capture locality was 600–4300 m (mean=2104 m, n=11). The two Heard Island pregnant females were taken by bottom trawl at depths of 248 and 259 m and bottom temperatures of 2.9 and 2.5°C, respectively. The Auckland Islands female was caught by midwater trawl at 160–164 m and a temperature of 11.9°C. Porbeagles have also been caught by bottom trawl near Macquarie Island at temperatures of 1°C (Williams[5]).

Length, weight, and growth

The relationships between PL and FL (both in cm) for New Zealand porbeagles were as follows:

$PL = -1.366 + 0.907\ FL$	(n=866, r^2=0.995,
$FL = 1.990 + 1.098\ PL$	range 61–223 cm FL, 54–208 cm PL

The relationships between TL and FL (both in cm) for Australian porbeagles were as follows:

$TL = 4.165 + 1.098\ FL$	(n=173, r^2=0.967,
$FL = -0.567 + 0.881\ TL$	range 63–180 cm FL, 71–202 cm TL)

Length-weight data were available for 641 New Zealand porbeagles (330 males, 309 females, and 2 unsexed) over the range 61–228 cm FL and 3–153 kg weight. However 96.7% of the sample was less than 150 cm FL; therefore the results represent only juveniles. There was no evidence from the raw data, or the residuals from a log-log regression, of a difference between the sexes. The regression equation for combined sexes was as follows:

[3] Moss, S. A. 1995. University of Massachusetts, North Dartmouth, MA 02747, USA. Personal commun.

[4] Newton, A. 1996. The Marine Laboratory, P.O. Box 101, Aberdeen, Scotland. Personal commun.

[5] Williams, R. 1997. Australian Antarctic Division, Tasmania, Australia. Personal commun.

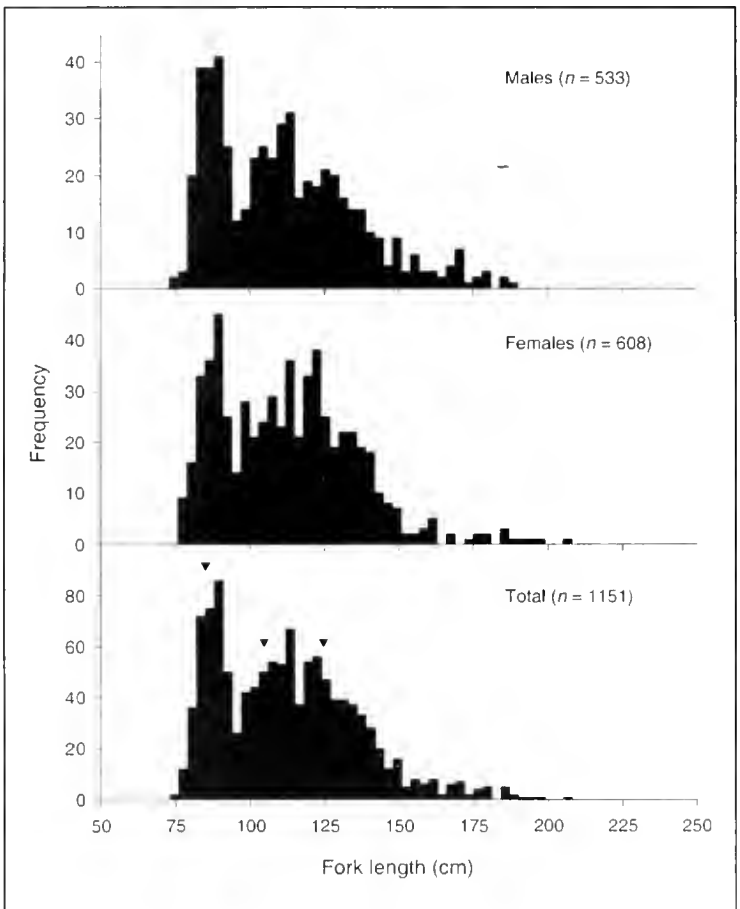

Figure 3A

Porbeagle length-frequency distributions by sex for April–July: (**A**) southwest New Zealand; (**B**) northeast New Zealand; (**C**) Australia. The bottom panel in each series includes some unsexed sharks. n = sample size. Triangles indicate mean lengths of the age classes identified by MIX modal decomposition.

$$\text{Log}_{10}(weight) = -5.050 + 3.128\ \text{Log}_{10}(FL), \quad (n = 641, r^2 = 0.956)$$

where weight is expressed in kg and FL in cm.

In New Zealand, length ranges were 64–228 cm for males and 61–206 cm for females (Fig. 3, A and B). Most were shorter than 150 cm. The size distributions were similar for males and females up to 150 cm, and the sex ratio (both subregions combined) was not significantly different from one (M:F=0.93:1; χ^2=1.99, P>0.1). However, males outnumbered females above 150 cm by 3.18:1 (χ^2=16.28, P<0.01).

In southwest New Zealand, there was a strong modal peak at 79–93 cm for both sexes, and for males there were also clear peaks at 100–115 cm and 118–133 cm (Fig. 3A). The best MIX fit to the combined sexes data consisted of three age classes whose mean lengths are shown in Fig. 3A. Sample sizes were small in northeast New Zealand; therefore no MIX model was applied. A strong mode was present at 67–88 cm (Fig. 3B), and indistinct modes were present for both sexes at about the same position as the second and third modes in southwest New Zealand.

In Australia, length ranges were 61–204 cm for males and 58–208 cm for females (Fig. 3C). Most were shorter than 150 cm, with a strong mode at 76–94 cm. The size distributions of males and females were similar. The sex ratio of sharks smaller than 150 cm did not differ significantly from one (1.07:1; χ^2=1.47, P>0.1), but males outnumbered females above 150 cm by 2.71:1 (χ^2=11.08, P<0.01). The best MIX fit to the combined sexes data consisted of five age classes whose mean lengths are shown in Figure 3C.

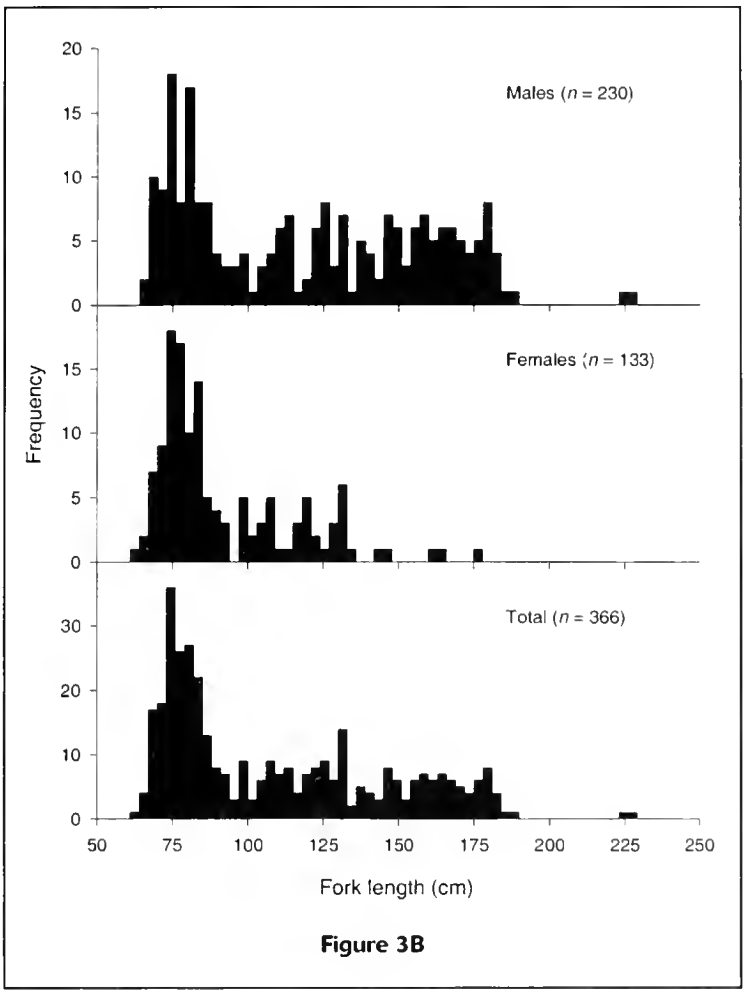

Figure 3B

The mean lengths of the modes for southwest New Zealand and Australia were plotted against age, which was calculated from a theoretical birth date of 1 June (see below) and mean sampling dates of 5 May and 16 June, respectively (Fig. 4). Thus the ages classes were sampled near their respective birth dates. We interpret the five Australian modes as representing sharks that were recently born, and 1–4 years old, and the three southwest New Zealand modes as those representing sharks that were 1–3 years old. The first length mode in the northeast New Zealand distribution was substantially shorter than the first southwest New Zealand mode and the second Australian mode, and we are uncertain about assigning an age to it. At age 1 year, southwest New Zealand and Australian porbeagles were similar in length, but for older ages New Zealand sharks were slightly larger. Growth in both regions was linear over the range of the data (Fig. 4):

southwest
New Zealand: $FL = 66.5 + 19.8\,(Age)$ $(r^2=1.000)$

Australia: $FL = 65.4 + 16.1\,(Age)$ $(r^2=0.997)$

Female length at maturity and reproductive development

Maturity status was not recorded; therefore we cannot estimated length at maturity. However, 37 pregnant females ranged from 167[6]–199 cm (mean=185 cm), suggesting that female maturity is reached around 165–180 cm.

The Macquarie Island female had four embryos 21.5–23.2 cm long. The right ovary was of the "internal" type, which is typical of lamnid sharks (Pratt, 1988). It weighed 2.75 kg (2.35% of total weight) and was undergoing active oogenesis. The entire ovary was packed with ova; other than a thin external envelope it had no macroscopically visible ovarian tissue. There was a single large efferent pore in the ovary, from which ova are shed (Stevens, 1983; Gilmore, 1993).

[6] FL of 167 cm was calculated from a PL of 151 cm.

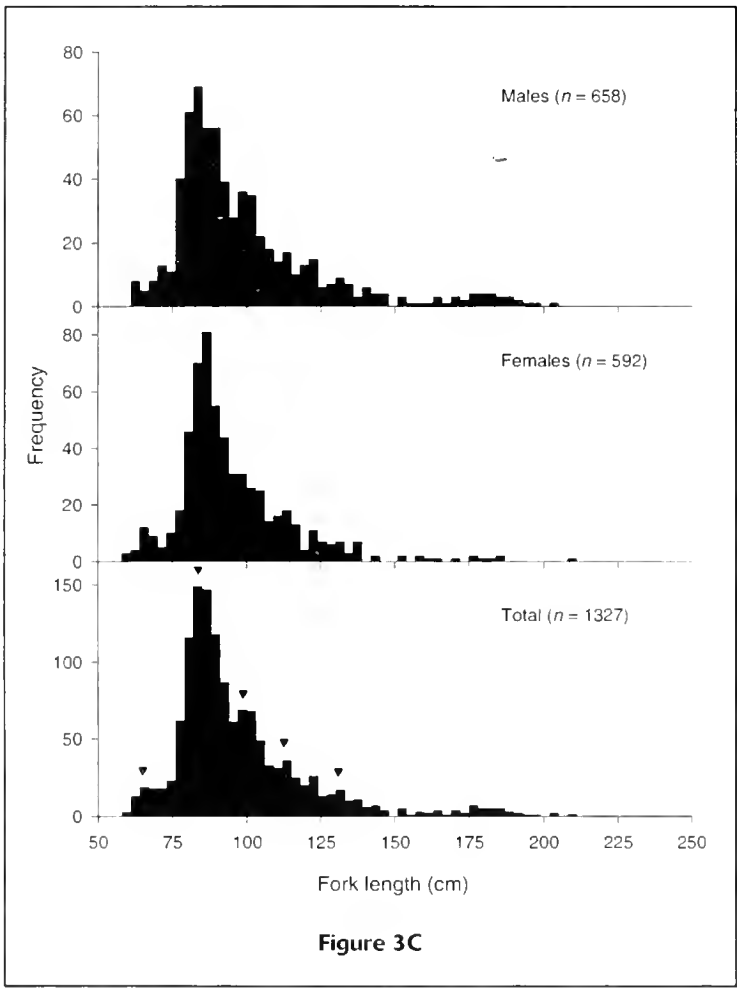

Figure 3C

The mean ovum count from six weighed subsamples was 72.2 ova per gram (SE=2.6), producing an estimated total number of 198,000 ova. Ova diameters were mostly 1.5–3.3 mm; a group of larger ova had diameters of 3.4–4.7 mm (Fig. 5). In addition to the embryos, the right uterus contained three egg capsules, and in the left uterus a 22.0-cm embryo had an egg capsule lodged in its mouth. Three of the capsules were empty and the fourth contained four ova (Fig. 6). Uterus width, estimated from a photograph containing a ruler, was about 10 cm. In other females with near-term embryos, uterus width was about 20 cm. The anterior quarter of the uterus had many longitudinal folds or pleats, and the rest was covered with small papillae and had a velvety texture.

Litter size, embryonic growth, and gestation

Data were obtained from 43 litters and 138 embryos (Table 1). All but four of the 40 litters for which litter size was known contained four embryos, two in each uterus. The exceptions were two litters reported by Graham (1939, 1956) with two and three embryos respectively, one reported by Hanchet [7] with three embryos, and a New Zealand longline-caught litter with two midterm embryos. Mean litter size was 3.85. Of 132 embryos that were sexed, 73 were males and 59 were females, producing a sex ratio not significantly different from one (χ^2=1.48, P>0.1).

Regression equations relating different embryo length measurements (in cm) were:

$PL = -0.125 + 0.885\ FL$ (n=97, r^2=0.999)
$TL_{nat} = 0.180 + 1.162\ FL$ (n=96, r^2=0.998)
$FL = -0.085 + 0.859\ TL_{nat}$ (n=96, r^2=0.998)
$TL_{flex} = 0.836 + 1.170\ FL$ (n=87, r^2=0.998)
$FL = -0.644 + 0.853\ TL_{flex}$ (n=87, r^2=0.998)

A log-log regression of yolk-free embryo weight (kg) against FL (cm) gave

[7] Hanchet, S. 1996. National Institute of Water and Atmospheric Research (NIWA), P. O. Box 893, Nelson, New Zealand. Personal commun.

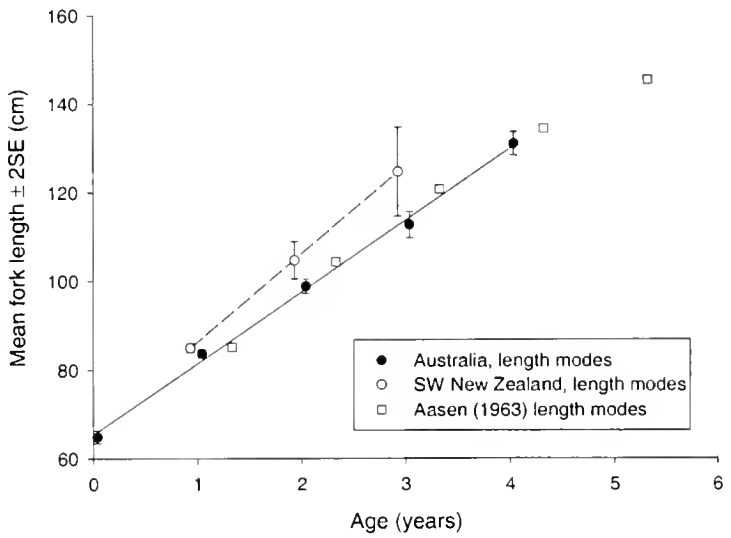

Figure 4

Porbeagle mean lengths-at-age determined by MIX analysis of the southwest New Zealand and Australian data in Figure 3, A and C, with fitted linear regressions. Also shown are Aasen's (1963) northwest Atlantic length-frequency modes, which were plotted assuming a 9 April theoretical birth date (1.7 months earlier than the Southern Hemisphere) and a mean sampling date of 9 August.

Table 1

Sources, numbers, collection periods and collection localities of Southern Hemisphere porbeagle embryos. NZ = New Zealand; NMNZ = Museum of New Zealand. Additional pregnant females reported by Graham (1956) were not included because of lack of data.

Source	Number of litters	Number of embryos	Collection period	Collection locality
Tuna longline	27	87	1992–98	New Zealand
Tuna longline	5	17	1991–95	Tasmania, Australia
Bottom trawl	2	8	1997	Heard Island
Bottom trawl	1	4	1995	Macquarie Island
Midwater trawl	1	4	1996	Auckland Island, NZ
NMNZ P22122	1	3	1987	Auckland Island, NZ
Hanchet[1]	2	2	1982–83	Otago, NZ
Berquist[2]	1	4	1998	Otago, NZ
Graham (1939, 1956)	2	5	1933	Otago, NZ
Duhamel and Ozouf-Costaz (1982)	1	4	1981	Kerguelen Island
Total	43	138		

[1] See Footnote 7 in the main text.
[2] Berquist, R. 1997 Department of Zoology, University of Otago, P.O. Box 56, Dunedin, New Zealand. Personal commun

$$\text{Log}_{10}(weight) = -4.719 + 2.916\ \text{Log}_{10}(FL) \quad (n=100,\ r^2=0.974)$$

The Kerguelen Island embryos reported by Duhamel and Ozouf-Costaz (1982) were the smallest in our sample, with estimated FLs of 9.6–10.4 cm. Our largest embryos were in litters of 62.0–67.0 cm, 64.2–65.6 cm, and 64.3–66.6 cm. Typically, all embryos in a litter were similar in length, but two litters each contained one unusually small embryo (runt) (Table 2). Variation in length within a litter increased with mean length, but the percentage range in length was relatively constant.

Table 2

Fork lengths and weights of stomach contents, intestinal contents, and livers of embryos from two litters that contained one unusually small embryo.

	Litter 1	Litter 2
Embryo fork lengths (cm)	22.5, 27.7, 29.0, 30.8	51.4, 55.3, 55.3, 63.8
Length range (cm)	8.3	12.4
Length range as percentage of mean length (%)	30.2	22.0
Smallest embryo		
Stomach contents (kg)	0.015	0.077
Intestine contents (kg)	0.007	0.069
Liver (kg)	0.003	0.056
Other three embryos		
Stomach contents (kg)	0.117–0.440	0.183–0.340
Intestine contents (kg)	0.114–0.296	0.092–0.130
Liver (kg)	0.006–0.017	0.151–0.364

All embryos were collected between 11 March and 16 July, reflecting the seasonality of the longline fisheries. The mean length of Southern Hemisphere embryos in a litter increased significantly ($P<0.01$) with sampling date (Fig. 7):

$$Mean\ FL\ (\text{cm}) = 9.36 + 7.48\ month,\quad (n=39,\ r^2=0.27)$$

where "month" is defined as the number of months elapsed since 1 January. There was considerable unexplained variability. For example, in April, mean embryo length varied between 20.3 and 63.5 cm. Inspection of the data by year of collection and sampling location showed that the variability was not caused by interannual or spatial differences. A regression equation fitted to North Atlantic embryo data (Fig. 7) was

$$Mean\ FL\ (\text{cm}) = 23.51 + 6.78\ month\quad (n=29,\ r^2=0.70)$$

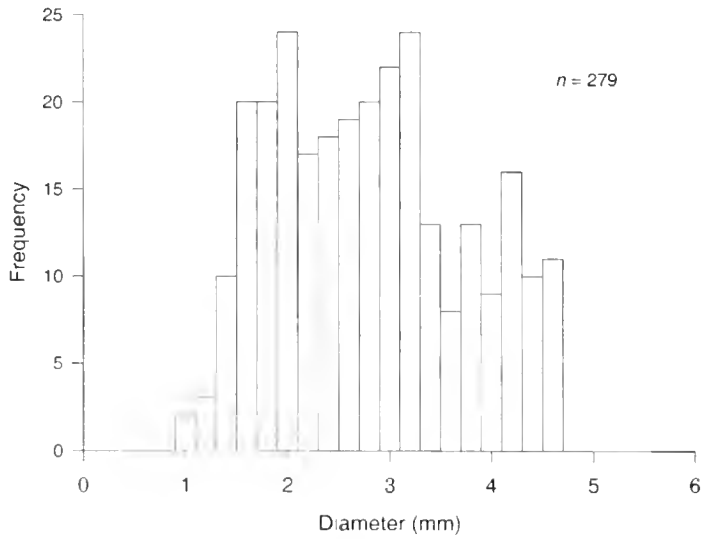

Figure 5

Frequency distribution of ovarian ova diameters from a pregnant porbeagle from Macquarie Island. n = sample size.

The North Atlantic regression explained a much higher proportion of the variation but displayed considerable length variability in early gestation. A homogeneity of slopes test showed that the regression slopes for the two hemispheres were not significantly different ($P=0.76$). The pooled data had a regression slope (=embryonic growth rate) of 7.1 cm per month, and the regression intercepts differed significantly (analysis of covariance, $P=0.004$) by 12.0 cm, which is equivalent to a temporal displacement of about 1.7 months.

Small, postnatal juveniles 58–68 cm long ($n=53$), were observed on Australian longlines between 22 May and 9 September, with a mean capture date of 15 July. Large embryos (up to 67 cm) were observed between mid-April and mid-June (Fig. 7). In the Southern Hemisphere, the large variation in embryo length at any one time, and the long period over which small juveniles, assumed to be newborn, were collected, indicate that the parturition period is lengthy. Parturition probably peaks in June–July (winter) but may

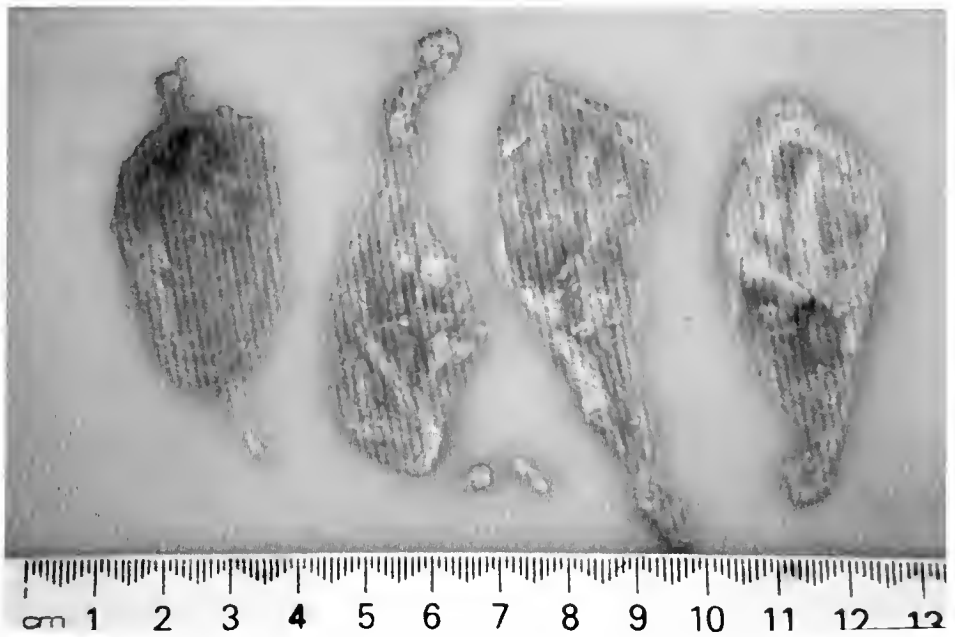

Figure 6

Four empty egg capsules found in the uteri and in the mouth of an embryo, from a pregnant porbeagle from Macquarie Island. Also shown are several loose ova found in one of the egg capsules. The largest egg case was 75 mm long.

extend from April to September. For aging purposes, we defined the theoretical birth date as 1 June. Based on the lengths of the smallest juvenile and the largest embryo, the length at birth is 58–67 cm. If a growth rate of 7.48 cm per month is maintained by Southern Hemisphere porbeagles throughout gestation, the gestation period is about 8–9 months. However, the unexplained variability in Fig. 7 compromises our ability to accurately estimate the gestation period.

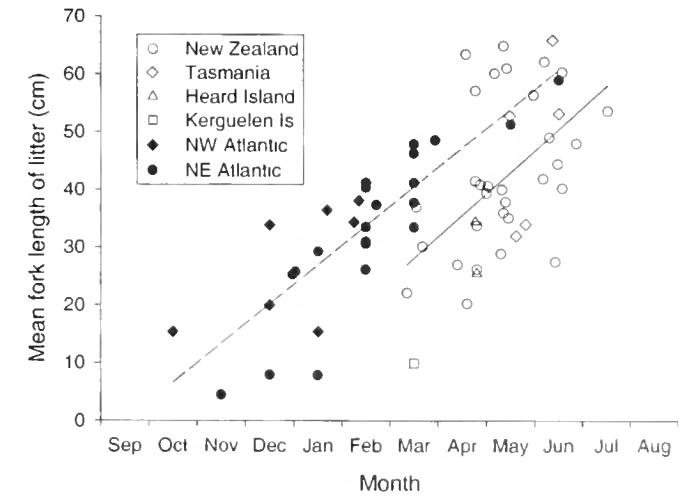

Figure 7

Monthly variation in the mean lengths of porbeagle embryos from four Southern Hemisphere locations (white symbols, n=39, r^2=0.27), and the northwest and northeast Atlantic (black symbols, n=29, r^2=0.70).

Embryonic development

Porbeagle embryos develop the distended yolk stomach that is characteristic of all oophagous lamnid sharks (Fig. 8). In the Kerguelen embryos (9.6–10.4 cm), such distension was already apparent. The caudal fin was notably curved, with the upper lobe much longer than the lower lobe, and there were no external gill filaments. At 19.8–20.7 cm, the bulging yolk stomach was the most noticeable feature, along with a marked lateral expansion of the head and branchial region (Fig. 8A). The body lacked pigmentation (except for the eyes), and appeared pink because of the presence of blood vessels under the skin. At 34.2 cm, the yolk stomach had become enormously distended, and measured 22.6 cm long by 15.9 cm high; the branchial and throat regions remained

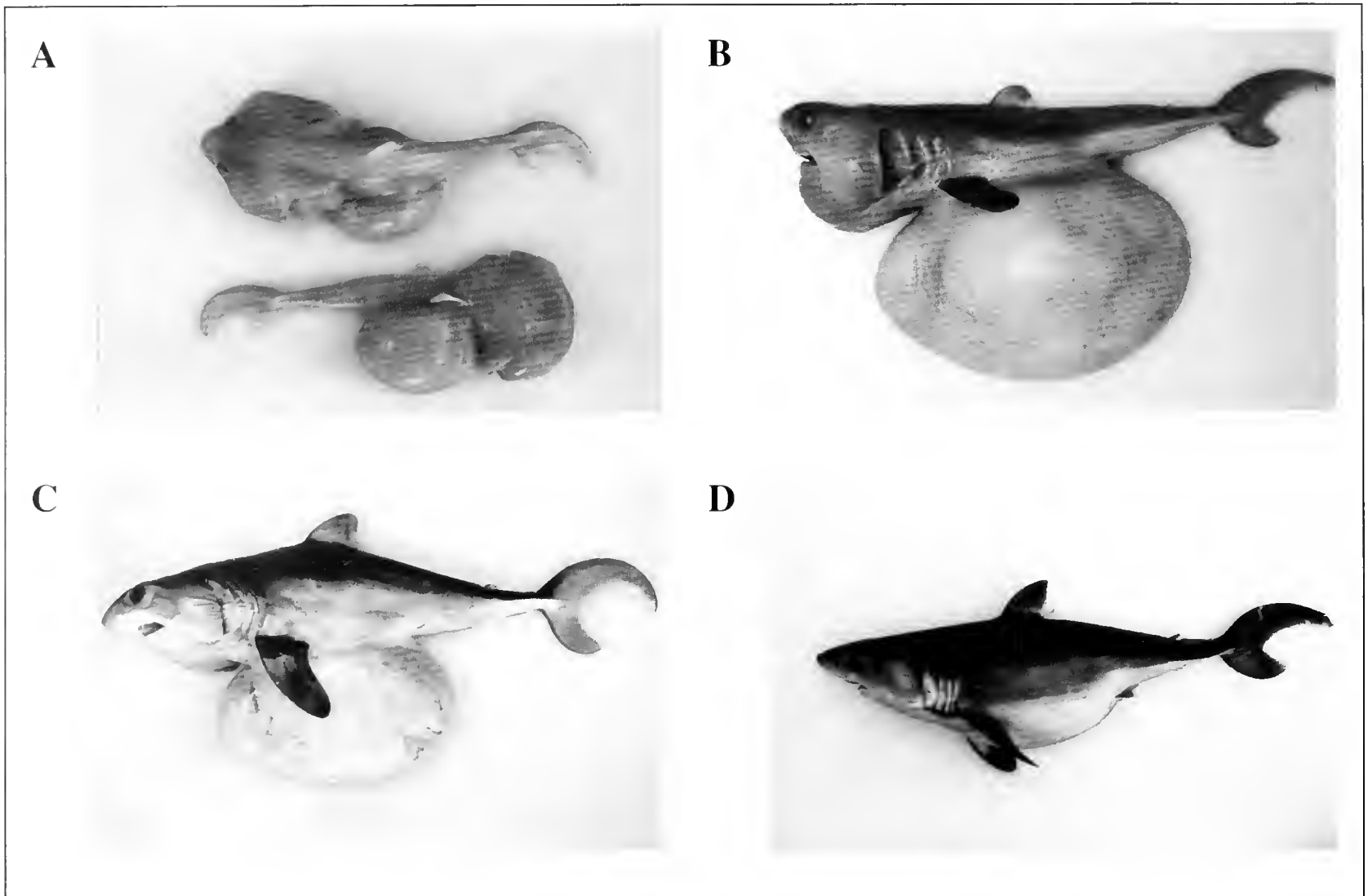

Figure 8

Changes in porbeagle embryo external shape with increasing size (not to same scale). (**A**) 20.7-cm female (top) and 19.8-cm male (bottom). (**B**) 34.2-cm female. (**C**) 40.3-cm female. (**D**) 58.0-cm female.

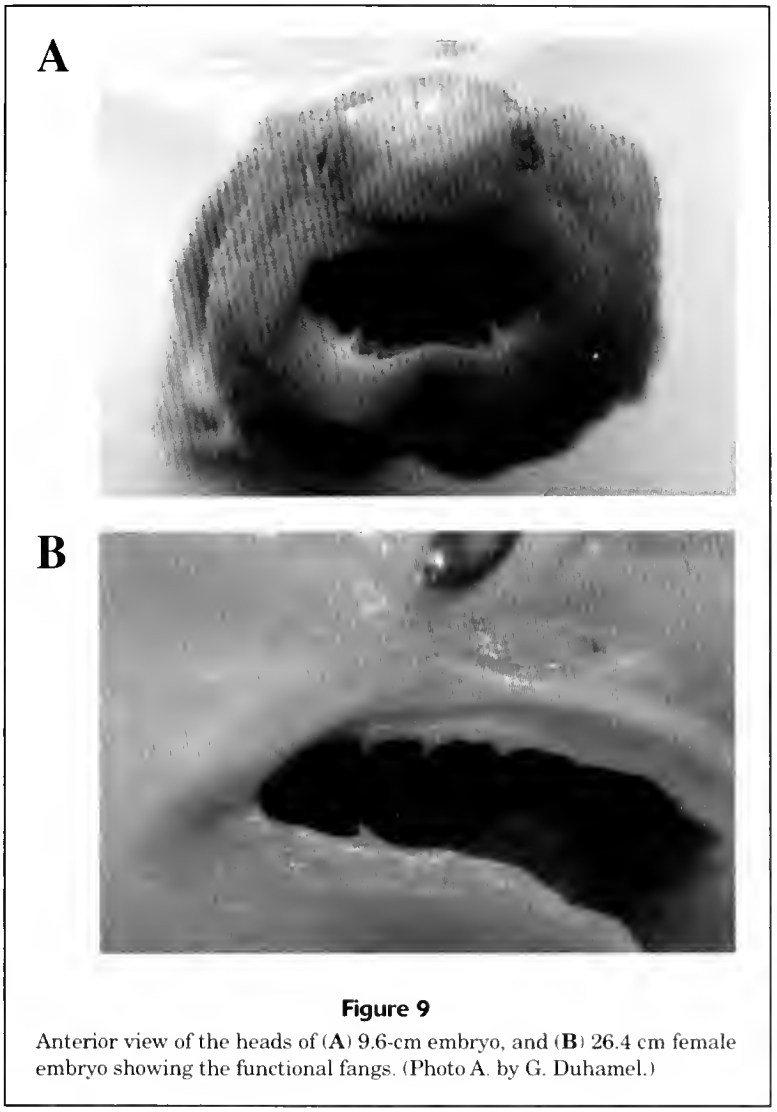

Figure 9

Anterior view of the heads of (**A**) 9.6-cm embryo, and (**B**) 26.4 cm female embryo showing the functional fangs. (Photo A. by G. Duhamel.)

swollen, and the upper body and pectoral fins had become pigmented (Fig. 8B). At 40.3 cm, pigmentation was essentially the same as in postnatal porbeagles, the swelling of the head had disappeared, and the yolk stomach had begun to shrink (Fig. 8C). At 58.0 cm the juvenile body form had been attained, apart from an enlarged abdomen (Fig. 8D). Other embryos around this size and larger had a more streamlined shape, with little noticeable abdominal distension.

Distension of the abdomen during early development causes the subdermal muscle layers to split along the ventral midline, extending anteriorly as far as the fifth gill slits. The expanding stomach protrudes between the muscle layers and stretches the abdominal skin. Later, the stomach shrinks back inside the muscle layers, and the stretched skin returns to its original shape. A distinct "scar" remains in the ventral midline in the area between the origins of the pectoral fins and the fifth gill slits, marking the anteriormost point of the split muscle layers.

Small embryos had large, erect, tubular, recurved "fangs" in both jaws (Fig. 9, A and B). These teeth, which were quite unlike those found in postnatal porbeagles, were clearly functional. In the Kerguelen embryos (9.6–10.4 cm), the tooth formula was (1+1/1+1), and the lower teeth were massive in relation to mouth size (Fig. 9A). Larger embryos (19.8–38.3 cm) had more functional upper teeth (3+3/1+1) (Fig. 9B). Additional minute teeth were visible under a light microscope, but they appeared vestigial and nonfunctional and were not included in the tooth formula. Replacement fangs were present behind the functional series, but they were irregularly spaced and usually located between the functional teeth. Oval scars on the gum of both jaws external to functional fangs indicated that fangs are progressively shed and replaced. The largest

embryo with fangs was 38.3 cm, and the smallest embryo without fangs was 33.9 cm. In the range of overlap, there were 12 embryos with fangs and 8 without fangs. Therefore, the fangs are shed between 34 and 38 cm.

Most of the larger embryos without fangs possessed several series of developing, nonerect, nonfunctional teeth shaped like those found in postnatal porbeagles, except that they lacked lateral cusps. One near-term litter had three embryos with nonfunctional upper teeth but partially erect lower teeth, whereas the fourth had nonfunctional teeth in both jaws.

The stomach contents consisted wholly or mostly of viscous, amorphous, light yellow yolk. In many embryos there were also discrete masses of clear, white or greyish gelatinous material, probably the remains of empty egg capsules, embedded in the yolk. This gelatinous material usually represented less than 10% of the stomach contents and has been included in the yolk weights reported below. Occasionally we found shed fangs in the stomachs, but the thick glutinous nature of the yolk made them difficult to find, and it was impossible to assess their frequency or abundance.

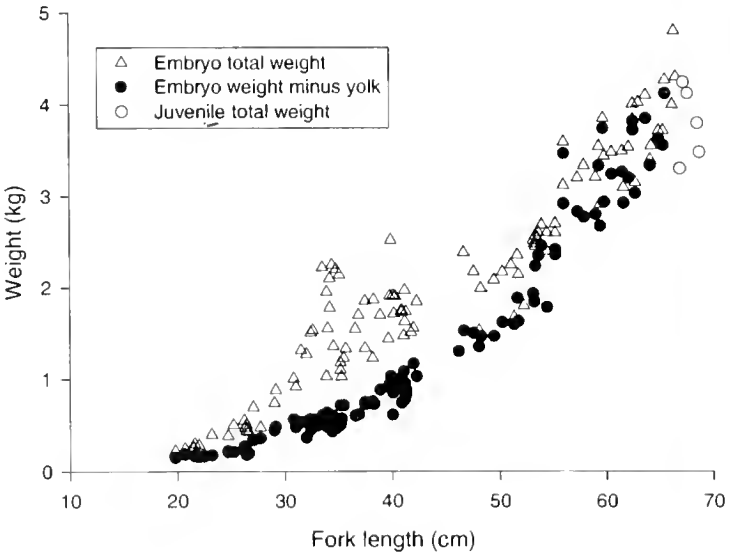

Figure 10

Variation in total weight and yolkfree weight with length for porbeagle embryos. Also shown are total weights of five small juveniles.

Embryonic total weight increased rapidly between 20 and 35 cm, changed little between 35 and 50 cm, then increased again during the rest of the gestation period (Fig. 10). Embryonic weight minus yolk weight increased steadily throughout gestation. The weights of five free-living juveniles shorter than 70 cm were similar to the yolk-free weights of the largest embryos.

The weight of yolk in the stomach increased steadily between 20 and 30 cm, before increasing rapidly to peak at 30–42 cm (Fig. 11). Yolk weight at 30–42 cm varied from 0.39 kg to 1.82 kg, representing 26.7–80.8% of total body weight. Absolute and percentage yolk weight both generally declined at lengths greater than 42 cm. Three embryos longer than 60 cm still had around 1 kg of yolk in their stomachs, but it represented a low proportion of their total weight (ca. 17–22%[8]). All embryos longer than 50 cm had yolk or gelatinous material in their stomachs, suggesting that the yolk may not be completely digested before birth.

The spiral valve of the intestine contained a thick, gritty, greenish-brown sludge that is the waste product of yolk digestion. The smallest embryos dissected (19.8–20.7 cm) contained small amounts of waste, and the quantity of waste increased steadily throughout gestation (Fig. 11). Intestinal contents composed the greatest percentage of yolk-free weight at 30–50 cm. Newborn porbeagles had smaller quantities of intestinal waste than large embryos, suggesting that the waste is retained until after birth.

Liver weight increased exponentially with FL, showing the most rapid increase above 55 cm (Fig. 11). Relative liver weight also increased to a maximum in the longest embryos. Postnatal porbeagles usually had smaller livers, both in absolute and relative terms, than those of the largest embryos, indicating that energy reserves stored in the liver are consumed by the young after birth.

The runts in two litters had low stomach and intestine contents, and liver weights (Table 2). The 22.5-cm runt in litter 1 had numerous short (1–3 mm) lacerations on its distended abdomen, and a few elsewhere on its body, presumably inflicted by the teeth of its larger sibling. However none of the gashes had penetrated the body cavity, and they did not appear to be life-threatening.

Five pairs of uteri containing embryos were obtained. The orientation of the embryos could be determined for only five of the 10 uteri; these five uteri contained embryos 38.2–62.6 cm long. In all cases, the two embryos were facing in opposite directions.

[8] Not shown in the percent yolk weight panel of Fig. 11 because embryo total weights were not measured accurately

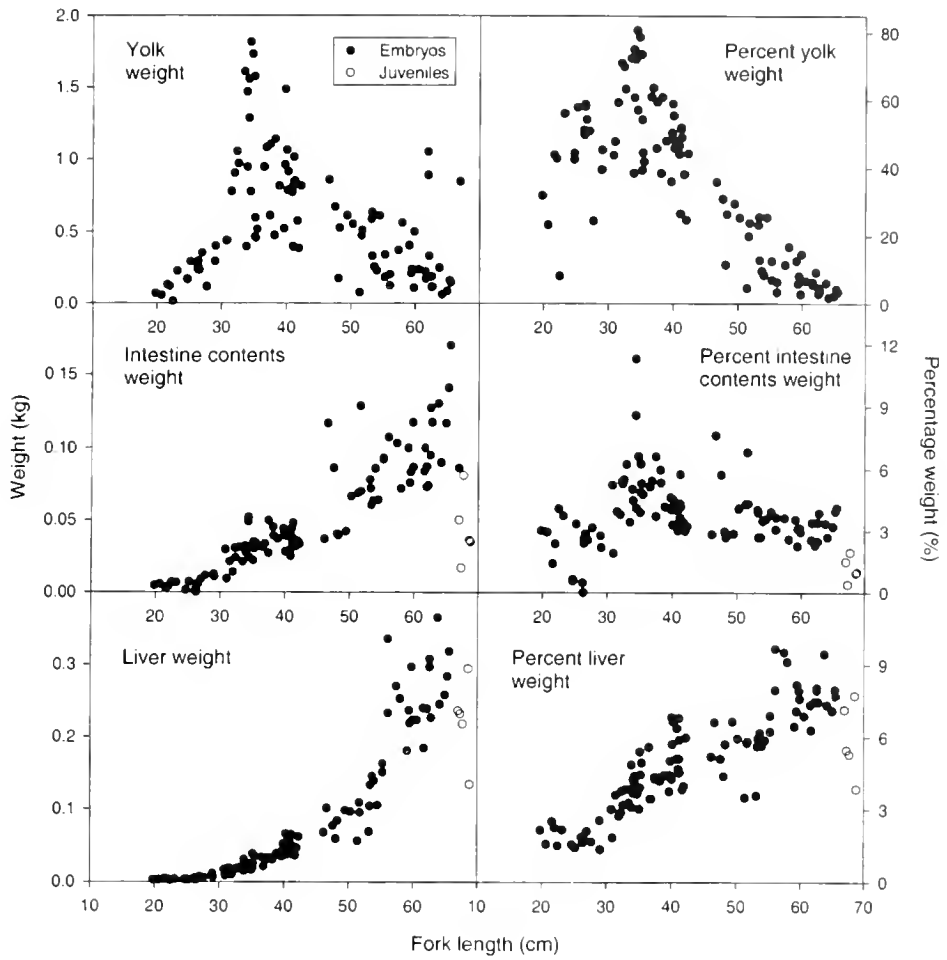

Figure 11

Variation in the weight of yolk, intestine contents, and liver with length (left panels), and the percentage of the total weight contributed by yolk, and percentages of yolkfree weight contributed by intestinal contents and liver (right panels) for porbeagle embryos. Comparable data for five small juveniles are also shown.

Discussion

Geographical distribution

Porbeagles occur throughout the New Zealand EEZ and the southern half of the Australian EEZ. On the east coast of Australia, they reach subtropical waters (to 23°44'S), but only during winter. At the other extreme, porbeagles are found in subantarctic waters in the Indian and southwest Pacific Oceans, reaching almost 54°S. Our results are consistent with observations of porbeagles between about 28 and 58°S across the entire South Pacific between New Zealand and Chile (Yatsu, 1995). Porbeagles are caught only north of 30°S in winter–spring (August–November), and they penetrate farther south during summer and autumn (Yatsu, 1995).

Sea surface temperature at locations where porbeagles were caught was 9.9–22.6°C, but catch rates were low above 19.5°C. This is similar to SSTs reported previously for porbeagles in the South Pacific by Stevens et al. (1983) (7.6–22.8°C, with most captures less than 16.7°C) and Yatsu (1995) (5–20°C with most captures less than 15 °C). Temperatures at the actual depth of capture would be similar to these because most longlines fished at 50–100 m depth, which is shallower than the depth of the mixed ocean layer in autumn–winter. Bottom temperatures for trawl-caught porbeagles were as low as 1–3°C, which is consistent with temperatures of 1.7°C (Svetlov, 1978) and 3.1–4.1°C (Templeman, 1963) reported elsewhere. Thus the temperature range inhabited by porbeagles in the Southern Hemisphere is probably about 1–23°C, with abun-

dance declining above about 19°C. The preferred temperature in the North Atlantic is less than 18°C (Aasen, 1963).

Porbeagles can maintain their body temperature up to 11°C above that of the surrounding water (Carey et al., 1985). Among the small group of endothermic sharks, they are exceeded in this capacity only by salmon sharks (Carey et al., 1985). The apparent preference for higher latitudes by large (Yatsu, 1995) and pregnant porbeagles may indicate an increased ability to thermoregulate in larger sharks. High body temperature is probably necessary for lamnid sharks to function as active predators of fast-moving prey in cold water (Goldman, 1997).

In the North Atlantic, porbeagle abundance varies seasonally and spatially (Aasen, 1961, 1963; Templeman, 1963; Mejuto and Garcés, 1984; Mejuto, 1985; Gauld, 1989), and there are indications of seasonal variability in their vertical distribution (Bigelow and Schroeder, 1948; Aasen, 1961, 1963). Limited tagging results show that they are capable of movements up to 2370 km (Aasen, 1962; Stevens, 1976, 1990). In combination with evidence of seasonal latitudinal migration in the South Pacific (Yatsu, 1995), this range of movement suggests that Southern Hemisphere porbeagles may exhibit complex seasonal, spatial, and length-related distribution patterns. Our data were collected mainly during April–July, and therefore provide little information on seasonality.

Length, weight, and growth

Several length-weight relationships have been published for the North Atlantic (Aasen, 1961; Mejuto and Garcés, 1984; Gauld, 1989; Stevens, 1990; Ellis and Shackley, 1995; Kohler et al., 1995). All were based on small samples, except those of Gauld (1989), who found a significant difference between males and females above 180 cm. Our New Zealand sample comprised mainly sharks less than 150 cm, and compared with the length-weight relationships of Mejuto and Garcés (1984), Gauld (1989) and Kohler et al. (1995), our length-weight relationship rises too steeply beyond 150 cm. Our relationship should therefore not be extrapolated beyond 150 cm.

The largest porbeagles in our samples were 228 cm (male) and 208 cm (female). The maximum length reached in the North Atlantic is not clear. Maxima of 253 cm (288 cm TL) and 278 cm (317 cm TL) for Scottish males and females, respectively, appear to be the largest reliable measurements (Gauld, 1989). Lengths of 294–325 cm ("estimated ... 11 feet", "ca 11–12 feet", or "340–370" cm TL) reported by McKenzie (1959) and Templeman (1963) were obviously not measured accurately and may have been overestimated. A TL of 12 feet equals 365.8 cm TL, which likely forms the basis for the maximum length of 365 cm TL reported by Pratt and Casey (1990). If Southern Hemisphere porbeagles grow as large as those in the North Atlantic, our samples do not include the larger size classes. Tuna longlines catch shortfin makos that exceed 300 cm FL (senior author, pers. obs.); therefore, they should be capable of retaining large porbeagles. The latter evidently inhabit latitudinal or depth ranges outside our sampling area, which is inhabited mainly by juveniles.

Males and females were equally represented at lengths up to 150 cm. At greater lengths, males significantly outnumbered females by about 3:1 in both New Zealand and Australia. Skewed sex ratios have been reported frequently in the North Atlantic, in favor of males (Mejuto and Garcés, 1984; Mejuto, 1985; Ellis and Shackley, 1995), females (Gauld, 1989), or either sex depending on the length range or sample (Aasen, 1963; O'Boyle et al., 1996). Aasen (1963) found that the overall sex ratio in large samples was close to 1:1. These results indicate that juveniles do not segregate by sex, but that larger sharks do.

MIX analysis discriminated 3 and 5 length modes respectively in southwest New Zealand and Australia, which we interpret as age classes. In northeast New Zealand, the mean sampling date was 25 June, over seven weeks after the mean sampling date for southwest New Zealand; therefore the first mode in the former could represent new-born sharks. Alternatively, it may represent slow-growing one-year-olds. The latter interpretation is supported by the similarity of the positions of modes 2 and 3 in both northeast and southwest New Zealand.

Juveniles grow linearly and rapidly, reaching 110–125 cm FL in three years. They may grow slightly faster in southwest New Zealand (20 cm/year) than in Australia (16 cm/year), but the standard errors were large for New Zealand 2- and 3-year-olds, and the comparison could be biased by incorrect determination of the number of modes in the length-frequency data. The modal lengths for Australian juveniles agree well with the first four modes for northwest Atlantic porbeagles presented by Aasen (1963) (Fig. 4), providing that our modes represent age classes. Aasen (1963) presented two growth curves—one based on length-frequency modes, and the other on back-calculated lengths-at-age from a single vertebra from a 226-cm female. [9] His two growth curves were practically identical.

Our growth estimates also agree with length-increment data for five tagged northeast Atlantic porbea-

[9] In a preliminary report, Aasen (1961) presented vertebral age data for 50 porbeagles. However the mean lengths-at-age differed substantially from those presented later, and Aasen (1963) stated that his earlier results "were not very accurate."

gles (Stevens, 1976, 1990). Their lengths at tagging and recapture were only estimated; therefore growth increments were approximate. The sharks were relatively small when released (84–105 cm), and were at liberty for 0.75–13 years. Annual growth increments were about 9–32 cm, with a mean of 20.4 cm. Despite good agreement among all sources of porbeagle growth data, a vertebral-based growth curve from adequate sample sizes and covering the full size range is still required for both hemispheres.

Longevity is unknown, but Aasen (1963) aged his 226 cm female as 19+ years and suggested that they may live around 30 years. This conclusion needs confirmation because longevity is often used to estimate the natural mortality rate, which is an important parameter in population models.

Length at maturity and reproductive development

The lengths of pregnant females (167–199 cm, mean 185 cm) suggest that females mature at about 165–180 cm. This estimate is consistent with reports of a 191-cm mature female from the South Atlantic (Svetlov, 1978), and immature females of 138, 139, and 150 cm from around New Zealand (Stevens et al., 1983; Duffy[10]). The length at maturity of North Atlantic females is controversial. Shann (1911) reported two pregnant females of "about five feet long" (152 cm TL, or 133 cm FL). In both cases, the length estimate was probably third-hand, and it is unlikely that the females were measured. That estimate of length at maturity, which we believe to be unreliable and too low, has permeated the literature (Bigelow and Schroeder, 1948; Compagno, 1984; Last and Stevens, 1994). Other authors have reported a wide maturity range of 175–220 cm FL (Aasen, 1961, 1963; Pratt and Casey, 1990). Templeman (1963) and Moss[3] reported females of 191 and 203 cm to be immature. The smallest mature females reported by Templeman (1963) and Gauld (1989) were 203 and 196 cm respectively, and Pratt (1993) examined one of 227 cm. Aasen (1961) showed that uterine width increased rapidly in females longer than 197 cm. These results suggest that North Atlantic females mature at about 195–205 cm (218–229 cm TL), which is higher than the range determined for the Southern Hemisphere. A similar between-hemisphere difference in length at maturity has been found for shortfin makos (Mollet et al.[11]).

There was no information on length at maturity in males in our data. On the basis of changes in clasper length and calcification, North Atlantic males apparently mature at a smaller size than do females, in the range 131–175 cm (150–200 cm TL) (Aasen, 1961; Ellis and Shackley, 1995).

The "internal" type ovary from our Macquarie Island pregnant female conformed with the morphology found in all lamnid and alopiid sharks examined so far (Pratt, 1988). It weighed 2.75 kg (2.35% of total weight). The ovary of Swenander's (1906, 1907) 246-cm North Atlantic pregnant female measured 41 by 28 cm, and weighed 6.3 kg, or 3.6% of estimated total weight. Mean embryo lengths in the two females were 22.1 cm and about 25 cm respectively. The embryo stomach contents peak at 30–42 cm, suggesting that ovarian size and ovulation may peak when embryos are about 25–30 cm long. In the shortfin mako, the ovary of an actively ovulating female with early-term embryos weighed about 5% of her total weight, whereas the ovaries of females carrying near-term embryos were spent and weighed as little as 0.2–0.3% of total weight (Mollet et al.[11]). In sandtiger sharks (*Carcharias taurus*), relative ovarian weight peaks at 6–7% of body weight, and then declines during the second half of gestation (Gilmore et al., 1983; Gilmore, 1993; Mollet et al.[11]). A low relative ovary weight was also reported in a longfin mako with near-term embryos (Gilmore, 1983).

The size-frequency distribution of ova from the Macquarie Island female indicated that they are ovulated at around 4–5 mm. Ova diameters measured in two pregnant North Atlantic females after preservation in 10% formalin were mainly in the range 2.3–4.3 mm, with the largest measuring 6.0 mm (Moss[3]). Swenander (1906, 1907) reported ova diameters between 1 and 5–6 mm in a North Atlantic pregnant female, and encapsulated 4–5 mm ova in the uteri of another female. Maximum ova diameters in other oophagous sharks range between 4 and 10 mm (Springer, 1948; Bass et al., 1975; Otake and Mizue, 1981; Gilmore, 1983; Gilmore et al., 1983; Stevens, 1983; Uchida et al., 1996; Chen et al., 1997).

Empty and near-empty egg capsules were found in the uteri of the Macquarie Island female, and in the mouth of one of its embryos. Moss[3] also found empty egg capsules in the mouths and gill slits of embryos measuring 33.8 and 36.2 cm. Apparently, embryos are capable of rupturing egg capsules and swallowing the contents, although the occasional presence of gelatinous material resembling egg capsules in embryo stomachs (Swenander, 1907; this study) suggests that whole or empty capsules are sometimes swallowed. Swenander (1906, 1907) found over 40 egg capsules, each measuring about 80 by 15 mm and containing

[10] Duffy, C. 1998. Department of Conservation, Private Bag 3072, Hamilton, New Zealand. Personal commun.

[11] Mollet, H. F., G. Cliff, H. L. Pratt, and J. D. Stevens. 1998. Reproductive biology of female shortfin mako *Isurus oxyrinchus* Rafinesque 1809. H. F. Mollet, Monterey Bay Aquarium, Monterey, California 93940, Unpubl. manuscript.

21–28 individual ova, in the uteri of a female that contained four embryos about 4.3–4.7 cm long. Duhamel and Ozouf-Costaz (1982) found 102 nonfertile eggs in the uteri of their Kerguelen Island female, which carried embryos of 9.6–10.4 mm. No photographs were taken of the eggs, and it is unclear whether they were egg capsules or individual ova (Duhamel[1]).

The emerging picture for oophagous sharks is that large numbers of nutritive egg capsules accumulate in the uteri during the early stages of gestation, and they are rapidly consumed as the embryos grow large enough to puncture and eventually swallow them (Gruber and Compagno, 1981; Otake and Mizue, 1981; Gilmore, 1983; Gilmore et al., 1983; Mollet et al.[11]). Ovulation peaks during midgestation, but full egg capsules are rarely found in the uteri, probably because they are eaten soon after entering the uteri. During later gestation, ovulation ceases and embryos metabolise their accumulated stomach contents for energy, growth, and storage in the liver.

Litter size, embryonic growth, and gestation

In 36 out of 40 of our pregnant females, litter size was four, with a mean of 3.85 embryos. Litters of two or three were occasionally recorded. In the North Atlantic, Shann (1911, 1923) stated that litters commonly consisted of two embryos (range 1–4), but his data almost certainly included several partial litters (see Table I in Shann, 1923). Templeman (1963) found three, four and four embryos in his three litters, and Gauld (1989) found four to be the most common number of embryos in a litter, with a mean of 3.7 (n=12).[12] One litter of five has also been reported (Bigelow and Schroeder, 1948). Our sample of Southern Hemisphere litters is the largest yet assembled, and Gauld's (1989) is the largest from the North Atlantic. Both samples had very similar mean numbers of embryos. We conclude that litter size is usually four, but smaller litters are occasionally found; litters larger than four are extremely rare. Some litters with fewer than four embryos were probably incomplete. Abortion of embryos during capture is common among nonlamnid sharks, but it is difficult to imagine midterm embryos with grossly distended abdomens being aborted, even when the mother is compressed in a trawl net. One of our New Zealand longline litters containing two midterm embryos, 37.5 and 38.3 cm long, was presumably complete. Abortion of near-term embryos is quite possible.

[12] Gilmore's Table 1 contains a number of errors. The reference to Aasen (1966) in the *Lamna nasus* section should presumably be Aasen (1963); the two Swenander (1907) litters contained four embryos each rather than 2; and the 219-cm TL shark with four embryos attributed to Nakaya (1971) was actually a male, and no embryos were mentioned by Nakaya.

Linear regressions fitted to the length-month data for both hemispheres suggest that embryos have a rapid growth rate of about 7 cm per month, but there was much unexplained variability (Fig. 7). The estimated growth rate is almost twice that of shortfin mako embryos (3.7 cm per month) (Mollet et al.[11]). The length of the gestation period appears to be about 8–9 months in both hemispheres. During July–September, Aasen (1963) found no embryos in the northwest Atlantic despite examining hundreds of mature females. He argued that the gestation period was 8 months, and that the females he examined were undergoing a short rest period between pregnancies. Our interpretation agrees with that of Aasen (1963).

A contrary hypothesis involving a gestation period of 1–2 years has been advanced by Shann (1923) and Gauld (1989). They argued that the high variability in embryo length and the apparent presence of two cohorts of embryos were inconsistent with a gestation period of less than one year. We cannot rule out their hypothesis, and we are conscious that our Southern Hemisphere data are limited in seasonal scope and that pooling data across locations and years is not desirable. However, we believe the data from both hemispheres are most consistent with a gestation period of less than one year. The implied rapid embryonic growth rate is not unreasonable given the abundant embryonic food supply and the relatively high growth rates of postnatal juveniles discussed above.

The high variability in the embryo length data might be explained by an extended mating period. In the northwest Atlantic, Aasen (1963) found males with seminal vesicles that were filling at the end of August, indicating that mating would begin in September. Pratt (1993) reported a mature female caught in October with moderate amounts of spermatozoa in the oviducal gland and with fresh vaginal abrasions. A mature male with haematose claspers was caught on the same longline, providing strong evidence of mating in October. Gauld (1989) found females with fresh bite marks, thought to be inflicted during mating, on females near the Shetland Islands in December–January. These observations suggest that mating lasts from September to January in the North Atlantic.

If our hypothesis of rapid embryonic growth and high intracohort variability is correct, parturition probably peaks in June–July (winter) in the Southern Hemisphere and possibly extends from April to September. Parturition in the Northern Hemisphere may peak around two months earlier (spring–summer). The presence of distinct length modes in juvenile length-frequency distributions from New Zealand, Australia, and the northwest Atlantic (Aasen, 1963) confirms that parturition is restricted to part of the year, rather than occurring year-round. Svetlov (1978) reported the capture

of a female in the South Atlantic in March and stated: "The shark had recently spawned, to judge by external characters (an inflamed area of the body around the anus) and the state of the ovaries." He did not elaborate further on the ovaries, so it is difficult to assess his report. If the female was postpartum, the timing is one month earlier than our suggested parturition period for Southern Hemisphere porbeagles. Another possibility is that the inflammation around the cloaca may have been the result of recent mating.

If the gestation and rest periods combined last one year, and females reproduce every year, annual fecundity is 3.85 young per female. If there is a resting period of just over one year between pregnancies, annual fecundity would be half that amount. It is therefore important to determine whether Aasen's (1963) suggestion of a one-year cycle is valid for both hemispheres. The gestation period in shortfin makos is thought to be 18 months, with a reproductive cycle of three years (Mollet et al.[11]). Interestingly, the greater average fecundity of makos would result in an annual fecundity of about four per female (Mollet et al.[11]), which is similar to the reproductive output of porbeagles assuming a one-year cycle.

For Southern Hemisphere porbeagles, the length at birth was estimated to be 58–67 cm (68–79 cm TL), based on the lengths of the largest embryos and the shortest postnatal juveniles. In the North Atlantic, the largest reported embryos were 60–64 cm (Pennant, in Shann, 1911) and 65 cm (Gauld, 1989). Bigelow and Schroeder (1948) reported a 55.7-cm specimen (66.0 cm TL; USNM 47528), but it was an embryo rather than a postnatal juvenile (Williams[13]). The embryo would have been about 58 cm before preservation. Postnatal porbeagles of 66 and 70 cm were reported by Imms and Day respectively (in Shann, 1911). These observations indicate that porbeagles are born at about the same length in both hemispheres.

Embryonic development

We assembled a comprehensive series of porbeagle embryos ranging from early gestation (9.6 cm long) to full-term, enabling us to describe the main morphological changes that occur during gestation. Previous studies that described and illustrated embryos were based on only a few embryos, most of which were midterm (Swenander, 1906, 1907; Shann, 1911; Nordgård, 1926; Bigelow and Schroeder, 1948; Templeman, 1963).The following review of embryonic development is derived from our observations, supplemented by literature reports.

[13] Williams, J. T. 1997. National Museum of Natural History, Washington DC 20560–0159. Personal commun.

Embryos 4.3–4.7 cm long have external gills and well-developed branchial regions (Swenander, 1907). They have nearly absorbed their yolk sacs and have a large spiral valve, but there is no yolk in the digestive system. Swenander (1907) stated that "these embryos are too small to be able to swallow entire egg capsules and their teeth are not sufficiently developed to tear open the egg capsules." They have not begun to feed at this stage, despite the large number of egg capsules present in the uteri, but precocial teeth have already formed. At 10 cm, the lower jaw contains two relatively massive fangs (Fig. 9A) that appear capable of tearing open egg capsules. The upper teeth are much less developed and there is only one functional tooth on each side of each jaw. Lower jaw teeth also develop earlier than upper jaw teeth in sandtiger sharks (Hamlett, 1983). The abdomen is swollen and the embryos have presumably begun feeding (the stomachs were not dissected). Large numbers of egg capsules are present in the uteri. The external gills have been resorbed. By 15 cm, the abdomen is distended, and the head and branchial region are gelatinous and grossly enlarged (Bigelow and Schroeder, 1948).

Between 20 and 42 cm, development is dominated by the consumption of large numbers of egg capsules, leading to a great increase in the relative size and distension of the yolk stomach (Swenander, 1907; Shann, 1911, 1923; Bigelow and Schroeder, 1948; Templeman, 1963; Moss[3]; Fig. 8). Large fangs are present in both jaws (Swenander, 1907; Templeman, 1963; Moss[3]; Fig. 9) and are used to open the egg capsules before removal of the contents; how this is accomplished is unknown. At 30–42 cm, yolk accounts for up to 81% of total weight (Fig. 11; Templeman, 1963). The stomach yolk in midterm embryos of shortfin makos peaks at about 60–70% of total weight (Mollet et al.[11]). Relative and absolute amounts of yolk in porbeagles and other oophagous sharks decline during the rest of gestation (Fig. 11; Mollet et al.[11]).

Porbeagle embryos shed their fangs at about 34–38 cm. Embryonic fangs (the "emb" teeth of Gilmore, 1993) have also been reported in salmon sharks, common and bigeye thresher sharks (*Alopias vulpinus* and *A. superciliosus*), shortfin makos and sandtiger sharks (Lohberger, 1910; Bass et al., 1975; Gruber and Compagno, 1981; Gilmore et al., 1983; Hamlett, 1983; Gilmore, 1993; Chen et al., 1997). They probably occur in all oophagous species, and in at least some species, they are shed part-way through gestation. In bigeye thresher sharks, fangs appear at about 11 cm TL and disappear at about 60 cm TL (Chen et al., 1997). In sandtiger sharks, they appear at 4–5 cm TL, and are lost some time before birth (Gilmore et al., 1983; Hamlett, 1983).

We suspect that female porbeagles cease ovulation at about the time the embryonic fangs are lost, as

has been reported for shortfin makos and sandtigers (Gilmore et al., 1983; Mollet et al.[11]). The embryos then rely on the yolk stored in their stomachs to provide the energy needed for growth and respiration during the rest of the gestation period. However it is also possible that females continue ovulating, and that the toothless embryos feed by swallowing whole egg capsules or by squashing them in their mouths. Whole egg capsules have been reported from the stomachs of near-term embryos of the bigeye thresher shark (Gilmore, 1983; Moreno and Morón, 1992), but not from near-term lamnid sharks. Clarification of this point requires examination of the ovaries of near-term females to assess their ovulatory state.

Above 35 cm, the waste products of yolk digestion continue to accumulate in the intestine. The greenish coloured waste is characteristic of oophagous sharks (Swenander, 1907; Lohberger, 1910; Shann, 1923; Springer, 1948; Uchida et al., 1996). The gritty nature of the intestinal contents was also mentioned by Swenander (1907) and has been reported to consist of "crystal-like pieces" in white shark embryos (Uchida et al., 1996). The composition of this material is unknown. The liver grows most rapidly in the second half of gestation as energy reserves are transferred to it for storage. An increase in the relative weight of the liver in larger embryos has also been observed in shortfin makos (Mollet et al.[11]).

During the second half of gestation, several series of "post-natal" teeth develop, but they are folded back in the jaws and are nonfunctional. In white sharks, some of these teeth are shed and swallowed by the embryos (Francis, 1996; Uchida et al., 1996). The teeth probably become erect near or soon after birth, as has been found in near-term white shark embryos (Francis, 1996; Uchida et al., 1996).

Typically, embryos in a porbeagle litter are of similar size, but occasionally a large size range is encountered. Gauld (1989) found one litter with embryos ranging from 55.6 to 65.0 cm, and Shann (1923) reported a litter with a range of 38.1–50.9 cm. The runts in our two litters had small quantities of stomach and intestinal contents, and small livers, but were otherwise developing normally. This suggests that sibling competition may occur when a dominant embryo with its snout nuzzled into the anterior end of the uterus consumes most of the egg capsules as they pass into the uterus, leaving few for its sibling. However, all four embryos are usually adequately nourished, and the two embryos in each uterus are usually oriented in opposite directions. This suggests that the direction of orientation within the uterus may be a problem only if the mother is unable to produce enough egg capsules to satisfy both embryos.

At birth, embryos may still have yolk in their stomachs. Near-term white shark embryos have been reported with either empty (apart from some ingested teeth and denticles) or yolk-filled stomachs (Francis, 1996; Uchida et al., 1996). Near-term shortfin mako embryos and new-born sandtiger sharks may also have small amounts of yolk in their stomachs (Cadenat, 1956; Bass et al., 1975; Gilmore et al., 1983; Mollet et al.[11]). Along with the energy stored in the liver, this yolk supplies the nutritional needs of the embryos until they learn to feed. However, the livers of porbeagle embryos never exceeded 10% of the yolk-free embryo weight, compared with 13.5–18.6% in near-term white shark embryos (Francis, 1996; Uchida et al., 1996).

Hubbs (1923) reported a 9.1 kg (20 lb) embryo collected in late August in Maine, USA. The weight is clearly too large to be a porbeagle embryo because they are not known to exceed 5 kg (Fig. 10). Moss[3] suggests that the embryo may have been from a sandtiger shark.

The presence of an "umbilical scar" or "yolk sac scar" in postnatal oophagous sharks has puzzled many scientists who were aware that the embryos have no placental connection to their mothers (Gilmore, 1983; Stevens, 1983; Klimley, 1985; Cliff et al., 1990, 1996; Pratt and Casey, 1990; Moreno and Morón, 1992; Francis, 1996; Uchida et al., 1996). Our observations show that distension of the stomach stretches the abdominal skin and separates subdermal muscle layers as far forward as the fifth gill slits. As yolk is consumed the stomach shrinks and the muscle layers return to their original position, leaving a scar in the pectoral-gill region. The scar is sometimes faint or absent.

In all lamnid sharks, embryos are nourished by oophagy. Contrary to earlier suggestions, there is no evidence that lamnid embryos indulge in uterine cannibalism (adelphophagy), an extreme extension of oophagy that has been confirmed only in the sandtiger shark (Gilmore, 1993). All lamnids, and most oophagous sharks, produce litters larger than two (one per uterus) (Francis, 1996), providing strong circumstantial evidence that adelphophagy does not occur in those species (Gilmore, 1993). One porbeagle embryo had nonlethal abdominal lacerations, probably resulting from incidental damage inflicted by its larger sibling while searching for egg capsules, which are about the same size as the smaller embryo's abdomen. This searching behavior could provide a mechanism for the development of adelphophagy from oophagy.

Unresolved questions

Two puzzling features of the reproduction of porbeagles demand further investigation. The first concerns

the gross abdominal distension during midgestation, a phenomenon that must create problems for the mother in accommodating them. It would seem energetically and hydrodynamically more efficient for a pregnant female to match her ovulation rate to the immediate growth and energy needs of the embryo, rather than to provide an over-supply of food during a short time period. We speculate that the answer lies in the availability of food resources. Porbeagles feed mainly on small to medium pelagic fishes and cephalopods, but also eat larger demersal teleosts and elasmobranchs (Bigelow and Schroeder, 1948; Graham, 1956; Aasen, 1961; Templeman, 1963; Stevens et al., 1983; Gauld, 1989; Yatsu, 1995). Oophagy may be an adaptation that allows pregnant porbeagles (and other oophagous species) to maximize their use of food resources that are abundant only during a short season.

The lack of a six-month phase shift between the reproductive cycles of Northern and Southern Hemisphere porbeagles is surprising, and suggests that water temperature and day length have little influence on reproduction. This may be due to porbeagles having a highly developed endothermic ability (Carey et al., 1985) which buffers body temperature against seasonal fluctuations in temperature. But why should the timing of reproduction be so similar in the two hemispheres? The shortfin mako is also endothermic, although not to such a high degree as porbeagles (Carey et al., 1985), and its reproductive cycles are six months out of phase in the two hemispheres (Mollet et al.[11]). In the northwest Atlantic, porbeagle parturition coincides with the arrival of migratory stocks of Atlantic mackerel, capelin and 0+ Atlantic herring (Moss[3]). Linking parturition with the period of peak abundance of the common prey species in each hemisphere would provide new-born young with their best chance of rapid growth and survival. Unfortunately, neither of these hypotheses can be tested, because there is no information on the existence or timing of abundance cycles of porbeagle prey in the Southern Hemisphere.

This study has clarified several important aspects of the reproductive biology of porbeagles, including the length of the gestation period, mean fecundity, length at birth, and the timing of parturition. Growth rates have been estimated for embryos and juveniles and are consistent with other studies. However considerable imprecision and uncertainty remain in all of these estimates, especially the lengths of the gestation period and reproductive cycle, and therefore the annual fecundity. Such information is crucial to the determination of stock productivity in porbeagles; therefore better estimates are required before effective stock assessment and management can be achieved.

Acknowledgments

We are indebted to the scientific observers who frequently operated under arduous conditions to collect data and specimens. Their enthusiasm and dedication made this study possible. Stephanie Kalish and Lynda Griggs provided database support, and arranged the delivery of specimens. The New Zealand Ministry of Fisheries allowed us access to the scientific observer database. Data, photographs and embryos were kindly provided by Guy Duhamel, Sandy Moss, Andrew Newton, Stuart Hanchet, Rachel Berquist, Dick Williams, Jeff Williams, and Clinton Duffy. Sabine Wintner, Henry Mollet, and Markus Leppä translated the important papers by Lohberger and Swenander. Henry also stimulated us with much discussion of lamnoid embryonic development. Three anonymous referees made helpful comments on the manuscript.

Literature cited

Aasen, O.
1961. Some observations on the biology of the porbeagle shark (*Lamna nasus* L.). ICES C. M. 1961. Near Northern Sea Comm. 109, 7 p.
1962. En interessant gjenfangst av merket håbrann. Fiskets Gang 14:221.
1963. Length and growth of the porbeagle (*Lamna nasus*, Bonnaterre) in the North West Atlantic. Fisk. Skrift. Ser. Havund. 13(6):20–37.
1966. Brugde, *Cetorhinus maximus* (Gunnerus), 1765. Saertrykk av Fishets Gang 49:909–920.

Anderson, E. D.
1990. Fisheries models as applied to elasmobranch fisheries. NOAA Tech. Rep. NMFS 90:473–484.

Bass, A. J., J. D. D'Aubrey, and N. Kistnasamy.
1975. Sharks of the east coast of southern Africa. IV. The families Odontaspididae, Scapanorhynchidae, Isuridae, Cetorhinidae, Alopiidae, Orectolobidae and Rhiniodontidae. Oceanogr. Res. Inst. Invest. Rep. 39, 102 p.

Bigelow, H. B., and W. C. Schroeder.
1948. Fishes of the Western North Atlantic. Part 1. Lancelets, cyclostomes, sharks. Mem. Sears Found. Mar. Res. 1:59–546.

Cadenat, J.
1956. Notes d'ichtyologie Ouest Africaine. XIV. Remarques biologiques sur le requin-sable *Carcharias* (*Odontaspis*) *taurus* Rafinesque 1810. Bull. l'Inst. Fran. d'Afr. Noire 18:1249–1256.

Carey, F. G., J. G. Casey, H. L. Pratt, D. Urquhart, and J. E. McCosker.
1985. Temperature, heat production and heat exchange in lamnid sharks. Mem. South. Calif. Acad. Sci. 9:92–108.

Chen, C.-T., K.-M. Liu, and Y.-C. Chang.
1997. Reproductive biology of the bigeye thresher shark, *Alopias superciliosus* (Lowe, 1839) (Chondrichthyes: Alopiidae), in the northwestern Pacific. Ichth. Res. 44:227–235.

Cliff, G., S. F. J. Dudley, and B. Davis.
1990. Sharks caught in the protective gill nets off Natal, South Africa. 3. The shortfin mako shark *Isurus oxyrinchus* (Rafinesque). S. Afr. J. Mar. Sci. 9:115–126.

Cliff, G., S. F. J. Dudley, and M. R. Jury.
1996. Catches of white sharks in KwaZulu-Natal, South Africa and environmental influences. *In* A. P. Klimley and D. G. Ainley (eds), Great white sharks: the biology of *Carcharodon carcharias*, p. 351–362. Academic Press, San Diego, CA.

Compagno, L. J. V.
1984. Sharks of the world. An annotated and illustrated catalogue of shark species known to date. FAO Fish. Synopsis 125, vol. 4, part 1, 249 p.

Duhamel, G., and C. Ozouf-Costaz.
1982. Presence de *Lamna nasus* (Bonnaterre, 1788) aux Iles Kerguelen. Cybium 6:15–18.

Ellis, J. R., and S. E. Shackley.
1995. Notes on porbeagle sharks, *Lamna nasus*, from the Bristol Channel. J. Fish Biol. 46:368–370.

Francis, M. P.
1996. Observations on a pregnant white shark with a review of reproductive biology. *In* A. P. Klimley and D. G. Ainley (eds), Great white sharks: the biology of *Carcharodon carcharias*, p. 157–172. Academic Press, San Diego, CA.

Francis, M. P., L. H. Griggs, S. J. Baird, T. E. Murray, and H. A. Dean.
1999. Fish bycatch in New Zealand tuna longline fisheries. NIWA Tech. Rep. 55, 70 p.

Gauld, J. A.
1989. Records of porbeagles landed in Scotland, with observations on the biology, distribution and exploitation of the species. Scot. Fish. Res. Rep. 45, 15 p.

Gilmore, R. G.
1983. Observations on the embryos of the longfin mako, *Isurus paucus*, and the bigeye thresher, *Alopias superciliosus*. Copeia 1983:375–382.
1993. Reproductive biology of lamnoid sharks. Env. Biol. Fish. 38:95–114.

Gilmore, R. G., J. W. Dodrill, and P. A. Linley.
1983. Reproduction and embryonic development of the sand tiger shark, *Odontaspis taurus* (Rafinesque). Fish. Bull. 81:201–225.

Goldman, K. J.
1997. Regulation of body temperature in the white shark, *Carcharodon carcharias*. J. Comp. Phys. B 167:423–429.

Graham, D. H.
1939. Breeding habits of the fishes of Otago Harbour and adjacent seas. Trans. Proc. Roy. Soc. N. Z. 69:361–372.
1956. A treasury of New Zealand fishes, 2nd ed. Reed, Wellington, 424 p.

Gruber, S. H., and L. J. V. Compagno.
1981. Taxonomic status and biology of the bigeye thresher, *Alopias superciliosus*. Fish. Bull. 79:617–640.

Hamlett, W. C.
1983. Maternal-fetal relations in elasmobranch fishes. Ph.D. diss., Clemson University, Clemson, SC, 228 p.

Hubbs, C. L.
1923. Notes on a small collection of fishes from Monhegan Island, Maine. Copeia 1923:101–103.

Klimley, A. P.
1985. The areal distribution and autecology of the white shark, *Carcharodon carcharias*, off the west coast of North America. Mem. South. Calif. Acad. Sci. 9:15–40.

Kohler, N. E., J. G. Casey, and P. A. Turner.
1995. Length-weight relationships for 13 species of sharks from the western North Atlantic. Fish. Bull. 93:412–418.

Last, P. R., and J. D. Stevens.
1994. Sharks and rays of Australia. CSIRO, Hobart, 513 p.

Lohberger, J.
1910. Uber zwei riesige embryonen von *Lamna* Sond. Abhand. Math.-Phys. Klasse Bayer. Akad. Wissen. IV suppl. bd. 2 abhand., 45 p.

MacDonald, P. D. M.
1987. Analysis of length-frequency distributions. *In* R. C. Summerfelt and G. E. Hall (eds.), The age and growth of fish, p. 371–384. Iowa State Univ. Press, Ames, IA.

MacDonald, P. D. M., and P. E. J. Green.
1988. User's guide to program MIX: an interactive program for fitting mixtures of distributions, Release 2.3. Ichthus data systems, Hamilton, Ontario, Canada.

MacDonald, P. D. M., and T. J. Pitcher.
1979. Age-groups from size-frequency data: a versatile and efficient method of analyzing distribution mixtures. J. Fish. Res. Board Can. 36:987–1001.

McKenzie, R. A.
1959. Marine and freshwater fishes of the Miramichi River and Estuary, New Brunswick. J. Fish. Res. Bd Can. 16:807–833.

Mejuto, J.
1985. Associated catches of sharks, *Prionace glauca*, *Isurus oxyrinchus*, and *Lamna nasus*, with NW and N Spanish swordfish fishery, in 1984. ICES C. M. 1985 H:42, 16 p.

Mejuto, J., and A. G. Garcés.
1984. Shortfin mako, *Isurus oxyrinchus*, and porbeagle, *Lamna nasus*, associated with longline swordfish fishery in NW and N Spain. ICES C. M. 1984 G:72, 9 p.

Moreno, J. A., and J. Morón.
1992. Reproductive biology of the bigeye thresher shark, *Alopias superciliosus* (Lowe, 1839). Aust. J Mar. Freshwater Res. 43:77–86.

Murray, T.
1994. A review of the biology and fisheries for albacore, *Thunnus alalunga*, in the South Pacific Ocean. FAO Fish. Tech. Pap. 336/2:188–206.

Nakaya, K.
1971. Descriptive notes on a porbeagle, *Lamna nasus*, from Argentine waters, compared with the North Pacific salmon shark, *Lamna ditropis*. Bull. Fac. Fish. Hokk. Univ. 21:269–279.

Nordgård, O.
1926. Trondhjems Biologiske Stasjon 1900–1925. Det Kong. Norske Viden. Selsk. Skriff. 1925:37–39.

O'Boyle, R. N., G. M. Fowler, P. C. F. Hurley, M. A. Showell, W. T. Stobo, and C. Jones.
1996. Observations on porbeagle shark (*Lamna nasus*) in the North Atlantic. DFO Atl. Fish. Res. Doc. 96/24, 29 p.

Otake, T., and K. Mizue.
1981. Direct evidence for oophagy in thresher shark, *Alopias pelagicus*. Jpn. J. Ichthyol 28:171–172.

Pratt, H. L.
1988. Elasmobranch gonad structure: a description and survey. Copeia 1988:719–729.
1993. The storage of spermatozoa in the oviducal glands of western North Atlantic sharks. Env. Biol. Fish. 38:139–149.

Pratt, H. L., and J. G. Casey.
1990. Shark reproductive strategies as a limiting factor in directed fisheries, with a review of Holden's method of estimating growth parameters. NOAA Tech. Rep. NMFS 90: 97–109.

Shann, E. W.
1911. A description of the advanced embryonic stage of *Lamna cornubica*. Ann. Rep. Fish. Bd Scotland 28(3):73–79.
1923. The embryonic development of the porbeagle shark, *Lamna cornubica*. Proc. Zool. Soc. Lond. 11:161–171.

Springer, S.
1948. Oviphagous embryos of the sand shark, *Carcharias taurus*. Copeia 1948:153–157.

Stevens, J. D.
1976. First results of shark tagging in the North-east Atlantic, 1972–1975. J. Mar. Biol. Assoc. U.K. 56:929–937.
1983. Observations on reproduction in the shortfin mako *Isurus oxyrinchus*. Copeia 1983:126–130.
1990. Further results from a tagging study of pelagic sharks in the North-east Atlantic. J. Mar. Biol. Assoc. U.K. 70:707–720.
Stevens, J. D., M. C. Dunning, and S. Machida.
1983. Occurrences of the porbeagle shark, *Lamna nasus*, in the Tasman Sea. Jpn. J. Ichthyol. 30:301–307.
Svetlov, M. F.
1978. The porbeagle, *Lamna nasus*, in Antarctic waters. J. Ichthyol. 18:850–851.
Swenander, G.
1906. Bidrag till kännedomen om Trondhjemsfjordens fiskar. Det Kong. Norske Viden. Selsk. Skrift. 1905(9):1–112.
1907. Uber die ernährung des embryos der *Lamna cornubica*. Zool. Stud. Toll. Tullberg, Upp. 1907:283–288.
Templeman, W.
1963. Distribution of sharks in the Canadian Atlantic (with special reference to Newfoundland waters). Bull. Fish. Res. Board Can. 140, 77 p.
Uchida, S., M. Toda, K. Teshima, and K. Yano.
1996. Pregnant white sharks and full-term embryos from Japan. *In* A. P. Klimley and D. G. Ainley (eds.), Great white sharks: the biology of *Carcharodon carcharias*, p. 139–155. Academic Press, San Diego, CA.
Yatsu, A.
1995. Zoogeography of the epipelagic fishes in the South Pacific Ocean and the Pacific sector of the Subantarctic, with special reference to the ecological role of slender tuna, *Allothunnus fallai*. Bull. Nat. Res. Inst. Far Seas Fish. 32, 145 p.

Abstract.—The retrospective assignment of collections of larval swordfish, *Xiphias gladius*, taken from 1973 to 1980, to water types and area of the Gulf Stream front, as well as three sets of contemporary collections taken in 1984, 1988, and 1997, indicated that larvae were collected most frequently within the western Gulf Stream frontal zone. Larval swordfish accumulate by localized hydrodynamic convergence, rather than localized spawning, and thus these rare, surface-oriented larvae are found more frequently within the frontal zone. Lengths of larval swordfish taken from curatorial collections, from contemporary collections, and from published records from the Caribbean Sea, the Gulf of Mexico, and the western North Atlantic, as well as assumptions about growth rates and Gulf Stream transport, indicated that swordfish may spawn as far north as Cape Hatteras.

Distribution of larval swordfish, *Xiphias gladius*, and probable spawning off the southeastern United States

John Jeffrey Govoni
National Marine Fisheries Service, NOAA
Southeast Fisheries Science Center
Beaufort Laboratory
101 Pivers Island Road
Beaufort, North Carolina 28516-9722
E-mail address Jeff.Govoni@noaa.gov

Bruce W. Stender

Oleg Pashuk
Marine Resources Research Institute
South Carolina Wildlife and Marine Resources Department
Charleston, South Carolina 29412

Swordfish, *Xiphias gladius*, is a cosmopolitan and highly migratory species that spawns year-round (Grall et al., 1983). Larvae of this fish do not account for high numbers of the ichthyoplankton or ichthyoneuston, and as a consequence, data that describe their spatial distribution are sparse. Grall et al. (1983) concluded from available data that, in the western North Atlantic, small larvae (<10 mm) occur most frequently in the eastern Caribbean and in the Straits of Yucatan and Florida in November, and that larger larvae (>10 mm) occur most often there, as well as in the Gulf Stream north to Cape Hatteras from January to March. Both length groups occur primarily in surface water over depths deeper than 200 m (Markle, 1974). Tibbo and Lauzier (1969) first speculated that larvae may be associated with horizontal temperature and salinity gradients. The collection of larvae along the apparent edges of the Gulf Loop Current in the Gulf of Mexico (Richards and Potthoff, 1980) and the Gulf Stream in the Atlantic (Potthoff and Kelley, 1982; Post et al., 1997) supports the notion that larvae occur in greater abundance within frontal zones. Yet, the rarity of larvae has hindered a clear understanding of such coarse and fine scale (Haury et al., 1978) spatial distribution.

The scarcity of larval swordfish has obscured an understanding of their spawning pattern as well. The mesoscale pattern of larval distribution (Grall et al., 1983) implies that swordfish spawn in the Caribbean and the Straits of Yucatan and Florida, and that their larvae are carried northward by the Gulf Stream. Occasional small larvae taken in the Atlantic imply that swordfish may spawn as far north as Cape Hatteras (Markle, 1974). Large, and presumably older larvae in any location may be the result either of local spawning and subsequent retention or of transport from a distant spawning locale. Small larvae at a specific locale must be the exclusive result of local spawning.

Hydrated oocytes within the ovaries of adult females indicate that swordfish spawn south of the Sargasso Sea, in the northern Caribbean Sea, and the Straits of Florida (Arocha and Lee, 1995), although Squires (1962) has suggested that

Manuscript accepted 22 June 1999
Fish. Bull. 98:64–74 (2000).

spawning may occur as far north as Cape Hatteras. Planktonic eggs have not been identified in the western North Atlantic.

Effective fisheries management requires knowledge of both the spatial distribution of larvae and the distribution of spawning adults. Contemporary stock status ascertained by virtual population analysis can be calibrated with larval abundance estimates, even for species with rare larvae (e.g. McGowan and Richards, 1989; Scott et al., 1993). Because this calibration depends on accurate estimates of larval abundance, the spatial and temporal distribution of larvae must be known. Knowledge of spawning distribution would be the first step toward protection of spawning habitat and, perhaps, the restriction of fishing within spawning seasons and locales.

Here we examine the coarse- and fine-scale distribution, and the lengths of swordfish larvae off the southeastern United States. Our focus is on the influence of the Gulf Stream in shaping the spatial distribution of larvae and in the determination of probable spawning locales.

Methods

We examined published records of larval swordfish (Arata, 1954; Arnold, 1955; Tibbo and Lauzier, 1969; Markle, 1974; Post et al., 1997), data from the Marine Resources Monitoring, Assessment and Prediction Program (MARMAP), data and specimens from the Southeast Area Monitoring and Assessment Program (SEAMAP), and new data from three surveys conducted between the Florida Straits and Cape Hatteras in 1984, 1988, and 1997 (CF8406, CH8807, and CH9703).

Spatial distribution of species

For spatial distribution, we examined exclusively neuston collections (the upper 0.5 m of water), because swordfish are surface-oriented as are larvae. Although some swordfish larvae have been collected in nets that fished principally below the surface (Grall et al., 1983), most have been collected at the surface (Tåning, 1955; Yabe et al., 1959; Gorbunova, 1969; Nishikawa and Ueyanagi, 1974). All swordfish larvae collected by MARMAP, SEAMAP, and CH8807 were collected in the neuston, none in accompanying, subsurface ichthyoplankton collections. Small larvae were occasionally taken from below the surface in CH9703, but these nets fished obliquely from 20 m and larvae were likely captured when nets were near the surface.

Collections of larvae were classified to water mass (or type)—shelf water (including Georgia water, Carolina Capes water, and occasionally Virginia coastal water [Pietrafesa, 1989]) or Gulf stream water—by applying measured hydrographic characteristics to the classifications of Matthews and Pashuk (1986) for MARMAP and CF8406 collections, and Pietrafesa et al. (1985) for CH8807 and CH9703 collections. Frontal zone water is a mixture of these water masses (Hitchcock et al., 1994). South of Cape Hatteras the Gulf Stream courses north-northeastward in juxtaposition with shelf water. Classically, the definition of the Gulf Stream front is a dynamic one: the Gulf Stream front is the point where the pressure gradient between Sargasso Sea water and slope water (north of Cape Hatteras) or shelf water (south of this Cape) is zero (Stommel, 1966). Practically, observed horizontally compressed surface isotherms and isohalines, accompanied by sharp discontinuities in sea-surface texture and color, define the Gulf Stream frontal zone (Olson et al., 1994). In our study, we used this observational definition to assign the surface position and to classify the water of the Gulf Stream frontal zone. Surface Gulf Stream water at its western front between the Florida Straits and Cape Hatteras has characteristic temperatures that range from 21° to 24°C in winter and from 27° to 29°C in summer, salinities that range from 35.7 to 36.4 psu and vary little seasonally, dissolved oxygen values that range from 4.5 to 5.0 mL/L, and nitrate values of 1.0 µM/L (Atkinson, 1985; Schmitz et al., 1993; Hitchcock et al., 1994; Xie and Pietrafesa, 1995). Shelf water is cooler and less saline (Pietrafesa et al., 1985). The course of the Gulf Stream along the continental shelf break is unstable; it meanders onshore and offshore and projects intrusions, filaments, and eddies onto the shelf (Pietrafesa, 1989; Lee et al., 1991). These processes complicate the position and distort the configuration of the frontal zone.

Retrospective examination of 1163 collections taken from the Straits of Florida to Cape Hatteras and offshore from the 9 m to 2000 m isobath (Fig.1) from 1973 to 1980 (MARMAP) afforded the determination of coarse-scale distribution. These collections were taken with neuston nets of two different dimensions and meshes: a 1.0 × 0.5 m net with 505-µm mesh and a 2.0 × 1.0 m net with 947-µm mesh. Both meshes collect swordfish larvae, which are reported to be at least 4 mm at hatching (Sanzo, 1910; Yasuda et al., 1978). Neuston nets were towed for 10 min at 5.6 km/h. Collections were made in all four seasons and at all times of day and night. Larvae were preserved in 5% formalin solution. The probable location of the Gulf Stream front for these collections was determined from 1) advanced, very high resolution, infra-red radiometer (AVHRR) satellite images of sea-surface temperature (SST) taken from 1976 to 1980; 2) expendable bathythermograph (XBT) profiles taken from 1973 to 1980;

3) sea-surface salinity, dissolved oxygen, and nitrate concentrations taken along with neuston collections (Mathews and Pashuk, 1986); 4) records of the National Oceanographic Data Center; and 5) records of U.S. Coast Guard visual observations from aircraft. The width of the frontal zone, and consequently the area occupied by frontal zone water, was determined as three times the standard deviation of the mean course of the front, i.e. ±10 nautical miles (18.5 km) of the estimated location of the frontal axis (Olson et al., 1983).

Forty-seven collections taken from 22 to 24 June 1984 with a 1.0 × 0.5 m neuston net with 909-µm mesh towed for 10 min at 5.6 km/h in the Gulf Stream and within its western frontal zone between Cape Canaveral and Cape Hatteras (CF8406) afforded an examination of coarse scale differences in occurrence of swordfish larvae within the frontal zone and in the body of the Gulf Stream. Six collections were taken during night, the remainder during the day. Larvae were preserved in 5% formalin. A sea-surface temperature plot, generated from composite AVHRR images of SST compiled on 20 June 1984 (Fig. 2), in conjunction with continuous temperature and salinity values from a hull-mounted thermosalinometer, was used to determine the position of the Gulf Stream and its frontal zone and to classify these collections to water mass.

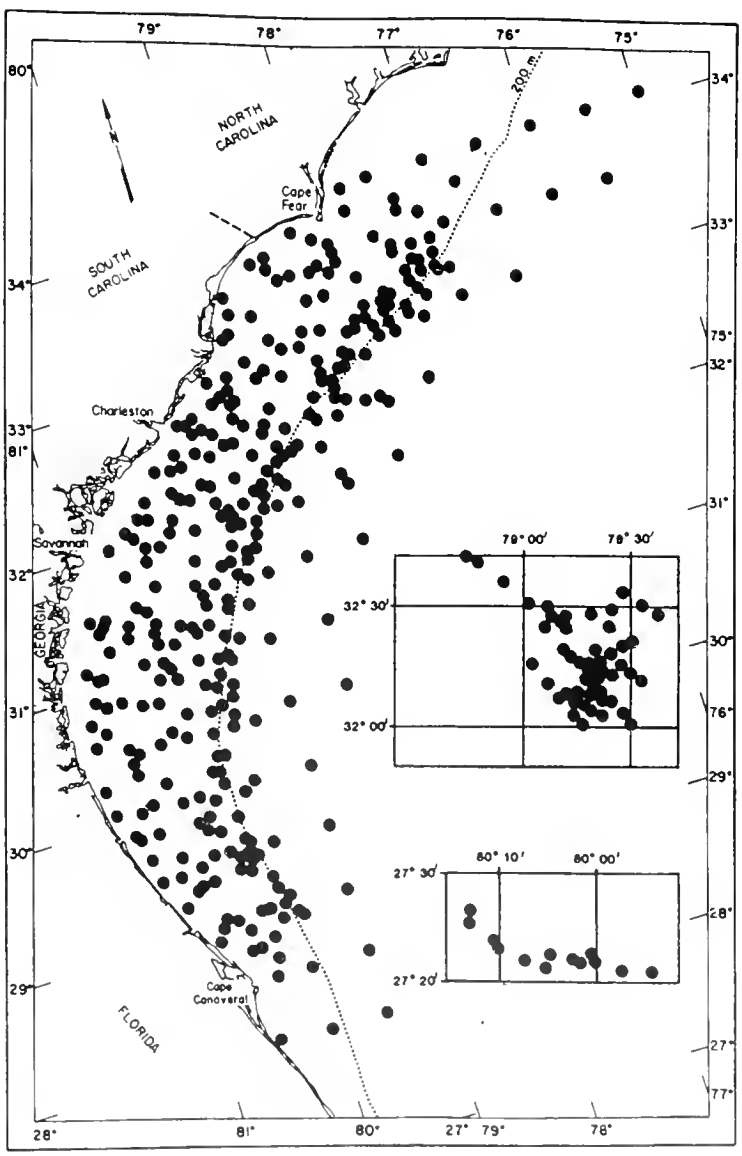

Figure 1

Nominal stations occupied by the Marine Resources Monitoring Assessment and Prediction Program from 1973 to 1980; each station was occupied at least once, some more than once.

One hundred and fifty-six collections (CH8807), taken from 13 to 24 September 1988 with a 2.0 × 1.0 m neuston net with 947-µm mesh along six cross-shelf and cross-slope transects (encompassed by 31°30.4N/080°16.5W, 30°45.0N/078°411.5W, 32 24°30.0N/076°19.5W, and 33°16.0N/077°54.0W), afforded examination of coarse- and fine-scale distribution of larval swordfish within and about the Gulf Stream frontal zone (Fig. 3). Neuston nets were towed for 10 min at 5.6 km/h. Ten stations were occupied along each transect (60 stations); 96 additional neuston collections were taken within the Gulf Stream or within its frontal zone. The 60 collections along transects were 18.5 km apart, whereas 94 of the additional 96 collections within the frontal zone or body of the Gulf Stream were clustered in groups of four to ten, with collections about 1 km apart. Surface salinity, two-dimensional sections of isotherms derived from XBT casts taken at each station along transects, and AVHRR images of SST were used to classify collections.

Six neuston collections taken on 31 May 1997 (CH9703) with a 2.0 × 1.0 m neuston net with 947-µm mesh within the Gulf Stream frontal zone in an area encompassed by 33°52.94'N/076°23.89'W, 33°52.30'N/076°24.77'W, and 33°52.92'N/076°22.27'W afforded examination of fine-scale distribution of larval swordfish within the Gulf Stream frontal zone (Fig. 4). Nets were towed for 10 min at 5.6 km/h, twice in the Gulf Stream frontal zone, and twice each on the shelf and Gulf Stream sides of the front. Larvae were preserved in 95% ethanol. Sea-surface temperature from a hull-mounted thermister in conjunction with XBT profiles and AVHRR images of SST were used to classify collections.

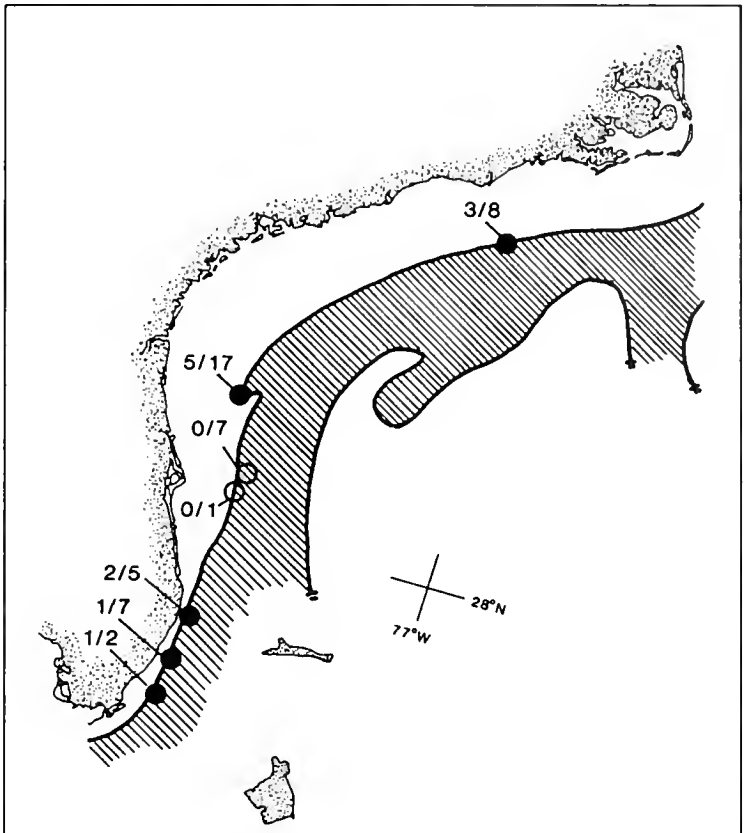

Figure 2

The position of the Gulf Stream (diagonal line pattern) illustrated from a 3-d average of sea-surface temperatures compiled on 20 June 1984 with data from infrared sensors on a Global Stationary Environmental Satellite operated by the National Weather Service (closed circles denote approximate locations of multiple neuston collections where swordfish larvae were present; open circles, locations where swordfish larvae were absent; fractions are the number of positive collections over the total number of collections).

Length of larvae

The overall distribution of the length of swordfish larvae in the Caribbean Sea, Gulf of Mexico, and off the southeastern Atlantic coast of the United States provided a view of the occurrence of the smallest larvae. Because most published have records reported either standard length (SL) or total length (TL), both measures are reported in our study. We employed no conversion, although the length of the caudal finfold or fin ranges from 3% to 12% of TL for larvae from 6 to 192 mm (calculated from Arata [1954]). We employed no correction for the shrinkage of larvae due to death or preservation, because preservation fluid was not routinely reported in the literature and some specimens were measured alive. Although the length from the anterior eye orbit to the tip of the notochord is perhaps a better measure of length in swordfish larvae, because the rostrum is often broken (Potthoff and Kelley, 1982), this measure was not uniformly available in published records. Standard or total lengths (anterior tip of the upper jaw to the posterior tip of the notochord or hypural plate (SL) or caudal fin (TL)) of swordfish larvae and locations of collection were taken from Arata (1954), Arnold (1955), Tibbo and Lauzier (1969), Markle (1974), Post et al. (1997) and MARMAP. Standard length was measured on larvae from SEAMAP, CF8408, CH8807, and CH9703 (from neuston as well as plankton collections taken within the Gulf Stream frontal zone with a MOCNESS (Wiebe, et al., 1976) system with 505 m mesh nets), and on a larva from a neuston collection taken in a *Sargassum* raft at 33°38.7'N/076°02.7'W in 1991. Specimens were considered larvae if they were <190 mm SL or TL, because

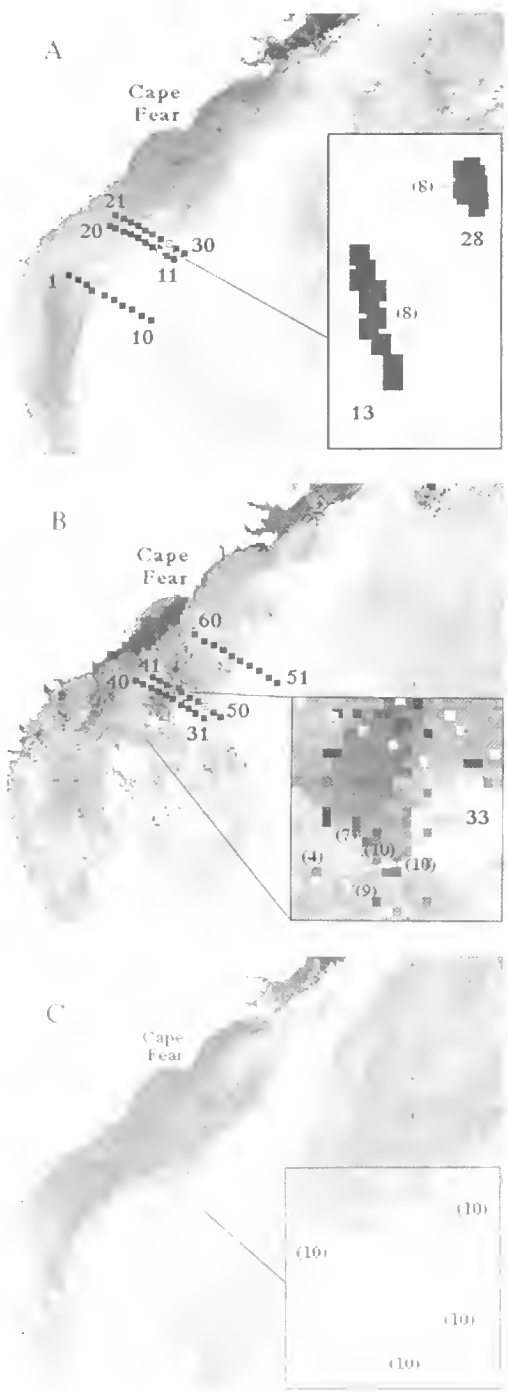

Figure 3

Advanced very high resolution infrared radiometer images of sea-surface temperatures off the southeastern Atlantic coast of the United States; five day composites from National Oceanic and Atmospheric Administration, National Environmental Satellite, Data and Information Service global orbiting satellites (**A**) 11 to 15 September; (**B**) 16 to 20 September; (**C**) 21 to 25 September 1988. Darker to lighter shades denote cooler to warmer water, squares denote locations of neuston collections; numbers denote station numbers, and parenthetical numbers within insets denote the number of overlapping stations.

swordfish retain larval characters (lower jaw at least half as long as the rostral cartilage; preorbital, supraorbital, posttemporal, and preopercular spines; enlarged and spinous dorsal and ventral scales; and a continuous and long dorsal fin) until they are at least 188 mm SL (Arata, 1954; Pothoff and Kelley, 1982; McGowan, 1988).

Approximate age of larvae

The age of swordfish larvae at length was approximated from published accounts of the age and lengths of laboratory-reared larvae, and from counts of apparent growth increments on otoliths excised from three specimens collected by CH9703. Larvae from the Mediterranean hatch at a length from 4.0 to 4.5 mm TL (measured alive) after 3 d of incubation and deplete their yolk and oil globule at a length of about 5 mm TL after 5 to 7 d at 22.5–25.2°C (Sanzo, 1910; Yasuda et al., 1978).

Results

Spatial distribution

The 1163 MARMAP collections yielded 55 swordfish larvae in 35 collections. Larvae were collected in all seasons and at all times of the day. Of the 35 collections that produced larvae, 21 were taken in the day, 5 at night, and 9 at dawn or dusk. As many as nine larvae were taken in a single collection. Between Cape Canaveral and Cape Hatteras, larvae were collected more frequently within the frontal zone of the Gulf Stream, than they were in shelf or Gulf Stream waters. Where the Gulf Stream jets through the Florida Straits (25° to 28° N latitude), larvae occurred across the narrow body of the Gulf Stream. If these Florida Straits collections are excluded from consideration, along with collections from single seasonal or annual surveys that did not produce any larvae, 21 of these 27 collections that yielded larvae were within the probable area of the Gulf Stream frontal zone, i.e. 18.5 km of the assigned position of the Gulf Stream surface frontal axis; one was in shelf water, and five were in Gulf Stream water (Fig. 5; Table 1). The probability of observing the presence or absence of larvae (calculated as frequency of occurrence), among the two water masses and the mixed frontal zone, with at least as much association was 0.000002% (Fisher's exact test, two-tailed distribution).

In June 1984 (CF8406), the frontal zone was defined by the 25° to 27°C surface isotherms. North of Florida, the western Gulf Stream front was smooth with no evidence of instabilities in the form of large intrusions (Fig. 2). Twelve of 47 collections of CF8406 yielded 16 swordfish larvae. Of these, two collections

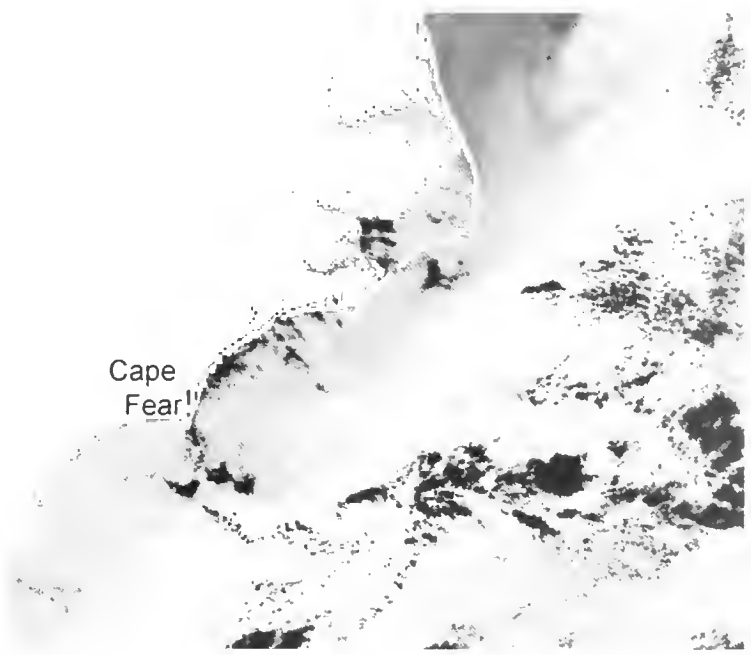

Figure 4

Advanced very high resolution infrared radiometer images of sea-surface temperatures off the southeastern Atlantic coast of the United States on 28 May 1997 from NOAA polar orbiting satellite (darker to lighter shades denote cooler to warmer water; circles denote locations of hydrographic stations occupied on 3 June 1997).

yielded more than one larva, i.e. two larvae in each. Ten collections with larvae present were within the frontal zone, whereas two collections were in the body of the Gulf Stream (Table 1). The probability of observing the presence or absence of larvae with a frequency at least this extreme was 0.176% (two-tailed test).

In September 1988 (CH8807), the Gulf Stream frontal zone was defined by 27° to 29°C surface isotherms. With the defining criterion of horizontally compressed surface isotherms within this temperature range, the width of this frontal zone ranged from 18 to 93 km. This area, however, encompassed a westward intrusion of the Gulf Stream that developed over the transect grid (Fig. 3) in the wake of the Charleston Bump, a topographic rise at the continental shelf break that typically forces an eastward deflection of the Gulf Stream (Pietrafesa et al., 1985). Isolated surface pools of 27° to 29°C water inshore of the Gulf Stream front proper (Fig. 6, B and F) indicated this intrusion. This convolution of the Gulf Stream front proper manifested three fronts across the shelf, but these were considered a composite single front for analysis. Shear zones (determined by rapid increases in the ship's set), drift lines of *Sargassum*, and discontinuities in sea-surface texture, were embedded within the frontal zone and evidenced probable convergence of surface water (Stommel, 1966; Olson et al., 1994). The 156 collections of CH8807 yielded 12 swordfish larvae. One collection yielded three larvae; another two. Larvae were collected exclusively within the frontal zone (Table 1), one at the tip of the intrusion (station 58; Fig. 6F). The probability of observing the presence or absence of larvae at least this extreme was 0.020%.

In May 1997 (CH9703), the Gulf Stream frontal zone was defined by 27° to 29°C surface isotherms. The frontal zone was moving rapidly eastward. On 23 May, 8 d before the collection of swordfish larvae within the frontal zone, an elongate filament of a Gulf Stream intrusion lay inshore of the collection area (Fig. 4). The isolated pool of 25°C water at the surface and eastward of the frontal zone (Fig. 7) indicated that this intrusion was extant on 31 May 1997 when collections of CH9703 were taken. The six neuston collections of CH9703 yielded nine larvae. One collection taken along the frontal axis and one collection taken on the Gulf Stream side of the axis yielded two larvae each; the other collection taken along the axis yielded three. Larvae were present in two collections along the frontal axis, two collections 1 km to the Gulf Stream side of the axis, and one of two collections taken 0.5 km

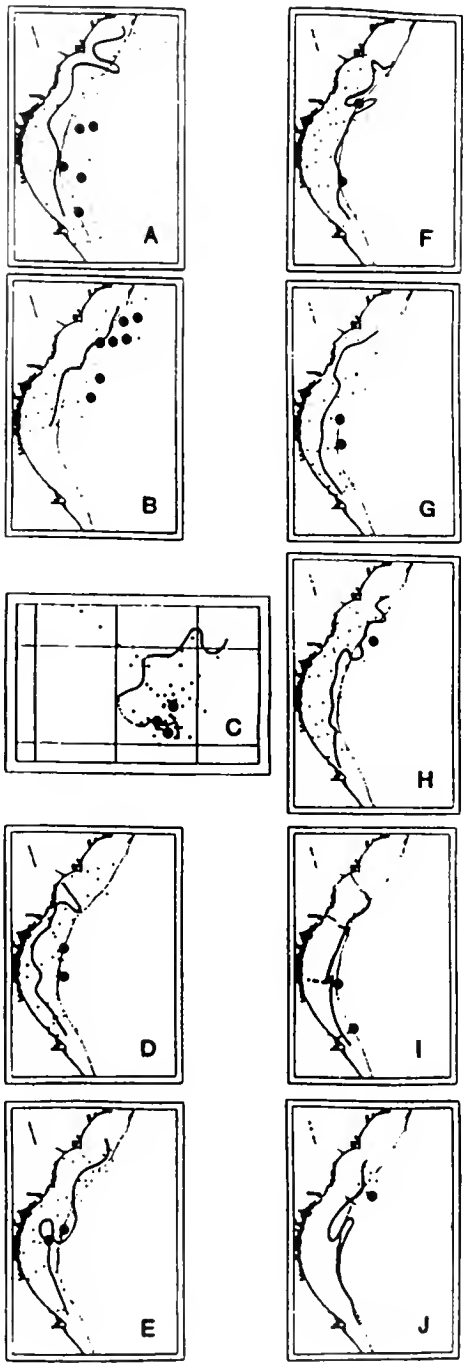

Figure 5

Position of the Gulf Stream front and locations of neuston collections of surveys when swordfish larvae were collected from 1973 to 1980 (solid lines denote assigned axis of the Gulf Stream front, small circles locations of neuston collections; large circles locations of swordfish larvae: (**A**) March 1973; (**B**) May 1973; (**C**) July 73; (**D**) November 1973; (**E**) August and September 1974; (**F**) August and September 1975; (**G**) January and February 1976; (**H**) August and September 1976; (**I**) September 1978; (**J**) April 1979

Table 1

Contingency tables of the absence and presence of larval swordfish, *Xiphias gladius*, in Gulf Stream frontal zone, the Gulf Stream, and shelf water in the southeastern Atlantic bight off the United States.

Frequency	Frontal zone water	Gulf Stream water	Shelf water	Total
1973–80				
Absent	158	25	175	358
Present	21	5	1	27
Total	179	30	176	385
1984				
Absent	21	14	35	
Present	10	2	12	
Total	31	16	47	
1988				
Absent	77	46	24	147
Present	9	0	0	9
Total	86	46	24	156
1997				
Absent	0[1]	0[2]	1[3]	1
Present	2[1]	2[2]	1[3]	5
Total	2[1]	2[2]	2[3]	6

[1] Taken along the frontal axis.
[2] Taken along offshore side of the axis.
[3] Taken on inshore side of the axis.

to the shoreward side of the frontal axis. Larvae were evenly distributed within the frontal zone (Table 1).

Length of larvae

Swordfish larvae ranged from 2.8 mm SL to 110 mm TL. The two largest larvae, >100 mm TL, were collected in the Atlantic and in the Caribbean. The smallest and youngest larvae, those ≤5 mm SL (Fig. 8), were collected in the eastern Gulf of Mexico in the vicinity of the Gulf Loop Current between 24° and 28°N (here, 39 of 152 larvae were ≤5 mm), and off the southeast coast from Georgia north to Cape Hatteras between 30° and 35°N latitude (here, 15 of 62 larvae were ≤5 mm SL). Larval lengths were not correlated with latitude (Pearson product-moment correlation coefficient=–0.1360).

Approximate age of larvae

The smallest larva measured (after preservation in 95% ethanol), taken in the Gulf of Mexico from SEAMAP, was appreciably smaller than the length at hatching for larvae (measured alive, 27 h after fertilization) from the Mediterranean (Yasuda et al., 1978). One larva 2.8 mm SL from the eastern Gulf of Mexico, and

one 3.8 mm SL (4.3 mm TL) taken off North Carolina (CH9703), had recognizable yolk and oil globule remnants. These lengths were smaller than the reported length of larvae at the completion of yolk and oil globule absorption, about 5 mm TL for larvae (measured alive, 65 h after fertilization) from the Mediterranean (Yasuda et al., 1978).

Counts of increments on sagittae from larvae 4, 5, and 6 mm SL, taken in CH9703, were 4, 3, and 6 (increments on swordfish otoliths have not been validated as daily intervals [Price et al., 1991]).

Discussion

North of the Florida Straits, larval swordfish were collected most frequently within the western frontal zone of the Gulf Stream. This observation corroborates the speculation that larvae are associated with water within sharp horizontal gradients of temperature and salinity (Tibbo and Lauzier, 1969). Convergence of surface water is a possible mechanism for their accumulation within the Gulf Stream front. The Gulf Stream front south of Cape Hatteras is cyclonically sheared with shelf water that directly opposes Gulf Stream water (Pietrafesa et al., 1985). The retrograde, hydrographic discontinuity between Gulf Stream and shelf water and their hydrodynamic opposition results in convergence of surface water within the frontal zone (Garvine, 1980; Olson et al., 1994). Convergence of surface water has been implicated in the accumulation of adult fishes with depth-keeping abilities (Olson and Backus, 1985). Positively buoyant or surface-seeking larval fishes will be entrained in converging water and will be advected toward the front where they will accumulate as they resist downwelling along the frontal axis (Govoni and Grimes, 1992). Swordfish larvae are unquestionably surface-seeking larvae. Convergence of surface water within oceanic frontal zones should produce accumulations of larvae on spatial scales of 10 to 100 km (Olson et al., 1994). At a coarse scale, larvae were more abundant within the frontal zone; no fine-scale pattern was evident within the frontal zone. Adaptive sampling (Lo et al., 1997) may be a more efficient means of estimating larval swordfish abundance than simple random sampling, because of the rarity and the spatial aggregation of larvae.

Small swordfish larvae were collected most often in the eastern Gulf of Mexico and off the east coast of the United States as far north as Cape Lookout, North Carolina. Swordfish apparently spawn in the eastern Gulf, but the present observations corroborate the speculation of spawning off the Carolinas (Squires, 1962; Markle, 1974) as well. Off the Carolinas, larvae

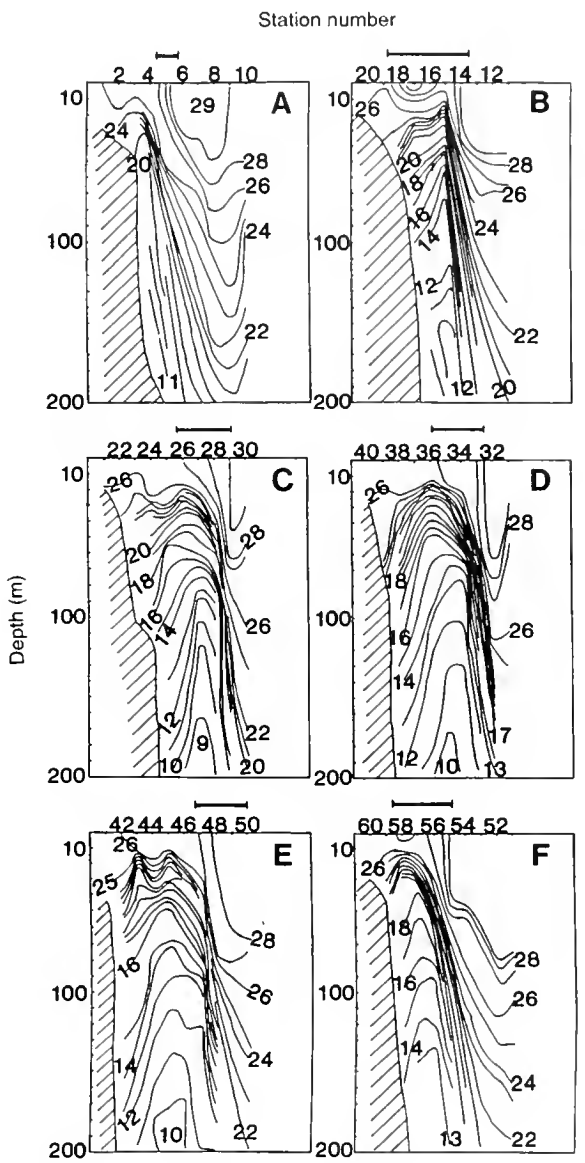

Figure 6

Sections of isotherms along transects occupied in September 1988: (**A**) 13 September; (**B**) 14 September; (**C**) 15 September; (**D**) 16 September; (**E**) 17 September; (**F**) 18 September (bars above station numbers indicate the Gulf Stream frontal zone).

5 mm SL or less occurred in 25° and 26°C water. Larvae that were 4 to 5 mm SL had 3 and 4 apparent growth increments on their sagittae. In water from 22° to 25°C, larvae that were 5 mm TL would be approximately 6 d old (Yasuda et al., 1978). Given an egg incubation period of 3 d at 24°C (Yasuda et al., 1978) and an additional 3 or 4 d for posthatch growth, along with a average axial velocity of the Gulf Stream of 1.5

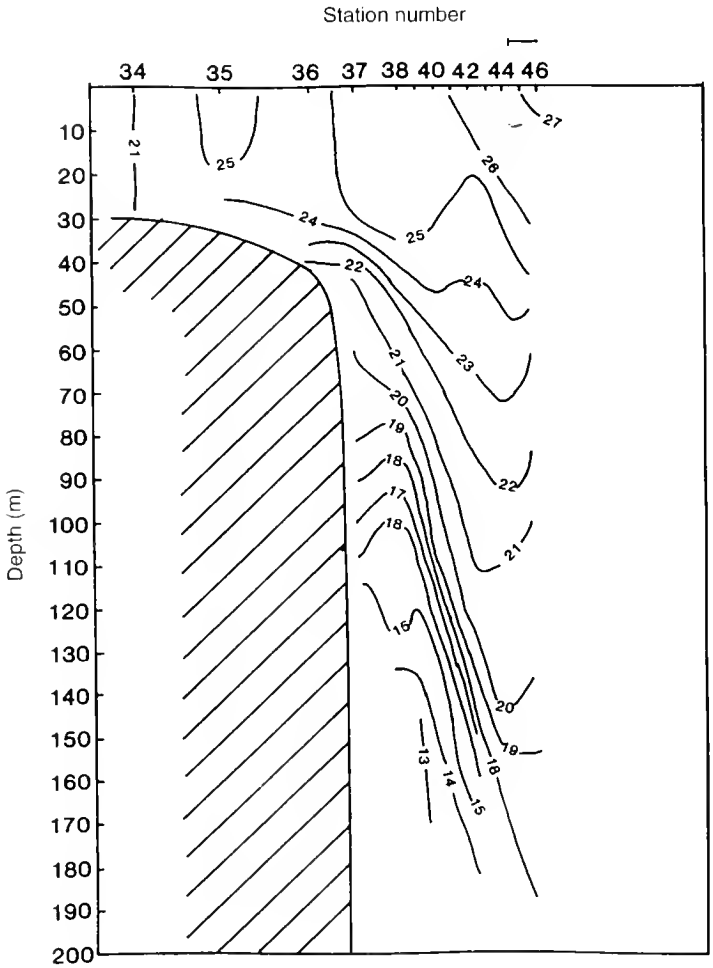

Figure 7

Section of isotherms along a transect occupied on 3 June 1997. Bar above station numbers indicates the Gulf Stream frontal zone and the location of larval swordfish collections.

m/s (Olson et al., 1994), larvae that were 4 to 5 mm SL in the Atlantic could have been transported from as far away as 900 km. A similar trajectory was projected for small larvae of bluefin tuna, *Thunnus thynnus* (McGowan and Richards, 1989). Larvae that were ≤5 mm in length, collected off North Carolina could have been spawned in the Florida Straits if they remained in the core of the Gulf Stream. Current velocities within the western Gulf Stream frontal zone, where larvae most frequently reside, are less than axial velocities (Lillibridge et al., 1990; Song et al., 1995; Limouzy-Paris et al., 1997). Further, departures from a smooth, along slope, Gulf Stream trajectory, in the form of meanders, intrusions, and filaments along the western Gulf Stream frontal zone are frequent (Pietrafesa, 1989). We collected swordfish larvae frequently within these Gulf Stream anomalies (Figs. 4–7). Water within these features veers and reverses direction (Lee et al., 1991), the result being that the northward translocation of swordfish larvae within the frontal zone is checked and their northward transport delayed. The possibility of spawning between Cape Canaveral and Cape Hatteras is real, but not certain.

Acknowledgments

We thank J. A. Hare and L. R. Settle (NOAA) for the collection of some of the swordfish specimens reported herein, J. A. Hare for manipulation of satellite images, E. H. Laban for the extraction of otoliths, and C. W. Lewis, R. L. Ferguson, and J. D. Christensen for preparation of figures. J. A. Hare, J. V. Merriner, and

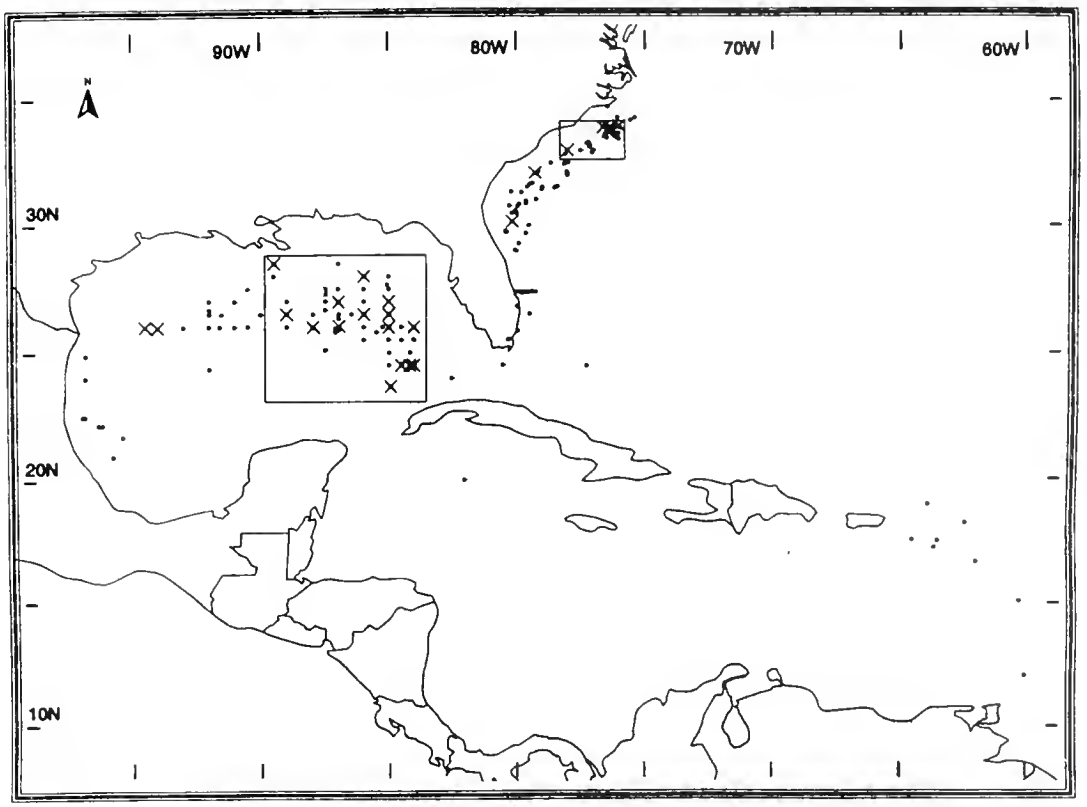

Figure 8

Locations of larval swordfish collection in the Caribbean Sea, Gulf of Mexico, and off the southeast coast of the United States north to Cape Hatteras (crosses depict larvae 2.8 through 5 mm standard (SL) or total length (TL); circles, larvae 5.1 through 110 mm SL or TL; within the box in the Gulf of Mexico, coincidental crosses represent 39 larvae ≤5 mm and 113 >5 mm SL; within the Atlantic, coincidental crosses represent 15 larvae ≤5 mm and coincidental circles 47 >5mm SL).

D. S. Vaughan provided reviews of the manuscipt. J. M. Leiby loaned SEAMAP specimens and data. JJG thanks W. J. Richards for first suggesting where to find swordfish larvae and the late F. G. Carey who supported initial work.

Literature cited

Arata, G. F.
1954. A contribution to the life history of the swordfish, *Xiphias gladius* Linnaeus, from the south Atlantic coast of the United States and the Gulf of Mexico. Bull. Mar. Sci. Gulf Caribb. 4:183–243.

Arnold, E. L.
1955. Notes on the capture of young sailfish and swordfish in the Gulf of Mexico. Copeia (1955)2:150–151.

Arocha, F., and D. W. Lee.
1995. The spawning of swordfish from the northwest Atlantic. Int. Comm. Conserv. Atl. Tuna, Collect. Vol Sci. Pap. 44:179–183.

Atkinson, L. P.
1985. Hydrography and nutrients of the southeastern U.S. continental shelf. *In* L. P. Atkinson, D. W. Menzel, and K. A. Bush (eds.), Oceanography of the southeastern U.S. continental shelf, p. 77–92. American Geophysical Union, Washington.

Garvine, R. W.
1980. The circulation dynamics and thermodynamics of upper density fronts. J. Phys. Oceanogr. 10:2058–2081.

Gorbunova, N. N.
1969. Breeding grounds and food of the larvae of the swordfish *Xiphias gladius* Linneus (Pisces, Xiphiidae). Prob. Ichthyol. 9:375–387.

Govoni, J. J., and C. B. Grimes.
1992. The surface accumulation of larval fishes by hydrodynamic convergence within the Mississippi River plume front. Cont. Shelf Res. 12:1265–1276.

Grall, C., D. P. de Sylva, and E. D. Houde.
1983. Distribution, relative abundance, and seasonality of swordfish larvae. Trans. Am. Fish. Soc. 112:235–246.

Haury, L. R., J. A. McGowan, and P. H. Weibe.
1978. Patterns and processes in the time-space scales of plankton distributions. *In* J. H. Steele (ed.), Spatial pattern in plankton communities, p. 277–327. Plenum, New York.

Hitchcock, G. L., T. Rossby, J. L. Lillibridge, E. J. Lessard, E. R. Levine, D. N. Connors, K. Y. Borsheim, and M. Mork.
1994. Signatures of stirring and mixing near the Gulf Stream front. J. Mar. Res. 52:797–836.

Lee, T. N., J. A. Yoder, and L. P. Atkinson.
1991. Gulf Stream frontal eddy influence on productivity

of the southeast U S. continental shelf. J. Geophys. Res. 96:22191–22205.

Lillibridge, J.L., G. Hitchcock, T. Rossby, E. Lessard, M. Mork, and L. Golmen.
1990. Entrainment and mixing of shelf/slope waters in the near-surface Gulf Stream. J. Geophys. Res. 95:13065–13087.

Limouzy-Paris, C. B., H. C. Graber, D. L. Jones, A. W. Röpke, and W. J. Richards.
1997. Translocation of larval coral reef fishes via sub-meso-scale spin-off eddies from the Florida Current. Bull. Mar. Sci. 60:966–983.

Lo, N. C. H., D. Griffith, and J. R. Hunter.
1997. Using restricted adaptive cluster sampling to estimate Pacific hake larval abundance. Calif. Coop. Oceanic Fish. Invest. Rep. 38:103–113.

Markle, G. E.
1974. Distribution of larval swordfish in the Northwest Atlantic Ocean. U.S. Dep. Commer., NOAA Tech. Rept NMFS-SSRF 675:252–260.

Mathews, T. D., and O. Pashuk.
1986. Summer and winter hydrography of the U.S. south Atlantic bight (1973–1979). J. Coast. Res. 2:311–336.

McGowan, C.
1988. Differential development of the rostrum and mandible of the swordfish (*Xiphias gladius*) during ontogeny and its possible functional significance. Can. J. Zool. 66:496–503.

McGowan, M. F., and W. J. Richards.
1989. Bluefin tuna, *Thunnus thynnus*, larvae in the Gulf Stream off the southeastern United States: satellite and shipboard observations of their environment. Fish. Bull. 87:615–631.

Nishikawa, Y., and S. Ueyanagi.
1974. The distribution of the larvae of swordfish, *Xiphias gladius*, in the Indian and Pacific oceans. U.S. Dep. Commer., NOAA Tech. Rep.NMFS-SSRF 675:261–264.

Olson, D. B., O. T. Brown, and S. R. Emmerson.
1983. Gulf Stream frontal statistics from Florida Straits to Cape Hatteras derived from satellite and historical data. J. Geophys. Res. 88:4569–4577.

Olson, D. B., and R. H. Backus.
1985. The concentrating of organisms at fronts: a cold-water fish and a warm-core Gulf stream ring. J. Mar. Res. 43:113–137.

Olson, D. B., G. L. Hitchcock, A. J. Mariano, C. J. Ashjian, G. Peng, R. W. Nero, and G. P. Podestá.
1994. Life on the edge: marine life and fronts. Oceanography 7:52–60.

Pietrafesa, L. P.
1989. The Gulf Stream and wind events on the Carolina Capes shelf. National Undersea Research Program. U.S. Dep. Commer., NOAA-NURP Rep. 89-2:89–100.

Pietrafesa, L. P., G. S. Janowitz, and P. A. Wittman.
1985. Physical oceanographic processes in the Carolina Capes. *In* L. P. Atkinson, D.W Menzel, and K. A. Bush (eds.), Oceanography of the southeastern U.S. continental shelf, p. 23–32. American Geophysical Union, Washington.

Potthoff, T., and S. Kelley.
1982. Development and structure of the vertebral column, fins and fin supports, branchiostegal rays and squamation in the swordfish *Xiphias gladius*. Fish. Bull. 80:161– 186.

Post, J. T., J. E. Serafy, J. S. Ault, T. R. Capo, and D. P. de Sylva.
1997. Field and laboratory observations on larval Atlantic sailfish (*Istiophorus platypterus*) and swordfish (*Xiphias gladius*). Bull. Mar. Sci. 60:1026–1034.

Prince, E. D., D. W. Lee, J. R. Zweifel, and E. B. Brothers.
1991. Estimating age and growth of young Atlantic blue marlin *Makaira nigricans* otolith microstructure. Fish. Bull. 89:441–459.

Richards, W. J., and T. Potthoff.
1980. Larval distributions of scombrids (other than bluefin tuna) and swordfish in the Gulf of Mexico in the spring of 1977 and 1978. Int. Comm. Conserv. Atl. Tuna, Coll. Vol. Sci. Pap. 9: 680–694..

Sanzo, L.
1910. Uovo e larva di pesce-spada (*Xiphias gladius* L.). Riv. Mens. Pesca Idrobiol. 12:206– 209.

Schmitz, W. J., J. R. Luyten, and R. W. Schmitt.
1993. On the Florida Current T/S envelope. Bull. Mar. Sci. 53:1048–1065.

Scott, G. P., S. L. Turner, C. B. Grimes, W. J. Richards, and E. B. Brothers.
1993. Indices of larval blue-fin tuna, *Thunnus thynnus*, abundance in the Gulf of Mexico; modelling variability in growth, mortality, and gear selectivity. Bull. Mar. Sci. 53:912–929.

Song, T., T. Rossby, and E. Carter.
1995. Lagrangian studies of fluid exchange between the Gulf Stream and surrounding waters. J. Phys. Oceanogr. 25:46–63.

Squires, J. L.
1962. Marlin and swordfish in oceanic waters of the western North Atlantic. Copeia (1962) 1:216–219.

Stommel, H.
1966. The Gulf Stream. Univ. California Press, Berkeley, CA, 248 p.

Tåning, Å.
1955. On the breeding areas of the swordfish (*Xiphias*). Deep-Sea Res. 3(suppl.):438–450.

Tibbo, S. N., and L. M. Lauzier.
1969. Larval swordfish (*Xiphias gladius*) from three localities in the western Atlantic. J. Fish. Res. Board Can. 26:3248–3251.

Wiebe, P.H., K.H. Burt, S.H. Boyd, and A.W. Morton.
1976. A multiple opening/closing net and environmental sensing system for sampling zooplankton. J. Mar. Sci. 34:313–326.

Yabe, H., S. Ueyanagi, S. Kikawa, and H. Watanabe.
1959. Study on the life-history of the sword-fish, *Xiphias gladius* Linnaeus. Rep. Nankai Reg. Fish. Res. Lab. 10:107–150.

Yasuda, F., H. Kohno, A. Yatsu, H. Ida, P. Arena, F. L. Greci, and Y. Taki.
1978. Embryonic and early larval stages of the swordfish, *Xiphias gladius*, from the Mediterranean. J. Tokyo Univ. Fish. 65:91–97.

Xie, L., and L. J. Pietrafesa.
1995. Shoreward intrusion of upper-layer warm water by prescribed shelf-break temperature perturbation and surface wind stress. Geophys. Res. Letters 22:2585–2588.

A biological reference point based on the Leslie matrix

Daniel B. Hayes
Department of Fisheries and Wildlife
13 Natural Resources Building
Michigan State University
East Lansing, Michigan 48824-1222
E-mail address hayesdan@msu.edu

Abstract.—For fish populations with an annual breeding cycle, a biological reference point based on the Leslie matrix is presented and compared with percent maximum spawning potential (%MSP) and F_{med} reference points. For deterministic population projections, the reference point is defined as the level of fishing mortality (F_{st}) that results in a Leslie matrix with a dominant eigenvalue (i.e. finite rate of increase or λ) of 1.0. It is shown that for the same input data, F_{st} is similar to a reference point based on a %MSP approach. For populations that are growing or declining, however, populations with the same λ but with different age-specific selectivities have different levels of %MSP. Previous applications of this reference point are extended to include situations where recruitment is a stochastic process. In stochastic projections, F_{st} is defined as the level of fishing mortality that results in an average finite rate of increase of 1.0. In an example with Georges Bank haddock, a deterministic analysis with mean birth and death rates resulted in an estimate of F_{st} of 0.52. The same estimate of F_{st} was obtained in a stochastic projection in which the growth rate of the mean population size was used. Stochastic projections using the mean of the finite rates of increase resulted in a lower estimate of F_{st} (0.45). When the value of recruits per unit of spawning stock biomass used in the %MSP analysis was calculated as Σrecruits/Σspawning stock biomass, the estimated reference point was the same as the stochastic projection. On the basis of these results, I recommend calculating the reference point based on a stochastic projection for which the mean of the simulated growth rates is used. A reference point based on a %MSP approach using the Σrecruits/Σspawning stock biomass results in an equivalent estimate of the reference point but does not convey important information on the expected population growth rate at higher or lower rates of fishing mortality.

Manuscript accepted 17 August 1999.
Fish. Bull. 98:75–85 (2000).

Advice to fishery managers on desirable harvest or exploitation rates is ideally based on full knowledge of fishery dynamics, including information on the fish population's stock-recruitment relationship, growth and maturation schedule, and bioeconomic considerations. With a lack of such complete information, guidance to fishery managers often takes the form of providing an estimate of fishing mortality and a comparison of that rate to one or more biological reference points (e.g. Clark, 1991; Anonymous[1]). Numerous biological reference points exist, each concerned with a somewhat different aspect of population response to harvesting. One class of reference points focuses on yield per recruit as a function of fishing mortality. The general goal of this class of reference points is to optimize harvest rates in relation to natural mortality and growth (i.e. prevent growth overfishing; Beverton and Holt, 1957). For example, F_{max} is the fishing mortality rate at which yield per recruit is maximized (Beverton and Holt, 1957). A related reference point is $F_{0.1}$, which is the fishing mortality rate where the slope of the yield per recruit curve is 10% of the slope at the origin (Gulland and Boerema, 1973). Fishing at F_{max} or $F_{0.1}$ results in maximal or nearly maximal yield from a fishery when recruitment is independent of stock size. A limitation of this class of reference points, however, is that reductions in recruitment are often evident when stocks are depleted to low levels (e.g. Overholtz et al., 1986). Thus, management advice based on F_{max} or $F_{0.1}$ can result in declines in abundance through recruitment overfishing (Sissenwine and Shepherd, 1987), ultimately resulting in reduced total yield from a stock.

As a counterpart to reference points based on yield per recruit, several reference points based on stock-recruitment considerations have been developed. The goal of these reference points is to provide a measure of fishing mortality that will likely avoid recruitment overfishing. An example of this type of reference point is F_{med} which is based on the median of the observed levels of recruits produced per unit of spawning stock biomass (R/SSB) (Sissenwine and Shepherd, 1987). The rationale behind this reference point is that fish abundance is maintained when the spawning stock biomass produced by a cohort over its lifetime is equal to the spawning stock biomass of the parent population when the cohort was spawned. Related to F_{med} is a set of reference points based on the spawning stock biomass per recruit (SSB/R) in relation to the SSB/R that would be produced if the

[1] Anonymous. 1996. Report of the 20th Northeast Regional Stock Assessment Workshop (20th SAW): SAW Public Review Workshop. Northeast Fisheries Science Center Reference Document 95-19. National Oceanic and Atmospheric Administration, National Marine Fisheries Service, Woods Hole, MA, 52 p.

stock were not fished (Gabriel et al., 1989; Clark, 1991). These reference points are termed percent maximum spawning potential (%MSP) or spawning per recruit (SPR) reference points. As an example, Gabriel et al. (1989) found that fishing at F_{med} for Georges Bank haddock results in a SSB/R ratio of about 30% ($F_{30\%}$) of the SSB/R that would be produced if the stock were not fished.

There are several limitations to this group of reference points. First, the population-level effect of fishing above or below a given reference point is not immediately obvious. For example, if fishing at $F_{30\%}$ results in a stable population, the rate of population decline when fishing mortality results in a 20% MSP is not clear. Secondly, although the use of the median SSB/R is an attempt to determine the SSB/R ratio with a robust estimator, the effects of variability in recruitment have not been closely examined in the estimation process. There is also an implication that two fishing mortality patterns (i.e. combination of fishing intensity and age at entry into the fishery) that produce the same SSB/R will result in equivalent impacts on the population. To my knowledge, this implication has not been investigated. Finally, these reference points treat the R/SSB ratio as being independent of stock size. Although the stock-recruitment relationship for many stocks is so weak and highly variable that this is a reasonable approach (Clark, 1991), this assumption should be examined on a case-by-case basis.

The goal of this paper is to explore a method for computing a reference point based on stock-recruitment data that overcomes some of the limitations of F_{med} and related reference points concerned with recruitment overfishing. In particular, this method allows for 1) a direct determination of the population-level impact of fishing above or below the reference point and, 2) incorporation of information on recruitment variability into the estimated reference point. This method does not, however, take into account any curvature in the stock-recruitment relationship (i.e. this method assumes that recruitment is proportional to spawning stock biomass). Although this assumption is not always met, the reduction in abundance that occurs for most exploited fish stocks results in a reduced magnitude of density-dependent effects on recruitment. Thus, the use of this reference point is likely to be reasonable for fish stocks that have already been exploited (Francis, 1997).

Methods

The proposed method is founded on an eigenvalue analysis of Leslie matrices representing the population's dynamics under exploitation. As such, the model is specifically intended for use for fish with a single breeding season per year. The underlying model is based on one developed by Quinn and Szarzi (1993), which led to determination of the fishing mortality (F_{st}) that resulted in a stationary population in a Leslie matrix setting. Their results are extended by examining the effects of recruitment variability on the reference point and the relationship between this method and %MSP methods. This model is conceptually similar to those used for environmental impact assessment of power plants (e.g. DeAngelis et al., 1977; Cohen et al., 1983; Goodyear and Christensen, 1984) but differs in that it focuses on sustainable harvest rates across several age classes, whereas environmental impact assessment models typically focus on mortality of early life stages. Related methods have also been presented by Getz and Haight (1989). Their methods, however, are not explicitly framed toward providing a reference point for a fishery. Further, their methods are based on catch (in numbers or weight) whereas my methods are based on fishing mortality rates.

Developing a Leslie matrix representation of harvesting: deterministic case

Consider initially a population with no harvest, and where abundance estimates are available on an annual basis at the time of breeding. If we assume that the vital rates (i.e. age-specific reproduction and survival) are constant, the dynamics of the population can be represented by a Leslie matrix L_u; (see Table 1 for a list of symbols and their definitions):

$$L_u = \begin{bmatrix} E(0) & E(1) & E(2) & \dots & E(s) \\ S(0) & 0 & 0 & \dots & 0 \\ 0 & S(1) & 0 & \dots & 0 \\ 0 & 0 & S(2) & \dots & 0 \\ \dots & \dots & \dots & \dots & \dots \\ 0 & 0 & 0 & S(s-1) & 0 \end{bmatrix}$$

where $E(i)$ is age-specific fecundity, $S(i)$ is the annual survival rate from age i to $i+1$ and s is the maximum age. With this projection matrix, the population at time $t+1$ can be determine from the population at time t by the equation:

$$N_{t+1} = L_u N_t.$$

Note that estimates of natural mortality rate are also necessary to compute the previously mentioned reference points and are typically available for species where quantitative stock assessments are performed. Also note that although age-specific fecundity is not always measured in fish stock assessments, spawning stock biomass is commonly used as a surrogate

Table 1
Symbols used and their definitions.

	Definition
$E(i)$	Fecundity at age i.
$F(i)$	Instantaneous fishing mortality rate from age i to $i+1$.
F	Fishing mortality rate on fully recruited age class(es).
F_{st}	Sustainable fishing mortality rate on fully recruited age class(es).
L_e	Leslie matrix representing exploited population.
L_u	Leslie matrix representing unexploited population.
λ_e	Dominant eigenvalue of L_e.
λ_u	Dominant eigenvalue of L_u.
$M(i)$	Instantaneous natural mortality rate from age i to $i+1$.
$N(i)$	Number at age i.
N_t	Total population size at time t.
i	Age index.
$PM(i)$	Proportion of females mature at age i.
R/SSB	Recruits per unit of spawning stock biomass.
SSB	Spawning stock biomass.
SSB/R	Spawning stock biomass per recruit
s	Maximum age.
$S(i)$	Annual survival rate from age i to $i+1$.
t_c	Age at recruitment when vulnerability to the fishery is knife-edge.
$W(i)$	Weight at age i.
$X(i)$	Fecundity equivalents for fish of age i.

(see Rothschild and Fogarty (1989) for cautions on this practice, however). Because data on spawning stock biomass are more commonly presented in fishery assessments than data on fecundity, I will present the model using age-specific fecundity equivalents (i.e. spawning biomass of individual fish) rather than fecundity. In this representation, the survival rate of age-0 fish is expressed as recruits per unit of spawning stock biomass (R/SSB) rather than as actual survival rate from egg to age 1, and SSB is used in place of egg production. It is easily shown that the use of R/SSB and SSB in the Leslie matrix is algebraically equivalent to using fecundity and survival from egg to age 1.

Given the mapping of the vital rates $[E(i), S(i)]$ of the unexploited population into a Leslie matrix, it is straightforward to represent the dynamics of the population under exploitation. Observe that for the unexploited population $S(i)=e^{-M(i)}$, where $M(i)$ is the instantaneous natural mortality rate. For an exploited population, $S(i)=e^{-[M(i)+F(i)]}$ where $F(i)$ is the age-specific instantaneous rate of fishing mortality. The Leslie matrix for the population under exploitation (L_e) is thus formed in exactly the same manner as for the unexploited population except that annual survival rates are decreased through fishing mortality.

It is important to emphasize that in this analysis, fecundity and natural mortality (including age-0 survival or R/SSB) are assumed to be constant. As such, the determination of a reference point based on an analysis of L_e is valid over the range of stock sizes for which these age-specific fecundity and mortality rates apply.

Methods of analyzing the Leslie matrix are well established (e.g. Keyfitz, 1977; Caswell, 1989). Properties of the Leslie matrix under certain regularity conditions include the following:

1 The Leslie matrix has at least one positive root (eigenvalue);
2 The largest of these roots (the dominant eigenvalue or λ) determines the population growth rate, except in cases where the population is inherently cyclical and the largest roots are of equal magnitude;
3 If $\lambda > 1$ the population will increase;
If $\lambda = 1$ the population will remain steady;
If $\lambda < 1$ the population will decrease.

(Pielou, 1974; Caswell, 1989; Getz and Haight, 1989). Of particular importance to this reference point is the dominant eigenvalue which, in the deterministic case, is sufficient to determine the long-term trend in population abundance (Keyfitz, 1977; Cohen et al., 1983). Given these properties, the following assertion for the deterministic case can be made:

1 A population under exploitation can maintain itself at or above a given level of abundance only if the dominant eigenvalue of L_e (i.e. λ_e) ≥ 1.

From this assertion arises the proposed reference point: F_{st} (for F steady, after Quinn and Szarzi, 1993) is a fishing mortality pattern where $\lambda_e = 1$. Note that F_{st} is actually a vector comprising two components: an overall level of fishing mortality (often termed fully recruited F) and the relative fishing mortality between age classes (often referred to as the partial recruitment vector or selection pattern), and that F_t = (fully recruited F) × (selection on age i). By convention, I will use the fully recruited F as an index of the overall level of fishing mortality, but stress that specification of the partial recruitment function is also necessary to determine the impact of harvesting on a population. Also note that there is an infinite set of fishing mortality patterns for which the condition that $\lambda_e=1$ is satisfied. For a given partial recruitment func-

tion, however, only one level of fishing will satisfy this condition. Note that the converse is not true; for a given level of fully recruited fishing mortality, numerous partial recruitment functions can satisfy the above condition. Because of the nature of these relationships, I will focus on those situations where the partial recruitment function is specified and solve for the level of fishing that is sustainable. Once the selection pattern and fully recruited fishing mortality are set, λ_e can be found by the power method as described by Johnson and Riess (1981).

Example of maintenance fishing mortality: deterministic case

Data from Georges Bank haddock (*Melanogrammus aeglefinus*) are used to illustrate the computation and application of this reference point. For ease of discussion, I first present general results assuming knife-edge recruitment to the fishery at age t_c with full vulnerability thereafter.

Age-specific fecundity equivalents ($X(i)$; Table 2) were computed as

$$X(i) = W(i) \times PM(i),$$

where $W(i)$ = mean weight (kg) at age i; and
$PM(i)$ = proportion of females mature at age i.

and spawning stock biomass was computed as the product of fecundity equivalents and number of fish at age. Mean weight at age ($W(i)$) and proportion of females mature ($PM(i)$) reported by O'Brien and Brown[2] were used in this analysis. The instantaneous natural mortality rate ($M(i)$) of haddock age 1 and older is 0.2 (Clark et al., 1982), and a maximum age of 15 was used following Gabriel et al. (1989).

I computed annual R/SSB (Table 3) from the ratio of number of female fish at age 1 to their parental female spawning stock biomass (Clark et al., 1982; O'Brien and Brown[2]; Hayes and Buxton[3]) for the period 1931–94. For the entire data series, R/SSB averaged 0.5902. As noted by Gabriel et al. (1989), however, the R/SSB ratio (reflecting age-0 survival) appears to have declined following the collapse of the Georges Bank haddock stock during the early 1960s.

Table 2

Age-specific characteristics of Georges Bank haddock. Fecundity equivalents (i.e. spawning biomass per individual) are denoted as X, instantaneous natural mortality rate as M, and partial recruitment as PR. The proportion mature and mean weights at age are from O'Brien and Brown (see Footnote 2 in the main text).

Age	Proportion mature	Mean weight (kg)	X	M	PR
0	0.00	—	0.000	—	0.00
1	0.08	0.486	0.039	0.2	0.00
2	0.46	0.676	0.311	0.2	0.07
3	0.88	1.197	1.053	0.2	0.65
4	1.00	1.621	1.621	0.2	1.00
5	1.00	2.021	2.021	0.2	1.00
6	1.00	2.424	2.424	0.2	1.00
7	1.00	2.780	2.780	0.2	1.00
8	1.00	3.192[1]	3.192	0.2	1.00
9	1.00	3.548[1]	3.548	0.2	1.00
10	1.00	3.924[1]	3.924	0.2	1.00
11	1.00	4.297[1]	4.297	0.2	1.00
12	1.00	4.667[1]	4.667	0.2	1.00
13	1.00	5.034[1]	5.034	0.2	1.00
14	1.00	5.398[1]	5.398	0.2	1.00
15	1.00	5.758[1]	5.758	0.2	1.00

[1] Predicted from von Bertalanffy growth equation fitted to observed data for ages 1 to 7.

At present the causes of the decline in the R/SSB ratio are not known. Several hypotheses explaining the observed decline in R/SSB have been put forth, including depensatory mortality on age-0 haddock (Collie and Spencer, 1993), changes in oceanographic conditions (Myers and Pepin, 1994), and increased predation or competition with elasmobranchs (Collie and Spencer, 1993). Although the cause is not known, a crucial consideration is the choice of an appropriate time period where R/SSB is representative of current population abundance and biomass and current environmental conditions.

One strategy to obtain a mean R/SSB value representative of "current" conditions is to average R/SSB from the most recent data point back several years. The philosophy behind this strategy is to smooth annual variations in R/SSB by averaging over a sufficiently long time period. The problem, however, is to define a time period sufficiently long to achieve adequate precision without introducing excessive bias. Averages over short time periods suffer from low precision and can vary considerably because of annual variation in R/SSB. If averages are taken over a time period spanning a wide range of population levels or

[2] O'Brien, L., and R. W. Brown. 1996. Assessment of the Georges Bank haddock stock for 1994. Northeast Fisheries Science Center Reference Document 95-13. National Marine Fisheries Service, Northeast Fisheries Science Center, Woods Hole, MA. 107 p.

[3] Hayes, D. B., and N. G. Buxton. 1991. Assessment of the Georges Bank haddock stock. Papers of the Northeast Regional Stock Assessment Workshop, Research Document SAW13/1, 126 p.

Table 3

Stock-recruitment data for Georges Bank haddock, 1931 to 1990. Data for 1931 to 1962 Hayes and Buxton (see Footnote 3 in the main text), and from 1963 to 1994 from O'Brien and Brown (see Footnote 2 in the main text).

Year	Spawning stock biomass (t) females only	Number of age-1 females produced (millions)	R/SSB	Year	Spawning stock biomass (t) females only	Number of age-1 females produced (millions)	R/SSB
1931	75,767	22.793	0.3008	1963	82,128	235.939	2.8728
1932	61,586	26.052	0.4230	1964	64,278	16.577	0.2579
1933	52,643	30.239	0.5744	1965	72,512	2.013	0.0278
1934	47,187	29.436	0.6238	1966	90,260	6.426	0.0712
1935	52,104	29.323	0.5628	1967	56,051	0.211	0.0038
1936	54,967	53.173	0.9674	1968	37,546	0.494	0.0132
1937	52,872	39.626	0.7495	1969	25,589	2.330	0.0911
1938	60,434	29.875	0.4943	1970	19,255	0.184	
1939	70,067	55.903	0.7979	1972	13,456	9.707	0.7214
1940	67,418	57.052	0.8462	1973	6,135	5.270	0.8590
1941	76,187	30.731	0.4034	1974	10,906	3.827	0.3509
1942	77,248	11.783	0.1525	1975	9,190	51.616	5.6165
1943	75,511	32.411	0.4292	1976	11,031	6.891	0.6247
1944	68,957	20.806	0.3017	1977	20,717	3.029	0.1462
1945	62,785	46.548	0.7414	1978	34,427	41.941	1.2183
1946	65,712	30.486	0.4639	1979	33,841	5.052	0.1493
1947	57,269	16.676	0.2912	1980	31,703	3.600	0.1136
1948	55,659	62.918	1.1304	1981	27,757	1.230	0.0443
1949	45,791	29.447	0.6431	1982	22,682	1.519	0.0670
1950	55,919	52.810	0.9444	1983	17,531	8.548	0.4876
1951	54,039	21.795	0.4033	1984	12,583	0.865	0.0687
1952	55,497	66.748	1.2027	1985	10,313	7.233	0.7013
1953	54,772	26.276	0.4797	1986	10,186	0.882	0.0866
1954	65,764	46.429	0.7060	1987	9,540	8.024	0.8411
1955	68,949	30.534	0.4428	1988	8,781	0.580	0.0661
1956	78,979	31.155	0.3945	1989	9,061	1.244	0.1373
1957	75,364	29.630	0.3932	1990	9,762	0.991	0.1015
1958	75,995	63.270	0.8326	1991	8,682	4.125	0.4751
1959	77,394	61.685	0.7970	1992	6,231	7.219	1.1586
1960	93,667	26.950	0.2877	1993	5,001	3.754	0.7507
1961	113,366	19.368	0.1708	1994	7,324	3.938	0.5377
1962	109,001	95.348	0.8747				

spanning a trend in environmental conditions, the estimate of future R/SSB may be biased. For this stock, mean R/SSB for periods of 5 to 15 years appear relatively stable. Over longer periods of time, mean R/SSB shows an upward trend, punctuated by sharp increases corresponding to the 1963 and 1975 year classes when R/SSB ratios were much higher than in any other years. Because of the trends observed over longer periods of time, I chose the time period from 1976 to 1994 as representative of "current" conditions for R/SSB, or equivalently, age-0 survival. For this time period, R/SSB averaged 0.4092, and had a median of 0.1493.

Based on the mean R/SSB for 1976 to 1994, the haddock population would be expected to grow at a rate of 18.0% per year with no exploitation (i.e. λ_u=1.180). For knife-edge recruitment, I computed λ_e for fishing mortality rates ranging from 0 to 2.0 (Fig. 1) and for ages at entry (t_c) from 1 to 5 years and for the commercial fishery age selectivity observed in 1993–94 (Table 2). Additionally, I determined F_{st} and %MSP (following the methods of Gabriel et al., 1989) for each age at entry (Table 4). It is apparent from this analysis that as age at entry is delayed, the impact of fishing on the population is decreased (Fig. 1). Thus, higher fishing mortality rates can be sustained when recruitment to the fishery is delayed (Table 4). In fact, when the age at entry is 5 or greater, any level of fishing mortality is sustainable.

These conclusions are not new; analysis of SSB/R yields similar insights into the response of populations

to harvesting. The analysis of the Leslie matrix offers information not available in the analysis of SSB/R, however. First, the consequences of overfishing or "underfishing" are clearly evident from the graph of λ_e against fishing mortality rate. For example, for an age at entry of 3 years, F_{st} is 0.465. If the fishing mortality rate was limited to 0.20 (for example), the population would be expected to increase at a rate of about 8.8% per year (Fig. 1). Likewise if fishing mortality was increased to 1.0, the population would be expected to decline at a rate of about 10.3% per year (Fig. 1).

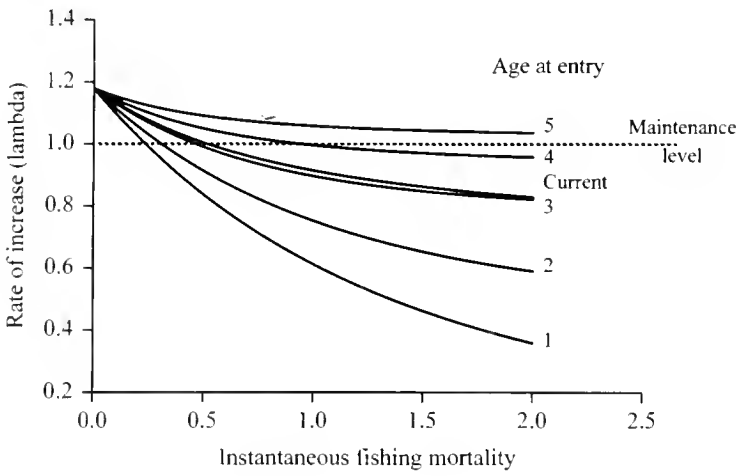

Figure 1

Rate of population increase (lambda) in relation to instantaneous fishing mortality (F) for a range of age at entry into the fishery.

When %MSP is plotted against lambda resulting from various levels of fishing mortality and ages at entry into the fishery, it is apparent that equal %MSP values are obtained for the same lambda only at two points along each of the curves. The first point is for the unfished population when lambda is at a maximum and there is 100% MSP. The second point where all %MSP values are equal is when lambda is equal to 1.00 (Fig. 2). These results demonstrate the assertion that fishing mortality rates that result in equal %MSP values do not necessarily result in the same population dynamics (i.e. the same rate of increase or decrease). The reason for this disparity is that in a growing or declining population, the timing of reproduction during the lifetime is important, as well as the total lifetime egg production. For example, when a population is growing, earlier realization of lifetime spawning potential contributes more to population growth than later reproduction. This relationship is evident when the formula for lifetime spawning stock biomass (on which %MSP is based) is compared to the formula for reproductive value, upon which the rate of population change depends. Observe that lifetime spawning stock biomass per newborn individual is (Gabriel et al., 1989)

$$SSB/N_0 = S(0)W(1)PM(1) + S(0)S(1)W(2)PM(2) + S(0)S(1)S(2)W(3)PM(3) + \ldots .$$

This formula is equivalent to that for the "net reproductive rate" (Caswell, 1989) which is the expected number of offspring produced by a newborn over its lifetime. With the above notation, the reproductive value (Caswell, 1989) of an age-1 individual can be expressed as

$$\textit{Reproductive value} = S(0)S(1)W(2)PM(2)\lambda^{-1} + S(0)S(1)S(2)W(3)PM(3)\lambda^{-2} + S(0)S(1)S(2)S(3)W(4)PM(4)\lambda^{-3} + \ldots .$$

Table 4

Sustainable fishing mortality (F_{st}) and %MSP as a function of age at entry (t_c) for Georges Bank haddock.

t_c	F_{st}	%MSP
1	0.236	27.20
2	0.309	27.20
3	0.465	27.20
Current	0.519	27.20
4	0.956	27.20
5	>2.0	—

These formulae are similar except for the addition of the term λ^{-i}, where i is the age index. Classical demographic theory shows that the growth rate of a population is dependent on the reproductive value rather than on the net reproductive rate (Caswell, 1989). These two quantities are clearly related, however.

Currently, Georges Bank haddock become vulnerable to the fishery at age 2 but are not fully recruited until age 4 (Table 2). With this partial recruitment vector, F_{st} is 0.519. The graph of λ_e against F (Fig. 1) indicates that if F is held at its 1994 value of about 0.29, the population would be expected to increase at a rate of 6.35% per year. If F is reduced to 0, the stock would be expected to increase at a rate of 18.0% per year. The expected rate of increase when F is below F_{st} is particularly pertinent to cases where stock rebuilding is desired because this analysis allows the de-

termination of how rapidly the stock will be rebuilt under various levels of fishing mortality.

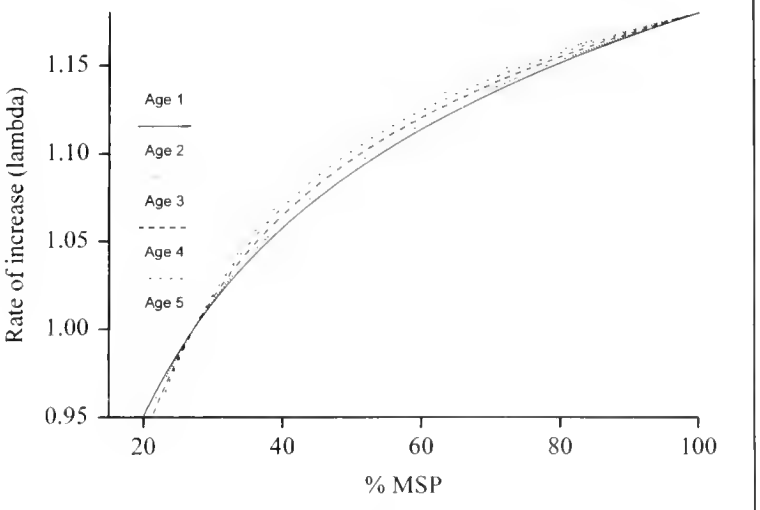

Figure 2

Relationship between rate of population increase (lambda) and percent maximum spawning potential (%MSP) for a range of age at entry.

Developing a Leslie matrix representation of harvesting: stochastic case

One of the major challenges facing fishery managers is to determine appropriate reference points for fish populations that show variable recruitment. When one or more elements of the Leslie matrix vary in a stochastic fashion, no general closed-form expressions for the growth rate of the population are available (Tuljapurkar, 1989). Results of theoretical studies of stochastic Leslie matrices are useful, however, in guiding the analysis and interpretation of matrices with entries that vary over time. Two results summarized by Tuljapurkar (1989) that are particularly useful in this analysis are

1 The analog to lambda for deterministic matrices is the mean population growth rate, in contrast to the growth rate of the average population. This is equivalent to the mean rate of change in the logarithm of population size (N).
2 The distribution of projected population size (N) over time tends towards a lognormal distribution when the dynamics are governed by a stochastic matrix.

From these results, maintenance fishing mortality can be defined as the fishing mortality that results in an average population growth rate of 0 (equivalent to λ_e=1). Because this measure is analogous to lambda, I will use the symbol λ for its representation but emphasize that computationally the measures for deterministic and stochastic Leslie matrices differ. An important corollary of the above two results is

3 A population growing deterministically at the mean growth rate does not produce the mean of the population sizes produced in the stochastic representation. Nor does a deterministic matrix composed of the means of the stochastic matrices produce a population with the same dynamics as applying the stochastic matrices.

To illustrate these theoretical results, I performed a simulation of the Georges Bank haddock stock dynamics using a stochastic Leslie matrix. In this case, I focused on the effects of stochastic age-0 survival as represented by R/SSB. I performed this simulation by projecting a starting population forward in time, with the value for R/SSB for each year selected with equal probability from observed values from 1976 to 1994. Five thousand replicates were simulated for a 150-year period.

Results of these simulations are in accord with the theoretical assertion that N_t is distributed lognormally; for times greater than 110 years, the $\ln(N_t)$ did not differ significantly from a normal distribution at α=0.05. It is interesting to note that N_t is lognormally distributed, even though the stochastic element (R/SSB) was not normally or lognormally distributed itself. The lognormal distribution of N_t arises from the fact that N_t is the result of the process of sequential multiplications of random elements (Aitchison and Brown, 1976). When the distribution of population size is plotted over time (Fig. 3), it is clear that the variance increases rapidly. When year-to-year population growth rates (i.e. N_{t+1}/N_t) are computed for individual simulation results, the distribution of growth rates shows an initial transient response for the first 5 years but thereafter settles into a stable distribution from year to year (Fig. 4). Because of the transient dynamics, I began the evaluation of long-term dynamics with year 10.

One of the critical theoretical results is that the growth rate of a population governed by stochastic rates tends towards a single value in the long run. This is what Tuljapurkar (1989) terms the "almost sure population growth rate." When the growth rate is computed over progressively longer intervals, the distribution shows a convergence on nearly the same

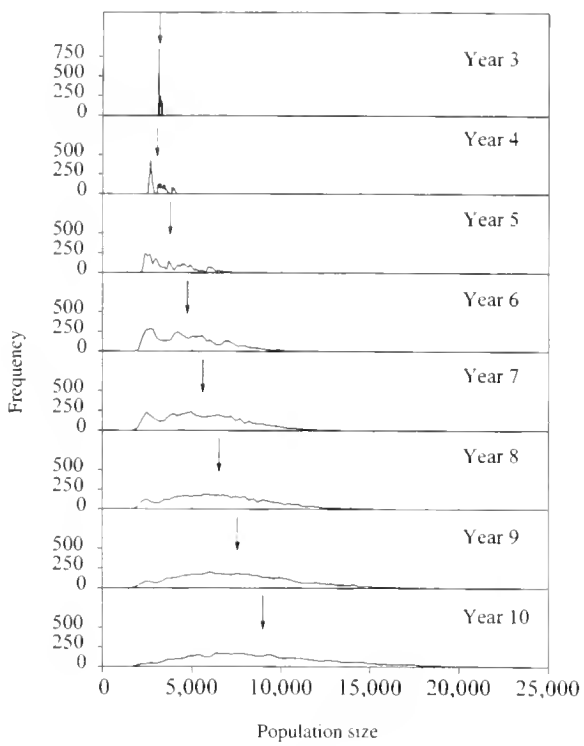

Figure 3

Distribution of population sizes to year 10 for a stochastic projection of the Georges Bank haddock stock. The distribution of population sizes for each time interval is based on 5000 simulations. Arrows indicate mean for each year.

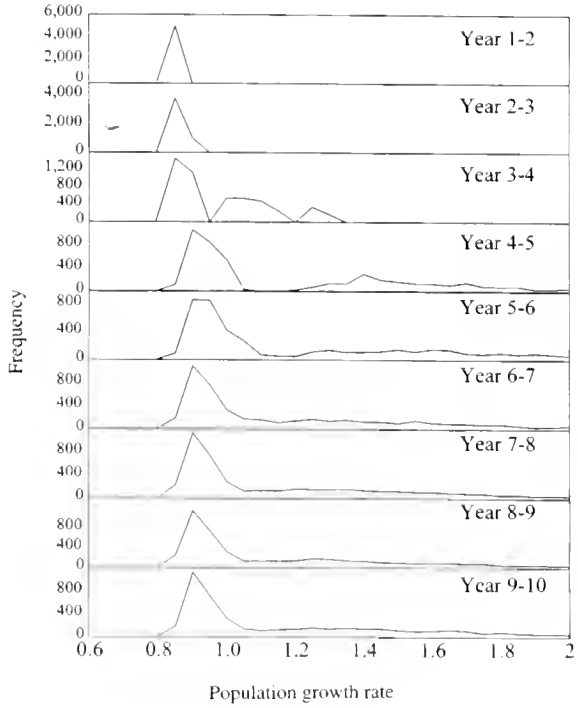

Figure 4

Distribution of annual population growth rates (lambda) to year 10 for a stochastic projection of the Georges Bank Haddock stock. The distribution of growth rates for each time interval is based on 5000 simulations.

mean value (Table 5) with a decreasing variance (Fig. 5). This result has both theoretical and pragmatic implications. Of theoretical importance is the concept that although the variance of projected population abundance increases over time, the variance of the growth rates declines over time. Thus mean population growth rate can be used in defining a maintenance fishing mortality rate. The practical consequence of the above result is that at least two different strategies can be used to compute λ for a stochastic population. One strategy is to project the population for a long period of time (e.g. hundreds of years) to make a precise estimate of the long-term population growth rate. This strategy makes use of the fact that the variance of the long-term population growth declines as the period of projection is lengthened. A problem with this approach, however, is that for projections over a long period of time, population abundance can become so large or small that it cannot be directly represented on a digital computer, causing a numeric overflow or underflow. A preferable strategy is to compute λ for a large number of simulations over a shorter time period (e.g. 150 years). This method avoids the problem of numeric overflow and achieves precision in the estimate of mean λ by having a large number of simulations.

Based on the current partial recruitment vector to the fishery, a fishing mortality of 0.450 (F_{st}) would result in an average population growth rate of zero (Table 6). The fishing mortality that results in a zero growth rate for the mean population size was higher, at 0.517 (Table 6). Interestingly, this is nearly the same as F_{st} computed for the deterministic case by using the mean R/SSB. The estimate of F_{med} with these same data is much lower than F_{st}— only 0.069 (Table 6). When a deterministic Leslie matrix analysis was made with the corresponding median R/SSB, it resulted in an estimate of F_{st} that was nearly the same as F_{med} (Table 6). This finding illustrates the basic connection between these methods when they are operating on the same inputs. As an additional comparison, I computed SSB/R as the ratio ΣSSB/ΣR instead of the mean (or median) of the individual year ratios. This method is based on sampling theory that suggests that the ratio of the sums is a less biased estima-

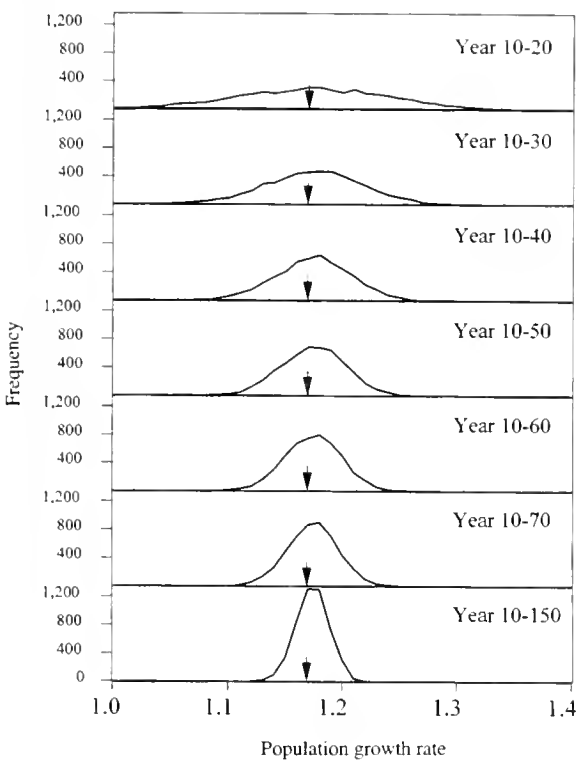

Figure 5

Distribution of population growth rates over various time scales for a stochastic projection of the Georges Bank haddock stock. The distribution of growth rates for each time interval is based on 5000 simulations. Arrows indicate mean for each year.

Table 5

Mean and coefficient of variation (CV) of 5000 simulations of long run population growth rate for Georges Bank Haddock without fishing.

Time interval	Mean	CV
Year 10–20	0.1552	37.02
Year 10–30	0.1555	23.28
Year 10–40	0.1558	18.03
Year 10–50	0.1559	15.23
Year 10–60	0.1559	13.34
Year 10–70	0.1560	12.07
Year 10–150	0.1563	7.60

Table 6

Comparison of F_{st} with deterministic analyses, stochastic analyses, and with %MSP calculations.

Type of simulation	Recruitment input	F_{st}
Deterministic	Mean R/SSB	0.519
Deterministic	Median R/SSB	0.070
Stochastic (mean of rates)	Uniform probability	0.450
Stochastic (mean of populations)	Uniform probability	0.517
%MSP	Mean SSB/R	0.519
%MSP	Median SSB/R	0.069
%MSP	$SSB/R = \Sigma SSB/\Sigma R$	0.449

tor of the "true" ratio than is the mean of the individual ratios (e.g. Cochran, 1977). The value for SSB/R obtained with this method was 2.685, and when used in place of the median SSB/R in the F_{med} calculations, resulted in an estimated reference point of 0.449—essentially the same as in the stochastic simulation where the mean population growth rate was zero (Table 6).

Discussion

The primary purpose of this paper was to demonstrate how the Leslie matrix can be used to compute a reference point for harvested populations and to contrast this method with the SSB/R method currently in use. One of the major findings was that the SSB/R method and the Leslie matrix approach produce similar estimates of sustainable fishing mortality when they are based on the same inputs. This is not surprising given the similarity between reproductive value, on which the Leslie matrix is based, and lifetime spawning stock biomass per recruit which the SSB/R approach uses.

Although the two methods produce similar estimates of sustainable fishing mortality, the Leslie matrix approach is preferable because of the additional direct information it provides regarding the population response to fishing at levels different from the reference point. Furthermore, when population growth rate is different from zero, equal levels of SSB/R do not result in the same population growth rate for different partial recruitment vectors. These differences are small, however, in relation to changes in population growth rate owing to changes in fishing mortality.

Given the various approaches illustrated (e.g. deterministic vs. stochastic), the basic question is what method to use. On the basis of theoretical advances in the population dynamics literature and results presented here, I recommend the use of a stochastic analysis where the mean of the population growth rates is used as the "best" measure of growth for harvested populations. A stochastic analysis is preferable be-

cause it can fully represent the information contained in the distribution of observed R/SSB values. Also, a stochastic simulation can be used to provide a measure of the uncertainty associated with estimates of the biological reference point. The use of the mean population growth rates instead of the mean of the population sizes is justified on theoretical grounds (Tuljapurkar, 1989). As shown in Table 6, use of the mean R/SSB in a deterministic analysis or the rate of growth of the mean population size in a stochastic simulation tends to result in higher estimates of sustainable fishing mortality (or, alternatively, a higher estimate of population growth rate for a given fishing mortality rate) than does the stochastic simulation where the mean of population growth rates are used as the output. I feel that the reason for this difference hinges on the distinction between projections and forecasts (Caswell, 1989). If we view the long-term simulation results as forecasts, this implies that we could use the distribution of population size (and the mean of the distribution) as the best estimate of the future state of the population. In these simulations, however, the mean population size is strongly influenced by the very high values that occur in the right-hand tail of the lognormal distribution. These estimates are far above what has ever been observed for this stock, and are probably not biologically realistic. As such, they should not be treated as true forecasts of the future population. In contrast, if we view the analysis as a projection, the goal is not to forecast future population size but rather to use the results to determine the population growth rate that is represented by the current Leslie matrix. By knowing the current population growth rate, it is possible to find the fishing mortality rate that maintains an expected value for population growth of zero, which would result in a statistically stationary population.

In a stochastic setting, the entire distribution of R/SSB ratios is used to portray the reproductive success for the stock. When a deterministic analysis is desired, however, it is necessary to choose among several possible measures of central tendency for the R/SSB ratio. Sissenwine and Shepherd (1987) advocated the use of the median R/SSB ratio as a way of robustly portraying the reproductive success of a stock. Their rationale was that the frequency of relatively poorer recruitment is balanced by years of better recruitment when the median R/SSB is used. Table 6 illustrates, however, that using the median of the observed R/SSB ratios can result in estimates of sustainable fishing mortality that are substantially different from the stochastic simulations, which are arguably the best to represent the population's dynamics. The use of the mean of the observed R/SSB ratio as the measure of central tendency can likewise result in estimates of sustainable fishing mortality that differ from the standard set by stochastic simulations. The primary reason for this difference is that use of a mean of the observed ratios is biased high in relation to the preferred estimator of the ratio (in this case the sum of recruitment over the sum of spawning stock biomass; Cochran, 1977). As such, the use of the mean of the observed R/SSB values can also be inaccurate. Among the measures presented here, the estimator Σrecruitment/Σspawning stock biomass should be used as the measure of central tendency for the R/SSB ratio in deterministic analyses. The use of this measure results in point estimates of sustainable fishing mortality that are essentially the same as a full stochastic analysis.

Although the Leslie matrix is a useful tool to portray the dynamics of harvested populations and to determine appropriate reference points, several issues arise that are of considerable practical importance. As alluded to earlier, a significant challenge is how to determine what is an appropriate distribution for the R/SSB ratio. Because of the variability in R/SSB over time and the occurrence of occasional large year classes, it is very difficult to determine what time frame is representative of the present. Although the answer to this question is beyond the scope of this paper, I feel that the best approach is to plot the mean R/SSB ratio over progressively longer time periods back from the present to determine if there are any temporal trends or epochs in the data set. The analyst should then use his or her judgment based on other biological information over time (such as stock size, mean weight per individual at age, and maturation schedule) to determine an appropriate period to use as the basis for stochastic simulations. It is important to emphasize that the dilemma of choosing a representative time period is not unique to analyses in which the Leslie matrix is used, and the same problem arises for computing any biological reference point.

In addition to the difficulty of determining what is a representative time period for the present population, a fundamental question is how to represent the dynamics of populations with a density-dependent stock-recruitment relationship. In principle, this can be approached by altering the R/SSB ratio as a function of stock size (e.g. Quinn and Szarzi, 1993). Although I agree with Quinn and Szarzi's (1993) approach, the challenge of accurately specifying the distribution of R/SSB ratios at different stock sizes is even greater than specifying the current distribution.

As a final comment, biological reference points for fish populations are not necessarily targets for fishery management (Mace, 1994), nor are they inviolate boundaries that may not be crossed. Rather, they are most useful as a means of comparing the consequences

of different choices among fishery management options. For example, it is appropriate to allow fishing mortality to exceed the biological reference point if the goal is to reduce an overly abundant fish stock. Likewise, they can be useful in projecting the likely growth of a population under more restrictive fishery management measures. In the end, however, they may be most useful as a reminder and a warning that there are limits to the productive capacity of fish population and that if we consistently exceed their limits, population declines are almost certain to occur (Francis, 1997; Myers, 1997).

Acknowledgments

I wish to thank Jim Bence, Mike Jones, Mike Rutter, and Terrance Quinn II for their insightful reviews of this manuscript. The support of the National Marine Fisheries Service, the Michigan State University Agricultural Experiment Station, the Fisheries Division of the Michigan Department of Natural Resources, and the Department of Fisheries and Wildlife at Michigan State University is also gratefully acknowledged.

Literature cited

Aitchison, J., and J. A. C. Brown.
1976. The lognormal distribution with special reference to its uses in economics. Cambridge Univ. Press, Cambridge, England, 176 p.

Beverton, R. J. H., and S. J. Holt.
1957. On the dynamics of exploited fish populations. U.K. Ministry of Agriculture, Fisheries and Food Fishery Investigations (series 2) 19, 533 p.

Caswell, H.
1989. Matrix population models. Sinauer Associates, Sunderland, MA, 328 p.

Clark, S. H., W. J. Overholtz, and R. C. Hennemuth.
1982. Review and assessment of the Georges Bank and Gulf of Maine haddock fishery. J. Northwest Atl. Fish. Sci. 3:1–27.

Clark, W. G.
1991. Groundfish exploitation rates based on life history parameters. Can. J. Fish. Aquat. Sci. 48:734–750.

Cochran, W. G.
1977. Sampling techniques. Wiley and Sons, New York, NY, 428 p.

Cohen, J. E., S. W. Christensen, and C. P. Goodyear.
1983. A stochastic age-structured population model of striped bass (*Morone saxatilis*) in the Potomac River. Can. J. Fish. Aquat. Sci. 40:2170–2183.

Collie, J. S., and P. D. Spencer.
1993. Management strategies for fish populations subject to long-term environmental variability and depensatory predation. *In* G. Kruse, D. M. Eggers, R. J. Marasco, C. Pautzke, and T. J. Quinn, II (eds.), Proceedings of the international symposium on management strategies for exploited fish populations, p. 629–650. Alaska Sea Grant College Program Report 93-02, Univ. Alaska, Fairbanks, AK.

DeAngelis, D. L., S. W. Christensen, and A. G. Clark.
1977. Responses of a fish population to young-of-the-year mortality. J. Fish. Res. Board Can. 34:2124–2132.

Francis, R. I. C. C.
1997. Comment: How should fisheries scientists and managers react to uncertainty about stock-recruit relationships? Can. J. Fish. Aquat. Sci. 54:982–983.

Gabriel, W. L., M. P. Sissenwine, and W. J. Overholtz.
1989. Analysis of spawning stock biomass per recruit: an example for George Bank haddock. N. Am. J. Fish. Manage. 9:383–391.

Getz, W. M., and R. C. Haight.
1989. Population harvesting: demographic models of fish, forest and animal resources. Princeton Univ. Press, Princeton, NJ, 391 p.

Goodyear, C. P., and S. W. Christensen.
1984. Bias-elimination in fish population models with stochastic variation in survival of the young. Trans. Am. Fish. Soc. 115:627–632.

Gulland, J. A., and L. K. Boerema.
1973. Scientific advice on catch levels. Fish. Bull. 71:325–335.

Johnson, L. W., and R. D. Riess.
1981. Introduction to linear algebra. Addison-Wesley, Reading, MA, 358 p.

Keyfitz, N.
1977. Introduction to the mathematics of populations with revisions. Addison-Wesley, Reading, MA, 490 p.

Mace, P. M.
1994. Relationships between common biological reference points used as thresholds and targets of fisheries management strategies. Can. J. Fish. Aquat. Sci. 51:110–122.

Myers, R. A.
1997. Comment and reanalysis: paradigms for recruitment studies. Can. J. Fish. Aquat. Sci. 54:978–981.

Myers, R. A., and P. Pepin.
1994. Recruitment variability and oceanography stability. Fish. Oceanogr. 3:246–255.

Overholtz, W. J., M. P. Sissenwine, and S. H. Clark.
1986. Recruitment variability and its implication for managing and rebuilding the Georges Bank haddock (*Melanogrammus aeglefinus*) stock. Can. J. Fish. Aquat. Sci. 43:748–753.

Pielou, E. C.
1974. Population and community ecology. Gordon and Breach Science Publishers, New York, NY, 424 p.

Quinn, T. J., II, and N. J. Szarzi.
1993. Determination of sustained yield in Alaska's recreational fisheries. *In* G. Kruse, D. M. Eggers, R. J. Marasco, C. Pautzke, and T. J. Quinn, II (eds.), Proceedings of the international symposium on management strategies for exploited fish populations, p. 61–84. Alaska Sea Grant College Program Report 93-02. Univ. Alaska, Fairbanks, AK.

Rothschild, B. J., and M. J. Fogarty.
1989. Spawning-stock biomass: a source of error in recruitment/stock relationships and management advice. J. Cons. Int. Explor. Mer 45:131–135.

Sissenwine, M. P., and J. G. Shepherd.
1987. An alternative perspective on recruitment overfishing and biological reference points. Can. J. Fish. Aquat. Sci. 44:913–918.

Tuljapurkar, S.
1989. An uncertain life: demography in random environments. Theor. Pop. Biol. 35:227–294.

Biological effects of shellfish harvesting on oyster reefs: resolving a fishery conflict by ecological experimentation

Hunter S. Lenihan
Beaufort Laboratory
National Marine Fisheries Service, NOAA
101 Piver's Island Road, Beaufort, North Carolina 28516
Present address: Institute of Marine Sciences
University of North Carolina at Chapel Hill,
3431 Arendell St., Morehead City, North Carolina
E-mail address: hslenihan@email.unc.edu

Fiorenza Micheli
National Center for Ecological Analysis and Synthesis
Santa Barbara, California 93101

Abstract.—We conducted a large-scale field experiment to test whether clam and oyster harvesting applied alone and in combination on intertidal oyster reefs have impacts on resident shellfish populations. This experiment was conducted to resolve a long-standing conflict between oyster (*Crassostrea virginica* (Gmelin, 1791)) and clam (*Mercenaria mercenaria* (Linneaus, 1758)) fishermen who contend that the other fishery causes high rates of mortality to their respective species. Intertidal oyster reefs located in two estuarine creeks near Wilmington, North Carolina, were harvested for clams only, oysters only, both clams and oysters, or were left undisturbed as controls. Experimental harvesting was conducted over a one-year period by a professional shellfisherman who used realistic fishing techniques (clam rakes and oyster tongs), intensity, and frequency. Harvesting impact on hard clam and oyster populations was assessed by sampling naturally occurring oysters before and after harvesting, and sampling both naturally occurring clams (all size classes) and transplanted, hatchery-raised clams (20–37 mm in length) after harvesting. Clam and oyster harvesting had obvious negative effects on populations of oysters. There was a substantial decrease in the number of live oysters on clam-harvested and oyster-harvested reefs compared with unharvested, control reefs. Clam and oyster harvesting, applied together, reduced oyster densities and killed unharvested oysters at a level similar to that caused by each type of harvesting applied separately. The effects of the shellfish harvesting on populations of hard clams varied between the two sites (i.e. creeks). In both creeks, clam harvesting, alone and combined with oyster harvesting, significantly decreased the number of live, naturally occurring clams. Oyster harvesting alone decreased the number of live, naturally occurring clams only at one site. Clam harvesting also decreased the number of live, transplanted clams on reefs, but there was no effect of oyster harvesting, because the transplanted clams were juveniles too small to be harvested with oyster tongs. Overall, the combined effect of both types of harvesting applied together did not have a negative synergistic effect on clam and oyster populations. Consequently, both clamming and oyster harvesting should be permitted on some reefs, but maintaining large populations of oysters and clams on intertidal oyster reefs will require protection of some reefs from both types of harvesting.

Manuscript accepted 24 March 1999.
Fish. Bull. 98:86–95 (2000).

Marine fisheries are an important source of employment and protein for humans but can negatively affect marine organisms and ecosystems (Dayton et al., 1995; Engel and Kvitek, 1995; Botsford et al., 1997). The most obvious negative ecological effects of fishing result from over-harvesting of target species, incidental mortality of nontarget species ("bycatch"), and fishery-related disturbances to marine habitat (FAO, 1993; Dayton et al., 1995). Of course, fisheries over-exploitation and habitat destruction also threaten the sustainability of the fishing industry. At present, 44% of the worlds fish stocks are fully to heavily exploited, and 22% are overexploited or depleted, indicating most fisheries are not managed for long-term sustainability (Botsford et al., 1997). The degradation and destruction of marine biogenic habitat (e.g. coral reefs, seagrass beds, mangrove forests, and oyster reefs) by dredging, trawling, use of explosives, and poisoning reduces fishery production by removing habitat essential for the recruitment, growth, and survival of fishery and prey organisms (Winslow 1881, a and b; Peterson et al., 1987; Norse, 1993; Rothschild et al., 1994; NRC, 1995; Lenihan and Peterson, 1998). The sustainability of a fishery is often threatened when competing fisheries exploit a common resource or negatively impact a commonly used habitat. For example, when the bycatch of one fishery is within a food web supporting another fishery (West and Gordon, 1994), or when a fishery destroys habitat important to the life history of other fishery species (Russ and Alcala, 1996), heated political battles arise and the livelihood of many people may be lost. Resolving such fishery conflicts has important ecological and economic consequences and is of major concern to fisheries managers and ecologists worldwide (McAllister and Peterman, 1992). This paper presents the results of an experimental analysis of whether two economically valuable fisheries conflict and provides management recommendations to resolve the conflict.

High productivity of fishery stocks in estuaries and shallow water coastal habitats often induces intense exploitation of a common species or habitat by multiple, potentially conflicting fisheries (Peterson et al., 1987). In many estuaries along the Atlantic coast of the USA, intertidal oyster reefs are harvested for hard clams (*Mercenaria mercenaria*) year round,

and for oysters (*Crassostrea virginica*) in the fall and winter (i.e. October–March). In recent years, clam and oyster (i.e. "shellfish") harvesting on oyster reefs has led to conflict between the two fisheries, and between fishermen and habitat managers over the issue of habitat degradation, especially in the southeastern United States (e.g. Frankenberg[1]; Noble[2]). Oyster fishermen claim that the harvesting of clams from intertidal oyster reefs decreases resident oyster populations, and vice-versa, because each type of fishing kills or removes the other species. Rakes and hand tongs used for the two types of shellfishing appear to increase the mortality of the sessile reef animals by burying them beneath sediments, fracturing their shells, or causing other physical damage (Noble[2]). In addition, bodies of dead and wounded animals left behind may attract scavengers and predators, thereby increasing predation intensity on healthy live animals (Dayton et al., 1995). Habitat and fishery managers are concerned that the physical destruction of oyster reefs caused by shellfishing will negatively affect many other fishery organisms that recruit to and utilize oyster reef habitat, including many species of fishes (Breitburg et al. 1995, Lenihan et al., 1998, Luckenbach et al., 1998) and the blue crab (*Callinectes sapidus* (Rathbun)) (Bahr and Lanier, 1981; Zimmerman et al., 1989; Lenihan et al., 1998; Micheli and Peterson, 1999). Shellfishing also reduces the overall size of reefs because shell material is broken or removed along with the target species (Lenihan and Peterson, 1998; Coen[3]). Reducing the size of reefs is thought to decrease the abundance of clams because less habitat is available for adults and recruits (Arnold, 1984; Sponaugle and Lawton, 1990; Peterson et al., 1995). Decreasing the size (i.e. height) of oyster reefs also reduces oyster production because flow speed over reefs diminishes, causing sediment to accumulate and oyster growth and survival to decrease (Lenihan, 1999; Lenihan et al., 1999). In contrast to the negative effects of shellfish harvesting, many fishermen claim that "turning over" the shell matrix of oyster reefs during harvesting improves clam and oyster production because it removes accumulated sediment. In North Carolina and many other Atlantic coast states, both types of shellfishing are allowed on reefs and conflicts between the fisheries continue (e.g. Frankenberg[1]; Marshall[4]). Whether oyster harvesting, clam harvesting, or both types of fishing activities together have negative impacts on shellfish populations of intertidal oyster reefs is a matter of opinion and has not been tested experimentally.

A comparison of the biological impact of various fishing practices by using large-scale field experiments is an efficient method of resolving many fishery-related conflicts (McAllister and Peterman, 1992) and is an important component of adaptive management strategies (Walters, 1986). Such experiments are usually designed so that replicate areas (i.e. treatments) are fished, by using each technique separately and by using a combination of techniques, while other areas (i.e. controls) are closed to fishing. For these experiments to be meaningful, they must be conducted on realistic temporal and spatial scales, and the fishing treatments must be applied through the actual fishery (McAllister and Peterman, 1992). The success of such experiments also depends heavily on close working relationships among fishermen, fishery ecologists, and fishery managers (Grumbine, 1997). For adaptive management, the results of initial (i.e. "prototype") experiments are used to design new management strategies that are subsequently tested on even larger temporal and spatial scales. Such adaptive management strategies and the use of experimental approaches are often discussed in fisheries management, but in reality are rarely attempted (e.g. Walters, 1986; Botsford et al., 1997).

We conducted a large-scale field experiment to test the effects of hard clam and oyster harvesting, separately and in combination, on oyster and hard clam populations living on intertidal oyster reefs in North Carolina. Specifically, we tested whether 1) the density of live and dead oysters varied among oyster reefs that were harvested for clams, harvested for oysters, harvested for clams and oysters, or were unharvested; 2) the density of live and dead clams varied among oyster reefs subjected to the same four harvesting treatments; and 3) the joint application of both shellfish harvesting practices has a synergistic (i.e. a multiplicative) effect on each species. If applying both types of harvesting to the same reefs enhances potential negative effects of each harvesting type, a possible management option would be to allow clam and oyster harvesting only on separate reefs. This experiment was designed and conducted with the combined effort of a clam and oyster fisherman,[5] ecologists,[6] and habitat

[1] Frankenberg, D. 1995. Report of North Carolina Blue Ribbon Advisory Council on oysters. North Carolina Department of Environmental Health, and Natural Resources, Raleigh, NC, 101 p.

[2] Noble, E. B. 1995. Destruction of oyster rocks by individuals taking clams by legal hand harvest methods. Report of the North Carolina Division of Marine Fisheries, Morehead City, NC, 11 p.

[3] Coen, L. D. 1995. A review of the potential impacts of mechanical harvesting on subtidal and intertidal shellfish resources. A report prepared by the South Carolina Department of Natural Resources, Marine Resources Research Institute, SC, 111 p.

[4] Marshall, M. 1996. North Carolina Division of Marine Fisheries, 3431 Arendell St., Morehead City, NC, 28557. Personal commun.

[5] Cummings, R. A. 1996. For address contact H. S. Lenihan, Institute of Marine Sciences, 3431 Arendell, Morehead City, NC 28557. Personal commun.

[6] Peterson, C. H., and H. C. Summerson. 1997. Institute of Marine Sciences, 3431 Morehead City, NC 28557.

managers,[7] and is a prototype experiment for adaptive management of shellfisheries in southeastern North America.

Methods

Study sites

The intertidal oyster reefs used in this study were located in two large tidal creeks, Pages and Whiskey Creeks, situated on the Intercoastal Waterway near Masonborough Inlet, Wilmington, North Carolina. The two creeks consisted of well-flushed sandy to muddy bottom tidal channels 0–2 m in water depth. Channels in each creek were separated by small to large patches of marsh (*Spartina alterniflora*) habitat surrounded by oyster reefs created by *Crassostrea virginica*. The two creeks were chosen because they have been permanently closed to fishing for about the last ten years owing to high coliform bacteria counts caused by the seepage of septic tanks from surrounding homes. Both creeks are highly productive, supporting large populations of fishes, birds, crabs, clams, and oysters. Tides in each creek are predominantly M-2 lunar tides, and the tidal range is 1–2 m in both creeks. Four large oyster reefs (9–13 m wide × 45–55 m long), each containing relatively high densities of oysters and hard clams, were chosen in each creek. The reefs were situated 150–200 m from the mouth of each creek. The salinity near the experimental reefs was 22–34 psu throughout the course of the experiment and water temperature was 3–30°C.

Three to five permanent 6-m long × 1-m wide transects were established haphazardly on each oyster reef by using PVC poles with rebar anchors between 1–14 June 1996. A total of sixteen transects were established in each creek at approximately 0.5 m above the mean low tide level. The sixteen transects provided a total of four replicates of each of the following four harvest treatments: clam harvesting only, oyster harvesting only, clam harvesting and oyster harvesting combined, and no harvesting. Reefs and transects were located in areas where disturbances caused by shellfishing, boat traffic, or other human activities did not normally occur. We found no evidence suggesting that experimental reefs were physically or chemically disturbed throughout the course of the experiment.

Sampling of clams and oysters

The density of live and dead oysters on each experimental oyster reef was measured between 5 and 10 July 1996 before harvest treatments were applied. Oyster density was measured by counting (but not removing) oysters in three 0.25-m^2 permanent plots established in each of the sixteen transects in each creek. Plots were established by stretching a measuring tape between the two PVC poles marking each transect and by placing a PVC quadrat at 0.5-, 2.5-, and 3.5-m distance. All live and dead oysters were counted in each quadrat. The density of naturally colonized clams was not determined prior to the application of harvest treatments to avoid disturbing the reefs and potentially influencing the condition of the remaining clams and oysters. Instead, between 5 and 10 July, 16 hatchery-raised clams provided by ARC, Inc. of Atlantic, North Carolina, were placed in each of three 1-m^2 quadrats established within each 6-m transect. This introduction of transplanted clams was done to assure that enough clams were present for the experiment. The 1-m^2 quadrats were also placed at 0.5, 2.5, and 3.5 m distance along the transects. Before being transplanted, hatchery clams were dyed in Alizarin red dye in order to distinguish them from natural clam populations (Peterson et al., 1995). Of the 16 clams in each plot, eight were 20–25 mm in length, and eight were 27–32 mm in length.

Between October 1996 and March 1997, oysters were harvested with hand tongs during low tides within the 1) oyster harvesting and 2) clam and oyster harvesting treatments. Oysters were harvested for the same total period of time (3.75–4.0 h/transect) along the entire length of each transect. From August 1996 to May 1997, clams were harvested during low tides with clam rakes and clam tongs from the 1) clam harvesting and 2) clam and oyster harvesting treatments, and for approximately the same total period of time (i.e. 3.75–4.0 h/transect). The total number of naturally occurring and transplanted clams and oysters removed during the harvest was recorded. All harvesting was conducted by R. A. Cummings, a professional shellfisherman.

The density of live and dead clams and oysters remaining on experimental reefs was sampled 10–23 July 1997, after termination of the harvesting treatments. Clams and oysters were sampled several months after the last clam harvesting in May so that any potential long-term effects of harvesting were realized. For example, unharvested clams and oysters remaining on reefs may have been injured during harvesting and died after several weeks. Oysters were sampled by placing a measuring tape along the transects and counting all oysters within the three 0.25-m^2 quadrats at 0.5-, 2.5-, and 3.5-m distance along each transect. Clams were sampled by digging up the top 25 cm of sediment from each 1-m^2 sampling plot. The sediment was then passed through a 1-mm sieve to remove all clams.

[7] Carpenter, R., and M. Marshall. 1996. North Carolina Division of Marine Fisheries, 3431 Arendell St., Morehead City, NC 28557.

Table 1

Mean square errors (MS), F ratios, and corresponding significance levels (P) of two-way fixed factor ANOVAs comparing densities of live and dead oysters, and proportions of dead oysters (per 0.25 m^2) among intertidal oyster reefs before application of experimental harvest treatments (sampled 5–10 July 1996). The main factors in ANOVAs were creeks (Pages and Whiskey Creeks) and harvest treatment (clamming, oystering, both, and neither).

		Live			Dead			Proportion dead		
Source	df	MS	F	P	MS	F	P	MS	F	P
Creek (C)	1	277.50	6.17	0.02	378.10	34.58	0.0001	0.03	30.11	0.0001
Harvest treatment (H)	3	31.03	0.69	0.57	0.41	0.04	0.99	0.001	0.48	0.70
C × H	3	31.74	0.71	0.56	12.27	1.12	0.36	0.001	1.19	0.33
Residual	24	45.01			10.93			0.001		

Statistical analyses

The density of live and dead oysters, and the proportion of the total number of oysters that were found dead before harvesting, were compared among treatments by using two-way, fixed factor analysis of variance (ANOVA) tests. The two main factors in the ANOVAs were creeks (Pages and Whiskey Creeks) and harvest treatments (clam harvesting, oyster harvesting, both, or neither). The same ANOVA model was used to test for differences in 1) the density of live and dead oysters, and the proportion of dead oysters (i.e. number of dead oysters/live + dead oysters) after harvesting, 2) the density of live and dead, and proportion of dead, naturally occurring clams after harvesting, and 3) the density of live and dead, and number of missing transplanted, hatchery-raised juvenile clams after harvesting. Before all ANOVAs, homogeneity of variances was tested by using Cochran's test (at α=0.05). When variances were heterogeneous, data were log transformed and homogeneity was retested. After ANOVAs, *post hoc* tests for differences among treatment means were conducted with Student-Newman-Keuls method (SNK) tests (at α=0.05).

Results

In July 1996, prior to the application of experimental harvests, the number of live and dead oysters (those observed with naked eye; >1 mm in length) and the proportion of dead oysters in experimental plots did not vary with the interaction of creeks and harvest treatment (ANOVA, *creek × harvest treatment interaction*, P=0.33–0.56; Table 1), nor among harvest treatments (P=0.57–0.99), but differed significantly between creeks (P=0.02–0.0001). Whiskey Creek had greater numbers of live and dead oysters and proportion of dead oysters than Pages Creek (Figs. 1 and 2).

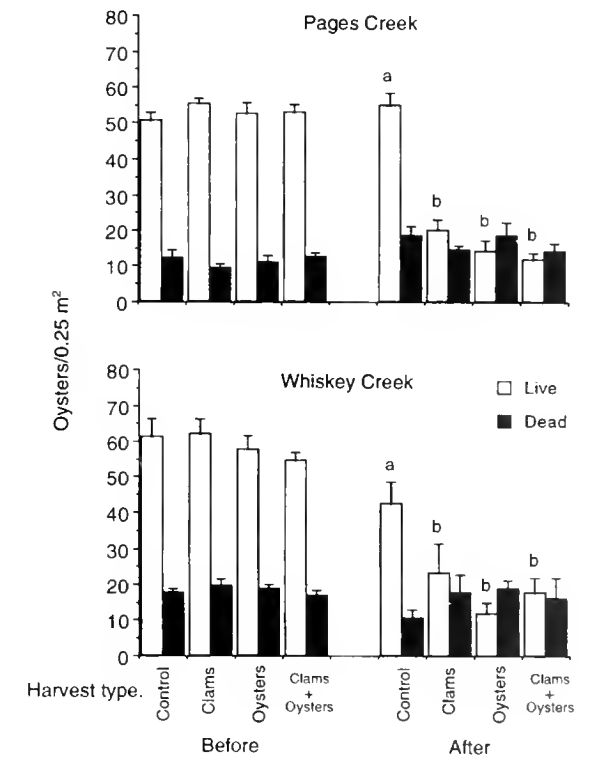

Figure 1

Mean density of live and dead oysters (>1 mm in length) before (5–10 July 1996) and after (10–23 July 1997) application of experimental harvest treatments in Pages and Whiskey Creeks, NC. Data are means and one standard error (n=4) of counts taken within 0.25-m^2 quadrats. Results of SNK *post hoc* comparisons are illustrated with letters above bars (a>b at P<0.05). Separate ANOVAs and SNK tests were used to compare numbers of live and dead oysters both before and after harvesting.

Experimental clam harvesting conducted from August 1996 to May 1997 removed only hard clams from experimental plots (Table 2). In contrast, a few clams

were caught in oyster tongs during oyster harvesting, which was conducted from October 1996 to March 1997. In both creeks, two to three times the number of clams were harvested during clam harvesting treatments than during oyster harvesting. Similar numbers of clams were removed from reefs in the clam harvesting and the combined clam and oyster harvesting treatments. Similar numbers of oysters were removed from plots harvested for oysters only and from those harvested for both oysters and clams (Table 2). According to visual observations, both types of harvesting inflicted obvious wounds (holes and cracks) to the shells of oysters (range: 5–13 individuals within each plot) that were not removed by harvesting.

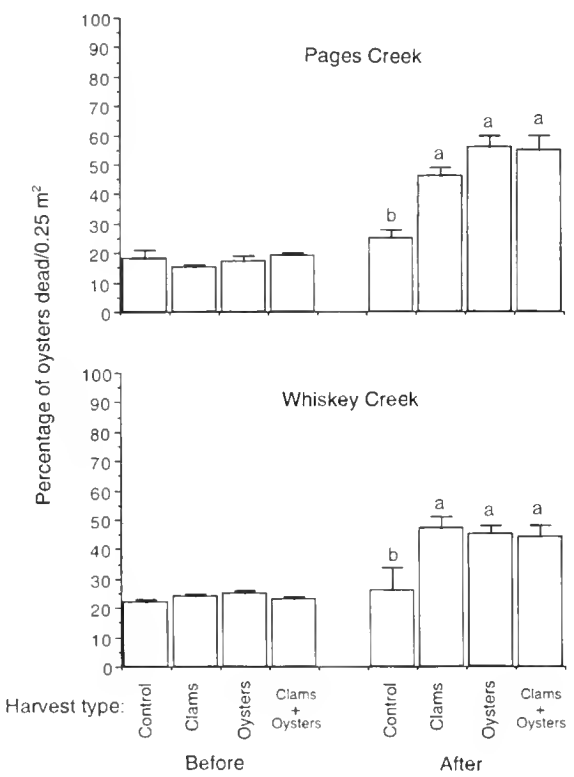

Figure 2

Mean percentage of oysters found dead before (5–10 July 1996) and after (10–23 July 1997) application of experimental harvest treatments in Pages and Whiskey Creeks, NC. Data are means and one standard error (n=4) of counts taken within 0.25-m² quadrats. Results of SNK *post hoc* comparisons are illustrated with letters above bars (a>b at P<0.05). Separate ANOVAs and SNK tests were used to compare numbers of dead oysters before and after harvesting.

In July 1997, after experimental clam and oyster harvesting, the density of live and dead oysters, and the proportion of dead oysters did not vary with the interaction of creeks and harvest treatment (ANOVA; *creek × harvest treatment interaction*, P=0.23-0.44; Table 3). There was also no significant difference in the density of live and dead oysters and the proportion of dead oysters between the two creeks (P=0.16–0.65; Table 3). In contrast, there was a highly significant effect of harvest treatment on the density of live oysters and the proportion of oysters found dead (P=0.0001; Table 3). At both sites, plots harvested for clams, oysters, or both had 2–4.5 times lower densities of live oysters and 2–2.5 times higher proportions of dead oysters than did unharvested control plots (SNK, P<0.05 for both contrasts; Figs. 1 and 2). There were no differences in the number of dead oysters among harvest treatments.

In July 1997, after experimental harvesting, the density of live, naturally occurring hard clams varied with the interaction of creeks and harvest treatments (ANOVA, *creek × harvest treatment interaction*, P=0.015; Table 4). At Pages Creek, there were greater numbers of live, naturally occurring clams in control reefs than in plots harvested for clams, oysters, or both (SNK; P<0.05; Fig. 3). At Whiskey Creek, there were more live, naturally occurring clams in both control and oyster-harvested plots than in plots harvested for clams and for both species (SNK, P<0.05 for both contrasts; Fig. 3). The number and proportion of dead, naturally occurring clams found in July 1997 did not vary with the interaction of creeks and harvest treatment (ANOVA, *creek × harvest treatment interaction*, P=0.09–0.87; Table 4), or between creeks (P=0.16–0.10; Table 4). There was also no significant effect of harvest treatment on the density of dead, naturally occurring clams (P=0.17; Table 4). However, there was a significant effect of harvest treatment on the pro-

Table 2

Mean number of clams and oysters removed from intertidal oyster reefs during experimental harvesting. Reefs were harvested for clams (clamming), oysters (oystering), both (clamming and oystering), or neither (controls). Transplanted, hatchery-raised clams were not removed during harvesting.

	Pages Creek		Whiskey Creek	
Harvest treatments	Clams	Oysters	Clams	Oysters
Controls	0	0	0	0
Clamming	3.47 ±1.1	0	11.77 ±7.37	0
Oystering	1.15 ±0.22	69.20 ±9.20	5.05 ±2.89	43.27 ±14.10
Clamming and oystering	3.46 ±0.75	89.40 ±58.32	12.59 ±5.84	34.97 ±8.26

Table 3

Mean square errors (MS), F ratios, and corresponding significance levels of (P) two-way fixed factor ANOVAs comparing densities of live and dead oysters, and proportions of dead oysters (per 0.25 m^2) among intertidal oyster reefs after application of experimental harvest treatments (10–23 July 1997). The main factors in ANOVAs were creeks (Pages and Whiskey Creeks) and harvest treatment (clamming, oystering, both, and neither).

		Live			Dead			Proportion dead		
Source	df	MS	F	P	MS	F	P	MS	F	P
Creek (C)	1	18.45	0.21	0.65	55.52	1.02	0.32	0.02	2.10	0.16
Harvest treatment (H)	3	2192.00	25.25	0.0001	4.45	0.08	0.97	0.12	13.86	0.0001
C × H	3	132.90	1.53	0.23	67.70	1.24	0.32	0.01	0.93	0.44
Residual	24	86.82			54.54			0.01		

Table 4

Mean square erros (MS), F ratios, and corresponding significance levels (P) of 2-way fixed factor ANOVAs comparing densities of live and dead hard clams, and proportions of dead clams (per 1.0 m^2) among intertidal oyster reefs after application of harvest treatments (10–23 July 1997) The main factors in ANOVAs were creeks (Pages and Whiskey Creeks) and harvest treatment (clamming, oystering, both, and neither).

		Live			Dead			Proportion dead		
Source	df	MS	F	P	MS	F	P	MS	F	P
Creek (C)	1	277.5	6.17	0.02	378.1	34.58	0.0001	0.03	30.11	0.0001
Creek (C)	1	0.13	0.03	0.85	10.7	2.15	0.16	0.07	2.94	0.10
Harvest treatment (H)	3	36.55	10.01	0.0002	8.97	1.80	0.17	0.16	6.19	0.003
C × H	3	15.60	4.27	0.015	12.28	2.47	0.09	0.01	0.23	0.87
Residual	24	3.65			4.98			0.03		

portion of dead, naturally occurring clams (P=0.003; Table 4). The proportion of dead clams in both creeks was much higher on harvested than on unharvested (i.e. control) reefs (SNK, P<0.05 for both contrasts; Fig. 4) but was similar among the three harvest treatments (SNK, P>0.05 for both contrasts; Fig. 4).

After harvesting, the density of live and dead hatchery-raised clams transplanted to reefs at the beginning of the experiment tended to vary with the interaction of creeks and harvest treatment, although not significantly (ANOVA, creek × harvest treatment interaction, P=0.07-0.08; Table 5). However, the density of live transplanted clams varied between creeks (P=0.03; Table 5) and among harvest treatments (P=0.04; Table 5). More transplanted clams were recovered alive in Pages Creek (mean ± 1SD: 3.21 ±1.62/m^2) than in Whiskey Creek (2.22 ±1.45/m^2). Fewer live transplanted clams were recovered from clam-harvested plots than from control plots in both creeks (SNK, P the interaction of <0.05; Fig. 5). The number of dead transplanted clams found after harvesting also varied between creeks (Pages Creek>Whiskey Creek; P=0.0001; Table 5) but did not vary significantly with harvest treatment (P=0.10; Table 5). At Pages Creek, there was a slight trend for greater mortality of transplanted clams on clam-harvested and clam- and oyster-harvested plots than in oyster-harvested and control plots only (Fig. 5). Most transplanted clams placed on reefs at the beginning of the experiment were not found at the end of the experiment ("missing" clams; Fig. 5). The number of missing transplanted clams differed with the interaction of creeks and harvest treatment (ANOVA, *creek × harvest treatment interaction*, P=0.03; Table 5) because fewer clams were recovered in our census in the oyster-harvested plots than in clam-harvested plots at Whiskey Creek only (SNK; P<0.05; Fig. 5).

Discussion

Our results clearly demonstrate that both clam and oyster harvesting significantly reduce oyster popula-

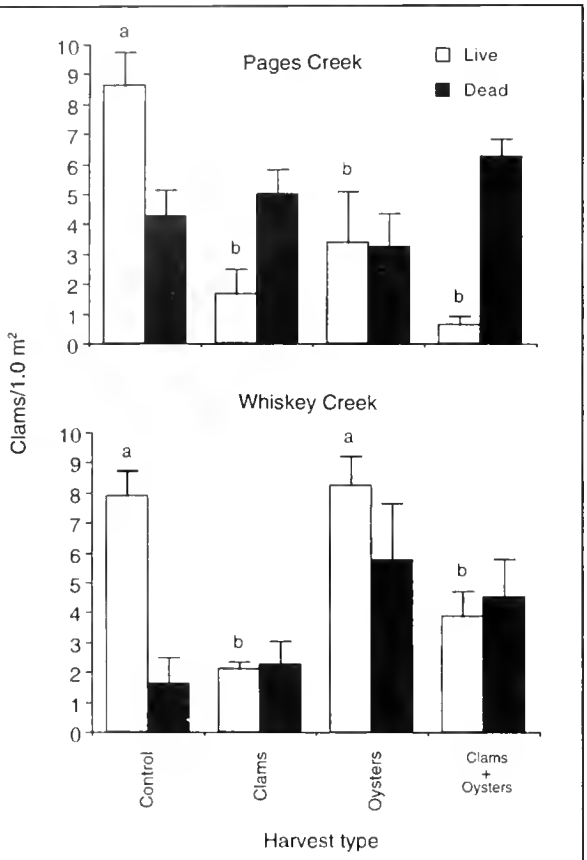

Figure 3

Mean density of live and dead naturally-occurring hard clams found after (10–23 July 1997) application of experimental harvest treatments in Pages and Whiskey Creeks, NC. Data are means and one standard error (n=4) of counts taken within 1.0-m^2 quadrats. Results of SNK *post hoc* comparisons are illustrated with letters above bars (a>b at P<0.05). Separate ANOVAs and SNK tests were used to compare numbers of live and dead clams.

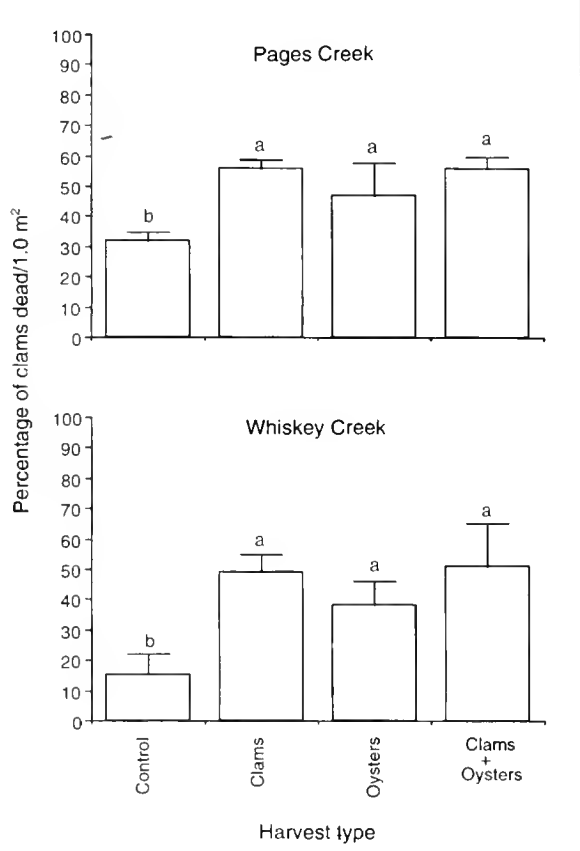

Figure 4

Mean percentage of naturally-occurring hard clams found dead after (10–23 July 1997) application of experimental harvest treatments in Pages and Whiskey Creeks, NC. Data are means and one standard error (n=4) of counts taken within 1.0-m^2 quadrats. Results of SNK *post hoc* comparisons are illustrated with letters above bars (a>b at P<0.05).

Table 5

Mean square errors (MS), F ratios, and corresponding significance levels (P) of 2-way fixed factor ANOVAs comparing numbers of live, dead, and missing hatchery-raised hard clams (per 1.0 m^2) among intertidal oyster reefs after application of harvest treatments (sampled 10–23 July 1997). Before application of harvest treatments, hatchery-raised juvenile clams were placed at equal densities (16 clams/m^2) on each reef. The main factors in ANOVAs were creeks (Pages and Whiskey Creeks) and harvest treatment (clamming, oystering, both, and neither).

		Live			Dead			Proportion dead		
Source	df	MS	F	P	MS	F	P	MS	F	P
Creek (C)	1	0.14	5.48	0.03	14.45	26.54	0.0001	41.63	19.33	0.0002
Harvest treatment (H)	3	0.08	3.24	0.04	1.28	2.35	0.10	2.03	0.94	0.44
C × H	3	0.07	2.67	0.07	1.40	2.58	0.08	7.65	3.55	0.03
Residual	24	0.03			0.54			2.15		

tions on intertidal oyster reefs. Both types of shellfish harvesting, applied separately or together, reduced the densities of live oysters by 50–80% compared with densities at unharvested reefs. Surprisingly, there was no difference among the effects of clam harvesting only, oyster harvesting only, and clam and oyster harvesting combined on the density of live oysters. We expected oyster harvesting to reduce oyster populations more than clam harvesting because oyster harvesting removes oysters whereas clam harvesting targets clams only (see Table 2). We do not know the effect of clam and oyster harvesting on oysters <1 mm in length; therefore further experiments should be conducted to determine their fate. Results of our experiment show conclusively that the density of live, adult oysters was significantly reduced on reefs that were harvested for clams only (Fig. 1). Therefore, clam harvesting has important negative effects on oysters, most likely through increased oyster mortality.

We did not investigate the specific mechanisms underlying the negative effect of clam harvesting on oyster populations, but observations made during experimental harvesting indicated that clamming with rakes killed oysters in two ways. First, during the process of clamming oyster shells were cracked or punctured (senior author, personal obs.) Severely wounded oysters probably died. Oysters were also indirectly killed during clamming when they were buried or smothered beneath sediments that were removed in the process of digging for buried clams (senior author, personal obs.). Another potential, but unobserved, mechanism potentially leading to enhanced oyster mortality during clamming was that predators (e.g. blue crab and the sheepshead fish, *Archosargus probatochephalus*) were attracted to the reefs by wounded oysters and by sediment disruption, thereby enhancing predation intensity on oysters (e.g. Dayton et al., 1995). It did not appear that oysters were spread around on the experimental reefs by clam harvesting, thus reducing their densities in sampling plots.

Effects of clam and oyster harvesting on naturally occurring populations of hard clams were less clear than effects of clam and oyster harvesting on oysters. Clam harvesting, both alone and in combination with oyster harvesting, decreased densities of live clams by 50–90% compared with unharvested reefs. This result was expected because clam harvesting removes large numbers of clams (see Table 2). Because clams are motile, it is possible that some clams emigrated from sampling plots following the harvest disturbance, thereby accounting for some reduction in clam density. However, this movement is unlikely to have accounted for a large proportion of the reduction in clam densities because the sampling plots covered much of the area on reefs inhabited by clams. Oyster harvesting

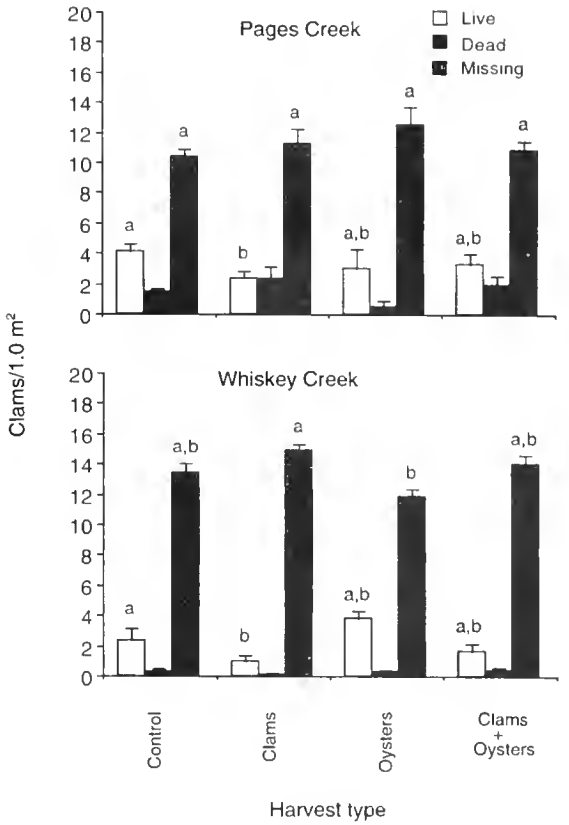

Figure 5

Mean density of live, dead, and missing hatchery-raised hard clams after (10–23 July 1997) application of experimental harvest treatments in Pages and Whiskey Creeks, NC. Sixteen clams were placed in each 1.0-m² quadrat between 5–10 July 1996. Data are means and standard errors (n=4) of counts taken within 1.0-m² quadrats. Results of SNK *post hoc* comparisons are illustrated with letters above bars (a>b at P<0.05). Separate ANOVAs and SNK tests were used to compare numbers of live, dead, and missing clams.

alone also reduced the density of live clams but only at one site, Pages Creek. At Whiskey Creek, the density of live clams after harvesting was similar between oyster-harvested and control plots, indicating that oyster harvesting had little effect on clam survival (Fig. 3). A negative effect of oyster harvesting on clams may be caused both by direct removal of clams as bycatch (Table 2) and enhanced clam mortality through mechanisms analogous to those hypothesized for oysters (see above). Some clams may also have emigrated from the oyster harvesting treatments following harvesting.

Patterns of survival and mortality of hatchery-raised clams transplanted to experimental reefs varied with site and harvest type (Table 5). Fewer live and dead transplanted clams were recovered from reefs at Whiskey Creek than at Pages Creek (Fig. 5). In con-

trast, there were greater numbers of missing transplanted clams at Pages Creek than at Whiskey Creek. Harvest type, specifically clam harvesting, influenced the number of live transplanted clams but had no significant effect on the number of dead or missing transplanted clams. Fewer live, transplanted clams were found in clam-harvested plots than were found in control plots at both sites (Fig. 5). Because few of the transplanted clams were removed from reefs by experimental harvesting, the negative effects of clam harvesting on densities of live, transplanted clams may be explained by increased clam mortality caused by clam harvesting. Overall, the effects of shellfish harvesting appear to be more variable and unpredictable for clams than for oysters. Our results indicate that both types of shellfish harvesting can have negative impacts on clam populations, but that this is a site-specific phenomenon.

Results of this study do not support the hypothesis that harvesting reefs for both clams and oysters has a negative synergistic impact on clam and oyster populations. Clam and oyster harvesting alone had similar negative effects on densities of live oysters, and the joint harvesting of both species on the same reefs did not decrease the density of live oysters any further. Similarly, the negative effects of clam harvesting on the density of live clams, and on survival of hatchery-raised clams were not enhanced when oyster harvesting was applied in combination with clam harvesting. Thus, the combined harvesting of both clams and oysters on intertidal reefs does not cause greater direct or indirect mortality of shellfish populations than that caused by clam or oyster harvesting conducted separately.

This experimental analysis has important implications for the management of intertidal oyster reefs and their associated molluscan fishery resources. First, maintaining high densities of oysters on some intertidal reefs, by preventing both clam and oyster harvesting, may help to preserve future oyster harvests and brood stock. Protecting some reefs from shellfishing will also help preserve the many ecological services that oysters and oyster reefs provide, such as improving water quality through the filtration of suspended particles (Officer et al., 1982; Dame et al., 1984; Newell, 1988) and creating essential recruitment, refuge, and foraging habitat for economically valuable fishes and crabs (Bahr and Lanier, 1981; Zimmerman et al., 1989; Lenihan et al., 1998). Preventing oyster and clam harvesting on some intertidal reefs will also potentially conserve clam populations from both the direct and indirect negative effects of shellfish harvesting, thereby protecting future clam harvests and brood stock. Overall, allowing the harvest of both clams and oysters on some natural and restored oyster reefs is a rational option because the combined effect of both clam and oyster harvesting is no greater than the effect of each harvesting activity conducted alone. Thus, we recommend that both types of harvesting be allowed on some reefs but that other reefs be protected as refuges for shellfish populations and other reef-associated fauna.

In adaptive fishery and habitat management, the results of relatively small-scale, prototype experiments, like the one reported here, are used to design larger-scale comparisons of potential management options. Therefore, we recommend that the results of our experiment be used to design alternative shellfishery management options that can be implemented and monitored on relatively large spatial and temporal scales in North Carolina and other coastal states of North America. Our recommendation that some natural and restored oyster reefs be closed from shellfish harvesting and others opened or restored for the purpose of both clam and oyster harvesting can be used to identify potential management options. Further testing of the generality of our findings on larger spatial and temporal scales is necessary because our study was conducted at only two sites and over a one-year period. Therefore, our results may not apply to areas with different environmental conditions (e.g. different flow and sedimentary regimes, areas of low recruitment) and harvesting intensities (e.g. very low and high levels of harvesting). It is necessary to determine with experiments and simulation models how much oyster reef habitat should be preserved from harvesting to maintain sustainable oyster and clam brood stock populations and habaitat for the successful recruitment and survival of other fishery organisms.

The following steps should now be taken by fishery and habitat managers to improve management of the clam and oyster populations and intertidal oyster reef habitat: 1) identify overall management goals and possible options; 2) derive specific predictions based, at least in part, on the experiment results reported in this study; and 3) design monitoring programs to quantify the effect of each management option. Whenever possible, it is highly recommended that fishermen, fishery managers, and ecologists be included in designing and monitoring large-scale management experiments because collectively they will provide the highest level of rigor and reality.

Acknowledgments

We thank R. A. Cummings for helping to design and conducted the experimental harvests. We thank M. Marshall, D. Meyers, C. H. Peterson, H. C. Summerson, and G. W. Thayer for advice; R. Carpenter for helping to select experimental sites; and D. Bockus,

L. Hill, C. Ingram, and C. Lund for help in the field. We thank J. B. Pearce, J. Merriner, and three anonymous reviewers for improving the manuscript. This work was funded by a Fishery Resource Grant awarded to F. Micheli, H. S. Lenihan, and R. A. Cummings by the North Carolina Marine Fisheries Commission. H. S. Lenihan also received support from a National Research Council Postdoctoral Associateship.

Literature cited

Arnold, W. S.
1984. The effects of prey size, predator size, and sediment composition on the rate of predation of the blue crab, *Callinectes sapidus* Rathbun, on the hard clam, *Mercenaria mercenaria* (Linne'). J. Exp. Mar. Biol. Ecol. 80:207–219.

Bahr, L. M. and W. P. Lanier.
1981. The ecology of intertidal oyster reefs of the South Atlantic Coast: a community profile. U.S. Fish and Wildlife Service, Biological Services Program FWS/OBS/81/15, 63 p.

Botsford, L. W., J. C. Castilla, and C. H. Peterson.
1997. The management of fisheries and marine ecosystems. Science (Wash. D.C.) 277:509–514.

Breitburg, D. L, M. A. Palmer, and T. Loher.
1995. Larval distributions and the spatial patterns of settlement of an oyster reef fish: response to flow and structure. Mar. Ecol. Prog. Ser. 125:45–64.

Dame R. F., R. G. Zingmark, and E. Haskin.
1984. Oyster reefs as processors of estuarine materials. J. Exp. Mar. Biol. Ecol. 83:239–247.

Dayton P. K., S. F. Thrush, M. T. Agardy, and R. J. Hofman.
1995. Environmental effects of marine fishing. Aquat. Cons. 5:205–232.

Engel, J., and R. G. Kvitek.
1995. Effects of otter trawling on a benthic community in Monterey Bay National Marine Sanctuary. Conserv. Biology 12:1204–1214.

FAO (Food and Agriculture Organization of the United Nations).
1993. Annual report. Food and Agriculture Organization, Rome, Italy, 321 p.

Grumbine, R.E.
1997. Reflections on "What is ecosystem management?" Conserv. Biol. 11:41–47.

Lenihan, H. S.
1999. Physical-biological coupling on oyster reefs: how habitat structure influences individual production. Ecol. Monogr. 69:251–276.

Lenihan, H. S., J. H. Grabowski, and G. W. Thayer.
1998. Recruitment to and utilization of oyster reef habitat by fishes and blue crabs. National Research Council, National Marine Fisheries Service, Beaufort, NC. Tech. Rep., 130 p.

Lenihan, H. S., F. Micheli, S. W. Shelton, and C. H. Peterson.
1999. The influence of multiple environmental stressors on susceptibility to parasites: an experimental determination with oysters. Limnol. Oceanogr. 910–924.

Lenihan, H. S., and C. H. Peterson.
1998. How habitat degradation through fishery disturbance enhances impacts of hypoxia on oyster reefs. Ecol. Appl. 8:128–140.

Luckenbach, M. A., R. Mann, and J. E. Wesson (eds).
1998. Oyster reef restoration: a symposium and synthesis of approaches. Virginia Institute of Marine Sciences Press, Gloucester Pt., VA, 266 p.

McAllister, M. K., and R. M. Peterman.
1992. Experimental design in the management of fisheries: a review. N. Am. J. Fish. Manage. 12:1–18.

Michelli, F., and C. H. Peterson.
1999. Estuarine vegetated habitats as corridors for predator movements. Conserv. Biol. 13:869–881.

NRC (National Research Council).
1995. Understanding marine biodiversity: a research agenda for the nation. National Academy Press, Washington, D.C., 203 p.

Newell, R. I. E.
1988. Ecological changes in Chesapeake Bay: Are they the result of overharvesting the American oyster, *Crassostrea virginica*? *In* Understanding the estuary: advances in Chesapeake Bay research: proceedings of a conference, p 536–546. Chesapeake Research Consortium Publication 129, CBP/TRS 24/88, Baltimore, MD.

Norse, E. A. (ed.).
1993. Global marine biological diversity strategy. Center for Marine Conservation, Washington, D.C., 321 p.

Officer C. B., T. J. Smaya, and R. Mann.
1982. Benthic filter feeding: a natural eutrophication control. Mar. Ecol. Prog. Ser. 9:203–210.

Peterson, C. H., H. C. Summerson, and S. R. Fegley.
1987. Ecological consequences of mechanical harvesting of clams. Fish. Bull. 85:281–298.

Peterson, C. H., H. C. Summerson, and J. Huber.
1995. Replenishment of hard clam stocks using hatchery seed: importance of bottom type, seed size, planting season, and density. J. Shell. Res. 14:293–300.

Rothschild B. J., J. S. Ault, P. Goulletquer, and M. Heral.
1994. Decline of the Chesapeake Bay oyster population: a century of habitat destruction and overfishing. Mar. Ecol. Prog. Ser. 111:29–39.

Russ, G., and Alcala, R.
1996. Marine reserves: rates and patterns of recovery and decline of large predatory fish. Ecol. Appl. 6:947–961.

Sponaugle, S., and P. Lawton.
1990. Portunid crab predation on juvenile hard clams: effects of substrate type and prey density. Mar. Ecol. Prog. Ser. 67:43–53.

Underwood, A. J.
1990. Experiments in ecology and management: their logic, functions and interpretation. Austr. J. Ecol. 15:365–389.

Walters, C. J.
1986. Adaptive management of renewable resources. MacMillan Press, New York, NY, 415 p.

West, R. J., and G. N. G. Gordon.
1994. Commercial and recreational harvest of fish from two Australian coastal rivers. Austr. J. Mar. Fish. Res. 45:1259–1279.

Winslow, F.
1881a. Deterioration of American oyster beds. Pop. Sci. Mon. 20:29–43.
1881b. Deterioration of American oyster beds. Pop. Sci. Mon. 20:45–156.

Zimmerman, R., T. J. Minello, T. Baumer, and M. Castiglione.
1989. Oyster reef as habitat for estuarine macrofauna NOAA Tech. Mem.NMFS-SEFC-249, 217 p.

Abstract.—In 1996 we surveyed the fishes living on and around seven offshore oil platforms in the Santa Barbara Channel area. We conducted belt transects at various depths in the midwater and around the bottoms of each platform using the research submersible *Delta*. The bottom depths of these platforms ranged from 49 to 224 m and the midwater beams ranged from 21 to 196 m. We found that there were several distinct differences in the fish assemblages living in the midwater and bottom habitats around all of the platforms. Both midwater and bottom assemblages were dominated by rockfishes. Platform midwaters were dominated by young-of-the-year (YOY) or juveniles up to two years old. Rockfishes larger than about 18 cm total length were rarely seen in the midwater. The fish assemblages around the bottoms of the platforms were dominated by larger individuals, primarily subadults or adults. Density of all fishes was similar between the bottoms and midwater of any given platform. However, the total biomass was much greater on the bottoms, owing to larger fish living there. There was a consistently greater number of species on the bottom than in the midwater of each platform, likely because of a larger variety of habitat types on the bottom. The fish assemblages also differed among platforms. We found significantly higher densities of young-of-the-year rockfishes around platforms north of Pt. Conception compared with those in the Santa Barbara Channel, probably because the more northerly platforms are located in the more productive waters of the California Current.

Manuscript accepted 16 August 1999
Fish. Bull. 98:96–117 (2000).

Fish assemblages around seven oil platforms in the Santa Barbara Channel area

Milton S. Love
Jennifer E. Caselle
Linda Snook
Marine Science Institute
University of California
Santa Barbara, California 93106
E-mail address: (for M. S. Love) love@lifesci.ucsb.edu

Petroleum production has been a part of the southern California economy since the nineteenth century. The earliest drilling took place on land, but by the early twentieth century a large number of piers lined the coast, tapping into offshore oil deposits. Hazel, the first offshore oil platform, was constructed off Summerland in 1958 (Carlisle et al., 1964). At the peak of oil drilling in the early 1980s, there were 30 platforms operating in southern and central California. Currently, there are 19 platforms in operation in the Santa Barbara Channel and off Point Conception (Fig. 1).

Oil platforms provide considerable habitat for marine organisms. The earliest structures were relatively small (23 m long at the surface), newer platforms, however, are over 100 m long (MBC[1]). Sessile invertebrates (primarily mussels, barnacles and anemones) encrust the pilings and well pipes and cover the bottom to form additional habitat.

Oil platforms have a finite economic lifespan and a number of them are becoming uneconomical to operate. In 1996, four platforms were removed from the Santa Barbara Channel, although not without controversy. There is considerable debate regarding the fate of these structures. Some interest groups would like to leave part or all of them in place, claiming protection of fish habitat; others favor complete removal. Understanding the biological communities on the platforms is crucial to making rational decisions regarding the fates of these structures. In addition, research on these platforms could also address questions regarding the role that artificial reefs might play in coastal fish communities. Ultimately, this research will allow us to contrast the fish assemblages on platforms with those of nearby reefs.

Currently, very little is known about the fish fauna around these platforms. One relatively comprehensive SCUBA survey examined fish populations around two shallow inshore platforms, Hazel and Hilda, during Hazel's first three years and Hilda's first year of operation (Carlisle et al., 1964). Additional cursory surveys were conducted around these two platforms in 1970 and 1975; Bascom et al., 1976; Allen and Moore[2]). With the exception of a short-term study of fishes around platform Hidalgo using a remotely operated vehicle (ROV) (Love et al., 1994) and a survey of recreational fishing around Santa Bar-

[1] MBC (Marine Biology Consultants). 1987. Ecology of oil/gas platforms offshore California. Outer Continental Shelf (OCS) Study Minerals Management Service (MMS) 86-0094

[2] Allen, M. J., and M. D. Moore. 1976. Fauna of offshore structures. South. Calif. Coast. Water. Res. Proj. Annu. Rep., Long Beach, CA, p. 179–186.

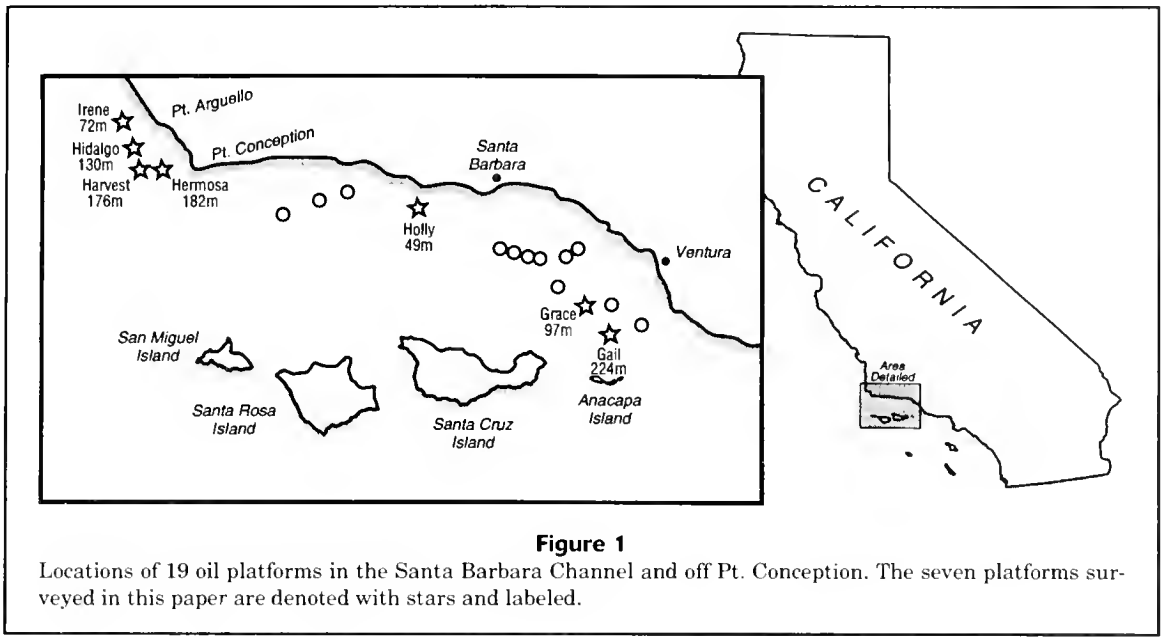

Figure 1
Locations of 19 oil platforms in the Santa Barbara Channel and off Pt. Conception. The seven platforms surveyed in this paper are denoted with stars and labeled.

bara Channel platforms (Love and Westphal, 1990), no other research has been published on the fishes of any California oil platform.

In 1995, we began a survey of the fishes living on and around several platforms in the Santa Barbara Channel area. The surveys were of two types: a scuba-based study in the surface waters (to 30 m) of the platforms and a submersible survey that examined the deeper sections of these structures. However, in 1995, we could not survey any platform bottoms because of inclement weather. This paper discusses the results of the 1996 deep survey.

Materials and methods

Study sites

We surveyed fish assemblages around oil platforms situated in and just northwest of the Santa Barbara Channel. Surveys were conducted around the bottom of six platforms and in the midwater of seven platforms in 1996 (Fig. 1; Table 1). The bottom depth of these platforms ranged from 49 to 224 m. The midwater depths ranged from 21 to 196 m.

The platforms are situated in an area with a complex oceanographic regime. The Santa Barbara Channel is semi-enclosed, faces east-west, and is bordered by the Northern Channel Islands on the south and the mainland on the west. It is embedded within the much larger California-Baja California coastal current regime (Brink and Muench, 1986; Hickey, 1992). Surface waters to the north and west of the Channel are typically cool because the California Current flows equatorward from high latitudes year-round and upwells in the Point Conception and Point Arguello areas during spring and summer. At the same time, the cyclonic circulation pattern in the southern California bight brings warm water flowing poleward along the coast from the east and south of the Santa Barbara Channel. In general, water is cooler and more productive in the area of Points Arguello and Conception than in the Santa Barbara Channel, particularly compared with the more eastern end of the channel.

Surveys

Using the submersible *Delta*, we conducted belt transects around each platform. The submersible maintained a speed of approximately 0.5 knots and stayed approximately 2 m from the structure. Transects were made around the bottom of the platform (from the substrata to approximately 2 m above the substrata) and around each set of cross beams to a minimum depth of about 20 m below the surface. Dives were conducted during daylight hours, between one hour after sunrise and two hours before sunset.

During the transects, researchers made their observations from the central starboard-side viewing port. An externally mounted Hi 8-mm video camera with associated lights filmed the same viewing field as seen by the observers. Observers identified and counted all fishes and verbally recorded those data on the video. All fishes within 2 m of the submarine were counted. Fish lengths were estimated by using

Table 1

Latitude, longitude, bottom and midwater depths, and date of sampling of the seven oil platforms. Platforms listed from northwest to southeast.

Platform	Location	Bottom depth (m)	Midwater depths (m)	Date surveyed
Irene	34°36.62'N, 120°43.77'W	72	29, 50	2 Nov 1996
Hidalgo	34°29.70'N, 120°42.13'W	130	36, 59, 83, 107	28 Oct 1996
Harvest[1]	34°28.15'N, 120°40.85'W	176	38, 61, 84, 113, 141	28 Oct 1996
Hermosa	34°27.33'N, 120°38.78'W	182	63, 84, 106, 131, 156	28 Oct 1996
Holly	34°23.38'N, 120°54.33'W	49	21, 35, 50	29 Oct 1996
Grace	34°10.77'N, 120°28.12'W	97	45, 69, 82	30 Oct 1996
Gail	34°07.50'N, 120°24.02'W	224	71, 95, 115, 141, 166, 196	30 Oct 1996

[1] Midwater survey only.

a pair of lasers mounted on either side of the external video camera. The projected reference spots were 20 cm apart and were visible to the observer. An environmental monitoring system aboard the submarine continuously recorded date and time, depth, and altitude of the vessel above the sea floor. After the dive, these data were overlaid on the original videotape.

Transect videos were reviewed either aboard the research vessel or in the laboratory. For each fish, we recorded 1) its species, to lowest identifiable taxa; 2) its estimated total length to the nearest cm; and 3) the microhabitat it occupied (e.g. pipe, sand, mussel shell mounds, mud). We defined young-of-year fishes (YOYs) from published estimates of size at age. Subadults are defined as juveniles in their second year up to, but not including, maturity.

During the survey at platform Gail, all greenspotted (*Sebastes chlorostictus*) and greenblotched rockfishes (*S. rosenblatti*) were inadvertently identified as greenspotted rockfish. In reviewing the videotape, it was clear that some of the individuals that were recorded as greenspotted rockfish were in fact greenblotched rockfish. In order to correct for this potential misidentification, the total number of both species was adjusted by using the proportion of greenblotched to greenspotted rockfishes (ratio=2.2) observed at platform Gail during the following year's survey (Love, unpub. data). Similar numbers of the two species combined were observed during the two years (1996: n=186,1997: n=209).

Analyses

We estimated length of those transects conducted on the bottom by first determining the submersible speed. This was done by evaluating a ten-second segment for every one minute of transect. The video was manually forwarded frame by frame and the number of 20-cm segments passing the lasers in a ten-second section was counted. The number of 20 cm segments per 10 seconds was divided by 2 to obtain speed in centimeters per second. All subsamples were then averaged to obtain mean transect speed (cm/s). The mean speed was then multiplied by the number of seconds in the transect and divided by 100 to obtain transect length in meters. The length was then multiplied by 2 m (the transect width) to obtain transect area, allowing us to present both densities (fish/m^2) and biomass (kg/m^2). Biomass was estimated for all species by using length-weight relationships derived empirically or obtained from the literature. No biomass estimates were made for species that could not be identified to the family level.

In the midwater, we could not see the lasers pass before fixed points; therefore, we could not directly measure the length of the midwater transects. Without knowledge of the length of the midwater transects, we could not calculate density or biomass per unit area as done on the bottom transects. However, we were able to estimate the length of midwater transects for use in estimating both fish density and biomass. We did this by converting density and biomass on the midwater transects from number and kilogram per minute to number and kilogram per m^2, respectively. This conversion was accomplished by calculating the equation for the regression of density in terms of number per m^2 on density in terms of number per minute for the bottom transects where both values were known (Fig. 2A). The same relationship was calculated for biomass (Fig. 2B). Given the regression equations, density per m^2 and biomass per m^2 could be calculated from number per minute and kilograms per minute. We called these

calculations "estimated density" (number/m^2) and "estimated biomass "(kg/m^2).

This method of estimating transect length and hence fish density and biomass relies on the assumption that the submersible travels at the same speed in both habitats. Although we did not have data on submersible speed, every attempt was made to maintain the submersible at the same speed on all transects during the survey. However, because of debris on the bottom and water currents in the midwater, if there were differences in speed, the submersible was likely to travel slightly faster in the midwater habitats than on the bottoms. In this case, the submersible would cover more area per unit time and the true fish density in the midwater may actually be slightly lower than our estimated density. We consider the potential bias introduced by differences in submersible speed to be minor in relation to the magnitude of the observed differences in fish densities between the midwater and bottom transects (see "Results" section).

We calculated both species richness (number of species) and species diversity. We used the Shannon-Weiner diversity index (H') for all species diversity comparisons (Shannon and Weaver, 1949). We also calculated a percent similarity index (PSI) that quantifies how similar two assemblages are in terms of their species composition (i.e. the relative abundance of those species). The index ranges from 0 (no species shared) to 100% (identical composition and relative abundances). The formula for PSI is

$$PSI = \left\{ \sum \min(p_{xi}, p_{yi}) \right\} \times 100,$$

where, p_{xi} and p_{yi} are the proportion of the ith species in habitat x and habitat y. PSI was calculated for each pair of platform bottom assemblages.

Results

Bottom versus midwater transects

We found that there were several distinct differences in the fish assemblages living in the midwater and bottom habitats around all of the platforms. We calculated percent similarity indices (PSI) between the bottom and midwater assemblages for each platform. These PSIs ranged from 1% to 34% (mean 13.3%). Although both midwater and bottom assemblages were dominated by rockfishes, platform midwaters were dominated by young-of-the-year (YOY) or slightly older juveniles (<10 cm). Rockfishes larger than about 20 cm were rarely seen in the midwater

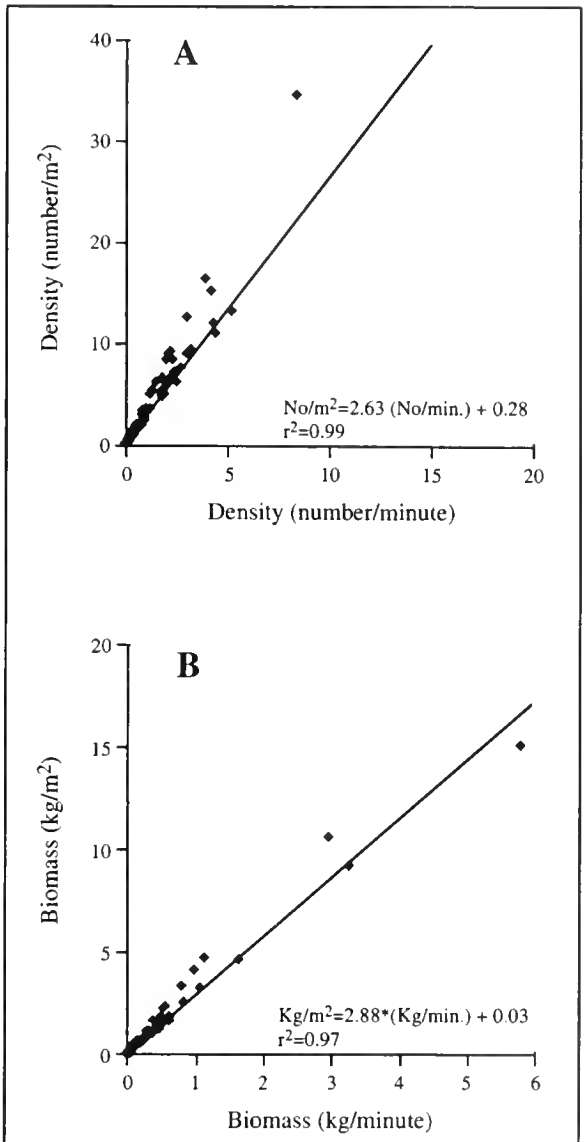

Figure 2

Regressions of (**A**) density in terms of number per minute on density in terms of number per m^2 and (**B**) biomass in terms of kilograms per minute on biomass in terms of kilogram per m^2 for bottom transects on all platforms. The regression equations were used to calculate density and biomass from number and kilogram per minute into number and kilogram per m^2 on the midwater transects. See "Methods" section for explanation of the conversion.

(Fig. 3). The fish assemblages around the bottoms of the platforms were dominated by subadults or adults (11–20 cm) and occasionally harbored very large individuals (up to 48 cm) (Fig. 3).

Average density per platform of all fishes combined was not significantly different on the bottom versus the midwater transects (bottom mean density

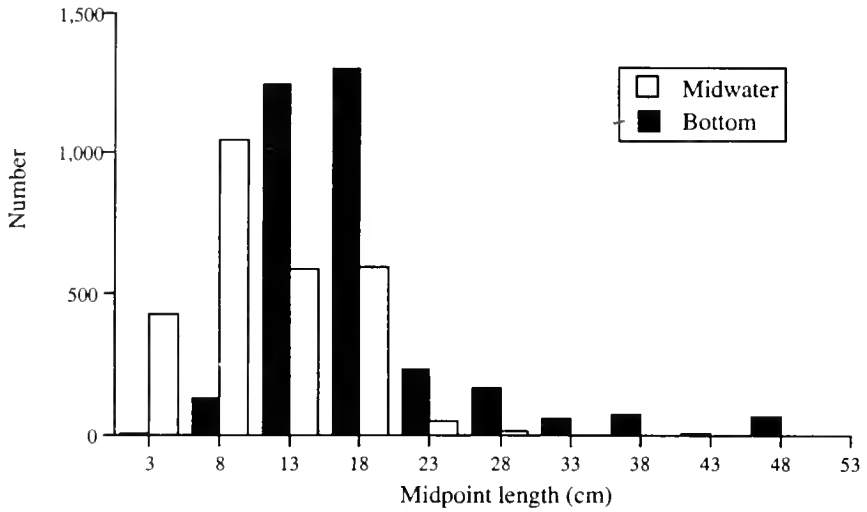

Figure 3
Length-frequency distribution for all rockfish species and all platforms combined. Midpoint length is the midpoint of 5-cm length bins.

(SE)=141.4 fish/100m^2 (49.0), n=6 platforms; midwater mean density (SE)=115.8 fish/100m^2 (32.2), n=7 platforms; t-test, t=0.44, P=0.66). On three platforms, density was higher on the bottom than in midwater and on three other platforms the reverse was true. However, there was a much larger and consistent difference in biomass between bottom and midwater transects. For most families and all platforms, total biomass was higher on bottom than midwater transects (Table 2). Average biomass per platform (SE) for all species combined was 19.06 kg/m^2 (2.5) on the bottom and 6.47 kg/m^2 (2.3) in the midwater (t-test, t=3.75, P=0.003). This consistent difference was due to the lack of adult fishes in the midwater.

Fewer species lived on the midwater structures than on the bottom. Species richness for all rigs combined was 24 in the midwater versus 40 on the bottom. Average species richness per platform was significantly higher on the bottom than in the midwater (bottom mean richness (SE)=14.7 species (1.5); midwater mean richness (SE)=8.2 species (1.4); t-test, t=3.26, P=0.008). Average species diversity (H') across platforms was identical between bottoms and midwaters (bottom mean H' (SE)=1.2 (0.2); midwater mean H' (SE)=1.2 (0.2); t-test, t=0.09, P=0.99). We present the remaining results for bottom and midwater habitats separately.

Bottom habitat

All platforms We identified at least 40 fish species around the platform bottoms (Table 2). Twenty-seven species were rockfishes; they were by far the most speciose group. Rockfishes made up 92.7% of all fishes on the bottom (Table 3) and represented 96.7% of the biomass (Table 2).

Halfbanded, greenspotted, copper, vermilion, widow, and flag rockfishes, and bocaccio were among the most commonly observed rockfishes (Table 3). Our observations indicated that vermilion rockfish, flag rockfish, and bocaccio of all sizes were always closely associated with the platform structure (Fig. 4A). Larger copper and greenspotted rockfishes also were more likely to be very close to the platform. In particular, flag rockfish were most often seen tucked well into the space formed by the bottom of the lowest crossbeam and the bottom (Fig. 4B). Flag and greenspotted rockfishes were almost always seen on or very close to the bottom. Halfbanded rockfish, as well as smaller greenspotted and copper rockfishes, were less bound to the platform and were often seen well away from the structure. Juvenile greenspotted and copper rockfishes were usually nestled within or just above the mussel, shell-covered substrata. Vermilion rockfish, and to a certain extent copper rockfish and bocaccio, would occasionally ascend up platform legs as much as 5 m.

Flag rockfish, as well as larger bocaccio and vermilion rockfish, often were solitary or found in small groups. The exception occurred at platform Gail, where one school of bocaccio comprised at least 100 individuals. Smaller adult or subadult vermilion and copper rockfishes tended to aggregate, often in mixed groups containing 50 or more individuals. The few

Table 2

Biomasses of fishes observed, by species, around all platforms in October–November of 1996. Biomasses are given for bottoms of platforms and midwater, with percent of totals for those parts of the platforms. Biomass is kilograms/m^2. Family totals are given in boldface. YOY means "young-of-year."

			Bottom		Midwater	
Family	Common name	Scientific name	Biomass	% Total	Biomass	% Total
Scorpaenidae	Rockfishes		**96.83**	**84.66**	**38.81**	**85.90**
	Kelp rockfish	*Sebastes atrovirens*	0	0	0.34	0.75
	Brown rockfish	*S. auriculatus*	0.82	0.71	0	0
	Gopher rockfish	*S. carnatus*	0.01	<0.1	0.23	0.51
	Copper rockfish	*S. caurinus*	12.12	10.59	0.47	1.04
	Greenspotted rockfish	*S. chlorostictus*	8.80	10.94	0.56	1.23
	Starry rockfish	*S. constellatus*	0.02	<0.1	0	0
	Darkblotched rockfish	*S. crameri*	0.07	<0.1	0	0
	Calico rockfish	*S. dalli*	1.40	1.22	0.08	0.18
	Greenstriped rockfish	*S. elongatus*	0.32	0.28	0	0
	Swordspine rockfish	*S. ensifer*	0.03	<0.1	0.08	0.17
	Widow rockfish	*S. entomelas*	1.86	1.62	24.08	53.15
	Yellowtail rockfish	*S. flavidus*	0.08	<0.1	0	0
	Chilipepper	*S. goodei*	0	0	0.82	1.82
	Squarespot rockfish	*S. hopkinsi*	0.46	0.40	0.51	1.12
	Vermilion rockfish	*S. miniatus*	20.84	18.22	0	0
	Blue rockfish	*S. mystinus*	0.74	0.65	0.29	0.64
	Bocaccio rockfish	*S. paucispinis*	14.35	12.55	3.68	8.12
	Canary rockfish	*S. pinniger*	1.18	1.03	0	0
	Rosy rockfish	*S. rosaceus*	0.46	0.40	0.07	0.15
	Greenblotched rockfish	*S. rosenblatti*	3.89	0.15	0	0
	Yelloweye rockfish	*S. ruberrimus*	0.06	<0.1	0	0
	Flag rockfish	*S. rubrivinctus*	1.44	1.26	0.55	1.21
	Bank rockfish	*S. rufus*	0.29	0.25	0	0
	Halfbanded rockfish	*S. semicinctus*	26.21	22.91	0.04	<0.1
	Olive rockfish	*S. serranoides*	0.03	<0.1	0	0
	Treefish	*S. serriceps*	0.19	0.17	0.04	<0.1
	Pygmy rockfish	*S. wilsoni*	0.04	<0.1	0	0
	Sharpchin rockfish	*S. zacentrus*	0.10	<0.1	0.04	<0.1
	Shortspine thornyhead	*Sebastolobus alascanus*	<0.1	<0.1	0	0
	Sebastomus group[1]		0.31	0.27	0.37	0.82
	Rockfish YOY	*Sebastes* spp.	0.72	0.63	6.56	14.47
Hexagrammidae	Greenlings		**12.88**	**11.25**	**2.72**	**6.01**
	Kelp greenling	*Hexagrammos decagrammus*	0	0	<0.1	<0.1
	Lingcod	*Ophiodon elongatus*	12.35	10.80	0	0
	Painted greenling	*Oxylebius pictus*	0.51	0.44	2.72	6.01
	Shortspine combfish	*Zaniolepis frenata*	0.01	<0.1	0	0
	Combfish sp.	*Zaniolepis* sp.	0.01	<0.1	0	0
Pomacentridae	Damselfishes		**0**	**0**	**0.54**	**1.20**
	Blacksmith	*Chromis punctipinnis*	0	0	0.54	1.20
Embiotocidae	Seaperches		**4.57**	**3.99**	**3.02**	**6.65**
	Pile perch	*Damalichthys vacca*	3.71	3.24	1.18	2.60
	Sharpnose surfperch	*Phanerodon atripes*	0.49	0.43	1.84	4.05
	Unident. sea perches		0.20	0.17	0	0
	Pink surfperch	*Zalembius rosaceus*	0.17	0.15	0	0
Gadidae	Cods		**0**	**0**	**0.20**	**0.44**
	Pacific hake	*Merluccius productus*	0	0	0.20	0.44

continued

Table 2 (continued)

Family	Common name	Scientific name	Bottom		Midwater	
			Biomass	% Total	Biomass	% Total
Cottidae	Sculpins		**0**	**0**	**0.03**	**0.07**
	Unidentifed sculpin		0	0	0.03	0.07
Bathymasteridae	Ronquils		**0.03**	**0.03**	**0**	**0**
	Unidentified ronquil		0.03	0.03	0	0
Agonidae	Poachers		**0.01**	**0.01**	**0**	**0**
	Unidentified poacher		0.01	0.01	0	0
Flatfish	Flatfish		**0.06**	**0.06**	**0**	**0**
	Sanddabs	*Citharichthys* sp.	0.01	0.01	0	0
	Unident. flatfish		0.05	0.05	0	0

[1] *Sebastomus* group may include greenblotched, greenspotted, pinkrose, rosethorn, rosy, starry, or swordspine rockfishes

canary rockfish we noted tended to associate with vermilion rockfish. Halfbanded rockfish were almost always seen in schools, sometimes containing hundreds of individuals (Fig. 4C).

In the greenling family, Hexagrammidae, both lingcod and painted greenling, were common; together they represented about 5.3% of all fishes seen. Larger lingcod were solitary and tended to remain near the bottom of the platform (Fig. 4D). They were usually seen sitting motionless on the bottom or slowly swimming just above it. Juvenile lingcod rarely came within a meter of the platform, they were usually seen lying among the mussel shells away from the structure (Fig. 4E). Painted greenling sat on the crossbeams, along the pilings and on the mussel shells, always found as solitary individuals.

Among platform comparisons The bottom fish assemblages around each platform were all different (Tables 4 and 5). Pairwise percent similarity indices (PSI) for each combination of platforms ranged from 0% (platforms Gail and Holly) to 70.1% (platforms Grace and Hidalgo) (Table 4). The average percent similarity was 20.0%. Despite a low average similarity value, rockfishes, as measured by number, density and biomass, dominated the bottom assemblages around all of the platforms (Table 5). Lingcod were the only nonrockfish species among the top four most common species at any platform.

Around platform Irene, subadult and adult copper and vermilion rockfishes were most abundant. Irene also was unique among the platforms in having large numbers of juvenile lingcod. Halfbanded rockfish, painted greenling, and pile perch were also commonly seen. Halfbanded and greenspotted rockfish were most common at platform Hidalgo, along with flag rockfish, lingcod, bocaccio, and vermilion rockfish. Similar to that around Hidalgo (PSI=60%), the bottom fish assemblage around platform Hermosa was characterized by greenspotted and halfbanded rockfish, with lesser numbers of flag rockfish and lingcod (Table 4). Vermilion, calico, widow, copper, and squarespot rockfishes were most often seen at Holly, along with lesser numbers of halfbanded rockfish, pile perch, rosy rockfish, and painted greenling. Very large schools of halfbanded rockfish were observed at Grace, along with some flag, greenspotted, and vermilion rockfishes. The dominance of halfbanded rockfish at Hidalgo and Grace resulted in the highest PSI among platform pairs (70.1%). Members of the rockfish subgenus *Sebastomus*, primarily greenblotched and greenspotted rockfishes and bocaccio were most abundant at platform Gail. Gail had by far the highest number and density of bocaccio of any of the platforms.

We observed between 8 and 21 species around the bottom of the platforms (Fig. 5A). We found no significant relationship between species number or diversity (H') and platform bottom depth (linear regression: species richness vs. depth, r^2=0.58, P=0.07, diversity (H') vs. depth, r^2=0.19, P=0.37, Fig. 5A). Although neither relationship was significant, there was a tendency for platforms in shallower water to have both higher species richness and species diversity. Location of the platforms within the Santa Barbara Channel and Santa Maria Basin also did not explain the differences among platforms. There was no correlation between northwest to southeast orientation and either species richness or diversity (Spearman rank correlation: species richness vs. orientation, r_s=–0.26, P=0.6, diversity (H') vs. orientation, r_s=–0.6, P=0.2). In fact, the two most

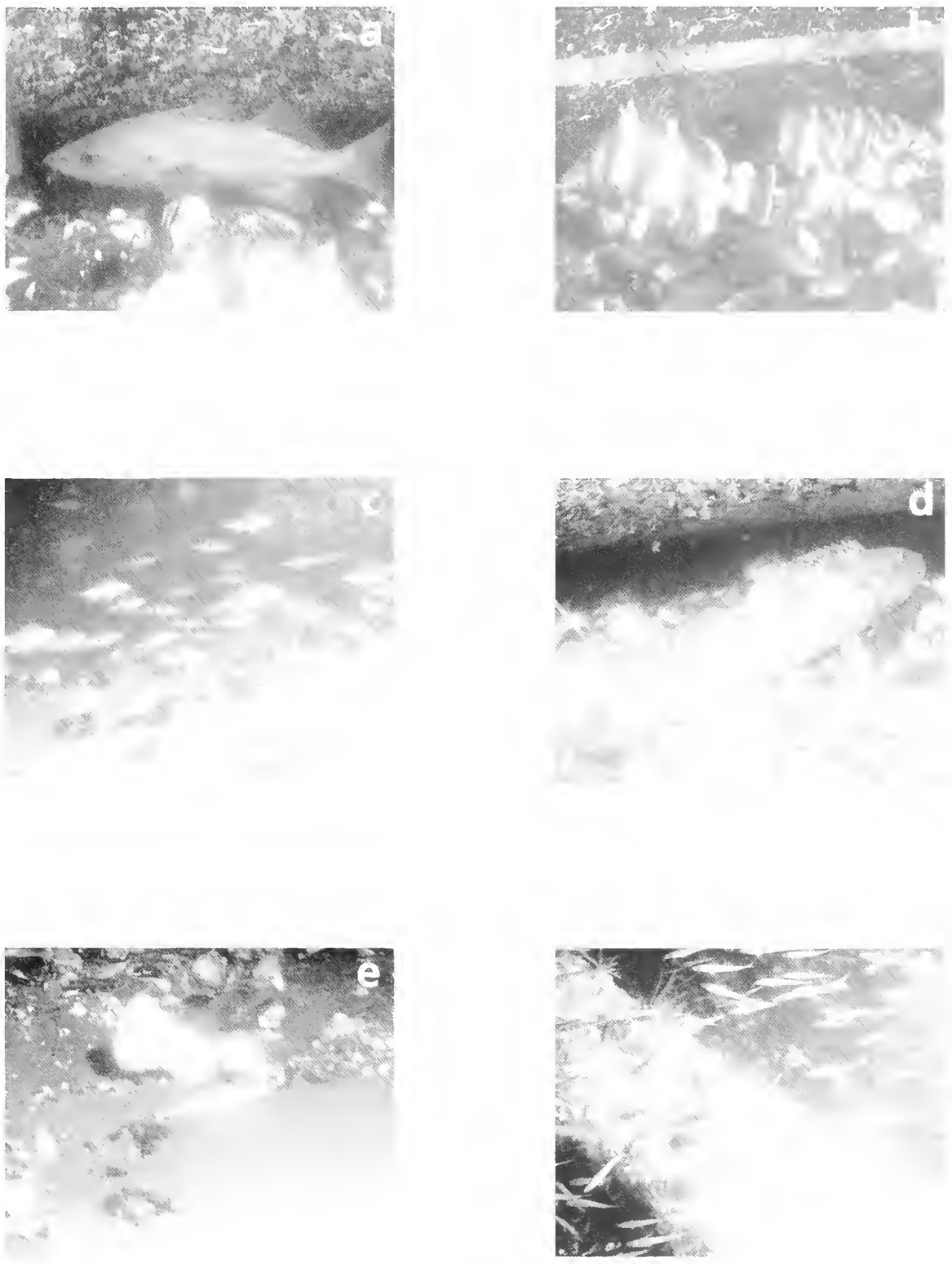

Figure 4

Fishes typical of offshore oil platforms in the Santa Barbara Channel and Santa Maria Basin: (**A**) bocaccio, *Sebastes paucispinis*, (**B**) flag rockfish, *S. rubrivinctus*, (**C**) halfbanded rockfish, *S. semicinctus*, (**D**) adult lingcod, *Ophiodon elongatus*, (**E**) juvenile lingcod, A–E all on bottom transects, and (**F**) young-of-the-year rockfish, *Sebastes* spp., on midwater crossbeam.

Table 3

Numbers of fishes observed, by species, around all platforms in October–November of 1996. Numbers are given for bottoms of platforms and midwater, with percent of totals for those parts of the platforms. Family totals are given in boldface. YOY means "young-of-year."

			Bottom		Midwater	
Family	Common name	Scientific name	Biomass	% Total	Biomass	% Total
Scorpaenidae	Rockfishes		**4212**	**92.7**	**2753**	**91.4**
	Kelp rockfish	*Sebastes atrovirens*	0	0	1	<0.1
	Brown rockfish	*S. auriculatus*	7	0.2	0	0
	Gopher rockfish	*S. carnatus*	2	<0.1	4	0.1
	Copper rockfish	*S. caurinus*	347	7.6	11	0.4
	Greenspotted rockfish	*S. chlorostictus*	365	8.0	18	0.6
	Starry rockfish	*S. constellatus*	1	<0.1	0	0
	Darkblotched rockfish	*S. crameri*	1	<0.1	0	0
	Calico rockfish	*S. dalli*	68	1.5	2	<0.1
	Greenstriped rockfish	*S. elongatus*	12	0.3	0	0
	Swordspine rockfish	*S. ensifer*	2	<0.1	2	<0.1
	Widow rockfish	*S. entomelas*	115	2.5	1054	35.0
	Yellowtail rockfish	*S. flavidus*	1	<0.1	0	0
	Chilipepper	*S. goodei*	0	0.00	68	2.3
	Squarespot rockfish	*S. hopkinsi*	47	1.0	22	0.7
	Vermilion rockfish	*S. miniatus*	307	6.8	0	0
	Blue rockfish	*S. mystinus*	7	0.2	6	0.2
	Bocaccio rockfish	*S. paucispinis*	85	1.9	264	8.8
	Canary rockfish	*S. pinniger*	10	0.2	0	0
	Rosy rockfish	*S. rosaceus*	31	0.7	1	<0.1
	Greenblotched rockfish	*S. rosenblatti*	129	2.8	0	0
	Yelloweye rockfish	*S. ruberrimus*	2	<0.1	0	0
	Flag rockfish	*S. rubrivinctus*	113	2.5	15	0.5
	Bank rockfish	*S. rufus*	2	<0.1	0	0
	Halfbanded rockfish	*S. semicinctus*	2491	54.8	1	<0.1
	Olive rockfish	*S. serranoides*	1	<0.1	0	0
	Treefish	*S. serriceps*	5	0.1	1	<0.1
	Pygmy rockfish	*S. wilsoni*	4	<0.1	0	0
	Sharpchin rockfish	*S. zacentrus*	11	0.2	1	<0.1
	Shortspine thornyhead	*Sebastolobus alascanus*	1	<0.1	0	0
	Sebastomus group[1]		19	0.4	13	0.4
	Rockfish YOY	*Sebastes* spp.	26	0.6	1269	42.1
Hexagrammidae	Greenlings		**244**	**5.4**	**187**	**6.2**
	Kelp greenling	*Hexagrammos decagrammus*	0	0	1	<0.1
	Lingcod	*Ophiodon elongatus*	193	4.3	0	0
	Painted greenling	*Oxylebius pictus*	46	1.0	186	6.2
	Shortspine combfish	*Zaniolepis frenata*	2	<0.1	0	0
	Combfish sp.	*Zaniolepis* sp	3	<0.1	0	0
Pomacentridae	Damselfishes		**0**	**0**	**12**	**0.4**
	Blacksmith	*Chromis punctipinnis*	0	0	12	0.4
Embiotocidae	Seaperches		**65**	**1.4**	**20**	**0.7**
	Pile perch	*Damalichthys vacca*	46	1.0	6	0.2
	Sharpnose surfperch	*Phanerodon atripes*	9	0.2	14	0.5
	Unident. sea perches		1	<0.1	0	0
	Pink surfperch	*Zalembius rosaceus*	9	0.2	0	0
Gadidae	Cods		**2**	**<0.1**	**18**	**0.6**
	Pacific hake	*Merluccius productus*	2	<0.1	18	0.6

continued

Table 3 (continued)

Family	Common name	Scientific name	Bottom		Midwater	
			Biomass	% Total	Biomass	% Total
Cottidae	Sculpins		**0**	**0**	**1**	**<0.1**
	Unidentifed sculpin		0	0	1	<0.1
Bathymasteridae	Ronquils		**2**	**<0.1**	**0**	**0**
	Unidentified ronquil		2	<0.1	0	0
Agonidae	Poachers		**2**	**<0.1**	**0**	**0**
	Unidentified poacher		2	<0.1	0	0
Flatfish	Flatfish		**13**	**0.3**	**0**	**0**
	Sanddabs	*Citharichthys* sp.	1	<0.1	0	0
	Unident. flatfish		12	0.3	0	0

[1] *Sebastomus* group may include greenblotched, greenspotted, pinkrose, rosethorn, rosy, starry, or swordspine rockfishes.

similar assemblages were on platforms near the geographic extremes (Hidalgo and Grace).

Density and biomass of all species combined also varied among rigs but in a pattern different from species richness and diversity (Fig. 5B). However, similar to richness and diversity, density and biomass differences could not be explained by bottom depth or by geography (linear regression: density vs. depth, r^2=0.22, P=0.35, biomass vs. depth, r^2=0.06, P=0.64; Spearman rank correlation: density vs. orientation, r_s=-0.31, P=0.54, biomass vs. orientation, r_s=-0.37, P=0.46).

Although bottom depth did not explain the patterns of abundance of all species combined, the abundance patterns of individual species did relate more strongly to bottom depth. Among the more commonly observed species, eight showed depth-related patterns of abundance (Fig. 6). Copper and vermilion rockfishes, lingcod, and painted greenling were most dense around the bottoms of some of the shallower platforms (especially platform Irene). Halfbanded and flag rockfishes were most dense on the bottoms of the middepth structures and bocaccio and greenspotted rockfish were most common at the bottom of the deeper platforms.

Table 4

Percent similarity indices for each pair of platforms for the bottom only in 1996. No bottom surveys were done on platform Harvest.

Platform	Gail	Grace	Holly	Hermosa	Hidalgo
Grace	2.3				
Holly	0	8.5			
Hermosa	24.7	34.5	8.5		
Hidalgo	17.9	70.1	11.8	60.0	
Irene	1.4	4.7	41.5	3.8	10.0

Midwater habitat

All platforms Rockfishes also dominated the midwater portions of the platforms, but were primarily YOYs and slightly older juveniles. Rockfishes represented 91.4% of the individuals (Table 3) and 85.9% of the biomass (Table 2) in the midwater. Although it was difficult to identify many of the smaller individuals, widow rockfish were by far the most common species, representing 35.0% of all fishes seen. It is likely that many of the small, unidentifiable YOYs also were widow rockfish. YOY bocaccio also were fairly abundant around some of the platforms and occasionally schooled with widow rockfish. Both species formed relatively tight, polarized schools, loosely associated with the pilings and crossbeams (Fig. 4F). When disturbed, the schools immediately swam inward underneath the platform structure. We also saw small numbers of what we tentatively identified as YOYs of the complex of kelp, copper, gopher and black-and-yellow rockfishes (*S. chrysomelas*). These were found in smaller, much less coherent aggregations and were more likely to move in closer to the substrata when disturbed.

Painted greenling, primarily small individuals, were the most commonly seen nonrockfish species. We often saw solitary individuals resting on the crossbeams. Other species occasionally seen near or

Table 5

Number, densities, and biomasses of fishes observed around the bottoms of six oil platforms off central and southern California. Platforms are listed geographically, from northwest to southeast. Species are ranked by number observed. YOY means "young-of-year." We computed minimum number of species by assuming that each unidentified taxa (flatfish, poacher, ronquil and seaperch) represented one species.

Platform	Species	Number	Density (fish/100m^2)	Biomass (kg/m^2)
Irene	Copper rockfish	297	55.99	10.01
	Vermilion rockfish	198	37.33	11.81
	Lingcod	152	28.65	1.23
	Halfbanded rockfish	25	4.71	0.16
	Painted greenling	20	3.77	0.24
	Pile perch	20	3.77	0.83
	Rosy rockfish	4	0.75	0.02
	Sebastomus group[1]	2	0.38	0.01
	Brown rockfish	2	0.38	0.05
	Bocaccio	1	0.19	0.24
	Flag rockfish	1	0.19	0.01
	Gopher rockfish	1	0.19	0.00
	Rockfish YOY	1	0.19	0.01
	Widow rockfish	1	0.19	0.02
	Yellowtail rockfish	1	0.19	0.08
	Total	**726**	**136.86**	**24.73**
	Minimum number of species	13		
Hidalgo	Halfbanded rockfish	552	94.62	9.35
	Greenspotted rockfish	109	18.68	3.48
	Flag rockfish	58	9.94	1.00
	Lingcod	29	4.97	6.52
	Bocaccio	17	2.91	2.10
	Vermilion rockfish	13	2.23	2.83
	Rosy rockfish	10	1.71	0.27
	Sharpchin rockfish	10	1.71	0.09
	Canary rockfish	7	1.20	1.03
	Greenstriped rockfish	7	1.20	0.11
	Painted greenling	5	0.86	0.07
	Pygmy rockfish	4	0.69	0.04
	Widow rockfish	4	0.69	0.64
	Squarespot rockfish	3	0.51	0.03
	Rockfish YOY	2	0.34	0.06
	Shortspine combfish	2	0.34	0.01
	Yelloweye rockfish	2	0.34	0.06
	Sebastomus group [1]	1	0.17	0.01
	Bank rockfish	1	0.17	0.02
	Unidentified poacher	1	0 17	0.01
	Total	**837**	**143.47**	**27.73**
	Minimum number of species	18		
Hermosa	Greenspotted rockfish	179	25.72	3.24
	Halfbanded rockfish	98	14 08	0.71
	Flag rockfish	16	2.30	0.20
	Lingcod	7	1.01	2.60
	Rockfish YOY	5	0.72	0.10
	Copper rockfish	4	0.57	0.03
	Pacific hake	2	0.29	0.00
	Sebastomus group[1]	1	0.14	0.04
	Greenblotched rockfish	1	0.14	0.15

continued

Table 5 (continued)

Platform	Species	Number	Density (fish/100m^2)	Biomass (kg/m^2)
Hermosa continued	Greenstriped rockfish	1	0.14	0.01
	Unidentified poacher	1	0.14	0.00
	Sharpchin rockfish	1	0.14	0.01
	Starry rockfish	1	0.14	0.02
	Widow rockfish	1	0.14	0.02
	Total	**318**	**45.70**	**7.13**
	Minimum number of species	12		
Holly	Vermilion rockfish	87	21.98	5.87
	Calico rockfish	68	17.18	1.40
	Widow rockfish	47	11.88	1.14
	Copper rockfish	45	11.37	2.05
	Squarespot rockfish	43	10.87	0.41
	Halfbanded rockfish	29	7.33	0.12
	Pile perch	26	6.57	2.88
	Rosy rockfish	16	4.04	0.11
	Painted greenling	15	3.79	0.17
	Sharpnose surfperch	9	2.27	0.49
	Blue rockfish	7	1.77	0.74
	Pink surfperch	7	1.77	0.15
	Unident. flatfish	6	1.52	0.02
	Brown rockfish	5	1.26	0.77
	Sebastomus group [1]	4	1.01	0.08
	Canary rockfish	3	0.76	0.15
	Rockfish YOY	3	0.76	0.15
	Treefish	2	0.51	0.10
	Ronquils	1	0.25	0.00
	Unident. sea perches	1	0.25	0.20
	Combfish sp.	1	0.25	0.00
	Gopher rockfish	1	0.25	0.01
	Olive rockfish	1	0.25	0.03
	Shortspine thornyhead	1	0.25	0.00
	Unidentified fish	1	0.25	•
	Total	**429**	**108.40**	**17.04**
	Minimum number of species	21		
Grace	Halfbanded rockfish	1787	351.16	15.87
	Flag rockfish	30	5.90	0.18
	Greenspotted rockfish	18	3.54	0.38
	Vermilion rockfish	9	1.77	0.33
	Rockfish YOY	7	1.38	0.05
	Unident. flatfish	6	1.18	0.03
	Painted greenling	6	1.18	0.03
	Widow rockfish	5	0.98	0.05
	Treefish	3	0.59	0.09
	Combfish sp.	2	0.39	0.01
	Lingcod	2	0.39	0.03
	Pink surfperch	2	0.39	0.01
	Ronquils	1	0.20	0.03
	Copper rockfish	1	0.20	0.03
	Greenblotched rockfish	1	0.20	0.02
	Rosy rockfish	1	0.20	0.06
	Sanddabs	1	0.20	0.01
	Squarespot rockfish	1	0.20	0.01

continued

Table 5 (continued)

Platform	Species	Number	Density (fish/100m^2)	Biomass (kg/m^2)
Grace continued	Unidentified fish	1	0.20	•
	Total	**1884**	**370.22**	**17.21**
	Minimum number of species	16		
Gail	Greenblotched rockfish	127	19.8	3.71
	Bocaccio	67	10.46	12.01
	Greenspotted rockfish	59	9.2	1.70
	Sebastomus group [1]	10	1.9	0.18
	Rockfish YOY	5	0.78	0.35
	Greenstriped rockfish	4	0.62	0.20
	Lingcod	3	0.47	1.96
	Flag rockfish	2	0.31	0.03
	Swordspine rockfish	2	0.31	0.03
	Bank rockfish	1	0.16	0.27
	Darkblotched rockfish	1	0.16	0.07
	Total	**281**	**44.17**	**20.51**
	Minimum number of species	9		

[1] *Sebastomus* group may include greenblotched, greenspotted, pinkrose, rosethorn, rosy, starry, or swordspine rockfishes

on midwater structure included juvenile greenspotted and flag rockfishes, as well as sharpnose seaperch, pile perch, and blacksmith.

Among platform comparisons The midwater assemblages also differed among rigs, although the variability was less than among the bottom assemblages. Species richness ranged from 6 to 11 species per platform (Fig. 7A). Species diversity also showed less variability among platform midwaters than platform bottoms (midwater H' range: 0.7 to 1.8, Fig. 7A).

The midwater around platform Irene was dominated by widow rockfishes (primarily YOYs, but also one-year-old fishes), unidentified YOY rockfishes (probably primarily widow rockfish) and YOY bocaccio. Almost no other fishes were noted (Table 6). The species composition at platforms Hidalgo and Harvest was similar to that at platfrom Irene, although painted greenling were also occasionally seen. Far fewer fishes were noted at platform Hermosa, although the species composition was similar, with the addition of small numbers of Pacific hake. Fewer fishes were seen at platform Holly. Here, YOY rockfish (probably widow rockfish), painted greenling, sharpnose seaperch and squarespot rockfish were the most common species. Smaller numbers of juvenile widow rockfish, YOY rockfish, and juvenile chilipepper characterized platform Grace. We saw fewest fishes in the midwaters around platform Gail where YOY rockfish (again probably widow rockfish) were the most common.

In general, the platforms at the western end of the Santa Barbara Channel harbored a higher density of fishes in the midwater than did those towards the east (Fig. 7B). There was a significant relationship between density and northwest-southeast rank (Spearmans r_s=0.89, P=0.006). This pattern was due to higher density of YOY rockfishes, especially widow rockfish and bocaccio, at platforms Irene and Hidalgo. YOY rockfishes were abundant only at Irene and Hidalgo, they were much less common at the platforms farther east. There was not a significant relationship between biomass and northwest-southeast rank (Spearmans r_s=0.64, P=0.11).

Length-frequency comparisons

Relatively few species were abundant in both the midwater and bottom assemblages. For those species that were found in both environments, such as copper, flag, and greenspotted rockfishes, there was a tendency for juveniles to be found in the midwater and older individuals on the bottom. Bocaccio were the extreme example, with smaller juveniles occurring only in midwater and larger individuals only on the bottom (Fig. 8). The painted greenling was one of the few species that occurred in virtually all size classes in both the midwater and on the bottom (Fig. 8).

There were considerable differences in the size frequencies of the major species around the platforms (Fig. 8). Some species, such as copper rockfish and vermilion rockfish, were found primarily as juveniles and subadults. At the extreme, we did not identify any mature widow rockfish. Numerous other species (i.e. painted greenling, bocaccio, greenspotted rockfish,

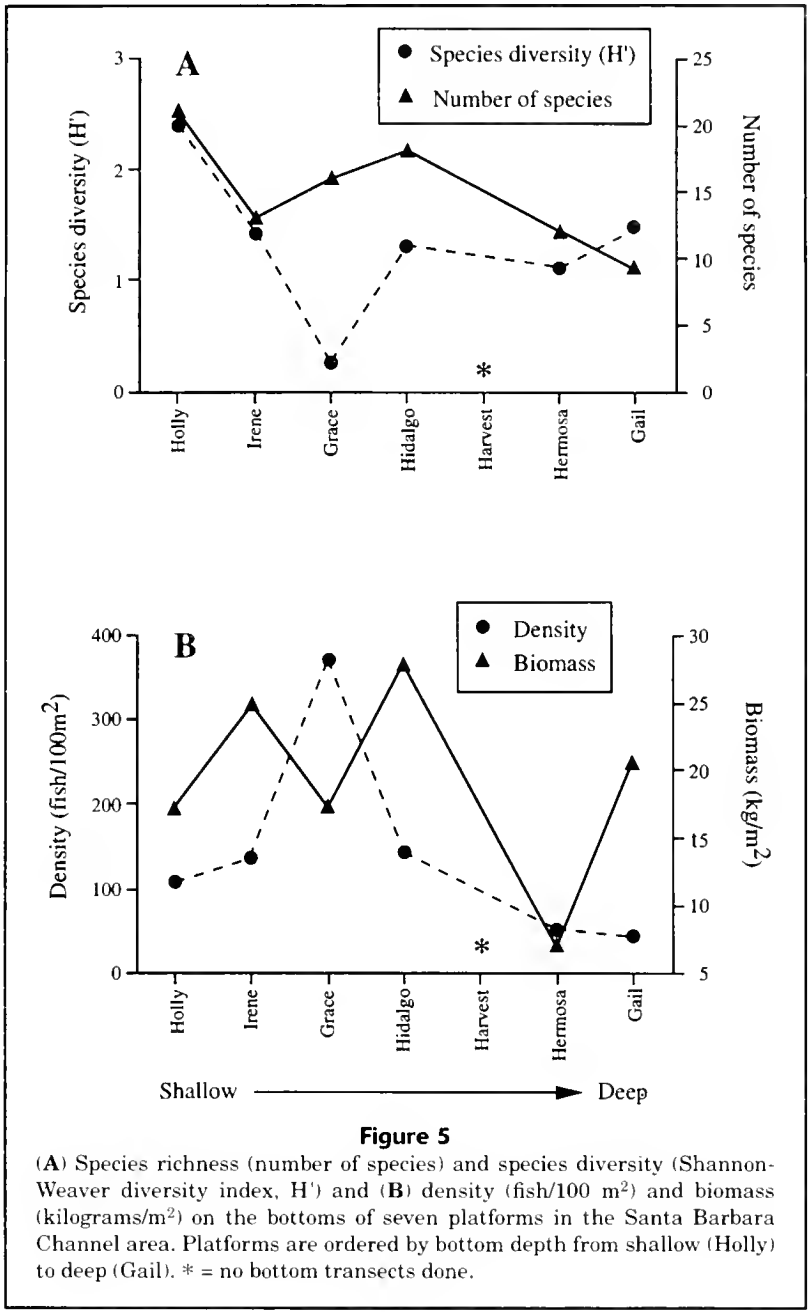

Figure 5

(**A**) Species richness (number of species) and species diversity (Shannon-Weaver diversity index, H') and (**B**) density (fish/100 m^2) and biomass (kilograms/m^2) on the bottoms of seven platforms in the Santa Barbara Channel area. Platforms are ordered by bottom depth from shallow (Holly) to deep (Gail). * = no bottom transects done.

flag rockfish, and halfbanded rockfish) were found over a wide size range, encompassing most life stages. Although a wide size range of lingcod was observed, it is noteworthy that most of the small fish were found around platform Irene; relatively few of these young individuals inhabited the other platforms.

Discussion

Although we found large variability in many of the attributes of the fish assemblages living around these seven oil platforms, several consistent patterns were evident. Around all of these structures, the midwater fish assemblage was quite different from that inhabiting the platform bottoms. Juvenile rockfishes were by far the dominant group occupying the midwater. Although the density of all species combined was similar between the bottom and midwater of any given platform, the biomass was much greater on the bottom, owing to larger fish living around the bottom. In addition, there was a consistently greater number of species on the bottom than in the midwater around each platform. The bottom of the

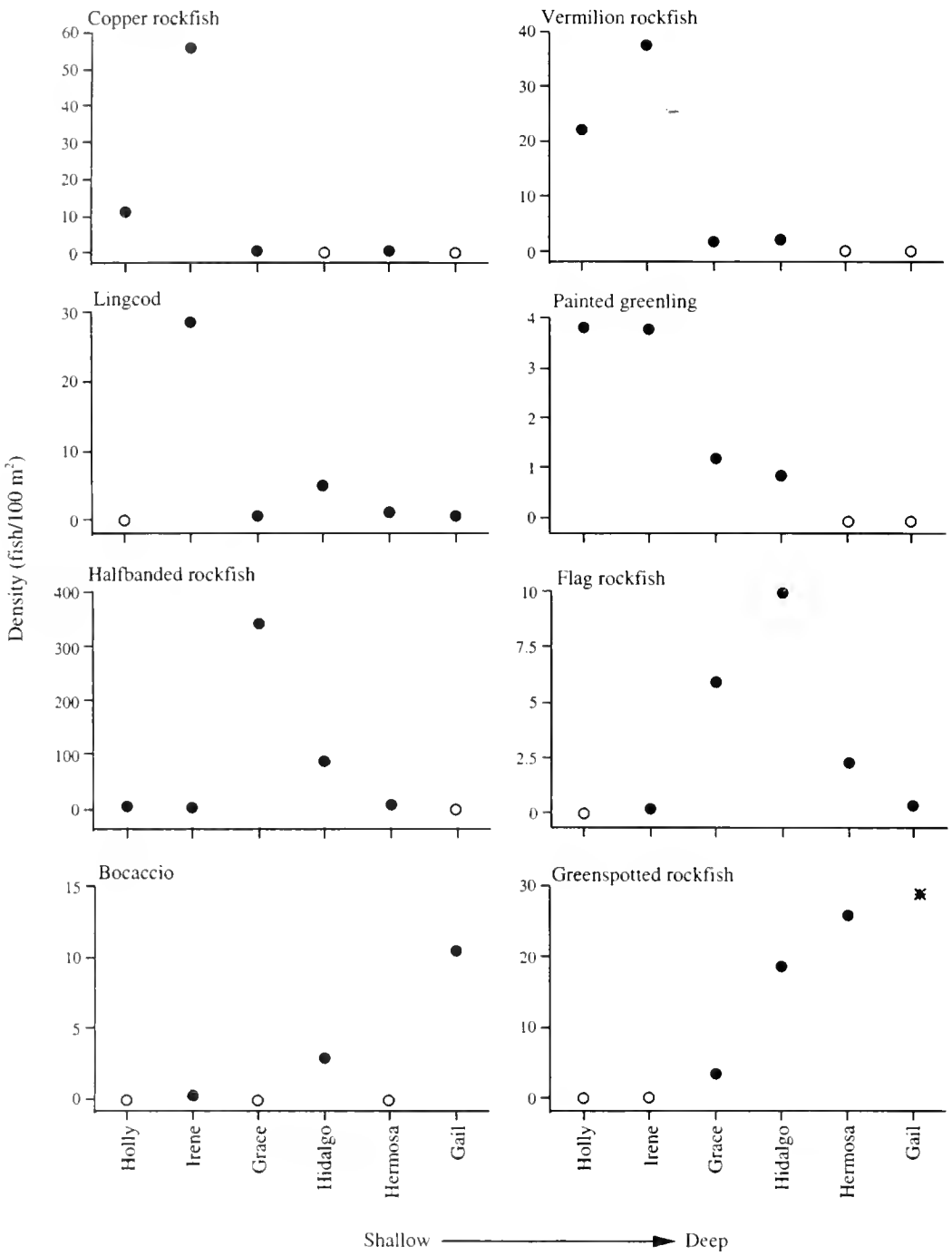

Figure 6

Densities (fish/100m²) of eight common species on the bottoms of seven platforms in the Santa Barbara Channel area. Platforms are ordered by bottom depth from shallow (Holly) to deep (Gail). Data for greenspotted rockfish around platform Gail (noted by *), may include observation of greenblotched rockfish. Empty symbols represent zero values.

platforms provided a larger variety of habitat types than did the midwater. Bottoms are often largely composed of shell mounds that have fallen from the upper parts of the platforms. These mounds, in com-

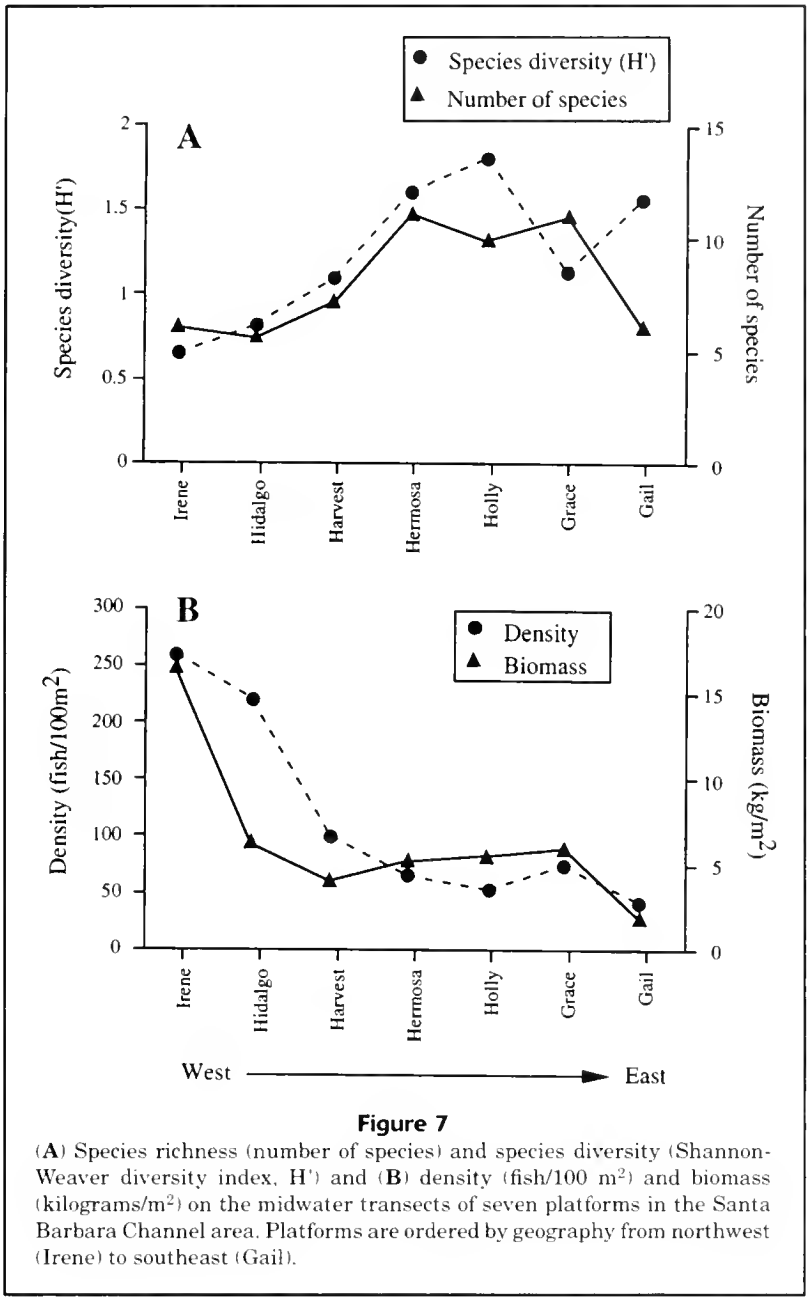

Figure 7

(**A**) Species richness (number of species) and species diversity (Shannon-Weaver diversity index, H') and (**B**) density (fish/100 m^2) and biomass (kilograms/m^2) on the midwater transects of seven platforms in the Santa Barbara Channel area. Platforms are ordered by geography from northwest (Irene) to southeast (Gail).

bination with the wells, crossbeams, and pilings provide a greater degree of habitat complexity and thus, may allow a greater number of species to coexist.

Platforms north of Pt. Conception in the Santa Maria Basin contain far more YOY rockfishes than those in the Santa Barbara Channel to the south. This geographic difference is almost certainly due to the difference in water masses of the two areas. Platforms north of Pt. Conception are more exposed to the California Current; those south of the Point are more influenced by Southern California Bight water (Brink and Muench, 1986; Hickey, 1992). There is considerable evidence that, within much of the Southern California Bight, juvenile rockfish recruitment has been poor for a number of years (Stephens et al., 1984, 1994; Love et al., 1998), probably due to decadal-long changes in oceanographic conditions. Since the late 1970s, waters off Southern California have warmed significantly and upwelling has declined. This situation has led to reduced zooplankton production (Roemmich and McGowan, 1995) and a reduction in the survival of many marine fish species in early life stages (Holbrook and Schmitt, 1996). The present regime is probably part of a long-term

Table 6

Number, densities, and biomasses of fishes observed on the midwater transects of seven oil platforms off central and southern California. Platforms are listed geographically, from northwest to southeast. YOY means "young-of-year." We computed minimum number of species by assuming that each unidentified taxa (flatfish, poacher, ronquil, and seaperch) represented one species. Both density and biomass on midwater transects are estimates calculated from transect minutes (see text for explanation of the conversion).

Platform	Species	Number	Estimated density (fish/100m^2)	Estimated biomass (kg/m^2)
Irene	Widow rockfish	447	127.25	12.47
	Rockfish YOY	271	78.22	1.36
	Bocaccio	162	46.56	2.73
	Blue rockfish	2	0.85	0.07
	Copper rockfish	2	0.85	0.11
	Pile perch	2	1.14	0.19
	Painted greenling	1	0.57	0.04
	Total	**887**	**255.44**	**16.97**
	Minimum number of species	6		
Hidalgo	Rockfish YOY	647	137.88	1.80
	Widow rockfish	286	50.57	3.62
	Bocaccio	78	19.70	0.29
	Painted greenling	29	8.60	0.28
	Greenspotted rockfish	2	0.71	0.04
	Unident. sculpin	1	0.53	0.03
	Flag rockfish	1	0.46	0.04
	Total	**1044**	**218.46**	**6.10**
	Minimum number of species	6		
Harvest	Widow rockfish	171	39.45	2.51
	Rockfish YOY	102	24.80	0.42
	Bocaccio	43	11.53	0.18
	Painted greenling	36	11.78	0.51
	Unidentified fish	17	5.09	•
	Blacksmith	8	2.27	0.05
	Greenspotted rockfish	5	1.80	0.11
	Cahco rockfish	1	0.55	0.05
	Flag rockfish	1	0.45	0.03
	Total	**384**	**97.72**	**3.87**
	Minimum number of species	7		
Hermosa	Painted greenling	77	21.24	1.06
	Rockfish YOY	63	17.70	1.41
	Widow rockfish	36	11.01	0.99
	Pacific hake	18	3.76	0.20
	Bocaccio	16	4.60	0.38
	Greenspotted rockfish	6	1.94	0.17
	Squarespot rockfish	6	2.67	0.20
	Sebastomus group [1]	4	1.56	0.12
	Blue rockfish	3	1.46	0.16
	Unidentified fish	3	1.45	•
	Copper rockfish	1	0.46	0.08
	Flag rockfish	1	0.46	0.04
	Hallbanded rockfish	1	0.45	0.04
	Sharpchin rockfish	1	0.46	0.04
	Total	**236**	**69.20**	**4.90**
	Minimum number of species	11		
Holly	Rockfish YOY	62	20.22	0.54
	Painted greenling	33	13.75	0.53

continued

Table 6 (continued)

Platform	Species	Number	Estimated density (fish/100m^2)	Estimated biomass (kg/m^2)
Holly continued	Sharpnose seaperch	14	6.22	1.84
	Squarespot rockfish	11	4.02	0.12
	Copper rockfish	8	3.77	0.28
	Blacksmith	4	1.82	0.49
	Gopher rockfish	4	2.13	0.23
	Pile perch	4	2.23	0.99
	Widow rockfish	3	1.80	0.31
	Bocaccio	1	0.57	0.04
	Kelp rockfish	1	0.67	0.34
	Total	**145**	**57.21**	**5.70**
	Minimum number of species	10		
Grace	Widow rockfish	103	28.92	3.90
	Rockfish YOY	76	25.18	0.32
	Chilipepper	25	6.73	0.64
	Sebastomus group[1]	9	4.67	0.25
	Painted greenling	8	3.37	0.16
	Squarespot rockfish	5	1.58	0.18
	Flag rockfish	2	0.88	0.03
	Greenspotted rockfish	2	0.80	0.06
	Swordspine rockfish	2	1.09	0.08
	Calico rockfish	1	0.62	0.04
	Kelp greenling	1	0.54	0.05
	Rosy rockfish	1	0.54	0.07
	Treefish	1	0.54	0.04
	Total	**236**	**75.47**	**5.76**
	Minimum number of species	11		
Gail	Rockfish YOY	48	21.49	0.72
	Flag rockfish	10	4.92	0.40
	Widow rockfish	8	3.77	0.27
	Bocaccio	7	3.07	0.25
	Greenspotted rockfish	3	1.42	0.18
	Painted greenling	2	1.29	0.14
	Unidentified fish	2	1.10	•
	Blue rockfish	1	0.63	0.06
	Total	**81**	**37.69**	**2.00**
	Minimum number of species	6		

[1] *Sebastomus* group may include greenblotched, greenspotted, pinkrose, rosethorn, rosy, starry, or swordspine rockfishes.

alternation of warm- and cold-water conditions that have occurred over millennia (MacCall, 1996).

Previous surveys of rockfishes at the two most inshore platforms of the Santa Barbara Channel, Hilda and Hazel, provide some evidence for the plasticity of rockfish populations in the Santa Barbara Channel. In the late 1950s, Carlisle et al. (1964) found large numbers of bocaccio and olive, copper, and brown rockfishes. Most of these fishes were either YOYs or older juveniles. By 1975, olive and brown rockfishes were still abundant, but bocaccio and copper rockfishes were uncommon (Bascom et al., 1976). In this latter survey, blue rockfish, not reported by Carlisle et al. (1964), were abundant.

Thus, we believe that the relative dearth of juvenile rockfishes around Southern California Bight platforms is not a permanent condition but represents a fluctuating system. It is likely that as oceanographic conditions in the Southern California Bight become more favorable to rockfish recruitment, offshore platforms in the Santa Barbara Channel may well harbor far greater numbers of juvenile rockfishes than at present. In fact, indirect evidence implies that juvenile rockfishes were at one time

far more abundant around southern California platforms. This conclusion comes from observations we made in the mid-1970s, a period of relatively strong juvenile rockfish recruitment off California (Love and Westphal, 1990). During that period, we observed a significant recreational fishery directed at juvenile widow rockfish and bocaccio (and to a certain extent olive and blue rockfishes) at platform Holly, as well as at a number of other Santa Barbara Channel platforms. We estimate that tens of thousands of these YOY and 1- and 2-yr-old fishes were caught over the course of about three years.

The absence or relative rarity of such common nearshore species as kelp bass (*Paralabrax clathratus*), opaleye (*Girella nigricans*), black seaperch (*Embiotoca jacksoni*), and white seaperch (*Phanerodon furcatus*) from the upper waters was particularly striking. This is in contrast to the inshore platforms and reefs of this area that harbor many of these species (Carlisle et al., 1964; Ebeling et al., 1980; Schroeder[3]). A most important cause for the absence of nearshore species is the isolation of these offshore structures; relatively deep water separates them from the mainland. This distance may effectively cut these species off from source populations of many shallow-water species. Thus, it may be difficult for the young of many species to either reach these platforms or become established there. Seaperches are viviparous and produce fully developed

[3] Schroeder, D. 1997. Marine Science Institute, University of California, Santa Barbara, CA 93106. Personal commun.

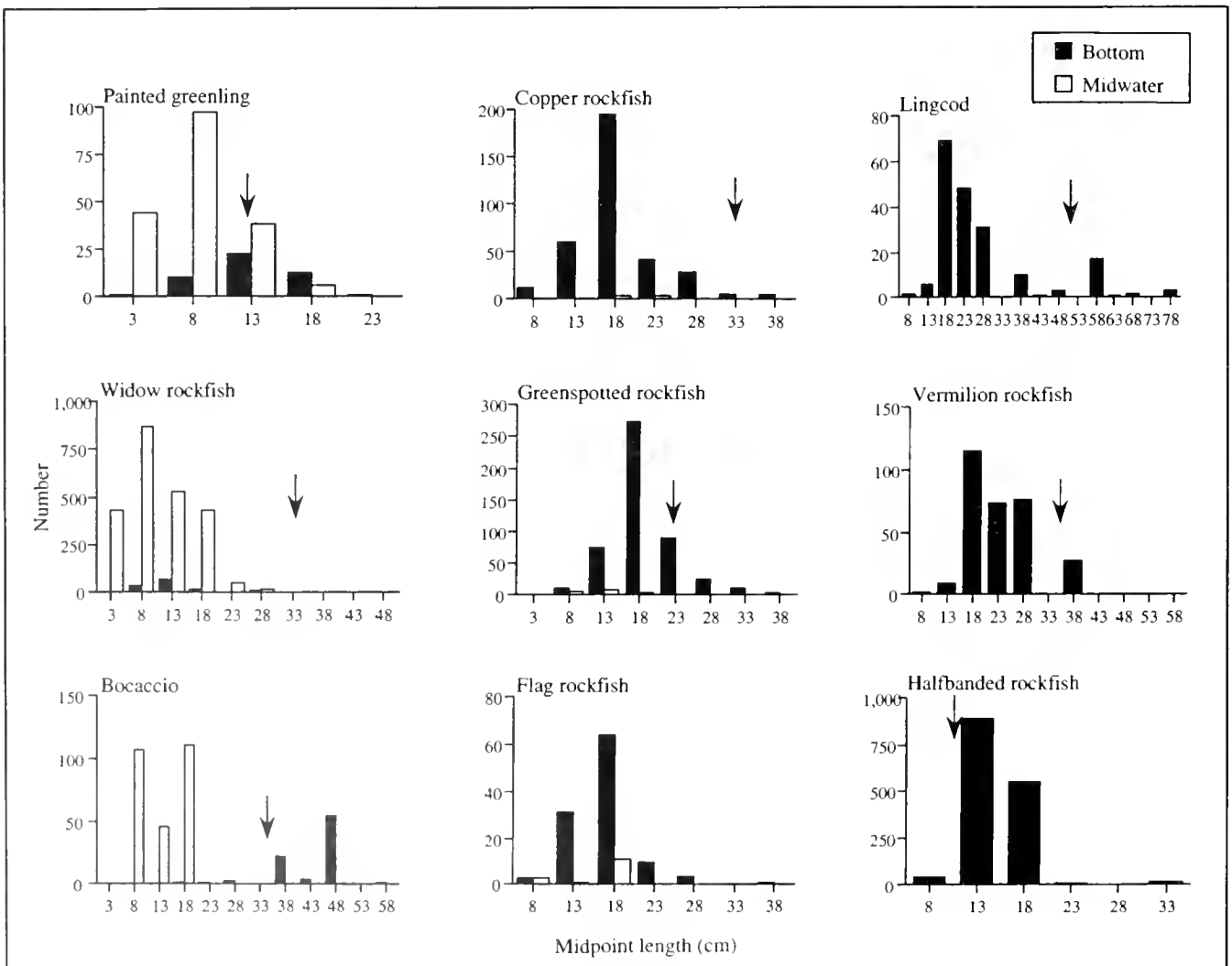

Figure 8

Length-frequency distributions of nine common species on midwater and bottom transects on all platforms combined. Midpoint length is the midpoint of 5-cm length bins.

young that do not disperse widely, making it unlikely that they commonly find their way to platforms. Kelp bass and opaleye produce pelagic larvae and although it is likely that some may settle to the platforms, conditions at these structures may preclude their survival after settlement. Young opaleye seem to require quiet intertidal waters and kelp bass YOY may need algae or thick benthic turf to avoid predation (Carr, 1994; Stephens[4]). Both of these conditions are lacking at platforms. Moreover, in the study area kelp bass recruitment is only sporadic and may not have occurred in the recent past. Thus, strong currents and lack of suitable habitat around platforms may reduce the amount of successful recruitment of these and other nearshore species.

A few species, notably painted greenling, do seem to be well adapted to a substrate-associated life in the midwaters. Judging from the very small individuals we observed, it is likely that larvae of this species recruit directly to the platform and settle out in the shallower portions. We saw a wide range of sizes, from newly settled individuals to adults, sitting on the crossbeams and hanging vertically on the pilings. Other than painted greenling, only a few juvenile flag, greenspotted, copper, swordspine, gopher, and rosy rockfishes were seen sitting on the platform in midwater.

Although juvenile rockfishes dominated the platform midwater, for some species platform bottoms tended to harbor a wider range of life stages. For some rockfishes (such as copper and greenspotted rockfishes), the entire range of stages from YOY to adults were present. In these species, the smaller individuals tended to live somewhat away from the legs and crossbeams and more among those parts of the mussel shell mounds a few meters from the platform. Although juvenile vermilion rockfish were common on several of the shallower platforms, we saw no YOYs around any of these structures. Vermilion rockfish tend to settle out in the nearshore, relatively shallow waters, and it is likely that even the shallowest of the surveyed platforms were situated in waters too deep for successful recruitment. This supposition was born out in our SCUBA diver surveys of platform Gina, located off Port Hueneme, southern California. Platform Gina is located in waters about 33 m deep. Divers have surveyed the entire structure and on several occasions have noted YOY vermilion rockfish at the bottom of the platform.

The situation with lingcod is particularly interesting. Including observations from all platforms, we observed all life stages from YOYs to large adults. However, almost all the young fish lived around platform Irene, in relatively high densities. From the lengths of these animals (Miller and Geibel, 1973), we determined that these fish were either YOYs or one-year-olds. We noted that most were sitting in the mussel shells on the bottom slightly away from the structure. In an underwater survey that encompasses seven platforms and 61 natural reefs in central and southern California, we have never encountered juvenile lingcod densities approaching the levels noted around platform Irene. Similar submersible research farther north, off Big Sur-Monterey (Yoklavich[5]) and Alaska (O'Connell[6]) also implies that such aggregations are very rare. The aggregation around Irene may also be relatively stable because we saw similar high densities in the subsequent 1997 survey. It is unclear what attracts young lingcod to this location. A large juvenile aggregation was noted off Big Sur on a sandy bottom covered with ripple marks (Yoklavich[4]). Perhaps young lingcod seek out substrate with at least some vertical relief and, at Irene, mussel shell mounds provide this type of relief.

Many bottom fishes tended to be patchily distributed around individual platforms. This is particularly true of the aggregating species, such as bocaccio and vermilion and halfbanded rockfishes. Whether this is in response to current pattern, variations in platform structure, or to other parameters is not clear at this point. We have also observed a tendency for small individuals, such as halfbanded rockfish or juvenile greenspotted rockfish, to be found away from larger, presumably predacious, individuals. Smaller fishes also tend to be found farther away from the platform, again probably to avoid the larger fishes nestled in the structure.

Fishing pressure is intense over most of the natural reefs in southern California and platforms may act as refuges for rockfishes and lingcod. An example is the relatively high numbers of bocaccio living around platform Gail. Historically, bocaccio were very important recreational and commercial fish along all of California and owing to a combination of over-fishing and poor juvenile recruitment, their populations have drastically decreased (Ralston et al., 1996). Our survey of the fish assemblages of 61 natural reefs off southern and central California shows that platform Gail has by far the highest density of adult bocaccio of all of these sites (10.5 fish/100 m^2 on platform Gail

[4] Stephens, J. 1997. Department of Biology, Occidental College, 1600 Campus Rd., Los Angeles, CA 90041. Personal commun.

[5] Yoklavich, M. 1997. Pacific Fisheries Environmental Laboratory, National Marine Fisheries Service, 1352 Lighthouse Ave., Pacific Grove, CA, 93950. Personal commun.

[6] O'Connell, T. 1998. Alaska Department of Fish and Game, 304 Lake St., Rm. 103, Sitka, AK, 99835. Personal commun.

compared with 4.4 fish/100 m^2 on the highest density natural reef). The reef was located on the northern side of the passage between San Miguel and Santa Rosa islands. The average density of bocaccio across all natural reefs surveyed in 1996 was only 1.26 fish/100 m^2. The large numbers of bocaccio around Gail may reflect the minimal fishing pressure around this platform. Fishing by recreational or commercial vessels near platforms is generally discouraged by platform operators. In addition, because larger fishes tend to live close to or inside the platforms, they are difficult to catch because the habitat close to or inside the platforms eludes most fishing gear.

We realize that the data presented in this paper represent a "snapshot" in time and thus issues of seasonality or interannual variation in assemblage structure remain to be addressed. Longer-term surveys of the fish fauna on two platforms in the Gulf of Mexico as well as one in the Santa Barbara Channel showed considerable diel and seasonal variation in the number of species present (Carlisle et. al 1964; Hastings et. al. 1975). In addition, monthly SCUBA observations on one shallow-water platform indicate that there may be large temporal changes in assemblage structure (Schroeder[2]). Despite this, the differences we observed in fish assemblages among and within platforms suggest that each platform may have unique characteristics.

There has been considerable discussion regarding the role of artificial structures in aggregation or enhanced production of marine species (or both) (Carr and Hixon, 1997). Based on this study, it appears that oil platforms may serve to do both. First, large adult fishes of several species were present on several platforms where no juveniles of those species had previously been observed, e.g. vermilion rockfish. It appears that those adults may have settled away from the platforms and migrated to them at some life stage. On the other hand, several platforms had very large numbers of very young fish that presumably settled to the platforms directly from the plankton, e.g. widow rockfish. If we assume that some of these young fishes would not have found appropriate settling habitat, then platforms, at least in the short term, do play some role in enhancing production. To ultimately assess the role of platforms in production of reef fishes, it will be necessary to understand the fate of the young fish settling to them.

Acknowledgments

We would like to thank Bob Lea, Mary Nishimoto, Donna Schroeder, Rick Starr, and Mary Yoklavich, all of whom were instrumental in helping us collect data. We would also like to express our appreciation to the crew of the RV *Cavalier*, Douglas Morse, Jonathan Blackman, Don Chesnut, Don Tondro, Nancy Stewart, Erik Kohnhorst, and the pilots of the submersible *Delta*, Chris Ijames, and Dave Slater, for their very professional handling of the technical aspects of this survey. Lyman Thorsteinson was, as always, extremely supportive and we thank him. This research was based on an information need identified by the Minerals Management Service's Pacific OCS Region and funded through the U. S. Geological Survey Biological Resources Division's National Offshore Environmental Studies Program (1445-CA-0995-0386).

Literature cited

Bascom, W., A. J. Mearns, and M. D. Moore.
1976. A biological survey of oil platforms in the Santa Barbara Channel. J. Pet. Tech. 28:1280–1284.

Brink, K. H., and R. D. Muench.
1986. Circulation in the Point Conception-Santa Barbara Channel region. J. Geophys. Res. 91(C1):877–895.

Carlisle, J. G., Jr., C. H. Turner, and E. E. Ebert.
1964. Artificial habitat in the marine environment. Calif. Dep. Fish and Game, Fish. Bull. 124, 93 p.

Carr, M. H.
1994. Effects of macroalgal dynamics on recruitment of a temperate reef fish. Ecology 75:1320–1333.

Carr, M. H., and M. A. Hixon.
1997. Artificial reefs: the importance of comparisons with natural reefs. Fisheries 22:28–33.

Ebeling, A. W., R. J. Larson, W. S. Alevizon, and R. N. Bray.
1980. Annual variability of reef-fish assemblages in kelp forests off Santa Barbara, California. Fish. Bull. 78:361–77.

Hastings, R. W., Ogren, L. H., and M. T. Mabry.
1975. Observations on the fish fauna associated with offshore oil platforms in the Northeastern Gulf of Mexico. Fish. Bull. 74:387–402

Hickey, B. M.
1992. Circulation over the Santa Monica-San Pedro basin and shelf. Prog. Oceanog. 30:37–115.

Holbrook, S. J., and R. J. Schmitt.
1996. On the structure and dynamics of temperate reef fish assemblages—are resources tracked? *In* M. L. Cody and J. A. Smallwood (eds.), Long-term studies of vertebrate communities, p. 19–48. Academic Press, San Diego, CA.

Love, M. S., J. Caselle, and K. Herbinson.
1998. Declines in nearshore rockfish recruitment and populations in the southern California Bight as measured by impingement rates in coastal electrical generating stations. Fish. Bull. 96:492–501.

Love, M. S., J. Hyland, A. Ebeling, T. Herrlinger, A. Brooks, and E. Imamura.
1994. A pilot study of the distribution and abundances of rockfishes in relation to natural environmental factors and an offshore oil and gas production platform off the coast of southern California. Bull. Mar. Sci. 55:1062–1095.

Love, M. S., and W. Westphal.
1990. Comparison of fishes taken by a sportfishing party vessel around oil platforms and adjacent natural reefs near Santa Barbara, California. Fish. Bull. 88:599–605.

MacCall, A. D.
1996. Patterns of low-frequency variability in fish populations of the California Current. Calif. Coop. Oceanic Fish. Invest. Rep. 37:100–110.

Miller, D. J., and J. J. Geibel.
1973. Summary of blue rockfish and lingcod life histories; a reef ecology study; and giant kelp, *Macrocystis pyrifera*, experiments in Monterey Bay, California. Calif. Dep. Fish Game, Fish Bull. 158, 137 p.

Ralston, S., J. N. Ianelli, R. A. Miller, D. E. Pearson, D. Thomas, and M. E. Wilkins.
1996. Status of bocaccio in the Conception/Monterey/Eureka INPFC areas in 1996 and recommendations for management in 1997, Appendix B. *In* Status of the Pacific Coast groundfish fishery through 1996 and recommended acceptable biological catches for 1997, stock assessment and fishery evaluation, p. 1–48. [Available from Pacific Fisheries Management Council, 2130 SW 5th Ave, Suite 224, Portland, OR 97201.]

Roemmich, D., and J. McGowan.
1995. Climatic warming and the decline of zooplankton in the California Current. Science (Wash. D.C.) 267:1324–1323.

Shannon, C. E., and W. Weaver.
1949. The mathematical theory of communication. Univ. Illinois Press, Urbana, IL, 117 p.

Stephens, J. S. Jr., P. A. Morris, D. J. Pondella, T. A. Loonce, and G. A. Jordan.
1994. Overview of the dynamics of an urban artificial reef fish assemblage at King Harbor, USA, 1974–1991: a recruitment driven system. Bull. Mar. Sci. 55:1224–1239.

Stephens, J. S. Jr., P. A. Morris, K. Zerba, and M. Love.
1984. Factors affecting fish diversity on a temperate reef: the fish assemblage of Palos Verdes Point, 1975–1981. Env. Biol. Fish. 11:259–275.

Spawning site fidelity in Atlantic bluefin tuna, *Thunnus thynnus*: the use of size-frequency analysis to test for the presence of migrant east Atlantic bluefin tuna on Gulf of Mexico spawning grounds

David Nemerson
National Audubon Society
550 South Bay Avenue
Islip, New York 11751
Present address: Marine Field Station
Institute of Marine and Coastal Sciences
Rutgers University
132 Great Bay Boulevard
Tuckerton, New Jersey 08087-2004
E-mail address: nemerson@imcs.rutgers.edu

Steven Berkeley
Oregon State University
Hatfield Marine Science Center
Oregon State University
Newport, Oregon

Carl Safina
National Audubon Society
550 South Bay Avenue
Islip, New York 11751

Abstract.—The Gulf of Mexico is the only known spawning area for bluefin tuna (*Thunnus thynnus thynnus*) in the western Atlantic. Although it is known from tag recaptures that eastern Atlantic bluefin tuna travel to the western Atlantic, whether or not these fish spawn in the western Atlantic is of critical importance in interpreting the significance of this movement. East Atlantic bluefin tuna mature at a younger age (4–5 yr) and smaller size (45 kg) than western bluefin tuna (8 yr and 135 kg), and tag recaptures indicate that some young fish make the trans-Atlantic swim. Thus the presence of small (<135 kg) bluefin tuna in the Gulf of Mexico during spawning season would constitute evidence that bluefin tuna of east Atlantic origin spawn in the west. We used size-frequency analysis to test the hypothesis that Atlantic bluefin tuna of eastern and western origins mingle on the Gulf of Mexico spawning grounds. We created a simple model to estimate the proportion of small eastern spawning fish that should be found in the Gulf of Mexico catch, assuming a 2% east-to-west transfer rate and complete mixing of eastern and western fish. Using conservative assumptions, the model predicts that between 5% and 10% of the bluefin tuna catch in the Gulf should consist of fish that are less than 135 kilograms in weight, and thus are presumably eastern migrants. We analyzed Gulf of Mexico catch records from 1980 to 1992 for the presence of bluefin tuna less than 135 kg. These small fish represented from 0% to 0.9% of the catch annually, and only 0.3% for the entire period. We conclude that eastern migrant tuna do not mix completely, if at all, with western bluefin tuna on the Gulf of Mexico spawning grounds.

Manuscript accepted 1 December 1998.
Fish Bull. 98:118–126 (2000).

Atlantic bluefin tuna (*Thunnus thynnus thynnus*) is a highly migratory pelagic species that ranges throughout the Atlantic between 60°N latitude and the equator, although it has not been encountered south of 20°N since the 1960s. Two bluefin tuna breeding sites are known in the North Atlantic: the Gulf of Mexico and the Mediterranean Sea. No other regular spawning site has been identified in the North Atlantic (Richards, 1976; McGowan and Richards, 1989; NRC, 1994). Intensive fisheries exist for bluefin tuna along the North American and European coasts, and to a lesser degree in the high seas of the North Atlantic. Although fish tagged on both sides of the ocean have been recovered on the side opposite from their release, it is not known if bluefin tuna return to their natal spawning ground to reproduce (Turner and Powers, 1995; Cooke and Lankester, 1996). This question is of utmost importance in evaluating the significance of trans-Atlantic movement and the scale at which management must operate to be effective.

The behavior of trans-Atlantic migrating bluefin tuna is unknown, but the possibilities are bounded by two extremes. At one extreme, an emigrant may join the population on the side of the ocean to which it migrates, becoming indistinguishable from the population it joins with respect to the probability, timing, and locale of future life history events, such as maturation, spawning, and migration. At the other extreme, a migrant may always return to its natal side prior to the next spawning season.

These two extremes, and the terms used to describe them, have been the subject of some confusion in the bluefin tuna literature. The permanent transfer of individuals from one side of the Atlantic to the other has been called the "no-memory condition" (Punt and Butterworth, 1995; Powers and Cramer, 1996) or the "diffusion model" (Cooke and Lankester, 1996). The case where migrants always return to their natal side prior to the next spawning season is termed the "overlap model" by Cooke and Lankester (1996). We follow the convention of Cooke and Lankester (1996) and use the terms diffusion and overlap to refer to the two models. We use "transfer rate" to refer to the permanent transfer of an emigrant from one population to the other and "migration rate" to refer generally to the trans-Atlantic movement of individuals. Finally, we use the term "memory" to refer only to an individual's behavior with respect to spawning location, not to other life history attributes. That is, under the diffusion (no-memory) model, a migrant will spawn on the side of the ocean to which it migrates, regardless of its birth location, but will retain other life history attributes such as size or age at maturity.

The permanent transfer of individuals can be considered a migration for dispersal (Greenwood and Harvey, 1982), whereas the overlap model can be assumed to be a feeding migration, and is free of implications for reproductive mixing. One can envision intermediate scenarios combining varying degrees of memory, or philopatry. For example, migrants may remain on the opposite side for a period of years, while either participating in or foregoing spawning, before ultimately returning to their natal side. Furthermore, some migrants may exhibit spawning site fidelity while others may stray, joining previously established spawning populations (e.g. Curry, 1994).

Simulation models have shown that the dynamics of the two populations are potentially very sensitive to even low trans-Atlantic migration rates, particularly for east-to-west transfer (NRC, 1994; Porch et al., 1995; Punt and Butterworth, 1995; Powers and Cramer, 1996) because the average size of the eastern population has been about 6 to 13 times that of the western population over the past 20 years (ICCAT[1,2]; Fig. 1). Recent spawning biomass estimates for the western population are based on

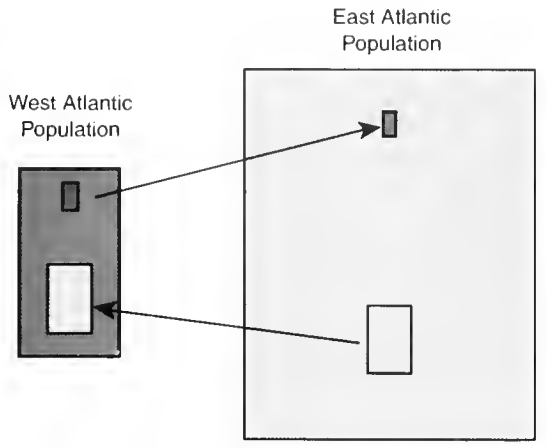

Figure 1

Representation of the effect of migration on the eastern and western populations of bluefin tuna. Migration from the larger eastern population to the west has a larger effect on the western population than does migration from the smaller western population to the east. In this schematic, the eastern population is about six times the size of the western population, and the migration rates are about 1% in each direction.

catches throughout the fishing area, which includes the entire North Atlantic west of 45°W longitude. If fish of eastern origin are included in these catch statistics but do not spawn in the west Atlantic, then western spawning biomass will be substantially overestimated (Powers and Cramer, 1996; American Fisheries Society[3]).

Determining the spawning site fidelity of iteroparous pelagic species that occur over a wide area of open ocean is difficult. Population differentiation can be inferred from tag-return data, comparisons of life history parameters and morphometric characters, or from genotypic variation. Several studies have attempted to analyze the population structure of Atlantic bluefin tuna with these methods (Calaprice, 1986; NRC, 1994; Cooke and Lankester, 1996).

Several investigators have reviewed and analyzed trans-Atlantic tag returns to estimate rates of migration (NRC, 1994; Punt and Butterworth, 1995; Turner and Powers, 1995; Cooke and Lankester, 1996). These studies have estimated annual migration rates of between 1% and 10% and have considered both diffusion and overlap models. Generally, these studies have sought to find interpretations of tag-return data that agree best with other estimates of population size.

[1] ICCAT (International Commission for the Conservation of Atlantic Tunas). 1994a. West Atlantic bluefin tuna. Biennial report of the ICCAT Standing Committee on Research and Statistics, 41 p. ICCAT, Estebanez Calderon 3, E-28020, Madrid, Spain.

[2] ICCAT (International Commission for the Conservation of Atlantic Tunas). 1994b. East Atlantic bluefin tuna. Biennial report of the ICCAT Standing Committee on Research and Statistics, 31 p. ICCAT, Estebanez Calderon 3, E-28020, Madrid, Spain.

[3] American Fisheries Society. 1995. Marine Fisheries Section statement on bluefin tuna, 2 p. Am. Fish. Soc., 5410 Grosvenor Lane, Ste. 110, Bethesda, MD 20814-2199.

Punt and Butterworth (1995) estimated west-to-east transfer at about 7% and east-to-west transfer at about 1.5–3%, assuming a diffusion model. They also state that the higher end of the range (3%) suggests a far larger size for the western population than do models that assume no migration. Cooke and Lankester (1996) test both diffusion and overlap models and concluded that the overlap model fits the data better. Under that model, they estimated exchange rates at 7.3% east-to-west and 9.8% west-to-east, but with no statistical difference between the two. Powers and Cramer (1996) examined the implications of a range of migration rates and degrees of spawning site fidelity. Although they made no conclusions about which scenario is most likely, they pointed out the extreme sensitivity of the results to the assumptions.

Eastern and western Atlantic bluefin tuna populations have markedly different life history parameters (Turner, 1994). The western population spawns from mid-April to mid-June (Richards, 1976). Western bluefin tuna sometimes mature as early as age 6 and are considered fully mature by age 8, at a weight of 135 kg (Baglin, 1982; NRC, 1992). The eastern population spawns from June through August (Dicenta and Piccinette, 1980) and matures at an earlier age and smaller size than the western population. Eastern bluefin tuna mature as early as age 3, at a weight of 15 kg (Rodriguez-Roda, 1967; Baglin, 1982), and are fully mature by age 5 (Rodriguez-Roda, 1967; Baglin, 1982; ICCAT[2]).

The contrast in size and age at maturity of western and eastern Atlantic bluefin tuna allows an inferential test of spawning site fidelity. Because the Gulf of Mexico is the only known spawning ground for western Atlantic bluefin tuna, and the vast majority of fish collected in the Gulf are large adults that are present only during and just prior to the spawning season (January–June), we assumed that all bluefin tuna in the Gulf during this time period are there to spawn.

If eastern Atlantic bluefin tuna that migrate to the west mature according to the eastern Atlantic maturation schedule, then the size distribution of bluefin tuna in the Gulf of Mexico should reveal the presence of eastern migrants within the western spawning population. Finding small fish (<135 kg) on the Gulf of Mexico spawning grounds would support the diffusion hypothesis and suggest that trans-Atlantic migrants from the east mix with western fish during spawning. In contrast, the absence of small fish on the Gulf of Mexico spawning grounds would imply that eastern migrants do not spawn in the west, supporting the overlap model and indicating strong spawning site fidelity. We know that small bluefin tuna from the east Atlantic swim west at least occasionally. All tagged eastern Atlantic bluefin tuna recaptured in the west have been small fish (n=19, all captured outside the Gulf), although very few large fish, and relatively few bluefin tuna overall, have been tagged in the east, compared with tagging in the west (NRC, 1994).

Methods

We analyzed the size distribution of bluefin tuna caught in the Gulf of Mexico prior to and during the spawning season (the only time of year when bluefin tuna are present in the Gulf) for fish between the known size of first breeding in the Mediterranean and the known size of first breeding for west Atlantic bluefin tuna. Any individuals smaller than the known size of first spawning in the west would presumably be of eastern Atlantic origin.

A weight-frequency distribution (WFD) of bluefin tuna on the Gulf spawning grounds was constructed by using data reported to National Marine Fisheries Service (NMFS) by the commercial fishing industry operating in the Gulf. This data set included the weight and date of capture for every bluefin tuna legally caught and landed in the Gulf. We used data from 1980 through 1992, because beginning in 1993 only bluefin tuna over 178 centimeters (70 inches) fork length were legally permitted to be retained and sold.[4]

To estimate the proportion of smaller eastern spawning fish expected at a given east-to-west annual transfer rate (i.e. fish remain with the western population), we created a simple model of the number of sexually mature eastern migrants that arrive in the west each year:

$$S^E_y = \sum P_a T^E N^E_{a,y},$$

where S^E_y = the number of age-7 or younger spawning fish of eastern origin arriving in year y;
P_a = the percentage of sexually mature adults in eastern age class a;
T^E = the east-to-west transfer rate; and
$N^E_{a,y}$ = the number in eastern age class a in year y.

East-to-west transfer was modeled as an instantaneous process that occurs prior to the spawning season. The parameter P was taken from the lit-

[4] National Marine Fisheries Service. 1995. Supplemental draft environment impact statement for a regulatory amendment for the western Atlantic bluefin tuna. U.S. Dep. Commer., NMFS, NOAA, Silver Spring, MD, 131 p.

erature, and is 0 for ages 0–3, 0.5 for age 4, and 1 for ages 5 and beyond (Baglin, 1982; ICCAT[2]). We assumed that any migrant of age 8 or greater would be the same size as western spawning fish and would not be distinguishable from western spawning fish of the same size (Cort, 1991; Turner et al., 1991; Table 1). We used a transfer rate T of 2% per year, east-to-west. This rate is at the low range of published estimates. In this initial test, we did not consider fish less than age 4 that could have migrated to the west as immature fish in prior years and then reached age 4 and maturity in the current year. Thus, our estimate of the expected number of spawning fish of eastern Atlantic origin in the western Atlantic should represent a minimum estimate and provide a conservative test for the presence of eastern migrants. $N^{E}_{a,y}$ was taken from yearly age-specific population estimates supplied by NMFS from a run of the ADAPT virtual population analysis (VPA) program with 2% east-to-west and a 1% west-to-east transfer rates, assuming no memory. Note that the population estimates from this VPA run resulted in poor fits to the indices of abundance used to tune the VPA.[5] We used these population estimates because they provided a conservative test of our assumptions.

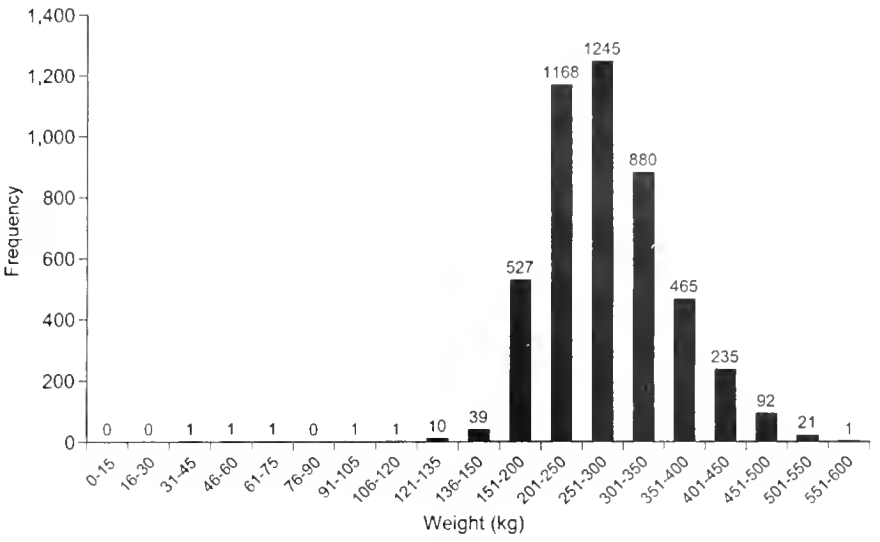

Figure 2

Weight-frequency distribution of bluefin tuna caught in the Gulf of Mexico between 1980 and 1992. The numbers over the bars indicate the total number of fish caught in the weight interval indicated.

Table 1

Estimated length at age for eastern (Cort, 1991) and western (Turner et al., 1991) Atlantic bluefin tuna.

	Length (cm)	
Age (yr)	East	West
1	53.4	48.6
2	77.0	73.8
3	98.4	97.0
4	118.0	118.5
5	135.8	138.4
6	152.1	156.8
7	166.9	173.7
8	180.4	189.4

Results and discussion

Bluefin tuna smaller than the accepted size at first spawning of western fish are very rare in the Gulf. Catches of fish less than 135 kg ranged from 0% to 0.9% of annual catch from 1980 to 1992 and averaged 0.3% over the entire period (Table 2). A complete weight frequency distribution is presented in Figure 2.

These percentages are not consistent with the low end of published migration rate estimates under the diffusion model. That is, if 2% of each age class migrated from east to west and joined the western population, we would expect to see many more small fish, i.e. fish of eastern origin, spawning in the west. (Recall that the diffusion, or no-memory model, implies that the migrant does not "remember" its natal spawning ground but does "remember" its maturation schedule.) The model predicts that between 8483 and 14,655 sexually mature migrants smaller than 135 kg would have arrived each year in 1980–92. We compared these numbers with the numbers of sexually mature fish estimated for the west from the

[5] Porch, C. 1995. National Marine Fisheries Service, Southeast Fisheries Science Center, 75 Virginia Beach Drive, Miami, FL 33149. Personal commun.

Table 2

Comparison of the number and proportion of spawning fish less than 135 kg actually caught in the Gulf of Mexico from 1980 to 1992 and predictions on the basis of a hypothesized 2% annual trans-Atlantic transfer rate. The number of small spawning fish observed is significantly less than the predicted number (χ^2=353, P<0.0001). Data in columns 2 and 3 from NMFS ADAPT VPA with 2% east-to-west and 1% west-to-east transfer rates and no memory; columns 4 and 5 are unpublished data, NMFS.

Year	Western population age 8 or greater	Predicted migrant spawning fish	Number of bluefin tuna <135 kg caught in the Gulf	Total bluefin tuna caught in the Gulf	Actual proportion of catch in the Gulf <135 kg	Predicted proportion of catch in the Gulf <135 kg
1980	97,824	10,745	0	19	0	0.099
1981	97,698	9,732	0	255	0	0.091
1982	88,781	9,402	0	228	0	0.096
1983	96,739	8,483	0	316	0	0.081
1984	92,440	8,691	0	320	0	0.086
1985	83,659	10,623	0	429	0	0.113
1986	89,444	13,151	1	395	0.003	0.128
1987	106,182	14,561	3	474	0.006	0.121
1988	117,440	14,655	3	516	0.006	0.111
1989	134,585	13,035	1	273	0.004	0.088
1990	167,115	10,631	4	469	0.009	0.060
1991	191,036	8,525	1	596	0.002	0.043
1992	260,192	9,436	1	399	0.003	0.035

ADAPT VPA run supplied by NMFS (Table 2). Table 2 shows that, if the no-memory assumption is correct and the trans-Atlantic transfer rate is at least 2%, we would expect about 5% to 10% of fish spawning in the west to be smaller than 135 kg. (Note that for this comparison to be valid, either all mature fish in the west and all small migrant spawning fish must go to the Gulf of Mexico to spawn or the same proportion of each group must go there each year.) In fact, only 0% to 0.3% of fish on the Gulf spawning grounds between 1980 and 1992 weighed less than 135 kg (Fig. 3), significantly less than predicted (χ^2=353, P<0.0001). Of 4688 fish for which NMFS has recorded weights, 15 were less than 135 kg, and 10 of those were between 120 and 135 kg (Fig. 2).

Note that this analysis considered only newly arrived migrants each year, and ignored the possible accumulation of sexually mature migrants from previous years that had not yet reached 135 kg. The continued presence of prior migrants would have raised the expected number of small spawning fish. Even without the cumulative effect of small migrants, the actual proportion of small spawning fish in the Gulf catch was about 5–10% of that predicted by the model with a 2% transfer rate. Higher transfer rates would imply that even greater numbers of small spawning fish should appear in the Gulf.

It is clear from our results that small bluefin tuna are not present among spawning fish in the Gulf of Mexico in the numbers that would be expected for even the lowest of hypothesized trans-Atlantic transfer rates. Our interpretation is that young adult bluefin tuna of eastern origin seldom or never spawn in the Gulf of Mexico and presumably do not contribute significantly to the spawning biomass of the western population. There are at least three possible alternatives: 1) eastern migrants may either delay spawning in the west until they reach 135 kg or remain in the east until they reach 135 kg, making them indistinguishable from western spawning fish; 2) migrant eastern tuna may be spawning in the west but not in the Gulf of Mexico; or 3) small migrants may be spawning in the Gulf but are avoiding detection or are being under-reported.

Size and age at maturity

If size and age at maturity are environmentally determined, then eastern migrants might follow the west Atlantic maturity schedule and thus be undetected with our methods. For example, changes in size and age at maturity may be a response to differences in interspecific or intraspecific population density. A lower population density reduces competition for food and increases per capita food intake, resulting in faster growth. When experiencing such low inter- or intraspecific population densities and enhanced growth, fish may mature at about the same size but would attain this size at a younger age (Trippel, 1995). However, for bluefin tuna, the reported dif-

ference in size and age at maturity between east and west Atlantic populations does not appear related to differences in growth rate because recent growth models indicate little difference between populations (Cort, 1991; Turner et al., 1991; Table 1).

Similarly, if differences in age or size at maturity are affected by environmental conditions, for example temperature, we would expect this effect to be manifested primarily by changes in growth rate. Again, the similarity in growth rate between east and west Atlantic bluefin tuna suggests that environmental conditions are unlikely to explain the difference in size and age at maturity.

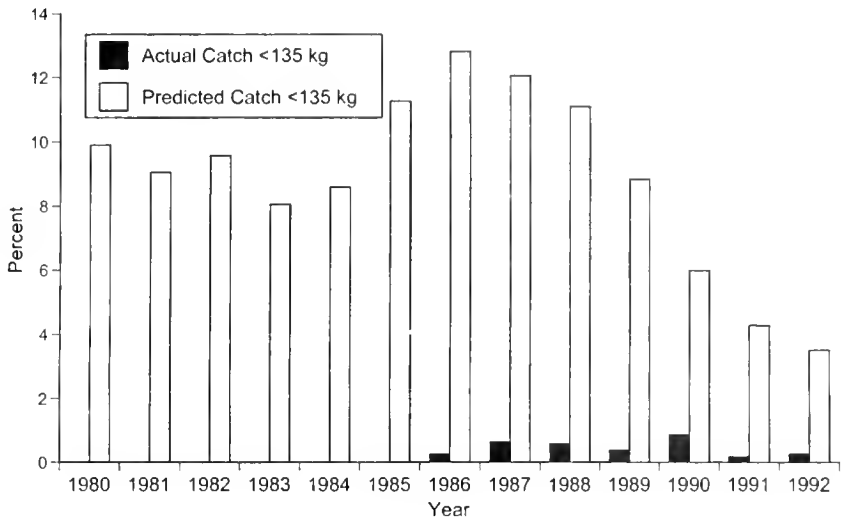

Figure 3

Comparison of actual catch of bluefin tuna less than 135 kg in the Gulf of Mexico between 1980 and 1992 and catch predicted with a 2% annual eat-to-west transfer rate and the diffusion model.

Alternatively, if age at maturity is a heritable trait, then a long period of size-selective fishing mortality could shift genotype frequencies in the population because few late-maturing fish are likely to survive to reproduce (Trippel, 1995), resulting in a younger age or smaller size at maturity, or both (Policansky, 1993; Trippel, 1995). Experiments with guppies indicate that increased mortality (as through fishing) selects for earlier maturity at smaller size (Reznick, 1993). Bluefin tuna in the east Atlantic has a longer history of exploitation and a much larger population than west Atlantic bluefin tuna. Assuming that the very large difference in population sizes results in a comparable difference in stock density, then an eastern bluefin tuna with a genetic propensity to mature at or before age 5 in the east Atlantic should, upon migrating to the west Atlantic, find itself in a relatively resource-rich, lower-density environment, which should certainly not delay maturation or inhibit spawning. Thus, although genetic effects are difficult to establish, such a large difference in size and age at maturity as between east and west Atlantic bluefin tuna is unlikely to be a result of density-dependent or environmental differences. Further, it seems unlikely that a sexually mature five- or six-year-old east Atlantic bluefin tuna would revert to immaturity upon migrating to the west Atlantic, and then remain immature for two or three years until finally spawning at age eight.

Another possible explanation for these results is that the size-at-maturity data on which this analysis depends are incorrect. In fact, Clay (1990) criticized both the Baglin (1982) and Rodriguez-Roda (1967) studies, citing small sample sizes and inadequate temporal and spatial coverage. As Clay (1990) pointed out, the Rodriguez-Roda (1967) study dealt with fish that were on their way to the spawning grounds and thus may have over-estimated the percentage of small, mature fish in the total population. Although this is a valid criticism, it is worth noting that the collection of Rodriguez-Roda also contained immature fish, implying that not all fish in his sample were on their way to the spawning grounds.

Further, although our method clearly relies on the assumption that bluefin tuna of eastern origin first spawn at a smaller size than western fish, only a small proportion of age classes 4 through 7 need be mature for our results to prevail. We investigated the sensitivity of our model to a ten-fold reduction in the maturity parameter P (i.e. to 0.05 on age-4 and 0.1 on ages 5 through 7) and found that small bluefin tuna would still be significantly rarer (chi-square test, $P<0.005$) in the Gulf than predicted under the diffusion model with a 2% east-to-west transfer rate, given our assumptions.

Finally, for the purpose of this study, we have made the most conservative assumption, i.e. that any bluefin tuna (except larvae) found in the Gulf of Mexico is spawning. Thus, it is possible that some of the smaller bluefin tuna in the Gulf of Mexico landing records were not actually spawning fish, or were of west Atlantic origin, or both.

Alternative spawning grounds

Our results might also be otabined if small migrant tuna of eastern origin spawn elsewhere in the west other than the Gulf of Mexico. A recently discovered concentration of medium and large tuna off the coast of North Carolina from January through April caused speculation that perhaps this concentration represents another spawning area. However, the lack of gonad development in a sample of seventeen fish (weighing between 65 and 183 kg) suggested that these fish were unlikely to spawn in the year they were captured and were probably immature (Belle[6]).

Several other workers have searched for evidence of bluefin tuna spawning in the west Atlantic. Mather et al. (1995) reported finding ripening small fish but no larvae. If the overlap hypothesis does prevail, then these potentially mature but nonspawning smaller fish may be eastern migrants that although capable of spawning, will return to the Mediterranean before actually doing so. McGowan and Richards (1989) reported on the sporadic presence of larvae in the Gulf Stream as far north as North Carolina but concluded that most larvae found in the Gulf Stream were either advected out of the Gulf or spawned by tuna exiting the Gulf. Furthermore, they stated that conditions are poor for larval development in the Gulf Stream and that the occasional occurrence of larvae there does not indicate an additional spawning ground. On the matter of alternative spawning grounds, the National Research Council concludes that "extensive searching has detected only two spawning localities: the Gulf of Mexico and the Mediterranean Sea" (NRC, 1994, p. 18).

Underreporting or low catchability

Two other possibilities for the lack of small bluefin tuna in the Gulf of Mexico catch are that they are present in the Gulf of Mexico and are either being caught but not recorded, or are not being caught owing to a lack of appropriate fishing effort. To test for the first possibility, we acquired records of all bluefin tuna recorded by longline observers in the Gulf of Mexico during 1993–95. Of 31 bluefin tuna recorded by observers for which actual or estimated weights were recorded, all were greater than 135 kg. We also reviewed ICCAT data for the Japanese longline fishery in the Gulf of Mexico for the period 1973 to 1981 and found that only 58 records out of 14,530 (0.4%) were for fish under 180 cm (135 kg). These data are particularly significant in light of the fact that there were no regulations concerning the retention and sale of small bluefin tuna during this period as there have been in recent years. Therefore, the Japanese would have had no incentive to intentionally misidentify or underreport small bluefin tuna. Mather et al. (1995), after reviewing longline catches in the Gulf and Caribbean prior to 1973, found only fish larger than 185 cm. They also reported very young bluefin tuna (less than 2 kg) in the Gulf of Mexico from July into November (Mather et al., 1995); fish presumably spawned a few months earlier. Similarly, Hisada and Suzuki (1982) presented length-frequency distributions of Japanese longline catches from the Gulf of Mexico which appear to show essentially no fish smaller than 200 cm.

The possibility that small bluefin tuna are present in the Gulf but are not being caught cannot be completely eliminated. However, there is a considerable accumulation of evidence that suggests that this is highly unlikely. For example, although there currently is no directed fishery for either small or large bluefin tuna in the Gulf, there is a widespread, yearround yellowfin tuna (*Thunnus albacares*) longline fishery. This fishery targets yellowfin tuna of the same size as the small bluefin tuna of east Atlantic origin that we hypothesize would be present in the Gulf if the diffusion model is correct. This fishery does have a bycatch of bluefin tuna, none of which have ever been recorded by observers as less than 175 cm.[7]

Furthermore, longline operations in the northwest Atlantic do catch small bluefin tuna, indicating that they are potentially vulnerable to this gear. Cramer and Turner[8] reported length frequencies for observer data from the U.S. longline fishery in the northwest Atlantic from 1992 to 1995, showing that over 30% of fish hooked were less than 150 cm straight fork length (Fig. 4). Similarly, catch data from the Japanese northwest Atlantic longline fishery in the 1970s and 1980s show that the catch dominated by bluefin tuna between 100 and 150 cm in several years (Fig. 8 in Hisada and Suzuki, 1982). Although failure to catch a given species or size class in an area can never rule out its presence, given the extent and diversity of fishing activity in the Gulf, it is unlikely that any significant aggregation of small bluefin tuna

[6] Belle, S. 1996. Biological sampling of bluefin tuna off Cape Hatteras, North Carolina Final report to the New England Aquarium Corporation (NOAA requisition no. 43AANF503279), Boston, MA, 12 p.

[7] Lee, D. 1996. National Marine Fisheries Service, Southeast Fisheries Science Center, 75 Virginia Beach Drive, Miami, FL 33149. Personal commun.

[8] Cramer, J., and S. C. Turner. 1996. Standardized catch rates for bluefin tuna, *Thunnus thynnus*, from the U.S. pelagic longline fishery in the northwest Atlantic. ICCAT working document SCRS/96/69.

there would have been entirely missed.

Finally, we tested the sensitivity of our results to a range of selectivities of longline gear set in the Gulf of Mexico. With selectivities on fish smaller than 135 kg ranging from 0 to 1 (where the selectivity on fish greater than 135 kg is 1), the sensitivity analysis indicated that at selectivities greater than about 0.13, small fish were significantly less abundant (chi-square test, $P<0.05$) in the catch in the Gulf than would be expected given our assumptions and a 2% east-to-west transfer rate.

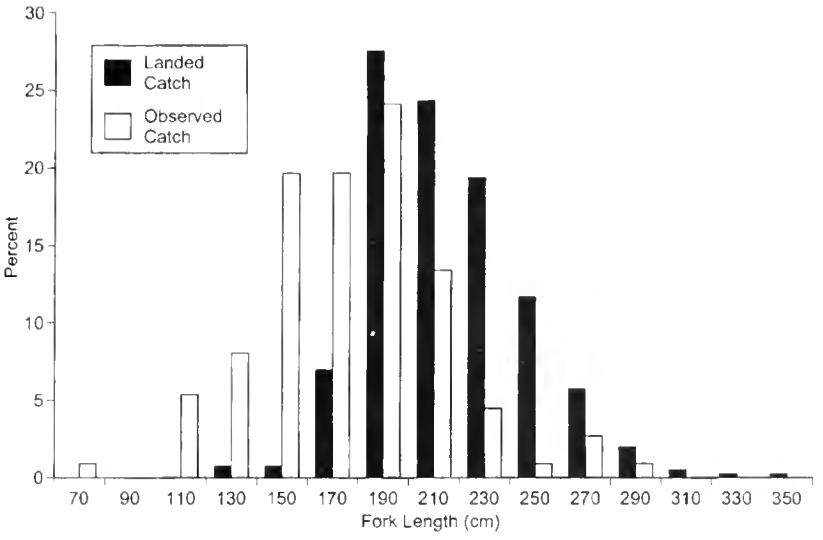

Figure 4

Length-frequency distributions of bluefin tuna caught on longlines in the northwest Atlantic (landings, n=403) and measured by observers on longline vessels (observer, n=112) between 1992 and 1995 (see Footnote 7 in the main text).

Future research on this topic must seek to address both the annual rate of trans-Atlantic movement as well as the degree of philopatry exhibited by migrants to achieve a full understanding of the population dynamics of east and west Atlantic bluefin tuna. Currently, there are studies underway to identify nuclear and mitochondrial DNA markers that may have variations specific to east and west populations (Graves et al., 1995). Examinations of otolith chemistry (microconstituent analysis) may provide information on stock differentiation and mixing rates, and researchers are currently deploying archival tags on bluefin tuna caught in the west Atlantic, primarily off Cape Hatteras, North Carolina.[9,10] These tags will record geolocation data and, if recovered, should yield a complete record of each fish's movement since its release. Finally, additional studies on the maturation schedules of fish in the east and west are still needed.

Clearly, it will take years before these studies yield sufficient information on transfer rates and philopatry to provide robust management advice. The depleted state of bluefin tuna populations worldwide, and in the west Atlantic particularly (Safina, 1993), make these issues of considerable practical importance. Until such time as these questions are answered definitively we believe that spawning site fidelity should be assumed and the stocks managed accordingly.

[9] Prince, E. 1996. National Marine Fisheries Service, Southeast Fisheries Science Center, 75 Virginia Beach Drive, Miami, FL 33149. Personal commun.

[10] Block, B. 1997. Hopkins Marine Station, Stanford University, Oceanview Boulevard, Pacific Grove, CA 93950-3094. Personal commun.

Acknowledgments

We would like to thank Clay Porch and Dennis Lee of the Southeast Fisheries Science Center, National Marine Fisheries Service, for kindly providing assistance in acquiring the data sets that made this paper possible.

Literature cited

Baglin, R. E.
1982. Reproductive biology of western Atlantic bluefin tuna. Fish. Bull. 80:121–134.

Calaprice, J. R.
1986. Chemical variability and stock variation in northern Atlantic bluefin tuna. ICCAT Coll. Vol. Sci. Pap. 24(2): 222–254.

Clay, D. (ed.).
1990. Atlantic bluefin tuna (*Thunnus thynnus* (L.)): a review. *In* World bluefin tuna meeting, May 25–31, La Jolla, CA, p. 89–180.

Cooke, J. G., and K. Lankester.
1996. Examination of alternative stock distribution models for the interpretation of bluefin tuna (*Thunnus thynnus*) tag-recovery data. ICCAT Coll. Vol Sci. Pap. 45(2):135–138.

Cort, J. L.
1991. Age and growth of the bluefin tuna, *Thunnus thynnus* (L.) of the northeast Atlantic. ICCAT Coll. Vol. Sci. Pap. 35(2):213–230.

Curry, P.
1994. Obstinate nature: an ecology of individuals. Thoughts on reproductive behavior and biodiversity. Can. J. Fish. Aquat. Sci. 51(7):1,664–1,673.

Dicenta, A., and C. Piccinetti.
1980. Comparison between the estimated reproductive stocks of bluefin tuna (*Thunnus thynnus*) of the Gulf of Mexico and western Mediterranean. ICCAT Coll. Vol. Sci. Pap. 9:442–448.

Graves, J. E., J. R. Gold, B. Ely, J. M. Quattro, C. Woodley, and J. M. Dean.
1995. Population genetic structure of bluefin tuna in the north Atlantic ocean. I. Identification of variable genetic markers. ICCAT Coll. Vol. Sci. Pap. 45(2):155–157.

Greenwood, P. J., and P. H. Harvey.
1982. The natal and breeding dispersal of birds. Annu. Rev. Ecol. Syst. 13:1–21.

Hisada, K., and Z. Suzuki.
1982. Catch, fishing effort and length composition of the Atlantic bluefin tuna caught by Japanese longline fishery. ICCAT Coll. Vol. Sci. Pap. 17:307–314.

Mather, F. J., J. M. Mason, and A. C. Jones.
1995. Historical document: life history and fisheries of Atlantic bluefin tuna. U.S. Dep. Commer., NOAA Tech. Memo. NMFS-SEFSC 370, 165 p.

McGowan, M. F., and W. J. Richards.
1989. Bluefin tuna, *Thunnus thynnus*, larvae in the Gulf stream off of the southeastern United States: satellite and shipboard observations of their environment. Fish. Bull. 87:615–631.

National Research Council (NRC).
1994. An assessment of Atlantic bluefin tuna. National Academy Press, Washington, D.C., 148 p.

Policansky, D.
1993. Fishing as a cause of evolution in fishes. *In* T. K. Stokes, J. M. McGlade, and R. Law (eds.), The exploitation of evolving resources, p. 2–18. Springer-Verlag, Berlin.

Porch, C. E., V. R. Restrepo, S. C. Turner, and G. P. Scott.
1995. Virtual population analyses of Atlantic bluefin tuna incorporating movement and tagging data. ICCAT Coll. Vol. Sci. Pap. 44(1):183–190.

Powers, J., and J. Cramer.
1996. An exploration of the nature of bluefin tuna mixing. ICCAT Coll. Vol. Sci. Pap. 45(2):173–181.

Punt, A. E., and D. S. Butterworth.
1995. Use of tagging data within a VPA formalism to estimate migration rates of bluefin tuna across the north Atlantic. ICCAT Coll. Vol. Sci. Pap. 44(1):166–182.

Reznick, D. N.
1993. Norms of reaction in fishes. *In* T. K. Stokes, J. M. McGlade, and R. Law (eds.), The exploitation of evolving resources, p. 72–90. Springer-Verlag, Berlin.

Richards, W. J.
1976. Spawning of bluefin tuna (*Thunnus thynnus*) in the Atlantic Ocean and adjacent seas. ICCAT Coll. Vol. Sci. Pap. 5(2):267–278.

Rodriguez-Roda, J.
1967. El atun, *Thunnus thynnus* (L.) del sur de Espana, en la campana almadrabera del ano 1966. Invest. Pesq. 31(2):349–359.

Safina, C.
1993. Bluefin tuna in the west Atlantic: negligent management and the making of an endangered species. Conserv. Biol. 7(2):229–233.

Trippel, E. A.
1995. Age at maturity as a stress indicator in fisheries. Bioscience 45(11):759–771.

Turner, S. C.
1994. A review of recent information on size at age and the calculation of age from size for Atlantic bluefin tuna. ICCAT Coll. Vol. Sci. Pap. 42(1):97–99.

Turner, S. C., and J. E. Powers.
1995. Review of information related to Atlantic bluefin tuna east-west movement. ICCAT Col. Vol. Sci. Pap. 44(1): 191–197.

Turner, S. C., V. R. Restrepo, and A. M. Eklund.
1991. A review of the growth of Atlantic bluefin tuna, *Thunnus thynnus*. ICCAT Coll. Vol. Sci. Pap. 35(2):271–293.

An analysis of genetic population structure in red drum, *Sciaenops ocellatus*, based on mtDNA control region sequences

Seifu Seyoum
Michael D. Tringali
Theresa M. Bert
Department of Environmental Protection
Florida Marine Research Institute
100 Eighth Avenue SE
St. Petersburg, Florida 33701-5095
E-mail address (for S. Seyoum, contact author): Seyoum_S@epic7.dep.state.fl.us

Doug McElroy
Department of Biology
Western Kentucky University
Bowling Green, Kentucky 42101

Rod Stokes
Department of Marine Science
University of South Florida
140 7th Avenue S.
St. Petersburg, Florida 33701-5095

Abstract.—Genetic information pertaining to stock structure in red drum (*Sciaenops ocellatus*) is equivocal, complicating attempts to develop sound fishery management and stock enhancement plans. In this study, genetic stock structure was examined by using mitochondrial DNA (mtDNA) control region sequences of 209 individual red drum from six locations in the Gulf of Mexico and five locations in the nearshore Atlantic Ocean off the southeastern United States. Eighty-one polymorphic sites within a 369 base-pair portion of the control region defined 134 different haplotypes which differed by up to 26 nucleotide substitutions. Red drum showed high average within-sample haplotype (0.98) and nucleotide (0.030) diversities. Sequence divergences between pairs of haplotypes ranged from 0.27% to 7.06% ($\bar{x}$=3.17%). Cluster analysis of haplotypes revealed very little phylogeographic structure among mtDNA lineages. However, a neighbor-joining tree based on nucleotide divergence between pairs of samples showed cohesion among Atlantic samples and, to a lesser degree, among Gulf samples. In contrast to a prior study, we found no evidence that red drum in Mosquito Lagoon, Florida, constitute a self-contained, reproductively isolated population. Hierarchical analysis of molecular variance supported the hypothesis that red drum are subdivided into two weakly diverged populations with a genetic transition in south Florida between Sarasota Bay and Mosquito Lagoon. This area forms a zone of differentiation between two genetically semi-isolated populations between which the structuring of heterogeneity differs from that under the assumption of panmixia. In addition, the analysis of molecular variance also indicated that red drum from Apalachicola Bay are genetically divergent from all other samples. The Atlantic and Gulf red drum populations are likely to respond independently to harvest regulations; these fisheries should continue to be managed separately. Additional subdivision of the Gulf stock between peninsular Florida and the northern and western Gulf may also be warranted.

Manuscript accepted 5 March 1999.
Fish. Bull. 98:127–138 (2000).

Red drum (*Sciaenops ocellatus*) is a pelagic marine fish that is distributed over a large geographic range that extends throughout the northern Gulf of Mexico and along the Atlantic coast of the southeastern United States to Cape Cod, Massachusetts (Ross et al., 1983). Juveniles grow rapidly in estuarine nurseries and reach reproductive maturity by age 4. At this age they join large schools of highly dispersing adults and for the remainder of their approximately 35-year life span (Murphy and Taylor, 1990), maintain a pelagic existence except to spawn during annual congregations at the mouths of bays and estuaries. The census size of the breeding population in the Gulf of Mexico has been estimated to be greater than 7 million individuals (Nichols[1]). Abundance in the Atlantic is thought to be of a similar magnitude (Gold et al., 1993).

Red drum supports highly valuable commercial and recreational fisheries throughout its range (Mercer, 1984). Fishing pressure is directed principally on subadult year classes (ages 2–4). A high rate of annual mortality among some cohorts (Murphy and Taylor, 1990) and an overall decline in abundance and recruitment during the 1980s (Goodyear[2]) have led to concerns regarding the status of red drum spawning stocks. Because there have been no prolonged offshore fisheries for adult red drum, biological and fishery-dependent data pertaining to their spawning stocks have been limited. Therefore, fishery managers have had to rely principally on virtual population analysis and simi-

[1] Nichols, S. 1988. An estimate of the size of the red drum spawning stock using mark/recapture. Southeast Fisheries Center, Natl. Mar. Fish. Serv., Pascagoula, MS.
[2] Goodyear, C. P. 1989. Status of the red drum stocks of the Gulf of Mexico. Report for 1989. Contract no. CRD 88/89-14. Coastal Resources Div., Miami Laboratory, Southeast Fisheries Center, Natl. Mar. Fish. Serv., Miami, FL.

lar analyses (e.g. Vaughan[3]) to manage the red drum fishery. Knowledge of stock structure in red drum, i.e. the geographic relation between spawning and recruitment, is needed to facilitate the management of this fishery.

Molecular studies have been used to define appropriate geographic scales for monitoring and managing exploited animal populations (Moritz, 1994), including marine fishes (e.g. Bentzen et al., 1996; Graves, 1996; Tringali and Bert, 1996). Although several population genetic studies have been conducted on red drum, the existing data are equivocal. On the basis of significant differences in allele frequencies at a single allozyme locus, Bohlmeyer and Gold (1991) concluded that red drum are weakly subdivided between the Atlantic Ocean (North Carolina and South Carolina) and the Gulf of Mexico. However, data from other allozyme surveys (Ramsey and Wakeman, 1987; Campton[4]) did not permit the rejection of the null hypothesis that red drum form a single panmictic gene pool. In contrast, on the basis of small but statistically significant differences in the frequencies of several composite mitochondrial DNA (mtDNA) haplotypes between red drum collected from North Carolina and South Carolina waters and red drum collected from the Gulf of Mexico, Gold and Richardson (1991) and Gold et al. (1993, 1994) reasserted that red drum are weakly subdivided between these regions, ostensibly along the south Florida coast. In addition, Gold et al. (1993) reported a pattern of mtDNA differentiation in Gulf red drum consistent with the isolation by distance model (Wright, 1943) for samples ranging from Florida to Texas. However, samples from a significant portion of the species range, including locations near the putative Atlantic-Gulf division (i.e. the eastern Florida seaboard), were not assayed in any of the above studies. An equally tenable but untested hypothesis is that isolation by distance occurs over the entire range of the species, perhaps in the absence of a genetic break at a particular geographic location.

Localized population subdivision in red drum has also been postulated. From comparisons with samples from North Carolina and South Carolina waters and samples from the Gulf of Mexico, Gold and Richardson (1994) proposed that red drum inhabiting Mosquito Lagoon, Florida, form a genetically distinct population. Red drum in Mosquito Lagoon reportedly have a life history uncharacteristic of other red drum. Adults occupy this coastal lagoon throughout the year and may complete their life cycle within the lagoon (Johnson and Funicelli, 1991). Adult red drum also occur throughout the year in other coastal lagoons adjacent to Mosquito Lagoon (e.g. Banana, Indian, and Halifax Rivers), but these have not been surveyed genetically. Rather than forming a self-contained population, red drum from Mosquito Lagoon may belong to a larger subpopulation occupying Florida Atlantic waters.

Owing to the perceived decline of red drum abundance in the 1980s, state agencies in Alabama, Florida, South Carolina, and Texas studied the feasibility of stock enhancement as a means of supplementing wild populations. Hatcheries in Florida, South Carolina, and Texas currently employ stocking on a large scale (McEachron et al., 1995; FDEP[5]). Hatchery programs potentially affect the gene pools of indigenous red drum populations by way of an inappropriate introduction of non-native individuals (Hindar et al., 1991) and by hatchery-induced inbreeding effects (Tringali and Bert, 1998). For example, because broodstocks for large-scale stock enhancement programs along the Atlantic seaboard have been obtained from Mosquito Lagoon and nearby estuaries (Halstead[6]), there is a potential for artificial genetic exchange between putatively separate gene pools (e.g. those of Mosquito Lagoon and the Carolinas).

State and regional fishery managers (Vaughan[3]; FDEP[5]) and hatchery managers (FDEP[7]) have adopted the stock structure scenario proposed by Gold et al. (1993) and Gold and Richardson (1994) in which red drum are divided into Gulf of Mexico and Atlantic populations, and those fish in Mosquito Lagoon comprise a unique, self-contained Atlantic subpopulation. However, several important questions regarding the genetic structure of red drum remain unanswered; each has serious implications for fishery management and stock enhancement programs. First, are red drum populations in the Gulf of Mexico and Atlantic really subdivided or do the observed genetic differences solely reflect isolation by distance over the range of the species? Second, if a genetic break does exist somewhere between the Gulf and the coast of the Carolinas, where is it?

[3] Vaughan, D. S. 1995. Status of the red drum stock on the Atlantic coast: stock assessment report for 1995. Southeast Fisheries Science Center, Natl. Mar. Fish. Serv., Beaufort, NC, 50 p.

[4] Campton, D. E. 1992. Gene flow estimation and population structure of red drum (*Sciaenops ocellatus*) in Florida. Final report, cooperative agreement no. 14-16-009-1522, National Fisheries Research Center, U.S. Fish and Wildlife Serv., Gainesville, FL.

[5] FDEP (Florida Department of Environmental Protection). 1993. A stock assessment of red drum (*Sciaenops ocellatus*) in Florida. Florida Marine Research Inst., Dep. Natural Resources, 100 Eighth Ave. SE, St. Petersburg, FL, 24 p.

[6] Halstead, B. 1997. Stock Enhancement Research Facility, Florida Department of Environmental Protection, 14495 Harlee Road, Port Manatee, FL 34221. Personal commun.

[7] FDEP (Florida Department of Environmental Protection). 1993. Marine fish stock enhancement and hatchery executive summary. Report to the legislature. FDEP, St. Petersburg, FL, 17 p.

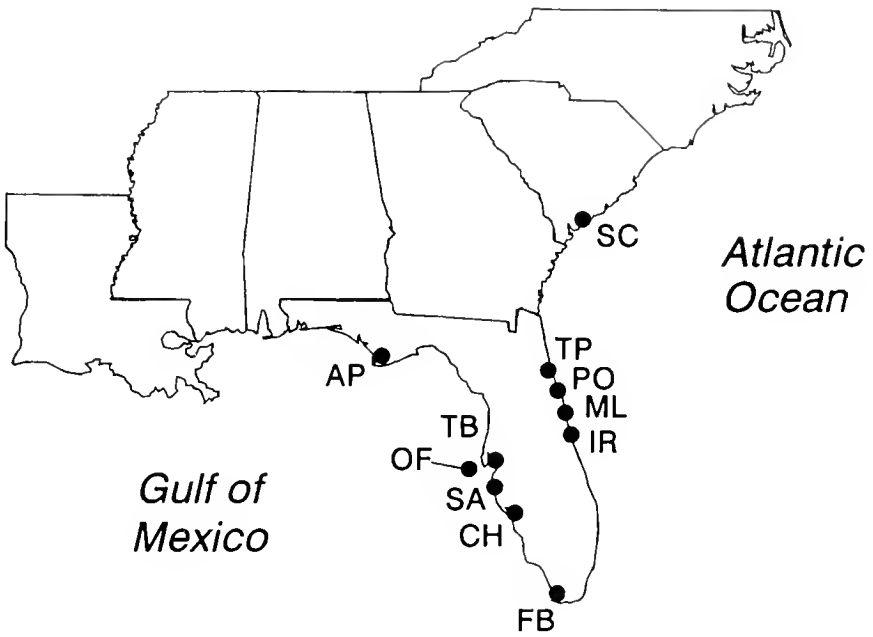

Figure 1

Sampling sites for red drum in waters off the southeastern United States. Florida: AP = Apalachicola Bay; TB = Tampa Bay; OF = offshore, Tampa Bay; SA = Sarasota Bay; CH = Charlotte Harbor; FB = Florida Bay; IR = Indian River; ML = Mosquito Lagoon; PO = Ponce de Leon inlet; TP = Tomoka Basin. South Carolina: SC = Charleston Harbor.

Third, are red drum in Mosquito Lagoon reproductively and genetically distinct or do they belong to a larger and heretofore unsampled east Florida population? To examine these questions, we obtained sequence data from the rapidly mutating mtDNA control region. Sequencing the control region has proven useful in intraspecific phylogeographic and population genetic studies of fishes (e.g. Fajen and Breden, 1992; Brown et al., 1993; Stepien, 1995; Stabile et al., 1996). We employed sampling and analytical regimes designed to test the various competing hypotheses of red drum population structure. In addition, by gathering baseline data for mtDNA control region diversity in red drum populations, we explored the potential for using the control region as a marker to assess and monitor ongoing stocking programs for wild red drum populations.

Materials and methods

Sample collection and DNA purification

Samples of red drum were collected with hook-and-line gear, trammel nets, and purse seines from riverine, estuarine, and offshore waters of the South Carolina coast (one location) and the east coast of Florida (four locations, sampled prior to stock enhancement activities), referred to collectively as the Atlantic samples; and the west coast of Florida (six locations), referred to collectively as the Gulf samples (Fig. 1). All specimens were collected between February 1992 and February 1997. Somatic muscle and liver tissue were dissected from each individual. Total length (range 280–1070 mm) of each individual was recorded prior to dissection. Tissues were frozen in liquid nitrogen and stored at –80°C in the laboratory until processing.

Approximately 100–400 milligrams of muscle or liver tissue were digested in 900 microliters of lysis buffer (0.1M Tris, pH 8.0, 0.05M ethylenediaminetetraacetid acid (EDTA), 0.2M NaCl, 1% weight by volume of sodium dodecyl sulfate (SDS), containing 1–2 milligrams of proteinase K) with moderate shaking for 3–5 h at room temperature. Following the addition of 150 microliters of chilled 8M potassium acetate, the SDS and cellular debris were precipitated for 30 min at 4°C and removed by centrifugation. Total genomic DNA was purified by phenol/chloroform extraction (Sambrook et al., 1989).

The DNA was concentrated by isopropanol precipitation, resuspended in 75 microliters of sterile water, and stored at –20°C.

mtDNA control region sequencing

Initially, we used the polymerase chain reaction (PCR; Saiki et al., 1988) and published primer sequences L15926 (Kocher et al., 1989) and H16498 (Meyer et al., 1990) to amplify a portion of the mtDNA control region of red drum. Double-stranded PCR was performed with Perkin Elmer AmpliTaq in a 50-µL reaction volume for 32 cycles in a DeltaCycler II System (Ericomp Inc., San Diego, CA), according to the methods described by Kocher et al. (1989). We amplified a 455-base-pair (bp) fragment of the control region for several individuals of red drum. However, because direct sequencing of the amplicon with the same PCR primers in the sequencing reaction yielded unsatisfactory results, we used a process of cloning and sequencing to design specific primers for red drum.

The 455-bp amplicon was cloned in pBluescript by TA cloning (Marchuk et al., 1990). Following denaturation of the plasmid DNA (Hattori and Sakaki, 1986), sequencing was done from both directions by the dideoxy termination method (Sanger et al., 1977) by using Sequenase version 2.0 (U.S. Biochemicals, Cleveland, OH) and [α-S^{35}] dATP (Dupont Biotechnology Systems, Wilmington, DE). Products of the sequencing reactions were resolved in 6% polyacrylamide/7-M urea gels that were vacuum dried at 80°C and autoradiographed with Kodak X-Omat AR film. We used the ESEE program (Cabot and Beckenbach, 1989) to align sequences. From these sequences, (Genbank accession no. AF054671), highly specific internal primers were designed for the control region of red drum. These primers partially overlapped the initial primers and were designated L15943 (5'-GTA AACCGGATGTCGGGGGTTAG-3') and H16484 (5'-GGAACCAGATACCAGGAATAGTTCA-3').

We used these custom primers to amplify a portion of the control region for 209 individuals in 50-µL reaction volumes. The PCR products were run on 1.2% low-EEO (Fisher Scientific, Norcross, GA) agarose gel during electrophoresis. The resulting bands were excised and then purified with GeneClean (Bio 101, La Jolla, CA). Double-stranded sequencing was conducted as described by O'Foighil et al. (1996).

Data analyses

Base composition, number of transitions (TSs), and number of transversions (TVs) were determined by using MEGA 1.01 (Kumar et al., 1993). Further analysis of base substitutions was conducted as in Brown and Clegg (1983). Each different haplotype was assigned a number, and the distribution of the different haplotypes was determined for each sample.

We used MEGA to generate a pairwise matrix of sequence divergence values between pairs of haplotypes and to construct an unrooted neighbor-joining tree; 200 replicates were used to estimate bootstrap values for the nodes. Sequence divergences were computed by using the pairwise-deletion option in MEGA; this distance estimator excludes sites at which indels occur on a pairwise basis. Haplotype and nucleotide diversity within samples and nucleotide divergence (D) between pairs of samples were estimated according to Nei and Tajima (1981) and Nei (1987) by using the DA option of REAP 4.0 (McElroy et al., 1992). The nucleotide divergence values were clustered by using the NJTREE program (Jin and Ferguson, 1990) based on the neighbor-joining method of Saitou and Nei (1987).

Geographic structuring of molecular variance among samples was examined by using the matrix of sequence divergences between all pairs of haplotypes in AMOVA 1.55 (Excoffier et al., 1992). In this analysis, the haplotype correlations (ϕ statistics) and their variance components were estimated in a hierarchical fashion: between regions, among samples within a region, and among individuals within samples. Statistical significances of ϕ values were computed by performing randomization tests with 500 replicates. Gold et al. (1993) concluded that red drum was subdivided into Atlantic and Gulf of Mexico populations. To determine the validity of this conclusion, we examined the spatial partitioning of molecular variance as follows. The between-region component of variance and ϕ_{CT} was first calculated for red drum samples divided into Atlantic (SC, TP, PO, ML, and IR) and Gulf (FB, CH, SA, OF, TB, and AP) regions. The compositions of the two groups were then adjusted by sequentially adding Atlantic samples to the Gulf group and then sequentially adding Gulf samples to the Atlantic group. After each addition, the apportioning of molecular variance between the resulting groups was recalculated. For example, IR (the Atlantic sample closest to the Gulf) was added to the Gulf group and tested against the remaining Atlantic samples (ML, PO, TP, and SC). ML (the second closest sample) was then added to the Gulf-plus-IR group; that grouping was then tested against PO, TP, and SC. This process was repeated until only a single sample remained in one group.

Finally, to test for an association between interpopulation D values and geographic distance (isolation-by-distance), we performed the Mantel test (BIOMstat, version 3.0; Rohlf and Slice, 1995) for samples grouped

by region (Atlantic or Gulf) and for all samples combined. The statistical significance of the association was tested by random permutation analysis by using 500 replicates (Sokal and Rohlf, 1995).

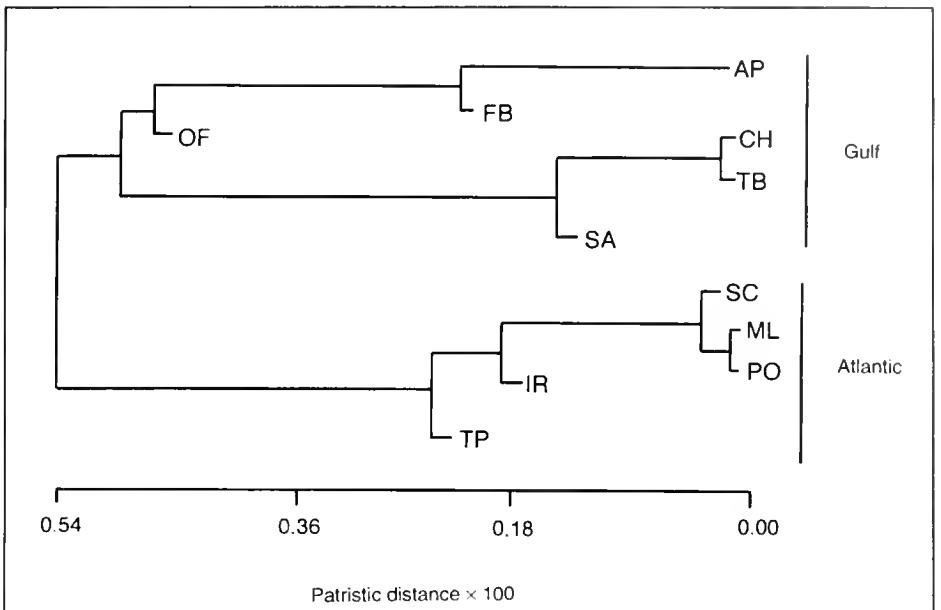

Figure 2

Neighbor-joining tree based on mtDNA nucleotide divergence between samples of red drum from Florida and South Carolina nearshore waters. Sample location and abbreviates are defined in Figure 1.

Results

We analyzed sequence data from a 369-bp portion of the mtDNA control region for 209 red drum. A total of 81 polymorphic sites were observed among all individuals. Of these, 67 sites had single-state, 11 had double-state, and 3 had triple-state transformations, totaling 98 polymorphisms and including two indels. The first indel consisted of an insertion of a pyrimidine (T or C) at position 160 and occurred in 10 individuals; the second indel consisted of a deletion of a purine (A) at position 210 and occurred in one of these individuals (Table 1). Seventy-three of the substitutions were TSs and 22 were TVs. As with control regions of other fishes (Stepien, 1995), the relative frequencies of the four nucleotide bases differed; adenine was the most prevalent (39%), followed by thymine (27%), cytosine (23%), and guanine (11%). The TS:TV ratio was 3.4:1 and was similar to ratios reported for marine and freshwater fishes (Stepien, 1995; but see Brown et al., 1993).

We observed 134 different haplotypes in the 209 individuals sequenced (Table 1). Sequences of these haplotypes have been deposited in GenBank under the accession numbers AF054672–F054805. Twenty-nine haplotypes were shared by more than one individual. Two haplotypes, no. 56 and no. 83, were shared by nine and nineteen individuals, respectively, which were widely dispersed among seven samples. Twenty-six haplotypes occurred infrequently, 25 in two to five individuals scattered among two to five samples, and one in two members of a single sample. Of the 19 individuals with haplotype no. 83, 17 were from the Atlantic and two from the Gulf. The percentage of different haplotypes in any one sample varied from 76% to 100% ($\bar{x}$=87%). Haplotype diversity within samples ranged from 0.95 to 1.00 ($\bar{x}$=0.98, SE=0.00) and nucleotide diversity ranged from 0.025 to 0.037 ($\bar{x}$=0.030, SE=0.003).

Percent sequence divergences between pairs of different haplotypes ranged from 0.3% to 7.1% ($\bar{x}$= 3.2%; SE=0.017). Between any two different haplotypes, the number of nucleotide differences varied from one to 26 ($\bar{x}$=12). The topology of the unrooted tree neighbor-joining (not shown) revealed that the 134 haplotypes were not phylogeographically structured. Haplotypes observed in Gulf and Atlantic samples were scattered throughout the tree; with the exception of two terminal groupings, nodes on the tree had low statistical support. Internal branch lengths of the tree were generally short; however, one interior branch was relatively long, and it defined the only well-supported major clade (bootstrap value=85). This clade consisted of 23 haplotypes, including the 10 haplotypes that had the insertion at position 160. The 10 insertion-bearing haplotypes were found in nine Atlantic individuals but in only one Gulf individual.

The D values between pairs of samples ranged from –0.08% to 0.10%. In the neighbor-joining cluster analysis, cohesion of the samples within geographic regions was generally observed (Fig. 2). All Atlantic samples formed a distinct clade which was separated by the longest branch of the tree from the clade formed by the Gulf samples. Less cohesion was observed among the Gulf samples, although the geographically proximal SA, TB, and CH samples clustered closely together.

Table 1

Distribution of red drum mitochondrial DNA control region haplotypes from 11 locations. Abbreviations for sample locations are defined in Figure 1

	Gulf						Atlantic				
Haplotype	AP	TB	OF	SA	CH	FB	IR	ML	PO	TP	SC
1	1										
2	3					1					
3	1						1		1	1	
4	1										
5	1										
6	1								1		
7	1		1		1	1			1		
8	1										
9	1										
10	1										
11	1										
12	1										
13	1										
14	1										
15	1										
16	1					1					
17	1										
18	1										
19		1									
20		1									
21[1]		1									
22		1									
23		1									
24		1									
25		2									
26		1									
27		1									
28		1									
29		1									
30		1									
31		1									
32			1							1	
33			1								1
34			1								
35			1								
36			1								
37		1	1								
38			1								
39			1								
40			1								
41			1								
42				1							
43				1							
44				1							
45				2							
46				1							
47				1							
48				1							
49					1						
50					1						
51					1						
52					1						
53					1	2			1	1	
54					1						

continued

Table 1 (continued)

	Gulf						Atlantic				
Haplotype	AP	TB	OF	SA	CH	FB	IR	ML	PO	TP	SC
55		3			3	1					
56		2			1	1	1	1		2	1
57		1			1						
58					1			1			
59					1						
60					1						
61					1					1	
62					1						
63			1		1						
64					1						
65					1						
66						1					
67						1					
68						1					
69						1					
70						1					
71						1					
72			1			1			1		
73						1			1		
74						1					
75						1					
76						1					
77						1					
78						1					
79							1				
80							2		1		1
81							2				1
82							1				
83		1	1				3	5	3	3	3
84[1]							1			1	
85							1				
86							1		1	1	1
87							1				
88							1				
89[1]							1				
90								1			
91								1			
92								1			
93[1]								1			
94								1			
95[1]								1			
96								1			
97								1			
98								1			
99								2			
100								1			
101[1]								1			
102								1			
103									1		1
104									1		
105									2		2
106									1		
107									1		
108									1		
109									1		
110									1		

continued

Table 1 (continued)

	Gulf						Atlantic				
Haplotype	AP	TB	OF	SA	CH	FB	IR	ML	PO	TP	SC
111									1		
112									1		
113										1	
114										1	
115										1	
116										1	
117[1,2]										1	
118										1	
119										1	
120										1	
121										1	
122[1]										1	
123										1	
124										1	1
125											1
126											1
127											1
128											1
129											1
130[1]											1
131											1
132											1
133											1
134											1
Total	20	22	14	8	20	20	17	21	22	23	22

[1] Haplotypes with an insertion at position 160.
[2] Haplotype with an insertion at position 210.

The D value between the ML sample and the remaining pooled Atlantic samples was –0.05%. In contrast, the D value between the ML sample and the Gulf samples ranged from –0.02% to 0.076%.

The analysis of molecular variance (AMOVA) for all samples yielded a ϕ_{ST} value of –0.001, indicating that no significant heterogeneity was detected between any two samples. For the geographic analysis, in which samples were divided into shifting regional subsets, the variance components among samples within groups and among individuals within samples were not significant for any grouping. Significant values of ϕ_{CT} were observed in five of the 10 groupings (Table 2). In four of the five significant groupings, the division occurred in peninsular south Florida. Overall, results of the AMOVA suggest that a genetic transition occurs in red drum along the Florida coast between Sarasota Bay in the Gulf and Mosquito Lagoon in the Atlantic. However, the highest ϕ_{CT} value and between-group variance component were observed when samples were grouped according to their actual Atlantic and Gulf locations (Table 2, grouping 1). The significant ϕ_{CT} value for the AP sample versus all other samples suggests that an additional genetic discontinuity occurs in Gulf waters off northwest Florida.

In the Mantel test between interpopulational D and geographic distance, no association was observed among the Atlantic samples (P=0.20) or among the Gulf samples (P=0.053). However, a significant association was observed for all red drum samples (P<0.01), reflecting the genetic transition that occurs in south Florida.

Discussion

Genetic population structure

Because there are few absolute barriers to gene flow in the ocean, it is generally expected that marine species with continuous distributions, large populations, and high levels of larval and adult dispersal should have very little intraspecific population structure over large geographic areas (Avise, 1987; Palumbi, 1992).

Table 2

Geographic analysis of molecular variance in the mtDNA control region of red drum. The table lists the ϕ_{CT} values and between-group variance components for the ten possible geographical groupings and the probability P of finding a more extreme variance component by chance (500 permutations). In each group, the letter G represents samples from the Gulf of Mexico (G_1=AP, G_2=TB, G_3=OF, G_4=SA, G_5=CH, G_6=FB) and the letter A represents samples from the Atlantic Ocean (A_1=IR, A_2= ML, A_3=PO, A_4=TP, A_5=SC). Abbreviations for sample locations are defined in Figure 1.

Grouping	First group	Second group	Variance between groups (%)	Φ_{CT}	P
1	$G_1G_2G_3G_4G_5G_6$	$A_1A_2A_3A_4A_5$	1.96	0.020	<0.002
2	$G_1G_2G_3G_4G_5G_6A_1$	$A_2A_3A_4A_5$	1.40	0.014	0.012
3	$G_1G_2G_3G_4G_5G_6A_1A_2$	$A_3A_4A_5$	0.39	0.004	NS
4	$G_1G_2G_3G_4G_5G_6A_1A_2A_3$	A_4A_5	–0.17	–0.002	NS
5	$G_1G_2G_3G_4G_5G_6A_1A_2A_3A_4$	A_5	–0.54	–0.005	NS
6	$G_1G_2G_3G_4G_5$	$G_6A_1A_2A_3A_4A_5$	1.48	0.015	0.004
7	$G_1G_2G_3G_4$	$G_5G_6A_1A_2A_3A_4A_5$	0.78	0.008	0.044
8	$G_1G_2G_3$	$G_4G_5G_6A_1A_2A_3A_4A_5$	0.73	0.007	NS
9	G_1G_2	$G_3G_4G_5G_6A_1A_2A_3A_4A_4$	0.74	0.007	NS
10	G_1	$G_2G_3G_4G_5G_6A_1A_2A_3A_4A_5$	1.50	0.015	<0.002

Red drum is a pelagic marine fish with these demographic and life history characteristics. However, although some genetic exchange may occur between red drum from distant locations, populations differ from the expectation of genetic homogeneity. Hierarchical analysis of the structuring of genetic variance supports the hypothesis that the species is weakly subdivided between the Atlantic Ocean and the Gulf of Mexico. The existence of the subdivision is also supported by cluster analysis of sequence divergence values. The geographic coverage of our samples, particularly the inclusion of samples from Florida's eastern seaboard, allowed us to infer that the genetic break separating these two populations occurs in south Florida. Another genetic discontinuity apparently occurs in Gulf waters off northwest Florida.

The Atlantic-Gulf subdivision in red drum may result from a combination of extrinsic and behavioral factors. Gold et al. (1993, 1994) summarized a number of potentially important oceanographic and geographic factors. Because the southernmost portion of the east Florida shelf is extremely narrow and provides little of the neritic habitat (Jones et al., 1985) generally occupied by adult red drum, it may represent a significant barrier to adult migration. Biotic factors largely preclude large-scale passive dispersal of eggs and larvae (Peters and McMichael, 1987), and widespread dispersal at the juvenile stage is rare (Murphy and Taylor[8]). If partitioning of genetic variation in red drum results from adult migration or vagrant movement between spawning locations, it is not evident from studies of fish movement. Although very few tagged adult red drum have been recaptured after spending significant periods at large, the evidence suggests that some are highly mobile and may disperse to distances of up to 320 km (Woodward and Nicholson, 1997; Crabtree[9]). However, movement of red drum between the Atlantic and Gulf regions has not been documented. In apparent contrast to the mark-recapture data, recent ultrasonic tracking studies of adults provide limited evidence for spawning fidelity to certain Atlantic estuaries over two-to-three-year periods, and potentially longer (Nicholson and Jordan[10]). Overall, the available movement data for adult red drum are not adequate to draw conclusions relating to regional recruitment processes and patterns of dispersal. Nevertheless, it is clear from the genetic data that reproductive exchange between spawning populations in the Atlantic and Gulf regions is limited.

Because red drum from Mosquito Lagoon were used to produce hatchery populations for at least two stock enhancement programs along the Atlantic seaboard, it was important to determine whether the spawning aggregation within that system represented a self-contained, genetically divergent popu-

[8] Murphy, M. D., and R. G. Taylor. 1989. Tag/recapture and age validation of red drum in Florida. Final report, NOAA grant NA86-WC-H-06136, National Marine Fisheries Service, Pascagoula, MS, 27 p.

[9] Crabtree, R. 1997. Florida Marine Research Institute, Department of Environmental Protection, St. Petersburg, FL. Unpublished data.

[10] Nicholson, N., and S. R. Jordan. 1994. Biotelemetry study of red drum in Georgia, November 1989–June 1993. Coastal Resources Division, Georgia Department of Natural Resources, Brunswick, GA, 65 p.

lation. Contrary to the study of Gold et al. (1994), we found no evidence to support the hypothesis that red drum in Mosquito Lagoon are reproductively isolated from other Atlantic red drum. In our survey of the mtDNA control region, there was no nucleotide divergence between Mosquito Lagoon and other Atlantic samples, whereas divergence values between the Mosquito Lagoon and the Gulf samples were among the highest. Furthermore, other investigators also found no significant differences at the allozyme loci that putatively distinguish Mosquito Lagoon red drum from other red drum (Campton[4]; Crawford and Bert[11]). This lack of difference suggests that the allozyme frequency differences observed by Gold and Richardson (1994) may not be temporally stable. A lack of samples geographically proximal to Mosquito Lagoon may have also influenced the outcome of that study. Considering all the evidence, it seems more likely that red drum from Mosquito Lagoon belong to the larger genetic population occupying nearshore Atlantic waters of the southern United States. Although it is generally better to obtain hatchery broodstock from locations within or near the intended release site (Utter, 1998), the use of Mosquito Lagoon red drum as a source of broodstock in Atlantic coast stock enhancement programs should not produce a negative genetic impact on wild red drum.

Implications for fishery and hatchery management

Because red drum support valuable fisheries throughout the Gulf of Mexico and Atlantic seaboard, the species is of special concern to state and regional fishery management agencies. Our results support the hypothesis that a genetic transition in red drum population structure occurs in south Florida. In theory, it requires the regular exchange of only a few individuals between breeding populations to homogenize their genetic composition (Slatkin, 1987). Thus, genetic exchange between Atlantic and Gulf stocks by any recruitment process must be sufficiently low to allow genetic differences to accumulate or, if the differences reflect a historical disassociation, for them to be maintained. The two red drum stocks can best be described genetically as demes, separate semi-isolated groups between which the structuring of heterogeneity differs from the assumption of panmixia (Hartl and Clark, 1989). Therefore, the Atlantic and Gulf stocks are likely to respond independently to harvest regulations and these fisheries should continue to be managed separately.

[11] Crawford, C., and Bert, T. 1997. Florida Marine Research Institute, Department of Environmental Protection, St. Petersburg, FL. Unpublished data.

Gold et al. (1993) observed a pattern of isolation by distance in the distribution of mtDNA haplotypes among Gulf samples that ranged from the southeast coast of Texas to the southwest coast of Florida. Although we did not observe a similar pattern for Gulf samples ranging from Apalachicola Bay to Florida Bay, the probability value for the Mantel coefficient was nearly significant at the 0.05 level and the AMOVA value for the Apalachicola sample versus all other samples was highly significant. This indicates that the minimum geographic scale at which the isolation-by-distance mechanism operates is greater than the distance between Apalachicola Bay and Florida Bay (approximately 670 km) or that genetic discontinuity also exists between Florida Gulf red drum and red drum inhabiting the northern and western Gulf of Mexico. Accordingly, cooperative management of the Gulf fishery on a regional basis is appropriate. No pattern of isolation-by-distance was evident for red drum along the southern Atlantic seaboard; the fishery between South Carolina and southeast Florida should be managed as a single unit.

Our principal objective for undertaking this study was to improve upon available genetic information relating to red drum population structure for fishery management purposes. Our most informative statistical tools were those that assessed relationships among the samples. Genotype frequency differences accumulate quickly in subdivided populations compared with the rate at which distinct phyletic lineages emerge and sort geographically. Moreover, mitochondrial DNA restriction fragment length polymorphism and sequence data for marine populations are typically characterized by haplotype distributions which consist of a few numerically and geographically prevalent haplotypes and many rare, geographically restricted haplotypes that may be important with respect to population structure. Therefore, as our results and the results of Tringali and Bert (1996) demonstrate, genetically-based management units (*sensu* Moritz, 1994), especially in marine fishery stocks, may be more easily identified by applying population-level analyses that take full advantage of both differences in genotype frequencies among samples and phylogenetic relatedness of individual genotypes. Statistical tests of association when applied to skewed haplotype distributions often lack the power to detect the low levels of population divergence that may characterize marine populations. Moreover, these tests ignore the interrelatedness of haplotypes in terms of sequence similarity or difference. The two principal analytical methods we employed, clustering of intersample nucleotide divergence values and AMOVA, are based on both the occurrence of haplotypes at particular locations and their sequence similarity to other

haplotypes at those locations. This approach may be particularly important in studies of pelagic marine species because, like red drum, genetic divergence separating populations is often buried within a high background of overall genetic diversity.

Finally, Moritz (1994) described the potential of using mtDNA as a marker for evaluating the success of stock enhancement programs. For this application, the mtDNA haplotypes borne by hatchery fish should be sufficiently rare in wild populations. The portion of control region we examined provides an excellent source of naturally occurring genetic markers. Because the percentage of wild red drum individuals with different haplotypes in any given sample averaged 87% and ranged up to 100%, a genetic monitoring program using this mtDNA fragment to track haplotypes borne by hatchery-released red drum after release should allow for assessment of the survival and reproductive output of these fish in the natural environment. In addition, nucleotide substitutions in this portion of the control region could be used to estimate the contribution of each female parent to the broods. This information will be important in the evaluation of breeding protocols designed to optimize levels of genetic variability in hatchery broods, in the assessment of genetic risk posed to wild red drum populations by hatchery stocking programs (e.g. Tringali and Bert, 1998), and in the evaluation of stock supplementation programs.

Acknowledgments

We thank M. Murphy and R. Taylor for valuable discussions regarding red drum life history, R. Muller for advice on statistical analyses, and L. Barbieri for providing information on biotelemetry studies of red drum in Georgia. We also thank C. Crawford for technical assistance and R. Crabtree, B. Falls, A. McMillen-Jackson, S. Lotz, A. Redford, R. Ruiz-Carus, and T. Thompson for assistance with field collections. We thank the editorial staff of the Florida Marine Research Institute, J. Gold, D. O'Foighil, and D. Winkelman for valuable comments that improved the manuscript. Financial support was provided by the State of Florida and the U.S. Fish and Wildlife Service, Department of the Interior, Federal Aid for Sportfish Restoration Project Grant F-69 to TMB.

Literature cited

Avise, J. C.
1987. Identification and interpretation of mitochondrial DNA stocks in marine species. *In* H. Kumpf (ed.), Proceedings of the stock identification workshop, p.105–136. U.S. Dep. Commer., NOAA Tech. Memo. NMFS-SEFC-199.

Bentzen, P., C. T. Taggart, D. E. Ruzzante, and D. Cook.
1996. Microsatellite polymorphism and the population structure of Atlantic cod (*Gadus morhua*) in the northwest Atlantic. Can. J. Fish. Aquat. Sci. 49:2,527–2,537.

Bohlmeyer, D. A., and J. R. Gold.
1991. Genetic studies in marine fishes. II. A protein electrophoretic analysis of population structure in the red drum, *Sciaenops ocellatus*. Mar. Biol. 108:197–206.

Brown, A. H. D., and T. M. Clegg.
1983. Analysis of variation in related DNA sequences. *In* M. Dekker (ed.), Statistical analysis of DNA sequence data, p.107–132. Marcel Dekker, New York, NY.

Brown, J. R., A.T. Beckenbach, and M. J. Smith.
1993. Intraspecific DNA sequence variation of the mitochondrial control region of white sturgeon (*Acipenser transmontanus*). Mol. Biol. Evol.10(2):326–341.

Cabot, E. L., and T. Beckenbach.
1989. Simultaneous editing of multiple nucleic acid and protein sequences with ESEE. Comput. Appl. Biosci. 5: 233–234.

Excoffier, L., P. E. Smouse, and J. M. Quattro.
1992. Analysis of molecular variance inferred from metric distances among DNA haplotypes: application to human mitochondrial DNA restriction data. Genetics 131:479–491.

Fajen, A., and F. Breden.
1992. Mitochondrial DNA sequence variation among natural populations of the Trinidad guppy, *Poecilia reticulata*. Evolution 46(5):1,457–1,465.

Gold, J. R., T. L. King, L. R. Richardson, D. A. Bohlmeyer, and G. C. Matlock.
1994. Allozyme differentiation within and between red drum (*Sciaenops ocellatus*) from the Gulf of Mexico and Atlantic ocean. J. Fish Biol. 44:567–590.

Gold, J. R., and L. R. Richardson.
1991. Genetic studies in marine fishes. IV. An analysis of population structure in the red drum (*Sciaenops ocellatus*) using mitochondrial DNA. Fish. Res. (Amst.) 12:213–241.
1994. Genetic distinctness of red drum (*Sciaenops ocellatus*) from Mosquito Lagoon, eastern Florida. Fish. Bull. 92: 58–66.

Gold, J. R., L. R. Richardson, C. Furman, and T. L. King.
1993. Mitochondrial DNA differentiation and population structure in red drum (*Sciaenops ocellatus*) from the Gulf of Mexico and Atlantic Ocean. Mar. Biol. (Berl.) 116:175–185.

Graves, J. E.
1996. Conservation genetics of fishes in the pelagic marine realm. *In* J. C. Avise and J. L. Hamrick (eds.), Conservation genetics: case histories from nature, p.335–366. Chapman and Hall, New York, NY.

Hartl, D. L., and A. G. Clark.
1989. Principles of population genetics. 2nd ed. Sinaeur Associates, Sunderland, MA.

Hattori, M., and Y. Sakaki.
1986. Dideoxy sequencing method using denatured plasmid templates. Ann. Rev. Biochem. 152:232–238.

Hindar, K., N. Ryman, and F. Utter.
1991. Genetic effects of cultured fishes on natural populations. Can. J. Fish. Aquat. Sci. 48:945–957.

Jin, L., and J. W. H. Ferguson.
1990. Neighbor-joining tree and UPGMA tree software. vers. 2.0. Center for Demographic and Population Genetics, Univ. Texas Health Science Center, Houston, 16 p.

Johnson, D. R., and N. A. Funicelli.
1991. Spawning of the red drum in Mosquito Lagoon, east central Florida. Estuaries 14:74–79.

Jones, A. C., S. A. Berkeley, J. A. Bohnsack, S. A. Bortone, D. K. Camp, G. H. Darcey, J. C. Davis, K. D. Haddad, M. Y. Hedgepeth, E. W. Irby, Jr., W. C. Jaap, F. S. Kennedy, Jr., W. G. Lyons, E. L. Nakamura, T. H. Perkins, J. K. Reed, K. A. Steidinger, J. T. Tilmant, and R. O. Williams.
1985. Ocean habitat and fishery resources of Florida. *In* W. Seaman Jr. (ed.), Florida aquatic habitat and fishery resources, p. 437–543. Special publication of the Florida Chapter, Am. Fish. Soc., Kissimee, FL.

Kocher, T. D., W. K. Thomas, A. Meyer, S. V. Edwards, S. Pääbo, F. X. Villablanca, and A. C. Wilson.
1989. Dynamics of mitochondrial DNA evolution in animals: amplification and sequencing with conserved primers. Proc. Nat. Acad. Sci. USA 86:6,196–6,200.

Kumar, S., K. Tamura, and M. Nei.
1993. MEGA: molecular evolutionary genetic analysis, vers. 1.01. Pennsylvania State Univ., University Park, PA, 412 p.

Marchuk, D., M. Drumm, A. Saulino, and F. S. Collins.
1990. Construction of T-vectors, a rapid and general system for direct cloning of unmodified PCR products. Nucleic Acids Res. 19(5):1,154.

McEachron, L. W., C. E. McCarty, and R. P. Vega.
1995. Beneficial uses of marine fish hatcheries: enhancement of red drum in Texas coastal waters. Am. Fish. Soc. Symp. 15:161–166.

McElroy, D., P. Moran, E. Bermingham, and I. Kornfield.
1992. REAP: an integrated environment for the manipulation and phylogenetic analysis of restriction data. J. Hered. 83:157–158.

Mercer, L.
1984. A biological and fisheries profile of red drum, *Sciaenops ocellatus*. N. Carolina Dep. Natl. Res., Div. Mar. Fish. Spec. Sci. Rep. 41:1–89.

Meyer, A., T. D. Kocher, P. Basasibwaki, and A. C. Wilson.
1990. Monophyletic origin of Victoria cichlid fishes suggested by mitochondrial DNA sequences. Nature 347:550–553.

Moritz, C.
1994. Application of mitochondrial DNA analysis in conservation: a critical review. Mol. Ecol. 3:401–411.

Murphy, M. D., and R. G. Taylor.
1990. Reproduction, growth, and mortality of red drum, *Sciaenops ocellatus* in Florida. Fish. Bull. 88:531–542.

Nei, M.
1987. Molecular evolutionary genetics. Columbia Univ. Press, New York, NY.

Nei, M., and F. Tajima.
1981. DNA polymorphisms detectable by restriction endonucleases. Genetics 97:145–163.

O'Foighil, D., T. J. Hilbish, and R. M. Showman.
1996. Mitochondrial gene variation in *Mercenaria* clam sibling species reveals a relict secondary contact zone in the western Gulf of Mexico. Mar. Biol. 126:675–683.

Palumbi, S. R.
1992. Marine speciation on a small planet. Trends Ecol. Evol. 7:114–118.

Peters, K. M., and R. H. McMichael.
1987. Early life history of *Sciaenops ocellatus* (Pisces: Sciaenidae) in Tampa, Florida Estuaries 10(2):92–107.

Ramsey, P. R., and J. M. Wakeman.
1987. Population structure of *Sciaenops ocellatus* and *Cynoscion nebulosus* (Pisces: Sciaenidae): Biochemical variation, genetic subdivision and dispersal. Copeia 3:682–695.

Rohlf, F. J., and D. E. Slice.
1995. BIOMstat for windows, statistical software for biologists, vers. 3.0. (manual). Applied Biostatistics, Setauket, NY, 57 p.

Ross, J. L., J. S. Pavela, and M. E. Chittenden Jr.
1983. Seasonal occurrences of black drum *Pogonias cromis*, and red drum, *Sciaenops ocellatus*, off Texas. Northeast Gulf Sci. 6(1):67–70.

Saiki, R. K., D. H. Gelfand, S. Stoffel, S. Scharf, R. H. Higuchi, G. T. Horn, K. B. Mullis, and H. A. Erlich.
1988. Primer-directed enzymatic amplification of DNA with a thermostable DNA polymerase. Science (Wash. D.C.) 239:487–491.

Saitou, N., and M. Nei.
1987. The neighbor-joining method: a new method for reconstructing phylogenetic trees. Mol. Biol. Evol. 4:406–425.

Sambrook, J., E. F. Fritsch, and T. Maniatis.
1989. Molecular cloning: a laboratory manual, 2nd ed. Cold Spring Harbor Laboratory Press, Cold Spring Harbor, NY.

Sanger, F., S. Nicklon, and A. R. Coulson.
1977. DNA sequencing with chain termination inhibitors. Proc. Natl. Acad. Sci. USA 74:5,463–5,467.

Slatkin, M.
1987. Gene flow and the geographic structure of natural populations. Science (Wash. D.C.) 236:782–792.

Sokal, R. R., and F. J. Rohlf.
1995. Biometry, 3rd ed. W. H. Freeman, New York, NY, 887 p.

Stabile, J., J. R. Waldman, J. Hart, and I. Wirgin.
1996. Stock structure and homing fidelity is high in Gulf of Mexico sturgeon (*Acipenser oxyrinchus desotoi*) based on restriction fragment length polymorphism and sequence analyses of mitochondrial DNA. Genetics 144:767–775.

Stepien, C.
1995. Population genetic divergence and geographic patterns from DNA sequences: examples from marine and freshwater fishes. Am. Fish. Soc. Symp. 17:263–287.

Tringali, M. D., and T. M. Bert.
1996. The genetic stock structure of common snook (*Centropomus undecimalis*). Can. J. Fish. Aquat. Sci. 53:974–984.
1998. Risk to effective population size should be an important consideration in fish stock-enhancement programs. *In* Proceedings of marine stock enhancement: a new perspective, p. 641–660. Bull. Mar. Sci. 62(2).

Utter, F.
1998. Genetic problems of hatchery-reared progeny released into the wild, and how to deal with them. *In* Proceedings of marine stock enhancement: a new perspective, p. 623–640. Bull. Mar. Sci. 62(2).

Woodward, A. G., and N. Nicholson.
1997. Movement of adult red drum in the central south Atlantic Bight (abstract). *In* 1997 Southern Div., Am. Fish. Soc., February 13–16, San Antonio, TX, 28 p.

Wright, S.
1943. Isolation by distance. Genetics 28:114–138.

Mortality and hematology of blue crabs, *Callinectes sapidus*, experimentally infected with the parasitic dinoflagellate *Hematodinium perezi**

Jeffrey D. Shields
Christopher M. Squyars
Department of Environmental Sciences
Virginia Institute of Marine Science
The College of William and Mary
P.O. Box 1346, Gloucester Point, VA 23602
E-mail address (for J. D. Shields): jeff@vims.edu

Abstract.—On the eastern seaboard of the United States, populations of the blue crab, *Callinectes sapidus*, experience recurring outbreaks of a parasitic dinoflagellate, *Hematodinium perezi*. Epizootics fulminate in summer and autumn causing mortalities in high-salinity embayments and estuaries. In laboratory studies, we experimentally investigated host mortality due to the disease, assessed differential hematological changes in infected crabs, and examined proliferation of the parasite. Mature, overwintering, nonovigerous female crabs were injected with 10^3 or 10^5 cells of *H. perezi*. Mortalities began 14 d after infection, with a median time to death of 30.3 ±1.5 d (SE). Subsequent mortality rates were greater than 86% in infected crabs. A relative risk model indicated that infected crabs were seven to eight times more likely to die than controls and that decreases in total hemocyte densities covaried significantly with mortality. Hemocyte densities declined precipitously (mean=48%) within 3 d of infection and exhibited differential changes in subpopulations of granulocytes and hyalinocytes that lasted throughout the course of the infection. Crabs that did not present infections after injection (i.e. "immune" hosts) did not show hemocytopenia and exhibited significant long-term (21–27 d) granulocytemia. Detection of the parasite in the hemolymph of infected crabs increased from approximately 30% after 14 d to 60% after 21 d to 100% after 35 d. Plasmodial stages were, however, detectable in histological preparations of the heart within 3 days of infection and increased in number over 5 and 7 days. Sporulation of the parasite occurred over a short time (at least 4 d, after 43 d of infection) and did not culminate in the immediate death of the host. *Hematodinium perezi* represents a significant threat to the blue crab fisheries in high-salinity estuaries. Although the parasite infects male and female crabs, it may have a greater impact on mature females as they move to higher salinities to breed.

Manuscript accepted 23 August 1999.
Fish. Bull. 98:139–152 (2000).

Hematodinium perezi is a parasitic dinoflagellate that proliferates in the hemolymph of several crab species. In the blue crab, *Callinectes sapidus*, *H. perezi* is highly pathogenic and usually kills the host. The main symptom of the infection is lethargy. Heavy infections are characterized by discolored (brown, yellow, milky or chalky) hemolymph that does not clot. The disease occurs in blue crabs in high-salinity (>11‰) waters from Delaware to Florida, and in the Gulf of Mexico (Newman and Johnson, 1975; Messick and Sinderman, 1992). In 1975, Newman and Johnson (1975) reported a prevalence of 30% in blue crabs from Florida; the effect of this disease on the blue crab population was thought to be high.

In 1991 and 1992, prevalences of infection up to 100% were found in blue crabs (mean prevalence=43%, several locations from 70% to 100%, n=971) from coastal bays in Maryland and Virginia (Messick, 1994). Commercial watermen reported reduced catches, lethargic and moribund crabs in pots and shedding facilities, and crabs that died soon after capture (Rux, Oesterling[1]). In 1996 and 1997, 10% to 40% of adult crabs from the eastern portions of Chesapeake Bay in Virginia were infected.[2] The disease has a low prevalence or does not occur in the larger, riverine ("bayside") fishery; it appears most detrimental to the coastal ("seaside") crab fisheries.

Outbreaks of infestation by *Hematodinium* spp. have caused concerns to several major crustacean fisheries. Significant population declines and economic losses have been reported for the Tanner (*Chionoecetes bairdi*) and snow (*C. opilio*) crab fisheries of Alaska and Newfoundland (Meyers et al., 1987, 1990; Taylor and Khan, 1995),[3] the Norway lobster (*Nephrops norvegicus*) fishery of western Scotland (Field et al., 1992), and the velvet crab (*Necora puber*) fishery of western France (Wilhelm and Miahle, 1996). The parasite causes a condi-

* Contribution 2241 from the Virginia Institute of Marine Science, The College of William and Mary, Gloucester Point, VA 23602.

[1] Rux, S. 1993. Red Bank Seafood Co., Box 37 Marionville, VA 23408. Personal commun.; Oesterling, M. 1993. VASG, Virginia Inst. Marine Science, Gloucester Point, VA 23062. Personal commun.

[2] Shields, J. D. 1997. An investigation into the epizootiology of *Hematodinium perezi*, a parasitic dinoflagellate in the blue crab, *Callinectes sapidus*. Saltonstall-Kennedy Program, National Marine Fisheries Service, NOAA. Final Report.

[3] Prevalences in Newfoundland are now at 1–15% in the northern bays. Taylor, D. 1998. DFO, CP 5567, White Hills, St. Johns, Newfoundland, Canada, A1C 5X1. Personal commun.

tion known as bitter crab disease in snow and Tanner crabs (Meyers et al., 1987). Low prevalences (1–4%) of another species, *H. australis*, have been reported in sand (*Portunus pelagicus*) and mud (*Scylla serrata*) crabs from Australia (Shields, 1992; Hudson and Shields, 1994).

Infections of *Hematodinium* spp. or *Hematodinium*-like species have been reported from a variety of different hosts (see Shields, 1994, for review). There are, however, only two described species of *Hematodinium*: *H. perezi* Chatton and Poisson, 1931, and *H. australis* Hudson and Shields, 1994. By convention (Newman and Johnson, 1975; MacLean and Ruddell, 1978) and from its distinct morphological features, we concur that *Hematodinium perezi* is the infectious species in the American blue crab.

Blue crabs sustain one of the largest fisheries in Chesapeake Bay. Current management plans and state regulations are based on population assessments that include numbers of juvenile and adult crabs found during winter, spring, and summer surveys (Lipcius and Van Engel, 1990; Abbe and Stagg, 1996; Rugolo et al., 1998). Although these projections include estimates of natural mortalities, they do not account for the potential epizootics and mortalities caused by *Hematodinium perezi*. In this study, we examined host mortality in controlled laboratory experiments and documented changes in the hemograms (total cell counts, and differential counts) of inoculated crabs versus uninfected crabs. We also examined proliferative growth of *H. perezi* at approximately weekly intervals and made observations on the biology and life history of the parasite.

Materials and methods

Blue crabs were collected from Chesapeake Bay and several of its subestuaries during the annual VIMS Winter Dredge Survey (part of the Chesapeake Bay Stock Assessment Program) with a 1.83-m-wide Virginia crab dredge fitted with 0.5-inch (1.25-cm) Vexar mesh dragged on the bottom for one minute at three knots. Crabs were also taken with commercial crab pots from two reference locations on the Delmarva Peninsula, Red Bank and Hungars Creeks, Virginia. Uninfected crabs were housed together for three to seven days prior to treatment to ensure acclimation and absence of overt bacterial or protozoal diseases (as assayed below). During the experiments, crabs were fed fish and squid semiweekly and held individually in aquaria (5 gal., 19 liter) at 20° to 21°C, and 24 ppt salinity. Although *H. perezi* infects both sexes, only mature, nonovigerous female crabs (healthy, orange maturing gonads, little to no shell damage, 120–160 mm carapace width including epibranchial spines) were used in the experiments. Females were used to limit the number of treatment effects (e.g. potential differences between sexes) and to improve sample sizes given the laborious nature of the experiments.

Hematodinium perezi was maintained in the laboratory by serial passage of infected hemolymph. Hemolymph from naturally infected crabs was injected directly into uninfected crabs. Naïve (unexposed) crabs and crabs used for inoculation experiments were obtained from low-salinity non-enzootic locations. Infected and inoculated crabs were housed separately and used as hemolymph donors to inject naïve hosts (10^5–10^6 parasites per host). Injections were given in the arthrodial membrane of the fifth leg at the juncture of the basis with the carapace. We have maintained *H. perezi* for over seven months using this method with no apparent loss from pathogenicity.

Two mortality experiments and one early life history experiment were undertaken. The mortality-I experiment used raw, infected hemolymph as the inoculant. Although appropriate for maintaining infections in the laboratory, raw hemolymph cannot be adjusted to manipulate parasite densities without the use of physiological buffers, nor can it be guaranteed as sterile without appropriate assessment (see Welsh and Sizemore, 1985). Preliminary experiments with sterile sea water, physiological buffers, and infected hemolymph indicated that buffer-washed parasites remained infectious, and could, therefore, be adjusted to consistent densities appropriate to controlled experiments. The mortality-II experiment used buffer-washed parasites adjusted to a density similar to that used in the mortality-I experiment. Mortality-II experiment closely resembled mortality-I experiment except for 1) handling (buffer washes with centrifugation) and 2) the use of plasmodial versus uninucleate stages of the parasite. Uninfected crabs served as controls in both experiments. Controls were used to assess handling effects and to establish baseline densities of hemocytes. The early infection experiment was designed to examine the effects of early infections on the hematology of the host and the early life history of the parasite. Experimental densities in the early infection experiment were four times higher than those in the previous experiments (4.1×10^5 vs. approx. 1.0×10^5 parasites/crab, respectively) and were arbitrarily higher to insure observation of parasites prior to their proliferation.

In the mortality-I and mortality-II experiments different proportions of trophonts and plasmodia were used (for definitions see below). The mortality-I experiment consisted of a control group of uninfected crabs (n=22) injected individually with 100 µL

of hemolymph from an uninfected donor crab and an experimental group (n=20) injected individually with 100 µL of infected hemolymph from a donor crab containing an estimated 1.3×10^6 trophonts/mL (1.3×10^5 trophonts per crab).

The mortality-II experiment consisted of a control group (n=8) injected individually with 100 µL of physiological saline buffer (modified from Appleton and Vickerman, 1998; NaCl, 19.31 g/L; KCl 0.65 g/L; $CaCl_2 \cdot 2H_2O$ 1.38 g/L; $MgSO_4 \cdot 7H_2O$ 1.73 g/L; Na_2SO_4 0.38 g/L; HEPES 0.82 g/L;) adjusted to pH 7.8, with added glucose (1.0 mg/mL) and two experimental treatments (high dose=1.0×10^5 parasites/crab; low dose=1.0×10^3 parasites per/crab, n=10, 10 respectively). To prepare the inoculum for the experimental treatments, 2.0 mL of infected hemolymph were drawn from a donor crab infected with 6.15×10^7 parasites/mL (comprising 97% plasmodia; 3% trophonts). The infected hemolymph was diluted 1:1 with buffer, centrifuged at 4000 rpm for 10 minutes, the supernatant was decanted, and the cells were resuspended in buffer. The cells were then adjusted to 1.0×10^7 parasites/mL, centrifuged through two more washes, and serially diluted to attain densities of 1.0×10^6 parasites/mL and 1.0×10^4 parasites/mL (for inoculum of 100 µL, 1.0×10^5 parasites/crab and 1.0×10^3 parasites/crab, respectively).

In both experiments, crabs were monitored daily for mortalities. Deaths within the first nine days of each experiment were excluded because of handling stress arising from infrequent, bacterial infections (e.g. Johnson, 1976). None of the crabs in the experiments were infected with amoebae, microsporans, or overt bacterial infections (but see Welsh and Sizemore, 1985 for background levels of *Vibrio* spp. in hemolymph of *C. sapidus*). Ten crabs from each treatment in the mortality-I experiment, and all of the crabs in the mortality-II experiment were bled approximately weekly to assess infection status. In the mortality-I experiment, the same ten crabs were bled approximately weekly until they died; other crabs from within the experiment were added as replacements.

Crab hemolymph was taken by using a tuberculin syringe (1 mL) with a 25.5-ga. needle from the arthrodial membrane at the juncture of the basis and the ischium of the 5th pereopod (swimming leg). Ethanol (70%) was used to sterilize the site of inoculation and blood letting. Total and differential counts of host hemocytes and estimates of parasite density were obtained from individual crabs with a hemocytometer (Neubauer improved, Bright Line, two counts per crab) with phase contrast microscopy at 400×. Host hemocytes were identified as granulocytes, semigranulocytes (intermediate cells with relatively few granules, Bodammer, 1978; Johnson, 1980) and hyalinocytes (cell types defined in Söderhäll and Cerenius, 1992). Hemocyte and parasite densities higher than 1.0×10^7 cells/mL were diluted 1:5 with buffer and recounted to provide better estimates of cell density. For comparative purposes, total hemocyte densities and differential counts from naturally infected male and female crabs were also obtained.

Parasites were easily distinguished from host cells by using phase contrast microscopy (Fig. 1): uninucleate trophonts (9–15 µm) possessed few small, refractile vacuoles and were rounded or amoeboid, without filopodia; multinucleate plasmodia (20–100 µm) were slender, vermiform, and motile. The density of infection refers to the number of parasites per mL of hemolymph. Total hemocyte density refers to the number of hemocytes per mL of hemolymph. Mean intensity refers to the mean number of parasites per quantity of *infected* host tissue (Margolis et al., 1982).

Permanent preparations of hemolymph were processed and stained as described in Messick (1994). Briefly, acid-cleaned, poly-l-lysine-coated microslides were smeared with fresh hemolymph, allowed to stand for 2–3 minutes, and fixed in Bouin's fixative. The smears were processed through a routine Harris hematoxylin and eosin-Y procedure (Humason, 1979, p. 123 without acid destain).

The early infection experiment consisted of a control group (n=5 crabs) injected individually with 100 µL of hemolymph from an uninfected donor crab and an experimental group (n=20) injected with 100 µL of hemolymph from a donor crab containing an estimated 4.1×10^6 parasites/ml (4.1×10^5 parasites per crab; comprising 79% plasmodia, 21% trophonts). Three days prior to infection, cell counts were conducted on all crabs to serve as a benchmark (presample) for before-after comparisons. On days 3, 5, and 7 after inoculation, five infected crabs were bled and dissected. Differential cell counts were conducted and tissue samples taken for histological analysis. Tissue samples were processed through a routine hematoxylin and eosin procedure and included muscle, hepatopancreas, heart, and, in some cases, foregut. The control crabs were bled and tissue samples taken 10 days after injection.

For statistical analyses, the proportional hazards model with the Weibull distribution was used to examine survival data and associated variables (Cox and Oakes, 1984). The Tarone-Ware log-rank test was used to examine differences between survival curves (Wilkinson, 1997). ANOVA was used to analyze relationships in hemocyte densities and proportion of cell type (cell type density divided by total hemocyte density) between inoculated and uninfected crabs. Simi-

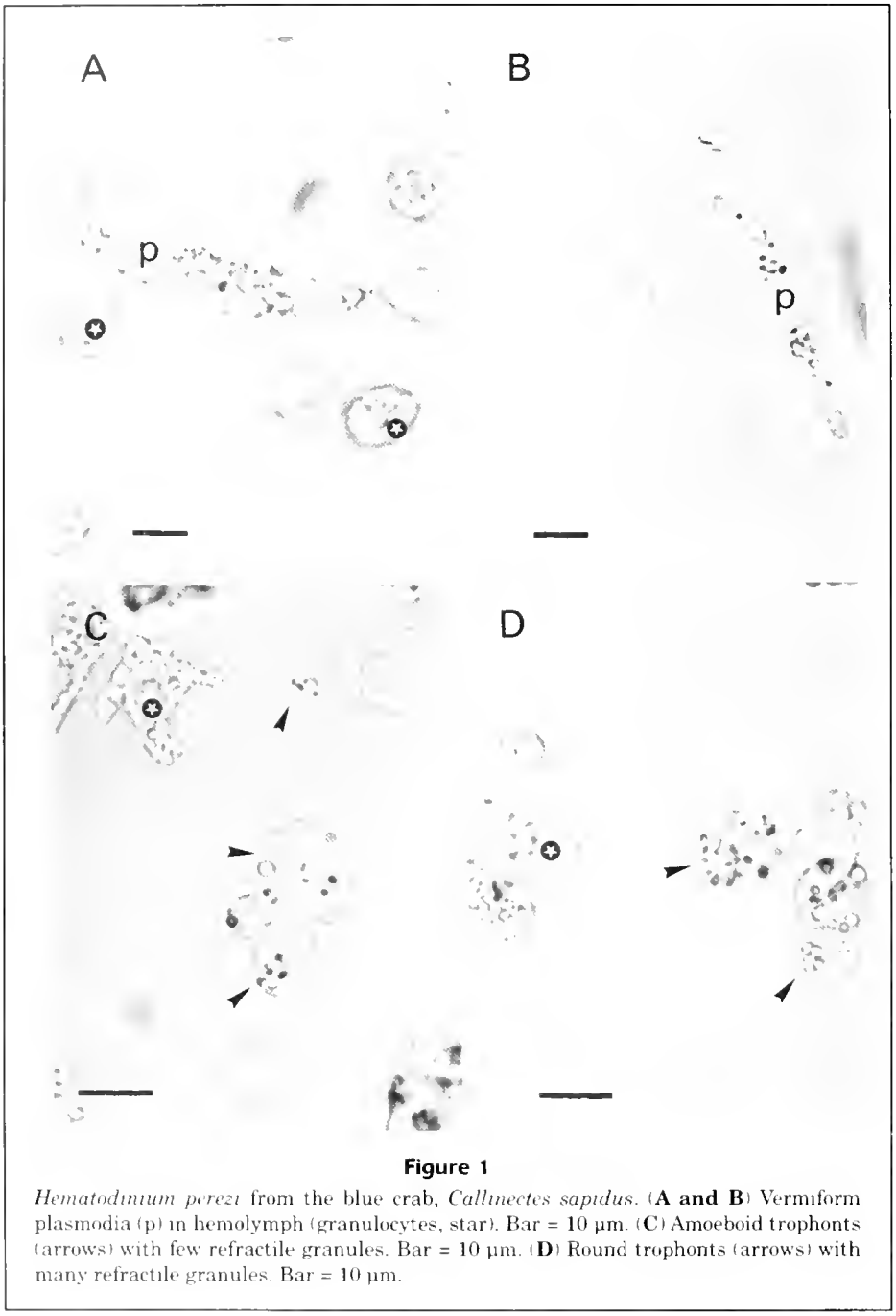

Figure 1

Hematodinium perezi from the blue crab, *Callinectes sapidus*. (**A and B**) Vermiform plasmodia (p) in hemolymph (granulocytes, star). Bar = 10 µm. (**C**) Amoeboid trophonts (arrows) with few refractile granules. Bar = 10 µm. (**D**) Round trophonts (arrows) with many refractile granules. Bar = 10 µm.

lar densities and proportions of cell types were noted in hematology and survival between the mortality-I and mortality-II experiments; hence, data were combined *a posteriori* for the analyses. Where similar trends were noted between statistics for injection dosage (10^3 vs. 10^5), data were also combined for the analysis (i.e. survivorship, hematology). SYSTAT (Wilkinson, 1997) and SAS (SAS, 1988) were used for the analyses. A probability level of $P < 0.05$ was accepted as significant.

Results

Inoculated crabs that became infected with *Hematodinium perezi* began dying two weeks after inoculation (Fig. 2). Mortalities peaked at three weeks after injection and continued to accumulate from weeks 3 through 5. The mortality rate of the infected crabs was 86%, whereas less than 20% of the controls died. Crab mortalities were similar over the time course of infection between mortality-I (infected

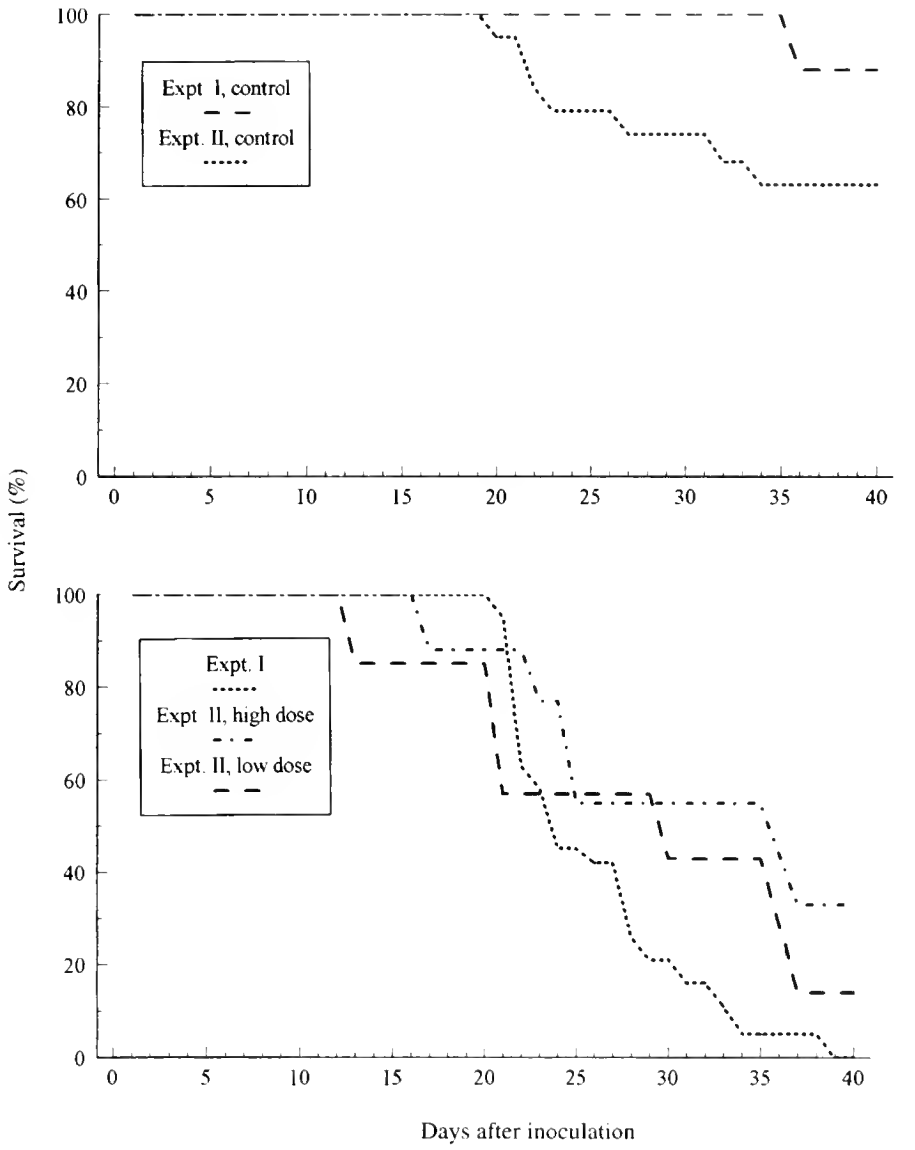

Figure 2

Survivorship curves for uninfected crabs and crabs infected with *H. perezi* (high dose=10^5 parasites/crab, low=10^3 parasites/crab). Sample sizes were 22 and 8 uninfected controls; 20 (mortality-I experiment), 10 and 10 (high and low dose, mortality-II experiment) respectively.

hemolymph, uninucleate trophonts) and mortality-II (buffer-washed parasites, vermiform plasmodia) experiments (Tarone-Ware, χ^2=1.21 with 1 df, P=0.27), even between different initial doses of the parasite (Fig. 2; Tarone-Ware, χ^2=0.74 with 1 df, P= 0.39). Uninfected crabs (controls) experienced significantly fewer mortalities than did infected hosts (Fig. 3; Tarone-Ware, χ^2=, 19.27 with 1 df, P<0.001). The controls for the mortality-II experiment did, however, exhibit background mortalities (Fig. 2); but the mortality rate was not significantly different from controls in the mortality-1 experiment (Tarone-Ware, χ^2=0.65 with 1 df, P= 0.42). None of the control crabs developed infections with *H. perezi*. Because mortalities within treatments were similar between experiments, data were grouped for further analysis.

The median time to death for infected crabs was 30.3 ±1.5 (SE) days. Because the controls exhibited few mortalities, the median time to death for the uninfected controls could not be calculated. Infected crabs had a significantly higher mortality rate, seven to eight times greater than that of the uninfected con-

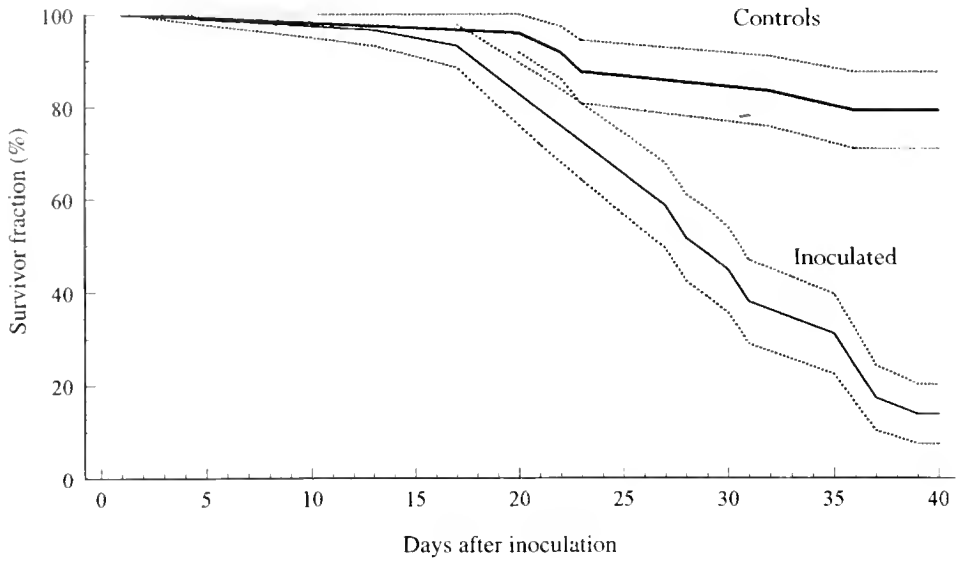

VARIABLE	ESTIMATE	SE	χ^2	P
Intercept	2.933	0.106	763.33	0.0001
Uninfected	1.055	0.287	13.50	0.0002
Injected	0	0		
Scale	0.517	0.083		

Figure 3

Survival function (Kaplan-Meier estimation) for uninfected crabs and crabs infected with *H. perezi*. Dashed lines are upper and lower standard errors. Data include all crabs from mortality-I and mortality-II experiments. Sample sizes are given in Figure 1.

trols (Fig. 3; proportional hazards, χ^2=13.50, P<0.001; relative risk=$e^{1.055/0.5174}$). Hemocyte and parasite density were jointly analyzed as covariates in the proportional hazards model. For injected crabs, the decline in ln(total hemocyte density) was significantly associated with mortality (ln *day of death* = 0.875 + 0.145 ln *total hemocyte density* – 0.017 ln *Parasite density* + 0.409 W; χ^2=4.47 with 1 df, P<0.05). Hemocyte density (untransformed), and parasite density (ln, and untransformed) were not associated with mortality (χ^2, P=0.07, 0.61, and 0.47, respectively); thus, decreases in hemocyte density (ln), not parasite density, were associated with imminent death.

Direct observations from crabs used to maintain infections and experimental results indicated that the parasite was detectable in the hemolymph approximately two weeks after injection (Fig. 4). Although the parasite could be detected as early as one week after inoculation, detectability (the percentage of infected crabs exhibiting detectable parasites in the hemolymph) was relatively low (30–35%) after 14 to 18 days, reaching 80–85% after 26 to 32 days, and 100% after 35 days. (Detectability was based solely on inoculated animals that developed infections. The four crabs from the mortality-II experiment that did not present infections, hereafter referred to as "immune" crabs, were excluded from the analysis of detectability.) Proliferation and growth of the parasite followed a similar pattern as detectability, and the two variables were clearly related (Table 1; Fig. 4).

Growth of the parasite showed a marked increase in the mean density of vermiform plasmodia over days 18 to 26 (Table 1). The mean density of trophonts increased markedly over days 32 to 35. Note, however, that to avoid mortalities from other causes (e.g. secondary infections), sampling could not be done on a daily basis.

Plasmodia were found within the hearts of 93% (n=14/15) of the injected crabs in the early infection experiment. Plasmodia were found in 4 of 5 crabs as early as day 3 (Table 2). Uninucleate trophonts were observed in the heart on and after day 7. Rel-

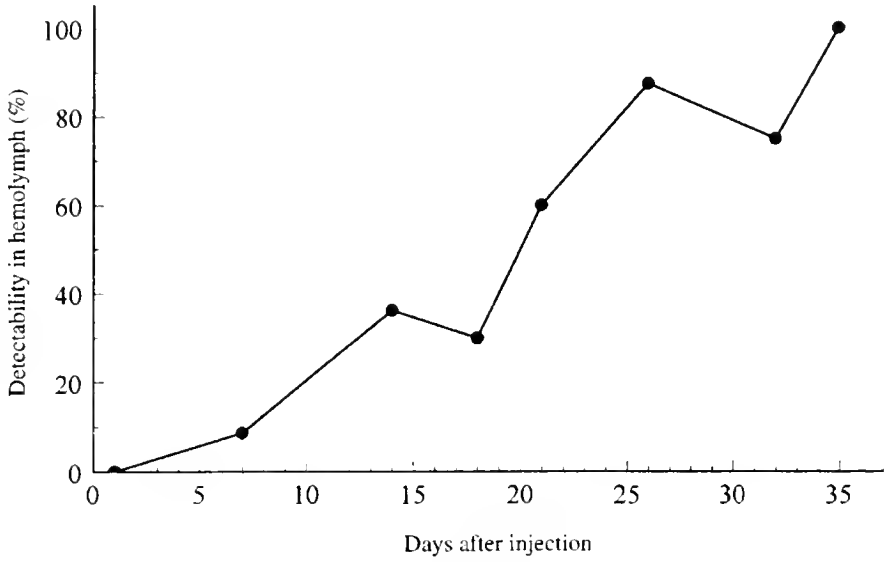

Figure 4

Detectability of parasites in hemolymph of infected blue crabs over the course of infection. Data were combined from mortality-I and mortality-II experiments and include only infected crabs. Samples sizes were 21, 11, 10, 10, 16, 4, and 4 crabs on days 7, 14, 18, 21, 26, 32, and 35, respectively.

Table 1

Parasite intensity ($\times 10^5$ parasites/mL per infected host) in the hemolymph in relation to days after inoculation. Counts combined for mortality-I and mortality-II experiments. N_{plas} = crabs with plasmodia, N_{troph} = crabs with trophonts, $N_{infected}$ = infected crabs exhibiting parasites. See Table 3 for sample sizes for hemocytometry.

		Plasmodia	log(plasmodia)		Trophont	log(trophont)	
Days	N_{plas}	Mean ±SE	Mean ±SE	N_{troph}	Mean ±SE	Mean ±SE	$N_{infected}$
7	1	0.50 ±0.00	4.70 ±0.00	1	0.25 ±0.00	4.40 ±0.00	1
14	4	1.44 ±0.53	5.09 ±0.16	3	1.25 ±0.29	5.06 ±0.11	4
18	1	1.25 ±0.00	5.10 ±0.00	2	1.00 ±0.25	4.99 ±0.11	3
21	5	7.70 ±4.61	5.61 ±0.24	5	8.65 ±4.17	5.87 ±0.18	5
26	11	14.98 ±6.07	5.85 ±0.17	12	8.19 ±3.86	5.40 ±0.22	14
32	2	8.38 ±1.63	5.92 ±0.09	3	4.25 ±1.32	5.59 ±0.14	3
35	4	7.88 ±3.89	5.69 ±0.25	4	49.81 ±36.82	6.35 ±0.31	4

atively more parasites were observed in the heart tissue over time (Table 2); but no effort was made to standardize area in the histological preparations. Growth of the parasite was rapid in the heart. The dosage in the early infection experiment was, however, four times higher than that in the mortality-I and mortality-II experiments; thus, results between experiments were not directly comparable.

Sporulation from the trophont stage to the dinospore stage was observed only in crabs that were used to maintain infections. Parasites in one crab sporulated at least twice and each event lasted less than 4 d. Parasite density was extraordinarily high (1.6×10^8 dinospores/mL) during sporulation, and dropped to moderate levels (3.3×10^6 trophonts/mL) thereafter. Dinospores were observed five times over the course of 26 d, beginning 43 d after injection. Additionally, some crabs injected with only the trophont (vegetative) stage were observed with plasmodia after 3 to 4 weeks of infection.

Hemograms of infected crabs were significantly different from those of uninfected controls (Tables

3 and 4, Fig. 5). Total hemocyte density was significantly depressed in infected crabs (Fig. 5A; 2-way ANOVA by group and day, F=5.03, P<0.001). Total hemocyte density was not significantly different between crabs inoculated with different initial doses (2-way ANOVA, 10^3 vs. 10^5 parasites per crab and day, F=3.19, df=1, 64, P=0.079). Crabs that were injected and did not acquire the infection ("immune" hosts) did not have significant decreases in hemocyte densities (Table 3, Fig. 5; 2-way ANOVA, F=1.46, df = 13, 105, P=0.145). In the early infection experiment, the decrease in total hemocyte densities occurred within three days of inoculation (Table 5).

In addition to a decrease in cell density, the proportions of different host cell types (density of cell type divided by total hemocyte density) in infected crabs shifted to those with proportionally more granulocytes than hyalinocytes (Table 6, Fig. 5, B and D) (2-way ANOVA, F=1.83; df=20, 149, P<0.05). Significant shifts in the population of semigranulocytes were also noted (F=2.51, df =20, 149, P<0.001).

Table 2

Relative intensity of plasmodia in histological preparations of heart sections of mature, nonovigerous female blue crabs from the early infection experiment. Mean intensities represent direct counts of plasmodia and are not standardized by tissue area.

Day	$N_{Infected}/N_{Injected}$	Mean intensity (±SD)	Range
Control	0/4	0.0 ±0.0	—
3	4/5	3.6 ±3.9	1–10
5	5/5	12.0 ±11.0	1–26
7	5/5	55.8 ±26.1	15–74

Table 3

Total mortality-hemocyte densities ($\times 10^6$ hemocytes/mL) in relation to days after inoculation. Hemocyte counts were combined from mortality-I and mortality-II experiments. (-- = not done, no infected crabs survived to day 40).

	Uninfected control crabs		Inoculated, infected crabs		Inoculated, immune crabs	
		Hemocyte density		Hemocyte density		Hemocyte density
Days	N	Mean ±SE	N	Mean ±SE	N	Mean ±SE
7	18	29.17 ±3.09	22	14.39 ±2.05	4	22.99 ±2.32
14	8	32.81 ±3.01	11	16.10 ±3.19	4	33.25 ±2.76
18	9	32.28 ±6.72	10	12.24 ±1.51	--	--
21	8	23.83 ±2.20	10	17.68 ±4.39	4	32.72 ±1.04
26	18	26.65 ±2.15	16	7.64 ±1.49	4	26.29 ±8.00
32	12	20.97 ±3.41	4	4.21 ±2.04	--	--
35	8	23.37 ±4.48	4	10.86 ±6.73	4	23.61 ±11.72
40	10	20.35 ±2.12	--	All dead	4	22.53 ±5.69

Table 4

Total and differential hemocyte densities (mean ±SE; × 10^6 hemocytes/mL) in naturally infected male and female blue crabs in relation to severity of infection (light < 4.0 × 10^5 parasites/mL; moderate = 4.0 · 10^5 to 2.0 · 10^6 parasites/mL; heavy > 2.0 · 10^6 parasites/mL; -- = not done).

Severity	n	Hemocyte density	Granulocyte density	Semigranulocyte density	Hyalinocyte density
Mature males					
Light	4	16 16 ±2.67	5.46 ±1.41	7.69 ±2.07	3.02 ±0.61
Moderate	6	7.46 ±1.74	1.92 ±0.63	4.10 ±1 10	1.45 ±0.46
Heavy	16	6 66 ±2.53	1.34 ±0.53	3.39 ±1.35	1.93 ±0.76
Mature females					
Light	--	--	--	--	--
Moderate	5	22.41 ±11.25	9.32 ±5.15	5.44 ±2.85	7 65 ±3.66
Heavy	5	14.37 ±7.37	5.98 ±3.09	4.01 ±1 63	4.39 ±2.89

"Immune" crabs exhibited a fluctuation in cell types with significantly higher proportions of granulocytes to semigranulocytes during the first five weeks after inoculation (F=4.35, df =5, 18, P<0.01). By day 40, the hemograms of "immune" hosts were virtually identical to those of the uninfected controls (Table 7, Fig. 5, C and D).

In the early infection experiment, hemocyte populations shifted within the first three days of infection (Tables 5 and 6; ANOVA, log hemocytes, F=9.16; df =3, 31, P<0.01); the proportion of granulocytes in infected crabs increased significantly compared with the proportion of semigranulocytes (ANOVA, F=4.39, P<0.05). Uninfected crabs exhibited minor fluctuations in the proportion of granulocytes to that of hyalinocytes but the proportions were similar to those observed in the mortality-I and mortality-II experiments (Tables 6 and 7).

Discussion

In laboratory experiments, *Hematodinium perezi* caused significant mortality to infected mature, nonovigerous blue crabs. Infections were not always fatal (four crabs survived inoculation without developing infections), but the overall mortality to laboratory-inoculated crabs was high at 86% over 40 days. The proportional hazards model indicated that infected crabs were seven to eight times more likely to die than uninfected crabs. Infections in Tanner crab, *Chionoeeetes bairdi*, and Norway lobster, *Nephrops norvegicus*, are frequently fatal to the host (Meyers et al., 1987; Field et al., 1992). The mortality of naturally infected Tanner crabs held in aquaria for 97 days was 67% (n=11) and hosts survived from 20 to 158 days in the laboratory. Uninfected Tanner crabs experienced no mortality during the course of the experiment (Meyers et al., 1987). Naturally infected Norway lobsters suffered mortality rates of 86% to 100% over 27 d and 75 d, respectively, and had mortality rates 2–4 times higher than uninfected lobsters, and most of the deaths occurred early in the course of the experiment (Field et al., 1992).

During epizootics, juvenile blue crabs have a higher prevalence of *H. perezi* than do mature hosts (Messick, 1994). Male blue crabs have a prevalence of infection similar to that for females along the

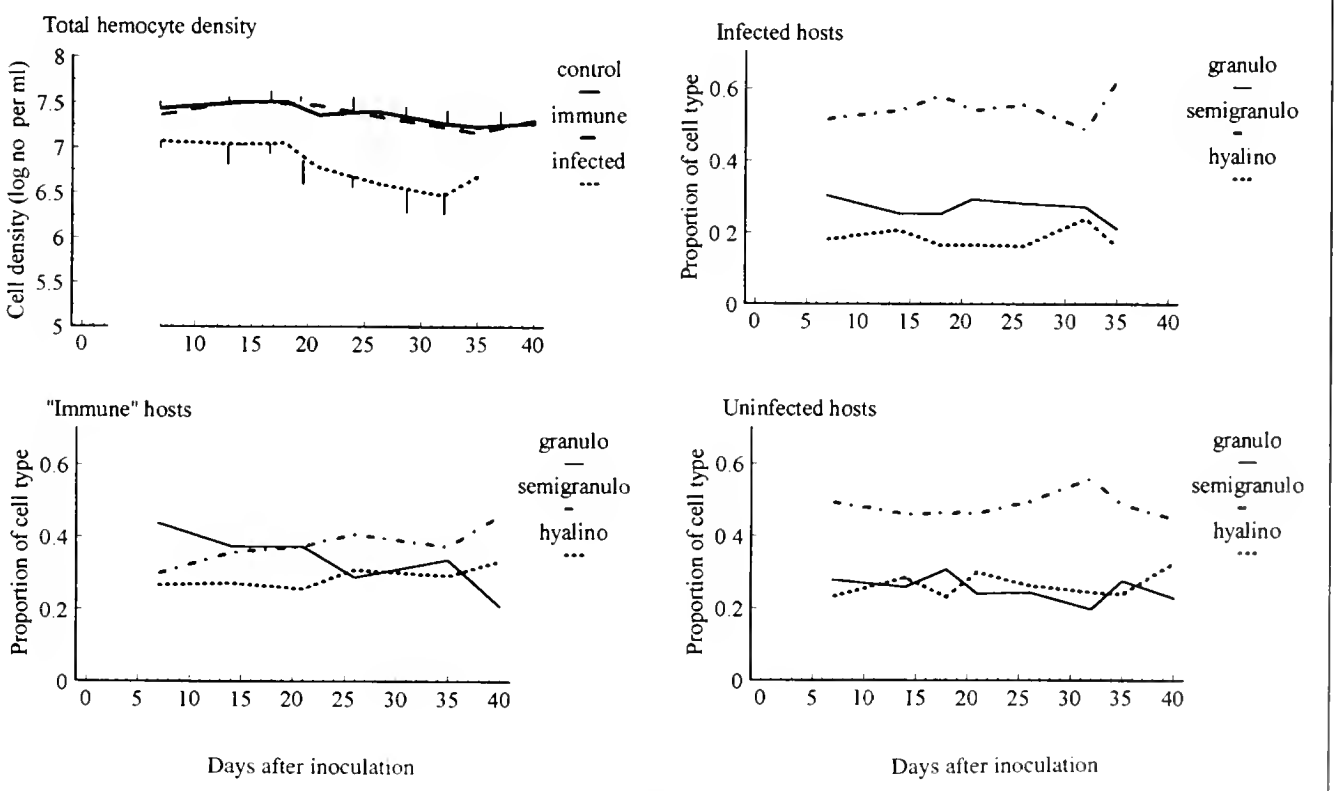

Figure 5

Total hemocyte densities and proportions of host cell types in uninfected, infected and "immune" crabs. Data combined from mortality-I and mortality-II experiments. Bars = SE. Standard errors (not shown) for proportion of host cell types were low (0.02–0.05). "Immune" crabs were survivors from mortality-II experiment that never developed infections. Sample sizes given in Table 3

Table 5

Differential densities of hemocytes ($\times 10^6$ hemocytes/ml) in relation to days after inoculation for crabs in the early infection experiment. Sample sizes are given in Table 2.

	Granulocyte density	Semigranulocyte density	Hyalinocyte density
Days	Mean ±SE	Mean ±SE	Mean ±SE
Uninfected control crabs			
Presample	3.72 ±0.31	7.66 ±0.50	4.53 ±0.79
10	7.48 ±1.60	11.20 ±1.94	5.30 ±1.47
Inoculated, infected crabs			
Presample	6.88 ±0.92	11.43 ±1.00	4.97 ±0.40
3	4.95 ±0.40	4.36 ±0.31	2.80 ±0.15
5	2.51 ±0.91	5.40 ±1.60	1.49 ±0.51
7	2.93 ±0.68	6.92 ±0.80	1.56 ±0.31

Delmarva Peninsula (Messick, 1994; Messick and Shields[4]) and show significantly greater changes than females in certain blood parameters.[5] Infected blue crabs apparently die before acquiring the bitter flavor found in infected Tanner and snow crabs.

Survival analysis indicated that parasite density was not associated with mortality. Similarly, survival time of Norway lobsters did not show a significant relationship with severity of infection, but host mortality did increase with the progression of the disease (Field et al., 1992). In blue crabs, absolute declines in ln(total hemocyte density) were associated with host mortality. Hence, the cellular defensive response of the host appeared seriously compromised by infection. Anecdotal evidence from hosts used to maintain the parasite suggests that infections established with plasmodia are more pathogenic than those established with trophonts; this may explain the similar mortality curves for the high and low doses of plasmodia in the mortality-II experiment. Observations on naturally and experimentally infected crabs indicate three possible outcomes to the disease:

1 Crabs with acute infections, such as those reported here, show rapid mortalities, typically dying within 40 d. Acute infections rarely lead to heavy infections (10^{7+} parasites/mL), and may not lead to the development of dinospores.

Table 6

Total hemocyte densities ($\times 10^6$ hemocytes/mL) in relation to days after inoculation (-- = not done) in the early infection experiment.

	Uninfected control crabs		Inoculated, infected crabs	
		Hemocyte density		Hemocyte density
Days	n	Mean ±SE	n	Mean ±SE
Presample	5	15.91 ±1.25	20	23.28 ±2.06
3	--	--	5	12.11 ±0.50
5	--	--	5	9.39 ±2.94
7	--	--	5	11.40 ±0.96
10	5	23.98 ±4.87	--	--

2 Crabs with chronic infections (observed in very cases, n=4) endure the acute stage, survive for longer periods (up to 90 days), and develop infections that lead to massive numbers of dinospores (Fig. 6).
3 Some crabs successfully resist the parasite or are refractory to the infection. Preliminary experiments (not shown) suggest that resistant crabs (n=10) may become refractory to further inoculations with *H. perezi*.

Blue crab catches fluctuate yearly in Chesapeake Bay but causes for these fluctuations are not well understood. Since salinity appears to limit the distribution of *H. perezi* (Newman and Johnson, 1975), the dinoflagellate could feasibly infect and cause significant mortalities to juvenile and adult crabs

[4] Messick, G. and J. D. Shields. 1999. The epizootiology of the parasitic dinoflagellate *Hematodinium perezi* in the blue crab, *Callinectes sapidus*. Oxford Cooperative Laboratory, 904 S. Morris St., Oxford, MD 21654. Unpubl. data.

[5] Shields, J. D. 1999. Mortality and pathophysiology studies of blue crabs infected with the parasitic dinoflagellate *Hematodinium perezi*. Saltonstall-Kennedy Program, NOAA/National Marine Fisheries Service. Final Report.

Table 7

Differential densities of hemocytes ($\times 10^6$ hemocytes/mL) in relation to days after inoculation. Hemocyte counts were combined from mortality-I and mortality-II experiments (-- = no data, no infected crabs survived to day 40). Sample sizes are given in Table 3.

	Granulocyte density	Semigranulocyte density	Hyalinocyte density
Days	Mean ±SE	Mean ±SE	Mean ±SE
Uninfected control crabs			
7	8.13 ±0.97	13.88 ±1.28	7.16 ±1.10
14	8.34 ±1.17	15.13 ±1.66	9.34 ±0.94
18	8.99 ±1.42	15.37 ±3.33	7.83 ±2.18
21	5.88 ±0.93	10.86 ±0.93	7.09 ±0.91
26	6.56 ±0.73	13.06 ±1.04	7.04 ±0.76
32	4.10 ±0.81	12.14 ±2.21	4.73 ±0.53
35	5.64 ±1.15	11.67 ±2.34	6.05 ±1.37
40	4.66 ±0.61	9.29 ±1.13	6.39 ±0.68
Inoculated, infected crabs			
7	5.28 ±1.04	6.18 ±0.71	2.92 ±0.56
14	5.59 ±1.34	6.90 ±1.26	3.62 ±0.94
18	3.29 ±0.67	6.76 ±0.65	2.20 ±0.47
21	4.77 ±1.23	8.37 ±1.75	4.60 ±1.54
26	2.10 ±0.45	4.25 ±0.83	1.28 ±0.36
32	1.11 ±0.57	2.19 ±1.14	0.90 ±0.41
35	3.11 ±2.13	6.11 ±3.58	1.64 ±1.06
40	--	--	--
Inoculated, immune crabs			
7	9.73 ±0.65	7.08 ±1.58	6.19 ±0.93
14	12.31 ±0.83	11.91 ±1.34	9.03 ±1.00
18	--	--	--
21	11.34 ±2.51	11.94 ±3.44	9.44 ±4.75
26	8.16 ±3.73	10.00 ±2.55	8.14 ±2.80
32	--	--	--
35	7.98 ±4.03	8.03 ±3.89	7.61 ±3.82
40	4.59 ±1.35	10.00 ±2.30	7.94 ±2.71

where salinities are greater than 11‰; i.e. much of the mainstem of Chesapeake Bay. Current models for blue crab populations in Chesapeake Bay are based on population assessments from various surveys (Lipcius and Van Engel, 1990; Abbe and Stagg, 1996; Rugolo et al., 1998). These models project crab abundance for the fishery as a whole but do not separate the larger, low-salinity "bayside" fishery from the smaller, high-salinity "seaside" fishery where mortalities due to *H. perezi* occur. Such projections include estimates of natural mortalities but do not account for the potential epizootics and resulting mortalities caused by *H. perezi*. Differential models of exploitation by region may be warranted, especially during or immediately following epizootics. Disease estimates must, however, account for the variation in the prevalence of detection because the prevalence in field samples may be significantly underreported (see Fig. 3).

The life cycle of *H. perezi* from *C. sapidus* has not been fully documented. Several morphological and life history differences, however, distinctly separate *Hematodinium* sp. ex *N. norvegicus* (Appleton and Vickerman, 1998) from *H. perezi* ex *C. sapidus*. For example, the syncytial and network forms of *Hematodinium* sp. ex *N. norvegicus* (Field and Appleton, 1995) have not been observed with *H. perezi* (Messick, 1994; present study); nor do the plasmodia (cf. filamentous trophonts of Appleton and Vickerman, 1998) of *H. perezi* develop as "gorgonlocks"; rather, they undergo budding to produce additional plasmodia, and schizogony (cf. segmentation in malaria life cycles) to produce uninucleate trophonts (senior author, unpubl. data). The trophonts then undergo further fission. Such differences may warrant generic separation between the two parasites.

Hematodinium perezi was successfully transmitted to blue crabs by injection. Transmission experiments

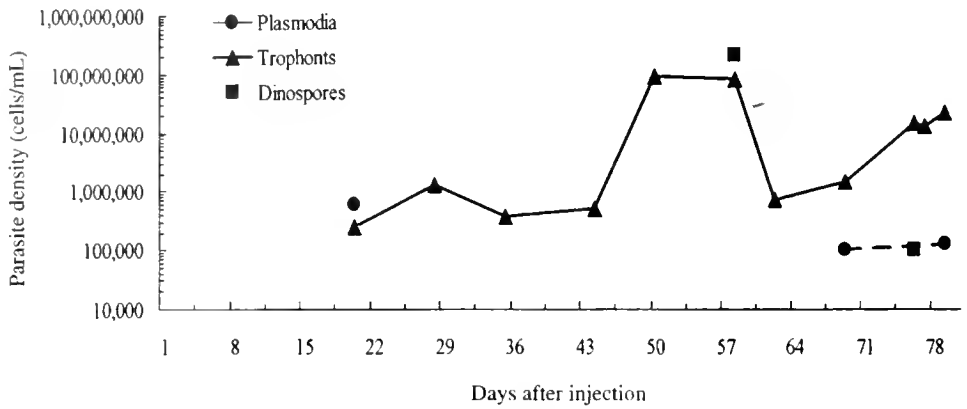

Figure 6

Crab no. 3977 presenting a chronic, experimentally induced infection of *H. perezi* (plasmodia, circles; trophonts, triangles; dinospores, boxes). The crab died after 80 days.

with the parasite in Tanner crabs and Australian sand crabs (*Portunus pelagicus*) have been partially successful. Parasites from primary cell culture (with sterile hemolymph) were successful in establishing infections in Tanner crabs, but inoculation with vegetative stages did not produce infections (Meyers et al., 1987). Injections of trophonts (vegetative stages) were successful in producing infections in the sand crab, but other stages were not investigated (Hudson and Shields, 1994). Infection experiments with Norway lobster have not been reported. Transmission with cultured dinospores has yet to be achieved (Appleton and Vickerman, 1998). Sporulation is a rapid event with *H. perezi*, presumably occurring over several hours instead of several days or weeks as reported for *Hematodinium* sp. from Tanner crabs (Meyers et al., 1987, 1990). At lower temperatures and salinities, *H. perezi* apparently ceases to grow or slows its proliferation in naturally infected blue crabs.[6]

Densities of circulating hemocytes declined rapidly in infected blue crabs. The decline occurred within the first three days and progressed to a 48% decrease in total hemocyte densities within the first week of infection. After three weeks, absolute declines of up to 80% were noted for total hemocyte densities. The loss of cells was evident early in the infection even though the parasites were not detectable in hemolymph. Declines in hemocyte densities have been reported for starved lobsters (33–60% loss) (Stewart et al., 1967), *Aeromonas*-infected lobsters (80–84% loss) (Stewart et al., 1983), *Fusarium*-infected brown shrimp, *Penaeus californiensis* (approximately 88% loss) (Hose et al., 1984), and *Vibrio*-infected *Cancer irroratus* (95% loss) (Newman and Feng, 1982). Reductions in hemocytes were noted for Norway lobster, *N. norvegicus*, infected with *Hematodinium* sp. (Field and Appleton, 1995), and for blue crabs, *C. sapidus*, infected with *Paramoeba perniciosa* (Sawyer et al., 1970), but the degree of loss, and differential counts were not quantified. Declines in hemocyte counts occur quickly in crayfish, *Pacifastacus leniusculus*, (10 min) and are associated with loss of resistance to *Aphanomyces* infections; the declines are dependent upon the stimuli (yeast vs. zymosan vs. buffers), and are evident over the course of several days (Perrson et al., 1987).

Crustacean cell types probably represent maturation of a single lineage (e.g. Bodammer, 1978; Bachau, 1981; Hose et al., 1990). Hyalinocytes represent younger cells that become semigranulocytes (intermediate hemocytes), then granulocytes. Infected crabs exhibited marked shifts in subpopulations of different hemocyte stages (cell types). Because there was an absolute decline in the total number of circulating hemocytes and relative declines in hyalinocytes and semigranulocytes, we suggest that cell death and differential sequestration occur in response to the disease. General declines in hemocyte density in *N. norvegicus* infected with *Hematodinium* sp. may occur from sequestration, other defense reactions, and hydrostatic effects of heavy infections or clogging of hemal sinuses (Field and Appleton, 1995). In our study, the rapid decline in total hemocyte density (within three to seven days) argues against hydrostatic effects and clogged sinuses. The shift towards proportionally more granulocytes than hyalinocytes may result from mobilization of tissue-dwelling reserves, differential cell death (Mix and

[6] Messick, G. 1998. Oxford Cooperative Laboratory, 904 S. Morris St., Oxford, MD 21654. Personal. commun.

Sparks, 1980), changes in mitotic stimuli of hemopoetic tissue (Hose et al., 1984), or sequestration of specific cell types in defense of the infection (e.g. nodule formation, Johnson, 1976, 1977). Hyalinocytes and semigranulocytes are the major phagocytic hemocytes in crustaceans (Bachau, 1981; Hose et al., 1990). Such hemocytes form nodules in bacterial, amoebic, and *Hematodinium* infections in blue crabs, *Hematodinium* infections in *N. norvegicus*, and gaffkemia infections in *Homarus americanus* (Johnson, 1976, 1977; Johnson et al., 1981; Messick, 1994; Field and Appleton, 1995) are thus removed from circulation, and may account, in part, for the observed declines. In fungal infections of crayfish, *P. leniusculus*, hemocytic nodules do not dissociate in the presence of zymosan, a yeast derivative, and may last several days (Perrson et al., 1987). In *Aeromonas*-infected lobsters, the hyalinocytes increase in proportion to the other cell types, presumably by increased mitotic activity in hemopoeitic centers, but there is a significant decline in hemocytes after five days of infection (Stewart et al., 1983).

Lastly, several blue crabs (n=4) successfully fought off the infection. These "immune" crabs exhibited significant sustained levels of granulocytes, did not suffer hemocytopenia, their hemolymph clotted normally, and they did not exhibit gross changes in morbidity. Histological preparations of heart, hepatopancreas, muscle, and hemopoeitic tissues were negative for latent infections in the "immune" animals. The relative increase in semigranulocytes and sustained densities of hyalinocytes over time (Fig. 5) suggests an increase in mitotic activity in hemopoetic tissue in response to the infection. This increase may not be sufficient to counter the parasite in susceptible hosts. In *N. norvegicus* infected with *Hematodinium* sp., the hemopoeitic tissues show marked increases in activity. Although changes in host cell densities were not quantified, apparent stem cells were present in the active nodes (Tables 1 and 2 in Field and Appleton, 1995). The role of the granulocytes in the defense against *Hematodinium* infections and the underlying mechanisms leading to refractory hosts warrant further study.

Acknowledgments

We wish to thank Seth Rux and Mike Seebo for their generous help. Seth Rux and members of the VIMS Dredge Surveys ably provided crabs. We thank Mary Anne Vogelbein, Romuald Lipcius, and Morris Roberts for technical advice, as well as Mike Newman for assistance with the survival analyses. Gretchen Messick and John Pearce improved the manuscript. This work was supported by NOAA, Saltonstall-Kennedy Grant NA76FD0148.

Literature cited

Abbe, G. R., and C. Stagg.
1996. Trends in blue crab (*Callinectes sapidus* Rathbun) catches near Calvert Cliffs, Maryland from 1968 to 1995 and their relationship to the Maryland commercial fishery. J. Shellfish Res. 15:751–758.

Appleton, P. L., and K. Vickerman.
1998. In vitro cultivation and developmental cycle of a parasitic dinoflagellate (*Hematodinium* sp.) associated with mortality of the Norway lobster (*Nephrops norvegicus*) in British waters. Parasitology 116:115–130.

Bachau, A. G.
1981. Crustaceans. *In* N. A. Ratcliffe and A. F. Rowley (eds.), Invertebrate blood cells, vol. 2, Arthropods to urochordates, invertebrates and vertebrates compared, p. 385–420. Academic Press, London, 641 p.

Bodammer, J. E.
1978. Cytological observations on the blood and hemopoietic tissue in the crab, *Callinectes sapidus*. Cell Tiss. Res. 187:79–96.

Cox, D. R., and D. Oakes.
1984. Analysis of survival data. Chapman and Hall, NY, 201 p.

Field, R. H., and P. L. Appleton.
1995. A *Hematodinium*-like dinoflagellate infection of the Norway lobster *Nephrops norvegicus*: observations on pathology and progression of infection. Dis. Aquat. Org. 22: 115–128.

Field, R. H., C. J. Chapman, A. C. Taylor, D. M. Neil, and K. Vickerman.
1992. Infection of the Norway lobster *Nephrops norvegicus* by a *Hematodinium*-like species of dinoflagellate on the west coast of Scotland. Dis. Aquat. Org. 13:1–15.

Hose, J. E., D. V. Lightner, R. M. Redman, and D. A. Danald.
1984. Observations on the pathogenesis of the imperfect fungus, *Fusarium solani*, in the California brown shrimp, *Penaeus californiensis*. J. Invertebr. Pathol. 44:292–303.

Hose, J. E., G. G. Martin, and A. S. Gerard.
1990. A decapod hemocyte classification scheme integrating morphology, cytochemistry, and function. Biol. Bull. 178: 33–45.

Hudson, D., and J. D. Shields.
1994. *Hematodinium australis* n. sp., a parasitic dinoflagellate of the sand crab, *Portunus pelagicus*, and mud crab, *Scylla serrata*, from Moreton Bay, Australia. Dis. Aquat. Orgs., 19:109–119.

Humason, G. L.
1979. Animal tissue techniques, 4th ed. Freeman and Co., San Francisco.

Johnson, P. T.
1976. Bacterial infection in the blue crab, *Callinectes sapidus*: course of infection and histopathology. J. Invertebr. Pathol. 28:25–36.
1977. Paramoebiasis in the blue crab, *Callinectes sapidus*. J. Invertebr. Pathol. 29: 308–320.
1980. Histology of the blue crab, *Callinectes sapidus*: a model for the Decapoda. Praeger Scientific, NY, 440 p.

Johnson, P. T., J. E. Stewart and B. Arie.
1981. Histopathology of *Aerococcus viridans* var. *homari* infection (Gaffkemia) in the lobster, *Homarus americanus*,

and a comparison with histological reactions to a Gram-negative species *Pseudomonas perolens*. J. Invertebr. Pathol. 38:127–148.

Lipcius, R. N., and W. A. Van Engel.
1990. Blue crab population dynamics in Chesapeake Bay: variation in abundance (York River, 1972–1988) and stock-recruitment functions. Bull. Mar. Sci. 46:180–194.

Margolis, L., G. W. Esch, J. C. Holmes, A. M. Kuris, and G. A. Schad.
1982. The use of ecological terms in parasitology. J. Parasitol. 68:131–133.

MacLean, S. A., and C. L. Ruddell.
1978. Three new crustacean hosts for the parasitic dinoflagellate *Hematodinium perezi* (Dinoflagellata: Syndinidae). J. Parasitol. 64:158–160.

Messick, G. A.
1994. *Hematodinium perezi* infections in adult and juvenile blue crabs *Callinectes sapidus* from coastal bays of Maryland and Virginia, USA. Dis. Aqua. Org., 19:77–82.

Messick, G. A., and C. J. Sinderman.
1992. Synopsis of principal diseases of the blue crab, *Callinectes sapidus*. U.S. Dep. Commer., NOAA Tech. Memo. NMFS-F/NEC-88.

Meyers, T. R., C. Botelho, T. M. Koeneman, S. Short, and K. Imamura.
1990. Distribution of bitter crab dinoflagellate syndrome in southeast Alaskan Tanner crabs *Chionoecetes bairdi*. Dis. Aquat. Org. 9:37–43.

Meyers, T. R., T. M. Koeneman, C. Botelho, and S. Short.
1987. Bitter crab disease: a fatal dinoflagellate infection and marketing problem for Alaskan Tanner crabs *Chionoecetes bairdi*. Dis. Aquat. Org. 3:195–216.

Mix, M. C., and A. K. Sparks.
1980. Tanner crab *Chionoecetes bairdi* Rathbun haemocyte classification and an evaluation of using differential counts to measure infection with a fungal disease. J. Fish Dis. 3:285–293.

Newman, M. C., and S. Y. Feng.
1982. Susceptibility and resistance of the rock crab, *Cancer irroratus*, to natural and experimental bacterial infection. J. Invertebr. Pathol. 40:75–88.

Newman, M. W., and C. A. Johnson.
1975. A disease of blue crabs (*Callinectes sapidus*) caused by a parasitic dinoflagellate, *Hematodinium* sp. J. Parasitol. 61:554–557.

Persson, M., L. Cerenius, and K. Söderhäll.
1987. The influence of haemocyte number on the resistance of the freshwater crayfish, *Pacifastacus leniusculus* Dana, to the parasitic fungus *Aphanomyces astaci*. J. Fish Dis. 10:471–477.

Rugolo, L. J., K. S. Knotts, A. M. Lange, and V. A. Crecco.
1998. Stock assessments of Chesapeake Bay blue crab (*Callinectes sapidus* Rathbun). J. Shellfish Res. 17:493–517.

SAS Institute, Inc.
1988. SAS, STAT user's guide, release 6.03. SAS Institute, Inc., Cary, NC, 1028 p.

Sawyer, T. K., R. Cox, and M. Higginbottom.
1970. Hemocyte values in healthy blue crabs, *Collinectes sapidus*, and crabs infected with the amoeba, *Paramoeba perniciosa*. J. Invertebr. Pathol. 15:440–446.

Shields, J. D.
1992. The parasites and symbionts of the blue sand crab, *Portunus pelagicus*, from Moreton Bay, Australia. J. Crust. Biol. 12:94–100.
1994. The parasitic dinoflagellates of marine Crustacea. Ann. Rev. Fish Dis. 4:241–271.

Söderhäll, K., and L. Cerenius.
1992. Crustacean immunity. Ann. Rev. Fish Dis. 2:3–23.

Stewart, J. E., B. Arie, and L. Marks.
1983. Hemocyte patterns during gaffkemia infections and induction of resistance in *Homarus americanus*. Rapp. P.-V. Reun. Cons. Int. Explor. Mer. 182:126–129.

Stewart, J. E., J. W. Cornick, D. M. Foley, M. F. Li, and C. M. Bishop.
1967. Muscle weight relationship to serum proteins, hemocytes, and hepatopancreas in the lobster, *Homarus americonus*. J. Fish. Res. Board Can. 24:2339–2354.

Taylor, D. M., and R. A. Khan.
1995. Observations on the occurrence of *Hematodinium* sp. (Dinoflagellata: Syndinidae), the causative agent of bitter crab disease in Newfoundland snow crab (*Chionoecetes opilio*). J. Invertebr. Pathol. 65:283–288.

Wilhelm, G., E. Mialhe.
1996. Dinoflagellate infection associated with the decline of *Necora puber* crab populations in France. Dis. Aquat. Orgs. 26:213–219.

Wilkinson, L.
1997. SYSTAT 7.0: new statistics. SPSS, Inc., Chicago, IL, 303 p.

Welsh, P. C., and R. K. Sizemore.
1985. Incidence of bacteremia in stressed and unstressed populations of the blue crab, *Callinectes sapidus*. Applied Environ. Microbiol. 50:420–425.

Age determination and growth of Hudson River Atlantic sturgeon, *Acipenser oxyrinchus**

Jill T. Stevenson
David H. Secor
Center for Environmental Science
Chesapeake Biological Laboratory
University of Maryland
P.O. Box 38
Solomons, Maryland 20688-0038
Present address (for J. Stevenson): Highly Migratory Species Management Division, F/SF1
National Marine Fisheries Service
1315 East-West Highway
Silver Spring, MD 20910
Email address (for J. Stevenson): jill.stevenson@noaa.gov

Abstract.—Atlantic sturgeon (*Acipenser oxyrinchus*) are a large anadromous fish which is especially vulnerable to overharvesting owing to its late age of maturity and low rate of reproduction. Age determination methods and growth rates are poorly described for this species. Pectoral-fin spine sections and sagittal otolith sections were examined to determine whether one of these structures would be useful in estimating the age and growth of Atlantic sturgeon. Otoliths have been difficult to collect, process, and interpret. Interpretation of annuli in sectioned pectoral spines has proven to be an unbiased method for aging juvenile and adult Hudson River Atlantic sturgeon. Marginal increment analysis has indicated an annual cycle of annulus deposition. Microchemical analysis with an electron microprobe of the periphery of fin spines has shown seasonal patterns of calcium and phosphorus concentrations related to the translucent and opaque zones of the annuli. Formation of yearly annuli was verified in 4-year-old laboratory-reared sturgeon. Von Bertalanffy growth models (based upon fin-spine interpretations) were fitted for the Hudson River population. Models predicted a more rapid growth rate for males than for females (females: K=0.07, L_∞=251 cm; males: K=0.25, L_∞=180 cm). Females, however, attained a greater maximum age (42 yr) and size (TL=277 cm). We believe that exploitation has had a large but unquantifiable bias on growth estimates for male and female Atlantic sturgeon. As the Hudson River population recovers, age structure and growth rate estimates should be refined to predict population recovery rates more accurately in the absence of a directed fishery.

Manuscript accepted 13 January 1999.
Fish. Bull. 97: 153–166 (1999).

Atlantic sturgeon (*Acipenser oxyrinchus*) are a large anadromous fish that ranges the East Coast of North America and spawns in rivers from Florida to Canada. Population levels throughout the range of the species declined appreciably in the late 19th century owing to increased harvest of sturgeon for caviar following the Civil War (Murawski and Pacheco, 1977; Secor and Waldman, in press). Overfishing and deterioration of habitat, predominantly the blockage of spawning runs, have contributed to the extirpation of several Atlantic sturgeon populations (Taub, 1990; Waldman and Wirgin[1]). The life history strategy of the anadromous Atlantic sturgeon indicates that age structure and vital rates are especially critical to conservation. Atlantic sturgeon exhibit high maximum age, late maturation (females 14–17, males 10–12; Van Eenennaam et al., 1996), and probable low mortality rates; growth, however, is rapid. These traits, as well as low relative fecundity and less-than-annual spawning frequency, make sturgeon especially susceptible to overexploitation (Boreman, 1997). Therefore, models of Atlantic sturgeon population dynamics may be expected to be sensitive to biases in estimated vital rates and reproductive schedules. Atlantic sturgeon growth rates have been estimated in several studies, but results are divergent (Table 1). Poorly validated techniques have been employed to estimate age; and rates of growth, reproduction, and mortality have not been developed sufficiently to support resource management models (Taub, 1990).

Studies of acipenserid age have employed annuli in calcified structures including scutes, pectoral-fin spines, otoliths, operculi, and other skeletal parts (Harkness, 1923; Greeley, 1937; Brennan and Cailliet, 1989, 1991; Guenette et al., 1992; Rien and Beamesderfer, 1994). The term "fin ray," previously used to describe the leading (primary) ray of the pectoral fin supporting element, was revised by Feindeis (1997) because this element becomes fully ensheathed with dermal bone early in ontogeny, and therefore should be termed a spine. Pectoral-fin spine sections have been preferred for aging because annuli in sections can be consistently interpreted, and fin spines are easily col-

* Contribution 3272 of the University of Maryland Center for Environmental Science, Solomons, MD 20688-0038.

[1] Waldman, J. R., and I. I. Wirgin. 1998. Status and restoration options for Atlantic sturgeon in North America. ICES Council Meeting/T 16.

Table 1

Imprecision in aging studies of various long-lived species, reported as coefficient of variation (CV).

Species	Study	CV	Maximum age observed
Atlantic sturgeon (*Acipenser oxyrinchus*) (fin spines)	This study	4.8	42
White sturgeon (*Acipenser transmontanus*)	Rien and Beamesderfer (1994)	7.8	104
Yellowfin sole (*Pleuronectus asper*)	Kimura and Lyons (1991)	3.2	26
Sablefish	Kimura and Lyons (1991)	12.9	29
Pacific ocean perch (*Sebastes alutus*)	Kimura and Lyons (1991)	4.9	78
Tarpon (*Megalops atlanticus*)	Cyr (1991)	12.0	50

lected and processed without sacrifice of fish. They have been used in the past to age Atlantic sturgeon, but authors have described difficulty in aging older fish (>20 yr; Magnin, 1964; Huff, 1975; Dovel and Berggren, 1983). Aging based upon fin spines has been validated for white sturgeon, *Acipenser transmontanus* (Brennan, 1988; Brennan and Cailliet, 1991) and lake sturgeon, *A. fulvescens* (Rossiter et al., 1995); however, no studies have validated the periodicity of annulus deposition in Atlantic sturgeon.

Otoliths are often preferred for estimating fish age, but rate of otolith annulus formation has not been evaluated in sturgeons. Greeley (1937) enumerated ridges on the external surface of otoliths without examination of an internal section. Subsequent studies have indicated that annuli on an internal section of otoliths do not provide age estimates as precise as those from fin-spine sections (Schneberger and Woodbury, 1944; Brennan and Cailliet, 1991). Otolithic material, however, does not resorb, which is desirable for accurate aging, especially of long-lived fishes.

The objectives of this study were to identify an appropriate calcified structure and develop a precise and unbiased method for determining age of Atlantic sturgeon and to model growth rates of Hudson River Atlantic sturgeon on the basis of juvenile and adult fish collected in 1992–96.

Materials and methods

Adult Atlantic sturgeon were collected during 1992–95 from fishery harvests in the Hudson River and New York Bight, in cooperation with New York State Department of Environmental Conservation and New Jersey Department of Environmental Protection. Fish were collected by using drift and anchored gill nets (25–36 cm stretched mesh) and otter trawls. During the period of collection, a minimum size limit of 152 cm total length (TL) was imposed on the New York fishery. In New Jersey, the minimum size limit of 107 cm TL was replaced with a 152-cm size limit in 1993.

We collected pectoral-fin spines from sturgeon smaller than the minimum commercial size limit (≤149 cm TL) in the Hudson River during 1993–95, using monofilament anchored gill nets (3–13 cm stretched mesh). Because few fish less than 152 cm were collected, other mid-Atlantic Bight regions were sampled. Fin spines were obtained from sturgeon collected from Chesapeake Bay commercial pound nets and gill nets in 1996 (n=11), from National Marine Fisheries Service trawl surveys in the Mid-Atlantic Bight (1994 and 1996; n=4), and from U.S. Fish and Wildlife Service gillnet surveys of the Delaware Bay (n=8). Because the Hudson River stock is the dominant reproducing stock in the Mid-Atlantic area (Waldman et al., 1996), subadults from areas other than the Hudson River were assumed to be predominantly of Hudson River origin.

Removal and preparation of hard parts

Pectoral-fin spines (n=634) were removed at the point of articulation, air-dried, and sectioned less than one centimeter distal to the articulation point. Soft tissue adhering to the fin spines was allowed to decompose through microbial decay. A one-centimeter-wide section of each fin spine was then embedded in a block of Spurr epoxy, sectioned with an Isomet saw (Buehler, Lake Bluff, IL), and mounted on glass slides (see Secor et al., 1991). Some fin spines (64%) were not embedded but were sectioned with a jeweller's saw. All sections were mounted with thermoplastic glue on glass slides and polished with an automated polishing wheel (MINIMET 1000, Buehler, Lake Bluff, IL) with fine grit carborundum paper and a 0.3-µm alumina slurry on a polishing cloth. Final sections were 1–2 mm thick.

Sagittal otoliths were removed from the severed heads of Atlantic sturgeon collected in 1994–95

(n=114). Sagittae were cleaned in 10% bleach, rinsed several times with deionized water, and air-dried. One sagittal otolith from each pair was embedded in Spurr epoxy and sectioned as described in Secor et al. (1991). Owing to their fragility, otolith sections were polished by hand with a variety of fine sandpapers and a 0.03-µm alumina slurry.

Annuli in thin sections of fin spines and otoliths were viewed under reflected light at 15× magnification by two experienced readers. An annulus was defined as a bipartite zone comprising an opaque and a translucent zone (Fig. 1). The first translucent zone was counted as the beginning of the first year of life. In some instances, a secondary fin spine was embedded within the primary fin spine (Feindeis, 1997), in which case care was taken to enumerate annuli only in the primary spine. False annuli were consistently observed in fin-spine sections of older individuals and were excluded from annulus counts. These structures were not continuous around the entire circumference of the section and were thus distinguishable from annuli to be counted (Prince et al., 1985).

Precision and bias

Readers counted annuli without knowing collection date, fish size, or previous age determination. They were trained with the aid of an imaging system that permitted simultaneous observation of annular growth zones. Paired difference tests were used to statistically evaluate bias and precision among readers in a single blind test. The coefficient of variation (CV) was used to measure precision; bias was assessed visually using age-bias plots (Fig. 2). An age-bias plot showed paired estimates of age for the same fish (Campana et al., 1995), with the estimates of reader 2 represented as mean age, and 95% confidence intervals corresponding to each of the age classes estimated by reader 1. For example, if reader 1 estimated five fish to be 15 years old, the age-bias plot indicated the mean age of those five fish as estimated by reader 2. Divergence from the equivalence line, where $Age_{Reader\ 1} = Age_{Reader\ 2}$, indicates a systematic difference between readers. Paired age estimates for either fin-

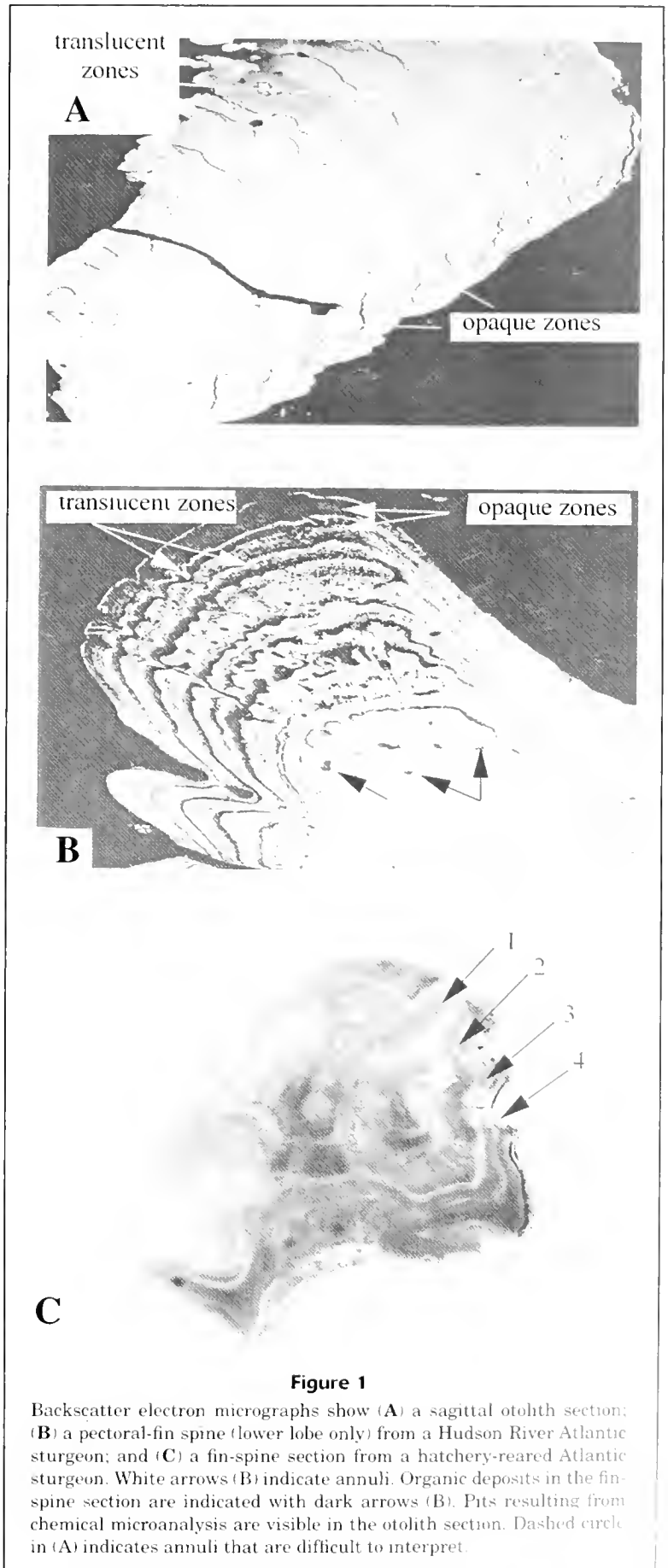

Figure 1

Backscatter electron micrographs show (**A**) a sagittal otolith section; (**B**) a pectoral-fin spine (lower lobe only) from a Hudson River Atlantic sturgeon; and (**C**) a fin-spine section from a hatchery-reared Atlantic sturgeon. White arrows (B) indicate annuli. Organic deposits in the fin-spine section are indicated with dark arrows (B). Pits resulting from chemical microanalysis are visible in the otolith section. Dashed circle in (A) indicates annuli that are difficult to interpret.

spine sections or otolith sections made by two readers were contrasted. In addition, for each reader, ages estimated from fin spine sections were compared with ages estimated from otolith sections from the same fish.

Validation of annulus formation

The periodicity of annulus formation in Atlantic sturgeon fin spines and otoliths was studied by using measurements and chemical microanalysis of marginal increments, and observation of annuli in juvenile hatchery-reared sturgeon marked with oxytetracycline (OTC) at a known age. Efforts were concentrated on fin-spine age validation because annuli were difficult to consistently interpret in otolith sections.

Marginal increment analysis measures the opaque zone deposited after the last identifiable translucent zone at the margin of a structure used for age estimation (Kalish, 1995). Seasonal growth of that opaque zone is used to determine the timing of annulus formation (Cailliet et al., 1986; Beamish and McFarlane, 1987; Brennan and Cailliet, 1989). In our analysis, marginal increments were measured with image analysis software (Optimas, Inc., 1994) to the nearest 0.001 mm. Marginal increment ratio (MIR) was calculated as

$$MIR = MI \times 1/A,$$

where MI = the width of the outermost opaque zone (marginal increment); and
A = the mean width of the three annuli deposited previous to the marginal increment.

Mean MIR was computed for each month separately, with ages and sexes combined. Because very few fish were collected for several months, monthly samples were pooled for four three-month seasons. The winter season (December–February) was eliminated owing to very low sample size.

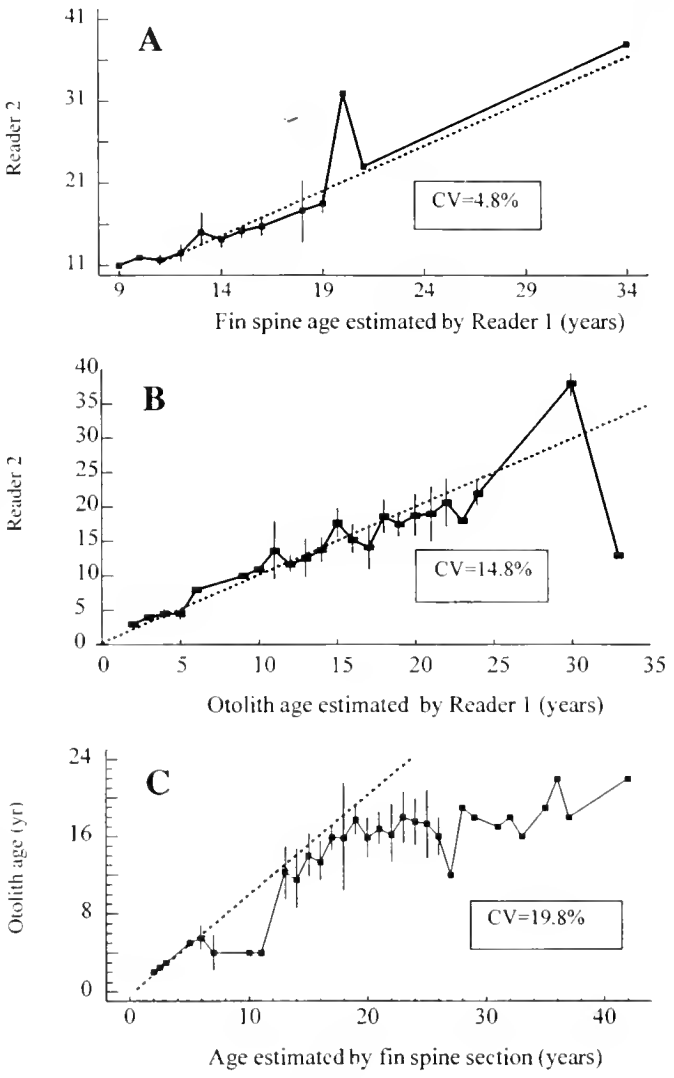

Figure 2

Bias in age estimates for Hudson River Atlantic sturgeon are evaluated by age-bias plots that compare estimates made by two readers interpreting the same (**A**) fin-spine sections and (**B**) otolith sections; and (**C**) made by one reader interpreting fin-spine and otolith sections taken from the same fish. Dashed lines are "equivalence lines" indicating the hypothetical case where both estimates are identical. Error bars represent the 95% confidence interval about the mean age (reader 2) for all fish assigned a given age by reader 1.

Microchemical analysis of calcified structures can verify the periodicity of annuli (Jones and Geen, 1977; Casselman, 1983; Radtke and Targett, 1984; Cailliet and Radtke, 1987). Calcium concentration is correlated with optically defined growth zones in the hard part (e.g. calcium is increased in the opaque zone and decreased in the translucent zone; Cailliet and Radtke, 1987; Lai et al., 1996). For instance, the most recently formed material in fin spines might contain high or low concentrations of calcium in fish collected during summer (rapid growth) or winter (slower growth), respectively (Cailliet and Radtke, 1987). In this instance, fin-spine microanalysis of calcium across annuli might show nadirs in calcium associated with translucent zones.

Calcium concentration in fin-spine sections was measured using a JEOL JXA-840A wavelength-dis-

persive (WDS) electron microprobe at the Center for Microanalysis, College Park, MD. Phosphorus was also measured because it makes up a large fraction of the fin spine's hydroxyapatite structure (Stevenson, 1997). Accelerating voltage was 25 kV and cup current was 20 nA. Each measurement represented rastering or scanning by the probe over a 5 × 5 µm area of the hardpart section. Molar weights of calcium and phosphorus were measured in peripheral regions of fin spines for 20 fish aged 3–18 years (fin-spine estimate) collected in March, June, September, and November. The mean of three peripheral points was calculated for each individual, and means were contrasted by month of collection with ANOVA.

Microprobe measurements were used to construct elemental chronologies of 15 fin spine sections taken from sturgeon aged 12–36 years (fin-spine estimate) and 164–236 cm TL. For each chronology, a series of point measurements was taken along an axis that traversed several annuli, with five points per annulus; points were assumed to sample seasons in linear proportion.

A solution of OTC (25 milligrams per kilogram of body weight) was injected into the dorsal musculature of five juvenile laboratory-reared fish of known age (55–65 cm TL) from Hudson River broodstock. Juveniles had been reared in circular fiberglass tanks in a recirculating system and fed a mixture of commercial pellet feeds. They were subjected to a twelve-hour photoperiod; water temperature ranged from 15° to 20°C. Three months after injection, the first fin spine section was removed from three fish with a jeweller's saw, and silver nitrate was applied to encourage clotting of the wound. Fifteen months after injection, a second section was removed from the opposite pectoral-fin spine of one fish only. Fin-spine segments were dried, sectioned, mounted on glass slides, and polished. Thin sections were viewed with epifluorescent microscopy to identify OTC marks. The position of OTC marks with respect to opaque and translucent zones was recorded and a micrograph was taken. In all cases, the reader was aware that the fish had received an injection of OTC but had no knowledge of the date of section collection.

Growth

Reported measurements of dressed carcasses were converted to total length based upon conversion metrics derived for Hudson River Atlantic sturgeon (Stevenson, 1997). Sturgeon included in the conversion metric sample (n=235) were collected during spawning season in the Hudson River; all but five possessed mature gonads. Ages derived from fin-spine and otolith sections were used to fit von Bertalanffy growth models by using a Marquardt iterative estimation procedure for the three model parameters. Length-at-age relationships were first examined to determine variance structure and progression of modal length with age. Growth parameters were estimated iteratively for males and females with a least-squares method. Because of high variance at the point of growth inflection, it was unlikely that a single growth model would fit all portions of the growth curve. Therefore, the juvenile portion (42–152 cm TL) was modeled separately with a power function based upon the best fit of residuals.

PC-SAS (SAS Institute, Inc., 1994) and Statgraphics Plus (STSC, Inc., 1992) were used for all statistical tests. Data that did not satisfy the assumption of heteroscedasticity (Bartlett's test, α=0.05) were transformed to satisfy this assumption. Transformed data that did not satisfy this assumption were analyzed with a Kruskal-Wallis nonparametric test to examine differences among groups.

Results

Comparison of hard parts

Otoliths were irregularly shaped and their annuli were difficult to interpret. In contrasting several sectioning planes, we observed that annuli on transverse sections yielded the most consistent interpretations. The first three to nine growth zones showed a clear alternation of opaque and translucent zones. Thereafter, translucent zones were irregularly spaced and often appeared to overlap (Fig. 1A). Low optical contrast between opaque and translucent zones reduced the readers' confidence in assigning annuli, especially in sections with more than twenty annuli.

In contrast, fin-spine sections exhibited concentric narrow translucent zones and wide opaque zones when viewed with transmitted light. Fin spines contained a vascularized core and deposits of organic material in lobe regions (Fig. 1B). Interspersed were fibrils that we interpreted as collagen or some other structural protein. Annuli became narrower toward the outer edge in larger (and presumably older) fish. Secondary fin spines (84% of fin-spine sections) and false annuli were observed but were simple to identify and disregard. Belts of two to five narrow annuli were apparent in most female fin-spine sections (96% of a subsample of 48). These belts were not apparent in the juvenile sturgeon examined.

Imprecision (CV) in age estimates was 4.8% between two readers of the same fin-spine section (Fig. 2A). Mean imprecision was 1.2 years (t=–1.97, P>0.05); estimates by the two readers were not significantly

different. Age estimates from otolith sections were less precise than from fin-spine sections (Fig. 2B). Absolute imprecision was 3.3 years and the CV on paired differences was 14.8%. No significant bias occurred in otolith interpretations between readers. In a comparison of ages estimated by a single reader from otolith sections and from corresponding fin-spine sections (i.e. from the same fish), the former were significantly lower than the latter (Fig. 2C; mean difference=5 yr, t=9.01, P<0.05). The bias was most apparent for presumed by older fish.

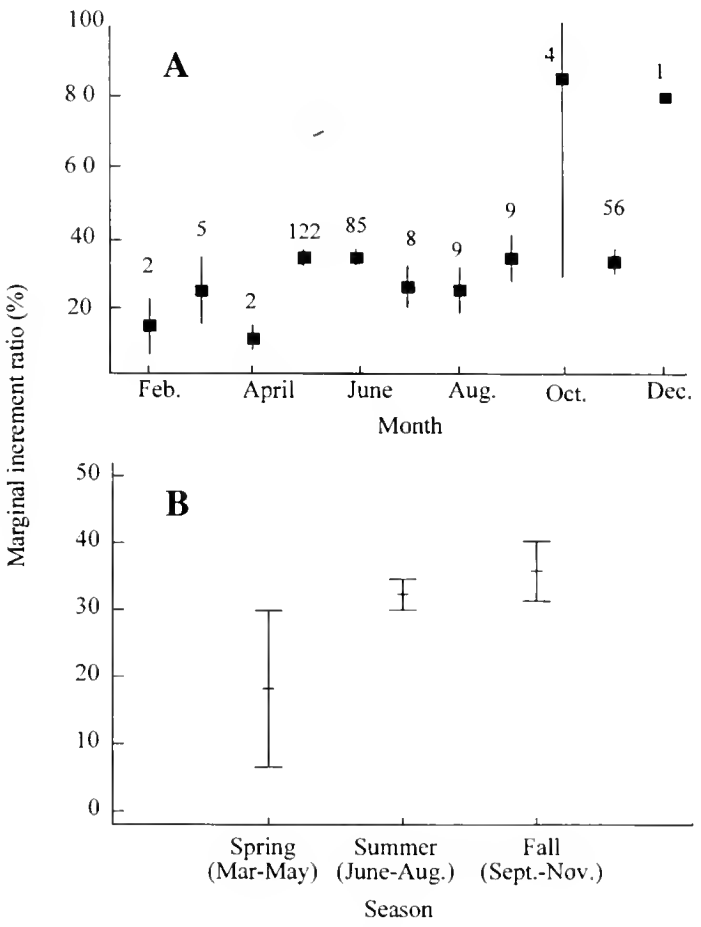

Figure 3

(**A**) Marginal increment ratios (MIR) ± one standard error for sectioned Hudson River Atlantic sturgeon pectoral fin spines evaluate current season's growth. Numbers represent sample size. (**B**) Marginal increment ± 95% confidence interval for data grouped by season. *MIR* = *MI* × 1/*A*, where *MI* = the width of the outermost opaque zone (marginal increment) and *A* = the mean width of the three annuli deposited previous to the marginal increment.

Validation of the fin-spine aging method

Marginal increment ratios for fish collected in late winter and spring (February–April) were significantly lower than those for summer and fall (Fig. 3; Kruskal-Wallis test; P=0.04). Mean MIR was 18% in spring, 33% in summer, and 36% in fall. The highest rate of marginal increment completion was observed for winter months (December–February), although sample size was very small for these months (n=3).

Readings of annuli from hatchery-reared sturgeon resulted in exact age estimates. The sturgeon were 4+ years old and annuli were clearly defined. There was a distinct difference in the shape of fin spines from hatchery-reared and wild juvenile sturgeon (Fig. 1C). Hatchery-reared fish exhibited irregularly shaped, compressed annuli which could indicate erosion or injury, but were nonetheless easily recognized. In OTC-injected fish, a distinct OTC mark followed by an opaque zone was apparent in all fin spines examined three months after injection. The fish did not show any symptoms of stress following fin-spine removal. The only sample examined at fifteen months after injection exhibited a clear OTC mark that was followed by opaque and translucent zones.

Microchemical analysis

The concentrations of calcium and phosphorus in peripheral regions of fin spines showed significant seasonality (Kruskal-Wallis test, P≤0.04; Fig. 4). Fin spines collected in November were significantly lower in calcium and phosphorus than those collected in March, June, and September. Calcium-to-phosphorus ratios increased significantly from March through November (Kruskal-Wallis test, P=0.04). Plots of calcium and phosphorus in fin spines revealed cyclical trends in both elements, with peaks associated with translucent zones (Fig. 5).

Growth

The size-age relationship for prespawning fish, as judged by interpretations of annuli in fin spines, was best fitted by a power regression (r^2= 0.75; Fig. 6). Von Bertalanffy models for both males and females considerably underestimated length at age for subadults. Over all life history portions, the fit of the von Bertalanffy model was better for females (ages 2–42; r^2=0.56) than for males (ages 4–36; r^2=0.33) owing to the broader range of ages and lengths in our sample

of females (Fig. 7A). Males grew faster but reached a smaller asymptotic length at a younger age than did females. Females grew more slowly (K=0.07) toward a significantly larger maximum length (251 ±12.8 cm). The asymptotic growth phase for females and males was 12–42 and 11–28 years, respectively. Estimates of growth coefficients, K, were significantly different between sexes (t=73.2, df=431, P<0.05). Log transformation of the data did not correct for the error structure. Residuals from the models were designated as corresponding either to fish of the size at entry into the fisheries (152 cm TL in New York and after 1993 in New Jersey), or to larger or smaller fish. The resulting residual plots indicated that the faster-growing males were harvested just as they reached size at entry (positive residuals) and that the slower-growing females entered the fishery at much older ages (negative residuals; Fig. 7B). The modeled growth pattern for females appeared more biased than that for males owing to a sharp shift in residuals from positive to negative at about 15 years. At older ages, the von Bertalanffy model underestimated the size of females. These patterns in residuals were also apparent in males, albeit less pronounced.

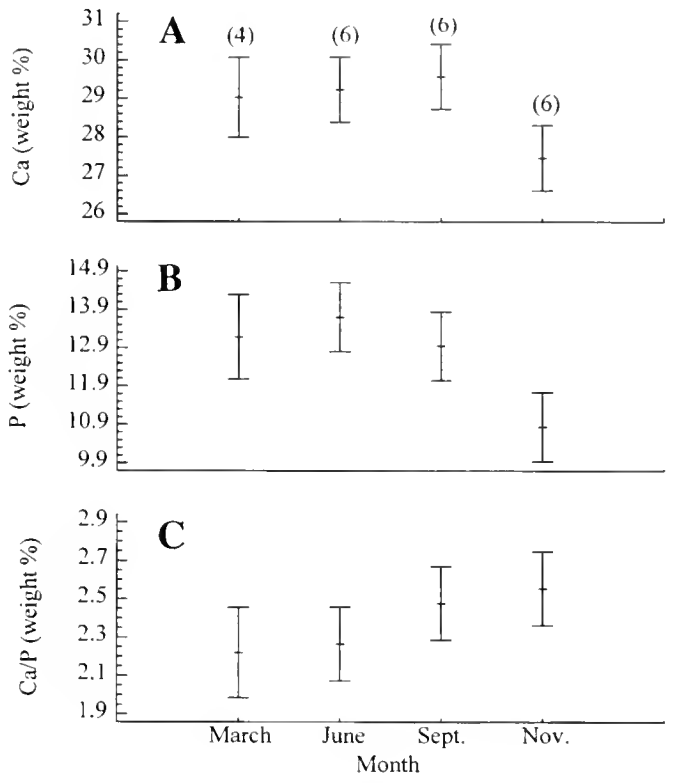

Figure 4

Microchemical analysis of marginal increments of fin spine sections taken from Hudson River Atlantic sturgeon show significant seasonality in (**A**) calcium; (**B**) phosphorus; and (**C**) calcium-to-phosphorus ratio. Means and 95% confidence intervals are depicted. Three points were analyzed per section. Numbers in parentheses indicate how many fin-spine sections were analyzed for fish collected in each of the four months (these apply to all three graphs).

Discussion

Fin spines or otoliths?

Owing to ease of collection and processing, as well as precision and accuracy in aging, we recommend the use of fin spines rather than otoliths for demographic analysis of Atlantic sturgeon. Preparation techniques used in this study (embedding, sectioning, and polishing) may have improved the visual resolution of annuli in pectoral-fin spines over that reported in earlier investigations.

Annuli in sturgeon otoliths and, as a result, growth rates, have been grossly misinterpreted in the past owing to examination of the external surface of hard parts only (Greeley, 1937). Especially in presumed older individuals, otoliths should not be used to verify age estimates based on fin spines. Annular clarity diminishes towards the distal end of the otolith (more recent growth), which may result in lower age estimates. In addition, individuals must be sacrificed to collect otoliths. Concern over declining sturgeon populations should restrict the size of otolith samples.

Precision and accuracy

Age estimates based on fin spines were unbiased and precise. Aging imprecision for Atlantic sturgeon was similar or better than imprecision reported for other long-lived (>20 yr) species, for which precision is often affected by narrow annuli, which result from reduced growth rates in older fish (Rien and Beamesderfer, 1994; Table 1). The annual patterns of marginal increment ratio (MIR), observations on fish of known age, and microchemistry have supported the hypothesis that a pair of opaque and translucent zones forms annually in Atlantic sturgeon fin spines. A small sample of OTC-marked juveniles also indicated annual annulus growth (Stevenson, 1997). Results for Atlantic sturgeon were similar to Huff's (1975) analysis of Gulf sturgeon (*Acipenser oxyrinchus desotoi*) fin-spine sections, in which a higher percentage of fin-spine sections showed that a completely formed

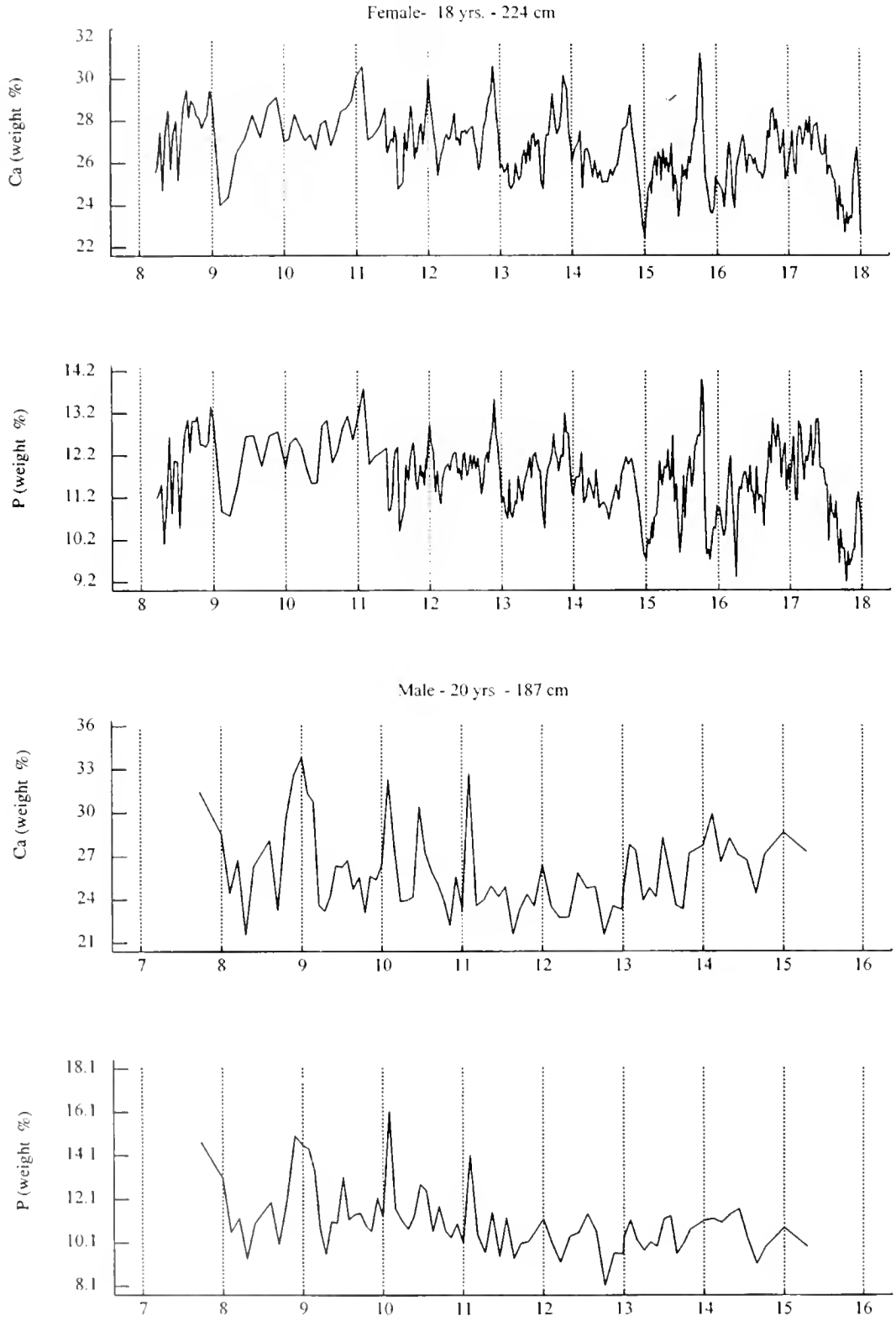

Figure 5

Series of microprobe analyses for calcium and phosphorus across annuli in fin-spine sections were used to construct elemental chronologies for Hudson River Atlantic sturgeon. In these two representative chronologies, dashed lines correspond with translucent zones.

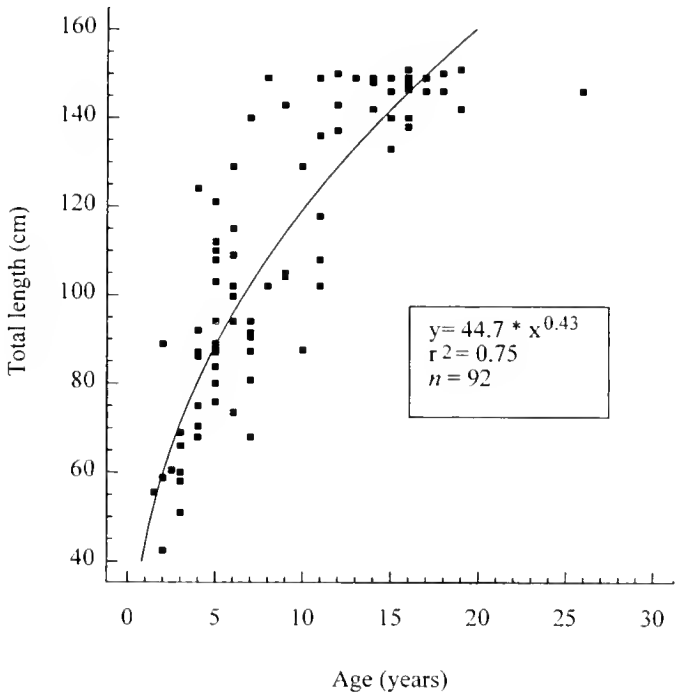

Figure 6

A power regression best describes the growth of juvenile and subadult Hudson River Atlantic sturgeon (TL<152 cm), based on ages derived from fin spine sections.

marginal annulus was completely formed in the fall rather than in the spring. Ideally, marginal increment analysis should be performed on separate age classes to ensure that annulus formation occurs for all ages (Casselman, 1983). However, owing to the relative scarcity of older individuals and the unavailability of fish in some seasons and because marginal increments are often difficult to discern in fin-spine sections taken from older individuals, age classes were pooled in our study. Accuracy of age estimation at older ages remains untenable. An attempt to validate longevity estimates of Hudson River Atlantic sturgeon using radiometric $^{210}Pb/^{226}Ra$ dating was unsuccessful (Burton et al., 1999). Recapture of hatchery-released Atlantic sturgeon (Secor[2]) has provided an opportunity to verify age determinations in older or mature individuals. Fin spines taken from juvenile sturgeon did not exhibit belts of annuli; such belts may provide information about spawning behavior in females.

Chemical microanalysis of hard parts is a promising tool for age verification (Jones and Geen, 1977; Casselman, 1983; Cailliet and Radtke, 1987). However, seasonal cycles were not consistently observed in elemental chronologies of Atlantic sturgeon fin spines. The technique assumes that the hard part is a closed system, and there is no resorption or remodeling. Burton et al. (1999) using radiometric tracers, found that Atlantic sturgeon fin spines appear to be open systems. In our study, we may have observed a corrupted seasonal signal.

Growth

Sexually dimorphic growth patterns in Atlantic sturgeon may be a result of differential reproductive schedules and migration patterns. The age-length relationship shows substantial variability in both males and females. Males mature earlier (12 yr) and spawn annually. Females mature later at a much larger size and are thought to spawn every 3–5 years (Smith, 1985). Lower growth rates and larger achieved sizes are typical for large, long-lived fish that broadcast numerous offspring (Adams, 1980; Moreau, 1987; Roff, 1988, Winemiller and Rose, 1992).

[2] Secor, D. H. 1998. Habitat utilization patterns of mid-Atlantic Bight juvenile Atlantic sturgeon. Final report on project 1445-CT-09-0189 to National Biological Survey, 30 p. Ref. no. [UMCES] CBL 98-019. [Available from David Secor, Chesapeake Biological Laboratory, 1 Williams St., Solomons, MD 20688-0038.]

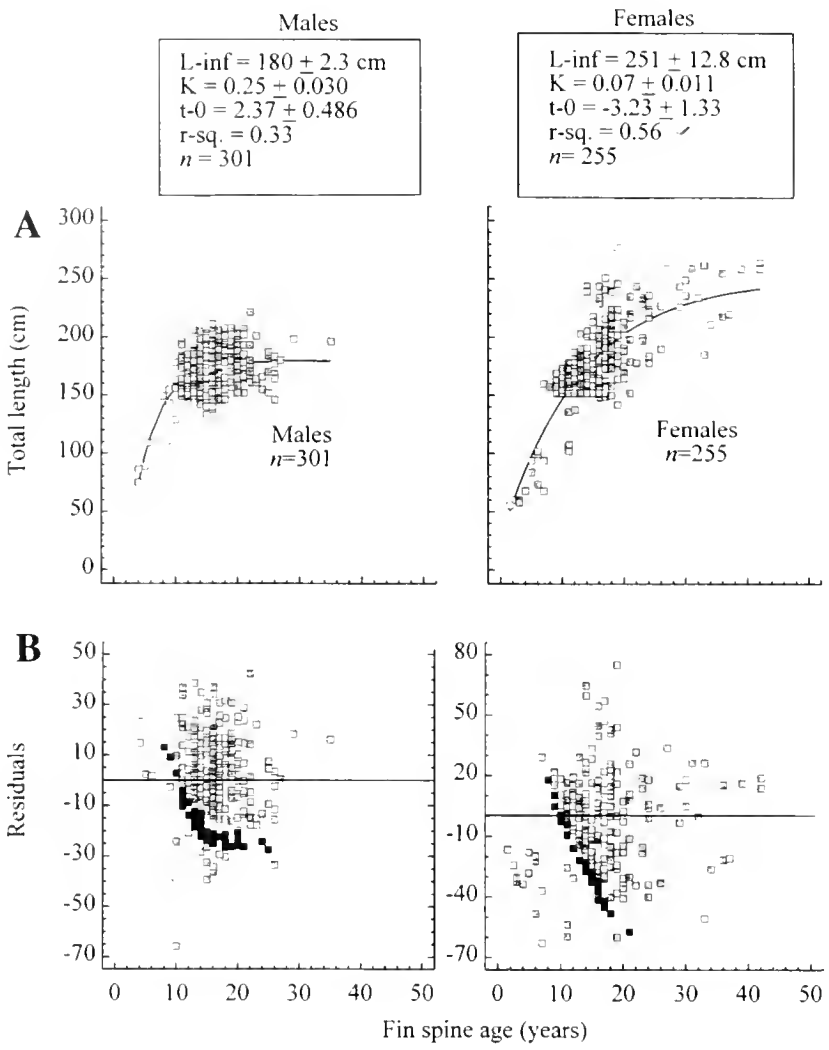

Figure 7

(**A**) Predictions of length at age from von Bertalanffy models for male and female Atlantic sturgeon (black curves) fitted observed length at age (grey squares) for females better. (**B**) Plots of residuals from the growth models reveal a difference between fish of size-at-entry (152 ±5 cm TL; black squares); and fish of TL above or below size-at-entry (gray squares). Note different *y*-axis scales for males and for females. Ages derived from fin-spine sections.

Growth is difficult to model accurately in long-lived species (Mulligan et al., 1987). Because little bias was detected in our readings (aging precision was unaffected by age), discrepancies in age estimates should not introduce systematic error in estimates of population parameters such as mortality rate, K, and L_∞. High variability in observed length at age indicates that length may be a poor predictor of age for Atlantic sturgeon. This high variability may result from amplification of early growth differences over a long life span. Variance in size at age may also have resulted from the nature of the Hudson River Atlantic sturgeon fishery. The imposed minimum size limit on Atlantic sturgeon commercial fisheries (>152 cm TL) may have biased the sample used for growth estimates and could have caused K and L_∞ to be over- and under-estimated, respectively (Fig. 8). The von Bertalanffy curve may have been driven upwards at younger ages by the potential maximum growth rate of the population. For instance, as soon as the fastest growing members of an age class exceeded the minimum size limit, they were harvested. At later ages, the curve is pulled downward as slower growing individuals enter the

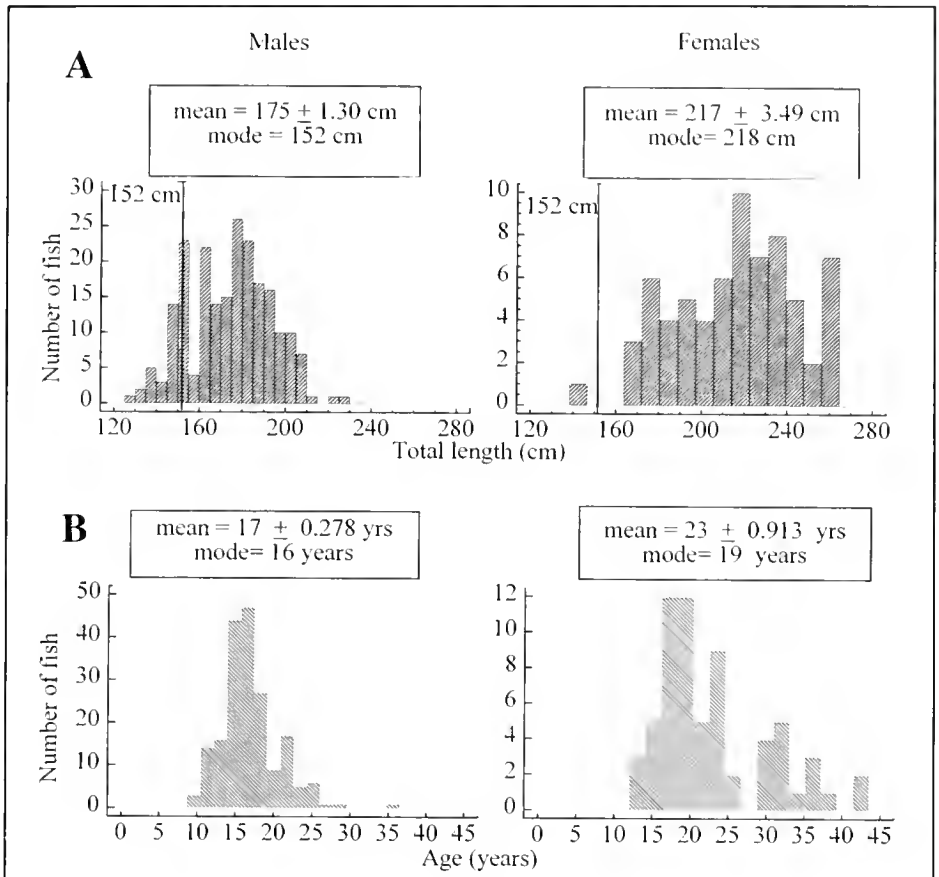

Figure 8

(**A**) Total length and (**B**) age of male and female Atlantic sturgeon caught in the Hudson River gillnet fishery (1992–95). Sublegal fish (<152 cm) were a result of a minimum dressed carcass length of 91 cm. Conversion from dressed length to total length may have resulted in "undersized" fish.

fishery (as evidenced by residual patterns), increasing K and decreasing L_∞.

Growth parameter estimates reported here for females are consistent with another study of the same population (Doroshov et al.[3]) but do not agree with an earlier study (with sexes combined) of the population (Dovel and Berggren, 1983). Recent reduction of the accumulated biomass by fishing, and resultant age and size truncation of the population, would cause lower apparent L_∞ and higher K values than in an unexploited population. Maximum length (L_∞) determined for females was substantially smaller than historical records of maximum size for this species (427 cm; Murawski and Pacheco, 1977), which may be a result of increased fishing pressure on the largest (female) component of the population during the past ten years. The historical longevity of females in the Hudson River also probably exceeded our estimate of 42 years; Magnin (1964) reported a 60-year-old female in the St. Lawrence estuary.

Because the largest male sampled (72 kg) was only 22 years of age, yet much smaller males were older than 30 years, male longevity in the unexploited population was also probably higher than in the population we sampled. Consideration of possible bias in von Bertalanffy growth parameters should direct managers to undertake sensitivity analyses in developing demographic-based stock assessments. Because L_∞ and K are inversely related (Kimura, 1980), age and size truncation would result in an over-estimated K (a lower L_∞ is approached more rapidly).

We found L_∞ values that were relatively low compared with estimates in previous studies of Hudson River Atlantic sturgeons (Greeley, 1937; Dovel and Berggren, 1983). These low values may indicate

[3] Doroshov, S., J. Van Eenennaam, G. Moberg, and G. Waton. 1994. Reproductive conditions of the Atlantic Sturgeon (*Acipenser oxyrinchus*) stock in the Hudson River. Report for year two to Hudson River Foundation. Animal Science Department, University of California, Davis, 65 p.

age truncation of the population by directed fishing effort. However, Dovel and Berggren (1983) reported difficulty in aging fish greater than 153 cm TL and may have misidentified annuli in both juveniles and adults. Greeley's (1937) study was based on enumerating annuli in otoliths. Likewise, K estimates from our study are higher than those estimated previously. Our growth estimates are consistent, however, with those of Doroshov et al.,[3] who aged the same population in the early 1990s.

Comparative studies of fish populations along a latitudinal gradient have shown an inverse relation between latitude and rates of growth and mortality (e.g. Leggett and Carscadden, 1978; Jennings and Beverton, 1991). Among Atlantic sturgeon populations, the most rapid growth was exhibited by fish sampled in southern latitudes. Maximum size increased with increasing latitude, which may indicate postponement of maturation (Magnin, 1964). Values of K for the Hudson River population did not differ significantly from those for any other population (α=0.05), whereas L_∞ values estimated for the Hudson River population were statistically different from those estimated for all other populations (α=0.05) along a latitudinal gradient (Table 2).

Table 2

Growth parameters have been calculated in various studies of Atlantic sturgeon populations (combined sexes). For Smith (1985), n=number of age classes. Smith's (1985) data were converted from fork length to total length (FL= 1.11×TL; Beamesderfer, 1993) and were presented as mean length by age class in the literature.

Location	Study	n	K	L_∞ (cm)
St. Lawrence River	Magnin, 1964	582	0.03	315
Kennebec, ME	Smith, 1985	7	0.06	236
Hudson River, NY	This study	634	0.08	225
Winyah Bay, SC	Smith, 1985	24	0.12	242
Suwannee River, FLA	Smith, 1985	17	0.14	184

Implications for stock restoration

Growth rates of acipenserid species are apparently affected by migratory behavior (Roff, 1988). Anadromous species of sturgeons exhibit higher growth coefficients than do semi-anadromous or freshwater resident species, although the semi-anadromous white sturgeon achieves a higher maximum length than do anadromous sturgeons (Table 3). Atlantic sturgeon undergo an ontogenetic habitat shift from estuarine nursery grounds to marine waters (Gilbert, 1989). We believe these species grow rapidly as juveniles (as shown by their high K coefficient) to outgrow predation in marine waters. Unfortunately, rapid growth may affect the timing of juvenile migration and increase their susceptibility to coastal fisheries at an early age.

Estimates of growth traits for Hudson River Atlantic sturgeon indicate that they are extremely vulnerable to overfishing. Slow growth following maturation, high longevity, and presumed low natural mortality indicate that year classes in this population reach their maximum biomass at relatively old ages (Alverson and Carney, 1975). Therefore, maximum fishing yield from sturgeon would be achieved at low

Table 3

Growth parameters (von Bertalanffy parameters unless otherwise indicated) estimated for North American sturgeons. Parameters were estimated for both sexes combined except where otherwise noted.

Species	Study	Location	n	L_∞ (cm TL)	K	t_0
Atlantic sturgeon (*A. oxyrinchus*)	This study[1]	Hudson River, NY	634	256 (female) 180 (male)	0.07 0.25	–3.2 2.4
White sturgeon (*A. transmontanus*)	DeVore et al., 1995	Unimpounded Columbia River, OR	783	307	0.03	–1.13
Green sturgeon (*A. medirostris*)	USFWS[1]	Klamath River, CA	173	238	0.05	2.0
Shortnose sturgeon (*A. brevirostris*)	Dadswell, 1979	St John's River, Canada	446	144[2]	0.04	2.0
Lake sturgeon (*A fulvescens*)	Thuemler, 1985[3]	Menominee River, WI–MI	1464	156	0.07	–0.02

[1] Growth parameters estimated for males and females separately.
[2] United States Fish and Wildlife Service. 1982. Klamath River Fisheries Investigation Program annual report, p. 123–141.
[3] Converted from fork length (FL= 1.11 × TL; Beamesderfer, 1993).
[4] Growth parameters derived from plot of mean TL at age.

rates of fishing or harvest of large, mature individuals (Bullock et al., 1992; Stevenson, 1997). A moratorium on commercial sturgeon fishing in the New York Bight was instituted in 1996; however, Atlantic sturgeon continue to be caught incidentally in many coastal fisheries. Continued research and monitoring of recruitment and bycatch mortality will be necessary to ensure the restoration of this population.

Acknowledgments

We would like to thank I. Burliuk, D. Bush, E. Nack, and S. Nack, commercial sturgeon fishermen, as well as M. Mangold of the U.S. Fish and Wildlife Service (USFWS), J. Fields (National Marine Fisheries Service), and J. Mohler (USFWS), for their help in the collection of sturgeon fin spine samples. J. Van Eenennaam (University of California, Davis), J. Mohler and M. Mangold (USFWS), K. McKown and B. Young (New York State Department of Environmental Conservation), and B. Andrews (New Jersey Department of Environmental Protection) provided additional previously collected fin spine samples. M. Bain (Cornell University) provided resources for sampling subadult sturgeon in the Hudson River. J. Van Eenennaam provided valuable insight on aging techniques for white sturgeon and Atlantic sturgeon. Anne Henderson-Arzapalo reared and sampled juvenile known-age sturgeon for validation. The Hudson Riverkeeper provided onsite laboratory facilities. This research was funded by a grant to D. Secor by the Hudson River Foundation.

Literature cited

Adams, P. B.
1980. Life history patterns in marine fishes and their consequences for fisheries management. Fish. Bull. 78:1–11.

Alverson, D. L., and M. J. Carney.
1975. A graphic review of the growth and decay of population cohorts. J. Cons. Int. Explor. Mer 36:133–143.

Beamesderfer, R. C.
1993. A standard weight (Ws) equation for white sturgeon. Calif. Dep. Fish Game 79:63–69.

Beamish, R. J., and G. A. MacFarlane.
1987. Current trends in age determination methodology. *In* P. C. Summerfelt and G. E. Hall (eds.), The age and growth of fish, p. 35–42. Iowa State Univ. Press, Ames, IA.

Boreman, J.
1997. Sensitivity of North American sturgeons and paddlefish to fishing mortality. Environ. Biol. Fishes 48:399–405.

Brennan, J. S.
1988. Age determination and verification of California white sturgeon (*Acipenser transmontanus*): a comparative analysis. M.S. thesis, San Jose State Univ., CA, 70 p.

Brennan, J. S., and G. M. Cailliet.
1989. Comparative age-determination techniques for white sturgeon in California. Trans. Am. Fish. Soc. 118:296–310.

1991. Age determination and validation studies of white sturgeon in California. *In* P. Williot (ed.), Acipenser: sectes du premier colloque international sur l'esturgeon, p. 209–234. French Institute of Agriculture and Environmental Engineering Research (CEMAGREF), Gazinet, France.

Bullock, L. H., M. D. Murphy, M. E. Mitchell.
1992. Age, growth, and reproduction of jewfish, *Epinephelus itajara*, in the eastern Gulf of Mexico. Fish. Bull. 90:243–249.

Burton, E. J., A. H. Andrews, K. H. Coale, G. M. Cailliet.
1999. Application of radiometric age determination to three long-lived fishes using ^{210}Pb:^{226}Ra disequilibria in calcified structures: a review. *In* J. A. Musick (ed.), Life in the slow lane: ecology and conservation of long-lived marine animals, p. 77–87. Am. Fish. Soc. Symp. 23.

Cailliet, G. M., and R. L. Radtke.
1987. A progress report on the electron microprobe analysis technique for age determination and verification in elasmobranches. *In* R. C. Summerfelt and G. E. Hall (eds.), The age and growth of fish, p. 359–369. Iowa State Univ. Press, Ames, IA.

Cailliet, G. M., R. L. Radtke, and B. A. Welden.
1986. Elasmobranch age determination and verification, a review. *In* T. Uyeno, R. Arai, T. Taniuchi, and K. Matsuura (eds.), Proceedings of the second international conference of Indo-Pacific Fishes, p. 345–360.

Campana, S. E., M. C. Annand, and J. I. McMillan.
1995. Graphical and statistical methods for determining the consistency of age determinations. Trans. Am. Fish. Soc. 124:131–138.

Casselman, J. M.
1983. Age and growth assessment of fish from their calcification tissue-techniques and tools. *In* E. D. Prince and L. M. Pulos [eds.], Proceedings of the international workshop on age determination of oceanic pelagic fishes, tunas, billfishes, and sharks, p. 1–17. U.S. Dep. Commer., NOAA Tech. Rep. NMFS 58.

Cyr, E. C.
1991. Aspects of the life history of the tarpon, *Megalops atlanticus*, from South Florida. Ph.D. diss., Univ. S. Carolina, Columbia, SC, 60 p.

Dadswell, M. J.
1979. Biology and population characteristics of the shortnose sturgeon, *Acipenser brevirostrum* LeSueur 1818 (Osteichthyes: Acipenseridae), in the Saint John River Estuary, New Brunswick, Canada. Can. J. Zool. 57:2,186–2,210.

DeVore, J. D., B. W. James, C. A. Tracy, and D. A. Hale.
1995. Dynamics and potential production of white sturgeon in the Columbia River downstream from Bonneville Dam. Trans. Am. Fish. Soc. 124:845–856.

Dovel, W. L., and T. J. Berggren.
1983. Atlantic sturgeon of the Hudson Estuary, New York. NY Fish Game J. 30:140–172.

Feindeis, E. K.
1997. Osteology and phylogenetic interrelationships of sturgeons (Acipenseridae). Environ. Biol. Fishes 48:73–126.

Gilbert, C. R.
1989. Atlantic and shortnose sturgeons. U.S. Fish Wildl. Serv. Biol. Rep. 82, 28 p.

Greeley, J. R.
1937. Fishes of the area with annotated list. A biological survey of the lower Hudson watershed. Rep. NY State Conserv. Dep. 26:45–103.

Guenette, S., D. Goyette, R. Fortin, J. Leclerc, N. Fournier, G. Roy, and P. Dumont.
1992. La periodicite de la croissance chez la femelle [illegible]

l'esturgeon jaune (*Acipenser fulvescens*) du fleuve Saint Laurent est-elle reliee a la periodicite de la reproduction? Can. J. Fish. Aquat. Sci. 49:1,336–1,342.

Harkness, W. J. K.
1923. The rate of growth and the food of the lake sturgeon (*Acipenser rubicundus*). Univ. Toronto Studies Publ. Ont. Fish. Res. Lab. 18: 15–42.

Huff, J. A.
1975. Life history of Gulf of Mexico sturgeon, *Acipenser oxyrhynchus desotoi*, in Suwannee River, Florida. Fla. Mar. Res. Publ. 16, 32 p.

Jennings, S., and R. J. H. Beverton.
1991. Intraspecific variation in the life history tactics of Atlantic herring (*Clupea harengus* L.) stocks. ICES J. Mar. Sci. 48:117–125.

Jones, B. C., and G. H. Geen.
1977. Age determination of an elasmobranch (*Squalus acanthias*) by x-ray spectrometry. J. Fish. Res. Board Can. 34:44–48.

Kalish, J. M.
1995. Glossary for otolith studies. *In* D. H. Secor, J. M. Dean, and S. E. Campana (eds.), Recent developments in fish otolith research, p. 723–729. Univ. S. Carolina Press, Columbia, SC.

Kimura, D. K.
1980. Likelihood methods for the von Bertalanffy curve. Fish. Bull. 77:765–773.

Kimura, D. K., and J. J. Lyons.
1991. Between reader bias and variability in the age determination process. Fish. Bull. 89:53–60.

Lai, H. L., V. F. Gallucci, and D. R. Gunderson.
1996. Age determination in fisheries: methods and applications to stock assessment. *In* V. F. Gallucci, S. B. Saila, D. J. Gustafson, and B. J. Rothschild (eds.), Stock assessment: quantitative methods and applications for small-scale fisheries, p. 82–178. Lewis Publishers, New York, NY.

Leggett, W. C., and J. E. Carscadden.
1978. Latitudinal variation in reproductive characteristics of American shad (*Alosa sapidissima*): evidence for population specific life history strategies in fish. J. Fish. Res. Board Can. 35:1,469–1,478.

Magnin, E.
1964. Croissance en longueur de trois esturgeons d'Amerique du Nord: *Acipenser oxyrhynchus* Mitchill, *Acipenser fulvescens* Raffinesque, et *Acipenser brevirostris* Le Sueur. Verh. Internat. Verein. Limnol. 15:968–974.

Moreau, J.
1987. Mathematical and biological expressions of growth in fishes: recent trends and further developments. *In* R. C. Summerfelt and G. E. Hall (eds.), The age and growth of fish, p. 81–114. Iowa State Univ. Press, Ames, IA

Mulligan, T. J., F. D. Martin, R. A. Smucker, and D. A. Wright.
1987. A method of stock identification based on the elemental composition of striped bass *Morone saxatilis* (Waldbaum) otoliths. J. Exp. Mar. Biol. Ecol. 114:241–248.

Murawski, S. A., and A. L. Pacheco.
1977. Biological and fisheries data on the Atlantic sturgeon, *Acipenser oxyrynchus* (Mitchill). U.S. Dep. Commer., NOAA NMFS Tech. Ser. Rep. 10, 59 p.

Optimas Corp.
1994. Optimas user's manual. Optimas Corp., Bothell, WA.

Prince, E. D., D. W. Lee, C. A. Wilson, and J. M. Dean.
1985. Longevity and age-validation of a tag-recaptured Atlantic sailfish, *Istiophorus platypterus*, using dorsal spines and otoliths. Fish. Bull. 84:493–502.

Radtke, R. L., and T. E. Targett.
1984. Rhythmic structural and chemical patterns in otoliths of the Antarctic fish *Notothenia larseni*: their application to age determination. Polar Biol. 3:203–210.

Rien, T. A., and R. C. Beamesderfer.
1994. Accuracy and precision of white sturgeon age estimates from pectoral fin spines. Trans. Am. Fish. Soc. 123:255–265.

Roff, D. A.
1988. The evolution of migration and some life history parameters in marine fishes. Environ. Biol. Fishes 22:133–146.

Rossiter, A., D. L. G. Noakes, and F. W. H. Beamish.
1995. Validation of age estimation for the lake sturgeon. Trans. Am. Fish. Soc. 124:777–781.

SAS Institute, Inc.
1994. User's guide, version 6.02. SAS Institute, Inc., Cary, NC.

Schneberger, E., and L. A. Woodbury.
1944. The lake sturgeon (*Acipenser fulvescens* Rafinesque) in Lake Winnebago, Wisconsin. Trans. Wis. Acad. Sci. Arts Lett. 36:131–140.

Secor, D. H., J. M. Dean, and E. H. Laban.
1991. Manual for otolith removal and preparation for microstructural examination. Univ. South Carolina Press, Columbia, SC, 85 p.

Secor, D. H., and J. R. Waldman.
1999. Historical abundance of Delaware Bay Atlantic sturgeon and potential rate of recovery. *In* J. A. Musick (ed.), Life in the slow lane: ecology and conservation of long-lived marine animals, p. 203–216. Am. Fish Soc. Symp. 23.

Smith, T. I. J.
1985. The fishery, biology, and management of Atlantic sturgeon, *Acipenser oxyrhynchus*, in North America. Environ. Biol. Fishes 14:61–72.

STSC, Inc.
1992. User's manual, version 6. Manugistics, Inc., Rockville, MD.

Stevenson, J. T.
1997. Life history characteristics of Hudson River Atlantic sturgeon and an age-based model for management. M.S. thesis, Univ. Maryland, College Park, MD, 221 p.

Taub, S. H.
1990. Fishery management plan for Atlantic sturgeon. Atlantic States Marine Fisheries Commission Fish. Manage. Rep. 17, Washington, D.C., 73 p.

Thuemler, T. F.
1985. The lake sturgeon, *Acipenser fulvescens*, in the Menominee River, Wisconsin–Michigan. Environ. Biol. Fishes 14:73–78.

Van Eenennaam, J., S. I. Doroshov, G. P. Moberg, J. G. Watson, D. S. Moore, and J. Linares.
1996. Reproductive conditions of the Atlantic sturgeon (*Acipenser oxyrinchus*) in the Hudson River. Estuaries 19:769–777.

Waldman, J. R., J. T. Hart, I. I. Wirgin.
1996. Stock composition of the New York Bight Atlantic sturgeon fishery based on analysis of mitochondrial DNA. Trans. Am. Fish. Soc. 125:364–371.

Winemiller, K. O., and K. A. Rose.
1992. Patterns of life-history diversification in North American fishes: implication for population regulation. Can. J. Fish. Aquat. Sci. 49:2,196–2,218.v

Settlement and nursery habitats for demersal fishes on the continental shelf of the New York Bight*

Brian P. Steves
Marine Sciences Research Center
State University of New York at Stony Brook
Stony Brook, New York 11794-5000
Present address: Marine Invasions Laboratory
Smithsonian Environmental Research Center
648 Contees Wharf Road
Edgewater, Maryland 21037
E-mail address: Steves@serc.si.edu

Robert K. Cowen
Marine Sciences Research Center
State University of New York at Stony Brook
Stony Brook, New York 11794-5000

Mark H. Malchoff
New York Sea Grant Program
3059 Sound Avenue
Riverhead, New York 11901

Abstract.—Although juvenile fish are studied extensively in estuarine and nearshore environments, surprisingly little is known about the basic habitat requirements of juveniles for offshore settlement and nursery areas. Between June 1996 and July 1997, settlement and nursery habitats of age-0 (early juvenile) demersal fish on the continental shelf of the New York Bight were investigated by using a two-meter beam trawl. Replicate tows at 21 stations along three cross-shelf transects (20–95 m depth), were sampled on a near monthly basis to determine general ecology (21,309 fish collected in 659 tows). Of the 47 species collected, 33 included age-0 juveniles, and 25 included near-settlement size individuals. The two dominant species, *Pleuronectes ferrugineus* and *Merluccius bilinearis*, constituted 88.9% of the total catch of age-0 fish. Of all age-0 fish, 94% were collected during summer and fall. Comparisons of weighted means and the use of canonical correspondence analysis determined that settlement and nursery habitats across the shelf are primarily delineated by depth, temperature, and time of year. Three zones across the shelf (inner, middle, and outer) each had distinct juvenile fish assemblages. Knowledge gained about the distribution and quality of juvenile habitat for commercially important offshore species should facilitate their improved management.

Manuscript accepted 7 December 1998.
Fish. Bull. 98:167–188 (1999).

With the decrease in fish abundance in the latter half of the twentieth century, particularly in the Northwest Atlantic (McHugh, 1972; NEFSC, 1992), fisheries managers have been concerned with both overfishing and habitat degradation. Much effort has been put into understanding the abundance, distribution (Colton, 1972; Colvocoresses and Musick, 1984), and environmental preferences (Scott, 1982; Auster et al., 1991; Felley and Vecchione, 1995) of adult groundfishes in the northwestern Atlantic. Although information on adult groundfishes is useful, events during the early life history of fish may be more important in determining recruitment variability (Sissenwine, 1984; Houde, 1987; Peterman et al., 1988; Bradford, 1992; Miller, 1994). Several ichthyoplankton surveys have helped to increase our understanding of egg and larval distributions of groundfishes in the Mid-Atlantic Bight (MAB; Morse et al., 1987; Cowen et al. 1993). However, less is known about the juvenile stage, which represents a dramatic change in lifestyle for groundfishes: they leave the three-dimensional environment of the plankton and settle onto the two-dimensional world of the sea floor (Chambers and Leggett, 1992).

Within this two-dimensional environment, the growth, survival, and recruitment of groundfishes are affected by various factors associated with the quality (value for growth) and quantity (area) of their nursery habitat (Gibson, 1994). Research involving the nurseries of groundfishes has been limited to estuaries and nearby coastal habitats where they can readily be studied (Riley et al., 1981; Able et al., 1989; Bolle et al., 1994; Henderson and Seaby, 1994; Nash et al., 1994;

* Contribution 1179 of the Marine Sciences Research Center, State University of New York at Stony Brook, Stony Brook, NY 11794-5000.

but see Toole et al., 1997). However, Able et al. (1989) have suggested that there is a lack of studies that examine the continental shelves of the MAB as potential nursery grounds. This is remarkable because the early life history stages of many species of groundfish are believed to inhabit almost the entire shelf as well as the slope (Fahay, 1983; Miller et al., 1991).

A wide assortment of biotic and abiotic variables may have a role in determining the distribution of continental shelf nursery grounds. Variations of abiotic parameters, such as temperature, salinity, and oxygen, can affect the metabolism of marine flatfishes during the juvenile stage (Malloy and Targett, 1991; Pihl et al., 1991; Gibson, 1994; Neill et al., 1994). Changes in temperature, for example, can have a marked effect on feeding rate and growth; thus lower temperatures may slow growth and consequently increase susceptibility to mortality due to size-selective predation (Van der Veer et al., 1994). Salinity seems to have a small influence on the growth rate of fish, but it is often effective in controlling their distribution (Rodgers, 1992). By adjusting their position in relation to local abiotic factors, fish may modify their growth rate and survival with respect to average environmental parameters (Gibson, 1994).

Biotic factors, particularly food resources and shelter related to biological activity, may also be a potent determinant of nursery habitat. Auster et al. (1991) found that several biotic microhabitat types, including amphipod tube mats, shells, and biogenic depressions, significantly affected the abundance of fishes and other megafauna. Other biotic factors that influence the distribution of juvenile fishes include the presence of potential predators (Bailey, 1994) and the availability of potential prey species. Biotic factors may be ephemeral; however their presence or absence at a given time and space may control the distribution of associated fish species. The spatial distribution of amphipod tubes in particular have been shown to have a strong influence on the abundance of age-0 silver hake (*Merluccius bilinearis*) during fall in the MAB (Auster et al., 1997).

Recent recruitment research has emphasized factors that affect survival of the early life history stages of fishes. Identification of the habitats preferred by juvenile fishes in offshore waters will allow for a more complete understanding of recruitment variation. Although shelf habitat is magnitudes larger in area than the nearshore habitat traditionally studied, there is currently little knowledge of its role as a nursery. For many flatfish species, the size of nursery habitat and year-class strength have been correlated (Rijnsdorp et al., 1992; Gibson, 1994). Our objectives were to provide a first-order analysis of the species that use the shelf as settlement and nursery habitat during the course of a year and to address the relation of these distributions to environmental correlates.

Description of the study area

The New York Bight (NYB), a central portion of the MAB, encompasses an area of 39,000 km^2 on the East Coast of the United States. Its boundary extends out to the 200-m isobath between Montauk Point, New York, and Cape May at the southern end of New Jersey. The bathymetry of the NYB varies on several geographical scales. Although the continental shelf in this area is, to the most extent, gently sloping, large-scale features do exist. The Hudson River Canyon, which almost bisects the NYB, is the most obvious of these. Imposed on this bathymetry are the convoluted isobaths of the ridge and the swale topography that dominates the NYB (Freeland and Swift, 1978). Surficial sediments range from fine sand along the southern shore of Long Island to pebbly gravel off the coast of New Jersey (Schlee, 1964). On a somewhat smaller scale, the sediments vary in color from yellow ochre to greenish gray and in composition from biogenic calcium carbonate to quartz and feldspar (Freeland and Swift, 1978).

The hydrography of the NYB changes seasonally. During the winter months, the entire water column is well mixed, but the coldest waters are found nearshore (Bowman and Wunderlich, 1977). Stratification begins in the spring and peaks in the summer. During stratification, a body of cold dense water, known as the cold pool, remains trapped on the bottom under the pycnocline on the midshelf. This cold pool forms a distinct band of midshelf temperature minima (about 4–5°C in midsummer) from Georges Bank to Cape Hatteras, persisting from late spring to early autumn (Houghton et al., 1982). Outside the cold pool, bottom temperatures in the NYB range inshore from less than 1°C in the winter to above 21°C in the summer. Deeper bottom water, near the 100-m isobath, is less variable, ranging from 7° to 12°C (Ketchum and Corwin, 1964). Salinity in the NYB varies less, with only a mild seasonal cycle. The lowest salinities (<31 psu) are found near the apex of the NYB, southeast of the Hudson River. However, salinities as high as 35 psu are found at the 200-m isobath. As with temperature, the largest seasonal fluctuations in salinity are found nearshore (Bowman and Wunderlich, 1977). Overall, nearshore habitats are less stable than those offshore in terms of both salinity and temperature.

Materials and methods

Sample collection

Ten sampling cruises were conducted between June 1996 and July 1997 on board an 85-foot commercial fishing vessel, the *Illusion*. Summer and fall cruises were conducted monthly, and winter and spring cruises were conducted every other month (Table 1). The 21 stations sampled during each cruise were arranged in three transects (west, central, and east), each with seven stations ranging in depth from about 20 meters to 90 meters (Fig. 1). Stations on each transect were located according to bathymetry so that six stations were distributed evenly across the range of depths (one approximately every 15 m of depth). The seventh station was placed to fill any large distance between stations that was due to variability in the slope. The distance from shore of stations at a particular depth varied between transects.

Not all stations were sampled during every cruise (Table 1). Owing to weather, only five stations were sampled during cruise 6 (December 1996) and only two of the three transects were sampled during the February 1997 and April 1997 cruises. Because less than 25% of the stations were sampled during cruise 6, we did not include these data in some of the analyses. However, cruises 7 and 8 were included because of their broader range of coverage (between the two cruises all three transects were covered at least once).

Temperature and salinity data were collected after trawling at each station by using an internally recording conductivity-temperature-depth (CTD) probe (Applied Microsystems Inc. model AMS-STD 12). Care was taken to collect data from as close to the bottom as possible without risking damage to the CTD. Because a backup CTD was unavailable and the CTD used was not always reliable, gaps in the physical data exist. Expendable bathythermograph (XBT) data collected nearby in early August by the MV *Oleander* as part of the NOAA Ship of Opportunity Program (SOOP) were substituted for missing temperature data for the central transect in that month.

Juvenile groundfishes were collected with a modified 2-m beam trawl with 4-mm stretch mesh net (and 5-cm stretch mesh outer net for chaffing), towed at about 2–2.5 knots. The addition of a meter wheel allowed us to measure the area swept as the distance trawled, multiplied by the width of the trawl (as in Carney and Carey, 1980). At each station, three 5-min tows were made; a fouled trawl was discounted and another trawl was repeated. The mean area swept during a 5-min tow was 698 m^2 ±35.1 m^2 (95% CI).

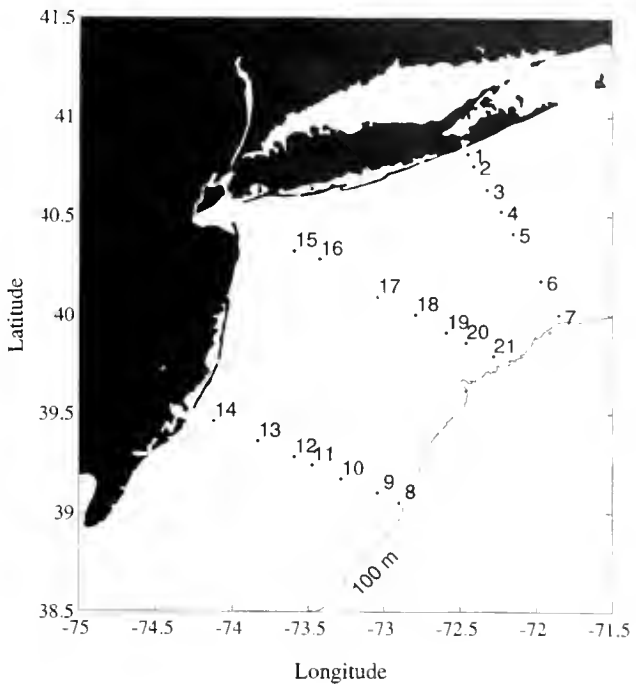

Figure 1

Twenty-one stations (numbers) on the continental shelf of the New York Bight were sampled with a two-meter beam trawl.

Table 1

Dates and sampling stations in the New York Bight for each of the ten cruises in this study. For each of the three transects, numbers indicate the stations sampled on a given cruise (sample locations are depicted in Figure 1).

Cruise number	Dates	West transect	Center transect	East transect
1	14–17 Jun 1996	8–13	16–21	1–7
2	9–11 Jul 1996	8–14	15–21	1–7
3	9–11 Aug 1996	8–14[1]	15–21[2]	1–7[1]
4	20–22 Sep 1996	8–14	15–21	1–7
5	25–27 Oct 1996	8–14	15–21	1–7
6	10 Dec 1996	—	—	1–5
7	26–27 Feb 1997	8–14	—	1–7
8	16–17 Apr 1997	8–14	15–21	—
9	11–13 Jun 1997	8–14	15–21	1–7
10	15–17 Jul 1997	8–14	15–21	1–7

[1] During the August cruise, no temperature or salinity data were collected.

[2] The center transect was supplemented by XBT data

A 2-m beam trawl is the recommended standard trawl for juvenile groundfish research because its fixed width allows for ready quantification of the area trawled (Kuipers et al., 1992). Our trawl had skids that were heavier than those on most stan-

dard 2-m beam trawls in order to reduce the amount of time the trawl took to reach the bottom and to ensure that it was heavy enough to remain there. To accommodate the increased weight (about 38 kg) and prevent the trawl from digging into the sediment, the skids were also longer (0.85 m) and wider (0.1 m). Typically, 2-m beam trawls are not used in depths greater than seven meters (Rodgers, 1992; Gibson, 1994; but see Pearcy, 1978); however, these modifications enabled us to trawl easily in waters as deep as 100 m.

Fish samples were sorted on deck and all recently settled juvenile fishes (age-0) were preserved in 95% denatured ethanol. These fish were measured in the laboratory to the nearest tenth of a millimeter standard length (SL) with digital calipers. Older fish were measured on deck to the nearest millimeter and returned to the water. With the exception of *Sebastes* and *Urophycis* spp., all age-0 fishes were identified to species. Fish stages were identified according to morphological changes such as squamation and, for flatfish, eye migration, as well as analysis of length frequencies of cohorts. The relative abundance and composition of the remaining sample (shell hash, sand dollars, and shrimp) were estimated from subsamples.

Length-frequency distributions of each species collected were calculated for each cruise. To account for differences in sampling effort among cruises, abundance data were standardized to the average cruise, which had 63 tows (21 stations × 3 tows each) lasting five minutes each. Length frequencies were then used to estimate the size range of the age-0 fishes collected during each cruise, as well as to infer some growth rates of the age-0 cohort between cruises.

Distribution analysis

Abundance data were standardized to the average number of fish per 1000 m^2. Because we were specifically interested in early juveniles, and adults were not efficiently collected, we limited our analysis to age-0 fishes. All species of age-0 fishes collected were included in the analyses. The distribution of age-0 fishes was evaluated with respect to a suite of environmental data (bottom temperature, bottom salinity, and depth) by comparing weighted means for each species (Scott, 1982). For a given species, an environmental variable such as temperature was weighted by the abundance of that species at each sampling station. The sums of each weighted variable were then divided by the total abundance of that species collected to yield a mean value for that species on that environmental parameter.

Cross-shelf migrations with ontogeny are a common feature of demersal fishes, particularly flatfish (Riley et al., 1981; Toole et al., 1997). To determine changes in cross-shelf distribution with size, weighted mean depths by size class were calculated for the more abundant species collected. In particular, distinct differences between the location of near-settlement size fishes and larger age-0 fishes might indicate migration between settlement and nursery habitats.

Environmental correlates

Distribution and abundance of fishes in relation to underlying multivariate environmental gradients were analyzed by canonical correspondence analysis (CCA) by using the software program CANOCO (ter Braak, 1992). This analysis has been widely applied in the field of community ecology (ter Braak, 1995; ter Braak and Verdonshot, 1995; Rakocinski et al., 1996); it entails reciprocal averaging of species and environmental data based on the assumption of a unimodal response of species abundance to the environment (Palmer, 1993; ter Braak, 1995). In a comparison of ordination techniques, Palmer (1993) found that CCA was robust, being less susceptible to spurious results such as the "arch effect" often common to principal components analysis (PCA). Furthermore, Palmer's (1993) simulations of CCA illustrated that noisy or skewed species data could be compensated for, and a variety of data types and sampling design were possible.

In total, 25 environmental variables (Table 2) were sampled during the cruises and included in the CCA analysis. Bottom temperature and salinity (from CTD casts), station depth (from an onboard depth sounder), latitude and longitude (global positioning system [GPS]), and distance from shore (nautical charts) were employed as continuous measures during the analysis. The relative abundances of nonfish constituents collected by the trawl were also considered to be environmental variables. Information on surficial sediment character at each station, another environmental variable we employed, was obtained from published data from the Marine EcoSystems Atlas (MESA) program's New York Bight Project (Freeland and Swift, 1978). Although these data are independent of this study, the MESA sampling area was the same and the spatial resolution of its sediment sampling was fine enough to obtain general information suitable for our analysis. The data on nonfish trawl constituents and surficial sediments were entered into the analysis as scaled values (i.e. as a number describing relative abundance among stations and tows). Because collections of both species and environmental data were made year-round, seasonal variables were also included and coded in the analysis as a set of nominal variables: spring (March–May), summer (June–August), fall (September–November),

Table 2
List of environmental variables used in the canonical correspondence analysis (CCA).

Environmental variable	Code	Type	Units
Spring	Spr	seasonal	true-false
Summer	Sum	seasonal	true-false
Fall	Fall	seasonal	true-false
Winter	Win	seasonal	true-false
Latitude	Lat	physical	° latitude
Longitude	Long	physical	° longitude
Bottom temperature	T	physical	° Celsius
Bottom salinity	Sal	physical	psu
Distance from shore	D	physical	km
Depth	Z	physical	m
Median grain size	MePhi	physical	Φ-scale
% organics in sediment	%Org	physical	percent
% calcium carbonate in sediment	%CaCO3	physical	percent
Northern sea stars, *Asterias forbesi*	noss	biological	relative volume of sample
Sand dollars, *Echinarchnius parma*	snd	biological	relative volume of sample
Margined sea stars, *Pontaster tenuispinus*	marg	biological	relative volume of sample
Small shell fragments	hash	biological	relative volume of sample
Large mollusk shells and shell pieces	shell	biological	relative volume of sample
Sea scallops, *Placopecten magellanicus*	scall	biological	relative volume of sample
Sand shrimp, *Crangon septemspinosa*	crang	biological	relative volume of sample
Boreal shrimp, *Pandalus montagui*	borsh	biological	relative volume of sample
Rock crabs, *Cancer* spp.	crab	biological	relative volume of sample
Amphipods	amph	biological	relative volume of sample
Fig sponges, *Suberites ficus*	spon	biological	relative volume of sample
Large biogenic tubes	tube	biological	relative volume of sample

and winter (December–February). Each environmental variable was standardized to have a mean of zero and a standard unit of variance so that all variables had equal weight despite differences in the scales of their usual units.

Although seasonal patterns are likely to be important in juvenile fishes, these patterns are likely to be influenced by the spawning patterns of adult fishes rather than by habitat selection of settling fishes. These seasonal effects may dilute the variation explained as due to other factors. Some environmental factors such as temperature, salinity, and the presence of ephemeral biota that vary with season are possibly of more interest than simply accounting for settlement timing. To this end, a partial CCA was conducted using season as a covariable. Partial CCA allows environmental variables to be treated as covariables, thus removing their influence from the rest of the data set (ter Braak and Verdonschot, 1995).

A forward selection of environmental variables was used to select a minimum set of environmental variables that best explained the distribution and abundance of age-0 fishes (ter Braak, 1992). Forward selection begins by the selection of the variable that explains the most variation in the data set. This variable is then treated as a covariable, the data set is then reevaluated, and the next most important variable is selected. This procedure continues until the desired subset of variables has been selected. To test the advisability of adding variables, Monte Carlo permutation simulations are conducted. Variables are added as long as their addition continues to contribute significantly to the explained variance ($P<0.05$). Forward selection was performed on the data set, with season treated as a covariable. The combination of partial CCA and forward selection is not considered problematic with regard to the assumptions of the analysis (ter Braak, 1992).

Results

Faunal composition and distribution

A total of 21,309 fish representing 47 species and 32 families were collected over the course of the ten cruises and the 659 tows. Of these 47 species, 33 were collected as age-0 juveniles, including 25 spe-

Table 3

Minimum, mean, and maximum standard length (mm) of the 32 species of age-0 demersal fish collected. Maximum larval size (Fahay, 1983) and sample size (n) are also indicated. Maximum sizes estimated from size-frequency distributions are included (see Figs. 4–6). Species are ordered by decreasing total abundance. An asterisk next to minimum standard length indicates that the species was collected at near-settlement size.

Species	Species code	Max larval size (mm)	Min. SL (mm)	Avg. SL (mm)	Max. SL (mm)	n
Pleuronectes ferrugineus	PLEFER	11–16	5.7*	17.4	34.9	10,452
Merluccius bilinearis	MERBIL	17–20	12.6*	28.2	145.0	3,195
Liparis inquilinus	LIPINQ	12–13	9.6*	20.4	49.0	595
Raja erinacea	RAJERI	80–90	87.2*	117.6	146.4	281
Urophycis spp.	UROSPP	20–25	8.8*	32.5	49.0	224
Macrozoarces americanus	MACAME	30	32.0*	89.1	119.0	213
Citharichthys arctifrons	CITARC	13–15	10.8*	18.8	29.7	120
Lepophidium profundorum	LEPPRO	20	85.5	85.5	115.0	117
Ophichthus cruentifer	OPHCRU	83.5	70.0*	111.0	146.0	80
Gadus morhua	GADMOR	20–30	20.0*	36.8	49.0	62
Peprilus triacanthus	PEPTRI	12–18	6.8*	15.2	45.0	61
Glyptocephalus cynoglossus	GLYCYN	22–35	13.5*	30.0	47.5	40
Helicolenus dactylopterus	HELDAC	20	21.0*	28.9	35.0	38
Enchelyopus cimbrius	ENCCIM	20	9.1*	26.7	47.0	35
Etropus microstomus	ETRMIC	10–12	14.7*	23.6	29.0	26
Prionotus carolinus	PRICAR	20	11.1*	30.1	49.0	26
Myoxocephalus octodecemspinosus	MYOOCT	15	15.9*	22.2	44.0	22
Scophthalmus aquosus	SCOAQU	9	9.1*	59.8	143.0	19
Paralichthys oblongus	PAROBL	10–12	9.4*	15.8	37.0	15
Hippoglossoides platessoides	HIPPLA	18–34	20.1*	23.7	26.1	13
Ophidion marginatum	OPHMAR	35–50	52.1*	64.4	75.3	10
Stenotomus chrysops	STECHR	17	52	64.4	75	10
Sebastes spp.	SEBSPP	24	25.5*	28.1	33.1	8
Lophius americanus	LOPAME	50	56.0*	74.2	96.5	5
Melanogrammus aeglefinus	MELAEG	20	39.0	44.7	48.0	4
Centropristis striata	CENSTR	8.3	25.0	29.8	35.5	3
Hemitripterus americanus	HEMAME	19	27.0	28.0	29.0	2
Astroscopus guttatus	ASTGUT	20	9.8*	9.8	9.8	1
Monolene sessilicauda	MONSES	33	41.0	41.0	41.0	1
Pholis gunnellus	PHOGUN	30–35	39.0*	39.0	39.0	1
Tautogolabrus adspersus	TAUADS	8	8.7*	8.7	8.7	1
Citharichthys cornutus	CITCOR	13–15	53.2	53.2	53.2	1
Pleuronectes americanus	PLEAME	10–13	81.2	81.2	81.2	1

cies collected at near-settlement sizes on the shelf (Table 3). Two species represented 88.9% of the age-0 fishes collected: yellowtail flounder (*Pleuronectes ferrugineus*, 67.8%) and silver hake (*Merluccius bilinearis*, 21.1%). Overall, densities of these dominant species on the shelf during peak settlement averaged 55.7 and 26.23 per 1000 m^2, respectively (Table 4), although maximum densities of 771.4 and 660.9 per 1000 m^2, respectively, occurred during peak settlement in individual tows. In addition to age-0 juveniles, both larval (n=267, <2% total), and adult (n=2765, 13.0% total) fishes were captured with the trawl. Of the 25 species collected at or near-settlement size, 11 included individuals smaller than predicted settlement size, based on published maximum larval size (Fahay, 1983).

Most (94%) age-0 fishes were collected in the summer and fall (Table 4). *P. ferrugineus* and *M. bilinearis*, the two dominant species, settled almost exclusively during summer and fall, respectively (Fig. 2). However, if species richness is considered rather than species abundance, summer and fall are still the primary

Table 4

Mean seasonal density (fish/1000 m^2) of 21 abundant age-0 fishes over the entire continental shelf of the New York Bight. Winter and spring cruises are combined. Species are grouped by their season of highest density and only species with a density greater than 0.1 in at least one season are included.

	Summer 1996	Fall 1996	Winter 1996–Spring 1997	Summer 1997
Summer				
Pleuronectes ferrugineus	55.68	0.53	—	1.29
Citharichthys arctifrons	3.84	2.25	0.66	0.09
Macrozoarces americanus	0.94	0.36	0.16	0.20
Gadus morhua	0.40	0.03	0.14	—
Helicolenus dactylopterus	0.09	0.03	—	0.26
Peprilus triacanthus	0.24	0.04	—	0.17
Glyptocephalus cynoglossus	0.21	0.03	—	0.05
Enchelyopus cimbrius	0.21	0.03	—	0.05
Myoxocephalus octodecemspinosus	0.11	0.07	0.11	0.09
Fall				
Merluccius bilinearis	0.07	26.23	1.04	0.22
Liparis inquilinus	1.19	1.89	0.09	1.75
Urophycis spp.	0.26	1.88	1.05	0.07
Lepophidium profunforum	0.09	0.77	—	—
Ophichthus cruentifer	0.02	0.61	—	0.11
Etropus microstomus	0.11	0.40	0.79	0.05
Paralichthys oblongus	0.06	0.13	—	0.05
Winter–Spring				
Raja erinacea	0.60	0.56	0.90	0.54
Prionotus carolinus	0.04	0.22	0.46	—
Centropristis striata	—	0.15	0.20	—
Ophidion marginatum	—	—	0.11	—
Scophthalmus aquosus	0.02	0.07	0.11	0.05

time of settlement on the shelf (Fig. 2). Although many species settled between August and October, *Macrozoarces americanus* and *Gadus morhua* settled, and *Raja erinacea* hatched, on the shelf starting in midwinter.

Juvenile fish were colleced at all 21 stations sampled. Mean depths of all species of age-0 fish, weighted by abundance, are shown in Figure 3. Although the depth distributions cover the entire depth range of the surveyed shelf, for convenience of discussion we separate species into three depth groups (inner, middle, and outer shelf; Table 5). Inner shelf species included two flounders (*Etropus microstomus* and *Paralichthys oblongus*), searobin (*Prionotus carolinus*), and fourbeard rockling (*Enchelyopus cimbrius*). Little skate (*Raja erinacea*) was collected on the inner shelf at sizes near to hatching size. Midshelf settlers were dominated by *Pleuronectes ferrugineus* but also included large numbers of inquiline snailfish (*Liparis inquilinus*) and phycid hakes (*Urophycis* spp.). The dominant fish that settled on the outer shelf were silver hake (*Merluccius bilinearis*), Gulf Stream flounder (*Citharichthys arctifrons*), margined snake eel (*Ophichthus cruentifer*), fawn cusk eel (*Lepophidium profundorum*), and black-bellied rose fish (*Helicolenus dactylopterus*).

Generally, distributions along depth (Fig. 3A) and salinity (Fig. 3B) gradients showed similar but inverse trends; this finding was expected because of high correlation between bottom depth and bottom salinity. Weighted average distributions with respect to bottom temperature (Fig. 3C) did not show similar trends; seasonal variation in temperature and the presence of minimum temperatures midshelf during the summer precludes temperature and depth trends from being similar. Midshelf species such as *P. ferrugineus* and *Liparis inquilinus*, which settle in summer, had the coldest mean temperatures of collection. Outer-shelf species found in slope water had slightly warmer preferences, and those of inner-shelf species were even warmer.

Individual year classes were distinct, based on length frequencies for the more abundant species (Fig. 4–6). For several species (e.g. *P. ferrugineus* and

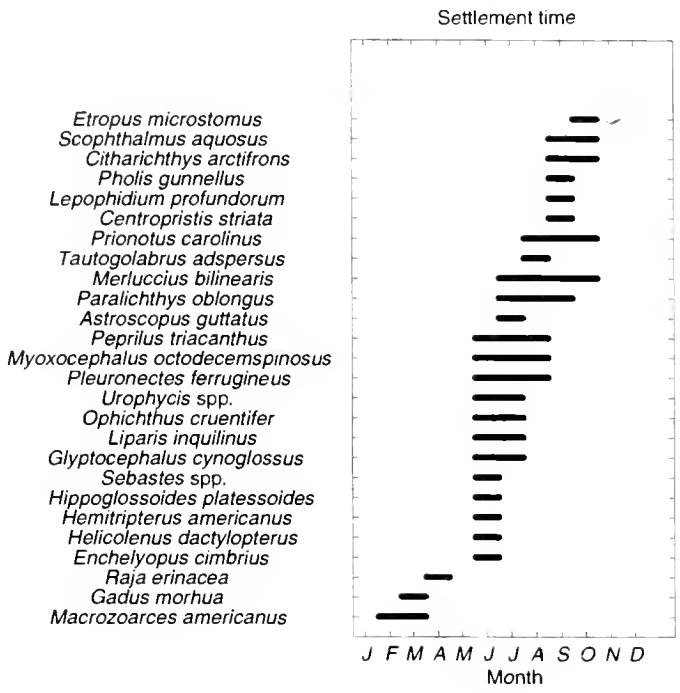

Figure 2

Timing of settlement for age-0 fish collected. For each species, a black horizontal bar marks the months in which cruises collected fish at or near settlement size. In some months there was no cruise (Table 1), and any settlement that might have occurred was not witnessed.

M. bilinearis), large decreases in abundance were observed following initial settlement, whereas abundance decreased at a more modest rate for other species such as *C. arctifrons*, *Macrozoarces americanus*, and *L. inquilinus*.

For species such as *P. ferrugineus* and *L. inquilinus* that settled during the summer (Fig. 4), the cohort could be followed for the entire first year after settlement (June 1996–July 1997). For other species that did not settle in the summer (Figs. 5 and 6), the cohort from the previous year was observed until the new cohort settled in the fall, winter, or spring. Inferred growth rates from the length-frequency distributions varied from two millimeters per month for species such as *P. ferrugineus* and *L. inquilinus* (Fig. 4), to about 15 mm per month for *Merluccius bilinearis* (Fig. 5) and *Macrozoarces americanus* (Fig. 6).

Cross-shelf movement between and within settlement and nursery areas was evident for some species but not for others. *Pleuronectes ferrugineus*, *Etropus microstomus*, and *Lepophidorum profundorum* are examples of species with consistent mean depths of distribution during their first year after settlement (Fig. 7, A–C). However, *M. americanus* exhibited a gradual migration towards deeper waters, whereas *C. arctifrons* and *Merluccius bilinearis* moved rapidly after settlement to waters about 30 meters deeper for the remainder of the first year (Fig. 7, D–F).

Habitat characteristics

Bottom temperatures in the NYB were dynamic (Fig. 8), and seasonal shifts in temperature were more varied at nearshore stations (5–20°C at the 25-m isobath) than at offshore stations (7–11°C at 90 m). Midshelf bottom temperatures showed a moderate seasonal range (4.3–14°C at 50 m). During the summer, bottom temperatures were stable, and there was only a slight increase of about 1°C per month. The highest rate of increase in bottom temperatures was recorded at the inshore stations: 8°C between August and September, associated with an early fall turnover in 1996. This was followed by the highest rate of cooling (–3°C) at the same nearshore locations between the September and October cruises. During fall turnover, the bottom temperatures increased by about 4°C per month over the midshelf, for a total of 8°C in two months. Following this

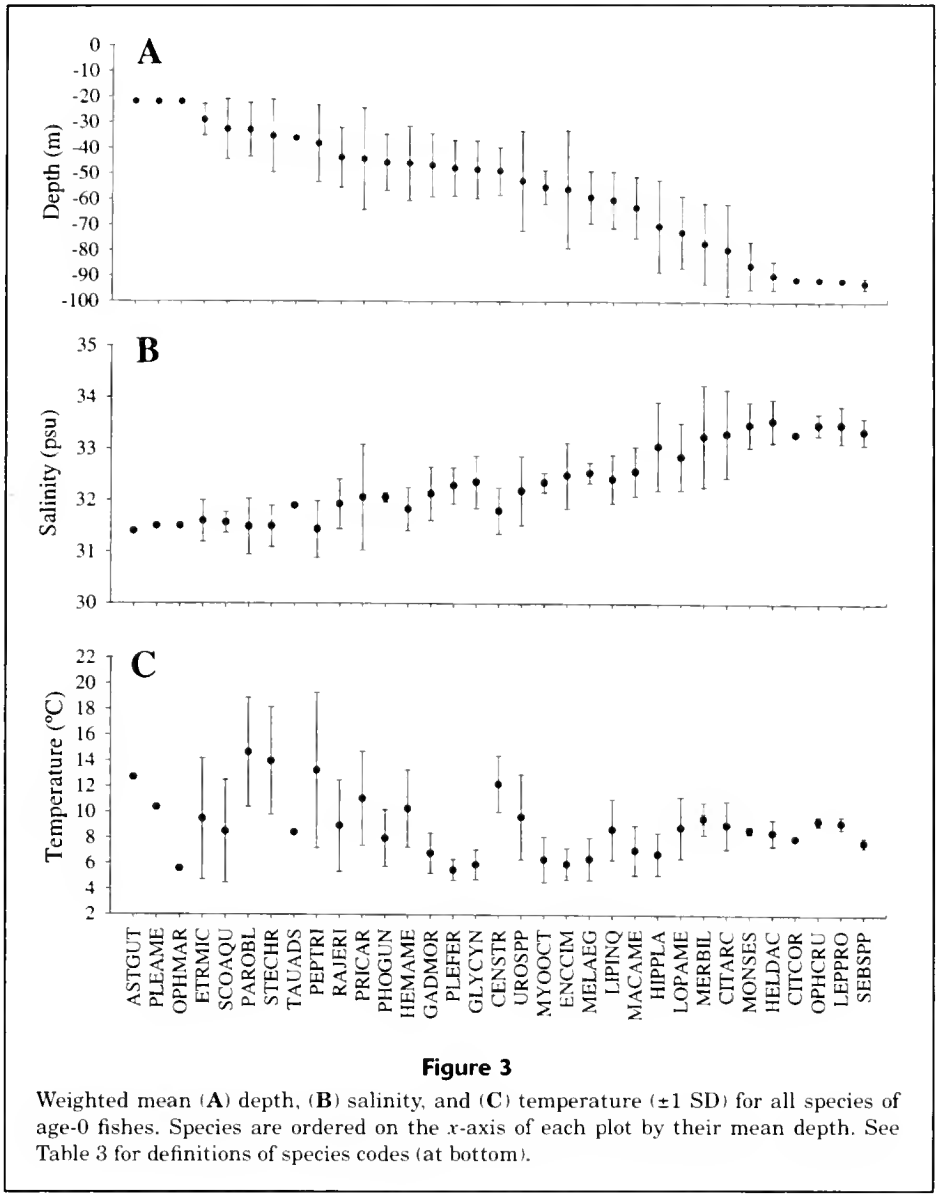

Figure 3

Weighted mean (**A**) depth, (**B**) salinity, and (**C**) temperature (±1 SD) for all species of age-0 fishes. Species are ordered on the *x*-axis of each plot by their mean depth. See Table 3 for definitions of species codes (at bottom).

warming trend, temperatures decreased by about 1°C per month until they reached their minimum in April. Late winter bottom temperatures in 1997 were not as cold as midshelf temperatures during summer 1996.

Salinity was a more conservative hydrographic variable than temperature. Variation in seasonal bottom salinity was slight; all cruises had a salinity range of approximately 31–35.5 psu. Bottom salinities were lowest inshore near inlets (station 1) and the Hudson River (station 15). The correlation between bottom salinity and bottom depth was high (r=0.87). Higher bottom salinities (>34 psu) offshore showed some fluctuation in their distribution on the outer shelf associated with similar fluctuations in warmer bottom temperatures. These warm, high-salinity bottom waters are representative of slope water intrusions (Churchill, 1985; Flagg et al., 1995).

The total catch of benthic organisms from the trawl varied greatly between stations, but there were generally three major groups or types of trawl samples. Groups were delineated to some extent by the depth at which they were collected. Inner-shelf stations (<40 m) typically included such organisms as the common sea star (*Asterias forbesi*) and fig sponge (*Suberites ficus*). Gammarid amphipods, sand shrimp (*Crangon septemspinosa*), and northern moon snail (*Euspira heros*) constituted much of the rest of the nonfish fauna collected there. Sand dollar (*Echina*

rachnius parma) and valves of surf clams (*Spisula solidissima*) dominated the midshelf group (40–70 m) of benthic organisms. Shell hash collected midshelf consisted of fine fragments of sand dollar tests and larger pieces of clam valves. Small, recently settled rock crabs (*Cancer borealis*) were found in high numbers (>100 per 5-min trawl) during the summer in this type of sample. Margined sea stars (*Pontaster tenuispinus*) and sea scallops (*Placopecten magellanicus*) made up most of the trawl catch for deeper outer-shelf stations (70–90 m). Young pandalid shrimp (*Pandalus montagui*) constituted a large fraction (30–90%) of samples from these stations in late summer and fall. Larger crustaceans such as American lobsters (*Homarus americanus*) and large rock crabs (*C. borealis*) were occasionally abundant (>10 per 5-min trawl) at these stations. Several were collected during each cruise.

Table 5

Mean density (fish/1000 m^2) of 21 abundant age-0 fishes within each of three depth strata: inner shelf (<40 m), middle shelf (41–70 m), and outer shelf (71–95 m) across all sampling periods. Species are grouped by stratum of their highest abundance; only species from Table 4 are included.

	Inner shelf	Middle shelf	Outer shelf
Inner shelf			
Raja erinacea	1.01	0.81	0.03
Etropus microstomus	0.88	0.01	—
Prionotus carolinus	0.21	0.11	0.01
Paralichthys oblongus	0.12	0.03	—
Enchelyopus cimbrius	0.10	0.06	0.08
Scophthalmus aquosus	0.09	0.01	—
Ophidion marginatum	0.06	—	—
Middle shelf			
Pleuronectes ferrugineus	15.31	49.81	2.25
Liparis inquilinus	0.03	1.94	1.11
Urophycis spp.	0.83	0.84	0.58
Macrozoarces americanus	0.03	0.79	0.69
Gadus morhua	0.16	0.38	0.01
Glyptocephalus cynoglossus	0.02	0.23	0.01
Peprilus triacanthus	0.05	0.19	0.05
Myoxocephalus octodecemspinosus	—	0.11	0.01
Centropristis striata	0.04	0.10	—
Outer shelf			
Merluccius bilinearis	0.40	5.42	14.69
Citharichthys arctifrons	0.29	0.64	5.63
Lepophidium profundorum	—	—	0.68
Ophichthus cruentifer	—	—	0.51
Helicolenus dactylopterus	—	—	0.14

Other groups of macrobenthos were ubiquitous. Hermit crabs and cancer crabs of intermediate sizes were found throughout the stations sampled. Although they dominated the midshelf, sand dollars were also collected at inner-shelf stations. Other large benthic fauna such as horseshoe crabs (*Limulus polyphemus*) and spider crabs (*Libinia emarginata*) were collected, but these collections were sporadic.

Species assemblages and environmental variables

Four canonical axes, each representing a linear combination of the environmental data, were calculated from the data set. These four axes together accounted for 36.7% of the variation in species abundance and 82.1% of the cumulative variation, in relation to the total variation explained by the environmental variables. A summary of eigenvalues and the variance accounted for by each axis is given in Table 6A. The variance explained by the entire ordination, as well as the first axis, was more significant than expected by chance, as calculated by a Monte Carlo permutation test (n=99 iterations, P=0.01 for both tests).

Interpretation of the relationships between environmental variables and the CCA axes involves determining which variables are most correlated to the axes. One intuitive and effective method of accomplishing this is to examine an ordination plot of environmental variables (Fig. 9). Environmental variables with large components along a CCA axis have high correlations to that axis. However, the results of the ordination with 25 environmental variables were difficult to interpret because of inherent covariability of variables with one another (Fig. 9, A–B).

Forward selection of environmental variables resulted in selection of five environmental variables (bottom temperature, depth, the relative abundance of scallops, longitude, and the relative abundance of margined sea stars). Eigenvalues of the forward selection of these five variables (Table 6B) are predictably lower than for the CCA with all 25 variables included (Table 6A). However, 59% of the variability explained with all 25 variables included was explained by these five environmental variables alone. Temperature represented 23% of the entire variability explained by the environmental data, depth contributed 18%, scallop abundance explained 8%, and longitude and margined sea star abundance combined explain an additional 5%. The remaining variables, which did not add significantly to the resulting explanation, each explained less than 4% of the variation. Because only five variables were selected, the four synthetic gradients (CCA axes) are each highly correlated with one of the environmental variables (Table 6A). Thus, to some extent each axis

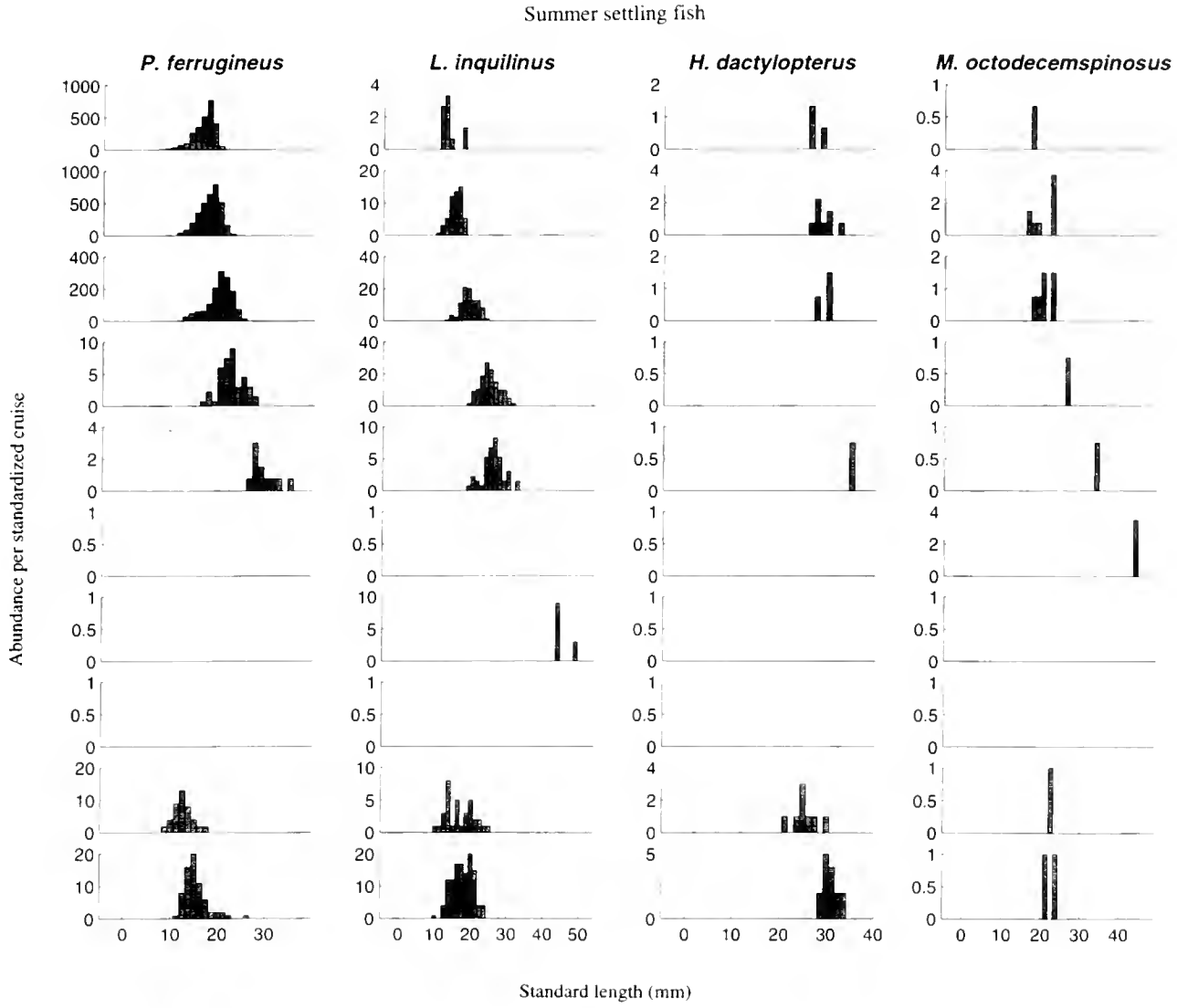

Figure 4

Length frequency by cruise of four species (*Pleuronectes ferrugineus*, *Liparis inquilinus*, *Helicolenus dactylopterus*, and *Myoxocephalus octodecemspinosus*) that settled to the shelf between early summer and midsummer. Plots for each species are ordered from top to bottom according to the order of the 10 cruises (see Table 1 for cruise dates). Abundance on each cruise was standardized to the number of fish collected during 63 5-min tows (21 stations with 3 tows each).

is a proxy for the environmental variable to which it is highly correlated.

Examination of species-environment biplots revealed relationships between environmental variables and species distributions. The species-environment biplot for the first two axes represents the majority of the species-environment relationships that resulted from the partial CCA (Fig. 9C). The importance of depth and temperature to these two canonical axes (see Table 7) indicates that temperature and depth are the two most important determinants of the species data. Inner-shelf species such as *Stenotomus chrysops*, *Paralichthys oblongus*, *Centropristis striata*, and *Etropus microstomus* are located near the upper right-hand quadrant of the ordination (positive values for both of the first CCA axes). Outer-shelf species, such as the rockfishes, *Sebastes* spp., and *Helicolenus dactylopterus* and the snake and cusk eels (*Ophichthus cruentifer* and *L. profundorum*) are found in the lower right-hand quadrant (positive CCA 1 and negative CCA 2). Species from the middle shelf, particularly *Pleuronectes ferrugineus* and *Liparis inquilinus*, are located near the origin of the ordination diagram.

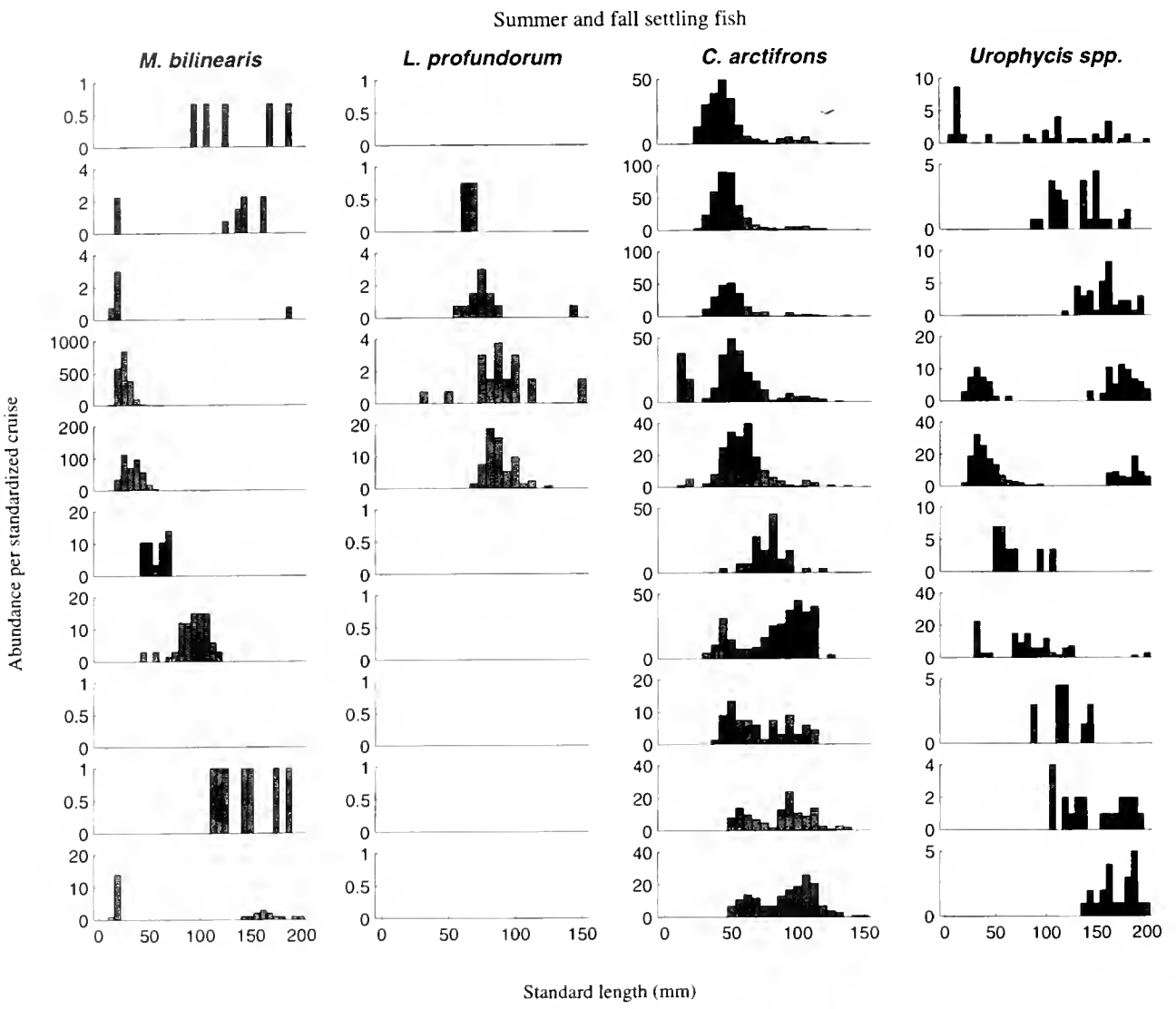

Figure 5

Length frequencies by cruise of four species (*Merluccius bilinearis, Lepophidium profundorum, Citharichthys arctifrons*, and *Urophycis* spp.) that settled to the shelf between late summer and midfall. Plots for each species are ordered from top to bottom according to the order of the 10 cruises (see Table 1 for cruise dates). Abundance on each cruise was standardized to the number of fish collected during 63 5-min tows (21 stations with 3 tows each).

The origin represents the mean for each environmental variable, and those means are weighted by species abundance. Because of the numerical dominance of *P. ferrugineus* in the samples, its mean temperature and depth of collection is driving the location of the origin. Consequently, the location of *P. ferrugineus* is just slightly left of the origin. The mean depth distribution of *P. ferrugineus*, however, was midshelf and thus its abundance did not skew the species distributions about the second axis, CCA 2.

One of the largest effects of the forward selection of variables is that the third and fourth CCA axes (Fig. 9D) now have definite environmental correlates. When 25 variables were used during full CCA, no one variable stood out as a clear contributor to the variation along these axes (Fig. 9B). With the abundance of scallops being the important environmental gradient describing the third CCA axis, one important species association is made clear: the abundances of juvenile inquiline snailfish and scallops. The fourth CCA axis, representative of longitude, accounted for only 5% of the total environmental explanation of the species patterns. This pattern might be considered as the subtle variation among the three transects (west, central, and east).

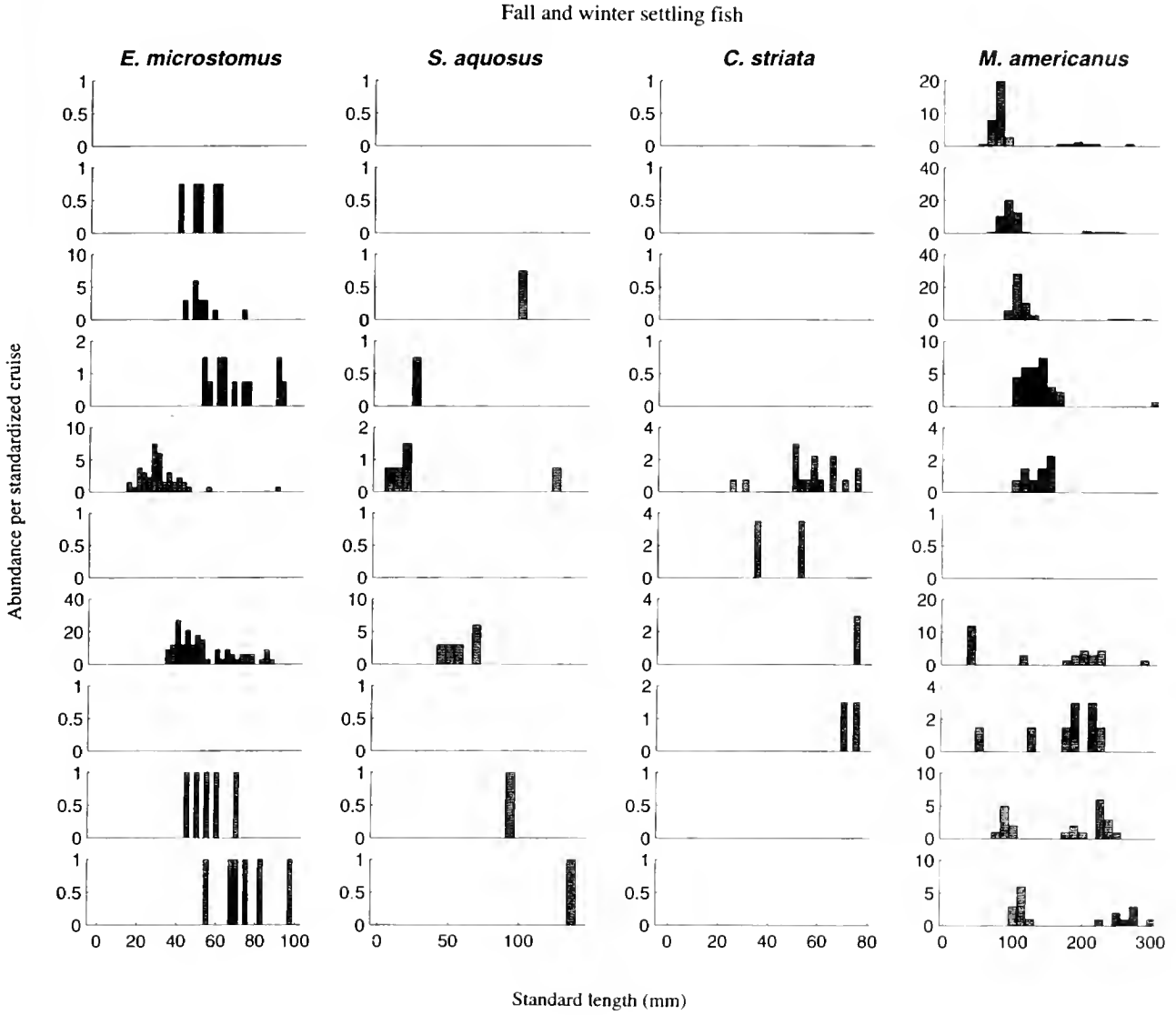

Figure 6

Length frequencies by cruise of four species (*Etropus microstomus*, *Scophthalmus aquosus*, *Centropristis striata*, and *Macrozoarces americanus*) that settled to the shelf between midfall and winter. Plots for each species are ordered from top to bottom according to the order of the 10 cruises (see Table 1 for cruise dates). Abundance on each cruise was standardized to the number of fish collected during 63 5-min tows (21 stations with 3 tows each).

Discussion

Many commercially and ecologically important species of demersal fishes in the NYB settle onto the continental shelf throughout the course of the year. In some cases settlement densities on the shelf may rival those of nearshore and estuarine species. For example, at some stations yellowtail flounder (*P. ferrugineus*) was found to have settlement densities as high as the long-term average for a congeneric estuarine species, plaice (*Pleuronectes platessa*), at approximately one per m^2 (Modin and Phil, 1994). Yet given the large areal extent of *P. ferrugineus* settlement on the shelf, its relative total abundance is potentially much larger. Similarly dense settlement may occur within portions of the shelf environment for other species such as *Merluccius bilinearis*. Even for those species collected in relatively low numbers, the large areas of NYB in which they settle suggests that total numbers are substantial.

Evidence that settlement does occur on the shelf is from two sources. The minimum size of collected

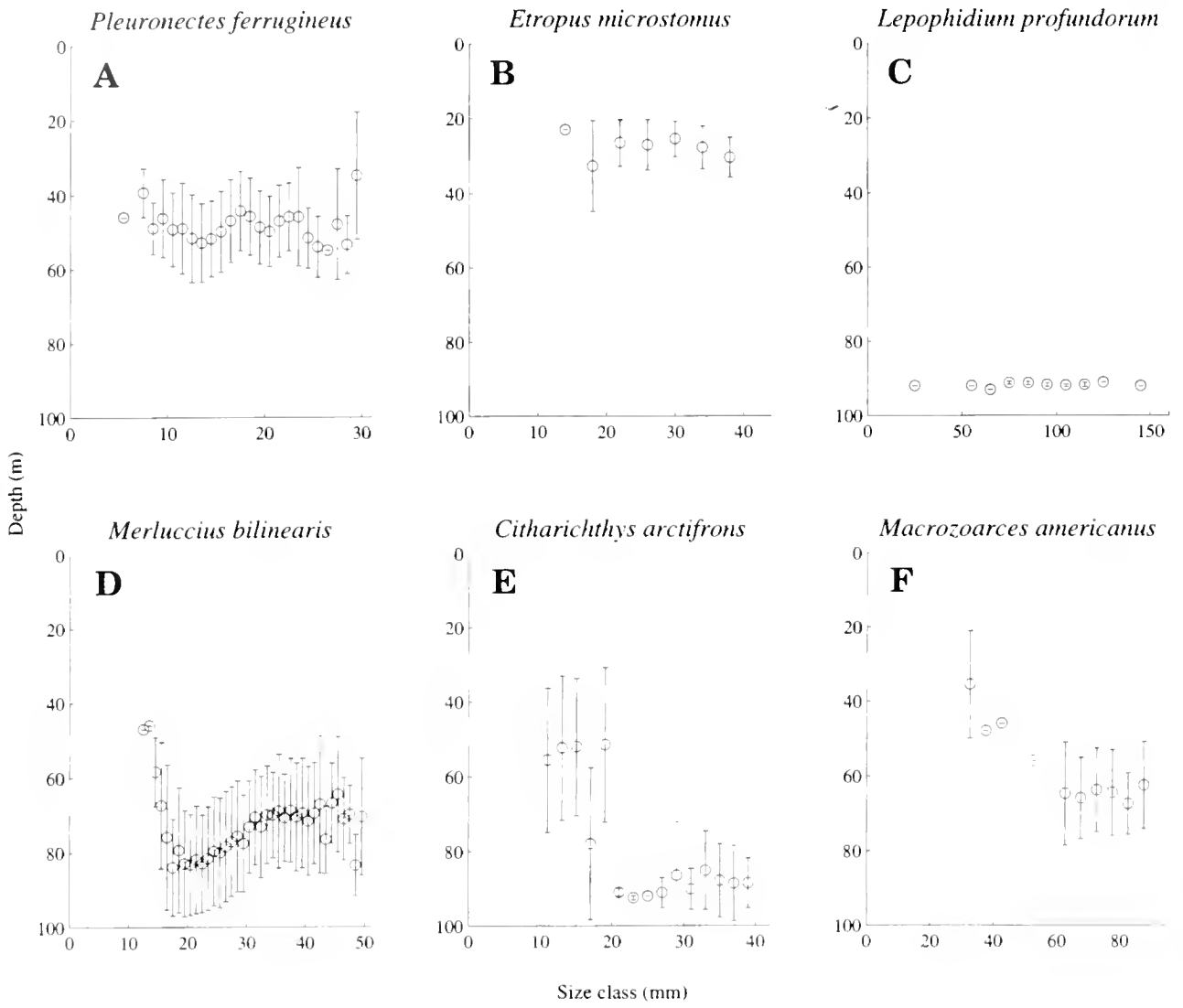

Figure 7

Mean depth (±1 SD) by size class for three species that do not show strong migration (A–C) and three species that do show migration with increased size (D–F).

age-0 fishes (Table 3; Figs. 4–6) were near (and occasionally below) that reported for size at the end of the larval stage (Fahay, 1983). Moreover, although the total contribution of larvae to the trawl catch was low (<2% of numeric abundance), the presence of these specimens in our samples strengthens the assertion that they were collected near first settlement. Most fish larvae collected were metamorphosing or post-flexion flounder, particularly *P. ferrugineus*. Larvae from nondemersal fish species known to be present in the water column at this time of year (Kendall and Naplin, 1981; Cowen et al., 1993; Cho, 1996) were not collected by the trawl. Collected larvae, therefore, were likely taken near the bottom rather than during the deployment or recovery of the net.

Compared with settlement areas, nursery areas for groundfishes on the continental shelf are more problematic to define. Gibson (1994) described nursery habitat as being an area where the scope for growth is enhanced for settled juveniles. Scope for growth is a function of habitat quality and quantity, but these parameters, particularly quality, are difficult to measure. Nursery habitats are generally spatially and temporally species-specific, but two or more species may have similar nurseries. Within a single species, nursery and settlement habitats may

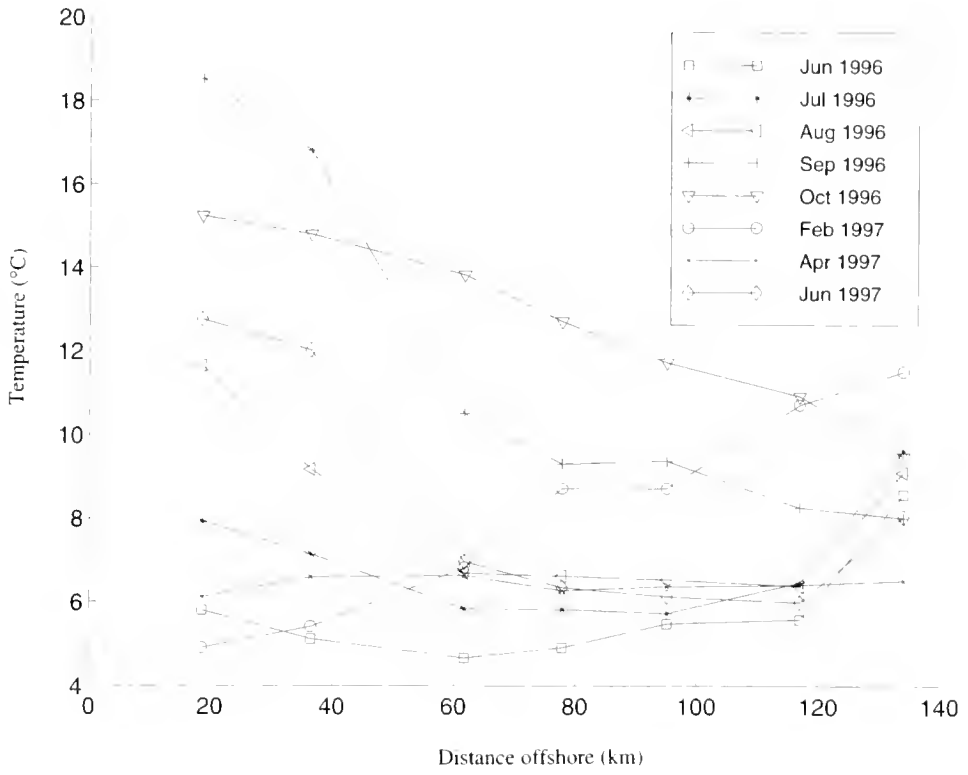

Figure 8

Bottom temperature by distance offshore for the center transect between June 1996 and June 1997.

occur in the same area, include just a slight overlap with one another, or may be entirely separate spatial entities. Although association with settlement habitat is not a given, an area in which postsettled juvenile fishes persist and grow prior to first spawning must be considered to be nursery habitat. Evaluation of nursery habitat quality requires the comparison of growth rates among stations for individual settlement cohorts (Sogard, 1992; Jenkins et al., 1993)—information not presented in our study. For many species, however, growth certainly occurs on the shelf after settlement (Figs. 4–6).

For several of the species collected during this study in the NYB, nursery and settlement habitats are synonymous. For example, *P. ferrugineus*, *E. microstomus*, and *L. profundorum* were limited in their distributions, remaining unchanged from settlement throughout the first year of life (Fig. 7, A–C). Several other species, *M. bilinearis*, *C. arctifrons*, and *M. americanus* (Fig. 7, D–F) showed some movement in depth between settlement and nursery areas, as well as some indication of within-nursery migration across the shelf. Toole et al. (1997) observed similar migration between the settlement and nursery areas of Dover sole (*Microstomus pacificus*) and suggested that such movements were actively pursued by the juveniles, but the ultimate migratory cues remained unclear.

Within the NYB, several environmental gradients describe the spatial and temporal distributions of settlement habitats. Species-environment relationships from the ordination analysis reveal that temperature and depth explain most of the among-species variance in habitat associations. Previous studies of adult fishes in the NYB have shown the importance of temperature and depth in describing species assemblages (Colvocoresses and Musick, 1984). This is in contrast to the west coast of the United States, where fish habitat associations have been studies extensively for rockfish (*Sebastes* spp.) and to a lesser extent for flatfish. There, for many species, more importance has been attributed to geological features such as sediment size and bathymetric heterogeneity (Pearcy, 1978; Stein et al., 1992; Adams et al., 1995). Considering the higher level of geological diversity on the West Coast than in the NYB, this conclusion is not surprising.

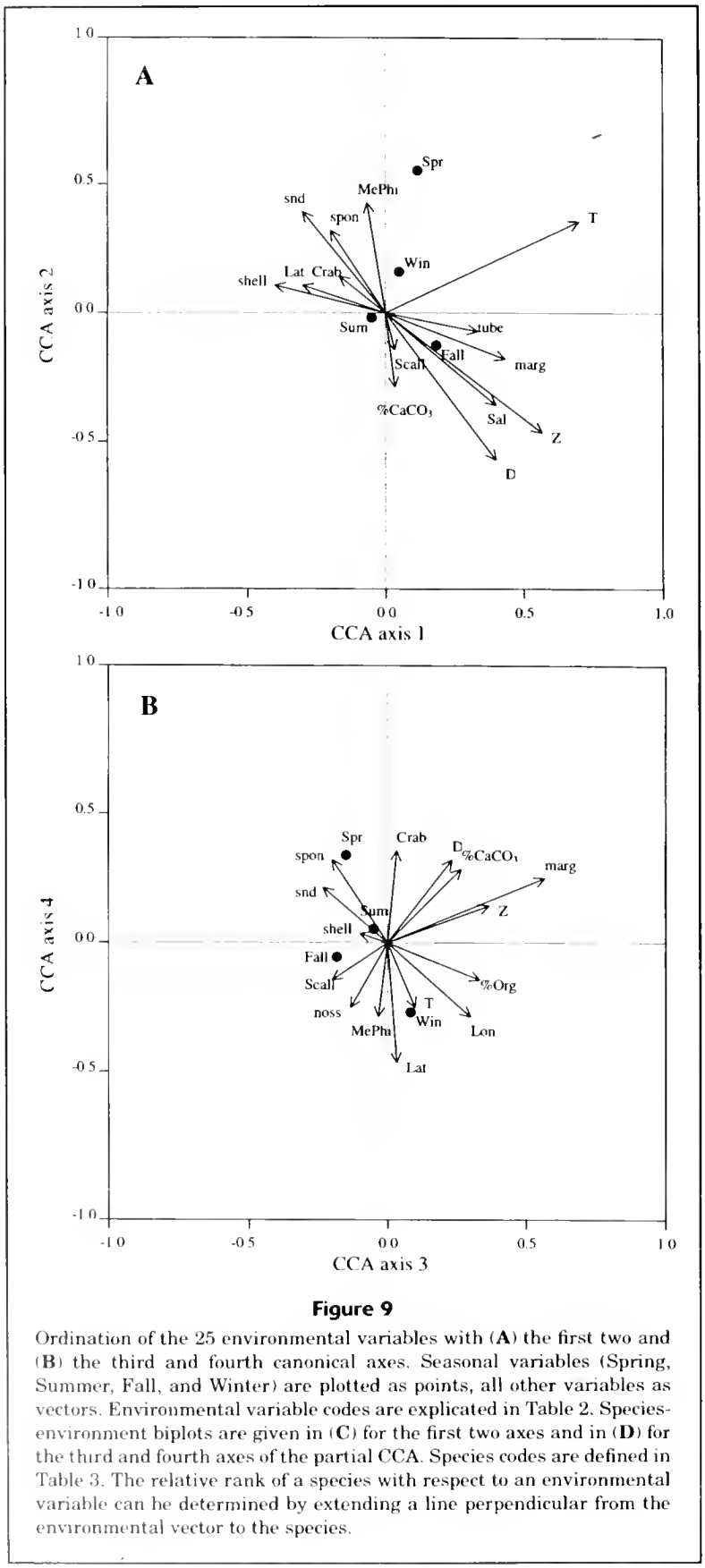

Figure 9

Ordination of the 25 environmental variables with (**A**) the first two and (**B**) the third and fourth canonical axes. Seasonal variables (Spring, Summer, Fall, and Winter) are plotted as points, all other variables as vectors. Environmental variable codes are explicated in Table 2. Species-environment biplots are given in (**C**) for the first two axes and in (**D**) for the third and fourth axes of the partial CCA. Species codes are defined in Table 3. The relative rank of a species with respect to an environmental variable can be determined by extending a line perpendicular from the environmental vector to the species.

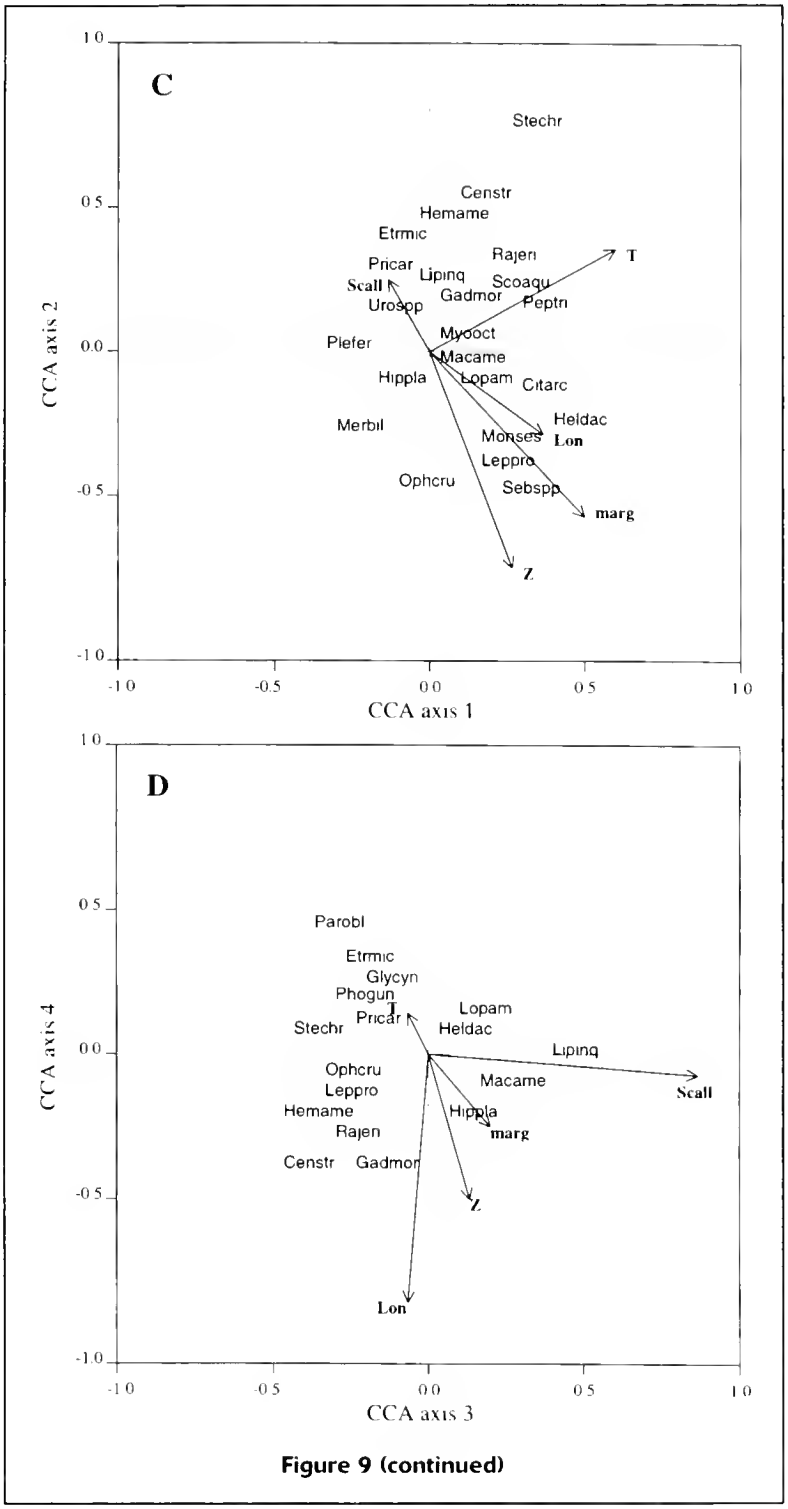

Figure 9 (continued)

Other variables such as salinity, the abundance of benthic organisms, mean sediment size, as well as the proximate location of other essential habitats (e.g. estuaries), were correlated to distance offshore and depth and are thus possible contributors to observed habitat preferences. It is doubtful that a species would prefer habitat based on distance offshore or depth alone because both variables are spatial indices and as such, they can have no direct effect on habitat quality. The indirect effects of these spatial variables on habitat quality may be associated with how they correlate with the distribution of

Table 6

(A) Results from the CCA including all 25 environmental variables. The sum of all canonical eigenvalues (2.187) was 44.7% of the total inertia (4.891). (B) Results of the CCA with forward selection (5 environmental variables) and season treated as a covariable. The sum of the unconstrained eigenvalues (3.825) is 78.2% of the total inertia, indicating that the seasonal component contributed 21.8% of the variance. The sum of all canonical eigenvalues (0.636) is 16% that of the sum of all unconstrained eigenvalues and 13% of total inertia. See text for explanation of terms.

	Axes				
	1	2	3	4	Total inertia
A					
Eigenvalues	0.809	0.464	0.284	0.238	4.891
Species-environment correlations	0.961	0.873	0.704	0.691	
Cumulative percentage variance					
of species data	16.5	26.0	31.9	36.7	
of species-environment relation	37.0	58.2	71.2	82.1	
Sum of all unconstrained eigenvalues					4.891
Sum of all canonical eigenvalues					2.187
B					
Eigenvalues	0.269	0.230	0.078	0.047	4.891
Species-environment correlations	0.721	0.735	0.518	0.365	
Cumulative percentage variance					
of species data	7.0	13.0	15.1	16.3	
of species-environment relation	42.3	78.5	90.8	98.3	
Sum of all unconstrained eigenvalues (after fitting covariables)					3.825
Sum of all canonical eigenvalues (after fitting covariables)					0.636

important factors or combinations of factors, or with both. For example, age-0 inquiline snailfish (*L. inquilinus*) are found almost exclusively in association with the presence of sea scallops, with which they have their inquiline relationship (Able and Musick, 1976). The distribution of these fishes on the mid to outer shelf is therefore not necessarily directly affected by any physiological response to depth or distance offshore; rather, they are probably most affected by their dependence on sea scallops for shelter. The distribution of scallops in turn may be affected by such variables as temperature, salinity, circulation pattern, and the production of phytoplankton (Stewart and Arnold, 1994). Temperature, however, may have a direct effect on the quality of habitat for a given species because many physiological functions such as respiration, metabolism, and growth are directly controlled by changes in temperature (Neill et al., 1994).

Temperature and depth not only seem to provide the best description of the overall variance within this data set, but, along with salinity and time of year, form the basis for the hydrographic description of the NYB. In general, the bottom waters of the NYB can be broken down by location into three regions: inner-shelf waters, middle shelf (cold pool), and outer shelf. This breakdown of the continental shelf for the NYB is consistent with that of other shelf systems (McRoy et al., 1986; Werner et al., 1997). During the summer, waters overlaying these regions of the shelf are divided by two frontal features: the inner front, dividing the inner and middle

Table 7

Weighted correlations between the five environmental variables selected during the CCA with forward selection and the axes of from the analysis. Numbers in bold indicate the strongest correlation for each of the four axes. See Table 2 for meaning of environmental variable codes

Axis	Temp	Z	Scall	Long	Marg
CCA 1	0.8262	0.4257	−0.0796	0.3723	0.6508
CCA 2	0.4932	−0.7895	0.1636	−0.2067	−0.5973
CCA 3	−0.0819	0.1485	0.9711	−0.0620	0.1028
CCA 4	0.0863	−0.3690	−0.1399	−0.8822	−0.0934

shelves, and the middle front, dividing the middle and outer shelves. A third front, the shelf-break front, separates the outer shelf from the continental slope (McRoy et al., 1986). These three hydrographic features can be utilized as an effective means for describing the general nursery areas for groundfishes within the NYB.

Differences in environmental conditions occur not only along the shelf, but also temporally. Patterns in surficial sediments and bathymetry change on the order of hundreds to thousands of years. These characteristics are relatively stable in their distributions on the shelf. Other factors such as benthic faunal distributions may change from year to year but should remain unvarying during the first year of a fish's life. Hydrographic variables and the presence of ephemeral predator and prey species, however, may change on a seasonal or even daily basis. The scale and extent to which these variables change are important in understanding the nature of the settlement and nursery areas.

The turnover of the cold pool in the fall represents an abrupt change in bottom temperature that subsequently may have biological significance. In our study, higher mean catch of age-0 *P. ferrugineus* corresponded to the distribution of the cold pool, and catch dropped dramatically in the fall as bottom temperature increased during cold pool turnover. For a species with a preference for low temperatures, increased temperature may be a density-independent source of mortality. In at least one case, an increase in mortality of larval *P. ferrugineus* on Georges Bank has been associated with an increase in temperature from a warm-core ring (Colton, 1959). Although such abrupt temperature fluctuations at greater depths are not common, they may occasionally occur near the edge of the shelf in some areas, perhaps associated with Gulf Stream meanders (Able et al., 1993). Able et al. (1993) found a temperature increase of 6°C over a two-day period, and they suggested that such temperature fluctuations may cause a cessation of feeding for tilefish, *Lopholatilus chamaeleonticeps*. In contrast, some species may benefit from increased bottom temperatures associated with turnover. For example, in our study, settlement of *M. bilinearis* did not peak until after turnover, when bottom temperature was greater than 9°C. Likewise, spawning distribution for Atlantic croaker (*Micropogonias undulatus*) in the southern portions of the MAB has a positive association with the presence and location of warmer waters coincident with the cold pool turnover (Norcross and Austin, 1988).

This study and another from Georges Bank (Frank et al., 1992) indicate that the distribution of *P. ferrugineus* corresponds well with bottom temperature. The presence of *P. ferrugineus* is negatively correlated with bottom temperature in the NYB, with highest abundance in the coldest waters (<8°C). However, on the Grand Banks the correlation with temperature was positive, with most fish collected above the warmest bottom waters (>3°C). Juveniles from the Grand Banks, however, were collected off the bottom, and highest abundances were found just below the thermocline, in waters closer to 6°C. Temperatures between 4° and 8°C have been noted as the preferred temperatures for older *P. ferrugineus* (Scott, 1982; Ross and Nelson, 1992; Walsh, 1992), and the evidence from these studies suggests that this may be true for age-0 *P. ferrugineus* as well.

Besides *P. ferrugineus*, several other boreal species, American plaice (*Hippoglossoides platessoides*), haddock (*Melanogrammus aeglefinus*), and Atlantic cod (*Gadus morhua*), were collected in our samples from the cold pool. Although not as numerically dominant as *P. ferrugineus*, the presence of these species this far down the coast suggests that the cold pool may act as a temporary refuge from the warmer waters normally associated with lower latitude. Metapopulations of such species, wherein local populations occupy small areas of suitable habitat outside the main population, are a potential confounding factor to the management of these species (Bailey, 1997). In the extreme, these juveniles may not be viable additions to the population if environmental conditions are not suitable for them to reach maturity. Just as warm-core eddies and eddy streamers may bring expatriates into this area from the south in the summer (Hare and Cowen, 1991), the cold pool may allow boreal species to temporarily extend their range southward during the summer. It is possible that conditions may occasionally enhance survival in such potentially marginal habitats to the extent that success of the population year class is facilitated.

In our study, we used trawl data to describe the general distribution and large-scale habitat associations of age-0 fishes. The resolution obtainable from trawl data is limited to the area swept (about 700 m^2). Such resolution is sufficient to determine differences between stations that are 10 km apart but not to deterine the heterogeneity in habitat within a station. *In situ* methods, including the use of manned submersibles, are required for these types of small-scale studies (see Auster et al., 1991, 1997; Adams et al., 1995). One other drawback of using a trawl to quantify fish abundance is that trawls are inherently poor at collecting all fishes present in a given area; gear selection is size- and species-specific. However, if gear selection is constant between sites, trawl samples should be comparable (Kuipers et al., 1992). The

relative efficiency of our 2-m beam trawl on offshore nursery areas for juvenile flatfish and other demersal species was unknown, although it was likely that our trawl was relatively inefficient but consistent in collecting demersal fishes. Consistent inefficiency among trawl samples would not affect the general patterns that we found but could have led to underestimation of abundances.

For a trawl to be efficient, demersal fishes must remain near the bottom. Recently settled juveniles of some species, such as *M. bilinearis*, have been shown to make nightly excursions away from the bottom to feed (Fahay, 1974). For a fusiform juvenile like *M. bilinearis* this ability is not surprising. However, the pleuronectiform *P. ferrugineus* has been collected well off the bottom on the Grand Banks, not only as larvae but also as juveniles (Frank et al., 1992). These "pelagic juveniles" were of the same size classes (10–34 mm) as the postmetamorphic flounder we collected on the bottom with a 2-m beam trawl in our study. In extensive studies in the MAB with comparable or larger midwater sampling gear, few *P. ferrugineus* larger than 15 mm were collected (Morse, 1989; Cowen et al., 1993). For the NYB, however, juvenile *P. ferrugineus* do not appear to exhibit such trawl-avoiding behavior. This regional difference in vertical distribution of >20-mm postmetamorphic young may be due either to differences in the temperature structure of the water column (i.e. depth of optimal temperature, as discussed above) or to some other unknown latitudinal difference in developmental rate, settlement size, or behavior (Miller et al., 1991; Fuiman and Higgs, 1997; Osse and Boogaart, 1997).

In summary, age-0 demersal fishes utilize the continental shelf of the NYB as both settlement and nursery habitat. According to our findings, the shelf of the NYB can be divided into three broad nursery areas (inner, middle, and outer shelves) and can be described by species assemblage as well as by hydrography. There is a need for more research concerning the quality of habitats for age-0 fishes in the NYB. Information on smaller-scale variation in habitat for age-0 fishes may be just as revealing as that for larger macrobenthos (see Auster et al., 1991). Manned submersibles may be used to determine such small-scale habitat associations, even for small juveniles. Differences in growth rates of given species among habitats should also shed light on habitat quality within the NYB. Nursery habitats play an important role in the life history of marine fishes, and knowledge gained about the distribution and quality of these areas for commercially important offshore species should help to improve management of these areas..

Acknowledgments

We thank all those who have contributed to the various aspects of this work. The fieldwork was made possible with the help of numerous volunteers, particularly Mark Sullivan and Teresa Rotunno. Captain Mark Phillips and the crew of the FV *Illusion* gave much to the practical aspects of the cruises. This manuscript benefited from critical reviews from Tom Grothues, Ken Able, and Robert Cerrato, as well as from valuable discussions with Michael Fahay, Al Stoner, and Brenda Norcross. Supplemental temperature data for August 1996 was kindly provided by Jack Jossi. This paper resulted from research sponsored by the National Oceanic and Atmospheric Administration's Saltonstall-Kennedy program, award number NA66FD0012. The views expressed herein are those of the authors and do not necessarily reflect the views of NOAA or its subagencies.

Literature cited

Able, K. W., C. B. Grimes, R. S. Jones, and D. C. Twichell.
1993. Temporal and spatial variation in the habitat characteristics of tilefish (*Lopholatilus chamaeleonticeps*) off the east coast of Florida. Bull. Mar. Sci. 53(3):1,013–1,026.

Able, K. W., R. E. Matheson, W. W. Morse, M. P. Fahay, and G. Shepard.
1989. Patterns of summer flounder *Paralichthys dentatus* early life history in the Mid-Atlantic Bight and New Jersey estuaries. Fish. Bull. 88:1–12.

Able, K. W., and J. A. Musick.
1976. Life history, ecology, and behavior of *Liparis inquilinus* (Pisces: Cyclopteridae) associated with the sea scallop *Placopecten magellanicus*. Fish. Bull. 74(2):409–412.

Adams, P. B., J. L. Butler, C. H. Baxter, T. E. Laidig, K. A. Dahlin, and W. W. Wakefield.
1995. Population estimates of Pacific coast groundfishes from video transects and swept-area trawls. Fish. Bull. 93:446–455.

Auster, P. J., R. J. Malatesta, and C. L. S. Donaldson.
1997. Distributional responses to small-scale habitat variability by early juvenile silver hake, *Merluccius bilinearis*. Environ. Biol. Fish. 50:195–200.

Auster, P. J., R. J. Malatesta, S. C. LaRosa, R. A. Cooper, and L. L. Stewart.
1991. Microhabitat utilization by the megafaunal assemblage at a low relief outer continental shelf site—Middle Atlantic Bight, USA. J. Northwest Atl. Fish Sci. 11:59–69.

Bailey, K. M.
1994. Predation on juvenile flatfish and recruitment variability. Neth. J. Sea. Res. 32(2): 175–189.
1997. Structural dynamics and ecology of flatfish populations. Neth. J. Sea Res. 37:269–280.

Bolle, L. J., R. Dapper, J. I. Witte, and H. W. Van der Veer.
1994. Nursery grounds of dab (*Limanda limanda* L.) in the southern North Sea. Neth. J. Sea Res. 32:299–307.

Bowman, M. J., and L. D. Wunderlich.
1977. Hydrographic properties. MESA New York. Bight Atlas

Monograph 10. New York Sea Grant Institute, Albany, NY.

Bradford, M. J.
1992. Precision of recruitment predictions from early life stages of marine fishes. Fish. Bull. 90:439–453.

Carney, R. S., and A. G. Carey Jr.
1980. Effectiveness of metering wheels for measurement of area sampled by beam trawls. Fish. Bull. 78:791–796.

Chambers, R. C., and W. C. Leggett.
1992. Possible causes and consequences of variation in age and size at metamorphosis in flatfishes (Pleuronectiformes): an analysis at the individual, population, and species levels. Neth. J. Sea Res. 29:7–24.

Cho, R. D.
1996. Vertical distributions of ichthyoplankton in the New York Bight with relation to potential cross-shelf transport and retention mechanisms. M.S. thesis, State University of New York at Stony Brook, Stony Brook, NY, 173 p.

Churchill, J. H.
1985. Intrusions of outer shelf and slope water within the nearshore zone off Long Island, New York. Limnol. Oceanogr. 30(5):972–986.

Colton, J. B. Jr.
1959. A field observation of mortality of marine fish larvae due to warming. Limnol. Oceanogr. 4:219–222.
1972. Temperature trends and the distribution of groundfish in continental shelf waters, Nova Scotia to Long Island. Fish. Bull. 70:637–657.

Colvocoresses, J. A., and J. A. Musick.
1984. Species associations and community composition of Middle Atlantic Bight continental shelf demersal fishes. Fish. Bull. 82:295–313.

Cowen, R. K., J. A. Hare, and M. P. Fahay.
1993. Beyond hydrography: can physical processes explain larval fish assemblages within the Middle Atlantic Bight. Bull. Mar. Sci. 53:567–587.

Fahay, M. P.
1974. Occurrence of silver hake, *Merluccius bilinearis*, eggs and larvae along the middle Atlantic continental shelf during 1966. Fish. Bull. 72(3):813–834.
1983. Guide to the early stages of marine fishes occurring in the western North Atlantic Ocean, Cape Hatteras to the southern Scotian Shelf. J. Northwest Atl. Fish. Sci. 4:1–423.

Felley, J. D., and M. Vecchione.
1995. Assessing habitat use by nekton on the continental slope using archived videotapes from submersibles. Fish. Bull. 93:262–273.

Flagg, C. N., R. W. Houghton, and L. J. Pietrafesa.
1995. Summertime thermocline salinity maximum intrusions in the Mid-Atlantic Bight. Deep-Sea Res. 41(2/3):325–340.

Frank, K. T., J. W. Loder, J. E. Carscadden, W. C. Leggett, and C. T. Taggart.
1992. Larval flatfish distributions and drift on the southern Grand Bank. Can. J. Fish. Aquat. Sci. 49:467–483.

Freeland, G. L., and D. J. P. Swift.
1978. Surficial sediments. MESA New York Bight Atlas Monograph 10. New York Sea Grant Institute, Albany, NY, 93 p.

Fuiman, L. A., and D. M. Higgs.
1997. Ontogeny, growth, and the recruitment process. *In* R. C. Chambers and E. A. Tripple (eds.), Early life history and recruitment in fish populations, p. 225–250. Chapman and Hall, London.

Gibson, R. N.
1994. Impact of habitat quality and quantity on the recruitment of juvenile flatfishes Neth. J. Sea Res. 32:191–206.

Hare, J. A., and R. K. Cowen.
1991. Expatriation of *Xyrichtys novacula* (Pisces: Labridae) larvae: evidence of rapid cross-shelf exchange. J. Mar. Res. 49:801–923.

Henderson, P. A., and R. M. H. Seaby.
1994. On the factors influencing juvenile flatfish abundance in the lower Severn Estuary, England. Neth. J. Sea Res. 32:321–330.

Houde, E. D.
1987. Fish early life dynamics and recruitment variability. Am. Fish. Soc. Symp. 2:17–29.

Houghton, R. W., R. Schlitz, R. C. Beardsley, B. Butman, and J. L. Chamberlin.
1982. The Middle Atlantic Bight cold pool: evolution of the temperature structure during the summer of 1979. J. Phys. Ocean. 12:1,019–1,029.

Jenkins, G. P., M. Shaw, and B. D. Stewart.
1993. Spatial variation in food-limited growth of juvenile greenback flounder, *Rhombosolea tapirina*: evidence from otolith daily increments and otolith scaling. Can. J. Fish. Aquat. Sci. 50:2,558–2,567.

Kendall, A. W., and N. A. Naplin.
1981. Diel-depth distribution of summer ichthyoplankton in the Middle Atlantic Bight. Fish. Bull. 79(4):705–726.

Ketchum, B. H., and N. Corwin.
1964. The persistence of "winter" water on the continental shelf south of Long Island, New York. Limno. Oceanogr. 9(4):467–475.

Kuipers, B. R., B. MacCurrin, J. M. Miller, H. W. Van der Veer, and J. I. Witte.
1992. Small trawls in juvenile flatfish research: their development and efficiency. Neth. J. Sea Res. 29:109–117.

Malloy, K. D., and T. E. Targett.
1991. Feeding, growth, and survival of juvenile summer flounder *Paralichthys dentatus*: Experimental analysis of the effects of temperature and salinity. Mar. Ecol. Prog. Ser.. 72:213–223.

McHugh, J. L.
1972. Marine fisheries of New York State. Fish. Bull. 3:585–610.

McRoy, C. P., D. W. Hood, L. K. Coachman, J. J. Walsh, and J. J. Goering.
1986. Processes and resources of the Bering Sea shelf (PROBES): the development and accomplishments of the project. Continental Shelf Res. 5:5–21.

Miller, J. M.
1994. An overview of the second flatfish symposium: recruitment in flatfish. Neth. J. Sea Res. 32:103–106.

Miller, J. M., J. S. Burke, and G. R. Fitzhugh.
1991. Early life history patterns of Atlantic North American flatfish: likely (and unlikely) factors controlling recruitment. Neth. J. Sea Res. 27:261–275.

Modin, J., and L. Pihl.
1994. Differences in growth and mortality of juvenile plaice, *Pleuronectes platessa* L, following normal and extremely high settlement. Neth. J. Sea Res. 32 (3/4):331–341.

Morse, W. W.
1989. Catchability, growth, and mortality of larval fishes. Fish. Bull. 87(3):417–446.

Morse, W. W., M. P. Fahay, and W. G. Smith.
1987. MARMAP surveys of the continental shelf from Cape Hatteras, North Carolina, to Cape Sable, Nova Scotia (1977–1984). Atlas No. 2. Annual distribution patterns of fish larvae. U.S. Dep. Commer., NOAA Tech. Memo. NMFS-F/NEC-47, 215 p.

Nash, R. D. M., A. J. Geffen, and G. Hughes.
1994. Individual growth of juvenile plaice (*Pleuronectes platessa* L.) on a small Irish Sea nursery ground (Port Erin Bay, Isle of Man, UK). Neth. J. Sea Res. 32:369–378.

NEFSC (Northeast Fisheries Science Center).
1992. Status of fishery resources off the northeastern United States for 1992. U.S. Dep. NOAA Tech. Memo. NMFS-F/NEC-95, 133 p.

Neill, W. H., J. M. Miller, H. W. Van der Veer, and K. O. Winemiller.
1994. Ecophysiology of marine fish recruitment: a conceptual framework for understanding interannual variability. Neth. J. Sea Res. 32(2):135–152.

Norcross, B. L., and H. M. Austin.
1988. Middle Atlantic Bight meridional wind component effect on bottom water temperatures and spawning distribution of Atlantic croaker. Continental Shelf Res. 8(1):69–88.

Osse, J. W. M., and J. G. M. Boogaart.
1997. Size of flatfish larvae at transformation, functional demands and historical constraints. J. Sea Res. 37:229–239.

Palmer, M. W.
1993. Putting things in even better order: the advantages of canonical correspondence analysis. Ecology 74(3):2,215–2,230.

Pearcy, W. G.
1978. Distribution and abundance of small flatfish and other demersal fishes in a region of diverse sediments and bathymetry off Oregon. Fish. Bull. 76(3):629–640.

Peterman, R. M., M. Bradford, N. C. Lo, and R. Methot.
1988. Contribution of early life stages to interannual variability in recruitment of northern anchovy (*Engraulis mordax*). Can. J. Fish. Aquat. Sci. 45:8–16.

Pihl, L., S. P. Baden, and R. J. Diaz.
1991. Effects of periodic hypoxia on distribution of demersal fish and crustaceans. Mar. Biol. 108:34–360.

Rakocinski, C. F., J. Lyczkowski-Schultz, and S. L. Richardson.
1996. Ichthyoplankton assemblage structure in Mississippi Sound as revealed by canonical correspondence analysis. Est. Coast. Shelf Sci. 43:237–257.

Riley, J. D., D. J. Symonds, and L. Woolner.
1981. On the factors influencing the distribution of age-0 demersal fish in coastal waters. Rapp. P.-V. Réun. Cons. int. Explor. Mer 178:223–228.

Rijnsdorp, A. D., F. A. Van Beek, S. Flatman, R. M. Millner, J. D. Riley, M. Giret, and R. De Clerck.
1992. Recruitment of sole stocks, *Solea solea* (L.), in the Northeast Atlantic. Neth. J Sea Res. 29:173–192.

Rodgers, S. I.
1992. Environmental factors affecting the distribution of sole (*Solea solea* (L.)) within a nursery area. Neth. J. Sea Res. 29(1–3):153–161.

Ross, M. R., and G. A. Nelson.
1992. Influences of stock abundance and bottom-water temperature on growth dynamics of haddock and yellowtail flounder on Georges Bank. Trans. Am. Fish. Soc. 121:578–587.

Schlee, J.
1964. New Jersey offshore gravel deposit. Pit and Quarry 1964:13–21.

Scott, J. S.
1982. Selection of bottom type by groundfish of the Scotian Shelf. Can. J. Fish. Aquat. Sci. 39:943–947.

Sissenwine, M. P.
1984. Why do fish populations vary? *In* R. M. May (ed.), Exploitation of marine communities, p. 59–94. Dhlem Konferenzen. Springer-Verlag, NY.

Sogard, S. M.
1992. Variability in growth rates of juvenile fishes in different estuarine habitats. Mar. Ecol. Prog. Ser. 85:35–53.

Stein, D. L., B. N. Tissot, M. A. Hixon, and W. Barss.
1992. Fish-habitat association on a deep reef at the edge of the Oregon continental shelf. Fish. Bull. 90:540–551.

Stewart, P. L., and S. H. Arnold.
1994. Environmental requirements of the sea scallop (*Placopecten magellanicus*) in eastern Canada and its response to human impacts. Can. Tech. Rep. Fish. Aquat. Sci. 2,005:ix +36 p.

ter Braak, C. J. F.
1992. CANOCO—a FORTRAN program for canonical community ordination. Microcomputer Power, Ithaca, New York, 95 p.
1995. Ordination. *In* R. H. G. Jongman, C. J. F. ter Braak, and O. F. R. van Tongeren (eds.), Data analysis in community and landscape ecology, p. 91–174. Cambridge University Press, New York, NY.

ter Braak, C. J. F., and P. F. M. Verdonshot.
1995. Canonical correspondence analysis and related multivariate methods in aquatic ecology. Aquat. Sci. 57(3):255–289.

Toole, C. L., D. F. Markle, and C. J. Donohoe.
1997. Settlement timing, distribution, and abundance of Dover sole (*Microstomus pacificus*) on an outer continental shelf nursery area. Can. J. Fish. Aquat. Sci. 54:531–542.

Van der Veer, H. W., R. Berghahn, and A. D. Rijnsdorp.
1994. Impact of juvenile growth on recruitment in flatfish. Neth. J. Sea Res. 32:153–173.

Walsh, S. J.
1992. Factors influencing the distribution of juvenile yellowtail flounder (*Limanda ferruginea*) on the Grand Bank of Newfoundland. Neth. J. Sea Res. 29(1–3):193–203.

Werner, F. E., J. A. Quinlan, B. O. Blanton, and R. A. Luettich Jr.
1997. The role of hydrodynamics in explaining variability in fish populations. J. Sea Res. 27:195–212.

Assemblage of deep-sea sharks on Chatham Rise, New Zealand

Bradley M. Wetherbee
Zoology Department
2538 The Mall
University of Hawaii
Honolulu, Hawaii 96822
Present address: Northeast Fisheries Science Center
National Marine Fisheries Service, NOAA
28 Tarzwell Dr., Narragansett, Rhode Island 02882
E-mail address: brad.wetherbee@noaa.gov

Abstract.—The distribution and abundance of deep-sea sharks on Chatham Rise, New Zealand, are described. Sharks were collected as bycatch in two deep-water trawl fisheries at a total of 390 stations, which ranged in depth from 740 to 1503 m. Sixteen species of shark were caught: *Deania calcea*, *Centroscymnus crepidater*, *Etmopterus granulosus*, and *Centroscymnus owstoni* accounted for the largest portion of the shark catch. Species that would provide the highest yield of commercially important liver lipids were not abundant in trawls. All sharks combined formed only 4.2% of overall biomass captured in trawls. Depth is a major determinant of the composition of the shark assemblage; both density of sharks (kg/km^2) and species diversity were inversely proportional to depth. Distributional patterns of the shark community varied with location on Chatham Rise, and species composition of the shark catch varied with the species of teleost targeted in deep-water trawls.

Manuscript accepted 12 July 1999.
Fish. Bull. 98:189–198 (2000).

Sharks are common bycatch in deep water fisheries around the world, forming as much as 50% of the catch in deep-sea trawls in areas such as New Zealand and Australia (Deprez et al., 1990; Clark and King[1]). Most sharks captured in the New Zealand and Australian deep-water fisheries are dead by the time they are brought to the surface and are discarded, but some sharks are retained for their liver oil. In Japan and Australia, several species of deep-sea shark in the family Squalidae are targeted in fisheries and their liver oil is utilized. Although the short-term potential of fisheries directed towards deep-sea sharks has been investigated for a few species (Summers, 1987; Davenport and Deprez, 1989), little information on even basic biology is available for the species captured in these fisheries. Thus, the effects that deep-water fisheries have on shark populations that are either targeted directly or caught incidentally are unknown. Information on abundance, distribution, community structure, reproduction, and age and growth of deep-sea sharks would improve understanding of these effects.

Shark liver oil contains commercially important lipids, such as squalene and diacyl glycerol ether, which are used in cosmetic, pharmaceutical, and other industries (Deprez et al., 1990; Bakes and Nichols, 1995). The lipid composition of liver oil is quite variable among and within species, and consequently the most desirable sharks are those individuals and species that have the highest potential as a source for these valuable lipids (Davenport and Deprez, 1989; Bakes and Nichols, 1995). Therefore, understanding the distribution and abundance of different species of deep-sea shark, in conjunction with knowledge of the lipid composition of their liver oil, is important for optimal use of these resources.

Some deep-sea sharks prey upon commercially important teleosts (Clark et al., 1989; Clark and King[1]), but the impacts of shark predation on fish populations in terms of the overall economic impact on the fishery are unknown. Diet varies considerably among even closely related species of deep-sea shark (Compagno et al., 1991; Ebert et al., 1992), and the level of predation on commercially important species of teleost by sharks also varies among species (author's unpubl. data). Information on the distribution and abundance of deep-sea sharks, in conjunction with knowl-

[1] Clark, M. R., and K. J. King. 1989. Deep water fish resources off the North Island, New Zealand: results of a trawl survey, May 1985 to June 1986. New Zealand Fisheries Technical Report 11, 56 p. MAF Fisheries Research Center, P.O. Box 297, Wellington, New Zealand

edge of their feeding habits, would improve our understanding of interactions between sharks and commercially important teleosts.

A variety of species of shark inhabit the deep water off New Zealand, where they form part of the bycatch of deep-sea fisheries that target teleosts such as orange roughy (*Hoplostethus atlanticus*) and smooth oreo (*Pseudocyttus maculatus*) (Clark and Tracey, 1994; Clark and King[1]). Access to this bycatch provided an opportunity to examine a multispecies complex of sharks, which might be termed an assemblage—"a group of co-occurring populations—not necessarily interacting" as defined by Crowder (1990). The purpose of this study was to investigate the abundance and distribution of sharks on Chatham Rise to increase understanding of the effects of fishing on shark populations, the potential of shark fisheries and utilization of bycatch, and interactions between sharks and commercially important teleosts.

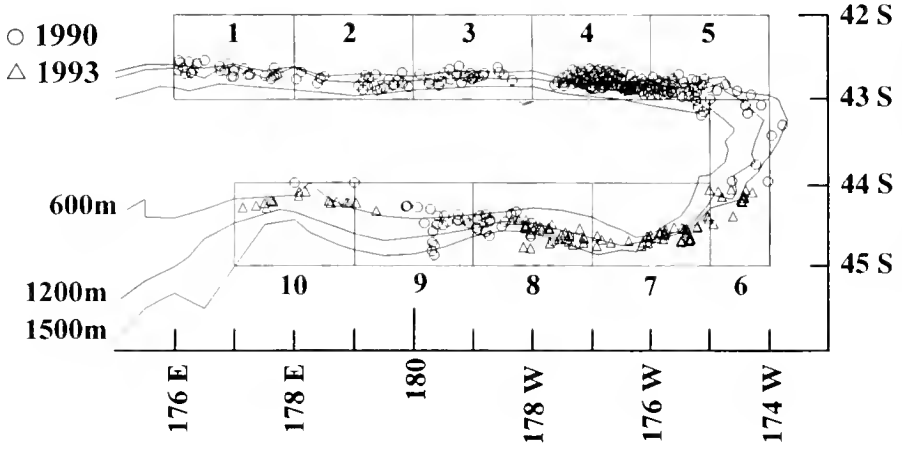

Figure 1

Map of Chatham Rise, New Zealand, showing depth contour lines and locations of trawls in a 1990 orange roughy survey and a 1993 smooth oreo survey. Trawls were grouped into 10 areas on the basis of major latitude and longitude meridians.

Materials and methods

Data for this study were collected from deep-water bottom trawls during two cruises conducted by the Ministry of Agriculture and Fisheries on Chatham Rise, New Zealand (Fig. 1). The first survey (15 June to 5 August 1990) consisted of 281 trawls for orange roughy (*H. atlanticus*) and was conducted primarily on the north of Chatham Rise from the FV *Cordella*. The second survey (24 October to 9 November 1993) consisted of 109 trawls for smooth oreo (*P. maculatus*), primarily on the south of Chatham Rise from the RV *Tangaroa*. Fishing during both surveys was conducted at depths of 740–1503 m throughout the day and night (Fig. 2).

Each survey consisted of a stratified random trawl design intended to provide relative biomass estimates and to illustrate patterns of distribution of deep-water species on Chatham Rise. Six-panel bottom otter-trawls with cut-away lower wings were used in each survey. The door-spread was 75 m for orange roughy trawls and 119 m for smooth oreo trawls, and distance between the net wings for both trawls was approximately 26 m. Codend mesh sizes were 110 mm for orange roughy trawls and 100 mm for smooth oreo trawls. Towing speed for both vessels was approximately 3.0 kn. Orange roughy trawls were roughly 1 h in duration, and smooth oreo trawls ranged from several minutes to 45 min. For density estimates (kg shark/km^2) it was assumed that herding by, and escape from, nets were minimal, and that trawls sampled different species of shark with equal effort.

For each trawl, the catch was sorted into bins by species, and the total weight of each species caught at each station was recorded. Latitude, longitude, water temperature, minimum and maximum depth of fishing, towing speed, and start and end time were also recorded for each trawl. When the author was present on the research vessel (at all times other than from 15 June to 10 July 1990), all individuals of each species of shark were weighed and measured, except when large numbers of sharks were caught and a lack of time prevented examination of every shark. Because of size varied among species, an estimate of the total number of individuals captured in all fishing was derived by using the average weight for each species. Because there were differences in fishing methods (net characteristics, trawl duration) and time (season, year) between the two surveys, catch data from surveys were examined separately. When possible, comparisons were made between common areas fished during both surveys. For comparison of the composition of the shark community at different locations on Chatham Rise, ten areas were designated based on major latitude and longitude meridians (Fig. 1).

Consideration of sharks as an assemblage, which is separate from the rest of Chatham Rise community, is an artificial division. However, because the primary interest of this study was to describe the abundance and distribution of the sharks on Chatham Rise, several ecological indices were employed to compare different locations, depths, and species of shark. Abundance was expressed as density (kg shark/km^2) and was calculated for each species within each trawl based on the total weight of sharks caught, net width, towing speed, and trawl duration. Three features of distribution were examined for sharks: diversity, similarity, and randomness. Diversity was expressed as the number of species of sharks per trawl (Stephens et al. 1984; Garcia et al. 1998). The Bray-Curtis similarity index was used for comparisons among the ten areas on Chatham Rise, depth intervals, and between the two surveys:

$$S = 1 - \left(\sum_{i=1}^{s} |Y_{ij} - Y_{ik}| / \sum_{i=1}^{s} (Y_{ij} + Y_{ik}) \right),$$

where Y_{ij} = score for i^{th} species in the j^{th} sample; and
Y_{ik} = score for the i^{th} species in the k^{th} sample (Field et al. 1982; Sedberry and Van Dolah 1984).

This index ranges from 0 (no species in common) to 1 (identical species in each sample). Morisita's index of dispersion (I_d) was calculated for each species of shark as an indicator of the randomness of their distributions:

$$I_d = n\left(\sum X^2 - N / N(N-1)\right),$$

where n = number of plots;
N = total number of individuals counted in all n plots; and
ΣX^2 = squares of the number of individuals per plot summed over all plots.

If the dispersion is random, then I_d = 1.0; if perfectly uniform, I_d = 0; and if maximally aggregated (all individuals in the same trawl), I_d = the number of trawls (Brower and Zar, 1984). To minimize the dominant effect of anomalous catches, each value of shark density (kg/km^2) was converted to ln(x +1) prior to calculation of these ecological indices (Field et al., 1982; Bianchi, 1991) and comparisons of means were made by using either a two-tailed t-test or one-way ANOVA.

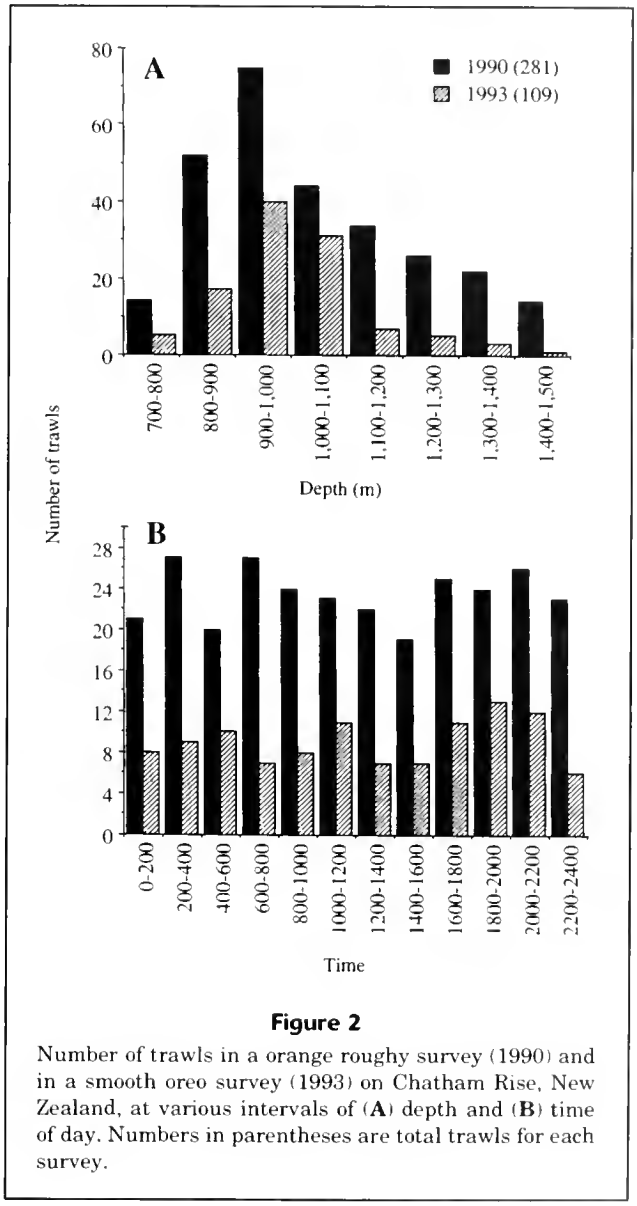

Figure 2

Number of trawls in a orange roughy survey (1990) and in a smooth oreo survey (1993) on Chatham Rise, New Zealand, at various intervals of (**A**) depth and (**B**) time of day. Numbers in parentheses are total trawls for each survey.

Results

Seven species of shark belonging to the family Squalidae and five undescribed species of catsharks in the genus *Apristurus* (family Scyliorhinidae) were regularly captured in deep-water trawls (Table 1). For the purpose of this study, all sharks of the genus *Apristurus* were treated as a single group. Several other species of shark were captured (*Chlamydoselachus anguineus*, *Centroscymnus coelolepis*, *Scymnodon squamulosus*, *Etmopterus lucifer*), but only one or two individuals of each species were captured and these are not discussed further. Although the composition of the catch varied throughout the day, there was no apparent correlation between density

Table 1

Catch data for eight taxa of sharks from trawls on Chatham Rise, New Zealand, 1990 (June–August, 281 trawls, depth range = 743–1503 m) and 1993 (November, 109 trawls, depth range = 780–1463 m). D.c. = *Deania calcea*, C.c. = *Centroscymnus crepidater*, E.g. = *Etmopterus granulosus*, C.o. = *Centroscymnus owstoni*, C.s. = *Centrophorus squamosus*, A.s. = *Apristurus* spp., S.p. = *Scymnodon plunketi*, D.l. = *Dalatias licha*. (SD = standard deviation).

	kg shark caught					% of total biomass			% of trawls			Avg. density (kg/km^2)			
Species	1990	1993	Total	Avg. wt. (kg)	Estimated no. of individuals	1990	1993	Total	1990	1993	Total	1990	1993	Total	SD
D.c.	6721.6	3618.7	10340.3	2.757	3750	1.38	2.10	1.57	65.7	50.5	61.5	172.5	343.5	220.3	590.3
C.c.	6058.0	351.3	6409.3	1.980	3237	1.25	0.20	0.97	58.6	39.2	53.2	151.2	61.8	126.2	266.5
E.g.	3072.2	2881.4	5953.6	1.416	4203	0.63	1.67	0.90	75.7	88.8	79.3	93.5	960.8	335.9	1624.5
C.o.	3731.9	25.5	3757.4	5.023	748	0.77	0.01	0.58	46.8	3.7	34.9	88.9	2.3	64.7	205.8
C.s.	181.0	81.7	262.7	8.209	32	0.04	0.05	0.04	7.1	7.5	7.2	4.7	33.1	12.6	115.2
A.s.	144.1	89.9	234.0	1.245	188	0.03	0.05	0.04	30.7	38.3	32.8	3.5	17.3	7.4	33.3
S.p.	128.7	105.8	234.5	9.770	24	0.03	0.06	0.04	5.0	6.5	5.4	3.0	23.0	8.6	88.9
D.l.	173.1	41.0	214.1	9.309	23	0.04	0.02	0.03	6.8	4.7	6.2	4.3	7.7	5.3	39.9
All sharks	22200.6	9188.3	27405.9		12205	4.15	4.17	4.16	90.3	97.2	92.2	521.8	1449.5	781.1	1786.6

and time of day for all sharks combined (ANOVA, P=0.77). Water temperature decreased linearly with depth (r^2=0.61) and ranged from 5.9° to 9.0°C.

The most abundant shark (by weight) was the shovelnose dogfish (*Deania calcea*), which represented 32.5% of the shark catch in 1990, 50.5% in 1993, and 37.2% overall. The longnose velvet dogfish (*Centroscymnus crepidater*), southern lantern shark (*Etmopterus granulosus*), and Owston's dogfish (*Centroscymnus owstoni*) also formed large proportions of the shark catch (Table 1). The largest catch (by weight) for any species of shark in a single trawl was 850 kg for *D. calcea* (area 5), followed by 441 kg for *C. owstoni* (area 1). Although sharks dominated the catch in some trawls, they formed only 4.2% of total biomass collected in trawls. Even the most abundant species (*D. calcea*) accounted for only 1.6% of total biomass caught (Table 1). The highest estimate for number of individuals of any species of shark captured in a single trawl was 308 for *D. calcea*, followed by 194 for *E. granulosus*.

The most abundant shark in terms of number of individuals captured was *E. granulosus*, which was present in 79.3% of trawls (Table 1). *Deania calcea* and *C. crepidater* were also captured in large numbers and appeared in a high proportion of the trawls. For three of the larger species of squalids (the leafscale gulper shark, *Centrophorus squamosus*; the Plunket shark, *Scymnodon plunketi*; and the kitefin shark, *Dalatias licha*) few individuals were captured, and these species occurred in a low percentage of the trawls (Table 1). Preliminary examination of stomach contents revealed that orange roughy were most common in stomachs of *E. granulosus* and *C. owstoni*, but were also consumed by *C. squamosus* and *D. licha*.

Abundance

There was a significant difference between mean densities (kg/km^2) caught in the two surveys for *E. granulosus*, *C. owstoni*, *C. crepidater*, and *Apristurus* spp., but not for the other species (ANOVA, P<0.01). A comparison of common areas that were fished in both surveys (areas 6, 8, 9, and 10) showed that there was no significant difference between the densities of any of the species for the two surveys (t-test, P>0.01), and data from common areas for the two surveys were therefore combined. In the orange roughy survey, there was a significant difference among areas for densities of all species except *D. licha*, whereas in the oreo survey, significant differences were observed among areas for only two species, *C. crepidater* and *D. calcea* (ANOVA, P<0.05). The highest densities for all sharks combined were recorded at the eastern tip of Chatham Rise, in areas 5 and 6 (1003.4 and 2249.1 kg/km^2), and the lowest were in the southwestern areas 8 and 10 (257.7 and 254.4 kg/km^2).

Composition of the shark catch varied considerably with location fished. In areas on the north of Chatham Rise, closest to New Zealand (areas 1 and 2), the catch was dominated by *C. owstoni* and *C. crepidater*, which accounted for 84% of the shark catch by weight (Fig. 3). On the mid-north of Chatham Rise (area 3), *C. owstoni* and *C. crepidater* still formed the majority of the catch; however *D. calcea* was also abundant and all eight major taxa were recorded. The northeast of Chatham Rise included those areas (4 and 5) where the most trawls were conducted. Here, *C. crepidater* still formed a large

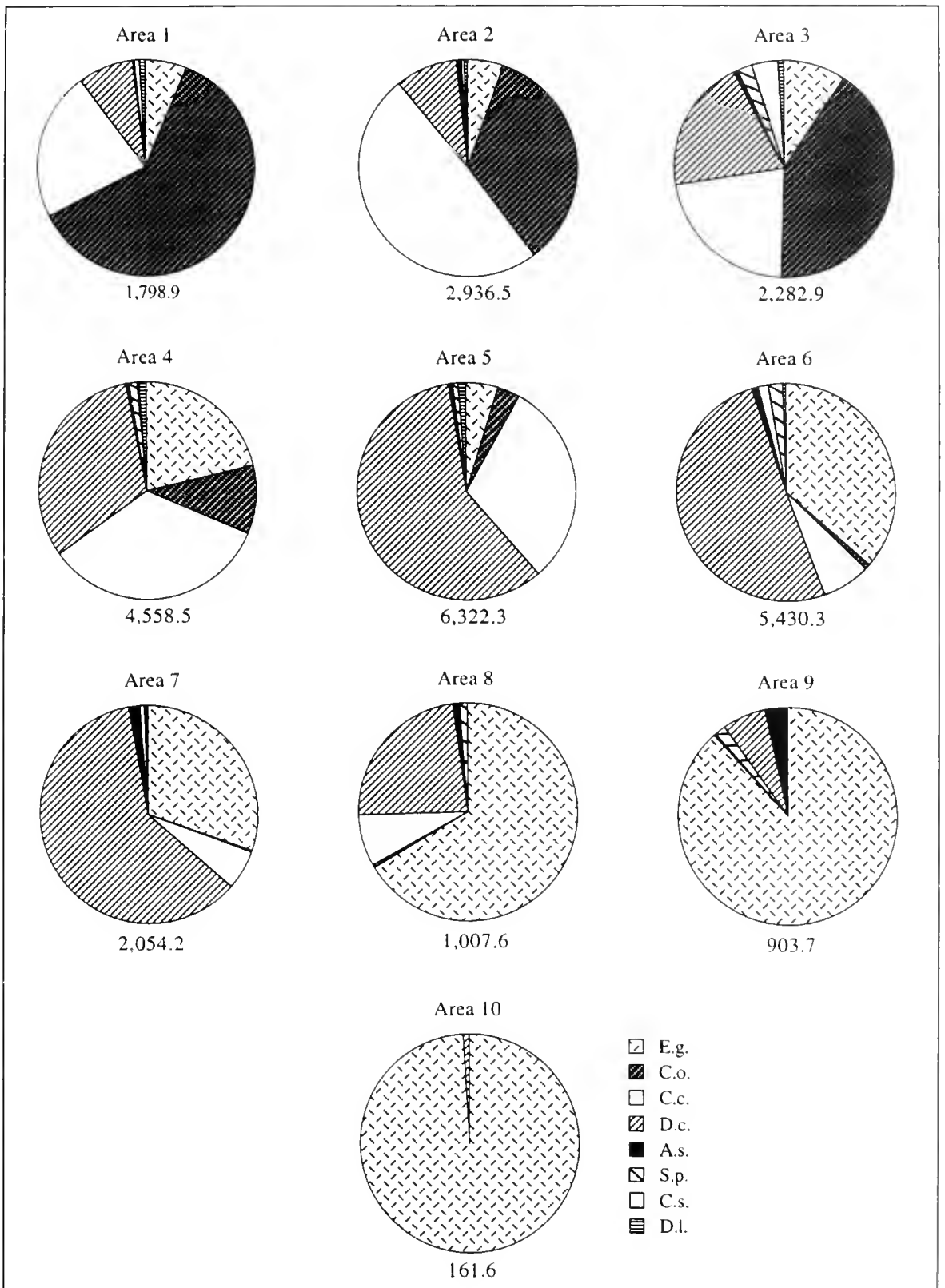

Figure 3

Species composition (as percent of total kg of shark caught) of the shark catch for both surveys combined in each of the 10 areas on Chatham Rise, New Zealand. Numbers below each area are the total weight (kg) of sharks caught in that area. E.g. = *Etmopterus granulosus*; C.o. = *Centroscymnus owstoni*; C.c. = *Centroscymnus crepidater*, D.c. = *Deania calcea*; A.s. = *Apristurus* spp.; S.p. = *Scymnodon plunketi*; C.s. = *Centrophorus squamosus*; and D.l. = *Dalatias licha*.

part of the catch, but the catch of *C. owstoni* declined substantially, and *D. calcea* began to dominate the shark catch. Along the eastern tip and southeast portion of Chatham Rise (areas 6 and 7), *D. calcea* accounted for the highest percentage of the catch, but *E. granulosus* was also prominent, and these two species formed over 85% of the shark catch by weight. *Etmopterus granulosus* dominated catches in areas along the south of Chatham Rise (areas 8–10); the proportion of the total catch increased with proximity to New Zealand (Fig. 3). The three large squalids (*C. squamosus*, *S. plunketi*, *D. licha*) were sporadically caught in areas 1–8, each with a peak density in area 6, but no squalids were recorded from the southwest of Chatham Rise (areas 9 and 10). *Apristurus* spp. were caught in small numbers throughout Chatham Rise, but their presence was more dependent upon depth than location (Fig. 3).

Composition of the catch also varied with depth (Fig. 4) and several natural divisions were apparent. The three large squalids (*C. squamosus*, *S. plunketi*, *D. licha*) appeared to have shallow distributions, and were not captured deeper than 1100 m (with the exception of one *S. plunketi* caught at 1170 m, and one *C. squamosus* at 1201 m). Densities (kg/km^2) of the other species were fairly high at depths of 700–1200 m, although *D. calcea* was most abundant at depths of less than 1000 m, *E. granulosus* peaked at 900–1200 m, and *Apristurus* spp. densities were highest at depths greater than 1000 m (Fig. 4). At depths greater than 1200 m, *Apristurus* spp. were the only sharks regularly caught in the trawls. There was a significant difference among three depth intervals (700–1000 m, 1000–1300 m, and 1300+ m) for mean densities (kg/km^2) of each species in the orange roughy survey, but only for the three most abundant species (*D. calcea*, *C. crepidater*, and *E. granulosus*) in the oreo survey (ANOVA, $P<0.05$). Density (kg/km^2) for all sharks combined gradually declined with depth between 700 and 1200 m, but was low at depths greater than 1200 m (Fig. 5).

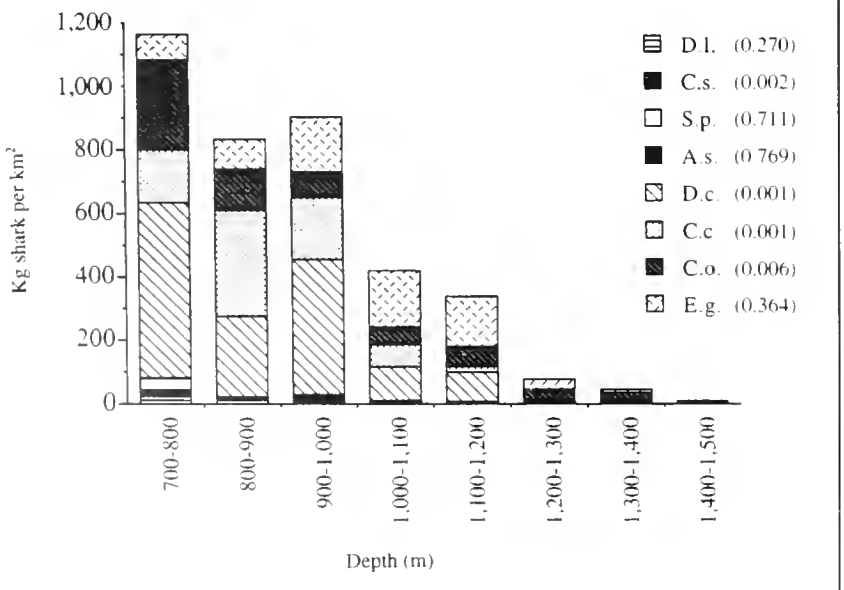

Figure 4

Density (kg/km^2) of sharks collected at all locations on Chatham Rise, New Zealand, at various depth intervals for both surveys combined. For abbreviations of species see Figure 3. For each species, P -values are given in parentheses for ANOVA comparisons of densities among depth intervals.

Distribution

Diversity (number of species per trawl) was significantly higher for the orange roughy survey than for the oreo survey (t-test, $P=0.0003$), but diversity in areas common to both surveys (areas 6, 8, 9, 10) did not differ (t-test, $P=0.14$, 0.77, 0.81, and 0.63 respectively). There was a significant difference among areas for mean diversity values in both surveys (ANOVA, $P<0.01$). Area 3 had the highest mean diversity value (4.2, SD=1.6) and area 10 had the lowest value (1.1, SD=0.9). Diversity differed significantly among the three major depth intervals (700–1000 m, 1000–1300 m, 1300+ m) for the oreo survey (ANOVA, $P=0.007$), but not for the orange roughy survey (ANOVA, $P=0.50$). The total number of species of shark caught in trawls was inversely proportional to depth, and declined by half from a maximum of ten (800–900 m) to only five species at depths of 1200–1300 m (Fig. 5).

The index of similarity (S) between the two surveys was high (0.89), and for each survey there was a high degree of similarity between areas, except for those most distant from each other, particularly between area 10 and other areas (Table 2). Indices of similarity between depth intervals were very similar for both surveys: high (0.80 for the orange roughy survey and 0.81 for the oreo survey) for the two shallowest depth intervals (700–1000 m versus 1000–1300 m), moderate (0.57 and 0.63) for the 1000–1300 m vs 1300+ m intervals, and much lower (0.42 and 0.47) for

700–1000 m versus 1300+ m intervals.

Morisita's index of dispersion (I_d) indicated that all species of sharks tended to be aggregated on Chatham Rise to some degree. The three large squalid sharks were the most aggregated: *S. plunketi* (I_d=104.5), *C. squamosus* (82.4), *D. licha* (55.4), followed by *E. granulosus* (24.3), *Apristurus* spp. (21.2), *C. owstoni* (10.9), *D. calcea* (8.2), and the most randomly distributed was *C. crepidater* (I_d=5.4).

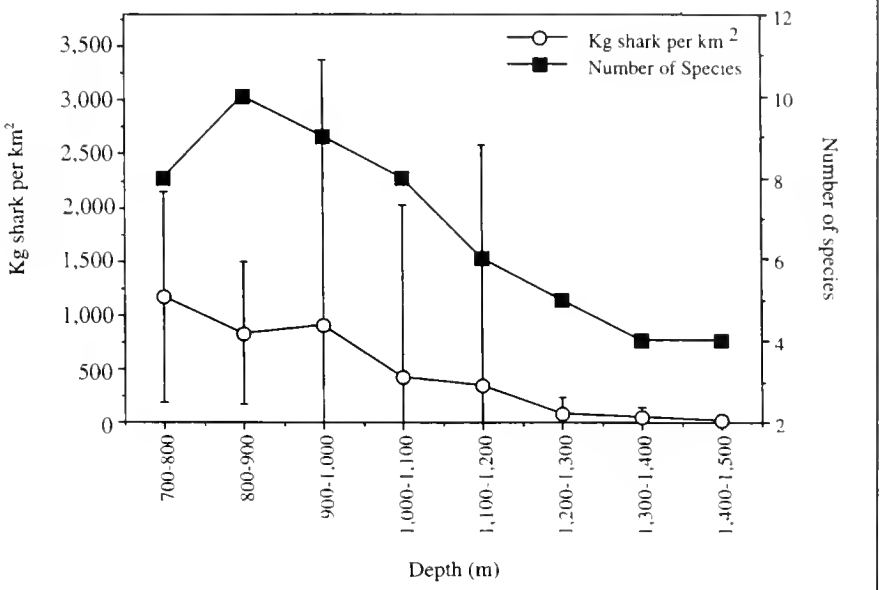

Figure 5

Average density (kg/km^2 ±SD) of all sharks combined and number of species captured within various depth intervals on Chatham Rise, New Zealand, for both surveys combined. For comparison of mean densities among intervals with ANOVA, P = 0.011, df = 389.

Discussion

Sharks are abundant and widely distributed on Chatham Rise. Even though sharks form a relatively small percentage of the overall catch in deep-water trawls they are frequently caught by the hundreds and occasionally dominate catches. The most abundant shark (by weight) on Chatham Rise, *D. calcea*, was often caught in large numbers, which suggests the presence of large aggregations. However, this species was caught in a high percentage of trawls and was widely distributed on Chatham Rise, which resulted in a fairly low index of dispersion (I_d). *D. calcea* is abundant elsewhere in New Zealand waters, accounting for as much as 70% of the shark catch off the North Island (Clark and King[1]). Kobayashi (1986) reported that *D. calcea* was one of the most common sharks in deep-water catches from Japan as well. The most ubiquitous shark in terms of presence at nearly all depths and locations on Chatham Rise was *E. granulosus*, although this species may have a fairly limited distribution outside of New Zealand and southeast Australia. Tachikawa et al. (1989) synonymized the New Zealand lantern shark, *E. baxteri*, with the widely-distributed southern lantern shark, *E. granulosus*; however, there may be several species within the *E. granulosus* group and *E. baxteri* may well be a valid species (Compagno et al., 1991; Wetherbee, 1996).

Catsharks captured in trawls were keyed out to five undescribed species (A–E) belonging to the genus *Apristurus* (Paulin et al., 1989). That several hundred specimens of these undescribed sharks were collected, underscores the paucity of information on deep-sea sharks. This genus also contains many undescribed species in other locations, such as Australia (Last and Stevens, 1994), and may eventually be recognized as one of the most speciose genera of sharks.

Table 2

Bray-Curtis index of similarity between geographical areas on Chatham Rise, New Zealand for a 1990 orange roughy survey and a 1993 smooth oreo survey. For location of areas see Figure 1.

Orange roughy survey Area	2	3	4	5	6	7	9	10
1	0.87	0.84	0.84	0.74	0.69	0.71	0.56	0.38
2		0.89	0.87	0.85	0.78	0.71	0.56	0.36
3			0.84	0.82	0.82	0.68	0.53	0.34
4				0.87	0.85	0.75	0.61	0.42
5					0.89	0.65	0.58	0.36
6						0.72	0.64	0.42
8							0.81	0.60
9								0.71

Oreo survey Area	7	8	9	10
6	0.76	0.71	0.35	0.32
7		0.76	0.47	0.37
8			0.57	0.53
9				0.85

Very few individuals of three species of relatively large squalid sharks (*Centrophorus squamosus*, *Scymnodon plunketi*, and *Dalatias licha*) were captured on Chatham Rise. These three species also happen to have liver oil that is high in squalene, or that has a high diacyl glycerol ether to triglycerol ratio, and the liver oil of these sharks is thus of high quality for industrial purposes (Bakes and Nichols, 1995; Wetherbee, 1998). Because each of these species formed less than 1% of the total shark catch in all fishing, targeting of any of these species by commercial fisheries on Chatham Rise does not appear to be practical. However, these species have been captured in greater numbers in fishing that was conducted at shallower depths and that targeted different fishes at locations other than Chatham Rise in New Zealand (Clark and King[1]).

The consistency in catch rate, regardless of time of day, indicates that there are few changes in the distribution of the deep-sea shark community on a diurnal basis. However, capture in a trawl may not provide information on activity patterns or feeding periodicity. For example, Kobayashi (1986) found that capture rate of sharks was higher at night than during the day in deep-sea fishing with baited lines. The present study was conducted over a three-month period and does not provide much information on seasonal differences in the distribution of deep-sea sharks. Some studies have suggested that there is continual movement of reproductive groups, or age classes, out of a particular area (Yano, 1991; Wetherbee, 1996). Other studies have maintained that community structure, temperature, and salinity of the deep-sea environment vary little throughout the year (Kobayashi, 1986; Clark and King[1]).

Orange roughy appear to be common prey of two species of sharks (*E. granulosus* and *C. owstoni*) and are also consumed by two of the less common, large squalids (*C. squamosus* and *D. licha*). *Centroscymnus owstoni* may exert the greatest predation pressure on orange roughy populations because both species are found in large numbers on the north of Chatham Rise. An expanded investigation of the feeding habits of sharks would provide more information on the relationship between sharks and commercially important teleosts on Chatham Rise.

Abundance

Differences in abundance of sharks between the orange roughy and oreo surveys appear to be attributable to the location at which fishing was concentrated in each survey. For the oreo survey, fishing was restricted to the south of Chatham Rise, and during the orange roughy survey, fishing was concentrated on the north of Chatham Rise (although trawls were made throughout Chatham Rise). The observation that there were no significant differences between the catches in areas common to both surveys indicates that overall differences between the surveys were probably not due to differences in fishing methods (duration of trawls and net specifications) or time (season or year). The contribution of sharks to total biomass of each survey was also remarkably similar.

The composition of the shark community was dependent upon the area of Chatham Rise that was sampled. Moving from west to east on the north of Chatham Rise, the dominant species in trawls changed from *C. owstoni* to *D. calcea*. Fishing areas at the eastern tip of Chatham Rise were the most diverse. There, the highest densities (kg/km^2) were recorded for six of the eight species of sharks and for all sharks combined. *Etmopterus granulosus* was the most abundant shark on the south of Chatham Rise, completely dominating the catch in the westernmost areas. Variation in the composition of the deep-sea shark community with location has been observed in other areas off New Zealand, and also in Japan and southern Africa (Kobayashi, 1986; King and Clark, 1987; Compagno et al., 1991). In several studies, the community of deep-sea sharks was thought to vary with latitude (Merrett and Marshall, 1981; Nakaya and Shirai, 1992; Yano and Kugai, 1993). The distribution of sharks on Chatham Rise may be influenced by a number of physical and biological factors. However, the lack of information on the deep-sea environment in this area precluded examination of the relationship between shark abundance and either biotic or abiotic factors; in contrast to other studies (Graham and Hastings, 1984; Bianchi, 1991; 1992; Garcia et al., 1998). Large portions of Chatham Rise are as shallow as 500 m, and sharks with fairly deep distributions might not move freely between the north and south slopes. Thus, the patterns of distribution observed for several species of sharks near Chatham Rise may be related to this physical barrier.

In this study, shark abundance also varied with depth. The depth range at which maximum shark density was recorded in the present study (700–800 m) was deeper than that reported by Kobayashi (1986) (300–500 m), and shallower than that found by Yano and Kugai (1993) (1100–1200 m). Depth distributions of sharks caught on Chatham Rise are characterized by several patterns. Some of the larger species were rare at depths greater than 1100 m, which may approximate their maximum depth of occurrence. The density of other species declined abruptly beyond 1200 m, and the proportion of *Apris-*

turus spp. in the catch increased at depths greater than 1200 m. The depths fished in the present study did not appear to reveal the minimum depth of occurrence for any species of shark. Compagno et al. (1991) noted the importance of determining minimum depth of occurrence describing the depth distribution of a particular species.

On Chatham Rise, density (kg/km^2) of all sharks combined was fairly constant up to about 1200 m but dropped drastically beyond this depth. Nakaya and Shirai (1992) observed a similar dramatic decrease in shark density at 500 m, and Merrett and Marshall (1981) at 1000–1100 m. An inverse relation between shark abundance and depth has been described for a number of species in other regions of New Zealand, and in other parts of the world (Merrett and Marshall, 1981; Kobayashi, 1986; King and Clark, 1987; Yano and Kugai, 1993).

Distribution

Diversity (species of shark/trawl) was higher for the orange roughy surveys than for the oreo surveys, but there was no significant difference in mean diversity between areas common to both surveys. These observations support the contention that differences in the shark catch between surveys are related to sampling location, rather than to temporal or methodological differences between surveys. However, there were generally more trawls within each area during the orange roughy survey than for the oreo survey, which may have increased the total number of species caught on the north of Chatham Rise. Hill (1973) predicated that as the size of a sample is increased, so almost without limit will the diversity. Diversity also declined with increased depth on Chatham Rise, and Crowder (1990) suggested that such a decline in species diversity might be due to changes in the level of competition, predation, or environmental homogeneity.

In this study, only 16 species of shark were caught, although many more species of deep-sea shark have been captured in New Zealand (Paulin et al., 1989). The total of only 16 species caught in the present study is also low in comparison to numbers (>30) of species caught in deep-water surveys in other parts of the world (Kobayashi, 1986; Compagno et al., 1991; Nakaya and Shirai, 1992; Yano and Kugai, 1993). Much of the fishing on Chatham Rise was conducted at depths of greater than 1000 m, which may be beyond the depth limit of a number of species of squalid sharks found in New Zealand waters (Yano, 1985; Compagno et al., 1991).

The index of similarity between the orange roughy and oreo surveys was high, again suggesting that differences introduced as a result of variable fishing methods or time were probably not substantial. The nearly identical indices of similarity between depth intervals for each survey also support this conclusion. The high indices of similarity between areas for most species, along with the fairly low indices of dispersion, indicate that although their abundance is variable, most species have fairly wide distributions on Chatham Rise.

Sharks within the genera *Etmopterus* and *Centrophorus* are thought to segregate by species in Japanese waters (Kobayashi, 1986; Baba et al., 1987; Yano and Tanaka, 1983). In the present study there was little evidence to suggest that any two species displayed such segregation. Compagno et al. (1991) found that *Centroscymnus* spp. were sympatric but had very different food habits. An examination of dietary overlap among sharks common on Chatham Rise may reveal whether these sympatric species compete for the same food resources.

Although the sharks captured during this study were incidental to commercially important fishes, such as orange roughy and smooth oreo, the data collected from these trawls have provided information on the abundance and distribution of a number of species of deep-sea shark on Chatham Rise. Distributional patterns of sharks vary among species, and the composition of the deep-sea shark community varies with depth and location. Therefore, the overall impact of deep-water trawl fisheries on shark populations would be expected to vary among species and to depend on the particular fishery, which in turn influences the location and depth where fishing is concentrated.

Acknowledgments

I thank A. Bush, T. Clarke, K. Holland, S. Kajiura, C. Lowe, C. Meyer, C. Mostello, and J. Parrish for their comments on the manuscript. P. Grimes, P. McMillan, and K. Mulligan were tremendously helpful with collection of specimens and access to trawl data. K. Fields, J. Fenaughty, M. Clarke, A. Hart, and the captains and crews of the RV *Tangaroa* and FV *Cordella* were instrumental in collection of data. J. Parrish, D. Yount, and B. Flannigan made funds available for travel to New Zealand.

Literature cited

Baba, O., T. Taniuchi, and Y. Nose.
1987. Depth distribution and food habits of three species of small squaloid sharks off Chosi. Nippon Suisan Gakkaishi 53(3):417–424.

Bakes, M. J., and P. D. Nichols.
1995. Lipid, fatty acid and squalene composition of liver oil from six species of deep-sea sharks collected in southern Australian waters. Comp. Biochem. Physiol. 110(B) :267–275.

Bianchi, G.
1991. Demersal assemblages of the continental shelf and slope edge between the Gulf of Tehuantepec (Mexico) and the Gulf of Papagayo (Costa Rica). Mar. Ecol. Prog. Ser. 73: 121–140.
1992. Demersal assemblages of the continental shelf and upper slope of Angola. Mar. Ecol. Prog. Ser. 81:101–120.

Brower, J. E., and J. H. Zar.
1984. Field and laboratory methods for general ecology. W.C. Brown Publishers, Dubuque, IA, 226 p.

Clark, M. R., K. J. King, and P. J. McMillan.
1989. The food and feeding relationships of black oreo, *Allocyttus niger*, smooth oreo, *Pseudocyttus maculatus*, and eight other fish species from the continental slope of the south-west Chatham Rise, New Zealand. J. Fish Biol. 35:465–484.

Clark, M. R., and D. M. Tracey.
1994. Changes in a population of orange roughy, *Hoplostethus atlanticus*, with commercial exploitation on the Challenger Plateau, New Zealand. Fish. Bull. 92:236–253.

Compagno, L. J. V., D. A. Ebert, and P. D. Cowley.
1991. Distribution of offshore demersal cartilaginous fish (class Chondrichthyes) off the west coast of southern Africa, with notes on their systematics. S. Afr. J. Mar. Sci. 11:43–139.

Crowder, L.B.
1990. Community ecology. *In* C. B. Schreck and P. B. Moyle (eds.), Methods for fish biology, p. 609–632. Am. Fish. Soc., Bethesda, MD.

Davenport, S., and P. Deprez.
1989. Market opportunities for shark liver oil. Aust. Fish. 11:8–10.

Deprez, P. P., J. K. Volkman, and S. R. Davenport.
1990. Squalene content and neutral lipid composition of livers from deep-sea sharks caught in Tasmanian waters. Aust. J. Mar. Freshwater Res. 41:375–387.

Ebert, D. A., L. J. V. Compagno, and P. D. Cowley.
1992. A preliminary investigation of the feeding ecology of squaloid sharks off the west coast of southern Africa. S. Afr. J. Mar. Sci. 12:601–609.

Field, J. G., K. R. Clarke, and R. M. Warwick.
1982. A practical strategy for analysing multispecies distribution patterns. Mar. Ecol. Prog. Ser. 8:37–52.

Garcia, C. B., L. O. Duarte, and D. von Schiller.
1998. Demersal fish assemblages of the Gulf of Salamanca, Columbia (southern Caribbean Sea). Mar. Ecol. Prog. Ser. 174:13–25.

Graham, J. H., and R. W. Hastings.
1984. Distributional patterns of sunfishes on the New Jersey coastal plain. Env. Biol. Fish. 10:137–148.

Hill, M. O.
1973. Diversity and evenesss: a unifying notation and its consequences. Ecology 54:427–432.

King, K., and M. Clark.
1987. Sharks from the upper continental slope—are they of value? Catch (May):3–6.

Kobayashi, H.
1986. Studies of deep-sea sharks in Kumano-nada Region. Bull. Fac. Fish. Mie Univ. 13:25–133.

Last, P. R., and J. D. Stevens.
1994. Sharks and rays of Australia. Commonwealth Scienfiic Industrial Research Organization (CSIRO), 513 p.

Merrett, N. R., and N. B. Marshall.
1981. Observations on the ecology of deep-sea bottom-living fishes collected of northwest Africa (08°–27°N). Prog. Oceanogr. 9:185–244.

Nakaya, K., and S. Shirai.
1992. Fauna and zoogeography of deep-benthic chondrichthyan fishes around the Japanese Archipelago. Jpn. J. Ichthyol. 39(1):37–48.

Paulin, C., C. Roberts, A. Stewart, and P. McMillan.
1989. New Zealand fish: a complete guide. National Museum of New Zealand Miscellaneous Series 19, Wellington, 279 p.

Sedberry, G. R., and R. F. Van Dolah.
1984. Demersal fish assemblages associated with hard bottom habitat in the South Atlantic Bight of the U.S.A. Env. Biol. Fish. 11:241–258.

Stephens, J. S. Jr., P. A. Morris, K. Zerba, and M. Love.
1984. Factors affecting fish diversity on a temperate reef: the fish assemblage of Palos Verdes Point, 1974–1981. Env. Biol. Fish. 11:259–275.

Summers, G.
1987. Squalene—a potential shark by-product. Catch (October) 1987:29.

Tachikawa, H., T. Taniuchi, and R. Arai.
1989. *Etmopterus baxteri*, a junior synonym of *E. granulosus* (Elasmobranchii, Squalidae). Bull. Nat. Sci. Mus., Tokyo Ser. A 15:235–241.

Wetherbee, B. M.
1996. Distribution and reproduction of the southern lantern shark from New Zealand. J. Fish Biol. 49:1186–1196.
1998. Biochemical and physiological buoyancy adaptations in deep-sea sharks. Ph.D. diss., Univ. Hawaii, Honolulu, HI, 144 p.

Yano, K.
1985. Studies on morphology, phylogeny, taxonomy and biology of Japanese squaloid sharks, order Squaliformes. Ph.D. diss., Tokai University, Shimizu, 335 p.
1991. Catch distribution, stomach contents and size at maturity of two squaloid sharks, *Deania calceus* and *D. crepidalbus* from the southeast Atlantic of Namibia. Bull. Jpn. Soc. Fish. Oceanogr. 55:189–196.

Yano, K., and K. Kugai.
1993. Deep-sea chondrichthyans collected from the waters around the Okinawa Islands: results of catch analysis of bottom longlines. Bull. Seikai National Fish. Res. Inst. 71:51–65.

Yano, K., and S. Tanaka.
1983. Portuguese shark, *Centrophorus coelolepis* from Japan, with notes on *C. owstoni*. Jpn. J. Ichthyol. 30:208–216.

Growth, population age structure, and aspects of the reproductive biology of snowy grouper, *Epinephelus niveatus*, off North Carolina and South Carolina*

David M. Wyanski
D. Byron White
Charles A. Barans
South Carolina Department of Natural Resources
Marine Resources Research Institute
P.O. Box 12559
Charleston, South Carolina 29422-2559
E-mail address (for D. M. Wyanski): wyanskid@mrd.dnr.state.sc.us

Abstract.—Sagittae (n=2,263) and gonads (n=870) from snowy grouper, *Epinephelus niveatus*, caught primarily with longlines, Kali poles, snapper reels, and chevron traps off North Carolina and South Carolina were examined 1) to compare growth rates, population age structure, and sex ratio between two periods 1979–85 and 1993–94, and 2) to determine reproductive seasonality, size and age at maturity, and size and age at sex change. There were several indications that the population off North Carolina and South Carolina is overfished: 1) size at age of specimens caught with longlines and snapper reels has increased noticeably since the 1980s (possibly a a density-dependent population response to a high level of fishing mortality); 2) 81% of the fish caught with commercial longlines during 1993–94 were ages 1–6, the majority (56%) of which were immature females; 3) the percentage of males in the population appears to have decreased significantly, from 7–23% in the 1970s and 1980s to 1% in the 1990s; and 4) mean length of fish landed in the longline fishery has steadily decreased from 65–80 cm in the early 1980s to 50–60 cm in the mid-1990s. There was a positive trend between water depth and total length in fishery-independent samples. Histological examination of gonads revealed that mature gonads were present in 4% of the females at age 3, 52% at age 5, 95% at age 7, and 100% at ages >7 during 1993–94. The smallest mature female was 469 mm TL, and the largest immature female was 575 mm. Estimates of $Length_{50}$ and Age_{50} were 541 mm (95% CI=529–553 mm) and 4.92 yr (95% CI=4.65–5.21 yr), respectively. Spawning females were caught during April through September on the upper continental slope off South Carolina at depths of 176–232 m. The size (767–1090 mm) and age (8–29 yr) of 97 male specimens and the capture of two specimens undergoing sex change provided conclusive evidence that snowy grouper are protogynous hermaphrodites.

Manuscript accepted 26 August 1999.
Fish. Bull. 98:199–218 (2000).

The snowy grouper, *Epinephelus niveatus*, is a commercially important deepwater species that occurs in the western Atlantic from North Carolina (Cape Hatteras) to Brazil, including the Gulf of Mexico and the Bahamas (Smith, 1971). It also occurs in the eastern Pacific from California to Mexico (Miller and Lea, 1976; Fitch and Schultz, 1978). Along the coast of the southeast United States, adult snowy grouper are predominantly found on the upper continental slope (>75 m; Lee et al., 1985) at depths of 116–259 m (Low and Ulrich, 1983; Moore and Labisky, 1984; Parker and Ross, 1986), whereas juveniles are more common at shallower depths (Moore and Labisky, 1984). Low and Ulrich (1983) noted a positive correlation between total length (TL) and water depth off South Carolina. Most fishing for this species occurs in habitats characterized by rocky ledges, cliffs, and swift currents (Matheson and Huntsman, 1984).

Snowy grouper are captured primarily in commercial fisheries of the southeastern United States (Parker and Mays, 1998). Most are caught with bottom longlines and snapper reels[1] (handlines). Starting in 1991, the longline fishery was restricted to waters deeper than 91 m by the South Atlantic Fishery Management Council (SAFMC, 1991). Fishing for snowy grouper has occurred off North Carolina and South Carolina (the Carolinas) since the mid-1950s (Huntsman, 1976); annual landings from the Carolinas averaged 119,657 kg during 1981–96 (Moran[2]). According to the spawning stock ratio (SSR), the population off the Atlantic coast of the United States is considered to be overfished (SAFMC, 1993).

Population age structure and individual growth rates in the snowy grouper population have not been assessed since the mid-1980s and should be assessed again given the sustained fishing pressure on the population. Studies of other fish populations have shown that size at age is often affected by the level and duration of exploitation (Haug and Tjemsland, 1986; Harris and McGovern, 1997; Helser and

* Contribution 430 of the South Carolina Marine Resources Center, P.O. Box 12559, Charleston, SC 29422.

[1] Snapper reels are commonly known as "bandits" or "one-armed bandits" by fishermen owing to the remote similarity between early snapper reels and gambling slot machines, and because luck is involved in what is caught. The early mechanical reels have typically been replaced by 12 volt DC automobile starter motors or hydraulic systems.

[2] Moran, J. 1996. S. Carolina Dept. of Natural Resources, P.O. Box 12559, Charleston, SC 29422. Personal commun.

Almeida, 1997; Zhao et al., 1997; Goodyear and Schirripa[3]), thus trends in growth can be indicators of population stability. Additionally, nothing is known about trends in sex ratio. Recent studies along the southeast Atlantic coast and in the Gulf of Mexico have documented sharp decreases in the proportion of males in other grouper, gag (*Mycteroperca microlepis*) and scamp (*M. phenax*), populations (Coleman et al., 1996; McGovern et al., 1998). This and other factors have led to reduced genetic diversity in the gag population along the southeast coast, a cause for serious concern, although the ramifications are not clearly understood (Chapman et al., 1999).

Little is known about the reproductive biology of snowy grouper off the Carolinas because the only previous study (Moore and Labisky, 1984) was conducted in the Florida Keys. Using a histological technique, Moore and Labisky (1984) showed that the snowy grouper is a protogynous hermaphrodite; females reach sexual maturity at ages 3–5 and change to males as early as age 6. The objectives of the present study were 1) to compare individual growth rates, population age structure, and sex ratio between two periods, 1979–85 and 1993–94, and 2) to determine reproductive seasonality, size and age at maturity, and size and age at sex change for snowy grouper off the Carolinas.

Materials and methods

Specimen acquisition

Snowy grouper were obtained from commercial boats, research vessels, and headboats, primarily off North Carolina and South Carolina (Table 1). All specimens were collected between 31°09'N and 34°44'N at depths of 42–302 m. Only seven specimens were caught south of 32°04'N. Fishery-independent samples were collected during cruises of the MARMAP (Marine Resources Monitoring Assessment and Prediction) program with bottom longlines, Kali poles (an off-bottom longline; Russell et al., 1988), snapper reels, rods and reels, and chevron traps (Collins, 1990). Specimens caught with longlines were collected primarily off South Carolina, whereas specimens caught with snapper reels were collected off South Carolina in the 1980s and primarily off North Carolina in the 1990s (Fig. 1). Total length (mm) was measured for all specimens and all length measurements in the text refer to total length (TL).

During 1993–94, samples from the commercial fishery usually included the total catch of snowy grouper from a vessel or a random subsample; on three of 20 occasions, the catches from vessels that landed fish in South Carolina were subsampled to collect otoliths from small and large specimens. No documentation on sampling design was available for fishery-dependent samples that were collected with snapper reels during 1979–85.

Age and growth

The left sagitta, and the right sagitta when time permitted, was removed and stored dry prior to processing. Each otolith was embedded in paraffin (1979–85) or Araldite epoxy resin (1993–94) and sectioned along a dorsoventral plane through the focus with a single high-concentration diamond wheel on a Buehler Isomet low-speed saw. Otolith sections were mounted on glass slides with Crystalbond thermoplastic or Accu-mount 60, covered with cedar wood oil, and examined under a dissecting microscope (10–63×) with reflected and transmitted light.

We examined otoliths from 1937 specimens and used the age determinations (n=326) of Waltz[4] for specimens collected with snapper reels from 1979 to 1985. The width of the translucent zone along the margin of the section was measured to assess the periodicity of increment formation. Increments were counted independently by two readers for 1853 of 1937 specimens. In older fish, all increments could not be counted along one axis in many specimens. Counting commenced on one of three axes (ventral, ventromedial, or adjacent to the sulcus acousticus) and shifted to another axis by following an increment to the new axis. If counts differed, both readers examined the otolith by projecting the image onto a TV monitor. The otolith was rejected if agreement could not be reached.

A small portion (n=129) of the 1937 otoliths that we examined were used for an earlier MARMAP study (Waltz[4]). Age assessments were compared to determine if annual increment structure was being interpreted in a similar manner. The specimens selected for the comparison were collected with longlines or Kali poles on research cruises during 1982–85. Age data from specimens collected with these two gear types were combined because they were fished simultaneously in the same area and were deployed with the same hook type and bait.

The sagittae of three young-of-the-year (YOY) specimens were hand-polished to thin (approx. 5μm)

[3] Goodyear, C. P., and M. J. Schirripa. 1993. The red grouper fishery of the Gulf of Mexico. Report MIA 92/93-75. Miami Laboratory, Southeast Fisheries Science Center, National Marine Fisheries Service, 75 Virginia Beach Dr., Miami, FL 33149.

[4] Waltz, W. 1986. The size and age of snowy grouper (*Epinephelus niveatus*) in the South Atlantic Bight. MARMAP Analytical Report, 16 p. S. Carolina Department of Natural Resources, P.O. Box 12559, Charleston, SC 29422.

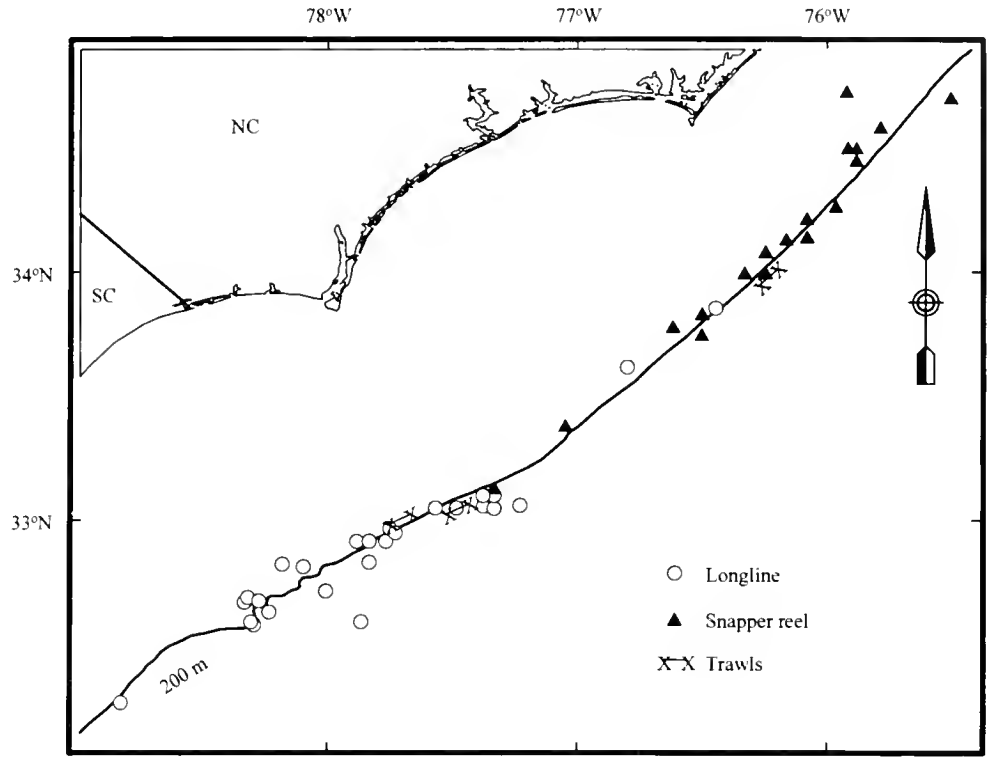

Figure 1

Approximate locations of commercial fishing effort with longlines and snapper reels for snowy grouper off North Carolina and South Carolina between June 1993 and September 1994. Snowy grouper were also caught in trawls in June 1978 during an exploratory squid cruise conducted by the government of Spain and the National Marine Fisheries Service on the RV *Pescapuerta Segundo*. Trawl site off Georgia is not shown.

Table 1

Numbers of specimens of snowy grouper for which otoliths and gonad samples were examined by gear type. C = commercial landings; H = headboats sampled by National Marine Fisheries Service, Beaufort, North Carolina; R = research cruises conducted by Marine Resources Monitoring Assessment and Prediction Program (MARMAP).

Gear	Source	Period	Otoliths	Gonads
Snapper reel	C, R	1979–85	326	309
Longline and Kali pole	most R, C	1982–85	190	180
Rod and reel	most H, R	1973–81	0	90
Other	C, R	1980–84	0	10
Snapper reel	C	1991–95	335	32
Longline	C	1993–94	1332	146
Chevron trap	R	1991–95	78	100
Other	R	1993–95	2	3
Total			2263	870

transverse sections according to the methods of Secor et al. (1992) and examined with a compound microscope. We counted the regular concentric rings, similar to those reported as daily growth increments in other species, to estimate age. Assumed daily rings were visible, with the exception of a large opaque core area, on the smallest otolith but were only distinguishable at discrete locations on the other two otoliths. For these two otoliths, age was estimated by extrapolating the increment count per unit distance to the total radial measurement of the ventral axis, excluding the core. Radial measurement

from the core to the first annulus was made for a subsample of 23 specimens that were age 1 and compared with the measurements from the three YOY to establish the position of the first annulus.

Age-length keys were formed by obtaining a matrix of numbers at age by length interval for each gear type (longline and snapper reel) in two periods (1980s and 1990s). Besides the differing selectivities of longlines and snapper reels, another reason for developing keys by gear type was the difference in sampling area in 1993–94 (Fig. 1) and potential differences in sampling depth due to the restriction (SAFMC, 1991) that limits the use of longlines to waters deeper than 91 m. Additional keys were generated to address two questions: 1) Do data from specimens with age estimates of lower precision affect the accuracy of the key for specimens caught with longlines in the 1990s? and 2) Are there differences in the keys for specimens caught with longlines or Kali poles during 1982–85 that were examined in the present study and in an earlier study by Waltz?[4] To address the first question, keys based on all specimens and specimens for which there was a difference of 0–1 increments between readers were compared.

All analysis of age and growth data was conducted with SAS software (SAS Institute, Inc., 1990). Fisher's exact test (Siegel, 1956) was used to compare the age distributions of two age-length keys by 25-mm length intervals. The FREQ procedure was used to run this test. A comparison was made only if each key had >6 specimens in an interval because of the low power associated with small sample sizes (Bennett and Hsu, 1960). The large number of tests required to compare age-length keys necessitated compensating for experimentwise error by computing an adjusted significance level (α^*) using the formula presented by Hayes (1993).

Nonlinear regression analysis with Marquardt's algorithm (NLIN procedure) and the NLIN weight statement were used to fit the von Bertalanffy growth model to observed length at age data (von Bertalanffy, 1938). Lengths were weighted by the inverse of the number of fish at each age to moderate the effect of large and small sample sizes on the estimates of growth parameters. Age-length keys were applied to length data collected through the Trip Interview Program (TIP) in the Carolinas to generate an age-frequency distribution. TIP is a commercial fisheries data collection program funded by the National Marine Fisheries Service (NMFS).

Reproduction

Gonads were obtained during 1979–95 from 870 specimens collected on research cruises and from fish landed whole by fishermen (Table 1). Ninety gonad samples from the headboat fishery during 1973–1981, collected in association with the study of Matheson and Huntsman (1984), were obtained from the Beaufort Laboratory of the NMFS. The posterior portion of the gonad was fixed in 10% seawater-formalin for 1–2 weeks and transferred to 50% isopropanol for 1–2 weeks. Gonad samples were processed, sectioned, and stained with double-strength Gill hematoxylin and eosin-y by using the methods of Schmidt et al. (1993).

Sex and reproductive state were assessed primarily by one reader using histological criteria (Table 2), without reference to body length or date of capture. A second reader examined sections from 75 specimens to ensure accurate interpretations. If the assessments of the two readers differed, the section was viewed simultaneously by the readers and rejected if agreement could not be reached. Specimens with developing, ripe, spent, or resting gonads were considered sexually mature. For females, this definition of sexual maturity included specimens with oocyte development at or beyond the cortical granule stage and specimens with beta, gamma, or delta stages of atresia (see Hunter and Macewicz, 1985). To ensure that females were correctly assigned to either the immature or resting categories, the length-frequency histogram of females with evidence of certain maturity (e.g. those that were developing, ripe, or spent) was compared with the histograms for immature and resting females. Females of uncertain maturity (Table 2) were excluded from data analyses. To estimate length at 50% maturity (L_{50}) and age at 50% maturity (A_{50}), the PROBIT procedure (SAS Institute, Inc., 1990) was used to fit gompit, logit, or probit models to maturity data in 25-mm length intervals or one year increments. The LOGISTIC procedure was used to determine which model to use in the PROBIT procedure.

Females with hydrated oocytes or postovulatory follicles were considered to be in spawning condition. Macroscopic observations of snowy grouper caught in June 1978 during trawls (Fig. 1) of an exploratory squid cruise conducted jointly by the government of Spain and the Northeast Fisheries Center of NMFS in Woods Hole, Massachusetts, on the RV *Pescapuerta Segundo* were also used to define the area and timing of spawning.

Results

Age and growth

An age was assigned to 91.6% of 1937 otoliths that we examined (Table 1). Otoliths were rejected if the

Table 2

Histological criteria used to determine reproductive stage in snowy grouper (see Hunter and Goldberg, 1980; Wallace and Selman, 1981; Hunter and Macewicz, 1985; Wenner et al., 1986; West, 1990).

Reproductive stage	Criteria
Immature	Previtellogenic oocytes only, no evidence of atresia. In comparison with resting female, most previtellogenic oocytes are <70 µm, area of transverse section of ovary is smaller, lamellae lack muscle and connective tissue bundles and are not as elongate, oogonia are abundant along margin of lamellae, and ovarian wall is thinner.
Developing	Oocytes undergoing cortical granule (alveoli) formation through nucleus migration and partial coalescence of yolk globules.
Ripe	Completion of yolk coalescence and hydration in the most advanced oocytes. Zona radiata becomes thinner.
Developing, recent spawning	Developing stage as described above plus presence of postovulatory follicles.
Spent	More than 50% of vitellogenic oocytes in alpha or beta stage of atresia.
Resting	Previtellogenic oocytes only with traces of atresia possible. In comparison with immature female, most previtellogenic oocytes >70 µm, area of transverse section of ovary is larger, lamellae have muscle and connective tissue bundles, lamellae are more elongate and convoluted, oogonia are less abundant along margin of lamellae, and ovarian wall is thicker and exhibits varying degrees of expansion owing to previous spawning.
Uncertain maturity	Immature or resting. Inactive ovaries, previtellogenic oocytes only. Reproductive stage is uncertain.
Transitional	Proliferation of spermatogonia through limited spermatogenesis within lamellae of resting ovary, accompanied by development of peripheral sinuses in musculature of ovarian wall.

readers could not agree on the age or if the section was not adequate. Ages ranged from 1 to 29 yr and lengths from 226 to 1137 mm. From a subsample (n=274) of 3–10 yr old specimens, we found that the mean width of the sagittal marginal translucent zone was smallest in April and May, indicating the period of increment formation (Fig. 2). The unimodal nature of the data indicated that one increment was deposited per year.

Data from longlines and snapper reels showed that size at age was greater during 1993–94 than during the previous decade (Figs. 3 and 4). Snowy grouper captured with longlines in 1993–94 exhibited a nearly constant growth rate until approximately age 10, after which there was a notable decrease. A similar growth pattern was noted for snowy grouper caught with snapper reels, although the trend was less definitive owing to smaller sample sizes. Estimates of theoretical maximum length (L_∞) were reasonable when compared with maximum observed lengths (Table 3). Data from both gear types indicated that L_∞ has increased 169–231 mm in the last decade. The application of the age-length key for samples caught with longlines during 1993–94 to TIP length data for the same period revealed recruitment to the fishery as early as age 1, and a modal age for recruitment of 5 (Table 4).

The increase in size at age since the 1980s was also evident in comparisons of age-length keys between

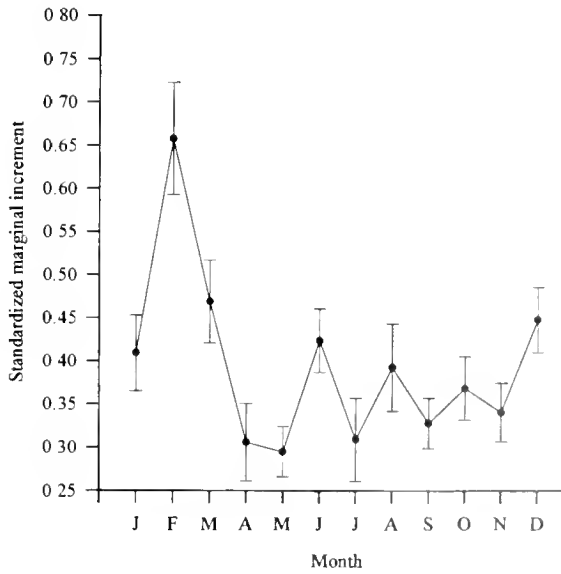

Figure 2

Mean width (±SE) of marginal translucent zone in transverse sections of sagittae from 248 snowy grouper that were 3–10 yr old.

periods for each gear type. For longline gear, the comparisons in 8 of 8 length intervals exceeded the adjusted significance level (P<0.00639; Table 5). The

Table 3

Von Bertalanffy parameters (± SE) describing the growth in mm total length of snowy grouper collected with snapper reels and longlines and Kali poles (LL, KP) during two decades. Mean observed length at age data were used to generate parameter estimates. Estimates from two earlier studies, generated using back-calculated lengths, are included for comparison.

Study	Gear and source	Period	n	Maximum observed length	L_∞	k	t_0
Waltz (1986)	Snapper reels commercial, research	1979–85	326	1090	970 (24)	0.109 (0.001)	−2.123 (0.336)
Present	Snapper reels commercial	1993–94	311	1110	1201 (34)	0.103 (0.008)	−1.149 (0.231)
Present	LL, KP, research	1982–85	163	1034	948 (28)	0.122 (0.017)	−0.668 (0.681)
Present	LL, commercial	1993–94	1218	1137	1117 (13)	0.119 (0.004)	−1.409 (0.121)
Matheson and Huntsman (1984)	Hook and line, headboat	1972–79	536	1130	1255	0.074	−1.92
Moore and Labisky (1984)	Hook and line, research	1978–81	118	1180	1320	0.087	−1.013

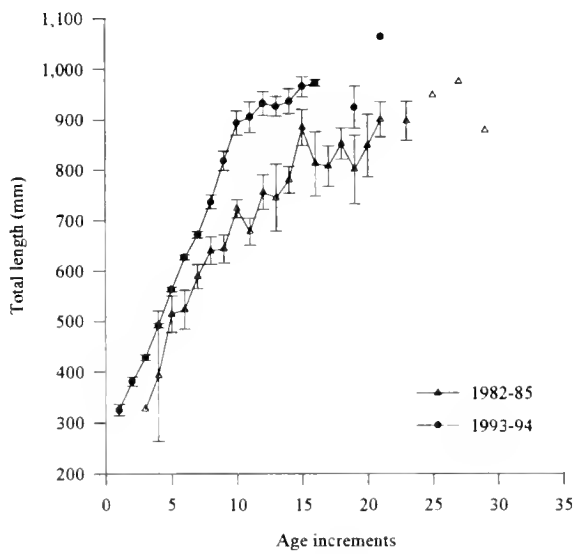

Figure 3

Mean observed size at age (±SE) for snowy grouper collected with longlines and Kali poles during 1982–85 (n=163) and longlines during 1993–94 (n=1,218) off North Carolina and South Carolina.

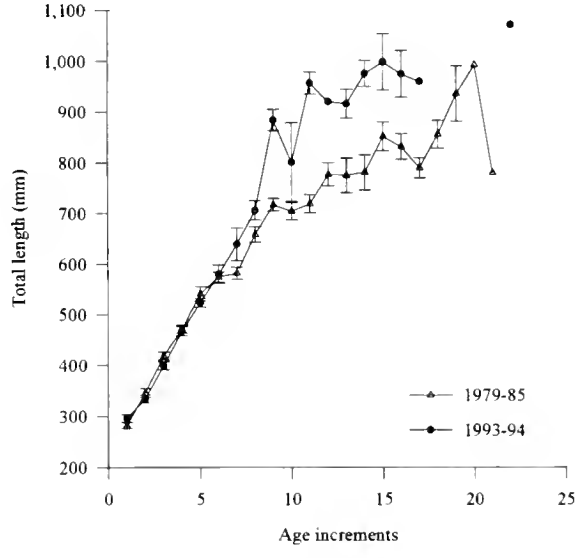

Figure 4

Mean observed size at age (±SE) for snowy grouper collected with snapper reels during 1979–85 (n=326) and 1993–94 (n=311) off North Carolina and South Carolina.

trend was not as strong for snapper reel gear because comparisons in 5 of 13 intervals exceeded the 0.05 level; only one comparison exceeded the adjusted significance level (P<0.00394; Table 5). The age-length keys for the two gear types were very similar in 1993–94 because comparisons in only 3 of 17 intervals exceeded the 0.05 level, none of which exceeded the adjusted significance level (P<0.00284; Table 5).

Initial agreement between independent readers was 24.2% for the 1853 otoliths examined by two readers; however, there was a difference of 0–1 increments between readers for 61.3% of the otoliths. The difference was >1 increment for 30.8% of the otoliths and 7.9% were rejected as uninterpretable. The inclusion in the data sets of age data for otoliths that were difficult to interpret did not affect the assessment of population age distribution for snowy grou-

Table 4

Population age structure of snowy grouper captured with longlines in North Carolina and South Carolina from July 1993 through May 1994. Age-length key was applied to length data from the same period collected during Trip Interview Programs.

Age	Number
1	5
2	32
3	77
4	172
5	209
6	163
7	82
8	23
9	13
10	8
11	6
12	7
13	4
14	2
15	3
16+	3
Total	809

per caught with longlines in 1993–94. Comparisons of age-length keys based on all specimens and specimens for which there was a difference of 0–1 increments between readers revealed a strong similarity in age distribution for 20 intervals (P>0.00256; Table 6).

Slightly less initial agreement was noted when our age estimates were compared with those of Waltz[4] for specimens caught in 1982–85 with longlines and Kali poles. Ages were assigned to 85.3% of 129 specimens that were examined in both studies. The same age was assigned to 18.2% of the specimens and there was a difference of 0–1 increments between studies for 40.0% of the specimens. Although the percent agreement was low, the estimates of mean size at age were similar (Fig. 5). Age distributions in the five length intervals that could be tested were similar (P>0.01021; Table 6). Given the similarity of age distributions, we decided to use the age data of Waltz[4] for snowy grouper caught with snapper reels in 1979–85 without reexamining the otoliths.

The low initial agreement between readers was due to a lack of a readily discernible growth pattern in many otoliths. Typical abnormalities included crystalline areas that obscured increments (Fig. 6A) and rounded opaque deformities that distorted increment spacing (Fig. 6B). In addition, the axis of otolith growth frequently changed direction at least once after 6–7 increments (Fig. 6C). Despite our inability to make linear measurements for back calculations, counts of increments were usually possible, although easily interpreted otoliths (Fig. 6D) were the exception.

We attempted to identify the first annulus 1) by examining daily increment structure in the sagittae of three specimens that were most likely YOY, and

Table 5

Comparison of age distributions by length interval with Fisher's exact test for snowy grouper collected off North Carolina and South Carolina with snapper reels during two periods (1979–85 and 1993–1994), with longlines during two periods (1982–85 and 1993–94), and with longlines and snapper reels during 1993–94. Dashed lines indicate that the sample size was less than seven in one or both groups.

mm TL	Snapper reel, 1979–85 vs. 1993–94	Longline, 1982–85 vs.1993–94	Longline vs. snapper reel, 1993–94
226–250	—	—	—
251–275	—	—	—
276–300	—	—	0.177
301–325	0.570	—	0.841
326–350	—	—	0.074
351–375	0.020	—	0.488
376–400	0.933	—	0.730
401–425	0.057	—	0.407
426–450	1.000	—	0.502
451–475	0.021	—	0.036
476–500	0.630	—	0.595
501–525	0.430	—	0.043
526–550	0.019	—	0.753
551–575	0.001*	—	0.323
576–600	0.209	—	0.972
601–625	0.045	<0.001	0.200
626–650	—	<0.001	0.668
651–675	0.064	<0.001*	0.438
676–700	—	<0.001*	—
701–725	—	<0.001	0.005
726–750	—	0.002*	—
751–775	—	<0.001	—
776–800	—	—	—
801–825	—	0.003	—
826–850	—	—	—
851–875	—	—	—
876–900	—	—	—
901–925	—	—	—
926–950	—	—	—
951–975	—	—	—
976–1000	—	—	—
α^1	0.00394	0.00639	0.00284

* $P < \alpha^1$. α^1 = adjusted significance level

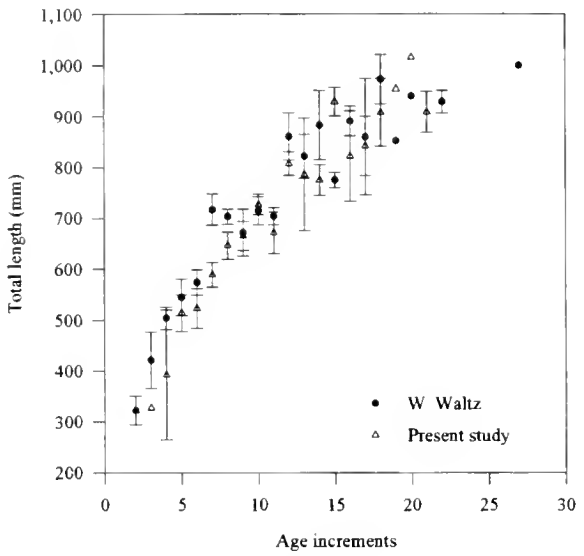

Figure 5

Mean observed size at age (±SE) for snowy grouper caught with longlines and Kali poles in the 1980s. The sagittae were examined by Waltz (n=132; see Footnote 3 in the main text) and investigators in the present study (n=129).

2) by comparing the measurements of otolith radius in these three specimens with the radial measurement to the first annulus in a subsample of 23 specimens that were age 1. Examination of sagittae from YOY revealed that fish lengths of 37, 156, and 172 mm were associated with estimated ages of 35, 159–201 and 191–291 days, respectively. Radial measurement to the edge in these three otoliths was less than the radial measurement to the first annulus in a subsample of 23 age-1 specimens.

Reproduction

Histological examination of 599 sexually mature snowy grouper in four data sets from three periods (1970s, 1980s, and 1990s) suggested that the number of males in the population has substantially decreased. The percentage of males was 7.2%, 19.5%, and 22.9% for samples collected with hook and line during 1973–81, snapper reels during 1980–84, and longlines and Kali poles during 1982–85, respectively, whereas males represented 1.2% of samples collected with longlines during 1993–94 (Table 7). Although sample sizes were <100 for two data sets, especially the 1993–94 data set, the mean total length ($\bar{x}$=63.6 cm, SE=1.0) of specimens in the 1993–94 data set was larger than the mean length of specimens measured through the TIP in North Carolina (1993: $\bar{x}$=58.0 cm, SE=0.6; 1994: $\bar{x}$=56.0, SE=1.4) and South Carolina (1993: $\bar{x}$=59.1, SE=0.7; 1994: $\bar{x}$=53.8, SE=0.6) for the same years, indicating that our data set was not biased toward smaller specimens.

There were ninety-seven males and two transitional specimens in the four sex-ratio data sets.

Table 6

Comparison of age distributions by length interval with Fisher's exact test for snowy grouper collected off North Carolina and South Carolina. These comparisons included 1) all specimens that were caught with longlines during 1993–94 and assigned an age versus those for which the difference in age assignment between readers was 0–1 increments (Best), and 2) specimens caught with longlines during 1982–85 that were examined in the present study and by Waltz (Footnote 4 in the main text). Dashed lines indicate that the sample size was less than seven in one or both groups.

mm TL	Best vs. all	Longline, present study vs. Waltz
251–275	—	—
276–300	—	—
301–325	—	—
326–350	1.000	—
351–375	1.000	—
376–400	0.852	—
401–425	0.855	—
426–450	0.980	—
451–475	0.978	—
476–500	0.951	—
501–525	0.853	—
526–550	0.966	—
551–575	0.932	—
576–600	0.997	—
601–625	0.993	0.669
626–650	1.000	0.669
651–675	0.955	—
676–700	0.663	—
701–725	0.832	0.242
726–750	0.943	1.000
751–775	0.902	0.660
776–800	—	—
801–825	1.000	—
826–850	0.795	—
851–875	—	—
876–900	—	—
901–925	—	—
926–950	—	—
951–975	—	—
976–1000		—
α^1	0.00256	0.01021

α^1 = adjusted significance level.

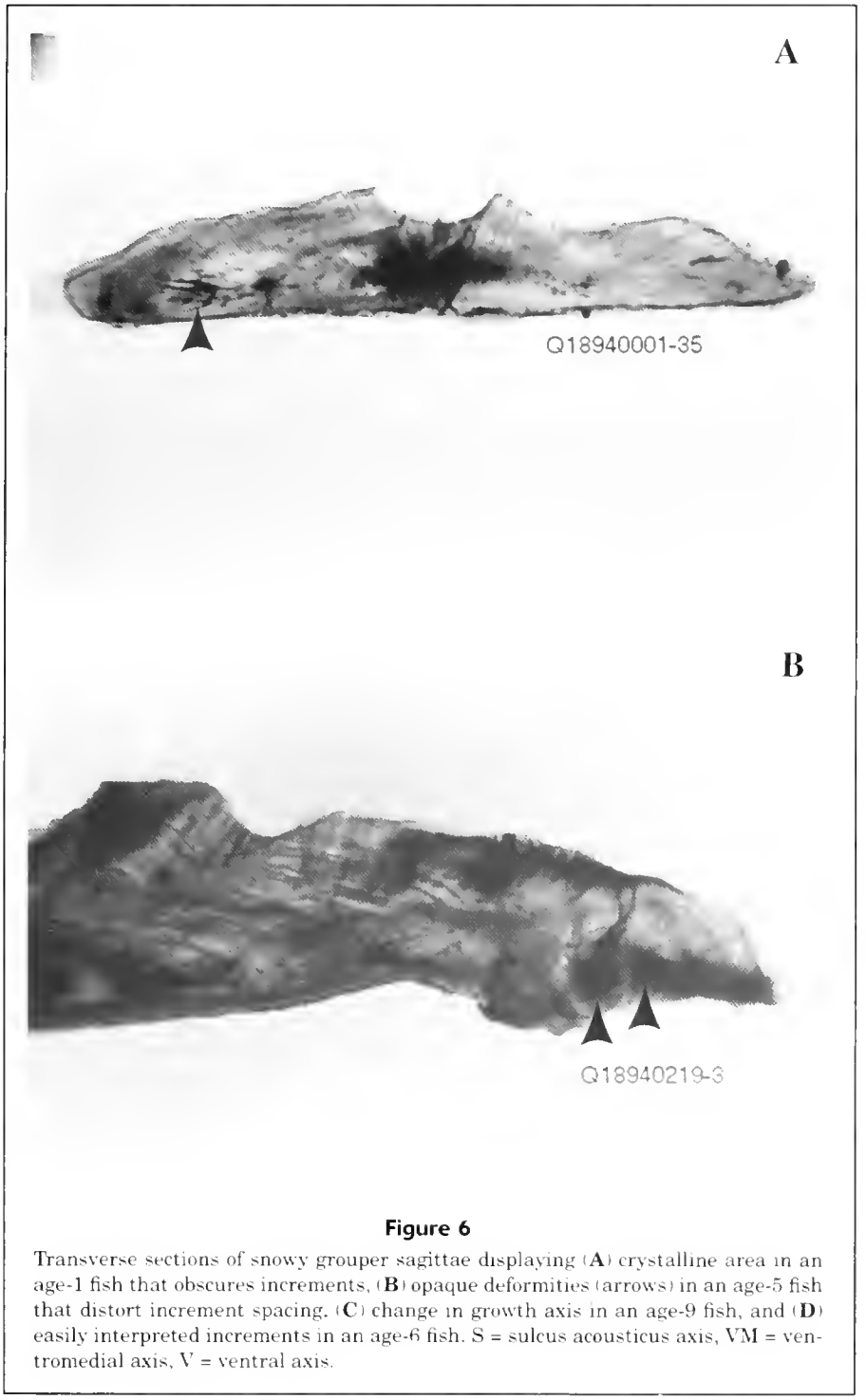

Figure 6

Transverse sections of snowy grouper sagittae displaying (**A**) crystalline area in an age-1 fish that obscures increments, (**B**) opaque deformities (arrows) in an age-5 fish that distort increment spacing, (**C**) change in growth axis in an age-9 fish, and (**D**) easily interpreted increments in an age-6 fish. S = sulcus acousticus axis, VM = ventromedial axis, V = ventral axis.

Males were collected during March through September and their length range was 767–1090 mm (median=918, $\bar{x}$=919 mm, SE=7). Age was assessed for 47 males and ranged from 8 to 29 yr (median=16, $\bar{x}$=16.87, SE=0.63). Transitional specimens (787 mm and unknown age, 1000 mm and age 13) were collected in July and September. The 787 mm specimen was in the latter stage of sexual change (Fig. 7); male tissue was predominant, although previtellogenic oocytes were still numerous.

The near overlap in the length distributions of female snowy grouper that were definitely mature and females that were resting indicated that specimens were correctly assigned to immature and rest-

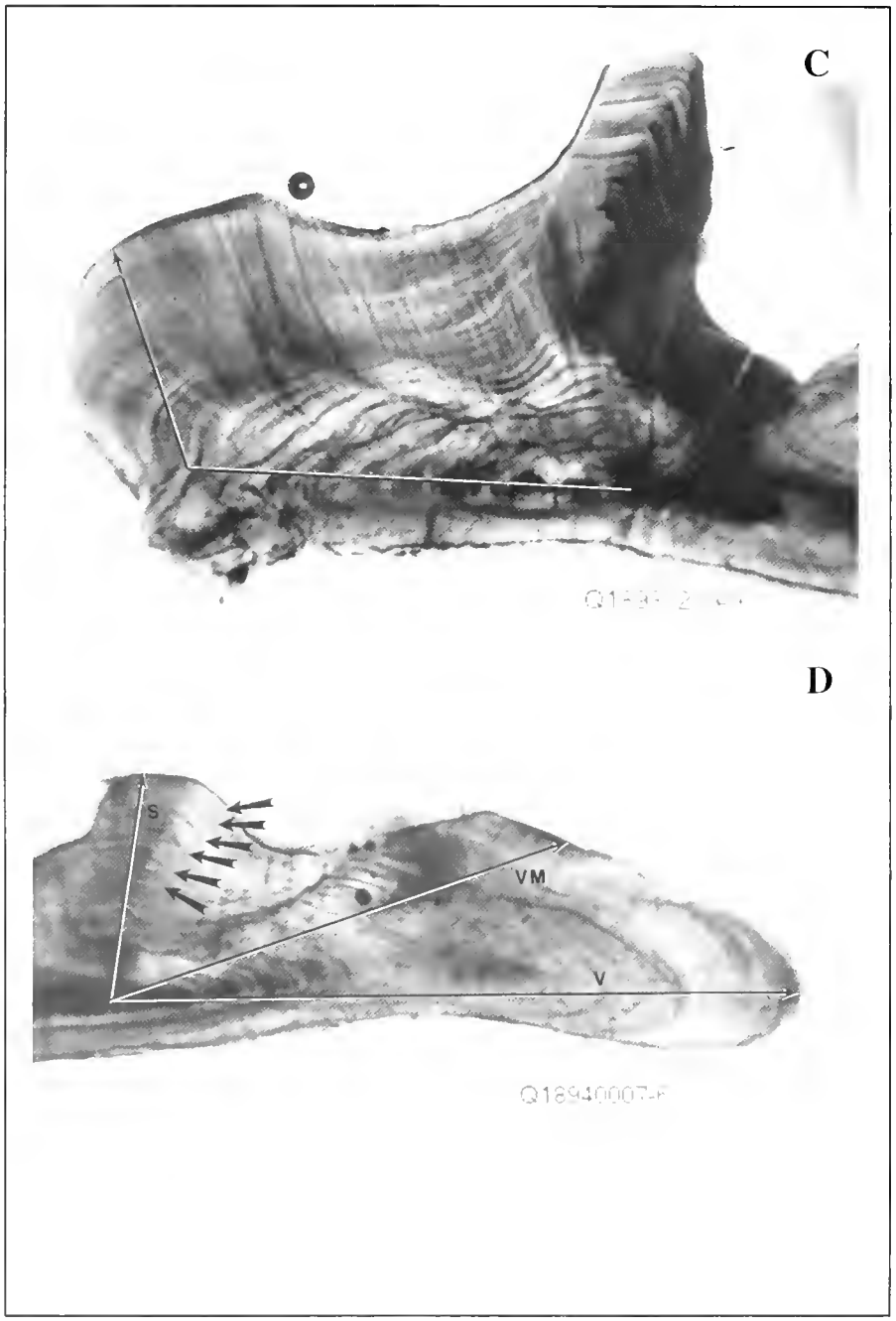

ing categories (Fig. 8); only 29 females of uncertain maturity were excluded from analyses. Samples collected primarily with longlines and chevron traps in 1991–95 revealed that snowy grouper become sexually mature at lengths of 451 to 575 mm (ages 3–7; Tables 8 and 9). Mature gonads were present in 4% of females at age 3, 52% at age 5, 95% at age 7, and 100% at ages >7 (Table 9). The smallest mature female was 469 mm, and the largest immature female was 575 mm. Estimates of L_{50} and A_{50} were 541 mm (gompit model; 95% CI=529–553 mm) and 4.92 yr (probit model; 95% CI=4.65–5.21 yr).

Samples collected primarily with bandit reels and longlines in 1980–85 showed that snowy grouper reached sexual maturity at similar lower limits of length and age, 476–500 mm and age 3, although sample sizes were small (<10) in the length and age intervals near the lower limit (Tables 8 and 9). Upper limits of size and age at maturity were higher, 626–650 mm and age 9, during this period and better defined owing to larger sample sizes in comparison to those for 1991–95. Mature gonads were present in 33% of females at age 3, 62% at age 5, 91% at age 7, 95% at age 9, and 100% at ages >9 (Table 9). The smallest

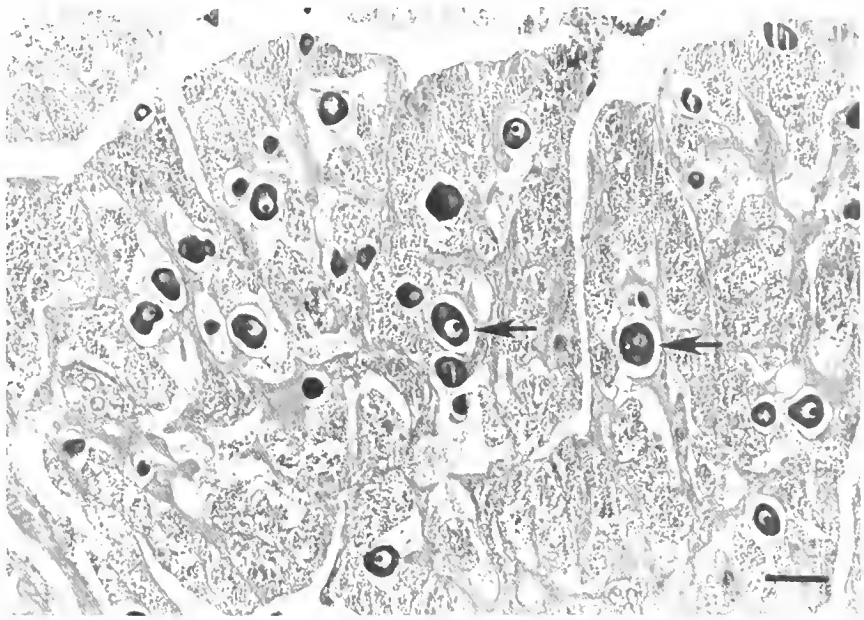

Figure 7

Histological section of gonad tissue from a 787-mm-TL snowy grouper captured in July in which transition to male is nearly completed. Chromatin nucleolar (arrows) and perinucleolar oocytes are still present. Bar = 100µ.

Table 7

Sex ratios of snowy grouper, *Epinephelus niveatus*, (M= male; F=female; T=transitional) collected off North Carolina and South Carolina during 1973–94. Ratios based on sexually mature individuals. LL=longline; KP=Kali pole.

Gear and source	Period	*n*	%*M*	%*F*	%*T*
Rod and reel headboat	1973–81	83	7.2	91.6	1.2
Snapper reels commercial, research	1980–84	281	19.5	80.5	0.0
LL, KP, research	1982–85	153	22.9	76.4	0.7
LL, commercial	1993–94	82	1.2	98.8	0.0

mature female was 483 mm, and the largest immature female was 634 mm. The estimate of L_{50} was 486 mm (logit model; 95% CI=449–509 mm) and A_{50} was not estimated owing to the absence of specimens younger than age 3. A third data set, specimens collected by NMFS during 1973–81 primarily from headboats, exhibited a pattern of size at maturity similar to that found for the 1980–85 samples, though sample sizes were <10 in every length interval and only three specimens were <551–575 mm (Table 8).

Snowy grouper were in spawning condition from April through September based on the presence of hydrated oocytes (Fig. 9A) and postovulatory follicles (Fig. 9B), with no obvious peak period (Fig. 10). Given the small sample sizes for October through March, the spawning season could be longer. Ninety-nine female specimens were captured in spawning condition. Seventy-two percent of the specimens were collected on research vessels off South Carolina (32°28' to 32°50'N) at depths of 176–232 m, primarily during May and July through September. The remaining 27 fish in spawning condition were collected during April through August on headboats off South Carolina, on research vessels off North Carolina between Cape Fear and Cape Lookout, and by commercial fishermen on the upper continental slope off North and South Carolina; exact location data were not recorded. Commercial fishermen reported approximate locations of 32°36' to 33°51'N and depths of 189–302 m for spawning fish.

Trawl collections during exploratory squid cruises in June 1978 also provided evidence that snowy grouper spawn on the upper continental slope (Fig. 1). Four large catches (1160 fish/8776 kg), which were made at depths of 180–316 m off North Carolina, South Carolina, and Georgia (not shown), ranged from 90 to 520 snowy grouper per tow. Tow distance ranged from 7.4 to 18.5 km and estimates of snowy grouper density ranged from 2.2 fish/ha to 10.9 fish/ha (13.5 kg/ha to 79.5 kg/ha). Although the reproduc-

Table 8

Percentage of mature specimens by length interval for female snowy grouper collected off North Carolina and South Carolina with 1) primarily bandit reels and longlines during 1980–85, 2) primarily longlines and chevron traps during 1991–95, and 3) primarily from headboats during 1973–81. Specimens in the developing, ripe, spent, or resting stages were considered mature. All specimens were examined histologically. n = number of specimens.

mm TL	1980–85 n = 372 % (n)	1991–95 n = 235 % (n)	1973–81 n = 74 % (n)
251–275	0 (1)	0 (3)	—
276–300	—	0 (6)	—
301–325	0 (1)	0 (10)	—
326–350	0 (1)	0 (12)	—
351–375	—	0 (10)	0 (1)
376–400	0 (5)	0 (11)	—
401–425	0 (3)	0 (11)	—
426–450	0 (1)	0 (17)	0 (1)
451–475	0 (2)	4 (22)	—
476–500	67 (6)	35 (17)	—
501–525	88 (8)	18 (17)	—
526–550	80 (15)	29 (7)	0 (1)
551–575	100 (20)	70 (20)	100 (7)
576–600	90 (21)	100 (13)	86 (7)
601–625	92 (24)	100 (9)	100 (6)
626–650	97 (31)	100 (12)	100 (8)
651–675	100 (25)	100 (7)	100 (9)
676–700	100 (31)	100 (7)	100 (7)
701–725	100 (39)	100 (7)	100 (3)
726–750	100 (35)	100 (4)	100 (6)
751–775	100 (28)	100 (3)	100 (7)
776–800	100 (15)	100 (1)	100 (3)
801–1025	100 (59)	100 (3)	100 (8)
No length	100 (1)	100 (5)	—

tive stage of individual fish was not determined, it was noted that milt flowed freely from males in a collection of 420 fish from a depth of 278 m off South Carolina (32°57' to 33°02'N). Nearly all of the specimens were sexually mature as the mean lengths of subsamples collected off North Carolina and off South Carolina and Georgia combined were 67.3 (48–96 cm; n=89) and 79.2 (60–97 cm; n=98), respectively.

Depth distribution

There was a moderately positive trend (r^2=0.53) between water depth and total length in fishery-independent samples. Snowy grouper were caught at depths of 46–258 m. Larger adults were caught more frequently in upper continental slope waters >100 m,

Table 9

Percentage of mature specimens by age class for female snowy grouper collected off North Carolina and South Carolina with 1) primarily bandit reels and longlines during 1980–85, and 2) primarily longlines and chevron traps during 1991–95. Specimens in the developing, ripe, spent, or resting stages were considered mature. All specimens were examined histologically. n = number of specimens.

Age (yr)	1980–85 n = 219 % (n)	1991–95 n = 197 % (n)
1	—	0 (5)
2	—	0 (22)
3	33 (3)	4 (26)
4	80 (5)	23 (43)
5	62 (8)	52 (40)
6	86 (21)	83 (29)
7	91 (32)	95 (21)
8	93 (30)	100 (7)
9	95 (20)	100 (1)
10	10 (26)	100 (1)
11	100 (15)	100 (1)
>11	100 (59)	100 (1)

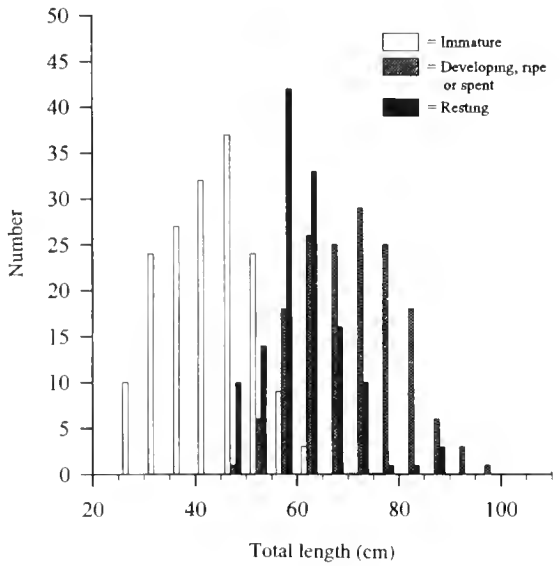

Figure 8

A comparison of length-frequency histograms for snowy grouper specimens collected during 1973–95 that were categorized as immature (n=166), definitely mature (n=158), or resting (n=130). Definitely mature specimens were developing, ripe, or spent.

whereas small adults and juveniles (<600 mm) were caught more frequently at depths <100 m (Fig. 11).

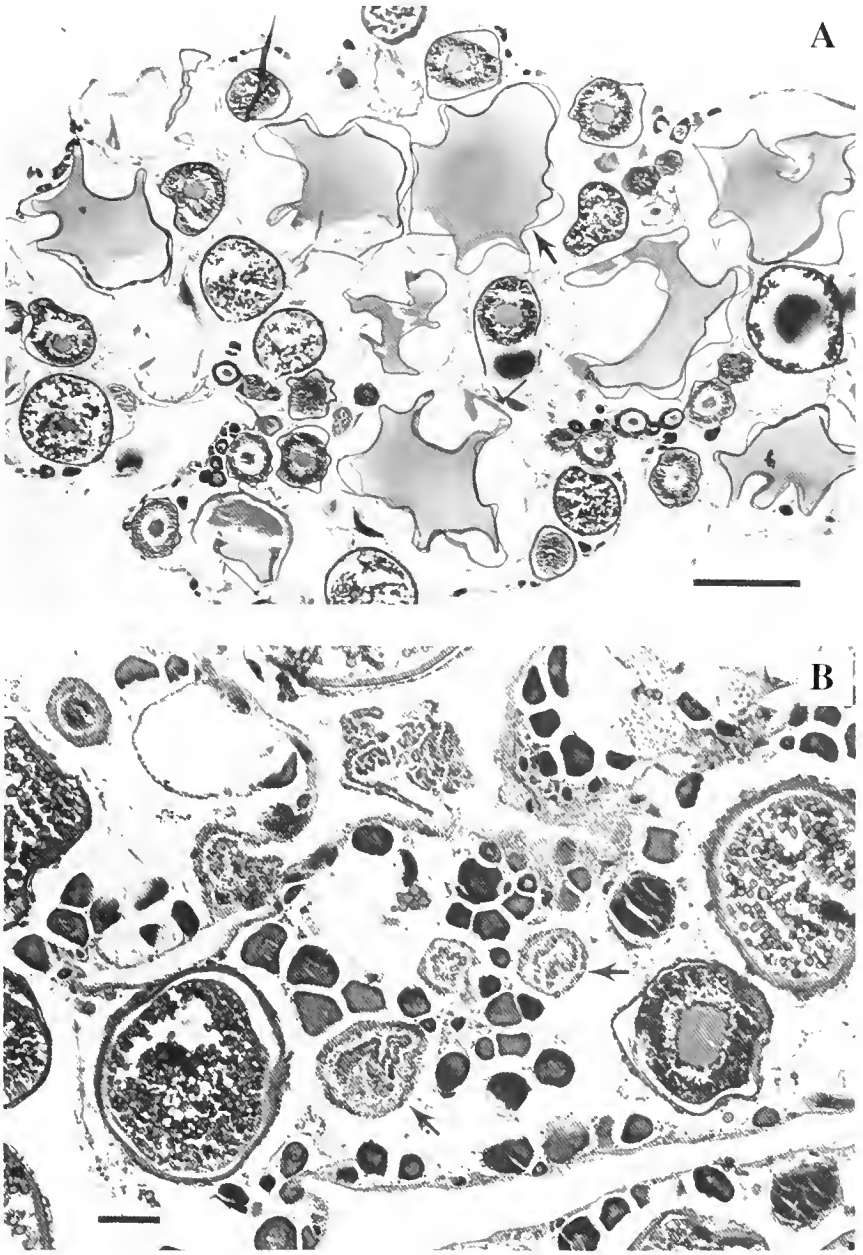

Figure 9

Histological sections of ovarian tissue from female snowy grouper with evidence of imminent or recent spawning: (**A**) hydrated oocytes (arrow) in a 744-mm-TL specimen captured in May (bar=400μ), and (**B**) age 24–48 h postovulatory follicles (arrows) in a 546-mm-TL specimen captured in August (bar=100 μ).

The fishery

Historically, most snowy grouper landings along the Atlantic coast of the United States, as reported through TIP, have occurred in North Carolina and South Carolina (Fig. 12). Although landings statistics are reported by state, fish are often caught throughout the region, especially by vessels fishing with longlines. Landings have varied widely, with peaks noted in 1983 and 1990 for South Carolina and in 1990 and 1992 for North Carolina. These fluctuations have often been the result of changes in effort. For example, the peak in 1983 reflected an approximate doubling in the number of vessels as

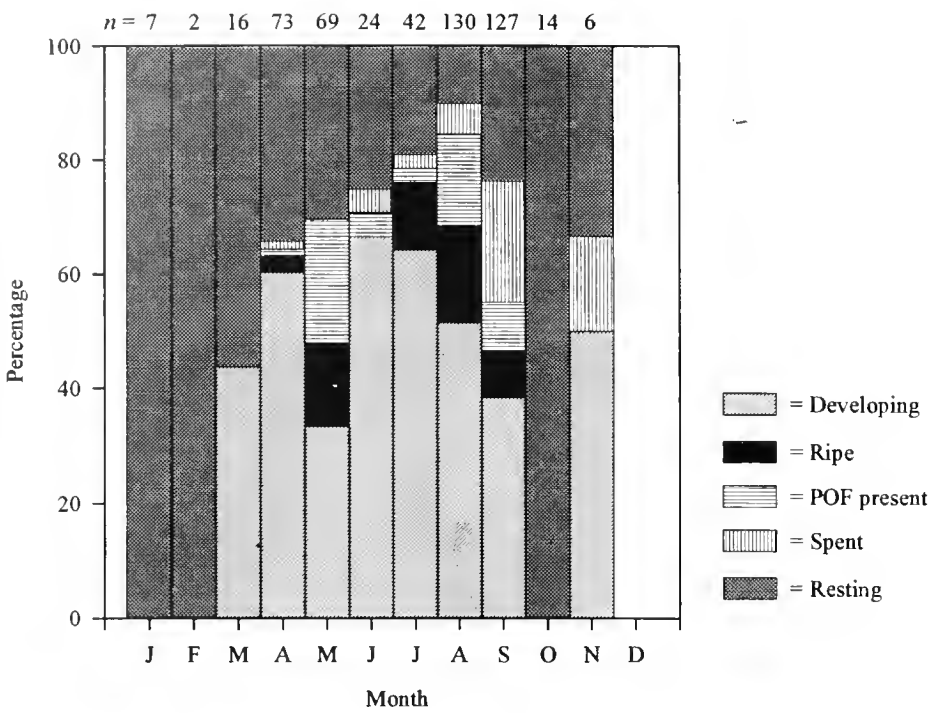

Figure 10

Percentage composition (based on histological criteria) of reproductive stages by month for 510 female snowy grouper. Number of specimens examined is above each bar. POF = postovulatory follicle.

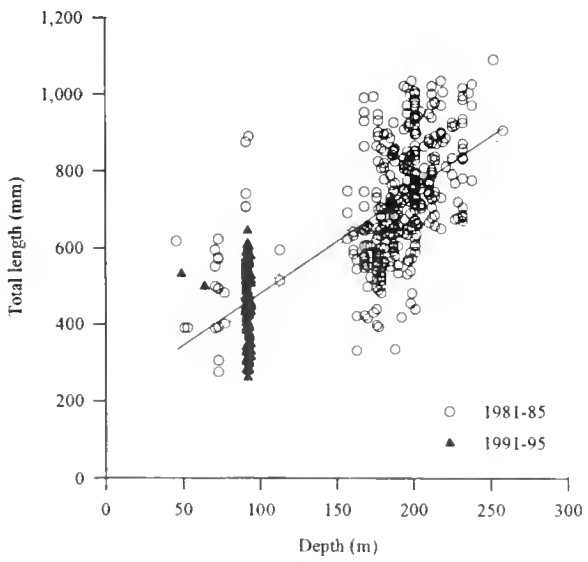

Figure 11

Relationship between length of snowy grouper and depth of capture in fishery-independent sampling off North Carolina and South Carolina primarily with longlines, Kali poles, and snapper reels during 1981–85 (n=359) and primarily with chevron traps during 1991–95 (n=114).

the bottom longline fishery developed. The decreases in 1984 and 1985 reflect a shift in effort to the pelagic longline fishery for swordfish (Low et al., 1987).

In South Carolina, the mean length of snowy grouper caught with longlines decreased steadily from 66 to 72 cm during 1983–84 to a low of 49 cm in 1996 (Fig. 13). No trend was evident in the length data for snowy grouper caught with snapper reels. The snowy grouper caught with snapper reels were consistently smaller than those caught with longlines because snapper reels were deployed in shallower water (Fig. 14).

Length data from North Carolina for snowy grouper caught with longlines showed a similar decreasing trend, though with greater interannual variation (Fig. 15). The mean length of snowy grouper caught with snapper reels has fluctuated, with peaks noted in 1985 and 1993.

Discussion

Status of the fishery

There are several indications that the snowy grouper population off the Carolinas is overfished: 1) size

at age of specimens caught with longlines and snapper reels has increased noticeably since the 1980s (Table 3), which could be a density-dependent population response to a decrease in competition for resources, 2) 81% of the specimens caught with longlines were ages 1–6, the majority (56%) of which were immature females (Tables 4 and 9), 3) the percentage of males appears to have decreased significantly, from 7% to 23% in the 1970s and 1980s to 1% in the 1990s (Table 7), 4) spawning stock ratio for the snowy grouper population in the South Atlantic Bight was 0.15 in the most recent assessment (SAFMC, 1993)—below the 0.30 level which means that the SAFMC considers the stock overfished, and 5) mean length of fish landed in the longline fishery has steadily decreased from 65 to 80 cm in the early 1980s to 50–60 cm in the mid-1990s (Figs. 13 and 15; see also Low, 1998).

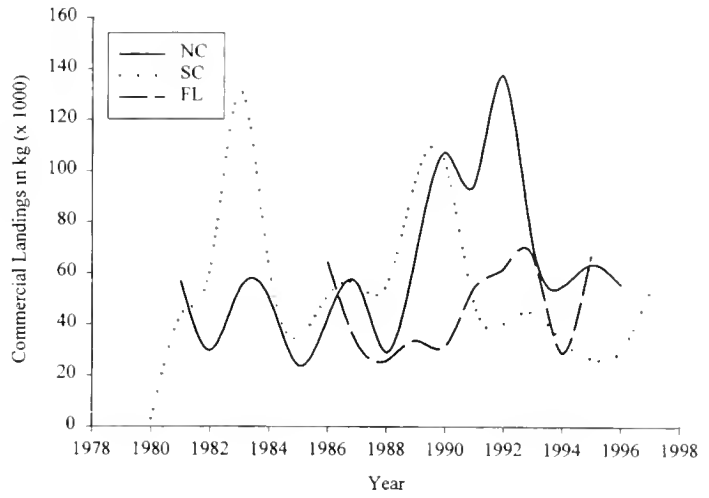

Figure 12

Commercial landings of snowy grouper in North Carolina, South Carolina, and Florida for all gear types, primarily longlines and snapper reels. Data were collected in individual states through their Trip Interview Program (TIP).

Snowy grouper are susceptible to rapid depletion in a localized area through fishing efforts. A study on a previously unexploited deep reef off North Carolina found that fishing can remove 3% of the reef population daily (Epperly and Dodrill, 1995). In less than three months, the catch per unit of effort and mean size of snowy grouper at that reef were reduced to levels comparable to other exploited sites. The mean size of snowy grouper landed in North and South Carolina during most of the 1990s (Figs. 13 and 15) is comparable to the size Epperly and Dodrill (1995) reported for exploited sites.

The increase in size at age over a ten-year period for fish from both gear types is noteworthy because this trend has been documented in populations that had experienced moderate to high levels of fishing mortality. Increases in size at age have been noted for silver hake (Helser and Almeida, 1997) and Atlantic halibut (Haug and Tjemsland, 1986) in the north Atlantic and several reef fish species (gag, red grouper, and red porgy) off the southeast coast of the United States and in the Gulf of Mexico (Johnson et al., 1993; Johnson and Collins, 1994; Harris and McGovern, 1997; Goodyear and Schirripa[3]). In our study, the increase in size at age may represent density-dependent growth in response to an increase in fishing mortality (Rothschild, 1986). Decreases in the abundance (Low, 1998) of co-occurring species on a similar trophic level, such as gray tilefish (*Caulolatilus microps*) and tilefish (*Lopholatilus chamaeleonticeps*), also may reduce competition for food and shelter in deepwater habitats. Snowy grouper and gray tilefish feed on macroinvertebrates, particularly crabs (Brachyura), and fishes closely associated with the substrate (Ross, 1982; Dodrill et al., 1993).

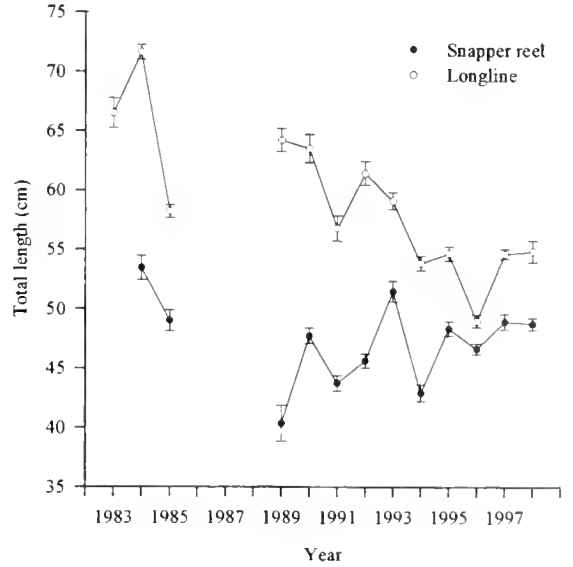

Figure 13

Mean length (±SE) of snowy grouper landed in South Carolina in the longline and snapper reel fisheries. Data were collected through the Trip Interview Program (TIP) at the South Carolina Department of Natural Resources. Sample sizes ranged from 22 to 851.

Density-dependent increases in growth rate generally indicate that a population or community is heav-

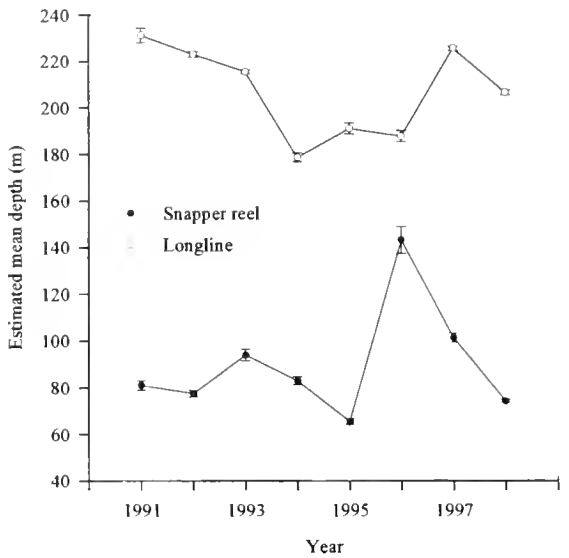

Figure 14

Estimated mean water depth (±SE), based on minimum and maximum depths provided by captains, during fishing efforts in the longline and snapper reel fisheries. Data were collected through the Trip Interview Program (TIP) at the South Carolina Department of Natural Resources from vessels landing their catches in South Carolina. Sample sizes ranged from 141 to 851.

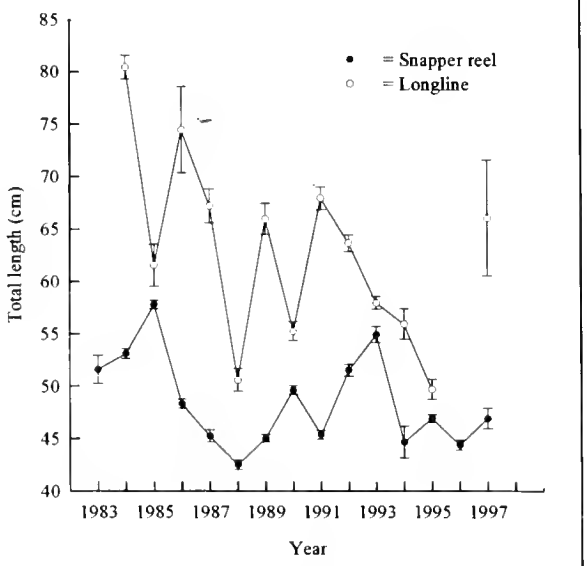

Figure 15

Mean length (±SE) of snowy grouper landed in North Carolina in the longline and snapper reel fisheries. Data were collected through the Trip Interview Program (TIP) at the North Carolina Department of Health, Environment, and Natural Resources. Sample sizes ranged from 5 to 1908 fish.

ily exploited and possibly overexploited. A situation of greater concern would be one where size at age has decreased after a sustained high level of fishing-induced mortality, as has been reported for red porgy, *Pagrus pagrus*, and vermilion snapper, *Rhomboplites aurorubens*, in our study region (Harris and McGovern, 1997; Zhao et al., 1997). There is evidence that faster-growing individuals in the populations of red porgy and vermilion snapper have been effectively eliminated, thus causing a decrease in size at age. Red porgy exhibited a density-dependent response after an initially high level of fishing mortality, but the sustained high level of mortality eventually removed the faster-growing individuals. Size at age should be monitored to ensure that this does not occur in the snowy grouper population.

The age composition of the snowy grouper landings also needs to be monitored because the longline fishery is presently supported by younger age classes (1–6). The present study showed that snowy grouper can attain an age of 29 yr, but only 19% of the fish caught on longlines were >age 6 (Table 4). The low percentage of older age classes in the landings supports the preliminary sex ratio data from the 1990s, showing that the percentage of males had significantly decreased.

Age and growth

A comprehensive comparison of growth data in our study with previously published results was not possible because 1) lack of large and old specimens and small sample sizes, and 2) differences in study area (Florida Keys in Moore and Labisky [1984]). One or more of these factors could explain the differences in size at age, k, and L_∞ between the results of two published studies (Matheson and Huntsman, 1984; Moore and Labisky, 1984) and our results for longline and snapper reel data from the 1980s. A primary reason for higher values of L_∞ in the published studies (Table 3) is that the growth curves do not exhibit asymptotes, which is probably due to low numbers of specimens greater than approximately 900 mm and older than 15–17 yr. In our study, all the data sets (2 bandit reel and 2 longline) had individuals over 1000 mm and at least 21 yr old. Sample sizes in two data sets were very small (<200): our longline or Kali pole data set (n=163) and the data set of back calculations (n=118) in Moore and Labisky (1984). Important factors that could not be evaluated on the basis of previous publications were 1) similarity of fishing gear, 2) method of increment interpretation, and 3) whether or not a weighting factor was used when fitting the von Bertalanffy growth model.

We feel confident that our assessment of the age structure in the snowy grouper population off the Carolinas was accurate, even though interpretation of growth increments was difficult and a minimal number of YOY specimens was available. The difficulty of assigning an age to the sagittae of snowy grouper had not been reported by other investigators, although it has been reported for other deepwater species of continental slopes. The clarity of the hyaline and opaque zones in otoliths (presumably sagittae) from hoki, *Macruronus novaezelandidae*, off New Zealand is highly variable and is divided into six categories based on internal features which are related to the ease of counting increments (Kuo and Tanaka, 1984). When otoliths are difficult to interpret, one option is to base population age structure only on the specimens for which age is easily assessed. Alternatively, ages can be estimated for nearly all specimens despite the difficulties, as we did in our study, with the assumption that the larger sample will represent the population better. We found that limiting the data set to only those specimens for which the difference in counts between readers was 0–1 increments did not improve the accuracy of the age-length key for specimens caught with longlines (Table 6). Thus, we advocate using the entire sample of specimens assigned an age. Crabtree and Bullock (1998) found that rejected otoliths tend to be from slower-growing older specimens, which could introduce bias into analyses. This bias was minimal in their study of growth in black grouper, *M. bonaci*, where each otolith was examined three times by two independent readers. Parameter estimates for the von Bertalanffy model based on all black grouper with ages were within one standard error of those based only on specimens for which the coefficient of variation of the six readings was ≤12%.

An important consideration in age determination is positive identification of the first annulus and any settling mark that may be deposited prior it. We believe that we have identified the first annulus because the largest YOY specimen (172 mm) had an estimated age of 191–291 days and the measurements of otolith radius for all YOY (n=3) were less than radial measurements to the first annulus in a subsample of 23 specimens that were age 1. Evidence to support our conclusion that these three specimens were YOY was found in another sampling effort, where six specimens 4–5 cm in length were caught with a trawl during August and September (Machowski[5]), the last two months of the spawning season. Moore and Labisky (1984) considered 150–175 mm specimens to be YOY, although they did not examine daily increments.

Validation of a technique for aging snowy grouper with otoliths has been weakly supported by previous studies. We found that marginal increments form annually and there is a peak in April and May that corresponds to the beginning of the spawning season. This finding concurs with the limited results of Matheson and Huntsman (1984) and Moore and Labisky (1984) who found that increment formation appeared to begin in April and peaked in June. Matheson and Huntsman (1984) measured marginal increments in 18 specimens collected during April through October and Moore and Labisky (1984) examined specimens collected during March through July (n not reported). Waltz[4] found a wider period of increment formation, April through September, although he was not able to conclude that increments form annually because samples were lacking for four months.

Reproduction

The reproductive pattern of snowy grouper needs to be investigated more comprehensively and the sex ratio should be assessed again, given the small sample size in 1993–94 (n=82), because there is evidence that reef fish species, particularly grouper, which change sex and aggregate to spawn, are more susceptible to size-selective mortality and overexploitation (Bannerot, 1987; Huntsman and Schaaf, 1994; Coleman et al., 1996). The capture of only one male in the 1993–94 samples, which appeared to be representative of the population based on commercial landings, is reason for concern because the percentage of males has apparently decreased from the 7–23% for samples collected with three gear types in the 1970s and 1980s (Table 7).

Large decreases in the number of males have been documented for two other grouper species in the southeast region. Percentages of males in populations of gag and scamp in the Gulf of Mexico, groupers that are known to form small spawning (10's to 100's of individuals) aggregations, decreased from 17% to 1% and 38% to 18%, respectively, between the 1970s and early 1990s (Coleman et al., 1996). A similar decrease, from 20% to 6%, was noted for gag along the Atlantic coast of the southeastern United States during the same period (McGovern et al., 1998). The resultant decrease in genetic diversity has been documented for gag (Chapman et al., 1999), and its ramifications are currently of great concern to many fishery scientists in the southeast region.

The size (767–1090 mm) and age (8–29 yr) of 97 male specimens in the present study and the capture

[5] Machowski, D. 1998. S. Carolina Department of Natural Resources, P.O. Box 12559, Charleston, SC, 29422. Personal commun.

of two specimens in the process of changing from female to male is conclusive evidence that snowy grouper are protogynous hermaphrodites. Moore and Labisky (1984) reported males as young as age 6 and some males with evidence of recent sex change. It is likely that we collected only two transitional specimens because sex change occurs after a female finishes spawning, during months when sample sizes in our study were small. Sex change in other grouper species, gag for example, occurs primarily during the first two to three months after the spawning season (McGovern et al., 1998), before males and females become spatially separated (Coleman et al., 1996).

Our findings on age at maturity and spawning season are in general agreement with the results of Moore and Labisky (1984) for snowy grouper in the Florida Keys. They found that the smallest mature female and largest immature female were age 3 and age 5, respectively, whereas the smallest mature female from 1980 to 1985 in our study was also age 3, but small percentages (<10%) of the age 7–9 females were immature (Table 9). Females and males in the Florida Keys were in spawning condition from April through July, although no mature fish were sampled in other months (Moore and Labisky, 1984). We found that females off the Carolinas spawn from April through September—possibly longer owing to small sample sizes in October through March.

The capture of 1160 specimens, some of which were assessed macroscopically as spawning, in four trawl collections on the exploratory squid cruise in June 1978 suggests that snowy grouper may form spawning aggregations. Estimates of density would have been much higher than 13.5–79.5 kg/ha calculated from the trawl data if the fish were caught in only a small part of the area sampled during tows of 7.4–18.5 km. Dodrill and Epperly (1995) reported that the initial density of exploitable snowy grouper on a 2700-m^2 virgin reef off North Carolina was 11 kg/m^2.

Depth distribution

Fishery-independent data collected over several years and with various gear types show that fish length is positively correlated with water depth (Fig. 11). Longlines, Kali poles, and snapper reels were the primary gear types deployed in waters >150 m and the waters <100 m were sampled primarily with chevron traps. Chevron traps are not known to be selective for snowy grouper <600 mm. Dodrill et al. (1993) speculated that the low abundance of adults in shallow waters may in part reflect years of intensive fishing pressure in 40–120 m depths and only relative recent fishing activity at depths >183 m off North Carolina. Alternatively, we propose that snowy grouper may migrate to deeper water toward the end of the juvenile stage.

Fish length and water depth data from the commercial fisheries (Figs. 13 and 14) concurred with the positive correlation noted in the Florida Keys (Moore and Labisky, 1984) and off Georgia and South Carolina (Low and Ulrich, 1983), although depth data from fishermen may be less accurate than fishery-independent data. We found small juveniles in shallow water, a finding that agrees with the results of Moore and Labisky (1984) and with observations from submersible dives that documented juvenile snowy grouper (<300 mm) between 46 and 91 m, but not in deeper waters (Parker[6]).

Accurate assessment of population parameters requires knowledge of juvenile and adult distributions of snowy grouper as well as characteristics of the fishery. The snapper reel fishery catches a greater proportion of younger age classes than does the longline fishery because fishing efforts are generally restricted to areas <100 m in depth (Figs. 13 and 14). The longline fishery presently catches a greater proportion of older age classes than does the snapper reel fishery because regulations established by the SAFMC restrict longlines to waters deeper than 91 m.

Conclusions

As other investigators have suggested, rebuilding grouper populations may require a novel approach such as long-term area closures or individual transferable quotas (Epperly and Dodrill, 1995; Coleman et al., 1996). At present, the regulations enacted to rebuild the snowy grouper population include an annual quota of 245,082 kg, with a trip limit of 1134 kg (SAFMC, 1993). Traditional management measures such as minimum size limits will not be effective because snowy grouper experience fatal embolisms while being brought to the surface from deep waters (Matheson and Huntsman, 1984). Future research should focus on improving our understanding of reproductive pattern (e.g. spawning behavior, spatial and temporal aspects of distribution) and include a thorough assessment of sex ratio and an updated assessment of population age structure.

Acknowledgments

We thank F. Rhode, J. Francesconi, and other assisting members of the North Carolina Department of Health,

[6] Parker, R., Jr. 1997. National Marine Fisheries Service, 101 Pivers Island Rd., Beaufort, NC, 28516. Personal commun.

Environment and Natural Resources for obtaining otoliths and gonads from snowy grouper in North Carolina. In South Carolina, the personnel of the MARMAP program of the S.C. Department of Natural Resources assisted with port sampling. Captains D. Juel, S. Juel, J. Murray, S. Shelley, and the late J. D. Skipper III let us remove otoliths from their catches of snowy grouper and brought in whole specimens for the study of reproductive biology. We very much regret the loss of Captain Skipper, his vessel, and a crew member. C. Jackson and T. Prince of the Southport Fish Market, and F. McGinn and R. McGinn of the Little River Fish House, allowed us to process specimens at their businesses. R. Dixon and G. Huntsman provided gonad samples collected by the National Marine Fisheries Service Beaufort Laboratory. K. Grimball and O. Pashuk prepared the histological sections. B. Zhao generated the parameter estimates for the von Bertalanffy model. T. Azarovitz, T. Reisinger, and D. Machowski contributed to the retrieval of data from the 1978 squid cruise originally collected by E. Gutherz. Earlier drafts of the manuscript were examined by P. Harris, J. McGovern, and three anonymous reviewers. This project was funded through the National Marine Fisheries Service MARFIN grant NA37FF0046-01 and the MARMAP contract 50WCNF006002.

Literature cited

Bannerot, S., W. W. Fox Jr., and J. E. Powers.
1987. Reproductive strategies and the management of snappers and groupers in the Gulf of Mexico and Caribbean. *In* J. J. Polovina and S. Ralston (eds.), Tropical snappers and groupers: biology and fisheries management, p. 561–603. Westview Press, Boulder, CO.

Bennett, B. M., and P. Hsu.
1960. On the power function of the exact test for the 2×2 contingency table. Biometrika 47:393–397.

Chapman, R. W., G. R. Sedberry, C. C. Koenig, and B. M. Eleby.
1999. Stock identification of gag, *Mycteroperca microlepis*, along the southeast coast of the United States. Mar. Biotechnol. 1:137–146.

Coleman, F. C., C. C. Koenig, and L. A. Collins.
1996. Reproductive styles of shallow-water groupers (Pisces: Serranidae) in the eastern Gulf of Mexico and the consequences of fishing spawning aggregations. Environ. Biol. Fishes 47:129–141.

Collins, M. R.
1990. A comparison of three fish trap designs. Fish. Res. 9:325–332.

Crabtree, R. E., and L. H. Bullock.
1998. Age, growth, and reproduction of black grouper, *Mycteroperca bonaci*, in Florida waters. Fish. Bull. 96:735–753.

Dodrill, J., C. S. Manooch III, and A. B. Manooch.
1993. Food and feeding behavior of adult snowy grouper, *Epinephelus niveotus* (Valenciennes) (Pisces: Serranidae), collected off the central North Carolina coast with ecological notes on major food groups. Brimleyana 19:101–135.

Epperly, S. P, and J. W. Dodrill.
1995. Catch rates of snowy grouper, *Epinephelus niveatus*, on the deep reefs of Onslow Bay, southeastern U.S.A. Bull. Mar. Sci. 56:450–461.

Fitch, J. E., and S. A. Schultz.
1978. Some rare and unusual occurrences of fishes off California and Baja California. Calif. Fish Game 64:74–92.

Harris, P. J., and J. C. McGovern.
1997. Changes in the life history of the red porgy, *Pagrus pagrus*, from the southeastern United States, 1972–1994. Fish. Bull. 95:732–747.

Haug, T., and J. Tjemsland.
1986. Changes in size- and age-distributions and age at sexual maturity in Atlantic halibut, *Hippoglossus hippoglossus*, caught in north Norwegian waters. Fish. Res. 4:145–155.

Hayes, D. B.
1993. A statistical method for evaluating differences between age-length keys with application to Georges Bank haddock, *Melanogrammus aeglefinus*. Fish. Bull. 91:550–557.

Helser, T. E., and F. P. Almeida.
1997. Density-dependent growth and sexual maturity of silver hake in the north-west Atlantic. J. Fish Biol. 51:607–623.

Hunter, J. R., and S. R. Goldberg.
1980. Spawning incidence and batch fecundity in northern anchovy, *Engraulis mordax*. Fish. Bull. 77:641–652.

Hunter, J. R., and B. J. Macewicz.
1985. Rates of atresia in the ovary of captive and wild northern anchovy, *Engraulis mordax*. Fish. Bull. 83:119–16.

Huntsman, G. R.
1976. Offshore headboat fishing in North Carolina and South Carolina. Mar. Fish. Rev. 38(3):13–23.

Huntsman, G. R., and W. E. Schaaf.
1994. Simulation of the impact of fishing on reproduction of a protogynous grouper, the graysby. North Am. J. Fish. Manage. 14:41–52.

Johnson, A. G., and L. A. Collins.
1994. Age-size structure of red grouper, *Epinephelus morio*, from the eastern Gulf of Mexico. Northeast Gulf Sci. 13:101–106.

Johnson, A. G., L. A. Collins, and J. J. Isley.
1993. Age-size structure of gag, *Mycteroperca microlepis*, from the northeastern Gulf of Mexico. Northeast Gulf Sci. 13:59–63.

Kuo, C. L., and S. Tanaka.
1984. Otolith features and reliability for age-determination of hoki, *Macruronus novaezelandidae* (Hector), in waters around New Zealand. Bull. Jpn. Soc. Sci. Fish. 50:1349–1355.

Lee, T. N., V. Kourafalou, J. D. Wang, W. J. Ho, J. O. Blanton, L. P. Atkinson, and L. J. Pietrafesa.
1985. Shelf circulation from Cape Canaveral to Cape Fear during winter. *In* L. P. Atkinson, D. W. Menzel, and K. A. Bush (eds.), Oceanography of the southeastern U.S. continental shelf, p. 33–62. American Geophysical Union, Washington, D.C.

Low, R. A.
1998. South Carolina marine fisheries, 1996. South Carolina Mar. Resour. Center Data Rep. 27, 78 p.

Low, R. A., and G. F. Ulrich.
1983. Deep-water demersal finfish resources and fisheries off South Carolina. South Carolina Mar. Resour. Center Tech. Rep. 57, 24 p.

Low, R. A., D. Theiling, and E. B. Joseph.
1987. South Carolina marine fisheries. South Carolina Mar. Resour. Center Tech. Rep. 67, 78 p.

Matheson, R. H., III, and G. R. Huntsman.
1984. Growth, mortality, and yield-per-recruit models for speckled hind and snowy grouper from the United States South Atlantic Bight. Trans. Am. Fish. Soc. 113:607–616.

McGovern, J. C., D. M. Wyanski, O. Pashuk, C. S. Manooch, III, and G. R. Sedberry.
1998. Changes in the sex ratio and size at maturity of gag, *Mycteroperca microlepis*, from the Atlantic coast of the southeastern United States during 1976–1995. Fish. Bull. 96:797–807.

Miller, D. J., and R. N. Lea.
1976. Guide to the coastal marine fishes of California. Calif. Dep. Fish Game Fish Bull. 157, 235 p.

Moore, C. M., and R. F. Labisky.
1984. Population parameters of a relatively unexploited stock of snowy grouper in the lower Florida Keys. Trans. Am. Fish. Soc. 113:322–329.

Parker, R. O., Jr., and R. W. Mays.
1998. Southeastern United States deepwater reef fish assemblages, habitat characteristics, catches, and life history summaries. U.S. Dep. Commer., NOAA Tech. Rep. NMFS 138, 41 p.

Parker, R. O., Jr., and S. W. Ross.
1986. Observing reef fishes from submersibles off North Carolina. Northeast Gulf Sci. 8:31–49.

Ross, J. L.
1982. Feeding habits of the gray tilefish, *Caulolatilus microps* (Goode and Bean, 1878) from North Carolina and South Carolina waters. Bull. Mar. Sci. 32:448–454.

Rothschild, B. J.
1986. Dynamics of marine fish populations. Harvard Univ. Press, Cambridge, MA, 277 p.

Russell, G. M., E. J. Gutherz, and C. A. Barans.
1988. Evaluation of demersal longline gear off South Carolina and Puerto Rico with emphasis on deepwater reef fish stocks. Mar. Fish. Rev. 50(1):26–31.

SAFMC (South Atlantic Fishery Management Council).
1991. Amendment 4, regulatory impact review, initial regulatory flexibility analysis and environmental assessment for the snapper grouper fishery of the South Atlantic region, 177 p. SAFMC, Charleston, SC.
1993. Amendment 6, regulatory impact review, initial regulatory flexibility analysis and environmental assessment for the snapper grouper fishery of the south Atlantic region, 202 p. SAFMC, Charleston, SC.

SAS Institute, Inc.
1990. SAS/STAT® user's guide, version 6, part 2, 4th ed., 1686 p. SAS Institute, Cary, NC.

Schmidt, D. J., M. R. Collins, and D. M. Wyanski.
1993. Age, growth, maturity, and spawning of Spanish mackerel, *Scomberomorus maculatus* (Mitchill), from the Atlantic coast of the southeastern United States. Fish. Bull. 91:526–533.

Secor, D. H., J. M. Dean, and E. H. Laban.
1992. Otolith removal and preparation for microstructural examination. *In* D. K. Stevenson and S. E. Campana (eds.), Otolith microstructure examination and analysis, p. 19–57. Can. J. Fish. and Aquat. Sci. Special Publ. 117.

Siegel, S.
1956. Nonparametric statistics for the behavioral sciences. McGraw-Hill, New York City, NY, 312 p.

Smith, C. L.
1971. A revision of the American groupers: *Epinephelus* and allied genera. Bull. Am. Mus. Nat. Hist. 146:228–241.

von Bertalanffy, L.
1938. A quantitative theory of organic growth. II. Inquiries on growth laws. Human Biol. 10:181–213.

Wallace, R. A., and K. Selman.
1981. Cellular and dynamic aspects of oocyte growth in teleosts. Am. Zool. 21:325–343.

Wenner, C. A., W. A. Roumillat, and C. W. Waltz.
1986. Contributions to the life history of black sea bass, *Centropristis striata*, off the southeastern United States. Fish. Bull. 84:723–741.

West, G.
1990. Methods of assessing ovarian development in fishes: a review. Aust. J. Mar. Freshwater Res. 41:199–222.

Zhao, B., J. C. McGovern, and P. J. Harris.
1997. Age, growth, and temporal change in size at age of the vermilion snapper from the South Atlantic Bight. Trans. Am. Fish. Soc. 126:181–193.

Notes on the biology of *Cephalurus cephalus* and *Parmaturus xaniurus* (Chondrichthyes: Scyliorhinidae) from the west coast of Baja California Sur, México

Eduardo F. Balart
División de Biología Marina, Centro de Investigaciones Biológicas del Noroeste, S.C.
Apdo. Postal 128, La Paz, B.C.S., México 23000
E-mail address: ebalart@cibnor.mx

Jeanette González-García
Carlos Villavicencio-Garayzar
Laboratorio de Elasmobranquios, Universidad Autónoma de Baja California Sur
Apdo. Postal 19-B, La Paz, B.C.S., México 23000

The head, or lollipop, shark *(Cephalurus cephalus)* and filetail catshark *(Parmaturus xaniurus)* are found in the eastern Pacific in waters ranging from 245 to 828 m and from 91 to 1251 m depth, respectively (Castro, 1983). Little is known of their biology because they are rarely captured. *Cephalurus cephalus* is a benthic catshark and has been recorded from southern California, Gulf of California, the Revillagigedo Archipelago, and off the coasts of Peru and Chile (Kato et al., 1967; Meléndez and Meneses, 1989; Pequeño, 1989). Mathews and Ruíz (1974) reported it from the upper Gulf of California, México, and Castro-Aguirre (1981) gave basic information about its morphology, taxonomy, and ecology based on 11 specimens from this locale.

Parmaturus xaniurus is distributed from central California to the Gulf of California (Castro, 1983). Cross (1988) has described its general biology and Lee (1969) reported that, in the Santa Barbara basin, it consumed myctophids. Cailliet[1] concluded that juveniles were mesopelagic, adults demersal, and noted that efforts to determine their age have failed because of the absence of annual rings on the vertebrae.

The objective of this study was to provide additional data on the biology of *C. cephalus* and *P. xaniurus*, with information on length-weight relationships, and notes on reproductive biology, including the sizes of oocytes and embryos, the sex ratio of embryos, and clasper length, for specimens from the west coast of Baja California Sur, México.

Materials and methods

Fish were sampled by bottom trawling with commercial shrimp nets (20-m mouth, 30-mm mesh size) during the oceanographic expedition EP9505 along the Pacific coast of Baja California Sur, México. Trawls were made at depths of 50–280 m from the RV *El Puma* during May 1995. On 5 May two scyliorhinid species (*C. cephalus* and *P. xaniurus*) were collected and whole specimens were frozen. All specimens were captured at the following three stations: 26°01.9'N, 113°26.9'W (280 m); 25°59.6'N, 113°20.5'W (260 m); 26°00.7'N, 113°18.3'W (230 m). Bottom temperature at the collection sites was 10.0°C. Total weight (W, g), and total length (TL, mm) were recorded. Females were dissected, the diameter of all visible oocytes were recorded, and embryos were removed. For the subsequent analysis of *C. cephalus*, previously published data were also used. The length-weight relationship was determined with STATISTICA software (StatSoft, Inc., 1995) by using the exponential function of the form

$$W = aTL^b,$$

as used by Cross (1988) for the filetail catshark. Length-weight relationships were compared between males and females by using an analysis of covariance.

Results and discussion

Seventy-five catsharks were obtained: 51 *P. xaniurus* and 24 *C. cephalus*. The latter species is recorded for the first time along the west coast of the Baja California peninsula. At one station, *C. cephalus* was captured together with *P. xaniurus*, as reported by Mathews and Ruiz (1974). Other organisms collected at the three stations were the fishes *Merluccius angustimanus*, *Physiculus rastrelliger*, *Kathetostoma averruncus*, *Synodus lucioceps*, *Hippoglossina stomata*, and *Lepophidium* spp., and the crustaceans *Pleuroncodes planipes* and *Cancer johngarthii*.

Cephalurus cephalus

Of the 24 specimens, 23 were female, with a range of 224 and 295 mm TL ($\bar{x}$=249 mm TL). The single male specimen was 298 mm TL. Previously reported maximum total

[1] Cailliet, G. 1981. Ontogenetic changes in the depth distribution and feeding habits of two deep-dwelling demersal fishes of California: sablefish and filetail cat sharks. Paper presented at the sixty-first annual meeting of the Am. Soc. Ichtyol. Herpetol.

Manuscript accepted 17 August 1999
Fish. Bull. 98:219–221 (2000).

lengths for females and males were 295 and 245 mm TL respectively (Castro-Aguirre, 1981). The length-weight relationship suggested allometric growth and was described by the following equation

$$W = 0.000012\ TL^{2.84} \qquad \text{(Fig. 1A)}.$$

The b coefficient was not significantly different ($F_{1,36}$= 2.15) between the sexes.

Females of this species have two functional ovaries and oviducts. Sixteen (70%) of the females had mature oocytes in their ovaries and a mean oocyte diameter of 10.5 mm (range 2.0–21.8 mm). The relationship of mean oocyte diameter with TL indicated that all females were mature (Fig. 1B). The size at first maturity has previously been estimated to be 190 mm TL (Compagno, 1984). The large diameter of the oocytes suggested that spawning occurs in early summer.

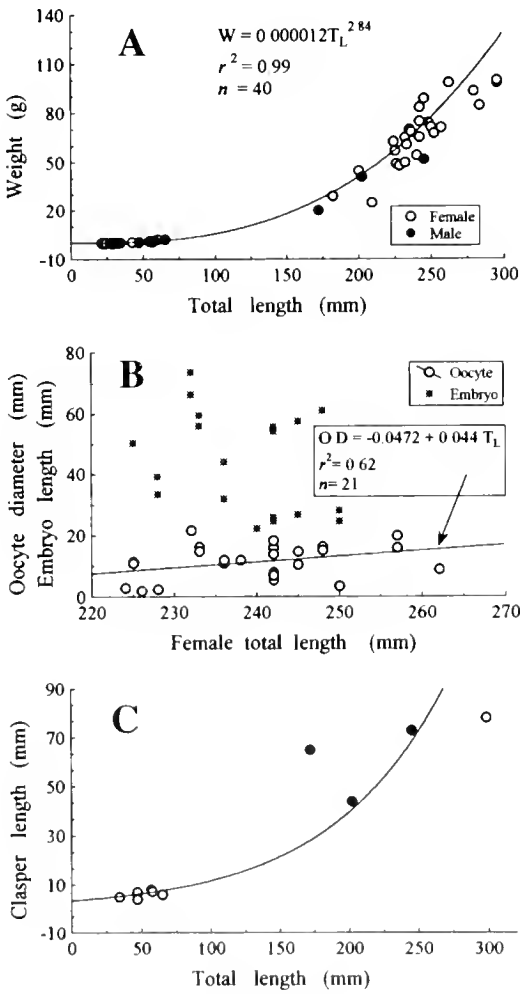

Figure 1

Cephalurus cephalus. (**A**) Length-weight relationship. (**B**) Relationships between oocyte diameter and embryo total length with female total lengths. (**C**) Relationship between total length and clasper length. Data less than 75 mm TL are from embryonic material. Data from Castro-Aguirre (1981) are denoted by solid circles.

Embryonic development of *C. cephalus* occurs in the uterine tract and is described as aplacental viviparity or ovoviviparity (Wourms, 1977, 1981; Compagno, 1984). The thin-walled egg cases of *C. cephalus*, which are retained in the oviducts, were observed in 11 individuals. The three largest females had neither eggs in the oviducts nor large oocytes in their ovaries and may have finished their reproductive cycle.

The mean size of the 19 embryos was 43 mm TL (size range 21 to 65 mm TL), which is less than the estimated size at birth (100 mm; Compagno, 1984), and the sex ratio of embryos (9 males, 10 females) was aproximately equal. The relation between clasper length and total length of adults and embryos is illustrated in Figure 1C.

Parmaturus xaniurus

Of 51 specimens captured, 22 were female and 29 were male. Females measured 108 to 350 mm TL ($\bar{x}$=184 mm TL), males 117 to 380 mm TL ($\bar{x}$=233 mm TL). The largest recorded lengths are 574 mm TL for females and 600 mm TL for males (Springer, 1979). The length-weight relationship of *P. xaniurus* indicated allometric growth (Fig. 2A) and was described by the following equation:

$$W = 5.5 \times 10^{-7}\ TL^{3.34}.$$

The analysis by sex (males: W= 6.76 × 10^{-7} $TL^{3.31}$; females: W=9.53 × 10^{-7} $TL^{3.22}$) did not reveal significant differences in the b coefficient ($F_{1,45}$=0.14) as reported by Cross (1988) for specimens from the upper continental slope off southern California.

All females examined were immature and did not contain mature oocytes. Cross (1988) noted that females first reached maturity at 425–475 mm TL in southern California waters. *Parmaturus xaniurus* is oviparous, and the egg cases of this species have been described by Cox (1963). Embryonic development lasts approximately one year (Compagno, 1984; Cross, 1988). The relationship between total length and clasper length suggested that males matured at 340 mm TL (Fig. 2B), and this size at first maturity was smaller than that previously recorded (375 to 425 mm TL; Cross, 1988). This may reflect latitudinal differences in the reproductive biology of *P. xaniurus*.

Acknowledgments

We thank Edgar Amador, Carolina Downton, Dinorah Herrero, M. Angeles Cobarrubias, and Carmiña A.

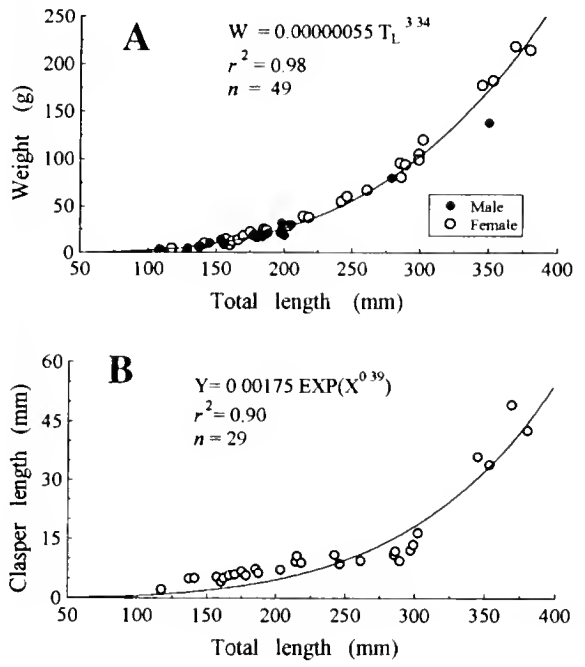

Figure 2

Parmaturus xaniurus. (**A**) Length-weight relationship. (**B**) Relationship between total length and clasper length.

Fernández, and the crew of the RV *El Puma* who were always helpful in our work. We gratefully acknowledge the valuable comments of Gregor Cailliet, Robert N. Lea, Jim Ellis. and two anonymous referees. We thank Ellis Glazier for editing the text in English. We also thank the Universidad Nacional Autónoma de México, especially Ingvar Emilsson, for supporting the projects of CIBNOR, UABCS, and CICIMAR and providing the RV *El Puma* for the cruise EP9505 at no cost.

Literature cited

Castro, J. I.
1983. The sharks of North american waters. Texas, A&M. University Press, Austin, TX, 180 p.

Castro-Aguirre, J. L.
1981. Especies de la Familia Scyliorhinidae (Elasmobranchii, Galeoidea), de la Costa Occidental de México, con especial referencia a *Cephalurus cephalus* (Gilbert). An. Esc. Nac. Cienc. Biól. Méx. 24:71–93.

Compagno, L. J. V.
1984. FAO species catalogue. Sharks of the world: an annotated and illustrated catalogue of shark species known to date. Part 2: Carcharhiniformes. FAO Fish. Biol. Synop. (125), vol. 4, pt 2: 251–655.

Cox, K. W.
1963. Egg-cases of some elasmobranchs and a cyclostome from California waters. Calif. Fish and Game 49(4):271–289.

Cross, J. N.
1988. Aspects of the biology of two scyliorhinid sharks, *Apristurus brunneus* and *Parmaturus xaniurus*, from the upper continental slope off southern California. Fish. Bull. 86 (4):691–702.

Kato, S., S. Springer, and M. H. Wagner.
1967. Field guide to Eastern Pacific and Hawaiian sharks. U.S. Fish and Wildl. Serv., Circ. 271:1–47.

Lee, R. S.
1969. The filetail catshark, *Parmaturus xaniurus*, in midwater in the Santa Barbara basin off California. Calif. Fish and Game 55(1):88–90.

Mathews, C. P., and M. F. Ruiz.
1974. *Cephalurus cephalus*, a small shark, taken in the northern Gulf of California, with a description. Copeia 1974(2): 556–560.

Meléndez, C. R., and D. R. Meneses.
1989. Tiburones del talud continental recolectados entre Arica (18°19'S) e Isla Mocha (38°30'S), Chile. Invest. Mar., Valparaíso, 17:3–73.

Pequeño, R. G.
1989. Peces de Chile. Lista sistemática revisada y comentada. Rev. Biol. Mar. 24(2):1–132.

Springer, S.
1979. A revision of the catsharks, family Scyliorhinidae. U.S. Dep. Commer., NOAA Tech. Rep. NMFS Circ. 422, 152 p.

StatSoft, Inc.
1995. STATISTICA for Windows. StatSoft, Inc., Tulsa, OK, 3782 p.

Wourms, J. P.
1977. Reproduction and development in chondrichthyan fishes. Am. Zool. 17:379–410.

1981. Viviparity: the maternal-fetal relation in fishes. Am. Zool. 2:473–515.

Penaeid shrimp landings in the upper Gulf of California in relation to Colorado River freshwater discharge

Manuel S. Galindo-Bect
Instituto de Investigaciones Oceanologicas
Universidad Autonoma de Baja California
Km 103 carretera Tijuana-Ensenada
Ensenada, Baja California, México

Edward P. Glenn
Environmental Research Laboratory
2601 East Airport Drive
Tucson, Arizona 85706
E-mail address (for E. P. Glenn, contact author): eglenn@ag.arizona.edu

Henry M. Page[1]
Kevin Fitzsimmons[2]
Luis A. Galindo-Bect[3]
Jose M. Hernandez-Ayon[3]
Robert L. Petty[1]
Jaqueline Garcia-Hernandez[2]
David Moore[2]

A commercial trawl fishery in the upper Gulf of California provides the principle source of income for the coastal communities of the region, but catches of estuarine-dependent crustaceans and fish have declined in recent years (Hernan, 1997; Cudney-Bueno and Turk-Boyer, 1998). Declines in shrimp landings, mainly *Litopenaeus stylirostris* (formerly classified as *Penaeus stylirostris*) (Perez-Farfante and Kinsley, 1997) have been attributed primarily to over-exploitation of the resource and to viral diseases (Rosas-Cota et al., 1996; Hernan, 1997).

The Biosphere Reserve of the upper Gulf of California and Colorado River Delta was created in 1993 to address some fisheries management problems. A more fundamental problem, however, may be the lack of river flow after construction of upstream dams. Historic reductions in river discharge have caused dramatic increases in salinity in the estuary and changes in the distribution of nutrients (Alvarez-Borrego et al., 1975; Hernandez-Ayon et al., 1993). Since 1979, occasional flood releases have entered the upper Gulf of California by means of the Colorado River when upstream impoundments are filled (Glenn et al., 1996).

Effects of freshwater on penaeid shrimp population development are controversial (Garcia and Le Reste, 1981; Day et al., 1989), but recruitment of spawning stocks of white shrimp (*Penaeus setiferus*) has been positively correlated with river discharge in the southwestern Gulf of Mexico and has been attributed to an expansion in estuarine nursery habitat for white shrimp (Garcia, 1991). River discharge also can stimulate the migration of subadults from estuaries (Deben et al., 1990; Vance et al., 1998). Fishermen have a strong perception that shrimp and fish catches in the northern Gulf of California are related to freshwater discharge from the Colorado River (Cudney-Bueno and Turk-Boyer, 1998). To evaluate their perception we conducted a correlation analysis of shrimp landings at San Felipe Baja California (nearest shrimping station to the delta) with freshwater discharges from the Colorado River to the northern Gulf of California.

Materials and methods

Data on annual shrimp landings and number of trawlers legally fishing from San Felipe were obtained from the Secretary of Environment, Natural Resources and Fish (SEMARNAP), San Felipe, Mexico. Landings were available from 1977 and number of trawlers from 1982. The artisanal catches by small boats (pangas) or the significant illegal shrimp fishery are not accounted for in reported shrimp landings. Annual shrimp landings serve as indicators of the variability in the total landings and are reported for all species of shrimp, even though landings are >90% *L. stylirostris* in San Felipe (Rosas-Cota et al., 1996). Data on freshwater discharge of the Colorado River were from the Southerly International Border (S.I.B.) gauging station which is below the last diversion on the river and were obtained from the United States

[1] Marine Science Institute
University of California
Santa Barbara, California 93106
[2] Environmental Research Laboratory
2601 East Airport Drive
Tucson, Arizona 85706
[3] Instituto de Investigaciones Oceanologicas
Universidad Autonoma de Baja California
Km 103 carretera Tijuana-Ensenada
Ensenada, Baja California, México

Manuscript accepted 25 August 1999.
Fish. Bull. 98:222–225 (2000).

Bureau of Reclamation, Yuma, Arizona (Williams[1]). We assumed that this flow entered the delta and the upper Gulf of California.

Annual shrimp landings and landings divided by numbers of trawlers (normal catch per unit of effort, CPUE) were correlated with river flow and number of trawlers. Our normal CPUE was a crude approximation of stock abundance or catchability. We lacked actual fishing time (days, weeks, hours of net deployment), size frequency of the legal vessels, and number of small boats (pangas) fishing. We made landings lag river discharge by one year because the life cycle of shrimp from hatching to capture is approximately one year (Gracia-Pamanes[2]). Transformed river flow ($\log_{10}$) was tested for nonlinearity; then we conducted a multiple regression analysis to predict shrimp landings from variables that were individually correlated ($P<0.05$) with landings.

Results

Annual shrimp landings ranged from 701 metric tons (t) (1983–84) to 217 t (1992–93), decreasing significantly from 1977 to 1996 ($r=0.78$, $P<0.001$, Fig. 1A). The reported number of trawlers legally fishing from San Felipe ranged from a high of 59 in 1988 to a low of 20 in 1995 (Fig. 1B). Catch per unit of effort (CPUE) increased from 1982 to 1984, then markedly decreased back to the 1982–83 level in 1985, remaining low until 1993, after which a positive trend was achieved and the highest CPUE ever was recorded in 1995 (Fig. 1C). There were substantial flows (>700 million cubic meters, Mm^3) in 8 of the 21 years from 1976 to1996 and varied over 10^4-fold, ranging from 1 Mm^3 in 1990 and 1996 to 15,657 Mm^3 in 1984 (Fig. 1D). Highest volume occurred between 1980 and 1987 as a result of overflow from Lake Powell in the United States (Glenn et al., 1996). The flow spike in 1993 was due to releases from Painted Rock Dam on the Gila River in Arizona. Periods of significant river flow at the S.I.B. were closely matched to El Nino Southern Oscillation (ENSO) events that occurred in 1983 and 1993.

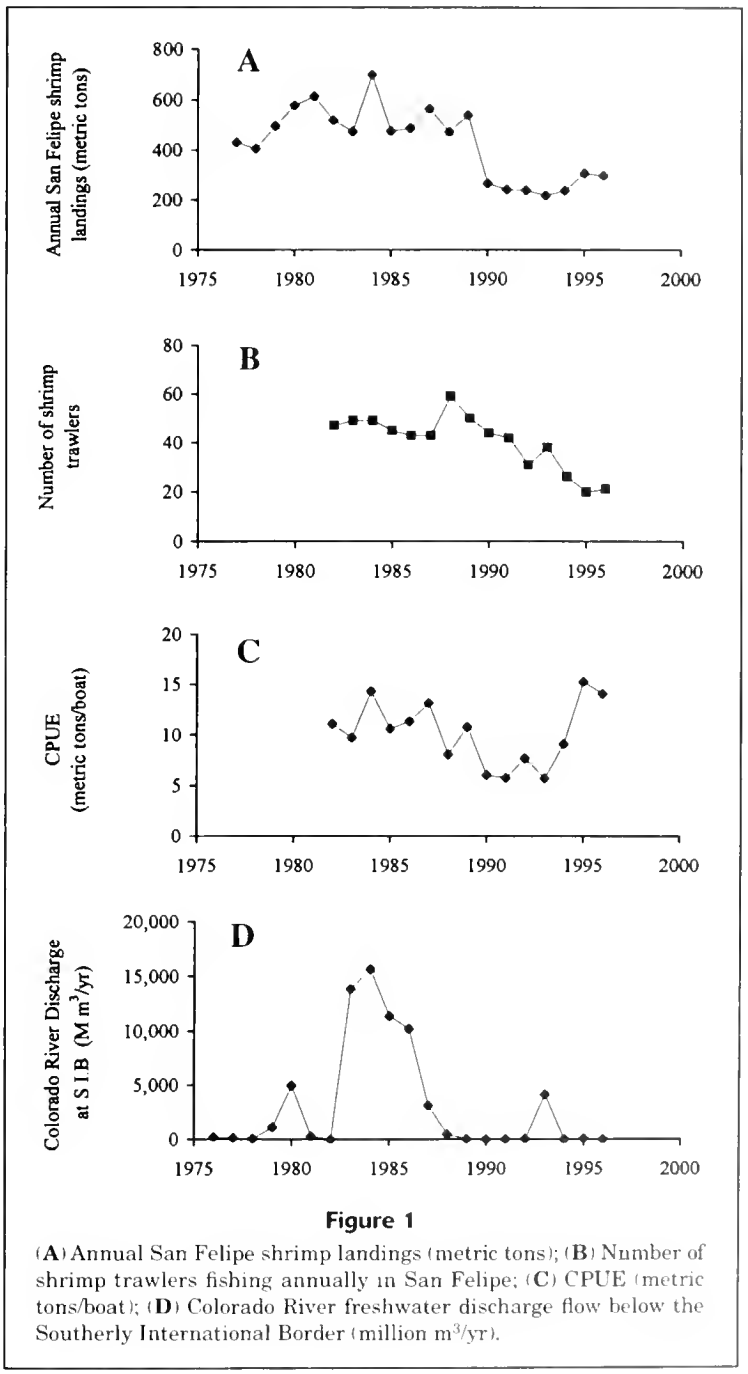

Figure 1

(**A**) Annual San Felipe shrimp landings (metric tons); (**B**) Number of shrimp trawlers fishing annually in San Felipe; (**C**) CPUE (metric tons/boat); (**D**) Colorado River freshwater discharge flow below the Southerly International Border (million m^3/yr).

Shrimp landings were significantly ($P<0.05$) correlated with same year river discharge, but $\log_{10}$-transformed river discharge in the year prior to shrimp harvest produced the highest correlation coefficient ($r=0.67$, $P<0.001$) (Table 1). The number of trawlers also significantly correlated with shrimp landings ($r=0.77$, $P<0.001$), as expected. The best correlation (r) of shrimp landings was the product

[1] Williams, B. 1998. United States Bureau of Reclamation, Yuma, Arizona. Personal commun.

[2] Garcia-Pamanes, F. C. 1992. Biologia reproductiva y dinamica poblacional del camaron azul Penaeus stylirostris en el Alto Golfo de California. Instituto de Investigaciones Oceanologicas, Universidad Autonoma de Baja California, Ensenada. Unpubl. final report.

Table 1

Correlation coefficients (r) and significance levels (P) from regression analysis relating San Felipe annual shrimp landings (1977–96) and CPUE (1982–96) to rainfall and discharge of the Colorado River at the Southern International Border. A "1-year lag" indicates that shrimp landings were paired with the previous year's river discharge in the correlation analysis.

	Correlation with shrimp landings		Correlation with CPUE	
Variable	r	P	r	P
River discharge	0.47	0.0362	0.25	0.3360
Log_{10} river discharge	0.54	0.0112	0.25	0.3368
River discharge (1-yr lag)	0.52	0.0127	0.34	0.1826
Log_{10} of river discharge (1-yr lag)	0.67	0.0006	0.38	0.1304
Number of shrimp trawlers	0.77	0.0003	0.18	0.4804
Log_{10} of river discharge (1-yr lag) × number of shrimp trawlers	0.80	0.0004	0.29	0.8771

of log_{10}-lagged river discharge and number of trawlers (r=0.80, P<0.001). CPUE was not significantly (P>0.05) correlated with river flow or number of trawlers (Table 1), nor with total landings (r=–0.26, P=0.31). The equation of best fit (0.64) for predicting shrimp landings took the form

$$Y = a + m(X_1X_2),$$

where X_1 = log_{10}-lagged river discharge (Mm^3/yr);
X_2 = number of trawlers;
Y = shrimp landings (t/yr);
M = the slope of the equation (1.67); and
a = the Y-intercept (232 t/yr).

Discussion

Our analyses represent a first attempt to identify relationships between variability in shrimp landings in the upper Gulf of California and factors influencing these landings. Total shrimp landings and the size of the shrimping fleet at San Felipe have declined over the past 15 years. Social and economic changes have affected shrimping. In the late 70s and early 80s shrimping was reserved for social units (cooperatives), with the result that privately owned shrimp trawlers were banned from the fishery. In addition, the government subsidized building of additional vessels and many new unskilled fishermen entered the industry. Then policies were reversed in the late 1980s, private boats returned, interest rates increased, and many of the shrimp trawlers were removed from the fleet.

We found a significant relationship (P<0.001) between total catch and the rate of freshwater discharge of Colorado River water into the marine ecosystem, although the mechanisms through which river discharge might affect the shrimp fishery are unknown. Lower salinity may improve the survival of early life stages by providing "enlarged nursery" protected habitat (Garcia, 1991), even though *L. stylirostris* and *P. californiensis* are generally considered euryhaline species (Hernan, 1997), having large numbers of postlarvae and juveniles in hypersaline habitats (Brusca, 1980; Page[3]). Salinity and nutrient gradients in the estuary and upper Gulf during river flows have not been reported to our knowledge.

Future plans for the Colorado River will likely decrease freshwater discharge into the estuary as more water is diverted upstream for farms and domestic use (Morrison et al., 1996). Our analyses suggest that decreases in river discharge to the delta and estuary may adversely affect shrimp landings. The United States and Mexican governments should initiate a research program on the effects of river flow on ecologically and commercially important species in the upper Gulf of California and incorporate these findings into a comprehensive management plan for the Biosphere Reserve as well as the Colorado River Basin at large.

Literature cited

Alvarez-Borrego, S., B. P. Flores-Báez, and L. A. Galindo-Bect.
1975. Hidrología del Alto Golfo de California II. Condiciones durante invierno, primavera y verano. Ciencias Marinas 2(1):21–36.

Brusca, R. C.
1980. Common intertidal invertebrates of the Gulf of California. Univ. Arizona Press, Tucson, AZ, 513 p.

[3] Page, M. 1999. Marine Science Institute, University of California, Santa Barbara, CA 93106. Unpubl. data.

Cudney-Bueno, R., and P. J. Turk-Boyer.
1998. Pescando entre mareas del Alto Golfo de California. Centro Intercultural de Estudios de Desiertos 7 Oceanos, Puerto Penasco, Sonora, Mexico, 166 p.

Day, J. W., Jr., C. A. S. Hall, W. M. Kemp, and A. Yanez-Aranchibia.
1989. Estuarine ecology. Wiley, New York, NY, 558 p.

Deben, W., W. Clotheir, G. Ditsworth and D. Baumgartner.
1990. Spatiotemporal flucuations in the distribution and abundance of demersal fish and epibenthic crustaceans in Yaquina Bay, Oregon. Estuaries 13(4):469–478.

Garcia, A.
1991. Spawning stock recruitment relationships of white shrimp in the southwestern Gulf of Mexico. Trans. Am. Fisheries Soc. 120(4):519–527.

Garcia, S., and L. Le Reste.
1981. Life cycles, dynamics, exploitation and management of coastal penaeid shrimp stocks. FAO Fish. Tech. Paper 203, 215 p.

Glenn, E. P., Ch. Lee, R. Felger, and S. Zengel.
1996. Effects of water management on the wetlands of the Colorado River Delta, Mexico. Conserv. Biol. 10(4):1175–1186.

Hernan, A.
1997. Morphologic and genetic characterization of wild populations of shrimp of the genus *Penaeus* within the Gulf of California, Mexico: new social, political and management dilemmas for the Mexican shrimp fishery. Univ. of Arizona, Tucson, AZ, 323 p.

Hernández-Ayno, J. M., M.S. Galindo-Beet, B.P. Flores-Báez, and S. Alvarez-Borrego.
1993. Nutrient concentrations are high in the turbid waters of the Colorado River Delta. Estuarine Coastal Shelf Sci., 37:593–602.

Morrison, J., S. Postel, and P. Gleick.
1996. The sustainable use of water in the Lower Colorado River Basin. Pacific Institute for Studies in Development, Environment, and Security, Oakland, California.

Perez-Farfante, I., and B. Kinsley.
1997. Panaeoid and sergestoid shrimps and prawns of the world: keys and diagnoses for the families and genera. Memoires du Museum National D'Histoire Naturelle 175:1–233.

Rosas-Cota, J. A., V. M. Garcia-Tirado, and J. R. Gonzalez-Camacho.
1996. Analisis de la pesqueria del camaron de altamar en San Felipe, B.C., durante la temporada de pesca 1995–1996. Secretaria de Medio Ambiente Recursos Naturales y Pesca, Instituto Nacional de la Pesca, Centro Regional de Investigacion Pesquera de Ensenada, Boletin 2, 23–30 p.

Vance, D. J., M. Haywood, D. Heales, R. Kenyon, and N. Loneragan.
1998. Seasonal and annual variation in abundance of postlarval and juvenile banana prawns *Penaeus merguiensis* and environmental variation in two estuaries in tropical northeastern Australia: a six year study. Mar. Ecol. Progress Ser. 163:21–36.

Fishery Bulletin

Guide for Contributors

Content

Articles published in *Fishery Bulletin* describe original research in fishery marine science, engineering and economics, and the environmental and ecological sciences, including modeling. Articles may range from relatively short to extensive.

Notes are reports of 5 to 10 pages without an abstract and describing methods or results not supported by a large body of data.

Although all contributions are subject to peer review, responsibility for the contents of papers rests upon the authors and not upon the editor or the publisher. It is therefore important that the contents of the manuscript are carefully considered by the authors.

Submission of an article is understood to imply that the article is original and is not being considered for publication elsewhere. Manuscripts should be written in English. Authors whose native language is not English are strongly advised to have their manuscripts checked by English-speaking colleagues prior to submission.

Preparation

Title page should include authors' full names and mailing addresses, the corresponding author's telephone, FAX number, and e-mail address, and a list of key words to describe the contents of the manuscript.

Abstract should not exceed one double-spaced typed page. It should state the main scope of the research but emphasize its conclusions and relevant findings. Because abstracts are circulated by abstracting agencies, it is important that they represent the research clearly and concisely.

Text must be typed double-spaced throughout. A brief introduction should portray the broad significance of the paper; the remainder of the paper should be divided into the following sections: **Materials and methods, Results, Discussion** (or **Conclusions**), and **Acknowledgments**. Headings within each section must be short, reflect a logical sequence, and follow the rules of multiple subdivision (i.e. there can be no subdivision without at least two items). The entire text should be intelligible to interdisciplinary readers; therefore, all acronyms, abbreviations, and technical terms should be spelled out the first time they are mentioned. The scientific names of species must be written out the first time they are mentioned; subsequent mention of scientific names may be abbreviated. Follow *Scientific Style and Format: the CBE Manual for Authors, Editors, and Publishers* (6th ed.), for editorial style, and the most current issue of the American Fisheries Society's *Common and Scientific Names of Fishes from the United States and Canada*, for fish nomenclature. Dates should be written as follows: 11 November 1991. Measurements should be expressed in metric units, e.g. metric tons as t; if other units of measurement are used, please make this fact explicit to the reader. The numeral one (1) should be typed as a one, not as a lower-case el (l). Use of appendices is discouraged.

Text footnotes should be numbered with Arabic numerals and inserted at the bottom of text. Footnote all personal communications, unpublished data, and unpublished manuscripts with full address of the communicator or author, or, as in the case of unpublished data, where the data are on file. Authors are advised to avoid references to nonstandard (gray) literature, such as internal, project, processed, or administrative reports. Where these references are used, please include whether they are available from NTIS (National Technical Information Service) or from some other public depository.

Literature cited comprises published works and those accepted for publication in peer reviewed literature (in press). Follow the name and year system for citation format. In the text, cite as follows: Smith and Jones (1977) or (Smith and Jones, 1977). If there is a sequence of citations, list alphabetically by author(s): Smith, 1987; Smith and Jones, 1985; Smith and Peterson, 1986. Abbreviations of serials should conform to abbreviations given in *Serial Sources for the BIOSIS Previews Database*. Authors are responsible for the accuracy and completeness of all citations.

Tables should not be excessive in size and must be cited in numerical order in the text. Headings within tables should be short but ample enough to allow the table to be intelligible on its own. All unusual symbols must be explained in the table legend. Other incidental comments may be footnoted with italic numerals. Use the asterisk only to indicate probability in statistical data. Zeros should precede all decimal points for values less than one.

Figures must be cited in numerical order in the text. The senior author's last name and the figure number should be written on the back of each one. Hand-drawn illustrations should be submitted as originals and not as photocopies. Submit photographs as glossy prints or slides with good contrast, otherwise we cannot guarantee a good final printed copy. Graphs should be submitted as laser-printed copies, not as photocopies. Label all figures with Helvetica typeface and capitalize the first letter of the first word in axis labels. Italicize species name and variables in equations. Use zeros before all decimal points. Use uppercase Times Roman bold typeface to label the parts of a figure, e.g. A, B, C, etc. Each figure legend should explain all symbols and abbreviations in the figure and should be double-spaced and placed at the end of the manuscript.

Copyright law Government publications are not copyrighted; they fall within the public domain. If an author reproduces any part of a government publication in his work, reference to source is appreciated.

Submission

Send printed copies (original and three copies without staples) to the Scientific Editor:

Dr. John V. Merriner
Southeast Fisheries Science Center
National Marine Fisheries Service
101 Pivers Island Road
Beaufort, NC 28516

Once the manuscript has been accepted for publication, you will be asked to submit an electronic copy of your manuscript to the Managing Editor. The electronic copy should be submitted in *WordPerfect* or *Microsoft Word* text format and placed on a 3.5-inch disk that is double-sided, double or high density, and that is compatible with either DOS or Macintosh systems.

A copy of page proofs will be sent to the author for final approval prior to publication.

Reprints (copies of published articles and notes) are available free of charge to the senior author (50 copies) and to his or her laboratory (50 copies). Additional copies may be purchased in lots of 100 when the author receives page proofs.

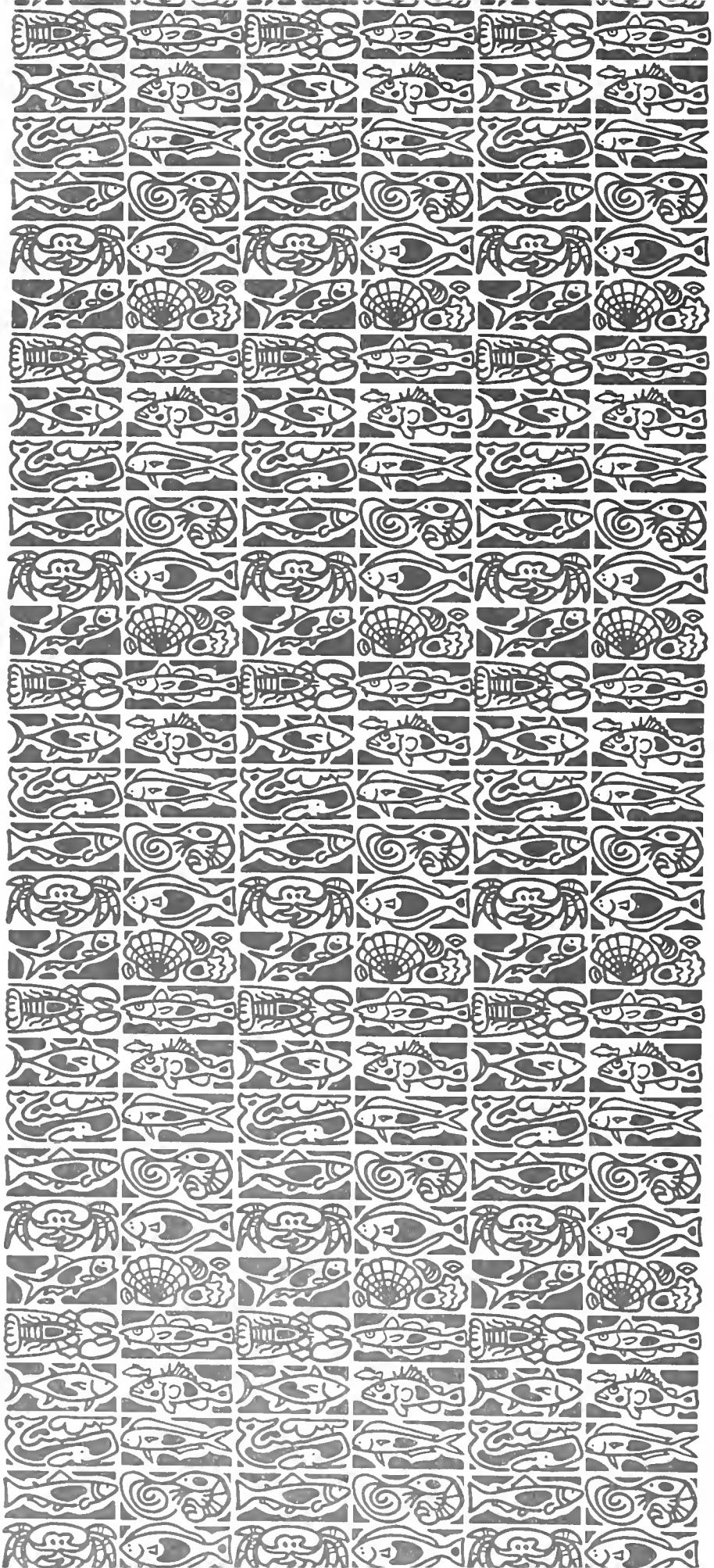

U.S. Department
of Commerce

Volume 98
Number 2
April 2000

Fishery Bulletin

The *Fishery Bulletin* (ISSN 0090-0656) is published quarterly by the Scientific Publications Office, National Marine Fisheries Service, NOAA, 7600 Sand Point Way NE, BIN C15700, Seattle, WA 98115-0070. Periodicals postage is paid at Seattle, WA, and at additional mailing offices. POSTMASTER: Send address changes for subscriptions to Fishery Bulletin, Superintendent of Documents, Attn: Chief, Mail List Branch, Mail Stop SSOM, Washington, DC 20402-9373.

The Secretary of Commerce has determined that the publication of this periodical is necessary according to law for the transaction of public business of this Department. Use of funds for printing of this periodical has been approved by the Director of the Office of Management and Budget.

For sale by the Superintendent of Documents, U.S. Government Printing Office, Washington, DC 20402. Subscription price per year $50.00 domestic and $62.50 foreign. Cost per single issue $19.00 domestic and $23.76 foreign. **See back for order form.**

Fishery Bulletin

***Fishery Bulletin* web site: fishbull.noaa.gov**

The *Fishery Bulletin* carries original research reports and technical notes on investigations in fishery science, engineering, and economics. It began as the Bulletin of the United States Fish Commission in 1881; it became the Bulletin of the Bureau of Fisheries in 1904 and the *Fishery Bulletin* of the Fish and Wildlife Service in 1941. Separates were issued as documents through volume 46, the last document was No. 1103. Beginning with volume 47 in 1931 and continuing through volume 62 in 1963, each separate appeared as a numbered bulletin. A new system began in 1963 with volume 63 in which papers are bound together in a single issue of the bulletin. Beginning with volume 70, number 1, January 1972, the *Fishery Bulletin* became a periodical, issued quarterly. In this form, it is available by subscription from the Superintendent of Documents, U.S. Government Printing Office, Washington, DC 20402. It is also available free in limited numbers to libraries, research institutions, State and Federal agencies, and in exchange for other scientific publications.

U.S. Department of Commerce
Seattle, Washington

Volume 98
Number 2
April 2000

Fishery Bulletin

Contents

Articles

Spawning of Brazilian menhaden, *Brevoortia aurea*, in the Río de la Plata estuary off Argentina and Uruguay*

Eduardo M. Acha
Dto Ciencias Marinas
Universidad Nacional de Mar del Plata
Funes 3350
(7600) Mar del Plata, Argentina
Present address: Instituto Nacional de Investigación y Desarrollo Pesquero (INIDEP)
Paseo V Ocampo N° 1
(7600) Mar del Plata, Argentina
E-mail address: macha@inidep.edu.ar

Gustavo J. Macchi
Consejo Nacional de Investigaciones Científicas y Técnicas (CONICET)
Rivadavia 1917
(1033) Buenos Aires, Argentina

Abstract.—Brazilian menhaden, *Brevoortia aurea*, is the only species of the genus *Brevoortia* in South American Atlantic waters and is abundant in the Río de la Plata estuary. We found that *B. aurea* in this area spawns almost exclusively in this estuary. We studied the temporal and spatial reproductive pattern of this menhaden and related the pattern to the major hydrographic features of the region. We based evidence of spawning activity on the presence of females with hydrated oocytes and on the occurrence of menhaden eggs in plankton samples. Our results show that *B. aurea* spawn during virtually every month of the year, but that they spawn mainly from September (late winter) to January (early summer). In the Río de la Plata estuary, spawned eggs occur in a thermohaline range of 13–23°C and 10–25 psu, mainly in stratified waters. *Brevoortia aurea* spawn very near the bottom salinity front, probably in a convergent flow between the riverine and estuarine waters that helps to retain eggs. In contrast to menhaden of the northern hemisphere (*B. tyrannus* and *B. patronus*), which spawn offshore and which drift during early life history stages, *Brevoortia aurea* in the Río de la Plata estuary are spawned and held in estuarine waters near spawning sites. The latter reproductive pattern is also shared by *Micropogonias furnieri* (whitemouth croaker), the most abundant fish species in the area.

Manuscript accepted 29 November 1999.
Fish. Bull. 98:227–235 (2000).

The Río de la Plata drains the second largest basin of South America. It flows into the Atlantic Ocean with an average discharge of 22,000 m^3/s, generating a large estuary of about 35,000 km^2 and 5–15 m in depth, located at 36°S, 56°W (Framiñan and Brown, 1996). Brazilian menhaden, *Brevoortia aurea*, is abundant in this estuary (Cousseau, 1985; Boschi, 1988); it also inhabits coastal and estuarine environments from 13°S (Brazil) to 40°S (Argentina). Historically, two species of menhaden were thought to inhabit Brazilian–Argentine waters (de Ciechomski, 1968; Weiss et al., 1976; Weiss and Krugg, 1977; Whitehead, 1985; Lasta and de Ciechomski, 1988); however, Cousseau and Díaz de Astarloa (1993) concluded that *B. aurea* is the only species that inhabits South American Atlantic waters.

Little is known about the reproductive biology of *B. aurea*. De Ciechomski (1968) described eggs and early larval stages of *B. aurea* and reported a period of 86–88 hours from the time of spawning to hatching at 13–14°C. Spawning has been detected in the Río de la Plata estuary (Lasta and de Ciechomski, 1988). Although their planktonic eggs also have been found in inshore waters along the Uruguayan and Argentine coasts (de Ciechomski, 1968; Hubold and Ehrlich, 1981; Cassia and Booman, 1985; Sánchez and de Ciechomski, 1995), Samborombón Bay (a shallow area inside the estuary) seems to be the locus of intensive spawning, where *B. aurea* eggs are exposed to low salinities (5–15 psu) (Lasta and de Ciechomski, 1988). Estuarine spawning by species producing pelagic eggs is uncommon (Dando, 1984; Haedrich, 1992; Potter et al., 1993); however no attempts have been made to describe the basic spawning habitat requirements of *B. aurea*. Furthermore, in the Río de la Plata, *Micropogonias furnieri*, the species with the largest biomass, releases pelagic eggs in the inner zone of the estuary (Macchi et al., 1996; Acha et al., 1999).

The life cycles of Northern Hemisphere menhaden, mainly *Brevoortia tyrannus* and *Brevoortia pat-*

* Contribution 1130 of the Instituto Nacional de Investigación y Desarrollo Pesquero (INIDEP), (7600) Mar del Plata, Argentina.

ronus (the Atlantic and gulf menhaden, respectively) are well understood. Both species are typical representatives of estuarine dependent species that spawn in the marine environment (Lawler et al., 1988; Day et al., 1989) in contrast to the Brazilian menhaden, which spawns in an estuarine environment.

Since 1983 the coastal resources of the Argentine–Uruguayan Common Fishing Zone have been monitored by a number of cruises, and results pertaining to menhaden form the basis for this paper. Our objectives were to describe the timing and spatial occurrence of spawning in relation to the major hydrographic features of the region in order to gain insight into the spawning habitat requirements of the Brazilian menhaden. Whenever possible, comparative analyses with other species of the estuary and menhaden of the Northern Hemisphere were performed.

Materials and methods

Samples from 47 cruises from 1983 through 1998 were analyzed in our study. Twenty-two of these cruises were on research vessels of the National Institute for Fisheries Research and Development (INIDEP), covering the Río de la Plata estuary and adjacent coastal waters, throughout which stations were randomly distributed. Twenty-five cruises took place in Samborombón Bay, on small fishing boats using a systematic sampling design. Monthly distribution of the sampling effort is shown in the insert of Figure 1. During 1983 and 1987, nineteen cruises in Samborombón Bay were performed every 30–45 days during the entire year. The remaining six cruises in this bay correspond only to spring months (October, November, and December). Cruises were made with several objectives, hence covering different periods, but sampling effort was higher in spring (October–November) when cruises for stock assessment were performed. The high number of plankton samples in May was due mainly to one cruise, designed to study physical variables and plankton in the estuary. Cruises on the small boats and on the research vessels were not simultaneous. All data were employed as a composite representing mean conditions.

Plankton was collected at 980 sampling stations by oblique tows of 60-cm bongo nets, 20-cm bongo nets, or a Nackthai sampler (a modified Gulf V high-speed plankton net, see Nellen and Hempel, 1969). All nets were equipped with flowmeters. The volume filtered in each tow ranged from 10 to 400 m^3. Sampling depth was estimated from measurements taken with an angle indicator (inclinometer) and a wheelout meter. All samples were preserved in 5% buffered formalin. Plankton samples were sorted and analyzed in the laboratory. *Brevoortia aurea* eggs were identified following the description of de Ciechomski (1968).

Estimates of egg density from the different samplers were not intercalibrated. They were arranged into four broad density classes (<10, 10 to 99, 100 to 999, ≥1000 eggs/m^3), and marked on a map to delineate the geographic location of the spawning area. Monthly distribution of the average number of eggs per tow (catch per unit of effort, CPUE) and the percentage of positive stations for menhaden eggs were plotted to identify the spawning season. Stations with no catch were included in the CPUE estimates.

Data from the November 1995 cruise were useful for gaining insight into the vertical distribution of menhaden eggs. During that cruise, plankton was sampled at five stations in a small area near Montevideo, where schools of spawning *B. aurea* were previously detected. In each of those stations, two tows were conducted with the Nackthai net, one to sample the surface and the other to sample the bottom layers as defined by a strong halocline. The depth of the halocline was previously measured with a conductivity-temperature-depth (CTD) profiler.

On all cruises, menhaden were collected with bottom trawls, and the presence of females with hydrated oocytes (macroscopic examination) was considered evidence of imminent spawning. The percentage of females with hydrated oocytes for each tow was also indicated on the map to identify the location of the spawning area. In addition, the mean monthly percentage of females with hydrated oocytes was used to determine the spawning season.

Temperature and salinity information was taken from the oceanographic database created by Guerrero et al. (1997a), which included all the CTD stations sampled during the cruises that we performed. Bottom salinity and temperature data for spring–summer were used because they could be matched to the vertical distribution of the eggs and the main reproductive period. Salinity is expressed as psu (practical salinity units; Anonymous, 1981). Horizontal and vertical salinity contour lines were made to compare the spawning area with the salinity field. Egg density was plotted into a temperature-salinity diagram to show the environmental ranges of the spawning habitat of the Brazilian menhaden.

Results

Eggs in the plankton

Brazilian menhaden eggs were detected virtually all year round (Fig. 1). The highest CPUE occurred from

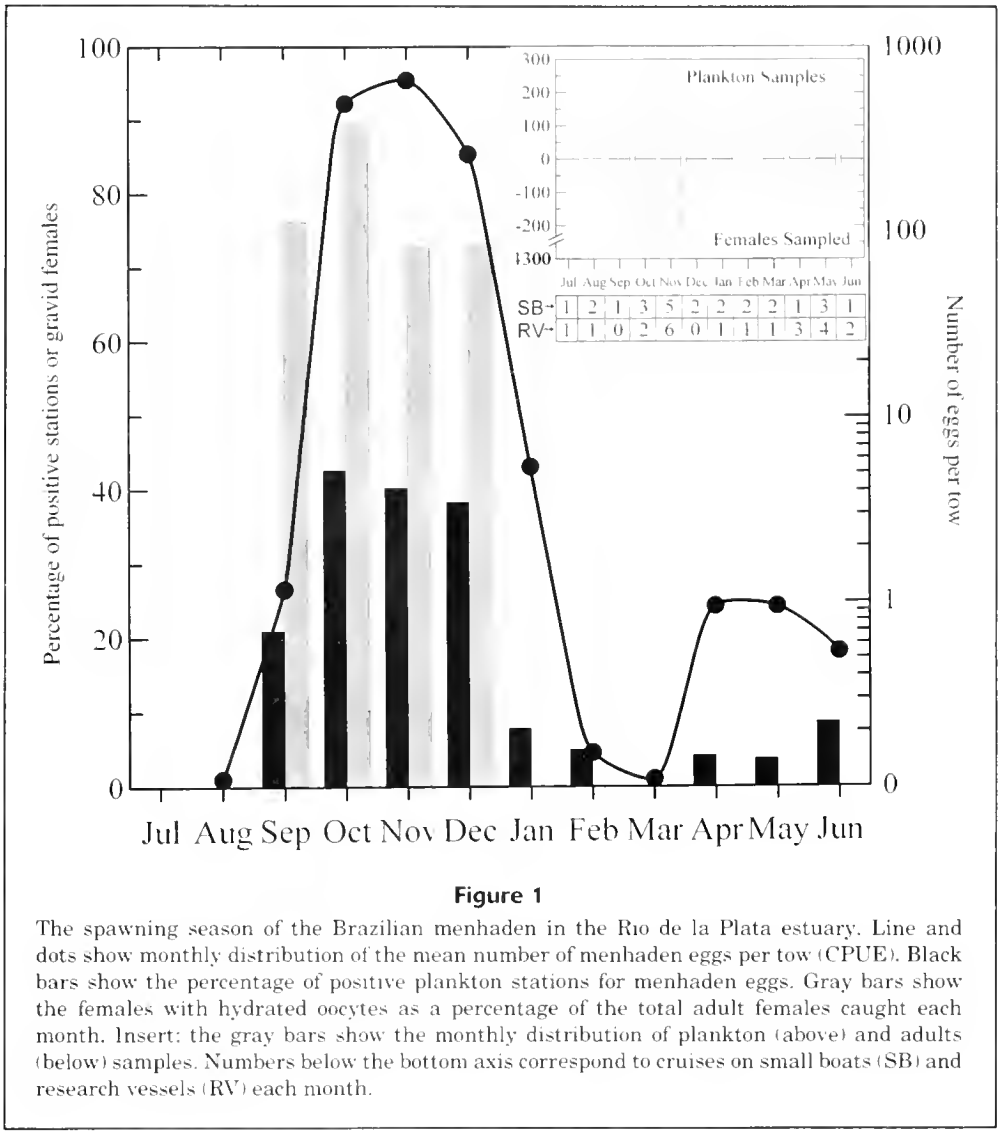

Figure 1

The spawning season of the Brazilian menhaden in the Rio de la Plata estuary. Line and dots show monthly distribution of the mean number of menhaden eggs per tow (CPUE). Black bars show the percentage of positive plankton stations for menhaden eggs. Gray bars show the females with hydrated oocytes as a percentage of the total adult females caught each month. Insert: the gray bars show the monthly distribution of plankton (above) and adults (below) samples. Numbers below the bottom axis correspond to cruises on small boats (SB) and research vessels (RV) each month.

September through January and diminished during late summer, followed by a secondary peak during the fall (April–June). The percentage of positive stations for menhaden eggs had a similar pattern to that of the CPUE. There was no plankton sampling in July.

Menhaden eggs were identified in 220 samples that represented 22.5% of all samples analyzed. The eggs were found mainly in estuarine waters (Fig. 2A), especially at depths <10 m. Highest densities of eggs were found in Samborombón Bay and west of Montevideo in the innermost part of the estuary, where salinity values ranged between 10 and 20 psu. Medium egg densities were found along the Uruguayan coast between Montevideo and Atlántida (55°45'W) and in the middle area of the river between Montevideo and Punta Piedras. Lowest densities (<10 eggs/m^3) were present in the rest of the estuary and adjacent coastal waters.

The study area (5 stations) of the vertical distribution of *B. aurea* eggs is shown by an arrow in Figure 2A. Total depth in this area was 6.5–7.5 m and halocline depth was 4.8–6.5 m. Menhaden eggs were present in the water layer below the halocline but were extremely scarce in the upper layer. In the bottom layer, egg density ranged from 50–2100 eggs/m^3. Eggs were found within a thermohaline range of 9.7–27.3 psu and 18.5–20.2°C. The upper layer was less saline (0.7–10.8 psu) and warmer (19.7–21.7°C). Strong haloclines up to 21.5 psu/m were observed. Figure 3 shows the vertical distribution of salinity and *B. aurea* eggs along a transect in the estuary. This transect includes four of the five plankton stations sampled above and below the halocline. Menhaden eggs were detected in the region where the salt wedge intersects the bottom (the bottom salinity front). In this area of stratified

waters, depth of bottom layer (measured from the halocline to the bottom) was less than 3 m, and menhaden eggs were located below the halocline.

Menhaden eggs occurred in a wide environmental range (Fig. 4). Densities of >100 eggs/m^3 were found in a salinity range of 10 to 25 psu; minor densities were located in waters with salinities reaching 33 psu (continental shelf waters). The low salinity boundary for egg distribution seems more abrupt than the high salinity boundary; very few eggs were detected below 10 psu. Most eggs produced over the prolonged spawning season were found at temperatures between 13 and 23°C.

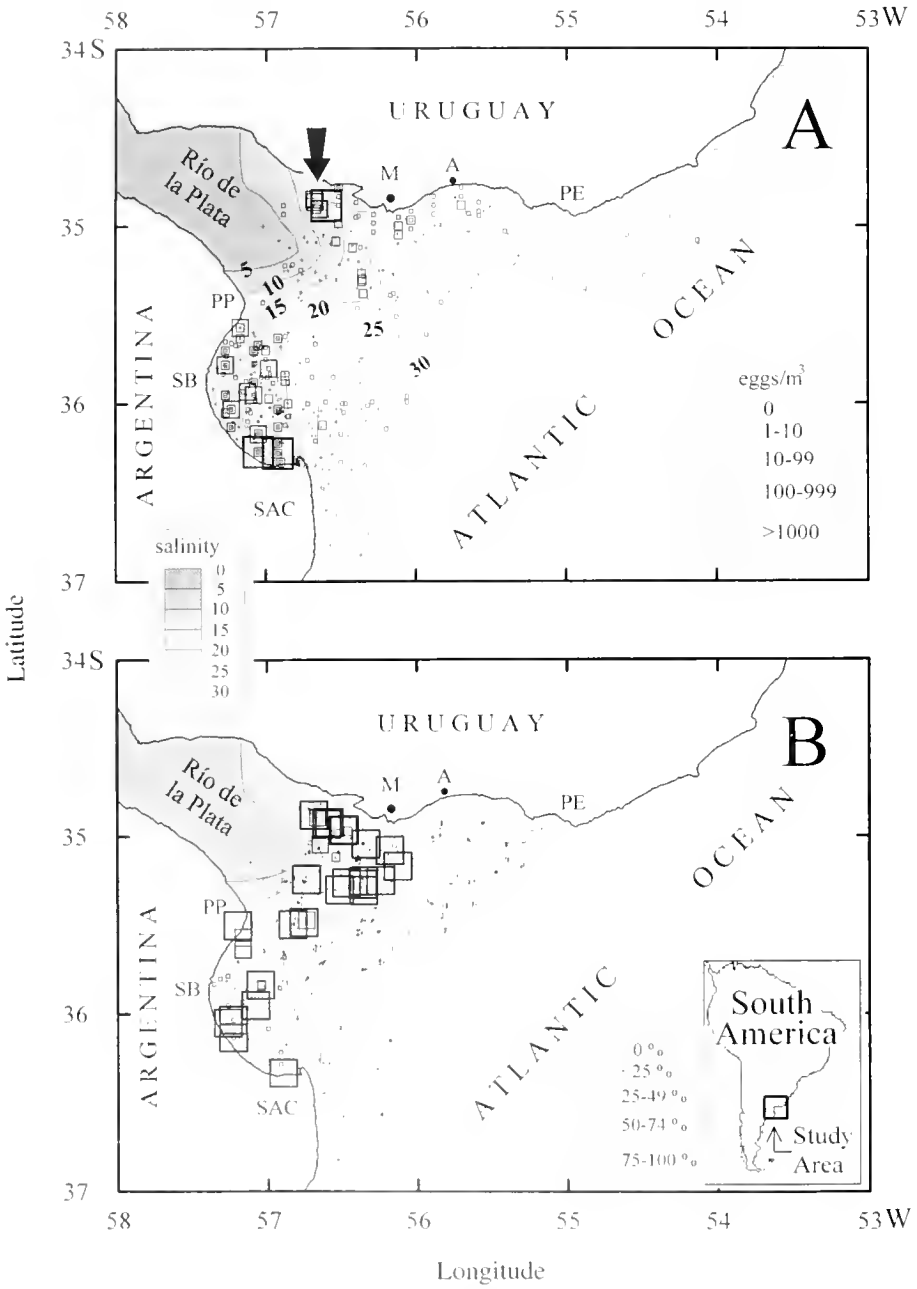

Figure 2

Location of the spawning area of the Brazilian menhaden. (**A**) The size of the symbols is proportional to the egg density from the plankton samples; the arrow shows the study site for examining the vertical distribution of eggs (see the text). (**B**) The size of the symbols is proportional to the percentage of females with hydrated oocytes. In both maps, the isohalines (expressed as psu) represent the bottom salinity field for spring-summer. PE = Punta del Este; A = Atlantida; M = Montevideo; PP = Punta Piedras; SB = Samborombon Bay; SAC = San Antonio Cape.

Gravid females

A total of 375 sampling stations were analyzed, in which 1084 gravid females were identified. All the gravid females were caught from September through December. In these months, the total percentage of females with hydrated oocytes ranged from 72.8% to 89.4% (Fig. 1).

Gravid females were detected across the river between Montevideo and Punta Piedras, and in Samborombón Bay (Fig. 2B). In that region, percentages of gravid females in each tow were >50%. The highest percentages of females with hydrated oocytes appeared to be associated with the highest horizontal salinity gradient (the salinity front). No females with hydrated oocytes were detected in continental shelf waters.

Discussion

The distribution of eggs and gravid females reveals that *B. aurea* spawn in the estuary (Fig. 2). Gravid females were found in a more restricted area than that where eggs were found, thus providing a more accurate picture of the spawning spatial pattern, because currents may move eggs to more distant areas. An echo sounder showed Brazilian menhaden below the halocline on all cruises, including the occasions when spawning individuals were collected. The halocline was detected by

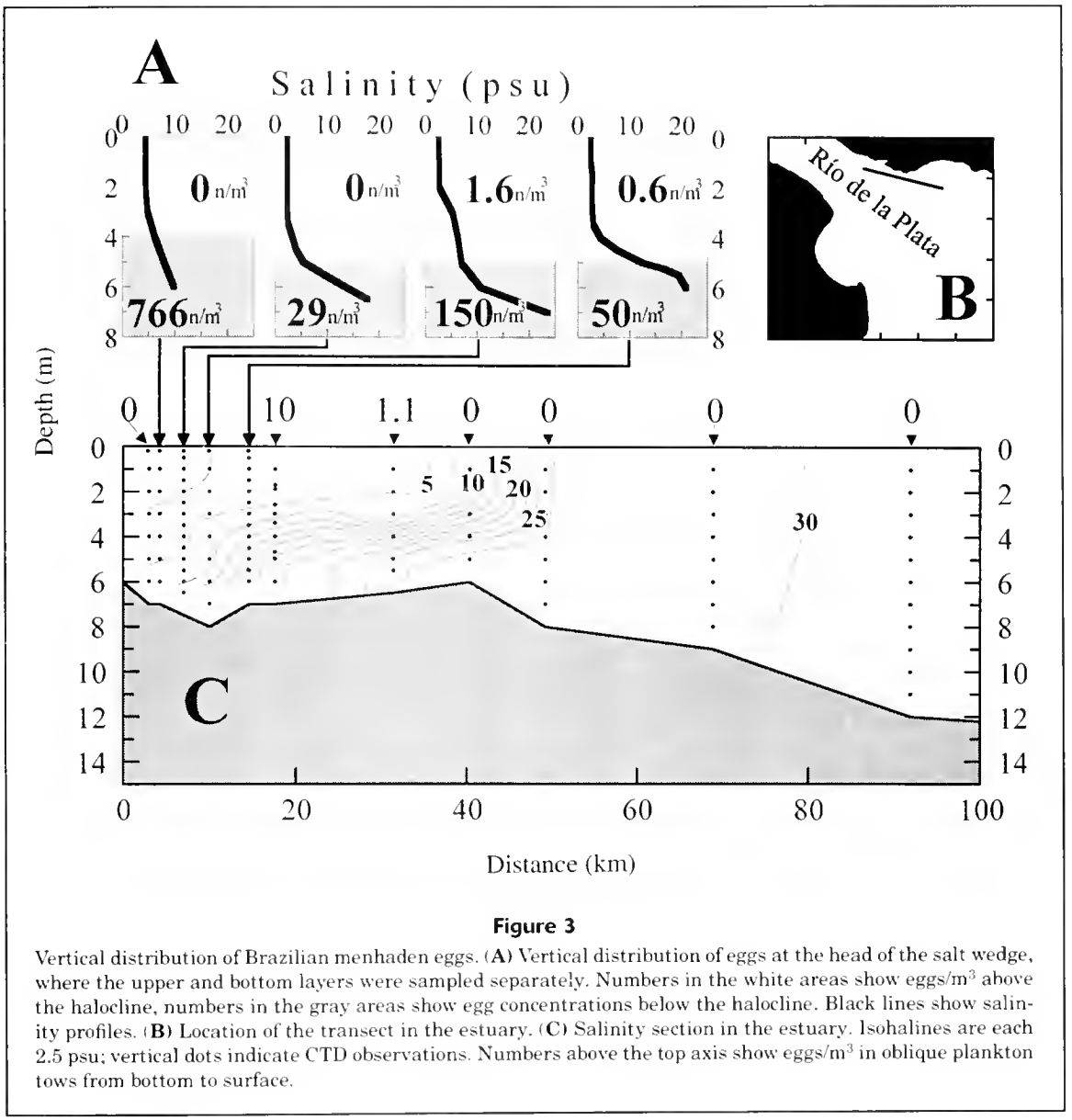

Figure 3

Vertical distribution of Brazilian menhaden eggs. (**A**) Vertical distribution of eggs at the head of the salt wedge, where the upper and bottom layers were sampled separately. Numbers in the white areas show eggs/m^3 above the halocline, numbers in the gray areas show egg concentrations below the halocline. Black lines show salinity profiles. (**B**) Location of the transect in the estuary. (**C**) Salinity section in the estuary. Isohalines are each 2.5 psu; vertical dots indicate CTD observations. Numbers above the top axis show eggs/m^3 in oblique plankton tows from bottom to surface.

the echo sounder as a scattering layer, owing to the concentration of zooplankton (Madirolas et al., 1997). Brazilian menhaden appears to spawn close to the bottom, at the salinity front. The mean position of this front is strongly related to bottom topography (Guerrero et al., 1997a), having a relatively fixed location. This spawning area extends into the stratified waters of the estuary between Montevideo and Punta Piedras, and along Samborombón Bay. However, because waters of the inner zone of the bay are vertically homogeneous, or weakly stratified (Guerrero et al., 1997a), some high egg concentrations occur in nonstratified waters.

Menhaden eggs occurred in a wide range of salinities and temperatures. Because the bottom front is a zone of major salinity changes, the eggs are exposed to a wide range of salinity values, and because the reproductive season extends over a long period, eggs are exposed further to a wide thermal range (Fig. 4). Low egg densities at low temperatures and high salinities represent samples taken in continental shelf waters, which were cooler than the estuarine waters during the warm season (Guerrero et al., 1997a, 1997b).

Presence of Brazilian menhaden eggs in the plankton year-round (Fig. 1) is strong evidence that they have a protracted reproductive season. Major spawning activity, based on incidence of eggs and hydrated ovaries (gravid females), occurs from September to January. Other reports of menhaden eggs, based on

partial temporal or spatial coverage, or both, fall within the temporal limits that we detected (de Ciechomski, 1968; Hubold and Ehrlich, 1981; Cassia and Booman, 1985; Lasta and de Ciechomski, 1988).

Brevoortia aurea eggs remain in the bottom layer of the water column, near where the halocline intersects the bottom (Fig. 3). At this frontal interface, a convergent flow near the bottom (Largier, 1993) would serve to retain eggs near the confluence of river and marine waters, minimizing their drift. Thus, specific gravity of the eggs seems to be an important feature of the reproductive strategy of *B. aurea*, allowing the eggs to stay in the saltier (and denser) bottom waters. Typically, bottom waters move landward in salt-wedge estuaries (Kjerfve, 1989; Mann and Lazier, 1991). Lower egg concentrations in the rest of the estuary probably indicate some dispersion of eggs or reduced spawning in these areas.

Disruptive events such as storms, which destroy the halocline (Guerrero et al., 1997a), intermittently occur in this region. These meteorological events are characterized by strong winds over 13 m/s from the southeast (Balay, 1961). The events have a characteristic duration of 1–3 (occasionally 5) days, occur throughout the year, and are usually the strongest from May to October (Anonymous, 1995). During these events, the estuarine circulation is modified, thus altering the egg retention properties of the system as well. The protracted reproductive season and multiple spawning of *B. aurea* (Macchi and Acha, 2000) may help to ensure that enough eggs survive in this unpredictable environment.

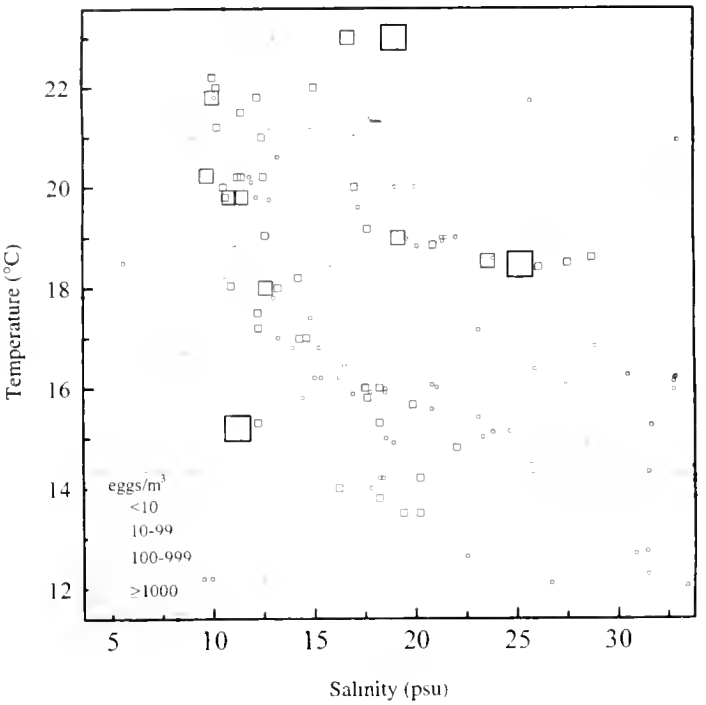

Figure 4

Thermohaline range of Brazilian menhaden eggs determined from plankton samples taken from the Río de la Plata estuary and adjacent coastal waters. The size of the symbols is proportional to egg density.

The four menhaden species in the Northern Hemisphere are the small-scaled menhaden *B. smithi* and *B. gunteri* and the large-scaled menhaden *B. tyrannus* and *B. patronus* (Ahrenholz, 1991). There is little information on the biology of *B. smithi* and *B. gunteri*. Conversely, *B. tyrannus* and *B. patronus* have been intensively studied, and the information on their life histories has been broadly reviewed (Ahrenholz, 1991; Powell, 1994). Both species have protracted reproductive seasons and a main spawning period in winter (Nelson et al., 1977; Shaw et al., 1985; Powell, 1994). Spawning of these menhaden takes place in marine waters. Larvae swim and drift with tides and currents toward estuaries where metamorphosis from larvae to juveniles takes place. In the case of *B. tyrannus*, larvae must be transported from the intensive spawning area south of Cape Hatteras, up to 100 km to estuarine nursery areas (Warlen, 1992; Powell, 1994). *Brevoortia patronus* seems to spawn relatively close to estuarine nursery areas (Shaw et al., 1985).

Brevoortia aurea, *B. tyrannus*, and *B. patronus* all have protracted spawning periods. The southern species is a spring–summer spawner; the northern ones spawn during cooler months. In the case of *B. tyrannus*, however, adults search for temperatures ≥17°C to spawn, and as larvae are transported nearer the coast, they enter cooler water (Warlen, 1992). Notwithstanding, the reproductive thermal range of the northern species (12.9–21.2°C for *B. patronus*, and ≥17°C for *B. tyrannus* (Warlen, 1988; 1992) lies close to that of *B. aurea*. The proposed advantage of winter spawning refers to maximum onshore transport during that season, providing a mechanism for transporting larvae of both species into the vicinity of estuaries (Nelson et al., 1977; Warlen, 1988).

The main differences between *B. aurea* and those northern menhaden seem to be the population biomass and the spawning habitat. *Brevoortia tyrannus* and *B. patronus* exhibit large population sizes and are a significant component of United States fishery landings (Vaughan, 1991; Powell, 1994). Although there is no biomass assessment for *B. aurea*, it has

little importance as a fishery species (Argentine landings in 1997 were 893 t (Anonymous, 1998). Life history characteristics of *Brevoortia aurea* are probably more similar to those of *B. smithi* and *B. gunteri*, which tend to be more nearshore and estuarine-oriented species, form loose aggregations in coastal waters, and have protracted spawning periods during fall–winter months (Ahrenholz, 1991). Not enough information, however, on their reproductive biology exists to make further comparisons.

Drift of early life history stages is a major feature in the life cycle of *B. patronus*, and especially of *B. tyrannus*. On the contrary, egg retention seems to be a main property of the life cycle of the Brazilian menhaden in the Río de la Plata estuary. However, in southern Brazil, *B. aurea* does not seem to be an estuarine spawner (reported as *B. pectinata*, Weiss et al., 1976; Weiss and Krug, 1977; Weiss, 1981; Sinque and Muelbert, 1997). The greatest number of eggs occurred in nearshore waters, in a saline range of 33.04–35.50 psu. Several eggs were also found in the access channel to Lagoa dos Patos (a large coastal lagoon in southern Brazil, 32°S) during high salinity events, although its larvae and juveniles were distributed throughout the estuary in low salinity conditions (Weiss et al., 1976; Weiss, 1981; Sinque and Muelbert, 1997). The spawning area of *M. furnieri*, the most abundant fish species in the Río de la Plata, partially overlaps that of *B. aurea*, and the eggs of *M. furnieri* are retained in the estuary below the halocline (Acha et al., 1999). Like *B. aurea*, *M. furnieri* is an estuarine spawner in the Río de la Plata (Macchi et al., 1996) but seems to be a saltwater spawner in southern Brazil (Sinque and Muelbert, 1997). Both species have the potential for estuarine reproduction, but the eventual spawning site depends on the dynamic properties of the environment.

Major reviews of the role of estuaries for fishes state that spawning of pelagic eggs within estuaries is an unusual episode (e.g. Day et al., 1981; Day et al.,1989; Haedrich, 1992). Owing to the net seaward movement of estuarine waters, export of early life-history stages from the estuaries seems to be a major problem for estuarine spawners (Boehlert and Mundy, 1988).

In the Río de la Plata estuary, at least two fish species (*B. aurea* and *M. furnieri*) spawn pelagic eggs, taking advantage of the retention properties at the head of the salt wedge. These retention properties are not a feature unique to the Río de la Plata because estuaries with salt wedges are well known features (e.g. Mann and Lazier, 1991; Officer, 1992); however spawning of pelagic eggs at those locations is an uncommon event. Retention of eggs and larvae in the convergence zone may not be complete and the net nontidal flows (residual currents) may drive them seaward. Given the large size of the Río de la Plata estuary, distance from the spawning area to the offshore limit of the salt wedge may reach 250 km (Guerrero et al., 1997a, 1997b). Therefore, larvae probably have enough time to develop to the stage where they become able to control their vertical position in the water column. The migratory behavior of larvae is manifested mostly in the vertical rather than horizontal plane (Norcross and Shaw, 1984). Thus, larval menhaden could take advantage of the two-layered circulation pattern and through vertical migrations compensate for the horizontal transport. This movement would be an important adaptation to maintain population (as the reproductive unit) coherency (Boucher, 1988; Sinclair and Iles, 1989).

Literature cited

Acha, E. M., H. W. Mianzan, C. A. Lasta, and R. A. Guerrero.
1999. Estuarine spawning of the whitemouth croaker *Micropogonias furnieri* in the Rio de la Plata, Argentina. Mar. Freshwater Res. 50(1):57–65.

Anonymous.
1981. Background papers and supporting data on the Practical Salinity Scale 1978. Tec. Pap. Mar. Sci. 37, UNESCO, Paris, 144 p.
1995. Derrotero Argentino. Parte 1 Río de la Plata, 10th ed. Servicio de Hidrografía Naval, Armada Argentina, Buenos Aires, 273 p.
1998. Capturas maritimas totales 1997. Ministerio de Economía y Obras y Servicios Públicos. Secretaria de Agricultura, Ganadería, Pesca y Alimentación. Subsecretaría de Pesca. Dirección Nacional de Pesca Acuicultura, Buenos Aires, 45 p.

Ahrenholz, D. W.
1991. Population biology and life history of the North American menhadens, *Brevoortia* spp. Mar. Fish. Rev. 53(4): 3–19.

Balay, M. A.
1961. El Rio de la Plata entre la atmósfera y el mar. Servicio de Hidrografía Naval, Argentina, Público H-621, 153 p.

Boehlert, G. W., and B. C. Mundy.
1988. Roles of behavioral and physical factors in larval and juveniles fish recruitment to estuarine nursery areas. Am. Fish. Soc. Sym. 3:51–67.

Boschi, E. E.
1988. El ecosistema estuarial del Rio de la Plata. An. Inst. Cienc. del Mar y Limnol., Univ. Nal. Autón. Mexico 15(2): 159–182.

Boucher, J.
1988. Space-time aspects in the dynamics of planktonic stages. *In* Toward a theory of biological-physical interactions in the world ocean: proceedings of the NATO advanced workshop, Casteria Verduzan, France, 15 June 1987 (B. J Rothschild, ed.), p. 203–214 Kluwer Academic Press, Dordrecht.

Cassia, M. C., and C. I. Booman.
1985. Distribución del ictioplancton en el Mar Argentino en los años 1981–1982. Physis 43(105):91–111.

Cousseau, M. B.
1985. Los peces del Río de la Plata y su Frente Marítimo. *In* Fish community ecology in estuaries and coastal lagoons: towards an ecosystem integration (A.Yáñez-Arancibia, ed.), p. 515–534. DR(R) UNAM Press, México.

Cousseau, M. B., and J. M. Díaz de Astarloa.
1993. El género *Brevoortia* en la costa Atlántica Sudamericana. Frente Marítimo 14:49–57.

Dando, P. R.
1984. Reproduction in estuarine fish. *In* Fish reproduction: strategies and tactics (G. W. Potts and R. J. Wootton, eds.) p. 155–170. Academic Press, London.

Day, J. H., S. J. M. Blaber, and J. H. Wallace.
1981. Estuarine fishes. *In* Estuarine ecology with particular reference to southern Africa (J. H. Day, ed.), p.197–221. A.A. Balkema, Rotterdam.

Day Jr., J. W., C. A. S. Hall, W. M. Kemp, A. Yáñez-Arancibia, and L. A. Deegan.
1989. Nekton, the free-swimming consumers. *In* Estuarin ecology (Day et al., eds.), p. 377–437. John Wiley and Sons, New York, NY.

de Ciechomski, J. D.
1968. Huevos y larvas de tres especies de peces marinos, *Anchoa marinii*, *Brevoortia aurea* y *Prionotus nudigula* de la zona de Mar del Plata. Bol. Inst. Biol. Mar. 17, 28 p.

Framiñan, M. B., and O. B. Brown.
1996. Study of the Río de la Plata turbidity front. Part I: spatial and temporal distribution. Cont. Shelf Res. 16(10):1259–1282.

Guerrero, R. A., E. M. Acha, M. B. Framiñan, and C. A. Lasta.
1997a. Physical oceanography of the Río de la Plata Estuary, Argentina. Cont. Shelf Res. 17(7):727–742.

Guerrero, R. A., C. A. Lasta, E. M. Acha, H. W. Mianzan, and M. B. Framiñan.
1997b. Atlas hidrográfico del Río de la Plata. Comisión Administradora del Río de la Plata-Instituto Nacional de Investigación y Desarrollo Pesquero, Buenos Aires-Montevideo, 109 p.

Haedrich, R. L.
1992. Estuarine fishes. *In* Ecosystems of the world, vol. 26, Estuaries and enclosed seas (B. H Ketchum, ed.), p. 185–207. Elsevier, Amsterdam.

Hubold, G., and M. D. Ehrlich.
1981. Distribution of eggs and larvae of five clupeoid fish species in the Southwest Atlantic between 25°S and 40 S. Meeresforschung 29:17–29.

Kjerfve, B.
1989. Estuarine geomorphology and physical oceanography. *In* Estuarine ecology (J. W. Day, C. A S. Hall, W. M. Kemp, and A. Yáñez-Arancibia, eds.), p.47–78. John Wiley & Sons, New York, NY.

Largier, J. L.
1993. Estuarine fronts: How important are they? Estuaries 16(1):1–11.

Lasta, C. A., and J. D. de Ciechomski.
1988. Primeros resultados de los estudios sobre la distribucion de huevos y larvas de peces en Bahía Samborombon en relacion a temperatura y salinidad. Publ. Com. Tec. Mix. Fr. Mar. 4 133–141.

Lawler, J. P., M. P. Weinstein, W. Y. Chen, and T. L. Englert.
1988. Modelling of physical and behavioral mechanisms influencing recruitment of spot and Atlantic croaker to the Cape Fear estuary. Am. Fish. Soc. Sym. 3:115–131.

Macchi, G. J., and E. M. Acha.
2000 Spawning frequency and batch fecundity of Brazilian menhaden, *Brevoortia aurea*, in the Río de la Plata estuary off Argentina and Uruguay. Fish. Bull. 98:283–289.

Macchi, G. J., E. M. Acha, and C. A. Lasta.
1996. Desove y fecundidad de la corvina rubia (*Micropogonias furnieri*, Desmarest, 1826) en el estuario del Río de la Plata, Argentina. Bōl. Inst. Español Oceanogr. 12:99–113.

Madirolas, A., E. M. Acha, R. A. Guerrero, and C. A. Lasta.
1997. Sources of scattering near an estuarine frontal system. Sci. Mar. 61(4):431–438.

Mann, K. H., and J. R. N. Lazier.
1991. Dynamics of marine ecosystems: biological-physical interactions in the oceans. Blackwell Science Publications, Boston, MA, 466 p.

Nellen, W., and G. Hempel.
1969. Versuche zur Fangigkeit des "Hai" und des modifizierten Gulf-V-Plankton-Samplers "Nackthai." Ber. Deuts. Wiss. Komm. Meeres. 20:141–154.

Nelson, W. R., M. C. Ingham, and W. E. Schaaf.
1977. Larval transport and year-class strength of Atlantic menhaden, *Brevoortia tyrannus*. Fish. Bull. 75(1):23–41.

Norcross, B. L., and R. F. Shaw.
1984. Oceanic and estuarine transport of fish eggs and larvae: a review. Trans. Am. Fish. Soc. 113:153–165.

Officer, C. B.
1992. Physics of estuarine circulation. *In* Ecosystems of the world, vol. 26, Estuaries and enclosed seas (B. H. Ketchum, ed.), p. 15–41. Elsevier, Amsterdam.

Potter, I. C., G. A. Hyndes, and F. M. Baronie.
1993. The fish fauna of a seasonally closed Australian estuary. Is the prevalence of estuarine-spawning species high? Mar. Biol. 116:19–30.

Powell, A. B.
1994. Life history traits of two allopatric clupeids, Atlantic menhaden and gulf menhaden, and the effects of harvesting on these traits. N. Am. J. Fish. Manage. 14:53–64.

Sánchez, R. P., and J. D. de Ciechomski.
1995. Spawning and nursery grounds of pelagic fish species in the sea-shelf off Argentina and adjacent areas. Sci. Mar. 59(3-4):455–478.

Shaw, R. F., J. H. Cowan Jr, and T. L. Tillman.
1985. Distribution and density of *Brevoortia patronus* (gulf menhaden) eggs and larvae in the continental shelf waters of western Louisiana. Bull. Mar. Sci. 36(1):96–103.

Sinclair, M., and T. D. Iles.
1989. Population regulation and speciation in the oceans. J. Cons. Int. Explor. Mer 45:165–175.

Sinque, C., and J. H. Muelbert.
1997. Environment and biota of the Patos Lagoon Estuary: ichthyoplankton. *In* Subtropical convergence environments: the coast and sea in the Southwestern Atlantic (Seeliger et al., eds.), p. 51–56. Springer-Verlag, Heidelberg.

Vaughan, D. S.
1991. Menhaden: the resource, the industry, and a management history. Preface. Mar. Fish. Rev. 53(4):1–2.

Warlen, S. M.
1988. Age and growth of larval gulf menhaden, *Brevoortia patronus*, in the northern Gulf of Mexico. Fish. Bull. 86(1):77–90.
1992. Age, growth and size distribution of larval Atlantic menhaden off North Carolina. Trans. Am. Fish. Soc. 121: 588–598.

Weiss, G.
1981. Ictioplancton del estuario de Lagoa dos Patos, Brasil. Ph.D diss., Univ. Nacional de La Plata, Facultad de Ciencias Naturales y Museo, La Plata, Argentina, 164 p.

Weiss, G., and L. C. Krug.
1977. Caracteristicas do desenvolvimento e metamorfose de *Lycengraulis olidus* (Engraulidae) e *Brevoortia pectinata* (Clupeidae) no estuario da Lagoa dos Patos, Brasil. Atlântica 2(1):83–117.

Weiss, G., J. A. Souza, and A. Santos.
1976. Contribuição ao conhecimento do ictioplancton marinho da plataforma sul do Brasil. Atlântica 1(1/2):7–78.

Whitehead, P. J. P.
1985. Clupeoid fishes of the world: an annotated and illustrated catalogue of the herrings, sardines, pilchards, sprats, anchovies and wolf-herrings. Part 1: Chirocentridae, Clupeidae and Pristigasteridae. FAO Fisheries Synopsis 125, vol. 7, 303 p.

Abstract.—Sandbar sharks (*Carcharhinus plumbeus*) support an important commercial fishery. They are managed as a component of a multispecies group, termed large coastal sharks, by the National Marine Fisheries Service (NMFS) under the Fishery Management Plan (FMP) for Atlantic sharks. Currently, large coastal sharks, generally, and sandbar sharks, specifically, are considered overfished. Several management options, including nursery ground closures and size limits, are being considered to conserve the fishery. We explored the implications of management options for large coastal sharks within the framework of a stage-based model. Based on biological criteria, the life cycle of the sandbar shark was represented as five stages: neonate, juvenile, subadult, pregnant adults, and resting adults. The model followed only females. From a fishing mortality rate (F) of 0.20, estimated in the 1996 stock evaluation workshop (SEW), the model projects a population decline to 13% of its current abundance within 20 years. The population is not stabilized until F is reduced to 0.07. In one run of the model, we assumed that F on neonates and pregnant adults was zero in order to assess the impact of a "perfect" nursery ground closure. Under this scenario, the population continued to decline unless F on the remaining stages was reduced to 0.097. Even with the closure of nursery grounds or the introduction of size limits to protect neonates and juveniles, F has to be reduced substantially. The model is highly sensitive to the dynamics of juveniles and subadults, which implies that management should protect these immature sharks to rebuild the stock.

Manuscript accepted 26 November 1999.
Fish. Bull. 98:236–249 (2000).

Management of the sandbar shark, *Carcharhinus plumbeus*: implications of a stage-based model*

Karyl K. Brewster-Geisz
Highly Migratory Species Management Division
National Marine Fisheries Service
1315 East West Highway
Silver Spring, Maryland 20910
E-mail address: Karyl.Brewster-Geisz@noaa.gov

Thomas J. Miller
Chesapeake Biological Laboratory
University of Maryland Center for Environmental Sciences
P. O. Box 38
Solomons, Maryland 20688-0038

The sandbar shark (*Carcharhinus plumbeus*) is a species of primary importance in the Atlantic and Gulf of Mexico shark fishery (NMFS, 1993; NMFS[1]; Branstetter and Burgess[2]). It is managed as a part of the large coastal shark group defined under the Atlantic shark Fishery Management Plan (FMP; NMFS, 1993). Since the mid 1980s, the demand for shark has increased (NMFS, 1993). The fishery peaked in 1989 with landings of approximately 4600 metric tons (t) dressed weight (dw; NMFS[3]). Catch per unit of effort of large coastal sharks declined rapidly during the 1970s and 1980s. To prevent overfishing, the FMP imposed an annual quota of 2570 t dw from 1994 to 1996 for the large coastal fishery, required mandatory reporting of landings, and prohibited the removal of fins (NMFS, 1993). At the 1996 stock evaluation workshop (SEW), scientists found no evidence of improvements in the large coastal stocks and recommended reducing fishing mortality by 50% (NMFS, 1996). In response, the National Marine Fisheries Service (NMFS) reduced the annual quota in 1997 by 50% to 1285 t dw and reported to Congress that large coastal sharks were overfished (NMFS, 1997). The most recent data indicate that fishing mortality rates have not declined as much as expected and may still be too high to stabilize the sandbar shark stock (NMFS[4]). A size limit equivalent to approximately 12–13 years of age (140 cm fork length) was recommended.

The NMFS is mandated, through the Magnuson-Stevens Fishery Conservation and Management Act, to

* Contribution 3264 of the University of Maryland Center for Environmental Sciences Series, Chesapeake Biological Laboratory, University of Maryland, Solomons, MD 20688-0038.

1 1996. Report of the shark evaluation workshop. Southeast Fisheries Science Center, Natl. Mar. Fish. Serv., NOAA, Miami, FL, 80 p.

2 Branstetter, S., and G. Burgess. 1997. Continuation of an observer program to characterize and compare regional efforts in the directed commercial shark fishery in the eastern Gulf of Mexico and South Atlantic. Gulf and South Atlantic Fisheries Development Foundation, Inc., Tampa, FL. University of Florida, Gainesville, FL., 83 p.

3 1997. Shark evaluation annual report. Southeast Fisheries Science Center, Natl. Mar. Fish. Serv., NOAA, , Miami, FL, 12 p.

4 1998. Report of the shark evaluation workshop. Southeast Fisheries Science Center, Natl. Mar. Fish. Serv., NOAA, Panama City, FL.

rebuild the large coastal stocks to the optimum yield level. In October 1998, the NMFS released a draft FMP for Atlantic tunas, swordfish, and sharks. The measures in this FMP were designed to halt overfishing and to rebuild these stocks. Management options under consideration for large coastal sharks included restrictions on effort, size limits, and area closures that were focused on nursery grounds.

Many traditional approaches that could be used to compare management options, such as surplus production models or age- and size-structured approaches, rely on catch or effort data, or both. However, because logbook reporting in the shark fishery was not mandatory until 1993, fishery-dependent time series have been insufficiently long to permit reliable application of these approaches. Yet a comparison of the efficacy of the potential management options is still required. The paucity of fishery-dependent data suggests that demographic approaches, such as life-table or stage-based analyses, may be the appropriate tools to explore the potential response of shark populations to management actions.

Life-table analysis is a common age-structured demographic approach with a long history in population dynamics (Kingsland, 1985). It is a matrix projection approach that estimates the contribution of each age class to future generations. Sminkey and Musick (1996) applied a life-table approach to sandbar sharks. From the intrinsic rate of natural increase, r, predicted by the model, they concluded that the population could not sustain the observed rates of fishing mortality. Heppell et al. (1999) developed matrix-based life tables for leopard (*Triakis semifasciata*) and angel (*Squatina californica*) sharks. Heppell et al. calculated the elasticity or proportional sensitivity of the population growth rate to changes in survival and fecundity and concluded that the two species differ in the degree to which each can compensate for changes in exploitation. Simpfendorfer (1999) developed a life table for the dusky shark (*Carcharhinus obscurus*). He concluded that in the absence of exploitation, dusky shark populations in southwestern Australia would increase at 4.3% annually. Analysis also indicated that current patterns of exploitation were sustainable. However, there are problems in application of life-table analysis to long-lived marine species. The intrinsic rate of natural increase predicted is dependent on the products of survival and fecundity for all ages and the estimated generation time. Thus, life tables require estimates of the schedules of mortality (survival) and fecundity over the entire age range (Gotelli, 1995). Consequently, in a long-lived species such as the sandbar shark, small errors in parameter estimates can become magnified.

Stage-based modeling is a matrix-based demographic approach that considers aggregate stages (defined in terms of size or life history stages) that represent functional biological units (Gotelli, 1995). It too has a long history in the field of ecological population dynamics (Kingsland, 1985). A stage-based model can be formed by collapsing a life table into discrete stages. Thus, unlike the life-table analysis that requires estimates for every year the organism lives, the stage-based model requires only estimates for each stage. Therefore, the realism of a many-staged model can be balanced with the precision of a simpler model when parameter estimation error is of concern. As with life tables, stage-based projection models can easily be solved analytically to permit formal sensitivity analysis (Caswell, 1989). Anderson (1990), and Hoenig and Gruber (1990) have suggested that stage-based models may provide a more realistic view of the dynamics of some populations.

The population dynamics of several marine species, including sandbar sharks (Cortés, 1999), sea turtles (Crouse et al., 1987; Crowder et al., 1994), blue crabs (Miller and Houde[5]), sardines (Lo et al., 1995), and anchovies (Pertierra et al., 1997) have been explored by using stage-based models. Cortés (1999) developed a stochastic stage-based model for sandbar sharks in the western North Atlantic. He used the model to explore the implications of three different harvest strategies on population viability when fecundity varies. He concluded that in the absence of exploitation, the sandbar shark population should increase slowly by about 1.3% annually. Additionally, Cortés concluded that all three patterns of exploitation would cause declines in population abundance. Cortés' model and results indicate the utility of stage-based models in exploring potential management alternatives for sandbar sharks.

Here, we develop a deterministic stage-based model for sandbar shark populations. The model includes the two-year reproductive cycle of fertile and resting periods known to occur in sandbar sharks, but which were not included in Cortés's (1999) original description. We chose to use a deterministic framework to permit a formal elasticity (proportional sensitivity) analysis of the basic model. Stages to which the population dynamics are most sensitive can be interpreted either as being stages at which management action is likely to have the most impact or as stages at which parameter estimates have to be most precise because of impacts of potential environmental stochasticity. We use the model to examine the expected change in population growth resulting from

[5] Miller, T. J., and E. D. Houde. 1998. Blue crab targeting. U.S. EPA Chesapeake Bay Program Report, Annapolis, MD, 167 p.

two particular management options, nursery ground closures and size limits. We exercised the general model framework to address four fundamental questions. What is the intrinsic rate of increase of sandbar shark populations under current patterns of exploitation? What is the sustainable level of fishing mortality ($F_{CRITICAL}$)? What is the effect of eliminating fishing mortality on early stages, either through nursery ground closures or through the introduction of size limits? For each question, we provide the results, predictions, and interpretation of sensitivity analyses to indicate the reliability of our conclusions.

Materials and methods

Life history of sandbar sharks

The first step in developing a stage-based model is to review the life history of a species to identify appropriate stages. Results of tagging and age and growth studies (Springer, 1960; Casey et al., 1985; Casey and Natanson, 1992; Sminkey and Musick, 1995, 1996) indicate that sandbar sharks are a long-lived species with low fecundity. These studies also indicate that females, males, and juveniles segregate by water depth and distance from shore. However, estimates of key vital rates are inconsistent. The generally accepted estimate of mortality and fecundity schedules indicates that sandbar sharks mature between 12 and 15 years of age and live to around 30 years of age (Casey et al., 1985; Sminkey and Musick, 1996). Another estimate suggests that sandbar sharks may not mature until age 29 and may live past 50 (Casey and Natanson, 1992). In our model we used an age at maturity of 15 years. From the biological function and the migration pathways determined by these studies, we identified five stages in the life history of the sandbar shark: neonates, juveniles, subadults, pregnant adults, and resting adults (Fig. 1).

Neonates are young-of-the-year sharks. Sandbar shark neonates are born fully developed at a fork length (FL) between 43 and 52 cm (Castro, 1983; Branstetter and Burgess[1]). They remain in this stage for one year before becoming juveniles. Juveniles are the first stage to show a seasonal pattern of movement. In the winter, juveniles migrate to warmer waters, often to the edge of the Gulf Stream off North Carolina. In the summer, juveniles return to their nursery grounds. They continue this seasonal migration until they are between 6 and 10 years old (Casey et al., 1985; Branstetter and Burgess[1]). In contrast, subadults, while still not yet mature, follow the adult migration pattern. This migration pattern consists of swimming along the Atlantic coast of the United States as far north as New England

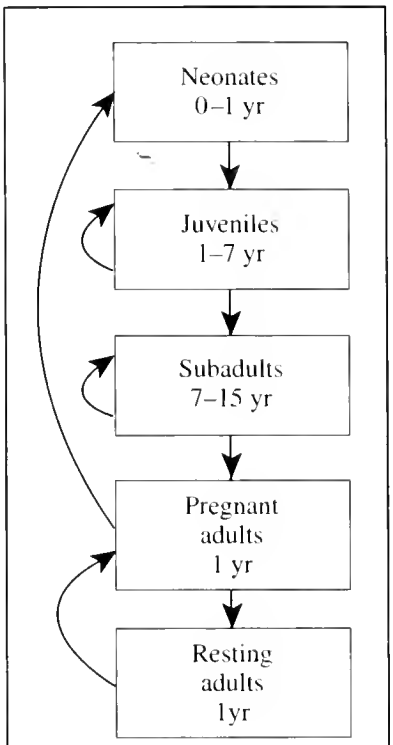

Figure 1

Diagram of the five-stage model. Arrows indicate individuals surviving and growing to the next stage or surviving and remaining in the same stage.

in the summer and traveling south to warmer waters in the winter (Castro, 1983). In this model, individuals remain in the subadults stage for 8 years, at which point they may be 15 years of age, and then join the reproductive population.

Fifty percent of female sandbar sharks are mature at about 150 cm FL (Springer, 1960; Casey et al., 1985; Sminkey and Musick, 1996) or 12 to 15 years of age depending on the von Bertalanffy model. Female sandbar sharks give birth at an average of 8 or 9 pups once every other year (Springer, 1960; Sminkey and Musick, 1996). Larger sharks do not appear to give birth to a greater number of pups (Sminkey and Musick, 1996). Gestation lasts between 9 and 12 months (Castro, 1983). Pregnant females pup in shallow bays and estuaries along the east coast of North America, including Chesapeake Bay (Sminkey and Musick, 1996), Delaware Bay (Pratt and Merson[6]) and the waters off the coast of South Caro-

[6] Pratt Jr., H. L., and R. R. Merson. 1996. Report of the 1996 apex predators investigation: sandbar shark nursery grounds project. Apex predators investigation. Northeast Fisheries Science Center, Natl. Mar. Fish. Serv., NOAA, Narragansett, RI.

lina (Castro, 1993). In the model, females alternate between pregnant and resting adult stages, spending one year in each. Thus, the stage durations used in the model were the following: 1 year for neonates; 6 years for juveniles; 8 years for subadults; 1 year for pregnant females; and 1 year for resting females.

Model development

The approach we present below is based on the general framework presented by Caswell (1989). Details on the general background of the approach can be found in Caswell (1989). In all equations, matrices and vectors are shown in boldface type, parameters in italic type.

The model is a postbreeding census, follows only females, and uses a yearly time step. The total number of sharks in the population at time t can be expressed in vector form as $\mathbf{N}_t$. Each element of $\mathbf{N}_t$ represents the number of sharks in the appropriate stage at time t. There are three possible transitions for each individual in each stage: the probability of surviving and growing to the next stage, G_t; the probability of surviving yet remaining in the same stage, P_t; or the probability of dying, $1-G_t-P_t$. The individual transition probabilities G_t and P_t may range between 0 and 1. The sum of G_t and P_t is further constrained such that when a stage is not subject to mortality, $G_t + P_t = 1$. One other parameter, stage-specific fecundity, is required to estimate the number of young females produced per breeding female per year.

The vital rates governing the dynamics of the shark population can be expressed mathematically in a 5×5 transition matrix, $\mathbf{A}$. The fundamental equation to estimate the stage-structure in the population at any time t is given by

$$\mathbf{N}_t = \mathbf{A}^t - \mathbf{N}_0, \tag{1}$$

where $\mathbf{N}_t$ = a vector of the number of individuals in each stage at time t; and

$\mathbf{A}$ = the transition matrix $\mathbf{A}$ for sandbar sharks given by

$$\begin{bmatrix} 0 & 0 & 0 & G_4 \times f_4 & 0 \\ G_1 & P_2 & 0 & 0 & 0 \\ 0 & G_2 & P_3 & 0 & 0 \\ 0 & 0 & G_3 & 0 & G_5 \\ 0 & 0 & 0 & G_4 & 0 \end{bmatrix}. \tag{2}$$

For large values of t, $\mathbf{AN}_t = \lambda \mathbf{N}_t = \mathbf{N}_{t+1}$, where the scalar λ is the finite rate of population increase. Further, $\ln\lambda = r$, the intrinsic rate of increase.

The columns of the matrix represent the fates of individuals in each stage. For example, surviving neonates can grow only to the juvenile stage (G_1) whereas surviving juveniles can either remain a juvenile (P_2) or survive and grow into a subadult (G_2). Surviving pregnant adults can give birth and become resting adults (G_4). Surviving resting adults (G_5) can grow only into a pregnant female. The rows represent the origins of individuals in each stage. Neonates arise from pregnant adults who survive ($G_4 \times f_4$) whereas juveniles arise from neonates surviving and growing into juveniles (G_1) or from juveniles surviving and remaining juveniles (P_2). Pregnant adults can arise from subadults surviving and growing into a pregnant female (G_3) or from resting adults surviving and becoming pregnant adults (G_5). Resting adults can arise only from pregnant adults that survive (G_4).

The transition probabilities, P_t and G_t, can be calculated from estimates of the probability that during a single time step an individual of stage i survives, σ_t, and an individual of stage i grows, γ_t. In this way G_t, the probability of surviving and growing to the next stage is given by

$$G_t = \sigma_t \gamma_t. \tag{3}$$

Consequently P_t, the probability of surviving, but not growing to the next stage is given by

$$P_t = \sigma_t (1 - \gamma_t). \tag{4}$$

The probability of survival, σ_t, over a single time step can be expressed as

$$\sigma_t = e^{-Z_t}. \tag{5}$$

Following traditional fisheries models, total mortality (Z_t) is calculated by using the equation $Z_t = F_t + M_t$, where F_t is the rate of fishing mortality and M_t is the rate of natural mortality at stage i.

Estimates of γ_t can be obtained in several different ways. Caswell (1989) recommended assuming constant stage duration for all individuals in the stage when only a relatively crude estimate of survival over broad age ranges is available. For this approach, individuals entering the stage have an equal probability of survival as individuals nearing the end of the stage. Employing this assumption yields an estimate of γ_t as

$$\gamma_t = \frac{(\sigma_t \lambda_{mat})^T - (\sigma_t \lambda_{mat})^{T-1}}{(\sigma_t \lambda_{mat})^T - 1}, \tag{6}$$

where T = the expected stage duration of a single stage; and

λ = the finite rate of population increase given by the dominant eigenvector of A ($\ln\lambda=r$, the intrinsic rate of increase).

We began with an initial value of $\lambda_{init} = 1$. We then iterated λ until the value of λ given by an eigenanalysis of the matrix **A** (see below), equaled the value of λ_{init} used in Equation 6. Together, Equations 1–6 described above allow estimates of G_i and P_i within **A** to be defined.

Fecundity must also be defined. The fecundity term, f_i, is simply the expected number of female offspring produced by a female in stage i. For sandbar sharks only one stage is reproductively active and thus the only fecundity term in the matrix **A** is $f_4 = 4.5$. This estimate is based on an equal sex ratio, 9 pups per brood, and one brood per year. However, as the model is a postbreeding census, the fecundity has to be discounted by the probability that a pregnant female will survive the gestation year to pup. Thus the realized fecundity term used in the model is $G_4 \times f_4$. All parameters within the matrix **A** are now defined.

One feature of stage-based projection models that motivated their use was that they allowed us to solve **A** analytically in order to calculate important demographic features and find the sensitivity of the model to parameter estimates. The two demographic features that can be calculated from **A** are the stable stage distribution and the reproductive value of each stage. Once the stable stage distribution has been reached, the relative proportion of individuals in each stage remains constant over time. The reproductive value is the relative number of offspring that are yet to be born by individuals in a given age (Gotelli, 1995). This value depends on individuals surviving to maturity and reproducing. Thus, the youngest stages should have the lowest reproductive values because individuals in those stages must survive and reach maturity before they can reproduce. Both features can be calculated from an eigenanalysis of **A**. For any $(n\times n)$ matrix one may define up to n scalar values ($\lambda_{1\ldots n}$) and n-associated right and left vectors such that

$$\mathbf{Aw} = \lambda\mathbf{w} \tag{7}$$

$$\mathbf{vA}^{\mathrm{T}} = \lambda\mathbf{v} \tag{8}$$

where $\mathbf{A}^{\mathrm{T}}$ = the transpose of **A**;
λ = the eigenvalue; and
w and **v** = the right and left eigenvectors of **A**.

The sandbar shark transition matrix has five possible eigenvalues and eigenvectors. However, our interpretation is simplified for the sandbar shark transition matrix, **A**, because it is non-negative, irreducible, and primitive. Thus, we are guaranteed that there is a single, dominant eigenvalue, λ_1, that is real, positive, and strictly greater than all other possible λs. This dominant eigenvalue, λ_1 will eventually describe the population rate of increase and $\ln \lambda_1 = r$, the intrinsic rate of increase of the population. Moreover, the right and left eigenvectors associated with λ_1 will be strictly positive. The population structure will eventually become proportional to a single stable stage distribution, given by $\mathbf{w}_1$. Finally, there will be a single vector, $\mathbf{v}_1$, associated with λ_1, that expresses the relative contributions of each stage to the future population—a vector of reproductive values. Reproductive values are standardized so that the reproductive value of an individual in the first stage is one.

We were interested in calculating the change in λ following a change in vital rates expressing a transition from stage i to any other stage (including remaining in i) that may have been caused by management activities. This change reflects the sensitivity of λ to the transition probability. If entries in the transition matrix **A** are represented as a_{ij}, it can be shown that

$$\frac{\partial\lambda}{\partial a_{ij}} = \frac{v_i w_j}{\langle w,v\rangle}. \tag{9}$$

where <**w**,**v**> = the scalar product of the two vectors.

Simply stated, the sensitivity of the population growth rate to changes in any vital rate is the product of the reproductive value of stage i and the proportional level of stage j in the stable stage distribution.

Because transition probabilities are censored parameters, varying only between 0 and 1, and fecundity is noncensored, it is more helpful to report the elasticity of λ. This is defined as the proportional change in λ for proportional changes in a_{ij}. Elasiticities are calculated as

$$e_{ij} = \frac{a_{ij}}{\lambda}\frac{\partial\lambda}{\partial a_{ij}}. \tag{10}$$

Importantly, elasticities are additive, such that the sum of elasticities for each stage defines the proportional contribution of a_{ij} to overall population growth, λ, as

$$\sum_i\sum_j e_{ij} = 1.$$

Elasticities depend on a stable stage distribution and should be compared qualitatively.

Transition probability estimation for management options

Current conditions Fishing mortality (F) and especially natural mortality (M) are difficult to estimate. Owing to the uncertainty in estimates and in order to simplify the model, we used an estimate of $M = 0.1$ for all stages and all projections (NMFS[1]; Sminkey and Musick, 1996). We projected the population forward using $F = 0.20$ for juveniles and older stages, as estimated in the 1996 shark evaluation workshop (SEW) for sandbar sharks only (NMFS[3]). For neonates a lower value of $F = 0.10$ was used because small sharks may be, but are not as likely to be, caught on the same gear as older sharks (Branstetter and Burgess[1]). Using these values of F and M and f_4=4.5, we iterated Equation 6 to estimate all P_t and G_i values. We initialized the population with 1000 neonates. Then we estimated the initial number in subsequent stages using the 90% survival schedule for sandbar sharks given in Sminkey and Musick (1996). These calculations yielded an initial population of 9640 sharks (N_0).

Estimate of $F_{CRITICAL}$ We defined $F_{CRITICAL}$ as the limiting level of fishing mortality that is sustainable, i.e. the F for which $r = 0$ or $\lambda = 1$, where $r = \ln\lambda$. We systematically reduced F on all stages to define the relationship between F and r. For our estimations, F_1 remained 0.10 as long as $F_{2,3,4,5}$ was ≥0.10. For any $F_{2,3,4,5}$ <0.10, $F_1 = F_{2,3,4,5}$. Thus, the fishing mortality of neonates was never greater than the fishing mortality on other stages.

Protecting neonates and pregnant adults: an extreme example We used the model to determine how efficient protecting different stages would be in promoting recovery of sandbar shark stocks. We asked the question: If neonates and pregnant adults are removed from the commercial fishery, how much will F on other stages need to be reduced to arrive at a sustainable population level? To address this question, we modified the model to remove all mortality on neonates (F_1=0, M_1=0) and to protect all pregnant adults from fishing pressure (F_4=0). In reality, we could not completely protect neonates from mortality (i.e. M_1>0) and we could not fully protect pregnant adults from commercial fishing. Thus the scenario represents an idealized nursery closure scheme. Fishing mortality on juveniles, subadults, and resting adults remained at 0.20. The fecundity for pregnant adults was left at 4.5.

Nursery closures and size limits We also ran the model using more realistic scenarios. In this case F on neonates and juveniles was 0, and F on the older stages was 0.20. Natural mortality for all stages remained at 0.10. This scenario is a fairly realistic size limit or nursery ground closure because sandbar sharks segregate by size. This scenario is similar to, but not as strict as, the 1998 SEW's recommended size limit.

Size limits protecting only one stage are another management option available. This method can be used to reduce the fishing mortality on any range of sizes. In this paper, two scenarios of this type are presented: 1) a size limit which reduces the F on juveniles to 0; and 2) a size limit which reduces the F on subadults to 0. Fishing mortality was equal to 0.20 in all other stages except neonates, where F=0.10. Implementing such management actions would be difficult because the gear (longlines) cannot realistically avoid catching only the restricted stage, but the results would be indicative of the potential of these mechanisms to improve stocks.

Using the relationships (Eqs. 1–10) and vital rate estimates defined above, we now proceed with an analysis of the population dynamics of sandbar sharks. For each scenario, we calculate the stable stage distribution, the proportional reproductive value for each stage, and the elasticity of λ to changes in each matrix parameter, and compare the population growth rate and potential population reduction after 20 years for each scenario.

Results

Current conditions

When $F = 0.20$ for all stages except neonates, the population decreases (Table 1). The model predicts the intrinsic rate of natural increase, r, of the population as $r = -0.124$. The population is 13% of the initial abundance when projected 20 years forward. Population growth rate, stable stage distribution, and reproductive values are not affected by choice of the actual numbers used for initial abundance. The stable stage distribution is reached after 21 years in this scenario.

The largest proportion of the population (>0.56) are juveniles (Table 2). The smallest proportions (0.04, 0.03) are pregnant and resting adults, respectively. Adults have much larger reproductive values than prereproductive stages (Table 3).

The pattern of model proportional sensitivity is shown in Figure 2. The elasticity of λ to a small change in fecundity was expressed only in the preg-

Table 1

The reduction in population abundance after 20 years of each scenario.

Scenario	Fishing and natural mortality rates used	Intrinsic rate of increase, r	Reduction (%) in population abundance after 20 years[1]
Current conditions	F_1=0.10; F_{2-5}=0.20 M=0.10	–0.124	87
Protecting neonates and pregnant adults	$F_{1,4}$=0; $F_{2,3,5}$=0.20 M_1=0; M_{2-5}=0.10	–0.079	62
Protecting neonates and juveniles	$F_{1,2}$=0; F_{3-5}=0.20 M=0.10	–0.058	51
Protecting juveniles only	F_1=0.10; F_2=0 F_{3-5}=0.20; M=0.10	–0.069	62
Protecting subadults only	F_1=0.10; F_3=0 $F_{2,4,5}$= 0.20; M=0.10	–0.048	50

[1] This percent reduction in population abundance is based on numbers generated in the model. Population abundance can also be calculated by using the equation

$$1 - e^{rt},$$

where r = the intrinsic rate of increase; and
t = the number of years.

Use of this equation results in a greater reduction in the population abundance.

Table 2

The stable stage distributions for each stage of the model and each scenario. The values of all stages under a scenario should sum to one.

Model stage	Current conditions, unstablized	Current conditions, stablized	Protecting neonates and pregnant adults	Protecting neonates and juveniles	Protecting juveniles	Protecting subadults
Neonate	0.15	0.16	0.15	0.10	0.12	0.19
Juvenile	0.56	0.54	0.60	0.54	0.51	0.51
Subadults	0.22	0.22	0.18	0.31	0.31	0.21
Pregnant adults	0.04	0.04	0.03	0.03	0.03	0.05
Resting adults	0.03	0.04	0.03	0.02	0.03	0.04

nant adult stage (because this is the only stage that is reproductively active). The highest elasticities were for the transition from neonate to juvenile and juvenile to subadult stages (Fig. 2). The elasticities for sharks remaining in the stage were equal for neonate, juvenile, subadult, and pregnant female stages. As discussed, the individual elasticities can be summed to estimate the overall contribution of each stage to λ. It is clear from Figure 2 that the peak elasticity occurs in the subadult stage. Estimates of elasticity suggest that the model is 2.3 times more sensitive to changes in this stage than in pregnant adults.

Estimate of $F_{CRITICAL}$

The relation between F and r is linear (Fig. 3). $F_{CRITICAL}$ = 0.071 when M = 0.10. Therefore, the population is sustainable if F = 0.071. The value of $F_{CRITICAL}$ will vary with the value of M that is chosen. Our analyses showed that total mortality (Z) must be less than 0.17 for all stages if the population is to increase (Fig. 4). The population will increase at a rate r = 0.05 if Z = 0.122, and the population will decrease at a rate r = –0.05 if Z = 0.222.

At $F_{CRITICAL}$, the population abundance stabilizes and the population reaches a stable stage distribu-

Table 3

The proportional standardized reproductive values of each stage under each scenario. Neonates will always equal one.

Model stage	Current conditions, unstablized	Current conditions, stablized	Protecting neonates and pregnant adults	Protecting neonates and juveniles	Protecting juveniles	Protecting subadults
Neonate	1.00	1.00	1.00	1.00	1.00	1.00
Juvenile	1.08	1.19	0.92	1.04	1.26	1.29
Subadults	3.10	3.32	3.48	1.34	1.52	5.83
Pregnant adults	12.72	13.06	20.44	9.23	9.65	8.84
Resting adults	10.67	11.00	16.38	7.25	7.66	6.87

tion (Table 2). In this scenario, the proportion of neonates, pregnant adults, and resting adults in the population has increased compared with the proportion of stages in previous scenarios. The pattern in reproductive values remains largely unchanged (Table 3). As with the baseline scenario, the elasticities show the model to be the most sensitive to changes at the juvenile and subadult stages.

In summary, these model runs suggest that to stabilize and increase the sandbar shark population, F needs to be reduced below 0.07 ($Z \leq 0.17$). An F of this magnitude requires more than the full 50% quota reduction to be implemented.

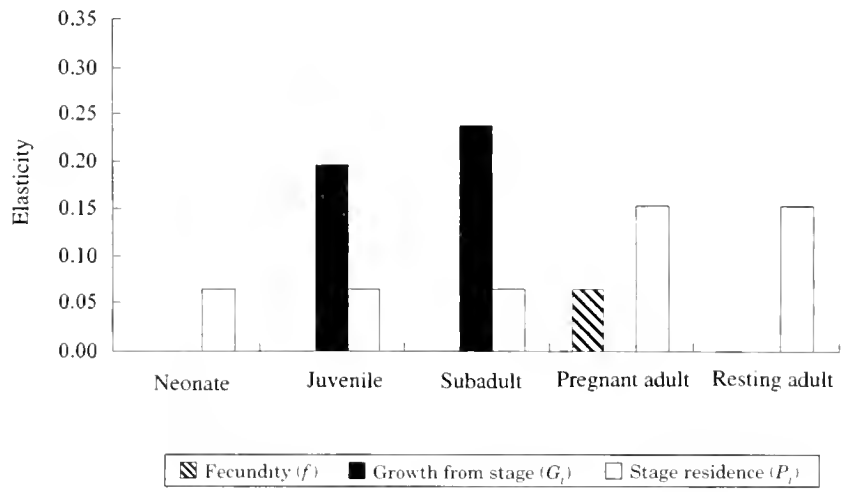

Figure 2

The proportional sensitivities (elasticity) of each stage to fecundity, growth, and stage residence under current fishing conditions (F=0.20).

Protecting neonates and pregnant adults: an extreme example

Results show that, even after protection of neonates and pregnant females, at current levels of F the population still decreases rapidly (r=–0.079). The population, projected 20 years forward, is only 38% of the initial abundance (Table 1). This percentage compares with reductions to 13% of initial abundance and r=–0.124 in the base run, where $F_{2,3,4,5} = 0.2$. In order to have a stable population (r=0) under this scenario, we needed to decrease F to 0.097. Without protecting neonates and pregnant females, F must be reduced to 0.07. Thus, protecting neonates and pregnant females provides a 37% increase in the F required to maintain a sustainable population (Table 4). However, it must be emphasized that although this option does provide some protection, implementation would still require a 52% reduction in F over those levels currently estimated to be operating in the fishery. This reduction is in contrast to the 64% reduction in F required to reach sustainable rates of exploitation in the absence of this protection.

Juveniles had the highest proportion of individuals in the stable stage distribution (Table 2). Pregnant females and resting adults have the highest reproductive values (Table 3). Similar to the previous scenario, projections show the highest overall sensitivity to transitions involving the abundance of subadults (Fig. 5). However, in contrast with earlier simulations, projections show additional substantial sensitivity to transitions into the resting adult stage (Fig. 5).

Nursery ground closures and size limits

Results of this scenario show that the protection of neonates and juveniles from all fishing mortality slowed the decline (r=–0.058) but could not stabilize the population. When projected forward 20 years, the population abundance is 49% of the initial abundance (Table 1). In order to stabilize this model, F had to be reduced on subadults and adults to 0.109. Thus, this closure provides a 54% increase in the F required to maintain a sustainable population over that required in the absence of nursery closures and a 12% increase in F over the extreme option modeled above (Table 4). Protecting neonates and juveniles through nursery ground closures or size limits would require a 46% reduction in F over those levels currently estimated to be operating in the fishery.

Juveniles have the highest proportion of individuals in the stable stage distribution (Table 2). Pregnant adults and resting adults have the highest reproductive values (Table 3). Again, the model shows the highest sensitivities to the juvenile and subadults stages (Fig. 6).

Protecting either juveniles or subadults alone still leads to a declining population. When F_2=0, after 20 years the population is 38% that of the initial population (Table 1). When F_3=0, the population at 20 years is 50% that of the initial population (Table 1). Further runs indicated that the population is stabilized if $F_{3,4,5}$ = 0.101 (when F_2=0) or if $F_{2,4,5}$ = 0.120 (when F_3=0). Quota reductions of 50% and 40%, respectively, are required to achieve these critical levels of F. In both cases the stable stage distribution is achieved within 24 years. The stable stage distribution proportions and reproductive values of each stage are listed in Tables 2 and 3. Figure 7 shows the sensitivity of the model to fecundity, growth, and stage residence when F_2 = 0. These sensitivities were approximately the same when F_3 = 0. As in the other models, juveniles and subadults have the highest sensitivity.

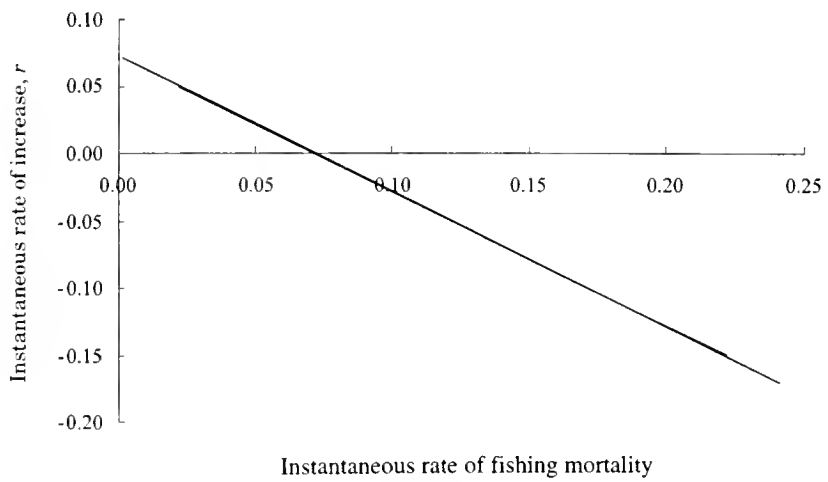

Figure 3

The relation between the intrinsic rate of increase (r) and fishing mortality (F). $F_{critical}$ is reached at 0.071. If F is less than $F_{critical}$, the population will increase. If F is greater than $F_{critical}$, the population will decrease.

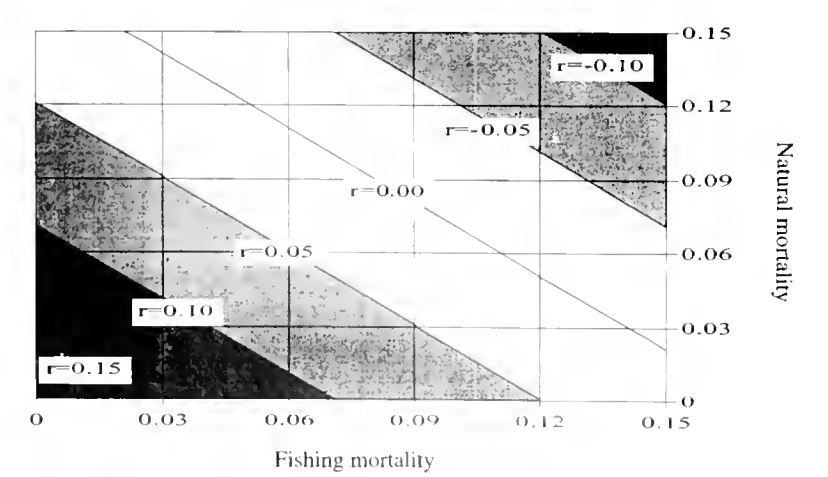

Figure 4

Isoclines showing the intrinsic rate of increase (r) at different rates of fishing (F) and natural mortality (M). The population will increase if r is greater than zero. The population will decrease if r is less than zero.

Discussion

The model projects that the sandbar shark population is unlikely to increase unless F is reduced below $F_{CRITICAL}$. The value calculated here is less than the $F_{CRITICAL}$ value of 0.10 that Sminkey and Musick (1996) predicted by using a life table. Both Sminkey and Musick's (1996) and Cortés's (1999) results and those presented here indicate that current estimates of F are

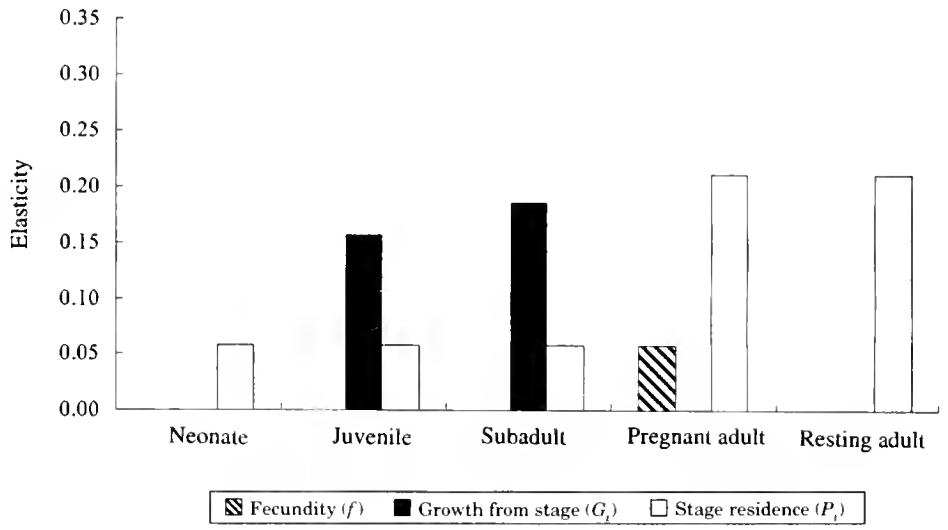

Figure 5

The proportional sensitivities (elasticity) of each stage to fecundity, growth, and stage residence if neonates and pregnant adults are protected ($F_{1,4}$=0; $F_{2,3,5}$=0.20).

Table 4

The percent reduction in fishing mortality needed to stabilize the population if $F_{Current}$ = 0.20. $F_{Critical}$ is the fishing mortality level at which the population abundance is stable. $F_{Current}$ is the fishing mortality level estimated in the 1996 stock assessment.

Scenario	Fishing and natural mortality rates used	$F_{Critical}$	% reduction needed
Current conditions	F_1=0.10; F_{2-5}= 0.20 M=0.10	0.071	64
Protecting neonates and pregnant adults	$F_{1,4}$=0; $F_{2,3,5}$=0.20 M_1= 0; M_{2-5}=0.10	0.097	52
Protecting neonates and juveniles	$F_{1,2}$=0; F_{3-5}=0.20 M=0.10	0.109	46
Protecting juveniles only	F_1=0.10; F_2=0 F_{3-5}=0.20; M=0.10	0.101	50
Protecting subadults only	F_1=0.10; F_3=0 $F_{2,4,5}$=0.20; M=0.10	0.120	40

too high to maintain the population and must be reduced. At the 1996 SEW, it was determined that reducing F levels by 50% was likely to increase the chances of recovering the large coastal stock (NMFS[1]). In response to this, NMFS reduced the quota in 1997 for Atlantic large coastal sharks by 50% in order to reduce F by 50%. Assuming that the estimate of F from the SEW is accurate, that a 50% quota reduction is equivalent to a 50% decrease in F, and that the reduction in F is equally distributed across age classes, we believe our results indicate that a 50% quota reduction may not stabilize the stock. Our model predicts that without alternative management strategies, the population will not begin to recover unless F on sandbar sharks is reduced to below 0.07, requiring a reduction in current estimates of F of greater than 50%.

Nursery ground closures and size limits are possible management strategies. These strategies would protect neonates, pregnant adults who are in the

nursery grounds to pup, and any juveniles who may have returned for the summer. One of the scenarios we ran is extreme in that every neonate survives (Z=0) and pregnant adults are not fished for the entire time they are pregnant. But in this scenario, juveniles are not protected. If F is not reduced on juveniles, subadults, and resting adults, the model shows that the population will decrease until F is reduced to 0.097. This is higher than the F = 0.07 which would be needed to stabilize the population without any protection for neonates, and would almost be met by the 50% reduction in quota as suggested by the 1996 SEW. However, these scenarios assume complete protection of protected stages from either fishing or natural mortality. Thus, they probably over-estimate the effectiveness of the potential management action. Overall, these models indicate that nursery ground closures or size limits that protect only neonates and juveniles, or neonates and pregnant adults, are not likely to be the ultimate solution. Additional measures will need to be taken to protect the sandbar shark.

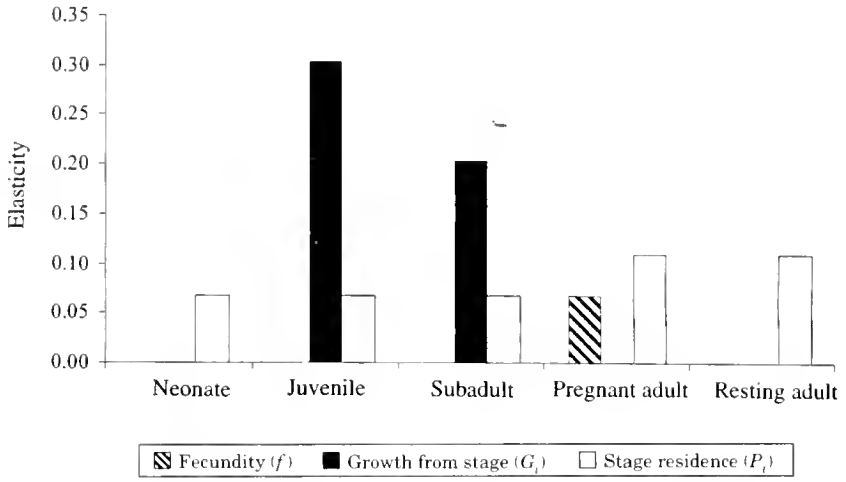

Figure 6

The proportional sensitivities (elasticity) of each stage to fecundity, growth, and stage residence if neonates and juveniles are protected ($F_{1,2}$=0; $F_{3,4,5}$=0.20).

Subsequent runs of the model showed that size limits that protect juvenile and subadult stages will not act to rebuild the population alone, despite the fact that the model indicates these stages are the most sensitive to survival. In these cases, F needs to be reduced to 0.10 or 0.12, respectively. If the current F estimate of 0.20 is correct and if a 50% reduction in quota reduces F by 50%, size limits to protect either stage and a reduction in quota of between 40% and 50% may be sufficient to stabilize the population.

All scenarios indicate that the sandbar shark stock will most likely be rebuilt through a combination of management strategies. With nursery closures or size limits that protect only one stage, the stock will decline if fishing mortality remains the same as that currently estimated. Because the model's estimates of population growth are sensitive to survival at the juvenile and subadult stages, because these stages have the highest proportion of the population in the stable stage distribution, and because subadults have relatively high reproductive values, ideally any management strategies selected should be those that conserve these stages.

Most of the model projections indicate that the total sensitivities of juveniles and subadults are the greatest. The sensitivity of population growth to events during these stages suggests two things: management needs to focus on protecting juveniles and subadults, and scientists need to collect accurate estimates of F and M for juveniles and subadults. Possible conservation efforts could include minimum sizes to protect immature sandbar sharks or time-area closures to protect both juveniles and subadults during their migrations. If our model is correct, it is important to take measures to protect these stages soon, not only because the model shows that the population abundance decreases quickly at current estimates of F, but also because there is evidence of strong year classes of immature sandbar sharks entering the fishery (Branstetter and Burgess[1]). In 1994, Sminkey suggested that the 1987, 1989, and 1992 year classes in Chesapeake Bay were exceptionally strong. It will be easier for the fishery to recover if we have strong year classes on which to build.

This is not the first time the use of a stage-based model has concluded that conservation efforts should target juveniles and subadults of a long-lived species more than newborns. Rates of population growth in many marine species are effected more by changes in survival of juvenile and subadult stages than by changes in survival of other stages, or by changes in fecundity (Heppell et al., 1999). For example, Crouse et al. (1987) and Crowder et al. (1994) concluded that population growth rate was most sensitive to the survival of large juvenile loggerhead sea turtles.

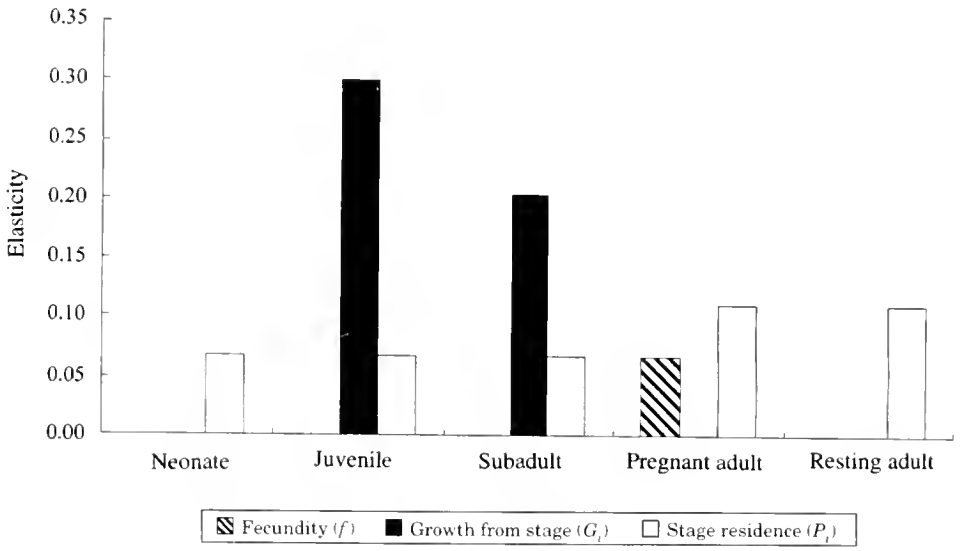

Figure 7

The proportional sensitivities (elasticity) of each stage to fecundity, growth, and stage residence if only juveniles are protected (F_2=0; F_1=0.10; $F_{3,4,5}$=0.20).

They suggested that the use of turtle excluder devices would protect juvenile sea turtles and aid in conservation and recovery of this species. Additionally, Heppell et al. (1996) indicated that population enhancement by means of hatchery production of sea turtles would likely not be successful. In contrast, marine mammals show a different pattern of sensitivity. For these taxa, population growth appears most sensitive to events occurring during the adult stages (Heppell et al., 1999). Studies indicate that marine fish may also show a different pattern of sensitivity, where there is increased sensitivity to events in the early life history (Heppell et al. 1999; Quinlan and Crowder, 1999).

Three features of our approach require one to use caution in interpreting our conclusions. First, there are problems in using stage-based models, or demographic models of all types, with highly migratory animals such as sharks. For instance, most demographic models assume that the population is closed. In the case of the sandbar shark this assumption may not hold true. Tagging studies show that a small percentage of sandbar sharks tagged in U.S. waters are caught in Mexican waters. Because it is currently unknown if there are nursery grounds in Mexican waters, this migration to Mexico may represent an additional source of loss to the population that may not be replaced. The model does not consider this loss. If a significant number of sandbar sharks are found to migrate to Mexican waters, current estimates of F may be underestimates. If this is the case, even greater reductions in F may be necessary to help the stock recover.

Second, we have presented a deterministic model of sandbar shark population dynamics. Thus, we have ignored uncertainty of and plasticity in vital rates such as growth and fecundity. Tuljapurkar (1997) and Nations and Boyce (1997) have discussed the potential biases that may result from basing harvest strategies on results from a deterministic model, particularly when juvenile survival is closely tied to environmental conditions. In addition to potential biases in the results, a deterministic model yields only a point estimate of population growth rate. Cortés (1999) included a stochastic term for fecundity in his model for sandbar sharks. Subsequently, he used Monte Carlo simulations to generate distributions of predicted population growth rates when fecundity varies stochastically. His results indicate that predicted population growth rates may vary by 2–3% when fecundity is allowed to vary. The impact of stochasticity in survival and growth on the predicted population growth rates is unknown. However, given the sensitivity of the model to transition involving growth and survival for juvenile and subadult animals, its impact may be substantial.

Finally, unlike many traditional fishery models, our demographic model does not take into account density dependence or compensation. However, given the longevity and age to maturity of sandbar sharks, and sharks in general, compensation may not be as signif-

icant or as observable as that for teleost fish. Sminkey and Musick (1995) have suggested three mechanisms of compensation in sharks: decreases in natural mortality of younger sharks as the abundance of predatory larger sharks is reduced; compensatory increases in fecundity when food is more available or when uterine mortality is reduced; and an increase in growth rate and thus a decrease in natural mortality and possibly earlier maturity when food is abundant. In Chesapeake Bay, they found evidence of a slight increase in growth rate of juvenile sharks after the population had been depleted but were not able to ascertain if the age of maturity had also been reduced. Late age at maturity due to relatively slow growth rates reduces the probability that small increases in growth or increased neonate survival through density-dependent mechanisms will compensate for fishing mortality (Heppell et al., 1999).

In summary, the results when $F = 0.20$ for older stages indicate that sandbar shark stocks are currently being fished above their ability to replace themselves (i.e. r is negative for the best estimate of F). Thus, management action (e.g. time area closures, reduced quota, minimum size) is needed to reduce F to the level where r is zero or positive. Because the model is highly sensitive to juvenile and subadult survival, management actions that reduce the mortality rates of these stages would likely be more effective than nursery closures that protect only neonates and pregnant females.

Although our study suggests that the protection of juvenile and subadult sandbar sharks may aid in recovery of sandbar sharks, our method may not work as well on other shark species, because life history traits differ. Sandbar sharks are often confused with other shark species such as the dusky shark; therefore, whichever management strategy is chosen, it should work for all large coastal shark species. These problems, combined with a paucity of data on pupping grounds, age at maturity, and other traits, make selection of a conservation method difficult. The model in our study should be viewed as a starting point for looking at the effect of the different options available and for comparing these options among the shark species involved.

Acknowledgments

We thank Selina Heppell, Pamela Mace, Michael Fogarty, John Musick, Thomas Sminkey, Ed Houde, and Steve Branstetter for comments on an earlier draft of this manuscript. Support for this work comes from the Chesapeake Bay Program USEPA (grant CB-993080-02), the Hudson River Foundation (grant 008/98A), and the University of Maryland Center for Environmental Sciences.

Literature cited

Anderson, E. D.
1990. Fishery models as applied to elasmobranch fisheries. *In* Elasmobranchs as living resources: advances in the biology, ecology, systematic, and the status of the fisheries (H. L. Pratt, S. H. Gruber, T. Taniuchi, eds.), p. 473–484. U.S. Dep. Commer., NOAA Technical Report NMFS 90.

Casey, J. G., and L. J. Natanson.
1992. Revised estimates of age and growth of the sandbar shark (*Carcharhinus plumbeus*) from the western North Atlantic. C. J. Fish. Aquat. Sci.49:1474–1477.

Casey, J. G., H. L. Pratt Jr., and C. E. Stillwell.
1985. Age and growth of the sandbar shark (*Carcharhinus plumbeus*) from the western North Atlantic. Can. J. Fish. Aquat. Sci. 42:963–975.

Castro, J.
1983. The sharks of North American waters. Texas A&M Univ. Press, College Station, TX, 180 p.
1993. The shark nursery of Bulls Bay, South Carolina, with a review of the shark nurseries of the southeastern coast of the United States. Environ. Biol. Fish. 38:37–48.

Caswell, H.
1989. Matrix population models. Sinauer Associates, Inc., Sunderland, MA, 328 p.

Cortés, E.
1999. A stochastic stage-based population model of the sandbar shark in the western North Atlantic. Am. Fish. Soc. Symp. 23:115–136.

Crouse, D. T., L. B. Crowder, and H. Caswell.
1987. A stage-based population model for loggerhead sea turtles and implications for conservation. Ecology 68:1412–1423.

Crowder, L. B., D. T. Crouse, S. S. Heppell, and T. H. Martin.
1994. Predicting the impact of turtle excluder devices on loggerhead sea turtle populations. Ecol. Appl. 4:437–445.

Gotelli, N. J.
1995. A primer of ecology. Sinauer Associates, Sunderland, MA, 206 p.

Heppell, S. L., L. B. Crowder, and D. T. Crouse.
1996. Models to evaluate headstarting as a management tool for long-lived turtles. Ecol. Appl. 6:556–565.

Heppell, S., L. B. Crowder, T. R. Menzel.
1999. Life table analysis of long-lived marine species, with implications for conservation and management. Am. Fish. Soc. Symp. 23:137–148.

Hoenig, J. M., and S. H. Gruber.
1990. Life history patterns in the elasmobranchs: implications for fisheries management. *In* Elasmobranchs as living resources: advances in the biology, ecology, systematic, and the status of the fisheries (H. L. Pratt, S. H. Gruber, T. Taniuchi, eds.), p. 1–16. U.S. Dep. Commer., NOAA, Tech. Report NMFS 90.

Kingsland, S. E.
1985. Modeling nature: episodes in the history of population ecology. Chicago Univ. Press, Chicago, IL, 267 p.

Lo, N. C. H., P. E. Smith, and J. L. Butler.
1995. Population growth of northern anchovy and Pacific sardine using stage-specific matrix models. Mar. Ecol. Prog. Ser. 127:15–26.

NMFS (National Marine Fisheries Service).
1993. Fishery management plan for sharks of the Atlantic ocean. Office of Sustainable Fisheries. U.S. Dep. Commer., National Oceanic and Atmospheric Administration (NOAA), NMFS, Silver Spring, MD, 173 p.
1997. Report to Congress: status of fisheries of the United States. U.S. Dep. Commer., NOAA, Silver Spring, MD, 75 p.

Nations, C. S., and M. S. Boyce.
1997. Stochastic demography for conservation biology. *In* Structured models in marine, terrestrial and freshwater systems (S. Tuljapurkar and H. Caswell, eds.), p. 450–469. Chapman and Hall. New York, NY, 643 p.

Pertierra, J. P., J. Lleonart, and N. C. H. Lo.
1997. Application of a stage-specific matrix model and length-cohort based analysis to assess the anchovy fishery in Catalan coastal waters (NW Mediterranean Sea). Fish. Res. 30:127–137.

Quinlan, J. A., and L. B. Crowder.
In press. Searching for sensitivity in the life history of Atlantic menhaden: inferences from a matrix model. Fish. Oceanog.

Simpfendorfer, C. A.
1999. Demographic analysis of the dusky shark fishery in southwestern Australia. Am. Fish. Soc. Symp. 23:149–160.

Sminkey, T. R., and J. A. Musick.
1995. Age and growth of the sandbar shark, *Carcharhinus plumbeus*, before and after population depletion. Copeia 4:871–883.
1996. Demographic analysis of the sandbar shark, *Carcharhinus plumbeus*, in the western North Atlantic. Fish. Bull. 94:341–347.

Springer, S.
1960. Natural history of the sandbar shark, *Eulamia milberti*. U.S. Fish Wildl. Serv. Fish. Bull. 61:1–38

Tuljapurkar, S.
1997. Stochastic matrix models. *In* Structured models in marine, terrestrial and freshwater systems (S. Tuljapurkar and H. Caswell, eds.), p. 59–87. Chapman and Hall. New York, NY, 643 p.

Food habits of the South American sea lion, *Otaria flavescens*, off Patagonia, Argentina

Mariano Koen Alonso

Enrique A. Crespo

Susana N. Pedraza

Centro Nacional Patagónico (CONICET)
and Universidad Nacional de la Patagonia
Boulevard Brown 3600
(9120) Puerto Madryn, Chubut, Argentina
E-mail address: koen@cenpat.edu.ar

Néstor A. García

Centro Nacional Patagónico (CONICET)
Boulevard Brown 3600
(9120) Puerto Madryn, Chubut, Argentina

Mariano A. Coscarella

Centro Nacional Patagónico (CONICET)
and Universidad Nacional de la Patagonia
Boulevard Brown 3600
(9120) Puerto Madryn, Chubut, Argentina

Abstract.—Food habits of the South American sea lion (*Otaria flavescens*) off Patagonia were studied by means of stomach content analysis. The samples were collected during 1982–1987 and 1990–1998 in northern and central Patagonia. The samples (n=59) came from individuals found dead on beaches and from animals recovered in incidental catches of the fishery. Forty-one prey species (including fishes, cephalopods, crustaceans, gastropods, polychetes, sponges, and tunicates) were identified; most important were Argentine hake (*Merluccius hubbsi*), red octopus (*Enteroctopus megalocyathus*), Argentine shortfin squid (*Illex argentinus*), "raneya" (*Raneya brasiliensis*), Patagonian squid (*Loligo gahi*), and Argentine anchovy (*Engraulis anchoita*). Differences in diet were found between sexes but not between geographical area of sampling, period of sampling, or source of samples. Females fed mostly on benthic species, whereas males fed mostly on demersal-pelagic species. The difference in diet between sexes was associated with different feeding grounds or different home ranges and could be produced by different constraints in the feeding behavior of each sex. These different constraints and restrictions could lead females to feed in more coastal and shallower waters than those waters where males feed. Some of the important prey were commercial species (Argentine hake, Argentine shortfin squid, Patagonian squid) consumed at both commercial and noncommercial sizes by sea lions. The presence of gastroliths was independent of the presence of stomach parasites; however, gastrolith weight was positively correlated with individual sea lion's length, indicating that gastroliths could be involved in buoyancy control. In summary, these stomach content analyses indicate that South American sea lions feed primarily on demersal and benthic species and, in general terms, use resources according to their environmental availability.

Manuscript accepted 9 August 1999.
Fish. Bull. 98:250–263 (2000).

The South American sea lion (*Otaria flavescens*) is one of the most common and abundant marine mammal species in the southwestern Atlantic and is distributed along the coasts of South America from Peru to southern Brazil in both the Pacific and Atlantic Oceans (Vaz Ferreira, 1982; Crespo[1]). Most investigations on South American sea lions have been focused on social behavior, breeding biology, and population dynamics (Vaz Ferreira, 1982; Campagna and Le Boeuf, 1988; Cappozzo et al., 1991; Crespo and Pedraza, 1991; Crespo[1]). Recent research has provided new data on the interactions between South American sea lions and fisheries (Crespo et al., 1994, 1997), on population size and trends (Reyes et al., 1999; Dans et al.[2]), and on diving behavior of lactating females (Werner and Campagna, 1995).

South American sea lions are considered opportunistic and broad-spectrum feeders, feeding on fish, squid, crustaceans, and occasionally on sea birds (Vaz Ferreira, 1982; George-Nascimento et al., 1985; Crespo et al., 1997). In Chilean waters, their most important prey are the Patagonian grenadier (*Macruronus magellanicus*) and the kingclip (*Genypterus* spp.); no relationship has been found between predator and prey sizes (George-Nascimento et al., 1985). For Patagonian waters, only preliminary information has been published about feeding (Crespo et al., 1997). Several studies (Hamilton, 1934; Vaz Fer-

[1] Crespo, E. A. 1988. Dinámica poblacional del lobo marino del sur *Otaria flavescens* (Shaw, 1800) en el norte del litoral patagónico. Doctoral thesis, Facultad de Cs. Exáctas y Naturales, Universidad Nacional de Buenos Aires, Buenos Aires, Argentina, 298 p.

[2] Dans, S., E. A. Crespo, S. Pedraza, R. González, and N. García. 1996. Estructura y tendencia de los apostaderos de lobos marinos de un pelo (*Otaria flavescens*) en el norte de Patagonia. Informes Técnicos del Plan de Manejo Integrado de la Zona Costera Patagónica. Fundación Patagonia Natural (Puerto Madryn, Argentina) 13:1–21.

Table 1

Number of South American sea lion stomachs analyzed in our study by period of time, geographical area, sex, and source of sampling. The number of empty stomachs is given in parentheses.

		Males		Females	
Period	Area	Dead on shore	Caught incidentally	Dead on shore	Caught incidentally
1982–87	Northern Patagonia	6 (1)		3 (1)	
	Central Patagonia			1 (0)	
1990–98	Northern Patagonia	13 (4)		20 (4)	
	Central Patagonia	1 (1)	8 (0)	4(0)	3(0)

reira, 1982; George-Nascimento et al., 1985) have reported the presence of gastroliths in this species, and others (Taylor, 1993) have suggested functions for them (food processing, buoyancy control, elimination of internal parasites, and alleviation of hunger).

The marine ecosystem in Patagonia supports one of the most intense fisheries in the world, with approximately one million tons of catch per year during the 1990s (Anonymous, 1996). South American sea lions are reported to be caught incidentally in the trawl fisheries for Argentine hake (*Merluccius hubbsi*) and Argentine red shrimp (*Pleoticus muelleri*) (Crespo et al., 1994, 1997). Some of the target and bycatch species of these and other fisheries, such as the Argentine shortfin squid (*Illex argentinus*) fishery, are consumed by South American sea lions (Crespo et al., 1997). The development of the fisheries may have been one factor that slowed the recovery of the South American sea lion population after harvesting of this marine mammal species ended in the mid 1960s (Crespo and Pedraza, 1991).

The objectives of this research were to describe the diet of South American sea lions off Patagonia, to evaluate some hypotheses on the function of gastroliths, and to explore the possibility of trophic competition with commercial fisheries.

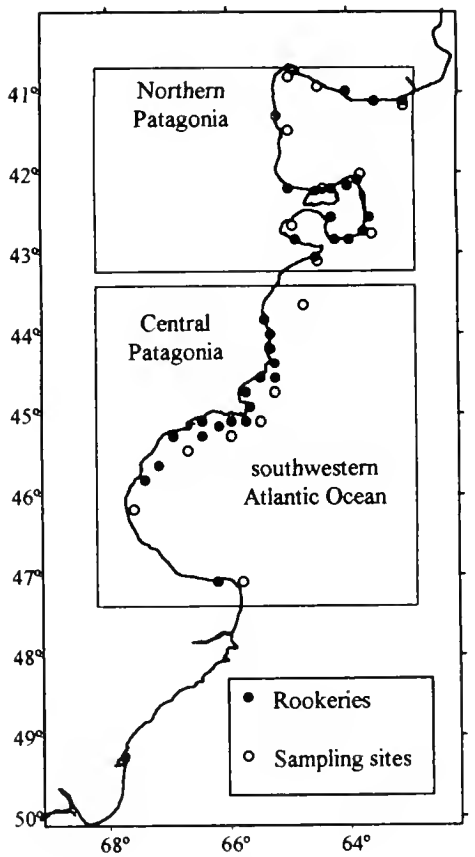

Figure 1

Study area, showing the two geographical areas considered in this work: northern and central Patagonia. The filled circles indicate the location of rookeries of South American sea lion and the empty circles indicate sampling sites.

Materials and methods

Sample studied

The total sample was composed of 59 stomachs from 28 males and 31 females, obtained in the periods 1982–1987 and 1990–1998 (Table 1). Most of the 1982–1987 sample (n=10) was collected in the northern area of Patagonia (Fig. 1). These animals were found dead on shore. The 1990–1998 sample (n=49) was collected in the northern and central Patagonian areas (Fig. 1). During this period, the animals were obtained from two sources: shores where animals were found dead (14 males and 24 females) and fisheries where animals were caught incidentally (8 males and 3 [illegible] (Table 1). Samples were clumped

into geographical areas based on the spatial distribution of rookeries (Fig.1) and the reported animal movements between rookeries in northern Patagonia (Crespo and Pedraza, 1991; Crespo[1]; Dans et al.[2]). Sex and standard length (SL, cm) were recorded when possible. Males ranged from 114 to 243 cm SL, whereas females ranged between 102 to 196 cm SL (Fig. 2).

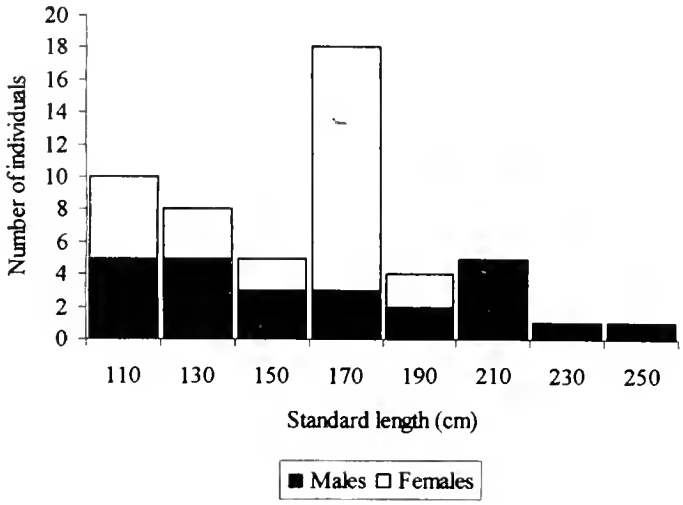

Figure 2

Length-frequency distribution of the total sample of South American sea lions analyzed in this work. Three males and four females were not included in this figure because their standard lengths could not be obtained.

Stomach content analysis

Stomach contents were preserved in 70% alcohol or frozen at –20°C. Hard pieces were recovered by using sieves of different mesh sizes (from 0.5 to 10 mm) flushed with water and by using decantation trays. Fish otoliths and bones, cephalopod beaks, crustacean exoskeletons and other hard remains were used to quantify and identify the prey species. Identification was made by using local species reference collections at the Marine Mammal Laboratory, Centro Nacional Patagónico, CONICET, and available catalogues (Clarke, 1986; Menni et al., 1984; Roper et al., 1984; Boschi et al., 1992; Gosztonyi and Kuba[3]). Complete and undigested elements (complete prey, otoliths and beaks) were measured with digital calipers. When digested and broken hard pieces were found in a stomach, the measurements for these elements were assigned from a random sample of undigested and whole parts of the same species obtained within the same stomach (Koen Alonso et al., 1998).

Size (total length ([TL]) of fish and dorsal mantle length ([DML]) of squid, cm) and wet weight (W, g) of prey were estimated from hard pieces by using allometric regressions (Clarke, 1986; George-Nascimento et al., 1985; Koen Alonso et al., 1998) (Table 2). In those cases where regressions were not available, regressions of related species were employed (Table 2). When related species regressions did not exist, weight was assigned by direct comparison with measured and weighed individuals of similar size for the same species or by weighing the fragments found in the stomach. The presence of stomach stones and parasites was recorded and all the gastroliths were weighed in each stomach.

Data analysis

The relative importance of prey species was evaluated by means of the index of relative importance (IRI) (Pinkas et al., 1971). The IRI was calculated for each prey species as

$$IRI = (\%N + \%W)\%FO,$$

Where $\%FO$ = the percent frequency of occurrence;
$\%N$ = the percentage by number; and
$\%W$ = the percentage by regression-estimated wet weight.

This IRI is a modified version of the index where the original term of percentage by volume was replaced by the $\%W$ term (Koen Alonso et al., 1998). In order to make easier the interpretation of the IRI, this index was expressed on a percent basis ($\%IRI$) (Cortés, 1997). Graphical representation of the diet was also employed to present some results (Cortés, 1997).

Two overlap indices, the general overlap index (GO) and the specific overlap index (SO) (Petraitis, 1979; Ludwig and Reynolds, 1988), were used to examine dietary differences. These indices were selected because they are based on the same theoretical framework, have associated statistical tests (Petraitis, 1979), and the GO presents a small bias even when the sample size is small (Smith and Zaret, 1982).

[3] Gosztonyi, A., and L. Kuba. 1996. Atlas de huesos craneales y de la cintura escapular de peces costeros patagonicos. Informes Tecnicos del Plan de Manejo Integrado de la Zona Costera Patagónica. Fundación Patagonia Natural (Puerto Madryn, Argentina) 4:1-29.

Table 2

Regressions used to estimate size and wet weight of prey of the South American sea lion off Patagonia, with their sample size (n), coefficient of determination (r^2), and source. Total length (TL) and dorsal mantle length (DML) are given in centimeters, otolith length (OL), lower rostral length (LRL), and lower hood length (LHL) are given in milimeters, and wet weight (W) is in grams.

Prey species	Regressions	n	r^2	Source
Teleosts				
Engraulis anchoita	$TL=2.36817+3.56OL$	79	0.70	Koen Alonso et al., 1998
	$W=0.0025TL^{3.353}$	81	0.93	Koen Alonso et al., 1998
Sciolella punctata	$TL=-0.1533+4.1987OL$	45	0.8956	present study
	$W=0.0182TL^{2.8635}$	22	0.8782	present study
Stromateus brasiliensis	$TL=3.042OL^{1.159}$	51	0.98	Koen Alonso et al., 1998
	$W=0.0006418TL^{3.917}$	63	0.98	Koen Alonso et al., 1998
Nemadoctylus bergi	$TL=-3.8317+5.6735OL$	56	0.9079	present study
	$W=0.0144TL^{2.9301}$	23	0.9824	present study
Merluccius hubbsi	$TL=1.823OL^{1.072}$ if $OL<15$	447	0.93	Koen Alonso et al., 1998
	$TL=1.984OL^{1.05}$ if $OL\geq15$	693	0.91	Koen Alonso et al., 1998
	$W=0.00476TL^{3.061}$ if $OL<15$	469	0.92	Koen Alonso et al., 1998
	$W=0.00972TL^{2.886}$ if $OL\geq15$	742	0.96	Koen Alonso et al., 1998
Acanthistius brasilianus	$TL=10.4444+1.8673OL$	23	0.7816	present study
	$W=0.0082TL^{3.1713}$	11	0.9654	present study
Pseudopercis semifasciata[1]	$TL=-12.9242+4.6425OL$	27	0.9789	present study
	$W=0.005TL^{3.2066}$	13	0.9807	present study
Genypterus blacodes	$TL=-18.3696+5.6394OL$	45	0.7890	present study
	$W=0.0016TL^{3.2251}$	24	0.9783	present study
Raneya brasiliensis	$TL=-0.7671+3.1968OL$	52	0.6819	present study
	$W=0.0022TL^{3.2685}$	26	0.9349	present study
Patagonotothen spp.[2]	$TL=-3.33204+4.21936OL$	121	0.7175	present study
	$W=0.0013TL^{3.668}$	75	0.9729	present study
Triathalassothia argentina	$TL=0.8116+2.775OL$	4	0.4278	present study
	$W=0.1987TL^{2.1123}$	4	0.6161	present study
Paralichthys isosceles	$TL=-0.9035+4.6962OL$	17	0.9436	present study
	$W=0.0013TL^{3.6036}$	8	0.9975	present study
Agnathans				
Mixine sp.	$W=0.003TL^{2.81089}$	7	0.9314	present study
Cephalopods				
Illex argentinus	$DML=-3.178+5.617LHL$	27	0.93	Koen Alonso et al., 1998
	$DML=0.08257+6.009LRL$	63	0.87	Koen Alonso et al., 1998
	$W=0.00982DML^{3.238}$	66	0.98	Koen Alonso et al., 1998
Loligo gahi[3]	$DML=-0.712+4.622LHL$	98	0.76	Koen Alonso et al., 1998
	$W=0.026DML^{2.753}$	102	0.93	Koen Alonso et al., 1998
Octopus vulgaris[4]	$W=e^{1.82+3.03\mathrm{Ln}(\mathrm{LHL})}$	108	—	Clarke, 1986
Eledone sp.	$W=e^{1.68+2.85\mathrm{Ln}(\mathrm{LHL})}$	214	—	Clarke, 1986

[1] These regressions were also used for *Pinguipes brasilianus*

[2] These regressions were used for *Patagonotothen cornucola*

[3] These regressions were also used for *Loligo sanpaulensis*

[4] This regression was used for *Enteroctopus megalocyathus* and *Octopus tehuelchus*

The GO evaluates the probability of obtaining the utilization curve of each group from the common utilization curve of all groups (Petraitis, 1979). This index has a minimum value which depends on the sample size and the number of prey species considered. To compare the index obtained from different samples, it was adjusted to vary between 0 and 1 (GO_a) (Ludwig and Reynolds, 1988). The null

hypothesis of a complete overlap (GO=1) can be statistically tested by using the *V*-statistic (Ludwig and Reynolds, 1988).

The SO is a pairwise nonsymmetric index which evaluates the probability of obtaining the utilization curve of one group from the utilization curve of the other (Petraitis, 1979; Ludwig and Reynolds, 1988). The probability of obtaining the utilization curve of the group i from the utilization curve of group k is denoted by SO_{ik}. The null hypothesis of a complete overlap (SO_{ik}=1) can be tested with the *U*-statistic (Ludwig and Reynolds, 1988).

The comparisons made were 1) geographical area of sampling (between northern Patagonia and central Patagonia), 2) period of sampling (between 1982–1987 and 1990–1998), 3) source of sampling (between dead animals on shore and entangled animals in the fishery), and 4) sex (between males and females). Because entangled individuals were mostly males and were obtained only during the 1990–1998 period (Table 1), comparisons were made between entangled and nonentangled males in the period 1990–1998.

The data employed for this analysis were those data on the occurrences of prey species that presented an %IRI greater than 2% in the pooled sample. Inherent in the use of occurrences of prey species is the assumption that each prey species in a stomach was consumed independently. For this reason, the correlations between the prey species used in our analyses were evaluated with the Spearman rank correlation coefficient (r_s) (Siegel and Castellan, 1995). The use of occurrences of prey species as data also increases the sample size for these comparisons because the stomach of one sea lion usually contained more than one prey species.

Differences in prey sizes consumed were tested by using the nonparametric two-sample Mann-Whitney *U* test in those cases where differences were detected (Siegel and Castellan, 1995).

The relationship between mean length of prey in each stomach and predator SL was evaluated using the r_s (Siegel and Castellan, 1995). This analysis was performed by using the pooled sample and analyzed by sex of predator.

The function of gastroliths

The role of gastroliths in eliminating stomach parasites and the potential function of gastroliths in buoyancy control were investigated. The independence between the presence of gastroliths and the presence of parasites in the stomachs was tested with Fisher's exact test. The relationship between SL and total weight of gastroliths found in the stomach (GW) was evaluated with the Spearman rank correlation coefficient (r_s) (Siegel and Castellan, 1995). This relationship was analyzed by considering each sex and the pooled sample.

Results

Prey species

Forty-eight of 59 stomachs analyzed contained food remains (Table 1). Aproximately 37 prey species were identified, mostly fishes and cephalopods (Table 3). Additionally, the stomach of one female found dead on the beach contained two sponge species, tube polychetes, nudibranchs and hagfish (*Mixine* sp.). Because this specimen was considered sick and anomalous, it was excluded from the analysis.

The collection analyzed was composed of 1449 individual prey, and the total estimated weight was 209.9 kg.

Males consumed a broader trophic spectrum of 32 prey species (Table 3), dominated by Argentine hake, followed by Patagonian squid, *Loligo gahi*, Argentine shortfin squid, "raneya," *Raneya brasiliensis*, and red octopus, *Enteroctopus megalocyathus*. Only the Argentine hake had a %IRI greater than 10%. The total number of prey found in male sea lions stomachs was 738 and the total estimated biomass was 91.4 kg. The five most important prey represented 74.0% by number and 74.6% by weight.

Twenty-nine species were found in female sea lion stomachs. The important prey were red octopus, Argentine shortfin squid, Argentine hake, "raneya," and Argentine anchovy (*Engraulis anchoita*) (Table 3). Only the first three species had %IRIs greater than 10%. The total number of prey found in the female stomachs was 711 and the estimated weight of this collection was 118.5 kg. The five most important prey represented 75.5% by number and 91.3% by weight.

Homogeneity of the sample

Six species (Argentine hake, red octopus, Argentine shortfin squid, Patagonian squid, "raneya," and Argentine anchovy) had an %IRI greater than 2% in the pooled sample (Fig. 3). All pairwise correlations for these prey species were nonsignificant (P>0.05). Data on the occurrences of these species were used in the overlap analysis.

Considering the GO, no differences in diet were found between geographical areas and between periods of sampling (Table 4). However, the SO indicates differences in diet between the periods 1990–1998 and

Table 3

Number (*n*), percent frequency of occurrence (*%FO*), percent number (*%N*), percent estimated wet weight (*%W*), and percent index of relative importance (*%IRI*) of prey of the South American sea lion off Patagonia. The ecological group for each species is shown in parentheses (P=pelagic, B=benthic, DP=demersal pelagic, DB=demersal benthic, NA=not assigned). Ecological groups were assigned following Angelescu (1982), Menni (1983), Menni et al. (1984), Angelescu and Prenski (1987), and Boschi et al. (1992).

	Females					Males				
Prey	*n*	*%N*	*%W*	*%FO*	*%IRI*	*n*	*%N*	*%W*	*%FO*	*%IRI*
Teleosts										
Merluccius hubbsi (DP)	101	14.2	9.0	34.6	11.9	286	38.8	52.4	72.7	68.6
Raneya brasiliensis (DB)	151	21.2	3.0	19.2	6.9	67	9.1	2.8	40.9	5.0
Engraulis anchoita (P)	123	17.3	2.0	15.4	4.4	33	4.5	0.8	27.3	1.5
Patagonotothen cornucola (DB)	34	4.8	0.3	7.7	0.6	40	5.4	0.4	22.7	1.4
Paralichthys isosceles (B)	18	2.5	0.7	7.7	0.4	8	1.1	2.6	18.2	0.7
Triathalassothia argentina (B)	13	1.8	0.4	15.4	0.5	5	0.7	0.2	9.1	0.1
Genypterus blacodes (DB)	12	1.7	0.7	3.8	0.1	3	0.4	3.4	9.1	0.4
Pseudopercis semifasciata (DB)	3	0.4	0.9	3.8	0.1	3	0.4	11.4	9.1	1.1
Stromateus brasiliensis (DP)	5	0.7	0.7	3.8	0.1	5	0.7	1.4	9.1	0.2
Acanthistius brasilianus (DB)	1	0.1	0.4	3.8	<0.1	2	0.3	1.4	9.1	0.2
Seriolella punctata (DP)	—	—	—	—	—	9	1.2	0.5	4.5	0.1
Iluocoetes fimbriatus (DB)	—	—	—	—	—	7	0.9	0.2	4.5	0.1
Percophis brasiliensis (DB)	1	0.1	0.8	3.8	0.1	1	0.1	0.6	4.5	<0.1
Pinguipes brasilianus (DB)	2	0.3	<0.1	3.8	<0.1	1	0.1	0.1	4.5	<0.1
Unidentified fish (NA)	1	0.1	<0.1	3.8	<0.1	1	0.1	0.1	4.5	<0.1
Nemadactylus bergi (DB)	—	—	—	—	—	3	0.4	0.2	4.5	<0.1
Prionotus punctatus (B)	—	—	—	—	—	1	0.1	0.1	4.5	<0.1
Trachurus picturatus (P)	1	0.1	0.1	3.8	<0.1	—	—	—	—	—
Elasmobranchs (DB)	6	0.8	3.0	7.7	0.4	1	0.1	0.5	4.5	<0.1
Agnathans										
Mixine sp. (B)	—	—	—	—	—	18	2.4	0.7	13.6	0.4
Cephalopods										
Enteroctopus megalocyathus (B)	54	7.6	61.7	53.8	55.0	21	2.8	9.3	27.3	3.4
Illex argentinus (DP)	108	15.2	15.7	38.5	17.5	27	3.7	8.2	54.5	6.7
Loligo gahi (DP)	18	2.5	0.2	26.9	1.1	145	19.6	1.9	40.9	9.1
Octopus tehuelchus (B)	6	0.8	0.1	11.5	0.2	9	1.2	0.4	22.7	0.4
Eledone sp. (B)	6	0.8	0.1	7.7	0.1	18	2.4	0.3	13.6	0.4
Loligo sanpaulensis (DP)	3	0.4	<0.1	7.7	0.1	1	0.1	<0.1	4.5	<0.1
Semirossia tenera (DB)	2	0.3	<0.1	3.8	<0.1	3	0.4	<0.1	4.5	<0.1
Crustaceans										
Crabs (B)	9	1.3	<0.1	15.4	0.3	4	0.5	<0.1	13.6	0.1
Pleoticus muelleri (DB)	3	0.4	<0.1	3.8	<0.1	6	0.8	0.1	9.1	0.1
Amphipods (P)	12	1.7	<0.1	3.8	0.1	—	—	—	—	—
Munida subrugosa (B)	2	0.3	<0.1	3.8	<0.1	1	0.1	<0.1	4.5	<0.1
Munida gregaria (B)	—	—	—	—	—	2	0.3	<0.1	9.1	<0.1
Serolis sp. (B)	—	—	—	—	—	2	0.3	<0.1	9.1	<0.1
Peisos petrunkevitchi (DB)	—	—	—	—	—	5	0.7	<0.1	4.5	<0.1
Heterosquilla platensis (B)	1	0.1	<0.1	3.8	<0.1	—	—	—	—	—
Polychetes										
Eunice argentinensis (B)	8	1.1	<0.1	3.8	0.1	—	—	—	—	—
Tunicates										
Pedicle tunicate (B)	7	1.0	<0.1	7.7	0.1	—	—	—	—	—

1982–1987 (Table 4). The Argentine anchovy was not found in the small sample for the period 1982–1987, and was the least important of the six prey species selected for the overlap analysis. When the analysis was performed excluding this prey species, no differences were found between periods in either of the

two overlap indices (Table 4). No differences were also found between entangled and nonentangled males in the period 1990–1998 (Table 4).

When the difference in feeding between sexes was analyzed, no differences were found with the GO, but the SO indicated significant differences in diet (Table 4). Taking into account that the GO analyzes the differences between the utilization curves of the groups with reference to a common utilization curve, whereas the SO analyzes one utilization curve with respect to the other one, our data suggest that there are some differences in the diet between sexes.

Prey size

No differences were found in the sizes of Argentine hake (U=13,785.5; n_{males}=286; $n_{females}$=101; P=0.496), Argentine shortfin squid (U=1,331.5; n_{males}=27; $n_{females}$=108; P=0.486), and Argentine anchovy (U=1,627; n_{males}=33; $n_{females}$=123; P=0.080) consumed by the two sexes. Seventy-four percent of the Argentine hake eaten by sea lions were less than 30 cm TL. Argentine shortfin squid consumed by sea lions had a DML greater than 15 cm, whereas Argentine anchovy consumed by sea lions were mostly between 12 and 17 cm of TL (Fig. 4). Red octopus consumed by males weighed significantly less than those consumed by females (U=194.5; n_{males}=21; $n_{females}$=54; P<0.0001). Patagonian squids consumed by males were larger than those consumed by females (U=880; n_{males}=145; $n_{females}$=18; P=0.024), but the range of DMLs of squid consumed by females was greater than that of squid eaten by males. Larger "raneya" was consumed by male sea lions than "raneya" eaten by female sea lions (U=2,681; n_{males}=67; $n_{females}$=151; P<0.0001) (Fig. 5).

No relationships were found between mean length of prey and predator SL with the pooled sample (r_s=0.007; n=37; P=0.964), with males only (r_s=0.004; n=19; P=0.985) or with females only (r_s=0.118; n=18; P=0.641).

Gastroliths

Of the stomachs analyzed, 60.4% had gastroliths and 87.9% had parasites. The parasites found in the stomachs were mostly nematodes. The presence of parasites and gastroliths was independent (Fisher exact test; P=0.999). A positive correlation was found between the SL of South American sea lions and GW (r_s=0.572; n=45; P<0.0001) (Fig. 6).

Gastroliths were found in 56.7% of females sea lions and 90.0% of females had parasites. The presence of gastroliths and parasites was independent (Fisher exact test; P=0.5645). A positive correlation was found between SL and GW (r_s=0.66; n=23; P=0.0006).

Gastroliths were found in 85.7% of the male sea lion stomachs, and 64.3% of males had parasites. The independence between the presence of gastroliths and parasites could not be rejected (Fisher exact test; P=1), and a positive correlation was found between SL and GW (r_s=0.599; n=22; P=0.0032).

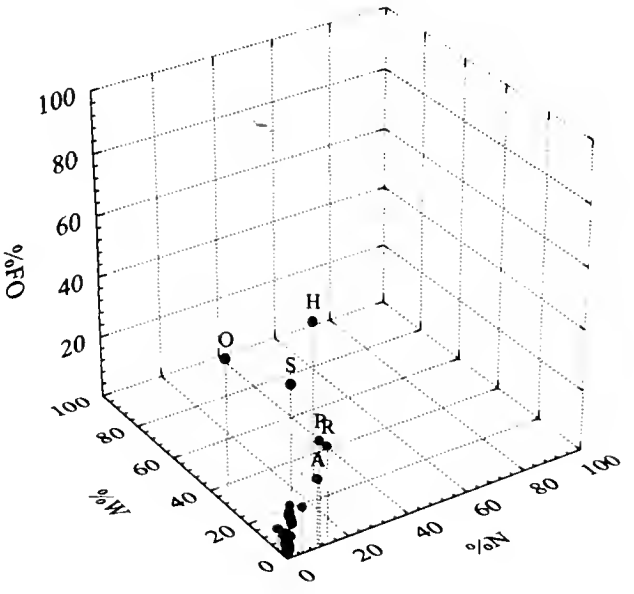

Figure 3

The diet of South American sea lions. The axes are %FO = percent frequency of occurrence, %N = percentage by number, and %W = percentage by regression-estimated wet weight. Only the labeled species had an %IRI>2%, and they were H = Argentine hake, O = red octopus, S = Argentine shortfin squid, P = Patagonian squid, R = "Raneya," and A = Argentine anchovy.

Discussion

The samples analyzed was collected over a broad range of time and space and were derived from two sampling sources. For that reason several subsamples were tested for homogeneity before a sample could be considered to be representative of the diet of South American sea lions. Those subsamples were tested by means of the GO and SO indices because they have associated statistical tests. The GO has only a small bias related to the difference in sample sizes even when the total sample size is relatively small (Smith and Zaret, 1982), and both overlap measures do not change if the resources are divided

Table 4

Diet overlap analyses between the major sources of variation in the sample studied. GO = general overlap index; GO_a = adjusted general overlap index; V = the statistic to test the null hypothesis that GO = 1; df = degrees of freedom; P = probability of the statistic; SO_{ik} = specific overlap of group i onto group k; U = statistic to test the null hypothesis that $SO_{ik} = 1$. The number of prey occurrences in each category are indicated in parentheses.

	General overlap index				
Source of variation	GO	GO_a	V	df	P
Period of time	0.987	0.953	2.870	5	0.720
Period of time[1]	0.997	0.990	0.585	4	0.965
Geographic area	0.986	0.971	2.989	5	0.702
Source of sampling	0.983	0.966	1.715	5	0.887
Sex	0.970	0.940	6.514	5	0.259

	Specific overlap index					
Source of variation	i	k	SO_{ik}	U	df	P
Period of time	1982–1987 (11)	1990–1998 (96)	0.869	3.078	5	0.688
	1990–1998 (96)	1982–1987 (11)	0.197	311.532	5	<0.001
	1982–1987[1] (11)	1990–1998[1] (86)	0.971	0.658	4	0.956
	1990–1998[1] (86)	1982–1987[1] (11)	0.969	5.367	4	0.252
Geographic area	central Patagonia (38)	northern Patagonia (69)	0.942	4.545	5	0.474
	northern Patagonia (69)	central Patagonia (38)	0.937	8.951	5	0.111
Source of sampling	nonentangled males (29)	entangled males (22)	0.932	4.066	5	0.540
	entangled males (22)	nonentangled males (29)	0.933	3.037	5	0.694
Sex	females (49)	males (58)	0.870	13.606	5	0.018
	males (58)	females (49)	0.894	13.029	5	0.023

[1] Analysis performed excluding the Argentine anchovy.

into classes below the organism's level of discrimination (Petraitis, 1979). However, one cannot evaluate the interaction between sources of variation with these analyses. For this reason, as in any statistical test, the lack of a difference for a particular source of variation does not indicate the absence of a difference, it means only that there is not enough information to affirm that this source of variation is significant.

The marine communities for both areas in this study comprise the same species and are considered to be relatively homogeneous along the entire geographical areas range covered by the study area (Fig. 1) (Menni, 1983; Menni and López, 1984; Angelescu and Prenski, 1987). In addition, the trend of sea lion stocks in northern and central Patagonia has followed a pattern of decline and recovery during recent decades. The northern Patagonia stock declined to one fifth of its original population size between 1930 and the mid-1960s as a consequence of intense harvesting. Then it remained stable between 1972 and 1990, when it began to recover (Crespo and Pedraza, 1991). The central Patagonia stock had not been harvested but declined in a similar proportion during the mid-century and has shown evidence of population increase in recent years—a fact that suggests a strong connection and interchange of individuals between these regions (Reyes et al., 1999). In addition, preliminary results based on electrophoresis analysis of blood enzymes and proteins codified by 10 loci have indicated that nine of these loci are monomorphic, suggesting that South American sea lions from both areas have had a strong gene flux between them and possibly constitute an unique biological population (Crespo[4]).

Regarding the two sampling periods, the differences in the diet detected with the SO are surely associated with the absence of Argentine anchovy in the 1982–1987 samples. The SO indicated that the utilization curve of food resources of the period 1990–1998 could not be drawn from the utilization

[4] Crespo, E. A. 1998. Laboratorio de Mamíferos Marinos, Centro Nacional Patagónico (CONICET), Boulevard Brown 3600, (9120) Puerto Madryn, Chubut, Argentina. Personal commun

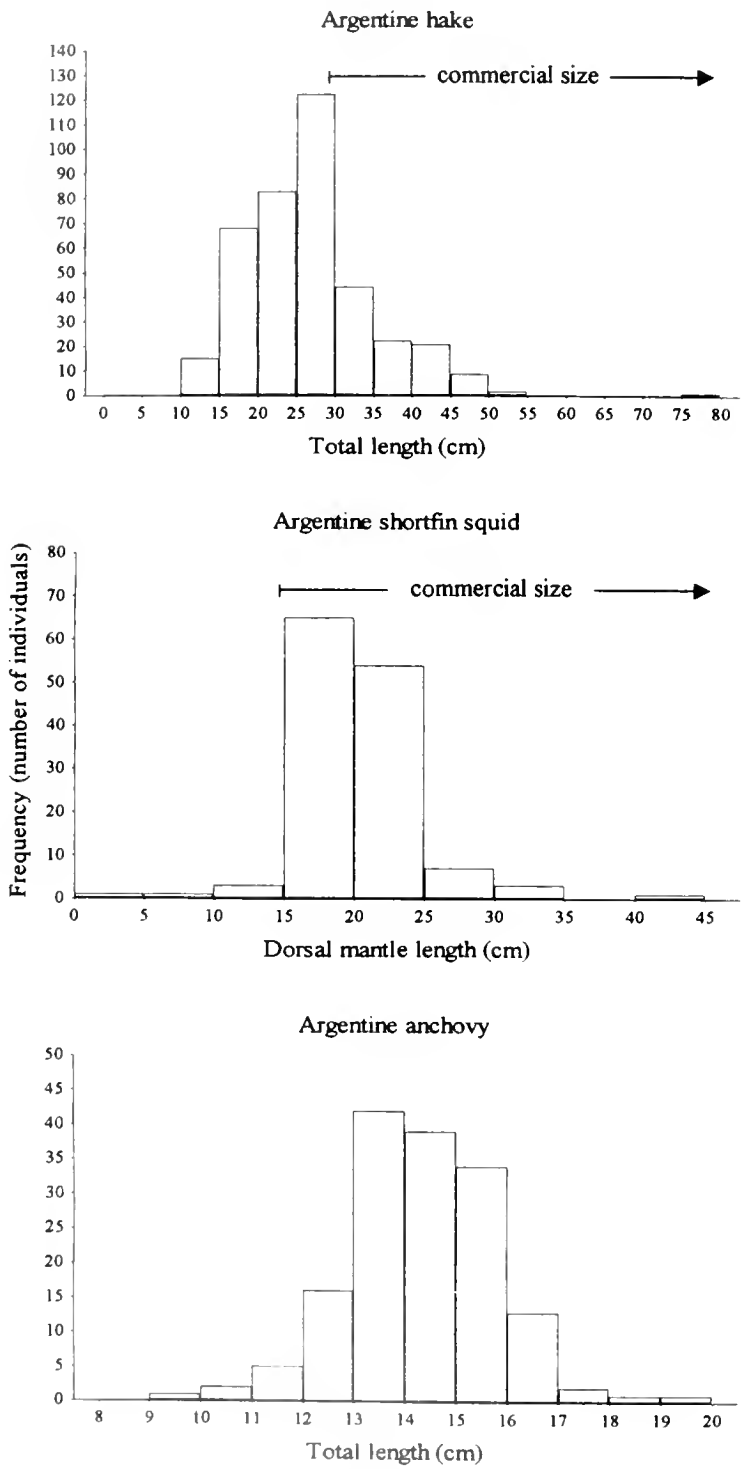

Figure 4

Regression-estimated size-frequency distribution of Argentine hake (*Merluccius hubbsi*), Argentine shortfin squid (*Illex argentinus*), and Argentine anchovy (*Engraulis anchoita*) consumed by South American sea lions off Patagonia collected in our study. The arrows indicate commercial sizes for Argentine hake and Argentine shortfin squid. All the sizes for Argentine anchovy are commercial.

curve in the period 1982–1987. Nevertheless, when the Argentine anchovy is excluded from the analysis, no differences were found between the two periods in either at the two overlap indices. Probably, the absence of Argentine anchovy in the period 1982–1987 is related to the small size of the sample collected and to the fact that Argentine anchovy was the least important prey species among the six prey species selected for the overlap analysis (Fig. 3) because the available information indicates that the abundance of Argentine anchovy was high and roughly constant during the entire study period (Ciechomski and Sánchez, 1988; Pájaro et al.[5]).

No differences in diet were detected when shore and entangled individuals were analyzed, even though several sources of bias could be operating at the same time. The diet information obtained from individuals found dead onshore could be biased, depending on the degree of digestion of the stomach contents. In our study, the use of several (and complementary) hard remains, such as otoliths and bones, allowed us to reduce this source of bias. Even when a small otolith was totally digested, the fish bones (mostly skull bones) permitted us to identify and quantify these prey. Thus, estimating prey size by regressions avoided underestimating the importance of small or highly digested prey. In some cases, when we used the regression of a related species, the results were likely partially biased. Samples from entangled sea lions probably did not hold any of these biases because all the stomach contents were presumably composed of fresh materials. The source of bias in this case would have been due to individuals that fed inside the net. Nevertheless, a comparison

[5] Pájaro, M., R. Sánchez and G. Macchi. 1997. Evaluación de la biomasa de adultos desovantes de la población norteña de anchoíta (*Engraulis anchoita*) en el período 1993–1996. Abstracts of the XII Simposio Científico-Tecnológico de la Comisión Técnica Mixta del Frente Marítimo, Montevideo, Uruguay, November 12–14, 1997, 4 p.

of dead, beached males with entangled males did not show any significant difference.

The only difference in diet found between subsamples was that shown by sexes. In this case differences in behavior and feeding habits could reflect differences in diet. Even if each sample source may have had different potential biases and the overlap analysis between them did not detect differences, we consider our sample to be, even with its limitations, a reasonable approximation of the diet of South American sea lions in Patagonia.

The diversity of prey species (Table 3) found in the diet of the South American sea lion indicates that it is a broad-spectrum predator. Some of these prey species (Argentine hake, Argentine shortfin squid, and Argentine anchovy) are abundant key species in the Patagonian continental shelf ecosystem and have commercial value (Angelescu, 1982; Angelescu and Prenski, 1987; Brunetti, 1990; Bezzi et al., 1994).

Argentine hake and Argentine shortfin squid are the two major target species of the Argentine fleet (Anonymous, 1996), and Patagonian squid is also exploited in the Falkland (Malvinas) Islands (Hatfield, 1996). Sea lions ate these prey species at both commercial and noncommercial sizes (Fig. 4).

The fishery catches Argentine hake with length modes between 35 and 40 cm TL (Cañete et al., 1986), and the minimum commercial size of this species is 30 cm TL. Mostly noncommercial sizes of Argentine hake (less than 30 cm TL) were consumed by South American sea lions (Fig. 4). Estimates of stock number by age by using virtual population analysis indicated that the most abundant Argentine hakes are those of age-1 and age-2 year classes (approximately 30 cm or less in TL), which represent around 56% in number of the estimated hake stock (Bezzi et al., 1994). These data indicate that sea lions are feeding on this species according to prey-size distribution and availability in the environment. Hakes smaller than 10 cm

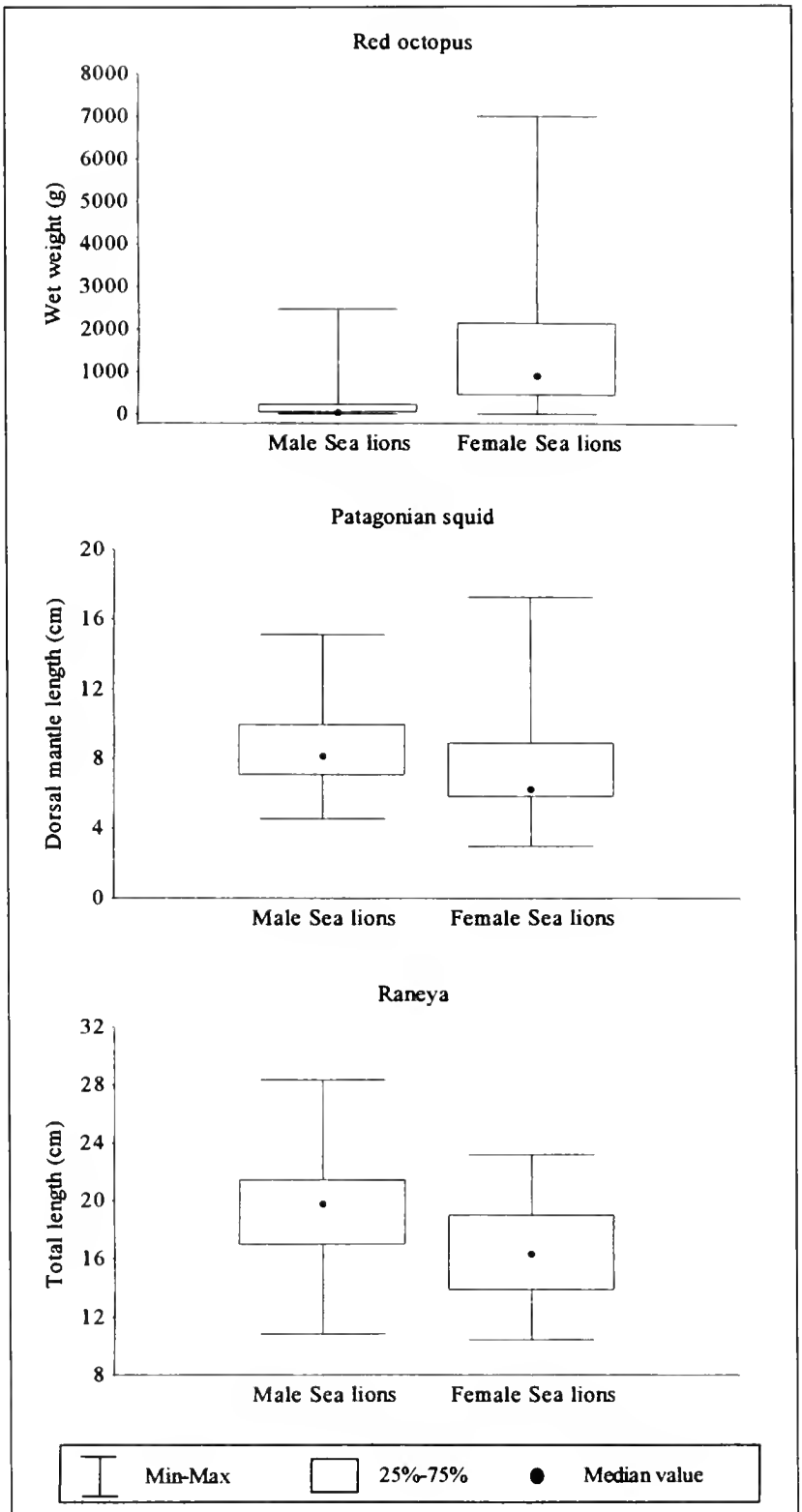

Figure 5

Box plots of regression-estimated size of red octopus (*Enteroctopus megalocyathus*), Patagonian squid (*Loligo gahi*), and "raneya" (*Raneya brasiliensis*) consumed by male and female South American sea lions collected in our study.

TL are not caught by either sea lions or the fishery because of the pelagic behavior of fish in this size range (Angelescu and Prenski, 1987).

The commercial squid species found in the diet of sea lions (Argentine shortfin and Patagonian squid) form schools of restricted size range (Brunetti and Ivanovic, 1992; Hatfield, 1996). Therefore, it is difficult to determine if the consumed sizes represent the environmental availability of these prey species. The commercial size of shortfin squid is approximately 15 cm DML, and this species was consumed by sea lions at commercial sizes (Fig. 4). Patagonian squid was consumed mostly at noncommercial sizes (less than 10 cm DML) because that most of the squid catches in the Falkland fishery were between 10 and 15 cm DML (Hatfield, 1996).

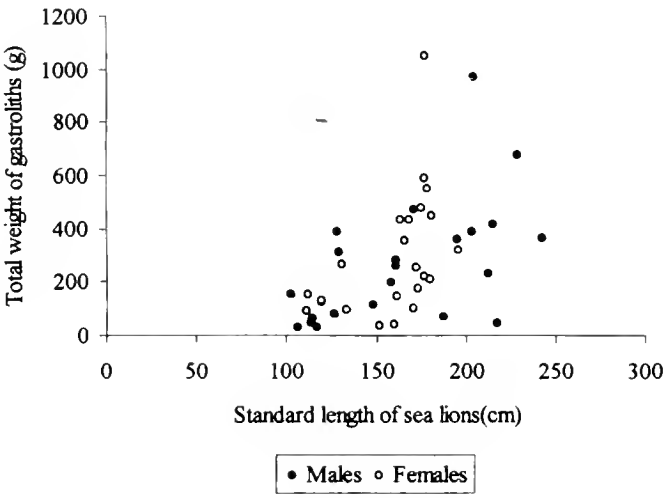

Figure 6

Scatterplot of total weight of gastroliths versus standard length for South American sea lions, by sexes.

These results indicate some overlap between the South American sea lion diet and fishery catches but not enough to conclude that competition exists with the fishery. The population of South American sea lions in northern Patagonia has been increasing during recent years at a rate of increase greater than 3% (Crespo and Pedraza, 1991; Dans et al.[2]). There is no indication that fishery catches affect the availability of food for sea lions at the present time. More detailed estimates of food consumption by South American sea lions are needed. Also, estimates of the catch and bycatch of the fishery are needed to evaluate conclusively the existence of ecological competition.

Differences in the diet between sexes are probably associated with different utilization of common and frequent food resources, suggesting some kind of differential feeding behavior between the sexes. The South American sea lion is a dimorphic and polygamous species. Therefore each sex must have different ecological constraints. Adult female feeding trips last for about three days during reproductive (Cappozzo et al., 1991) and nonreproductive (Reyes and Crespo[6]) seasons. Nursing pups may limit the distance that females can travel to feeding ground. Males are not restricted by nursing pups and their feeding trips seem to be less constant (Reyes and Crespo[6]). There is also some evidence obtained from sightings from fishing vessels that males move farther offshore than do females which remain closer to the coast (Crespo et al., 1997). Thus, differences in the diet could be associated with different feeding grounds or different home ranges between the sexes.

The prey of female South American sea lions were more evenly distributed within ecological groups than the prey of males (Fig. 7). The prey of females were mostly benthic and demersal-pelagic species. The mean dive depth recorded by lactating females in Patagonia was 60.9 m, and 69% of the dives were flat-bottomed and U-shaped (Werner and Campagna, 1995)—data that agree with the bottom and coastal feeding behavior suggested by the stomach contents. On the other hand, the most important prey of males were demersal-pelagic species (Fig. 7).

The Patagonian squid spawns in shallow waters, and the new generation migrates offshore to feed, grow, and mature (Hatfield, 1996). This migration pattern implies that small Patagonian squid must be more abundant in shallow, coastal waters than in deeper, offshore areas, but their size range in the coastal area must be broader than that in offshore areas because mature (and large) squids return to shallow waters to spawn. The consumption of larger Patagonian squid by male sea lions and the broader range size of Patagonian squid eaten by female sea lions agree with the hypothesis that females feed in more coastal and shallower waters than do males.

The red octopus lives mostly in caves on rocky bottoms (Ré, 1998) and is the most important prey species of female South American sea lions. Red octopus reach maturity around 120 mm DML and 850 g of total weight (Ré, 1998); male sea lions consumed

[6] Reyes, L. M., and E. A. Crespo. 1993. Variaciones diarias y lunares y viajes de alimentacion en el lobo marino del sur *Otaria flavescens* en el norte de Patagonia. Abstracts of the Jornadas Nacionales de Ciencias del Mar "93," 19–25 September 1993, Puerto Madryn, Argentina, 156 p.

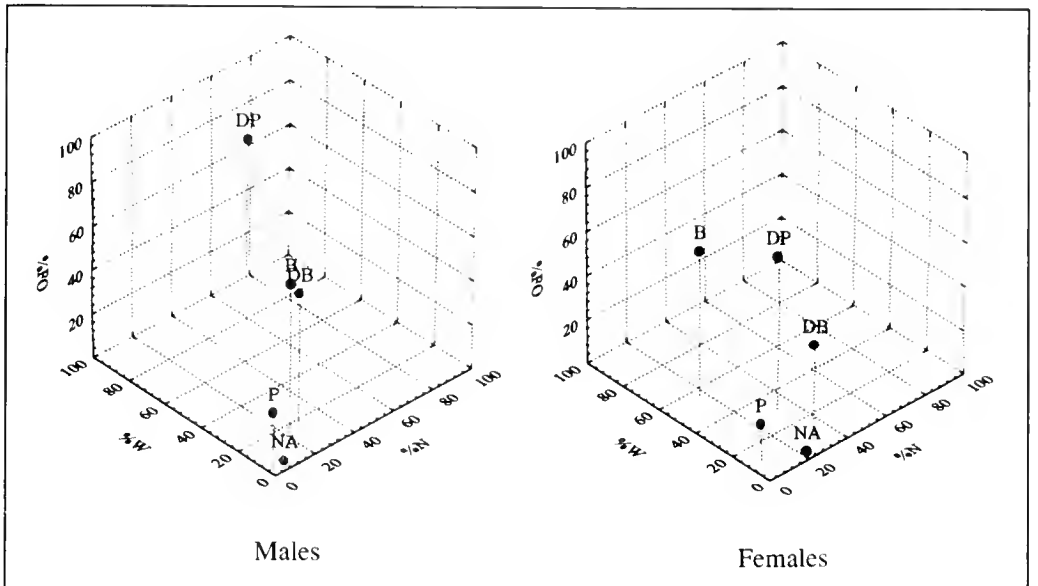

Figure 7

Ecological groups in the diet of male and female South American sea lions in our study. %FO = percent frequency of occurrence, %N = percentage by number, and %W = percentage by regression estimated wet weight. P = pelagic, B = benthic, DP = demersal pelagic, DB = demersal benthic, NA = not assigned.

mostly immature individuals whereas female sea lions consumed mature ones. If females search for prey on rocky bottoms, they will catch the mature and larger red octopus. Instead, if male South American sea lions feed mostly in the water column near the bottom, they could catch the younger red octopus when they are actively moving on the bottom. Younger octopus could be more vagrant than adults, and in some species, posthatching octopuses do exhibit pelagic behavior (Boletzky, 1977). The difference in the size of red octopus that South American sea lion consumed could be associated with this characteristic in prey biology, thus supporting the hyphothesis of different feeding behavior between the sexes.

In regard to gastrolith function, the hypothesis of buoyancy control has been postulated with the evidence of the presence of gastroliths in several living and extinct tetrapods that swim using their limbs in the form of an underwater fly (Taylor, 1993). Taylor (1993), in an extensive comparative study, demonstrated that there is no correlation between the presence of gastroliths and diet, but he found a correlation between gastroliths and underwater flying. Another explanation for the ingestion of stones is that gastroliths "grind up" parasitic worms that usually infest seals (Riedman, 1990). The role of stomach stones seems to be better explained as "buoyancy control" than as "elimination of stomach parasites" because of the independence between the presence of parasites and gastroliths, and the significant correlations between predator size and gastrolith weight. Gastroliths found in the South American sea lions could be considered "ballasts" that allow the sea lions to regulate their buoyancy. Moreover, the gastroliths can also be quickly swallowed and vomited, allowing sea lions to change buoyancy according to their needs (Harrison and Kooyman, 1968).

In summary, these stomach content analyses indicate that South American sea lions feed primarily on demersal and benthic species and, in general terms, use resources according to their environmental availability. Males and females appear to have different constraints in their feeding behavior and these restrictions could lead females to feed in more coastal and shallower waters than those where males feed. These potential differences in feeding grounds or home ranges, or both, could explain the observed differences in diet between the sexes.

Acknowledgments

The authors wish to thank Pablo Mariotti, Bárbara Berón Vera, Nancy Mora, Pablo Nepomnaschy and Laura Reyes for their help with the stomach contents analysis; Silvana L. Dans, Pablo Yorio and Guillermo Harris for their critical reading and useful comments on earlier versions of the manuscript; and all of the

fishermen and wildlife wardens for their help aboard ship and in the field. Three anonymous reviewers (especially no. 817) and Sarah Shoffler made important and useful comments that enhanced the analysis of results and the expression of the ideas. As always, Sharyn Matriotti gave us important help with this article. Institutional support was provided by Centro Nacional Patagónico (CONICET), Universidad Nacional de la Patagonia, Fundación Patagonia Natural, Prefectura Naval Argentina, and the government of Chubut Province. The fishing companies Harengus S.A. and Alpesca S.A. collaborated with the authors in the retrieval of entangled sea lions and gave their permission for work onboard their fishing vessels. This work was carried out with the financial support of the National Geographic Society (Grant 5548/95 to E.A. Crespo and A.C.M. Schiavini), the Whale and Dolphin Conservation Society, the Patagonian Coastal Zone Management Plan (GEF/UNEP FPN/WCS) and the Programa de Cooperación Científica con Iberoamérica (1996–1998).

Literature cited

Angelescu, V.
1982. Ecología trófica de la anchoita del Mar Argentino (Engraulidae, *Engraulis anchoita*). Parte II. Alimentación, comportamiento y relaciones tróficas en el ecosistema. INIDEP (Instituto Nacional de Investigación y Desarrollo Pesquero), Contribution 409, 83 p.

Angelescu, V., and L. B. Prenski.
1987. Ecología trófica de la merluza común del Mar Argentino (Merlucciidae, *Merluccius hubbsi*). Parte 2. Dinámica de la alimentación analizada sobre la base de las condiciones ambientales, la estructura y las evaluaciones de los efectivos en su área de distribución. INIDEP, Contribution 561, 205 p.

Anonymous.
1996. Captura 95. Redes 88:24–40.

Bezzi, S., G. Cañete, M. Pérez, M. Renzi, and H. Lassen.
1994. Report of the INIDEP working group on assessment of hake (*Merluccius hubbsi*) north of 48°S (Southwest Atlantic Ocean). INIDEP Doc. Cient. 3:5–28.

Boletzky, S. V.
1977. Post-hatching behavior and mode of life in cephalopods. Symp. Zool. Soc. Lond. 38:557–567

Boschi, E. E., C. E. Fischbach, and M. I. Iorio.
1992. Catálogo ilustrado de los crustáceos estomatópodos y decápodos marinos de Argentina. Frente Marítimo 10 (sec. A):7–94.

Brunetti, N. E.
1990. Evolucion de la pesqueria de *Illex argentinus* (Castellanos, 1960). Inf. Técn. Inv. Pesq. 155, 19 p.

Brunetti, N. E., and M. L. Ivanovic.
1992. Distribution and abundance of early life stages of squid (*Illex argentinus*) in the south-west Atlantic. ICES J. Mar. Sci. 49:175–183.

Campagna, C., and B. J. Le Boeuf.
1988. Reproductive behavior of Southern sea lions. Behaviour 104:233–261.

Cañete, G. R., R. G. Perrotta, and J. A. Pérez Comas.
1986. Aspectos comparativos entre muestreos de desembarque y muestreos en alta mar de la especie merluza (*Merluccius hubbsi*), considerando el descarte efectuado por la flota marplatense en el período julio 1979–Setiembre 1980. Publ. Com. Téc. Mix. Fr. Mar. 1:447–453.

Cappozzo, H. L., C. Campagna, and J. Monserrat.
1991. Sexual dimorphism in newborn Southern sea lions. Mar. Mamm. Sci. 7(4):385–394.

Clarke, M. R.
1986. A handbook for the identification of cephalopods beaks. Clarendon Press, Oxford, 273 p.

Cortés, E.
1997. A critical review of methods of studying fish feeding based on analysis of stomach contents: application to elasmobranch fishes. Can. J. Fish. Aquat. Sci. 54:726–738.

Crespo, E. A., J. F. Corcuera, and A. López Cazorla.
1994. Interactions between marine mammals and fisheries in some coastal fishing areas of Argentina. *In* Gillnets and cetaceans (W. F. Perrin, G. P. Donovan, and J. Barlow, eds.), p. 269–281. Rep. Int. Whal. Comm. (special issue 15).

Crespo, E. A., and S. N. Pedraza.
1991. Estado actual y tendencia de la población de lobos marinos de un pelo (*Otaria flavescens*) en el litoral norpatagónico. Ecología Austral 1:87–95.

Crespo, E. A., S. N. Pedraza, S. L. Dans, M. Koen Alonso, L. M. Reyes, N. A. García, M. Coscarella, and A. C. M. Schiavini.
1997. Direct and indirect effects on the high seas fisheries on the marine mammal populations in the northern and central patagonian coast. J. Northwest Atl. Fish. Sci., 22:189–207.

de Ciechomski, J. D., and R. P. Sanchez.
1988. Análisis comparativo de las estimaciones de biomasa de la anchoita (*Engraulis anchoita*) en el Atlántico Sudoccidental en diferentes años y con distintas metodologías. Publ. Com. Téc. Mix. Fr. Mar. 4:117–132.

George-Nascimento, M. F., R. A. Bustamante, and R. C. Oyarzun.
1985. Feeding ecology of the Southern sea lion *Otaria flavescens* Shaw, 1800: food contents and food electivity. Mar. Biol. Prog. Ser. 21:135–143.

Hamilton, J. E.
1934. The Southern sea lion *Otario byronia* (de Blainville). Discovery Rep. 8:269–318.

Harrison, R. J., and G. L. Kooyman.
1968. General physiology of the Pinnipedia. *In* The behavior and physiology of pinnipeds (R. J. Harrison, R. C. Hubbard, R. S. Peterson, C. E. Rice, and R. J. Schusterman, eds.), p 221–296. Appleton-Century-Crofts, New York, NY.

Hatfield, E. M. C.
1996. Towards resolving multiple recruitment into loliginid fisheries: *Loligo gahi* in the Falkland Islands fishery. ICES J. Mar. Sci. 53:565–575.

Koen Alonso, M., E. A. Crespo, N. A. García, S. N. Pedraza, and M. Coscarella.
1998. Diet of dusky dolphins, *Lagenorhynchus obscurus*, in waters off Patagonia, Argentina. Fish. Bull. 96:366–374.

Ludwig, J. A., and J. F. Reynolds.
1988. Statistical ecology. John Wiley and Sons, New York, NY, 337 p.

Menni, R. C.
1983. Los peces en el medio marino. Estudio Sigma S.R.L., Buenos Aires, Argentina, 169 p.

Menni, R., and H. L. López.
1984. Distributional patterns of Argentine marine fishes. Physis 42 (issue 103, sec. A):71–85.

Menni, R. C., R. A. Ringuelet, and R. A. Aramburu.
1984. Peces marinos de la Argentina y Uruguay. Editorial Hemisferio Sur S.A., Buenos Aires, Argentina, 359 p.

Petraitis, P. S.
1979. Likehood measures of niche breadth and overlap. Ecology 60(4):703–710.

Pinkas, L., M. S. Oliphant, and I. L. K. Iverson.
1971. Food habits of albacore, bluefin tuna and bonito in California waters. U.S. Dep. Fish. Game, Fish Bull. 152:1–105.

Ré, M. E.
1998. Pulpos octopódidos (Cephalopoda, Octopodidae). *In* El mar argentino y sus recursos pesqueros (E. Boschi, ed.), tomo 2: Los moluscos de interés pesquero. Cultivos y estrategias reproductivas de bivalvos y equinoideos, p 99–114. Instituto Nacional de Investigación y Desarrollo Pesquero, Secretaría de Agricultura, Ganadería, Pesca y Alimentación, Mar del Plata, 231 p.

Reyes, L. M., E. A. Crespo, and V. Szapkievich.
1999. Distribution and population size of the southern sea lion (*Otaria flavescens*) in central and southern Chubut, Patagonia, Argentina. Mar. Mamm. Sci. 15(2):478–493.

Riedman, M.
1990. The pinnipeds: seals, sea lions and walruses. Univ. California Press, Berkeley, CA, 439 p.

Roper, C. F. E., M. J. Sweeney, and C. E.Nauen.
1984. FAO species catalogue: an annotated and illustrated catalogue of species of interest to fisheries, vol. 3: Cephalopods of the world. FAO Fish. Synop. 125, 277 p.

Siegel, S., and N. J. Castellan.
1995. Estadística no paramétrica aplicada a las ciencias de la conducta, 4th Spanish edition. Editorial Trillas S.A., Mexico D.F., Mexico, 437 p.

Smith, E. P., and T. M. Zaret.
1982. Bias in estimating niche overlap. Ecology 63(5): 1248–1253.

Taylor, M. A.
1993. Stomachs stones for feeding or buoyancy? The occurrence and function of gastroliths in marine tetrapods. Philos. Trans. R. Soc. Lond. (B Biol. Sci.) 341:163–175.

Vaz Ferreira, R.
1982. *Otaria flavescens* (Shaw), South American sea lion. *In* Mammals of the world, FAO Fish. Series 5(IV), p 447–495. FAO, Rome.

Werner, R. and C. Campagna.
1995. Diving behavior of lactating southern sea lions (*Otaria flavescens*) in Patagonia. Can. J. Zool. 73:1975–1982.

Modeling statistical performance of an airborne lidar survey system for anchovy

Nancy C. H. Lo

John R. Hunter

Southwest Fisheries Science Center
National Marine Fisheries Service, NOAA
P.O. Box 271, La Jolla, California 92038
E-mail address (for N.C.H. Lo): NancyLo@noaa.gov

James H. Churnside

Ocean Remote Sensing Division
Environmental Technology Laboratory
325 Broadway, Boulder, Colorado 80303

Abstract.—The objective of our study was to model the performance of an airborne lidar survey system for northern anchovy in terms of survey accuracy and precision. Our analyses indicated that swath width would have little or no effect on the probability that at least one fish school would be encountered. In typical coastal waters off California (attenuation coefficient=0.1/m), about half of the schools were detected by the lidar during the day and about 64% during the night. A greater proportion of schools were detected during the night because anchovy have a shallow vertical distribution, whereas in the day, schools may extend down to 155 m; schools below about 40 m depth were not detectable to the laser. Although schools tended to be more diffuse during the night than during the day, even the very diffuse schools of anchovy (0.5 fish/m^3) were detectable at night throughout the upper 20 m of the water column with a lidar. With a substantial increase in instrument and survey costs, it would be possible to increase the equivalent laser-pulsed power by a factor of 10 over that of the "off-the-shelf system," as used in our model. Such a change would increase the maximum detection depth of the lidar system by about 10 m but would have a negligible effect on the probability of detecting schools during the day owing to the skewed vertical distribution of anchovy schools. More effective approaches for improving the accuracy and precision of potential lidar surveys for fisheries would be to improve school detection algorithms and to develop a lidar survey model based on line transect theory to obtain an unbiased estimate of abundance. To produce an accurate reconstruction of the average vertical distribution of schools for a particular season and region, a synthesis of acoustic and lidar surveys of school distribution is required.

Manuscript accepted 18 November 1999
Fish. Bull. 98:264–282 (2000).

Airborne lidar surveys are an attractive alternative to the methods presently used in fishery-independent surveys of epipelagic fishes (Hunter and Churnside[1]). They would cost much less per survey mile than ship-based methods (acoustic-trawl, ichthyoplankton), and the survey would extend to greater depths than present aerial methods. A lidar, (li[ght] d[etecting] and r[anging]) system, in its most basic form, produces short pulses of laser light that pass through the water surface and reflect off fish and particles in the water; a receiver measures the returning reflected pulse; the strength of the returning pulse separates fish targets from small particles, and the elapsed time from start to return of pulses indicates the range (depth below the surface) of the target. The application of lidar technology to fishery surveys is still in its infancy. Fish schools have been detected with a variety of lidar systems (Churnside and Hunter, 1996), but schools have never been systematically studied with lidar, nor has existing lidar technology been adapted to fish-survey needs; formal fish surveys have never been conducted.

A lidar survey system for fishery-independent monitoring of epipelagic fish stocks is being developed jointly by two laboratories of the National Oceanic Atmospheric Administration (NOAA): Environmental Technical Laboratory, Boulder, CO; and Southwest Fisheries Science Center, La Jolla, CA. The approach is to combine evaluations of prototype instruments at sea with modeling of survey performance to develop an optimal lidar survey system. The goal is to develop a system that will deliver the greatest statistical precision for the lowest survey cost, while minimizing potential biases. In our study, we modeled a lidar survey with the objective of evaluating how instruments would affect survey precision or accuracy. Two classes of instrument design were considered, those affecting fish schools in the horizontal plane (swath width) and those affecting the detection of fish schools in the vertical plane (depth-specific detection). We also analyzed a trade-off between swath width and penetration depth, which is analogous to changing from a visual-based aerial survey (wide swath, shallow penetration) to a lidar-based

[1] Hunter, J. R., and J. H. Churnside, eds. 1995. Airborne fishery assessment technology—a NOAA workshop report. SWFSC Admin. Rep. LJ-95-02, 33 p. Southwest Fish. Sci. Ctr., NMFS, NOAA, P.O. Box 271, La Jolla, CA 92038.

aerial survey (narrow swath, deeper penetration). We discuss each.

Precision of an airborne lidar survey will depend upon the number of transects flown and the probability of encountering schools along them. The width of the transect lines (swath width), may affect the probability of encountering schools and therefore could be one of the few factors affecting precision that involve instrument design. Swath width could be increased in a variety of ways (flying higher, scanning or optically expanding the laser beam), but such changes are accompanied by disadvantages (loss in penetration depth, reduced resolution, increased instrument cost and weight). In our study, we modeled how the width of the swath (width of transect line) cut by the survey instrument affects the probability of encountering fish schools, and therefore the precision of the survey estimate, assuming fish are uniformly distributed in the water column.

The accuracy of a biomass survey depends on the extent to which the entire stock is vulnerable to the counting technique and on the variability in size of the uncounted fraction (Gunderson, 1993). The key issue for accuracy of a lidar survey is the vulnerability of a stock to being counted in the vertical plane. Depth-specific detection by a lidar depends upon laser power, sensitivity of the detection system, the rate of exponential decay of the laser pulse with water depth, the way the fish-detection function of the instrument changes with signal attenuation, fish size and reflectivity, school packing density, and, of course, the vertical distribution of the fish. Using a set of models and taking into account many of these variables, we evaluated the effect of instrument and survey design on the accuracy of an aerial lidar survey for measuring fish abundance. We considered how variations in laser power, school size, diel changes in vertical distribution of schools and school packing density (number of fish per m^3) would affect the accuracy of the survey. We also used these models to estimate the maximum depth at which schools might be detected by a single lidar pulse. For our study, we chose to use anchovy because more data exist on anchovy schools than most other species. Lo et al.[2] have, however, recently applied the same models to sardine and herring schools.

Materials and methods

We used various models to evaluate the potential effects of instruments on survey design. To evaluate how swath width may affect survey accuracy, simulation runs were used for a school-group encounter model. To evaluate the relation between laser power and maximum detection depth for fish schools, we computed the probability of detecting schools as a function of the signal-to-noise-ratio and estimated laser power and the laser attenuation coefficient. School parameters, size, distribution and density, and survey area (46,204 km^2=333 km (180 nmi) × 138.75 km (75 nmi)) were taken from acoustic surveys of northern anchovy in the Southern California Bight (Mais, 1974; Fiedler, 1978; Smith, 1981; MacCall[3]). For daytime profiles, vertical distributions of schools were based on northern anchovy off California (Holliday and Larsen, 1979); for nighttime profiles we used the distribution of early stage anchovy eggs (Pommeranz and Moser, 1987) and acoustic data for anchoveta off Peru (Castillo Valderrama, 1995). Signal-to-noise ratio was based on information on packing density of schools provided by Aoki and Inagaki (1988) and Graves (1977).

Many pelagic fish schools form distinct aggregations or school groups (Cram and Hampton, 1976; Fiedler, 1978). The area of an anchovy school (expressed by school diameter in our study) is highly variable, as are the size and number of schools within a school group. Because of this complexity, simulations were used to compute the probability of encountering anchovy schools in a survey area (Fiedler, 1978).

In the simulation, school groups were randomly assigned in the survey area. The sizes of the anchovy schools within a group were generated from the frequency distribution of the diameters of northern anchovy schools in the Southern California Bight (Fiedler, 1978; Smith, 1981; Table 1). The number of anchovy schools within an anchovy school group was generated from the area occupied by the group and the density of schools. Both the diameters of school groups and the density of schools within a school group were assumed to follow the lognormal distributions measured for anchovy in the Southern California Bight (Fiedler, 1978; Smith, 1981) (Fig. 1). Simulations were used to compute the encounter probability (p_y) for various swath widths (y).

The locations of school groups were randomly allocated in north–south (n–s) and east–west (e–w) directions. When school groups overlapped (intersected) in the north–south directions, they were combined as a "single" school group for computing the encoun-

[2] Lo, N. C. H., J. R. Hunter, and J. H. Churnside. 1999. Modeling properties of airborne lidar surveys for epipelagic fish. Admin. Rep. LJ-99-01. Southwest Fish. Sci. Ctr. NMFS, NOAA. P.O. Box 271, La Jolla, CA 92037.

[3] MacCall, A. 1975. Anchovy population survey simulation: a report of CalCOFI Anchovy Workshop Group on methods of estimating anchovy abundance, July 21–22, 1975, Contribution 4, 9 p. Marine Life Research Group, Scripps Institution of Oceanography, 9500 Gilman Drive, La Jolla, CA 92037-0227.

Table 1

The frequency distribution of school sizes of anchovy in the Los Angeles Bight based on sonar mapping conducted by the California Department of Fish and Game (Mais, 1974; Smith,1981).

School diameter (m)	Frequency	Sample proportions
10	9906	0.4338
30	9002	0.3942
50	1822	0.0798
70	706	0.0309
90	824	0.0361
110	178	0.0078
130	217	0.0095
150	50	0.0022
170	40	0.0018
190	51	0.0022
210	19	0.0008
230	7	0.0003
250	3	0.0001
270	1	<0.0001
290	2	0.0001
310	1	<0.0001
330	3	0.0001
350	0	0
370	0	0
390	2	0.0001

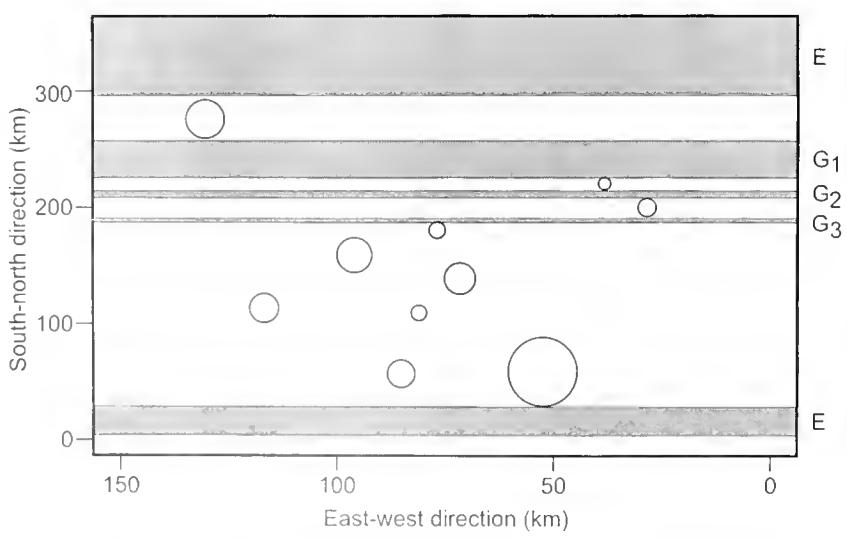

Figure 1

A spatial distribution of school groups from one simulation run. Circles indicate areas covered by school groups for a population of 80,000 schools. This graph was generated from lognormal distributions with mean = 3.91 and variance = 0.51 for school density (number of schools/nmi^2) and from lognormal distribution with mean = 2.319 and variance = 0.676 for diameter (nmi) of school group (nmi was later converted to km). G1, G2, G3, and E are the gaps used to compute the encounter probability (Eq. 1).

ter probability. Only the north–south direction was relevant because the transect was run from east to west. Similarly, schools were randomly allocated within a school group and when schools overlapped in the north–south direction, they were combined as a "single" school for computing purposes. This process continued until all schools were separated in the north–south direction and termed "disjoint" schools. The distance (gaps) between disjoint schools in the north–south direction were summed for each school group and later summed for all fish groups. The sum of n–s gaps within school groups was termed "total gap within." Similarly, a "total gap between" (disjoint school groups) was also computed. Both "total gap within" and "total gap between" were used to compute the encounter probability (p_y) (the probability that at least one fish school is detected):

$$p_y = 1 - (\textit{total gap within} + \textit{total gap between})/L$$

or

$$p_y = 1 - \frac{\sum_{i}^{n}\sum_{j}^{J_i-1}(g_{ij} - y) + \sum_{i}^{n-1}(G_i - y) + E}{L}, \quad (1)$$

where y = the swath width in meter;

g_I = the gap length between j^{th} and $j+1^{th}$ disjoint school within a school group and the quantity of $g_{ij} - y$ is set to zero if g_{ij} is less than y;

G_I = the gap length between i^{th} and $i+1^{th}$ disjoint school groups and $G_i - y$ is set to zero if G_i is less than y;

E = the distance between the north and south end of the survey area and their nearest anchovy schools;

N = number of school groups disjoint in the north–south direction; and

L = 333 km (180 nautical miles [nmi]) which is about the length of the coastline along the Southern California Bight.

Smith (1981) reported that the diameter (nmi) of a school group followed a lognormal distribution and had a logarithmic mean of 2.319 and a logarithmic variance

of 0.676, and that the density of fish schools/nmi^2 in a school group had a logarithmic mean of 3.91 and a logarithmic variance of 0.51 based on data from MacCall.[3] The number of schools within a school group is the product of the area of the school group and the density of schools within. Thus, the mean number of schools was 10,274[4] in a school group (Table 2). The diameter of anchovy schools was generated from the frequency distribution of the diameters of anchovy fish schools in the Southern California Bight (Table 1).

On average, there were 150,000 anchovy schools in the Southern California Bight in the 1970s (Mais, 1974). In recent years, the population has decreased to one fifth of that level (Jacobson et al., 1994). In the simulation, we constructed populations comprising 80,000, 32,000, and 16,000 schools with an average biomass of 12 metric tons (t). At each population level of anchovy, we simulated school groups for nine combinations of three school diameters and three school densities, each with a multiplier of 0.5, 1, and 1.5 applied to both mean and standard deviation of ln(*school diameters*) and of ln(*density of schools*) respectively (Table 2). For example, for a population of 32,000 schools, a multiplier of 0.5 applied to both mean and standard deviation of ln(*diameter*) (an area of 9.45 nmi^2 or 32.34 km^2) for a school group,[5] and a multiplier of 1.5 applied to the mean and standard deviation of ln(density) (625 schools /nmi^2 or 182 schools/km^2),[6] would yield an average number of 5914 schools per school group and an average of six school groups (32,000/5914) (Table 2). This population was denoted as 32,000 (0.5,1.5). The encounter probabilities for seven swath widths (1, 10, 50, 200, 500, 900, and 1600 m for a total of 63 ($3 \times 3 \times 7$) sets of scenarios) were simulated (in computation, numeral 1 was used to represent diameters less than or equal to 1 m). For each of the three populations, 500 iterations were run for each of 63 sets. The mean of the encounter probabilities from 500 runs was used to estimate the mean encounter probability.

For multiple swaths (n), the probability ($p_{y,n}$) that at least one of the swaths intercepts schools is computed as

$$p_{y,n} = 1 - (1 - p_y)^n, \tag{2}$$

where p_y is computed from Equation 1.

Table 2

The average number of school groups for three population sizes and the average number of schools per school group for combinations of different multipliers for the school densities and the school diameters (see text).

Multipliers for diameter of school groups	Multipliers for school density		
	0.5	1.0	1.5
Average number of school groups for three population sizes:			
Population: 16000 schools			
0.5	224.79	26.28	2.71
1.0	13.32	1.56	0.16
1.5	0.56	0.07	0.01
Population: 32000 schools			
0.5	449.58	52.56	5.41
1.0	26.64	3.11	0.32
1.5	1.13	0.13	0.01
Population: 80000 schools			
0.5	1123.94	131.41	13.53
1.0	66.59	7.79	0.80
1.5	2.81	0.33	0.03
Average number of schools per school group			
0.5	71.18	608.77	5914.65
1.0	1201.33	10274.66	99826.39
1.5	28429.65	243150.98	2362398.24

Estimating the number of swaths needed in a survey

Typically, the optimal sample size for a survey is computed by minimizing the variance of the estimate subject to a fixed cost. Because this information was not available, we defined a desirable sample size in terms of the minimum number of transect lines or swaths needed to guarantee at least one positive sighting at an acceptable probability. Therefore, from p_y in Equation 1, one can compute the number of swaths (n) needed for a desired value of $p_{y,n}$ by using

$$n = \frac{\ln(1 - p_{y,n})}{\ln(1 - p_y)}. \tag{3}$$

Probability of detecting fish by depth with signal-to-noise ratios (SNR)

The signal level of a lidar system decays exponentially with depth. The decaying signal of a single pulse can be expressed by the equation

$$S(z) = S_0 \frac{\beta_w(z) + \beta_f(z)}{\beta_0} \exp(-2\alpha z), \tag{4}$$

[4] The mean diameter is 14.25 nmi = exp(2.319+0.676/2) and the mean density of fish schools is 64.39 schools/nmi^2 = exp(3.91+0.51/2), the mean number of fish schools in a school group = $(14.25/2)^2$ 64.39 =10,274.

[5] [exp(2.319 × 0.5 + 0.676 × 0.5 × 0.5/2)/2]^2 × 3.1416 = 9.45 nmi^2.

[6] exp(3.91 × 1.5 + 0.51 × 1.5 × 1.5/2) = 625.62 schools/nmi^2.

where z = depth in meters;
S_0 = the signal level at the surface;
β_w = the clear-water backscatter coefficient;
β_f = the backscatter coefficient of a school of fish;
β_0 = the backscatter coefficient at the surface; and
α = the lidar attenuation coefficient.

The backscatter coefficients, β, have units of 1/m and represent the fraction of the energy that would be scattered upward by a 1-m layer of either clear water or fish. By clear water we mean natural sea water with its attendant load of yellow substance, plankton, silt, etc., but without fish. The lidar attenuation coefficient is related to the absorption and scattering coefficients of the water, in a way that is not completely understood, but depends on the field of view of the lidar. In an operational system, this parameter can be obtained directly from the lidar data. A very narrowly collimated system (defined as one where the field of view is much smaller than the average scattering angle in the water and much smaller than the ratio of the beam attenuation coefficient to the lidar height) will have an attenuation that is very close to the sum of the absorption and scattering. A wide field of view collects multiple scattered photons, and the attenuation is closer to the absorption coefficient.

The noise in a lidar system can come from several different processes. One of these is likely to predominate in any particular set of circumstances. One source is thermal noise in the receiver. This is an additive noise that is independent of the signal level. It is Gaussian with a zero mean. Another source of noise is the shot noise from the sum of the signal current, background-light-generated current, and detector dark current. This is a Poisson process that depends on the total detector current. However, except for very low illumination levels, the Poisson distribution is nearly Gaussian, and we made this approximation. Also, we noted that if the signal from the fish school is very large, the detection probability is nearly unity, and accurate modeling of the noise distribution is not critical. If the fish signal is small, the shot-noise variance will be very nearly the same whether fish are present or not. This is the situation that must be treated accurately, and so we assumed that shot noise could be approximated by an additive signal-independent Gaussian process for the purposes of our study. The final noise source is caused by variations of the optical properties of the water with depth. Variations that are slow in comparison with the depth resolution of the lidar can be estimated and eliminated. However, more rapid fluctuations would be indistinguishable from noise. In the absence of a better model for these fluctuations, we also assumed that they were Gaussian. Thus, an additive signal-independent Gaussian noise was considered, and the source of this noise was not considered further. The final results would not be very different if the dominant noise was not Gaussian. Non-Gaussian noise would change the numerical values of the detection and false-alarm integrals. Because of the strong exponential decrease in signal level with depth, small changes in these values would correspond to small changes in detection depth. A similar effect was caused by our choice of threshold level, which also changed the detection and false-alarm integrals. We show that the results are not very sensitive to our choice of threshold level for the same reason. It is possible that the variations in optical properties produce a highly non-Gaussian noise that will have a significant effect, but we have no evidence for this.

The probability density function (pdf) of the instantaneous signal (s) for a single pulse at some depth can therefore be approximated by a normal pdf with mean = S and variance = σ^2. For illustration, we assumed that σ was not depth dependent, although s clearly was.

Detection was accomplished by setting a threshold signal level above which we asserted that fish were present. The detection probability is the probability that the instantaneous signal is above this threshold when fish are present (i.e. when $\beta_f > 0$). Thus,

$$p(detection) = P(s > T) = 1 - \Phi\left(\frac{T - S_f}{\sigma}\right),$$

where T = the threshold level;
S = a normal random variable with mean= S_f and variance = σ^2;
S_f = the signal level with fish present; and
$\Phi(u)$ = $P(U<u)$ is normal distribution function of U with mean = 0 and variance = 1.

Specifying that fish are present whenever the received signal exceeds some threshold value entails some probability of a "false alarm." This probability can be calculated from

$$P(false\ alarm) = P(s > T) = 1 - \Phi\left(\frac{T - S_w}{\sigma}\right),$$

where S_w = the signal from clear water.

To reduce the number of free parameters, we normalized everything by the noise level. Thus, we defined a signal-to-noise ratio, $SNR = (S_f - S_w)/\sigma$

and a threshold-to-noise ratio, $TNR = (T - S_w)/\sigma$. Then $P(detection) = 1 - \Phi(TNR - SNR)$ for signals following normal distribution with mean SNR and variance 1 when fish are present, and $P(false\ alarm) = 1 - \Phi(TNR)$ for signals following normal distribution with mean = 0 and variance = 1 when no fish are present.

The maximum detection depth, z_{max}, was defined as the depth at which the detection probability is 0.5, i.e. the SNR_z is equal to the TNR because of the sharp drop in detection probability from 1 to 0 with depth (Fig. 2).

$$TNR = SNR_z = SNR_0 e^{(-2\alpha z)}. \quad (5)$$

We could rearrange the terms in Equation 5 and calculate that

$$z_{max} \approx -\frac{1}{2\alpha} \ln\left(\frac{TNR}{SNR_0}\right). \quad (6)$$

We investigated the degree that maximum detection depth for schools is affected by the setting of the false-alarm rate by calculating z_{max} as a function of the false-alarm probabilities and determining the value of TNR to be used in Equation 6. The detection probability ($P(detection)$) can be approximated by unity for depths above this z_{max} and by zero for depths below it (Fig. 2). That is

$$P(detection) = 1 \text{ for } SNRz > TNR \text{ or } z < z_{max}$$
$$= 0 \text{ otherwise.}$$

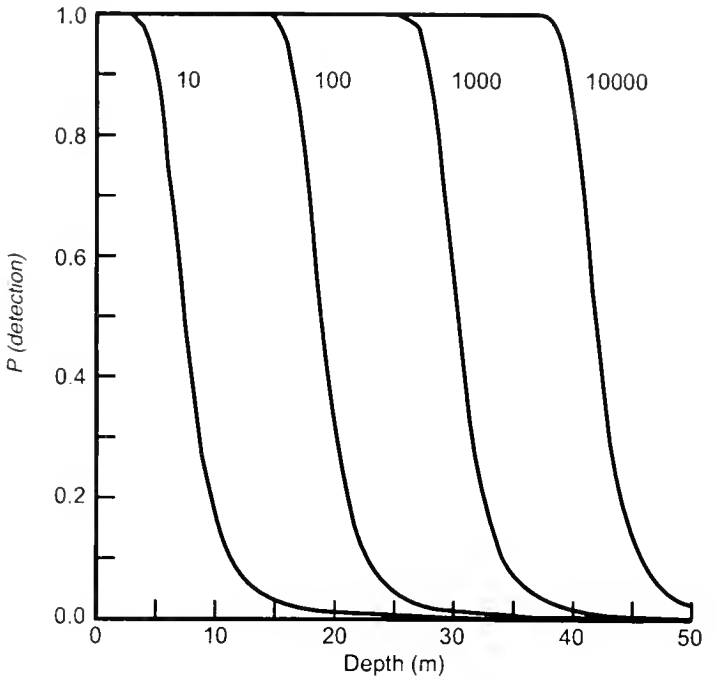

Figure 2

Detection probability as a function of depth for a lidar system with a false-alarm probability of 0.01 operating in water with an attenuation coefficient of 0.1/m. Curves are labeled by the value of the signal-to-noise-ratio (SNR_0) at the surface.

Laser power and penetration depth

To get an idea of the ranges of depths that might be available to the lidar for a reasonable cost, we calculated the maximum penetration depth (z_{max}) with a lidar model that was developed to perform engineering trade-offs quickly and easily. Input parameters and lidar components can be changed easily by the user, and the computer program automatically calculates all of the affected quantities. Plots can be quickly generated within the program to allow the results to be immediately viewed. The lidar system was assumed to be similar to that currently used by NOAA (Churnside et al., 1997). Actual parameters are presented in Table 3.

Only laser power effects were considered. Clearly, other factors were also important. These included receiver telescope diameter, detector sensitivity, background light conditions, fish species, density, etc. However, a full investigation of the effects of all pertinent parameters was beyond the scope of our study. The effects of some of these parameters, however, could be estimated. Doubling the receiver telescope area, detector sensitivity, or fish density, for example, is equivalent to doubling the laser power, and we could have considered an equivalent laser energy that included differences in these parameters. Because of the assumptions used in our calculations, our calculations should be taken as representative and are not necessarily precise.

Because of the interference with the surface, it was difficult to actually calculate SNR_0. Instead, we noted that

$$SNR_0 = SNR_z \exp(2\alpha z), \quad (7)$$

where z = any arbitrary depth; and
SNR_z = the signal-to-noise ratio at that depth.

The calculations were done with a fish school deep enough so that surface effects (e.g. specular reflections of the tail of the laser pulse) did not contribute to the received signal from the school. Equation 7 does not hold for fish within about 1 m of the surface.

but the errors are negligible for the depth distributions of fish used in our study.

The signal and noise levels can be defined at any one of a number of points in the receiver, including optical power on the detector, current out of the detector, the voltage generated by that current through a standard 50-Ω resistance, the output of the log-amplifier, or the integer value that this produces when digitized. We consistently used the voltage across 50 Ω, which is the input voltage to the log-amplifier. For an infinitesimally short laser pulse, this signal varies in time as the pulse propagates through the water. We could relate this time to the depth at which the light was scattered back to the receiver because we knew the speed at which light travels through water. Therefore, we could write the signal as a function of depth as for a nadir-pointing:

$$S'(z) = \frac{P(z)\pi d^2 R\beta(\pi)}{4(z+nh)^2}\exp(-2\alpha z), \quad (8)$$

Table 3

Baseline model parameters for computing laser power and penetration depth.

Parameter	Value
Transmitter	
Wavelength	532 nmi
Pulse length	15 nsec
Pulse energy	1 mJ–1 kJ
Pulse repetition rate	10 Hz
Height above surface	100 m
Beam divergence	25 mrad
Receiver	
Aperture diameter	20 cm
Field of view	25 mrad
Optical bandwidth	10 nm
Electronic bandwidth	100 MHZ
Sample rate	1 GHz
Receiver noise	140 microvolts
Detector type	R5800 photomultiplier tube @ 1200 V
Polarization	Unpolarized
Environment	
Aircraft height	100 m
Water type	IB, III
Background light	1/4 moon
Background light fluctuations	2 percent
Fish school	
Fish type	anchovy
Length	10 cm
Reflectivity	
Packing density	0.5/ m^3
School thickness	10 m

where S' = the received signal per unit depth at depth z;
P = the laser power;
R = the responsivity of the detector and load in V/W;
$\beta(\pi)$ = the backscatter coefficient of the water plus any fish present at that depth;
h = the height of the aircraft above the surface;
n = the index of refraction of water (1.33); and
α = the lidar attenuation coefficient.

To get the actual signal voltage, we had to integrate Equation 8 over the finite duration of the laser pulse. To get the short pulses desired, it was necessary to use Q-switching. With this technique, the laser resonator is blocked electro-optically while the energy is stored in the lasing medium. The cavity is then quickly opened. Lasing begins rapidly, and the output power quickly builds to a high value. As the energy in the lasing medium is depleted, the output power decreases back to zero. This technique produces a characteristic pulse shape that can be approximated by

$$P(t) = \frac{Et}{\tau^2}\exp\left(-\frac{t}{\tau}\right), \quad (9)$$

where E = the total pulse energy; and
τ = 0.408 times the full width of the pulse at one half of its maximum value.

We converted this time to distance through the speed of light, and integrated Equation 8 over depth.

Two water types were used. These were Jerlov (1968) types IB and III. These specify only the diffuse attenuation coefficient K_D. To obtain an estimate of lidar attenuation we needed to have an estimate of the volume scattering function $\beta(\vartheta)$, where ϑ is the scattering angle. We used the general functional form of Petzhold (Petzhold, 1972; Mobley, 1995) with the exact values scaled by the value of the scattering coefficient inferred from the different values for K_D. We first noted that

$$K_D = a + 2\pi b\int_{\frac{\pi}{2}}^{\pi}\frac{\beta(\theta)}{b}\sin(\theta)d\theta, \quad (10)$$

where a = the absorption coefficient of sea water;
b = the scattering coefficient; and
$\beta(\vartheta)/b$ = the normalized scattering function of Petzhold.

From this expression, we obtained the scattering coefficient and the backscatter coefficient for each of the Jerlov water types. The beam attenuation coefficient is given by

$$C = a + b. \qquad (11)$$

The lidar attenuation coefficient lies somewhere between the diffuse attenuation coefficient and the beam attenuation coefficient in such a way that it depends on the beam divergence of the lidar and on the spot size of the laser at the surface. The details of this dependence are not completely understood, and therefore we made what we hoped were reasonable estimates. Following Feigels and Kopilevich (1994), we estimated the divergence angle effect for a beam of negligible size by assuming that photons scattered at angles greater than the lidar divergence angle $\Phi/2$ are lost. We then applied a correction to this value for the finite size of the spot at the surface based on a curve fitted to the results of Gordon (1982). The final result was an estimate for the lidar attenuation coefficient given by

$$\alpha = K_D + 2\pi b \exp(-0.8c\phi h) \int_{\frac{\phi}{2}}^{\frac{\pi}{2}} \frac{\beta(\theta)}{b} \sin(\theta) d\theta, \qquad (12)$$

where h = the height of the lidar above the surface.

The results were fairly sensitive to this parameter; a factor of 2 in α is equivalent to a factor of 2 in depth penetration. The values used in our study were consistent with observations in the Southern California Bight, and are representative of what can be expected. However, more work is needed before accurate predictions of detection probability can be made for a specific water mass based on measurements of the optical properties. Direct measurements of α can provide better detection predictions and can also be used to refine this relationship.

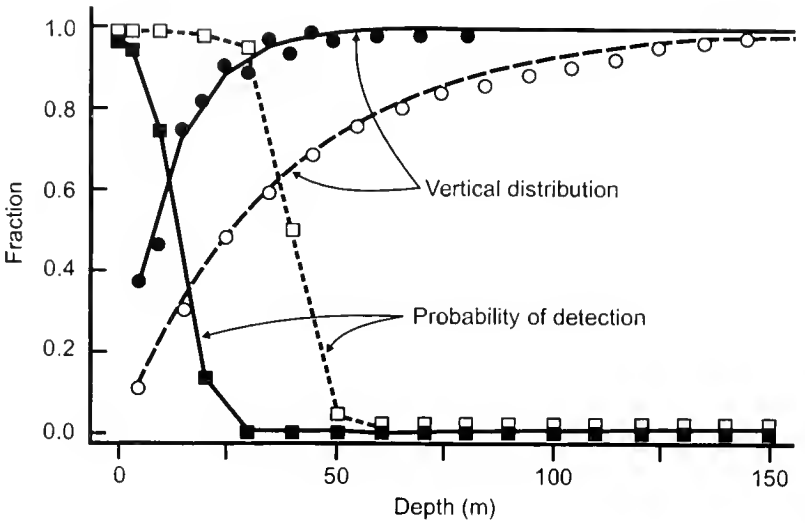

Figure 3

Vertical distribution and probability of detection (Eq. 16) by lidar of anchovy during day (open symbols) and night (solid symbols). The mean depth of anchovy schools was 38.98 m during the day and 11.64 m during the night (Eq. 13).

Vertical distribution and packing density of fish schools

The vertical distributions of schools below the surface, their packing density, and fish size are critical biological properties affecting detection of schools with a lidar. Two vertical distributions of anchovy fish schools were used in our analyses. One represented an average distribution of anchovy schools during the day and the other, average distribution of anchovy schools during the night (Fig. 3). The daytime vertical distribution fitted the average of the cumulative proportion of fish schools during the May 1997 and September 1997 surveys of Holliday and Larson (1979), who used the acoustic reflection from the bottom as a better way to probe the upper 10–20 m than that afforded by conventional acoustic methods. The nighttime vertical distribution curve fitted the cumulative proportions of newly spawned anchovy eggs from two California sites (Pommeranz and Moser, 1987) and anchovy schools from three anchoveta acoustic surveys in Peru (Castillo Valderrama, 1995). The depth of early-stage anchovy eggs may indicate school depth because anchovy spawn during the night. Vertical distributions during the daytime and nighttime were fitted to an exponential distribution function:

$$F(z) = p(Z < z) = 1 - \exp(-z/\lambda), \qquad (13)$$

where $F(z)$ = the proportion of fish schools in the upper z meter depth; and
λ = the mean depth of the fish schools.

Direct measurements of school packing density (numbers of fish/m^3) for anchovy were taken from the literature (Table 4). Graves (1977) deployed a

Table 4

Estimated mean, standard deviation (SD) of packing density(x; fish/m^3) of anchovy and herring, and the log-transformed data (y=ln(x)) during day and night. Coefficient of variation (CV)= SD/mean.

		Packing density(x)			y=ln(x)			
Species	Night or day	mean	SD	CV	mean	SD[1]	Fish length (cm)	Reference
Anchovy	night	53	0.257 n=5	0.48	-0.74	(0.52) 1.11	10	Aoki and Inagaki, 1988
Anchovy	day	114.8	99 n=10	0.86	4.505	(0.67) 1.11	10	Graves, 1977
Herring	day	2.57	3.99 n=20	1.55	0.0725	1.344	3	Misund, 1993

[1] 1.11=sqrt(ln(1.55^2 + 1)), where 1.55 is the CV for 34-cm herring (Eq. 14). Values in parentheses were computed from original data sets.

"dropped" camera by day and Aoki and Inagaki (1988) used a tethered camera by night and obtained the packing density of anchovy with an average length of 10 cm.

The standard deviations (SD) of packing density of anchovy computed from data collected by Aoki and Inagaki (1988) and Graves (1977) measured only the variation among schools and would underestimate the overall variation of packing density. For this reason, we used the coefficient of variation of packing density of herring (1.55) (Misund, 1993; Lo et al.[2]), a more realistic measurement of the variation of packing density, together with the mean packing density of anchovy to estimate the mean (μ_y) and variance (σ_y^2) of log-transformed data: $y = \ln(x)$, where x is the packing density for 10-cm anchovy:

$$\hat{\sigma}_y^2 = \ln\left[cv^2(x)+1\right], \tag{14}$$

$$\begin{aligned}\hat{\mu}_y &= \ln(\bar{x}) - \hat{\sigma}_y^2/2 \\ &= \ln(\bar{x}) - \ln\left(cv^2(x)+1\right)/2,\end{aligned} \tag{15}$$

where $cv(x)$ was that of herring (=1.55). Equations 14 and 15 were derived from the following two relations:

$$\mu_x = \exp(\mu_y + \sigma_y^2/2) \text{ and}$$

$$\sigma_x^2 = \exp(2\mu_y + \sigma_y^2)\left[\exp(\sigma_y^2) - 1\right].$$

Depth-specific probability of detection ($p_a(z)$) based on packing density

As mentioned in an earlier section, $P(detection) = 1$ for $SNRz > TNR$, and zero otherwise, because the steep drop of $P(detection)$ around z_{max}, the proportion of fish that can be detected and identified at depth z, $p_a(z)$, was modeled by the $P(SNR_z > TNR)$. The probability of detection ($p_a(z)$) was computed by means of the probability density function of fish packing density (x) at depth z, assuming that SNR_0 is proportional to the packing density (x), i.e. $SNR_0 = Ax$, where A is the proportionality and is a function of fish size and reflectivity. If reflectivity is the same for all fishes, then A is a function of fish size only, $A \sim 10^4 \times L^2$, where L is the fish length in meters (Churnside et al., 1997). The packing density, x, is a lognormal random variable. We could write $SNR_z = SNR_0 \exp(-2z\alpha) = Ax \exp(-2z\alpha)$; thus $SNR_z > TNR$ is equivalent to $x > (TNR/A)\exp(2z\alpha)$, and we approximated the proportion of fish detected at depth z on the basis of the lognormal distribution of packing density (x) by

$$\begin{aligned}p_a(z) &= \int_{\exp(2\alpha z)TNR/A} p(x)dx \\ &= p\left(\ln(x) > \left[2\alpha z + \ln(TNR/A)\right]\right) \\ &= 1 - \Phi\left(\frac{2\alpha z + \ln(TNR/A) - \mu}{\sigma}\right),\end{aligned} \tag{16}$$

where $\Phi(u) = P(U<u)$ for the normal random variable, U, with mean = 0 and variance = 1; and

$\ln(x)$ has mean μ and variance σ^2.

Equation 16 was computed through SNR_z, the mean of each individual normalized signal (or pulse). In the appendix of this paper, we computed $P_a(z)$ through individual normalized signals. We also assumed with this computation that the effects of shadowing could be neglected. Although more work on this issue is needed, our results suggest that it is not a serious effect. We observed multiple layers of fish in our

data, suggesting that light was penetrating the first layer. We also observed that the water returned from below and above schools of fish and found that the additional attenuation caused by the fish was small in comparison with the background water attenuation.

Proportion of fish schools detected (q)

The proportion of fish schools detected in the upper z meters (q_z) depends on the depth-specific probability of detection ($P_a(z)$; Eq. 16) and the vertical distribution of fish schools (Eq. 13).

The quantity (q_z) was computed by numerical integration:

$$q_z = \int_0^x P_a(u) f(u) du = \int_0^z \left[1 - \Phi\left(\frac{2\alpha u + \ln(TNR / A) - \mu}{\sigma} \right) \right] \frac{1}{\lambda} e^{-\left(\frac{u}{\lambda}\right)} du, \quad (17)$$

where $p_a(u)$ is derived from Equation 16 and $f(u)$ is the exponential pdf derived from Equation 13:

$$f(u) = \frac{1}{\lambda} e^{-\left(\frac{u}{\lambda}\right)}. \quad (18)$$

The quantity, q_z, increases with depth z and reaches an asymptote at z_{max} (q; q<=1) and q is defined as the proportion of fish schools detected.

Criterion for evaluating trade-offs between penetration depth and swath width

If laser power is held constant, an increase in swath width would decrease the maximum depth of penetration of the laser pulse. In this section, we established a criterion for comparing various instruments having different combinations of swath width and laser power (maximum penetration depth). The effectiveness of the width of a swath (y) can be measured by the probability that some fish schools will be encountered (p_y) in the swath (Eq. 1 from simulation). The effectiveness of a lidar in detecting schools within the swath is measured by the proportion of fish schools detected (q) (Eq. 17). The product of p_y q (Eqs. 1 and 17) is then used to evaluate the overall effectiveness of any instruments with a given swath width (y).

Results

Effects of swath width on encounter probability

We assumed that schools were aggregated into school groups in the survey area (42,204 km^2) and that school diameters and densities were equal to, or less than, those reported by Smith (1981). Our simulation results indicated that swath width had little effect on the probability of encountering schools. This was true for all three population sizes: 16,000, 32,000, and 80,000 schools (Fig. 4). Encounter probability was affected by the swath width only when the diameters of the school groups were small and the school density within the school group was so low (both multipliers were 0.5) that their distribution became nearly random rather than aggregated. In these cases, the encounter probability increased sharply when the swath width increased from 1 m to 50 m. Even this very limited effect of swath width diminished as the number of schools in the survey area increased. The encounter probability for swath widths greater than 50 m was almost constant regardless of conditions.

For the multiple swaths, the probability that at least one of them would intercept anchovy schools (Eq. 2) was high in general. The lowest probability was 0.65, for the case where fish were aggregated in few large school groups of low population, i.e. 16,000 (1.5,1.5) for n=5 (Eq. 2). For n=10, the probability ($p_{y,n}$) was close to one for all cases.

Depth-specific detection probability

The depth at which a lidar is capable of detecting a school or target will depend in part on the threshold setting of the instrument in relation to the noise (TNR). To illustrate these relationships we fixed a false-alarm rate ($P(false\ alarm)$) for the detection of schools, used an alarm rate to determine the threshold level, and then calculated the detection probability for schools ($P(detection)$). The results of such a calculation are presented in Figure 5, where the detection probability for fish schools was plotted as a function of the probability of a false alarm for signal-to-noise ratios of 1 and 3. Zero, the lower limit of the plot, corresponds to a very high threshold (TNR) setting, where the probability of a false alarm and the probability of detecting a school are both zero. We concluded that fish are never present at a setting of zero. The upper limit of Figure 5 corresponds to a very low threshold setting, where $P(false\ alarm)$ and $P(detection)$ are both unity; at a setting of 1, we concluded that fish are always present.

If one selects a reasonable false-alarm rate and a signal-to-noise ratio at the surface, one can calculate the detection probability as a function of depth. This was done for a false-alarm probability of 1% and a lidar attenuation coefficient of 0.1/m, and the results are plotted in Figure 2 for several values of the surface signal-to-noise ratio. There are several interest-

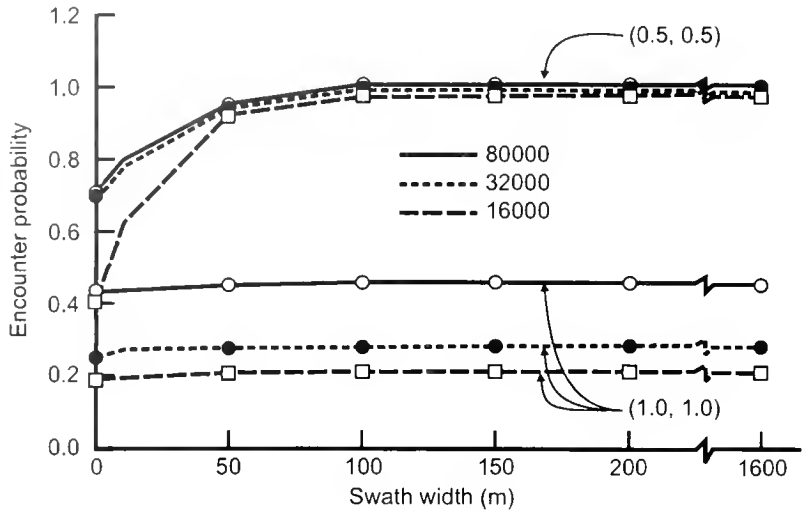

Figure 4

Simulated encounter probability of anchovy schools in Los Angeles Bight (Table 2) for 16,000, 32,000, and 80,000 schools. The swath width ranged from 1 m to 1600 m. The multiplier for mean and standard deviation of the log of diameter of school group and the log of school density in a school group are given in parentheses. Values for populations with multiplier (1.5,1.5), similar to populations with multiplier (1.0,1.0), are not shown.

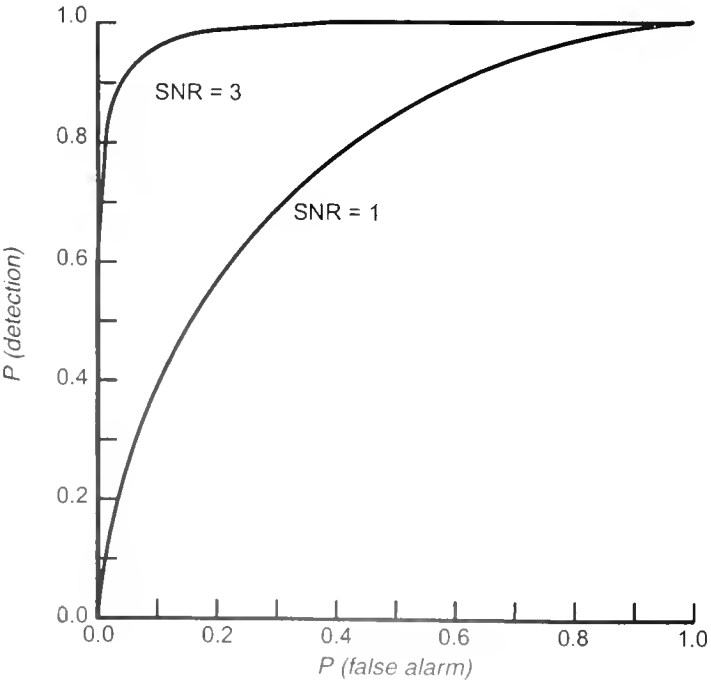

Figure 5

Detection probability as a function of the false-alarm probability for lidar systems with signal-to-noise-ratios (SNR) of 1 and 3.

ing features of these results. The first is that when a critical depth is reached, the detection probability drops abruptly from nearly unity to nearly zero over a narrow, 5–10 m span of depth. Because of this sharp transition, we defined a maximum detection depth (z_{max}) as the depth at which the detection probability is 0.5. The depth z_{max} depends logarithmically on signal level because of the exponential attenuation of the signal with depth. Thus, each order-of-magnitude increase in signal level (illustrated in Fig. 2) provides an increase in z_{max} of just over 10 m in depth. Ten meters is just about 1 lidar attenuation depth, defined as $1/\alpha$ (Eq. 6). We can rewrite Equation 6 as $z_{max} = \ln(SNR_0/TNR) \times 0.5/\alpha$. Therefore, if the attenuation coefficient (a) is different from 0.1/m, the value used in our study, these z_{max} depth values scale linearly with lidar attenuation depth ($1/\alpha$).

To examine the sensitivity of z_{max} (Eq. 6) to TNR and thus the false alarm probability (Eq. 6), we used the same values of the surface signal-to-noise ratio as those used in Figure 2. This calculation indicated that the maximum detection depth (z_{max}) was relatively insensitive to changes in false-alarm probabilities. Decreasing the false alarm rate by a factor 10 from 0.01 to 0.001 would only increase the maximum detection depth by a few meters (Fig. 6). Thus, a fairly low rate of false alarms for a system could be selected without seriously degrading the detection performance. It also implied that we could select a nominal threshold level and obtain a simple expression for the maximum detection depth. A value of $TNR = 3$ results in a false-alarm probability of just above 0.1%. Therefore, according to Equation 6, z_{max} is determined by

$$z_{\max} \approx -\frac{1}{2\alpha}\ln\left(\frac{3}{SNR_0}\right). \qquad (19)$$

We then considered the depth in the water colum at which schools can be detected by

a single lidar pulse and computed, using Equation 16, the proportion of fish schools that could be detected for anchovy (Fig. 3). During the daytime, and at a depth of 30 m, 97% of 10-cm anchovy would be detected ($p_a(z)$, when α=0.1/m). Moreover, one can also compute a signal-to-noise ratio from the packing density(x): $SNR_z = Ax \exp(-2\alpha z)$ for a fish length of 10 cm and compare it to the threshold target-to-noise ratio (TNR) of 3. At the surface, SNR_0 was 11,480 for 10-cm anchovy and z_{max} = 41.24 m. At a depth of 30 m, SNR_{30} (α=0.1) was 28.5, which was above TNR = 3, indicating that most of the schools in the upper 30 m could be detected. The detection probability for anchovy was unity over the upper 30 m (Fig. 3), which was consistent with the results we obtained from Equation 16 (Fig. 3).

For the schools at night, we used a very low packing density (0.53 anchovy/m^3). The signal-to-noise ratio at the surface (SNR_0) for such diffuse schools was 53, substantially above a TNR of 3, and z_{max} = 14 m. At 20 m, the SNR_{20} for anchovy schools declined to 0.97 with a probability of detection of only 13%. At 30 m, the detectability of anchovy was less than 1%.

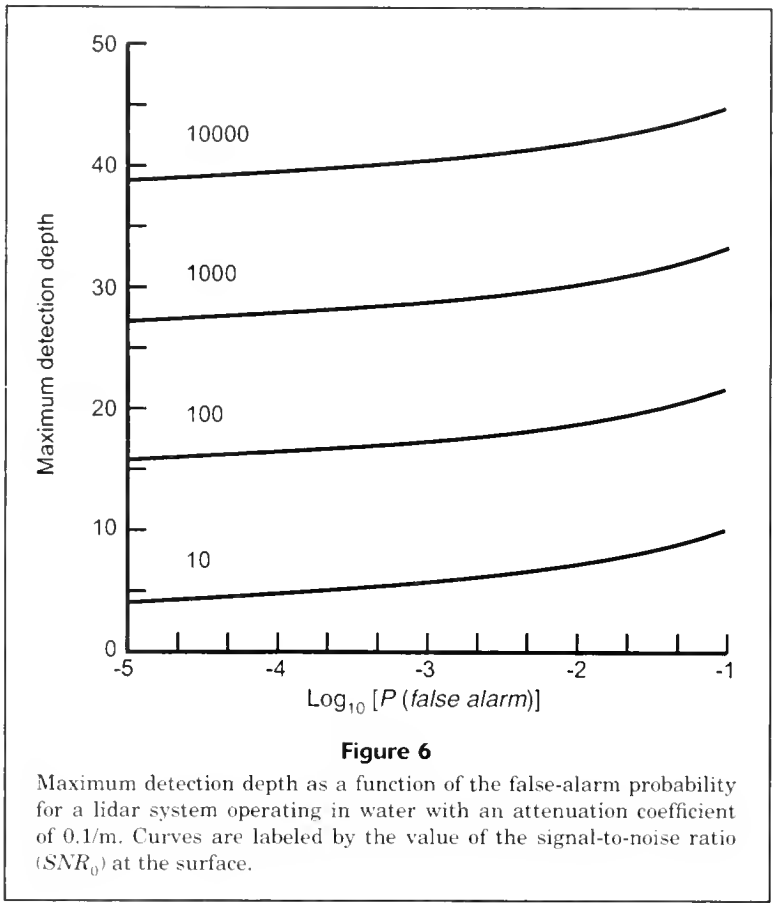

Figure 6

Maximum detection depth as a function of the false-alarm probability for a lidar system operating in water with an attenuation coefficient of 0.1/m. Curves are labeled by the value of the signal-to-noise ratio (SNR_0) at the surface.

Overall vulnerability of schools to lidar detection in the vertical plane

We estimated the cumulated proportion of schools of anchovy that might be detected by a lidar assuming constant day and night vertical distributions. As the first step in the discussion that follows, we focused on the two components used to make the estimate: 1) the average vertical distributions of schools of anchovy during the day and the night (Fig. 3; Eq. 13); and 2) the depth-specific probability of detecting a school, which was discussed in the previous section (Eq. 16). These two components were combined to obtain the final estimates .

The probability of detecting a school during the day declined from about 1 at the surface to 0.50 at 40 m and approached zero at 60 m (α=0.1, Eq. 16; Fig. 3). Because of the lower packing density of the school, the depth-specific probability of detecting a school was much lower at night (with the detection probability dropping from 1 at the surface to 0.10 at 20 m and zero at 30 m). Thus, even the very diffuse nighttime aggregations of anchovy (0.53 fish/m^3) observed by Aoki and Inagaki (1988) could be distinguished from background noise. That shallow nighttime schools can readily be detected by an airborne lidar despite their low packing density means that during the night lidar surveys are feasible.

By combining the detection probabilities with the vertical distributions (Eq. 17), we could calculate the proportion of anchovy schools that could be detected (q) by the lidar (Fig. 7). This calculation indicated that a lidar survey at night would be more accurate than one during the day because the cumulated proportion of schools detected during the night was 60% in the upper 20 m, whereas during the day, it was 40% in the upper 20 m. Thus, despite the higher packing density in the day (115 fish/m^3) which permitted detection down to about 50 m, schools were detected more often at night. This feature was due to the difference in vertical distributions between night and day.

Up to this point we have discussed only cases in which the lidar attenuation coefficient, α, equals 0.1/m, a typical value for the coastal waters of southern California. To illustrate the effect of water clarity, we varied α from 0.05 to 0.6, where the attenuation coefficient for the most turbid coastal water was 0.52. Generally, the proportion of anchovy schools detected (q) declines rapidly with increasing α, although detection also depends on the design

and settings of the lidar as well. Some generalizations can be made. During the night the lidar field of view can be large because less background light exits to interfere with the signal. Under these conditions, the lidar attenuation coefficient (α) will be very nearly equal to the diffuse attenuation coefficient. For the Jerlov open-ocean water types at 532 nmi, α varies from about 0.05/m (type I) to about 0.11/m (type III). The values for the Jerlov coastal water types range from 0.15 (type 1) to about 0.53 (type 9). From our analysis, we expected that most anchovy schools would be detected during the night in the open ocean for $\alpha \leq 0.1$.

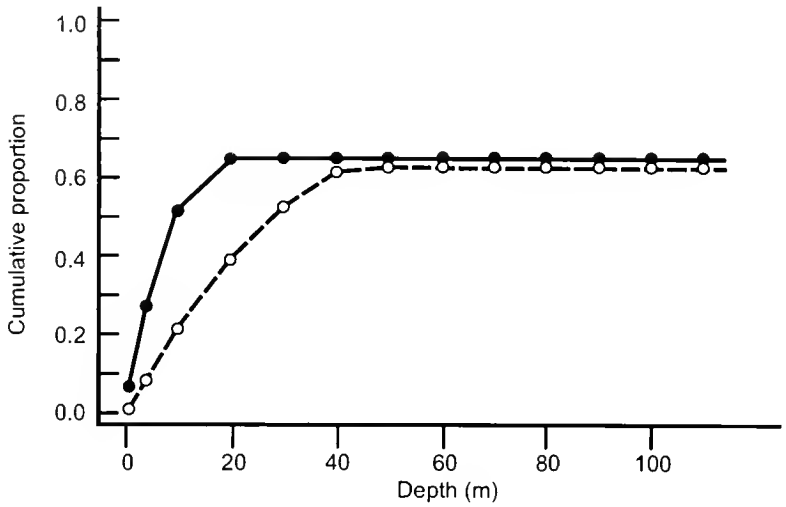

Figure 7

Proportion of fish schools detected in the upper meter depth (Eq. 17) for 10-cm anchovy during the day (open circles) and night (solid circles). The attenuation coefficient is 0.1/m.

During the day, the situation is more complicated. A lidar system with a large field of view will have a smaller signal-to-noise ratio because scattered sunlight reaches the receiver. We could have increased the signal to noise by decreasing the field of view, but this would tend to increase α. Besides, an increase in the signal-to-noise ratio during the day would have little effect on q, because the vertical distribution of schools during the day has a long tail extending down to 155 m (Castillo Valderrama, 1995). At night, an increase in the signal strength that extends the maximum depth of a return by 10 m or so could have an important consequence because of shallow vertical distribution (82% of the school are in the upper 20 m).

Comparisons with vision-based methods

We compared the ability of a human observer to count fish schools with the capability of a lidar. Hara (1990) reported that an observer flying at 500 m would be able to detect sardine schools along a 1600-m swath and to a depth of about 4 m. We assumed that all schools at 4 m could be detected visually and none was detected below that depth. For the lidar, we used a swath width of 7 m, and we considered the product of encounter probability (p_y) (Eq. 1) depicted by swath width and the maximum proportion of schools detected (q) depicted by depth (Eq. 17) to be a measure of the overall performance.

A human observer detects somewhat more schools in the horizontal plane than does a lidar system because of the relatively large swath width provided by aerial viewing (Table 5). The encounter probabilities in the horizontal plane (Eq. 1) obtained from simulation for a population of 32,000 schools was 0.51 for visual detection and 0.42 for lidar detection. In the vertical plane, however, our analysis demonstrated that lidar is superior in detecting schools both during the day and night. During the night, the proportion of anchovy schools detected (q) by the lidar was 0.65, whereas it was 0.28 for the human observer. The difference between visual detection and lidar detection was much greater during the day (q was 0.63 for the lidar), whereas that for the observer was only 0.095.

The $p_y q$ (an overall measure of detection performance) for a lidar was at least 1.9 times that of an aerial observer. This means on the average that the proportion of anchovy schools detected during a survey would be about twice as great for a lidar as it would be for an aerial observer.

We have considered here, however, only one aspect of the two systems—detection rates. Many other differences also exist in relation to species identifications, biomass, and effects of environmental conditions on the observing system.

Laser power and penetration depth

A set of parameters used to compute the laser power and penetration depth for schools of anchovy is listed in Table 3. The lidar signal was computed by using Equation 8, and the penetration depth was computed from the attenuation coefficient estimated from Equation 12. The relation of penetration

Table 5

Comparison of the effectiveness of lidar and aerial observation with different swath width (y) and depth penetration for 10-cm anchovy during the night and day. p_y is the probability of encountering schools for a population of 32,000 schools and swath width y. q proportion of fish school detected for $\alpha = 0.1$ and 0.05, where α is the instantaneous attenuation rate per meter. The product, $p_y q$ is used to evaluate the efficiency of instruments.

Lidar aerial ratio	Maximum detection depth (m)	Swath width (y) (m)	p_y	Proportion of fish schools detected (q)		Overall efficiency ($p_y q$)	
				night	day	night	day
α=0.1							
Lidar		7	0.42	0.65	0.63	0.27	0.26
Aerial	4	1600	0.51	0.28	0.095	0.14	0.048
Ratio						1.92	5.410
α=0.05							
Lidar		7	0.42	0.84	0.85	0.35	0.35
Aerial	4	1600	0.51	0.28	0.095	0.14	0.048
Ratio						2.44	7.50

depth and the logarithmic laser energy for both open ocean and coastal waters was obtained (Fig. 8). Calculations of SNR_0 were made at two laser power levels, and logarithmic dependence was used to generate the curves.

We calculated the maximum penetration depth for the NOAA lidar with a power of 67 mJ and scaled that depth with laser power (Churnside and Hunter, 1996; Table 3). For this calculation, we assumed the presence of 10-cm anchovy with a packing density of 0.5/m^3 (Table 3). Night flights at 100 m altitude were also assumed. Two water types were used, one typical of open ocean water (Jerlov type IB) and one more typical of coastal water (Jerlov type III) (Jerlov, 1968).

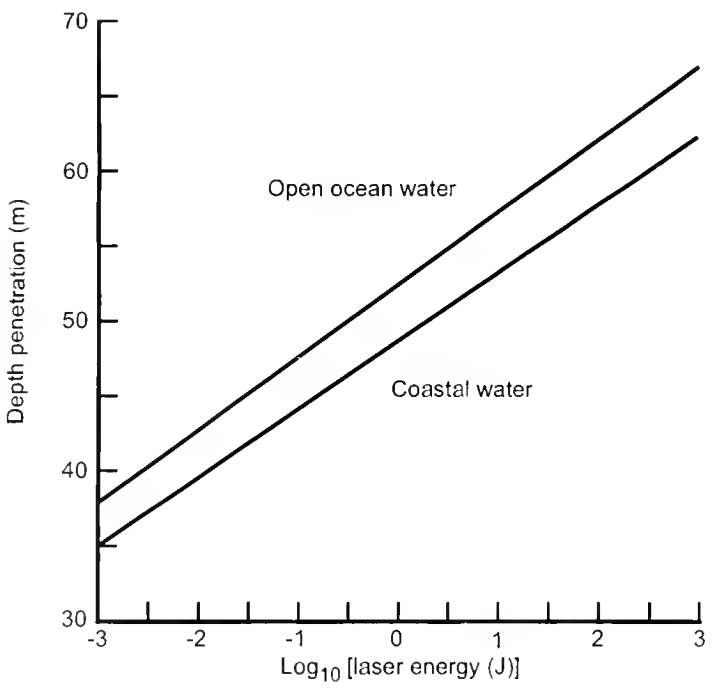

Figure 8

Depth penetration (m) for different laser energy levels (J) on a logarithmic scale for open ocean water and coastal water.

The NOAA lidar presently in use is capable of operating from a single-engine plane; it weighs about 100 kg, requires less than 1 kW of power, and the cost of its components is about $50K. The penetration depth for this system under these somewhat optimum conditions is estimated to be about 45 m at 67 mJ (Fig. 8). Some cost can be saved by using a lower-power laser and smaller telescope, but not a great deal. A savings of only about $10K is likely even if one uses an equivalent energy of 1 mJ. This amount of energy still provides close to 32 m of depth penetration for the conditions assumed in our study.

On the other end, one can obtain approximately 57 m of penetration by using a system with an equivalent pulse energy of 100 J (Fig. 8), but such a system would be a very large and expensive to set up and operate. Part of the equivalent energy could be obtained by using a larger telescope at a power only a little over an order of magnitude of that currently used—one that would emit a laser energy of 10J. This type of laser would require a custom design, with a cost that we estimated to be in the order of one million dollars. In addition, it would require about 100 kW of power, which cannot be supplied by a small,

single-engine aircraft. An aircraft something like the DeHaviland Twin Otter may be necessary to accommodate the size and power requirements of the NOAA lidar system. The system size and cost would probably increase significantly at an equivalent energy of about 1 J. Thus, a practical range for penetration depths would be between about 35 and 50 m.

Discussion

Interpretation of modeling results

Our goal was to model various aspects of a lidar survey system for anchovy with a focus on features that might affect survey accuracy and precision. We learned from our modeling of swath width that this width has little or no effect on the rate at which schools are encountered when they are aggregated into school groups, as is commonly the case with small pelagic fish, like sardines and anchovy, except under very low biomass levels. Under conditions of very low biomass, schools may become scattered rather than aggregated, in which case encounter rates would increase with swath width. Our analyses also showed that the chance that all the transects would not intercept any fish school was extremely small because the number of transect lines is likely to be much greater than 5, owing to the high speed of the survey airplane. Thus, from the standpoint of survey precision, swath width may be given a low priority.

Lack of full vulnerability to the counting technique is one of the most important potential sources of bias for biomass surveys. Fish may not be fully vulnerable because the survey does not extend over the full geographic range of the stock and because there are limitations to the counting system. Nearly all fishery-independent surveys suffer to some extent from these problems. In the case of an airborne lidar survey, the depth limits of the sensing system could produce a large potential bias, particularly if the system is used during the day. Our model indicated that, on average, 36% of schools of anchovy during the day would be expected to be below the maximum detection depth of the lidar (z_{max}=41 m) (Figs. 3 and 8). Because the vertical distribution of schools can vary considerably between surveys, the undetected fraction would vary, thus affecting survey accuracy. This computation is driven by our vertical distribution curve for the daytime and the rapid attenuation of light in water; packing density and fish size have negligible effects. Thus, a reliable estimation of the biomass of such small schooling fishes during the day in offshore waters does not seem practical unless a reliable unbiased estimate of vertical distribution of schools is available. On the other hand, in water up to 30 m depth over the shelf, accurate estimates of biomass for the daytime are practical because the vertical movements of the fish would be restricted.

If a lidar survey were restricted to night flights, when schools are closer to the surface, the bias caused by the uncounted fraction of deep schools would be considerably reduced. During the night, however, schools may become very diffuse and consequently have a much lower target strength which reduces their detectability. The good news from our modeling work was that even the very diffuse schools of 10-cm Japanese anchovy (0.53/m^3, Aoki and Inagaki, 1988) at night were detectable over the upper 20 m. Our model indicated that 65% of all anchovy schools would be detected during the night.

In our study, we focused only on 10-cm anchovy schools at two known and widely differing packing densities and vertical distributions. We ran our models with other packing densities and fish sizes, using data from herring, sardine, and mackerel but keeping the vertical distributions the same as that for anchovy.[2] These results indicated that packing density is an important factor in the detection of schools at night when the vertical distribution is shallow but is unimportant during the day when fish have a deeper vertical distribution. The effect of packing density at night can be significant. For example, at night at 30 m the *SNR* for schools of 10-cm anchovy (packing density 0.53) was only 0.97, whereas that for 13-cm sardine (4.0 packing density) was 12.38 (their detectability was 13% and 77%, respectively). Schools of small fishes may be inherently more detectable than those of larger fish because the decline in average packing densities of schools with increasing fish size is not completely compensated by the increase in reflective area of the fish (packing density changes in proportion to $1/L^3$ (Misund, 1993), whereas the reflective area changes in proportion to L^2). However, this theoretical relationship is eclipsed by the huge variation in packing density due to behavioral factors. The density of anchovy schools at night varies from compact schools suitable for capture by the purse-seine fishery (Squire, 1972) to schools so diffuse that many authors have concluded that schooling ceases (Whitney, 1969; Baxter and Hunter, 1982). The packing density used in our example of an anchovy school at night from Aoki and Inagaki (1988) represents such an extremely dispersed state, but dense concentrations of anchovy do occur at night, only their packing density has not been measured. In fact, 4 fish/m^3 used in the sardine night example might be equally appropriate for anchovy. Unfortunately, because field measurements of packing densities at night are so infrequent, it is impossible to tell at this

point where the mean may fall or what differences might exist between species.

Detection of schools during the night would improve if maximum schooling depth and α were correlated as Hunter and Nicholl (1985) speculated. They determined the visual threshold for schooling in northern anchovy ($6\times10^{-11}W/cm^2$) and suggested that maximum nighttime depth was a function of the ability of fish to see one another. They estimated that the visual threshold for schooling would occur at 38 m during a full moon and at 30 m on a starlit night where chlorophyll was 0.2 mg Chla/m^3 and at 8 m (starlit) and 20 m (full moon) when chlorophyll was 2.0 mg Chla/m^3. If Hunter and Nicholl (1985) are correct, then the maximum lidar detection depth should increase as the schooling depth increases at night, as long as survey flights are made under the same moon phase. This relationship between visual threshold and moon phase also indicates that it may also be important to exclude survey nights during a full moon—a rule long observed by pilots who locate schools for the fishing industry.

It may be possible in practice to detect schools somewhat deeper than those that our model indicates because the model estimates the detection of a single pulse at one range gate or depth. In practice, a lidar will generate a composite image of a school derived from a number of such pulses over a range of gates (depths) analogous to an echogram trace. Such a composite image produced from multiple returns and gates can be more readily separated from background noise than can a single pulse, but such a separation involves a more complex, and at the present time, somewhat more qualitative discrimination process. Signal-processing algorithms can be developed for this application, but their performance would depend on the exact algorithm used. More accurate estimates of detection depth would depend upon the development of such signal-processing algorithms. Development of such algorithms is one of the most promising directions for future research on fisheries lidar. Their development would greatly improve both the accuracy and precision of future lidar surveys for fisheries, as well as reduce the work in processing images. Similarly, a more thorough understanding of the causes of the observed variation in the vertical distribution of fish could improve survey accuracy and precision. The phase of the moon, time of day, mixed layer depth, temperature, location of forage, fish size, season, and spawning habitats, may all influence where in the water column a school may be found.

It seems unlikely that depth of detection will be greatly improved by increasing sensitivity or power of a lidar system over the basic radiometric system used in our model. Our analysis indicated that an order of magnitude increase in equivalent laser power (laser power plus sensor changes) would gain about 10 m in detection depth. Such a change would require a custom, rather than an "off-the-shelf" laser, which would cost around a million dollars, in addition to associated costs, including a larger aircraft to satisfy the new power and weight requirements. In addition, increasing the depth of penetration by 10 or 20 m, on the average, would not increase the numbers of schools detected by more than about 10% during the day because school distributions tend to be skewed with a long tail extending to depths far beyond the practical limits of lidar detection in coastal waters. A 10-m gain would be more significant during the night but may not be worth the additional cost.

We have treated the failure of a lidar to count deep schools as a potential bias, which is true unless an unbiased estimate of the mean vertical distribution of schools exists for the particular survey region and season and an appropriate statistical model is used for the survey. When these conditions are met, the failure of a lidar to count deep schools becomes a matter of precision rather than bias. An unbiased estimate of the mean vertical distribution of schools could be estimated from data generated by lidar and acoustic surveys for the same region because by combining the two surveys, one corrects for the vertical bias in each. The appropriate statistical model for a lidar survey would be one based on line transect theory (Buckland et al., 1993). Line transect theory usually deals with encounter rates on the horizontal plane, and animals are assumed to be uniformly distributed in space. In the case of lidar, we turned the model on its side and used an average vertical distribution of anchovy schools in the survey area. An empirically derived vertical distribution does not seem to be subject to any more bias than a uniform, horizontal distribution, one that is commonly assummed in line transect surveys.

To provide indices of relative abundance based on airborne lidar is an important fishery application that is less demanding than that of estimating biomass. For an index of abundance, the extent to which schools are available for counting is not a major concern. Lidar seems uniquely well-suited for taking an inventory of the juveniles of small pelagic fishes (prerecruits) because they are extremely patchy and tend to inhabit shallow water near the coast in areas difficult to sample with a research vessel. Lidar surveys can provide useful indices of adult biomass as well. Aerial observations (Lo et al., 1992) and passive imaging (Nakashima, 1990; Nakashima and Borstad[7])

[7] Nakashima, B. S., and G. A. Borstad. 1993. Detecting and measuring pelagic fish schools using remote sensing techniques. ICES Report C.M. 1993/B:7, session T, Fish Capture Committee, 18 p.

from aircraft are currently used in several fisheries as indices of the abundance of small pelagic fishes and a lidar-based system would have several advantages over these passive methods. Our computation with a deterministic model showed that a lidar survey may be about twice as efficient in detecting schools as a vision-based system during the night and five times more efficient during the day. At night, a lidar will detect more schools than an observer, but the difference is not huge because the very wide swath width (1600 m) of our hypothetical aerial observer compensated, to some degree, for the observer not seeing farther beneath the surface. During the day, the efficiency of lidar detection, in contrast to visual detection, increases greatly because schools inhabit deeper water. In addition to increased detection efficiency, lidar has several other advantages over aerial observers: lidar images can be better quantified than those based on visual detection or cameras because the school volume rather than school area can be estimated, thereby improving the precision of the index; in addition, detection is less dependent on sea state and is little affected by sun angle or moon phases. On the other hand, skilled fishermen working in aerial surveys can identify species of schooling fish with remarkable accuracy; a remote species identification algorithm for a lidar will be difficult, if not impossible, to develop.

As with hydroacoustic methods, species identification with lidar is a major concern. Even after 50 years of hydroacoustic research, the only method for identifying acoustic targets with certainty is by securing voucher specimens. Radiometric backscatter has no magical properties in relation to those of acoustic back scatter that might allow a rapid solution to the problem of species identificaton. The lesson learned from hydroacoustics is that for species identification to be a reality in lidar surveys, additional sensing systems will be needed. That skillful humans make accurate species identifications visually provides the hope that species recognition algorithms eventually will be practical. We believe it will be possible over the long term to develop species recognition algorithms for lidar in combination with advanced lidar signal processing, digital video cameras, and local knowledge, but at present species identifications must depend upon combining lidar survey data with other information. From the lidar data, we could distinguish reliably between small (about 30 cm length) and large (about 1-m) fish. Identification of intermediate lengths may become possible with more practical experience. One possible approach for obtaining additional information is to use visual identifications of fish schools by aerial observers prorated to lidar targets. Other possible approaches are to combine airborne lidar survey with a research trawler that can provide voucher specimens or to combine airborne lidar with simultaneous sampling of fish eggs from a research vessel (Checkley et al., 1997). The latter approach has been used successfully in a test of the NOAA lidar (Churnside, 1999).

Future application of airborne lidar

An airborne lidar survey could provide a census of epipelagic fishes an order of magnitude faster than that provided by ships, thus reducing costs in dollars (based on 1999 dollar amounts) from about $100 per ship-survey mile to $3 per aerial-survey mile (research ship cost=$12,000 per day, net ship speed including stopping at stations=5 kn; airplane=$600 per hour at 200 kn).

Faster surveys not only cost less but improve accuracy because steady state assumptions are reduced, vessel avoidance is eliminated, and, most important, high speed makes it practical to survey a much larger area, thereby eliminating the errors associated with partial coverage. No major technical barrier exists in acquiring a suitable instrument; adequate fish detection lidars already exist. Fish-detecting lidars may be purchased from one or more vendors or a radiometric lidar may be assembled from "off the shelf" components as has been done with the NOAA lidar (Churnside and Hunter, 1996). However, to implement routine surveys, signal-processing algorithms for rapid quantification of targets are needed, and if the fish targets are to be converted to biomass, direct calibrations of target strength will be needed.

The depth limitation of lidar is not a major barrier to implementation. Our analysis demonstrates, as does our practical experience, that school detection depths of 30–40 m can be expected for California coastal waters using off-the-shelf instrumentation. In fact, more powerful systems are unlikely to do much better owing to the rapid attenuation of signal with depth. The 30–40 m depth limitation is less important at night because most epipelagic fish schools are found within the volume of water that is to be detected by lidar. Our analysis demonstrated that schools can be detected at night despite a much lower packing density. To deal most effectively with the fraction of undetected schools, survey design should be based on line transect theory and should require an estimate of the average vertical distribution of schools under the specific survey conditions (region, species, season, time of day).

In conclusion, the census of epipelagic fish schools with airborne lidar would be practical and useful today if three conditions could be met: assumptions regarding species identity are acceptable; a line transect survey design is used in conjunction with

the known vertical distribution of schools; and algorithms are developed to process the data.

Acknowledgments

We thank Edgeworth Wester and Wynn Eberhard of Environmental Technology Laboratory, Boulder, Colorado, for reading an early draft, and two anonymous reviewers for their constructive comments and suggestions that improved the presentation of the manuscript. Partial support for J. Churnside was provided by the Advanced Sensor Applications Program of the U.S. Department of Defense.

Literature cited

Aoki, I., and T. Inagaki.
1988. Photographic observations on the behaviour of Japanese anchovy *Engraulis japonica* during the night in the sea. Mar. Ecol. Prog. Ser. 43:213–221.

Baxter, J. H. S., and J. R. Hunter.
1982. The biology of the clupeoid fishes. *In* Advances in marine biology, p. 1–223. Academic Press, New York, NY.

Buckland, S. T., D. R. Anderson, K. P. Burnham, and J. L. Laake.
1993. Distance sampling: estimating abundance of biological populations. Chapman and Hall, London, 446 p.

Castillo Valderrama, P. R.
1995. Disribucion de los principales recursos pelagicos durante los veranos de 1992 a 1994. Instituto Del Mar Del Peru Informe 114:17–18.

Checkley, D. M., P. B. Ortner, L. R. Settle, and S. R. Cummings.
1997. A continuous, underway fish egg sampler. Fish. Oceanogr. 6(2):58–73.

Churnside, J. H.
1999. Can we see fish from an airplane? *In* Airborne and in-water underwater imaging (Gary D. Gilbert, ed.), p. 45–48. Proc. SPIE (Society of Photo-Optical Instrumentation Engineers) 3761. SPIE, Bellingham, WA.

Churnside, J. H., and J. R. Hunter.
1996. Laser remote sensing of epipelagic fishes. *In* Laser remote sensing of natural waters: from theory to practice (V. I. Feigels and Y. I. Kopilevich, eds.), p. 38–53. SPIE, Bellingham, WA.

Churnside, J. H., J. J. Wilson, and V. V. Tatarskii.
1997. Lidar profiles of fish schools. Appl. Opt. 36:6011–6020.

Cram, D. L., and I. Hampton.
1976. A proposed aerial/acoustic strategy for pelagic fish stock assessment. J. Const. Int. Explor. Mer 37(1):91–97.

Feigels, V. I., and Yu. I. Kopilevich.
1994. Applicability of lidar remote sensing methods for vertical structure investigation of ocean optical properties distribution. *In* Ocean optics XII (J. Jaffe, ed.), p. 449–457. Proc. SPIE 2258.

Fiedler, P. C.
1978. The precision of simulated transect surveys of northern anchovy, *Engraulis mordax*, school groups. Fish. Bull. 76(3):679–685.

Gordon, H. R.
1982. Interpretation of airborne oceanic lidar: effects of multiple scattering. Appl. Opt. 21:2996–3001.

Graves, J.
1977. Photographic method for measuring spacing and density within pelagic fish schools at sea. Fish. Bull. 75: 230–234.

Gunderson, D. R.
1993. Surveys of fisheries resources. John Wiley and Sons, Inc., New York, NY, 248 p.

Hara, I.
1990. Comparison of ship and aerial surveys of sardine schools. IEEE (Institute of Electrical and Electronic Engineers) Trans. Geosci. Remote Sens. 28(4):693–695.

Holliday D. V., and H. L. Larsen.
1979. Thickness and depth distributions of some epipelagic fish schools off southern California. Fish. Bull. 77(2):489–494.

Hunter, J., and R. Nicholl.
1985. Visual threshold for schooling in northern anchovy *Engraulis mordax*. Fish. Bull. 83(3):235—242.

Jacobson, L. D., N. C. H. Lo, and J. T. Barnes.
1994. A biomass-based assessment model for northern anchovy, *Engraulis mordax*. Fish. Bull. 92:711–724.

Jerlov, N. G.
1968. Optical oceanography. Elsevier, Amsterdam, 194 p.

Lo, N. C. H., I. D. Jacobson, and J. L. Squire.
1992. Indices of relative abundance from fish spotter data based on delta-lognormal models. Can. J. Fish. Aquat. Sci. 49:2515–2526.

Mais, K. F.
1974. Pelagic fish surveys in the California Current. Calif. Dep. Fish Game, Fish. Bull. 162, 79 p.

Misund, O. A.
1993. Dynamics of moving masses: variability in packing density, shape, and size among herring, sprat, and saithe schools. ICES J. Mar. Sci. 50:145–160.

Mobley, C. D.
1995. The optical properties of sea water. *In* Handbook of optics, second ed., vol.1, chap. 43 (M. Bass, ed.), p. 36. McGraw-Hill, New York, NY.

Nakashima, B. S.
1990. Capelin school surface area index for NAFO Div. 3L during the 1989 spawning season. Northwest Atlantic Fisheries Organization (NAFO) SCR Doc. 90/59, serial no. N1780.

Petzhold, T. J.
1972. Volume scattering functions for selected ocean waters. SIO (Scripps Institution of Oceanography) Ref. Doc. 72-78. Scripps Inst. Oceanogr., La Jolla, CA, 82 p.

Pommeranz, T., and H. G. Moser.
1987. Data report on the vertical distribution of the eggs and larvae of northern anchovy, *Engraullis mordax*, at two stations in the Southern California Bight March–April 1980. U.S. Dep. Commer., NOAA Tech. Memo. NOAA-TM-NMFS- SWFC-75, 140 p.

Smith, P. E.
1981. Fisheries on coastal pelagic schooling fish. *In* Marine fish larvae: morphology, ecology and relation to fisheries (R. Lasker, ed.), 1–31 p. Washington Sea Grant Program, Univ. Washington Press, Seattle, WA.

Squire, J. L., Jr.
1972. Apparent abundance of some pelagic marine fishes off the southern and central California coast as surveyed by an airborne monitoring program. Fish. Bull. 70:1005–1019.

Whitney, R. R.
1969. Schooling of fishes relative to available light. Tran. Am. Fish. Soc. 98(3):497–504.

Appendix

The detection probability by depth ($p_a(z)$) was defined as the proportion by which the mean values of SNR_z exceed the threshold, TNR (Eq. 16). Strictly speaking, one should define the detection probability as the expected probability that each signal exceeds the threshold. The expectation would be computed by integrating over the pdf of mean SNR_z. For a lognormal distribution of mean SNR_z, we would have

$$P_a(z) = \int P(s > TNR \mid SNR_z)\text{lognormal}(SNR_z)dSNR_z$$

$$= \int_0^\infty [1 - \Phi(TNR - SNR_z)]\frac{1}{\sqrt{2\pi}\sigma SNR_z}$$

$$\exp\left(-0.5\left(\frac{\ln(SNR_z) - \mu_z}{\sigma}\right)^2\right)d(SNR_z), \qquad (20)$$

where s = the signal-noise-ratio which follows normal ($SNRz$, 1); and

SNR_z = a lognormal random variable with mean $\mu_z = \ln(A) + E(\ln(x)) - 2\alpha z$; and

standard deviation σ = SD($\ln(x)$) where x is the packing density.

Our exercise indicated that both detection probabilities from Equations 16 and 20 were very similar. Equation 16, although an approximation, was used in our computation because of its simplicity.

Abstract.—The reproductive biology of Brazilian menhaden, *Brevoortia aurea*, inhabiting the estuarine waters of the Río de la Plata (Argentina–Uruguay), was studied by using histological analysis of the ovaries. The samples were collected during the peak of the spawning period of this species (November) during 1994, 1995, and 1997. *Brevoortia aurea* is a multiple spawner with indeterminate annual fecundity. Spawning frequency, determined from the percentage of females with postovulatory follicles, was about 12% during November 1995. At this frequency, each female on average spawned a new batch of eggs about every 8 days. Batch fecundity, estimated from counts of hydrated oocytes, was fitted to a power function of length and a linear function of ovary-free female weight. Batch fecundity estimates ranged from 20,000 (27 cm fork length) to 130,000 (34 cm fork length) hydrated oocytes. Annual differences in the size-fecundity relationship were observed. Relative fecundity estimates obtained from the different years sampled ranged from 60 to 212 hydrated oocytes/g of female (ovary-free weight).

Spawning frequency and batch fecundity of Brazilian menhaden, *Brevoortia aurea*, in the Río de la Plata estuary off Argentina and Uruguay*

Gustavo J. Macchi
Consejo Nacional de Investigaciones Científicas y Técnicas (CONICET)
Rivadavia 1917
(1033) Buenos Aires, Argentina
Present address: Instituto Nacional de Investigación y Desarrollo Pesquero (INIDEP)
Paseo Victoria Ocampo No. 1
Mar del Plata (7600), Argentina
E-mail address: gmacchi@inidep.edu.ar

Eduardo M. Acha
Dto. Ciencias Marinas
Universidad Nacional de Mar del Plata
Funes 3350
(7600) Mar del Plata, Argentina

The Brazilian menhaden (*Brevoortia aurea*) is a pelagic coastal species of the southwest Atlantic ranging from Salvador de Bahía, Brazil (13°S), to the south of Buenos Aires province, Argentina (40°S) (Cousseau and Díaz de Astarloa, 1993). It is abundant in the estuarine waters of the Río de la Plata area, where it is caught by the commercial fleets of Argentina and Uruguay, although it is a resource of little economic value (Argentine landings in 1997 were 893 metric tons (t); Anonymous, 1998). Maximum body size is about 41 cm total length (36 cm fork length), which corresponds to an age of 11 years (López Cazorla, 1985). These attributes are similar to those for Atlantic menhaden (*Brevoortia tyrannus*) from the Atlantic coast of the United States, which attains a maximum body size of 36–37 cm fork length and a maximum age of about 10 years (Powell, 1994). Estimation of size at sexual maturity of Brazilian menhaden has not been documented, but the minimum length at maturity for female is 22.5 cm TL (Cassia et al., 1979). Previous reports on life history attributes include descriptions of embryonic and larval development (de Ciechomski, 1968; Weiss and Krug, 1977), growth (López Cazorla, 1985), taxonomy (Cousseau and Díaz de Astarloa, 1993; Díaz de Astarloa and Cousseau, 1993), and feeding (Sánchez, 1989; Giangiobbe and Sánchez, 1993). Comprehensive information on reproduction of Brazilian menhaden does not exist. Recently, we reported that major spawning in the Río de la Plata area occurs from September to December, in estuarine waters across a wide range of salinities (Acha and Macchi, 2000). Cassia et al. (1979) reported total fecundity estimates based on the assumption that the number of eggs spawned by a female is fixed prior to the onset of spawning. Brazilian menhaden may be a multiple spawner, in which case

Manuscript accepted 20 October 1999.
Fish. Bull. 98:283–289 (2000).

* Contribution 1128 of the Instituto Nacional de Investigación y Desarrollo Pesquero, Mar del Plata, Argentina.

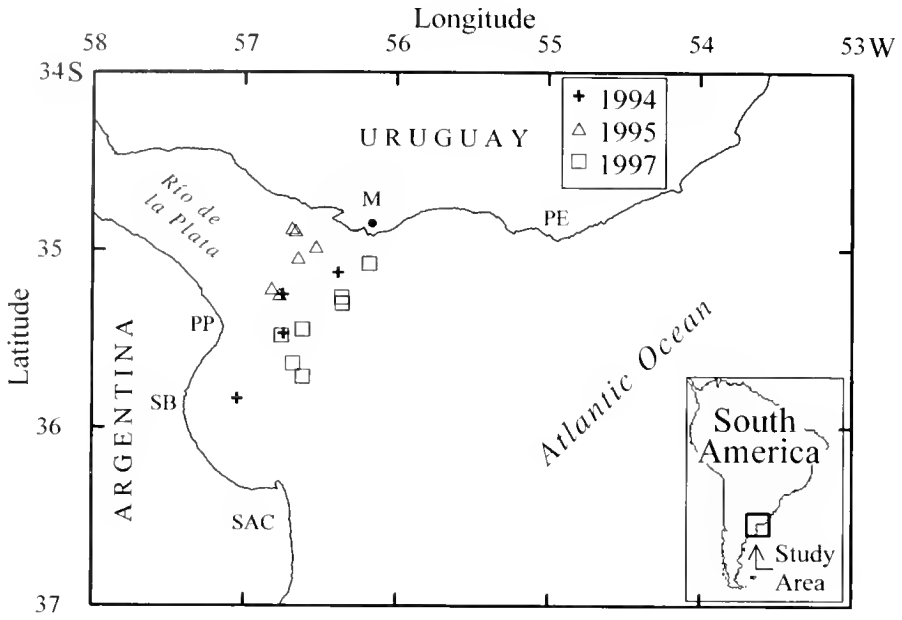

Figure 1

Sample locations for female Brazilian menhaden taken in the Río de la Plata estuary, during November 1994, 1995, and 1997. PE = Punta del Este, M = Montevideo, PP = Piedras Point, SB = Samborombón Bay, SAC = San Antonio Cape.

batch fecundity and spawning frequency must be estimated to determine annual fecundity (Hunter and Goldberg, 1980).

Through histological analysis of the ovaries, we investigated the reproductive biology of *B. aurea* from the Río de la Plata estuary to determine the pattern of spawning and estimate spawning frequency and batch fecundity during the main spawning peak.

Materials and methods

Brevoortia aurea females were collected from the Río de la Plata estuary during three fortnightly research cruises in November 1994, 1995, and 1997 (Fig. 1). Fish samples and oceanographic data (temperature and salinity) were taken for each trawl station from 6 to 20 m depths. Fork length (FL, cm) and total weight (TW, g) were recorded for each fish sampled. Length distributions obtained for the three years were compared with a Kolmogorov-Smirnov Test (KS) (Sokal and Rohlf, 1969). During 1994, only gravid females with hydrated oocytes (n=54) for fecundity estimation were sampled. Females collected in 1995 (n=169) and 1997 (n=92) were randomly selected including different maturity stages. The ovaries were removed and fixed in 10% neutral-buffered formalin for one week. In the laboratory, the gonads were weighed, and a portion of tissue (about 2,0 g) was removed from the center of each ovary, dehydrated in methanol, cleared in benzol, and embedded in paraffin. Tissues were cut into 4-µm sections, and stained with Harris's hematoxylin followed by eosin counterstain. Classification of ovaries was based on the stage of oocyte development and on the occurrence of postovulatory follicles (POF) according to Hunter and Goldberg (1980). Our description of the stages of POF degeneration was adapted from that given by Fitzhugh and Hettler (1995) for *B. tyrannus* and these stages were classified as day-0 and day-1, according to the elapsed time from spawning. A day-0 POF (elapsed time from spawning <24 h) has an irregular, convoluted shape; the granulosa cells are aligned, and many folds and the lumen are clearly visible (Fig. 2, A and B). A Day-1 POF (elapsed time from spawning >24 h) shows degenerative process, the linear appearance of the granulosa cells is not distinct and the lumen becomes reduced (Fig. 2, C and D).

Oocyte diameters for five gravid ovaries were measured after fixation (40 ±µm) with an ocular micrometer (n=749). Spawning frequency was estimated from samples (n=169) collected during November 1995. Daily fraction of spawning females was estimated by the incidence of fish with day-0 and day-1 POFs (Hunter and Goldberg, 1980) and spawning frequency was determined from the average of the percentages of day-0 and day-1 spawning females (Fitzhugh et al., 1993; Macchi, 1998).

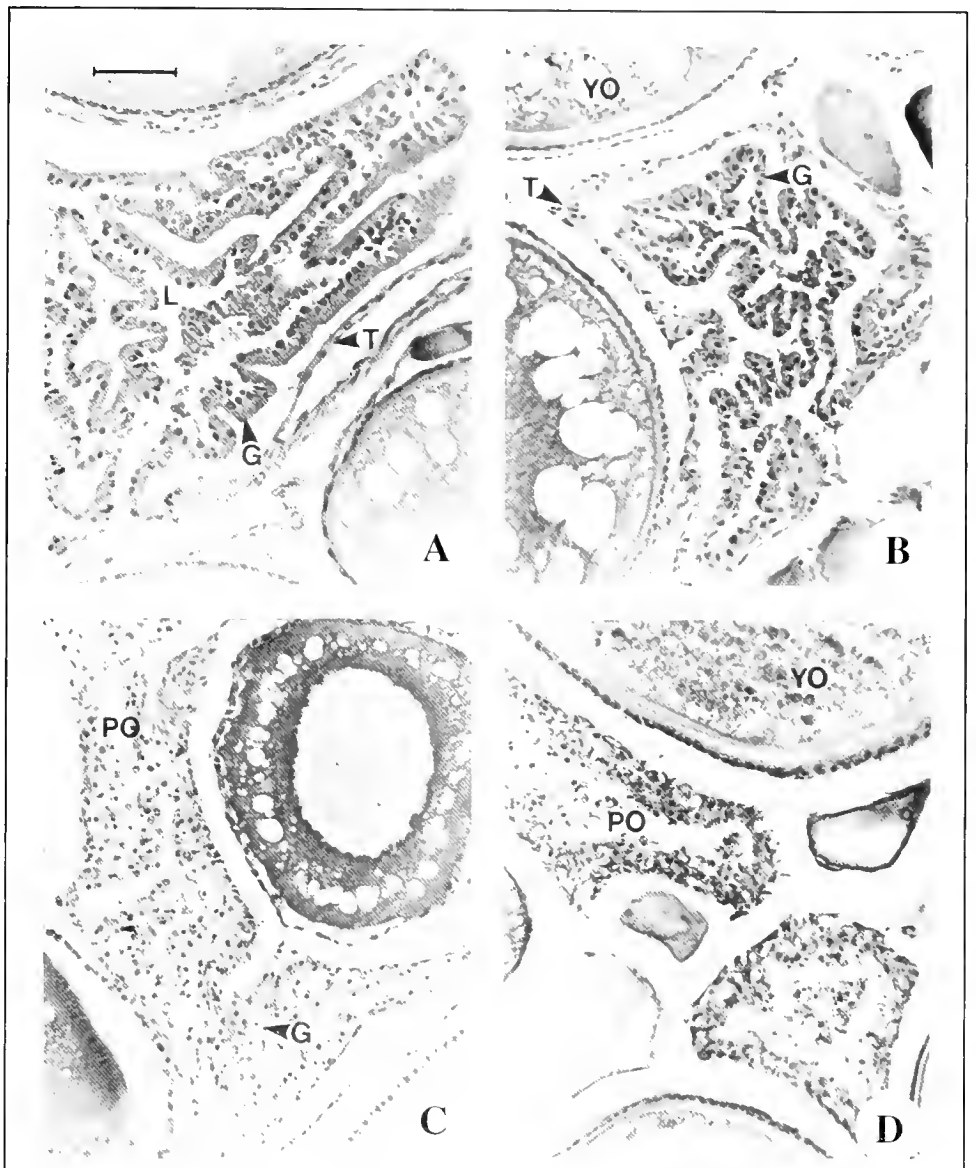

Figure 2

Postovulatoty follicles from female Brazilian menhaden at different stages: (**A** and **B**) day-0, cordlike appearance of the granulosa layer can be observed; (**C** and **D**) day-1, reduction in size and degeneration of follicles are evident. T = thecal layer; G = granulosa layer; L = lumen; YO = yolked oocytes; PO = postovulatory follicles. Bar = 50 µm.

Batch fecundity (BF; number of oocytes released per spawning) was estimated gravimetrically by the hydrated oocyte method (Hunter et al., 1985) for 112 females (44 from 1994, 38 from 1995, and 30 from 1997). The hydrated ovaries showed no evidence of recent spawning (no POFs). Three pieces of ovary, approximately 0.1–0.2 g each, were removed from the anterior, middle, and posterior parts of one gonad, weighed (±0.1 mg), and the number of hydrated oocytes were counted. Batch fecundity for each female was the product of the mean number of hydrated oocytes per unit of weight and the total weight of the ovaries. Relative fecundity (RF; hydrated oocytes per gram of body weight) was determined as the batch fecundity divided by female weight (without ovary). The relationships of batch fecundity to fork length and to total weight (ovary free) were described by regression analysis (Draper and Smith, 1981), and the significance evaluated by testing whether the slope of the regression was significantly different from zero. Interannual comparisons were based on coincident length ranges in the

three years, and an analysis of covariance to log-transformed data was applied (Draper and Smith, 1981).

Results

Length distributions for Brazilian menhaden ranged from 26 to 36 cm FL and did not differ among the years sampled (P>20). All individuals collected were adult mature females with yolked or hydrated oocytes; no immature ovaries were observed.

The oocyte diameter distribution of gravid *B. aurea* females (with hydrated oocytes) showed four groups of oocytes (Fig. 3). The smallest group was composed mainly of primary growth oocytes (smaller than 120 µm). The next larger group was composed of cortical alveolus stage and partially yolked oocytes (primary yolk stage) ranging from 120 to 500 µm. A third group included advanced yolked oocytes (secondary yolk stage) ranging from 500 to 700 µm. The fourth group was the largest and corresponded to the hydrated oocytes measuring 1100 to 1500 µm. The continuous distribution from primary growth oocytes to advanced yolked oocytes is a characteristic pattern in multiple spawning fishes.

Spawning frequency was estimated by examining ovarian tissue from 169 mature females sampled between 21 and 23 of November 1995 during the main spawning peak. Of all specimens examined, about 14% had new postovulatory follicles (day-0) and 10% had day-1 postovulatory follicles (Table 1), the average was 11.98% (SD=7.53%).

Batch fecundity estimates ranged from 20,000 hydrated oocytes for a 27-cm-FL female to 130,000 hydrated oocytes for a 34-cm-FL female. A power model and a linear model were fitted to the relationships BF versus FL and BF versus TW, respectively (Fig. 4). Analysis of covariance indicated that the slope of the regression of fecundity on length did not differ between years, but the intercepts were significantly different (1994–95, $F_{(1, 74)}$=6.68, P<0.05; 1994–97, $F_{(1, 68)}$ = 26.02, P<0.01; 1995–97, $F_{(1, 61)}$=4.53, P<0.05). Relative fecundity ranged from 60 to 212 hydrated oocytes per gram of female (ovary free). These values were different (P<0.05) between the years 1994 (107 ±29 hydrated oocytes) and 1995 (135 ±34 hydrated oocytes), and 1994 versus 1997 (149 ±30 hydrated oocytes), but not between 1995 and 1997.

Discussion

Brevoortia aurea is a multiple spawner with indeterminate annual fecundity, according to our observations of maturing ovaries with postovulatory follicles and yolked oocytes (partially spent stage). These observations suggest that after one batch of eggs is spawned, a new batch develops and is released (Hunter et al., 1992). Further, the oocyte size-frequency distribution of gravid females shows different batches of growing oocytes, including hydrated eggs. Fractional spawning has been suggested for other congeners, such as Atlantic menhaden and gulf menhaden (*Brevoortia patronus*), on the basis of oocyte diameter distributions (Lewis and Roithmayr, 1980; Lewis et al., 1987). These species have a long reproductive season, 6–8 mo. (Powell, 1994), similar to that of *B. aurea*. Atlantic and gulf menhaden spawn during the fall and winter (Powell, 1994), whereas Brazilian menhaden spawn in spring–summer, as do most of the fishes inhabiting the Río de la Plata estuary (Macchi and Acha, 1998).

During November the temperature ranges from 19° to 21°C in the spawning area of Brazilian menhaden. Because duration of the POF stage varies at different temperatures, disappearance of the lumen

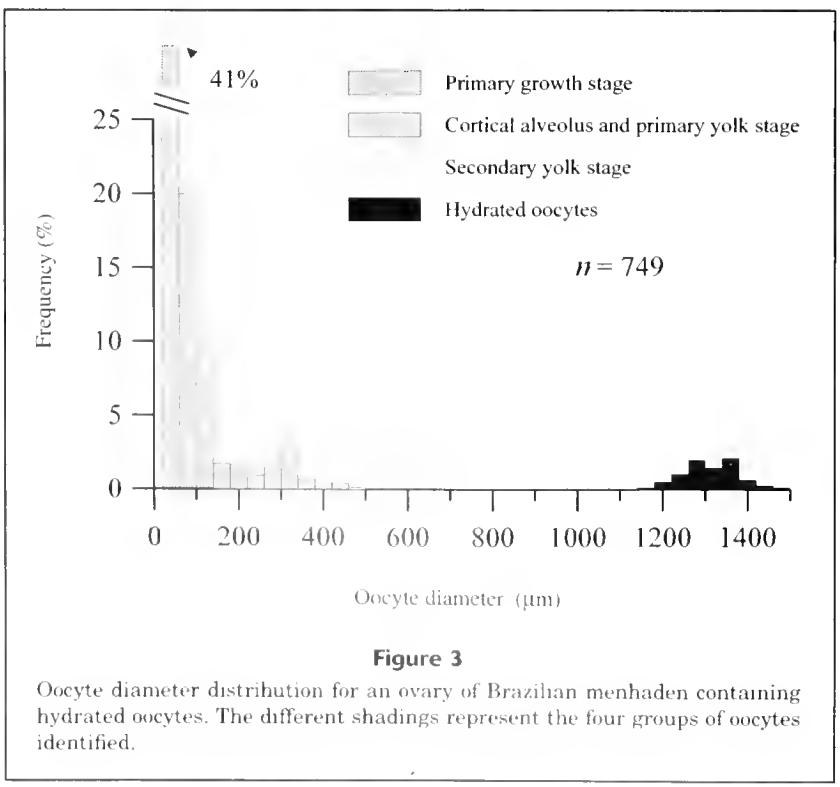

Figure 3

Oocyte diameter distribution for an ovary of Brazilian menhaden containing hydrated oocytes. The different shadings represent the four groups of oocytes identified.

Table 1

Number of Brazilian menhaden females in reproductive activity from the Río de la Plata estuary that were histologically staged for estimation of spawning frequency. POF = postovulatory follicles; CI = confidence interval.

Day of month (November 1995)	Yolked oocytes and no POF	Hydrated oocytes	Day-0 POF	Day-1 POF	Total mature females
21	2	13	3	2	20
21	1	11	1	2	15
22	0	19	1	0	20
22	4	13	0	3	20
22	4	0	9	7	20
22	8	9	3	0	20
23	1	18	1	0	20
23	5	12	1	2	20
23	9	0	4	1	14
Total	34	95	23	17	169
% (average)			13.7	10.1	
95% CI			±9.43	±7.19	

after the loss of the alignment of the granulosa layer was used as the main characteristic to distinguish day-0 from day-1 postspawning ovaries, according to Fitzhugh and Hettler (1995). They concluded that this is the most important feature for classification of POFs in Atlantic menhaden spawning at about 20°C. Spawning frequency estimated from the average between day-0 and day-1 POF percentages (11.98%, SD=7.53%) indicated that *B. aurea* spawn once every eight days during the peak of the reproductive season (November). This value should be considered a preliminary estimate because we did not have samples during other months in the spawning period. Daily spawning fraction of Brazilian menhaden was similar to that of other clupeoids inhabiting temperate waters, such as *Engraulis mordax* (Hunter and Goldberg, 1980), *E. ringens* (Alheith et al., 1984), *Sardinops sagax* (Herrera and Claramunt, 1990), *Sardina pilchardus* (Pérez et al., 1992), *E. capensis* (Melo, 1994), and *E. anchoita* (Pájaro et al., 1997).

Cassia et al. (1979) reported Brazilian menhaden fecundity by counts of yolked oocytes (diameter >540 µm) from ovaries in an advanced maturity stage. They estimated a potential fecundity of 120,000 oocytes for one 30-cm-FL female but did not consider a multiple spawning pattern. Our estimated batch fecundity for females of this length was about 60,000 hydrated oocytes. During the main reproductive period (September–December), a female Brazilian menhaden with a spawning frequency of 8 days would spawn 15 times. Although total fecundity has been calculated for Atlantic menhaden (Higham and Nicholson, 1964; Dietrich, 1979; Lewis et al., 1987) and gulf menhaden (Lewis and Roithmayr, 1980), batch fecundity estimates have not been reported, and gravid females in wild population have rarely been observed (Ahrenholz, 1991).

Batch fecundity was fitted to a power function of fork length and a linear function of ovary-free body weight. Analysis of covariance showed significant differences ($P<0.05$) in regression coefficients among the three years considered (1994, 1995, and 1997). The low coefficients of determination in regressions were similar to those obtained for Atlantic menhaden (Lewis et al., 1987), possibly as a consequence of different ages occurring within length classes after sexual maturity (Lopez Cazorla, 1985). Mean relative fecundities for *B. aurea* (107 [in 1994], 135 [in 1995], and 149 [in 1997] oocytes/g ovary-free body weight) were much lower than those for *Engraulis anchoita* (about 600 oocytes/g ovary-free body weight), the most abundant clupeoid of the Argentine Sea (Pájaro et al., 1997). The difference may reflect the larger egg size of *B. aurea* (1500–1600 µm), compared with *E. anchoita* (about 900 µm; de Ciechomski and Weiss, 1973). The reproductive strategy of some species indicates that egg size takes priority over fecundity (Kjesbu et al., 1996). The larger eggs may be advantageous during the first days of life because hatchlings have larger yolk reserves, contributing to higher growth rates, and may avoid predation more effectively (Hinckley, 1990; Wootton, 1994). Our paper provides the first estimation of spawning frequency and batch fecundity of Brazilian menhaden during the spawning peak. These parameters should also be estimated at the end of the reproductive season to evaluate possible variations and their effect over the annual egg production. Future stud-

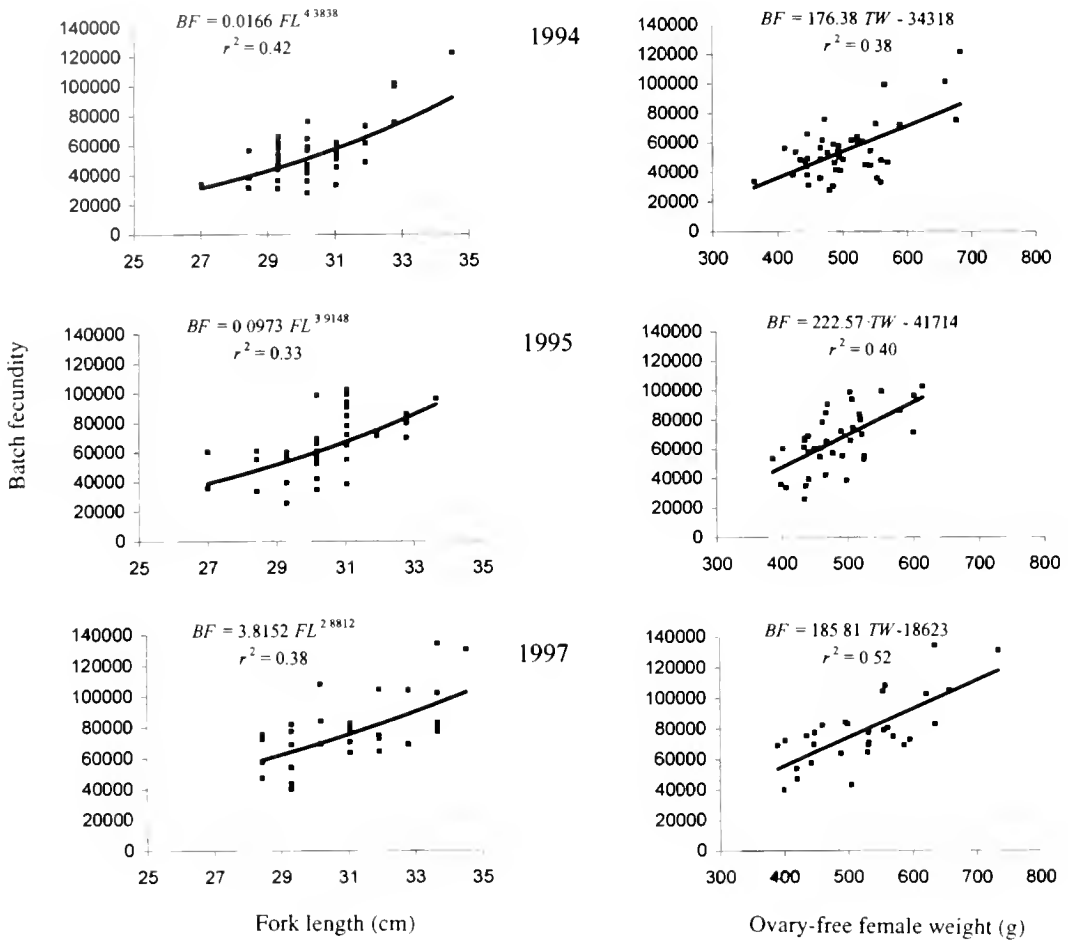

Figure 4

Batch fecundity as a function of fork length and total weight (without ovary) obtained from the different sampled years.

ies about egg quality of *B. aurea* compared with that of *E. anchoita* should include determination of oocyte dry weight, ash dry weight, and total lipid and fatty acid composition.

Acknowledgments

This research was conducted within the INIDEP's Coastal Project. We thank Teresa Carlé and Haraldo E. Christiansen for the preparation of histological sections and Marcela Tobio who was responsible for the photographic procedures. We would also like to thank Norberto Scarlato and two anonymous reviewers for a critical review of our manuscript.

Literature cited

Acha, E. M., and G. J. Macchi.
2000. Spawning of Brazilian menhaden, *Brevoortia aurea*, in the Rio de la Plata estuary off Argentina and Uruguay. Fish. Bull. 98:227–235.

Ahrenholz, D. W.
1991. Population biology and life history of the North American menhadens, *Brevoortia* spp. Mar. Fish. Rev. 53(4): 3–19.

Alheith, J., V. H. Alarcón, and B. J. Macewicz.
1984. Spawning frequency and sex ratio in the Peruvian anchovy *Engraulis ringens*. CalCOFI Rep. 25:43–52.

Anonymous.
1998. Capturas marítimas totales 1997. Ministerio de Economía y Obras y Servicios Publicos. Secretaría de Agricultura, Ganadería, Pesca y Alimentacion. Subsecretaría de

Pesca, Dirección Nacional de Pesca y Acuicultura, Buenos Aires, 45 p.

Cassia, M. C., J. D. de Ciechomski, and H. E. Christiansen.
1979. Estudios sobre la reproducción y fecundidad de la saraca, *Brevoortia aurea* (Agassiz, 1829) Hildebrand, 1948 (Pisces, Clupeidae) y la comparación de dos métodos utilizados. Physis 94:39–46.

Cousseau, M. B., and J. M. Díaz de Astarloa.
1993. El género Brevoortia en la costa atlántica sudamericana. Frente Marítimo 14:49–58.

de Ciechomski, J. D.
1968. Huevos y larvas de tres peces marinos: anchoa marini, *Brevoortia aurea* y *Prionotus nudigula* de la zona de Mar del Plata. Boletin Instituto Biología Marina 17:1–27.

de Ciechomski, J. D., and G. Weiss.
1973. Desove y fecundidad de la anchoita argentina, *Engraulis anchoita*, Hubbs & Marini. Physis 32 (84):137–153.

Díaz de Astarloa, J. M., and M. B. Cousseau.
1993. Caracteristicas regionales de la saraca (*Brevoortia aurea*) dentro del área costera bonaerense. Frente Marítimo 14:59–62.

Dietrich, Ch. S., Jr.
1979. Fecundity of the Atlantic menhaden, *Brevoortia tyrannus*. Fish. Bull. 77(1):308–311.

Draper, N., and H. Smith.
1981. Applied regression analysis, second edition. J. Wiley and Sons, New York, NY, 709 p.

Fitzhugh, G. R., and W. F. Hettler.
1995. Temperature influence on postovulatory follicle degeneration in Atlantic menhaden, *Brevoortia tyrannus*. Fish. Bull. 93:568–572.

Fitzhugh, G. R., B. A. Thompson, and T. G. Snider III.
1993. Ovarian development, fecundity, and spawning frequency of black drum *Pogonia cromis* in Louisiana. Fish. Bull. 91:244–253.

Giangiobbe, A., and F. Sánchez.
1993. Alimentación de la saraca (*Brevoortia aurea*). Frente Marítimo 14:71–80.

Herrera, G., and G. Claramunt.
1990. Estimaciones de la fecundidad parcial y frecuencia de desove de *Sardinops sagax* durante 1987 y 1988, en el norte de Chile. Invest. Cient. y Tec., Serie: Ciencias de Mar 1:55–68.

Higham, J., and W. R. Nicholson.
1964. Sexual maturation and spawning of Atlantic menhaden. Fish. Bull. 63(2):255–271.

Hinckley, S.
1990. Variation of egg size of walleye pollack *Theragra chalcogramma* with a preliminary examination of the effect of egg size on larval size. Fish. Bull. 88:471–483.

Hunter, J. R., and S. R. Goldberg.
1980. Spawning incidence and batch fecundity in northern anchovy, *Engraulis mordax*. Fish. Bull. 77(3):641–652.

Hunter, J. R., N. C. H. Lo, and R. J. H. Leong.
1985. Batch fecundity in multiple spawning fishes. *In* An egg production method for estimating spawning biomass of pelagics fish: application to the northern anchovy, *Engraulis mordax* (R. M. Lasker, ed.), p. 67–77. U.S. Dep. Commer., NOAA Tech. Rep. NMFS 36.

Hunter, J. R., B. J. Macewicz, N. C. H. Lo, and C. A. Kimbrell.
1992. Fecundity, spawning, and maturity of female Dover sole *Microstomus pacificus*, with an evaluation of assumptions and precision. Fish. Bull. 90:101–128.

Kjesbu, O. S., P. Solemdal, P. Bratland, and M. Fonn.
1996. Variation in annual egg production in individual captive atlantic cod (*Gadus morhua*). Can. J. Fish. Aquat. Sci. 53:610–620.

Lewis, R. M., D. W. Ahrenholz, and S. P. Epperly.
1987. Fecundity of Atlantic menhaden, *Brevoortia tyrannus*. Estuaries 10(4):347–350.

Lewis, R. M., and Ch. M. Roithmayr.
1980. Spawning and sexual maturity of Gulf menhaden, *Brevoortia patronus*. Fish. Bull. 78(4):947–951.

López Cazorla, A.
1985. Edad, crecimiento y comportamiento migratorio de *Brevoortio aurea* (Agassiz, 1829) (Osteichthyes, Clupeidae) de Bahía Blanca (Argentina). Inv. Pesq. 49(2):297–313.

Macchi, G. J.
1998. Preliminary estimate of spawning frequency and batch fecundity of striped weakfish, *Cynoscion striatus*, in coastal waters off Buenos Aires province. Fish. Bull. 96:375–381.

Macchi, G. J., and E. M. Acha.
1998. Aspectos reproductivos de las principales especies de peces muestreadas durante la campaña costera H-13/94. INIDEP Inf. Téc. 21:67–89

Melo, Y. C.
1994. Spawning frequency of the anchovy *Engraulis capensis*. S. Afr. J. Mar. Sci. 14: 321–331.

Pájaro, M., G. J. Macchi, and R. P. Sánchez.
1997. Fecundidad y frecuencia reproductiva de las poblaciones bonaerense y patagónica de anchoita argentina (*Engraulis anchoita*). Rev. Invest. Des. Pesq. 11:19–38.

Pérez, N., I. Figueiredo, and B. J. Macewicz.
1992. The spawning frequency of sardine, *Sardina pilchardus* (Walb.), off the Atlantic Iberian coast. Bol. Inst. Esp. Oceanogr. 8 (1):175–189.

Powell, A. B.
1994. Life history traits of two allopatric clupeids, Atlantic menhaden and Gulf menhaden, and the effects of harvesting on these traits. N. Am. J. Fish. Manage. 14:53–64.

Sánchez, M. F.
1989. Caracteristicas morfológicas del aparato digestivo y espectro trófico de la saraca (*Brevoortia aurea*, Clupeiformes, Pisces). Physis 47(112):21–33.

Sokal, R. R., and F. J. Rohlf.
1969. Biometry: the principles and practice of statistic in biological research. W. H. Freeman, San Francisco, CA, 776 p.

Weiss, G., and L. C. Krug.
1977. Caracteristicas do desenvolvimento e metamorfose de *Lycengraulis olidus* (Engraulidae) e *Brevoortia pectinota* (Clupeidae) no estuario da Lagoa dos Patos, Brasil. Atlántica 2(1):83–117.

Wootton, R. J.
1994. Life histories as sampling devices: optimum egg size in pelagic fishes. J. Fish Biol. 45.1067–1077.

Age and growth of the yellowedge grouper, *Epinephelus flavolimbatus*, and the yellowmouth grouper, *Mycteroperca interstitialis*, off Trinidad and Tobago

Sherry C. Manickchand-Heileman
Institute of Marine Affairs
P.O. Box 3160
Carenage, Trinidad, West Indies
Present address: c/o L. Heileman
United Nations Environment Programme
P.O. Box 47074
Nairobi, Kenya
E-mail address: sh_heileman@yahoo.com

Dawn A. T. Phillip
Institute of Marine Affairs
P.O. Box 3160
Carenage
Trinidad, West Indies

Abstract.—Age and growth were determined for the yellowedge grouper, *Epinephelus flavolimbatus*, and the yellowmouth grouper, *Mycteroperca interstitialis*, off Trinidad and Tobago. Age was determined from cross sections of sagittae and opaque rings were counted as annuli. From the monthly variation in marginal increment ratio (marginal increment divided by the distance between the penultimate and outermost annulus), rings were found to be deposited annually from October to February in the yellowedge grouper. Monthly variation in the frequency of otoliths with an opaque margin showed that opaque rings were deposited from September to January in the yellowmouth grouper. Both species were found to grow slowly, to have long lifespans, and to achieve high asymptotic lengths. Ages between 3 and 35 years (282–985 mm TL) were found for the yellowedge grouper, for which the von Bertalanffy growth equation was $L_t = 963\ (1-e^{-0.099(t+0.08)})$, where L_t is length (mm) at time t (yr). Yellowmouth groupers between ages 5 and 41 years (335–827 mm FL) were found and the von Bertalanffy growth equation was $L_t = 854\ (1-e^{-0.057(t+4.6)})$. The length-weight relationship for the yellowedge grouper was $Wt = 5 \times 10^{-5} TL^{2.80}$, where Wt is body weight (g) and TL is total length (mm). For the yellowmouth grouper this relationship was $Wt = 1.88 \times 10^{-5} FL^{2.94}$, where FL is fork length (mm). Both species appear to grow more slowly and to achieve a greater asymptotic size and age than populations in higher latitudes, in contrast to what was expected based on differences in environmental temperature. This may be attributed to differences in fishing pressure because the populations in this study might have been subjected to a lower level of exploitation over a shorter period of time.

Manuscript accepted 26 November 1999.
Fish. Bull. 98:290–298 (2000).

The yellowedge grouper (*Epinephelus flavolimbatus*) and the yellowmouth grouper (*Mycteroperca interstitialis*) are two large serranids commonly caught in the trap fishery off Trinidad and Tobago. The yellowedge grouper has been recorded from North and South Carolina (Huntsman, 1976), the Gulf of Mexico, the West Indies, and the north coast of South America to Brazil at depths of 35–370 m (Smith, 1978). The yellowmouth grouper is found in rocky areas from the shoreline to depths of at least 55 m and is distributed from Bermuda, the South Atlantic Bight, the Gulf of Mexico, throughout the West Indies, Venezuela and Brazil (Smith, 1978), replacing the northern species *M. phenax* in some areas.

Both species are of significant commercial value in Venezuela (Smith, 1971; Gonzalez and Celaya[1]). The yellowmouth grouper is also commercially exploited in Bermuda (Smith, 1971) and the eastern Gulf of Mexico (Bullock and Murphy, 1994). Groupers are also of commercial importance in Trinidad and Tobago where they form part of a lucrative export trade in chilled fish. Yellowedge and yellowmouth groupers are the most commonly caught groupers in traps and are also caught by handlines (Manickchand-Heileman and Phillip, 1993). Historically, these species have been fished on the continental shelf and shelf edge northwest of Tobago and along the north and northeastern coasts of Trinidad by artisanal vessels from Trinidad and Tobago, as well as from Venezuela (Mendoza and Larez, 1996). Due to the decline in catch rates in these areas (Manickchand-Heileman and Phillip, 1993; Mendoza and Larez, 1996), the fishery has expanded to

[1] Gonzalez, L.W., and J. Celaya. 1986. Diagnostico socio-economico de la pesqueria de media altura pargo-mero del estado Nueva Esparta. Contrib. 8, Centro de Investigaciones Cientificas, Univ. Oriente, Venezuela. 31 p. Univ. del Oriente, Apdo. Postal 245, Cumana, Sucre, Venezuela.

the offshore continental shelf and shelf edge to the east of Trinidad. At present, this fishery is not managed and the decline in catches in the traditional fishing areas emphasizes the need for proper management. However, lack of data is an impediment to the development of appropriate management strategies for this important fishery.

Groupers are relatively long-lived and slow-growing and are protogynous hermaphrodites, making them especially susceptible to overexploitation (Bannerot et al., 1987; Shapiro, 1987; Bohnsack[2]). In reviewing the status of grouper stocks in the western central Atlantic, Sadovy (1990) found that these stocks are heavily fished throughout the region and that many are growth or recruitment overfished, or both. Sadovy also emphasized the need for management to ensure their continued commercial and recreational viability.

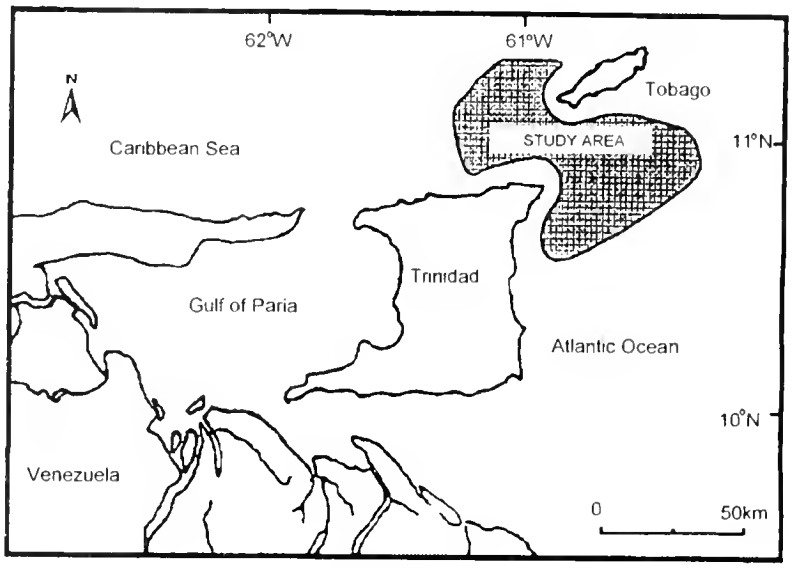

Figure 1
Location of study area.

Published information on the yellowedge and yellowmouth grouper is scarce. Age, growth and reproduction of the yellowedge grouper in South Carolina have been investigated by Keener (1984) and in the eastern Gulf of Mexico by Bullock and Godcharles.[3] Randall (1967) documented the food habits of yellowmouth grouper from the Bahamas and Thompson and Munro (1978) recorded the occurrence of spawning individuals in Jamaica. Aspects of the life history, including age and growth, of yellowmouth grouper in the eastern Gulf of Mexico have been reported by Bullock and Smith (1991) and Bullock and Murphy (1994).

In Trinidad and Tobago, information on reproduction, age, and growth of the yellowedge and yellowmouth groupers have been presented by Manickchand-Heileman and Phillip.[4] However, age was not validated and results were only preliminary. Our study reports on the age and growth of these two species off Trinidad and Tobago. It was carried out as part of a national fish stock assessment project, in collaboration with the Fisheries Division, Ministry of Agriculture, Lands and Marine Resources (Trinidad and Tobago), the United Nations Development Program (UNDP), and the Food and Agriculture Organization (FAO).

Materials and methods

Study area

Trinidad and Tobago, a twin-island Republic, are the southernmost of the Caribbean chain of islands (Fig. 1). Both islands are situated on the South American continental shelf; Tobago is about 32 km to the northeast of Trinidad. Topographically, the shelf in this area is relatively featureless; a substratum of fine mud is interspersed with occasional patches of shell debris and fine sand (Kenny and Bacon, 1981). The shelf edge lies along the 90–100 m contour (Gade[5]) which ranges from a distance of approximately 12 km from the northwest coast of Tobago to approximately 50 km from the north coast of Trinidad.

This area experiences a dry season from December to May and a wet season from June to November. Bottom temperatures at depths of about 100 m vary from a maximum of 25°C in the dry season to a minimum of 22°C in the wet season (Gade[5]). During the wet season the large input of fresh water from

[2] Bohnsack, J. A. 1989. Protection of grouper spawning aggregations. Coastal Resour. Div. Contrib. Rep. CRD 88-89-06, NMFS Southeast Fish. Sci. Cent., Miami, FL, 8 p.

[3] Bullock, L. H., and M. F. Godcharles. 1984. Life history aspects of the yellowedge grouper, *Epinephelus flavolimbatus* (Pisces: Serranidae) from the eastern Gulf of Mexico. Annual Report, Fla. Dep. Nat. Resour., Mar. Res. Lab., St. Petersburg, FL, 28 p. Unpubl. data.

[4] Manickchand-Heileman, S., and D. A. T. Phillip. 1992. Preliminary stock assessment of the fishpot fishery of Tobago. Technical report of the Project for the Establishment of Data Collection Systems and Assessment of the Fisheries Resources. Report FAO/UNDP:TRI/91/001/TR12, 38 p.

[5] Gade, H. 1989. The environmental-ecological regimes. *In* Report on surveys of the fish resources in the shelf areas between Suriname and Colombia with the R/V *Dr. Fridtjof Nansen*, p. 8–41. Institute of Marine Research, Bergen.

local precipitation and runoff from South American rivers, particularly the Orinoco River, affect surface salinity which ranges from 35.5‰ in the dry season to less than 27‰ in the wet season. However, the salinity of deeper waters is not greatly affected and ranges from about 36.8‰ in the wet season to 36.5‰ in the dry season (Gade[5]).

Methods

Monthly samples of yellowedge and yellowmouth grouper were obtained from commercial fish landings at a fish processing plant on the island of Tobago. Fish were caught by Antillean fish traps (Munro et al., 1971) on the continental shelf and slope to the northeast of Trinidad and northwest of Tobago in depths of 37–128 m (Fig. 1). A total of 729 yellowedge and 116 yellowmouth groupers were obtained during the study period.

Total length (mm) was recorded for the yellowedge grouper, whereas fork length (FL) was recorded for the yellowmouth grouper because, in most cases, the filamentous rays of the caudal fin of this species were damaged. Total body weight (g) was recorded for both species. For most fish the left sagittal otolith was removed unless broken or lost, in which case the right was obtained. Otoliths were stored dry in labelled envelopes.

For sectioning, otoliths were embedded in Spurr resin (Spurr, 1969) and allowed to harden overnight. One or two 0.5-mm transverse sections of each otolith were taken through the focus along a dorsoventral plane with a high-speed circular saw. Sections were ground and polished with several grades of silicon carbide paper. They were placed in glycerol and viewed against a black background with reflected light under a dissecting microscope at a magnification of 20×. Alternating opaque and translucent bands were visible and the former were counted as annuli.

For each species, otolith radius (distance from the core to the otolith edge) and the distance from the core to the distal edge of each opaque ring were measured under a binocular microscope with an ocular micrometer (1 micrometer unit=0.125 mm). All measurements were taken along the ventral surface of the sulcus acousticus. In order to validate that rings were formed annually in the yellowedge grouper, the monthly mean marginal increment ratio, that is, the marginal increment (distance between the distal edge of the outermost annulus and the otolith margin) divided by the distance between the distal edge of the penultimate annulus and proximal edge of the outermost annulus (Bullock et al., 1992), was calculated. Because of difficulty in measuring annulus radius in the yellowmouth grouper, it was not possible to carry out this analysis in sufficiently large monthly samples. Instead, for this species the monthly frequency of occurrence of otoliths with an opaque edge was determined. Mean monthly marginal increment ratios in the yellowedge grouper and frequency of occurrence of opaque edges in the yellowmouth grouper were compared by using the chi-square goodness-of-fit test for circular data (Zar, 1974). Least squares linear regression of otolith radius on fish length was carried out and the relationship used to backcalculate lengths of fish at earlier ages.

The von Bertalanffy growth function was used to describe growth (Ricker, 1975):

$$L_t = L_\infty\left(1-e^{-K(t-t_0)}\right),$$

where L_t = total or fork length (mm) at time t (years);
L_∞ = the asymptotic length;
K = the growth coefficient; and
t_0 = theoretical age at zero length.

This function was fitted to observed lengths at age by using the FISHPARM program (Prager et al., 1987). The length-weight relationship was determined by least squares linear regression with logarithmically transformed data:

$$W = aL^b,$$

where W = body weight (g);
L = fish length (mm); and
a and b are constants.

Results

Validation

Satisfactory annuli counts were made on 326 of the 367 yellowedge grouper otoliths examined. A randomly chosen subsample of 63 otoliths was read by an independent reader and a 95% agreement was found. This species showed a significant difference among monthly mean marginal increment ratios ($P<0.001$), with elevated values (greater than 50%) occurring from March to September (Fig. 2). This finding suggests that there is one main period of annulus formation during the year from October to February, even though otoliths with opaque edges were observed throughout the year.

Growth of the otolith was proportional to growth in length of the fish and the relationship between total length (TL) and otolith radius (OR) was

$$TL = 111.4OR - 105.2 \qquad (n=330,\ r^2=0.93).$$

Number of rings increased with fish length; 3–35 rings were found in yellowedge grouper between 282 and 985 mm TL.

Of the 90 otoliths read for the yellowmouth grouper, satisfactory annuli counts were made on 80. A random subsample of 33 otoliths was read by an independent reader and a 98% agreement was found. For this species frequency of otoliths with an opaque edge showed significant monthly variation ($P<0.001$), with elevated values occurring from September to January (Fig. 3). Growth of the otolith was proportional to growth in length and the relationship between fork length (FL) and otolith radius was

$$FL = 162.97 + 90.86OR \qquad (n=57,\ r^2=0.81).$$

The number of rings increased with fish length; 5–41 rings were found in yellowmouth grouper between 335 and 827 mm FL.

The monthly sample sizes shown in Figures 2 and 3 indicate the seasonal pattern of catches for both species in this study area. At the extremities of the year, catches were low because fishing is restricted to shallow waters owing to rough seas that prevail at this time.

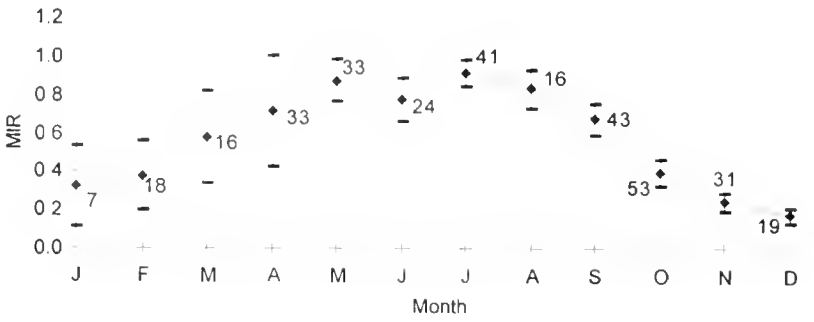

Figure 2

Monthly variation in mean marginal increment ratio (MIR) for yellowedge grouper, *E. flavolimbatus*. Sample sizes are given next to means and standard deviation is represented by the horizontal bars.

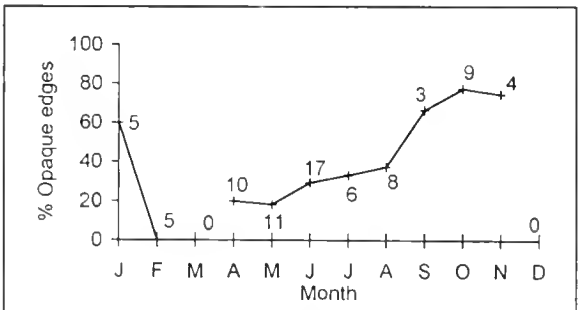

Figure 3

Monthly variation in the frequency of occurrence of otoliths with opaque margin for yellowmouth grouper, *M. interstitialis*. Sample sizes are given next to data points.

Age and growth

For both species, the growth parameters are presented for combined sexes because in some instances otoliths were obtained from fish that were gutted at sea and thus of unknown sex. The relationship between fish length and otolith radius was used to backcalculate lengths of fish at earlier ages. Owing to the narrowing of the space between successive annuli in older individuals and the resulting difficulty in making accurate measurements, radii were measured in 231 yellowedge grouper with 3 to 15 rings. Mean backcalculated lengths for yellowedge grouper are given in Table 1. Close agreement was found between the observed, backcalculated, and theoretical growth curves for this species, although for some age groups the backcalculated lengths were greater than observed lengths (Fig. 4). The von Bertalanffy growth parameters (asymptotic standard error) for observed length and age data for the yellowedge grouper were L_∞ = 963 mm TL (18.8 mm), K= 0.099/yr (0.01 yr), t_0= –0.08 years (0.28 yr).

Owing to narrowing of the space between annuli in older individuals and difficulty in making accurate measurements, it was possible to measure radii in only 20 yellowmouth grouper, with 5 to 19 rings. Mean backcalculated lengths for yellowmouth grouper are given in Table 2. Close agreement was also found between the observed, backcalculated and theoretical growth curves for this species, although some backcalculated lengths were greater than observed lengths, particularly for the younger age groups (Fig. 5). For the yellowmouth grouper, the von Bertalanffy growth parameters (asymptotic standard error) for observed length at age data were L_∞ = 854 mm FL (59.9 mm), K= 0.057/yr (0.01/yr), t_0= –4.6 years (2.29 yr).

Length-weight relationship

For the yellowedge grouper, the relationship between total body weight (Wt) and length (TL) was

Table 1

Observed and backcalculated mean total lengths (TL mm) at age (yr) for the yellowedge grouper, *E. flavolimbatus*. Roman numerals represent annulus number, beginning at the focus of the otolith.

Age (yr)	*n*	Mean TL (mm)	SD (mm)	I	II	III	IV	V	VI	VII	VIII	IX	X	XI	XII	XIII	XIV	XV
3	3	317	14	185	251	313												
4	2	299	23	123	198	241	294											
5	15	389	24	136	203	269	331	381										
6	29	438	35	128	206	277	340	395	431									
7	41	469	47	120	194	265	334	389	434	465								
8	33	534	50	126	209	281	350	412	461	502	530							
9	26	586	61	135	221	300	363	426	478	519	552	579						
10	22	618	44	135	220	292	360	420	469	513	552	578	605					
11	32	638	36	124	202	281	353	411	466	511	550	583	612	629				
12	13	666	74	129	197	259	333	400	451	497	537	577	610	638	659			
13	6	696	61	162	215	290	354	408	452	492	534	573	610	644	669	690		
14	5	725	72	129	197	250	317	369	423	474	517	545	586	623	661	694	718	
15	4	769	57	121	201	264	327	382	442	482	519	562	603	640	677	709	743	766
Total	231																	
Weighted backcalculated mean TL (mm)				129	207	278	345	403	453	497	542	577	607	633	664	696	728	766
Growth increment (mm)					78	71	67	58	50	44	45	35	30	26	31	32	32	38

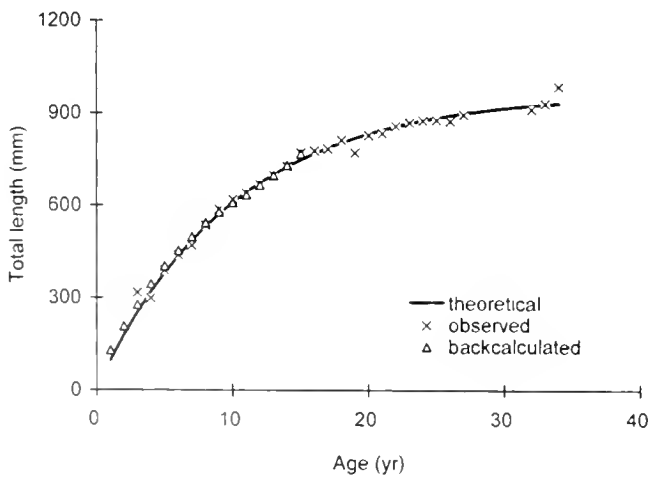

Figure 4

Observed, backcalculated, and theoretical lengths at age for yellowedge grouper, *E. flavolimbatus*.

$$Wt = 5.0 \times 10^{-5}\mathrm{TL}^{2.80} \qquad (n=335,\ r^2=0.88).$$

The exponent b was significantly different from 3 (t-test, $t=17.98$, $P<0.001$). For the yellowmouth grouper this relationship was

$$Wt = 1.88 \times 10^{-5}FL^{2.94} \qquad (n=50,\ r^2=0.94),$$

with b being significantly different from 3 (t-test, $t=5.19$, $P<0.001$).

Discussion

The annual formation of opaque rings was demonstrated in both yellowedge and yellowmouth groupers in the study area. Deposition of annuli occurs over a protracted period of about five months, beginning in the wet season and continuing into the early part of the dry season. A protracted period of annulus deposition has been observed in other grouper populations, e.g. *Mycteroperca phenax* (Matheson et al., 1986), *Epinephelus itajara* (Bullock et al., 1992), and *M. microlepis* (Hood and Schlieder, 1992). Factors affecting annulus formation in groupers have been discussed by Moe (1969), who attributed annulus formation in red grouper to spawning and related physiological processes. In contrast, in our study area, annulus formation in the yellowmouth and yellowedge groupers occurred after the period of peak spawning from about April to July for both species (Manickchand-Heileman and Phillip[4]). Formation of annuli after spawning was also reported for the Nassau grouper, *E. striatus*, in the Cayman Islands (Bush et al., 1996). Annulus formation has also been found to occur out of phase with spawning in other grou-

Table 2

Observed and backcalculated mean fork lengths (FL mm) at age (yr) for the yellowmouth grouper, *M. interstitialis*. Roman numerals represent annulus number.

Age (yr)	*n*	Mean TL (mm)	SD (mm)	I	II	III	IV	V	VI	VII	VIII	IX	X	XI	XII	XIII	XIV	XV	XVI	XVII	XVIII	XIX
5	3	335	3	234	273	298	320	332														
6	1	355	—	236	262	302	322	335	349													
8	2	482	23	269	315	355	380	411	436	456	474											
9	1	516	—	271	310	349	379	398	428	457	487	506										
10	1	557	—	290	337	372	406	430	453	476	511	534	557									
12	3	566	48	279	321	360	394	418	445	469	492	511	525	544	558							
13	1	603	—	273	346	395	432	456	481	505	530	554	566	579	591	603						
14	5	605	38	277	324	359	382	404	427	449	469	489	508	528	544	555	564					
15	1	559	—	331	321	341	371	391	410	430	450	480	499	519	529	539	549	559				
17	1	634	—	289	335	381	404	427	450	473	496	508	531	554	565	577	588	600	611	623		
19	1	700	—	336	380	405	431	457	475	492	509	527	544	553	579	605	622	626	631	635	639	644
Total	20																					
Weighted backcalculated mean TL (mm)				274	316	351	378	399	434	462	484	506	524	540	555	566	572	595	621	629	639	644
Growth increment (mm)					42	35	27	22	35	28	22	22	18	16	15	11	6	23	26	8	11	4

pers in higher latitudes, e.g. *M. phenax* in the South Atlantic Bight (Matheson et al., 1986), *E. itajara* (Bullock et al., 1992) and *M. microlepis* (Hood and Schlieder, 1992) in the eastern Gulf of Mexico, and *M. bonaci* in south Florida (Crabtree and Bullock, 1998). For the two species in our study, annulus formation may be associated with changes in environmental factors, notably reduced bottom temperature during the wet season. On the continental shelf, where our study was conducted, bottom temperature has been found to decrease to a minimum of about 22°C in the wet season (Gade[5]).

Annual rings were found in otoliths of yellowedge and yellowmouth groupers in other geographical areas, although time of annulus formation differed, which may be attributed to differences in annulus measurement techniques. For yellowedge grouper in the South Atlantic Bight, annulus formation occurred in March–September and coincided with time of peak spawning (Keener, 1984), whereas in the eastern Gulf of Mexico it occurred from May to November (Bullock and Godcharles[3]). The yellowmouth grouper formed annuli in August–October in the eastern Gulf of Mexico (Bullock and Murphy, 1994).

Some backcalculated lengths were larger than observed lengths, especially for the younger age groups. This reverse "Rosa Lee" phenomenon may have resulted from increased survival of fast-growing fish (Ricker, 1975). For the yellowmouth grouper, the small number of fish available for ring measurements may have also contributed to discrepancies in the backcalculated lengths.

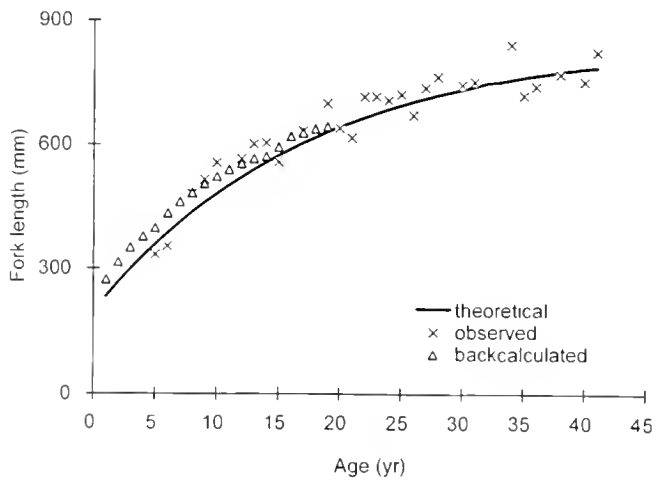

Figure 5

Observed, backcalculated, and theoretical lengths at age for yellowmouth grouper, *M. interstitialis*.

The growth pattern of these two species is similar to that reported for other groupers, in that they are long-lived and have low growth rates and high asymptotic lengths (e.g. *M. phenax*, Matheson et al., 1986; *M. bonaci*, Manooch and Mason, 1987, Crabtree and Bullock, 1998; *E. itajara*, Bullock et al., 1992; *M. micro-*

lepis, Hood and Schlieder, 1992; *E. guttatus*, Sadovy et al., 1992). In the southern United States, the yellowedge grouper has a lower asymptotic length and higher growth rate (L_∞=891mm TL, K=0.163, Keener, 1984; L_∞=831 mm TL, K=0.191, Bullock and Godcharles[3]) than those found in our study. Our maximum observed age (35 years) was greater than those (15 and 27 years) reported by Keener (1984) and Bullock and Godcharles,[3] respectively.

Comparison of growth curves using Φ', where $\Phi' = \log K + 2\log L_\infty$ (Munro and Pauly, 1983; Pauly and Munro, 1984) showed close agreement with those in other areas (Φ'=2.96, our study, Φ'=3.11 and 3.12, southern United States with growth parameters of Keener, 1984, and Bullock and Godcharles[3], respectively). This comparison suggests that the general growth pattern of yellowedge grouper observed in our study is similar to that for the southern United States and further validates the results obtained in our study.

The yellowmouth grouper also showed a higher L_∞ (854 mm FL or 934 mm TL) and lower K than reported for the eastern Gulf of Mexico where L_∞ was 828 mm TL and K was 0.076 (Bullock and Murphy, 1994). The maximum observed age (41 years) was higher than that (28 years) reported by Bullock and Murphy (1994). Comparison of growth curves using Φ' showed close agreement between the growth curve obtained in our study (Φ'=2.70) and that obtained by Bullock and Murphy (1994) whose growth parameters resulted in Φ' of 2.72.

Results suggest that the growth curve of each species belongs to the same family of curves as their counterparts in other geographical areas, i.e. the relationship between L_∞ and K is similar (Pauly, 1991). However, comparison of actual growth rates and asymptotic lengths indicates that each species grows slower and achieves a greater size and age than those reported for populations in the southern United States. This finding is in contrast to what is expected in the growth patterns of tropical versus subtropical and temperate populations. Tropical fish generally grow faster and reach smaller sizes than populations in higher latitudes, mainly because of differences in environmental temperature (Longhurst and Pauly, 1987). It appears that factors other than those related to the environment may be responsible for the differences observed, or may mask the real growth pattern. Such factors may include intrinsic differences between populations, or differences in fishing patterns between the two areas. The latter may contribute significantly to differences in growth because grouper populations in the southern United States have been fished since the late 1970s (Bullock and Murphy, 1994; Bullock et al., 1996) for a longer period of time than the populations in our study. Populations subjected to high exploitation rates for long time periods generally exhibit changes in growth and reproductive patterns, such as faster growth and smaller sizes (Gulland, 1983), as well as smaller size at maturity (McGovern et al., 1998) than populations that have not been as heavily fished.

The slow growth, long life spans, and presumed low natural mortality rates of yellowedge and yellowmouth grouper reported for our study, imply that they are highly susceptible to overfishing (Bullock et al., 1992). These characteristics suggest that maximum yield would be obtained at either low exploitation rates or with capture of only large individuals (Bullock et al., 1992). In addition, the protogynous hermaphroditic strategy of some groupers may also make them more susceptible to overfishing than gonochoristic species (Bannerot et al., 1987). Evidence of hermaphroditism has been reported for the yellowedge grouper (Keener, 1984; Bullock et al., 1996) and other species of *Mycteroperca* (Matheson et al., 1986; Collins et al., 1987; Hood and Schlieder, 1992; Crabtree and Bullock, 1998). We did not consider differences in growth patterns and population dynamics specific to an alternative reproductive strategy in our study. For protogynous hermaphrodites, the pooling of data for combined sexes may mask certain growth patterns such as enhanced growth rates following sexual transition and could lead to errors in the predictions obtained from standard yield models (Bannerot et al., 1987). Thus, subsequent studies should consider the effects of an alternative reproductive strategy on population parameters and the predictions for management of these species in Trinidad and Tobago.

Acknowledgments

This project was accomplished with financial and technical assistance from the United Nations Development Programme and the Food and Agricultural Organization. The authors wish to thank the following: Edward Brothers for assistance with otolith reading; Daniel Pauly for technical advice; Maxwell Sturm for reviewing earlier drafts of the manuscript; and the Yeates brothers for allowing access to fish catches and for facilitating field sampling. Two anonymous reviewers contributed comments that significantly improved the manuscript.

Literature cited

Bannerot, S. P., W. W. Fox Jr., and J. E. Powers.
1987. Reproductive strategies and the management of snappers and groupers in the Gulf of Mexico and Caribbean. *In* Tropical snappers and groupers: biology and fisheries man-

agement (J. J. Polovina and S. Ralston, eds.), p. 561-603. Westview Press, Boulder.

Bullock, L. H., M. F. Godcharles, and R. E. Crabtree.
1996. Reproduction of yellowedge grouper *Epinephelus flavolimbatus*, from the eastern Gulf of Mexico. Bull. Mar. Sci. 59(1):216–224.

Bullock, L. H., and M. D. Murphy.
1994. Aspects of the life history of the yellowmouth grouper, *Mycteroperca interstitialis*, in the eastern Gulf of Mexico. Bull. Mar. Sci. 55(1):30–45.

Bullock, L. H., M. D. Murphy, M. F. Godcharles, and M. E. Mitchell.
1992. Age, growth, and reproduction of jewfish *Epinephelus itajara* in the eastern Gulf of Mexico. Fish. Bull. 90: 243–249.

Bullock, L. H., and G. B. Smith.
1991. Seabasses (Pisces: Serranidae). Mem. Hourglass Cruises 8(2):1–243.

Bush, P. G., G. C. Ebanks, and E. D. Lane.
1996. Validation of ageing technique for Nassau grouper (*Epinephelus striatus*) in the Cayman Islands. *In* Biology, fisheries and culture of tropical snappers and groupers (F. Arreguin-Sanchez, J. L. Munro, M. C. Balgos and D. Pauly, eds.), p.150–157. ICLARM Conf. Proc. 48.

Collins, M. R., C. W. Waltz, W. A. Roumillat, and D. L. Stubbs.
1987. Contribution to the life history and reproductive biology of gag, *Mycteroperca microlepis* (Serranidae), in the South Atlantic Bight. Fish. Bull. 85:648–653.

Crabtree, R. E., and L. H. Bullock.
1998. Age, growth and reproduction of black grouper, *Mycteroperca bonaci*, in Florida waters. Fish. Bull. 95:735–753.

Gulland, J.A.
1983. Fish stock assessment. A manual of basic methods, vol.1. FAO/Wiley series on Food and Agriculture, 223 p.

Hood, P. B., and R. C. Schlieder.
1992. Age, growth and reproduction of gag, *Mycteroperca microlepis*, in the eastern Gulf of Mexico. Bull. Mar. Sci. 51(3):337–352.

Huntsman, G. R.
1976. Offshore bottom-fisheries of the United States south Atlantic coast. *In* Proc. Coll. on snapper-grouper fishery resources of the western central Atlantic Ocean (H. R. Bullis and A. C. Jones, eds.), p. 192–221. Florida Sea Grant Rep. 17, Gainesville, FL.

Keener, P.
1984. Age, growth, and reproductive biology of the yellowedge grouper, *Epinephelus flavolimbatus*, off the coast of South Carolina. M.S. thesis, College of Charleston, Charleston, SC, 65 p.

Kenny, J. S., and P. R. Bacon.
1981. Aquatic resources. *In* The natural resources of Trinidad and Tobago (St. G. C. Cooper and P. R. Bacon, eds.), p. 112–144. Edward Arnold Ltd., London.

Longhurst, A. R., and D. Pauly.
1987. Ecology of tropical oceans. Academic Press Inc. Ltd., London, 407 p.

Manickchand-Heileman, S., and D. A.T. Phillip.
1993. Description and status of the snapper grouper fishery of Trinidad and Tobago. Gulf and Caribb. Fish. Inst. 45th Annual Meeting, 11 p. Harbour Branch Oceanographic Institute, Fort Pierce, FL.

Manooch, C. S. III, and D. L. Mason.
1987. Age and growth of the Warsaw grouper and black grouper form the southeast region of the United States. Northeast Gulf Science 9(2):65–75.

Matheson, R. H. III, G. R. Huntsman, and C. S. Manooch III.
1986. Age, growth, mortality, food and reproduction of the scamp, *Mycteroperca phenax*, collected off North Carolina and South Carolina. Bull. Mar. Sci. 38(2):300–312.

McGovern, J. C., D. M. Wyanski, O. Pashuk, C. S. Manooch, and G. R. Sedberry.
1998. Changes in sex ratio and size at maturity of gag, *Mycteroperca microlepis*, from the Atlantic coast of the southeastern United States during 1976–1995. Fish. Bull. 96:797–807.

Mendoza, J. J., and A. Larez.
1996. Abundance and distribution of snappers and groupers targeted by the artisanal medium range fishery off northeastern Venezuela (1981–1992). *In* Biology, fisheries and culture of tropical snappers and groupers (F. Arreguin-Sanchez, J. L. Munro, M. C. Balgos, and D. Pauly, eds.), p. 266–275. ICLARM Conf. Proc. 48.

Moe, M. A.
1969. Biology of the red grouper *Epinephelus morio* (Valenciennes) from the eastern Gulf of Mexico. Fla. Dep. Nat. Resour. Mar. Res. Lab. Prof. Pap. Ser. 10, 95 p.

Munro, J. L., and D. Pauly.
1983. A simple method for comparing growth of fishes and invertebrates. ICLARM Fishbyte 1(1):5–6.

Munro, J. L., P. H. Reeson, and V. C. Gaut.
1971. Dynamic factors affecting the performance of the Antillean fish trap. Proc. Gulf and Caribb. Fish. Inst. 23: 184–194.

Pauly, D.
1991. Growth performance in fishes: rigorous description of patterns as a basis for understanding causal mechanisms. Aquabyte 4(3):3–6.

Pauly, D., and J. L. Munro.
1984. Once more on the comparison of growth in fish and invertebrates. ICLARM Fishbyte 2(1):21.

Prager, M. H., S. B. Sailer, and C. W. Recksiek.
1987. FISHPARM: a microcomputer program for parameter estimation of nonlinear models in Fishery Science. Oceanography Technical Report. 87–10, 18 p. Old Dominion University, Norfolk, VA.

Randall, J. E.
1967. Food habits of reef fishes of the West Indies. Stud. Trop. Oceanogr. Inst. Mar. Sci. Univ. Miami, 5:665–847.

Ricker, W. E.
1975. Computation and interpretation of biological statistics of fish populations. Fish. Res. Board Can. Bull. 191, 382 p.

Sadovy, Y.
1990. Grouper stocks of the western central Atlantic: the need for management and management needs. Gulf and Caribb. Fish.Inst. 43rd Annual Meeting, 17 p. Harbour Branch Oceanographic Institute, Fort Pierce, FL.

Sadovy, Y., M. Figuerola, and A. Roman.
1992. Age and growth of the red hind *Epinephelus guttatus* in Puerto Rico and St. Thomas. Fish. Bull. 90:516–528.

Shapiro, D. Y.
1987. Reproduction in groupers. *In* Tropical snappers and groupers: biology and fisheries management (J. J. Polovina and S. Ralston, eds.), p. 295–327. Westview Press, Boulder, CO.

Smith, C. L.
1971. A revision of the American groupers: *Epinephelus* and allied genera. Bull. Am. Mus. Nat. Hist. 146(2):69–241.
1978. Serranidae. *In* FAO species identification sheets for fisheries purposes (W. Fischer, ed.), vol. IV. Western Central Atlantic (fishing area 31). FAO, Rome.

Spurr, A. R.
1969. A low-viscosity epoxy resin embedding medium for electron microscopy. J Ultrastructure Res. 26:31–43.
Thompson, R., and J. Munro.
1978. Aspects of the biology and ecology of Caribbean reef fishes: Serranidae (hinds and groupers). J. Fish. Biol. 12: 115–146.
Zar, J. H.
1974. Biostatistical analysis. Prentice Hall Inc., Englewood Cliffs, NJ, 620 p.

Reproductive biology of the female shortfin mako, *Isurus oxyrinchus* Rafinesque, 1810, with comments on the embryonic development of lamnoids

Henry F. Mollet
Monterey Bay Aquarium
886 Cannery Row
Monterey, California 93940
E-mail address: mollet@mbay.net

Geremy Cliff
Natal Sharks Board
Private Bag 2
Umhlanga Rocks 4320, South Africa

Harold L. Pratt Jr.
Narragansett Laboratory
28 Tarzwell Drive
Narragansett, Rhode Island 02882

John D. Stevens
CSIRO Marine Research
P O Box 1538
Hobart, Tasmania 7001, Australia

Abstract.—Reproductive data from 95 mature female shortfin mako sharks, *Isurus oxyrinchus* Rafinesque, 1810, including 35 pregnant females, together with data on 450 postnatal fish were collected from around the world. Size at birth was approximately 70 cm total length (TL) and litter size varied from 4 to 25, increasing with maternal size. Embryo length-at-capture data predicted a gestation period of 15–18 months and late winter to midspring parturition in both hemispheres. A temporal analysis of uterus width index and gonadosomatic index of pregnant and postpartum females indicated that the reproductive cycle is three years. The median TL-at-maturity of females from the western North Atlantic (2.98 m) was greater than that of females from the Southern Hemisphere (2.73 m) and they were 16–19% heavier in the TL range of 2.5–3.5 m.

Recently ovulated females and a litter with 2.6–3.3 cm TL embryos having external gills, a large yolk sac, and still inside their egg cases, are described. We describe a litter of embryos (52.0 cm TL) with huge yolk-filled stomachs. Litters of 59.9- and 68.8-cm-TL embryos showed a decline in the mass of the yolk-filled stomach from 29.1% to 10.9% of total mass and an increase in hepatosomatic indices from 3.7% to 7.0% as gestation advances. When the mass of the yolk-filled stomach was excluded, the mass-length relationship of shortfin mako embryos could be fitted with a power regression similar to that for postnatal fish. The condition factor of lamnid embryos (including yolk-stomach mass) reaches a maximum between 20 and 35 kg/m^3 when the embryos are midterm and have the largest yolk stomachs. The condition factor of alopiid embryos remains constant, indicating that no large yolk-filled stomach develops.

Manuscript accepted 23 November 1999.
Fish. Bull. 98:299–318 (2000).

The shortfin mako, *Isurus oxyrinchus* Rafinesque, 1810, is a pelagic species with a circumglobal distribution in tropical and temperate seas (Garrick, 1967). It is frequently taken by commercial fisheries, mainly as bycatch of tuna and swordfish longlining, and is an important recreational species (e.g. Casey and Kohler, 1992; Pepperell, 1992). It is one of five species in the family Lamnidae comprising the genera *Isurus*, *Carcharodon*, and *Lamna* (Compagno, 1984). All lamnids are large, active pelagic sharks that regulate their body temperature (Carey et al., 1985; Goldman, 1997). Reproduction in lamnids is oophagous (Swenander, 1907; Lohberger, 1910; Bass et al., 1975; Gilmore, 1993; Francis, 1996).

Our knowledge of shortfin mako biology and reproductive parameters has increased considerably in the last 30 years. Garrick (1967) showed that the 12 nominal species of *Isurus* represent a single worldwide species, *I. oxyrinchus*; these findings were confirmed by Heist et al. (1996). Both males and females were thought to mature at around 1.8 m TL (Bigelow and Schroeder, 1948; Gubanov, 1978; Cailliet et al., 1983). With the collection of more extensive data it has become apparent that females mature at a much larger size than males (2.7–2.8 m; Pratt and Casey, 1983; Stevens, 1983; Cliff et al., 1990).

Our review of available reproductive data showed that female shortfin makos have similar reproductive characteristics in all regions. Based on a small number of mostly near-term litters, litter size is 4–16 in Australia (Stevens, 1983) and 9–14 in South Africa (Cliff et al., 1990). Litter sizes from other parts of the world are reported to be between 6 and 18, with the exception of a

litter of 25–30 from the Mediterranean Sea (Sanzo, 1912; Mollet et al.[1]). Pratt and Casey (1983) reported April parturition at a size of 65–75 cm TL in the western North Atlantic. Stevens (1983) and Cliff et al. (1990) suggested November parturition at about 70 cm TL in New South Wales and KwaZulu-Natal, respectively. The data presented by Gilmore (1993) showed no clear time of parturition, but investigation during the course of our study revealed several data errors (see Table 1). Cliff et al. (1990) proposed a 6- or 18-month gestation but indicated that 18 months appeared more feasible, based on a gestation of a little over 1 year postulated by Pratt and Casey (1983). Pratt and Casey (1983) reported first year growth rates of about 50 cm per year in the western North Atlantic, whereas Cailliet et al. (1983) suggested growth rates half as fast off California. Recent tagging results from California[2] and New Zealand (Saul and Holdsworth, 1992; Saul[3]) have shown that growth rates in the Pacific are similar to those reported for the Atlantic.[4] The size-frequency modes reported by Hanan et al. (1993) and O'Brian and Sunada (1994) confirmed high juvenile growth rates for California sharks.[4]

Currently there is growing concern over the extent of pelagic shark catches worldwide, both as targeted fishing and, particularly, as bycatch of high-seas longlining. Further attempts to manage resources of shortfin makos will require, among other demographic data,[4] information on reproductive parameters. Although this species is commonly caught in a variety of fisheries (Bonfil, 1994), few pregnant females have been documented and extensive biological data from a single location do not exist. Given all these factors and assuming reproductive synchronism of mating and gestation, spring parturition, and consistency in growth and size at birth of sharks from several widely spaced regions, we decided to combine all available information, adjusting for seasonal shifts between hemispheres. Our study documents the reproductive biology of female shortfin mako sharks from around the world.

[1] Mollet, H. F., A. D. Testi, L. J. V. Compagno, and M. P. Francis. 1999. Re-identification of a lamnid shark embryo. In review.

[2] Laughlin, L. 1997. California Department of Fish and Game, 330 Golden Shore, Long Beach, CA 90802. Personal commun.

[3] Saul, P. 1997. Blue Water Marine Research, RD 3, Whangarei New Zealand. Personal commun.

[4] Mollet, H. F., and G. M. Cailliet. 1997. Preliminary demographic analysis of the shortfin mako shark, *Isurus oxyrinchus*. Program and Abstract of the American Society of Ichthyologists and Herpetologists (ASIH) and American Elasmobranch Society (AES) Annual Meeting, University of Washington, Seattle WA, June 26–July 1, 1997, 336 p.

Materials and methods

Materials examined

Reproductive and morphometric data from 95 mature females, including 35 pregnant individuals (Table 1), together with data on 450 postnatal fish, including almost 200 age-0+ fish, were collected from around the world. Much of the data came from the western North Atlantic (largely unpublished, with the exception of data on three pregnant females), from eastern Australia (all unpublished, except four pregnant females reported by Stevens [1983]), and from KwaZulu-Natal, South Africa (either unpublished or providing substantially more detailed information than that reported by Cliff et al. [1990]). For methods of collection, measurement, and assessment of maturity see Pratt and Casey (1983); Stevens (1983); Cliff et al. (1990); and Stevens and McLoughlin (1991).

Morphometrics

We used total length (TL, expressed in meters or cm) for our length measurement following Stevens (1983) and calculated TL of western North Atlantic and some South African sharks from the relationship with fork length (FL) (Casey and Kohler, 1992) or precaudal length (PCL) (Cliff et al., 1990), respectively. Total length of embryos, if not measured, was estimated from TL-FL ratios (1.156 at TL 60 cm; 1.203 at TL 35 cm) and the TL-PCL ratio (1.294 at TL 60 cm) of similar-size specimens.

We defined power regression as a linear y-on-x regression of log-transformed data. We used Student residuals and leverage, an index of the leverage of each observation on the size of the mean square error, to carry out linear regression residual analyses (Wilkinson, 1986). We fitted power regressions to our mass-length data of females weighing more than 55 kg (TL=~2 m) from the western North Atlantic and the Southern Hemisphere (no maternal data were available from Brazilian litters) and reported back-transformed equations in the form M (kg)=a TL^b (m). The prepower coefficient "a" predicts the mass of a 1-m-TL shortfin mako because we used meters as the unit of length in all such calculations (Mollet and Cailliet, 1996). We were interested only in possible mass differences of adolescent and mature females from different regions and chose 55 kg as the suitable minimum. A geometrical mean (GM) regression gives the correct functional relationship (Mollet and Cailliet, 1996), but we wanted to compare our results with previously reported back-transformed y-on-x power regressions. An F-test and the linear interaction model were used to check for statisti-

Table 1

Summary of *Isurus oxyrinchus* litter data. SST = sea surface temperature. ECS = eggcases with single egg; NIA = not included in analysis; WY = without yolk (yolk-stomach punctured).

No.	TL embryo[1] (cm)	Mass embryo[1] (kg)	Litter size	TL female (m)	Mass female (kg)	Capture date	Capture location	SST (°C)	References and comments
1	0 (ECS)		11	2.92	236	19 Mar 87	KwaZulu-Natal	23.0	This study; Cliff et al. (1990)
2	0 (ECS)		14	2.88	217	10 Jun 86	KwaZulu-Natal	21.1	This study; Cliff et al. (1990)
3	2.6–3.3 (5)		9	3.09[2]	270[4]	9 Jan 93	W. North Atlantic		This study
4	25–31		18	~3.05	334	22 Aug 78	DeSoto Canyon, FL		Branstetter (1981); Gilmore (1993)
5	29.5–39.5		15	3.37[4]	363	5 Dec 92	Daytona Beach, FL		Putz[6]; Colket[7]; this study
6	36 I(1)	0.80(1)	25–30	3.85[4]	~500	~Aug 1903	Strait of Messina, Italy		Sanzo (1912); Gilmore (1993); Mollet et al.[8]; this study
7	34.8 mean		13	2.88[2]	217[4]	late Jun 93	Gulf of Guinea (1.5N, 1W)	28.5	Castro and Mejuto (1995)
8	39.4 mean	1.456 mean	16(11F)	3.37	380	15 Nov 84	Okinawa Japan		Uchida et al. (1987); Gilmore (1993, embryo TL range reported were means of L and R uterus)
9			6	3.15[4]	~270	~Apr 79	New South Wales, Au	18–21	Stevens (1983)
10	~41 NIA		18	~3.66(12')	547	2 Mar 90	Kona, HI	27.8	This study; Rizzuto[9]; Hodson[10]
11	42.3–49.2		12(6F)			1 Apr 85	Florida Straits		Gilmore (1993), Putz[6]
12	45.0–48.5	0.60–0.90(WY)	12(8F)	2.97[2]	224[3]	18 Sep 92	S. Pacific (24S, 155E)	~20	This study
13			9	2.84[4]	195[3]	10 Aug 81	Port Edward, SA	19.5	Cliff et al. (1990)
14	~50(1)	~3.25(1)				pre-1832	Marseille, Med. Sea		Vaillant (1889)
15	49.5–53.0(2)	1.63–2.30(2)	12(6F)	3.04[2]	271	17 Aug 92	S. Pacific (30S, 156E)	~20	This study
16	50.4–54.0	1.435–2.370	15(5F,9M)	3.25	313	15 Jan 92	Puerto Rico	26.3	This study; Gilmore (1993, incorrect TL for mother and embryos)
17	53.0–60.8		14	2.77[4]	180[3]	10 Jul 84	KwaZulu-Natal	21.0	Cliff et al. (1990)
18	53.0–59.0		12	3.31	337[3]	13 Feb 94	WNA, 20.4N, 73.5 W		This study; Castro[11]
19	59.0(1)	3.53(1)	5	2.69[2]	165[3]	24 Aug 92	S. Pacific (30S, 160E)	~20	This study
20	56.8–62.0	2.100–2.800	9(5F)	3.34	284	27 Aug 97	KwaZulu-Natal	19.3	This study
21	~60		4	3.11[4]	259	Sep 79	New South Wales, Au	18–21	Stevens (1983); Gilmore (1993)
22	~60		14	3.39[4]	340	4 Oct 80	New South Wales, Au	18–21	Stevens (1983); Gilmore (1993)
23	60	fully developed	6	2.63	153[4]		Red Sea		Gohar and Mazhar (1964)

Continued

Table 1 (continued)

No.	TL embryo[1] (cm)	Mass embryo[1] (kg)	Litter size	TL female (m)	Mass female (kg)	Capture date	Capture location	SST (°C)	References and comments
24	60.5(1)	~1.134(10)	10	2.93[3]	229	20 Feb 52	Cat Cay, Bahamas		Depperman[12]; Garrick (1967); Gilmore (1993, incorrect embryo TL); this study
25	60.5(1)					26 Mar 09	Nagasaki, Japan		Garrick (1967)
26	58.2–64.0(5)	1.42–1.72(5)	16	2.80[3]	186	28 Sep 80	New South Wales, Au	18–21	Stevens (1983); Gilmore (1993)
27	65.0(1)					1971–73	Atlantic (off NW Cuba)		Guitart-Manday (1975)
28	63.5–69.8		10(5F)						IGFA[13]; this study
NIA			10						Gubanov (1978)
29	64.5–70.4	1.84–2.49(13[5])	10(6F)			Oct 92	S/SW Brazil		Costa et al.[14]; this study
30	64.6–70.7	2.300–3.125	13(6F)	3.14[2]	266[3]	15 Aug 97	S. Pacific 24.5S, 156.5E	21.2	This study
31	66–70		10				S. W. Indian Ocean		Bass et al. (1975)
32	65.5–73.8(15)	2.30–2.84(15)	16(9F, 6M)			Sep 94	S/SW Brazil		Costa et al.[15]; this study
33	66.1–69.3(2)		14			Oct 92	S/SW Brazil		Costa et al.[14]; this study
34	71.2(1)					Oct 92	S/SW Brazil		Costa et al.[14]; this study
35	~75 NIA	fully developed	11			late Jan 83?	Green Canyon, LA		Branstetter[16]; this study

[1] Number in parentheses gives number of embryos of litter investigated if not all were available;

[2] Estimated from $FL = 0.9286\ TL - 0.0171$ (Casey and Kohler, 1992);

[3] Estimated from $M = 7.658\ TL^{3.1}$ (Stevens, 1983), Southern Hemisphere, $M = 9.933\ FL^{3.1546}$ (Casey and Kohler, 1992), northern hemisphere;

[4] Used data given in Cliff et al. (1990) to calculate TL from PCL;

[5] Mass range of 3 litters with 10, 2, and 1 embryo (stored in same bag and weighed later).

[6] Putz, O. 1995. Grolmanstrasse 48, 10623 Berlin, Germany. Personal commun.

[7] Colket, T. 1996. 2020 Cordova Ave., Vero Beach, FL 32960. Personal commun.

[8] Mollet, H. F., A. D. Testi., L. J. V. Compagno, and M. P. Francis. 1999. Re-identification of a lamnid shark embryo. In review.

[9] Rizzuto, J. 1996. Kona mako the world's biggest? New Zealand Fishing News 19(7):22, 102.

[10] Hodson, G. 1996. Hustler Sportfishing, P.O. Box 4976, Kailua-Kona, HI 96755.

[11] Castro, J. 1998. NOAA/NMFS, SEFC, 75 Virginia Beach Dr., Miami, FL 33149. Personal commun.

[12] Depperman, B. 1953. Maternity mako model. Sports Afield, March 1953:86-7.

[13] International Game Fish Association (IGFA). 1979. Game Fish Yearbook, p. 138. 300 Gulf Stream Way, Dania Beach, FL 33004.

[14] Costa, F. E. S., F. M. S. Braga, A. F. Amorim, C. A. Arfelli. 1994. Analysis of mako sharks, *Isurus oxyrinchus*, from Santos longliners off South and Southeast Brazil. Program and Abstracts ASIH and AES Annual Meeting. USC Los Angeles, California, June 1994, 217 p. Dates from A. F. Amorim 1995. CPPM Santos, São Paulo-Brazil. Personal commun.

[15] Costa, F. E. S., F. M. S. Braga, A. F. Amorim, C. A. Arfelli. 1995. Reproductive biology of shortfin mako, *Isurus oxyrinchus*, Rafinesque 1809. Resumos VII Reunião do Grupo de Trabalho sobre Pesca e Pesquisa de Tubaroes e Raias do Brasil, Rio Grande, November 20–24, 1995.

[16] Branstetter, S. 1996. NMFS Southeast Regional Office, 9721 Executive Center Dr. N., St. Petersburg, FL 33702. Personal commun.

cally significant differences between hemispheres (Neter and Wassermann, 1974). The condition factor (CF=*total mass*/TL^3, in units of kg/m^3) was used as a qualitative estimate of the size of the yolk-filled stomach in lamnid and alopiid embryos.

The calculation of gonadosomatic index (GSI) (ovary mass as percentage of total mass) and hematosomatic index (HSI) (liver mass as percentage of total mass) required a mass estimate if the shark was not weighed. For a few sharks only the mass was available and a TL estimate was required. We estimated mass or TL (from FL) of western North Atlantic and Southern Hemisphere sharks from the equations of Casey and Kohler (1992) and Stevens (1983), respectively. Only two dimensions (length and width) were available for the ovaries of western North Atlantic sharks and the mass had to be estimated. The estimates were calibrated with an ovary of dimensions 19.6×8.7 cm and mass of 0.630 kg (Fig. 2C in Stevens, 1983). The resulting GSI values proved to be comparable with those obtained from weighed ovaries of mature Southern Hemisphere sharks.

Size at maturity

In the absence of embryos or egg cases, the maturity of nonpregnant females was determined from GSI, maximum ova diameter (MOD), oviducal gland diameter (measured in western North Atlantic specimens only), uterus width, and absence of a hymen. We fitted a logistical model $Y=[1+e^{-(a+bX)}]^{-1}$ to our binomial maturity data (immature=0, mature=1) of female specimens with TL > 2.0 m (Wilkinson, 1986; Welch and Foucher, 1988). Two meaningful parameters to characterize maturation, namely median TL-at-maturity ($MTL=-a/b$) and slope at MTL ($S=b/4$), can be expressed in terms of a and b as given. An F-test was used to check for statistically significant differences between hemispheres (Neter and Wassermann, 1974).

Litters, gestation, and parturition

Data collected on litters included number of embryos , length and mass of embryos, maternal length and mass, capture date and location, and sea surface temperature (Table 1). Data for 21 litters, either not previously published or published with errors, are presented. We fitted a power regression to the litter size and maternal length data. For two recently fertilized South African fish, the number of uterine egg cases containing a single blastodisc ovum was assumed to be the litter size. The gestation period was estimated from seven litters from the western North Atlantic, one from the Gulf of Guinea, one from the Mediterranean Sea, two from Japan, seven from Australia, four from South Africa, and four from Brazil (n=26). The litters from Hawaii (no. 10 in Table 1) and the Gulf of Mexico (no. 35) were not included because of uncertain length data. We defined early-, mid-, and near-term litters as having embryo size between 0 to 20, 20 to 45, and 45 to 70 cm TL, respectively. Embryos of a term litter had TLs between 65–75 cm. Capture dates and TL estimates of 188 age-0+ fish from the western North Atlantic (extrapolations based on Fig. 3 in Pratt and Casey [1983] [n=45]), from California (Cailliet et al., 1983; Cailliet[5]) (n=16), and from New South Wales, Australia (Pepperell, 1992; Pepperell[6]) (n=119), and South Africa (n=8), were also considered in the estimation of size at birth and time of parturition.

Capture dates from Northern and Southern Hemisphere fish were combined on a single time scale based on seasons. For example, spring was defined as 21 March to 21 June in the north and from 23 September to 23 December in the south. Seasons were further divided into three periods of equal length to define the terms early, mid, and late (e.g. early spring in the north lasts from 21 March to 20 April).

To support the combination of Northern and Southern Hemisphere data for the shortfin mako, we examined sandtiger shark (*Carcharias taurus*) data from South Africa (Bass et al., 1975) and the eastern United States (Gilmore et al., 1983). These data were also used to support our use of a linear regression to estimate gestation and parturition from the slope of the embryo TL versus seasonal time regression, as well as size at birth. Bass et al. (1975) reported that 100-cm neonate sandtiger sharks were born from June through August after a gestation of 8–9 months. Gilmore et al. (1983) reported that 100-cm neonates were born from December through March after 9–12 months of gestation. We analyzed reported length-at-capture data by using a linear regression which yielded similar estimates for time of parturition and gestation period from intercept and slope:

South Africa: Jul.–Aug. parturition, 10 months gestation, n=27, r^2=0.93;
Eastern United States: Jan.–Feb. parturition, 8 months gestation, n=14, r^2=0.83;
Combined data: midwinter parturition, 9 months parturition, n=41, r^2=0.93.

[5] Cailliet, G. M. 1997. Moss Landing Marine Laboratory, PO Box 530, Moss Landing, CA 95039. Personal commun.

[6] Pepperell, J. G. 1997. Pepperell Research and Consulting Pty, PO Box 818, Caringbah, NSW 2229, Australia. Personal commun.

These results justified combining shortfin mako data from different regions and the use of a linear regression. Embryonic development may, however, deviate from a straight line and be more S-shaped; therefore a straight line may underestimate time of fertilization and overestimate parturition. These deviations cancel each other and a straight line still provides a good estimate of gestation.

Reproductive cycle

We lacked sufficient numbers of females in all reproductive stages to determine the reproductive cycle from a stage-frequency distribution. For many litters, little or no maternal data were available, which precluded the use of a more rigorous multivariate statistical analysis in determining the reproductive cycle. We used temporal uterus width index data (UWI, uterus width as % of TL) of pregnant and postpartum females with a graphical comparison of 2- and 3-year reproductive cycles. The uterus of postpartum shortfin mako sharks shrinks after parturition. We chose the reproductive cycle compatible with this, given that our results suggested an extended gestation period of 15–18 months. For easier graphic interpretation, we plotted the 19 March (1988) Southern Hemisphere specimen a few days later. This procedure assured that the specimen appeared at the beginning of the gestation period (fall) on the far left-hand side of the temporal graphs. The use of polar coordinates did not provide a better presentation.

Results

Pregnant females and details of selected litters

There were 35 pregnant females on record (Table 1), with mean length of 3.1 m (range 2.63–3.85 m, n=24) and mass range of 153–547 kg. Capture dates ranged from pre-1832 (Vaillant, 1889; no. 14, Table 1) to 27 August 1997 (no. 20, Table 1). Capture locations were distributed worldwide and corresponding sea surface temperatures, where available, ranged from 18 to 28.5 C. Detailed information was available for six females, three in very early pregnancy and three with well-developed embryos (Table 2).

Two recently fertilized South African sharks of 2.92 and 2.88 m were caught in late summer and late fall of 1987 and 1986 (nos. 1 and 2 in Tables 1 and 2, respectively). A 3.09-m female was caught near Puerto Rico in January (early winter) with a litter of nine early-term embryos (no. 3 in Tables 1 and 2). The 2.6–3.3 cm embryos, each still inside an egg case, had external gills and a large yolk sac (Fig. 1A). The size of the yolk sac was estimated from Fig. 1A to be 0.9 × 0.6 cm, assuming the embryo in the center of the figure was 3.0 cm. There were over 40 nutritive egg cases in each uterus (Fig. 1B).

A 3.25-m female with a near-term litter was caught in the same month and location (January and Puerto Rico, respectively) by a commercial swordfish longliner (no. 16 in Table 1, no. 4 in Table 2). This female carried 15 embryos of around 52 cm, each with a similarly large yolk-filled stomach (Fig. 1C). No uterine compartments were observed and no egg cases remained in the uterus. A 3.34-m female shark stranded on the beach at Umhlanga, South Africa, in late winter (no. 20 in Table 1; no. 5 in Table 2). This female carried a litter comprising nine embryos of about 60 cm. Emerging adultlike teeth were present in both jaws of the embryo examined. The stomachs of four embryos that were cut open had no shed teeth but had large amounts of yolk (Fig. 1D). No uterine compartments were observed and no egg cases remained in the uterus. About one liter of clear, viscous fluid (not seawater) was found in each uterus but was not analyzed. A Japanese longliner caught a 3.14-m female in the southern Pacific in midwinter (no. 30 in Table 1, no. 6 in Table 2). The 13 full-term embryos had a length of about 69 cm and a total mass of 36.8 kg, 14% of the estimated maternal mass of 266 kg. The embryo stomachs were slightly distended and contained small but variable amounts of yolk.

Litter size

The majority of the litters examined for this study were near-term. The mean number of embryos per litter (litter size) was 12.5 (range: 4 to 27.5, n=30). The largest litter comprised 25–30 embryos (we used 27.5 in our calculations) in a female caught in the Mediterranean Sea in about August of 1903 (Sanzo, 1912). The capture date was inferred from the observation that it occurred during a long holiday period (summer) at the University of Messina.[7] A summer date agrees with the dates of the traditional swordfish fishery, in which this shark was probably caught.[8] One of these embryos was described by Sanzo (1912) as being a great white shark, *Carcharodon carcharias*, but a recent re-examination has shown it to be a shortfin mako shark.[1] The male to female ratio of 10 litters was 57:68 and is not significantly different from 1:1 (pooled χ^2=0.80, Yates corrected, P=0.37).

[7] Notarbartolo di Sciara, G. 1997. Instituto Centrale per la Ricerca Applicata al Mare (ICRAM), via di Casalotti 300, 00166 Rome, Italy. Personal commun.

[8] Fergusson, I. 1998. The Shark Trust, 36 Kingfisher Court, Hambridge Road, Newbury, UK RG14 5SJ. Personal commun.

Table 2

Details for pregnant *Isurus oxyrinchus*. (1–3) Females in very early pregnancy with blastodisc and nutritive egg cases. Observations appear in proposed chronological order. (4–6) Females with well-developed embryos. (L=left; R=right.) GSI = gonadosomatic index; HSI = hematosomatic index.

No.	TL (m)	Date	Location	Observations
1	2.92	19 Mar. 1987	KwaZulu-Natal	6(L)+5(R) egg cases with single egg; no blastodisc observed; 4(L)+8(R) nutritive egg cases with numerous burst eggs; capsule being formed in left oviducal gland; GSI = 1.13%, HSI = 10.6%; mating bites.
2	2.88	10 June 1986	KwaZulu-Natal	7(L)+7(R) egg cases with single egg (some blastodisc); 12(L+R) nutritive egg cases with up to 14 eggs of 4 mm diameter; several ova being encapsulated in right oviducal gland; GSI = 1.21%, HSI = 10.3%; mating bites.
3	3.09	9 Jan. 1993	Puerto Rico	7(L) empty egg cases; 4(L) blastodisc egg cases at least, with one embryo each (~3.0 cm TL, badly disintegrated when measured); 5(R) blastodisc egg cases (3–10 cm) with one embryo each (2.6, 2.9, 3.0, 3.0, & 3.3 cm TL); 43(L) + 42(R) nutritive egg cases (3×5 cm) with 16–20 eggs per capsule, 7–9 g each capsule, 334 g total (R); 2(L) egg cases in lower oviduct; GSI ~5% (estimate from ovary dimensions 44×27 cm).
4	3.25	15 Jan. 1992	Puerto Rico	7(L) embryos (1 female, 5 males, and 1 lost), 51.0–54.0 cm, 1.660–2.300 kg; 8(R) embryos (4 females), 50.5–53.8 cm, 1.435–2.370 kg; mean length and mass of 14 embryos 52.0 cm (SE 0.4) and 2.000 kg (SE 0.071); uteri dimensions 103×22 cm (L), 111×22 cm (R); GSI ~0.3% (estimate from ovary dimensions 27×9 cm), spent ovary.
5	3.34	27 Aug. 1997	KwaZulu-Natal	9(L+R) embryos (5 females), 56.8–62.0 cm (mean 59.9 cm, SE 0.6), 2.100–2.800 kg (mean 2.416 kg, SE 0.094); embryo stomachs with 551–846 g yolk, 26.2–32.0% of total embryo mass (n=4); embryo livers 75-110 g, HSI range 3.4–4.1% (n=4); GSI = 0.185% (spent ovary), HSI = 2.465%.
6	3.14	15 Aug. 1997	South Pacific	13 (L+R) embryos (6 females), 64.6–70.7 cm (mean 68.8 cm, SE 0.5); 2.300–3.125 kg (mean 2.830 kg, SD 0.062); embryo stomachs with 73–478 g yolk, 2.6–15.3% of embryo mass; embryo spiral valve with 68–88 g yolk, 2.4–3.3% of embryo mass (mean 2.9%); embryo livers 146–234 g, HSI range 5.2–8.0% (mean 7.0%, SE 0.2); GSI and HSI of female not available.

Litter size (LS) increased with maternal TL according to

$$LS=0.810\ TL^{2.346} \qquad (n=24,\ P=0.013,\ r^2=0.25)$$

and fell within the band of a model calculation (LS=(0.26 to 0.46) $TL^{3.10}$). The model was derived from the maternal mass-length relationship (M= 7.658 $TL^{3.10}$; Stevens, 1983) by postulating that the litter mass is a constant fraction of the pregnant female mass (10–15%, based on available data) and by using an estimate of the embryo mass at birth (2.5–3.0 kg, based on available data). The power regression was still significant (P=0.029) if the smallest litter of four (an outlier) and the largest litter of 27.5 were excluded.

There were no significant differences between the mean litter size of Northern (14.0, n=13) and Southern Hemisphere females (11.1, n=17, ANOVA, P=0.09) or between western North Atlantic (12.8, n=8) and Southern Hemisphere females (ANOVA, P=0.28).

Indicators of sexual maturity

The size of reproductive organs increased as the shortfin mako approached maturity (Fig. 2). A logarithmic scale was necessary to present the large GSI range between 0.00044% and ~5.0% (Fig. 2A), reflecting ovaries weighing less than 10 g in immature sharks smaller than 2.4 m, up to an estimated 11.3–13.5 kg in a female in early pregnancy (no. 3 in Table 2). There was considerable overlap in the GSI of adolescent females (range: 0.005–0.28%, n=28) and that of mature, nonpregnant females with inactive ovaries (range: 0.08–0.81%, n=38) or pregnant females with near-term embryos and spent ovaries (GSI=0.185% and ~0.3%, n=2). The GSI (1.1%) of recently fertilized females with egg cases and the GSI (~5%) of the female with the 3-cm embryos were the largest observed (Fig. 2A).

Oocytes of noticeable size (1 mm) appeared in maturing females larger than 2.4 m (Fig. 2B). The MOD of immature fish ranged from 1.0 to 4.0 mm

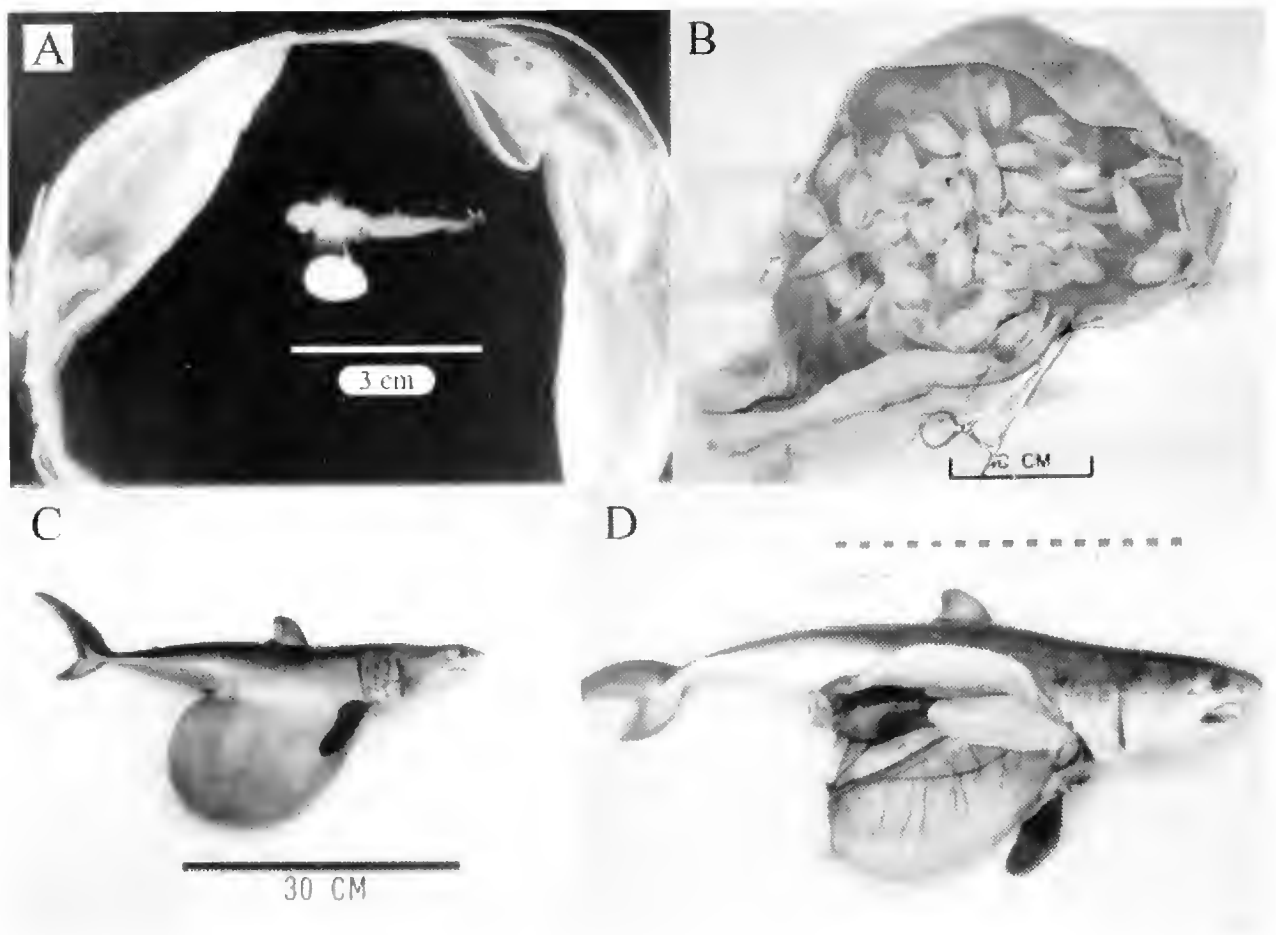

Figure 1

Isurus oxyrinchus embryos and egg cases. (**A**) 3-cm-TL embryos with external gills, large yolk sac, and still within the egg cases from right uterus of pregnant female (no. 3 in Tables 1 and 2). Embryo in the center was removed from egg case. (**B**) Right uterus containing 42 nutritive egg cases from female with embryos shown in A. Scale bar, 10 cm (**C**) Embryo from a litter of 15 with mean TL=52.0 cm and mean mass=2.000 kg with large yolk stomach of estimated dimensions 19 × 12 cm (no. 16 in Table 1). (**D**) Embryo from a litter of 9 (mean TL=59.9 cm, mean mass=2.426 kg, mean yolk mass=29.1%, mean HSI=3.7%) dissected to show yolk stomach, spiral valve, and right liver lobe. Upper jaw cartilage is visible and emerging adultlike teeth are present in both jaws (no. 20 in Table 1). Scale bar, 30 cm.

(n=17) and overlapped considerably with that in mature sharks which had a range of 1–8 mm (n=26). The blastodisc ova appeared to be 6–8 mm in diameter, given the MOD of 8 mm and the estimated spherical diameter of 7 mm of the yolk sac of a 3-cm embryo (Fig. 2B). Nutritive eggs appeared to have a slightly smaller diameter at 4–6 mm. This diameter was based on a MOD of 6 mm for the female in early pregnancy (Fig. 2B) and on the 4-mm ova found in the uteri of two fertilized South African females (Table 2). A spent ovary in a female with large embryos also contained 6-mm ova (Fig. 2B).

The oviducal gland remained undeveloped until the onset of maturity and then increased rapidly in diameter in females of 2.7–3.0 m, as they matured (Fig. 2C, western North Atlantic specimens only). The range in immature fish was from 0.1 to 1.1 cm (n=32). There was considerable overlap in the diameter of the adolescent oviducal gland, ranging from 2.5 to 4.7 cm (n=11) and in the diameter of mature females, ranging from 2.3 to 5.1 cm (n=19). The oviducal gland diameter of two pregnant females, one with early-term, the other with near-term embryos, were similar (4.9 and 4.2 mm, respectively) to that of nonpregnant mature females.

Uterus width provided the best indication of maturity. There was little overlap between immature females in the range of 0.3–6.5 cm (mean 1.6, SE=0.2,

n=58) and mature females in the range of 5.0–22.7 cm (mean 10.7, SE 0.7, n=44) (Fig. 2D). The uterus widths of pregnant (with egg cases or embryos) and nonpregnant females overlapped.

The HSI of immature and mature females in the TL range of 0.73–3.66 m varied from 1.2 to 17.9% and the overall mean HSI of 6.7% (SE=0.25%, n=161) was a little lower than the HSI of near-term embryos (see below). The large HSI range of immature females (1.2–17.6%, n=125) was almost the same as that of mature females (2.5–17.9%, n=36).

Gestation and parturition

The capture of two females with litters containing 3.0- and 52-cm embryos (Table 2, nos. 3 and 4) in the same month (January) and location (Puerto Rico) suggested that gestation is longer than one year. Assuming a gestation in excess of 12 months, the mean embryo length for 26 litters and the length for 188 age-0+ fish from both the Northern and Southern Hemisphere were graphed against season of capture (Fig. 3A). Based on the three females caught in early pregnancy (Table 2), ovulation takes place in fall. Parturition occurs in late winter to mid-spring at ca. 70 cm. The length-at-capture data of the age-0+ fish indicated a smooth continuation of the growth rate evident *in utero*.

The relationship between embryo length and time of capture of all western North Atlantic litters (n=7, slope=3.7 cm/month, SE=0.6 cm/mo., P=0.002, r^2=0.87) predicted a gestation of 19 months. The combined Northern Hemisphere data, which include five mid-term litters, yielded a gestation of 20 months (n=11, slope=3.4 cm/month, SE=0.05 cm/mo., P<0.001, r^2=0.84).

There were no mid-term litters from the Southern Hemisphere. If the two females with recently fer-

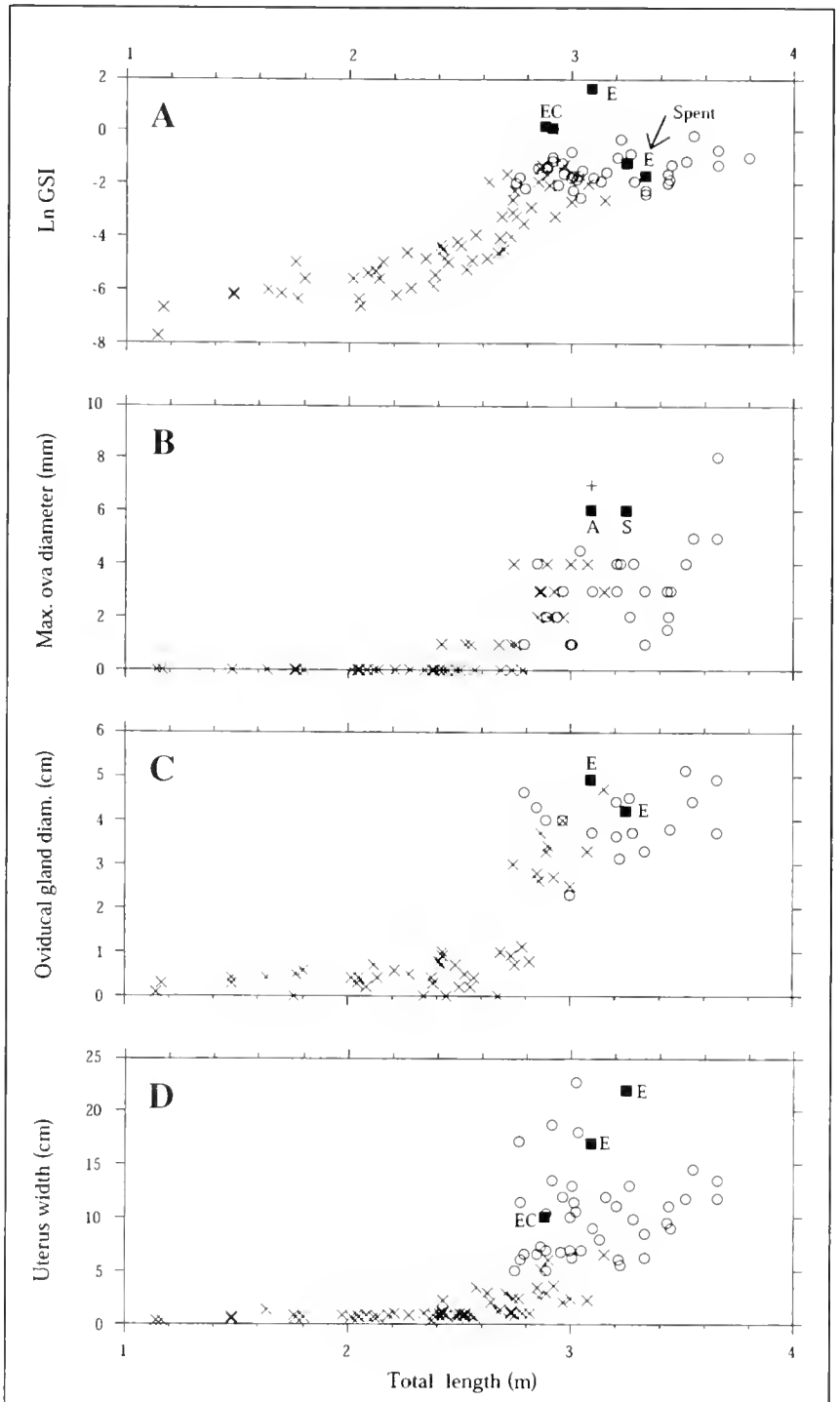

Figure 2

The relationships between four reproductive parameters and length of female *Isurus oxyrinchus*. (**A**) Natural logarithm (Ln) of gonadosomatic index (GSI) was used. (**B**) Maximum ova diameter. Lack of, or very small oocytes, are indicated by 0 diameter. A = female with active ovary and 3-cm-TL embryos; + = diameter of yolk sac of 3-cm-TL embryo; S = female with spent ovary and 52-cm-TL embryos. (**C**) Oviducal gland diameter of western North Atlantic specimens. (**D**) Uterus width. (■ = pregnant; ○ = mature, not pregnant; × = immature and adolescent; E=embryos present; EC=egg cases with single ovum present.)

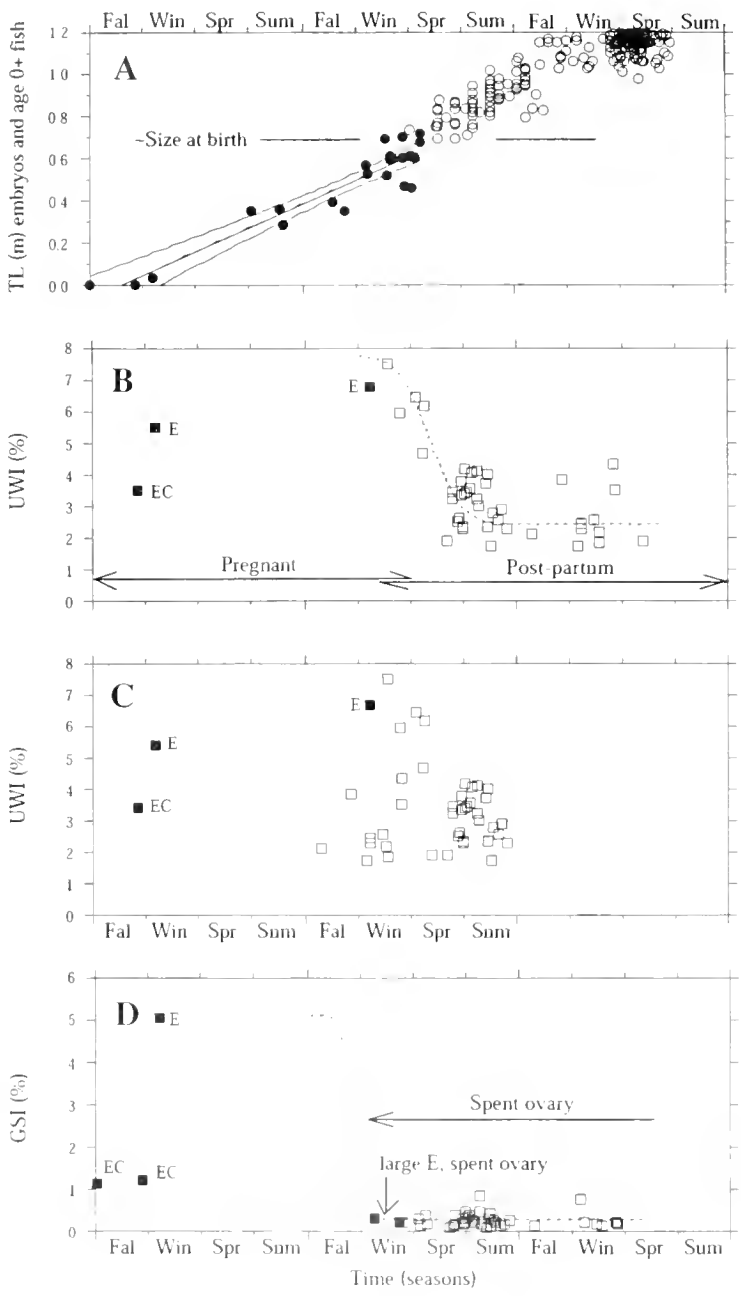

Figure 3

Gestation, parturition, and reproductive cycle of *Isurus oxyrinchus*. (**A**) The relationships between length of embryos and age-0+ fish, and time of capture. Regression with 95% confidence band for the line of combined embryo data from Northern and Southern Hemispheres is shown. ●=embryos; ○=age-0+ fish. (**B**) Temporal uterus width index (UWI) of mature females based on a 3-year reproductive cycle. The dotted line was fitted to the data by eye. (**C**) Temporal UWI of mature females based on a 2-year reproductive cycle. (**D**) Temporal gonadosomatic index (GSI) based on a 3-year reproductive cycle. The dotted line shows suggested decrease of GSI during last third of gestation. (■=pregnant, □=mature, not pregnant, E=embryos present, EC=egg cases with single ovum present.)

ova (Table 2, nos. 1 and 2) are more than one year apart from the near-term litters (on the basis of the Northern Hemisphere data), the regression predicted a 19-mo. gestation period (n=15, slope=3.7 cm/mo., SE=0.3 cm/mo., P<0.001, r^2=0.92). It is also possible to fit these data with a regression that predicts a 6.7-mo. gestation period (n=15, slope=10.4 cm/mo., SE=1.8 cm/mo., P<0.001, n=15, r^2=0.73).

The intercept and slope of Northern and Southern Hemisphere regressions, assuming a gestation longer than 12 months, were not significantly different (P=0.8 and 0.7, respectively) and the combined regression was

$$Embryo\ TL\ (\text{cm}) = 3.71\ (\text{SE}=0.27)T,$$
$$(P<0.001,\ r^2=0.89\ n=26)$$

where T = the number of months since midfall.

It predicted a gestation period of 15–24 months (19 for the line) with 70 cm for the size-at-birth (Fig. 3A). However, we suggest the shorter estimate is more realistic because parturition appears to be a little earlier than what was indicated by the regression. The GM regression line (not shown) was slightly steeper than the y-on-x regression and predicted a gestation of 17.8 months. The GM regression reflects the functional relationship better because of the uncertainties of several dates. Therefore, we concluded that the best estimate for the gestation is 15–18 months. When the three early-term litters with fairly high leverage (L=0.2–0.35) were excluded, the gestation was still around 18 months based on a significant regression (P=0.001) with a slope of 3.8 cm/month (SE= 0.6, n=23).

Reproductive cycle

A three-year reproductive cycle provided the best fit to the temporal UWI data. UWI increased in early-term females and reached a maximum of 7–8% at parturition (Fig. 3B). The pregnant female with the 52-cm embryos and UWI of 6.8% would be expected to give birth

about 3–4 months later and have a UWI around 7% at that time. The UWI decreased in postpartum females over a 6 month period to values around 2–4% (Fig. 3B, curve fitted by eye). With a 2-year cycle, UWI showed no decreasing pattern for postpartum females and low UWI values between 2% and 4% extended over almost the entire second year of the reproductive cycle (Fig. 3C). This result would suggest aseasonal parturition; however, this conclusion is in conflict with the observed seasonal parturition indicated by Figure 3A.

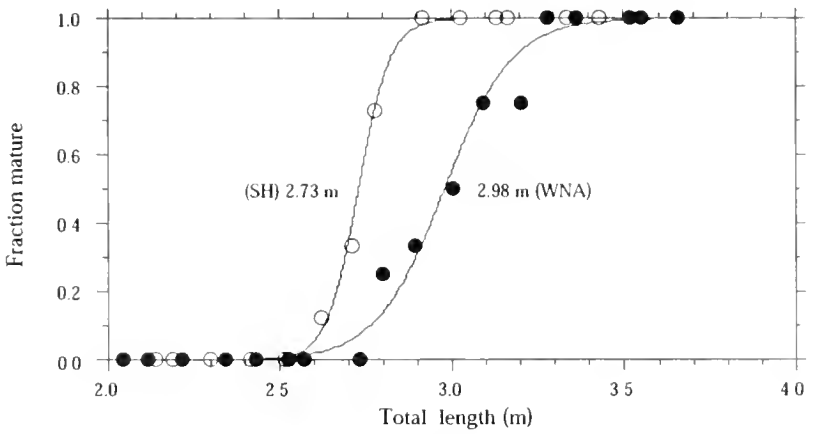

Figure 4

The relationships between maturity and length of female *Isurus oxyrinchus* from the western North Atlantic and the Southern Hemisphere. A logistical model was fitted to the binomial maturity data (0=immature, 1=mature). Mean TL and mean fraction mature of 10-cm-TL ranges (instead of individual data points) were plotted for clarity. Estimated TLs when 50% are mature (MTL) are included. ● = western North Atlantic (n=61); ○ = Southern Hemisphere (n=82).

The GSI was not as useful in determining the length of the reproductive cycle because it decreased during pregnancy. Recently ovulated females had a GSI of 1.1% and an early-term female had an estimated GSI of about 5% (Fig. 3D). We suggest that the GSI remains high until the embryos are about 40–50 cm long, and then decreases (Fig. 3D, curve fitted by eye). Two females with large embryos (mean: 52.0 and 59.9 cm) had low GSIs of ~0.3% and 0.185%, respectively, indicating that ovulation had ceased (spent ovary). The GSI during at least the last quarter of gestation (i.e. ≥4 months) was similar to that of postpartum females (mean: 0.26%, SE=0.03%, n=38). When we tried to fit the GSI data with a 2-year cycle, we found that data for six postpartum females caught in winter (five from South Africa) overlapped with those for the two pregnant females with large embryos. This would extend parturition into fall and would conflict with convincing seasonal parturition data (Fig. 3A).

The remaining reproductive parameters were not helpful in determining the reproductive cycle. No temporal pattern was evident for MOD. Oviducal gland diameters were available mostly for summer captures only and possible temporal changes could not be investigated. There was no clear temporal pattern in the HSI because we had few data for preovulating and early-term pregnant females.

Regional differences

The scarcity of data precluded a meaningful statistical comparison of many reproductive parameters for female shortfin makos from different regions. However, we were able to substantiate differences for mass and length-at-maturity for females from the western North Atlantic and the Southern Hemisphere (South Africa and Australia; no data were available from Brazil).

Western North Atlantic females were significantly heavier by 19–66 kg or 16–19% than Southern Hemisphere females (P<0.001 in TL range 2.5–3.5 m). The latter data were combined because the power regressions for South African (n=47) and Australian females (n=22) were not statistically different (P=0.164, $F^* < F$ (0.95,2,65)). The back-transformed M-TL relationships were

M=7.299 $TL^{3.224}$ (n=63, r^2=0.94, western North Atlantic females 2.0–3.7 m TL);

M=6.824 $TL^{3.137}$ (n=69, r^2=0.90, Southern Hemisphere females 2.0–3.4 m TL).

The median TL-at-maturity (MTL) of 61 western North Atlantic females (2.98 m, SE=0.045) was significantly larger by 25 cm (P<0.001, $F^* >> F$ (0.95,2,147), than that of 82 Southern Hemisphere females (2.73 m, SE=0.02 m) (Fig. 4). The data from South Africa and Australia were combined because MTL in South Africa was only 11 cm smaller than MTL in Australia and the length of these fish was not measured consistently. The maturation size of western North Atlantic sharks extended from 2.76 m, when 10% were mature, to 3.20 m when 90% were mature and was 16–35 cm larger than that in the Southern Hemisphere, where the range was 2.60–2.85 m. The largest immature female from the western

North Atlantic (3.15 m) was a virgin. The smallest mature female from the Southern Hemisphere of 2.63 m was pregnant (no. 23 in Table 1).

Liver-, yolk-, and total mass of embryos

There was a significant positive relation between the HSI and the length of near-term embryos, rising from 3.8% in a litter with a mean length size of 59.9 cm to 7.0% in a litter with a mean length size of 68.8 cm. The slope was 0.34%/cm (SE=0.04%/cm, $P<0.001$, $r^2=0.83$, $n=17$). The TL range of the embryos in these two litters was small (12.5 cm) but they covered almost 50% of the HSI range. The increasing HSI was accompanied by a corresponding decrease in the amount of yolk in the stomach from 29.1% to 10.9% of total mass. The yolk percentage versus TL regression was significant with slope –1.64%/cm (SE= 0.33%/cm, $P<0.001$, $r^2=0.62$, $n=17$).

The mass-length relationship of embryos is complicated owing to the highly variable mass of the yolk-filled stomach. The scarce data indicated that the yolk mass amounts to 60–70% of total mass for mid-term litters and then decreases to around 10% in a full-term litter (Fig. 5, *y*-axis on left). When the mass of the yolk-filled stomach was subtracted from the total mass, a power regression could be fitted to net embryo mass (M_{net}) (Fig. 5, *y*-axis on right). The back-transformed equation was

$$M_{net}=8.198\ TL^{3.117}$$

($n=21$, $r^2=0.98$, TL range= 0.36–0.71 m).

The mass of the smallest free-swimming fish agreed with the predicted mass based on the extrapolated curve beyond the upper limit of the embryo data (Fig. 5). The corresponding condition factors of shortfin mako embryos ($CF_{net}=M_{net}/TL^3$) were between 7.3 and 7.9 kg/m^3 and were similar to postnatal values. If the mass of the yolk-filled stomach was included, the condition factor ($CF=M/TL^3$) reached values as large as 26 kg/m^3 when the embryos were mid-term and had the largest yolk stomachs (Fig. 6, *I. oxyrinchus* data).

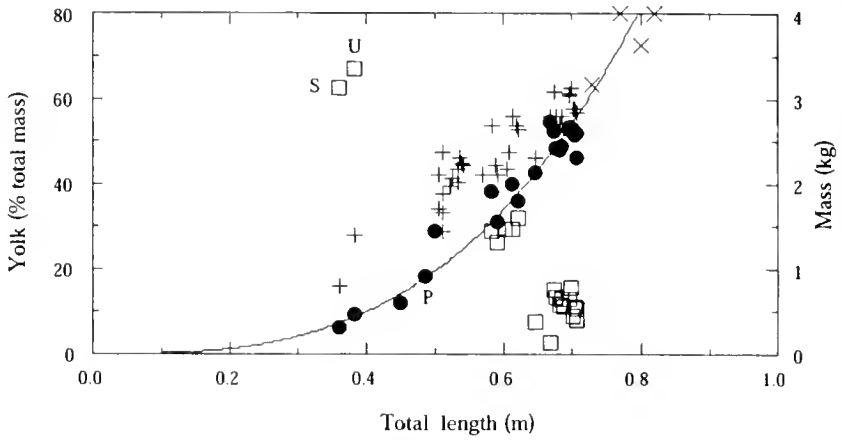

Figure 5

The relationships between 1) yolk % (left *y*-axis), 2) embryo mass with and without yolk (right *y*-axis), and length of *Isurus oxyrinchus* embryos. A power regression was fitted to embryo mass without yolk data. □ = yolk %; ● = embryo mass without yolk; + = embryo mass with yolk; × = mass of free swimmers; S = Sanzo (1912); U = Uchida et al. (1987); remaining data from this study including P = upper and lower limit of mass range of litter with punctured yolk-stomachs.

Discussion

Embryonic development

Our data documented early and late embryonic development of the shortfin mako. As expected, it was similar to that reported for other lamnids (Swenander, 1907; Lohberger, 1910; Otake, 1990; Gilmore, 1993; Francis and Stevens, 2000) in which the embryos hatch at about 6 cm TL and then feed on nutritive eggs (oophagy) until the beginning of the last third of the gestation period. Embryonic nutrition may also include egg jelly absorbed through the external gill filaments in the prehatching phase and uterine milk in the posthatching phase (Hamlett, et al. 1985; Gilmore, 1993; Koob and Straus, 1998).

After mating, the largest of the relatively small ova are ovulated, fertilized, and packaged into egg cases (one blastodisc ovum per egg case) as evident in three cases in our study (Table 2). The diameter of these blastodisc ova appears to be slightly larger (~7 mm) than the nutritive ova (4–6 mm) and the ova remaining in the ovary (4–6 mm); this larger diameter may also apply to other lamnids and lamnoids. Mating may stimulate the enlargement of the largest ova in the ovary and trigger subsequent ovulation. The capsules with nutritive ova are formed after the blastodisc ova have been encapsulated. Blastodisc egg cases with only one fairly large ovum were observed in the bigeye thresher shark, *Alopias superciliosus* (Moreno and Morón, 1992). In

the sandtiger shark, the blastodisc capsules contain up to 14 blastodisc ova, but only one egg develops and absorbed material and other encapsulated ova contribute more to initial development than does the yolk sac (Gilmore et al., 1983). A possible early-term great white shark had a total of 192 egg cases of three types of different size and mass in the left uterus, but the size and number of the ova were not reported (Uchida et al., 1987).

We observed 3-cm-TL shortfin mako embryos still attached to a relatively large yolk sac and inside egg cases (Fig. 1A). It is not clear at what size the embryos hatch from the egg cases, possibly 5–6 cm, the size at which porbeagle (*Lamna nasus*) and sandtiger sharks hatch (Swenander, 1907; Gilmore et al., 1983). This estimate agrees with an estimate of the embryo TL calculated from the diameter of the blastodisc ovum (Mollet, unpubl. data). Bigeye thresher embryos hatch at a slightly larger size (7–8 cm FL) because their yolk sac diameter (11 mm) is greater than that of porbeage and sandtiger sharks (Chen et al., 1997).

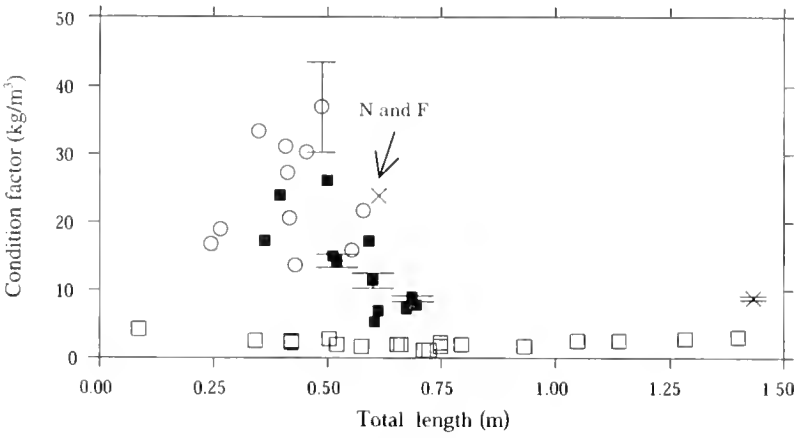

Figure 6

The relationship between condition factor (M/TL^3) and TL of lamnid and alopiid embryos. Error bars give ±2 SE of mean, if available. ■ = *Isurus oxyrinchus*; ○ = *Lamna spp.*; × =*Carcharodon carcharias*; □ = *Alopias spp.* See Table 1 for sources of *I. oxyrinchus* data. *Lamna* spp. data from Lohberger (1910); Templeman (1963); Otake (1990); Francis;[9] Otake[10]. *Carcharodon carcharias* data from Norman and Fraser (1938, NandF); combined Francis (1996) and Uchida et al. (1996). *Alopias* spp. data from Joseph (1954); Cadenat (1956); Gubanov (1972); Hixon (1979); Gilmore (1983); Moreno and Morón (1992); Otake (1990).

During the oophagous embryonic phase, lamnids develop huge yolk-filled stomachs, sandtiger sharks develop large yolk-filled stomachs, and alopiids develop only slightly extended yolk-filled stomachs according to photographs and our calculated condition factors (Nakamura, 1935; Gilmore et al., 1983; Moreno and Morón, 1992; our Fig. 6 for lamnids and alopiids). The condition factors of the shortfin mako (our data and references in Table 1), the porbeagle (Templeman, 1963; Francis[9]), the salmon shark, *Lamna ditropis* (Lohberger, 1910; Otake, 1990), and the great white shark (Norman and Fraser, 1938) reach a maximum between 20 and 35 kg/m^3 when the embryos are midterm. The condition factor decreases in the last third of gestation and approaches values similar to those of postnatal lamnids (our data for the shortfin mako; Francis and Stevens (2000) for the porbeagle; Uchida et al., 1996; Francis, 1996 for the great white shark). The yolk-stomach in the sandtiger shark reaches its largest size between 33.4 and 80 cm TL, but no embryo masses were reported by Gilmore et al. (1983) and therefore the condition factor could not be calculated. The condition factors of thresher shark embryos are much smaller if TL rather than PCL is used as the length parameter. However, if the alopiids were to develop a large yolk-filled stomach, then the condition factor of mid-term embryos would be considerably larger compared with that of early- and near-term embryos, which is not the case (Fig. 6). The embryonic development of alopiids proceeds at a steady rate without development of a large yolk-filled stomach and we expect ovulation of nutritive ova right up to parturition. Francis and Stevens (2000) have suggested that the puzzling gross abdominal distention observed in porbeagle embryos (and other lamnids) is energetically inefficient for the pregnant female.

The HSIs of shortfin mako embryos from a full-term litter were between 5% and 8 % and the yolk-stomach constituted 3–15% of body mass. These combined nutrient reserves may provide neonates with nutrition while they improve their hunting ability. From the metabolic rate of a shortfin mako pup reported by Graham et al. (1990) (1.5% of bodymass/d), we estimated that a 20% reserve would enable pups to survive for about 20–30 days. This

[9] Francis, M. P. 1997. National Institute of Water and Atmospheric Research (NIWA), P.O. Box 14-901, Wellington, New Zealand. Personal commun.

[10] Otake, T. 1998. Mie University, 1515 Kamihama, Tsu, Mie 514, Japan. Personal commun.

estimate agrees with the observation that a sandtiger pup born in captivity at Sea World of Orlando did not eat until 25 d after birth (Gilmore et al., 1983). By comparison, HSI values of 13–19% were recorded in three great white shark full-term embryos with stomach yolk mass between 0% and 4% (Francis, 1996; Uchida et al., 1996). A near-term 97-cm-TL longfin mako, *Isurus paucus*, embryo had a large liver but surprisingly small amounts of yolk in the cardiac stomach (0.54%) (Gilmore, 1983).

There is no convincing evidence[11] to confirm that older shortfin mako embryos eat smaller ones while in the uterus, as claimed by Tricas et al. (1997). They possibly inferred this conclusion from a misleading statement in Compagno (1988, p. 83).[12] Costa et al.[13] suggested that uterine cannibalism occurs on the basis of a piece of lower jaw found in the stomach of a term embryo. This behavior is difficult to explain, and Francis (1996) observed only shed teeth in the stomach of a great white shark full-term embryo. We expected to but did not find any shed teeth in the stomach of near-term embryos. Embryonic cannibalism has only been documented in the sandtiger shark (Gilmore et al., 1983) and seems unlikely in the shortfin mako with a litter size as high as 25–30.

Litter size

Data on litter size of shortfin makos were scarce and possibly biased by low values due to abortion during capture and the reported large value of 25–30 in Sanzo (1912). The lowest values of 4–6 were for near-term litters (TL~60 cm) reported anecdotally by game fishermen. Although we are sure they are reliable, they should be taken as minimum estimates because such low values suggest abortion during capture, especially for near-term litters. Abortion is unlikely for mid-term embryos with their huge yolk stomachs.[11] A means model test was not conclusive because litter size also depends on maternal size, which was not available for five near-term litters. The number of embryos in the Sanzo (1912) litter was also based on information from a fisherman; however, a study of the original Italian text has suggested that the value of 25–30 is reliable.[7] Although western North Atlantic females are slightly heavier than females of similar size from South Africa and Australia, there were no regional differences in litter size between the two regions.

The mean litter size of 12.5 is larger than that for other lamnids, although data for some species are scarce. The longfin mako has a mean litter size of four (range 2–8, n=3, Compagno, 1984; Killam and Parsons, 1986; Casey[14]). The mean litter size of the great white shark is 8.9 (range: 4–14, n=11; Francis, 1996; Uchida et al., 1996). A single litter of four was reported for the salmon shark (Otake, 1990). The litter size of the porbeagle is 2–5, mostly 4 (e.g. Swenander, 1907; Templeman, 1963; Francis and Stevens, 2000). A weak relationship between litter size and maternal length in the shortfin mako also exists for the great white shark (based on data in Francis, 1996). A positive relation between litter size and maternal size has been observed for many carcharhinids (Compagno, 1988).

Indicators of sexual maturity

The GSI was not conclusive in determining sexual maturity in lamnids because near-term and postpartum females both have low values. In oophagous sharks the ovary continues production to nourish the embryos well into gestation, thus producing high GSIs. The large variations in ovary size in mature shortfin makos (0.2–12 kg; GSI ~0.1–5.0%) were as expected. Data from other lamnids are scarce. A longfin mako with near-term embryos had a spent ovary with GSI=0.46% (Gilmore, 1983). Active ovaries in mid-term porbeagles weighed 2.75 kg (GSI 2.35%) and 6.3 kg (GSI 3.6%) (Francis and Stevens, 2000; Swenander, 1907). Arfelli and de Amorim[15] observed a 12-kg ovary (GSI 0.48%) in a nonpregnant 5.3-m-TL great white shark.

We found that MOD was not useful for determining maturity in shortfin makos, whereas it is in sharks without oophagy (e.g. Pratt, 1979; Peres and Vooren, 1991; Parsons, 1993). The values near the upper limit of the observed range (1–8 mm, Fig. 2B) were similar to values (5–11 mm) reported for other lamnids (Swenander, 1907; Gilmore, 1983; Bruce,

[7] Gilmore, R. G. 1999. Dynamic Corp., Kennedy Space Center, FL 32899. Personal commun.

[11] Compagno, L. V. C. 1998 and 1999. Shark Research Centre, P.O. Box 61, 8000 Cape Town, South Africa. Personal commun.

[12] Costa, F. E. S., F. M. S. Braga, A. F. Amorim, and C. A. Arfelli. 1995. Reproductive biology of shortfin mako, *Isurus oxyrinchus*, Rafinesque 1809. Resumos VII Reunião do Grupo de Trabalho sobre Pesca e Pesquisa de Tubaroes e Raias do Brasil, Rio Grande, November 20–24, 1995. Fundacao Universidade do Rio Grande, FURG Rio Grande, RS Brasil.

[14] Casey, J. 1986. Distribution of the longfin mako (*Isurus paucus*) in the northwest Atlantic. Program and Abstracts ASIH and AES Annual Meeting, Victoria BC, Canada, 15–21 June 1986, no page numbers.

[15] Arfelli, C. A., and A. F. de Amorim. 1993. Notes on the white shark (*Carcharodon carcharias*) caught off Cananeia, São Paulo-Brazil. Program and Abstracts ASIH and AES Annual Meeting. The University of Texas at Austin, 27 May–2 June 1993, 348 p.

1992; Francis and Stevens, 2000) and lamnoids (Matthews, 1950; Gilmore et al., 1983; Chen et al., 1997; Yano et al., 1999). The report of a 50-mm diameter egg in the ovary of a 3.37-m-TL shortfin mako with an empty uterus (Applegate, 1966) is inexplicable.

Uterus width was the most suitable reproductive parameter for distinguishing between immature and mature female shortfin makos and also between different reproductive stages of mature females. Our data indicated that immature shortfin mako have UWIs between 0.17% and 2.1%, whereas mature shortfin makos have UWIs between 1.7% and 7.5%, with the largest values occurring at parturition and in early postpartum females (Fig. 3B). Little comparative data for other lamnids were available. Two immature great white sharks of 4.8 m and 4.9 m had a UWI of 2.1% and 1.6%, respectively.[12, 16] A 5.2-m-TL great white shark had a UWI of 7.7%; this fish may have recently given birth (Stevens, unpubl. data). However, a 5.2-m, 1520 kg female reported by Bruce (1992) to be mature, and bearing possible mating scars had UWIs of only 0.88–1.0% (left) and 0.44–0.56% (right); these values appear to be far too small for a mature shark of this size.

Our study failed to confirm the potential of HSI as a good indicator of reproductive status. Our sample size was large (immature, n=125; mature, n=35); however, we had few data for pregnant fish. Cliff et al. (1990) observed the highest HSIs in two recently fertilized females, which also had high GSIs. Their observations suggested that HSI might be useful as an indicator of reproductive status; however, their sample size was small (n=12). They also noted that the HSIs of males were just as variable and covered about the same range (2.9–13.7%). For sharks with long gestation period, the HSI may not be tied closely to the reproductive cycle. Because the shortfin mako has a high metabolic rate (Graham et al., 1990), reserves in the liver cannot be expected to last longer than a few weeks.

Gestation period

A small number of early and mid-term litters from the western North Atlantic and the Northern Hemisphere supported a gestation period in excess of 12 months. By contrast, the absence of measured mid-term litters from the Southern Hemisphere made it possible also to fit the data with a 6–7 month gestation period. It is highly unlikely that a regional difference of this magnitude could exist in a widely distributed species such as the shortfin mako. It is therefore most probable that the duration of gestation is 15–18 months in both hemispheres.

Is a 6–7 month gestation possible for the Northern Hemisphere? Reproductive asynchrony (where individuals in an accessory population are out of phase with the principal population) is a possibility for wide-ranging oceanic sharks, and was suggested for the great white shark (Lineaweaver and Backus, 1970). For our shortfin mako data, we would have to propose that the early-term (no. 3 in Table 1) and all five mid-term litters (nos. 4–8) belong to the accessory population(s). However, the gestation period becomes indeterminate when these litters are excluded from the calculations. It is far more probable that these pregnant females belong to the principal populations, should this theory apply to the shortfin mako, and that the gestation period is 15–18 months. Additional data would be needed to test the hypothesis of reproductive asynchrony for elasmobranchs.

No embryo length data were available for an early fall litter from the Southern Hemisphere (no. 9 in Table 1). If the gestation period were 6–7 months, this litter would have been at the blastodisc stage (as were litters no. 1 and no. 2 in Table 2) and might have been overlooked without detailed examination of the uterus. If the gestation period was 18 months, the embryos of this litter would have been 35–45 cm long and would have been observed (as they were) during gutting of the pregnant fish on the boat.

Body temperature may account for some of the difference in the gestation between the shortfin mako (15–18 months) and the porbeagle (9 months in both hemispheres; Francis and Stevens, 2000). The porbeagle and the salmon shark possess a sizable kidney rete, which is not found in the shortfin mako, and body temperatures are in general higher in *Lamna* than in *Isurus*.[17] Cloacal temperature measurements from 21 salmon sharks had a mean of 23.3°C (SD=1.1°) which is probably most representative of the uterus area.[17] This temperature could be 5°C higher than the temperature of the uterus in the shortfin mako, which prefers water temperatures around 18°C and is known for vertical movements into colder water (Casey and Kohler, 1992; Carey and Scharold 1990; Holts and Bedford, 1993).

Our litter of 3.0-cm-TL embryos confirmed slow shortfin mako embryonic development, at least during the early stage. These very early-term embryos were found next to more than 40 nutritive egg cases in each uterus (Fig. 1B, Table 2). Gilmore (1993) reported that

[16] Bruce, B. 1998. CSIRO Marine Research, P.O. Box 1538, Hobart, Tasmania 7001. Personal commun.

[17] Goldman, K. 1998. Virginia Institute of Marine Science (VIMS), P.O. Box 1346, Gloucester Pt., VA 23062. Personal commun.

production of empty and blastodisc egg cases preceded that of nutritive egg cases in the sandtiger shark and that each oviducal gland produced one egg case per day. We observed that blastodisc egg cases preceded the nutritive egg cases in the shortfin mako (no. 2 in Table 2). Therefore, the 2.7–3.3 cm TL embryos would be about 40–50 days old. They were at a very early stage of development because the yolk sac was almost intact, and oophagy may not begin until the embryos are about 3–4 months old and 5–6 cm long.

The gestation period of the shortfin mako is about twice as long as that of the sandtiger shark (9 months; Cliff, unpubl. data), which has a term litter mass (13 kg), about half that of the shortfin mako (25–40 kg). Scant ovary data for the shortfin mako and extensive ovary data for the sandtiger shark (Gilmore et al., 1983; Cliff, unpubl. data) suggested that the masses of ovulating ovaries are similar in the two species. The shortfin mako would therefore require about twice as long to nourish a litter double the weight of that of the sandtiger shark.

Our interpretation of reported great white shark data suggested that the gestation is longer than one year and probably similar to that of the shortfin mako. Parturition is in late spring (Klimley, 1985; Francis, 1996; Uchida et al., 1996). Uchida et al. (1987; 1996) suggested that a 5.55-m-TL, 1970-kg female captured in mid-February had aborted an entire litter of near-term embryos. However, the presence of almost 200 egg cases in the left uterus (weighing 9 kg) and the robust appearance of the specimen, probably due to a large liver, suggest that this great white shark was at an early stage of gestation. Further support for our gestation estimate of about 18 months was the capture of a great white shark with a midterm litter of nine embryos in the summer of 1934 (Norman and Fraser, 1938). Length and mass of these embryos (61 cm TL, 5.4 kg as suggested by Ellis and McCosker, 1991) were as expected for midterm embryos with a large yolk-filled stomach (M/TL^3=23.8 kg/m^3, Fig. 6) and birth was expected 9 months later in spring.

Gestation periods longer than 12 months were reported for the whitetip reef shark, *Triaenodon obesus* (13.5 mo.), the tiger shark, *Galeocerdo cuvier* (13–16 and 15–16 mo.), the dusky shark, *Carcharhinus obscurus* (22 mo.), and the spiny dogfish, *Squalus acanthias* (18–24 mo.) (Compagno, 1984; Uchida et al., 1990; Randall, 1992; Musick et al., 1993; Crow[18]). The basking shark, *Cetorhinus maximus*, probably has a gestation period longer than 12 months, but we agree with Pauly[19] that the reported gestation period of 3.5 years by Parker and Stott (1965) was based on fallacious reasoning.

Parturition in Northern and Southern Hemispheres

Based on a few full-term litters and a large number of neonates, parturition occurred mainly in late winter to midspring in both hemispheres (Fig. 3A). Pratt and Casey (1983) reported "late spring parturition" in the western North Atlantic, but April should be called early spring; and the data in their Figure 3 suggest that parturition begins as early as late February (late winter). Other large pelagic and nearshore sharks have seasonal parturition in late spring to early summer in both hemispheres (e.g. Bass et al., 1973; Pratt, 1979; Klimley, 1985; Randall, 1992; Musick et al., 1993; Francis, 1996; Crow[18]). Parturition of the porbeagle peaks in June–July in both hemispheres which Francis and Stevens (2000) found puzzling.

Reproductive cycle and resting period

Given a gestation period of about 18 months and a distinct seasonal spring parturition, the reproductive cycle for shortfin makos is either 2 or 3 years. There were insufficient data to determine its duration conclusively, but a 2-year cycle would only allow a recovery period of some 6 months, which would appear to be insufficient. Our temporal UWI data (Fig. 3B) support a 3-year reproductive cycle, which would mean an 18-month resting period.

There is conflicting evidence about the need for a resting period after parturition in elasmobranchs. For many medium to large sharks a resting period has been documented. Peres and Vooren (1991) reported a 3-year reproductive cycle for the soupfin shark, *Galeorhinus galeus*, off southern Brazil with a gestation of 12 months. The gestation for the whitetip reef shark is 13.5 months and the reproductive cycle is 2 or 3 years (Uchida et al., 1990). Musick et al. (1993) suggested that the sandbar shark, *Carcharhinus plumbeus* (with one-year gestation), must have a resting period of at least one year, requiring a 2-year reproductive cycle. The 2-year reproductive cycle for the sandtiger shark with 8–9 mo. gestation period is well documented (Branstetter and Musick, 1994; Cliff, unpubl. data). Tagging and cap-

[18] Crow, G. L. 1995. The reproductive biology of the tiger shark, *Galeocerdo cuvier*, in Hawaii: a compilation of historical and contemporary data. Program and Abstract ASIH and AES Annual Meeting, University of Alberta, Edmonton, Alberta, Canada, June 15–19 1995, 229 p.

[19] Pauly, D. 1978. A critique of some literature data on the growth, reproduction and mortalities of the lamnid shark *Cetorhinus maximus* (Gunnerus). Report to the Pelagic Fisheries Commission, International Council for the Exploration of the Seas, CM 1978/H17, Copenhagen.

tive grow-out studies indicated that the nurse shark *Ginglymostoma cirratum* has a 2-year reproductive cycle with a 3.5–4.5 months gestation and a ~20 months resting period.[20] A 3-yr reproductive cycle was proposed for the dusky shark and the tiger shark with 22-mo. and 15–16 mo. gestation periods, respectively (Musicke et al., 1993; Crow[18]). Francis and Stevens (2000) reported that gestation in the porbeagle lasts 9 months, which would allow for only a very short resting period if they have pups every year. Francis (1996) suggested that the great white shark might have little or no resting period because mating was observed immediately after parturition.

In the 3-year cycle of the shortfin mako, mating could occur either after parturition, which would require sperm storage, or after the resting period and before ovulation. Two recently fertilized shortfin makos from South Africa caught in March and June had fresh mating scars, suggesting mating takes place in late summer–fall before ovulation. It may be selectively advantageous for mating to occur in summer–fall prior to ovulation when the females appear to be in a different geographical area, rather than after parturition in spring of the previous year near the pupping grounds, because both sexes may be feeding actively at that time.

There was an uneven distribution of reproductive stages in our shortfin mako data. Pre-ovulating and early to mid-term pregnant females were poorly represented. Casey and Kohler (1992) suggested that adult females remain far offshore in more tropical waters. We propose that this suggestion applies particularly to pre-ovulating females ready to be mated and early to midterm females. Because the shortfin mako prefers 18°C water (Casey and Kohler, 1992), these females are likely to be found in deeper water and are less likely to be caught.

Regional differences

The studies of Garrick (1967) and Heist et al. (1996) have suggested that there is only one circumglobal species of shortfin mako, *Isurus oxyrinchus*. Despite this conclusion, we found that there were significant differences in the median TL-at-maturity of females and in their mass-length relationship between the Northern and Southern Hemispheres. Small regional differences in size at maturity have been reported for a number of other elasmobranch species, including widely distributed species such as the sandbar shark (Last and Stevens, 1994), scalloped hammerhead shark, *Sphyrna lewini* (Branstetter, 1987; Chen et al., 1990), soupfin shark (Peres and Vooren, 1991), and dusky shark, *Carcharhinus obscurus* (Natanson and Kohler, 1996). Our estimates of the duration of gestation and reproductive cycle are unlikely to be greatly affected by these differences.

Determining reproductive parameters for the large, wide-ranging and oceanic shortfin mako proved difficult. A dedicated sampling program conducted throughout the year within a particular region may still not provide the necessary data. We believe our approach of combining scarce data from widely spaced localities was justified.

Acknowledgments

The data collected by Abner Kingman as an observer on a swordfish longliner proved to be very useful. We are most grateful to Malcolm P. Francis and Ken J. Goldman for many suggestions and for data on porbeagles and salmon sharks. We thank Fabio E. S. Costa and Alberto F. Amorim for litter data from Brazil, David W. Welch for help with the statistical analysis, Nancy E. Kohler for providing HSI data, Dave B. Holts for the California drift gillnet fishery data, and Gregor M. Cailliet for reviewing the manuscript. A large number of people provided data and useful suggestions, and we acknowledge Shelton P. Applegate, Steven Branstetter, Barry D. Bruce, José I. Castro, Tris Colket; Leonard J. V. Compagno; Gerald L. Crow; David A. Ebert, Ian K. Fergusson, R. Grant Gilmore and Oliver Putz, William C. Hamlett, Glen Hodson, Leanne Laughlin, Robert N. Lea, Jean R. C. de Marignac, Sanford A. and Barbara Moss, John A. Musick, Gavin J. P. Naylor, Giuseppe Notarbartolo di Sciara, Tsuguo Otake, Daniel Pauly, Julian G. Pepperell, John E. Randall, Peter Saul, Jeffrey A. Seigel, Colin A. Simpfendorfer, Antonio D. Testi, and Senzo Uchida. GC wishes to thank his colleagues at the Natal Sharks Board for assistance in providing and examining specimens. HFM wishes to thank Cherilyn Chin, Juan E. Ezcurra, Scott R. Greenwald, John B. O'Sullivan, and Gilbert Van Dykhuizen at the Monterey Bay Aquarium for help and support. Anne L. Mollet proofread the manuscript. Comments by four anonymous and two NMFS reviewers helped us to focus and strengthen our findings.

Literature cited

Applegate, S. P.
1966. A possible record-sized bonito shark, *Isurus oxyrinchus* Rafinesque, from Southern California. Calif. Fish Game 52:204–207.

[20] Carrier, J. C., and H. L. Pratt. 1998. Albion College, 4705 Kellogg Ctr., Albion, MI 49224. Unpubl. data

Bass, A. J., J. D. D'Aubrey, and N. Kistnasamy.
1973. Sharks of the east coast of southern Africa. 1. The genus *Carcharhinus* (Carcharhinidae). Oceanogr. Res. Inst. Invest. Rep. 33:1–168.
1975. Sharks of the east coast of southern Africa. IV. The families Odontaspididae, Scapanorhynchidae, Isuridae, Cetorhinidae, Alopiidae, Orectolobidae and Rhiniodontidae. Oceanogr. Res. Inst. Invest. Rep. 39:1–102.

Bigelow, H. B., and W. C. Schroeder.
1948. Part 1: sharks. *In* Fishes of the western North Atlantic, p. 59–546. Sears Foundation for Marine Research, Yale Univ.

Bonfil, R.
1994. Overview of world elasmobranch fisheries. FAO Fisheries Technical Paper 341:1–119.

Branstetter, S.
1981. Biological notes on the sharks of the north central Gulf of Mexico. Contribb. Mar. Sci. 24:13–34.
1987. Age, growth and reproductive biology of the silky shark, *Carcharhinus falciformis*, and the scalloped hammerhead, *Sphyrna lewini*, from the northwestern Gulf of Mexico. Env. Biol. Fish. 19:161–173.

Branstetter, S., and J. A. Musick.
1994. Age and growth estimates for the sandtiger in the northwestern Atlantic Ocean. Trans. Am. Fish. Soc. 123: 242–254.

Bruce, B. D.
1992. Preliminary observation on the biology of the white shark, *Carcharodon carcharias*, in South Australian waters. *In* Sharks: biology and fisheries (J. G. Pepperell, ed.), p. 1–11. Aust. J. Mar. Freshwater Res. 43.

Cadenat, J.
1956. Note d'ichthyologie ouest-africaine. Vol. XV: Sur un requin-renard nouveau pour la faune d'afrique occidentale francaise *Alopius superciliosus* (Lowe) 1840? Bull. Inst. Fr. Afr. Noire 18A:1257–1266.

Cailliet, G. M., L. K. Martin, J. T. Harvey, D. Kusher, and B. A. Weldon.
1983. Preliminary studies on the age and growth of the blue shark, *Prionace glauca*, common thresher, *Alopias vulpinus*, and shortfin mako, *Isurus oxyrinchus*, from California waters. *In* Proceedings of the international workshop on age determination of oceanic pelagic fishes: tunas, billfishes, and sharks (E. D. Prince and L. M. Pulos, eds.), p. 179–188. U. S. Dep. Commer., NOAA Tech. Rep. NMFS 8.

Carey, F. G., J. G. Casey, H. L. Pratt, D. Urquhart, and J. E. McCosker.
1985. Temperature, heat production and heat exchange in the lamnid sharks. Memo. S. Cal. Acad. Sci. 9:92–108.

Carey, F. G., and J. V. Scharold.
1990. Movements of blue sharks (*Prionace glauca*) in depth and course. Mar. Biol. 106:329–342.

Casey, J. G., and N. E. Kohler.
1992. Tagging studies on the shortfin mako shark (*Isurus oxyrinchus*) in the western North Atlantic. *In* Sharks: biology and fisheries (J. G. Pepperell, ed.), p. 45–60. Aust. J. Mar. Freshwater Res. 43.

Castro, J. A., and J. Mejuto.
1995. Reproductive parameters of blue shark, *Prionace glauca*, and other sharks in the Gulf of Guinea. Mar. Freshwater Res. 46:967–73.

Chen, C. T., T. C. Leu, S. J. Joung, and N. C. H. Lo.
1990. Age and growth of the scalloped hammerhead, *Sphyrna lewini*, in northeastern Taiwan waters. Pac. Sci. 44: 156–170.

Chen C. T., K. M. Liu, and Y. C. Chang.
1997. Reproductive biology of the bigeye thresher shark, *Alopias superciliosus* (Lowe, 1839) (Chondrichthyes: Alopiidae), in the northwestern Pacific. Ichthyological Research 44:227–235.

Cliff, G., S. F. J. Dudley, and B. Davis.
1990. Sharks caught in the protective gill nets off Natal, South Africa. 3. The shortfin mako, *Isurus oxyrinchus* (Rafinesque). S. Afr. J. Mar. Sci. 9:115–126.

Compagno, L. J. V.
1984. FAO species catalogue; sharks of the world. An annotated and illustrated catalogue of shark species known to date. FAO Fisheries Synopsis (125), vol. 4, part 1: Hexanchiformes to Lamniformes, 249 p. FAO, Rome.
1988. Sharks of the order Carcharhiniformes. Princeton Univ. Press, Princeton, NJ, 467 p.

Ellis, R., and J. E. McCosker.
1991. Great white shark. Harper Collins Publishers, New York NY, 270 p.

Francis, M. P.
1996. Observations on a pregnant white shark with a review of reproductive biology. *In* Great white sharks: the biology of *Carcharodon carcharias* (A. P. Klimley and D. G. Ainley, eds.), p. 157–172. Academic Press, San Diego CA.

Francis, M. P., and J. D. Stevens.
2000. Reproduction, embryonic development, and growth of the porbeagle shark, *Lamna nasus*, in the Southwest Pacific Ocean. Fish. Bull. 98(1):41–63.

Garrick, J. A. F.
1967. Revision of sharks of genus *Isurus* with description of a new species (Galeoidea, Lamnidae). Proc. U. S. Nat. Mus. 118:663–694.

Gilmore, R. G.
1983. Observation on the embryos of the longfin mako, *Isurus paucus*, and the bigeye thresher, *Alopias superciliosus*. Copeia 1983:375–382.
1993. Reproductive biology of lamnoid sharks. Env. Biol. Fish. 38:95–114.

Gilmore, R. G., J. W. Dodrill, and P. A. Linley.
1983. Reproduction and embryonic development of the sandtiger shark, *Odontaspis taurus* (Rafinesque). Fish. Bull. 81:201–225.

Gohar, H. A. F., and F. M. Mazhar.
1964. The elasmobranchs of the north-western Red Sea. Publ. Mar. Biol. Stat. Al-Ghardaqa (Red Sea) No. 13:1–144.

Goldman, K. J.
1997. Regulation of body temperature in the white shark, *Carcharodon carcharias*. J. Comp. Physiol. B 167:423–429.

Graham, J. B., H. Dewar, N. C. Lai, W. R. Lowell, and S. M. Arce.
1990. Aspects of shark swimming performance determined using a large water tunnel. J. Exp. Biol. 151.175–192.

Gubanov, Ye. P.
1972. On the biology of thresher shark (*Alopias vulpinus*) in the North-west Indian Ocean. J. Ichthyol. 12:591–600
1978. The reproduction of some species of pelagic sharks from the equatorial zone of the Indian ocean. J. Ichthyol. 18:781–792.

Guitart-Manday, D.
1975. Las pesquerias pelagico-oceanicas de corte radio de accion en la region noroccidental de Cuba [Short-range marine pelagic fishing of northeast Cuba]. Seria Oceanologica, Oceanographic Institute Academy of Sciences of

Cuba 31, p. 3–26. [Translated for the National Science Foundation and the US Department of Commerce, NOAA, NMFS by the Agence Tunisiennes de Public-Relations, Tunis.]

Hamlett, W. C., D. J. Allen, M. D. Stribling, F. J. Schwartz, and L. J. A. DiDio.
1985. Permeability of external gill filaments in the embryonic shark. Electron microscopic observations using horseradish peroxidase as a macromolecular tracer. J. Submicrosc. Cytol. 17:31–40.

Hanan, D. A., D. B. Holts, and A. L. Coan Jr.
1993. The California drift gill net fishery for shark and swordfish 1981–82 through 1990–91. Fish. Bull. 175: 1–93.

Heist, E. J., J. A. Musick, and J. E. Graves.
1996. Genetic population structure of the shortfin mako (*Isurus oxyrinchus*) inferred from restriction fragment length polymorphism analysis of mitochondrial DNA. Can. J. Fish. Aquat. Sci. 53:583–538.

Hixon, M. A.
1979. Term fetuses from a large common thresher shark, *Alopias vulpinus*. Calif. Fish Game 65:191–2.

Holts, D. B., and D. W. Bedford.
1993. Horizontal and vertical movements of the shortfin mako shark, *Isurus oxyrinchus*, in the Southern California Bight. Aust. J. Mar. Freshwater Res. 44:501–509.

Joseph, D. C.
1954. A record-size thresher from Southern California. Calif. Fish Game 40:433–435.

Killam, K., and G. Parsons.
1986. First record off the longfin mako, *Isurus paucus*, in the Gulf of Mexico. Fish. Bull. 84:748–749.

Klimley, A. P.
1985. The areal distribution and autoecology of the white shark, *Carcharodon carcharias*, off the west coast of North America. Mem. S. Cal. Acad. Sci. 9:15–40.

Koob, T. J., and J. W. Straus.
1998. On the role of egg jelly in *Raja erinacea* egg capsule. Bull. Mt. Desert Island Biol. Lab. 37:117–119.

Last, P. R., and J. D. Stevens.
1994. Sharks and rays of Australia. Commonwealth Scientific and Industrial Research Organization (CSIRO), Australia, 513 p. + 84 color plates.

Lineaweaver, T. H., and R. H. Backus.
1970. The natural history of sharks. 1984 reprint, Nick Lyons Books/Schocken Books, New York, NY, 256 p.

Lohberger, J.
1910. Uber zwei riesige Embryonen von *Lamna*. Abh. K. Bayer. Akad Wiss. IV. Suppl. Bd. 2:1–45.

Matthews, L. H.
1950. Reproduction in the basking shark, *Cetorhinus maximus*, (Gunnerus). Phil. Trans. B. Royal Soc. Lond. 234: 247–316.

Mollet, H. F., and G. M. Cailliet.
1996. Using allometry to predict body mass from linear measurements of the white shark. *In* Great white sharks: the biology of *Carcharodon carcharias* (A. P. Klimley and D. G. Ainley, eds.), p. 81–89. Academic Press, San Diego CA.

Moreno, J. A., and J. Morón.
1992. Reproductive biology of the bigeye thresher shark, *Alopias superciliosus* (Lowe, 1839). *In* Sharks: biology and fisheries (J. G. Pepperell, ed.), p. 77–86. Aust. J. Mar. Freshwater Res. 43.

Musick, J. A., S. Branstetter, and J. A. Colvocoresses.
1993. Trends in shark abundance from 1974 to 1991 for the Chesapeake Bight region of the U.S. mid-Atlantic coast. *In* Conservation biology of elasmobranchs (S. Branstetter, ed.), p. 1–19. U.S. Dep. Commer., NOAA Tech. Rep. NMFS 115.

Nakamura, H.
1935. On the two species of the thresher shark from Formosan waters. Mem. Fac. Sci. Agric. Taihoku Imp. Univ. 14:1–6.

Natanson, L. J., and N. E. Kohler.
1996. A preliminary estimate of age and growth of the dusky shark *Carcharhinus obscurus* from the south-west Indian Ocean, with comparison to the western North Atlantic population. S. Afr. J. Mar. Sci. 17:217–224.

Neter, J., and W. Wassermann.
1974. Applied linear statistical models. Richard D. Irwin Inc., Homewood, IL, 842 p.

Norman, J. R., and F. C. Fraser.
1938. Giant fishes, whales and dolphins. W. W. Norton and Company Inc., New York, NY, 361 p.

O'Brian, J. W., and J. S. Sunada.
1994. A review of the southern California experimental drift longline fishery for sharks, 1988–1991. CalCOFI Rep. 35: 222–229.

Otake, T.
1990. Classification of reproductive modes in sharks with comments on female reproductive tissues and structures. *In* Elasmobranchs as living resources: advances in the biology, ecology, systematics and the status of fisheries (H. L. Pratt, S. H. Gruber, T. Taniuchi, eds.), p. 113–130. U.S. Dep. Commer., NOAA Tech. Rep. NMFS 90.

Parker, H. W., and F. C. Stott.
1965. Age, size, and vertebral calcification in the basking shark *Cetorhinus maximus* (Gunnerus). Zool. Meded. (Leiden) 40:305–319.

Parsons, G. R.
1993. Geographic variation in the reproduction between two populations of the bonnethead shark, *Sphyrna tiburo*. Env. Biol. Fish. 38:25–35.

Pepperell, J. G.
1992. Trends in the distribution, species composition and size of sharks caught by gamefish anglers off South-eastern Australia, 1961–90. *In* Sharks: biology and fisheries (J. G. Pepperell, ed.), p. 213–225. Aust. J. Mar. Freshwater Res. 43.

Peres, M. B., and C. M. Vooren.
1991. Sexual development, reproductive cycle, and fecundity of the school shark *Galeorhinus galeus* off southern Brazil. Fish. Bull. 89:655–667.

Pratt, H. L., Jr.
1979. Reproduction in the blue shark, *Prionace glauca*. Fish. Bull. 77:445–70.

Pratt, H. L., Jr., and J. G. Casey.
1983. Age and growth of the shortfin mako, *Isurus oxyrinchus*, using four methods. Can. J. Fish. Aquat. Sci. 40:1944–1957.

Randall, J. E.
1992. Review of the biology of the tiger shark (*Galeocerdo cuvier*). *In* Sharks: biology and fisheries (J. G. Pepperell, ed.), p. 21–31 Aust. J. Mar. Freshwater Res. 43.

Sanzo, L.
1912. Embrione di *Carcharodon Rondeletii* M. Hle. (?) con particolare disposizione del sacco vitellino. Regio Comitato Talassografico Italiano, Memoria XI. 1–12.

Saul, P., and J. Holdsworth.
1992. Cooperative gamefish tagging in New Zealand waters 1975–90. New Zealand Fisheries Technical Report No. 33, 24 p.

Stevens, J. D.
1983. Observations on reproduction in the shortfin mako *Isurus oxyrinchus*. Copeia 1983:126–130.

Stevens, J. D., and K. J. McLoughlin.
1991. Distribution, size and sex composition, reproductive biology, and diet of sharks from Northern Australia. Aust. J. Mar. Freshwater Res. 42:151–199.

Swenander, G.
1907. Uber die Ernäherung des Embryos der *Lomno cornubico*. Zoologiske Studier Tollagnade Tullberg Uppsala 1907:283–289.

Templeman, W.
1963. Distribution of sharks in the Canadian Atlantic (with special reference to Newfoundland waters). Bull. Fish. Res. Board Can. 140:1–77.

Tricas, T. C., K. Deacon, P. Last, J. E. McCosker, T. I. Walker, and L. Taylor.
1997. The Nature Company guides. Sharks and rays (L. Taylor, consultant ed.). Time-Life Books, Time Life Inc. San Francisco, CA, 288 p.

Uchida S., M. Toda, and Y. Kamei.
1990. Reproduction of elasmobranchs in captivity. *In* Elasmobranchs as living resources: advances in the biology, ecology, systematics, and the status of fisheries (H. L. Pratt, S. H. Gruber, T. Taniuchi, eds.), p. 211–237. U.S. Dep. Commer., NOAA Tech. Rep. NMFS 90.

Uchida, S., M. Toda, K. Teshima, and K. Yano.
1996. Pregnant white sharks with near-term fetuses from Japan. *In* Great white sharks. The biology of *Carchorodon corchorios* (A. P. Klimley and D. G. Ainley, eds.). Academic Press, San Diego, CA, p. 139–155.

Uchida, S., F. Yasuzumi, M. Toda, and N. Okura.
1987. On the observation of reproduction in *Carcharodon carchorias* and *Isurus oxyrinchus*. Rep. of Japanese Group for Elasmobranch Studies 24:5–6.

Vaillant, L.
1889. Note sur un foetus gigantesque d'*Oxyrhina spallanzani* Bonap. Bull. Soc. Philom. Paris 1:38–39.

Welch, D. W., and R. P. Foucher.
1988. A maximum likelihood methodology for estimating length-at-maturity with application to Pacific cod *(Gadus macrocephalus)* population dynamics. Can. J. Fish. Aquat. Sci. 45:333–343.

Wilkinson, L.
1986. SYSTAT: The system for statistics. SYSTAT Inc., Evanston IL, 18 chapters and 4 appendices without continuous page numbers.

Yano K., Y. Yabumoyo, S. Tanaka, O. Tsukada, and M. Furuta.
1999. Capture of a mature female megamouth shark, *Megachasma pelagios*, from Mie, Japan. *In* Proc. 5th Indo-Pac. Fish Conf., Noumea 3–8 November 1997 (B. Seret and J. Y. Sire, eds.), p. 351–365. Société Francaise d'Ichtyologie and Institut de Recherche pour le Développement, Paris.

The relation between early marine growth of pink salmon, *Oncorhynchus gorbuscha*, and marine water temperature, secondary production, and survival to adulthood

Donald Mortensen

Alex Wertheimer

Sidney Taylor

Joyce Landingham

Auke Bay Laboratory
Alaska Fisheries Science Center
National Marine Fisheries Service, NOAA
11305 Glacier Highway
Juneau, Alaska 99801-8626

E-mail address (for D. Mortensen): don.mortensen@noaa.gov

Abstract.—Juvenile pink salmon, *Oncorhynchus gorbuscha*, from four consecutive brood years were tagged as they emigrated to the estuarine waters of Auke Bay, and information was obtained on the relationships between early marine growth, environmental conditions, and survival to adulthood. Juveniles that emigrated from Auke Creek later in the spring spent significantly less time in the estuary. Individual growth rates of tagged fish recovered in Auke Bay ranged from 3.1% to 7.1% per day. In all study years, juvenile pink salmon grew more slowly in early April than in late April and early May. Water temperature and growth were significantly correlated in all years, but growth did not consistently correlate with the biomass of epibenthic prey or zooplankton available to the fish. Comparisons of expected and observed growth rates suggested that low prey availability, as well as low temperatures, may have limited growth for early spring emigrants. Although early emigrants encountered poorer growth conditions, survivors were larger at a given date than later emigrants, their larger size possibly protecting them from size-selective predation. Early marine growth was significantly related to intra-annual cohort survival to adults (r^2=0.65, P<0.05). Larger fish consistently survived better than their smaller cohorts for all years. Although early marine growth was an important determinate of survival within a cohort of pink salmon, other factors, such as predator abundance, contributed to the large interannual variability observed.

Manuscript accepted 29 November 1999.
Fish. Bull. 98:319–335 (2000).

Pink salmon, *Oncorhynchus gorbuscha*, are the most abundant Pacific salmon species native to the west coast of the United States and Canada (Morrow, 1980). In southeastern Alaska pink salmon typically mature after 15 to18 months at sea and return to their native streams to spawn in late summer and early fall. Pink salmon usually spawn in the lower portions of streams just above the intertidal zone and in intertidal areas at stream mouths (Bailey, 1969). Eggs hatch in January or February and the embryos (alevins) continue to develop within the gravel of the stream bed. In late March or early April juvenile pink salmon (fry) emerge from the gravel and emigrate downstream to salt water and begin feeding on epibenthic organisms and small zooplankton. They form schools and reside in the nearshore marine habitat for several weeks (Heard, 1991). This early marine residency is evidently a critical stage in the early life history of salmon and can significantly affect year-class strength (Parker, 1968; Walters et al., 1978; Bax, 1983; Nichelson, 1986). Rapid growth during this early marine period may be a mechanism by which size-selective mortality is reduced (Parker, 1971; Hargreaves and LeBrasseur, 1985).

Growth and mortality of juvenile fish is thought to be coupled with the magnitude and timing of primary and secondary production (Cushing, 1976; Pitcher and Hart, 1982; D'Amours, 1987). Slight variations in migration timing and the developmental rate of juvenile fish in relation to secondary production influence feeding success and may in turn affect growth and survival. Subarctic estuarine ecosystems are characterized by high levels of primary and secondary production in spring (Russell-Hunter, 1970; Larrance, 1971; Goering et al., 1973). Consequently, the timing of emigration of species such as juvenile pink and chum, *O. keta*, salmon may have evolved so that this highly productive period maximizes growth and survival (Murphy et al., 1988; Holtby et al., 1989). This concept is somewhat

intuitive and there is little direct supportive evidence. To test this idea, we designed our study with the following objectives: 1) to examine emigration timing and growth of tagged individual juvenile pink salmon in relation to secondary production and water temperature and 2) to investigate the relation between timing of emigration, early marine growth, and intra- and interannual variability in marine survival.

Methods

This research focused on the Auke Creek pink salmon population. Auke Creek is a small, lake-fed stream that empties into Auke Bay in southeast Alaska (Fig. 1). The National Marine Fisheries Service maintains a permanent two-way counting weir (where both seaward-migrating and returning salmon are counted) at the confluence of Auke Creek with Auke Bay. The pink salmon run at Auke Creek is bimodal, that is it has a distinct early and late spawning component. Salmon in the early run begin spawning in late July through August and salmon in late run spawn from September through mid-October. The emigration of fry in the spring lasts from late March to mid-May and is relatively unimodal. The peak emigration usually occurs in late April (Taylor, 1980)

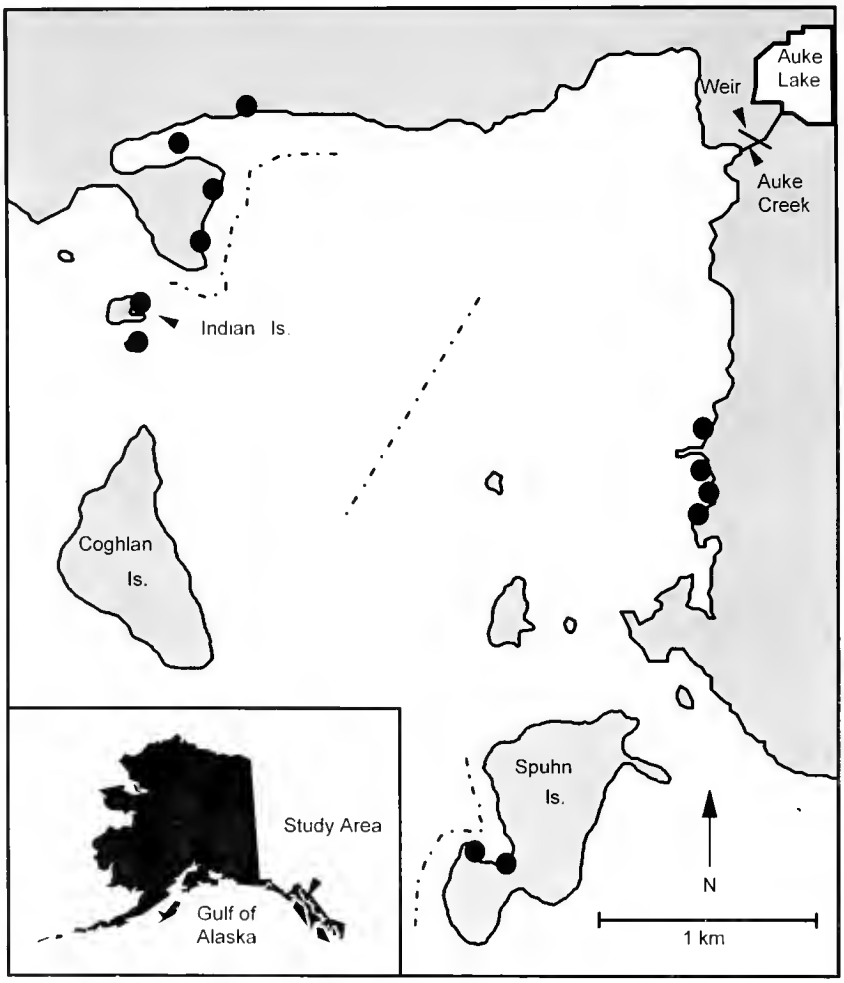

Figure 1

Map of Auke Bay, Alaska, showing beach seine sites (circles) and surface trawl transects (dashed lines).

The downstream emigration of wild pink salmon juveniles from Auke Creek into Auke Bay generally begins in early March, peaks between mid-April and early May, and ends by mid-May. From 1986 to 1989, 53,526, 17,249, 38,149, and 42,599 juvenile pink salmon emigrated from Auke Creek respectively. Each day all captured emigrants were counted and samples were measured to the nearest millimeter fork length.

Each year a portion of the emigrants was marked. Marking involved the excision of the entire adipose fin after a 0.5-mm binary coded wire was injected into the snout. Tag codes were assigned in lots of 10,000; therefore to use all the tags in a particular code-lot, tagging was conducted over several days each week. The 1985 brood was tagged in five-day emigration periods when sufficient numbers of fish were captured. The 1986 through 1988 broods were tagged in two to three-day emigration periods. After having been tagged, the fish were held for one day (1985 and 1986 broods) or three days (1987 and 1988 broods) to assess mortality and tag loss. Dead fish and those missing tags were deducted from the total tagged in each group. Release dates were similar each year.

Nearshore areas of Auke Bay were sampled for juvenile pink salmon from late March to early July with a 37-m long × 3-m deep beach seine. All captured juvenile salmon were identified to species, counted, and checked for evidence of tagging at the capture site; recaptured tagged fish were retained for tag recovery and size measurements. Random samples of up to 100 unmarked fish from each beach seine from sites on Spuhn and Indian Islands in Auke Bay were retained for length and weight measurements and stomach analysis. Other species (nonsalmonid) that were captured in the beach seines were enumerated and measured to the nearest millimeter (fork length

[FL] or total length [TL] depending upon the species). These fish have the potential to be either predators on or competitors with pink salmon juveniles.

Beginning in 1987, offshore areas of Auke Bay (>100 m from shore) were sampled weekly, at night, with a 6.1-m wide × 3.0-m deep surface trawl (Bax et al.[1]). All tagged salmon and a sample of up to 100 untagged juvenile pink salmon from each tow were retained for length and weight measurements and stomach analysis. All other fish captured in each tow were identified, enumerated, and measured.

Water temperature at 1-m depth was recorded daily in Auke Bay. Spuhn Island was sampled weekly for littoral epibenthic crustaceans in 1987–1989, with an epibenthic pump (1987) (Simenstad et al.[2]) or an epibenthic sled (1988 and 1989) (Celewycz and Wertheimer, 1996b). Zooplankton data for the upper 5-m and upper 40-m water column in Auke Bay were collected concurrently with our study by University of Alaska researchers (Coyle and Paul, 1990).

Stomachs of a subsample of untagged juvenile pink salmon retained from beach seine and trawl catches were examined to determine feeding habits. Stomach contents were weighed, and prey items were identified, measured, and counted. A mean volume and dry weight were calculated for each prey category, and the index of relative importance (IRI; Pinkas et al., 1971) was then computed by using the formula

$$IRI = (N + V)F,$$

where N = the numerical percentage;
V = the volumetric percentage of each prey item in the diet; and
F = the percent frequency of occurrence of the prey item.

The importance of individual prey groups were compared as a percentage of the total *IRI* for all prey.

The maximum residence of tagged fish from each weekly release group in Auke Bay was calculated by subtracting the actual release date for a particular lot of tagged fish from the last recovery date of a tagged juvenile from the same lot of tagged fish, yielding the number of days from release to recapture. The weighted mean residence time for each tag release group ($\overline{D}_{res_i}$) was calculated by subtracting the weighted mean release date for each weekly release group from the weighted mean recovery date for each release group. The weighted mean release date ($\overline{D}_{rel_i}$) for weekly release group i was calculated from the formula

$$\overline{D}_{rel_i} = \frac{\sum_{d=1}^{d=n} d_{rel} N_{d_{rel}}}{\sum_{d=1}^{d=n} N_{d_{rel}}},$$

where n = the number of release days per week;
d_{rel} = the actual release day (Julian date); and
$N_{d_{rel_i}}$ = the number of tagged fish from that day that were released. The weighted mean residence for each weekly group was then calculated by subtracting the weighted mean release date of a juvenile for a given week from the weighted mean recovery date. The weighted mean recovery date ($\overline{D}_{rec_i}$), for a particular release group was calculated as

$$\overline{D}_{rec_i} = \frac{\sum_{d=1}^{d=n} d_{rec} N_{d_{rec}}}{\sum_{d=1}^{d=n} N_{d_{rec}}},$$

where n = the number of recovery days per week;
d_{rec} = the actual recovery day (Julian date) of a tagged juvenile; and
$N_{d_{rec_i}}$ = the number of tagged fish recovered on day d.

The weighted mean residence time ($\overline{D}_{res_i}$) was regressed against release date for each year. Analysis of covariance (ANCOVA) was used to determine whether significant differences existed among years, followed by the Newman-Keuls multiple comparison test to determine if significant differences (α=0.05) existed within years.

The instantaneous growth rate, g, for individual tagged pink salmon juvenile was calculated as

$$W_2 = W_1 \exp^{gt},$$

where t = the period in days from the mean release date, over which the growth rate was calculated; and
W_1 and W_2 = the fish weight at the beginning and end of the period, respectively.

In addition the natural log of the weight of tagged fish at capture was regressed against days from

[1] Bax, N. J., E. O. Salo, B. P. Snyder, C. A. Simenstad, and W. J. Kinney. 1978. Salmonid outmigration studies in Hood Canal. Final Report FRI-UW-7819, Phase III, January to July 1977, University of Washington, College of Fisheries, Fisheries Research Institute, Seattl, WA.

[2] Simenstad, C. A., C. D. Tanner, and R. M. Thom. 1989. Estuarine wetland restoration and monitoring protocol. Report FRI-UW-8918, University of Washington, College of Fisheries, Fisheries Research Institute, Seattle, WA.

release to recovery to provide the growth rate (the slope of the regression line) for each release group. Using g we then calculated the relative growth, h, as the percentage of body weight per day (%bwd) for each fish and for each group was calculated from the formula

$$h = (\exp^g - 1)\ 100.$$

Tagged juveniles that were recaptured within a week of the mean release date from the Auke Creek weir were not used in growth rate calculations. It was assumed that after a week the fish had acclimated to the marine environment and were recovered from prerelease tagging stress. In addition to the above calculations, the weights of tagged and untagged juveniles at successive capture dates were logarithmically transformed and regressed against days from the mean release day to the day of capture.

To determine how water temperature and food abundance relate to growth in the estuary, individual growth rates of tagged fish were correlated with average surface water temperature and prey biomass over the period between release and recapture. The average daily biomass of prey organisms was calculated for three habitats: the upper 5-m of the water column, the upper 40-m of the water column, and the littoral zone (harpacticoid copepods only). Correlation analysis and stepwise regression (Zar, 1974) were employed to determine significant correlations and provide partial correlation coefficients for each of the above parameters.

To test the possibility that estuarine growth of juvenile pink salmon could be limited by prey availability, the residual (difference) between expected and actual growth of individual juvenile pink salmon at given water temperatures was calculated and plotted against average water temperature. Expected maximum growth rates for given temperatures were obtained from (Mortensen and Savikko, 1993).

Growth of the tagged juvenile pink salmon was also computed for two periods or stanzas. Each year, the early period was that before and including 5 May, and the late period was that after 5 May. These dates were chosen because of the distinct change in size of juveniles between the two periods and the distribution of tag recoveries. Each year a dramatic increase in length was noted in the tagged fish at the beginning of May. Growth for each tagged group within a year was calculated for the early period; this rate was then used to estimate the initial weight for each tag group for computation of growth in the late period. Differences in growth between periods and years were tested by using analysis of covariance (ANCOVA) and the Newman-Keuls multiple comparison or Dunnet's tests (Zar, 1974). Significance levels were set at $\alpha = 0.05$.

Survival of fish from each release group for each emigrant year, 1986–1989 (brood years 1985–1988) was determined from the number of adult salmon returning to the Auke Creek weir. Each pink salmon adult passing through the weir was examined for a coded wire tag (cwt) on the adipose fin. Clipped fish were killed and their heads removed. Fish with adipose fins were returned to the creek to spawn. Coded-wire tags were removed from heads of the clipped fish later at the laboratory. Fish that showed a clip mark but were missing cwts were assigned to an emigration group that was based upon the proportion of all tag codes recovered each return week. Therefore, the return of each emigration group was the number of known tagged fish plus an expansion for clipped fish that had lost their tags. The total return of pink salmon adults to Auke Creek was the product of weir recoveries and a fishery correction factor. The fishery correction factor for each brood year was determined as

$$1/(1 - h),$$

where h = harvest rate determined as the proportion of the total return that is caught in the commercial fishery according to estimates by Alaska Department of Fish and Game (ADF&G) commercial fisheries management personnel.

Fishery correction factors obtained from the commercial fisheries branch of ADF&G for the 1985–1988 broods at Auke Creek were 1.45, 1.03, 1.53, and 1.43, respectively.[3] Growth and survival of the individual release groups within each year were standardized as a proportion of the highest rates observed. The proportional growth rate for each release group was regressed against proportional survival to determine the degree to which growth rate was a predictor of intra-annual survival. Survival rates were regressed against growth rates to determine the relation between growth and interannual survival.

Results

Catch and residency times

Juvenile pink salmon use Auke Bay as a nursery area throughout the spring and early summer and reside nearshore from late March until mid-June. Pink salmon

[3] Ingledue, D. 1987–90. Alaska Department of Fish and Game, Division of Commercial Fisheries, Southeast Regional Office, 802 Third Street, Douglas, Alaska 99609. Personal commun.

were most abundant in late April and early May; 70–80% of the catch occurred between 5 May and 1 June. Most pink salmon left the nearshore area by late May. Salmon catch offshore tended to increase coincidentally with the decline in catch near shore; offshore catches peaked between May and mid-June, depending on the year (Fig. 2). Most tagged juveniles were recaptured near shore; only 11 and 2 fish were recaptured offshore in 1987 and 1988, respectively (no fish were recaptured in 1989, and no offshore sampling occurred in 1986). By mid-July of each year, juveniles were not present in nearshore or offshore catches.

Estuarine residence time (based on recaptures of tagged fish) generally decreased with progressive release dates. The exception was 1988, when residence time was similar between all release groups. Mean residence time ranged from a high of 30 d for the early release in 1986 and 1987 to about 7 d for the late release in 1989. The mean residence was also significantly longer in the first two weeks of 1986 and 1987 than in 1988 and 1989 (Table 1). Mean residence times did not differ significantly by release week between 1986 and 1987 or between 1988 and 1989, but were significantly different between 1987 and 1988. Based on recaptured tagged fish, maximum residence times in Auke Bay ranged from 19 d for juveniles from the 3 May release in 1988 to 72 d for the juveniles from the 13 April release in 1987 (Table 1).

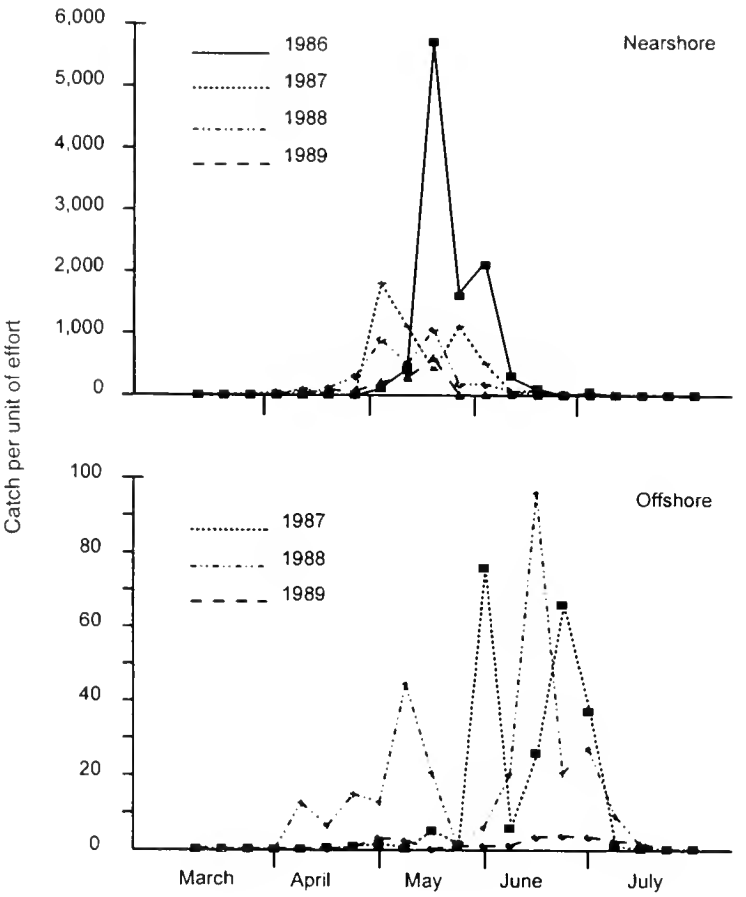

Figure 2

Catch per unit of effort (CPUE) of juvenile pink salmon at nearshore and offshore transects in Auke Bay, Alaska.

Nearshore catches consisted primarily of juvenile pink and chum salmon (Fig. 3). In even years, pink salmon juveniles were more abundant than chum salmon juveniles; pink salmon juveniles made up 83% and 65% of the catch in 1986 and 1988, versus 16% and 17% for chum salmon juveniles. In contrast, the ratios of pink and chum salmon in odd years were nearly equal (52–43%, 1987, and 52–44%, 1989). Coho (*O. kisutch*) and sockeye (*O. nerka*) salmon smolts and juvenile and adult Dolly Varden (*Salvelinus malma*) were also captured each year. Other nonsalmonid fishes captured included juvenile Pacific herring (*Clupea pallasi*) sculpins (Cottidae,) juvenile flatfish (Pleuronectidae), and juvenile walleye pollock (*Theragra chalcogramma*). Juvenile Pacific herring made up a significant proportion of the nearshore catch (14%) only in 1988.

Offshore catch composition for 1987 through 1989 consisted primarily of Pacific herring and capelin (*Mallotus villosus*). Pink salmon were the most abundant salmonid captured in offshore sampling. In 1987 and 1988, pink salmon made up 10% and 13% of the offshore catch respectively. Juvenile herring and capelin accounted for 76% and 74% of the offshore catch in 1987 and 1988, respectively. In 1989, pink salmon accounted for only 0.1% of the offshore catches, whereas juvenile Pacific herring were abundant and accounted for 97% of the total fish numbers. Fewer chum salmon juveniles and sockeye, coho, and chinook (*O. tshawytscha*) smolts were caught offshore than inshore. Other fish caught included juvenile and adult walleye pollock, sculpins, Pacific sandfish (*Trichodon trichodon*) and starry flounder (*Platichthys stellatus*).

Predators

Coho salmon smolts, medium (fork length $15 \geq x \geq 30$ mm) and large (fork length >30 cm) Dolly Varden, and three sculpin species (great sculpin, *Myoxoceph-*

Table 1

Release dates, number released, maximum and weighted mean residence (days), growth rate (percent body weight per day), and adult survival of coded-wire-tagged Auke Creek pink salmon for each release year followed by brood year in parentheses. Standard deviations for mean residence and growth are given in parentheses.

	Release week						
	1 April	7 April	15 April	22 April	29 April	6 May	13 May
1986 (1985)							
Number released	4322	8697	7416	10,136	11,446	10,866	643
Number recaptured	1	32	11	27	22	9	0
Maximum residence	29	47	35	65	31		—
Mean residence	29 (0)	30.5 (10.6)	17.6 (10.1)	18.3 (14.7)	12.8 (9.6)	10.6 (8.7)	—
Growth rate	—	3.6 (0.01)	4.0 (0.06)	4.0 (0.07)	3.7 (0.06)	3.4 (0.10)	—
Survival rate	1.14	1.44	2.62	2.17	3.14	1.18	0
1987 (1986)							
Number released	3442	4646	7684	1477	—	—	—
Number recaptured	17	54	53	8	—	—	—
Maximum residence	62	71	72	28	—	—	—
Mean residence	27.5 (16.3)	23.2 (8.7)	20.2 (12.2)	14.9 (9.3)	—	—	—
Growth rate	3.8 (0.08)	4.3 (0.07)	4.6 (0.09)	4.6 (0.05)	—	—	—
Survival rate	1.97	3.10	3.41	3.76	—	—	—
1988 (1987)							
Number released	5207	6031	8548	10,513	7880	—	—
Number recaptured	25	33	27	47	34	—	—
Maximum residence	26	34	33	41	19	—	—
Mean residence	15.5 (5.4)	12.0 (11.3)	16.8 (10.9)	15.4 (8.3)	13.5 (7.6)	—	—
Growth rate	3.5 (0.08)	4.3 (0.08)	5.6 (0.14)	5.8 (0.06)	6.4 (0.08	—	—
Survival rate	0.48	0.69	1.03	1.44	1.83	—	—
1989 (1988)							
Number released	—	3670	5113	8819	10,160	11,467	3370
Number recaptured	—	5	2	27	56	120	21
Maximum residenc	—	33	27	31	34	27	22
Mean residence	—	14.0 (15.1)	21.7 (5.2)	10.0 (8.7)	12.5 (10.6)	9.4 (12.3)	6.9 (11.1)
Growth rate	—	4.5 (0.05)	5.6 (0.02)	5.3 (0.06)	6.1 (0.07)	5.9 (0.06)	4.2 (0.09)
Survival rate	—	2.58	4.33	5.34	5.88	4.86	3.30

alus polyacanthocephalus, Pacific staghorn sculpin, *Leptocottus armatus*, and buffalo sculpin, *Enophrys bison*) were captured in beach seines and surface trawls along with juvenile salmon. We also observed these fish striking at schools of juvenile pink salmon in nearshore areas. Examination of the stomachs of a few of these predators showed that pink salmon juveniles were indeed a dietary item. The abundance of potential predators captured in beach seines and tow net trawls was similar for all study years. Temporally, the number of predators initially increased slowly in April, then rose sharply in late April, peaked by late May, and declined sharply in June (Fig. 4). The period of rapid increase and decline each year was due primarily to the pulse of coho salmon smolts entering Auke Bay in May and leaving in June. Dolly Varden and sculpin numbers increased more gradually in the spring and remained steady throughout late spring and early summer.

Water temperature and prey

Water temperature generally increased rapidly during April, May, and early June (Wing and Pella, 1998). Temperatures ranged from 3 to 5 C in late March to 10–14 C in June (Fig. 5). Temperature in 1986 and 1987 remained below 8°C for at least a week longer in April compared with temperature in 1988 and 1989.

Prey organisms of the juvenile salmon consisted primarily of zooplankton and littoral harpacticoid copepods. The seasonal dynamics of the biomass of zooplankton prey in the upper 40 m and upper 5 m of the Auke Bay water column have been discussed

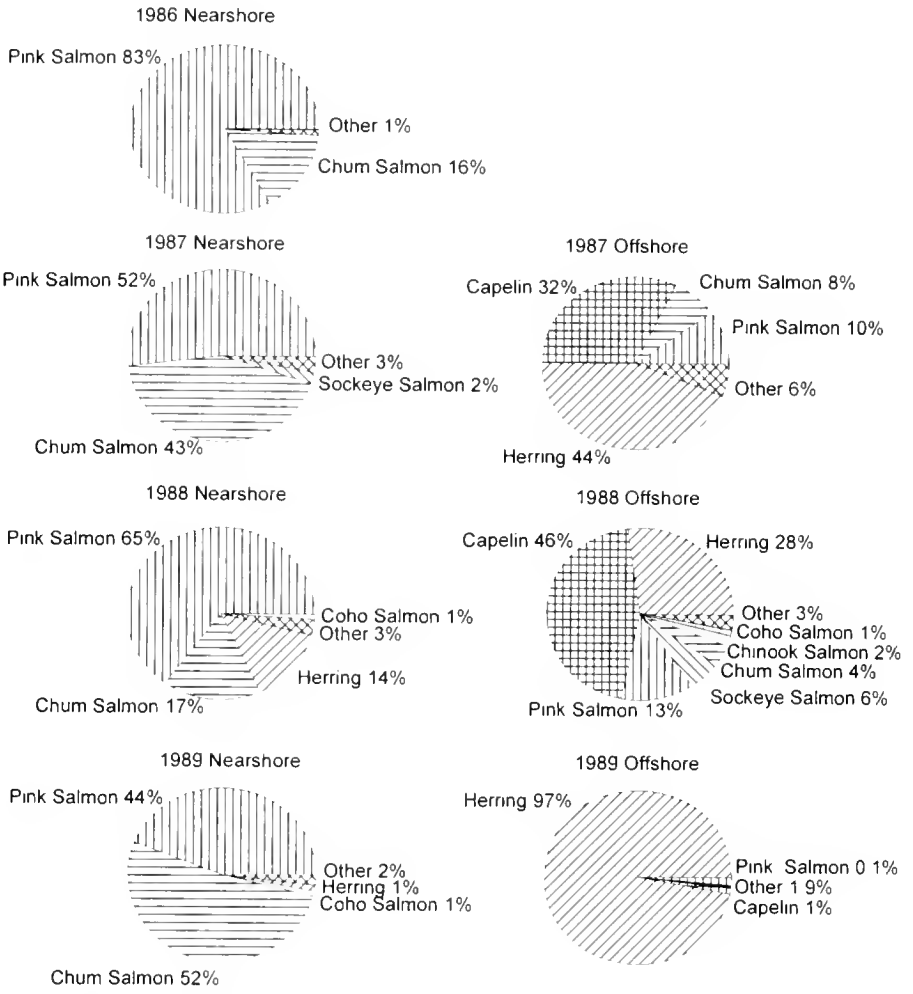

Figure 3

Species composition of nearshore and offshore catches from Auke Bay, Alaska, 1986–89.

by Coyle and Paul (1990), and we used their data to develop these profiles. Generally the biomass of zooplankton prey in the upper 40 and the upper 5 m of the water column began rising in mid-April and peaked in mid-June. However, in 1986 the biomass of prey in the upper 5 m remained low throughout the spring (Fig. 5).

Littoral harpacticoids were sampled at Spuhn Island in 1987, 1988, and 1989. Although the sampling method changed between 1987 and 1988, an indication of the dynamics of the harpacticoid population is achieved by presenting indices of biomass as a proportion of the highest value within each year. In 1987, harpacticoid copepod biomass was characterized by rapid fluctuations but remained low, except for a peak in mid-May. The biomass in 1988 again fluctuated rapidly, with peaks in late April and early May. In 1989, the biomass peaked in early April and again in early May.

Diet

Harpacticoid copepods and zooplankton (principally calanoid copepods, euphausid larvae, *Oikopleura* sp., and fish eggs and larvae) were eaten by the pink salmon juveniles captured near shore (Fig. 6). Between April and May, pink salmon consumed epibenthic prey more than pelagic prey; by mid-May they switched to a predominately pelagic diet.

Pink salmon juveniles captured offshore in Auke Bay exhibited a predominately pelagic diet, but some epibenthic organisms were still present. This finding may indicate that at times epibenthic prey are transported to offshore areas by water currents, or that the juvenile salmon optimize feeding by moving between pelagic and epibenthic areas in Auke Bay.

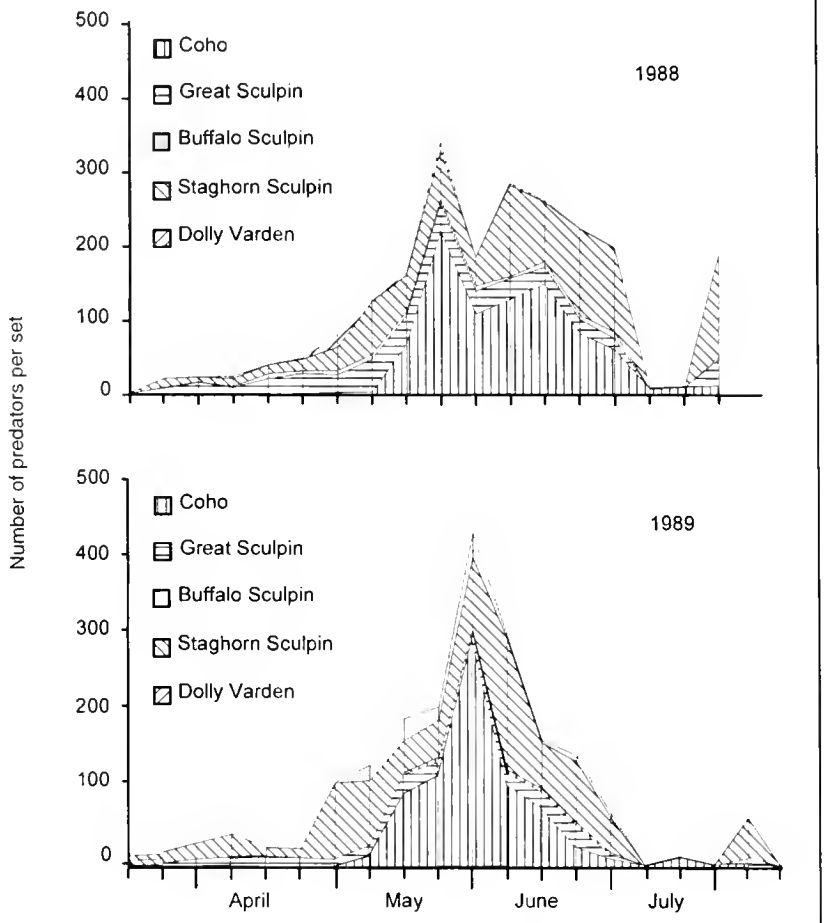

Figure 4

Mean catch per set of potential predators of juvenile pink salmon in the nearshore areas of Auke Bay, Alaska, 1988 and 1989.

Growth rates

Growth (as a percentage [bwd]), of tagged and untagged juvenile pink salmon was examined in two periods, 1 April to 6 May (early) and 7 May to 16 June (late) in all study years (Table 2). Growth of tagged fish in the early period ranged from 2.93% bwd in 1986 to 4.88% in 1989 and of untagged fish from 1.21% bwd in 1987 to 2.10% in 1989. In the late period, growth of tagged fish ranged from 4.82% bwd in 1986 to 6.66% in 1988, and of untagged fish from 2.87% bwd in 1989 to 4.86% in 1988. Tagged and untagged juvenile pink salmon grew significantly slower in the early period than in the late period in all years.

Growth rates calculated for tagged juvenile pink salmon in any given period in a year were consistently higher than the apparent growth rates calculated from the mean weights of samples of untagged pink salmon (Table 2). Continuous recruitment of newly emigrated juveniles (fork length <33 mm) into the untagged population caused this pattern. The number of untagged juvenile pink salmon shorter than 33 mm that were captured by beach seine ranged from highs between 59% and 100% in late March each year to below 10% by 20 May of each year except 1989, when they remained at 11% until 12 June. Such variations in the number of new recruits and the number of larger fish leaving the nearshore juvenile pink salmon population resulted in a bias for growth rate calculations from untagged populations. Tagged fish provided a more realistic assessment of growth in relation to the environment.

Factors limiting growth

Fish growth can be limited by low water temperatures (Weatherley and Gill, 1995) and low prey abundance (Brant et al., 1992). To determine when growth

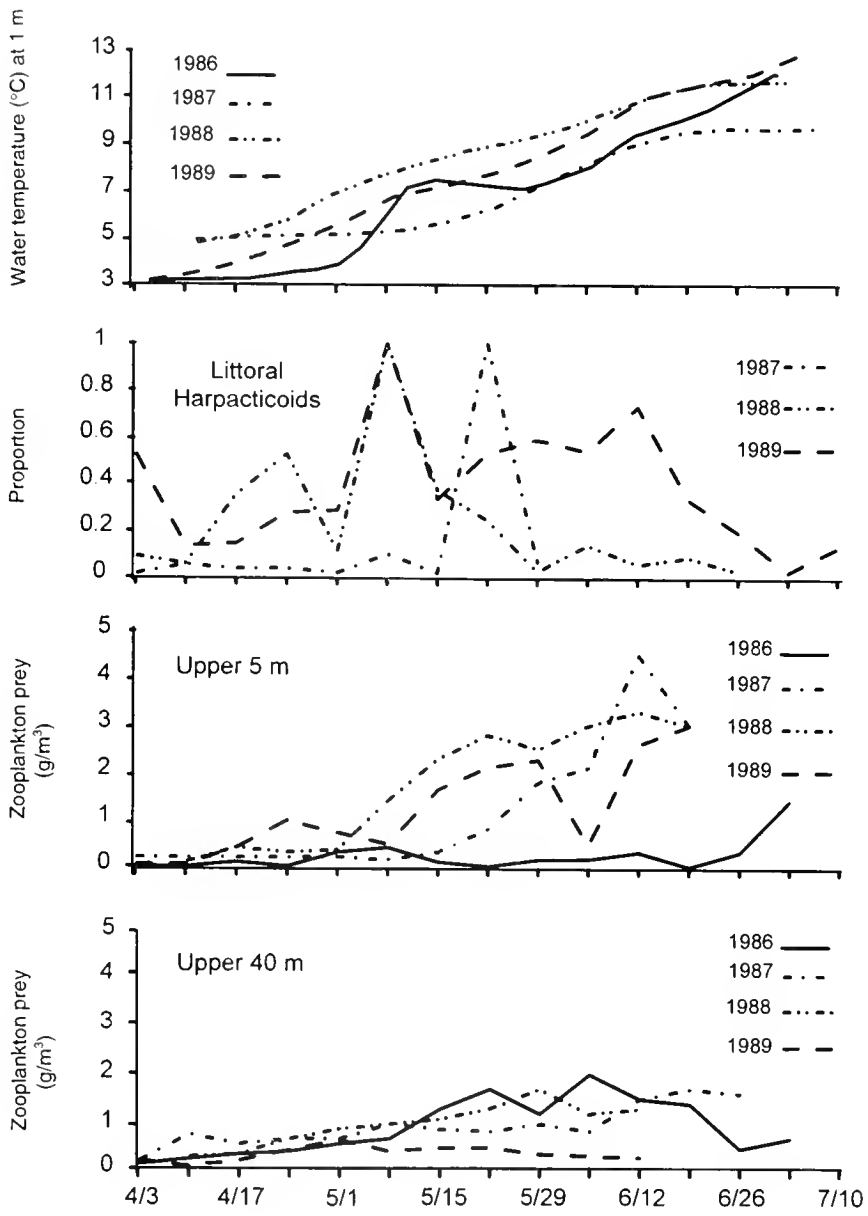

Figure 5

Water temperature, biomass of zooplankton and harpacticoid copepod prey of juvenile pink salmon from the epibenthos, upper 5 m, and 40 m of Auke Bay, Alaska. Owing to differences in collection technique between years, the values depicted for littoral harpacticoids are expressed as a proportion of the highest biomass within each year. Littoral harpacticoids were not collected in 1986. Zooplankton data for the upper 5 m and 40 m were taken from Coyle and Paul (1990).

of juvenile pink salmon might be restrained by prey abundance, the observed growth of each tagged fish was compared to maximum expected growth at similar water temperatures. In all years, the residuals between observed and expected growth (observed–expected) had significant positive slopes (Fig. 7), indicating that a higher proportion of early emigrants (rearing in relatively cool water) were below expected growth rates compared with fish at higher water temperatures (later emigrants). If abundance of prey is not growth-limiting, the growth rate of juvenile pink salmon at 5°C water temperature in

Table 2

Growth rate (as percent body weight per day [% bwd]), of tagged and untagged juvenile pink salmon caught in Auke Bay in early and late growth periods (1 April–6 May and 7 May–16 June). Growth of tagged juveniles was calculated between release and recapture within the early period and the number of days from the end of the early period to recapture within the late period. To calculate the rate of growth of tagged fish, the average weight of the fish from release to recapture within the early period was used, whereas in the late period the estimated weight of fish at the end of the early period and at the date of recapture within the late period was used. The growth of untagged fish was calculated similarly, except that the number of days from the beginning to the end of a specific growth period was used. The standard deviation (SD), coefficient of determination (r^2), and sample size (n) are also shown.

Growth period	Tagged	Growth rate (% bwd)	SD	r^2	n	Growth period	Tagged	Growth rate (% bwd)	SD	r^2	n
1986						1988					
Early	tagged	2.93	0.237	0.84	76	Early	tagged	2.95	0.208	0.62	134
	untagged	1.41	0.213	0.71	422		untagged	1.51	0.398	0.50	2019
Late	tagged	4.82	0.221	0.83	23	Late	tagged	6.66	0.274	0.60	32
	untagged	3.21	0.391	0.65	955		untagged	4.86	0.341	0.42	2535
1987						1989					
Early	tagged	3.14	0.203	0.78	101	Early	tagged	4.88	0.287	0.44	173
	untagged	1.21	0.333	0.62	569		untagged	2.10	0.335	0.36	462
Late	tagged	5.40	0.173	0.94	31	Late	tagged	5.40	0.202	0.82	58
	untagged	4.34	0.433	0.77	1658		untagged	2.87	0.387	0.36	1030

early April should be about 2.0% or more (Mortensen and Savikko, 1993). Examination of growth residuals from tagged juveniles in relation to those at "maximum" feeding levels, indicates that fish in early April tended to have lower than expected growth rates, up to 2% lower depending upon the year. The slope of the residuals was lowest in 1988, when a higher proportion of the observations fell below the zero line throughout the temperature range observed.

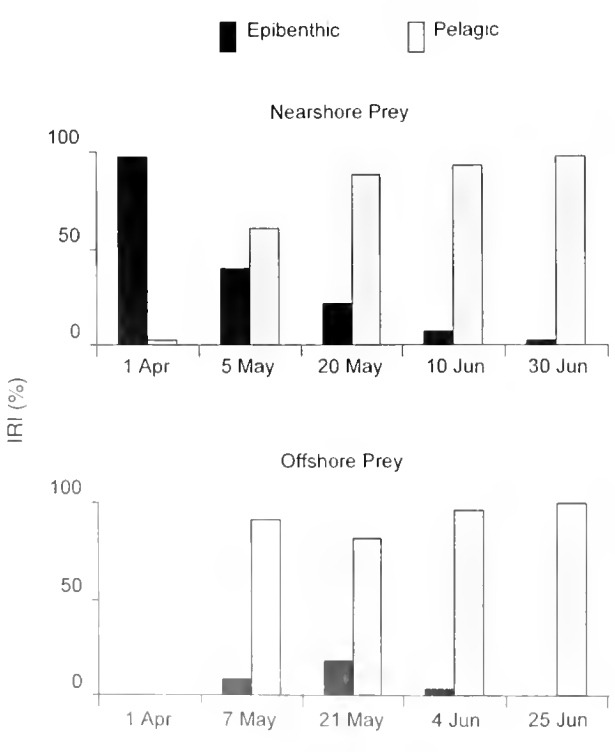

Figure 6

Index of relative importance (IRI) of pink salmon prey during residence in the nearshore and offshore areas of Auke Bay, Alaska.

Intra-annual growth of tagged pink salmon

Growth of tagged juvenile pink salmon generally increased each year with successive release dates, reaching a maximum in late April, and then declining for later emigrants (Table 1). Recovery year is specified in the following sections, and brood year (BY) is given in parentheses. In our study, brood year corresponded to the spawning year of the parental generation and was always the year prior to the year when the sample was taken. Growth of weekly release groups varied from a low of 3.38% bwd in 1986 (1985 BY) to a high of 6.39% in 1988 (1987 BY). The decline in growth of emigrants from late releases was not observed in 1987 (1986 BY) and 1988 (1987 BY), when emigration ended before the end of April. In 1986 (1985 BY), the lowest growth rates were observed for the latest fish emigrating in the first week of May. In 1989 (1988 BY), the lowest growth rates were also observed for the last emigrants. However, these fish emigrated in the second week in May; fish emigrating in the first week in May in 1989 (1988 BY) had growth rates similar to those at the midpoint of the emigration timing.

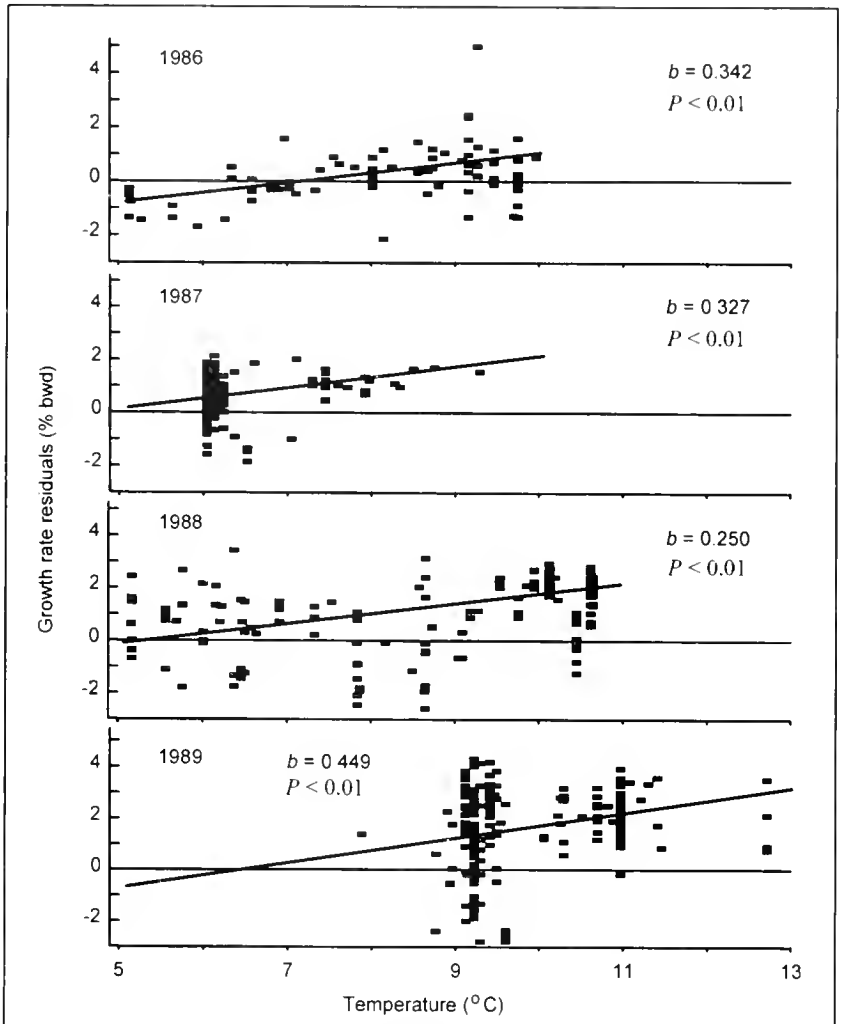

Figure 7

Residuals between the observed growth rate of tagged juvenile pink salmon and expected growth rate of juvenile pink salmon fed excess ration. Year shown refers to recovery year.

Interannual growth of tagged pink salmon

The growth rates of juvenile pink salmon from individual release groups varied substantially between years (Table 1). All release groups of juvenile pink salmon in recovery year 1986 (1985 BY) grew significantly slower than those of juveniles in subsequent years. In 1987 (1986 BY) and 1988 (1987 BY), the only years when tagged juveniles from the 1 April group were recovered, growth was not significantly different. Similarly the growth of juveniles from the 7 April groups were not significantly different between years. Juvenile pink salmon from the 15 April and 22 April releases grew significantly slower in 1987(1986 BY) than in 1988 (1987 BY) or 1989 (1988 BY), by nearly 1%. Growth was significantly slower (about 0.5% bwd) for the 22 April release group in 1989 (1988 BY) than in 1988 (1987 BY). The juveniles from the 29 April release grew significantly faster (0.3% bwd) in 1988 (1987 BY) than in 1989 (1988 BY).

Growth in relation to water temperature and prey biomass

Water temperature was the only environmental parameter measured that was significantly correlated with growth rate over all years (Table 3). Both simple and partial correlations were significant (<0.05) in each year for water temperature, and in every year except 1988, temperature explained the most variation in the parameters tested.

Table 3

Simple and partial (S/P) correlation coefficients between the instantaneous growth rate of juvenile pink salmon and average water temperature; average harpacticoid biomass; average biomass of prey integrated from 40 m to surface; average biomass of prey in the upper 5 m; and average biomass of harpacticoids + prey from the integrated water column. An * indicates a significant ($P<0.05$) correlation. NA = not available.

Year	Average water temperature	Average harpacticoid biomass	Average integrated column biomass	Average biomass in upper 5 m
1986	0.696*/0.696*	NA	0.630*/0.187*	–0.187/-0.046
1987	0.312*/0.312*	–0.201*/-0.017*	0.193/0.248	0.228/0.046
1988	0.423*/0.047*	0.337/0.000	0.505*/0.505*	0.472/0.228
1989	0.354*/0.354*	–0.226*/-0.118*	0.057/0.003	0.254/0.128*

The 5-m depth zooplankton biomass was not significantly related to growth in any year, whereas biomass from the 40-m integrated water column was significantly correlated in two of the four years. In 1988, the biomass from the 40-m integrated water column was the parameter most correlated with growth.

The biomass of littoral harpacticoids was significantly correlated with juvenile pink salmon growth for two of the three years for which data were available. In both cases, the relationship was negative (Table 3). Because feeding habits showed that the pink salmon were switching between epibenthic and zooplankton resources during the nearshore phase, growth rate was also correlated with a combined index of the biomass of littoral harpacticoids and the 40-m depth zooplankton. This combined index did not fit the growth data as well as either water temperature or zooplankton biomass considered independently (Table 3).

Growth and survival

Mid- to late April emigrants had significantly higher survival than the earliest emigrants within a year (Table 1). Brood year is specified in the following paragraphs unless otherwise noted. When emigration extended into May (1985 and 1988 brood years), survival decreased by as much as 2% from the groups released from mid- to late April. The last emigrants from both the 1985 and 1988 broods, which had the lowest growth rates of those years, also had significantly lower survival than emigrants from mid- to late April.

The intra-annual survival of cwt juvenile pink salmon exhibited a pattern similar to that for growth rates. Regression of growth rate against survival (as proportions within each year) indicated a highly significant relationship (r^2=0.65, $P<0.003$; Fig. 8). Within-year survival generally increased with growth rate.

To examine the relation between growth and survival interannually, growth rate (%bwd) was regressed against survival rate of each release group. Although survival appears to increase with increasing growth rate, there was no relationship when all years were considered (r^2=0.02, $P>0.397$). Fish from the 1987 brood year (1988 emigrants, 1989 adults) had a distinctly different growth versus survival trajectory than fish for other years (Fig. 9). Data from brood years 1985, 1986, and 1988 fitted well (r^2=0.88, slope=1.82, P=0.001). Survivals of the 1987 brood were also significantly related to growth when considered separately from the other years (r^2=0.93, slope=0.40, P=0.001).

Discussion

Pink salmon juveniles were abundant in the nearshore areas of Auke Bay in April and May; by the end of May or early June, the fish had moved farther offshore. This pattern is typical for juvenile pink salmon, which generally follow shorelines during their first weeks in the marine environment, then migrate offshore as they grow (Heard, 1991; Celewycz and Wertheimer, 1996a).We found water temperature to be the main factor that determined the growth rate of juvenile pink salmon during their early marine existence. The metabolism and growth of fish are influenced extensively by water temperature and prey density (Brett et al., 1969; Weatherley and Gill, 1995). To attain maximum growth at a particular temperature, prey concentrations must be adequate (Bailey et al., 1975; Cooney et al., 1981). In our study there were indications in early spring of each year that the growth of juvenile pink salmon was limited by abundance of prey. These early fish enter the Auke Bay estuary before the spring zooplankton bloom and rely on overwintering epibenthic prey organisms such as harpacticoid copepods.

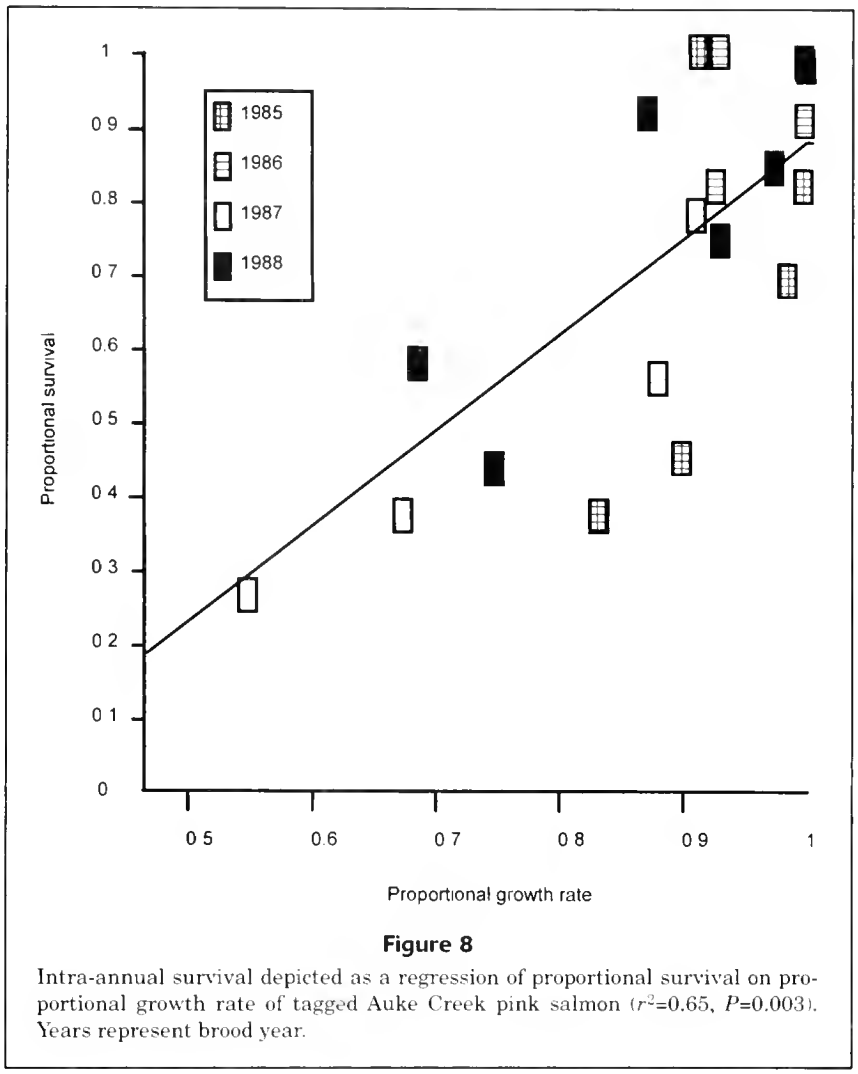

Figure 8

Intra-annual survival depicted as a regression of proportional survival on proportional growth rate of tagged Auke Creek pink salmon (r^2=0.65, P=0.003). Years represent brood year.

The relatively sparse population of potential predators in early spring allow a portion of the juveniles to survive the period of low growth. Growth was strongly related to adult survival within each of the study years; however, this relationship did not hold true between years.

Growth of fish in the tag groups over all recovery years ranged from 3.4% (8 May 1986 release) to 6.4% (29 April 1988 release). These rates are within the 1.5–7.6% range of growth rates previously reported for pink salmon during their initial marine residency (LeBrasseur and Parker, 1964; Healey, 1980). Willette (1996) also observed growth rates of 3.5–5.2% for cwt pink salmon in Prince William Sound.

Variations in the feeding activity of salmonids is characteristic of opportunistic and broad-spectrum predators, which optimize their food consumption in response to prey density (Parker and Vanstone, 1966; Parker, 1969; Ware, 1972; Hunter and Thomas, 1974; Godin, 1981). Both epibenthic crustaceans and zooplankton were important components of the prey of juvenile pink salmon during their nearshore residence in Auke Bay. In previous studies, harpacticoid copepods, among other epibenthic organisms, have been reported as the primary prey of pink salmon juveniles in nearshore marine habitats (Healey, 1980; Godin, 1981; Landingham, 1982; Webb, 1991). In Alaska waters, however, planktonic prey often predominate in the early diet of pink salmon (Bailey et al., 1975; Cooney et al., 1981; Sturdevant et al., 1996; Willette, 1996). Some of these differences are due to the types of beaches where juvenile pink salmon are sampled. In studies where harpacticoid copepods are the primary dietary component, the fish are sampled at low-gradient beaches with substantial epibenthic production (e.g. Kaczynski et al., 1973; Godin, 1981; Webb, 1991). Sturdevant et al. (1996) also found that a higher proportion of epibenthic prey was consumed by juvenile pink salmon captured on lower-gradient than on steep-gradient beaches. In Auke

Bay, pink salmon samples for diet analysis were taken from low-gradient beaches where there is a high production of epibenthic harpacticoid copepods (Landingham, 1982; Cordell, 1986). However, even at this habitat type, pelagic zooplankton was an important dietary component. Similarly, Sturdevant et al. (1996) found zooplankton to be the dominant dietary component of pink salmon juveniles from all nearshore habitat types sampled in Prince William Sound, Alaska.

From a bioenergetics standpoint, prey density and water temperature are critical factors affecting fish growth by influencing consumption rate, metabolic rate, and gastric evacuation rate (Willette, 1996). Temperature was significantly correlated with observed growth of juvenile pink salmon, but indices of prey abundance were not consistently correlated with growth and were even inversely related in the case of harpacticoid copepods. This lack of correlation may be due to the typically high and variable productivity of zooplankton and littoral epibenthos found in subarctic ecosystems such as Auke Bay (Cordell, 1986; Coyle and Paul, 1990). Assuming there is some threshold level of prey density required to sustain maximum growth of juveniles, then the pronounced spikes in biomass of prey populations associated with the spring bloom would mean that much of the variability in prey occurs above the density threshold, thereby masking a relationship between prey biomass and juvenile pink salmon growth. Any such relationship should occur primarily before or after the prey population peaks. Analysis of residuals between expected growth of pink salmon and observed initial growth indicated that food abundance did limit growth at low water temperatures, (i.e. growth rates observed in the early period of nearshore residency were possibly constrained by food availability as well as lower temperatures (Fig. 7).

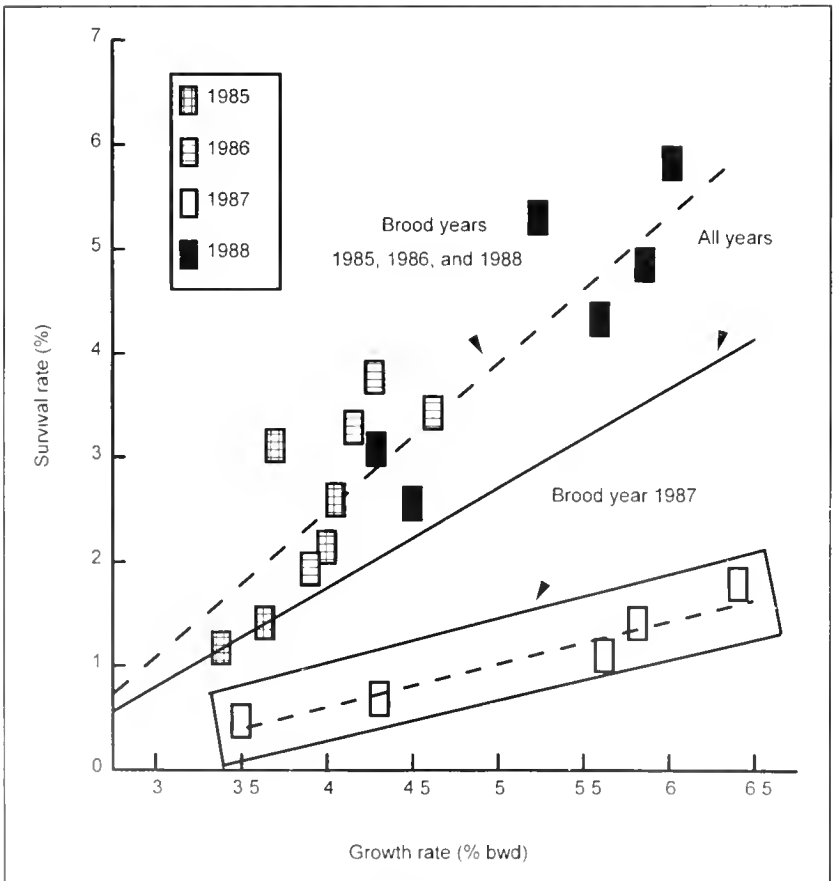

Figure 9

Interannual survival depicted as the regression of survival (adjusted for catch rate) versus growth rate of tagged Auke Creek pink salmon. When all four brood years are included in the regression, a poor relationship results (r^2=0.02, P=0.397). However, when brood year 1987 is excluded from the regression, the relationship between survival and growth rate improves (r^2=0.88, P=0.001). This relationship is also very good when based on data from just brood year 1987 (r^2=0.93, P=0.001).

The emigration of Auke Creek pink salmon extended from late March to mid-May; most of the fish emigrated within 2–3 weeks in mid- to late April. Holtby et al. (1989) proposed that the synchronous timing of emigration of chum salmon may be an adaptive feature based upon advantageous growth conditions in the estuarine environments, with synchrony acting as a mechanism to saturate predators and enhance survival. By this premise, it would be beneficial for all Auke Creek juveniles to emigrate together, later in the spring, within a narrow time window, so as to ensure optimum growth conditions. Each year, however, a portion of the Auke Creek pink salmon juveniles emigrate in early spring and they consistently encounter poor growth conditions. Water temperatures are usually 4 C, and zooplankton abundance is very low. These juveniles take longer to reach a particular size than do later emigrants and generally reside longer in estuarine nursery areas than the later, faster-growing emigrants (Table 1). Even though predator populations are relatively low in early spring, the early emigrants are exposed to predation over a longer period than are later

emigrants. Despite spending more time in low-growth conditions, they will have the advantage of being larger at a given date than subsequent, faster-growing emigrants (Fig. 10). Thus, there is an adaptive advantage in lessening size-selective predation by being on the "leading edge" of the synchronous emigration to marine waters. However, this advantage is constrained by poorer growth early in the spring and poorer survival to adulthood.

The abundance of potential predators (coho salmon, Dolly Varden, and sculpins) near shore increases rapidly in May, emphasizing the importance of larger size and larger numbers for pink salmon to avoid predation. Late emigrants, although encountering what appear to be good conditions for growth, may not be able to effectively outgrow increasing predation pressure or may not be abundant enough to saturate the predator population. Other factors may combine to affect the growth and ultimately the survival of the late emigrants. The abundance of competitors such as young-of-the-year and juvenile herring and capelin may affect the availability of prey at critical times and could explain the lower growth rates observed for late-emerging pink salmon.

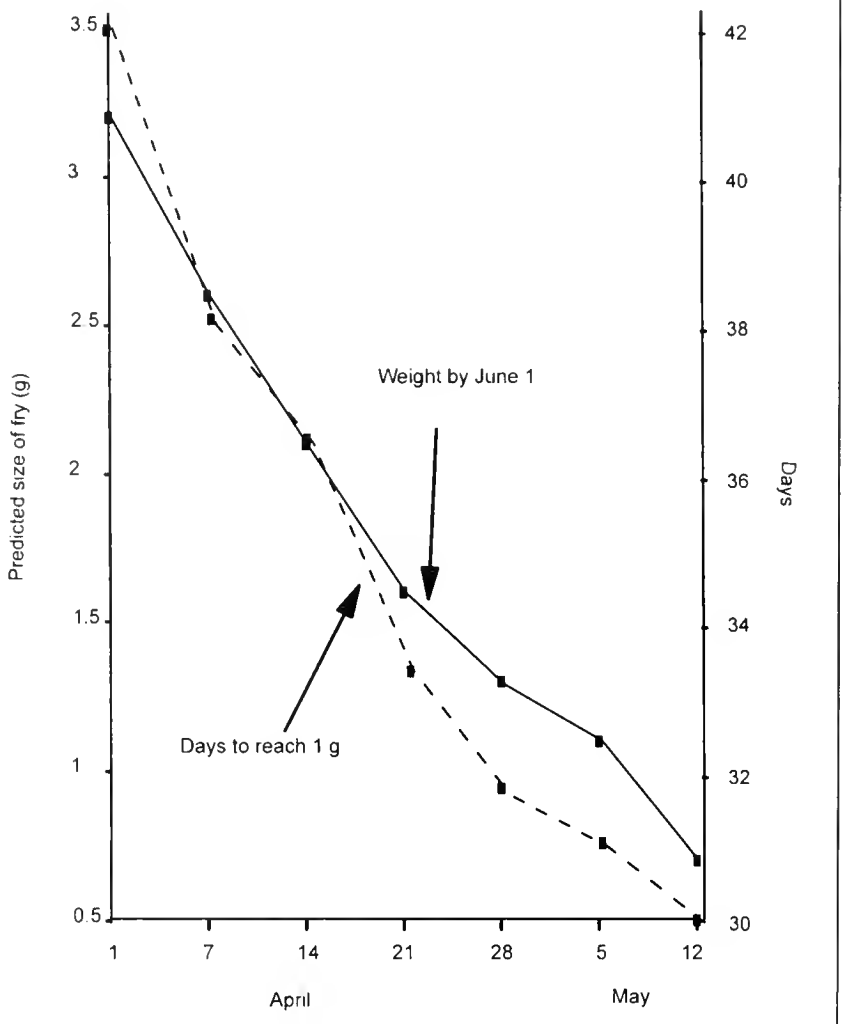

Figure 10

The predicted size of pink salmon fry by 1 June and the number of days to reach 1 g for emigration dates between 1 April and 12 May.

Growth rate of pink salmon juveniles in Auke Bay was consistently related to survival within a given year. This finding is consistent with the concept that high growth rates during early marine residency give a survival advantage by minimizing the intensity of predation (Parker, 1971; Heard, 1991). Following the *Exxon Valdez* oil spill in Prince William Sound in 1989, Willette (1996) found a direct relationship between growth and survival of pink salmon juveniles. However, he did not observe this association for juveniles captured in 1990 or 1991 and speculated that changes in the feeding habits of predators due to the absence of alternate prey obscured the relationship between growth and survival. Correlations of parameters for scale growth rates with run size of pink salmon in northern southeastern Alaska indicated that nearshore growth conditions are a significant contributor to the interannual variation in marine survival. Early scale growth (Jaenicke et al., 1994) was positively correlated with survival, indicating that high early marine growth lessens mortality due to predation. In our study, for three of the four years, growth rate was an excellent predictor of survival interannually, explaining 85% of the observed variability. The anomalous year was 1988 (1987 brood), which was also the year of highest overall growth rates. Fish from all release groups of the 1987 brood returned to the weir at consistently lower rates than fish from the other brood years. Fishery exploitation on returning adults may be a factor. We corrected the rate of survival each year for those fish taken in the commercial fishery with the correction factor used by the Alaska Department of Fish and Game; however, the correction factor was relatively crude with no measure of variance. It is conceiv-

able that fishery exploitation could still have affected the growth and survival relationship. Changes in nearshore predation or conditions (both environmental and biological) after the fish had moved offshore could also have been the cause. Although we noted no unusually high concentrations of piscivorous sea birds or marine mammals in the Auke Bay area in the spring of 1987, that observation does not preclude the possibility that larger than normal populations of predators may have caused significant mortality on the juveniles beyond our study area of Auke Bay. Identification of the elements causing such anomalous years would provide insight into how these factors interact with growth conditions to drive interannual variation.

Acknowledgments

We thank our colleagues at the Auke Bay Laboratory who participated in this project. We are particularly indebted to Joe Orsi, Adrian Celewycz, Molly Sturdevant, Herbert Jaenicke, and Judy Lum. Without their unfailing dedication, expertise, and excellent attitudes this project would not have been as successful or enjoyable. Additionally, we extend our appreciation to Mark Carls, Jon Heifetz, and John Joyce who provided in-house reviews of this manuscript.

Literature cited

Bailey J. E.
1969. Alaska's fishery resources—the pink salmon. U. S. Fish and Wildlife Serv., Bur. of Comm. Fish. Leaflet 619.

Bailey, J. E., B. L. Wing, and C. R. Mattson.
1975. Zooplankton abundance and feeding habits of fry of pink salmon, *Oncorhynchus gorbuscha*, and chum salmon, *Oncorhynchus keta*, in Traitor's Cove, Alaska, with speculations on the carrying capacity of the area. Fish. Bull. 73:846–861.

Bax, N. J.
1983. Early marine mortality of marked juvenile chum salmon (*Oncorhynchus keta*) released into Hood Canal, Puget Sound, Washington, in 1980. Can. J. Fish. Aquat. Sci. 40:426–435.

Brant, S. B., D. M. Mason, and E. V. Patrick.
1992. Spatially-explicit models of fish growth rate. Fisheries 17(2):23–33.

Brett, J. R., J. E. Shelbourn, and C. T. Shoop.
1969. Growth rate and body composition of fingerling sockeye salmon, *Oncorhynchus nerka*, in relation to temperature and ration size. J. Fish. Res. Board Can. 26:2363–2394

Celewycz, A. C., and A. C. Wertheimer.
1996a. Abundance and growth of juvenile pink salmon in oiled and non-oiled locations of western Prince William Sound after the *Exxon Valdez* oil spill. Am. Fish. Soc. Symp. 18:518–532.
1996b. Prey availability to juvenile salmon after the *Exxon Valdez* oil spill. Am. Fish. Soc. Symp. 18:564–577.

Cooney, R. T., D. Urquhart, and D. Barnard.
1981. The behavior, feeding biology and growth of hatchery-released pink and chum salmon fry in Prince William Sound, Alaska. Univ. Alaska, Sea Grant Report 81-5, 114 p.

Cordell, J. R.
1986. Structure and dynamics of an epibenthic harpacticoid assemblage and the role of predation by juvenile salmon. M.S. thesis, Univ. Washington, Seattle, WA, 134 p.

Coyle, K. O., and A. J. Paul.
1990. Interannual variations in zooplankton population and biomass during the spring bloom in an Alaskan subarctic embayment. *In* APPRISE—Interannual variability and fisheries recruitment (D. A. Ziemann and K. W. Fulton-Bennett, eds.), p. 179–228. The Oceanic Institute, Honolulu, HI, and The School of Fisheries and Ocean Sciences, Fairbanks, AK.

Cushing, D. H.
1976. Biology of fishes in the pelagic community. *In* The ecology of the seas (D. H. Cushing and J. J. Walsh, eds.), p. 317–340. W. B. Saunders Co., Philadelphia.

D'Amours, D.
1987. Trophic phasing of juvenile chum salmon (*Oncorhynchus keta* Walbaum) and harpacticoid copepods in the Fraser River estuary, British Columbia. Ph.D. diss., Univ. British Columbia, Canada, 163 p.

Godin, J.-G. J.
1981. Effects of hunger on the daily pattern of feeding rate in juvenile pink salmon (*Oncorhynchus gorbuscha* Walbaum). J. Fish. Biol. 19:63–71.

Goering, J. J., W. E. Shiels, and C. J. Patton.
1973. Primary production. *In* Environmental studies of Port Valdez (D. W. Hood, W. E. Shiels, and E. J. Kelley, eds.), p. 253–279. Univ. Alaska, Fairbanks, Inst. Mar. Sci. Occas. Publ. 3.

Hargreaves, N. B., and R. J. LeBrasseur.
1985. Species selective predation on juvenile pink (*Oncorhynchus gorbuscha*) and chum (*O. keta*) by coho salmon (*O. kisutch*). Can. J. Fish. Aquat. Sci. 42:659–668.

Healey, M. C.
1980. The ecology of juvenile salmon in Georgia Strait, British Columbia. *In* Salmonid ecosystems of the North Pacific (W. J. McNeil and D. C. Himsworth, eds.), p. 203–229. Oregon State Univ. Press, Corvallis, OR.

Heard, W. R.
1991. Life history of pink salmon (*Oncorhynchus gorbuscha*). *In* Pacific salmon life histories (C. Groot and L. Margolis, eds.), p. 119–230. Univ. British Columbia Press, Vancouver, Canada.

Holtby, L. B., T. E. McMahon, and J. C. Scrivener.
1989. Stream temperatures and inter-annual variability in the emigration timing of coho salmon (*Oncorhynchus kisutch*) smolts and fry and chum salmon (*O. keta*) fry from Carnation Creek, British Columbia. Can. J. Fish. Aquat. Sci. 46:1396–1405.

Hunter, J. R., and G. L. Thomas.
1974. Effect of prey distribution and density on the searching and feeding behaviour of larval anchovy *Engraulis mordax*. *In* The early life history of fish (J. S. H. Blaxter, ed.), p. 559–574. Springer-Verlag, New York, NY.

Jaenicke, H. W., M. J. Jaenicke, and G. T. Oliver.
1994. Predicting northern southeast Alaska pink salmon returns by early marine scale growth. *In* Proceedings of the 16th Northeast Pacific Pink and Chum Salmon Workshop, p. 97–109. Alaska Sea Grant College Program Report 94-02.

Kaczynski, V. W., R. J. Feller, and J. Clayton.
1973. Trophic analysis of juvenile pink and chum salmon (*Oncorhynchus gorbuscha* and *O. keta*), in Puget Sound. J. Fish. Res. Board Can. 30:1003–1008.

Landingham, J. H.
1982. Feeding ecology of pink and chum salmon fry in the nearshore habitat of Auke Bay, Alaska. M.S. thesis, Univ. Alaska, Juneau, AK, 132 p.

Larrance, J. D.
1971. Primary production in the mid-subarctic Pacific region 1966–68. Fish. Bull. 69:595–613.

LeBrasseur, R. J., and R. R. Parker.
1964. Growth rate of central British Columbia pink salmon (*Oncorhynchus gorbuscha*). J. Fish. Res. Board Can. 21:1101–1128.

Morrow, J. E.
1980. The freshwater fishes of Alaska. Alaska Northwest Publishing Company, Anchorage, AK, 248 p.

Mortensen, D. G., and H. Savikko.
1993. Effects of water temperature on growth of juvenile pink salmon (*Oncorhynchus gorbuscha*). U.S. Dep. Commer., NOAA Tech. Memo. NMFS-AFSC-28, 12 p.

Murphy, M. L., J. F. Thedinga, and K V. Koski.
1988. Size and diet of juvenile Pacific salmon during seaward migration through a small estuary in southeastern Alaska. Fish. Bull. 86:213–222.

Nichelson, T. E.
1986. Influences of upwelling, ocean temperature, and smolt abundance on marine survival of coho salmon (*Oncorhynchus kisutch*) in the Oregon production area. Can. J. Fish. Aquat. Sci. 43:527–535.

Parker, R. R.
1968. Marine mortality schedules of pink salmon of the Bella Coola River, central British Columbia. J. Fish. Res. Board Can. 25:757–794.
1969. Foods and feeding of juvenile pink salmon in central British Columbia waters. I. 1966 diel series. Fish. Res. Board Can. Manuscr. Rep. Ser. 1017, no pages given.
1971. Size selective predation among juvenile salmonid fishes in a British Columbia inlet. J. Fish. Res. Board Can. 28:1503–1510.

Parker R. R., and W. E. Vanstone.
1966. Changes in chemical composition of central British Columbia pink salmon during early sea life. J. Fish. Res. Board Can. 23:1353–1384.

Pinkas, L., M. S. Oliphant, and I. L. K. Iverson.
1971. Food habits of albacore, bluefin tuna, and bonito in California waters. California Dep. Fish and Game, Fish. Bull. 152, 64 p.

Pitcher, T. J., and P. J. B. Hart.
1982. Fisheries ecology. AVI Publishing Co., Westport, CT, 414 p.

Russell-Hunter, W. D.
1970. Aquatic productivity. Macmillan Co., New York, NY, 306 p.

Sturdevant, M. V., A. C. Wertheimer, and J. L. Lum.
1996. Diets of juvenile pink and chum salmon in oiled and non-oiled nearshore habitats in Prince William Sound, 1989 and 1990. Am. Fish. Soc. Symp. 18:578–592.

Taylor, S. G.
1980. Marine survival of pink salmon fry from early and late spawners. Trans. Am. Fish. Soc. 109:79–82.

Walters, C. J., R. Hilborn, R. M. Peterman, and M. J. Staley.
1978. Model for examining early ocean limitation of Pacific salmon production. J. Fish. Res. Board Can. 35:1303–1315.

Ware, D. M.
1972. Predation by rainbow trout (*Salmo gairdneri*): the influence of hunger, prey density, and prey size. J. Fish. Res. Board Can. 29:1193–1201.

Weatherley, A. H., and H. S. Gill.
1995. Growth. *In* Physiological ecology of Pacific salmon (C. Groot, L. Margolis, and W. C. Clarke, eds.), p. 101–158. Univ. British Columbia Press, Vancouver, Canada.

Webb, D. G.
1991. Effect of predation by juvenile Pacific salmon on marine harpacticoid copepods. I. Comparisons of patterns of copepod mortality with patterns of salmon consumption. Mar. Ecol. Progr. Ser. 72:25–36.

Willette, M.
1996. Impacts of the *Exxon Valdez* oil spill on the migration, growth, and survival of juvenile pink salmon in Prince William Sound. Am. Fish. Soc. Symp. 18:533–550.

Wing, B. L., and J. J. Pella
1998. Time series analysis of climatological records from Auke Bay, Alaska. U.S. Dep. Commer., NOAA Tech. Memo. NMFS-AFSC-91, 90 p.

Zar, J. H.
1974. Biostatistical analysis. Prentice-Hall, Inc., Englewood Cliffs, NJ, 620 p.

Genetic structure of tautog (*Tautoga onitis*) populations assayed by RFLP and DGGE analysis of mitochondrial and nuclear genes

Elizabeth A. Orbacz
Patrick M. Gaffney
College of Marine Studies
University of Delaware
Lewes, Delaware 19958
E-mail address (for P. M. Gaffney, contact author) pgaffney@udel.edu

Abstract.—The tautog (*Tautoga onitis*) is one of two temperate labrid species commonly inhabiting the coastal marine and estuarine waters of the mid-Atlantic coast of the United States. To delineate population structure throughout its primary range, we examined samples collected from three sites (Rhode Island, Delaware, Virginia). Five regions of the mitochondrial genome (COI, ATPase 6, cyt *b*, ND2 and control region) and one nuclear intron were amplified by PCR and screened for sequence variation with a battery of restriction enzymes (RFLP analysis), or by denaturing gradient gel electrophoresis (DGGE).

With RFLP analysis an average of 129 restriction sites per individual were revealed and 532 bases per individual were surveyed. Polymorphisms were observed in the ND2 and control region fragments, but not in the COI, ATPase 6, or cyt *b* fragments. Mean within-sample haplotype diversity was 0.6905 (±0.00184), within the range of values reported for other marine species. However, mean nucleotide diversity was 0.000782, one of the lowest values reported for a marine teleost. Corrected nucleotide divergence between samples was essentially zero, suggesting the absence of population structuring along the mid-Atlantic Coast. DGGE analyses of COI, cyt *b*, and a lactate dehydrogenase (LDH) intron revealed little additional variation; each product possessed a single common haplotype and occasional rare variants.

The low level of genetic diversity observed in the tautog may reflect a small effective population size resulting from historical population bottlenecks or large variance in reproductive success. The apparent absence of geographic differentiation suggests that tautog from Rhode Island to Virginia form a single genetic stock; data from additional genetic polymorphisms are needed to confirm or disprove this conclusion.

Manuscript accepted 27 September 1999
Fish. Bull. 98:336–344 (2000).

The tautog (*Tautoga onitis*) is one of two temperate labrid species commonly inhabiting the coastal marine and estuarine waters of the mid-Atlantic coast of the United States. Although the species range extends from the outer coast of Nova Scotia to Georgia, tautog are most abundant from Cape Cod to Chesapeake Bay (Bigelow and Schroeder, 1953). They are generally found in high relief, reeflike habitats such as those associated with jetties, breakwaters, and wrecks (Auster, 1989).

In the northern part of the their range, adult tautog generally overwinter in a state of torpor in sheltered areas in deep water offshore and move inshore during the spring to spawn in estuaries and nearshore waters (Cooper, 1966; Olla et al., 1974). Some tautog remain offshore throughout the year, particularly in the southern part of their range (Olla and Samet, 1977; Eklund and Targett, 1991). Those that migrate offshore do not always return to the same sites to overwinter (Olla et al., 1979). Juveniles and some adults have been found to overwinter at inshore sites off Virginia (Hostetter and Munroe, 1993) and Delaware (Eklund and Targett, 1991). In a tagging study, Cooper (1966) found that adult tautog tagged in Narragansett Bay tended to return to the same spawning site each year, and adult movement into and out of the area was negligible. In general, tautog do not appear to undergo extensive along-coast migration (Cooper, 1966; Olla et al., 1974; Briggs, 1977).

Tautog spawn between mid-May and mid-August; spawning activity peaks in June (Colton et al., 1979). Eggs are buoyant and generally confined to coastal waters. Hatching occurs in 42–45 hours at 20–22°C, and pelagic larval duration is approximately 20–30 days (Victor, 1986). Although spawning occurs primarily in estuaries, offshore spawning has been reported (Eklund and Targett, 1990; Hostetter and Munroe, 1993).

Tautog support important recreational and small commercial fisheries throughout their range. After peaking in 1986, annual harvests have declined, and the species is believed to be overexploited, particularly in the northern part of its range, between New York and Massachusetts.[1]

Despite the economic importance of tautog, little information is available regarding stock structure of the species. Tagging studies suggest that there is little mixing of adult fish between geographical regions (Cooper, 1966; Briggs, 1977). Hostetter and Monroe (1993) reported latitudinal variation in size-at-age; fish from Virginia were found to grow

[1] Atlantic States Marine Fisheries Commission. 1996. Fishery management plan for tautog, April 1996. Fishery Management Report 25 of the Atlantic States Marine Fisheries Commission. 1444 Eye Street, N.W., 6th Floor, Washington D.C. 20005.

Table 1

List of primer sequences used in polymerase chain reaction amplifications for RFLP and DGGE-heteroduplex analyses. All sequences are in 5′→3′ orientation. Approximate size of product includes primers.

Primer	Sequence	Region	Reference
CO1a-H	AGTATAAGCGTCTGGGTAGTC	cytochrome oxidase subunit 1 (≈680 bp)	Palumbi et al., 1991
CO1f-L	CCTGCAGGAGGAGGAGAYCC		
CB2-H	CCCTCAGAATGATATTTGTCCTCA	cytochrome *b* (≈380 bp)	Palumbi et al., 1991
CB1-L	CCATCCAACATCTCAGCATGATGAAA		
t-Met	AAGCTATCGGCCCCATACCC	NADH dehydrogenase subunit 2 (≈1270 bp)	Park et al., 1993
c-Trp	CTGAGGGCTTTGAAGGCCC		
12SAR-H	ATAGTGGGGTATCTAATCCCAGTT	control region (≈1250 bp)	Palumbi et al., 1991
L15995	AACTCTCACCCCTAGCTCCCAAAG		Meyer et al., 1994
ATPase6-F	ATAAATAGGCTAATTGTTTCG	ATP synthase 6 (≈680 bp)	Quattro[1]
ATPase6-R	AAGCACTACGGTTTTAAGC		
LDHA6F1	TACACTTCCTGGGCSATYGGBATG	LDH A intron 6 (≈240 bp)	Quattro and Jones, 1999
LDHA6R	CGCTSAGGAASACCTCRTCCTTCAC		

[1] Courtesy of J. Quattro, Department of Biological Sciences, University of South Carolina, Columbia, SC 29208.

more than twice as fast as fish from Rhode Island during their first year of life. However, in a common-garden experiment with fish from Rhode Island, Delaware, and Virginia, Martin (1993) found no genetic basis for the difference in growth rates. To date, there have been no published genetic analyses of population structure in this species.

The purpose of this study was to evaluate patterns of genetic variation in tautog across the primary range of the species, by examining DNA sequence variation in several mitochondrial and nuclear genes. We used restriction fragment length polymorphism (RFLP) analysis to examine several regions of the mitochondrial genome amplified by the polymerase chain reaction (PCR). These included portions of four protein-coding genes (cytochrome *b*, cytochrome *c* oxidase subunit I, ATP synthetase subunit 6, and NADH dehydrogenase subunit 2) and a segment including the entire control region, $tRNA^{Phe}$, and part of the 12S rRNA gene. In addition, we used denaturing gradient gel electrophoresis (DGGE) heteroduplex analysis to examine a nuclear gene intron and portions of the mitochondrial cytochrome *b* and cytochrome *c* oxidase subunit I genes.

Materials and methods

Sample collection and DNA extraction

Juvenile tautog under age two were collected between 1991–1993 from three sites in the northern, middle, and southern portions of the tautog's primary range: Narragansett Bay, Rhode Island; Delaware Bay, Delaware; and Chesapeake Bay, Virginia (for details regarding collection techniques see Martin, 1993). Fish were stored at –20°C. In addition, fin clips were taken from adult fish collected from Delaware Bay in 1996.

Total DNA extracts were prepared from white muscle tissue and fin clip samples from 24 fish from each of the three sites by using a Puregene DNA isolation kit (Gentra Systems, Inc., Minneapolis, MN) following the protocol specified for animal tissue.

Polymerase chain reaction amplification of DNA

The polymerase chain reaction (PCR) was used to amplify parts of five regions of the mitochondrial genome: cytochrome *c* oxidase subunit I (COI), ATP synthetase 6 (ATPase 6), cytochrome *b* (cyt *b*), NADH dehydrogenase subunit 2 (ND2), and the control region (D-loop). In addition, intron 6 of the LDH-A gene was amplified. Amplifications were performed in a Perkin-Elmer 480 thermocycler under conditions optimized for each primer pair. Primer sequences are listed in Table 1. To create PCR products suitable for use in DGGE, primers CO1f-L, CB1-L ,and LDH849R were modified through the addition of a 15 base pair (bp) GC clamp (5′-CCCGCCGCCGCCGCC-3′) to the 5′ ends.

An approximately 680-bp portion of the COI gene was amplified with universal primers CO1a-H and CO1f-L (Palumbi et al., 1991) by using an initial

denaturation step of 2 min at 94°C followed by 35 cycles of 1 min at 95°C, 1 min at 50°C, and 1 min at 72°C, with a final step of 5 min at 72°C. Reaction volumes of 100 µL contained 1 µL of DNA extract, 2 mM $MgCl_2$, 200 µM each dNTP, 2.5 units *Taq* polymerase (Promega), and 0.17 µM of each primer. An approximately 380-bp fragment of the cyt *b* gene was amplified with universal primers CB2-H and CB1-L (Palumbi et al., 1991) by using the same protocol, except that the final primer concentrations were 0.2 µM.

An approximately 680-bp fragment of the ATPase 6 gene was amplified with primers ATPase6-F and ATPase6-R by using an initial denaturation step of 2 min at 94°C followed by 30 cycles of 45 sec at 94°C, 1 min at 52°C, and 2 min at 72°C, with a final step of 5 min at 72°C. Reagent and template concentrations were identical to those used to amplify the cyt *b* fragment. This PCR reaction protocol was also used to amplify an approximately 1270-bp fragment of ND2 with universal primers t-Met and c-Trp (Park et al., 1993) and an approximately 1455-bp fragment containing the entire control region, $tRNA^{Phe}$, as well as part of the 12S rRNA gene with universal primers L15995 (L-Pro; Meyer et al., 1994) and 12SAR-H (Palumbi et al., 1991).

An approximately 240-bp fragment of the LDH intron 6 was amplified with primers LDHA6F1 and LDHA6R (Quattro and Jones, 1999) by using an initial denaturation step of 2 min at 94°C followed by 35 cycles of 1 min at 95°C, 1 min at 52°C, and 1 min at 72°C, and a final step of 2 min at 72°C. Reaction volumes of 100 µL contained 3 µL of DNA extract, 2 mM $MgCl_2$, 200 µM each dNTP, 2.5 units *Taq* polymerase, and 0.2 µM of each primer.

Restriction endonuclease digestion of PCR products

Restriction enzyme digestions were performed as specified by the manufacturer (New England BioLabs, Inc., Beverly, MA) in 20 µl reactions containing 5 units of enzyme per reaction. Digestions were incubated for a minimum of 5 hours before being stopped with loading dye (20% Ficoll 400, 0.1 M Na_2EDTA pH 8, 1% SDS, 0.25% bromophenol blue, 0.25% orange G). The digests were run for electrophoresis on 2% agarose gels for at least 2 hours at 100 volts. Gels were stained with ethidium bromide and photographed under UV light. Fragment sizes were determined from migration distances in relation to known standards [*Bst*N I digest of pBR322 (New England Biolabs) and *Hae* III digest of pUC18 (Sigma, St. Louis, MO)] with the computer package Anagel (Mrázek and Spanova, 1992).

A subset of 24 fish, eight from each geographical region, was screened for polymorphisms in the five amplified mitochondrial DNA segments with the following 16 restriction enzymes: *Alu* I, *Aci* I, *Bsm*A I, *Bst*U I, *Dde* I, *Dpn* II, *Hae* III, *Hha* I, *Hinf* I, *Mnl* I, *Mse* I, *Msp* I, *Nla* III, *Rsa* I, *αTaq* I, and *Tsp*509 I. Restriction enzyme and mtDNA region combinations that revealed variation in the initial screening, ND2-*Hinf I* and control region-*Hae* III, were repeated for the entire sample of 72 fish, 24 from each geographic region.

Denaturing gradient gel electrophoresis

Perpendicular gradient denaturing gels were run to determine the approximate denaturing points of the COI, cyt *b*, and LDH intron PCR products. For each fragment, PCR product was mixed with an equal volume of neutral loading dye (20% sucrose; 10 mM Tris-HCl, pH 7.8; 1 mM ethylenediaminetetraacidic acid [EDTA]; 0.1% bromophenol blue) and run on 6.5% acrylamide gels (14 cm × 19 cm, 0.75 mm thick) containing a perpendicular gradient of 0 to 80% denaturant [100% denaturant was defined as 7 M urea/ 40% (v/v) formamide]. Gels were electrophoresed at 150 volts for a minimum of 5 hours in a recirculating 1 × TAE buffer bath at 60°C (CBS Scientific, Inc., Del Mar, CA). Gels were visualized with ethidium bromide staining and photographed under UV light.

The entire sample of 72 fish was screened for polymorphisms in COI, cyt *b*, and the LDH intron by means of parallel DGGE. The parallel gradient gels spanned a range of 10% denaturant on either side of the experimentally determined melting point of each region: 40% to 60% gels were used to screen COI and cyt *b*, and 20% to 40% gels to screen the LDH intron. Parallel denaturing gels were run at 150 volts under conditions identical to those used for the initial perpendicular DGGE; the running times were optimized for resolution of each region: 4 hours for the LDH intron, 5 hours for cyt *b*, and 6 hours for COI.

In addition, heteroduplex analysis was performed on each individual from each of the three regions. Heteroduplexes were formed by heating samples containing equal volumes of PCR product from two individuals to 95°C for 5 min and then incubating them at –20°C for at least 30 min. Each heteroduplex sample was allowed to thaw slowly at room temperature and was run on the appropriate gradient. To create a chain of comparison linking each individual to all of the others, the samples were sequentially combined: the first was mixed with the second, the second with the third, etc., including the last sample which was combined with the first. Pairs of samples that exhibited a single homoduplex band and no het-

Table 2

Frequencies of composite haplotypes from restriction digestion of the COI, cyt *b*, ATPase 6, ND2, and the control region amplified fragments from *T. onitis*. Restriction enzymes used for each PCR product are listed. RI = Rhode Island, DE = Delaware, VA = Virginia. All individuals had identical haplotypes for COI, cyt b, and ATPase 6 for the enzymes surveyed.

COI: *Hae* III, *Hinf* I, *Nla* III, *Dde* I, *Mnl* I, *Aci* I and *Tsp509* I

cyt *b*: *Hae* III, *Hha* I, *αTaq* I, *Nla* III, *Bst*U I, *Mse* I, *Dde* I, *Mnl* I, *Aci* I, and *Tsp*509 I

ATPase 6: *Alu* I, *Rsa* I, *Hae* III, *Hha* I, *αTaq* I, *Hinf* I, *Nla* III, *Bst*U I, *Mse* I, *Dde* I, *Mnl* I, *Aci* I, and *Tsp*509 I

ND 2:*Alu* I, *Hae* III, *Rsa* I, *Hha* I, *Msp* I, *Hinf* I, *Dpn* II, *Nla* III, *Bst*U I, *Mse* I, *Dde* I, *Mnl* I, *Aci* I and *Tsp*509 I

control region: *Alu* I, *Rsa* I, *Hae* III, *Hha* I, *αTaq* I, *Msp* I, *Hinf* I, *Dpn* II, *Nla* III, *Bst*U I, *Mse* I, *Dde* I, *Mnl* I, *Aci* I and *Tsp*509 I

Haplotype				
ND 2	Control region	RI	DE	VA
AAAAAAAAAAAAAA	AAAAAAAAAAAAAAA	4	5	4
AAAAA**B**AAAAAAAA	AAAAAAAAAAAAAAA	2	2	2
AAAAAAAAAAAAAA	AA**B**AAAAAAAAAAAA	2	1	1
AAAAAAAAAAAAAA	AA**C**AAAAAAAAAAAA	0	0	1

eroduplex bands were considered to possess identical haplotypes.

DNA sequencing

Haplotypes identified by DGGE-heteroduplex screening of the cytochrome *b* fragment were sequenced by using an ABI 373 automated DNA sequencer with dye terminator chemistry. Sequencing was done in both directions with the original PCR primers.

Statistical analysis of RFLP data

Restriction patterns were analyzed with the Restriction Enzyme Analysis Package (REAP, version 4.0) (McElroy et al., 1992). For each of the three geographical samples, haplotype diversities were calculated following Nei (1987), and nucleotide diversities were calculated following Nei and Miller (1990). Haplotype diversity ranges from zero (all individuals share a common haplotype) to one (every individual has a unique haplotype) and estimates the probability that two randomly selected individuals in a sample will have different haplotypes. Nucleotide diversity estimates the average number of nucleotide substitutions for a pair of haplotypes randomly drawn from a sample. Nucleotide divergences among samples were estimated and corrected for within-sample variation according to Nei (1987). Heterogeneity of haplotype frequencies across samples was tested with exact R × C tests of independence using the software program StatXact (Cytel, 1992). Additional analyses of population differentiation were conducted using Arlequin 1.1 (Schneider et al.[2]). Power analysis of R × C tests was performed with Power and Precision 1.0 (Borenstein et al., 1997).

Results

Restriction site variation

Digestion with 16 restriction enzymes revealed polymorphisms in the ND2 and control region fragments, but not in the COI, ATPase 6, or cyt *b* fragments. Restriction enzyme digestion revealed an average of 129 restriction sites per individual and surveyed an average of 532 bases in each fish.

ND2 gene sequence variation was revealed by digestion with *Hinf* I, and sequence variation in the control region fragment was revealed by digestion with *Hae* III. The remaining enzymes produced invariant patterns. The 16 enzymes revealed four composite haplotypes attributable to restriction site gains or losses in the 24 individuals surveyed (Table 2). No additional haplotypes were uncovered by increasing the sample size to 24 individuals from each geographic region for the ND2-*Hinf* I and control region-*Hae* III combinations (Table 3). No evidence of mitochondrial genome size variation or heteroplasmy was observed in the regions analyzed.

[2] Schneider, S., J.-M. Kueffer, D. Roessli, and L. Excoffier. 1997. Arlequin: a software for population genetic data analysis, vers. 1.1. Genetics and Biometry Lab., Department of Anthropology, Univ. Geneva, Geneva.

One of the composite haplotypes was found only in a single individual from Virginia, whereas the remaining three were found in all three geographical regions. Mean within-sample haplotype diversity was 0.6905 (±0.00184), and mean nucleotide diversity was 0.000782 (Table 4).

Corrected nucleotide divergence between samples varied between –0.0077 and –0.0081%, suggesting the absence of population structuring along the mid-Atlantic Coast. This inference is further supported by exact log-likelihood analysis of the distribution of the four composite haplotypes across the three sites (likelihood ratio statistic=2.82, 6 df, exact P=1.00). A similar analysis of the larger data set (n=72, only polymorphic sites examined) indicated no significant heterogeneity (likelihood ratio statistic=6.05, 6 df, exact P=0.469). Lack of population differentiation was further supported by a mean F_{ST} value of –0.005 (i.e. zero), and the analysis of molecular variance (AMOVA), which found 100% of total haplotype variation to occur within populations.

Table 3

Composite haplotypes from restricted gene and restriction enzyme combinations (ND2-*Hinf* I and control region-*Hae* III) for entire sample (n=72).

Haplotype	Rhode Island	Delaware	Virginia
AA	13	14	14
BA	6	9	7
AB	5	1	2
AC	0	0	1
Total	24	24	24

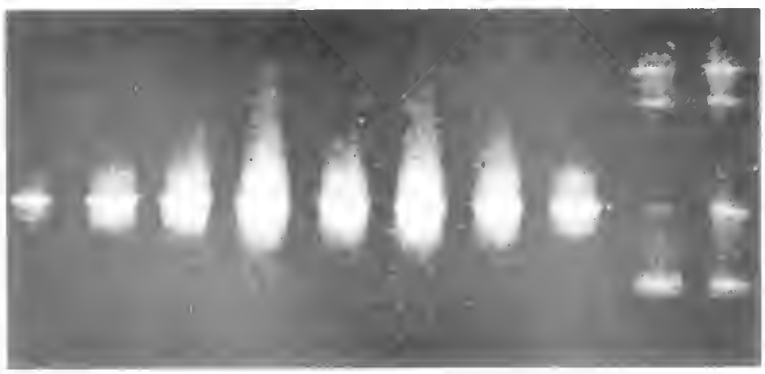

Figure 1

Denaturing gradient gel of tautog cyt *b* PCR products. Each lane represents the pooling of PCR products from two individuals, treated to induce heteroduplex formation when two different DNA sequences were present. The single homoduplex bands in lanes 1–8 (from left to right) indicate sequence identity for the nine tautog examined in pairwise combinations. Lanes 9–10 (the two lanes farthest to the right) illustrate the combination of the common haplotype and one rare haplotype. The two lower (faster-migrating) bands represent alternative homoduplex molecules; the upper two bands are the heteroduplex molecules.

DGGE-heteroduplex analysis

For the entire sample of 72 individuals, analysis of the cyt *b* fragment revealed a total of three haplotypes, two of which were unique and found only in single individuals from Delaware and Virginia (Fig. 1). Sequence analysis of the three cyt *b* haplotypes revealed that the two unique haplotypes differed from the dominant haplotype by synonymous single base substitutions. The unique Virginia haplotype differed from the common haplotype by an A to G transition at base 276, whereas the unique Delaware haplotype resulted from the same substitution at base 291 (Fig. 2).

All 72 tautog appeared to possess a single COI haplotype, a result consistent with the extensive restriction enzyme screening of this region performed on the original subset of 24 individuals. The LDH intron was also relatively invariant. Of the 72 fish screened, DGGE-heteroduplex analysis revealed only a single heterozygous individual, collected in the Delaware region.

Discussion

RFLP analysis revealed a mean mtDNA haplotype diversity value (0.6905 ±0.00184) for tautog that is intermediate within the range of values reported for other marine fishes. However, the overall nucleotide diversity value (0.078%) for the tautog is one of the lowest reported for a marine fish. It should be noted that values for haplotype diversity are affected by the number of restriction enzymes used and should be compared across studies with caution. In addition, values for haplotype and nucleotide diversity may be biased upwards in analyses that include only polymorphic enzymes.

Low levels of intraspecific sequence diversity in mitochondrial genes are generally attributed to low effective population size (N_e) or to reduced rates of mutation (Ovenden, 1990). Effective population sizes inferred from mtDNA data are often orders of magnitude smaller than present-day census estimates; this disparity may reflect the

Table 4

Summary statistics from the analysis of variation in the mitochondrial COI, cyt *b*, ATPase 6, ND2, and control region genes. Samples are pooled according to geographic region.

Population	Sample size	Haplotype diversity	Nucleotide diversity
Rhode Island	8	0.7143 ±0.12275	0.000816
Delaware	8	0.6071 ±0.16398	0.000648
Virginia	8	0.7500 ±0.13913	0.000883
Overall	24	0.6905 ±0.00184	0.000782

action of historical fluctuations in population size, such as bottlenecks caused by disease epidemics or environmental change, as well as a large variance in reproduction among females (Bowen and Avise, 1990). Low levels of nucleotide sequence diversity observed in some teleost fish have also been attributed to rates of sequence evolution that are lower than those estimated for birds and mammals (Bernatchez and Danzmann, 1993).

The Pleistocene glaciation is believed to have decreased the genetic diversity of many species through bottleneck effects (Bernatchez et al., 1989; Avise, 1992). During the Pleistocene era, ten or more glacial advances and retreats that caused changes in sea level and climate are believed to have had significant impacts on the distributions of coastal and marine fauna (Avise, 1992). Tautog population size may have been reduced through the reduction of suitable habitats for both themselves and their food resources. During the most recent glacial event, ice covered all waters north of Long Island and would have forced temperate populations southward into regions where high relief, hard substrate habitats are patchier and less abundant. Glacial advances also resulted in drops in sea level that would have reduced the availability of estuarine environments. In addition, postglacial dispersal from southern refugia may have created population bottlenecks if current populations were founded by a limited number of propagules. The same considerations may apply to the black sea bass *Centropristis striata*, an estuarine-dependent species with low nucleotide diversity (0.03%), corresponding to an estimate of ≈5,000 for N_{fe}, the effective number of females (Bowen and Avise, 1990).

```
TTT GGC TCC CTA CTA GGC CTC TGC TTA GTC GCA CAA ATT CTT ACA  45
 F   G   S   L   L   G   L   C   L   V   A   Q   I   L   T

GGG CTT TTC CTA GCC ATA CAC TAC ACC TCG GAT ATC GCC ACA GCC  90
 G   L   F   L   A   M   H   Y   T   S   D   I   A   T   A

TTT TCA TCA GTC GCC CAC ATC TGC CGC GAC GTT AAT TAC GGC TGA 135
 F   S   S   V   A   H   I   C   R   D   V   N   Y   G   W

CTA ATT CGA AAC ATA CAT GCA AAC GGC GCC TCC TCC TTC TTC ATC 180
 L   I   R   N   M   H   A   N   G   A   S   S   F   F   I

TGC ATC TAC CTA CAC ATT GCA CGG GGC CTT TAC TAC GGC TCA TAC 225
 C   I   Y   L   H   I   A   R   G   L   Y   Y   G   S   Y

CTC CAC AAA GAA ACG TGA AGC ATC GGC GTT GTT CTC CTC CTC CTT 270
 L   H   K   E   T   W   S   I   G   V   V   L   L   L   L

GTT ATa ATA ACT GCC TTC GTa GGC TAT GTC CTC CCC             306
 V   M   M   T   A   F   V   G   Y   V   L   P
```

Figure 2

Nucleotide sequence and deduced amino acid sequence of a 306-bp portion of the mitochondrial cyt *b* gene in *T. onitis*. Reading frame was inferred from alignment with published teleost cyt *b* sequences. Two rare haplotypes possessed synonymous A→G transitions at nucleotides 276 and 291 (indicated by lower case letters).

In addition to the low levels of within-population nucleotide diversity observed, this analysis also failed to detect genetic heterogeneity among tautog samples from different geographical regions. The uncorrected mean nucleotide sequence divergences among tautog samples were of the same magnitude as mean nucleotide diversities within samples; the mean difference between haplotypes randomly drawn from a single sample was equivalent to the mean difference between haplotypes drawn from different samples.

Low levels of intraspecific genetic variation do not preclude the detection of genetic differentiation among stocks. Shulman and Bermingham (1995) detected significant population subdivision within the Caribbean reef fish *Stegastes leucostictus*, for which they reported a mean within-sample sequence diversity of 0.07%. Bowen and Avise (1990) reported a mean within-sample sequence diversity of 0.03%

for black sea bass but detected significant divergence between Gulf of Mexico and Atlantic populations.

The results of our study are consistent with the null hypothesis that the tautog form a single genetic stock within the species range. Although tagging studies in Rhode Island have suggested that adult movement into and out of the area is negligible (Cooper, 1966), tautog have a relatively long pelagic larval stage of approximately three weeks which could result in enough gene flow among geographic regions to prevent the genetic differentiation of subpopulations.

The current system off of the mid-Atlantic coast of the United States consists of three major features: the northeastward flow of the Gulf Stream, the southwestward flow of the along-shelf current, and the across-shelf-flowing warm-core ring streamers that split off from the Gulf Stream (Brooks, 1996). The direction of flow is also influenced by local river runoff, seasonal wind patterns and meteorological events, and by the onshore movement of Ekman currents. The flow patterns in the mid-Atlantic region suggest that a high degree of transport of larvae among regions is possible (Hare and Cowen, 1993), especially for species such as the tautog that spawn in nearshore waters and have pelagic eggs. Larval transport has been suspected as the cause of genetic homogeneity over wide geographic ranges for many marine species (Avise, 1994; Hedgecock, 1994).

Other mtDNA analyses of stock structuring of coastal fish species in the mid-Atlantic region have likewise detected no population subdivision, e.g. weakfish (Graves et al., 1992b), bluefish (Graves et al., 1992a), summer flounder (Jones and Quattro, 1999), and Atlantic croaker (Lankford et al., 1999). None of these studies detected significant genetic heterogeneity among samples collected at different sites within the geographical region spanning from Rhode Island to Chesapeake Bay. For many fish species, the extensive mobility of juveniles and adults coupled with larval dispersal is likely to result in substantial gene flow.

We were unable to reject the null hypothesis of genetic homogeneity among three sites in the northern, middle, and southern portions of the tautog's range but we did not not conclusively prove that tautog in the mid-Atlantic region constitute a single genetic stock. Population structure not resolved by our study might be detected by an examination of additional polymorphisms, with rapidly evolving markers better suited for detecting recent subpopulation divergence. Improved resolution would also be gained by increasing sample sizes; the current analysis with a sample size of 24 individuals per population had limited power (40%) to detect significant heterogeneity among populations with the observed haplotype-frequency distributions. However, it is unlikely that by simply increasing sample sizes with the same set of molecular markers the picture of minimal geographic heterogeneity would alter substantially. If we had found the same haplotype proportions in a study with quadrupled sample sizes (n=96 individuals per site), estimates of gene flow (Nm) would still be substantial (Nm=8.6 between RI and DE; 28 for VA–RI; 73 for DE–VA). We conclude that the sampled populations are probably genetically homogeneous, as the result of contemporary or recent gene flow.

In many genetic studies of population structure, PCR amplification of DNA is coupled with a restriction fragment length polymorphism (RFLP) analysis or direct sequencing. Although PCR is relatively simple, the subsequent analyses can become expensive and time-consuming when large numbers of individuals must be evaluated. These drawbacks can be alleviated through the use of mutation detection techniques such as DGGE and DNA heteroduplex mobility assays (Lessa 1992; Grompe, 1993; Lessa and Applebaum, 1993). These methods can be used to compare DNA fragments to determine rapidly which individuals have the same haplotype. Only one representative of each haplotype needs to be further characterized, and large numbers of individuals can be rapidly and efficiently screened. High-resolution DNA screening techniques such as DGGE and heteroduplex analysis provide the sensitivity of DNA sequencing and make it possible to screen greater numbers of individuals for less cost and effort than standard sequencing techniques.

Our study employed a DGGE-heteroduplex assay to screen regions of the mitochondrial and nuclear genomes of the tautog for polymorphisms useful for the analysis of population structure. Both the cytochrome *b* and cytochrome *c* oxidase products, as well as the LDH intron, appeared to be invariant in the tautog samples, raising the question of whether the DGGE-heteroduplex technique was providing the high degree of resolution anticipated.

In order to provide an independent assessment of the DGGE-heteroduplex technique, we examined the cytochrome *b* fragment from eight spot (*Leiostomus xanthurus*), a species that has been shown to have a high genetic diversity in a RFLP analysis of the ATPase 6 and control regions (Lankford et al., 1999), with the same protocol used to evaluate tautog samples. Four to six haplotypes were observed in the eight individuals. It is clear that DGGE-heteroduplex analysis is capable of revealing DNA sequence diversity in amplified mtDNA, as has been reported by other investigators (e.g. Campbell et al. 1995; Michikawa et al. 1997; Tek Kay et al. 1997).

Additionally, this study shows that DGGE-heteroduplex analysis is a powerful technique that makes it possible to screen large numbers of samples and to identify haplotypes that differ by as little as a single nucleotide. The unique tautog cytochrome *b* haplotypes identified by DGGE-heteroduplex analysis result from single base substitutions that would not have been revealed by a RFLP analysis because of the lack of restriction enzyme target sequences spanning the mutation sites.

The low level of genetic variation in the tautog mitochondrial genome suggests that further mtDNA analyses would likely prove to be unsuccessful in delineating tautog population structure. It might be more productive to focus instead on highly variable nuclear DNA sequences such as microsatellite loci, major histocompatibility complex genes, and introns. In addition, more thorough tagging studies and observations of tautog egg and larval transport should prove valuable in determining the amount of exchange among regions within the species range. However, until further studies are undertaken, the null hypothesis that tautog populations between Rhode Island and Virginia constitute a single genetic stock cannot be rejected.

Acknowledgments

This work was performed in partial fulfillment of the requirements for the M.S. degree at the College of Marine Studies, University of Delaware. We thank John Graves and Timothy Targett for their help in project design, execution, and analysis. Laboratory assistance was kindly provided by Ami Wilbur and Thomas Lankford. This research was funded by NOAA Saltonstall-Kennedy Project NA46FD0329 to PMG.

Literature cited

Auster, P. J.
1989. Species profiles: life histories and environmental requirements of coastal fishes and invertebrates (North and Mid-Atlantic)—tautog and cunner. U. S. Fish and Wildlife Service Biological Report 82 (11.105), 13 p.

Avise, J. C.
1992. Molecular population structure and the biogeographic history of a regional fauna: a case history with lessons for conservation biology. Oikos 63:62–76.
1994. Molecular markers, natural history and evolution. Chapman Hall, New York, NY, 511 p.

Bernatchez, L., and R. G. Danzmann.
1993. Congruence in control-region sequence and restriction-site variation in mitochondrial DNA of brook char (*Salvelinus fontinalis* Mitchell). Mol. Biol. Evol. 10:1002–1014.

Bernatchez, L., J. J. Dodson, and S. Boivin.
1989. Population bottlenecks: influence on mitochondrial DNA diversity and its effect in coregonine stock discrimination. J. Fish. Biol. 35(A):233–244.

Bigelow, H. B., and W. C. Schroeder.
1953. Fishes of the Gulf of Maine. Fish. Bull. 77:1–576.

Borenstein, M., H. Rothstein, and J. Cohen.
1997. Power and precision, release 1.0. Dataxiom Software Inc., Los Angeles, CA, 219 p.

Bowen, B. W., and J. C. Avise.
1990. Genetic structure of Atlantic and Gulf of Mexico populations of sea bass, menhaden, and sturgeon: influence of zoogeographic factors and life-history patterns. Mar. Biol. 107:371–381.

Briggs, P. T.
1977. Status of tautog populations at artificial reefs in New York waters and effect of fishing. N.Y. Fish Game J. 24:154–167.

Brooks, D. A.
1996. Physical oceanography of the shelf and slope seas from Cape Hatteras to Georges Bank: a brief overview. *In* The Northeast shelf system: assessment, sustainability, and management (K. Sherman, N. A. Jaworski, and T. J. Smayda, eds.), p. 47–74. Blackwell Science, Inc., Cambridge, MA.

Campbell, N. J. H., F. C. Harriss, M. S. Elphinstone, and P. R. Baverstock.
1995. Outgroup heteroduplex analysis using temperature gradient gel electrophoresis: high resolution, large scale, screening of DNA variation in the mitochondrial control region. Mol. Ecol. 3:407–418.

Colton, J. B., Jr., W.G. Smith, A. W. Kendall, Jr., P. L. Berrien, and M. P. Fahay.
1979. Principal spawning areas and times of marine fishes, Cape Sable to Cape Hatteras. Fish. Bull. 76:911–915.

Cooper, R. A.
1966. Migration and population estimation of the tautog, *Toutoga onitis* (Linnaeus), from Rhode Island. Trans. Am. Fish. Soc. 95:239–247.

Cytel.
1992. StatXact for SYSTAT, ver. 1.0. Cytel Software Corp., Cambridge, MA, 358 p.

Eklund, A.M., and T.E. Targett.
1990. Reproductive seasonality of fishes inhabiting hard bottom areas in the Middle Atlantic Bight. Copeia 1990: 1180–1184,
1991. Seasonality of fish catch rates and species composition from the hard bottom trap fishery in the Middle Atlantic Bight (US east coast). Fish. Res. 12: 1–22.

Graves, J. E., J. R. McDowell, A. M. Beardsley, and D. R. Scoles.
1992a. Stock structure of the bluefish *Pomatomus saltatrix* along the mid-Atlantic coast. Fish. Bull. 90:703–710.

Graves, J. E., J. R. McDowell, and M. L. Jones.
1992b. A genetic analysis of weakfish *Cynoscion regalis* stock structure along the mid-Atlantic Coast. Fish. Bull. 90:469–475.

Grompe, M.
1993. The rapid detection of unknown mutations in nucleic acids. Nature Genetics 5:111–117.

Hare, J. A., and R. K.Cowen.
1993. Ecological and evolutionary implications of the larval transport and reproductive strategy of bluefish *Pomotomus saltatrix*. Mar. Ecol. Prog. Ser. 98:1–16.

Hedgecock, D.
1994. Temporal and spatial genetic structure of marine

animal populations in the California Current. CalCOFI Rep. 35:73–81.

Hostetter, E. B., and T. A. Munroe.
1993. Age, growth, and reproduction of tautog *Tautoga onitis* (Labridae: Perciformes) from coastal waters of Virginia. Fish. Bull. 91:45–64.

Jones, W. J., and J. M Quattro.
1999. Genetic structure of summer flounder (*Paralichthys dentatus*) populations north and south of Cape Hatteras. Mar. Biol. 133:129–135.

Lankford, T. E., Jr., T. E. Targett, and P. M. Gaffney.
1999. Mitochondrial DNA analysis of population structure in the Atlantic croaker, *Micropogonias undulatus* (Perciformes: Sciaenidae). Fish. Bull. 97:884–890.

Lessa, E. P.
1992. Rapid surveying of DNA sequence variation in natural populations. Mol. Biol. Evol. 9:323–330.

Lessa, E. P., and G. Applebaum.
1993. Screening techniques for detecting allelic variation in DNA sequences. Mol. Ecol. 2:119–129.

Martin, D. L.
1993. Latitudinal growth variation in juvenile and larval *Tautoga onitis* (Pisces: Labridae). M.S. thesis, Univ. Delaware, Newark, DE, 62 p.

McElroy, D., P. Moran, E. Bermingham, and I. Kornfield.
1992. REAP: the restriction enzyme analysis package, version 4.0. Univ. Maine, Orono, ME, 40 p.

Meyer, A., J. M. Morrissey, and M. Schartl.
1994. Recurrent origin of a sexually selected trait in *Xiphophorus* fishes inferred from a molecular phylogeny. Nature 368:539–542.

Michikawa, Y., G. Hofhaus, L. S. Lerman, and G. Attardi.
1997. Comprehensive, rapid and sensitive detection of sequence variants of human mitochondrial tRNA genes. Nucleic Acids Research 12:2455–2463.

Mrázek, J., and A. Spanova.
1992. ANAGEL. Comput. Appli. Biosci. 8:524.

Nei, M.
1987. Molecular evolutionary genetics. Columbia Univ. Press, New York, NY, 512 p.

Nei, M., and J. C. Miller.
1990. A simple method for estimating average number of nucleotide substitutions within and between populations from restriction data. Genetics 125:873–879.

Olla, B. L., A. J. Bejda, and A. D. Martin.
1974. Daily activity, movements, feeding, and seasonal occurrences in the tautog, *Tautoga onitis*. Fish. Bull. 72: 27–35.

Olla, B. L., and C. Samet.
1977. Courtship and spawning behavior of the tautog, *Tautoga onitis* (Pisces: Labridae), under laboratory conditions. Fish. Bull. 75:585–599.

Olla, B. L., A. L. Studholme, A. J. Bejda, and C. Samet.
1979. Seasonal dispersal and habitat selection of cunner, *Tautogolabrus adspersus*, and young tautog, *Tautoga onitis*, in Fire Island Inlet, Long Island, New York. Fish. Bull. 77:255–261.

Ovenden, J. R.
1990. Mitochondrial DNA and marine stock assessment: a review. Aust. J. Mar. Freshwater. Res. 41:835–853.

Palumbi, S. R., A. Martin, S. Romano, W. O. McMillan, L. Stice and G. Grabowski.
1991. The simple fool's guide to PCR, version 2.0. Univ. Hawaii, Honolulu, HI, 47 p.

Park, L.K., M. A. Brainard, D.A. Dightman, and G.A. Winans.
1993. Low levels of intraspecific variation in the mitochondrial DNA of chum salmon (*Oncorhynchus keta*). Molec. Mar. Biol. Biotech. 2:362–370.

Quattro, J. M., and W. J. Jones.
1999. Amplification primers that target locus-specific introns in actinopterygian fishes. Copeia 99:191–196.

Shulman, M. J., and E. Bermingham.
1995. Early life histories, ocean currents, and the population genetics of Caribbean reef fishes. Evolution 49:897–910.

Tek Kay, W., J. M. Cook, D. J. Rowe, and R. H. Crozier.
1997. Migration between nests in the Australian arid-zone ant *Rhytidoponera* sp. revealed by DGGE analyses of mitochondrial DNA. Molecular Ecology 6:403–411.

Victor, B. C.
1986. Duration of the planktonic stage of one hundred species of Pacific and Atlantic wrasses (family Labridae). Mar. Biol. 90:317–326.

Age and growth of dolphinfish, *Coryphaena hippurus*, off Puerto Rico

Glauco A. Rivera

Richard S. Appeldoorn

Department of Marine Sciences
University of Puerto Rico
Mayagüez, Puerto Rico 00681-9013

E-mail address (for R. S. Appeldoorn, contact author): R_Appeldoorn@rumac.upr.clu.edu

Abstract.—Dolphinfish, *Coryphaena hippurus*, off Puerto Rico were sampled over an 8-month period to study age and growth from daily increments recorded in the sagittae. A total of 121 otoliths were analyzed. Growth was rapid and nonlinear. No significant differences in growth rate were observed based on sex or on location of capture (north or south coast). The von Bertalanffy growth parameters were L_∞ = 1457 mm *FL*, K = 2.19/yr, and t_0 = –0.046 yr. With these values, extrapolated growth over the first year averaged 3.6 mm FL/day. An existing hypothesis of two separate stocks (north and south) in the vicinity of Puerto Rico predicts that fish from the north coast caught primarily in the winter would show a much slower growth rate than fish from the south coast caught primarily in the spring. The absence of growth differences between coasts does not match this prediction; however previous growth estimates for the northern stock may have been underestimated. On the basis of these results, the stock structure and migration pattern of dolphinfish are likely to be more complicated than originally postulated.

Manuscript accepted 26 November 1999.
Fish. Bull. 98:345–352 (2000).

The dolphinfish, *Coryphaena hippurus* L., is a pelagic and migratory fish, distributed worldwide throughout tropical and subtropical waters (Gibbs and Collette, 1959; Shcherbachev, 1973). Migrating stocks support important sport and commercial fisheries. In the northwestern Atlantic they are fished off North Carolina (Rose and Hassler, 1968), Florida (Beardsley, 1967), in the Gulf of Mexico (Gibbs and Collette, 1959), off Puerto Rico (Erdman, 1956; Pérez and Sadovy, 1996), off the U.S. Virgin Islands and the Windward Islands (Mahon et al., 1981), and off Barbados (Oxenford and Hunte, 1986).

Age and growth for dolphinfish have been studied in detail by Beardsley (1967), Rose and Hassler (1968), Wang (1979), Oxenford and Hunte (1983), Uchiyama et al. (1986), and Bentivoglio (1988). No such studies have been conducted for fish off Puerto Rico. For the Caribbean region, the most relevant studies are those of Beardsley (1967), off Miami, and Oxenford and Hunte (1983) in Barbados. Beardsley (1967), using annuli on scales, found dolphinfish distributed among five age groups: 379 in group 0, 121 in group I, 9 in group II, 1 in group III, and 1 in group IV. In that study, the mean growth rate in the first year was 1.82 mm SL/day. Oxenford and Hunte (1983) assumed daily increment formation in the otolith and obtained a linear growth rate of 4.71 mm SL/day for all fish. The rate for adult fish (±700 mm SL) was 1.43 mm SL/day. Oxenford and Hunte's assumption of daily increment formation was validated indirectly by comparing their estimated growth rates to modal progression in length frequency distributions; their study was subsequently validated directly by Uchiyama et al. (1986) in a study of Hawaiian dolphinfish. Determination of age from annuli has not been validated and remains subjective.

Dolphinfish have sexually dimorphic growth; older male fish show an enlargement of the forehead (Schuck, 1951; Lozano-Cabo, 1961). Oxenford (1985) and Uchiyama et al. (1986) reported differences in the growth rate in length between sexes, but other studies have reported growth as a combination of both sexes; specifically, Rose and Hassler (1968) found no differences in length at age between males and females.

Oxenford and Hunte (1986) proposed a migration circuit in the western Central Atlantic for two separate northern and southern stocks (Fig. 1). One stock is located southeast, and the other northwest, of Puerto Rico and the Virgin Islands. Abundance of dolphinfish in Puerto Rico peaks from November to January and again (albeit to a lesser degree) from April to June (Pérez and Sadovy, 1996). The U.S. Virgin Islands also has a bimodal distribution in abundance, with a large peak in April–May and small

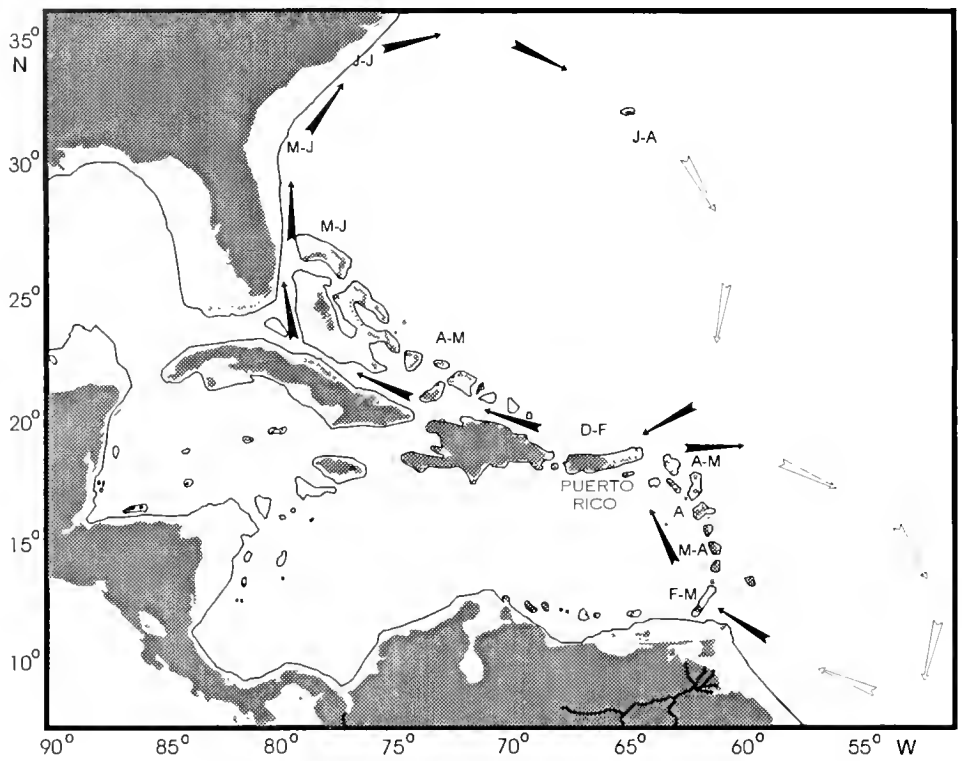

Figure 1

Proposed migration circuits for northern and southern stocks of dolphinfish, *Coryphaena hippurus*. Solid arrows indicate proposed migration route, open arrows indicate proposed migration route where catch data are not available. Letter symbols indicate months of peak catch. Redrawn from Oxenford and Hunte (1986).

peak in November. Assuming the migration circuit of the two-stock hypothesis (Oxenford and Hunte, 1986), we interpret the major peak in Puerto Rico as coinciding with the presence of the northern stock, whereas the minor peak coincides with the appearance of the southern stock in the Virgin Islands. The two-stock hypothesis is based on three main observations. First, there are differences in life-history parameters between dolphinfish from the southeast United States (North Carolina and Florida) and those from Barbados. Southern dolphinfish grow faster, attain sexual maturity at a larger size, have lower fecundity for size, and have smaller eggs than northern dolphinfish (Oxenford and Hunte, 1986). Second, the gene flow between both groups is slight. The difference in allele frequencies of the IDH-2 locus in heart extracts and in phenotypic frequencies at the IDH-2,3 loci in liver extracts indicates infrequent breeding between the stocks (Oxenford and Hunte, 1986). Third, the seasonality of catch between regions is different (Oxenford and Hunte, 1986). Because Puerto Rico lies along the boundary for the two proposed stocks, it is an ideal location to test the two-stock hypothesis.

The purpose of our study was to determine age and growth of dolphinfish in Puerto Rico. Comparison of growth rates between Puerto Rico and other areas (Florida, Barbados) was used to test the two-stock hypothesis. Of specific interest was the comparison of growth between fish from the north and fish from the south coasts. All fish from the north coast were caught during the period when abundance first peaked, whereas 92% of the fish from the south coast were caught during the period of the second peak in abundance.

Materials and methods

Dolphinfish were collected from sportfishing tournaments and commercial fishing villages from September 1991 to April 1992. Twelve dolphin tournaments were held in Puerto Rico, five on the north coast and seven on the south coast. Fifteen billfish tournaments were visited for additional samples. Purchased fish or fish heads supplemented samples when necessary. Fish were caught by trolling lines. Data on date and site of collection, standard, fork, and total lengths,

weight, and sex were recorded. All fish were measured to the nearest millimeter and weighed to the nearest 50 grams. Heads were separated from the body at the site of collection and kept frozen.

The removal and preservation of otoliths followed the methods of Panella (1980) and Brothers (1987). A sagittal (longitudinal) cut through the midline of the frozen head was made with an electric band saw. Under a dissection microscope, sagittae were removed from the sacculi and extraneous tissue was removed. Sagittae were used owing to their relatively larger size in comparison with the lapillus and asteriscus. Each pair of sagittae was stored in glycerin for clearing in labeled vials.

Examination of external otolith microstructure was used to determine age (Panella, 1971). Sagittae were placed on glass slides in glycerin. Otolith structure was examined and the radius measured under a compound light microscope with transmitted light at 200×. Translucent and opaque lines were counted following the procedure of Oxenford and Hunte (1983). Otolith rings were assumed to be daily lines (Uchiyama et al., 1986) and were counted from the focus to the edge of the posterior rostrum.

All otoliths were read twice at random. If there was any difference in reading (10% or more), the otolith was discarded. A subsample of ten otoliths was sent to Hazel Oxenford (Bellairs Research Institute of McGill University, in Barbados) for additional reading and verification of counts. Otoliths were sent in coded vials with no information about length, weight, or sex. Fish length, from which otoliths were sent, ranged from 630 mm FL to 1325 mm FL.

The relation between fish fork length and daily increment of the sagittae was determined with a predictive linear regression of length on number of rings (Ricker, 1975, Francis, 1990). Following Oxenford and Hunte (1983) and Bentivoglio (1988), growth rates were calculated from the linear regressions and reported as mm/day. Analyses were done by coast (north and south) and by sex (male and female). Differences between growth-rate estimates were compared by using a homogeneity of slopes test (ANOVA) (Sokal and Rohlf, 1981).

For a more realistic representation of growth, age-length data were also modeled by using the von Bertalanffy growth function,

$$l_t = L_\infty\left(1 - e^{-k(t-t_0)}\right),$$

where l_t = length (mm) at time t (years);
L_∞ = asymptotic length;
k = the growth coefficient; and
t_0 = the hypothetical age at which length equals zero.

Parameters were estimated by a nonlinear regression with SYSTAT (Wilkinson, 1987).

Results

A total of 170 dolphinfish were collected during the eight-month sampling period. From this total, 80 were captured off the north coast and 90 were captured off the south coast. The size range from the south coast was broader than that from the north: north = 475 mm FL (1.25 kg) to 1283 mm FL (18.50 kg); south = 381 mm FL (0.70 kg) to 1479 mm FL (25.00 kg); in addition, the largest fish were found on the south coast. From the total sample, 55 were male and 115 were female. Males were slightly larger than females: males = 630 mm FL (2.50 kg) to 1479 mm FL (25.00 kg); females = 381 mm FL (0.07 kg) to 1283 mm FL (19.75 kg).

The relation between standard length (SL) and fork length (FL) was linear and expressed by the equation

$$SL = -1.37 + 0.92\,FL \qquad (r=0.99).$$

The relation between the logarithms of fish weight (W) and fork length was linear and expressed by the equation

$$\log W = -4.42 + 2.78 \log FL \qquad (r=0.98).$$

Otoliths were collected from 22 males and 38 females from the north coast, and from 21 males and 40 females from the south coast. Otoliths were not collected from all fish owing to difficulties in making the longitudinal cut through the head, to breakage during dissection, or to loss during extraction from the cranial tissue. Thus, for the age and growth determinations, fork lengths ranged on the north coast from 746 mm FL to 1283 mm FL for males and from 475 mm FL to 1222 mm FL for females. Males on the south coast ranged from 625 mm FL to 1325 mm FL, and females ranged from 550 mm FL to 1275 mm FL.

Examination of the external structure of the otolith showed clear growth increments. On large otoliths, increments tended to be tightly spaced on the edge of the rostrum. Reading daily increments in this area was difficult owing to poor resolution even after clearing in glycerin; however, independent readings by Oxenford were within 10%. The oldest individual had 336 increments.

Figure 2 shows the length and number of otolith increments for all fish. Linear growth rate was 2.52 mm FL/day for all fish (Table 1, Fig. 2). Differences in linear growth rates by sex or coast (Table 1) were not

significant. For the comparison by sex, however, the test approached significance, with P=0.138. Given the variability in data, the power of this test was probably low. Furthermore, growth was clearly nonlinear and decreased over time. To reach a size of 600 mm FL in 100 days, cumulative growth would have to be 6 mm FL/day. The maximum observed cumulative growth rate was 9.5 mm FL/day for a fish of 1303 mm FL and 137 increments. On average, fish of 110–150 days grew 3.3 mm FL/day, those 170–220 days old grew 2.9 mm FL/day and those 230–270 days of age grew 2.1 mm FL/day. Parameter values for the von Bertalanffy model (Fig. 2) are shown in Table 2. It was not possible to fit the model to the data sorted by both coast and sex, owing to reduced sample size in relation to large amount of variance. Differences between sexes were the greatest, and the confidence limits on k indicated statistical significance would occur at a P-value of approximately 0.06. Extrapolation of the von Bertalanffy equation for all individuals predicted a cumulative growth rate of 3.59 mm FL/day over the first year.

Table 1

Summary of results for linear regressions of sagittal rings on fork length. All = all aged fish, M = male, F = female, N = north coast, S = south coast, n = number of fish. r = coefficient of correlation.

Group	Slope	(SE)	Intercept	(SE)	r	n
All	2.52	(0.26)	497	(141)	0.66	121
MN	2.14	(0.67)	535	(134)	0.58	22
FN	2.35	(0.46)	493	(130)	0.65	38
MS	2.23	(0.72)	641	(144)	0.58	21
FS	2.34	(0.45)	535	(142)	0.64	40
N	2.28	(0.37)	506	(129)	0.63	60
S	2.37	(0.39)	558	(146)	0.62	61
M	2.54	(0.50)	518	(148)	0.62	43
F	2.46	(0.31)	493	(136)	0.67	78

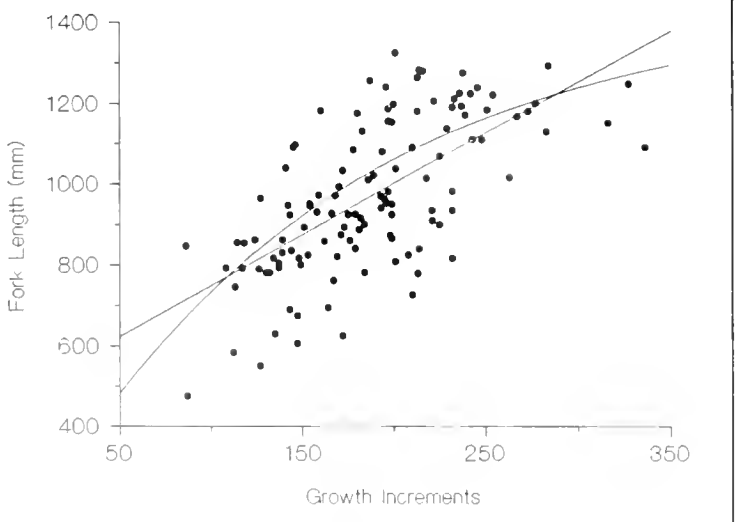

Figure 2

Relation between fork length and number of sagittal rings for dolphinfish from Puerto Rico. Straight line indicates linear growth over all fish. Curved line indicates growth according to the von Bertalanffy model (see text).

Discussion

All linear growth rates for dolphinfish (Table 1) were greater than those reported by Beardsley (1967) and Rose and Hassler (1968) (Table 3). However, use of linear growth estimates is justified largely by the high variability observed in fork lengths for a given age; high variability masks any underlying growth pattern, thus making a linear model the simplest and most parsimonious, but not necessarily the most realistic model. A better approach is to use a biologically realistic model, in this case the von Bertalanffy model. The resulting parameters of the von Bertalanffy model for the Puerto Rico data are consistent with the known biology of dolphinfish. Asymptotic lengths were in accord with known maximum lengths, values of t_0 were very close to zero, even though they represented extrapolations of three months (=25% of maximum age observed), and growth coefficients were high. Growth rates predicted for dolphinfish from these equations give a different picture from those provided by the linear model. For all fish, growth averaged over 1 year was 3.59 mm FL/day (3.31 mm SL/day); growth averaged over the first 6 months was 5.57 mm FL/day (5.13 mm SL/day). These rates are comparable to the higher values reported in Table 3.

Growth rates for dolphinfish reported from previous studies (Table 3) are of questionable value when they lack uniformity in length units and in the time over which growth is evaluated, when growth is not portrayed accurately, and when the size for which growth is reported is unclear. The use of the von Bertalanffy growth function allows standardization for comparison of growth. Parameters for the von Bertalanffy model were calculated for four previous studies in which length-at-age data were reported (Table 4). Comparisons using Φ' (=log$K$ + 2logL_∞), the growth performance index of Pauly and Munro (1984), suggests

Table 2

Von Bertalanffy growth parameters (L_∞ = asymptotic length, K = growth coefficient, t_0 = length at age = 0) and standard errors (in parentheses) calculated from captured dolphinfish. n = number of fish.

Group	n	L_∞ (mm FL)	K (per yr)	t_0 (yr)
All fish	121	1457 (59)	2.19 (<0.365)	−0.046 (0.037)
North coast	60	1289 (66)	2.19 (<0.365)	−0.090 (0.054)
South coast	61	1493 (69)	2.19 (<0.365)	−0.006 (0.046)
Male	43	1380 (92)	2.55 (0.365)	0.023 (0.064)
Female	78	1506 (79)	1.82 (<0.365)	−0.087 (0.048)

Table 3

Estimated growth rates (mm/day) for *Coryphaena hippurus* at various locations. n = number of fish, P = period of sampling in months (adapted from Oxenford and Hunte, 1983; and Bentivoglio, 1988).

Location	n	P	Aging method	Growth rate	Reference
Gulf of Mexico	19	5	otolith count	0.49 SL	Bentivoglio, 1988 for fish >900 mm FL
North Carolina	26	3	days known	1.07 TL	Hassler and Rainville, 1975
Barbados	25	18	otolith count	1.43 SL	Oxenford and Hunte, 1983 for fish 700–1100 mm SL
North Carolina	593	3	scale annuli	1.64 SL	Rose and Hassler, 1968
Straits of Florida	121	12	scale annuli	1.82 SL	Beardsley, 1967
Taiwan	?	19	modal progression	2.96 SL	Wang 1979
Hawaii	7	6	days known	2.82 SL	Uchiyama et al., 1986
	11	14	otolith count	3.19 SL	
Florida	?	?	days known	3.03 SL	Schekter, personal commun. in Oxenford and Hunte, 1983
Puerto Rico	121	8	otolith count	3.31 SL	Our study
Hawaii	94	2–3	days known	3.56 SL	Hagood et al., 1981
Gulf of Mexico	81	5	otolith count	3.88 SL	Bentivoglio, 1988
Barbados	50	18	otolith count	4.71 SL	Oxenford and Hunte, 1983
Florida Marineland	2	?	days known	4.80 SL	Herald, 1961
Miami Seaquarium	1	?	days known	5.28 SL	Beardsley, 1971
North Carolina	30	1–2	days known	5.88 SL	Hassler and Hogarth, 1977

Table 4

Von Bertalanffy growth parameters calculated for dolphinfish from previous studies. $\Phi' = \text{Log}(K)+2\text{Log}(L_\infty)$.

Location	L_∞ (mm FL)	K (per yr)	Φ'	Reference
North Carolina	1733	0.31	5.59	Rose and Hassler, 1968
Straits of Florida	1650	0.68	6.27	Beardsley, 1967
Gulf of Mexico	1427	3.13	6.80	Bentivoglio, 1988
Puerto Rico	1457	2.19	6.67	Our study
Barbados	1436	2.87	6.77	Oxenford and Hunte, 1983

that dolphinfish in North Carolina and Florida grow more slowly than in the Gulf of Mexico, Puerto Rico (Φ'=6.67), and Barbados, or that values of K in the northern areas are underestimated (Table 4). These slower growth rates are derived from unvalidated studies of scales. Furthermore, the age at the time of first annulus formation may be significantly less than one year, depending on the difference between

the period of annulus formation (presumably in winter) and the spawning season. It is distinctly possible that otolith studies in these areas might show significantly faster growth and younger fish. This possibility is also raised by the rapid growth rates of dolphinfish from these areas when maintained in aquaria (Herald, 1961; Beardsley, 1971; Hassler and Hogarth, 1977), which are among the highest reported (Table 3).

The two-stock hypothesis of Oxenford and Hunte (1986) predicts that fish sampled off Puerto Rico from November to March (north coast fish) should show distinctly different growth rates from fish sampled from March to May (south coast fish). However, no such differences were found, and in general growth rates were similar to those reported for the proposed southern stock (Oxenford and Hunte, 1983). Figure 3 shows that most fish sampled may have belonged to a single cohort whose distribution shifted over time. The size differences between fish from the north coast (primarily January–February) and those from the south coast (March–April) can be explained by growth over the 8-month sampling period. There is an influx of small fish in April off the south coast; the growth rates of these fish are equal to those of the rest of the sample. Although these fish may represent the appearance of a different (e.g. southern) stock, an equally likely explanation is that they represent the entry of a new cohort. Dolphinfish are known to spawn several cohorts over the year (Beardsley, 1967; Oxenford, 1985; Pérez and Sadovy, 1996), and a similar appearance of small fish occurs off Barbados in June, where only one stock is hypothesized. Annual length-frequency data from the south coast of Puerto Rico (Fig. 4 in Pérez and Sadovy, 1996) show considerable variation in the most abundant size class landed (from 800–1100 mm FL), which may reflect variations in the relative strengths of the two cohorts.

These observations do not necessarily negate the two-stock hypothesis if, as postulated above, growth rates for northern dolphinfish are much greater than previously reported. In addition to growth rate, the hypothesis is also based on differences in other life-history parameters, but more recent studies cast doubt on the significance of most of these. Data in Pérez et al.[1] show trends in several parameters related to reproduction. Both the range and mean size of mature oocytes show a gradual increase in fish from Florida, Puerto Rico, and Barbados, although sizes were identical for the north and south coasts of Puerto Rico. A trend of increasing slope among length-fecundity relationships was also evident.[1] Length of minimum maturity in females also increased along the same gradient, from 324 SL mm for Florida (Beardsley, 1967), 400 mm FL (369 mm SL) for Puerto Rico,[1] to 610 mm SL for Barbados (Oxenford and Hunte, 1986). These results, however, could equally be interpreted as representing a cline, as opposed to data for distinct stocks (Mahon and Mahon, 1987). Genetic data showing differences is based on the extremes of the distribution (Florida, Barbados) and thus cannot be used to interpret what occurs at a mid location such as Puerto Rico.

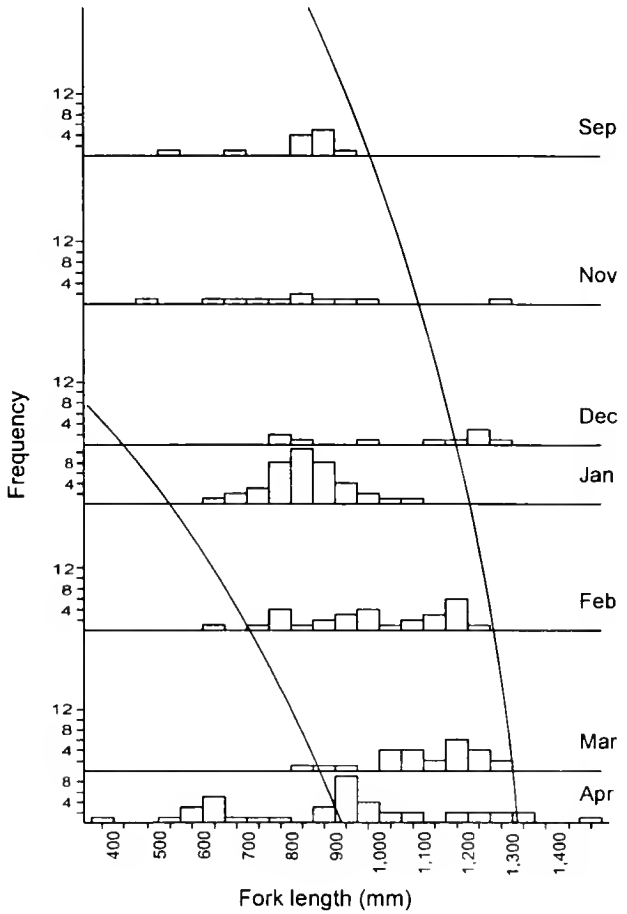

Figure 3

Length-frequency distributions of dolphinfish from Puerto Rico by month. Vertical position of the horizontal axes represents the mean sampling date for each month. Curves indicate the von Bertalanffy growth rate estimated from otoliths and are positioned to indicate the main cohort of fish sampled.

[1] Pérez, R. N., A. Román, and G. A. Rivera. 1992. Investigation of the reproductive dynamics and preliminary evaluation of landings data of the dolphinfish *Coryphaena hippurus*, L. Puerto Rico Department of Natural Resources, Puerto Rico Fisheries Research Laboratory, P.O. Box 3665, Mayaguez, Puerto Rico 00680. Final Report D-J F26-1, 95 p.

Furthermore, the perceived movements of dolphinfish in the vicinity of Puerto Rico is complex. In Puerto Rico, fish generally are caught in abundance first on the north coast and then on the south coast. Fish are caught in the Mona Passage on the west side of Puerto Rico but not off the east coast over the Puerto Rican–Virgin Islands shelf.[1] Off the U.S. Virgin Islands there is a bimodal distribution of catch over time similar to that for Puerto Rico. For recreational boats operating out of St. Croix, increases in catch rates, particularly in the spring are first observed to the southeast, then move progressively closer to St. Croix and then St. Thomas-St. John.[2] The implied direction of movement is from southeast to northwest, opposite to that predicted by the two-stock hypothesis. The temporal distribution of dolphinfish along the southeast coast of the Dominican Republic is similar to that off the south coast of Puerto Rico,[3] but in contrast, off the southwest coast, dolphinfish catch rates show a single sharp peak in the month of November.[4] In agreement with Mahon and Mahon (1987), the real stock structure and migration pattern of dolphinfish are likely to be more complicated than originally proposed, a point well appreciated by Oxenford and Hunte (1986).

Acknowledgments

Data collection was aided by M. Figuerola, R.N. Pérez, and A.M. Román of the Fisheries Research Laboratory, Puerto Rico Department of Natural and Environmental Resources, and by the Puerto Rico sportfishing community. We thank H. Oxenford for her help and willingness to verify otolith counts. D.A. Hensley and V. Vicente gave valuable criticism.

Literature cited

Beardsley, G. L., Jr.
1967. Age, growth and reproduction of the dolphin, *Coryphaena hippurus*, in the Straits of Florida. Copeia 1967: 441–451.
1971. Dolphin spectacular. Sea Front. 17:194–201.

Bentivoglio, A. A.
1988. Investigations into the growth, maturity, mortality rates and occurrence of the dolphin (*Coryphaena hippurus*, Linnaeus) in the Gulf of Mexico. M.S. thesis, Univ. College of North Wales, Bangor, United Kingdom, 37 p.

Brothers, E. B.
1987. Methodological approaches to the examination of otoliths in aging studies. *In* Age and growth of fish (R. C. Summerfelt and G. E. Hall, eds.), p. 319–330. Iowa State Univ. Press, Ames, IA.

Erdman, D. S.
1956. Recent fish records from Puerto Rico. Bull. Mar. Sci. Gulf Caribb. 6(4):315–340.

Francis, R. I. C. C.
1990. Back calculation of fish length: a critical review. J. Fish Biol. 36:883–902.

Gibbs, R. H., and B.B. Collette.
1959. On the identification, distribution, and biology of the dolphins, *Coryphaena hippurus* and *C. equiselis*. Bull. Mar. Sci. Gulf Caribb. 9(2):117–152.

Hagood, R. W., G. N. Rothwell, M. Swafford, and M. Tosaki.
1981. Preliminary report on the aquacultural development of the dolphin fish, *Coryphaena hippurus* (Linnaeus). J. World Maricul. Soc. 12(1):135–139.

Hassler, W. W., and W. T. Hogarth.
1977. The growth and culture of dolphin (*Coryphaena hippurus*) in North Carolina. Aquaculture 12:115–122.

Hassler, W. W., and R. P. Rainville.
1975. Techniques for hatching and rearing dolphin, *Coryphaena hippurus*, through larvae and juvenile stages. Univ. North Carolina, Sea Grant Program Publ. UNC-SG-75-31, 16 p.

Herald, E. S.
1961. Living fishes of the world. Doubleday, Garden City, NY, 304 p.

Lozano-Cabo, F.
1961. Biometría, biología y pesca de la Lampuga (*Coryphaena hippurus* L.) de las islas Baleares. Memorias de la Real Academia de Ciencias Exactas, Físicas y Naturales de Madrid. Serie de Ciencias Naturales, tomo XXI, 93 p.

Mahon, R., W. Hunte, H. Oxenford, K. Storey, and F. E. Hastings.
1981. Seasonality in the commercial marine fisheries of Barbados. Proc. Gulf Caribb. Fish. Inst. 34:28–37.

Mahon, R., and S. Mahon.
1987. Seasonality and migration of pelagic fishes in the eastern Caribbean. *In* Report and proceedings of the expert consultation on shared fishery resources of the Lesser Antilles region (R. Mahon, ed.), 192–273 p. Mayaguez, Puerto Rico. 8–12 September 1986. FAO Fish. Rep. 383.

Oxenford, H. A.
1985. Biology of the dolphin *Corhphaena hippurus* and its implications for the Barbadian fisheries. Ph.D. diss., Univ. West Indies, Cave Hill, Barbados, 366 p.

Oxenford, H. A., and W. Hunte.
1983. Age and growth of dolphin, *Coryphaena hippurus*, as determined by growth rings in otoliths. Fish. Bull. 81(4): 906–909.
1986. A preliminary investigation of the stock structure of the dolphin, *Coryphaena hippurus*, in the western central Atlantic. Fish. Bull. 84(2):451–459.

Panella, G.
1971. Fish otoliths: daily growth layers and periodical patterns. Science (Wash. D.C.) 173:1124–1127.
1980. Methods of preparing fish sagittae for the study of growth patterns. *In* Skeletal growth of aquatic organisms: biological records of environmental change (D. C. Rhoades and R. A. Lutz, eds.), p. 619–624. Plenum Press, New York, NY.

Pauly, D., and J. L. Munro.
1984. Once more on growth comparisons in fish and invertebrates. Fishbyte 2(1):21.

[2] Adams, A. 1997. Virgin Islands Division of Fish and Wildlife, 101 Estate Nazareth, St. Thomas, USVI 00802. Personal commun.

[3] Felix, E. 1998. Office of the Navy, Santo Domingo, Dominican Republic. Personal commun.

[4] Colom, R. 1995. PROPESCAR-SUR, Apartado 120, Barahona, Dominican Republic. Personal commun.

Pérez, R. N., and Y. Sadovy.
1996. Preliminary data on the reproductive dynamics and landing records of *Coryphaena hippurus* L., in Puerto Rico. Proc. Gulf Caribb. Fish. Inst. 44:651–670.

Ricker, W. E.
1975. Computations and interpretations of biological statistics of fish populations. Bull. Fish. Res. Board Can. 191, 382 p.

Rose, C. D., and W. W. Hassler.
1968. Age and growth of the dolphin, *Coryphaena hippurus* (Linnaeus), in North Carolina waters. Trans. Am. Fish. Soc. 97:271–276.

Schuck, H. A.
1951. Notes on the dolphin (*Coryphaena hippurus*) in North Carolina waters. Copeia 1951:35–39.

Shcherbachev, Y. N.
1973. The biology and distribution of the dolphins (Pisces, Coryphaenidae). J. Ichthyol. 13:182–191.

Sokal, R. R., and F. J. Rohlf.
1981. Biometry, 2nd ed. W. H. Freeman, San Francisco, CA, 859 p.

Uchiyama, J. H., R. K. Burch, and S. A. Kraul.
1986. Growth of dolphins, *Coryphaena hippurus* and *C. equiselis*, in Hawaiian waters as determined by daily increments in otoliths. Fish. Bull. 84:186–191.

Wang, C. H.
1979. A study of population dynamics of dolphin fish (*Coryphaena hippurus*) in waters adjacent to eastern Taiwan. Acta Oceanogr. Taiwan 10:233–251.

Wilkinson, L.
1987. SYSTAT: the system for statistics. SYSTAT Inc., Evanston, IL.

Abstract.—Five rockfish juveniles (15.0–30.4 mm SL) collected in midwater trawls from offshore banks off the coast of California were identified by using a combination of morphological and molecular characters. All had pigment patterns consistent with members of the subgenus *Sebastomus*, but each required the use of molecular markers for species identification. Using DNA sequence data from the mitochondrial cytochrome *b*, we identified the juveniles as a transforming larva of *Sebastes constellatus* and a transforming larva and three pelagic juveniles of *S. ensifer*. We provide detailed descriptions of the specimens and compare our results with the developmental stages of other species of *Sebastes* of the subgenus *Sebastomus*. We found some differences in structure and pigmentation that might allow identification of these young stages by traditional means, but more descriptive work is necessary. The use of molecular tools can thus be successfully used to complement traditional identification efforts to solve problems unassailable by morphological and pigment characters alone.

Manuscript accepted 28 September 1999.
Fish. Bull. 98:353–363 (2000).

Molecular identification and description of pelagic young of the rockfishes *Sebastes constellatus* and *Sebastes ensifer*

Axayácatl Rocha-Olivares
Scripps Institution of Oceanography
University of California San Diego
9500 Gilman Dr., La Jolla, California 92093-0208
Present address. Louisiana State University
Department of Biological Sciences
508 Life Sciences Building
Baton Rouge, Louisiana 70809-1715
E-mail address arocha@lsu.edu

H. Geoffrey Moser

Jason Stannard
La Jolla Laboratory
Southwest Fisheries Science Center
National Marine Fisheries Service, NOAA
P.O. Box 271, La Jolla California 92038

Live-bearing rockfishes of the genus *Sebastes* constitute the largest genus of scorpaeniform fishes with about 110 species worldwide, 72 of which reside in the Northeast Pacific (Eschmeyer and Herald, 1983; Kendall, 1991; Nelson, 1994). In this geographic region, rockfishes are very important in the bottom trawl fishery as well as in recreational fisheries (Lenarz, 1986; Leet et al., 1992; Low, 1993). Newborn rockfishes are extruded as first-feeding larvae from viviparous females (Yoklavich and Boehlert, 1991), and they rank among the most frequent and abundant of all fish larvae in plankton collections off the coasts of California and Oregon (Moser et al., 1993; Moser, 1996; Doyle[1]). The juvenile stages of *Sebastes* are also important ecologically as prey of larger fishes and birds (Love et al., 1991; Moser and Boehlert, 1991; Ainley et al., 1993). In addition to their biological significance, rockfish larvae and early juveniles have received much attention for their potential use in estimating spawning biomass and recruitment (Moser and Butler, 1987; Hunter and Lo, 1993; Ralston and Howard, 1995).

Species identification has been the most challenging aspect in the study of the early life history stages of *Sebastes*. For instance, of the 59 species distributed in the California Cooperative Oceanic Fisheries Investigations (CalCOFI) region, complete developmental series are available for only thirteen and partial series are available for an additional eight (Moser, 1996). Several factors have influenced this lack of a complete developmental series, including a very large number of sympatric species, the preponderance of small larvae, and the limited number of taxonomic characters identifiable in the early stages (Sakuma and Laidig, 1995; Moser, 1996; Moser et al., 1977). Alternative methods involving the analysis of electrophoretic patterns or DNA

[1] Doyle, M. 1992. Patterns in distribution and abundance of ichthyoplankton off Washington, Oregon, and northern California (1980–1987). U.S. Dep. Commer., NOAA NMFS Alaska Fish. Sci. Center Process Report 92-14, 344 p.

have been proposed to overcome this obstacle (e.g. Seeb and Kendall, 1991; Rocha-Olivares, 1998b). In our paper we describe new developmental stages of two species of *Sebastes* identified using mitochondrial DNA (mtDNA) sequence data.

Materials and methods

Sample collection

Specimens were collected in the vicinity of Tanner (32°69'N119°12'W) and Cortes (32°61'N119°33'W) Banks in August 1995 during a rockfish sampling cruise aboard the Scripps Institution of Oceanography RV *Robert Gordon Sproul*. Four specimens were sampled in oblique tows with a 5-m^2 Isaacs-Kidd midwater trawl. The fifth specimen was retrieved, intact, from the digestive tract of an adult greenspotted rockfish, *Sebastes chlorostictus*, caught with hook and line. Fish were preserved in 95% ethanol. Except for one specimen that completely dried out upon evaporation of the preserving fluid, the shrinkage effect of ethanol preservation on the length of the specimens has been assumed to be negligible owing to their relatively large size (15.0–30.4 mm SL, Radtke, 1989). The dehydrated specimen was rehydrated in water before description.

Molecular analyses

Total genomic DNA was extracted and purified from liver or muscle tissue with a GlasPac/GS (U.S. National Scientific Supply CO., San Rafael, CA) DNA purification kit as described in Rocha-Olivares (1998b). Universal primers, and versions customized for *Sebastes*, were used for the polymerase chain reaction (PCR) and automated cycle sequencing (see Rocha-Olivares, 1998a for a complete list of primers). A region spanning 781 base pairs (bp) of the mitochondrial cytochrome *b* (cyt-*b*) was amplified by PCR as described in Rocha-Olivares et al. (1999a). Briefly, 50-mL reactions were performed following Kocher et al. (1989), with 100 ng of genomic DNA and 2 units of Taq DNA polymerase (Perkin Elmer Cetus, Foster City, CA, or Gibco BRL, Rockville, MD). Thermal cycling was performed as follows: hot start at 90°C for 2 min., followed by 36 cycles of 50 s at 94°C; 2 min at 51 C; 1.5 min at 72°C, and a final extension of 3 min at 72°C to ensure complete amplification of products. PCR products were purified with microconcentrators (Microcon® 100, Millipore, Bedford, MA) or purification columns (QIAquick® 250, Qiagen, Valencia, CA) following manufacturers' protocols. Automated DNA sequencing was performed with ABI PRISM (Perkin Elmer Cetus) DyeDeoxy® dRhodamine chemistry on an ABI 377 DNA sequencer in 12 µL reactions (30–100 ng double stranded PCR product, 3 pmol primer, 1.6–2.0 µL terminator ready reaction mix); cycle sequencing annealing was 10 seconds at 55°C; we followed the manufacturer's protocol in respect to all other experimental conditions. Sequence data were obtained by sequencing both DNA strands of the PCR products.

Molecular identification

The mtDNA data from the unknown pelagic young was aligned with a database of orthologous sequences obtained from adult specimens of congeneric species generated at the genetics and physiology laboratory of the Southwest Fisheries Science Center in La Jolla (Rocha-Olivares, 1998a).[2] Because the morphological and pigmentation patterns of the specimens revealed that they belonged to the subgenus *Sebastomus* (Chen, 1971; 1975), the DNA sequence data were compared to 89 sequences obtained from all 15 species of this subgenus (Rocha-Olivares et al., 1999a; 1999c). Species identification was determined on the basis of the most similar haplotype among the species compared. Sequence comparisons were carried out by using pair-wise measures of sequence divergence calculated as the total number of different nucleotides.

Results

Molecular identification

The mtDNA sequence data confirmed morphological observations that the five pelagic young were members of the subgenus *Sebastomus*. The number of conspecific DNA sequences used in the reference database ranged from 1 to 13 (*S. notius*, *S. lentiginosus*, n=1; *S. spinorbis*, n=3; *S. capensis*, n=4; *S. oculatus*, *S. exsul*, *S. helvomaculatus*, n=5; *S. rosaceus*, n=6; *S. chlorostictus*, *S. ensifer* n=7; *S. umbrosus*, *S. constellatus*, *S. simulator*, *S. eos*, n=8; *S. rosenblatti*, n=13). Two juveniles (CA3 and CA4) had identical mtDNA cyt-*b* sequences. On the basis of the number of nucleotide differences, one specimen (CA1, Fig. 1) was identified as starry rockfish, *S. constellatus*, and the other four as swordspine rockfish, *S. ensifer* (CA2-CA5, Fig. 1). The mitochondrial haplotypes of three specimens (CA1, CA3, and CA4) were identical to adult reference sequences, providing unequivocal

[2] Rocha-Olivares, A., and R. D. Vetter. 1998. Unpubl. data.

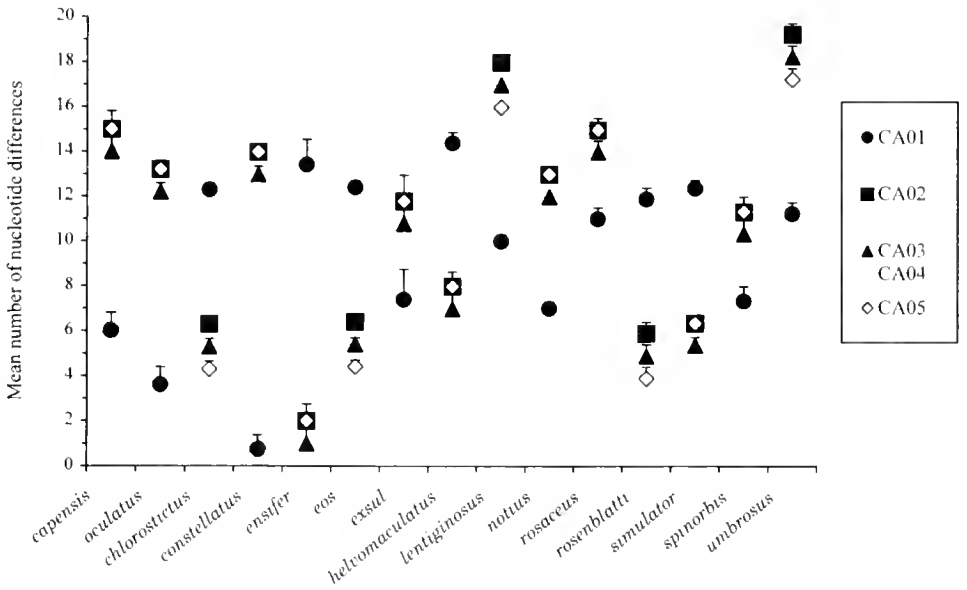

Figure 1

Plot of the mean number of nucleotide differences (+SE) in 781 base pairs of the cytochrome *b* gene of the four haplotypes found among five unidentified *Sebastes* pelagic young (CA1-CA5) with orthologous sequences from known adults of congeneric species of the subgenus *Sebastomus*.

evidence of species identity. The others differed from reference data by 1 to 3 nucleotides (Fig. 1).

Cluster analyses (unweighted pair-group method using averages [UPGMA]) performed on the pairwise distance matrices generated from the molecular data clustered CA1 with *S. constellatus* and CA2-CA5 with *S. ensifer* (not shown).

Description of specimens

Sebastes constellatus (Jordan and Gilbert 1880) Transforming larva: CA1 (15.0 mm SL), Figure 2A

Literature Transforming larvae and pelagic juveniles of *S. constellatus* have not been described in the published literature.[3] Larval stages up to notochord flexion (~7.1 mm) show features typical of preflexion larvae of other *Sebastomus* species: robust head and body with strong serrated parietal ridges and spines; strong postocular ridge and spine; heavy pigment on top of head, on jaws, and on paired fins, with heaviest pigment on distal edge of pectoral fin; postanal ventral midline series of 11–17 melanophores (Moser et al., 1977; Moser, 1996).

General morphology Body moderately deep and compressed; head, jaws, and eyes large (Table 1).

Fins and other meristic features Full complements of spinous and soft rays present; dorsal- and anal-fin rays moderate in length; anteriormost 5 scales of lateral line just beginning to form but visible only after staining with alizarin red-S (Table 2).

Spination Supraocular crest and associated spines (preocular, supraocular, postocular) prominent; parietal crests well developed, weakly serrate parietal spine slightly longer than nuchal spine; tympanic spine not yet formed on the upper margin of sensory canal pore but a slight prominence, indicating initial spine development, is noticeable; posterior preopercular series well developed with spine at angle longer than others and finely serrated along the longitudinal flange (dorsal and ventral margins of spine smooth); first and third spines weakly developed in anterior preopercular series; first and second lower infraorbitals present; first and fourth spines in upper series visible only after staining; presence of other spines as listed in Table 3.

[3] A fully pigmented "pelagic juvenile" (length not given) ascribed to *S. constellatus* is illustrated and briefly described *in* Laroche, W. A. 1987. Guide to the larval and juvenile rockfishes (*Sebastes*) of North America. Unpublished manuscript. Stonefish Environm. & Taxon. Serv., Enosburg Falls, VT 05450.

Table 1

Morphometric characters of pelagic young of three *Sebastes* (subgenus *Sebastomus*) species. Average values (in percent) are given for each proportion, followed by the standard deviation and the range. Proportions for *S. helvomaculatus* derived from data in Richardson and Laroche (1979). Abbreviations: HL= Head length; SL= standard length.

	Transforming specimens			Pelagic juveniles	
Proportions	*S. constellatus* n = 1 15.0 mm SL	*S. ensifer* n = 1 19.8 mm SL	*S. helvomaculatus* n = 5 17.8–18.6 mm SL	*S. ensifer* n = 3 27.3–30.4 mm SL	*S. helvomaculatus* n = 8 19.8–41.6 mm SL
Body depth at pectoral fin base/SL	33.3	33.3	31.6 ±0.50 (31.0–32.1)	32.9 ±1.23 (31.5–33.9)	31.2 ±1.57 (28.4–32.9)
Body depth at anus/SL	26.0	26.8	23.8 ±0.86 (23.1–25.3)	27.1 ±1.15 (26.0–28.3)	23.2 ±1.24 (21.2–25.0)
Snout to anus length/SL	64.0	63.1	61.4 ±2.12 (59.8–64.5)	63.6 ±2.12 (61.2–65.1)	62.8 ±2.44 (59.8–66.0)
Snout to pelvic fin origin/SL	41.3	39.9	41.7 ±4.15 (38.0–47.3)	40.3 ±1.85 (38.5–42.2)	42.8 ±3.17 (39.3–48.2)
Head length/SL	37.3	39.9	40.3 ±2.62 (36.4–43.0)	32.5 ±0.52 (31.9–32.9)	40.1 ±1.48 (37.5–41.9)
Eye diameter/HL	39.3	38.0	34.4 ±2.73 (32.0–37.5)	36.8 ±0.79 (36.0–37.5)	33.6 ±1.76 (30.9–36.9)
Upper jaw length/HL	50.0	46.8	43.4 ±2.80 (39.7–47.2)	51.8 ±2.29 (49.4–54.0)	45.2 ±2.63 (40.2–47.6)
Snout length/HL	26.8	26.6	32.3 ±4.50 (25.0–36.0)	25.6 ±1.29 (24.7–27.1)	31.7 ±2.52 (26.7–34.2)
Interorbital distance/HL	30.4	24.1	24.9 ±2.04 (23.3–28.4)	26.4 ±1.57 (25.0–28.1)	21.6 ±3.83 (13.3–25.6)
Angle gill raker length/HL	17.9	16.5	15.0 ±0.97 (13.8–16.4)	17.9 ±0.88 (17.0–18.8)	14.2 ±1.10 (12.7–15.7)
Longest dorsal spine length/HL	28.6	36.7	33.2 ±3.77 (30.7–37.5)	40.3 ±1.21 (39.3–41.7)	30.9 ±2.95 (28.0–35.7)
Longest dorsal ray length/HL	ray broken	39.2	36.8 ±4.05 (32.5–41.7)	44.7 ±3.26 (42.0–48.3)	35.8 ±2.23 (31.7–38.1)
Longest anal spine length/HL	tip broken	31.7	31.3 ±3.34 (28.4–36.1)	45.5 ±2.64 (42.7–47.9)	32.4 ±5.69 (23.8–38.8)
Pectoral fin length/SL	22.7	broken	26.2 ±1.28 (25.1–28.3)	26.5 ±1.53 (24.9–28.0)	25.3 ±3.44 (16.8–26.9)
Pectoral fin base depth/SL	9.3	8.6	9.6 ±0.33 (9.0–9.8)	8.5 ±0.42 (8.1–8.9)	9.0 ±0.34 (8.2–9.3)
Pelvic fin length/SL	17.3	20.7	19.6 ±1.44 (17.9–21.4)	19.5 ±1.06 (18.3–20.2)	19.2 ±1.37 (17.3–21.4)
Pelvic spine length/SL	16.0	16.2	18.1 ±0.76 (17.3–19.1)	16.0 ±0.57 (15.4–16.5)	16.4 ±2.01 (13.5–18.9)
Parietal spine length/HL	8.6	5.6	11.5 ±2.30 (9.0–14.3)	not present	5.6 ±3.32 (1.1–9.5)
Nuchal spine length/HL	6.1	5.6	4.2 ±0.90 (3.0–5.4)	6.0 ±0.32 (5.6–6.3)	3.6 ±1.15 (1.7–5.2)
Preopercular spine length/HL	23.2	10.6	18.3 ±1.94 (16.3–20.9)	13.3 ±0.38 (13.0–13.5)	11.7 ±6.25 (2.6–15.9)

Table 2

Meristics from transforming larval specimens and pelagic juveniles of *Sebastes* (subgenus *Sebastomus*) from southern California. CA 1, CA 2, etc. are identification labels for individual fish.

Features counted	CA 1 *S. constellatus* transforming specimen	CA 2 *S. ensifer* transforming specimen	CA 3 *S. ensifer* pelagic juvenile	CA 4 *S. ensifer* pelagic juvenile	CA 5 *S. ensifer* pelagic juvenile
Standard length (mm)	15.0	19.8	30.4	30.1	27.3
Dorsal-fin spines and rays	XIII, 13	XIII, 12	XIII, 13	XIII, 12	XIII, 13
Anal-fin spines and rays	III, 6	III, 6	III, 6	III, 6	III, 6
Pectoral-fin rays	17/17	17/17	17/17	17/17	17/17
Pelvic-fin spines and rays	I, 5	I, 5	I, 5	I, 5	I, 5
Gill rakers	7 + 19 = 26	9 + 25 = 34	11 + 25 = 36	11 + 27 = 38	11 + 25 = 36
Lateral line pores	5 visible	~10 visible	scales forming; some missing in series	~40	39
Procurrent caudal-fin rays	9 + 9	10 + 11	10 + 11	11 + 11	11 + 11

Pigmentation Solid sheath over gut; solid patch over brain; shallow, internal, dorsal, and dorsolateral melanophores on snout and some at tip of lower jaw; large postorbital patch continues posteriad to cover opercle; patch of melanophores continuous with dorsal brain sheath, extending back on dorsum to sixth dorsal-fin spine and ventrad to lateral line region to form a saddle; separate patch below the saddle forming at horizontal septum region; melanophore on each side of dorsum at ninth dorsal-fin spine; bar at caudal peduncle complete except at ventral midline; melanistic pigment scattered over pectoral and pelvic fins.

Sebastes ensifer Chen 1971
Transforming larva: CA2 (19.8 mm SL), Figure 2B
Pelagic juveniles CA5 (27.3 mm), Figure 2C; CA3 (30.4 mm SL) and CA4 (30.1 mm SL) not illustrated

Literature Transforming larvae and pelagic juveniles of *S. ensifer* have not been described in the published literature.[4] A 4.2-mm first-feeding larva has been illustrated (Moser et al., 1977; Moser, 1996), showing features typical of first-feeding *Sebastomus* larvae as summarized above for *S. constellatus*.

General morphology Body moderately deep and compressed; head, jaws, and eyes large; relative head length, and eye diameter decrease after transformation to pelagic juveniles; relative interorbital distance dorsal spine and ray length, and anal spine length increase after transformation (Table 1).

Fins and other meristic features Full complements of spinous and soft rays present; dorsal and anal-fin rays moderate in length; anterior scales in lateral line series forming, ~10 visible after staining in transforming specimen, full complements of lateral line scales forming in pelagic juveniles (Table 2).

Spination Supraocular crest and associated spines well developed; parietal crests well developed, weakly serrate, and parietal and nuchal spines subequal in transforming specimen; in pelagic juveniles the nuchal spine forms the terminus of the parietal ridge and only a remnant of the parietal spine can be seen; tympanic spine present; posterior preopercular series well developed with spine at angle longer than others but not serrated; anterior preopercular spines absent; first and second lower infraorbitals present; upper infraorbitals faintly visible after staining in transforming specimen but not in pelagic juveniles; cleithral spine present in pelagic juveniles but not in transforming specimen; presence of other spines as listed in Table 3.

Pigmentation *Transforming specimen*: solid sheath over gut; solid covering over brain; scattered melanophores on snout and some at tip of lower jaw; large postorbital and opercular patches; patch of melanophores continuous with dorsal brain sheath extending back on dorsum to 11th dorsal-fin spine

[4] A 35.5-mm pelagic juvenile ascribed to *Sebastes ensifer* is illustrated and briefly described *in* Laroche, W. A. 1987. Guide to larval and juvenile rockfishes (*Sebastes*) of North America. Unpublished manuscript. Stonefish Environm. & Taxon. Serv., Enosburg Falls, VT 05450

Table 3

Head spines in pelagic young of *Sebastes* (subgenus *Sebastomus*) from southern California. Symbols: + = present; – = absent; ☆ = weakly developed or initial development. CA 1, etc. are identification labels for individual fish.

	Specimen (standard length)				
Spine	CA 1 (15.0 mm)	CA 2 (19.8 mm)	CA 3 (30.4 mm)	CA 4 (30.1 mm)	CA 5 (27.3 mm)
Parietal	+	+	In these specimens the parietal spines are degenerating and the nuchal spine is becoming the terminus of each parietal ridge.		
Nuchal	+	+	+	+	+
Anterior preopercular-1	☆	–	–	–	–
Anterior preopercular-2	–	–	–	–	–
Anterior preopercular-3	☆	–	–	–	–
Posterior preopercular-1	+	+	+	+	+
Posterior preopercular-2	+	+	+	+	+
Posterior preopercular-3	+	+	+	+	+
Posterior preopercular-4	+	+	+	+	+
Posterior preopercular-5	+	+	+	+	+
Opercular-upper	+	+	+	+	+
Opercular-lower	+	+	+	+	+
Interopercular	☆	☆	–	–	–
Subopercular	–	–	–	–	–
Preocular	+	+	+	+	+
Supraocular	+	+	+	+	+
Postocular	+	+	+	+	+
Lower infraorbital-1	+	+	+	+	+
Lower infraorbital-2	+	+	+	+	+
Lower infraorbital-3	–	–	–	–	–
Upper infraorbital-1	+	☆	–	–	–
Upper infraorbital-2	–	☆	–	–	–
Upper infraorbital-3	–	☆	–	–	–
Upper infraorbital-4	☆	☆	–	–	–
Nasal	+	+	+	+	+
Coronal	–	–	–	–	–
Tympanic	☆	+	+	+	+
Pterotic	☆	–	–	–	–
Upper posttemporal	+	+	+	+	+
Lower posttemporal	+	+		☆	+
Supracleithral	+	+	+	+	+
Cleithral	–	–	+	+	+

and ventrad to lateral line region to form a broad saddle; saddle continues ventrad faintly to horizontal septum; wide bar at caudal peduncle, complete except at ventral midline; scattered melanophores on pelvic fin and at base of pectoral fin. Embedded pigment, barely visible through the musculature of the body, lies on the upper surface of the vertebral column. *Pelagic juveniles*: general melanistic pigment filling in previously unpigmented regions except ventrally on head, chest, and region above anal fin; heavy along dorsum; saddle somewhat variegated, with pale regions that become white patches in adults; caudal peduncle bar enlarged anteriorly, blending with saddle, darkest on peduncle region with several chevrons forming; some pigment on paired fins.

Table 4

Geographic ranges and meristic characters for the species of *Sebastes*, subgenus *Sebastomus*, in the eastern North Pacific. All species have three anal spines, one pelvic spine with five rays, and 8+7 principal caudal-fin rays. Data are derived primarily from Miller and Lea (1972), Chen (1971, 1975, 1986), Matarese et al. (1989), Moser (1996). Abbreviations: BCA = Baja California; C = central; CA = California; G of AK = Gulf of Alaska; G of CA = Gulf of California; N = northern; S = southern; WA = Washington. GR = gill rakers.

		Fin rays						
		Dorsal						
Species	Distribution	Spines	Rays	Anal	Pectoral	Vertebrae	GR (first arch)	Lateral line pores
S. chlorostictus	WA to C BCA	XIII	11–15	5–7	16–18	26–27	31–36	35–43
S. constellatus	C CA to S BCA	XIII–XIV	12–14	5–7	16–18	25–26	25–30	37–47
S. ensifer	C CA to C BCA	XIII	12–14	5–7	16–18	26	34–40	34–44
S. eos	C CA to C BCA	XIII	11–13	5–7	17–18	26	26–31	34–42
S. exsul	G of CA	XIII	12–13	5–6	16–18	26	32–37	35–43
S. helvomaculatus	G of AK to S CA	XII–XIV	12–14	6–7	15–18	26	28–33	34–45
S. lentiginosus	S CA to N BCA	XIII	12–13	6–7	16–18	26	34–39	33–41
S. notius	C BCA	XIII	11–13	5–7	15–18	26	33–38	34–44
S. rosaceus	N WA to C BCA	XIII–XIV	11–14	5–7	16–18	26–27	29–34	36–46
S. rosenblatti	C CA to C BCA	XIII–XIV	11–13	5–6	16–18	26	28–34	34–42
S. simulator	S CA to C BCA	XIII	12–14	5–6	16–18	26	28–33	33–40
S. spinorbis	G of CA	XIII	13–14	6	18	26	30–33	33–38
S. umbrosus	C CA to S BCA	XII–XIV	11–13	5–7	15–18	26	31–38	33–44

Discussion

Molecular identification

The genetic information encoded in the rockfish mitochondrial cytochrome *b* has been found useful in the study of phylogenetic relationships of the species in the genus *Sebastes* (Rocha-Olivares, 1998a). The degree of genetic variability is large enough to recognize diagnostic mutations characteristic of several species (Rocha-Olivares, 1998a; Rocha-Olivares and Vetter[2]). The use of this information in blind tests of species identification of adult *Sebastes*, independently determined by morphological and genetic techniques, has given satisfactory results (Rocha-Olivares and Lea[5]). Diagnostic mutations have been used to design a method of species identification based on multiplex PCR (Rocha-Olivares, 1998b). In our study we relied on raw DNA sequence data to determine the species identity of five wild-caught pelagic young of *Sebastes*. The very small sequence divergence of their mtDNA with that of known adults (ranging from zero to three bp) provided very strong evidence supporting the identity of the unidentified specimens. Moreover, the small intraspecific genetic variation, indicated by the reduced standard errors in Figure 1, suggests that the possibility of species misidentification with our molecular approach is also very small.

Faster-evolving regions of the mtDNA have been successfully used to study the genetic structure of rockfish populations in both hemispheres (Rocha-Olivares et al., 1999b; Rocha-Olivares and Vetter, 1999); therefore, it is conceivable that molecular tools can also be applied intraspecifically to study, for example, the relative contribution of juvenile recruits from genetically differentiated populations.

Species comparisons

Transforming specimens of *S. constellatus* and *S. ensifer* The specimens of *S. constellatus* and *S. ensifer* are remarkably similar. The meristic similarity reflects the general overlap among species documented for the subgenus (Table 4; Chen, 1971, 1975). The distinctly lower gill raker count for the transforming specimen of *S. constellatus*, compared with that of *S. ensifer* specimens (Table 2), matches the gill raker counts of adults (Table 4; Chen, 1971). Slight differences in spination between the trans-

[5] Rocha-Olivares, A., and Lea, R. N. 1998. Unpubl. data.

forming specimens of the two species (e.g. a longer serrate third preopercular spine in *S. constellatus*, more infraorbitals in *S. ensifer* only visible after staining) may be due to ontogenetic stage or individual variation (Table 3). However, the relatively longer fin rays in *S. ensifer* appear to be a species difference. The relative size and position of the parietal and nuchal spines differs in the two transforming specimens; however, this may be due to difference in stage of development. In the *S. ensifer* series the nuchal spine gradually replaces the parietal spine as the terminus of the parietal ridge and this may also occur in *S. constellatus*. Transforming specimens of the two species differ slightly in pigmentation (e.g. wider dorsal saddle and peduncle patch in *S. ensifer*); however, this difference can not be confirmed without additional specimens.

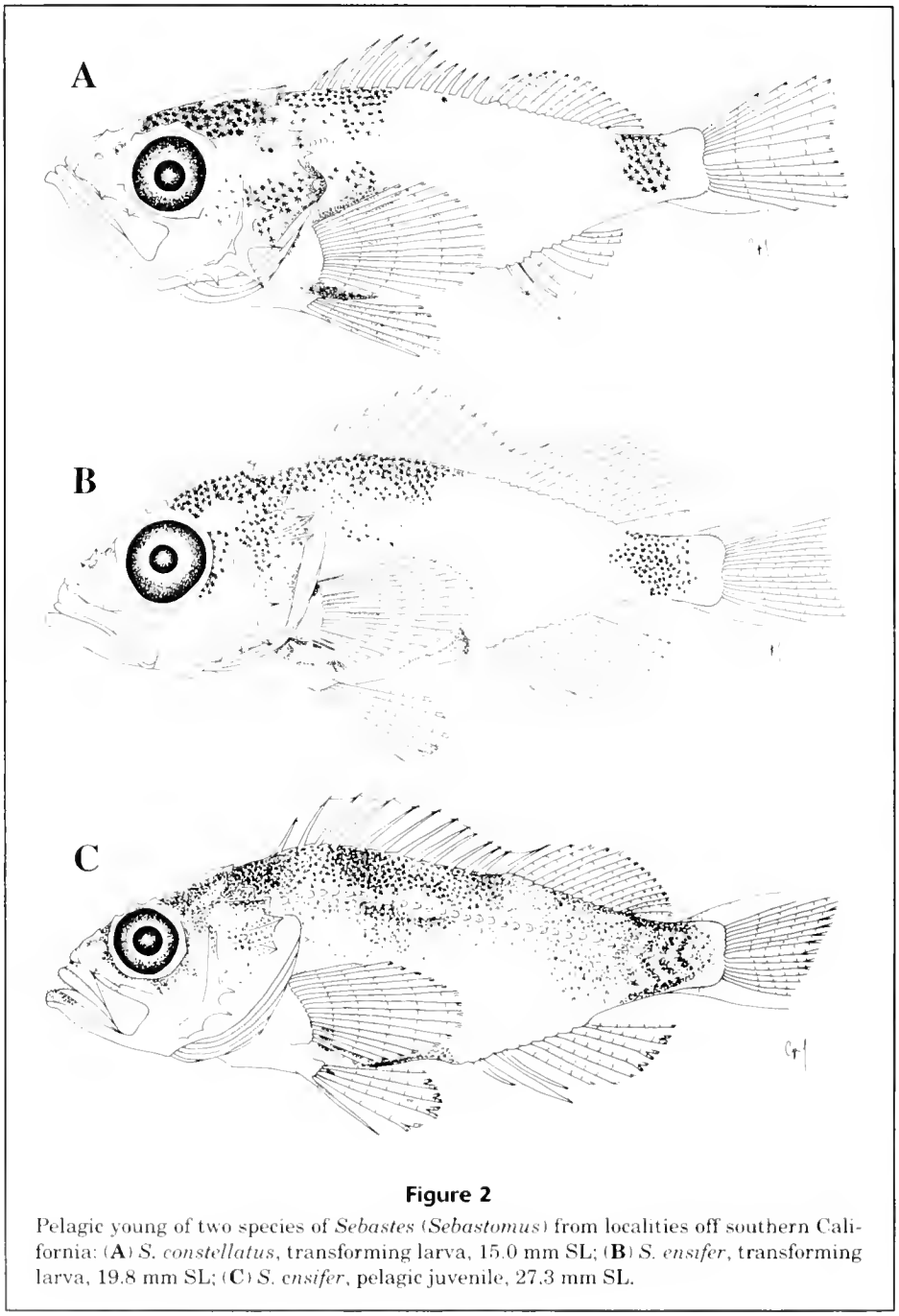

Figure 2

Pelagic young of two species of *Sebastes* (*Sebastomus*) from localities off southern California: (**A**) *S. constellatus*, transforming larva, 15.0 mm SL; (**B**) *S. ensifer*, transforming larva, 19.8 mm SL; (**C**) *S. ensifer*, pelagic juvenile, 27.3 mm SL.

Transforming specimens and pelagic juveniles of *S. ensifer* and *S. helvomaculatus*

The species differ markedly in morphometry (Table 1). *S. ensifer* has a deeper-body than field-caught *S. helvomaculatus* described and illustrated in Richardson and Laroche (1979), as shown by the greater relative body depth measured at the anus (Table 1; Figs. 2 and 3). The two species are different in other morphometric features. Eye diameter, jaw length, and fin ray and spine lengths in the dorsal and anal fins are relatively greater in transforming specimens and pelagic juveniles of *S. ensifer* compared with *S. helvomaculatus*, whereas relative snout length is greater in *S. helvomaculatus*. In pelagic juveniles, relative head length is greater in *S. helvomaculatus* than in *S. ensifer*, whereas relative interorbital length is less compared with that in *S. ensifer*. The two species differ in stage of development at length. The illustrated 18.4-mm transforming specimen of *S. helvomaculatus* lacks a melanistic saddle on the trunk, and the caudal peduncle bar is just beginning to form, whereas these features are well established in the 19.8-mm specimen of *S. ensifer* (Figs. 2 and 3). The pigment saddle is present in the 22.4-mm pelagic juvenile of *S. helvomaculatus* but does not extend ventrad more than about half-way to the lateral line. Moreover, the complex pattern of bars and clear areas present on late-stage pelagic juveniles of *S. ensifer* is not present on *S. helvomaculatus* (Fig. 3). Also, the

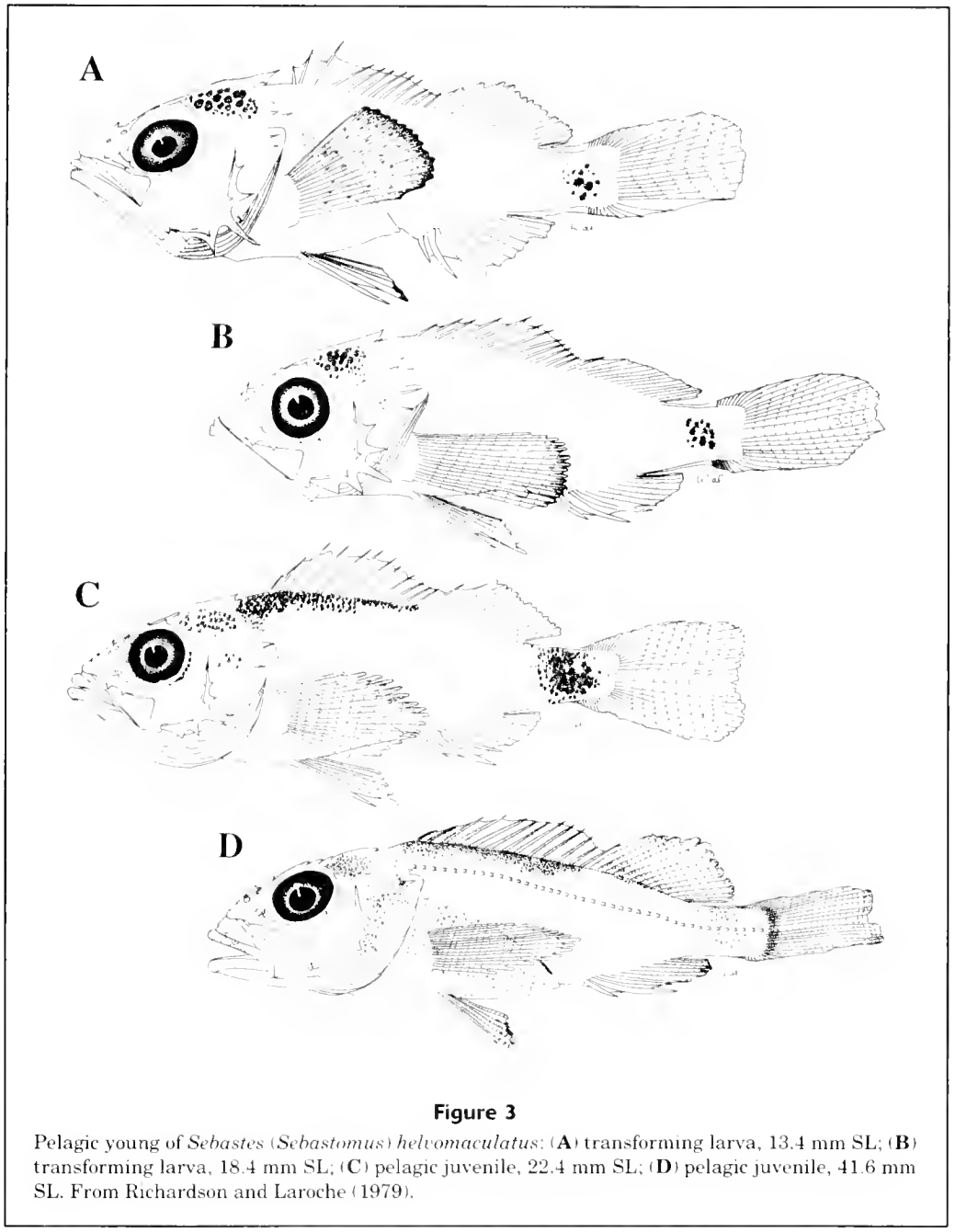

Figure 3

Pelagic young of *Sebastes* (*Sebastomus*) *helvomaculatus*: (**A**) transforming larva, 13.4 mm SL; (**B**) transforming larva, 18.4 mm SL; (**C**) pelagic juvenile, 22.4 mm SL; (**D**) pelagic juvenile, 41.6 mm SL. From Richardson and Laroche (1979).

ontogenetic changes in head spines (e.g. loss of infraorbitals and anterior preopercular; decrease in the relative size of the parietals) occur in *S. helvomaculatus* larger than *S. ensifer* (Figs. 2 and 3).

Pelagic juveniles of other *Sebastomus* species A field-caught 21.0-mm pelagic juvenile of *S. chlorostictus* illustrated in Matarese et al. (1989) and Kendall (1991) is generally similar to specimens of *S. constellatus* and *S. ensifer* described in this study. In contrast to these species, the nape area in *S. chlorostictus* appears to lack pigment. In *S. chlorostictus* the dark pigment saddle extends from the first to sixth dorsal-fin spines, becomes wider mid-laterally on the trunk and appears to extend to the abdominal region. The caudal peduncle pigment is equally heavy and forms a complete band around the peduncle in the 21.0-mm specimen. Also, the dorsal and anal fin rays appear to be shorter than those in *S. ensifer*.

Comments on the identification of pelagic young of *Sebastomus* The transforming larvae and pelagic

juveniles of *S. constellatus* and *S. ensifer* identified by molecular methods, although conforming to the general facies known for *Sebastomus* pelagic young, show some differences in morphological features and pigmentation that may permit their identification by traditional means. The possibility of identifying the pelagic young of this species-rich subgenus is further suggested by the striking differences between pelagic young of *S. ensifer* and *S. helvomaculatus*. Further advancement will require: 1) the collection of fresh specimens of pelagic young of all species of *Sebastomus* in the waters off California and Baja California; 2) the establishment of ontogenetic series positively identified by molecular methods; and 3) a detailed description and series of illustrations published for each species. Pelagic young of this subgenus are common constituents of the midwater fauna of the continental borderland of the Southern California Bight (Moser and Ahlstrom, 1978; Moser and Boehlert, 1991), and specimens are readily available from midwater trawls.

In conclusion, this paper reports a novel approach to the study of young rockfishes. We have used molecular data in conjunction with morphological descriptions to increase knowledge on the identification of elusive early life history stages of *Sebastes*.

Acknowledgments

This research was supported by NOAA Fisheries by core funding and a Saltonstall-Kennedy Fisheries Development Grant to R. D. Vetter, H. G. Moser, and W. Watson. Ship time on board the RV *Robert Gordon Sproul* was granted to A. Rocha-Olivares by the Ship Operations Office of the Scripps Institution of Oceanography. Additional support for A. Rocha-Olivares was provided by the Consejo Nacional de Ciencia y Tecnología (México) and the Shirley-Boyd Memorial Fellowship through the Scripps Institution of Oceanography. D. W. Foltz read an earlier version of the manuscript. William Watson and three anonymous reviewers offered helpful suggestions. We are indebted to C. Manning and W. Watson for preparing the illustrations of Figure 2.

Literature cited

Ainley, D. G., W. J. Sydeman, R. H. Parrish, and W. H. Lenarz.
1993. Oceanic factors influencing distribution of young rockfish (*Sebastes*) in central California—a predators perspective. Calif. Coop. Oceanic Fish. Invest. Rep. 34:133–139.

Chen, L.-C.
1971 Systematics, variation, distribution, and biology of the subgenus *Sebastomus* (Pisces, Scorpaenidae, *Sebastes*). Bull. Scripps Inst. Oceanogr. Univ. Calif. 18:1–115.

1975. The rockfishes, genus *Sebastes* (Scorpaenidae), of the Gulf of California, including three new species with a discussion of their origin. Proc. Calif. Acad. Sci. Ser.4, 40(6):109–141.

1986. Meristic variation in *Sebastes* (Scorpaenidae), with an analysis of character association and bilateral pattern and their significance in species separation. U.S. Dep. Commer., NOAA Tech. Rep. NMFS 45, 25 p.

Eschmeyer, W. N., and E. S. Herald.
1983. A field guide to Pacific coast fishes North America. Houghton Mifflin Company, Boston, MA, 336 p.

Hunter, J. R., and N. C. H. Lo.
1993. Ichthyoplankton methods for estimating fish biomass. Introduction and terminology. Bull. Mar. Sci. 53:723–727.

Kendall, A. W., Jr.
1991. Systematics and identification of larvae and juveniles of the genus *Sebastes*. Environ. Biol. Fishes 30(1-2): 173–190.

Kocher, T. D., W. K. Thomas, A. Meyer, S. V. Edwards, S. Pääbo, F. X. Villablanca, and A. C. Wilson.
1989. Dynamics of mitochondrial DNA evolution in animals: amplification and sequencing with conserved primers. Proc. Nat. Acad. Sci. U.S.A. 86(16):6196–6200.

Leet, W. F., C. M. Dewees, and C. W. Haugen (eds.).
1992. California's living marine resources and their utilization. Univ. Calif. Sea Grant Rep. UCSGEP- 92-12, 257 p.

Lenarz, W. H.
1986. The rockfish fishery, a California perspective. Rockfish: a focus for research? Proceedings of a California Sea Grant Workshop. Report No. T-CSGCP-015, p. 3–9. Univ. Calif., Davis, CA.

Love, M. S., M. H. Carr, and L. J. Haldorson.
1991. The ecology of substrate-associated juveniles of the genus *Sebastes*. Environ. Biol. Fishes 30(1–2):225–243.

Low, L., (ed.).
1993. Status of living marine resources off the Pacific coast of the United States for 1993. U.S. Dep. Commer., NOAA Tech. Memo. NMFS-AFSC-26, 90 p.

Matarese, A. C., A. W. Kendall Jr., D. M. Blood, and B. M. Vinter.
1989. Laboratory guide to early life history stages of northeast Pacific fishes. U.S. Dep. Commer., NOAA Tech. Rep. NMFS 80, 652 p.

Miller, D. J., and R. N. Lea.
1972. Guide to the coastal marine fishes of California. Calif. Dep. Fish Game Fish Bull. 157, 249 p.

Moser, H. G.
1996. Scorpaenidae: Scorpionfishes and rockfishes. *In* The early stages of fishes in the California Current Region (H. G. Moser, ed.), p. 733–795. Calif. Coop. Oceanic Fish. Invest. Atlas 33.

Moser, H. G., and E. H. Ahlstrom.
1978. Larvae and pelagic juveniles of blackgill rockfish, *Sebastes melanostomus*, taken in midwater trawls off southern California and Baja California. J. Fish. Res. Board Can. 35(7):981–996.

Moser, H. G., E. H. Ahlstrom, and E. M. Sandknop.
1977. Guide to the identification of scorpionfish larvae (family Scorpaenidae) in the eastern Pacific with comparative notes on species of *Sebastes* and *Helicolenus* from other oceans. U.S. Dep. Commer., NOAA Tech. Rep. NMFS Circ. 402, 71 p.

Moser, H. G., and G. W. Boehlert.
1991. Ecology of pelagic larvae and juveniles of the genus *Sebastes*. Environ. Biol. Fishes 30(1– 2):203–224.

Moser, H. G., and J. L. Butler.
1987. Descriptions of reared larvae of six species of *Sebastes*. *In* Widow rockfish, Proceedings of a workshop, Tiburon, California, Dec. 11–12, 1980 (W. H. Lenarz and D. R. Gunderson, eds.) p. 19–29. U.S. Dep. Commer., NOAA Tech. Rep. NMFS 48.

Moser, H. G., R. L. Charter, P. E. Smith, D. A. Ambrose, S. R. Charter, C. A. Meyer, E. M. Sandknop, and W. Watson.
1993. Distributional atlas of fish larvae and eggs in the California current region: taxa with 1000 or more total larvae, 1951 through 1984. Calif. Coop. Oceanic Fish. Invest. Atlas 31, 233 p.

Nelson, J. S.
1994. Fishes of the world, third ed. John Wiley & Sons, Inc., New York, NY, 600 p.

Radtke, R. L.
1989. Larval fish age, growth, and body shrinkage: information available from otoliths. Can. J. Fish. Aquat. Sci. 46:1884–1894.

Ralston, S., and D. F. Howard.
1995. On the development of year-class strength and cohort variability in two northern California rockfishes. Fish. Bull. 93(4):710–720.

Richardson, S. L., and W. A. Laroche.
1979. Development and occurrence of larvae and juveniles of the rockfishes *Sebastes crameri*, *Sebastes pinniger*, and *Sebastes helvomaculatus* (Family Scorpaenidae) off Oregon. Fish. Bull. 77(1):1–46.

Rocha-Olivares, A.
1998a. Molecular evolution, systematics, zoogeography and levels of intraspecific genetic differentiation in the species of the antitropical subgenus *Sebastomus*, *Sebastes* (Scorpaeniformes, Teleostei) using mitochondrial DNA sequence data. Ph.D. diss., Scripps Institution of Oceanography, Univ. of California, San Diego, CA, 240 p.

1998b. Multiplex haplotype-specific PCR: a new approach for species identification of the early life stages of rockfishes of the species-rich genus *Sebastes* Cuvier. J. Exp. Mar. Biol. Ecol. 231(2):279–290.

Rocha-Olivares, A., C. A. Kimbrell, B. J. Eitner, and R. D. Vetter.
1999a. Evolution of a mitochondrial cytochrome *b* gene sequence in the species-rich genus *Sebastes* (Teleostei, Scorpaenidae) and its utility in testing the monophyly of the subgenus *Sebastomus*. Mol. Phylogenet. Evol. 11(3):426–440.

Rocha-Olivares, A., R. H. Rosenblatt, and R. D. Vetter.
1999b. Cryptic species of rockfishes (*Sebastes*: Scorpaenidae) in the Southern Hemisphere inferred from mitochondrial lineages. J. Hered. 90(3):404–411.

1999c. Molecular evolution, systematics, and zoogeography of the rockfish subenus *Sebastomus* (*Sebastes*, Scorpaenidae) based on mitochondrial cytochrome *b* and control region sequences. Mol. Phylogenet. Evol. 11(3):441–458.

Rocha-Olivares, A., and R. D. Vetter.
1999. The effects of oceanographic circulation on the gene flow, genetic structure, and phylogeography of the rosethorn rockfish *Sebastes helvomaculatus*. Can. J. Fish. Aquat. Sci. 56(5):803–813.

Sakuma, K. M., and T. E. Laidig.
1995. Description of larval and pelagic juvenile chilipepper, *Sebastes goodei* (family Scorpaenidae), with an examination of larval growth. Fish. Bull. 93(4):721–731.

Seeb, L. W., and A. W. Kendall Jr.
1991. Allozyme polymorphisms permit the identification of larval and juvenile rockfishes of the genus *Sebastes*. Environ. Biol. Fishes 30(1-2):191–201.

Yoklavich, M. M., and G. W. Boehlert.
1991. Uptake and utilization of 14C-glycine by embryos of *Sebastes melanops*. Environ. Biol. Fishes 30(1–2):147–153.

Shape, volume, and resonance frequency of the swimbladder of yellowfin tuna, *Thunnus albacares*

Kurt M. Schaefer
Inter-American Tropical Tuna Commission
8604 La Jolla Shores Drive
La Jolla, California 92037-1508
E-mail address: kschaefer@iattc.ucsd.edu

Charles W. Oliver
Southwest Fisheries Science Center
National Marine Fisheries Service, NOAA
P.O. Box 271, La Jolla, California 92038

Abstract.—The shapes and volumes of swimbladders of yellowfin tuna, *Thunnus albacares*, were measured from freshly caught fish from the eastern Pacific Ocean. Direct measurements of swimbladder volumes were obtained from a geometric reconstruction with morphometric measurements of intact bladders and by volumetric displacements of the same intact bladders excised from 46 fish (57 to 157 cm in length). The estimates of the swimbladder volumes obtained from geometric reconstruction were not significantly different from those obtained with the corresponding volumetric displacements. There is a nonlinear relationship between yellowfin swimbladder volumes and fish lengths. The mean swimbladder volume was 1.33% of body volume with a minimum of 0.30% and a maximum of 2.84%. A comprehensive model, based on the data from this study and those from a previous investigation, is presented for the relationship of yellowfin swimbladder volumes, estimated from geometric reconstruction and fish lengths for 108 specimens (35 to 157 cm). This predictive model was then used with other formulae to estimate yellowfin tuna swimbladder resonance frequencies for fish lengths and fish depths. Because these resonance frequencies are within the range of frequencies audible to yellowfin tuna, we speculate on the potential distance at which dolphins could be detected by yellowfin tuna.

Manuscript accepted 19 November 1999
Fish. Bull. 98:364–374 (2000).

The shape and volume of the swimbladder of yellowfin tuna, *Thunnus albacares*, is obviously important because it functions as a hydrostatic organ, which lowers the energy costs of locomotion (Magnuson, 1973; Alexander, 1993). The yellowfin swimbladder may also function in acoustic detection, providing increased sensitivity in hearing, thus enhancing the ability of fishes to detect other organisms, such as dolphins and prey (Iverson, 1967; Hawkins, 1993). In addition, the swimbladder may also function in acoustical detection of tuna by other species. At low frequencies (< 2 kHz), the maximum acoustic target strength occurs at a resonance frequency determined by the volume of the swimbladder (Love, 1978). At high frequencies (2–200 kHz), the swimbladder has been reported to account for 50% (Harden Jones and Pearce, 1958) to as much as 95% (Foote, 1980) of the acoustic target strength for some fish.

Low-frequency acoustic detection and tracking of yellowfin tuna schools is being investigated by the U.S. National Marine Fisheries Service as an alternative method of locating yellowfin tuna independent of dolphins. Studies suggest that yellowfin tuna schools could be detected at much greater ranges (20 to 40 km) than are currently feasible (Rees, 1998). Development of an acoustic detection system could greatly increase the efficiency of commercial fishing and might also provide a fishery-independent method for assessing yellowfin tuna or other large pelagic fish.

Nero[1] used two acoustic-scattering models to estimate the target strengths of yellowfin tuna schools: a model for very low frequencies (50–1000 Hz) assumed to be near swimbladder resonance (Feuillade et al., 1996; Feuillade and Nero, 1998), and a high-frequency (2–200 kHz) model for frequencies well above swimbladder resonance (Love, 1977; Love, 1981). Yellowfin swimbladders were modeled as gas-filled spheres (Feuillade et al., 1996). Nero's models (1996) included swimbladder volume estimates of approximately 5% of fish volume for yellowfin tuna in excess of 80 cm in length, extrapolated from Magnuson's (1973) relationship of swimbladder volume to fish length for yellowfin tuna 44 to 82 cm in length.

The objectives of our study were 1) to obtain direct measurements

[1] Nero, R. W. 1996. Model estimates of acoustic scattering from schools of large yellowfin tuna. Report NRL/MR/774-95-7708. Naval Research Laboratory, Ocean Acoustics Branch, Acoustics Division, Stennis Space Center, MS 39529-5004, 21 p.

of swimbladder shapes and volumes from freshly caught yellowfin tuna 50 to 150 cm in length, 2) to compare the swimbladder displacement volumes with volumes estimated from geometric reconstruction, 3) to compare the swimbladder volumes estimated from geometric reconstruction for freshly caught and frozen-and-thawed specimens, and 4) to calculate swimbladder resonance frequencies as functions of fish length and depth.

All four objectives are directly related to designing a low-frequency, long-range acoustic detection system to locate large yellowfin tuna. The first objective provides direct measurements of the relation between swimbladder volume and fish length, upon which are based acoustic target strength estimates. The previously modeled relationship was based upon smaller yellowfin tuna (Magnuson, 1973; Nero, 1996). The second and third objectives were to ascertain the practicality of obtaining swimbladder volumes by means other than volumetric displacement of the swimbladder from freshly caught fish, thus providing both a simpler method and wider sampling opportunities. The last objective allows incorporation of fishery information (fish size and swimming depth) to select a particular frequency, or frequency range, in order to optimize an acoustic detection system.

Materials and methods

Yellowfin tuna specimens were caught by rod and reel. Seventeen specimens, 57 to 70 cm in length, were collected from a skiff during October 1997, in the vicinity of the Frailes Islands (lat. 7°20'N, long. 80°08'W). An additional 29 specimens, 71 to 157 cm in length, were collected aboard the MV *Royal Polaris*, a San Diego-based long-range sportfishing boat, during January and February 1998, primarily in the vicinities of Alijos Bank (lat. 24°49'N, long. 115°56'W) and Hurricane Bank (lat. 16°52'N, long. 117°30'W).

Freshly caught specimens were assigned an identification number. Fish length was measured with a caliper to the nearest millimeter and fish weight was measured with an electronic balance to the nearest pound. Cutting the abdominal cavity open from the anus to the isthmus and removing most of the viscera exposed the swimbladder. A photograph of the intact swimbladder was then taken with a digital camera. Morphometric measurements of length and three widths (rostral, medial, and caudal) were taken for each intact swimbladder, with a dial caliper, to the nearest tenth of a millimeter. The inflated swimbladder and some extraneous tissue were excised from the abdominal cavity, and the volumetric displacement was measured in a graduated cylinder to the nearest 5 mL. The swimbladder was then punctured and the volumetric displacement of the tissue measured. The estimated volume of gas in the swimbladder was calculated as the difference between displacement volumes of the inflated and deflated swimbladder, including the attached extraneous tissues. The volume of the swimbladder wall was not determined and should be considered insignificant, being extremely thin, with respect to volumetric displacement.

Estimates of swimbladder volumes were also computed by a geometric reconstruction from the bladder's length and width measurements. Based on the above four measurements of each bladder, an algorithm was employed to estimate the volumes between several cross sections. Cross sections of the swimbladder were assumed to be elliptical. The rostral and caudal ends of the bladders were assumed to be hemispheres. The total estimate of the volume of gas within the swimbladder was the sum of all the geometrical units. Estimates of swimbladder volumes by a geometric reconstruction for 62 frozen and thawed yellowfin tuna, ranging in length from 35 to 149 cm (Schaefer, 1999), were included in this study for both comparative and comprehensive analyses.

Results

Swimbladder shape and volume

Photographic images of the ventral, dorsal, left, and right profiles of an excised intact swimbladder of yellowfin tuna provided definitive views of the overall shape (Fig. 1). The swimbladder is cylindrically shaped and has medial bulging and hemispheric ends. There are paired protuberances on the rostral-dorsal surface. The protuberances are commonly of unequal size (the left is larger than the right) and they fit into sockets located on each side of the vertebral column. As size increased in the yellowfin specimens we examined (Table 1), the ratio of the swimbladder length to the width remained fairly constant, around a mean of 3.1 (range: 2.2–4.8). The swimbladder shape, however, changed noticeably, particularly at the caudal end (Fig. 2).

The swimbladder has thin elastic walls except for the thicker walls of the protuberances. The dorsal surface of the swimbladder is attached to a sheet of thick connective tissue, situated along the dorsal wall of the abdominal cavity adjacent to the vertebral column. In larger specimens, there is a prominent cord of connective tissue originating from the posterior area of this tissue and extending anteriorly to the area of the sockets at the rostral end of the swimbladder. This distinct cord of connective tissue

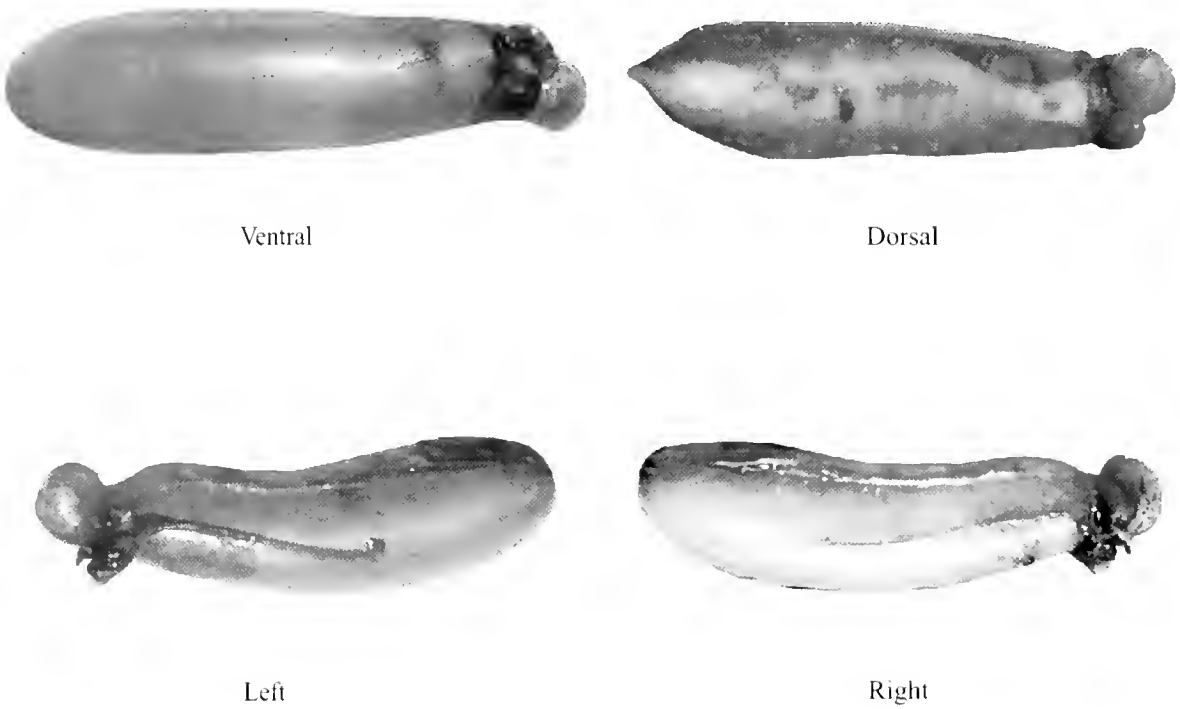

Figure 1

Profiles of an excised intact yellowfin tuna swimbladder. The actual length of the swimbladder was 165 mm, the maximum width 69.1 mm, and the displacement volume 245 cc. The fish was 784 mm in length and 8.6 kg in weight.

is situated directly adjacent to the dorsal wall of the swimbladder.

The relationship of swimbladder volume obtained from volumetric displacement, to fish length for the freshly caught yellowfin tuna is shown in Figure 3. The relationship is described by a power function:

$$Y_x = 0.000000005\, x^{3.5715}, \quad (r^2=0.87, n=46) \quad (1)$$

where Y_x = swimbladder volume at fish length x.

The relationship of swimbladder volume, obtained from volumetric displacement and expressed as a percentage of the body volume (estimated from body weight) to weight for freshly caught yellowfin tuna is shown in Figure 4. The mean volume was 1.33% (95% CI=0.16%) with minimum and maximum values of 0.30% and 2.84%, respectively. The relation between the swimbladder volume, expressed as the percentage of body volume to body weight is described by the following linear function:

$$Y_x = 1.0822 + 0.0146x, \quad (r^2=0.17, n=46) \quad (2)$$

where Y_x = swimbladder volume, expressed as a percentage of body volume, at weight x.

The relationship of swimbladder volume (estimated from geometric reconstruction) to volume obtained from volumetric displacement for freshly caught yellowfin tuna is shown in Figure 5. The relationship was described and analyzed by the following linear function, with the intercept set to zero:

$$Y_x = 1.0735x, \quad r^2=0.96, n=46 \quad (3)$$

where Y_x = swimbladder volume estimated from geometric reconstruction for the corresponding volumetric displacement x.

The regression coefficient is significantly different from 1 ($t_{0.05(2),44}$=2.41; P<0.05). However, it is apparent from Figure 5 that the two techniques produce similar estimates, providing credence to the estimation of volume from geometric reconstruction.

Analysis of covariance applied to the log-transformed swimbladder volumes by geometric recon-

Table 1

Measurements of fresh yellowfin tuna and their swimbladders. The volumes are volumetric displacements in seawater.

Fish		Swimbladder		
Length (mm)	Weight (kg)	Length (mm)	Maximum width (mm)	Volume (cc)
572	3.7	102.0	31.3	38
590	4.1	114.9	32.3	43
591	4.1	109.9	36.9	53
591	3.7	107.0	25.9	36
600	3.9	100.8	26.7	26
601	3.9	103.6	36.1	41
608	4.2	112.6	31.0	56
611	4.3	110.2	35.0	46
614	4.6	119.2	34.6	71
624	4.6	115.6	30.2	54
624	4.4	123.3	25.8	31
636	4.9	101.4	34.4	35
650	5.2	111.3	38.3	78
671	5.7	118.1	39.7	33
675	6.0	136.7	42.4	111
681	6.5	128.7	45.0	71
704	8.1	109.3	41.9	66
705	7.3	132.0	54.1	91
736	7.3	143.0	48.2	51
751	8.2	135.0	47.3	81
784	8.6	165.0	69.1	245
789	8.6	114.0	51.3	26
824	9.5	163.0	58.4	166
842	11.3	164.0	50.6	161
861	13.2	158.0	44.9	136
917	13.6	178.0	64.9	260
933	15.4	168.0	64.9	106
940	16.8	184.0	51.6	280
964	17.2	174.0	52.3	161
977	19.1	205.0	61.6	410
1033	20.4	195.0	61.9	320
1039	21.8	228.0	61.7	260
1047	21.3	196.0	48.5	147
1069	23.6	193.0	61.7	310
1087	24.9	240.0	79.1	610
1129	27.2	205.0	66.3	495
1130	30.4	195.0	66.9	250
1179	33.6	205.0	75.9	500
1190	33.1	235.0	69.8	540
1197	29.5	207.0	71.1	390
1218	34.0	213.0	76.8	500
1236	35.4	215.0	75.6	540
1290	37.2	260.0	74.5	830
1346	44.5	270.0	79.5	915
1519	62.6	230.0	104.6	800
1569	68.0	295.0	114.2	1530

struction and fish-length data truncated to a length range of 60 to 119 cm from the present study (n=36) and from Schaefer (1999) (n=24) indicated no significant difference in the test for equality of slopes (F=2.50, P=0.12) or equality of adjusted means (F=2.38, P=0.13). In addition, an approxi-

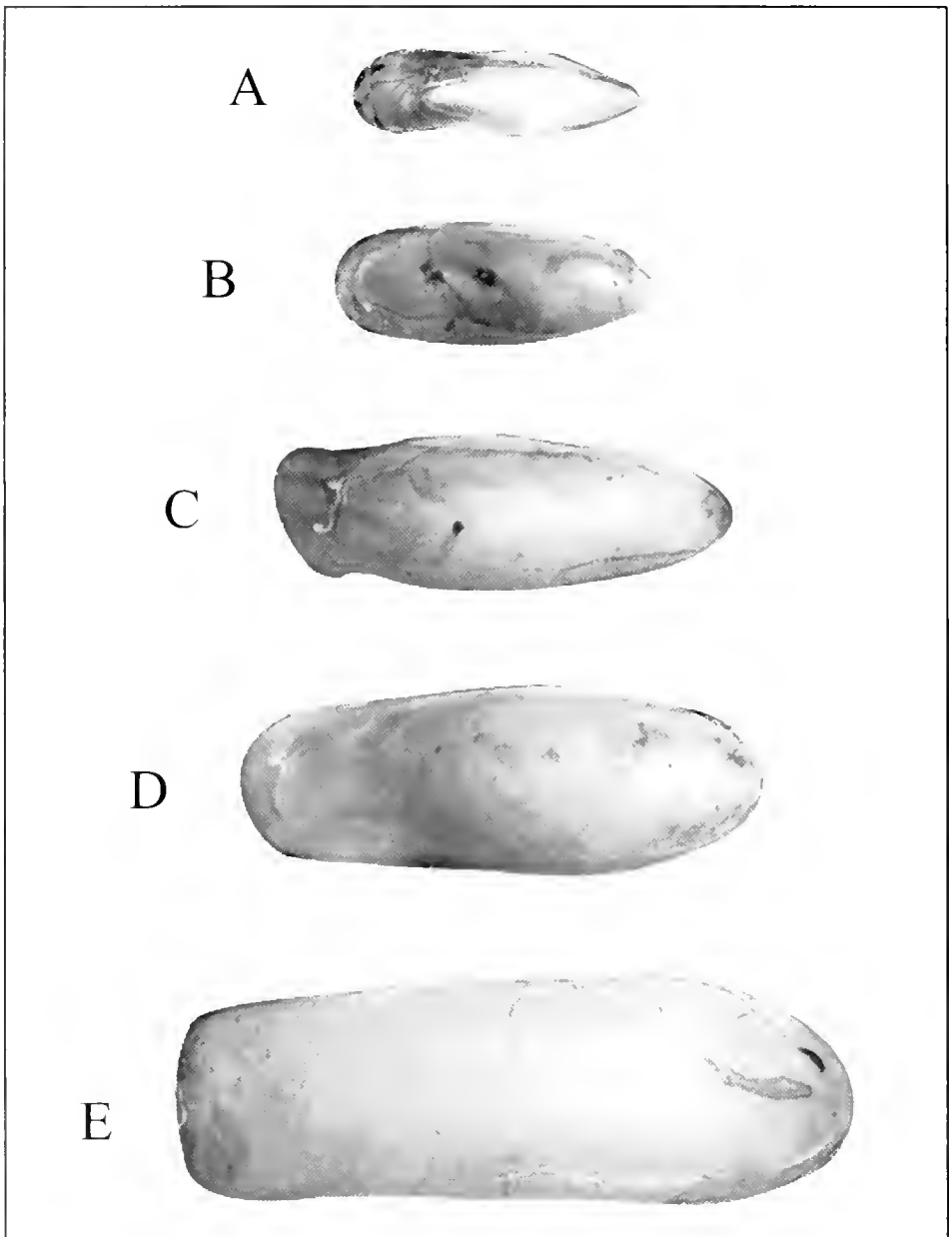

Figure 2

Ventral profiles of excised intact yellowfin tuna swimbladders scaled to relative size. Values given for each image are measured lengths and displacement volumes of bladders, fish length, and fish weight. (**A**) 115 mm and 43 cc, 590 mm, 4.1 kg. (**B**) 135 mm and 81 cc, 751 mm, 8.2 kg. (**C**) 184 mm and 280 cc, 940 mm, 16.8 kg. (**D**) 205 mm and 495 cc, 1129 mm, 27.2 kg. (**E**) 270 mm and 915 cc, 1346 mm, 44.5 kg.

mate F-ratio statistic (Zar, 1974) indicated that the sample power functions fitted to the data of percentage of swimbladder volume (obtained from geometric reconstruction) to fish length (57 to 157 cm, n=46) from our study and (35 to 149 cm, n=62) from Schaefer's study (1999) are estimating the same population regression function (F=2.65, P>0.10). It thus appears appropriate to pool the two sets of data for yellowfin tuna swimbladder volumes obtained from geometric reconstruction, in order to provide the most comprehensive model possible.

The relation of swimbladder volume (estimated by geometric reconstruction) and length of the yellowfin tuna from our study, combined with that from Schae-

fer's (1999) is shown in Figure 6. The relationship is well described by a power function fitted to the nontransformed data by means of a weighted regression procedure:

$$Y_x = 0.00000002\, x^{3.0601}, \quad (r^2=0.83,\ n=108 \text{ (fish length range: 353 to 1569 mm)}) \qquad (4)$$

where Y_x = a swimbladder volume at fish length x.

The weighting employed consisted of the reciprocal of the variance about the volumes within each 200-mm length interval.

Swimbladder resonance frequency

The monopole-dominant resonance frequency of a swimbladder (Andreeva, 1964) is approximated by using a spherical volume of gas (Love, 1978) as follows:

$$\text{Resonance frequency} = \sqrt{\frac{3\Gamma P}{4\pi^2 r^2 D}} \qquad (5)$$

where Γ = 1.4;
r = radii of equivalent sphere in meters;
D = density of fish flesh (1050 kg/m^3); and
P = sound speed parameter at depth Z defined as

$$P = \left[1 + \left[\frac{Z_{\text{meters}}}{10_{\text{meters}}}\right]\right] \times 10100 \text{ Pascals}. \qquad (6)$$

Because yellowfin tuna swimbladders are not spherical, the predicted resonance frequency must be adjusted to account for the approximate prolate spheroid shape of the swimbladder (Figs. 1 and 2). Weston (1967) has provided a formula and figure (Chap. 5, p 59, Fig. 5.2) for this adjustment using the ratio of the swimbladder's maximum (a) and minimum (b) radii (e.g. 1/2 length and 1/2 width). From the figure, we interpolated the magnitude of the upward adjustment at various depths, incorporating Boyle's Law to account for changes in volume with depth. The swimbladder's maximum radius (a) was held constant at all depths because it is firmly attached to the connective tissue sheet adjacent to the dorsal wall of the abdominal cavity. We calculated the expected minimum radii (b) at various depths, using the predictive regression function for swimbladder

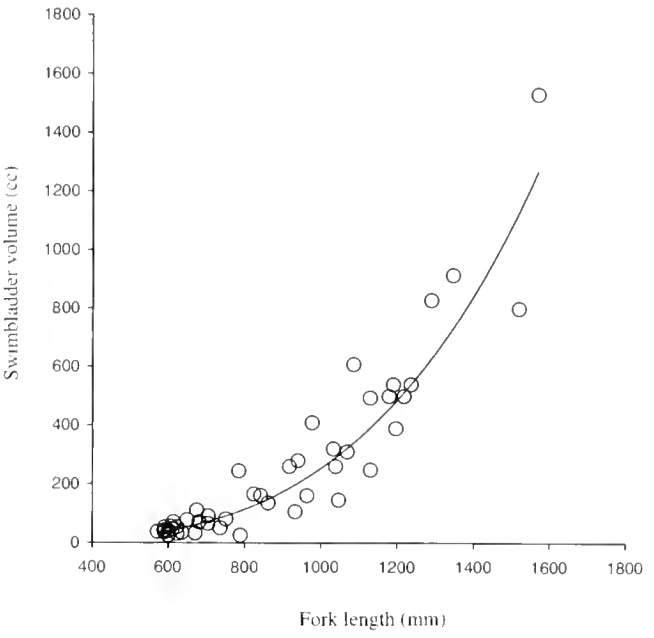

Figure 3

Relation between swimbladder displacement volume and length for yellowfin tuna. The fitted line is for a power function given in the text.

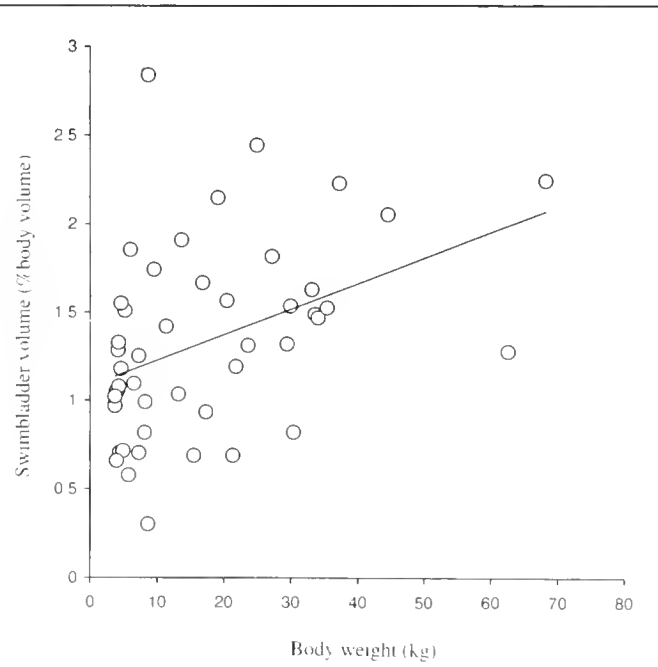

Figure 4

Relation between swimbladder displacement volume, as a percentage of estimated body volume, and body weight in air for yellowfin tuna. The fitted line is for a linear function given in the text.

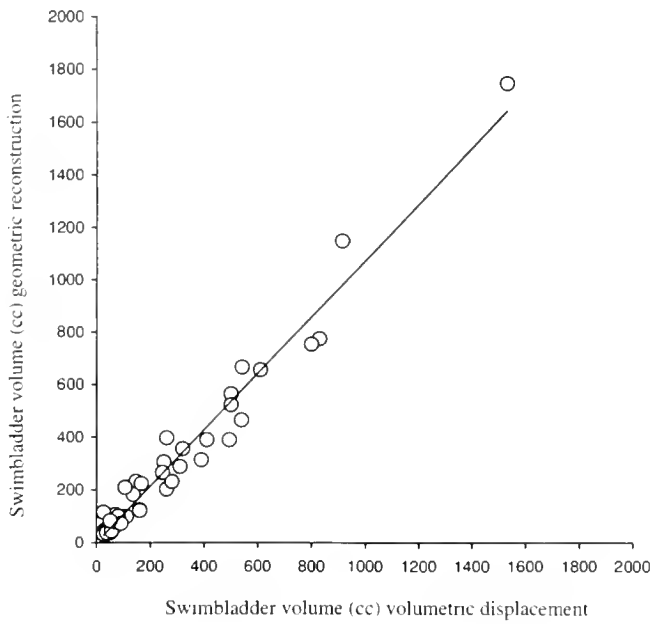

Figure 5

Relation between estimated swimbladder volume, from geometric reconstruction, and swimbladder displacement volume for yellowfin tuna. The fitted line is for a linear function given in the text.

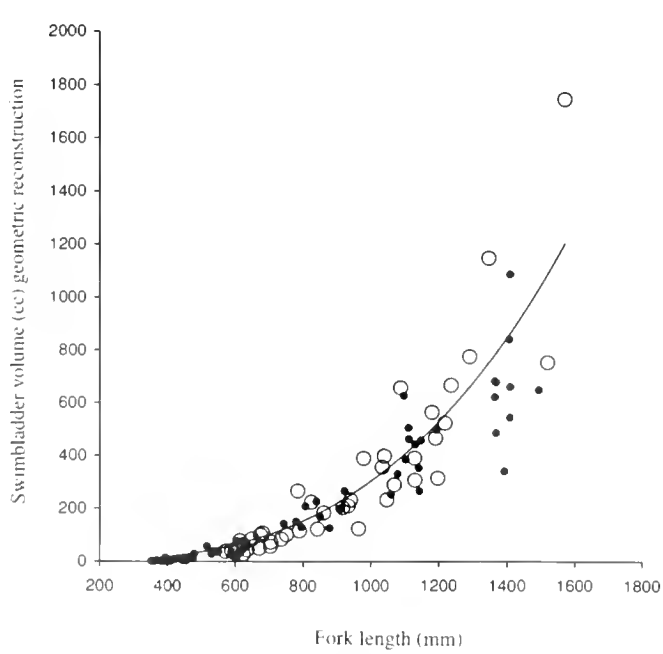

Figure 6

Relation between estimated swimbladder volume, from geometric reconstruction, and length for yellowfin tuna. The open circles are for the data from this study and the solid circles are from Schaefer (1999). The fitted line is for a power function given in the text.

volumes at the surface for fish lengths (Fig. 6), and determined the percent increase in the expected resonance frequency. The regression coefficient (b=1.053) for the linear relationship of swimbladder volume estimated by geometric reconstruction to the volume estimated from the equation for a prolate spheroid is not significantly different from 1 ($t_{0.05(2),106}$=1.84; P>0.05). Solving for b yields:

$$b_{\text{depth}} = \sqrt{\frac{V_{\text{depth}}}{\frac{4}{3}\pi a}} \qquad (7)$$

Resonance frequencies for swimbladders of yellowfin tuna of various lengths and at various depths were estimated (Fig. 7), using the above equations and the predictive regression function for swimbladder volumes for fish lengths (Fig. 6). Applying this correction increased resonance frequencies between 5% and 26% for yellowfin tuna from 40 to 150 cm at depths from 0 to 120 m.

Discussion

Swimbladder shape and volume

Godsil and Byers (1944) described the shape of the swimbladder of yellowfin tuna. Additional information regarding yellowfin tuna swimbladder shape is provided through the digital images of the various views of the swimbladder (Figs. 1 and 2) and the morphometric information presented in Table 1.

The swimbladder volume estimates derived by geometric reconstruction in this study and in Schaefer (1999) appear to provide realistic representations for swimbladders of live yellowfin tuna swimming at the surface of the ocean. All of the intact swimbladders within the abdominal cavities for those specimens were sufficiently inflated so that the bladders were taut, rather than flaccid. Many of the yellowfin tuna stomachs were relatively full, and there was a broad range in the stage of gonadal development. There was no extrusion of the bladder or other organs from the initial incision into the abdominal cavity for any specimen. Thus, it does not appear there were any deformations or reduction in swimbladder volumes within the body cavity similar to those described for cod (Ona, 1990). In addition, yellowfin tuna are physoclistous, and the

inflation and deflation of the swimbladder is controlled through special glands that function in the secretion or resorption of gases from, or to, the blood (Alexander, 1993). Virtually nothing is known about inflation and deflation rates in swimbladders of tunas, but it would appear from studies of other fishes (Alexander, 1993) that swimbladder volume adjustments would be extremely slow in relation to the rapid swimming speeds during vertical forays by these species (Holland et al., 1990).

Geometric reconstruction of swimbladders in yellowfin tuna was previously derived from radiographs to estimate volumes, which were validated by volumetric displacement (Chang and Magnuson, 1968). It is apparent from the results of that study and our study that the geometric reconstruction method is sufficiently accurate for deriving estimates of volumes of swimbladders of yellowfin tuna, and possibly other tunas as well. Obtaining swimbladder volumetric data by geometric reconstruction is more practical than by volumetric displacement because of the additional time required and potential of puncturing the swimbladder when excising for determination of volumetric displacement. Furthermore, unless there are instances where it is not feasible to cut open the abdominal cavity of specimens, it does not appear to be necessary to employ an x-ray unit for obtaining these estimates.

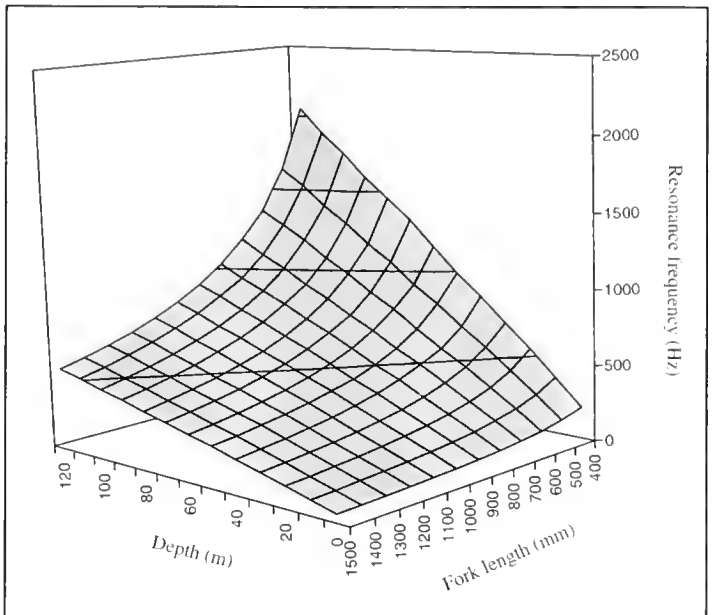

Figure 7
Relation between estimated swimbladder resonance frequency, fish length, and fish depth for yellowfin tuna.

Magnuson (1973) reported that swimbladder volumes for 11 yellowfin tuna specimens, 44 to 82 cm in length, ranged from around 0.25% to 4.0% of body volume (estimated from Fig. 4a of Magnuson, 1973). The swimbladder volumes in our study, derived from volumetric displacements, expressed as a percentage of the estimated body volumes (Fig. 4) had a mean of about 1.3%, with a range of about 0.3% to 2.84%, and almost no relation with increasing mass. Swimbladder volumes, from the present study, for yellowfin tuna in the length range presented in Magnuson (1973) appear to be significantly lower (Fig. 4). The data of Magnuson (1973) were based upon measured volumetric displacements of the fish, whereas in the present study body volume was estimated, without adjusting for fish density because those values were not available for these specimens. However, we calculated the body volumes from weights for specimens from the present study, using an adjustment factor for density of 1.05 g/mL (Magnuson, 1973) and found swimbladder volumes, expressed as a percentage of body weight, would be increased by only 0.07% on average. This small increase in volume does not account for the apparent differences in swimbladder volumes between the present study and those in Magnuson (1973). In addition, although Magnuson (1973) reported that specimens of 2 kg or less have no gas in the bladder, Schaefer (1999) reported yellowfin swimbladders are inflated with measurable quantities of gas in specimens as small as 0.85 kg (353 mm) (Fig. 6).

Swimbladder resonance frequency

Acoustic tracking studies have shown that yellowfin tuna occupy the lower mixed layer during daylight and waters closer to the surface at night (Carey and Olson, 1982; Holland et al., 1990; Block et al., 1997). Although they appear to make frequent short excursions toward the surface, they spend very little time at the surface. In the area of the eastern Pacific surface fishery (Bayliff, 1998), the thermocline depth ranges from about 40 to 120 meters (Fiedler, 1992). Resonance frequency will change with depth because volume is the primary determinant of the resonance frequency of a swimbladder. Thus, the acoustic target strength of a tuna, or school of tunas, will vary as the swimbladder volumes vary at depth for low-frequency acoustic detection systems.

Nero (1996) modeled target strengths for schools of larger yellowfin tuna for both high frequencies (2–200 kHz), and low frequencies (below 2 kHz), using an assumed swimbladder volume equal to 5% of fish volume for calculating resonance frequencies. Nero's (1996) high-frequency model predicted target strengths of 2.5, 1.6, and 0.9 dB re 1μPa for yellowfin

tuna schools of 80, 100, and 130-cm fish respectively. The decreasing trend in school target strength as fish length and bladder volume increases, as shown in Nero (1996), results primarily from the reduced number of fish in a modeled 15-kg school. Some decrease in Nero's reported school target strengths could result from the smaller swimbladder volumes that we measured for fish of similar lengths, depending upon the swimbladder's contribution to target strength at high frequencies (Harden Jones and Pearce, 1958; Foote, 1980).

Nero (1996) estimated low-frequency target strengths for schools of yellowfin tuna at various depths, fish lengths, and packing densities but noted school target strength was complicated because of interference and coupled resonance effects dependent on the fish size, numbers, aspect, and packing density. We expect Nero's reported school target strengths, for low frequencies, to decrease as a result of the smaller swimbladder volumes we report. Because resonance frequency varies inversely with swimbladder volume, overestimating volume results in predicted lower resonance frequencies. Direct measurement of resonance frequency and target strength of *in situ* swimbladders would eliminate the need to model these parameters and provide better information to optimize an acoustic detection system for large yellowfin tuna.

Yellowfin tuna monitor their environment through the use of sensory organs for visual, chemoreceptive, and acoustic information. Although vision (Guthrie and Muntz, 1993) and chemoreception (Hara, 1993) are presumably important to yellowfin tuna in foraging, sex, and social communication, acoustic sensory capacities probably provide greater detection potential because of the light attenuation and chemical dilution effects in the ocean (Hawkins, 1993). Sounds can travel great distances in the sea, depending upon the sound propagation characteristics of the water and the sound frequency and source level. Reception and processing of sounds by fish presents the potential for detection at a greater distance than that by either visual or chemoreceptive senses (Hawkins, 1993). Although the swimbladder of yellowfin tuna may enhance their acoustic detection and their ability to detect sounds, the size and shape of their swimbladder does not appear to provide for any directional information. Directionality in hearing, however, may exist in yellowfin tuna based on the anatomy and organization of the inner ears (Hawkins, 1993).

The physiological behavior of yellowfin tuna and the affect that it potentially has on the acoustic characteristics of the swimbladder should be considered. For instance, the swimming behavior of yellowfin tuna, exemplified by vertical excursions, may enable individuals to actively control the resonance frequencies of their swimbladders (Fig. 7) and to potentially enhance their ability to sense their environment, as previously proposed by Feuillade and Nero (1998) for other fish with swimbladders. By varying the resonance frequency of the swimbladder, yellowfin tuna may be able not only to amplify acoustic signals but also filter auditory signals and thus improve acoustic detection in the presence of high levels of ambient noise (Hawkins, 1993).

Because estimates of yellowfin tuna swimbladder resonance frequencies presented in our study were within the range of frequencies audible to yellowfin tuna (Iverson, 1967) and because swimbladders may enhance yellowfin tuna hearing (Blaxter and Tytler, 1978; Blaxter, 1980), it is tempting to speculate about the potential distance at which yellowfin tuna could become aware of dolphins (*Stenella* spp. and *Delphinus delphis*) or prey, predators, or conspecifics through sound reception. Identification of a mechanism that facilitates the yellowfin tuna and porpoise bond in the eastern Pacific (National Research Council, 1992) may provide a means of breaking the bond prior to setting nets that encircle dolphins, thus enabling the capture of yellowfin tuna without catching dolphins. If the mechanism is an attractant (i.e. yellowfin tuna move towards the sounds of dolphins or other oceanic sounds, or towards the sounds of both), then the possibility exists to attract larger yellowfin tuna artificially with acoustical devices. Active sounds produced by dolphins include clicks, bangs, and whistles (Schevill, 1964; Tavolga, 1965; Norris and Mohl, 1983; Watkins and Wartzok, 1985; Marten et al., 1988) at peak frequencies as high as 160 kHz and peak source levels up to 228 dB re 1μPa (Au, 1993). Passive sounds resulting from tail-slaps, breaches, and other behaviors have also been described as loud (Hult, 1982; Smolker and Richards, 1988). The energy at frequencies between 50 and 1100 Hz is of particular interest because yellowfin tuna have been shown to respond to sounds in this range—the most sensitive responses occurring between 300 and 500 Hz (Iverson, 1967).

Sound intensity decreases with range as a sound propagates through the water, primarily because of transmission loss associated with spherical spreading of the wavefront and absorption (Richardson et al., 1995). At 500 Hz, absorption loss is approximately 0.013 dB/km (Urick, 1983) and total transmission loss can be approximated from spreading loss alone over relatively short distances. We used the best hearing sensitivity at 500 Hz reported by Iversen (1967) for small yellowfin tuna (83 dB re 1μPa) as the minimum received source level (SL) a tuna can hear. In the absence of published data on SL at 500 Hz associated with low-frequency sounds

produced by *Stenella* and *Delphinus*, we use the maximum SL measured for jaw pops of *Tursiops truncatus*, 163 dB re 1µPa (Finneran et al., 2000). Maximum detection range under spherical spreading conditions is calculated as:

$$Range = 10\,(SL_{initial} - SL_{received}) / 20. \quad (8)$$

In the absence of other sounds (e.g. ambient noise), we estimated that yellowfin tuna in the eastern Pacific Ocean may be able to detect a 500-Hz sound of 163 dB re 1µPa out to a distance of approximately 10 km.

Ambient noise in offshore waters results primarily from wind and waves (Richardson et al., 1995) and can mask reception of other sounds. In the region of the eastern Pacific Ocean, where a yellowfin tuna fishery exists, the sea surface is characterized by frequent periods of light winds with wind speed less than 5 m/s (sea state 2) more than 60% of the time (Webb, 1998). At 500 Hz and with sea state 2, broadband ambient noise is approximately 85 dB re 1µPa (Richardson et al., 1995), and would probably mask the ability of tuna to detect our hypothetical 83-dB dolphin sound at the maximum distance we calculated. We are unaware of any data on critical ratios or critical band widths associated with tuna hearing, from which we could estimate the effective received level required for a tuna to detect our sound in the presence of this ambient noise. However, the source level received by a yellowfin tuna would have to be higher than ambient noise level, thus reducing detection distance.

The swimbladder of yellowfin tuna may function as a key mechanism in the formation of the bond between yellowfin tuna and dolphins in the eastern Pacific Ocean. Whether larger yellowfin tuna actively search for dolphins to increase their probability of remaining within food-rich habitat (Fiedler et al., 1998) or whether the dolphin's sonar echolocation ability detects yellowfin tuna (Au, 1993), the swimbladder may play an important role in both sound reception and detectability as an acoustical target. Further research should be conducted on yellowfin tuna bioacoustics, including hearing sensitivity in larger yellowfin tuna, determination of the role of the swimbladder in hearing sensitivity, and measurements of source level sounds produced by dolphins and other marine organisms at frequencies below 1 kHz, referenced to a source.

Acknowledgments

We thank R. Deriso and E. Edwards for their encouragement and support of this investigation. We are grateful to F. LoPreste and S. Loomis, and also the crew and passengers of the *Royal Polaris*, for their invaluable assistance in obtaining these data. We also gratefully acknowledge R. Allen, W. Bayliff, R. Nero, D. Rees, and three anonymous reviewers for helpful suggestions and comments on the manuscript. This paper is dedicated to the memory of James "Rollo" Heyn (1960–1999) who taught me, K. Schaefer, a great deal over the years aboard the *Royal Polaris* about how to kill large yellowfin tuna with rod and reel, in the name of science.

Literature cited

Alexander, R. M.
1993. Buoyancy. *In* The physiology of fishes (D. H. Evans, ed.), p. 75–97. CRC Press, Inc., Boca Raton, FL.

Andreeva, I. B.,
1964. Scattering of sound by air bladders of fish in deep sound-scattering ocean layers. Sov. Phys. Acoust. 10:17–20.

Au, W. W. L.
1993. The sonar of dolphins. Springer-Verlag New York, Inc., New York, NY, 277 p.

Bayliff, W. H. (ed.).
1998. Inter-Amer. Trop. Tuna Comm., Ann. Rep. for 1996, 306 p.

Blaxter, J. H. S.
1980. The swimbladder and hearing. *In* Hearing and sound communication in fishes (W. N. Tavolga, A. N. Popper, and R. R. Fay, eds.), p. 61–71. Springer-Verlag, New York, NY.

Blaxter, J. H. S., and P. Tytler.
1978. Physiology and function of the swimbladder. Adv. Comp. Phys. Biochem. 7:311–367.

Block, B. A., J. E. Keen, B. Castillo, H. Dewar, E. V. Freund, D. J. Marcinek, R. W. Brill, and C. Farwell.
1997. Environmental preferences of yellowfin tuna (*Thunnus albacares*) at the northern extent of its range. Mar. Biol. 130:119–132.

Carey, F. G., and R. J. Olson.
1982. Sonic tracking experiments with tuna. International Commission for the Conservation of Atlantic Tunas (ICCAT), Collective Volume of Scientific Papers 17:458–468.

Chang, R. K. C., and J. J. Magnuson.
1968. A radiographic method for determining gas bladder volume of fish. Copeia 1968:187–189.

Feuillade, C, and R. W. Nero.
1998. A viscous-elastic swimbladder model for describing enhanced-frequency resonance scattering from fish. J. Acoust. Soc. Am. 103:3245–3255.

Feuillade, C., R. W. Nero, and R. H. Love.
1996. A low frequency acoustic scattering model for small schools of fish. J. Acoust. Soc. Am. 99:196–208.

Fiedler, P. C.
1992. Seasonal climatologies and variability of eastern tropical Pacific surface waters. U.S. Dep. Commer., NOAA Tech. Rep. NMFS 109:1–65.

Fiedler, P. C., J. Barlow, and T. Gerrodette.
1998. Dolphin prey abundance determined from acoustic backscatter data in eastern Pacific surveys. Fish. Bull. 96:237–247.

Finneran, J. J., C. W. Oliver, K. M. Schaefer, and S. H. Ridgway.
2000. Source levels and estimated yellowfin tuna (*Thunnus albacares*) detection ranges for dolphin jaw pops, breaches, and tail slaps. J. Acoust. Soc. Am. 107(1):649–656.

Foote, K. G.
1980. Importance of the swimbladder in acoustic scattering by fish: a comparison of gadoid and mackerel target strength. J. Acoust. Soc. Am. 67:2084–2089.

Godsil, H. C., and R. D. Byers.
1944. A systematic study of Pacific tunas. Calif. Div. Fish Game, Fish Bull. 60, 131 p.

Guthrie, D. M., and W. R. A. Muntz.
1993. Role of vision in fish behaviour. *In* Behaviour of teleost fishes, second ed. (T. J. Pitcher, ed.), p. 89–128. Chapman and Hall, London.

Hara, T. J.
1993. Role of olfaction in fish behaviour. *In* Behaviour of teleost fishes, second ed. T. J. Pitcher, ed.), p. 171–199. Chapman and Hall, London.

Harden Jones, F. R., and G. Pearce.
1958. Acoustic reflexion experiments with perch (*Perca flariatilis* Linn.) to determine the proportion of the echo returned by the swimbladder. J. Exp. Biol. 35:437–450.

Hawkins, A. D.
1993. Underwater sound and fish behaviour. *In* Behaviour of teleost fishes, second ed. (T. J. Pitcher, ed.), p. 129–169. Chapman and Hall, London.

Holland, K. N., R. W. Brill, and R. K. C. Chang.
1990. Horizontal and vertical movements of yellowfin and bigeye tuna associated with fish aggregating devices. Fish. Bull. 88:493–507.

Hult, R.
1982. Another function of echolocation for bottlenose dolphins (*Turstops truncatus*). Cetology 47:1.

Iverson, R. T. B.
1967. Response of yellowfin tuna (*Thunnus albacares*) to underwater sound. *In* Marine bio-acoustics, vol 2 (W. N. Tavolga,. ed.), p.105–121. Pergamon, New York, NY.

Love, R. H.
1977. Target strength of an individual fish at any aspect. J. Acoust. Soc. Am. 62:1397–1403.
1978. Resonant acoustic scattering by swimbladder-bearing fish. J. Acoust. Soc. Am. 64:571–580.
1981. A model for estimating distributions of fish school target strengths. Deep-Sea Res. 28A:705–725.

Magnuson, J. J.
1973. Comparative study of adaptations for continuous swimming and hydrostatic equilibrium of scombroid and xiphoid fishes. Fish. Bull. 71:337–356.

Marten, K., K. Norris, P. W. B. Moore, and K. A. Englund.
1988. Loud impulse sounds in odontocete predation and social behavior. *In* Animal sonar: processes and performance (P. E. Nachtigall and P. W. B. Moore, eds.) p. 567–579. Plenum, New York, NY.

National Research Council.
1992. Committee on reducing porpoise mortality from tuna fishing, dolphins and the tuna industry. National Academy Press, Washington, D.C., 176 p.

Norris, K. S., and B. Mohl.
1983. Can odontocetes debilitate prey with sound? Am. Nat. 122:85.

Ona, E.
1990. Physiological factors causing natural variations in acoustic target strength of fish. J. Mar. Biol. Assoc. U.K. 70:107–127.

Rees, C. D.
1998. Active towed-array acoustic system design study for yellowfin tuna in the eastern tropical Pacific fishery area. U.S Dep. Commer, NOAA Tech. Memo. TM-NMFS-SWFSC-251, 65 p. plus appendices.

Richardson, J. W., C. R. Greene, C. I. Malme, and D. H. Thomson.
1995. Marine mammals and noise. Academic Press, San Diego, CA, 576 p.

Schaefer, K. M.
1999. Comparative study of some morphological features of yellowfin (*Thunnus albacares*) and bigeye (*Thunnus obesus*) tunas. Inter-Am. Trop. Tuna Comm., Bull. 21:489–525.

Schevill, W. E.
1964. Underwater sounds of cetaceans. *In* Marine bioacoustics, vol. 1 (W. N. Tavolga, ed.), p. 307–316. Pergamon, New York, NY.

Smolker, R., and A. Richards.
1988. Loud sounds during feeding in Indian Ocean bottlenose dolphins. *In* Animal sonar: processes and performance (P. E. Nachtigall and P. W. B. Moore, eds.), p. 703–706. Plenum, New York, NY.

Tavolga, W. N.
1965. Review of marine bio-acoustics, state of the art. U.S. Naval Training Device Center Tech. Report 1212-1, 100 p.

Urick, R. J.
1983. Principles of underwater sound, third ed. McGraw-Hill, New York, NY, 423 p.

Watkins, W. A., and D. Wartzok.
1985. Sensory biophysics of marine mammals. Mar. Mamm. Sci. 1:219–260.

Webb, S. C.
1998. Broadband seismology and noise under the ocean. Rev. Geophys. 36:105–142.

Weston, D. E.
1967. Sound propagation in the presence of bladder fish. *In* Underwater acoustics, vol. 2 (M. Albers, ed.), p. 55–88. Plenum, New York, NY.

Zar, J. H.
1974. Biostatistical analysis. Prentice-Hall, Englewood Cliffs, NJ, 620 p.

Abstract.—Genetic variation at the liver *MDH** locus was used to describe the species composition and the geographic distribution of the larvae of the two redfish species, (*Sebastes mentella* and *S. fasciatus*) in the Gulf of St. Lawrence in 1991 and 1992. In both years, redfish larvae were more abundant at the junction of the Laurentian and the Esquiman Channels than in other areas surveyed. Electrophoretic analysis of 697 larvae in 1991 and 1041 in 1992 showed that larvae of both species were present in the Gulf during the two years of the study although in very different proportion. Larvae belonging to the genotype *MDH*A1A1* (*S. mentella*) represented at least 61% of the redfish larvae collected in the Gulf in 1991 and 77% in 1992. Strong spatial heterogeneity in the frequency of the two *MDH** alleles was observed; a higher proportion of *S. mentella* occurred in the central and deeper part of the channels and a higher proportion of *S. fasciatus* in shallower zones. Larvae of the genotype *MDH*A1A1* (*S. mentella*) were significantly larger than those of the genotype *MDH*A2A2* (*S. fasciatus*) for both years of the study, suggesting that the extrusion times differ between the two redfish species. The sizes and geographic distributions of the heterozygous larvae (*MDH*A1A2*) did not differ from those of *S. mentella* (*MDH*A1A1*).

Identification and distribution of larvae of redfish (*Sebastes fasciatus* and *S. mentella*: Scorpaenidae) in the Gulf of St. Lawrence

Jean-Marie Sévigny
Direction des Invertébrés et de la Biologie expérimentale
Institut Maurice-Lamontagne
Ministère des Pêches et des Océans
850 Route de la Mer
Mont-Joli
Québec G5H 3Z4, Canada
E-mail address: SevignyJM@dfo-mpo.gc.ca

Patrice Gagné
Département de Biologie
Faculté des Sciences et de Génie
Université Laval
Québec G1K 7P4, Canada

Yves de Lafontaine
Environment Canada
Centre Saint-Laurent, 105 McGill, suite 7400
Montréal, Québec H2Y 2E7, Canada

Julian Dodson
Département de Biologie
Faculté des Sciences et de Génie
Université Laval
Québec G1K 7P4, Canada

The Gulf of St. Lawrence redfish consist of a complex of three putative species, currently identified as deepwater redfish, *Sebastes mentella*, and Acadian redfish, *S. fasciatus*, that dominate the commercial fishery (Atkinson, 1984; 1987; Rubec et al., 1991) and golden redfish, *S. norvegicus*, formerly named *S. marinus* (Fernholm and Wheeler, 1983) which occurs only sporadically and at very low abundance, namely at <1% of the catch (Ni and McKone, 1983; Rubec et al., 1991).

Although *S. fasciatus* differs morphologically from *S. mentella*, the overlap in meristic and morphometric characters is such that the two redfish species are difficult to separate and, frequently, individuals cannot be unequivocally identified (Ni, 1981; 1982; Kenchington, 1986; Rubec et al., 1991). Discrimination among redfish larvae is even more complex because the morphological characters used for adults and juveniles cannot be used for identifying species during the larval stages (Penney, 1987). The taxonomic confusion, as well as the absence of reliable morphological characters to identify the larvae, has limited our understanding of the ecology and population dynamics of redfish in the North Atlantic.

Electrophoretic analysis is an appropriate tool for identifing *Sebastes* species at all stages of their life cycle, including larvae (Payne and Ni, 1982; McGlade et al., 1983; Nedreaas and Naevdal, 1991; Rubec et al., 1991; Seeb and Kendall, 1991;

Manuscript accepted 26 November 1999.
Fish. Bull. 98: 375–388 (2000).

Sévigny and de Lafontaine, 1992; Gagné, 1995; Seeb, 1998). In the Northwest Atlantic, differences in the electrophoretic mobility patterns of the dimeric protein malate dehydrogenase (MDH; EC 1.1.1.37) from liver tissue appear to distinguish *S. fasciatus* from *S. mentella* (Payne and Ni, 1982; McGlade et al., 1983; Rubec et al., 1991). The presence of two alleles (*MDH*A1* and *MDH*A2*) segregating at this locus results in three genotypes that can easily be identified by electrophoresis. A low-mobility banding pattern, corresponding to the genotype *MDH*A2A2* predominates in *S. fasciatus* whereas a high-mobility pattern, corresponding to the genotype *MDH*A1A1*, is more characteristic of *S. mentella*. However, there are two restrictions to using this approach. First and foremost, the heterozygous individuals sharing alleles of both *S. fasciatus* and *S. mentella* cannot be assigned unambiguously to one species. Second, electrophoretic mobility of MDH does not differ between *S. mentella* and *S. norvegicus* (McGlade et al., 1983). Despite these limitations and until a more reliable taxonomic tool becomes available, electrophoretic mobility patterns of liver MDH remain the best approach for identification of redfish species in the Gulf of St. Lawrence, especially at larval stages. However, one should remember that the taxonomic status of redfish is still under debate and although, for convenience, we use and refer to the species names *S. fasciatus* and *S. mentella* throughout the text, these may be putative species.

Redfish of the North Atlantic are ovoviviparous; their eggs are fertilized by sperm stored in the oviducts. Although the reproductive biology of the redfish of the Gulf of St. Lawrence is not well understood, mating (transfer of spermatozoa from male to female) probably takes place during late fall or early winter. Fertilization and embryogenesis take place in winter, and larvae hatch internally and are extruded during late spring and early summer (St-Pierre and de Lafontaine, 1995, and references therein). In consequence, the location of larval extrusion may differ significantly from the location where copulation has taken place. In order to avoid confusion, the term "larval extrusion," rather than "spawning," is used to distinguish between the hatching-extrusion phase and the mating phase of the redfish reproductive cycle. The importance of gene flow within and between species is established during the mating and fertilization phase of the reproductive cycle, whereas the location of larval hatching and extrusion will determine the geographic distribution of the species at the larval stage.

It is commonly assumed that the life cycle of the two species of redfish is completed inside the Gulf and that the redfish larval population represents a mixture of *S. fasciatus* and *S. mentella*. Although the presence of newly hatched redfish larvae in plankton samples from the Gulf did confirm that redfish extrude larvae in this area (de Lafontaine, 1990, and references therein; de Lafontaine et al., 1991), the species composition of these larvae has never been elucidated and their distribution in the Gulf has never been described. The objectives of the present study were 1) to describe the species composition of larval redfish in order to verify that the two species use the Gulf of St. Lawrence as an extrusion site, 2) to determine the spatial co-occurrence of *S. fasciatus* and *S. mentella* within the Gulf, and 3) to describe the larval size distribution of the two species as an indication of the variability in extrusion times.

Materials and methods

Sample collection

Sampling was conducted at 32 stations along three transects on the western and eastern side of Anticosti Island in the Gulf of St. Lawrence between 22 June and 4 July 1991 and at 74 stations, located mainly to the east of Anticosti Island, between 10 June and 20 June 1992 (Figs. 1 and 2). Numerous sampling stations were selected in order to obtain the largest spatial coverage for larval redfish distribution in the Gulf of St. Lawrence. Plankton samples were collected with a modified opening-closing 1-m^2 rigid "Tucker" trawl equipped with two, 333-m mesh nets and two G.O. model 2030 flowmeters. The gear was hauled in double-oblique tows from the ship's side at a cruising speed of 2.5–3.0 knots. Sampling was restricted to the 0–50 m upper layer where redfish larvae are concentrated (Kenchington, 1991; Runge and de Lafontaine, 1996). Maximum sampling depth was determined by a Vemco acoustic transducer attached to the gear frame and by calculation from the amount of wire length deployed and the wire angle. Tow duration varied between 6 and 10 min. Once back on board, nets were rapidly rinsed and samples were concentrated in codends and transferred to the laboratory on the vessel for larval sorting.

Upon collection, a visual examination of the samples was made. When the estimated number of larvae in one sample was greater than fifty, a subsample was taken for further sorting. All redfish larvae from the subsample were sorted individually and placed gently, while alive, in a drop of water on a plexiglass plate (95 mm diameter and 0.61 mm thickness) next to an inscribed number that served to identify individuals for the videotape recordings (see below)

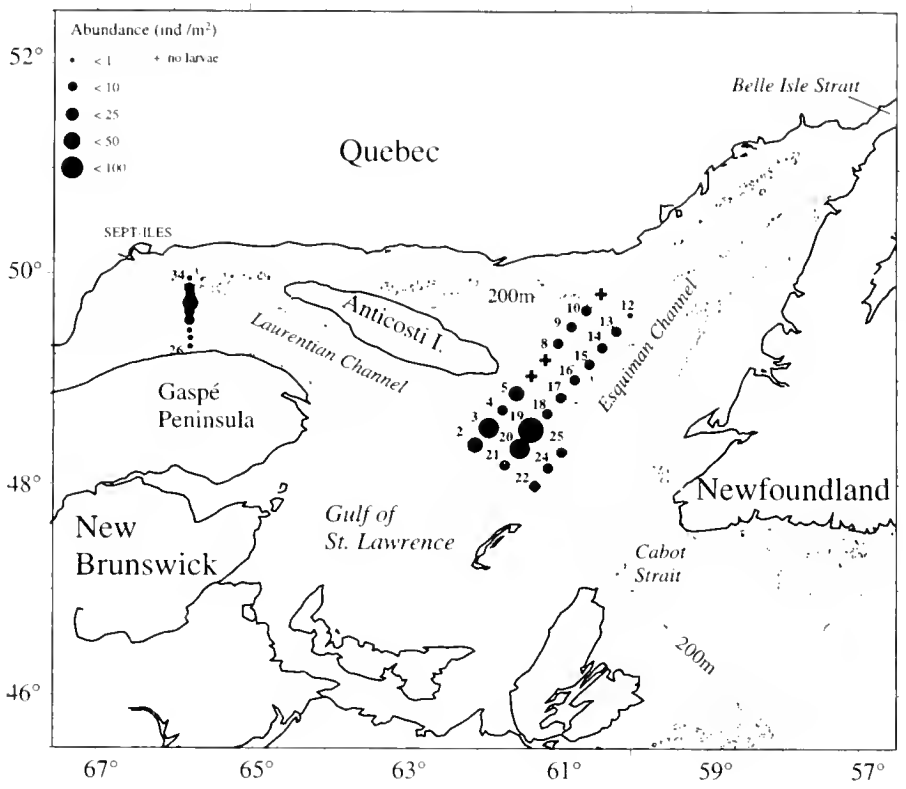

Figure 1

Geographic distribution and abundance of redfish larvae at stations sampled in June–July 1991 in the Gulf of St. Lawrence.

and for genotype determination. This procedure was adopted to minimize possible bias towards selection of larger larvae during sorting. A maximum of 10 larvae were placed on each plate. The total number of larvae so treated varied between stations owing to variable larval abundance at each station. The remaining sample with unsorted larvae and plankton was preserved in a 10% formalin seawater solution (4% formaldehyde) for subsequent laboratory sorting. Re-examination of the samples and subsamples in the laboratory showed that the proportion of larvae remaining in the samples was always less than 5% and that in most cases, larvae had been effectively sorted during the initial onboard sorting process.

The larvae placed on plates were individually video-recorded with a Hitachi black and white camera mounted on a stereomicroscope at 6× and 9× magnification and connected to a Sony Beta videotape recording machine. Periodic calibration of the magnification was made by filming a stage micrometer. The overall procedure (from sorting to filming) was completed in less than 5 min. and care was taken to ensure that larvae were alive during the video recording. The fish were sorted and video-taped on board while still alive so that morphometric measurements represented real values; these fish were later used for genetic analyses. This procedure eliminated the necessity of having one subsample for morphometric analyses and another one for biochemical analyses and did not introduce any measurement bias due to postmortem and preservation shrinkage (Magnússon[1]). Afterwards, each plate with larvae was immersed for a few seconds in liquid nitrogen, then placed in a petri dish and stored on board at –40°C. Samples were transferred to a –80°C freezer in the laboratory until electrophoresis analyses were carried out.

Laboratory analyses

Standard lengths of individual larvae was measured from the video recordings that were digitized with a Bioquant M8 image analyzing system. Repeated measurements of individual larvae indicated a measurement error of less than 3% (de Lafontaine, unpubl. data). Plankton samples were examined completely and the redfish larvae were sorted and enu-

[1] Magnusson, J. V. 1982. Shrinkage of dying redfish larvae. Int. Counc. Explor. Sea (ICES) Council Meeting 1982/G:23.

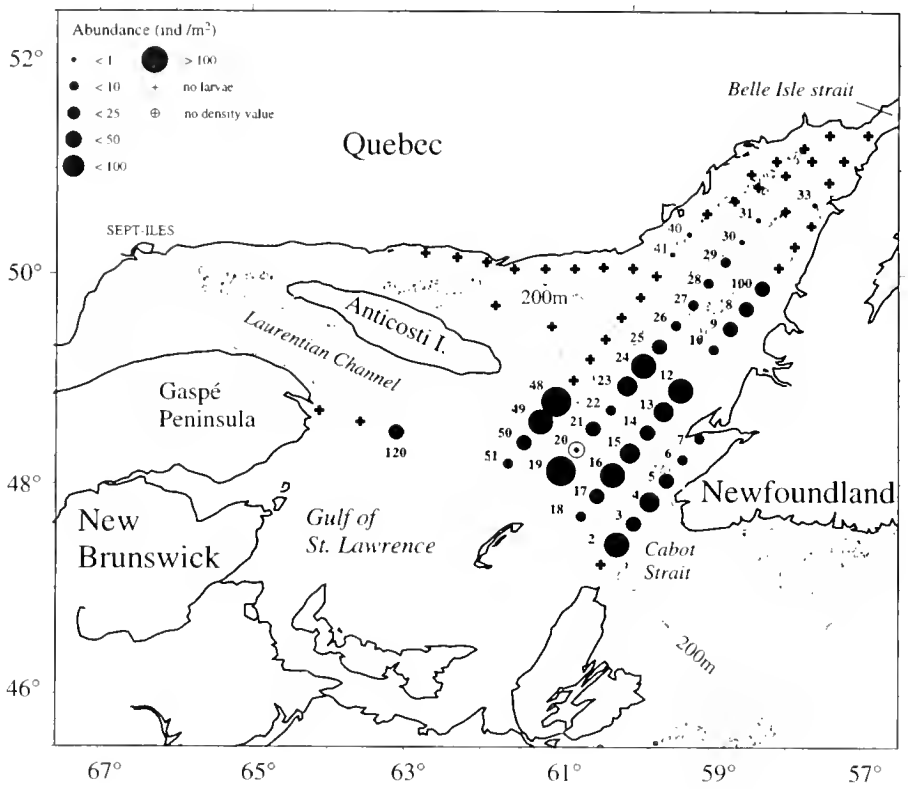

Figure 2

Geographic distribution and abundance of redfish larvae at stations sampled in June 1992 in the Gulf of St. Lawrence.

merated. The number of larvae frozen on board and those later sorted from the plankton samples were summed to provide estimates of the total abundance of redfish larvae (individuals/m^2) at each station.

Electrophoretic analyses

All electrophoretic analyses were performed within two to three months after specimen collection. The plexiglass plates supporting the larvae were always kept on ice during laboratory examination and analysis. The tissue in the liver area of individual larva was dissected under a stereomicroscope, placed directly into an individual sample well, and homogenized in an extraction solution containing 10 µL of a 0.01M Tris-HCl (pH 8.0) composed of 30% sucrose, 0.005M dithiothreitol (DTT), 0.5% polyvinylpyrrolidone (PVP) and 0.001M phenylmethylsulfonyl fluoride (PMSF). The tissue was homogenized with a fine glass rod and an aliquot was applied on the cellulose acetate gels. Cellulose acetate gel electrophoresis and gel staining were carried out as described by Hebert and Beaton (1989). A specimen of genotype *MDH*A1A2* was used as a standard on every gel to assess both the quality of the electrophoretic separation and to ensure allele identification. In 1991, a total of 735 larvae was frozen and analyzed for genotypic variation. Interpretable results were obtained for 697 specimens. In 1992, 1041 larvae were analyzed and scored.

Two alleles segregated at the *MDH** locus, resulting in the presence of three phenotypes (Rubec et al. 1991 and references therein). Homozygotes for the slow allele (*MDH*A2*) were assigned to *S. fasciatus*, and the homozygotes for the fast allele (*MDH*A1*) were classified as *S. mentella*. Heterozygotes at the *MDH** locus were left unclassified (see "Results" and "Discussion" sections).

Statistical analyses

The adequacy of genotypic proportions to Hardy-Weinberg expectations was tested for each sampling station where genotypic variation was observed by using the *G*-test of goodness-of-fit (Tables 1 and 2).

Standard length data were either not homoscedastic or not normally distributed. Therefore, comparisons of larval standard length between 1991 and 1992, between the different sampled areas of the Gulf, were carried out with a Mann Whitney *U*-test. Heterogeneity in the distribution of standard lengths

Table 1

Observed (Obs.) and expected (Exp.) number of larvae with each of the three genotypes and allelic frequencies in samples taken during June–July 1991. The mean standard length of the larvae and its coefficient of variation (CV, as a percentage) and the *G*-test values for deviation from Hardy-Weinberg expectations are given. * indicates that results were significant at $P<0.05$; ** indicates that results were significant at $P<0.001$.

Sampling station	Depth (m)	Larval density (no./m²)	Genotype *A1A1* Obs.	*A1A1* Exp.	*A1A2* Obs.	*A1A2* Exp.	*A2A2* Obs.	*A2A2* Exp.	Allelic frequency *A1	*A2	*n*	*G*-test value	Fish length Mean (mm)	Fish length CV (%)
2	340	19.9	20	20.0	9	9.0	1	1.0	0.817	0.183	30	0	9.63	10.12
3	437	28.5	23	22.7	12	12.5	2	1.7	0.784	0.216	37	0.274	9.28	8.58
4	380	7.2	10	9.8	5	5.5	1	0.8	0.781	0.219	16	-0.103	8.72	9.77
5	246	20.6	33	34.1	19	16.8	1	2.1	0.802	0.198	53	0.514	8.60	10.18
8	225	1.4	0	0	0	0	10	10.0	0	1	10	—	7.50	8.08
9	290	2.1	2	0.4	1	4.2	13	11.4	0.156	0.844	16	*6.982	6.99	9.28
10	267	1.6	0	0	0	0	9	9.0	0	1	9	—	6.98	11.78
13	216	1.4	6	3.2	1	6.5	6	3.2	0.500	0.500	13	*11.340	7.14	7.41
14	276	9.7	30	20.4	10	29.2	20	10.4	0.583	0.417	60	*27.865	8.17	14.29
15	244	4.5	1	0.2	1	2.7	13	12.2	0.100	0.900	15	2.884	7.29	8.55
16	146	1.5	7	6.4	2	3.2	1	0.4	0.800	0.200	10	1.207	8.80	15.92
17	174	5.5	24	24.0	14	14.0	2	2.0	0.775	0.225	40	0	9.46	11.06
18	375	5.9	11	10.2	8	9.5	3	2.2	0.682	0.318	22	0.772	9.64	13.33
19	416	62.6	30	27.8	5	9.4	3	0.8	0.855	0.145	38	*6.187	9.25	1.074
20	405	36.1	14	14.3	9	8.4	1	1.2	0.771	0.229	24	0.284	10.07	6.91
21	405	1.1	3	1.5	0	3.0	3	1.5	0.500	0.500	6	*8.318	8.91	13.64
22	64	1.4	6	6.0	0	0	0	0	1	0	6	—	7.16	31.04
24	369	3.8	13	12.4	7	8.2	2	1.4	0.750	0.250	22	0.440	9.80	16.52
25	475	7.0	33	32.4	6	7.2	1	0.4	0.900	0.100	40	0.856	10.36	11.99
26	222	0.4	0	0	0	0	4	4.0	0	1	4	—	6.47	11.89
27	350	0.6	0	0	0	0	7	7.0	0	1	7	—	6.97	8.19
28	346	0.5	0	0	0	0	4	4.0	0	1	4	---	6.83	4.83
29	330	4.0	1	0.5	5	6.0	19	18.4	0.140	0.860	25	0.782	7.69	15.13
30	329	7.5	38	33.6	10	18.8	7	2.6	0.782	0.218	55	*10.593	9.25	11.24
31	338	13.8	36	31.8	10	18.5	7	2.7	0.774	0.226	53	*9.965	8.96	14.35
32	335	3.6	13	7.5	4	15.0	13	7.5	0.5	0.5	30	*18.028	7.92	11.24
33	274	3.8	1	0.1	3	4.7	43	42.2	0.053	0.947	47	3.526	7.15	11.15
34	170	0.9	2	1.2	1	2.5	2	1.2	0.500	0.500	5	2.254	8.67	12.67
East sites			266	219.8	109	201.2	92	46.0	0.686	0.314	467	**95.410	8.93	15.79
West sites			91	50.2	33	114.5	106	65.3	0.467	0.533	230	*128.856	8.24	16.46
All sites			357	262.8	142	330.4	198	103.8	0.614	0.386	697	*234.634	8.70	16.42

among the three genotypes within and between sampled areas and between years was tested with a Kruskal-Wallis test. Nonparametric multiple comparisons (Dunn test) were used *a posteriori* to determine which genotypes had significantly different sizes of larvae. Differences between genotypic pairs were considered significant when $P<0.05$; the statistics Q is thus not provided in our text.

The relative proportion of *S. mentella* and of *S. fasciatus* in the sampled larval population was estimated by using two different approaches depending on the taxonomic status of the heterozygous individuals. With the first approach, the heterozygous individuals were not taken into account and the contribution of *S. mentella* and of *S. fasciatus* was based on the frequencies of the genotypes *MDH*A1A1* and *MDH*A2A2*, respectively. This approach yielded a conservative estimate. With the second approach, the heterozygous individuals were attributed to *S. mentella*. This procedure can be justified by the lack of difference in the size distribution of the *MDH*A1A1* and *MDH*A1A2* individuals and by the similar geographic distribution of these two genotypes (see "Results" and "Discussion" sections).

Table 2

Observed (Obs.) and expected (Exp.) number larvae with each of the three genotypes and allelic frequencies in samples taken during June 1992. The mean standard length of the larvae and its coefficient of variation (CV, as a percentage) and the *G*-test values for deviation from Hardy-Weinberg equilibrium are given. * indicates that results were significant at $P<0.05$; ** indicates that results were significant at $P<0.001$; nd = density value was not determined; therefore, this sampling station was not considered in the calculation of the contribution of each genotype to the larval population.

Sampling station	Depth (m)	Larval density (mo./m²)	Genotype *A1A1* Obs.	*A1A1* Exp.	*A1A2* Obs.	*A1A2* Exp.	*A2A2* Obs.	*A2A2* Exp.	Allelic frequency *A1	*A2	*n*	*G*-test value	Fish length Mean (mm)	Fish length CV (%)
2	427	51.0	23	21.4	8	11.1	3	1.4	0.794	0.206	34	2.650	8.36	5.90
3	531	22.1	19	19.3	5	4.5	0	0.3	0.896	0.104	24	0.458	8.07	10.99
4	464	33.8	25	24.0	8	9.9	2	1.0	0.829	0.171	35	1.404	8.74	6.62
5	196	12.5	24	23.1	8	9.9	2	1.1	0.824	0.176	34	0.816	8.82	5.63
6	126	9.2	28	27.3	4	5.5	1	0.3	0.909	0.091	33	1.278	8.99	6.64
7	93	1.3	18	17.9	8	8.1	1	0.9	0.815	0.185	27	0.212	8.77	5.42
8	110	19.6	23	20.8	8	12.3	4	1.8	0.771	0.229	35	*4.130	9.00	4.83
9	128	16.0	18	15.6	10	14.9	6	3.6	0.676	0.324	34	*24.690	9.01	8.69
10	141	3.2	15	9.5	6	16.9	13	7.5	0.529	0.471	34	*15.577	8.30	12.01
12	115	51.2	26	25.5	6	7.0	1	0.5	0.879	0.121	33	0.546	8.58	8.23
13	158	33.4	28	26.5	4	7.1	2	0.5	0.882	0.118	34	*4.038	8.44	5.34
14	282	13.9	26	24.0	6	9.9	3	1.0	0.829	0.171	35	*4.745	8.35	7.18
15	418	46.1	26	26.4	7	6.3	0	0.4	0.894	0.106	33	0.681	8.66	5.10
16	490	87.6	27	27.5	8	7.1	0	0.5	0.886	0.114	35	0.919	8.53	7.06
17	451	14.1	24	23.4	5	6.2	1	0.4	0.883	0.117	30	0.897	7.11	7.91
18	69	2.3	30	29.1	1	2.9	1	0.1	0.953	0.047	32	*4.303	8.74	8.80
19	401	125.4	29	28.4	5	6.3	1	0.4	0.900	0.100	35	0.734	8.56	8.79
20	447	nd	30	30.2	5	4.6	0	0.2	0.929	0.071	35	0.435	8.70	8.24
21	393	20.2	29	28.3	4	5.5	1	0.3	0.912	0.088	34	1.277	7.91	7.31
22	317	1.8	3	0.8	2	6.3	14	11.8	0.211	0. 789	19	*8.128	6.93	14.99
23	321	39.9	29	27.5	4	7.1	2	0.5	0.886	0.114	35	*4.035	8.36	8.69
24	290	74.6	29	26.6	3	7.8	3	0.6	0.871	0.129	35	*8.934	8.21	9.42
25	271	22.4	23	21.4	8	11.1	3	1.4	0.794	0.206	34	2.650	8.65	8.87
26	246	4.6	22	15.6	2	14.9	10	3.6	0.676	0.324	34	**27.526	8.32	12.86
27	225	1.2	8	8.0	0	0	0	0	1	0	8	—	6.40	5.22
28	218	1.5	7	4.9	0	4.2	3	0.9	0.700	0.300	10	**12.217	7.20	12.35
29	263	4.1	7	1.4	0	11.1	27	21.4	0.206	0.794	34	**35.084	6.89	6.33
33	269	0.9	0	0	0	0	10	10.0	0	1	10	—	6.70	8.65
48	257	101.1	28	27.5	6	7.1	1	0.5	0.886	0.114	35	0.375	8.39	8.22
49	413	69.5	29	27.5	4	7.1	2	0.5	0.886	0.114	35	*4.035	8.44	8.81
50	415	14.3	26	24.9	7	9.3	2	0.9	0.843	0.157	35	1.464	8.53	12.35
51	179	4.6	25	24.5	6	7.0	1	0.5	0.875	0.125	32	0.547	8.10	10.26
100	123	11.9	19	15.1	8	15.8	8	4.1	0.657	0.343	35	8.536	8.85	9.49
120	92	14.8	21	20.2	2	3.7	1	0.2	0.917	0.083	24	2.389	7.74	10.65
All sites			744	657.9	168	339.3	129	43.7	0.795	0.205	1041	**226.100	8.35	10.91

Larval abundance at each station was taken into account when calculating the contribution of each genotype. The contribution for the entire sampling area was estimated by the sum of the relative contribution of each genotype at each station calculated by the formula:

$$TC = S[(N_{MDH} / n) \times larval\ abundance],$$

where TC = the total contribution of a genotype to the sampled larval population;

N_{MDH} = the number of individuals of a genotype at the *MDH** locus for a given station; and

n = the total number of individuals analyzed for MDH variation for a given station.

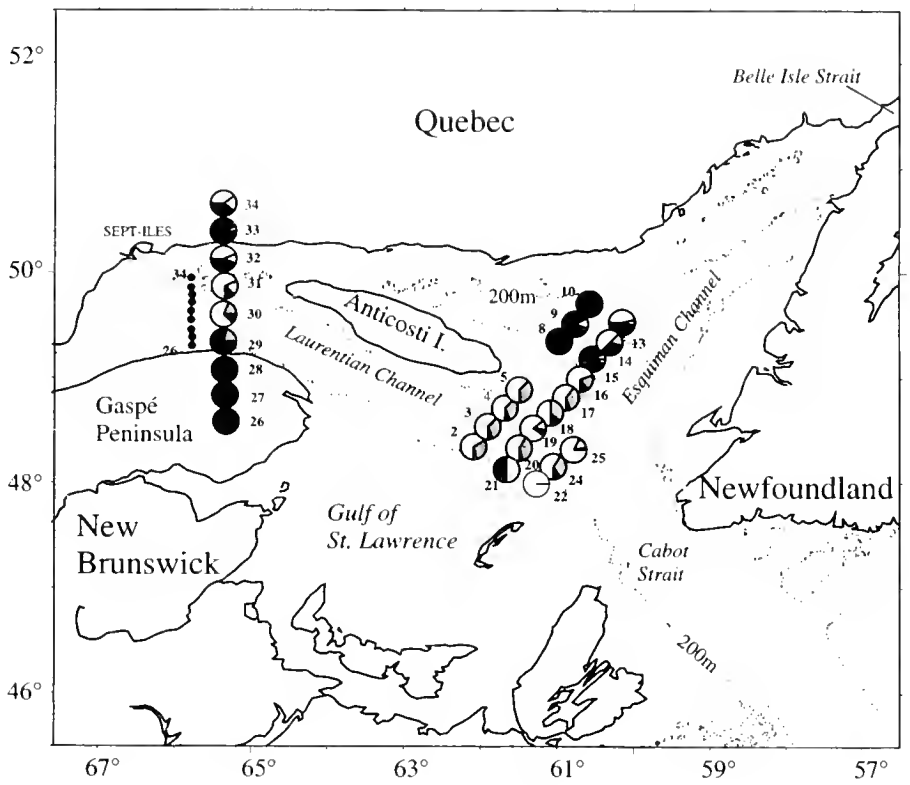

Figure 3

Geographic distribution of the larval genotypes *MDH*A1A1* characteristic of *S. mentella* (white), *MDH*A2A2* caracteristic of *S. fasciatus* (black) and *MDH*A1A2* (gray) in June–July 1991.

Results

Larval distribution, abundance, and size

In 1991, redfish larvae were caught at all but three sampling stations that were shallower than 200 m (Fig. 1). Larval abundance was highest (max.=62.6 individuals/m^2) over the central portion of the Laurentian Channel, on the southeastern side of Anticosti Island, and decreased northward along the Esquiman Channel. Only one larva was captured at the northeasternmost sampling station (12) (Fig. 1; Table 1). On the western side of Anticosti Island, larval abundance was highest (max.=13.8/m^2) at the central stations of the transect. Few larvae were caught at coastal stations within the Gaspé current (stations 26–28) or at the northernmost sampling station (<200 m deep) (Fig. 1; Table 1).

In 1992, larvae were collected at 34 of the 74 sampling stations (Fig. 2), and centers of abundance (max =125.4 larvae/m^2) were again located in the Laurentian Channel. Abundance gradually declined northwards along the Esquiman Channel. Larval redfish were virtually absent at the mouth of the Belle Isle Strait, along the Quebec north shore, at the shallow (<200 m) sampling stations on the north side of Anticosti Island or at the tip of the Gaspé peninsula (Fig. 2; Table 2).

The size of larvae ranged from 5.0 mm to 12.3 mm in 1991 and from 5.6 mm to 10.9 mm in 1992 (Tables 1 and 2). Larvae collected in 1991 were significantly larger than those collected in 1992 (Mann-Whitney *U*-test, $P<0.0001$; Table 1). Larvae from the eastern sector in 1991 were larger than those collected in the western sector (Mann-Whitney *U*-test, $P<0.0001$), and larvae collected in the eastern sector in 1991 were significantly larger than those collected in approximately the same region in 1992 (Mann-Whitney *U*-test, $P<0.0001$).

Spatial and temporal genotypic variations

The three genotypes were found in larval redfish and their relative proportion varied between sites and years (Figs. 3 and 4; Tables 1 and 2). In 1991, two groups of stations could be identified on the western side of Anticosti Island (stations 26–34) based on the frequencies of the genotypes observed. The first

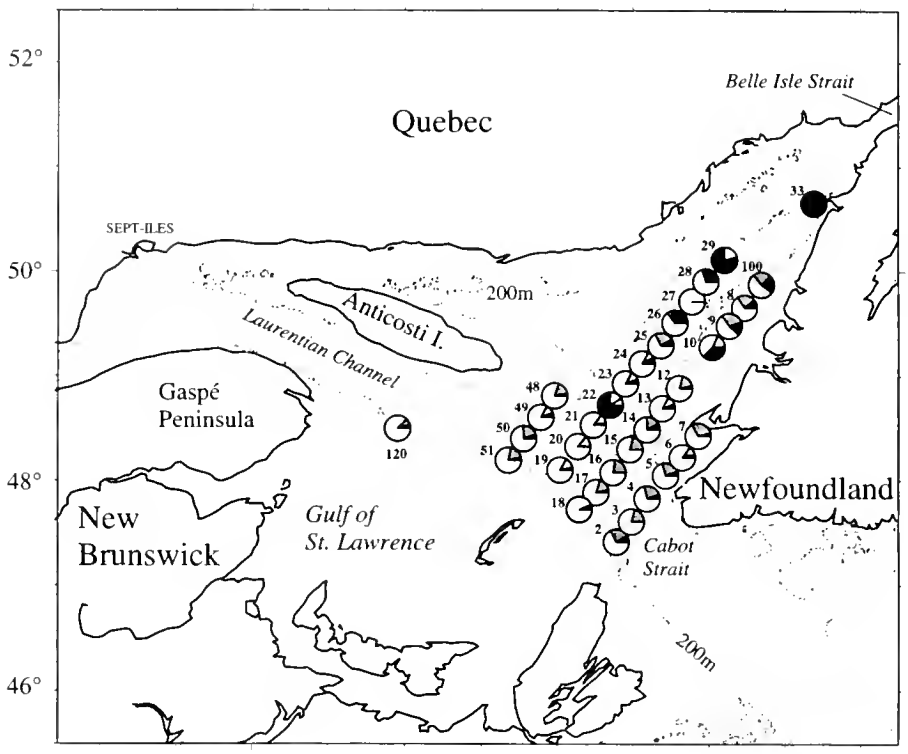

Figure 4

Geographic distribution of the larval genotypes *MDH*A1A1* characteristic of *S. mentella* (white), *MDH*A2A2* caracteristic of *S. fasciatus* (black) and *MDH*A1A2* (gray) in 1992. Sampling station numbering does not correspond with that for 1991.

group comprised stations 26–29 and 33–34 where the *MDH*A2A2* genotype is generally the most frequent. The frequency of allele *MDH*A2* at stations 26–29 within the Gaspé current system along the north shore of the Gaspé peninsula was very high, ranging from 0.860 to 1.0. At the northernmost station (33), the allele *MDH*A2* predominated and the frequency of both alleles was equal (0.500) at station 34. There was no significant deviation from Hardy-Weinberg expectations at the stations of this group. The second group comprised the central stations (30 31, 32). At theses stations, the three genotypes were represented but there was an abrupt inversion of the most frequent allele. At these stations, the frequency of allele *MDH*A1* ranged from 0.500 to 0.782. The frequency of this allele never equaled 1.0. Significant departure from Hardy-Weinberg expectations was also observed at these three central stations (Table 1).

On the eastern side of Anticosti Island, the genotype *MDH*A1A1* was most frequent in a group of stations located at the south-east end of the island near the junction of the Laurentian and Esquiman channels. The three genotypes were observed at each site except for station 22, where only *MDH*A1A1* was observed, and at station 21, where the heterozygous genotype was absent (Fig. 3; Table 1). Deviation from Hardy-Weinberg expectation was observed at stations 19 and 21 only (Table 1). The northern stations (8, 9, 10, 13, 14, 15) at the north-eastern end of Anticosti Island formed a distinct group where the genotype *MDH*A2A2* dominated. The frequency of allele *MDH*A2* varied from 0.417 to 1.0 (Table 1). The three genotypes were observed at stations 9, 13, 14, and 15 where significant deviation from Hardy-Weinberg was observed at all but sampling station 15 (Table 1).

In 1992, the genotype *MDH*A1A1* was also the most frequent genotype observed throughout the study area, except for stations 22, 29, and 33, where the genotype *MDH*A2A2* was dominant (Fig. 4). The allele *MDH*A1* was thus the most frequent except at these three sampling stations (Table 2). Statiens 29 and 33 were the northernmost stations where larvae were found during our study. The frequency of the genotype *MDH*A2A2* increased towards the north within the sampling area although it was not the most frequent genotype. This trend was also observed in 1991 (Fig. 3). In general, the three genotypes were represented at all stations except at stations 3, 15, 16, 27, and 33, where only one or two genotypes

were observed. As noted in 1991, heterozygous individuals co-occurred with those of the *MDH*A1A1* genotype. The frequency of allele *MDH*A1* varied from 0.794 to 0.953 (Table 2). Allelic frequency of 1.0 was observed at stations 27 (*MDH*A1*) and 33 (*MDH*A2*) only. Deviations from Hardy-Weinberg expectations caused by a deficit in the number of heterozygous individuals were observed at 14 sampling stations (Table 2). When data for the entire study area were pooled, a significant departure from the Hardy-Weinberg equilibrium, also due to a deficit in heterozygotes, was noted for both years and for the eastern and western sectors of the Gulf in 1991 (Tables 1 and 2). Such deviations from Hardy-Weinberg equilibrium at any given station, within the different sectors of the Gulf or over the entire sampling area, indicate that redfish larval populations do not form a panmictic group in the Gulf of St. Lawrence but rather consist of a mixture of at least the two most frequent species, *S. mentella* and *S. fasciatus*.

A strong spatial heterogeneity in the distribution of genotypes was observed. The genotype *MDH*A2A2* dominated or was more frequent at stations located in the northern part of the Gulf whereas *MDH*A1A1* dominated in the southern part of the Gulf. The frequency distribution of the genotypes over the entire area in 1991 differed significantly between the eastern and the western Gulf of St. Lawrence (χ^2=53.0; P<0.0001), indicating important spatial variation on a large scale.

Genotype and larval-size distribution

In 1991, the size of the larvae varied significantly between the three genotypes (Kruskal-Wallis, P<0.0001); the *MDH*A2A2* larvae were smaller than those of the other two genotypes (Fig. 5). The size distribution of the larvae was not significantly different between the genotypes *MDH*A1A1* and *MDH*A1A2*. The size distribution of larvae of each genotype did not differ between the eastern and the western sectors of the Gulf. The obvious bimodal distribution of larval size (all genotypes confounded) observed on the west side of Anticosti Island can thus be explained by the difference in size of larvae of the different genotypes.

Similar results were obtained in 1992, where the size of the homozygous larvae *MDH*A2A2* was significantly smaller than those of the genotypes *MDH*A1A1* and *MDH*A1A2*. There was again no significant difference in the standard length between larvae of the *MDH*A1A1* and *MDH*A1A2* genotypes (Fig. 6).

A significant difference in the size of larvae between 1991 and 1992 (Kruskal-Wallis, P<0.0001; Fig. 6) was however noted and can be attributed to the smaller size of the *MDH*A1A1* and *MDH*A1A2* larvae in 1992 compared with those in 1991. The size distribution of the homozygous *MDH*A2A2* larvae was similar in both years.

In 1991, the genotype *MDH*A2A2* was more frequently represented in recently extruded larvae (<8.5 mm) and the genotype *MDH*A1A1* was most frequent for larvae >8.5 mm. In 1992, the genotype *MDH*A1A1* was the most frequent genotype in all size classes except for larvae <6.5 mm which were dominated by the genotype *MDH*A2A2*. In both years, the genotypic composition varied between the size classes of larval redfish, indicating that a larval cohort may be dominated by individuals belonging to a single species (Fig. 6). These differences are most likely associated with a difference in the extrusion time between *S. fasciatus* and *S. mentella*.

Relative proportion of each genotype in the overall larval population

Larvae of the *MDH*A1A1* genotype accounted for 61.8% and 77.6% of all collected larvae in 1991 and 1992 respectively. The contribution of the *MDH*A2A2* genotype was 14.4% in 1991 but dropped to 5.6% in 1992. The heterozygote genotype accounted for 23.8% in 1991 and 16.8% in 1992. The combined contributions of the genotypes *MDH*A1A1* and *MDH*A1A2* thus represented 85.6% and 94.4% of the larval population in 1991 and 1992, respectively.

Discussion

Our results clearly show that the larval redfish population in the Gulf of St. Lawrence is not genetically homogeneous but rather is multispecific and composed of at least two genetically distinct species currently identified as *S. mentella* and *S. fasciatus*. As previously indicated in the introduction, *S. norvegicus* may also occur in the Gulf but at very low abundance and cannot be distinguished from *S. mentella* at the *MDH** locus. The co-existence and the larval extrusion of the two species of redfish, identified by the number of anal-fin rays, have been inferred for Gulf species in previous studies based on the presence of gravid adults (Ni and Sandeman, 1984) and on the presence of sexually mature females in spawning and postspawning condition for both species (St-Pierre and de Lafontaine, 1995). We report here the first evidence that the two species are clearly identified in the larval population.

The taxonomic status of the heterozygous individuals is however problematic. Rubec et al. (1991) suggested that the presence of heterozygotes was best

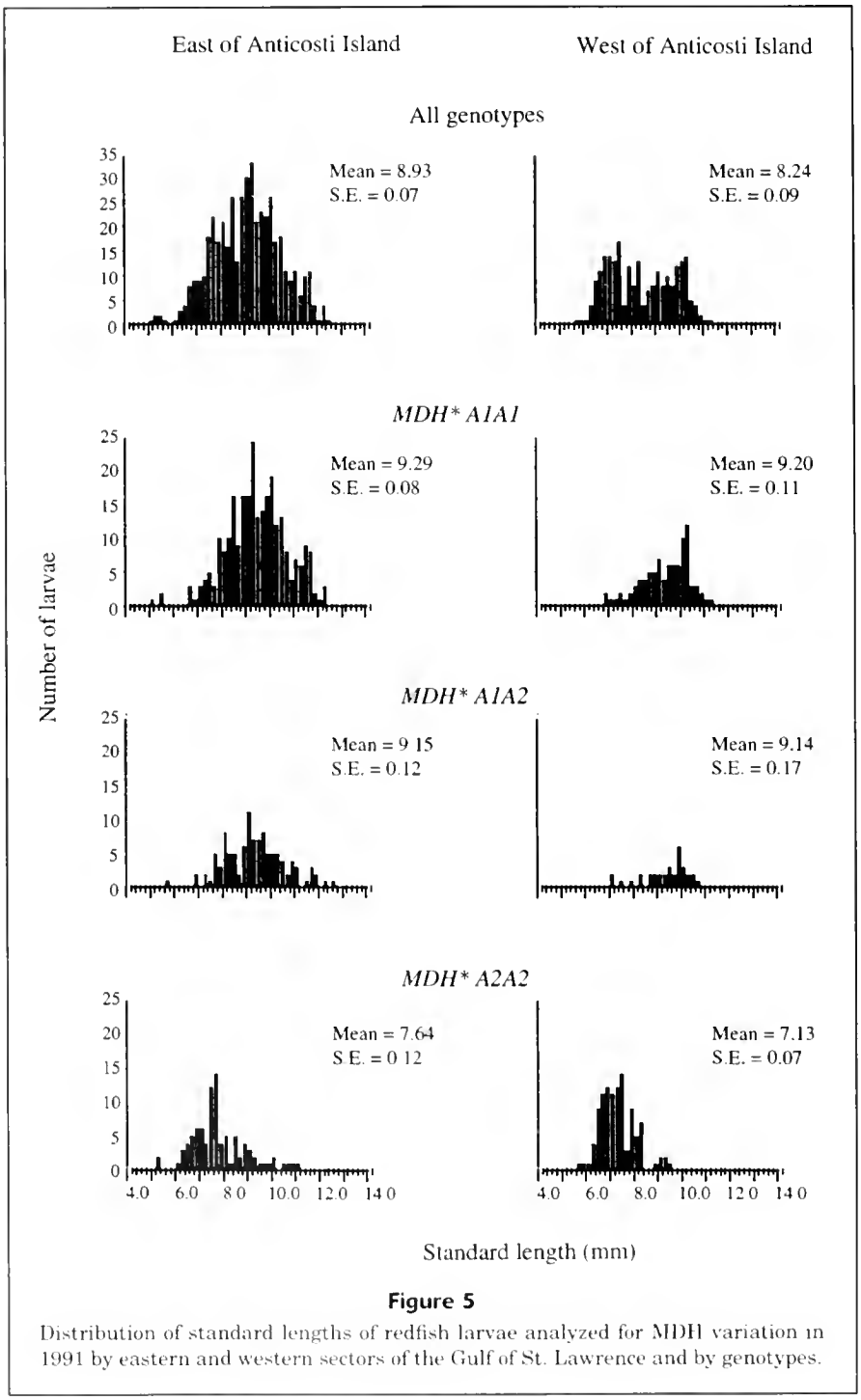

Figure 5

Distribution of standard lengths of redfish larvae analyzed for MDH variation in 1991 by eastern and western sectors of the Gulf of St. Lawrence and by genotypes.

explained by introgressive hybridization between *S. fasciatus* and *S. mentella* in the Gulf. Our results do not rule out this possibility. Hybridization between *S. fasciatus* and *S. mentella* was also suggested as one possibility to explain the RFLP patterns of rDNA observed in adult redfish from the Gulf of St. Lawrence (Desrosiers et al., 1999), where individuals with the rDNA hybrid type had more affinities with *S. mentella* than with *S. fasciatus*. In fact, hybridization between *Sebastes* species may not be an uncommon phenomenon because introgression was recently observed between three rockfish species in Puget Sound (Seeb, 1998). In our study, the similar size distribution of larvae of the *MDH*A1A1* and *MDH*A1A2* genotypes suggests that heterozygous individuals have more affinity with the *S. mentella*

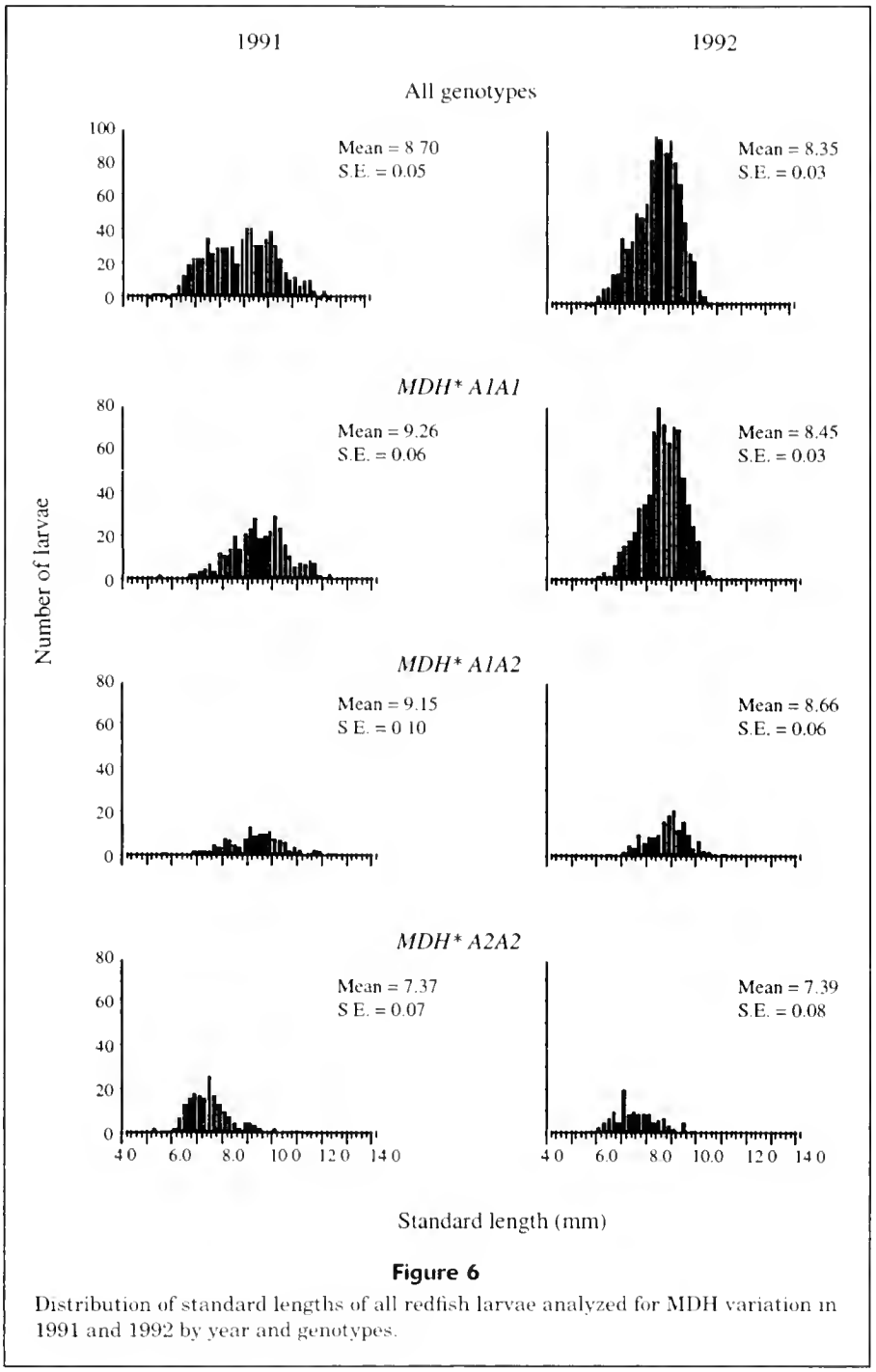

Figure 6

Distribution of standard lengths of all redfish larvae analyzed for MDH variation in 1991 and 1992 by year and genotypes.

than with *S. fasciatus*. The geographic distribution of the heterozygote larvae also matched closely that of the genotype *MDH*A1A1*.

Overall, clear geographic patterns in the abundance and the geographic distribution of redfish larval genotypes were observed in the Gulf of St. Lawrence. In both sampling years redfish larvae were mainly concentrated in offshore areas associated with the deep (>200 m) waters of the Laurentian and Esquiman Channels, as previously reported (Kenchington, 1991; de Lafontaine et al., 1991; Runge and de Lafontaine, 1996). The high abundance of redfish larvae on the southeastern side of Anticosti Island is consistent with the observed occurrence of gravid redfish during May and June in the same area (St-Pierre and de Lafontaine, 1995). High abundance of larval redfish east of Anticosti Island has been frequently observed from mid-May to mid-June

and would correspond to the seasonal peak in larval extrusion as indicated by the maturity cycle of adults (Ni and Templeman, 1985; St-Pierre and de Lafontaine, 1995). On the western side of Anticosti Island, the highest larval abundance is associated with a cyclonic residual circulation (El-Sabh, 1976) as found in previous studies (de Lafontaine, 1990; de Lafontaine et al., 1991). Our data suggest however, that in 1991 and 1992 the contribution of the western sector to the entire redfish larval production of the Gulf of St. Lawrence was small and less important than that of the eastern sector. The western sector contributed approximately up to 10.2% of the *S. mentella* (*MDH*A1A1 +MDH*A1A2*) and up to 34.4% of the *S. fasciatus* larvae in the 1991 samples. This observation is in agreement with the estimated lower biomass of adult redfish in the western Gulf of St. Lawrence in relation to the eastern sector (Atkinson, 1984; Morin and Bernier[2]). The proportionally higher contribution of *S. fasciatus* in the western sector would be indicative of slightly higher abundance of *S. fasciatus* periodically observed in that part of the Gulf (Morin[3]).

The different geographic distributions of the various larval genotypes strongly suggest differences in the preferred extrusion sites of *S. fasciatus* and *S. mentella* (Figs. 3 and 4). *Sebastes mentella* seems to prefer zones located in the central and deeper parts of the channels whereas *S. fasciatus* preferably uses shallower zones near the shelf break and along the sides of the channels. This observation is consistent with the reported summer distribution patterns of adult redfish in the Gulf of St. Lawrence (Rubec et al. 1991; St-Pierre and de Lafontaine, 1995). The apparent low proportion of *S. fasciatus* in the southern part of the Gulf may be due to the relative lack of shallower stations. Attempts to infer more precisely the locations of extrusion sites from the observed larval distributions would, however, require that the size frequency of sampled larvae be considered. In this case, size at extrusion would therefore be the best basis from which to infer the vicinity of the extrusion sites. The size at extrusion for redfish larvae in the Gulf of St. Lawrence is unknown. Penney and Evans (1985) indicated that newly extruded redfish (presumably *S. mentella*—see Penney, 1987) larvae from Flemish Cap (east of Newfoundland Grand banks) ranged between 6.2 and 8.9 mm. From the age-length relationships, these authors estimated that the mean size of newly extruded larvae was 7.68 and 8.23 mm in two consecutive years. Magnusson and Magnusson[4] also reported considerable variation in the size at extrusion (5.5–7.2 mm) of redfish larvae from the Northeast Atlantic waters. Penney (1985) indicated that the mean size of pre-extruded larvae in gravid females of *S. fasciatus* and *S. mentella* collected in southern Newfoundland waters was 7.34 and 7.89 mm, respectively. The size range of larvae in our study was 5.0 to 12.3 mm in 1991 and 5.6 to 10.9 mm in 1992. The proportion of larvae <8.5 mm was 46% and 54% in 1991 and 1992, respectively, suggesting that a large number of sampled larvae were recently extruded. Assuming an average size at extrusion of 7.5 mm and given the estimated growth rates (0.1 to 0.15 mm/day) reported in the literature (Penney and Evans, 1985; Herra, 1989), the maximum length of larvae in our samples would correspond to larvae of approximately 22 to 45 days old. The majority of larvae being <10 mm long, the sampled population was certainly less than 1 month old. Although the period of time between larval extrusion and time of collection may allow for some horizontal drift of larvae by the surface currents, the relatively small size and the presumably young age of the larvae would tend to indicate that these larvae did not disperse much (in relation to the large area sampled in our study) and would have been collected close to their extrusion sites. Consequently, the differences in the relative distribution of the genotypes of larvae indicate that the extrusion sites of the two species do not overlap to a large extent within the Gulf of St. Lawrence.

The mean and the range of the size of larvae varied between genotypes where larvae of the *MDH*A2A2* were significantly smaller (by 1.5 to 2.0 mm) than those of the two other genotypes (Fig. 6). This finding is consistent with other observations, suggesting that the length of *S. fasciatus* at extrusion is smaller than that of *S. mentella*, although considerable variability exists (Penney, 1985; 1987; Penney and Evans, 1985). The similar results obtained in the two sampling years of our study would tend to reveal a species-specific characteristic. In addition, the difference between the mean (and modal) size of each homozygote genotype was larger than that for the reported size at extrusion between the two species (0.5–0.6 mm; see Penney, 1985; Penney and Evans,

[2] Morin, B., and B. Bernier. 1997. The status of redfish in Unit 1 (Gulf of St. Lawrence). Can. Stock Assess. Sec. Res. Doc. 97/112, 23 p. Sciences Branch, Department of Fisheries and Oceans, Maurice Lamontagne Institute, 850 Route de la Mer, Mont-Joli, Quebec, Canada G5H 3Z4.

[3] Morin, B. 1998. Unpubl. results. Sciences Branch, Department of Fisheries and Oceans, Maurice Lamontagne Institute, 850 Route de la Mer, Mont-Joli, Quebec, Canada G5H 3Z4.

[4] Magnusson, J. V., and J. Magnusson. 1977. On the distinction between larvae of *S. marinus* and *S. mentella*: preliminary report. Int. Counc. Explor. Sea (ICES) Council Meeting 1977/F:48.

1985). This finding suggests that the larvae of *S. fasciatus* were extruded slightly later than those of *S. mentella* in the Gulf of St. Lawrence. Once again assuming that larval growth rates can vary between 0.10 mm and 0.15 mm/day, one can conlude that the peak in larval extrusion as determined by the modal size groups of each homozygote genotype (7.5 mm for *MDH*A2A2* and 10.2 mm for *MDH*A1A1* in 1991) would be approximately 15–25 days apart. From age estimates of larvae from otolith microstructure, Penney (1987) concluded that extrusion time of *S. mentella* was earlier than that of *S. fasciatus* in Flemish Cap area. Previous larval collections made over three consecutive summers at a fixed site along the Gaspé coast in the Gulf of St. Lawrence also showed that larvae extruded earlier tend to be larger than those extruded later in the season (Jean, 1955). Such a sampling strategy combined with genetic identification of the larvae (as presented our paper) would permit a more precise description of the seasonal variability in the extrusion of the two redfish species in the Gulf of St. Lawrence. The significantly smaller larvae collected in 1992, compared with 1991, is probably due to the earlier sampling time in 1992.

Sebastes mentella dominated the redfish larval population in the Gulf of St. Lawrence, contributing 61.8% and 77.6% of all larvae collected in 1991 and 1992, respectively. If we assume that the heterozygous individuals belong to *S. mentella*, the proportion of *S. mentella* increases to 85.6% and 94.4% for these years, respectively. Furthermore, if the heterozygous individuals belong to *S. mentella*, it might be expected that a small proportion of homozygous *MDH*A2A2* individuals were actually *S. mentella*, although misclassified as *S. fasciatus*. In which case, we would have slightly underestimated the abundance of *S. mentella*. The presence of these individuals in the *MDH*A2A2* group might correspond to the largest individuals of this group (Figs. 5 and 6). In any case, the values we obtained for larval stages are very close to those (90.3%) for adult *S. mentella* from samples in the Gulf of St. Lawrence in 1989 and 1990 (St-Pierre and de Lafontaine, 1995).

These results contrast with those of Sévigny and de Lafontaine (1992) who showed that *S. fasciatus* dominated the population of juveniles sampled in the northeastern sector of the Gulf in summer 1990 and 1991. Those juveniles mostly belonged to the 1988 cohort whose origin is not known, and Sévigny and de Lafontaine (1992) did not rule out the possibility that these fish may have originated from outside the Gulf. This rather distinct variation in the genotypic frequency among the various life stages of redfish in the Gulf of St. Lawrence remains unexplained in the light of present knowledge of the ecology of redfish over the entire distribution area. Change in the relative proportion and the geographic distribution of these two species (both at the larval and juvenile stage) may result from variable annual recruitment or from different larval drift and retention patterns among species. The mechanisms responsible for these recruitment patterns are not known but are consistent with the view that the Gulf of St. Lawrence does not form a homogeneous environmental unit but rather may consist of distinctly different pelagic ecosystems in the eastern and western sectors (de Lafontaine et al., 1991).

Acknowledgments

This study would not have been made possible without the support, technical skill and expertise of several people to whom we wish to express our sincere gratitude: Pierre Joly, Geneviève Ross, Éric Parent, and Yves Morin for assistance during work at sea and in the laboratory. We also acknowledge the captain and crew of the CSS *Alfred Needler*, for technical help during sampling cruises. A particular and very sincere thank you to M. Jean-François Saint-Pierre who participated in all aspects of this study and who suggested and developed the video camera system for filming larvae at sea. Dominique Gascon and Jean-Denis Dutil made useful comments on an early version of the manuscript. We also want to thank three anonymous reviewers for their useful comments. This study was supported by the Department of Fisheries and Oceans, Canada.

Literature cited

Atkinson, D. B.
1984. Distribution and abundance of beaked redfish in the Gulf of St. Lawrence, 1976–81. J. Northwest Atl. Fish. Sci. 5:189–197.
1987. The redfish ressources off Canada's east coast. *In* Proceedings of the International Rockfish Symposium, Anchorage, Alaska, October 1986, p. 15–33. Lowell Wakefield Fisheries Symposium Series, Alaska Sea Grant College Program Report 97-2.

de Lafontaine, Y.
1990. Ichthyoplankton communities in the St. Lawrence Estuary: composition and dynamics. *In* Oceanography of a large scale estuarine system, the St Lawrence (M. I. El-Sabh and N. Silverberg, eds.), p. 321–343. Coastal and Estuarine Studies 39.

de Lafontaine,Y., S. Demers, and J. A. Runge.
1991. Pelagic food web interactions and productivity in the Gulf of St-Lawrence: a perspective. *In* The Gulf of St-Lawrence: small ocean or big estuary? (J. C. Therriault, ed.), p. 99–123. Can. Spec. Publ. Fish. aquat. Sci. 113.

Desrosiers, B., J.-M. Sévigny, and J.-P. Chanut.
1999. Restriction fragment length polymorphism of rDNA

in the redfish *Sebastes fasciatus* and *S. mentella* (Scorpaenidae) from the Gulf of St. Lawrence. Can. J. Zool. 77: 267–277.

El-Sabh, M. I.
1976. Surface circulation pattern in the Gulf of St. Lawrence. J. Fish. Res. Board Can. 33:124–138.

Fernholm, B., and A. Wheeler.
1983. Linnaean fish specimens in the Swedish Museum of Natural History, Stockholm. Zool. J. Linn. Soc. 78:199–286.

Gagné, P.
1995. Variation génotypique et distribution spatio-temporelle des larves de sébaste, *Sebastes fasciatus* et *S. mentella* dans le golfe du Saint-Laurent. Mémoire de Maitrise, Université Laval, Québec, 96 p.

Hebert, P., and M. Beaton.
1989. Methodologies for allozyme analysis using cellulose acetate. Practical handbook. Educational service of Helena labs, Beaumont, TX, 31 p.

Herra, T.
1989. Larval redfish drift migration in relation to hydrographic features. Rapp. P-V. Réun. Cons. Int. Explor. Mer 191:92–99.

Jean, Y.
1955. Présence de larves de *Sebastes marinus* dans la Baie-des-Chaleurs et leurs caractères distinctifs. Nat. Can. 82: 33–43.

Kenchington, T. J.
1986. Morphological comparison of two northwest Atlantic redfishes, *Sebastes fasciatus* and *S. mentella*, and techniques for their identification. Can. J. Fish. Aquat. Sci. 43:781–787.
1991. Vertical distribution and movements of larval redfishes (*Sebastes* spp.) in the southern Gulf of St. Lawrence. J. Northwest Atl. Fish. Sci. 11:43–49.

McGlade, J. M., C. M.. Annand, and T. J. Kenchington.
1983. Electrophoretic identification of *Sebastes* and *Helicolenus* in the Northwestern Atlantic. Can. J. Fish. Aquat. Sci. 40:1861–1870.

Nedreaas, K., and G. Naevdal.
1991. Identification of 0-and 1-groups redfish (genus *Sebastes*) using electrophoresis. ICES J. Mar. Sci. 48:91–99.

Ni, I.-H.
1981. Separation of sharp-beaked redfish, *Sebastes fasciatus* and *S. mentella*, from northeastern Grand Bank by morphology of extrinsic gasbladder musculature. J. Northwest Atl. Fish. Sci. 2:7–12.
1982 Meristic variation in beaked redfishes, *Sebastes mentella* and *S. fasciatus*, in the Northwest Atlantic. Can. J. Fish. Aquat. Sci. 39:1664–1685.

Ni, I.-H., and W. D. McKone.
1983 Distribution and concentration of redfishes in Newfoundland and Labrador waters. North Atlantic Fisheries Organization (NAFO) Sci. Coun. Studies 6:7–14.

Ni, I.-H., and E. J. Sandeman.
1984. Size at maturity for northwest Atlantic redfishes (*Sebastes*). Can. J. Fish. Aquat. Sci. 41:1753–1762.

Ni, I.-H., and W. Templeman.
1985. Reproductive cycles of redfishes (*Sebastes*) in southern Newfoundland waters. J. Northwest Atl. Fish. Sci. 6:57–63.

Payne, R. H., and I.-H. Ni.
1982. Biochemical population genetics of redfishes (*Sebastes*) off Newfoundland. J. Northwest Atl. Fish. Sci. 3:169–172.

Penney, R. W.
1985. Comparative morphology of preextrusion larvae of the North Atlantic sharp-beaked redfishes, *Sebastes mentella* and *Sebastes fasciatus* (Pisces: Scorpaenidae). Can. J. Zool. 63: 1181–1188.
1987. Development of deep-water redfish (*Sebastes mentella*) larvae, with comparative notes on newly extruded Acadian redfish (*Sebastes fasciatus*) from the Flemish Cap. Can. J. Zool. 65:1167–1180.

Penney, R. W., and G. T. Evans.
1985. Growth histories of larval redfish (*Sebastes* spp.) on an offshore Atlantic fishing bank determined by otolith increment analysis. Can. J. Fish. Aquat. Sci. 42:1452–1464.

Rubec, P. J., J. M. McGlade, B. L. Trottier, and A. Ferron.
1991. Evaluation of methods for separation of Gulf of St. Lawrence beaked redfishes, *Sebastes fasciatus* and *S. mentella*: malate dehydrogenase mobility patterns compared with extrinsic gasbladder muscle passages and anal fin ray counts. Can. J. Fish. Aquat. Sci. 48:640–660.

Runge, J. A., and Y. de Lafontaine.
1996. Characterization of the pelagic ecosystem in surface waters of the northern Gulf of St. Lawrence in early summer: the larval redfish-*Calanus*-microplankton interaction. Fish. Oceanogr. 5:21–37

Seeb, L. W.
1998. Gene flow and introgression within and among three species of rockfishes, *Sebastes auriculatus*, *S. caurinus* and *S. maliger*. J. Heredity 89:393–403.

Seeb, L. W., and A. W. Kendall Jr.
1991. Allozyme polymorphism permit the identification of larvae and juvenile rockfishes of the genus *Sebastes*. Env. Biol. Fish. 30:191–201.

Sévigny, J.-M., and Y. de Lafontaine.
1992 Identification of redfish juveniles in the Gulf of St. Lawrence using genotypic specific variations. *In* Juvenile stages: the missing link in fisheries research (Y. de Lafontaine, T. Lambert, G. R. Lilly, W. D McKone, and R. J. Miller, eds.), p. 69–73. Can. Tech. Rep. Fish. Aquat. Sci. 1890.

St-Pierre, J.-F., and Y. de Lafontaine.
1995. Fecundity and reproduction characteristics of beaked redfish (*Sebastes fasciatus* and *S. mentella*) in the Gulf of St. Lawrence. Can. Tech. Rep. Fish. Aquat. Sci. 2059:32 + vii p.

Ghost fishing by Tanner crab (*Chionoecetes bairdi*) pots off Kodiak, Alaska: pot density and catch per trap as determined from sidescan sonar and pot recovery data

Bradley G. Stevens
Alaska Fisheries Science Center
National Marine Fisheries Service, NOAA
301 Research Ct.
Kodiak, Alaska 99615
e-mail address: bradley.g.stevens@noaa.gov

Ivan Vining

Susie Byersdorfer
Alaska Department of Fish and Game
211 Mission Road
Kodiak, Alaska 99615

William Donaldson
P.O. Box 271
Dublin, New Hampshire 03444

Abstract.—Sidescan sonar was used to locate 189 putative lost crab pots in a 4.5 km^2 area of Chiniak Bay, near Kodiak, Alaska. Subsequent observations of 15 such objects by submersible and ROV verified that they were indeed crab pots. In 1995 and 1996, 147 pots were recovered from the surveyed and adjacent nonsurveyed areas by grappling, and their condition and contents were examined. Tanner crabs, *Chionoecetes bairdi*, were the most abundant organism, with 227 found in 24 pots (16% frequency of occurrence); sunflower sea stars (*Pycnopodia helianthoides*) were the most frequent (42%) occupant and second most abundant (189 in 62 pots). Octopuses (*Octopus dofleini*) were significantly associated with pots containing Tanner crabs. Occurrence of crabs in pots was primarily a function of background crab density and differed between the surveyed and nonsurveyed areas. Recently lost pots (< 1yr old) had significantly more male crabs, significantly larger male crabs, and contained seven times more total crabs than older pots (those lost two or more years prior to recovery). The proportion of pots with damaged webbing increased with pot age, but holes in pot webbing did not significantly affect catch per pot.

Manuscript accepted 18 November 1999.
Fish. Bull. 98:389–399 (2000).

Lost and derelict fishing gear is a problem because of concerns about aesthetics at sea, entanglement of marine fauna, and ghost fishing by the gear (Sheldon and Dow, 1975; Smolowitz, 1978a; Breen, 1990). Marine mammals, birds and reptiles (Laist, 1996), nontargeted fish and shellfish (Carr et. al., 1990), and even boats (Kirkley and McConnell, 1997) have become entangled in fishing gear. In this paper ghost fishing is "the ability of fishing gear to continue fishing after all control of that gear is lost by the fisherman," as defined by Smolowitz (1978a).

Attempts to quantify the extent and impacts of ghost fishing have met with variable success (Sheldon and Dow, 1975; Smolowitz, 1978b; High and Worlund, 1979; Muir et al., 1984; Breen, 1987; Parish and Kazama, 1992; Guillory, 1993). Parish and Kazama (1992) concluded that ghost fishing of Hawaiian spiny lobsters (*Panulirus marginatus*) was unimportant because the lobsters could escape from pots easily. Conversely, Sheldon and Dow (1975) estimated that approximately one third of all American lobsters (*Homarus americanus*) entering lost pots would perish. Other studies have identified ghost fishing as a concern or possible problem and have identified potential solutions to reduce resource loss (High, 1976; Pecci et al., 1978; Smolowitz, 1978b; High and Worlund, 1979; Carr and Harris, 1997). The impact of ghost fishing by lost crab pots in Alaska waters has been studied by High and Worlund (1979), Kimker (1994), Stevens (1996), Kruse and Kimker,[1] and Ste-

[1] Kruse, G. H. and A. Kimker. 1993. Degradable escape mechanisms for pot gear: a summary report to the Alaska Board of Fisheries. Regional information report 5J93-01. Alaska Department of Fish and Game (ADFG), 211 Mission Rd., Kodiak, AK 99615, 23 p.

vens et al.[2] High and Worlund (1979) placed red king crab in unbaited square pots; after 16 days, 20% of legal-size crabs remained in the pots. Those crabs that escaped after prolonged enclosure were recaptured at lower rates than those that escaped quickly. Crabs that were placed in closed unbaited square pots exhibited mortalities from 4% to 12% after 16 days.

In our report we examined ghost fishing by lost crab pots in specific areas off the northeast shore of Kodiak Island, Alaska. In Chiniak Bay, the locations of 189 putative lost pots were discovered in April 1994 with sidescan sonar. With this sonar survey as a guide, we estimated the extent of ghost fishing by recovering lost pots and examining their contents. Three studies were conducted: 1) a pilot study within Chiniak Bay in 1995 to develop methods for pot recovery; 2) a targeted study in 1996 to recover specifically identified pots from known locations within Chiniak Bay; and 3) a nontargeted study in 1996 within Chiniak, Kalsin, Womans, and Ugak Bays, to recover pots from areas known to have been heavily fished during past crab fisheries, without attempting to target specific pots. These efforts were carried out jointly by the Alaska Department of Fish and Game (ADF&G) and the National Marine Fisheries Service (NMFS), with assistance from the U.S. Army Corps of Engineers (USACE) and the Kodiak Island Borough (KIB).

Materials and methods

Sidescan sonar survey and *in-situ* observations

The sonar survey was conducted by scientists at SAIC, Inc., using a dual frequency (100/500 KHz) sidescan sonar system (Klein model 595), with both a paper chart and digital data signal processor. Positions were recorded with a differential GPS receiver. The sonar was operated from the Alaska Department of Fish and Game (ADF&G) RV *Resolution* during 6–8 April 1994, in a portion of Chiniak Bay at depths of 100–150 m. Transects 3 km in length were run at a spacing of 75 m, such that the scanning of each line overlapped those on each side by 50%, providing a total coverage of 150%. A total area of approximately 4.5 km^2 was surveyed. From 22 April to 2 May 1995, the two-person submersible *Delta* was used to survey the area for a study of crab behavior (Stevens et al., in press); pots that were encountered accidentally during that study were examined. On 27 April 1995, a remotely operated vehicle (model S2 ROV Phantom, Deep Ocean Engineering, Inc.) equipped with a sector-scanning sonar was also used to locate and examine crab pots.

1995 pilot study

Pots identified from the sidescan sonar survey were plotted on a map (Fig. 1), then numbered. A random sample of 23 single pots was chosen for trial recovery in April 1995. A short (7.6-m) grappling chain, designed to hook the pot or its floating line, or both, was towed from the main boom of the RV *Resolution*. The grappling chain was lowered into the water when the ship was approximately 250 m from the estimated position of the targeted pot, then towed past the position at less than 5.6 km/h (3 kn). If the recovery operation was not successful, the vessel would continue to tow the grappling chain in a circle around the same position until the pot was hooked or until we gave up. When a pot was hooked, it was brought onboard with the ship's crane. Information about the pot and its contents was recorded, including pot type, condition, damage to the frame or webbing, and presence of bait jars and biodegradable mesh. In most cases the grapple snagged the steel frame of the pot and it was not possible to determine if snagging action caused additional damage to the webbing.

In our paper, we use the terms "trap" and "pot" interchangeably. The three types of crab traps most commonly used in the Gulf of Alaska are square, pyramidal, and conical (see High and Worlund, 1979, for detailed descriptions). Square pots are the most commonly used type in the Bering Sea and are made with steel frames, usually >2 × 2 m, with two funnel-shaped entrance tunnels on opposite sides. Pyramidal and conical pots are slightly smaller and have a single square or round entrance at the top, which is usually fitted with a plastic collar. All three of these types of pots are covered with nylon twine webbing. Cod pots are square pots that have been modified for cod fishing by the addition of restriction devices to prevent entry of crabs and escapement of cod. Subsistence pots, used to capture crabs for personal consumption, may be any of the above styles of pots or variations thereof. Pot conditions were rated on a subjective five-point scale from "very poor" to "excellent." Criteria used to evaluate condition included the condition of webbing (presence of holes or major gaps), numbers of broken frames and corner joints, and estimated age of the pot. Pots coded as "good" or "excellent" were assumed to have been lost less than one year and were probably placed for subsis-

[2] Stevens, B. G., J. A. Haaga, and W. E. Donaldson. 1993. Underwater observations on behavior of king crabs escaping from crab pots. Alaska Fisheries Science Center processed report 93-06, Alaska Fisheries Science Center, NMFS, 7600 Sand Point Way NE, Seattle, WA 98115, 14 p.

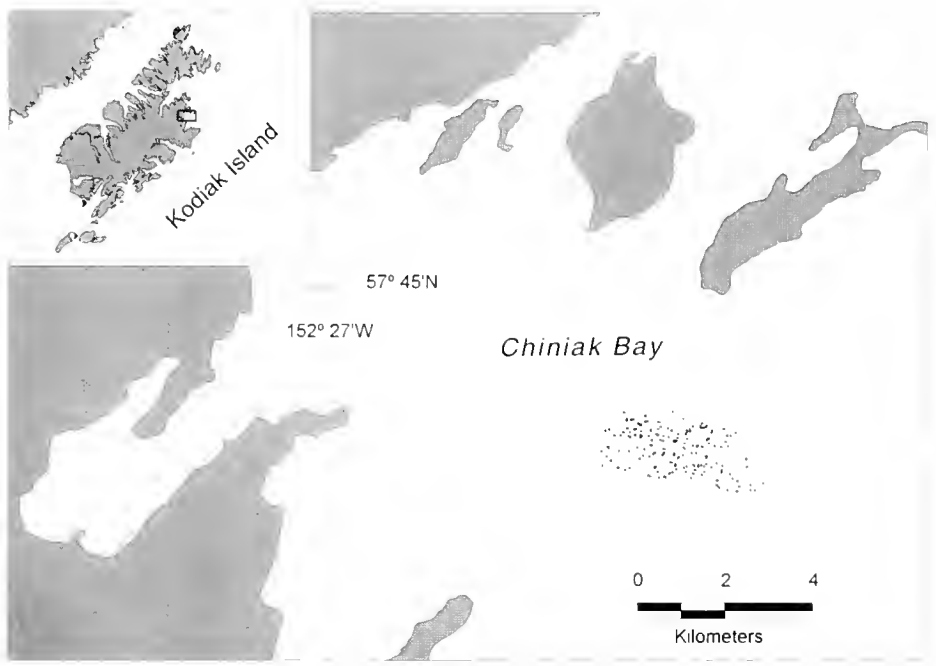

Figure 1

Chart of Chiniak Bay, Kodiak Island, Alaska, showing position of pots discovered by sidescan sonar survey. Inset shows location of Chiniak Bay on Kodiak Island.

tence use, whereas pots coded as "fair," "poor," or "very poor" were assumed to have been lost more than one year. Commercial fishing for Tanner crabs around the northeast quadrant of Kodiak Island has been closed since January 1994, and for king crab since 1983[3]; therefore no commercial crab pots have been used in the region since that time, although subsistence pots are still allowed. Therefore, recovered pots would have to have been lost at least 2 years previously (prior to April 1993), unless used for subsistence purposes. Since 1977, the state of Alaska has required that all crab pots contain an 18-inch (45.7-cm) segment of biodegradable twine that degrades within 90 days (Alaska Statutes, 1996). For this reason, all pots were examined for the presence and condition of degradable twine. However, it was not our goal to study the effectiveness of biodegradable twine because suitable control pots were not available. Furthermore, absence of biodegradable twine was inconclusive when holes were present in the webbing, because it could have indicated either that the twine had already degraded or that no twine had been present and holes resulted from some other cause.

[3] ADF&G (Alaska Dept. Fish and Game). 1996. Annual management report for the shellfish fisheries of the Westward Region, 1996. Regional information report 4K97-41. ADF&G, 211 Mission Rd. Kodiak, AK 99615.

For all crabs found in pots, carapace width (CW) was measured to the nearest mm with vernier calipers across the widest part of the carapace, excluding spines. Abundance of all other species inside the pot and size of commercially important species was also recorded. These procedures were repeated for each pot. All retrieved pots had their webbing cut and were disposed of at a location designated by the USACE and the KIB.

Targeted study

From 17 June to 18 July 1996, the procedures developed during 1995 were again used, with some modifications. The study was conducted by biologists aboard the contracted fishing vessel *Big Valley*. Pots were randomly selected for retrieval from the list of putative pot positions. Gear used for this study was a grappling beam made of 6.4 m long, 5.1 cm diameter steel pipe, and was pulled by a braided steel wire cable with a synthetic bridle. A 183-m tag line and buoy were attached to the beam to retrieve the device if the tow line was broken. Attached to the beam were six grapples, each consisting of a 1.2-m long "V" bar with two 30-cm arms welded so as to project forward and down. After the first week, a second set of arms was welded to the grapples facing upward, and on 8 July 1996, 7.6-cm barbs were welded to the ends of each arm to prevent snagged lines or pot

frames from slipping off during recovery. The grapple beam was lowered into the water with enough cable to maintain a 2:1 scope (ratio of wire out to depth), and towed through the suspected pot position. If no pot was hooked, additional transects were run parallel to the first, or the vessel was set into a sharp turn and the beam was towed in a circle. Hooked pots were retrieved with the ship's crane, while the vessel ran at a slow speed. Recovered pots were designated by the number of the most likely sonar position where they were found, and information was recorded as during the pilot study. The southeast section of the sonar-surveyed area could not be sampled owing to underwater cables and rocks.

Nontargeted study

The nontargeted study was conducted by the skipper and crew of the FV *Big Valley* without biologists aboard during 19–31 August 1996 and 5–21 October 1996. Previous attempts to snag randomly selected (i.e. targeted) pots were not particularly efficient because only 43 pots were recovered during 32 days of fishing. Therefore, instead of targeting specific pots for recovery, the skipper was instructed to fish haphazardly at his own discretion in areas where commercial crab fishing had previously been conducted, but without knowing specific pot locations. This method was more efficient and productive. The grapple beam was damaged, however; therefore it was replaced with a 30-m long weighted chain, to which were attached six short grapples, each with four barbed tines. The long grapple chain was towed at 2.8 km/h in a constant 10 turn until a pot was hooked. Recovered pots were given sequential numbers, and data were recorded as before.

Data analysis

Because Tanner crabs were the target species for most pots, associations between the presence of Tanner crabs and other species were tested by contingency table (chi-square) analysis. To reduce empty cells, Tanner crabs were combined into logarithmic categories (0, 1–9, 10–99, >99) before analysis. Association between pot condition and sex of the crabs was also tested by means of chi-square. For this purpose, pots were regrouped into two categories designated "best" (including pots coded as "excellent" or "good") and "worst" (including "fair," "poor," or "very poor" pots). Mean sizes of crabs in various condition categories are given as mean ±SE and were compared by means of the Mann-Whitney *U*-test (MWU) because variances were typically unequal (Zar, 1984). Catch of crabs or other organisms is expressed as catch per pot (CPP, i.e. crab per pot). CPP was not standardized by time because we could not adequately determine how long each pot had been in the water. The effect of holes in pot webbing on crab CPP was tested with the MWU-test; additionally, binomial confidence intervals were calculated for the proportion of pots with crabs and compared for overlap between pots with holes and those without. The null hypothesis was that torn pot webbing had no effect on CPP.

Results

Sonar survey and *in-situ* observations

Submersible observations in 1995 and previous years showed that seafloor substrates in the surveyed area were primarily sandy silt with occasional areas of compacted mud, and bottom contour was relatively flat below 100 m depth (senior author, personal obs.). The soft mud bottom absorbed most of the transmitted sonar energy and reflected very little. As a result, crab pots and other anthropogenic objects were easily distinguishable with the sidescan sonar. At least 189 objects were believed to be crab pots; 177 were single and 12 were connected together in groups of 2 to 5. In some cases attached lines could also be distinguished by sonar. Density of crab pots in the 4.5-km^2 area examined was 42 pots/km^2. At least 15 of these objects were later observed with the submersible *Delta* and the ROV, and all were verified to be crab pots, including a group of five pots connected together by tangled lines. Also noticeable were several large linear features up to 2 km long; one was later observed from the *Delta* to be a drag scar or ditch, approximately 0.5 m deep and 3–5 m wide.

Condition of pots recovered

A total of 147 pots of varying age, size, and type were retrieved during the three studies (Table 1; Fig. 2). Detailed information on location, condition, and contents of each pot is contained in a separate data report.[4] Seventy-two pots were recovered from inside the sonar-surveyed portion of Chiniak Bay (these are subsequently referred to as "inside" pots), including

[4] Vining, I., S. Byersdorfer, W. E. Donaldson, B. G. Stevens, and G. Edwards. 1997. Lost crab and cod pot recovery and ghost fishing in Chiniak Bay and other areas in the waters around Kodiak Island, Alaska. Regional information report 4K97-42. Alaska Dept. of Fish and Game, 211 Mission Rd., Kodiak, Alaska 99615, 93 p.

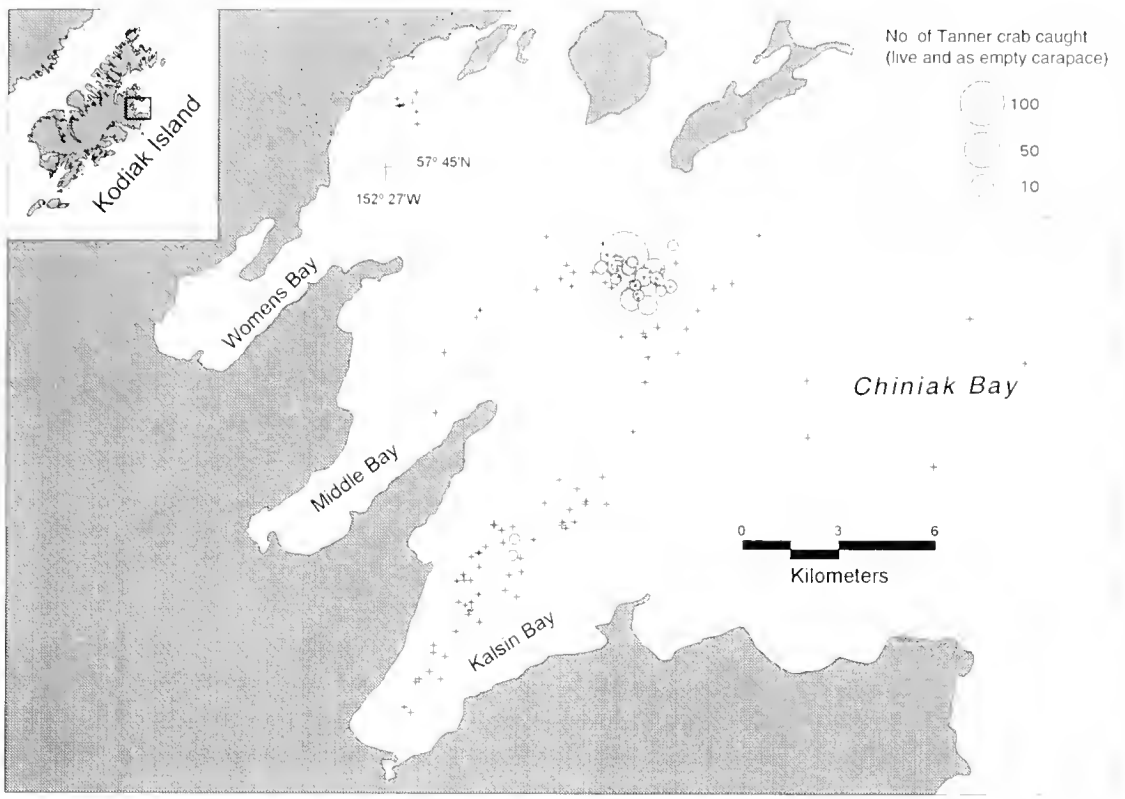

Figure 2

Location of pots retrieved from Chiniak Bay and adjacent areas during all studies, and index of Tanner crab catch per pot (crab per pot). Smallest circles represent one crab, and crosses represent pots with no crabs. Location of the three pots retrieved from Ugak Bay is not shown.

7 pots recovered during the pilot study and 43 pots recovered during the targeted study. Three of these were not previously detected by sonar and were presumed to be subsistence pots less than a year old, lost after the sonar survey was conducted, because commercial fishing had been closed in this area for over two years. An additional 22 inside pots were recovered during the nontargeted study. The remaining 75 pots were recovered from outside the surveyed area ("outside" pots) during the nontargeted study. Square pots were the most common (50%, including two cod pots), followed by pyramidal (24%) and conical (16%). Nine round pots (6%) were recovered, all of which were less than 1.07 m in diameter and were covered with a wire mesh that does not degrade easily; these were probably intended to catch Dungeness crabs (*Cancer magister*). Additional pots included two small subsistence type pots, one rectangular shrimp pot, and one made from a 55-gal oil drum.

Intact biodegradable twine was found in only eight commercial pots (3 square, 2 pyramid, 3 conical). Of those eight, four were classified as being in good condition, two as fair, one as poor, and for one pot, data on its condition were not available (Table 2). Three of these had other holes in the webbing. Eighty-eight pots had holes in the webbing; for 85 of these pots, the holes might have been the result of the degradation of biodegradable twine (excluding the three mentioned above with intact twine). However, as stated previously, without evidence of biodegrad-

Table 1

Types of pots recovered from Chiniak Bay and other bays during pilot, targeted, and nontargeted studies.

Pot type	Number of pots	% of total pots
Square	73	50
Pyramid	35	24
Conical	24	16
Cod	2	1
Round	9	6
Subsistence	2	1
Shrimp	1	1
55-gal. drum	1	1
Total	147	

Table 2

Presence of biodegradable twine and damaged pot webbing, by condition of pot. Only 133 commercial style pots were included.

Condition	Intact bio-twine	Damaged webbing	Total	% damaged
Excellent	0	0	2	0
Good	4	16	33	48
Fair	2	33	49	67
Poor	1	20	29	69
Very poor	0	15	16	94
Unknown	1	4	4	100
Total	8	88	133	

able twine, we were not able to determine if gaps in the webbing resulted from short-term degradation of biodegradable twine, longer-term degradation of nylon webbing, encounters with other fishing gear, damage during grappling and recovery, or from some other process. Generally, the proportion of pots with damaged webbing increased as the condition of the pot degraded (Table 2). Forty-five (34%) of the commercial pots had no biodegradable twine or gaps in the webbing that would have allowed crabs to escape and therefore were probably illegally set; 19 of these were rated as good or excellent, and 26 as fair to very poor.

Organisms

Organisms were found within 97 pots, including 40 (56%) of the inside pots and 57 (76%) of the outside pots. Tanner crab was the most abundant species (227 caught, mean 1.54 CPP), and second most frequent occurring in 24 pots (16%) (Table 3). The majority of Tanner crabs occurred in just two inside pots that contained 125 and 22 crabs, respectively; both pots were in good condition and were presumed to have been lost less than a year, so they were probably set for subsistence purposes. Excluding these two pots, Tanner crab CPP was only 0.55. Sunflower stars (*Pycnopodia helianthoides*) occurred most frequently (42%) and were the second most abundant species (189 caught, mean 1.29 CPP). The next most abundant species were hairy tritons (*Fusitriton oregonensis*), 174 were caught (15% occurrence), and white anemones (*Metridium senile*), 64 were caught (3% occurrence), although some of the latter may have been epibionts that were detached from the webbing during pot retrieval. In addition, we found, but did not count, many more individuals and species attached to the exterior of the pot and attached lines, including barnacles, tubiculous polychaetes, anemones, bryozoans, brachiopods, mussels, clams, snails, seastars, and basket stars (*Gorgonocephalus* sp.)

During the pilot study, 3 octopuses (*Octopus dofleini*) were found in 4 pots with Tanner crabs, suggesting that octopuses, which are known predators of Tanner crabs (senior author, personal obs.), entered the pot to prey on the crabs. Of 16 octopuses recovered during the entire study, 6 occurred in pots with Tanner crabs, and all 4 pots with 10 or more Tanner crabs (accounting for 181 of 227 crabs) contained at least one octopus, including the pot with 125 Tanner crabs. Presence and absence of octopuses was significantly associated with Tanner crabs (in logarithmic categories; χ^2=26.3). This association may have been underestimated because octopuses were not always located inside the pot. Using the ROV, we observed one octopus sitting on top of a pyramidal pot; in such a position, it probably would have been lost during grappling and recovery.

Crabs

The recovered pots contained a total of 195 live Tanner crabs, 2 dead crabs, and 30 empty carapaces. From their size and condition, these empty carapaces were considered to be the result of death or predation, rather than molting, and were not measured. Twenty-three of 32 empty carapaces or dead crabs (72%) were found in pots with octopuses. Of the live crabs, 191 were found in inside pots, and 4 in outside pots. Mean CW of all Tanner crabs was 129.8 ±1.8 mm for males (n=160), and 85.1 ±3.0 mm for females (n=35).

Pot condition, an indicator of time elapsed since it was lost, was examined for its effect on the size of crabs caught. No excellent pots contained crabs, but 152 crabs were recovered from 4 good pots. A total of 166 Tanner crabs were found in 7 out of 42 best pots (17% frequency of occurrence), whereas 61 Tanner crabs were found in 17 of 105 worst pots (16%) (Table 4); mean CPP was 6.8 times greater in best pots (3.95) than in worst pots (0.58), but this difference was not significant (MWU, Z=0.152, P>0.5). Mean CW of 141 male Tanner crabs from best pots (135.6 ±1.3 mm) was significantly larger than for 19 males from worst pots (87.1 ±6.0 mm: MWU, Z=6.29, P<0.001; Table 4). This difference was significant even after excluding pot no. 301, which contained 125 crabs; in this case, mean CW of 26 male crabs in best pots was 130.6 ±5.7 mm (MWU, Z=4.194, P<0.001). Seventy males larger than legal size (138 mm CW), with a mean CW of 144.9 mm were found in best pots; no legal males were found in worst pots. There was no significant difference in mean CW of

Table 3

Abundance of organisms found inside recovered pots. Mean values for all pots, with and without the pot containing the highest number of individuals.

Common name	Species name	Total	Maximum no. per pot	Average no. per pot	Average without max	Total no. pots with species	% of pots with species
Tanner crab	*Chionoecetes bairdi*	227	125	1.54	0.69	24	16
sunflower sea star	*Pycnopodia helianthoides*	189	13	1.29	1.2	62	42
hairy triton	*Fusitriton oregonensis*	174	50	1.18	0.84	22	15
anemone (white)	*Metridium senile*	64	50	0.44	0.1	5	3
tube worms	*Crucigera* spp.	50	50	0.34	0	1	1
green sea urchin	*Strongylocentrotus droebachiensis*	38	17	0.26	0.14	11	7
decorator crab	*Oregonia gracilis*	17	3	0.12	0.1	10	7
sun star	*Solaster* spp.	16	12	0.11	0.03	4	3
giant Pacific octopus	*Octopus dofleini*	16	3	0.11	0.09	14	10
sea cucumber	Holothuroidea	12	3	0.08	0.06	8	5
Neptune snail	*Neptunea* spp.	9	3	0.06	0.04	5	3
lyre crab	*Hyas lyratus*	9	5	0.06	0.03	4	3
kelp crab	*Pugettia gracilis*	7	3	0.05	0.03	4	3
candlefish	*Mallosus villosus*	6	6	0.04	0	1	1
rough-eye rockfish	*Sebastes aleutianus*	5	2	0.03	0.02	4	3
hermit crab	*Pagurus* sp.	5	2	0.03	0.02	4	3
sculpin	Cottidae	5	1	0.03	0.03	5	3
Hind's scallop	*Chlamys rubida*	4	2	0.03	0.01	3	2
yellow Irish lord	*Hemilepidotus jordani*	4	2	0.03	0.01	2	1
red king crab	*Paralithodes camtschaticus*	4	3	0.03	0.01	2	1
rockfish	*Sebastes* spp.	3	1	0.02	0.01	3	2
Pacific cod	*Gadus macrocephalus*	3	1	0.02	0.01	3	2
arrowtooth flounder	*Atheresthes stomias*	1	1	0.01	0	1	1
basket star	*Gorgonocephalus eryi*	1	1	0.01	0	1	1
Beringius snail	*Beringius* sp.	1	1	0.01	0	1	1
blue mussel	*Mytilus trossulus*	1	1	0.01	0	1	1
dogwinkle	*Nucella lamellosa*	1	1	0.01	0	1	1
flathead sole	*Hippoglossoides elassodon*	1	1	0.01	0	1	1
red urchin	*Strongylocentrotus franciscanus*	1	1	0.01	0	1	1
ribbed Neptune	*Neptunea lyrata*	1	1	0.01	0	1	1
mottled sea star	*Evasterias troschelii*	1	1	0.01	0	1	1

Table 4

Comparison of Tanner crab catch, sex, and size, by pot condition. ("Best" pots include those coded as good or excellent; "worst" pots include those coded as fair, poor, very poor, or in unknown condition.)

Parameter	Best pots	Worst pots	Mann Whitney *U*-test
Number of pots	42	105	
Number with Tanner crabs	7 (17%)	17 (16%)	
Number of Tanner crabs	166	61	
Crabs per pot	3.95	0.58	Z= 0.152, P>0.5
Number of legal males	70	0	
Total males	141	19	
Mean CW (SE), males	135.6 (1.3)	87.1 (6.0)	Z=6.29, P<0.001
Total females	11	24	
Mean CW (SE), females	81.3 (7.5)	86.9 (2.7)	Z=1.48, P>0.1

females from best pots (81.3 ±7.5 mm, n=11) or worst pots (86.9 ±2.7 mm, n=24) (MWU, Z=1.48, P>0.1). Numbers of male crabs were significantly associated with best pots, whereas female crabs were associated with worst pots χ^2=53.7, P<0.001); however, this result was highly dependent on two pots with the highest number of males (117) and females (8) respectively. Exclusion of those two pots reduced the χ^2 value to insignificance (3.4, P>0.05). Males composed 93% of crabs in best pots and 44% in worst pots. This result may be due primarily to the fact that pots in good condition retained large males that could have escaped more easily from damaged pots.

Even though we could not determine whether holes in webbing were caused by the degradation of biodegradable twine, recovery, or some other process, we examined their influence on crab CPP. The four highest CPPs for Tanner crabs (10, 17, 22, and 125) occurred in pots without holes, but there was no significant difference in CPP between pots with intact or torn webbing (MWU=1.17, P>0.26). Therefore, we could not reject the hypothesis that pot holes have no effect on CPP. The 95% confidence intervals around the proportion of intact pots containing crabs (10 of 41; P=0.244, 95% CI range: 0.124–0.403) overlapped those for holed pots with crabs (14 of 106; P=0.132, 95% CI range: 0.074–0.211) and included the mean of the latter. Thus the binomial test also failed to reject the null hypothesis. Lack of significance in these tests may be partly due to the high number of pots without crabs in both groups.

In addition to Tanner crabs, four male red king crabs (*Paralithodes camtschaticus*) were found in two outside pots. One pot contained 3 legal-size red king crabs with a mean CW of 161 mm and a recently dead Pacific cod which probably acted as bait; the other pot contained a single red king crab of 54 mm CW.

Discussion

Sidescan sonar has been used to assess the coverage of fishing grounds by bottom trawlers (Krost et al., 1989) but, to our knowledge, has not previously been used to determine the prevalence of ghost fishing by pots or other lost gear. Sonar is a very effective tool in this regard; lost crab pots could easily be identified by their shape and attached lines were often visible on the sonar plots. Occasionally other unidentified objects were observed; some of these could have been extremely degraded pots and one looked like the chassis of a truck or shipping van. Since this study was conducted, we have also tested a laser line-scanning system; its resolution (±1 cm) is much better than that afforded by sonar and allowed us to identify crabs and other organisms on the bottom as well as inside crab traps (Tracey et al., 1998).

The mean CPP (1.54 crab/pot) for all Tanner crabs does not seem particularly excessive. However, much of these data were obtained from an area where heavy fishing pressure had not occurred for 2.5 years. CPP in the best (i.e. most recently lost) pots was almost seven times that in the worst (i.e. oldest) pots; even though this difference was not statistically significant, it represents an important trend. Thus, examining lost pots soon after an active fishery has closed would probably yield high estimates of trapped crabs, and more males of larger sizes.

In addition to catch rates, it is necessary to know the number of actively fishing ghost pots. One "ballpark" estimate of pot loss rates in the eastern Bering Sea is 20,000 pots per year (Alaska Board of Fisheries, cited in Paul et al., 1994), but this estimate was made at a time when up to 100,000 pots were being used in Bering Sea crab fisheries annually. In 1997, the Alaska Board of Fisheries imposed pot limits in the Bering Sea and required all pots to be registered for each crab fishery, partly to reduce loss of pots when weather or ice prevented their recovery. Since then, fewer pots have been used in the Bering Sea, and pot loss rates are presumably lower. In 1999, 50,720 pots were registered for the Bering Sea snow crab (*C. opilio*) fishery; preliminary information indicates that about 1% of these may be lost and replaced during the fishery, as boats return to port for unloading.[5] However, not all lost pots are replaced during intensive fisheries, and during short (<1 week) king or Tanner crab fishery openings, boats do not return to port (a 2-d round trip) or replace pots until after the fishery closes; such losses are not reported. Pot losses as low as 10% per year would contribute 5000 lost pots each year. Subsistence pots, on the other hand, are not accounted for, are not required to be registered, and have practically no restricted locations.

Stevens (1996) concluded that the number of active ghost pots would reach a maximum over time, due to the arithmetic increase in lost pots and exponential decay processes. If 7000 pots with a half-life of 4 years were lost annually, the number of active ghost pots would stabilize at 44,000 after 40 yr, although most would begin to accumulate by year 25 (Stevens, 1996). This is a reasonable time frame for accumulation, because pot fishing for crabs in the Bering Sea has been conducted since at least 1966. However,

[5] Morrison, R. 1999. ADF&G, P.O. Box 308, Dutch Harbor, AK 99692. Personal commun.

extrapolation of ghost pot densities in Chiniak Bay to a 40,000 km^2 area of the Bering Sea (where fishing for king, Tanner, and snow crab is particularly intensive) would yield 1.68 million pots in various stages of degradation. The actual number is probably somewhere between these extremes.

If a reliable estimate of pot loss existed, it would be tempting to speculate on the numbers of crabs killed owing to ghost fishing. However, our estimate of 3.95 Tanner crabs per "best" pot represents only a "snapshot" of the ghost fishing process and does not account for cumulative mortality over time. The difference in CPP between best (3.95) and worst pots (0.58) illustrates that numbers of trapped crabs decline over time, due to escapement, predation, mortality, and reduced capture or retention rates. Starvation may account for a large part of the mortality. Kimker (1994) found 39% mortality among legal-size (>139 mm CW) male Tanner crabs that were kept in closed crab pots for 119 days; some of this mortality was undoubtedly due to cannibalism of weaker crabs (Kimker, 1994). Mortality was low for the first 30 days, then increased linearly through the remainder of the experiment. Starvation may be delayed even longer; Paul et al. (1994) held Tanner crabs in laboratory tanks for fixed periods without food, then gave them unlimited access to food. Only 10% mortality occurred among crabs during 90 d while they were held without food, but 100% mortality occurred during the following 140 days during which time they had access to food. Overall mortality ranged from 40% for those starved 60 days to 100% for those starved 90 days (Paul et al., 1994), which is consistent with the findings of Kimker (1994). Predation by octopus (High, 1976) and sunflower seastars (Breen, 1987) has also been implicated as a cause of mortality of crabs in pots. Octopus were important predators in our study and may cause a significant portion of initial mortality. In a year-long study of blue crab (*Callinectes sapidus*) ghost fishing, Guillory (1993) concluded that, of crabs that were recruited after loss of bait, 51% escaped and 45% died. Although mean CPP was only 1.0 (similar to our study) during weekly pot retrievals, the average total CPP for the entire year was 48 crabs, of which 26 (55%) died (Guillory, 1993).

Escapement probably accounts generally for the decline in numbers of crabs found in lost pots. Escapement of legal-size (>165 mm CW) king crabs from pots tended toward an asymptotic value of 80%, whereas escapement of smaller crabs was 92% after periods of 14 to 16 d (High and Worlund, 1979). Escapement rate probably depends upon behavioral differences between species. Video observations of crabs in square pots showed that both Tanner and king crabs tended to aggregate in the corners of pots, but during random movements some crabs accidentally found the entrance tunnel and escaped through it.[2] Tanner crabs are too small to reach the tunnel unless there are large numbers in the pot, allowing them to climb on top of one another to reach the tunnel opening. In addition, degradable twine in Tanner crab pots should create gaps in the webbing within weeks or months after loss, although 34% of our pots had intact webbing even after 1–2 years in the water. That such a large proportion contained no degradable twine suggests that, at a minimum, one third of the commercial crab pots used in the Kodiak region prior to 1994 were illegally constructed. Apparently, fishermen were taking advantage of the very sparse law enforcement presence in Alaskan ports.

Crabs continue to enter lost pots, even without bait. High and Worlund (1979) showed that king crabs continue to enter unbaited pots for up to 16 days. Breen (1987) showed that unbaited traps caught Dungeness crab (*Cancer magister*) at the same rate one year after becoming lost as they did when first set. He estimated that lost traps caught 17 Dungeness crabs per year, of which almost half (9.3) died, and the remainder escaped. Tanner and king crab traps are quite different from Dungeness crab pots, which are made with stainless steel webbing that degrades very slowly. Nevertheless, Breen's (1987) study clearly demonstrates that entry, escapement, and mortality rates of crabs in lost pots is a dynamic process.

Seasonality is also an important factor in ghost fishing. Breen (1987) found varying crab numbers in pots at different times of the year and concluded that a study must be conducted all year round to obtain the best estimate of crab ingress rates. Guillory (1993) found that recruitment of blue crabs to ghost pots, mortality, and escapement all varied seasonally. High turnover rates can lead to high capture and mortality rates; 2/3 of blue crabs entering traps died or escaped within 2 weeks (Guillory, 1993). Thus it is not possible to estimate mortality from a single observation of recovered traps because the number of crabs in the trap represents a balance of continuous ingress, egress, and mortality rates.

During the 1996 ADF&G annual Gulf of Alaska crab trawl survey,[6] the density of Tanner crabs was approximately 1685 crab/km^2 in Chiniak Bay, 97 in Kalsin Bay, and 76 in Middle Bay, for an average

[6] Urban, D. 1997. Bottom trawl survey of crab and groundfish: Kodiak Island, Chignik, and South Peninsula areas, 1996. Regional Information Rep. 4K97-58. Alaska Dept. of Fish and Game, 211 Mission Rd. Kodiak, AK 99615.

density of 943 crab/km^2 in the sonar-surveyed and nonsurveyed study areas combined. Relative CPP of pots recovered during our study reflected the trawlable densities in each bay; CPP was 2.70 for pots in Chiniak Bay, 0.04 in Kalsin Bay, and 0 in Middle Bay. For both the 1996 trawl survey and our pot retrieval studies, the Chiniak area had the highest density of Tanner crabs, with Kalsin Bay second, and Middle Bay last. Chiniak Bay is also a site where female Tanner crabs aggregate continuously and form high density spawning aggregations in the spring (Stevens et al., 1994).

Knowledge of the abundance of lost pots and numbers of crabs in these pots is required to estimate the impact of ghost fishing, but are not enough in themselves. A more complete assessment of ghost fishing by crab pots will require estimates for rates of ingress, egress, as well as mortality rates of crabs and studies on the degradation rates of biodegradable twine and other structural components of crab traps. Improved enforcement of existing regulations could help reduce ghost fishing. Current estimates of total pot losses are just guesses but could be substantially improved by surveying fishermen or requiring them to report pot losses.

Acknowledgments

We are indebted to Capt. Gary Edwards of the FV *Big Valley*, who built and operated the grappling devices during the targeted and nontargeted portions of this study. The pilot study was conducted with the aid of Capt. Ron Kutchick, of the ADF&G RV *Resolution*. We also thank the many "ghost (pot) busters" who assisted us in our effort, including J. Haaga, R. Otto, R. MacIntosh, P. Cummiskey, and K. Phillips. This report benefited from the thoughtful comments of Bob Wilbur and two anonymous reviewers. This study was partially funded by the U.S. Army Corps of Engineers. Funding for use of sidescan sonar was provided by the West Coast and Polar Regions Undersea Research Center, University of Alaska, Fairbanks, AK.

Literature cited

Alaska Statutes.
1996. Alaska statutes, vol. 5, Alaska Legislature Council. Michie Law Publishers, Charlottesville, VA.

Breen, P.A.
1987. Mortality of Dungeness crabs caused by lost traps in the Fraser River Estuary, British Columbia. N. Am. J. Fish. Manage. 7:429–435.
1990. A review of ghost fishing by traps and gillnets. *In* Proceedings of the second international conference on marine debris, 2–7 April 1989, Honolulu, Hawaii (R.S. Shomura and M. L. Godfrey, eds.), p. 571–599. U.S. Dep. Commer., NOAA Tech. Memo. NMFS-SWF-SC-154.

Carr, H. A., and J. Harris.
1997. Ghost-fishing gear: Have fishing practices during the past few years reduced the impact? *In* Marine debris: sources, impacts and solutions (J. M Coe and D. B. Rogers, eds.), p. 171–186. Springer, New York, NY.

Carr, H. A., E. H. Amaral, A. W. Hulbert, and R. Cooper.
1990. Underwater survey of simulated lost demersal and lost commercial gill nets off New England. *In* Proceedings of the second international conference on marine debris, 2–7 April 1989, Honolulu, Hawaii (R. S. Shomura and M. L. Godfrey, eds.), p. 438–447. U.S. Dep. Commerce, NOAA Tech. Memo. NMFS-SWF-SC-154.

Guillory, V.
1993. Ghost fishing by blue crab traps. N. Am. J. Fish. Manage. 13:459–466.

High, W. L.
1976. Escape of Dungeness crabs from pots. Mar. Fish. Rev. 38(4):19–23.

High, W. L., and D. D. Worlund.
1979. Escape of king crab, *Paralithodes camtschatica*, from derelict pots. U.S. Dep. Commer., NOAA Tech. Rep. NMFS-SSRF-734, 11 p.

Kirkley, J., and K. E. McConnell.
1997. Marine debris: benefits, costs and choices. *In* Marine debris: sources, impacts and solutions (J. M Coe and D. B. Rogers, eds.), p. 171–186. Springer, New York, NY.

Kimker, A.
1994. Tanner crab survival in closed pots. Alaska Fish. Res. Bull. 1(2):179–183.

Krost, P., M. Brenhard, F. Werner, and W. Hukriede.
1989. Otter trawl tracks in Kiel Bay (Western Baltic) mapped by side-scan sonar. Meeresforsch. 32:344–353.

Laist, D. W.
1996. Marine debris entanglement and ghost fishing: a cryptic and significant type of bycatch. *In* Solving bycatch: considerations for today and tomorrow, p 33–39. Alaska Sea Grant College Program Report 96-03, Univ. Alaska, Fairbanks, AK.

Muir, W. D., J. T. Durkin, T.C. Coley, and G.T. McCabe Jr.
1984. Escape of captured Dungeness crabs from commercial crab pots in the Columbia River estuary. N. Am. J. Fish. Manage. 4:552–555.

Parish, F. A., and T. K. Kazama.
1992. Evaluation of ghost fishing in the Hawaiian lobster fishery. Fish. Bull. 90:720–725.

Paul, J. M., A. J. Paul, and A. Kimker.
1994. Compensatory feeding capacity of 2 brachyuran crabs, Tanner and Dungeness, after starvation periods like those encountered in pots. Alaska Fish. Res. Bull. 1(2):184–187.

Pecci, K. J., R. A. Cooper, C. D. Newell, R. A. Clifford, and R. J. Smolowitz.
1978. Ghost fishing of vented and unvented lobster, *Homarus americanus*, traps. Mar. Fish. Rev. 40(5-6):9–43.

Sheldon, W. W., and R. L. Dow.
1975. Trap contributions to losses in the American lobster fishery. Fish. Bull. 73:449–451.

Smolowitz, R. J.
1978a. Trap design and ghost fishing: an overview. Mar. Fish. Rev. 40(5–6):2–8.
1978b. Trap design and ghost fishing: discussion. Mar. Fish. Rev. 40(5–6):59–67.

Stevens, B. G.
1996. Crab bycatch in pot fisheries. *In* Solving bycatch: considerations for today and tomorrow, p.151–158. Alaska Sea Grant Program Report No. 96-03. Univ. Alaska Fairbanks, AK.

Stevens, B. G., J. A. Haaga, and W. E. Donaldson.
1994. Aggregative mating of Tanner crabs *Chionoecetes bairdi*. Can. J. Fish.Aquat. Sci. 51: 1273–1280.
In press. Mound formation by Tanner crabs (*Chionoecetes bairdi*): Tidal phasing of larval launch pads? *In* The biodiversity crisis and crustacea: proceedings of the fourth international crustacean congress, Amsterdam, Netherlands, July 20–24, 1998, vol 2. (F. R. Schram and J. C. von Vaupel Klein, eds). Crustacean Issues 12.

Tracey, G. A., E. Saade, B. Stevens, P. Selvitelli, and J. Scott.
1998. Laser line scan survey of crab habitats in Alaskan waters. J. Shellfish Res. 17(5):1483–1486.

Zar, J. H.
1984. Biostatistical analysis, 2nd ed. Prentice Hall, Inc. Englewood Cliffs, NJ, 718 p.

Spatial distributions of Pacific herring, *Clupea pallasi*, and walleye pollock, *Theragra chalcogramma*, in Prince William Sound, Alaska

Kevin D. E. Stokesbury
Institute of Marine Science
University of Alaska-Fairbanks
Fairbanks, Alaska 99775-7220
Present address: Center for Marine Science and Technology
University of Massachusetts Dartmouth
706 South Rodney French Boulevard
New Bedford, Massachusetts 02744-1221
E-mail address: kstokesbury@umassd.edu

Jay Kirsch
Prince William Sound Science Center
P.O. Box 705
Cordova, Alaska 99574

Evelyn D. Brown
Institute of Marine Science
University of Alaska-Fairbanks
Fairbanks, Alaska 99775-7220

Gary L. Thomas
Prince William Sound Science Center
P.O. Box 705
Cordova, Alaska 99574

Brenda L. Norcross
Institute of Marine Science
University of Alaska-Fairbanks
Fairbanks, Alaska 99775-7220

Abstract.—Nursery areas of Pacific herring, *Clupea pallasi*, and walleye pollock, *Theragra chalcogramma*, were identified by using acoustic surveys in October 1995, and in March and July 1996 in Prince William Sound, Alaska. Pacific herring and walleye pollock were aggregated in the east-northeast and west-southwest areas. Juvenile Pacific herring spent the first two years of their lives isolated within bays. Water temperatures within bays were cooler in the summer and warmer in the winter compared with temperatures measured along coastal passages and the open coast. Although these temperature differences were small and based on point observations their accumulative effect over the season may be considerable. The school structure of juvenile Pacific herring varied seasonally. Newly recruited age-0 Pacific herring were tightly aggregated, forming a few, dense schools within a single-size cohort, in shallow water at the heads of bays in July. Age-0 Pacific herring were still aggregated within bays in shallow water in October, but the school structure was less cohesive and size cohorts began to mix. School structure and distribution completely changed in March as age-0 Pacific herring moved away from the shores into deeper water and spread out forming sparse shoals of mixed-size cohorts. Juvenile Pacific herring joined the adult schools after their second winter, leaving as new recruits entered the bays. Juvenile walleye pollock also aggregated within bays and were spatially segregated from adults. However, there appeared to be little overlap between Pacific herring and walleye pollock juveniles because they occupied different portions of the water column within these bays.

Manuscript accepted 29 November 1999
Fish. Bull. 98:400–409 (2000).

In Prince William Sound, Alaska, Pacific herring (*Clupea pallasi*) and walleye pollock (*Theragra chalcogramma*) support major commercial fisheries and are primary forage for marine birds, mammals and other fishes (Clausen, 1983; Hatch and Sanger, 1992; Livingston, 1993; Brown et al., 1996). Recently the abundance of both these species in Prince William Sound has fluctuated, particularly that of Pacific herring, which suffered a population crash in 1993 resulting in the closure of the commercial fisheries (bait, sac-roe, and roe on kelp) (Meyers et al., 1994; Paine et al., 1996). Little is known of the spatial distributions and the physical and biological variables influencing Pacific herring and walleye pollock life histories in this biologically rich, high latitude ecosystem (Paine et al., 1996).

We identified Pacific herring and walleye pollock nursery areas by examining their small-scale (km) spatial distributions in Prince William Sound, Alaska. We hypothesized that juvenile Pacific herring and juvenile walleye pollock were contagiously distributed and that

their distributions varied seasonally in relation to the stage of life of fish, school structure, and coastal structure. We then examined the degree of overlap between juvenile Pacific herring and juvenile walleye pollock distributions. Further we determined if cohorts (age and size) of Pacific herring were spatially segregated. Adult Pacific herring and walleye pollock distributions were also observed; however, these fishes appeared to emigrate from Prince William Sound at certain times of the year.

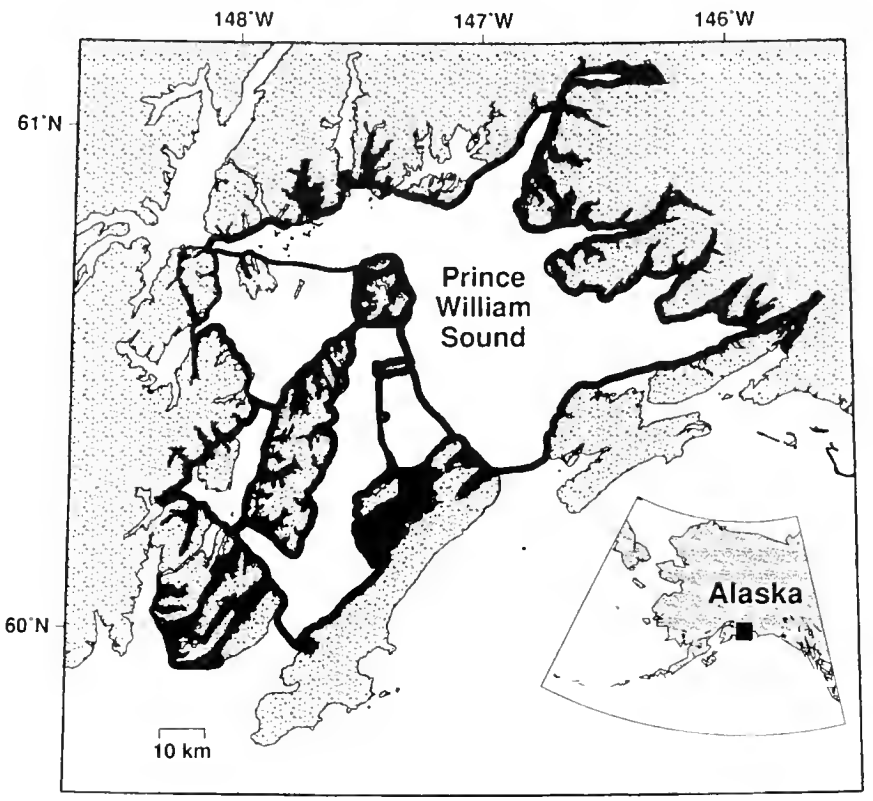

Figure 1

Location of the October 1995, March 1996, and July 1996 acoustic survey transects in Prince William Sound, Alaska. The dark areas represent the locations within which we conducted our zigzag transect survey.

Materials and methods

Prince William Sound is a large body of water separated from the Gulf of Alaska by a series of mountainous islands and deep passages (Fig. 1). The rocky coastline is highly irregular and has numerous islands, passages, bays, and deep fjords. The Sound had a semidiurnal tide with a maximum range of 4.4 m during the period of our study.

Prince William Sound coastal waters were acoustically surveyed in October 1995, and in March and July 1996 (Fig. 1). Five vessels were used during each 10-day survey (12 hours per day): three commercial seiners (≈16.8 m) deployed the acoustic and oceanographic equipment and fished the seines; a trawler (Alaska Department of Fish and Game RV *Pandalus*, ≈20 m) was used for midwater sampling; and a tour vessel (≈25 m) was used for processing samples. Surveys were conducted during the night (2000 to 0800 h) in October 1995 and March 1996, and during the day (0800 to 2000 h) in July 1996. Northern latitude conditions dictated this sampling design because there was little daylight in March and little darkness in July. Further, the summer cruises had to be coordinated with aerial surveys for forage fish that could only be flown during daylight (E. Brown, unpubl. data). We observed and collected both Pacific herring and walleye pollock in surface waters and near the sea floor, a range of area that coincides with the known diel distributions for these two species.

The acoustic vessel followed a zigzag transect pattern along the shore (MacLennan and Simmonds, 1992; Gunderson, 1993) to a distance of ≈1 km at a speed of 14 to 17 km/h. We attempted to survey the same bays, passages, and open coast during all three surveys. The vessel's sonar (50 kHz, 46°) was used to locate fish schools along these transects. When a fish school was encountered, the acoustic vessel slowed to 9 to 11 km/h and completed a series of parallel transects perpendicular to shore by using a 120-kHz BioSonics 101 echosounder with a preamplified dual-beam transducer (6°×15°). The transducer was mounted on a BioSonics 1.2-m BioFin and towed at ≈1 m depth. The acoustic signals were processed in real-time with BioSonics ESP 221 Echo square integration software and ESP 281 Dual beam software, and the raw signal was stored on digital audio tape (Thorne, 1983a; 1983b; MacLennan and Simmonds, 1992). The acoustic system was calibrated before each cruise with a standard target and the source level (SL) was 225.07 dB μPa. Acoustic noise was well below our lowest density of interest.

Fish schools observed with the acoustic equipment were sampled to determine species composition and size structure. Fish were captured with a modified bottom trawl in deep water (1.52 × 2.13 m Nor'Eastern Astoria V trawl doors, 21.3-m head rope, 29.0-m, foot rope, 3 × 20.0-m mouth, 10.2-cm mesh

wings, 8.9-cm middle, and a 32.0-mm codend liner), with one of two anchovy seines in surface water (250.0 × 34.0 m or 20.0 m, 25.0-mm stretch mesh), or with a small salmon fry seine in shallow water (50.0 × 8.0 m, 3.0-mm stretch mesh deployed from a 6-m skiff equipped with a 70-horsepower engine). Fish collections were directed by the acoustic survey and we attempted to sample every observed school. The catchability of the fish species sampled may vary with time of day, season, and between nets. However, we assumed that these collections reflected the actual species and age cohort ratios present within the acoustically observed fish school. A total of 220, 122, and 60 fish collections were made in 15, 29, and 28 locations in October 1995, March 1996, and July 1996, respectively. Each net collection was characterized by species, and 1000 individuals of the dominant fish species, usually Pacific herring, were randomly sampled. Fork lengths (mm) for 550 fish were measured immediately after capture, and 450 fish were frozen and later their fork length and wet weight (g) were measured in the laboratory. After subsampling the remaining fish were released unharmed from the seine.

A length-dependent scaling constant was used to convert estimated target strength (TS $-10 \log_{10} w$) from units of reflected acoustic energy (dB) to units of biomass density (kg/m^3):

$$TS - 10 \log_{10} w = -6.0 \log_{10} L - 24.2 \text{ dB m}^2/\text{kg},$$

where L = the mean fork length (cm) of the fish collected in the area (Thorne, 1977; 1983a 1983b; Thorne and Thomas, 1990).

This equation differs from the more standard regression equation (Foote, 1987) because it derives the target strength as a proportion of weight. Thorne's equation was developed for echo integration primarily with Pacific herring surveys from Alaska and Puget Sound (Thorne, 1983a).

For walleye pollock, that have a physoclistic swim bladder, the standard equation:

$$TS = 20 \log_{10} x - 66.0 \text{ dB}$$

was used (Foote and Traynor, 1988).

The acoustic estimates of Pacific herring and walleye pollock school densities were derived from these target strength equations. Many physical and biological variables (including morphologic features [such as physostomic, physoclistic, fat content], the orientation of the fish, water temperature, and depth) affect target strength (Thorne, 1983b; Foote, 1987; Rose and Leggett, 1988; Thorne and Thomas, 1990; MacLennan and Simmonds, 1992; Misund et al., 1995; Huse and Ona, 1996; McClatchie et al., 1996; Ona and Mitson, 1996; Misund, 1997; Misund et al., 1998).

Echo integration measurements were converted into data cells with lengths of 120 m, 40 m, or 20 m and width and depth of 1 m for the October 1995, March 1996, and July 1996 surveys, respectively. Cell length was determined by using the simultaneously recorded latitude and longitude from the GPS navigational system.

Species proportion and size modes per species were determined from the fish collections. The species proportions, based on the number of individuals per fish species in the random subsample, were multiplied by the echo integration densities (kg/m^3) and then converted by using length-weight regressions into the number of Pacific herring per size mode, or the number of walleye pollock. Walleye pollock were not divided into size modes because the standard deviations of the mean fork lengths of individual collections indicated that aggregations were unimodal.

A group of data cells was considered to be a fish school if the sum of the absolute differences between latitudes and longitudes of adjacent cells was >0.009°. We concluded that cells containing the equivalent of <0.5 fish/m^3 were probably zooplankton on the basis of frequency distributions of the data, and these cells were removed from the data set (MacLennan and Simmonds, 1992; Gunderson, 1993). If fish located near the bottom were difficult to distinguish acoustically, data cells for the bottom 5 m were removed.

Cohorts of Pacific herring and walleye pollock large-scale spatial distributions were examined by using circular statistics (Batschelet, 1981). The angle (0°=true north) for each data cell was determined from an origin in the center of Prince William Sound (60.6000°N, 146.9000°W). These angles represent distributions along the survey transect line and are influenced by inequalities in shoreline distance and sampling bias. Angle frequency distributions were compared with random distributions and with the distributions of other herring size modes along the same transect by using a chi-squared test at the 5% level of significance (Batschelet, 1981). Expected values were grouped according to Cochran's rule, which states that <20% of the expected frequencies should have a value <5 (Sokal and Rohlf, 1981).

Nursery areas were determined by examining the relation between juvenile fish spatial distributions and coastline structure. Bays were defined statistically from passages or open coast by calculating the sum of the three nearest shore distances (Σ3NSD). To determine this value, first the distance between the center of each fish school and the nearest shore was measured. The second distance was determined by

moving 90° on either side of the first line, measuring the distance to shore and selecting the shorter of the two lines. The third distance was determined by moving 90° on either side of the first and second lines, measuring the distance to shore, and selecting the shorter of the two lines. These three distances were summed. This measurement was calculated at specific points inside 26 bays and outside 17 bays to verify that it accurately distinguished between bays, passages, and open coast. The Σ3NSD for each fish school was compared with the same measurements from randomly selected points along the same survey transect by using a chi-squared test grouped according to Cochran's rule (Sokal and Rohlf, 1981). This technique removed sampling and shore structure discrepancies.

Differences in water conditions within bays compared with conditions in passages or along open coastline were examined. Vertical water profiles of temperature and salinity at 1-m intervals, measured with a SeaBird CTD instrument (SEACAT SBE19), were collected inside and outside bays. Differences between means were examined with a Mann-Whitney rank sum test (U).

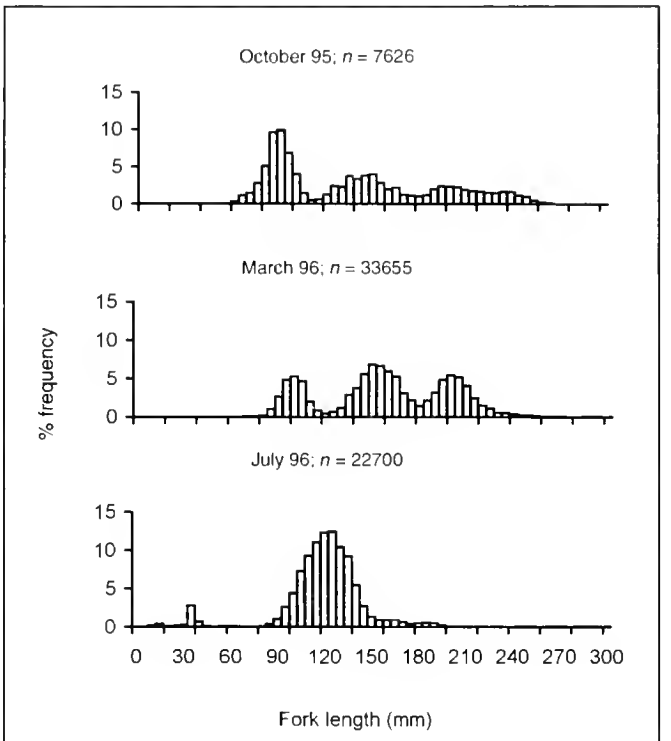

Figure 2

Percent size-frequency distributions of Pacific herring, *Clupea pallasi*, (fork length mm) collected during three acoustic surveys of Prince William Sound, Alaska, in 1995 and 1996 (n=count).

Results

Ninety-seven species of fish and macroinvertebrates were collected during the October 1995, and the March and July 1996 surveys. Pacific herring (65.0% of subsample collections) dominated the ichthyofauna followed by walleye pollock (19.2%).

Pacific herring and walleye pollock size frequencies differed. The Pacific herring population consisted of three size modes representing age-0, 1–2 year old, and adult fishes (Stokesbury et al. 1999) (Fig. 2). The walleye pollock population size distribution was bimodal, representing age-0 and adult fishes in October 1995 and March 1996, whereas only age-0 fish were collected during July 1996 (Fig. 3). Age-0 and adult pollock were always collected separately.

The proportion of Pacific herring schools consisting of a single size cohort varied among seasons. In October 1995, 49.0% of the Pacific herring schools sampled consisted of a single size class, mostly age 0. In March 1996, 38.9% of the Pacific herring schools sampled consisted of a single size, primarily 1–2 year olds. In July 1996, 83.3% of the Pacific herring schools sampled consisted of a single size, primarily 1–2 year olds.

Juvenile Pacific herring and walleye pollock were contagiously distributed in the east-northeast and the west-southwest of Prince William Sound (Fig. 4). Adult Pacific herring aggregated in the southwest (210°–240°) in October 1995, in the south (180°) and east (90°) in March 1996, and west (240°–270°) in July 1996 (Fig. 4).

Pacific herring schools had the lowest densities in March 1996 and the highest densities in July 1996 (Table 1). Walleye pollock schools had low densities in October 1995 and March 1996 compared with very high densities in July 1996 (Table 1).

Pacific herring were deeper in the water column in March 1996 (27.0–28.9 m) than in October 1995 (15.0–20.2 m) and July 1996 (14.1–16.7 m) (Fig. 5). Walleye pollock were distributed near the bottom during all three surveys (Fig. 5).

The 26 locations within bays had a mean Σ3NSD value of 3.8 km (SD=2.45), significantly smaller than 9.8 km (SD=6.69) for the 17 locations within passages and along the open coast (t=–3.61, df=41, P<0.001). The water conditions within these bays generally differed from conditions in passages and open coast (Table 2). The surface water temperatures (0–30 m) were cooler inside than outside the bays by 0.32°C and 0.20°C in October 1995 and July 1996, respectively. The surface water inside the bays was also less saline in October 95 but was similar inside

Table 1

Means and standard deviations (SD) of densities (fish/m^3) for the three Pacific herring, *Clupea pallasi*, size modes and for walleye pollock, *Theragra chalcogramma*, aggregations observed during three acoustic surveys of Prince William Sound, Alaska, in 1995 and 1996 (n=number of schools observed).

	October 1995 fish/m^3			March 1996 fish/m^3			July 1996 fish/m^3		
Herring	n	mean	SD	n	mean	SD	n	mean	SD
age-0	137	2.52	8.36	179	0.91	2.84	8	2.67	5.46
age 1–2	126	0.51	1.10	223	0.81	0.95	42	9.15	15.75
adult	54	1.35	3.21	147	0.51	0.95	32	3.62	0.86
Pollock	119	3.14	8.68	148	4.20	14.59	31	267.87	72.05

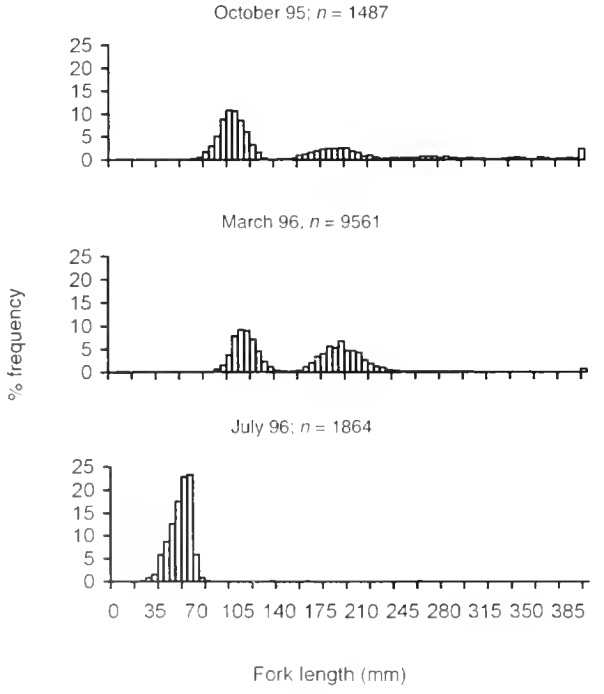

Figure 3

Percent size-frequency distributions of walleye pollock, *Theragra chalcogramma* (fork length mm), collected during three acoustic surveys of Prince William Sound, Alaska, in 1995 and 1996 (n=count).

and outside the bays in deeper water (31–60 m) and throughout the water columns in July 1996 (Table 2). Deeper waters, where Pacific herring were aggregated, inside the bays were warmer than outside the bays, 0.28 C (31–60 m) in March 1996.

Pacific herring and walleye pollock Σ3NSD distributions differed from randomly calculated Σ3NSD distributions during all three surveys (Table 3; Fig. 6). In October 1995, age-0 and 1–2 year old Pacific herring aggregated at the heads of bays with Σ3NSD values <3 km (Fig. 6). Adult Pacific herring were aggregated in passages or along the open coast (Fig. 6). Walleye pollock distribution was also significantly aggregated within bays but not as tightly as age-0 and 1–2 year old Pacific herring (Table 3; Fig. 6). In March 1996, all size modes of Pacific herring and walleye pollock had greater than expected Σ3NSD values, ranging between 4 and 10 km (Table 3; Fig. 6). In July 1996, age-0 Pacific herring were highly aggregated at the heads of bays (57.1% of Σ3NSD <1 km; Fig. 6). Age 1–2 year old Pacific herring were also aggregated at the head of bays (<2 km). Adult Pacific herring were aggregated within bays (<2 km), but more than expected had Σ3NSD values of 6 to 7 km (Fig. 6). In July 1996, walleye pollock were aggregated within bays and the majority of Σ3NSD values were <3 km (Table 3; Fig. 6).

Discussion

Pacific herring was the most abundant fish aggregating in the east-northeast and west southwest areas of Prince William Sound. Bays appeared to be nursery areas for age-0 and 1–2 year old Pacific herring. Water conditions within bays fluctuated less than conditions within passages and along the open coast. In October 1995 and July 1996 water temperatures in the upper 30 m were cooler inside these bays than within passages or along the open coast. In March this pattern was reversed and deeper waters, where the Pacific herring were aggregated, were warmer within the bays than within passages or along the open coast. Although, these fluctuations were small, they may have affected juvenile Pacific herring metabolic rates. Temperature and length of winter are critical factors in determining juvenile Pacific herring growth and over-winter survival (Paul and Paul, 1998; Paul et al., 1998; Foy and Paul, 1999).

When larval Pacific herring metamorphose into juveniles, they develop the ability to form and maintain schools (Blaxter, 1985; Gallego and Heath, 1994). Schooling behavior is the juvenile herring's primary defense against predation (Blaxter and Hunter, 1982). School structure results from the dynamic interaction of several variables causing opposing behaviors, primarily the availability of food, the physical size and condition of the fish, and the threat of predation (for a review see Pitcher, 1986). Newly recruited age-0 Pacific herring were tightly aggregated in shallow water at the heads of bays in July. These herring formed a few dense schools of a single-size cohort near the surface. This distribution possibly resulted from a high threat of predation (Stokesbury et al.[1]), coupled with an abundance of food as indicated by the fullness of herring stomachs (Foy and Norcross, 1999) and from zooplankton samples (Foy[2]).

Age-0 Pacific herring were aggregated within bays near the surface, in October. However, the number of schools increased, schools became less cohesive, and size cohorts began to mix in contrast to the highly aggregated unimodal schools observed in July. The distribution observed in October may have resulted from a decrease in food abundance, a decrease in the threat of predation, or both (Foy and Norcross, 1999, Stokesbury et al.[1]).

Age-0 Pacific herring school structure and distribution completely changed in March. These herring had just survived the winter when prey abundance is minimal and the risk of starvation is great (Paul and Paul, 1998; Paul et al., 1998; Foy and Paul, 1999). Herring moved away from the shores into deeper water and spread out forming sparse (<1 fish/m^3) shoals of mixed-size cohorts. Distance between fish within schools increases with hunger, reducing cohesion, and causing lower mean densities (Pitcher and Partridge, 1979; Robinson, 1995). This independent segregating behavior reduces competition for food and increases the chance of encountering food by

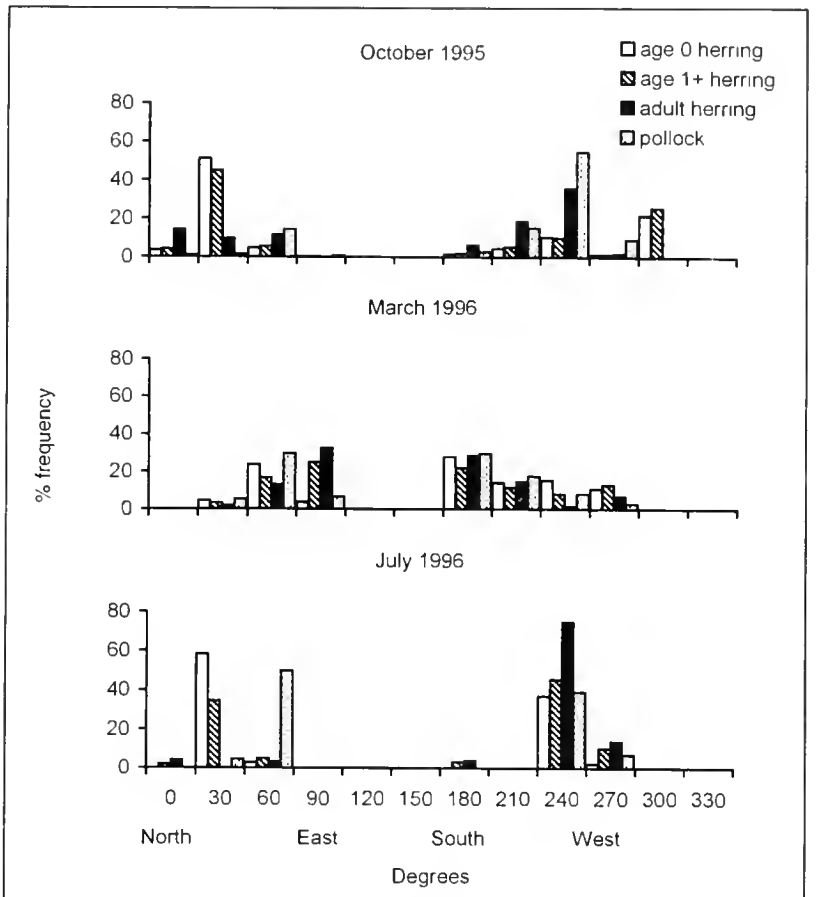

Figure 4

Angle percent-frequency distributions of Pacific herring, *Clupea pallasi*, and walleye pollock, *Theragra chalcogramma*, observed during three acoustic surveys of Prince William Sound, Alaska, in 1995 and 1996.

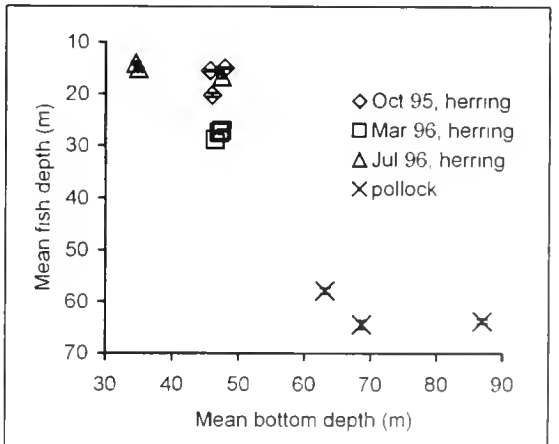

Figure 5

Mean depths (m) and standard error bars for Pacific herring, *Clupea pallasi*, and walleye pollock, *Theragra chalcogramma*, compared with mean bottom depths (m) during three acoustic surveys of Prince William Sound, Alaska, in 1995 and 1996.

[1] Stokesbury, K. D. E., J. Kirsch, and B. L. Norcross. 1999. Mortality estimates of juvenile Pacific herring (*Clupea pallasi*) in Prince William Sound, Alaska. Unpubl. manuscript.

[2] Foy, W. 1996–1998. Unpubl. data. Institute of Marine Science, Industrial Technology Center, University of Alaska, Fairbanks, 118 Trident Way, Kodiak, AK 99614-7401.

Table 2

Means and standard deviations (SD) of water conditions inside bays and outside bays in passages and along open coast during three surveys of Prince William Sound, Alaska, in 1995 and 1996 (n=count; Mann-Whitney rank sum test=U).

			Temperature (°C)			Salinity (‰)		
Water depth (m)		n	mean	SD		mean	SD	
October 1995								
0–30	inside	146	9.34	0.626	U=16135	28.77	1.111	U=18583
0–30	outside	180	9.66	0.821	P<0.001	29.29	1.063	P<0.001
31–60	inside	71	7.95	2.06	U=4212	30.62	0.749	U=8610
31–60	outside	186	9.87	0.393	P<0.001	30.36	0.21	P=0.303
March 1996								
0–30	inside	667	4.14	0.437	U=281130	31.65	0.225	U=305280
0–30	outside	509	4.06	0.357	P<0.001	31.66	0.219	P=0.320
31–60	inside	416	4.53	0.521	U=228192	31.83	0.106	U=209925
31–60	outside	512	4.25	0.344	P<0.001	31.80	0.106	P<0.001
July 1996								
0–30	inside	688	10.93	1.984	U=291730	28.98	1.772	U=287935
0–30	outside	480	11.10	1.569	P=0.049	29.09	1.642	P=0.194
31–60	inside	453	6.45	1.084	U=192162	31.02	0.479	U=213780
31–60	outside	492	6.94	1.238	P<0.001	31.08	0.265	P=0.911

Table 3

Chi-squared analysis in which the percent frequency distributions of the sum of the three near shore distances (Σ3NSD) for Pacific herring, *Clupea pallasi*, and walleye pollock, *Theragra chalcogramma*, aggregations were compared with values generated from a random distribution during three acoustic surveys in Prince William Sound, Alaska (Fig. 6 in main text); * = P<0.05, ** = P<0.01, df = degrees of freedom.

	October 1995		March 1996		July 1996	
	df	χ^2	df	χ^2	df	χ^2
Herring						
age-0	12	55.30	9	53.68	8	182.17
age 1–2	12	51.41	9	58.40	8	59.29
adult	12	123.26	9	84.55	8	52.18
Pollock	12	25.16	9	63.60	8	64.46

increasing the foraging area (Robinson and Pitcher, 1989; Robinson, 1995).

Age-1 Pacific herring repeated this contraction-expansion pattern of school structure and distribution during the year. After their second winter, herring appeared to join the adult schools, leaving as new recruits entered the bays.

Pacific herring and walleye pollock geographic distributions were roughly similar within Prince William Sound. Walleye pollock distribution was bimodal with aggregations in the east-northeast and the west-southwest areas. However, there appeared to be little spatial overlap between these species because they occupied different portions of the water column. Juvenile walleye pollock were highly aggregated, forming a few, very dense schools in July within bays. Juvenile walleye pollock distribution may be influenced by the cannibalistic behavior of adult walleye pollock (Livingston, 1993). Adult walleye pollock were primarily aggregated in the southern portion of Prince William Sound, although a smaller school was evident in the east-northeast.

Bays within Prince William Sound appear to be nursery areas for both Pacific herring and walleye pollock juveniles. Data presented here and growth studies suggest that these nursery areas are isolated (Stokesbury et al., 1999). This finding differs from that for other herring species distributions where juveniles from different populations appear to share a common nursery and feeding areas, separating only when adults begin to spawn (Blaxter and Hunter, 1982; Iles and Sinclair, 1982; Sinclair et

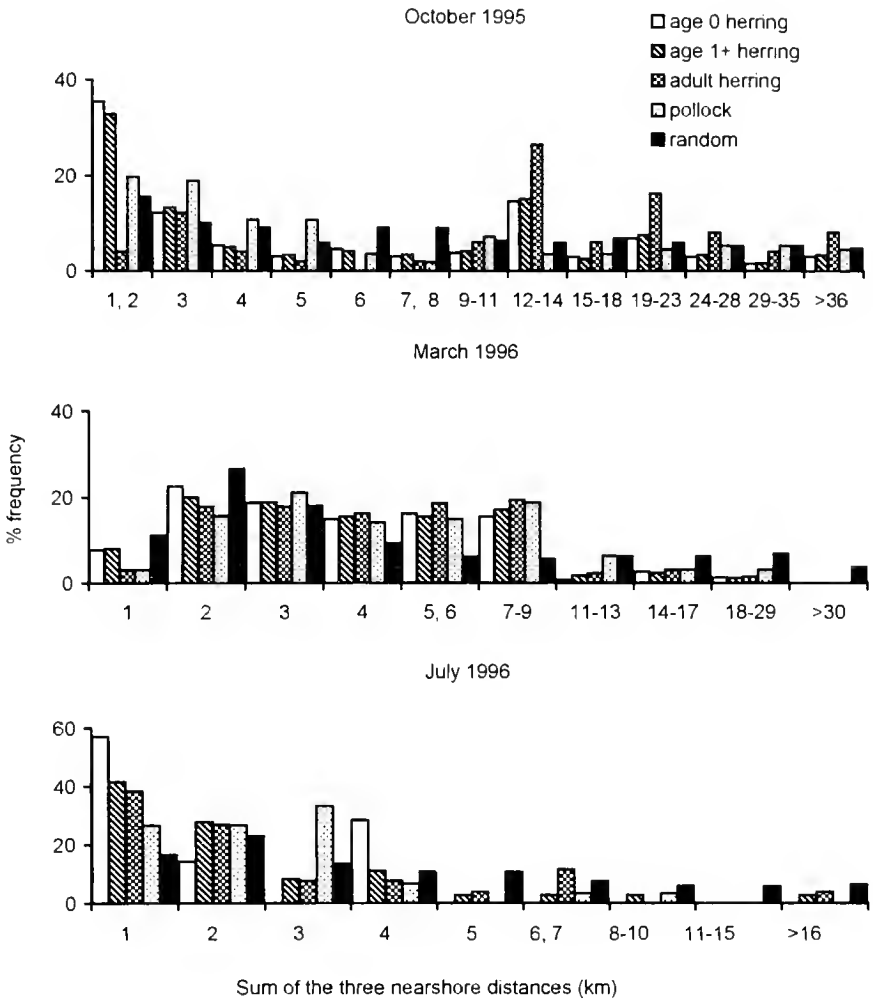

Figure 6

Percent frequency distributions of the sum of the three near shore distances (Σ3NSD) for Pacific herring, *Clupea pallasi*, age cohorts and walleye pollock, *Theragra chalcogramma*, aggregations and values generated from a random distribution, during three acoustic surveys in Prince William Sound, Alaska. Fish schools with sum of the three near shore distances <7 were usually within bays.

al., 1985; Sinclair, 1988). Future work should focus on determining the physical and biological variables influencing juvenile Pacific herring and walleye pollock within these bays to estimate population fluctuations that are critical for ecosystem models and effective fisheries management.

Acknowledgments

We thank R. Foy, M. McEwen, S. Gay, and L. Tuttle for assistance with field collections. N. Peters and G. B. Steinhart assisted in collecting and processing the acoustic data. S. Moreland and M. Vallerino assisted with data analyses. R. Foy, G. B. Steinhart, and S. Moreland provided helpful comments on the manuscript. The comments of three anonymous reviewers further improved this manuscript. We also thank the captains and crews of the FV *Temptation*, FV *Miss Kayley*, FV *Kyle David*, MV *Pacific Star*, FV *Pagan*, FV *Cape Elrington*, RV *Pandalus*, and the Alaska Department of Fish and Game, Cordova, for their help. The Exxon Valdez Oil Spill Trustee Council through the Sound Ecosystem Assessment (SEA) project at the University of Alaska, Fairbanks, and the Prince William Sound Science Center funded this project.

Literature cited

Batschelet, E.
1981. Circular statistics in biology. Academic Press, London, 371 p.

Blaxter, J. H. S.
1985. The herring: a successful species? Can. J. Fish. Aquat. Sci. 42 (suppl. 1):21–30.

Blaxter, J. H. S., and J. R. Hunter.
1982. The biology of clupeoid fishes. Adv. Mar. Biol. 20:1–223.

Brown, E. D., T. T. Baker, J. E. Hose, R. M. Kocan, G. D. Marty, M. D. McGurk, B. L. Norcross, and J. Short.
1996. Injury to the early life history stages of Pacific herring in Prince William Sound after the *Exxon Valdez* oil spill. *In* Proceedings of the *Exxon Valdez* oil spill symposium (S. D. Rice, R. B. Spies, D. A. Wolfe, and B. A. Wright, eds.), p. 448–462. Am. Fish. Soc. Symp. 18, Bethesda, MD, 931 p.

Clausen, D. M
1983. Food of walleye pollock, *Theragra chalcogramma*, in an embayment of southeastern Alaska. Fish. Bull. 81:637–642

Foote, K. G.
1987. Fish target strengths for use in echo integrator surveys. J. Acoust. Soc. Am. 82:981–987.

Foote, K. G., and J. J. Traynor.
1988. Comparison of walleye pollock target strength estimates determined from *in situ* measurements and calculations based in swimbladder form. J. Acoust. Soc. Am. 83:9–17.

Foy, R. J., and B. L. Norcross.
1999. Spatial and temporal variability in the diet of juvenile Pacific herring (*Clupea pallasi*) in Prince William Sound, Alaska. Can. J. Zool. 77:1–10

Foy, R. J., and A. J. Paul.
1999. Winter feeding and changes in somatic energy content for age-0 Pacific herring in Prince William Sound, Alaska. Trans. Am. Fish. Soc. 128:1193–1200.

Gallego, A., and M. R. Heath.
1994. The development of schooling behavior in Atlantic herring *Clupea harengus*. J. Fish. Biol. 45:569–588.

Gunderson, R. D.
1993. Surveys of fisheries resources. John Wiley and Sons, Inc., New York, NY, 248 p.

Hatch, S. A., and G. A. Sanger.
1992. Puffins as samplers of juvenile pollock and other forage fish in the Gulf of Alaska. Mar. Ecol. Prog. Ser. 80:1–14.

Huse, I., and E. Ona.
1996. Tilt angle distribution and swimming speed of overwintering Norwegian spring spawning herring. ICES J. Mar. Sci. 53:863–873.

Iles T.D., and M. Sinclair.
1982. Atlantic herring: stock discreteness and abundance. Science (Wash. D.C.) 215:627–633.

Livingston, P. A.
1993. Importance of predation by groundfish, marine mammals and birds on walleye pollock *Theragra chalcogramma* and Pacific herring *Clupea pallasi* in the eastern Bering Sea. Mar. Ecol. Prog. Ser. 102:205–215.

MacLennan, D. N., and E. J. Simmonds.
1992. Fisheries acoustics. Chapman and Hall, London, 325 p.

McClatchie, S., J. Alsop, and R. F. Coombs.
1996. A re-evaluation of relationships between fish size, acoustic frequency, and target strength. ICES J. Mar. Sci. 53:780–791.

Meyers, T. R., S. Short, K. Lipson, W. N. Batts, J. R. Winton, J. Wilcock, and E. Brown.
1994. Association of viral hermorrhagic septicemia virus with epizootic hemorrhages of the skin in Pacific herring *Clupea harengus pallasi* from Prince William Sound and Kodiak Island, Alaska, USA. Dis. Aquat. Org. 19:27–37.

Misund, O. A.
1997. Underwater acoustics in marine fisheries and fisheries research. Rev. Fish. Biol. Fish. 7:1–34.

Misund, O. A., A. Aglen, and E. Fronaes.
1995. Mapping the shape, size, and density of fish schools by echo integration and a high-resolution sonar. ICES J. Mar. Sci. 52:11–20.

Misund, O. A., A. Ferno, T. Pitcher, and B. Totland.
1998. Tracking herring schools with a high resolution sonar. Variations in horizontal area and relative echo intensity. ICES J. Mar. Sci. 55:58–66.

Ona, E., and R. B. Mitson.
1996. Acoustic sampling and signal processing near the seabed: the deadzone revisited. ICES J. Mar. Sci. 53:677–690.

Paine R.T., J. L. Ruesink, A. Sun, E. L. Soulanille, M. J. Wonham, C. D. G. Harley, D. R. Brumbaugh, and D. L. Secord.
1996. Trouble on oiled waters: lessons from the *Exxon Valdez* oil spill. Annu. Rev. Ecol. Syst. 27:197–235.

Paul, A. J., and J. M. Paul.
1998. Comparisons of whole body energy content of captive fasting age zero Alaskan Pacific herring (*Clupea pallasi* Valenciennes 1847) and cohorts over-wintering in nature. J. Exp. Mar. Biol. Ecol. 226:75–86.

Paul, A. J., J. M. Paul, and E. D. Brown.
1998. Fall and spring somatic energy content for Alaskan Pacific herring (*Clupea pallasi* Valenciennes 1847) relative to age, size and sex. J. Exp. Mar. Biol. Ecol. 223:133–142.

Pitcher, T. J.
1986. Functions of shoaling behavior in teleosts. *In* The behavior of teleost fishes (T. J. Pitcher, ed.) p. 294–338. Johns hopkins Univ. Press, Baltimore, MD, 553 p.

Pitcher, T. J., and B. L. Partridge.
1979. Fish school density and volume. Mar. Biol. 54:383–394.

Robinson, C. J.
1995. Food competition in a shoal of herring: the role of hunger. Mar. Behav. Physiol. 24:237–242.

Robinson., C. J., and T. J. Pitcher.
1989. Hunger motivation as a promoter of different behaviors within a shoal of herring: selection for homogeneity in fish shoal? J. Fish. Biol. 35:459–460.

Rose, G. A., and W. C. Leggett.
1988. Hydroacoustic signal classification of fish schools by species. Can. J. Fish. Aquat. Sci. 45:597–604.

Sinclair, M.
1988. Marine populations: an essay on population regulation and speciation. Washington Sea Grant Program, Univ. Washington Press, Seattle, WA, 252 p.

Sinclair, M., V. C. Anthony, T. D. Iles, and R. N. O'Boyle.
1985. Stock assessment problems in Atlantic herring (*Clupea harengus*) in the Northwest Atlantic. Can. J. Fish. Aquat. Sci. 42:888–898.

Sokal, R. R., and F. J. Rohlf.
1981. Biometry, 2nd ed. H. Freeman, San Francisco, CA, 859 p.

Stokesbury, K. D. E., R. J. Foy, and B. L. Norcross.
1999. Spatial and temporal variability in juvenile Pacific herring, *Clupea pallasi*, growth in Prince William Sound, Alaska. Environ. Biol. Fish. 56:409–418.

Thorne, R. E.
1977. A new digital hydroacoustic data processor and some observations on herring in Alaska. J. Fish. Res. Board Can. 34:2288–2294.
1983a. Assessment of population abundance by hydroacoustics. Biol. Oceanog. 2:253–262.
1983b. Hydroacoustics. *In* Fisheries techniques (L. A. Nielsen and D. L. Johnson, eds.), p. 239–259. Am. Fish. Soc., Bethesda, MD, 468 p.

Thorne, R. E., and G. L. Thomas.
1990. Acoustic observations of gas bubble release by Pacific herring (*Clupea harengus pallasi*). Can. J. Fish. Aquat. Sci. 47:1920–1928.

A method for estimating dredge catching efficiency for blue crabs, *Callinectes sapidus*, in Chesapeake Bay

Jon H. Vølstad
Versar, Inc.
9200 Rumsey Road
Columbia, Maryland 21045
E-mail address: Volstadjon@versar.com

Alexei F. Sharov
Maryland Department of Natural Resources
Tawes State Office Building B-2
580 Taylor Avenue
Annapolis, Maryland 21401

Glenn Davis

Brenda Davis
Maryland Department of Natural Resources
301 Marine Academy Drive
Stevensville, Maryland 21666

Abstract.—A winter dredge survey of blue crab (*Callinectes sapidus* Rathbun) is conducted annually in Chesapeake Bay as a key element of a long-term, bay-wide population dynamics study. Removal experiments are performed routinely as part of this stratified random survey of the blue crab population. We present a method for estimating the catching efficiency of the standard Virginia crab dredge used in the winter survey. Data from 88 experiments conducted between November 1992 and March 1995 were analyzed; up to 10 removals were completed in each experiment. Two models were used to estimate catching efficiency for each experiment: 1) the Leslie model, and 2) a log-linear model in which it is assumed that a fixed proportion of crabs is removed in each sweep of the experimental area, allowing for an error term ε. We estimated the catchability coefficient ($\bar{q}$) as a weighted mean of the point estimates from each experiment; its standard error was estimated with the jackknife method. The average catchability coefficients across years were 0.16 (SE=0.01) for model 1, and 0.15 (SE=0.02) for model 2. There were no significant differences in yearly estimates of dredge efficiency for the period investigated in our study. We show how the estimated catching efficiency can be used to calibrate catch per unit of effort in a dredge survey. The precision of estimates of absolute abundance could be improved significantly by increasing the precision of the estimates of catchability. Similar improvements of estimates of absolute abundance are expected for analogous dredging surveys of slow-moving or sedentary benthic species buried in the sediment, such as scallops and clams.

Manuscript accepted 29 November 1999.
Fish. Bull. 98:410–420 (2000).

Stratified random dredge surveys have been conducted in Chesapeake Bay yearly since 1989 during the coldest winter months to estimate abundance and other key statistics for the blue crab (*Callinectes sapidus* Rathbun). The survey design implemented during the winter of 1992–1993 became the standard. Three geographic strata were sampled every year thereafter: upper bay and rivers (61% of the total area), middle bay (27% of the total area), and lower bay (12% of the total area). The number of randomly selected stations in each stratum was proportional to the area of the stratum. The strata were designed to encompass major areas of habitat and to account for differences in spatial distribution of crabs by size and sex. Details of the design of the Chesapeake Bay blue crab winter survey, its characteristics, and history can be found in Vølstad et al.[1] and Rothschild and Sharov.[2] Survey results indicated that the distribution of blue crabs is highly patchy, and the coefficient of variation (CV) of average crab density is usually large. Nevertheless, catch per unit of effort (CPUE) from the annual dredge surveys generally provides accurate estimates of relative abundance because of efficient stratification and large sample sizes.

[1] Vølstad, J. H., B. J. Rothschild, and T. Maurer. 1994. Abundance estimation and population dynamics of the blue crab in the Chesapeake Bay. Ref. No. UMCEES [CBL] 94-014. Final report to the Maryland Department of Natural Resources, the Chesapeake Bay Stock Assessment Committee, and the National Oceanic and Atmospheric Administration (NOAA). Chesapeake Biological Laboratory, P.O. Box 38, Solomons, MD 21236.

[2] Rothschild, B. J., and A. F. Sharov. 1997. Abundance estimation and population dynamics of the blue crab in the Chesapeake Bay. Final report to the Maryland Department of Natural Resources and Chesapeake Bay Stock Assessment Committee. Center for Marine Science and Technology, University of Massachusetts, North Dartmouth, MA 02747-2300.

Accurate estimates of absolute abundance and population characteristics over time provide a means of ensuring a sustainable harvest of the Chesapeake Bay blue crab stock. CPUE must be adjusted for the dredge catching efficiency to estimate absolute abundance from the survey data. Catching efficiency (i.e. the fraction of crabs present in the path of the dredge that is captured) can be estimated from removal experiments (e.g. Seber, 1973; Ricker, 1975; Hilborn and Walters, 1992). In such experiments, a closed population is sampled repeatedly over a relatively short time. An estimate of the catching efficiency is typically based on the slope of a linear regression of CPUE on cumulative catch (Leslie and Davis 1939), or on log-transformed CPUE and cumulative effort (Delury, 1947). It is assumed that no emigration, immigration, or natural mortality occurs during the experiment and that all animals caught are not returned to the population (Otis et al., 1978; Schnute, 1983).

During the summer months, blue crabs are active swimmers; therefore, an otter trawl is more effective for sampling. Estimates of absolute abundance, however, are difficult to obtain during the summer. First, trawling at random locations may be difficult because of the presence of crab pots and trotlines throughout Chesapeake Bay. Second, the catching efficiency of trawls is difficult to estimate because it is affected by the swimming behavior of blue crabs. The key assumption for estimating catching efficiency of a closed population is likely to be violated in depletion experiments conducted with an otter trawl in small geographic areas because of migration.

Blue crabs in Chesapeake Bay are largely inactive and bury themselves in the bottom sediment from November through March (Van Engel, 1958); thus, they are less likely to escape the dredge by swimming. Orth and van Montfrans (1987) reported negligible catches in bottom trawls during winter, further supporting the premise that crabs are buried in the substrate. Blue crabs captured in removal experiments showed little signs of mobility when brought aboard the vessel. We, therefore, believe that the assumption of a closed population is fairly well met during the short time span of each experiment in winter. Also, fishing activity is at a minimum during winter; only crabs in the Virginia mainstem of the bay are harvested.

We report on the catching efficiency of the sampling dredge estimated from multiple removal experiments in the blue crab survey. We demonstrate that catchability estimates from a single or a few removal experiments will not be reliable for the entire bay. We show how the estimated catchability can be used to calibrate the relative estimate of abundance from the survey.

Material and methods

Removal experiments

Maryland Department of Natural Resources (MDNR), Chesapeake Biological Laboratory (CBL), and Virginia Institute of Marine Science (VIMS) conducted 88 removal experiments between November 1992 and March 1995 using the standard 1.83-m wide Virginia sampling dredge. The dredge was lined with either 12.7-mm hexagonal chicken wire or nylon mesh and is assumed to have "knife edged" selectivity for crabs with a carapace width (CW) of at least 15 mm (Sulkin and Miller, 1975).

Depletion experiments generally were conducted at locations that represent the variations in depth and sediment type typical of Chesapeake Bay (Fig. 1), taking into account up-to-date survey data. It is impractical to select sites for depletion experiments randomly because blue crabs have a patchy distribution, and the annual baywide dredge survey generally has a large number of zero catches. Because of cost considerations, removal experiments were conducted each year at a random subset of survey stations with positive catches.

Removal experiments were conducted within an area of approximately 100 m by 5.5 m in Maryland waters and 100 m by 9 m in Virginia waters. In both cases experimental areas were marked with buoys. Each removal from the experimental area (coverage) consisted of three (CBL and MDNR) or five (VIMS) parallel, nonoverlapping dredge tows conducted back and forth (Fig. 2) at a standard towing speed of 3 knots. A maximum of 10 removals was completed for each depletion experiment. The unit of effort was one coverage (i.e. the combined 3 or 5 hauls required to sweep the experimental area), and catch was recorded as the total number of crabs caught per coverage.

Estimating catchability

Hirst (1994) formulated the following standard assumptions for the removal method: 1) there is no immigration to or emigration from the enclosed area during the removal experiments; 2) each animal has an equal probability of being caught; 3) each removal is equally efficient (i.e. the probability of capture for each animal is constant from one removal to the next). The first of these assumptions is reasonable because crabs are largely inactive during winter, and each depletion experiment is conducted over a short time (2 to 4 hours). The latter two assumptions may be less likely to be true because crabs generally are clustered in distribution. In marine surveys the sampling unit is typically a fixed volume, or a unit

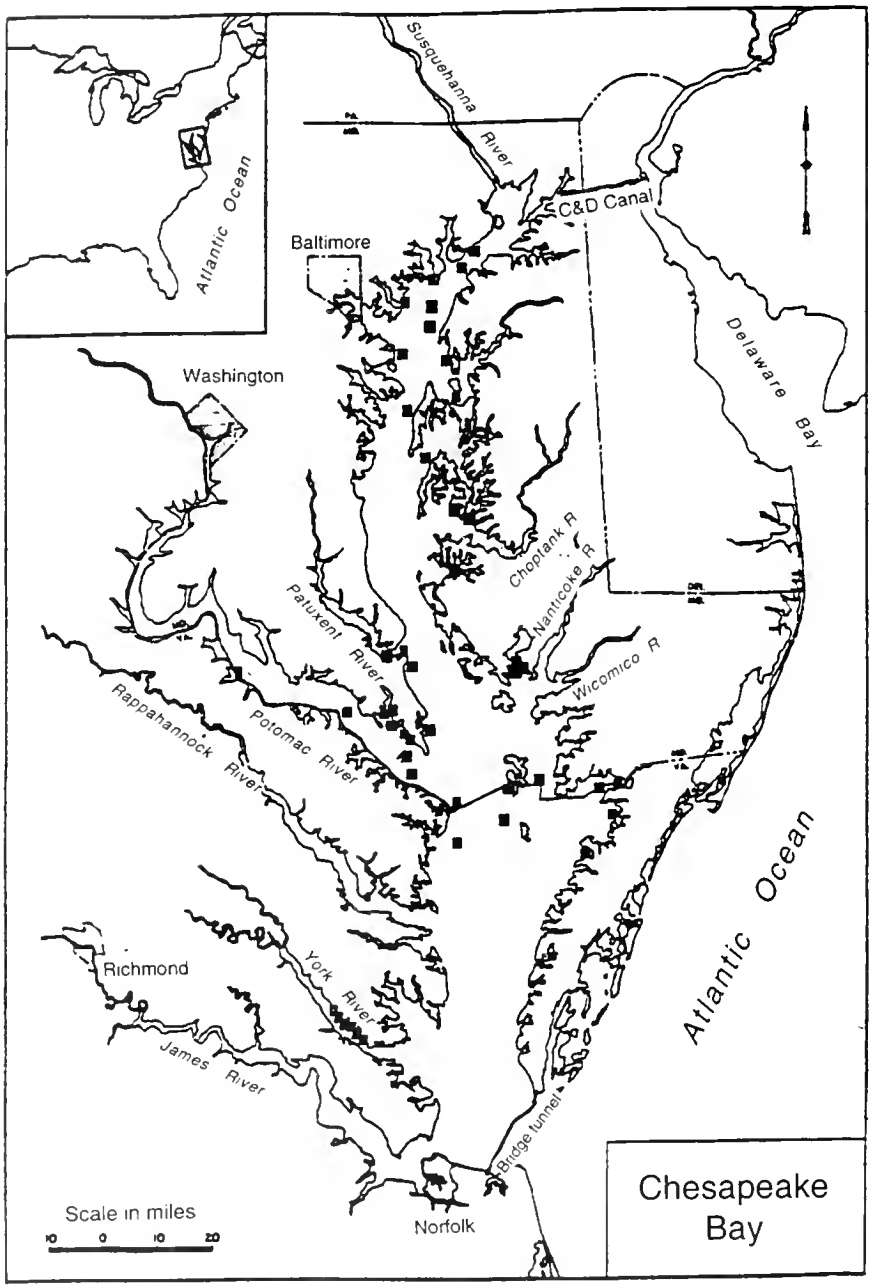

Figure 1

Map of Chesapeake Bay with positions of the dredge efficiency experiments conducted between November 1992 and March 1995.

of area swept by a standard tow (see Pennington and Volstad, 1994). As a result, sampling individuals randomly from the target population generally is not feasible. The possible dependence of animal capture probability on environmental conditions, or on the characteristics of individual animals, such as body size, is another important practical problem.

In our study we assumed that each crab has an equal probability of being caught by the dredge within each experimental area. The catching efficiency of the dredge, however, may vary significantly between experimental sites because of different bottom topography and sediment types. The possible effect of body size on catching efficiency was evaluated by comparing mean carapace width and size-frequency distributions between removals. Assume, for example, that large crabs have a higher probability of capture than small crabs. In this case the mean cara-

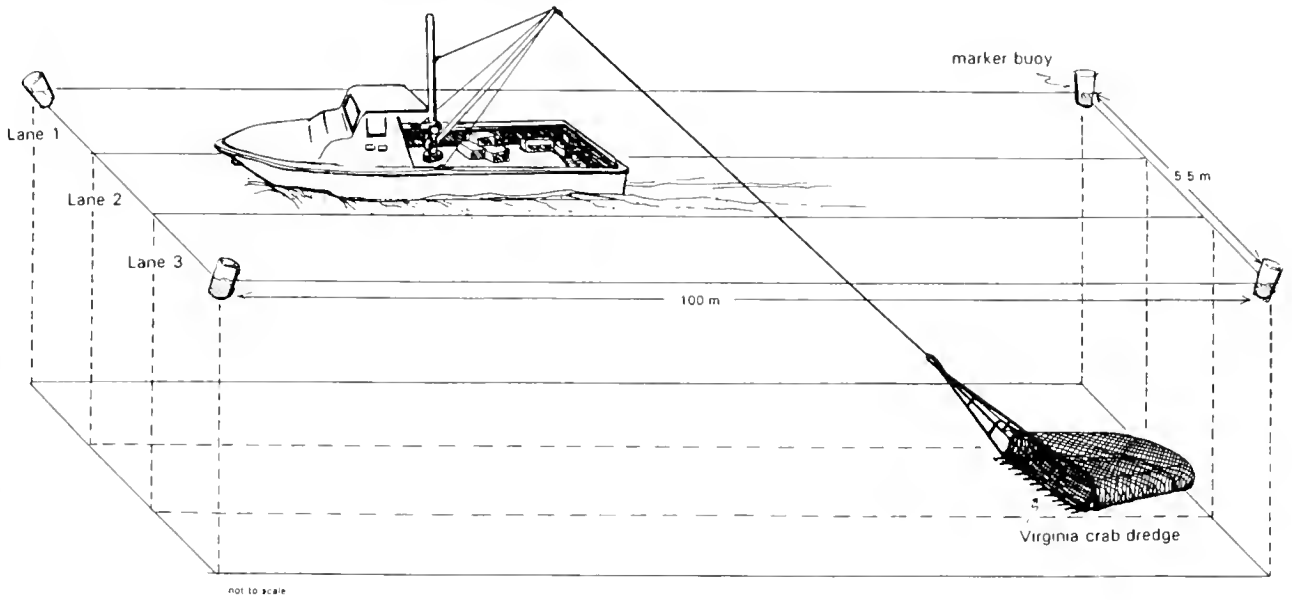

Figure 2

Schematic diagram of a standard removal experiment conducted in Maryland waters. Each removal from the area (coverage) consisted of three parallel tows conducted back and forth at a speed of 3 knots. A maximum of ten removals was completed for each experiment.

pace width of crabs in the first removals would, on average, be larger than in the final removals.

We used two models to estimate the dredge efficiency for each experiment. Model 1 is a standard Leslie model (Leslie and Davis, 1939)

$$y_i = q[P_0 - K_{i-1}] = qP_0 - qK_{i-1}, \quad (1)$$

where y_i = the catch from the ith removal; and
K_{i-1} = cumulative catch taken before each removal;
P_0 = the initial population in the area before the depletion experiment.

The catchability coefficient q = the slope of the linear regression estimated from Equation 1. The basic assumption of this model is that the number of crabs in each removal and the unit of effort is measured without error. An implication of using model 1 is that if the ith removal in a particular depletion experiment is zero, then the cumulative catch provides an absolute measure of the initial population P_0. Some crabs, however, may remain in the experimental area, even though no crabs are caught in an individual removal. This results in an underestimate of P_0 and an overestimate of q for this site.

A different technique may be used to estimate dredge efficiency. For each coverage (i) of the experimental area, we can assume that a fixed proportion (q) of the true population in the area is removed; therefore, the catch (y_1) in the first coverage is q multiplied by P_0, the initial population. For the ith coverage, we have

$$y_i = q(1-q)^{i-1}P_0\varepsilon$$

and

$$\ln(y_i) = \ln(q) + \ln(P_0) + [\ln(1-q)](i-1) + \ln(\varepsilon). \quad (2)$$

In this model, it is assumed (perhaps more realistically) that the fraction of the population removed for each unit of effort is estimated with an error ε. A simple regression of $\ln y_i$ against $(i-1)$ provides an estimate of the slope, $\ln(1-q)$. An estimate of the expected value of the catchability coefficient (q) is obtained after a retransformation, following the method of Finney (1941; see also Johnson et al., 1994, p. 221). The variance of the slope estimate in model 2 is taken into account in the estimation of $(1-q)$, and hence q. An approximation for estimating q for a single experiment is

$$\hat{q} = 1 - \exp\left(\hat{\beta} + s^2_{\hat{\beta}}/2\right)$$

where $\hat{\beta}$ = an estimate of the slope in Equation 2, with variance $S^2_{\hat{\beta}}$ (Gilbert 1987).

Characteristically, blue crabs have a patchy distribution, and the estimated CPUE from the dredge survey is driven by relatively few large catches. To estimate a mean catchability coefficient that is applicable to the entire survey area, estimates of catchability from each removal experiment were weighted by the abundance in the experimental area. An estimator for the overall catchability coefficient to use for calibrating CPUE in the dredge survey is

$$\bar{q} = \sum \frac{c_i q_i}{C},$$

where c_i = the total number of crabs caught in the ith experiment;
q_i = the corresponding estimated gear efficiency; and
C = total number of crabs caught in the n experiments.

Because n is small within each year, the jackknife estimate of average gear efficiency and its standard error were used (Cochran, 1977; Efron and Gong, 1983). The jackknife estimator of standard error is

$$\hat{\sigma} = \left\{ [(n-1)/n] \sum (\theta_{(i)} - \theta_{(\cdot)})^2 \right\}^{\frac{1}{2}},$$

where

$$\theta_{(i)} = \sum_{i \neq j} \frac{c_i q_i}{(C - c_j)}$$

is the weighted mean catchability deleting the nth experiment and

$$\theta_{(\bullet)} = \sum \frac{\theta_{(i)}}{n}$$

is the jackknife estimate of $\bar{q}$ for the n experiments.

For model 2 we also estimated the weighted mean and variance of the slopes from all n experiments. An estimate of q was obtained after retransformation with the method of Finney (1941); the standard error was estimated by jackknifing (Tukey, 1958; Manly, 1997).

In the annual winter dredge survey, a one-minute tow is standard. For soft sediments, the dredge may be saturated before the tow is completed. A randomized block experiment was conducted during the winter of 1992–1993 to investigate such gear-saturation effects on CPUE. Double tows were made at 77 randomly selected stations in the Maryland part of the bay. One tow of one-minute duration and one tow of 30-seconds duration were taken in random order at each station.

During the winter of 1994–1995, the chicken wire liner of the dredge was replaced with nylon mesh because the latter proved to be easier to operate and repair. To investigate any effect of the new liner on the catchability coefficient estimate, we conducted 9 removal experiments using a dredge with a chicken wire liner and 10 experiments using a dredge with a nylon liner.

Using the estimated catchability to calibrate CPUE

If r is the true blue crab density (number of crabs per m^2) in Chesapeake Bay at the time of the winter survey, and if we have an approximately unbiased estimate of the overall catching efficiency q that is uncorrelated with CPUE, an estimator for blue crab density is then

$$\hat{r} = CPUE / \hat{q},$$

where CPUE = the estimated mean number of crabs caught per m^2 swept.

A baywide estimate of the population total τ is

$$\hat{\tau} = A\hat{r},$$

where A = the area of blue crab habitat in Chesapeake Bay, which we estimated using geographic information system (GIS) to be approximately 11,000 km^2.

Using Taylor series approximations, we estimated the variance of $\hat{\tau}$ (Thompson, 1992, p 168) as

$$\mathrm{var}(\hat{\tau}) = \frac{A^2}{\hat{q}^2}\left[\hat{\mathrm{var}}(\bar{y}) + \frac{(1-\hat{q})}{\hat{q}}\bar{y} + \frac{\bar{y}^2}{\hat{q}^2}\hat{\mathrm{var}}(\hat{q}) \right],$$

where $\bar{y}$ = the estimated CPUE.

The relative precision of $\hat{\tau}$ is $k = \sqrt{\mathrm{var}}(\hat{\tau}) / \hat{\tau}$. The variance of estimated catching efficiency thus adds to the variance of absolute abundance estimates.

If sampling fractions differ between strata, the absolute abundance can be estimated separately for each stratum. Here, $\hat{q}$, CPUE, and hence $\hat{\tau}$ can be estimated by stratum, by using the same approach as above. The size of each stratum must also be known. If the sampling in each stratum is independent, the variance in the combined estimate of absolute abundance is additive. This approach would also be appro-

priate if the density of depletion experiments was higher for some strata than for others.

Results

Catching efficiency

Estimates of catching efficiency for the standard Virginia crab dredge from individual depletion experiments conducted during the winters between November 1992 and March 1995 are presented in Tables 1 through 3. There was large variation in catchability estimates among individual experiments (from −0.13 to 0.45); however, the difference among average annual catchability coefficients for the entire survey area was small; $\bar{q}$ varied from 0.13 to 0.18 for model 1 and model 2 (Fig. 3). For both depletion models, an analysis of variance revealed that yearly differences in q are not significant (ANOVA, $P>0.3$; we used a significance level of 5% for all tests in our study). Experiments from all years, therefore, were pooled to estimate an overall catchability coefficient for the dredge survey. The weighted mean catchability coefficients were 0.16 (SE=0.01) for model 1 (Eq. 1), and 0.15 (SE=0.02) for model 2 (Eq. 2). The means and standard errors were estimated by using the jackknife method; catchability coefficients from individual experiments were assumed to be independent. The two methods for estimating a mean catchability coefficient for model 2 produced identical estimates. The difference in estimates from the two models was not significant.

Mean carapace width of crabs in each removal for all years combined, which is plotted in Figure 4, did not show any significant trend (nonparametric Mann-Kendall test (Gilbert, 1987), $n=10$, $P=0.19$). Further, the size-frequency distributions of crabs for individual removals were similar (Fig. 5). These results support our assumption that probability of capture is independent of carapace width.

Our test for gear saturation effects resulted in an average catch per minute of 3.7 (SE=0.8) for the half-minute tows, and of 2.3 (SE=0.7) for the 1-minute tows. The higher CPUE for half-minute tows, although not significant, suggests saturation effects and might be explained by the period of time that the dredge continues to be towed along the bottom after it has begun to be hauled back. Such a delay would affect shorter tows more than longer tows.

For the experiments on the effect of the dredge liner, estimates of mean q for the dredge lined with chicken wire were 0.17 (SE=0.02) based on model 1, and 0.15 (SE=0.03) for model 2. For the nylon liner the estimates were 0.22 (SE=0.03) based on model 1, and 0.21 (SE=0.03) for model 2. Means and standard errors were estimated by using the jackknife method. The results indicated that nylon has a higher catching efficiency, but the difference in catchability between the two liners was not significant (ANOVA, $P>0.54$). Results from all 88 experiments combined showed no significant difference in catching efficiency between liners. The jackknife estimates of mean catchability across years for the

Table 1

Estimates of dredge efficiency ($\hat{q}$) from depletion experiments carried out during the winter of 1992–1993, with coefficients of determination (r^2) and degrees of freedom (df) for the regressions. The jackknife estimates of average $\hat{q}$ for the entire survey area were 0.13 (SE=0.02) for model 1, and 0.13 (SE=0.03) for model 2. CBL = Chesapeake Bay Laboratory; MDNR = Maryland Department of Natural Resources; and VIMS = Virginia Institute of Marine Science.

Institution	Number of crabs	Model 1 $\hat{q}$	Model 1 r^2	Model 2 $\hat{q}$	Model 2 r^2	df
CBL[1]	88	0.13	0.58	0.10	0.38	9
	327	0.06	0.30	0.06	0.31	9
	67	0.07	0.18	0.08	0.22	9
	23	0.13	0.39	0.06	0.39	8
	121	0.14	0.51	0.18	0.56	9
	89	0.01	0.02	0.01	0.04	9
	180	0.10	0.42	0.09	0.37	9
	223	0.22	0.66	0.32	0.73	9
	59	0.30	0.65	0.38	0.36	9
	102	0.30	0.91	0.27	0.77	9
	267	−0.01	0.00	0.03	0.03	9
	615	0.01	0.12	−0.03	0.17	9
	106	0.12	0.55	0.17	0.62	9
MDNR[1]	368	0.20	0.60	0.20	0.61	5
	137	−0.10	0.15	−0.11	0.14	5
	190	0.14	0.61	0.16	0.66	5
	203	0.23	0.83	0.31	0.85	5
	60	0.08	0.13	0.07	0.09	5
	109	0.17	0.24	0.11	0.11	5
	154	0.13	0.47	0.13	0.30	5
	96	0.11	0.29	0.11	0.29	5
	311	0.14	0.85	0.16	0.85	9
	312	0.22	0.41	0.24	0.48	4
VIMS[2]	139	0.24	0.88	0.22	0.85	4
	74	0.17	0.32	0.20	0.19	4
	129	0.17	0.71	0.16	0.55	4
	193	0.18	0.63	0.17	0.44	9
	132	0.20	0.31	0.20	0.34	4
	161	0.09	0.18	0.09	0.52	4

[1] Chicken wire liner used.
[2] Nylon mesh liner used.

Table 2

Estimates of dredge efficiency ($\hat{q}$) from depletion experiments carried out during the winter of 1993–1994, with coefficients of determination (r^2) and degrees of freedom (df) for the regressions. The jackknife estimates of average $\hat{q}$ for the entire survey area were 0.18 (SE=0.02) for model 1 and 0.18 (SE=0.02) for model 2. CBL = Chesapeake Bay Laboratory; MDNR = Maryland Department of Natural Resources; and VIMS = Virginia Institute of Marine Studies.

Institution	Number of crabs	Model 1 $\hat{q}$	Model 1 r^2	Model 2 $\hat{q}$	Model 2 r^2	df
CBL[1]	100	0.37	0.84	0.24	0.48	5
	118	0.05	0.11	0.05	0.12	5
	78	0.27	0.76	0.30	0.72	5
	55	0.09	0.55	0.10	0.59	5
	83	0.41	0.88	0.35	0.59	4
	11	0.40	0.89	0.23	0.60	3
	52	0.35	0.79	0.34	0.78	5
	34	0.39	0.85	0.43	0.86	5
	20	0.32	0.37	0.36	0.39	3
	92	0.13	0.64	0.13	0.68	5
	321	0.25	0.57	0.38	0.73	5
MDNR[1]	35	0.23	0.60	0.17	0.48	9
	89	0.27	0.65	0.18	0.31	9
	219	0.13	0.38	0.11	0.12	9
	145	0.12	0.64	0.14	0.59	9
	96	0.17	0.44	0.16	0.30	9
	48	0.30	0.81	0.28	0.59	7
VIMS[2]	376	0.22	0.71	0.19	0.73	8
	232	0.34	0.89	0.35	0.77	7
	110	0.13	0.62	0.17	0.41	8
	133	0.02	0.02	−0.04	0.08	8
	188	0.03	0.02	0.04	0.02	8
	244	0.13	0.79	0.14	0.64	8
	174	0.12	0.64	0.14	0.71	8
	346	0.10	0.31	0.14	0.43	8

[1] Chicken wire liner used.
[2] Nylon mesh liner used

Table 3

Estimates of dredge efficiency ($\hat{q}$) from depletion experiments carried out during the winter 1994–1995, with coefficients of determination (r^2) and degrees of freedom (df) for the regressions. The jackknife estimates of average $\hat{q}$ for the entire survey area were 0.18 (SE=0.02) for model 1 and 0.14 (SE=-0.03) for model 2. CBL = Chesapeake Bay Laboratory; MDNR = Maryland Department of Natural Resources; and VIMS = Virginia Institute of Marine Studies.

Institution	Number of crabs	Model 1 $\hat{q}$	Model 1 r^2	Model 2 $\hat{q}$	Model 2 r^2	df
CBL[1]	72	0.12	0.49	0.16	0.48	9
	29	0.21	0.34	0.28	0.48	5
	48	0.26	0.55	0.06	0.06	9
	99	0.12	0.42	0.06	0.13	9
	67	0.19	0.57	0.18	0.44	9
	63	0.28	0.84	0.22	0.77	9
	66	0.12	0.48	0.18	0.61	9
	40	0.13	0.39	0.13	0.41	9
	9	0.30	0.70	0.27	0.74	4
CBL[2]	83	0.31	0.96	0.35	0.94	7
	55	0.20	0.69	0.24	0.73	9
	28	0.16	0.26	0.24	0.41	5
	54	0.22	0.77	0.15	0.40	9
	12	0.22	0.60	0.08	0.30	9
	67	0.16	0.46	0.12	0.23	9
	66	0.30	0.84	0.26	0.74	9
	92	0.11	0.64	0.17	0.51	9
	58	0.23	0.68	0.13	0.29	9
	11	0.32	0.60	0.32	0.76	9
MDNR[2]	207	0.16	0.31	0.11	0.16	5
	151	0.22	0.42	0.19	0.48	5
	127	0.26	0.68	0.22	0.50	5
	145	0.22	0.83	0.21	0.69	5
	61	0.38	0.86	0.55	0.86	4
	64	0.45	0.93	0.33	0.64	5
	23	0.36	0.96	0.38	0.94	5
VIMS[2]	113	0.04	0.07	0.07	0.12	5
	114	0.11	0.79	0.11	0.81	5
	139	0.23	0.89	0.18	0.80	5
	121	0.15	0.24	0.13	0.12	5
	185	0.24	0.16	−0.13	0.11	5
	107	0.07	0.35	0.05	0.20	5
	167	0.03	0.03	0.02	0.01	5
	103	0.04	0.05	−0.10	0.19	5

[1] Chicken wire liner used
[2] Nylon mesh liner used

dredge lined with chicken wire were 0.16 (SE=0.02) for model 1, and 0.16 (SE=0.03) for model 2. For the nylon liner, estimates are 0.16 (SE=0.02) for model 1, and 0.13 (SE=0.02) for model 2.

An estimate of absolute abundance

A stratified random sample of 1412 stations was taken in the Chesapeake Bay during the winter of 1994–1995 (Rothschild and Sharov[2]). At each station, the standard Virginia crab dredge was towed for 1 minute at 3 knots. The sampling intensity was equal in all three geographic strata. The estimated baywide mean number of crabs (CW ≥15 mm) caught per 1000 m^2 swept was $\bar{y}$ = 8.53 (k=0.07). For age group 1+ (CW ≥60 mm) the estimate was $\bar{y}$ = 3.75 (k=0.08). With the catchability coefficient $\bar{q}$ = 0.16 and standard error 0.01 (from model 1), the absolute abundance estimate

for blue crab with CW ≥15 mm was $\hat{\tau}_1$= 5.86×10^8 (k=0.09), and 2.58×10^8 (k=0.10) for crabs with CW≥60 mm. Using $\bar{q}$=0.15 with standard error 0.02 (from model 2), we estimated absolute abundance for crabs with CW ≥15 mm to be $\hat{\tau}_2=6.26\times10^8$ (k=0.15), and 2.75×10^8 (k=0.16) for crabs with CW ≥60 mm. To check plausibility of these estimates, we compared the absolute abundance estimates of the 1+ age group (CW 60 mm) with estimated total landings for 1995. Blue crabs of age 1+ reach harvestable size (127 mm) the following fishing season. The reported total landings in the commercial fishery were 17,820 metric tons (t). Using an average weight per crab of 150 g (Knotts[3]), we estimated the total number of crabs caught to be 1.19×10^8 and the exploitation coefficient (as a ratio of catch in numbers and number of age 1+ crabs) to be about 45%.

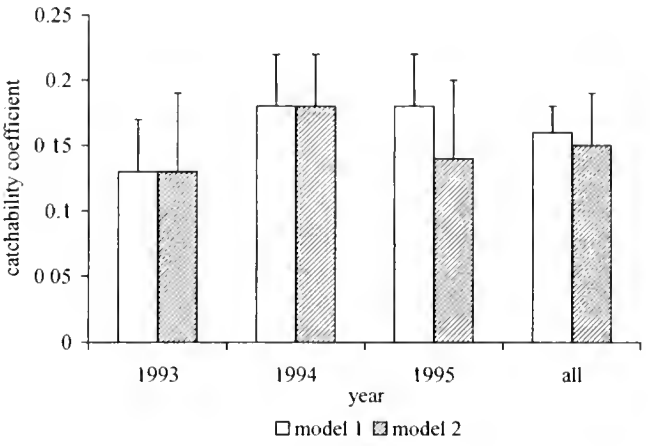

Figure 3

Jackknife estimates of average catchability ($\bar{q}$) by year for model 1 and model 2. The error-bars represent the half width of the confidence intervals.

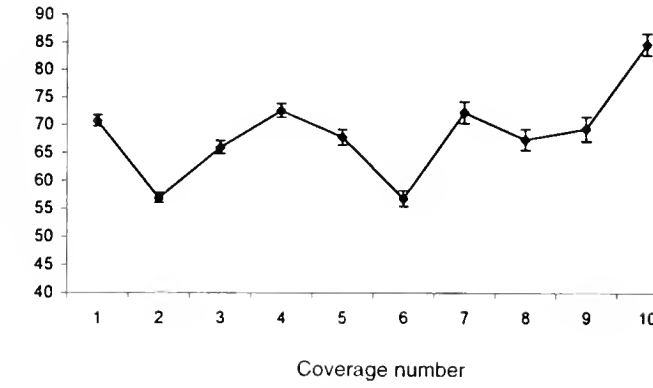

Figure 4

Mean carapace width for blue crabs by coverage in the Maryland depletion experiments. Data from all years are combined.

Exploitation rates can be calculated for males and females separately in similar fashion by using mean CPUE and landings by sex. These rates may be very valuable information because there is an evident disproportion in crab landings by sex; on average more males are landed per year (at least by weight) than females (Rugolo et al., 1998a). For example, 9320 t of males and 7230 t of females were landed in Maryland in 1995. If the average weights of males and females in the catch were similar, the exploitation rate for males would be higher than that for females. However, uncorrected for catchability, the density of age 1+ males (2.31 per 1000 m^2) observed in 1995 was higher than that of age 1+ females (1.44 per 1000 m^2), suggesting that females are being exploited at a higher rate. To obtain precise estimates of sex-specific exploitation rates, data on mean weight of crabs by sex in the harvest are required but are not available.

Discussion

Our method for estimating overall dredge catching efficiency provides consistent estimates over time (Fig. 3). The Leslie model produces the most precise estimate for catching efficiency, but the estimate could be slightly biased upwards if measurement error in effort occurs. In practice, given that the standard unit of effort in the depletion experiments is one complete coverage of the closed area, the three to five tows forming a coverage may partially overlap or extend outside the area because of navigational errors or effects of bottom currents. This measurement error in catch or effort inflates the average catchability coefficient estimates from the Leslie model (Gould et al., 1997). For model 2, the estimate of q for individual experiments depends on the regression slope and its variance and will decrease with increasing variance. The method for estimating q for individual experiments assumes that the distribution of the estimated slope tends toward normality; therefore estimates of based q on model 2 could be biased at low sample sizes, but

[3] Knotts, K. S. 1989. Preliminary stock assessment of the Chesapeake Bay blue crab population. M.S. thesis, Univ. Maryland, College Park, MD, 206 p.

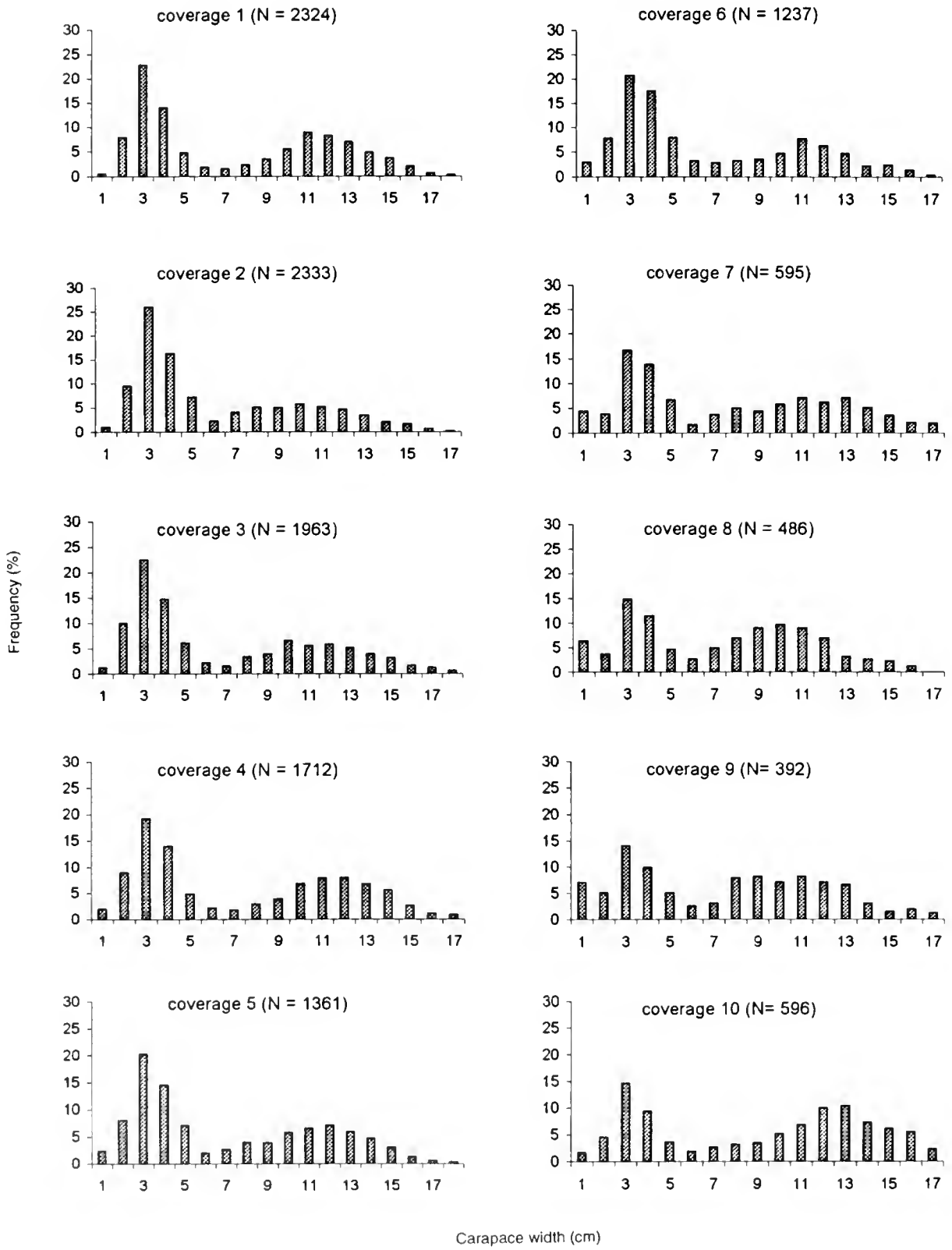

Figure 5

Carapace-width frequency distribution of blue crabs by coverage in Maryland depletion experiments. Data from all years are combined

the identical estimates of $\bar{q}$ from the two alternative methods indicate that such bias is small.

Obtaining reasonable estimates of catching efficiency from catch-effort techniques requires depleting a substantial proportion (usually more than 30%) of the population (see Gould and Pollock, 1997). Also, estimates of the regression slopes, and hence q, are likely to be more accurate for both models if the independent variables (i.e. cumulative catch, K_i, or coverage, i) have a wider range. For the depletion experiments with ten removals conducted in Maryland waters, estimates of q based on the first five removals were generally higher than estimates of q based on all ten removals. Thus, fewer removals per experiment can bias the estimates of gear efficiency just as vessel effects can. In experiments conducted from two similar vessels in Maryland waters, we did not detect significant differences in catchability between vessels. Environmental factors probably were the principal cause of variability in catchability estimates from different experiments because sediment type, bottom topography, intensity and direction of the current, towing speed, and crab distribution influence dredge performance.

When our overall estimates of catching efficiency are used to adjust CPUE from the baywide winter survey, plausible estimates of absolute abundance of blue crab in the Chesapeake Bay are obtained, resulting in an estimated exploitation rate of about 45% in 1995. The catchability coefficient estimate (q=0.26) presented in Zhang et al. (1993), in contrast, would result in an estimated exploitation rate of 75%. Their method eliminated removal experiments with low coefficients of determination (r^2) for the regressions, or with negative catchability estimates, which could result in a positive bias in the estimated overall catchability.

We have not accounted for landings from the recreational fishery or for natural mortality in our example; therefore the above exploitation rates were probably underestimates. Recreational harvest data are very scarce, but limited surveys conducted by the Maryland Department of Natural Resources in 1983, 1988, and 1990 have indicated that recreational harvest represented approximately 79%, 50%, and 26% of the reported commercial harvest (Rugolo et al. 1998b). The 1990 survey is considered the most reliable of the three. Assuming that the recreational harvest in 1995 represented 26% of the commercial harvest, then the corrected estimate of total blue crab exploitation rate is 56.7%. A bias in the opposite direction would result if the exploitable part of the stock were underestimated because of recruitment during the fishing season.

The results of this study demonstrate that improved estimates of catching efficiency can substantially increase the accuracy of estimates of absolute abundance. In our example based on survey data from the winter 1994–1995, the variance in the absolute abundance estimate for the 1+ age group is driven by the variance in $\hat{q}$. Size of sampling locations in the Chesapeake Bay winter dredge survey for blue crabs have ranged between 877 and 1412 stations per year, and relative precision (k) of the estimated CPUE (i.e. its standard error divided by the mean) has been around 10% for most years. Because of the asymptotic properties of k, it would be prohibitively expensive to significantly increase the precision of absolute abundance estimates by increasing the sample size in the survey. We believe a more cost-effective way to increase the precision of estimates of absolute abundance would be to improve the estimate of catchability by increasing the number of depletion experiments. Our results show that an estimate of catching efficiency based on a single experiment or on a few removal experiments would not represent the entire bay accurately because catchability is highly variable among sites owing to differences in bottom conditions and other factors. We included all the depletion estimates of catchability in our study, including those less than zero. We assumed that point estimates of catchability are estimated with a random error that is normally distributed around a mean: estimates in the tails of the distribution could be substantially higher or lower than the true mean catchability. An accurate estimate of catching efficiency, applicable to the entire Chesapeake Bay, requires conducting a large number of depletion experiments at representative locations. Although no statistical differences were found among the annual catchability coefficient estimates for the years analyzed in our study, we caution that interannual variation in q is likely. For example, an increase in water temperature during mild winters may affect crab behavior (they would cease hibernation) and hence probability of capture. We recommend, therefore, that depletion experiments be conducted yearly as part of an annual winter survey of blue crab population.

The conclusions of our study can be generalized and extended to similar resource assessment surveys of other slowly moving or sedentary bottom dwelling species with patchy distribution, such as scallops or clams. In surveys of target species, such as these, attention must be paid to variability in capture efficiency of the gear with respect to sediment type, depth, towing speed, and other factors (such as animal interactions) that affect the gear. Sediment or bottom type are often selected as stratification criteria in bottom surveys of benthic organisms. Properly designed removal experiments can provide reliable estimates of catchability coefficients for each sampling stratum, allowing adjustment of

strata CPUE used in the estimator of absolute abundance. Sediment distribution, however, is often very patchy, and the exact area on the bottom of any type of sediment is typically not known. Accurate mapping of bottom sediment is expensive and thus it makes sediment-based stratification impractical. An alternative approach for taking sediment into account is to conduct a series of depletion experiments at locations that are representative of the entire survey area. If a sufficient number of experiments are conducted, the effects of sediment on catching efficiency will be accounted for. Although we agree that efficient stratification is an important aspect of designing cost-effective marine resource surveys, we stress that careful estimation of sampling gear efficiency through a series of depletion experiments could significantly improve the accuracy of absolute abundance estimates. Both elements are essential in designing effective sample survey programs for estimating vital characteristics of a population.

Acknowledgments

This project was funded by the National Oceanic and Atmospheric Administration (NOAA) and Maryland Department of Natural Resources. J. H. Vølstad and A. Sharov are grateful to B. Rothschild for providing us the opportunity to work on this project. We thank T. Maurer, E. Connor, and captains A. Moore and D. Pierce for assisting with the field work in Maryland waters. We thank R. Lipcius and M. Montain for their research cooperation and for providing the data from depletion experiments conducted in Virginia. We greatly appreciate suggestions from two anonymous referees that helped improve the manuscript.

Literature cited

Cochran W. G.
1977. Sampling techniques. John Wiley and Sons, New York, NY, 428 p.

DeLury, D. B.
1947. On the estimation of biological populations. Biometrics 3:145–167.

Efron, B., and G. Gong.
1983. A leisurely look at the bootstrap, the jackknife and cross-validation. Am. Stat. 37:36–48.

Finney, D. J.
1941 On the distribution of a variate whose logarithm is normally distributed J Roy. Statist. Soc. (series B) 7:155–161.

Gilbert, R. O.
1987. Statistical methods for environmental pollution monitoring. Van Nostrand Reinhold, New York, NY, 320 p.

Gould, W. R., and K. H. Pollock.
1997 Catch-effort maximum likelihood estimation of important population parameters. Can. J. Fish. Aquat. Sci. 54: 890–897.

Gould, W. R., L. A. Stefanski, and K. H. Pollock.
1997. Effects of measurement error on catch-effort estimation. Can. J. Fish. Aquat. Sci. 54:898–906.

Hilborn, R., and C. J. Walters.
1992. Quantitative fisheries stock assessment. Chapman and Hall, New York, NY, 570 p.

Hirst, D.
1994. An improved removal method for estimating animal abundance. Biometrics 50:501–505.

Johnson, N. L., S. Kotz, and N. Balakrishnan.
1994. Continuous univariate distributions, vol. 1. John Wiley and Sons, New York, NY, 756 p.

Leslie, P. H., and D. H. S. Davis.
1939. An attempt to determine the absolute number of rats on a given area. J. Anim. Ecol. 8:94–113.

Manly, B. F. J.
1997. Randomization, bootstrap and Monte Carlo methods in biology. Chapman and Hall, New York, NY, 399 p.

Orth, R. J., and J. van Montfrans.
1987. Utilization of a seagrass meadow and tidal marsh creek by blue crabs, *Callinectes sapidus*. I. Seasonal and annual variation in abundance with emphasis on post-settlement juveniles. Mar. Ecol. Prog. Ser. 41:283–294.

Otis, D. L, K.P Burnham, G. C. White, and D. R. Anderson.
1978. Statistical inference from capture data on closed animal populations. Wildl. Monogr. 62. The Wildlife Society, Inc., Washington, D.C.

Pennington, M., and J. H.Vølstad.
1994. Assessing the effect of intra-haul correlation and variable density on estimates of population characteristics from trawl surveys. Biometrics. 50:725–732.

Ricker, W. E.
1975. Computation and interpretation of biological statistics of fish populations. Bull. Fish. Res. Board Can. 191.

Rugolo, L. J., K. S. Knotts, A. M. Lange, and V. A.Crecco.
1998a. Historical profile of the Chesapeake Bay blue crab (*Callinectes sapidus Rathbun*) fishery. J. Shellfish Res. 17(N2): 383–394.

1998b. Stock assessment of Chesapeake Bay blue crab (*Callinectes sapidus* Rathbun). J. Shellfish Res. 17 (N2): 493–518.

Schnute, J.
1983. A new approach to estimating populations by the removal method. Can. J. Fish. Aquat. Sci. 40:2153–2169.

Seber G.A.
1973. The estimation of animal abundance and related parameters. Griffin, London, 506 p.

Sulkin, S. D., and R. E. Miller.
1975. Modified commercial crab and oyster dredges as sampling devices for blue crab, *Callinectes sapidus* Rathbun. Ches. Sci. 16:137–139.

Thompson, S. K.
1992. Sampling. John Wiley & Sons, New York, NY, 342 p.

Tukey, J. W.
1958. Bias and confidence in not quite large samples. Ann. Math Statist. 29:614.

Van Engel, W. A.
1958. The blue crab and its fishery in Chesapeake Bay. Part 1. Reproduction, early development, growth and migration. Commer. Fish. Rev. 20:6–17.

Zhang, C. I., J. S. Ault, and S. Endo.
1993. Estimation of dredge sampling efficiency for blue crabs in Chesapeake Bay. Bull. Korean Fish. Soc. 26:369–379.

Periodicity of increment formation in otoliths of overwintering postlarval and prejuvenile Atlantic menhaden, *Brevoortia tyrannus*

Dean W. Ahrenholz
Beaufort Laboratory, Southeast Fisheries Science Center
National Marine Fisheries Service, NOAA
101 Pivers Island Road
Beaufort, North Carolina 28516-9722
e-mail address: dean.ahrenholz@noaa.gov

Deborah D. Squires

James A. Rice

Stephen W. Nixon
Department of Zoology, North Carolina State University
P.O. Box 7617
Raleigh, North Carolina 27695-7617

Gary R. Fitzhugh
Panama City Facility, Southeast Fisheries Science Center
National Marine Fisheries Service, NOAA
3500 Delwood Beach Road
Panama City, Florida 32408-7403

Hypotheses of fishery recruitment processes often have as their foundation studies of incremental otolith growth (e.g. Methot, 1983; Rice et al., 1987). Conclusions from these studies, however, are only as robust as their baseline otolith validation work. This is especially true for investigations on Atlantic menhaden (*Brevoortia tyrannus*), an estuarine-dependent, marine-migratory clupeid ranging from southeastern Florida to Nova Scotia (Reintjes, 1969; Ahrenholz, 1991). The spawning season for Atlantic menhaden is protracted, occurring wherever fish of spawning age are found (Judy and Lewis, 1983). Spawning is probably greatest from October to March (Higham and Nicholson, 1964). The spawning activity that occurs in south coastal U.S. waters normally occurs within this time period, usually peaking during mid- to late winter (Wilkens and Lewis, 1971; Nicholson, 1972). Owing to the extended spawn and seasonal movement of spawning adults, progeny from different temporal spawning periods experience different environmental conditions during similar early life history stages.

Daily age validation studies have been conducted on late larvae and juvenile Atlantic menhaden (Ahrenholz et al., 1995), but none of the specimens were reared in a water temperature regime that typified conditions experienced by fall-spawned larvae. Fall-spawned larvae enter inshore nurseries when estuarine waters are cooling, yet still warm enough for moderate somatic growth and development. These young fish then endure the coldest winter temperatures in a partially transformed condition, i.e. in a postlarval-prejuvenile stage. In contrast, larvae of winter and early spring spawnings ingress into relatively cold, but progressively warming waters, from late winter to midspring; although they probably do not enter during extreme winter cold spells (Reintjes and Pacheco, 1966). Differences in growth patterns in the otolith microstructure of larvae and juveniles from these different spawning periods are detectable (Fitzhugh et al., 1997).

Validation of the otolith daily aging technique should take into account the environmental conditions experienced by field-sampled specimens (Jones, 1986), especially when some field conditions affect the daily periodicity of otolith growth increments. The sagittal growth increments for the fall-spawned Atlantic menhaden are disproportionately narrower (±1 µm) during the coldest overwintering months. Moreover, increments <1 µm potentially indicate less than daily increment formation (Campana et al., 1987). Less than daily increment deposition associated with cold water and slow growth rates has been observed for juvenile summer flounder (*Paralichthys dentatus*), another estuarine-dependent, marine-migratory species (Szedlmayer and Able, 1992).

Previous otolith microstructure validation studies for larval Atlantic menhaden have used larvae collected in the field during April or laboratory-reared specimens spawned in February (Ahrenholz et al., 1995). Test conditions were set at higher salinities than are normally associated with larval to juvenile transformation. Hence, we designed a study to specifically address the periodicity of otolith increment formation in over-wintering, fall-spawned Atlantic menhaden postlarvae and prejuveniles under the thermal and salinity conditions they experience in North Carolinian estuaries.

Manuscript accepted 26 November 1999
Fish. Bull. 98:421–426 (2000).

Materials and methods

Atlantic menhaden larvae were collected while ingressing into the Newport River estuary during the week of 7 December 1994. In the laboratory, these larvae were immersed on 8 December, in 100 mg/L solution of alizarin-complexone (ALC) solution for 16 h (overnight) at 18°C. Nearly equal numbers of marked larvae were reared in two concrete ponds (6600 L). Pond one, the high-salinity pond, received flow-through seawater at ambient water temperatures. Pond two, the low-salinity pond, received flow-through seawater and freshwater from a well. Pond two was generally a few degrees warmer and about one-half the salinity of pond one. Menhaden larvae were fed powdered salmon starter, supplemented with brine shrimp larvae, for the first few weeks, followed by salmon starter only.

Two to six specimens were sacrificed periodically, and measured for fork length (FL) to the nearest mm. Sagittal otoliths were removed, mounted in droplets of epoxy resin, and sectioned obliquely with a slow-speed saw with dual diamond wafering blades (Ahrenholz et al., 1995). Polished otolith sections (10–15 µm thick) were viewed through a compound microscope (1000×) and on an image analysis video monitor (3800×). When the otolith sample was examined under blue light epifluoresence, the ALC-marked increment was seen as red-orange. The number of increments from the ALC mark to the otolith margin was estimated as the arithmetic mean of a series of independent counts tallied blindly with a hand-held counter. A section was counted twice when the two counts differed by 0 to 2 increments. A section was counted three to five times when the difference between the initial two counts was greater than two increments. Otoliths from one specimen from the high-salinity pond were deemed unreadable.

An image analysis system was used to measure increment widths in groups of 10, starting from the innermost increment, for a select number of otoliths from each test group. However, the increments measured just prior to the alizarin mark may have numbered from 5 to 10. This procedure was undertaken to separate pre- and postmark increments from width estimates. Measurements were taken from oblique-transverse sections (Ahrenholz et al., 1995) as opposed to similar measurements taken on transverse sections, as done by Fitzhugh et al. (1997). Owing to nearly concentric otolith growth for the life history stage sampled, the measurements taken in our study should be similar to, or slightly greater than, transverse-oriented measurements.

Estimates of the dates when eggs were spawned for the test groups were obtained by sacrificing eight larvae on the day of ALC-marking. Their otoliths were removed, mounted on microscope slides, and read whole. Three independent counts were made from the first increment following the first feeding mark to the margin. Five days were added to the mean counts to account for time from spawning to first increment formation (Warlen, 1992).

Statistical analyses of the results generally followed those of Ahrenholz et al. (1995). The null hypothesis tested was that the growth increments in the otoliths were formed daily during the rearing period. The hypothesis was not rejected if the slope of a regression of increment count on number of days since marking was not significantly different from one and the intercept was not significantly different from zero. The statistical power to test for differences in the slope was also calculated (Rice, 1987). Student's-*t* test was used to test for statistical significance of the regression parameters. Analysis of covariance (ANCOVA) and regression computations were performed with SAS statistical programs (SAS Institute, 1985). Ninety-five percent confidence intervals (CI) for individual age estimations (see discussion in Rice [1987]) were calculated for an inverse prediction condition (Sokal and Rohlf, 1981; note also discussions of inverse regression in Draper and Smith [1980]).

Results

Fish were sampled from pond two (the low-salinity regime) on postmarking days 35, 56, 74 (and 75), 98, 119, and 140 (total n=22). Fish from pond one (the high-salinity regime) were sampled similarly through day 75 (total n=13). Prior to day 75 (for about two weeks), many of the menhaden in pond one died. The remaining fish from the high-salinity regime were sampled on day 75.

Spawned-date estimates determined from larvae sacrificed before being reared ranged from 17 October to 20 October 1994, thus, verifying that the experimental tests were performed on larvae derived from fall-spawning activity.

Temperature and salinity regimes during the rearing period (Fig. 1) were adequate to attain the study's objectives. The cooling and warming pattern, as well as the actual water temperatures were well within the range observed for winters in North Carolina estuaries over a 15-year period (Hettler and Chester, 1982). Salinity levels in both rearing regimes were within ranges observed for larval or juvenile menhaden in the field (Wilkenson and Lewis, 1971; Turner and Johnson, 1973), although the larval forms are more highly associated with lower salinities. Water temperatures were relatively warm in the early por-

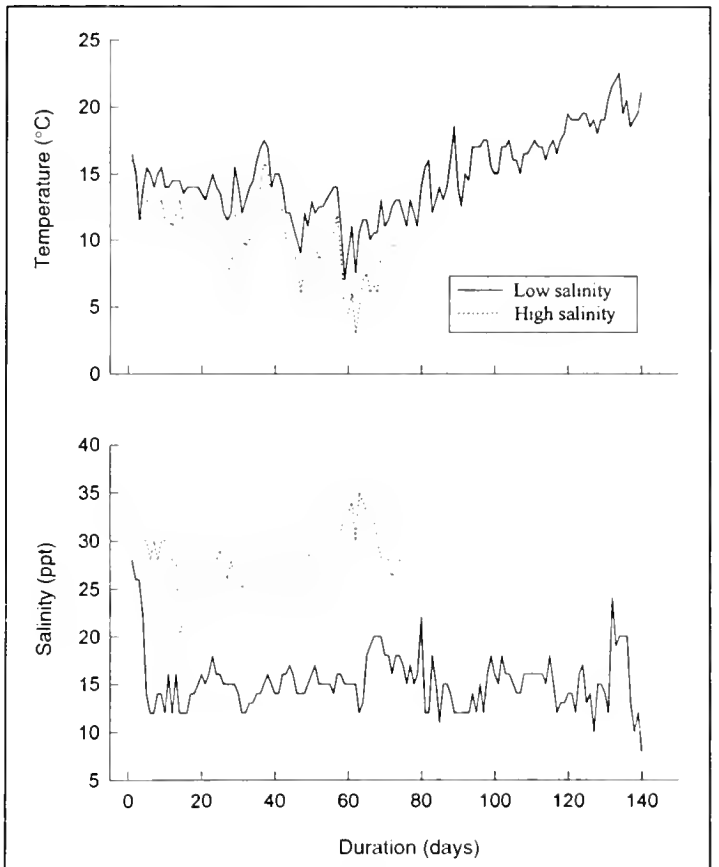

Figure 1

Environmental conditions experienced by two groups of ALC-marked larval-juvenile Atlantic menhaden (*Brevoortia tyrannus*) during the otolith validation study. The upper panel depicts temperature histories and the lower panel, the salinity histories. The high-salinity (low-temperature) rearing experiment ended after 75 days owing to high mortality rates.

tion of the study; larval menhaden advanced well into their transformation into juveniles. Through day 60 of rearing, water temperatures steadily declined to low winter minima. During the lower temperature period, the growth rates of fishes were reduced (Fig. 2). The mean width of the otolith growth increments for fish from the high-salinity group gradually dropped below 1 mm following the severe drop in temperature. During the same period, the increments for the low-salinity group reflected the higher growth rates for this group and were wider, with all mean widths above 1 μm (Fig. 3).

Similarity between regression parameters of increment counts versus days since marking between the high- and low-salinity regimes was tested over the shared range of duration (75 days). Tests for homogeneity of slopes showed no differences (P=0.679). A subsequent ANCOVA analysis revealed no differences between intercepts (P=0.712). Thus, the increment counts for the two rearing regimes were pooled and validation hypotheses were tested with a regression analysis. Results of this analysis revealed that the intercept was not significantly different from zero, and the slope was not significantly different from one (Fig. 4, Table 1). The confidence interval (95%) for estimates of daily age obtained from otoliths of fish which encountered conditions similar to those tested here, would be ±9 to 10 days over a range of 140 days (approximately 50 to 190 days of age).

Discussion

Growth increments on sagittal otoliths of fall-spawned Atlantic menhaden formed daily, even when experimental water temperatures declined to 3 C

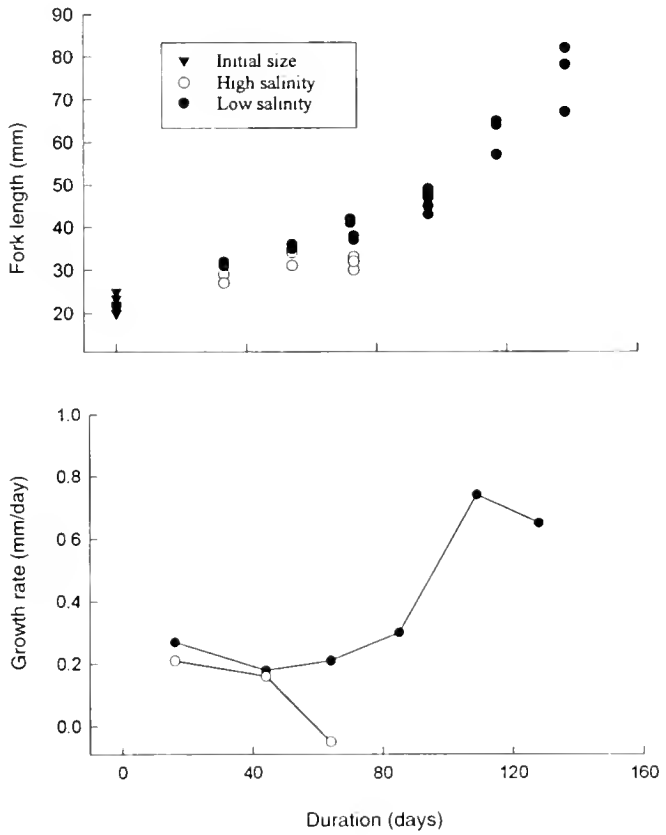

Figure 2

The body size (fork length) of ALC-marked juvenile Atlantic menhaden (*Brevoortia tyrannus*) sampled during the validation rearing study (upper panel) and rate of growth estimated from mean size of sampled fish (lower panel). The rates of growth are plotted at midpoints between sampling periods.

Table 1

Results of least squares linear regression analysis for marked Atlantic menhaden, *Brevoortia tyrannus*, otolith increment counts (n=34, r^2=0.984, and SE=standard error).

Parameter	Estimate	SE	P
Slope	1.0048	0.0224	0.168
Power[1]	99.1%	—	—
Intercept	0.3771	1.8257	0.162

[1] Statistical power to detect a deviation of 0.1 in the estimate of the slope at the P=0.05 level.

(Fig. 1). Even though growth rate declined to low levels during initial study weeks, especially for the high-salinity group (Fig. 2), an otolith increment continued to be formed daily even when increment widths fell below 1 µm for a number of days (Fig. 3). If a difference in increment formation rate had occurred between groups, we would not have been able to determine the cause because both temperature and salinity varied between groups. It seems likely that the faster growing fish responded to the higher temperatures. Regardless, both test groups experienced conditions that could be expected in the field during winter. The October-spawned larval menhaden used in our study displayed a growth increment mean width that ranged from values that were greater than those previously measured at sea to those that were less than previously measured in estuaries in a relatively short period of days (compare with Fitzhugh, et al. 1997).

The rearing conditions for specimens maintained during our study and earlier studies (Ahrenholz et al., 1995) should provide otolith increment validations for most, if not all, Atlantic menhaden that recruit

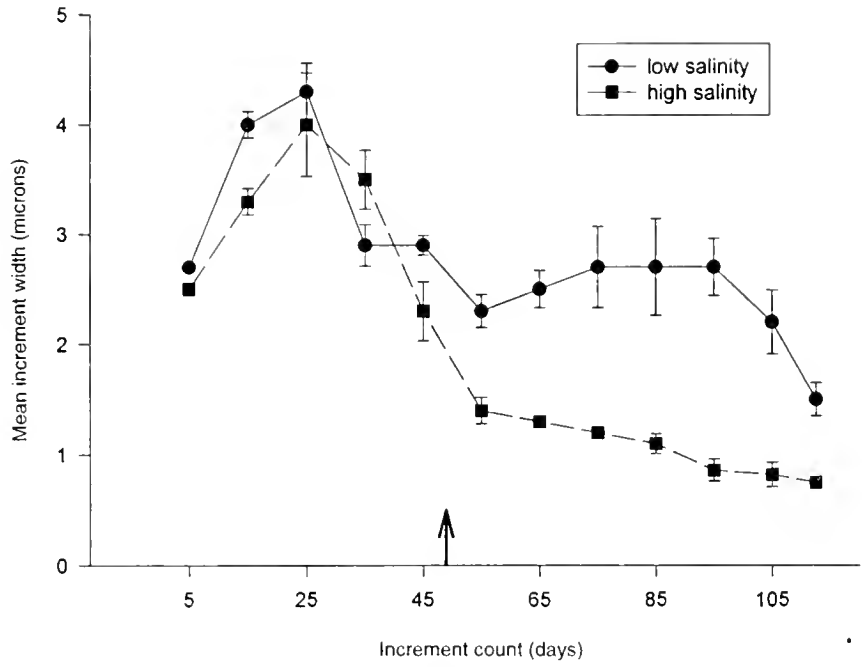

Figure 3

Estimates of mean width for otolith growth increments from larval-juvenile Atlantic menhaden (*Brevoortia tyrannus*) from each test-rearing group. The error bars represent ±1 SE, with n=3 for each data point (the error bars may be hidden by the symbol for some entries). The arrow denotes when the alizarin marking occurred. At-sea values are thus to the left of the arrow. (Note: after ALC marking, the low-salinity group was reared at a higher temperature than the high-salinity group.)

into estuarine systems from North Carolina to northern Florida. Additional studies may be necessary for more northern systems, such as Chesapeake and Delaware bays, especially for fall-spawned postlarval menhaden that may overwinter in even colder waters and for more extended periods of time.

Acknowledgments

Critical reviews of the manuscript were provided by A. B. Powell, J. W. Smith, and D. S. Vaughan. Support for the study was provided in part by the SABRE program of the National Oceanic and Atmospheric Administration's Coastal Ocean Program / Coastal Fisheries Ecosystems Studies.

Literature cited

Ahrenholz, D. W.

1991. Population biology and life history of the North American menhadens (Genus *Brevoortia*). Mar. Fish. Rev. 53(4):3–19.

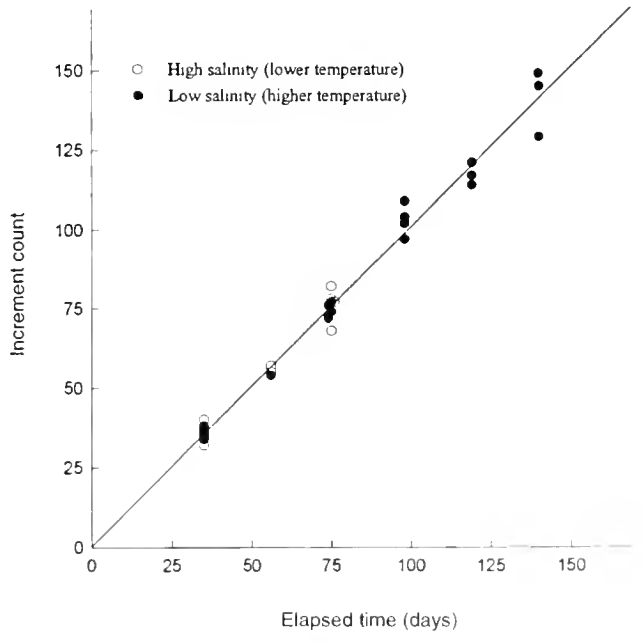

Figure 4

Scatterplot of growth increment count on elapsed time since ALC-marking for juvenile Atlantic menhaden (*Brevoortia tyrannus*). The fitted least squares regression line is shown.

Ahrenholz, D. W., G. R. Fitzhugh, J.A. Rice, S. W. Nixon, and W. C. Pritchard.
1995. Confidence of otolith ageing through the juvenile stage for Atlantic menhaden, *Brevoortia tyrannus*. Fish. Bull. 93:209–216.

Campana, S. E., J. A. Gagné, and J. Munro.
1987. Otolith microstructure of larval herring (*Clupea harengus*): image or reality? Can. J. Fish. Aquat. Sci. 44:1922–1929.

Draper, N. R., and H. Smith.
1980. Applied regression analysis, 2nd ed. John Wiley & Sons, Inc., New York, NY, 709 p.

Fitzhugh, G. R., S. W. Nixon, D. W. Ahrenholz, and J. A. Rice.
1997. Temperature effects on otolith microstructure and birth month estimation from otolith increment patterns in Atlantic menhaden. Trans. Am. Fish. Soc. 126:579–593.

Hettler, W. F., and A. J. Chester.
1982. The relationship of winter temperature and spring landings of pink shrimp, *Penaeus duorarum*, in North Carolina. Fish. Bull. 80:761–768.

Higham, J. R., and W. R. Nicholson.
1964. Sexual maturation and spawning of Atlantic menhaden. Fish. Bull. 63:255–271.

Jones, C.
1986. Determining age of larval fish with the otolith increment technique. Fish. Bull. 84:91–103.

Judy, M. H., and R. M. Lewis.
1983. Distribution of eggs and larvae of Atlantic menhaden, *Brevoortia tyrannus*, along the Atlantic coast of the United States. U.S. Dep. Commer., NOAA Tech. Rep. NMFS SSRF 774, 23 p.

Methot, R. D., Jr.
1983. Season variation in survival of larval northern anchovy, *Engraulis mordax*, estimated from the age distribution of juveniles. Fish. Bull. 81:741–750.

Nicholson, W. R.
1972. Population structure and movements of Atlantic menhaden, *Brevoortia tyrannus*, as inferred from back-calculated length frequencies. Chesapeake Sci. 13:161–174.

Reintjes, J. W.
1969. Synopsis of biological data on Atlantic menhaden, *Brevoortia tyrannus*. U.S. Dep. Interior, Fish Wildl. Serv., Circ. 320, 30 p.

Reintjes, J. W., and A. L. Pacheco.
1966. The relation of menhaden to estuaries. Am. Fish. Soc. Spec. Publ. 3:50–58.

Rice, J. A.
1987. Reliability of age and growth rate estimates from otolith analysis. *In* Age and growth of fish (R. C. Summerfelt and G. E. Hall, eds.), p. 167–176. Iowa State Univ. Press, Ames, IA.

Rice, J. A., L. B. Crowder, and M. E. Holey.
1987. Exploration of mechanisms regulating larval survival in Lake Michigan bloater: a recruitment analysis based on characteristics of individual larvae. Trans. Am. Fish. Soc. 116:703–718.

SAS Institute, Inc.
1985. SAS/STAT guide for personal computers, version 6 ed. SAS Inst., Cary, NC, 378 p.

Sokal, R. R., and F. J. Rohlf.
1981. Biometry, 2nd ed. W.H. Freeman and Co., New York, NY, 859 p.

Szedlmayer, S. T., and K. W. Able.
1992. Validation studies of daily increment formation for larval and juvenile summer flounder, *Paralichthys dentatus*. Can. J. Fish. Aquat. Sci. 49:1856–1862.

Turner, W. R., and G. N. Johnson.
1973. Distribution and relative abundance of fishes in Newport River, North Carolina. U.S. Dep. Commer., NOAA Tech. Rep. NMFS SSRF 666, 23 p.

Warlen, S. M.
1992. Age, growth, and size distribution of larval Atlantic menhaden off North Carolina. Trans. Am. Fish. Soc. 121: 588–598.

Wilkens, E. P. H., and R. M. Lewis.
1971. Abundance and distribution of young Atlantic menhaden, *Brevoortia tyrannus*, in the White Oak River estuary, North Carolina. Fish. Bull. 69:783–789.

Larval and pelagic juvenile fishes collected with three types of gear in Gulf Stream and shelf waters in Onslow Bay, North Carolina, and comments on ichthyoplankton distribution and hydrography*

Allyn B. Powell
Center for Coastal Fisheries and Habitat Research
Beaufort Laboratory
National Ocean Service, NOAA
101 Pivers Island Road
Beaufort, North Carolina 28516-9722
E-mail address allyn.powell@noaa.gov

David G. Lindquist
University of North Carolina at Wilmington
Department of Biological Sciences and
Center for Marine Science Research
601 South College Road
Wilmington, North Carolina 28403-3297

Jonathan A. Hare
Center for Coastal Fisheries and Habitat Research
Beaufort Laboratory
National Ocean Service, NOAA
101 Pivers Island Road
Beaufort, North Carolina 28516-9722

The fish fauna in waters off North Carolina is diverse, receiving contributions from the Virginian, Carolinian, and Caribbean faunal provinces (Gray et al., 1968; Schwartz, 1989). South of Cape Hatteras exist live-bottom habitats, small areas of rock outcroppings containing rich sessile invertebrate communities and many species of commercially and recreationally important subtropical and tropical fishes (Huntsman, 1976; Miller and Richards, 1979). Little is known about the patterns and source of recruitment of many of these and other fishes. Fahay (1975) sampled a transect off New River Inlet, North Carolina, and Cape Fear, North Carlina, at quarterly intervals with a surface-towed meter net. Eldridge et al. (1978) examined the performance of a 2 m × 1 m neuston net in waters off South Carolina. Powles and Stender (1976) surveyed ichthyoplankton from Cape Fear, North Carlina, to Cape Canaveral, Florida, with a standard ichthyoplankton bongo sampler. Ichthyoplankton research targeting live-bottom habitats in Onslow Bay, North Carlina, was recently conducted by Powell and Robbins (1998), who provided information on spatial and temporal spawning. The use of standard ichthyoplankton samplers, however, may introduce bias against the capture of late-larvae and early-juveniles owing to net avoidance (Shima and Bailey, 1994); therefore little information would be gained about recruitment sources and patterns.

The use of complementary gear that could collect a series of pelagic larval stages would be useful in understanding the source of recruits to live-bottom and other habitats off North Carolina. The spatial distributions of larval stages could indicate if recruitment is from local populations, or other sources, (Leis, 1994; Booth and Brosnan, 1995). However, the spatial distribution of larval stages needs to be coupled with oceanographic observations to interpret the source of recruits.

The major goal of our study was 1) to examine the effectiveness of three gear types in collecting a complete series of the pelagic larval phase of reef fishes and associated taxa, and 2) to examine the influence of short-term hydrographic conditions on fish distributions.

Materials and methods

Sampling was generally conducted in darkness aboard the RV *Cape Hatteras*, 14–16 September 1994, along an onshore-offshore transect in Onslow Bay (Table 1, Fig. 1). With some modifications, we followed Struhsaker (1969) in classifying habitat types: coastal (<18 m); middle-shelf (18–55 m); outer-shelf (55–185 m); and oceanic (>185 m). Station 1 (76°15.0'W, 33°54.0'N) was located in oceanic waters (water depth=341 m); station 2 (76°21.3'W, 33°58.5'N) was located in outer-shelf waters where smooth to highly broken bottom exists (water depth= 75–110 m); station 3 (76°27.8'W, 34°04.0'N) was located in middle-shelf waters (water depth=40 m); and stations 4 (76°34.2'W, 34°08.7'N) and 5 (76°35.5'W, 34°14.3'N) were located on the middle shelf adjacent to live-bottom habitat (water depth=33–35 m and 28–31 m, re-

* Contribution 186 of the Center for Marine Science Research, University of North Carolina, Wilmington, NC 28403-3297.

Manuscript accepted 8 November 1999.
Fish. Bull. 98:427–438 (2000).

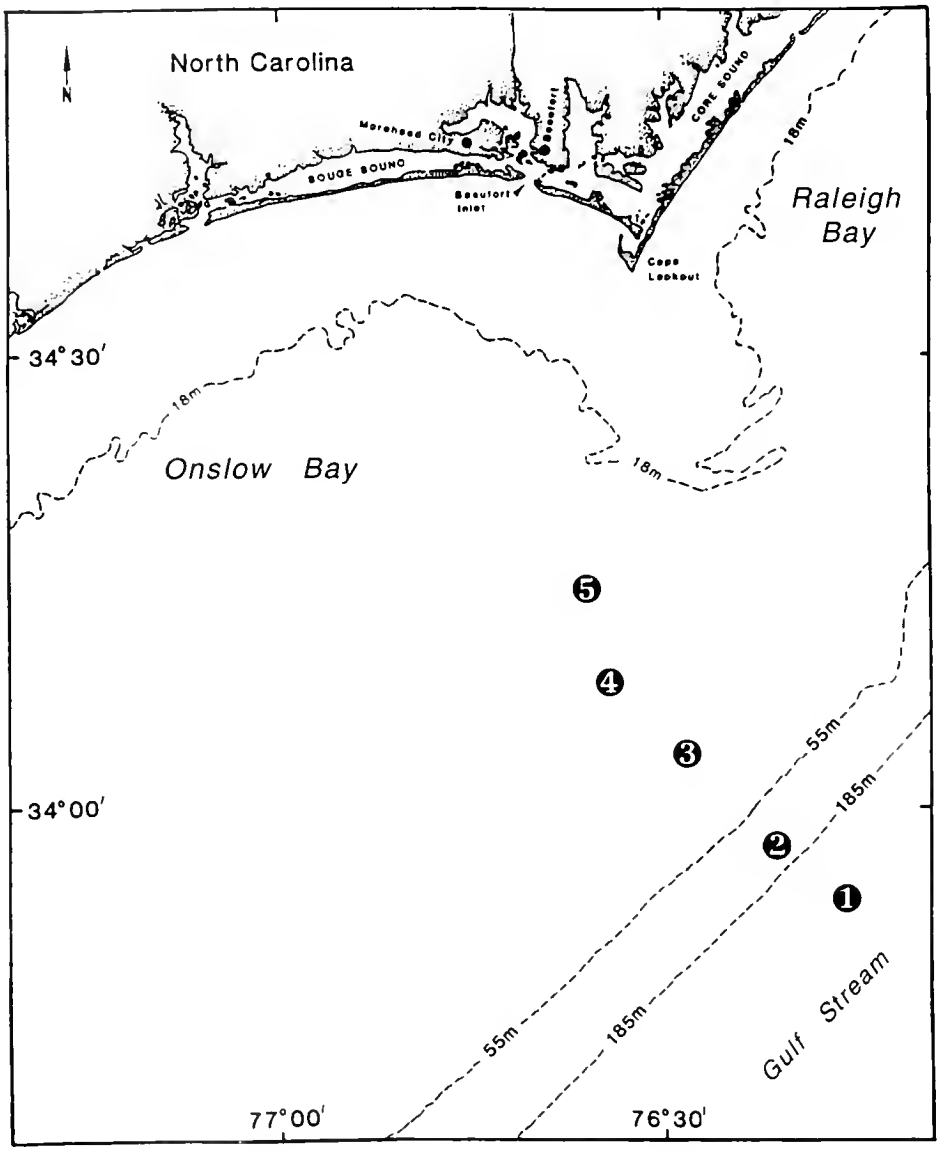

Figure 1
Location of sampling stations.

spectively). Stations 1 and 2 were influenced by the Gulf Stream.

Three samplers were used: a 60-cm diameter bongo sampler with 0.333-mm mesh nets, a 5-m^2 Methot frame trawl with 2×3 mm oval mesh (Methot, 1986), and a 1×2 m neuston net with 0.947-mm mesh. The bongo sampler was towed obliquely at 1.5 knots for a minimum of 5 min to insure 150 m^3 of water was sampled. The Methot frame trawl was towed obliquely at 4 knots for a minimum of 20 min to insure that >10,000 m^3 of water had been sampled, except for one tow of 10 min on 14 September 1994 at station 2 at 2111 hours. Both the bongo sampler and frame trawl were retrieved in a modified step oblique tow after deployment to a depth approximately 10 m from the bottom, except at station 1 where nets were deployed to a maximum depth of 170 m. The neuston net was towed for 10 min at 1.5 knots with approximately one-half of the net under water. Volume estimates for bongo nets and Methot frame trawl were based on General Oceanics flowmeter readings. No volume readings were taken for neuston tows. A summary of sample data is presented in Table 1. Samples were preserved in 95% ethyl alcohol. Body length measurements are notochord lengths (preflexion and flexion stages) or standard lengths (postflexion and juvenile stages).

At each station a conductivity-temperature-depth (CTD) probe (Sea-Bird model 911plus) was cast to within 1–3 m of the bottom. Temperature and salin-

Table 1

Summary of sample data taken in waters off North Carolina. For gear type: frame = 5 m^2-Methot frame trawl with 3×4 mm oval mesh (Methot, 1986); bongo = 60-cm bongo nets with 0.333-mm mesh; neuston = 1×2 m neuston net with 0.947-mm mesh. Density of larvae indicates numbers/100 m^3 for bongo nets; numbers/10,000 m^3 for frame trawl; and numbers/10-min tow for neuston net.

Date	Station	Time	Gear	Density of larvae
14 Sep 1994	2	2111	frame	27
		2149	frame	29
		2244	bongo	112
		2307	neuston	32
15 Sep 1994	3	0122	frame	15
		0204	bongo	79
		0224	neuston	33
	4	0401	frame	25
		0445	neuston	29
		0458	bongo	72
	5	0620	frame	3
	1	2108	frame	9
		2148	bongo	26
		2207	neuston	23
16 Sep 1994	2	2341	frame	16
		0024	neuston	26
		0040	bongo	82
	3	0201	frame	8
		0235	bongo	161
		0244	neuston	20
	4	0355	frame	23
		0427	neuston	58
		0443	bongo	156
	5	0541	frame	19
		0616	bongo	118
		0625	neuston	29

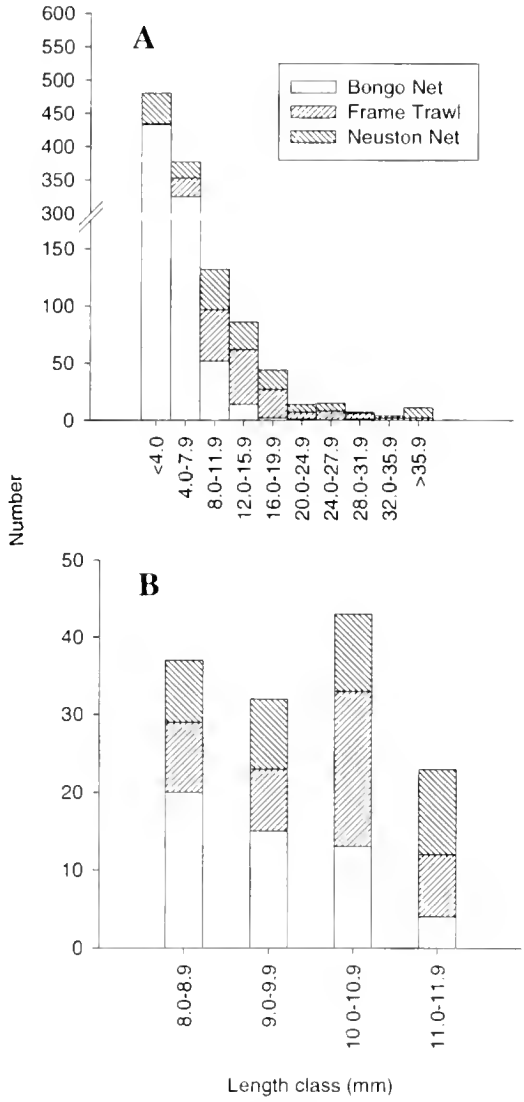

Figure 2

Length-frequency distributions by gear of (**A**) all ichthyoplankton (excluding leptocephali); and (**B**) ichthyoplankton between 8.0 and 12.0 mm in length.

ity measurements were reviewed for aberrant data points. Satellite-derived advanced very high resolution radiometer (AVHRR) data (NOAA/NESDIS CoastWatch node, NMFS Beaufort Laboratory) were used to examine sea surface temperature (SST) during the study period (1–20 September 1994). A nonparametric Kruskal-Wallis test (SAS Institute, Inc., 1987) was used to evaluate differences in fish lengths between gear types, and between days at specific stations.

Results

Larval length distributions by gear

There was a significant difference in length of larvae among gears (Kruskal-Wallace Test, P <0.01). The neuston net and frame trawl collected larger larvae, whereas the bongo net collected smaller larvae (Fig. 2A). The bongo net was more effective in collecting larvae <10.0 mm, and the frame trawl and neuston net were more effective in collecting larvae 10.0 mm (Fig. 2B). A wide range of size classes was obtained with the neuston net and frame trawl, but catches typically were low (Table 1, Fig. 2).

Some 40 reef fish taxa were collected (Table 2); approximately 25 with the bongo sampler, 24 with the frame trawl, and 14 with the neuston net. Five families were commonly collected (Table 3), but a size series of only two taxa (*Acanthurus* sp(p). and

Table 2

The frequency of occurrence from *n* samples and, in parenthesis, the density (bongo net=numbers/100 m^3, frame trawl= numbers/10,000 m^3, neuston net=numbers/10-min tow; summed over all stations) of reef-associated taxa collected with three different samplers in September, 1995, in waters off North Carolina.

Family	Taxa	Bongo net (*n*=10)	Frame trawl (*n*=8)	Neuston net (*n*=8)
Acanthuridae	*Acanthurus bahianus*		2(4.0)	
	A. bahianus/*chirurgus*		1(0.8)	
	A. chirurgus		1(1.1)	
	A. coeruleus	1 (0.8)	1(1.1)	
	Acanthurus sp(p).	1 (0.8)	2(1.4)	2(2.0)
Balistidae	*Balistes capriscus*		1(0.6)	2(2.0)
	unidentified	3 (2.0)	1(0.6)	1(1.0)
Carangidae	*Alectis ciliaris*		1(0.8)	
	Seriola sp(p).	1 (1.3)	1(0.6)	1(2.0)
Chaetodontidae	*Chaetodon ocellatus*		1(0.6)	
Diodontidae	unidentified		1(0.8)	
Fistularidae	*Fistularia* sp(p).	1 (1.5)	1(0.8)	
Gobiidae	*Ioglossus calliurus*	3 (2.8)		
Holocentridae	unidentified	2 (1.0)	2(1.3)	3(3.0)
Labridae	*Bodianus* sp.	1 (0.6)		
	Halichoeres sp(p).	2 (5.5)		
Lutjanidae	*Etelis oculatus*	1 (0.5)		
	Lutjanus campechanus	1 (0.7)		
	Pristipomoides aquilonaris	1 (0.7)		
	Rhomboplites aurorubens	5(11.7)		1(1.0)
	unidentified	4(15.2)		
Monacanthidae	*Aluterus scriptus*		1(0.8)	
	Aluterus sp.		1(0.8)	
	Cantherines sp.		1(0.6)	
	Monacanthus ciliatus		3(2.2)	
	M. hispidus	1 (1.3)	4(4.4)	2(6.0)
Muraenidae	*Gymnothorax moringa*		1(0.6)	
	G. ocellatus complex		3(5.5)	
	Gymnothorax sp(p).	1 (1.3)	1(1.5)	
	unidentified	1 (1.3)		1(1.0)
Ogcocephalidae	unidentified	1 (0.7)	2(2.2)	
Pomacanthidae	*Holacanthus* sp(p).	2 (4.0)		
	unidentified	1 (1.3)		
Pomacentridae	*Pomacentrus* sp(p).	3 (2.6)		
	unidentified	1 (0.7)		2(2.0)
Priacanthidae	*Pristigenys alta*		1(0.9)	
	unidentified	5 (8.4)	1(0.6)	
Scaridae	type A	6(15.6)		2(7.0)
	type B	5 (9.8)		1(1.0)
	unidentified	1 (1.5)		
Scorpaenidae	*Scorpaena* sp.		1(0.6)	
	unidentified	7 (9.0)		1(2.0)

continued

Table 2 (continued)

Family	Taxa	Bongo net (*n*=10)	Frame trawl (*n*=8)	Neuston net (*n*=8)
Serranidae	*Diplectrum formosum*	2 (1.3)		
	Epinephelus cruenatus		1(1.7)	
	E. niveatus / flavolimbatus	1 (0.8)		
	Hemanthias vivanus			1(1.0)
	Liopropoma sp(p).			2(2.0)
	Rypticus sp(p).	2 (1.3)		
	Serraninae type A	2 (2.7)		
	Serranus sp.		1(0.6)	
	subfamily Serraninae	3(11.8)		
	tribe Epinephelini			1(1.0)
Syngnathidae	*Hippocampus erectus*		2(1.4)	3(3.0)

Table 3

The range of body lengths, by gear, for the most commonly collected taxa, identified below the family level. Values in parentheses indicate the number of fish measured. Bongo = 60-cm bongo nets with 0.333-mm mesh; Frame = 5-m^2 Methot frame trawl with 3×4 mm oval mesh; and Neuston = 1×2 m neuston net with 0.947-mm mesh.

Taxa	Bongo net	Frame trawl	Neuston net
Reef fish taxa			
Acanthuridae			
Acanthurus sp(p).	2.5–8.6	4.7–10.2	3.0–3.3
	(11)	(10)	(2)
Labridae			
Halichoeres sp(p).	2.1–5.4	—	—
	(8)		
Lutjanidae			
Rhomboplites aurorubens	2.9–5.6	—	4.2
	(18)	—	(1)
unidentified	1.9–3.4	—	—
	(30)	—	—
Priacanthidae			
Pristigenys alta	—	10.3	
		(1)	
unidentified	1.8–4.4	—	3.1–4.1
	(19)	—	(4)
Scaridae			
type A	2.9–7.7	—	8.4–9.8
	(18)	—	(7)
type B	2.7–7.7	—	7.6
	(11)	—	(1)
Pelagic taxa			
Carangidae			
Decapterus punctatus	2.1–14.7	18.7	2.9–11.0
	(30)	(1)	(10)
Selar crumenophthalmus	3.7–6.7	7.3–16.2	4.1–5.0
	(5)	(16)	(2)

continued

Table 3 (continued)

Taxa	Bongo net	Frame trawl	Neuston net
Coryphaenidae			
Coryphaena equisetus	4.4–4.6	—	*10.0–19.2*
	(2)	—	(12)
C. hippurus	—	—	12.3–43.0
	—	—	(15)
Scombridae			
Auxis sp(p).	2.6–7.1	10.7	4.0–18.3
	(20)	(1)	(6)
Scomberomorus cavalla	2.8–6.2	13.5	4.2–7.9
	(38)	(1)	(4)
Thunnus sp(p).	2.6–6.2	4.6–5.7	4.7–5.7
	(12)	(2)	(14)
Demersal taxa			
Bothidae			
Bothus sp(p).	2.0–15.0	6.5–19.5	3.4–6.0
	(104)	(30)	(18)
Trichopsetta ventralis	30.0	13.5–29.8	—
	(1)	(20)	—
Callionymidae			
Diplogrammus pauciradiatus	1.2–3.4	—	—
	(66)	—	—
Paradiplogrammus bairdi	1.7–6.2	—	3.5–6.0
	(9)	—	(6)
Caproidae			
Antigonia sp(p).	2.8–6.3	3.4–8.3	2.7–4.0
	(16)	(6)	(2)
Labridae			
Xyrichtys novacula	2.4–9.9	6.2	6.8–13.5
	(46)	(1)	(2)
Ophidiidae			
Ophidion selenops	1.9–16.0	—	—
	(8)	—	—
Otophidion omostigmum	3.1–8.3	—	—
	(14)	—	—
Paralichthyidae			
Syacium papillosum	1.3–12.7	4.2–9.3	3.2–4.3
	(92)	(3)	(25)

Scaridae type A) were collected with complementary gear. The bongo sampler and frame trawl were effective in collecting a series of *Acanthurus* sp(p)., the bongo and neuston net in collecting Scaridae type A. Larvae of the economically important *Rhomboplites aurorubens* were collected almost exclusively with bongo nets and ranged from 2.9 to 5.6 mm (Tables 2 and 3). The unidentified lutjanid larvae were probably *R. aurorubens* because few *Lutjanus campechanus* were collected (n=3).

Of the seven commonly collected pelagic taxa, size series of four taxa (*Selar crumenophthalmus*, *Coryphaena equisetus*, *Auxis* sp(p)., and *Scomberomorus cavalla*) were collected with complementary gear (Table 3). Except *S. crumenophthalmus*, which was effectively collected with the bongo sampler and frame trawl, all others were collected with the bongo sampler and neuston net. *Coryphaena hippurus* specimens were large and collected solely with the neuston net.

The frame trawl effectively sampled large anguilliform leptocephali, and the bongo sampler was a good complementary gear for collecting smaller specimens (Fig. 3). Only one leptocephalus was captured with the neuston net. Taxa representing three families were collected: Congridae (*Ariosoma balearicum*, *Bathycongrus* sp(p)., *Heteroconger luteolus*, *Para-*

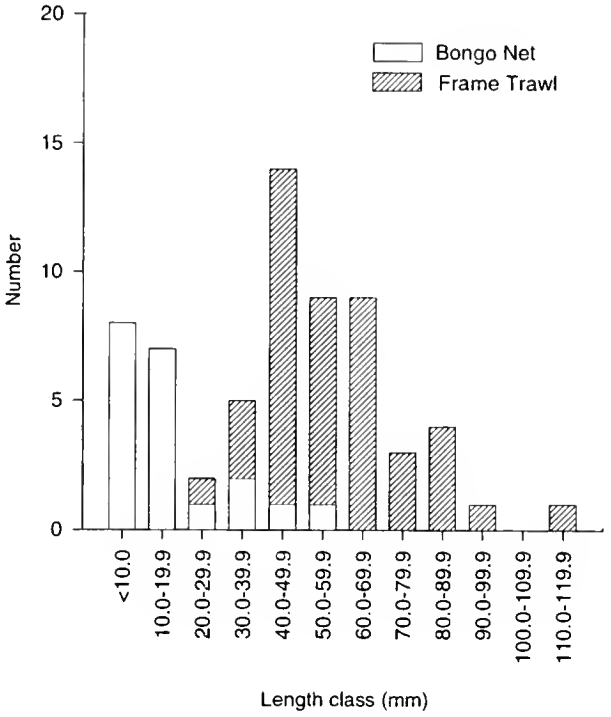

Figure 3
Length-frequency distribution of anguilliform leptocephali by gear.

conger caudilimbatus); Muraenidae (*Gymnothorax moringa*, *G. ocellatus* complex); and Ophichthidae (*Callechelys muraena*, *Gordiichthys ergodes*, *Letharchus aliculatus*, *Ophichthus gomesii*, *O. melanoporus*, *O. puncticeps*).

A size series of two demersal species (*Bothus* sp(p). and *Antigonia* sp(p).) was collected with the bongo net and frame trawl (Table 3). Because size of *Bothus* at metamorphosis is approximately 16–21 mm (Fahay, 1983), our collections represent a complete size series. Species most likely include *B. ocellatus* and *B. robinsi* (Robins and Ray, 1986), both of which inhabit middle-shelf waters as adults (Schwartz, 1989). The series of antigonids did not include the large pelagic stage (ca. 13–14 mm).[1] All the specimens that had developed meristic characters (ca. 5.0 mm) were *Antigonia capros*. On this basis, the smaller specimens might be *A. capros*, but *A. capros* and *A. combatia* exist sympatrically in the western North Atlantic (Berry, 1959).

[1] Richards, W. J. 1991. National Marine Fisheries Service, Southeast Fisheries Science Center, 75 Virginia drive, Miami, FL 33149. Unpubl. data.

Hydrography and ichthyoplankton distribution

A major hydrographic feature observed in SST imagery was a large frontal eddy that was propagating northeastward and associated with a Gulf Stream meander crest (Fig. 4). A warm filament of Gulf Stream derived water lay over the shelf and resulted from the cyclonic circulation of the frontal eddy. This filament was bounded inshore by cooler shelf water and separated from the Gulf Stream by cooler water of the frontal eddy.

Temperature and salinity were in concordance with the SST imagery (Fig. 5). On 15 September 1994 (day 1), domed-shaped isotherms and lower salinities were observed at station 2 indicating recent upwelling from the passage of the frontal eddy (Fig. 4). The warmer and more saline water on the shelf on day-1 (Fig. 5) was consistent with the presence of stranded Gulf Stream water resulting from the frontal eddy filament observed on the SST imagery (Fig. 4). Associated with this stranded Gulf Stream water on the middle-shelf was a diverse group of larvae that are not known to occur as adults or spawn in middle-shelf waters (Table 4). The frequency occur-

Figure 4

Sea-surface-temperature satellite imagery during (**A**) 12 and, (**B**) 15 and, (**C**) 16 September 1994 off North Carolina. Station locations are referenced. See Figure 1 for station numbers.

rence of these larvae appeared to be similar on both days as was the presence of Gulf Stream water.

On 16 September 1994 (day 2), hydrographic conditions had changed markedly offshore (Fig. 5). At the surface of station 2, warm, low-salinity water was present, indicating water of coastal origin. But the temperature was higher than observed over the Carolina shelf in the SST imagery (Fig. 4), indicating a more southern coastal origin for this water. Accompanying these changes in outer-shelf waters, the length-frequency distributions of the two most abundant taxa, *Bothus* sp(p). and *S. papillosum*, differed significantly between day 1 and day 2 (Kruskal-Wallace Test; $P<0.01$ for both taxa). Very small larvae of both middle-shelf taxa were abundant in outer-shelf waters on day 2 but absent on day 1 (Fig. 6).

Discussion

Gear comparison

A series of pelagic larvae and juveniles was collected with complementary gear for *Acanthurus* sp(p)., *Antigonia* sp(p)., *Bothus* sp(p)., Scaridae type A, and *Selar crumenophthalmus*. The Methot frame trawl was not successful in collecting large larvae or early juveniles of economically important reef fish species (snappers and groupers), probably due to the low abundance of adult populations. In other studies, the frame trawl has successfully collected large larvae and juveniles of those species whose adults are extremely abundant (i.e. *Theragra chalcogramma* [Shima and Bailey, 1994; Brodeur et al., 1995]) and *Engraulis mordax*, [Methot, 1986]). Economically important reef fish species are relatively rare and larger size pelagic larvae and juveniles are rarer than young larvae. Longer frame-trawl tow times (one hour) will be required, but this would limit the extent of the area to be sampled and decrease the quality of the specimens. The bongo sampler is generally limited in its ability to collect late-stage larvae or early pelagic juveniles owing to net avoidance (Shima and Bailey, 1994); however, it is a more effective sampler than either the neuston net or frame trawl in collecting early stage larvae, and it is needed to obtain information on spatial and temporal spawning.

The frame trawl is effective in capturing leptocephali, and because the leptocephalus is a true oceanic form regardless of habitat as an adult (Smith, 1989), it is a valuable indicator species in studies dealing with cross-shelf transport. Similarly, the frame trawl is effective in capturing *Trichopsetta ventralis*, a resident of the Gulf of Mexico (Robins

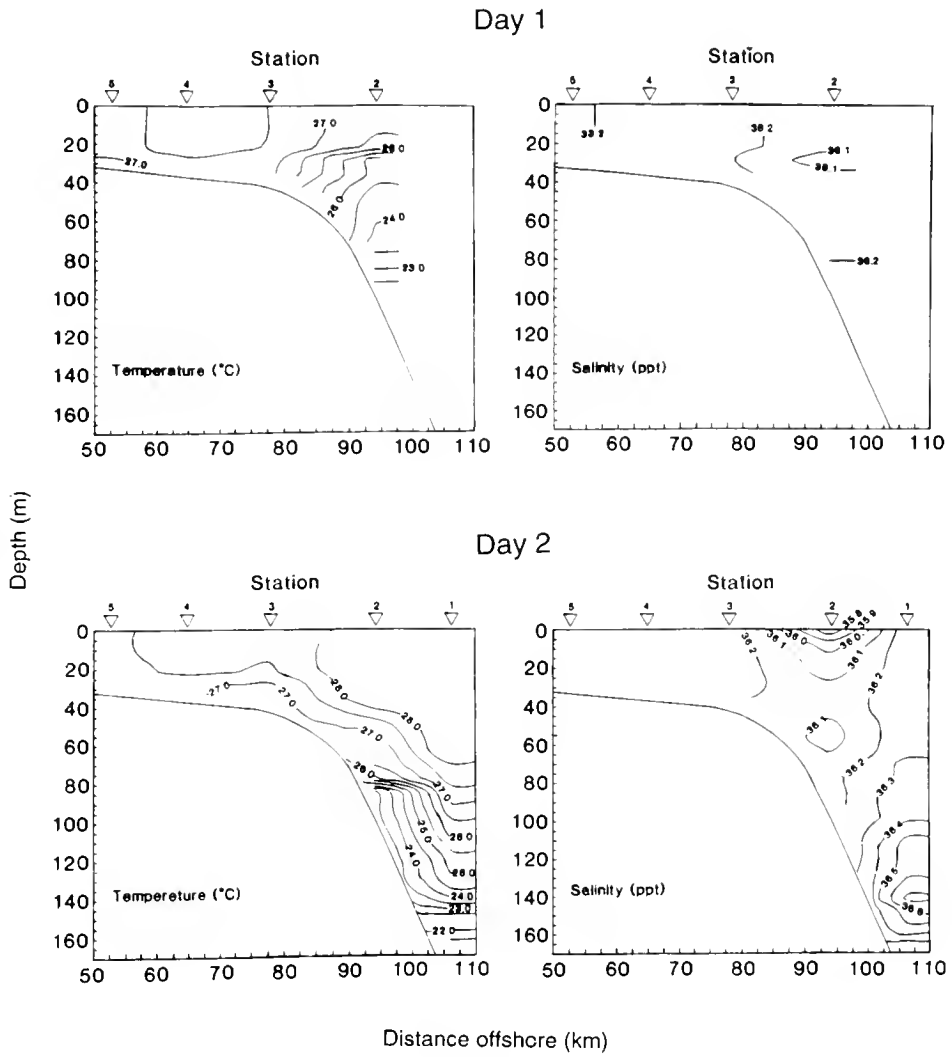

Figure 5

Temperature (°C) and salinity (ppt) sections across a transect from middle-shelf to Gulf Stream waters of 24-h duration. Sampling periods and locations: day 1 is from 14 September 1994, 2111 h (station 2) to 15 September, 0620 h (station 5); day 2 from 16 September, 2108 h (station 1) to 16 September, 0625 h (station 5). Station 1 was not sampled on day 1.

and Ray, 1986) and an indicator that certain larvae spawned in the Gulf of Mexico as well as other organisms (Pietrafesa, 1989) can be transported to shelf waters off North Carolina.

Our study and previous studies (Eldridge et al., 1978) indicate that the 1 m × 2 m neuston net is as effective in sampling large larvae and juveniles as is the frame trawl, although a comparison has not been made by using both nets as neuston nets. Eldridge et al. made a large number of neuston tows (24 day, 24 night) and, in some cases, collected larger fishes (e.g. *Decapterus* sp, *Selar crumenopthalmus* and Priacanthidae). However, they did not collect any Acanthuridae, *Trichopsetta*, and *Antigonia* sp(p)., taxa that were relatively common in frame trawl collections. A comparison between the two gear types for neuston tows could be informative.

Ichthyoplankton distribution in relation to hydrography

Factors influencing the hydrography of the waters off North Carolina are complex and dynamic (Pietrafesa, 1989; Pomeroy et al., 1993; Verity et al., 1993) and

Table 4

The occurrence of larvae (denoted by a "+" sign) from taxa that occur or spawn as adults in oceanic (>185 m) and outer-shelf waters (55–185 m) or that occur south of the study area (denoted by an asterisk) collected in middle-shelf waters (stations 3 and 4) during two sampling periods of 24-h duration (denoted by day 1 and day 2).

Family	Species	Day 1	Day 2	Family	Species	Day 1	Day 2
Acropomatidae	*Synagrops* sp.		+	Lutjanidae	*Etelis oculatus**		+
Balistidae	*Canthidermis maculatus*	+		Muraenidae	*Gymnothorax ocellatus* complex	+	
Bathypteroidae	unidentified		+			+	
Bothidae	*Trichopsetta ventralis**	+	+		unidentified		+
Caproidae	*Antigonia capros* (?)	+	+	Myctophidae	*Benthosema suborbitale*	+	
Carapidae	*Carapus bermudensis**		+		*Ceratoscopelus* sp(p).	+	+
Chiasmodontidae	unidentified		+		*Notolychnus valdiviae*		+
Congridae	*Ariosoma balearicum*	+	+		unidentified	+	+
	Bathycongrus sp(p).	+	+	Nomeidae	*Cubiceps pauciradiatus*	+	
	Heteroconger luteolis	+		Notosudidae	*Scopelosaurus smithii*		+
	Paraconger caudilimbatus	+		Ophichthidae	*Gordiichthys ergodes*		+
Gempylidae	*Gempylus serpens*	+		Paralepididae	*Lestidium atlanticum*	+	
	Nesiarchus nasutus		+		unidentified	+	
Gonostomatidae	*Cyclothone* sp(p).	+	+	Paralichthyidae	*Citharichthys gymnorhinus**	+	+
Lobotidae	*Lobotes surinamensis**		+	Phosichthyidae		+	

certainly influence the composition of ichthyoplankton on the continental shelf. A major feature is the intrusion of Gulf Stream waters onto the continental shelf. Additionally, during summer, southwest winds result in the advection of shelf waters south of North Carolina onto the North Carolina shelf (Pietrafesa, 1989). Intrusions of the Gulf Stream, along with the advection of Georgian shelf water, appeared to be evident in our study and could have influenced the composition of ichthyoplankton on the shelf—particularly evident at the outer-shelf station (station 2) where hydrographic conditions and size composition of the two most abundant taxa changed within a 24-h period.

We identified 21 species of larvae on the middle shelf from oceanic and outer-shelf waters and five species which, as adults, occur in shelf waters south of the study area (Table 4). The intrusion of these larvae is a common event that occurs throughout all seasons (Powell and Robbins, 1994; 1998; our study) and appears to be related to water expelled from frontal eddies created by Gulf Stream meanders that have stranded on the continental shelf. Nevertheless, we were unable to determine the role of cross shelf transport in the recruitment of subtropical and tropical reef fishes and other taxa to waters off North Carolina.

Our observations on larval fish distribution patterns in relation to hydrography are derived from five stations over a 48-h period. Longer-term studies, with extensive sampling, will be necessary to test assumptions made in our study, especially the transport of larvae from the middle shelf to the outer shelf. *Syacium papillosum* a middle-shelf species that is abundant from spring to early fall (Powell and Robbins 1994; 1998; our study) could serve as an indicator of transport in long-term studies. Such studies could test the hypothesis that circulation patterns during late spring, summer, and early fall in shelf waters off North Carolina retain larvae within the bays. The major goal of future research should be to develop a comprehensive model or scenario of larval transport based on circulation patterns (e.g. Hare and Cowen, 1996). Such a model could provide a lucid framework for testing larval transport hypotheses and be of heuristic value as new problems are discovered.

Acknowledgments

We wish to express our appreciation to the crew of the RV *Cape Hatteras* and those individuals who participated in the cruise, especially Mike Greene. We especially thank David Smith and Mark Leiby for leptocephali identification, Curtis Lewis for figure preparation, and Dave Colby and Jim Waters for computer assistance. Comments by Bill Hettler, Patti Marraro, and Dave Peters along with those of two anonymous reviewers greatly improved the manuscript.

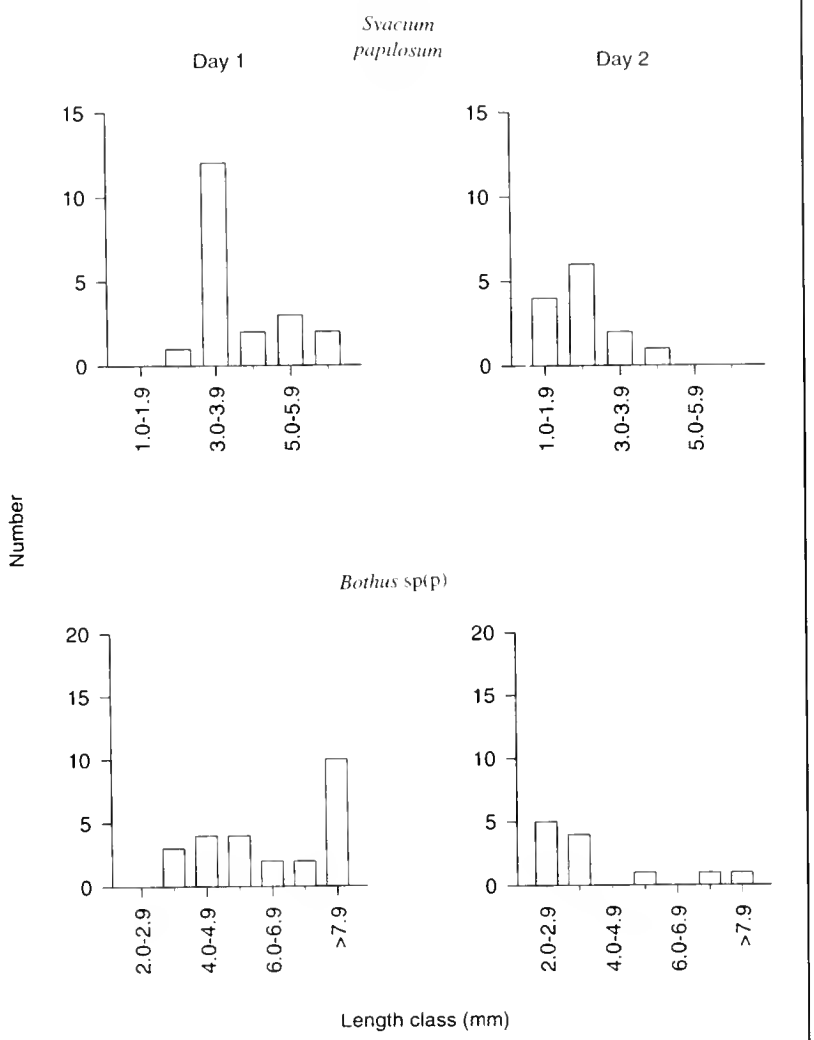

Figure 6

Length-frequency distributions of two commonly collected middle-shelf species at outer-shelf station 2 at a 24-h interval. See Figure 5 for dates and times of day 1 and day 2.

Literature cited

Berry, F. H.
1959. Boarfishes of the genus *Antigonia* of the western Atlantic. Bull. Fla. State Mus. 4:205–250.

Booth, D. J., and D. M. Brosnan.
1995. The role of recruitment dynamics in rocky shore and coral reef fish communities. Adv. Ecol. Res. 26:309–385.

Brodeur, R. D., M. S. Busby, and M. T. Wilson.
1995. Summer distribution of early life stages of walleye pollock, *Theragra chalcogramma*, and associated species in the western Gulf of Alaska. Fish. Bull. 93:603–618.

Eldridge, P. J., F. H. Berry, and M. C. Miller III.
1978. Diurnal variations in catches of selected species of ichthyoneuston by the Boothbay neuston net off Charleston, South Carolina. Fish. Bull. 76:295–297.

Fahay, M. P.
1975. An annotated list of larval and juvenile fishes captured with surface-towed meter net in the South Atlantic Bight during four RV *Dolphin* cruises between May1967 and February 1968. U.S. Dep. Commer., NOAA Tech. Rep. NMFS SSRF-685, 39 p.
1983. Guide to the early stages of marine fishes occurring in the western north Atlantic Ocean, Cape Hatteras to the southern Scotian Shelf. J. Northwest Atl. Fish. Sci. 4:1–423.

Gray, I. E., M. E. Downey, and M. J. Cerame-Vivas.
1968. Sea-stars of North Carolina. Fish. Bull. 67:127–164

Hare, J. A., and R. K. Cowen.
1996. Transport mechanisms of larval and pelagic juvenile bluefish (*Pomatomus saltatrix*) from South Atlantic Bight spawning grounds to Middle Atlantic Bight nursery habitats. Limnol. Oceanogr. 41:1264–1280.

Huntsman, G. R.
1976. Offshore headboat fishing in North Carolina and South Carolina. Mar. Fish. Rev. 38:13–23.

Leis, J. M.
1994. Coral Sea atoll lagoons: closed nurseries for the larvae of a few coral reef fishes. Bull. Mar. Sci. 54:206–227.

Methot, R. D.
1986. Frame trawl for sampling pelagic juvenile fish. CALCOFI Rep. 27:267–278.

Miller, G. C., and W. J. Richards.
1979. Reef fish habitat, faunal assemblages, and factors determining distributions in the South Atlantic Bight. Proc. Gulf Caribb. Fish. Inst. 32:114–130.

Pietrafesa, L. J.
1989. The Gulf Stream and wind events on the Carolina Capes shelf. *In* North Carolina coastal oceanography symposium (R. Y. George and A. Hulbert, eds.), p. 89–129. U.S. Dep. Commer., NOAA-NURP Rep. 89-2.

Pomeroy, L. R., J. O. Blanton, G.-A. Paffenhöfer, K. L. Von Damn, P. G. Verity, H. L. Windom, and T. N. Lee.
1993. Inner shelf processes. *In* Ocean processes: U. S. southeast continental shelf: a summary of research conducted in the South Atlantic Bight under the auspices of the U. S. Department of Energy from 1977 to 1991 (D. W. Menzel, ed.), p. 9–43. Office of Scientific and Technical Information, Rep. DOE/OSTI-11674.

Powell, A. B., and R. E. Robbins.
1994. Abundance and distribution of ichthyoplankton along an inshore-offshore transect in Onslow Bay, North Carolina. U.S. Dep. Commer. NOAA Tech. Rep. NMFS 120, 28 p.
1998. Ichthyoplankton adjacent to live-bottom habitats in Onslow Bay, North Carolina. U.S. Dep. Commer., NOAA Tech. Rep. NMFS 133, 32 p.

Powles, H., and B. W. Stender.
1976. Observations on composition, seasonality and distribution of ichthyoplankton from MARMAP cruises in the South Atlantic Bight in 1973. S.C. Mar. Res. Cent., Tech. Rep. Ser. 11.

Robins, C. R., and G. C. Ray.
1986. A field guide to Atlantic coast fishes of North America. Houghton Mifflin, Boston, MA, 354 p.

SAS Institute, Inc.
1987. SAS/STAT™ guide for personal computers, version 6 edition. SAS Institute Inc., Cary, NC, 1028 p.

Schwartz, F. J.
1989. Zoogeography and ecology of fishes inhabiting North Carolina's marine waters to depths of 600 meters. *In* North Carolina coastal oceanography symposium (R. Y. George and A. W. Hulbert, eds), p. 335–374. U.S. Dep. Commer., NOAA-NURP Rep. 89-2.

Shima, M., and K. M. Bailey.
1994. Comparative analysis of ichthyoplankton sampling gear for early life stages of walleye pollack (*Theragra chalcogramma*). Fish. Oceanogr. 3:50–59.

Smith, D. G.
1989. Introduction to leptocephali. *In* Fishes of the western north Atlantic, memoir 1, part 9, vol. 2, Leptocephali (E. A. Bohlke, ed.), p. 657–658. Sears Found. Mar. Res., Yale Univ.

Struhsaker, P.
1969. Demersal fish resources: composition, distribution, and commercial potential of the continental shelf stocks off the southeastern United States. Fish. Indust. Res. 4:261–300.

Verity, P. G., T. N. Lee, J. A. Yoder, G.-A. Poffenhöfer, J. O. Blanton, and C. R. Alexander.
1993. Outer shelf processes. *In* Ocean processes: U. S. southeast continental shelf: a summary of research conducted in the South Atlantic Bight under the auspices of the U.S. Department of Energy from 1977 to 1991 (D. W. Menzel, ed.), p. 45–74. Office of Scientific and Technical Information, Rep. DOE/OSTI-11674.

Fishery Bulletin

Guide for Contributors

Content

Articles published in *Fishery Bulletin* describe original research in fishery marine science, engineering and economics, and the environmental and ecological sciences, including modeling. Articles may range from relatively short to extensive.

Notes are reports of 5 to 10 pages without an abstract and describing methods or results not supported by a large body of data.

Although all contributions are subject to peer review, responsibility for the contents of papers rests upon the authors and not upon the editor or the publisher. It is therefore important that the contents of the manuscript are carefully considered by the authors.

Submission of an article is understood to imply that the article is original and is not being considered for publication elsewhere. Manuscripts should be written in English. Authors whose native language is not English are strongly advised to have their manuscripts checked by English-speaking colleagues prior to submission.

Preparation

Title page should include authors' full names and mailing addresses, the corresponding author's telephone, FAX number, and e-mail address, and a list of key words to describe the contents of the manuscript.

Abstract should not exceed one double-spaced typed page. It should state the main scope of the research but emphasize its conclusions and relevant findings. Because abstracts are circulated by abstracting agencies, it is important that they represent the research clearly and concisely.

Text must be typed double-spaced throughout. A brief introduction should portray the broad significance of the paper; the remainder of the paper should be divided into the following sections: Materials and methods, Results, Discussion (or Conclusions), and Acknowledgments. Headings within each section must be short, reflect a logical sequence, and follow the rules of multiple subdivision (i.e. there can be no subdivision without at least two items). The entire text should be intelligible to interdisciplinary readers; therefore, all acronyms, abbreviations, and technical terms should be spelled out the first time they are mentioned. The scientific names of species must be written out the first time they are mentioned; subsequent mention of scientific names may be abbreviated. Follow Scientific Style and Format: the CBE Manual for Authors, Editors, and Publishers (6th ed.), for editorial style, and the most current issue of the American Fisheries Society's Common and Scientific Names of Fishes from the United States and Canada, for fish nomenclature. Dates should be written as follows: 11 November 1991. Measurements should be expressed in metric units, e.g. metric tons as t; if other units of measurement are used, please make this fact explicit to the reader. The numeral one (1) should be typed as a one, not as a lower-case el (l). Use of appendices is discouraged.

Text footnotes should be numbered with Arabic numerals and inserted at the bottom of text. Footnote all personal communications, unpublished data, and unpublished manuscripts with full address of the communicator or author, or, as in the case of unpublished data, where the data are on file. Authors are advised to avoid references to nonstandard (gray) literature, such as internal, project, processed, or administrative reports. Where these references are used, please include whether they are available from NTIS (National Technical Information Service) or from some other public depository.

Literature cited comprises published works and those accepted for publication in peer reviewed literature (in press). Follow the name and year system for citation format. In the text, cite as follows: Smith and Jones (1977) or (Smith and Jones, 1977). If there is a sequence of citations, list alphabetically by author(s): Smith, 1987; Smith and Jones, 1985; Smith and Peterson, 1986. Abbreviations of serials should conform to abbreviations given in Serial Sources for the BIOSIS Previews Database. Authors are responsible for the accuracy and completeness of all citations.

Tables should not be excessive in size and must be cited in numerical order in the text. Headings within tables should be short but ample enough to allow the table to be intelligible on its own. All unusual symbols must be explained in the table legend. Other incidental comments may be footnoted with italic numerals. Use the asterisk only to indicate probability in statistical data. Zeros should precede all decimal points for values less than one.

Figures must be cited in numerical order in the text. The senior author's last name and the figure number should be written on the back of each one. Hand-drawn illustrations should be submitted as originals and not as photocopies. Submit photographs as glossy prints or slides with good contrast, otherwise we cannot guarantee a good final printed copy. Graphs should be submitted as laser-printed copies, not as photocopies. Label all figures with Helvetica typeface and capitalize the first letter of the first word in axis labels. Italicize species name and variables in equations. Use zeros before all decimal points. Use uppercase Times Roman bold typeface to label the parts of a figure, e.g. A, B, C, etc. Each figure legend should explain all symbols and abbreviations in the figure and should be double-spaced and placed at the end of the manuscript.

Copyright law Government publications are not copyrighted; they fall within the public domain. If an author reproduces any part of a government publication in his work, reference to source is appreciated.

Submission

Send printed copies (original and three copies without staples) to the Scientific Editor:

Dr. John V. Merriner
Southeast Fisheries Science Center
National Marine Fisheries Service
101 Pivers Island Road
Beaufort, NC 28516

Once the manuscript has been accepted for publication, you will be asked to submit an electronic copy of your manuscript to the Managing Editor. The electronic copy should be submitted in WordPerfect or Microsoft Word text format and placed on a 3.5-inch disk that is double-sided, double or high density, and that is compatible with either DOS or Macintosh systems.

A copy of page proofs will be sent to the author for final approval prior to publication.

Reprints (copies of published articles and notes) are available free of charge to the senior author (50 copies) and to his or her laboratory (50 copies). Additional copies may be purchased in lots of 100 when the author receives page proofs.

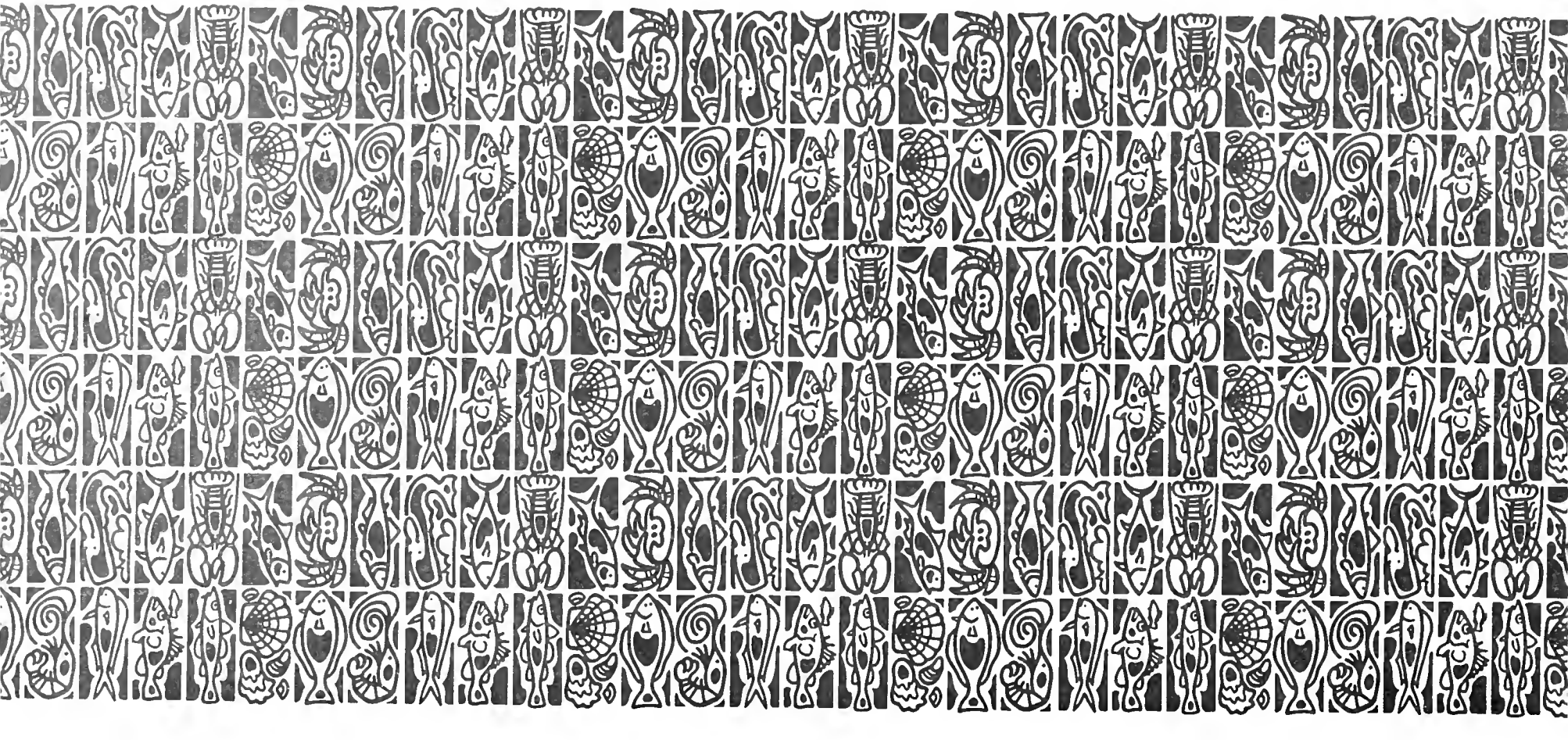

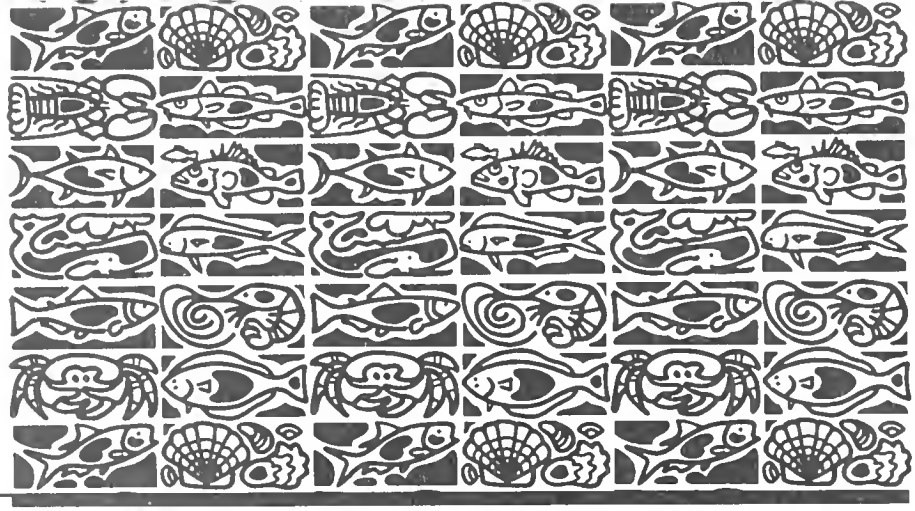

U.S. Department
of Commerce

Volume 98
Number 3
July 2000

Fishery Bulletin

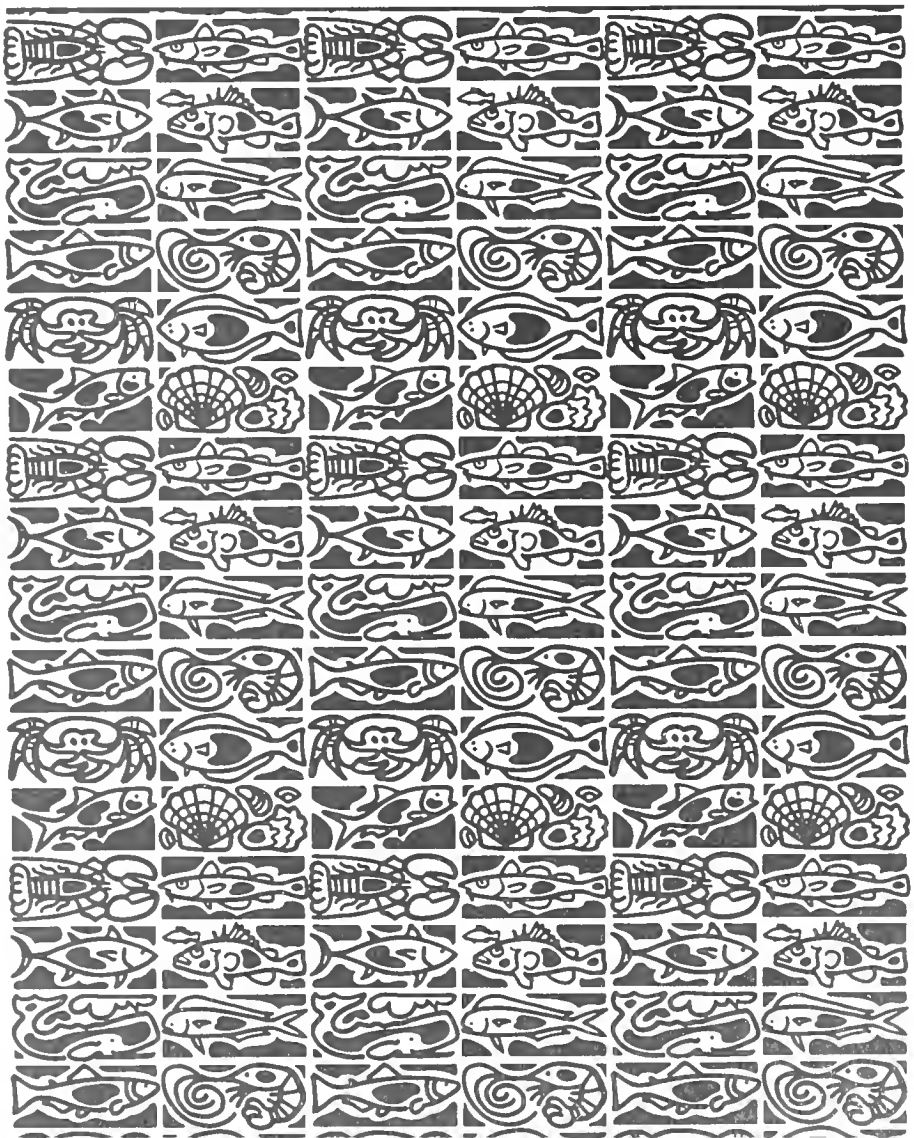

The *Fishery Bulletin* (ISSN 0090-0656) is published quarterly by the Scientific Publications Office, National Marine Fisheries Service, NOAA, 7600 Sand Point Way NE, BIN C15700, Seattle, WA 98115-0070. Periodicals postage is paid at Seattle, WA, and at additional mailing offices. POSTMASTER: Send address changes for subscriptions to Fishery Bulletin, Superintendent of Documents, Attn.: Chief, Mail List Branch, Mail Stop SSOM, Washington, DC 20402-9373.

The Secretary of Commerce has determined that the publication of this periodical is necessary according to law for the transaction of public business of this Department. Use of funds for printing of this periodical has been approved by the Director of the Office of Management and Budget.

For sale by the Superintendent of Documents, U.S. Government Printing Office, Washington, DC 20402. Subscription price per year: $50.00 domestic and $62.50 foreign. Cost per single issue: $19.00 domestic and $23.76 foreign. **See back for order form.**

Fishery Bulletin

***Fishery Bulletin* web site: fishbull.noaa.gov**

The *Fishery Bulletin* carries original research reports and technical notes on investigations in fishery science, engineering, and economics. It began as the Bulletin of the United States Fish Commission in 1881; it became the Bulletin of the Bureau of Fisheries in 1904 and the *Fishery Bulletin* of the Fish and Wildlife Service in 1941. Separates were issued as documents through volume 46; the last document was No. 1103. Beginning with volume 47 in 1931 and continuing through volume 62 in 1963, each separate appeared as a numbered bulletin. A new system began in 1963 with volume 63 in which papers are bound together in a single issue of the bulletin. Beginning with volume 70, number 1, January 1972, the *Fishery Bulletin* became a periodical, issued quarterly. In this form, it is available by subscription from the Superintendent of Documents, U.S. Government Printing Office, Washington, DC 20402. It is also available free in limited numbers to libraries, research institutions, State and Federal agencies, and in exchange for other scientific publications.

U.S. Department of Commerce
Seattle, Washington

Volume 98
Number 3
July 2000

Fishery Bulletin

Contents

Distinction between silver hake (*Merluccius bilinearis*) stocks in U.S. waters of the northwest Atlantic based on whole otolith morphometrics

Karen L. Bolles

Gavin A. Begg

Northeast Fisheries Science Center
National Marine Fisheries Service, NOAA
166 Water Street, Woods Hole, Massachusetts 02543
Present address: (for K. L. Bolles): Marine Research Institute
Skulagata 4, P.O. Box 1390
121 Reykjavik, Iceland

E-mail address (for K. L. Bolles): karen@hafro.is

Abstract.—A method for using whole otolith morphometrics to identify silver hake (*Merluccius bilinearis*) stocks in U.S. waters of the northwest Atlantic is described. Whole sagittal otolith morphometric variables of length, width, area, perimeter, circularity, and rectangularity were extracted by image processing and, in combination with age-specific discriminant analyses, were used to differentiate two stocks of silver hake: a northern stock from the Gulf of Maine to northern Georges Bank and a southern stock from southern Georges Bank to the Middle Atlantic. Further support for these groupings is supported by growth rate analyses: fish of the northern stock grew slower than those of the southern stock, resulting in typically larger otoliths for fish from the northern stock. This study demonstrates that whole otolith morphometrics, specific to fish age, are useful in identifying silver hake stocks and can be a useful tool in identifying other fish stocks.

Manuscript accepted 15 February 2000.
Fish. Bull. 98:451–462 (2000).

Accurate distinction between fish stocks is necessary for effective fisheries management to prevent overfishing of individual stocks, to preserve the reproductive and genetic diversity of stock complexes, and to determine optimal strategies for rebuilding stocks (Cushing, 1968; Booke, 1981; Grimes et al., 1987; Begg et al., 1999; Stephenson, 1999). Integral to attaining such management strategies and objectives, is the necessary requirement of reevaluating stock definitions when needed, particularly when the status of the resource changes, or when new technologies become available that may provide more effective stock discrimination tools than those already in use (Begg and Waldman, 1999). Because of the uncertainties surrounding the stock definitions for silver hake (*Merluccius bilinearis*) in U.S. waters of the northwest Atlantic, such a need for reevaluation of stock definitions arose. Furthermore, there was no efficient method for adequately discriminating between silver hake stocks that could also provide a fast and accurate way to determine levels of stock mixing for current fishery assessment and management. In our study, we focused on these issues by incorporating the technology and efficiency of image analysis systems, in combination with multivariate statistical analyses, to distinguish between silver hake stocks on the basis of phenotypic differences in whole otoliths.

Silver hake, (or whiting), is a principal groundfish species found along the continental shelf and slope from Newfoundland to South Carolina, inhabiting depths from shallow inshore waters to those greater than 400 m (Bigelow and Schroeder, 1953; Almeida, 1987; Helser et al., 1995). Silver hake are ecologically important both as a predator and prey in the northwest Atlantic ecosystem (Edwards and Bowman, 1979; Bowman and Michaels, 1984), and form an important part of the commercial fisheries throughout this region (Anonymous, 1998). With annual landings averaging 16,600 metric tons, silver hake are currently considered overexploited (Anonymous, 1998).

Two stocks of silver hake are currently defined in U.S. waters on the basis of analysis of research survey and commercial catch data, as well as multivariate analysis of external morphometric data: a northern stock (from the Gulf of Maine to northern Georges Bank) and a southern stock (from southern Georges Bank to the Middle Atlantic) (Almeida, 1987). Distributions of the two stocks vary seasonally and spatially, probably in response to temperature and depth (Helser et al., 1995). Silver hake that compose the northern stock overwinter in the deeper regions of the Gulf of Maine and during their peak spawning months of July and August, are found on northern Georges Bank and in coastal waters east of Cape Cod, north to Grand Manan (Big-

elow and Schroeder, 1953; Almeida, 1987). In contrast, the southern stock is found predominantly in waters from Cape Cod to Montauk Point, New York, and during peak spawning, which occurs in June and July, it is found on southern Georges Bank, in the New York Bight, and as far south as Cape Hatteras (Almeida, 1987; Helser et al., 1995).

Although silver hake in U.S. waters are currently assessed according to this two-stock scheme, uncertainty exists in the stock definitions. A variety of other stock identification techniques have also been used to identify these two stocks of silver hake, including examining external morphometrics (Conover et al., 1961), growth rate comparisons (Nichy, 1969), immunological analyses (Konstantinov and Noskov, 1969), research survey distribution studies (Anderson, 1974), and genetic analyses (Schenk, 1981). However, the stock boundaries suggested in each of these studies have all tended to vary from one another. More recently, Helser (1996) found that silver hake growth rates differed both between and within the two stocks—a finding that is inconsistent with the stock boundaries currently defined (Almeida, 1987) and that confounds the delineation of the stocks and the degree to which the two stocks mix. Given this finding, we believed further investigation into the stock structure of silver hake was needed to clarify the current management units defined for U.S. waters. In addition, we aimed to introduce a more efficient and accurate method for distinguishing between silver hake stocks than the previous methods that have been used, one which would have the potential to enable rapid and accurate in-season assessment of the degree of stock mixing for silver hake.

Figure 1

NEFSC spring survey stations where silver hake samples were collected for otolith morphometric-based stock discrimination analysis in 1992 (squares), 1994 (closed circles), and 1996 (open circles). GOM-NGB: Gulf of Maine to northern Georges Bank; SGB-MID: southern Georges Bank to the Middle Atlantic.

Otolith morphometric data have recently been used to identify stocks of marine fish, including Atlantic mackerel, *Scomber scombrus* (Dawson, 1991; Hopkins[1]), Atlantic herring, *Clupea harengus* (Messieh et al., 1989), and Atlantic salmon, *Salmo salar* (Friedland and Reddin, 1994). In contrast, otolith morphometric data have not been used to differentiate between stocks of silver hake, but because silver hake have been found to differ phenotypically (Almeida, 1987), and possibly genetically (Schenck, 1981), it was assumed that otolith morphometric characteristics may also vary. Dery (1988) observed that silver hake otoliths from the northern stock were narrower and thicker in cross-section than those of the southern stock, although no statistical analyses were used to test her observations. Accordingly, it was thought that otolith morphometrics could differ between the two silver hake stocks and could prove to be useful characters by which to differentiate stocks in the future. The collection of such data by means of image processing techniques has proven to be useful in stock identification, providing accurate and efficient measures that traditional morphometric methods have not been able to provide (Jearld, 1995; Cadrin and Friedland, 1999). Given these benefits and Dery's (1988) observations, our study aimed to identify whole otolith morphometric characteristics unique to silver hake stocks in U.S. waters of the northwest Atlantic by using image processing techniques. We address the advantages and limitations encountered when using this method to distinguish fish stocks, and reevaluate the current silver hake stock scheme given the recent within-stock growth differences observed by Helser (1996).

[1] Hopkins, P.J. 1986. Mackerel stock discrimination using otolith morphometrics. ICES Council Meeting 1986, 17 p.

Materials and methods

Sample collection

Silver hake were collected in 1992, 1994, and 1996 during the spring Northeast Fisheries Science Center (NEFSC) stratified random bottom-trawl surveys when the fish were assumed to be on their spawning grounds. Silver hake samples were obtained from the Gulf of Maine to northern Georges Bank (GOM–NGB), and from southern Georges Bank to the Middle Atlantic regions (SGB–MID) (Fig. 1, Table 1). Silver hake were measured (fork length [FL], cm),

sex was determined by macroscopic examination of the gonads, and sagittal otolith pairs were removed from each fish. One otolith from each pair was sectioned and assigned an age following methods in Dery (1988). The other otolith of the pair, either left or right, was then used for morphometric analysis. Samples were restricted to fish of ages 1 to 3 years, because older fish were infrequently collected in the surveys. This restriction also enabled both size- and age-related variation, which could have confounded discrimination analyses, to be minimized.

Otolith orientation was standardized by positioning the otolith with its proximal side down and the rostrum was used as a common starting point from which the perimeter was traced in a counterclockwise direction. Broken or visibly damaged otoliths were not measured. Whole otolith length, width, area and perimeter, and two shape indices—circularity and rectangularity, were collected for each otolith by using the OPTIMAS™ (version 6.2) image analysis system (OPTIMAS, 1996). Rectangularity is a measure of the otolith area divided by the area of its minimum enclosing rectangle, and circularity is the perimeter of the otolith squared divided by its area (OPTIMAS, 1996). All otolith measurements were performed at a magnification of 7×.

Table 1

Sampling information on silver hake.

Region	Age group (years)	Year class	Sex	Length range (cm)	*n*
North	1	1991	Females	—	—
			Males	12–18	45
South	1	1991	Females	11–19	22
			Males	11–20	22
North	2	1990	Females	17–28	50
			Males	16–24	31
South	2	1990	Females	18–22	6
			Males	17–26	11
North	3	1989	Females	23–32	15
			Males	22–29	12
South	3	1989	Females	26–36	9
			Males	26–28	5
North	3	1991	Females	23–31	50
			Males	23–29	26
South	3	1991	Females	23–35	50
			Males	23–32	50
North	3	1993	Females	20–32	53
			Males	22–29	24
South	3	1993	Females	21–34	53
			Males	22–33	25

Data analysis

Bottom ocean temperatures measured throughout the NEFSC spring and autumn bottom-trawl surveys from 1989 to 1996 were compared between the northern and southern regions to determine whether different thermal regimes exist between the two regions that could effect growth rates and subsequent otolith morphometric characteristics of silver hake inhabiting each of these regions. A two-way, fixed-factor, unbalanced analysis of variance (ANOVA) was used to compare bottom temperatures between the regions and time of the survey. Following a significant interaction between these factors, unpaired *t*-tests were used to compare bottom temperatures between regions for each survey, and one-way ANOVAs were used to compare bottom temperatures between surveys for each region. Significance levels were corrected for multiple testing by using the Bonferroni adjustment factor. Tukey's honestly significant difference (HSD) tests were used for *a posteriori* comparisons.

Growth rates of silver hake sampled throughout the NEFSC spring bottom-trawl surveys were calculated by using linear regressions for samples of each sex, year, and region of capture to determine if growth differences existed that might be indicative of stock separation. Analysis of covariance (ANCOVA) was used to compare differences in growth rates of silver hake between the sexes (same year and region), sampling years (same sex and region), and regions (same year and sex).

All otolith morphometric variables were first examined for normality and homogeneity of variances, and were $\log_e$-transformed prior to statistical analysis if these criteria were not satisfied. ANCOVA was then used to determine the effect of fish length on the magnitude of each otolith morphometric variable. "Region" was treated as the main factor and "length" was the covariate. Morphometric variables for which "region-length" interactions were significant were not included in any further analyses because they could not be corrected for fish length. Variables that were significantly correlated with fish length were corrected for variable fish length by using the common within-group slope (b).

Multivariate analysis of variance (MANOVA) was used to compare otoliths sampled for each sex (same region, year class, and age group) by using the appropriate length-corrected variables. One-way ANOVAs were then used to examine individual morphometric variables to explain any significant differences detected by the MANOVAs. Significance levels were corrected for multiple testing with the Bonferroni adjustment factor. Likewise, multi- and univariate analyses were then used to test the effects of year class (samples from the same region and age group) on otolith structure. Following these analyses, similar tests were used to investigate morphological differences in otolith samples from the northern and southern regions. Spatial comparisons were made between samples from the different regions for fish of the same age group, sex, and year class. Canonical discriminant analysis was then used to detect morphometric differences in otoliths of silver hake sampled from the northern and southern regions. Significant ($P<0.05$) canonical variates represented the optimal combination of regions and morphometric variables that provided the best overall discrimination between the groups. Standardized coefficients provided for each sig-

nificant variable represented the contribution of the respective morphometric variable to the discrimination of silver hake samples between regions. Jack-knifed cross-validation procedures were used to give unbiased estimates of classification success (SYSTAT, 1997).

Results

Bottom ocean temperatures differed significantly between region and time of survey (ANOVA interaction, F=11.7, df=15, 2931, P<0.0001). Generally, temperatures were significantly lower in the northern region than in the southern region for all surveys (t-tests, P<0.0001), except during the spring of 1994 and 1996 (although consistent differences were still maintained between regions during these times, albeit not significant) (Fig. 2). Within each region, bottom temperatures have a consistent seasonal pattern, tending to be significantly lower in spring than autumn for both regions (ANOVA, P<0.0001; HSD, P<0.05), with no apparent differences between years within seasons and regions (Fig. 2).

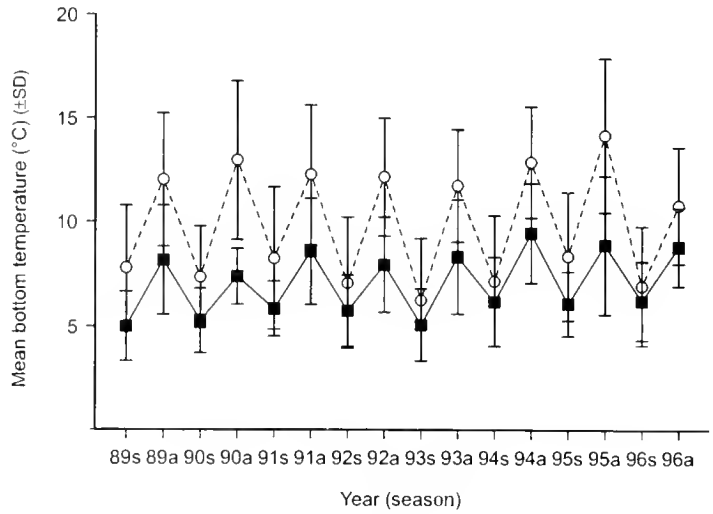

Figure 2

Mean ocean bottom temperatures (°C) (± standard deviation) of northern (squares) and southern (circles) regions collected from the spring (s) and autumn (a) NEFSC bottom-trawl surveys (1989–1996).

Silver hake had significantly different growth rates between sexes, year classes, and the regions from where they were sampled (Fig. 3). Female silver hake grew at a faster rate than males in both the northern and southern regions; and age-length differences between the sexes increased as the fish got older (ANCOVA, P<0.05). Growth rates of each sex, within each region, also differed between sampling years, indicative of the presence of a year class effect (ANCOVA, P<0.005). Likewise, significant differences in growth rates were found between silver hake from the northern and southern regions in each year for both males and females (ANCOVA, P<0.005).

The six otolith morphometric variables (length, width, area, perimeter, circularity, and rectangularity) that were measured for silver hake were $\log_e$-transformed, except for otolith width, to correct for non-normality and heterogeneity of variances. ANCOVAs detected significant (P<0.0001) "region-fish length" interactions for four (otolith area, length, width, and perimeter) of the six variables measured when all samples were examined together, irrespective of age group, year class, or sex. However, the use of individual ANCOVAs for fish of each age group reduced the number of interactions to only one variable for both 1-year-old (rectangularity) and 2-year-old silver hake (width), and two variables (area, length) for samples from 3-year-olds (Table 2). All the remaining variables for the different aged samples were significantly correlated with fish length (P<0.01), and therefore were corrected for variable fish length with their respective common within-group slope (Table 2). Consequently, length-corrected data determined from the individual ANCOVAs for each age group were used for the remaining analyses and indicated the strong effect different ages can have on these types of measurements. Typically, for any given fish length, silver hake from the northern region appeared to have larger otolith dimensions (area, length, width, and perimeter) than those fish from the southern region (Fig. 4).

Multi- and univariate analyses were used to examine confounding sources of variation that may have influenced regional patterns of silver hake (Table 3). In general, otolith morphometrics were not significantly different (P>0.05) between the sexes, indicating that their otoliths develop at a similar rate over the age range examined. In contrast, as for the growth rate analyses, significant differences were found among otolith morphometrics of the same-age silver hake sampled from different year classes for both males and females (Table 3). Likewise, similar year-class differences in otolith morphometrics were found when the sexes were pooled together, confirming congruency in rates of otolith development, and justifying assimilation of sexes for statistical purposes.

Silver hake sampled from the northern region tended to have larger otolith dimensions than those from the southern region (Fig. 4). Overall, when the appropriate length-corrected morphometric variables were examined together for silver hake of the same age group and year class, irrespective of sex, significant differences were found between samples from the northern and southern regions (MANOVA, P<0.001) (Table 4). Fewer multivariate significant differences were detected for samples from 3-year-olds, although these differences were probably the result of samples for this age group having fewer variables to examine compared with samples from the other age groups. This was supported by univariate tests where significant differences (P<0.05) between silver hake from the northern and southern regions were found for several variables, for all age groups, and for almost all of the age group, sex, and year class combinations (Table 4). Also, the oto-

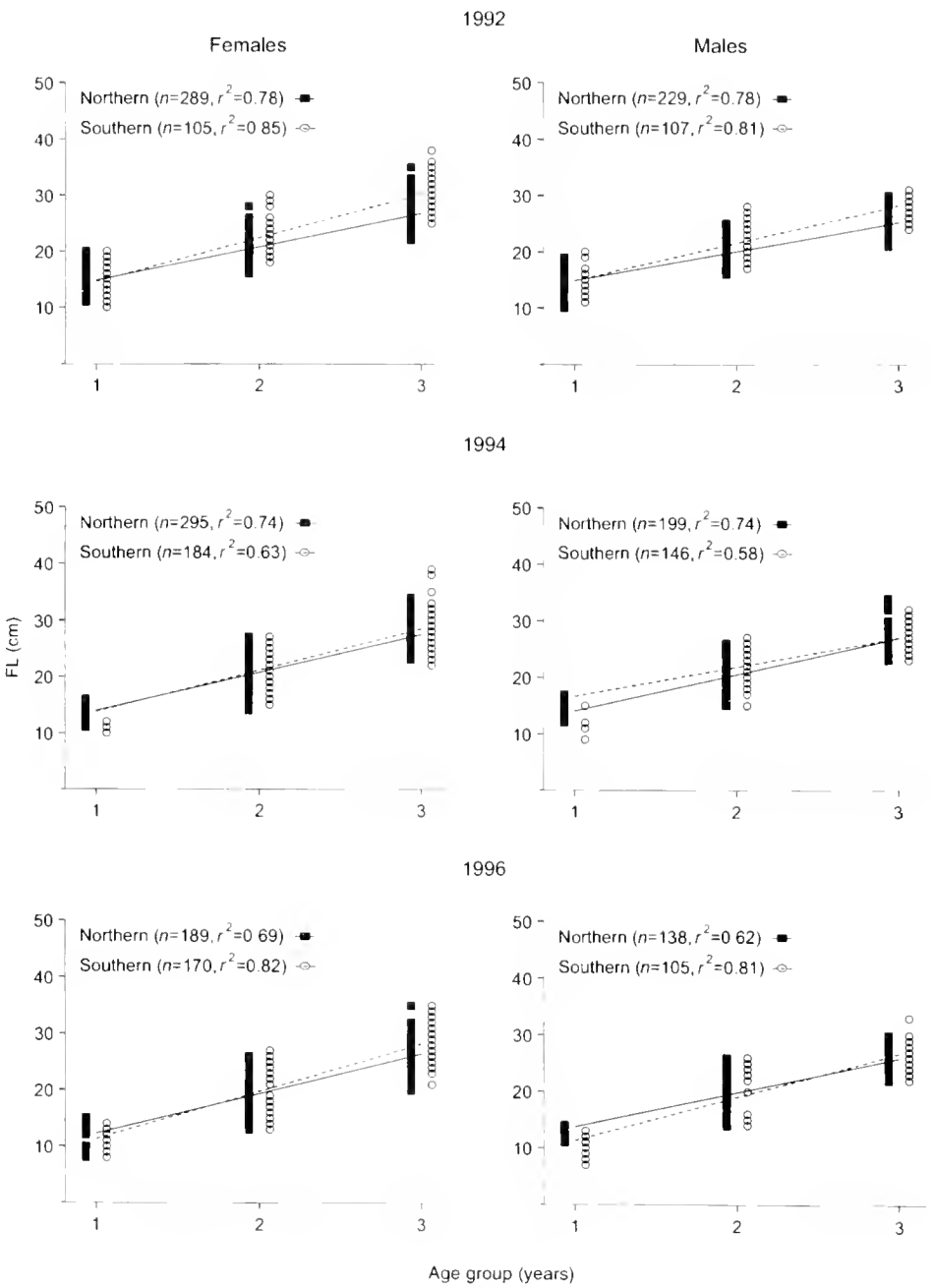

Figure 3

Linear growth relationships of silver hake samples (age groups 1 to 3) from the NEFSC 1992 (northern, F: S=6.41, I=8.15; M: S=4.97, I=9.98; southern, F: S=6.83, I=8.33, M: S=5.73, I=9.58), 1994 (northern, F: S=6.75, I=7.20; M: S=6.07, I=8.33; southern, F: S=7.10, I=6.99, M: S=4.84, I=12.25), and 1996 (northern, F: S=6.91, I=5.57; M: S=5.76, I=8.30; southern, F: S=8.03, I=3.72, M: S=7.15, I=4.65) spring surveys. (F=females; M=males; S=slope; I=intercept; n=sample size; r^2=coefficient of determination).

lith morphometric variables not included in the comparisons of 3-year-olds (those variables based on the ANCOVA results—area and length) were the most significant of the variables examined individually for the other age groups, emphasizing the potential importance of these two variables for stock discrimination.

Discriminant analyses provided further support for the separation between northern and southern stocks among

Table 2

Otolith morphometric variables that were significantly correlated with fish length for 1-, 2-, and 3-year-old silver hake samples. N.S. = not significant.

A 1-year-old silver hake

	Fish length · variable (df=2, 83)		Fish length (df=1, 85)		
Variable	*F*	*P*	*F*	*P*	*b*
Otolith length	0.10	N.S.	603.59	0.0001	0.0063
Width	2.65	N.S.	526.37	0.0001	0.0156
Area	1.24	N.S.	683.39	0.0001	0.0118
Perimeter	0.05	N.S.	471.07	0.0001	0.0067
Circularity	1.85	N.S.	15.99	0.0001	0.0016
Rectangularity	6.07	0.0035	—	—	—

B 2-year-old silver hake

	Fish length · variable (df=3, 90)		Fish length (df=1, 93)		
Variable	*F*	*P*	*F*	*P*	*b*
Otolith length	1.46	N.S.	621.48	0.0001	0.0047
Width	3.84	0.0123	—	—	—
Area	2.17	N.S.	715.78	0.0001	0.0084
Perimeter	0.78	N.S.	515.89	0.0001	0.0049
Circularity	0.80	N.S.	30.83	0.0001	0.0014
Rectangularity	1.11	N.S.	6.83	0.0104	–0.0002

C 3-year-old silver hake

	Fish length · variable (df=11, 348)		Fish length (df=1, 359)		
Variable	*F*	*P*	*F*	*P*	*b*
Otolith length	2.56	0.0040	—	—	—
Width	0.68	N.S.	561.32	0.0001	0.0102
Area	2.04	0.0239	—	—	—
Perimeter	1.10	N.S.	1024.62	0.0001	0.0037
Circularity	0.64	N.S.	144.02	0.0001	0.0020
Rectangularity	0.82	N.S.	12.78	0.0004	–0.0001

the silver hake samples, as indicated by the multi- and univariate analyses (Fig. 5). We found significant differences in the discriminant scores (CV 1) between those samples from the northern and southern regions for both 1-year-old (t=-6.3075, df=87, P<0.0001) and 2-year-old fish (t=4.7654, df=95, P<0.0001). However, as in the preceding analyses, poor separation was observed between the samples of 3-year-olds (t=1.7827, df=370, not significant). This was again probably due to the reduced number of variables in the analyses, particularly that of otolith area and length. Variation in otolith area, length, and circularity was mainly responsible for the north–south separation in samples of 1- and 2-year-olds, whereas otolith width and circularity accounted for most of the variation in the samples of 3-year-olds (Table 5).

Classification success, based on each particular discriminant model, decreased with each age group. Overall, individual samples of 1-, 2-, and 3-year-old silver hake were correctly classified 75%, 69%, and 49% of the times, respectively (Table 6). Classification rates increased slightly when samples from each age group were analyzed separately by sex (1-year-old fish, males—78%; 2-year-old fish, females—68%, males—71%; 3-year-old fish, females—54%, males—56%) and year class (3-year-old fish: 1989 year class—54%; 1991 year class—64%; 1993 year class—61%), indicating the confounding affects that these variables can have on these types of analyses when used for stock discrimination.

Discussion

We confirmed that two stocks of silver hake exist in U.S. waters of the northwest Atlantic from differences in whole otolith morphometrics and growth rates. Our method of

Table 3

Examination of confounding sources of variation (sex and year class) on the length-corrected otolith morphometric variables. N.S. = not significant.

	MANOVA				ANOVA		
Comparison	*F*	df	*P*	Significant variable	*F*	df	*P*
Sex							
Females vs. males (South; 1991 year class; age 1)	0.18	4, 39	N.S.	—	—	—	—
Females vs. males (North; 1990 year class; age 2)	2.59	4, 76	0.0434	circularity	8.02	1, 79	0.0059
Females vs. males (South; 1990 year class; age 2)	0.36	4, 12	N.S.	—	—	—	—
Females vs. males (North; 1989 year class; age 3)	1.49	4, 22	N.S.	—	—	—	—
Females vs. males (South; 1989 year class; age 3)	2.54	4, 9	N.S.	—	—	—	—
Females vs. males (North; 1991 year class; age 3)	1.74	4, 71	N.S.	—	—	—	—
Females vs. males (South; 1991 year class; age 3)	7.32	4, 95	0.0001	rectangularity	8.43	1, 98	0.0046
Females vs. males (North; 1993 year class; age 3)	0.53	4, 72	N.S.	—	—	—	—
Females vs. males (South; 1993 year class; age 3)	0.57	4, 73	N.S.	—	—	—	—
Year class							
1989; 1991 vs. 1993 (Females; North; age 3)	4.97	8, 226	0.0001	—	—	—	—
1989; 1991 vs. 1993 (Males; North; age 3)	5.45	8, 114	0.0001	width	4.80	2, 59	0.0118
1989; 1992 vs. 1993 (Females; South; age 3)	2.37	8, 214	0.0183	perimeter circularity	6.67 6.13	2, 109	0.0018 0.0030
1989; 1992 vs. 1993 (Males; South; age 3)	2.86	8, 150	0.0055	perimeter	6.18	2, 77	0.0033
1989; 1991 vs. 1993 (Sexes pooled; North; age 3)	8.60	8, 350	0.0001	width	7.81	2, 177	0.0006
1989; 1992 vs. 1993 (Sexes pooled; South; age 3)	3.23	8, 374	0.0014	perimeter circularity	9.65 5.94	2, 189	0.0001 0.0031

using otolith morphometrics, coupled with discriminant function analysis, when analyzed with respect to fish age, enabled us to distinguish between a northern stock (from the Gulf of Maine to northern Georges Bank) and a southern stock (from southern Georges Bank to the Middle Atlantic), thus providing a more efficient and accurate method for discriminating between silver hake stocks than had been used previously.

Typically, silver hake of the northern stock grew at a slower rate, and had larger otoliths than fish of the southern stock. Otoliths of silver hake from the northern stock tended to be longer, wider, and greater in area and perimeter than similar-size fish from the southern stock because, for any given fish length, northern stock fish were older and therefore had more time to accumulate otolith material than had southern stock fish. These results were consistent with previous growth studies where slower growing fish generally had larger otoliths than those of similar-size, faster growing fish (Templeman and Squires, 1956; Reznick et al., 1989; Fowler and Short, 1996).

Likewise, Helser (1996) found that silver hake from the northern stock grew at slower rates than those fish of the southern stock, and like Nichy (1969), Almeida (1978) and Pentilla et al. (1989) found that the northern stock reached larger asymptotic lengths. However, Helser (1996) also found results that did not support the current stock

Table 4

Spatial comparisons of the length-corrected otolith morphometric variables. N.S. = not significant.

	MANOVA				ANOVA		
Spatial comparison	*F*	df	*P*	Significant variable	*F*	df	*P*
Same sex, age group, and year class							
North vs. South (Males; age 1; 1991)	6.98	4, 62	0.0001	length	13.71	1, 65	0.0004
				width	8.12		0.0059
				area	18.06		0.0001
North vs. South (Females; age 2; 1990)	1.24	4, 51	N.S.	—	—	—	—
North vs. South (Males; age 2; 1990)	6.30	4, 37	0.0006	area	8.68	1, 40	0.0053
				circularity	13.93		0.0006
North vs. South (Females; age 3; 1989)	1.98	4, 19	N.S.	—	—	—	—
North vs. South (Males; age 3; 1989)	2.40	4, 12	N.S.	—	—	—	—
North vs. South (Females; age 3; 1991)	5.80	4, 95	0.0003	—	—	—	—
North vs. South (Males; age 3; 1991)	3.84	4, 71	0.0070	perimeter	10.48	1, 74	0.0018
				circularity	7.35		0.0083
North vs. South (Females; age 3; 1993)	2.16	4, 101	N.S.	—	—	—	—
North vs. South (Males; age 3; 1993)	2.38	4, 44	N.S.	width	7.03	1, 47	0.0109
Same age group, year class; sexes combined							
North vs. South (age 1; 1991)	9.60	4, 84	0.0001	length	17.18	1, 87	0.0001
				width	9.04		0.0035
				area	22.16		0.0001
				circularity	10.61		0.0016
North vs. South (age 2; 1990)	5.05	4, 93	0.0010	length	11.15	1, 96	0.0012
				area	12.78		0.0006
North vs. South (age 3; 1989)	0.78	4, 36	N.S.	—	—	—	—
North vs. South (age 3; 1991)	5.18	4, 171	0.0006	perimeter	10.44	1, 174	0.0015
				circularity	8.47		0.0041
North vs. South (age 3; 1993)	4.05	4, 150	0.0038	width	11.49	1, 153	0.0009

scheme; growth rates differed between silver hake from northern Georges Bank and the Gulf of Maine and between fish from southern Georges Bank and the Middle Atlantic. Such within-stock differences further emphasizes the uncertainty that currently exists over both stock boundaries and the degree of mixing between silver hake stocks in U.S. waters of the northwest Atlantic.

Similarly, the uncertainty in stock boundaries and the degree of stock mixing was evident in most of the past silver hake stock discrimination studies (Conover et al., 1961; Konstantinov and Noskov, 1969; Nichy, 1969; Anderson, 1974), although we believe that our approach has the potential to resolve some of these questions. A major reason for this uncertainty has been due to a lack of intensive genetic studies to investigate the population structure of the species, and therefore a subsequent lack of knowledge concerning the actual reproductive isolation of the species. Schenk (1981) demonstrated two genetically distinct groups but, owing to a limited geographic sample area, was not able to define boundaries between the groups. However, it must be remembered that a "stock" in its working definition for practical fisheries management is a management unit and not a discrete biological population unit. Consequently, stocks of fish with different phenotypic (i.e. morphometric) characteristics or life history (i.e. growth) dynamics should be considered as separate management units and modeled separately regardless of genetic characteristics for stock assessment and management purposes (Cadrin and Friedland, 1999). Although our study did not delineate actual stock bound-

aries or determine the mixing components between the silver hake stocks, further investigation into the application of this technique may show that otolith morphometrics, when coupled with image processing and discriminant analysis, is capable of achieving these objectives.

Subsequently, to understand better the fishery dynamics of silver hake stocks and to manage them accordingly, we must question what caused these differences—whether they are differences in fish growth, or internal or external morphometric characters, both between and within stocks. Otolith morphometric differences between silver hake stocks are probably the result of both environmental and genetic influences. For example, the hydrodynamics of northwest Atlantic waters are considered to be heterogeneous; environmental conditions differ between the Gulf of Maine and the Middle Atlantic (Brooks, 1996). Certainly, we observed significant and consistent differences in the bottom temperatures between the two stock regions inhabited by silver hake, where those fish in the northern region experience lower temperatures than those in the southern region. Because fish growth and external body morphometrics are known to be influenced by such environmental factors (Ihssen et al., 1981; Pawson and Jennings, 1996), one would also expect that internal morphometrics, such as otolith length and width, would also differ in response to these variables because fish growth and otolith growth tend to be related. In accord with these assumptions, otolith shape has been found to vary in response to environmental conditions and is also highly correlated with fish growth (Campana and Casselman, 1993). Similarly, the results of our study showed significant correlations between fish and otolith growth for all the otolith morphometric characteristics measured. Therefore, it is likely that the differences found between silver hake stocks in growth rates (Helser, 1996; our study), external morphometrics (Conover et al., 1961; Almeida, 1987), and internal morphometrics (our study) are to some extent reflective of localized environmental conditions.

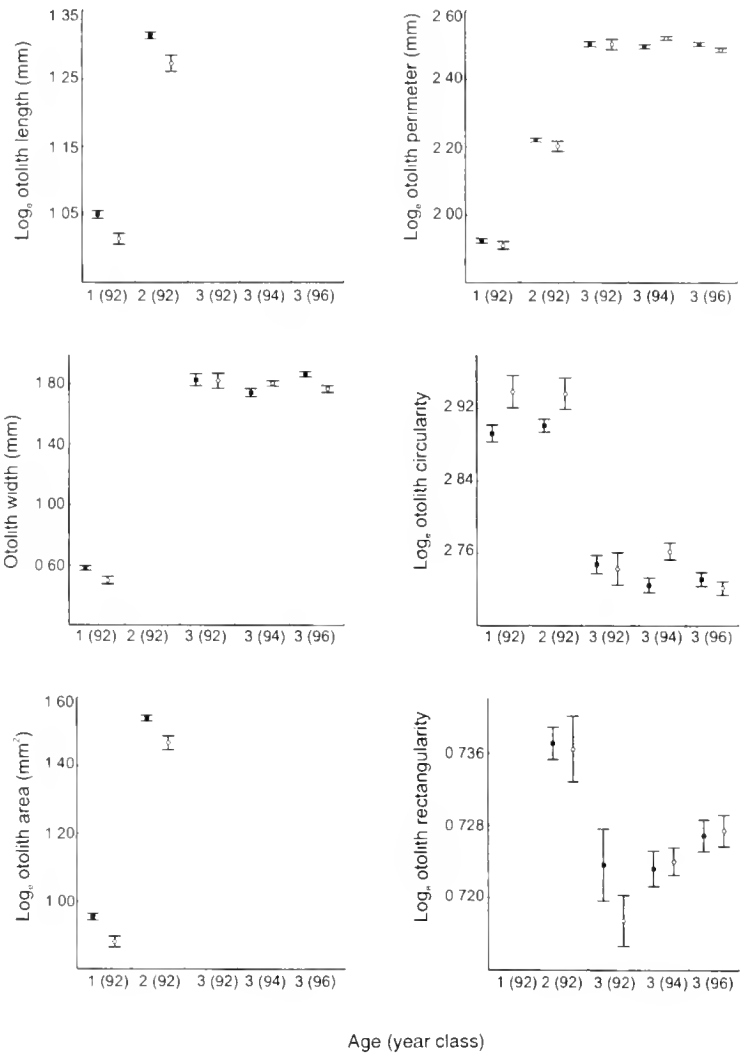

Figure 4

Otolith morphometrics (mean ±standard error) for 1-, 2-, and 3-year-old silver hake samples pooled across sexes for individual year classes showing differences between those fish from the northern (squares) and southern (circles) regions.

Assuming that environmental variables can effect otolith growth, we analyzed bottom ocean temperature between the two stock regions across the life history range of our samples to investigate whether the differences in otolith morphometrics found in this study were due to a weather phenomenon during any given sampling year (Fig. 2). Temperature was found to differ consistently on a seasonal basis during all years, as would be assumed, and there was no marked change in temperature between any given years, within any given season. As a result, the possibility of a severe temperature shift that could influence otolith morphometrics and make this method unsuitable for stock discrimination was not apparent in our study. However, because temperature was shown to differ between the proposed stock regions and because silver hake distribute themselves in response to temperature (Almeida, 1987; Helser, 1996), it can be assumed that this variable could effect otolith growth.

Alternatively, growth and otolith morphometric differences found between silver hake stocks could also be apparent, regardless of environmental variation, and reflect a genetic influence. This could be a valid assumption given

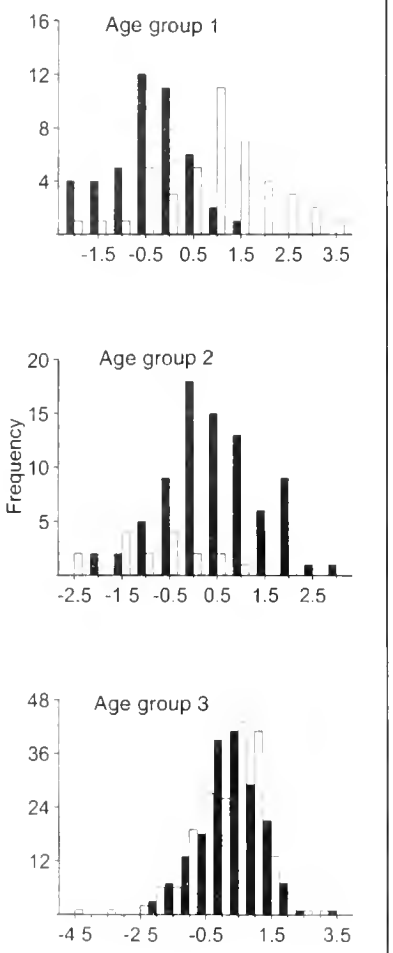

Figure 5

Discrimination of silver hake samples from the northern (solid bars) and southern regions (open bars) based on frequency of canonical variate scores (CV I) for 1-, 2-, and 3-year-old fish.

that a certain degree of reproductive isolation has been confirmed in spawning and postspawning silver hake (Almeida, 1987). Such isolation could restrict gene flow to a level that effectively isolates population units (Iles and Sinclair, 1982). However, some degree of intermixture probably occurs owing to the wide migratory patterns of silver hake (Almeida, 1987). Therefore, further investigations are required to interpret the degree to which morphological differences between silver hake stocks are caused by environmental or genetic influences, but as long as these differences persist between stocks, the use of otolith morphometrics remains a viable tool for stock discrimination.

Otolith morphometrics in combination with an image analysis system has been found to be a relatively inexpensive, objective, and efficient tool by which to distinguish fish stocks (Messieh et al., 1989; Jearld, 1995). Rapid and precise measurements can be obtained in less time with this technique, compared with alternative manual-based procedures, because all the measurements are automatically determined from an outline of the otolith perimeter traced with an edge-detection algorithm (OPTIMAS, 1996). In addition otolith morphometric data can easily be obtained because

Table 5

Length-corrected otolith morphometric variables responsible for the discrimination of 1-, 2-, and 3-year old silver hake samples determined by the standardized within-group variances of the canonical variates (CV I).

Otolith morphometric variable	Canonical variate 1		
	Age group 1	Age group 2	Age group 3
Length	−1.01	0.57	—
Width	0.04	—	0.62
Area	0.10	0.38	—
Perimeter	—	—	−0.32
Circularity	0.82	−0.66	−0.59
Rectangularity	—	−0.16	0.09

Table 6

Jack-knifed classification matrix of the frequency of assigned cases in each region (pooled sexes and year classes) used to differentiate samples.

	Classification of individual silver hake								
	Age group 1			Age group 2			Age group 3		
	Correct %	North	South	Correct %	North	South	Correct %	North	South
North	80	36	9	70	57	24	54	98	82
South	70	43	31	65	6	11	43	109	83
Total	75	49	40	69	63	35	49	207	165

otoliths are routinely collected by most fisheries agencies to determine the age of their respective principal fish species for assessment and management purposes. However, one drawback in using otolith morphometrics for stock discrimination is that otoliths frequently are broken or lost during routine collection and processing, effectively limiting the number of samples available for analysis.

In these types of studies, it is also essential to consider any confounding variation that may be present owing to differences between samples in age group, year class, or sex, so as to not mistake stock differences for sample differences. Failure to account for such extraneous influences may result in falsely attributing morphological differences between separate stocks to a "stock effect," whereas the differences may in fact simply be reflecting variation between samples in age structure, sex ratio, or sampling year (Castonguay et al., 1991). Significant variation in otolith morphometrics of silver hake observed in our study between different age groups, year classes, and to a lesser extent sex, emphasized the need to examine these factors before evaluating the stock status of the species with this technique. Likewise, significant differences in these effects have been detected in other morphometric-based stock identification studies for marine fish species, such as Atlantic salmon (L'Abée-Lund, 1988), Atlantic mackerel (Castonguay et al., 1991), and Atlantic cod, *Gadus morhua* (Campana and Casselman, 1993). Thus, although it is clearly necessary to correct for these confounding variables, which can influence any stock identification procedure, they do not limit the use of otolith morphometrics for stock discrimination provided they are examined and accounted for before making any conclusions about the stock structure of a species. Indeed, calculating linear discriminant functions of otolith morphometric characteristics for 1-year-old silver hake on a yearly basis, differentiated by sex, should provide a level of discrimination not yet seen for silver hake stocks in U.S. waters of the northwest Atlantic and may assist in estimating levels of stock mixing (an objective yet to be realized for silver hake or for most of our commercially exploited fish stocks).

There was clearly a need for a more advanced and efficient method in distinguishing between silver hake stocks or in determining mixing levels between stocks. Assessment and management of silver hake stocks are currently based on stock structure results from the late 1970s and early 1980s, on discriminant analysis of external morphometric characters, coupled with a qualitative analysis of research survey and commercial catch data (Almeida, 1987). Since that time, the status of silver hake has certainly changed—spawning stock biomass and recruitment levels have declined (Helser and Brodziak, 1998)—and stock discrimination technologies through image processing have certainly improved (Cadrin and Friedland, 1999). We suggest that the use of whole otolith morphometrics in the analysis of silver hake stocks will give fishery scientists and managers greater logistical benefits (in terms of time and expense), not to mention greater discrimination success, than the stock discrimination methods used previously.

Our study indicated that successful identification of silver hake stocks can be achieved by using whole otolith morphometrics in combination with image processing and discriminant function analysis. We are confident that this is a relatively inexpensive, objective method which can facilitate routine discrimination of silver hake stocks, as well as other marine fish species, by efficiently obtaining accurate measurements to produce valid, repeatable results. This method may prove to be particularly useful for rapid (in-season) assessments for determining levels of stock mixing that are often a requirement of contemporary management plans. Discrimination between stocks is important for fisheries stock-rebuilding strategies, such as those for silver hake, because genetic and stock biodiversity of the species needs to be maintained to ensure all divisions of a stock contribute to the replenishment of the resource.

Acknowledgments

We thank Fred Nichy for his support and guidance; John Boreman, Frank Almeida, Kathy Lang, and two anonymous reviewers for reviews of this manuscript; Nina Shepherd for aging silver hake; Jay Burnett for his helpful suggestions; Donald Hoagland and Jim Phillips for their support during the initial phase of the study; and the staff of the Fishery Biology Program for their assistance with the image analysis. This work was performed while G. A. Begg held a National Research Council (NOAA/NMFS/NEFSC) Research Associateship.

Literature cited

Almeida, F. P.
1978. Determination of the Von Bertalanffy growth equation for the southern New England-Middle Atlantic, Georges Bank, and Gulf of Maine stocks of silver hake. Woods Hole Lab. Ref. Doc. 78-13, Northeast Fisheries Science Center, Natl. Mar. Fish. Serv., NOAA, 15 p.
1987. Stock definition of silver hake in the New England Middle Atlantic area. N. Am. J. Fish. Manage. 7:169–186.

Anderson, E. D.
1974. Comments on the delineation of red and silver hake stocks in the ICNAF Subarea 5 and Statistical Area 6. Int. Comm. NW Atl. Fish. Res. Doc. 74/100, 8 p.

Anonymous.
1998. Status of the fishery resources off the Northeastern United States for 1998. U.S. Dep. Commer., NOAA Tech. Memo. NMFS-NE-115, 149 p.

Begg, G. A., K. D. Friedland, and J. B. Pearce.
1999. Stock identification and its role in stock assessment and fisheries management—an overview. Fish. Res. 43:1–8.

Begg, G. A., and J. R. Waldman.
1999. An holistic approach to fish stock identification. Fish. Res. 43:35–44.

Bigelow, H. B., and W. C. Schroeder.
1953. Fishes of the Gulf of Maine. U.S. Fish and Wildl. Serv. Bull. 74, vol. 53, 577 p.

Booke, H. E.
1981. The conundrum of the stock concept—are nature and nurture definable in fishery science? Can. J. Fish. Aquat. Sci. 38:1479–1480.

Bowman, R. E., and W. L. Michaels.
1984. Food of seventeen species of northwest Atlantic fish. U.S. Dep. Commer., NOAA Tech. Memo. F/NEC-28, 196 p.

Brooks, D. A.
1996. Physical oceanography of the shelf and slope seas from Cape Hatteras to Georges Bank: a brief overview. *In* The northeast shelf ecosystem: assessment, sustainability, and management (K. Sherman, N. A. Jaworski, and T. J. Smayda, eds.), p. 47–74. Blackwell Science, Inc., Cambridge.

Cadrin, S. X., and K. D. Friedland.
1999. The utility of image processing techniques for morphometric analysis and stock identification. Fish. Res. 43:129–139.

Campana, S. E., and J. M. Casselman.
1993. Stock discrimination using otolith shape analysis. Can. J. Fish. Aquat. Sci. 50:1062–1083.

Castonguay, M., P. Simard, and P. Gagnon.
1991. Usefulness of Fourier analysis of otolith shape for Atlantic mackerel (*Scomber scombrus*) stock discrimination. Can. J. Fish. Aquat. Sci. 48:296–302.

Conover, J. T., R. L. Fritz,, and M. Viera.
1961. A morphometric study of silver hake. U.S. Fish Wildl. Serv., Spec. Sci. Report, Fisheries 368.

Cushing, D. H.
1968. Fisheries biology, a study in population dynamics. Univ. Wisconsin Press, Madison, WI, 200 p.

Dawson, W. A.
1991. Otolith measurement as a method of identifying factors affecting first-year growth and stock separation of mackerel (*Scomber scombrus* L.). J. Cons. Int. Explor. Mer 47:303–317.

Dery, L. M.
1988. Silver hake, *Merluccius bilinearis*. *In* Age determination methods for northwest Atlantic species (J. Pentilla and L. M. Dery, eds.), p. 41–47. U.S. Dep. Commer., NOAA Tech. Rep. NMFS 72.

Edwards, R. L., and R. E. Bowman.
1979. Food consumed by continental shelf fishes. *In* Predator-prey systems in fish communities and their role in fisheries management (H. Clepper, ed.), p. 387–407. Sports Fishing Institute, Washington, D.C.

Fowler, A. J., and D. A. Short.
1996. Temporal variation in the early life-history characteristics of the king george whiting (*Sillaginodes punctata*) from analysis of otolith microstructure. Mar. Freshwater Res. 47:809–818.

Freidland, K. D., and D. G. Reddin.
1994. Use of otolith morphology in stock discriminations of Atlantic salmon (*Salmo salar*). Can. J. Fish. Aquat. Sci. 51:91–98.

Grimes, C. B., A. G. Johnson, and W. A. Fable Jr.
1987. Delineation of king mackerel (*Scomberomorus cavalla*) stocks along the U.S. east coast and in the Gulf of Mexico. *In* Proceedings of the stock identification workshop November 5–7, 1985 Panama City Beach, Florida (H. E. Kumpf, R. N. Vaught, C. B. Grimes, A. G. Johnson, and E. L. Nakamura, eds.), p. 186–187. U.S. Dep. Commer., NOAA Tech. Memo. NMFS-SEFC-199.

Helser, T. E.
1996. Growth of silver hake within the U.S. continental shelf ecosystem of the northwest Atlantic Ocean. J. Fish. Biol. 48:1059–1073.

Helser, T. E., F. P. Almeida, and D. E. Waldron.
1995. Biology and fisheries of north-west Atlantic hake (silver hake: *M. bilinearis*). *In* Hake: biology, fisheries and markets (J. Alheit, and T. J. Pitcher, eds.), p. 203–237. Chapman and Hall, London.

Helser, T. E., and J. K. T. Brodziak.
1998. Impacts of density dependent growth and maturation on assessment advice to rebuild depleted U.S. silver hake (*Merluccius bilinearis*) stocks. Can. J. Fish. Aquat. Sci. 55:882–892.

Ihssen, P. E., H. E. Booke, J. M. Casselman, J. M. McGlade, N. R. Payne, and F. M. Utter.
1981. Stock identification: materials and methods. Can. J. Fish. Aquat. Sci. 38:1838–1855.

Iles, T. D., and M. Sinclair.
1982. Atlantic herring: stock discreteness and abundance. Science (Wash. D.C.) 215:627–633.

Jearld, A. Jr.
1995. Clinic overview. Image analysis systems. *In* Recent developments in fish otolith research (D. H. Secor, J. M. Dean and S. E. Campana, eds.), p. 655–670. Univ. South Carolina Press, Columbia, SC.

Konstantinov, K. G., and A. S. Noskov.
1969. U.S.S.R research report, 1968. ICNAF (International Commission for the Northwest Atlantic Fisheries) Redbook II:99–117.

L'Abée-Lund, J. H.
1988. Otolith shape discriminates between juvenile Atlantic salmon, *Salmo salar* L., and brown trout, *Salmo trutta* L. J. Fish Biol. 33:899–903.

Messieh, S. N., C. MacDougall, and R. Taylor.
1989. Separation of Atlantic herring (*Clupea harengus*) stocks in the southern Gulf of St. Lawrence using digitized otolith morphometrics and discriminant function analysis. Can. Tech. Rep. Fish. Aquat. Sci. 1647:iv + 22 p.

Nichy, F. E.
1969. Growth patterns on otoliths from young silver hake, *Merluccius bilinearis* (Mitchell). Int. Comm. NW Atl. Fish. Res. Bull. 6:107–117.

OPTIMAS. 6.
1996. User guide and technical reference, 8th ed., vol. I: xiii + 474 p. vol. II: viii + 630 p. Media Cybernetics, Silver Spring, MD.

Pawson, M. G., and S. Jennings.
1996. A critique of methods for stock identification in marine capture fishes. Fish. Res. 25:203–217.

Pentilla, J. A., G. A. Nelsen, and J. M. Burnett.
1989. Guidelines for estimating lengths at age for 18 northwest Atlantic finfish and shellfish species. U.S. Dep. Commer., NOAA Tech. Memo. NMFS-F/NEC-66, 30 p.

Reznick, D., E. Lindbeck, and H. Bryga.
1989. Slower growth results in larger otoliths: an experimental test with guppies (*Poecilia reticulata*). Can. J. Fish. Aquat. Sci. 46:108–112.

Schenk, R.
1981. Population identification of silver hake (*Merluccius bilinearis*) using isoelectric focusing. Woods Hole Lab. Ref. Doc. 81-44, Northeast Fisheries Science Center, NOAA, 31 p.

Stephenson, R. L.
1999. Stock complexity in fisheries management: a perspective of emerging issues related to population sub-units. Fish. Res. 43:247–249.

SYSTAT.
1997. SYSTAT 7.0 statistics. SPSS Inc., Chicago, IL., 751 p.

Templeman, W., and H. J. Squires.
1956. Relationship of otolith lengths and weights in the haddock *Melanogrammus aeglefinus* (L.) to the rate of growth of the fish. J. Fish. Res. Board Can. 13:467–487.

Abstract.—The influences on catches and bycatches due to 1) an increase in size of mesh and 2) a reduction in twine diameter in the body of prawn trawls were investigated in Gulf St. Vincent, Australia. Compared with a conventional trawl body (mesh size 45 mm) attached to a composite square-mesh codend, two new trawl bodies, made with 53-mm mesh but with different twine diameters (1 and 1.7 mm, respectively) and each attached to identical composite square-mesh codends, were equally effective in significantly reducing the numbers of a range of small fish (by between 23.7% and 67%) and in not significantly reducing the weight of targeted prawns. Because there were no significant differences in the selectivity parameters of both new trawl bodies, these results indicated that the main cause of bycatch reduction was the increase in size of mesh in the body of the trawl. The escape of large numbers of unwanted small fish and prawns is discussed in terms of their probable behavior in the body of the trawl and the extent to which this behavior was influenced by the operational characteristics of the gear.

Manuscript accepted 1 December 1999.
Fish. Bull. 98:463–473 (2000).

Effects of twine diameter and mesh size in the body of prawn trawls on bycatch in Gulf St. Vincent, Australia

Matt K. Broadhurst

Departamento de Pesca, Laboratório de Oceanografia Pesqueira
Universidade Federal Rural de Pernambuco-UFRPE
Av. Dom Manuel de Medeiros, s/n
Dois Irmãos, Recife-PE, Brasil, CEP: 52.171-900
E-mail address: fhvhazin@truenet.com.br

Paul E. McShane

South Australian Aquatic Sciences Centre
P.O. Box 120
Henley Beach, South Australia 5022, Australia

Roger B. Larsen

University of Tromsø
Breivika N-9037
Tromsø, Norway

In many of the world's prawn-trawl fisheries, large numbers of organisms are captured incidentally with the targeted catch (collectively termed "bycatch" *sensu* Saila, 1983). This bycatch comprises a diverse assemblage of small fish, cephalopods, and crustaceans, including prawns that are smaller than optimum size (for reviews see Saila, 1983; Andrew and Pepperell, 1992; Alverson et al., 1994). Concerns over the negative effects that the mortality of these fish and small organisms may cause on the yield of stocks has led to the application of various management strategies designed to minimize bycatch (Andrew and Pepperell, 1992). The most common approach has been to change the conventional trawls to improve overall selectivity of the gear. Depending on the sizes and species to be targeted and excluded, these changes have involved the sizes and types of mesh used, and the application of physical modifications, collectively termed bycatch reducing devices (BRDs) (see Broadhurst, 2000, for review).

Inherent variations among the characteristics of different prawn-trawl fisheries have resulted in a range of modifications to conventional trawls. Regardless of design, however, the majority of functional modifications have been applied within or immediately anterior to the codend (e.g. Isaksen et al., 1992; Thorsteinsson, 1992; Broadhurst and Kennelly, 1997; Rogers et al., 1997) mainly because observations suggest that most of the selection process for many species occurs in this area (Armstrong et al., 1990; MacLennan, 1992; Wileman et al., 1996). Moreover, because codends often are similar among the different trawl designs within a particular fishery (e.g. Broadhurst and Kennelly, 1997), any modifications to improve selectivity are more easily implemented, adopted, and regulated throughout the fishery.

Although alterations to codends have been successful in reducing various subsets of bycatch, there is evidence suggesting that individuals of some species, particularly those of prawns, escape from the bodies of prawn trawls (High et al., 1969; Sumpton et al., 1989; Vendeville, 1990). For example, High et al. (1969) attached various covers to the upper, lateral, and posterior bodies of trawls to isolate areas that could be modified to passively separate fish from prawns (*Pandalus* sp.). Although there was little evidence of fish escaping, large numbers of small prawns were retained in the covers, particularly in the posterior sections. Similarly, in one

of the few studies on the effects of changes in the types of twine used in the body of trawls on catches, Sumpton et al. (1989) showed that compared with multifilament twine (1.1 mm diameter), significantly more smaller-size prawns (*Penaeus* spp.) and squid (*Loligo* spp.) escaped through the bodies of trawls made from monofilament twine (0.9 mm diameter).

Despite these results and although nearly all prawn-trawl fisheries are regulated by means of legally defined minimum mesh sizes (typically ranging from 40 to 50 mm stretched mesh, Vendeville, 1990), there is a paucity of information on the effects of different sizes of mesh used in the bodies of trawls on selectivity. This is particularly the case in Australian prawn-trawl fisheries, where despite extensive research to develop BRDs (see Broadhurst, 2000), no published studies have quantified the effects of different sizes of mesh. In a recent experiment in Gulf St. Vincent, South Australia (Broadhurst et al., 1999), we provided evidence to suggest, however, that the minimum size mesh (45 mm) throughout the trawls was too small. As a first step in addressing this issue, we investigated modifications to the codends and demonstrated that new designs comprising composite panels of different-size square-shape mesh (52 and 80 mm mesh hung on the bar) were effective in significantly reducing bycatches of undersize western king prawns (*Penaeus latisulcatus*) and small fish without reducing the weight of the commercial catch.

These results, combined with the simplicity of the new codend, led to the immediate and unanimous adoption of a design, based on those tested, by Gulf St. Vincent prawn trawlers. Encouraged by the performance of simple changes in mesh type and size to improve selectivity, commercial fishermen sought assistance to examine other refinements to their trawls. Given evidence to suggest that the mesh size used in Gulf St. Vincent was inappropriate and that selection for some species may occur in the body of prawn trawls, our aims in the present study were to quantify the influences on selection in this area due to 1) increasing the mesh size (from approx. 45 mm to 53 mm) and 2) reducing the diameter of twine used.

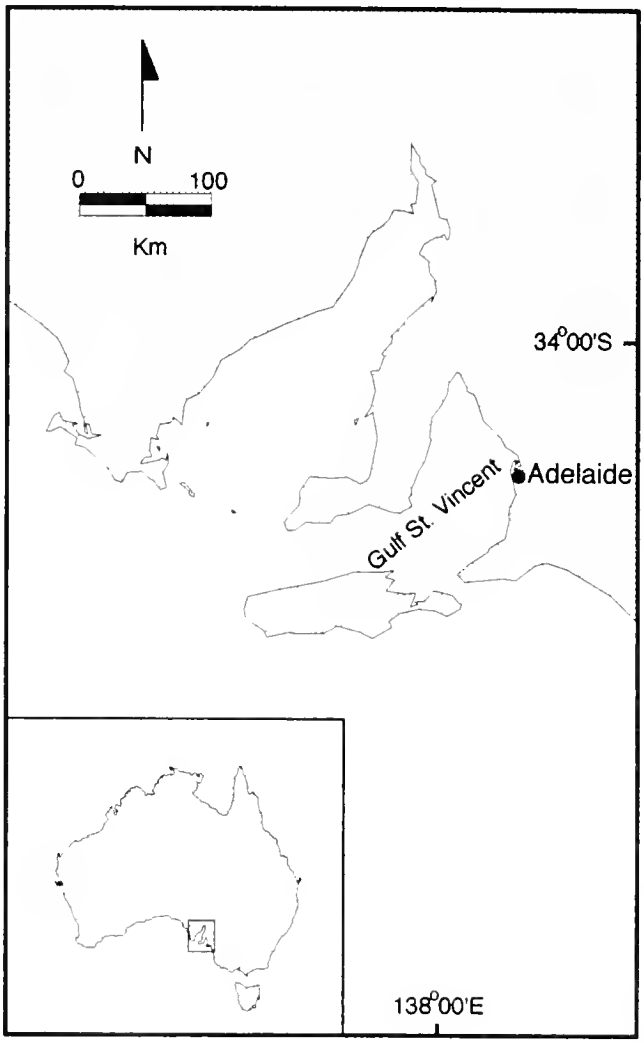

Figure 1
Location of study at Gulf St. Vincent, South Australia.

Materials and methods

Our work was done in Gulf St. Vincent, South Australia (Fig. 1), in October, 1998, with a chartered commercial prawn trawler rigged to tow three trawls in a standard triple gear configuration (see Andrew et al., 1991, for details). Three different trawl bodies were examined. The first (termed the "control") represented conventional trawl bodies (see Broadhurst et al., 1999, for specifications) and was constructed of 1.7-mm-diameter, 24-strand, polyethylene twisted twine with a mean mesh size (stretched distance between the knots) of 44.42 mm (see "Results" section). The second and third trawl bodies (termed "spectra-1-mm" and "momoi-1.7-mm") were identical in design, in headrope and footrope length, in rigging and tapers to the control trawl body but were made from 1-mm-diameter, polyethylene cabled twine (brand name "spectra") and 1.7-mm-diameter, 30-ply, polyethylene twisted twine (brand name "momoi"), respectively, with mean mesh sizes of 52.43 and 52.96 mm, respectively (see "Results" section).

All three trawl bodies were attached to identical composite square-mesh codends (Broadhurst et al., 1999) consisting of two sections, each measuring 80 bars in circumference, 70 bars in length, and constructed of 52-mm mesh (3-mm-diameter, braided polyethylene twine) cut on the bar (Fig. 2, A–C). Each square-mesh section consisted of an upper and lower panel sewn together so that the direction of the knots on the upper panel were opposite those on the lower panel (Fig. 2A). A panel of 104-mm netting, measuring 6 bars × 10 bars, was inserted into the tops of the posterior sections of each square-mesh codend, starting at the leading edge and ending about 1.3 m anterior to the last row of meshes (Fig. 2, A and B). Lengths of 12-mm-diameter, polyethylene 3-strand rope (termed "last-ridge ropes") were firmly laced at a hanging ratio of 0.9 to each of the two lateral seams of the codends (to provide length-wise strength) (Fig. 2B).

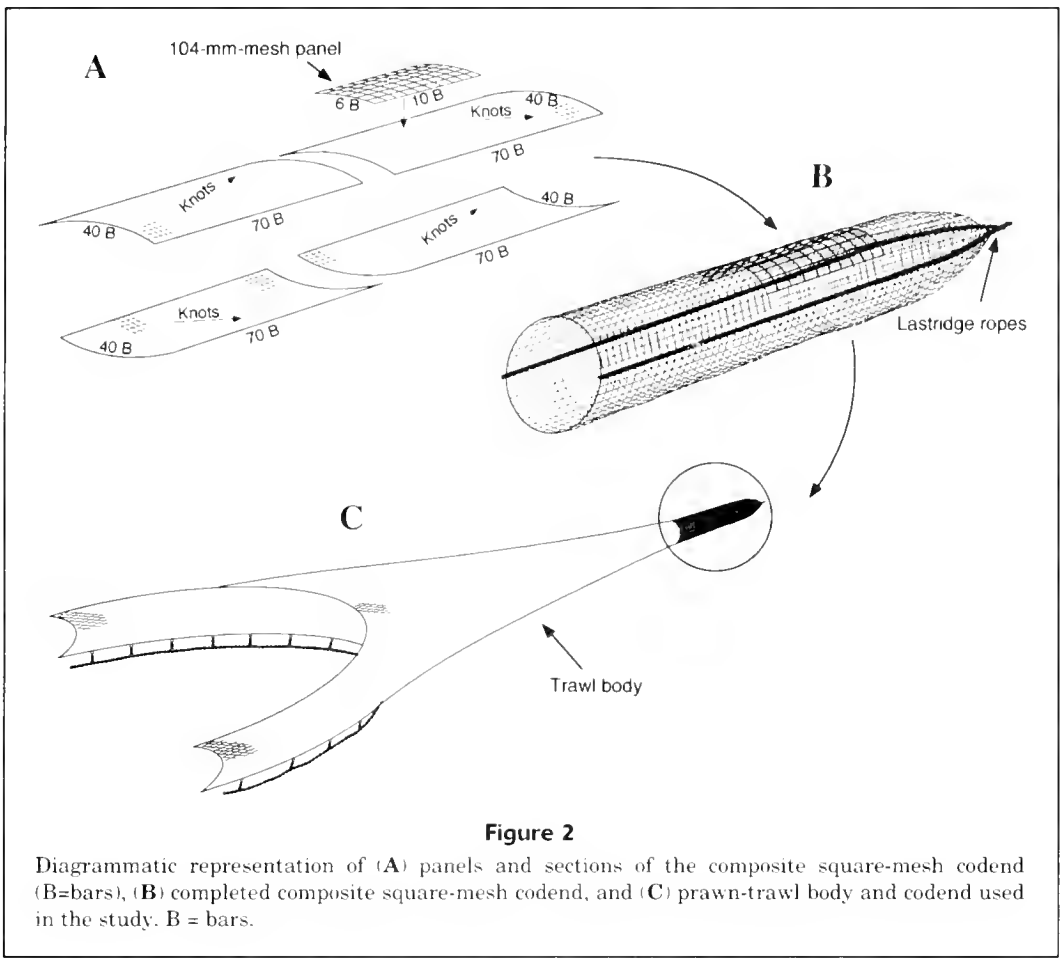

Figure 2

Diagrammatic representation of (**A**) panels and sections of the composite square-mesh codend (B=bars), (**B**) completed composite square-mesh codend, and (**C**) prawn-trawl body and codend used in the study. B = bars.

Experimental procedure

Before starting the experiment, all trawls were towed for a short period to allow knots and bindings to stretch. To obtain accurate information on mesh sizes, a set of dial calipers was used to measure 30 randomly located meshes (stretched length in mm, between the inside knots) at four separate locations (starboard wing, footrope, headrope, and posterior body) in each trawl body.

The spectra-1-mm and momoi-1.7-mm trawls were compared separately against the control trawl. In each paired comparison, the trawls were shackled to the outside sweeps of the sleds and otterboards of the triple rigged gear and towed simultaneously. A conventional trawl body was used as the center net in all comparisons, but because it was not rigged in exactly the same manner as the outside nets, its catch was excluded from analysis. The triple gear was towed in normal commercial tows of 25-min duration at 3 knots (1.5 m/s) over a combination of sandy and light coral bottoms. Each of the outside trawls were randomly assigned after each tow (to eliminate any potential biases), so that three paired comparisons of each new trawl against the control trawl were made on each night (i.e. a total of six tows per night). Over five nights, we completed a total of 15 replicate comparisons of each configuration.

After each tow, the catches from the two outside trawls were emptied onto a partitioned tray. Data collected from each tow were the following: the total weight of western king prawns and a subsample (100 prawns from each trawl) of their carapace lengths (to the nearest 1 mm); the total number of prawns (estimated from the weight of the subsample); the total weight of discarded bycatch and discarded noncommercial bycatch; the weights and numbers of commercially or recreationally (or both) important bycatch species; and the sizes (to the nearest 0.5 cm) of commercially or recreationally (or both) important fish. A random sample of prawns (approximately 12 kg) from each trawl in each tow was separated and sent to A. Raptis & Sons PTY LTD (seafood processing plant) in Adelaide for grading into "commercial categories" (based on a system of numbers per pound) with a locally built "dynamic grading machine."

Several commercially important species were caught in sufficient quantities to enable meaningful comparisons. These were western king prawns (*Penaeus latisulcatus*), blue swimmer crabs (*Portunus pelagicus*), sand trevally (*Pseudocaranx wrighti*), red mullet (*Upeneichthys porosus*), leatherjacket (*Thamnaconus degeni*), southern sand flathead (*Platycephalus bassensis*), small-toothed flounder (*Pseudorhombus jenynsii*), and southern calamari (*Sepioteuthis australis*). With the exception of western king prawns

and southern calamari (which fishermen are legally permitted to retain), all remaining species comprised those that are considered commercially important bycatch (e.g. to other fisheries) and that are normally discarded.

Analysis of mesh sizes

The mesh-size measurements collected from the trawl bodies were analyzed for heteroscedasticity with Cochran's test and a two-factor, balanced analysis of variance (ANOVA) with trawl body and location of meshes considered fixed and random factors, respectively. Significant differences detected in these analyses were investigated by Tukey's multiple comparisons of means test.

Analysis of catch data

Catch data for all replicates that had sufficient numbers of each variable (i.e. 1 individual in at least 10 replicates) were analyzed with paired t-tests ($P \leq 0.05$). Except for the weights and numbers of blue swimmer crabs and small-toothed flounder (species that could not pass through the meshes in any of the trawls), all variables were analyzed with one-tailed tests to test the hypothesis that the larger-mesh trawl bodies retained fewer individuals than the control. Catches of blue swimmer crabs and small-toothed flounder were compared with two-tailed tests. To examine the relative effectiveness of the spectra-1-mm and momoi-1.7-mm trawl bodies, differences in catches (between each trawl and their respective controls) for those variables that had data in all tows were analyzed by using Cochran's test for homogeneity of variances and a balanced, two-factor ANOVA. In these analyses, trawl-type and nights were considered fixed and random factors, respectively. Where there were sufficient data ($n>25$ in each trawl, pooled across all tows), size frequencies of commercially or recreationally important fish (or both) were plotted and compared with two-sample Kolmogorov-Smirnov tests ($P=0.05$).

Analysis of prawn sizes

Size-frequencies of prawns retained in each of the three trawls were combined across all tows. Using an estimated split model (Millar and Walsh, 1992), we fitted logistic curves to these data by maximum likelihood method (Pope et al., 1975). Logistic curve parameters, associated standard errors and 95% confidence limits were calculated for each large-mesh trawl body. Model deviance values were determined for a goodness-of-fit hypothesis (i.e. to test H_0: that the curves were logistic). Size categories of commercially graded prawns from each trawl were plotted and analyzed with two-sample Kolmogorov-Smirnov tests ($P=0.05$).

Results

Analysis of mesh sizes

There were significant differences detected in size of mesh between the three trawl bodies (Table 1). Tukey's comparison of means test showed no significant differences between the spectra-1-mm and momoi-1.7-mm trawl bodies (mean mesh sizes ±SE of 52.43 ±0.08 mm and 52.96 ±0.09 mm, respectively). The mean size of mesh in the control trawl was significantly less at 44.42 ±0.13 mm. Mesh size was not significantly different among the various locations (e.g. wing, footrope, head rope, and posterior body) examined in any of the trawl bodies.

Table 1

Summaries of F ratios from two-factor analysis of variance to determine differences in size of mesh in the trawls and at various locations and results of Tukey's comparison of means test for the significant difference detected in size of mesh between trawls (spectra-1-mm=momoi-1.7-mm>control). Data were treated in the raw form. ** = $P<0.01$.

Treatment	df	Mesh size (mm)
Trawls (T)	2	2494.7**
Location of mesh in trawl (L)	3	0.85
$T \times L$	6	1.4
Residual	346	

Analysis of catch data

Compared with the control, the spectra-1-mm and momoi-1.7-mm trawl bodies significantly reduced the numbers of western king prawns caught (means reduced by 13.7% and 15.6%, respectively), without significantly reducing the weights of prawns (although mean catch from the spectra-1-mm was 6.3% lower than that from the control) (Table 2; Fig. 3, A and B). The spectra-1-mm and momoi-1.7-mm trawl bodies also significantly reduced the weights of total discarded bycatch (by 29.3% and 20.3%); numbers of leatherjacket (by 32.5% and 23.7%) and their weights (by 24.2% and 19.6%); numbers of sand trevally (by 56.2% and 40.4%) and their weights (by 52.8% and 40.4%); and the numbers of southern sand flathead (by 59.8% and 40.2%) and red mullet (by 67.2% and 59.3%) (Fig. 3, C, E, F, G, and I; Table 2). The spectra-1-mm trawl body also significantly reduced the weights of southern sand flathead (by 31.8%), red mullet (by 57%), and the numbers of southern calamari (by 33.6%) (Fig. 3, H, J, and L; Table 2). ANOVA of the differences in catches between the new trawl bodies and their controls showed no significant interactions nor main effects for any of the variables examined (Table 3).

Two-sample Kolmogorov-Smirnov tests for comparing the size-frequency distributions of fish measured from the control and new trawl bodies detected significant differences in the relative size compositions of southern sand flathead retained by both new trawl bodies and in the relative size compositions of sand trevally retained by the momoi-1.7-mm trawl body (the new trawl bodies retained proportionally fewer small-size fish) (Fig. 4, A and B). There were no other significant differences detected.

Table 2

Summaries of paired *t*-tests in which the control and the new trawl bodies were compared. Weights and numbers of blue swimmer crabs and small-toothed flounder were analyzed with two-tailed paired *t*-tests whereas the remaining variables were analyzed with one-tailed paired *t*-tests. pt-v = paired *t*-value; *n* = number of replicates; disc = discarded; n-comm = noncommercial. * = $P<0.05$; ** = $P<0.01$.

	Spectra-1-mm versus control			Momoi-1.7-mm versus control		
	pt-v	*P*	*n*	pt-v	*P*	*n*
No. of prawns	−2.368	0.016*	15	−2.389	0.016*	15
Wt. of prawns	−1.755	0.051	15	−0.044	0.483	15
Wt. of total disc bycatch	−4.127	0.0005**	15	−2.662	0.009**	15
Wt. of disc n–comm bycatch	−1.709	0.055	15	−1.38	0.095	15
No. of leatherjacket	−3.627	0.001**	15	−2.447	0.014*	15
Wt. of leatherjacket	−4.542	0.0002**	15	−2.181	0.023*	15
No. of sand trevally	−1.987	0.033*	15	−2.491	0.013*	15
Wt. of sand trevally	−1.960	0.035*	15	−2.253	0.020*	15
No. of southern sand flathead	−3.516	0.002**	14	−2.939	0.006**	14
Wt. of southern sand flathead	−2.994	0.005**	14	0.445	0.668	14
No. of red mullet	−3.116	0.004**	15	−2.610	0.013*	11
Wt. of red mullet	−2.157	0.024*	15	−0.882	0.199	11
No. blue swimmer crab	1.505	0.156	14	0.725	0.482	13
Wt. of blue swimmer crab	1.524	0.152	14	1.462	0.169	13
No. of small–toothed flounder	−0.395	0.699	13	−1.977	0.068	15
Wt. of small–toothed flounder	−0.082	0.936	13	−0.150	0.883	15
No. of southern calamari	−2.210	0.022*	15	−0.846	0.206	15
Wt. of southern calamari	0.026	0.510	15	−0.837	0.208	15

Table 3

Summaries of *F* ratios from two-factor analyses of variance to determine effects on variables due to fishing with different trawl bodies on different nights. The transforms used to stabilize the variances where required are listed. N-comm = noncommercial, disc = discarded.

				Bycatch (wt. in g)							
		Prawns		Total	N-comm	Leatherjacket		Trevally		Southern calamari	
Treatment	df	no. $1/(x+1)$	wt.	disc	disc	no. $\ln(x+1000)$	wt.	no.	wt.	no.	wt.
Trawl bodies (*T*)	1	0.01	3.97	0.64	0.44	0.64	0.64	1.36	1.36	1.15	1.31
Nights (*N*)	4	1.50	1.79	0.40	0.41	0.40	0.42	0.72	0.72	1.47	0.18
$T \times N$	4	1.00	0.48	0.86	1.27	0.86	0.23	0.73	0.29	2.20	0.36
Residual	19										

Analysis of prawn sizes

The logistic length selection curves derived for each of the new trawl bodies are provided in Figure 5. Model deviance indicated sufficient goodness of fit for both curves (Table 4). The 95% confidence limits of the selectivity parameters showed that there were no statistically significant differences between the two new trawl bodies (Table 4).

Significant differences were detected in Kolmogorov-Smirnov tests on the commercial-size categories of prawns

graded from the control and new trawl bodies (Fig. 6). Both trawls with the larger meshed bodies retained proportionally fewer smaller prawns.

Discussion

The results from this study showed that both new trawl bodies were effective in excluding under-size prawns and large numbers of small fish (by up to almost 60%) and in not reducing the weight of targeted prawns. These results provide evidence to suggest that simple changes to the body of prawn trawls can have a contributing effect on overall trawl selectivity. The escape of large numbers of small fish and prawns from this area may be due to their behavior in the trawl and the extent to which they were influenced by the operational characteristics of the gear.

It is well established that fish exhibit specific responses to stimuli from trawls and attempt to avoid contact with the trawl body by maintaining position at the opening (Wardle, 1983; Watson, 1989). After some period, depending on species- and size-specific swimming abilities (Wardle, 1975), fish invariably tire and turn towards the codend, allowing the trawl to pass around them (Watson, 1989) or alternatively, maintain swimming in the direction of the tow, but gradually fall back along the taper of the body panel towards the codend opening (Wardle, 1983). As the taper of the trawl body narrows and the density of fish increases, some fish may rise in the trawl and attempt escape through the meshes or pass into the codend and resume swimming immediately anterior to the catch (Wardle, 1983). In contrast, benthic invertebrates like prawns tend to display limited responses during capture. SCUBA observations by Watson (1976) showed that after contact with the leading edge of the trawl, penaeid prawns contracted their abdomens ventrally, propelling themselves backwards. This initial response was repeated three to five times but because prawns are not capable of maintaining such activity, the speed of the trawl through the water quickly forced them against the meshes of the trawl body and they eventually tumbled down the net into the codend.

In view of these behavioral patterns, gear-related factors, such as the fast towing speed (1.5 m/s) and taper of the trawl body in our study, may have increased the probability of small fish and prawns being selected in this area. For example, the sizes of most of the fish encountered, and particularly sand trevally, leatherjackets, and small southern sand flathead (5–15 cm, [Fig. 4]), means that they would have been unable to maintain position in the moving trawls. Studies quantifying the swimming speeds of teleost fish suggest that although individuals 5 and 15 cm long may be expected to have burst speeds of 0.5 m/s and 1.5 m/s over very short periods, their normal maximum swimming performance (or maximum cruising speed, Wardle, 1983) would be much less (Bainbridge, 1958; Wardle, 1975, 1983; Beamish, 1978). As a consequence, in our study some fatigued individuals probably came in contact with meshes in the body panels as they were herded towards the codend opening. Further, the relatively steep tapers (i.e. 1N4B—see Broadhurst et al., 1999) of the trawl bodies (compared with those used in most other prawn-trawl fisheries, FAO,

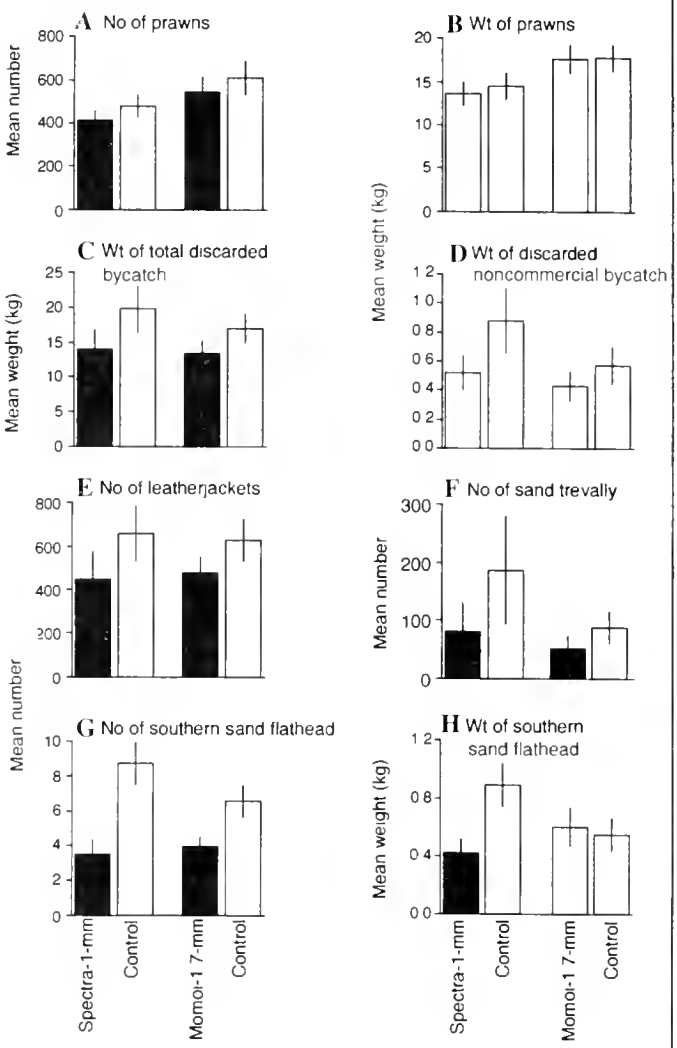

Figure 3

Differences in mean catches (per 25 min tow ±SE) between the new trawl bodies and control for the (**A**) numbers and (**B**) weights of king prawns (*Penaeus latisulcatus*); the weights of (**C**) total discarded bycatch and (**D**) discarded noncommercial bycatch; the numbers of (**E**) leatherjackets (*Thamnaconus degeni*), (**F**) sand trevally (*Pseudocaranx wrighti*) and (**G**) southern sand flathead (*Platycephalus bassensis*); the weights of (**H**) southern sand flathead; the numbers (**I**) and weights (**J**) of red mullet (*Upeneichthys porosus*); the numbers of (**K**) blue swimmer crabs (*Portunus pelagicus*); the numbers (**L**) and weights of (**M**) southern calamari (*Sepioteuthis australis*); and the numbers of small-toothed flounder (*Pseudorhombus jenynsii*). Significant differences are indicated by shaded histograms.

Table 4

Computed selectivity parameters for prawns (carapace length in mm) from the two new trawl bodies and deviance values for the goodness-of-fit logistic curve. Standard errors are given in parentheses. a, b = logistic parameters (Pope et al., 1975). P = split proportion from estimated split model

	Momoi-1.7-mm		Spectra-1-mm	
a	−8.99		−13.00	
b	0.26		0.39	
P	0.59		0.56	
		95% confidence limits		95% confidence limits
25% retention (L25)	30.26 (0.67)	25.43–34.91	29.92 (0.49)	26.72–32.92
50% retention (L50)	34.47 (0.92)	32.93–37.06	32.68 (0.57)	31.69–34.13
75% retention (L75)	38.68 (1.56)	34.11–45.51	35.44 (0.92)	32.46–39.55
Selection range (SR)	8.42 (0.44)	5.48–11.42	5.52 (0.16)	3.71–7.33
Deviance	22.58		29.49	
df	34		32	
P-value	0.932		0.594	

1972), probably contributed to contact of both fish and prawns with meshes in this section of the trawl. A combination of the above effects in the larger-mesh spectra-1-mm and momoi-1.7-mm trawl bodies may have facilitated the escape of smaller individuals.

It is also likely that a reduction in twine area associated with the larger mesh sizes in both new trawl bodies allowed a faster release of water than did the control trawl body,[1] possibly contributing to the effects discussed above. In partial support of this hypothesis and although no significant differences were detected between the spectra-1-mm and the momoi-1.7-mm trawl bodies for those variables examined (Table 3), the narrower-twine spectra-1-mm trawl body consistently reduced a larger percentage of bycatch across a greater range of variables. These variables included the weights of southern sand flathead and red mullet and the numbers of southern calamari (Table 2; Fig 3). Further investigation, involving a greater number of replicate tows would be required, however, to validate the potential for this effect.

A contributing operational factor towards the escape of fish from both large-mesh trawl bodies may have been the period between the time when the vessel was slowed and when the gear was hauled to the surface (termed "haulback") (Watson, 1989; Broadhurst et al., 1996). Watson (1989) showed that differences in geometry of the trawl and associated water flow during haulback caused fish (that were still swimming in the trawl) to become disorientated and to attempt escape through the surrounding meshes. More specifically, Workman and Taylor (1989) observed that numerous small individuals of schooling species such as Carangidae (e.g. *Trachurus lathami* and *Decapterus punctalus*) escaped during this period and that larger individuals were often caught by their gills in

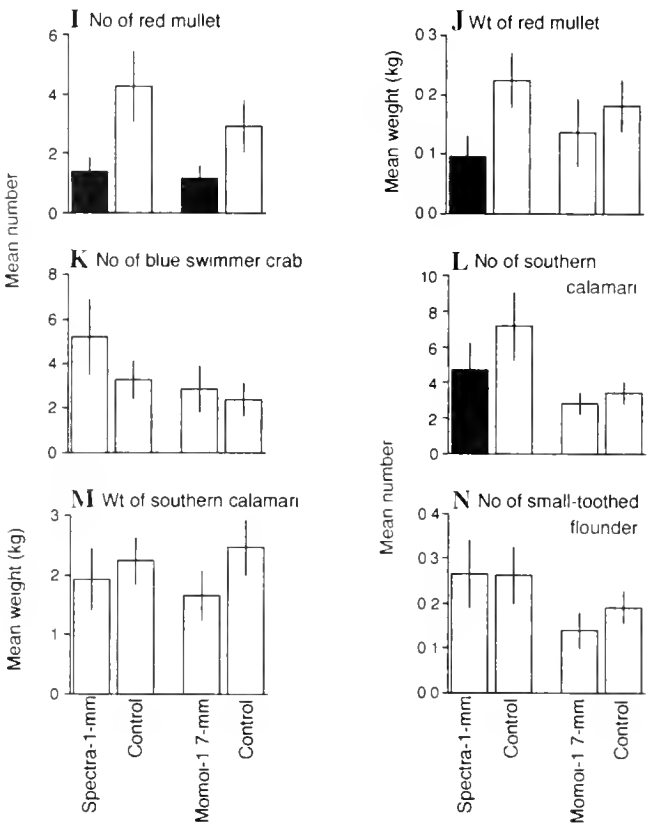

Figure 3 (continued)

[1] Harrington, D. L., J. W. Watson, L. G. Parker, J. B. Rivers, and C. W. Taylor. 1988. Shrimp trawl design and performance, 37 p. University of Georgia Marine Extension Service, 715 Bay St., Brunswick, Georgia 31520-4601.

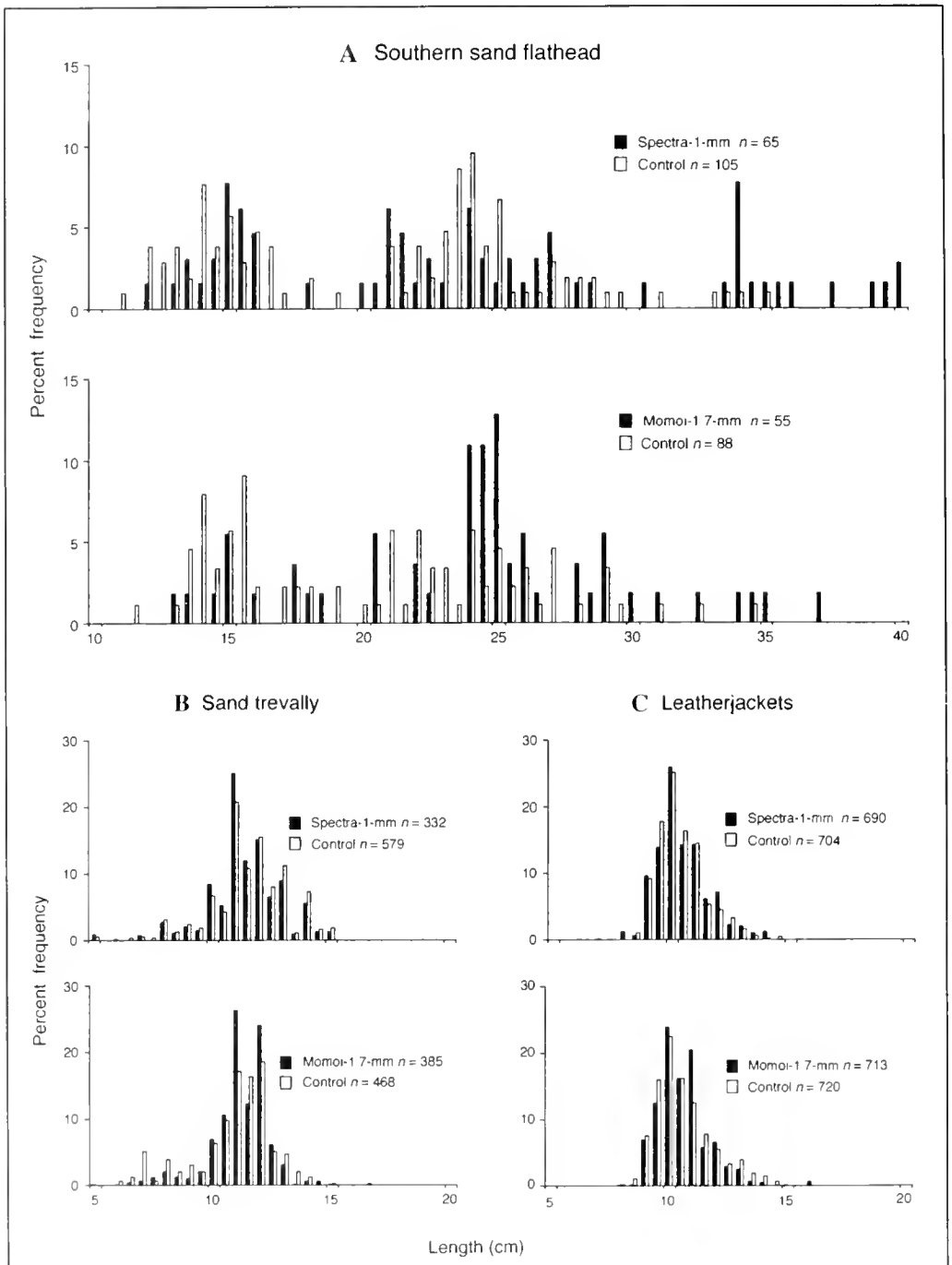

Figure 4

Size-frequency distributions of the new and control trawl bodies for (**A**) southern sand flathead (*Platycephalus bassensis*), (**B**) sand trevally (*Pseudocaranx wrighti*) and (**C**) leatherjacket (*Thamnaconus degeni*).

the meshes of the body panels. Likewise in our study, we observed numerous larger individuals of southern sand flathead, leatherjackets, and particularly larger sand trevally (10–15 cm) trapped in the meshes of the posterior sections of both large-mesh trawl bodies.

Although the results showed that significantly more smaller prawns escaped from the new trawl bodies than from the control trawl body, the selectivity parameters and associated 95% confidence limits (Fig 5; Table 4) were within the range calculated in a previous study (Broadhurst et al., 1999) for a

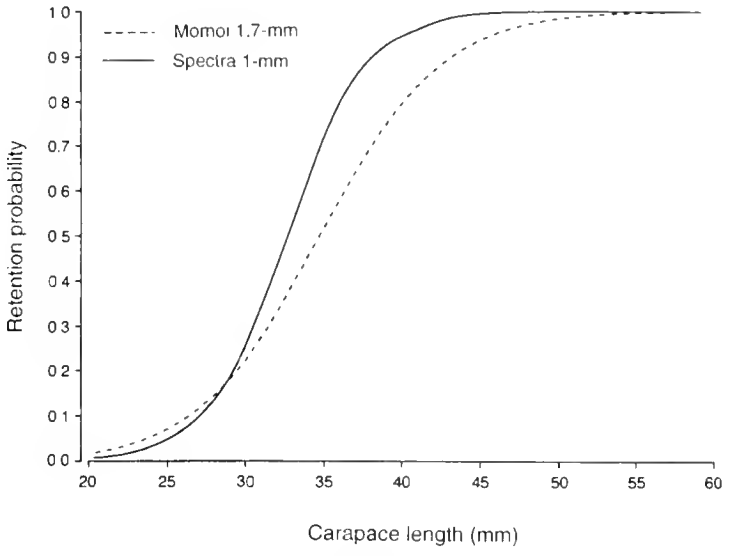

Figure 5

Plots of the selection curves of western king prawns (*Penaeus latisulcatus*) for the spectra-1-mm and momoi-1.7-mm trawl bodies.

trawl comprising a body of 45-mm mesh attached to a similar composite square-mesh codend. During this previous study, the codend that showed the most appropriate size-selectivity for prawns tapered from a circumference of 70 bars at the start of the anterior section to 58 bars at the end of the posterior section. After extensive commercial testing, however, it was reported that the slight taper in this codend occasionally "wedged" the catch in the posterior section, making it difficult to remove the catch when the codend was retrieved and the draw-strings were opened. To address this problem, fishermen widened the circumference to 80 bars throughout the codend. Although such an alteration solved the problems associated with buildup of catch in the codend (by allowing it to distribute more horizontally), it probably lowered the selectivity for prawns (Broadhurst and Kennelly, 1996). Any contributing effects on trawl selectivity due to the larger mesh in the spectra-1-mm and momoi-1.7-mm trawl bodies may have been slightly negated by a reduction in overall selectivity of the composite square-mesh codends. This result illustrates the need for ongoing assessments of influences on selectivity of trawls due to subtle modifications to facilitate operational procedures.

Like the results from other related studies, the significant reduction in numbers of prawns caught, but not in their weights, has shown that increases in mesh sizes or in openings (or in both) can facilitate an increase in catches of target-size individuals (Walsh et al., 1992; Broadhurst and Kennelly, 1997; Broadhurst et al., 1999). Possible hypotheses to explain this effect include 1) a faster release of water from the larger-mesh trawls resulted in prawns quickly passing into the trawl after initial contact, with less chance of escaping over the head rope and out through the mouth of the trawl or alternatively, 2) less drag in the larger-mesh trawls, due to less twine area and amount of bycatch, allowed the mouth of the trawl to spread wider, thereby covering more of the sea bed and capturing more prawns. Of these two hypotheses, the potential for an increase in spread is less likely because there were no significant differences in the catches of blue swimmer crabs or small-toothed flounder (species that could not pass through either the trawl bodies or composite square-mesh codends) between any of the trawls examined.

Because there were no significant differences detected in the weights of prawns captured between the various trawls, a further increase in the size of mesh in the body of the trawl (e.g. 60 mm) warrants investigation. Given the results presented in our study, this increase in mesh size could facilitate a greater release of small fish and further improve size selectivity for the targeted prawns. Alternatively, it may be feasible to examine the utility of trawl bodies comprising composite panels of larger mesh, particularly in the posterior section, because it is apparent that as fish are herded together in this area their densities increase, resulting in random attempts at escape through the sides of the trawl (Wardle, 1983). In addition, any fatigued fish still swimming in the posterior section of the trawl during haulback may have an opportunity to escape through these larger meshes.

Although not mandated, the results from our study have led to the use of large-mesh trawl bodies by many of the fishermen operating in Gulf St. Vincent. Combined with the contributing effects on bycatch reduction due to the composite square-mesh codend, this modification should result in a comparatively more selective prawn-trawl fishery. For example, in a review of literature quantifying bycatches from prawn-trawl fisheries throughout the world, Andrew and Pepperell (1992) reported that typical bycatch-to-prawn ratios in similar temperate fisheries were in the order of 5:1. From the mean catch per tow from the control and the new trawl bodies in our study,

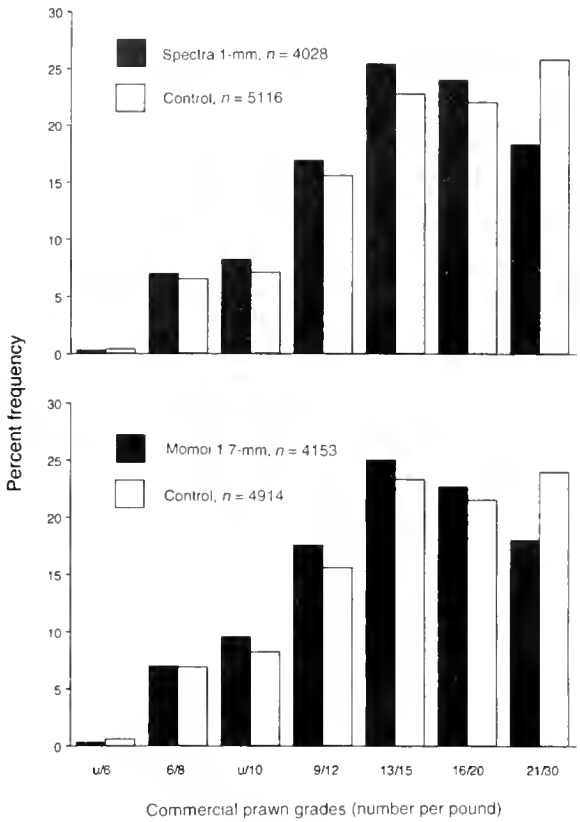

Figure 6

Commercial size categories of western king prawns (*Penaeus latisulcatus*) caught with the (**A**) spectra-1-mm and control trawls and (**B**) momoi-1.7-mm and control trawls (u=under).

discarded bycatch-to-prawn ratios were 1:1 for the spectra-1-mm and 1:1.3 for the momoi-1.7-mm trawl bodies. Ongoing monitoring is still required, however, to assess any potential effects on selectivity associated with operational refinements to the current trawl configurations.

Acknowledgments

This study was funded by the Australian Fishing Industry Research and Development Corporation. We thank Simon Boxshall and Brian McDonald for logistical support and assistance in the field and Jim Raptis (A. Raptis and Sons, PTY LTD) for the use of his vessel *Jillian Sandra*. We are grateful for the assistance and advice provided by Less Lowe (Gulf Net mending PTY LTD), Kim Redman, Hec Kavenagh, and all Gulf St. Vincent prawn trawlers. We would also like to acknowledge the Conselho National de Ensino e Pesquisa (CNPq) in Brazil for their contribution to the involvement of Matt Broadhurst.

Literature cited

Alverson, D. L., M. H. Freeberg, S. A. Murawski, and J. G. Pope.
1994. A global assessment of fisheries bycatch and discards. FAO Fish. Tech. Paper 339, Rome, 233 p.

Andrew, N. L., K. J. Graham, S. J. Kennelly, and M. K. Broadhurst.
1991. The effects of trawl configuration on the size and composition of catches using benthic prawn trawls off the coast of New South Wales, Australia. ICES J. Mar. Sci. 48:201–209.

Andrew, N. L., and J. G. Pepperell.
1992. The bycatch of shrimp trawl fisheries. Oceanogr. Mar. Biol. Annu. Rev. 30:527–565.

Armstrong, D. W., R. S. T. Ferro, D. N. MacLennan, and S. A. Reeves.
1990. Gear selectivity and the conservation of fish. J. Fish Biol. 37A:261–262.

Bainbridge, R.
1958. The speed of swimming of fish as related to size and to the frequency and amplitude of the tailbeat. J. Exp. Biol. 35:109–133.

Beamish, F. W. H.
1978. Swimming capacity. *In* Fish physiology, vol: VII, Locomotion (W. S. Hoar and D. J. Randall, eds.), p. 101–187. Academic Press, New York, NY.

Broadhurst, M. K.
In press. Modifications to reduce bycatch in prawn trawls: a review and framework for development. Rev. Fish Biol. Fish.

Broadhurst, M. K., and S. J. Kennelly.
1996. Effects of the circumference of codends and a new design of square-mesh panel in reducing unwanted bycatch in the New South Wales oceanic prawn-trawl fishery, Australia. Fish. Res. 27:203–214.
1997. The composite square-mesh panel: a modification to codends for reducing unwanted bycatch and increasing catches of prawns throughout the New South Wales oceanic prawn-trawl fishery. Fish. Bull. 95:653–64.

Broadhurst, M. K., S. J. Kennelly, and G. O'Doherty.
1996. Effects of square-mesh panels in codends and of haul-back-delay on bycatch reduction in the oceanic prawn-trawl fishery of New South Wales, Australia. Fish. Bull. 94:412–22.

Broadhurst, M. K., R. B. Larsen, S. J. Kennelly, and P. McShane.
1999. Use and success of composite square-mesh codends in reducing bycatch and in improving size-selectivity of prawns in Gulf St. Vincent, South Australia. Fish. Bull. 97:434–48.

FAO (Food and Agriculture Organization of the United Nations).
1972. Catalogue of fishing gear designs. Fishing news books Ltd., Farnham, Surrey, England, 160 p.

High, W. L., J. E. Ellis, and L. D. Lusz.
1969. A progress report on the development of a shrimp trawl to separate shrimp from fish and bottom-dwelling animals. Comm. Fish. Rev. 31:20–33.

Isaksen, B., J. W. Valdemarsen, R. B. Larsen, and L. Karlsen.
1992. Reduction of fish bycatch in shrimp trawl using a rigid separator grid in the aft belly. Fish. Res. 13:35–52.

MacLennan, D. N.
1992. Fishing gear selectivity: an overview. Fish. Res. 13: 201–204.

Millar, R. B., and S. J. Walsh.
1992. Analysis of trawl selectivity studies with an application to trouser trawls. Fish. Res. 13:205–220.

Pope, J. A., A. R. Margetts, J. M. Hamley, and E. F. Akyuz.
1975. Manual methods for fish stock assessment. Part III: selectivity of fishing gear. FAO Fisheries Technical Report 41 (revision 1), 65 p. FAO, Rome.

Rogers, D. R., B. D. Rogers, J. A. de Silva, and V. L. Wright.
1997. Effectiveness of four industry-developed bycatch reduction devices in Louisiana's inshore waters. Fish. Bull. 95:552–565.

Saila, S. B.
1983. Importance and assessment of discards in commercial fisheries. FAO Fish. Circ. 765, 62 p.

Sumpton, W. D., P. J. Smith, and B. G. Robotham.
1989. The influence on catch of monofilament and multifilament netting in otter prawn-trawls. Fish. Res. 8:35–44.

Thorsteinsson, G.
1992. The use of square mesh codends in the Icelandic shrimp (*Pandalus borealis*) fishery. Fish. Res. 13:255–266.

Vendeville, P.
1990. Tropical shrimp fisheries: types of fishing gear used and their selectivity. FAO Fish. Tech. Paper 261 (revision 1), 75 p. FAO, Rome.

Walsh, S. J., R. B. Millar, C. G. Cooper, and W. M. Hickey.
1992. Codend selection in American plaice: diamond versus square mesh. Fish. Res. 13:235–254.

Wardle, C. S.
1975. Limit of fish swimming speed. Nature (Lond.) 255: 725–7.
1983. Fish reactions to towed fishing gears. *In* Experimental biology at sea (A. MacDonald and I. G. Priede, eds.), p. 167–195. Academic Press, New York, NY.

Watson, J. W.
1976. Electrical shrimp trawl catch efficiency for *Penaeus duorarum* and *Penaeus aztecus*. Trans. Am. Soc. 105:135–148.
1989. Fish behaviour and trawl design: potential for selective trawl development. *In* Proceedings of the world symposium on fishing gear and fishing vessels (C. M. Campbell, ed.), p. 25–29. Marine Institute, St Johns, Canada.

Wileman, D. A., R. S. T. Ferro, R. Fonteyne, and R. B. Millar.
1996. Manual methods of measuring the selectivity of towed fishing gears. ICES, Copenhagen, 126 p.

Workman, I. K., and C. W. Taylor.
1989. The fish funnel: a trawl modification to reduce fish escapement. Mar. Fish. Rev. 51:23–27.

A new approach to validation of periodicity and timing of opaque zone formation in the otoliths of eleven species of *Lutjanus* from the central Great Barrier Reef*

Mike Cappo
Australian Institute of Marine Science, PMB 3
Townsville MC, Queensland, Australia 4810
E-mail address: m.cappo@aims.gov.au

Peter Eden
Mote Pty Ltd
423 Elizabeth Drive
Vincentia, Jervis Bay, New South Wales, Australia 2540

Stephen J. Newman
Western Australian Marine Research Laboratories
Fisheries Western Australia
PO Box 20, North Beach, Western Australia 6020

Simon Robertson
Central Ageing Facility
Marine and Freshwater Resources Institute
Queenscliff, Victoria 3225, Australia

Abstract.—A model was proposed for validation studies of the periodicity and timing of growth checks on fish otolith sections, based on measurements of otolith radii around tetracycline (OTC) marks. Continuous variables were obtained by expressing measurements of the marginal increment and distance between the OTC mark and the subsequent opaque zone as "fractions" of the width of a completed increment cycle within an otolith. The sum of these fractions and the counts of whole cycles completed outside the OTC mark, divided by the known time at liberty, produced estimates of the periodicity of opaque zone completion. Given this rate of completion and known dates of OTC marking and sacrifice, the marginal increment was used to estimate a date on which the outermost opaque zone was completed. The model was applied to 82 marked fish of 11 *Lutjanus* species recovered after 6–22 months at liberty, and an hypothesis of annual periodicity, about a mean of 0.96 ±0.32 cycles/yr, was retained for the pooled species along the best, ventral reading axis. Model estimates for *L. erythropterus*, *L. johnii*, *L. malabaricus*, and *L. sebae* were in the range of 0.78 ±0.22 cycles/yr to 1.03 ±0.29 cycles/yr along this axis. Median ages of these fish were 3+ for *L. erythropterus* and *L. sebae* and 5+ for *L. johnii*. A two-fold difference in somatic and otolith growth detected between field-tagged and captive fish did not affect periodicity. Extension of the model suggested false annuli were induced by changes in salinity or adverse weather. On average, annuli were completed within 1–3 months after the minima in water temperature, in the austral spring–early summer, around early September for *L. erythropterus* and *L. johnii*, late September for *L. malabaricus* and late October for *L. sebae*. Results from the model were only preliminary for the small samples of *L. argentimaculatus*, *L. bohar*, *L. carponotatus*, *L. monostigma*, *L. rivulatus*, and *L. vitta*, although the common validation approach indicated annual periodicity of opaque zone completion for these species.

Manuscript accepted 1 December 1999.
Fish. Bull. 98:474–488 (2000).

There have been recent developments in the use of thin sections of otoliths for counting annual increments in otolith macrostructure as accurate and precise indicators of age for a variety of tropical reef species (see Fowler, 1995 for review). Lifespans of 15–30 years were estimated for tropical snappers in Mexico (Rocha-Olivares, 1998) and the central Great Barrier Reef (GBR) region (Sheaves, 1995; Newman et al., 1996). In contrast, Milton et al. (1995) applied a radiometric aging technique and estimated longevities of <10 years for the "red snappers" *Lutjanus erythropterus*, *L. malabaricus* and *L. sebae* in the Gulf of Carpentaria (lat. <14°S). These results were one third to one half of the maximum ages estimated by Newman et al. (in press) from sectioned otoliths for the same species in the central GBR (lat. 18–20°S).

These differences have produced uncertainty about the nature of potential development of northern Australian fisheries and raised important questions regarding intraspecific, latitudinal variation in otolith interpretation and demographic parameters. There is a clear need to validate age estimates from both regions.

Francis (1995) proposed that validation is the process of estimating the accuracy of an aging method and that a first stage in the validation involves confirming the temporal meaning of the zones. A three-step conceptual approach to direct age validation studies with tetracycline (OTC) marking and recapture has also been used (Fowler, 1990, 1995; Fowler and Short, 1998), but no corresponding protocols have been published for the statistical analysis

Contribution 930 of the Australian Institute of Marine Science, Townsville, Queensland, Australia.

and reporting of the periodicity and timing of annulus formation outside OTC marks.

The most common analysis of periodicity has been that of informally comparing the observed number and position of annuli distal to the OTC mark with an expected number of annuli chosen from the whole number of years or seasons elapsed between marking and recapture. The most extensive studies, comprising large numbers of long-term recoveries of marked fish, reported the results as either percentage agreement (MacLellan and Fargo, 1995) or as a *t*-test (McFarlane and Beamish, 1995). Both approaches could not include fish recovered at liberty for less than one year and did not allow exploration of the sources of error evident in the comparisons. Low recovery rates of fish at liberty for more than 2–3 years are a feature of such tagging programs (Campana and Jones, 1998) and sample sizes are usually small. A median of only 21 fish was reported by Francis et al. (1992) from 14 earlier OTC mark-recapture studies. Such characteristics prevent the use of linear regressions, such as those used in validating daily microincrements (e.g. Foreman, 1996). The timing of opaque zone formation is most commonly inferred by informally noting the relative position of opaque zones, OTC marks, and the otolith margins on diagrams and photomicrographs (Choat and Axe, 1996; Ferreira and Russ, 1992, 1994; Fowler and Doherty, 1992; Murphy et al., 1998).

We propose that validation can be formalized into models to develop separate estimators of both the periodicity and timing of formation of opaque zones based on ratios of increment measurements around OTC marks. Our primary goals were to determine directly if the distinct opaque zones in sectioned otoliths of 11 species of *Lutjanus* from the central GBR were formed once per year and to estimate the dates of completion of these zones. Long-term recovery of useful sample sizes of GBR lutjanids marked with OTC is difficult because of ontogenetic changes in habitat of many species, the low levels of fishing effort, and tag shedding. Therefore we held captive fish to complement recoveries from a field-tagging program.

Our objectives were to develop a model for otolith growth past OTC marks that would allow tests of the null hypothesis of annual periodicity of opaque zone formation and that would provide mean estimates and measures of variation of the date of completion of these zones for comparison with environmental variables. These objectives required that we compare interpretations of otoliths and otolith growth between captive and wild fish, that we compare different reading axes and readers, and that we compare model estimates with the earlier validation approaches.

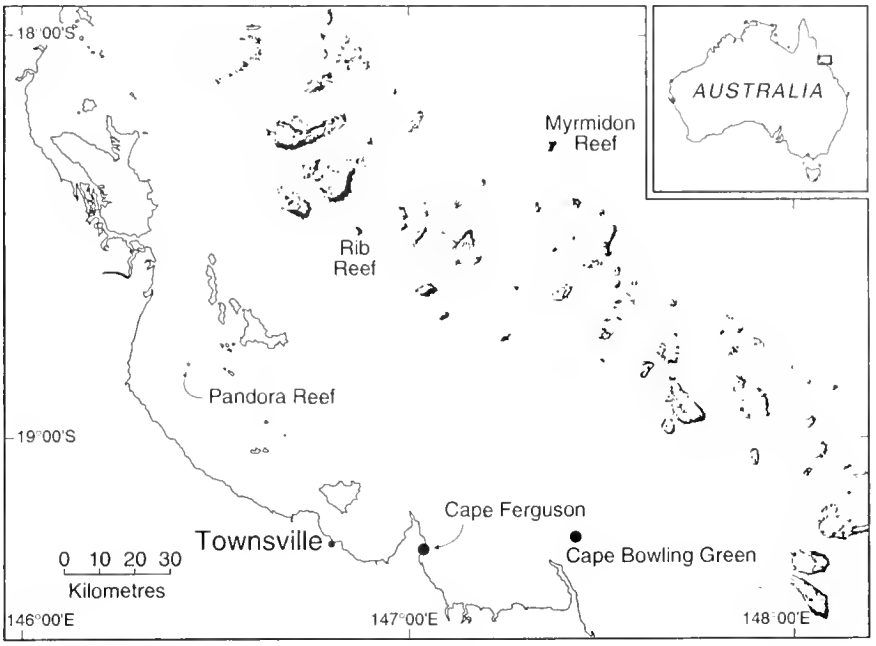

Figure 1
Central section of Great Barrier Reef Marine Park, showing sampling locations.

Materials and methods

Field techniques

Fish were collected with baited lines or traps (see Newman and Williams, 1995) in shallow water (<10 m) around the wharf at Cape Ferguson and Pandora Reef, and in deeper water (<37 m) in the GBR lagoon off Cape Bowling Green and the bases of Rib and Myrmidon Reefs (Fig. 1). There were two separate groups of fish used in the study. One group (n=170) of seven species were tagged and released in the shallow locations, where commercial and recreational fishing was prohibited, and repeated visits were made under research permits to recapture tagged fish. A second group (n=251) of 12 species were transported from the deeper locations and housed in two sea cages at Cape Ferguson wharf. The cages had a volume of 17.7 m^3 (cage dimensions: 2.95 m long × 2.45 m deep × 2.45 m wide) and were constructed from 25-mm galvanized steel tube covered in square, galvanized weldmesh (50 mm or 25 mm). Fish in each cage were fed with 2.5 kg of chopped pilchards (*Sardinops sagax*) each night.

Tetracycline was administered to both groups of fish in the form of Terramycin/MA injectable solution (oxytetracycline hydrochloride at 100 mg/mL) into the coelomic cavity at a dosage rate of 50 millilitres of Terramycin/MA per kilogram of estimated fish weight. In the field-tagging program, the fork length (FL mm) of all fish was measured and they were double-tagged below the spinous dorsal fin with numbered "T-bar" anchor tags or nylon-tipped dart tags. Tag legends advised retaining the whole fish upon recapture, but some fish recaptured after short times at liberty were injected and released again. Batches of captive fish were measured and injected once with OTC. Some *L. erythropterus* were injected

Table 1

Details of release, numbers of fish recovered (n), and ranges in age, length at recovery (FL mm) and time at liberty (months) of fish with visible OTC marks. Field = fish released in shallow locations where commercial and recreational fishing was prohibited; cage = fish held captive in sea cages.

Species	Release group	Place of capture	n	Age (yr)	FL	Liberty
L. argentimaculatus	field Sep 92–Mar 93	Cape Ferguson	3	6–7+	435–520	13.2–19.3
L. bohar	cage Mar 94	Myrmidon Reef	1	6+	386	11.6
L. carponotatus	cage Jul 93	Rib Reef	1	7+	326	19.9
L. carponotatus	cage Mar 94	Pandora Reef	1	4+	288	11.6
L. erythropterus	cage Aug 93	Cape Bowling Green	21[1]	2–5+	335–496	9.0–18.5
L. erythropterus	cage Nov 93	Cape Bowling Green	13[1]	3–4+	427–481	15.4
L. gibbus	cage Mar 94	Myrmidon Reef	1	4+	296	11.6
L. johnii	cage Feb 94	Cape Ferguson	10	4–7+	422–598	12.7
L. johnii	field Feb 93–Apr 94	Cape Ferguson	10[1]	3–7+	376–740	6.0–21.7
L. malabaricus	cage Mar 94	Pandora Reef	4	3+	402–466	11.2–11.6
L. monostigma	cage Mar 94	Pandora Reef	1	4+	306	11.6
L. rivulatus	cage Feb 94	Cape Ferguson	1	4+	312	12.7
L. rivulatus	cage Mar 94	Cape Ferguson	1	5+	401	12.0
L. sebae	field Mar 93	Pandora Reef	2	3+	280–296	12.3
L. sebae	cage Aug 93	Cape Bowling Green	3	2–4+	371–446	18.5
L. sebae	cage Mar 94	Pandora Reef	8	2–5+	331–444	11.6
L. vitta	cage Aug 93	Cape Bowling Green	2	4–6+	284–315	18.5

[1] Five of these fish were injected twice.

again about 3 months later. Most individuals were identified before release into the cages by tagging with anchor tags or by clipping of fin spines or rays. Some rarer species were not identified this way to reduce handling stress, and other individuals shed tags before recapture. The histories of these captive fish were recognizable from unique combinations of cage and species or, for some *L. erythropterus*, from twin OTC marks visible on otolith sections (Table 1).

Monthly measurements of surface seawater temperature and salinity recorded next to the cages and continuous records from the Australian Institute of Marine Science weather stations nearby on the GBR were used to derive information on environmental stressors and wind speed and direction. Caged fish were subject to extremes of wave energy, water temperature, turbidity, and salinity that are characteristic of the inshore habitat in the cyclone belt of the dry tropics. Water temperatures rose by 11°C from the austral winter to summer, and freshwater plumes from cyclonic rains caused fluctuations in salinity and turbidity. These influences extended out to Pandora Reef, but not to Rib and Myrmidon Reefs where there were clear waters and only a 6°C seasonal change in water temperature.

Laboratory techniques

For each fish after death, the FL was measured where possible and both sagittae (hereafter referred to as the otoliths) were removed, weighed, and measured. One otolith from each fish was randomly selected and embedded in soft epoxy resin. Three transverse sections were cut with a low-speed saw and diamond wafering blade in the vicinity of the primordium. The sections were 0.25–0.50 mm thick, depending on width of the otolith, and were lightly polished on wet ebony paper (1000 grade) and lapping film (9 and 3 µm). The sections were mounted on microscope slides under cover slips in a colorless epoxy casting resin and stored in darkness between short periods of examination.

The counts and measurements of otolith features made at the Australian Central Ageing Facility (CAF) were used in the analyses in our study to avoid possible bias from familiarity with the treatment of the individual fish. These data were compared with counts made by the senior author to assess precision and bias in otolith interpretation. Opaque zones were counted under magnifications from 7.5× to 25.2× with a stereo-dissecting microscope with transmitted white light, or under reflected light against a dark background (Newman et al., 1996). The position of the OTC mark was then measured by using epifluorescence illumination with a compound microscope at 20× to 40× magnification.

Video images were obtained, enhanced, and digitized with Bioscan's Optimas™ and Optimate™ software by using customized macros (Morison et al., 1998) along two planes (Fig. 2), from the primordium to the ventral apex of the otolith (ventral L1 axis), and from the primordium to the proximal edge parallel to the sulcus on the crista inferior (sulcal L3 axis). To define the position of the opaque

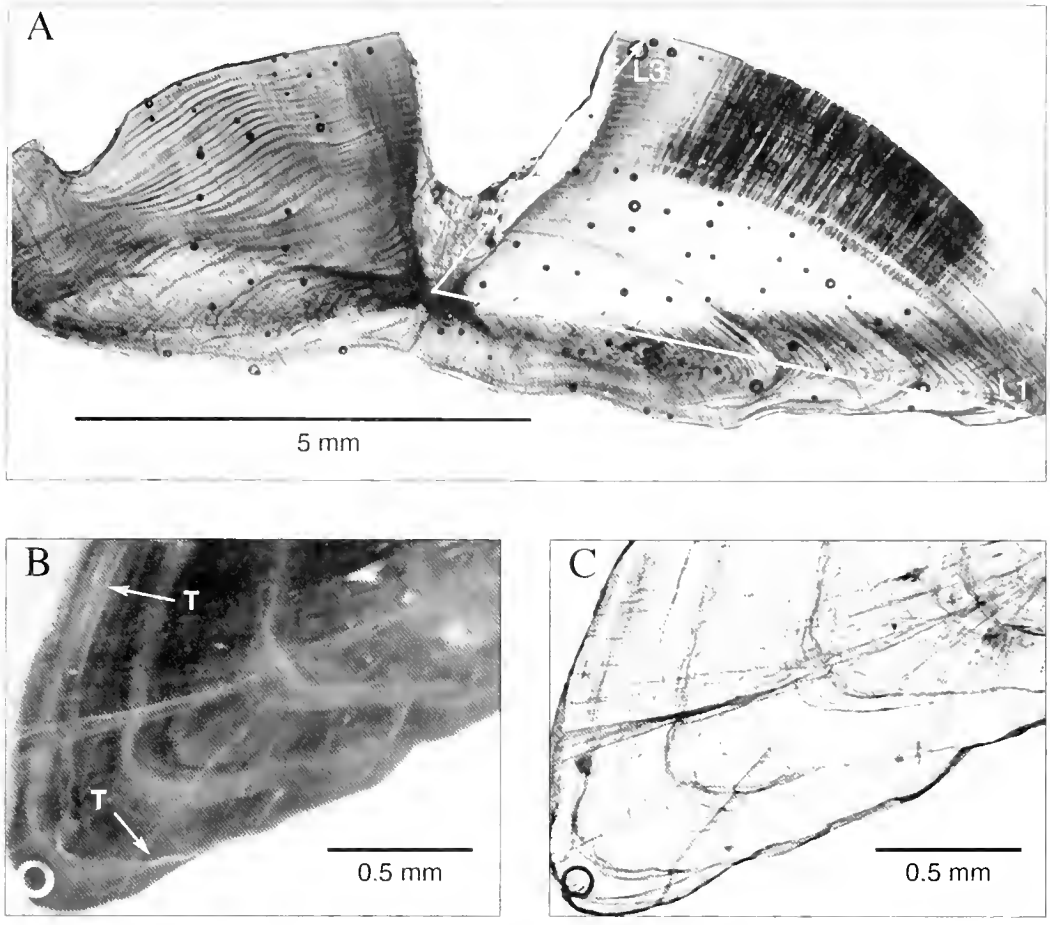

Figure 2

Photomicrographs of transverse sections of the sagittae of (**A**) *L. erythropterus* s1799 (21+yr) by transmitted white light showing the ventral L1 and sulcal L3 axes used for counting opaque zones; (**B**) the outer L1 axis of *L. rivulatus* (s1996) showing the position of an OTC mark (T) by reflected ultraviolet light; (**C**) the same outer L1 axis of *L. rivulatus* (s1996) showing narrow opaque zones by transmitted white light.

zones along these axes we recognized sharply defined "structural check rings" (sensu Gauldie, 1988) that could be followed from the ventral leading edge of the otolith around to the sulcus. These check rings were evident on the outermost edges of the opaque zones and were counted and measured after adjustment for aspect ratios. The position of the OTC mark was measured from the primordium to the outside edge of the mark and from there to the edge of the otolith along the L1 and L3 axes. The distance between twin OTC marks was measured from the distal edge of the first mark to the proximal edge of the second.

Data analyses

Analyses of the results for periodicity and timing of increment formation each comprised both an informal approach analogous to those used in earlier validation studies and a model of otolith growth. The informal validation of periodicity assumed a calendar date of 1 October for completion of opaque zones, based on previous Australian studies (Fowler, 1995), to report frequency distributions of the observed number of zones minus the expected number of zones formed outside OTC marks. The informal, "method of best fit" approach to estimate timing of completion of opaque zones was to assume that formation was completed annually on a particular day of the year. For each otolith section, and for every single day of the year, the number of opaque zones expected to be completed during time at liberty was calculated from the dates elapsed between marking and sacrifice. Only those dates for which the expected number of opaque zones formed past the OTC mark equalled the number actually observed were retained for analysis. The mean dates (MD) from frequency distributions of these possible calendar dates were selected as best informal estimates of time of completion of opaque zones.

We defined an "increment cycle" as the complete formation of adjacent translucent and opaque zones visible on an otolith section (Fig. 3). Two models were developed in a "direct method" to estimate the periodicity and timing

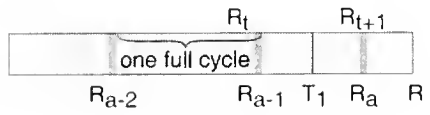

Figure 3

Positions of radii used to estimate initial and final fractions of otolith growth in Equations 1–3 shown across an otolith section of width R from a fish of age $a+$ with an OTC mark at T_1. In this example the radii of opaque zones at R_{a-1} and R_a are equivalent to radii of opaque zones immediately before (R_t) and after (R_{t+1}) the OTC mark. A full increment cycle is indicated.

of opaque zone completion based on the following observations. First, otoliths grow at a measurable rate that allows both counts of annuli and measurements of otolith weight to be converted to an estimate of age, with an associated error (Worthington et al., 1995). Second, this is a continuous process best represented by a continuous variable (*sensu* Zar 1996)—not a discrete variable such as the (whole) number of opaque zones. Third, the widths of outer increment cycles become similar for older fish (see figures in Fowler, 1995). We therefore proposed that ratios of otolith widths could be equated to ratios of corresponding time intervals in a model if two approximations were assumed:

1 the rate of otolith growth throughout the formation of an increment cycle was constant; and
2 the widths of increment cycles on outer margins of otoliths were the same.

We obtained continuous variables by expressing measurements of the marginal increment and distance between the OTC mark and subsequent opaque zone as "fractions" of widths of a completed increment cycle within an otolith. The sum of these fractions and the counts of whole cycles completed outside the OTC mark, divided by the known time at liberty, produced estimates of the rate, or periodicity, of opaque zone completion. Given this rate of completion, and known dates of OTC marking and sacrifice, the marginal increment could be used to estimate a date on which the outermost opaque zone was completed.

The number of increment cycles completed per year was the "cycle frequency" (V) and its inverse was the "cycle period" in units of years. The "closing date" (CD) of an increment cycle was defined as the date on which the formation of the opaque zone was completed. The time elapsed between OTC injection and the day on which the fish was sacrificed was referred to as the "time at liberty" (L) measured in decimal units of years.

The "initial fraction" (IF) and the "final fraction" (FF) of otolith growth were the two ratios of widths modelled to estimate time intervals with this direct method. Following the measurements shown in Figure 3, these two values were calculated as

$$IF = (R_{t+1} - T_1) / (R_{t+1} - R_t), \quad (1)$$

where R_t = the radius to the opaque zone formed immediately before OTC injection; and
R_{t+1} = the radius to the opaque zone formed immediately after OTC injection;

and as

$$FF = (R - R_a) / (R_a - R_{a-1}), \quad (2)$$

where a = age of the fish;
R_a = the radius to the final opaque zone; and
R_{a-1} = the radius to the penultimate opaque zone.

The terms R_a and R_{t+1} were equivalent, and R_{a-1} and R_t were equivalent, where there was only a single opaque zone measured past the OTC mark.

The cycle frequency (V) was estimated for all sections with at least one opaque zone past the OTC mark as

$$V = (IF + N + FF) / L, \quad (3)$$

where N = the number of full increment cycles visible outside the OTC mark; and
L = the time at liberty; the term N = an integer and $N = 0$ in Figure 3.

The "liberty fraction" (LF) was calculated as the sum of the full cycles and partial cycles that formed during time L, and was expressed in decimal fractions of cycles as

$$LF = IF + N + FF. \quad (4)$$

The cycle frequency was investigated using linear regression (SAS Institute Inc., 1989a) of the model

$$LF = \beta L. \quad (5)$$

This assumed an intercept value of zero (there was no time for otolith growth to occur when $L=0$) and the slope $\beta = 1$ when cycles had an annual periodicity. Confidence intervals for β were calculated from t distributions (Montgomery, 1991).

The second model, to estimate closing dates (CD) of the last cycle fully completed, assumed that for each otolith section the cycles that finished during time L had equal cycle periods. Closing dates were calculated as

$$CD = K - 365(FF/V), \quad (6)$$

where K = the date on which the fish was sacrificed, coded by SAS in units of days (SAS Institute Inc., 1989b).

The calendar day of the year on which the cycle ended (calendar closing date CCD) was derived from CD by

using SAS date functions as an integer between 1 and 365. The closing dates of anomalous extra cycles for comparison with environmental stressors were estimated by using

$$CD_{t+i} = TET_1IN + 365(i - 1 + IF) / V, \quad (7)$$

where TET_1IN = the date of the first OTC injection coded in SAS internal format in units of days; and
$t + i$ = the i_{th} opaque zone completed after the OTC mark.

The mean of the *CCD* estimates could be used as an estimate of the calendar date (*MCCD*) on which the opaque zones were most likely to have been completed. Days or months of the year are circular scales of measurement and best expressed in Polar coordinates as angles and radius unity. Means, angular deviations (analogous to the linear standard deviation), and confidence intervals were therefore calculated for circular von Mises distributions of *CCD* for each species by using the methods of Zar (1996). The Hotelling paired sample test was used to determine the significance of differences in angular *CCD* data between reading axes.

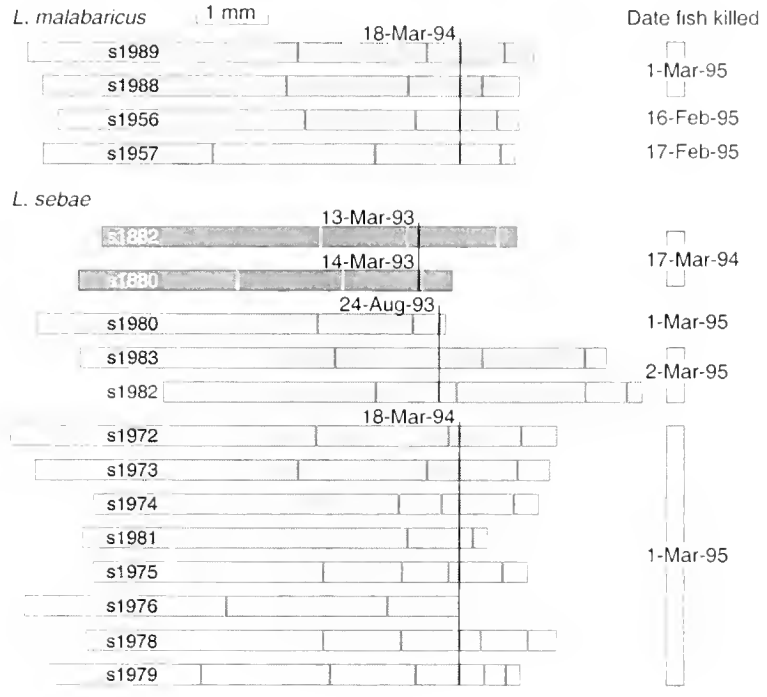

Figure 4

Measurements of the position of opaque zones and the OTC marks (unbroken or extended vertical bar) on the ventral L1 axis from the primordium to the otolith edge for *L. malabaricus* and *L. sebae*, identified by slide numbers. Bars representing field-tagged recaptures are shaded darker than those for captives. Dates of injection and sacrifice are shown. Otoliths marked on the same date are arranged with OTC marks aligned vertically, with a subjective horizontal scale for the spread of injection dates.

Results

Recoveries of marked fish

A total of 82 individuals from 11 species were recovered with OTC marks visible on sections of their otoliths (Table 1), equating to a recovery rate of less than 20% from the field-tagged and captive groups. Times at liberty were less than 22 months and the marked fish were all in younger year classes, less than 8+, in relation to the longevities estimated in some current studies (e.g. Williams et al.[1]). The median ages estimated for the most numerous species were only 3+ for *L. erythropterus*, *L. malabaricus*, and *L. sebae*, and 5+ for *L. johnii*. Apart from a few early recoveries of fatalities in the cages, all captive fish were sacrificed in the beginning of March 1995. Fish were recaptured in the field mainly over the summer period between September 1994 and April 1995.

Recoveries of field-tagged *L. johnii*, *L. argentimaculatus* and *L. sebae* were low (only 8–10% of the initial number released were recovered, and tag loss was evident (60% of field recoveries had lost one tag and three others, not included in our study, had an OTC mark but no tags). Of the captive group, only 60 fish from 10 species, including six dead fish, were recovered. None of the smallest species, *L. fulviflamma* and *L. kasmira*, and only 5% of the numerous *L. vitta* remained at the end of captivity. Only eight captive fish had retained anchor tags, and individual lengths at release for captive fish without tags were generally not distinguishable. One field-tagged *L. johnii* and four captive *L. erythropterus* had two OTC marks visible on their otoliths.

Otolith growth and interpretation near OTC marks

The strength of the working assumptions used in the models developed in our study depended on the sources of variability apparent in rate of growth of the otoliths outside the OTC mark amongst species, age classes, field-tagged and captive groups, and individuals in Figures 4–7. This region generally comprised only a small proportion of the otolith width, especially in the oldest fish, *L. johnii* (Fig. 6),

[1] Williams, D. McB., S. J. Newman, M. Cappo, and P. J. Doherty. 1995. Recent advances in the ageing of coral reef fishes. South Pacific Commission, Forum Fisheries Agency Workshop on the Management of South Pacific Inshore Fisheries. South Pacific Commission Integrated Coastal Fish Management Project Technical Document 12. Forum Fisheries Agency, P.O. Box 629, Honiara, Guadalcanal, Solomon Islands.

L. argentimaculatus, *L. gibbus*, and *L. bohar* (Fig. 7). There were no opaque zones visible past the OTC mark on both axes of one *L. gibbus*, and *L. monostigma* had no OTC mark visible on the ventral axis. An opaque zone was coincident with the OTC mark on the ventral axis, but not the sulcal axis, of *L. bohar*.

The ease of interpretation of opaque zones in the otolith preparations was tested by comparing the pairs of counts made by the two otolith readers. Nonparametric, Wilcoxon signed rank tests showed significant differences between readers in estimates of fish age along both reading axes (ventral axis n=82 S=285.0 $P>|S|$=0.0001; sulcal axis n=82 S=285.5 $P>|S|$=0.0001) but not in interpretation of the number of opaque zones past the OTC mark (ventral axis n=61 S=21.0 $P>|S|$=0.5034; sulcal axis n=62 S=15.0 $P>|S|$=0.6476). An age bias plot (Campana et al., 1995) showed that the mean and standard deviation of the CAF estimates were 2.9 ±0.5 for 2+ fish, 3.5 ±0.6 for 3+ fish and 4.2 ±0.4 for 4+ fish aged by the senior author. We inferred that there was similar interpretation amongst readers of the area of interest outside the OTC mark and that the definition of the first opaque zone was a source of bias for youngest fish.

Sections from *Lutjanus* otoliths have been read along the sulcal L3 axis in a protocol developed by Newman et al. (1996), but opaque zones may be closest together in this area and measurements of growth past OTC marks might best be made elsewhere. To justify our choice of measurement axes for subsequent analyses we compared the mean growth and variance from the two axes in Table 2. Growth rates along the ventral axis were consistently twice as high as those along the sulcal axis; therefore we judged that errors in measurement of zone radii would be least, and interpretation best, along the ventral axis. The coefficients of variation were similar for both axes, with the exception of those for *L. sebae*.

Lutjanus sebae showed the highest mean growth rates and variability along both reading axes (Table 2) which led us to investigate artifacts of captivity. The growth rates of otoliths of *L. johnii* and *L. sebae* in the field were much lower than those of captives (Figs. 4 and 6). Captive *L. johnii* had mean otolith growth rates of 0.78 mm/yr along the ventral axis—twice as high as those tagged in the field (0.36 mm/yr). These differences were highly significant (n=20 ndf=1 ddf=18 F=22.49 $P>F$=0.0002), but no significant difference in otolith weight was detected when fish length was used as a covariate (n=20, ndf=1 ddf=18 F=0.19 $P>F$=0.6704). This latter finding indicated that faster otolith growth rates were correlated with the faster somatic growth of captive fish.

Further evidence of this correlation and the effects of captivity on somatic growth were an increase in mean FL of captives by about 7 mm/month for *L. johnii* and about 12 mm/month for *L. sebae*, compared with field growth rates of 0.2–6.2 mm/month for *L. johnii* and only 2.6–3.9 mm/month for *L. sebae*. One field-tagged *L. johnii* (s6667, Fig. 6) showed both an apparent decline in FL and no otolith growth outside the OTC mark on the ventral axis.

Plots of increment cycle width (W) along the ventral axis against cycle number (a) were made to examine

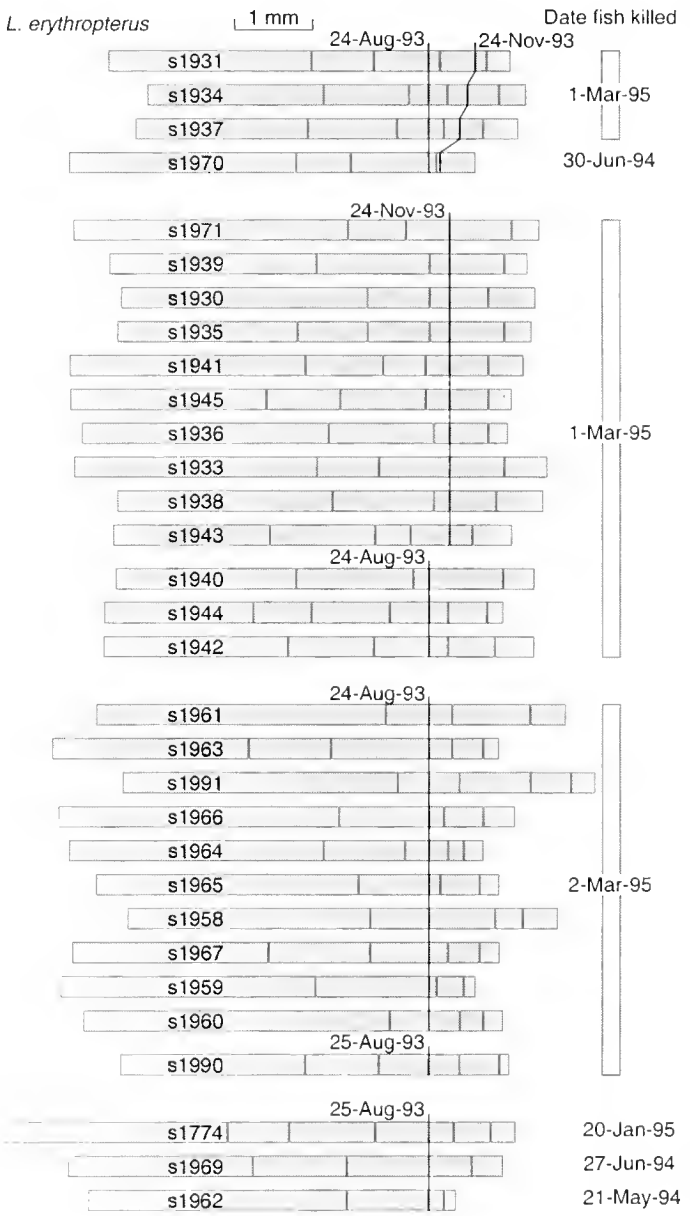

Figure 5

Measurements of the position of opaque zones and the OTC marks on the ventral L1 axis for *L. erythropterus*. Date of the second injection with OTC is shown to the right of the continuous line joining OTC marks. All conventions as in Figure 4.

Table 2

Mean growth rates of otoliths (mm/yr) outside OTC marks and measures of dispersion from sample size (n) of the most numerous species along the ventral L1 and sulcal L3 axes. Captive = fish held in sea cages; field = fish released in shallow locations where commercial and recreational fishing was prohibited.

Group	Age range (yr)	Axis	n	Growth rate	SD	CV (%)
L. johnii—captive	4–7+	L1	10	0.78	0.21	27
		L3	10	0.31	0.08	25
L. johnii—field	3–7+	L1	10	0.36	0.18	51
		L3	10	0.21	0.09	45
L. sebae—captive	2–5+	L1	11	1.00	0.61	61
		L3	11	0.43	0.15	36
L. sebae—field	3+	L1	2	0.91	0.62	69
		L3	2	0.52	0.17	33
L. erythropterus—captive	2–5+	L1	27	0.77	0.22	28
		L3	27	0.33	0.08	24
L. malabaricus—captive	3+	L1	2	0.94	0.15	16
		L3	2	0.36	0.07	20

our second working approximation that outer cycles had equal widths on the marked otoliths. The plots were fitted best by exponential curves: $W = 0.38 + 4.92e^{-0.81a}$ for species pooled; $W = 0.70 + 11.44e^{-1.68a}$ for *L. erythropterus*; $W = 0.30 + 3.21e^{-0.5a}$ for *L. johnii*; and $W = 0.75 + 9.12e^{-1.26a}$ for *L. sebae*. On average, there was a small decrease in cycle width from the third to the fourth cycle and then successive cycles were similar; however captivity or tagging may have caused anomalous growth of some otoliths. Two *L. sebae* showed no (s1976), or insignificant (s1980), growth along the ventral axis (Fig. 4) but their otoliths did continue to thicken. The largest *L. sebae* and *L. erythropterus* showed substantial growth along the ventral axis in relation to other individuals (Figs. 4 and 5), contributing to the high coefficients of variation shown in Table 2. For some captives this phenomenon led to a progressive or irregular increase in cycle width, most notable for *L. erythropterus* marked in August 1993 (eg. s1937, s1943, s1954, and s1958 in Fig. 5), that violated the second approximation of our model.

Periodicity of zone formation

Using the informal validation approach, and assuming a springtime completion date of 1 October, we estimated the frequency distributions shown in Table 3 that indicated an annual periodicity of deposition of opaque zones in the majority of otolith sections. However, there was a small minority of fish with more or less zones than expected, and information about the opaque zones counted for these individuals was available by applying the "direct method" developed in our study by rewriting Equation 3 as

$$V = (IF + FF)/L + N/L. \quad (8)$$

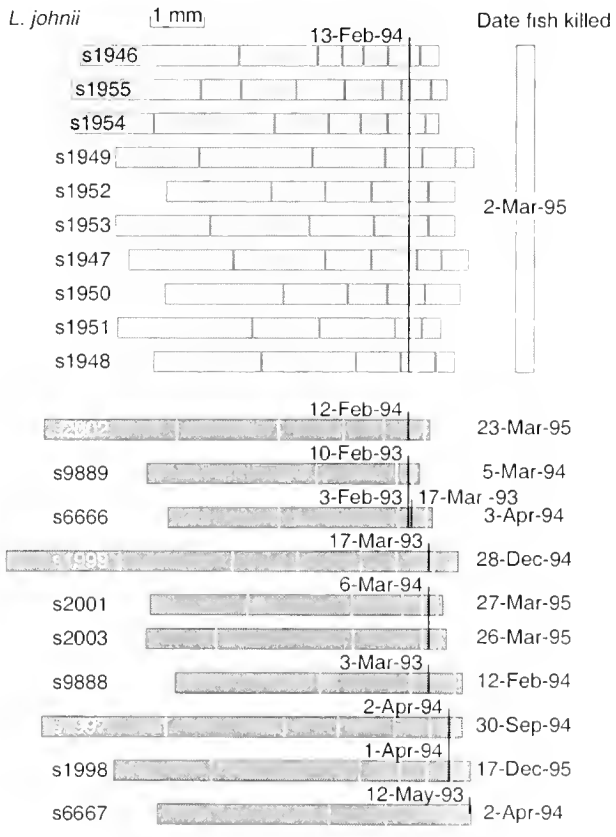

Figure 6

Measurements of the position of opaque zones and the OTC marks on the ventral L1 axis for *L. johnii*. All conventions are the same as those in Figures 4 and 5.

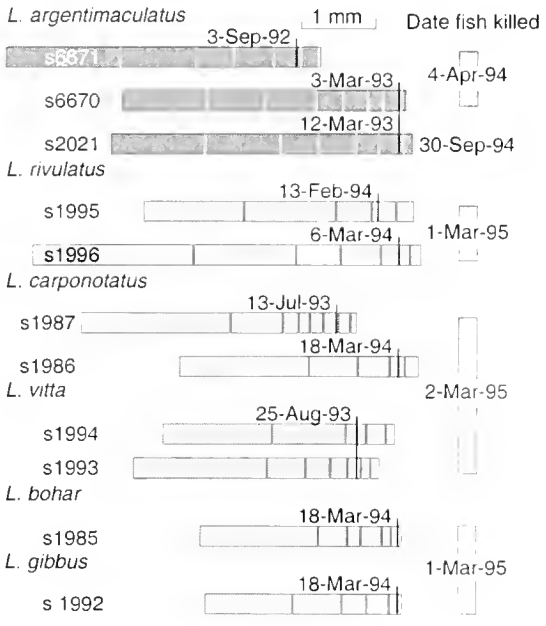

Figure 7

Measurements of the position of opaque zones and the OTC marks on the ventral L1 axis for six species represented by three individuals or less in the study. All conventions are the same as those in Figure 4.

Table 3

Frequency distribution of the difference between observed (obs) and expected (exp) number of opaque zones past the first OTC mark where a nominal date of 1 October was used for completion of zone formation.

			Difference between obs and exp no. of opaque zones			
Species	*n*	Axis	−2	−1	0	1
L. argentimaculatus	3	L1	0	0	3	0
		L3	0	0	3	0
L. bohar	1	L1	0	1	0	0
		L3	0	0	1	0
L. carponotatus	2	L1	0	0	2	0
		L3	0	0	2	0
L. erythropterus	31	L1	0	1	29	1
		L3	0	2	27	2
L. gibbus	1	L1	0	1	0	0
		L3	0	1	0	0
L. johnii	20	L1	0	0	16	4
		L3	0	0	16	4
L. malabaricus	4	L1	0	0	4	0
		L3	0	0	4	0
L. monostigma	1	L1	—	—	—	—
		L3	0	0	1	0
L. rivulatus	2	L1	0	0	2	0
		L3	0	0	2	0
L. sebae	13	L1	1	1	8	3
		L3	1	0	8	4
L. vitta	2	L1	0	0	2	0
		L3	0	0	2	0

This procedure allowed us to determine objectively outliers in the values of N estimated for fish in groups with similar times at liberty. Fish with the same values of liberty, L, and number of complete increment cycles, N, lay on a line of slope $1/L$ in the plot of cycle frequency (V) against the sum of the initial and final fractions ($IF+FF$) in Figure 8. Fish with the same value of L and an estimate of N larger or smaller by one complete increment cycle were offset from this line by $1/L$ cycles per year.

In addition, this procedure allowed us to exclude 18 fish from the "direct method" of estimating periodicity along either reading axis, under three criteria. First, fish with anomalies in opaque zone formation, such as "false annuli" (e.g. *L. erythropterus* s1991, *L. johnii* s1947, *L. sebae* s1982), or with other errors in otolith interpretation were included only in analyses exploring the possible relationships between formation of false annuli and environmental conditions. Second, fish with $FF>1.0$ (e.g. *L. erythropterus* s1958, s1964 in Fig. 5) were excluded because they violated our second working approximation of the equal spacing of outer zones. Third, other fish were excluded because the OTC marks were absent along one axis (*L. monostigma*) or were visible outside the outermost opaque zones (*L. sebae* s1980, *L. gibbus*).

When these outliers were removed, the "direct method" produced a normal distribution of cycle frequency along the ventral axis about a mean of 0.96 ±0.32 cycles/yr (n=66 Shapiro-Wilk w=0.98 $P<w$=0.71) for all species pooled. Data from the sulcal axis produced a mean of 1.02 cycles/yr (n=64 w=0.95 $P<w$=0.04), but this was not normally distributed.

The estimated cycle frequencies were grouped loosely about one cycle/yr for *L. erythropterus*, *L. johnii*, *L. rivulatus*, and *L. sebae*, with *L. malabaricus*, *L. argentimaculatus*, and *L. bohar* having a lower estimate and *L. carponotatus* and *L. vitta* having a higher frequency (Fig. 9). All means lay within the range 0.78–1.21 cycles/yr; apparently a lower cycle frequency was estimated when radii measured along the ventral axis (Table 4) were used. Analysis of variance showed no significant differences in cycle frequencies among these species and between reading axes, but a nonparametric Wilcoxon signed-rank test for paired data found significant differences between axes (n=61 S=−363.5 prob >|S|=0.008).

Simple linear regression of the number of whole and partial cycles formed after OTC marking (liberty fraction LF) on time at liberty showed significant linear relationships along both the ventral axis (n=66 ndf=1 ddf=64 F=739.37 $P>F$=0.0001) (Fig. 10) and the sulcal axis (n=64 ndf=1 ddf=62 F=913.36 $P>F$=0.0001). The slopes were β=1.01

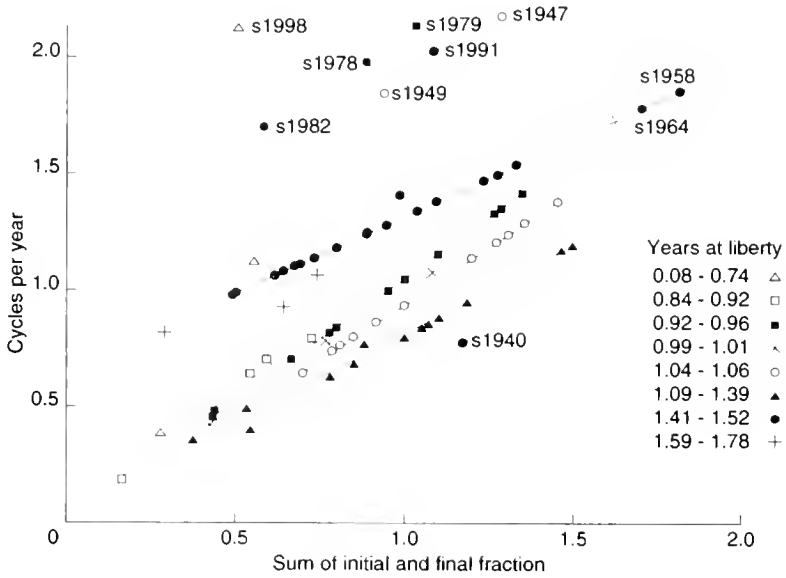

Figure 8

Number of increment cycles per year plotted against the sum of the initial (*IF*) and final fractions (*FF*) measured along the ventral L1 axis. Data labelled with slide numbers have extra or fewer cycles than expected. Circled data on the end of the line represents fish whose otolith growth in the final increment cycle markedly exceeds the previous deposition rate.

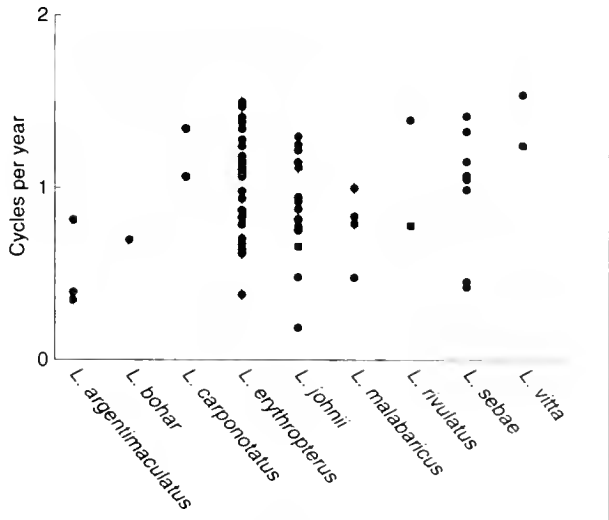

Figure 9

Number of increment cycles per year along the ventral L1 axis estimated for 61 fish of nine study species with the direct method.

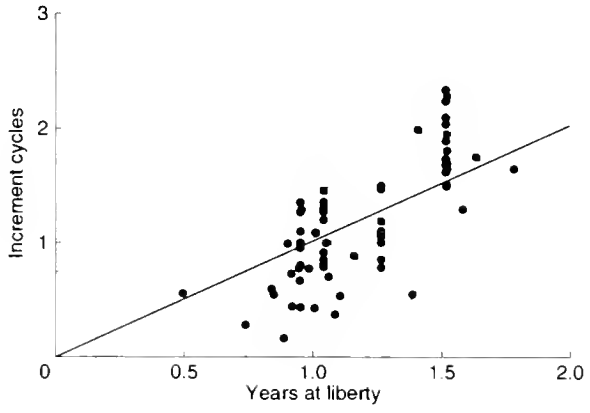

Figure 10

Linear regression and 95% confidence intervals ($LF=\beta L$) for the number of whole and partial increment cycles formed during time at liberty *LF* (liberty fraction, ventral L1 axis) against time at liberty *L* for 66 fish of 9 species from Figure 9.

along the ventral axis ($t_{0.025,\,64}=1.99$; confidence interval $0.94<\beta<1.09$) and $\beta=1.09$ along the sulcal axis ($t_{0.025,\,62}=1.99$; confidence interval $1.02<\beta<1.16$). The regression residuals were normally distributed only along the ventral axis ($n=66$ $w=0.981428$ $P<w=0.7105$), and were influenced by a group of positive residuals around 1.5 years at liberty, corresponding to $V > 1$ cycles/yr. These were mainly *L. erythropterus*, for which Equation 6 consistently estimated

that the 1993 zones were completed later in the calendar year than those formed in 1994. The hypothesis that the frequency of zone completion, as the slope of the regression, was equal to one cycle/yr was therefore retained for the ventral axis for all species pooled.

Timing of zone formation

Four *L. erythropterus* had otoliths with two OTC marks that bracketed a fully formed opaque zone (Fig. 5), indicating that these annuli were formed in the austral spring in September–November 1993. A Hotelling paired sample test for equality of means in circular distributions showed that there were significant differences in estimates of calendar closing dates (*MCCD*) from the direct method between reading axes (n=60 ndf=2 ddf=58 F=3.41 $P>F$=0.04). There was also variability amongst species, with the most numerous species completing an annulus along the ventral axis in mid-August by *L. johnii*, in early September by *L. erythropterus*, and in early November by *L. sebae*.

Table 4

Mean increment cycle frequency (increment cycles/yr) and standard deviation along the ventral L1 and sulcal L3 axes for the species represented by four or more marked individuals.

Species	L1 axis	L3 axis
L. erythropterus	1.03 ±0.29	1.15 ±0.25
L. johnii	0.88 ±0.29	0.85 ±0.22
L. malabaricus	0.78 ±0.22	0.88 ±0.15
L. sebae	0.99 ±0.37	1.21 ±0.33

By pooling data from the ventral and sulcal axes by taking the mean of each pair we were able to overcome problems associated with anomalous otolith growth, resolve differences in the estimates, and not significantly change the degrees of freedom in any subsequent tests for significance of timing of zone formation. This procedure tightened the estimates of closing date for *L. sebae* and generally gave a best estimate of spring–early summer for formation of the annulus in the most numerous species (Table 5). Results from the "method of best fit" were inside the bounds of the confidence limits of the direct method for *L. johnii* and *L. sebae* and were similar for *L. malabaricus*, *L. monostigma*, and *L. rivulatus* but were significantly later in the year for *L. erythropterus* (Table 5). The discrepancies between methods for *L. argentimaculatus*, *L. bohar*, *L. carponotatus*, and *L. vitta* reflected both the small number of fish and difficulties in measurement and interpretation of their smaller otoliths. The estimates for the less numerous species must be considered to be tentative.

There was a marked coincidence between the August 2nd minimum in water temperature and a peak in August for frequency of 1994 closing dates (Fig. 11). Extra opaque zones counted or deemed to be false annuli may have formed after storms and salinity fluctuations at Cape Ferguson. To investigate this possibility, we estimated closing dates using Equation 7 from the radii of anomalous "extra" opaque zones visible on both reading axes in otoliths of *L. johnii* (s1947, s1949, s1998, Fig. 6), *L. sebae* (s1979, s1982, Fig. 4), and *L. erythropterus* (s1991, Fig. 5) identified as outliers on Figure 8. All but one of these fish (s1998) were in the group of captives. Compared with salinity and sea state during the months of captivity, there appeared to be a relationship between a sharp fall and rise in salinity of at least 1.4 ppt for March–May 1994 and the completion of these "extra" zones in the following month, although periods of rough and very rough sea conditions also occurred most commonly at this time. Salinity dropped

Table 5

Mean calendar closing dates (*MCCD*), angular deviation (s) in days, and lower (*LCL*) and upper (*UCL*) 95% confidence limits pooled and averaged for the ventral and sulcal axes, from the "direct method," compared with the mean date (*MD*) estimated from the "method of best fit" for n fish of each study species.

Species	n	(*LCL* < *MCCD* <*UCL*)	s	*MD*
L. argentimaculatus	3	26 Oct	54	26 Dec
L. bohar	1	14 May	—	8 Sep
L. carponotatus	2	14 Aug	13	29 Oct
L. erythropterus	27	14 Aug< 2 Sep<20 Sep	42	31 Oct
L. gibbus	1	—	—	9 Mar
L. johnii	17	3 Aug< 5 Sep <8 Oct	53	16 Aug
L. malabaricus	4	30 Sep	26	3 Sep
L. monostigma	1	8 Sep	—	8 Sep
L. rivulatus	2	27 Aug	5	23 Aug
L. sebae	9	9 Sep < 19 Oct < 29 Nov	47	23 Oct
L. vitta	2	17-Sep	71	27 Nov

from 36.0 ppt on 3 February to 34.8 ppt on 1 April and rose again to 36.2 ppt on 1 May. The closing dates for these false annuli were distributed in March (n=1), April (n=2), and May (n=3).

Discussion

The use of increment widths on otolith sections to examine timing of opaque zone formation underpins marginal increment analysis (Fowler and Short, 1998) and informal inferences made from the relative position of OTC marks (Choat and Axe, 1996; Ferreira and Russ, 1992, 1994; Francis et al., 1992). The direct method developed in our study has essentially formalized and extended this use to allow for robust parametric tests and has three advantages over previous approaches to direct validation. First, the use of fractions of otolith growth allows linear regression of the number of whole or partially completed (or whole *and* partially completed) increment cycles on time at liberty, and both measures are expressed correctly as continuous variables. This method allows periodicity to be estimated directly from all recaptures with at least one opaque zone outside the OTC mark, including those fish at liberty for less than one year. Second, there is no need for subjective choice of a fixed date of completion of opaque zones to allow for comparisons between expected and observed counts of opaque zones. Third, the calendar date of completion of outer opaque zones can be estimated independently of the dates of marking or sacrifice for all recaptures with at least one opaque zone outside the OTC mark. Previous inferences about timing have been limited to the opaque zones that are immediately adjacent to OTC marks. Such contrasts are not always readily available, especially when tagging and recaptures cannot be spread throughout the year because of seasonal differences in fishing effort or vulnerability of fish to capture.

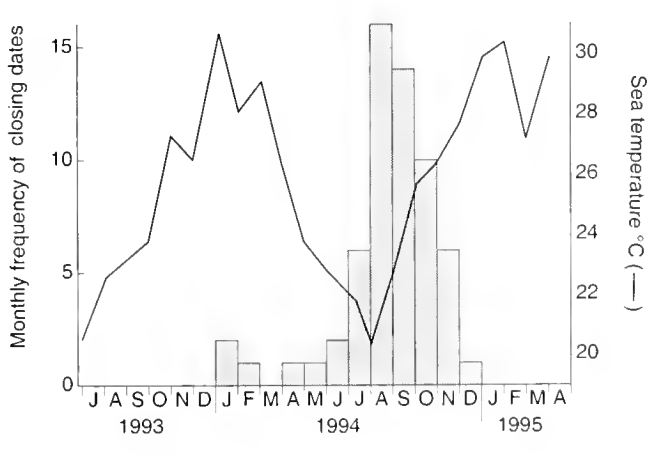

Figure 11

Monthly sea surface temperature (°C) in the cages during captivity of marked fish, plotted with the monthly frequency of closing dates (*CD*) in 1994 estimated with the "direct method" with Equation 6 for nine species from Figure 9. The estimates have been pooled and averaged for the ventral and sulcal axes for each of 61 fish.

Periodicity and timing of opaque zones

We tested, and retained, the hypothesis that there was an annual periodicity of formation of opaque zones for the pooled study species, around a mean of 0.96 ±0.32 increment cycles/yr. Anomalous sections and "false" annuli were identified objectively and could be related to periods of environmental stress in six cases. The model also identified interannual difference in timing of zone completion by a group of *L. erythropterus*, which clearly inflated overall estimates of periodicity. Despite this difference, estimates of periodicity in the range of 0.78–1.21 cycles/yr for both reading axes, accompanied by confidence intervals, were robust for *L. erythropterus*, *L. johnii*, *L. malabaricus*, and *L. sebae*. This result supported the use of thin sections of otoliths for accurate age estimates of lutjanids in the central GBR and supported estimates of longevity proposed for some of our study species (eg Sheaves, 1995; Newman et al., in press; Loubens[2]). The results for the other species showed similar trends, and no interspecific differences in periodicity were detected, but the numbers of marked fish were low for *L. argentimaculatus*, *L. bohar*, *L. carponotatus*, *L. gibbus*, *L. monostigma*, *L. rivulatus*, and *L. vitta*. Twofold differences in otolith growth rate between captive and tagged *L. johnii* and *L. sebae* did not affect the periodicity of annulus formation, further demonstrating the capacity of these otoliths to accurately reflect age under varying conditions of somatic growth.

Substantial variability in the timing of opaque zone formation has been noted by Beckman and Wilson (1995), at the individual, population, and species levels. Our best estimates of closing dates indicated that, on average, opaque zones recognized as annuli in lutjanid otoliths were completed within months of the austral spring and early summer, around early September for *L. erythropterus* and *L. johnii*, late September for *L. malabaricus*, and late October for *L. sebae*. These differences were significant and indicated a timing of formation that is somewhat earlier for *L. erythropterus* and *L. johnii* than the spring–summer peak of opaque zone formation in tropical fishes identified by Fowler (1995) and Beckman and Wilson (1995). Other studies have concluded that lutjanids and serranids on the GBR form opaque zones in winter–spring (Ferreira and Russ, 1992, 1994; Newman et al., 1996).

Lack of definition of the term "formation" makes it difficult to compare our results with those of previous studies. Our use of single OTC marks and measurements of only the outside edges of opaque zones allowed inferences about the timing of completion, not commencement, of annuli. We could

[2] Loubens, G. 1980. Biologie de quelques de poissons du lagon Neo-Caledonian. III. Croissance. Cahiers de l'Indo-pacifique 2(2): 101–153. Foundation Singer-Polignac, 43, avenue Georges-Mandel, 75016 Paris. ISSN 0180-9954.

estimate a formation time of less than 3 months for opaque zones on otoliths from *L. erythropterus* marked twice in 1993. Those individuals clearly showed springtime formation of the opaque zones in that year, but we also concluded that completion occurred earlier in the following year, about 1–2 months after the minimum water temperature in August, indicating that commencement and formation could have occurred during winter 1994. This difference was not explained by interannual variation in the occurrence of minimum water temperatures and may have been due to changes in metabolism and physiology induced by capture, transport, handling, and captivity. These are plausible artifacts, given that opaque zone formation is under control of a poorly understood combination of environmental and endogenous factors that influence endolymph fluid chemistry (Beckman and Wilson, 1995; Romanek and Gauldie, 1996). The location of the cages may have contributed to mortality or lack of growth of the otoliths of *L. bohar*, *L. fulviflamma*, *L. gibbus*, *L. kasmira*, and *L. vitta* transported inshore from their reef habitats, whereas the other inshore species were expected to be more tolerant of the cage environment.

The models produced similar, but more informative, conclusions to the application of the informal approaches. Analyses following MacLellan and Fargo (1995) indicated an annual periodicity of opaque zone formation for 10 study species with few exceptions. The "method of best fit" estimated mean calendar completion dates that were inside the confidence intervals of the direct method, with the exception of *L. erythropterus*, for which the method was sensitive to the interannual variability in timing of annulus completion.

Sources of bias

Assumptions concerning otolith growth rate in the direct method were the best available approximations, given both our observations and the current understanding of otolith growth, and we were confident that their main effects were accounted for by excluding outliers and by measures of variation reported about the mean results.

Earliest models of otolith growth presumed that no net accretion occurred when fish stopped growing, and these "no-growth" horizons provided the foundation for the recognition of annual winter marks in otoliths (Romanek and Gauldie, 1996). However, otolith growth is not directly coupled to somatic growth (e.g. Mosegaard et al., 1988) and has been observed to show complexities correlated by various authors with factors such as food intake, life-history stage, temperature, and metabolic rate (Romanek and Gauldie, 1996; Schirripa and Goodyear, 1997). Most recently, Romanek and Gauldie (1996) proposed that otolith growth along the main growth axis is continuous, with the rate of deposition (that is, the microincrement width) being modulated by temperature and pH of the endolymph. This model was based on the known physiology of the endolymph and the physical chemistry of aragonite, and was tested by Payan et al. (1997) and Gauldie and Romanek (1998).

We therefore assumed a constant rate of otolith growth, while recognizing that a number of factors might be expected to vary regularly during continuous growth of the otolith, including the widths of daily micro-increments, trace element concentrations, matrix proteins, and aragonite crystal structure (Gauldie and Nelson, 1990; Gauldie et al., 1990). It remains unknown which combination of such variable characteristics integrate into the optical macrostructure of otolith sections viewed as opaque and translucent zones (Fowler, 1995).

If alternating periods of slow and fast otolith growth occurred regularly throughout each increment cycle, in violation of our working approximation, errors would tend to cancel one another during calculation of periodicity. In Equations 1–3, the initial fraction of otolith growth (*IF*) was estimated by using a numerator from the last part of a cycle, but the final fraction (*FF*) was estimated from the first part of a cycle by using the marginal increment as a numerator. If *IF* was underestimated because the otolith grew slowly at the end of a cycle, it would be countered by an overestimation of *FF* caused by faster otolith growth at the start of a cycle. Our method was most vulnerable to interannual differences in otolith growth rate, which were evident for some fish as anomalous otolith growth, possibly as a physiological response to captivity or tagging.

The widths of outer increment cycles were assumed to be the same in our second working approximation because an exponential decrease in growth along otolith reading axes and equidistant outer zones are a feature of several families from the central GBR, including lutjanids (Fowler and Doherty, 1992; Choat and Axe, 1996; Newman et al., 1996). The exponential curves presented in our study supported the approximation for the 50 marked fish that had completed their fourth increment cycle but did not support so well for the younger fish sacrificed during their fourth (n=28) and third cycles (n=4). Finally, the model assumption that the increment cycles had the same time period of formation in an individual otolith was supported for our estimation of closing dates by the determination of the annual periodicity of opaque zone formation.

There was bias in interpretation of the position of the first annulus, causing significantly higher estimates of total age by the unfamiliar reader, but not of the number of annuli past the OTC marks. The structural check rings at the outer edges of opaque zones were the best feature of the large lutjanid otoliths, and the potential for errors in interpreting the annuli on outer margins (Francis et al., 1992) was reduced by sacrificing most fish in late summer and autumn. The longer ventral axis was the most useful because of the variability in growth, measurement errors, and significant differences in estimates of closing dates from measurements along the shorter sulcal axis. However, growth in older otoliths with complex prismatic structure becomes restricted by the otic cleft (Gauldie and Nelson, 1990), and the sulcal axis may provide the only straight axis for measurement in future applications of the models.

Related studies

In contrast to our results for the "red snappers" *L. erythropterus*, *L. malabaricus*, and *L. sebae*, Milton et al. (1995)

concluded from disequilibria in ^{210}Pb to ^{226}Ra ratios of pooled otoliths that shorter lifespans obtained from whole otolith readings (*sensu* McPherson and Squire, 1992) were more accurate than the higher estimates from section counts. This independent method of age determination had previously helped differentiate between very different age interpretations of deep-water *Hoplostethus* and *Sebastes* that were thought to attain high longevities. However, Campana and Jones (1998) noted that radiochemical dating was too imprecise for detailed or individual age determinations, and West and Gauldie (1994) also concluded that the method held promise but was inadequate to validate fish ages.

Regional differences in the ease of interpretation of otolith macrostructure have been reported in tropical species separated by only four degrees of latitude (Fowler, 1995) and may partly explain the differences between our results. The lack of interpretable macrostructure in an otolith section from *L. erythropterus* from the Gulf of Carpentaria is evident when Figure 5b in Milton et al. (1995) is compared with the well-defined incremental structure for the same species in our Figure 2A. Alternatively, there may be real latitudinal differences in the demography of these species. Comparisons of the relationships between otolith weight and age estimates from the Gulf of Carpentaria and the central GBR, and further validation with the "radiocarbon bomb chronometer" (Kalish, 1995; Campana and Jones, 1998), OTC marking, or other independent techniques, may account more precisely for the differences between the validation studies.

Models with ratios of increment measurements around OTC marks in order to estimate time intervals could provide a statistical protocol to accompany the emerging definitions of various levels of validation. Francis (1995) proposed that the highest degree of validation requires demonstration that inner and outer zones are formed annually and that quantitative estimates of accuracy are provided for the process of converting a count of zones to an age estimate. This method requires knowledge of hatching dates and the age at completion of the first annulus, as well as decisions about the nominal calendar dates when opaque zones can be distinguished on otolith margins. The approach presented in our study could allow precise estimates of the timing of some of these latter events if improved theoretical models of growth of opaque zones are developed. We conclude that, for at least the three "reds" species and *L. johnii*, we have attained Francis's (1995) second level of validation—namely, that the opaque zones were formed annually and completed from spring through early summer, but there remains a need to produce quantitative estimates of the accuracy of this aging method.

Acknowledgments

This work was supported by grants to D. McB. Williams and G. Russ from the Australian Research Council. Fieldwork was greatly assisted by the fishing skills of S. Boyle, J. Dalling, A. Mead, G. Muller and D. Moore. The sea cages were designed and built by P. Speare, and we are grateful to the officers of Argus Security Pty Ltd for feeding the captive fish. At the Central Ageing Facility we wish to thank K. Hall for sample registration and database entry and C. Green for advice on interpretation and photomicrography of otoliths. M. Fimeri offered support with image analysis and M. Eden and T. Simmonds drafted the figures. We are particularly grateful for the improvement of the manuscript by three anonymous referees, and for critique of our first working approximation by A. J. Fowler and R. W. Gauldie.

Literature cited

Beckman, D. W., and C. A. Wilson.
1995. Seasonal timing of opaque zone formation in fish otoliths. *In* Recent developments in fish otolith research (D. H. Secor, J. M. Dean, S. E. Campana, eds.), p. 27–44 Univ. South Carolina Press, Columbia, SC.

Campana, S. E., M. C. Annand, and J. I. McMillan.
1995. Graphical and statistical methods for determining the consistency of age determinations. Trans. Am. Fish. Soc. 124:131–138.

Campana, S. E., and C. M. Jones.
1998. Radiocarbon from nuclear testing applied to age validation of black drum, *Pogonias cromis*. Fish. Bull. 96:185–192.

Choat, J. H., and L. M. Axe.
1996. Growth and longevity in acanthurid fishes; an analysis of otolith zones. Mar. Ecol. Prog. Ser. 134:15–26.

Ferreira, B. P., and G. R. Russ.
1992. Age, growth and mortality of the inshore coral trout *Plectropomus maculatus* (Pisces: Serranidae) from the central Great Barrier Reef, Australia. Aust. J. Mar. Freshwater Res. 43:1301–1312.
1994. Age validation and estimation of growth rate of the coral trout, *Plectropomus leopardus*, (Lacepede 1802) from Lizard Island, northern Great Barrier Reef. Fish. Bull. 92:46–57.

Foreman, T.
1996. Estimates of age and growth, and an assessment of ageing techniques, for northern bluefin tuna, *Thunnus thynnus*, in the Pacific Ocean. Int.-Am. Trop. Tuna Comm. Bull. 21(2):123.

Fowler, A. J.
1990. Validation of annual growth increments in the otoliths of a small, tropical coral reef fish. Mar. Ecol. Progr. Ser. 64:25–38.
1995. Annulus formation in otoliths of coral reef fish—a review. *In* Recent developments in fish otolith research (D. H. Secor, J. M. Dean, S. E. Campana, eds.), p. 45–64. Univ. South Carolina Press, Columbia, SC.

Fowler, A. J., and P. J. Doherty.
1992. Validation of annual growth increments in the otoliths of two species of damselfish from the southern Great Barrier Reef. Aust. J. Mar. Freshwater Res. 43:1057–1068.

Fowler, A. J., and D. A. Short.
1998. Validation of age determination from otoliths of the King George whiting *Sillaginodes punctata* (Perciformes). Mar. Biol. 130:577–587.

Francis, R. I. C. C.
1995. The analysis of otolith data—a mathematician's perspective (what, precisely, *is* your model). *In* Recent developments in fish otolith research (D. H. Secor, J. M. Dean, S. E. Campana, eds.), p. 81–95. Univ. South Carolina Press, Columbia, SC

Francis, R. I. C. C., L. J. Paul, and K. P. Mulligan.
1992. Ageing of adult snapper (*Pagrus auratus*) from otolith annual ring counts: validation by tagging and oxytetracycline injection. Aust. J. Mar. Freshwater Res. 43:1069–1089.

Gauldie, R. W.
1988. Similarities in fine structure of annual, and non-annual, check rings in the otolith of the New Zealand snapper (*Chrysophrys auratus*). N.Z. J. Mar. Freshwater Res. 22:273–278.

Gauldie, R.W., N. M. Davies, G Coote, and I. Vickridge.
1990. The relationship between organic material and check rings in fish otoliths. Comp. Biochem. Physiol. 97A:461–474.

Gauldie, R. W., and D. G. A. Nelson.
1990. Otolith growth in fishes. Comp. Biochem. Physiol. 97A:119–135.

Gauldie, R. W., and C. R. Romanek.
1998. Orange roughy otolith growth rates: a direct experimental test of the Romanek-Gauldie otolith growth model. Comp. Biochem. Physiol. 120A:649–653.

Kalish, J. M.
1995. Radiocarbon and fish biology. *In* Recent developments in fish otolith research (D. H. Secor, J. M. Dean, S. E. Campana, eds.), p. 637–654. Univ. South Carolina Press, Columbia, SC.

MacLellan, S. E., and J. Fargo.
1995. Validation of age and growth for English sole (*Parophrys vetulus*) in Hecate Strait, British Columbia. *In* Recent developments in fish otolith research (D. H. Secor, J. M. Dean, S. E. Campana, eds.), p. 341–355. Univ. South Carolina Press, Columbia, SC.

McFarlane, G. A., and F. W. H. Beamish.
1995. Validation of the otolith cross-section method of age determination for sablefish (*Anoploma fimbria*) using oxytetracycline. *In* Recent developments in fish otolith research (D. H. Secor, J. M. Dean, S. E. Campana, eds.), p. 319–329. Univ. South Carolina Press, Columbia, SC.

McPherson, G. R., and L. Squire.
1992. Age and growth of three dominant *Lutjanus* species of the Great Barrier Reef inter-reef fishery. Asian Fish. Sci. 5:25–36.

Milton, D. A., S. A. Short, M. F. O'Neill, and S. J. M. Blaber.
1995. Ageing of three species of tropical snapper (Lutjanidae) from the Gulf of Carpentaria, Australia, using radiometry and otolith ring counts. Fish. Bull. 93:103–115.

Montgomery, D. C.
1991. Design and analysis of experiments, 3rd ed. Wiley, New York, NY, p. 486–489.

Morison, A. K., S. G. Robertson, and D. C. Smith.
1998. An integrated system for production fish ageing: image analysis and quality assurance. N. Am. J. Fish. Manage. 18:587–598.

Mosegaard, H., H. Svedang, and K. Taberman.
1988. Uncoupling of somatic and otolith growth rates in Arctic char (*Salvelinus alpinus*) as an effect of differences in temperature response. Can. J. Fish. Aquat. Sci. 45:1514–1524

Murphy, M. D., D. H. Adams, D. M. Tremain, and B. L. Winner.
1998. Direct validation of ages determined for adult black drum, *Pogonias cromis*, in east-central Florida, with notes on black drum migration. Fish. Bull. 96:382–387.

Newman, S. J., and D. McB. Williams.
1995. Mesh size selection and diel variability in catch of fish traps on the central Great Barrier Reef, Australia: a preliminary investigation. Fish. Res. 23:237–253.

Newman, S. J., D. McB. Williams, and G. R. Russ.
1996. Age validation, growth and mortality rates of the tropical snappers (Pisces; Lutjanidae) *Lutjanus adetii* (Castelnau, 1873) and *L. quinquelineatus* (Bloch, 1790) from the central Great Barrier Reef, Australia. Mar. Freshwater Res. 47:575–584.

Newman, S. J., M. Cappo, and D. McB. Williams.
In press. Comparison of age, growth, mortality rates and corresponding yield estimates using counts of annuli in whole and sectioned otoliths of the tropical red snappers *Lutjanus erythropterus*, *L. malabaricus* and *L. sebae* from the central Great Barrier Reef, Australia. Fish. Res.

Payan, P., H. Kossmann, A. Watrin, N. Mayer-Gostan, and G. Bouef.
1997. Ionic composition of endolymph in teleosts: origin and importance of endolymph alkalinity. J. Exp. Biol. 200:1905–1912.

Rocha-Olivares, A.
1998. Age, growth, mortality, and population characteristics of the Pacific red snapper, *Lutjanus peru*, off the southeast coast of Baja California, Mexico. Fish. Bull. 96:562–574

Romanek, C. S., and R. W. Gauldie.
1996. A predictive model of otolith growth in fish based on the chemistry of the endolymph. Comp. Biochem. Physiol. 114A:71–79.

SAS Institute Inc.
1989a. SAS/STAT user's guide, version 6, 4th ed., vol. 2. SAS Institute Inc., Cary, NC, p. 1352–1455.
1989b. SAS language and procedures: usage, version 6, 1st ed. SAS Institute Inc., Cary, NC, p. 185–197.

Schirripa, M. J., and C. P. Goodyear.
1997. Simulation of alternative assumptions of fish otolith-somatic growth with a bioenergetics model. Ecol. Modelling 102:209–223.

Sheaves, M. J.
1995. Large lutjanid and serranid fishes in tropical estuaries: Are they adults or juveniles? Mar. Ecol. Progr. Ser. 129:31–40.

West, I. F., and R. W. Gauldie.
1994. Determination of fish age using ^{210}Pb:^{225}Ra disequilibrium methods. Can. J. Fish. Aquat. Sci. 51:2333–2340.

Worthington, D. G., A. J. Fowler, and P. J. Doherty.
1995. Determining the most efficient method of age determination for estimating the age structure of a fish population. Can. J. Fish. Aquat. Sci. 52:2320–2326.

Zar, J. H.
1996. Biostatistical analysis, 3rd ed. Prentice Hall, Upper Saddle River, NJ, p. 591–662.

Sexual maturity, sex ratio, and size composition of swordfish, *Xiphias gladius*, caught by the Hawaii-based pelagic longline fishery

Edward E. DeMartini

James H. Uchiyama

Happy A. Williams

Honolulu Laboratory
Southwest Fisheries Science Center
National Marine Fisheries Service, NOAA
2570 Dole Street
Honolulu, Hawaii 96822-2396

E-mail address (for E. E. DeMartini): Edward.Martini@noaa.gov

Abstract.—Swordfish (*Xiphias gladius*) caught by the Hawaii-based pelagic longline fishery during March 1994–June 1997 were examined at sea by observers of the National Marine Fisheries Service, Southwest Region. Observers provided unbiased size and sex composition data for 4.8% of the swordfish catch and 4.9% of the effort in number of hooks of the fishery during the 40-mo. period. Observers measured body lengths for more than 8600 swordfish brought aboard participating vessels; sex, based on macroscopic appearance of gonads, was identified aboard ship for 77% of measured fish. Sex identifications were later verified (0.5% error rate) and gonadal developmental stage described for 1336 fish whose sex was identified in the field. Logistic regression was used to estimate sex-specific, median body size at sexual maturity (L_{50}) by using microscopic morphological evidence for gonadal development. L_{50} was 102 cm ±2.5 (95% CI) cm eye-to-fork length (EFL) and 144 ±2.8 cm EFL for males (n=506) and females (n=822), respectively. Sex ratios were an increasing power function between 100 and 220 cm, and nearly all fish >220 cm EFL were females. Sex composition and body size varied temporally and spatially, especially the latter. Relatively more males were caught south of 27° N; females dominated catches north of 27° N. Small-bodied fish of both sexes prevailed year-round below 22° N. A greater percentage of large-bodied (>156-cm [males], >172-cm [females] EFL) fish were caught north of 35° N during the late summer–early winter. The latter observations are consistent with several nonmutually exclusive hypotheses of migration energetics and body muscle heat conservation, both of which are discussed.

Manuscript accepted 1 December 1999.
Fish. Bull. 98: 489–506 (2000).

Rapid expansion of the Hawaii-based pelagic longline fishery for swordfish (*Xiphias gladius*) during the late 1980s and early 1990s has generated a need for an explicit management plan and assessment of swordfish stocks in the Pacific. Assessments for swordfish might be improved by using size- or age-structured, rather than surplus production, models for several reasons. Size- and age-structured models are less dependent on effort statistics (Gulland and Rosenberg, 1992) and in the Pacific as in the Atlantic, adequate effort statistics are largely unavailable for pelagic longline catches. Effort data are further complicated by geographically separated fisheries that differentially target swordfish or other pelagic fishes and by multiple jurisdictions with varying data collection standards. In the Atlantic these difficulties might be overcome by using nonequilibrium production models and virtual population analyses (ICCAT, 1997).

Estimates of body size and age at sexual maturity are of fundamental importance for the determination of fishery management thresholds based on size- and age-structured stock assessments. In particular, determination of the spawning potential ratio (SPR: Goodyear, 1993) depends on size at maturity. Sex-specific size composition data are also needed to stratify catch and effort statistics, thereby reducing the variances of CPUE estimates.

Information on reproductive biology is inadequate for swordfish in the Pacific. Nakamura et al. (1951) were the first to infer spawning seasonality in the western Pacific based on net collections of swordfish larvae. Yabe et al. (1959) further described swordfish eggs and larvae and used plots of gonad weight versus body length for fish on spawning grounds to approximate body size at sexual maturity for female swordfish in the western Pacific. Kume and Joseph (1969) estimated body size at sexual maturity for female swordfish in the eastern Pacific, and Sosa-Nishizaki (1990) estimated body size at sexual maturity for female swordfish throughout the North Pacific. Uchiyama and Shomura (1974) estimated total fecundities for eight fish and provided anecdotal evidence of swordfish spawning near the Hawaiian Archipelago. Adult-size swordfish caught in the eastern North Pacific were described by Weber and Goldberg (1986) as reproductively inactive during late August–November. Hinton and Deriso's (1998) more recent evaluation of swordfish gonadal index data from the Japanese longline fishery, however, has documented the seasonal presence of reproductively active swordfish near Baja California during May–August. Although largely nonexistent for the Pacific, reproductive and related growth parameters have recently been estimated for swordfish in the Northwest Atlantic (Arocha et al., 1994; Arocha and Lee, 1995, 1996; Ehrhardt et al., 1996; Arocha, 1997).

Catch and effort data for swordfish in Pacific fisheries have been summarized by Miyabe and Bayliff (1987) and Nakano and Bayliff (1992) and reviewed

by Sosa-Nishizaki (1990) and Sosa-Nishizaki and Shimizu (1991). DiNardo and Kwok (1998) have provided a preliminary description of catch statistics and the body size and sex composition of swordfish caught by the Hawaii-based longline fishery in the central North Pacific.

Our study had several complementary objectives, and the ultimate goal of providing accurate and precise information for stock assessments of Pacific swordfish. In our study, we estimated size at sexual maturity for swordfish captured by the Hawaii-based pelagic longline fishery in the central North Pacific. Because the growth rates of adult male and female swordfish differ in the Pacific (Uchiyama et al., 1998), as elsewhere (Ehrhardt et al., 1996), size at maturity was characterized separately for males and females. We classified maturity on the basis of histological analyses of gonads subsampled from a larger sample of field-sexed fish and used this maturity classification as the basis for our estimates of size at maturity. The latter are compared with a complementary characterization of reproductive activity using gonad indices (Hinton et al., 1997). Data on body size (length), date, and location of capture of swordfish in the parent sample of field-sexed fish were used to provide preliminary descriptions of temporal and spatial patterns of size- and sex-specific catch. These patterns of sex and size composition identified factors that could be used for stratifying catch and effort data for the Hawaii-based longline fishery, thereby reducing the variance of population parameter estimates based on logbook records used in future stock assessments. Finally, we interpreted spatial and temporal variations in catch in terms of possibly different migratory behaviors by swordfish of different body sizes and sexes.

Methods and materials

Shipboard collections and measurements

About 90% of the swordfish analyzed were caught by commercial vessels fishing pelagic longlines in the central North Pacific from March 1994 to June 1997. Most (65%: Ito and Machado, 1996,[1] 1997,[2] 1999[3]) swordfish were caught on trips on which swordfish were targeted. Another 34% were caught on "mixed sets" (both tuna and swordfish targeted), and the remaining 1% on "tuna sets" (Boggs and Ito, 1993; He et al., 1997). The remaining 10% of swordfish examined were caught on swordfish research cruises of the NOAA ship *Townsend Cromwell* during 1992–97 in the region of the commercial fishery.

Commercial fishermen dressed all swordfish as the fish were brought aboard ship; observers noted that about 10% were alive and 90% moribund or dead upon retrieval. Viability of fish when sampled is important for interpreting the quality of histological specimens. Observers (NMFS SWR) were assigned to participating longline vessels according to a stratified random design based on vessel size (effort). Observers recorded eye-to-fork length (EFL, cm) for most swordfish caught. For most swordfish that were measured, sex was identified on the basis of macroscopic appearance of the gonads, and, for a random subsample of sexed fish, a gonad tissue sample (2 cm^3, including gonad wall) was collected from the middle of either gonad lobe and immediately fixed in 10% buffered formalin. Swordfish gonad samples were collected during most months of four consecutive years (172 trips sampled during March 1994–June 1997), complemented by specimens collected by research cruises in April–May of 1992 and 1993, September 1996, and March–April 1997. Specimens examined histologically thus spanned several annual cycles; overall 81% of the fish examined were collected during March–July spawning periods (Fig. 1). Fish were sampled throughout the spatial range of the longline fishery during March 1994–June 1997, mostly between lat. 17–41°N and long. 141–180°W (Fig. 2).

During spring 1997, SWR observers collected whole ovaries of approximately 100 swordfish as they were being dressed aboard ship. For each pair of ovaries, a fresh tissue specimen was collected and fixed for later histological evaluation of developmental stage (as described below), and the remainder of the ovaries were frozen for weighing ashore. The latter samples were used in analyses of gonad indices.

Laboratory processing

Field-classified sex was verified and reproductive condition evaluated based on gonadal developmental stage determined by microscopic examination of histological preparations and oocyte size frequencies. Fixed gonad specimens were stored for at least 60 days before oocytes were measured or a subsample was prepared for histological analyses. A single series of sequential, histological sections (6 µm thick) (2–8: mode=3[ovaries], mode=4[testes]) was cut and stained with Harris's hematoxylin, followed by eosin counterstain (Hunter and Macewicz, 1985). Slide sections were examined with a compound microscope at 60–300× and developmental stage categorized following the stage criteria of Murphy and Taylor (1990). For females, the following characteristics were noted for the largest size mode of oocytes present: presence and relative quantity of eosinophilic yolk, partly to moderately yolked oocytes, and fully yolked oocytes. If oocytes were fully yolked, we further noted the presence of hydrating or hydrated oocytes (HYDs), postovulatory follicles (POFs), and fully

[1] Ito, R. Y., and W. A. Machado. 1996. Annual report of the Hawaii-based longline fishery for 1995. Southwest Fish. Sci. Cent. Admin. Rep. H-96-12, Honolulu Laboratory, Southwest Fish. Sci. Cent., Natl. Mar. Fish. Serv., NOAA, Honolulu, HI 96822-2396, 45 p.

[2] Ito, R. Y., and W. A. Machado. 1997. Annual report of the Hawaii-based longline fishery for 1996. Southwest Fish. Sci. Cent. Admin. Rep. H-97-12, Honolulu Laboratory, Southwest Fish. Sci. Cent., Natl. Mar. Fish. Serv., NOAA, Honolulu, HI 96822-2396, 48 p.

[3] Ito, R. Y., and W. A. Machado. 1999. Annual report of the Hawaii-based longline fishery for 1998. Southwest Fish. Sci. Cent. Admin. Rep. H-99-06, Honolulu laboratory, Southwest Fish. Sci. Cent., Natl. Mar. Fish. Serv., NOAA, Honolulu, HI 96822-2396, 62 p.

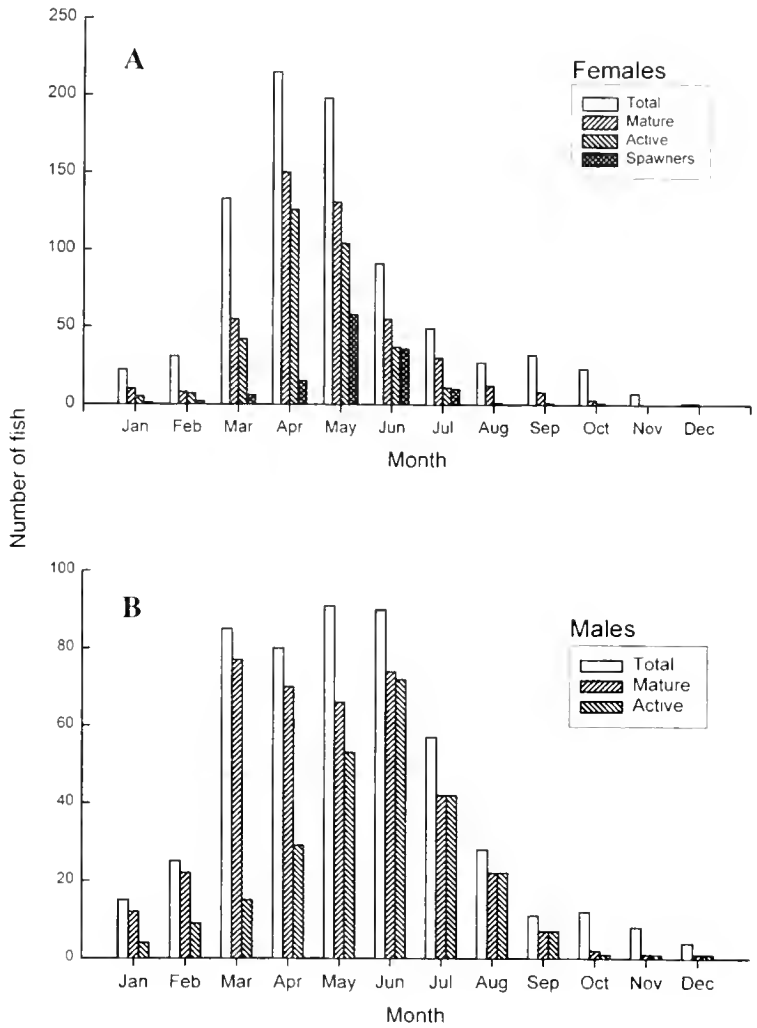

Figure 1

Numbers of (**A**) female and (**B**) male swordfish (*Xiphias gladius*) that were immature, mature, active, or imminent spawners (females only), which were caught on occasional research cruises and by the Hawaii-based pelagic longline fishery each month during March 1994–June 1997. Maturity and reproductive activity were assessed based on gonad developmental stages scored histologically.

yolked oocytes undergoing α-, or β- and later atresia (Table 1). Female individuals were designated as "immature" if their most advanced oocytes were unyolked or only partly to moderately yolked without substantial atresia, or as "mature" if their most advanced oocytes were fully yolked with or without atresia ("active-mature") or if their most advanced oocytes were less than fully yolked but with alpha or beta atretic stages present. Developmental stages were further described according to the diameters of the largest size class mode of oocytes present. Among mature females, fish were deemed "ripening mature" if fully yolked but lacking HYDs or POFs, "ripe mature" (imminent spawners) if POFs or HYDs were present, or "resting mature" if a majority of yolked oocytes were atretic.

Oocyte diameters were measured by using formalin-fixed whole oocytes or oocyte cross sections on histological slides. For formalin-fixed specimens, diameters of 25 of the largest oocytes were measured with a dissecting microscope (random axis, 25–50×). The median of 25 random diameters provides a cost-efficient estimator of average maximum oocyte size for multiple-spawning fishes (Lau and DeMartini, 1994); swordfish are multiple-spawners (Uchiyama and Shomura, 1974; Arocha, 1997). Histological slides were prepared for a random subset of these specimens; diameters of oocyte cross sections on slides were measured at 60–300× and for each fish ovary examined, maximum and minimum diameters were averaged for 5–10 of the largest oocyte sections present

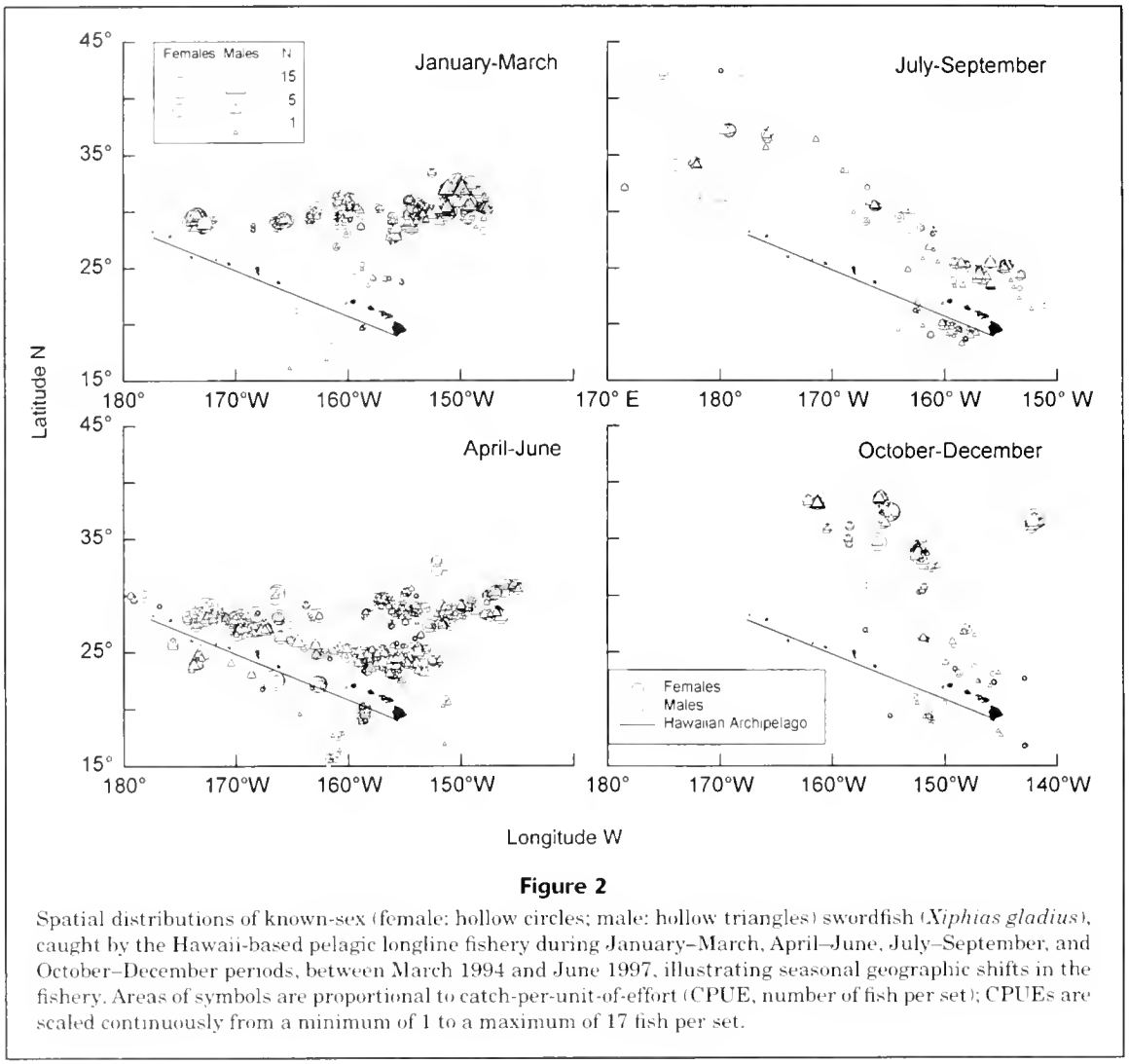

Figure 2

Spatial distributions of known-sex (female: hollow circles; male: hollow triangles) swordfish (*Xiphias gladius*), caught by the Hawaii-based pelagic longline fishery during January–March, April–June, July–September, and October–December periods, between March 1994 and June 1997, illustrating seasonal geographic shifts in the fishery. Areas of symbols are proportional to catch-per-unit-of-effort (CPUE, number of fish per set); CPUEs are scaled continuously from a minimum of 1 to a maximum of 17 fish per set.

that included a central nucleus and were spherical (least deformed by processing), so that the coefficient of variation (CV) of the diameter estimate was <10%. Diameters measured for a subset of matched (formalin-fixed, histology) specimens were used to convert between the two types of measurements.

The gonadal development of males was classified by using the criteria of Grier (1981) as specified for billfish by de Sylva and Breder (1997). Males were scored as "immature" if spermatogenesis (meiosis) was absent or, when occurring, if ripe (fully tailed) spermatozoa were restricted to crypts and lobules (tubules) of testes. Males were deemed mature only if ripe sperm were present in spermatic ducts, as well as in crypts and lobules, or as spent or resting if they had developed lobules but no spermatogenesis present (Table 1).

Sex was histologically verified for 506 males and 830 females. The sex of only 23 swordfish (8 males: 70–153 cm EFL, March–December; 15 females: 98–212 cm EFL, April–December) was misclassified from gross visual inspection of gonads by observers aboard commercial longliners. Misclassification error was unrelated to true sex (χ^2=0.02; df=1; P=0.9), and appeared unrelated to fish size or period of capture, although the data were too few to formally evaluate size and period effects. Because the misclassification rate was so low (0.5%), we ignored it in further analyses of the sex composition of swordfish catch where field-sexed fish were used.

For ovary specimens collected in spring 1997, frozen specimens were thawed overnight in a refrigerator. Each lobe of bilobed ovaries was weighed damp; accuracy was 1 g (if total ovary weight ≤500 g) or 20 g (if >500 g). Seven of 95 females caught during the spring 1997 spawning period lacked weights for one ovary lobe; total ovary weights of these fish were estimated by using the relationship between both ovaries (total gonad weight, GW) and right (RO) and left (LO) ovary weights (in g): $GW = 1.807RO$, and $GW = 2.170LO + 133.6$ (both r^2>0.98; n=88). Right ovaries of the swordfish examined were 28% heavier than left ovaries (matched-pair t-test; t=6.9; n=88).

Table 1

Histological criteria for classification of gonadal developmental stages and maturation in male and female swordfish, *Xiphias gladius*, caught in the central North Pacific during the period April 1992–June 1997. Maturity stages are based on the criteria of Murphy and Taylor (1990). Median observed oocyte diameters are for 10% formalin-fixed (sea water) specimens.

Maturity stage by sex		Histological appearance of the most advanced gamete stage present in gonads
Females		
1	vestigial	Primitive oogonia only; 80 µm
2	developing	Primary oocytes (basophilic) only present; 133 µm
3	maturing	Early vitellogenesis; beginnings of nucleus breakdown and development of fat inclusions; no chorionic membrane (zona pellucida); 211 µm
4	ripening	Oocytes well-yolked (completely eosinophilic); nuclear membrane indistinct; prominent chorionic membrane, with fat inclusions distributed throughout cytoplasm; 547 µm
5	spawning	Migratory (eccentric) nucleus, hydrating or hydrated oocytes present; 1012 µm
6	recently spawned	Postovulatory follicles present; 1197 µm
7	spent or resting	A majority of classes 4–5 yolked oocytes present undergoing α- β-, or later atresia; 201 µm
Males		
1	undeveloped	Spermatocytes only present; spermatogenesis (meiosis) lacking
2–3	maturing	Spermatogenesis present; some to many ripe (fully tailed) spermatozoa present in crypts and lobules (tubules), but none in spermatic ducts
4	ripe	Ripe sperm present in spermatic ducts as well as crypts and lobules; relatively little spermatogenic activity
5	spent	Developed lobules containing few remaining sperm

Statistical analyses

We estimated body length at median sexual maturity (L_{50}) for males and females separately using nonlinear regression. A derivative-free maximum likelihood method (Proc NLIN; SAS, 1989) was used to fit percentage maturity by 5-cm length class to the two-parameter logistic model,

$$P_x = 100 / (1+\exp^{(a-bEFL)}),$$

where P = percentage mature at length x; and
L_{50} = $(-a/b)$.

Sex ratios (females/total) also were related to 5-cm length class by using nonlinear regression. Regressions were weighted by the square root of the number of fish examined in each length class. Ninety-five percent confidence intervals on L_{50}'s were calculated by using SAS Proc PROBIT. Logistic regression (STATISTIX, vers. 4.1; Analytical Software, 1994) was used to relate ovarian developmental stage to oocyte diameter and to predict reproductive readiness with gonad weight plus body size. Contingency chi-square and unbalanced fixed-factor ANOVAs (Zar, 1984; SAS, 1989) were used to compare sex ratios and the relative body size compositions of swordfish catches, pooled by 1° lat. by 1° long. bins, during spawning (March–July) and nonspawning (August–February; see "Results" section) periods. Least-squares regression was used to regress median body length versus latitude after body length distributions were made linear by rank transformation. Analyses of sex ratios and size composition were limited to observer-sampled trips and should be considered a first approximation of patterns for the total Hawaii-based longline catches of swordfish during March 1994–June 1997. Significance was based on an alpha level of 0.05.

Results

Sex and maturity composition of sampled fish

During the 40-mo. sampling period, an estimated 142,000 swordfish were caught by the Hawaii-based pelagic longline fishery (2.26 million hooks: Ito and Machado, 1996,[1] 1997,[2] 1999[3]). Data for the 6639 field-sexed fish examined herein thus represent about 4.8% of the commercial landings of swordfish, with the samples reflecting about 4.9% of the total longline effort (2.26 million out of 45.7 million hooks) expended during the period. The sex ratio (females as fraction of total) of the field-sexed commercial catch was 0.533 (SE=0.006; $P<0.001$). About 64% of the 1336 swordfish examined histologically were sexually mature (stages ≥4, Table 1). The two sexes differed in maturity composition based on histological classification ($\chi^2=67.4$; $P<0.001$): 78% of 506 confirmed males but only 56% of 828 confirmed females were mature.

About 73% of 463 mature females were reproductively active (stages 4–6; including 28% stages 5–6 imminent spawners) and 27% were spent or resting (stage 7, Table 1). Of a total 130 spawning females, 33 had ovaries containing oocytes that were hydrating or hydrated, indicating imminent spawning. The ovaries of 122 fish contained POFs, suggesting ovulation within several days prior to capture. The exact age of POFs was inestimable because the likely temperature-dependent (Fitzhugh and Hettler, 1995) degradation rate of swordfish POFs is unknown and because gonad samples were collected from fish that had been hooked for differing lengths of time at varying water temperatures. Twenty-five of the 130 fish had ovaries containing both unovulated, hydrated oocytes and POFs from a previous spawning (Fig. 3, A and B). Of a total 395 mature (stage ≥4) males, 65% were reproductively active (stage 4) and 35% were spent or resting (stage 5, Table 1).

Oocyte size and developmental stage

Ovarian developmental stage was closely related to diameter of the largest size class mode of oocytes present in ovaries. The diameters of formalin-fixed whole oocytes (OD, in μm) and oocyte cross sections (XS, in eyepiece units [epu], where 1 epu=0.1544 μm) on histological slides were best related by the linear regression

$$OD = 11.9 + 6.320XS \qquad (r^2=0.948, n=182, P<0.001).$$

With logistic regression, ovarian development as an indicator of reproductive activity (where active=stages 4–6; inactive=stages 1–3, 7) was predicted with 97.5% accuracy for 828 fish collected during both spawning and nonspawning periods. The predictive relationship was

$$\ln(p/(1-p)) = -6.318 + 0.0180OD,$$

where OD = whole oocyte diameter (in μm); and
p = the probability of active stages 4–6.

The threshold (p=0.5) for stages 4–6 is predicted at a whole oocyte diameter of 351 μm. Oocyte size distributions are related graphically to ovarian stages in Figure 4. Median oocyte diameters for the respective stages are listed in Table 1.

Body lengths at sexual maturity

Estimates of L_{50} with all females were indistinguishable (<1 cm different: G-test; P=0.3) from those where females were used that had been caught during the 5-mo. (March–July) spawning periods when reproductively active females (stages 4–6) were present. L_{50} estimates for males were improved if immature (most likely less-than-year-old) fish, many of which were available only during nonspawning periods, were included. We therefore felt it preferable to describe L_{50}'s using all gonad sample fish collected year-round.

L_{50}'s were 102.0 ± 2.5 (95% CI) cm EFL for males (r^2=0.98; n=506) and 143.6 ± 2.8 cm EFL for females (r^2=0.97; n=816; Fig. 5). Fits to the logistic model were as follows:

$$\text{Males:} \quad \%\ Mature = 100/(1 + e^{(14.4011 - 0.1412EFL)})$$
$$\text{Females:} \quad \%\ Mature = 100/(1 + e^{(14.8569 - 0.1034EFL)}).$$

Females attained ≥95% sexual maturity at 173 cm EFL. The corresponding value for males was 123 cm EFL. The smallest reproductively active female whose ovaries contained hydrated oocytes or postovultory follicles was 134 cm EFL. Sample sizes ranged from 2 to 45 fish of each sex per 5-cm EFL class; only 6 out of 36 and 12 out of 31 classes contained <10 fish for females and males, respectively. Median sample sizes were 22 (for females) and 17 (for males) for each 5-cm class (Fig. 5).

Indices of spawning readiness

Reproductive readiness (verified by histological staging of ovaries) of female swordfish in the Hawaii-based fishery could be predicted by logistic regressions with body size (length, weight) and ovary weight (or with length- or weight-based gonad indices). Although the spawning activity of female swordfish was predictable from body size and ovary weight alone, the accuracy of prediction was improved if a measure of ovary maturation (such as size of the largest oocytes present) was included. Overall, about 96% of 95 females (range 8–295 kg, 76–247 cm EFL; Table 2A) were correctly classified (with reference to histological stages 4–6) as either reproductively active (1) or not (0) by the logistic regression

$$\ln(p/(1-p)) = \ln(RW) + \ln(GW) + \ln(EV),$$

where RW = round weight in kg;
GW = gonad weight in g; and
EV = oocyte volume in $mm^3 = 4/3\pi r^3$; and
r = diameter/2 (Table 2A).

The fit of this model was similar to those where oocyte volume plus any of several length- or weight-based gonad indices were used. Among the latter, the index, $GI(2') = [\ln(GW)/\ln(RW)]$, was best (90% accurate), and overall classification accuracy increased to 97% if oocyte volume was added to the model (Table 2B). The index, $GI(2) = [\ln(GW)/\ln(EFL)]$ of Hinton et al. (1997), plus oocyte volume, showed comparable accuracy (94%; Table 2C), and retained 87% accuracy even if oocyte volume was excluded (Table 2D). The latter length-based gonad index itself (Table 2D) should have the widest applicability, despite some loss in predictive power because an oocyte volume term is lacking, because data on swordfish body lengths and gonad weights are often available but body weight and egg size data are not. We also provide (Table 3) several key regressions of swordfish length-on-length and weight-on-length, summarized from Uchiyama et al. (1999), to enable conversions between the different index-based predictors of reproductive readiness.

Temporal and spatial spawning patterns

Swordfish caught by the Hawaii-based longline fishery during March 1994–June 1997 included both reproductively inactive and active adult fish, in addition to imma-

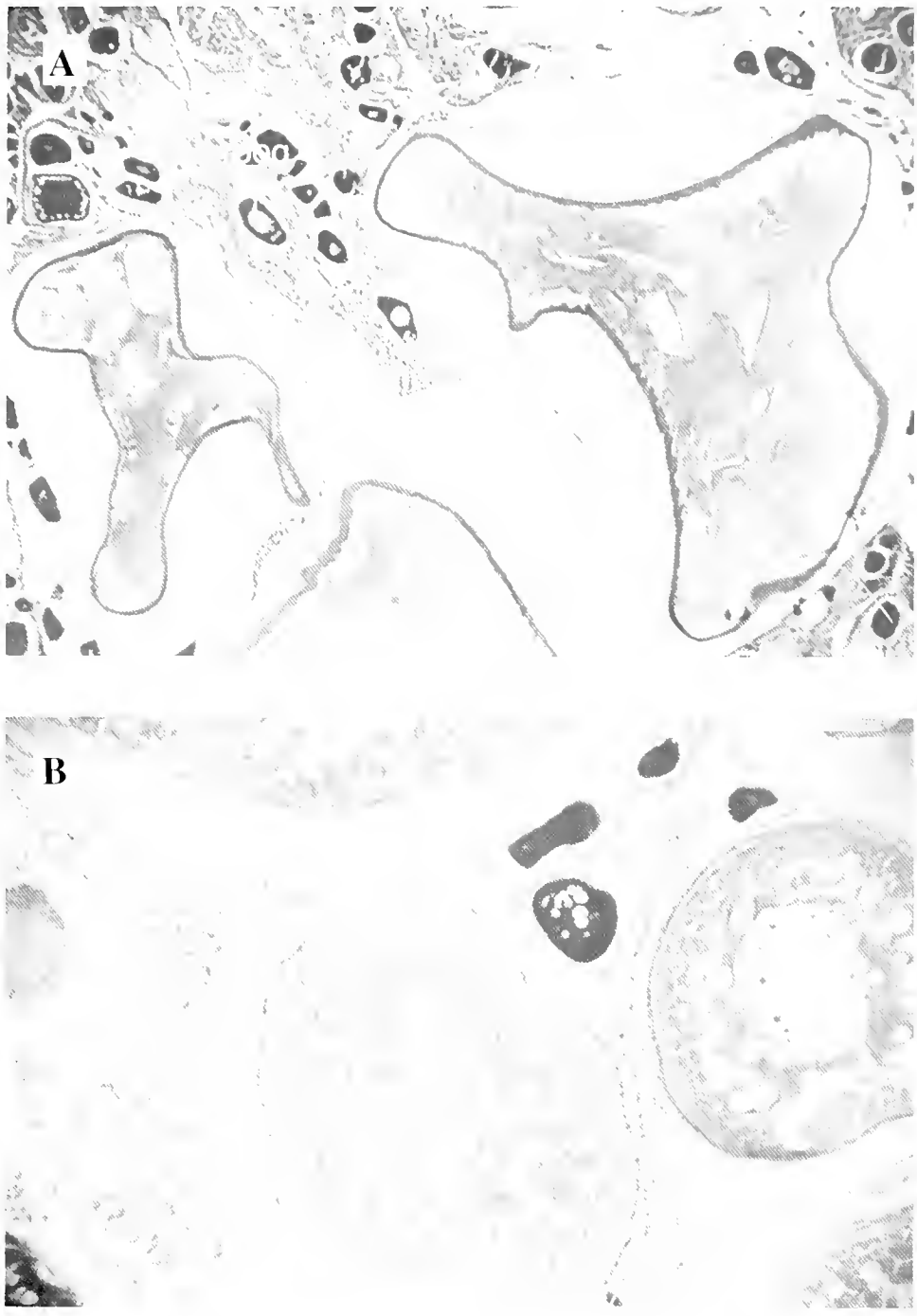

Figure 3

Histological sections of the ovaries of imminently spawning swordfish (*Xiphias gladius*) illustrating (**A**) hydrated oocytes (hyd; stage 5) and (**B**) postovulatory follicles (pof; stage 6). Several other developmental stages of oocytes are also present, including primitive oogonia (pog; stage 1); previtellogenic oocytes (poc; stage 2); early vitellogenic (evo; stage 3) and vitellogenic (vo; stage 4) oocytes; and atretic oocytes (atret, stage 7; an α-atretic, vitellogenic oocyte indicated by arrow in 3A).

ture, mostly female fish. Reproductively active females (stages 4–6) were caught primarily during spring (Fig. 6). Ninety-eight percent of all imminently spawning females were caught during March–July periods, and 73% were caught during May–June (Fig. 6). POFs and hydrated oocytes often co-occurred in ovaries (in 25 out of 33 cases;

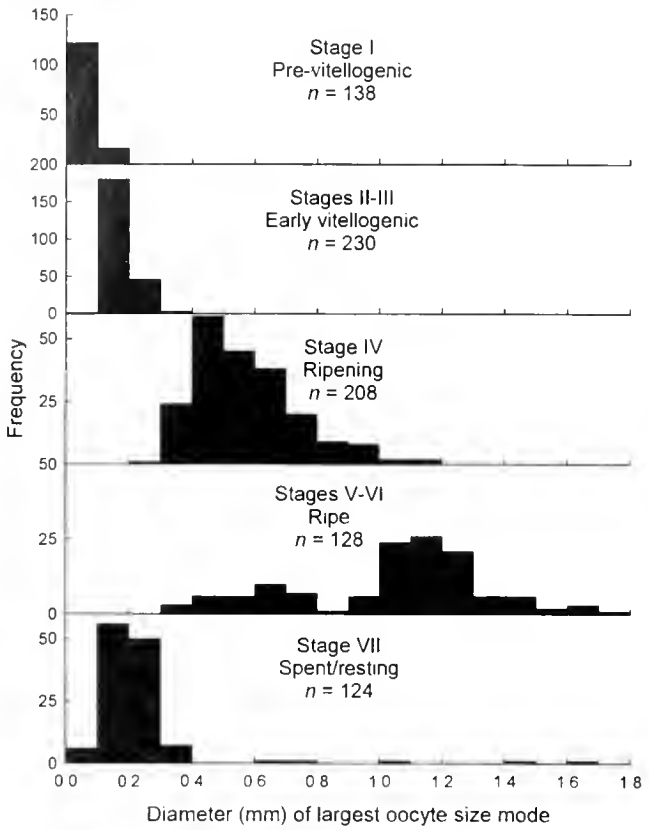

Figure 4

Size distribution of oocyte stages in ovaries of swordfish (*Xiphias gladius*) caught by the Hawaii-based pelagic longline fishery during March 1994–June 1997, which were examined histologically. Diameters (mm) are for the largest size class mode of viable (not atretic) oocytes present. Sample sizes refer to the numbers of specimens with ovaries in each stage.

χ^2=23.1; df=1; P<0.001). The relative numbers of active females and imminent spawners were independent of moon phase (Table 4), although indicating no lunar spawning periodicity. Eighty-two percent of all reproductively active (stage 4) males were caught during March–July. Many imminently spawning females were caught within several hundred km of the Hawaiian Archipelago (Fig. 6), not far beyond the borders of the 75- and 50-mile closures to pelagic longlining in the main Hawaiian and Northwestern Hawaiian Islands, respectively.

Size, sex, and maturity composition of catches

The size and sex composition of swordfish catches were related (Table 5; Fig. 7). Most (0.55) of the swordfish caught that were <140 cm were male, most (0.64) of those >150 cm were female, whereas the sex ratio (females/total) of fish between 140 and 150 cm EFL was indistinguishable from 0.5 (Fig. 8). Sex ratios fluctuated around 0.5 without pattern at lengths <100 cm, were an increasing power function of fish length between 100 and 220 cm (proportion female=$0.0018EFL^{1.1418}$; r^2=0.87; n=24 5-cm classes; P<0.001) and were consistently >0.9 at lengths >220 cm EFL (Fig. 7). Overall, males represented about 39.5% of the March 1994–June 1997 observer-sampled swordfish catch by weight. The female catch by weight was 60.5%.

The maturity composition of swordfish catches differed between the sexes. During March 1994–June 1997, mature fish represented about 56% and 77% of the sampled female catch in terms of numbers and weight, respectively. Mature fish comprised 88% (numbers) and 96% (weight) of the sampled male catch. Overall, 71% and 85% of the total sampled catch (both sexes) were mature by numbers and weight, respectively.

Both the sex and size composition of swordfish catches varied spatially (Fig. 9; Table 6). Latitude had a stronger influence on sex ratio and size composition than did longitude (Table 6, A and B). A large majority (61%) of all swordfish caught south of 27 N were males. The body size (hence sex) of swordfish caught might vary with depth and time

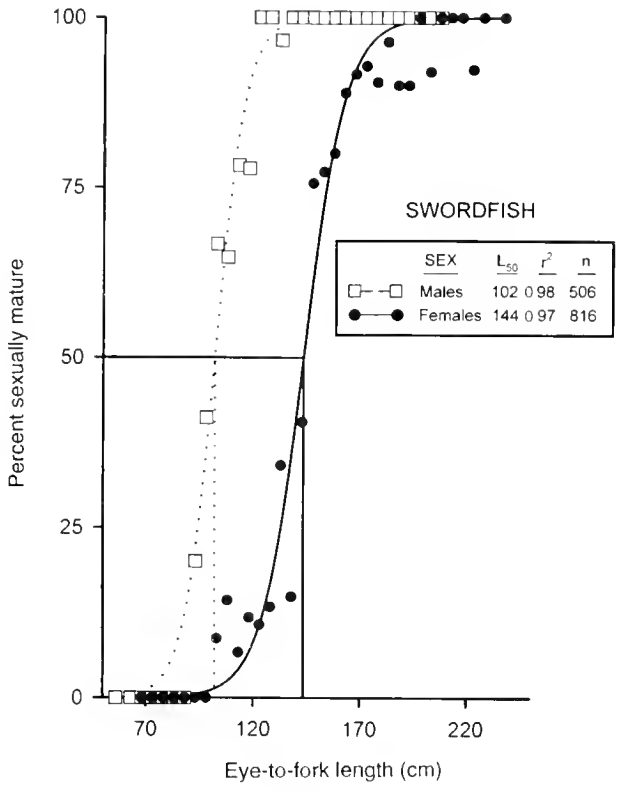

Figure 5

Nonlinear regression fits of the logistic model for percentage sexually mature versus eye-to-fork length (5-cm EFL class), weighted by square root of sample size per length class, for male and female swordfish (*Xiphias gladius*) caught by the Hawaii-based pelagic longline fishery during March 1994–June 1997. Solid and dashed best-fit lines are predicted relationships, and analogous perpendicular lines are median body size at sexual maturity (L_{50} intercepts), for females and males, respectively. Symbols represent mean percentages mature per 5-cm EFL class.

of day fished, and relatively more "tuna sets" (deep, daytime soak) are made during the peak summertime tuna season, particularly at latitudes at and below the Hawaiian Archipelago (He et al., 1997). We therefore reevaluated the sex composition of swordfish catches south and north of 27° N using only the fish caught on sets on which swordfish were targeted (He et al., 1997). A total of 5547 fish were caught on swordfish sets, representing 84% of all swordfish present in the parent sample. The male proportion of 585 swordfish caught on swordfish sets south of 27° N was the same (61%) as for all observer-sampled sets. Proportions of females in catches at and north of 27° N also were the same (56%) for total and swordfish-targeted sets.

Sex and size composition of the swordfish catch varied with season (Table 6A). Small-bodied males and females dominated lower-latitude catches during spawning as well as nonspawning periods (Table 6B). Overall, about 64% by numbers and 65% by weight of all swordfish were caught during March–July spawning periods.

Several interesting spatial patterns were apparent in the size composition data. Relatively greater numbers of "small-bodied" (<25th length percentile; females: <126 cm; males: <118 cm EFL) swordfish were caught south of 22° N (Table 6B). Relatively greater numbers of "large-bodied" (>75th percentile; females: >172 cm; males: >156 cm EFL) fish were caught north of 35° N (Table 6C). Median body sizes of swordfish caught increased with latitude (regressions of ranked median EFL on 1° bins, r^2>0.8 for each sex, n=21, P<0.001) with the proportions of catch that were small-bodied (and mostly male) greater south of about 22° N (Fig. 9).

Discussion

Sex-specific sizes at maturity

Effects of methods Ninety-five percent confidence intervals on our estimates of median body size (L_{50}) at sexual

Table 2

Summary results of logistic regressions predicting reproductive activity (histological stages 4–6) versus inactivity (stages 1–3, 7; see Table 1) based on (**A**) round weight (RW), gonad weight (GW), plus egg volume (EV); (**B**) a weight-based gonad index [GI(2')] plus EV; (**C**) a length- based gonad index [GI(2)] plus EV; or (**D**) GI(2) alone; for female swordfish, *Xiphias gladius*, sampled from the Hawaii-based pelagic longline fishery during May–June of 1997.

A $\ln(p/(1-p)) = \ln(RW) + \ln(GW) + \ln(EV)$

Predictor variables	Coefficient	Standard error	*P*-value
ln(*RW*)	−10.740	3.437	0.0018
ln(*GW*)	4.228	1.899	0.0260
ln(*EV*)	2.073	0.610	0.0007

Classification table			Proportion correctly classified		
	Predictions		0	1	overall
Actual	0	1	0.900	0.973	0.958
0	18	2			
1	2	73			

B $\ln(p/(1-p)) = GI(2') + \ln(EV)$, where $GI(2') = [\ln(GW)/\ln(RW)]$

Predictor variables	Coefficient	Standard error	*P*-value
GI (2')	−21.464	5.176	0.0001
ln(*EV*)	2.822	0.610	0.0001

Classification table			Proportion correctly classified		
	Predictions		0	1	overall
Actual	0	1	0.850	1.000	0.968
0	17	3			
1	0	75			

C $\ln(p/(1-p)) = GI(2) + \ln(EV)$, where $GI(2) = [\ln(GW)/\ln(EFL)]$

Predictor variables	Coefficient	Standard error	*P*-value
GI (2)	−15.916	3.847	0.0001
ln(*EV*)	1.934	0.444	0.0001

Classification table			Proportion correctly classified		
	Predictions		0	1	overall
Actual	0	1	0.700	1.000	0.937
0	14	6			
1	0	75			

D $\ln(p/(1-p)) = GI(2)$

Predictor variables	Coefficient	Standard error	*P*-value
GI (2)	20.559	4.823	0.0001
Intercept	−24.968	6.008	0.0001

Classification table			Proportion correctly classified		
	Predictions		0	1	overall
Actual	0	1	0.650	0.933	0.874
0	13	7			
1	5	70			

Table 3

Predictive equations and summary statistics for best-fit regressions relating various body length and weight metrics for swordfish, *Xiphias gladius*, in the central North Pacific. Source: Uchiyama et al. (1999). Eye-to-fork length (EFL) and lower jaw-to-fork length (LJFL) are cm; and round weight (RW) and dressed weight[1] (DW) are kg. Sample size (*n*) is number of fish (sexes pooled). All equations are significant at $P<0.001$.

Model	Equation	SE *b*	SE *a*	*n*	r^2
$EFL = a + b \cdot LJFL$	$EFL = -6.543 + 0.927 \cdot LJFL$	0.006	0.849	179	0.992
$LJFL = a + b \cdot EFL$	$LJFL = 8.009 + 1.071 \cdot EFL$	0.007	0.865	179	0.992
$RW = a \cdot EFL^b$	$RW = 1.299 \cdot 10^{-5} \cdot EFL^{3.074}$	0.041	$3.010 \cdot 10^{-6}$	166	0.967
$DW = a \cdot RW^b$	$DW = 0.646 \cdot RW^{1.032}$	0.051	0.016	73	0.987

[1] Dressed weight is defined as round (total) weight minus the head, entrails, vertical and pectoral fins, and with caudal fin (including caudal peduncle and keel) removed by a cut made between the 22nd and 23rd vertebrae (Uchiyama et al., 1999).

maturity were within ±2–3% of their respective estimate and provide reasonably precise input parameters for stock assessment. Occasional estimates of less-than-complete maturity in some larger length classes of females (Fig. 5) likely reflect chance indetection of relatively rare, large atretic oocytes in the ovaries of inactive but mature females. Such may be expected when only a single region of ovary is examined histologically. We feel that the evalu-

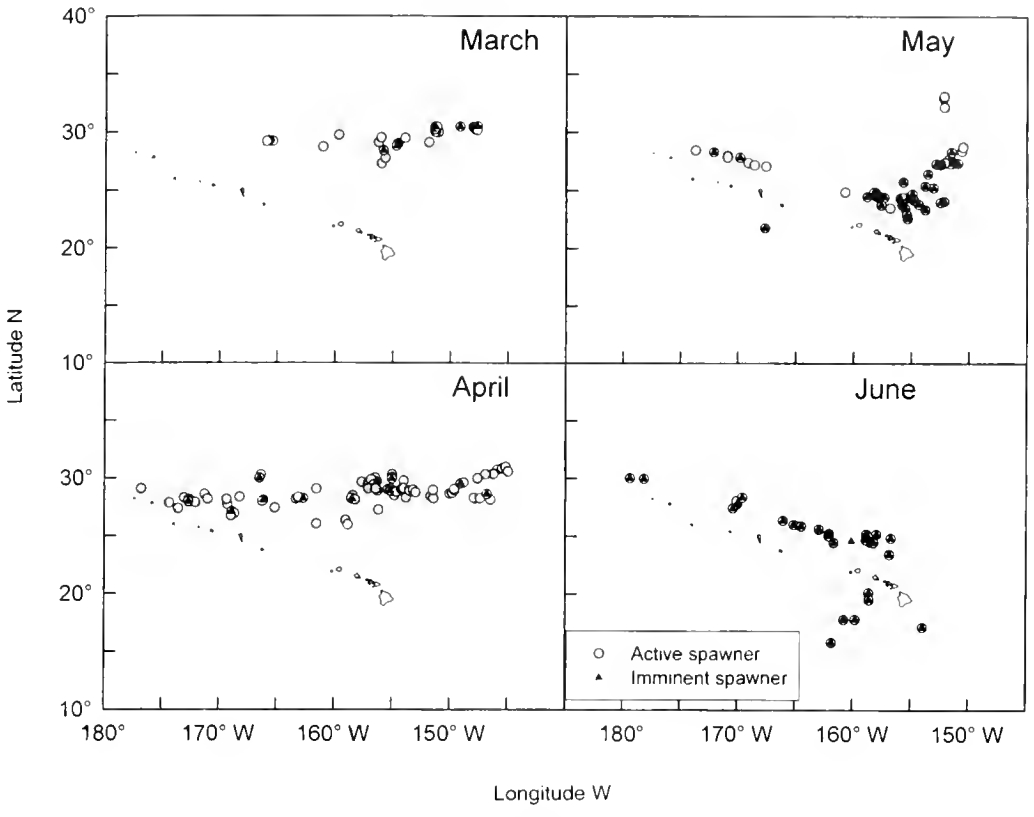

Figure 6

Capture locations of imminent spawners (stages 5–6; solid triangles) overlaid on locations of all reproductively active females (stages 4–6; shaded circles), for swordfish (*Xiphias gladius*) caught by the Hawaii-based pelagic longline fishery during March 1994–June 1997. Monthly plots from March, April, May, and June depict the increasing proximity of imminent spawners to the Hawaiian Archipelago as the spawning season progresses.

ation of greater numbers of females by using only a single ovary section offsets the rare failure to detect maturity in mature but inactive females.

Histological examination of gonadal developmental stage is the most accurate and expensive method of characterizing sexual maturity, and cost-effective alternatives are desirable (West, 1990). Gonad indices (GIs) represent one such general (West, 1990) and specific (Hinton et al., 1997) option. Our findings indicate that swordfish body weight plus ovary weight together can predict reproductive activity with >90% accuracy in swordfish caught by the Hawaii-based fishery. Our observations support the conclusion of Hinton et al. (1997) that GIs can provide useful proxies of reproductive activity in swordfish. We reiterate, however, that GIs alone are limited to detection of reproductive activity (Hinton et al., 1997); without ancillary data such as gonad development or oocyte size, GIs are often not reliable measures to distinguish reproductively inactive but mature females from immature females during the nonspawning season (West, 1990; Mejuto and Garcia, 1997). GIs are most often used for determining spawning seasons; if nonspawning season fish are to be included in a size-at-maturity evaluation, a relatively inexpensive alternative to histological staging (such as oocyte size) should be used for deducing maturation stages. Oocyte size can provide an accurate proxy for gonadal developmental stage

Table 4

Results of 2×3 χ^2 test comparing relative frequency with which imminently spawning (stages 5–6) female swordfish, *Xiphias gladius*, were caught, among all reproductively active females (stages 4-6) caught during new, quarter, and full moon periods by the Hawaii-based pelagic longline fishery during March 1994–June 1997. χ^2 = 3.28, df = 2, P = 0.20.

Period	Active	Spawning	Both
New	34	27(44%)	61
Quarter	76	39(34%)	115
Full	74	59(44%)	133
All	184	125	309

Table 5

Monthly sex ratios (females/total), effort (positive swordfish sets), and summary statistics for body sizes of female and male swordfish, *Xiphias gladius*, used to describe sex and size composition of catch. n = number of fish in sample. EFL = eye-to-fork length (cm).

Month	Sex	n	Sex ratio	Trips (sets)	25th percentile	Median EFL	75th percentile
Jan	F	182	0.56	3 (35)	132	153	176
	M	142		3 (32)	125	144	163
Feb	F	334	0.56	9 (66)	129	148	165
	M	264		11 (60)	125	141	159
Mar	F	883	0.55	13 (161)	129	151	175
	M	723		13 (165)	121	136	159
Apr	F	746	0.58	15 (170)	128	150	175
	M	531		17 (164)	118	134	152
May	F	359	0.51	14 (110)	120	151	181
	M	340		14 (108)	115	129	148
Jun	F	183	0.44	12 (71)	118	148	171
	M	237		14 (83)	118	139	160
Jul	F	174	0.46	11 (51)	118	152	178
	M	204		10 (60)	114	135	157
Aug	F	39	0.39	4 (17)	106	136	152
	M	62		7 (29)	102	125	151
Sep	F	41	0.53	6 (24)	93	105	122
	M	36		6 (21)	68	102	126
Oct	F	159	0.45	11 (50)	120	140	155
	M	193		10 (50)	119	138	164
Nov	F	283	0.56	6 (49)	124	151	167
	M	218		5 (47)	108	133	152
Dec	F	156	0.51	7 (36)	136	159	180
	M	150		6 (39)	121	140	160
All	F	3539	0.533	111 (840)	126	149	172
	M	3100		116 (858)	118	136	156

in swordfish (Taylor and Murphy, 1992; Arocha and Lee, 1995; our study). Gonad weights scaled for body length (because body lengths, not weights, are typically collected for swordfish at sea) deserve further evaluation as predictors of spawning readiness, particularly because our findings for swordfish in the central North Pacific are so similar to those of Hinton et al. (1997) for Atlantic swordfish.

Other maturity estimates Prior reported estimates of body size at sexual maturity for female swordfish in the Pacific in general do not agree with ours, but dissimilarities likely reflect the different measures used to gauge sexual maturity used by various researchers. For example, Yabe et al. (1959) concluded, from length distributions and gonad weights, that "most [female] swordfish" in the western Pacific mature sexually between 150 and 170 cm EFL. Kume and Joseph (1969) observed that female swordfish "in spawning condition" (defined as having a greater than defined threshold value of gonad index) were not "regularly encountered" until about 170 cm EFL. Sosa-Nishizaki's (1990, p. 64) estimate of sexual maturity at about 160 cm EFL for "most individuals" was also inferred from a length-based GI. In contrast to females, ours is the first estimate of any kind for body size at sexual maturity of male swordfish in the Pacific Ocean. Our results overall underscore the importance of sex-specific, histologically validated estimates of median body size at sexual maturity as data for stock assessments.

Our estimates of L_{50} for swordfish caught by the Hawaii-based longline fishery appear comparable (for males) to slightly smaller (females) than estimates for swordfish caught in several regions of the Atlantic. For swordfish from the Straits of Florida, Taylor and Murphy (1992) observed L_{50}'s of 112 and 182 cm lower jaw-to-fork length (LJFL) for males and females, respectively, equivalent to 96 and 161 cm EFL. Arocha and Lee (1996) estimated L_{50}'s of 129 (males) and 179 cm LJFL (females), equivalent to 112 and 158 cm EFL, respectively, for swordfish caught throughout the western Atlantic. We caution that these L_{50} estimates for swordfish in the Atlantic may not be totally comparable to ours because studies might differ in whether estimates apply to fish caught throughout the entire year or during spawning periods only.

Female swordfish in the Mediterranean presently mature at an L_{50} of about 142 cm LJFL (de la Serna et al., 1996),

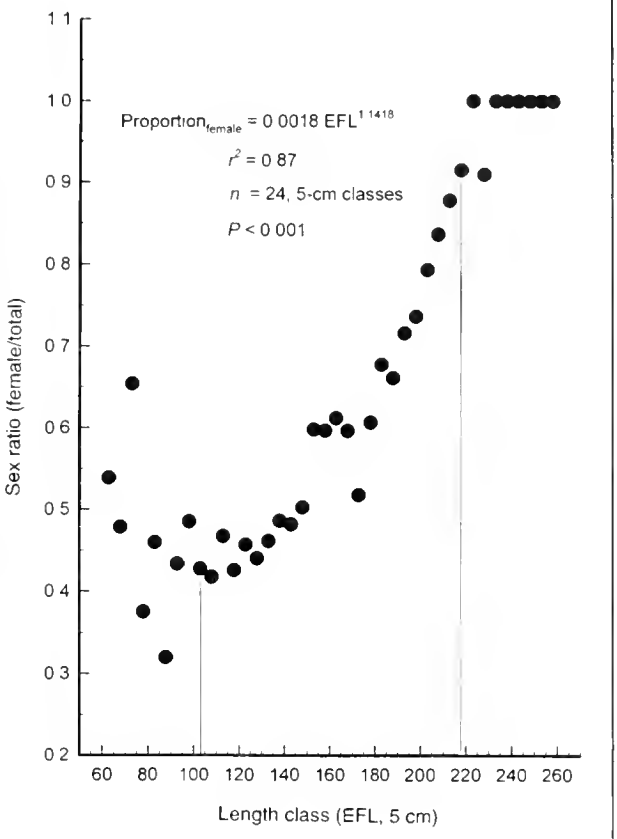

Figure 7

Relationship between sex ratios (females/total) estimated from catches and eye-to-fork length (EFL, 5-cm classes) for swordfish (*Xiphias gladius*) caught by the Hawaii-based pelagic longline fishery during March 1994–June 1997. Vertical lines depict the bounds (100≤EFL≤220 cm) used to regress proportion female on fish length.

equivalent to an estimated 124 cm EFL, considerably smaller than that documented for females in any other fishery. This estimate by de la Serna et al. (1996) was based on length-based gonad indices that were histologically validated.

For swordfish caught by the Hawaii-based longline fishery, the disparate body lengths at median sexual maturity of males and females are equivalent to a threefold difference between 55 kg RW (40 kg dressed-head off weight, DW) for females and 19 kg RW (14 kg DW) for males. Corresponding ratios of female:male body weights at L_{50} for swordfish in the tropical and western North Atlantic are 4.4 (Taylor and Murphy, 1992) and 2.7 (Arocha and Lee, 1996). Details of computation notwithstanding, these disparities in mass clearly represent biologically meaningful differences between the sexes in swordfish. Sexual differences in rates of biomass accrual—likely due to sexually dimorphic growth rates—translate to important differences in the sustainable fisheries yield provided by each sex. With later maturation, the period of rapid prereproductive somatic growth of female swordfish extends several or more years longer than that of males. Taylor and Murphy (1992) for example estimate ages-at-sexual maturity of swordfish from the Straits of Florida, corresponding to median sizes-at-maturity, as 5.5 yr (for females) and 1.4 yr (for males).

At present our characterization of maturity in North Pacific swordfish is limited to body size. Age-at-maturity estimates must await completion of size-at-age studies being conducted at the Honolulu Laboratory of the National Marine Fisheries Service.

Sex and size composition

Sex ratios of swordfish caught by the Hawaii-based longline fishery vary temporally and spatially. These variations may partly reflect different availabilities or catchabilities resulting from sexual differences in behavior that change seasonally (e.g. during spawning periods). Variations in the sex composition of catches must partly reflect different natural distributions of the sexes. Sex ratios of catches follow recurrent seasonal patterns among years, and spatial differences in the sex composition of catches repeat annually. Neither of these two observations would be likely if, for example, the sex composition of catches represented simple targeting of larger (female) fish by fishermen.

Similarities in sex ratios-at-length between North Atlantic (Stone and Porter, 1997) and central North Pacific swordfish (our study) suggest that size-specific sex ratios of swordfish catches can be predicted with adequate precision from data on the length composition of catches. If true, this could obviate the need for a direct characterization of the sex composition of swordfish catches—a task complicated in fisheries like Hawaii's in which swordfish are landed fully dressed. Sex ratios of swordfish caught by the Hawaii-based fishery are identical for swordfish-targeted and nonswordfish-targeted sets. Estimates of the sex ratio of swordfish catches in the Hawaii-based fishery thus seem robust to the specifics of capture, at least for the period sampled. Further comparisons of sex ratio estimates for catches with different gear types over a longer sampling period would be required to thoroughly evaluate possible sexual differences in catchability and expand inferences on sex ratios beyond catch to stock.

Seasonal patterns Temporal changes in the sex ratios and related size composition of swordfish catches in the Hawaii-based longline fishery resemble those observed for swordfish in other known spawning areas. Taylor and Murphy (1992) observed analogous temporal differences in catches of male and female swordfish in and near the Straits of Florida, where the fraction of males in catches was significantly greater than that of females only during peak (spring–summer) spawning periods. Temporal patterns of changes in sex ratios thus are consistent with sexual differences in migratory and spawning or other reproductive behaviors such as the greater propensity for males to aggregate in group-spawning pelagic species (Hunter and Macewicz, 1986) and other fishes.

Spatial patterns Arocha and Lee (1995) observed spatial variations, complementary to Taylor and Murphy's (1992)

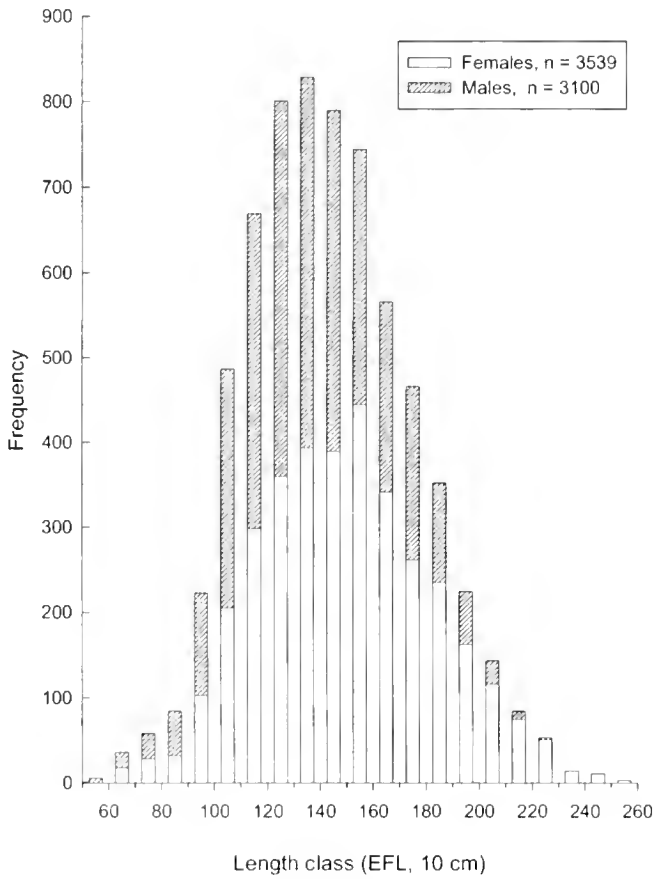

Figure 8

Size-specific sex ratios of swordfish (*Xiphias gladius*), used to evaluate sex and size composition of catch of the Hawaii-based pelagic longline fishery during March 1994–June 1997. For readability, lengths (EFL) have been pooled by 10-cm classes.

temporal variations in swordfish sex ratios elsewhere in the western Atlantic. The sex ratios of adult-size swordfish (>125 cm LJFL, but smaller than very large adults [>195 cm], the size at which the numbers of males diminish greatly in Atlantic swordfish stocks) are strongly male-biased only in the subtropical region (19–35°N) in which most spawning occurs (Arocha et al., 1994; Arocha and Lee, 1995). Spatial patterns similar to the latter also have been observed in spawning regions of the tropical western Atlantic (Mejuto et al., 1998) and western Indian Ocean (Mejuto et al., 1995).

Spatial differences in the sex and size composition of swordfish also may be related to sex-specific foraging migrations. Differences in the sex and size composition of swordfish catches have been noted by others in western Atlantic fisheries. Males predominate in catches made at tropical latitudes but females dominate in waters <18°C (Beckett, 1974). Most swordfish caught in the western North Atlantic off New England and the Canadian maritime provinces are large female fish (Tibbo et al., 1961).

Distributional ecology and energetics of migration

Limited tag-recapture data[4] suggest that some swordfish move great distances within the North Pacific. Swordfish also display marked diel vertical migrations that appear to vary among fish of different sizes and that inhabit continental shelf versus open ocean areas (Carey and Robison, 1981; Carey, 1990). As they migrate between warm mixed layer and cold subthermocline waters, swordfish encounter changes in water temperature as great as 19° in 2.5 h (8–27°C; Carey and Robison, 1981). A vascular rete system enables swordfish to dampen the rate of temperature loss in swimming muscles on deep dives, and it is likely that body mass importantly influences this ability (Carey, 1990) and the metabolic costs of inhabiting cold water masses

[4] Boggs, C. H. 1998. Unpubl. data. Honolulu Laboratory, Southwest Fish. Sci. Cent., Natl. Mar. Fish. Serv., NOAA, Honolulu, HI 96822-2396.

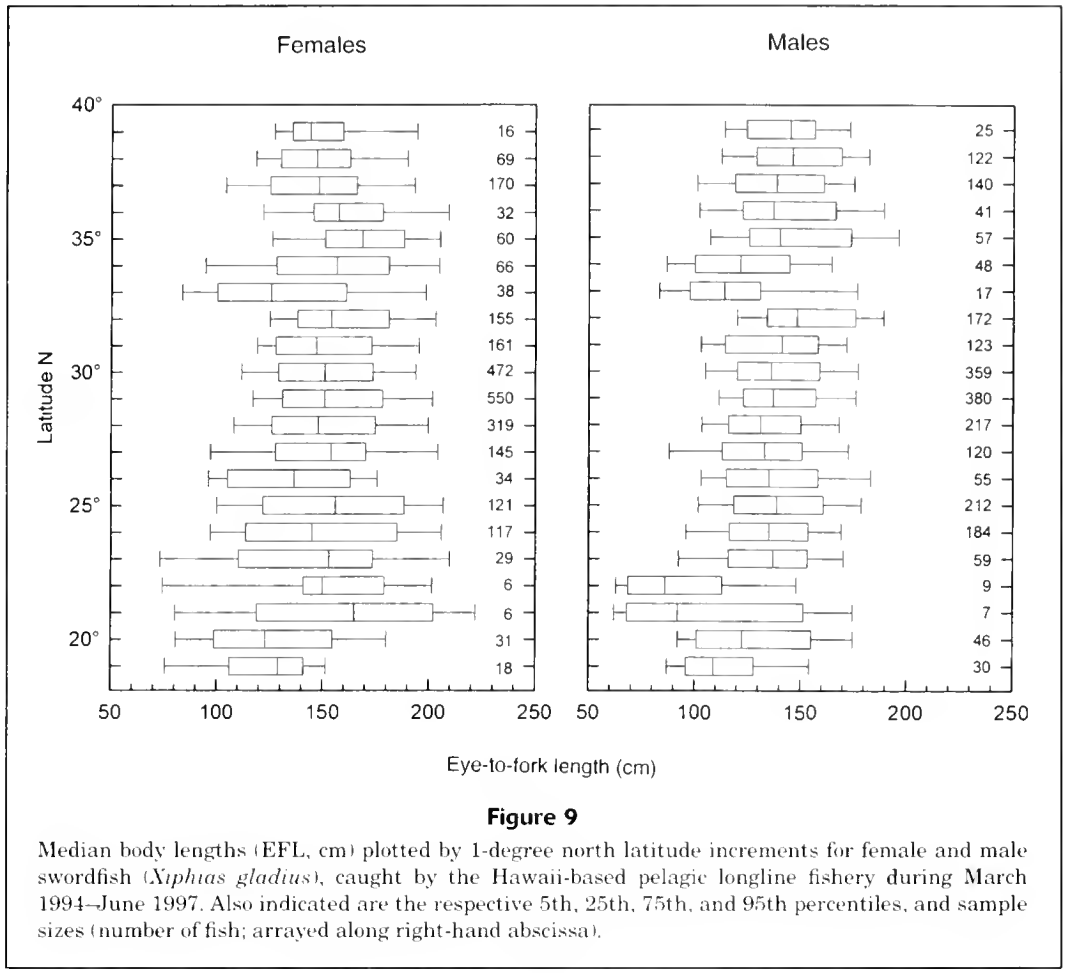

Figure 9

Median body lengths (EFL, cm) plotted by 1-degree north latitude increments for female and male swordfish (*Xiphias gladius*), caught by the Hawaii-based pelagic longline fishery during March 1994–June 1997. Also indicated are the respective 5th, 25th, 75th, and 95th percentiles, and sample sizes (number of fish; arrayed along right-hand abscissa).

(first hypothesized as a "size-temperature mediated physiological mechanism" by Hoey, 1991).

Horizontal movements also incur different energetic costs, as well as other types of costs, for fishes of different body sizes (Roff, 1988). It is plausible that feeding and spawning migrations involve different costs for individual swordfish ranging over the broad spectrum of body sizes (90–210 cm EFL, 13–180 kg; Fig. 8) commonly caught by the Hawaii-based fishery. Because most small swordfish are males and most large swordfish are females, it is further likely that the costs of migration differ between the sexes as well as among fish of varying body sizes that might migrate different distances. The significant relationships observed between latitude and sex ratio and between latitude and body size for swordfish of both sexes in the central North Pacific are consistent with the latter hypothesis.

Recurrent patterns of variation in the sex composition of swordfish catches throughout the world's longline fisheries remain poorly understood. Observed patterns may reflect natural differences in distributions of the sexes, may represent consistent artifacts of different catchabilities of the sexes during spawning periods, or both. A challenging topic for future research will be the evaluation of whether the differences reflect sexually distinct costs versus benefits for vertical or horizontal migration that result from the disparate body masses of males and females.

Implications for stock assessment

It is clear that stratifying swordfish catch statistics by sex could appreciably reduce the variances of catch and effort estimates, and future research should include simulation studies that explore the quantitative effects of sex stratification on stock assessments (Restrepo, 1991). Further, if our observations for swordfish caught by the Hawaii-based longline fishery have identified patterns that are relevant to swordfish caught elsewhere, age-structured stock assessments for swordfish in the Pacific should evaluate explicitly the potentially great importance of temporal and spatial dynamics in the sex and size composition of catches. It will likely be necessary to stratify catches by latitude of capture (and perhaps spawning and nonspawning period), in addition to standardizing CPUE statistics for environmental variables and targeting (e.g. see He et al., 1997; Hinton and Deriso, 1998; Bigelow et al., 1999), in order to reduce the variances of abundance indices used in stock assessments.

Table 6

Results of fixed-factor ANOVAs relating (**A**) sex ratio (females/total) versus period (spawning = Mar–Jul, nonspawning = Aug–Feb), latitude class (North: ≥27 N, South: <27 N) and longitude class (East: ≤160 W, West: >160 W); (**B**) the relative number of fish smaller than the 25th length percentile (RNQ1, see text) versus period and latitude class (Far S: ≤22 N, Other: >22 N); and (**C**) the relative number of fish larger than the 75th percentile (RNQ3, see text) vs sex and latitude class (Far N: ≥35°N, Other: <35 N) on sets with swordfish present, for swordfish, *Xiphias gladius*, caught by the Hawaii-based pelagic longline fishery during March 1994–June 1997. NS terms (e.g. longitude) are unspecified. SS = sum of squares; MS = mean square; LSMEAN = least square mean; SE LSMEAN = Standard error of least square mean.

A Source		df	SS	MS	*F*-value	*Pr>F*
Latitude		1	6.634	6.634	23.13	0.0001
Period × Latitude		2	4.297	2.149	7.49	0.0006
			Sex ratio			
Case	Period × Latitude		LSMEAN	SE LSMEAN	Contrasts	
1	Nonspawning	N	0.532	0.012		
2	Nonspawning	S	0.472	0.048	3>1=2=4	
3	Spawning	N	0.584	0.009		
4	Spawning	S	0.392	0.016		
B Source		df	SS	MS	*F*-value	*Pr>F*
Period		1	2.634	2.634	10.64	0.0011
Latitude		1	14.179	14.179	57.29	0.0001
Period · Latitude		1	2.009	2.009	8.12	0.0044
			RNQ1			
Case	Period · Latitude		LSMEAN	SE LSMEAN	Contrasts	
1	Nonspawning	FarS	0.696	0.073		
2	Nonspawning	Other	0.248	0.011	1>3>2=4	
3	Spawning	FarS	0.433	0.043		
4	Spawning	Other	0.230	0.008		
C Source		df	SS	MS	*F*-value	*Pr>F*
Sex		1	0.486	0.486	2.31	0.13
Latitude		1	1.569	1.569	7.47	0.0063
Sex · Latitude		1	1.254	1.254	5.97	0.0146
			RNQ3			
Case	Sex · Latitude		LSMEAN	SE LSMEAN	Contrasts	
1	Female	FarN	0.253	0.023		
2	Female	Other	0.248	0.008	3>1=2=4	
3	Male	FarN	0.321	0.023		
4	Male	Other	0.232	0.009		

Acknowledgments

We thank Don Peterson, Tim Price, and Lyle Enriquez of the NMFS, Southwest Region (SWR, Long Beach, CA) office and Tom Shearer, Kevin Busscher, and numerous shipboard observers (anonymous for confidentiality) of the SWR, Honolulu Office, for the organized collection of specimens and data management necessary to complete our study. Eric Yamanoha (Pathology Department, Queen's Hospital, Honolulu) ably supervised the histological work. We also thank Chris Boggs, Gerard DiNardo, Kurt Schaefer, and two anonymous reviewers for constructive criticisms of manuscript drafts and Debra Yamaguchi for help with the figures.

Literature cited

Analytical Software, Inc.
1994. STATISTIX, user's manual, vers. 4.1. Analytical Software, P.O. Box 12185, Tallahassee, Florida, 329 p.

Arocha, F.
1997. The reproductive dynamics of swordfish *Xiphias gladius* L. and management implications in the northwestern Atlantic. Ph.D. diss., Univ. Miami, Florida, 383 p.

Arocha, F., and D. W. Lee.
1995. The spawning of swordfish from the Northwest Atlantic. Int. Comm. Conserv. Atl. Tunas, Coll. Vol. Sci. Pap., vol. 44(3):179–186.
1996. Maturity at size, reproductive seasonality, spawning frequency, fecundity and sex ratio in swordfish from the Northwest Atlantic. Int. Comm. Conserv. Atl. Tunas, Coll. Vol. Sci. Pap., vol. 45(2):350–357.

Arocha, F., D. W. Lee, and J. R. Grubich.
1994. Observations on sex ratio, maturity stages, and fecundity estimates of swordfish, *Xiphias gladius*, in the Northwest Atlantic Ocean. Int. Comm. Conserv. Atl. Tunas, Coll. Vol. Sci. Pap., Vol. 42(1):309–318.

Beckett, J. S.
1974. Biology of swordfish, *Xiphias gladius* L., in the Northwest Atlantic Ocean. *In* Proc. Int. Billfish Symp., Part 2, Review and contributed papers (R. S. Shomura, and F. Williams, eds.), p. 105–106. U. S. Dep. Commer., NOAA Tech. Rep. NMFS SSRF-675.

Bigelow, K. A., C. H. Boggs, and X. He.
1999. Environmental effects on swordfish and blue shark catch rates in the U.S. North Pacific longline fishery. Fish. Oceanogr. 8:179–198.

Boggs, C. H., and R. Y. Ito.
1993. Hawaii's pelagic fisheries. Mar. Fish. Rev. 55:69–82.

Carey, F. G.
1990. Further acoustic telemetry observations of swordfish. *In* Planning the future of billfishes: research management in the 90s and beyond, Proc. 2nd Int. Billfish Symp., Kailua-Kona, Hawaii, August 1–5, 1988; Part 2: Contributed papers (R. H. Stroud, ed.), p. 103–122.

Carey, F. G., and B. H. Robison.
1981. Daily patterns in the activities of swordfish, *Xiphias gladius*, observed by acoustic telemetry. Fish. Bull. 79:277–292.

de la Serna, J. M., J. M. Ortiz de Urbina, and D. Macias.
1996. Observations on sex ratio, maturity and fecundity by length-class for swordfish (*Xiphias gladius*) captured with surface longline in the Western Mediterranean. Int. Comm. Conserv. Atl. Tunas, Coll. Vol. Sci. Pap., vol. 45(1): 115–139.

de Sylva, D. P., and P. R. Breder.
1997. Reproduction, gonad histology, and spawning cycles of North Atlantic billfishes (Istiophoridae). Bull. Mar. Sci. 60:668–697.

DiNardo, G. N., and W. Kwok.
1998. Spatiotemporal dynamics of swordfish (*Xiphias gladius*) landings in the Hawaii-based North Pacific longline fishery. *In* Biology and fisheries of swordfish, *Xiphias gladius* (I. Barrett, O. Sosa-Nishizaki, and N. Bartoo, eds.), p. 51–64. U.S. Dep. Commer., NOAA Tech. Rep. NMFS 142.

Ehrhardt, N. M., R. J. Robbins, and F. Arocha.
1996. Age validation and growth of swordfish, *Xiphiasgladdius*, in the Northwest Atlantic. Int. Comm. Conserv. Atl. Tunas, Coll. Vol. Sci. Pap., vol. 45(2):358–367.

Fitzhugh, G. R., and W. F. Hettler.
1995. Temperature influence on postovulatory follicle degeneration in Atlantic menhaden, *Brevoortia tyrannus*. Fish. Bull. 93:568–572.

Goodyear, C. P.
1993. Spawning stock biomass per recruit in fisheries management: foundation and current use. *In* Risk evaluation and biological reference points for fisheries management (S. J. Smith, J. J. Hunt, and D. Rivard, eds.), p. 67–81. Can. Spec. Publ. Fish. Aquat. Sci. 120.

Grier, H. J.
1981. Cellular organization of the testis and spermatogenesis in fishes. Am. Zool. 21:345–367.

Gulland, J. A., and A. A. Rosenberg.
1992. A review of length-based approaches to assessing fish stocks. FAO Fish. Tech. Pap. 323, 100 p. FAO, Rome.

He, X., K. R. Bigelow, and C. H. Boggs.
1997. Cluster analysis of longline sets and fishing strategies within the Hawaii-based fishery. Fish. Res. 31:147–158.

Hinton, M. G., and R. B. Deriso.
1998. Distribution and stock assessment of swordfish, *Xiphias gladius*, in the eastern Pacific Ocean from catch and effort data standardized on biological and environmental parameters. *In* Biology and fisheries of swordfish, *Xiphias gladius* (I. Barrett, O. Sosa-Nishizaki, and N. Bartoo, eds.), p. 161–179. U.S. Dep. Commer., NOAA Tech. Rep. NMFS 142.

Hinton, M. G., R. G. Taylor, and M. D. Murphy.
1997. Use of gonad indices to estimate the status of reproductive activity of female swordfish, *Xiphias gladius*: a validated classification method. Fish. Bull. 95:80–84.

Hoey, J.
1991. Sex ratio data for western North Atlantic swordfish. Int. Comm. Conserv. Atl. Tunas, Coll. Vol. Sci. Pap., vol. 35(2):429–436.

Hunter, J. R., and B. J. Macewicz.
1985. Measurement of spawning frequency in multiple spawning fishes. *In* An egg production method for estimating spawning biomass of pelagic fish: application to the northern anchovy, *Engraulis mordax* (R. Lasker, ed.), p. 79–94. U.S. Dep. Commer., NOAA Tech. Rep. NMFS 36.
1986. The spawning frequency of skipjack tuna, *Katsuwonus pelamis*, from the South Pacific. Fish. Bull. 84:895–903.

ICCAT (International Commission for the Conservation of Atlantic Tunas).
1997. 1996 detailed report on swordfish. Report of the ICCAT Swordfish Stock Assessment Session (Halifax, N.S., Canada, October 2–9, 1996). ICCAT Coll. Vol. Sci. Pap., vol. 46(3):165–188.

Kume, S., and J. Joseph.
1969. Size composition and sexual maturity of billfish caught by the Japanese longline fishery in the Pacific Ocean east of 130° W. Bull. Far Seas Fish. Res. Lab. (Shimizu) 2:115–162 [In Engl., Jpn. summ.]

Lau, B. B., and E. E. DeMartini.
1994. An evaluation of oocyte size in multiple regressions predicting gonad weight from body weight: a test using Hawaiian ehu, *Etelis carbunculus*. U.S. Dep. Commer., NOAA Tech. Memo. NMFS-SWFSC-212, 17 p.

Mejuto, J., J. M. de la Serna, and B. Garcia
1995. An overview of the sex ratio at size of the swordfish (*Xiphias gladius*) around the world: similarity between different strata. Int. Comm. Conserv. Atl. Tunas, Coll. Vol. Sci. Pap., vol. 44(3):197–205.
1998. Some considerations on the spatial and temporal variability in the sex-ratio at size of the swordfish (*Xiphias gla-*

dius). Int. Comm. Conserv. Atl. Tunas, Coll. Vol. Sci. Pap., vol. 48(4):205–215.

Mejuto, J., and B. Garcia.
1997. A preliminary analisis [sic] of gonadal indices of the swordfish (*Xiphias gladius* L.) in the Atlantic Ocean. Int. Comm. Conserv. Atl. Tunas, Coll. Vol. Sci. Pap., vol. 46(3):336–344.

Miyabe, N., and W. H. Bayliff.
1987. A review of the Japanese longline fishery for tunas and billfishes in the eastern Pacific Ocean, 1971–1980. Inter-Am. Trop. Tuna Comm., Bull. 19(1):1–163.

Murphy, M. D., and R. G. Taylor.
1990. Reproduction, growth, and mortality of red drum *Sciaenops ocellatus* in Florida waters. Fish. Bull. 88:531–542.

Nakamura, H., T. Kamimura, Y. Yabuta, A. Suda, S. Ueyanagi, S. Kikawa, M. Honma, M. Yukinawa, and S. Morikawa.
1951. Notes on the life history of the sword-fish, *Xiphias gladius* Linnaeus. Jpn. J. Ichthyol. 1:264–271.

Nakano, H., and W. H. Bayliff.
1992. A review of the Japanese longline fishery for tunas and billfishes in the eastern Pacific Ocean, 1981–1987. Inter-Am. Trop. Tuna Comm., Bull. 20(5):183–355.

Restrepo, V.
1991. Some possible biases in swordfish VPAs due to sexually dimorphic growth. Int. Comm. Conserv. Atl. Tunas, Coll. Vol. Sci. Pap., vol. 35(2):338–345.

Roff, D. A.
1988. The evolution of migration and some life history parameters in marine fishes. Environ. Biol. Fish. 22:133–146.

Sosa-Nishizaki, O.
1990. A study of the swordfish *Xiphias gladius* stocks in the Pacific Ocean. Ph.D. diss., Fac. Agric., Univ. Tokyo, Tokyo, 246 p.

Sosa-Nishizaki, O., and M. Shimizu.
1991. Spatial and temporal CPUE trends and stock unit inferred from them for the Pacific swordfish caught by the Japanese tuna longline fishery. Bull. Nat. Res. Inst. Far Seas Fish. (Shimizu) 28:75–89.

SAS (Statistical Analysis System).
1989. SAS/STAT user's guide, version 6, 4th ed., vol. 2. SAS Inst., Cary, NC, 846 p.

Stone, H. H., and J. M. Porter.
1997. Development of a swordfish sex ratio-at-size relationship for catches from the Canadian fishery. Int. Comm. Conserv. Atl. Tunas, Coll. Vol. Sci. Pap., vol. 46(3):311–314.

Taylor, R. G., and M. D. Murphy.
1992. Reproductive biology of the swordfish *Xiphias gladius* in the Straits of Florida and adjacent waters. Fish. Bull. 90:809–816.

Tibbo, S. N., L. R. Day, and W. F. Doucet.
1961. The swordfish (*Xiphias gladius* L.), its life-history and economic importance in the northwest Atlantic. Fish. Res. Board Can. Bull. 130:1–47.

Uchiyama, J. H., E. E. DeMartini, and H. A Williams.
1999. Length-weight interrelationships for swordfish, *Xiphias gladius* L. caught in the central North Pacific. U.S. Dep. Commer., NOAA Tech. Memo. NMFS NOAA-TM-NMFS-SWFSC-284, 82 p.

Uchiyama, J. H., and R. S. Shomura.
1974. Maturation and fecundity of swordfish, *Xiphias gladius*, from Hawaiian waters. *In* Proc. Int. Billfish Symp., part 2, Review and contributed papers (R. S. Shomura and F. Williams, eds.), p. 142–147. U.S. Dep. Commer., NOAA Tech. Rep. NMFS SSRF-675.

Uchiyama, J. H., R. A. Skillman, J. D. Sampaga, and E. E. DeMartini.
1998. A preliminary assessment of the use of hard parts to age central Pacific swordfish, *Xiphias gladius*. *In* Biology and fisheries of swordfish, *Xiphias gladius* (I. Barrett, O. Sosa-Nishizaki, and N. Bartoo, eds.), p. 261–273. U.S. Dep. Commer., NOAA Tech. Rep. NMFS 142.

Weber, E. C., and S. R. Goldberg.
1986. The sex ratio and gonad indices of swordfish, *Xiphias gladius*, caught off the coast of southern California in 1978. Fish. Bull. 84:185–186.

West, G.
1990. Methods of assessing ovarian development in fishes: a review. Austr. J. Mar. Freshwater Res. 41:199–222.

Yabe, H. S., S. Ueyanagi, S. Kikawa, and H. Watanabe.
1959. Studies of the life history of the swordfish, *Xiphias gladius* Linnaeus. Rep. Nankai Reg. Fish. Res. Lab., 10:107–150. [In Jpn., Engl. summ.; transl. by CEP Multilingual Serv. Div., Dep. Sec. of State, Canada.]

Zar, J. H.
1984. Biostatistical analysis, 2nd ed. Prentice-Hall, Englewood Cliffs, NJ, 718 p.

Larval development of red snapper, *Lutjanus campechanus*, and comparisons with co-occurring snapper species

Denice M. Drass
National Marine Fisheries Service, NOAA
3209 Frederick St
Pascagoula, Mississippi 39567
E-mail address: ddrass@triton.pas.nmfs.gov

Kevin L. Bootes
Marine Science Institute
University of Texas at Austin
750 Channel View Drive
Port Aransas, Texas 78373

Joanne Lyczkowski-Shultz
National Marine Fisheries Service, NOAA
3209 Frederick St
Pascagoula, Mississippi 39567

Bruce H. Comyns
Gulf Coast Research Laboratory
E. Beach Blvd
Ocean Springs, Mississippi 39564

G. Joan Holt
Marine Science Institute
University of Texas at Austin
750 Channel View Drive
Port Aransas, Texas 78373

Cecilia M. Riley
Gulf Coast Bird Observatory
103 West Highway 332
Lake Jackson, Texas 77566

Ronald P. Phelps
Department of Fisheries and Allied Aquaculture
Auburn University
Auburn, Alabama 36849

Abstract.—The larval development of red snapper, *Lutjanus campechanus*, is described from reared larvae and from specimens collected in the Gulf of Mexico (GOM). Snapper larvae are pelagic and are characterized by the following features: a deep and compressed, lightly pigmented body; moderately short gut; 24 myomeres; and elongated dorsal and pelvic fins that form early in development. Specimens of *L. campechanus* (1.9 to 26.1 mm) also showed the presence of weak serrations on pelvic-fin spines, absence of serrations on preopercular or dorsal spines, early forming pigment in dorsal and pelvic fins, and notochord flexion between 3.6 and 5.5 mm. Preflexion larvae of the snapper subfamily Lutjaninae in GOM collections cannot be reliably identified to species despite recent larval descriptions. Species-specific differences in number, spacing, and size of melanophores in the postanal ventral series are evident in the youngest larvae of species from the GOM whose development has been described (*Ocyurus chrysurus*, *L. analis*, *L. synagris*, *L. griseus*, *L. campechanus*, and *Rhomboplites aurorubens*) but further evaluation of the utility of these characters is needed. Characteristics that distinguish mid- to late-flexion larvae of these species are compiled in our study and discussed. Among known GOM lutjanine larvae, body depth, pelvic-ray length and serrations on the angle spine of the preopercle can be used in combination with pigmentation to identify larvae to species. Presence of melanistic pigment (and size at first appearance) or absence of melanistic pigment in the following locations are useful characters for larval snapper identification: anterior surface of the visceral mass, ventral to notochord flexure; internal area over the notochord; dorsal midline of caudal peduncle; soft dorsal fin; anal-fin base or membrane; and pelvic fin.

Manuscript accepted 7 February 2000.
Fish. Bull. 98:507–527 (2000).

In the Gulf of Mexico (GOM), the red snapper, *Lutjanus campechanus*, supports lucrative commercial and recreational fisheries that have been under increasingly restrictive regulation since the 1980s (Workman and Foster, 1994; Schirripa and Legault[1]). Responsible management decisions should be based on an understanding of all life history stages, but until recently the larval development of only three of the 18 species of snappers found in the GOM were known. Collins et al. (1980) described *L. campechanus* from wild larvae with substantial fin development that allowed identification by meristic counts and Rabalais et al. (1980) described reared red snapper eggs and larvae that developed only until 4 days after hatching. Substantial fin development also allowed identification by meristic counts for larvae of the vermilion snapper, *Rhomboplites aurorubens* (Laroche, 1977), and a third lutjanid, the gray snapper (*L. griseus*), was described by Richards and Saksena (1980) from reared specimens. More recently, descriptions by Clarke et al., 1997 (*Ocyurus chrysurus*, *L. analis* and *L. synagris*), Riley et al., 1995 (*O. chrysurus*), Leis and Lee, 1994 (*Etelis* spp., *Pristipomoides aquilonaris* and *P. freemani*?) and the summary compilation by Richards et al. (1994) added three genera and four species to the list of known snapper larvae. Our paper describes for the first time the complete sequence of larval development of red snapper from reared specimens and compares the structure and shape of reared and wild larvae. Additionally, we present a summary of developmental characteristics to separate snapper larvae in field collections from the Gulf of Mexico.

[1] Schirripa, M. J., and C. M. Legault. 1997. Status of the red snapper in U.S. waters of the Gulf of Mexico: updated through 1996. Unpublished contribution report MIA-97/98-05, 37 p. Miami Laboratory, Southeast Fish. Sci. Cent., Natl. Mar. Fish. Serv., NOAA.

Materials and methods

A total of 96 reared larvae, ranging in body length (BL) from 1.9 to 26.1 mm, and a total of 118 wild larvae, ranging from 2.6 to 20.0 mm BL, were used to describe larval development of red snapper. Reared larvae came from the Marine Science Laboratory, University of Texas at Austin, Port Aransas, Texas (TX), and the Claude Peteet Mariculture Center in Gulf Shores, Alabama (AL). Spawning and rearing methods used are described by Riley et al. (1995) at the Texas facility and by Bootes (1998) at the Alabama facility. Notable differences in the rearing methods at the two facilities that could have contributed to different developmental rates include higher salinities in the TX study (33–38 ppt vs. 31–33 ppt), higher temperatures in the AL study (27–32°C vs. 27–28°C) and natural light conditions in the AL study. Several larvae were preserved each day during the Texas rearing study whereas only one larva was preserved each day during the Alabama rearing experiments. Specimens from AL were fixed in 2% formalin and specimens from TX were fixed in 80% ethanol (EtOH) and together formed the developmental series described in our study. Age in days after hatching (DAH) is included in parentheses after BL for reared larvae. In addition, observations on the development of pigment characters were augmented with 96 larvae reared at the Gulf Coast Research Laboratory (GCRL) in Ocean Springs, MS, under conditions similar to the AL study.

Wild red snapper larvae were obtained from plankton samples collected in the GOM by the Southeast Area Monitoring and Assessment Program (SEAMAP) and GCRL. Samples were collected with bongo and neuston nets at stations 56 km apart by using standard SEAMAP collection procedures (Richards, 1984; Richards et al., 1993). Samples were fixed in 10% formalin and transferred to 70% EtOH after 48 h.

All specimens described in our study are considered larvae because they exhibit specializations for pelagic life (head spination, long fin elements) and are pigmented differently than juveniles and adults are pigmented (Leis, 1987; Leis and Trnski, 1989; Leis et al., 1997). Myomere and fin-ray counts were made on the left side of the body. Illustrations were made with a camera lucida. Preserved eggs and larvae were measured to the nearest 0.1 mm with an ocular micrometer fitted to a dissecting microscope. Body length (BL) as defined in Leis and Rennis (1983) is equivalent to notochord length or standard length depending on the stage of development of the larvae. Notochord length is the straight line distance from the tip of the snout to the posterior tip of the notochord and is used as the standard measurement before and during flexion. Standard length is the distance from the tip of the snout along the midline to a vertical line through the posterior edge of the hypural plate. Other common measurements and abbreviations follow Leis and Rennis (1983). Additional abbreviations used here are as follows:

avm = anterior surface of the visceral mass;
BD = body depth;
IPo = inner border of the preopercle (=anterior border of some authors);
OPo = outer border of the preopercle (=posterior border of some authors);
pav = postanal-ventral.

Results

Description of reared larvae

General development (Table 1, Figs. 1–5) Red snapper eggs (AL) were 0.72–0.76 mm in diameter (n=4) at one hour after fertilization and contained a single oil globule (diameter 0.11–0.13 mm). Larvae hatched in approximately 24 h and had a large, elongate yolk sac extending anteriorly beyond the head with a single oil globule. The oil globule was the last portion of the yolk to be absorbed at 4 days after hatching (DAH). Body lengths of the youngest larvae measured were 1.9 mm at hatching (n=1), 2.5 mm at 12 h (n=1), and 2.8 mm at 28 h (n=1). The eyes were pigmented and the mouth was functional by the end of 2 DAH when larvae began to swim actively and feed. Larvae were initially elongate (10% BD at 2.9 mm) but became deeper bodied (43% BD at 4.9 mm) and laterally compressed with development. The smallest larvae (2.5–3.1 mm) showed no fin development or spination. Head length increased from 9% BL in preflexion larvae (2.4 mm) to 42% BL in postflexion larvae (7.5 mm). Teeth appeared along the premaxilla and dentary by 3.5 mm. The gut was initially straight but began to coil at 2.4 mm (6 DAH) and was fully coiled by 3.6 mm (9 DAH). Preanal length increased from 38% BL (2.4 mm) in preflexion larvae to 69% BL in postflexion larvae (16.5 mm). Gas bladder inflation occurred at 4 DAH, and in our study the gas bladder was visible in the 2.4-mm (6 DAH) larva. Notochord flexion began at 3.8 mm (12 DAH) and was complete by 5.5 mm (15 DAH). Scales were present on the largest specimen (26.3 mm, 34 DAH).

Spination (Figs. 1–5) All spines described here were easily visible without clearing and staining. Head spination began by 3.0 mm with the development of preopercular spines, with one spine on the inner border of the preopercle (IPo) and two spines (including the angle spine) on the outer border of the preopercle (OPo). At 3.6 mm, there were two spines on the IPo and four spines on the OPo, one above the angle spine and two below. Spines increased to three on the IPo and five on the OPo by 3.8 mm. At 5.6 mm, there were four spines on the IPo and six spines on the OPo, four below and one above the angle. Spines on the IPo increased to six by 12.2 mm, and on the OPo increased to eight with six below and one above the angle. Spines on the preopercle in the two largest specimens were smaller (reduced in size) and more numerous than in smaller specimens. One interopercular spine was observed between the angle spine and the upper OPo spine by 3.5 mm and was present throughout the rest of the series. An opercular spine was present by 4.4 mm and a postcleithral spine was present just above the pectoral-fin base by 9.6 mm. One supracleithral spine formed by 3.6 mm on the 9-DAH specimen and two supracleithral spines were present on the 3.6-mm (10-DAH) specimen. There were three supra-

Table 1

Measurements (mm) of reared larval red snapper. — = not measured owing to damage. TX = Texas; AL = Alabama.

Source	Age (DAH)	Body length (BL)	Head length	% Head length/BL	Preanal length	% Preanal length/BL	Body depth at cleithrum	% Body depth/BL	Eye diameter	% Eye diameter/BL
TX	4–6	1.93	0.48	24.87	0.84	43.52	0.35	18.13	0.21	10.88
TX	1	2.02	0.20	9.90	1.01	50.00	0.56	27.72	—	—
TX	5	2.06	0.42	20.39	0.80	38.83	0.30	14.56	0.18	8.74
TX	4–6	2.07	0.42	20.29	0.83	40.10	0.35	16.91	0.23	11.11
TX	1	2.10	0.24	11.43	0.99	47.14	0.38	18.10	—	—
TX	4–6	2.16	0.51	23.61	1.11	51.39	0.32	14.81	0.21	9.72
AL	6	2.16	0.46	21.30	1.03	47.69	0.39	18.06	0.22	10.19
AL	6	2.16	0.52	24.07	1.05	48.61	0.43	19.91	0.25	11.57
TX	4–6	2.21	0.39	17.65	0.93	42.08	0.35	15.84	0.21	9.50
TX	5	2.24	0.50	22.32	0.90	40.18	0.32	14.29	0.20	8.93
TX	3	2.30	0.39	16.96	0.90	39.13	0.29	12.61	0.20	8.70
AL	6	2.33	0.42	18.03	0.95	40.77	0.37	15.88	0.22	9.44
AL	6	2.34	0.48	20.51	1.08	46.15	0.40	17.09	0.23	9.83
AL	6	2.35	0.46	19.57	1.02	43.40	0.43	18.30	0.25	10.64
TX	1	2.35	0.21	8.94	1.17	49.79	0.51	21.70	—	—
TX	10	2.40	0.59	24.58	0.92	38.33	0.35	14.58	0.24	10.00
TX	4–6	2.40	0.41	17.08	0.99	41.25	0.30	12.50	0.20	8.33
AL	6	2.42	0.49	20.25	1.08	44.63	0.46	19.01	0.25	10.33
TX	1	2.44	0.29	11.89	1.19	48.77	0.42	17.21	—	—
TX	4–6	2.44	0.42	17.21	1.08	44.26	0.33	13.52	0.23	9.43
TX	1	2.44	0.35	14.34	1.17	47.95	0.56	22.95	—	—
TX	4–6	2.44	0.53	21.72	1.14	46.72	0.36	14.75	0.23	9.43
TX	5	2.47	0.53	21.46	0.96	38.87	0.38	15.38	0.23	9.31
TX	1	2.49	0.27	10.84	1.19	47.79	0.42	16.87	—	—
TX	4–6	2.49	0.48	19.28	1.11	44.58	0.36	14.46	0.20	8.03
AL	6	2.53	0.54	21.34	1.11	43.87	0.43	17.00	0.26	10.28
AL	6	2.53	0.51	20.16	1.09	43.08	0.46	18.18	0.25	9.88
TX	3	2.53	0.50	19.76	1.13	44.66	0.32	12.65	0.23	9.09
AL	6	2.53	0.52	20.55	1.08	42.69	0.45	17.79	0.25	9.88
TX	3	2.54	0.44	17.32	0.99	38.98	0.32	12.60	0.21	8.27
TX	1	2.54	0.30	11.81	1.20	47.24	0.44	17.32	—	—
TX	1	2.54	0.33	12.99	1.25	49.21	0.53	20.87	—	—
TX	1	2.54	0.27	10.63	1.22	48.03	0.42	16.54	—	—
TX	1	2.54	0.32	12.60	1.22	48.03	0.53	20.87	—	—
TX	3	2.59	0.41	15.83	1.08	41.70	0.36	13.90	0.21	8.11
TX	4–6	2.59	0.51	19.69	1.11	42.86	0.32	12.36	0.22	8.49
TX	3	2.59	0.35	13.51	1.11	42.86	0.32	12.36	0.18	6.95
TX	3	2.59	0.47	18.15	1.14	44.02	0.29	11.20	0.20	7.72
TX	4–6	2.59	0.49	18.92	1.08	41.70	0.38	14.67	0.21	8.11
TX	4–6	2.59	0.50	19.31	1.16	44.79	0.33	12.74	0.20	7.72
AL	6	2.60	0.55	21.15	1.12	43.08	0.48	18.46	0.25	9.62
AL	7	2.60	0.70	26.92	1.20	46.15	0.60	23.08	0.31	11.92
TX	3	2.63	0.51	19.39	1.26	47.91	0.32	12.17	0.17	6.46
TX	3	2.63	0.51	19.39	1.17	44.49	0.30	11.41	0.23	8.75
TX	4–6	2.63	0.48	18.25	1.08	41.06	0.38	14.45	0.21	7.98
TX	1	2.63	0.29	11.03	1.23	46.77	0.45	17.11	—	—
TX	1	2.63	0.27	10.27	1.19	45.25	0.39	14.83	—	—

continued

Table 1 (continued)

Source	Age (DAH)	Body length (BL)	Head length	% Head length/BL	Preanal length	% Preanal length/BL	Body depth at cleithrum	% Body depth/BL	Eye diameter	% Eye diameter/BL
TX	10	2.63	0.62	23.57	1.10	41.83	0.40	15.21	0.26	9.89
TX	12	2.65	0.63	23.77	1.22	46.04	0.44	16.60	0.18	6.79
TX	10	2.67	0.63	23.60	1.17	43.82	0.38	14.23	0.27	10.11
TX	4–6	2.68	0.53	19.78	1.13	42.16	0.40	14.93	0.21	7.84
TX	4–6	2.68	0.54	20.15	1.13	42.16	0.36	13.43	0.24	8.96
TX	3	2.68	0.47	17.54	1.08	40.30	0.32	11.94	0.18	6.72
TX	4–6	2.68	0.56	20.90	1.20	44.78	0.35	13.06	0.20	7.46
TX	4–6	2.68	0.54	20.15	1.16	43.28	0.39	14.55	0.23	8.58
TX	1	2.68	0.26	9.70	1.23	45.90	0.51	19.03	—	—
TX	3	2.68	0.51	19.03	1.13	42.16	0.30	11.19	0.21	7.84
TX	4–6	2.68	0.47	17.54	1.10	41.04	0.34	12.69	0.21	7.84
TX	6	2.73	0.60	21.98	1.22	44.69	0.33	12.09	0.23	8.42
TX	3	2.73	0.50	18.32	1.17	42.86	0.33	12.09	0.23	8.42
TX	6	2.73	0.60	21.98	1.20	43.96	0.36	13.19	0.23	8.42
TX	3	2.73	0.48	17.58	1.11	40.66	0.32	11.72	0.23	8.42
TX	10	2.73	0.65	23.81	1.23	45.05	0.41	15.02	0.27	9.89
TX	3	2.73	0.41	15.02	1.31	47.99	0.30	10.99	0.23	8.42
TX	3	2.77	0.51	18.41	1.17	42.24	0.30	10.83	0.21	7.58
TX	5	2.80	0.54	19.29	1.17	41.79	0.30	10.71	0.20	7.14
TX	3	2.82	0.45	15.96	1.17	41.49	0.30	10.64	0.21	7.45
TX	13	2.91	0.83	28.52	1.23	42.27	0.66	22.68	0.36	12.37
TX	3	2.91	0.53	18.21	1.26	43.30	0.30	10.31	0.23	7.90
TX	12	2.99	0.70	23.41	1.37	45.82	0.45	15.05	0.30	10.03
TX	17	3.00	0.77	25.67	1.43	47.67	0.59	19.67	0.30	10.00
TX	12	3.05	0.68	22.30	1.34	43.93	0.48	15.74	0.30	9.84
TX	12	3.11	0.69	22.19	1.28	41.16	0.47	15.11	0.29	9.32
TX	13	3.20	0.81	25.31	1.39	43.44	0.63	19.69	0.33	10.31
TX	13	3.28	0.82	25.00	1.41	42.99	0.53	16.16	0.32	9.76
TX	16	3.30	0.96	29.09	1.49	45.15	0.65	19.70	0.36	10.91
AL	11	3.38	1.06	31.36	1.73	51.18	1.18	34.91	0.43	12.72
TX	16	3.42	0.96	28.07	1.59	46.49	0.72	21.05	0.31	9.06
AL	9	3.51	1.06	30.20	1.68	47.86	1.03	29.34	0.41	11.68
AL	10	3.51	1.06	30.20	1.70	48.43	1.01	28.77	0.41	11.68
TX	13	3.52	0.95	26.99	1.68	47.73	0.68	19.32	0.33	9.38
AL	12	3.64	1.22	33.52	1.93	53.02	1.41	38.74	0.52	14.29
TX	16	3.65	1.08	29.59	1.70	46.58	1.00	27.40	0.41	11.23
TX	16	3.80	1.16	30.53	1.82	47.89	1.00	26.32	0.50	13.16
AL	13	4.42	1.73	39.14	2.50	56.56	1.80	40.72	0.62	14.03
AL	14	4.81	1.74	36.17	2.68	55.72	2.07	43.04	0.66	13.72
AL	15	5.27	2.07	39.28	3.01	57.12	2.16	40.99	0.75	14.23
AL	16	5.40	1.97	36.48	3.15	58.33	2.16	40.00	0.75	13.89
AL	19	7.54	3.15	41.78	4.70	62.33	2.91	38.59	1.03	13.66
AL	17	9.49	3.42	36.04	5.58	58.80	3.42	36.04	1.35	14.23
AL	26	12.20	4.23	34.67	7.74	63.44	4.23	34.67	1.53	12.54
AL	21	15.34	5.20	33.90	9.23	60.17	5.59	36.44	1.95	12.71
AL	33	16.50	6.63	40.18	11.44	69.33	6.76	40.97	2.47	14.97
AL	35	18.10	6.37	35.19	11.57	63.92	6.89	38.07	2.47	13.65
AL	26	20.50	7.02	34.24	13.00	63.41	7.28	35.51	2.60	12.68
AL	34	26.10	9.62	36.86	16.90	64.75	9.62	36.86	3.25	12.45

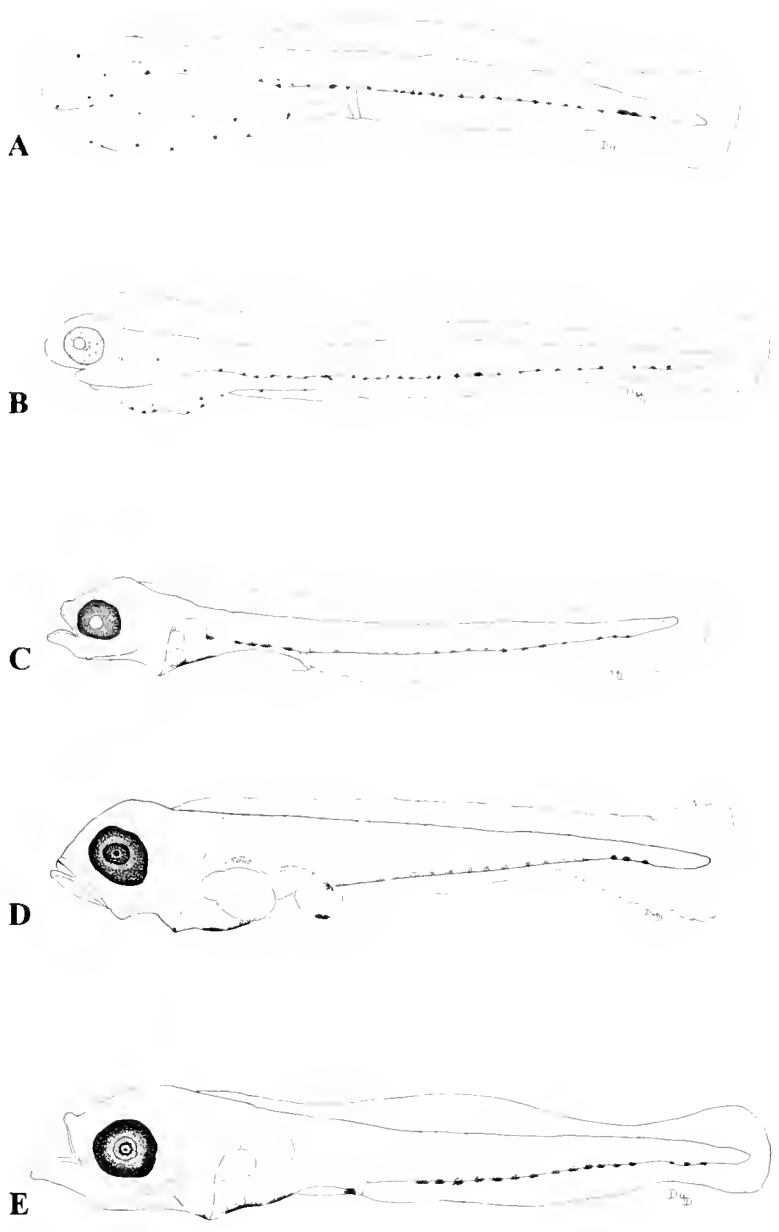

Figure 1

Preflexion larvae of reared *Lutjanus campechanus*: (**A**) 2.5 mm, 1 DAH, from TX; (**B**) 2.6 mm, 3 DAH, from TX; (**C**) 2.8 mm, 5 DAH, from TX; (**D**), 2.4 mm, 6 DAH, from AL; (**E**) 3.1 mm, 12 DAH, from TX.

cleithral spines on the 3.5-mm (11-DAH) specimen and by 4.9 mm (14 DAH), four supracleithral spines were present. A posttemporal spine had developed by 3.8 mm (12 DAH), and by 5.5 mm (15 DAH) there were two posttemporal spines. A supraocular ridge formed by 3.8 mm and one spine developed on the ridge by 4.4 mm (13 DAH). Two, three, and four additional spines were present on the supraocular ridge by 4.9 mm (14 DAH), 5.6 mm (16 DAH), and 9.6 mm (17 DAH), respectively.

Fin development (Table 2, Figs. 1–5) Sequence of fin-ray formation can be characterized either by initial or completed development of fin elements. The order of development, based on initial development as reported by Potthoff et al. (1988), for red snapper is first dorsal, then pelvic, caudal, second dorsal, anal, pectoral. Order by completed development as reported by Johnson (1984) for lutjanids in general is first dorsal, then pelvic, second dorsal, anal, pectoral. Elements of the dorsal and pelvic fins began forming

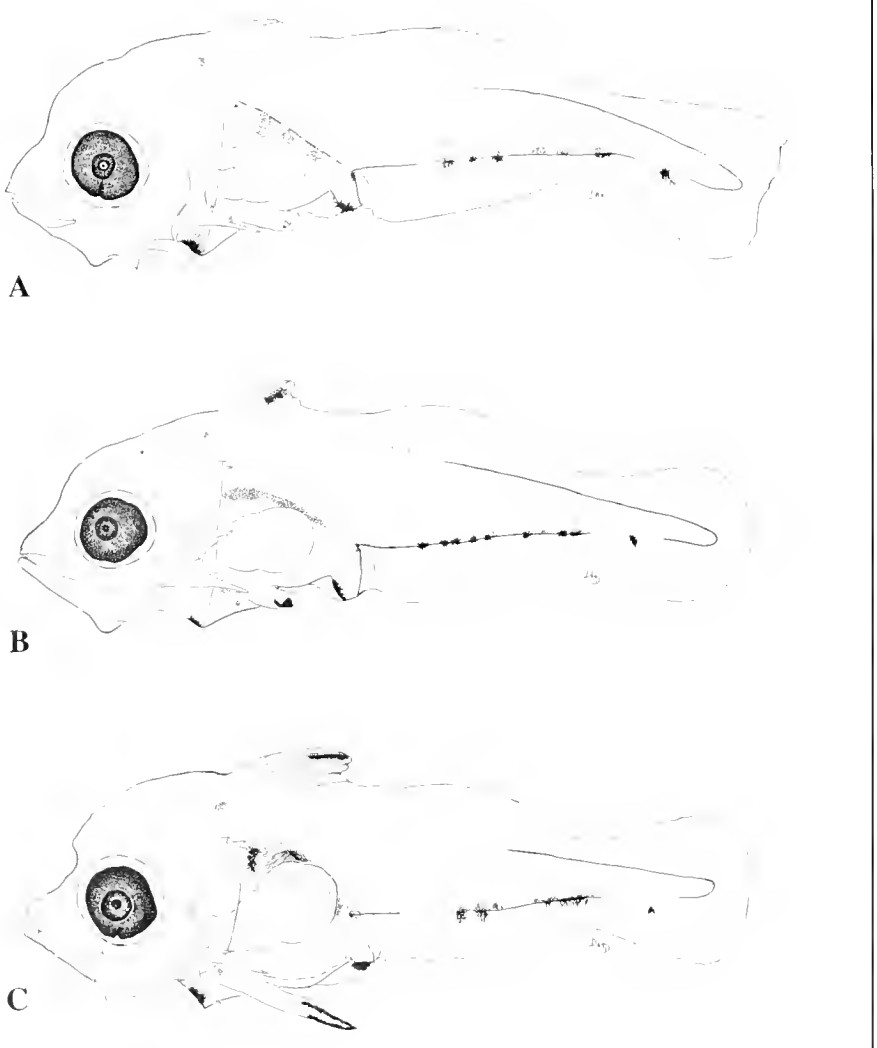

Figure 2

Preflexion reared *Lutjanus campechanus* larvae. (**A**) 3.6 mm, 9 DAH, from AL; (**B**) 3.6 mm, 10 DAH, from AL; (**C**) 3.5 mm, 11 DAH, from AL.

at >3.6 mm between 9 and 11 DAH. The second spine of the dorsal fin was first to develop followed by the third, then the first and fourth spines. Development of the remaining dorsal-fin elements proceeded posteriorly; the tenth dorsal spine initially formed as a raylike element. Fine serrations were present on the leading edge of the pelvic spine at 3.8 mm (12 DAH). Anal-fin development began by 3.6 mm (11 DAH) and by 3.8 mm (12 DAH) the first anal spine began to form. Development of the remaining anal-fin elements proceeded posteriorly; the third anal spine initially forming as a raylike element. All fin spines were V-shaped in cross section. Caudal rays were first noticeable at 4.4 mm (13 DAH) and pectoral-fin rays began forming at 5.5 mm (15 DAH). By 9.6 mm (17 DAH), all elements in the dorsal, pelvic, and anal fins were formed. Formation of pectoral rays and both principal and procurrent rays of the caudal fin was completed by 12.2 mm.

Pigmentation (Figs. 1–5) *Head* Small melanophores were scattered over the head of day-old yolksac larvae at 2.5 mm. These melanophores were not present in 3 DAH larvae but small melanophores were present in the otic capsule of 2.6- and 2.8-mm larvae (3 and 5 DAH). A melanophore appeared over the midbrain at 3.6 mm and with development, both internal and external head pigment increased until at 9.6 mm, most of the surface of the head above the midbrain was covered with small melanophores. Pigment on the surface of the head over the forebrain was

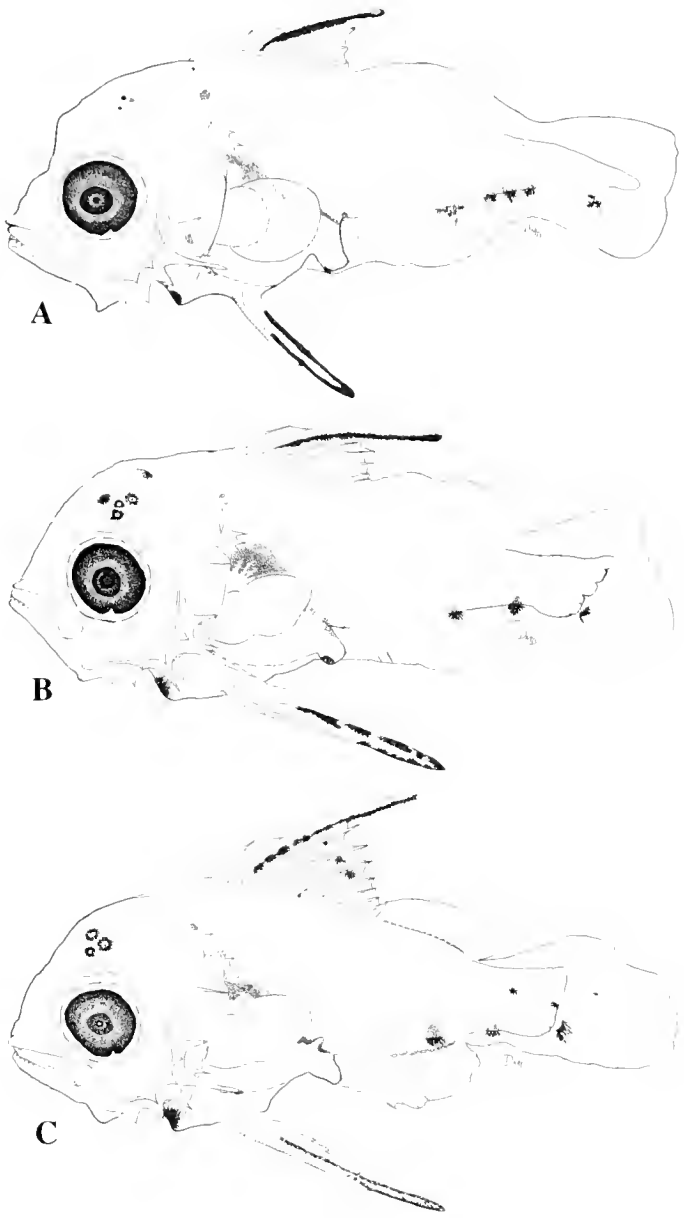

Figure 3

Early flexion and flexion reared *Lutjanus campechanus* larvae: (**A**) 3.8 mm, 12 DAH, from AL; (**B**) 4.4 mm, 13 DAH, from AL; (**C**) 4.9 mm, 14 DAH, from AL.

present by 9.6 mm, and by 12.2 mm the forebrain region was covered with many small melanophores. An internal nape melanophore was present at 3.1 mm and persisted until overlying tissue obscured it. Pigment did not appear on the operculum until 5.5 mm, and by 9.6 mm additional small melanophores were present dorsal to the operculum pigment and posterior to the orbit. Pigment first appeared on the tip of the premaxilla at 9.6 mm and increased over the snout and on the lower jaw by 12.2 mm. The head region and jaws of the 26.3-mm specimen were densely covered with pigment. A melanophore lying just anterior to the cleithral symphysis first appeared by 2.4 mm (6 DAH) and remained visible throughout the developmental series until becoming obscured by tissue in fish larger than 12.0 mm.

Body Numerous melanophores were scattered over the yolk sac and dorsal surface of the gut in the smallest larvae. The number of melanophores over the gut and

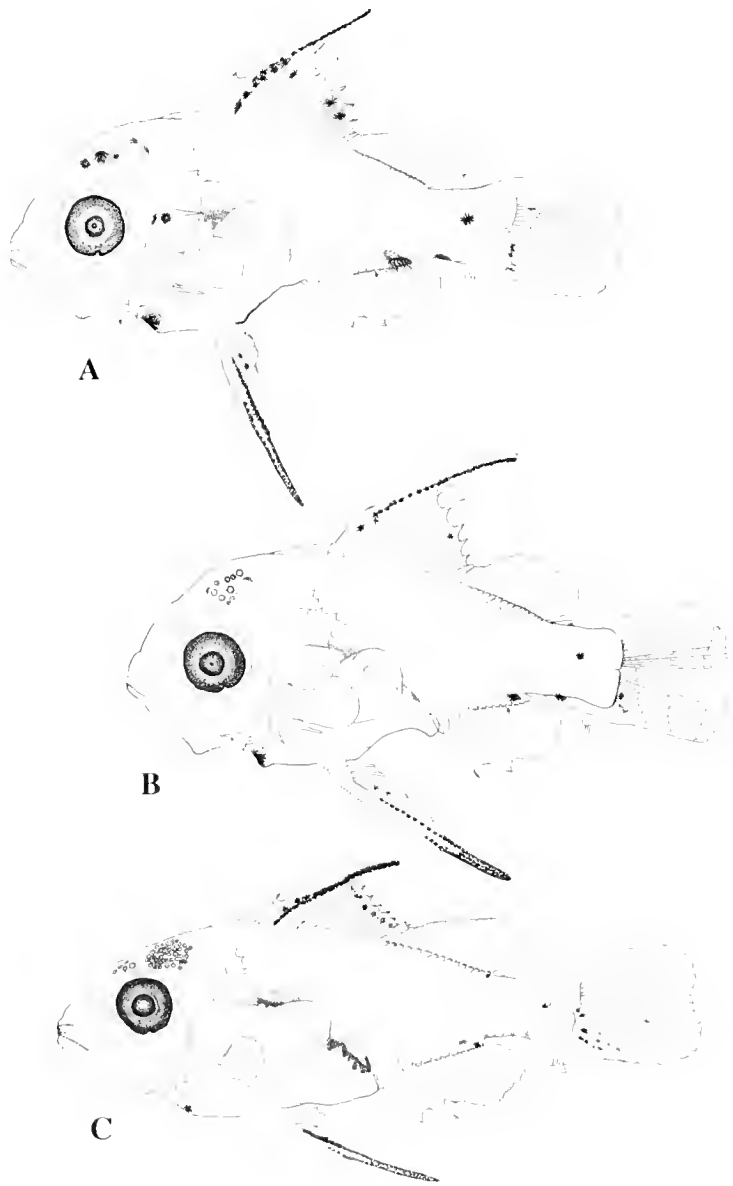

Figure 4

Flexion and postflexion reared *Lutjanus campechanus* larvae: (**A**) 5.5 mm, 15 DAH, from AL; (**B**) 5.6 mm, 16 DAH, from AL; (**C**) 9.6 mm, 17 DAH, from AL.

gas bladder increased until 3.6 mm when this pigment appeared as a solid melanistic patch. Pigment on the ventral surface of the trunk (between the cleithrum and the anus) consisted of one or two melanophores that were present until the pelvic fin bud emerged. As the pelvic fin developed, this pigment migrated internally to a position anterodorsal to the insertion of the pelvic fin and remained discernible through the body wall of specimens up to 4.9 mm. One melanophore was also present on the ventral surface of the hindgut just anterior to the anus over the size range of 2.4 mm to 4.4 mm. A melanophore was present in the peritoneum on the anterior surface of the visceral mass (avm) at the level of the pectoral-fin base and was visible through the operculum in the 3.6-, 3.8-, 4.4-, and 5.6-mm specimens. This melanophore was more easily observed when the operculum was lifted. Additional data from larvae (n=96) raised at GCRL showed that the avm melanophore was first present in larvae as small as

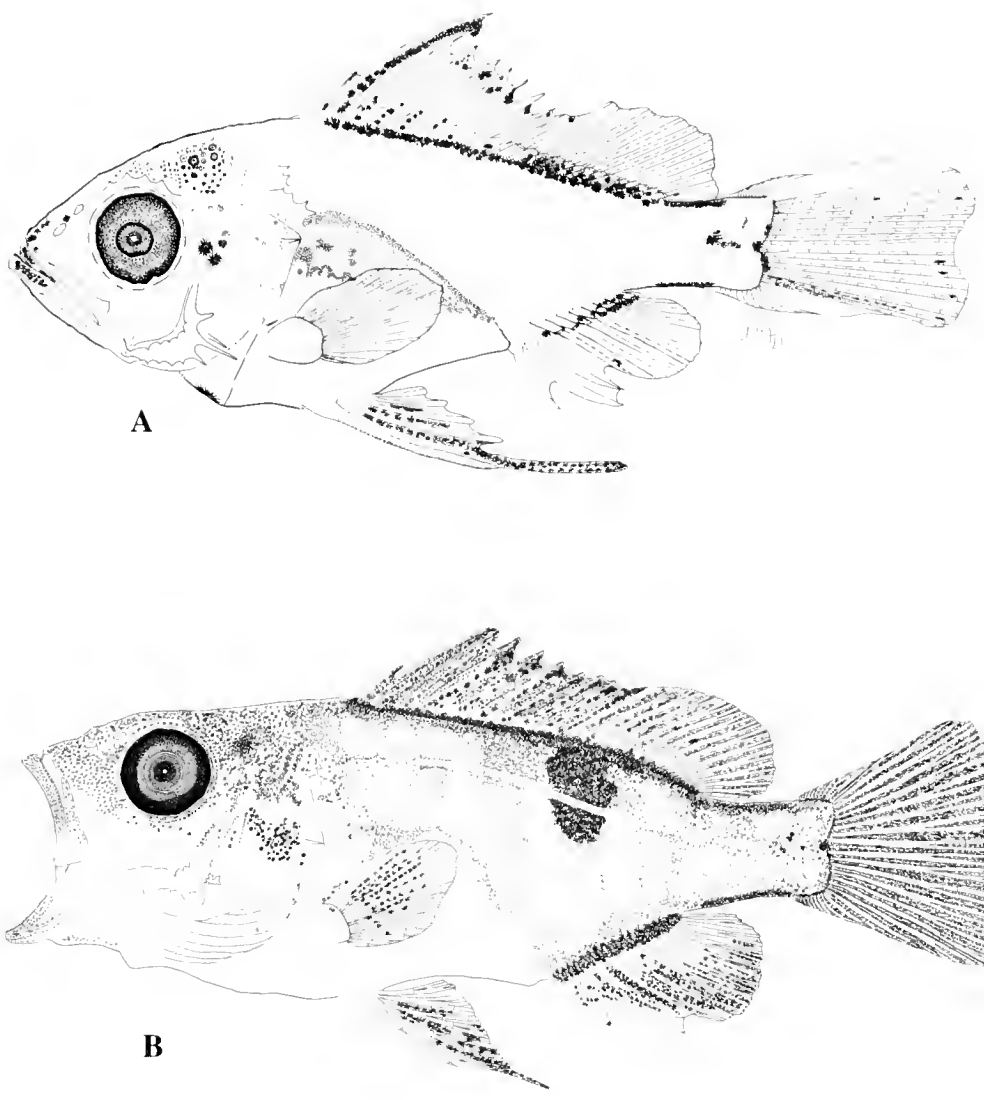

Figure 5

Postflexion reared *Lutjanus campechanus* larvae: (**A**) 12.2 mm, 26 DAH, from AL; (**B**) 26.3 mm, 34 DAH, from AL. Scales omitted from illustration.

3.4 mm (preflexion) and was found in all specimens ≥3.6 mm. When present, this spot lies above the internal melanophore that is located anterodorsal to the insertion of the developing pelvic fin.

Melanophores that form a postanal ventral (pav) series on the tail were most numerous (18–20) in the smallest larvae and decreased in number with development. The pav series is further characterized by the presence of a gap posteriorly and by the presence of one to four melanophores (typically three) located after the gap in the hypural area. As flexion began (3.8 mm), three melanophores were present on the caudal peduncle, but these melanophores coalesced to form a single ventral spot on the caudal peduncle in postflexion larvae up to 9.6 mm. In larger larvae, additional melanophores lined the entire ventral edge of the caudal peduncle. At the beginning of flexion, one to three melanophores were present over the ventral edge of the hypural plate anlagen. As flexion progressed, this pigment bent up with the hypural elements and came to lie at the base of the ventral caudal rays. A melanophore at the flexure of the notochord on the caudal peduncle first appeared in the 4.9-mm larva. It remained prominent until extensive surface pigment on the body obscured it in the largest specimen. Dorsal pigment on the caudal peduncle appeared in the 3.8-mm early flexion larva in the form of a single internal melanophore. This

Table 2

Meristics and spine lengths of reared larval red snapper. nd = not developed, i = incipient ray(s) or spine(s). AL = Alabama; TX = Texas. P_2 = pelvic fin.

Source	Body length (BL)	Dorsal fin spines and rays	2nd dorsal spine length	% 2nd dorsal spine length/BL	3rd dorsal spine length	% 3rd dorsal spine length/BL	P_2 spine length	% P_2 spine length/BL	P_2 ray length	% P_2 ray length/BL	Anal fin spines and rays
AL	3.57	ii	nd	nd	nd	nd	bud	nd	bud	nd	nd
AL	3.57	IIi	0.32	8.96	0.21	5.88	bud	nd	bud	nd	nd
AL	3.57	IIii	0.53	14.85	0.38	10.64	0.24	6.72	0.45	12.61	nd
TX	3.65	III	0.36	9.86	0.21	5.75	0.26	7.12	0.42	11.51	nd
AL	3.76	Vii	0.89	23.67	0.60	15.96	0.55	14.63	0.86	22.87	i
TX	3.80	IIIi	0.54	14 21	0.29	7.63	0.27	7.11	0.50	13.16	nd
AL	4.40	VIIi	1.45	32.95	0.91	20.68	1.05	23.86	1.64	37.27	Iii
AL	4.85	IXi,(14i)	1.75	36.08	1.06	21.86	1.22	25.15	1.82	37.53	II,(9i)
AL	5.47	IXi,(14i)	1.85	33.82	1.32	24.13	1.32	24.13	2.16	39.49	II,(9i)
AL	5.64	IXi,(14i)	2.16	38.30	1.42	25.18	1.37	24.29	2.09	37.06	II,(10i)
AL	7.54	IXi,(14i)	2.49	33.02	1.74	23.08	2.11	27.98	3.02	40.05	III,8
AL	9.59	X,15	2.91	30.34	2.02	21.06	2.07	21.58	3.10	32.33	III,9
AL	12.20	X,14	3.15	25.82	2.44	20.00	2.82	23.11	3.38	27.70	III,8
AL	15.34	X,14	3.71	24.19	3.06	19.95	2.96	19.30	4.61	30.05	III,9
AL	16.50	X,13	3.76	22.79	3.24	19.64	3.71	22.48	4.95	30.00	III,8
AL	18.10	IXi,14	3.71	20.50	3.20	17.68	3.10	17.13	12.87	71.10	III,9
AL	20.50	X,14	4.42	21.56	3.90	19.02	4.51	22.00	2.91	14.20	III,9
AL	26.10	X,14	4.56	17.47	4.47	17.13	4.32	16.55	6.75	25.86	III,8

pigment was absent in the next two larvae in the series (4.4 and 4.9 mm) but it was present in the remaining larvae of the series. Additional melanophores were added until the entire dorsal surface of the caudal peduncle was lined with pigment by 12.2 mm.

Fins Melanophores were present on the pelvic fin bud at its emergence in the 3.6-mm (9 DAH) specimen. This pigment became concentrated on the first ray and in the membrane between the first and second rays as fin elements developed. Melanophores appeared on the membrane between the second and third rays by 5.5 mm and continued to increase until pigment was present between the first four pelvic rays by 12.2 mm. Pigment appeared in the dorsal-fin membrane behind the second dorsal spine by 3.6 mm (10 DAH) and continued to increase as that spine grew, so that pigment extended out along the entire length of the spine. At 4.9 mm, additional melanophores were present near the distal margin of the dorsal-fin membrane between the third and fourth, fourth and fifth, and fifth and sixth spines. This latter condition was not consistent over the series; the 5.5-mm specimen had pigment between the third and fourth, fifth and sixth, sixth and seventh spines, whereas the 5.6-mm specimen had pigment only between the fifth and sixth spines. As seen in the largest specimens of the series, pigment eventually developed in the membrane between all of the dorsal spines but pigment was consistently most extensive behind the second dorsal spine. By 12.2 mm, melanophores appeared in the proximal region of the fin membrane at the base of the spines. One melanophore was present at the base of the last dorsal ray by 9.6 mm, and by 12.2 mm pigment covered the entire base of the dorsal fin. As the anal fin formed, one to four melanophores from the pav series persisted over the posterior pterygiophores. At sizes larger than 9.6 mm, additional melanophores began to form on the anal fin base, and by 12.2 mm the pterygiophores of the last six rays were pigmented and eventually the entire anal-fin base was covered. The distal region of the anal fin and the pectoral fin were extensively pigmented in the 26.3-mm specimen. Pigment on the caudal-fin rays first developed on the ventralmost rays and subsequently near the posterior margin of the fin until in the 26.3-mm specimen, the membrane between the rays was pigmented from the base out to the edge of the fin.

Comparison of reared and wild larvae

Reared and wild red snapper larvae were examined and compared to determine variability and usefulness of various developmental characters (Figs. 1–6; Tables 1–4). Field-collected larvae were identified as red snapper by the presence of morphological and pigmentational features described in Collins et al. (1980) and Richards et al. (1994), as well as by their general resemblance to the reared larvae described in our study. All wild larvae were collected in shelf waters in the northcentral GOM, where

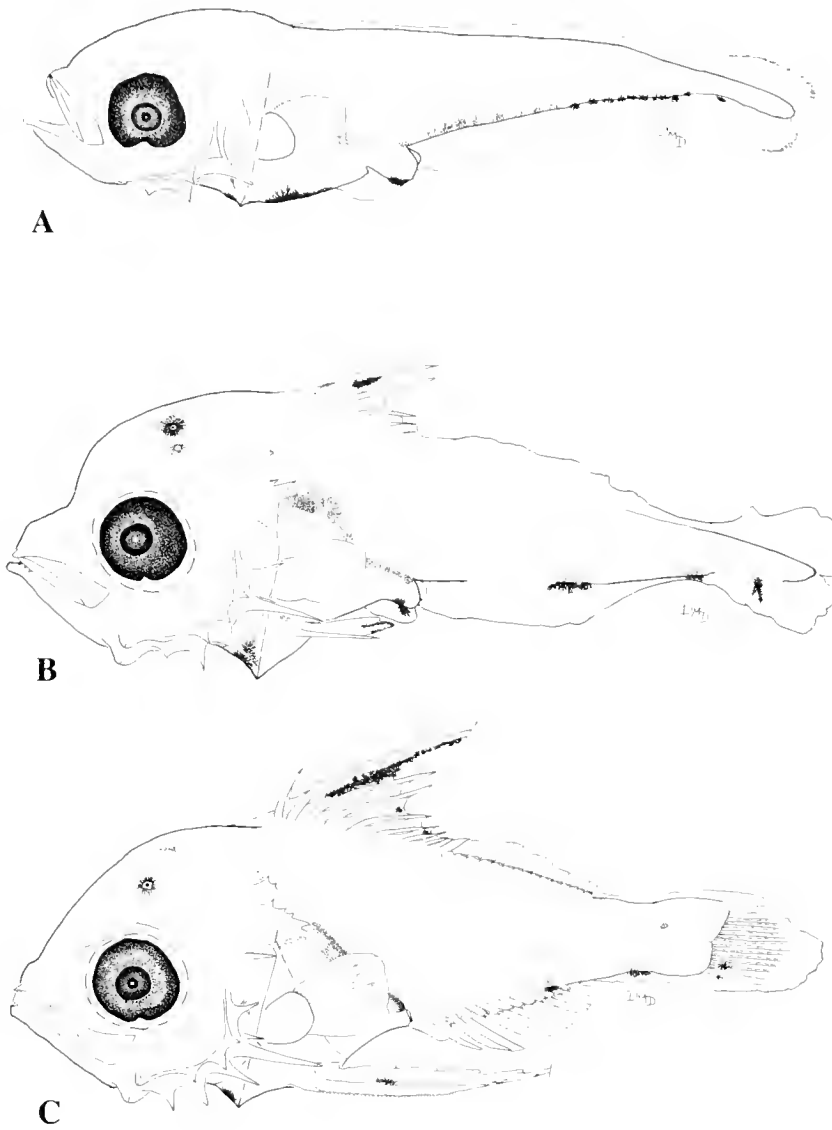

Figure 6

Preflexion and flexion wild *Lutjanus campechanus*: (**A**) 2.6 mm., GCRL 1708; (**B**) 3.5 mm, SEAMAP 14766; (**C**) 5.2 mm, GCRL 1753B.

relatively few species of lutjanids (larvae or adults) occur in abundance [SEAMAP Atlas 1985–1995 (Thompson et al., 1988; Sanders et al., 1990a, 1990b, 1991a, 1991b, 1992; Donaldson et al. 1993, 1994, 1996, 1997a, 1997b); longline data, (Jones[2]); video data, (Gledhill[3])].

There were no notable or consistent differences between laboratory-reared and field-caught red snapper larvae in pigmentation, development or morphometry at similar stages of development. Presence of avm pigment, number of pav spots, and arrangement of median fin pigment among wild larvae matched the appearance of these features in reared larvae at about the same stage of development (Figs. 2–6). Differences in size at stage of development that were evident were probably caused by net-related shrinkage or abrasion, or by both (Theilacker, 1980). We observed no consistent differences in pigment that could have been caused by rearing conditions. Median fin element development in wild red snapper larvae appeared at smaller sizes

[2] Jones, L. M. 1998. Personal commun. Mississippi Laboratories, Southeast Fisheries Science Center, National Marine Fisheries Service, PO Drawer 1207, Pascagoula, MS 39568-1207.

[3] Gledhill, C. T. 1998. Personal commun. Mississippi Laboratories, Southeast Fisheries Science Center, National Marine Fisheries Service, PO Drawer 1207, Pascagoula, MS 39568-1207.

Table 3

Measurements (mm) of wild larval red snapper. — = not measure owing to damage. GCRL = Gulf Coast Research Laboratory; SEAMAP = Southeast Area Monitoring and Assessment Program.

Source	Body length (BL)	Head length	% Head length/BL	Preanal length	% Preanal length/BL	Body depth at cleithrum	% Body depth/BL	Orbit diameter	% Orbit diameter/BL
GCRL	2.60	0.79	30.38	1.39	53.46	0.77	29.62	0.34	13.08
GCRL	2.60	0.75	28.85	1.36	52.31	0.66	25.38	0.30	11.54
GCRL	2.60	0.77	29.62	1.27	48.85	0.79	30.38	0.34	13.08
GCRL	2.73	0.79	28.94	1.30	47.62	0.74	27.11	0.29	10.62
GCRL	2.73	0.84	30.77	1.44	52.75	0.79	28.94	0.36	13.19
GCRL	2.86	0.72	25.17	1.25	43.71	0.77	26.92	0.31	10.84
GCRL	2.86	0.77	26.92	1.44	50.35	0.72	25.17	0.34	11.89
SEAMAP	2.86	1.27	44.41	1.41	49.30	1.18	41.26	0.47	16.43
GCRL	2.99	0.89	29.77	1.46	48.83	0.82	27.42	0.43	14.38
GCRL	2.99	0.91	30.43	1.61	53.85	0.89	29.77	0.36	12.04
GCRL	2.99	0.99	33.11	1.74	58.19	1.08	36.12	0.38	12.71
SEAMAP	2.99	1.08	36.12	1.63	54.52	0.98	32.78	0.38	12.71
SEAMAP	2.99	1.10	36.79	1.56	52.17	1.15	38.46	0.41	13.71
SEAMAP	2.99	1.37	45.82	1.97	65.89	1.32	44.15	0.46	15.38
GCRL	3.12	0.85	27.24	1.46	46.79	0.89	28.53	0.33	10.58
GCRL	3.12	0.91	29.17	1.56	50.00	0.86	27.56	0.41	13.14
GCRL	3.12	0.98	31.41	1.56	50.00	0.89	28.53	0.38	12.18
GCRL	3.12	0.89	28.53	1.42	45.51	0.86	27.56	0.31	9.94
SEAMAP	3.12	1.08	34.62	1.63	52.24	0.96	30.77	0.41	13.14
SEAMAP	3.12	1.13	36.22	1.50	48.08	1.18	37.82	0.47	15.06
SEAMAP	3.12	1.27	40.71	1.65	52.88	1.13	36.22	0.52	16.67
GCRL	3.25	1.13	34.77	1.61	49.54	1.01	31.08	0.38	11.69
GCRL	3.25	0.89	27.38	1.55	47.69	0.89	27.38	0.38	11.69
GCRL	3.25	1.13	34.77	1.79	55.08	1.22	37.54	0.42	12.92
SEAMAP	3.25	1.27	39.08	1.69	52.00	1.13	34.77	0.47	14.46
GCRL	3.38	0.91	26.92	1.61	47.63	1.03	30.47	0.36	10.65
GCRL	3.38	0.94	27.81	1.49	44.08	0.91	26.92	0.36	10.65
GCRL	3.38	1.20	35.50	1.68	49.70	1.03	30.47	0.41	12.13
SEAMAP	3.38	0.98	28.99	1.51	44.67	1.13	33.43	0.41	12.13
SEAMAP	3.38	1.15	34.02	1.58	46.75	1.15	34.02	0.43	12.72
SEAMAP	3.38	1.13	33.43	1.70	50.30	1.22	36.09	0.38	11.24
SEAMAP	3.38	1.27	37.57	1.75	51.78	1.25	36.98	0.48	14.20
SEAMAP	3.38	1.41	41.72	1.83	54.14	1.41	41.72	0.45	13.31
SEAMAP	3.38	1.41	41.72	1.93	57.10	1.36	40.24	0.52	15.38
GCRL	3.51	1.13	32.19	1.75	49.86	0.98	27.92	0.43	12.25
GCRL	3.51	1.22	34.76	1.83	52.14	1.13	32.19	0.38	10.83
GCRL	3.51	1.15	32.76	1.85	52.71	1.20	34.19	0.43	12.25
SEAMAP	3.51	1.25	35.61	—	—	1.20	34.19	0.41	11.68
SEAMAP	3.51	1.22	34.76	1.69	48.15	1.22	34.76	0.47	13.39
SEAMAP	3.51	1.41	40.17	1.93	54.99	1.36	38.75	0.52	14.81
SEAMAP	3.51	1.41	40.17	2.07	58.97	1.41	40.17	0.47	13.39
GCRL	3.64	0.79	21.70	1.44	39.56	0.86	23.63	0.38	10.44
GCRL	3.64	1.10	30.22	1.75	48.08	1.08	29.67	0.43	11.81
GCRL	3.64	1.10	30.22	1.75	48.08	1.13	31.04	0.41	11.26
SEAMAP	3.64	1.32	36.26	1.88	51.65	1.27	34.89	0.47	12.91
SEAMAP	3.64	1.50	41.21	1.97	54.12	1.50	41.21	0.52	14.29

continued

Table 3 (continued)

Source	Body length (BL)	Head length	% Head length/BL	Preanal length	% Preanal length/BL	Body depth at cleithrum	% Body depth/BL	Orbit diameter	% Orbit diameter/BL
SEAMAP	3.64	1.27	34.89	1.83	50.27	1.22	33.52	0.52	14.29
GCRL	3.77	1.18	31.30	1.80	47.75	1.15	30.50	0.43	11.41
GCRL	3.77	1.03	27.32	1.74	46.15	1.18	31.30	0.42	11.14
GCRL	3.77	1.13	29.97	1.83	48.54	1.13	29.97	0.47	12.47
GCRL	3.77	1.27	33.69	1.87	49.60	1.22	32.36	0.46	12.20
SEAMAP	3.77	1.66	44.03	2.28	60.48	1.56	41.38	0.53	14.06
SEAMAP	3.77	1.20	31.83	1.73	45.89	1.42	37.67	0.58	15.38
SEAMAP	3.77	1.56	41.38	2.11	55.97	1.49	39.52	0.55	14.59
SEAMAP	3.77	1.41	37.40	1.88	49.87	1.46	38.73	0.56	14.85
SEAMAP	3.77	1.41	37.40	2.02	53.58	1.50	39.79	0.52	13.79
SEAMAP	3.77	1.65	43.77	2.21	58.62	1.55	41.11	0.52	13.79
SEAMAP	3.81	1.55	40.68	2.21	58.01	1.41	37.01	0.52	13.65
SEAMAP	3.84	1.50	39.06	2.12	55.21	1.46	38.02	0.47	12.24
SEAMAP	3.90	1.36	34.87	1.97	50.51	1.46	37.44	0.47	12.05
GCRL	3.90	1.46	37.44	2.16	55.38	1.46	37.44	0.56	14.36
SEAMAP	3.90	1.32	33.85	1.93	49.49	1.36	34.87	0.56	14.36
SEAMAP	3.90	1.46	37.44	2.07	53.08	1.55	39.74	0.52	13.33
SEAMAP	3.90	1.41	36.15	2.02	51.79	1.55	39.74	0.52	13.33
GCRL	4.03	1.36	33.75	1.97	48.88	1.27	31.51	0.52	12.90
SEAMAP	4.03	1.32	32.75	2.11	52.36	1.44	35.73	0.43	10.67
GCRL	4.03	1.41	34.99	2.16	53.60	1.46	36.23	0.52	12.90
SEAMAP	4.03	1.50	37.22	2.12	52.61	1.55	38.46	0.56	13.90
SEAMAP	4.03	1.60	39.70	2.21	54.84	1.55	38.46	0.61	15.14
SEAMAP	4.03	1.50	37.22	2.07	51.36	1.46	36.23	0.56	13.90
SEAMAP	4.03	1.56	38.71	2.23	55.33	1.63	40.45	0.60	14.89
GCRL	4.16	1.27	30.53	2.02	48.56	1.22	29.33	0.47	11.30
GCRL	4.16	1.20	28.85	1.63	39.18	1.10	26.44	0.41	9.86
GCRL	4.16	1.41	33.89	2.21	53.13	1.50	36.06	0.52	12.50
GCRL	4.16	1.60	38.46	2.26	54.33	1.50	36.06	0.56	13.46
SEAMAP	4.16	1.55	37.26	2.16	51.92	1.60	38.46	0.56	13.46
SEAMAP	4.16	1.55	37.26	2.30	55.29	1.69	40.63	0.56	13.46
SEAMAP	4.16	1.65	39.66	2.30	55.29	1.55	37.26	0.56	13.46
SEAMAP	4.16	1.65	39.66	2.16	51.92	1.65	39.66	0.56	13.46
SEAMAP	4.29	1.50	34.97	2.07	48.25	1.41	32.87	0.52	12.12
SEAMAP	4.29	1.65	38.46	2.35	54.78	1.65	38.46	0.56	13.05
GCRL	4.29	1.50	34.97	2.30	53.61	1.46	34.03	0.56	13.05
SEAMAP	4.42	1.50	33.94	2.26	51.13	1.50	33.94	0.51	11.54
SEAMAP	4.42	1.60	36.20	2.07	46.83	1.65	37.33	0.56	12.67
SEAMAP	4.42	1.79	40.50	2.49	56.33	1.79	40.50	0.56	12.67
SEAMAP	4.42	1.50	33.94	2.44	55.20	1.69	38.24	0.61	13.80
GCRL	4.42	1.79	40.50	2.54	57.47	1.79	40.50	0.71	16.06
SEAMAP	4.55	1.55	34.07	2.44	53.63	1.65	36.26	0.52	11.43
SEAMAP	4.55	1.55	34.07	2.35	51.65	1.74	38.24	0.61	13.41
GCRL	4.55	1.79	39.34	2.49	54.73	1.74	38.24	0.66	14.51
SEAMAP	4.55	1.88	41.32	2.54	55.82	2.02	44.40	0.66	14.51
GCRL	4.68	1.65	35.26	2.54	54.27	1.74	37.18	0.56	11.97
GCRL	4.68	1.55	33.12	2.44	52.14	1.69	36.11	0.61	13.03
SEAMAP	4.68	1.69	36.11	2.44	52.14	1.65	35.26	0.56	11.97

continued

Table 3 (continued)

Source	Body length (BL)	Head length	% Head length/BL	Preanal length	% Preanal length/BL	Body depth at cleithrum	% Body depth/BL	Orbit diameter	% Orbit diameter/BL
SEAMAP	4.68	1.83	39.10	2.59	55.34	1.79	38.25	0.66	14.10
SEAMAP	4.81	1.69	35.14	2.44	50.73	1.74	36.17	0.56	11.64
SEAMAP	4.81	1.97	40.96	2.82	58.63	1.97	40.96	0.71	14.76
SEAMAP	4.81	1.93	40.12	2.77	57.59	1.97	40.96	0.56	11.64
SEAMAP	4.94	1.93	39.07	2.63	53.24	1.93	39.07	0.66	13.36
SEAMAP	4.94	1.97	39.88	2.73	55.26	2.12	42.91	0.71	14.37
GCRL	5.07	1.79	35.31	2.68	52.86	1.79	35.31	0.71	14.00
SEAMAP	5.07	1.88	37.08	2.73	53.85	1.88	37.08	0.61	12.03
SEAMAP	5.07	1.65	32.54	2.44	48.13	2.02	39.84	0.61	12.03
SEAMAP	5.07	1.93	38.07	2.73	53.85	1.79	35.31	0.71	14.00
GCRL	5.20	1.74	33.46	2.73	52.50	1.83	35.19	0.66	12.69
SEAMAP	5.20	1.93	37.12	2.77	53.27	1.93	37.12	0.71	13.65
SEAMAP	5.20	1.88	36.15	2.82	54.23	2.02	38.85	0.71	13.65
GCRL	5.46	1.97	36.08	3.01	55.13	1.97	36.08	0.71	13.00
SEAMAP	5.46	2.35	43.04	3.29	60.26	2.21	40.48	0.71	13.00
GCRL	5.46	1.88	34.43	3.15	57.69	2.16	39.56	0.61	11.17
SEAMAP	5.46	2.12	38.83	3.10	56.78	2.12	38.83	0.71	13.00
GCRL	5.59	1.97	35.24	3.15	56.35	2.16	38.64	0.71	12.70
SEAMAP	5.59	2.16	38.64	3.10	55.46	2.21	39.53	0.80	14.31
SEAMAP	5.85	1.97	33.68	3.10	52.99	2.54	43.42	0.71	12.14
GCRL	6.37	2.26	35.48	3.57	56.04	2.26	35.48	0.85	13.34
GCRL	9.49	3.85	40.57	5.67	59.75	3.57	37.62	1.36	14.33
SEAMAP	10.01	4.03	40.26	5.85	58.44	3.48	34.77	1.32	13.19
SEAMAP	20.02	7.15	35.71	12.09	60.39	7.02	35.06	2.60	12.99

(2.9 mm) than in reared larvae, whereas fin pigmentation seemingly appeared later in development (Tables 1–4). Comparisons of the ratios of head length, preanal length, body depth, and orbit diameter to body length indicated that development in the laboratory resulted in larvae that mirrored development in the wild.

Discussion

The larvae of as many as eighteen species of snappers in three subfamilies can occur in the western Central Atlantic which includes the Gulf of Mexico and Caribbean Sea. The early life stages of the subfamily Apsilinae are mostly unknown but the low number of dorsal soft rays (10, rarely 9) should separate late-stage larvae and juveniles of *Apsilus dentatus* from larvae of species in the other two subfamilies (Leis et al., 1997; Leis and Lee, 1994; Richards et al., 1994). Eteline snappers are represented by four species in GOM collections, *Etelis oculatus* and three species of *Pristipomoides*. The larvae of these taxa should be separable from lutjanine larvae by body shape and spine structure because eteline larvae are slender bodied and have weaker median fin spines (Leis and Lee, 1994; Richards et al., 1994). The lower dorsal count of etelines (21) will also distinguish larvae from lutjanines (22–24) in specimens whose total dorsal elements can be counted (Leis and Lee, 1994; Richards et al., 1994). The majority of snappers (13 species) found in the area belong to the subfamily Lutjaninae (Richards et al., 1994). Distinguishing the lutjanine larvae from each other is difficult despite published larval descriptions for six taxa: *Rhomboplites aurorubens* (Laroche, 1977); *Lutjanus griseus* (Richards and Saksena, 1980); *Ocyurus chrysurus* (Riley et al., 1995; Clarke et al., 1997); *L. synagris* (Clarke et al., 1997); *L. analis* (Clarke et al., 1997); and *L. campechanus* (Rabalais et al., 1980; Collins et al., 1980; and our study). We undertook a synthesis of these published descriptions and illustrations to better evaluate the usefulness of various characters in distinguishing the larvae of lutjanine species occurring in the Gulf of Mexico (Table 5).

Our tabulated character list is not exhaustive and represents only those features for which known GOM lutjanine larvae appear to differ. Dorsal-fin meristics can be used to narrow the possible choices among species once total fin element number is established and even before spines and rays are completely differentiated. Only four species have 22 or 23 total dorsal elements and of these, *R. aurorubens* is the only species with 12 dorsal spines; the other three usually have 10 spines. Body shape may also

Table 4

Meristics and spine lengths of wild larval red snapper. nd = not developed, — = not measured owing to damage, i = incipient ray(s) or spine(s), P_2 = pelvic fin. SEAMAP = Southeast Area Monitoring and Assessment Program; GCRL = Gulf Coast Research Laboratory.

Source	Body length (BL)	Dorsal fin spines and rays	2nd dorsal spine length	2nd dorsal spine length/BL	3rd dorsal spine length	3rd dorsal spine length/BL	P_2 spine length	P_2 spine length/BL	P_2 ray length	P_2 ray length/BL	Anal fin spines and rays
SEAMAP	2.86	II	0.30	10.49	0.24	8.39	bud	nd	bud	nd	anlage
SEAMAP	2.99	i	0.09	3.01	nd	nd	bud	nd	bud	nd	nd
SEAMAP	2.99	IIi	0.44	14.72	0.36	12.04	0.21	7.02	0.29	9.70	anlage
SEAMAP	2.99	IVi	0.58	19.40	0.38	12.71	0.26	8.70	0.26	8.70	anlage
SEAMAP	3.12	ii	0.17	5.45	0.12	3.85	bud	nd	bud	nd	nd
SEAMAP	3.12	IIii	0.44	14.10	0.36	11.54	0.23	7.37	0.23	7.37	anlage
SEAMAP	3.12	IVi	0.54	17.31	0.39	12.50	0.32	10.26	0.38	12.18	anlage
GCRL	3.25	IIIi	0.29	8.92	0.18	5.54	bud	nd	bud	nd	anlage
SEAMAP	3.25	IIIi	0.48	14.77	0.36	11.08	0.26	8.00	0.38	11.69	anlage
SEAMAP	3.38	IIi	0.38	11.24	0.32	9.47	0.18	5.33	0.38	11.24	anlage
SEAMAP	3.38	IIii	0.50	14.79	0.41	12.13	0.19	5.62	0.26	7.69	anlage
SEAMAP	3.38	IVii	0.53	15.68	0.36	10.65	0.22	6.51	0.26	7.69	anlage
SEAMAP	3.38	IVii	0.55	16.27	0.38	11.24	0.26	7.69	0.31	9.17	anlage
SEAMAP	3.38	V	0.66	19.53	0.42	12.43	0.42	12.43	0.47	13.91	anlage
SEAMAP	3.38	Vi	0.80	23.67	0.52	15.38	0.52	15.38	0.61	18.05	anlage
GCRL	3.51	IIii	0.29	8.26	0.22	6.27	1.06	30.20	0.58	16.52	na
SEAMAP	3.51	IIii	0.38	10.83	0.24	6.84	0.19	5.41	0.19	5.41	anlage
SEAMAP	3.51	IIIii	0.55	15.67	0.36	10.26	0.29	8.26	0.34	9.69	anlage
SEAMAP	3.51	V	0.61	17.38	0.56	15.95	0.38	10.83	0.52	14.81	anlage
SEAMAP	3.51	VIi	0.99	28.21	0.61	17.38	0.33	9.40	0.56	15.95	i
SEAMAP	3.64	IIIii	0.66	18.13	0.38	10.44	0.56	15.38	—	—	anlage
SEAMAP	3.64	Vi	0.72	19.78	0.48	13.19	0.50	13.74	0.50	13.74	anlage
SEAMAP	3.64	VI	0.55	15.11	0.38	10.44	0.26	7.14	0.34	9.34	anlage
GCRL	3.77	II	0.20	5.31	0.17	4.51	bud	nd	bud	nd	nd
GCRL	3.77	IIi	0.31	8.22	0.24	6.37	bud	nd	bud	nd	nd
GCRL	3.77	IIii	0.24	6.37	0.17	4.51	bud	nd	bud	nd	anlage
GCRL	3.77	IVi	0.36	9.55	0.29	7.69	bud	nd	bud	nd	anlage
SEAMAP	3.77	Vi	1.08	28.65	0.70	18.57	0.70	18.57	0.89	23.61	anlage
SEAMAP	3.77	VI	0.87	23.08	0.53	14.06	0.53	14.06	0.56	14.85	anlage
SEAMAP	3.77	VI	0.94	24.93	0.67	17.77	—	—	—	—	anlage
SEAMAP	3.77	VIi	0.82	21.75	0.55	14.59	0.48	12.73	0.50	13.26	anlage
SEAMAP	3.77	VIi	1.08	28.65	0.65	17.24	0.70	18.57	0.79	20.95	anlage
SEAMAP	3.77	VIi	1.18	31.30	0.75	19.89	0.80	21.22	0.99	26.26	ii
SEAMAP	3.81	Vi	0.56	14.70	0.47	12.34	0.21	5.51	0.68	17.85	anlage
SEAMAP	3.84	Vi	0.71	18.49	0.42	10.94	0.47	12.24	0.66	17.19	anlage
SEAMAP	3.90	IVii	0.82	21.03	0.53	13.59	0.55	14.10	0.77	19.74	anlage
GCRL	3.90	Vi	0.72	18.46	0.46	11.79	0.43	11.03	0.43	11.03	anlage
SEAMAP	3.90	Vii	0.89	22.82	0.50	12.82	0.60	15.38	0.63	16.15	anlage
SEAMAP	3.90	VIi	1.03	26.41	0.61	15.64	0.65	16.67	0.70	17.95	anlage
SEAMAP	3.90	VIi	1.03	26.41	0.71	18.21	0.71	18.21	0.89	22.82	i
GCRL	4.03	IVi	0.54	13.40	0.35	8.68	0.30	7.44	0.57	14.14	anlage
SEAMAP	4.03	IVii	0.68	16.87	0.44	10.92	0.29	7.20	0.60	14.89	anlage
GCRL	4.03	Vi	0.66	16.38	0.48	11.91	0.50	12.41	0.57	14.14	anlage
SEAMAP	4.03	Vi	0.94	23.33	0.56	13.90	0.66	16.38	1.03	25.56	anlage
SEAMAP	4.03	VIi	1.03	25.56	0.65	16.13	0.62	15.38	0.82	20.35	anlage

continued

Table 4 (continued)

Source	Body length (BL)	Dorsal fin spines and rays	2nd dorsal spine length	2nd dorsal spine length/BL	3rd dorsal spine length	3rd dorsal spine length/BL	P_2 spine length	P_2 spine length/BL	P_2 ray length	P_2 ray length/BL	Anal fin spines and rays
SEAMAP	4.03	VIii	0.85	21.09	0.49	12.16	0.52	12.90	0.80	19.85	anlage
SEAMAP	4.03	VIIIi	1.22	30.27	0.77	19.11	0.94	23.33	1.22	30.27	i
GCRL	4.16	IVii	0.53	12.74	0.33	7.93	0.26	6.25	0.33	7.93	anlage
GCRL	4.16	Vi	0.62	14.90	0.47	11.30	0.45	10.82	0.45	10.82	anlage
GCRL	4.16	Vi	0.82	19.71	0.50	12.02	0.46	11.06	0.55	13.22	anlage
GCRL	4.16	Vi	0.70	16.83	0.43	10.34	0.31	7.45	0.53	12.74	anlage
SEAMAP	4.16	VIi	1.13	27.16	0.38	9.13	0.75	18.03	0.89	21.39	ii,(9i)
SEAMAP	4.16	VIi	1.27	30.53	0.85	20.43	0.94	22.60	0.85	20.43	anlage
SEAMAP	4.16	VIIi,(16i)	1.13	27.16	0.80	19.23	0.80	19.23	0.99	23.80	anlage
SEAMAP	4.16	VIIii,(15i)	1.32	31.73	0.85	20.43	0.42	10.10	0.75	18.03	ii,(9i)
SEAMAP	4.29	Vi	0.82	19.11	0.67	15.62	0.54	12.59	0.72	16.78	anlage
SEAMAP	4.29	Vii	0.94	21.91	0.66	15.38	0.75	17.48	0.80	18.65	anlage
GCRL	4.29	VIi	0.86	20.05	0.58	13.52	0.53	12.35	0.79	18.41	anlage
SEAMAP	4.42	VIi	0.94	21.27	0.52	11.76	0.56	12.67	0.71	16.06	anlage
SEAMAP	4.42	VIi,(17i)	1.25	28.28	0.82	18.55	0.72	16.29	0.96	21.72	ii,(9i)
SEAMAP	4.42	VIii,(16i)	1.18	26.70	0.79	17.87	—	—	—	—	II,(9i)
SEAMAP	4.42	VIIIi	0.33	7.47	0.89	20.14	1.03	23.30	1.32	29.86	IIi
GCRL	4.42	VIIii,(13i)	1.44	32.58	0.96	21.72	1.15	26.02	1.49	33.71	ii,(8i)
SEAMAP	4.55	VIi	1.00	21.98	0.65	14.29	0.77	16.92	0.78	17.14	anlage
SEAMAP	4.55	VIIi	1.13	24.84	0.71	15.60	0.56	12.31	1.03	22.64	i
SEAMAP	4.55	VIIIi	1.65	36.26	0.80	17.58	0.38	8.35	1.41	30.99	IIi,(8i)
GCRL	4.55	VIIii,(14i)	1.04	22.86	0.69	15.16	0.93	20.44	1.41	30.99	ii,(9i)
SEAMAP	4.68	IXi,(14i)	1.74	37.18	1.08	23.08	1.20	25.64	1.46	31.20	IIi,(8i)
GCRL	4.68	VIi	0.98	20.94	0.46	9.83	0.62	13.25	0.77	16.45	anlage
GCRL	4.68	VIi,(16i)	0.98	20.94	0.65	13.89	0.91	19.44	0.98	20.94	ii
SEAMAP	4.68	VIIIi,(15i)	1.55	33.12	0.94	20.09	1.03	22.01	1.34	28.63	ii,(9i)
SEAMAP	4.81	IXi,(14i)	1.60	33.26	0.94	19.54	1.20	24.95	1.78	37.01	ii,(9i)
SEAMAP	4.81	VIi,(15i)	1.18	24.53	0.80	16.63	0.94	19.54	1.08	22.45	ii,(9i)
SEAMAP	4.81	VIIii,(14i)	0.61	12.68	0.89	18.50	0.24	4.99	1.22	25.36	ii,(8i)
SEAMAP	4.94	IXi,(14i)	0.94	19.03	1.08	21.86	1.36	27.53	1.83	37.04	IIi,(9i)
SEAMAP	4.94	VIIii	1.46	29.55	0.94	19.03	1.03	20.85	1.60	32.39	ii,(10i)
GCRL	5.07	VIIi,(16i)	1.20	23.67	0.79	15.58	0.93	18.34	0.82	16.17	ii,(9i)
SEAMAP	5.07	VIIIi,(13i)	1.27	25.05	0.89	17.55	0.99	19.53	1.13	22.29	ii,(9i)
SEAMAP	5.07	VIIIii	1.55	30.57	1.03	20.32	1.18	23.27	1.70	33.53	IIi,(8i)
SEAMAP	5.07	VIIIii,(14i)	1.66	32.74	1.01	19.92	1.08	21.30	1.75	34.52	IIi,(8i)
SEAMAP	5.20	IXi,(14i)	1.74	33.46	0.99	19.04	1.27	24.42	1.32	25.38	IIi,(8i)
GCRL	5.20	VIIii,(15i)	1.32	25.38	0.84	16.15	0.86	16.54	1.42	27.31	II,(9i)
SEAMAP	5.20	VIIIii,(14i)	1.54	29.62	0.94	18.08	1.08	20.77	1.39	26.73	IIi,(8i)
SEAMAP	5.46	IXi,(14i)	1.88	34.43	1.13	20.70	1.36	24.91	1.32	24.18	IIi,(8i)
SEAMAP	5.46	VIIii,(15i)	1.58	28.94	1.06	19.41	1.22	22.34	1.89	34.62	IIi,(8i)
GCRL	5.46	VIIii,(15i)	1.39	25.46	0.89	16.30	0.94	17.22	1.15	21.06	II,(9i)
GCRL	5.46	VIIIi,(15i)	1.10	20.15	0.91	16.67	0.74	13.55	0.74	13.55	II,(9i)
SEAMAP	5.59	IX,(15i)	1.92	34.35	1.32	23.61	1.61	28.80	2.04	36.49	IIi,(8i)
GCRL	5.59	VIIIii,(14i)	2.96	52.95	1.06	18.96	1.15	20.57	1.49	26.65	II,(9i)
SEAMAP	5.85	IXi,(14i)	1.74	29.74	1.32	22.56	1.46	24.96	1.97	33.68	IIi,(8i)
GCRL	6.37	IXi,(14i)	1.61	25.27	1.13	17.74	0.89	13.97	1.37	21.51	II,(9i)
GCRL	9.49	X,14	3.20	33.72	1.74	18.34	1.79	18.86	0.80	8.43	III,8
SEAMAP	10.01	X,14	2.96	29.57	2.26	22.58	2.87	28.67	3.85	38.46	III,9
SEAMAP	20.02	X,14	6.63	33.12	3.64	18.18	2.73	13.64	5.20	25.97	III,9

Table 5

Morphological comparison of *Rhomboplites aurorubens*, *Ocyurus chrysurus*, and *Lutjanus* spp. larvae based on presence (+), absence (–), and specimen size (BL in mm) at the first noted appearance of selected characters from published descriptions and illustrations. Abbreviations: D = dorsal; D_2 = soft dorsal fin; BD= body depth; sp = spine; a = anterior; p = posterior; P_2 = pelvic fin; Pr An sp = preopercular angle spine; avm = anterior visceral mass; pav = postanal ventral melanophore series; nv = not visible in published illustrations; ? = no published illustrations. "Spots" refer to melanophores. Dorsal fin counts in parentheses are rare values (Richards et al., 1994).

	Dorsal-fin count	BD to BL ratio	P_2 ray length	Avm pigment	Pr An sp serrations	D sp serrations	No. of pav spots in preflexion	Enlarged pav spot in preflexion	Gap in pav series in preflexion
R. aurorubens	XII,(10)11(12)	35% at 4.0	=P_2sp	–	+	+	8–18	–	–
L. apodus	X,14	?	?	?	?	?	?	?	?
L. cyanopterus	X,14	?	?	?	?	?	?	?	?
L. griseus	X,14	34% at 4.2	=P_2sp	nv	–	+	23–27	–	–
L. jocu	X,(13)14	?	?	?	?	?	?	?	?
L. mahogani	X,(11)12	?	?	?	?	?	?	?	?
O. chrysurus	(IX)X(XI),12-13(14)	26% at 4.5	2×P_2sp	3.3–4.0	–	+	13–19	–	–
L. synagris	X,12(13)	29% at 4.6	2×P_2sp	3.3–4.0	–	+	15–25	+	–
L. analis	X(XI),(13)14	23% at 4.6	2×P_2sp	3.3–4.0	–	+	13–23	+	+
L. buccanella	X,14	?	?	?	?	?	?	?	?
L. campechanus	(IX)X,(13)14(15)	36% at 4.2	2×P_2sp	3.4	–	–	8–22	–	+
L. purpureus	(IX)X,(13)14(15)	?	?	?	?	?	?	?	?
L. vivanus	X(XI),(13)14	?	?	?	?	?	?	?	?

	Spot ventral to notochord flexure	Internal spots over notochord	Dorsal midline caudal pigment	D_2 pigment	Anal-fin pigment base and membrane	Pelvic-fin pigment during flexion	Data sources
R. aurorubens	–	–	4.5	nv	5.1/nv	membrane ray 1	1,2,3
L. apodus	?	?	?	?	?	?	
L. cyanopterus	?	?	?	?	?	?	
L. griseus	–	–	–	by 9.6	by 6.2/by 7.1	spine+ray tips (?)	2,4
L. jocu	?	?	?	?	?	?	
L. mahogani	?	?	?	?	?	?	
O. chrysurus	–	6.3	6.3	11.5	5.3/6.3	membrane all rays	5,6
L. synagris	–	6.2	6.2	6.2	4.7/9.8	membrane ray 1	6
L. analis	5.8	–	8.1	11.5	6.2/16	membrane ray 1	6
L. buccanella	?	?	?	?	?	?	
L. campechanus	–	–	3.8 or 5.5	12.2	3.8/12.2	membrane ray 1	2,7,8
L. purpureus	?	?	?	?	?	?	
L. vivanus	?	?	?	?	?	?	

[1] Laroche (1977).

[2] Richards et al. (1994).

[3] Comyns, B.H., and J. Lyczkowski-Shultz. 1993. Spawning and early life history of snappers in the northcentral Gulf of Mexico. Final Report, MARFIN grant NA17FF0382-01, NMFS Southeast Regional Office, St. Petersburg, FL 33701.

[4] Richards and Saksena (1980).

[5] Riley et al. (1995).

[6] Clarke et al. (1997).

[7] Collins et al. (1980).

[8] Our study.

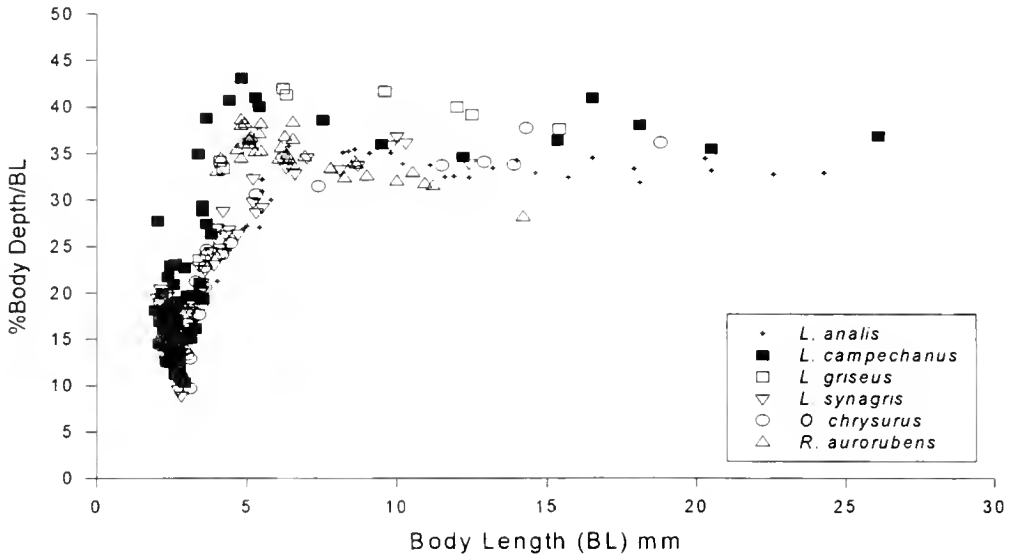

Figure 7

Comparison of body depth ratios among larvae of *L. analis*, *L. campechanus*, *L. griseus*, *L. synagris*, *O. chrysurus*, and *R. aurorubens*.

provide important diagnostic characters. Flexion larvae of *O. chrysurus*, *L. analis*, and *L. synagris* are shallow-bodied ranging from 23% to 29% of body length (Fig. 7), whereas body depth in flexion larvae of *L. campechanus*, *L. griseus*, and *R. aurorubens* is from 34% to 36% of body length. The approximately equal length of the longest pelvic-fin ray and pelvic spine helps distinguish *R. aurorubens* and *L. griseus* from *O. chrysurus*, *L. synagris*, *L. analis*, and *L. campechanus* larvae in which the longest pelvic ray is nearly twice the length of the pelvic spine.

Small preflexion larvae of *L. campechanus* can be consistently distinguished from larvae of *R. aurorubens* in northcentral GOM waters by the presence of the avm melanophore. This character first appeared in reared specimens at 3.4 mm but would be seen in somewhat smaller wild specimens because of the shrinkage experienced by net-captured larvae (Theilacker, 1980). Larvae of *O. chrysurus*, *L. synagris*, and *L. analis* also develop avm pigment at BLs between ~3 and 4 mm. The presence or absence of this character in *L. griseus* larvae could not be ascertained from published illustrations (Richards and Saksena, 1980), but avm pigment was present in all specimens of *L. griseus* that we examined. The presence of serrations on the angle spine of the preopercle in *R. aurorubens* larvae at sizes >3.4 mm distinguishes them from *O. chrysurus* and all *Lutjanus* larvae currently known in the GOM. Snapper larvae may develop serrations on the median fin spines to some degree or another, but at least three species of lutjanine snappers (*Hoplopagrus guntheri*, *L. novemfasciatus*, and *L. peru*) from the Pacific do not develop serrations on any fin spines (Brogan, 1996; Watson and Brogan, 1996). Larvae of the six species compared in Table 5 develop serrations on the pelvic spine and all species, except *L. campechanus*, develop serrations on dorsal-fin spines. Although not shown in the illustrations of Richards and Saksena (1980), the larvae of *L. griseus* do develop pronounced serrations on both dorsal and pelvic spines (Clarke et al., 1997; Richards et al., 1994). The relative size and extent of these serrations vary among species; *R. aurorubens* has the stoutest serrations among snapper larvae on both the leading and trailing edges of the spines (Laroche, 1977).

The postanal series of melanophores (pav) along the ventral midline is characteristic of many percoid larvae, including those of snappers. In snapper larvae, postanal pigmentation decreases dramatically during the flexion stage. Despite the dynamic nature of this pigment during development and the considerable overlap in number of pav melanophores among preflexion larvae (Table 5), Clarke et al. (1997) suggested that the "usual" number (not overall range) of pav melanophores would distinguish the larvae of *L. synagris* and *L. analis* from each other. Yolksac and preflexion larvae of these two species are further distinguished from other known lutjanine larvae by the presence of an enlarged melanophore in the pav series (Clarke et al., 1997). An additional pav-related character that differs among known lutjanine larvae is the gap in the pav series posteriorly, as seen in *R. aurorubens*, *L. campechanus*, and *L. analis*. The pav series of melanophores in *L. griseus*, *O. chrysurus*, and *L. synagris* is continuous in preflexion larvae.

Pigmentation associated with the notochord can be used to distinguish the larvae of *O. chrysurus*, *L. synagris*, and *L. analis* from other described GOM lutjanine larvae (Table 5). Although pigment overlying the point of notochord flexure develops by ~6 mm in all described GOM

lutjanine larvae, only *L. analis* simultaneously acquires pigment ventral to notochord flexure. Only the larvae of *O. chrysurus* and *L. synagris* develop internal melanophores over the notochord. Both species first acquire this pigment by ~6 mm but it becomes more extensive with development in *O. chrysurus* than in *L. synagris*. Pigment on the dorsal midline of the caudal peduncle develops in all lutjanine larvae except *L. griseus*. There is some interspecific variation in the size when this pigment first develops (Table 5). *Rhomboplites aurorubens* larvae as small as 4.5 mm have dorsal pigment on the caudal peduncle (Richards et al., 1994) and this pigment does not develop in *L. analis* larvae until ~8 mm. A single melanophore first appeared on the dorsal midline of the caudal peduncle in the 3.8-mm *L. campechanus* of our series. It was not present in the next two specimens but was present in the 5.5-mm specimen and all subsequent larvae.

Interspecific differences among known lutjanine larvae are apparent in the amount, location, and size at first appearance of dorsal-fin pigment. Pigment in the spinous dorsal fin first appears in the membrane behind the second spine in *L. campechanus*, *O. chrysurus*, *L. synagris*, and *L. analis*. Additional melanophores develop posteriorly behind successive spines in *L. synagris* throughout flexion, whereas in the other three species, pigment develops posteriorly behind successive spines only in late flexion or after flexion. It appears from the illustrations of Clarke et al. (1997) that although pigment between the first and second spines is present in *L. synagris* from 4.7 to 6.2 mm, it is consistently present only in *O. chrysurus* larvae from preflexion onward. Spinous dorsal-fin pigment in *L. griseus* differs notably from the other species of lutjanines; melanophores first form low in the fin at the base of the second or third spines, or at the base of both, and as development proceeds, melanophores are added distally (farther out onto the fin) and posteriorly. Pigment was present between the second and third dorsal-fin spines in the few *R. aurorubens* larvae that had intact dorsal-fin membranes. Dorsal-fin pigment was not indicated in illustrations by Laroche (1977), probably because these specimens did not have intact fin membranes. Among known GOM lutjanine larvae, only *L. synagris* larvae develop pigment in the second (soft) dorsal fin before ray formation is complete, at ~6 mm. In larvae of the remaining species, pigment in the second dorsal-fin first appears at larger sizes when fin ray development is well advanced (Table 5).

Anal- and pelvic-fin pigmentation is also useful in separating the larvae of GOM lutjanines. Pigment on the anal-fin base develops in all six species whose larvae have been described and of these, *L. campechanus* larvae develop this pigment at the smallest size, <4 mm (Table 5). There are greater differences among larvae in size at first appearance of pigment in the anal-fin membrane than in the anal base. *Lutjanus campechanus* and *L. analis* larvae can be distinguished from the other described larvae by later development of anal-fin pigment at sizes ≥12 mm (Table 5). Pigment on the pelvic fin bud has been indicated in all illustrated lutjanine larvae except *L. griseus*. It is likely that this exception is due, not to true absence of this feature in *L. griseus*, but to the limited number of larvae in the described series (Richards and Saksena, 1980). The 4.2-mm *L. griseus* larva illustrated by these authors had pigment at the distal tips of the pelvic fin, but this pigment was not present in larger larvae of the series or in the 7.1-mm specimen illustrated in Richards et al. (1994). Pelvic-fin pigment distinguishes *O. chrysurus* and *L. griseus* from other lutjanine larvae once the spine and first ray are formed. From illustrations in Clarke et al. (1997), it appears that starting in the preflexion stage, *O. chrysurus* larvae have pigment throughout the pelvic-fin membrane and not just around the first fin ray as in *L. campechanus*, *L. synagris*, and *L. analis*. The unique condition of pelvic-fin pigmentation that characterizes *L. griseus* is the "candycane stripe" pattern of melanophores that overlay the pelvic spine. Pigment on the pelvic spine is present in *L. griseus* larvae as small as 4.2 mm and the striped pattern is evident by at least 6.2 mm (Richards and Saksena, 1980).

In Table 9 of their recent publication, Clarke et al. (1997) provided a summary of distinguishing characters for the known larvae and juveniles of western Central Atlantic lutjanine snappers. We have noted some discrepancies in that summary that may cause confusion for those attempting to identify lutjanine snapper larvae from our area. In Table 9, the "usual" number of pav melanophores listed for *L. campechanus* was given as 16–18. The modal number of pav spots among preflexion *L. campechanus* larvae (2.2–3.8 mm BL; n=70) from the GCRL rearings was 15, and 50 specimens had 14 to 19 pav spots. Also in Table 9, for the character "serrations on dorsal and pelvic fin spines," the entry for *L. campechanus* states, "on anterior spine margin only." Larvae of *L. campechanus* develop serrations on the anterior margin of the pelvic spine only, not on the dorsal spines (Collins et al., 1980; Potthoff et al., 1988). Clarke et al. (1997) also note that *L. griseus* larvae develop internal melanophores ventral to the point of notochord flexure (their character "O"). This feature is not visible in any of the published illustrations of *L. griseus* larvae or in specimens we have examined. Finally, information in Table 9 that pertains to character "P"—"internal melanophores on antero-ventral surface of gut (peritoneum) dorsal to pelvic bone" noted as being absent in four species—was clearly present in the *R. aurorubens* and *L. campechanus* larvae that we examined and is visible in illustrations of *L. analis* and *O. chrysurus* in Clarke et al. (1997).

The descriptions of larval lutjanine snapper development now available will allow scientists to identify mid- to late-flexion and postflexion larvae of the most common lutjanids in the Gulf of Mexico. In an examination of over 1500 snapper larvae from Gulfwide collections in 1992 and 1993, we found that the larvae of *R. aurorubens*, *L. campechanus*, and *P. aquilonaris* made up 23%, 13%, and 13% of all snapper larvae captured, respectively. Other identified taxa consisted of *Lutjanus* spp. (3%), *L. griseus* (<1%), and *L. synagris* (<1%). However, 47% of snapper larvae in these collections, typically <3.5–4.0 mm in length, could not be identified beyond the family level because diagnostic characters are present only after flexion has begun.

Closer scrutiny of characters, such as the number of pav spots, the enlarged pav spot, and the gap in the pav series, may allow identification of preflexion and early flexion snapper larvae, if not to a single species, at least to a reduced number of possibilities. Of course, larvae of the remaining snapper species need to be described before all small "undifferentiated snapper larvae" can be reliably and consistently identified to the species level. Investigation of additional characters among preflexion larvae such as the presence and location of other chromatophores, may yield further useful species-specific traits (Riley et al., 1995). Initial observations of *L. campechanus* show yellow chromatophores in similar locations (head and gut area) as those reported for *O. chrysurus* (Riley et al., 1995). Among larger *L. campechanus* specimens, additional chromatophores were present in locations not noted for *O. chrysurus* larvae. More specific comparisons will have to await a larger sample size to determine variability in numbers of chromatophores and size at development. Additionally, biochemical techniques are currently being investigated for the purpose of species-specific identification of snapper larvae (Chow et al., 1993; Sarver et al., 1996; Schultz et al., 1996). Initial results seem to indicate that no single technique will distinguish between all species in the subfamily Lutjaninae. Use of these biochemical assay methods for routine identification of snapper larvae may not be feasible for specimens taken during broadscale surveys. Yet a positive species identification of subsamples of field-caught snapper larvae with biochemical methods may lead to recognition of morphological features that have been previously overlooked and determination of the error rate of morphologically based identifications.

Acknowledgments

Most of the work for this study was done while the primary author was employed by Johnson Controls World Services. Gratitude is expressed to the following individuals for their able assistance during the course of this study and the support of the institutions they represent: the staff of the Claude Peteet Mariculture Center, particularly Jim Duffy; John Ogle, Casey Nicholson, Jeff Lotz, Donald Barnes, Mae Blake and Pam Bond of the Gulf Coast Research Laboratory, University of Southern Mississippi; and Kim Williams of the SEAMAP Archiving Center at the Florida Marine Research Institute, St. Petersburg, FL. The Texas study was funded by Grant NA16RG0457-03 from the National Oceanic and Atmospheric Administration through The Texas Sea Grant College Program. We thank W. J. Richards for reading an earlier draft and two anonymous reviewers for comments on the manuscript.

Literature cited

Bootes, K. L.
1998. Culture and description of larval red snapper, *Lutjanus campechanus*. M.S. thesis, Department of Fisheries and Allied Aquacultures, Auburn Univ., Auburn, AL. 155 p.

Brogan, M. W.
1996. Larvae of the Eastern Pacific snapper *Hoplopagrus guntheri* (Teleostei: Lutjanidae). Bull. Mar. Sci. 58(2):329–343.

Chow, S., M. E. Clarke, and P. J. Walsh.
1993. PCR-RFLP analysis on thirteen western Atlantic snappers (subfamily Lutjaninae): a simple method for species and stock identification. Fish. Bull. 91:619–627.

Clarke, M. E., M. L. Domeier, and W. A. Laroche.
1997. Development of larvae and juveniles of the mutton snapper (*Lutjanus analis*), lane snapper (*Lutjanus synagris*) and yellowtail snapper (*Lutjanus chrysurus*). Bull. Mar. Sci. 61(3):511–537.

Collins, L. A., J. H. Finucane, and L. E. Barger.
1980. Description of larval and juvenile red snapper, *Lutjanus campechanus*. Fish. Bull. 77:965–974.

Donaldson, D. M., N. J. Sanders, and P. A. Thompson.
1993. SEAMAP environmental and biological atlas of the Gulf of Mexico, 1991. Gulf States Marine Fisheries Commission 29, 321 p.
1994. SEAMAP environmental and biological atlas of the Gulf of Mexico, 1992. Gulf States Marine Fisheries Commission 30, 293 p.

Donaldson, D. M., N. J. Sanders, P. A. Thompson, and R. Minkler.
1996. SEAMAP environmental and biological atlas of the Gulf of Mexico, 1993. Gulf States Marine Fisheries Commission 34, 284 p.
1997a. SEAMAP environmental and biological atlas of the Gulf of Mexico, 1994. Gulf States Marine Fisheries Commission 40, 277 p.
1997b. SEAMAP environmental and biological atlas of the Gulf of Mexico, 1995. Gulf States Marine Fisheries Commission 41, 280 p.

Johnson, G. D.
1984. Percoidei: development and relationships. *In* Ontogeny and systematics of fishes (H. G. Moser, W. J. Richards, D. M. Cohen, M. P. Fahay, A. W. Kendall Jr. and S. L. Richardson, eds.), p. 464–498. Am. Soc. Ichthyol. Herpetol. Spec. Publ. 1.

Laroche, W. A.
1977. Description of larval and early juvenile vermilion snapper, *Rhomboplites aurorubens*. Fish. Bull. 75:547–554.

Leis, J. M.
1987. Review of the early life history of tropical groupers (Serranidae) and snappers (Lutjanidae). *In* Tropical snappers and groupers: biology and fisheries management (J. J. Polovina and S. Ralston, eds.), p. 189–237. Westview Press, Boulder, Colorado.

Leis, J. M., and K. Lee.
1994. Larval development in the lutjanid subfamily Etelinae (Pisces): the genera *Aphareus*, *Aprion*, *Etelis* and *Pristipomoides*. Bull. Mar. Sci. 55(1):46–125.

Leis, J. M., and D. S. Rennis.
1983. The larvae of Indo-Pacific coral reef fishes. Univ. Hawaii Press, Honolulu, HI. 269 p.

Leis, J. M., and T. Trnski.
1989. The larvae of Indo-Pacific shorefishes. Univ. Hawaii Press, Honolulu, HI, 371 p.

Leis, J. M., S. Bullock, D. J. Bray, and K. Lee.
1997. Larval development in the lutjanid subfamily Apsilinae (Pisces): the genus *Paracaesio*. Bull. Mar. Sci. 61(3):697–742.

Potthoff, T., S. Kelley, and L. A. Collins.
1988. Osteological development of the red snapper, *Lutjanus campechanus* (Lutjanidae). Bull. Mar. Sci. 43(1):1–40.

Rabalais, N. N., S. C. Rabalais, and C. R. Arnold.
1980. Description of eggs and larvae of laboratory reared red snapper (*Lutjanus campechanus* Poey). Copeia 1980:704–708.

Richards, W. J.
1984. Kinds and abundances of fish larvae in the Caribbean Sea and adjacent areas. U.S. Dep. Commer., NOAA Tech. Rep. NMFS-SSRF-776, 54 p.

Richards, W. J., and V. P. Saksena.
1980. Description of larvae and early juveniles of laboratory-reared gray snapper, *Lutjanus griseus* (Linnaeus) (Pisces, Lutjanidae). Bull. Mar. Sci. 30:515–521.

Richards, W. J., M. F. McGowan, T. Leming, J. T. Lamkin, and S. Kelley.
1993. Larval fish assemblages at the Loop Current boundary in the Gulf of Mexico. Bull. Mar. Sci. 53(2):475–537.

Richards, W. J., K. C. Lindeman, J. L-Shultz, J. M. Leis, A. Ropke, M. E. Clarke, and B. H. Comyns.
1994. Preliminary guide to the identification of the early life history stages of lutjanid fishes of the western central Atlantic. U.S. Dep. Commer., NOAA Tech. Memo. NMFS-SEFSC-345, 49 p.

Riley, C. M , G. J. Holt and C. R. Arnold.
1995. Growth and morphology of larval and juvenile captive bred yellowtail snapper, *Ocyurus chrysurus*. Fish. Bull. 93:179–185.

Sanders, N. J., D. M. Donaldson, and P. A. Thompson.
1991a. SEAMAP environmental and biological atlas of the Gulf of Mexico, 1988. Gulf States Marine Fisheries Commission 23, 320 p.
1991b. SEAMAP environmental and biological atlas of the Gulf of Mexico, 1989. Gulf States Marine Fisheries Commission 25, 318 p.
1992. SEAMAP environmental and biological atlas of the Gulf of Mexico, 1990. Gulf States Marine Fisheries Commission 27, 311 p.

Sanders, N. J., P. A. Thompson, and D. M. Donaldson.
1990a. SEAMAP environmental and biological atlas of the Gulf of Mexico, 1987. Gulf States Marine Fisheries Commission 22, 337 p.

Sanders, N. J., P. A. Thompson, and T. Van Devender.
1990b. SEAMAP environmental and biological atlas of the Gulf of Mexico, 1986. Gulf States Marine Fisheries Commission 20, 328 p.

Sarver, S. K., D. W. Freshwater, and P. J. Walsh.
1996. Phylogenetic relationships of western Atlantic snappers (Family Lutjanidae) based on mitochondrial DNA sequences. Copeia 1996(3):715–721.

Schultz, D. R., P. I. Arnold, T. R. Capo, C. B. Paris-Limouzy, J. E. Serafy, and W. J. Richards.
1996. Immunologic methods for species identification of early life stages of lutjanid fishes from the western central Atlantic. Part I: Characterization of an interspecies protein. Fish. Bull. 94:734–742.

Theilacker, G. H.
1980. Changes in body measurements of larval northern anchovy, *Engraulis mordax*, and other fishes due to handling and preservation. Fish. Bull. 78:685–692.

Thompson, P. A., T. Van Devender, and N. J. Sanders Jr.
1988. SEAMAP environmental and biological atlas of the Gulf of Mexico, 1985. Gulf States Marine Fisheries Commission 17, 338 p.

Watson, W., and M. W. Brogan
1996. Lutjanidae: snappers. *In* The early stages of fishes in the California Current region (H. G. Moser, ed.), p. 977–989. California Cooperative Oceanic Fisheries Investigations Atlas 33.

Workman, I. K., and D. G. Foster.
1994. Occurrence and behavior of juvenile red snapper, *Lutjanus campechanus*, on commercial shrimp fishing grounds in the northeastern Gulf of Mexico. Mar. Fish. Rev. 56(2):9–11.

Consequences of dispersal of subtropically spawned crevalle jacks, *Caranx hippos*, to temperate estuaries*

Richard S. McBride
Rutgers University Marine Field Station
Institute of Marine and Coastal Sciences
800 Great Bay Boulevard
Tuckerton, New Jersey 08087
Present address: Florida Marine Research Institute
100 Eighth Avenue Southeast
St. Petersburg, Florida 33701-5095
E-mail address: richard.mcbride@fwc.state.fl.us

Kim A. McKown
New York State Department of Conservation
205 Belle Meade Road
East Setauket, New York 11733

Abstract.—*Caranx hippos* spawn at subtropical and tropical latitudes, but some of their propagules are dispersed hundreds of kilometers north of Cape Hatteras into temperate waters of the western North Atlantic. The effect that this northward dispersal pattern has upon the population depends on whether these juveniles return south during autumn to overwinter or whether they become expatriated from the spawning population and die from hypothermal winter conditions at temperate latitudes. We evaluated whether repatriation was possible by comparing *C. hippos* seasonal abundance and size-structure from New York to Florida. Young-of-the-year *C. hippos* occurred annually during summer and autumn but were uncommon in relation to other species in subtropical and temperate estuaries. Sizes of *C. hippos* at temperate latitudes were as large as conspecifics at subtropical latitudes and juveniles of other species that are known to migrate during autumn from temperate nursery grounds to subtropical latitudes. As *C. hippos* disappeared from estuaries of the middle Atlantic states in autumn, similar-size fish appeared on the inner continental shelf. We postulate that at least some of the *C. hippos* observed migrating from temperate estuaries during the autumn eventually overwinter at subtropical latitudes, where they can return to the spawning population. This is unusual, because individuals of many other species whose larvae are transported north of Cape Hatteras do not appear to successfully migrate back to subtropical overwintering habitats. This life-history pattern, in which fish begin their first year in the Carolinian biogeographic province, are dispersed to the Virginian province, and return to the Carolinian province before their first winter, has been demonstrated for only one other western North Atlantic finfish species: bluefish (*Pomatomus saltatrix*). A few other species are likely to occupy and reproduce within such large-scale oceanographic systems because they have a combination of spawning, larval, and juvenile traits that is similar to that of *P. saltatrix* and *C. hippos*.

Manuscript accepted 15 December 1999.
Fish. Bull. 98: 528–538 (2000).

In the western North Atlantic, many species spawn at tropical and subtropical latitudes, and their larvae are dispersed to temperate and even boreal regions (e.g. Gill, 1904; Markle et al., 1979; Curran, 1989). This transport of larvae occurs in association with the Gulf Stream (Wroblewski and Cheney, 1984; Hare and Cowen, 1991, 1996) and disperses propagules from the Carolinian to the Virginian biogeographic province (Briggs, 1974, 1996). This process, which involves the entrainment of eggs and larvae into oceanographic currents and the dispersal of propagules to various water masses, is understood for only a few species and may vary considerably between species. Perhaps the most famous example is that of catadromous freshwater eels (*Anguilla anguilla* and *A. rostrata*), which spawn in the Sargasso Sea and whose larvae are transported to coastal nurseries in North America and Europe (McCleave et al., 1987). Larval *A. rostrata* drift for up to one year (Kleckner and McCleave, 1985) through gyres in the southwestern Sargasso Sea, the Antilles Current, and the Florida Current and its Gulf Stream extension before moving into coastal waters (McCleave, 1993). In the case of a wrasse, *Xyrichtys novacula*, northward transport across hundreds of kilometers occurs in as little as eight days, and cross-shelf transport in the northern portion of the Carolinian province is aided by interactions between western-edge, warm-core eddies and the Gulf Stream itself (Hare and Cowen, 1991). Similar northward transport in association with the Gulf Stream occurs for "spring-spawned" bluefish, *Pomatomus saltatrix*, except that for this species dispersal time is longer—about 2 months (McBride and Conover, 1991)—and its juveniles may actively swim out of the Gulf Stream system (Hare and Cowen, 1996). Although some species are transported annually in this manner (e.g. *Pomatomus*), others are transported less regularly (*Xyrichtys*, *Bothus*, *Syacium*), and still other species do not move between slope and shelf water masses (Cowen et al., 1993).

Those individuals dispersed across biogeographic boundaries become expatriated, in terms of passing on their genes if they do not return to spawning grounds to reproduce. *Anguilla* species remain in coastal habitats for several years before migrating back to the Sargasso Sea (Tesch, 1977), but many species that spawn at subtropical latitudes are physiologically incapable of overwintering at temperate latitudes. To our knowledge, only *P. saltatrix* spawns at

* Contribution 2000-06 of the Institute of Marine and Coastal Sciences, Rutgers University, Tuckerton, New Jersey 08087.

subtropical latitudes and its propagules, once dispersed to temperate latitudes, are known to migrate south within the same year. This species is successful largely because it spawns early in the year in the subtropics and juveniles enter temperate estuaries at a time when their principal prey is becoming available (Juanes et al., 1994). Direct evidence of a successful autumn migration by young-of-the-year *P. saltatrix* is available from recaptures of tagged individuals and size-frequency analyses (Lund and Maltezos, 1970; McBride et al., 1993). This "spring-spawned" cohort of *P. saltatrix* was more abundant than other intraspecific cohorts in the western North Atlantic during the 1980s and early 1990s (Chiarella and Conover, 1990; McBride et al., 1993), and this species repeats this life-history pattern in several oceanographic systems worldwide (Juanes et al., 1996).

The effects of this transport process, from the Carolinian province to the Virginian province, is known for few other species and these examples suggest a different fate for these species than for *P. saltatrix*. Moss (1973) concluded that the "sluggish" swimming ability and the critical thermal minimum of 8.7°C for planehead filefish, *Monocanthus hispidus*, prevented individuals of this species from surviving once they had been dispersed to temperate latitudes. Hare and Cowen (1991) observed a wrasse, *Xyrichtys novacula*, settling on the continental shelf at temperate latitudes, but successive cruises could not find survivors from the initially observed cohort. And McBride and Able (1998) reported on the annual appearance of butterflyfishes (*Chaetodon* spp.) at temperate latitudes, but field collections and laboratory experiments led them to conclude that none of these individuals survived through their first winter. Sinclair (1988) would categorize these unfortunate individuals as "vagrants" from, as opposed to "members" of, a population.

Although the ecological information about these tropical forms as they occur in temperate waters is limited, the common paradigm is that "[the] Gulf Stream has a profound effect upon the distribution of shore animals in the western Atlantic . . . many tropical forms are left stranded along the inhospitable shores of northeastern North America." (Briggs, 1996; p. 238). We believe that Briggs's conclusion can be applied to most of these species; nonetheless, juveniles of several "southern" species grow and survive well at temperate latitudes during the summer and, based on their size by autumn and their general mobility, may migrate successfully back to subtropical latitudes before winter (see also Hare and Cowen, 1993). We propose that at least one other species is capable of following a dispersal-migration pattern that links the temperate and subtropical latitudes during its first year. The crevalle jack, *Caranx hippos* (Linnaeus), is a migratory, coastal species that is distributed worldwide at subtropical and tropical latitudes (Briggs, 1960; Kwei, 1978; Grosslein and Azarovitz, 1982). In the western North Atlantic, it occurs primarily in the southeastern United States and the Gulf of Mexico (U.S. Department of Commerce, 1986), and spawning is known to occur only in the subtropical Straits of Florida (Berry, 1959; Fahay, 1975) and in the tropical Caribbean Sea (Montolio, 1978). Young-of-the-year (YOY) *C. hippos* occur in subtropical estuaries of the south Atlantic states, and they use these habitats as nurseries before presumably migrating offshore in autumn (Berry, 1959). However, YOY *C. hippos* are also reported from many temperate estuaries north of Cape Hatteras (McBride[1]). Despite the broad geographic distribution of YOY *C. hippos*, little is known about their early life history at any latitude. From archived museum collections, recent field collections, and the literature, we assembled data about *C. hippos* in both southern and northern estuaries and postulate on the significance of dispersal of YOY *C. hippos* across two biogeographic provinces.

Materials and methods

Archival collections were examined at the New York State Museum, the American Museum of Natural History, and the Academy of Natural Sciences of Philadelphia, and collection dates, locations, and sizes of *C. hippos* from coastal habitats of New York and New Jersey were recorded (material examined is listed in McBride[1]). Similar data for *C. hippos* in subtropical estuaries (from Cape Hatteras, North Carolina, to Cape Sable, Florida) were taken from Berry (1959). Densities and size data from samples collected in Great South Bay (New York) and southern New Jersey embayments during 1987 and 1988 were also examined (see McBride and Conover [1991] for seine-survey design; weir-sample data from Rountree et al.[2]). Fish densities in these other estuaries and from the published literature were calculated as

$$CPUE = (Catch\ per\ unit\ of\ effort\ [number\ of\ fish\ per\ seine\ haul])$$

for the period May–October unless stated otherwise. Field sampling (described below) of temperate coastal habitats was also completed, and abundance, habitats, seasonality, and sizes of *C. hippos* were examined. Unless noted otherwise, fish size is reported to the nearest cm fork length (FL). A Gompertz model was used to model growth:

$$FL = L_{\infty} \exp\left(-\exp\left\{-G[DOY - X_0]\right\}\right),$$

where FL = fork length in mm;
L_{∞} = asymptotic length;
G = instantaneous rate of growth at age X_0;
DOY = day of the year, and
X_0 = inflection point of the curve.

[1] McBride, R. S. 1995. Perennial occurrence and fast growth rates by crevalle jacks (Carangidae: *Caranx hippos*) in the Hudson River estuary. *In* Final reports of the Tibor T. Polgar Fellowship Program, 1994 (E. A. Blair and J. R. Waldman, eds.), p. VI1–VI29. Hudson River Foundation, New York, NY.

[2] Rountree, R. A., K. J. Smith, and K. W. Able. 1992. Length frequency data for fishes and turtles from polyhaline subtidal and intertidal marsh creeks in southern New Jersey. Institute of Marine and Coastal Science (IMCS) report 92-34, Rutgers, the State Univ. of New Jersey, New Brunswick, NJ, 08903, 165 p.

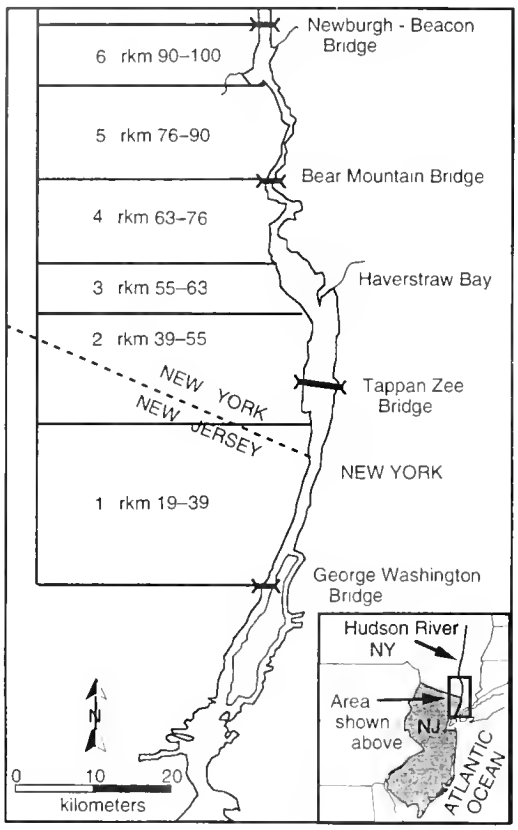

Figure 1

Sampling strata (1–6) in the Hudson River region where *Caranx hippos* was common. Haverstraw Bay is within strata 2–4. Strata 7–12 (river kilometers 100–246) are not shown. Jamaica Bay is located just east of the mouth of the Hudson River.

Growth modeling and other statistical analyses were performed by using SAS (SAS, 1990).

Field sampling—Hudson River

Recent data (1986–1993) were analyzed from an ongoing (since 1974) survey of the entire Hudson River (Fig. 1). Fish were collected during daylight over a 1-wk period every other week between mid-June and mid-November. During each sampling week, a 30.5-m · 2.4-m (max. mesh=10 mm) beach seine was set in an arc from a boat at approximately 100 stations. Station locations were selected in a stratified random design by using 12 strata between Manhattan and Albany, New York (from river kilometer [rkm] 19 to 246). The length of each stratum varied from 8 to 44 km, and typically 5–20 hauls were completed in each stratum during each biweekly period. Mean abundance, by month or stratum, was calculated from transformed values of the number of fish in each seine haul ($\log_e[n+1]$) and was expressed as a geometric mean (antilogged mean values of −1). Annual abundances were also calculated as geometric means but only for data from August to September (when *C. hippos* were consistently collected).

Field sampling—Haverstraw and Jamaica bays

Further analyses of the ecology of *Caranx hippos* in the Hudson River were based on data from an independent survey for the same 8-yr period (1986–1993) as the survey of the entire river. This additional survey focused on two subregions of the estuary: Haverstraw Bay and Jamaica Bay. Haverstraw Bay corresponds to strata numbers 2–4 of the Hudson River survey (Fig. 1); Jamaica Bay is a satellite embayment close to the mouth of the Hudson River.

Seining in Haverstraw Bay occurred biweekly from July to November (see also McKown and Young, 1992). Typically, 25 stations were sampled during daylight over a 2-d period; at each station, a single haul was made with a 61-m × 3-m beach seine (max. mesh=6.4 mm) set in an arc from a boat. This seine was used similarly in Jamaica Bay from May to November, but sampling frequency was generally monthly and only 4–5 stations were sampled each time. Temperature and salinity were measured with a hand-held thermometer and refractometer from surface-water samples after the net was hauled. Abundance of *C. hippos* was calculated as above (i.e. by geometric means).

Field sampling—the continental shelf

To determine seasonal abundance of *C. hippos* above the U.S. east coast continental shelf, we examined data collected during 1972–1996 in the National Marine Fisheries Service's bottom-trawling program. This program followed a stratified random statistical design to survey fish stocks of the continental shelf (9–366 m) from Cape Fear, North Carolina, to Nova Scotia, Canada. Standard methods were to tow a 24.4- or 30.5-m otter trawl (13-mm codend liner) for 30 min at randomly assigned stations within fixed strata (strata were delimited largely by depth and latitude). All samples combined covered all seasons, but sampling intensity was greatest during spring (March–May) and autumn (September–November), when about 350 stations were sampled during each 6–8 wk period. Fish were measured to the nearest cm. General survey design and its specific applications for other species can be found in many other studies (e.g. Grosslein and Azarovitz, 1982; Despres-Patanjo et al., 1988; McBride et al., 1998).

Results

Latitudinal comparisons

Young-of-the-year *C. hippos* occurred in subtropical estuaries between North Carolina and Florida from June to November and in temperate estuaries of New York and New Jersey during July–November (Fig. 2). On average, we observed only about one fish collected in three or more seine hauls, and these arithmetic mean densities were the same for temperate and subtropical estuaries (Fig. 3).

At subtropical latitudes, individuals <4.0 cm FL were present in all months, June–November (Fig. 2). Small individuals were also present for three months, July–September, at temperate latitudes. In both biogeographic regions,

some individuals had reached approximately 20 cm FL by October and November, suggesting that absolute growth could exceed 1 mm/d. The prolonged appearance of small fish in southern estuaries, in particular, and the lack of age-specific data precluded more detailed comparisons of growth rates.

Estuarine residency

In the Hudson River system, *C. hippos* occurred annually but its density varied by an order of magnitude among years (Table 1). This species occurred as far upstream as rkm 102 (i.e. lower part of stratum 7) but was most abundant in the upper portion of Haverstraw Bay (Fig. 4A). Seasonally, *C. hippos* resided in the Hudson River system from July to November and was most common from late July to early October (Figs. 4B, 5A). The median temperature for collections of *C. hippos* was 26°C in Haverstraw Bay and 24°C in Jamaica Bay (Fig. 6). Near Haverstraw Bay, where salinities were much lower than those of Jamaica Bay, *C. hippos* was capable of invading nearly freshwater regions of the Hudson River (Fig. 6). Abundance measured with a 61-m net, set in a comparable manner in both bays, showed that the abundance of *C. hippos* was much higher in Jamaica Bay than in Haverstraw Bay. Abundance in Great South Bay, New York, was also consistently higher than in Haverstraw Bay (Fig. 5A), even though a smaller, 30-m net was used.

Fork length of fish collected during 1986–1993 in the Hudson River estuary ranged from 2.9 to 17.6 cm. Growth rate was modeled by using data for New York and New Jersey estuaries (Fig. 5B; n=439), and the resulting equation,

$$FL = 136.6\exp\left(-\exp\left\{-0.0315\left[DOY - 211\right]\right\}\right), \quad (r^2=0.75),$$

predicted a peak instantaneous growth rate for July 30, after which growth slowed and fish reached a mean asymptotic length of 13.7 cm. The distribution of residuals for this growth model suggested that the asymptotic length was biased (i.e. lowered) by the presence of small, presumably young, juveniles in August–September; therefore we consider these growth estimates to be preliminary.

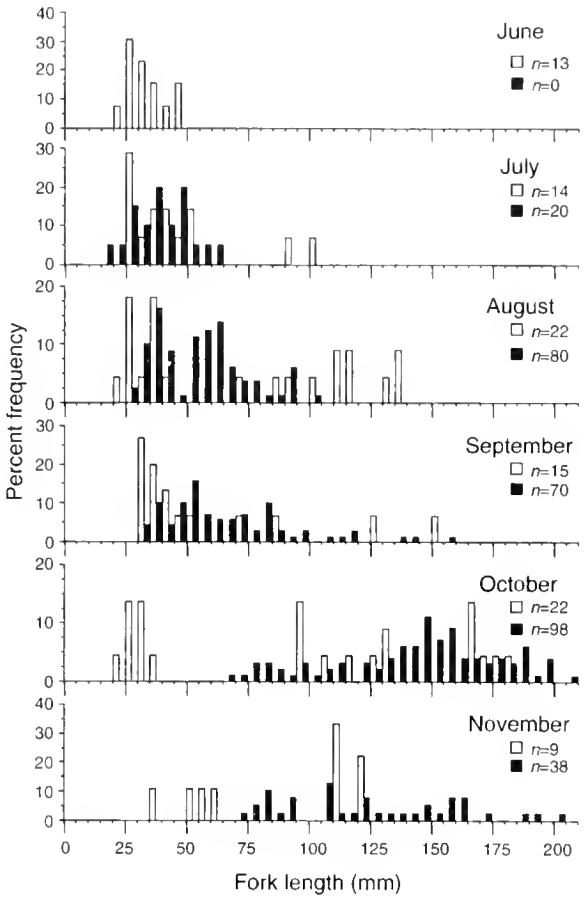

Figure 2

Monthly length frequencies of young-of-the-year *Caranx hippos* in estuaries from North Carolina to Florida (open bars) and New York or New Jersey (filled bars). Data for southern states are taken from Berry (1959; Table 23, Addenda, p: 534–535), and data for northern states are from material archived at the New York State Museum, Academy of Natural Sciences in Philadelphia, and American Museum of Natural History (listed in McBride[1]). n = number of fish measured.

Continental shelf distributions

A total of 657 *C. hippos* were collected at 134 stations between 33°47'N and 41°00'N and at depths from 6 to 38 m (Fig. 7A). Although present in all but four years during 1972–1996, *C. hippos* were collected only in the months of July (1 of 134 stations=0.8%), September (84.3%), October (14.2%), and November (0.8%) during this period. Fish ranged in size from 3 to 29 cm FL, and modal size (17 cm) was the same for fish collected both north and south of 36°00'N (Fig. 7B).

Discussion

Densities of *C. hippos* in Haverstraw Bay, where our study was focused, were generally low compared with other New York estuaries. We did observe considerable variation in densities of *C. hippos* between months, years, and estuaries, which we believe is at least partially the result of this species' relatively low density and shoaling (e.g. aggregating) behavior (Kwei, 1978). Larval dispersal processes or habitat may also affect juvenile *C. hippos* densities between temperate estuaries. This variability appears to have led to contradictory reports of *C. hippos* abundance at temperate latitudes: some investigators concluded that this species is "rare" or "scarce" (e.g. Bean, 1900; Greeley, 1937), whereas others have considered it to be "common" or "abundant" (DeKay, 1842; Smith, 1985).

Our review of seining data across a latitudinal range from 27°N to 41°N demonstrated that densities of *C. hippos* propagules transported to subtropical estuaries were not

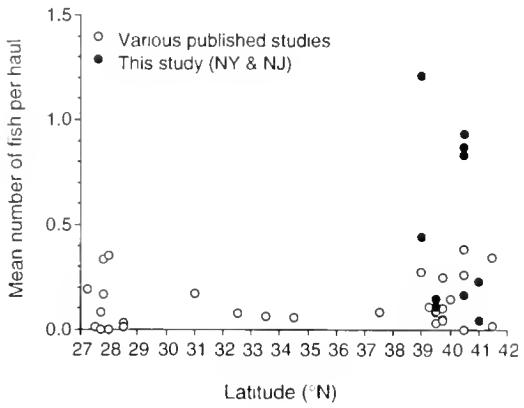

Figure 3

Densities (arithmetic mean number of fish caught per seine haul) of young-of-the-year *Caranx hippos* by sampling latitude (Rhode Island to Florida). Data were limited to seines from 10- to 90-m long, set during May–October and calculated per year if a study was conducted for multiple years. Data were taken from the following surveys (open circles), listed here by decreasing latitude (with seine length): Hoff and Ibara, 1977 (12 m); Briggs and O'Connor, 1971 (91 m); Briggs, 1975 (91 m); Ecological Analysts, Inc. 1981. Ecological studies at Oyster Creek Nuclear Generating Station. Feb. 1981 EA Report JCP91I3 Progress Report. September 1979–August 1980, prepared for Jersey Central Power and Light Company, Appendix D, E, unpaginated (46 m); Marcellus, 1972 (11 m); Thomas, D. L., and C. B. Milstein 1973. Ecological studies in the bays and other waterways near Little Egg Inlet and in the ocean in the vicinity of the proposed site for the Atlantic generating station, NJ. Progress Report for January–December, 1972, vol. I: Fishes and volume II: Appendices, Ichthyological Associates, Inc. Absecon, NJ, 1065 p. (76 m); Thomas, D. L., C. B. Milstein, T. R. Tatham, R. C. Bieder, D. J. Danila, H. K. Hoff, D. P. Swiecicki, R. P. Smith, G. J. Miller, J. J. Gift, and M. C. Wyllie. 1975. Ecological studies in the bays and other waterways near Little Egg Inlet and in the ocean in the vicinity of the proposed site for the Atlantic generating station, NJ. Progress Report for January–December, 1974. Volume I: Fishes, 490 p. Ichthyological Associates, Inc. Absecon, NJ. (76 m); de Sylva, D. P., F. A. Kalber, and C. N. Shuster. 1962. Fishes and ecological conditions in the shore zone of the Delaware River Estuary, with notes on other species collected in deeper water. University of Delaware Marine Laboratory. Information Series Publication 5. Technical Report to Delaware Board of Game and Fish Commissioners under Dingell-Johnson Federal Aid in Fish and Wildlife Restoration. Delaware Project F-13-R-1-2-3, 150 p. Contact senior Richard McBride (senior author) for data of this report (18 m); Richards and Castagna, 1970 (12 m); Tagatz and Dudley, 1961 (21 m); Ogburn et al., 1988 (15 m); Anderson et al., 1977 (20 m); Miller, G. L., and S. C. Jorgenson. 1969. Seasonal abundance and length frequency distribution of some marine fishes in coastal Georgia, 103 p. U. S. Fish Wildl. Ser. Data Rep. 35. Washington, D.C. (on two microfische) (21 m); Gilmore, 1988 (62 m); Schooley, 1977 (12 m); Peters, 1984 (9 m); Futch and Dwinell, 1977 (15 m); and Gunter and Hall, 1963 (15 m). Data from the present study, restricted to the years 1987 and 1988, are shown separately (filled circles) and include two southern New Jersey locales and Haverstraw, Jamaica, and Great South bays, New York (30 and 61 m seine nets). There was no significant relationship among the data (Spearman correlation coefficent, r_s=0.24, n=40; P=0.14).

higher, as would be expected for a "subtropical" species, than densities of those propagules transported to temperate estuaries. Not all CPUE values we examine in our study were directly comparable because of potential differences in deployment procedures, sampling habitats, and range of seine sizes. We hope that others will report more data for such comparative purposes in the future. We are also unaware of comparative data for tropical regions to determine if this species is more abundant in a more central portion of its latitudinal range. Young-of-the-year *C. hippos* abundance is generally low compared with other estuarine finfishes from Massachusetts to Florida (e.g. Ayvazian et al., 1992; Tremain and Adams, 1995; Able et al., 1996), and we conclude that this species is uncommon throughout this range.

Having found juvenile *C. hippos* in reasonable densities in temperate estuaries, we also observed them to occupy habitats similar to those of juvenile *C. hippos* in subtropical estuaries. In both temperate and subtropical regions, juveniles of this species appear to use estuaries as nurseries (see also Berry, 1959; Kwei, 1978). We observed individuals as far upstream as the freshwater interface (about 1 ppt), at about rkm 90–100 in the Hudson River during July–October (Cooper et al., 1988; Geoghegan et al., 1992). Several others have reported YOY *C. hippos* in oligohaline habitats (Christensen, 1965; Tagatz, 1968; Smith, 1985; Beebe and Savidge, 1988) but none in fresh water. The presence of *C. hippos* within the Hudson River was associated with warm temperatures; this species occurred in similarly warm temperatures in subtropical estuaries (18–33°C: Tagatz and Dudley, 1961; Christensen, 1965; Tagatz, 1968). The concentration of fish in and near Haverstraw Bay is probably due to this region's broad width and shallow bathymetry, which slows water-flow rates and responds rapidly to solar radiation (Cooper et al., 1988). In addition, three power plants that release heated effluent are located near Haverstraw Bay (Cooper et al., 1988). Temperature eventually becomes a very important parameter affecting YOY *C. hippos* distribution, and cold temperatures have been implicated in several cases of overwintering mortality for *C. hippos*. We know of no experimental study to document the lower lethal temperature for this species, but Bean (1903) noted that *C. hippos* could overwinter in aquarium conditions above 10°C, and Hoff (1971) observed dead *C. hippos* in waters colder than 9°C, whereas conspecifics in a downstream portion of the same Massachusetts river survived in waters above 9°C. Water temperatures fall below 10°C for at least the 4-mo. period of December–April near Haverstraw Bay and above the continental shelf of the middle Atlantic states (Cooper et al., 1988; Mountain and Holzwarth, 1989); therefore there is no suitable overwintering habitat for *C. hippos* north of Cape Hatteras. Yet although the predictability of the seasonal cycle may be an important determinant of a species' latitu-

Table 1

Catch data for all Hudson River sampling sites; a 30.5-m seine or 61-m seine net was used. Geometric mean (GM) number of *C. hippos* per seine haul is calculated only from collections during peak abundance (August–September).

Year	Total no. of hauls	No. of hauls containing *C. hippos*	Total no. of *C. hippos* collected	GM	Total no. of hauls	No. of hauls containing *C. hippos*	Total no. of *C. hippos* collected	GM
Entire Hudson River (30.5-m seine)	All sampling strata				Haverstraw Bay (strata 2–4)			
1986	1000	6	10	0.0058	429	4	8	0.0135
1987	1101	2	3	0.0038	473	2	3	0.0089
1988	1100	12	22	0.0235	407	6	12	0.0344
1989	1100	15	40	0.0198	429	14	39	0.0468
1990	1000	19	32	0.0284	364	13	23	0.0395
1991	1000	11	58	0.0134	364	11	58	0.0341
1992	1000	9	53	0.0084	364	8	50	0.0130
1993	1000	17	30	0.0171	364	15	27	0.0403
Total	8301	91	248	—	3,194	73	220	—
Haverstraw and Jamaica bays (61-m seine)	Haverstraw Bay				Jamaica Bay			
1986	222	6	21	0.0398	38	2	10	0.732
1987	225	7	9	0.0406	56	4	14	0.468
1988	220	21	45	0.1578	42	4	54	1.151
1989	225	17	64	0.0730	49	2	2	0.000
1990	217	16	39	0.1274	48	7	11	0.475
1991	215	9	20	0.0649	58	4	6	0.000
1992	221	5	5	0.0140	44	2	3	0.292
1993	225	11	20	0.0437	43	3	11	0.000
Total	1770	92	223	—	378	28	111	—

dinal range, sudden and irregular freezes are more likely agents for actual hypothermal mortality, regardless of latitude (Storey, 1937). There are, for example, several instances of hypothermal mortality of *C. hippos* on Florida's Atlantic and Gulf coasts (Storey and Gudger, 1936; Miller, 1940; Galloway, 1941; Gilmore et al., 1978; Snelson and Bradley, 1978; Provancha et al., 1986). If individuals dispersed to temperate estuaries react in a similar manner to those dispersed to subtropical estuaries and emigrate from estuaries during autumn, then they may successfully migrate south to suitable overwintering habitats. We observed similar sizes of YOY *C. hippos* disappearing from estuaries and appearing on the continental shelf during September and October, which is strong circumstantial evidence of a migration pattern before hypothermal temperatures are reached.

During the summer, coastal water temperatures at temperate and subtropical latitudes are similar (e.g. Mountain and Holzwarth, 1989) and produce a favorable growth climate for *C. hippos* across a wide latitudinal range. Monthly sizes of YOY *C. hippos* were similar across latitudes, and the apparent growth rates were high in relation to other YOY estuarine fish species in temperate waters (Rountree and Able, 1992). Our comparative data suggested no size disadvantage for individuals dispersed to temperate estuaries. Overwintering mortality is size-dependent for some species that migrate offshore (Conover, 1990), so that if *C. hippos* in temperate waters were smaller by autumn than those in subtropical estuaries, then their overwinter survival could be lower. Nevertheless, individuals in temperate waters may be at a disadvantage to equal-size individuals in subtropical waters because the latter do not need to migrate as far to reach overwintering habitats. Our preliminary growth model was confounded by a prolonged (about 3 months) presence of small fish, and presumably there was considerable age variation within our late-summer samples. The continued presence of small fish into September confounded analysis of length frequencies and created the appearance of sudden shifts in average fish size in late summer. The discrepancy between predicted size in temperate estuaries during autumn and the modal size observed on the shelf (e.g. 14 vs. 17 cm FL) could be the result of smaller fish having a higher mortality rate during this habitat shift. Further work with growth modeling will improve with age-specific data. The growth and size data of our study, however, suggest that *C. hippos* emigrated from estuaries largely as YOY and at the same time and sizes across latitudes. These data suggest that the same behavioral cue to migrate operated on individuals dispersed to both biogeographic regions.

By the time YOY *C. hippos* reach shelf habitats during autumn, we postulate that they are of adequate size to continue south to subtropical latitudes. For example, YOY *C. hippos* are as large as "summer-spawned" YOY *P. saltatrix*; McBride et al. (1993) concluded the latter migrate from temperate nursery grounds to subtropical overwintering habitats at sizes of 10–15 cm FL. Moreover, several fish species have been tagged in temperate waters and recaptured in subtropical waters at sizes similar to those of *C. hippos* in autumn, including Atlantic croaker, *Micropogonias undulatus* (Pearson, 1932; Haven, 1959); spot, *Leiostomus xanthurus* (Pearson, 1932); weakfish, *Cynoscion regalis* (Nesbit, 1954); Atlantic thread herring, *Opisthonema oglinum* (Pristas and Cheek, 1973); bluefish, *P. saltatrix* (Lund and Maltezos, 1970); and Atlantic menhaden, *Brevoortia tyrannus* (Kroger and Guthrie, 1973). We reject the hypothesis that YOY *C. hippos* migrate offshore to the shelf edge, because they are distributed close to shore (<38 m) during autumn and they are not collected in winter or spring sampling out to 366 m depths by the National Marine Fisheries Service's trawling program. We similarly reject the hypothesis that the YOY *C. hippos* observed in coastal habitats during autumn have moved inshore from "offshore" nursery grounds. This cohort was not evident in summer trawl samples and such a hypothesis would require an alternative life history tactic for using shelf habitats as nurseries—a tactic that up until now has not been reported for this species.

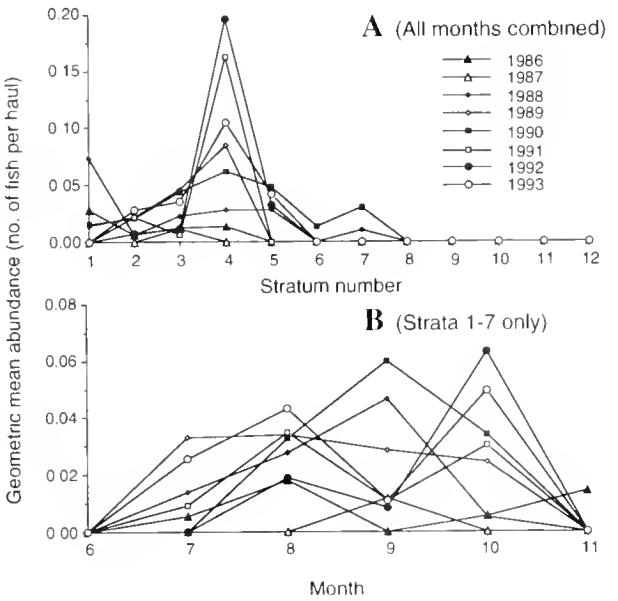

Figure 4

Variations in abundance of *Caranx hippos* from late June to early November: (**A**) Geometric mean abundance by sampling strata and year; (**B**) geometric mean abundance by month and year. All samples were collected with a 30.5-m seine and symbols denoting sampling year (1986–1993) in both A and B are the same. See Figure 1 for reference strata.

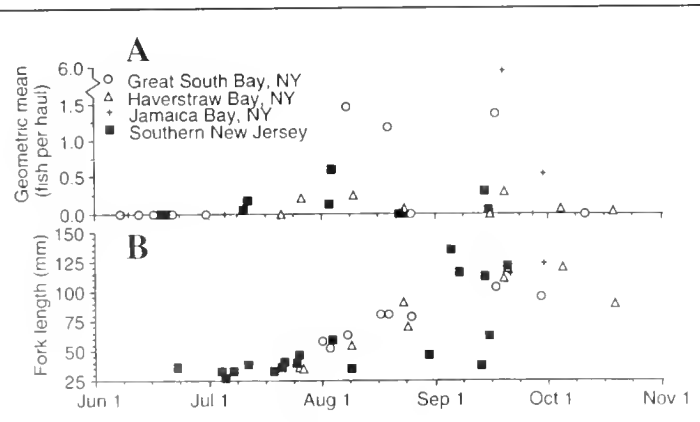

Figure 5

(**A**) Geometric mean abundance of *Caranx hippos* plotted for each sampling day during 1988 (seine-net collections only) for four estuarine systems in the New York and New Jersey region. (**B**) Mean length of *C. hippos* plotted for each sampling day during 1988 (same symbols used to denote each embayment as in A). Sampling gears differ between bays: Great South Bay—30.5-m seine, Haverstraw Bay—61-m seine, Jamaica Bay—61-m seine, and two southern New Jersey areas—30.5-m seine plus lengths from weir samples.

Direct evidence (e.g. mark-recapture) of successful migrations by marine fishes is rare, and the migration patterns of many species are inferred from seasonal changes in distribution (Leggett, 1977), as we have done in our study. In addition, we have examined growth rates and sizes to link the seasonal changes in geographic distribution to the YOY cohort. The above evidence indirectly links some YOY *C. hippos* that have dispersed to temperate estuaries back to suitable overwintering habitats and suggests that these individuals retain "membership" in the spawning population (*sensu* Sinclair, 1988). We do not, however, assume that all individuals leave temperate estuaries before hypothermal conditions can develop, nor that all individuals survive an autumn migration to subtropical latitudes. The relative importance of temperate estuaries over subtropical estuaries for YOY *C. hippos* depends on the relative contribution to future spawning by individuals dispersed to each biogeographic region, but this contribution can not be calculated without further study.

Cape Hatteras represents a major faunal (and floral) break along the U.S. east coast (Pielou, 1979; Briggs, 1996), but the larvae of many species that spawn in coastal habitats, particularly of those that broadcast their eggs into the water column and have moderate-to-long planktonic larval durations, are capable of being transported around this geographic barrier (e.g. Curran, 1989). Among these species, we postulate that there is a subset of species that have juvenile traits that allow them to exploit nursery habitats in both biogeographic provinces, and an additional subset of species for which some individuals can return

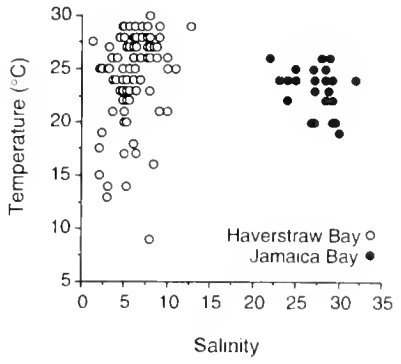

Figure 6

Scattergram of temperature and salinity measured at stations where young-of-the-year *Caranx hippos* were collected in Haverstraw (open circles) and Jamaica (filled circles) bays. Data were collected with 61-m seine nets and pooled for all years, 1986–1993.

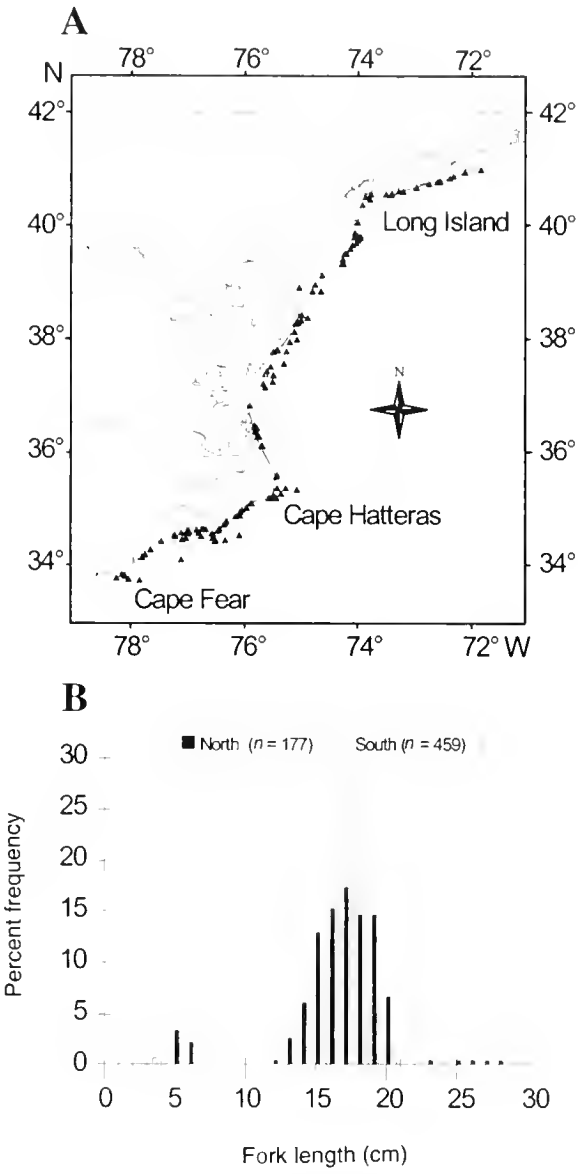

Figure 7

(**A**) Distribution of tows containing *Caranx hippos* based on sampling of the continental shelf between Cape Fear and southern New England. (**B**) Size frequency of *C. hippos* collected north (filled bars) and south (open bars) of 36°N. Samples are from bottom trawl collections for the years 1972–1996. There were no records of *C. hippos* farther north or east of Long Island (but see Bigelow and Schroeder, 1953). *n* = number of fish measured.

from temperate estuaries to reproduce. Traits such as early spawning season (i.e. winter or spring), fast growth rate, large YOY body size, generalized habitat requirements, and fast swimming speeds are favorable traits for any species attempting to complete a life-history circuit within one year between subtropical and temperate waters of the western North Atlantic. These traits are found in several finfish species in the Carangidae, Scombridae, and Mugilidae. Grouping species by spawning, larval, and juvenile characteristics and comparing their fate in these large oceanographic systems will help define the appropriate spatial scale for sampling these populations in the western North Atlantic, as well as in other systems such as the Sea of Japan (Nishimura, 1965), the Agulhas Current (Beckley, 1985), and the East Australian Current (Miskiewicz, 1981) where similar dispersal patterns of subtropically spawned species to temperate waters have been described. An initial screening for such characters allows researchers to begin to evaluate whether a specific "subtropical" species can or cannot survive once dispersed to temperate habitats.

Some of these subtropically spawned species are dispersed to temperate waters during less favorable conditions (e.g. winter) and, presumably, others do not grow to a sufficient size or have the behavior characteristics to migrate in autumn. A nonadaptive outcome of dispersal for many species on an ecological timescale is not, however, necessarily surprising. An examination of the paleontological record, which is most complete for invertebrates, shows that biogeographic assemblages lag notably behind environmental changes at an evolutionary timescale (Briggs, 1974; Pielou, 1979). A modeling and theoretical method, such as that used by Hare and Cowen (1993), could help explain why the larvae of so many species are dispersed into large oceanographic systems even when expatriation is likely, but more natural history data are necessary before such a method can be widely applied. A more complete record of which species are and are not expatriated within large-scale systems will contribute to understanding the processes underlying these biogeographic patterns, provide opportunities to examine further the evolution of

reproductive strategies, and help explain oceanographic effects on population dynamics.

Acknowledgments

R. Daniels, W. Saul, and C. L. Smith assisted with the collections at the New York State Museum, the Academy of Natural Sciences of Philadelphia, and the American Museum of Natural History, respectively. Data for the entire Hudson River were collected for Consolidated Edison and were made available by J. Young and G. Sentell of EA Engineering, Science, and Technology. B. Young, L. Pasciutti, M. Penski, and other biologists of the New York State Department of Environmental Protection helped collect data for Haverstraw Bay and Jamaica Bay. Trawling data were collected by the Northeast Fishery Science Center, National Marine Fisheries Service, and made available by T. Azarovitz and B. O'Gorman. Valuable discussions or comments were provided by K. Able, F. Berry, E. Blair, D. Conover, R. Crabtree, J. Hare, S. Kaiser, R. Loveland, W. Smith-Vaniz, and J. Waldman. Final data analyses and manuscript preparation were completed while R.S.M. was employed at he Florida Marine Research Institute. Editorial assistance was provided by L. French, J. Leiby, and J. Quinn. This research was supported in part by a Tibor T. Polgar Fellowship to R.S.M. from the Hudson River Foundation. We are grateful to all of the above.

Literature cited

Able, K. W., D. A. Witting, R. S. McBride, R. A. Rountree, and K. J. Smith.
1996. Fishes of polyhaline estuarine shores in Great Bay-Little Egg Harbor, New Jersey: a case study of seasonal and habitat influences. *In* Estuarine shores: environments and human alterations (K. F. Nordstrom and C. T. Roman, eds.), p. 335–355. John Wiley and Sons, Ltd. New York, NY.

Anderson, W. D., Jr., J. K. Dias, R. K. Dias, D. M. Cupka, and N. A. Chamberlain.
1977. The macrofauna of the surf zone off Folly Beach, South Carolina. U.S. Dep. Commer., NOAA Tech. Rep. NMFS-SSRF 704, 23 p.

Ayyazian, S. G., L. A. Deegan, and J. T. Finn.
1992. Comparison of habitat use by estuarine fish assemblages in the Acadian and Virginian zoogeographic provinces. Estuaries 15:368–383.

Bean, T. H.
1900. Report on the fishes of Long Island collected in the summer of 1898. N. Y. State Mus. Rep. 52, vol. 1, p. r103.
1903. Catalogue of the fishes of New York. Bull. N. Y. State Mus. 60, Zoology 9:428–429.

Beckley, L. E.
1985. The fish community of East Cape tidal pools and an assessment of the nursery function of the habitat. South African J. Zool. 20:21–27.

Beebe, C. A., and T. R. Savidge.
1988. Historical perspective on fish species composition and distribution in the Hudson River estuary. Am. Fish. Soc. Monogr. 4:25–36.

Berry, F. H.
1959. Young jack crevalles (*Caranx* species) off the southeastern Atlantic coast of the United States. Fish. Bull. 59:417–535.

Bigelow, H. B., and W. C. Schroeder.
1953. Fishes of the Gulf of Maine. U.S. Fish and Wildl. Serv. Bull. 74, vol. 53, 577 p.

Briggs, J. C.
1960. Fishes of worldwide (circumtropical) distribution. Copeia 1960:171–180.
1974. Marine zoogeography. McGraw-Hill Book Co, New York, NY, 475 p.
1996. Global biogeography. Elsevier, Amsterdam, The Netherlands, 452 p.

Briggs, P. T.
1975. Shore-zone fishes of the vicinity of Fire Island Inlet, Great South Bay, New York, N.Y. Fish Game J. 22:1–12.

Briggs, P. T., and J. S. O'Connor.
1971. Comparison of shore-zone fishes over naturally vegeetated and sand-filled bottoms in Great South Bay. N. Y. Fish Game J. 18:16–41.

Chiarella, L. A., and D. O. Conover.
1990. Spawning season and first-year growth of adult bluefish from the New York Bight. Trans. Am. Fish. Soc. 119:455–462.

Christensen, R. F.
1965. An ichthyological survey of Jupiter Inlet and Loxahatchee River, Florida. M.S. thesis. Fla. State Univ., Tallahassee, FL, 318 p.

Conover, D. O.
1990. The relation between capacity for growth and length of growing season: evidence for the implications of countergradient variation. Trans. Am. Fish. Soc. 119:416–430.

Cooper, J. C., F. R. Cantelmo, and C. E. Newton.
1988. Overview of the Hudson River estuary. Am. Fish. Soc. Monogr. 4:11–24.

Cowen, R. K., J. A. Hare, and M. P. Fahay.
1993. Beyond hydrography: can physical processes explain larval fish assemblages within the Middle Atlantic Bight? Bull. Mar. Sci. 53:567–587.

Curran, M. C.
1989. Occurrence of tropical fishes in New England waters. *In* Proceedings of the American Academy of Underwater Science; Ninth Ann. Sci. Diving Symp. Sept. 28–Oct. 1, 1989 (M. A. Lang and W. C. Jaap, eds.), p. 71–82. Am. Academy of Underwater Sciences, Costa Mesa, CA.

DeKay, J. E.
1842. Zoology of New York or the New York Fauna. Part III: reptiles and amphibia, p. 120–121. W. & A. White & J. Visscher, Albany, NY.

Despres-Patanjo, L. I., T. R. Azarovitz, and C. J. Byrne.
1988. Twenty-five years of fish surveys in the northwest Atlantic: the NMFS Northeast Fisheries Center's Bottom Trawl Survey Program. Mar. Fish. Rev. 50:69–71.

Fahay, M. P.
1975. An annotated list of larval and juvenile fishes captured with surface-towed meter net in the South Atlantic Bight during four RV *Dolphin* cruises between May 1967 and February 1968. U.S. Dep. Commer., NOAA Tech. Rep. NMFS-SSRF-685, 39 p.

Futch, C. R., and S. E. Dwinell.
1977. Nearshore marine ecology at Hutchinson Island, Florida 1971–1974. IV: Lancelets and fishes. Fla. Mar. Res. Publ. 24, 23 p.

Galloway, J. C.
1941. Lethal effect of the cold winter of 1939–40 on marine fishes at Key West, Florida. Copeia 1941:118–119.

Geoghegan, P., M. T. Mattson, J. J. Reichle, and R. G. Keppel.
1992. Influence of salt front position on the occurrence of uncommon marine fishes in the Hudson River Estuary. Estuaries 15:251–254.

Gill, T.
1904. State ichthyology of Massachusetts. Science (new series) 20:321–338.

Gilmore, R. G., Jr.
1988. Subtropical seagrass fish communities: population dynamics, species guilds and microhabitat associations in the Indian River Lagoon, Florida. Ph.D. diss., Fla. Inst. Tech. Melbourne, FL, 199 p.

Gilmore, R. G., Jr., L. H. Bullock, and F. H. Berry.
1978. Hypothermal mortality in marine fishes, south-central Florida, January, 1977. Northeast Gulf Sci. 2:77–97.

Greeley, J. R.
1937. Fishes of the area with annotated list. *In* Survey of the lower Hudson watershed, p. 45–103. State of New York Conservation Department, Albany, NY.

Grosslein, M. D., and T. R. Azarovitz.
1982. Fish distribution. MESA New York Bight Atlas Monograph 15. New York Sea Grant Institute, Albany, NY, 182 p.

Gunter, G., and G. E. Hall.
1963. Biological investigations of the St. Lucie estuary (Florida) in connection with Lake Okeechobee discharges through the St. Lucie canal. Gulf Res. Rep. 1:189–307.

Hare, J. A., and R. K. Cowen.
1991. Expatriation of *Xyrichtys novacula* (Pisces: Labridae) larvae: evidence of rapid cross-slope exchange. J. Mar. Res. 49:801–823.
1993. Ecological and evolutionary implications of the larval transport and reproductive strategy of bluefish, *Pomatomus saltatrix*. Mar. Ecol. Prog. Ser. 98:1–16.
1996. Transport mechanisms of larval and pelagic juvenile bluefish (*Pomatomus saltatrix*) from South Atlantic Bight spawning grounds to Middle Atlantic Bight nursery habitats. Limnol. Oceanogr. 41:1264–1280.

Haven, D. S.
1959. Migration of the croaker, *Micropogon undulatus*. Copeia 1959:25–30.

Hoff, J. G.
1971. Mass mortality of the crevalle jack, *Caranx hippos* (Linnaeus) on the Atlantic coast of Massachusetts. Chesapeake Sci. 12:49.

Hoff, J. G., and R. M. Ibara.
1977. Factors affecting the seasonal abundance, composition and diversity of fishes in a southeastern New England estuary. Estuarine Coastal Marine Sci. 5:665–678.

Juanes, F., J. A. Buckel, and D. O. Conover
1994. Accelerating the onset of piscivory: intersection of predator and prey phenologies. J. Fish Biol. 45 (suppl. A):41–54.

Juanes, F., J. A. Hare, and A. G. Miskiewicz.
1996. Comparing early life history strategies of *Pomatomus saltatrix*: a global approach. Mar. Freshwater Res. 47:365–79.

Kleckner, R. C., and J. D. McCleave.
1985. Spatial and temporal distribution of American eel larvae in relation to North Atlantic ocean current systems. Dana 4:67–92.

Kroger, R. L., and J. F. Guthrie.
1973. Migrations of tagged juvenile Atlantic menhaden. Trans. Am. Fish. Soc. 102:417–422.

Kwei, E. A.
1978. Food and spawning activity of *Caranx hippos* (L.) off the coast of Ghana. J. Nat. Hist. 12:195–215.

Leggett, W. C.
1977. The ecology of fish migrations. Ann. Rev. Ecol. Syst. 8:285–308.

Lund, W. A., and G. C. Maltezos.
1970. Movements and migrations of the bluefish, *Pomatomus saltatrix*, tagged in waters of New York and Southern New England. Trans. Am. Fish. Soc. 99:719–725.

Marcellus, K. L.
1972. Fishes of Barnegat Bay, New Jersey, with particular reference to seasonal influence and the possible effect of thermal discharge. Ph.D. diss., Rutgers Univ., New Brunswick, NJ, 172 p.

Markle, D. F., W. B. Scott, and A. C. Kohler.
1979. New and rare records of Canadian fishes and the influence of hydrography on resident and nonresident Scotian shelf ichthyofauna. Can. J. Fish. Aquat. Sci. 37:49–65.

McBride, R. S., and K. W. Able.
1998. Ecology and fate of butterflyfishes *Chaetodon* spp. in the temperate, western North Atlantic. Bull. Mar Sci. 63(2):401–416.

McBride, R. S., and D. O. Conover.
1991. Recruitment of young-of-the-year bluefish (*Pomatomus saltatrix*) to the New York Bight: Variation in abundance and growth of spring- and summer-spawned cohorts. Mar. Ecol. Prog. Ser. 78:205–216.

McBride, R. S., J. B. O'Gorman, and K. W. Able.
1998. Interspecific comparisons of searobins (*Prionotus* spp.) movements, size structure, and abundance in the temperate western North Atlantic. Fish. Bull. 96:303–314.

McBride, R. S., J. L. Ross, and D. O. Conover.
1993. Recruitment of bluefish (*Pomatomus saltatrix*) to estuaries of the South Atlantic Bight. Fish. Bull. 91:389–395.

McCleave, J. D.
1993. Physical and behavioural controls on the oceanic distribution and migration of leptocephali. J. Fish Biol. 43 (suppl. A):243–273.

McCleave, J. D., R. C. Kleckner, and M. Castonguay.
1987. Reproductive sympatry of American and European eels and implications for migration and taxonomy. Am. Fish. Soc. Symp. 1:286–297.

McKown, K. A., and B. H. Young.
1992. Effects of year class strength on size of young-of-the-year striped bass. *In* Estuarine research in the 1980's (C. L. Smith, ed.), p. 265–276. State Univ. New York Press. Albany, NY.

Miller, E. M.
1940. Mortality of fishes due to cold on the southeast Florida coast. Ecology 21:420–421.

Miskiewicz, A. G.
1981. The distribution of tropical/coral reef fish larvae in temperate waters along the New South Wales coast of Australia. Rapp. P.-V. Cons. Int. Explor. Mer 191:452.

Montolio, M.
1978. Algunos aspectos sobre el desove y las concentraciones larvarias de las especies de la familia Carangidae en el Mar Caribe. Rev Cubana Invest. Pesqueras 3:29–49.

Moss, S. A.
1973. The responses of planehead filefish, *Monocanthus hispidis* (Linnaeus), to low temperature. Chesapeake. Sci. 14:300–303.

Mountain, D. G., and T. J. Holzwarth.
1989. Surface and bottom temperature distribution for the northeast continental shelf. U.S. Dep. Commer., NOAA Tech. Memo. NMFS-F/NEC-73, 32 p.

Nesbit, R. A.
1954. Weakfish migration in relation to its conservation U.S. Fish Wildl. Spec. Sci. Rep.-Fish. 115, 81 p.

Nishimura, S.
1965. The zoogeographical aspects of the Japan Sea, part 1. Publ. Seto Mar. Biol. Lab. 13:35–79.
Ogburn, M. V., D. M. Allen, and W. K. Michener.
1988. Fishes, shrimps, and crabs of the North Inlet Estuary, SC: a four-year seine and trawl survey. Baruch Institute Tech. Rep. 88-1, Univ. South Carolina. Columbia, SC, 299 p.
Pearson, J. C.
1932. Winter trawl fishery off the Virginia and North Carolina coasts. U.S. Bur. Fish. Invest. Rep. 10, 31 p.
Peters, D. J.
1984. Seasonality, residency, and spatial distribution of juvenile surf zone fishes of the Florida east coast. M.S. thesis, Fla. Inst. Tech., Melbourne, FL, 66 p.
Pielou, E. C.
1979. Biogeography. John Wiley & Sons. New York, NY, 351 p.
Pristas, P. J., and R. P. Cheek.
1973. Atlantic thread herring (*Opisthonema oglinum*) movements and population size inferred from tag returns. Fish. Bull. 71:297–301.
Provancha, M. J., P. A. Schmalzer, and C. R. Hall.
1986. Effects of the December 1983 and January 1985 freezing air temperatures on select aquatic poikilotherms and plant species of Merritt Island, Florida. Fla. Sci. 49:199–212.
Richards, C. E., and M. Castagna.
1970. Marine fishes of Virginia's eastern shore (inlet and marsh, seaside waters). Chesapeake Sci. 11:235–248.
Rountree, R. A., and K. W. Able.
1992. Fauna of polyhaline subtidal marsh creeks in southern New Jersey: composition, abundance, and biomass. Estuaries 15:178–220.
SAS Institute, Inc.
1990. SAS/STAT user's guide, vols. 1 and 2. SAS Institute, Inc., Cary, NC, 1686 p.
Schooley, J. K.
1977. Factors affecting the distribution of the nearshore fishes in the lagoonal waters of the Indian River, Florida. M.S. thesis, Univ. Florida. Gainesville, FL, 165 p.
Sinclair, M.
1988. Marine populations: an essay on population regulation and speciation. Washington Sea Grant Program. Seattle, WA, 252 p.
Smith, C. L.
1985. The inland fishes of New York State. The New York State Department of Environmental Conservation. Albany, NY, 522 p.
Snelson, F. F., and W. K. Bradley Jr.
1978. Mortality of fishes due to cold on the east coast of Florida, January, 1977. Fla. Sci. 41:1–12.
Storey, M.
1937. The relation between normal range and mortality of fishes due to cold at Sanibel Island, Florida. Ecology 18:10–26.
Storey, M., and E. W. Gudger.
1936. Mortality of fishes due to cold at Sanibel Island, Florida, 1886–1936. Ecology 17:640–648.
Tagatz, M. E.
1968. Fishes of the St. Johns River, Florida. Quart. J. Fla. Acad. Sci. 30:25–50.
Tagatz, M. E., and D. L. Dudley.
1961. Seasonal occurrence of marine fishes in four shore habitats near Beaufort, N.C., 1957–60. U. S. Fish Wildl. Spec. Sci. Rep. Fish 390, 19 p.
Tesch, F.-W.
1977. The eel: biology and management of Anguillid eels. Chapman and Hall. London, United Kingdom, 434 p
Tremain, D. M., and D. H. Adams.
1995. Seasonal variations in species diversity, abundance, and composition of fish communities in the northern Indian River Lagoon, Florida. Bull. Mar. Sci. 57:171–192.
U. S. Department of Commerce.
1986. Marine recreation fishery statistics survey, Atlantic and Gulf coasts, 1985. Current Fishery Statistics 8327. Natl. Mar. Fish. Serv. Washington, D.C., 21 p.
Wroblewski, J. S., and J. Cheney.
1984. Ichthyoplankton associated with a warm core ring off the Scotian Shelf. Can. J. Fish. Aquat. Sci. 41:294–303.

Revision of the genus *Lepidopsetta* Gill, 1862 (Teleostei: Pleuronectidae) based on larval and adult morphology, with a description of a new species from the North Pacific Ocean and Bering Sea

James W. Orr

Ann C. Matarese

Resource Assessment and Conservation Engineering Division
Alaska Fisheries Science Center
National Marine Fisheries Service, NOAA
7600 Sand Point Way NE
Seattle, Washington 98115-0070
E-mail address (for J. W. Orr): James.Orr@noaa.gov

Abstract.—The endemic North Pacific pleuronectid genus *Lepidopsetta* Gill is revised to include three species: *L. bilineata* (Ayres), *L. polyxystra* n. sp., and *L. mochigarei* Snyder. Adults of *L. bilineata* can be distinguished by a low gill-raker count and high supraorbital pore count; larvae may be distinguished by four dorsal midline melanophores, heavy finfold pigment, a short snout-to-anus length, and a deep body. The species ranges from Baja California to the eastern Aleutian Islands and the extreme southeastern Bering Sea. Adults of *L. mochigarei* are distinguished from all other members of *Lepidopsetta* by higher scale and preopercular pore counts and lower gill-raker and supraorbital pore counts. Larvae are similar to larvae of *L. bilineata* but can be distinguished by their postanal pigment pattern and melanophores on pectoral-fin rays. *Lepidopsetta mochigarei* ranges from the southern Sea of Okhotsk to Korea. Adults of *L. polyxystra* n. sp. are diagnosed by a high gill-raker count and low supraorbital pore count; larvae are diagnosed by two dorsal midline melanophores, light finfold pigment, long snout-to-anus length, and a slender body. The species is found from Puget Sound through the Bering Sea and Aleutian Islands to the Kuril Islands, overlapping with *L. bilineata* from the extreme southeastern Bering Sea to Puget Sound and with *L. mochigarei* in the southern Sea of Okhotsk. Synonymies, diagnoses, descriptions, and geographic distributions are provided for adults and larvae of all species; keys are provided for adults. Descriptions of early juveniles of eastern North Pacific species are also presented. Under the name of *L. bilineata*, *L. polyxystra* n. sp. has been the subject of many studies of eastern North Pacific *Lepidopsetta*. All previous studies of specimens from the southeastern Bering Sea into Puget Sound should be considered applicable at the generic level only, unless voucher specimens are verifiable.

Manuscript accepted 22 February 2000.
Fish. Bull. 98:539–582 (2000).

The flatfishes (Pleuronectiformes) of the eastern North Pacific Ocean constitute a major component of the commercial fisheries of the region. In the Bering Sea, which encompasses the largest fisheries resource of the United States, the rock soles of the genus *Lepidopsetta* are the second most abundant flatfishes and the third most abundant commercial groundfish species, second only to yellowfin sole (*Limanda aspera*) and walleye pollock (*Theragra chalcogramma*) (NMFS, 1999).

At the species level, eastern North Pacific pleuronectids have been considered well known. Nearly all species were recognized and described during the latter half of the 1800s, primarily through the activities of California ichthyologists. Among the names that remain valid, the last species to be described was *Limanda sahkalinensis* Hubbs, 1915, although in the western Pacific *Microstomus shuntovi* Borets, 1983, was most recently described from the northwestern Hawaiian ridge. However, these earlier works were based on adult morphology, and only recently has a knowledge of the ontogeny of these species been acquired. Among the descriptions of early life history stages of eastern North Pacific pleuronectids, one morphological form could not be traced to a recognized species. Examination of this form led to the following revision of the genus *Lepidopsetta*.

Four nominal species have been described and allocated to the genus *Lepidopsetta*: *Platessa bilineata* Ayres, 1855a, was described from San Francisco material, and apparently without the knowledge of Ayres' slightly earlier description, a specimen collected near Puget Sound was described as *Platichthys umbrosus* Girard, 1856. Gill (1862) erected *Lepidopsetta* to contain *Platichthys umbrosus* and later (1864) indicated that *Platessa bilineata* Ayres, 1855a, was allied and perhaps congeneric. Lockington (1879b) published a redescription of *L. umbrosa*, describing the misidentified new species *Isopsetta isolepis* (Lockington, 1880a), which he ultimately removed from *Lepidopsetta* to his new genus *Isopsetta* (Lockington, 1883). In his description of *Lepidopsetta isolepis*, he treated *Platichthys umbrosus* Girard as a synonym of *L. bilineata*. Nearly 20 years after Gill's erection of *Lepidopsetta*, Cope (1873) described *Pleuronectes perarcuatus* from Alaska, later considered a synonym of *L. bilineata* by Jordan and Gilbert (1881). Jordan and Evermann (1898) considered each of these nominal species members of *Lepidopsetta* and further as synonyms of *L. bilineata*, although they recognized the northern populations ("Puget Sound and northward") as *L. bilineata umbrosa*. Finally, Japanese *Lepidopsetta* were described by Snyder (1911) as *L. mochigarei* and Jordan and Hubbs (1925) considered all Japanese *Lepidopsetta* to be representatives of this species.

More recently, the genus has been envisioned as containing either two spe-

cies, *L. bilineata* of the eastern North Pacific Ocean and Bering Sea and *L. mochigarei* of the western North Pacific around Japan (Hubbs, 1915; Sakamoto, 1984b), or a single species, *L. bilineata*, with two subspecies *L. b. bilineata* and *L. b. mochigarei* in the Bering Sea and western Pacific (Taranets, 1937; Schmidt, 1950). A third subspecies in the southeastern North Pacific was recognized by Moiseev (1953) and Wilimovsky et al. (1967). Although both authors split eastern Pacific populations into two subspecies, Moiseev (1953) considered the northern subspecies to be *L. b. bilineata* and the southern subspecies to be *L. b. umbrosa*, whereas Wilimovsky et al. (1967) applied the names *L. b. perarcuata* and *L. b. bilineata* to northern and southern populations, respectively.

Our study arose from an examination of collections from ichthyoplankton surveys conducted from the Bering Sea to northern California by the Recruitment Processes Task (referred to simply as "Task" in the following account) of the Alaska Fisheries Science Center (AFSC). In 1985, ichthyoplankton taxonomists began to routinely separate an unidentified pleuronectid from numerous collections. Larvae from the developmental series of this unidentified pleuronectid most closely resembled larvae previously described as *Psettichthys melanostictus* (Hickman, 1959; Pertseva-Ostroumova, 1961) and, for the following few years, larval pigment patterns and morphological characters were used to separate what were then considered *Psettichthys* into two readily distinguishable morphotypes. Thus in 1986, an early draft of the Task's laboratory guide (Matarese et al., 1989) included illustrations of an unidentified series referred to as a variant of *Psettichthys* ("*Psettichthys* 2").

During winter and spring 1987, larvae of both morphotypes of "*Psettichthys*" were collected from Puget Sound and reared through transformation and settlement stages, and upon examination of the reared juveniles, Kendall and Matarese[1] determined that larvae previously referred to as "*Psettichthys* 2" were, in fact, another form of *Lepidopsetta*. From the early results of this work, Matarese et al. (1989) decided to include a partial description of the unknown pleuronectid (referred to as "*Lepidopsetta* 2") and compared various stages with larvae of *Psettichthys* and other *Lepidopsetta*. Mulligan et al. (1995) finally verified the identity of *Lepidopsetta* 2 by rearing larvae spawned from *Lepidopsetta* adults collected in Puget Sound and conducted a morphological study of adults. Although they reported significant heterogeneity in shape, structure, and allozymes, they recommended the retention of Wilimovsky et al.'s (1967) subspecies designations.

Although previous authors (Townsend, 1936, 1937; Wilimovsky et al., 1967; Mulligan et al., 1995) concluded that observed variation represented a cline smoothly grading from California through the Bering Sea to Japan and supported subspecific designations, new data became available in 1992 with the development of a fishery for *Lepidopsetta* in the northern Gulf of Alaska. Domestic fisheries observers (see "Acknowledgments" section) experienced in sampling in the Bering Sea flatfish fisheries began to report the presence of two syntopic adult forms of *Lepidopsetta* in the northern Gulf of Alaska, one distinctly different from the form in the eastern Bering Sea. These observations spurred a further examination into the morphological differences of all life stages of *Lepidopsetta*. Our revision therefore incorporates evidence from adult, juvenile, and larval morphology and distribution to support the recognition of three species, one described as new, in the North Pacific. We describe morphological variation in adults, juveniles, and larvae; differentially diagnose adults, juveniles, and larvae; and describe geographic and bathymetric distributions of the three species.

Materials and methods

Unless indicated otherwise, standard length (SL) is used throughout. Institutional abbreviations follow Leviton et al. (1985) and Leviton and Gibbs (1988), as modified by Poss and Collette (1995), except for the Kamchatka Institute of Ecology, abbreviated as KIE.[2]

Adult morphology

Meristic data, except gill-raker counts, and morphometric data were taken from the ocular-side of adult material, following Hubbs and Lagler (1958) with the following exceptions. Standard, head, and snout length were measured from the anterior margin of the maxilla, with the mouth closed. Body depth was the greatest depth measured at the origin of the anal fin. Head length included only the opercle and not the opercular membrane. Snout length was measured to the anterior edge of the dorsal orbit. Cheek length was the greatest distance from the posterior rim of the ventral orbit to the edge of the preopercle, often the posterior angle of the preopercle. Interorbital width equals the least bony width. Pectoral-fin length was the length of the longest ray, often the third ray, and was measured for both ocular-side and blind-side fins. Lateral-line arch length was the distance between anterior and posterior flexion points, and this straight line was used as the base for the depth measurement. Greatest caudal peduncle depth was measured at the base of the caudal fin.

All rayed elements were included in counts of fin rays. The last two rays of the dorsal and anal fins were counted separately. Scales above the lateral line were counted on a diagonal at the greatest depth between the dorsal-fin base and lateral line. Scales below the lateral line were counted from the anal-fin origin on a diagonal to the lateral line. Total scales above and below the lateral line is the sum of the two counts. Cheek scales were counted at greatest cheek length. Ocular-side suborbital pores were counted

[1] Kendall, A. W., Jr., and A. C. Matarese. 1987. Unpubl. data. Resource Assessment and Conservation Engineering Division, Alaska Fisheries Science Center, Natl. Mar. Fish. Serv., NOAA, 7600 Sand Point Way NE, Seattle, WA 98115.

[2] Sheiko, B. 1997. Personal commun. Kamchatka Institute of Ecology, Partizanskaya 6, Petropavlovsk-Kamchatsky 683000, Russia. Present address: Department of Ichthyology, Zoological Institute, Russian Academy of Sciences, Universitetskaynab. 1, St. Petersburg 199034, Russia.

from the first pore branching from the temporal canal to the anteriormost pore; all pores were counted, including those dorsal and ventral to the canal. Blind-side suborbital pores were counted from the first pore branching from the postorbital canal to the anteriormost pores. Pore counts of the dorsal anterior and posterior branches of the accessory dorsal branch of the lateral line (ADB) began with the first pore of each branch and did not include the single pore typically found at the intersection of the two branches. Supraorbital pores include the first pore dorsal to the postorbital canal and include those pores at the posterior rim of the dorsal orbit (Fig. 1). Preopercular pores begin with the first pore posterior to the mandibular articulation and end at the last pore before the temporal canal. Caudal-fin terminology follows Sakamoto (1984a).

Larval collections

Most data were garnered from samples collected by the AFSC with standard bongo gear during ichthyoplankton surveys of the Bering Sea and Gulf of Alaska (1971–1994, Table 1, Appendix Table 1). In most cases, the identities of specimens collected prior to 1985 (when the unidentified pleuronectid developmental series was first separated) have been verified. All larval specimens used for illustrations and morphological descriptions have been cataloged at the University of Washington Fish Collection (UWFC); other material will be archived at the UWFC as well (see Appendix Table 1). Additional data for *Lepidopsetta* in Canadian waters were obtained from the Canadian Department of Fisheries and Oceans, Pacific Biological Station, Nanaimo (W. Shaw), and Vancouver Public Aquarium (J. Marliave; these specimens are now deposited at UWFC). The Washington Department of Fisheries also provided distribution and life history data for Puget Sound.[3] In addition, dip-net sampling in Puget Sound conducted by the AFSC from 1985 through 1995 resulted in 16 collections of *Lepidopsetta* larvae (Busby et al., 2000). Two larvae from the Washington, Oregon, and northern California survey area were examined—the only two *Lepidopsetta* larvae collected during the eight years (from 1980 to 1987) during which the AFSC conducted ichthyoplankton cruises in the region. Geoff Moser, NMFS Southwest Fisheries Science Center (SWFSC), provided data for *Lepidopsetta* collected during California Cooperative Fisheries Investigations (CalCOFI) cruises conducted along the coast of California.

Identification of juveniles

Recently transformed juveniles present particular problems in identification because adult characters, such as meristics and pigment patterns, are not completely developed and some aspects of larval shape, structure, and pigment patterns are retained. Thus, early juveniles (approximately 20–35 mm SL) were identified by a combination of characters, including gill-raker counts of the first arch, larval pigment characters retained on the blind side, and size at transformation. Although gill rakers were not fully formed, specimens with counts greater than seven on the lower arch were assumed to be the new species. Juveniles with counts of seven or less were identified in conjunction with other characters. Postsettlement juveniles greater than 30 mm SL were separated by using the above characters in addition to counts of the number of supraorbital pores. *Lepidopsetta bilineata* typically has 4–6 head pores along the supraorbital canal, whereas the new species typically has 1–3. Differences in gill-raker structure useful in distinguishing adults are usually not evident at sizes less than 200 mm SL.

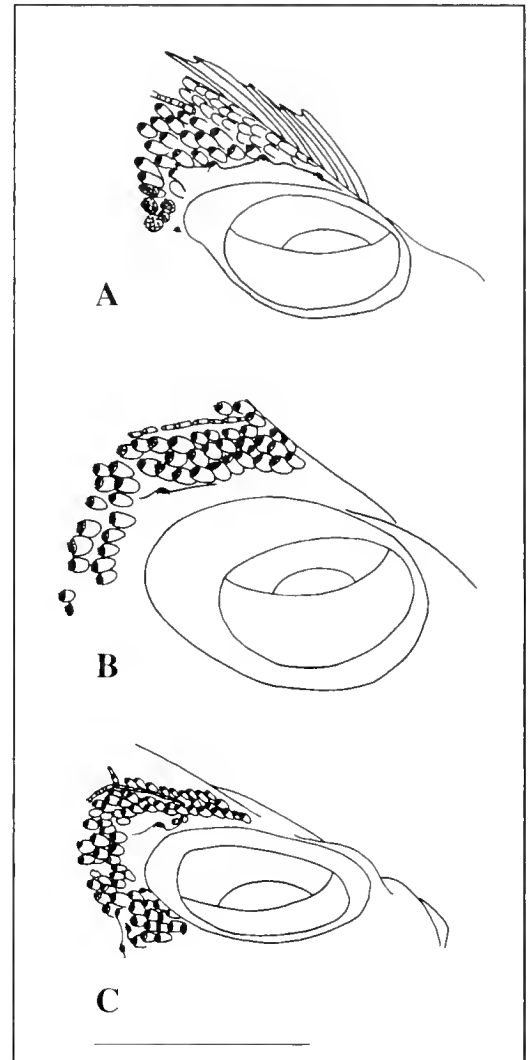

Figure 1

Supraorbital pores of *Lepidopsetta* species: **(A)** *L. bilineata*, UW 29670, 187.5 mm; **(B)** *L. polyxystra* n. sp., UW 044023, 239.5 mm; **(C)** *L. mochigarei*, USNM 68245, 174.0 mm, holotype. View of dorsal (right lateral) side. Scale bar equals 15 mm.

[3] Penttila, D. 1996. Personal commun. Puget Sound Forage Fish Unit, Washington Department of Fish and Wildlife, 1702 Anderson Road, Bay 4, Mt. Vernon, WA 98173.

Table 1

Collections of *Lepidopsetta* larvae examined for this study. AFSC = Alaska Fisheries Science Center, Seattle, WA; VPA = Vancouver Public Aquarium, Vancouver, BC; PBS = Pacific Biological Station, Nanaimo, BC; CalCOFI = California Current Oceanic Fisheries Investigations, La Jolla, CA.

General location	Source of data	Years	Months sampled	No. of samples
Bering Sea	AFSC	1971, 1977, 1979, 1988, 1992–94	Apr–Aug	152
Gulf of Alaska	AFSC	1972, 1978–79, 1981-94	Mar–Oct	1896
British Columbia	VPA, PBS	1983–88, 1991–93	Mar–July	72
Puget Sound	AFSC	1985–95	Mar–July	16
WA, OR, and N. CA	AFSC	1980–87	Apr–May	2
California	CalCOFI	1951–84	Feb–July	21

Identification of larvae

Identification of *Lepidopsetta* larvae was accomplished by a variety of methods because the more traditional serial approach was not possible. Initially, our unidentified pleuronectid series was grouped together on the basis of a continuous sequence of shared characters. This series, however, could not be linked with a recognized pleuronectid taxon whose larvae had not already been described. The unidentified series (*Psettichthys* 2) was similar to larvae previously described for *P. melanostictus*. Larvae of *Psettichthys* 2 were determined to be *Lepidopsetta* by rearing wild-caught larvae[1] and finally confirmed to be *Lepidopsetta* by rearing larvae spawned from *Lepidopsetta* adults collected in Puget Sound (Mulligan et al., 1995).

Nomenclature of larval developmental stages follows Kendall et al. (1984) where each stage is based on widespread, fundamental features of development. The early life history stages used in our study were based on the flexion of the notochord that accompanies the hypochordal development of the homocercal caudal fin. The onset of the juvenile stage is defined in our study as completion of eye migration and attainment of the adult complement of fin elements. Early juveniles (approximately 20–35 mm SL) are defined as those collected in the water column; many had remnants of larval pigmentation on their blind side. Postsettlement juveniles were collected with bottom gear and rarely retained any larval pigmentation on their blind side.

Only melanistic pigment is described in our study because formalin fails to preserve other pigments (live larvae have yellow, orange, and brown chromatophores associated with the melanophores). Previous descriptions of larval pigment patterns, particularly those of pleuronectids, have used confusing terminology. Postanal pigment patterns have been variously described as vertically oriented bands (Pertseva-Ostroumova, 1961; Moser et al., 1984; Matarese et al., 1989) and bars (Charter and Moser, 1996). The number of postanal bands and bars may or may not include the caudal or terminal notochord pigment. For clarity, in the descriptions of pigment patterns, the terms "band" and "bar" refer to aggregations of melanophores that approximate vertically oriented rectangles (including the caudal pigment). A band is always complete and a bar incomplete. A "stripe" approximates a line or elongate rectangle and is horizontally oriented. A "spot" is an approximately circular aggregation of melanophores. A "patch" is any other distinguishable aggregation of melanophores.

Larval morphology

A total of 115 eastern North Pacific *Lepidopsetta* larvae were measured with a calibrated digital image analysis system (larvae of the western North Pacific *L. mochigarei* were not available). This system consists of a video camera attached to a dissecting stereomicroscope or camera lens, a microcomputer with digital imaging board, and a video monitor. All measurements of larvae were taken from the left side. Unless otherwise noted, standard length (SL) is used throughout and is defined in our study as the length from snout tip to notochord tip (prior to development of the caudal fin) or to the posterior margin of hypural elements. Other measurements are defined as follows: head length (HL), snout tip to posterior edge of opercle (to pectoral-fin base in small larvae before opercular margin is visible); snout length (SNL), snout tip to anterior margin of orbit; orbit length (OL), greatest length of orbit; body depth (BD), vertical distance from dorsal to ventral body margin at a vertical line through center of anal opening; snout-to-anus length (SAL), distance along body midline from snout tip to a vertical line through center of anal opening. Standard proportional measurements were calculated (Table 2).

Distributional analysis of larvae

The dataset used for mapping and calculation of mean density of larvae (number per 10 m^2; Appendix Table 1) was a subset of the AFSC ichthyoplankton historical database (1972–1994) from the Bering Sea and Gulf of Alaska. This subset included all reidentified samples that had been originally identified as *Psettichthys* 2, *Lepidopsetta* 2, and *L. bilineata* and thus provided the only historic distributional records for larvae of *L. polyxystra* n. sp. Maps of material examined and distribution and mean density

Table 2

Proportional measurements for *Lepidopsetta* larvae. SL = standard length; HL = head length. Statistical significance of raw data was evaluated by an ANCOVA analysis. See Table 10 for *P*-values. NS = not significant; S = significant.

Developmental stage	*L. polyxstra* n. sp.	*L. bilineata*	Significance
Yolksac			
Sample size	6	13	
Snout-to-anus length /SL	32.1 ±1.7 (30.6–34.8)	32.9 ±1.8 (30.1–36.8)	NS
Body depth/SL	3.8 ±0.6 (2.7–4.3)	4.7 ±0.8 (3.9–6.7)	S
Head length/SL	11.6 ±1.0 (10.1–12.6)	13.3 ±1.4 (10.0–15.1)	NS
Snout length/HL	24.7 ±2.4 (21.2–27.1)	22.6 ±7.8 (13.1–36.5)	NS
Orbit length/HL	51.8 ±5.6 (43.8–58.9)	51.9 ±6.6 (36.7–61.5)	NS
Preflexion			
Sample size	11	13	
Snout-to-anus length /SL	33.5 ±1.3 (32.3–36.0)	30.7 ±2.3 (26.8–34.3)	S
Body depth/SL	4.8 ±0.7 (3.2–5.8)	5.0 ±0.9 (3.3–6.7)	NS
Head length/SL	13.0 ±1.3 (10.6–15.6)	12.7 ±1.8 (10.4–15.8)	NS
Snout length/HL	20.5 ±5.3 (13.3–29.7)	23.5 ±6.3 (15.1–35.8)	NS
Orbit length/HL	48.1 ±6.7 (34.1–61.9)	45.3 ±5.6 (37.1–53.0)	S
Flexion			
Sample size	26	17	
Snout-to-anus length /SL	35.5 ±2.5 (31.3–40.0)	33.8 ±2.1 (29.9–38.2)	S
Body depth/SL	10.5 ±4.1 (4.6–18.0)	11.1 ±5.1 (5.5–21.9)	S
Head length/SL	19.1 ±3.6 (13.3–26.4)	17.9 ±3.0 (14.6–24.4)	NS
Snout length/HL	20.5 ±3.3 (12.8–26.2)	22.5 ±4.7 (13.5–29.3)	NS
Orbit length/HL	31.1 ±6.9 (20.6–44.9)	33.6 ±4.1 (27.8–40.6)	NS
Postflexion			
Sample size	10	19	
Snout-to-anus length /SL	39.3 ±3.3 (35.3–45.7)	34.6 ±2.9 (29.3–38.2)	S
Body depth/SL	28.5 ±6.4 (20.0–38.6)	35.7 ±3.0 (27.8–39.9)	S
Head length/SL	26.7 ±2.4 (22.4–30.6)	29.3 ±1.7 (26.7–32.7)	S
Snout length/HL	22.8 ±2.1 (19.3–26.0)	20.7 ±2.3 (16.8–24.2)	NS
Eye length/HL	20.9 ±2.4 (17.5–24.0)	23.8 ±3.2 (19.6–31.8)	S
Total larvae measured	53	62	

of species were generated by using the geographic information system Arc/Info and ArcView (Environmental Systems Research Institute, 1996). Tables were produced with ArcView and Systat software (SPSS, Inc., 1996). Densities were mapped by dividing the geographic area into contiguous square polygons, 625 km^2 each. Catches per unit of effort (CPUEs) from all tows (including 0 catches) within each square polygon were averaged, yielding a mean density. Polygons were shaded according to their mean density, or left unshaded when no tows occurred within a polygon.

Adult statistical analyses

The software programs S-Plus (Statistical Sciences, 1993) or Statgraphics Plus 2.1 (Manugistics, 1997) were used in statistical analyses performed on juveniles and adults. Unless otherwise indicated, tests were considered significant at $P < 0.05$, as adjusted by the Bonferroni correction (Sokal and Rohlf, 1995). For all characters, Bartlett's test of homogeneity of variances (Sokal and Rohlf, 1995) was used to determine the appropriateness of an ANOVA to test for differences between species. When Bartlett's test found significant differences in variances, pairwise comparisons were made. Pairs with significant differences in variances were then tested for differences in medians by using the nonparametric Kruskal-Wallis test (Sokal and Rohlf, 1995). The following meristic characters did not differ significantly in variance among species pairs and were subjected to an ANOVA: gill rakers of the upper and lower first arch and lower second arch; dorsal- and anal-fin rays; ocular-side and blind-side pectoral-fin rays; posterior and anterior ADB pores; interorbital scales; cheek scales; scales above, below, and total around the lateral line; ocular-side and blind-side suborbital pores; supraorbital pores.

Table 3
Counts of gill rakers for species of *Lepidopsetta*.

	Upper first arch											
Species	1	2	3	4	5	6	*n*	*x*	SD			
L. bilineata	12	167	104	4			287	2.3	0.58			
L. mochigarei	1	18	8				27	2.3	0.53			
L. polyxystra n. sp.			135	183	15	3	336	3.7	0.61			
	Lower first arch											
	4	5	6	7	8	9	*n*	*x*	SD			
L. bilineata	5	105	160	17			287	5.7	0.62			
L. mochigarei	1	5	18	3			27	5.9	0.66			
L. polyxystra n. sp.			13	204	114	5	336	7.3	0.57			
	Lower second arch											
	5	6	7	8	9	10	11	12	13	*n*	*x*	SD
L. bilineata	1	52	170	38	12	2				275	7.1	0.76
L. mochigarei		2	14	10	1					27	7.4	0.69
L. polyxystra n. sp.			4	17	125	139	40	10	1	336	9.7	0.92

For morphometric characters, significant differences between species were identified using an ANOVA of arcsine-transformed ratios of the measurement divided by SL or HL (Sokal and Rohlf, 1995) and an analysis of covariance (ANCOVA) with SL or HL as covariates when assumptions of homogeneity of slopes were satisfied. The following morphometric characters did not significantly differ in variances among species pairs and were subjected to an ANOVA: head length, snout length, ocular-side maxilla length, blind-side maxilla length, ocular-side mandible length, cheek length, interorbital width, dorsal orbit length, ocular-side pectoral-fin length, body depth, caudal peduncle depth, and caudal-fin length. Snout length, blind-side maxilla length, ocular-side mandible length, and interorbital width were also subjected to ANCOVA.

To aid in the discrimination and classification of species, standard principal components analysis (PCA) was conducted on all morphometric and meristic characters for adults of all species together and on the eastern North Pacific material separately. Raw morphometric data were log-transformed and the covariance matrix was subjected to PCA, as was the correlation matrix of raw meristics. Differences between species were illustrated by separately plotting principal components (PC) 2 and 3 of the morphometric analyses, PC1 and PC2 of the meristic analyses, and PC1 of the meristic analyses against PC2 of the morphometric analyses (Stauffer and Hert, 1992). For eastern North Pacific species, data points were also identified by reference to 11 geographic regions: Sea of Okhotsk, western Bering Sea, eastern Bering Sea, Aleutian Islands, Gulf of Alaska, British Columbia, Puget Sound, Washington coast, Oregon coast, California coast, and Baja California coast.

Larval statistical analyses

In an effort to identify additional characters to distinguish larvae of the two eastern North Pacific species, morphometric characters of yolksac preflexion, flexion, and postflexion larvae were further analyzed. Scatter plots for each measurement versus SL were made. Morphometric data were analyzed by the ANCOVA model for each parameter at each developmental stage and at all stages combined, which included species as a factor, standard length as a covariate, and a species/SL interaction (e.g. $BD = C + Species + SL + (Species \times SL)$). A residual analysis was done for each model to determine the appropriateness of the model. Whenever the interaction was not significant (at the 5% level), a reduced model was used, and the interaction was dropped and the slopes were forced to be the same ($BD = C + Species + SL$). This procedure removed the effect of SL and allowed testing for significant differences between species. When the species were significantly different, the *P*-value was reported and graphs were generated to illustrate differences between elevations of the two regressions. Principal components analysis was also used to highlight differences.

Results

Adults

All three species differed significantly from each other in three meristic characters (Tables 3–7): posterior ADB pores (Table 5), total scales above and below the lateral

Table 4

Fin-ray counts for species of *Lepidopsetta*.

	Dorsal-fin rays																							
Species	64	67	68	69	70	71	72	73	74	75	76	77	78	79	80	81	82	83	84	85	86	89	*n*	*x*	SD
L. bilineata		1			4	1	6	5	10	7	15	22	21	11	8	5	3	1	1	1	4	1	127	77.14	3.57
L. mochigarei								1	5	3	10		3	1		3	1						27	76.52	2.46
L. polyxystra n. sp.	1	3	5	6	12	9	13	12	13	8	20	14	10	14	7	4	1	2					154	74.60	3.84

	Anal-fin rays																						
	49	50	51	52	53	54	55	56	57	58	59	60	61	62	63	64	65	66	*n*	*x*	SD
L. bilineata							7	2	13	26	17	29	15	9	4	1	2	1	126	59.3	2.15
L. mochigarei								1	3	5	4	5	6	1	1		1		27	59.6	2.02
L. polyxystra n. sp.	1	3	6	4	5	6	14	20	11	17	17	20	15	9	3	2			153	57.5	3.28

	Blind pectoral-fin rays								
	8	9	10	11	12	13	*n*	*x*	SD
L. bilineata			10	52	62	2	126	11.4	0.66
L. mochigarei			2	17	6	2	27	11.3	0.72
L. polyxystra n. sp.	1	2	36	82	30	2	153	10.9	0.77

	Ocular pectoral-fin rays							
	9	10	11	12	13	*n*	*x*	SD
L. bilineata	5	12	69	32	5	123	11.2	0.81
L. mochigarei		5	14	7	1	27	11.1	0.77
L. polyxystra n. sp.	5	47	74	25	2	153	10.8	0.79

line (Table 6), and ocular-side suborbital pores (Table 7). *Lepidopsetta polyxystra* n. sp. also differed from *L. bilineata* in number of gill rakers of the upper and lower first arch and lower second arch (Table 3), dorsal-fin rays (Table 4), ocular-side and blind-side pectoral-fin rays (Table 4), anterior ADB pores (Table 5), blind-side suborbital pores (Table 7), and supraorbital pores (Table 7), and differed from *L. mochigarei* in number of gill rakers of the upper and lower first arch and lower second arch (Table 3), blind-side pectoral-fin rays (Table 4), anterior and posterior ADB pores (Table 5), and cheek scales (Table 6).

All three species were found to differ significantly in the means of two morphometric characters with either ANOVA or ANCOVA: interorbital width and ocular-side mandible length (Table 8). *Lepidopsetta polyxystra* n. sp. also differed from *L. bilineata* in seven additional characters: head length, blind-side maxilla length, cheek length, body depth, ocular-side pectoral-fin length, caudal-fin length, and caudal peduncle depth; and differed in medians in ocular-side maxilla length, blind-side pectoral-fin length, and body depth. *Lepidopsetta polyxystra* n. sp. also differed from *L. mochigarei* in means of two characters: dorsal orbit length and cheek length; and in medians of head length, body depth, depth at caudal base, and caudal length. *Lepidopsetta bilineata* also differed from *L. mochigarei* in means of two additional characters: blind-side maxilla length and dorsal orbit length; and differed in medians in head length, ocular-side maxilla length, cheek length, body depth, caudal peduncle depth, and depth at caudal base. No differences in means were found in snout length or ocular-side maxilla length.

In the standard PCA of all three species together, loadings of morphometric PC1 were all positive and thus exhibited a strong size effect (Table 9), accounting for 95% of morphometric variation. Principal components 2 and 3 accounted for 56% of the remaining morphometric variation. Principal component 2 loadings described a gradient based on interorbital width and dorsal orbit length; PC3 loadings, a gradient on caudal peduncle depth, cheek depth, caudal depth at hypural margins, and body depth. The plot of PC2 versus PC3 revealed extensive overlap in morphometric characters (Fig. 2A). Principal components 1 and 2 of the meristics analysis accounted for 46% of the meristic variance: PC1 strongly loaded on lateral line pores and scales above and below the lateral line, preopercle pores, and suborbital pores, whereas PC2 strongly

Table 5

Counts of lateral-line and supratemporal pores for species of *Lepidopsetta*.

	Lateral-line pores																					
Species	70	71	72	73	74	75	76	77	78	79	80	81	82	83	84	85	86	87	88	89	90	91
L. bilineata	1			2		2	5	4	9	9	15	15	18	17	11	12	11	8	4	2	2	1
L. mochigarei																						
L. polyxystra n. sp.							2		2	1	5	6	3	12	12	24	15	14	16	10	7	10

	Lateral-line pores (cont'd)																							
	92	93	94	95	96	97	98	99	100	101	102	103	104	105	106	107	108	109	115	117	119	*n*	*x*	SD
L. bilineata																						148	82.1	3.67
L. mochigarei				1	1			3	2	2	3	2	1	2	1	4		2	1	1	1	27	104.4	5.84
L. polyxystra n. sp.	5	6	2	4		1	1	1	1													160	86.8	4.28

	Posterior supratemporal pores																																	
	6	8	9	10	11	12	13	14	15	16	17	18	19	20	21	22	23	24	25	26	27	28	29	30	31	33	34	35	*n*	*x*	SD
L. bilineata		1	1	1		4	7	6	13	5	15	14	12	11	6	8	5	6	7	4	1	2		4				1	134	19.1	4.73
L. mochigarei	2	3	2	1	3	2	3	3	3	1				1		2													26	12.6	4.28
L. polyxystra n. sp.				3	2	2		4	2	8	14	8	13	16	16	6	11	10	8	2	4	7	1	4	5	1	3	1	151	21.4	5.21

	Anterior supratemporal pores																
	2	3	4	5	6	7	8	9	10	11	12	13	14	15	*n*	*x*	SD
L. bilineata	1	4	11	33	19	23	23	7	9	2	2				134	6.6	1.99
L. mochigarei		1	5	1	6	5	1	3	2	1	1				26	6.8	2.38
L. polyxystra n. sp.		1	1	9	15	30	25	30	25	8	3	1	2	1	151	8.3	1.99

Table 6

Counts of total scales above and below lateral line, scales above lateral line, scales below lateral line, and cheek scales for species of *Lepidopsetta*.

	Total body scales																							
Species	65	66	67	68	69	70	71	72	73	74	75	76	77	78	79	80	81	82	83	84	85	86	87	88
L. bilineata	2	1	2	5	3	2	4	2	4	7	5	3	9	6	3	7	4	4	1	5	3	1	1	1
L. mochigarei																								
L. polyxystra n. sp.		1		1	1	1	3		1	3	6	6	4	5	5	9	10	3	7	7	3	1	3	1

	Total body scales (cont'd)																						
	89	90	91	92	93	94	95	96	97	98	99	100	101	102	103	104	105	106	107	108	*n*	*x*	SD
L. bilineata																					85	76.3	5.59
L. mochigarei			1	1	1			1	5	2		3	1	3	3	2	1	1	1	1	27	100.1	4.42
L. polyxystra n. sp.	5	2	2	2	1			1													94	80.8	5.95

	Scales above lateral line																						
	25	26	27	28	29	30	31	32	33	34	35	36	37	38	39	40	41	42	43	44	45	*n*	*x*	SD
L. bilineata	1	5	8	5	8	8	13	12	9	6	4	4			1			1	1			85	31.0	3.13
L. mochigarei											1	3		4	2	6	4	4	1	1	1	27	39.9	2.49
L. polyxystra n. sp.			5	5	5	11	9	16	17	7	9	6	2	1		1						94	32.2	2.69

	Scales below lateral line																																
	32	38	39	40	41	42	43	44	45	46	47	48	49	50	51	52	53	54	55	56	58	59	60	61	62	63	64	65	67	*n*	*x*	SD
L. bilineata	1	1	1	3	10	5	6	5	9	11	10	7	6	3	3	2	2													85	45.3	3.74
L. mochigarei																1		1		2	3	4	2	4	3	4	1	1	1	27	60.2	3.33
L. polyxystra n. sp.		1		2	1	3	1	2	7	7	15	5	12	11	11	4	2	1	2	5	1	1								94	48.6	3.95

	Cheek scales												
	7	8	9	10	11	12	13	14	15	16	*n*	*x*	SD
L. bilineata			7	14	18	21	15	6	2	1	84	11.6	1.55
L. mochigarei				2	8	9	7		1		27	11.9	1.11
L. polyxystra n. sp.	3	5	14	36	29	10	2				99	10.2	1.21

Table 7

Counts of ocular- and blind-side suborbital pores, preopercle pores, and supraorbital pores for species of *Lepidopsetta*.

	Ocular-side suborbital pores																													
Species	13	14	15	16	17	18	19	20	21	22	23	24	25	26	27	28	29	30	31	32	33	34	35	36	37	38	*n*	*x*	SD
L. bilineata		1		1		9	8	7	16	15	2	3	6		2	1	1										72	21.2	2.71
L. mochigarei										1			1			2	8	3	2	3	3		1		2	1	27	30 7	3.51
L. polyxystra n. sp	1		2		2	4	2	7	11	11	17	10	11	6	3	3	3										93	22 7	3.10

	Blind-side suborbital pores																	
	6	7	8	9	10	11	12	13	14	15	16	17	18	19	20	*n*	*x*	SD
L. bilineata	1	2	12	24	21	9	3	2								74	9.5	1.32
L. mochigarei					2	3	7	8	4	2					1	27	12.9	1.94
L. polyxystra n. sp			5	17	32	31	3	4	1							93	10.3	1.16

	Supraorbital pores											
	1	2	3	4	5	6	7	8	9	*n*	*x*	SD
L. bilineata		2	6	20	70	91	51	10	5	255	5.8	1 19
L. mochigarei	17	1	1							19	1.2	0.50
L. polyxystra n. sp	118	105	29	7	2	3	2			266	1.8	1.03

	Preopercle pores											
	5	6	7	8	9	10	11	12	13	*n*	*x*	SD
L. bilineata	2	60	9							71	11 6	1.55
L. mochigarei			1	4	2	8	6	1	2	24	11.9	1.11
L. polyxystra n. sp	1	32	53	3						89	10.2	1.21

Table 8

Proportional morphometrics of adults of *Lepidopsetta*. HL = head length; SL = standard length. Data are in hundreds of SL or HL with mean ± standard deviation (range). Statistical significance was evaluated by ANOVA and ANCOVA, when appropriate, at 0 05 level. All = Differences between all three species were significant; bp = Differences between *L. bilineata* and *L. polyxystra* n. sp. were significant; pm = Differences between *L. polyxystra* n. sp. and *L. mochigarei* were significant; ns = No significant differences were found.

	Species			Significance	
	L. bilineata	*L. mochigarei*	*L. polyxystra*	ANOVA	ANCOVA
Sample size	83	26	94		
Head length/SL	28.20±1.64 (24.01-32.86)	26.23±1.71 (23.23–30.54)	27.24±1.62 (21.75–31.54)	bp	
Snout length/HL	16.09±2.07 (12.37-22.45)	16.13±1.69 (12.72–20.21)	16.02±1.84 (12.06–20.12)	ns	ns
Ocular-side maxilla length/HL	27.88±1.25 (25.26-32.53)	27.21±1.41 (24.63–29.41)	26.30±1.89 (20.42–31.47)	ns	
Ocular-side mandible length/HL	41.91±1.69 (38.33-46.10)	39.61±1.83 (36.57–44.64)	40.73±2.20 (34.39–50.00)	bm	All
Interorbital width/HL	3.54±0.79 (2.14-6.02)	2.68±0.69 (1.32–4.17)	4.35±0.80 (2.49–6.56)	All	All
Dorsal orbit length/HL	28.06±1.91 (23.38-32.46)	30.08±1.83 (26.09–34.74)	28.13±1.95 (22.18–32.86)	pm/bm	
Ventral orbit length/HL	3.54±0.79 (2.14-6.02)	2.68±0.69 (1.32–4.17)	4.35±0.80 (2.49–6.56)		
Cheek length/HL	34.17±2.84 (28.06-41.84)	31.09±1.71 (28.57–34.98)	32.54±2.77 (26.67–38.52)	bp/pm	
Body depth/SL	46.98±2.84 (40.80-57.04)	51.79±3.23 (45.54–61.04)	49.02±3.44 (41.17–58.93)	bp	
Ocular-side pectoral length/SL	15.19±1.34 (12.20-18.20)	14.58±1.24 (12.60–17.42)	14.66±1.52 (10.73–18.23)	bp	
Caudal-fin length/SL	20.79±1.57 (17.62-23.63)	21.22±1.69 (18.77–25.14)	22.72±1.77 (17.78–29.13)	bp	
Caudal peduncle depth/SL	10.20±0.80 (8.18-12.29)	11.03±0.94 (9.71–13.96)	10.91±0.71 (9.36–13.13)	bp	
Caudal peduncle length/SL	9.11±0.72 (7.18-10.87)	8.89±0.54 (7.77–10.28)	8.90±0.62 (7.01–10.12)		
Ocular-side pelvic length/SL	9.83±0.98 (7.64-12.50)	9.82±0.94 (7.40–11.75)	9.95±0.97 (7.84–12.15)		
Sample size	77	26	93		
Blind-side maxilla length	31.26±2.25 (25.16-41.18)	29.73±1.56 (27.30–32.87)	28.70±2.01 (22.22–35.66)	bp/bm	bp/bm
Sample size	78	26	93		
Blind-side pectoral length/SL	9.91±0.77 (7.33-12.22)	9.58±0.90 (7.89–11.69)	10.16±1.17 (6.58–12.66)		
Sample size	67	26	92		
Cheek depth/HL	19.15±2.13 (13.92-24.19)	19.64±2.60 (14.83–25.53)	18.62±2.17 (13.56–22.73)		
Caudal depth at hypurals/SL	12.13±0.69 (10.46-14.25)	13.12±0.70 (11.66–14.61)	12.35±0.88 (10.06–16.91)		
Sample size	8	6	15		
Lateral line length/ lateral line depth	30.20±3.78 (24.84-37.06)	33.42±3.78 (27.86–38.98)	31.72±3.41 (26.29–38.20)		

Table 9

Character loadings for principal component analysis of morphometric characters of adult *Lepidopsetta bilineata*, *L. mochigarei*, and *L. polyxystra* n. sp.

	Loadings		
Characters	PC1	PC2	PC3
Standard length	0.22484	0.06236	0.15282
Head length	0.22819	0.03318	–0.06512
Snout length	0.21789	0.00863	–0.04715
Ocular-side maxilla length	0.23138	0.05417	–0.30392
Blind-side maxilla length	0.23849	0.0835	–0.30268
Ocular-side mandible length	0.2334	0.03438	–0.20318
Dorsal orbit length	0.21415	0.11385	–0.09032
Ventral eye length	0.20185	0.09275	–0.20682
Interorbital width	0.22077	–0.96363	–0.03502
Cheek length	0.24796	0.00482	–0.13585
Cheek depth	0.25623	0.08324	–0.39732
Body depth	0.23716	0.08671	0.33759
Ocular-side pectoral length	0.24489	0.0723	–0.01453
Blind-side pectoral length	0.24277	0.01015	0.184878
Ocular-side pelvic length	0.22725	0.0275	0.076978
Caudal peduncle length	0.22574	0.08882	0.121448
Caudal peduncle depth	0.22183	0.00716	0.401018
Caudal depth at hypurals	0.22707	0.07164	0.377584
Caudal-fin length	0.20981	–0.00818	0.20981

Table 10

Character loadings for principal component analysis of meristic characters for *Lepidopsetta bilineata*, *L. mochigarei*, and *L. palyxystra* n. sp. ADB = supratemporal branch of the lateral line.

	Loadings	
Characters	PC1	PC2
Upper 1st arch gill rakers	0.0722	0.4021
Lower 1st arch gill rakers	0.0646	0.4414
Upper 2nd arch gill rakers	0.0067	0.1393
Lower 2nd arch gill rakers	0.0181	0.406
Dorsal-fin rays	–0.1314	–0.1926
Anal-fin rays	–0.1265	–0.1939
Ocular-side pectoral-fin rays	–0.0975	–0.1331
Blind-side pectoral-fin rays	–0.0759	–0.1527
Lateral-line pores	–0.4017	0.1027
ADB1 pores	0.2092	0.1578
ADB2 pores	0.0079	0.1962
Interorbital scales	–0.0508	0.2163
Cheek scales	–0.1907	–0.2532
Scales above lateral line	–0.384	0.0291
Scales below lateral line	–0.392	0.0873
Ocular-side suborbital pores	–0.3635	0.0177
Blind-side suborbital pores	–0.3007	0.0961
Preopercle pores	–0.3643	0.0394
Supraorbital pores	0.203	–0.3731

loaded on gill rakers of the lower first and second arches and upper first arch and supraorbital pores (Table 10). By plotting PC1 of the meristic analysis and PC2 of the morphometric analysis (Fig. 2C), we found a distinct cluster representing *L. mochigarei* and an overlap of clusters representing *L. bilineata* and *L. polyxystra* n. sp.

In the PCA of only the eastern North Pacific species, loadings of morphometric PC1 were all positive and thus exhibited a strong size effect, accounting for 96% of morphometric variation. Principal components 2 and 3 accounted for 33% and 19% of the remaining morphometric variation, respectively. Principal component 2 loadings described a gradient based primarily on interorbital width, as well as on ventral orbit length and blind-side maxilla length; PC3 loadings described a gradient on interorbital width, caudal peduncle depth, and body depth. The plot of PC2 versus PC3 revealed extensive overlap in morphometric characters (Fig. 3A). Principal components 1 and 2 of the meristics analysis accounted for 28% and 17%, respectively, of the meristic variance; PC1 strongly loaded on gill rakers and supraorbital pores and PC2 strongly loaded on dorsal-fin rays, anal-fin rays, and cheek scales. The plot of meristic PC1 versus PC2 revealed two distinct clusters (Fig. 3B). By plotting PC1 of the meristic analysis and PC2 of the morphometric analysis (Fig. 3C), we found two distinct clusters representing *L. bilineata* and *L. polyxystra* n. sp.

When data points of eastern North Pacific species were identified by geographic regions, no significant clustering was apparent within groups of either *L. bilineata* or *L. polyxystra* n. sp. Extensive overlap was found between clusters representing each of these general geographic areas.

Larvae

Raw morphometric data were subjected to an ANCOVA analysis, which indicated differences in several morphological characters (snout-to-anus length, body depth, and orbit length) between larvae of *L. bilineata* and *L. polyxystra* n. sp. at various stages of development (Table 11). Several characters showed significant differences in postflexion larvae ($P<0.0001$), including snout-to-anus length, head length, and orbit length. Snout-to-anus length is shorter in larvae of *L. bilineata* during the preflexion, flexion, and postflexion stages (Fig.4). Larvae of *L. bilineata* are deeper-bodied during the yolksac, preflexion, and flexion stages of development (Fig. 5). The PCA plots of PC2 and PC3 for each developmental stage produced broadly overlapping clusters.

Systematics

Genus *Lepidopsetta* Gill, 1862

Lepidopsetta Gill, 1862:330 (type species *Platichthys umbrosus* Girard, 1856 [originally cited as *Psettichthys umbrosus* but subsequently corrected by Gill (1864)], by monotypy).

Diagnosis

Pleuronectid genus *Lepidopsetta* is distinguished by the following combination of characters in adults: lateral line with a high arch, 6–8 scale rows between highest point of arch and base of arch over the pectoral fin; supratemporal branch of lateral line with a moderately elongate posterior extension of up to 35 pored scales; mouth small, maxilla extending to anterior quarter of ventral orbit; expanded anteriormost anal pterygiophore ("anal spine") present, often projecting beyond body wall in damaged specimens; supraorbital pores present; scales on ocular side often tuberculate, especially on the head and anterior portion of body; scales on blind side always cycloid anteriorly.

Larvae are distinguished from other pleuronectid genera by the following combination of characters: dorsal and anal finfold pigment present, 1–3 postanal bars (2–4 distinctive pigment regions along dorsal midline), a series of ventral midline melanophores, absence of slashlike hypaxial pigment along the postanal body, few to many pigment spots around the notochord tip, and 37–44 total myomeres (Table 12).

Description of adults

Body ovate, greatest depth 31.7–61.0% SL, scales above lateral line 25–45, scales below lateral line 27–67; head acute to rounded, length 21.8–32.9% SL; dorsal margin of head concave to nearly linear, snout length 3.1–6.2% SL (12.1–22.4% HL); mouth small, premaxilla with fleshy lips and prominent, broad-based posterior lobe, maxilla extending to anterior rim of ventral orbit, ocular-side maxilla shorter than blind-side maxilla, ocular-side maxilla length 20.4–32.5% HL, blind-side maxilla length 22.2–41.2% HL; ocular-side mandible length 34.4–50.0% HL, about equal in length to blind-side mandible; teeth conical and slightly lobate or truncate, largest are anterior becoming gradually smaller posteriorly, fewer on ocular-side premaxilla and dentary, 4–10 on ocular-side premaxilla, 20–27 on blind-side premaxilla, 8–15 on ocular-side dentary, 20–29 on blind-side dentary; gill rakers of first arch moderately slender to broad and robust, 6–14 total, 1–6 on upper and 4–9 on lower arch; gill rakers of second arch broad and robust, 6–14 total, 0–4 on upper and 5–13 on lower arch; dorsal orbit round (nearly equal to eye length) to elliptical (posterior rim elongate and much greater than eye length), orbit lenth 22.2–34.7% HL,

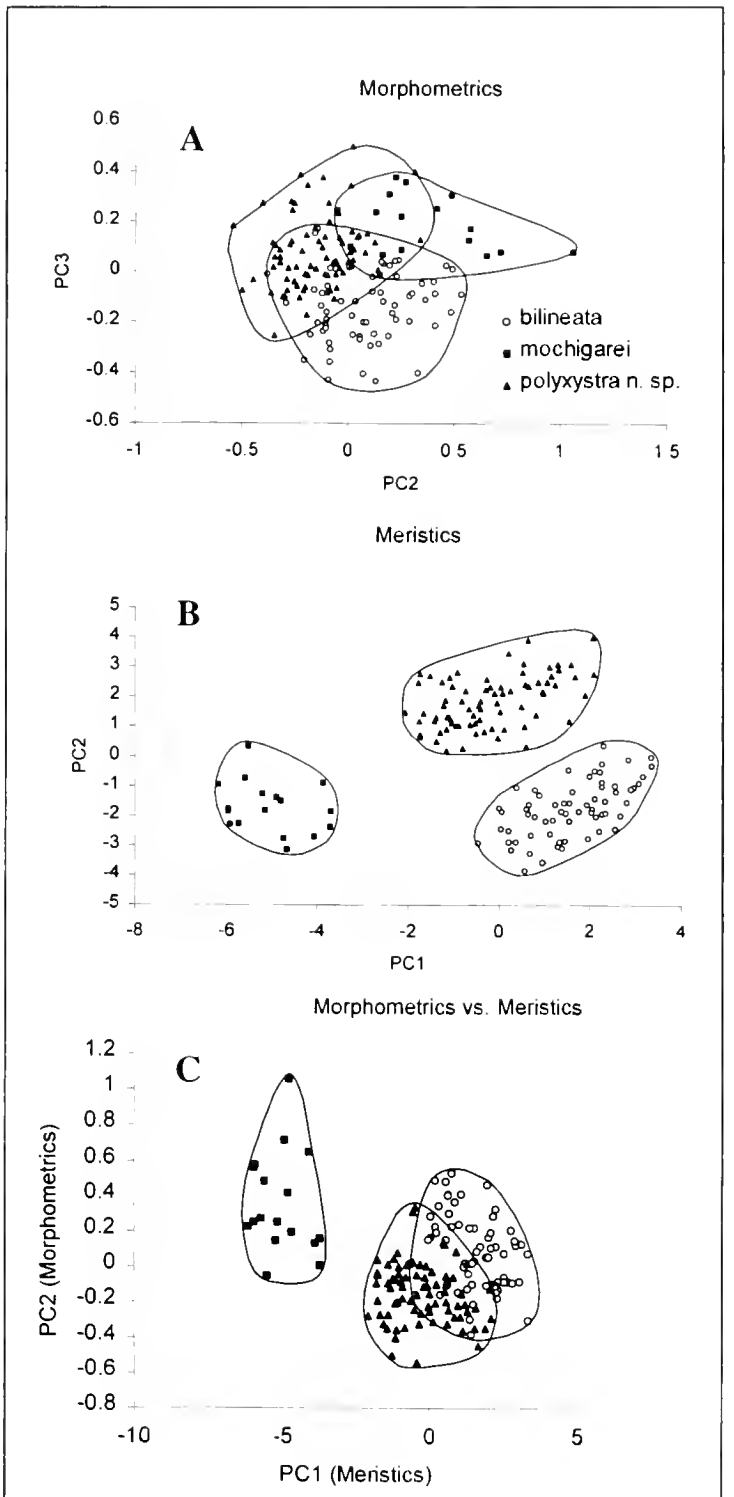

Figure 2

Plots of principal component scores for morphometric and meristic characters for *Lepidopsetta* species: *L. bilineata* (circle), *L. mochigarei* (square), *L. polyxystra* n. sp. (triangle). **(A)** Morphometric characters only; **(B)** meristic characters only; **(C)** morphometric characters (PC2) versus meristic characters (PC1).

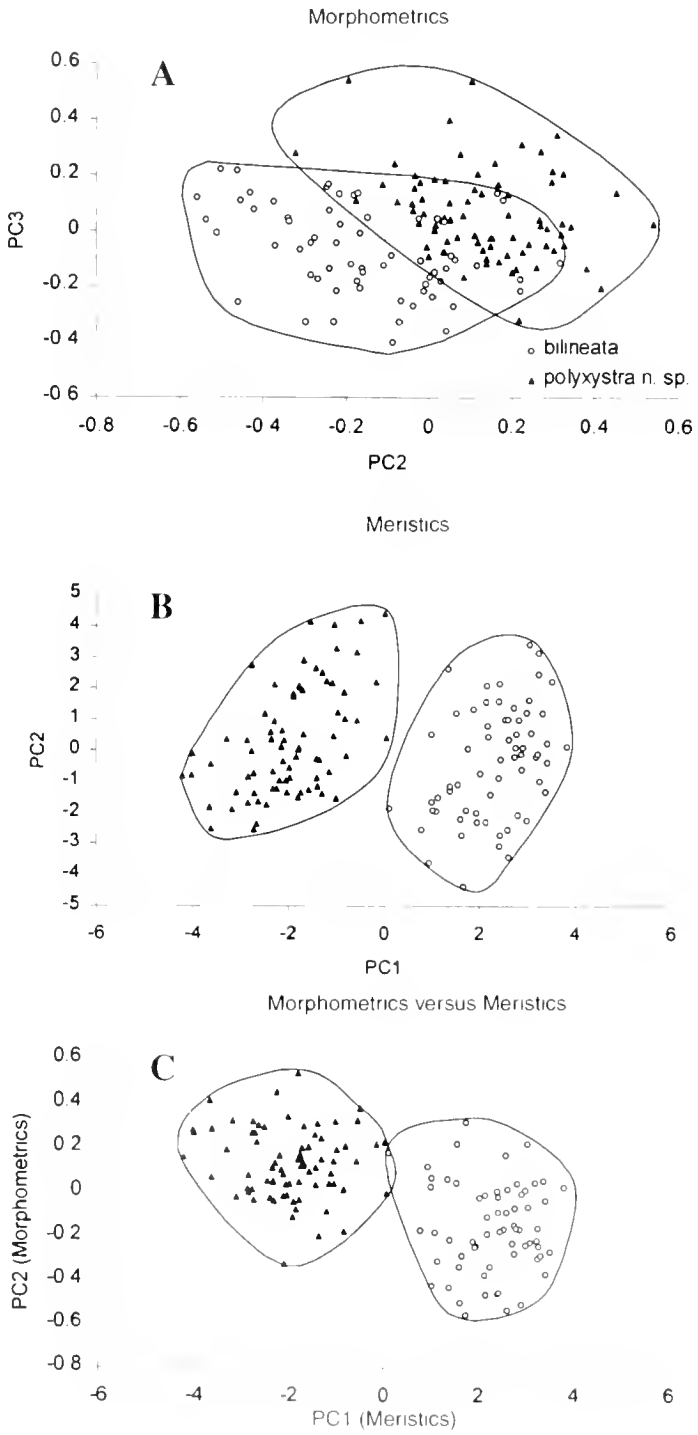

Figure 3

Plots of principal component scores for morphometric and meristic characters for eastern North Pacific *Lepidopsetta* species. *L. bilineata* (circle), *L. polyxystra* n. sp. (triangle). **(A)** Morphometric characters only; **(B)** meristic characters only; **(C)** morphometric characters (PC2) versus meristic characters (PC1).

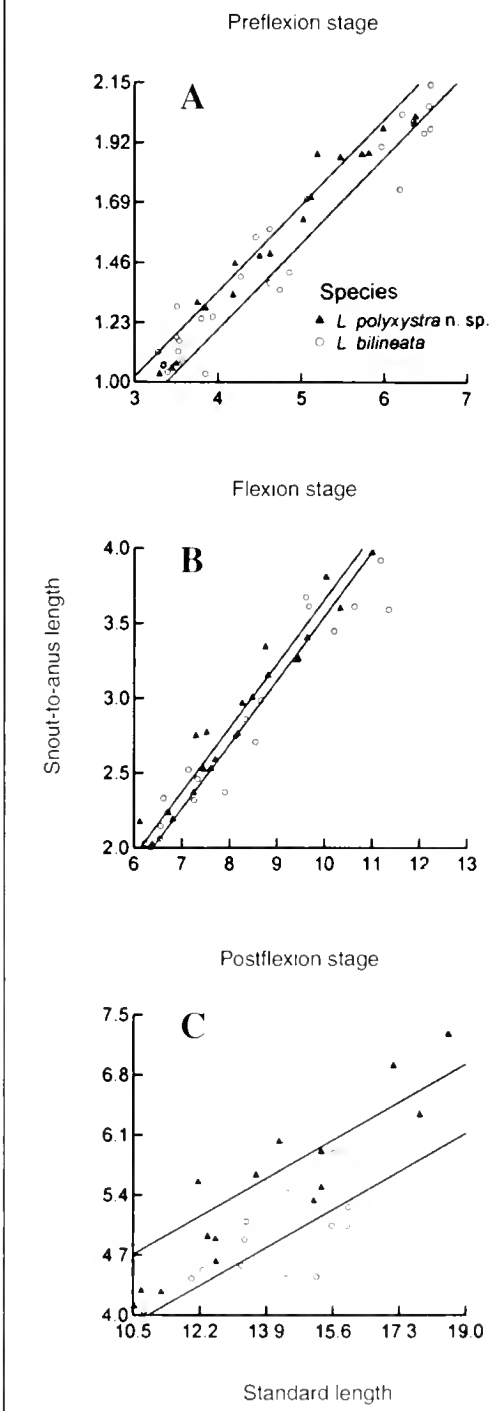

Figure 4

Comparison of snout-to-anus length versus standard length in developmental stages of *Lepidopsetta bilineata* (open circle) and *L. polyxystra* n. sp. (triangle). The lines represent a linear regression with both species having similar slopes. **(A)** preflexion, **(B)** flexion, **(C)** postflexion.

Table 11

P-values for ANCOVA of larvae of *Lepidopsetta bilineata* and *L. polyxystra* n. sp. Bold values indicate that the species are different from each other at the 0.05 significance level.

	Stage of development			
Character	Yolksac	Preflexion	Flexion	Postflexion
Snout-to-anus length	NS	***P*=0.001**	***P*=0.035**	***P*<0.001**
Body depth	***P*=0.001**	NS	***P*=0.037**	***P*<0.001**
Head length	NS	NS	NS	***P*=0.001**
Snout length	NS	NS	NS	NS
Orbit length	NS	***P*=0.020**	NS	***P*<0.001**

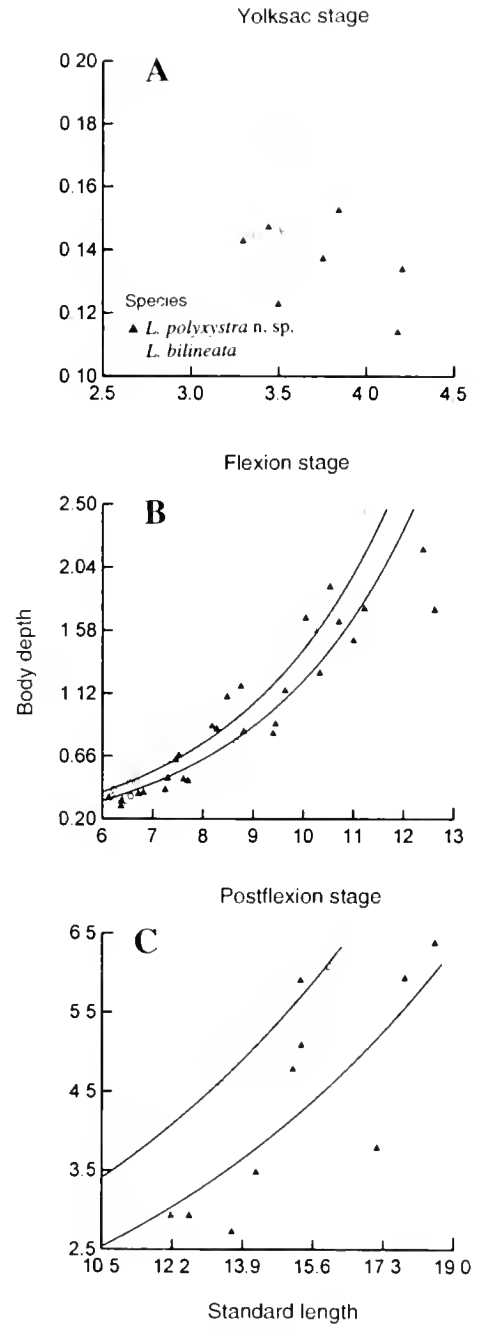

Figure 5

Comparison of body depth versus standard length in developmental stages of *Lepidopsetta bilineata* (open circle) and *L. polyxystra* n. sp. (triangle). The lines represent a nonlinear relationship between body depth and standard length: **(A)** yolksac (no relationship between body depth and standard length), **(B)** flexion, **(C)** postflexion.

dorsal eye length 17.9–32.9% HL; ventral eye approximately equal in length to ventral orbit, length 17.2–35.4% HL; interorbital with up to 5 scales (often lost in preserved material), width 1.3–6.6% HL; cheek with 7–16 scales, length 26.7–65.9% HL, depth 13.6–33.6% HL; preopercular pores 5–13; ocular-side suborbital pores 13–38; blind-side suborbital pores 6–20; lateral line with a high arch, 6–8 scale rows high over the pectoral fin, arch length about three times its depth, length 26.1–69.9% HL, lateral line pores 70–119; anterior supratemporal short, pores 2–15; posterior supratemporal branch moderately elongate, pores 6–35; supraorbital canal short or long, pores 1–9; pectoral fins with 8–13 rays, dorsal 2–3, and ventralmost simple and all others branched, ocular-side pectoral fin longer than blind-side pectoral fin, length 10.7–18.2% SL (38.3–70.4% HL), blind-side pectoral fin about equal in length to pelvic fins, length 6.6–12.7% SL (23.2–49.6% HL); pelvic fins with 6 branched rays, ocular-side pelvic-fin length about equal to blind-side pelvic-fin length, 7.4–12.5% SL (26.7–45.9% HL); dorsal-fin origin over anterior portion of dorsal orbit, dorsal fin with 64–89 simple soft rays, smallest rays anterior and posterior, longest rays at midbody, height 10.2–16.6% SL; dorsal-fin pterygiophores 68–78 in specimens with 64–83 dorsal-fin rays, 8–11 anterior to first neural spine, the first bifurcate and supporting two rays; anal fin with 49–77 simple soft rays in specimens with 54–63 anal-fin rays supported by 53–63 pterygiophores, fin about equal in height to dorsal fin; anal-fin rays 1 and 2 supported by greatly expanded anterior pterygiophore, sharp point of which often projects through skin between anal-fin origin and anus; caudal peduncle length 7.0–10.9% SL (25.5–42.2% HL); least caudal peduncle depth 8.2–14.0% SL (29.6–50.3% HL; 90.0–172.0% caudal peduncle length); greatest caudal peduncle depth 10.1–16.9% SL (37.2–57.7% HL); caudal fin truncate to rounded, with 18–19 rays, total of 8–10 both dorsally and ventrally, five on each of complex hypurals 1+2 and 3+4, 3 on hypural 5, one on the epural or preural 2 neural spine, and four on the parhypural, length 15.3–29.1% SL; vertebrae 39–42, 11 precaudal and 28–31 caudal, neural spines 1–3 and haemal spines 1–4 anteroposteriorly expanded, epineurals present on vertebrae 2–11, ribs present on vertebrae 3–11. Meristics are summarized in Tables 3–7.

Table 12

Summary of selected larval characters helpful in distinguishing eastern North Pacific pleuronectid larvae during preflexion and early flexion stages (Matarese et al., 1989, in part). Characters are presented for taxa where at least some early life-history stages are known. Only general trends are presented because pigment may vary among specimens. When specimens were not available, subjective decisions were based on previously published material. PVM = postventral melanophores.

	Pigment characters							
Genus	Postanal bars	Hypaxial	PVM	Notochord tip	Dorsal finfold	Anal finfold	Head spines	Total myomeres
Embassichthys	3	Absent	Absent	Present	Present	Present	Absent	57–65
Eopsetta	3	Absent	Absent	Present	Absent	Absent	Preopercular	41–45
Glyptocephalus	4	Absent	Absent	Present	Present/ absent	Present/ absent	Preopercular	52–66
Hippoglossoides	3–4	Present	Absent	Present	Present	Present	Absent	44–51
Isopsetta	3	Absent	Absent	Present	Absent	Present	Absent	41–42
Lepidopsetta	1–3	Absent	Present	Present	Present	Present	Absent	37–44
Microstomus	3–4	Absent	Absent	Present	Present	Present	Otic	50–55
Psettichtys	1	Absent	Absent	Present	Present	Present	Absent	38–41
Acanthopsetta	Absent	Present	Present	Present	Absent	Absent	Absent	39–40
Atheresethes	Absent	Absent	Absent	Present/ absent	Absent	Absent	Preopercular/ supraocular crest	47–50
Hippoglossus	Absent	Present	Absent	Present	Present	Present	Absent	49–51
Limanda	Absent	Present	Present	Absent	Absent	Present	Absent	40–41
Liopsetto	Absent	Absent	Absent	Present	Absent	Absent	Absent	37–41
Lyopsetta	Absent	Present	Absent	Present	Present	Present	Absent	43–47
Parophrys	Absent	Present	Present	Present	Absent	Present	Absent	42–47
Platichthys	Absent	Absent	Present	Present	Present	Present	Absent	35–38
Pleuronectes	Absent	Absent	Present	Absent	Absent	Present	Absent	41–42
Pleuronichthys	Absent	Absent	Absent	Present	Present	Present	Absent/otic	38–41
Reinhardtius	Absent	Present	Absent	Present	Present	Present	Absent	61–64

Ocular-side scales ctenoid, often tuberculate, especially on anterior portion of the body around the head and pectoral girdle; tubercules columnar, narrow from base to tip, up to 10 tubercules on scales of head, fewer on tuberculate body scales; blind-side scales nearly always cycloid except in ambicolored specimens, never tuberculate, posterior scales occasionally with central cteni along lateral midline; broad, flaplike urogenital pore on ocular side, dorsal to anus; anus just anterior to anal-fin origin; color of ocular side varies with substrate, in life olivaceous greenish brown with various blotches of dark brown and spots of light areas scattered over body, brown streaks in dorsal, anal, and caudal fins, often with a series of four to five large light spots at base of dorsal fin and four similar spots at base of anal fin; in preservation ocular side yellowish brown with blotches; blind side bright white to cream in life, cream to yellowish in preservation. Moderate sized pleuronectids, reaching a standard length of 600 mm (Hart, 1973).

Description of larvae

Snout-to-anus length remaining constant during development, length 32.1–39.3% SL; preflexion body slender, body depth increasing with development, sharply after flexion, from a depth of 3.8 to 35.7% SL; finfolds of moderate size; head length increasing with development, sharply after flexion, from a length of 11.6 to 29.3% SL; snout length remaining constant during development, length 20.5–24.7% HL; orbit length decreasing with development, from 51.9 to 20.9% HL.

Size at stage of development variable among species (Table 13). Larvae hatching at less than 3.0–4.45 mm; yolk absorbed by 2.7–4.5 mm. Preflexion larvae ranging in size from 3.8 to 6.6 mm; flexion larvae between 6.4 and 11.1 mm; postflexion larvae between 10.8 and 18.6 mm. Transformation occurring at sizes as small as 10.0 mm; juvenile stage usually attained by 35.0 mm (Table 13).

Preanal pigment present initially along lower jaw, increasing posteriorly with development. Pigment occurring ventrally along gut and dorsally on anus; by flexion a distinct patch of melanophores occurring along the posterior edge of the gut, with pigment increasing laterally with development. Pigment may be present or absent on pectoral-fin rays and base.

Postanal pigment in preflexion larvae may be present as melanophores along distal edges of dorsal and anal finfolds, but typically with isolated patches along finfolds and pigment spots or patches along distal edges of anal finfold; when present, two to four distinct pigment regions along

Table 13

Length at stage of development for species of *Lepidopsetta* (mm SL). For a more complete explanation of each developmental stage, see Kendall et al. (1984).

Stage	*L. bilineata*	*L. mochigarei*	*L. polyxystra* n. sp.
Egg	~1.0	0.90	~1.0
Hatch	<3.0	3.95–4.48	>3.0
Yolk absorption	2.7–4.5	unknown	3.3–4.2
Preflexion	3.8–6.6	unknown	4.2–6.2
Flexion	6.4–11.1	~8.9–10.6	6.2–12.6
Postflexion	10.8–16.0	unknown	12.2–18.6
Transformation	as small as 10.0	as small as 15.3	as small as 15.0
Early juvenile	complete as small as 13.0 (13.0–33.9)	unknown	complete as small as 26.0
Postsettlement juvenile	<35.0	unknown	>35.0

dorsal midline; a series of melanophores present from the gut along the ventral midline posterior to anus to just posterior to ventral stripe of posteriormost bar; a few melanophores on the caudal peduncle and above and below the notochord tip.

Distribution

The genus is endemic to the North Pacific and is widespread on the continental shelf (Figs. 6–13). Its range extends from Yongil Bay, Korea, in the southern Sea of Japan and along the northern coasts of Japan, north through the Sea of Okhotsk and the Bering Sea, the most northerly record being from the Gulf of Anadyr and the vicinity of St. Lawrence Island. It is recorded from the Aleutian Islands and into the eastern North Pacific throughout the Gulf of Alaska, south into Puget Sound and along the west coast of Washington, Oregon, California, and Mexico. Its most southerly record in the eastern Pacific is from the Cortez Banks of Baja California, Mexico.

Larvae of the eastern North Pacific species range from the Bering Sea and Aleutian Islands along the Pacific coast to Baja California (Figs. 12-13). Both species co-occur in the eastern Aleutian Islands to the Washington coast; only larvae of *L. polyxystra* n. sp. have been routinely collected from the Bering Sea and only larvae of *L. bilineata* have been collected from California and south in California Cooperative Oceanic Fisheries Investigations (CalCOFI) samples. A subset of larvae collected by AFSC surveys in the Gulf of Alaska and Bering Sea was examined to compare differences in temporal distribution and mean density (number/10 m^2; Appendix Table 1). During the 22-year sampling period, larvae of *L. polyxystra* n. sp. appear first in our March collections (Table 14), whereas larvae of *L. bilineata* first appear in April. The largest catches of *L. polyxystra* n. sp. occurred in May, whereas the largest catches of *L. bilineata* occurred in June. Overall, in the subset of cruises from 1972 to 1994 considered in our study, *L. polyxystra* n. sp. were more abundant and mean density was higher (5.34/10 m^2) than that of *L. bilineata* (0.414/10 m^2).

Habitat

Species of the continental shelf were collected over sand and gravel, commonly at depths of 200 m and less, to as deep as 575 m (Allen and Smith, 1988). For eastern North Pacific species, highest densities of larvae were found over depths of less than 500 m, although they were also collected over deeper water.

Life history

Described eggs of *Lepidopsetta* are demersal, off-round, and have a sticky chorion, causing them to adhere to each other or to a substrate, and range in size from 0.86 to 1.08 mm in diameter (Yusa, 1958; Pertseva-Ostroumova, 1961; Penttila, 1995). The reproductive season extends from winter to early summer, generally earlier in southern species, and spawning occurs at depths of less than 220 m. All sexually mature *Lepidopsetta* apparently migrate from shallow shelf areas in the fall to deeper upper slope waters during winter and migrate back into shallower shelf waters during spring and summer. Immature *Lepidopsetta* remain in shallow waters throughout the winter and migrate into shallower coastal waters in the spring and summer.

Garrison and Miller (1982) provided a summary of reproductive characteristics of *Lepidopsetta* from the western and eastern Pacific Ocean, which included *L. bilineata* and *L. polyxystra* n. sp. Blackburn (1973) described the ichthyoplankton from Skagit Bay, Washington, located in the northernmost region of Puget Sound and included descriptions and illustrations of larvae of *Lepidopsetta*. The Washington Department of Fisheries (WDF) has reported eggs of *Lepidopsetta* (*L. bilineata* or *L. polyxystra* n. sp., or both) from late December through early March in sandy gravel of upper intertidal beaches in several sites in central and

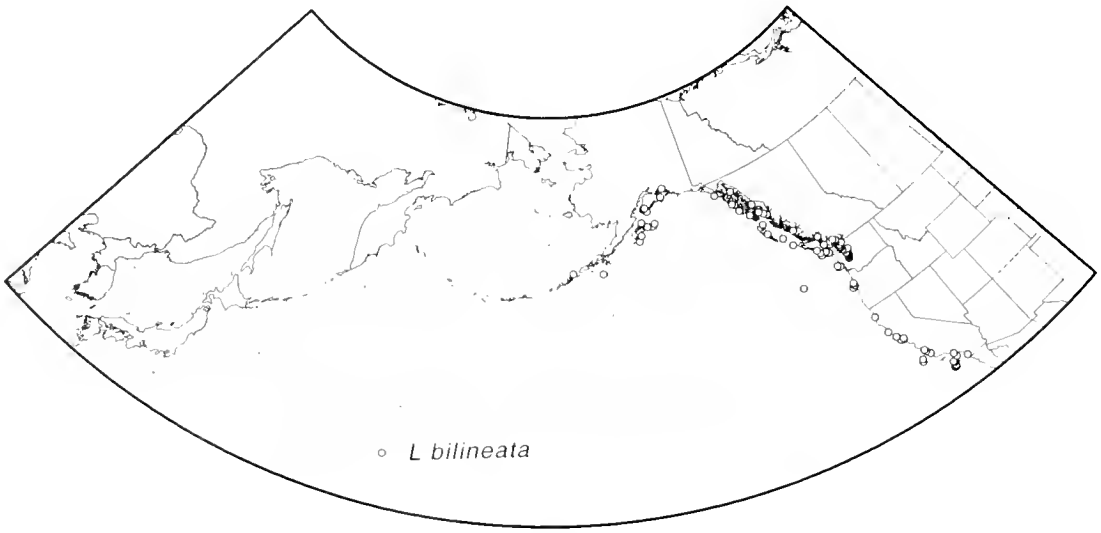

Figure 6

Distribution of adults of *Lepidopsetta bilineata* based on material examined. Each symbol may represent more than one capture.

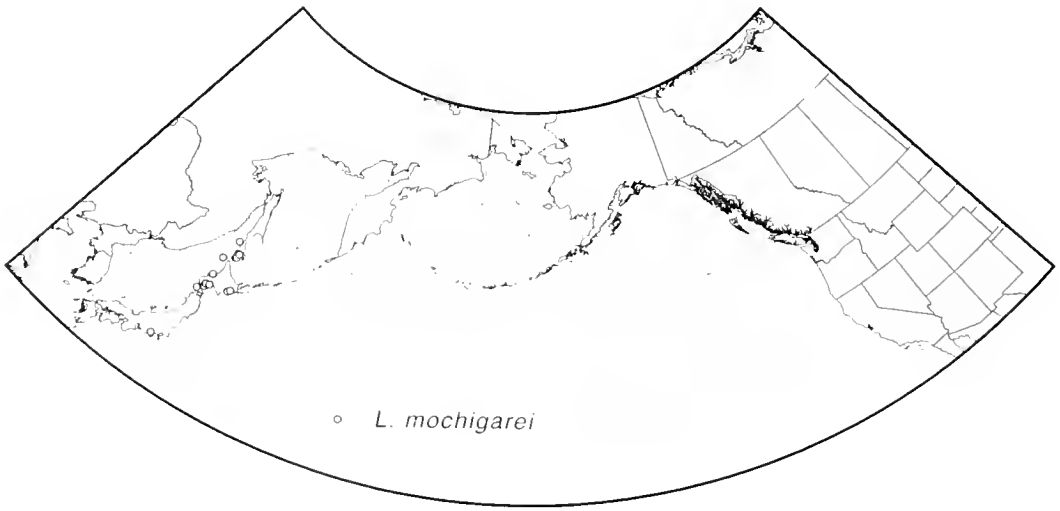

Figure 7

Distribution of adults of *Lepidopsetta mochigarei* based on material examined. Each symbol may represent more than one capture.

southern Puget Sound (Penttila, 1995). These eggs were described as demersal and adhesive ("clinging to upper beach surface material," p. 238). Eggs were collected at the same times and location as those of surf smelt (*Hypomesus pretiosus*) and Pacific sand lance (*Ammodytes hexapterus*).

Etymology

The name *Lepidopsetta* is derived from the Greek *lepido* meaning "scaled," a probable reference to the strongly ctenoid scales found on the ocular side of most individuals, and *psetta*, meaning "flatfish".

Comments

Sakamoto (1984a) synonymized *Lepidopsetta* (as well as five other pleuronectid genera: *Limanda*, *Parophrys*, *Isopsetta*, *Pseudopleuronectes*, and *Liopsetta*) with *Pleuronectes*, based on a phenetic analysis of detailed morphological data. Several recent authors have criticized Sakamoto's (1984a) phylogenetic techniques (Chapleau [1993]; Rass

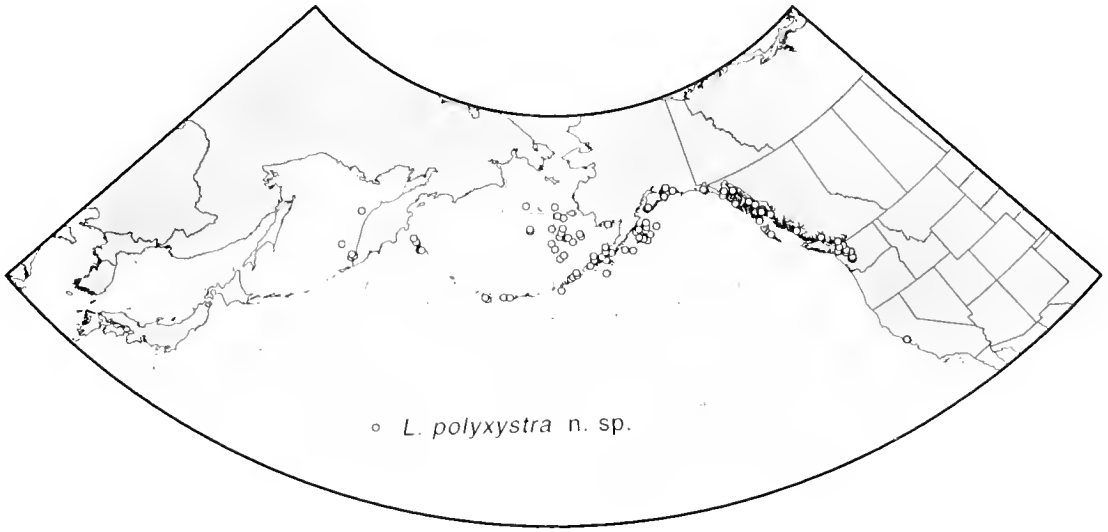

Figure 8

Distribution of adults of *Lepidopsetta polyxystra* n. sp. based on material examined. Each symbol may represent more than one capture.

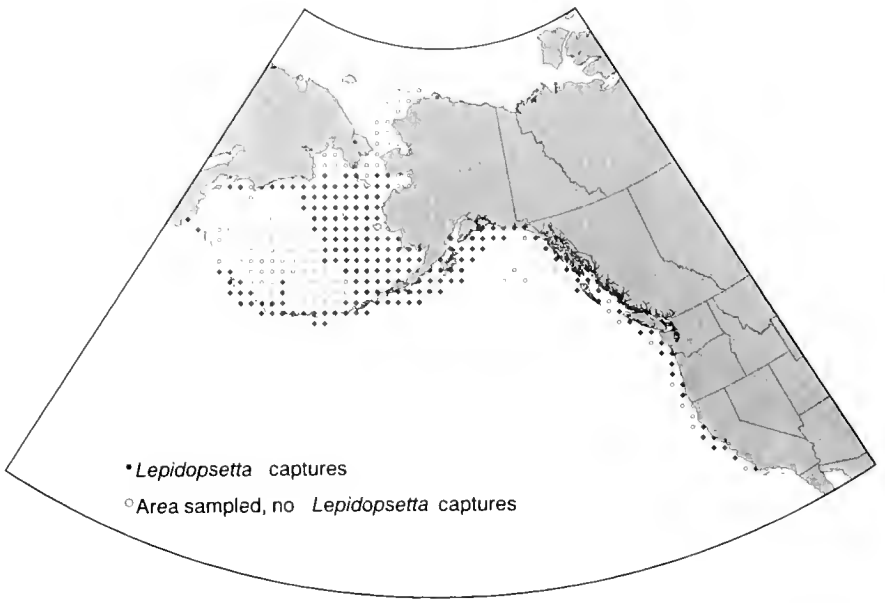

Figure 9

Records of *Lepidopsetta* from the National Marine Fisheries Service, Alaska Fisheries Science Center, Resource Assessment and Conservation Engineering survey database 1948–1997.

[1996]; Berendzen, [1998]; Cooper and Chapleau [1998]) and have refuted the monophyly of *Pleuronectes sensu* Sakamoto (Rass [1996]; Cooper and Chapleau [1998]). Cooper and Chapleau (1998) recently conducted a cladistic analysis and resurrected these genera from synonymy with *Pleuronectes*. We follow the consensus among most current scientists (Nelson, 1994; Cooper and Chapleau, 1996, 1998; Rass, 1996) and recognize each of these genera as distinct.[4]

[4] We do not recognize two other generic nomenclatural changes recommended by Cooper and Chapleau (1998) and have chosen to retain *Embassichthys* and *Atheresthes* as separate genera, distinct from *Microstomus* and *Reinhardtius*, respectively.

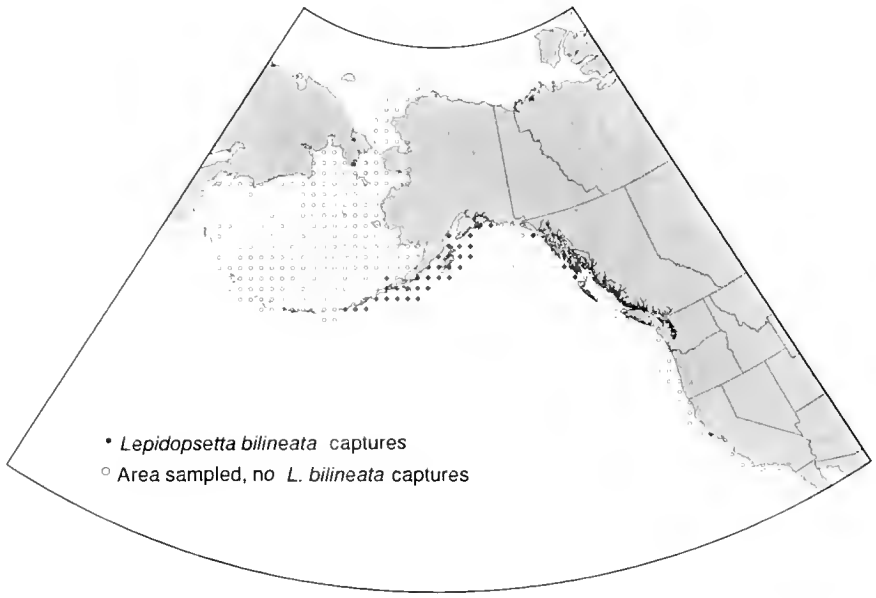

Figure 10

Records of *Lepidopsetta bilineata* from the National Marine Fisheries Service, Alaska Fisheries Science Center, Resource Assessment and Conservation Engineering survey database, 1995–1998.

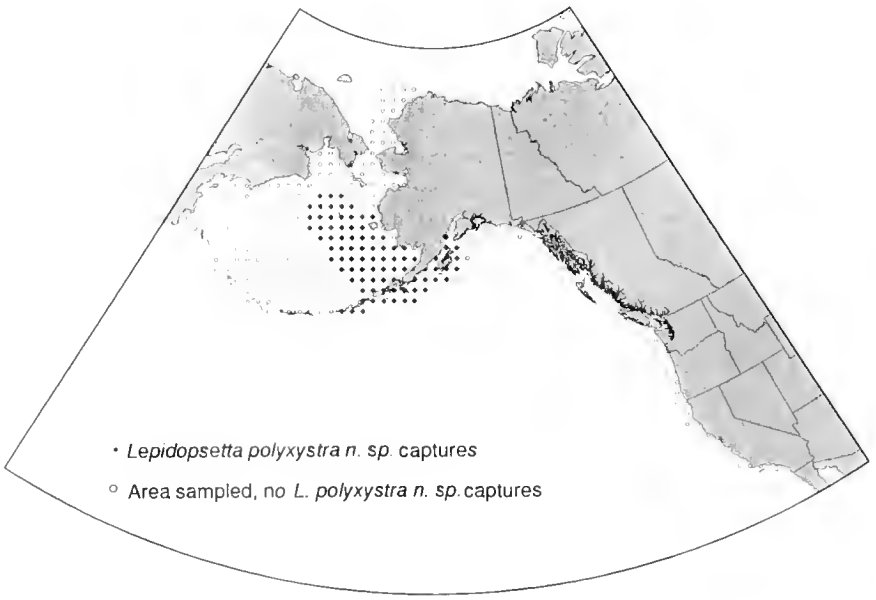

Figure 11

Records of *Lepidopsetta polyxystra* n. sp. from the National Marine Fisheries Service, Alaska Fisheries Science Center, Resource Assessment and Conservation Engineering survey database, 1995–1998.

Supraorbital pores have not been reported in other flatfishes. The supraorbital canal is an extension of a nerve branch arising from between the frontals at the posterior rim of the dorsal orbit. In *Lepidopsetta* the pores of the canal are supported by a series of 1–6 bones (Fig. 14), similar in size and shape to the suborbitals. Typically each bone shares in the support of one or two pores.

Among other North Pacific pleuronectids examined, *Parophrys vetulus*[5] has 6–11 pores and *Isopsetta isolepis* 2–12 pores, whereas *Limanda aspera* and *L. punctatissimus*,

Figure 12

Distribution of larvae of *Lepidopsetta bilineata* based on material examined. Each symbol may represent more than one capture. Sampling effort by the National Marine Fisheries Service, Alaska Fisheries Science Center, was limited in regions between Kodiak and Vancouver Islands; other data are not available from alternate sources.

Figure 13

Distribution of larvae of *Lepidopsetta polyxystra* n. sp. based on material examined. Each symbol may represent more than one capture. Sampling effort by the National Marine Fisheries Service, Alaska Fisheries Science Center, was limited in regions between Kodiak and Vancouver Islands; other data are not available from alternate sources.

[5] Cooper and Chapleau (1998) changed the specific epithet of *Parophrys vetulus* to *vetula* to agree in gender with *Parophrys*. However, because Girard's (1854) original description did not specify his treatment of *vetulus* and because it may also be treated as a noun in apposition, we consider this change an incorrect subsequent spelling and retain *P. vetulus*.

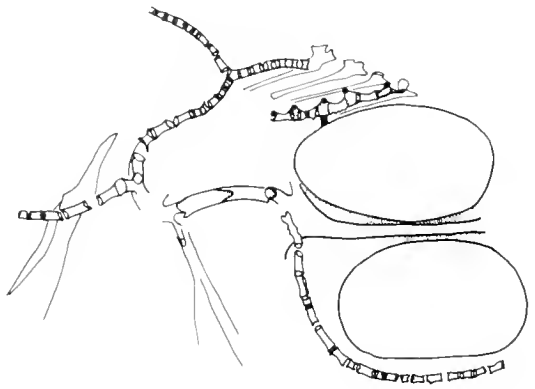

Figure 14

Supporting elements of the pores of the supraorbital canal of *Lepidopsetta bilineata*, UW 025197, 77.3 mm, Puget Sound, WA. View of dorsal (right lateral) side. Scale bar equals 5 mm.

Psettichthys melanostictus, and *Inopsetta ischyra* (a possible hybrid of *Platichthys stellatus* and *Parophrys vetulus*) have a single pore. In *Hippoglossoides elassodon* and *H. robustus*, a series of pores is found at the anterior extension of the supratemporal line, as depicted by Lindberg and Fedorov (1993) for *H. elassodon* (their Fig. 33). These pores are apparently part of the anterior extension of the trunk lateral line, but ventrally the pores extend near the dorsal orbital rim. In one specimen of *H. elassodon* examined (UW 040271), the pores extended nearly the same length along the rim of the dorsal orbit as the length for the same pores in some *L. bilineata*.

Pleuronectid larvae are difficult to diagnose on the basis of a simple set of characters. Pleuronectids are oviparous and spawn planktonic or demersal eggs (about 0.66–4.5 mm), with homogenous yolk that is either pigmented or not, and usually contains no oil. Among eastern North Pacific pleuronectids, *Lepidopsetta* is the only genus that produces demersal eggs, which are off-round and have a sticky chorion that causes them to adhere to each other or to a substrate (Pertseva-Ostroumova, 1961; Penttila, 1995). Pleuronectid larvae hatch between 1.7 and 16.0 mm; yolksac and preflexion larvae are slender, becoming deeper-bodied during the postflexion stage. Larvae of *Lepidopsetta* hatch at <3.0–4.5 mm; preflexion larvae are slender and have moderate-size finfolds.

Larval pigmentation (including finfold) varies considerably in pleuronectids. A combination of pigment pattern (postanal bands, bars, and finfold), meristic characters, and size at development is needed for identification (Matarese et al., 1989; Charter and Moser, 1996). Larvae with special characters (e.g. *Atheresthes* larvae with head spines) or high myomere counts (e.g. *Embassichthys*) are easily distinguished. Other pleuronectid larvae are usually distinguished by a combination of pigmentation characters including the number of postanal bands and bars and finfold pattern (Table 12).

No single early life history character distinguishes larvae of *Lepidopsetta* from other pleuronectid genera. Depending on developmental stage, larvae of *Lepidopsetta* generally are categorized by the presence of at least one postanal bar (Table 12). Larvae of *L. bilineata* have a postanal pigment pattern with four dorsal pigment patches (the posteriormost aligning with a ventral patch forming a caudal bar), larvae of *L. mochigarei* have three dorsal patches (the posteriormost aligns with a ventral pigment patch approximating a caudal bar), whereas larvae of *L. polyxystra* n. sp. have two dorsal pigment patches (the posteriormost aligns with a ventral pigment patch forming a bar located at about 2/3 of body length). Among other pleuronectid genera that have a postanal band and bar pattern, preflexion and early flexion larvae of *Lepidopsetta* may be distinguished by the presence of a series of postanal ventral midline melanophores and fewer pigment spots along the notochord tip (Table 12).

In general, larvae of *L. bilineata* closely resemble those of *Psettichthys* among other genera (Table 12). Both have alternating patches of pigment on dorsal and ventral body margins, although *Psettichthys* has a series of small patches on the dorsal and ventral finfold margins whereas *L. bilineata* has isolated patches along the finfolds. A series of postanal ventral melanophores is present in *L. bilineata* and absent in *Psettichthys*, in which postanal pigment is usually restricted to three or four large spots. Larvae of *L. bilineata* generally have much less pigment on the jaws and isthmus than do larvae of *Psettichtys*.

Size at stage of development varies among species (Table 13). Larvae of *L. bilineata* begin transformation at smaller lengths than larvae of *L. polyxystra* n. sp. or *L. mochigarei*. Larvae of *L. bilincata* also have a larger orbit, shorter snout-to-anus length, and a slenderer body (see Table 2).

The juvenile stages of most eastern North Pacific pleuronectids are poorly known. Traditional early life history descriptions typically describe developmental stages on the basis of eggs and larvae captured in plankton nets and usually do not include transitional larvae that undergo changes associated with a benthic existence. Plankton surveys routinely use nets that do not effectively sample bottom waters where many pleuronectid juveniles eventually settle.

Pleuronectid juveniles can be separated by several characters. Perhaps the most important character is the size at which transformation occurs, although data are scarce on when transformation is completed. Among taxa for which data are available, eastern North Pacific pleuronectids can be grouped into three categories based on approximate transformation sizes: <15 mm SL, 15–30 mm SL, and >30 mm SL. Genera with at least one species transforming at sizes <15 mm SL include *Limanda*, *Platichthys*, *Pleuronectes*, and *Pleuronichthys* (*sensu* Cooper and Chapleau, 1998). Genera with larvae that transform at much larger sizes (>30 mm SL) include *Atheresthes*, *Embassichthys*, *Glyptocephalus*, *Hippoglossoides*, *Microstomus*, and *Reinhardtius*. Larvae of *Lepidopsetta* generally undergo transformation between 15 and 25 mm SL. Other eastern North

Pacific pleuronectids that undergo transformation at similar sizes include *Acanthopsetta*, *Eopsetta*, *Hippoglossus*, *Isopsetta*, *Lyopsetta*, *Parophrys*, and *Psettichthys*.

Characters that separate juveniles further include meristics of vertebrae, median fin elements, and gill rakers (although gill rakers may not be fully formed); mouth size; and the shape of the lateral line. Generally juveniles of *Lepidopsetta* have lower meristics than juveniles of *Atheresethes*, *Eopsetta*, *Hippoglosssoides*, and *Hippoglossus*. Juveniles of *Lepidopsetta* develop the highly arched lateral line during this stage (15–25 mm SL). A combination of mouth size, residual larval pigment on the blind side of early juveniles, lateral line shape, and, in larger juveniles, number of gill rakers may help to separate other similar-looking eastern North Pacific pleuronectids (*Acanthopsetta*, *Isopsetta*, *Lyopsetta*, *Parophrys*, and *Psettichthys*).

Identification of early life history stages of *Lepidopsetta* has been confused in the literature for many years. Hickman (1959) described egg and larval development of the sand sole, *Psettichthys melanostictus*, on the basis of material collected from Puget Sound, Washington. He illustrated six larvae identified as *Psettichthys* from specimens reared from eggs (his Figs. 1 and 2) and from larvae collected by net (his Figs. 3–6). His Figures 3 and 4 can be identified as *L. bilineata* from the alignment of dorsal and ventral midline melanophores on the postanal body.

In her extensive study of reproduction and development in North Pacific flatfishes, Pertseva-Ostroumova (1961) described the early life history stages of *L. bilineata* and *L. mochigarei*. The description of *L. bilineata* is based on material from collections off the Kuril Islands, off the eastern and western coasts of Kamchatka, and in the western Bering Sea. Larvae from these geographic areas are *L. polyxystra* n. sp.

Blackburn (1973) provided figures of two specimens of *L. bilineata* (his appendix Fig. C-2, A and B) in his survey of ichthyoplankton from Skagit Bay, Puget Sound. His discussion, however, is clearly based on the larvae of both eastern North Pacific species.

Garrison and Miller (1982) reviewed the reproductive characteristics of *L. bilineata*, but their sources either represent both species (Smith, 1936; Forrester, 1969; Forrester and Thompson, 1969) or *L. polyxystra* n. sp. alone (Shubnikov and Lisovenko, 1964; Shvetsov, 1979). Ahlstrom et al. (1984) correctly illustrated *Psettichthys* larvae but presented data and a figure for *L. bilineata* (their Fig. 351b) based on Figure 22 (4) of Pertseva-Ostroumova (1961), now identified as *L. polyxystra* n. sp. Okiyama (1988) also presented material for *L. bilineata*, based on Figure 23(1) of Pertseva-Ostroumova (1961), which therefore represents *L. polyxystra* n. sp.

Matarese et al. (1989) separated larvae of *Lepidopsetta* from *Psettichthys*. Their description and figures of *L. bilineata* are based on what we now refer to as *L. polyxystra* n. sp., whereas the descriptions and figures of "*Lepidopsetta* 2" are now referred to as *L. bilineata*. Charter and Moser (1996) presented figures of both *Psettichthys melanostictus* and *L. bilineata* but, because Pertseva-Ostroumova (1961) was cited as a source for *L. bilineata*, some descriptive data are suspect. Data for *L. bilineata*, particularly in the introductory tables, may be based in part on *L. polyxystra* n. sp. (see tables "Pleuronectidae," pages 1370–1373, Charter and Moser, 1996).

Key to juveniles and adults >30 mm of species of *Lepidopsetta*

1a Preopercular pores 8–13; lateral-line pores 95–119; sum of scales above and below lateral line 91–103; supraorbital pores 1–3; total gill rakers on first arches ≤10, on upper part of first arch ≤3 . ***L. mochigarei***
southern Sea of Okhotsk to Korea

1b Preopercular pores 5–7; lateral-line pores 70–91; sum of scales above and below lateral line 65–88; supraorbital pores 1–8; total gill rakers on first arch 6–14 **2**

2a Total gill rakers on first arch typically ≥10, on upper part of first arch ≥3; supraorbital pores 1–2, rarely 3–7; blind side creamy white . ***L. polyxystra* n. sp.**
Puget Sound to Sea of Okhotsk

2b Total gill rakers on first arch typically ≤10, on upper part of first arch ≤3; supraorbital pores 3–8; blind side with extensive bright white highlights. . . ***L. bilineata***
Baja California to southeastern Bering Sea

Lepidopsetta bilineata (Ayres, 1855a) Southern rock sole Figs. 1–6, 10, 12, 14–18; Tables 2–11, 13–14

Platessa bilineata Ayres, 1855a:2 (original description, one specimen, apparently lost, sex and size unknown, fish markets of San Francisco Bay, California).

Platichthys umbrosus Girard, 1856:136 (original description, one specimen, apparently lost, sex unknown, ca. 190 mm TL, Cape Flattery, Washington).

Pleuronectes perarcuatus Cope, 1873:32 (original description, one specimen; holotype, ANSP 8725, sex undetermined, 108 mm SL, Gulf of Alaska, "Sitka" or "Unalaska").

Lepidopsetta bilineata umbrosa (in part) Jordan and Evermann, 1898:2643 (new combination, "Puget Sound and northward").

Lepidopsetta bilineata bilineata Taranets, 1937:144 (new combination, keys).

Pleuronectes bilineata Sakamoto, 1984a:99 (new combination, phylogenetics).

Neotype

CAS 42650, 1(207.6 mm), Calif., Gulf of the Farallones, Sta. F43(2)N, M. Moriguchi, August–September 1978.

Other material examined

A total of 380 adult and juvenile specimens, 22.7–426 mm, including the neotype listed above, was examined. Sixty-four larvae were examined.

Adults Bering Sea: UW 041696, 3(222–245 mm), N of Unimak I., 55.0213°N, 164.6009°W. Aleutian Islands: SIO 94-164, 1(167 mm) of 10(103–193 mm), Unimak Pass, 54°15.1'N, 165°57.6'W, 4 June 1994; UW 041695, 3(170-210), Aleutian Is., NE of Umnak I., 53.44°N, 168.4944°W; Gulf of Alaska: ABL uncat, 1(153 mm), Ursus Channel, San Fernando I., 1 November 1956; ABL 64-696, 1(138 mm), Gore Point, S of Kenai Peninsula, 28 July 1963; ABL 67-211, 4(197–234 mm), Auke Bay, 19.2 km NW of Juneau, 22 May 1962; ABL 71-5, 2(200.5–205.5 mm), Baranof I., Point Conclusion, 17 May 1971; OS 6447, 3(166.1–184.6 mm), 57°10'N, 151°40.5'W, 77 m, 20 September 1978; OS 2156, 1(75.0 mm), Revillagigedo I., Ward Cove, 26 July 1949; OS 2175, 1(102.4 mm), Revillagigedo I., Ward Cove, 26 August 1949; SIO 72-219, 1(251 mm), Lituya Bay, 9.3 km SW of Harbor Pt., 25 June 1961; SIO 72-258, 1(289 mm), Baranof I., Katlian Bay, 57°10'N, 135°20'W; SIO 72-225, 1(288 mm), 2°E of Kodiak I., 6 May 1962; SIO 76-300, 1(187.5 mm) of 28(145–280 mm), Kodiak shelf, 57°40'N, 150°37'W, 23 June 1976; SIO 69-478, 3(112–170 mm) of 7(51–195 mm), Afognak I., Kitoi Bay, NE of Kodiak I., 16–21 April 1968; UW 040267, 1(330 mm), off Kodiak; UW 044021, 1(255 mm), 55.8088°N, 158.7503°W, 67 m, 10 June 1996; USNM 054286, 1(358 mm), Ketchikan, Sta. TT2120, RV *Albatross*; USNM 130739, 1(252 mm), Prince William Sound, Macleod Harbor, 16 March 1941; UW 01666, 1(132 mm), Alexander Archipelago, off Wrangell I., 1 December 1931; UW 008376, 1(240 mm), Ketchikan, 23 September 1949; UW 040902, 1(182 mm), Prince William Sound, 1989; UW 008292, 1(162 mm), Southeast Alaska, 26–31 March 1950; UW 018837, 2(222.5–230.5 mm), 11.7 km NNW of Triangle I., 50°58.1'N, 129°4.9'W, 19 August 1960; UW 40264, 1(342 mm), 54.039°N, 165.8153°W; UW 27679, 23(20.5–57.4 mm), Prince William Sound; UW 044010, 1(240 mm), 59.4918°N, 151.6185°W, 41 m, 27 February 1996; UW 044028, 1(292 mm), 59.4885°N, 151.6062°W, 30 m, 27 February 1996; UW 044025, 2(210–285 mm), Kachemak Bay, 12 May 1996; UW 040268, 1(290 mm), Kodiak I.; UBC 65-525, 1(290 mm), off Baranof I.; UW 044013, 7(287–426 mm), 56.5°N, 153.5°W, R. Bonaduhr; UW 041801, 6(270–335 mm), 54°N, 160.74°W, British Columbia: UW 083483, 33.5 mm, off Vancouver Island, 48°39.5'N, 125°55.2'W, 19 September 1977. SIO 63-202, 1(247 mm), Strait of Georgia, Fraser R.; USNM 31993, 1(158.5 mm), Carter Bay, June 1882; UBC 53-85, 1(172 mm), Vancouver I.; UBC 53-50, 1(57.3 mm), Vancouver I.; UBC 53-68, 1(105 mm), Vancouver I.; UBC 53-50, 1(57.3 mm), Vancouver I., Departure Bay, 49.2167°N, 123.95°W; UBC 53-301, 7(101.5–177 mm), Vancouver I., Baynes Sound; UBC 53-245, 1(144.8 mm), Vancouver I., Burrard Inlet; UBC 55-281, 1(32.9 mm), Vancouver I., Departure Bay, 49.2167°N, 123.95°W; UBC 56-8, 1(220.5 mm); UBC 55-496, 3(217–235 mm), Point Gray, 3.2 km SE of North Arm of Fraser R.; UBC 56-519, 5(205–233 mm), Vancouver fish docks; UBC 61-393, 3(59–88 mm), Bute Inlet; UBC 61-484, 2(145–167 mm), Vancouver I., Burrard Inlet, 25 October 1961; UBC 61-609, 9(38.5–123 mm), Bute Inlet; UBC 61-232, 2(245 mm and one head only), Hecate Strait; UBC 60-416, 1(205 mm), Queen Charlotte Is., Gillat Arm; UBC 63-910, 1(148 mm), Howe Sound; UBC 63-732, 10(68–140 mm), off Keats I.; UW 044026, 1(306.5 mm), 48.57723°N, 124.7803°W, 25 August 1995; UW 044027, 2(293–308 mm), 48.74507°N, 125.9744°W, 28 August 1995; UBC 65-676, 6(44–142 mm), Graham I., McIntyre Bay; UBC 62-93, 6(80–142 mm), Nass Bay; UBC 61-686, 1(62.8 mm), S of Vargas I., 5 July 1934; UBC 61-621, 1(50.5 mm), Snake I., near Nanaimo, 8 May 1933; UBC 61-610, 2(139–142 mm), Work Channel, head of Trail Bay, 16 July 1951; UBC 61-674, 1(60 mm), Dean Channel, off Nescall Bay; UBC 62-94, 1(94 mm), Sydney Inlet; UBC 81-3, 1(201 mm), Vancouver I., Grappler Inlet; UBC 76-7, 1(135 mm), English Bay, 20 January 1962. Washington, Oregon, and California: USNM 054392, 1(292 mm), near Port Townsend, TT2838, RV *Albatross*; USNM 27299, 2(150-246 mm), Puget Sound, 1880; UW 041090, 2(196.0–196.5 mm), Agate Pass, 3 April 1950; UW 041089, 1(229 mm), Agate Pass, 3 April 1950; UW 6070, 7(61–133 mm), San Juan Islands, East Sound, 3 March 1937; UW 06134, 2(53–63.5 mm), N of Maury I., 4 December 1948; UW 014838, 2(65-68 mm), Golden Gardens Beach, 14–15 May 1952; UW 014380, 2(101–108 mm), near Hat I., 29 May 1936; UW 044011, 1(145 mm), San Juan Islands, East Sound, 18 February 1964; UW 017115, 1(178 mm), Port Orchard Channel, 2 February 1964; UW 015423, 1(169 mm), Shilshole Bay; UW 000782, 2(147–156.5 mm), Alki Point, 8 March 1930; UW 005522, 11(46.6–159.5 mm), Edmonds, 18 August 1947; UW 018663, 1(60.5 mm), San Juan Islands, East Sound, 11 December 1964; UW 040665, 2(54–58 mm), Port Townsend Bay, 5 January 1979; UW 040686, 6(114.3–167.3 mm), West Point, 3 October 1978; UW 025723, 4(52.1–230.5 mm), Port Townsend Bay, 5 December 1978–5 January 1979; UW 025721, 3(166–208 mm), Golden Gardens, 22 July 1981; UW 006109, 1(154.5 mm), Alki Point, 3 March 1939; UW 017840, 1(211 mm), S end of Port Susan, 6 May 1950; UW 025719, 12(103.2–164.5 mm), Murden Cove, 22 April 1980; UW 025727, 2(116.5–169.5 mm), West Point, 29 March 1979; UW 005135, 8(22.7–70.6 mm), Alki Point, 5 April 1938; UW 025197, 1(77.3 mm; cleared-and-stained), Meadow Point; UW 044006, 11(135–250.5 mm), Nisqually, 47.1578°N, 122.6693°W, 16 May 1996; UW 040269, 10(209–259 mm), Puget Sound, 47°19.48'N, 122°33.8'W, 10 May 1996; UW 029670, 49(125.3–283.5 mm), Colvos Passage off Vashon I., 47.5°N, 122.4167°W, 18 July 1949; UW 025726, 5(125–175 mm), Puget Sound, West Point, 3 October 1978; UW 025720, 7(130–185 mm), Puget Sound, West Point, 3 April 1979; UW 041319, 6(122–202 mm), Puget Sound, West Point; UW 041330, 1(225 mm), Puget Sound, Portage Bay; UW 041301, 1(245 mm), Puget Sound, Port Townsend Bay; OS 15509, 4(226.5–287.4 mm), Cobb Seamount, 46°50'N, 130°50'W, 20 August 1992; OS 13792, 1(180.3 mm), 44°54.2667'N, 124°10.0667'W; OS 13500, 1(417 mm), Cobb Seamount, 46°50'N, 130°50'W; OS 13499, 1(330 mm), 44°52.2667'N, 124°09.55'W; OS 7482, 1(223.3 mm), off Newport; OS 14732, 1(132.2 mm), 44°40.7'N, 124°09'W; OS 14690, 1(189.4 mm), 44°37'N, 124°11.1'W; OS 6208, 4(137.3–222.8 mm), off Newport, 30 September 1978; OS 7477, 1(173.7 mm), 44°37.4'N, 124°08.9'W; CAS 18553, 1(198.5 mm), Calif., San Francisco Bay, 14 May 1931; CAS 31832, 1(205 mm), Calif., Gulf of the Farallones, 37°44'N, 122°40'W, October 1973; CAS 40341, 1(347.4 mm), Calif., 22.6 km NW of Pt. Pinos, 34°47.5'N, 122°7.8167'W; CAS-SU 111615, 1(335.0 mm),

San Francisco Market, May 1895; CAS 49152, 1(229.5 mm), Calif., Sonoma, Bodega Bay, 18 October 1981; SIO 88-119, 1(277 mm), Calif., south of La Jolla; SIO H48-22, 1(261 mm), Calif., south of La Jolla; SIO 63-241, 1(243 mm), Tanner Bank, Calif., 32°42.5'N, 119°6.5'W, 17 May 1963; SIO 65-460, 1(284 mm), Calif., ridge between Tanner and Cortez Banks, 26 September 1965; SIO 65-6-64A, 1(210 mm), Calif., Tanner Bank, 32°42'N, 119°08'W, 15 January 1965; SIO 63-732-64A, 1(183 mm), Calif., Catalina I., off Avalon, 22 March 1962; SIO 85-145, 2(74–86 mm), Calif., Navarro Head, 39°05.7'N, 123°E44.95'W, 60.4–110.5 m, 17 August 1985; LACM W54-382, 7(178.5–247 mm), 1.6 km W of Santa Barbara I., 33°08.15'N, 119°04.1333'W, 31 October 1954; LACM W66-67, 1(198.5 mm), off San Simeon Point, 13 November 1966; LACM W54-380, 2(274–275 mm), 1.6 km E of Santa Barbara I., 30 October 1954; LACM 44390-1, 1(282 mm), off Palos Verdes, 22 February 1988; LACM 31966-8, 8(176.5–357 mm), Humboldt Co., 8 km S of Shelter Cove, 7 August 1971; LACM 241, 4(153–320 mm), Calif., San Francisco; OS 972, 1(201.2 mm), southern Calif.; LACM 35690-3, 2(83–164.5 mm), Calif., S end of Tanner Bank; UW 044009, 9(143–252.5 mm), 37.781°N, 122.9288°W, 26 June 1995; UW 040262, 1(250 mm), 48.74317°N, 125.7785°W, 27 September 1992; UW 041698, 1(223 mm), 35.0935°N, 120.7774°W, 15 June 1995; UW 041803, 1(358 mm), 47.0839°N, 124.748°W, 8 August 1995; UW 041802, 1(376 mm), 46.91147°N, 124.7292°W, 3 August 1995; UW 041903, 2(290–347 mm), 46.91308°N, 124.4756°W, 5 August 1995; Mexico: CAS 2484, 1(226.3 mm), Baja California, off Cortez Banks, 21 August 1932.

Larvae 64 specimens (2.7–19.0 mm) examined: Western Gulf of Alaska: UW 083400, 2(10.8–12.3 mm), 54°10.8'N, 165°24.3'W, 0–55 m depth, Methot net, 30 July 1991; UW 083401, 1(10.9 mm), 54°38.5'N, 160°51.2'W, 0–98 m depth, Methot net, 30 July 1991; UW 083402, 1(12.0 mm), 56°11.6'N, 157°21.7'W, 0–129 m depth, Methot net, 27 July 1991; UW 083403, 1(14.0 mm), 54°36.2'N, 162°16.2'W, 0–87 m depth, Methot net, 30 July 1991; UW 083404, 1(14.1 mm), 55°43.8'N, 157°34.6'W, 0–105 m depth, Methot net, 27 July 1991; UW 083405, 2(14.4–15.6 mm), 55°43.0'N, 159°49.4'W, 0–108 m depth, Methot net, 25 July 1991; UW 083406, 1(15.5 mm), 53°59.8'N, 165°51.0'W, 0–50 m depth, Methot net, 31 July 1991; UW 083407, 2(15.9–16.0 mm), 55°18.0'N, 160°11.4'W, 0–115 m depth, Methot net, 24 July 1991; UW 083408, 1(16.0 mm), 55°17.7'N, 160°11.7'W, 0–115 m depth, Methot net, 24 July 1991; UW 083445 1(13.3 mm), 56°11.6'N, 158°03.6'W, 0–141 m depth, Methot net, 25 July 1991; UW 072255, 5 of 6(2.7–8.6 mm), 57°01.1'N, 156°19.2'W, 0–95 m depth, bongo net, 3 June 1990; UW 072453, 2 of 4(6.2–6.5 mm), 57°17.2'N, 155°27.6'W, 0–102 m depth, bongo net, 5 June 1990; UW 072126, 2(6.6–7.3 mm), 56°54.0'N, 156°29.5'W, 0–84 m depth, bongo net, 3 June 1990; UW 071455, 1(6.7 mm), 57°60.0'N, 153°59.3'W, 0–103 m depth, bongo net, 28 May 1990; UW 072087, 1(8.1 mm), 56°39.8'N, 156°20.0'W, 0–102 m depth, bongo net, 3 June 1990; UW 072264, 1(8.7 mm), 57°09.1'N, 156°09.1'W, 0–100 m depth, bongo net, 3 June 1990; Gulf of Alaska: UW 083484, 1(19.0 mm), 59°37.8'N, 151°44.2'W, 34 m depth, 17 July 1996; UW 083409, 1(16.4 mm), 58°19.5'N, 150°53.0'W, 64 m depth, bongo net, 22 July 1977; UW 083410, 1(6.3 mm), 57°61.1'N, 151°17.4'W, 0–35 m depth, Tucker net, 26 June 1978; UW 083411, 1(9.7 mm), 56°42.3'N, 153°33.4'W, 28–70 m depth, Tucker net, 28 June 1978; UW 083412, 1(11.0 mm), 57°00.8'N, 153°28.3'W, 0 m depth, neuston net, 14 September 1978; UW 083413, 2(5.1–6.2 mm), 57°10.7'N, 156°01.3'W, 0–100 m depth, Tucker net, 4 June 1988; UW 083414, 1 (6.6 mm), 56°21.0'N, 157°03.8'W, 0–100 m depth, Tucker net, 6 June 1988; UW 083415, 1(6.4 mm), 56°47.3'N, 155°26.0'W, 0–105 m depth, Tucker net, 23 May 1988; UW 083416, 1(6.5 mm), 57°03.8'N, 156°01.8'W, 0–101 m depth, Tucker net, 4 June 1988; UW 083417, 1(6.6 mm), 56°47.3'N, 155°25.9'W, 0–101 m depth, Tucker net, 4 June 1988; UW 083418, 1(7.1 mm), 57°10.8'N, 156°29.9'W, 0–102 m depth, Tucker net, 4 June 1988; UW 083419, 1(8.3 mm), 56°38.9'N, 156°31.5'W, 0–101 m depth, Tucker net, 2 June 1988; UW 083420, 1(10.2 mm), 56°46.7'N, 156°18.3'W, 0–91 m depth, Tucker net, 2 June 1988; UW 083421, 1(10.6 mm), 57°15.0'N, 155°53.6'W, 0–101 m depth, Tucker net, 4 June 1988; UW 083422, 3(3.3–3.4 mm), 57°55.6'N, 151°02.3'W, 0–76 m depth, bongo net, 13 May 1991; UW 083423, 1(3.9 mm), 5°43.8'N, 154°02.1'W, 0–100 m depth, bongo net, 24 May 1991; UW 083424, 1(4.7 mm), 55°53.9'N, 155°59.8'W, 0–75 m depth, bongo net, 23 May 1991; UW 083425, 1(4.9 mm), 57°36.9'N, 155°28.3'W, 0–101 m depth, bongo net, 24 May 1991; UW 083426, 1(3.6 mm), 56°40.7'N, 155°10.7'W, 0–61 m depth, bongo net, 8 May 1992; UW 083427, 1(6.0 mm), 56°58.4'N, 156°06.2'W, 0–100 m depth, bongo net, 14 May 1992; UW 083428, 2(3.5–4.3 mm), 55°27.2'N, 157°39.3'W, 0–88 m depth, bongo net, 19 May 1992; UW 083429, 1(3.8 mm), 55°17.0'N, 157°44.8'W, 0–72 m depth, bongo net, 19 May 1992; UW 083430, 1(4.6 mm), 55°22.5'N, 156°56.8'W, 0–80 m depth, bongo net, 19 May 1992; UW 083431, 1(7.9 mm), 55°16.0'N, 156°15.0'W, 0–102 m depth, bongo net, 18 May 1992; UW 083432, 1(7.3 mm), 55°55.3'N, 156°15.3'W, 0–216 m depth, bongo net, 21 May 1992; UW 083443, 1(3.2 mm), 57°01.1'N, 156°19.2'N, 0–95 m depth, bongo net, 3 June 1990; Puget Sound: UW 083433, 1(9.6 mm), 47°34.15'N, 122°32.3'W, 0 m depth, dip net, 9 May 1994; UW 083434, 1(9.7 mm), 47°34.15'N, 122°32.3'W, 0 m depth, dip net, 5 May 1989; UW 083435, 1(11.2 mm), 47°34.15'N, 122°32.3'W, 0 m depth, dip net, 27 March 1991; UW 083436, 1(11.4 mm), 47°34.15'N, 122°32.3'W, 0 m depth, dip net, 16 July 1987; UW 083437, 1(13.3 mm), 48°1.0'N, 123°0.0'W, reared, 4 May 1989; UW 083438, 1(13.4 mm), 48°1.0'N, 123°0.0'W, reared, 4 May 1989; UW 083439, 1(14.4 mm), 48°1.0'N, 123°0.0'W, 0 m depth, dip net (26 April 1989), reared (20 May 1989); UW 083440, 1(15.2 mm), 48°1.0'N, 123°0.0'W, 0 m depth, dip net (26 April 1989), reared (20 May 1989); UW 083441, 1(15.6 mm), 48°1.0'N, 123°0.0'W, 0 m depth, dip net, 1 July 1989; UW 083442, 1(11.4 mm), 47°34.15'N, 122°32.3'W, 0 m depth, dip net, 16 July 1987; UW 083444, 1(9.3 mm), 47°34.15'N, 122°32.3'W, 0 m depth, dip net, 1 June 1989.

Diagnosis

This species of *Lepidopsetta* has the following combination of characters in adults: total gill rakers on first arch 6–11; on upper arch 1–3, rarely 4, with at least one rudi-

mentary; total gill rakers on second arch 6–11; supraorbital pores 3–9; preopercular pores 5–7; lateral-line pores 70–91; sum of scales above and below lateral line 65–88; interorbital narrow; blind-side coloration white, with glossy highlights along myotome margins increasing anteriorly.

Larvae are distinguished from other species of *Lepidopsetta* by the following characters: body deep, snout-to-anus length short; hatching, flexion, and transformation at comparatively smaller sizes; preflexion pigment pattern with pigment patches along distal edges of dorsal and anal finfolds, four prominent spots along dorsal midline (in a pattern resembling alternating dorsal and ventral spots, with posteriormost dorsal spot coalescing with a corresponding ventral patch to form a bar), and a series of small ventral midline melanophores extending from gut to last myomere; flexion pigment pattern with distinctive anterior dorsal midline spot and posteriormost dorsal spot forming a bar with corresponding ventral patch; pectoral-fin rays unpigmented.

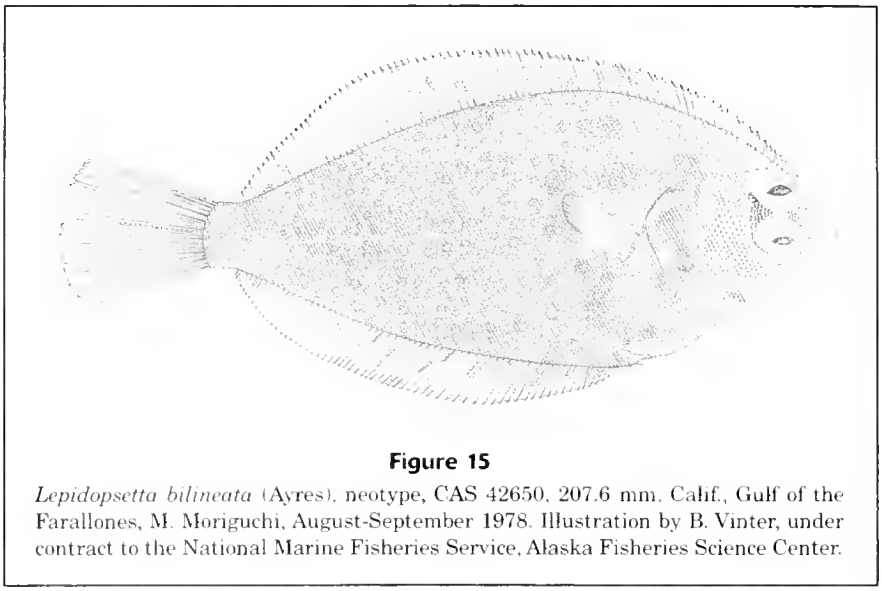

Figure 15

Lepidopsetta bilineata (Ayres), neotype, CAS 42650, 207.6 mm, Calif., Gulf of the Farallones, M. Moriguchi, August-September 1978. Illustration by B. Vinter, under contract to the National Marine Fisheries Service, Alaska Fisheries Science Center.

Description of adults (Fig. 15)

Body ovate, greatest depth 40.8–57.0 (47.0)% SL, scales above lateral line 25–43 and scales below lateral line 27–53; head relatively acute, length 24.0–32.9 (28.2)% SL; dorsal margin of head at dorsal-fin origin concave, snout length 3.1–6.1 (4.5)% SL (12.4–22.4 (16.1)% HL); ocular-side maxilla length 25.3–32.5 (27.9)% HL; blind-side maxilla relatively long, length 25.2–41.2 (31.3)% HL; ocular-side mandible length 38.3–46.1 (41.9)% HL; teeth 5–10 on ocular-side premaxilla, 20–27 on blind-side premaxilla and 10–12 on ocular-side dentary, 23–29 on blind-side dentary; gill rakers of first arch typically broad and robust, 6–11 total, 1–4 on upper arch, 5–7 on lower; gill rakers of second arch 6–11 total, 1 on upper and 5–10 on lower arch; dorsal orbit larger than eye length, orbit length 23.4–32.5 (28.1)% HL, dorsal eye length 17.9–30.3 (24.2)% HL; ventral eye length 18.2–35.4 (24.8)% HL; interorbital narrow, up to 3 scales at narrowest portion, 2.1–6.0 (3.5)% HL; cheek with 9–16 scales, length 28.1–41.8 (34.2)% HL, depth 13.9–24.2 (19.2)% HL; preopercular pores 5–7; ocular-side suborbital pores 14–29; blind-side suborbital pores 6–13; lateral-line pores 70–91, lateral-line arch length 49.3–58.1 (54.3)% HL, its depth 24.8–37.1 (30.2)% of its length; both anterior and posterior supratemporal branches relatively long, anterior pores 2–12, posterior pores 8–30; supraorbital canal long, extending to dorsal rim of dorsal orbit near insertions of dorsal-fin rays 3–4, pores 3–9; ocular-side pectoral-fin length 12.2–18.2 (15.2)% SL (43.6–66.2 (53.9)% HL); blind-side pectoral-fin length 6.7–12.2 (9.9)% SL (23.2–44.3 (35.0)% HL), about equal to ocular-side pelvic-fin length 7.6–12.5 (9.8)% SL (26.7–44.7 (34.8)% HL); dorsal fin with 67–89 rays, height 10.7–16.5 (13.3)% SL, in specimens with 72-79 rays supported by 71–78 pterygiophores, 9–11 anterior to first neural spine; anal fin with 54–77 rays, in specimens with 54–62 rays supported by 53–60 pterygiophores; caudal peduncle relatively slender, least depth 8.2–12.3 (10.2)% SL (29.6–43.0 (36.2)% HL; 90.0–152.4 (112.6)% caudal peduncle length); greatest depth 10.5–14.3 (12.1)% SL (37.2–53.0 (42.8)% HL); caudal peduncle length 7.2–10.9 (9.1)% SL (25.5–42.2 (32.4)% HL); caudal-fin length 15.3–23.6 (20.8)% SL. Vertebrae 40–41, with 11 precaudal and 29–30 caudal.

Scales around head and those scattered posteriorly on ocular side moderately rough with columnar tubercles in large adults; strong spines in small adults and juveniles. Urogenital flap darkly pigmented in 21–58 mm juveniles.

In life, blind side in adults translucent to bright white, with glossy highlights along edges of myotomes; in juveniles, primarily translucent, and having reduced glossy areas especially prominent over the head. When preserved, blind side of all individuals uniform creamy white to yellow-brown. Ocular side slightly more green than that of congeneric in Puget Sound.

Remaining description as for genus. Largest specimen examined 426 mm (UW 044012). Maximum size reported ca. 540 mm (580 mm TL[6]).

Description of juveniles (Fig. 16)

Most individuals were collected on bottom (Fig. 16A) by 19.0 mm; newly settled juveniles with dorsal eye completely migrated; median fin rays formed; lateral line nearly formed; expanded anteriormost anal-fin pterygiophore well devel-

[6] Resource Assessment and Conservation Engineering (RACE) Division. 1996. Unpubl. data from RACE database. Alaska Fisheries Science Center, Natl. Mar. Fish. Serv., NOAA, 7600 Sand Point Way NE, Seattle, WA 98115.

oped. Preanal pigment increased along head and gut; postanal pigment smaller and distributed in random patches; urogenital papilla darkly pigmented throughout its length. Blind side with pigment similar to that of postflexion larvae. Orbit length larger, mouth smaller, body depth less, gill-raker counts on lower arch less, and distance from pelvic-fin origin to anal-fin origin greater than in *L. polyxystra* n. sp. Pelvic- and pectoral-fin rays formed.

By 30.0 mm, pigmentation has increased along body, with darker patches and spots throughout (Fig. 16B) obscuring pigmented urogenital papillae. Lateral line more fully developed; supraorbital canal pores visible.

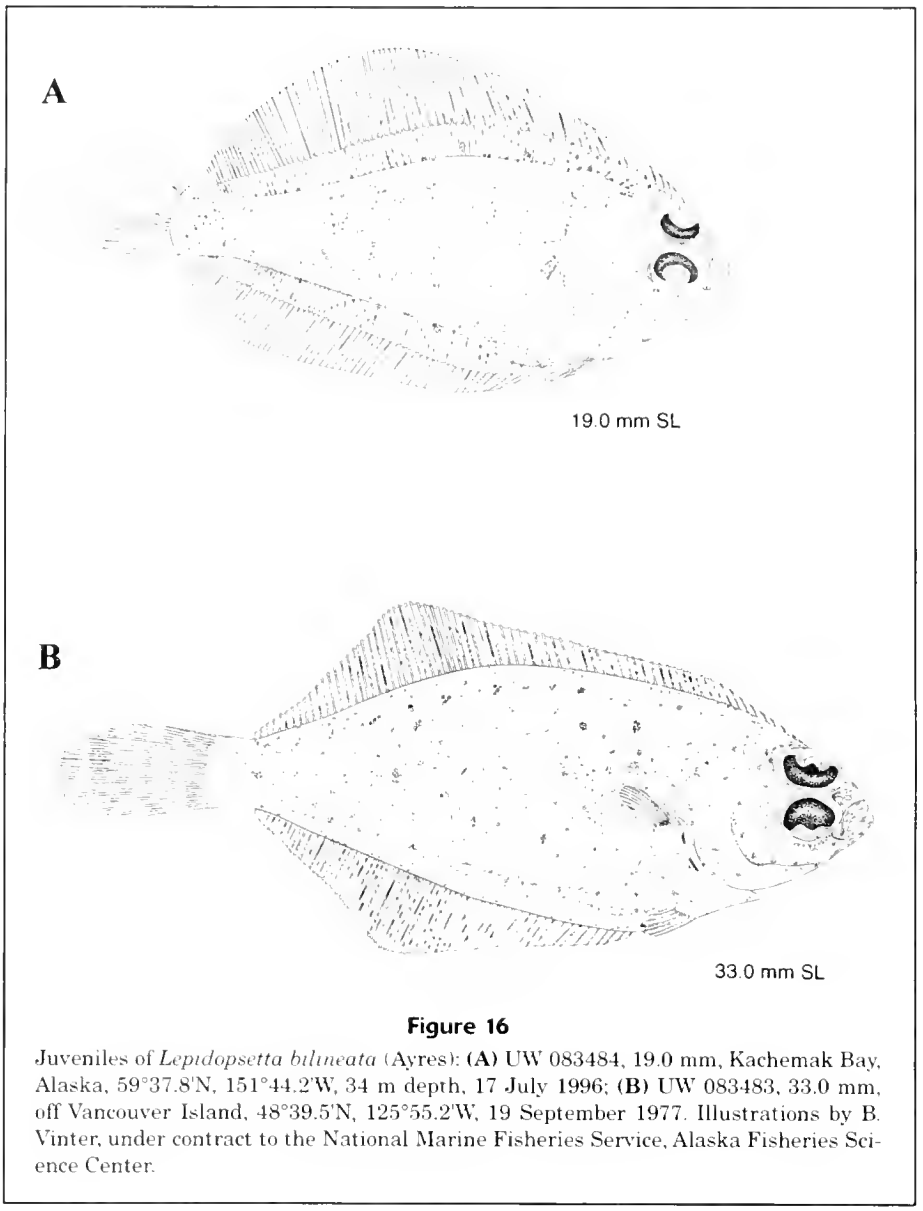

Figure 16

Juveniles of *Lepidopsetta bilineata* (Ayres): **(A)** UW 083484, 19.0 mm, Kachemak Bay, Alaska, 59°37.8'N, 151°44.2'W, 34 m depth, 17 July 1996; **(B)** UW 083483, 33.0 mm, off Vancouver Island, 48°39.5'N, 125°55.2'W, 19 September 1977. Illustrations by B. Vinter, under contract to the National Marine Fisheries Service, Alaska Fisheries Science Center.

Description of larvae (Fig. 17)

Snout-to-anus length is 32.9–34.6% SL, remaining constant during development; body depth 4.7–35.7% SL, increasing with development, sharply after flexion; head length 13.3–29.3% SL, increasing with development, sharply after flexion; snout length 22.6–20.7% HL, remaining constant during development; orbit length 51.9–23.8% HL, decreasing with development (Table 2). Total myomeres 37–44.

Larvae hatching at small lengths, at sizes less than 3.0 mm, yolk absorbed by 2.7–4.5 mm. Preflexion larvae ranging in size from 3.8 to 6.6 mm; flexion larvae, from 6.4 to 11.1 mm; postflexion larvae from 10.8 to 16.0 mm. Transformation occurring at lengths as small as 10.0 mm (often accompanied by a decrease in total body length); postsettlement juvenile stage usually attained by 20.0 mm (Table 13).

Preanal pigment present initially along lower jaw and ventral side of cleithral region, increasing with development to snout, upper jaw, and isthmus. Pigment ventrally along gut and dorsally on anus; by flexion a distinct patch of melanophores along the posterior edge of the gut; pigment increases laterally with development.

Postanal pigment present as melanophores along distal edges of dorsal and anal finfolds; four distinct pigment areas along the dorsal midline, anterior (first) spot begins 1–5 myomeres after anus at about myomere 12–16, second spot begins at about myomere 23–26, third spot begins at about myomere 33–46, and the fourth spot begins at about myomere 41–42 (after initially forming as a dorsal midline patch, the posteriormost spot coalesces with ventral patch to form a caudal bar); series of melanophores from the gut along the ventral midline beginning in a double row, changing to a single row posterior to the ventral stripe of the caudal bar; several additional melanophores along the ventral midline posterior to the caudal bar, pigment above and below the tip of the notochord. By transformation, the third dorsal midline patch and opposing ventral patch expand to form an indistinct bar; other patches of pigment form in myosepta and continue into the dorsal and anal pterygiophores and fin rays.

Distribution (Figs. 6, 10, 12, 18)

Lepidopsetta bilineata ranges from the continental shelf north and south of the Islands of Four Mountains in the eastern Aleutian Islands and in the southern Bering Sea

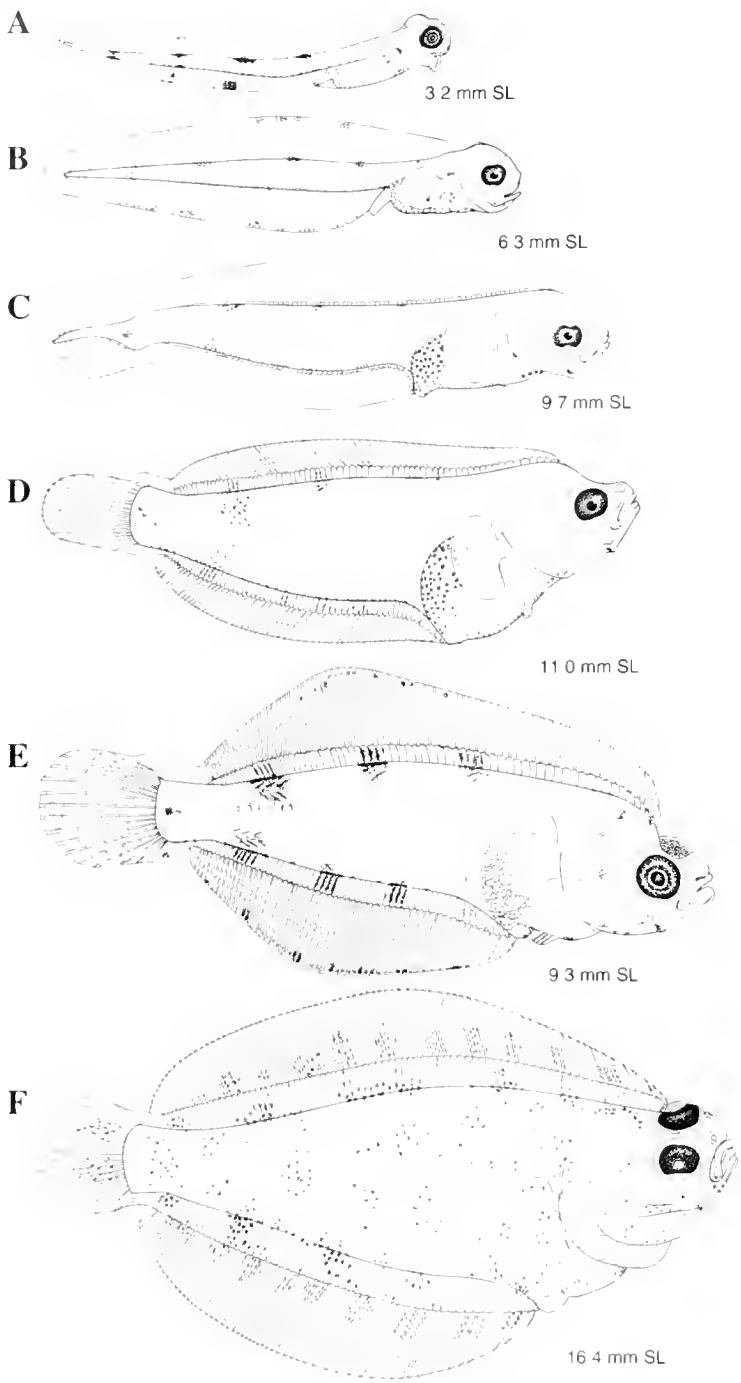

Figure 17

Larvae of *Lepidopsetta bilineata* (Ayres): **(A)** UW 083443, 3.2 mm, Gulf of Alaska, AFSC, 3 June 1990; **(B)** UW 083410, 6.3 mm, Gulf of Alaska, AFSC, 26 June 1978 (Matarese et al., 1989); **(C)** UW 083411, 9.7 mm, Gulf of Alaska (Matarese et al., 1989), AFSC, 28 June 1978; **(D)** UW 083112, 11.0 mm, Gulf of Alaska, AFSC, 14 Sept 1978; **(E)** UW 083444, 9.3 mm, Puget Sound, AFSC, 1 June 1989; **(F)** UW 083409, 16.4 mm, Gulf of Alaska, AFSC, 22 July 1977 (Matarese et al., 1989). Illustrations by B. Vinter, under contract to the National Marine Fisheries Service, Alaska Fisheries Science Center.

on the Slime Bank north of Unimak I., to Cortez Banks, Baja California, Mexico. It is common from the northern Gulf of Alaska to Puget Sound and is locally abundant along the coasts of Washington, Oregon, and California. Larvae have been collected from just south of the Aleutian Islands to Tanner Bank, Mexico (Moser et al., 1993; Charter and Moser, 1996).

Habitat

Adults were collected over sand and gravel substrates to depths of 339 m (RACE[6]). Larvae were collected over depths <1000 m.

During our 22-year sampling period, larvae were less common than those of *L. polyxystra* n. sp. in spring ichthyoplankton surveys conducted in the Gulf of Alaska. Larvae appeared in larger numbers later in the season (June) and the highest densities occurred from Kodiak Island to the eastern Gulf of Alaska (Table 14; Fig. 18). In the CalCOFI region, larvae were collected from February to July; peak abundance was in May (Charter and Moser, 1996). Larvae were collected more frequently and in higher densities closer to the coastline (within 55.6 km, Moser et al., 1993).

Life history

In *L. bilineata* taken off the coast of Oregon, brittlestars of the genus *Ophiura* dominated the diet, and polychaetes and mollusks constituted much of the remainder (Kravitz et al. 1976). Adults from the Gulf of Alaska and Aleutian Islands are often infested with the parasitic copepods *Nectobrachia indivisa* and *Naobranchia occidentalis*.[7] Both parasites were previously recorded in *Lepidopsetta* by Kabata (1988). For both parasite species, *L. bilineata* was significantly less infested than *L. polyxystra* n. sp.[6] The maximum recorded age for female *Lepidopsetta* is 18 yr at 49 cm FL and for a male is 17 yr at 40 cm FL (Levings, 1967; Forrester, 1969). For early life history information, see generic account.

[7] Zimmermann, M. and R. Harrison. 1998. Personal commun. Resource Assessment and Conservation Engineering Division, Alaska Fisheries Science Center, Natl. Mar. Fish. Serv., NOAA, 7600 Sand Point Way NE, Seattle, WA 98115.

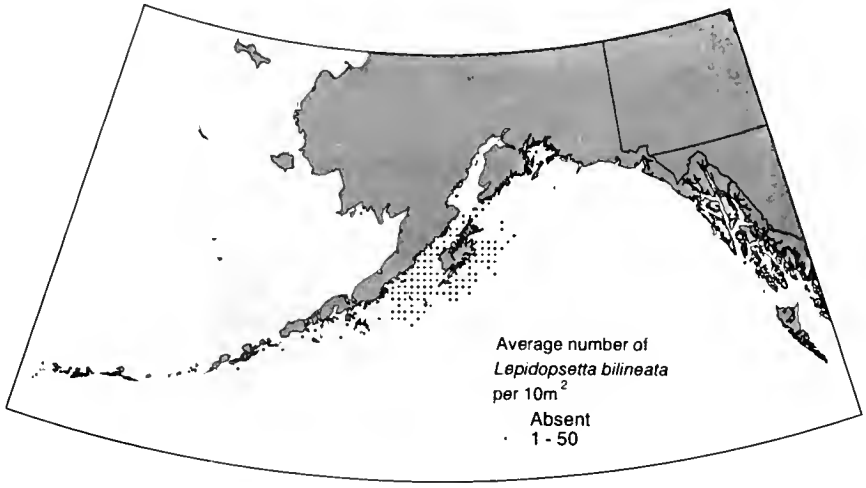

Figure 18

Distribution and density (average number per 10 m^2) of *Lepidopsetta bilineata* in the Gulf of Alaska and Bering Sea, 1972–1994.

Table 14

Monthly collections of larvae of *Lepidopsetta* in the Gulf of Alaska and Bering Sea (1972–1994). Mean density (number per 10 m^2) followed below by the standard deviation of the mean in parentheses.

	Month												
Taxon	Jan	Feb	Mar	Apr	May	Jun	Jul	Aug	Sep	Oct	Nov	Dec	Overall
L. bilineata	0	0	0	0.0139	0.568	1.73	0.15	0	0.116	0.0311	0	0	0.414
	(0)	(0)	(0)	(0.0059)	(0.0592)	(0.243)	(0.0553)	(0)	(0.0872)	(0.0311)	(0)	(0)	(0.0357)
L. polyxystra n. sp.	0	0	0.456	5.80	7.06	4.44	0.659	0	0.09	0.0386	0	0	5.34
	(0)	(0)	(0.204)	(0.633)	(0.383)	(0.481)	(0.018)	(0)	(0.0634)	(0.0386)	(0)	(0)	(0.289)
Total observations	115	163	704	2926	2678	861	333	0	144	138	585	11	7502

Etymology

The specific name is derived from the Latin *bilineata*, meaning "two lined", a reference to the bifurcate supratemporal branch of the lateral line.

Comments

Basing his work on an account first published in *The Pacific* (Ayres, 1855a) and subsequently reprinted in the Proceedings of the California Academy of Sciences (Ayres, 1855b), Ayres described his specimen of *Platessa bilineata* at the California Academy of Natural Sciences (CAS) in 1855. The specimen has not been located at CAS[8] (where it may have been destroyed in the 1906 San Francisco earthquake and subsequent fire, Springer and Anderson, 1998), ANSP,[9] LACM,[10] or USNM.[11] Because *L. bilineata* may be easily confused with *L. polyxystra* n. sp., especially in the Gulf of Alaska and Puget Sound, we therefore designated CAS 42650, collected in the Gulf of Farallones off California, as the neotype of *L. bilineata*. Ayres obtained his specimen from the San Francisco fish market and noted that, although not common, the species was taken in San Francisco Bay. Lockington (1879a) noted that *L. bilineata* was most commonly caught "at or near the Farallone Islands" for the San Francisco markets.

[8] Catania, D. 1996. Personal commun. Ichthyology Department, California Academy of Sciences, Golden Gate Park, San Francisco, CA 94118.

[9] Saul, W. 1996. Personal commun. Academy of Natural Sciences, 19th and The Parkway, Philadelphia, PA 19103.

[10] Feeney, R. 1996. Personal commun. Natural History Museum of Los Angeles County, 900 Exposition Blvd., Los Angeles, CA 90007.

[11] Jewett, S. 1995. Personal commun. Division of Fishes, Smithsonian Institution, Washington, D.C. 20560.

Girard (1856) described *Platichthys umbrosus* on the basis of a single specimen deposited at the USNM, which was collected at Cape Flattery, Washington, by Lieutenant W. P. Trowbridge. One lot listed in the catalog, USNM 607, bears the collector's name as Trowbridge and a collection date of 1856, and thus the single specimen of this lot appears to have been the one examined by Girard for his original description. From the original description, the specimen is approximately 190 mm TL. Unfortunately, this lot cannot be found and is presumed missing or destroyed.[11]

Girard was apparently unaware of Ayres' (1855a, 1855b) description of *L. bilineata* (Leviton and Aldrich, 1997). Although Günther (1862) considered *Platichthys umbrosus* distinct (basing his conclusion on the dried skins identified as *P. umbrosus* taken off Vancouver Island, Canada, and on the descriptions of *L. bilineata* provided by Ayres), later authors have treated *P. umbrosus* as a synonym of *L. bilineata* (Lockington, 1880a, 1880b; Jordan and Gilbert, 1881; Jordan and Evermann, 1898; Norman, 1934; Schmidt, 1950), and the name has not been used at the species level since Lockington's (1879b) misidentification of *Isopsetta isolepis*. *Lepidopsetta polyxystra* n. sp. also ranges south along the east coast of Vancouver Island, the "Inside Passage," to Puget Sound, and larvae of the new species have been recorded from the extreme northwest coast of Vancouver Island. Although *L. bilineata* is present, but uncommon, off the west coast of Vancouver Island, no adults or larvae of *L. polyxystra* n. sp. have been collected off Washington (Cape Flattery and south), despite the intensive survey efforts of the 1995 and 1998 NMFS triennial surveys, during which all captured *Lepidopsetta* were examined. Although the original description is insufficient to refer it to either of these species, the type locality lies well within the known range of *L. bilineata* and outside that of *L. polyxystra* n. sp. and we therefore consider *Platichthys umbrosus* to be a synonym of *L. bilineata*.

Cope's (1873) description of *Pleuronectes perarcuatus*, from a specimen taken somewhere along the eastern Pacific Ocean coast of Alaska, perhaps near Sitka or Unalaska Island, included a comparison with Girard's *Platichthys umbrosus* but not with Ayres's *Platessa bilineata*. Although the holotype is badly damaged, especially about the head, the gill-raker count and structure, as well as presence of at least one supraorbital pore at the dorsal margin of the orbit,[8] indicate the holotype is *L. bilineata*. The specimen has a high lateral-line pore count at the upper range of counts for *L. bilineata*. The name has been considered synonymous with, or a subspecies of, *L. bilineata* by later authors (Jordan and Gilbert, 1881; Jordan and Goss, 1889; Jordan and Evermann, 1898; Wilimovsky et al., 1967).

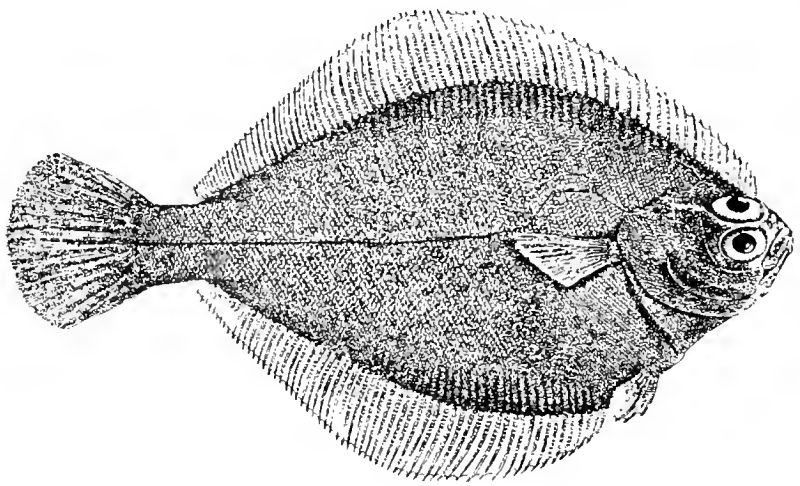

Figure 19

Lepidopsetta mochigarei Snyder, holotype, USNM 68245, 1(174 mm), Japan, Hokkaido, Otaru Market, 1906. After Snyder (1912).

Lepidopsetta mochigarei Snyder, 1911
Ricecake sole
Asabagarei
Figs. 1–2, 7, 19–20; Tables 3–10, 13

Lepidopsetta mochigarei Snyder, 1911:547 (original description, two specimens: holotype by original designation, USNM 68245, male, 174 mm, and "cotype," SU 21430, 145 mm TL, both from the market at Otaru, Hokkaido, Japan).

Lepidopsetta bilineata mochigarei Taranets, 1937:144 (new combination, keys).

Pleuronectes mochigarei Sakamoto, 1984a:99 (new combination, phylogenetics).

Material examined

Adults 27 specimens, 90.7–280.3 mm, including holotype listed above. Japan: CAS-SU 113378, 1(257.5 mm), Bomasiri Shima, off N end of Rebun To., 45°25.5'N,140°53'E, 22 September 1906; CAS-SU 122548, 1(146.7 mm), Tsugaru Strait/Sea of Japan, between Hakodate, Hokkaido and Ebisu, Sado I., S of Cape Tsiuka, 41°35.8333'N, 140°36.75'E, 16 July 1906; HUMZ 56717, 1(154 mm), Hokkaido, off Kushiro; HUMZ 58576, 1(189 mm), Hokkaido, off Otanoshike; HUMZ 58566, 1(197.5 mm), Otanoshike, off Hokkaido, 20 m; HUMZ 58563, 1(200.5 mm), Otanoshike, off Hokkaido, 20 m; HUMZ 58568, 1(171.5 mm), Otanoshike, off Hokkaido; HUMZ 58567, 1(184 mm), Hokkaido, off Otanoshike; HUMZ 87820, 1(175 mm), Hokkaido, off Muroran, 135 m; HUMZ 80974, 1(190.5 mm), Hokkaido, off Muroran; HUMZ 81056, 1(167.5 mm), Hokkaido, Usujiri, Minamikayabe; HUMZ 90912, 1(142.5 mm), Hokkaido, off Tomakomai, 300 m; HUMZ 64730, 1(116.6 mm), Hokkaido, Funkawan; HUMZ 15505, 1(107.2 mm), Hokkaido, Funka Bay; HUMZ

15456, 1(130.5 mm), Hokkaido, Funka Bay; HUMZ 15506, 1(90.7 mm), Hokkaido, Funka Bay; HUMZ 94034, 1(193.5 mm), Hokkaido, off Tomakomai, 300 m; UBC 58-355, 2(204–240 mm), Japan; USNM 150380, 1(130.6 mm), Hokkaido; USNM 077125, 1(166.1 mm), 104 km S of OseSaki, *Albatross* Sta. 5067, 35.0972°N, 138.6875°E, 536 m; Russia: USNM 77126, 1(244.2 mm), Gulf of Tartary, off SW coast of Sakhalin I., *Albatross* Sta. 4999, 47.6389°N, 141.65°E; USNM 77127, 1(247.4 mm), Aniwa Bay, approaching Korsokov, Sakhalin I., 73 m, *Albatross* Sta. 5008, 46.1306°N, 142.6222°E; USNM 77130, 1(280.3 mm), Gulf of Tartary, off SW coast of Sakhalin I., 57 m, *Albatross* Sta. 5000, 46.55°N, 142.7083°E; USNM 77128, 1(257 mm), Aniwa Bay, approaching Korsokov, Sakhalin I., 77 m, *Albatross* Sta. 5007, 46.05°N, 142.5167°E; USNM 77135, 1(246.8 mm), Sakhalin I., off Korsokov Lt., 39-56 m, *Albatross* Sta. 5010, 46.55°N, 142.725°E.

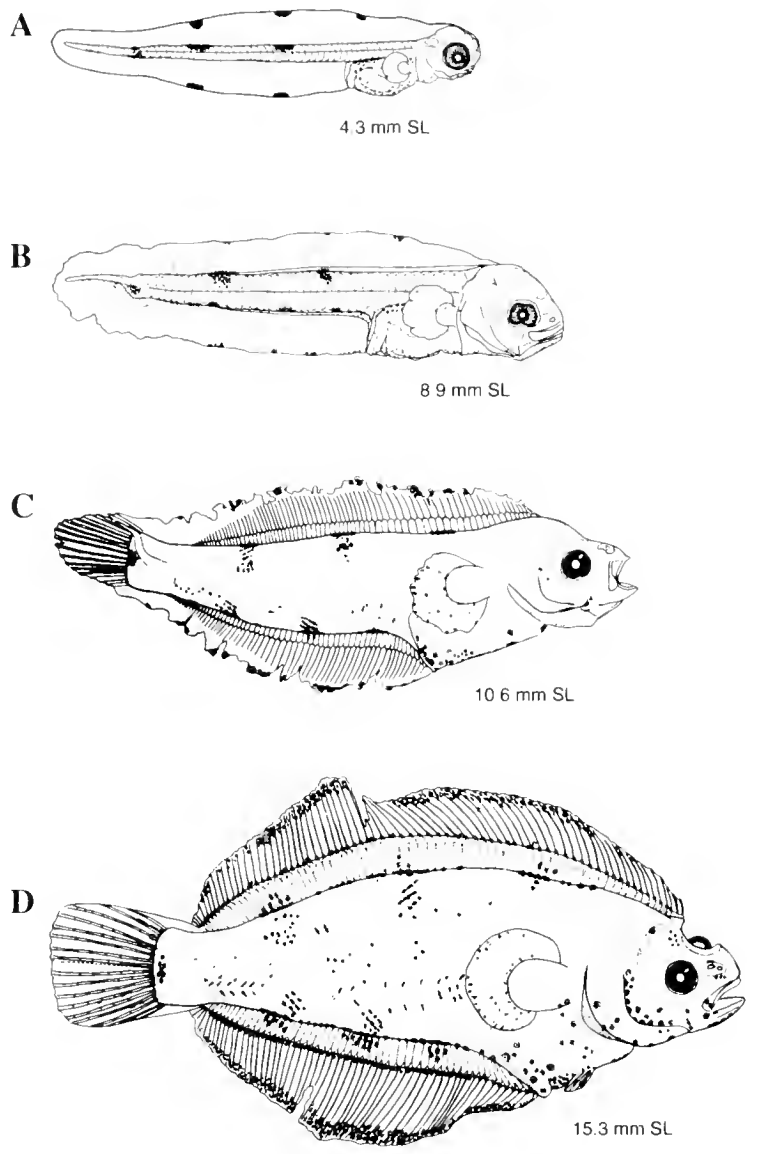

Figure 20

Larvae of *Lepidopsetta mochigarei* Snyder (figures reproduced from Okiyama, 1988): **(A)** 4.3 mm, Japan Sea (Okiyama and Takahashi, 1976); **(B)** 8.9 mm, Sea of Japan (Okiyama and Takahashi, 1976); **(C)** 10.6 mm, Sea of Japan (original illustration of Nagasawa, cited in Okiyama, 1988, locality implied in text); **(D)** 15.3 mm, Sea of Japan (original illustration of Nagasawa, cited in Okiyama, 1988, locality implied in text).

Diagnosis

Lepidopsetta mochigarei is a species of *Lepidopsetta* with the following combination of characters in adults: total gill rakers on first arch 6–10, on upper arch 1–3; total gill rakers on second arch 7–10; supraorbital pores 1–3; preopercular pores 8–13; lateral-line pores 95–119; sum of scales above and below lateral line 91–108; interorbital narrow; blind-side coloration white, and glossy highlights along myotome margins increasing anteriorly.

Larvae are distinguished from other species of *Lepidopsetto* by having the following combination of characters: body deep, increasing rapidly with development and snout-to-anus length moderate; larvae undergoing notochord flexion at comparatively larger sizes; preflexion pigment pattern with three prominent spots along margin of dorsal finfold and two spots along ventral finfold, three patches along postanal dorsal midline aligned with finfold spots to form slightly offset opposing patches, posteriormost dorsal spot coalescing with a corresponding ventral spot to form a bar; pectoral-fin rays pigmented (Okiyama and Takahashi, 1976; Nagasawa, cited in Okiyama, 1988).

Description of adults

Body ovate, relatively deep, greatest depth 45.5–61.1 (51.7)% SL, scales above lateral line 35–45 scales below lateral line 52–67; head relatively short and robust, length 23.3–30.5 (26.2)% SL; dorsal margin of head at dorsal-fin origin nearly linear, snout length 3.3–6.2 (4.3)% SL (12.7–20.2 (16.1)% HL); ocular-side maxilla length 24.6–29.4 (27.2)% HL; blind-side maxilla length 27.3–32.9 (29.7)% HL; ocular-side mandible length 36.6–44.6 (39.7)% HL; teeth 6–10 on ocular-side premaxilla, 23 on blind-side premaxilla and 8–15 on ocular-side dentary, 21–28 on blind-side dentary; gill rakers of first arch broad and robust, 6–10 total, 1–3 on upper arch, 4–7 on lower; gill

rakers of second arch 7–10 total, 1 on upper and 6–9 on lower arch; eyes relatively large, dorsal orbit slightly longer than eye length, orbit length 26.1–34.7 (30.1)% HL, eye length 21.4–30.0 (25.3)% HL; ventral eye length 21.6–31.1 (25.5)% HL; interorbital a narrow ridge, up to 2 scales at narrowest portion, 1.3–4.2 (2.7)% HL; cheek with 10–15 scales, length 28.6–35.0 (31.1)% HL, depth 14.8–25.5 (19.7)% HL; preopercular pores 8–13; ocular-side suborbital pores 22–38; blind-side suborbital pores 10–20; lateral line pores 95–119, lateral-line arch relatively long, 53.7–69.9 (62.7)% HL, its depth 23.8–35.7 (30.9)% its length; both anterior and posterior supratemporal branches relatively short, anterior pores 3–12, posterior pores 6–22; supraorbital canal short, reaching only to the posterior rim of the dorsal orbit at about the insertion of dorsal-fin rays 5–6, pores 1–3; ocular-side pectoral-fin length 12.6–17.4 (14.6)% SL (47.9–60.2 (55.6)% HL); blind-side pectoral-fin length 7.9–11.7 (9.6)% SL (30.3–42.8 (36.5)% HL); ocular-side pelvic-fin length 7.4–11.8 (9.8)% SL (31.8–43.5 (37.4)% HL); dorsal fin with 73–82 rays, height 11.2–14.7 (12.9)% SL, in specimens with 75–81 rays supported by 71–77 pterygiophores, typically 8 or rarely 9 anterior to first neural spine; anal fin with 56–65 rays, in specimens with 56–63 rays supported by 57–61 pterygiophores; caudal peduncle relatively deep, least caudal peduncle depth 9.7–14.0 (11.0)% SL (36.2-50.3 (42.2)% HL; 105.1–172 (124.3)% caudal peduncle length), greatest caudal peduncle depth 12.0–14.6 (13.2)% SL (44.7–56.0 (50.5)% HL); caudal peduncle length 7.8–10.3 (8.9)% SL (27.5–39.4 (34.1)% HL); caudal-fin length 18.8–25.1 (21.2)% SL. Vertebrae 39–42, with 11 precaudal and 28–31 caudal.

Scales on head, pectoral region, and those scattered posteriorly on ocular side slightly rough and having columnar tubercles in larger adults. Small spines present in small adults.

In life, blind side of adults translucent to white with glossy highlights along edges of myotomes (Amaoka et al., 1983, Fig. 220 as *L. bilineata*; Amaoka et al., 1995, Fig. 524 as *Pleuronectes bilineatus*). When preserved, blind side uniform creamy white to yellow-brown. Ocular side brownish with faint yellow highlights around small dark spots near bases of dorsal and anal fins and at midline (Amaoka et al., 1995, Fig. 524).

Remaining description as for genus. Largest specimen examined 280.3 mm (USNM 77130). Maximum size reported 400 mm SL (Sakamoto, 1984b).

Description of juveniles

No juveniles were examined for this study. Juveniles are not described in available literature.

Description of larvae

No larvae were examined in our study. The following description is based on Okiyama and Takahasi (1976, based on 3 specimens of 4.12–8.59 mm) and Pertseva-Ostroumova (1961; number and size of specimens examined not stated).

Snout-to-anus length 32.8–37.0% SL, decreasing with development according to Pertseva-Ostroumova, 1961 (34.2–32.5% SL); body depth 9.0–17.0% SL, increasing with development; head length 15.0–20.0% SL, increasing with development; orbit length 41.0–28.0% HL, decreases with development. Total myomeres 41–43.

Hatching occurring at relatively large sizes, at 3.95–4.48 mm (Yusa, 1958); flexion beginning by 8.9 mm (Fig. B of Okiyama, 1988); postflexion size between 10.6 mm and 15.3 mm (Figs. C and D of Okiyama, 1988); transformation occurring at sizes larger than 15.3 mm (Fig. D of Okiyama, 1988).

Preanal pigment (Fig. 20, based on Okiyama, 1988) present initially along lower jaw, extending ventrally along gut to anus. By flexion, melanophores appearing on pectoral-fin rays; pectoral-fin rays and base not pigmented in all earlier developmental stages; pectoral fin pigmented more heavily than *L. polyxystra* n. sp. by later stages (Pertseva-Ostroumova, 1961).

Postanal pigment of preflexion larvae in prominent patches of melanophores along finfold edges, three along dorsal and two along anal finfold, becoming more dispersed and less prominent with development; three distinct pigment patches along the dorsal midline, anterior patch begins at about myomere 20–22, posterior patch begins at about 33–36, and caudal patch, which aligns with a ventral patch to form a caudal bar, begins in the range of myomeres 40–44; these dorsal midline patches align vertically with the two posteriormost dorsal and both ventral finfold patches; a series of melanophores may occur along the postanal ventral midline (additional descriptions cannot be found in the literature); additional pigment spots above and below the notochord tip.

Distribution

Lepidopsetta mochigarei ranges in the western Pacific Ocean from the east coast of Korea, Yoglin Bay, in the Sea of Japan (Kim and Youn, 1994) to Iturup Island of the Kuril Islands in the southern Okhotsk Sea (Nikiforov et al., 1983), and to the west coast of northern Japan. Larvae have been collected in March along the coast of northern Honshu in the Sea of Japan (Okiyama, 1988).

Habitat

Adults have been collected over the continental shelf; spawning may occur in depths of about 120 m (Okada, 1955).

Life history

Fecundity ranges from 510,000 to 550,000 eggs (Okada, 1955). Spawned eggs are demersal and adherent, about 0.87–0.95 mm in diameter (Yusa, 1958; Pertseva-Ostroumova, 1961); oocytes at maturation stage IV were 0.440–0.655 mm in diameter (Nikiforov et al., 1983). Spawning occurs from December to June in waters around Hokkaido and the southern Kuril Islands (Minami, 1995). Embryonic and larval development to about 5.0 mm has been described by Yusa (1958).

Etymology

The species name *mochigarei* is derived from the Japanese, meaning "rice-cake flounder" (Snyder, 1911), probably a reference to the bright white blind side similar to white rice-cake common in Japan.[12]

Comments

Masutomi and Hamada (1966) described a fossil of *L. mochigarei*. It was subsequently described as the extinct *Chibapsetta dolichurostyli* by Sakamoto and Uyeno (1988).

Because early life history material was not available for examination, descriptions were based on the available literature (Yusa, 1957, 1958; Pertseva-Ostroumova, 1961; Okiyama and Takahashi, 1976; Okiyama, 1988). Several potentially important characters could not be gleaned from the available sources: an anterior pigment spot along the dorsal midline, important in distinguishing *L. bilineata* from *L. polyxystra* n. sp. (Figs. 17C, 17D), is not present in preflexion larvae (Figs. 20A and 20B). Because the sources were different, we needed verification that these figures constitute a series. Although present, the extent of the postanal ventral melanophores, important in distinguishing *Lepidopsetta* from *Psettichthys* in particular as well as from other pleuronectids, is not known. Additional data for morphological characters were also needed for all developmental stages. Larvae of *L. mochigarei* appear more similar to those of *L. bilineata* than *L. polyxystra* n. sp., but they are not sympatric with *L. bilineata*. Based on the present descriptions, larvae of *L. mochigarei* can be distinguished from those of *L. polyxystra* n. sp. by the distinctive vertically aligned dorsal midline and finfold pigment.

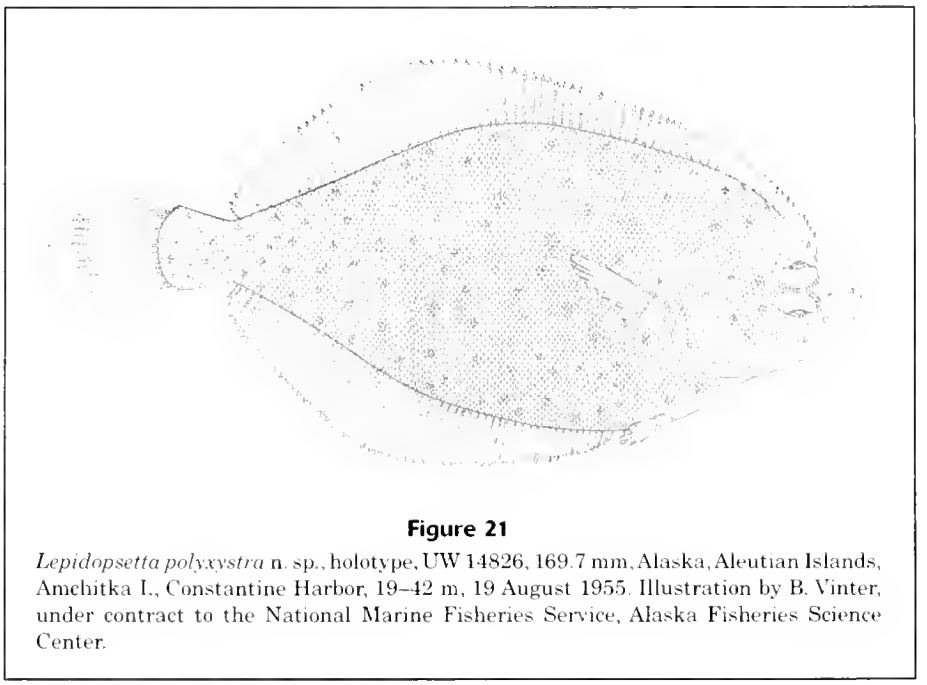

Figure 21

Lepidopsetta polyxystra n. sp., holotype, UW 14826, 169.7 mm, Alaska, Aleutian Islands, Amchitka I., Constantine Harbor, 19–42 m, 19 August 1955. Illustration by B. Vinter, under contract to the National Marine Fisheries Service, Alaska Fisheries Science Center.

Lepidopsetta polyxystra n. sp.
Northern rock sole
Figs. 1–5, 8, 11, 13, 21–24; Tables 2–11, 13–14

Lepidopsetta bilineata var. *umbrosa* Jordan and Evermann, 1898:2643 (in part, Fig. 928).

Lepidopsetta bilineata bilineata Taranetz, 1937:144 (in part, new combination, keys).

Holotype

UW 014826, 1(169.7 mm), Alaska, Aleutian Is., Amchitka I., Constantine Harbor, 19–42 m, 19 August 1955.

Material examined

A total of 843 adults and juveniles, including the holotype listed above, was examined. Sixty larvae were examined.

Paratypes

Adults 219 specimens, 26–427.5 mm. Okhotsk Sea: UW 042341 (orig. KIE 1147), 2(105.5–109.5 mm), western Kamchatka, 51°57'N, 156°25'E; UW 042342 (orig. KIE 1149), 3(144.5–195 mm), western Kamchatka, 52°02'N, 155°58'E, 6 June 1992; UW 042343 (orig. KIE 1151), 10(186–247 mm), 52°29'N, 153°40'E, 24 June 1992; KIE 1148, 1(89.5 mm), 51°43'N, 156°04'E, 5 June 1992; Southeast Kamchatka: CAS-SU 122549, 1(112.3 mm), Kamchatka, off Petropavlovsk, 18 June 1906; Bering Sea: KIE 1415, 1(289.5 mm), Bering I., SW of Cape Monati, 54°37'N, 166°31'E, 27 April 1996; KIE 1417, 1(258.5 mm), Bering I., SW of Cape Monati, 54°39'N, 166°29'E, 8 May 1996; KIE 1414, 1(260.5 mm), SW of Cape Monati, 54°40'N, 166°29'E; KIE 1268, 1(338.6 mm), NW of Bering I., 55°34'N, 164°55'E, 7 January 1994; KIE 1418, 1(289 mm), Bering I., SE of Cape Monati, 54.6667°N, 166.8333°E, 9 May 1996; KIE 1416, 1(261 mm), Kamchatka, SW of Cape Northwestern, 55.2833°N, 165.5333°E, 4 May 1996; KIE 1150, 1(238.5 mm), Kamchatka, 56.2333°N, 154.3°E, 18 June 1992; ABL 93-37, 1(193 mm), St. Paul I., Pribilof Is.; ABL 60-15, 1(265 mm), N of Pribilof Is., 58°33'N, 170°12'W, 17 July 1960; UW 041694, 3(150-177), Aleutian Is., NE of Umnak I., 53.44°N, 168.4944°W; SIO 94-164, 9(103–190 mm), Aleutian Is., off Unalaska I., 54°15.1'N, 165°57.6'W, 4 June 94; UW 041199, 1(267 mm), 60.6667°N, 169.65°W, 16 July 1979; UW 041697, 1(245 mm), Bering Sea, N of Unimak I., 55.0213°N, 164.6009°W; CAS 45562, 1(240.8 mm), WNW of Pribilof Is., NE end of Zhenchug Canyon, 58°15.8667'N,

[12] Amaoka, K. 1997. Personal commun. Laboratory of Marine Zoology, Faculty of Fisheries, Hokkaido University, Hakodate, Hokkaido, Japan.

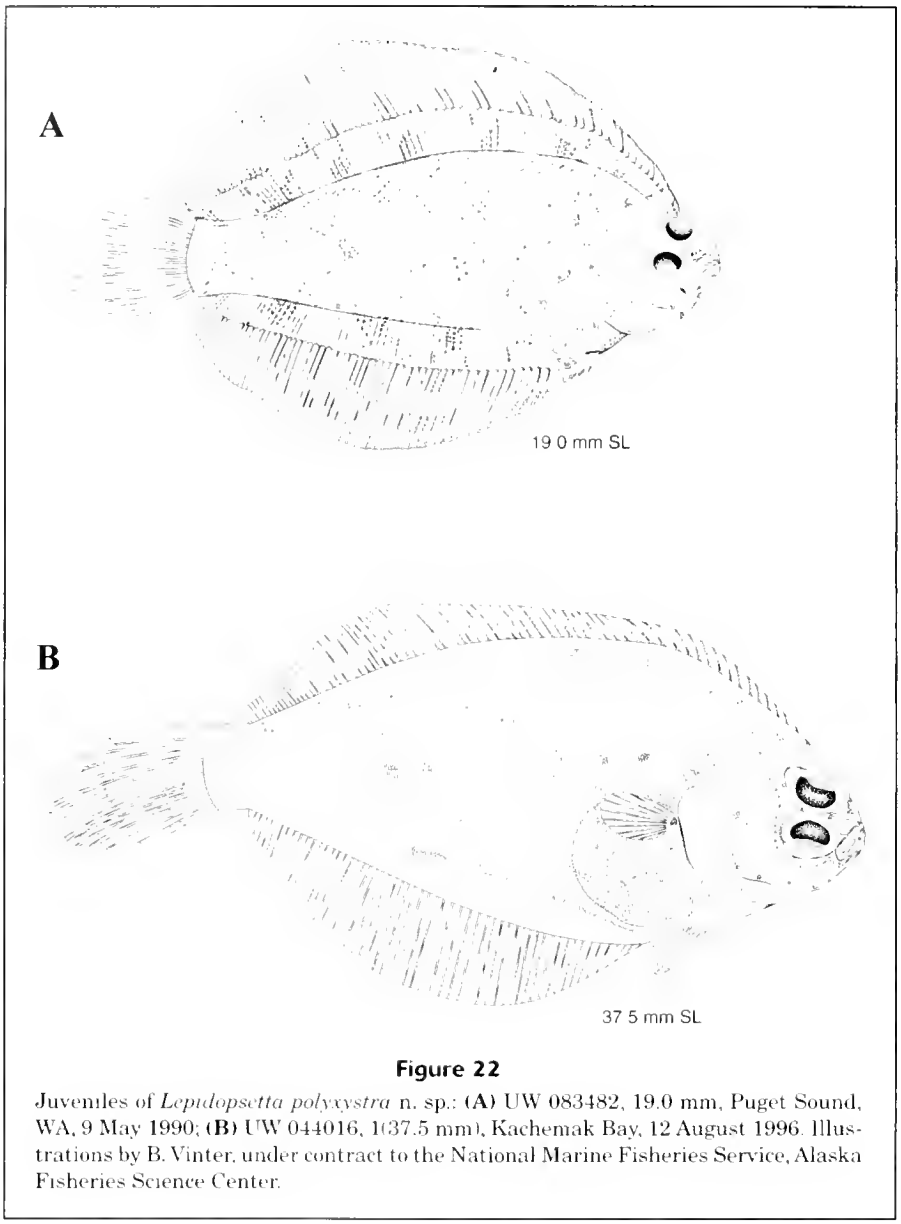

Figure 22

Juveniles of *Lepidopsetta polyxystra* n. sp.: **(A)** UW 083482, 19.0 mm, Puget Sound, WA, 9 May 1990; **(B)** UW 044016, 1(37.5 mm), Kachemak Bay, 12 August 1996. Illustrations by B. Vinter, under contract to the National Marine Fisheries Service, Alaska Fisheries Science Center.

174°0.3'W, 21 June 79; CAS 45567, 1(272.1 mm), SSW of Pribilof Is., 55°38.8667'N, 168°39.9833'W, 16 June 79; CAS 46676, 1(87.7 mm), Pribilof Is., St. George I., 56°35'N, 169°36'W, 27 July 1977; CAS 47531, 5(181.4–199.4 mm), Aleutian Is., 51°43.9'N,177°57.8833'W, 10 August 1980; CAS-SU 105731, 5(132.6–182.9 mm), Aleutian Is., Umnak I., off Nikolski, 31 July 1896; USNM 130725, 3(287–310 mm), 40 mi above Port Moller, 8 May 1941; USNM 060905, 1(316.5 mm), Karluk, TT2204, RV *Albatross*; UW 001378, 1(175.5 mm), Unalaska I., 1930; UW 003656, 1(100.5 mm), Alaska Peninsula. Cold Bay, 13 June 1932; UW 013667, 1(208.1 mm), Unimak I., False Pass, 1 July 1957; UW 016609, 1(191 mm), Pribilof Is., St. George I.; UW 025736, 3(28–45.7 mm), Port Moller; UW 016600, 3(83.9–130.9 mm), 58.5833°N, 168.1°W, 4 July 1949; UW 003100, 3(86.7–164.6 mm), Captains Bay, Unalaska I.; UW 10650, 2(81.6–112.8 mm), off Nunivak I., 59°36'N, 167°56'W; UW 14831, 1(83 mm), off Nunivak I., 59.82°N, 169.13°W, 4 July 1949; UW 25760, 1(193 mm), 57.65°N, 167.65°W; UW 25731, 1(178.9 mm), 57.6667°N, 167.2°W, 27 April 1987; UBC 65-39, 1(175 mm), Izembeck Bay, 31 August 1964; UBC 62-565, 2(198–229 mm), 120 km E of St. George I.; UBC 65-730, 2(220–245 mm), 57°45'N, 164°45'W, 16 August 1965; UBC 65-714, 1(160 mm), 57°45'N, 168°45'W, 1 August 1965; UBC 65-729, 1(150 mm), 55°45'N, 162°45'W, 14 August 1965; Gulf of Alaska: ABL 72-74, 6(26–59.3 mm), SE shore of Favorite Channel, 10 November 1972; ABL Uncat, 1(195 mm), Unalaska I., 18 June 1958; 86ABL 62-202, 3(83.5–88 mm), Auke Bay, ca. 17.6 km NW of Juneau, 23 May 1962; ABL 62-199, 1(52.3 mm), 19.2 km NW of Juneau; ABL 64-996, 2(65.6–69.5 mm), Auke Bay, ca. 17.6 km NW of Juneau, 30 April 1964; ABL 67-32,

1(265 mm), Baranof I., Katlian Bay, 19 April 1967; OS 17158, 20(227–315 mm), 55.3323°N, 161.3186°W, 32 m, 3 June 1996; OS 17157, 3(230–262 mm), Aleutian Is., 51.88373°N 179.7202°E, 95 m, 16 July 1997; OS 3497, 1(213 mm), False Pass, Ikatan Bay, 19 June 1956; OS out of 6447, 2(166.1–170.2 mm), 57°10'N, 151°40.5'W, 77 m, 20 September 1978; OS 2157, 1(92 mm), Kodiak I., Shelikof St., mouth of Sturgeon R., 9–10 September 1954; OS 2169, 1(64 mm), Moffet Pt. to Black Hill, 28 May 1957; OS 2173, 1(63.5 mm), Moffet Pt. to Black Hill, 3 June 1957; OS 3979, 1(94.6 mm), Little Port Walter, 8 August 1964; SIO 69-748, 3(51–195 mm) of 7(51–195 mm), Afognak I., Kitoi Bay, 16–21 April 1968; SIO 76-299, 1(270 mm), Kodiak shelf, 56°43'N, 153°22'W, 25 June 1976; SIO 72-227, 1(235 mm), 40 km NW of Juneau, Lynn Canal, 16 February 1963; USNM 130734, 1(254.5 mm), Ivanof Bay, 3 April 1941; USNM 27602, 1(261.8 mm), Kodiak I., 12 July 1880; USNM 27942, 1(260.2 mm), Cook Inlet, Port Chatham; USNM 116332, 2(293–295 mm), Canoe Bay, 17 September–15 October 1940; UW 003854, 1(355 mm), Alitak Bay, Kodiak I., 9 June 1932; UW 040498, 1(195 mm), Prince William Sound, 1989; UW 025740, 1(68.4 mm), Ugak Bay, Kodiak I.; UW 044029, 1(276 mm), 59.5743°N, 151.325°W, 11 m depth, 26 February 1996; UW 044001, 18(52.7–99 mm) [3(30–40 mm) of 18 used for illustration], Prince William Sound; UBC 59-485, 2(71–116.2 mm), Chief Cove, Spiridon Bay; UBC 65-572, 1(74 mm), Boussole Bay, 29 June 1965; UBC 63-174, 1(290 mm), Prince William Sound, off Cordova; UBC 65-148, 1(205 mm), W of Chirikof I., 3 August 1964. British Columbia: SIO 63-206-64B, 1(97 mm), Vancouver I., Stanley Park at Lumberman's Arch, 15 March 1963; UBC 56-83, 3(83.5–121.3 mm), Strait of Georgia, off Saturna I.; UBC 62-874, 1(120 mm), off Sooke, 20 June 1962; Puget Sound: OS 3565, 1(224 mm), Puget Sound, 3 February 1943; UW 041078, 2(126–144 mm), Nisqually Reach, 25 February 1949; UW 004411, 1(36 mm), Edmonds, 1 June 1938; UW 000203, 1(45.9 mm), Lopez I., 12 August 1929; UW 041678, 1(67.2 mm), San Juan Islands, East Sound, 11 December 1964; UW 041675, 3(53.7–166.5 mm), Port Townsend Bay, 5 December 1978–5 January 1979; UW 018096, 1(182.4 mm), Bellingham Bay, Chuckanut Bay, May 1964; UW 044014, 29(121–223 mm), 47°19.48'N,

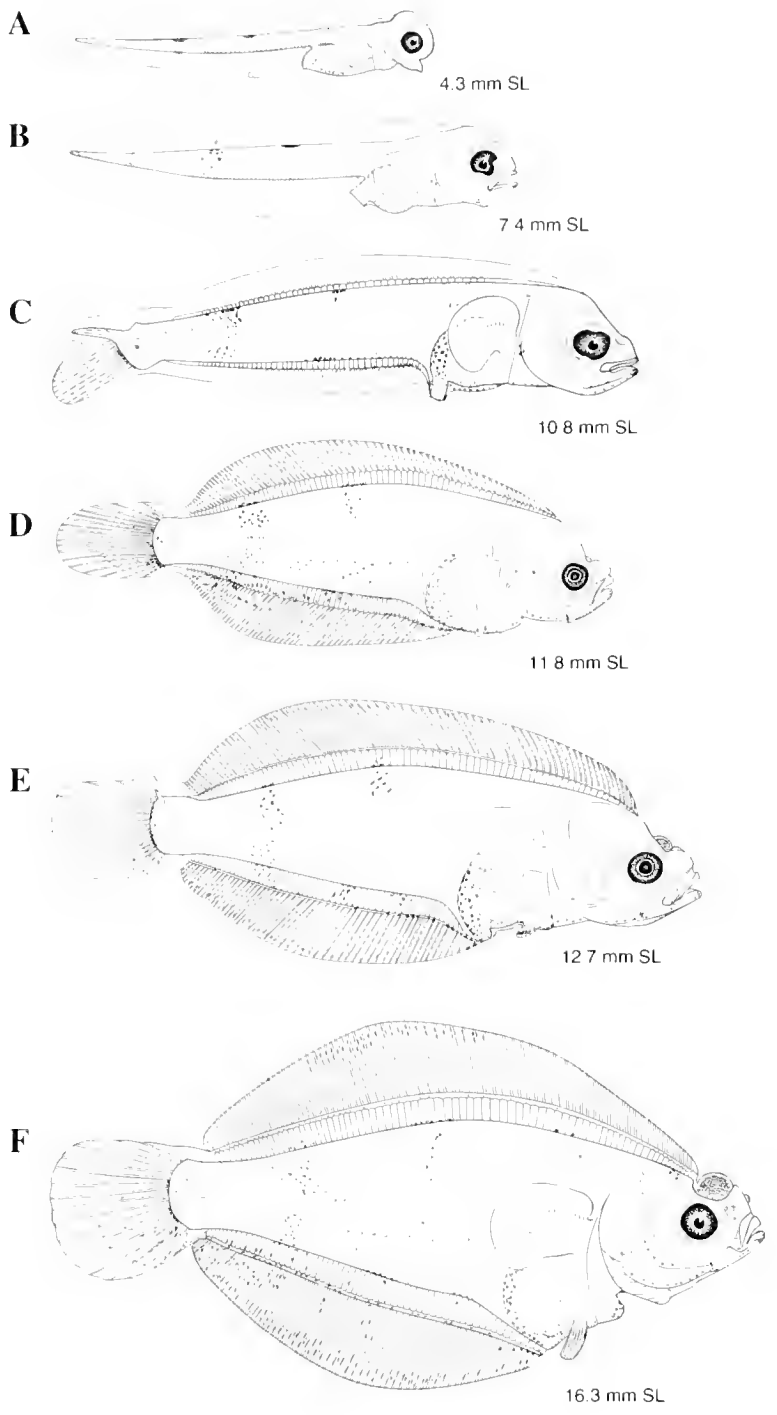

Figure 23

Larvae of *Lepidopsetta polyxystra* n. sp.: **(A)** UW 069346, 4.3 mm, Gulf of Alaska, 30 March 1978 (Matarese et al., 1989); **(B)** UW 083455, 7.4 mm, Gulf of Alaska, 15 May 1979 (Matarese et al., 1989); **(C)** UW 083446, 10.8 mm, Bering Sea, 26 July 1971 (Matarese et al., 1989); **(D)** UW 063735, 11.8 mm, Gulf of Alaska, 25 May 1985; **(E)** UW 083453, 12.7 mm, Gulf of Alaska, 24 June 1978; **(F)** UW 083454, 16.3 mm, Gulf of Alaska, 24 June 1978 (Matarese et al., 1989). Illustrations by B. Vinter, under contract to the National Marine Fisheries Service, Alaska Fisheries Science Center.

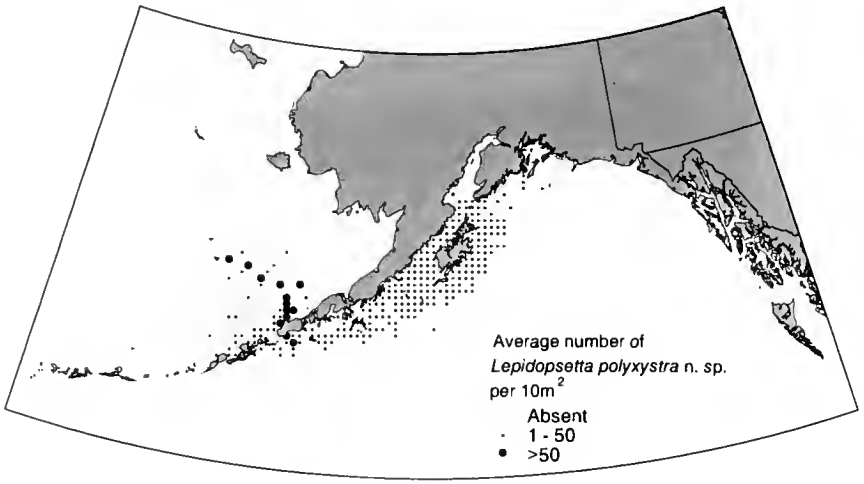

Figure 24

Distribution and density (average number per 10 m^2) of *Lepidopsetta polyxystra* n. sp. in the Gulf of Alaska and Bering Sea, 1972–1994.

122°33.8'W, 10 May 1996; UW 044007, 9(135–200 mm), Nisqually, 47°9.47'N, 122°40.16'W, 16 May 1996.

Larvae 18 specimens, 3.3–18.6 mm, examined. Bering Sea: UW 083475, 1(3.7 mm), 55°47.0'N, 165°59.0'W, 0–117 m depth, bongo net, 19 April 1991; Gulf of Alaska: UW 083456, 1(3.3 mm), 58°22.0'N, 150°06.0'W, 0–52 m depth, bongo net, 9 April 1991; UW 083479, 1(11.2 mm), 57°19.0'N, 156°09.0'W, 0–100 m depth, bongo net, 4 June 1990; UW 083457, 1(4.2 mm), 56°30.0'N, 157°00.2'W, 0–43 m depth, bongo net, 24 April 1991; UW 083476, 1(5.2 mm), 56°54.3'N, 156°15.3'W, 0–100 m depth, bongo net, 9 May 1992; UW 083461, 1(6.4 mm), 56°46.1'N, 156°47.9'W, 0–47 m depth, bongo net, 24 May 1991; UW 083472, 1(7.2 mm), 56°46.2'N, 156°33.6'W, 0–99 m depth, bongo net (333 mesh), 13 May 1992; UW 083471, 1(8.8 mm), 56°46.2'N, 156°33.6'W, 0–99 m depth, bongo net, 13 May 1992; UW 083478, 2 of 10 (10.0–10.7 mm), 56°56.7'N, 154°43.2'W, 0–42 m depth, bongo net, 5 June 1990; UW 083481, 2(13.6–14.2 mm), 56°54.0'N, 156°29.5'W, 0–84 m depth, bongo net, 3 June 1990; UW 083477, 1(5.7 mm), 55°57.0'N, 158°33.1'W, 0–100 m depth, bongo net, 21 May 1991; UW 083480, 2(12.4–12.6 mm), 55°39.1'N, 156°3.4'W, 0–100 m depth, bongo net, 31 May 1990; UW 083451, 1(17.8 mm), 55°18.1'N, 160°12.0'W, 0–115 m depth, Methot net, 24 July 1991; UW 083450, 1(15.3 mm), 54°39.2'N, 159°23.0'W, 0–54 m depth, Methot net, 29 July 1991; UW 083452, 1(18.6 mm), 54°36.2'N, 162°16.2'W, 0–87 m depth, Methot net, 30 July 1991.

Other material examined

Adults 629 adults and juveniles. Bering Sea: UW 044023, 6(173–292 mm), 60.6869°N, 175.4609°W, 11 July 1995; UW 044020, 2(331–368.5 mm), 58.45°N, 174.33°W; UW 044003, 2(226–249 mm), 58.12°N, 168.43°W; UW 041699, 1(108 mm), 58.66°N, 159.47°W; Gulf of Alaska: UW 044015, 307(18.2–190 mm), Kachemak Bay; UW 044016, 1(37.5 mm), Kachemak Bay; UW 044018, 54(26–90 mm), Kachemak Bay; SIO 76-300, 3(161–200 mm) of 28(145–280 mm), Kodiak shelf, 57°40'N, 150°37'W, 15 March 1963; ABL 68-505, 2(128–140 mm) of 15(15–140 mm) examined, Glacier Bay, 8 August 1968; UW 025735, 2(35.8–61.8 mm), "6/10/83, Sta. 14, Haul 52"; UW 04321, 1(230 mm), Fishing Vessel *Sulak*, Cruise 436, Robin Scheid; UW 002688, 83(56–107 mm), Shumagin Is., Baralof Bay, 27 June 1931; UW 002032, 30(75–137 mm), Yakutat Bay, 21 June 1932. UW 041674, 11(67.5–139 mm), Alexander Archipelago, off Wrangell I., 1 December 1931; UW 003841, 13(72–99 mm), Yakutat Bay, 21 June 1932; UW 004004, 7(77–100 mm), Yakutat Bay, 21 June 1932; UW 005047, 6(97–120 mm), Alitak Bay, 9 June 1932; UW 041681, 1(119.5 mm), Prince William Sound, 1989; UW 002069, 8(106–157.3 mm), Cold Bay, 6-26 May 1932; UW 022413, 5 cleared and stained of 14(53–110 mm), Adak I., Aleutian Is.; UW 040265, 16(159–350 mm), 54.03899°N, 165.8153°W; UW 003913, 5(113.4–167 mm), Prince William Sound, Orca Inlet, 2 April 1935; UW 044012, 6(275–384 mm), 56.5°N, 153.5°W, Bonaduhr; UW 020658, 7(56.1–135.7 mm), Kodiak I., Ugak Bay; UW 025763, 1(139.7 mm), off Amchitka I.; UW 040263, 3(214–255 mm), 54°N, 160.74°W. British Columbia: UBC out of 61-609, 3(44.8–56.6 mm), Bute Inlet; UBC out of 60–416, 6(181–230 mm), Queen Charlotte Is., Gillat Arm; UBC out of 62-93, 7(75–111 mm), Nass Bay; UBC out of 61-674, 7(64–81 mm), Dean Channel, off Nescall Bay. Washington, Oregon, and California: UW 041673, 5(68–110.5 mm), San Juan Is., East Sound, 3 March 1937; UW 047270, 6(60–240 mm), Puget Sound, Port Townsend Bay; CAS 19305, 1(246.5 mm), San Francisco (see comments).

Larvae 42 specimens (4.2–20.0 mm) examined: Bering Sea: UW 083446, 1(10.8 mm), 57°30.0'N, 169°30.0'W, depth unknown, bongo net, 26 July 1971; UW 083447, 1(4.5 mm), 54°01.3'N, 166°33.9'W, 0–100 m depth, bongo net, 25 April 1993; Western Gulf of Alaska: UW 083448, 1(15.1 mm),

55°17.7'N, 160°11.7'W, 0–115 m depth, Methot net, 24 July 1991; UW 083449, 1(15.3 mm), 54°39.2'N, 159°23.0'W, 0–54 m depth, Methot net, 29 July 1991; UW 071740, 1(12.0 mm; 11.0 mm as measured in this study), 55°38.6'N, 153°30.1'W, 0–102 m depth, bongo net, 31 May 1990; UW 071752, 1(10.0 mm; 9.4 mm as measured in this study), 55°31.6'N, 156°16.3'W, 0–100 m depth, bongo net, 31 May 1990; UW 072106, 1 of 2(17.1 mm), 56°46.2'N, 156°33.6'W, 0–100 m depth, bongo net, 3 June 1990; Gulf of Alaska: UW 069346, 1(4.3 mm) of 9, 58°22.0'N, 150°12.8'W, 0–47 m depth, bongo net, 30 March 1978; UW 083453, 1(12.7 mm), 56°41.9'N, 154°33.2'W, 0–16 m depth, bongo net, 24 June 1978; UW 083454, 1(16.3 mm), 57°19.5'N, 152°23.9'W, 0–48 m depth, bongo net, 24 June 1978; UW 083455, 1(7.4 mm), 56°23.7'N, 155°45.0'W, 0–79 m depth, bongo net, 15 May 1979; UW 063735, 1 of 12 (11.8 mm), 56°35.1'N, 153°43.6'W, 0–70 m depth, bongo net, 25 May 1985; UW 072459, 1 of 10 (9.4 mm), 57°10.7'N, 155°12.9'W, 0–100 m depth, bongo net, 5 June 1990; UW 072497, 6 of 10 (7.4–12.6 mm), 56°56.7'N, 154°43.2'W, 0–42 m depth, bongo net, 5 June 1990; UW 072502, 4 of 9 (7.3–10.3 mm), 56°49.4'N, 154°30.3'W, 0–60 m depth, bongo net, 5 June 1990; UW 072511, 1(12.2 mm), 57°28.6'N, 154°42.4'W, 0–60 m depth, bongo net, 5 June 1990; UW 072546, 1(8.1 mm), 57°40.6'N, 155°10.5'W, 0–287 m depth, bongo net, 6 June 1990; UW 083458, 1(6.8 mm), 57°15.6'N, 155°55.4'W, depth unknown, Mocness net, 14 May 1991; UW 083460, 1(6.4 mm), 56°16.4'N, 158°04.9'W, 0–64 m depth, bongo net, 22 May 1991; UW 083463, 1(4.2 mm), 57°52.3'N, 155°0.1'W, 0–82 m depth, bongo net, 7 April 1992; UW 083464, 1(5.0 mm), 57°42.2'N, 154°47.3'W, 0–219 m depth, bongo net, 7 April 1992; UW 083465, 1(5.5 mm), 57°16.5'N, 155°55.0'W, 0–100 m depth, bongo net, 8 May 1992; UW 083466, 1(5.8 mm), 56°54.3'N, 156°15.3'W, 0–100 m depth, bongo net, 9 May 1992; UW 083467, 3(4.6–6.0 mm), 56°51.8'N, 156°21.4'W, 0–99 m depth, bongo net, 9 May 1992; UW 083468, 1(6.1 mm), 56°53.3'N, 156°23.9'W, 0–102 m depth, bongo net, 9 May 1992; UW 083469, 1(8.5 mm), 56°42.2'N, 156°32.3'W, 0–100 m depth, bongo net, 13 May 1992; UW 083470, 1(6.7 mm), 56°44.4'N, 156°28.7'W, 0–102 m depth, bongo net, 13 May 1992; UW 083473, 1(7.6 mm), 56°09.4'N, 157°14.3'W, 0–101 m depth, bongo net, 22 May 1992; UW 083474, 1(7.5 mm), 56°40.6'N, 155°10.4'W, 0–59 m depth, bongo net, 15 May 1992; UW 083482, 2(19.0–20.0 mm), 47°34.15'N, 122°32.30'W, 0 m depth, dip net, 9 May 1990.

Diagnosis

Lepidopsetta polyxystra is a species of *Lepidopsetta* with the following combination of characters in adults: total gill rakers on first arch 9–14, on upper arch 2–6; total gill rakers on second arch 8–14; supraorbital pores 1–3, rarely 4–7; preopercular pores 5–8; lateral-line pores 76–100; sum of scales above and below lateral line 66–96; interorbital wide; blind side coloration in life creamy, without glossy highlights along margins of myotomes.

Larvae are distinguished from other species of *Lepidopsetta* by the following characters: body slender; snout-to-anus length long; larvae undergo hatching, flexion, and transformation at comparatively larger sizes; preflexion pigment pattern with light pigmentation along finfolds, limited mainly to the ventral finfold, and two pigment spots along the dorsal midline (the posteriormost aligning with a ventral patch forming a bar), a series of small melanophores extending from just posterior to the anus to just beyond the postanal bar (about 2/3 body); and flexion pigment pattern with a single bar located on the postanal body; pectoral-fin rays unpigmented.

Description of adults

Body ovate, greatest depth 41.2-58.9 (49.0)% SL, scales above lateral line 27–40, scales below lateral line 38–59; head relatively acute, length 21.8–31.5 (27.2)% SL; dorsal margin of head at dorsal-fin origin slightly concave, snout length 3.1–5.7 (4.4)% SL (12.1–20.1 (16.0)% HL); ocular-side maxilla length 20.4-31.5 (26.3)% HL; blind-side maxilla length 22.2–35.7 (28.7)% HL; ocular-side mandible length 34.4–50.0 (40.7)% HL; teeth 4–5 on ocular-side premaxilla, 23–24 on blind-side premaxilla and 8–9 on ocular-side dentary, 20–24 on blind-side dentary; gill rakers of first arch relatively slender, 9–14 total, 3–6 on upper arch, 6–9 on lower arch; gill rakers of second arch 8–14 total with 0–4 on upper and 7–13 on lower arch; dorsal orbit length often with posteriorly elongate rim and much longer than eye length, orbit length 22.2–32.9 (28.1)% HL, dorsal eye length 18.5–32.9 (23.0)% HL; ventral eye length 17.2–31.1 (24.2)% SL; interorbital wide, up to 5 scales at narrowest portion, 2.5–6.6 (4.4)% HL; cheek with 7–12 scales, length 26.7–38.5 (32.5)% HL, depth 13.6–22.7 (18.7)% HL; preopercular pores 5–8; ocular-side suborbital pores 13–29; blind-side suborbital pores 8–14; lateral line pores 76–100, lateral-line arch length 26.1–64.5 (52.3)% HL, its depth 26.3–38.2 (31.7)% its length; both anterior and posterior supratemporal branches relatively long, anterior pores 3–15, posterior pores 10–35; supraorbital canal short, reaching only to the posterior rim of the dorsal orbit at about the insertion of dorsal-fin rays 5–6, pores 1–3, rarely 4–7; ocular-side pectoral-fin length 10.7–18.2 (14.7)% SL (38.3–70.4 (53.9)% HL); blind-side pectoral-fin length 6.6–12.7 (10.2)% SL (24.2–49.6 (37.4)% HL); ocular-side pelvic-fin length 7.8–12.2 (9.9)% SL (27.6–45.9 (36.6)% HL); dorsal fin with 64–83 rays, height 10.2–16.6 (13.5)% SL, in specimens with 69–80 rays supported by 68–78 pterygiophores, typically 9 or rarely 8 anterior to first neural spine; anal fin with 49–64 rays, in specimens with 55–61 rays supported by 53–63 pterygiophores; caudal peduncle relatively slender, least depth 9.4–13.1 (10.9)% SL (32.2-48.8 (40.2)% HL, 101.2-144.2 (123)% caudal peduncle length), greatest depth 10.1–16.9 (12.3)% SL (38.1–57.7 (45.2)% HL); caudal peduncle length 7.0–10.1 (8.9)% SL (27.6–42.0 (32.7)% HL); caudal-fin length 17.8–29.1 (22.7)% SL. Vertebrae 39–41, with 10–11 precaudal and 29–30 caudal.

Scales around head and those scattered posteriorly on ocular side very rough, with columnar tubercles in large adults; strong spines in small adults and juveniles. Urogenital flap unpigmented or lightly pigmented in 23–80 mm juveniles.

In life, blind side in moderate to large adults creamy white, skin opaque (Amaoka et al., 1995, Fig. 525); in juveniles, blind side nearly completely translucent, with small, white glossy areas on head. When preserved, blind side of all individuals uniform creamy white to yellow-brown. Ocular

side slightly less green than that of congeneric in Puget Sound, often with faint yellow highlights around darker spots near bases of dorsal and anal fins and at midline.

Remaining description as for genus. Largest specimen examined 340 mm (427.5 mm TL) (UW 040265). Maximum size reported 588 mm (Fadeev, 1965) to 690 mm TL.[6]

Description of juveniles

Individuals of about 20 mm collected in water column (one 19.0-mm individual examined, UW 083482, not completely transformed; see comments); lateral line and pectoral-fin rays undeveloped; body pigmentation increasing throughout; bars and patches of postflexion larval pigmentation pattern visible; urogenital papilla light or speckled with an unpigmented tip. Eye length smaller, mouth larger, body deeper, gill-raker counts on lower arch higher, distance from pelvic-fin origin to anal-fin origin shorter, expanded anteriormost anal-fin pterygiophore less developed (not protruding beyond body wall in our material) than in similar-size *L. bilineata*.

By 35 mm, many individuals collected near bottom. Postsettlement juveniles (Fig. 22B) as developed as similar-size *L. bilineata*: increased body pigmentation giving juveniles a darker appearance (obscuring urogenital papillae pigment), rays of paired and median fins formed, lateral line formed, supraorbital pores present, expanded anteriormost anal-fin pterygiophore strongly developed.

Description of larvae

Snout-to-anus length 32.1–39.3% SL, remaining constant during development; body depth 3.8–28.5% SL, increasing with development, sharply increasing after flexion; head length 11.6–26.7% SL, increasing with development; snout length 22.8–24.7% HL, remaining constant during development; orbit length 51.8–20.9% HL, decreasing with development (Table 2). Total myomeres 38–42.

Larvae hatching at greater than 3.0 mm (3.6–4.0 mm, Pertseva-Ostroumova, 1961); yolk absorbed by 3.3–4.2 mm. Preflexion larvae ranging in size from 4.2 to 6.2 mm; flexion larvae, 6.2–12.6 mm; postflexion larvae, 12.2–18.6 mm. Transformation occurring at sizes as small as 15.0 mm; postsettlement stage usually not complete by 20.0 mm (Table 13).

Head pigment present initially along lower jaw and underside of chin (Fig. 23); increasing with development to snout, upper jaw, and isthmus. Pigment ventrally along gut and dorsally on anus; by flexion a distinct patch of melanophores along posterior edge of gut; pigment increasing laterally with development.

Postanal pigment light along the anal finfold, melanophores absent on dorsal finfold (Fig. 23); two pigment patches along the dorsal midline, anterior patch beginning about midbody at myomere 18–20, posterior patch beginning about myomere 30, posterior patch aligning with a ventral patch forming a postanal bar; series of melanophores along the ventral body midline beginning just posterior to the anus, extending to just beyond the postanal bar (about 2/3 body length); a few melanophores on caudal peduncle and above and below the notochord tip.

Distribution (Figs. 8, 11, 13, 24)

Ranging from the northern coast of Hokkaido throughout the Kuril Islands and the Okhotsk Sea of the western North Pacific, through the Bering Sea, from the Gulf of Anadyr[13] to off St. Lawrence Island (Allen and Smith, 1988), to Puget Sound, Washington, in the eastern North Pacific. Large concentrations have been reported from the west and southeast of the Kamchatka Peninsula, where it once composed 90% of the fisheries catches of pleuronectids (Shubnikov and Lisovenko, 1964), and from the southeastern Bering Sea. Minami and Nakamura (1978) also reported a single specimen of *L. bilineata* (=*L. polyxystra* n. sp. based on distribution) among many *L. mochigarei* from Wakasa Bay, Japan (ca. 35.7°N, 135.5°E); this specimen could not be located.[14] Larvae have been collected from Puget Sound, the east coast and northern tip of Vancouver Island, Hecate Strait, and north along the coasts of Alaska into the Bering Sea. According to Okiyama (1988), larvae occur along the coast of the Kuril Islands, the coast of Kamchatka, and into the Bering Sea.

The recorded locality of one adult (CAS 19305) from San Francisco Bay, over 1200 km south of the nearest verified capture in Puget Sound, is questionable. Although no evidence from catalog records[8] indicates that the specimen had been misplaced, the specimen was collected in 1888 and has an original catalog number from the Indiana University collection. Its morphology and meristics are distinctively that of more northerly populations.

Habitat

Lepidopsetta collected in the eastern Bering Sea are most commonly associated with sand, and least with "sand and mud," when compared with all other measured substrate types in the Bering Sea, including combinations of sand, gravel, and mud.[15] The maximum depth of collection was 246 m.[16] During the 22-year ichthyoplankton sampling period (all previously unidentified pleuronectid larvae were re-examined, thus providing the only historic distributional records for larvae of *L. polyxystra* n. sp.), larvae were common in spring surveys conducted in the Gulf of Alaska and Bering Sea, when they first appear in March collections; largest catches have been taken in May.

[13] Kessler, D. 1997. Personal commun. Under contract to Resource Assessment and Conservation Engineering Division, Alaska Fisheries Science Center, Natl. Mar. Fish. Serv., NOAA, 7600 Sand Point Way NE, Seattle, WA 98115.

[14] Saruwatari,T. 1997. Personal commun. Ocean Research Institute, University of Tokyo, Tokyo, Japan. Shinohara, G. 1997. Personal commun. Fish Section, Department of Zoology, National Science Museum (Natural History), Huankunin-cho, Shinjuku-ku, Tokyo, Japan.

[15] McConnaughey, R. 1997. Personal commun. Resource Assessment and Conservation Engineering Division, Alaska Fisheries Science Center, Natl. Mar. Fish. Serv., NOAA, 7600 Sand Point Way NE, Seattle, WA 98115.

[16] Resource Assessment and Conservation Engineering (RACE) Division. 1998. Unpubl. data from the RACE database, Alaska Fisheries Science Center, Natl. Mar. Fish. Serv., NOAA, 7600 Sand Point Way NE, Seattle, WA 98115.

Highest densities of larvae occur in the Bering Sea (Fig. 24), compared with the western Gulf of Alaska.

Life history

Lepidopsetta collected from the eastern Bering Sea and Sakhalin Island, presumed to be *L. polyxystra* n. sp., fed primarily on polychaetes and other marine worms; molluscs (Skalkin, 1959, 1963; Lang et al., 1995) or fishes, primarily *Ammodytes hexapterus* in depths >50 m (Lang et al., 1995), were a second significant component of the diet. Feeding took place primarily from May to September, falling to low levels during the winter (Shubnikov and Lisovenko, 1964) when spawning occurs (Fadeev, 1965). Spawning occurs in areas with good water circulation over hard bottoms of sand with gravel and peaks from early March to mid-April in waters off Kamchatka, possibly occurring as late as mid-June in the western Pacific (Pertseva-Ostroumova, 1961). Fecundity ranges from 151,700 to 404,200 eggs (Fadeev, 1965). Life history including spawning and development was discussed by Pertseva-Ostroumova (1961, as *L. bilineata bilineata*) and larval development was described by Okiyama (1988, as *L. bilineata*).

The Washington Department of Fisheries reported *Lepidopsetta* from late December through early March in sandy gravel of upper intertidal beaches at several sites in central and southern Puget Sound (Penttila, 1995). In January 1991, one beach site on the south shore of Dana Passage (the center of a relatively large area of documented *Lepidopsetta* spawning) was the source of six batches of field-collected spawned eggs (each about 1 mm in diameter) that were subsequently reared through hatching. We identified the reared larvae as *L. polyxystra* n. sp. Egg batches ranged in size from 40 to several hundred eggs and were incubated over about 14 days with ambient central Puget Sound water (about 9.0°C[3]). Larvae hatched between 4 and 5 mm and had yellow pigmentation associated with the melanophores. For additional early life history information, see generic account.

The maximum recorded age for female *L. polyxystra* n. sp. captured in the Bering Sea is 18 yr at 49 cm FL, and for males is 17 yr at 40 cm FL (Alton and Sample[17]). The gills of adults from the Gulf of Alaska have been found to be heavily infested with copepod parasites *Nectobrachia indivisa*, and *Naobranchia occidentalis*, previously recorded in *Lepidopsetta* by Kabata (1988). For both parasites, *L. polyxystra* n. sp. was significantly more heavily infested than *L. bilineata*.[7] The parasites *Acanthochondria vancouverensis* and *Haemobaphes* sp. were also recorded.

Etymology

The specific name *polyxystra* is derived from the Greek *poly*, meaning many, and *xystrus*, meaning raker, referring to the gill rakers being more numerous than those of congeneric species.

Comments

Under the name of *L. bilineata*, *L. polyxystra* n. sp. has been the subject of many studies. Work on specimens collected north of the extreme southeastern Bering Sea and west of the eastern Aleutian Islands in the western North Pacific may be presumed to be based on *L. polyxystra* n. sp. However, all studies conducted on specimens from the Gulf of Alaska into Puget Sound, regions of extensive overlap in the distributions of *L. polyxystra* n. sp. and *L. bilineata*, should be considered applicable at the generic level only, unless voucher specimens were collected and can be verified.

According to Pertseva-Ostroumova (1961), juveniles as small as 20 mm SL have been collected on the bottom. However, the species exhibits much plasticity in settling size, with specimens much greater than 20 mm SL routinely collected in plankton nets.

A widely published illustration identified as *L. bilineata* is based on a specimen of *L. polyxystra* n. sp. taken off Kodiak Island, Alaska ("St. Paul, Kodiak," USNM 27602), now badly damaged. First published in Goode (1884), it was subsequently reprinted in Jordan and Goss (1889), Jordan and Evermann (1900), Jordan and Starks (1906), and Evermann and Goldsborough (1907) among other publications.

Acknowledgments

Beverly Vinter first noticed an unidentified pleuronectid in our ichthyoplankton samples almost 15 years ago. With support from A. W. Kendall Jr., she persisted over the years in her belief that these larvae represented a new species of pleuronectid. We thank her for her insight as well as her identifications, illustrations, measurements, and numerous examinations of larvae. Early in our study, A. W. Kendall Jr. arranged for the collection of adults, the rearing of larvae (with D. Misitano, formerly of NWFSC), and electrophoretic analysis of samples (with F. Utter formerly of NWFSC). Helen Mulligan (first working at AFSC and later on contract to Humboldt State University) made several significant contributions to the study including a preliminary analysis of the geographic distribution of larval and adult *Lepidopsetta* that provided evidence supporting a taxonomic basis for the observed differences in larval shape and structure. Maryjane Cleveland, a domestic fisheries observer, provided detailed notes of her observations of *Lepidopsetta*, sparking independent early collections of adult samples. Other samples and data have been provided over the years by the AFSC's RACE Division (W. Flerx, G. R. Hoff, R. MacIntosh, G. Walters, and K. Weinberg), Resource Ecology and Fisheries Management Division's Observer Program (S. Barbeaux, M. Brown, S. Corey, K. Kruse, M. Loefflad, R. Narita, N. Raring, and K. Scott), and by the Alaska Department of Fish and Game (H. Sanborn and D. Urban). Biologists of the Washington Department of Fish and Wildlife, including W. A. Palsson, R. Pacunski, and G. Lippert, provided comparative photographs, specimens, and data for the Puget Sound. Jeff Marliave

[17] Alton, M. A., and T. Sample. 1976. Rock sole (family Pleuronectidae). *In* Demersal fish and shellfish resources of the eastern Bering Sea in the baseline year 1975 (W. T. Pereyra, J. E. Reeves, and R. G. Bakkala), p. 461–474. Northwest and Alaska Fish. Center Proc. Rep., Seattle, WA.

(Vancouver Public Aquarium) also provided Canadian larval material. Data on distribution and abundance of larvae and juveniles have been provided by H. G. Moser (SWFSC), W. Shaw (DFO, PBS), B. L. Norcross, A. A. Abookire, and B. Holladay (UA, Fairbanks), and D. Penttila (WDF). Several scientists at AFSC assisted throughout this study: D. M. Blood and M. S. Busby (collections at sea and technical assistance), L. Ciannelli (measurements), K. Mier (statistical analyses), S. Picquelle (mapping software and CPUE calculations), R. C. Harrison (translations), and W. Rugen (database support). For discussions on pleuronectid characters, osteology, and phylogeny, we thank J. A. Cooper and P. Berendzen. The following curators and collection managers generously provided loans and information on specimens under their care: D. Catania (CAS), W. G. Saul (ANSP), B. A. Brown (AMNH), R. F. Feeney and J. Seigel (LACM), J. D. McPhail, G. Haas, and E. Keeley (UBC), D. F. Markle (OS), B. Sheiko (KIE), T. W. Pietsch and B. K. Urbain (UWFC), S. Jewett and S. J. Raredon (NMNH), R. H. Rosenblatt, H. J. Walker, and C. Klepadlo (SIO), K. Amaoka (HUMZ), G. Shinohara (NSMT), I. Kinoshita (FRSKU), T. Minami (Japan Sea National Fisheries Institute), and B. L. Wing (ABL). We thank the following individuals for their reviews of the manuscript: T. W. Pietsch, W. Aron, G. R. Hoff, M. S. Busby, A. W. Kendall Jr., C. W. Mecklenburg, E. S. Brown, and H. H. Zenger.

Literature cited

Ahlstrom, E. H., K. Amaoka, D. A. Hensley, H. G. Moser, and B. Y. Sumida.
1984. Pleuronectiformes: Development. *In* Ontogeny and systematics of fishes (H. G. Moser, W. J. Richards, D. M. Cohen, M. P. Fahay, A. W. Kendall Jr., and S. L. Richardson, eds.), p. 640–670. Am. Soc. Ichthy. Herpet. Spec. Publ. 1.

Allen, M. J., and G. B. Smith.
1988. Atlas and zoogeography of common fishes in the Bering Sea and northeastern Pacific. U.S. Dep. Commer., NOAA Tech. Rep., NMFS 66, 151 p.

Amaoka, K., K. Nakaya, and M. Yabe.
1995. The fishes of northern Japan. Kitanihon Kaiyo Center Co., Sapporo, Hokkaido, 387 p.

Amaoka, K., K. Nakaya, and H. Yamamoto.
1983. Fishes and marine algae of northern Japan. Kitanihon Kaiyo Center Co., Sapporo, Hokkaido, 371 p.

Ayres, W. O
1855a. [Description of new fishes from California.] The Pacific 4(18).
1855b. [Description of a new flounder.] Proc. Calif. Acad. Sci. 1:39–40.

Berendzen, P. B.
1998. Phylogenetic analysis of the order Pleuronectiformes using molecular and morphological evidence. M.S. thesis, Univ. Kansas, Lawrence, KS, 61 p.

Blackburn, J. E.
1973. A survey of the abundance, distribution, and factors affecting distribution of ichthyoplankton in Skagit Bay. M.S. thesis, Univ. Washington, Seattle, WA, 136 p.

Busby, M. S., A. C. Matarese, and K. L. Mier.
2000. Annual, seasonal, and diel composition of larval and juvenile fishes collected by dip-net in Clam Bay, Puget Sound, Washington, from 1985 to 1995. U.S. Dep. Commer., NOAA Tech. Memo. NMFS-AFSC-111, 36 p.

Chapleau, F.
1993. Pleuronectiform relationships: a cladistic reassessment. Bull. Mar. Sci. 52(1):516–540.

Charter, S. R., and H. G. Moser.
1996. Pleuronectidae: righteye flounders. *In* The early stages of fishes in the California Current Region (H. G. Moser, ed.), p. 1369–1403. CalCOFI Atlas 33.

Cooper, J., and F. Chapleau.
1996. The monophyletic status of *Pleuronectes* (Pleuronectidae: Pleuronectiformes). *In* Abstracts of the 1996 Annual Meeting of the American Society of Ichthyologists and Herpetologists, New Orleans, LA, p. 114.
1998. Monophyly and intrarelationships of the family Pleuronectidae (Pleuronectiformes), with a revised classification. Fish. Bull. 96:686–726.

Cope, E. D.
1873. A contribution to the ichthyology of Alaska. Proc. Am. Phil. Soc. 13:24–32.

Environmental Systems Research Institute.
1996. Arcview GIS, ver. 3.0. Environmental Systems Research Institute, Redlands, CA, 614 p.

Evermann, B. W., and E. L. Goldsborough.
1907. The fishes of Alaska. Bull. Bur. Fish. 26:219–360.

Fadeev, N. S.
1965. Comparative outline of the biology of flatfishes in the southeastern part of the Bering Sea and condition of their resources. Soviet Fisheries Investigations in the northeast Pacific, Part 4. Pacific Scientific Research Institute of Marine Fisheries and Oceanography (TINRO). Izvestiya 58:112–129. [1968 transl. by Israel Prog. Sci. Transl.]

Forrester, C. R.
1969. Life history information on some groundfish species. Fish. Res. Board Can. Tech. Rep. 105, 17 p.

Forrester, C. R., and J. A. Thompson.
1969. Population studies on the rock sole (*Lepidopsetta bilineata* (Ayres)) of northern Hecate Strait, B.C. Fish. Res. Board Can., Tech. Rep. 108, 104 p.

Garrison, K. J., and B. S. Miller.
1982. Review of the early life history of Puget Sound fishes. Report FRI-UW-8216 of the Fish. Res. Inst., Univ. Washington, Seattle, WA, 729 p.

Gill, T. N.
1862. Note on some genera of fishes of western North America. Proc. Acad. Nat. Sci. Phila. 14:329–332.
1864. Synopsis of the pleuronectoids of California and northwestern America. Proc. Acad. Nat. Sci. Phila. 16:194–198.

Girard, C. F.
1854. Descriptions of new fishes, collected by Dr. A. L. Heermann, naturalist attached to the survey of the Pacific railroad route, under Lieut. R. S. Williamson, U.S.A. Proc. Acad. Nat. Sci. Phila. 7:129–140.
1856. Contributions to the ichthyology of the western coast of the United States, from specimens in the collection of the Smithsonian Institution. Proc. Acad. Nat. Sci. Phila. 8:131–137.

Goode, G. B.
1884. The fisheries and fishery industries of the United States. Section I. Natural history of useful aquatic animals with an atlas of two hundred and seventy-seven plates. Plates. Government Printing Office, Washington, D.C., 215 p.

Gunther, A.
1862. Catalogue of the fishes in the British Museum. Catalogue of the Acanthopterygii Pharyngognathi and Anacanthini in the collection of the British Museum, vol. 4, 534 p.

Hart, J. L.
1973. Pacific fishes of Canada. Bull. Fish. Res. Board Can. 180, 740 p.

Hickman, C. P., Jr.
1959. The larval development of the sand sole (*Psettichthys melanostictus*). Wash. Dep. Fish. Res. Pap. 2:38–47.
Hubbs, C. L.
1915. Flounders and soles from Japan collected by the United States Bureau of Fisheries steamer "*Albatross*" in 1906. Proc. U.S. Natl. Mus. 48:449–496.
Hubbs, C. L., and K. F. Lagler.
1958. Fishes of the Great Lakes region. Cranbrook Inst. Sci., Ann Arbor, MI, 213 p.
Ivankov, V. N.
1996. Review of the book by G. U. Lindberg and V. V. Fedorov, The fishes of the Sea of Japan and adjacent parts of the Sea of Okhotsk and the Yellow Sea. Part 6. Teleostomi, Osteichthyes, Actinopterygii. XXXI. Pleuronectiformes—Family Psettodidae—CCICFamily Cynoglossidae. J. Ichthyol. 36(7):549–550. [Transl. by P. A. Aleinikov.]
Jordan, D. S., and B. W. Evermann.
1898. The fishes of North and Middle America: a descriptive catalogue of the species of fish-like vertebrates found in the waters of North America, north of the Isthmus of Panama. Part III. Bull. U.S. Natl. Mus. 47:2183–3136.
1900. The fishes of North and Middle America: a descriptive catalogue of the species of fish-like vertebrates found in the waters of North America, north of the Isthmus of Panama. Part IV. Bull. U.S. Natl. Mus. 47:3137–3313.
Jordan, D. S., and C. H. Gilbert.
1881. List of the fishes of the Pacific Coast of the United States, with a table showing the distribution of the species. Proc. U.S. Natl. Mus. 3:452–458.
Jordan, D. S., and D. K. Goss.
1889. A review of the flounders and soles (Pleuronectidae) of America and Europe. Rep. U.S. Fish Comm. 14:225–342.
Jordan, D. S., and C. L. Hubbs.
1925. Record of fishes obtained by David Starr Jordan in Japan, 1922. Mem. Ann. Carnegie Mus. 10(2):93–346.
Jordan, D. S., and E. C. Starks.
1906. A review of the flounders and soles of Japan. Proc. U.S. Natl. Mus. 31(1484):161–246.
Kabata, Z.
1988. Copepoda and Branchiura. *In* Guide to the parasites of fishes of Canada, part II— Crustacea (L. Margolis and Z. Kabata, eds.), p. 3–127. Can. Spec. Publ. Fish. Aquat. Sci. 101.
Kendall, A. W., Jr., E. H. Ahlstrom, and H. G. Moser.
1984. Early life history stages of fishes and their characters. *In* Ontogeny and systematics of fishes (H. G. Moser, W. J. Richards, D. M. Cohen, M. P. Fahay, A. W. Kendall Jr., and S. L. Richardson, eds.), p. 11–22. Am. Soc. Ichthy. Herpet. Spec. Publ. 1.
Kim, I. S., and C. H. Youn.
1994. Taxonomic revision of the flounders (Pisces: Pleuronectiformes) from Korea. Korean J. Ichthy. 6(2):99–131.
Kravitz, M., W. G. Pearcy, and M. P. Guin.
1976. Food of five species of co-occurring flatfishes on Oregon's continental shelf. Fish. Bull. 74:984–990.
Lang, G. M., P. A. Livingston, and B. S. Miller.
1995. Food habits of three congeneric flatfishes: yellowfin sole (*Pleuronectes asper*), rock sole (*P. bilineatus*), and Alaska plaice (*P. quadrituberculatus*) in the eastern Bering Sea. Proc. InterNatl. Symp. N. Pac. Flatfish, Alaska Sea Grant Prog. Report AK-SG-95-04, p. 225–245.
Levings, C. D.
1967. A comparison of growth rates of the rock sole (*Lepidopsetta bilineata*) Ayres, in northeast Pacific waters. Fish. Res. Board Can., Tech. Rep. 36, 43 p.
Leviton, A. E., and M. L. Aldrich.
1997. Theodore Henry Hittell's "The California Academy of Sciences, a narrative history: 1853–1906." Calif. Acad. Sci., San Francisco, CA, 623 p.
Leviton, A. E., and R. H. Gibbs Jr.
1988. Standards in herpetology and ichthyology. Standard symbolic codes for institutional resource collections in herpetology and ichthyology. Suppl. 1: additions and corrections. Copeia 1988:280–282.
Leviton, A. E., R. H. Gibbs Jr., E. Heal, and C. E. Dawson.
1985. Standards in herpetology and ichthyology: part I. Standard symbolic codes for institutional resource collections in herpetology and ichthyology. Copeia 1985:802–832.
Lindberg, G. U., and V. V. Fedorov.
1993. The fishes of the Sea of Japan and adjacent parts of the Sea of Okhotsk and the Yellow Sea. Part 6. Teleostomi, Osteichthyes, Actinopterygii. XXXI. Pleuronectiformes—Family Pleuronectidae. Zool. Inst. Rossiiskoi Akad. Nauk, 271 p.
Lockington, W. N.
1879a. The flounders of our markets, No. 2. Mining and Scientific Press 39(4):70.
1879b. Review of the Pleuronectidae of San Francisco. Proc. U.S. Natl. Mus. 2:69–108.
1880a. Note on a new flat-fish (*Lepidopsetta isolepis*) found in the markets of San Francisco. Proc. U.S. Natl. Mus. 3:325.
1880b. Notes on new and rare fishes of the Pacific Coast. Am. Nat. 14:595–600.
1883. *Isopsetta isolepis*. *In* 1883 synopsis of the fishes of North America (D. S. Jordan and C. H. Gilbert, eds.), p. 1–1018. Bull. U. S. Natl. Mus. 16.
Manugistics.
1997. Statgraphics plus 2.1. Manugistics, Inc., Rockville, MD, 882 p.
Masutomi, K., and T. Hamada.
1966. Fossils in colour. Hoikusha Publishing Co., Osaka, 268 p. [Not seen; cited in Sakamoto and Uyeno (1988).]
Matarese, A. C., A. W. Kendall Jr., D. M. Blood, and B. M. Vinter.
1989. Laboratory guide to early life history stages of northeast Pacific fishes. U.S. Dep. Commer., NOAA Tech. Rep., NMFS 80, 652 p.
Minami, T.
1995. Spawning season of pleuronectid flatfishes in the coastal waters of Hokkaido, Japan [Review]. Bull. Hokkaido Natl. Fish. Res. Inst. 59:69–80.
Minami, T., and I. Nakamura.
1978. Seasonal occurrence of pelagic stages of flatfishes in the coastal waters of western Wakasa Bay. Mem. Coll. Agriculture, Kyoto Univ. 112:29–47.
Moiseev, P. A.
1953. [Cod and flounders of Far-Eastern Seas.] Izv. Tikhook. N.-I. Inst. Rybn.-Khoz. I Okeanogr. 40:1–287. Fish. Res. Board Can. Transl. 119.]
Moser, H. G., W. J. Richards, D. M. Cohen, M. P. Fahay, A. W. Kendall Jr., and S. L. Richardson, eds.
1984. Ontogeny and systematics of fishes. Am. Soc. Ichthy. Herpet. Spec. Publ. 1, 760 p.
Moser, H. G., R. L. Charter, P. E. Smith, D. A. Ambrose, S. R. Charter, C. A. Meyer, E. M. Sandknop, and W. Watson.
1993. Distributional atlas of fish eggs and larvae in the California Current region: taxa with 1000 or more total larvae, 1951 through 1984. CalCOFI Atlas 31, 233 p.
Mulligan, H. L., A. W. Kendall Jr., and A. C. Matarese.
1995. The significance of morphological variation in adults and larvae of the rock sole, *Pleuronectes bilineatus*, from the Bering Sea and northeastern Pacific Ocean. Proc. Int.

Symp. N. Pac. Flatfish, Alaska Sea Grant Coll. Prog. Report AK-SG-95-04, p. 133–150.

NMFS (National Marine Fisheries Service).
1999. Our living oceans: report on the status of U.S. living marine resources, 1999. U.S. Dep. Commer., NOAA Tech. Memo. NMFS-F/SPO-41, 301 p.

Nelson, J. S.
1994. Fishes of the world, 3rd ed. Wiley & Sons, New York, NY, 600 p.

Nikiforov, S. N., S. N. Safronov, and N. S. Fadeev.
1983. Distinguishing characters of rock sole, *Lepidopsetta bilineata*, and mochigar sole, *L. mochigarei* (Pleuronectidae). J. Ichthyol. 23:36–44.

Norman, J. R.
1934. A systematic monograph of the flatfishes (Heterosomata). Brit. Mus. Nat. Hist. 1:1–459.

Okada, Y.
1955. Fishes of Japan, illustrations and descriptions of fishes of Japan. Maruzen Co., Tokyo, 434 p.

Okiyama, M., ed.
1988. An atlas of the early stages of fishes in Japan. Tokai Univ. Press, Tokyo, 1154 p. [In Japanese.]

Okiyama, M., and K. Takahashi.
1976. Larval stages of right eye flounders (subfamily Pleuronectinae) occurring in Japan Sea. Bull. Japan. Sea. Reg. Fish. Res. Lab. 27:11–34.

Penttila, D. E.
1995. The WDFW's Puget Sound intertidal baitfish spawning beach survey project. *In* Puget Sound Research 95 Proceedings, vol. 1, Jan. 12–14, 1995, p. 235–241.

Pertseva-Ostroumova, T. A.
1961. The reproduction and development of far eastern flounders. Tr. Inst. Okeanol. Akad. Nauk SSR. [In Russian; English transl., Fish. Res. Board Can., Transl. Serv. 856, 1967.]

Poss, S. G., and B. B. Collette.
1995. Second survey of fish collections in the United States and Canada. Copeia 1995:48–70.

Rass, T. S.
1996. On taxonomy of Pleuronectini (Pleuronectidae). J. Ichthyol. 36:546–548.

Sakamoto, K.
1984a. Interrelationships of the family Pleuronectidae (Pisces: Pleuronectiformes). Mem. Fac. Fish., Hokkaido Univ. 31(1/2):95–215.
1984b. Pleuronectidae. *In* The fishes of the Japanese Archipelago (H. D. Masuda, K. Amaoka, C. Araga, T. Uyeno, and T Yoshino, eds.), p. 351–354. Tokai Univ. Press, Tokyo, Japan.

Sakamoto, K., and T. Uyeno.
1988. A new righteye flounder from the late Pleistocene Togane Formation, Chiba Prefecture, Japan. Bull. Nat. Sci. Mus., Tokyo, ser. C, 14(3):135–142.

Schmidt, P. Y.
1950. Fishes of the Sea of Okhotsk. Academy of Sciences of the USSR, Transactions of the Pacific Committee, vol. 6, Moscow-Leningrad, 392 p. [In Russian, 1965 transl. by Israel Prog. Sci. Trans. Available from the National Technical Information Service, Springfield, VA.]

Shubnikov, D. A., and L. A. Lisovenko.
1964. Data on the biology of rock sole of the southeastern Bering Sea. Soviet Fisheries Investigations in the northeast Pacific, Part 2. Pacific Scientific Research Institute of Marine Fisheries and Oceanography (TINRO). Izvestiya 49.220–226. [1968 transl. by Israel Prog. Sci. Transl.]

Shvetsov, F. C.
1979. Reproduction of the flounder *Lepidopsetta bilineata bilineata*, off the Okhotsk Sea coast near Paramoshiro and Shumushu Islands. J. Ichthyol. 19(5):61–62.

Skalkin, V. A.
1959. [Diet and food relations of flatfish on the Il'inskii Shoal.] Pacific Scientific Research Institute of Marine Fisheries and Oceanography (TINRO). Izvestiya 47. [In Russian; cited by Skalkin, 1963.]
1963. Diet of flatfishes in the southeastern Bering Sea. Soviet Fisheries Investigations in the Northeast Pacific, Part 1. Pacific Scientific Research Institute of Marine Fisheries and Oceanography (TINRO). Izvestiya 50:235–250. [1968 transl. by Israel Prog. Sci. Transl.]

Smith, R. T.
1936. Report on the Puget Sound otter trawl investigations. Wash. Dept. Fish. Biol. Rep. 36B:1–61.

Snyder, J. O.
1911. Descriptions of new genera and species of fishes from Japan and Riu Kiu Islands. Proc. U.S. Natl. Mus. 40:525–549.
1912. Japanese shore fishes collected by the United States Bureau of Fisheries Steamer "*Albatross*" expedition of 1906. Proc. U.S. Natl. Mus. 42:437–441.

Sokal, R. R., and F. J. Rohlf.
1995. Biometry, 3rd ed. W. H. Freeman and Co., New York, NY, 859 p.

Springer, V., and M. E. Anderson.
1998. Catalog of type specimens of recent fishes in the National Museum of Natural History, 8: Suborder Zoarcoidei (Anarhichadidae, Bathymasteridae, Pholidae, Ptilichthyidae, Scytalinidae, Stichaeidae, Zoarcidae). Smiths. Contr. Zool. 589, 27 p.

SPSS, Inc.
1996. SYSTAT for Windows, version 6.0. SPSS, Inc., Chicago, IL, 751 p.

Statistical Sciences.
1993. S-Plus for Windows, version 3.3. Statistical Sciences, Seattle, WA, 819 p.

Stauffer, J. R., Jr., and E. Hert.
1992. *Pseudotropheus callainos*, a new species of mbuna (Cichlidae), with analyses of changes associated with two intra-lacustrine transplantations in Lake Malawi, Africa. Ichthyol. Explor. Freshwaters 3:253–264.

Taranets, A. J.
1937. Handbook for identification of fishes of the Soviet Far East and adjacent waters. Bull. Pac. Sci. Fish. Inst. Vladivostok. 11:1–200+map.

Townsend, L. D.
1936. Variations in the meristic characters of flounders from the northeastern Pacific. Rep. Intern. Fish. Comm. 11:1–24.
1937. Geographical variation and correlation in Pacific flounders. Copeia 1937:92–103.

Wilmovsky, N. J., A. Peden, and J. Peppar.
1967. Systematics of six demersal fishes of the North Pacific Ocean. Fish. Res. Board Can. Tech. Rep. 34, 95 p.

Yusa, T.
1957. Eggs and larvae of flatfishes in the coastal waters of Hokkaido. II. Early development of the flatfish (*Lepidopsetta mochigarei* Snyder). Bull. Hokkaido Reg. Fish. Res. Lab. 15(2):15–21.
1958. Eggs and larvae of flatfishes in the coastal waters of Hokkaido. II. Post-embryonic development and larvae of the flatfish *Lepidopsetta mochigarei* Snyder. Bull. Hokkaido Reg. Fish. Res. Lab. 18:1–10.

Appendix Table 1

Summary of Alaska Fisheries Science Center cruises with positive tows for larvae of *Lepidopsetta* (1971–72, 1977–94). Cruises in boldface were not used in calculations of mean density. BS = Bering Sea; GA = Gulf of Alaska; WA = Washington. Bongo = bongo net of 60 cm diameter, 0.505-mm mesh (larvae were occasionally collected using alternative frame sizes, including 20-cm net diameter and 0.333-mm mesh, but these collections were not used for abundance calculations); Meth = Methot trawl net of 5-m2 frame (2 × 3 mm oval mesh); Tuck = Tucker trawl net of 1-m frame and 0.505-mm mesh.

						Total occurrences	
Year	Cruises	Region	Month	Gear[1]	Total stations	*L. polyxystra* n. sp.	*L. bilineata*
1971	**4DE71**	**BS**	**Jul–Aug**	**bongo**	**10**	**8**[2]	**0**
1972	2KE72	GA	Apr–May	bongo	67	27	0
1977	**MF77B-5,6**	**BS**	**Apr–May**	**bongo**	**75**	**35**	**0**
	9SEI77	**GA**	**Jul**	**bongo**	**99**	**0**	**1**[2]
1978	4DI78	GA	Mar–Apr	bongo,Tuck	225	80	0
	2MF78	GA	Jun–Jul	bongo,Tuck	267	41	66
	3MF78	GA	Sep	bongo	26	1	1
	4MF78	GA	Sep–Oct	bongo	66	2	0
	5MF78	GA	Oct–Nov	bongo	19	0	1
1979	1PO79	GA	Sep	bongo	18	0	1
	3MF79	BS	Jun–Jul	bongo, Tuck	271	35	0
	5TK79	GA	May	bongo	58	15	3
1980	**1MF80**	**BS**	**Jan–Feb**	**bongo**	**8**	**2**[2]	**0**
1981	**1PO81**	**WA**	**May–Jun**	**bongo**	**131**	**0**	**1**
	1SH81	GA	Mar	bongo	131	4	0
	2MF81	GA	Mar–Apr	bongo	89	1	0
	2SH81	GA	Apr	bongo	60	31	2
	3MF81	GA	Apr–May	bongo	79	37	2
	3SH81	GA	May	bongo	57	37	10
	4MF81	GA	May	bongo	80	52	8
1982	1DA82	GA	Apr	bongo	83	20	0
	2DA82	GA	May	bongo	62	29	1
1983	1CH83	GA	May	bongo	70	19	5
	1EQ83	**WA**	**Apr–May**	**bongo**	**124**	**0**	**1**
1984	1SH84	GA	Apr–May	bongo	157	22	1
1985	1PO85	GA	Mar–Apr	bongo	154	37	0
	2MF85	GA	May	bongo	62	4	0
	2PO85	GA	May–Jun	bongo	189	52	17
1986	1GI86	GA	Apr	bongo	149	53	0
	1MF86	GA	Apr	bongo	80	4	0
	2MF86	GA	May	bongo	107	53	0
1987	1BB87	GA	Mar–Apr	bongo	117	12	1
	2MF87	GA	Apr	bongo	142	9	0
	3MF87	GA	May	bongo	60	14	8
1988	1DN88	BS and GA	Mar–May	bongo	203	17	0
	1MF88	GA	Apr	bongo,Tuck	196	51	0
	2MF88	GA	Apr–May	bongo,Meth,Tuck	84	41	1
	3MF88	GA	May	bongo	13	2	0
	4MF88	GA	May–Jun	bongo,Meth,Tuck	209	69	75
1989	1MF89	GA	Apr	bongo,Tuck	140	21	0
	2MF89	GA	Apr–May	bongo,Tuck	107	55	1
	3MF89	GA	May	bongo,Meth,Tuck	221	127	2
	4MF89	GA	May–Jun	Tuck	95	87	9

Continued

Appendix Table 1 (continued)

Year	Cruises	Region	Month	Gear[1]	Total stations	Total occurrences	
						L. polyxystra n. sp.	*L. bilineata*
1990	1MF90	GA	Apr	bongo	107	17	0
	2MF90	GA	May	bongo,Tuck	92	52	2
	3MF90	GA	May	bongo	17	9	0
	4MF90	GA	May–Jun	bongo	130	83	21
1991	1MF91	GA	Apr	bongo,Tuck	98	5	0
	2MF91	GA	Apr	bongo,Tuck	156	24	0
	3MF91	GA	May	bongo	119	28	0
	4MF91	GA	May	bongo	98	19	8
	5MF91	WGA	July	Meth	62	40	12
1992	1MF92	GA	Apr	bongo,Tuck	103	7	0
	1MM92	BS and GA	Jul	Meth	11	3	2
	3MF92	GA	May	bongo,Tuck	188	59	7
	4MF92	GA	May	bongo, Meth,Tuck	154	46	31
1993	2MF93	GA	Apr	bongo, Meth,Tuck	135	12	0
	3MF93	BS	Apr	bongo,Tuck	135	21	0
	4MF93	GA	May	bongo, Meth,Tuck	168	44	7
	5MF93	GA	May–Jun	bongo,Meth	119	25	22
	6MF93	GA	Sep	Tuck	24	0	2
1994	3MF94	GA	Mar–Apr	bongo, Tuck	49	2	0
	4MF94	BS	Apr	bongo,Tuck	144	37	0

[1] Although larvae of *Lepidopsetta* were collected in neuston and Mocness tows (see "Material examined" section), these collections were not used for abundance calculations and are not listed here.

[2] Total occurrences for these cruises represent the minimum number collected. Complete records for these cruises are unavailable at this time.

An alternative method for estimating bycatch from the U.S. shrimp trawl fishery in the Gulf of Mexico, 1972–1995

Mauricio Ortiz

Christopher M. Legault

Nelson M. Ehrhardt

Division of Marine Biology and Fisheries
Rosenstiel School of Marine and Atmospheric Sciences
University of Miami
4600 Rickenbacker Causeway
Miami, Florida 33149
Present address (for M. Ortiz): Miami Laboratory
Southeast Fisheries Science Center
National Marine Fisheries Service, NOAA
75 Virginia Beach Dr., Miami, Florida 33149

E-mail address (for M. Ortiz): mauricio.ortiz@noaa.gov

Abstract.—Finfish bycatch taken by the U.S. Gulf of Mexico shrimp fishery is an important issue in the management of fisheries resources given the perceived high mortality of the different fish stocks taken as bycatch in the region. Bycatch data are characterized by a high number of low catches, a few high catches, and depending on the finfish species, a significant proportion of observations with zero bycatch. An evaluation of the current general linear model for generating bycatch estimates indicates that the bycatch data do not conform to the assumptions of this model because bycatch estimates depend upon choices within the model that can significantly change the results of the model. These choices include the constant value added to catch-per-unit-of-effort (CPUE) values prior to the logarithmic transformation (to avoid undefined logarithms with zero CPUEs) and the standard time-unit selection for calculating CPUE values from catch in numbers and variable tow times. Currently a value of one is added to observed CPUE, and a constant time unit of one hour has been used; however, these choices are somewhat arbitrary.

An alternative approach to model bycatch data is to use a delta distribution that has two components. Component one models the proportion of zeros, and component two models the positive catches. In our study, we applied the delta lognormal model to estimate finfish bycatch in the shrimp fishery. This model avoids the problems of 1) the addition of a constant positive value to log-transformed CPUEs, and 2) the selection of a standard time unit for CPUE calculations. Bycatch estimates determined with the current general linear model were compared with those determined with the delta lognormal model for Atlantic croaker (*Micropogonias undulatus*), red snapper (*Lutjonus campechanus*), Spanish mackerel (*Scomberomorus maculatus*), and all finfish from 1972 through 1995. Analysis and evaluation of the performance of the delta lognormal model indicated that this model fits the bycatch database better than the current general linear model.

Manuscript accepted 10 January 2000.
Fish. Bull. 98:583–599 (2000).

In recent years shrimp bycatch has become one of the most important issues in fishery management in the southeastern United States, including the U.S. Gulf of Mexico. In 1990, the U.S. Congress requested a 3-year research program to assess the impact of bycatch by the shrimp fishery on federally managed fishery resources along the south Atlantic and the U.S. Gulf of Mexico coasts (Public Law 101-627, sec110c[1]). As a result, the National Marine Fisheries Service (NMFS) created the Cooperative Shrimp Bycatch Characterization Project (NOAA[1]), a four-year program which focused on 1) characterizing onboard shrimp trawl bycatch, 2) developing and testing bycatch reduction devices (BRDs), and 3) evaluating alternative bycatch management options. Among the major objectives identified in this project were those of updating and expanding temporal and spatial bycatch estimates (offshore and inshore waters) (NOAA[1]).

Since 1987, the NMFS has provided bycatch estimates for several finfish species in the Gulf of Mexico by using a catch-per-unit-of-effort (CPUE) method, where bycatch CPUEs are estimated following a general linear approach (Nichols et al.[2]). Briefly, a bycatch CPUE rate is estimated for each fish species by year (1972–95), area, season, and depth-zone stratum. These bycatch CPUEs are multiplied by an estimated annual shrimping effort within the stratum, and the total annual bycatch is the sum of the bycatch for each stratum. To estimate bycatch, the sample unit is defined as the number of fish of a given species caught each net-hour during a tow. The current general linear model was evaluated by considering two main topics: 1) the assumptions entailed with using the model and the theoretical basis for generating the estimates, and 2) the appropriateness of the available data to the configuration and analysis of the model. More specifically, we examined the matrix structure used in the general linear model, the logarithm usage in the general linear model, and the standardization of effort in the CPUE's in the current general linear model.

[1] NOAA. 1995. Cooperative research program addressing finfish bycatch in the Gulf of Mexico and South Atlantic shrimp fisheries: a report to congress. National Marine Fisheries Service Southeast Regional Office, 9721 Executive Center Dr. N., St. Petersburg, FL 33702.

[2] Nichols S., A. Shah, G. J. Pellegrin, and K. Mullin. 1987. Estimates of annual shrimp fleet bycatch for thirteen finfish species in the offshore waters of the Gulf of Mexico. Report to the Gulf of Mexico Fishery Management Council. The Commons at Rivergate, 3018 U.S. Highway 301 N., Tampa, FL 33619.

Procedure for estimating bycatch with the general linear model

In the bycatch estimation procedure with CPUE, it is assumed that the estimated annual shrimping effort is known and no variance is associated with this value. Therefore, we restricted our evaluation to the general linear model method to estimate the bycatch rates (CPUE) within each stratum. The general linear model is defined for each bycatch species by Nichols et al. (1987[2]) as

$$\mathrm{Log}_{10}(CPUE+1)_{ijklm} = mean + dataset_i + year_j + season_k + area_l + depth_m + \varepsilon_{ijklm}, \quad (1)$$

where CPUE = the catch in numbers per trawl for each hour of shrimp fishing;
mean = the overall mean;
dataset (i) = a fixed effect term differentiating commercial shrimp fishing from research trawls; and
the terms *year (j)*, *season (k)*, *area (l)*, and *depth (m)* = also fixed-effect terms characterizing the spatiotemporal variability of shrimp bycatch.

This model assumes that the error terms are random, independent, and normally distributed, with equal variance throughout. Predicted catch per trawl net for each hour of shrimp fishing is then estimated for each stratum for the commercial shrimp fishery as

$$CPUE = 10^{\hat{Y}+1.1513\times RMS} - 1, \quad (2)$$

where $\hat{Y}$ = the general linear model predicted $\log_{10}$ *(CPUE+1)*; and
RMS = the residual mean square from the general linear model.

The *RMS* term is required to estimate the arithmetic mean from the geometric mean of the assumed lognormal distribution. The constant 1.1513 is a correction factor for estimations derived with log base 10 instead of the natural log.

The predicted CPUE in each stratum is then multiplied by the estimated shrimping effort in the corresponding stratum. CPUEs are estimated for each trawl net. An average of two trawl nets per commercial shrimp vessel for the 1972–95 time series is assumed owing to the lack of information on number of nets per boat for each stratum (cell in the matrix configuration) or other grouping category. Total annual bycatch estimates for a given species are then simply the sum of the commercial bycatch (i=1) in all strata for that year (j) as

$$Bycatch_j = 2 \times \sum_{klm} CPUE_{ijklm} \times f_{jklm}, \quad (3)$$

where f_{jklm} = the estimated total shrimping effort (hours of fishing) for year j, area k, season l, and depth zone m.

The general linear model estimates an approximate variance for the arithmetic mean CPUE for each cell as

$$\left(10^{2(\hat{Y}+1.15\times RMS)+2.3(S_{\hat{Y}}^2+2.65\times RMS^2/rdf)}\right)\left(10^{2.3(S_{\hat{Y}}^2+2.65\times RMS^2/rdf)}-1\right),$$

where $\hat{Y}$ and *RMS* = the predicted $\log_{10}$ *(CPUE+1)* and the residual mean square respectively;
$S_{\hat{Y}}^2$ = the estimate of variance of the predicted $\log_{10}$ *(CPUE+1)* for the cell; and
rdf = the residual degrees of freedom.

No variance estimates for the estimated shrimping effort are included in this model; thus effort is considered as if it were known exactly (Nichols et al.[2]).

The database for estimating shrimp bycatch CPUEs was derived from information collected in several projects. The current database comprises two types of data sources: 1) direct measurements of finfish catch by observers onboard of commercial shrimp vessels, and 2) catch rates from research surveys. Direct observations came from four main programs: the Sea Turtle Incidental Catch and Mortality Project (Henwood and Stuntz, 1987), the Excluder Trawl Device Evaluation Project (Henwood and Stuntz, 1987), the Shrimp Fleet Discards Project (Pellegrin, 1982), and the Cooperative Shrimp Bycatch Characterization Project (NOAA[1]). Direct observations were discontinuous in time and space; in particular, no onboard commercial vessels observations occurred between 1982 and 1991. Research observations came primarily from two annual trawling projects: the Fall Groundfish Surveys and the Summer SEAMAP Program. With over 22,000 tows documented from 1972 through 1995, research observations were the main source of the bycatch database. Research observations were restricted to tow surveys with the RV *Oregon II* equipped with a standard 40-ft shrimp trawl (Nichols et al.[3]).

For estimating bycatch, the U.S. Gulf of Mexico was divided into four geographic areas, two depth zones, and three seasons. Area 1 covered the Texas coastline, area 2 covered the Louisiana coast, area 3 covered the Alabama and Mississippi coasts, and area 4 covered to the Florida West Coast and the Lower Florida Keys. Two depth strata were defined by using the 10-fathom depth as the divider of inshore and offshore regions. Temporal variability of shrimp bycatch was taken into account by including three seasons: 1) January–April, 2) May–August, and 3) September–December.

Annual estimates of bycatch for the finfish category (i.e. all fish species, in weight units instead of numbers of fish), and for three fish species (Atlantic croaker, Spanish mack-

[3] Nichols S., A. Shah, G. J. Pellegrin and K. Mullin. 1990. Updated estimates of shrimp fleet bycatch in the offshore waters of the US Gulf of Mexico 1972–1989. Report to the Gulf of Mexico Fishery Management Council. The Commons at Rivergate 3018 U.S. Highway 301 N., Tampa, FL 33619.

Table 1

Distribution of number of cells and observations per cell for the general linear model and the modified models. The 3-area model refers to a reduced number of levels in the area factor of the general linear model (from 4 to 3) by combining areas 2 and 3 into a single area (see text for description of each area). The 2-season model refers also to a reduced number of levels in the season factor of the general linear model where season 1 is from September to April and season 2 is from May to August. The no-depth-zone model refers to the general linear model without the depth zone factor. The combined model refers to a model of 3 areas, 2 seasons, and no depth zone. The year and dset (data set) refers to a general linear model with only these two factors (i.e. excluding season, area, and depth-zone factors). Percent coverage refers to the proportion of cells in the matrix that have tow observations, both by type of data (commercial, research, and combined) as well as the number of positive bycatch tows with Spanish mackerel.

	Matrix structure of general linear model								
	Research			Commercial			Total		
Scenario	No. cells of matrix	Cells with tows	Cells with Spanish	No. cells of matrix	Cells with tows	Cells with Spanish	No. cells of matrix	Cells with tows	Cells with Spanish
General linear model	576	274	175	576	181	77	1152	455	252
3 areas	432	176	129	432	148	68	864	324	197
2 seasons	384	236	153	384	152	69	768	388	222
No depth zone	288	143	110	288	112	61	576	255	171
Combined	144	80	66	144	71	41	288	151	107
Year dset only	24	24	24	24	15	10	48	39	34
	Percentage coverage								
General linear model		47.6%	30.4%		31.4%	13.4%		39.5%	21.9%
3 areas		40.7%	29.9%		34.3%	15.7%		37.5%	22.8%
2 seasons		61.5%	39.8%		39.6%	18.0%		50.5%	28.9%
No depth zone		49.7%	38.2%		38.9%	21.2%		44.3%	29.7%
Combined		55.6%	45.8%		49.3%	28.5%		52.4%	37.2%
Year dset only		100.0%	100.0%		62.5%	41.7%		81.3%	70.8%

erel, and red snapper) were used to compare results of the sensitivity analysis. Atlantic croaker is a species commonly caught as bycatch, found in about 61% of tows. Red snapper and Spanish mackerel are important commercial and recreational fisheries in the U.S. Gulf of Mexico; the directed fishery management actions for these fisheries are influenced by the level of bycatch in the shrimp trawl fishery. Red snapper is caught as bycatch in the shrimp fishery in about 28% of tows, whereas Spanish mackerel is less commonly caught in only 5% of tows.

To evaluate the general linear model, we first describe some characteristics of the database that are important regarding assumptions entailed with the use of the model and analysis of the model , then we present a sensitivity analysis on the model structure and parameters. Three main analyses were performed: 1) analysis of the general linear model matrix structure, 2) analysis of the logarithmic scaling of the observed CPUE values, and 3) analysis of the standard tow time unit used to calculate observed CPUE values.

Evaluation of the general linear model

The present general linear model configuration for estimating bycatch created a matrix of 1152 cells, comprising data for 24 years, 2 datasets, 4 areas, 3 seasons, and 2 depth zones. Although there were a relatively large number of observations in the database (26,380), the percentage of cells in the matrix that had observations was only 39%, only 4160 tows (16%) were from commercial vessels during normal shrimp fishing operations, and the remaining 22,220 (84%) tows were from research vessels. In addition, the number of observations per cell varied largely, from 1 to 466 within research tows, and from 1 to 181 within the commercial tows.

Given the unbalanced distribution of observations per cell, we investigated the effects of the matrix structure on the general linear model. Our approach was to fit the model to scenarios with a reduced number of levels within factors or a reduced number of factors in the model (or to scenarios with both). For example, we combined seasons 1 and 3 to reduce the season factor to two levels or we eliminated the season factor from the model. Table 1 describes all the scenarios evaluated. Correspondingly, shrimping effort was adjusted to the new general linear model matrix by adding the annual shrimping effort within the modified strata, and annual bycatch was estimated as the product of the predicted CPUEs and the shrimping effort for each cell. Defining the percentage of coverage as the number of cells with observations divided by the total number of cells

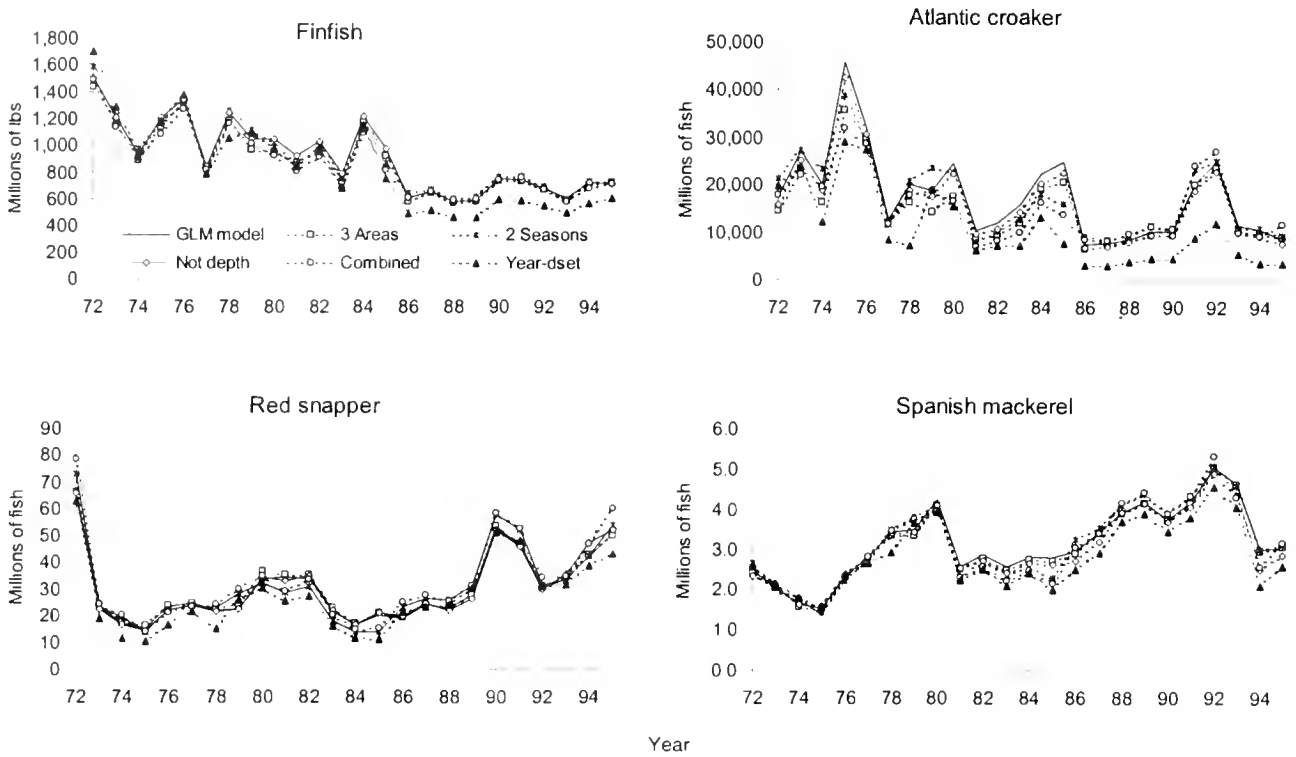

Figure 1

Estimated total bycatch with the general linear model and modified models of the general linear model for the finfish group, Atlantic croaker, red snapper, and Spanish mackerel. (See Table 1 for descriptions of the modified models.)

in the matrix, we found that this value increased from 39% in the base scenario of the current general linear model to 81%, in what was defined as the "minimum model" where only the factors year and dataset were included.

Overall, the results showed that total bycatch estimates did not vary substantially, although the assumed model was radically modified (Fig. 1). These results suggest that season, area, and depth zone are factors that do not significantly contribute to the explanation of the observed variability in the data. Although the F-values from the ANOVA tables were highly significant ($P<0.05$) for each factor in all general linear model matrix scenarios, this significance may be a response to the large number of degrees of freedom. Alternatively, it is possible that the structure of the general linear model does not reflect all the main factors that account for bycatch variability among years, except for dataset source. Indeed, interactions between the main factors may also be important. Given the limited data coverage, however, the inclusion of other factors or interactions among factors in the general linear model is clearly not advisable.

In summary, the simple model with year and dataset as factors produced similar estimates of bycatch in relation to the complex model, including season, area, and depth zone factors. In particular, for species that are not common as shrimp bycatch, a simple model avoids empty cells and highly unbalanced input matrix designs.

Use of logarithms in the general linear model

One of the assumptions in the linear regression model is that the error within the matrix cells should follow a normal distribution and have a constant equal variance. In the bycatch dataset, the CPUE variance increases as the mean CPUE increases, indicating a constant coefficient of variation. This condition suggests a logarithmic transformation of mean CPUE values. To avoid the problem of undefined logarithms for zero catches, a constant value c of 1 was added to all observed CPUE (Eq. 1) in the model. Then the linearization procedure was carried out on the log base 10 of the modified CPUE. This c value was then subtracted in the back transformation of the predicted means (Eq. 2). No particular explanation for the choice of 1 in the current general linear model has been given.

Thus, we considered the effects of using different c values in the general linear model. Three different c values where used: 10, 0.5, and the smallest positive CPUE-value for each species (i.e. 0.0178 for finfish, 0.0779 for Atlantic croaker, 0.0685 for red snapper, and 0.0685 for Spanish mackerel). The results showed that annual bycatch estimates vary dramatically depending upon the c value used in the algorithm (Fig. 2). Although the magnitudes varied with changes in the c value, the trends were the same for each species. However, the direction of change was not the same among spe-

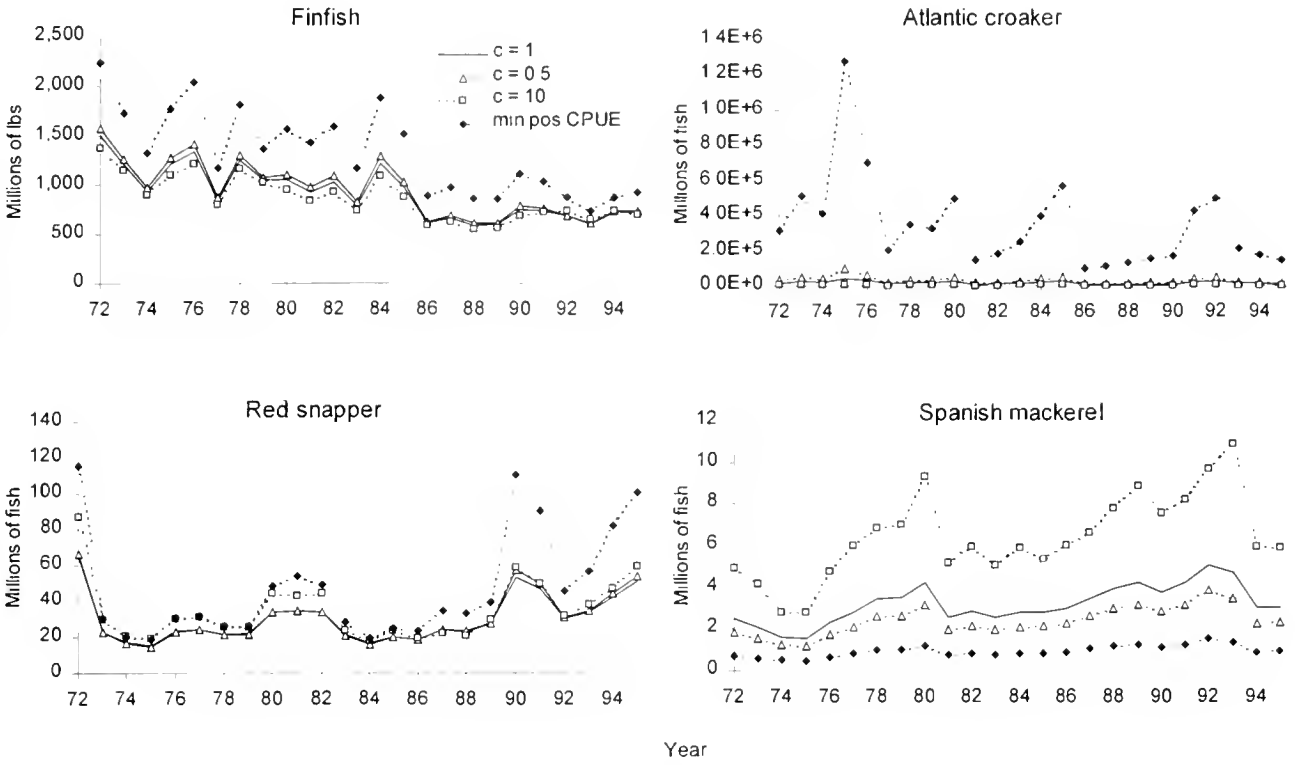

Figure 2

Estimated total with the general linear model with different c-values used in the logarithmic transformation of bycatch CPUE. Base scenario (c=1).

cies. For Spanish mackerel and red snapper, using c=10 increased the estimates of bycatch (100% and 15%, respectively). In contrast, bycatch estimates decreased for Atlantic croaker and finfish (75% and 6%, respectively). When the c was the smallest positive value of the data, annual estimates increased on average 47% for red snapper, 43% for finfish, and 1694% for Atlantic croaker, whereas bycatch estimates decreased on average 70% for Spanish mackerel.

These results show that the general linear model is highly sensitive to the logarithmic c value added to the observed CPUE values. Although it is known that logarithm transformations are affected by the selection of a c value, the large variations in magnitude of estimates for bycatch species should at least merit a review and analysis of the criteria for choosing an appropriate c value. In a review of logarithmic transformations, Berry (1987) suggested choosing a c that normalizes the log-transformed data. He specified an additive function of the skewness and the kurtosis of the data, where skewness and kurtosis are defined as

$$g_1(c) = \sum (y - \bar{y})^3 / (n\hat{\sigma}^3) \text{ and}$$

$$g_2(c) = \sum (y - \bar{y})^4 / (n\hat{\sigma}^4) - 3$$

respectively,

where $\bar{y}$ = the predicted means;
y = the observations; and
$\hat{\sigma}$ = the estimated standard deviation within the defined strata.

When the observations are normally distributed, then the g_1 function has a mean of zero, and the function g_2 has a mean equal to $-6/(d+2)$, where d is the number of degrees of freedom of the error. The additive function of skewness and kurtosis is then defined as

$$g_0(c) = |g_1(c)| + |g_2(c) + 6/(d+2)|.$$

Thus, the c value that minimizes $g_0(c)$ will make the residuals closer to a sample that follows a normal distribution. Using CPUE values for Spanish mackerel, we evaluated several c values ranging from 1.0E – 8 up to 1.0E + 3. We did not find a minimum solution for $g_0(c)$, but rather an asymptotic behavior with c values less than 0.05, indicating that it is not possible to normalize the Spanish mackerel bycatch data by using a logarithm transformation. Therefore, there is not an objective criterion for selecting a particular c value, and as shown before, even relatively small changes of the c value could cause significant variation of the annual bycatch estimates. Furthermore, independent of the method used to select the c constant in

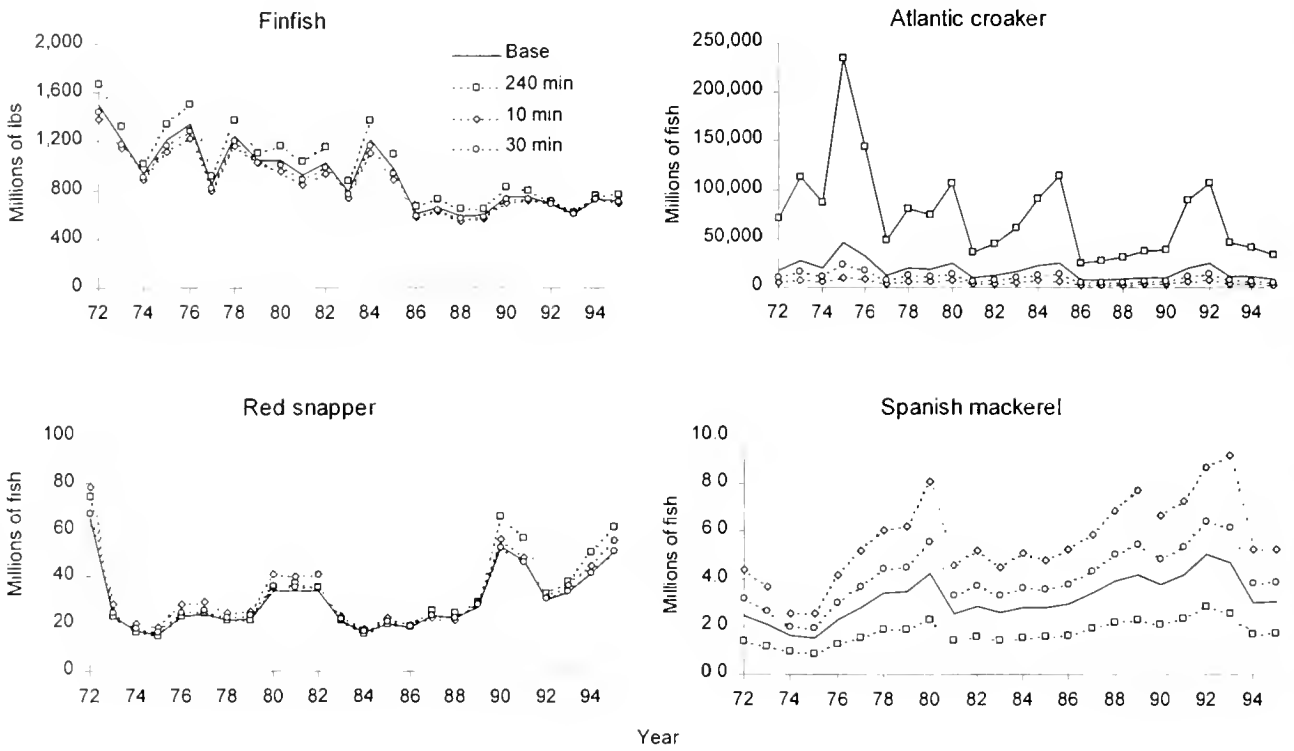

Figure 3

Estimated total bycatch with the general linear model when using different tow-time standard units. The current general linear model uses a one-hour tow time (base scenario).

the logarithmic transformation of the CPUE, the c values must be selected for each species independently. Therefore, the same c value might not be appropriate for different bycatch species, and if new bycatch data are added, then the c value must be re-evaluated.

Standardizing effort in the general linear model

The general linear model predicts bycatch CPUE by cell in units of number of fish caught in one shrimp trawl net per hour. Because actual observations of bycatch are the number of fish caught in a shrimp net during a tow and because tow times are variable, observations are converted to a standard unit of one hour tow time. This standardization procedure implies a direct linear relation between number of fish caught and tow time for all observations (i.e. if 10 fish were caught in a 30-min tow, the CPUE would be 20 fish per hour). However, the average tow time and the tow time distribution from commercial observations are considerably different from those from research observations. Most of the commercial tows range from 1 to 7 hours and have a mode of approximately 4 hours; a few tows are over 12 hours. In contrast, research tows are predominantly of 10-minute duration (73%), and the rest last 1 hour or less.

Given these differences in fishing and sampling time-effort between commercial and research observations, we estimated total bycatch by using different time units to convert the observed catch to CPUE values. We selected 10-, 30-, and 240-minute time units instead of the currently used one-hour unit. These were chosen on the basis of the most frequent tow time for research observations (10 min), the mean tow time of research observations (30 min), and the mode tow time for commercial observations (240 min). The predicted CPUEs were then multiplied by the shrimping effort per cell in the modified time units. Shrimping effort was given in 24-hour-day fishing effort. Therefore, if the predicted CPUE units were 0.5 hour (30 min), the 24-hour shrimping effort would be multiplied by 2. The c value was 1.0 for all these calculations.

Modifying the time unit for calculating CPUE values also had an effect on the annual estimates of shrimp bycatch from the general linear model (Fig. 3). Similar to the results of the evaluation of the logarithmic constant, the changes of estimated bycatch were different for each species and varied in the direction of the change. For example, for finfish and Atlantic croaker, a time unit of 10 minutes decreased estimated annual bycatch (5% and 68% on average, respectively). By contrast, red snapper and Spanish mackerel estimated bycatch increased with the 10 minute unit (12% and 78%, respectively). With the commercial mean tow time (240 min), bycatch estimates of Atlantic croaker increased on average 300%, and 10% for finfish. For red snapper, estimates changed only in the most recent

years (1990–95) by 20%. In contrast, the estimated bycatch of Spanish mackerel was reduced by 44% on average.

The estimated CPUE should be independent of the time unit used (because it is a constant factor for all observations). However, the differences seen in our study in estimated bycatch were due to the presence of zero CPUE values. By dividing by different time units, the relative distance between the groups of zero CPUE values and the positive CPUE values is changed; as a result, estimators of the central tendency for these data will vary. Although the end results of the time-unit and c value choices are similar (biased estimates), their mathematical origin is different. The time-unit choice is a multiplier of the positive catch data (zero catch /any time unit=zero CPUE), whereas the c value choice adds the c value to all CPUE data. Although a change in time unit could be exactly matched by the appropriate change on the c value, addition of more data, with the same time unit, would require recalculating the appropriate c value.

Procedure for estimating bycatch with the delta lognormal model

Delta models have been used to analyze fisheries data, in particular when there is a predominant group of zero observations. These models have been used to obtain estimates of abundance for highly aggregated organisms, such as planktonic samples (Pennington, 1983), in the analysis of catch-per-unit-of-effort data for the development of CPUE indices (Lo et al., 1992; Cooke and Lankester[4]), as well as in the analysis of ground trawl surveys to estimate total or relative abundance (Pennington, 1996; Stefánsson, 1996). The main advantage of delta models is that they allow for an explicit and finite probability of zero catch. In a delta model, the estimated values are the product of two independent components: the probability of nonzero observations, and the probability of effective density if there is a positive observation. In the case of fishery surveys, the nonzero probability can be analogous to the probability of encountering a fish aggregation, whereas the probability within the positive observations would correspond to the estimated density of a given fish aggregation (Cooke and Lankester[4]).

Delta models are multivariate distributions with a nonzero probability mass at the origin (Shimizu, 1988). Stefánsson (1996) presented a mathematical model based on a generalized delta lognormal model for analyzing groundfish survey data. This model defines the cumulative density function of abundance at a given sampling station as

$$F_i(\omega) = P[Y_i \leq \omega] = (1 - p_i) + p_i G_i(\omega),$$

where G_i = a continuous cumulative density function describing the distribution of positive values in a station I; and

p_i = the probability of finding fish in that station.

If p_i is constant and G_i is a lognormal distribution within a stratum, the function is the delta lognormal model. If p_i is set to one (i.e. excluding zero values), and G_i is set to a gamma or other exponential function with a parameterized mean, this model becomes a generalized linear model (GliM, Stefánsson, 1996). The advantage of this formulation is that each component in the delta model can be expressed in terms of a GLiM (McCullagh and Nelder, 1989). Thus, the choice of a particular density function in each of the delta model components can be related to other measured variables, such as tow times, location effects, and seasonal or year effects, through assumptions on distribution.

Bycatch data derived from observers in the Gulf of Mexico shrimp trawl fishery typically have a high proportion of zero bycatches and a skewed distribution of the positive bycatch CPUE rates, with a large number of low bycatches and very few large bycatches. The large catches most likely reflect the spatial-temporal distribution characteristics of fish stocks rather than are outliers of the data. This type of distribution is far from normal, and commonly used transformations are unable to make the data comply with the normal assumptions with the classical regression models. Furthermore, in the case of so-called "non-frequent bycatch species," the proportion of zero observations is markedly increased (above 95%); this significantly biases and reduces the efficiency of statistical estimators of central tendency and overestimates the variance (Pennington, 1996).

The delta lognormal model was used in our study to generate annual bycatch estimates for all finfish combined, as well as for three specific finfish species: Atlantic croaker, red snapper, and Spanish mackerel in the U.S. Gulf of Mexico shrimp trawl fishery. Briefly, bycatch CPUE rates of a given fish species in a given cell were estimated as the product of two components: 1) the proportion of tows with positive catch and 2) the mean catch rate if at least one fish was caught. Bycatch per cell is then the product of the estimated CPUE and the corresponding shrimping effort for that particular cell. Total annual bycatch is then the sum over all strata within a year for the commercial component, as in the general linear model (see Eq. 3).

Each component of the delta lognormal model, the proportion of positive tows and the mean bycatch rate, was estimated by following a general linear model approach with the procedure GENMOD in the SAS statistical software package (SAS Institute Inc., 1993). General linear models consist of three elements: 1) the *random* component which defines the error structure of the model, 2) the *systematic* component which defines a set of explanatory variables $x_1, x_2, \ldots, x_q$, and 3) the *link* function which defines the relation between the random and the systematic components (McCullagh and Nelder, 1989). We described the delta lognormal model for estimating shrimp bycatch on the basis of the assumptions entailed with each component of the model. To compare models, the same explanatory variables used in the current general linear model were used with the delta lognormal model.

[4] Cooke, J. G., and K. Lankester. 1995. Consideration of statistical models for catch-effort indices for use in tunning VPA's. ICCAT Collect. Vol. Sci. Pap. 45(2):125–131.

Proportion of positive tows

The proportion of positive tows for a particular fish species was estimated after classifying each tow as either 0 (no fish caught) or 1 (at least one fish caught). For the shrimp bycatch data, the model assumes that the data are independent results from n successive trials of a Bernoulli-type random variable with a probability p of catching a given fish species. In this case, it is assumed that the frequency distribution of observed zero and positive tows in each cell follows a binomial distribution. The error term is assumed to be constant and independent among the cells. The binomial distribution is then defined in terms of the proportion (y) of positive tows (r) to total tows (n) per cell, and the probability density function $f(y)$ and associated variance $Var(y)$ function are given by

$$\text{for } y = r/n,\ f(r) = \binom{n}{r}\mu^r(1-\mu)^{n-r} \text{ where } r = 1, 1, 2, \ldots\ldots, n$$

$$Var(y) = \mu(1-\mu)/n$$

where μ = the mean of y. The response variables y_i are independent for i=1,2,...., n tow trials.

The systematic component defines the set of explanatory variables $x_1, x_2, \ldots, x_q$ which produce a linear predictor η given by

$$\eta = \sum_{j=1}^{q} x_j \beta_j + \beta_0.$$

For the shrimp bycatch data, the linear predictor is a linear function of the fixed explanatory variables dataset, year, season, area, and depth zone, such that

$$\eta = \beta_0 + \beta_1 \cdot dataset + \beta_2 \cdot year + \beta_3 \cdot season + \beta_4 \cdot area + \beta_5 \cdot depth\ zone,$$

where the β_j are parameters to be estimated.

The link function that relates the linear predictor η to the expected value μ of observations y in each cell of the model must be a monotonic differentiable function g such that

$$g(\mu_1) = \eta.$$

In this case, the logit or logistic function expresses the relationship between the assumed binomial error distribution of μ and the given linear function of explanatory variables η, as

$$\eta = \log\left[\frac{\mu}{(1-\mu)}\right].$$

The GENMOD algorithm uses maximum-likelihood estimates for assumed binomial distributions, which are unbiased to a first order of approximation (McCullagh and Nelder, 1989).

Mean bycatch rate

In this section only positive tows were considered. The delta lognormal model assumed that for a given species the number of fish caught as bycatch relates to fixed variables: data source (commercial or research), year, season, area, and depth zone. The mean bycatch CPUE given a nonzero catch was also estimated following a generalized linear model approach. In this case, the random component for the estimated CPUE was assumed to follow a lognormal error distribution within cells. The probability density function is given by the normal function

$$f(y) = \frac{1}{\sqrt{2\pi\sigma^2}} e^{\left[-\frac{(y-\mu)^2}{2\sigma^2}\right]},$$

where μ = $E[y]$; and
σ^2 = $Var(y)$ with a logarithmic link function.

This specification is mathematically equivalent to defining the random component as lognormal with the identity as the link function.

The systematic component is defined as

$$\text{Log}(CPUE) = \beta_0 + \beta_1 \cdot dataset + \beta_2 \cdot year + \beta_3 \cdot season + \beta_4 \cdot area + \beta_5 \cdot depth,$$

where $CPUE$ = the catch rate in numbers of fish per net hour for nonzero catches;
β_0 = the overall mean;
$dataset$ = a fixed effect differentiating data sources from commercial shrimp fishing from those in research trawls, the terms *year*, *season*, *area*, and *depth* are also fixed effects; and
the β_j = parameters to be estimated.

The link function between the random and systematic components is the identity function:

$$\eta = \mu.$$

Estimation of bycatch

The overall model is then referred to as the delta lognormal model. This model generates the estimated proportion of positives tows ($\hat{p}_{ijklm}$) and the mean bycatch rate ($\hat{CPUE}_{ijklm}$) for a given species. Estimates of bycatch are calculated as the product of the proportion of positives tows ($\hat{p}_{ijklm}$) multiplied by the mean bycatch rate ($\hat{CPUE}_{ijklm}$) multiplied by the shrimping effort (f_{jklm}) multiplied by the two nets (assumed) per boat. Shrimping effort data are the same as those used in the current general linear model. Annual estimates of bycatch are simply the sum of bycatch per cell over the season, area and depth zone strata, for the commercial sector (i=1).

$$Bycatch = 2 \cdot \sum_{jklm} \hat{p}_{1jklm} \times \hat{CPUE}_{1jklm} \cdot f_{jklm}.$$

Evaluation of the delta lognormal model

Before comparing the annual bycatch estimates of total finfish, Atlantic croaker, red snapper, and Spanish mackerel from the general linear model (Nichols[5]) and the delta lognormal model, the delta lognormal model was evaluated and assessed. Because there is not yet a formal strategy for model verification, acceptance of a particular model should not be based exclusively on "goodness of fit" scores (McCullagh and Nelder, 1989).

In general, model assessments can be classified into two main groups. The first group checks for systematic departure from the underlying model, testing for additional factors, factor interactions, or covariates that could explain a significant proportion of the residual model variation. The second group involves evaluation of particular or isolated points in the data. McCullagh and Nelder (1989) and O'Brien and Kell[6] have described six specific tests for evaluating generalized linear models: 1) assessment of the scale of independent variables; 2) assessment of the link function adequacy; 3) assessment of variance function adequacy; 4) investigation of systematic departure from the assumed model; 5) investigation of outliers; and, 6) investigation of omitted predictor variables. Most of these analyses are based on the behavior of the model residuals, either as graphical or informal tests, rather than an exact statistical test. For the delta lognormal model, only tests evaluating systematic departure from the assumed model were performed on each of the model components (i.e. an estimation of the proportion of positive tows and the estimation of bycatch rates) separately.

With the delta lognormal model, an evaluation of the proportion of positive tows was restricted to a graphical analysis of the frequency distribution of positive tows of observed and predicted data. This restriction was warranted because most of the tests suggested for assessing model adequacy are uninformative for binomial data (McCullagh and Nelder, 1989; O'Brien and Kell[6]). Figure 4 shows the standardized frequency distributions of proportion of positive tows per cell for the combined finfish category, Atlantic croaker, red snapper, and Spanish mackerel. Each plot shows the observed and the predicted proportions estimated by the binomial distribution of the delta lognormal model. The predicted frequencies fitted closely those observed in all four cases. The assumed binomial distribution is able to predict appropriately the proportion of positive tows in a broad range (from the combined finfish category case where almost all tows were positive [97%] to the case of Spanish mackerel where only 5% of the tows were positive).

The suitability of the delta lognormal general linear model component for the positive tows was evaluated by the following graphical tests: 1) adequacy of the link function, 2) adequacy of the variance function, and 3) systematic departure from the assumed model.

By plotting the adjusted dependent variable (log CPUE) we were able to assess the link function against the estimated linear predictor ($\hat{\eta}$). A linear configuration is expected for normal, assumed Poisson or gamma error distributions. In our case, the delta lognormal model assumed a normal error distribution for log CPUE of positive catch. Figure 5A shows the plots of the linear predictor (lp-logcp) against the adjusted dependent variable (log CPUE) for red snapper. In the case of high density of points as in Figure 5A, locally weighted regression smoothing procedures (i.e LOESS smoothing) have been suggested for showing the trend of the response variable (McCullagh and Nelder, 1989).

Adequacy of the variance or assumed error distribution function was evaluated by using a plot of residuals against fitted values. The spread of residuals is expected to be approximately constant and independent of the fitted values, confirming the adequacy of the assumed error distribution in the model. Figure 5B shows the plots of residuals (R-logcpu) against the fitted values (P-logcpu) for red snapper. The residuals are evenly distributed about the zero line and are without any apparent trend with respect to the fitted values. Likewise, a plot of residuals versus the normalized cumulative residuals (QQ plot) can be used to assess the variance function adequacy. A linear relationship is expected for residuals from a normal error distribution.

A plot of standardized residuals (rs-logcp) against fitted values (log CPUE) was used to identify possible trends or curvatures that would suggest a departure from the assumed model (Fig. 5C). The null pattern of this plot is a linear configuration of the standardized residuals (O'Brien and Kell[6]). In conclusion, assessments of each of the delta lognormal model components did confirm the model choices and assumptions for the finfish group and the fish species examined (similar plots were created for finfish, Spanish mackerel, and Atlantic croaker but are not presented here for briefness).

As shown before, bycatch estimates from the current general linear model depend upon the standard time unit chosen to convert catches in numbers to CPUE values. Similarly, the same tow time evaluation with the delta lognormal model was performed as with the general linear model. CPUE values were calculated by using 10-, 30- and 240-min tow times, and concurrently, shrimping effort unit, given in hours, were multiplied by a scale factor to make the time unit compatible with the modified CPUE values. With the delta lognormal model, the annual bycatch estimates were exactly the same, independent of the time unit used to calculate the CPUE values, further demonstrating the benefits of using a model that separates the zero catch observations from the positive catch. In addition, delta models do not require adding a constant value to logarithmic transformed values because the estimated density component is restricted to positive catch only, thus avoiding the uncertainty in selecting a c value to log transform CPUE values as required in the general linear model.

Results and discussion

Because the bycatch database complied with the delta lognormal model specifications, a stepwise analysis of devi-

[5] Nichols, S. 1996. Estimates of annual shrimp fleet bycatch in the offshore waters of the Gulf of Mexico. Personal commun. NMFS Pascagoula laboratory, 3209 Frederic St. Pascagoula, MS 39567.

[6] O'Brien, C. M., and L. T. Kell. 1996. The use of generalized linear models for the modelling of catch-effort series. I Theory. ICCAT Collect. Vol. Sci. Pap. 46(4):476–482.

ance was performed to assess the importance of the factors selected in the delta model. Table 2 gives the percent change in deviance as each factor is added to the binomial fitted proportion of the zero versus positive tows component of the delta lognormal model. The deviance explained by the model is equivalent to the r^2 concept in linear models (McCullagh and Nelder, 1989; Stefánsson, 1996). Tests of significance were based on the χ^2 statistic for the binomial distribution of the proportion of positive tows (McCullagh and Nelder, 1989). Overall, the delta lognormal model, with all factors, explained between 55% and 75% of the total deviance for the finfish group and the three fish species. However, as expected, the percentage of deviance explained by each factor differed for each species. For example, the *dataset* factor appeared to be unimportant in estimating the proportion of positive tows for red snapper and Atlantic croaker. Instead, area and season factors were more important for red snapper, and area and depth zone for Atlantic croaker.

Table 3 shows the lognormal component of the delta model r^2 values, sum of squares error or residual deviance, residual degrees of freedom, and the P values. Similarly to the proportion of positive tows, a stepwise analysis of the r^2 shows that dataset, year, season, area, and depth zone are significant factors in explaining the overall variability of the model. An exception is the depth zone factor in estimating bycatch CPUE rates for red snapper. The delta lognormal estimated density model explained from 17% (Atlantic croaker) to 36% (Spanish mackerel) of the total variation, indicating that a significant portion of the bycatch CPUE variability is still unexplained by the model.

The annual shrimp bycatch estimates for the four species groups in the U.S. Gulf of Mexico differed in several aspects between the delta lognormal model and the current general linear model. Results varied for the finfish group and the fish species analyzed. Differences were found both in the absolute magnitude of bycatch estimates and in the trend over the time series 1972–95. For the total finfish bycatch, the delta lognormal model estimated an average of 795 million lbs. for the period 1972–95, or 14% lower than the equivalent general linear model estimate of 916

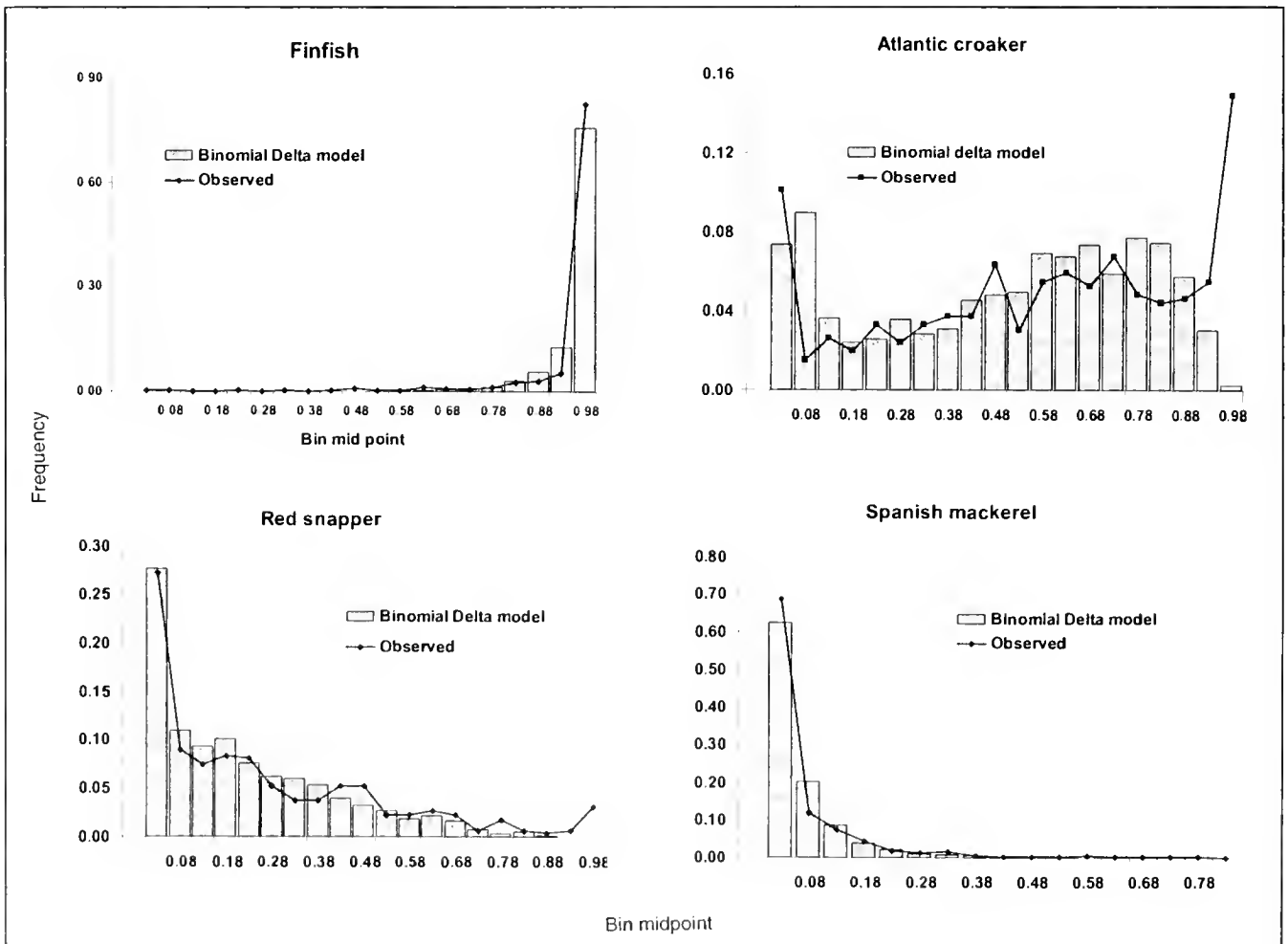

Figure 4

Standardized frequency distribution of the proportion of positive tows from the bycatch data 1972–95 and the proportions estimated by the binomial-based delta lognormal model component.

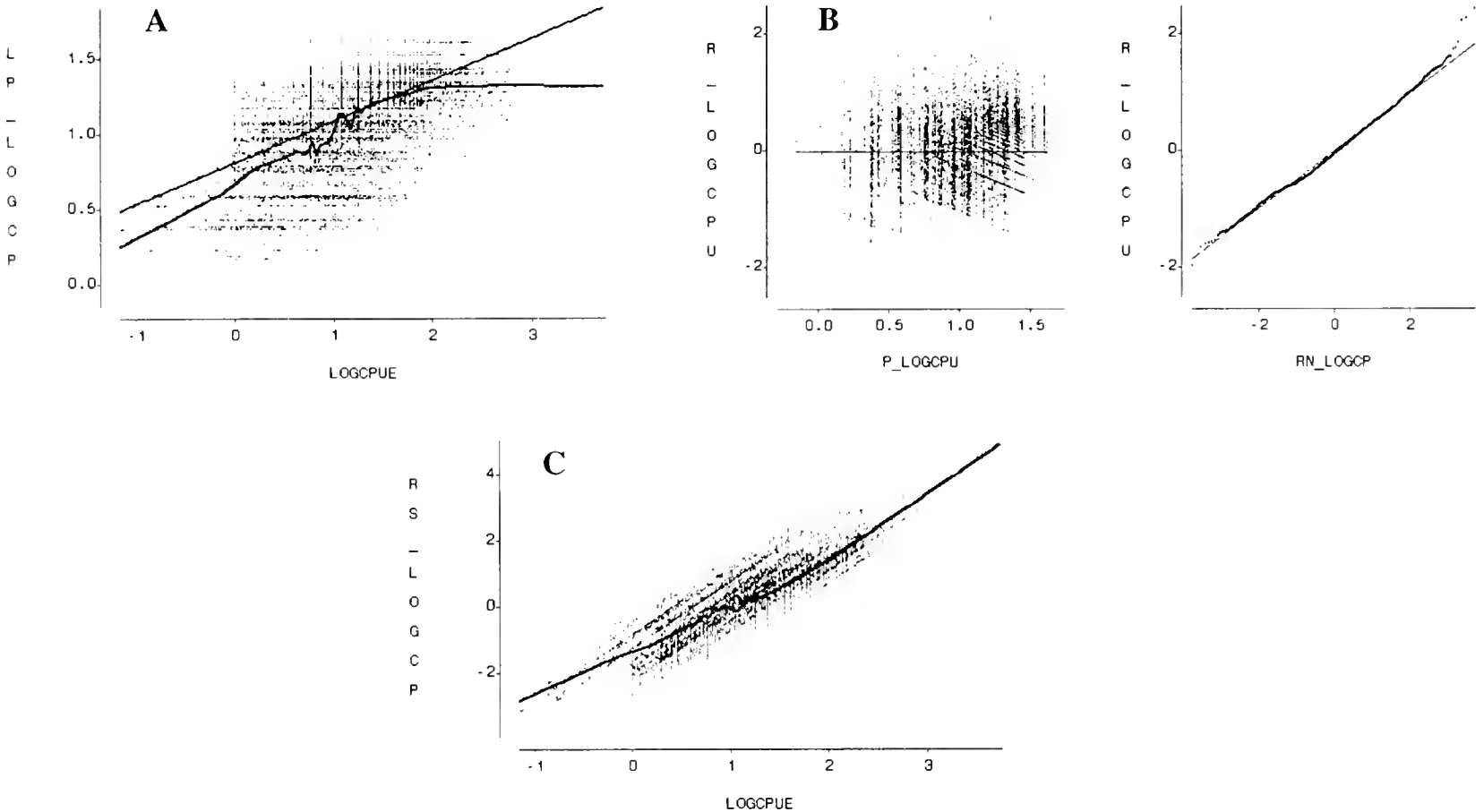

Figure 5

Evaluation plots for the positive catch component for red snapper with the delta lognormal model. (**A**) Plot of the linear predictor (lp_logcp) against the dependent variable (logCPUE). The straight line is the linear function of the variables for comparison purposes, the dark line is the LOESS smoothing procedure of the data. (**B**) Plot of the residuals (r_logcpu) against predicted values (p_logcpu) and the cumulative normalized-residuals or QQ plot. (**C**) Plot of the standardized residuals (rs_logcp) against the fitted values (logCPUE). The line represents the LOESS smoothing procedure to evaluate the data trend.

Table 2

Analysis of deviance table for different binomial-based delta lognormal models fitted to positive/total tows of each fish species and finfish category in the bycatch database for the U.S. Gulf of Mexico 1972–95. The models are fitted sequentially and the columns give the residual degrees of freedom for each model, the residual deviance, the resulting change in deviance, the percentage of total deviance change, and the *P*-value when χ^2 test was used for significance. Model 1 refers to estimating only the overall mean.

Model factors	Residual df	Residual deviance	Change in deviance	% of total deviance	*P*	Residul deviance	Change in deviance	% of total deviance	*P*
	Finfish					Atlantic croaker			
1	454	2403				8869			
Data set	453	1676	726.05	0.30	<0.001	8866	3.38	0.00	<0.0660
Data set + year	430	1113	563.93	0.23	<0.001	7890	976.05	0.11	<0.001
Data set + year + season	428	1079	33.70	0.01	<0.001	6194	1696.32	0.19	<0.001
Data set + year + season + area	425	1026	52.80	0.02	<0.001	3866	2327.89	0.26	<0.001
Data set + year + season + area + depth zone	424	1016	9.66	0.00	<0.001	3849	17.22	0.00	<0.001
	Red snapper					Spanish mackerel			
1	454	6390				2356			
Data set	453	6389	0.34	0.00	<0.5605	2086	270.00	0.11	<0.001
Data set + year	430	4935	1454.20	0.23	<0.001	1810	275.91	0.12	<0.001
Data set + year + season	428	4013	921.97	0.14	<0.001	1550	260.29	0.11	<0.001
Data set + year + season + area	425	2770	1243.33	0.19	<0.001	1468	81.92	0.03	<0.001
Data set + year + season + area + depth zone	424	1633	1136.46	0.18	<0.001	1065	402.92	0.17	<0.001

million lbs. (Table 4, Fig. 6). Total finfish bycatch estimates from the delta lognormal model were consistently lower for all years, and overall followed the same trend as the estimates from the current general linear model. The normalized plot of total finfish bycatch (i.e. year estimate minus the mean divided by the standard deviation of the time period) shows that the trends are identical between the two models up to 1990, but in 1991–95 some discrepancies were observed (Fig. 7). However, both models show a decreasing trend in the total finfish bycatch estimates from about 1,100 million lbs. (1972–84) to less than 700 million lbs. during the last 10 years (1985–95). This decline can be attributed to improvements in the selectivity of the shrimp trawl gear to retain less bycatch (i.e. introduction of TEDs and BRDs) or to an overall reduction of the trawlable fish stock biomass in the U.S. Gulf of Mexico.

For Atlantic croaker, bycatch estimates from the delta lognormal model were on average 4.5 billion fish for the 1972–95 period, 74.5% lower than estimates of 17.7 billion fish from the general linear model (Table 4, Fig. 6). Once more, the normalized plot shows a similar decreasing trend in bycatch estimates from both models in the 1972–95 period (Fig. 7). Atlantic croaker, together with longspine porgy (*Stenotomus caprinus*), are the most common finfish bycatch species in the Gulf of Mexico shrimp fishery, therefore a significant reduction in bycatch estimates of Atlantic croaker most likely correlates with a reduction in total estimated finfish bycatch.

Bycatch estimates of red snapper from the delta lognormal model were slightly greater in general from 1972 to 1982, and much lower from 1987 to 1995 compared with estimates yielded with the general linear model (Fig. 6). On average, the delta lognormal model bycatch estimates were 22.1 million fish for the years 1987–95, 40% lower than the equivalent average of 36.8 million fish estimated with the general linear model (Table 4). The normalized plot shows that since 1987, there has been an overall increasing trend in red snapper bycatch according to both the general linear model and delta model estimates, a peak in bycatch in 1990, subsequent low in 1992, and an increasing trend since then (Fig. 7). Prior to 1987, red snapper bycatch was relatively lower, with an exception of the highest bycatch peak in 1972 and some above average bycatch in 1980–82.

Delta lognormal estimates of Spanish mackerel bycatch were 97% higher on average than those from the general linear model (Fig. 6, Table 4) for the time period 1972–95. Spanish mackerel bycatch estimated by the delta lognormal model was on average 6.5 million fish, compared with 3.2 million fish estimated by the general linear model. In

Table 3

Analysis of deviance table for different lognormal-based delta models fitted to the positive bycatch CPUEs of each finfish species and the finfish category in the bycatch database for the US Gulf of Mexico 1972–95. The models were fitted sequentially and the columns give the residual degrees of freedom for each model, the residual deviance, the resulting change of deviance, the r^2 values, and the P-value when the F-test was used for significance. Model 1 refers to estimating only the overall mean.

Model factors	Residual df	Residual deviance	Change in deviance	% of total deviance	P	Residual df	Residul deviance	Change in deviance	% of total deviance	P
	Finfish					Atlantic croaker				
1	25,636	10,040.40				15,985	16,036			
Data set	25,635	8870.06	1170.34	0.12	<0.0001	15,984	15,238	798.03	0.05	<0.0001
Data set + year	25,612	7809.32	1060.74	0.22	<0.0001	15,961	13,855	1382.60	0.14	<0.0001
Data set + year + season	25,610	7685.07	124.25	0.23	<0.0001	15,959	13,790	65.09	0.14	<0.0001
Data set + year + season + area	25,607	7440.94	244.13	0.26	<0.0001	15,956	13,463	326.60	0.16	<0.0001
Data set + year + season + area + depth zone	25,606	7436.59	4.35	0.26	<0.0001	15,955	13,308	154.96	0.17	<0.0001
	Red snapper					Spanish mackerel				
1	7377	2491.32				1240	430.90			
Data set	7376	2122.94	368.38	0.148	<0.0001	1239	369.80	61.10	0.142	<0.0001
Data set + year	7353	1889.23	233.71	0.242	<0.0001	1216	329.53	40.27	0.235	<0.0001
Data set + year + season	7351	1847.03	42.20	0.259	<0.0001	1214	305.09	24.43	0.292	<0.0001
Data set + year + season + area	7348	1803.48	43.55	0.276	<0.0001	1211	288.32	16.77	0.331	<0.0001
Data set + year + season + area + depth zone	7347	1803.26	0.22	0.276	<0.0001	1210	273.54	14.78	0.352	<0.0001

our study, the delta lognormal model showed a larger year variability of bycatch with prominent peaks in 1980 and 1992. The normalized plot of Spanish mackerel bycatch illustrates that estimates from the general linear model and delta lognormal model followed similar trends from 1972 to 1981, and from 1988 to 1995 (Fig. 7). The time period from 1984 to 1987, the period of greatest oscillation in bycatch estimates for the delta lognormal model, corresponds with the years of no bycatch observations in the commercial fishery. Although delta lognormal bycatch estimates show a comparable trend to the general linear model estimates in the later years (1987–95), the magnitude of bycatch is much greater; the peak estimate of 14.4 million fish in 1993 is twice as high as the reported estimates from the general linear model (Nichols[5]).

The delta lognormal model protocol appears to be an improved alternative procedure for estimating shrimp bycatch in the U.S. Gulf of Mexico compared with the currently used general linear model. In theory, the delta model allows for an explicit probability for zero catches, which are highly common in the bycatch data set, especially when dealing within single species cases. Myers and Pepin (1990) stated that lognormal-based estimators are sensitive to violations of model assumptions, in particular if the number of observations is below 40 or if there is no confirmation that the sample came from a true lognormal distribution (or if both situations occur). However, their arguments are restricted to the positive tows (i.e. nonzero observations); they concluded that lognormal estimators should be used only in cases where the assumed lognormal distribution can be confirmed. Following their criteria, Myers and Pepin's arguments should then be applied to the delta lognormal model (more specifically to the density estimation component that models the nonzero catches) and to the current general linear model as well (if a lognormal distribution can be assumed for all observations, Nichols et al.[2]). In the bycatch database, there are a large number of cells with low number of observations (i.e. ≤40). Restricting the database to cases where the number of observations per stratum (year, area, season, depth, and dataset) were greater than 40, we were able to use cumulative CPUE distributions more approximate to lognormal

Table 4

Bycatch estimates from the general linear model and the delta lognormal model. Percentage of change is with reference to the bycatch general linear model estimates, negative percentages refer to lower estimates. The average values are over the 24-year period.

	Finfish			Atlantic croaker			Red snapper			Spanish mackerel		
	Millions of lbs.			Millions of fish			Millions of fish			Millions of fish		
Year	GLM	Delta	% change	GLM	Delta	% change	GLM	Delta	% change	GLM	Delta	% change
1972	1501.10	1305.45	−13	17,529.94	4736.80	−73	69.49	73.27	5	2.47	5.63	128
1973	1211.12	1093.34	−10	27,161.33	9034.68	−67	23.00	28.22	23	2.08	3.62	74
1974	934.85	826.66	−12	20,205.60	5396.10	−73	16.97	19.58	15	1.62	1.65	2
1975	1209.90	1098.10	−9	45,615.42	7337.83	−84	15.23	18.01	18	1.53	2.35	54
1976	1343.26	1177.58	−12	32,140.84	7806.93	−76	23.27	30.27	30	2.32	5.63	143
1977	843.11	772.07	−8	12,793.05	4405.55	−66	24.45	25.41	4	2.80	8.22	194
1978	1248.09	1113.57	−11	20,133.40	6648.36	−67	21.62	18.40	−15	3.43	6.27	83
1979	1045.06	957.10	−8	18,851.25	5121.00	−73	22.36	22.91	2	3.48	8.64	148
1980	1045.81	925.60	−11	24,707.77	5860.63	−76	34.07	38.35	13	4.24	16.93	299
1981	922.37	787.92	−15	10,431.83	4727.13	−55	34.21	37.99	11	2.57	5.94	131
1982	1028.24	878.77	−15	11,953.52	4264.06	−64	33.77	36.31	8	2.85	6.94	144
1983	790.33	680.57	−14	15,826.07	5940.60	−62	21.18	17.97	−15	2.58	3.08	19
1984	1217.03	1043.25	−14	22,381.82	7291.54	−67	16.44	13.57	−17	2.79	6.89	147
1985	975.74	821.60	−16	24,975.37	4558.15	−82	20.15	14.68	−27	2.79	2.17	−22
1986	606.40	513.85	−15	7453.91	2134.62	−71	18.80	14.31	−24	2.95	4.11	39
1987	656.50	556.19	−15	7778.19	1281.58	−84	23.88	11.99	−50	3.42	2.33	−32
1988	582.70	498.09	−15	8601.77	1732.06	−80	22.69	11.72	−48	3.94	8.33	111
1989	594.09	507.50	−15	10,286.57	2800.51	−73	27.51	18.10	−34	4.20	8.38	100
1990	748.97	639.65	−15	10,370.38	2414.03	−77	53.17	32.35	−39	3.77	6.64	76
1991	742.31	597.00	−20	20,449.99	3775.18	−82	46.93	27.03	−42	4.19	6.97	66
1992	684.74	430.25	−37	24,818.83	5298.03	−79	30.37	17.06	−44	5.05	10.74	113
1993	605.72	517.55	−15	11,556.16	1998.04	−83	33.71	18.77	−44	4.68	14.41	208
1994	729.20	660.36	−9	10,984.66	2177.96	−80	41.98	32.32	−23	3.01	4.11	37
1995	719.92	669.17	−7	8715.51	1500.90	−83	50.87	29.94	−41	3.06	5.32	74
Average	916.11	794.63	−14	17,738.47	4510.09	−74	30.26	25.36	−14	3.16	6.47	97

density function in the case of nonzero catches (i.e. delta lognormal model) than in the case when both zero and positive catches are included (i.e current general linear model). Thus, if departures from the assumed distribution produced biased lognormal estimates, certainly the current general linear model would be more prone to these biases than the delta lognormal model.

As stated by Pennington (1991) in his response to Myers and Pepin's (1991) article, the assumed lognormal data were contaminated with data from distributions that generated extremely small values, close to zero, which in a logarithmic scale become large negative values. These large negative values then biased estimates of the mean. In the case of the bycatch database this is not a problem because the smallest positive bycatch CPUE values are in most cases greater than 0.05.

Another point to consider when comparing the delta lognormal model and the current general linear model is the variance associated with the estimated bycatch. Smith (1988) described an exact variance for the delta lognormal distribution estimates. He also pointed out that the efficiency of the delta lognormal variance is a function of the sample size, the proportion of zero observations, and the variance within the nonzero observations. The variance of bycatch estimates are, however, restricted to the variance from the general linear model or the delta lognormal model because the shrimping effort multiplier is assumed to be exactly known (Nichols et al.[2]). Thus to compare true standard errors of bycatch estimates, one would require the variance of the shrimping effort and calculate an overall variance through a mathematical approach such as the delta method or use resampling techniques such as bootstrapping procedures. Because point estimates of bycatch are more frequently used in stock assessments of affected species rather than the confidence intervals, the present analysis focused on the point estimates of bycatch.

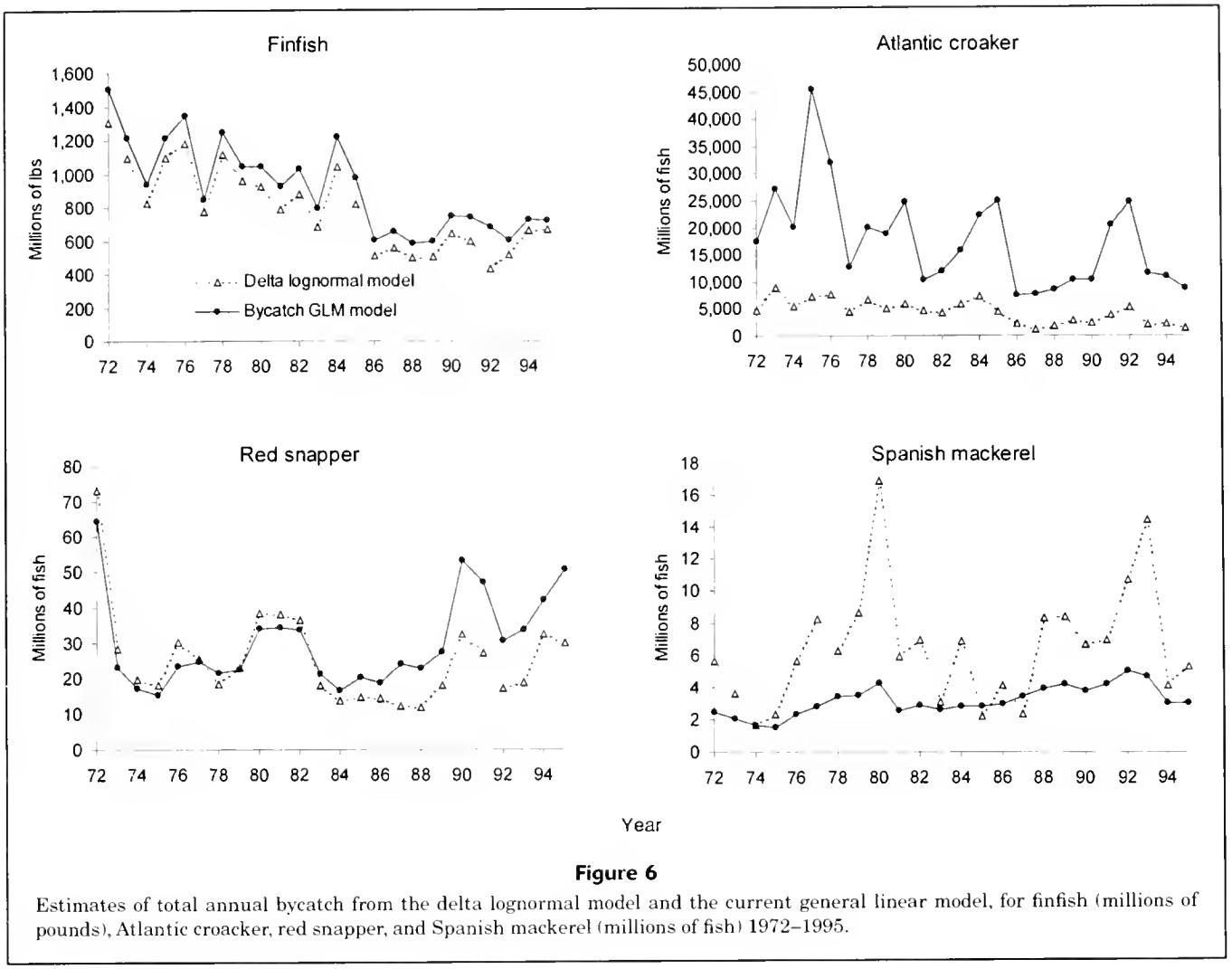

Figure 6

Estimates of total annual bycatch from the delta lognormal model and the current general linear model, for finfish (millions of pounds), Atlantic croacker, red snapper, and Spanish mackerel (millions of fish) 1972–1995.

Conclusions and recommendations

Analyses of the total finfish bycatch and the bycatch of Atlantic croaker, red snapper, and Spanish mackerel show that the delta lognormal model estimates differ both in magnitude and trends from those generated by the current general linear model. However, these differences are not consistent among species. In terms of absolute magnitude, they are substantially different for Atlantic croaker and Spanish mackerel over all years (1972–95), whereas for red snapper differences are greater in the most recent years of the time series (1987–95). Total finfish bycatch estimates are more similar in magnitude and trend for both models. Although the trends of bycatch in the time series from 1972 to 1995 are similar for the species examined, the absolute estimated values are highly variable. Because these estimates are included as additional catch (usually for age 0 and 1) in the stock assessments of directed fisheries, the uncertainty of the bycatch estimates will impact the results of these assessments. Further, this uncertainty will extend to management policies adopted from these assessment results for species like Spanish mackerel, king mackerel, and red snapper (Ehrhardt and Legault, 1997; Goodyear[7]).

As presented before, the general linear model estimates depend on choices about the constant added to the CPUE values prior to logarithmic transformation and on the standard time unit chosen for calculating CPUE values. These problems emerge from the noncompliance of the bycatch data with the assumptions associated with the general linear model. In particular, the observed CPUEs are not lognormally distributed owing to the significant proportion of zero observations within the data. In contrast, the delta lognormal model conforms better with the structure of the data and avoids the problems of choosing a c value for catches in the logarithm transformation and of selecting a standard time unit for the CPUE calculations. As

[7] Goodyear, C. P. 1995. Red snapper in U.S. waters of the Gulf of Mexico. Contribution report MIA 95/96-05, 171 p. Miami Laboratory, Southeast Fisheries Science Center, NMFS, NOAA, 75 Virginia Beach Dr., Miami, FL 33149.

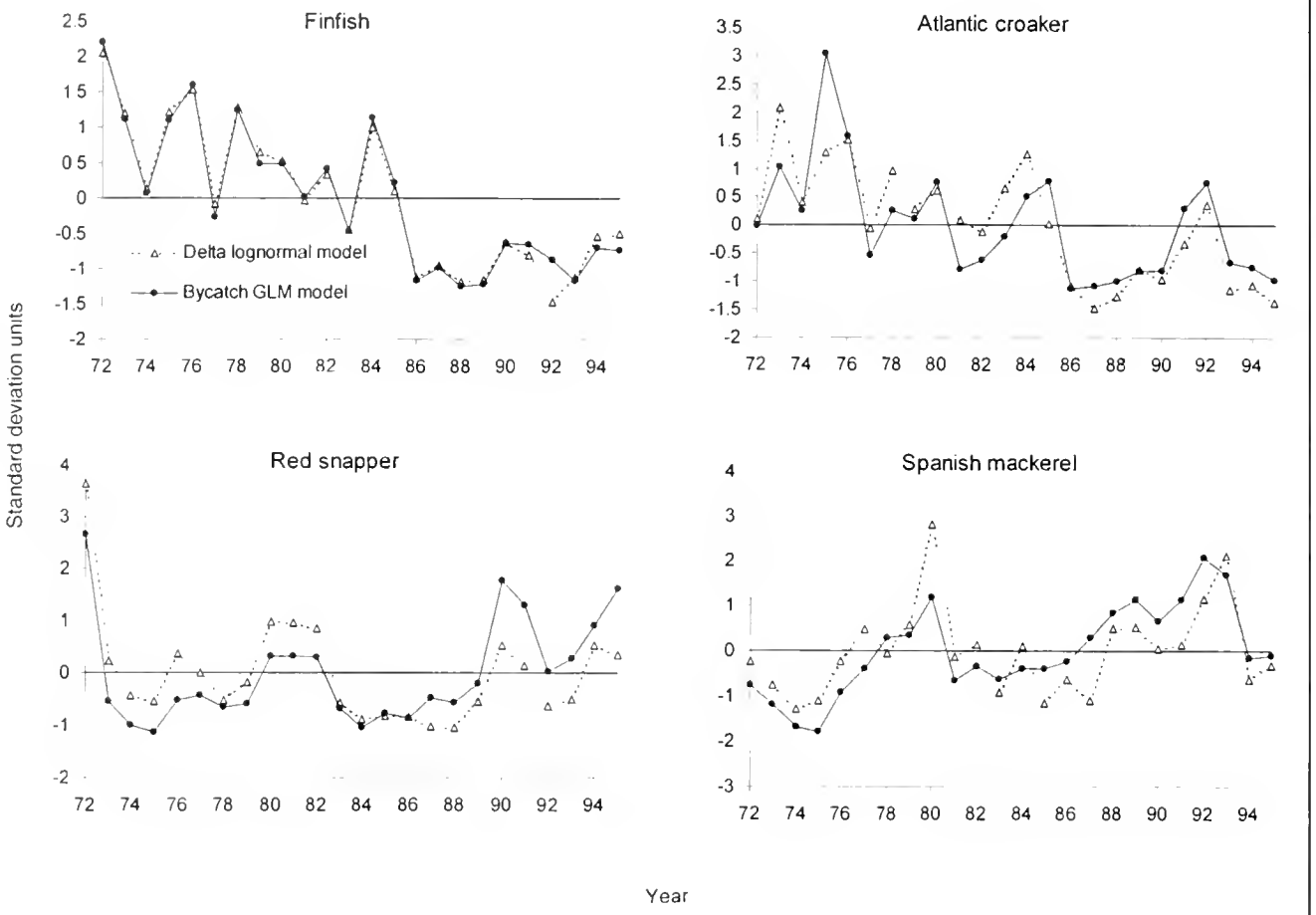

Figure 7

Normalized plots of bycatch estimates by species from the current general linear model and the delta lognormal model.

expected, both models agree better in the case of the finfish bycatch estimates where the proportion of zero CPUE values is the lowest (less than 3%).

Besides the problems related to zero observations, several other considerations must be addressed to generate annual bycatch estimates:

1 The matrix structure of area, season, year, and data source is inadequately covered by observations. This is true for any model that uses these same factors but in particular for the period 1985–90, when commercial observations were not available. It may be beneficial to limit the analysis to years, areas, and seasons where there are data from both commercial and research sources. This change, however, will require the redefinition of the objectives of the bycatch estimation procedure because the estimated annual bycatch will not be possible for the 1972–95 period.

2 Another important requirement is the standardization of the CPUE units for both the commercial and research observations. We feel that these CPUEs represent different units for each type of observation for each particular species and that a single linear relationship is not adequate. This standardization will require a thorough analysis of each fleet and additional information in order to convert the effort units from nominal to effective units for each fleet prior to bycatch estimation. It has been suggested that the more recent data obtained by the Bycatch Characterization Project (NOAA[1]) could be used for this type of analysis. As an alternative, we modified the delta lognormal model to incorporate the observed catch (i.e. numbers of fish) as the dependent variable, and we used the tow time (i.e. hours fishing) as a covariate in the systematic linear component of the delta lognormal model. With this modification, the total deviance explained by the model increased for red snapper. However, we would recommend standardizing the nominal CPUE instead of simply adding more variables to an already unbalanced matrix and avoid considering only goodness-of-fit as an indicator.

3 In the analysis of bycatch by species, it is presently assumed that estimated bycatch in number of fish belongs

to the same age class, usually the age-0 class. This may not be true for some species. Thus, bycatch estimates should take into account number of fish per age or size class.

Acknowledgments

This research was supported by a grant provided by MARFIN (NA57FF283-01); additional grants came from the Florida Sea Grant College Project (R/LR-8-37). We thank Victor Restrepo from the University of Miami RSMAS for his scientific advice, Scott Nichols from the Pascagoula laboratory of the NMFS for providing the bycatch database and algorithms, and Nancy Cummings from the NMFS Miami laboratory for her comments and suggestions. Three anonymous reviewers provided valuable comments on the final draft.

Literature cited

Berry, D. A.
1987. Logarithmic transformations in ANOVA. Biometrics 43:439–456.

Ehrhardt, N. M., and C. M. Legault.
1997. The role of uncertainty in fish stock assessment and management: a case study of the Spanish mackerel, *Scomberomorus maculatus*, in the US Gulf of Mexico. Fish. Res. 29:145–158.

Henwood, T. A., and W. E. Stuntz.
1987. Analysis of sea turtle captures and mortalities during commercial shrimp trawling. Fish. Bull. 85(4):813–17.

Lo, N. C., L. D. Jacobson, and J. L. Squire.
1992. Indices of relative abundance from fish spotter data based on delta-lognormal models. Can. J. Fish. Aquat. Sci. 49:2515–26.

McCullagh, P., and J. A. Nelder.
1989. Generalized linear models. Chapman & Hall, London, 512 p.

Myers, R. A., and P. Pepin.
1990. The robustness of lognormal-based estimators of abundance. Biometrics 46:1185–1192.
1991. Replay to: on testing the robustness of lognormal based estimators. Biometrics 47:1623–1624.

Pellegrin, G. J.
1982. Fish discards from the southeastern United States shrimp fishery: fish by-catch: bonus from the sea report of a technical consultation on shrimp by-catch utilization held in Georgetown, Guyana, 27–30 October 1981. International Development Research Center (IDRC), Ottawa, 163 p.

Pennington, M.
1983. Efficient estimators of abundance, for fish and plankton surveys. Biometrics 39:281–86.
1991. On testing the robustness of lognormal-based abundance estimators. Biometrics 47:1623.
1996. Estimating the mean and variance from highly skewed marine data. Fish. Bull. 94:498–505.

SAS Institute Inc.
1993. SAS/STAT® software: the GENMOD procedure, release 6.09. SAS® Technical Report P-243. SAS Institute Inc., Cary, NC, 88 p.

Shimizu, K.
1988. Point estimation. lognormal distributions: theory and applications. Department of Information Sciences, Faculty of Science and Technology, Science University of Tokyo, Japan Edwin L. Crow, and Kunio Shimizu. Marcel Dekker, Inc., New York, NY, 387 p.

Smith, S. J.
1988. Evaluating the efficiency of the Δ-distribution mean estimator. Biometrics 44:485–493.

Stefánsson, G.
1996. Analysis of groundfish survey abundance data: combining the general linear model and delta approaches. ICES J. Mar. Sci. 53:577–88.

Validation of annual growth increments in the otoliths of the lethrinid *Lethrinus mahsena* and the lutjanid *Aprion virescens* from sites in the tropical Indian Ocean, with notes on the nature of growth increments in *Pristipomoides filamentosus*

Graham M. Pilling
MRAG Ltd.
47 Prince's Gate
London SW7 2QA, United Kingdom
E-mail address: g.pilling@ic.ac.uk

Richard S. Millner
Michael W. Easey
Fisheries Laboratory
CEFAS
Pakefield Road
Lowestoft NR33OHT, United Kingdom

Christopher C. Mees
MRAG Ltd
47 Prince's Gate
London SW7 2QA, United Kingdom

Shyama Rathacharen
Albion Fisheries Research Centre
Albion, Petite Riviere, Mauritius

Roland Azemia
Seychelles Fishing Authority
P.O. Box 449
Victoria, Mahe, Seychelles

Abstract.—The lutjanids *Pristipomoides filamentosus* and *Aprion virescens* and the lethrinid *Lethrinus mahsena* are commercially important demersal bank and deep slope reef fish from the central Indian Ocean. To obtain von Bertalanffy growth parameter estimates for management purposes, length-based methods are commonly applied by the fisheries institutions of the region. Because the relatively long-lived, slow-growing nature of these species results in a lack of distinct modal progression in length-frequency data, such estimates are unreliable. In an attempt to obtain more reliable growth estimates, the feasibility of age-based methods (where age is determined from annual increments in otoliths) was investigated. Successful validation of annual or daily increments has been reported in two of these species (*P. filamentosus* and *A. virescens*), but not for the target areas of our study: the banks of the Seychelles and Mauritius.

A range of methods was used in an attempt to ensure that the otoliths fulfilled the criteria for use in aging. Two methods are described in this paper: back-calculation and a combination of marginal increment and edge analysis. The results of validation are presented, along with a description of the problems encountered. Marginal increment and edge analysis both indicated that the increments present in the otoliths of *L. mahsena* are annuli. For *A. virescens*, no pattern was present in the marginal increment analysis of older individuals. However, edge analysis offered evidence that the increments present in the otoliths were annuli. The combined marginal increment and edge analysis proved inconclusive for *P. filamentosus*; therefore the increments present in the otoliths of this species could not be validated. Conclusions are drawn regarding the justification of assuming periodicity of increments on the basis of validation achieved in other locations.

Manuscript accepted 4 January 2000.
Fish. Bull. 98:600–611 (2000).

Examination of hard body parts, such as otoliths, frequently reveals the presence of "rings." Laid down incrementally (whether daily, monthly, or annually), these structures provide a means of aging fish. For tropical species, however, the use of otoliths has become relatively common only since the early nineteen eighties (e.g. Loubens, 1978; Morales-Nin and Ralston, 1990; Ferreira and Russ, 1992; Francis et al., 1992; Milton et al., 1995; see also Manooch, 1987, and Fowler, 1995, for reviews). The lack of studies before this time is frequently attributed to the expectation that tropical fish grow consistently in an aseasonal environment. Hence hard parts in tropical fish species were not expected to contain internal structures that relate to fluctuations in growth resulting from the environment.

The physiological basis for the formation of distinct zones in calcified structures of tropical species has not been established conclusively (Ferreira and Russ, 1994). The formation of such zones has been associated with both abiotic and biotic factors (Beckman and Wilson, 1995), such as regular seasonal variances in water temperature (e.g. Reay, 1972; Panella, 1980), photoperiod, feeding, reproduction, and spawning period (e.g. Morales-Nin and Ralston, 1990)

"Indeterminate increments" (increments not related to the annual time scale) are found in all hard parts. These need to be distinguished from increments formed at regular intervals (Fowler and Doherty, 1992). Before increments can realistically be used for aging, they need to be "validated" (Beamish and McFarlane, 1983) to ensure that the structures, such as the otoliths used in our study, can be used as accurate chronometers. They must therefore fulfill a number of criteria (Fowler and Doherty, 1992): 1) the otolith must grow throughout the lifespan of the individual fish; 2) the otolith must show an internal incremental structure; and 3) this structure must correspond to a regular time scale.

Our study concentrated on macro-increments. Aging through micro-(daily)increment counts (e.g. Ralston and Miyamoto, 1983) requires considerable investment in time and equipment and is generally constrained to younger ages, where daily increments remain distinct. These constraints render such techniques unfeasible for stock assessment purposes, particularly in developing countries.

The local fisheries institutions in the study locations of the central Indian Ocean are, to date, limited to the use of length-based methods for aging fish. The results of these methods are felt to be uncertain when applied to long-lived, slow-growing species such as snappers and emperors, owing to modal overlap and a general absence of modal progression (e.g. Langi, 1990). Our study aimed to validate as annual the macro-increments seen in the sagittal otoliths of two species of snapper, *Aprion virescens* (Valenciennes 1830) and *Pristipomoides filamentosus* (Valenciennes 1830), and one species of emperor, *Lethrinus mahsena* (Forsskål, 1775). Validation of the annual nature of increments seen in the otoliths of these species would allow age-based methods of stock assessment to be applied to these commercially important demersal bank and deep-slope reef-fish species from the central Indian Ocean.

Compliance with the three criteria for validation was examined by using two methods: back-calculation (e.g. Manooch, 1987; Van Leewen and Rijnsdorp[1]) and a combination of marginal increment and edge analysis (e.g. Mason and Manooch, 1985; Manooch and Drennon, 1987; Manickchand-Heileman and Philipp, 1996). Back-calculation was used to test the validity of the first two criteria for aging. Marginal increment analysis and edge analysis were then used to validate mark periodicity, fulfilling the third criterion.

Materials and methods

Otoliths of the study species were obtained from commercial fish catches. In waters off both Mauritius and the Seychelles, fishing is frequently limited by rough seas during the SE trade wind period from May to October. Samples of *Lethrinus mahsena* were obtained during excursions of the Mauritian mothership-dory vessels on Nazareth Bank of the Mascarene Ridge (15°S, 61°E). On the Mauritian banks, this species composes about 80–90% of the total catch (Ardil, 1986; Bertrand[2]). In the Seychelles, fishing occurs from smaller vessels, which generally remain on the Mahé Plateau (05°S, 55°E). Otoliths from both *P. filamentosus* and *A. virescens* were obtained from this area.

Two methods were used to examine whether the otoliths fulfilled the requirements for aging: 1) back-calculation of growth from otolith increments; and 2) marginal increment and edge analysis. A general description of these methods is provided in Blacker (1974) and Williams and Bedford (1974).

Sagittal otoliths were selected for examination because a number of studies have used these structures to age snapper and emperor species successfully elsewhere (e.g. Manooch, 1982; Mason and Manooch, 1985; Morales-Nin, 1989; McPherson and Squire, 1992; Newman et al., 1996), including *Aprion virescens* and *Pristipomoides filamentosus* (Loubens, 1980; Ralston and Miyamoto, 1981, 1983).

One otolith from each fish was embedded in black polyester resin, and a 0.5-mm transverse section taken through the center ("nucleus") of the otolith by using a diamond cutting blade (Bedford, 1983). Sections were then either mounted in clear resin on a microscope slide or stained with acidified neutral red (Richter and McDermot, 1990) and left unmounted. Otoliths were examined with a Zeiss compound microscope equipped with zoom lens and magnification up to 60×. Reflected or transmitted light was used as necessary to identify and count the increments.

In our study, terminology was based on that recommended in Secor et al. (1995). The term "opaque zone" refers to the area that appeared milky under reflected light or dark under transmitted light in unstained samples.

Back-calculation of growth by means of otolith increments

For back-calculation, snapper otoliths were most easily assessed unstained, whereas *L. mahsena* otoliths were most easily assessed stained. Only otoliths that showed clear increment patterns were used for measurements; as a result, seven *A. virescens* otoliths, in which it was difficult to distinguish the first or second increment, were omitted from the samples. Measurements of the total otolith radius, from the nucleus to outside edge, and the distance along the selected growth axis between suspected annual increments were made with the tools described in Millner and Whiting (1996). Unstained *P. filamentosus* and *A. virescens* otoliths were assessed along a growth axis close to the sulcus acousticus (Figs. 1 and 2). This area provides the most consistent and easily interpretable

[1] Van Leeuwen, P. I., and A. D. Rijnsdorp. 1986. The analysis of the growth of turbot by back-calculation of otoliths. ICES Council Meeting 1986/G:50

[2] Bertrand, J. 1986. Pour une evaluation des resources en capitaine/dame berri (*Lethrinus mahsena*) des bancs de Saya de Malha. *In* Rapport du Groupe Travaile, French Institute of Research and Exploitation of the Sea (IFREMER)/Albion Fisheries Research Centre (Mauritius). 23–25 Juillet 1985, 39 p. [Available from Albion Fisheries Research Centre, Albion, Petite Riviere, Mauritius.]

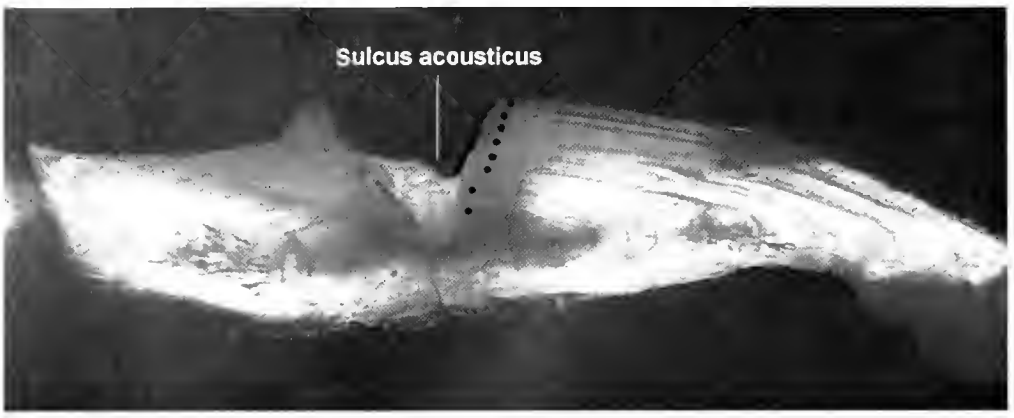

Figure 1

Unstained transverse 0.5-mm section through the sagittal otolith of *P. filamentosus* from Seychelles, viewed with transmitted light. Magnification: 16×. Black dots along sulcus acousticus mark are suspected annual increments.

Figure 2

Unstained transverse 0.5-mm section through the sagittal otolith of *A. virescens* from Seychelles, viewed with transmitted light. Magnification: 32×. Black dots along sulcus acousticus mark are suspected annual increments.

incremental pattern. Measurements on stained *L. mahsena* otoliths were performed out to the tip of the dorsal lobe, at approximately 90° to the *sulcus* (Fig. 3). In all species, when the increment structure became too closely spaced to measure individual increments accurately, the thickness of further increments was estimated by interpolation based on the remaining distance from the last measured increment to the outside edge of the otolith, the number of years expected in this zone, and the pattern found in the previous increment widths.

Following the recommendations of Francis (1990) and Ricker (1992), we calculated the geometric mean regression (GMR) of fork length at capture from otolith radius at capture for each species. Back-calculated lengths-at-age for each individual were then derived with the following formula (Ricker, 1992):

$$FL_i = \left(\frac{FL_c - b}{O_c} \times O_i \right) + b,$$

where Fl_i = the estimated fork length at age i;
Fl_c = the fork length at capture;
O_c = the otolith radius at capture;

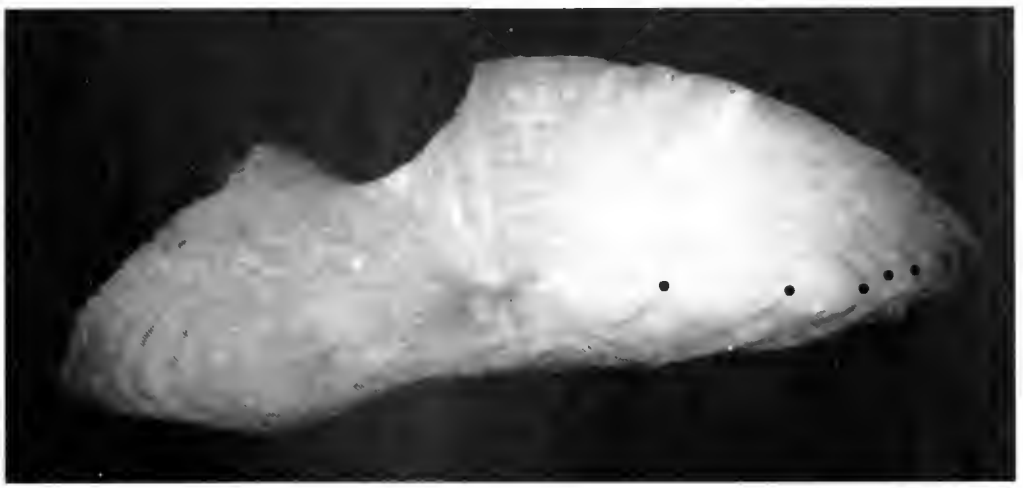

Figure 3

Transverse 0.5-mm section through the sagittal otolith of *L. mahsena* from Mauritius (Nazareth bank), stained with acidified neutral red (see text), and viewed with reflected light. Magnification: 23×. Black dots mark are suspected annual increments.

O_i = the otolith radius at age i; and
b = the intercept of the GMR calculated with the Ricker procedure.

For each species, a von Bertalanffy growth curve was fitted to the back-calculated mean length at age through least squares estimation.

Marginal increment analysis

The thickness of the outer zone in the otoliths was measured by using the image analysis system (see Millner and Whiting, 1996). Measurements were taken from the inside edge (start) of the last opaque band and the edge of the otolith. In stained *L. mahsena* otoliths (indeed in all three study species where otoliths were stained; see "Edge analysis," below), a band was stained on the border between the end of the "translucent zone," and the start of the next opaque zone. Measurements from the last stained band were therefore equivalent to those made for the snapper species. Because zones at the edge of sections taken from the unstained otoliths of both snapper species were not distinct, an average of four measurements was taken in the region of the sulcus (where zones were more easily distinguished). Zones at the edge of the stained *L. mahsena* otolith sections were clearly visible and, therefore, it was possible to obtain a single measurement along the same growth axis as that used for back-calculation.

The pattern expected in the marginal increment resulting from the development of an annual increment would be a minimal marginal increment at the start of the growth period, increasing with time until the measurement fell to a minimum again at the formation of the next period of growth.

The size of the growth zone varies both with time of sampling during the year and the age of the fish. Because younger fish grow faster than older individuals, a larger marginal increment is expected. For this reason, quantitative marginal increment analyses should be standardized for age. Our study was therefore carried out by age class. Owing to the wide range of ages encountered, however, there were insufficient samples to accomplish this standardization fully. It was necessary to combine the ages into two or three groups representing fast, moderate, and slow-growing individuals (Table 1). These classes were based on the growth curves derived from back-calculation, and hence on the assumption that the increments represented annual growth.

For *P. filamentosus*, because sample sizes were either small or because samples could not be obtained in specific months, data were grouped into bimonthly time periods. Sufficient *L. mahsena* and *A. virescens* samples were available to allow the analysis to occur on a monthly basis. For all three species, a mean marginal increment for each time period and growth category was calculated.

Edge analysis

The type of zone at the growing edge of the otolith was identified in each month of the year. Annuli were traceable as a developing single translucent and opaque zone on the edge of the otolith during that growth year.

Problems were encountered in identifying the edge type in unstained *P. filamentosus* and *A. virescens* from Seychelles because of poor resolution of the banding in otoliths, and what appeared to have been the seepage of resin either under or through the edge of the otolith. Staining trials were performed in an attempt to clarify the growth type at the edge of the otolith in these species, and stained otoliths were subsequently examined during edge analysis.

Thin sections of the stained otoliths were assessed for the presence of the band of stain on the growing tip of the

dorsal lobe. The percentage of otoliths with a stained band at the growing tip was calculated for each month. Although an extended data set was available for edge analysis, as a result of the seasonal nature of the Seychelles and Mauritius fisheries, sample sizes were either small or not available for certain months.

Results

Based on the assumption that the increments seen in the otoliths were annual, the length and age range of individuals from each species examined in each method is presented in Table 2. The sample size is also shown.

A greater number of samples were examined during edge analysis. This method was less intensive than that required for either back-calculation or marginal increment analysis, allowing more samples to be examined during the period of study and increased the range of lengths and ages examined.

Table 1

Age groups selected for marginal increment analysis, by species.

Species	Growth group	Age class (years)
L. mahsena	Fast	1–5
	Slow	6+
A. virescens	Fast	3–5
	Slow	6+
P. filamentosus	Fast	3–5
	Moderate	6–10
	Slow	11+

Back-calculation

A linear relationship existed between the fork length and otolith radius of fish in all three species, to which the geometric mean regression (GMR) of fork length from otolith radius was fitted (Figs. 4–6).

The von Bertalanffy growth parameters derived from mean back-calculated length-at-age data from *A. virescens*, *P. filamentosus* and *L. mahsena* are shown in Table 3. Initial L_∞ estimates for *L. mahsena* were low compared with the maximum lengths seen in length-frequency distributions from the region (52 cm). The asymptotic length, L_∞, was therefore constrained to levels in keeping with the maximum length found in the distributions, and the remaining von Bertalanffy growth parameters were re-estimated.

For the snapper species, both L_∞ and K estimates derived from the back-calculated length-at-age data were lower than those historical estimates derived with length-based methods. For *L. mahsena*, constraining L_∞ to a level in keeping with the maximum length found in catches resulted in estimates of K comparable to those estimated by Bautil and Samboo (1988).

Marginal increment and edge analysis

The number of individuals examined in marginal increment analysis are presented in Table 4 by species and time period.

Because the region between translucent and opaque zones took up the stain, the presence of a stained area at the otolith edge during edge analysis indicated the start of opaque band formation.

Table 2

The length range, age range, and sample size of individuals examined by method and species. Ages are based on the assumption that the increments identified in the otoliths are annuli.

	Method		
Species	Back-calculation	Marginal increment analysis	Edge analysis
L. mahensa			
Lenth range (cm)	22–42	22–42	20–50
Age range (yr)	3–14	3–14	3–16
n	222	220	568
A. virescens			
Lenth range (cm)	37–87	37–87	30–99
Age range (yr)	3–19	3–19	3–27
n	81	141	1259
P. filamentosus			
Lenth range (cm)	22–73	22–73	—
Age range (yr)	3–30	3–30	—
n	85	242	—

L. mahsena Marginal increment analysis indicated an overall increase in the marginal increment between January and May, falling in August (Fig. 7). This pattern was clearest in the younger, faster-growing growth group. A unimodal distribution was found in the plot of the proportion of stained edges found in each month, as well as a high proportion of individuals showing opaque growth commencing between May and August (Fig. 8).

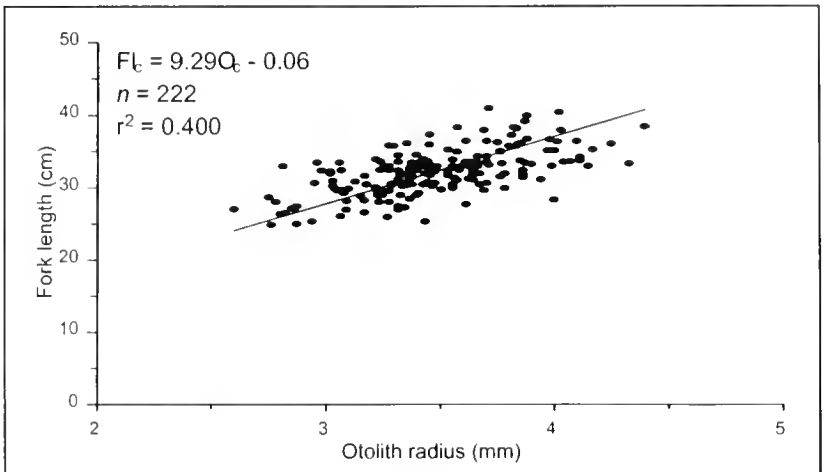

Figure 4

Geometric mean regression of fork length (cm) from otolith radius (mm) for *L. mahsena*.

A. virescens With relatively few samples at certain key times during the year, patterns in the marginal increment could not be identified clearly (Table 4). The width of the outer zone increased until June in younger, faster-growing individuals. In subsequent months, a lack of samples prevented the identification of an indicative pattern (Fig. 9). No pattern was found in the marginal increment of older individuals. Staining improved the clarity of the type of growth present on the edge of the otolith. Edge analysis of these specimens showed a unimodal distribution of the percentage of stained edges by month. A high proportion of individuals exhibited opaque zone formation in the period between October and March (Fig. 10).

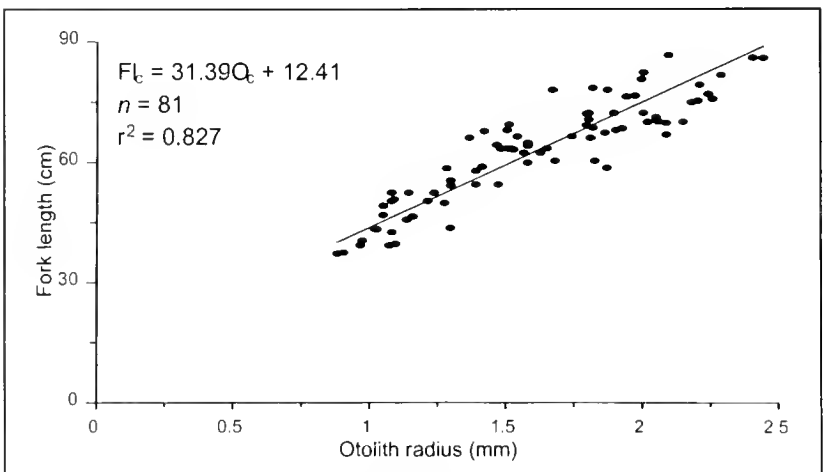

Figure 5

Geometric mean regression of fork length (cm) from otolith radius (mm) for *A. virescens*.

P. filamentosus No overall pattern of increase in the marginal increment was found (Fig. 11). This result was partly due to the lack of samples in the months of May and June. The legibility of the increments in the otoliths of this species was poor, and staining failed to improve the clarity of the otolith zones. Edge analysis was confused by indeterminate increments formed in the translucent growth period. Their presence on the edge of the stained otolith at the time of capture led to the misidentification of opaque zone formation and thus confused the identification of an overall pattern. As a result, validation could not be achieved with this method.

Discussion

Back-calculation indicated that there was a direct linear relationship between fork length and otolith radius. The otoliths of each species showed an internal structure, with increments widely spaced near the nucleus and narrower and more evenly spaced toward the edge. Growth curves derived from back-calculated length-at-age data indicated an exponential decrease in increment width with assumed increasing age. The otoliths of the three species therefore fulfilled the first two criteria for their use in aging, at least over the age range seen in the samples, in that the otolith grew throughout the life of the fish and showed an internal structure of increments. The pattern in *P. filamentosus* was, however, confused by the presence of indeterminate increments.

Confirmation of the third criterion (that increments seen in the otoliths corresponded to a regular time scale) was not demonstrated so readily. Validation could not occur through methods such as tetracycline injection owing to practical limitations imposed by the fisheries and to the depths inhabited by certain species. *Pristipomoides filamentosus*, for example, is caught at over 75 m depth. The majority of specimens would be dead or heavily stressed through barotrauma on reaching the surface (DeMartini et al., 1996) and useless for tagging programs. Marginal increment and edge analysis was therefore used.

Some evidence for the annual nature of the increments seen in the otoliths of *L. mahsena* was found in the pattern of the marginal increment through the year (Fig. 7). This evidence was confirmed by the unimodal distribution resulting from edge analysis (Fig. 8), indicating that opaque band formation was initiated once a year, from May to August.

For *A. virescens*, identification of the pattern in marginal increments (Fig. 9) was confused by the poor resolution of the unstained sections and the relatively small samples sizes, rendering the results inconclusive. However, the unimodal plot resulting from edge analysis on stained specimens from this species indicated that the transition between the translucent and opaque bands occurred once a year (Fig. 10), between October and March.

From this evidence, we considered the increments seen in the otoliths of both *L. mahsena* from Mauritius and *A. virescens* from Seychelles validated as annual deposits.

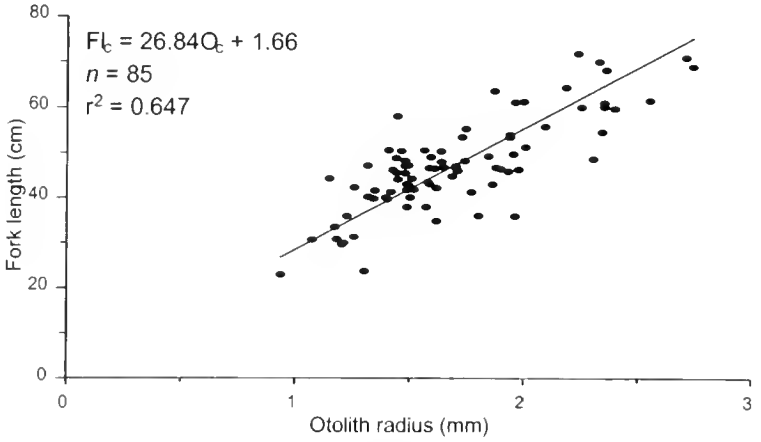

Figure 6

Geometric mean regression of fork length (cm) from otolith radius (mm) for *P. filamentosus*.

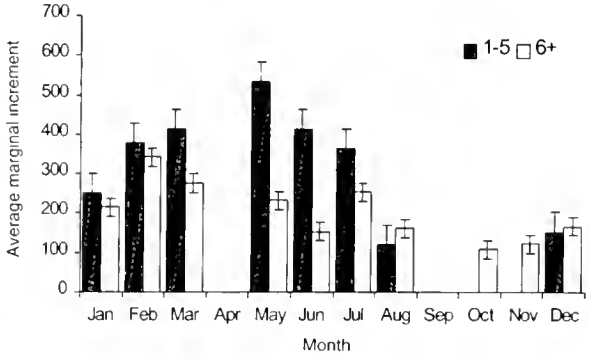

Figure 7

Marginal increment plot by month for *L. mahsena*. Marginal increment measured in VID units (pixels). Data segregated as in Table 1. Error bars denote one standard error.

Opaque zone deposition is thought to occur during periods of increased growth, whereas the corresponding "translucent zone" is formed during periods of low metabolic activity (Beckman and Wilson, 1995). The period of opaque zone initiation in *L. mahsena* from the Mauritian bank, from May to August, corresponded to the season of the southeast trade winds, a period of rough weather. The period of opaque zone deposition in *A. virescens* from Seychelles, from October to March, coincided with the northwest monsoon season from mid-November to mid-March.

In reviews of otolith studies in tropical latitudes, Beckman and Wilson (1995) and Fowler (1995) found that, for the majority of tropical species studied, the period of opaque growth coincided with spring and summer months, as seen in *L. mahsena* from the Mauritian bank. *Aprion virescens* from Seychelles appears to contradict this general pattern its opaque zone formation begins during winter months. The authors also performed edge analysis studies for 1090 *L. mahsena* individuals from Seychelles (not presented). These studies indicated that in this area, *L. mahsena* also exhibits opaque zone initiation during winter. Of the twenty-nine tropical species reviewed by Fowler (1995), only four showed opaque zone formation in the winter period. Timing of opaque zone formation in these two species may be driven by local phenomena. If opaque zone formation is linked with increased food availability, the monsoon periods experienced in Seychelles at this time, combined with local upwelling, may improve local productivity and feeding conditions. Although little empirical data exist to support this theory, algal blooms have been identified around Seychelles at this time of year.[3]

Although edge analysis indicated differences in the timing of opaque zone deposition at Nazareth bank (Mauritius), and Seychelles (Figs. 8 and 10), patterns in the marginal increment analysis for these locations were similar (Figs. 7 and 9). This similarity may result from the relatively small data sets available for marginal increment analysis, requiring ages to be grouped into age classes, and the difficulty experienced in measuring the marginal increment in *A. virescens* otoliths from Seychelles. Similarities may therefore result from inadequacies in the data that obscure the true pattern.

The results of marginal increment analysis for *P. filamentosus* were inconclusive because problems were experienced in identifying and measuring the outer zone in the otolith. Staining did not improve the clarity of the zones owing to the frequent appearance of "indeterminate increments." Validation was therefore considered to be unsuccessful for *P. filamentosus* in Seychelles and contrasts with that achieved in Hawaii where microincrements were used (Ralston and Miyamoto, 1981, 1983). During our study, ini-

[3] Tarbit, J. 1980. Demersal trawling in Seychelles waters. Fisheries Bulletin 5, Fisheries Division, Seychelles. Seychelles Fishing Authority, P.O. Box 449, Victoria, Mahe, Seychelles.

Table 3

Von Bertalanffy growth parameters estimated from back-calculated length data and published sources. Method: L = parameters derived through length-based methods, O = parameters derived from otoliths.

Species	K	L_∞ (FL)	n	Method	Reference
P. filamentosus	0.11	62.3	85	O	Our study
	0.29	81.7	—	L	Mees (1993)
	0.24	75.8	—	L	Mees and Rousseau (1997)
	0.146	78	—	O	Ralston and Miyamoto (1983)
	0.33–0.36	78-86	—	O	Hardman-Mountford et al. (1997)
A. virescens	0.13	79.0	81	O	Our study
	0.32	95-104	—	L	Mees (1993)
	0.31	65.6	—	O	Loubens (1980)
L. mahsena	0.38	34.1	222	O	Our study
	0.09	52.0	222	O	Our study, L_∞ = 52 cm
	0.1	61.7	—	L	Bautil and Samboo, (1988)
	0.32	58.9	—	L	Dalzell et al. (1992)

Table 4

Numbers of individuals examined for marginal increment analysis by monthly (*L. mahsena* and *A. virescens*) or bimonthly (*P. filamentosus*) interval.

	Age class						
	L. mahsena		*A. virescens*		*P. filamentosus*		
Month	1–5 yr	6+ yr	3–5 yr	6+ yr	3–5 yr	6–10 yr	11+ yr
Jan	14	8	—	4	95	29	20
Feb	13	5	—	—			
Mar	19	5	4	8	—	16	18
Apr	—	—	3	15			
May	15	9	10	17	—	—	—
Jun	4	11	6	11			
Jul	15	8	10	—	8	—	4
Aug	21	4	5	6			
Sep	—	—	—	8	11	19	5
Oct	—	17	—	4			
Nov	—	19	6	16	—	7	10
Dec	13	20	—	8			

tial examination of *P. filamentosus* otoliths was performed by using scanning electron microscopy, in an attempt to validate the "suspected" annuli through micro-increment counts (Brothers and Mathews, 1987). Unlike the results reported from studies in Hawaii, no consistent pattern of micro-increments was found, although it should be noted that our study was very limited in scope (n=4). Hardman-Mountford et al. (1997), also using specimens from the Seychelles, related assumed "monthly increments" to assumed annuli, finding approximately 12.4 monthly increments within each annual increment. Consistent banding of this type could not be found during our study for specimens collected from the same region, even though we had a larger sample size.

The lack of consistent annual increments in *P. filamentosus* may be due to the biology of the species. Spawning occurs throughout the year, with two peaks (Mees, 1993), and may not provide a sufficient stimulus for zone formation. *Pristipomoides filamentosus* is found at greater depths (between 75 and 150 m) than the other study species (around 30 m) in conditions that may be buffered against environmental change. Hardman-Mountford et. al. (1997), however, indicated that the 20–24.5°C temperature range at this depth (Mees, 1993) is sufficient to leave

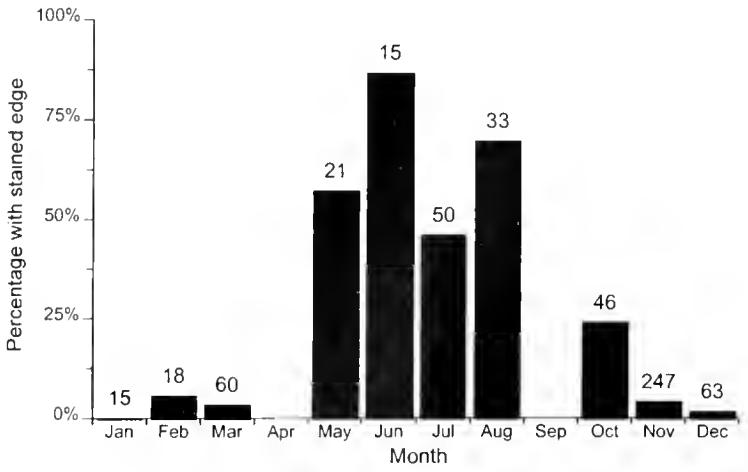

Figure 8

Proportion of *L. mahsena* otoliths with stained edges on the growing tip of the dorsal lobe, by month. Numbers denote sample size.

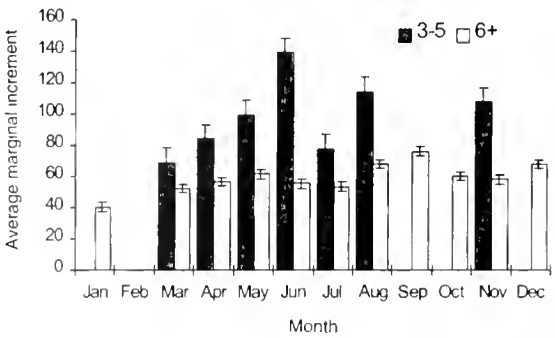

Figure 9

Marginal increment plot by month for *A. virescens*. Marginal increment measured in VID units (pixels). Data segregated as in Table 1. Error bars denote one standard error.

increments on scales in some species (Chey, 1933, in Panella, 1980). If this species is sensitive to relatively small changes in temperature, currents, food supply or food quality, relatively short periods of fluctuation in these factors may result in frequent "indeterminate increments." Even if validation had been achieved, *P. filamentosus* otoliths appear unsuitable for routine aging procedures owing to the difficulties in differentiating periodic increments from other increments not related to a regular time scale.

These difficulties highlight the dangers in assuming the periodicity of increments in otoliths on the basis of validation of that species or a similar species in another location (e.g. Smith and Kostlan, 1991) and also identify the need for thorough validation studies. For example, our study indicated that the assumption of annual, and possibly daily periodicity for increments in the otoliths for *P. filamentosus* in Seychelles, based on published data, would have been incorrect.

Published work (e.g. Sparre and Venema, 1998) suggests that consistent periodic increments do not form in otoliths of tropical species; this is particularly so in the case of low-latitude species. The validation results obtained by our study contrast sharply with this view; indeed, our results add to the expanding number of tropical species for which the validation of annual increments has been successful.

The results of models used in fisheries management, e.g. analytical yield per recruit models (Beverton and Holt, 1957), are sensitive to uncertainty in the estimates of input parameters such as the von Bertalanffy growth parameters (Mees and Rousseau, 1997). Current estimates of growth and mortality in fish in Seychelles and Mauritius

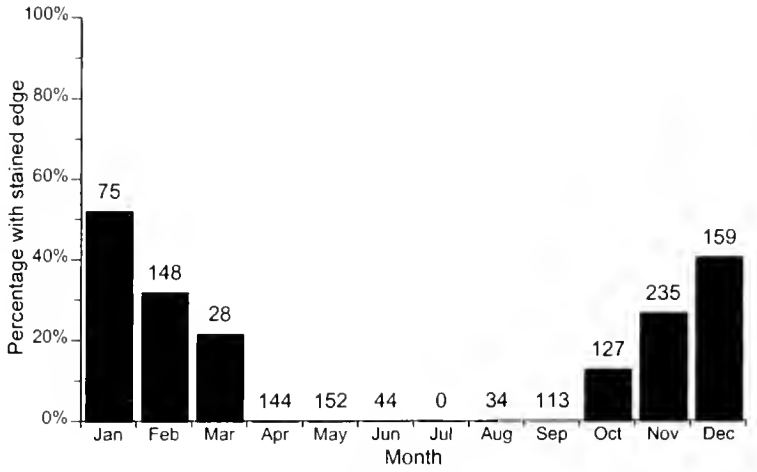

Figure 10

Proportion of *A. virescens* otoliths with stained edge on the growing tip of the dorsal lobe, by month. Numbers denote sample size.

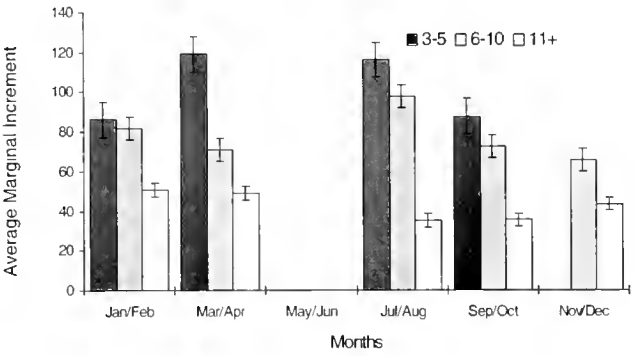

Figure 11

Marginal increment plot by month for *P. filamentosus*. Marginal increment measured in VID units (pixels). Data segregated as in Table 1. Error bars denote one standard error.

are derived through length-based methods, which for long-lived, slow growing species are considered uncertain. The preliminary back-calculated growth parameters from our study are the first otolith-based estimates of growth for the study species at these particular locations. Although these estimates are not definitive, they do suggest that current length-based growth estimates for *A. virescens* may have overestimated mean growth rate and asymptotic length. For *L. mahsena*, growth rate may have been underestimated, and asymptotic length overestimated. However, by constraining the value of L_∞ to levels in keeping with the maximum size found in length distributions from the region (52 cm), we obtained a similar growth rate to that identified by Bautil and Samboo (1988). If snappers do indeed have a longer life span than that indicated by length-based assessments, they may be more vulnerable to overfishing than previously thought. Future work will involve the estimation of more definitive growth parameters based on length-at-age data derived from otoliths.

Acknowledgments

The authors wish to thank the Directors and staff of CEFAS, Albion Fisheries Research Centre and the Seychelles Fishing Authority who collaborated on this project and provided the data necessary for this analysis. Three anonymous reviewers are thanked for their helpful comments on the manuscript. The project to which this paper relates was funded by the Department for International Development of the UK through the Fisheries Management Science Programme.

Literature cited

Ardil, J. D.
1986. Current status of the fishery in Mauritius. Food and Agriculture Organisation of the United Nations (FAO) Southwest Indian Ocean Project (SWIOP) document RAF/79/065/WP/37/87/E, 30 p.

Bautil, B., and C. R. Samboo.
1988. Preliminary stock assessment for the Mahsena emperor (*Lethrinus mahsena*) on the Nazareth Bank of Mauritius. *In* Proceedings of the workshop on the assessment of the fishery resources in the southwest Indian Ocean (M. J. Sanders, P. Sparre, and S. C. Venema, eds.), p. 260–267.

Beamish, R. J., and G. McFarlane.
1983. The forgotten requirement for age validation in fisheries biology. Trans. Am. Fish. Soc. 112:735–743.

Beckman, D. W., and C. A. Wilson.
1995. Seasonal timing of opaque zone formation in fish otoliths. *In* Recent developments in fish otolith research, no. 19 (D. H. Secor, J. M. Dean, and S. E. Campana, eds.), p. 27–43. The Bella W Baruch Library in Marine Science.

Bedford, B. C.
1983. A method for preparing sections of large numbers of otoliths embedded in black polyester resin. J. Cons. Int. Explor. Mer 41:4–12.

Beverton, R. J. H., and S. J. Holt.
1957. On the dynamics of exploited fish populations. Fish. Invest. Minist. Agric. Fish. Food GB (2 Sea Fish.) 19, 533 p.

Blacker, R. W.
1974. Recent advances in otolith studies. *In* Sea fisheries research (R. Harden-Jones, ed.), p 67–90. Elek Science, London.

Brothers, E. B., and C. P. Mathews.
1987. Application of otolith microstructural studies to age determination of some commercially valuable fish of the Arabian Gulf. Kuwait Bull. Mar. Sci. 9:127–157.

Dalzell, P., S. Sharma, and G. Naith.
1992. Estimation of exploitation rates in a multispecies emperor (Pisces: Lethrinidae) fishery in Fiji, based on length frequency data. *In* Papers on fisheries science from the Pacific Islands, vol. 1: Inshore fisheries research project, technical document 1, p. 43–50. South Pacific Commission, Noumea, New Caledonia.

DeMartini, E. E., F. A. Parrish, and D. M. Ellis.
1996. Barotrauma-associated regurgitation of food: implications for diet studies of Hawaiian pink snapper, *Pristipomoides filamentosus* (Family: Lutjanidae). Fish. Bull. 94:250–256.

Ferreira, B. P., and G. R. Russ.
1992. Age, growth and mortality of the inshore coral trout *Plectropomus maculatus* (Pisces: Serranidae) from the central Great Barrier Reef, Australia. Aust. J. Mar. Freshwater Res. 43:1301–1312.
1994. Age validation and estimation of growth rate of the coral trout *Plectropomus leopardus* from Lizard Island, Northern Great Barrier Reef. Fish. Bull. 92:46–57.

Fowler, A. J.
1995. Annulus formation in otoliths of coral reef fish—a review. *In* Recent developments in fish otolith research, vol. 19 (D. H. Secor, J. M. Dean, and S. E. Campana, eds.), p. 46–63. The Bella W Baruch Library in Marine Sciences.

Fowler, A. J., and P. J. Doherty.
1992. Validation of annual growth increments in the otoliths of two species of damselfish from the southern Great Barrier Reef. Aust. J. Mar. Freshwater Res. 43:1057–1068.

Francis, R. I. C. C.
1990. Back-calculation of fish length—a critical review. J. Fish Biol.:883–902.

Francis, R. I. C. C., L. J. Paul, and K. P. Mulligan.
1992. Ageing of adult snapper (*Pagrus auratus*) from otolith annual ring counts: validation by tagging and oxytetracycline injection. Aust. J. Mar. Freshwater Res. 43: 1069–1089.

Hardman-Mountford, N. J., N. V. C. Polunin, and D. Boullé.
1997. Can the age of tropical species be determined by otolith measurement? A study using *Pristipomoides filamentosus* (Pisces: Lutjanidae) from the Mahé Plateau, Seychelles. Naga 20:27–31.

Langi, S.
1990. The applicability of ELEFAN for use in analysing three species of deep-sea snappers (*Etelis corruscans*, *Pristipomoides flavipinnis* and *P. filamentosus*, Family Lutjanidae). Fishbyte 8(1):21–25.

Loubens, G.
1978. Biologie de quelque especes de poisson du lagon Neo-Caledonien. I. Determination de l'age (otolithometrie). Cahiers ORSTOM, Series Oceanographie 16:263–283.
1980. Biologie de quelques especes de poissons du lagon Neo-Caledonien III. Croissance. Cal. Indo-Pac. 2:101–153.

Manickchand-Heileman, S. C., and D. A. T. Philipp.
1996. Reproduction, age and growth of the Caribbean red snapper (*Lutjanus purpureus*) in waters off Trinidad and Tobago. *In* Biology, fisheries and culture of tropical groupers and snappers (F. Arreguin-Sánchez, J. L. Munro, M. C. Balgos, D. Pauly, eds.), p. 137–149. ICLARM, Manila, Philippines.

Manooch, C. S.
1982. Ageing reef fishes in the Southeast fisheries centre. *In* The biological basis for reef fishery management: proceedings of a workshop held October 7–10, 1980 at St. Thomas, Virgin Islands of the Unites States (G. R. Huntsman, W. R. Nicholson, and W. W. Fox, eds.), p. 24–43. U.S. Dep. Commer., NOAA, Beaufort, North Carolina 28516.
1987. Age and growth of snappers and groupers. *In* Tropical snappers and groupers: biology and fisheries management (J. J. Polovina and S. Ralston, eds.), p. 329–363. Westview Press Inc., Boulder, CO.

Manooch, C. S., and C. L. Drennon.
1987. Age and growth of yellowtail snapper and queen triggerfish collected from the US Virgin Islands and Puerto Rico. Fish. Res. 6:53–68.

Mason, D. L., and C. S. Manooch.
1985. Age and growth of the mutton snapper along the east coast of Florida. Fish. Res. 3: 92–104.

McPherson, G. R., and L. Squire.
1992. Age and growth of three dominant *Lutjanus* species of the Great Barrier Reef inter-reef fishery. Asian Fish Sci. 5 (1):25–36.

Mees, C. C.
1993. Population biology and stock assessment of *Pristipomoides filamentosus* on the Mahe Plateau, Seychelles. J. Fish Biol. 43:695–708.

Mees, C. C., and J. A. Rousseau.
1997. The potential yield of the lutjanid fish *Pristipomoides filamentosus* from the Mahe Plateau, Seychelles: Managing with uncertainty. Fish. Res. 33:73–87.

Millner, R. S., and C. L. Whiting.
1996. Long-term changes in growth and population abundance of sole in the North Sea from 1940 to the present. ICES J. Mar. Sci. 53:1185–1195.

Milton, D. A., S. A. Short, M. F. O'Neill, and S. J. M. Blaber.
1995. Ageing of three species of tropical snapper (Lutjanidae) from the Gulf of Carpentaria, Australia, using radiometry and otolith ring counts. Fish. Bull. 93(1):103–115.

Morales-Nin, B.
1989. Growth determination of tropical marine fishes by means of otolith interpretation and length frequency analysis. Aquatic Living Resources Nantes 2:241–253.

Morales-Nin, B., and S. Ralston.
1990. Age and growth of *Lutjanus kasmira* (Forsskal) in Hawaiian waters. J. Fish Biol. 36(2):191–203.

Newman, S. J., D. M. Williams, and G. R. Russ.
1996. Age validation, growth and mortality estimates of the tropical snappers *Lutjanus adetii* and *L. quinquelineatus* from the Central Great Barrier Reef, Australia. Mar. Freshwater Res. 47:575–584.

Panella, G.
1980. Growth patterns in fish sagittae. *In* Skeletal growth of aquatic organisms (D. C. Rhoads and R. A. Lutz, eds.), p. 519–560. Plenam Press, New York, NY.

Ralston, S., and G. T. Miyamoto.
1981. Estimation of the age of a tropical reef fish using the density of daily growth increments. *In* The reef and man (E. D. Gomez, C. E. Birkeland, R. W. Buddemeier, R. E. Johannes, J. A. Marsh, and R. T. Tsuda, eds.), p. 83–88. Proceedings of the fourth international coral reef symposium, Manila, 1981, vol. 1.
1983. Analyzing the width of daily otolith increments to age the Hawaiian snapper, *Pristipomoides filamentosus*. Fish. Bull. 81(3):523–535.

Reay, P. J.
1972. The seasonal pattern of otolith growth and its application to back-calculation studies in *Ammodytes tobianus*. J. Cons. P. Int. Explor. Mer 34:485–504.

Richter, H., and J. G. McDermot.
1990. The staining of fish otoliths for age determination. J. Fish Biol. 36:773–779.

Ricker, W. E.
1992. Back-calculation of fish lengths based on proportionality between scale and length measurements. Can. J. Fish. Aquat. Sci. 49:1018–1026.

Secor, D. H., J. M. Dean, and S. E. Campana.
1995. Recent developments in fish otolith research. Belle W. Baruch library in marine science no. 19, South Carolina Press, Columbia, SC, 735 p.

Smith, M. K., and E. Kostlan.
1991. Estimates of age and growth of Ehu *Etelis carbunculus* in four regions of the Pacific from density of daily increments in otoliths. Fish. Bull. 89:461–472.

Sparre, P., and S. C. Venema.
1998. Introduction to tropical fish stock assessment. Part 1, Manual, FAO Fisheries Technical Paper 306.1, rev 2. FAO, Rome, 407 p.

Williams, T., and B. C. Bedford.
1974. The use of otoliths for age determination. *In* Ageing of fish (T. B. Bagenal, ed.), p. 114–123. Unwin, Surrey, UK.

Age, growth, maturation, and protandric sex reversal in common snook, *Centropomus undecimalis*, from the east and west coasts of South Florida

Ronald G. Taylor
Florida Fish and Wildlife Conservation Commission
Florida Marine Research Institute
100 Eighth Avenue SE
St. Petersburg, Florida 33701-5095
E-mail address: ron.taylor@fwc.state.fl.us

James A. Whittington
Florida Fish and Wildlife Conservation Commission
Tequesta Field Laboratory
Florida Marine Research Institute
19100 SE Federal Highway
Tequesta, Florida 33469

Harry J. Grier
Florida Fish and Wildlife Conservation Commission
Stock Enhancement Research Facility
Florida Marine Research Institute
14495 Harllee Road
Port Manatee, Florida 34221

Roy E. Crabtree
National Marine Fisheries Service, F/SER23
9721 Executive Center Drive North
St. Petersburg, Florida 33702

Abstract.—During 1986–91, we examined 2088 common snook, *Centropomus undecimalis*, captured in Jupiter and Lake Worth inlets and adjacent waters on the east coast of Florida and 1784 common snook captured in Tampa Bay on the west coast of Florida. Of fish that were sexed, females ranged in length from 397 to 1105 mm FL, and males ranged from 124 to 925 mm FL. East coast fish were larger overall than west coast fish. Age of common snook was determined from sectioned otoliths. Results from the return of 80 oxytetracycline-marked otoliths combined with analyses of monthly patterns in marginal increments and the percentage of otoliths with an annulus on the edge, demonstrated that a single annulus is formed each year. Common snook can live to 21 years, but most of the fish in our sample were from 1 to 7 years old. The von Bertalanffy growth models were significantly different ($P<0.001$) for each coast and suggested that east coast snook grow faster than west coast snook. Common snook are protandric hermaphrodites. The gonads of 27 transitional specimens contained both degenerating spermatogenic and developing ovarian tissue, and sex reversal was observed in captive common snook. Common snook sex ratios and length-frequency distributions were also consistent with a diagnosis of protandric hermaphroditism. Females smaller than 500 mm FL were uncommon, and only one female less than 400 mm long was captured. The predicted lengths and ages at which 50% of the fish in the population would be females were 767 mm FL and 7.4 years for the east coast and 608 mm FL and 5.1 years for the west coast. Some males on both coasts were sexually mature at lengths less than 200 mm FL and at age 0; most age-1 males were mature on both coasts. All females were considered mature because they were derived from post-spawning males.

Manuscript accepted 6 January 2000.
Fish. Bull. 98:612–624 (2000).

Common snook, *Centropomus undecimalis*, (Perciformes: Centropomidae) are valuable euryhaline fishes that inhabit tropical and subtropical estuarine systems of the western Atlantic. They are abundant off the east coast of Florida from Cape Canaveral southward around the peninsula to Cedar Key off the west coast. They also inhabit waters off Galveston, Texas, south to Rio de Janeiro, Brazil (Gilmore et al., 1983; Rivas, 1986). They are commercially exploited throughout most of their range, except in Texas and Florida where they traditionally have supported large recreational fisheries (Matlock and Osburn, 1987). Snook are stenothermic; their northern range is limited by the winter 15°C isotherm (Shafland and Foote, 1983), similar to the distribution of mangroves which is their principal habitat (Marshall, 1958; Gilmore et al., 1983). Genetic studies of the stock structure suggest that in Florida, east coast and west coast populations are separate stocks (Tringali and Bert, 1996).

Anglers target common snook because of their fighting ability and culinary value (Tucker et al., 1985; Matlock and Osburn, 1987), and concerns about overfishing have resulted in a long history of regulation of the fishery off Florida (Bruger and Haddad, 1986). Size limits were first imposed on the fishery in 1953, and the sale of common snook in Florida has been prohibited since 1956. In 1994, a management goal was established to maintain a minimum spawning potential ratio (SPR) of 40% for

common snook stocks (Muller and Murphy[1]). In 1998, the Florida Marine Fisheries Commission enacted the current restrictive regulations to reduce the harvest of snook from Florida waters to maintain a 40% SPR.

Our study examined age, growth, maturation, and sex reversal of common snook which previously had not been diagnosed as being protandrous hermaphrodites. Earlier studies derived ages from either scales or whole otoliths, and ages were poorly validated (Volpe, 1959; Thue et al.[2]). Since these reports, studies on a variety of species have shown that scales are not reliable for aging long-lived fishes and that scale-derived and whole-otolith–derived age estimates are often lower than the validated estimates derived from sectioned otoliths (Beamish and McFarlane, 1983; Casselman, 1983; Lowerre-Barbieri et al., 1994; Crabtree et al., 1996). A validated method for aging snook is necessary to assess previous estimates of growth rates, mortality, and longevity. Our objectives were to describe validated aging techniques, length and age composition, and length and age at maturity of common snook populations from the east and west coasts of Florida. We also diagnosed common snook as protandrous hermaphrodites.

Methods

On the east coast of Florida, common snook were collected with hook-and-line gear during June–August 1987–91 in Sebastian, Jupiter, and Lake Worth Inlets. Young-of-the-year and juvenile common snook were collected on both coasts during April and May in 1989 and 1990 with a 3-m cast net (19-mm stretched mesh) from protected backwaters of coastal rivers. In December 1989, dead or moribund snook that had succumbed to low water temperatures were collected on both coasts. A detailed description of additional collections made with various nets on both coasts may be found in Taylor et al., 1998. Data, otoliths, and gonads collected and used in that study were used in the present study.

In the laboratory, total length (TL), fork length (FL), and standard length (SL) were measured to the nearest mm; all measurements reported in our study are fork lengths. Weights were measured to the nearest gram (g), and gonads were weighed to the nearest 0.01 g. Gonad samples were fixed in 10% buffered formalin for histological processing. Sagittal otoliths were removed and stored dry.

Age and growth

A Buehler Isomet low-speed saw was used to cut four sections approximately 0.5 mm thick that were mounted on a microscope slide (Chilton and Beamish, 1982). Annuli were counted on the section through the core by using compound microscopes and transmitted light. Two independent readers counted annuli on each otolith without knowledge of fish size or capture date. If the two readings disagreed, both readers read the otolith again, for a total of four readings. If three of the four readings agreed, then this reading was accepted as the annulus count; otherwise the otolith was excluded from further analysis.

An annual growth zone in a common snook otolith comprises a narrow, concentric opaque band, formed each winter as growth slows, and a wider, translucent band, formed each summer as growth increases. Opaque winter bands were enumerated as assumed annuli because they were the salient feature in each section. Ages were assigned to each fish on the basis of a 1 June birth date because most snook have completed annulus formation by 1 June and because June corresponds to the approximate beginning of the snook spawning season (Taylor et al., 1998). Annulus counts were adjusted on the basis of an assumed birth date of 1 June. All otoliths that had an annulus on the edge from fish captured between 1 December and 1 June were assigned an age of one less than the annulus count. Fish captured after 1 June and before 1 December were assigned ages equal to the annulus count.

In earlier studies (Volpe, 1959; Thue et al. 1982), whole otoliths or scales were used to estimate ages. To evaluate the validity of using these structures to estimate snook age, we examined whole and sectioned otoliths from 199 fish that included at least five individuals from each abundant age class and the oldest individuals. Whole otoliths were read three times by a single reader. Whole otoliths were submerged in glycerin and read over a dark background with reflected light. Scale impressions from 48 common snook of different ages and lengths were made on acetate slides and read under compound microscopes equipped with transmitted light. Ages from these scales were compared with ages derived from sectioned otoliths of the same fish.

The von Bertalanffy (1957) growth equation $FL_t = L(1 - e^{(-K(t-t_0))})$ was fitted to observed age-length data with nonlinear regressions. These predicted lengths at age were compared with the average observed lengths at age that included some seasonal growth that occurred after the formation of the final annulus. Likelihood-ratio tests were used to compare parameter estimates for males and females (Kimura, 1980). If coast had a significant effect, the equations were calculated for each coast. Length-weight regressions were calculated by linear regression of $\log_{10}$-transformed data. Length-length and length-weight regressions were calculated for common snook of both sexes with pooled data.

Age validation

We captured 754 common snook 327–961 mm and injected them with oxytetracycline (OTC) at a dosage of 25-mg OTC/kg of fish body weight. Fish were then double-tagged with dart and internal-anchor tags and released at the original capture site. We relied on anglers and our own fish-

[1] Muller, R. G., and M. D. Murphy. 1998. A stock assessment of common snook, *Centropomus undecimalis*. Rep. to the Florida Marine Fisheries Commission, Florida Dep. of Environ. Protection. Florida Marine Research Institute, 100 Eighth Ave. SE, St. Petersburg, Florida 33701, 53 p.

[2] Thue, E. B., E. S. Rutherford, and D. E. Buker. 1982. Age, growth and mortality of the common snook, *Centropomus undecimalis* (Bloch), in the Everglades National Park, Florida. U. S. National Park Service South Florida Research Center Report T-683, 32 p.

ery-independent sampling techniques to recapture tagged fish. Otoliths from recaptured OTC-injected common snook were processed, read, and measured according to Chilton and Beamish (1982) and Beamish and McFarlane (1983). The number of annuli formed after the OTC mark was then compared with the number of days since injection.

Measurements from the core to each assumed annulus and to the margin of the otolith were made with a digital image-processing system on an axis extending along the sulcal ridge to the proximal margin of each section. We expressed the distance from the final annulus to the edge of the otolith (the marginal increment) as a percentage of the distance between the last two annuli formed on the otolith, or for fish with only a single annulus, as a percentage of the distance between the otolith core and the first annulus. The monthly percentage of otoliths with an annulus on their margin was plotted by capture month to show when the annuli were formed and to reveal their repetitive seasonal trend in formation. The annularity of the assumed age mark was demonstrated for each age class by plotting monthly mean measurements for all ages pooled into three inclusive groups.

Reproduction

Sections of each gonad were prepared for histological analysis and scored according to the level of reproductive activity, or class. Gonad samples were processed with a modification of the periodic acid Schiff's (PAS) stain for glycol-methacrylate sections, with Weigert's iron-hematoxylin as a nuclear stain and metanil yellow as a counterstain (Quintero-Hunter et al., 1991). Seasonal spawning patterns and spawning frequency of the common snook that we examined were reported by Taylor et al. (1998). We considered common snook in Taylor et al.'s (1998) and Grier and Taylor's (1998) classes 2–5 to be sexually mature. For a more detailed description of common snook testicular maturation see Grier and Taylor (1998). These classes included snook that had testes with evidence of active spermatogenesis and regressed testes with evidence of previous gonadal development.

We diagnosed hermaphroditism in common snook by observing histological sections of transitional-sex-stage individuals and sex-specific age- and length-frequency distributions, according to the criteria of Sadovy and Shapiro (1987). We also conducted an experiment with captive snook to document sex reversal in individual fish. We raised common snook from eggs at the Florida Fish and Wildlife Commission's Stock Enhancement Research Facility. On 6 July 1995, 137 age-4 snook ranging from 445 to 608 mm (mean=534 mm) were identified as males on the basis of presence of flowing milt at the vent and were tagged with passive-integrated transponders (PIT tags). These fish were held for 13 months in a one-quarter acre outdoor pond that had constant exchange of ambient seawater. Water temperature and salinity ranged from 17 to 37°C and from 15 to 34‰, respectively. During December 1995 and January 1996, additional well water (17°C and 3‰) was added to maintain 17°C water temperature and to reduce the salinity to 15‰. Rations consisted of squid, sardines, and dried trout pellets. Fish were fed at the rate of 2% body weight per day.

These fish were examined and sexed on two occasions: after 2 months and after 13 months. Fish that could not be positively identified as males from the presence of flowing milt at the vent were sacrificed and examined by histological analysis.

A logistic function was fitted to the percentage of females in our samples by length and age to estimate the length and age at which 50% of the males in the population transformed into females. Regressions were performed with coast as a categorical effect. If coast was a significant effect, the equations were calculated for each coast. The inflection point of the logistic curves was used as an estimate of the length or age at which 50% of the population had undergone transition from male to female.

Results

The 3872 common snook that were examined ranged in length from 124 to 1105 mm (Fig. 1). Of the fish that we sexed, females ranged in length from 397 to 1105 mm (n=1448) and males ranged from 124 to 925 mm (n=2276; Fig. 2). East coast females were usually larger than west coast females (Fig. 2). East coast females ranged in length from 448 to 1105 mm (n=683), and west coast females ranged from 397 to 1032 mm (n=765; Fig. 2). East coast males ranged in length from 124 to 908 mm (n=1258) and west coast males ranged from 129 to 925 mm (n=1018; Fig. 2). The sex ratio (male to female) of the sample from the east coast (EC) was 1.8:1 and from the west coast (WC) was 1.3:1, significantly skewed towards males on both coasts (EC: χ^2=85, df=1, P<0.01; WC: χ^2=36, df=1, P<0.01). The length-length and length-weight regressions for common snook on each coast were significantly different (P<0.05); the relationship between SL, FL, and TL are presented in Table 1.

Age and growth

Common snook annuli are formed once each year, usually during late winter or spring. We recaptured 80 common snook that had been previously injected with OTC. At recapture, these fish ranged in length from 360 to 960 mm and ranged in age from 2 to 14 years. OTC-injected individuals were at large from 4 to 2505 days. All of the recaptured common snook that were at large long enough to have formed an annulus (n=51) showed the expected pattern of annulus formation: one per year. The fish at large for the longest period was 2 years old when it was injected and was recaptured 2505 days later (Fig. 3). This fish had formed seven annuli after the OTC mark and had been at large for 6 years and 11 months; thus the rate of annulus formation was consistent with our predicted rate of one annulus per year. The oldest fish recaptured was 8 years old when injected and was recaptured 5 years and 10 months later, at age 14. This fish had formed six annuli after the OTC mark.

Monthly patterns in marginal increments were also consistent with the formation of a single annulus each year. We plotted the monthly mean percentage of fish whose oto-

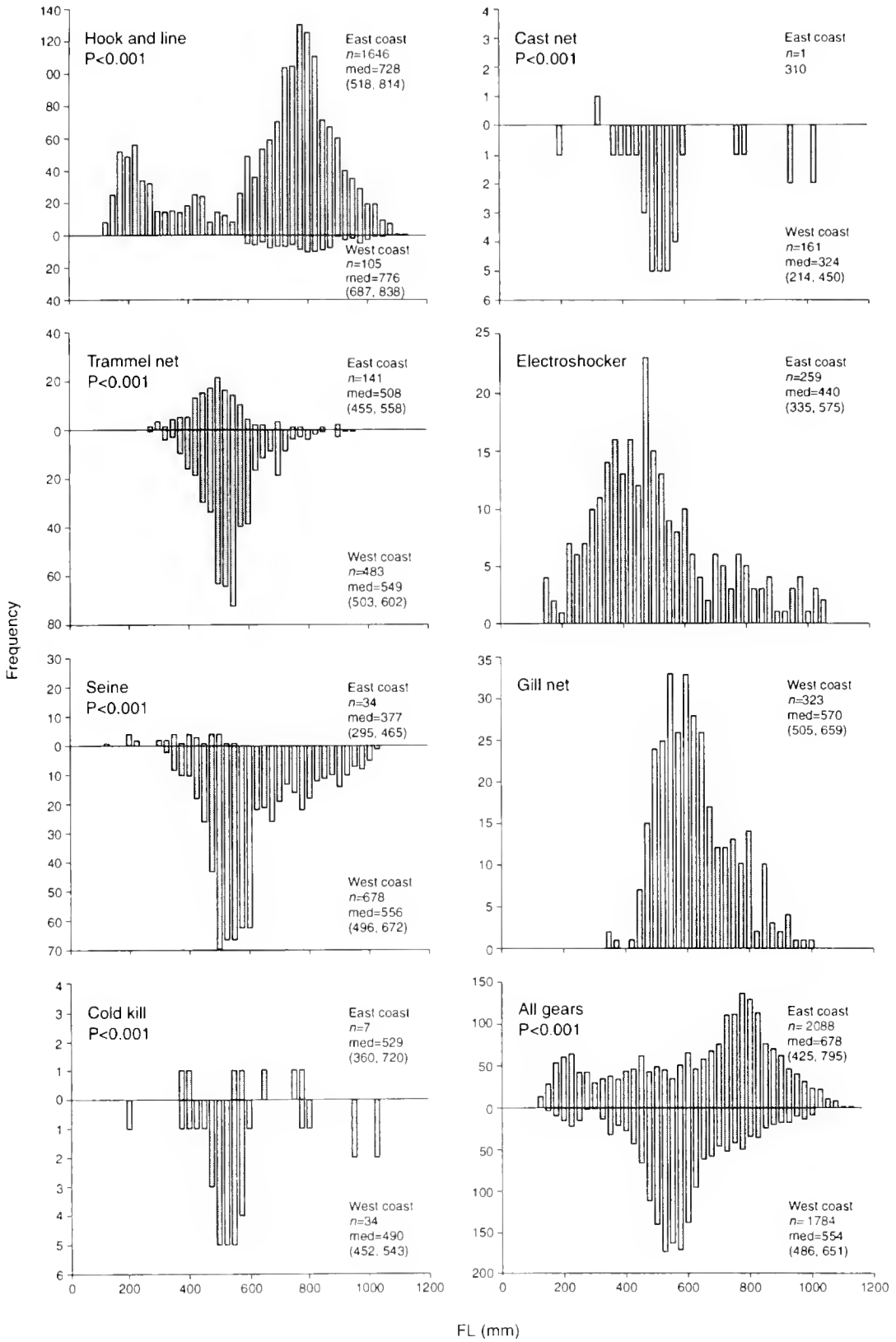

Figure 1

Length distributions, by gear type and coast, of common snook, *Centropomus undecimalis*, collected from South Florida waters during 1986–90. Med = median, numbers in parentheses are the 25th and 75th quartiles, and P is the Kolmogorov-Smirnov test value that compares the cumulative distribution of the two samples.

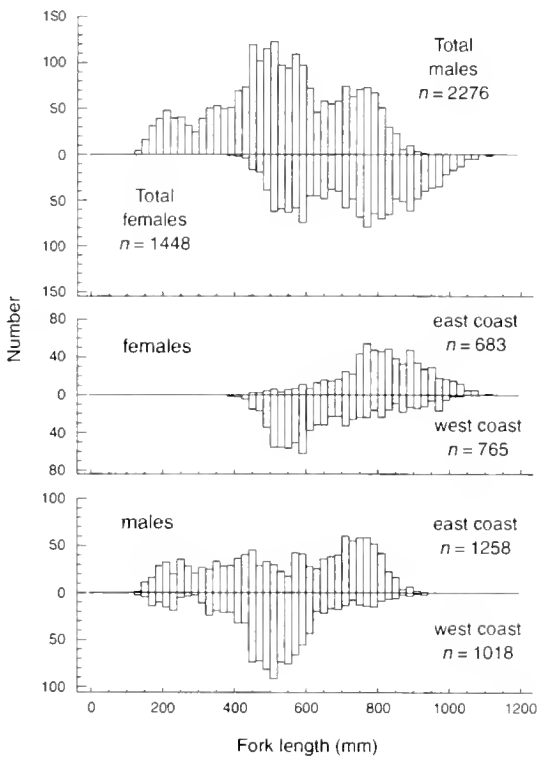

Figure 2

Lengths of male (n=2276) and female (n=1448) common snook, *Centropomus undecimalis*, sampled from South Florida waters.

liths had an annulus on the edge. The greatest percentages occurred during March–May of each year, confirming that annuli are formed then (Fig. 4). A cyclic annual pattern of margin deposition was consistent for common snook of all ages: three inclusive groups, with data pooled sufficient to reveal trends, showed a consistent annual cycle of narrowest margins during March–May and widest margins during late fall and early winter. By June, annulus formation was completed (Fig. 4).

Of the 3883 sectioned otoliths that we examined, 369 (9.5%) were rejected because of disagreements among readings. The length-frequency distribution of fish whose otoliths were rejected because they were unsuitable for age estimation was not significantly different from that of fish whose otoliths were readable (Kolmogorov-Smirnov two-sample test, two-sided test statistic=1.344, P=0.054).

Ages estimated from whole otoliths were significantly less than those estimated from sectioned otoliths (paired t-test, t=4.595, P<0.001). In addition, the slope of the regression of whole-otolith annulus counts on sectioned-otolith annulus counts was 0.873 (SE=0.014), which was significantly less than 1 (t-test=8.75, P<0.001; Fig. 5). Discrepancies between the ages estimated from the two structures were as great as five years, but usually the ages determined from whole otoliths were underestimated by 1–2 years for fish older than 10 years. Ages determined from the two structures agreed for 123 fish, whole-otolith-derived ages were greater for 15 fish, and sectioned-otolith-derived ages were greater for 72 fish. The oldest fish aged from the sectioned otoliths was estimated to be 21 years old and the oldest fish aged from whole otoliths was estimated to be 19 years old.

Table 1

The relationships between standard length, fork length, and total length and between length and weight of common snook, *Centropomus undecimalis*, from South Florida waters off the east and west coasts of Florida. *TL* = total length (mm), *FL* = fork length (mm), *SL* = standard length (mm), *WT* = whole weight (g). The fork length range for all length-length regressions was 112–1105 mm and for the length-weight regression was 124–1105 mm. Coast was a dummy variable equal to 1 for the east coast and 0 for the west coast used in the original regressions where both coasts were pooled, but only the simplified, two-parameter, coast-specific equations are presented here.

$Y = a + bX$						
Y	X	n	Coast	a	b	r^2
SL	*FL*	2416	east	−5.7186	0.8990	0.998
SL	*FL*		west	−14.7684	0.9338	
SL	*TL*	2023	east	−15.4246	0.8564	0.998
SL	*TL*		west	−21.8457	0.8566	
FL	*SL*	2416	east	7.1198	1.1109	0.998
FL	SL		west	20.0876	1.0630	
FL	*TL*	3343	east	−10.8259	0.9526	0.999
FL	*TL*		west	−14.8606	0.9512	
TL	*SL*	2023	east	19.3639	1.1652	0.998
TL	*SL*		west	26.5459	1.1648	
TL	*FL*	3343	east	11.826	1.0490	0.999
TL	*FL*		west	16.2241	1.0502	
$\log_{10}WT$	$\log_{10}FL$ 2919		east	−5.0821	3.0434	0.976
$\log_{10}WT$	$\log_{10}FL$		west	−5.3564	3.1117	

Because scales were difficult to interpret, we were unable to obtain consistent readings. Ages determined from scales were always younger than ages determined from sectioned otoliths by 1 to 3 years for snook less than 10 years. We were unable to reach agreement for the ages of the ten older snook whose structures were compared. Because of the difficulties in interpreting the banding patterns on scales, we did not attempt to analyze counts derived from scales.

The oldest common snook in our sample was a 21-year-old, unsexed (i.e. sex not determined), east coast fish that was 890 mm long (Table 2). This fish was identified as a male in the field but because no gonad sample was taken, we could not confirm the sex of the fish by histological analysis; consequently, we considered the fish to be of undetermined sex in all analyses. The oldest east coast male, other than the unconfirmed 21-year-old fish, was 15 years old (865 mm); the largest east coast male was 908 mm long and 11 years old. The oldest east coast female was 18 years old (1025 mm), and the largest east coast female was 1105 mm long and 16 years old (Table 2). The oldest west coast male was 12 years old (810 mm), and the largest west coast male was 925 mm long and 4 years old. The oldest west coast female was 15 years old (982 mm), and the largest west coast female was 1032 mm long and 10 years old (Table 3).

Common snook grew rapidly until age 5–7 years after which growth slowed considerably (Fig. 6). The most abundant age classes of males were from 2 to 7 years old and those of females were from 3 to 8 years old (Tables 2 and 3). Only 10 east coast specimens were estimated to be older than 16 years, and no west coast fish were older than 16 years. The smallest and youngest female was a 397-mm west coast fish estimated to be 1 year old (Table 3). On the east coast, the smallest and youngest female was a 448-mm fish estimated to be 2 years old (Table 2). The sex-specific age-frequency distributions for the two coasts were significantly different, and east coast fish were older overall than west coast fish (Kolmogorov-Smirnov two-sample, $P<0.05$). The coast-specific differences in age were more pronounced for females than for males (Table 2, Fig. 2).

The von Bertalanffy growth models suggest that east coast fish grow more rapidly than do west coast common snook (Fig. 6, Table 4). Results of likelihood-ratio tests showed a significant difference in the overall von Bertalanffy growth models for east coast and west coast snook ($\chi^2=284.90$, df=3, $P<0.001$). East coast estimates of K = 0.24, (95% confidence interval=0.22–0.25) and t_0 = –0.10 (95%CI=–0.01–(–0.19)) were significantly different from west coast estimates of K=0.18 (95% CI=0.14–0.21) and t_0 = –1.35 (95% CI=–1.68–(–1.01)), ($P<0.005$, $P<0.001$, respectively). The east coast estimate of L_∞ 989 mm (95% CI=966–1012) and 947 mm (95% CI=884–1010) for west coast fish were similar (P=0.342). For fish ages 1–2, the observed lengths at age of west coast fish were greater than those of east coast fish, but for fish in most of the older age classes, lengths of east coast fish were greater (Tables 2 and 3). Lengths at age predicted from the von Bertalanffy growth model for ages 0–2 were greater for west coast fish than for east coast fish, but those for all older age classes were greater for east coast fish than for west coast fish.

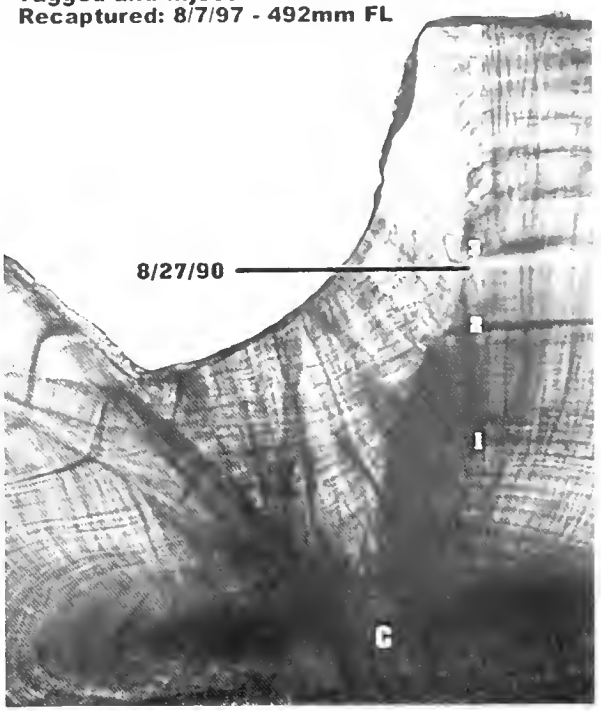

Figure 3

A transverse section of an otolith from an age-9 common snook, *Centropomus undecimalis*, that was injected with oxytetracycline (OTC) on 27 August 1990 and released at the entrance to Bishop's Harbor in lower Tampa Bay, Florida. The fish was recaptured 6 years and 11 months later at the same location and had formed seven annuli between the OTC mark and the otolith's edge.

Maturation and sex transition

Common snook present biological characteristics that are consistent with protandric hermaphroditism. We examined 27 wild-caught specimens that we considered were at the transitional-sex stage on the basis of simultaneous presence in the gonad of ovigerous lamellae and remnants of the dorsal sperm ducts that contained sperm. The mean length and age of these transitional-sex-stage common snook were 515 mm and 3.4 years. They ranged in length from a 240-mm, 1-year-old male specimen that had a prodigious number of ova in the peripheral portions of the testis, to an 824-mm, 7-year-old female with residual sperm in remnant sperm ducts. All ovaries, transitional and otherwise, contained remnants of the major dorsal sperm ducts, regardless of season or reproductive condition (Fig. 7). In addition, transitional gonads contained degenerating spermatogenic and developing ovarian tissue

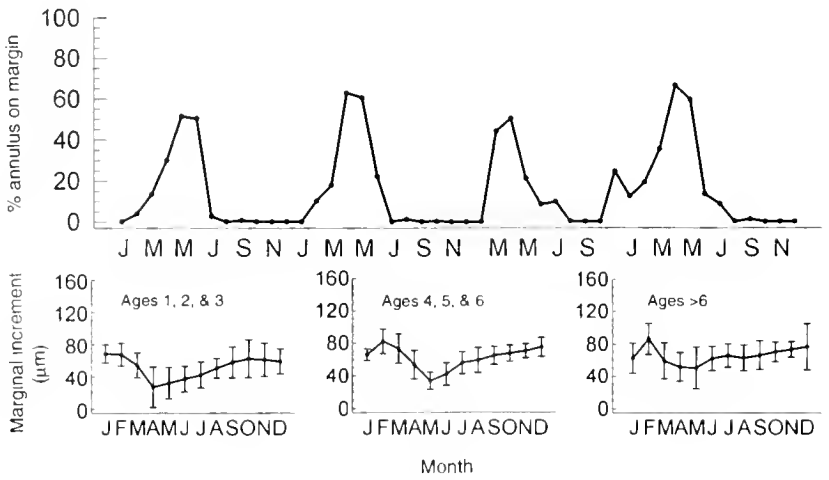

Figure 4

Percentage, by month, of otoliths with an annulus on the edge and mean monthly marginal increments with standard errors for all age classes pooled into three groups for common snook, *Centropomus undecimalis*, from south Florida waters.

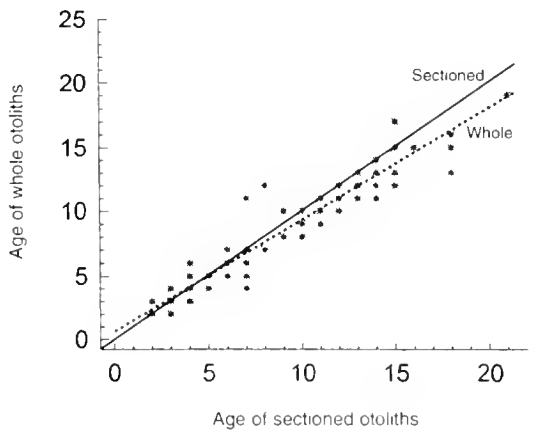

Figure 5

The relationship between annulus counts determined from sectioned and whole otoliths. The regression equation is $WO = 0.499 + SO \cdot 0.874$, where WO is the annulus count from whole otoliths and SO is the annulus count from sectioned otoliths (r^2=0.949, n=199).

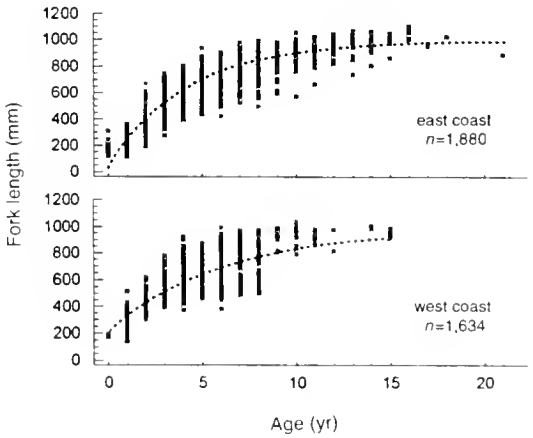

Figure 6

The von Bertalanffy growth curves for common snook, *Centropomus undecimalis*, from the east and west coasts of Florida. Parameter estimates are given in Table 4.

(Fig. 8). Most (74%) transitional-sex-stage fish were captured during September–November, shortly after the end of the spawning season, suggesting that sex reversal of postspawning males takes place shortly after spawning. The small number of transitional-sex-stage fish in our sample suggests that sex reversal occurs quickly.

During the 13-month experiment designed to document sex reversal, three males changed into females. The 137 four-year-old fish whose sex we monitored were initially sexed in July 1995 and ranged in length from 445 to 608 mm (mean=508 mm). In September 1995, we sexed the fish again and found that the largest individual (tag no. 96-344C, 617 mm) had completed sex reversal and that its ovary contained early vitellogenic oocytes. We examined these fish a final time on 17 August 1996 and found that they ranged in length from 467 mm to 649 mm (mean=534 mm). Two additional fish that were 622 mm (tag no. 10685C) and 584 mm (tag no. 13CB03) long had reversed sex, and their ovaries contained nonvitellogenic oocytes. The largest fish, a male, (tag no. 13BC2E) was

Table 2

Average observed and predicted (von Bertalanffy) fork lengths (mm) of east coast sexed and unsexed common snook, *Centropomus undecimalis*, and average observed lengths of females and males. The average observed length at age includes some seasonal growth that occurred after the formation of the final annulus. Values in parentheses are standard error and sample size.

Age (yr)	All snook		Females	Males
	Average observed	Predicted	Average observed	Average observed
0	185 (10.1;17)	22		228 (21.8;5)
1	211 (3.2;266)	225		231 (3.9;166)
2	359 (7.7;131)	385	580 (46.6;4)	357 (6.9;122)
3	514 (7.7;230)	511	644 (10.5;44)	484 (7.6;186)
4	629 (7.0;268)	611	695 (9.2;85)	597 (8.5;179)
5	698 (6.1;310)	690	760 (7.5;114)	661 (7.5;194)
6	755 (6.4;209)	753	809 (5.9;95)	711 (8.8;114)
7	792 (7.3;127)	802	841 (7.5;58)	748 (9.3;68)
8	820 (9.5;104)	841	874 (8.0;60)	747 (13.4;44)
9	849 (10.1;71)	872	902 (8.7;37)	782 (11.7;31)
10	903 (12.5;42)	897	936 (8.5;29)	807 (26.1;11)
11	911 (13.5;30)	916	943 (9.8;20)	832 (23.8;9)
12	948 (15.6;19)	932	973 (13.0;15)	854 (16.8;4)
13	959 (18.3;20)	944	989 (13.0;15)	832 (30.5;4)
14	960 (28.5;8)	953	994 (20.3;6)	857 (48.5;2)
15	987 (22.6;7)	961	1007 (11.8;6)	865 (1)
16	1048 (19.2;5)	967	1048 (19.2;5)	
17	961 (10.0;2)	971	961 (10.0;2)	
18	1024 (1.5;2)	975	1024 (1.5;2)	
19	978			
20	980			
21	890 (1)	982		

608 mm in 1995 and grew to be the largest fish in the study in 1996 (649 mm) but did not reverse sex. At the end of the experiment, the two fish that had reversed sex were the second-and third-largest snook.

Common snook sex ratios and length-frequency distributions were consistent with a diagnosis of protandric hermaphroditism. The overall sex ratio (male to female) for fish on both coasts, over the entire size range, was 1.6:1.0, significantly different from the expected 1:1 (χ^2=184, df=1, P<0.001). Females smaller than 500 mm were uncommon (4.63% of total observed), and only one female smaller than 400 mm was captured. Logistic curves were used to describe length- and age-related shifts in the common snook sex ratio. The predicted length at which 50% of the fish in the population were females was 767 mm on the east coast and 608 mm on the west coast (Fig. 9, Table 5). The predicted age at which 50% of the fish in the population were females was 7.4 years on the east coast and 5.1 years on the west coast (Fig. 9, Table 5).

Males reached sexual maturity at 150–200 mm on both coasts. The smallest mature east coast male was 175 mm long and the smallest mature west coast male was 152 mm long. The youngest mature male on both coasts was age 0. Our sample contained only 13 immature east coast males and 60 immature west coast males.

Discussion

We sampled common snook from a variety of fishery-independent and fishery-dependent sources. Some specimens were donated by recreational anglers, and others were caught by biologists using hook-and-line gear. We also used trammel and gill nets and haul seines to capture fish. On the east coast, most of the large common snook we sampled were caught by hook and line during the spawning season from spawning aggregations. In contrast, most west coast samples were collected with seines and trammel nets, and we did not regularly sample west coast spawning aggregations. We cannot quantify the potential biases resulting from the use of these different types of gears and sample sources, but our east coast material may have been biased towards larger fish because larger more aggressive individuals were harvested with hook and line. Our finding on the east coast of larger and older common snook and of larger observed and predicted lengths at age for most age classes

Table 3

Average observed and predicted (von Bertalanffy) fork lengths (mm) of west coast sexed and unsexed common snook, *Centropomus undecimalis*, and average observed lengths of females and males. The average observed length at age includes some seasonal growth that occurred after the formation of the final annulus. Values in parentheses are standard error and sample size.

Age (yr)	All snook		Females	Males
	Average observed	Predicted	Average observed	Average observed
0	179 (7.0;2)	200		179 (7.0;2)
1	272 (8.0;106)	320	460 (32.5;4)	264 (7.4;102)
2	442 (4.3;186)	421	487 (6.4;44)	428 (4.6;142)
3	521 (3.4;359)	505	548 (4.6;177)	494 (4.2;182)
4	587 (5.0;332)	576	623 (7.2;157)	555 (6.1;175)
5	625 (6.2;220)	636	664 (8.8;106)	589 (7.1;114)
6	651 (7.9;226)	686	720 (10.6;102)	594 (8.5;124)
7	719 (12.6;125)	728	796 (14.2;64)	637 (15.2;61)
8	751 (23.4;40)	763	827 (25.5;23)	647 (27.6;17)
9	928 (18.1;9)	793	928 (18.1;9)	
10	926 (24.7;10)	818	969 (15.1;7)	826 (19.1;3)
11	927 (12.0;10)	838	931 (12.6;9)	891 (1)
12	891 (81.0;2)	856	972 (1)	810 (1)
13	871			
14	995 (7.7;3)	883	995 (7.7;3)	
15	953 (12.6;4)	893	953 (12.6;4)	

Table 4

Parameter estimates of the von Bertalanffy growth model for common snook, *Centropomus undecimalis*, collected from the waters of South Florida. Values in parentheses are standard errors.

	n	L (mm FL)	K	t_0	Adjusted r^2
East coast	1880	989.3 (11.64)	0.235 (0.0076)	−0.0976 (0.04447)	0.835
West coast	1634	947.3 (32.15)	0.175 (0.0155)	−1.352 (0.1714)	0.610

Table 5

Relationships of percent female to fork length (mm) and age (years) for common snook, *Centropomus undecimalis*, from South Florida waters. *FL* = fork length (mm) and *Age* = age (years). P_{50} = the absolute value of $(a+b)/c$, which is the inflection point of the curve and is the length or age predicted by the logistic regression at which 50% of the common snook in our sample were females. Coast is a dummy variable equal to 1 for the east coast and 0 for the west coast. PD is the adjusted percentage of deviance explained by the model.

Percent female = $e^{(a+b(\text{coast})+cX)}/(1+e^{(a+b(\text{coast})+cX)})$

X	n	a	b	c	PD	P_{50}
FL	3723	−5.713 (0.2114)	−1.495 (0.1006)	0.0094 (0.00035)	0.269	767 mm east coast 608 mm west coast
Age	3380	−1.578 (0.0900)	−0.705 (0.0778)	0.307 (0.0171)	0.093	7.4 years east coast 5.1 years west coast

may reflect sampling bias rather than a true difference in the maximum fish sizes reached on the two coasts.

Other comparative studies on two inshore (Florida) Sciaenidae species also have found that east coast fishes attain greater sizes or grow at faster rates than do west coast fishes (Murphy and Taylor, 1990; Murphy and Taylor, 1994). Although gear biases may have confounded growth differences in these comparative studies, there is some basis for physiological differences in common snook. Tringali and Bert (1996) have provided evidence that common snook in Florida comprise two genetically different populations: one population in Atlantic waters and one in Gulf waters. They have reported that mtDNA divergence, both in haplotype diversity and in nucleotide sequence, supports the hypothesis that the two populations are reproductively isolated, which may account for a portion of the observed differences in biological parameters.

Age and growth

Our findings suggest that scales and whole otoliths may not be suitable for aging common snook older than 6–9 years, the point at which our length-at-age data began to reach an asymptote. Ages derived from whole otoliths were reasonably accurate for snook younger than about 10 years, but ages of older snook were consistently underestimated. Furthermore, whole otoliths were more difficult to read than sectioned otoliths and therefore readers' counts from whole otoliths often varied, principally because the closely spaced annuli on the edge of whole otoliths were difficult to differentiate. Our observations of common snook scales led us to conclude that they were not suitable for use in age estimation. Whole-otolith–derived estimates of longevity reported by Volpe (1959) and scale-derived estimates by Thue et al. (1982) of 7–8 years are considerably less than our sectioned-otolith–derived estimate of 21 years. Both Volpe (1959) and Thue et al. (1982) examined fewer fish than we did; therefore their samples would be expected to contain fewer old individuals than ours did. Their samples were also collected many years before ours, and additional regulations have been imposed on the fishery since their studies; however, the magnitude of the discrepancies in ages between our study and theirs is so great that we suspect they underestimated the ages of many fish. Thue et al. (1982) reported von Bertalanffy growth parameters for common snook, but their growth model did not reach an asymptote; consequently, their estimate of $L = 1615$ mm for combined sexes is much greater than our estimate for either coast and is far larger than the length reported for any common snook. We suspect that their growth curve did not reach an asymptote because they consistently underestimated the ages of old common snook.

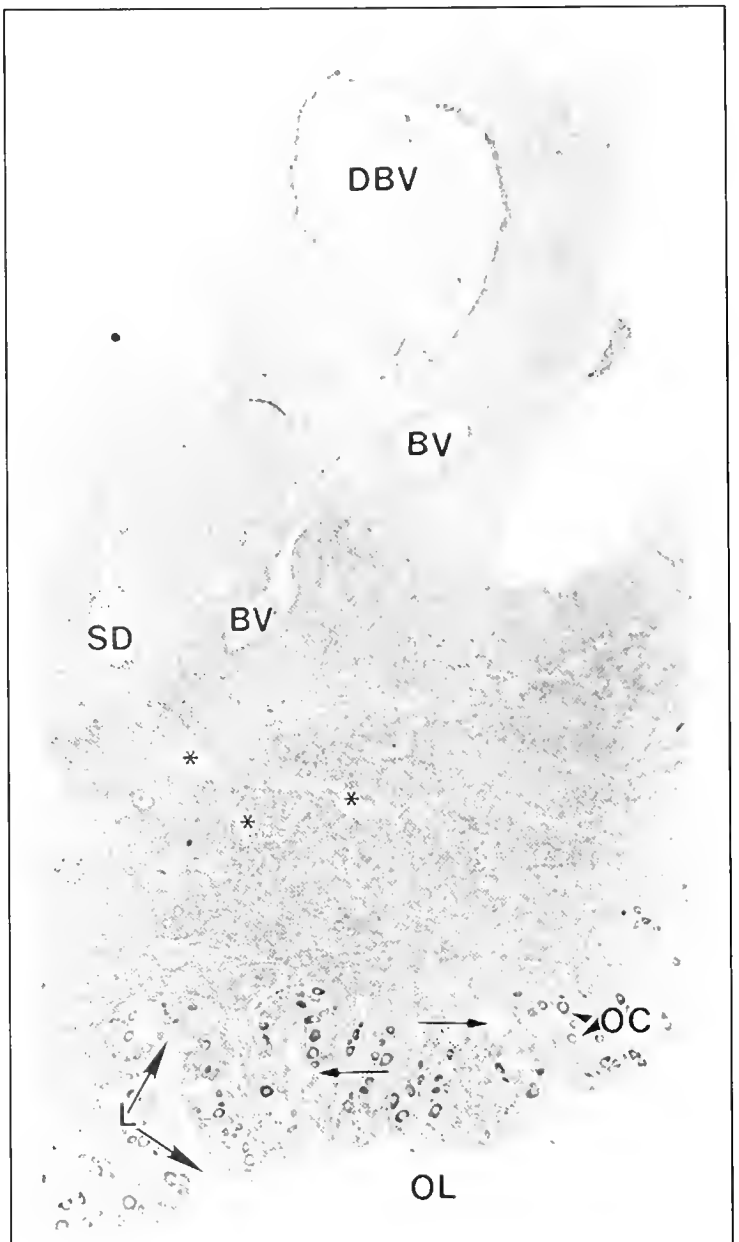

Figure 7

A histological section from a transitional-sex-stage common snook, *Centropomus undecimalis* (632 mm FL), captured in lower Tampa Bay in July 1989. Remnants of the major sperm duct (SD) and collecting tubules (*) are present in the dorsal matrix. Located throughout the peripheral ovigerous lamellae (L) are female germ cells that are either primary growth oocytes (OC) or meiotic and interphase oogonia (arrows). The dorsal (DBV) and lateral (BV) blood vessels are distinguished from the sperm ducts by the presence of red blood cells. OL = ovarian lumen.

Growth data for common snook in our study fitted the von Bertalanffy model well. The poor fit at age 0 for the east coast is explained by the collection of young-of-the-year fish in April and May, just prior to their first birthday when they were longest at age. The asymptotic values of

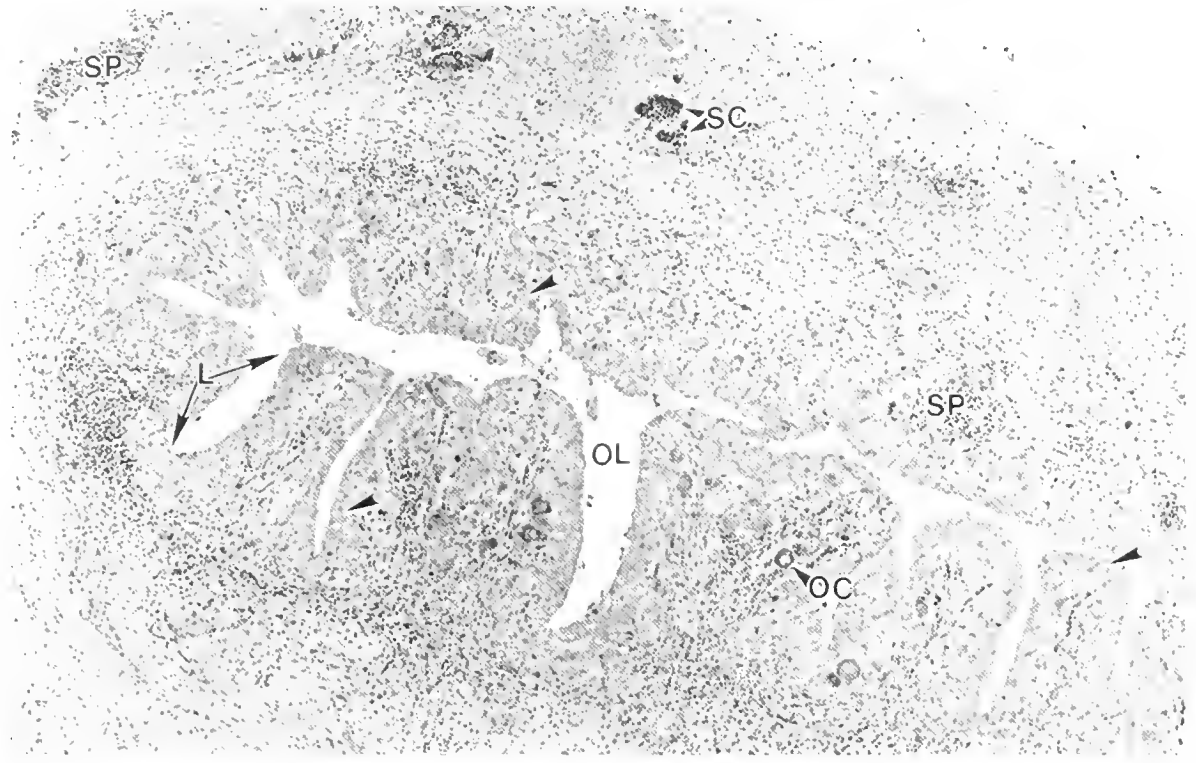

Figure 8

A histological section from a transitional common snook, *Centropomus undecimalis* (474 mm FL), captured in lower Tampa Bay in September 1989. Cysts that contain sperm (SP) and spermatocytes (SC) are visible in the peripheral wall of the gonad. Central lamellae (L) contain primary growth oocytes (OC) in addition to clusters of meiotic and interphase oogonia (arrow). OL = ovarian lumen.

approximately one meter may be a result of the difficulty of sampling large robust snook; trophy-size individuals are not uncommon in Florida and snook 1155–1194 mm are recorded (IGFA, 1998).

Maturation and sex transition

We based our determination that common snook are protandrous hermaphrodites on the following criteria presented by Sadovy and Shapiro (1987): 1) sex ratios shifted from exclusively male to predominantly female with increasing size and age, 2) transitional-sex-stage individuals were observed whose gonads contained both degenerating spermatogenic and developing ovarian tissue, and 3) sex change was documented in captive fish. Common snook have not previously been diagnosed as protandrous hermaphrodites, but another centropomid, the barramundi *Lates calcarifer*, has been diagnosed as a protandric hermaphrodite (Moore, 1979; Davis, 1982).

The male-to-female sex ratios previously reported for southwest Florida common snook (e.g. Volpe 1959, Thue et al., 1982), are similar to ours, with the exception of those reported by Marshall (1958). Thue et al. (1982) reported a 3:1 sex ratio for common snook smaller than about 500 mm and younger than age 2 in the Everglades National Park and a sex ratio 1:11 for common snook larger than 800 mm and older than age 8. Volpe (1959) reported a similarly skewed sex ratio of 1:3 for fish larger than 800 mm from southwest Florida. These shifts in the common snook sex ratio with increasing length and age are consistent with our diagnosis of protandrous hermaphroditism. In contrast, Marshall (1958) found that there were more females than males smaller than 500 mm (1.0:1.1) and that the overall sex ratio for common snook in southwest Florida was not significantly different from 1:1. It is possible that Marshall (1958) did not observe the actual sex ratio of the population he studied because 288 of the 531 total specimens in his sample had been gutted and were not included in the analysis.

Male common snook reach sexual maturity at surprisingly small lengths and ages, some at lengths less than 200 mm. We considered a fish to be sexually mature if mature sperm were present in the testis. According to this criterion, immature males made up <2% of our sample. Furthermore, most of the males we classified as immature were caught outside of the spawning season, and we may have misclassified some regressed mature fish as immature. Because our sample contained so few males that we could be certain were immature, we did not attempt to fit a logistic function to male maturity. The small mature

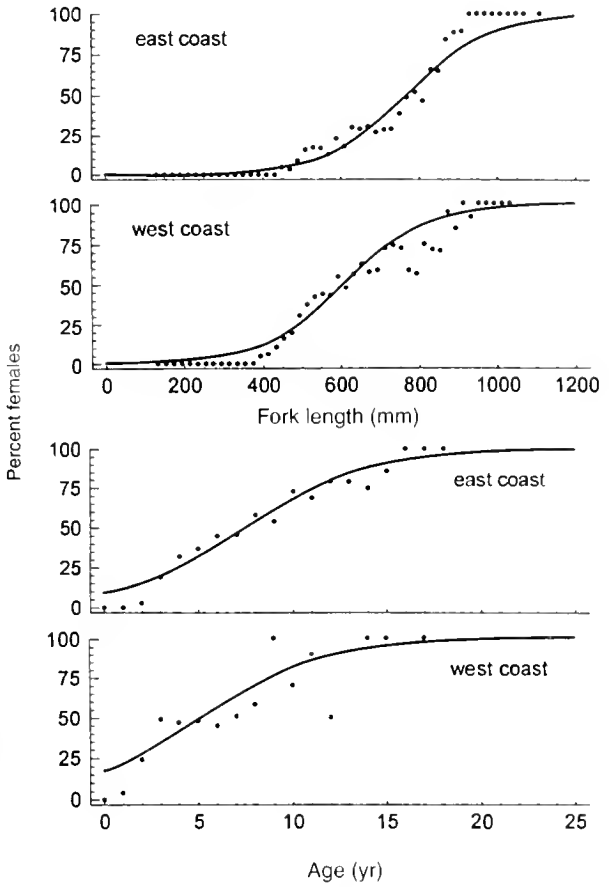

Figure 9

Logistic curves describing the percentage of females of common snook, *Centropomus undecimalis*, as a function of fork length (east coast n=1940, west coast n=1783) and age (east coast n=1742, west coast n=1638).

males we observed were smaller than those observed by previous workers; however, previous studies of maturation were based only on a macroscopic examination of gonads. Marshall (1958) examined 239 common snook from southwest Florida and concluded that 50% of the specimens of both sexes were mature at 400 mm and that all common snook, with few exceptions, were mature at 500 mm. Volpe (1959) used Marshall's lengths-at-maturity data to estimate the age at first maturity to be 3 years. It is unclear whether the small males we observed were spawning males, but they appeared to be capable of spawning; therefore we considered them to be sexually mature. Common snook typically spawn in large aggregations near passes and inlets (Taylor et al., 1998). We did not observe males smaller than 350 mm in spawning aggregations, and most spawning males were longer than 400 mm; however, we can not eliminate the possibility that some spawning involved smaller males outside these large aggregations. Additional research is needed to determine whether or not these small, precocious males are active members of the spawning population.

We considered all female common snook to be sexually mature on the assumptions that they develop directly from males that had previously spawned, that sex transition occurs shortly after spawning, and that they would be capable of spawning as females during the next spawning season. Among other centropomids, *L. calcarifer* also undergoes sex change near the end of the spawning season (Davis, 1982; Guiguen et al., 1994). Davis (1982) found that in *L. calcarifer*, oocytes first appear as the testes ripen for the final time and that sex reversal is completed shortly after spawning. This finding is consistent with our observations of common snook. Most transitional-sex-stage individuals were captured during September–November; we did not observe any transitional fish from April to June and only one transitional fish in February and one in March. Sex reversal appears to occur quickly and shortly after spawning, and we found no evidence to suggest that females do not spawn during their first spawning season after transition from male to female. This conclusion is supported by the captive fish that completed sex reversal and developed vitellogenic oocytes in only two months. Management decisions based on length and age at maturity of females should more appropriately focus on the size and age at sex transition, and all females should be included in estimates of spawning stock biomass.

Acknowledgments

We thank the many anglers and biologists who participated in this study. We especially thank Ed Irby, Kraig Krum, William Howard, and other staff at the Tequesta field laboratory. Iliana Quintero, Pamela Nagle, and Ruth Reese provided invaluable assistance. Buck Dennis, William Halstead, John Young, Patricia Hindle, and other staff at the Stock Enhancement Research Facility are kindly acknowledged. We thank David Harshany, Doug Haymans, Dan Merryman, Heather Patterson, Graham Gerdeman, and Connie Stevens for their assistance. This manuscript was greatly improved by the conscientious reviews of Jim Quinn, Judy Leiby, and Llyn French. This work was supported in part under funding from the Department of the Interior, U.S. Fish and Wildlife Service, Federal Aid for Sportfish Restoration, Project Number F-59.

Literature cited

Beamish, R. J., and G. A. McFarlane.
1983. The forgotten requirement for age validation in fisheries biology. Trans. Am. Fish. Soc. 112:735–743.

Bruger, G. E., and K. H. Haddad.
1986. Management of tarpon, bonefish, and snook in Florida. *In* Proceedings of the eleventh annual marine recreational fisheries symposium, Tampa, FL (R. H. Stroud, ed.), p. 53–57. National Coalition for Marine Conservation Inc., Savannah, GA.

Casselman, J. M.
1983. Age and growth assessment of fish from their calcified structures--techniques and tools. *In* Proceedings of the international workshop on age determination of oceanic pelagic fishes: tunas, billfishes, and sharks (E. D. Prince

and L. M. Pulos, eds.), p. 1–17. U.S. Dep. Commer., NOAA Tech. Rep. NMFS 8.

Chilton, D. E., and R. J. Beamish.
1982. Age determination methods for fishes studied by the groundfish program at the Pacific Biological Station. Can. Fish. and Aquat. Sci. Spec. Publ. 60, 102 p.

Crabtree, R. E., C. W. Harnden, D. Snodgrass, and C. Stevens.
1996. Age, growth, and mortality of bonefish, *Albula vulpes*, from the waters of the Florida Keys. Fish. Bull. 94:442–451.

Davis, T. L. O.
1982. Maturity and sexuality in barramundi, *Lates calcarifer* (Bloch), in the Northern Territory and south-eastern Gulf of Carpentaria. Aust. J. Mar. Freshwater Res. 33:529–545.

Gilmore, R. G., C. J. Donahoe, and D. W. Cooke.
1983. Observations on the distribution and biology of the common snook, *Centropomus undecimalis* (Bloch). Fla. Sci. 46:313–336.

Grier, H. J., and R. G. Taylor.
1998. Testicular maturation and regression in the common snook. J. Fish Biol. 53:521–542.

Guiguen, Y., C. Cauty, A. Fostier, J. Fuchs, and B. Jalabert.
1994. Reproductive cycle and sex inversion of the seabass, *Lates calcarifer*, reared in sea cages in French Polynesia: histological and morphological description. Environ. Biol. Fishes 39:231–247.

IGFA (International Game Fish Association).
1998. World record game fishes. IGFA, Ft. Lauderdale, FL, 352 p.

Kimura, D. K.
1980. Likelihood methods for the von Bertalanffy growth curve. Fish. Bull. 77:765–776.

Lowerre-Barbieri, S. K., M. E. Chittenden Jr., and C. M. Jones.
1994. A comparison of a validated otolith method to age weakfish, *Cynoscion regalis*, with the traditional scale method. Fish. Bull. 92:555–568.

Marshall, A. R.
1958. A survey of the snook fishery of Florida, with studies of the biology of the principal species, *Centropomus undecimalis* (Bloch). Fla. Board Conserv. Mar. Res. Lab. Tech. Ser. 22, 39 p.

Matlock, G. C., and H. R. Osburn.
1987. Demise of the snook fishery in Texas, USA. Northeast Gulf Sci. 9(1):53–58.

Moore, R.
1979. Natural sex inversion in giant perch, *Lates calcarifer*. Aust. J. Mar. Freshwater Res. 33:647–661.

Murphy, M. D., and R. G. Taylor.
1990. Reproduction, growth, and mortality of red drum *Sciaenops ocellatus* in Florida waters. Fish. Bull. 88:531–542.
1994. Age, growth, and mortality of spotted seatrout in Florida waters. Trans. Am. Fish. Soc. 123:482–497.

Quintero-Hunter, I., H. Grier, and M. Muscato.
1991. Enhancement of histological detail using metanil yellow as counterstain in periodic acid/Schiff's hematoxylin staining of glycol methacrylate tissue sections. Biotech. Histochem. 66:169–172.

Rivas, L. R.
1986. Systematic review of the perciform fishes of the genus *Centropomus*. Copeia 1986:579–611.

Sadovy, Y., and D. Y. Shapiro.
1987. Criteria for the diagnosis of hermaphroditism in fishes. Copeia 1987:136–156.

Shafland, P. L., and K. J. Foote.
1983. A lower lethal temperature for fingerling snook, *Centropomus undecimalis*. Northeast Gulf Sci. 6:175–178.

Taylor, R. G., H. J. Grier, and J. A. Whittington.
1998. Spawning rhythms of common snook in Florida. J. Fish Biol. 53:502–520.

Tringali, M. D., and T. M. Bert.
1996. The genetic stock structure of common snook (*Centropomus undecimalis*). Can. J. Fish. Aquat. Sci. 53:974–984.

Tucker, J. W., Jr., M. P. Landau, and B. E. Faulkner.
1985. Culinary value and composition of wild and captive common snook, *Centropomus undecimalis*. Fla. Sci. 48(4): 196–200.

Volpe, A. V.
1959. Aspects of the biology of the common snook, *Centropomus undecimalis* (Bloch) of southwest Florida. Fla. Board Conserv. Mar. Res. Lab. Tech. Ser. 31, 38 p.

von Bertalanffy, L.
1957. Quantitative laws in metabolism and growth. Q. Rev. Biol. 32:217–231.

Habitat associations of deep-water rockfishes in a submarine canyon: an example of a natural refuge

Mary M. Yoklavich
Pacific Fisheries Environmental Laboratory
National Marine Fisheries Service, NOAA
1352 Lighthouse Avenue
Pacific Grove, California 93950-2097
Present address: National Marine Fisheries Service
c/o Long Marine Laboratory
100 Shaffer Road
Santa Cruz, California 95060
E-mail address: mary.yoklavich@noaa.gov

H. Gary Greene
Gregor M. Cailliet
Deidre E. Sullivan
Moss Landing Marine Laboratories
8272 Moss Landing Road
Moss Landing, California 95039-9647

Robert N. Lea
California Department of Fish and Game
20 Lower Ragsdale Dr.
Monterey, California 93940

Milton S. Love
University of California Santa Barbara
Marine Science Institute
Santa Barbara, California 93106

Abstract.—A multidisciplinary assessment of benthic rockfishes (genus *Sebastes*) and associated habitats in deep water was conducted in Soquel Submarine Canyon, Monterey Bay, California. Rock habitats at depths to 300 m were identified by using bathymetric and side-scan sonar imaging, verified by visual observations from a manned submersible, mapped and quantified. Species composition, abundance, size, and habitat specificity of fishes were determined by using a video camera and parallel laser system along transects made by a submersible.

We counted 6208 nonschooling fishes representing at least 52 species from 83 10-min strip transects that covered an estimated 33,754 m^2. Rockfishes represented 77% of the total number of individuals, and included a minimum of 24 species. Six distinct habitat guilds of fishes were manifest from habitat-based clustering analysis: small species were associated with mud and cobble substrata of low relief, and larger species of rockfishes were associated with high-relief structures such as vertical rock walls, ridges, and boulder fields. There was remarkable concordance between some of the guilds identified in Soquel Canyon and the results of other habitat-specific assessments of fishes along the west coast of the United States from central California to Alaska. These generalities are valuable in predicting community structure and evaluating changes to that structure, as well as in applying small-scale species-habitat relationships to broader-scale fishery resource surveys. Additionally, establishment of these groups is critical when incorporating the concept of essential fish habitat (EFH), and negative impacts to it, into the management of fisheries in relatively deep water, as required by the Sustainable Fisheries Act of 1996.

High numbers of large rockfishes (e.g. *Sebastes chlorostictus*, *S. levis*, *S. melanoblattis*, and *S. ruberrimus*) were locally associated with rock ledges, caves, and overhangs at sites having little or no evidence of fishing activity. Abundance and size of several species were lower at fished than at unfished sites. We suggest that rock outcrops of high relief interspersed with mud in deep water of narrow submarine canyons are less accessible to fishing activities and thereby can provide natural refuge for economically important fishes, as exemplified in Soquel Canyon.

Manuscript accepted 17 December 1999.
Fish. Bull. 98:625–641 (2000).

Rockfishes (*Sebastes* spp.) are quite speciose, dominate coastal benthic fish assemblages on the west coast of the United States, and are among the most valuable fisheries in California. They have been harvested commercially in California as early as 1875 (Phillips, 1957). About 85% of the 57 or more rockfish species in California have some economic value, and landings have increased dramatically over the last 40 years (Lea, 1992). During the past decade (1988–97), commercial fishermen have landed an average of nearly 10,000 metric tons of rockfish at California ports per year, with an average exvessel value of $11.4 million per year (Thomson, 1999). During this period, recreational anglers on commercial passenger fishing vessels caught an additional 1.8 million individual rockfish per year (Thomson, 1999), at a value that far exceeds that of the commercial catch.

Many species of rockfishes are slow-growing, long-lived, and relatively old at maturity, making them particularly vulnerable to overfishing. Historically, rockfish landings have been especially high in Monterey (Phillips, 1939), and there are recent indications that numbers and sizes are decreasing for some species (Pearson and Ralston, 1990; Mason, 1995, 1998; Ralston, 1998). As with many coastal fisheries, the Monterey fleets have expanded their range to deeper and more remote areas as local stocks have become depleted in shallow water (Deimling and Liss, 1994; Karpov et al., 1995; Mason, 1995).

As increased fishing effort is applied to populations in deep coastal waters, it becomes critical to identify and protect areas of natural refuge for larger,

older individuals of valuable rockfish species. There is little information on the distribution, abundance, and habitat characteristics of mature rockfishes associated with deep-water benthic marine habitats off California. This type of habitat is below scuba depths (<30 m), and the rocky heterogeneous substrata inhabited by many rockfish species prohibit accurate estimates of fish abundance with conventional trawl surveys. Diversity, quality, and extent of habitat likely are among the most significant environmental determinants of distribution, abundance, and species richness of adult rockfishes (Larson, 1980; Richards, 1986; Pearcy et al., 1989; Carr, 1991; Stein et al., 1992). Characterizing and quantifying elements of suitable habitat, such as substratum type, texture, and relief, are therefore critical for evaluating the effectiveness of refugia, both natural and designated protected areas, to maintain regional marine resources.

Eight submarine canyons cut into the continental shelf off central California, placing deep-water habitats in close proximity to shore. We hypothesized that isolated rock outcrops in deep water along the steep walls of these canyons could serve as natural harvest refugia and allow certain rockfish species locally to attain large sizes and high abundances. Subsequent distribution of offspring from these mature fishes could help maintain viable populations and species diversity in adjacent areas of greater fishing activity.

Our general goal in this study was to characterize rockfish assemblages and their relationship to specific benthic habitats within submarine canyons by combining geophysical and *in situ* submersible surveys. Because temperate benthic habitats are often defined by geologic attributes, geophysical techniques are critical in determining habitat structure, depth, and lithology.

Within our general goal, this study had four specific objectives. Our first objective was to characterize the geomorphology of our study site in Soquel Canyon using bathymetric mapping and side-scan sonar imaging (i.e. sonographs) to classify the substrata and to locate rock outcrops on a spatial scale of 100s of meters to kilometers. Our second objective was to map and quantify the amount of exposed hard substrata at depths suitable to rockfishes within our study site. Third, using a manned submersible, we set out to verify our interpretations of the remotely sensed images of habitat on a smaller scale (i.e. 1 meter to 10s of meters) and determine frequency of occurrence, distribution and type of habitat that support assemblages of adult benthic rockfishes in Soquel Canyon. Our fourth objective was to estimate and compare species composition, abundance, size, and diversity of fishes among habitat types, depth zones, and locations that have been subject to various amounts of fishing activity within the canyon.

Materials and methods

Study site

Soquel Canyon (ca. 36°49'N, 121°59'W) is a submarine canyon of inactive sediment that cuts into the continental shelf in Monterey Bay nine miles south of Santa Cruz, at a water depth of 80 m. This canyon trends southwest for 10 km, at which point it intersects the larger Monterey Canyon at a depth of 915 m (Fig. 1A). Soquel Canyon is eroded from the generally flat-lying beds of the Pliocene Purisima Formation, a shallow-water marine deposit comprising interlayers of sandstone, mudstone, and shell hash (coquina). Previous undercutting of the canyon walls has caused extensive landslides and slumping; resultant rock exposures were the targets of our survey of rockfishes and their associated habitats.

Our study area covered about 17 km^2 of the headward part of the canyon, between 80 and 360 m water depth. This represents about two-thirds (6.7 km) of the length of the canyon's axis; at 6.7 km along the axis, the canyon is 3.5 km wide and 650 m deep.

Geophysical surveys

Side-scan sonar is a suitable method for distinguishing blocks of hard substrata from surrounding soft sediment by differences in intensity of reflected sound (Able et al., 1987; Greene et al., 1995; Yoklavich et al., 1997). Our sonographs of seafloor morphology resemble a black and white photographic negative. Topographic features such as ledges, vertical walls, and boulders produce dark and light images on the records, depending on the orientation and hardness of the feature. A strong signal or reflector (dark) is received from the side of a relatively hard feature facing the transducer, whereas a weak signal or shadow (light) is received from the side sloping away from the transducer.

We conducted a side scan sonar survey along 110 km of track lines using a 100 kHz acoustic signal with a swath width of 600 m (300 m per side). The sonographs along each track line were positioned precisely with navigational data from a differential global positioning system (GPS) to form a mosaic of rock type and texture within the canyon. Because of steep relief, only one side of the transducer received usable signals and 200% coverage was necessary to produce a complete mosaic.

We used the mosaic to quantify the amount of hard substrata at depths suitable to rockfishes. Our interpretations of the sonographs were verified by direct observations made by marine geologists (HGG and DS) during nine dives in the *Delta* submersible. Type, relief, and size and depth range of features were described; these field descriptions assisted the marine biologists in planning dives at each site and in assessment of habitat after the cruise.

We conducted a bathymetric survey of Soquel Canyon using a 3.5-kHz precision depth recorder integrated with Loran and GPS navigational data. The resultant high-resolution map (20-m intervals) was used to identify areas of high relief and potential slumps.

Fish and habitat surveys

We used the *Delta* submersible to assess benthic fish assemblages and associated habitat in Soquel Canyon in August 1992 and October 1993. The *Delta* is a small (4.75-m) submersible, accommodates one scientific observer and a pilot, has a maximum operating depth of 365 m, and a cruising speed of 1.5 knots. An acoustic track-point

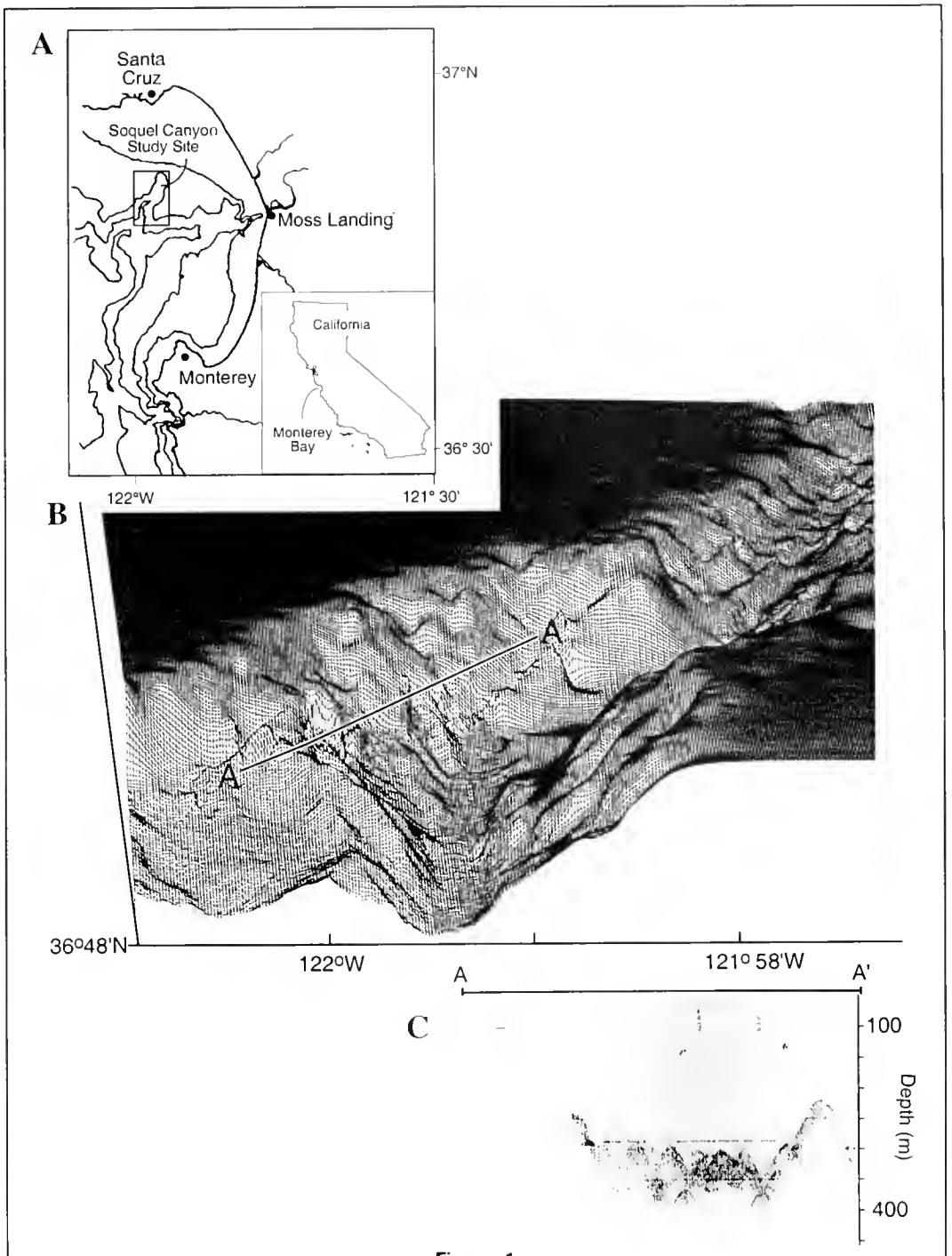

Figure 1

(**A**) Study area in Soquel Canyon, the northernmost tributary to the Monterey Submarine Canyon System. (**B**) A physiographic map of Soquel Canyon, produced from 3.5-kHz echo-sounding data. Transect A–A' is at the location of the seafloor profile (**C**), and displays the hummocky nature of slump deposits on the west wall of the Canyon.

system and differential GPS were used on board the support vessel to record the underwater location of the submersible. All dives were made during daylight to avoid potential bias due to diel activity patterns of some species (Hixon[1]; Yoklavich, pers. obs.)

To quantify fish abundance and habitat use, strip transects of 10-min duration were conducted 1–2 m off the

[1] Hixon, M. 1992. Personal commun. Department of Zoology, Oregon State University, Corvallis, OR 97331-2914.

bottom at 0.4–0.9 knots. Transects were purposely of short duration to maintain constant depth within the rock habitat at each station. Each transect was documented continuously with a high 8-mm video camera and associated lights that were externally mounted on the starboard side of the submersible. The scientific observer verbally annotated each videotape, identifying, counting, and estimating size of all fishes in front of the starboard viewing port. A hand-held dive sonar was aimed at objects (e.g. large fish and boulders) along the transects from inside the submersible to estimate distance from the observer to the object; this procedure helped us to estimate the width of the transect. After each dive, divers transcribed observations on fishes and habitat from video tapes into a computerized database on board the support vessel.

Two parallel lasers were mounted on either side of the external video camera at the fixed distance of 39.5 or 20.0 cm apart, in association with different laser systems each year. The laser spots were projected onto the seafloor habitats. They were visible to the observer, recorded onto the video tape, and were critical in accurately estimating the size of fishes, distance traveled along a transect and area of habitat patches. We made measurements by comparing the size of a fish or habitat feature to the known spacing of the two bright laser spots when the object was perpendicular to the camera and lasers (Tusting and Davis, 1993). We estimated the length of each transect, independent of submersible speed and bottom currents and type, by counting the number of laser-spot intervals as they moved along the substrata in the video transect (much like using a yardstick, end-over-end along the transect).

Microhabitat of each fish within the transect was characterized from the video tapes. Various combinations of substratum type, including mud, pebble, cobble, boulders, and rock ridge (see Greene et al., 1999, for definitions), were categorized according to primary (at least 50% of the area viewed) and secondary (>20% of the area viewed) microhabitat (conforming to Stein et al., 1992). Relief was categorized as flat (0–5°), low (5–30°), and high (>30°). Each surface area of uniform habitat (i.e. a patch) along the quantitative transect was measured to the nearest 0.1 m^2. Species-specific abundance was standardized per area of associated habitat patch. The habitat patch was used as our sample unit.

Data analyses

Similarity of assemblages of nonschooling fishes among the different combinations of substrata was evaluated with cluster analysis on the basis of abundance of each species standardized by area of associated bottom type in each patch. Only species representing ≥1% of the total abundance in each bottom type category and only bottom types representing ≥1% of the total area surveyed were used in this analysis. Only nonschooling (i.e. nonpolarized aggregations or solitary individuals) benthic fishes were included in our analyses because schooling fishes commonly were more abundant in midwater above our field of view and therefore could not be accurately enumerated. Clustering was performed with the average linkage method and with Euclidean distance as a measure of dissimilarity (SYSTAT, 1992). Dissimilarity among clusters ≥50% of the maximum overall distance was considered a major division and used to define distinct habitat guilds of fishes (*sensu* Root, 1967).

Further analyses were focused on nonschooling fish species that dominated the rock habitat guild, as defined by the cluster analysis. These are some of the species important in commercial and recreational catches (Weinberg, 1994; Mason, 1995, 1998). We used the incidence of fishing gear and associated debris, observed on the seafloor during the quantitative fish transects, as a relative index of fishing activity throughout our study area. Statistical differences in abundance (number of fish per 100 m^2 of habitat patch) of those species in the rock habitat guild were analyzed among five sites of varying fishing activity by using analysis of variance (ANOVA) with equal sample variances and otherwise by resampling statistics (Bruce et al., 1995). We used Cochran's test for homogeneity of variance (Winer, 1971).

Differences in size of selected dominant species were tested among two arbitrarily chosen 100-m depth categories (i.e. shallow [75–175 m] and deep [176–275 m]) and the five sites were tested by using two-factor ANOVA (with homogeneity of sample variances) where appropriate.

Overall species diversity was calculated as

$$H' = \sum_{i=1}^{s} [p_i][\ln p_i],$$

where s = number of species; and
p_i = proportional abundance of species i.

Richness (number of species), and evenness ($J' = H'/H'_{MAX}$), as well as species diversity, were evaluated for all habitat types (see Krebs, 1989) and then among sites just within the rock habitat guild in shallow and deep water. Sufficiency in the number of samples necessary to reliably characterize overall diversity for each habitat type was examined by plotting cumulative numbers of species against the sample unit (both for number of patches and area of habitat surveyed). These plots indicated that the number of samples was sufficient to yield a reliable estimate of diversity for comparisons among all habitats and for comparisons among sites in shallow and deep rock habitat (i.e. the number of samples evaluated for diversity always surpassed the number comprising 95% of the species; see data on Figs. 8 and 9).

Results

Geophysical mapping of habitats

A physiographic representation of the relatively high-resolution bathymetric data (Fig. 1B; production assisted by the U.S. Geological Survey, Menlo Park, CA) helped us to visualize canyon morphology, to identify areas of high relief and potential slumping, and to select submersible dive

sites for fish and habitat surveys. The bathymetry indicated that Soquel Canyon is steeper and more rugged than previously interpreted from NOAA's Seabeam data. From the 3.5-kHz bottom profiles we identified large slumps along both walls and in the axis of the canyon. These areas had a hummocky surface with little or no sediment cover and were bounded by sharp relief on either side (e.g. Fig. 1C); these characteristics indicated likely rockfish habitat.

Five study sites were defined (Fig. 2) on the basis of a series of side-scan images identified along the canyon walls. These images were interpreted as rock outcrops representing approximately 35 ha of the total area surveyed in Soquel Canyon. Area of rock outcrop in the five study sites ranged from 1.4 ha of isolated rocks in about 200 m water depth at site 5 to 19.6 ha of extensive rock in 90–350 m water depth at site 3. We considered these estimates to accurately represent the amount of exposed outcroppings within our study area.

From submersible observations we verified our interpretation of these reflectors as well-bedded rock outcrops of various resistance, lithologies, and bottom morphology (e.g., Fig. 3, A and B). Crescent-shaped slump scarps were imaged along the upper walls of the canyon, and extensive rockfalls comprising large (meters in diameter) angular to sub-rounded (having rounded corners but not spherical) blocks and smaller boulders (0.25–1.0 m diameter) were concentrated at the base and in the axis. Well-layered, friable sedimentary rocks were differentially eroded into overhangs (>90°), crevices, and caves. These rocks occurred as isolated outcrops (Fig. 3A), and as more extensive rock exposures (Fig. 3C) interspersed with soft mud along very steep walls from at least 150 to 330 m water depth.

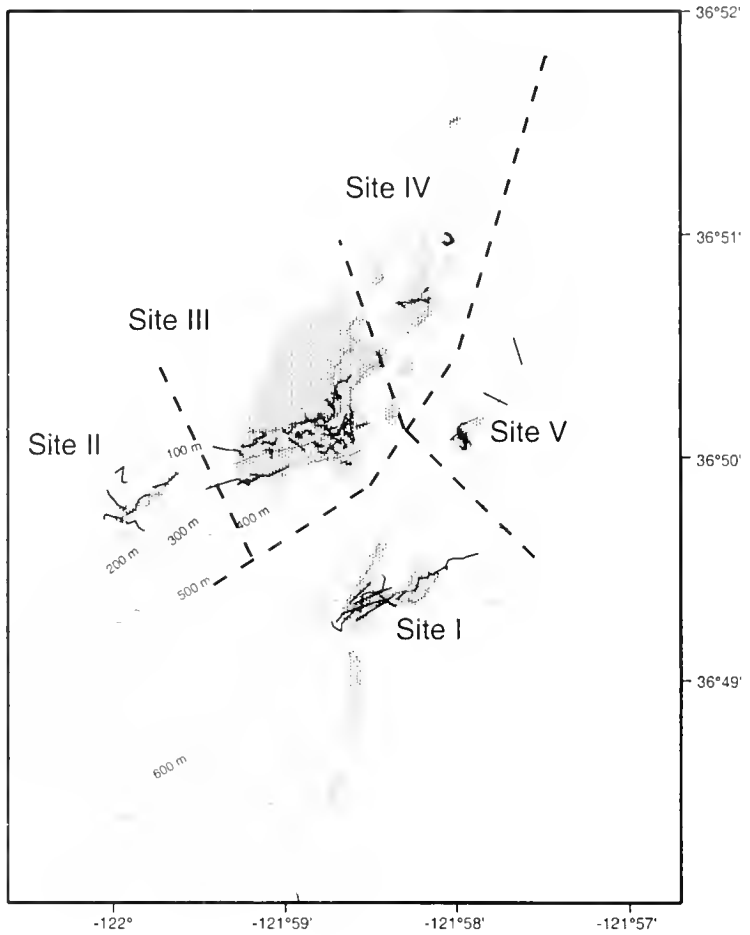

Figure 2

Schematic map constructed from interpretations of side-scan sonographs of rock outcrops (stippled areas) in Soquel Canyon. Submersible track lines during quantitative transects are mapped (lines), and the five main study sites are labeled.

Fish and habitat associations

Thirty-three submersible dives were made at five sites to assess rockfish assemblages and habitat associations in Soquel Canyon. We counted 6208 nonschooling fishes, representing at least 52 species (see Table 1 for both scientific and common names), from 83 10-min strip transects that covered an estimated 33,754 m^2. Rockfishes represented 77% of the total number of individuals, and included a minimum of 24 species. The 20 most abundant taxa (90% of total abundance) included 4540 individual rockfishes representing at least 12 species. Nonrockfish species were represented primarily by six species, which comprised 17.2% of the total abundance: *Microstomus pacificus*, *Ophiodon elongatus*, *Sebastolobus alascanus*, *Eptatretus stouti*, *Merluccius productus*, and an unidentified species (or possibly a complex of species) in the family Agonidae (most likely *Xeneretmus* spp.).

Major rockfish habitat types in Soquel Canyon included vertical cliffs with joints, fractures, and overhangs, small and large ledges, talus slopes, cobble, and boulder fields of exposed sandstone and mudstone interspersed with soft mud. Most rockfishes of all sizes were associated with some structure, including invertebrates such as crinoids, sea anemones and sponges, debris, and simple shallow depressions in the mud.

Cluster analysis (Fig. 4), which grouped standardized abundance of each fish species (number per 100 m^2) by bottom type, resulted in six habitat guilds. Most distinct were guild I, having small species found on uniformly mud bottom of flat or low relief, dominated by *S. saxicola* (42%) and to a lesser degree by *M. pacificus*, Agonidae, and *S. alascanus*, and guild VI, a rock-boulder habitat of low-to-high relief largely at 75–175 m depth, dominated by *S. wilsoni* (42%), and with less representation by *S. paucispinis*, *S. pinniger*, and *S. chlorostictus*.

The remaining four habitat guilds (guilds II, III, IV, and V; Fig. 4) were grouped two each into two clusters at Euclidian distances 0.058 and 0.063. Guilds II and III were characterized by combinations of mud and large-grain cobbles and pebbles that were of mostly flat or low relief (72% occurrence). These assemblages were relatively diverse,

evenly distributed (see results of diversity analysis that follows), and included mostly small species (i.e. *S. semicinctus*, *S. wilsoni*, and *S. elongatus*) and small members of a large species (*S. chlorostictus*). Most (88–95%) of habitat guild II occurred at shallow depth (75–175 m); about one-half of guild III occurred in water <175 m. Guilds IV and V represented habitats of large structure, high relief (78% occurrence), and both shallow and deep (>175 m) water. Although they both had similar top-ranked species, guild IV (boulder-mud) was much less diverse and was dominated by a single species (*S. helvomaculatus*). Economically valuable rockfish species made up most (52–77%) of guild V (rock habitat). The rock habitat guild, in particular, contained high numbers of large species up to 1 m in total length, such as *S. levis* (12% of total fish abundance in this habitat) and *S. ruberrimus* (5% total abundance). These fishes were closely associated with ledges, caves, crevices, and overhangs.

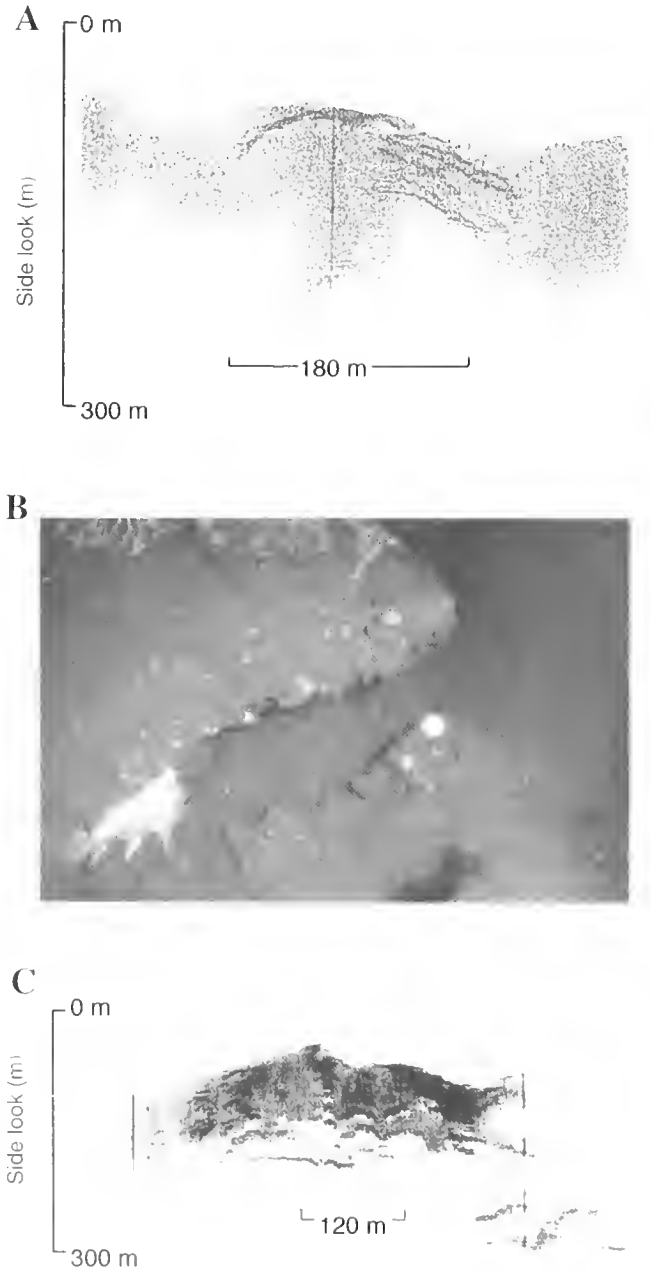

Figure 3

(**A**) Side-scan sonograph of isolated rock outcrop on steep wall of Soquel Canyon. Strong acoustic reflectors (dark areas) are from exposed bedding faces, white areas are shadows behind faces, and gray areas are nonreflective mud. (**B**) These eroded mudstone beds comprise habitat for benthic fishes, such as this adult greenspotted rockfish (*Sebastes chlorostictus*). (**C**) Side-scan sonograph of steep, well-bedded rock walls on southeast side of canyon from 150 to 330 m.

Fishes and habitat by site

In general, our study area in Soquel Canyon comprised five sites of exposed rock ridge, boulder, cobble, pebble, and mud bottom types (Fig. 5). From the mosaic of side scan sonographs, total area of outcrops ranged from 1.4 ha (site 5) to 19.6 ha (site 3), and the sampling effort (i.e. number of dives, transects) in these sites tended to vary accordingly. We quantitatively surveyed fish and habitat in 1025 sample patches (average area of a habitat patch was 34.0 m^2; SE=1.9 m^2), representing from 1285 to 13,626 m^2 per site. From analysis of 83 transects, 74–94% of the bottom types at these sites were characterized by mud, rock ridge, and combinations of both. Not surprisingly, nearly 50% of our survey was in areas of high relief, and almost all (97%) rock ridge was high relief. Mud habitats were largely (78%) of flat and low relief.

Site 1, located on the east canyon wall at a water depth from 98 to 305 m, was characterized as rock outcrop with moderate vertical fracturing, stepped rock ridges of 1–6 m height (habitat guild V), mud-cobble and mud-boulder fields (habitat guilds II and III), and mud terraces (habitat guild I). Directly opposite on the west wall, site 2 included a series of rock ledges, mud terraces, and vertical walls extending from 263 to 148 m depth; this site is heavily fished (see later criteria). Site 3 comprised small ledges interspersed with mud, boulder, cobble, and pebble slopes of low relief at 94–150 m, high-relief rock ledges with fractures cutting the bedding planes and massive vertical mudstone walls (150–250 m), and scattered boulder-mud fields at the base of the wall. Sites 4 and 5 were largely isolated outcrops of rock ridges surrounded by fields of mud at 152–226 m depth.

Rockfishes of various species ranked first in abundance at all of the five study sites (Table 1); over all habitat types and depth, at least three of the top five species were rockfishes (4–5 of 5 at most sites). Average abundance was highest at site 5 (42.4 fish per 100 m^2), 96% of which comprised economically valuable species (e.g. in rank order of abundance, *S. pau-*

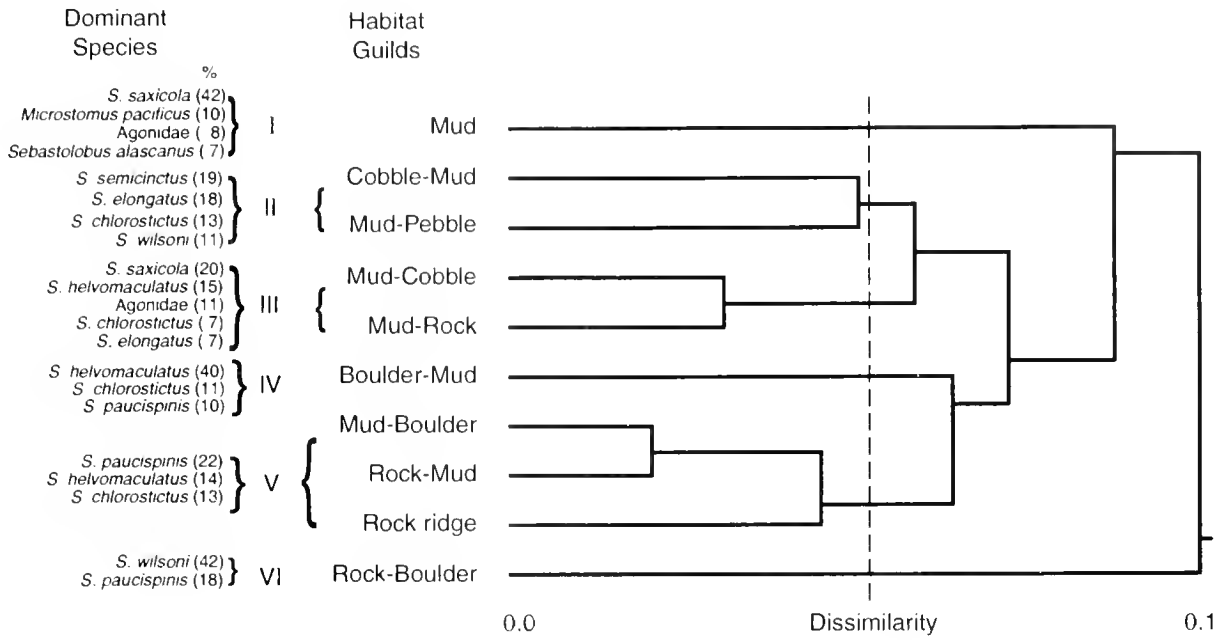

Figure 4

Cluster dendogram that groups standardized abundance (number per 100 m^2) of nonschooling benthic fish species in Soquel Canyon, based on associated type of bottom substrata. Dominant species (percent relative abundance in parentheses) of the six main habitat guilds are indicated. See Figure 8 for number of habitat patches sampled in each habitat.

cispinis, *O. elongatus*, *S. levis*, *S. rosenblatti*, *S. chlorostictus*, *S. ruberrimus*). These sedentary fishes were primarily sheltered under ledges, in crevices, and among large sea anemones (*Metridium giganteum*) on this isolated rock outcrop.

One objective of our study was to compare species composition, abundance, size, and diversity of fishes among sites receiving varying amounts of fishing pressure within the canyon. Seventy-five lines (polypropylene and monofilament; n=67) and cables (n=8) were observed on 83 transects during 13.5 h; no mesh nets, pots, or trawl tracks were found. Eighty-five percent of these sightings occurred at site 2, with 26.7 observations of gear made per hour of survey (or 0.9 sightings per 100 m^2). Observations of 1.5 and 0.7 per hour were made at sites 3 and 1, respectively. No evidence of fishing gear or activity was found at sites 4 and 5. These observations are supported by California Department of Fish and Game (CDFG) records of site-specific activities of commercial passenger fishing vessels (Reilly[2]).

From the cluster analysis, economically important rockfishes are largely represented by the rock habitat guild (V). After limiting statistical comparisons among sites to those species occurring on mud-boulder, rock-mud, and rock ridge bottom types (i.e. habitat guild V), we found abundance of each of the top eight species in this guild (Fig. 6) varied significantly among sites (ANOVA or randomization test; P<0.01). Large solitary and sedentary species, such as *S. chlorostictus*, *S. ruberrimus*, *and S. levis*, were most abundant at sites 1, 3, 4, and 5, which received minimal to no fishing pressure. Abundances of these three species were statistically less at site 2, the area of highest fishing activity.

Sebastes paucispinis, one of the most important species in commercial and recreational fisheries of Monterey Bay, occurred in high numbers at all sites but was significantly more abundant at site 5 (Fig. 6; randomization test, P<0.01). Although we limited our study to nonschooling individuals, *S. paucispinis* can be semipelagic and we sometimes encountered this species in loose groups of 50 or more fishes above rock outcrops. These groups were not included in our analysis but indicate that this species is more active and broad ranging than the solitary benthic rockfishes.

Interestingly, the most abundant species at the site most heavily fished (site 2) was *S. helvomaculatus*, a relatively small species and historically of minor interest to either commercial or recreational fisheries. This species also was significantly more abundant at this site than at any of the other four sites (Fig. 6; resampling test, P<0.01). *Sebastes crameri* and *S. rufus*, relatively important rockfish species in the commercial trawl fishery but rarely taken by hook and line, were abundant only at site 2 (ranking second and fifth, respectively). *Sebastes elongatus*, a relatively small species that was most abundant in the cobble-mud guild, was moderately abundant in the rock guild but only at sites 1–3.

Size of most of these species differed by site and depth category (shallow=75–174 m; deep=175–275 m; Fig. 7). Significantly smaller individuals of *S. chlorostictus*, *S. helvomaculatus*, *S. elongatus*, and *S. paucispinis* occurred

[2] Reilly, P. 1997. Personal commun. CDFG, 20 Lower Ragsdale Dr., Monterey, CA 93940.

Table 1

Abundance (mean number/100 m^2), total number and percentage, and mean total length of nonschooling fishes counted during 83 transects at five sites in Soquel Canyon. SE = standard error. Species names follow Robins et al. (1991).

		Site 1		Site 2		Site 3		Site 4		Site 5		Total		Length (cm)	
Species	Common name	Mean	SE	Mean	SE	Mean	SE	Mean	SE	Mean	SE	No.	%	Mean	SE
Sebastes saxicola[1]	stripetail rockfish	3.6	0.6	2.7	0.7	3.7	0.7	0.2	0.2	0.3	0.2	1005	16.2	16.4	0.2
Sebastes paucispinis	bocaccio	2.5	0.8	2.5	0.6	0.7	0.3	1.9	1.2	18.2	5.6	712	11.5	55.3	0.5
Sebastes helvomaculatus	rosethorn rockfish	2.9	0.5	5.5	1.0	1.3	0.3	<0.1	<0.1	0.3	0.2	542	8.7	22.1	0.3
Sebastes chlorostictus	greenspotted rockfish	2.0	0.4	0.6	0.2	5.6	0.9	4.0	1.2	2.3	0.6	426	6.9	32.5	0.6
Sebastes spp	unidentified rockfishes	0.7	0.2	3.6	0.6	1.4	0.6	1.0	0.6	0.3	0.1	349	5.6	21.1	0.8
Agonidae	poachers	1.5	0.4	1.2	0.2	2.4	0.4	0.4	0.2	0.1	0.1	324	5.2	16.8	0.3
Sebastes elongatus	greenstriped rockfish	0.9	0.3	1.9	0.5	1.4	0.2	<0.1	<0.1	<0.1	<0.1	289	4.7	25.7	0.5
Sebastes crameri	darkblotched rockfish	—	—	4.7	0.8	<0.1	<0.1	0.4	0.4	—	—	259	4.2	21.3	0.3
Sebastes semicinctus	halfbanded rockfish	1.1	0.5	—	—	0.8	0.2	—	—	—	—	230	3.7	12.7	0.2
Sebastes levis	cowcod	0.6	0.4	0.1	0.1	0.2	0.1	0.4	0.4	5.1	1.1	202	3.3	58.6	1.1
Sebastes wilsoni	pygmy rockfish	1.9	1.4	0.2	0.1	0.7	0.3	—	—	—	—	201	3.2	16.2	0.3
Microstomus pacificus	Dover sole	0.7	0.3	0.1	<0.1	0.6	0.2	0.1	<0.1	0.3	0.2	199	3.2	24.5	0.7
Ophiodon elongatus	lingcod	<0.1	<0.1	0.3	0.1	1.4	0.4	0.3	0.2	6.4	1.8	171	2.8	57.8	1.5
Sebastolobus alascanus	shortspine thornyhead	0.6	0.3	<0.1	<0.1	1.3	0.3	—	—	<0.1	<0.1	171	2.8	19.8	0.6
Eptatretus stouti	Pacific hagfish	0.5	0.2	<0.1	<0.1	0.8	0.3	0.2	0.2	0.4	0.2	115	1.9	23.6	0.7
Sebastes ruberrimus	yelloweye rockfish	0.3	0.1	0.1	0.1	0.3	0.1	0.5	0.5	1.7	0.6	104	1.7	56.1	1.9
Merluccius productus	Pacific hake	0.2	0.1	0.1	0.1	0.1	<0.1	1.7	1.0	0.1	0.1	83	1.3	18.4	0.6
Sebastomus complex[2]	unidentified rockfishes	<0.1	<0.1	0.4	0.1	0.2	0.1	0.1	0.1	—	—	83	1.3	24.8	1.5
Sebastes pinniger	canary rockfish	—	—	—	—	0.5	0.2	—	—	—	—	73	1.2	37.5	0.5
Sebastes rosenblatti	greenblotched rockfish	0.1	<0.1	0.3	0.1	0.1	<0.1	0.9	0.3	5.0	3.3	65	1.0	42.7	1.4
Pisces	unidentified fish	0.2	0.1	0.3	0.1	0.3	0.2	—	—	<0.1	<0.1	56	0.9	17.6	2.6
Pleuronectiformes	unidentified flatfishes	0.3	0.2	0.3	0.1	0.1	<0.1	—	—	—	—	53	0.9	22.1	1.3
Sebastes rufus	bank rockfish	—	—	0.7	0.2	—	—	—	—	—	—	48	0.8	28.6	1.7
Sebastes entomelas	widow rockfish	—	—	0.1	0.1	—	—	—	—	1.4	0.6	45	0.7	45	1.8
Sebastes flavidus	yellowtail rockfish	—	—	—	—	0.4	0.1	—	—	—	—	36	0.6	40.3	1.2
Zaniolepis frenata	shortspine combfish	0.1	<0.1	0.1	<0.1	0.1	<0.1	—	—	—	—	31	0.5	21.6	0.7
Zalembius rosaceus	pink seaperch	0.1	<0.1	—	—	0.1	<0.1	—	—	—	—	30	0.5	15.9	0.6
Hydrolagus colliei	spotted ratfish	0.1	0.1	0.1	0.1	0.3	0.3	0.1	0.1	—	—	29	0.5	32.9	1.8
Sebastes chlorostictus and *S. rosenblatti*	greenspotted and greenblotched rockfish	<0.1	<0.1	—	—	0.2	0.1	—	—	0.2	0.1	29	0.5	41.3	1.1
Sebastes babcocki	redbanded rockfish	—	—	0.1	<0.1	<0.1	<0.1	—	—	0.3	0.1	24	0.4	39.3	3.5
Zoarcidae	unidentified eelpouts	0.1	0.1	0.1	0.1	<0.1	<0.1	—	—	<0.1	<0.1	24	0.4	24.4	1.6
Sebastes diploproa	splitnose rockfish	<0.1	<0.1	0.1	0.1	<0.1	<0.1	—	—	<0.1	<0.1	20	0.3	25.5	4.1
Lycodes cortezianus	bigfin eelpout	0.1	0.1	<0.1	<0.1	<0.1	<0.1	0.1	0.1	<0.1	<0.1	18	0.3	29.7	1.9
Zaniolepis spp	unidentified combfish	—	—	0.1	<0.1	<0.1	<0.1	—	—	—	—	17	0.3	22	2

continued

Table 1 (continued)

Species	Common name	Site 1		Site 2		Site 3		Site 4		Site 5		Total		Length (cm)	
		Mean	SE	Mean	SE	Mean	SE	Mean	SE	Mean	SE	No.	%	Mean	SE
Errex zachirus	rex sole	<0.1	<0.1	—	—	<0.1	<0.1	<0.1	<0.1	—	—	15	0.2	21	0.8
Pleuronectes vetulus	English sole	—	—	<0.1	<0.1	0.1	<0.1	<0.1	<0.1	—	—	12	0.2	26.3	1.7
Icelinus filamentosus	threadfin sculpin	0.1	0.1	<0.1	<0.1	<0.1	<0.1	—	—	—	—	11	0.2	14.3	1.9
Eopsetta exilis	slender sole	—	—	0.1	<0.1	—	—	0.1	0.1	—	—	11	0.2	20	4.5
Sebastes miniatus	vermilion rockfish	0.1	0.1	—	—	—	—	—	—	0.1	<0.1	11	0.2	47	3.4
Sebastes ensifer	swordspine rockfish	—	—	0.2	0.1	—	—	—	—	—	—	9	0.1	22.9	2
Cottidae[1]	unidentified sculpins	—	—	0.1	<0.1	<0.1	<0.1	—	—	—	—	9	0.1	13.3	3.3
Chilara taylori	spotted cusk-eel	<0.1	<0.1	—	—	<0.1	<0.1	—	—	—	—	8	0.1	20	
Plectobranchus evides	bluebarred prickleback	<0.1	<0.1	—	—	0.2	0.2	—	—	—	—	7	0.1	10.8	1.4
Synodus lucioceps	California lizardfish	—	—	—	—	<0.1	<0.1	0.2	0.2	—	—	6	0.1	32.5	5.9
Anoplopoma fimbria	sablefish	<0.1	<0.1	—	—	—	—	—	—	<0.1	<0.1	5	0.1	32	3.6
Bathymasteridae	unidentified ronquil	<0.1	<0.1	<0.1	<0.1	<0.1	<0.1	—	—	—	—	5	0.1	11	2.1
Coryphopterus nicholsi	blackeye goby	—	—	—	—	<0.1	<0.1	—	—	—	—	5	0.1	9	0.9
Raja rhina	longnose skate	<0.1	<0.1	—	—	<0.1	<0.1	—	—	<0.1	<0.1	5	0.1	42	7.5
Porichthys notatus	plainfin midshipman	<0.1	<0.1	—	—	—	—	—	—	—	—	4	0.1		
Sebastes goodei	chilipepper	—	—	—	—	<0.1	<0.1	—	—	—	—	4	0.1	28.3	6.7
Zaniolepis latipinnis	longspine combfish	—	—	<0.1	<0.1	<0.1	<0.1	—	—	—	—	4	0.1	20	
Sebastes ovalis	speckled rockfish	—	—	—	—	<0.1	<0.1	—	—	—	—	3	<0.1	40	
Argentina sialis	Pacific argentine	—	—	<0.1	<0.1	—	—	—	—	—	—	2	<0.1	25	
Raja spp	unidentified skates	<0.1	<0.1	—	—	—	—	—	—	<0.1	<0.1	2	<0.1	30	10
Sebastes rubrivinctus	flag rockfish	—	—	<0.1	<0.1	—	—	—	—	—	—	2	<0.1	10	
Eopsetta jordani	petrale sole	—	—	0.1	0.1	—	—	—	—	—	—	1	<0.1	60	
Hexanchus griseus	sixgill shark	<0.1	<0.1	—	—	—	—	—	—	—	—	1	<0.1	200	
Sebastes hopkinsi	squarespot rockfish	—	—	—	—	<0.1	<0.1	—	—	—	—	1	<0.1	15	
Sebastes jordani	shortbelly rockfish	—	—	<0.1	<0.1	—	—	—	—	—	—	1	<0.1		
Torpedo californica	Pacific electric ray	—	—	—	—	—	—	—	—	<0.1	<0.1	1	<0.1	45	
Sum		21.3		26.8		25.7		12.8		42.4		6208			
Number of taxa		31		35		38		20		22		52			
Number rockfish species		12		17		18		9		12		24			

[1] Observations of this small species could include *Sebastes zacentrus*, a species with similar color patterns and body shape

[2] Rockfishes within the *Sebastomus* complex comprise seven species off central CA, several of which are difficult to identify without close examination

[3] Likely *Icelinus* spp

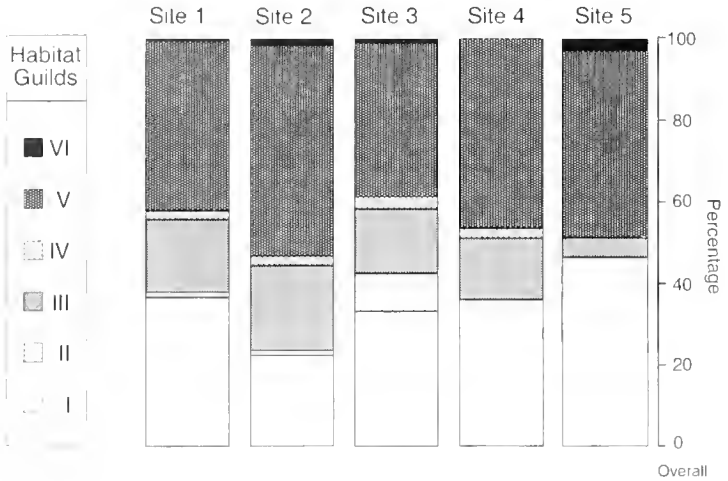

	Site 1	Site 2	Site 3	Site 4	Site 5	Overall
Number Dives	5	6	13	3	6	33
Number Transects	13	14	39	4	13	83
Number Habitat Patches	207	185	515	52	66	1,025
Depth Range (m)	98-305	148-263	94-296	153-210	152-226	94-305
Time Surveyed (h)	2 7	2 4	6.0	0.6	1 7	13 4
Area Surveyed (m^2)	7,638	7,256	13,626	1,285	3,949	33,754
Total Area (ha)	6 9	1 5	19 6	5.8	1 4	35 2

Figure 5

Percent cover of bottom types in habitat guilds (see Fig. 4 for identifications) at five study sites in Soquel Canyon. Number of dives, transects, and habitat patches, depth range, time and area covered, and total area (as estimated from mosaic of side scan sonographs in geographic information system) are listed for each site.

at shallow depths (ANOVA, $P<0.01$). Within depth category, site 2 generally had smaller fishes, and site 5 consistently had the largest fishes. *S. levis* and *S. ruberrimus* were abundant only in the deep category, and were significantly bigger at site 5.

Patterns of species richness (S), diversity (H′), and evenness (J′) were evident among the species assemblages associated with different bottom types (Fig. 8). The two most distinct habitat guilds in the cluster analysis (i.e. mud [guild I] and rock-boulder [guild VI]) ranked among the lowest in both H′ and J′, with a single species clearly dominating each guild. Diversity also was low in the boulder-mud guild (IV), although with somewhat more even proportions among species. The most diverse and evenly distributed assemblages were those in the remaining three guilds (II, III, and V).

Considering just the rock habitat guild (V), diversity measures were examined among sites having different fishing activity in both shallow and deep depth categories (Fig. 9). No patterns in diversity among the three sites in the shallow rock habitat guild were evident (Fig. 9A), although differences in relative abundance of each species were clear. In deep water, a shift in relative abundance occurred from site 2 to site 5, with large species playing a larger role at the less fished sites. The deep rock habitat guild at the iso-

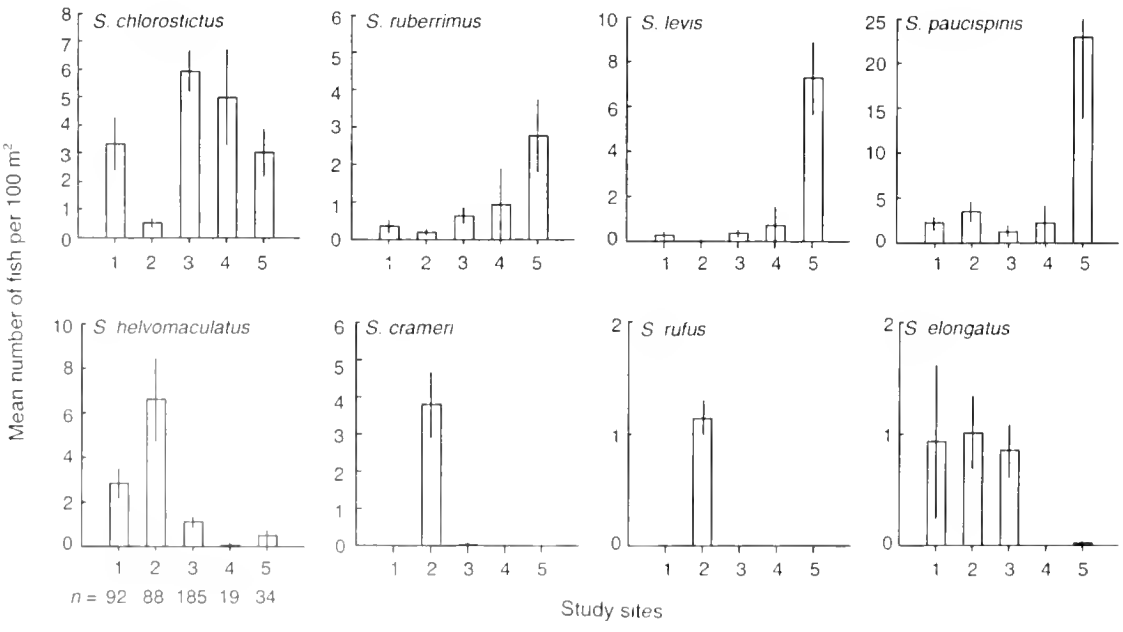

Figure 6

Index of abundance (mean number/100 m^2) of dominant species of nonschooling rockfishes in the rock habitat guild at five sites in Soquel Canyon. Vertical bars are 1 standard error; n = number of habitat patches at each site.

lated site 5 had the lowest diversity among all sites and depths, as measured by H′ and J′.

Discussion

Habitats

Several studies have described distinct fish-habitat associations for various species of benthic rockfishes during different stages of development (Carlson and Straty, 1981; Pearcy et al., 1989; Carr, 1991; Stein et al., 1992; O'Connell and Carlile, 1993). Although species composition may vary latitudinally, there is remarkable concordance between some of the habitat guilds identified in Soquel Canyon and the results of a habitat-based assessment of fishes using similar techniques and habitat characterizations on Heceta Bank off central Oregon (Stein et al., 1992). Mud, rock-boulder, and boulder habitats were most distinct in both studies and included the same dominant species; *M. pacificus*, *S. alascanus*, and Agonidae were abundant on mud, whereas *S. wilsoni* was the single most abundant species in the rock-boulder habitat of Soquel Canyon and the boulder habitat on Heceta Bank (Table 2). Fish assemblages in low relief, mixed habitats of mud, cobble, and pebble grouped together, and although dominant species were largely different (i.e. mud-cobble habitat dominated by *S. zacentrus* and *S. wilsoni* in Oregon and by *S. saxicola*, *S. helvomaculatus* and Agonidae in Soquel Canyon), the assemblages were made up of relatively small species in both studies. Several species common to both studies were characterized similarly in terms of habitats (e.g. associations of *S. pinniger* with rock-boulder combinations and *S. elongatus* with mud-cobble combinations).

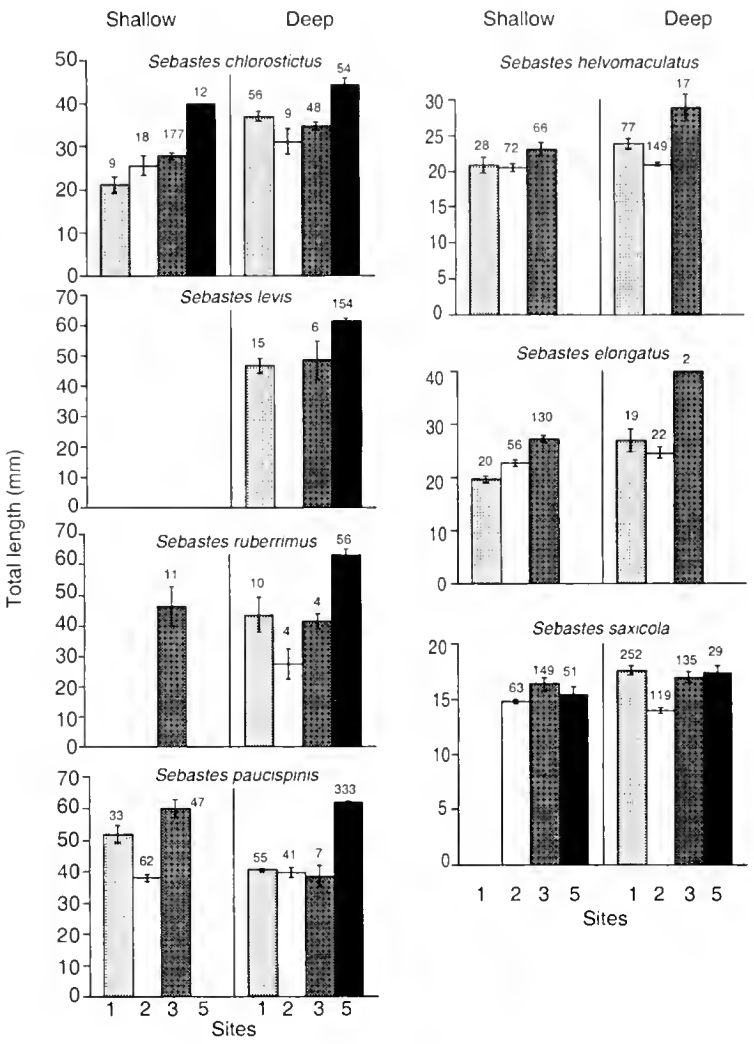

Figure 7

Mean size (vertical bars are 1 standard error) for dominant species in shallow and deep depth categories over all bottom types at study sites 1 to 3 and 5. Small numbers above bars are sample sizes.

Several of the species-habitat associations identified in Soquel Canyon also agreed with those described even farther north. From submersible observations off British Columbia, albeit made at shallower depths (21–150 m) and with less comprehensive habitat classifications than in Soquel Canyon or Heceta Bank, Murie et al. (1994) and Richards (1986) reported adult *S. ruberrimus* to be found exclusively on complex rock habitats, whereas *S. elongatus* was almost exclusively associated with sand-mud and mud-cobble substrata of low relief. In the eastern Gulf of Alaska, adult *S. ruberrimus* were found to be strongly associated with boulder fields, broken rock, overhangs, and crevices (O'Connell and Carlile, 1993), features similar to those of habitats described for this species in Soquel Canyon.

The generalities in habitat-specific associations, such as those described above for several rockfish species occurring along the entire west coast of the United States from central California to Alaska, can be valuable in predicting community structure and its response to perturbation. Identifying functional groups or habitat guilds that persist coastwide will be especially useful when applying these small-scale relationships between species and habitats to broader-scale resource surveys, potentially improving assessments of groundfish populations. Additionally, establishing these groups is critical to incorporating the concept of essential groundfish habitats, and negative impacts to them into the management of fisheries in relatively deep water, as required by the Sustainable Fisheries Act of 1996.

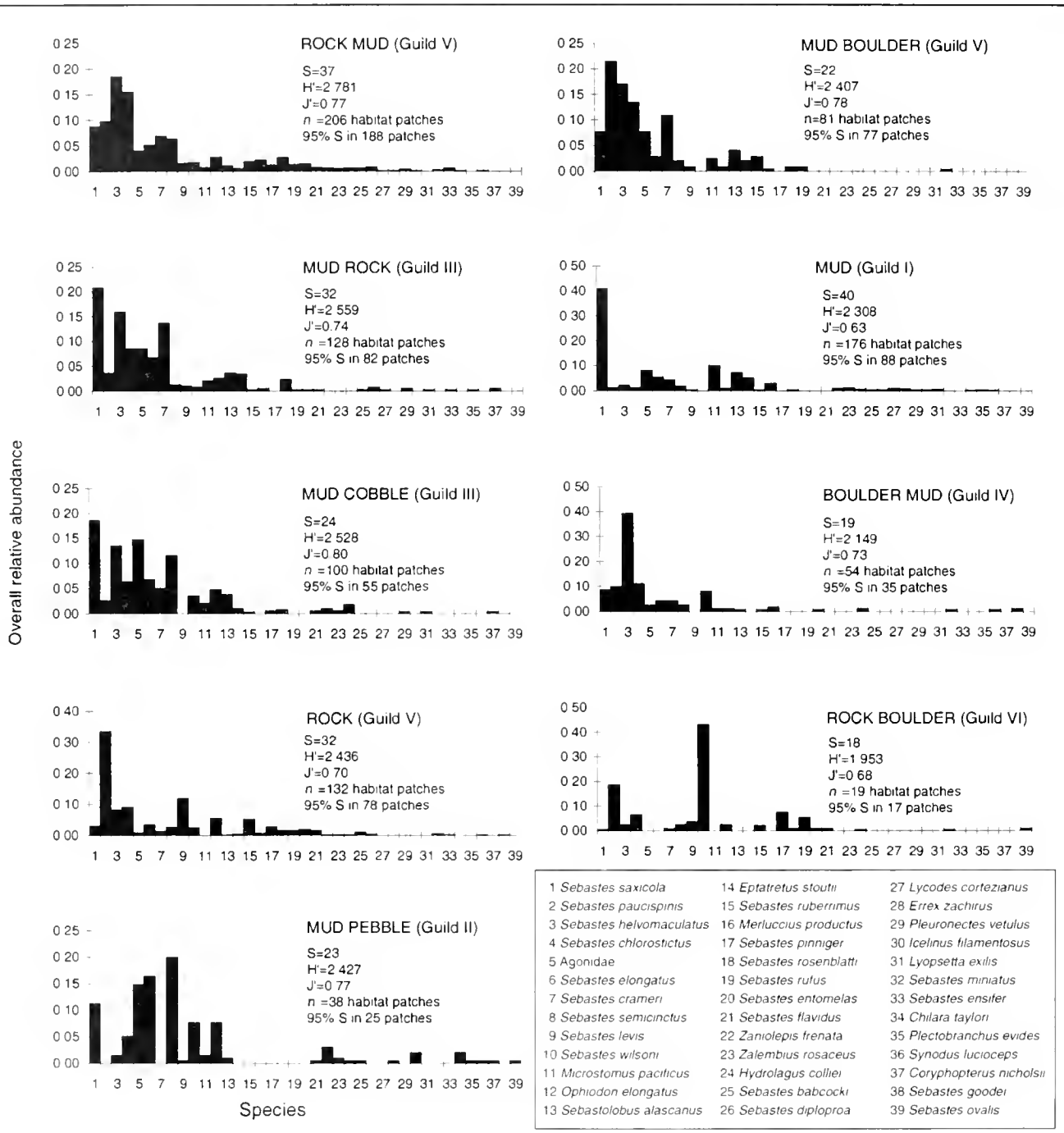

Figure 8

Overall relative abundance of each species associated with each type of habitat. Species richness (S), diversity (H'), and evenness (J') were calculated for each habitat guild (see Fig. 4 for identifications). *n* = the number of habitat patches sampled in each habitat. The number of patch samples required to detect 95% of the species is indicated.

Refugia

The high abundances of adult rockfishes associated with rock habitats along the sides of Soquel Submarine Canyon indicate that this canyon may in part serve as a natural harvest refuge, especially for those species of economic value. A comparison of average number of fish per hectare of habitat for the most abundant taxa in Soquel Canyon with the results of the habitat-based study on Heceta Bank (Stein et al., 1992), a longtime area of fishing activ-

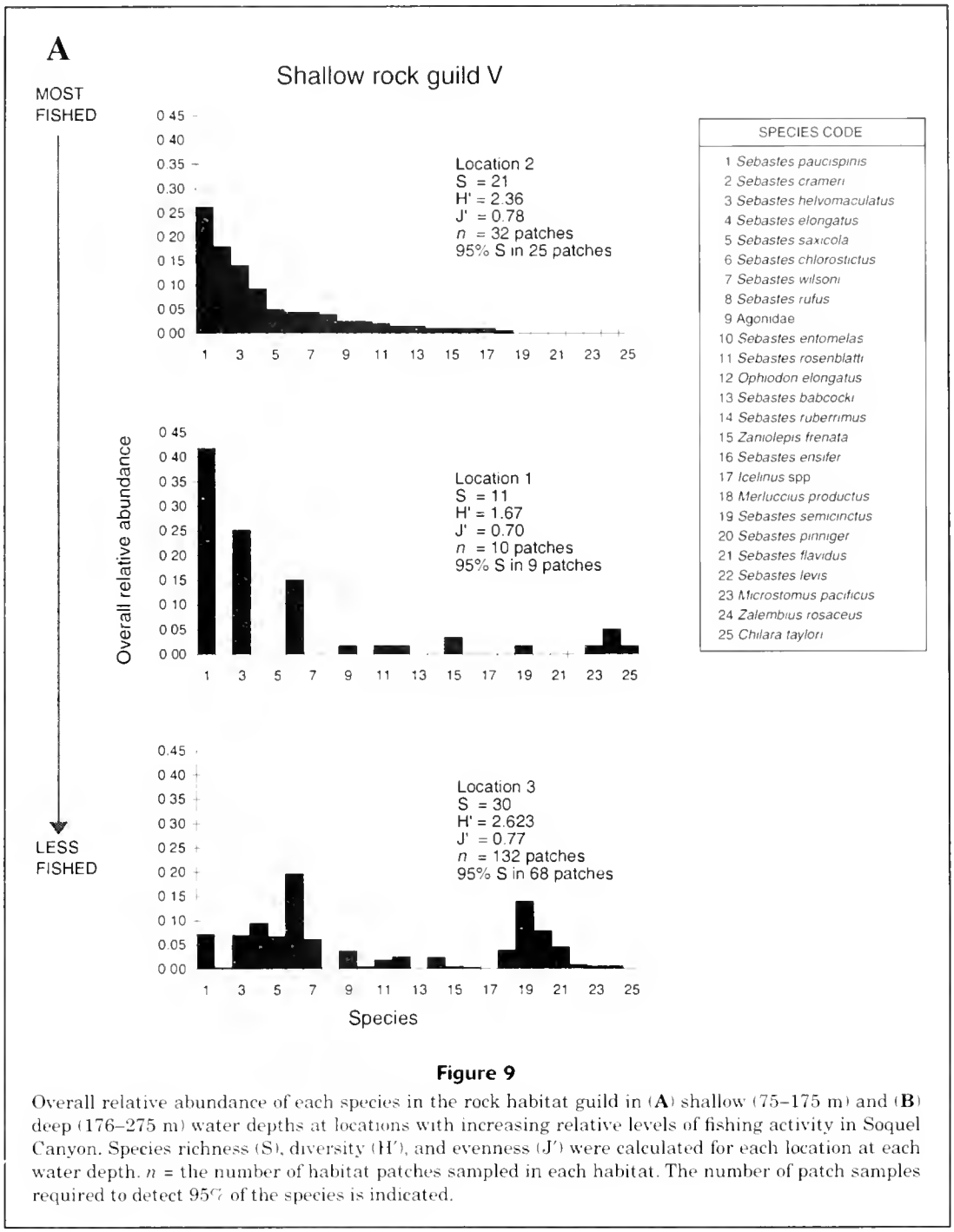

Figure 9

Overall relative abundance of each species in the rock habitat guild in (**A**) shallow (75–175 m) and (**B**) deep (176–275 m) water depths at locations with increasing relative levels of fishing activity in Soquel Canyon. Species richness (S), diversity (H'), and evenness (J') were calculated for each location at each water depth. *n* = the number of habitat patches sampled in each habitat. The number of patch samples required to detect 95% of the species is indicated.

ities, supports this conclusion. For example, our study site had several abundant, economically important benthic species (e.g. *O. elongatus*, *S. chlorostictus*, *S. levis*, *S. rosenblatti*, *S. ruberrimus*, *S. paucispinis*, *S. crameri*, and *S. rufus*; Table 2). These species generally dominated the rock, boulder, mud combination habitats in Soquel Canyon. Comparable habitats in Oregon were dominated by less valuable, small benthic rockfish species (e.g. *S. zacentrus*, *S. wilsoni* and *S. helvomaculatus*). The benthic species of highest abundance in the Oregon study were all in mud-cobble-boulder combination habitats, and most of these were not economically important. Large species of benthic rockfishes and *O. elongatus* did not occur in high numbers on Heceta Bank, Oregon. Although neither study estimated the abundance of active, semipelagic rockfishes, which generally aggregated above the submersible, commercially valuable species such as *S. flavidus* and *S. entomelas* occurred occasionally in high numbers in Soquel Canyon and more commonly over Heceta Bank.

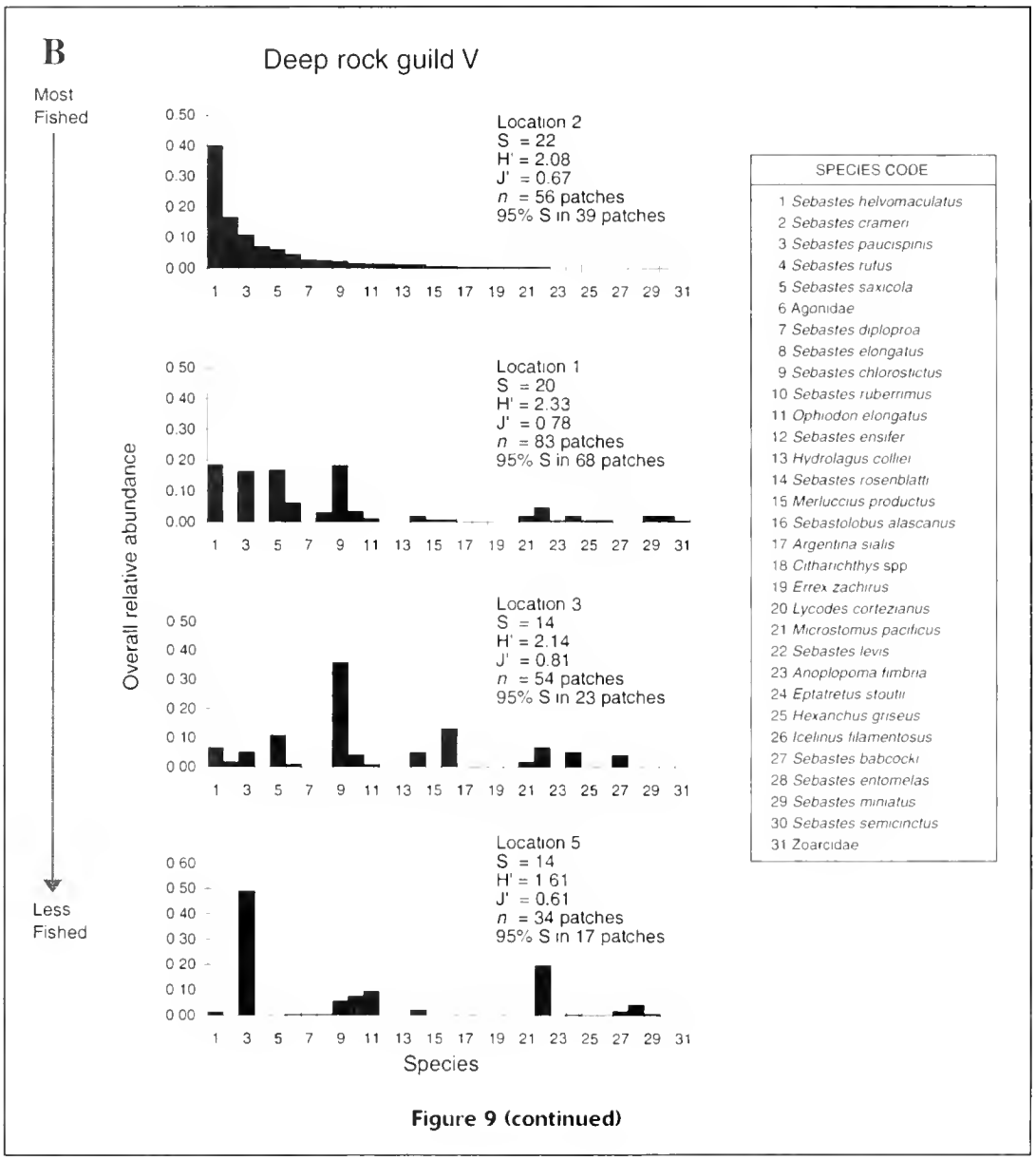

Figure 9 (continued)

The high abundances of large species of benthic rockfishes associated with complex habitats of rock, boulder, and mud combinations at several sites in Soquel Canyon are unique among other habitat-based groundfish assessments, lending further credibility to its designation as a natural harvest refuge. Other studies have reported relatively high numbers of various species of rockfishes associated with rock substrata (Richards, 1986; Stein et al., 1992; O'Connell and Carlile, 1993; Murie et al., 1994), but none have estimated abundances as high as those in Soquel Canyon. This is especially true when considering the extreme abundances of large fishes at site 5, an isolated outcrop on a steep section of the canyon wall surrounded by extensive fields of mud. For example, highest mean abundances of *S. ruberrimus* (number fish/100 m^2) on complex rock substrata were estimated to be about 0.3 off central Oregon (Stein et al., 1992), 0.9 in the Gulf of Alaska (O'Connell and Carlile, 1993), 1.4 off British Columbia (Richards, 1986), and 2.8 at site 5 in Soquel Canyon. Other economically valuable species (e.g. *S. paucispinis* and *O. elongatus*) had even higher abundances at some of the relatively unfished sites in the canyon (Table 1 and Fig. 6), but their abundances were not estimated in the other studies. Mean abundances of *S. elongatus*, a smaller species that is less frequently caught by anglers (Richards, 1986; Karpov et al., 1995), were similar off British Columbia, Oregon and in Soquel Canyon (about 1.5, 0.8, and 1.0 fish/100 m^2 of rock habitat, respectively).

The abundance of *Sebastes helvomaculatus*, another small species that is of minor value to regional fisheries, might be considered an indirect indicator of fishing activity. This benthic species was strongly associated with the same

Table 2

Average number of fish per hectare of habitat of most abundant taxa in Soquel Canyon study. Bold numbers are most common taxa in each habitat category. Number in brackets is abundance estimated in similar habitat off Oregon (Stein et al., 1992). Shading indicates economically valuable species that commonly occurred in relatively high abundance in Soquel Canyon but not off Oregon.

	Guild I	Guild II		Guild III		Guild IV	Guild V	Guild VI		
Species[1]	Mud	Cobble-mud	Mud-pebble	Mud-cobble	Mud-rock	Boulder-mud	Mud-boulder	Rock-mud	Rock-ridge	Rock-boulder
Agonidae	121 [186]	65 [-]	**228**	**251** [464]	110	53 [25]	147 [1122]	50 [-]	18 [18]	—
Eptatretus stouti	77	—	—	17	43	—	39	6	6	—
Merluccius productus	44	—	—	—	7	40	8	27	15	—
Microstomus pacificus	150 [499]	— [-]	24	34 [343]	27	26 [-]	46 [2295]	9 [-]	— [15]	—
Ophiodon elongatus	13 [-]	— [67]	118	81 [-]	33	26 [-]	15 [-]	35 [-]	117 [30]	123
S. chlorostictus and *S. rosenblatti*	5	—	—	—	3	13	15	11	18	20
Sebastes chlorostictus	19	**390**	78	106	110	237	**255**	**193**	**192**	328
Sebastes crameri	64	195	—	85	**176**	92	209	86	29	41
Sebastes elongatus	80 [64]	**325** [266]	**251**	115 [364]	87	92 [25]	54 [204]	64 [-]	74 [79]	—
Sebastes entomelas	1	—	—	—	3	13	—	18	42	41
Sebastes flavidus	— [-]	— [67]	8	8 [29]	3	— [176]	— [-]	9 [-]	34 [191]	41
Sebastes helvomaculatus	32 [26]	65 [933]	24	**229** [343]	**206**	**844** [161]	**325** [408]	**231** [474]	**172** [675]	123
Sebastes levis	5	—	8	—	13	—	15	20	**254**	184
Sebastes paucispinis	19	—	—	42	47	211	**410**	**122**	**714**	**922**
Sebastes pinniger	— [-]	— [-]	—	8 [14]	—	— [-]	— [102]	15 [158]	60 [82]	369
Sebastes rosenblatti	4	—	—	13	30	—	15	33	35	41
Sebastes ruberrimus	2 [-]	— [-]	—	4 [7]	3	13 [25]	54 [-]	23 [-]	111 [27]	102
Sebastes rufus	—	—	—	—	3	—	15	17	32	266
Sebastes saxicola[2]	**611** [60]	130 [133]	173	**314** [2930]	**270**	185 [-]	147 [2754]	109 [-]	62 [277]	20
Sebastes semicinctus	29	**325**	**306**	195	17	53	39	79	55	123
Sebastes wilsoni	1 [21]	260 [999]	118	59 [2129]	10	172 [2772]	— [8926]	21 [-]	51 [1785]	**2131**
Sebastolobus alascanus	108 [239]	— [-]	16	64 [443]	47	13 [-]	77 [2193]	14 [-]	2 [-]	—

[1] See Table 1 for common names

[2] Comparison is made with *Sebastes jacentrus* in Stein et al. (1992) study

complex rock habitats that harbor the larger, more valuable species, such as *S. ruberrimus*. *Sebastes helvomaculatus* ranked third in overall abundance both in Soquel Canyon and on Heceta Bank, Oregon (Stein et al., 1992). This was one of the dominant species in the complex rock habitats on Heceta Bank, as well as on site 2 (the area with the most fishing activity in Soquel Canyon). Interestingly, abundance of *S. helvomaculatus* was significantly lower in this same habitat at those sites having high numbers of larger species and less fishing activity in Soquel Canyon (i.e. sites 3–5; Fig. 6).

It is generally understood, especially in the broad literature on artificial and tropical reefs, that complex rock outcrops of high relief provide shelter and protection to reef fishes (Bohnsack, 1989; Potts and Hulbert, 1994, among others). O'Connell and Carlile (1993) noted that the occurrence of adult *S. ruberrimus* was higher in areas with more voids or refuge spaces, and that "extremely high" densities of this and other species were associated with isolated abrupt pinnacles comprising boulders and overhangs. This type of habitat, surrounded by fields of mud as is the case at Site 5 in Soquel Canyon, likely functions as a natural aggregating device for structure-oriented species such as many of the benthic rockfishes. Moreover, in seeking shelter near these rock outcrops in Soquel Canyon, large rockfishes may be excavating the semiconsolidated mudstone (Yoklavich, pers. obs.), thereby creating more of their own habitat (not unlike the construction of burrows in soft sediments by tilefish [*Lopholatilus chamaeleonticeps*; Able et al. 1982]). The extraordinary abundances estimated for several large species (*S. paucispinis*, *S. levis*, *S. rosenblatti*, *O. elongatus*) in a relatively small area of the canyon provide an insight into considerations of design and location when establishing protected areas as a management tool.

In addition to high abundances of valuable species on those rock outcrops in Soquel Canyon with little or no

evidence of fishing activities, the large sizes of individual fishes further support the concept of a natural harvest refuge in these areas. Although overall mean length of many species was similar and in some cases smaller in Soquel Canyon when compared with those on Heceta Bank (Stein et al., 1992), sizes were substantially larger for the large benthic species in the canyon (i.e. *S. ruberrimus, S. paucispinis, S. babcocki,* and *O. elongatus*).

Aggregations of young rockfishes were absent at any depth during our surveys of Soquel Canyon, leading us to conclude that although the canyon is likely a refuge for adult rockfishes it does not serve as a nursery ground. In contrast, from submersible observations of dense schools of young-of-the-year rockfishes associated with the shallow (100 m) ridge tops of Heceta Bank, Pearcy et al. (1989) suggested that rocky portions of the bank function as a nursery for young rockfishes. Heceta Bank is topographically isolated and located about 55 km off the Oregon coast; it is likely that there are no suitable nursery areas for rockfishes nearby. Soquel Canyon, however, is about 15 km offshore in Monterey Bay, and in close proximity to shallow rock outcrops, cobble fields, and kelp forests that function as nursery areas for many rockfish species (Carr, 1991; Johnson, 1997).

Aside from changes in population numbers and sizes, marine fisheries have been identified as one of the most critical environmental threats to marine biodiversity (Sobel, 1993; Boehlert, 1996), and it has been suggested that harvest refugia may contribute to the preservation of individual species, genotypes, and habitats (Bohnsack and Ault, 1996). Overall, the benthic fish assemblages in the various habitats of Soquel Canyon are relatively diverse; total species richness in the canyon was 52 (20 species comprising 90% of the total abundance) compared with 38 species on Heceta Bank (where only 10 species contributed to 90% of the abundance; Stein et al., 1992). Species diversity, as measured by H′ (Fig. 8), clearly varied among habitats; fish assemblages associated with complex habitats of rock, cobble, and mud maintained the highest diversity, whereas boulder habitats had lower diversity with a few dominant species. There was no clear influence of relative fishing activity on species diversity in the complex rock habitats of the canyon, but there was an influence on the relative abundance and sizes of the species themselves.

We conclude that some heterogeneous rocky habitats of high relief interspersed with soft mud in deep water of Soquel Submarine Canyon support high numbers of large adult rockfishes, in particular those species important to regional fisheries. These fishes are likely protected from excessive harvest because these habitat characteristics make them difficult to locate and target. These areas appear to function as a natural harvest refugium, potentially contributing new recruits to adjacent fished areas. We suspect that other such isolated high-relief rock habitat, as yet undetected or described, exists elsewhere in deep water on the continental shelf and slope of the west coast. The challenge now is to identify and characterize these habitats and associated fish assemblages, and to relate these small scale patterns to larger geographic areas relevant to benthic fishery stocks.

Acknowledgments

This multidisciplinary study required the time and effort of many people. In particular, we acknowledge the assistance of the following people: L. Browne, M. Ledbetter, G. Moreno, P. Reilly, R. Starr, P. Stipa, W. Wakefield, and D. Watters with field logistics and data collection; D. Caswell (Pelagos Corp.) with the side scan sonar survey; M. Boyle, T. Chase, C. Degnan, H. Lucky, and C. Steele (USGS) with geophysical data analyses and mapping; the captains and crews of the RVs *Jolly Roger, Cavalier,* and *Pt. Sur* for providing suitable research platforms; J. Barry and S. Etchemendy (MBARI) for logistical support; and all personnel from Delta Oceanographics, especially R. Slater, D. Slater, and C. Ijames, whose expertise and dedication provided for the safe and efficient use of the research submersible *Delta*. J. Mason, V. O'Connell, R. Parrish, P. Reilly, and three anonymous reviewers offered valuable comments on earlier drafts of this manuscript. This study was partially supported by NOAA's National Undersea Research Program, West Coast and Polar Regions Undersea Research Center, University of Alaska Fairbanks (grant nos. UAF-92-0063 and UAF-93-0036).

Literature cited

Able, K. W., C. G. Grimes, and J. R. Uzmann.
1982. Burrow construction and behavior of tilefish, *Lopholatilus chamaeleonticeps*, in Hudson Submarine Canyon. Environ. Biol. Fishes 7:199–205.

Able, K. W., D. C. Twitchell, C. G. Grimes, and R. S. Jones.
1987. Side scan sonar as a tool for detection of demersal fish habitats. Fish. Bull. 85:725–744.

Boehlert, G. W.
1996. Biodiversity and the sustainability of marine fisheries. Oceanography 9:28–35.

Bohnsack, J. A.
1989. Are the high densities of fishes at artificial reefs the result of habitat limitation or behavioral preference? Bull. Mar. Sci. 44:631–645.

Bohnsack, J. A., and J. S. Ault.
1996. Management strategies to conserve marine biodiversity. Oceanography 9:73–82.

Bruce, P. J. Simon, and T. Oswald.
1995. Resampling stats, version 4.0 edition. Resampling Stats, Inc., Arlington, VA, 127 p.

Carlson, H. R., and R. R. Straty.
1981. Habitat and nursery grounds of Pacific rockfish, *Sebastes* spp., in rocky coastal areas of Southeastern Alaska. Mar. Fish. Rev. 43:13–19.

Carr, M. H.
1991. Habitat selection and recruitment of an assemblage of temperate zone reef fishes. J. Exp. Mar. Biol. Ecol. 146: 113–137.

Deimling, E. A., and W. J. Liss.
1994 Fishery development in the eastern North Pacific: a natural-cultural system perspective, 1888–1976. Fish. Oceanogr. 3:60–77.

Greene, H. G., M. M. Yoklavich, R. M. Starr, V. M. O'Connell, W. W. Wakefield, D. E. Sullivan, J. E. McRea Jr., and G. M. Cailliet.
1999 A classification scheme for deep seafloor habitats. Oceanologica Acta 22(6):663–678.

Greene, H. G., M. M. Yoklavich, D. Sullivan, and G. M. Cailliet.
1995. A geophysical approach to classifying marine benthic habitats: Monterey Bay as a model. Alaska Fish Game Special Publication 9:15–30.

Johnson, K. A.
1997. Rockfish (*Sebastes* spp.) recruitment to soft bottom habitats in Monterey Bay, CA. M.S. thesis, California State University, Stanislaus, CA, 70 p.

Karpov, K. A., D. P. Albin, and W. H. Van Buskirk.
1995. The marine recreational finfishery in northern and central California: a historical comparison (1958–1986), status of stocks (1980–1986), and effects of changes in the California Current. Calif. Fish Game Fish Bull. 176:1–192.

Krebs, C. J.
1989. Ecological methodology. Harper and Row, Publishers, New York, NY, 654 p.

Larson, R. J.
1980. Competition, habitat selection, and the bathymetric segregation of two rockfish (*Sebastes*) species. Ecol. Monogr. 50:221–239.

Lea, R. N.
1992. Rockfishes: overview. *In* California's living marine resources and their utilization (W. S. Leet, C. M. Dewees, and C. W. Haugen, eds.), p. 114–116. Sea Grant Extension Publ. UCSGEP-92-12, University of California, Davis, CA.

Mason, J. E.
1995. Species trends in sport fisheries, Monterey Bay, California, 1959–86. Mar. Fish. Rev. 57:1–16.
1998. Declining rockfish lengths in the Monterey Bay, California recreational fishery, 1959–94. Mar. Fish. Rev. 60:15–28.

Murie, D. J., D. C. Parkyn, B. G. Clapp, and G. G. Krause.
1994. Observations on the distribution and activities of rockfish, *Sebastes* spp., in Saanich Inlet, British Columbia, from the *Pisces IV* submersible. Fish. Bull. 92:313–323.

O'Connell, V. M., and D. W. Carlile.
1993. Habitat-specific density of adult yelloweye rockfish *Sebastes ruberrimus* in the eastern Gulf of Alaska. Fish. Bull. 91:304–309.

Pearcy, W. G., D. L. Stein, M. A. Hixon, E. K. Pikitch, W. H. Barss, and R. M. Starr.
1989. Submersible observations of deep-reef fishes of Heceta Bank, Oregon. Fish. Bull. 87:955–965.

Pearson, D. E., and S. Ralston.
1990. Trends in landings, species composition, length-frequency distributions, and sex ratios of 11 rockfish species (Genus *Sebastes*) from central and northern California ports (1978–88). U.S. Dep. Commer., NOAA Tech. Memo. NMFS-SWFC-145, 65 p.

Phillips, J. B.
1939. The rockfish of the Monterey wholesale fish markets. Calif. Fish Game 25:214–225.
1957. A review of the rockfishes of California (Family Scorpaenidae). Calif. Fish Game Fish Bull. 104:1–158.

Potts, T. A., and A. W. Hulbert.
1994. Structural influences of artificial and natural habitats on fish aggregations in Onslow Bay, North Carolina. Bull. Mar. Sci. 55:609–622.

Ralston, S.
1998. The status of federally managed rockfish on the U.S. west coast. *In* Marine harvest refugia for west coast rockfish: a workshop (M. Yoklavich, ed.), p. 6–16. U.S. Dep. Commer., NOAA Tech. Memo. NMFS-SWFC-255, 159 p.

Richards, L. J.
1986. Depth and habitat distributions of three species of rockfish (*Sebastes*) in British Columbia: Observations from the submersible *PISCES IV*. Environ. Biol. Fishes 17:13–21.

Robins, C. R., R. M. Bailey, C. E. Bond, J. R. Brooker, E. A. Lachner, R. N. Lea, and W. B. Scott.
1991. Common and scientific names of fishes from the United States and Canada (5th ed.). Am. Fish. Soc. Spec. Publ. 20:1–183.

Root, R. B.
1967. The niche exploitation pattern of the blue-gray gnatcatcher. Ecol. Monogr. 37:317–350.

Sobel, J.
1993. Conserving biological diversity through marine protected areas. Oceanus 36:19–26.

Stein, D. L., B. N. Tissot, M. A. Hixon, and W. Barss.
1992. Fish-habitat associations on a deep reef at the edge of the Oregon continental shelf. Fish. Bull. 90:540–551.

SYSTAT.
1992. Statistics, version 5.2 edition. SYSTAT, Inc., Evanston, IL, 724 p.

Thomson, C. J.
1999. Economic and management implications of no-take reserves: an application to *Sebastes* rockfish in California. Calif. Coop. Oceanic Fish. Invest. Rep. 40:107–117.

Tusting, R. F., and D. L. Davis.
1993. Improved methods for visual and photographic benthic surveys. *In* Diving for science ... 1993. Proceedings of the American Academy of Underwater Sciences 13th Annual Scientific Diving Symposium, Pacific Grove, CA (J. N. Heine and N. L. Crane, eds.), p. 157–172. [Available from AAUS, 430 Nahant Rd., Nahant, MA 01908.]

Weinberg, K. L.
1994. Rockfish assemblages of the middle shelf and upper slope off Oregon and Washington. Fish. Bull. 92:620–632.

Winer, B. J.
1971. Statistical principles in experimental design. McGraw-Hill, Inc., New York, NY, 907 p.

Yoklavich, M., R. Starr, J. Steger, H. G. Greene, F. Schwing, and C. Malzone.
1997. Mapping benthic habitats and ocean currents in the vicinity of central California's Big Creek Ecological Reserve. U.S. Dep. Commer., NOAA Tech. Memo. NMFS-SWFC-245, 52 p.

Long-distance movement of a Nassau grouper (*Epinephelus striatus*) to a spawning aggregation in the central Bahamas

Stephania K. Bolden

Southeast Fishery Science Center
National Marine Fisheries Service, NOAA
75 Virginia Beach Drive
Miami, Florida 33133
E-mail address: stephania.bolden@noaa.gov

Smith (1972) first reported *Epinephelus striatus* (Nassau grouper) spawning aggregations. Since then, spawning aggregations from a few dozen individuals to perhaps 100,000 individuals have been reported from the Bahamas, Jamaica, Cayman Islands, Belize, the Virgin Islands, and Mexico (Olson and LaPlace, 1979; Colin et al., 1987; Carter, 1988; Colin, 1992; Aguilar-Perera and Aguilar-Davila, 1996). Colin (1992) investigated and documented actual spawning of *E. striatus* off Long Island, Bahamas. Colin et al. (1987) and Sadovy et al. (1994) have provided the only other observations of spawning aggregations of western Atlantic serranid species (*E. guttatus* and *Mycteroperca tigris*).

Epinephelus striatus spawning aggregation sites are transient, site specific, and are usually known by local fishermen who fish them intensely during the spawning period. *Epinephelus striatus* spawn in the southern Caribbean during the full moon of December and January (Smith, 1972; Olsen and LaPlace, 1979; Colin et al., 1987; Colin, 1992), and at more northern locales (i.e. Bermuda) from May to July (Bardach et al., 1958). Johannes (1978) suggested that the period and location of reef fish spawning is selected to favor larval survival; more recently Colin (1996) has suggested that aggregation sites may be "learned." Differing densities of *E. striatus* at spawning sites prior to, during, and following full moon periods indicate that individuals move to an aggregation site for a limited period of time (Colin, 1992). Timing, size, and sex composition of moving prespawning individuals are unknown.

Knowledge of the distance and direction of *E. striatus* movement to historic spawning sites is based on Colin (1992) where a single tagged specimen was recaptured by a fisherman at a known spawning site east of Long Island, Bahamas, after travelling approximately 110 km in two months. This contribution documents long-distance movement (220 km) of a tagged *E. striatus* to a spawning aggregation.

Materials and methods

The Exuma Cay Land and Sea Park (ECLSP, Fig. 1) was the study site for an investigation of the home range of *E. striatus*. The 456-km^2 ECLSP was established in the central Bahamas in 1958 and fishing was banned in 1986. A total of eleven individuals were captured by traditional Bahamian fish traps, tagged, and released for the home range study during summer 1997. An *E. striatus* (58.1 cm TL) captured on 24 June 1997, tagged on 25 June, held in a fish trap and released at 24°18.8′N and 76°33.6′W on 2 July 1997 was later recaptured by a fisherman.

Each fish had a unique Floy dart tag (Floy Tag & Manufacturing, Inc., Seattle, Washington) inserted below the anterior dorsal-fin rays, between the second and third scale rows.

Each fish also had an acoustic transmitter (VEMCO Limited, Nova Scotia, Canada) surgically implanted into its body cavity.

Daily water temperature data were obtained from Caribbean Marine Research Center (CMRC) at Lee Stocking Island (approximately 120 km NW of Long Island, Fig. 1) to correlate with spawning season. Mean monthly water temperature was calculated for the months of February 1998 (this investigation) and February 1989 (Colin, 1992). February 1988 data (Colin, 1992) were not available.

Fish were continuously tracked by their individual acoustic frequency 24 hours a day for a 3-week period. Subsequent daily diver observations identified individual fish by their external tags.

Results

The recaptured Nassau grouper was tracked by ultrasound at its presumed "home reef" from 2 to 31 July 1997. Daily visual observations (by divers) from 9 to 15 August confirmed the presence of the Nassau grouper at its home reef. The last observation was recorded at the tagging locale on 16 August 1997 at the end of the field season.

Three other individuals tagged during the summer 1997 investigation were observed at the exact patch reef where they were tagged in summer 1998. Two of these tagged individuals were considered to be mature adults when tagged (47.1 cm TL and 44.1 cm TL), and the third was deemed a juvenile (25.2 cm TL). Measurement of two individuals indicated an annual growth rate of 3–4 cm: from 47.1 to 50.1 cm TL, and from 25.2 to 29.0 cm TL. Seven other *E. striatus* tagged during summer 1997 were not observed during summer 1998.

A fisherman caught the tagged individual on 16 February 1998 in a fish trap at the Long Island, Bahamas, spawning location described by Colin (1992) as the "south point aggregation site" at 22°51.0′N and 74°51.5′W, approximately 220 km (in a straight ESE route) from the release point (Fig. 1). Physical features of the aggregation site are described by Colin (1992). The fish was at large for 185 days and was caught in 18–21 m of water. Because fishing was limited during the period "due to high seas and strong wind,"[1] the exact date the fish entered the trap or the soak time is unknown.

Manuscript accepted 16 February 2000.
Fish. Bull. 98:642–645 (2000).

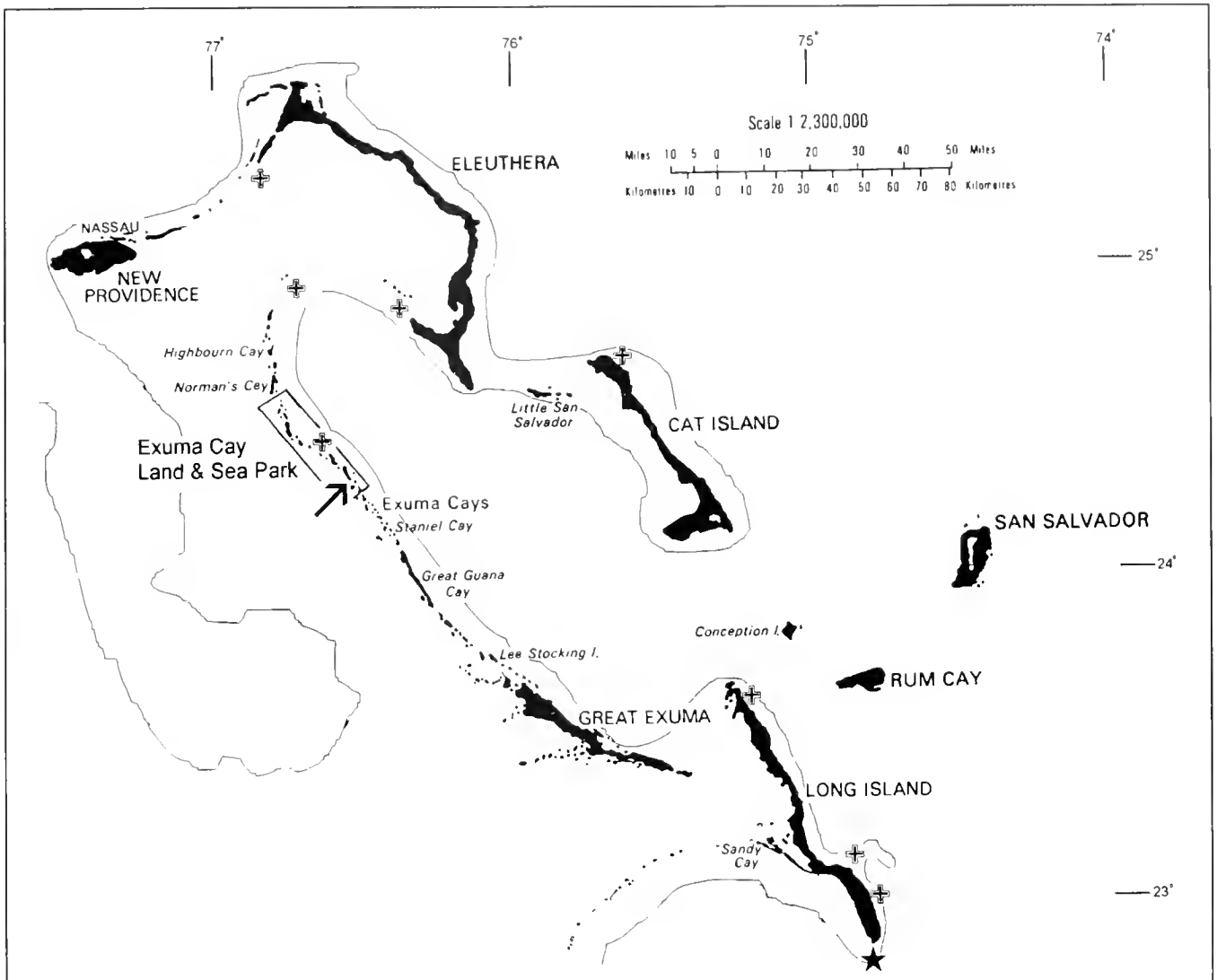

Figure 1

Map of the central Bahamas showing locations of tag and return sites of Nassau grouper (*Epinephelus striatus*). Longitude is west; latitude is north. The Exuma Cay Land and Sea Park is enclosed by a box. The site where the fish was captured, tagged, and released is designated by an arrow (↑); recapture site—denoted as the "south point aggregations site by Colin, 1992—by a star (★). Other possible *E. striatus* spawning sites noted by Bahamian government, local fishermen, and scientific literature are designated by a cross (✚). The 500-fathom depth contour, as determined by NOAA chart no. 23605, is designated by a solid line. This figure is modified with permission from a map produced by Department of Lands and Surveys for the Government of the Bahamas B.L.S. 1100.

Mean monthly water temperatures at CMRC dock were 23.94°C ±1.41 for February 1998, and $\bar{x}$ = 24.68°C ±0.75 for February 1989. Mean water temperature for the full moon period from 11 February 1998 to date of capture (16 February 1998) was 23.83°C ±0.63. The wide standard deviation for the February 1998 monthly mean was due to a 7-day (18–24 February) period of warm water temperature (>25°C every day).

[1] Cartwright, Capt. A. 1998. Personal commun. P.O. Box CB 11039, Nassau, Bahamas.

Discussion

Site fidelity for the recaptured Nassau grouper was 46 days; and perhaps a year for the three Nassau grouper at large, tagged in 1997 and resighted in 1998. Sexual maturity for *E. striatus* is reached at about 42 cm SL and 40 cm SL, for males and females respectively (Colin et al., 1987), thus the two larger fish seen again in 1998 were theoretically sexually mature. These two fish should have joined a spawning aggregation: they had either left the area and returned "home," or they were remarkably steadfast to that reef.

The south point aggregation site (where the tagged *E. striatus* was recaptured) has supported a seasonal fishery (fish trap, and hook and line) since before 1900 (Colin, 1992). During spawning aggregation periods, the site draws 2000–3000 *E. striatus*; density decreases during nonspawning periods (Colin, 1992). Notably, an *E. striatus* spawning aggregation site is known to have previously existed within the ECLSP boundaries at the "Wide Opening," approximately 20 km to the NNW of the tagging site.[2] However, it is not known if the site currently sustains spawning Nassau grouper. If this and other nearby spawning sites do exist (denoted by a cross (✚) in Fig. 1), one can only speculate as to why a fish would migrate a considerably greater distance to spawn.

I suggest that *E. striatus* learn the routes to historic spawning sites by local enhancement from older individuals (i.e. older animal directs attention of younger animal to a particular part or object in the environment), perhaps by socially transmitted traditions (see Helfman and Schultz, 1984, for definitions). The fact that traditions differ among subpopulations would account for both the number of spawning sites in an area and their historical nature. If spawning sites are learned from older individuals, then one could conjecture how this learning behavior affects recovering *E. striatus* populations; older individuals are required to socially transmit the location of spawning sites, and young adults need to be present to learn. Current and future studies of sensory systems and migration should provide insight into these hypotheses.

Because actual spawning was not observed and gonads were not available, the reproductive status of the recaptured *E. striatus* is unknown. Hence, fishermen reports and water temperature data were used to investigate the likelihood of *E. striatus* spawning at time of recapture. The recaptured fish was captured on 16 February from a spawning "school" five days after the full moon.[3] Local fishermen believe that spawning was occurring at this time because catches of *E. striatus* were abundant, the fishermen were targeting a known spawning site, and the fish were "full [of eggs]".[2] Spawning is usually synchronous with the full moon; thus it is speculated that the Nassau grouper use the moon as a visual cue in migrating to common spawning areas.

The geographic differences in spawning season of *E. striatus* are thought to correlate with water temperatures, of which optimal spawning temperature is most likely in the range of 25–26°C (Colin, 1992; Tucker et al., 1993). Mean monthly water temperature at the Long Island south point aggregation site was 24.68°C in February 1988 (no spawning; Colin, 1992) and 23.94°C in February 1998 (presumed spawning; present study). If spawning is correlated only with water temperature, then it is unlikely that the recaptured *E. striatus* grouper was actively spawning. However it is more likely that temperature is only one of many physical attributes influencing the spawning of *E. striatus* and if the fishermen reports are correct, it is entirely possible that the recaptured *E. striatus* was removed from a spawning aggregation.

ECLSP is a marine reserve for the preservation of animals, plant, and other marine life. For management purposes, the intent of a marine reserve is to provide spatial refuge from fishing, whereas the intent of traditional fishery restrictions on the resource is to allow a sufficient number of animals to reproduce. (Bohnsack, 1998). Evidence provided in the present study indicates that spatial refuge alone may be insufficient because the ECLSP reserve provided protection only until the animal migrated to spawn and thus was captured. If the Nassau grouper stock are to be preserved, protection throughout the animal's life history including spawning needs to be considered. Possible ways to provide this protection include closing documented spawning aggregation sites to fishing, enforcing seasonal closures, or providing protection for migrating and spawning individuals.

Acknowledgments

This research was conducted under a grant from NOAA Office of Protected Species, and a Research Permit from the Govt. of the Bahamas. I thank the National Marine Fisheries Service for financial support and the Nature Conservancy for field assistance. Special appreciation to Bell Island Ltd. and K. James for logistical support. Comments by W.J. Richards, J. Bohnsack, and three anonymous reviewers greatly improved the content. I would like to also thank Captain A. Cartwright and the Long Island fisherman who provided local fishing knowledge, L. Massey for creating the map, and N. Mehta of CMRC for temperature data. Field assistance by J. Kelly, H. Luciano IV, and K. Sullivan is appreciated.

Literature cited

Aguilar-Perera, A., and W. Aguilar-Davila.
1996. A spawning aggregation of Nassau grouper *Epinephelus striatus* (Pisces: Serranidae) in the Mexican Caribbean. Env. Biol. Fish. 45:351–361.

Bardach, J. E., C. L. Smith, and D. W. Menzel.
1958. Bermuda fisheries research program final report. Bermuda Trade Development Board, Hamilton, Bermuda, 59 p.

Bohnsack, J. A.
1998. Application of marine reserves to reef fisheries management. Aust. J. Ecol. 23:298–304.

Carter, J.
1988. Grouper mating ritual on a Caribbean reef. Underwater Natur. 17:8–11.

Colin, P. L.
1992. Reproduction of the Nassau grouper, *Epinephelus striatus* (Pisces: Serranidae) and its relationship to environmental conditions. Env. Biol. Fish. 34:357–377.
1996. Longevity of some coral reef fish spawning aggregations. Copeia 1996:189–191.

[2] Darville R. 1998. Personal commun. ECLSP Park Warden, P.O. Box N-4105 Nassau, Bahamas.

[3] Fishermen refer to the aggregations as "schools" because a large number of fishes are present in reproductive condition

Colin, P. L., D. Y. Shapiro, and D. Weiler.
1987. Aspects of the reproduction of two species of groupers, *Epinephelus guttatus* and *E. striatus*, in the West Indies. Bull. Mar. Sci. 40:220–230.
Helfman, G. S., and E. T. Schultz.
1984. Social transmission of behavioural traditions in coral reef fish. Anim. Behav. 32:379–384.
Johannes, R. E.
1978. Reproductive strategies of coastal marine fishes in the tropics. Env. Biol. Fish. 3:65–84.
Olsen, D. A., and J. A. LaPlace.
1979. A study of a Virgin Islands grouper fishery based on a breeding aggregation. Proc. Gulf Carib. Fish. Inst. 31:130–144.
Sadovy, Y., P. L. Colin, and M. L. Domeier.
1994. Aggregation and spawning in the tiger grouper, *Mycteroperca tigris* (Pisces: Serranidae). Copeia 1994:511–516.
Smith, C. L.
1972. A spawning aggregation of Nassau grouper, *Epinephelus striatus* (Bloch). Trans. Am. Fish. Soc. 2:257–261.
Tucker, J. W. Jr., P. G. Bush and S. T. Slaybaugh.
1993. Reproductive patterns of Cayman Islands Nassau grouper (*Epinephelus striatus*) populations. Bull. Mar. Sci. 52:961–969.

Concurrent scavenging off a whale carcass by great white sharks, *Carcharodon carcharias*, and tiger sharks, *Galeocerdo cuvier*

Sheldon F.J. Dudley
Michael D. Anderson-Reade
Greg S. Thompson
Paul B. McMullen

Natal Sharks Board
P Bag 2
Umhlanga Rocks 4320, South Africa
E-mail address (for S. Dudley): dudley@shark.co.za

The great white shark, *Carcharodon carcharias* (Lamnidae), and the tiger shark, *Galeocerdo cuvier* (Carcharhinidae), are two of the largest species of macropredatory sharks. Both are known to prey on dolphins (Delphinidae) off KwaZulu-Natal, South Africa (Cockcroft et al., 1989). Although scavenging off whale carcasses by white sharks (Carey et al., 1982; Pratt et al., 1982; McCosker, 1985; Long and Jones, 1996) and tiger sharks (Compagno et al., 1998) has been documented, the two species have not been recorded feeding concurrently on the same carcass. In August 1993, Natal Sharks Board (NSB) observers saw both species feeding on the carcass of a humpback whale, *Megaptera novaeangliae*, off Durban, but they were not seen scavenging concurrently (NSB[1]). In September 1997, elsewhere in the southwest Indian Ocean, tiger sharks were filmed feeding on a humpback whale carcass off the southern tip of Madagascar, but no white sharks were present. Compagno[2] subsequently viewed the footage and verified the identification of the tiger sharks.

This paper presents observations of white and tiger sharks scavenging off the floating carcass of a Bryde's whale, *Balaenoptera edeni*, off the coast of KwaZulu-Natal, South Africa. These observations are of a single event and hence should not be attributed more significance than they can support.

Methods

The National Sea Rescue Institute (NSRI) reported the presence of a Bryde's whale carcass to the NSB at midday on 26 April 1998. The NSRI, which had responded to a call reporting the carcass as a capsized yacht, found it floating 4 km east of the Durban harbor entrance (29°52′S, 31°24′E) with large sharks in its vicinity. The following day various reports were received that the carcass had drifted 25 km to the north and was several kilometers off the mouth of the Umdloti River (29°38′S, 31°07′E). Large sharks were reported to be feeding on it.

On 28 April, three of the authors launched a 5.5-m open-deck boat, equipped with photographic equipment and a shark cage, from the beach at Umhlanga Rocks (29°43′S, 31°05′E). The carcass was located 6 km offshore of the launch site and 10 km south of its position on the previous day. It was observed for 5 h. Conditions were excellent, with a glassy sea, light wind, little current, an estimated water temperature of 23°C and clarity of 15 m.

This account was written by S. F. J. Dudley (who did not witness the event) on the basis of separate interviews with the remaining authors and on viewing 27 min of video footage filmed by M. D. Anderson-Reade and an additional 4 min of footage filmed from another boat. All distances, times, and shark lengths (precaudal length, PCL) are approximate. The carcass was identified to species from the video footage, by the presence of prominent head ridges (Peddemors[3]).

Results

A white shark of 5 m was encountered 500 m from the carcass. The shark made numerous passes within 2 m of the stationary boat and just below the surface. This behavior continued for 15 min before the boat continued towards the carcass. This animal was not seen again.

Immediately upon reaching the carcass, two tiger sharks of 3.5 m were seen cruising 3 m below the surface. Two white sharks were present as well, one of about 4 m and the other a larger animal with a distinctive bite scar on the right side, located dorsolaterally and posterior to the first dorsal fin. A second boat was present and both shark species made approaches to each boat. The shark cage was deployed and occupied by two divers. A number of tiger sharks with distended abdomens were seen feeding on the carcass, usually singly but sometimes in groups of two or more. Their approaches to the carcass were leisurely and gave no evidence of intraspecific aggression. The white sharks, which were not seen feeding during this period, moved off soon after the cage was deployed and the animal with the bite scar was not seen again.

For 20 min the boat and cage were maneuvered around the carcass in an attempt to film the feeding process. Large quantities of organic debris reduced water clarity and because visibility was better from the surface, the divers returned to the boat and the cage was retrieved.

A 4-m female white shark, possibly the smaller animal seen at the carcass

[1] NSB (Natal Sharks Board). 1993. Unpubl. data. Natal Sharks Board, P. Bag 2, Umhlanga Rocks 4320, South Africa.

[2] Compagno, L. J. V. 1999. Personal commun. South African Museum, P.O. Box 61, Cape Town 8000, South Africa.

[3] Peddemors, V. M. 1998. Personal commun. Natal Sharks Board, P. Bag 2, Umhlanga Rocks 4320, South Africa.

Manuscript accepted 6 January 2000.
Fish. Bull. 98:646–649 (2000).

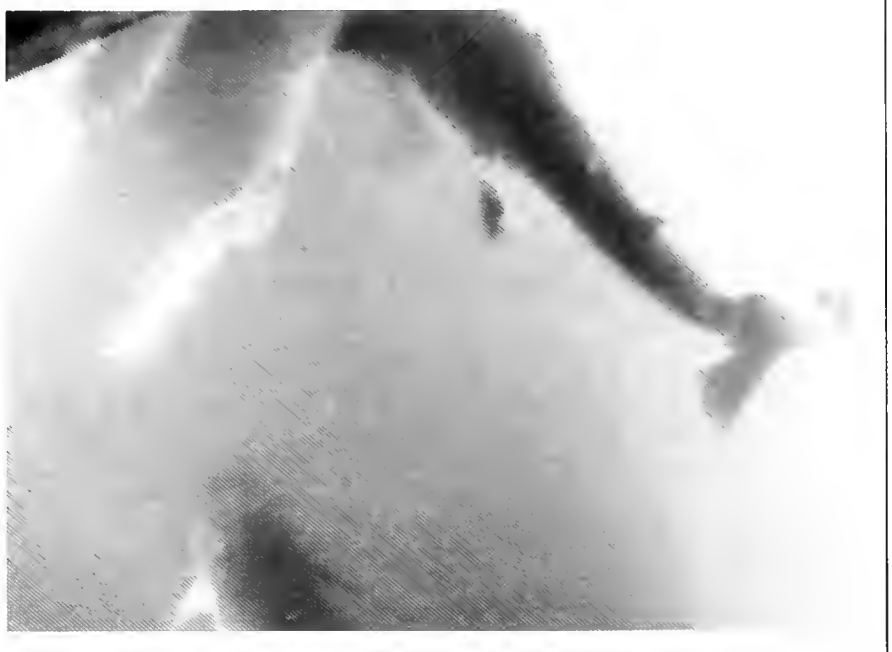

Figure 1

A 4-m PCL white shark feeding on the carcass of a Bryde's whale, and a 3.5-m tiger shark swimming below it. The head of the white shark, out of picture, is above water. The boat hull is at upper left, and strands of whale tissue are hanging beneath it. (Frame from Hi8 videotape).

initially, was observed surfacing 100 m from the carcass and regurgitating its stomach contents. It then circled the floating matter. While being approached by the boat, it began to feed on the regurgitated material. This was the only time that regurgitation was observed but, on other occasions, clouds of what appeared to be regurgitated matter were seen in the water near the carcass, indicating that regurgitation may have occurred more frequently.

Subsurface filming of the white shark was conducted over the gunwale. On five or six occasions the shark approached the camera (which was enclosed in a yellow housing) such that the cameraman was forced to lift the camera out of the water just prior to the shark's snout making contact. The shark would then mouth (lightly and briefly grasp) the boat or motors before moving off. On one occasion it damaged its head on the motor and the resulting laceration, immediately anterior to the right eye, was used subsequently as an identification mark.

A small (3–3.5 m), red, semirigid, inflatable boat arrived and the white shark immediately showed interest in it, approaching it from the rear several times and mouthing the motor.

After 40 min, the observers (coauthors) returned to close proximity of the carcass, where there now appeared to be between 7 and 10 tiger sharks, all 3.5 m. Feeding on the carcass continued, but the animals showed more interest in the boat than previously. Typically, a shark would leave the boat, feed on the whale and then return slowly to the vicinity of the boat. The motors were bumped three times and a propeller was mouthed once. As with the white shark, the tiger sharks approached the camera directly, and on several occasions the cameraman depended upon warnings from his co-observers to ensure timely evasion. Only one interaction between individual tiger sharks was observed. Two animals, swimming one above the other, converged slowly to within 1 m, at which point they diverged rapidly. Immediately prior to this event, one of the animals had been investigating the camera and it is possible that it had been unaware of the other shark's presence.

Soon after returning to the carcass, the observers noted the arrival of the white shark with the wounded snout. There appeared to be a slight increase in the swimming speed of the tiger sharks but no other reaction was observed. The white shark fed on three occasions and on each occasion one or more tiger sharks fed at the same time. On one occasion two tiger sharks swam within 3 m of the feeding white shark—one of these was captured on videotape, together with the white shark (Fig. 1). The white shark removed a piece from the carcass, then abandoned the piece and returned to the carcass. A tiger shark then fed on the piece but moved off when the white shark came back to it.

Both species fed on the carcass at the water line, but the tiger sharks fed below the water line as well. Tiger sharks were observed to thrust their heads out of the water to feed (Fig. 2) as has been observed previously (Gilbert, 1963;

Figure 2

A 3.5-m PCL tiger shark feeding on a Bryde's whale carcass at the water line. The shark's eye is covered by the nictitating membrane.

Moss, 1972; Strong, 1991). One approach behavior exhibited by the white shark and captured on film conformed with that described by Tricas (1985) as an underwater approach, in which the shark approached the carcass just below the surface until approximately 1 m away and then attacked by deflecting the head upward, emerging out of the water to bite. When feeding above the water line, both species tended to bite twice in quick succession, apparently gaining better purchase with the second bite. This procedure was followed by slow and deliberate shaking, twisting, and turning to cut away the mouthful. The tiger sharks demonstrated more thrashing than the white shark, sometimes rolling onto their backs while biting. The white shark behavior described by Pratt et al. (1982), in which the shark bit a whale carcass ventral-surface-up before rolling upright to cut a mouthful, was not seen.

When tiger sharks fed below the surface, the carcass was penetrated vertically and a swaying motion of the body, rather than twisting, followed the bite. As many as five individual tiger sharks fed on the carcass at one time, some hanging below the carcass and some biting at the waterline.

The tiger sharks tended to remain at or near the carcass at all times, whereas the wounded white shark approached the carcass to feed and then moved off again, sometimes out of sight of the observers. A white shark of 3.5–4 m, believed to have been an individual not previously observed, made a brief appearance near the carcass during this period. The tiger sharks were generally more active than the wounded white shark, although both species were unhurried and deliberate. The white shark increased swimming speed only when investigating the camera.

The red inflatable boat which had been present earlier, returned, and the wounded white shark again showed particular interest in it. On one occasion the shark held the rear of the starboard pontoon in its mouth and kept the boat stationary despite the crew of the boat engaging gear and running the 40-hp motor at speed. After 10 sec the shark released the pontoon, the only damage to which was a single, small puncture, perhaps the result of exploratory mouthing behavior.

Discussion

White sharks feeding on whale carcasses appear to feed until satiated (McCosker, 1985). The observed regurgitation of food suggests that feeding may continue even after satiation.

Observations suggest agonistic encounters amongst white sharks when feeding on a whale carcass. Observers saw at least four and possibly up to nine different white sharks in the vicinity of a fin whale carcass, *Balaenoptera physalus*, over a 30-h period but never more than two together (Pratt et al., 1982). When two did co-occur their behavior appeared agonistic, and some of the sharks had tooth cuts and slashes (some previous wounds, some freshly inflicted). Similarly, Long and Jones (1996) reported that about five different white sharks fed on the carcass of a blue whale, *Balaenoptera musculus*, but only one fed at a time. McCosker (1985) observed an agonistic encounter between two white sharks feeding on horsemeat bait; the smaller shark was forced to depart after receiving a minor bite. Strong et al. (unpubl. data in Strong [1996]), also

noted that feeding attempts by individual white sharks may be thwarted by larger conspecifics. In our study, although three, possibly four, white sharks were seen at or near the carcass, only one was seen feeding. Although the observation period was brief, this type of behavior is consistent with the existence of intraspecific competitive exclusion. The animal seen feeding was smaller than at least two of its conspecifics, and it is possible that the larger individuals had fed previously.

The tiger sharks exhibited no evidence of intraspecific competition, despite the presence of up to 10 individuals in the vicinity of the carcass and up to five feeding concurrently. The abundance of food or the similarity in size of the sharks may have prevented the establishment of the size-dependent hierarchy discussed by Bres (1993).

Interspecific competition for food amongst reef-dwelling, carcharhinid species has been recorded (Nelson and Johnson, 1980), as have apparent interspecific hierarchies comprising 1) the silvertip shark, *Carcharhinus albimarginatus*, the Galapagos shark, *C. galapagensis*, and the blacktip shark, *C. limbatus*, (Limbaugh, 1963); 2) the oceanic whitetip shark, *C. longimanus*, and the silky shark, *C. falciformis*; and 3) hammerhead sharks (Sphyrnidae) and various other species (Springer, 1967). Pratt et al. (1982) noted that the locally abundant blue shark, *Prionace glauca*, and shortfin mako, *Isurus oxyrinchus*, were conspicuously absent from the vicinity of the fin whale carcass, and a fish spotter pilot observed no blue sharks within a 3.2-km radius. These authors suggested that this was a consequence of territorial exclusion by white sharks. Similarly, Long and Jones (1996) suggested that white sharks excluded blue sharks, a species known to scavenge on whale carcasses, from the blue whale carcass. McCosker (1985) observed a single white shark feeding on the carcass of a grey whale, *Eschrichtius robustus*, and saw no other shark species nearby. The white and tiger sharks, however, did not appear to compete at the Bryde's whale carcass. Springer (1967) noted that mixed-species feeding aggregations tend to consist of sharks of similar sizes. If it is hypothesized, therefore, that the single 4-m white shark would have competitively excluded a single 3.5-m tiger shark, the presence of several tiger sharks may have prevented this from occurring. McKibben and Nelson (1986) speculated that juvenile gray reef sharks grouping in a loose aggregation or as a polarized pack may obtain protection from larger sharks. The tiger sharks, attracted by a single stimulus, may have derived an incidental defensive benefit.

Literature cited

Bres, M.
1993. The behaviour of sharks. Rev. Fish Biol. Fish. 3:133–159.

Carey, F. G., J. W. Kanwisher, O. Brazier, G. Gabrielson, J. G. Casey, and H. L. Pratt.
1982. Temperature and activities of a white shark, *Carcharodon carcharias*. Copeia 1982(2):254–260.

Cockcroft, V. G., G. Cliff, and G. J .B. Ross.
1989. Shark predation on Indian Ocean bottlenose dolphins *Tursiops truncatus* off Natal, South Africa. S. Afr. J. Zool. 24(4):305–310.

Compagno, L. J. V., C. Simpfendorfer, J. E. McCosker, K. Hollaud, C. Lowe, B. Wetherbee, A. Bush, and C. Meyer.
1998. Sharks. (Reader's Digest explores). Reader's Digest, Pleasantville, NY, 160 p., illustr.

Gilbert, P. W.
1963. The visual apparatus of sharks. *In* Sharks and survival (P. W. Gilbert, ed.), p. 283–326. D.C. Heath and Co., Boston, MA.

Limbaugh, C.
1963. Field notes on sharks. *In* Sharks and survival (P. W. Gilbert, ed.), p. 63–94. D.C. Heath and Co., Boston, MA.

Long, D. J., and R. E. Jones.
1996. White shark predation and scavenging on cetaceans in the Eastern North Pacific Ocean. *In* Great white sharks: the biology of *Carcharodon carcharias* (A. P. Klimley and D. G. Ainley, eds.), p. 293–307. Academic Press, San Diego, CA.

McCosker, J. E.
1985. White shark attack behavior: observations of and speculations about predator and prey strategies. Mem. Southern Calif. Acad. Sci. 9:123–135.

McKibben, J. N., and D. R. Nelson.
1986. Patterns of movement and grouping of gray reef sharks, *Carcharhinus amblyrhynchos*, at Enewetak, Marshall Islands. Bull. Mar. Sci. 38(1):89–110.

Moss, S. A.
1972. The feeding mechanism of sharks of the family Carcharhinidae. J. Zool. Lond. 167:423–436.

Nelson, D. R., and R. H. Johnson.
1980. Behavior of the reef sharks of Rangiroa, French Polynesia. Natl Geog. Soc. Res. Rep. 12:479–499.

Pratt, H. L, J. G. Casey, and R. B. Conklin.
1982. Observations on large white sharks, *Carcharodon carcharias*, off Long Island, New York. Fish. Bull. 80(1):153–156.

Springer, S.
1967. Social organisation of shark populations. *In* Sharks, skates, and rays (P.W. Gilbert, R. F. Mathewson, and D. P. Rall, eds.), p. 149–174. Johns Hopkins Press, Baltimore, MD.

Strong, W. R.
1991. Instruments of natural selection: How important are sharks? *In* Discovering sharks (S. H. Gruber, ed.), p. 70–73. Am. Littoral Soc., Highlands, NJ.
1996. Repetitive aerial gaping: a thwart-induced behavior in white sharks. *In* Great white sharks: the biology of *Carcharodon carcharias* (A. P. Klimley, and D. G. Ainley, eds.), p. 393–400. Academic Press, San Diego, CA.

Tricas, T. C.
1985. Feeding ethology of the white shark, *Carcharodon carcharias*. Mem. Southern Calif. Acad. Sci. 9:81–91.

Validation of age estimates from otoliths of larval and juvenile spotted seatrout, *Cynoscion nebulosus*

Allyn B. Powell

Elisabeth H. Laban

Center for Coastal Fisheries and Habitat Research
National Ocean Service
National Oceanic and Atmospheric Administration
101 Pivers Island Road
Beaufort, North Carolina 28516-9722
E-mail address (for A. B. Powell): allyn.powell@noaa.gov

Scott A. Holt

G. Joan Holt

University of Texas Marine Science Institute
750 Channelview Drive
Port Aransas, Texas 78373

Otolith microstructure analysis has been shown to be valuable for relating biotic and abiotic factors to growth and survival (Crecco and Savoy, 1985; Thorrold and Williams, 1989; Maillet and Checkley, 1991; Jenkins et al., 1993) and determining size-specific mortality (Gleason and Bengtson, 1996; Sabo and Orth, 1996; Hare and Cowen, 1997) for the early life history stages of fishes. Prior to using otolith microstructure analysis, it is important that otolith validation studies be undertaken to examine the rate of increment formation and the timing of initial increment formation, and to check the interpretive skills of the otolith reader (Geffen, 1992).

Our validation study dealt with spotted seatrout, *Cynoscion nebulosus*, an economically important sciaenid. Otolith increment deposition rates from spotted seatrout have been validated by using tetracycline marking of wild-caught fish larvae and juveniles collected in Tampa Bay, Florida (McMichael and Peters, 1989). Because known-age larvae were not used, the timing of initial increment formation was not determined. The purpose of our study was to determine the rate of increment formation and timing of initial increment formation as well as to provide confidence to otolith readers by using known-age larvae and wild-caught juveniles. Our study is ancillary to spotted seatrout early life history studies in Florida Bay, Everglades National Park.

Materials and methods

Spotted seatrout eggs were obtained from the Texas Parks and Wildlife GCCA/CPL Marine Development Center hatchery from adults collected from upper Laguna Madre, Texas. Eggs were transported to the University of Texas Marine Science Institute (UTMSI), Port Aransas, Texas, in May 1997. Eggs were incubated in 600-L tanks at egg densities of 100 eggs/L. Tanks were held in greenhouses, illuminated with natural sunlight and 40-W overhead flourescent lights at a 24-h (15L:9D) photoperiod. A closed system was used, but water was continuously recirculated through a biofilter. During the rearing process, ambient temperatures ranged from 25.0 to 28.0°C; salinities, from 32 to 33 ppt. Larvae to age 12 d were fed rotifers (5/mL), which in turn were provided the algae *Isochrysis*. At age 13 d, brine shrimp nauplii, enriched with oil emulsion (Leger et al., 1986), were introduced (4 rotifers/mL; 2 nauplii/mL on a daily basis), and from age 15 d until the end of the experiment, 2–3 nauplii/mL were maintained on a daily basis. Food density was estimated twice a day and food added to the required density. Frozen adult brine shrimp and red drum, *Sciaenops ocellatus*, eggs were added on a daily basis from age 23 d to the end of the experiment. Otoliths of reared larvae were marked with alizarin complexone (ALC) at concentrations of 50 mg/L for four hours at age 9 and 16 d. Fifty larvae were sacrificed at ages 6, 9, 14, 20, 23, and 32 d and preserved in 95% ethyl alcohol. Larvae sacrificed at ages 6 and 9 d were not immersed in ALC.

Wild-caught juveniles were collected in Aransas Bay, Texas, in August 1997 with a 6-m bag seine (4.5-mm mesh in both the wings and the bag). Juveniles were placed in 45-L tanks and transported to the rearing facility at UTMSI, Port Aransas, Texas. Juveniles were held in 3-m raceways in 1100-L water at temperatures 27.0–28.0°C and a salinity of 36 ppt. Juveniles were segregated by size to avoid cannibalism. Two days after capture, otoliths were marked with ALC (100 mg/L for 4 h). Otoliths were similarly remarked 7 d later (9 d after capture). Mortality associated with the marking process was nil. All fish were sacrificed and preserved in 95% ethyl alcohol at 21 d after capture.

Otoliths were removed with probes and fine-tipped forceps. Polarized light was used to facilitate location of otoliths from fish <6 mm standard length (SL). All otoliths, except for the right sagitta, were placed on a slide, covered with mounting media and archived. The right sagittal otolith was embedded for transverse sectioning or polishing (or for both procedures). The left sagitta was embedded for transverse sectioning if the right was damaged during preparation.

Sagittae were read with a light microscope at 1000× magnification under oil immersion with blue light epifluorescence to detect ALC marks that fluoresce as reddish orange. The first increment was determined as that following the core increment, the latter a well-defined dark increment surrounding the core. Sagittae were read by one

Manuscript accepted 29 December 1999.
Fish. Bull. 98:650–654 (2000).

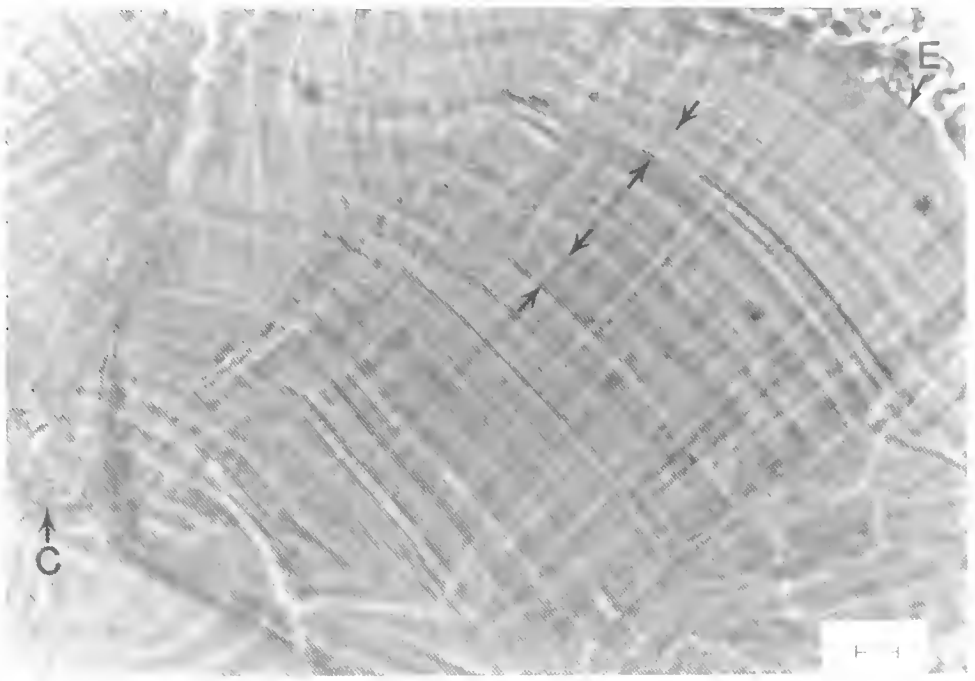

Figure 1

Photomicrograph of a transverse section of a spotted seatrout otolith from a 32-d-old laboratory-reared fish (SL=23.6 mm). C = the core; E = edge. The arrows point to daily increments that were determined as those rings that maintained relatively equal spacing as the fine focus was manipulated. The rings between the arrows were considered subdaily rings or optical artifacts. These rings did not maintain equal spacing when the fine focus was manipulated, were not continuous, and generally were poorly defined. Scale bar = 10 µm.

reader without knowledge of age of fish. Two to three readings were made and the counts averaged. Following Rice et al. (1985) and Ahrenholz et al. (1995), counts were regressed on age (SAS Institute, Inc., 1985), and Student's *t*-test used to determine if the slope was significantly different (α=0.05) than one. The null hypothesis is that the slope of increment counts on known age equals one. The null hypothesis is rejected if the slope is significantly different from one. A summary of the increment count data from known-age fish is shown in Table 1.

In our initial analysis, the slope of increment count regressed on known-age was significantly greater than one (α=0.05), but there were problems in aging the oldest juveniles (32 d)—problems that we related to variability in fish sizes (16.2 to 34.6 mm).Using linear regression, we examined the relation between increment count on size for all age groups. Only for the 32-d-old juveniles was the slope of increment count on size significantly different from zero (α=0.05), indicating that greater counts were observed as size increased. This result suggested that we interpreted subdaily rings as daily rings. We then examined otoliths from known-age juveniles in great detail to establish criteria to separate subdaily from daily rings. Although reading the older age (32-d-old) juveniles was difficult, daily rings maintained relatively equal spacing as the fine focus was manipulated. Subdaily rings or optical artifacts were not continuous, did not maintain equal spacing when focus was manipulated, and were not well defined (Fig. 1). Juvenile otoliths (23-d and 32-d-old) were reread (two blind readings per sagitta, with a hand counter). The reader avoided making mentally sequential counts, relying solely on the results of the hand counter.

Table1

Mean, standard deviation (SD), number of fish (n), total number of readings (nr), and range of increment counts from known-age laboratory-reared *Cynoscion nebulosus*.

Age (days)	n	nr	Mean	SD	Range
6	10	25	4.7	0.7401	2–6
9	10	30	6.0	0.8383	5–8
14	10	30	12.1	0.6641	10–15
20	10	30	20.2	0.8409	17–24
23	12	24	21.9	1.3046	18–25
32	15	30	30.5	1.1568	28–33

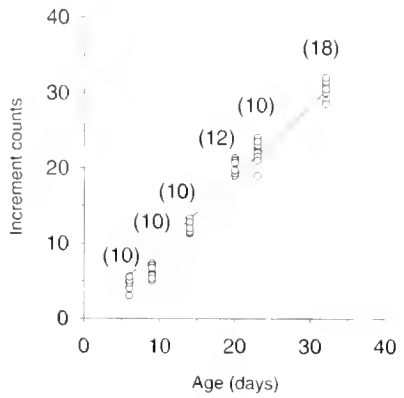

Figure 2

The relation between increment counts and known-age for spotted seatrout, *Cynoscion nebulosus*. Solid line represents regression line; dotted, 45° line. Values in parentheses indicate number of specimens.

Results

The slope of the line describing the relation between increment counts and known age was not significantly different from one (Table 2; Fig. 2). This result indicated that rings were being deposited daily and that we were correctly interpreting daily rings from subdaily rings or optical artifacts, a problem that was encountered with juveniles in our initial readings (see "Materials and methods" section).

A large percent of the laboratory-spawned and laboratory-reared fish that were marked with ALC failed to take up the stain on their otoliths. Only 15% (n=61) of the known-age fish exhibited a readable mark and only for two age groups. On the other hand, the majority (75%) of wild-caught juveniles exhibited a readable mark on their otoliths.

Increments were estimated to form at age 2–3 d. An inverse regression (counts regressed on age) yielded an intercept with a value of 2.3 d (Table 2). The intercept was significantly different from zero. Analysis of increment counts on ALC-marked otoliths from known-age larvae also revealed the first increment formed on day 2 or 3. For 14-d-old larvae marked at age 9 d, seven increments were counted; for 23-d-old larvae marked at age 9 d, six and seven were counted.

Increment counts on marked otoliths were fairly accurate. On 14-d-old larvae (n=4) marked at day 9, we counted seven increments from the core to the ALC mark, and four to six ($\bar{x}$=5.0; five expected) from the mark to the otolith edge. On 23-d larvae (n=5) that were marked on day 9 and day 16, we counted six to seven ($\bar{x}$=6.6) increments from the core to the first mark, 14 to 15 ($\bar{x}$=14.7) from the core to the second mark, and four to nine ($\bar{x}$=7.6) from the second mark (16-d-old) to the edge (23-d-old). For wild-caught larvae (n=12) (which ranged from 34.4 to 70.2 mm SL, were marked at 7-d intervals, and which were preserved 14 d after marking), we observed seven to eight ($\bar{x}$=7.0) increments between marks and 13–15 ($\bar{x}$=14.2) increments between the last mark and the edge.

Table 2

Analysis of variance results for increment counts versus age, and inverse regression for age versus increment counts (inverse regression) for all larvae and juveniles (n=69) of known-age spotted seatrout, *Cynoscion nebulosus*. SE = standard error.

Dependent variable	Slope	SE	Intercept	SE	P
Counts	1.0296	0.0172	−1.9867	0.3574	0.0001
Age	0.9538	0.0159	2.2273	0.3135	0.0001

Discussion

Our overestimation of ages, in our initial analysis (see "Materials and methods" section), from increment counts of older juveniles is difficult to relate to environmental factors. Overestimation of age is not common, although Fives et al. (1986) reported that larger bay anchovies, *Anchoa mitchelli*, in any known age group generally had more growth increments than smaller fish. Nielson and Geen (1982, 1985) noted that for salmonids, feeding frequency, exposure to warm or cool temperature cycles twice in a 24-h period, and an enforced increase in activity increased the rate of increment formation. Fish in our study did not undergo such cyclic events.

Campana and Moksness (1991), from a detailed appraisal of accuracy and precision of age estimates derived from otoliths, concluded that accuracy of age determination from validation experiments is probably "optimistic" owing in part to the constraints and limitations of validation studies done under laboratory conditions. The marked size difference of our known-age 32-d-old juveniles (16.2–34.6 mm SL) was undoubtedly a result of laboratory rearing conditions and indicated that even with appropriate photoperiod and feeding conditions, caution should be used when interpreting rings from older laboratory-reared juveniles, especially when size ranges are highly variable as in our study. For older known-age laboratory-reared material, multiple markings should be employed to discern those areas where interpretation is difficult and to discern subdaily rings.

Previous validation studies of spotted seatrout have indicated that rings are deposited daily, but central rings are difficult to interpret (McMichael and Peters, 1989). McMichael and Peters (1989) used otoliths mounted whole from tetracycline-marked wild-caught larvae and juveniles (7–10 mm). Although they were able to observe the formation of daily rings, they had difficulty in interpreting central rings. They used the average measurement to the tenth ring (50 µm, SD=2) taken from few exception-

ally clear juveniles. Our measurements from 23-d (n=12) and 32-d-old (n=15) juveniles averaged 52.4 µm (SD=8.1). Although our data were more variable, because we did not select only clear otoliths, our measurement to the tenth increment was similar to that of McMichael and Peters (1989), indicating we were interpreting the central increments fairly accurately.

Our relative lack of success in marking known-age larvae could be due to an inadequate concentration of ALC (50 mg/L) or insufficient immersion time at that concentration. Thomas et al. (1995) produced high mark quality on 6.0–9.0 mm red drum larvae at concentrations of 100 mg/L for as little as 2-h immersions. Fish mortality was minimal (and mark quality high) for immersion times up to 24 h at that concentration. A concentration of 50 mg/L for 4 h appears to be inadequate, however, for spotted seatrout larvae. Because of the relative lack of success in marking small larvae at 50 mg/L, larger juveniles were immersed in a concentration of 100 mg /L and marking success was relatively high after 4-h immersion, but still not 100%. Thomas et al. (1995) found that mortality of larvae was fairly high (>65%) at concentrations of 250 mg/L or higher; therefore longer immersion times are probably necessary for 100% marking success. Other investigators have had difficulties in marking larvae with tetracycline immersion that were related to divalent cations in full strength seawater (Campana and Nielson, 1982; Hettler, 1984; Gleason and Recksiek, 1990).

In conclusion, we caution investigators that our interpretation of increment counts for spotted seatrout may not be valid for other studies. The skill of the otolith reader is a critical component in otolith microstructure analysis (Campana and Moksness, 1991); therefore, microstructure analysis studies on spotted seatrout should require a separate validation study for each reader.

Acknowledgments

We are grateful to Cameron Pratt for collecting wild-caught fish, Patti Pickering for rearing and marking the fish, and Curtis Lewis for photographing and preparing the otolith figure. Dean Ahrenholz, Jon Hare, and two anonymous reviewers reviewed the manuscript and provided many valuable comments. This research was supported by the NOAA Coastal Ocean Program.

Literature cited

Ahrenholz, D. W., G. R. Fitzhugh, J. A. Rice, S. W. Nixon, and W. C. Pritchard.
1995. Confidence of otolith ageing through the juvenile stage for Atlantic menhaden, *Brevoortia tyrannus*. Fish. Bull. 93:209–216.

Campana, S. E., and E. Moksness.
1991. Accuracy and precision of age and hatch date estimates from otolith microstructure examination. ICES J. Mar. Sci. 48:303–316.

Campana, S. E., and J. D. Nielson.
1982. Daily growth increments in otoliths of starry flounder (*Platichthys stellatus*) and the influence of some environmental variables in their production. Can. J. Aquat. Sci. 39:937–942.

Crecco, V. C., and T. F. Savoy.
1985. Effects of biotic and abiotic factors on growth and relative survival of young American shad, *Alosa sapidissima*, in the Connecticut River. Can. J. Fish. Aquat. Sci. 42:1640–1648.

Fives, J. M., S. M. Warlen, and D. E. Hoss.
1986. Aging and growth of larval bay anchovy, *Anchoa mitchelli*, from the Newport River Estuary, North Carolina. Estuaries 9:362–367.

Geffen, A. J.
1992. Validation of otolith increment deposition rate. *In* Otolith microstructure examination and analysis (D. K. Sevenson and S. E. Campana, eds.), p. 101–113. Can. Spec. Publ. Fish. Aquat. Sci.

Gleason, T. R., and D. A. Bengtson.
1996. Size-selective mortality of inland silversides: evidence from otolith microstructure. Trans. Am. Fish. Soc. 125:860–873.

Gleason, T. R., and C. W. Recksiek.
1990. Preliminary field validation of daily growth increments in lapillar otoliths of juvenile cunner. *In* Fish marking techniques (N. C. Parker and five coeditors), p. 562–565. Am. Fish. Soc., Symposium 7, Bethesdsa, MD.

Hare, J. A., and R. K. Cowen.
1997. Size, growth, development and survival of planktonic larvae of *Pomatomus saltatrix* (Pisces: Pomatomidae). Ecology 78:2415–2431.

Hettler, W. F.
1984. Marking otoliths by immersion of marine fish larvae in tetracycline. Trans. Am. Fish. Soc. 113:370–373.

Jenkins, G. P., M. Shaw, and B. D. Stewart.
1993. Spatial variation in food-limited growth of juvenile greenback flounder, *Rhombosolea tapirina*: evidence from otolith daily increments and otolith scaling. Can. J. Fish. Aquat. Sci. 50:2558–2567.

Leger, P. H., D. A. Bengtson, K. L. Simpson, and P. Sorgeloos.
1986. The use and nutritional value of *Artemia* as a food source. Oceanogr. Mar. Biol. Rev. 24:521–623.

Maillet, G. L., and D. M. Checkley Jr.
1991. Storm-related variation in the growth rate of otoliths of larval Atlantic menhaden *Brevoortia tyrannus*: a time series analysis of biological and physical variables and implications for larva growth and mortality. Mar. Ecol. Prog. Ser. 79:1–16.

McMichael, R. H., and K. M. Peters.
1989. Early life history of spotted seatrout, *Cynoscion nebulosus* (Pisces: Sciaenidae), in Tampa Bay, Florida. Estuaries 12.98–110.

Nielson, J. D., and G. H. Geen.
1982. Otoliths of chinook salmon (*Oncorhynchus tshawytscha*): daily growth increments and factors influencing their production. Can. J. Fish. Aquat. Sci. 39:1340–1347.
1985. Effects of feeding regimes and diel temperature cycles on otolith increment formation in juvenile chinook salmon, *Oncorhynchus tshawytscha*. Fish. Bull 83:91–101.

Rice, J. A., L. B. Crowder, and F. P. Binkowski.
1985. Evaluating otolith analysis for bloater, *Coregonus hoyi*: do otoliths ring true. Trans Am. Fish. Soc. 114:532–539.

Sabo, M. J., and D. J. Orth.
1996. Absence of size-selective mortality among larval smallmouth bass in a Virginia stream. Trans. Am. Fish. Soc. 125: 920–924.

SAS Institute, Inc.
1985. SAS/STAT guide for personal computers, version 6 ed. SAS Institute, Inc., Cary, NC, 378 p.

Thomas, L. M., S. A. Holt, and C. Arnold.
1995. Chemical marking techniques in larval and juvenile red drum (*Sciaenops ocellatus*) otoliths using different flourescent markers. *In* Recent developments in fish otolith research (D. H. Secor, J. M. Dean, and S. E. Campana, eds.), p. 703–717. Univ. South Carolina Press, Columbia, SC.

Thorrold, S. R., and D. M. Williams.
1989. Analysis of otolith microstructure to determine growth histories in larval cohorts of a tropical herring (*Herklotsichthys castelnaui*). Can. J. Fish. Aquat. Sci. 46:1615–1624.

Consumption of Pacific herring (*Clupea pallasi*) eggs by greenling (Hexagrammidae) in Prince William Sound, Alaska

Christopher N. Rooper

Lewis J. Haldorson

Juneau Center for Fisheries and Ocean Sciences
University of Alaska Fairbanks
11120 Glacier Hwy, Juneau, Alaska 99801
Present address (for C. N. Rooper): Fishery Sciences Building
Box 355020
University of Washington
Seattle, Washington 98195

E-mail address (for C. N. Rooper): rooper@fish.washington.edu

Predation is an important process regulating egg survival in marine systems (Bailey and Houde, 1989). Pacific herring (*Clupea pallasi*) spawn demersal adherent eggs on shallow subtidal and intertidal substrates. Consequently, their eggs are available to a variety of predators throughout incubation. Documented predators of herring eggs include birds, invertebrates, marine mammals, and fish (Palsson, 1984). Avian predators were responsible for over 95% of the herring eggs lost in the intertidal zone in Holmes Harbor, Washington, in 1946 (Cleaver and Franett, 1946), 39% of the intertidal herring eggs lost on the west coast of Vancouver Island from 1947 to 1950 (Outram, 1958), and 70% of the herring eggs lost in Yaquina Bay, Oregon, in 1970 (Steinfeld, 1971). Estimates of egg predation by birds at two sites in British Columbia in 1988 and 1989 were 3.0% and 3.5% of the total eggs deposited by herring (Haegele and Schweigert, 1989; 1991).

Much less is known about the effects of other predators because studies to quantify Pacific herring egg loss from predators other than birds have been rare. In Barkeley Sound, British Columbia, predation by invertebrates accounted for 13.0% of the total herring eggs deposited, whereas gray whales consumed 3.0% of the total eggs deposited (Haegele and Schweigert, 1989). In 1989, herring egg loss due to epibenthic invertebrates was 4.1% of the total eggs spawned in Georgia Strait, British Columbia (Haegele and Schweigert, 1991).

Fish predation on Pacific herring eggs has not been studied in the northeast Pacific, although some studies have been done on the deeper-spawning Atlantic herring (*Clupea harengus*). Historically, abundance of North Sea haddock (*Melanogrammus aeglefinus*) and saithe (*Pollachius virens*) with stomachs containing Atlantic herring eggs were used as indicators of the concentrations of herring eggs (Hempel and Hempel, 1971); in years of light spawning, cod and haddock can consume up to 60% of the total eggs deposited.[1] Stomachs of sand eels (*Ammodytes marinus*) have been observed to be full of Atlantic herring eggs (Rankine and Morrison, 1989), and perch (*Perca fluviatilis*) has been found to be the most important consumer of herring eggs in the Archipelago Sea (Rajasilta et al., 1993). For Atlantic herring off the coast of Norway, egg loss due to haddock consumption has been estimated at 4.2% of the total eggs spawned (Toreson, 1991). Total Atlantic herring egg loss due to consumption by winter flounder (*Pseudopleuronectes americanus*) was at least 7% of the total egg abundance at a site in the Northwest Atlantic (Tibbo et al., 1963).

[1] Johannessen, A. 1980. Predation on herring (*Clupea harengus*) eggs and young larvae. International Council for the Exploration of the Sea, Council Meeting/1980, H:33, 12 p.

Lack of knowledge about fish predation on Pacific herring eggs and the importance of herring as a forage fish in the Northeast Pacific Ocean, led us to study predation on herring eggs in Prince William Sound, Alaska. The objective of our study was to estimate total consumption of herring eggs by some fish predators with the Elliot-Persson model (Elliot and Persson, 1978).

Materials and methods

Our study was conducted after herring spawning was completed on northern Montague Island in Prince William Sound, Alaska (Fig. 1), during late April and early May, 1995. Two variable mesh gill nets, 30.5 m long and 2.4 m deep, were used to collect fish near incubating herring eggs in the subtidal and intertidal zones at eight transects. Stretched-mesh sizes ranged from 2.5 to 12.7 cm. Panels of same-size mesh were equal length and depth (6.1 m × 2.4 m), and a total of five panels per net were used. A standardized fishing plan was carried out from one to three transects per day. Two nets were set at the bottom parallel to the shoreline at each transect. Depths fished depended on tide stage; at high tide, depths fished were 0.0 m and –3.0 m, whereas at low tide, depths fished were –1.5 m and –3.0 m in relation to mean low water. Logistical constraints limited fishing to one series of gillnet samples centered around the daylight high tide, and one series of samples centered around the daylight low tide. Each series consisted of three one-hour sets of the two nets, for a total of six gillnet sets over each tide stage, and a total of 96 sets equally spread over the eight transects.

Fish captured were identified by species and measured for fork length. Time of catch, net soak time, and tide stage were also recorded for each fish. Fish stomachs were removed and preserved in 10% buffered formalin. Stomach contents were categorized by type of prey (herring eggs, vegetation, crustaceans, etc.) and weighed to the nearest 0.01 g. Wet weights of each group of stomach contents were recorded, and herring eggs were subsampled to determine the

Manuscript accepted 1 December 1999.
Fish. Bull. 98:655–659 (2000).

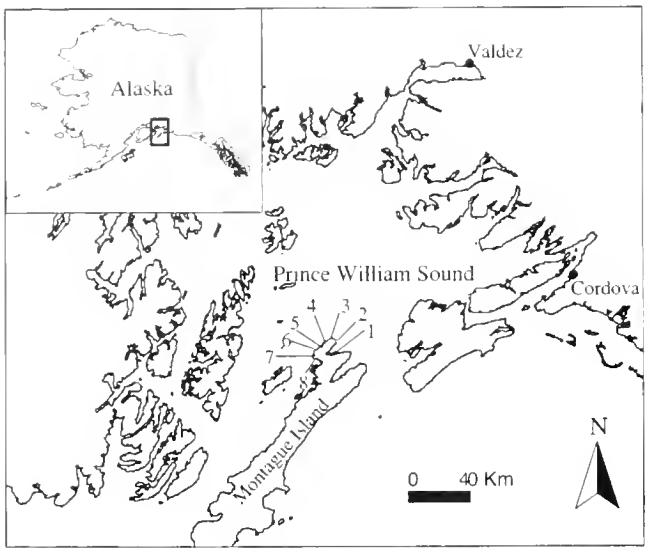

Figure 1

Study transects on Montague Island in Prince William Sound, Alaska, where gill nets were used to collect fish predators of herring spawn in 1995.

number of eggs per g. By multiplying the wet weight of herring eggs contained in each stomach by the number of eggs per g, the total number of herring eggs in each stomach was estimated.

Based on stomach-content analysis, estimates of daily ration were calculated only for greenling species. Because of the small number of each greenling species caught, these species were combined to estimate herring egg consumption. Estimates of daily ration were calculated by using the Elliot and Persson (1978) model,

$$C_t = \frac{(S_t - S_0 e^{-Rt}) \times Rt}{1 - e^{-Rt}}, \quad (1)$$

where C_t = food consumption during daylight hours;
R = the calculated gut clearance rate;
t = the number of daylight hours; and
S_0 and S_t = average stomach contents at time 0 and time t, respectively.

Estimates of stomach contents were obtained by examining fish caught during gillnet sampling and were assumed to be constant over daylight hours. The gut clearance rate (R) was calculated from a relationship of species evacuation rate versus temperature for marine and freshwater fish:

$$R = 0.0175T - 0.0442 \quad \text{(Worobec, 1984)}. \quad (2)$$

The average temperature (T) over the incubation period at a Montague Island transect was used in Equation 2. We had to extrapolate the equation in Worobec (1984) because their temperature range was warmer than ours. Initial consumption of food at the onset of daylight was calculated according to the Elliot-Persson model by using the equation

$$C_{initial} = S_{average} - S_0 e^{-Rt}, \quad (3)$$

where $S_{average}$ = the average eggs per stomach from gillnet samples; and
t = the nighttime hours.

Adding $C_{initial}$ and C_t gives an estimate of the daily consumption (C_d) of herring eggs over 24 h. Total consumption over the incubation period was then calculated by

$$C_{total} = C_d \times D \times I, \quad (4)$$

where C_d = the calculated daily consumption in numbers of eggs;
D = predator density; and
I = length of the incubation period in d.

Two previous studies estimated nearshore fish abundance on Montague Island. The first study estimated greenling density by using SCUBA surveys (Jewett et al.[2]) and the second study estimated nearshore fish biomass (Rosenthal[3]). We used both these estimates in separate calculations of Equation 4 to derive consumption estimates for greenling.

In the first calculation we used greenling density estimates in the subtidal zone from Jewett et al. (1995); total consumption per m^2 was compared directly with the average number of eggs per m^2 estimated in 1995. To use the biomass estimates from Rosenthal (1980), we changed the daily ration in egg numbers to a daily ration in egg biomass. Assuming isometric growth for greenling and using the end points of greenling length and weight ranges reported in Rosenthal (1980), we calculated the weight of each greenling caught during gillnet sampling. Using these two calculations for each fish sampled, we then estimated the daily ration as a percentage of body weight. Then, incorporating biomass estimates for greenling in Prince William Sound from Rosenthal (1980) and the number of incubation days for herring eggs in 1995, we calculated the total weight of eggs consumed per km^2 by converting Equation 4 to

$$C_t = B_g \times C_w \times I, \quad (5)$$

[2] Jewett, S. C., T. A. Dean, R. O. Smith, M. Stekoll, L. J. Haldorson, D. R. Laur and L. McDonald. 1995. The effects of the *Exxon Valdez* oil spill on shallow subtidal communities in Prince William Sound, Alaska 1989–93. *Exxon Valdez* Oil Spill Restoration Project Final Report (Restoration Project 93047; subtidal study number 2A), Alaska Dept. of Fish and Game, Habitat and Restoration Division, Anchorage, Alaska, 178 p.

[3] Rosenthal, R. J. 1980. Shallow water fish assemblages in the northeastern Gulf of Alaska: habitat evaluation, species composition, abundance, spatial distribution and trophic interaction. *In* Environmental assessment of the Alaskan continental shelf, p. 451–540. Final reports of principal investigators, 17: biological studies, NOAA/NOS, Office of Oceanography & Marine Services.

Table 1

Total gillnet hours fished and mean catch per hour for each fish species captured at Montague Island, Alaska, in 1995. Numbers in parentheses indicate total number of fish captured during sampling.

		Catch (no. of fish) per hour				
Transect	Hours fished	Greenling (two species)	Dolly Varden	Starry flounder	Red Irish lord	Great sculpin
1	13:48	(0)	0.435 (6)	0.072 (1)	(0)	(0)
2	14:26	(0)	0.069 (1)	(0)	(0)	(0)
3	13:28	0.446 (0)	(0)	(0)	(0)	(0)
4	13:52	0.072 (1)	(0)	(0)	(0)	0.072 (0)
5	13:32	0.296 (4)	(0)	(0)	0.074 (1)	0.074 (1)
6	12:15	0.082 (1)	(0)	(0)	(0)	(0)
7	14:34	0.069 (1)	0.069 (1)	(0)	(0)	(0)
8	14:39	(0)	(0)	(0)	(0)	0.068 (1)
Average CPUE		0.120 (13)	0.072 (8)	0.009 (1)	0.009 (1)	0.027 (1)

where C_t = the total biomass of eggs consumed per km^2;
B_g = the biomass of greenling;
C_w = the daily ration as a percentage of fish weight; and
I = the length of the incubation period in d.

This estimate of egg biomass consumed was applied to the biomass estimates of eggs spawned on Montague Island to obtain a percentage of the total herring eggs consumed by greenling.

Results

Six fish species were caught during gillnet sampling: rock greenling (*Hexagrammos lagocephalus*), kelp greenling (*Hexagrammos decagrammus*), Dolly Varden char (*Salvelinus malma*), starry flounder (*Platichthys stellatus*), red Irish lord (*Hemilepidotus hemilepidotus*) and great sculpin (*Myoxocephalus polyacanthocephalus*). The most common fish caught were the two greenling species, followed by Dolly Varden and great sculpin; only one red Irish lord and one starry flounder were caught. Average catch for all species was relatively low, ranging from 0.009 fish per h (SE=0.008) for starry flounder and red Irish lord to 0.120 fish per h (SE=0.052) for the greenling species combined (Table 1). Only greenling and Dolly Varden consumed herring eggs; all 13 greenling stomachs contained eggs, whereas just 4 of 8 Dolly Varden stomachs contained eggs. Stomachs of other fish species contained a combination of unidentifiable fish and invertebrates. The average number of eggs per stomach was 87 (SE=40.4) for Dolly Varden, and 8785 (SE=2107.6) for greenling. The number of herring eggs per greenling stomach increased exponentially with length (Fig. 2).

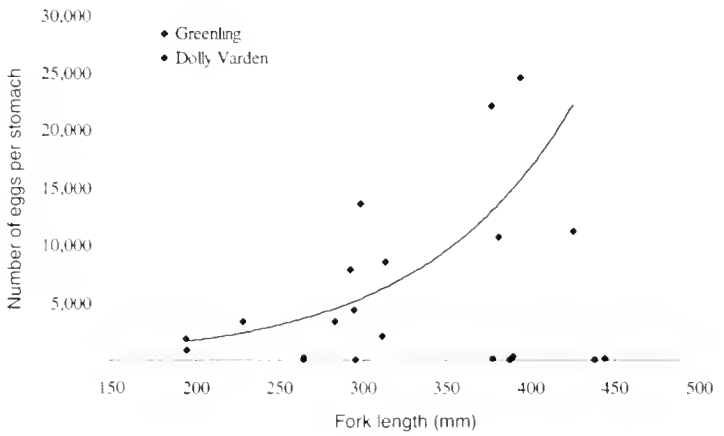

Figure 2

Number of eggs per stomach for combined greenling species (n=13) and Dolly Varden char (n=8) captured by gillnetting at herring spawning bed transects in 1995. The line represents the predicted exponential increase in eggs per stomach with increasing fork length; r^2 for the predicted versus the observed relationship was 0.55.

A pattern in greenling and Dolly Varden catch distributions was apparent; Dolly Varden were caught exclusively in embayments, whereas all greenling, except one, were caught on the outer coast of Montague Island. The average temperature during incubation at −1.5 m depth was 5.8°C at transect 4, resulting in an estimated instantaneous evacuation rate of 0.057 per h. The daily ration calculated with that evacuation rate was 11,984 eggs per d (Table 2).

Subtidal surveys of fish abundance in Prince William Sound found an average of 0.0889 greenling per m^2 on

Table 2

Calculations for estimating daily consumption of herring eggs by greenling with the Elliot-Persson model.

Elliot-Persson model for estimating daily consumption (Eq. 1)	
1 Consumption during daylight hours (assuming constant stomach fullness), C	
t = average daylight hours from 29 April to 20 May 1995	16.67
Instantaneous evacuation rate (R)	0.057
S_0	9264
S_t	9264
C_t	8816
2 Initial consumption at onset of feeding, $C_{initial}$	
Decrease in stomach contents during night, $S_t = S_0 e^{-Rt}$	
S_0	9264
t = average nighttime hours from 20 April to 20 May 1995	7.33
Instantaneous evacuation rate (R)	0.057
S_t	6096
$C_{initial} = S_0 - S_t$	3168
3 Total consumption over 24 hours = $C_{initial} + C_t$	11,984

island points in shallow waters from 2 to 20 m deep on Montague Island (Jewett et al., 1995). According to the daily ration calculated above, daily consumption of herring eggs by greenling would be 1065 eggs per m^2. In 1995, the incubation period for herring eggs was 21 d in Prince William Sound; therefore total removal during incubation would have been 22,373 eggs per m^2. In 1995, the average number of eggs per m^2 was 606,831, on Montague Island.[4] Therefore, using the daily consumption above, we estimated that 3.7% of the eggs deposited were consumed by greenling over the course of incubation.

The weight of the estimated daily ration (11,984 eggs) for greenling was 38.3 g, or weight of the eggs in a greenling stomach multiplied by 1.29. From this conversion factor, daily ration as a percentage of greenling body weight was estimated as 6% per d. Results from dive surveys from Rosenthal (1980) have shown a greenling biomass at Zaikoff Point on Montague Island of approximately 35,000 kg/km^2. Multiplying this biomass estimate by the daily ration as a percentage of body weight and by the number of incubation days in 1995, yields an egg consumption estimate of 44,100 kg/km^2. In 1995, an estimated 5,922,673 kg of eggs were deposited over a 3.05-km^2 area on Montague Island.[2] If one assumes that all greenling move into subtidal and intertidal areas to feed on eggs deposited there, then greenling would have consumed 2.3% of the total eggs deposited.

Discussion

Calculation of daily ration by the Elliot-Persson method presented here assumes that greenling maintain a full stomach throughout the entire daylight period. The exponential increase in eggs per stomach with greenling length suggests that our assumption that greenling maintain a constant state of gut fullness is correct because greenling stomach volume should increase exponentially with body length. Our method for estimating total consumption of herring eggs by greenling also assumes that there is no numerical response to availability of eggs. If greenling move from deeper water to the band of herring eggs, the estimate of consumption may be higher. Migration of greenling to the spawning beds from areas where no spawn was deposited would also have increased the consumption estimate.

By sampling during slack tide periods, total consumption of eggs may have been underestimated. If greenling were actively feeding during the time when they encountered gill nets, their stomach contents may not have been representative of the entire daylight period. Greenling stomach contents may have been less during times of active feeding than during the rest of the day. Gill nets are also known to be both size selective and species selective (Hay et al., 1986; Methven and Schneider, 1998). Selectivity, therefore, probably influenced our results both on account of the nets selecting for a small range of greenling sizes and selecting only species that exhibited behaviors that made them susceptible to capture. If the average length of greenling captured during sampling was larger than the average length of greenling in the total population, we may have overestimated the total consumption of eggs. However, the estimate of total consumption of herring eggs is likely to have been underestimated for Prince William Sound, because the estimate is only for two species of fish. Because greenling make up only 56% by number and 59% by biomass of the fish species at Montague Island (Rosenthal, 1980), many other species inhabiting the zone covered by herring eggs would have access to the rich food source the eggs provide. Our results are similar to other studies in the Atlantic where predation on herring eggs by fish has typically been estimated at less than 10% of the total herring eggs (Tibbo et al., 1963; Toreson, 1991).

A concurrent study of egg loss in Prince William Sound has shown that herring egg loss from spawning beds increases at shallower depths (Rooper et al., 1999). Consumption of eggs by bird species indicate avian predators may be responsible for removals of large numbers of eggs (27%),[5] most of which are lost in the intertidal zone. The different levels of predation in the intertidal and subtidal zones by birds and fish may be the underlying cause of the higher egg loss rates observed at shallower depths. If predation is an important factor regulating survival of eggs to time of hatching, then herring behavior may lend itself to depensatory mortality. Concentration of herring

[4] Wilcock, J., and K. Hyer. 1998. Personal commun. Alaska Department of Fish and Game, P.O. Box 669, Cordova, AK 99754

[5] Bishop, M. A., and P. Green. 1998. Unpubl. data. USFS-CRDI, PO Box 1460, Cordova AK 99574.

stocks into a relatively small area during spawning and the resulting spatial concentration of eggs in the spawning beds could lead to high egg losses owing to predation even in years of low herring biomass. This in turn could drive the abundance of herring eggs even lower, as predators continued to concentrate on an ever-dwindling resource.

In summary, our study estimated that two greenling species consumed between 2.3% and 3.7% of the total herring eggs deposited on Montague Island in Prince William Sound in 1995. Greenling represent only a portion of the fish species in Prince William Sound; therefore predation by other fish species would probably increase the consumption estimates. Although consumption of herring spawn by fish species has not been extensively studied in the Pacific, the results of our study indicate the importance of predation by fish species on the mortality of herring eggs in spawning beds.

Acknowledgments

We thank John Wilcock and Karen Hyer, Alaska Department of Fish and Game, for providing the egg abundance data, as well as Dr. Terrance Quinn II and Jennifer Boldt, University of Alaska Fairbanks, for their technical support. Funds for this study were provided by the Exxon Valdez Trustee Council through the Alaska Department of Fish and Game, Herring Natal Habitats Project no. 95166.

Literature cited

Bailey, K. M., and E. D. Houde.
1989. Predation on eggs and larvae of marine fishes and the recruitment problem. Adv. Mar. Biol. 25, 82 p.

Cleaver, F. C., and D. M. Franett.
1946. The predation by sea birds upon the eggs of the Pacific herring (*Clupea pallasi*) at Holmes Harbor during 1945. Washington State Dept. Fish. Biol. Rep. 46B, 18 p.

Elliot, J. M., and L. Persson.
1978. The estimation of daily rates of food consumption for fish. J. Animal Ecol. 47:977–991.

Haegele, C. W., and J. F. Schweigert.
1989. Egg loss from Pacific herring spawns in Barkeley Sound in 1988. Can. Manage. Rep. Fish. Aquat. Sci. 2037, 40 p.
1991. Egg loss in herring spawns in Georgia Strait, British Columbia. *In* Proceedings of the International Herring Symposium, Anchorage, Alaska, October 23–25, 1990, p. 309–322. Univ. Alaska, Fairbanks, AK

Hay, D. E., K. D. Cooke, and C. V. Gissing.
1986. Experimental studies of Pacific herring gillnets. Fish. Res. 4:191–211.

Hempel, I., and G. Hempel.
1971. An estimate of mortality in eggs of North Sea herring (*Clupea harengus* L.). Rapp. P.-V. Reun. Cons. Int. Explor. Mer 160:24–26.

Methven, D. A., and D. C. Schneider.
1998. Gear-independent patterns of variation in catch of juvenile Atlantic cod (*Gadus morhua*) in coastal habitats. Can. J. Fish. Aquat. Sci. 55:1430–1442.

Outram, D. M.
1958. The magnitude of herring spawn losses due to bird predation on the west coast of Vancouver Island. Fish. Res. Board Can. Pac. Biol. Stat. Prog. Rep. 111:9–13.

Palsson, W. A.
1984. Egg mortality upon natural and artificial substrata within Washington state spawning grounds of Pacific herring (*Clupea harengus pallasi*). M.S. thesis, Univ. Washington, Seattle, WA, 191 p.

Rajasilta, M., J. Eklund, J. Hanninen, M. Kurkilahti, M., J. Kaaria, P. Rannikko, and M. Soikkeli.
1983. Spawning of herring (*Clupea harengus membras* L.) in the Archipelago Sea. ICES J. Mar. Sci. 50:223–246.

Rankine, P. W., and J. A. Morrison.
1989. Predation on herring larvae and eggs by sand-eels *Ammodytes marinus* (Rait) and *Hyperoplus lanceolatus* (Lesauvage). J. Mar. Biol. Assoc. U. K. 69:493–498.

Rooper, C. N., L. J. Haldorson, and T. J. II Quinn.
1999. Habitat factors controlling Pacific herring (*Clupea pallasi*) egg loss in Prince William Sound, Alaska. Can. J. of Fish. Aquat. Sci. 56:1133–1142.

Steinfeld, J. D.
1971. Distribution of Pacific herring spawn in Yaquina Bay, Oregon, and observations on mortality through hatching. M.S. thesis, Oregon State University, Corvallis, OR, 75 p.

Tibbo, S. N., D. J. Scarratt, and P. W. G. McMullon.
1963. An investigation of herring (*Clupea harengus* L.) spawning using free-diving techniques. J. Fish. Res. Board Can. 20:1067–1079.

Toreson, R.
1991. Predation on the eggs of Norwegian spring-spawning herring (*Clupea harengus* L.) on a spawning ground on the west coast of Norway. ICES J. Mar. Sci. 48:15–21.

Worobec, M. N.
1984. Field estimates of the daily ration of winter flounder, *Pseudopleuronectes americanus* (Walbaum), in a southern New England salt pond. J. Exp. Mar. Biol. Ecol. 77:183–196.

Fishery Bulletin

Guide for Contributors

Content

Articles published in *Fishery Bulletin* describe original research in fishery marine science, engineering and economics, and the environmental and ecological sciences, including modeling. Articles may range from relatively short to extensive.

Notes are reports of 5 to 10 pages without an abstract and describing methods or results not supported by a large body of data.

Although all contributions are subject to peer review, responsibility for the contents of papers rests upon the authors and not upon the editor or the publisher. It is therefore important that the contents of the manuscript are carefully considered by the authors.

Submission of an article is understood to imply that the article is original and is not being considered for publication elsewhere. Manuscripts should be written in English. Authors whose native language is not English are strongly advised to have their manuscripts checked by English-speaking colleagues prior to submission.

Preparation

Title page should include authors' full names and mailing addresses, the corresponding author's telephone, FAX number, and e-mail address, and a list of key words to describe the contents of the manuscript.

Abstract should not exceed one double-spaced typed page. It should state the main scope of the research but emphasize its conclusions and relevant findings. Because abstracts are circulated by abstracting agencies, it is important that they represent the research clearly and concisely.

Text must be typed double-spaced throughout. A brief introduction should portray the broad significance of the paper; the remainder of the paper should be divided into the following sections: Materials and methods, Results, Discussion (or Conclusions), and Acknowledgments. Headings within each section must be short, reflect a logical sequence, and follow the rules of multiple subdivision (i.e. there can be no subdivision without at least two items). The entire text should be intelligible to interdisciplinary readers; therefore, all acronyms, abbreviations, and technical terms should be spelled out the first time they are mentioned. The scientific names of species must be written out the first time they are mentioned; subsequent mention of scientific names may be abbreviated. Follow Scientific Style and Format: the CBE Manual for Authors, Editors, and Publishers (6th ed.), for editorial style, and the most current issue of the American Fisheries Society's Common and Scientific Names of Fishes from the United States and Canada, for fish nomenclature. Dates should be written as follows: 11 November 1991. Measurements should be expressed in metric units, e.g. metric tons as t; if other units of measurement are used, please make this fact explicit to the reader. The numeral one (1) should be typed as a one, not as a lower-case el (l). Use of appendices is discouraged.

Text footnotes should be numbered with Arabic numerals and inserted at the bottom of text. Footnote all personal communications, unpublished data, and unpublished manuscripts with full address of the communicator or author, or, as in the case of unpublished data, where the data are on file. Authors are advised to avoid references to nonstandard (gray) literature, such as internal, project, processed, or administrative reports. Where these references are used, please include whether they are available from NTIS (National Technical Information Service) or from some other public depository.

Literature cited comprises published works and those accepted for publication in peer reviewed literature (in press). Follow the name and year system for citation format. In the text, cite as follows: Smith and Jones (1977) or (Smith and Jones, 1977). If there is a sequence of citations, list alphabetically by author(s): Smith, 1987; Smith and Jones, 1985; Smith and Peterson, 1986. Abbreviations of serials should conform to abbreviations given in Serial Sources for the BIOSIS Previews Database. Authors are responsible for the accuracy and completeness of all citations.

Tables should not be excessive in size and must be cited in numerical order in the text. Headings within tables should be short but ample enough to allow the table to be intelligible on its own. All unusual symbols must be explained in the table legend. Other incidental comments may be footnoted with italic numerals. Use the asterisk only to indicate probability in statistical data. Zeros should precede all decimal points for values less than one.

Figures must be cited in numerical order in the text. The senior author's last name and the figure number should be written on the back of each one. Hand-drawn illustrations should be submitted as originals and not as photocopies. Submit photographs as glossy prints or slides with good contrast, otherwise we cannot guarantee a good final printed copy. Graphs should be submitted as laser-printed copies, not as photocopies. Label all figures with Helvetica typeface and capitalize the first letter of the first word in axis labels. Italicize species name and variables in equations. Use zeros before all decimal points. Use uppercase Times Roman bold typeface to label the parts of a figure, e.g. A, B, C, etc. Each figure legend should explain all symbols and abbreviations in the figure and should be double-spaced and placed at the end of the manuscript.

Copyright law Government publications are not copyrighted; they fall within the public domain. If an author reproduces any part of a government publication in his work, reference to source is appreciated.

Submission

Send printed copies (original and three copies without staples) to the Scientific Editor:

Dr. John V. Merriner
Southeast Fisheries Science Center
National Marine Fisheries Service
101 Pivers Island Road
Beaufort, NC 28516

Once the manuscript has been accepted for publication, you will be asked to submit an electronic copy of your manuscript to the Managing Editor. The electronic copy should be submitted in WordPerfect or Microsoft Word text format and placed on a 3.5-inch disk that is double-sided, double or high density, and that is compatible with either DOS or Macintosh systems.

A copy of page proofs will be sent to the author for final approval prior to publication.

Reprints (copies of published articles and notes) are available free of charge to the senior author (50 copies) and to his or her laboratory (50 copies). Additional copies may be purchased in lots of 100 when the author receives page proofs.

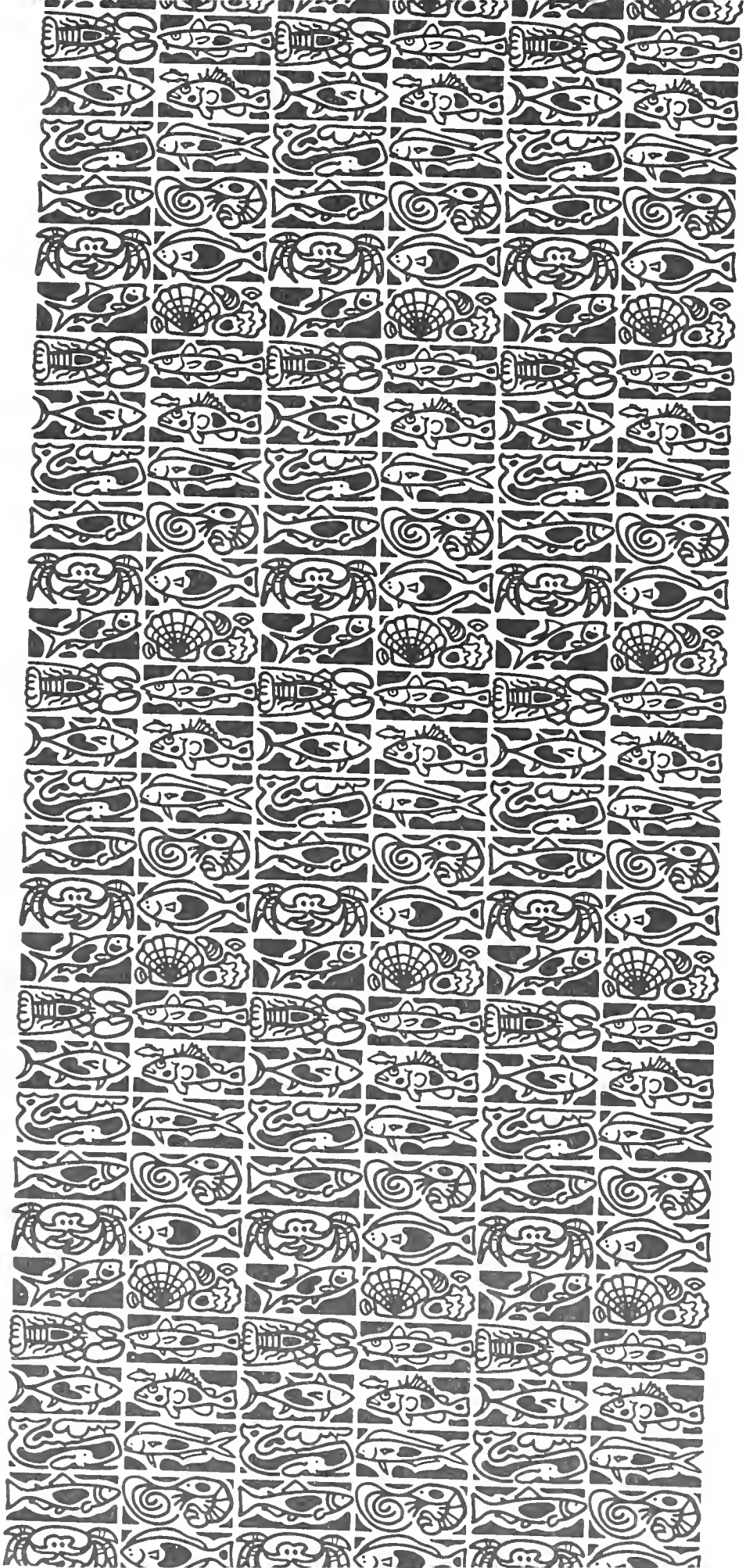

U.S. Department
of Commerce

Volume 98
Number 4
October 2000

Fishery Bulletin

The *Fishery Bulletin* (ISSN 0090-0656) is published quarterly by the Scientific Publications Office, National Marine Fisheries Service, NOAA, 7600 Sand Point Way NE, BIN C15700, Seattle, WA 98115-0070. Periodicals postage is paid at Seattle, WA, and at additional mailing offices. POSTMASTER: Send address changes for subscriptions to Fishery Bulletin, Superintendent of Documents, Attn.: Chief, Mail List Branch, Mail Stop SSOM, Washington, DC 20402-9373

The Secretary of Commerce has determined that the publication of this periodical is necessary according to law for the transaction of public business of this Department. Use of funds for printing of this periodical has been approved by the Director of the Office of Management and Budget.

For sale by the Superintendent of Documents, U.S. Government Printing Office, Washington, DC 20402. Subscription price per year: $50.00 domestic and $62.50 foreign. Cost per single issue: $19.00 domestic and $23.76 foreign. **See back for order form.**

Fishery Bulletin

***Fishery Bulletin* web site: fishbull.noaa.gov**

The *Fishery Bulletin* carries original research reports and technical notes on investigations in fishery science, engineering, and economics. It began as the Bulletin of the United States Fish Commission in 1881; it became the Bulletin of the Bureau of Fisheries in 1904 and the *Fishery Bulletin* of the Fish and Wildlife Service in 1941. Separates were issued as documents through volume 46, the last document was No. 1103. Beginning with volume 47 in 1931 and continuing through volume 62 in 1963, each separate appeared as a numbered bulletin. A new system began in 1963 with volume 63 in which papers are bound together in a single issue of the bulletin. Beginning with volume 70, number 1, January 1972, the *Fishery Bulletin* became a periodical, issued quarterly. In this form, it is available by subscription from the Superintendent of Documents, U.S. Government Printing Office, Washington, DC 20402. It is also available free in limited numbers to libraries, research institutions, State and Federal agencies, and in exchange for other scientific publications.

U.S. Department of Commerce
Seattle, Washington

Volume 98
Number 4
October 2000

Fishery Bulletin

Contents

Abstract—Variation in the life history parameters of Dover sole (*Microstomus pacificus*) off the coasts of Washington, Oregon, and northern California was investigated by using research survey data. We compared growth, maturation, and length-weight curves of Dover sole within the International North Pacific Fisheries Commission (INPFC) statistical areas of Monterey, Eureka, Columbia, and Vancouver. We found strong evidence of dimorphism in growth and maturation rates between sexes. In addition, geographic variation in both growth and maturation rates was also suggested. Male and female Dover sole from the Columbia area had lower Brody growth coefficients and larger asymptotic lengths than Dover sole from other areas. Further, there was an apparent latitudinal cline in maturation rates because males and females matured at smaller size and younger ages at higher latitudes. In contrast, no difference between male and female length-weight relationships was detected. In comparison with other pleuronectids, we found that Dover sole matured at relatively larger sizes and younger ages. These differences likely reflect adaptation of Dover sole to the inherent variability of the California Current.

Manuscript accepted 15 March 2000.
Fish. Bull. 98:661–673 (2000).

Variation in life history parameters of Dover sole, *Microstomus pacificus*, off the coasts of Washington, Oregon, and northern California

Jon Brodziak

Hatfield Marine Science Center
Northwest Fisheries Science Center
National Marine Fisheries Service, NOAA
2030 SE Marine Science Drive
Newport, Oregon 97365
Present address: Northeast Fisheries Science Center
166 Water Street
Woods Hole, Massachusetts 02543
E-mail address: Jon.Brodziak@noaa.gov

Robert Mikus

Hatfield Marine Science Center
Oregon Department of Fish and Wildlife
2040 SE Marine Science Drive
Newport, Oregon 97365

Dover sole (*Microstomus pacificus*) is a deep-water pleuronectid fish that ranges from Baja, California, to the Bering Sea (Hart, 1973) at depths from 10 m to 1200 m (Pearcy et al., 1982; Allen and Smith, 1988). Dover sole are demersal and have a complex life history that includes an extended pelagic larval phase of one year or more (Pearcy et al., 1977; Markle et al., 1992; Toole et al., 1993; Butler et al., 1996) and an ontogenetic migration range from continental shelf to continental slope (Jacobson and Hunter, 1993). Dover sole support an important commercial fishery off the coasts of Washington, Oregon, and California, where annual landings have averaged about 12,000 t during 1956–96 (Brodziak et al., 1997).

Previous research on life history parameters of Dover sole off the west coast of the United States was conducted during the late 1940s and the 1980s. Hagerman (1952) estimated growth, maturation rates, and length-weight curves of Dover sole from commercial fishery samples collected from the ports of Eureka and Fort Bragg, California during 1948–49. Harry (1959) estimated maturation rates of Dover sole from commercial fishery samples collected at the port of Astoria, Oregon, during 1948–49. More recently, Hunter et al. (1990) have estimated growth and maturation rates of Dover sole from research survey samples collected between Point Conception and Half Moon Bay, California, during 1985–88. Hunter et al. (1992) refined maturation rate estimates of female Dover sole through histological analysis of survey data collected off the coasts of Oregon and California during 1985–89.

In this study, we investigated variation in life history parameters of Dover sole off the coasts of Washington, Oregon, and northern California from samples collected during research surveys during 1984–85 and 1990–93. Dover sole samples were partitioned into geographic regions based on International North Pacific Fisheries Commission statistical areas in order to investigate latitudinal differences among potential management units. We used length-at-age data to estimate growth and to quantify sexual dimorphism and geographic variation in growth. Maturation of male and female Dover sole as a function of length and age was estimated and geographic variation in maturity was quantified. Sexual dimorphism and geographic variation on weight at length were also explored. We discuss apparent differences between life history parameters of Dover sole and other pleuronectids.

Materials and methods

Length-at-age samples

A total of 4780 Dover sole were collected for age determination during 1984–93 from bottom trawl surveys of the upper continental slope (Raymore and Weinberg, 1990; Parks et al., 1993; Lauth et al., 1997). Biological samples were collected from three depth strata (183–549 m, 550–914 m, and 915–1280 m) within the International North Pacific Fisheries Commission (INPFC) statistical areas (Table 1; Fig. 1) of Monterey (38°24′N–40°30′N), Eureka (40°30′N–43°00′N), Columbia (43°00′N–47°30′N), and Vancouver (47°30′N–48°29′33″N). The survey area was length- and depth-stratified to ensure adequate coverage for otolith sampling. For each fish collected, sex was determined, total length (to the nearest cm) was measured, and otoliths were extracted for age determination.

Maturity stage was determined for 4490 Dover sole by visual inspection of gonads. Only samples from surveys conducted by the RV *Miller Freeman* (Table 1) were used for analyzing maturity rates because these samples were collected prior to the spawning season during winter when gross anatomical features provide a reasonably accurate measure for determining whether a fish is mature or not (Hagerman, 1952; Hunter et al., 1992). Total fish weights (to the nearest gram) were also recorded for 3019 samples from surveys conducted by the MV *Half Moon Bay* and the RV *Miller Freeman*; these data were used for length-weight analyses.

Fish ages were determined by the break and burn method, which is the standard for Dover sole (Pikitch and Demory, 1988), although the method has not been validated. In our study, the initial otolith increment was assumed to be an age-1 marker in accordance with the convention for aging adult Dover sole (Chilton and Beamish, 1982). Increments in each otolith were counted two or more times and assigned a single age by one of four readers. In some cases, a mark within the otolith core was counted as the initial increment because it met the identification criteria of an annual increment. A paired comparison of age readings between the most experienced reader and the other readers indicated that there was a mean difference of μ=0.22 years (σ_μ=0.13) based on a blind sample of 474 Dover sole; this difference was almost significant at the 5% level (P=0.08).

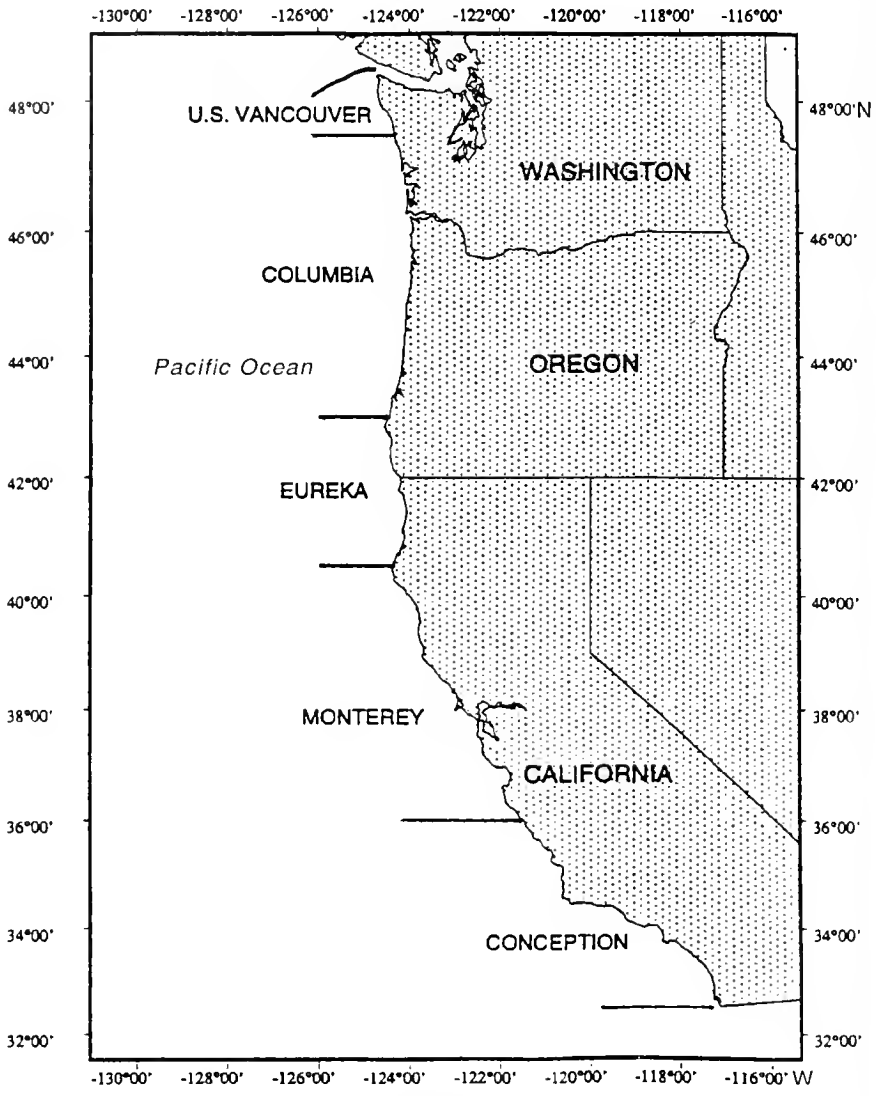

Figure 1

International North Pacific Fisheries Commission statistical areas in the North Pacific Ocean.

Empirical comparisons of mean ages, lengths, and weights by sex within each INPFC area were performed. The GT2 test is appropriate for unplanned comparisons of populations with unequal sample sizes (Sokal and Rohlf, 1981) and it was used to test for differences in mean age, length, and sex among INPFC areas.

Growth curves

Bartlett's test of homogeneity of variance was used to test whether variance in length at age varied by sex for Dover sole from ages 3 to 30 years. Test results were used to select an appropriate error structure for growth curve estimation. Growth curves for male, female, and pooled-sex samples were estimated by maximum likelihood (see Kimura, 1980). We used an alternative parameterization of the von Bertalanffy growth curve (Schnute

Table 1

Dover sole samples used for growth, maturity,[1] and length-weight[2] analyses by INPFC area, vessel, month and year of collection, and depth range of capture.

INPFC area		Number of males	Number of females	Total	Vessel	Month and year	Depth range (m)
Vancouver		94	97	191	FV *Marathon*	Apr 1985	221–406
		41	59	100	FV *Mys. Babushkina*	May 1985	188–280
		77	60	137	RV *Miller Freeman*	Oct 1992	225–854
	Total	212	216	428			
Columbia		329	54	383	FV *Poseydon*	Apr 1984	320–450
		596	331	927	MV *Half Moon Bay*	Sep 1984	110–856
		419	248	667	FV *Marathon*	Apr 1985	188–448
		230	88	318	FV *Mys. Babushkina*	May 1985	115–262
		162	236	398	RV *Miller Freeman*	Oct 1992	210–1211
		182	240	422	RV *Miller Freeman*	Oct 1993	192–1132
	Total	1918	1197	311			
Eureka		226	303	529	RV *Miller Freeman*	Oct 1990	252–1189
		37	39	76	RV *Miller Freeman*	Oct 1991	229–1176
		54	75	129	RV *Miller Freeman*	Oct 1993	243–1163
	Total	317	417	734			
Monterey		209	294	503	RV *Miller Freeman*	Oct 1991	198–1130

[1] Maturity analyses comprised data from surveys conducted by the RV *Miller Freeman*.
[2] Length-weight analyses comprised data from surveys conducted by the RV *Miller Freeman* and the MV *Half Moon Bay*.

and Fournier, 1980; Ratkowsky, 1983) because its parameters were simpler to interpret and because it exhibited better statistical properties than other parameterizations of the von Bertalanffy model. This form was

$$L(t_i) = L_{min} + (L_{max} - L_{min}) \frac{(1 - c^{t_i - t_{min}})}{(1 - c^{t_{max} - t_{min}})} + \varepsilon_i, \quad (1)$$

where t_i = age of the i^{th} sample;
L_{min}, L_{max}, and c = parameters;
t_{min} and t_{max} denote the youngest and oldest ages observed in the length-at-age sample;
L_{min} and L_{max} denote the predicted lengths at ages t_{min} and t_{max}; and
ε_i = independent and identically distributed normal error terms with zero mean and constant variance $\varepsilon_i \sim N(0, \sigma^2)$.

There is a one-to-one relationship between parameters of the alternative form and the standard von Bertalanffy model (see Ratkowsky, 1983). Residuals from estimated growth models were tested for normality with the Shapiro and Wilk (1965) test. Standard errors of parameter estimates were computed by using the conditional bootstrap with 1000 bootstrap replicates (Efron and Tibshirani, 1993), except for the pooled-sex analysis, where asymptotic standard error estimates were used owing to the large sample size.

As found in previous research, some sexual dimorphism in growth was expected, but there was no information about geographic variation in growth. A likelihood-ratio test (Kimura, 1980) was applied to determine whether growth curves differed by sex or by INPFC area. This test compared two hypotheses: H_0, the hypothesis of identical growth parameters between sexes or among areas; and H_1, the hypothesis of different growth parameters. The test statistic (χ^2) was

$$X^2 = -N \log\left(\frac{\sigma_1^2}{\sigma_0^2}\right), \quad (2)$$

where σ_0^2 and σ_1^2 = sample estimates of residual variance for growth curves estimated under H_0 and H_1.

The likelihood-ratio test was applied to male and female samples from all INPFC areas and was then separately applied to male and female samples for paired adjacent INPFC areas. When there was no difference between adjacent areas, samples were grouped and the process was repeated. Standard errors of parameter estimates of the final groups were computed by using the conditional bootstrap with 1000 replicates.

Maturation curves

Maturation by length and by age were estimated for female (n=934) and male (n=1232) Dover sole with logistic regression (McCullagh and Nelder, 1989). Significance of fish length or age as a predictor of fraction mature was tested with the likelihood-ratio chi-square test. Standard errors for model parameters were estimated by using the nonparametric bootstrap method with 1000 replicates.

Geographic differences in maturation rates were also evaluated for male and female samples by using logistic regression. Step-wise model selection was used to determine the best model of length or age and the factors INPFC area and sex, and all possible higher order interactions between these terms. The full model with all possible interactions was

$$\log\left(\frac{\pi}{1-\pi}\right) = (\beta_0 + \beta_A + \beta_S + \mathrm{B}_{AS}) + (\beta_1 + \beta_{1A} + \beta_{1S} + \beta_{1AS})X, \quad (3)$$

where π = the probability of being sexually mature;

β_A, β_S, and β_{AS} = coefficients of area, sex, and their interaction; and

β_{1A}, β_{1S}, and β_{1AS} = coefficients of first- and second-order interactions between area, sex, and the variable length (or age), denoted by X.

Akaike's information criterion (AIC) was used to compare competing nested models in a step-wise manner (Hastie and Pregibon, 1993). We also evaluated whether overdispersion due to cluster sampling was present (McCullagh and Nelder, 1989). If the ratio of observed to expected sampling variation (ϕ) for the estimated model was less than 1, we concluded that overdispersion was not present. Nonparametric bootstrapping based on 1000 replicates was used to estimate standard errors for parameter estimates.

Length-weight curves

We estimated length-weight relationships for pooled-sex, male (n=1549), and female (n=1470) samples based on the allometric equation

$$W_i = AL_i^B \exp(\varepsilon_i), \quad (4)$$

where W_i and L_i = the observed total weight (grams) and total length (centimeters) of the i^{th} fish;

A and B = parameters; and

ε_i = independent and identically distributed normal error terms with zero mean and constant variance.

A natural logarithmic transformation was applied to length and weight measurements and linear regression was applied to estimate parameters, denoted as b_0=log$A$ and b_1=B. Because lognormal errors were assumed, the retransformed intercept needs to be adjusted to give an accurate predictive equation for mean weight, and the adjusted intercept was computed as A=exp(b_0)exp((σ^2– $\sigma_0{}^2$)/2), where σ^2 is the residual variance from the regression and $\sigma_0{}^2$ is the variance of b_0 (Hayes et al., 1995). Nonparametric bootstrapping with 1000 replicates was used to estimate standard errors of parameters and to provide nominal estimates of parameter bias (Efron and Tibshirani, 1993).

Geographic variation and sexual dimorphism in the length-weight relationship for Dover sole were investigated by a step-wise procedure among generalized linear models relating the log-transformed length-weight observations to the factors INPFC area and sex, and all possible higher order interactions between these terms. The full model with all possible interactions was

$$\log W_i = (\log A + \beta_A + \beta_S + \beta_{AS}) + (B + \beta_{AL} + \beta_{SL} + \beta_{ASL})\log L_i + \varepsilon_i, \quad (5)$$

where β, β_S, and β_{AS} = coefficients of area, sex, and their interaction;

β_{AL}, β_{SL}, and β_{ASL} = coefficients of first- and second-order interactions between area, sex, and the natural logarithm of length; and

ε_i = a normally distributed error with zero mean and constant variance.

As in the maturity analyses, the AIC criterion was used to choose among competing models in a step-wise manner (Hastie and Pregibon, 1993). Estimates of standard errors of parameters and nominal estimates of parameter bias were computed with the nonparametric bootstrap with 1000 replicates. Bootstrap estimates of residual variance and $\sigma_0{}^2$ = Var[b_0]=Var[log$A$+β_A+β_S+β_{AS}] were used to compute the adjusted intercept.

Results

Length-at-age samples

Female and male age and total length distributions differed across areas. On average, females were 1 to 2 years older than males (Table 2). Mean ages of males and females were significantly different for all areas combined and within the Vancouver, Columbia, and Eureka areas (P<0.05). Mean ages were lowest in the Vancouver area and highest in the Eureka area. The youngest males were 2 years old and had lengths of 19, 22, and 25 cm, whereas the oldest male was 42 years old and 41 cm long. The youngest female was 2 years old and 21 cm long, whereas the oldest female was 48 years old and 51 cm long. Maximum observed ages of females were greater than those of males in all areas except the Vancouver area where the fewest samples were collected. Females were 4 to 5 cm longer than males on average (Table 2). Mean female

Table 2

Dover sole mean, minimum (Min), and maximum (Max) ages (yr), total lengths (cm), and total weights (g) by INPFC area and sex. Standard errors (SE) of mean values appear in parentheses.

		Age (yr)			Length (cm)			Weight (g)		
INPFC area	Sex	Min	Mean (SE)	Max	Min	Mean (SE)	Max	Min	Mean (SE)	Max
Vancouver	Male	3	10.2 (0.3)	39	20	33.1 (0.4)	49	97	505 (32)	1195
	Female	4	11.1 (0.3)	29	21	37.4 (0.5)	57	114	704 (55)	1850
Columbia	Male	3	11.9 (0.1)	42	17	33.6 (0.1)	51	40	467 (9)	1325
	Female	3	14.0 (0.2)	48	15	38.8 (0.2)	66	33	660 (14)	2479
Eureka	Male	2	13.0 (0.4)	35	16	35.4 (0.4)	49	48	485 (15)	1182
	Female	3	14.5 (0.4)	40	21	40.6 (0.4)	56	75	789 (23)	2296
Monterey	Male	3	12.7 (0.5)	31	19	35.4 (0.5)	49	55	499 (19)	1240
	Female	2	13.6 (0.4)	42	20	39.4 (0.5)	55	65	741 (27)	2157
All areas	Male	2	12.0 (0.1)	42	16	33.9 (0.1)	51	40	478 (7)	1325
	Female	2	13.7 (0.1)	48	15	39.1 (0.2)	66	33	712 (11)	2479
	Pooled	2	12.7 (0.1)	48	15	36.2 (0.1)	66	33	598 (7)	2479

length was significantly greater than mean male length for all areas combined and within each area ($P<0.05$). Mean lengths were greatest within the Eureka and Monterey areas and smallest in the Vancouver area. The smallest male (16 cm) was 4 years old, whereas the two largest males (51 cm) were 25 and 37 years old. The smallest female (15 cm) was 2 years old and the largest female (66 cm) was 38 years old.

Weight distributions differed by sex across areas. Mean female weights exceeded male values by 200 to 300 g. Significant differences between male and female weight were detected for all areas combined and within each area ($P<0.05$). Individual fish weights were more variable for females than for males. Mean weights were greatest within the Eureka and Monterey areas and lowest in the Columbia area. The lightest male weighed 40 g and was 5 years old, whereas the heaviest male was 1325 g and 26 years old. The lightest female weighed 33 g and was 5 years old, whereas the heaviest female was 2479 g and 38 years old.

Growth curves

Variances in length at age of male and female Dover sole were homogeneous. For male samples (n=2613), the coefficient of variation (CV) of length at age ranged from 6 to 14% and averaged 10%, with an average variance of 12.5 cm. Male variance in length was homogeneous across ages (P=0.83, χ^2=20.97). For female samples (n=2514), the CV ranged from 6 to 16% and averaged 11%, with an average variance of 17.5 cm. Similar to that for males, female variance in length was homogeneous across ages (P=0.59, χ^2=25.64). As a result, we used an additive normal error term for estimating growth curves.

There was sexual dimorphism in growth of Dover sole when samples were pooled across areas. Maximum likelihood estimates and standard errors (SE) for pooled-sex samples were as follows: L_{max} = 51.3 cm, SE = 0.5; L_{min} = 20.9 cm, SE = 0.3; c = 0.9337, SE = 0.0030 with corresponding von Bertalanffy values: L_∞ = 52.6 cm, K = 0.069, and t_0 = –5.4. Male and female growth parameters for all areas (Table 3) were significantly different ($P<0.001$, χ^2=1079) and showed that females grow more rapidly than males and attain larger sizes. There was greater variation in female size at age, and residual variance from the female curve was roughly twice that value from the male curve. Both female and male curves for samples pooled across areas did not satisfy the assumption of normally distributed residuals ($P<0.01$). Thus, neither male nor female growth was adequately described by a single growth curve representing all areas.

Geographic variation was evident in male growth curves estimated for each area (Table 3). The hypothesis of identical growth parameters for all areas was rejected ($P<0.001$, χ^2=96.25). Male samples from adjacent INPFC areas were grouped and growth curves were estimated. Homogeneous growth was rejected for Vancouver and Columbia samples ($P<0.001$, χ^2=25.88) and for Columbia and Eureka samples ($P<0.001$, χ^2=42.31) but was accepted for the Eureka and Monterey samples (P=0.28, χ^2=3.85). Homogeneous growth was rejected for combined samples from Eureka, Monterey, and Columbia ($P<0.001$, χ^2=80.98) but was accepted for combined male samples from Eureka, Monterey, and Vancouver (P=0.35, χ^2=6.65).

We found that growth of male Dover sole differed between the Columbia area and the combined Vancouver, Eureka, and Monterey areas (Table 3) and that male growth curves from the Vancouver, Eureka, and Monterey

areas were not statistically distinguishable. Males from the Columbia area grew more slowly and reached larger sizes, on average, than males from the Vancouver, Eureka, and Monterey areas (Fig. 2A). Estimates of L_∞ and K for the Columbia area differed from estimates for the combined Vancouver, Eureka, and Monterey areas by 3% and −26%, respectively. Parameters of the alternative growth curve were more precisely determined with CVs of 1–3% for the Columbia and combined areas in comparison to the standard von Bertalanffy model where CVs were 2–14%. Residual variance for the Columbia area was lower than that for the three areas combined. However, residuals from the Columbia area curve did not satisfy the normality assumption (P=0.01), whereas residuals from the combined areas did (P=0.83). Overall, there was no latitudinal cline in growth parameters.

Similarly, we found geographic variation in growth of female Dover sole by area (Table 3). The hypothesis of identical female growth parameters across areas was rejected (P<0.001, χ^2=91.70). Female samples from adjacent INPFC areas were grouped and growth curves were estimated. Homogeneous growth was rejected for Vancouver and Columbia samples (P=0.002, χ^2=14.92) and for Columbia and Eureka samples (P<0.001, c=56.90) but was accepted for Eureka and Monterey samples (P=0.09, χ^2=6.45). Homogeneous growth was rejected for combined samples from Eureka, Monterey, and Columbia (P<0.001, χ^2=89.15) and weakly supported for combined samples from Eureka, Monterey, and Vancouver (P=0.025, χ^2=14.47).

Growth of female Dover sole exhibited geographic variation (Fig. 2B). In particular, females from the Columbia

Table 3

Estimated growth curves for length (cm) at age (yr) of male and female Dover sole by INPFC area. Parameters L_{max} L_{min} and c are from the empirical von Bertalanffy curve. Corresponding values for the standard von Bertalanffy curve (L_∞, t_0, and K) are also listed. Bootstrap estimates of standard errors appear immediately below each estimate in parentheses. Other table entries are the residual variance from the nonlinear regression (σ^2) and the probability that residuals were normally distributed (P(normal)) based on the Shapiro and Wilk (1965) test.

Growth curves by INPFC area	L_{max}	L_{min}	c	σ^2	P(normal)	L_∞	t_0	K
Male growth curves								
All areas[1]	46.6	21.2	0.9315	11.45	<0.01	48.2	−6.2	0.071
	(0.5)	(0.4)	(0.0042)			(0.8)	(0.5)	(0.005)
Vancouver	45.9	21.8	0.9102	13.03	0.51	47.8	−3.7	0.094
	(1.6)	(1.0)	(0.0157)			(2.3)	(1.3)	(0.017)
Columbia	46.4	23.0	0.9347	10.92	0.01	48.2	−6.6	0.068
	(0.6)	(0.4)	(0.0053)			(1.1)	(0.7)	(0.006)
Eureka	45.7	20.8	0.9182	11.37	0.71	47.3	−4.8	0.085
	(0.9)	(0.8)	(0.0102)			(1.5)	(0.9)	(0.011)
Monterey	43.7	22.6	0.8910	10.21	0.95	44.6	−3.1	0.115
	(0.8)	(0.8)	(0.0146)			(1.2)	(0.9)	(0.016)
Vancouver, Eureka, and Monterey	45.7	20.4	0.9121	11.53	0.83	46.6	−4.3	0.092
	(0.7)	(0.6)	(0.0072)			(0.9)	(0.6)	(0.008)
Female growth curves								
All areas	51.7	19.7	0.9131	20.06	<0.01	52.2	−3.2	0.091
	(0.5)	(0.6)	(0.0042)			(0.6)	(0.4)	(0.005)
Vancouver	51.0	24.5	0.9135	24.18	0.87	54.1	−2.7	0.091
	(1.9)	(1.5)	(0.0219)			(5.1)	(1.7)	(0.024)
Columbia	51.8	22.5	0.9206	19.93	0.63	52.5	−3.8	0.083
	(0.7)	(0.7)	(0.0057)			(0.9)	(0.6)	(0.006)
Eureka	50.8	20.8	0.8879	17.94	0.24	51.1	−1.4	0.119
	(0.7)	(1.0)	(0.0091)			(0.8)	(0.6)	(0.010)
Monterey	49.7	19.1	0.8819	15.03	0.99	49.9	−1.9	0.122
	(0.8)	(1.1)	(0.0103)			(0.9)	(0.6)	(0.012)
Vancouver, Eureka, and Monterey	51.0	18.5	0.8965	18.64	0.58	51.4	−2.1	0.109
	(0.8)	(0.8)	(0.0060)			(0.7)	(0.4)	(0.007)

[1] INPFC areas sampled in the study: Vancouver, Columbia, Eureka, and Monterey

area appeared to grow more slowly and achieve greater sizes than females from the other areas. Estimates of female L_∞ and K from the Columbia area were 2% and −24% different from estimates for the combined Vancouver, Eureka, and Monterey areas (Table 3). As with the results for males, female growth parameters were more precisely estimated for the alternative growth curve with CVs of 1–6% in comparison with CVs of 2–65% for the standard von Bertalanffy curve. In contrast to males, residuals of female growth curves were normally distributed and there was an apparent increase in L_∞ with latitude. Overall, geographic variation of male and female growth was similar, with the exception that asymptotic female size appeared to increase with latitude.

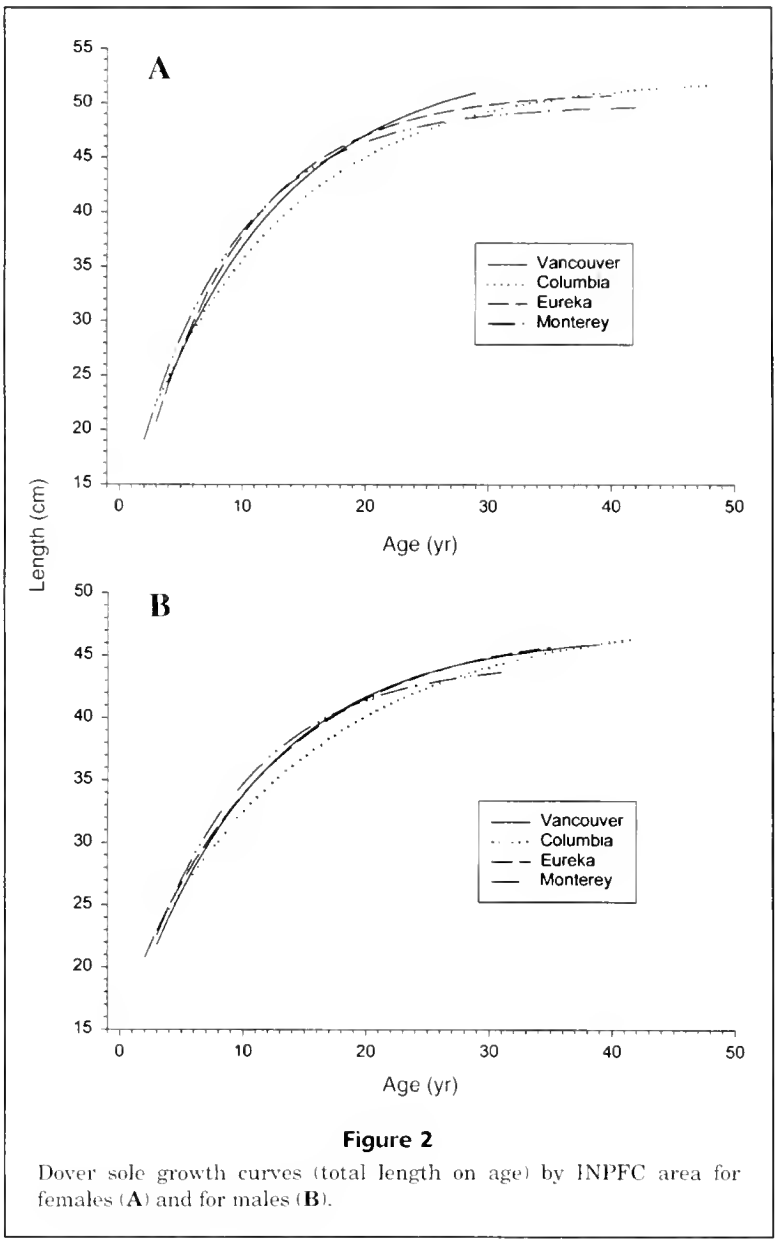

Figure 2

Dover sole growth curves (total length on age) by INPFC area for females (**A**) and for males (**B**).

Maturation curves

We found that male Dover sole matured at smaller sizes than did females when samples were combined across areas (Table 4). Predicted female median length at maturity (L_{50}) exceeded male L_{50} by 6 cm (23%), and the ratio of median length at maturity to asymptotic size (L_{50}/L_∞) of females exceeded that of males by 14%. The estimate of male L_{50} (CV=2%) was more variable than the female L_{50} (CV=1%).

Maturity-at-age curves for all areas (Table 5) indicated that males matured at younger ages than females. Predicted female median age at maturity (A_{50}) exceeded male A_{50} by three years (57%), whereas the ratio of female median age at maturity to maximum observed age (A_{50}/A_{max}) exceeded that of males by about 42%. The estimate of male A_{50} (CV=10%) was less precise than the female estimate (CV=3%).

Geographic variation was evident in maturity at length by INPFC area (Fig. 3). The best logistic model for maturity at length included terms[1] for length, sex, area, length×sex, and length×area and had a dispersion parameter of ϕ = 1.28 (Table 4). This factor indicated a moderate degree of overdispersion in the maturity-at-length data. Male maturity curves by INPFC area showed a geographic cline in L_{50}, and median size at maturity decreased with latitude. Male L_{50} values ranged from 22 to 29 cm with CVs of 2% to 9%. Similarly, the ratio L_{50}/L_∞ decreased from 0.66 in Monterey to 0.47 in Vancouver. Female L_{50}'s showed a similar geographic cline, although female L_{50}'s were more precisely estimated than male L_{50}'s. Female L_{50} values ranged from 35 cm in Monterey to 28 cm in Vancouver. Female values of L_{50}/L_∞ also decreased as latitude increased. Overall, median length at maturity of both male and female Dover sole decreased with increasing latitude.

Maturity at age also varied by INPFC area (Fig. 4). The best logistic model included terms for age, sex, area, age×sex, and age×area (Table 5). Dover sole maturity-at-age data were highly overdispersed and the ratio of observed-to-expected sampling variance for the selected model was ϕ = 4.86. Male maturity ogives by INFPC area suggested a latitudinal cline in A_{50}. Male A_{50} values ranged from 3 to 7 years and decreased with increasing latitude, except for the Columbia area. CVs of male A_{50} values were high and ranged from 8% to 70%. The ratio A_{50}/A_{max} showed a clear latitudinal trend and decreased from 0.22 in Monterey to 0.09 in Vancouver. Female A_{50} values decreased as latitude increased and ranged from 9 years in Monterey to 6 years in Vancouver. Estimates of female A_{50} by INPFC area were more precise than those for males (with CVs of 5–20%). Female ratios of A_{50}/A_{max}

[1] XY denotes an interaction between X and Y.

had no obvious latitudinal pattern and were relatively similar (0.16 to 0.21) across areas. Overall, median age at maturity of both male and female Dover sole appeared to decrease with increasing latitude.

Length-weight curves

Length-weight curves for all areas combined were highly significant ($P<0.001$) for pooled-sex, male, and female samples (Table 6). Males had a larger length exponent than females but there was little apparent difference between male and female curves. For pooled-sex samples, the length exponent exceeded 3 and showed that Dover sole weight in autumn was more than proportional to the cube of length. CVs of intercept parameters ranged from 3% to 5% for pooled-sexes, males, and females, whereas CVs of length exponents were all less than 1%. Bootstrap estimates of parameter bias were low compared with standard errors and were less than 0.3% of point estimate in all cases. For the intercept parameter, ratios of bias to standard error were −1%, 5%, and 6% in pooled-sex, male, and female samples. Corresponding ratios for the length exponent were 2%, −2%, and −4%.

Geographic variation in length-weight relationships of Dover sole was suggested by the generalized linear model analyses. The best model contained the terms for log(*length*), *area*, and log(*length*)×*area*. Although length-weight curves by INPFC area exhibited some geographic variation (Fig. 5), there was no detectable difference between male and female weight at length. Predicted weight at length was smallest for the Vancouver area and greatest for the Monterey area, whereas length-weight curves from the Columbia and Eureka areas were very similar. Length exponents exceeded 3 for all areas except Vancouver, where few length-weight data were available. As above, the length exponent (with CVs less 2%) was more precisely estimated than the intercept (with CVs of 5–19%). Estimates of parameter bias were less than 1.6% of the parameter estimate in all cases. For each area, the ratio of estimated bias to standard error for the intercept parameter was also low: Vancouver (9%), Columbia (0%), Eureka (0%), and Monterey (5%). Corresponding ratios for the length exponent were also low: 1%, 2%, 7%, and −2%. Thus, parameter bias for the length-weight curves was inconsequential.

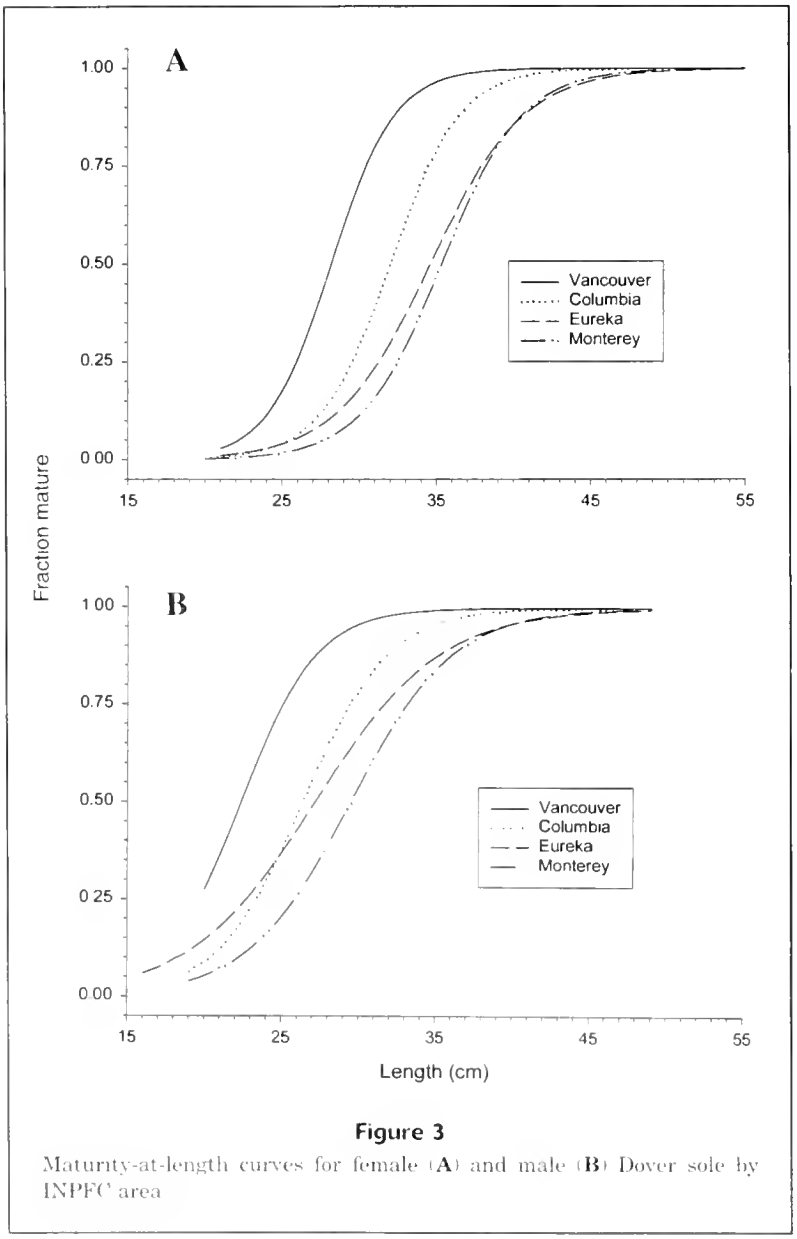

Figure 3

Maturity-at-length curves for female (**A**) and male (**B**) Dover sole by INPFC area

Discussion

We found that the use of the alternative form of the von Bertalanffy growth curve gave satisfactory parameter estimates that had greater precision than those of the standard form. Bootstrap estimates of standard errors and corresponding coefficients of variation were lower with the alternative form. Ratkowsky (1983) recommended the alternative form used in our study because its parameters were more readily interpreted, it had close-to-linear behavior that facilitated comparisons among data sets, and it was insensitive to the choice of initial parameter values. Our results provide further support for its use.

Variance in size at age of females was 40% greater than that of males. This may result from differences in seasonal patterns of movement between females and males. In particular, Hagerman (1952) noted that commercial Dover sole catches were often segregated by sex and that Dover sole appeared to undertake an inshore feeding migration

Table 4

Maturity-at-length (cm) curves for male and female Dover sole by INPFC area. Standard errors appear immediately below estimates in parentheses. The ratio L_{50}/L_{∞} is reported for comparison with other Pleuronectiformes.

curves by INPFC area	Maturity-at-length L_{50}	β_0	β_1	L_{50}/L_{∞}	n
Male maturity-at-length curves					
All areas[1]	27.1	−6.256	0.2305	0.56	934
	(0.5)	(0.533)	(0.0173)		
Vancouver	22.4	−9.122	0.4078	0.47	77
	(2.1)	(3.854)	(0.1371)		
Columbia	26.4	−9.627	0.3649	0.55	331
	(0.6)	(0.995)	(0.0333)		
Eureka	27.2	−6.717	0.2473	0.57	317
	(0.9)	(0.915)	(0.0291)		
Monterey	29.5	−8.926	0.3029	0.66	209
	(0.7)	(1.051)	(0.0315)		
Female maturity-at-length curves					
All areas	33.4	−9.969	0.2988	0.64	1232
	(0.3)	(0.598)	(0.0169)		
Vancouver	28.2	−13.811	0.4904	0.52	60
	(1.0)	(3.880)	(0.1376)		
Columbia	32.0	−14.315	0.4475	0.61	464
	(0.4)	(1.224)	(0.0367)		
Eureka	34.6	−11.405	0.3299	0.68	415
	(0.5)	(0.878)	(0.0232)		
Monterey	35.3	−13.614	0.3855	0.71	293
	(0.5)	(1.220)	(0.0350)		

[1] INPFC areas sampled in this study: Vancouver, Columbia, Eureka, and Monterey.

Table 5

Maturity-at-age (yr) curves for male and female Dover sole by INPFC area. Standard errors appear immediately below estimates in parentheses. The ratio A_{50}/A_{max} is reported for comparison with other Pleuronectiformes where A_{max} is maximum observed age in our study.

INPFC area	A_{50}	β_0	β_1	A_{50}/A_{Max}
Male maturity-at-age curves				
All areas[1]	5.1	−1.254	0.2438	0.12
	(0.5)	(0.240)	(0.0271)	
Vancouver	3.3	−1.620	0.4838	0.09
	(2.3)	(1.336)	(0.1820)	
Columbia	5.4	−2.314	0.4273	0.13
	(0.5)	(0.456)	(0.0555)	
Eureka	5.2	−1.323	0.2563	0.15
	(0.7)	(0.397)	(0.0467)	
Monterey	6.7	−2.361	0.3510	0.22
	(0.5)	(0.425)	(0.0470)	
Female maturity-at-age curves				
All areas	8.0	−2.733	0.3423	0.17
	(0.2)	(0.256)	(0.0276)	
Vancouver	5.6	−3.353	0.5985	0.19
	(1.1)	(1.343)	(0.1809)	
Columbia	7.5	−4.046	0.5419	0.16
	(0.3)	(0.515)	(0.0588)	
Eureka	8.2	−3.055	0.3710	0.21
	(0.4)	(0.354)	(0.0362)	
Monterey	8.8	−4.094	0.4657	0.21
	(0.4)	(0.496)	(0.0587)	

[1] INPFC areas sampled in this study: Vancouver, Columbia, Eureka, and Monterey.

during spring and an offshore spawning migration in late autumn. Westrheim et al. (1992) inferred from tag recoveries that two major concentrations of Dover sole were present during summer: an inshore group composed of females and small males and an offshore group primarily composed of large males. Jacobson and Hunter (1993) also found that Dover sole segregated by sex in their analysis of bathymetric patterns in population structure. Overall, if large male Dover sole undertake seasonal movements less frequently than females, their growth rates may be expected to be less heterogeneous than those of females that move from the continental slope to the more productive waters of the continental shelf during spring. Seasonal sampling of Dover sole population structure at depth would improve understanding of the relative movements of male and female Dover sole.

As others have suggested (Hagerman, 1952; Hunter et al., 1990; Turnock et al., 1994), we found that Dover sole exhibit sexual dimorphism in growth. In particular, there was a significant difference between male and female growth curves because females attain larger sizes. Mean length of females increased more rapidly than that of males at roughly 5 years of age. The result that females attain greater lengths than males is consistent with Hunter et al. (1990) who also found that values of L_{∞} were greater for females. Although our results were not directly comparable to those of Hunter et al. (1990) because of differences in otolith aging technique and sampling design, asymptotic lengths of females were estimated to be 8% greater than those for male samples in both studies. Some of the growth differences between sexes may result from behavioral differences in feeding and habitat use. Although Dover sole feed more intensively and less selectively on the continental shelf during summer (Pearcy and Hancock, 1978), some older fish may remain in deeper water year round (Hunter et al., 1990). Sexually mature Dover sole are commonly found in the oxygen minimum zone at depths of 600–1000 m (Hunter et al., 1990; Jacobson and Hunter, 1993), where low food and oxygen levels depress metabolism and growth potential (Vetter et al., 1994). Differences between male and female patterns of

growth may result from a differential use of deep-water habitat, where adult males spend more time, on average, in the oxygen minimum zone, or may result from the effects of egg production and spawning on growth and deposition of rings in the annuli of females. In summary, Dover sole exhibit a moderate degree of sexual dimorphism, and differences between sexes become apparent, on average, at about 5 years of age.

In addition to differences between sexes, moderate levels of geographic variation in growth of Dover sole off the west coast were apparent. Growth curves for the Columbia area and for the combined Vancouver, Eureka, and Monterey areas differed for both male and female Dover sole. Asymptotic lengths of males and females from the Columbia area were 3% and 2% greater than those for the combined Vancouver, Eureka, and Monterey areas. Male and female Dover sole from the Columbia area also had lower Brody growth coefficients and larger asymptotic lengths than other areas. These differences, however, were relatively minor and would not be expected to have a substantial impact on target harvest rates if the Dover sole fishery were managed by INPFC areas rather than as a coastwide unit.

The reason for geographic variation in growth is unknown but probably stems from regional differences in productivity within the California Current. In particular, oceanographic properties of the California Current differ north and south of Cape Blanco (U.S. GLOBEC, 1994), the southern boundary of the Columbia area, and physical differences in the strength and duration of upwelling may affect the growth potential of Dover sole inhabiting these regions. The fact that adult Dover sole are benthic feeders (Pearcy and Hancock, 1978) and are relatively sedentary, having negligible north–south movements (Westrheim et al., 1992), indicates that geographic variation in physical habitat and benthic community structure are probably important determinants of Dover sole growth. Indeed, Jacobson and Hunter (1993) showed that there is relatively more Dover sole habitat off Oregon than off central California.and that depth preferences of Dover sole appear to differ between these regions.

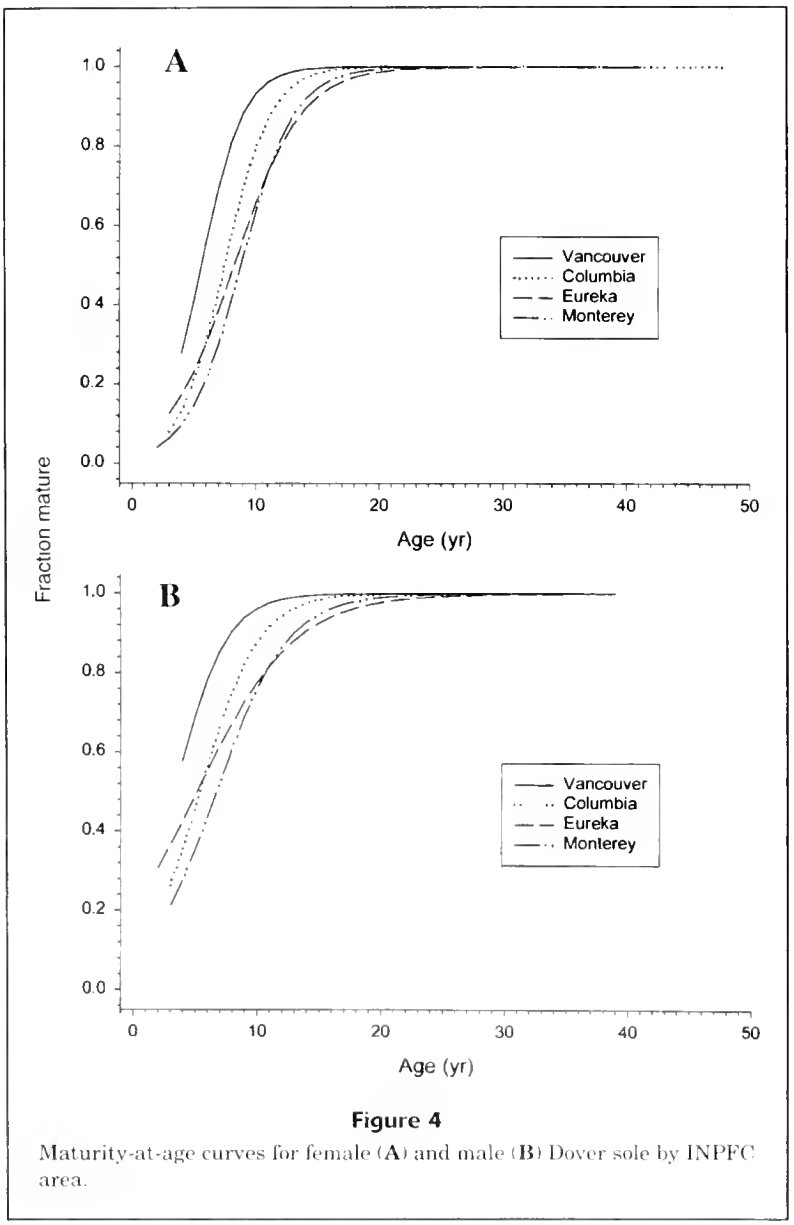

Figure 4

Maturity-at-age curves for female (**A**) and male (**B**) Dover sole by INPFC area.

Alternatively, the cumulative effects of long-term harvest may have also affected the geographic pattern of Dover sole growth because commercial harvests by INPFC area have differed through time. Landings of Dover sole in the Eureka area peaked in the early 1970s, whereas landings in the Columbia, Monterey, and U.S. Vancouver areas peaked in the 1980s (Brodziak, et al. 1997). Although historic size at age of Dover sole has not been documented, some otolith aging data collected off California in the 1940s have provided evidence that mean size at age of males and females may have changed through time (Hagerman, 1952). In particular, Hagerman reported mean sizes at age-5 and age-9 of male Dover sole were 32.3 and 35.5 cm, whereas mean sizes of age-5 and age-9 females were 33.6 and 41.5 cm. In comparison with our estimates, these data suggest that growth may have declined since the 1940s and are consistent with reductions in mean size at age due to fishery-size selection (see Ricker, 1968). Thus, geographic patterns in Dover sole growth may also have been affected by differences in harvest pressure among regions.

Temporal variability of the California Current (Ware, 1995) may have also influenced observed growth, as well as maturation patterns. Research survey samples collected during the 1980s had a higher percentage of

Dover sole that had been spawned prior to a regime shift in the late 1970s (see McGowan et al., 1998) than samples collected during the 1990s. Although temporal changes in growth due to ocean regime may have occurred, such changes would be difficult to detect given the unbalanced temporal and spatial coverage of the available research survey data. Regardless of the mechanism, continued sampling of Dover sole for data on size at age and maturity will be needed to understand whether the observed geographic variation is stable through time.

We found that maturation rates differed between sexes. On average, males matured at a smaller size and at a younger age than did females. This difference might be expected given the sexual dimorphism in Dover sole growth and is consistent with conclusions drawn by Beverton (1992, Fig. 2), who reported that males generally have smaller size at 50% maturity than females within the Pleuronectiformes.

In addition to differences between sexes, we found geographic variation in maturity rates and an apparent latitudinal cline in the median length at maturity of male and female Dover sole. Results were similar for maturity-at-age curves, with the exception of results for Columbia area males. In his review of latitudinal patterns in flatfish reproductive life history, Castillo (1995) found no evidence of a latitudinal trend in age or length at first maturity of Dover sole off Oregon and California. In our study, results suggested that Dover sole mature at smaller size and younger ages at higher latitudes. This finding contrasts with expectations that Dover sole would mature at larger size and older age at higher latitudes (e.g. Castillo, 1995). The apparent trend in Dover sole maturation rates may reflect local adaptation to latitudinal differences in oceanographic properties of the California Current (U.S. GLOBEC, 1994). Nonetheless, sample sizes from some areas (e.g. Vancouver) may have been insufficient to accurately characterize the pattern of maturation in length or age. Also, effects of potential latitudinal differences in the timing of spawning were not accounted for in our study. Thus, although we found some evidence of geographic variation, we recommend further sampling to verify our observed geographic patterns in maturation.

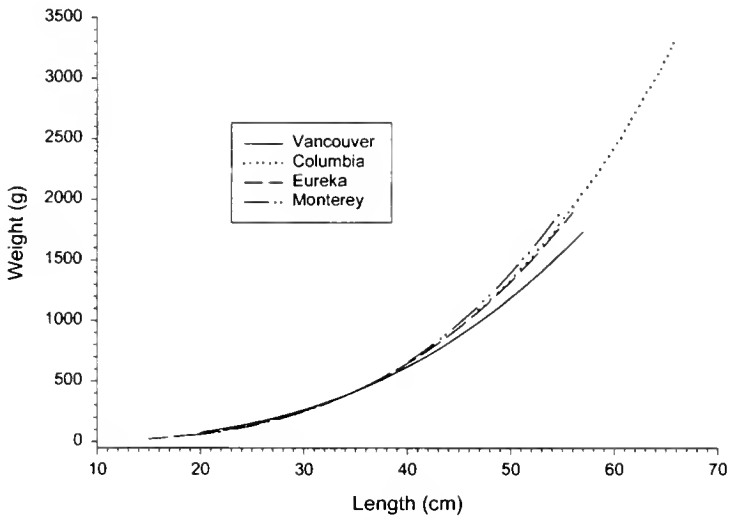

Figure 5

Pooled-sex total length-total weight curves of Dover sole by INPFC area.

Table 6

Estimated parameters and residual variance[1] of Dover sole total length (cm)-total weight (g) curves by INPFC area. Estimated standard errors appear immediately below each estimate in parentheses.

INPFC area	A	B	σ^2	n
All areas	4.0659×10^{-3}	3.2479	1.295×10^{-2}	3019
	(0.1366×10^{-3})	(0.0093)	(0.044×10^{-2})	
Male—all areas	3.7064×10^{-3}	3.2736	1.322×10^{-2}	1470
	(0.1992×10^{-3})	(0.0151)	(0.056×10^{-2})	
Females—all areas	4.4149×10^{-3}	3.2254	1.266×10^{-2}	1549
	(0.2073×10^{-3})	(0.0128)	(0.063×10^{-2})	
Vancouver[1]	13.5571×10^{-3}	2.9093	1.252×10^{-2}	137
	(2.5797×10^{-3})	(0.0521)	(0.040×10^{-2})	
Columbia	3.7610×10^{-3}	3.2676		1645
	(0.1958×10^{-3})	(0.0144)		
Eureka	4.9630×10^{-3}	3.1934		734
	(0.4313×10^{-3})	(0.0235)		
Monterey	2.8550×10^{-3}	3.3484		503
	(0.2146×10^{-3})	(0.0208)		

[1] Residual variance estimates from the generalized linear model are identical for each INPFC area

Maturity-at-length estimates from our study were consistent with those from other studies of Dover sole maturation. Although maturation criteria and sampling design differed between our study and those of Hunter et al. (1992), estimated median lengths for female maturity were remarkably consistent. In particular, Hunter et al. (1992) estimated female L_{50} to be 33.2 cm, whereas in our study, female L_{50} was estimated to be 33.4 cm. These female L_{50} estimates contrast with earlier estimates that were based on commercial fishery samples in which fish were 36 cm (Hagerman [1952] reported within Hunter et al. [1990]) and 38 cm (Harry [1959]). Although it is unknown whether the earlier estimates are directly comparable to

those of our study because of differences in sampling and maturation criteria, they suggest, however, the possibility that female size at maturity may have declined since the 1950s.

We found no difference between male and female length-weight curves. Male and female length-weight curves were virtually identical for fish less than 50 cm in length. Comparisons between large mature females (>50 cm) and males were not possible because maximum observed size of male Dover sole is about 51 cm. In addition, some geographic variation in length-weight relationships was detected. Estimated length exponents from the allometric equation exceeded 3 for all INPFC areas, with the exception of the Vancouver area, where relatively few samples were collected. Overall, it appeared that Dover sole weight during late autumn, when samples were collected, was not proportional to the cube of fish length. In contrast, Hagerman (1952) found that Dover sole weight was roughly proportional to the cube of length in commercial fishery samples collected throughout the year. Hagerman's estimates may not be comparable to ours owing to differences in sampling and analysis. We recommend year-round collection of Dover sole samples for length-weight analysis to determine whether seasonal and geographic variation are important in predicting mean weight at length in the population.

In comparison with other pleuronectids, we found that Dover sole matured at relatively larger sizes and younger ages. Beverton (1992) reported average ratios of L_{50}/L_{∞} of 0.47 and 0.52 for male and female pleuronectids, whereas comparable values in our study were 0.56 and 0.64. Similarly, male and female ratios of A_{50}/A_{max} of 0.28 and 0.39 from Beverton (1992) were higher than corresponding values of 0.12 and 0.17 in our study. Observed differences with other pleuronectids likely result from the complex life history pattern of Dover sole in the California Current. Dover sole are a relatively late-maturing flatfish. The age at first reproduction (α) that maximizes expected lifetime fecundity for this species is roughly α=15 years, where $\alpha=\log(1+(3K/M))/K$ (see Roff, 1991) using K=0.091 for females from our study and a natural mortality rate of M=0.09/yr (Brodziak et al., 1997). In contrast, observed ages at first reproduction for Dover sole range from 4 to 6 years (Castillo, 1995), or roughly 1/3 of the optimal age that would maximize fitness. However, these equilibrium calculations do not account for environmental forcing, and differences between the optimal and observed values probably reflect the importance of environmental variation (Roff, 1982) on the reproductive success of Dover sole. It may be necessary for Dover sole to reproduce as soon as possible to hedge their bets against natural cycling in the survival of pelagic larvae in the California Current (Parrish et al., 1981). In comparison to the pleuronectids reviewed in Beverton (1992), the lower A_{50}/A_{max} ratio of Dover sole may reflect the lack of growth experienced by adults that inhabit the oxygen minimum zone. Similarly, Dover sole may have a higher L_{50}/L_{∞} ratio than other pleuronectids because they achieve most of their potential growth as juveniles while resident on the continental shelf. Overall, maturation rates of Dover sole appear to differ from other pleuronectids and we believe that these differences reflect adaptation of Dover sole to the inherent variability of the California Current.

Acknowledgments

We thank the Captains, crew, and scientific staff of the FV *Marathon*, the FV *Mys. Babushkina*, the RV *Miller Freeman*, the FV *Poseydon*, and the MV *Half Moon Bay* for collecting the samples used in our study. We thank Richard Methot and three anonymous reviewers for their helpful comments on the draft manuscript. We also thank Mark Saelens of the Oregon Department of Fish and Wildlife (ODFW) and Marion Mann, Joseph O'Malley, and Bruce Pederson of the ODFW and National Marine Fisheries Service Cooperative Ageing Project for their support and assistance in aging Dover sole. This work was partially supported by Grants NA37FN0063 and NA67FN0174 from the National Marine Fisheries Service of the National Oceanic and Atmospheric Administration to the Oregon Department of Fish and Wildlife.

Literature cited

Allen, M. J., and G. B. Smith.
1988. Atlas and zoogeography of common fishes in the Bering Sea and northeastern Pacific. U.S. Dep. Commer., NOAA Tech. Rep. NMFS 66, 151 p.

Beverton, R. J. H.
1992. Patterns of reproductive strategy parameters in some marine teleost fishes. J. Fish. Biol. 41:137–160.

Brodziak, J., L. Jacobson, R. Lauth,, and M. Wilkins.
1997. Assessment of the Dover sole stock for 1997. *In* Pacific Fishery Management Council appendix: status of the Pacific coast groundfish fishery through 1997 and recommended biological catches for 1998: stock assessment and fishery evaluation. Pacific Fishery Management Council, 2130 SW Fifth Avenue, Suite 224, Portland, OR 97201, 135 p.

Butler, J. L., K. A. Dahlin, and H. G. Moser.
1996. Growth and duration of the planktonic phases and a stage based population matrix of Dover sole, *Microstomus pacificus*. Bull. Mar. Sci. 58(1):29–43.

Castillo, G.
1995. Latitudinal patterns in reproductive life history traits of northeast Pacific flatfish. *In* Proceedings of the international symposium on North Pacific flatfish, p. 52–72. Alaska Sea Grant College Program. AK-SG-95-04, Anchorage, AK.

Chilton, D. E., and R. Beamish.
1982. Age determination methods for fishes studied by the Groundfish Program at the Pacific Biological Station. Can. Spec. Publ. Fish. Aquat. Sci. 60.

Efron, B., and R. J. Tibshirani.
1993. An introduction to the bootstrap. Chapman and Hall, New York, NY, 436 p.

Hagerman, F. B.
1952. The biology of the Dover sole (*Microstomus pacificus*). Calif. Dep. Fish. Game. Bull. 85, 48 p.

Harry, G.Y.
1959 Time of spawning, length at maturity, and fecundity of the English, petrale, and Dover soles (*Parophrys vetulus*,

Eopsetta jordani, and *Microstomus pacificus*, respectively). Fish. Comm. Oregon. Res. Briefs 7(1)5–13.

Hart, J. L.
1973. Pacific fishes of Canada. Fish. Res. Board. Can. Bull. 180, 740 p.

Hastie, T. J., and D. Pregibon.
1993. Generalized linear models. *In* Statistical models in S (J. M. Chambers and T. J. Hastie, eds.), p. 195–247. Chapman and Hall, New York, NY, 608 p.

Hayes, D. B., J. K. T. Brodziak, and J. B. O'Gorman.
1995. Efficiency and bias of estimators and sampling designs for length-weight relationships of fish. Can. J. Fish. Aquat. Sci. 52:84–92.

Hunter, J. R., J. L. Butler, C. Kimbrell, and E. A. Lynn.
1990. Bathymetric patterns in size, age, sexual maturity, water content, and caloric density of Dover sole, *Microstomus pacificus*. CalCOFI Rep. 31:132–144.

Hunter, J. R., B. J. Macewicz, N. C. Lo,, and C. A. Kimbrell.
1992. Fecundity, spawning, and maturity of female Dover sole, *Microstomus pacificus*, with an evaluation of assumptions and precision. Fish. Bull 90:101–128.

Jacobson, L. D., and J. R. Hunter.
1993. Bathymetric demography and management of Dover sole. N. Am. J. Fish. Manage. 13:405–420.

Kimura, D.
1980. Likelihood methods for the von Bertalanffy growth curve. Fish. Bull. 77:765–776.

Lauth, R. R., M. E. Wilkins, and P. R. Raymore Jr.
1997. Results of trawl surveys of groundfish resources of the West Coast upper continental slope. U.S. Dep. Commer., NOAA Tech. Memo. NMFS-AFSC-79, 342 p.

Markle, D. F., P. M. Harris, and C. L. Toole.
1992. Metamorphosis and an overview of early-life-history stages in Dover sole *Microstomus pacificus*. Fish. Bull. 90:285–301.

McGowan, J. A., D. R. Cayan, and L. M. Dorman.
1998. Climate-ocean variability and ecosystem response in the Northeast Pacific. Science (Washington D.C.) 281:210–217.

McMullagh, P. and J. A. Nelder.
1989. Generalized linear models, 2nd ed. Chapman and Hall, New York, NY, 511 p.

Parks, N. B., F. R. Shaw, and R. L. Henry.
1993. Results of a 1988 trawl survey of groundfish resources of the upper continental slope off Oregon. U.S. Dep. Commer., NOAA Tech. Memo. NMFS-AFSC-23, 164 p.

Parrish, R. H., C. S. Nelson, and A. Bakun.
1981. Transport mechanisms and reproductive success of fishes in the California Current. Biol. Oceanogr. 1 175–203.

Pearcy, W. G., and D. Hancock.
1978. Feeding habits of Dover sole, *Microstomus pacificus*; rex sole, *Glyptocephalus zachirus*, slender sole, *Lyopsetta exilis*, and Pacific sanddab, *Citharichthys sordidus*, in a region of diverse sediments and bathymetry off Oregon. Fish. Bull. 76:641–651.

Pearcy, W. G., M. J. Hosie, and S. L. Richardson.
1977. Distribution and duration of pelagic life of Dover sole, *Microstomus pacificus*, rex sole, *Glyptocephalus zachirus*, and Petrale sole, *Eopsetta jordani*, in waters off Oregon. Fish. Bull. 75:173–183.

Pearcy, W. G., D. L. Stein, and R. S. Carey.
1982. The deep-sea benthic fish fauna of the northeastern Pacific ocean on Cascadia and Tufts abyssal plains and adjoining continental slopes. Biol. Oceanogr. 1(4):375–429.

Pikitch, E. K., and R. L. Demory.
1988. Assessment of scales as a means of aging Dover sole. Trans. Am. Fish. Soc. 117:345–349.

Ratkowsky, D. A.
1983. Statistical properties of alternative parameterizations of the von Bertalanffy growth curve. Can. J. Fish. Aquat. Sci. 43:742–747.

Raymore, P. A., Jr., and K. L. Weinberg.
1990. 1984 spring and autumn surveys of Pacific West Coast upper continental slope groundfish resources. U.S. Dep. Commer., NOAA Tech. Memo. NMFS F/NWC-179, 196 p.

Ricker, W. E.
1968. Effects of size-selective mortality and sampling bias on estimates of growth, mortality, production, and yield. J. Fish. Res. Board Canada 26:479–541.

Roff, D. A.
1982. Reproductive strategies in flatfish: a first synthesis. Can. J. Fish. Aquat. Sci. 39:1686–1698.
1991. The evolution of life-history variation in fishes, with particular reference to flatfishes. Neth. J. Sea. Res. 27:197–207.

Schnute, J., and D. Fournier.
1980. A new approach to length-frequency analysis: growth structure. Can. J. Fish. Aquat. Sci. 37:1337– 1351.

Shapiro, S. S., and M. B. Wilk.
1965. An analysis of variance test for normality (complete samples). Biometrika 52:591–611.

Sokal, R. R., and F. J. Rohlf.
1981. Biometry, 2nd ed. W.H. Freeman and Co., New York, NY, 859 p.

Toole, C. L., D Markle, and P. Harris.
1993. Relationships between otolith microstructure, microchemistry, and early life history events in Dover sole, *Microstomus pacificus*. Fish. Bull. 91:732–753.

Turnock, J., M. Wilkins, M. Saelens, and R. Lauth.
1994. Status of the west coast Dover sole in 1994. *In* Pacific Fishery Management Council appendix C: status of the Pacific coast groundfish fishery through 1994 and recommended biological catches for 1995: stock assessment and fishery evaluation. Pacific Fishery Management Council, 2130 SW Fifth Avenue, Suite 224, Portland, OR 97201, 62 p.

GLOBEC (U.S. Global Ocean Ecosystem Dynamics).
1994. A science plan for the California Current. Report 11, U.S. GLOBEC Office, Univ. of Calif., Berkeley, CA, 134 p.

Vetter, R. D., E. A. Lynn, M. Garza, and A S. Costa.
1994. Depth zonation and metabolic adaptation in Dover sole, *Microstomus pacificus*, and other deep-living flatfishes: factors that affect the sole. Mar. Biol. 120:145–159.

Ware, D. M.
1995. A century and a half of change in the climate of the NE Pacific. Fish. Oceanogr. 4:267–277.

Westrheim, S. J., W. H. Barss, E. K. Pikitch, and L. F. Quirollo.
1992. Stock delineation of Dover sole in the California-British Columbia region, based on tagging studies conducted during 1948–1979. N. Am. J. Fish. Manage. 12.172–181.

Genetic structure of two commercial penaeids (*Penaeus californiensis* and *P. stylirostris*) from the Gulf of California, as revealed by allozyme variation

Jorge de la Rosa-Vélez

Facultad de Ciencias Marinas
Universidad Autónoma de Baja California
Km. 106 carretera Tijuana-Ensenada
Ensenada, Baja California 22800, Mexico
E-mail address: jdrosa@bahia.ens.uabc.mx

Roberto Escobar-Fernández

Francisco Correa

Instituto de Investigaciones Oceanológicas
Universidad Autónoma de Baja California
Km. 106 carretera Tijuana-Ensenada,
Ensenada, Baja California 22800, Mexico

Mercedes Maqueda-Cornejo

Javier de la Torre-Cueto

Facultad de Ciencias Marinas
Universidad Autónoma de Baja California
Km. 106 carretera Tijuana-Ensenada
Ensenada, Baja California 22800, Mexico

Abstract—Two commercial shrimp species (*Penaeus californiensis and P. stylirostris*) were sampled along the Gulf of California and crude extracts were assayed electrophoretically to assess allozyme variation and population genetic structure. *Penaeus californiensis*, a more oceanic species, displayed a 12.5% polymorphism (P_{95}) and a 0.023–0.037 expected heterozygosity (H_e) in three sampled populations, whereas *P. stylirostris*, a more coastal species, showed a north–south clinelike pattern in its genetic variability parameters: P_{95} from 15.63% to 31.25% and H_e from 0.038 to 0.086. Differences between species in levels of genetic variation and genotype distribution may be related to differences in habitat during important life cycles stages which reflect the remarkable changes of environmental conditions of coastal lagoons in the Gulf of California. *Penaeus stylirostris* subpopulations appeared more structured (F_{st}=0.372) than those of *P. californiensis* (F_{st}=0.182). A number of private alleles and alternation of the most common allele in several loci account for the outstanding high results of both species. Nei's genetic similarities were computed within species (*P. californiensis* subpopulations, I=0.988–0.997; *P. stylirostris* subpopulations, I=0.929–0.954) and between species (*P. californiensis* × *P. stylirostris*, I=0.674). A dendrogram generated from Nei's genetic similarities segregated the upper Gulf populations of both species from the other two populations (middle Gulf and mouth of the Gulf). This segregation may be the result of the "Island Barrier" hypothesized as segregating other decapods inhabiting the Gulf of California.

Manuscript accepted 12 July 2000.
Fish. Bull. 98:674–683 (2000).

Penaeid shrimp fisheries and hatcheries have undergone an accelerated development during the past three decades (Rosenberry, 1996). Yields of such productive activities are highly appreciated worldwide and have resulted in the economic development of prawn farming in several eastern (e.g. Thailand, Indonesia, Vietnam, China, India, etc.) and Latin American (e.g. Ecuador, Mexico, Colombia, Peru, Panama, etc.) countries.

Business based on penaeid shrimp trading may be considered as having two components: 1) heavy producers, countries, such as those mentioned above, which are mainly exporters, and 2) heavy importers, countries such as those of Europe and the United States of America, where the consumption of imported shrimp has long exceeded landings from their domestic fisheries (Lightner et al., 1997). Moreover, in the way of production (fishing on wild populations vs. rearing in hatcheries), three kinds of producer countries can be recognized: 1) countries that base their shrimp production mainly on their fishery yields (for example, the United States, where farmed shrimps make up only 1% of its production); 2) countries that have focused their shrimp production efforts almost exclusively on hatcheries (for example, Ecuador, where farmed shrimps make up 95% of its shrimp production); and 3) countries that produce shrimps in similar percentages from both wild stocks and hatcheries (for example, Mexico, China, India, and Indonesia) (Lightner et al., 1997).

Shrimp-producing countries, no matter their main way of production, need increasingly to take into account the resource's genetic structure and the variability of fisheries or hatcheries management (Allendorf et al., 1987). Two key questions must be outlined

when a resource is desired to be characterized genetically: 1) What amount of genetic variation is present across its populations? 2) Is the variation homogeneously distributed? This line of research has impelled a number of studies on populations of shrimp species to ensure adequate exploitation and optimal rearing (for a review see Rodríguez-Romero and Rosa-Vélez, 1993).

Our study aimed to characterize the genetic variability and structure of two wild populations of shrimp species, to recognize the actual genetic pool currently segregating in them, and to render information to design rearing strategies based on existing genetic variability.

Penaeus (Farfantepenaeus) californiensis Holmes is an oceanic species distributed in the eastern Pacific, San Francisco Bay, U.S.A., to Sachura Bay, Peru and Galapagos Islands, Ecuador (Rodriguez de la Cruz, 1976). Adults are found up to 220 m deep, although the peak of abundance occurs at 55 m on silt-clay or sand-silt bottoms (Rodríguez de la Cruz and Rosales, 1970). *Penaeus (Litopenaeus) stylirostris* Stimpson is a more coastal species distributed from the upper Gulf of California, Mexico, to Tumbes, Peru. Adults are found in shallow waters around the mouth of coastal lagoons, up to 40 m deep (CICTUS, 1985), where they are more abundant.

Life cycles are similar for both species but there is one very distinctive difference: *P. californiensis* can complete its whole life cycle in the marine environment, whereas *P. stylirostris* must spend part of its life cycle (postlarval and juvenile stages) as an inhabitant of coastal lagoons. In brief, for both species, females deposit eggs in demersal zones where they undergo total segmentation in 12–15 hours. The outcome is a planktonic larva that metamorphoses through five naupliar, three protozoean, and three mysis stages, before reaching the semibenthic postlarval stage. Once the rostral form is accomplished, the animal is considered a juvenile and is totally benthic. The complete cycle may take12–17 days (Rodríguez de la Cruz and Rosales, 1970).

In our study we ascertained different levels of genetic variation between species, a clinelike pattern of genetic variability in the more coastal species, and significant genetic structure among subpopulations of both species.

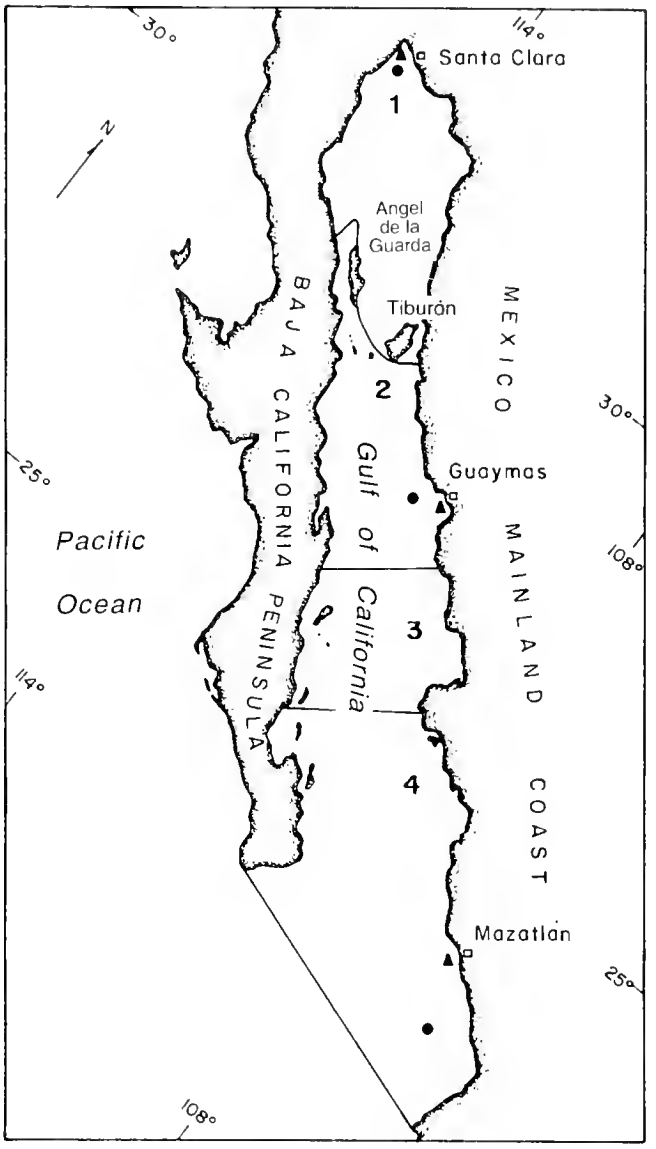

Figure 1

Map of the Gulf of California showing its subdivision (after Round, 1967): 1 = upper Gulf; 2 = middle Gulf; 3 = lower Gulf; and 4 = mouth of the Gulf; and the sampling locations: ▲ = *Penaeus stylirostris*, and ● = *Penaeus californiensis*.

Materials and methods

Samples of *Penaeus californiensis* were obtained in November 1995 by means of bottom trawling nets operated from commercial shrimp fishing vessels performing standard catching efforts (average trawling time: 1 hour; trawling speed: 2 knots), in the following locations: south of Santa Clara Port (31°34′N, 114°19′W); west of Guaymas Port (27°50′N, 111°05′W); and southwest of Mazatlan Port (22°27′N, 106°44′W). Samples of *P. stylirostris* were caught in September 1995 with a cast net thrown from small boats in the following shallow coastal areas: off Santa Clara Port (31°44′N, 114°19′W); off Guaymas Port (27°54′N, 110°55′W); and off Mazatlan Port, (23°12′N, 106°30′W). The samples covered three out of four distinctive areas (called here "upper Gulf, middle Gulf, lower Gulf, and mouth of the Gulf") according to Round (1967; Fig. 1). Samples were frozen (–20°C) and shipped to the laboratory, where they were stored at –75°C until dissection.

Soft tissues from head and abdominal muscle from adult specimens were separated and homogenized in 1 to 2 volumes of cold buffer prepared with 0.1 M Tris-HCl, pH 7.00 + NAD^+ + $NADP^+$ + PVP (10:1:1:100; v:p:p:p). Homogenates were spun (12,000 × g) at 4°C, for 20 min. Supernatants were stored at –75°C until needed.

Electrophoretic assays were performed on 12.5% starch gels (Sigma Chemical Co., St. Louis, MO) in a horizontal apparatus that was placed in the refrigerator (4°C). Three

buffer systems were used to resolve 16 enzymatic systems and muscular protein: continuous tris-citrate buffer, pH 8.0 (TC8) following Selander et al. (1971), 150 V, 6 h; discontinuous tris-citrate, pH 8.3-sodium borate buffer, pH 8.65 (POU) according to Poulik (1957), 250 V, 5 h; and continuous tris-EDTA-borate, pH 8.0 (TEB) following Shaw and Koen (1968), 200 V, 6 h. Tissue sources, electrophoresis systems employed to resolve each enzyme or muscular protein, and number of loci resolved in each enzyme system are listed in Table 1. Staining procedures were accomplished according to the methods of Schaal and Anderson (1974), Shaw and Prasad (1970), Shaw and Koen (1968), Abreu-Grobois (1983), and Rosa-Velez (1986).

Allelomorphs were named A to F depending on their anodal mobility, A being the fastest one. Zymogram interpretation was achieved following recommendations by Utter et. al (1987). In those cases where more than one zone of activity was present in the gel, genetic hypotheses were constructed to ensure correct interpretation. The more complex pattern was displayed by the group of esterases, which was interpreted by standardizing procedures. These involved gel staining with each of the esters used in the staining mixture (a-naphtyl acetate [black bands] and b-napthyl acetate [red bands]), but in separate assays, followed by a joined assay of the same sample, as Laubier et al. (1984) suggested.

Swofford's (1989) BIOSYS-1 software was fed with raw genotypic data from electropherograms to obtain allelic frequencies, proportion of polymorphic loci at the 95% level, observed and unbiased expected (Nei, 1978) heterozygosity, chi-square goodness-of-fit test for testing conformity to the Hardy-Weinberg equilibrium (H-W equilibrium) of variable loci, and Nei's (1978) unbiased genetic similarity and distance.

The same set of raw data was used with GENEPOP (versus 1.2) (Raymond and Rousset, 1995), to compute an unbiased estimate of the *P*-value of an F_{st}-based exact test for the distribution of genotypes by means of the Markovian chain method. PHYLIP's software (versus 3.5) was used to perform bootstrap resampling of gene frequencies to obtain a genetic distance UPGMA (unweighted pair-group method with arithmetic averaging) dendrogram. A Bonferroni correction was applied where multiple tests were carried out.

Results

A total of 32 loci were resolved from 16 enzyme systems and muscular protein. Twenty loci (*Acph-1, Aph-2, Gdh, Got-1, Got-2, G3pd, Gpd, Idh, Ldh, Mdh-1, Mdh-2, Me, Pt-1, Pt-2, Pt-4, Pt-5, Pt-6, Sdh-1, Sdh-2,* and *Xdh*) were monomorphic across all populations sampled. Protein polymor-

Table 1

Electrophoretic conditions, tissues assayed and number of loci resolved in the allozymic variation study of *Penaeus californiensis* and *P. stylirostris*. E.C. = Enzyme Commission.

Enzyme	E.C. no.	Tissue[1]	Buffer system[2]	Staining recipe[3]	Genetic locus	No. of loci scored
Acid phosphatase	3.1.3.2	C	B	SP	*Acph*	2
Alkaline phosphatase	3.1.3.1	C,M	A	SK	*Aph*	3
Esterase	3.1.1.1	C	C	SP	*Est*	5
Glucose-6-phosphate dehydrogenase	1.1.1.49	M	C	SA	*G6pd*	1
Glutamate dehydrogenase	1.4.1.3	M	C	SA	*Gdh*	1
Glutamic oxalacetic transaminase	2.6.1.1	M	A	SA	*Got*	2
Glyceraldehyde-3-phosphate dehydrogenase	1.2.1.12	M	C	SA	*G3pd*	1
α-Glycerophosphate dehydrogenase	1.1.1.8	M	C	SA	*Gpd*	1
Isocitrate dehydrogenase	1.1.1.42	M	C	AG	*Idh*	1
Lactate dehydrogenase	1.1.1.27	M	C	SP	*Ldh*	1
Leucinamino peptidase	3.4.11.1	C	A	SP	*Lap*	1
Malate dehydrogenase	1.1.1.37	M	C	SA	*Mdh*	2
Malic enzyme	1.1.1.40	M	A	SA	*Me*	1
Phosphoglucomutase	5.4.2.2	M	A	SA	*Pgm*	1
Total protein	—	C,M	B	RV	*Pt*	6
Sorbitol dehydrogenase	1.1.1.14	M	A	SA	*Sdh*	2
Xantine dehydrogenase	1.2.1.37	M	A	SA	*Xdh*	1

C = cephalothorax, M = muscle

A = tris-citrate, pH 8.0 (Selander et al., 1971), B = tris-citrate, pH 8.3-sodium borate, pH 8.65 (Poulik 1957, C = Tris-EDTA-borate, pH 8.0 (Shaw and Koen 1968)

SA = Schaal and Anderson (1974); SP = Shaw and Prasad (1970); SK = Shaw and Koen (1968); AG = Abreu-Grobois (1983); RV = Rosa-Velez (1986)

phism ($P \leq 0.95$) was 0.125 for *P. californiensis* in the three populations sampled along the Gulf of California, unlike *P. stylirostris* that showed a clinelike pattern with increasing polymorphism from 0.156 in the upper Gulf population to 0.312 in the mouth of the Gulf. The genetic diversity, reported as expected heterozygosity, was quite homogeneous along the surveyed distribution of *P. californiensis* and showed a gradual northern–southern increase in *P. stylirostris*. (Table 2).

After the Bonferroni correction for multiple tests was applied ($\alpha' = 0.00142$), only *Est-2* was out of H-W equilibrium in at least one population of each species, and *Pgm* and *Pt-3* displayed the same pattern in *P. stylirostris*, all of them accounting for heterozygote deficiency (Table 2).

Four loci (*Aph-3, Est-1, Est-4*, and *Est-5*) in the upper population of *P. stylirostris* showed $D = -1.000$ values (see Table 2); however, four loci had to be considered monomorphic because the polymorphism criterion applied was the most conservative (P_{95}; a locus is considered polymorphic only when the frequency of the most common allele is ≤ 0.95). In most of these cases only one or two individuals were scored as homozygotes for the alternative allele. Such a low frequency may not be significant for the evolutionary process owing to the high probability of disappearance through random processes in just a few generations.

On the other hand, in spite of the high frequencies of both alleles ($p \approx 0.5$), only one heterozygous individual was scored for the diallelic locus *Aph-1* in the upper population of *P. stylirostris*, resulting in a highly significant heterozygote deficiency.

Standardized variance (F_{st}) analysis was achieved among subpopulations within species (Table 3). *Penaeus californiensis* showed a lesser degree of genotypic differentiation among its populations ($F_{st} = 0.182$) than *P. stylirostris* ($F_{st} = 0.372$). This result is possibly related to the mean frequency of private alleles (*sensu* Barton and Slatkin, 1986) in their populations ($p = 0.096$ in *P. californiensis*; and $p = 0.214$ in *P. stylirostris*), even though both figures were notably high. Three loci accounted for differences in the subpopulations of *P. californiensis*: *Aph-3, Est-1*, and *Est-2*. The higher genetic variability displayed by *P. stylirostris* produced a more complex pattern of genotypic differentiation where ten loci accounted for significant differences among subpopulations (*Acph-3, Est-1, Est-2, Est-3, Est-4, Est-5, G6pd, Lap, Pgm, and Pt-3*).

Genetic similarities among subpopulations showed a similar pattern in both species (Table 4); there was a closer resemblance between the middle Gulf and the mouth of the Gulf populations of both species than with the upper Gulf population. This pattern can be visualized in the dendrogram (Fig. 2), where the upper Gulf population of both species segregates from the other two, which are clustered together.

Furthermore, a different level of similarity among subpopulations within species is clearly noticeable (Table 4). *Penaeus californiensis* showed a higher level of similarity among its subpopulations (*I* range: 0.988–0.997) than *P. stylirostris* (*I* range: 0.929–0.954). Genetic similarities between species rendered a clustering level of 0.674 (Fig. 2, Table 4).

Discussion

Two results are of particular interest: a north–south clinelike gradual increase in genetic variability in the more coastal species and the finding of a heterogeneous distribution of genotype frequencies in both assayed species. Most of the previous studies on *Penaeus* species around the world have depicted a general pattern of low homogeneous genetic variability. For example, Mulley and Latter (1980) reported heterozygosity values ranging between 0.006 and 0.033 in Australian penaeids (four species of *Metapenaeus* and six of *Penaeus*). These data were confirmed by subsequent studies: Richardson (1982) found an average heterozygosity of 0.028 in six populations of *P. latisculatus*, and Tam and Chu (1993) reported an observed heterozygosity range of 0.007–0.049 in some species of *Penaeus* and *Metapenaeus* from the South China Sea. *Penaeus japonicus* exhibited one of the highest heterozygosity values ($H_0 = 0.047 \pm 0.029$) among the species surveyed in that study. However there are other reports of even greater heterozygosity in populations of that species transported to European hatcheries as broodstock ($H_0 = 0.102$, Sbordoni et al., 1986; $H_0 = 0.071$, Laubier et al., 1984).

For penaeid species occurring in the western hemisphere, Lester (1979) reported heterozygosities between 0.070 and 0.089 for three commercial penaeids of the Gulf of Mexico. Very similar data for the same species were later reported by Labacena et al. (1994). Lester (1983) also studied one population of each species, *P. vannamei* (from Chomes, Costa Rica) and *P. stylirostris* (from Guaymas, México), which dwell along the northeastern Pacific coast, and reported heterozygosity values of 0.02 and 0.06, respectively. Sunden and Davis (1991) reported heterozygosity values for *P. vannamei* samples from Mexico, Panama, Ecuador, and one farmed population at a Texas hatchery, which were 0.0173, 0.0172, 0.0208, and 0.0111, respectively.

Levels of genetic variability of the species that we studied were not out of the range of those of previous estimations. It must be noticed, in addition, that *P. californiensis* showed a lower, narrower heterozygosity range (0.023 ± 0.014–0.037 ± 0.012) than *P. stylirostris* (0.038 ± 0.021–0.086 ± 0.027). The latter might be explained by the different habitats that each species occupies during its life cycle. This important difference may also be related to the clinelike pattern of the heterozygosity values in *P. stylirostris*, whereas the genetic variability of *P. californiensis* could be evidence of the more stable oceanic conditions that this species experiences during its life span. *Penaeus stylirostris* appears to reflect the environmental variability of the coastal lagoons, which it penetrates during a critical stage of its life cycle. Latitudinal variability of hydrological, ecological, and productivity conditions characterize coastal lagoons along the eastern coast of the Gulf of California. The upper zone's coastal lagoons (Fig. 1) are located in an arid region where vegetation is scarce; around the lagoons, some halophytes and sea grasses predominate. Productivity in these basins depends almost exclusively on microalgae (phytoplankton and microphytobenthos) (Contreras, 1985). To the south, through the

Table 2

Genetic variation of six naturally occurring populations of *Penaeus californiensis* (3) and *P. stylirostris* (3) throughout the Gulf of California (upper, middle and mouth of Gulf). Population names correspond to designated zones of the Gulf (see Fig. 1); n = the number of genes assayed, H = the frequency of observed heterozygotes, D = Selander's coefficient of deviation. Significances of goodness-of-fit chi-square tests (after Bonferroni correction) are given as usual (*=$P \leq 0.05$; ***=$P \leq 0.001$).

			Penaeus californiensis			*Penaeus stylirostris*		
Locus		Allele	Upper	Middle	Mouth	Upper	Middle	Mouth
Acph-3	*n*		76	44	92	96	42	28
		A	1.000	1.000	1.000	1.000	1.000	0.429
		B	0.000	0.000	0.000	0.000	0.000	0.321
		C	0.000	0.000	0.000	0.000	0.000	0.250
	H		0.000	0.000	0.000	0.000	0.000	0.429
	D		0.000	0.000	0.000	0.000	0.000	–0.365
Aph-1	*n*		90	48	96	96	48	32
		A	1.000	1.000	1.000	0.510	0.250	0.406
		B	0.000	0.000	0.000	0.490	0.750	0.594
	H		0.000	0.000	0.000	0.021	0.417	0.438
	D		0.000	0.000	0.000	–0.959***	0.088	–0.121
Aph-3	*n*		90	34	90	92	48	32
		A	0.067	0.000	0.021	0.978	1.000	1.000
		B	0.889	0.765	0.947	0.022	0.000	0.000
		C	0.044	0.000	0.032	0.000	0.000	0.000
		D	0.000	0.235	0.000	0.000	0.000	0.000
	H		0.178	0.235	0.022	0.000	0.000	0.000
	D		–0.136	–0.365	–0.662	–1.000***	0.000	0.000
Est-1	*n*		76	38	96	84	36	28
		A	0.737	0.342	0.156	0.976	0.389	0.643
		B	0.171	0.632	0.646	0.024	0.500	0.214
		C	0.092	0.026	0.198	0.000	0.111	0.143
	H		0.237	0.211	0.333	0.000	0.444	0.286
	D		–0.443	–0.576	–0.365	–1.000***	–0.263	–0.471
Est-2	*n*		82	48	96	88	44	32
		A	0.024	0.000	0.000	0.000	0.000	0.000
		B	0.012	0.104	0.083	0.000	0.000	0.000
		C	0.061	0.229	0.052	0.398	0.023	0.344
		D	0.573	0.667	0.854	0.602	0.909	0.625
		E	0.329	0.000	0.010	0.000	0.068	0.031
	H		0.244	0.625	0.292	0.159	0.182	0.125
	D		–0.569*	0.243	0.107	–0.672*	0.055	–0.753
Est-3	*n*		72	38	96	74	44	32
		A	0.083	0.053	0.052	0.203	1.000	1.000
		B	0.889	0.947	0.948	0.797	0.000	0.000
		C	0.028	0.000	0.000	0.000	0.000	0.000
	H		0.111	0.105	0.104	0.351	0.000	0.000
	D		0.458	0.028	0.044	0.072	0.000	0.000
Est-4	*n*		76	42	94	86	34	24
		A	1.000	1.000	1.000	0.953	0.853	0.292
		B	0.000	0.000	0.000	0.047	0.147	0.708
	H		0.000	0.000	0.000	0.000	0.176	0.250
	D		0.000	0.000	0.000	–1.000**	–0.317	–0.420

continued

mouth of the Gulf, subtropical conditions prevail; abundant fringing vegetation, dominated by four species of mangroves, contributes a huge amount of organic matter that triggers a complementary source of organic production within the detritus chain. Biodiversity indices rise and trophic resources become diversified (González-Farias and Mee, 1988; Flores-Verdugo, 1990). Hence, it is plausible to assume that complexity of ecological webs increases from the northern to the southern coastal zone of the Gulf of California. A parallel gradual increment in heterozygosity in the populations of *P. stylirostris* may be related to that ecological feature. However, Burton (1983) has stated that a direct relation between high heterozygosity and high ecological complexity is very difficult to demonstrate,

Table 2 (continued)

Locus		Allele	*Penaeus californiensis* Upper	Middle	Mouth	*Penaeus stylirostris* Upper	Middle	Mouth
Est-5	*n*		96	46	96	94	46	30
		A	1.000	1.000	1.000	0.957	0.022	0.767
		B	0.000	0.000	0.000	0.043	0.717	0.200
		C	0.000	0.000	0.000	0.000	0.261	0.033
	H		0.000	0.000	0.000	0.000	0.130	0.133
	D		0.000	0.000	0.000	−1.000***	−0.694	−0.653
G6pd	*n*		96	48	96	90	38	30
		A	1.000	1.000	1.000	1.000	1.000	0.767
		B	0.000	0.000	0.000	0.000	0.000	0.100
		C	0.000	0.000	0.000	0.000	0.000	0.133
	H		0.000	0.000	0.000	0.000	0.000	0.267
	D		0.000	0.000	0.000	0.000	0.000	−0.329
Lap	*n*		96	48	96	92	48	32
		A	1.000	1.000	1.000	0.272	0.458	0.688
		B	0.000	0.000	0.000	0.728	0.542	0.313
	H		0.000	0.000	0.000	0.543	0.500	0.500
	D		0.000	0.000	0.000	0.358	−0.014	0.127
Pgm	*n*		96	48	94	88	48	32
		A	1.000	1.000	1.000	0.125	0.104	0.094
		B	0.000	0.000	0.000	0.795	0.292	0.281
		C	0.000	0.000	0.000	0.000	0.188	0.531
		D	0.000	0.000	0.000	0.000	0.333	0.094
		E	0.000	0.000	0.000	0.034	0.083	0.000
		F	0.000	0.000	0.000	0.045	0.000	0.000
	H		0.000	0.000	0.000	0.136	0.208	0.315
	D		0.000	0.000	0.000	−0.613*	−0.728*	−0.513
Pt-3	*n*		96	48	96	96	48	32
		A	1.000	1.000	1.000	0.000	0.250	0.063
		B	0.000	0.000	0.000	1.000	0.750	0.938
	H		0.000	0.000	0.000	0.000	0.083	0.000
	D		0.000	0.000	0.000	0.000	−0.782	−1.000
Number of loci studied			32	32	32	32	32	32
Mean number of individuals per locus			45.8 ±0.6	22.3 ±0.7	46.2 ±1.5	44.7 ±1.1	22.0 ±0.6	15.7 ±0.2
Mean number of alleles per locus			1.31 ±0.16	1.19 ±0.09	1.25 ±0.13	1.38 ±0.12	1.44 ±0.16	1.53 ±0.16
Polymorphism (P_{95})			12.50	12.50	12.50	15.63	25.00	31.25
H_0			0.024 ±0.012	0.037 ±0.021	0.023 ±0.014	0.038 ±0.021	0.067 ±0.025	0.086 ±0.027
H_e			0.044 ±0.023	0.046 ±0.024	0.030 ±0.018	0.075 ±0.027	0.109 ±0.038	0.145 ±0.041

and therefore, correlation should not be taken as conclusive evidence for causation.

Several reports have stated a small probability of encountering genetically "differentiated" stocks in *Penaeus* species, mainly due to their low variability and the apparent homogeneous allele distributions among the subpopulations (Lester, 1979, 1983; Mulley and Latter, 1981a, 1981b; Richardson, 1982). However, Sunden and Davis (1991) could trace a slight geographic differentiation across the range of *P. vannamei*. They detected at least one unique allele in each wild population. Tam and Chu (1993) attributed the higher genetic similarity shown between the species pair *P. merguiensis* and *Metapenaeus ensis* to the genetic differentiation among populations of the same species. In addition, some allozyme variation was observed among populations of *Metapenaeus benettae* (Salini, 1987) in Australia and *P. kerathurus* in the Mediterraenean (Mattocia et al., 1987). From later studies, it was noticed that when the allozymes surveys were performed over larger geographical scales, substantially higher significant variation and differentiation among populations was found. Such is the case for the wild populations of *P. monodon* along the Australian coast (Benzie et al., 1992), where expected heterozygosities have ranged between 0.053 and 0.103, and significant genetic differences have existed among Australian populations.

The use of more variable markers such as mtDNA genes have confirmed the allozymic findings on the structuring of *P. monodon* populations in Australia (Benzie et al., 1993), and *P. notialis* and *P. schmitti* in the South American Atlantic coast (Machado et al., 1993).

From our data, subpopulations of both species appear genetically differentiated in terms of significant values of standardized variance of their genotypic distributions (Table 3). Two reasons seem to account for such a result: 1) private alleles exist in about every polymorphic locus (75% in both species), and 2) the most frequent allele alternates among subpopulations of the same species in several loci (see Table 2).

Heterogeneity among subpopulations is commonly explained as a lack of genetic flow (see Slatkin, 1985, for a review). Nonetheless, penaeids can be considered vagile species because they have two dispersal phases, the planktonic larvae and the vagile adult. Lester (1979) imputes this characteristic to the high levels of genetic similarity among the penaeids populations of the Gulf of Mexico.

Although penaeids are capable of being displaced, geographical barriers must prevent their movement. The Gulf of California is now considered as a much more complex ecosystem than it was formerly believed: Santamaría-Del Angel et al. (1995) proposed 14 biogeographic subdivisions in the Gulf on the basis of satellite images describing concentrations of photosynthetic pigments. Likewise, González-Farias et al. (1995) described complicated patterns of carbon turn-over throughout the Gulf from the analysis of organic matter and heterotrophic bacteria. The upper Gulf region is a very unique environment where the Colorado River drained until about fifty years

Table 3

Wright's standardized variance (F_{st}) of populations within species. Statistical significance in brackets (ns=not significant; **=$P \leq 0.01$; ***=$P \leq 0.001$).

Loci	*P. californiensis*	*P. stylirostris*
Acph-3	—	0.510(***)
Aph-1	—	0.054(ns)
Aph-3	0.094(***)	−0.022(ns)
Est-1	0.278(***)	0.384(***)
Est-2	0.134(***)	0.128(**)
Est-3	−0.005(ns)	0.756(***)
Est-4	—	0.514(***)
Est-5	—	0.650(***)
Gdh-1	—	−0.009(ns)
G6pd	—	0.207(***)
Lap	—	0.149(***)
Pgm	—	0.264(***)
Pt-3	—	0.210(**)
Mean values	0.182(***)	0.372(***)

Table 4

Nei's genetic similarity (above diagonal ****) and distance (below diagonal *****) among six populations of two penaeid species, *Penaeus californiensis* and *P. stylirostris*, throughout the Gulf of California (upper, middle, and mouth of Gulf).

		Penaeus californiensis			*Penaeus stylirostris*		
	Population source	Upper	Middle	Mouth	Upper	Middle	Mouth
Penaeus californiensis	Upper	****	0.991	0.988	0.690	0.654	0.691
	Middle	0.009	****	0.997	0.632	0.656	0.686
	Mouth	0.012	0.003	****	0.672	0.655	0.679
Penaeus stylirostris	Upper	0.371	0.383	0.397	*****	0.929	0.936
	Middle	0.425	0.422	0.423	0.074	*****	0.954
	Mouth	0.370	0.377	0.387	0.067	0.047	*****

ago, when the Hoover Dam was constructed up river and flow was severely restricted. Presently, hypersaline conditions prevail in the upper Gulf region. This dynamic and extreme environment is topographically bounded to the south by a submarine range. Tiburón and Angel de la Guarda Islands are the heights of this submarine range (Fig. 1); south of these islands the Gulf increases in depth to around 3000 m in the Guaymas Basin. Thus, the islands may be considered a geographical or ecological boundary that reduces the free flow of penaeids. Correa-Sandoval and Carvacho-Bravo (1992) came to a similar conclusion when they described the distribution pattern of brachyuran crabs in the Gulf of California.

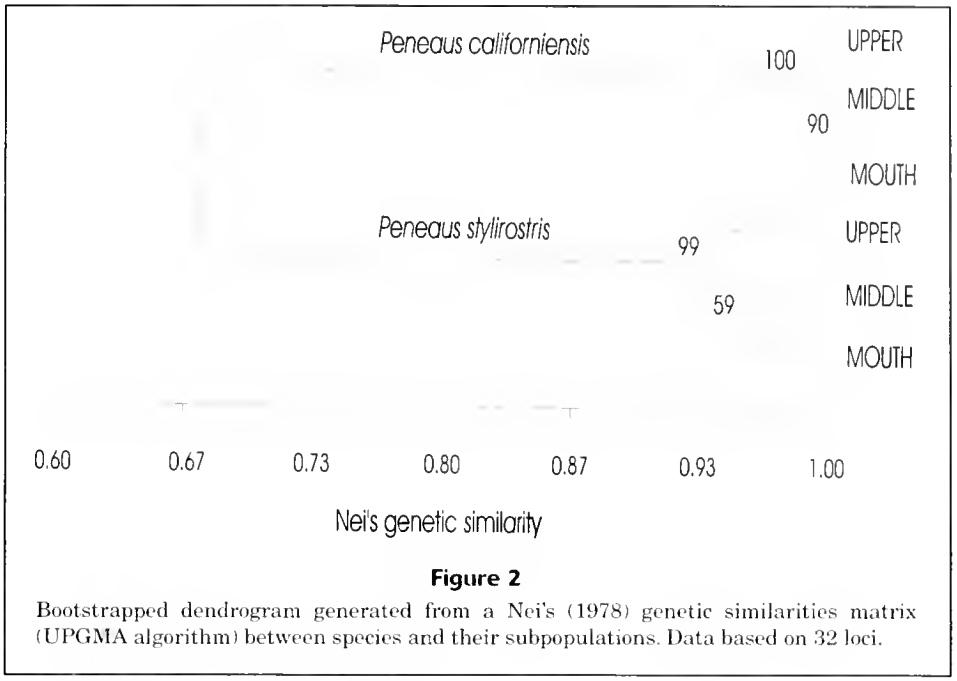

Figure 2

Bootstrapped dendrogram generated from a Nei's (1978) genetic similarities matrix (UPGMA algorithm) between species and their subpopulations. Data based on 32 loci.

In some populations of both species, three loci (*Aph-1*, *Est-2*, and *Pgm*) were found to be out of H-W equilibrium according to the chi-square goodness-of-fit test. Two of the common causes of heterozygote deficiency, as discussed by Zouros and Foltz (1984), can be invoked here: 1) the Wahlund effect, because some genetic structure has been demonstrated in both species, at least in the geographic range that we studied; thus, different genetic compositions taking part in reproductive events, will yield such a pattern; and 2) selection against heterozygotes, a hypothesis that is difficult to prove, but is feasible owing to very recent environmental modification (ca. half a century). Homozygous genotypes may be selected if they perform better under extreme conditions with no drastic gene erosion during the little time elapsed since environmental alterations began. For example, *Aph-1* displays a ca. 50% frequency of the two segregating alleles, which allows us to expect high heterozygote frequency. However, the sample lacked these genotypes almost completely. With no additional evidence to discard either of the above, a third one, i.e. the presence of a null allele segregating in this population, may also be invoked. Further evidence from breeding experiments among individuals of this population is needed to evaluate this supposition.

Additional evidence of the divergence of populations (remarkably, populations of both species dwelling in the upper Gulf) is given by Nei's genetic similarity (Table 4; Fig. 2). It is evident from the dendrogram that 1) there is a clear subdivision in both within-populations dendrograms that distinguishes the populations inhabiting the upper Gulf (hence, it is not only the previously discussed characteristic of heterozygote deficiency that segregates these populations from the rest, but the distribution of their genes too) and 2) a subdivision between species where the degree of genetic similarity is similar to those previously reported in other penaeid species. Average genetic similarities among species within *Penaeus* genera were 0.65 ±0.08, and 0.69 ±0.08 within *Metapenaeus* (Mulley and Latter, 1980). Similar values (I=0.66) were found between two forms of brachyuran freshwater crabs from South Africa (Stewart and Cook, 1998).

The characteristic genetic features we found provide additional support for the recent scheme proposed by Pérez-Farfante and Kensley (1997). Their proposition, regarding the reorganization of American shrimps in the family Penaeidae, involves the promotion of an existing subgenus to genus, i.e. *Penaeus californiensis* would become *Farfantepenaeus californiensis*, and *Penaeus stylirostris* would change to *Litopenaeus stylirostris*. However, more evidence must be compiled to support this reclassification.

Complexity of the Gulf of California ecosystem, as well as the biological features described for each species, may account for the greater degree of genetic structure in the species that inhabit it. Fisheries and hatcheries managers can take advantage of such information, for example, by defining stocks or selecting the more variable populations to be submitted to artificial selection programs in the aquaculture scheme.

Acknowledgments

We thank the useful and insight comments of two anonymous reviewers which substantially improved the paper. M. A. Cervantes and L. M. Enriquez processed the data and prepared the tables and figures. This study was partially funded by Centro Internacional de Biologia Molecular y Celular, A. C. One of us (R.E.-F.) received support from Consejo Nacional de Ciencia y Tecnologia during the study.

Literature cited

Abreu-Grobois, A.
1983. Population genetics of *Artemia*. Ph.D. diss., Univ. College of Swansea, Wales, 438 p.

Allendorf, F. W.; N. Ryman, and F. M. Utter.
1987. Genetics and fishery management: past, present and future. Chap. 1 *in* Population genetics and fishery management (N. Ryman and F. Utter, eds.), p. 1–19. Washington Sea Grant Program, Univ. Wash. Press, Seattle and London.

Barton, N. H., and M. Slatkin.
1986. A quasi-equilibrium theory of the distribution of rare alleles in a subdivided population. Heredity 56:409–415.

Benzie, J. A. H., E. Ballment, and S. Frusher.
1993. Genetic structure of *Penaeus monodon* in Australia: preliminary data from allozymes and mtDNA. Aquaculture 11:89–93.

Benzie, J. A. H., S. Frusher, and E. Ballment.
1992. Geographical variation in allozyme frequencies of *Penaeus monodon* (Crustacea: Decapoda) populations in Australia. Aust. J. Mar. Freshwater Res. 43:715–725.

Burton, R. S.
1983. Protein polymorphisms and genetic differentiation of marine invertebrate populations. Mar. Biol. Letters 4:193–206.

CICTUS (Centro de Investigación Cientifica y Tecnológica de la Universidad de Sonora).
1985. El cultivo del camaron azul *Penaeus stylirostris* (Stimpson). Universidad de Sonora, Hermosillo, Sonora, Mexico, 125 p.

Contreras, F.
1985. Las lagunas costeras Mexicanas. Centro de Ecodesarrollo, Secretaria de Pesca, Mexico, D.F., 263 p.

Correa-Sandoval, F., and A. Carvacho-Bravo.
1992. Efecto de la "Barrera de las Islas" en la distribucion de los braquiuros (Crustacea: Decapoda) en el Golfo de California. Proc. San Diego Soc. Nat. Hist. 26:1–4.

de la Rosa-Velez, J.
1986. Variabilidad genetica poblacional en ostiones de la especie *Crassostrea virginica* del Golfo de Mexico. Ph. D. diss., Univ. Nal. Auton, Mexico, 124 p.

Flores-Verdugo, F. J.
1990. Algunos aspectos sobre la ecologia, uso e importancia de los ecosistemas de manglar. Chap. 2 *in* Temas de oceanografia biologica en Mexico, vol. I (J. de laRosa-Vélez and F. Gonzalez-Farias, eds.), p. 21–56. Universidad Autonoma de Baja California, Ensenada, Mexico.

Gonzalez-Farias, F., M. Hernandez-Garza; F. Flores-Verdugo, and O. Calvario-Martinez.
1995. Distribucion de la materia organica particulada y bacterias heterotrofas en aguas superficiales del mar de Cortes. Chap. 4 *in* Temas de oceanografia biologica en Mexico, vol. II (F. Gonzalez-Farias and J. de la Rosa-Velez, eds.), p. 87–110. Universidad Autonoma de Baja California, Ensenada, Mexico.

Gonzalez-Farias, F., and L. Mee.
1988. Effect of mangrove humic-like substances on biodegradation rate of detritus. J. Exp. Mar. Biol. Ecol. 119:1–13.

Labacena, M. E., M. Torres and G. Espinoza.
1994. Variabilidad y distancia genetica en especies de *Penaeus*. Rev. Invest. Mar. 15(1):80–87.

Laubier, A., N. Pasteur, and M. Moriyasu.
1984. Estimation du polymorhisme enzymatique d'une population de *Penaeus japonicus* maintenue en elevage depuis quatre générations. Oceanol. Acta 7(4):451–456.

Lester, L. J.
1979. Population genetics of penaeid shrimp from the Gulf of Mexico. J. Hered. 70(3):175–180.
1983. Developing a selective breeding program for penaeid shrimp mariculture. Aquaculture 33:41–50.

Lightner, D. V., R. M. Redman; B. T. Poulos; L. M. Nunan, J. L. Mari, and K. W. Hasson.
1997. Risk of spread of penaeid shrimp viruses in the Americas by the international movement of live and frozen shrimp. Rev. sci. tech. Off. Int. Epiz. 16(1):146–160.

Machado, E. G., N. Dennebouy, M. O. Suarez; J.-C. Mounolou, and M. Monnerot.
1993. Mithocondrial 16S-rRna gene of two species of shrimps: sequence variability and secondary structure. Crustaceana 65 279–286.

Mattocia, M., G. La Rosa, E. De Matthaeis, M. Cobolli-Sbordoniand, and V. Sbordoni.
1987. Patterns of genetic variability in Mediterranean populations of *Penaeus kerathurus* (Crustacea: Decapoda). *In* Selection, hybridization and genetic engineering in aquaculture (K. Tiews, ed.), p. 131–142. Heenemann Verlag, Berlin.

Mulley, J. C., and B. D. H. Latter.
1980. Genetic variation and evolutionary relationships within a group of thirteen species of penaeid prawns. Evolution 34:904–916.
1981a. Geographical differentiation of eastern Australian penaeid prawn populations. Aust. J. Mar. Freshwater Res. 32:889–895.
1981b. Geographic differentiation of tropical Australian penaeid prawn populations. Aust. J. Mar. Freshwater Res. 32:897–906.

Nei, M.
1978. Estimation of average heterozygosity and genetic distance from a small number of individuals. Genetics 89:583–590.

Perez-Farfante, I., and B. Kensley.
1997. Penaeoid and Sergestoid Shrimps and Prawns of the World. Keys and diagnoses for the families and genera. (Memoires du Muséum National d'Histoire Naturel, tome 175). Backhuys Publishers, The Netherlands, 233 p.

Poulik, M. D.
1957. Starch gel electrophoresis in a discontinuous system of buffers. Nature 180:1477–1479.

Raymond, M., and F. Rousset.
1995. GENEPOP (version 1.2): a population genetics software for exact test and ecumenisism. J. Hered. 86:248–249.

Richardson, B. J.
1982. Geographical distribution of electrophoretically detected protein variation in Australian commercial fishes. III. Western king prawn, *Penaeus latisulcatus* Kishinouye. Aust. J. Mar. Freshwater Res. 33:927–931.

Rodriguez de la Cruz, M. C.
1976. Sinopsis biologica de las especies del género *Penaeus* del Pacifico Mexicano. Mem. Simp. Biol. Y Din. Pobl. Cam. Guaymas, Son. 1:282–316.

Rodriguez de la Cruz, M. C., and F. J. Rosales.
1970. Sinopsis de *Penaeus californiensis* Holmes. FAO, Rome, 35 p.

Rodriguez-Romero, F., and J. de la Rosa-Velez.
1993. Prespectivas de la genètica aplicada a la camaronicultura en las costas mexicanas. Chapter 6 *in* Camaronicultura bases tecnicas y cientificas para el cultivo de camarones peneidos (L.R. Martinez Cordoba, ed.), p. 221–233. CICTUS Hermosillo, Sonora, Mexico.

Rosenberry, B. (ed.)
1996. World shrimp farming, 1996. Aquaculture Digest. San Diego, CA, 164 p.

Round, F. E.
1967. The phytoplankton of the Gulf of California – part 1. Its composition, distribution and contribution to the sediments. J. Exper. Mar. Biol. Ecol. 1:76–97.

Salini, J. C.
1987. Genetic variation and population subdivision in the greentail prawn *Metapenaeus benettae*. Aust. J. Mar. Freshwater Res. 38:339–349.

Santamaría-Del Angel, E., S. Alvarez-Borrego, and F. E. Muller.
1995. Regiones biogeográficas del Golfo de California basadas en las imágenes del *Coastal Zone Color Scanner*. Chapter 3 *in* Temas de oceanografía biológica en Mexico, vol. II (F. González-Farías, and J. de la Rosa-Vélez, eds.), p. 63–83. Universidad Autónoma de Baja California, Ensenada, Mexico.

Sbordoni, V., E. de Matthaeis, M. Cobolli-Sbordoni, G. La Rosa, and M. Mattoccia.
1986. Bottleneck effects and the depression of genetic variability in hatchery stocks of *Penaeus japonicus* (Crustacea, Decapoda). Aquaculture 57:239–251.

Schaal, B. A., and W. W. Anderson.
1974. An outline of techniques for starch gel electrophoresis of enzymes from the American oyster *Crassostrea virginica* Gmelin. Tech. Rep. Ser. Georgia Mar. Sci. Cent. 74(3), 18 p.

Selander, R. K., M. H. Smith, S. Y. Yang, W. E. Johnson and J. B. Gentry.
1971. Biochemical polymorphisms and systematics in the genus *Peromyscus* I. Variation in the old field mouse (*Peromyscus polonatus*). Stud. Genet. 6. Univ. Texas Publ. 7103: 49–90.

Shaw, C. R., and A. L. Koen.
1968. Starch gel zone electrophoresis of enzymes. Chapter 9 *in* Chromatographic and electrophoresis techniques, vol. II (I. Smith, ed.), p. 325–364. Interscience Publ, New York, NY.

Shaw, C. R., and R. Prasad.
1970. Starch gel electrophoresis of enzymes: a compilation of recipes. Biochem. Genet. 4 297–320.

Slatkin, M.
1985. Gene flow in natural populations. Ann. Rev. Ecol. Syst. 16:393–430.

Stewart, B. A., and P. A. Cook.
1998. Identification of a new species of river crab (Decapoda: Brachyura: Potamonautidae) from South Africa using morphological and genetic data. J. Crust. Biol. 18(3): 556–571.

Sunden, S. L. F., and S. K. Davis.
1991. Evaluation of genetic variation in domestic population of *Penaeus vannamei* (Boone): a comaprision with three natural populations. Aquaculture 97:131–142.

Swofford, D. L.
1989. BIOSYS-1: a computer program for the analysis of allelic variation in population genetics, a biochemical systematics. Univ. of Illinois, Urbana, IL, 43 p.

Tam, Y K. and K. H. Chu.
1993. Electrophoretic study on the phylogenetic relationships of some species of *Penaeus* and *Metapenaeus* (Decapoda: Penaeidea) from the South China Sea. J. Crust. Biol. 13 (4) 697–705.

Utter, F., P. Aebersold, and G. Winans.
1987. Interpreting genetic variation detected by electrophoresis. Chapter 2 *in* Population genetics and fishery management (N. Ryman and F. Utter, eds.), p. 21–46. Washington Sea Grant Program, Univ. Washington Press, Seattle and London.

Zouros, E., and D. W. Foltz.
1984. Possible explanations of heterozygote deficiency in bivalve molluscs. Malacologia 25(2):583–591.

Indices of larval king mackerel (*Scomberomorus cavalla*) abundance in the Gulf of Mexico for use in population assessments

Christopher T. Gledhill

Joanne Lyczkowski-Shultz

Southeast Fisheries Science Center
National Marine Fisheries Service, NOAA
3209 Frederic St.
Pascagoula, Mississippi 39568-1207
E-mail address (for C. T. Gledhill): Christopher.T.Gledhill@noaa.gov

Abstract—The stock status of the Gulf of Mexico migratory group of king mackerel (*Scomberomorus cavalla*) is currently evaluated by using age-based sequential virtual population analysis (VPA). We examined king mackerel larval occurrence and abundance indices from annual ichthyoplankton surveys, developed an age-adjusted abundance index, and questioned whether larval indices of abundance are useful for calibrating the king mackerel VPA. Gulf of Mexico king mackerel larval occurrence and abundance increased over a fourteen-year time series from 1982 to 1995 and were highly correlated with spawning stock size. Correlations between stock size and larval occurrence, and between stock size and larval abundance, were 0.82 and 0.84, respectively. The correlation between larval occurrence and stock size for the years 1986–95 increased to 0.91, owing to the addition in 1986 of a fall survey with added coverage during peak spawning. Daily instantaneous mortality rate (Z) was estimated by regression of larval catch curves. Although a large amount of interannual variability in mortality rates was noted, no statistical differences were detected among years. The instantaneous daily mortality rate estimated by pooling all years, $Z = 0.53$, was used to develop an age-adjusted index for king mackerel in order to eliminate the influence of variable larval age composition among years. This adjusted index did not improve correlations between stock size and larval abundance (r=0.78). For now, indices of larval occurrence and unadjusted larval abundance from ichthyoplankton collections reflect trends in spawning stock size and provide useful variables for calibrating the king mackerel VPA.

Manuscript accepted 4 April 2000.
Fish. Bull. 98:684–691 (2000).

The king mackerel (*Scomberomorus cavalla*), a western Atlantic member of the family Scombridae, ranges from Massachusetts to Brazil (Shipp, 1986). This highly migratory, coastal pelagic species can attain a maximum size of 1.7 m and 45 kg (Robins and Ray, 1986) and ages of more than 20 years (DeVries and Grimes, 1997). King mackerel support valuable commercial and recreational fisheries that are regulated in the southeastern coastal states and Gulf of Mexico under the Coastal Migratory Pelagic Resources Fishery Management Plan. These fisheries were largely unregulated in the late 1970s and early 1980s when fishing mortality was high, and thus stock size was reduced. As a result, management by quota was implemented in the 1985–86 fishing year. The current management regime for king mackerel fisheries recognizes only two stocks off the U.S. southeast coast: an Atlantic migratory group and a Gulf of Mexico migratory group. There is, however, some disagreement as to whether there are one or two distinct stocks in the Gulf of Mexico (Johnson et al., 1994; DeVries and Grimes, 1997; Gold et al., 1997; Roelke and Cifuentes, 1997).

Reproduction in this highly fecund, serial spawning species occurs from May through early October and peaks in September along both the U.S. Gulf of Mexico and southeast Atlantic coasts (McEachran et al., 1980; Finucane et al., 1986; Grimes et al., 1990). Data on the abundance and distribution of king mackerel larvae indicate that spawning occurs chiefly over the mid to outer continental shelf of the northern Gulf of Mexico (McEachran et al., 1980; Grimes et al., 1990). Grimes et al. (1990) suggested that spawning occurs over shallower depths in the region from west Louisiana to northwest Florida and may be associated with oceanographic features, especially the discharge plume of the Mississippi River. Absolute growth rates of king mackerel larvae were observed to range from 0.54 to 1.33 mm per day and were slightly higher for larvae from the Mississippi River plume when compared to other locations in the Gulf and southeast Atlantic coast (DeVries et al., 1990).

Population size of Gulf-group king mackerel is estimated biennially by scientists of the Mackerel Stock Assessment Panel (Gulf of Mexico and South Atlantic Fishery Management Councils) using an age-based sequential virtual population analysis (VPA). This VPA is implemented by using ADAPT (Conser and Powers, 1990; Powers and Restrepo, 1993). The king mackerel VPA is calibrated or tuned by using various indices of abundance based on fisheries dependent catch-per-unit-of-effort and fisheries independent resource survey data. Survey estimates of annual abundance and frequency of occurrence of king mackerel larvae were first considered as tuning variables for the king mackerel VPA by the 1996 Mackerel Stock Assessment Panel.[1] Although fre-

[1] Mackerel Stock Assessment Panel. 1996. 1996 Report of the Mackerel Stock Assessment Panel. Gulf of Mexico Fishery Management Council, Lincoln Center, Suite 331, 5401 West Kennedy Blvd, Tampa, FL 33609 and South Atlantic Fishery Management Council, Southpark Bldg., Suite 306, 1 Southpark Circle, Charleston, SC 29407.

quency of occurrence was ultimately accepted as a tuning variable, abundance was not because larval catches had not been adjusted for age. Interannual differences in age composition of sampled larvae could contribute a large amount of variation in estimates of mean annual abundance because of the exponential decline in numbers of larvae with age. Furthermore, it was thought that survey estimates of larval abundance would be too variable to be of value as an index of stock size owing to the highly variable nature of larval mortality rates.[2] In our study, we developed an age-adjusted larval index for king mackerel and evaluated the appropriateness of using larval indices in calibrating the king mackerel VPA.

Materials and methods

King mackerel larvae in the Gulf of Mexico have been collected annually since 1982 during Southeast Area Monitoring and Assessment Program (SEAMAP) ichthyoplankton surveys conducted by the states of Florida, Alabama, Mississippi, Louisiana, and by the National Marine Fisheries Service. Larvae were captured in oblique tows from near bottom to the surface with a 61-cm, 0.333-mm-mesh bongo net by following standardized SEAMAP collection procedures (Richards et al., 1993). Survey stations were typically located 55.56 km apart in a fixed grid, and sampled at all times of day or night. Collections were taken west of 88°W longitude in June and July from 1982 to 1985. Starting in 1986, gulf-wide samples were also collected in late August, September, and early October. Catches of king mackerel larvae were standardized to account for sampling effort and expressed as number of larvae under 10 m^2 of sea surface (no./10 m^2). Annual mean abundances, i.e. the indices not adjusted for age composition of larval catches, were based on arithmetic means. Use of the delta-distribution (Pennington, 1983) did not lower estimates of standard error.

The age composition of king mackerel larvae captured at each station was estimated by converting lengths to ages with a least squares regression model based on the length and age of larvae (n=47) collected in September 1986 from the Gulf of Mexico and Atlantic Ocean and aged by counting otolith growth increments[3] (DeVries et al., 1990). Two additional techniques for assigning larval ages from lengths were considered, namely a probability age-classification matrix (Scott, et al., 1993) and discriminant analysis, but these were found to be ineffective owing to the small number of aged larvae. Once ages were assigned, individual catch curves for each year of the time series from 1982 to 1995 were constructed from the descending arm of $\log_e$-transformed catch-at-age data (Ricker, 1975) by using the regression procedure of SAS (SAS Institute Inc., 1990). A dummy-variable model was used in the regression procedure to fit a single model for all years with test statements that tested for homogeneity of intercepts and of slopes. Instantaneous daily mortality rates and an age-adjusted index of abundance were then calculated.

The age-adjusted index for king mackerel was based on the abundance of a single age class to eliminate the influence of variable larval age composition among years. We arbitrarily chose one-day-old larvae as the standard age class on which to base the age-adjusted index. We estimated the density of one-day-old larvae at each station by back-calculating and summing their numbers from older age classes using an estimate of daily instantaneous mortality rate. The density of one-day-old king mackerel larvae at each station was estimated as

$$I_{y,s} = \sum_{i=1}^{k} N_{y,s,i} e^{Z(i-1)},$$

where $I_{y,s}$ = the number of one-day-old larvae under 10 m^2 of sea surface (y=year; s=station); and

$N_{y,s,i}$ = the number of larvae under 10 m^2 of sea surface of each age class represented in the sample (i=age class).

Annual mean age-adjusted index of larval abundance was estimated as the average of station values.

Annual estimates of spawning stock size (ages 1 through 11+ years) were obtained from a VPA of king mackerel.[4] No king mackerel larval occurrence data from SEAMAP were used to tune this VPA. However, the VPA used for the most recent stock assessment was calibrated with larval occurrence data. Residual plots from regressions between the VPA estimate of stock size indices of larval abundance exhibited no particular pattern; therefore data were not transformed for correlation analyses. Correlation between the VPA estimate of spawning stock size and three SEAMAP larval indices were then estimated by using the correlation procedure of SAS (SAS Institute Inc., 1990). Larval indices used were 1) frequency of occurrence; 2) mean abundance of all larvae captured unadjusted for age; and 3) mean abundance of age one-day larvae.

Results

The SEAMAP survey king mackerel larval frequency of occurrence index ranged from 0.02 (SE=0.017, CV=100%) in 1983 to 0.32 (SE=0.038, CV=12%) in 1995 (Table 1). The survey larval abundance index (no./10 m^2) ranged from 0.23 (SE=0.228, CV=100%) in 1983 to 5.15 (SE=0.924; CV=18%) in 1995 (Table 1). Mean frequency of occurrence and abundance of king mackerel larvae varied more during the first four years of the time series when observations were available from only the early part of the spawning season, i.e. summer months. However, both frequency of occurrence and abundance have increased over

[2] Powers, J. E. 1996. Personal commun. Southeast Fisheries Science Center, Miami Laboratory, Miami, FL 33149.

[3] DeVries, D. 1996. Personal commun. Southeast Fisheries Science Center, Panama City Laboratory, Panama City, FL 32407.

[4] Legault, C. 1998. Personal commun. Southeast Fisheries Science Center, Miami Laboratory, Miami, FL 33149.

the fourteen-year time series (Fig. 1A, Table 1). Variability decreased after 1986, when the fall SEAMAP ichthyoplankton survey was added which both extended coverage into the time period of peak king mackerel spawning and increased the number of samples. Coefficients of variation (100 × SE/mean) have been less than 20% for both frequency of larval occurrence (1989–95) and larval abundance (1992–95) for the most recent years of the time series (Table 1). Also an expansion in the areal distribution of king mackerel larvae has been apparent since 1986 (Fig. 2).

A total of 798 king mackerel larvae ranging in length from 1.6 to 10.1 mm were collected from 1982 to 1995 (Table 2). A quadratic equation best described the relationship between larval king mackerel age and length data (Fig. 3). Catch-at-age was calculated from the estimates of larval density and age frequencies and then used to construct annual catch-at-age curves for survey-captured king mackerel larvae. Over the time series, larvae ranged in age from 2 to 11 days, and estimates of instantaneous daily mortality rates for individual years ranged from 0.35 in 1985 to 0.70 in 1992 (Table 3). A single catch-at-age regression for all years combined indicated no significant difference among slopes (i.e. instantaneous mortality rates) or among intercepts. Therefore, a pooled regression model was fitted. The slope of the pooled regression gave an estimate of instantaneous daily mortality rate (Z) of 0.53 (Table 3) and was subsequently used to backcalculate the abundance of one-day-old larvae and generate the age-adjusted index of king mackerel larval abundance.

VPA estimates of king mackerel spawning stock size ranged from 46.03 × 10^5 individuals in 1985 to 101.93 × 10^5 individuals in 1995 (Fig. 1A). Survey larval frequency of occurrence and estimates of stock size corresponded with a correlation of 0.82 over the entire time series, 1982–95, and 0.92 for the period 1986–95 (Fig. 1A). The king mackerel survey index of larval abundance (unadjusted for age) was also highly correlated with spawning stock size (Fig. 1A). The correlation, 0.84, was the same for both periods of comparison, all survey years, and years since 1986. Our attempt to adjust larval abundance for age did not improve the correlation between the abundance index and spawning stock size. The correlation with spawning stock size was, however, higher after fall surveys began, 0.78 versus 0.65, but these values were both lower than those for the "uncorrected" abundance index and the index based on frequency of occurrence (Fig. 1B).

Discussion

Hunter and Lo (1993) asserted that fish eggs and larvae can be used not only to estimate the biomass of a fish stock but also to monitor trends in relative stock abundance. Indices of relative abundance are less costly to produce than biomass estimates from ichthyoplankton data, but they are also less precise. The CVs of the most precise biomass estimates based on ichthyoplankton data range between 20% and 30%. Whether adjusted for growth and mortality of larvae or not, ichthyoplankton indices are "surprisingly sensitive to major changes in stock abundance" (Hunter and Lo, 1993). It should be of no surprise that our indices based on abundance and frequency of occurrence of king mackerel larvae from SEAMAP collections in the Gulf of Mexico closely tracked trends in adult abundance over the time

Table 1

SEAMAP annual estimates of king mackerel larval mean abundance and frequency of occurrence (n=number of stations, CV=100×SE/mean).

		Number/10 m^2			Frequency of occurrence		
Year	n	Mean	SE	CV (%)	Mean	SE	CV (%)
1982	77	0.83	0.464	56	0.09	0.033	36
1983	59	0.23	0.228	100	0.02	0.017	100
1984	74	1.19	0.413	35	0.18	0.045	25
1985	94	0.36	0.178	49	0.06	0.025	40
1986	225	1.10	0.286	26	0.10	0.020	20
1987	216	0.69	0.161	23	0.12	0.022	19
1988	125	0.97	0.319	33	0.11	0.028	25
1989	129	2.08	0.711	34	0.19	0.034	18
1990	129	1.67	0.357	21	0.21	0.036	17
1991	129	1.33	0.368	28	0.18	0.034	19
1992	167	2.00	0.338	17	0.28	0.035	12
1993	175	3.22	0.546	17	0.30	0.035	12
1994	176	2.82	0.503	18	0.26	0.033	13
1995	155	5.15	0.924	18	0.32	0.038	12

series. Annual estimates of mean king mackerel occurrence were more precise than the estimates of larval abundance, and CV's for both king mackerel indices were comparable to CVs of ichthyoplankton-based estimates for other species (Hunter and Lo, 1993). Larval abundance of Atlantic bluefin tuna, a species that poses a more intractable sampling problem than does king mackerel, namely an immense spawning area (the open Gulf) and lower overall abundance, has been used as a tuning variable in population assessments by VPA (Scott et al., 1993).

The use of a simple larval index for monitoring stock size is not unprecedented. Data from larval surveys of Atlantic herring (*Clupea harengus harengus*) in the North Sea have been used since 1967 as the sole source of information on stock size or in combination with catch statistics or acoustic surveys, or both (Heath, 1993). One of the two larval indices for North Sea herring, the larval abundance index, employs only larvae less than 10 mm in length (up to 15 days old). The correlation between this larval index and stock size became weaker with increasing age of larvae owing, it was surmised, to interannual variation in mortality and dispersal. The potential influence of varying mortality rates and dispersal were likewise minimized in our study because most king mackerel larvae collected during the SEAMAP surveys were less than 5 mm and no more than ten days old. The other larval herring abundance index for the North Sea, the larval production estimate, utilizes all size and age groups to estimate the abundance at hatching and requires estimates of growth and mortality rates. Both herring indices are calculated annually; however, the actual use of each in VPA assessment is dependent on survey coverage in time and space in relation to spawning events for that year.

Our attempt to account for differences in larval age composition among years by adjusting the index for mortality of larvae did not improve the correlation with stock size. There are a number of reasons for this outcome. It is very likely that the limited age-at-length data available for conversion of king mackerel lengths to age probably resulted in imprecise assignment of ages. Overestimation of age by a single day would result in a 70% error in the backcalculated abundance of age one-day fish, and a 41% error if underestimated. Hauser and Sissenwine (1991) noted that estimates of larval production using "back-calculation techniques," as we did to estimate the abundance of one-day-old king mackerel larvae, will be biased if the growth rate used is incorrect or if mortality is size dependent, or both conditions transpire. It is also likely that the assumption of constant mortality rate, an integral part of catch curve analysis, did not hold for king mackerel larvae. Bailey et al. (1996a; 1996b) found that early mortality rates of walleye pollack larvae were not only highly variable among years but declined as larvae became older. Furthermore, the observation that instantaneous mortality rates of king mackerel larvae among years were not significantly different may be caused by the low number of larvae caught and the small number of age classes represented in collections (Comyns, 1997). However, an age-adjusted index calculated with annual estimates of mortality rate had a much poorer correlation with stock size; therefore we did not report these data. Our estimate of mortality (Z=0.53) may be biased high owing to net selectivity, i.e. avoidance of the net by larger larvae. To correct this bias, we truncated the upper 20% of the size distribution and recalculated mortality rates and an age-adjusted index. Although the mortality estimate was lower (Z=0.43), the correlation between stock size and the age-adjusted index based on this mortality rate did not differ from the correlations based on nontruncated distributions.

Another measure of king mackerel stock size was considered, namely the VPA-generated estimate of egg pro-

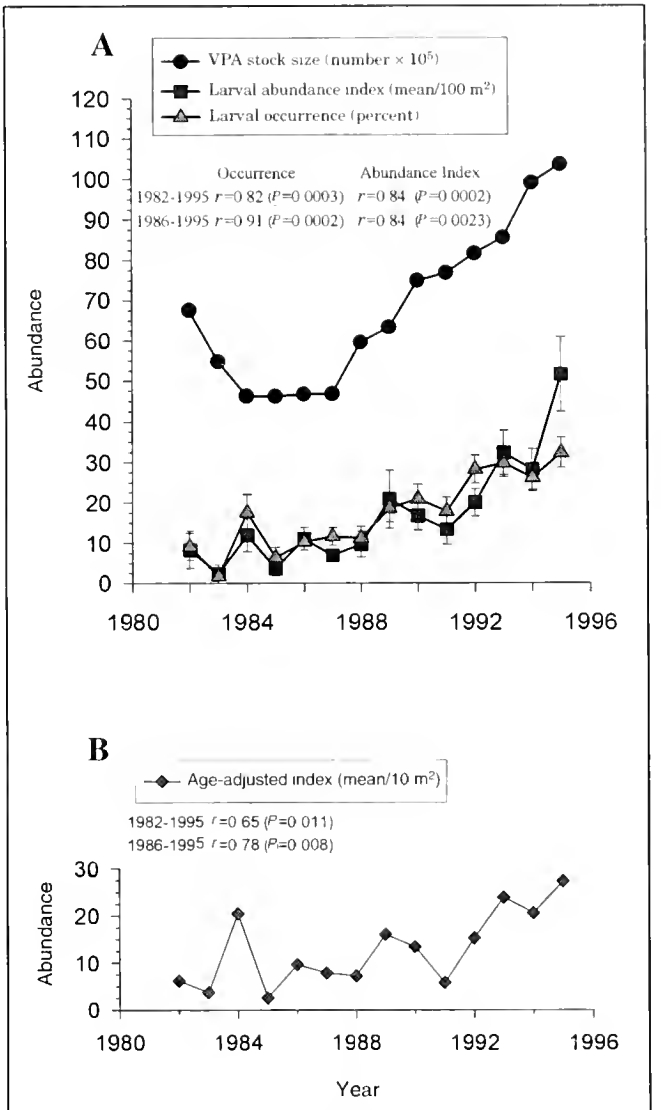

Figure 1

(**A**) King mackerel adult spawning stock size (number × 10^5 of fish in the 1 through 11+ age groups) estimated by VPA, survey larval index of abundance (mean number under 100 m^2 of sea surface ±SE), and survey larval frequency of occurrence (percent of stations where larvae were captured ±SE). (**B**) Annual age-adjusted larval index of abundance (mean number under 10 m^2 of sea surface).

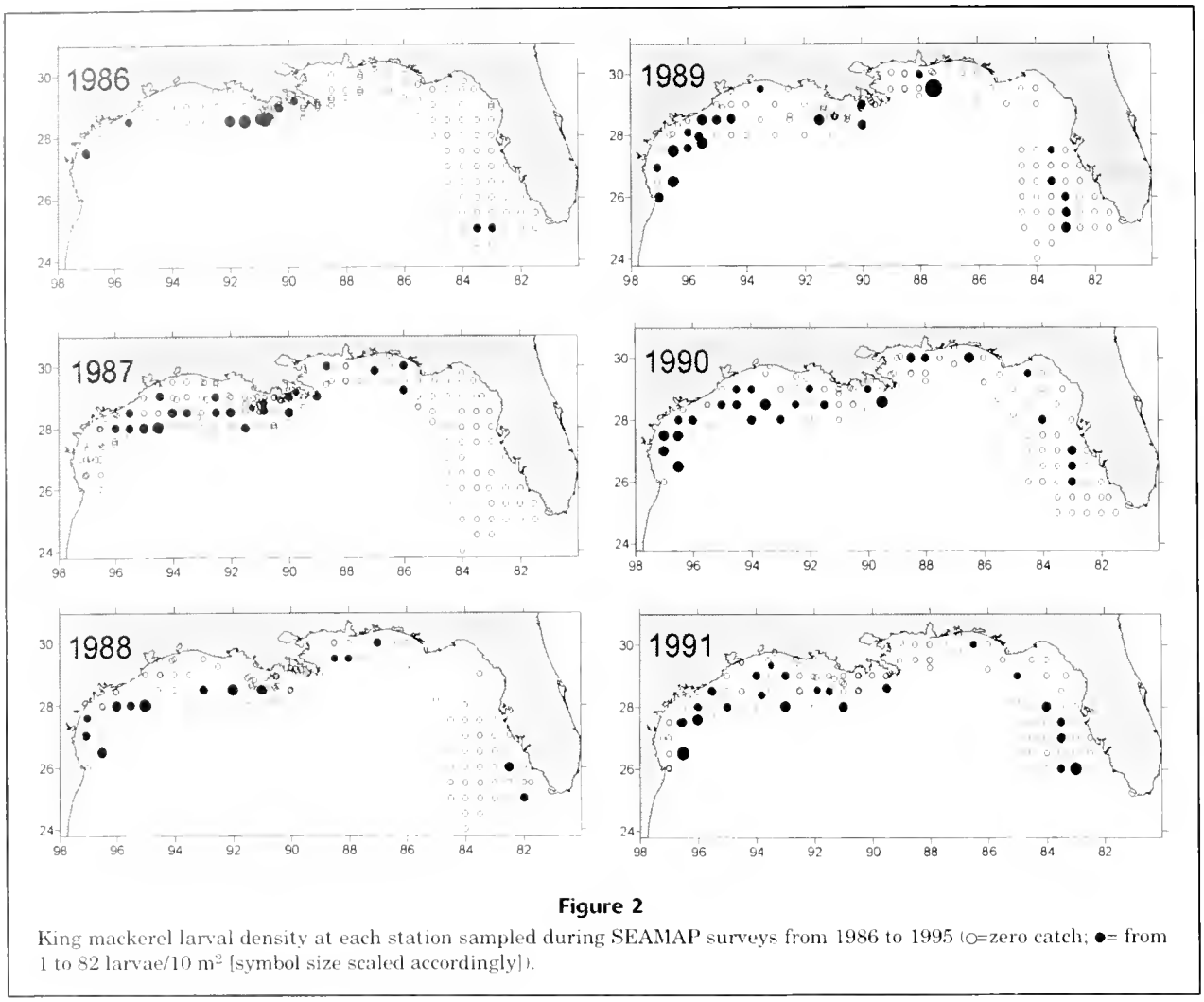

Figure 2

King mackerel larval density at each station sampled during SEAMAP surveys from 1986 to 1995 (○=zero catch; ●= from 1 to 82 larvae/10 m^2 [symbol size scaled accordingly]).

duction (number-at-age × relative fecundity-at-age). This measure accounts for the presumably greater contribution of older and larger fish to overall reproductive output; therefore it would seem a better correlate of larval occurrence and abundance than numbers of fish. However, we found egg production to be somewhat less correlated with larval indices than were numbers of fish, perhaps owing to the use of a constant fecundity-at-age distribution to estimate king mackerel egg production. Significant interannual differences in relative fecundity have been demonstrated for a wide variety of fishes (Bagenal, 1966; 1967; Bagenal and Braum, 1971; Hunter et al., 1985; Rijnsdorp, 1991; Koslow et al., 1995). But there is insufficient data on fecundity of king mackerel over the time series to ascertain the influence of interannual variability on this parameter, and in turn, on larval production.

Application of growth and mortality rates to refine or adjust larval indices of relative abundance may be moot because determinants of larval survival, i.e. predation or starvation rates, or both, appear to be unrelated to spawning stock abundance (Hunter and Lo, 1993). It has been argued that larval occurrence provides a more useful index of stock size because stock size and the geographic area occupied by eggs and larvae may be correlated, as is the case for Pacific sardines (*Sardinops sagax*) and northern anchovy (*Engraulis mordax*), especially at low population levels. (Mangel and Smith, 1990; Smith, 1993; Hunter and Lo, 1993; MacCall, 1988). However, Mangel and Smith (1990) suggest that a switch from presence and absence data to actual counts would be necessary when the spawning biomass increases to a level where "virtually all stations have eggs."

King mackerel in the Gulf of Mexico are rebounding from the low levels of the late 1970s and early 1980s (Powers and Restrepo, 1993), and the increases are reflected in larval occurrence and abundance. A switch to a larval abundance index may be required to follow trends in stock size as larval abundance rises if the uncorrected abundance index at some future time no longer corresponds to stock size. Adjustment of the king mackerel larval abundance index would require annual estimates of mortality and growth rates by direct aging of survey-caught larvae. For now, both the index of larval occurrence and the unadjusted index of abundance from SEAMAP collec-

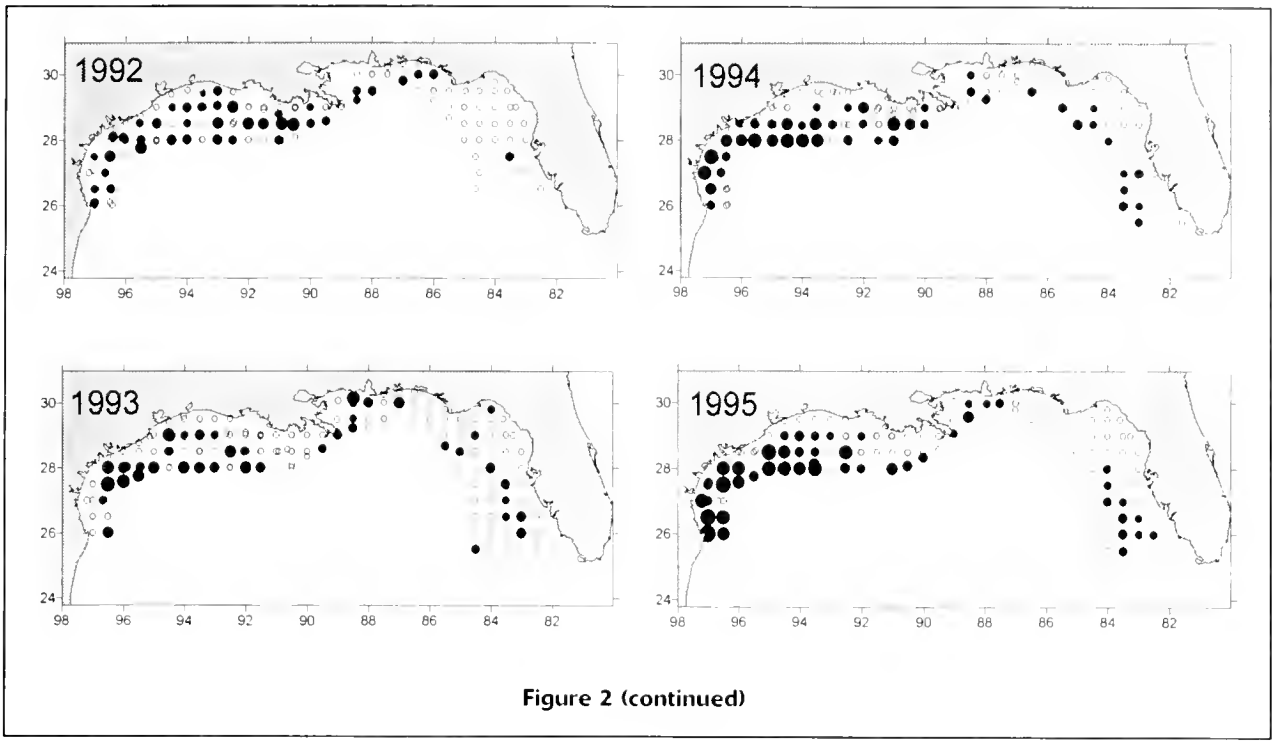

Figure 2 (continued)

Table 2

Average length (mm) and age (days) of king mackerel larvae collected during annual surveys (n=number of larvae measured).

		Length				Age			
Year	n	Mean	SE	Min	Max	Mean	SE	Min	Max
1982	29	3.4	0.231	2.0	6.0	4.47	0.257	2.81	7.25
1983	4	4.9	0.860	4.0	7.5	6.08	0.880	5.13	8.71
1984	20	4.7	0.467	2.2	8.7	5.84	0.494	3.05	9.81
1985	12	3.8	0.330	1.9	5.5	4.89	0.369	2.69	6.74
1986	63	3.9	0.170	1.8	8.0	4.94	0.183	2.57	9.18
1987	35	4.3	0.267	1.9	7.5	5.39	0.297	2.69	8.71
1988	28	3.6	0.245	2.0	6.8	4.62	0.270	2.81	8.04
1989	58	3.5	0.171	2.0	10.0	4.53	0.182	2.81	10.91
1990	49	3.6	0.232	1.6	9.8	4.64	0.249	2.32	10.74
1991	33	3.1	0.209	1.8	6.0	4.06	0.236	2.57	7.24
1992	86	3.3	0.157	1.7	8.5	4.28	0.171	2.45	9.63
1993	137	3.3	0.133	1.7	10.1	4.27	0.142	2.45	10.99
1994	105	3.4	0.164	1.8	9.6	4.35	0.177	2.57	10.58
1995	139	3.2	0.100	1.8	8.1	4.18	0.111	2.57	9.27

tions reflect trends in spawning stock size and provide useful variables for calibrating the king mackerel VPA.

Acknowledgments

The authors wish to thank Doug DeVries at the NMFS Panama City Laboratory for giving us his larval king mackerel age and length data. Joe Powers and Chris Legault of the NMFS Miami Laboratory supplied king mackerel VPAs for the various iterations of this manuscript. Rosanne Brasher supplied indispensable assistance with the SEAMAP database. Scientists at the Polish Sorting and Identification Center in Szczecin, Poland, sorted and identified larvae from collections. Kim Williams, Collections Manager of the SEAMAP Archiving

Center in St. Petersburg, Florida, facilitated our work by furnishing king mackerel specimens and data. This time series would not have been possible without the labor of the crews of the NOAA ships *Chapman* and *Oregon II*, and field biologists of the NMFS laboratories and state agencies participating in SEAMAP cruises. Scott Nichols, Director of the NMFS Mississippi Laboratories, gave us encouragement, incentive and comments on an early draft of the manuscript. We greatly appreciate the comments and suggestions of Chris Legault, James H. Cowan, Bruce Comyns, and one anonymous reviewer who improved the manuscript.

Table 3

Individual annual and pooled catch curve parameters. ($\log_e$(number) = $\beta_0 + \beta_1$ *Age*; n=number of age groups.)

Year	n	β_0	β_1	r^2
1982	4	0.323	−0.444	0.86
1983	2	0.063	−0.366	1.00
1984	4	1.657	−0.505	0.51
1985	3	−0.824	−0.345	0.09
1986	7	1.343	−0.638	0.83
1987	5	−0.032	−0.431	0.41
1988	6	−0.631	−0.557	0.82
1989	5	1.638	−0.629	0.67
1990	7	1.642	−0.654	0.88
1991	6	0.643	−0.573	0.63
1992	7	1.757	−0.700	0.71
1993	8	1.485	−0.509	0.94
1994	8	1.332	−0.574	0.91
1995	7	2.187	−0.636	0.84
Pooled (1982–1995)	78	0.940	−0.529	0.65

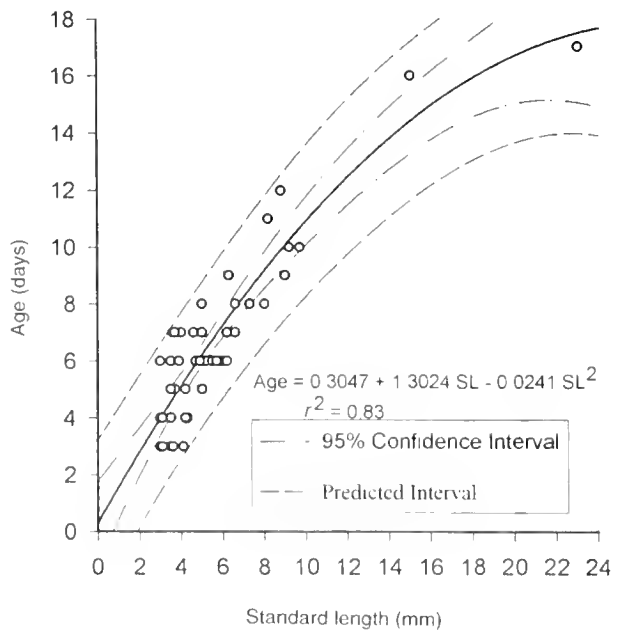

Figure 3

Relation between age and standard length (SL) with 95% confidence limits for king mackerel. Data from DeVries et al. (1990).

Literature cited

Bagenal, T. M.
1966. The ecological and geographical aspects of the fecundity of the plaice. J. Mar. Biol. Assoc. U.K. 46:161–186.
1967. A short review of fish fecundity. *In* The biological basis of freshwater fish production (Shelby D. Gerking, ed.), p. 89–111. Blackwell, Oxford, England.

Bagenal, T. M., and E. Braum.
1971. Eggs and early life history. *In* Methods for assessment of fish production in fresh waters (W.E. Ricker, ed.), p. 166–198. International Biological Programme (IBP) Handbook 3, second ed. Blackwell Scientific Publications, Oxford, England.

Bailey, M., A. L Brown, M. M Yoklavich, and K. L. Mier.
1996a. Interannual variability in growth of larval and juvenile walleye pollock *Theragra chalcogramma* in the western Gulf of Alaska, 1983–91. Fish. Oceanog. 5(suppl. 1):137–147.

Bailey, K. M., S. J. Picquelle, and S. M. Spring.
1996b. Mortality of larval walleye pollock *Theragra chalocogramma* in the western Gulf of Alaska, 1988–1991. Fish. Oceanog. 5(suppl. 1):124–136.

Comyns, B. H.
1997. Growth and mortality of fish larvae in the northcentral Gulf of Mexico and implications to recruitment. Ph.D. diss., Louisiana State Univ., Baton Rouge, LA, 199 p.

Conser, R. J., and J. E. Powers.
1990. Extensions of the ADAPT VPA tuning method designed to facilitate assessment work on tuna and swordfish stocks. International Commission for the Conservation of Atlantic Tunas. Coll. Vol. Sci. Pap. 28:203–220.

DeVries, D. A., and C. B. Grimes.
1997. Spatial and temporal variation in age and growth of king mackerel, *Scomberomorus cavalla*, 1977–1992. Fish. Bull. 95:694–708.

DeVries, D. A., C. B. Grimes, K. L. Lang, and D. B. White.
1990. Age and growth of king and Spanish mackerel larvae and juveniles from the Gulf of Mexico and U.S. South Atlantic Bight. Env. Biol. Fish. 29:135–143.

Finucane, J. H., L. A. Collins, H. A. Brusher, and C. H. Saloman.
1986. Reproductive biology of king mackerel, *Scomberomorus cavalla*, from the southeastern United States. Fish. Bull. 84.841–850.

Gold, J. R., A. Y. Kristmundsdóttir, and L. R. Richardson.
1997. Mitochondrial DNA variation in king mackerel (*Scomberomorus cavalla*) from the western Atlantic Ocean and Gulf of Mexico. Mar. Biol. 129:221–232.

Grimes, C. B., J. H. Finucane, L. A. Collins, and D. A. DeVries.
1990. Young king mackerel, *Scomberomorus cavalla*, in the Gulf of Mexico, a summary of the distribution and occurrence of larvae and juveniles, and spawning dates for Mexican juveniles. Bull. Mar. Sci. 46.640–654

Hauser, J. W., and M. P. Sissenwine.
1991. The uncertainty in estimates of the production of larval fish derived from samples of larval abundance. ICES J. Mar. Sci. 48:23–32.

Heath, M.
1993. An evaluation and review of the ICES herring larval surveys in the North Sea and adjacent waters. Bull. Mar. Sci. 53(2):795–817.

Hunter, J. R., and N. C. -H. Lo.
1993. Ichthyoplankton methods for estimating fish biomass introduction and terminology. Bull. Mar. Sci. 53(2):723–727.

Hunter J. R., N. C. H. Lo, and R. J. H. Leong.
1985. Batch fecundity in multiple spawning fishes. *In* An egg production method for estimating spawning biomass of pelagic fish: application to the northern anchovy, *Engraulis mordax* (R. Lasker, ed.), p. 67–77. U.S. Dep. Commer., NOAA Technical Report NMFS 36.

Johnson, A. G., W. A. Fable Jr., C. B. Grimes, L. Trent, and J. V. Perez.
1994. Evidence for distinct stocks of king mackerel, *Scomberomorus cavalla*, in the Gulf of Mexico. Fish. Bull. 92: 91–101.

Koslow, J. A., J. Bell, P. Virture, and D. C. Smith.
1995. Fecundity and its variability in orange roughy: effects of population density, condition, egg size, and senescence. J. Fish Biol. 47(6):1063–1080.

MacCall, A. D.
1988. Dynamic geography of marine fish populations. Univ. Washington Press, Seattle, WA, 153 p.

Mangel, M., and P. E. Smith.
1990. Presence-absence sampling for fisheries management. Can. J. Fish. Aquat. Sci. 47:1875–1887.

McEachran, J. D., J. H. Finucane, and L. S. Hall.
1980. Distribution, seasonality, and abundance of king and Spanish mackerel larvae in the northwestern Gulf of Mexico (Pisces: Scombridae). Northeast Gulf Sci. 4:1–16.

Pennington, M.
1983. Efficient estimators of abundance for fish and plankton surveys. Biometrics 39:281–286.

Powers, J. E., and V. R. Restrepo.
1993. Evaluation of stock assessment research for Gulf of Mexico king mackerel: benefits and costs to management. N. Am. J. Fish. Manage. 13:15–26.

Richards, W. J., M. F. McGowan, T. Leming, J. T. Lampkin, and S. Kelley.
1993. Larval fish assemblages at the Loop Current boundary in the Gulf of Mexico. Bull. Mar. Sci. 53:475–537.

Ricker, W. E.
1975. Computations and interpretation of biological statistics of fish populations. Fish. Res. Board Can., Bull. 191, 382 p.

Rijnsdorp, A. D.
1991. Changes in fecundity of female North Sea plaice (*Pleuronectes platessa* L.) between three periods since 1900. ICES J. Mar. Sci. 48(3):253–280.

Robins, C. R. and G .C. Ray.
1986. A field guide to Atlantic coast fishes of North America. Houghton Mifflin, Boston, MA, 354 p.

Roelke, L. A., and L. A. Cifuentes.
1997. Use of stable isotopes to assess groups of king mackerel, *Scom beromorus cavalla*, in the Gulf of Mexico and southeastern Florida. Fish. Bull. 95:540–551.

SAS Institute Inc.
1990. SAS/STAT user's guide, vers. 6, fourth ed., vol. 2. SAS, Institute, Inc., Carry, NC, 1686 p.

Scott, G. P., S. C. Turner, C. B. Grimes, W. J. Richards, and E. B. Brothers.
1993. Indices of larval bluefin tuna, *Thunnus thynnus*, abundance in the Gulf of Mexico: modeling variability in growth, mortality, and gear selectivity. Bull. Mar. Sci. 53(2):912–929.

Shipp, R. L.
1986. Guide to fishes of the Gulf of Mexico. 20th Century Printing Co., Mobile, AL, 256 p.

Smith, P. E.
1993. Balancing sampling precision and fisheries management objectives: minimal methods. Bull. Mar. Sci. 53(2):930–935.

Evasive behavior of spotted and spinner dolphins (*Stenella attenuata* and *S. longirostris*) during fishing for yellowfin tuna (*Thunnus albacares*) in the eastern Pacific Ocean

Gisela Heckel

Facultad de Ciencias Marinas
Universidad Autónoma de Baja California
Plácido Mata 2309 Depto D-5
Condominio Las Fincas
22820 Ensenada
Baja California, México
E-mail address gheckel@telnor.net

Kim E. Murphy

Facultad de Ciencias Marinas
Universidad Autónoma de Baja California
Km 103 Carretera Tijuana-Ensenada
22800 Ensenada,
Baja California, México

Guillermo A. Compeán Jiménez

Programa Nacional de Aprovechamiento del Atún y
de Protección de Delfines
Km 107 Carretera Tijuana-Ensenada
Campus CICESE
22800 Ensenada
Baja California, México

Abstract—This study examines the question of whether the evasive behavior of northeastern offshore spotted dolphins (*Stenella attenuata*) during fishing for tuna (by the Mexican fleet) varies in geographic areas of the eastern Pacific Ocean (EPO). It also investigates whether evasion differs between northeastern offshore spotted and eastern spinner dolphins (*Stenella longirostris orientalis*). Observations recorded in the database of the Mexican Programa Nacional de Aprovechamiento del Atún y de Protección de Delfines (PNAAPD) from 1992 to 1995 were analyzed. The calculated evasion index was the estimated percentage of dolphins that evaded capture in relation to the herd's estimated initial size in each set.

Evasion index by set was averaged in 2×2 quadrants and then used to draw a contour map. Three areas were outlined with low (25%), medium (44.44%), and high (71.80%) median evasion indices. These areas were significantly different ($P<0.0001$) according to the Kruskal-Wallis nonparametric multisample test, thus indicating a spatial pattern in evasive behavior of northeastern offshore spotted dolphins during fishing operations of the Mexican fleet. Spatial patterns in evasive behavior might be related to the dolphins' learning capacity, hence experience of individual dolphins or herds with tuna purse-seining in the EPO should be estimated to demonstrate this. To be representative, future research should utilize available historical fishing effort data for the international fleet. Furthermore, a multivariate approach to this issue is necessary.

One of the investigated areas (mouth of the Gulf of California) was further analyzed regarding differences between two stocks of dolphins. Evasion indices for eastern spinners were significantly different from those for northeastern offshore spotted dolphins ($P<0.0001$, Kolmogorov-Smirnov two-sample test). This difference may correspond to different evasive strategies used by the two stocks to evade capture in the net, such as evasion under the net and dispersion (division of herd into subgroups during the set). Eastern spinners apparently evaded more frequently than northeastern offshore spotted dolphins by diving under the net. During the three set stages of tuna fishing (before chase, during chase, and during encirclement), eastern spinner dolphins dispersed less often than spotted dolphins, behavior that may permit them to coordinate their evasive movements more effectively than northeastern offshore spotted dolphins. Evasion over the net was rarely observed in either stock.

Manuscript accepted 1 July 2000
Fish. Bull. 98:692–703 (2000).

The tuna fishery in the eastern Pacific Ocean (EPO) sets purse seines in three major modes: school, log, and dolphin fishing. Yellowfin tuna (*Thunnus albacares*) and certain species of dolphins are found to associate in the EPO. The spotted dolphin (*Stenella attenuata*) is by far the most important species from the point of view of its frequency of association with tuna and its use by fishermen for catching tuna (Perrin, 1969). The frequent appearance of spinner dolphins (*Stenella longirostris*) in sets also makes this species significant, although in almost all cases it appears in mixed herds with the spotted dolphin (National Research Council, 1992).

During "dolphin fishing" or "fishing on dolphins," the net is set around the tuna and the dolphins after a period of chase. Once a dolphin herd is sighted with high-power binoculars (25×), four to six speedboats are lowered, and the chase begins. The speedboats herd the dolphins and the accompanying tuna into a tight group that can be encircled by the seiner. The dolphins may try to evade the boats to avoid capture. Those that do not succeed are released by the fishing crew during the "backdown" procedure (a procedure in which the vessel is run in reverse to pull the corkline underwater and thus release the dolphins) (Barham et al., 1977).

Impact of the fishery on cetacean populations has been assessed by estimating cetacean abundance and distribution involved in tuna purse-seining, as well as by estimating mortality rates. By 1988, the estimated abundance of the northeastern offshore spotted dolphin had been reduced to between 19% and 28% and that of the eastern spinner dolphin and to between 32% to 58%

in relation to estimated pre-exploitation levels (Wade, 1993; Wade[1]). Therefore, these stocks have been designated as depleted under the U.S. Marine Mammal Protection Act. However, when compared to abundance estimates from 1986–90 research surveys (Wade and Gerrodette, 1993), preliminary estimates from the most recent surveys (Gerrodette[2]) show a noticeable increase in the abundance of the northeastern offshore spotted and the eastern spinner dolphin compared to previous estimates (Wade and Gerrodette, 1993).

In addition to abundance estimation, the total incidental mortality (all species and stocks involved in the fishery and for the international fleet) was estimated at 3274 for 1995, which represents 0.03% of the total population (Hall and Lennert, 1997) of 9.6 million for all dolphin species involved in the tuna fishery (Wade and Gerodette, 1993). The Mexican Programa Nacional para el Aprovechamiento del Atún y de Protección de Delfines (PNAAPD) estimated the incidental mortality (of all species and stocks) of the Mexican fleet to be 1819 dolphins in 1994 (Compeán et al.[3]).

Important efforts have been aimed at reducing mortality rates, such as improving fishing gear (Barham et al., 1977; Coe et al., 1984), placing quotas on the number of dolphins killed for each stock (Wade[4]), placing a quota on the number of dolphins killed by fishing vessel and making the backdown procedure mandatory (Colson, 1992).

Other efforts in reducing mortality have been directed towards research on dolphin behavior during tuna purse-seining (Norris et al., 1978; Pryor and Kang[5]). Mortality rates may also be reduced by understanding more about the dolphins' behavior, so that they are less likely to injure themselves or die during fishing practices (Norris et al., 1978).

Some research indicates that some dolphin stocks may have reduced mortality through behavioral adaptations. The first ethological research on *Stenella attenuata* and *Stenella longirostris* during fishing operations was accomplished by Norris et al. (1978). They focused on overall herd movements and interanimal distances and developed the first ethogram for these animals during a net set for tuna. Pryor and Kang (1980) also made observations during seining operations but focused more on individual and subgroup behavior. Although Norris et al. (1978) described high stress levels in dolphins that were involved in sets, Pryor and Kang interpreted their own data as indicating much learned adaptive behavior and low stress levels. By analyzing records from observers on tuna boats, Stuntz and Perrin[6] noted and discussed the fact that dolphins (*Stenella* spp.) were more difficult to capture in areas where fishing effort had been higher and the authors concluded that dolphins had been able to learn to evade capture from tuna boats.

Data collected by observers on board tuna purse-seiners from 1992 to 1995 (PNAAPD database) were used to investigate whether the evasive behavior[7] of northeastern offshore spotted dolphins (*Stenella attenuata*) during fishing for yellowfin tuna varied geographically in the EPO. Differences in evasive behavior between the northeastern offshore spotted and the eastern spinner dolphin (*Stenella longirostris orientalis*) were also assessed. Furthermore, differences in evasive strategies[8] between these two stocks were described.

Methods

Data collection

Data from 1992 to 1995 from the PNAAPD database (Mexican fleet) were used to study evasive behavior of two stocks of different species in the EPO: the northeastern offshore spotted dolphin, a stock of the pantropical spotted dolphin (*Stenella attenuata*), and the eastern spinner dolphin (*Stenella longirostris orientalis*), a subspecies and stock of the spinner dolphin (*Stenella longirostris*) (Dizon et al., 1994; Perrin and Gilpatrick, 1994; Perrin et al., 1994).

Observers (also referred to as scientific technicians) from the Inter-American Tropical Tuna Commission (IATTC)

[1] Wade, P. R. 1993. Estimation of historical population size of the northeastern stock of offshore spotted dolphin (*Stenella attenuata*). Southwest Fisheries Science Center Administrative Report LJ-93-18, 18 p. Southwest Fisheries Science Center, Natl. Mar. Fish. Serv., NOAA, 8604 La Jolla Shores Drive, La Jolla, CA 92038-0271.

[2] Gerrodette, T. 1999. Preliminary estimates of 1998 abundance of four dolphin stocks in the Eastern Tropical Pacific. http://swfsc.ucsd.edu/IDCPA/Abund98.html. Southwest Fisheries Science Center., Natl. Mar. Fish. Serv., NOAA, P.O. Box 271. La Jolla, CA 92038

[3] Compeán J., G. A., I. Méndez G.-H. and I. Méndez R. In preparation. Annual estimates of incidental mortality for dolphin species associated with the Mexican tuna fishery during 1992–1995. Programa Nacional para el Aprovechamiento del Atún y de Protección de Delfines (PNAAPD). Km 107 Carretera Tijuana-Ensenada, Campus CICESE, 22800 Ensenada, B.C., México.

[4] Wade, P. R. 1993. Revised estimates of fisheries kill of dolphin stocks in the eastern tropical Pacific, 1959–1972. Southwest Fisheries Science Center Administrative Report LJ-93-17, 19 p. Southwest Fisheries Science Center, Natl. Mar. Fish. Serv., NOAA, 8604 La Jolla Shores Dr., La Jolla, CA 92038-0271.

[5] Pryor, K., and I. Kang. 1980. Social behavior and school structure in pelagic porpoises (*Stenella attenuata* and *S. longirostris*) during purse seining for tuna. Southwest Fisheries Center. Admin. Rep. LJ-80-11C. Southwest Fisheries Science Center, 8604 La Jolla, Shores Drive, La Jolla, CA 92038-0271.

[6] Stuntz, W. E., and W. F. Perrin. 1979. Learned evasive behavior by dolphins involved in the eastern tropical Pacific tuna purse seine fishery. Unpubl. abstract. Third Biennial Conference on the Biology of Marine Mammals, October 7–11, 1979, Seattle, WA.

[7] Evasive behavior: In this study, calculated as a percentage of the estimated number of dolphins that avoided capture in the net relative to the best estimate of the initial herd size (before the set started) by the observer or scientific technician. See "Methods" section.

[8] Evasive strategies: movements of the herd or subgroups of dolphins in relation to seiner, speedboats, and net (when it has been set and before rings up) by which dolphins attempt to avoid capture in the net.

and corresponding national programs have worked on board tuna vessels. Since 1991, the PNAAPD has placed observers on board 50% of the trips by Mexican tuna boats (the remaining 50% is covered by IATTC observers). Observers record data during dolphin sets, using standardized data forms and instructions provided by the PNAAPD (which are very similar to those used by the IATTC). A detailed description of data collection and procedures can be found in Perrin et al. (1983) and Polachek.[9] In summary, in the "Daily Activity Record" (DAR), observers keep a daily log on events (date, time of day, departure, arrival, sightings, sets, geographic position, aerial assistance during a set, etc.), weather conditions (cloud cover, sea state, visibility, water temperature), and tuna catch. In other forms they also record the vessel's features and all data concerning marine mammal sightings and sets, school and log sets, sea turtle sightings, and more recently, bycatch.

When a marine mammal group is sighted (which might lead to a net set for tuna catch), observers fill out the "Record of Marine Mammal Observations and Set Data" (RMMOSD). Herd size and composition (percent and species or stock identification) is annotated as estimated by the observer (usually with 7×50 or 10×50 binoculars), a crew member on board (with 20× or 25× binoculars), and another crew member from the helicopter. At the end of a set, the observer has to decide on his "best estimate" of the herd size and composition before the actual set occurred. During a set, the observer estimates the number of dolphins (identified by species or stock) that actively evade the boats and net before the chase, during the chase, and during the encirclement, as well as the number of groups within the herd during each of the three set stages. The number of dolphins deliberately cut out by the skipper, those that evade by diving under the net or escape by leaping out of the net are also estimated and identified by the observer All these data were of interest for our study (except dolphins deliberately cut out because this action was not considered evasion actively achieved by dolphins). Other data recorded by the observer are chase and set times, number of speedboats used, whether or not explosives were used, the number and composition of captured marine mammals (those that were encircled), number of animals rescued and the manner of their rescue, start and end of backdown, number of dolphins hurt or killed, and further details about the fishing procedure.

The observers' estimates of herd size and number of dolphins evading capture may be biased owing to differing experience and estimation between observers. However, they attend a complete training course at the institution they work for (IATTC, PNAAPD, or other national programs), where they learn to identify fauna species they may encounter at sea (marine mammals, fish, birds, and sea turtles), how the fishing operation proceeds, and how to collect data. At the end of each trip, experienced editors at the institutions review the observers' collection of data. These procedures give credence to the data collected. Moreover, reactions of dolphins to approaching survey vessels have been studied previously by means of field experiments (Au and Perryman, 1982; Hewitt, 1985). Their results might be compared to the dolphins' behavior "before chase" because sighting distance in those studies (as during the fishing operation) was usually between 2 and 6 or 7 nmi (nautical miles), aided with 20× or 25× binoculars. Dolphins started to react (by changing their swimming speed and course) between 1.5 to 3 nmi distance to the ship (Hewitt, 1985) with one exception, where the herd reacted at 6 nmi (Au and Perryman, 1982). Almost half of the herds observed by Hewitt (1985) did not react at all. Therefore, the observer's estimate of initial herd size (which is also compared to the estimate by a crew member on board and by the crew member in the helicopter) was assumed to be reliable. We also relied on the observer's estimation of number of dolphins evading capture during all set stages (before chase, during chase, and during encirclement) because of their training and experience.

The logbooks with these observations are collected by the institution for which the observer works. To improve the accuracy and reliability of the observers' records, careful debriefing and editing is accomplished by skilled technicians (with considerable experience at sea) at the institutions (in our study, the PNAAPD). The observations are then entered into the corresponding computerized databases which are also checked for errors that might have occurred during "capture" (entry) of the data into the database (Perrin et al., 1983; Polacheck[9]).

Confidence in the databases of the IATTC and national programmes (PNAAPD and the U.S National Marine Fisheries Service) is acknowledged with the publication of studies that have analyzed some of these data. A few examples of such studies are the following: dolphin distribution (Perrin et al., 1983; Perrin et al., 1985), dolphin abundance estimation (Anganuzzi et al., 1992; Polachek[9]), incidental kill of dolphins in tuna fishing nets (Hall and Lennert, 1997; Wade[4]), dolphin life history (Chivers and De Master, 1994), tuna-dolphin association (Edwards, 1992; Scott and Cattanach, 1998), blue whale distribution in the eastern tropical Pacific (Reilly and Thayer, 1990), and aspects of the Mexican tuna fishery (Compeán and Dreyfus, 1996).

In our study, spatial patterns in evasive behavior of the northeastern offshore spotted dolphin were described, as well as differences in evasive behavior and strategies (herd dispersion,[10] evasion under and over the net) between

[9] Polachek, T. 1984. Documentation of the time sequential file created from the tuna boat observer data bases for analyzing the relative abundance of dolphins in the eastern tropical Pacific. Southwest Fisheries Science Center Admin. Report LJ-84-33, 26 p. National Marine Fisheries Service.

[10] Herd dispersion: to establish if a herd dispersed during a set, the grouping codes applied by the observers in paragraph 3 of the RMMOSD were used. The codes are the following: 1, herd is in one group; 2, herd has divided into two or three groups; 3, herd consists of more than three groups. These codes are recorded during three set stages: before chase, during chase, and during encirclement. For each species, the number of sets where the specified grouping code occurred was counted during each set stage. If codes were in ascending order, this was interpreted as herd dispersion during the fishing operation.

the northeastern offshore spotted and the eastern spinner dolphin (*Stenella longirostris orientalis*). A subset of the PNAAPD database (1992–95) was extracted from sections of the DAR (those referring to date and set position) and the RMMOSD (observer's best estimation of herd size and composition by species and stock, number and identification [also by species and stock] of evading and escaping dolphins, as described previously), and grouping codes. Data from sets that were interrupted (due to loss of tuna catch because all dolphins escaped from the chase or mechanical problems of the vessel or net performance, etc.) were excluded from the analyses.

Because data collected by the Mexican observer program (PNAAPD) represented 50% of the Mexican fleet's effort in the EPO, we assumed that the data set in our study was sufficiently large to represent the dolphins' evasive behavior in relation to Mexican tuna fishing boats during the sampled period.

Data analysis

Evasion index by set Evasion index by set was calculated in order to search for spatial patterns in evasive behavior of the northeastern offshore spotted dolphin and to analyze differences between northeastern offshore spotted and eastern spinner dolphins. This index is defined as the estimated percentage of dolphins that evaded capture during each set in relation to the herd's estimated initial size:

$$\hat{I}_{ij} = \left(\frac{\hat{E}}{\hat{H}}\right)100,$$

where $\hat{I}_{ij}$ = estimated evasion index during set i in quadrant j;
$\hat{E}$ = number of dolphins that evaded capture during set i in quadrant j, i.e. the sum of escaping dolphins estimated by the observer before the chase, during the chase, and during the encirclement as recorded in the RMMOSD;
$\hat{H}$ = herd size before chase started during set i in quadrant j, i.e. the observer's best estimate as recorded in the RMMOSD.

Evasion index by set was stratified by stock by selecting from the database only sets on pure herds (i.e. those herds composed 100% of a species) of northeastern offshore spotted dolphins and sets on pure herds of eastern spinner dolphins. Because only these two stocks were studied, results should not be considered representative of the corresponding species (pantropical spotted dolphin, *Stenella attenuata*, and spinner dolphin, *Stenella longirostris*).

Sets in which no dolphins escaped and therefore the calculated evasion index was zero were included in all analyses because they indicated that evasive behavior did not occur or failed. This action is contrary to common practice where "zeros" are often eliminated because they represent missing data that tend to bias calculations.

Spatial patterns in evasive behavior of northeastern offshore spotted dolphins To evaluate if there were spatial patterns in evasive behavior for the data in our study a computer program based on Matlab version 4.2c was used to plot the evasion index by set of the northeastern offshore spotted dolphin on a map of the EPO. The program calculated average evasion index by set in 2 × 2 quadrants to smooth the data which were then used to draw a contour map with the commercial surface mapping program Surfer version 6.01 (Smith et al., 1995). This software interpolated the average evasion index by set in 2 × 2 quadrants to form a regular rectangular array of grid values. This procedure was chosen because the smoothness of contours on a contour map is partially a function of the number of X and Y lines in the grid. When a grid is created, reducing the number of lines in the X and Y directions can result in more angular contours on the contour map. Most of the gridding methods in Surfer use a weighted average interpolation algorithm. The gridding method called "Kriging" with a linear variogram was chosen because it incorporates anisotropy and underlying trends in an efficient and natural manner and has been proven to be quite effective for many data sets in different fields (Smith et al., 1995).

A geographic difference in evasive behavior was observed in the contour map (see "Results" section, Fig. 1), and the 60%, 50%, and 40% contours were considered the limits between three areas with different evasive behavior (as defined by the evasion index) during the study period and for the Mexican fleet. In addition, the following statistical procedures were applied to test for significant differences in mean evasion indices of the three areas.

Analysis of variance (ANOVA) can be used to compare the mean of three groups of proportions (i.e. for each area) (Zar, 1999). Because proportions (like the evasion index) have a binomial distribution, the individual data should be transformed as follows in order to meet normality and homoscedasticity assumptions (Zar, 1999):

$$\hat{I}'_{ij} = 0.5\left(\arcsin\sqrt{\frac{\hat{E}}{\hat{H}+1}} + \arcsin\sqrt{\frac{\hat{E}+1}{\hat{H}+1}}\right),$$

where $\hat{I}'_{ij}$ = estimated transformed evasion index during set i in quadrant j;
$\hat{E}$ = estimated number of dolphins that evaded capture during set i in quadrant j; and
$\hat{H}$ = estimated herd size before chase during set i in quadrant j.

After transformation, the data still did not have a normal distribution (Kolmogorov-Smirnov goodness-of-fit test, D=0.0704, P<0.01, n=808; Zar, 1999). Therefore, distribution-free tests were used to search for significant differences between the three evasion areas (Conover, 1980; Neave and Worthington, 1988).

To search for significant differences between the medians (usual group average measure in nonparametric statistics) of three groups (evasion areas), the nonparametric Kruskal-Wallis multisample test seemed to be the most appropriate for the data in our study. The reasons for this

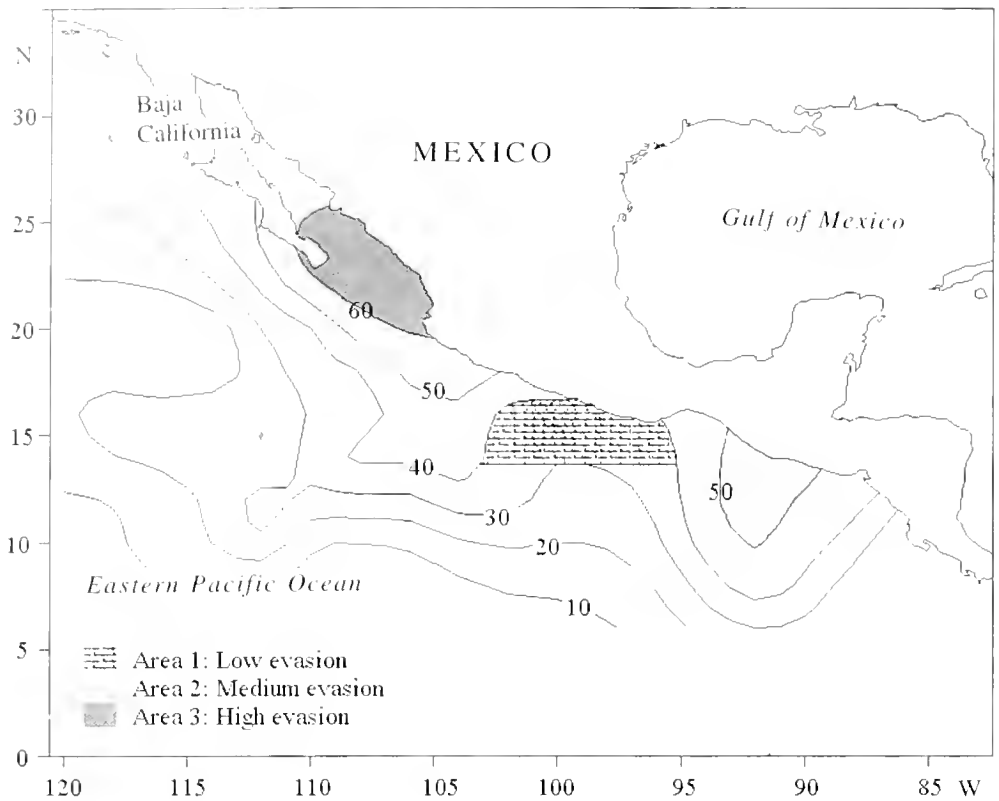

Figure 1

Estimated evasion index by set (estimated percentage of dolphins that evaded capture during each set in relation to estimated initial herd size) for northeastern offshore spotted dolphins (1992–95, Mexican fleet, PNAAPD data). Three areas were delimited according to 60%, 50%, and 40% evasion index contours.

are that data were measured in an interval scale (the test requires at least an ordinal scale), and samples are considered to be independent when it is assumed that dolphins remain approximately in the same area. Even though the swimming capacity of dolphins is well known, it is difficult to establish how fast or far they are able to travel. The Kruskal-Wallis test was preferred over the median test (with simpler calculations) because the latter uses the data more crudely than the former, and so the median test will generally be somewhat less powerful (Conover, 1980).

The Kruskal-Wallis test ranks all observations from 1 to n, and its statistic (H) is based on comparing each group's mean rank with the mean of all the ranks, weighted by the appropriate sample size to compensate for the effect of unequal sample sizes (Neave and Worthington, 1988). If the differences among the three evasion areas proved to be significant, nonparametric multiple comparisons could be executed to find which areas could be most confidently claimed to have different medians from each other (Conover, 1980; Neave and Worthington, 1988). The statistic for multisample comparisons (T) is obtained by calculating the absolute differences between the means of ranks assigned to the samples and then dividing these difference by their standard deviations. The T statistic has approximately the standard normal distribution; therefore H_0 will be rejected if $T>z$ (Conover, 1980; Neave and Worthington, 1988). Statistical procedures were performed with computing packages Statistica version 4.2 (StatSoft, 1993) and BMDP (Dixon, 1990).

Differences between stocks To evaluate differences in evasive behavior between eastern spinner and northeastern offshore spotted dolphins, estimated evasion indices by set for both stocks in evasion area 3 (as outlined in Fig. 1) were compared. Areas 1 and 2 were excluded from the analysis because eastern spinner sample sizes were smaller than 30 and these sizes were considered insufficient for statistical analysis when compared to sample sizes in area 3. Northeastern offshore spotted data were not normally distributed, and nonparametric tests were again used to compare the two independent samples (two stocks).

To decide which test was the most appropriate, "box-and-whisker" plots (Du Toit et al., 1986) were drawn to look for general distribution similarities or differences between both data sets (Fig. 2). The apparent difference in the medians would be worthwhile testing with the Mann-Whitney two-sample test (Conover, 1980; Neave and Worthington, 1988). However, data sets seemed to be different in spread (Mann-Whitney assumes equal spread); therefore a more

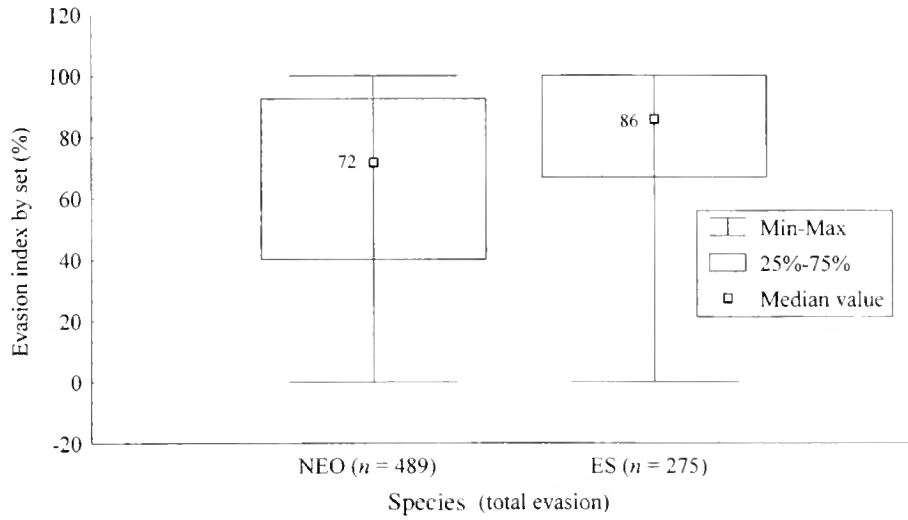

Figure 2

"Box and whiskers" plot for estimated total evasion index by set (estimated percentage of evaded dolphins that evaded capture during each set related to estimated initial herd size) for northeastern offshore spotted (NEO) and eastern spinner (ES) dolphins (Mexican fleet, PNAAPD data

cautious approach would be to apply the nonparametric Kolmogorov-Smirnov two-sample test because differences in location (average) and spread are tested simultaneously (Conover, 1980; Neave and Worthington, 1988). The Kolmogorov-Smirnov test compares the cumulative distribution function of two samples and uses the maximum vertical difference between them as the test statistic D (Neave and Worthington, 1988).

Eastern spinner and northeastern offshore spotted dolphins were also compared with respect to the dolphins' evasive strategies, such as evasion under and evasion over the net. The Kolmogorov-Smirnov test for two independent samples was used to evaluate estimated evasion indices by set between the stocks when they evaded capture by swimming under the net. The one-sided test was used to confirm if the evasion indices by set in one stock were larger than in the other. Differences in estimated evasion indices by set, when dophins evaded capture by swimming over the net, were not tested owing to very low sample sizes (n=3 in the northeastern offshore spotted, n=5 in the eastern spinner dolphin).

Furthermore, differences between the two stocks were described with respect to the dolphins' dispersion, i.e. the ability of the herds to "explode" (separate suddenly) (Allen et al., 1980) into subgroups in relation to the herds' configuration before the chase. For this description, the grouping codes applied by the observers in paragraph 3 of the RMMOSD were used. The codes used were the following: 1, herd is in one group; 2, herd has divided into two or three groups; 3, herd consists of more than three groups. These codes were recorded during three set stages: before chase, during chase, and during encirclement. For each stock, the number of sets where the specified grouping code occurred was counted during each set stage. If codes were found in ascending order, this was interpreted as herd dispersion during the fishing operation.

To test for significant differences in dispersion behavior between northeastern offshore spotted and eastern spinner dolphins, only data for evasion area 3 (Fig. 1) were used because sample sizes for both stocks were largest there. A multiway frequency table seemed to be the appropriate statistical tool, since counts of grouping codes was the response variable during each set stage and for each stock. However, one of the most important assumptions of multiway frequency analysis, independence, was not met. Only designs for comparisons between subjects may be analyzed with this analysis, so that the frequency in each cell is independent of the frequencies in all other cells. If the same case contributes values to more than one cell, those cells are not independent (Tabachnik and Fidell, 1996). In our study, each case (i.e. each set) contributed to three different cells (the three set stages).

Consequently, to test for differences in dispersion behavior between the stocks, data were rearranged by using the grouping code as the response variable and set stages as the repeated measures in each set (Table 1). Therefore, this design resembled a repeated-measures analysis with one among-subjects factor (stocks) and one within-subjects factor (set stage). If the response variable were in interval scale, a repeated-measures analysis of variance (ANOVA) would have been appropriate to test for differences between stocks (Zar, 1999). However, the response variable in our study was the grouping code, a categorical variable in ordinal scale.

The plausible alternative to apply was logistic regression, often referred to as linear probability models (Tabach-

nik and Fidell, 1996). This technique is similar to multiple regression analysis in that one or more independent variables (the three set stages in our study) are used to predict a single dependent, categorical variable (the stocks). Linear probability models accommodate all types of independent variables (numerical and categorical) and they do not have to be normally distributed, linearly related, or of equal variance within each group. The assumptions of multivariate normality and equal variance-covariance matrices across groups do not have to be met, either. Furthermore, logistic regression might be preferable to multiple discriminant analysis because it is similar to regression with its straightforward statistical tests, ability to incorporate nonlinear effects, and wide range of diagnostics (Tabachnik and Fidell, 1996).

The model produced by logistic regression is nonlinear, and the outcome variable is the probability of having one outcome or another (in our study: one stock or the other) based on a nonlinear function of the best linear combination of predictors, with two outcomes (Tabachnik and Fidell, 1996):

$$\hat{Y}_i = \frac{e^u}{1+e^u},$$

where $\hat{Y}_i$ = the estimated probability that the ith case is in one of the categories and u is the usual linear regression equation:

$$u = A + B_1X_1 + B_2X_2 + \ldots + B_kX_k,$$

with constant A, coefficients B_j, and predictors, X_j (independent variables, the set stages in this study) for k predictors (j=1, 2, ..., k).

This linear regression equation creates the log of the odds, that is, the linear regression equation is the (natural log of the) probability of being in one group divided by the probability of being in the other group. The procedure for estimating coefficients is maximum likelihood, and the goal is to find the best linear combination of predictors to maximize the likelihood of obtaining the observed outcome frequencies. Logistic regression can be used to fit and compare models. The researcher uses goodness-of-fit tests to choose the model that does the best job of predictions with the fewest predictors. (Tabachnik and Fidell, 1996).

Therefore, logistic regression analysis was applied to test the predictability of stock membership (the dependent or grouping variable) by grouping codes (response variables) during three set stages (independent variables). The simplest model (constant-only model) was compared with the full model (with the three independent variables) by computing their log-likelihoods and by using χ^2. Degrees of freedom were the difference between degrees of freedom for the full and the constant-only models. The constant-only model has 1 df (for the constant) and the full model for our study had 3 df (1 df for each individual effect and one for the constant); therefore χ^2 was evaluated with 3 df. If χ^2 was significant, the full model would be reliable (Tabachnik and Fidell, 1996).

Results

Spatial patterns in evasive behavior of northeastern offshore spotted dolphins

The evasion index by set of northeastern offshore spotted dolphins was averaged in 2 × 2 quadrants and the resulting contour map is shown in Figure 1. The highest evasion index by set contour was 60% and extended approximately from south of the Baja California peninsula, across the Gulf of California mouth, and to the Mexican mainland (approx. 20 northern latitude). The 55% and 50% evasion

Table 1

Repeated-measures design to test for differences in dispersion behavior[1] between northeastern offshore spotted and eastern spinner dolphins. The data (response variable) are grouping codes for case i, during set stage j, for species k (=X_{ijk}). (Mexican fleet, 1992–95, PNAAPD data.)

Case (herd in each set)		Species	Set stages 1 (before chase)	2 (during chase)	3 (during encirclement)
1 to 308	1	northeastern offshore spotted dolphin	$X_{1\,1\,1}$	$X_{1\,2\,1}$	$X_{1\,3\,1}$
			$X_{308\,1\,1}$	$X_{308\,2\,1}$	$X_{308\,3\,1}$
309 to 544	2	eastern spinner dolphin	$X_{309\,1\,2}$	$X_{309\,2\,2}$	$X_{309\,3\,2}$
			$X_{544\,1\,2}$	$X_{544\,2\,2}$	$X_{544\,3\,2}$

[1] Herd dispersion: to establish if a herd dispersed during a set, the grouping codes applied by the observers in paragraph 3 of the RMMOSD were used. The codes are the following: 1, herd is in one group, 2, herd has divided into two or three groups; 3, herd consists of more than three groups. These codes were recorded during the three set stages: before chase, during chase, and during encirclement. If observers documented an ascending order in the codes (1, 2, 3), this feature was interpreted as herd dispersion during the fishing operation.

index contours were approximately parallel to the 60% contour and in addition formed a triangle-shaped area off the coast of Guatemala. Evasion indices 40% and lower extended south and offshore west of Mexico (Fig. 1). Therefore, the 60%, 50%, and 40% contours were considered the limits between three areas with different evasive behavior of the northeastern offshore spotted dolphin for our study. Three areas were identified (shaded areas in Fig. 1):

1) Low evasion: south of Mexico (30% to 40% estimated evasion index by set)
2) Medium evasion: coastal area south of Guatemala (50% to 55% estimated evasion index by set)
3) High evasion: mouth of the Gulf of California (60% and higher estimated evasion index by set)

Not all data between these contours were used because of difficulty in extracting data throughout the geographic range and because sample sizes for each area (n>100) seemed to be adequate for the analysis. Average mean evasion indices differed significantly between the three areas (Kruskal-Wallis, n_1=206, n_2=111, n_3=491; total n=808, H=93.13, 2 df, P<0.0001). Hence, nonparametric multiple comparisons between all pairs of areas were executed, and all pairs were found to be significantly different (Table 2).

According to these results, there seemed to be a spatial pattern in evasive behavior (measured in our study as the estimated median evasion index by set in each evasion area) of northeastern offshore spotted dolphins during fishing operations of the Mexican fleet from 1992 to 1995.

Differences between stocks

The eastern spinner dolphin seemed to evade capture more effectively than the northeastern offshore spotted dolphin in evasion area 3 when estimated evasion indices by set for both stocks were compared (Fig. 2). The differences were significant according to the Kolmogorov-Smirnov one-sided test for two independent samples (spinner: n=275, spotted: n=489; D=0.2031, P<0.001).

With respect to the evasive strategies of these two stocks, evasion index when the dolphins escaped under the net was compared by set. Eastern spinner dolphins apparently escaped more effectively under the net than northeastern offshore spotted dolphins (spinner n=177, spotted n=125, D=0.4097, P<0.001, Kolmogorov-Smirnov two-sample test; Fig. 3).

Dispersion behavior of northeastern offshore spotted and eastern spinner dolphins is presented for evasion area 3 (mouth of the Gulf of California, Fig. 4). Herds of both stocks tended to disperse from one set stage to the next; during encirclement, grouping code 3 (herd divided into more than 3 subgroups) had increased and was the most frequently recorded grouping code for northeastern offshore spotted dolphins in area 3 during our study. Northeastern offshore spotted herds tended to be more fragmented than eastern spinner herds before chase and to disperse in greater numbers during subsequent set stages (Fig. 4). Logistic regression analysis revealed a reliable full model (χ^2=60.209, P<0.001, df 3, n=544), i.e. the outcome of stock was predicted by the three independent variables (set stages). The prediction of stock outcome might further be interpreted as a difference between northeastern offshore spotted and eastern spinner dolphins with respect to dispersion behavior in our study.

In contrast, both stocks presumably escaped only on rare occasions by leaping out of the net because eastern spinners did so in only 5 of 275 sets (1.82%) and northeastern offshore spotted dolphins in 3 of 489 sets (0.61%) during the study period. Estimated evasion indices by set could not be compared because the samples were too small for any statistical test.

Discussion

Spatial patterns in evasive behavior

An apparent significant geographic difference in evasive behavior of northeastern offshore spotted dolphins was found between three areas in the EPO (Mexican fleet data, 1992–95, Fig. 1, Table 2). The lowest evasion area was located south of Mexico (area 1), the medium evasion area was in a relatively small coastal area south of Guatemala (area 2), and the highest evasion area was in the Gulf of California mouth (area 3, Fig. 1). About twenty years ago, fishermen noticed that dolphins were more difficult to capture in some areas than in others. Certain coastal dolphin

Table 2

Nonparametric multiple comparisons (according to Conover, 1980; Neave and Worthington, 1988) of estimated average (median) evasion index by geographic area (see Fig. 2) for the northeastern offshore spotted dolphin (1992–95, Mexican fleet, PNAAPD data). The null hypothesis (i.e. the median of two groups is equal) is rejected if the T statistic is larger than the critical Z value. All pairwise comparisons were significant (*indicates significant at P<0.05, where the critical Z-value for 3 groups (k–1)=2.39).

Area	n	Estimated median evasion index (%)	25–75% quartiles	Pairwise comparisons	T
1 (low)	206	25.00	0–66.67	1 and 2	3.17*
2 (medium)	111	44.44	20–83.33	1 and 3	9.49*
3 (high)	491	71.80	40–92.50	2 and 3	3.86*

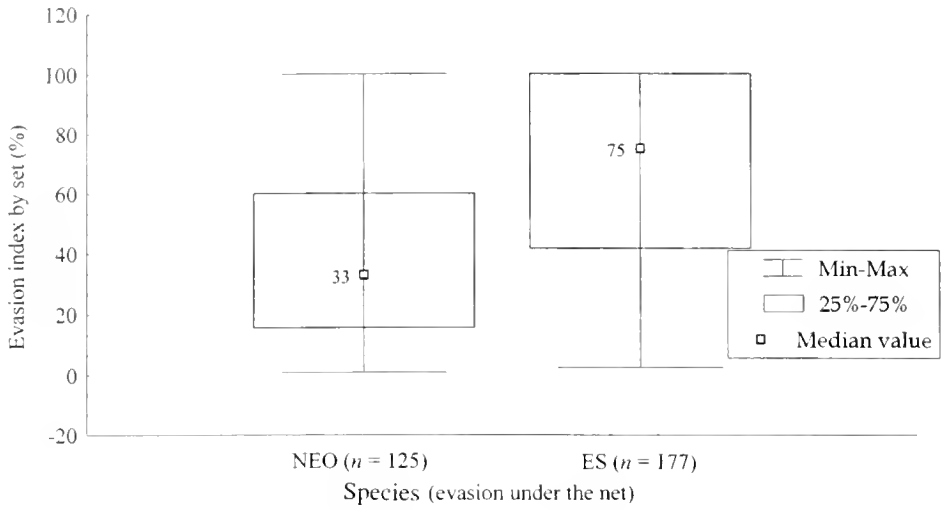

Figure 3

"Box and whiskers" plot for estimated evasion index by set for northeastern offshore spotted (NEO) and eastern spinner (ES) dolphins when dolphins evaded under the net (Mexican fleet, PNAAPD data 1992–95).

herds were called "the untouchables" by fishermen (Pryor and Norris, 1978) because the animals were capable (and still are) of completely evading the fishing operation even before the net has been set (National Research Council, 1992).

Several authors have suggested that the reasons for the detectable spatial patterns in evasive behavior seem to be related to the learning capacity of these mammals. Stuntz and Perrin[5] stated that dolphins (*Stenella* spp.) were more difficult to capture in areas where fishing effort had been greatest, therefore concluding that dolphins have learned to evade capture more effectively. Hewitt (1985) pointed out that the dolphins' reaction distance to survey vessels "may vary between geographic areas with the degree of animal naivete." This possibility was also considered by Hall and Boyer (1986) as an explanation for the spatial heterogeneity of mortality rates.

Although dolphin learning seems to be a logical explanation for geographic differences in evasive behavior, adequate measures for the dolphins' experience (i.e. their exposure to the tuna fishery) have to be designed. A measure may be the historical fishing effort (no. of chases per one-, two- or five-degree quadrant by the international fleet on the northeastern offshore spotted dolphin accumulated from 1959, when the tuna purse-seining fishery started, until today) standardized with respect to herd density (as described by Polachek, 1987; Reilly, 1990; or Reilly and Fiedler, 1994). Standardization is necessary because dolphins in areas with fewer herds will presumably have more opportunities to practice evading capture in comparison with areas where there are more herds (higher density) and effort has apparently been the same (number of chases per quadrant).

Furthermore, the number of dolphins that evaded capture during a set might also be affected (reduced) by the number of speedboats, the fishing vessel's power, and the presence of a helicopter; explosives were also used to herd dolphins several years ago. In addition, the dolphins' distribution (and hence possibly the fleet's effort) is influenced by changes in oceanographic features between seasons (Au and Perryman, 1985; Reilly, 1990) and years (Fiedler and Reilly, 1994; Reilly and Fiedler, 1994). Therefore, all variables recorded by the observers regarding the fishing operation (vessel power, number of speedboats, aerial assistance, use of explosives), time, and environmental features should be considered. However, this thorough analysis, including the important (according to the literature) variable "fishing effort" was not performed with the available data because the effort of the Mexican fleet should not be considered representative of the international fleet (Mexican vessels tend to fish closer to Mexico than do other fleets). Our future research aims to consider these variables and the effort of the complete international fleet, which is possible only with data from the IATTC.

Differences between stocks

In the mouth of the Gulf of California (area 3, Fig. 1), eastern spinner dolphins (*Stenella longirostris orientalis*) showed significantly higher estimated evasion indices than those for northeastern offshore spotted dolphins (*Stenella attenuata*) in our study (Fig. 2). A stronger evasion behavior by the eastern spinner dolphin has been described by other authors (Norris et al., 1978; Pryor and Kang, 1980) and may relate to different evasive strategies used by the two stocks to evade capture in the net, some of which were analyzed in our study.

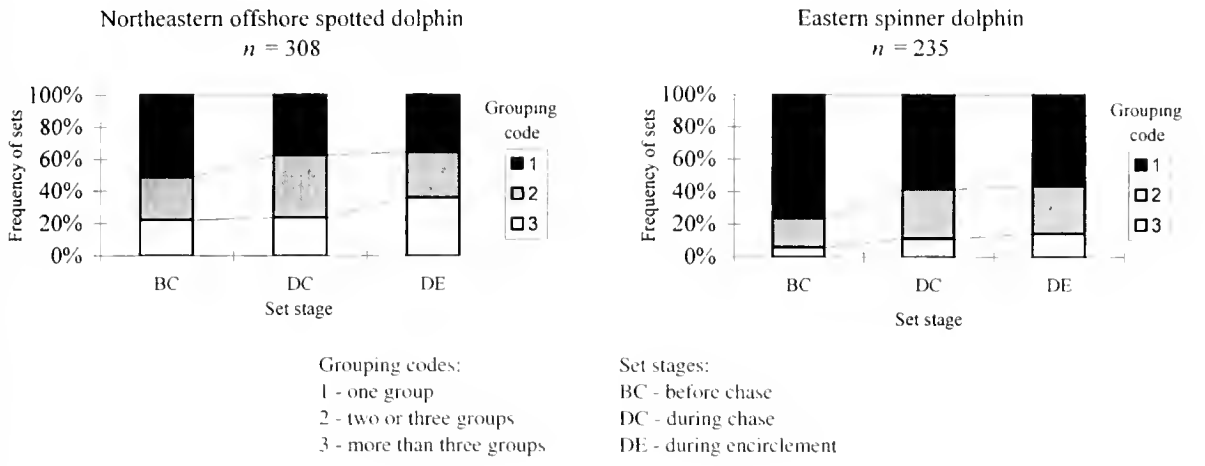

Figure 4

Dispersion (the ability of herds to "explode" (separate suddenly) into subgroups in relation to their configuration before chase) of northeastern offshore spotted and eastern spinner herds in evasion area 3 (Gulf of California mouth, Mexican fleet, PNAAPD data 1992–95).

Analysis of evasive strategies indicated that eastern spinner dolphins seemed to evade capture more effectively under the net than northeastern offshore spotted dolphins (Fig. 3). According to stomach-content analyses of spinner and spotted dolphins, the spinner dolphin is thought to forage deeper (approx. 250 m) than the spotted dolphin (approx. 30 m) (Fitch and Brownell, 1968). Therefore, the spinner dolphin may be more habituated to dive deeply enough to escape under the bottom of the net approximately 200 m from the surface, before the net is pursed.

In addition, even though herds of both stocks tended to disperse from one set stage to the next, there seemed to be a significant difference in dispersion between the stocks (according to logistic regression analysis results), i.e. eastern spinner dolphins apparently dispersed less often than the northeastern offshore spotted (Fig. 4). This evasive strategy (previously described as "school exploding" by Allen et al., 1980) also might have contributed to the eastern spinner dolphin's higher estimated evasion index in our study (Fig. 2). Because they disperse less and also tend to form larger subgroups than spotted dolphins during the fishing operation (Pryor and Kang, 1980), eastern spinner dolphin herds could be more cohesive and this behavior may coordinate their evasive movements more effectively than northeastern offshore spotted dolphins.

Moreover, the apparent higher evasive ability of eastern spinner dolphins might also be associated with different activity levels in these dolphins. Spinner dolphin activity level during the set tends to be higher than that of the spotted dolphin (Schramm, 1997) and could probably enhance evasion by spinners.

The frequency of evasion over the net was negligible in both stocks (spotted dolphins leaped over the net in only 0.61% of the sets analyzed; spinners, in 1.8%). Fishermen and scientists (Pryor and Kang, 1980) have also observed that dolphins encountered in fishing for tuna seldom attempt to leap out of the net to escape, even though individuals of both dolphin species are capable of doing so. The reasons why this event seems to be so rare are still unknown. Norris et al. (1978) mentioned that oceanic dolphins (like spinners and spotted) in captivity may take more time than coastal dolphins (like bottlenose dolphins, *Tursiops truncatus*) to cross a white line or a sunken rope on the tank bottom; this behavior might be explained by the fact that the animals may come from open waters where no barriers are present at all and there is no confinement. Thus, confinement in a tuna set may be foreign to these animals, as are the corkline and other features of a set (Norris et al., 1978).

Acknowledgments

Data were provided by the PNAAPD. M. Hall and M. Scott (IATTC) made thorough revisions of early drafts of the manuscript. The final version was considerably improved thanks to three anonymous reviewers. I. Méndez (PNAAPD) and A. Trujillo (Universidad Autónoma de Baja California) gave statistical advise. J. A. Delgado (Centro de Investigación Científica y Educación Superior de Ensenada) shared his mapping program. G. Heckel was financially supported by Consejo Nacional de Ciencia y Tecnología, Mexico, the Baitenmann family, and C. Jordan.

Literature cited

Allen, R. L., D. A. Bratten, J. L. Laake, J. F. Lambert, W. L. Perryman, and M. D. Scott.
1980. Report on estimating the size of dolphin schools, based on data obtained during a charter cruise of the M/V

Gina Anne, October 11–November 25, 1979. Data Report 6, Inter-Am. Trop. Tuna Comm., La Jolla, CA, 56 p.

Anganuzzi, A .A., K. L. Cattanach, and S. T. Buckland.
1992. Relative abundance of dolphins associated with tuna in the eastern tropical Pacific in 1990 and trends since 1975, estimated from tuna vessel sightings data. Rep. Int. Whal. Comm. 42:541–546.

Au, D., and W. Perryman.
1982. Movement and speed of dolphin schools responding to an approaching ship. Fish. Bull. 80(2):371–379.
1985. Dolphin habitats in the eastern tropical Pacific. Fish. Bull. 83:623–642.

Barham, E. G., W. K. Taguchi, and S. B. Reilly.
1977. Porpoise rescue methods in the yellowfin purse seine fishery and the importance of Medina panel mesh size. Mar. Fish. Rev. 39(5):1–10.

Chivers, S. J., and D. P. DeMaster.
1994. Evaluation of biological indices for three eastern Pacific dolphin species. J. Wildl. Manage. 58(3):470–478.

Coe, J. M., D. B. Holts, and R. W. Butler.
1984. The "tuna-porpoise" problem: National Marine Fisheries Service dolphin mortality reduction research, 1970–81. Mar. Fish. Rev. 46:18–33.

Colson, D. A.
1992. US policy on tuna-dolphin issues. U.S. Department of State Dispatch 3(34):667–671.

Compeán, G. A., and M. J. Dreyfus L.
1996. Interaction between vessels fishing for northern and southern yellowfin tuna (*Thunnus albacares*) in the northeastern and southeastern Pacific. *In* Status of Interactions of Pacific Tuna Fisheries in 1995 (R. Shomura, J. Majkowski, and R. Harman, eds.), p. 339–349. FAO Fish. Tech. Papers. 365.

Conover, W. J.
1980. Practical nonparametric statistics, 2nd ed. John Wiley & Sons, New York, NY, 493 p.

Dixon, W. J.
1990. BMDP statistical software manual, vol. 1. Univ. California Press, Berkeley, CA, 1385 p.

Dizon, A E., W. F. Perrin, and P. A. Akin.
1994. Stocks of dolphins (*Stenella* spp. and *Delphinus delphis*) in the eastern tropical Pacific: a phylogeographic classification. U.S. Dep. Commer., NOAA Technical Report NMFS 119, 20 p.

Du Toit, S. C., A. G. W. Steyn, and R. H. Stumpf.
1986. Graphical exploratory data analysis. Springer-Verlag New York, NY, 307 p.

Edwards, E. F.
1992. Energetics of associated tunas and dolphins in the eastern tropical Pacific Ocean: a basis for the bond. Fish. Bull. 90.678–690.

Fiedler, P. C., and S. B. Reilly.
1994. Interannual variability of dolphin habitats in the eastern tropical Pacific. II: effects on abundances estimated from tuna vessel sightings, 1975–1990. Fish. Bull. 92:451–463.

Fitch, J. E., and R. L. Brownell Jr.
1968. Fish otoliths in cetacean stomachs and their importance in interpreting feeding habits. J Fish. Res. Board Canada. 25(12):2561–2574.

Hall, M. A , and S. D. Boyer.
1986. Incidental mortality of dolphins in the eastern tropical Pacific tuna fishery: description of a new method and estimation of 1984 mortality. Rep. Int. Whal. Comm 36:375–381

Hall, M. A., and C. Lennert.
1997. Incidental mortality of dolphins in the Eastern Pacific Ocean tuna fishery in 1995. Rep. Int. Whal. Comm. 47:641–644.

Hewitt, R. P.
1985. Reaction of dolphins to a survey vessel: effects on census data. Fish. Bull. 83(2):187–193.

National Research Council.
1992. Dolphins and the tuna industry. National Academy Press, Washington, D.C., 175 p.

Neave, H. R., and P. L. B. Worthington.
1988. Distribution-free tests. Unwin Hyman Ltd., London, United Kingdom, 430 p.

Norris, K. S., W .E. Stuntz, and W. Rogers.
1978. The behavior of porpoises and tuna in the eastern tropical Pacific yellowfin tuna fishery—preliminary studies. Marine Mammal Commission. Contract MM6AC022, Publication PB-283-970, p. 86. [Available from the National Technical Information Service. Springfield, VA.]

Perrin, W. F.
1969. Using porpoise to catch tuna. World Fishing. 18(6): 42–45.

Perrin, W. F., and J. W. Gilpatrick Jr.
1994. Spinner dolphin, *Stenella longirostris* (Gray, 1828). *In* Handbook of marine mammals, vol. 5 (S. H. Ridgeway and R. Harrison, eds.), p. 99–128. Academic Press, San Diego, CA.

Perrin, W. F., G. D. Schnell, D. J. Hough, J. W. Gilpatrick Jr., and J. V. Kashiwada.
1994. Reexamination of geographic variation in cranial morphology of the pantropical spotted dolphin, *Stenella attenuata*, in the eastern Pacific. Fish. Bull. 92:324–346.

Perrin, W. F., M. D. Scott, G. J. Walker, and V. L. Cass.
1985. Review of geographical stock of tropical dolphins (*Stenella* spp. and *Delphinus delphis*) in the Eastern Pacific. U.S. Dep. Commer., NOAA Tech. Report NMFS 28.

Perrin, W .F., G. J. Scott, J. Walker, F. M. Ralston, and D. W. K. Au.
1983. Distribution of four dolphins (*Stenella* spp. and *Delphinus delphis*) in the eastern tropical Pacific, with an anotated catalog of data sources. U.S. Dep. Commer., NOAA Tech. Memo. SWFC-TM-NMFS-38, 65 p.

Polachek, T.
1987. Relative abundance, distribution and inter-specific relationship of cetacean schools in the eastern tropical Pacific. Mar. Mamm. Sci. 3(1):54–77.

Pryor, K., and K. S. Norris.
1978. The tuna/porpoise problem: behavioral aspects. Oceanus. 21(2):31–37.

Reilly, S. B.
1990. Seasonal changes in distribution and habitat differences among dolphins in the eastern tropical Pacific. Mar. Ecol. Prog. Ser. 66:1–11.

Reilly, S. B., and P. C. Fiedler.
1994. Interannual variability of dolphin habitats in the eastern tropical Pacific. I: research vessel surveys, 1986–1990. Fish. Bull. 92:434–450.

Reilly, S. B., and V. G. Thayer.
1990. Blue whale (*Balaenoptera musculus*) distribution in the eastern tropical Pacific. Mar. Mamm. Sci. 6(4):265–277.

Schramm, Y.
1997. Activity levels of offshore spotted (*Stenella attenuata*) and eastern spinner (*S. longirostris*) dolphins in tuna nets in the Eastern Pacific Ocean. M.Sc. thesis, Universidad Autonoma de Baja California. Ensenada, B.C., Mexico, 59 p.

Scott, M. D., and K. L. Cattanach.
1998. Diel patterns in aggregations of pelagic dolphins and tunas in the eastern Pacific. Mar. Mamm. Sci. 14(3): 401–428.
Smith, D., W. Wall, Z. Chen, R. Barnes, and B. Simons.
1995. Surfer (Win 32), vers. 6.01, surface mapping system. Golden Software, Inc., Golden, CO.
StatSoft.
1993. Statistica for Windows, version 4.2. StatSoft, Inc., Tulsa, OK, 1371 p.
Tabachnik, B. G., and L. S. Fidell.
1996. Using Multivariate statistics, third ed. Harper Collins College Publs., New York, NY, 880 p.
Wade, P. R.
1993. Estimation of historical population size of the eastern spinner dolphin (*Stenella longirostris orientalis*). Fish. Bull. 91:775–787.
Wade, P. R., and T. Gerrodette.
1993. Estimates of cetacean abundance and distribution in the eastern tropical Pacific. Rep. Int. Whal. Comm. 43: 477–493.
Zar, J.H.
1999. Biostatistical analysis, 4th ed. Prentice Hall, Upper Saddle River, NJ, 663 p.

Larval growth of the anchoveta *Engraulis ringens* during the winter spawning season off central Chile

Eduardo H. Hernandez

Leonardo R. Castro*

Departamento de Oceanografia
Universidad de Concepcion
Casilla 160-C, Concepcion, Chile

E-mail address (for L. R. Castro, contact author): lecastro@udec.cl

Abstract—Larval growth rates of the anchoveta *Engraulis ringens* were determined for two periods during the winter spawning season off Talcahuano, central Chile. Because winter is the season of minimum plankton production during the year, we hypothesized that larval growth rates during winter should be constantly low because of decreased larval fish food availability. Our results, however, indicate that 1) mean larval growth rates determined from three growth models in winter (mid-July through mid-September) were as high as in other periods of the year (linear, Gompertz, and von Bertalanffy; 0.47 mm/d, 0.50 mm/d, and 0.48 mm/d, repectively); 2) differences in larval growth rates occurred in two groups of cohorts spawned in the two periods during the spawning season (0.40 mm/d vs. 0.57 mm/d); and, 3) larval food (dinoflagellates, copepod eggs, and copepod nauplii) concentrations in the field were relatively high and not very variable during the study. Hydrography of the water column, however, varied throughout the season. During the last weeks of the study seawater temperature was higher, indicating intrusion of offshore warmer waters into the coastal zone. The presence of these warmer waters suggests that differences in growth rates between groups of cohorts may have resulted from larval development in water with different characteristics. Consequently, for a coastal upwelling species such as the anchoveta, increased growth rates in some cohorts may be advantageous considering that its main spawning season occurs in winter when the environmental conditions fluctuate markedly in short time scales.

Manuscript accepted 11 April 2000
Fish. Bull. 98:704–710 (2000).

The anchoveta *Engraulis ringens* (also known as "Peruvian anchoveta," FAO, 1988) has traditionally been one of the most important pelagic resources in the world in terms of landings (Pauly and Palomares, 1989). After strong fluctuations in abundance during the last three decades, especially marked during the anchoveta collapse in the early seventies, the stocks have rebounded. Catches in recent years have reached over 12 million tons and constitute one of the largest fisheries of the world.

Within its long latitudinal distribution range from 4°S to 40°S, several major spawning areas have been reported. The most important spawning areas have been traditionally located off Northern Peru, from off Southern Peru to off Northern Chile, and off Central Chile (Bernal et al., 1983). Despite its wide latitudinal range and paramount economic importance for the world fish markets, other than distribution and abundance, little information exists on basic biological parameters during the larval phase. For the larval stage, reseachers have documented information on the age of onset of feeding, feeding habits, and validation of daily deposition of ring increments in the otoliths (Rojas de Mendiola and Gómez, 1980, 1981; Ware et al., 1981; Muck et al., 1989; Morales-Nin, 1989; Villavicencio, 1989; Llanos, 1990). Information on larval growth rates in the wild, however, have been reported only for the southern stock and, unfortunately, only for seasons other than the major winter spawning seasons (Herrera et al., 1985).

There is a marked seasonality in the southern spawning area of the anchoveta. During spring, summer, and early fall, southerly winds predominate and lead to very intense upwelling events. During winter, intense northerly winds dominate, and upwelling events develop only occasionally. This marked seasonality in the oceanography also leads to changes in environmental conditions that may affect larval growth. During winter, due to the low frequency of upwelling events, the general production of the area is lower than in summer. Similarly, the very intense north winds may produce high levels of turbulence in the water column, thus dispersing the potential larval food patches (Lasker 1975, 1978). On the basis of these harsh environmental conditions, it has been proposed that food for larval anchoveta off Talcahuano might be limited during winter (Herrera et al., 1985; Bernal et al., 1990). However, because the anchoveta has been historically an important fishery of central Chile (1996 landings in the area reached ca. 300,000 metric tons, SERNAPESCA, 1996), there must be some mechanisms by which relatively high levels of larval survival can be achieved: either feeding conditions are not permanently harsh or factors other than food enhance larval survival, at least for some periods within the winter spawning season.

The objectives of our study were 1) to determine whether intraseasonal differences in growth rates occur between groups of cohorts of larval anchoveta spawned throughout the winter spawning season, and 2) to assess the role of two environmental factors (larval food and temperature) as potential factors affecting larval growth rates. Because some basic information for the deter-

mination of growth rates was still missing, we first determined the age of deposition of the first ring increment on larval otoliths and then described the growth functions of larvae caught in the wild, using three common growth models (the linear, Gompertz, and von Bertalanffy). Finally, we determined the mean growth rates for larval anchoveta spawned over the entire sampling winter season, and for two groups of cohorts spawned during that season but which faced different environmental conditions.

Methods

Larval growth in the wild

Larval anchoveta were collected in eight cruises from a grid of nine stations in the coastal zone off Talcahuano, central Chile (Fig. 1), during the winter of 1995 (12, 18 July; 1, 8, 17, 30 August; 4, 11 September). In each cruise, ichthyoplankton samples were collected with a bongo net (mesh size: 500 µm, diameter of mouth of net: 60-cm) equipped with a flow meter to quantify the volume of water sampled from the surface to a depth of 40 m. Once on board, half of the samples were preserved in 4% formalin and the other half in 96% ethanol for otolith analysis. At all stations, sea water samples were collected from nine depths (0, 5, 10, 15, 20, 30, 40, 60, 80 m) in 4-liter Niskin bottles for determination of temperature and salinity, and for identification and quantification of microplankton (dinoflagellates, copepod eggs, and copepod larvae) as potential larval food.

In the laboratory, anchovy larvae from both subsamples were identified, sorted, and counted. From the subsamples preserved in ethanol, 112 larvae within a size range between 5.68 and 20.74 mm (corrected for shrinkage, see below) were measured and their otolits were extracted and mounted in immersion oil. Otolith ring counts and otolith diameters were determined with the aid of a light microscope attached to a video camera and monitor to facilitate the reading of daily rings. Each otolith was counted twice and those counts where the readings differed in three or more rings were discarded. Larval lengths were corrected for shrinkage by using the algorithms proposed by Theilacker (1980) for larval northern anchovy (*Engraulis mordax*). Three models were used to describe the growth and growth rates of larval anchovy: the linear, Gompertz, and von Bertalanffy models. These models were used to describe growth for 1) all larvae spawned during winter (1 July–11 September) of 1995, and 2) for two groups of cohorts spawned during a) 1 July through 17 August, and b) from 18 August through 11 September. To classify the larvae as belonging to the first or second period, spawning dates were backcalculated as "the number of rings + 2" (see day of first ring deposition in the "Results" section). All statistical tests (regressions, analyses of variance, covariance, and models) were carried out with the commercial statistical software package STATISTICA, 1993.

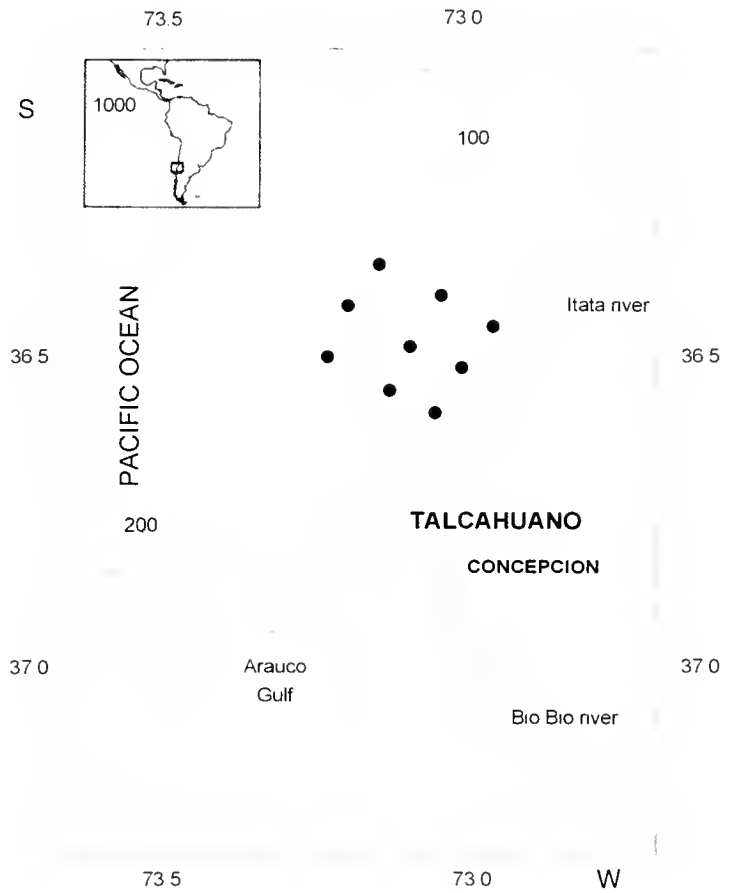

Figure 1

Survey area of ichthyoplankton during the 1995 anchoveta winter spawning season off Central Chile. Dots represent sampling stations.

First increment deposition

Anchovy eggs were collected from a coastal station off Talcahuano during the winter spawning season on 1997. At that station, gentle vertical tows were carried out with a bongo net from 0 to 40 m for collections of ichthyoplankton. The samples were placed in a 20-gal cooler at 12–13°C and transported to the Universidad de Concepcion Marine Station at Dichato. The transit time to the station took about 45 min. At the laboratory, between 20 and 60 anchovy eggs were sorted and placed in ten, 700-mL transparent plastic jars and incubated at 10°C and 14°C in light and dark cycles of 14:10 h and 12:12 h, respectively. One third of the water contained in the jars was replaced daily throughout the duration of the study. All larvae hatched in a given day were transplanted to new jars containing water at the same temperature as that used for hatching and in which *Isocrysis* sp. and powdered larval food were added daily. Every day a variable number of larvae were extracted from the jars for determination of fresh larval length, preserved in ethanol, remeasured, and dissected for otolith analysis (ring counts and diameter).

Results

First increment deposition

Only thirteen larvae from the rearing experiments in the laboratory were analyzed for determination of age at the first increment deposition, and because of the low number of larvae, the data from the treatments were analyzed together. These preliminary experiments showed that no larvae formed the first ring on the otoliths at hatching (two larvae were analyzed at hatching). Although the first ring on the otoliths was first observed in a larva at end of the first larval day after hatching (two larvae were analyzed), most larvae formed their first ring during the third day after hatching (four out of six larvae, 3-days-old or older). The larva analyzed at the end of the fourth day had two rings deposited; therefore it formed its first ring during the third day. At the end of the third day after hatching, all larvae had deposited their first ring. The mean diameter of the otolith focus for those larvae hatched in our experiments was 10.23 (SD=1.25) µm and the mean diameter of the otolith with their first increment formed was 12.83 (SD=1.56) µm.

The relation between the number of rings and otolith diameters from anchoveta larvae collected in the wild was well described by a linear regression (r^2=0.90; n=112; P<0.001)(Fig. 2). From this relationship, a larval anchoveta with one ring should have an estimated otolith diameter of 12.6 micrometers, which is close to the mean otolith diameter measured from larvae reared in our laboratory (mean=12.83 µm, SD=1.56). A power model was used to describe the relation between otolith diameter and larval length (corrected for shrinkage after Theilacker 1980) of wild larvae (r^2=0.79; n=112; P<0.001) (Fig. 3). According to these two relationships, a larva with one increment (12.6-µm otolith diameter) should have a larval length of 5.6 mm.

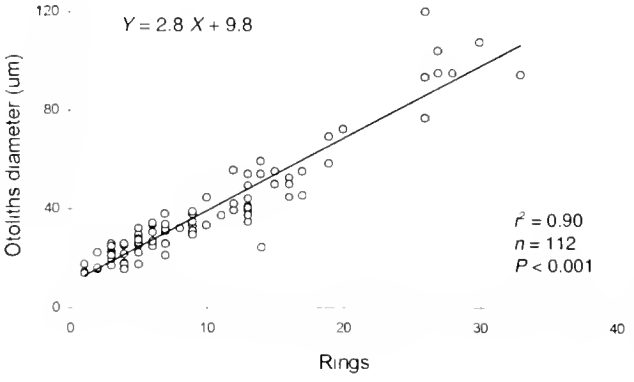

Figure 2

Linear regression showing the relation between the number of otolith rings formed and the otolith diameters of anchoveta larvae caught in the wild.

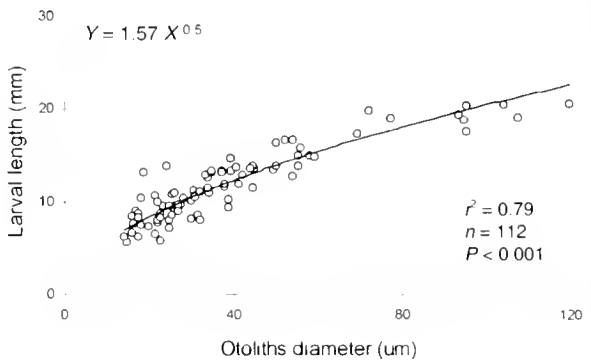

Figure 3

Relation between otolith diameter and length in larval anchoveta during the winter spawning season of 1995.

Larval growth of larvae caught in the wild

Because deposition of the first ring in most larvae occurred during the third day after hatching, age of larvae caught in the wild was estimated by adding two days to the number of rings in their otoliths. The standard lengths of larvae used in the growth models varied between 5.68 mm and 20.71 mm, and their age ranged from 3 to 35 days.

The three growth models used to describe anchovy larval growth during the winter of 1995 were highly significant (P<0.001) (Fig. 4, Table 1). The linear model yielded a daily growth rate of 0.47 mm/d (n=112 larvae; r^2=0.82); the Gompertz model yielded a mean daily growth rate of 0.50 mm/d (n=112 larvae; r^2=0.84); and the von Bertalanffy model yielded a mean daily growth rate of 0.48 mm/d (n=112 larvae; r^2=0.84). Estimated larval length at the end of the third day after hatching (day of the first ring deposition) varied from 7.81 mm with the linear model to 7.17 mm with the Gompertz model and 6.13 mm with the von Bertalanffy model.

The results of the analyses of growth rates between groups of cohorts spawned early versus late in the winter season varied according to the models used to describe growth. The larval growth rates determined from the linear model revealed that the group of daily cohorts spawned earlier in the season grew slower (1 Jul–17 Aug: 0.40 mm/d; n=63) than the group of larvae spawned later in the season (18 Aug–11 Sep: 0.57 mm/d; n=49) (ANCOVA, F=26.2, n=112, P<0.001; Zar, 1984). For both groups of cohorts, the linear regressions used to describe larval growth were significant (P<0.001) and explained over 78% and 74% of the variance in the respective data sets. A comparison of larval growth rates between periods using the Gompertz and von Bertalanffy models, however, showed no differences between larvae spawned early versus larvae spawned later in winter (Gompertz: F=1.08, n=112, P>0.05; von Bertalanffy: F=0.82, n=112, P>0.05; analysis of residual sum of squares, ARSS; Chen et al., 1992).

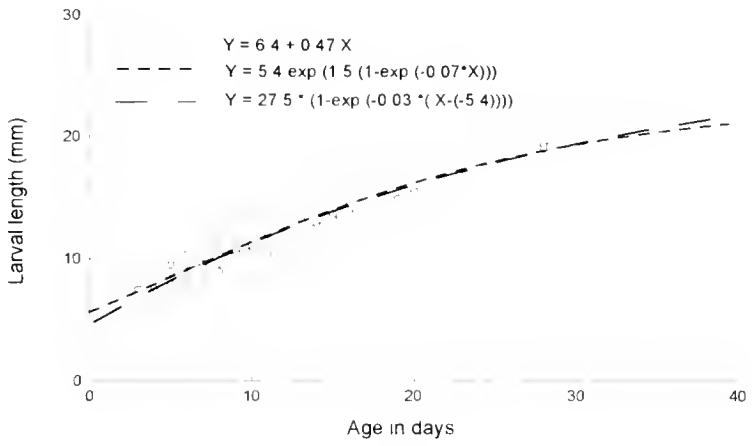

Figure 4

Models usedd to describe larval growth of the anchoveta *Engraulis ringens* during the 1995 winter spawning season off central Chile: linear model (—); Gompertz model (– – –); and von Bertalanffy model (— — —). Basic statistics for each model are shown in Table 1.

Table 1

Growth models used to determine growth rates for larval anchoveta off central Chile during the 1995 winter spawning season (mid July through mid September). RSS = residual sum of squares; r^2 = coefficient of determination.

	Model	Parameters	RSS	r^2	P
Linear	$Y = a + bX$	$a = 6.4$ $b = 0.47$	254.1	0.82	<0.001
Gompertz	$L = L_0 \exp(G(1 - \exp(-gt)))$	$L_0 = 5.4$ $G = 1.5$ $g = 0.07$	227.7	0.84	<0.001
von Bertalanffy	$L = L_\infty(1 - \exp(-K(t-t_0)))$	$L_\infty = 27.5$ $K = 0.03$ $t_0 = -5.4$	227.1	0.84	<0.001

Larval food (dinoflagellates, copepod eggs, and nauplii) occurred in relatively high concentrations throughout the season (Fig. 5). No differences in dinoflagellate densities (Mann-Whitney U=4.00; P=0.296), copepod egg densities (Mann-Whitney U=7.00; P=0.861), and copepod nauplii densities (Mann-Whitney U=5.00; P=0.456), were detected between the periods used to classify both groups of larval cohorts during the season. Sea surface temperature, another factor that may affect larval growth, was higher (Mann-Whitney U=19; P=0.025) during the second period of the spawning season (maximum, sea surface temperature: 13.5°C), probably as a result of the intrusion of offshore warmer waters to the coastal zone (Fig. 6) During the first period of the season, instead, when some of the upwelling events and the river plume were stronger and farther offshore (Castro et al., 2000), the sea surface temperature reached a minimum (11.1°C) in the coastal area.

Discussion

The deposition of the first ring in the larval otoliths has been associated with events in the early life history of fishes, such as the onset of feeding or eye pigmentation. For northern anchovy, *Engraulis mordax*, for instance, the deposition of the first increment takes place at the initiation of exogenous larval feeding or after yolksac absorption which occurs five or six days after hatching (Brothers et al., 1976; Methot and Kramer, 1979). Bay anchovy, *Anchoa mitchilli*, completes its first otolith ring

at the end of the second day after hatching—a time which corresponds to the time of yolksac depletion (Leak and Houde, 1987). Mediterranean anchovy, *Engraulis encrasicolus*, deposits its first increment during the second day after hatching with completion of yolk absorption (Palomera et al., 1988). In our rearing experiments larval anchoveta finished forming their first otolith increment at the end of the third day after hatching, which coincides with the end of the eye pigmentation.

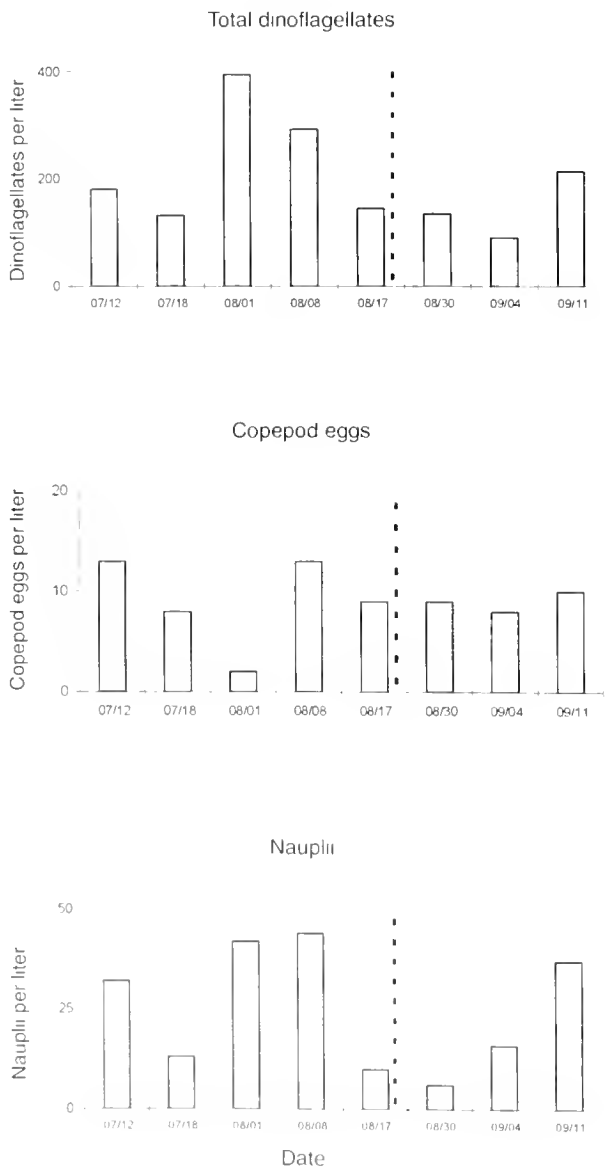

Figure 5

Mean density of potential larval food items in field during the winter spawning season of the anchoveta *Engraulis ringens* off Talcahuano, central Chile, in 1995. dinoflagellates, copepod eggs, and copepod nauplii. The vertical dashed line indicates the separation of periods considered in the groups of larval cohorts.

Larval anchoveta finished forming their first otolith increment at a larval length of 5.6 mm (estimated from the rings and otolith diameter and from the otolith diameter and larval length relationships). Observations of laboratory-reared anchoveta (*E. ringens*) larvae off Peru indicated that the mouth and eyes become functional at 64 h after hatching at a larval length of 4.03 mm (Ware et al., 1981). Initiation of larval feeding, however, varied from 3.5 to 6.8 days after hatching (mean 4.4 d), which corresponded to estimated larval lengths between 4.10 and 4.16 mm. If the deposition of the first ring in larval anchoveta coincided with the onset of feeding, then our estimations of 5.6 mm at the end of the third day after hatching were slightly higher than those estimated by Ware et al., (1981).

The three models used to fit the age and larval length data of anchoveta larvae collected during the winter spawning season in 1995 fitted the age and larval anchovy length data appropriately for the winter spawning season of 1995. A visual inspection, however, revealed a slight decrease in growth rate as the larvae increased in age, which suggests that the nonlinear models (von Bertalanffy and Gompertz) would describe larval growth better beyond the ages determined in our study.

Growth rates calculated with the three growth models (linear=0.47 mm/d; Gompertz=0.50 mm/d; and von Bertalanffy=0.48 mm/d) were very similar to estimations for anchoveta in other seasons (larval size range 5.0–20mm=0.45 mm/d, 12.5°C, Herrera et al., 1985) and within ranges reported for other engraulids. Methot and Kramer (1979) estimated northern anchovy larval growth rates between 0.34 and 0.55 mm/d between 13.0° and 16.2°C; for bay anchovy, *Anchoa mitchilli*, larval growth rates between 22° and 30°C ranged from 0.25 to 0.58 mm/d (Fives et al., 1986; Leak and Houde, 1987; Castro and Cowen, 1991); and for Mediterranean anchovy, *Engraulis encrasicolus*, growth rates ranged between 0.9 and 0.96 mm/d for 8-mm larvae at 20°C (Palomera et al., 1988). If only the larval anchovies from the upwelling areas of California and central Chile are compared, then the growth rates determined for the anchoveta in our study (0.40–0.57 mm/d at sea temperatures between 11.1° and 13.5°C), are slightly higher than those estimated for the northern anchovy at similar temperatures (0.39–0.47 mm/d at 13.0–13.2°C; Methot and Kramer 1979).

Some intraseasonal variability in growth rates of the anchoveta was observed between groups of cohorts during the winter spawning season, when rates from linear growth models were compared. Larval growth rates determined with the linear model (0.40 vs. 0. 57 mm/d) were within the same range reported for cohorts of other clupeiforms spawning at different times during the year or under different environmental conditions within the same spawning season (Methot and Kramer, 1979, Leak and Houde, 1987). Larval food, as a potential factor affecting larval growth rates, did not seem to be limited throughout the

entire sampling season. In fact, observed larval food concentrations may be considered high compared with concentrations reported for the same species in lower latitudes (Walsh et al., 1980). Differences in seawater temperature experienced by both groups of cohorts spawned during winter, however, may have accounted for the apparent differences in larval growth rates. An increase in water temperature occurred during the last weeks of sampling owing to an intrusion of offshore warmer waters into the coastal zone (Castro et al., 2000). Response to changes in seawater temperature as the spawning seasons progress is known for other anchovy species (*A. mitchilli*, Leak and Hode, 1987; Rilling and Houde, 1999). However, earlier evidence may have not been so conclusive for larval anchovy at upwelling areas (i.e. *E. mordax*, Methot and Kramer, 1979; Butler, 1989), probably because of the difficulties of determining the temperature of the water where the larvae actually developed, especially given the frequent changes in hydrographic conditions common in coastal upwelling areas.

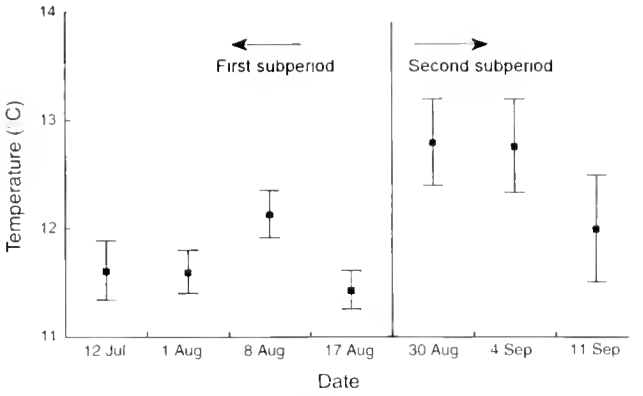

Figure 6

Mean sea surface temperature during the winter spawning season of the anchoveta *Engraulis ringens* off Talcahuano, central Chile, in 1995.

Because growth may be dependent on environmental factors (Pepin, 1991), seasonal variations in growth rates were expected among the cohorts spawned during the year. In our study, we documented potential differences in growth rates of groups of cohorts spawned a few weeks apart during the main spawning season. For coastal species living in upwelling areas, changes in growth rates among cohorts may be beneficial because environmental conditions may change markedly in short time scales (from days to a few weeks). With this scenario, increases in growth rates in some cohorts (given the right conditions during a few weeks) may be advantageous because the main spawning season for *E. ringens* occurs in winter. At the end of the season we expected a large pool of late larvae and early juveniles within a similar size range that had grown at different rates because they were exposed to different conditions. Given the relationship between environmental conditions and larval development, and the wide distribution range of the anchoveta (from 4°S to 40°S), differences in growth rates are to be expected in larval anchovies growing in different latitudes. Future studies should evaluate whether the models and growth rate changes determined off Talcahuano (37°S), close to the southern limit of distribution for the anchoveta, also apply for larvae growing in lower latitudes, such as spawning areas off northern Chile (18–24°S) and Peru (4–14°S).

Acknowledgments

The authors of this paper wish to thank G. Salinas, for helping in the collection of samples and in processing these samples, and C. Maturana for helping in the larval rearing experiments in the laboratory. An early version of this manuscript was reviewed by J. Butler. Funds for the field work were provided by FONDECYT and Fundacion Andes through grant numbers 3950024 and 12999-8, respectively, to L. R. Castro. During the writing of the manuscripts, L. R. Castro was also supported by FONDAP: Subprogram Advanced studies on the Humboldt Current System.

Literature cited

Bernal, P., G. Herrera, V. Troncoso, H. Gonzalez, and M. George-Nascimento.
1990. Cuantificacion de la mortalidad larval de *Sardinops sagax* y de *Engraulis ringens*. Efecto de inanicion y su control causal. Final Research Report FONDECYT 0372-88. P, Universidad Catolica de Chile, Talcahuano, Chile, 67 p.

Bernal, P. A., F. L. Robles, and O. Rojas.
1983. Variabilidad fisica y biologica en la region meridional del sistema de corrientes Chile-Peru. FAO Fish. Report 291:683–711.

Brothers, E. B., C. P. Mathews, and R. Lasker.
1976. Daily growth increments in otoliths from larvae and adult fishes. Fish. Bull. 74:1–8.

Butler, J. L.
1989. Growth during the larval and juvenile stages of ther northern anchovy, *Engraulis mordax*, in the California Current during 1980–84. Fish. Bull. 87:64–652.

Castro, L. R., and R. K. Cowen.
1991. Environmental factors affecting the early life history of bay anchovy *Anchoa mitchilli* in Great South Bay, New York. Mar. Ecol. Prog. Ser. 76:235–247.

Castro, L. R., E. H. Hernandez, and G.R. Salinas.
2000. Environmental influences on winter spawning of the anchoveta *Engraulis ringens* off central Chile. Mar. Ecol. Prog. Ser. 197:247–258.

Chen, Y., D. A. Jackson, and H. H. Harvey.
1992. A comparizon of von Bertalanffy and polynomial functions in modelling fish growth data. Can. J. Fish. Aquat. Sci. 49:1228–1235.

Fives, J. M., S. M. Warlen, and D. E. Hoss.
1986. Aging and growth of larval bay anchovy *Anchoa mitchilli*, from the Newport River Estuary, North Carolina. Estuaries 9(4b):362–367.

FAO (Food and Agriculture Organization of the United Nations).
1988. FAO species catalogue. Vol. 7: Clupeoid fishes of the

world (suborder Clupeoidei): an annotated and illustrated catalogue of the herrings, sardines, pilchards, sprats, shads, anchovies, and wolfherrings. Part 2: Engraulididae. Prepared by P. J. P. Whitehead, G. J. Nelson, and T. Wongratana. FAO, Rome, p. 322.

Herrera, G., E. Aguilera, G. Castillo, and P. Bernal.
1985. Growth of anchovy larvae *Engraulis ringens* in central Chile, determined by daily increment counts in otoliths. Biología Pesquera 14:11–15.

Lasker , R.
1975. Field criteria for survival of anchovy larvae: the relation between inshore chlorophyll maximum layers and succesfull first feeding. Fish. Bull. 73:453–462
1978. The relation between oceanographic conditions and larval anchovy food in the California Current: identification of factors contributing to recruitment failure. Rapp. P.-V. Reun. Cons. Perm. Int. Explor. Mer 173:212–230.

Leak, J. C., and E. D. Houde.
1987. Cohort growth and survival of bay anchovy *Anchoa mitchilli* larvae in Biscayne Bay, Florida. Mar. Ecol. Prog. Ser. 37:109–122.

Llanos, A.
1990. Sobreposición dietaria de estados larvales de cuatro especies de clupeiformes, en la Bahía de Concepción. Tesis para optar al grado de Licenciado en Ciencias Biológicas. Pontificia Universidad Católica de Chile, Talcahuano, Chile, 54 p.

Methot, R. D., and D. J. Kramer.
1979. Growth of northern anchovy, *Engraulis mordax*, larvae in the sea. Fish. Bull. 77(2):413–423.

Morales-Nin, B.
1989. Age and growth of the southern stock of Peruvian anchoveta based on otolith microstructures and length frequency analysis. *In* The Peruvian upwelling ecosystem: dynamics and interactions (D. Pauly, P. Muck, J. Mendo and I. Tsukayama, eds.), p. 179–188. ICLARM Conference Proceeding 18.. Instituto del Mar del Peru (IMARPE), Callao, Peru, 438 p.

Muck, P., B. Rojas De Mendiola, and E. Antonietti.
1989. Comparative studies on feeding in larval anchoveta (*Engraulis ringens*) and sardine (*Sardinops sagax*). *In* The Peruvian upwelling ecosystem: dynamics and interactions (D. Pauly, P. Muck, J. Mendo and I. Tsukayama, eds.), p. 86–96. ICLARM Conference Proceeding 18, Instituto del Mar del Perú (IMARPE), Callao, Peru, 438 p.

Palomera, Y., B. Morales-Nin, and J. Lleonart.
1988. Larval growth of anchovy, *Engraulis encrasicolus*, in the western Mediterranean Sea. Mar. Biol. 99:238–291.

Pauly, D., and M. L. Palomares.
1989. New estimate of monthly biomass, recruitment and related statistics of anchoveta *Engraulis ringens* off Peru (4–14°S), 1953–1985. *In* The Peruvian upwelling ecosystem: dynamics and interactions (D. Pauly, P. Muck, J. Mendo and I. Tsukayama, eds.), p. 189–206. ICLARM Conference Proceeding 18, Instituto del Mar del Perú (IMARPE), Callao, Perú, 438 p.

Pepin, P.
1991. Effect of temperature and size on development, mortality and survival rates of pelagic early life history stages of marine fish. Can. J. Fish. Aquat. Sci. 48:503–518.

Rilling, G. C., and E. D. Houde.
1999. Regional and temporal variability in growth and mortality of bay anchovy, *Anchoa mitchilli*, larvae in Chesapeak Bay. Fish. Bull. 97:555–569.

Rojas de Mendiola, B., and O. Gómez.
1980. Food, survival and time of inactivity of larval anchovy (*Engraulis ringens*). International Oceanographic Commission (IOC) Workshop Report 28:241–258.
1981. Daily rings in otoliths of larval anchovy (*Engraulis ringens*). J. Reun. Cons. Explor. Mer 178:565–566.

SERNAPESCA (Servicio Nacional de Pesca).
1996. Anuario estadistico de pesca 1996. Servicio Nacional de Pesca, Ministerio de Economia, Fomento y Reconstruccion, Valparaiso, Chile, 224 p

STATISTICA.
1993. Statistica for Windows. Release 4.5 Statsoft, Inc., Tulsa, OK.

Theilacker, G. H.
1980. Changes in body measurements of larval northern anchovy, *Engraulis mordax*, and other fishes due to handling and preservation. Fish. Bull. 78(3):685–692.

Villavicencio, Z.
1989. Tetracycline labeling for age and growth studies in fish, with emphasis on the peruvian anchoveta. *In* The peruvian upwelling ecosystem: dynamics and interactions (D. Pauly, P. Muck, J. Mendo and I. Tsukayama, eds.), p. 174–178. ICLARM Conference Proceeding 18. Instituto del Mar del Perú (IMARP), Callao, Perú, 438 p.

Walsh, J. J., T. E.Whitledge, W. E. Esaias, R. L.Smith,
S. A. Huntsman, H. Santander, and B. R. de Mendiola.
1980. The spawning habitat of the peruvian anchovy, *Engraulis ringens*. Deep Sea Res. 27A:1–27.

Ware, D. M., R. De Mendiola, B. and D. S. Newhouse.
1981. Behaviour of first-feeding Peruvian anchovy larvae, *Engraulis ringens* J. *Reprinted from* Symposium on early life history of fish (K. Sherman and G. Hempel, eds.), p. 467–474. Conseil International pour l Exploration de la Mer, Rapports et Proces-Verbaux des Reunions 178.

Zar, J. H.
1984. Bioestatistical analysis, 2nd ed. Prentice-Hall, Englewood Cliffs, NJ, 718 p.

Biology and ecology of threaded sculpin, *Gymnocanthus pistilliger*, in the eastern Bering Sea

Gerald R. Hoff

National Marine Fisheries Service
Alaska Fisheries Science Center
7600 Sand Point Way NE
Seattle, Washington 98115
E-mail address: jerry.hoff@noaa.gov

Abstract—The threaded sculpin (*Gymnocanthus pistilliger*) is distributed in the North Pacific from Norton Sound south to Southeast Alaska and west to Russia and Japan. It reaches its greatest abundance in the eastern Bering Sea in Bristol Bay where it is typically found in waters less than 50 m deep. Alaska Fisheries Science Center groundfish surveys in the eastern Bering Sea have estimated densities of up to 102 fish per hectare (catch per unit of effort, CPUE) for 1997 and 1998. Population estimates for 1997 were 111.20 million and for 1998 were 51.70 million. The population estimate drop is reflected in length-frequency data that suggest a complete lack of 2-year-old fish for 1998. *Gymnocanthus pistilliger* is a short-lived species (age estimates from otoliths range up to 10 years for males and up to 9 years for females), and the maximum size is 161 mm and 201 mm total length for males and females, respectively. During June, when specimen collections were made, ovaries are in the resting stage and contain some residual eggs from a previous spawning. The diet of *G. pistilliger* changes from predominantly gammarid amphipods and polychaetes to crangonid shrimp and fish with increased total length. Comparisons with studies from the western North Pacific on *G. pistilliger* suggest biological differences between populations, which may reflect adaptation to different habitats.

Manuscript accepted 2 June 2000.
Fish. Bull. 98:711–722 (2000).

Gymnocanthus pistilliger (Pallas), the threaded sculpin, is a small marine cottid that inhabits waters from Southeast Alaska north to Norton Sound and west to Russia and Japan (Wilson, 1973). It is found in shallow waters (<50 m) over soft sandy to muddy bottoms and is the most abundant cottid in the Bristol Bay region (>15 m) of the eastern Bering Sea. *Gymnocanthus pistilliger* may compete for resources with juvenile stages of commercially important flatfish in the shallow bays and nearshore areas used as nursery grounds (Grigorev and Fadeev, 1995). Although *G. pistilliger* is an abundant species, little life history information is available on Bristol Bay populations. The present study reports on the ecology and biology of *G. pistilliger* from Bristol Bay, Alaska, and compares it to ecology studies conducted on western North Pacific populations.

Methods

Specimens of *G. pistilliger* were collected in June of 1997 and 1998 during the National Marine Fisheries Service, Alaska Fisheries Science Center (AFSC), eastern Bering Sea survey. The survey area extended from the Alaska Peninsula north to Nunivak and St. Matthew Islands, and west to the 200-m shelf break (Fig. 1). Trawls were conducted on a grid of 356 fixed stations (20 nmi × 20 nmi) fished during daylight hours throughout the Bering Sea survey area. Thirty-minute trawls towed at 3.0 knots were conducted at each station. The shallowest depth surveyed was 15 m in Bristol Bay and the deepest was 178 m near the shelf edge. Trawling was conducted with the AFSC 83-112 eastern trawl, which is a low-opening two-seam trawl with a 26.5-m headrope and 34.1-m cable footrope (Rose and Walters, 1990) wrapped with rubber stripping and chain hangings that contact the bottom while the trawl is towed. Height and width measurements of the net were recorded with an acoustic SCANMAR net mensuration system. Global positioning system was used to record latitude and longitude data at the start and end of the trawl in order to determine distance fished.

The entire catch was sorted to species, enumerated and weighed, or a weighed subsample was used if there was a very large catch. Catch per unit of effort (CPUE) was calculated as number of fish per hectare (no./ha) by dividing the number of fish caught for each haul by the estimate of the area swept (net width × distance fished). *Gymnocanthus pistilliger* occurred in the survey area only at stations less than 50 m in depth (Fig. 1); therefore only this area was used for calculating population estimates. A population estimate was calculated by first determining a mean CPUE from all hauls combined (<50 m) and then expanded to the area. The biomass estimates were calculated in a similar manner by using weight in metric tons. The population and biomass estimates were made under the assumption that all fish in the path of the trawl were caught and were a representative sample for each station grid. However, given that there may be gear selectivity for fish size and given the patchy nature of fish distributions, the populations and biomass stated in this study are best estimates.

In May of 1995 and June of 1988–91 exploratory trawling was conducted in the shallow bays (<30 m) within Bristol

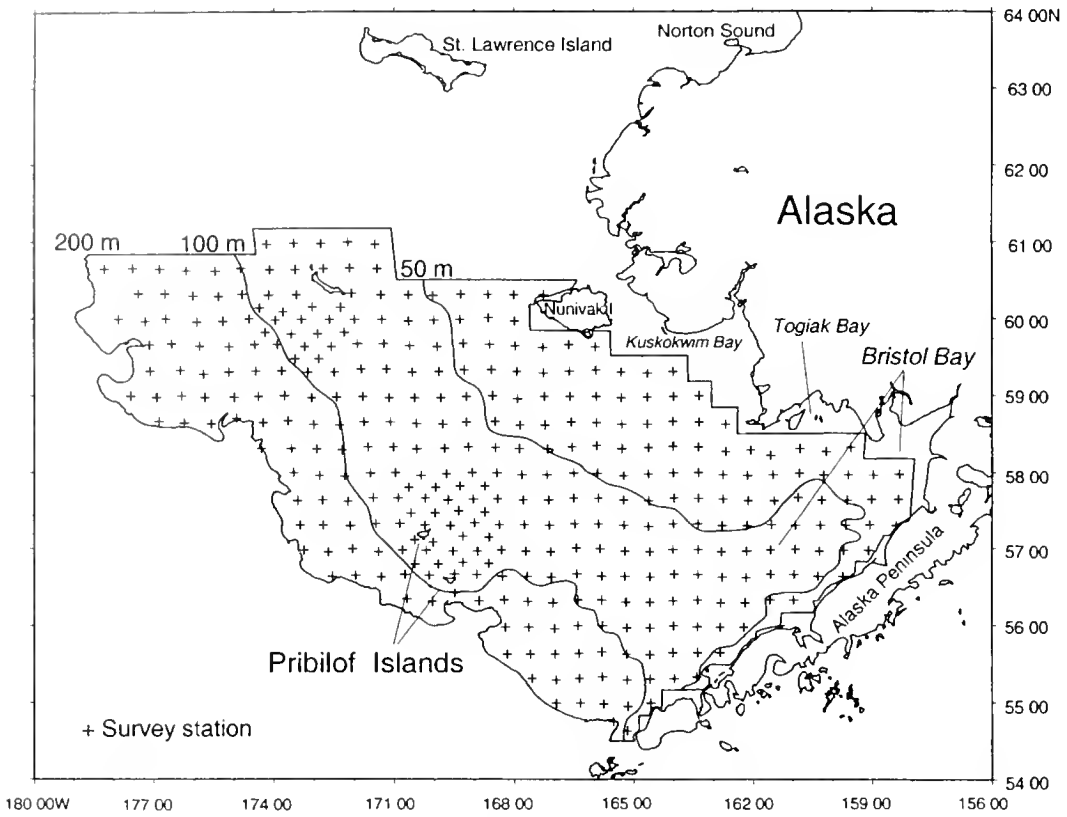

Figure 1

Map of the area in the eastern Bering Sea surveyed by the National Marine Fisheries Service. All stations (+) shown were trawled in 1997 and 1998. Map includes contour lines at 50-, 100-, and 200-m depths.

Bay by the National Marine Fisheries Service. Trawling methods, population, and density estimates were performed as described above.

Gymnocanthus pistilliger samples collected during 1997 and 1998 were preserved at sea by freezing or by preserving in a 10% formalin-seawater solution buffered with sodium bicarbonate. Frozen samples were partially thawed, and total length (TL, in mm), standard length (SL, in mm), total fish weight (TFW, in mg), gonad weight (GW, in mg), and sex were recorded. Sagittal otoliths were removed and placed in 50% ethanol. Parameters from formalin-preserved specimens with stomachs and ovaries removed were recorded in a similar manner and placed in 50% ethanol.

Dark bands on otoliths were evident under reflected light and were counted by the break-and-burn method to ensure inclusion of all ring structures. Length at age was described by using nonlinear regression to fit the von Bertalanffy (1957) growth model for male and females separately with pooled data from the two years.

The von Bertalanffy growth curve is

$$L_t = L_\infty [1 - e^{-K(t - t_0)}].$$

Fish numbers for length-frequency samples were combined for all hauls by sex and year.

The relationships of total fish length (TL) to total fish weight (TFW) were investigated with the model

$$TFW\,(\mathrm{g}) = a\,TL(\mathrm{mm})^b.$$

Ovaries were removed and weighed to the nearest milligram from formalin-preserved fish. The gonosomatic index (GSI) was calculated from TFW and ovary weight was calculated as

$$100(ovary\ weight/TFW).$$

Stomach contents were recorded to the lowest practical taxon, and enumerated and weighed to the nearest milligram. For analysis, prey items were grouped into seven logical or taxonomic categories (Table 1). *Gymnocanthus pistilliger* were grouped into four length groups (<100 mm, 100–124 mm, 125–149 mm, and 150–201 mm TL). Percent frequency of occurrence, total count, and total weight were calculated for individual prey items and for each prey item group. Statistical analysis and graphing were conducted with the computer programs Statgraphics 2.0 and SigmaPlot 4.0, and distributional maps were produced with the software Arcview 3.0.

Table 1

Diet composition of *Gymnocanthus pistilliger*. Prey items are grouped into major taxonomic or similar groups and frequency of occurrence (freq.), total count, and total weight percentages were calculated for both individual items and for groups. (Total lengths 73–201 mm, n=93).

Prey items	Frequency of occurrence	Total count	Total weight
Wormlike organisms			
Polychaeta	47.19	1.21	14.27
*Echiur*us sp.	7.87	0.36	1.43
Opheliidae	2.25	0.03	0.48
Annelida	1.12	0.01	0.01
Goniadae	1.12	0.07	0.08
Total	52.81	1.69	16.26
Amphipoda			
Gammaridea	82.02	92.74	15.43
Caprellidea	2.25	0.04	0.05
Amphipoda unidentified	1.12	0.03	0.26
Total	83.15	92.84	15.74
Shrimp			
Crangonidae	32.58	0.7	31.23
Total	32.58	0.7	31.23
Other Crustacea			
Ostracoda	1.12	0.06	0.01
Mysidacea	1.12	0.01	0.03
Cumacea	17.89	0.4	0.47
Isopoda	1.12	0.01	0.07
Euphausiacea	1.12	0.01	0.02
Crustacea unidentified	1.12	0.01	0.07
Total	21.35	0.52	0.67
Mollusca			
Gastropoda	10.11	0.27	0.64
Naticacea	2.25	0.04	0.99
Bivalvia	31.46	1.39	1.5
*Clinocardi*um sp.	1.12	0.01	1.1
Octopus sp. (beaks)	2.25	0.03	0.01
Total	39.33	1.75	4.24
Fish			
*Lumpen*us sp.	1.12	0.01	2.24
*Ammodytes hexa*pterus	4.49	0.07	12.03
Teleostei unidentified	2.25	0.03	1.24
Total	7.87	0.12	15.5
Miscellaneous			
Forminifera	3.37	0.07	0.02
Anthozoa	2.25	0.03	0.05
Urochordata	1.12	0.03	0.03
unidentified eggs	10.11	0.48	0.06
organic material unidentified	85.39	1.15	12.28
wood	1.12	0.01	0.19
rocks	38.2	0.51	2.61
sand	4.49	0.06	1.06
material unidentified	1.12	0.01	0.04
Total	88.76	2.37	16.35

Results

Distribution

The distribution of *G. pistilliger* during the 1997 and 1998 eastern Bering Sea surveys was limited to depths <50 m; areas of highest concentration were located around southern Kuskokwim and Togiak Bays for both survey years (Fig. 2). In 1997, *G. pistilliger* were caught in 60% of the trawls <50 m (n=86 for each year), compared with 51% in 1998. The 1997 CPUE ranged from 0.19 to 101, with a mean of 15.81 (SD=22.78); the population estimate for

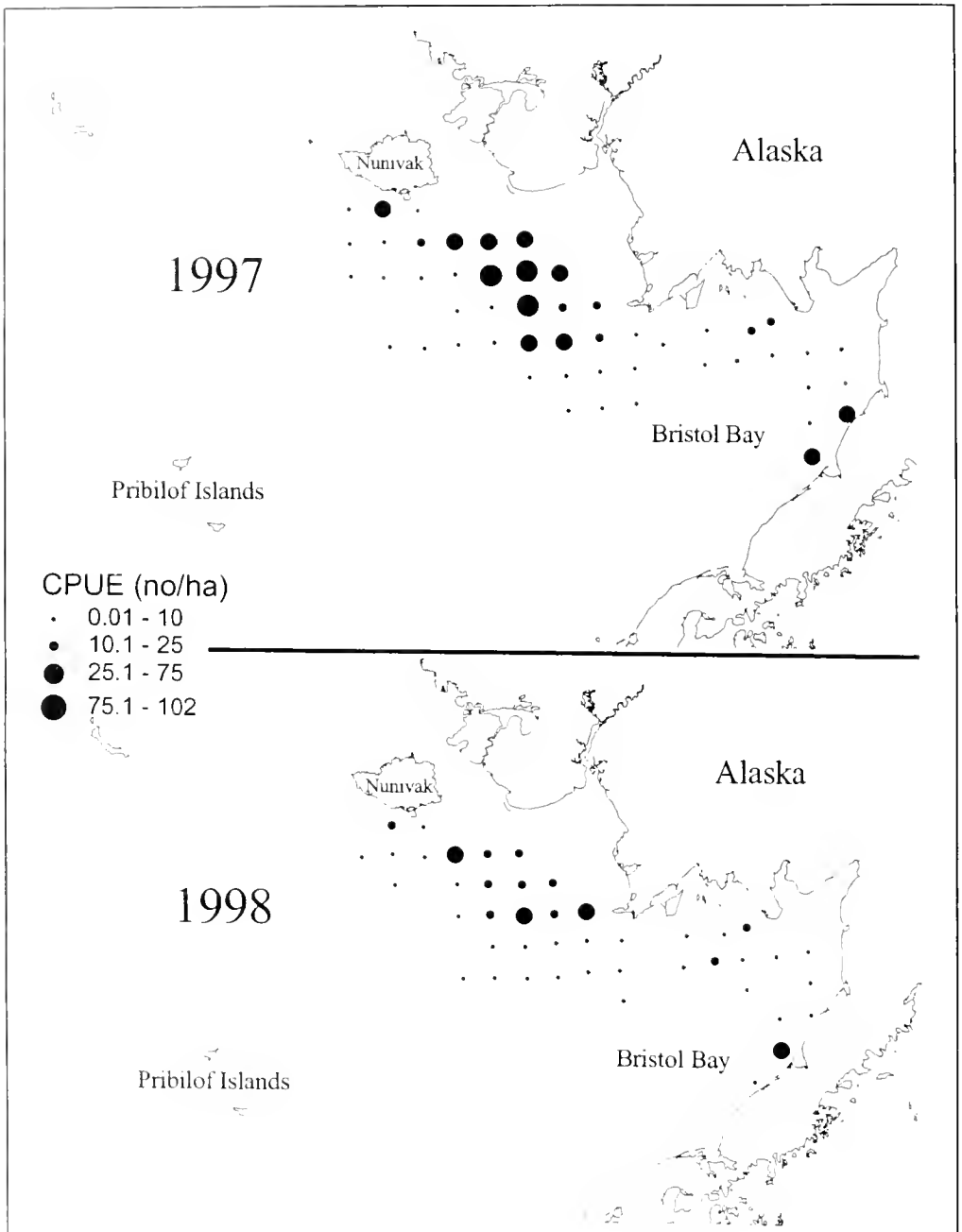

Figure 2

Trawling stations (coded by density [CPUE=number fish per hectare] for 1997 and 1998), where *Gymnocanthus pistilliger* were collected during the Alaska Fisheries Science Center Eastern Bering Sea Groundfish Survey.

the entire survey area was 110.24 million fish and the biomass estimate was 4254 metric tons (t). The 1998 CPUE ranged from 0.1 to 55 with a mean of 7.37 (SD=5.23); the population estimate was 51.70 million fish and the biomass estimate was 1956 t.

The distribution of females and males differed by depth (Fig. 3) with the proportion of females decreasing with depth. Catch rates at depth indicated that *G. pistilliger* inhabited nearshore areas and were most abundant in the shallowest depths covered by this survey (Fig. 4).

Trawling in Kuskokwim Bay and Togiak Bays resulted in mean CPUEs of 6 and 24 for each bay, respectively (n=9 trawls per bay, CPUEs of 1 to 17, SD=5.54 for Kuskokwim Bay; CPUEs of 1 to 79, SD=30.32 for Togiak Bay). During

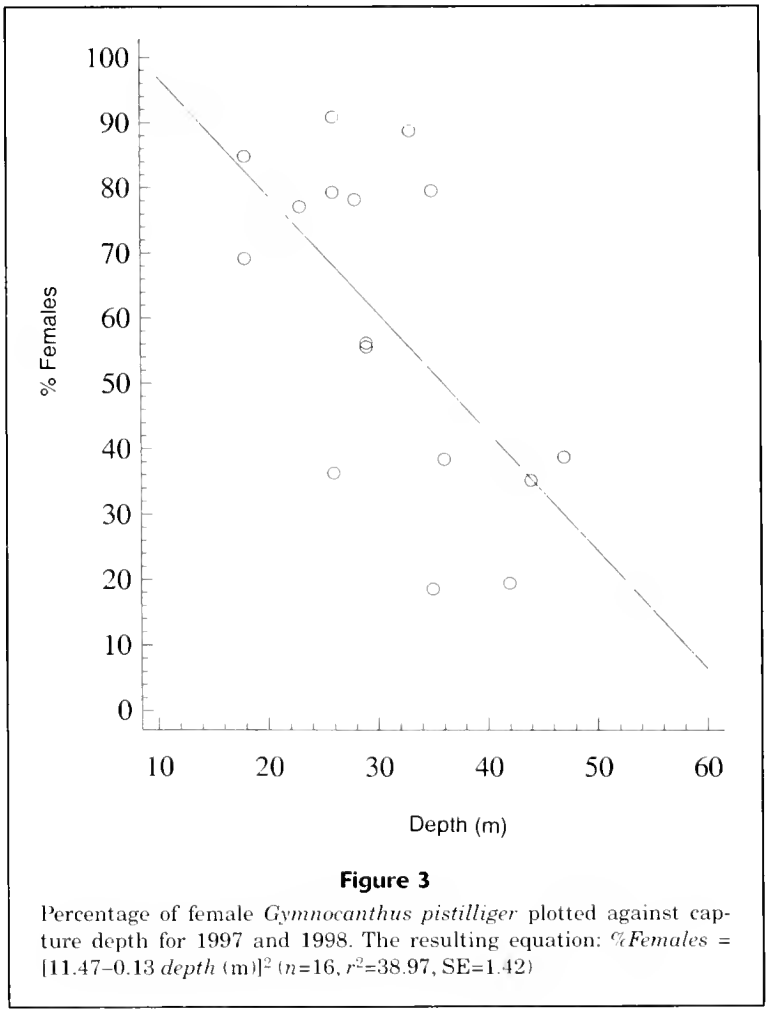

Figure 3

Percentage of female *Gymnocanthus pistilliger* plotted against capture depth for 1997 and 1998. The resulting equation: $\%Females = [11.47 - 0.13\ depth\ (\mathrm{m})]^2$ (n=16, r^2=38.97, SE=1.42)

these years, catches peaked in Togiak Bay (CPUEs of 71 to 79) at some of the shallowest depths trawled (13–15 m). Trawls conducted in Togiak Bay again in 1995, during late May, resulted in densities up to 249 at 19.8 m in depth (n=28 trawls, CPUEs from 4 to 249, $\bar{x}$=65.68, SD=74.68, depth range: 4–30 m).

Age and growth

A von Bertalanffy growth curve was fitted to pooled length-at-age data for 1997b and 1998 and analyzed separately for males and for females (Fig. 5). The growth models were the following:

males $L_t = 165.5\ [1-e^{-0.375299\,(t\,+\,0.0704311)}]$
(n=395, r^2=0.78, SE=8.08);

females $L_t = 223.8\ [1-e^{-0.228048\,(t\,+\,0.226626)}]$
(n=595, r^2=0.84, SE=9.85).

Females grew faster than males, and by three years of age, a difference in length at age was established (Fig. 5). Females reached >200 mm TL and a maximum age of 9 years; males reached 160 mm and a maximum age of 10 years.

Age groups from 1997 consisted of 2- to 10-year-old fish; the strongest age group was 4 years (>50% of individuals) and there were large groups of 2- and 3-year-old fish. In 1998 however, ages ranged from 3 to 9-year-old fish. The strongest age group (>50% of individuals) was 5 years. Two-year-old fish were absent (Fig. 6). Length-frequency histograms (Fig. 7) for 1997 and 1998 male and female *G. pistilliger* show the age modes as well as the age groups that were absent in 1997 and 1998.

Weight-length relationships for males and females and between years showed no significant difference (P>0.05) and were pooled for analysis (Fig. 8). The pooled weight-length equation was statistically significant (P<0.01, r^2=0.97, n=992):

$$TFW\ (\mathrm{gm}) = 2.40317 \times 10^{-6} TL\ (\mathrm{mm})^{3.30692}.$$

Ovaries were not developed in June when fish were collected; few large females contained residual eggs from the previous spawning. The GSI ranged from 0.5% to1.9% for fish collected from 1997 (females n=108, 70–190 mm TL).

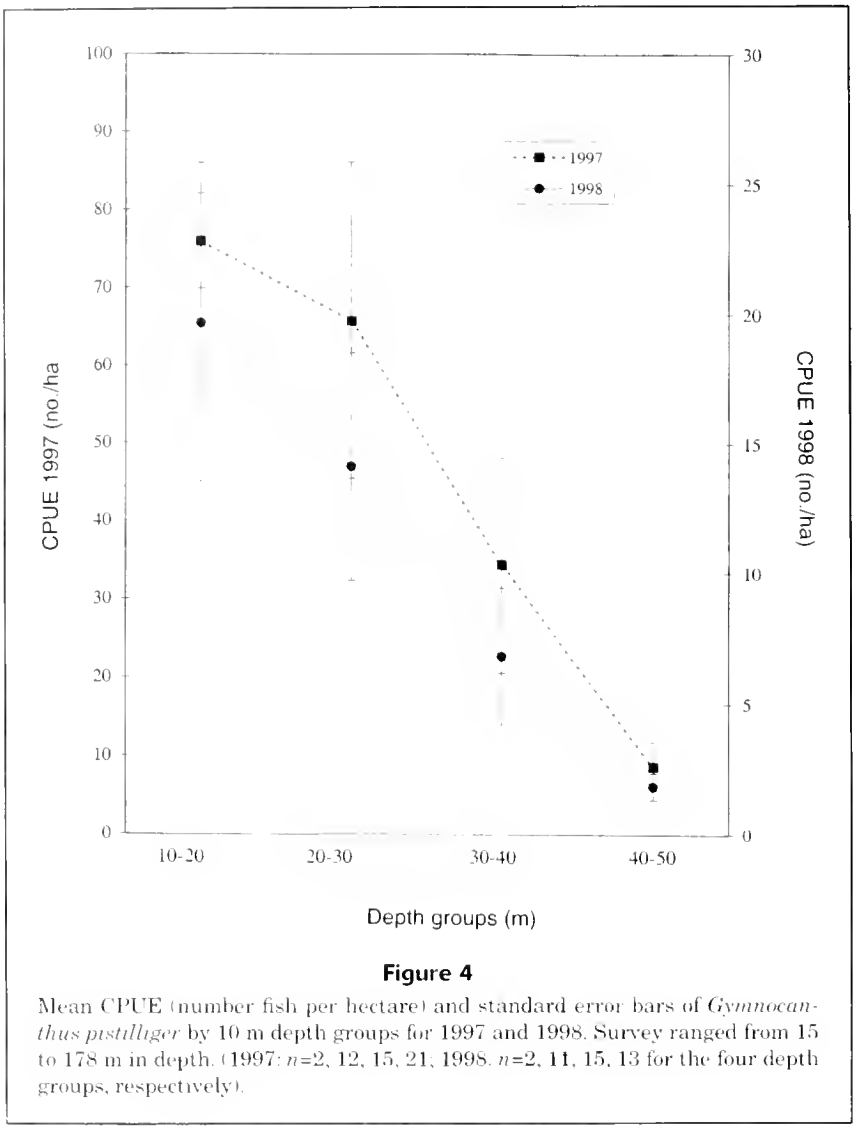

Figure 4

Mean CPUE (number fish per hectare) and standard error bars of *Gymnocanthus pistilliger* by 10 m depth groups for 1997 and 1998. Survey ranged from 15 to 178 m in depth. (1997: n=2, 12, 15, 21; 1998. n=2, 11, 15, 13 for the four depth groups, respectively).

Diet

A total of 32 different prey items were identified from 93 stomachs of fish collected in 1997 (Table 1). Frequency of occurrence analysis indicated that gammarid amphipods and polychaete worms were the most common prey items; crangonid shrimp and bivalves were encountered less frequently. Similarily prey total count indicated that gammarid amphipods were the most numerous prey items encountered but no other single item was found in large numbers. Crangonid shrimp predominated by total weight. Pacific sandlance (*Ammodytes hexapterus*), gammarid amphipods, and polycheates were secondarily important and were of approximately equal weight.

The relation between fish size and diet composition showed a shift from predominantly small benthic amphipods to increasingly larger prey items, such as crangonid shrimp and fish with increased fish TL (Fig. 9). Total diet weight proportion showed similar trends; crangonid shrimp and fish became more important and gammarid amphipods decreased in diet weight proportion as fish increased in TL (Fig. 10).

Discussion

Distribution

Gymnocanthus pistilliger is abundant in the spring to early summer (May and June) near the mouth of Kuskokwim and Togiak Bays and throughout the shallow areas of Bristol Bay. This area is characterized by relatively shallow water (<50 m) and has a sandy to muddy bottom (McDonald et. al, 1981). The Togiak River and Kuskokwim River discharge large amounts of fresh water into the shallow estuarine environment creating fluctuating tem-

peratures and salinities; thus, during winter the entire area may be covered in thick ice sheets. *Gymnocanthus pistilliger* may move in and out of the shallow local bays seasonally to sustain a suitable habitat. However the nearshore distribution was difficult to assess for *G. pistilliger* from the present study owing to limited sampling in very shallow coastal waters and single season collections. The timing of spawning movements, however, may significantly affect population estimates if the species moves between depths seasonally and may help to explain a 50% decline in fish from 1997 to 1998. Although water temperature is often associated with fish movements, there was no significant difference between the means (*t*-test P=0.18) in bottom water temperatures in the survey area <50 m in depth for the two years sampled (1997, $\bar{x}$=4.22°C, SD=1.88; 1998, $\bar{x}$=4.48°C, SD=0.87).

Vdovin et al. (1994) suggested that *G. pistilliger* remains within shallow water and except for spawning, probably remains in the nearshore area most of the year. Spawning migrations in winter resulted in both sexes aggregating in deeper bay areas of Peter the Great Bay (Vdovin et al., 1994); however, the proportion of females increased with increasing depth (a depth range of 80 to 110 m was maintained during spawning) (Tokranov, 1987; Vdovin et al., 1994).

If Bristol Bay populations are similar to Peter the Great Bay populations, then at the time of capture (June) *G. pistilliger* has already spawned and dispersed in the nearshore areas. Females probably migrate to join the males in the deeper part of Bristol Bay (around 50 m depth) during late winter to early spring to spawn, although it is unlikely that Bristol Bay populations reach the spawning depths of populations in Peter the Great Bay. Distributional data from Alaska indicate that *G. pistilliger* are rarely found deeper than 50 m, except occasionally in coastal areas of the Gulf of Alaska (Hoff, unpubl. data).

Age and growth

Age data gathered from otoliths suggest that *G. pistilliger* is short lived (to 10 years), the females exhibit faster growth, and that this species reaches a maximum size of 205 mm for females and 160 mm for males. The age structure of western Bering Sea populations has shown older populations than those for Bristol Bay (a strong mode from 7 to 9 years (range 3–13 years) and a larger maximum size of 270 mm TL for females and 220 mm TL for males (Tokranov, 1987). Length-at-age data for fish collected off Kamchatka (Tokranov, 1987) were similar to those reported in the present study, suggesting that similar aging techniques were used and similar growth rate estimates were calculated for the two populations of *G. pistilliger*. Therefore, different size composition and age groups for eastern Bering Sea and western Pacific populations appear real.

The ovaries from females collected in June from Bristol Bay were deflated and a few large females contained residual eggs from a previous spawn. Wilson (1973) stated that *G. pistilliger* spawn in spring but provided no evidence for this. Ovaries collected from eastern Bering Sea populations in June of 1997 suggest that *G. pistilliger* is a late winter to early spring spawner. Tokranov (1987) reported that *G. pistilliger* spawn in winter, are single batch spawners in shallow waters, and produce adhesive eggs.

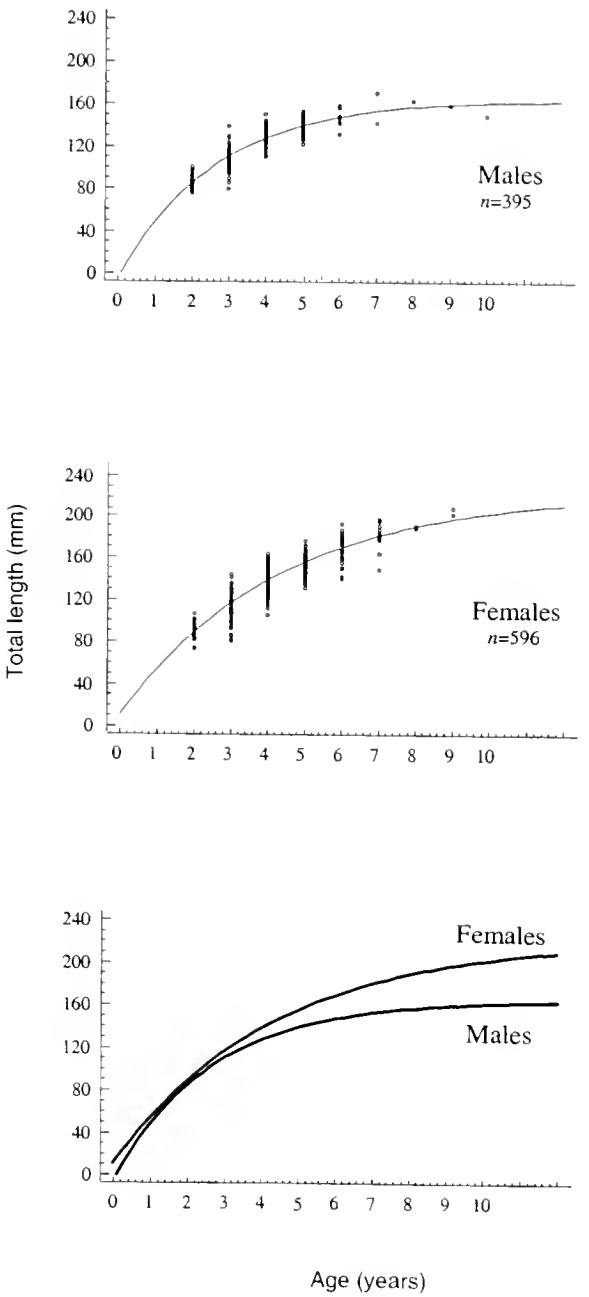

Figure 5

Von Bertalanffy growth curves and individual data for male and female *Gymnocanthus pistilliger* collected during 1997 and 1998, combined with curves plotted together for comparison. Length-at-age data were gathered from sagittal otoliths by the break-and-burn method

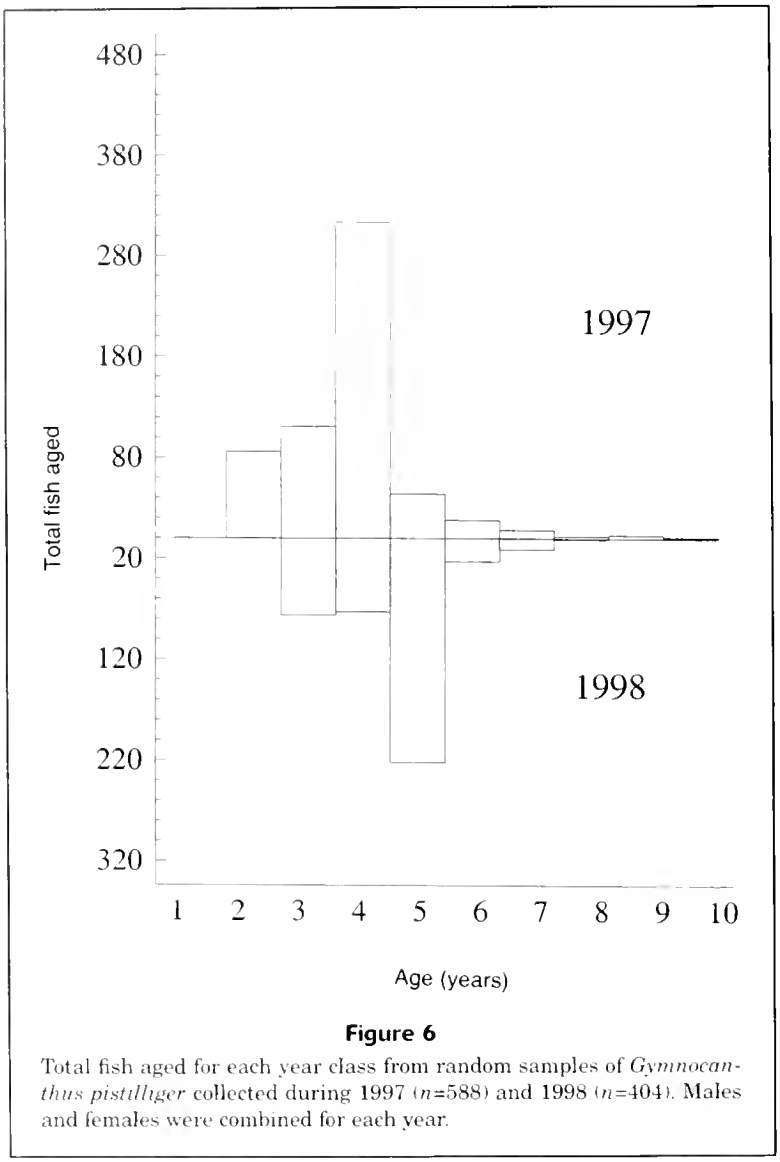

Figure 6

Total fish aged for each year class from random samples of *Gymnocanthus pistilliger* collected during 1997 (n=588) and 1998 (n=404). Males and females were combined for each year.

Diet

Gymnocanthus pistilliger preys upon benthic amphipods, polychaetes, crangonid shrimp, and fish. A diet shift from amphipods to shrimp and fish with increased body size represents the sculpin's ability to capture and ingest larger prey items with increased body size, an ability that lessens the likelihood of intraspecific competition and increases efficiency in feeding.

Tokranov (1985) reported on the diets of *G. pistilliger* from off the western coast of the Kamchatka Peninsula. He found diets consisted mainly of polychaete and *Echiurus* (~70% frequency and weight) and amphipods (contributing little to the diet). *Gymnocanthus pistilliger* from Kamchatka increasingly consumed mollusks, decapods, and juvenile capelin as it grew, and polychaetes and *Echiurus* decreased as important items in the diet. Tokranov (1985) also found a shift to larger prey items with increasing fish size.

Commercially important flatfish also use shallow waters in Bristol Bay as spawning and nursery grounds (Fadeev, 1968; Grigorev and Fadeev, 1995). The diet composition of *G. pistilliger* overlaps with that of flatfish species, such as *Limanda aspera* (yellowfin sole), *Limanda proboscidea* (long-head dab), *Pleuronectes bilineatus* (rock sole), and *Pleuronectes quadrituberculatus* (Alaska plaice), where competitive interactions may occur. These flatfish diets also consist of benthic amphipods, polychaetes, and *Echiurus* (>50% by weight) (Livingston et al., 1986; Brodeur and Livingston, 1988; Corcobado-Onate, 1991; Lang et al., 1995). However, Holladay and Norcross (1995) found that these flatfish species exhibit a diverse diet (10–57 groups) and show diet preferences based on substrate. Dietary shifts such as these may lessen the likelihood of prey competition in densely populated areas such as Bristol Bay.

Gymnocanthus pistilliger is also potentially an important resource to larger predators because of its small size

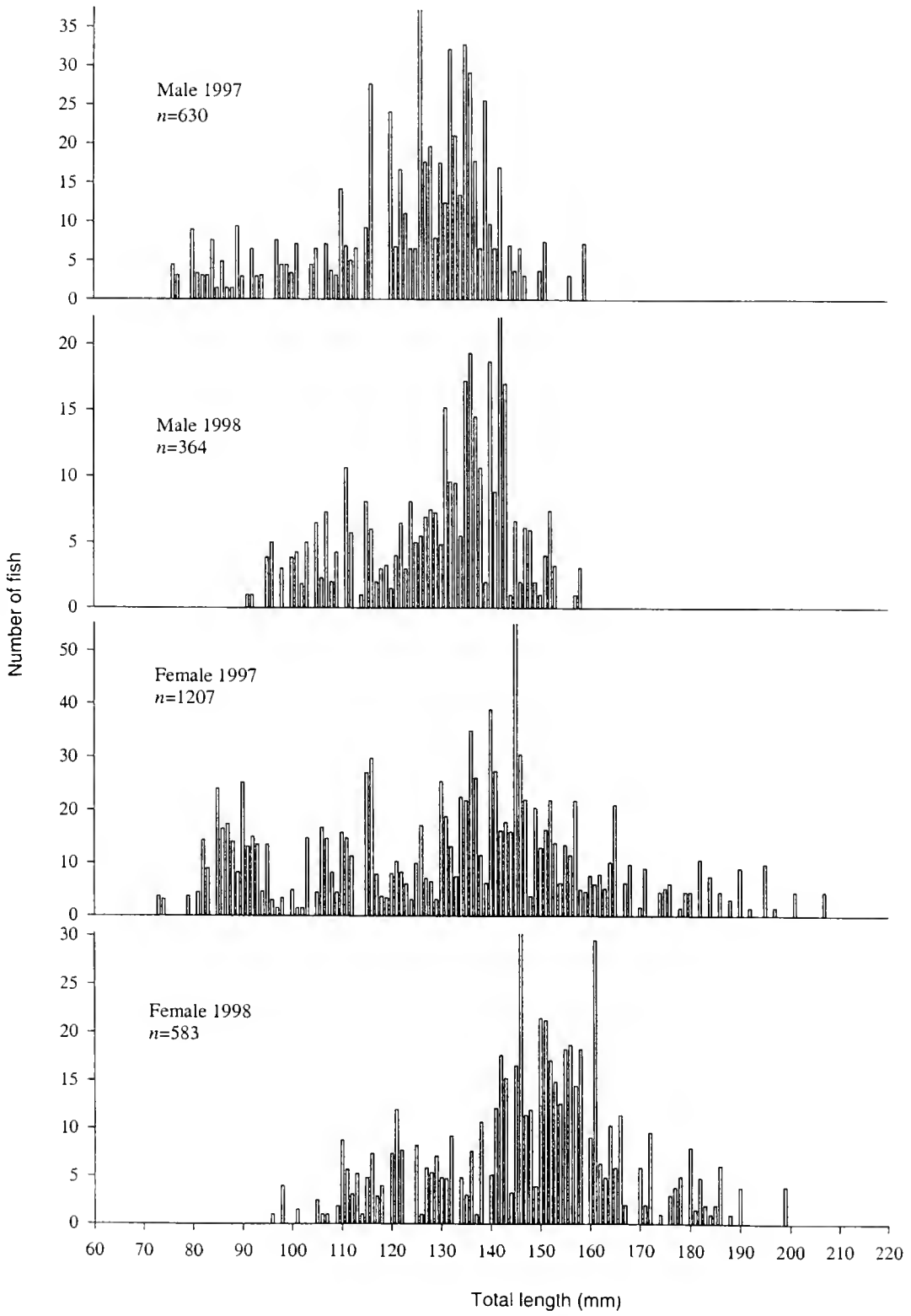

Figure 7

Length frequencies for male and female *Gymnocanthus pistilliger* for 1997 and 1998.

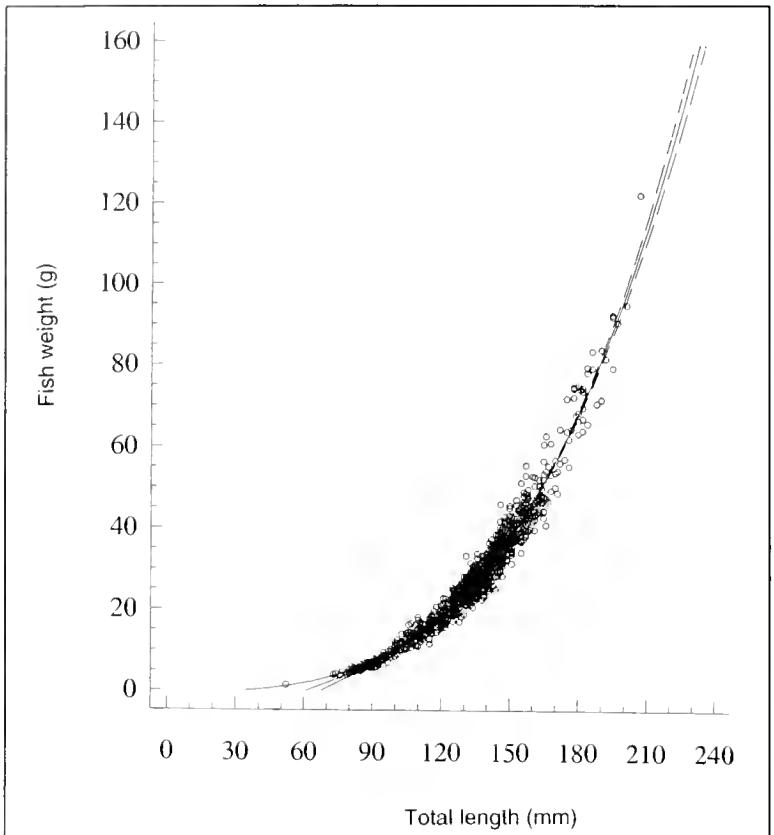

Figure 8

Weight-length relationship for *Gymnocanthus pistilliger* for 1997 and 1998 males (n=394) and females (n=596) combined. Solid line is the fitted model, dashed line represents the 95% confidence intervals. (P<0.01, SE=0.097).

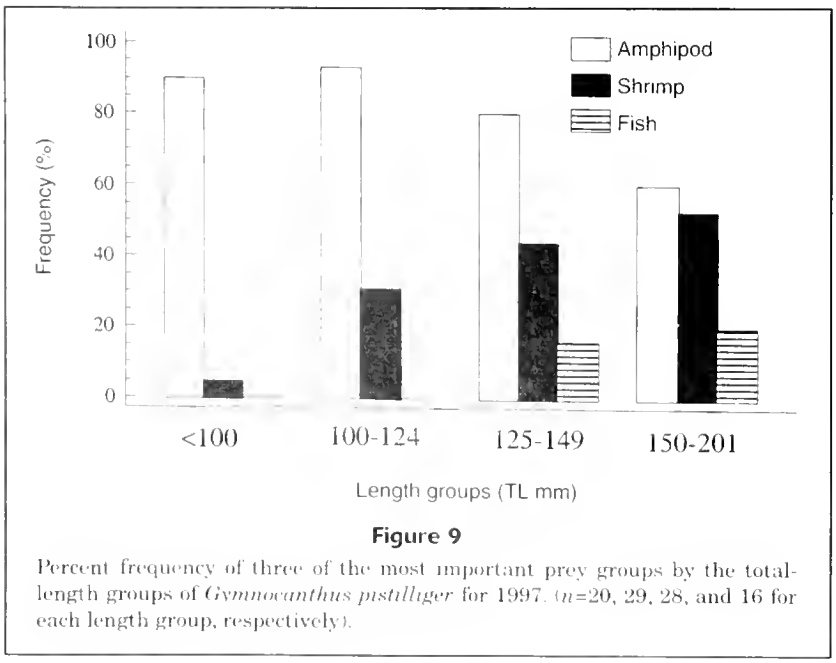

Figure 9

Percent frequency of three of the most important prey groups by the total-length groups of *Gymnocanthus pistilliger* for 1997. (n=20, 29, 28, and 16 for each length group, respectively).

and relative abundance. Pacific cod from Bristol Bay have been found to occasionally feed on *G. pistilliger*.[1] Bearded seals, *Erignathus barbatus*, whose distribution overlaps with *G. pistilliger*, consume sculpin species (>80% by volume) (Lowry et al., 1980) and may exploit *G. pistilliger*. However, many feeding studies on seals do not document which species of sculpins were found as prey items.

Gymnocanthus pistilliger is an abundant, short-lived cottid species occurring in shallow waters of the Bristol Bay area. Owing to its great abundance, it may make up an important part of the biomass resource in its range. There are distinct biological differences, such as male-to-female ratios with depth, maxi-

[1] Buckley, T. 1998. Personal commun. Alaska Fisheries Science Center, National Marine Fisheries Service, NOAA, 7600 Sand Point Way N E., Seattle, WA 98115

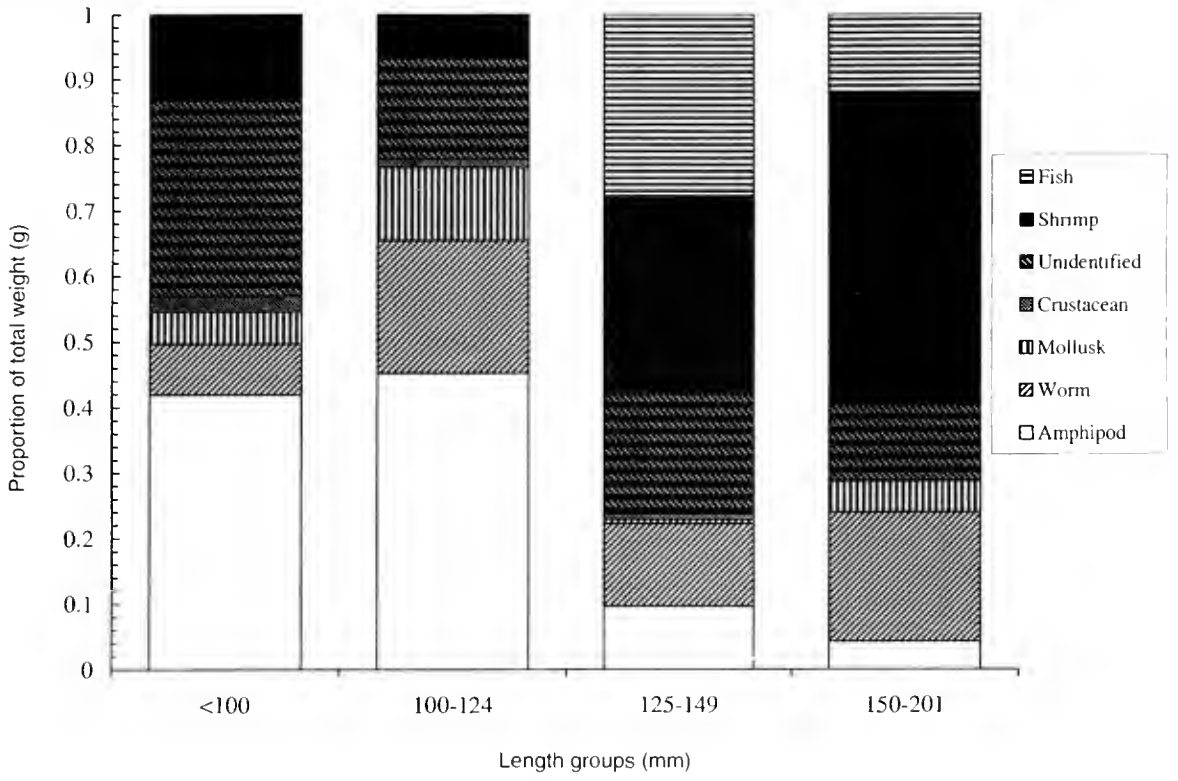

Figure 10

Proportion of the total weight of all prey groups by the total-length groups of *Gymnocanthus pistilliger* for 1997. (n=20, 29, 28, and 16 for each length group, respectively).

mum depth, maximum age and size, and diet preferences between western and eastern North Pacific populations. The eastern Bering Sea and Kamchatka shelf habitats have different currents, salinities, sediment types, shelf area, and temperatures (Pavlov and Pavlov, 1996) and these different oceanographic features may be reflected in the local adaptation patterns of *G. pistilliger* in this area.

Smith et. al (1997) reported on the biology of *Gymnocanthus tricuspis*, a congener of *G. pistilliger*, which is abundant in the Chukchi Sea and Norton Sound, Alaska (Allen and Smith, 1988). The two species of *Gymnocanthus* are very similar and probably occupy the same ecological niche in different environments. Smith et. al (1997) reported similar ages up to 9 years of age and similar densities and interannual variations in populations of *G. tricuspis* as were found for *G. pistilliger*. The ecological importance of *Gymnocanthus* throughout its range is not well understood but undoubtedly significant because of its high abundance and role as prey and competitive predator.

Acknowledgments

I would like to thank the crew and scientific parties of the vessels *Arcturus* and *Aldebaran* for their efforts in collecting data and in collecting biological specimens. I would also like to thank the reviewers Troy Buckley, Bill Gale, Doug Markle, Dave Somerton, Gary Stauffer, and Gary Walters and the unidentified journal reviewers. All gave many helpful suggestions that improved the content of the manuscript.

Literature cited

Allen, M. J., and G. B. Smith.
1988. Atlas and zoogeography of common fishes in the Bering Sea and Northeast Pacific. U.S. Dep. Commer., NOAA Tech. Report NMFS-66, 151 p.

Brodeur, R. D., and P. A. Livingston.
1988. Food habits and diet overlap of various eastern Bering Sea Fishes. U.S. Dep. Commer., NOAA Tech. Memo. NMFS/NWC-127, 76 p.

Corcobado-Onate, F.
1991. Food and daily ration of the rock sole *Lepidopsetta bilineata* (Pleuronectidae) in the eastern Bering Sea. Mar. Biol. 108:185–191.

Environmental Systems Research Institute.
1996. Arcview GIS, ver. 3.0. Environmental Systems Research Institute, Redlands, CA, 614 p.

Fadeev, N. S.
1968. Comparative outline of the biology of flatfishes in the southeastern part of the Bering Sea and condition of their

resources. *In* Soviet fisheries investigations in the northeast Pacific, part iV (P.A. Moiseev, ed.), p. 112–129. Translated from Russian by Isr. Prog. Sci. Transl., 1968. [Avail. Natl. Tech. Inf. Serv., Springfield, VA, as TT 67-51206.]

Grigorev, S. S., and N. S. Fadeev.
1995. Distribution of Alaska plaice, flathead sole, and Bering flounder eggs in the eastern Bering Sea during April–July, 1988–1990. *In* Proceedings of the international symposium on North Pacific flatfish p. 89–100. Alaska Sea Grant College Program Report 95-04, Univ. Alaska, Fairbanks, AK.

Holladay, B. A., and B. L. Norcross.
1995. Diet diversity as a mechanism for partitioning nursery grounds of pleuronectids. *In* Proceedings of the international symposium on North Pacific flatfish, p. 177–204. Alaska Sea Grant College Program 95-04, Univ. Alaska Fairbanks, AK.

Jandell.
1995. Sigmaplot 4.0. Jandell Scientific, P.O. Box 7005, San Rafael, CA 94912-7005.

Lang, G M., P. A Livingston, and B. S. Miller.
1995. Food habits of three congeneric flatfishes: yellowfin sole (*Pleuronectes asper*), rock sole (*P. bilineatus*), and Alaska plaice (*P. quadrituberculatus*) in the eastern Bering Sea. *In* Proceedings of the international symposium on North Pacific flatfish, p. 225–246. Alaska Sea Grant College Program 95-04, Univ. Alaska Fairbanks, AK.

Livingston, P. A., D. A. Dwyer, D. L. Wencker, M. S. Yang, and G. M. Lang.
1986. Trophic interactions of key fish species in the eastern Bering Sea Int. North Pac. Fish. Comm. Bull. 47:49–65.

Lowry, L. F., K. J. Frost, and J. J. Burns.
1980. Feeding of bearded seals in the Bering and Chukchi Seas and trophic interaction with Pacific walruses. Arctic 33(2):330–342.

Manugistics.
1997. Statgraphics Plus 2 1. Manugistics, Inc. Rockville, MD, 822 p.

McDonald, J., H. M. Feder, and M Hoberg.
1981 Bivalve mollusks of the southeastern Bering Sea. *In* The eastern Bering Sea shelf: oceanography and resources, vol. 2 (D. W. Hood and J.A. Calder, eds.), p. 1155–1204. U.S. Dep. Commer., NOAA., Washington, D.C.

Pavlov, V. K., and P. V. Pavlov.
1996. Oceanographic description of the Bering Sea. *In* Ecology of the Bering Sea: a review of Russian literature (O. A. Mathisen and K. O. Coyle (eds.), p. 1–96. Univ. Alaska Sea Grant College Program Report 96-01, Univ. Alaska. Fairbanks, AK.

Rose, C. S., and G. E. Walters.
1990. Trawl width during bottom trawl surveys: causes and consequences. *In* Proceedings of the symposium on application of stock assessment techniques to gadids (L.-L. Low, ed.), p. 57–67. Int. North Pac. Fish. Comm. Bull. 5.

Smith, R. L., W. E. Barber, M. Vallarino, J. Gillispie, and A. Ritchie.
1997. Population biology of the arctic staghorn sculpin in the northeastern Chukchi Sea. *In* Fish ecology in Arctic North America (J. Reynolds, ed), p. 133–139. Am. Fish. Soc. Symp. 19.

Tokranov, A.M.
1985. Feeding in species of sculpins of the genus *Gymnocanthus* (Cottidae) from Kamchatka waters. J. Ichthyol. 25(4):46–51.
1987. Reproduction of sculpins of the genus *Gymnocanthus* (Cottidae) in the coastal waters of Kamchatka. J. Ichthyol. 28(3):124–128.

Vdovin, A. N., G. V. Shvydkii, N. I. Afanas'eva, V. I. Rachkov, and N. M. Skokleneva.
1994. Spatial and temporal variability of distribution of staghorn sculpin in Peter the Great Bay. Russian J. Ecol. 25(4):53–59.

von Bertalanffy, L.
1957. Quantitative laws in metabolism and growth. Q. Rev. Biol. 2:217–231.

Wilson, D. E.
1973. Revision of the cottid genus *Gymnocanthus*, with a description of their osteology. M.S. thesis, Univ. British Columbia, Vancouver, Canada, 223 p.

Age, growth, mortality, and reproduction of red porgy, *Pagrus pagrus*, from the eastern Gulf of Mexico

Peter B. Hood

Florida Marine Research Institute
Florida Department of Environmental Protection
100 Eighth Avenue SE, St. Petersburg, Florida 33701-5095
Present address: Gulf of Mexico Fishery Management Council
3018 U.S. Hwy 301 North, Suite 1000
Tampa, Florida 33619-2266

E-mail address: peter.hood@gulfcouncil.org

Andrea K. Johnson

College of Veterinary Medicine
North Carolina State University
4700 Hillsborough St.
Raleigh, North Carolina 27606

Abstract—The red porgy (*Pagrus pagrus*) is an important component of the Gulf of Mexico reef-fish fishery, yet little information is available on this species's life history. We sampled 877 red porgy (194–489 mm TL) from the eastern Gulf of Mexico during 1995 and 1996 to assess their age structure, growth, mortality, spawning season, size and age at maturity, and batch fecundity. The average length of males was significantly greater than that of females, and the overall sex ratio (1:1.6 in favor of females) was significantly different from 1:1. Marginal-increment analysis indicated that one opaque ring is formed on red porgy otoliths during the late spring or early summer of each year. Ages ranged from 1 to 17 years, and most fish were 3 and 8 years old. Von Bertalanffy growth model parameters were L_∞=459 mm TL, K=0.111/yr, and t_0=–6.6 years for all aged fish. Growth rates in our study were lower than those in previous studies of Gulf of Mexico red porgy—perhaps the result of size-selective fishing. Pooled estimates of total instantaneous mortality were 0.62–0.87/yr based on recreational landings data and 0.54/yr based on commercial landings data. Red porgy are protogynous hermaphrodites. The length and age at which males composed 50% of the population was 345.5 mm TL and 5.3 years. Few immature females were observed in our collections (n=10). All females greater than 302 mm TL and age 4 were mature. Red porgy spawn during the winter and spring, and ripe females were caught from January to April.

Manuscript accepted 21 April 2000
Fish. Bull. 98:723–735 (2000).

The red porgy, *Pagrus pagrus*, occurs in the eastern Atlantic from the British Isles south to Angola and in the western Atlantic from New York to Argentina (Manooch and Hassler, 1978; Randall and Vergara, 1978). In the Gulf of Mexico (GOM), red porgy are usually found near hard-bottom areas off the west-central Florida coast and the Florida Middle Ground, and the Flower Garden Banks off Texas (Smith et al., 1975; Nelson, 1988). Studies of reef habitat along the southeastern United States indicate that red porgies are most common over inshore live-bottom habitats and over shelf-edge, rocky-rubble, and rock outcrop habitats (Grimes et al., 1982; Barans and Henry, 1984; Chester et al., 1984; Sedberry and Van Dolah, 1984).

Most red porgy caught in the GOM are landed in Florida. From 1986 to 1991, an average of 83.6% of the commercially caught and 76.7% of the recreationally caught red porgy were landed there (Goodyear and Thompson[1]). Red porgy are an important component of the Florida west coast commercial reef-fish fishery and rank thirteenth in total weight of reef fish landed in this area (Goodyear and Thompson[1]). In Florida commercial landings data, red porgy are not distinguished from other porgies. However, assuming that red porgies made up 50% of all porgies landed (Goodyear and Thompson[1]), the combined west coast 1995 and 1996 Florida landings of this species were estimated at 0.5 million pounds and had an estimated dockside value of $487,000 (Marine Fisheries Information System[2]). Over the same period, an estimated 242,000 red porgy were landed by anglers in Florida (Marine Recreational Fishery Statistics Survey[3]), 80% by charter boats or headboats (Goodyear and Thompson[1]).

Currently there are no regulations on red porgy harvest in the GOM. Fishery managers are concerned that the harvest of reef-fish species, such as red porgy, may increase if the fishery shifts effort from red snapper to these species because of increasing restrictions

[1] Goodyear, C. P., and N. B. Thompson. 1993. An evaluation of data on size and catch limits of red porgy in the Gulf of Mexico. Contribution report MIA-92/93-67. National Marine Fisheries Service, Southeast Fisheries Center, Miami Laboratory, Miami, FL.

[2] Marine Fisheries Information System. 1997. Unpubl. data. Florida Fish and Wildlife Conservation Commission, 100 Eighth Avenue SE, St. Petersburg, FL 33701-5095.

[3] Marine Recreational Fishery Statistics Survey (MRFSS). 1997. Unpubl. data. Fisheries Statistics Division, National Marine Fisheries Service, Department of Commerce, Silver Springs, MD 20910.

on the GOM red snapper fishery (Anonymous[4]). The red porgy fishery shifted from a predominately recreational fishery to a predominately commercial fishery between 1988 and 1991 (Goodyear and Thompson[1]). Owing to these changing dynamics within the red porgy fishery, the Reef Fish Stock Assessment Panel of the Gulf of Mexico Fishery Management Council recommended that age, growth, and reproduction studies be initiated for future stock assessments (Anonymous[4]). Red porgy are protogynous hermaphrodites and may be more susceptible to overfishing than gonochoristic reef-fish species such as snappers if size-selective fishing reduces the number of males available for spawning and thus limits the amount of sperm available for fertilization (Bannerot et al., 1987; Koenig et al., 1996).

Existing age and growth data for this species in the GOM are inadequate. Nelson (1988) used scales to age red porgy collected from the Flower Garden Banks off Texas in the early 1980s and reported a maximum age of 6 years. This value is much lower than maximum ages reported from other regions. Maximum ages, determined from scales, whole otoliths, and sectioned otoliths have ranged from 13 to 18 years (Manooch and Huntsman, 1977; Vassilopoulou and Papaconstantinou, 1992; Pajuelo and Lorenzo, 1996; Harris and McGovern, 1997; Vaughan[5]). Nelson (1988) suggested that the reason he did not observe fish as old as those observed by Manooch and Huntsman (15 years; 1977) was that fishing had removed older fish from the GOM. However, mortality rates in the South Atlantic Bight (SAB) are now greater than those reported by Nelson (1988) for the GOM, and SAB fish as old as age 18 have recently been reported by Vaughan.[5]

Little information is available on the reproductive biology of red porgy in the GOM. Female red porgy begin to transform into males at 221 mm fork length; however, the length at which females begin to mature in the GOM is unknown because the smallest female sampled by Nelson (1988) was 272 mm fork length and all females that he examined were mature. Spawning occurs in the winter and spring in the GOM, as has been reported for the SAB, Canary Islands, and Mediterranean Sea (Manooch, 1976; Nelson, 1988; Vassilopoulou and Papaconstantinou, 1992; Pajuelo and Lorenzo, 1996), although Ciechomski and Weiss (1973) reported, on the basis of larval collections, that red porgies may spawn in the Argentine Sea during the summer (December and January).

Basic life-history information is needed for use in assessments of red porgy stocks in the GOM. Although Nelson (1988) examined red porgy age, growth, and reproduction in the GOM; his study was limited by area (Flower Garden Banks off Texas), sample size (n=126), and aging structure (scales). Accurate ages are needed to develop growth models, develop age-length keys, and estimate total mortality. In addition, the annual periodicity of ring deposition in otoliths has not been validated for red porgy in the GOM. With the increasing reliance on estimates of spawning-potential ratios to describe a stock's condition, information on maturation schedules and sex ratios are also needed. The purpose of our study was to age eastern GOM red porgy accurately in order to develop age-length keys and growth models, to construct catch curves for deriving estimates of total mortality, and to describe the reproductive biology of this species.

Methods

Collections

Eastern GOM red porgy were sampled from headboat and commercial catches between October 1995 and September 1996. Total length (TL), fork length (FL), and standard length (SL) were measured to the nearest millimeter. Whole weight and gutted weight were measured to the nearest gram (g). The relationships between lengths, weights, and $\log_{10}$-transformed total lengths and weights were determined by least-squares regression (SAS Institute, Inc., 1985). Male and female regression lines of $\log_{10}$-transformed total lengths and weights were compared by using analysis of covariance (Snedecor and Cochran, 1971). Length-frequency distributions were compared by sample source and by sex by using the Kolmogorov-Smirnov test for goodness of fit (Sokal and Rohlf, 1981). All length data are reported as total length unless stated otherwise.

Age, growth, and mortality

Thin sections of otoliths (sagittae) were used to determine the ages of fish. Otoliths were removed and stored dry in culture wells. The left otolith was serially sectioned across its anterior-posterior midpoint at 0.5-mm intervals by making a transverse cut with an Isomet diamond saw. Mounted sections were placed on a black field, illuminated with reflected light, and examined with a binocular dissecting microscope. The magnified images of otolith sections were transmitted by means of video camera to a video monitor. The number of opaque zones and the radial measurements from the core to the last opaque zone and to the edge of the otolith (otolith radius, Fig. 1) were recorded from the monitor by using a computer-driven, data-acquisition software package (Optimas Corp., 1996). Marginal increments were measured as the distance between the last opaque zone and the edge of the otolith.

To determine if zone counts were repeatable between investigators, two readers independently examined sectioned otoliths collected from fish collected during July and August 1996 (n=241). After the first reading, readers examined the sections together and compared zone counts to form a consensus about what constituted a zone. The two readers then re-examined the sectioned otoliths independently, and counts were compared again. Because agreement between

[4] Anonymous. 1993. Final report of the reef fish stock assessment panel. Gulf of Mexico Fishery Management Council, 3018 U.S. Highway 301 N, Suite 1000, Tampa, FL 33619-2266.

[5] Vaughan, D. S. 1999. Population characteristics of the red porgy *Pagrus pagrus* from the U.S. Southern Atlantic Coast. Report prepared for the South Atlantic Fishery Management Council. National Marine Fisheries Service, Beaufort Laboratory, 101 Pivers Island Road, Beaufort, NC 28516.

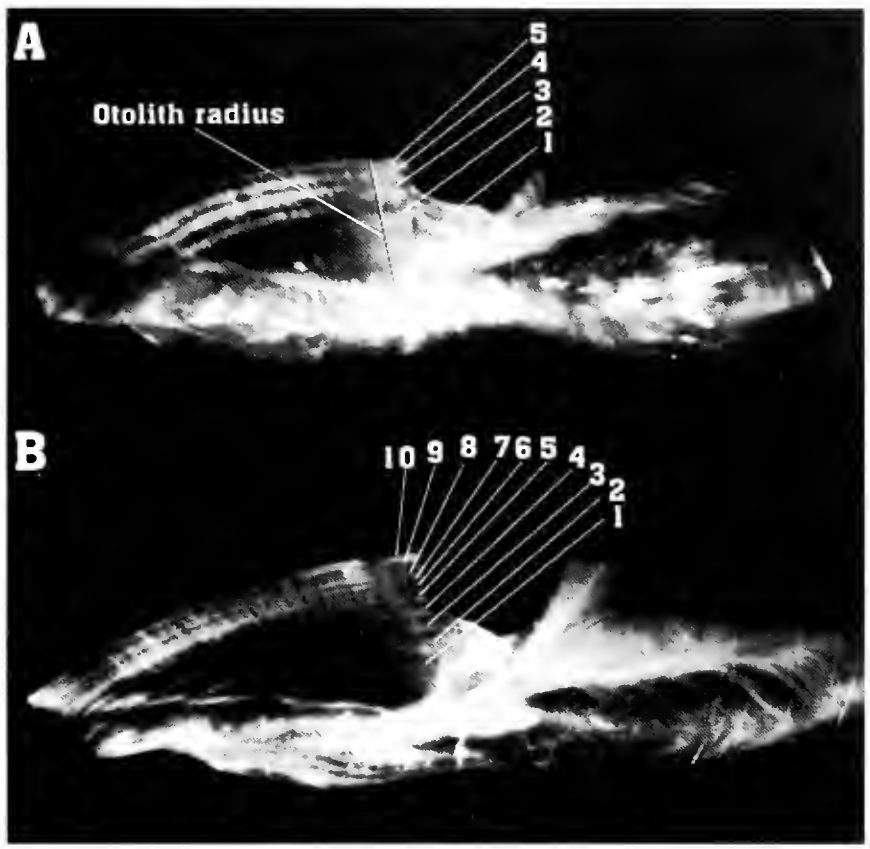

Figure 1

Sectioned sagittae from (**A**) a 5-year-old (345-mm-TL) and (**B**) a 10-year-old (485-mm-TL) eastern Gulf of Mexico red porgy. The 5-year-old fish was caught in September 1996, and the 10-year-old fish was caught in April 1996.

readers was high (86%) for the second readings, one reader read the remaining otoliths to determine age. Each of the remaining otolith sections was read three times, and annulus counts were accepted for ages only if at least two of the three separate readings were the same. Age was considered to be the count with the highest frequency of occurrence. To validate annulus periodicity, marginal increments and their medians were plotted by month for each age and compared for consistent temporal patterns.

Age in years was estimated as the number of opaque rings; therefore, length at age included any growth that occurred after the last opaque ring was formed. Length at age between sampling sources was compared by using an unbalanced two-way analysis of variance (SAS Institute, Inc., 1985). Mean observed length at age was calculated for males, females, and for all aged fish. Age and length data were fitted to a von Bertalanffy growth model with nonlinear regression (SAS Institute, Inc., 1985). We calculated an adjusted r^2 for the resulting curve by using methods described by Helland (1987).

We used age-frequency data from this study to estimate mortality rates from Florida commercial and recreational length data for Florida. Because the number of red porgy measured by the Trip Interview Program[6] and MRFSS[3] were low, we pooled the data from the most recent years for which data were available. Length data from commercial landings were obtained from the TIP[6] from 1992 to 1994 and in 1996. Length data from recreational landings were obtained from the MRFSS[3] and the National Marine Fisheries Service's Headboat Survey[7] and were pooled for years 1990–1996. Because red porgies are protogynous hermaphrodites, we pooled sexed and unsexed fish to generate the catch curves. Instantaneous mortality and survivorship rates were estimated by the Chapman-Robson method (Youngs and Robson, 1978). Age at full recruitment was estimated from the catch curve as being one year older than the age with the greatest catch.

[6] Trip Interview Program (TIP). 1997. Unpubl. data. Florida Fish and Wildlife Conservation Commission, 100 Eigth Avenue, SE, St. Petersburg, FL 33701-5095.

[7] National Marine Fisheries Service Headboat Survey. 1999. Unpubl. data. Beaufort Laboratory, 101 Pivers Island Rd., Beaufort, NC 28516-9722.

Reproduction

Reproductive analyses were based on gonad weights and a histological examination of gonadal tissue. Fish sampled were put on ice soon after capture, and we sampled fish within 36 hours after their capture by the recreational fishery and 10 days after their capture by the commercial fishery. Whole gonads were weighed to the nearest 0.1 g. Some fish were gutted before they were landed. If a portion of gonad was present, it was removed for histological preparation; if none was present, the sex of the fish was listed as unknown. Gonads were fixed in 10% buffered formalin for approximately one week, rinsed in water, and then transferred to 70% ethanol. We removed a sample of tissue from the middle of the preserved gonad and embedded it in paraffin. Several 5.0-µm sections were serially cut from the sample, stained with Harris's haematoxylin, counterstained with eosin (Humason, 1972), and examined under a compound microscope to determine sex and developmental state of the gonads. For ovaries, we staged oocytes as being primary growth, cortical alveoli, or vitellogenic oocytes, or as mature oocytes by using criteria developed by Moe (1969), Wallace and Selman (1981), and West (1990). The frequency of occurrence of oocyte developmental stages (including atretic bodies and postovulatory follicles) was tabulated for approximately 300 oocytes from each ovary by using a computer-driven data-acquisition software package (Optimas Corp., 1996). Mature ovaries were distinguished from immature ovaries by the presence of atretic bodies, advanced oocyte development stages (vitellogenic or mature oocytes), or both. Testes were assigned to development classes (Table 1) by using a modified classification scheme developed from Hyder (1969) and Moe (1969). Transitional males (individuals with gonads in transition from ovaries to testes) were identified according to the criteria of Sadovy and Shapiro (1987).

Sex ratios for all sexed fish were compared for significant differences from 1:1 by using the chi-square test (Snedecor and Cochran, 1971). The length and age at which 50% of the population consisted of males was estimated by fitting a logistic curve to length and age data with sex as a binary response equal to zero for females and to one for males. The curves were fitted to the data by using nonlinear regression (Jandel Corp., 1992).

Reproductive seasonality was determined by examining the monthly changes in gonad stages, the monthly distribution of oocyte stages, and the monthly changes in the gonosomatic index (GSI). The GSI was calculated by using the following equation:

$$GSI = gonad\ weight/(whole\ weight - gonad\ weight).$$

Table 1
Development classes for testes of red porgy.

Classes	Testes
Transitional	Massive atresia of oocytes. Spermatogonia, spermatocytes, and (or) spermatids developing in lumen of testicular lumen. Tailed sperm may be present.
Resting	Mostly spermatogonia and spermatocytes present in the central lobules. Free spermatozoa in the lumen of the lobule, and brown bodies (Grier, 1987) may be present.
Developing	Mostly spermatocytes and spermatids present in the central lobules, free spermatozoa in the lumen of the lobule.
Ripe	Mostly spermatozoa found in the central lobules and in the lumen of the lobule; all or later stages of spermatogenesis occurring in the peripheral lobules.
Spent	Few free spermatozoa in the lumen of the lobule; early stages of spermatogenesis in the peripheral lobules.

Results

Collections

We sampled 877 red porgy that ranged from 194 to 489 mm in length. Although we did not record the locations where fishermen caught their fish, most fishing effort was directed in the Florida Middle Ground and off west central Florida. Most fish (92%) were in length classes between 251 and 400 mm long and had a modal length class of 326–350 mm (Fig. 2). Relationships between lengths, between whole weight and gutted weight, and between TL and weight are shown in Table 2. Male and female data were pooled for the weight-length relationship because sex-specific regression equations were not significantly different (ANCOVA, $P>0.05$). Most of the fish sampled were from the recreational fishery (n=601), and they ranged in length from 205 to 455 mm (Fig. 2). Fish from the commercial fishery (n=276) ranged from 265 to 489 mm (Fig. 2). The mean length of recreationally caught fish (321 mm, SE=40) was significantly less than the mean length of commercially caught fish (350 mm, SE=40; t-test, $P<0.001$). The length-frequency distributions for commercially and recreationally caught fish were significantly different (D=0.287, $P<0.001$). Males (n=331) ranged in length from 248 to 470 mm and females (n=456) from 205 to 455 mm (Table 3). The mean length of males (341 mm, SE=36.3) was significantly greater than that of females (316.2 mm, SE=40.5; t-test, $P<0.001$). The length-frequency distributions for males and females were significantly different (D=0.317, $P<0.001$). The largest fish examined (489 mm) had been gutted; therefore the sex of the specimen was unknown.

Age, growth, and mortality

Under reflected light, alternating opaque (white) and translucent (dark) zones were evident in red porgy otoliths (Fig. 1). Two readers examined a subsample of 241 otoliths, and 50% of their readings were in agreement. Most of the disagreements (71%) differed by only one

Table 2

The linear relationships among lengths, among weights, and between weight and length, and the logistic proportion of males by age and total length for red porgy from the eastern Gulf of Mexico. SL = standard length (mm), FL = fork length (mm), TL = total length (mm), WT = whole weight (gm), GWT = gutted weight (gm). n = the number of fish sampled, and the standard error is given in parentheses.

			$Y = a + bX$		
Y	X	n	a	b	r^2
SL	*FL*	876	−5.3 (1.4)	0.89 (0.005)	0.97
SL	*TL*	869	−10.1 (1.6)	0.78 (0.005)	0.97
FL	*SL*	876	13.0 (1.5)	1.09 (0.005)	0.97
FL	*TL*	867	−4.9 (1.0)	0.87 (0.003)	0.99
TL	*SL*	869	24.5 (2.0)	1.24 (0.01)	0.97
TL	*FL*	867	8.9 (1.1)	1.13 (0.004)	0.99
WT	*GWT*	121	6.0 (3.4)	1.05 (0.008)	0.99
$\log_{10}WT$	$\log_{10}TL$	572	−4.51 (0.053)	2.86 (0.216)	0.97
$\log_{10}GWT$	$\log_{10}TL$	272	−4.45 (0.08)	2.82 (0.32)	0.97
			$Y = 1/(1+e^{(a(x-b))})$		
Proportion male	*Age*	781	−0.703 (0.067)	5.332 (0.118)	
Proportion male	*TL*	784	−0.017 (0.002)	345.5 (5.1)	

zone. A second independent reading of the subsample by both readers resulted in a higher agreement rate of 86% and indicated that both readers were consistently identifying the same features as opaque zones. Of 877 sectioned otoliths examined, 852 (97%) could be assigned ages. Of the otoliths that could be aged, measurements for marginal-increment analyses could not be made for 40 (4.6%) because of broken or occluded areas along the otolith radius.

Analyses of marginal-increment data for fish ages 2–10 yr suggested that opaque zones were formed once a year during the late spring to early summer (Fig. 3). Because of small sample sizes, we pooled marginal-increment data for ages 8 to 10. During the spring and early summer, the widest increments (ring formation was imminent) and the narrowest increments (ring formation was just completed) were present, indicating that rings were being formed during this period. In addition, monthly median marginal increments for ages 2–10 had a consistent yearly pattern of high median values from October to April and low values from June to August (Fig. 3).

Ages ranged from 1 to 17 years and most fish (83%) were between ages 3 and 8. No females older than 10 years were observed. Initial growth of red porgy was rapid, and fish attained a mean length of 260 mm during their second year (age 1; Table 4). Subsequent increases in length, however, were low (<40 mm/yr). Average lengths at age were not significantly different between males and females ($F_{8,741}$=1.5, P=0.155) or between sampling sources ($F_{8,817}$=0.96, P=0.462). The

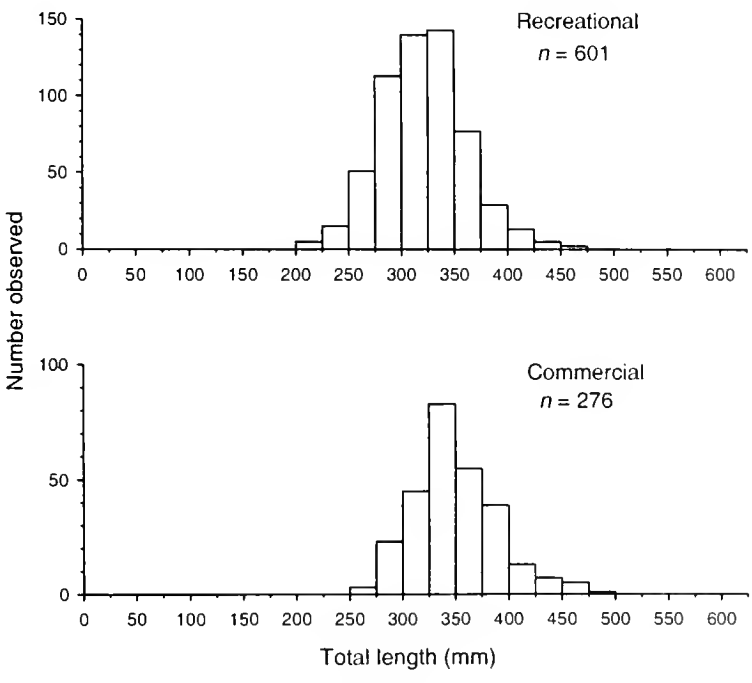

Figure 2

Total lengths of red porgy from the eastern Gulf of Mexico by sampling source.

estimated von Bertalanffy growth parameters (standard error) for all aged fish (n=854) were L_∞=459(31) mm, K=0.111 (0.028)/yr, and t_0=–6.6 (1.3) yr. Predicted lengths at age were similar to mean lengths at age (Table 4, Fig. 4). The adjusted r^2 for the growth model was 0.40.

Fishery-based length-frequency data were transformed into age frequencies by using age- length keys constructed from the ages of the fish in our study. Full recruitment into both the recreational and commercial fisheries occurred at age 4. Survivorship (standard error) of red porgy was estimated to be 0.42(0.001) from the headboat fishery data, 0.54(0.046) from the recreational fishery data and 0.58(0.014) from the commercial fishery data. Instantaneous mortality estimates (Z=–ln survivorship) were 0.87

Table 3

Number of males, number of females, and percentage of male red porgy in relation to the total number of sexed individuals by length and age from the eastern Gulf of Mexico.

Length (mm TL)	No. of females	No. of males	% males	Age (yr)	No. of females	No. of males	% males
<200	1	—	—	1	6	1	14.29
201–225	4	—	—	2	55	5	8.33
226–250	14	1	6.67	3	100	20	16.67
251–375	48	6	11.11	4	124	38	23.46
276–300	98	37	27.41	5	89	89	50.00
301–325	113	60	34.68	6	49	63	56.25
326–350	95	113	54.33	7	15	64	81.01
351–375	46	63	57.80	8	6	28	82.35
376–400	22	29	56.86	9	2	9	81.82
401–400	7	16	69.57	10	3	10	76.92
426–450	3	5	62.50	11+		5	100
451–475	2	1	33.33				

Table 4

Mean empirical and predicted total lengths (mm TL) of female, male, and all red porgy sampled from the eastern Gulf of Mexico. Standard error is given in parentheses, and n = number of fish examined

	Female			Male			All fish			
Age (yr)	n	Mean empirical	Range	n	Mean empirical	Range	n	Mean empirical	Range	Predicted
1	6	253 (36.7)	194–290	1	298	—	7	260 (37.4)	194–298	262
2	55	292 (31.8)	205–363	5	311 (40.9)	285–382	61	294 (32.6)	205–382	283
3	99	288 (29.1)	230–368	20	300 (28.9)	248–350	124	291 (31.2)	220–378	302
4	122	315 (29.9)	245–402	38	318 (30.0)	258–372	171	316 (29.7)	245–402	318
5	88	337 (36.5)	265–455	87	337 (32.4)	276–435	189	339 (34.8)	265–455	333
6	48	344 (25.3)	290–405	63	346 (26.1)	300–420	134	348 (26.9)	290–426	347
7	15	360 (21.9)	330–397	62	351 (32.0)	288–425	88	357 (33.3)	288–489	358
8	6	364 (33.1)	326–415	27	340 (20.2)	295–380	38	348 (27.0)	295–425	369
9	2	410 (46.0)	377–442	9	379 (36.7)	330–450	13	388 (40.0)	330–452	379
10	3	379 (39.6)	334–407	9	407 (38.5)	348–470	18	396 (46.5)	321–470	387
11				1	405		4	415 (20.9)	390–436	395
12				1	397	—	2	393 (5.7)	389–397	402
13				1	393	—	1	393	—	408
14				1	389	—	2	377 (17.7)	364–389	413
15							1	445	—	418
17				1	438	—	1	438	—	426

for the headboat fishery, 0.62 for the recreational fishery, and 0.54 for the commercial fishery.

Reproduction

Red porgy are protogynous hermaphrodites. We classified 68 males (8% of the sexed fish) as transitional-sex-stage fish because of the simultaneous presence of deteriorating ovarian tissue and proliferating male tissue. We determined that the gonadal structure was delimited (Sadovy and Shapiro, 1987) because connective tissue separated testicular from ovarian tissue. Sex ratios and length and age data were consistent with monandric protogyny. The overall sex ratio of males to females was 1.0:1.6, which was significantly different from 1:1, χ^2=51.0, df=1, P<0.001). In addition, the modal length class and age of females (301–325 mm; 4 yr) were less than the modal length class and age of males (326–350 mm; 5 yr; Table 3). We also did not observe any males less than 298 mm, whereas the smallest female was 194 mm. The estimated age and length at which 50% of fish in our samples were males were 5.3 years and 345.5 mm (Table 2).

Few immature female (n=10) red porgies were observed in our samples. We did not find any age-1 (n=6) immature female red porgy, and most age-2 (91%, n=55) and age-3 (96%, n=99) females were sexually mature. All females age 4 or older were sexually mature. Immature females ranged in length from 194 to 302 mm and the smallest mature female was 230 mm. More than half (69%) of the fish observed were mature by the length class 226–250 mm (n=17).

Red porgy in the eastern GOM spawn from December to April. During this time period, ovaries containing either mature oocytes (spawning is imminent) or postovulatory follicles (spawning has recently occurred) were observed (Fig. 5). Throughout the rest of the year, ovaries progressed from containing only primary growth oocytes (May to August) to containing cortical alveoli and vitellogenic oocytes (September to November; Fig. 5). Ripe males were observed in every month except July and September (Fig. 6). Immature (transitional-sex-stage) males were captured throughout most of the year, but they were absent or rare just prior to and during the spawning season (November to April). For both sexes, median GSI's were low from May to October (<0.015 for females and <0.005 for males; Fig. 7). In January, median GSI's increased dramatically (0.035 for females and 0.019 for males) and then gradually decreased through August.

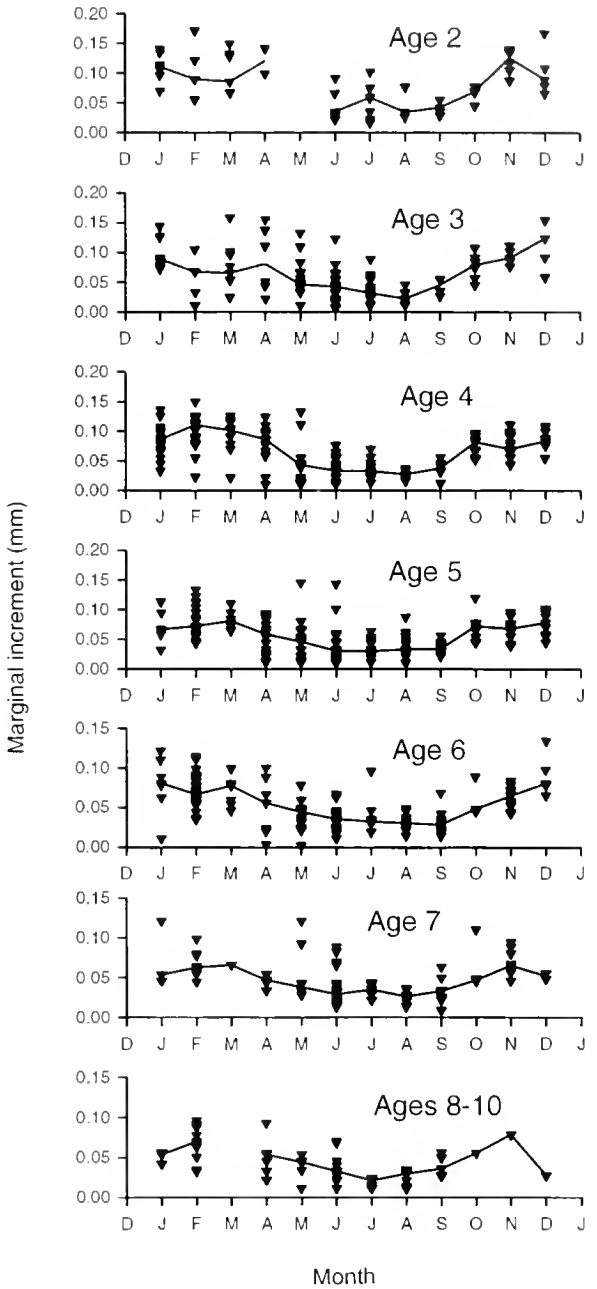

Figure 3

Marginal increments from sectioned otoliths of red porgy ages 2–10 years from the eastern Gulf of Mexico. Median monthly increments are identified by the solid line. Because of low sample sizes, ages 8–10 were pooled.

Discussion

Collections

There appeared to be a trend towards smaller red porgy in the GOM from the 1980s to the 1990s. Although landings have not increased since the early 1980s (Gulf-wide average annual landings of approximately 250,000 lbs; [Goodyear and Thompson[1]]), the length structure of the population has changed. Between 1990 and 1992, modal lengths of commercially caught fish have decreased from 357 mm to 279 mm for fish landed in Florida and from 381 mm to 254 mm for fish landed in Louisiana and Texas (Goodyear and Thompson[1]). In addition, there has been a decline from 508 mm to 381 mm in the maximum length of fish caught from headboats during 1979–91 (Goodyear and

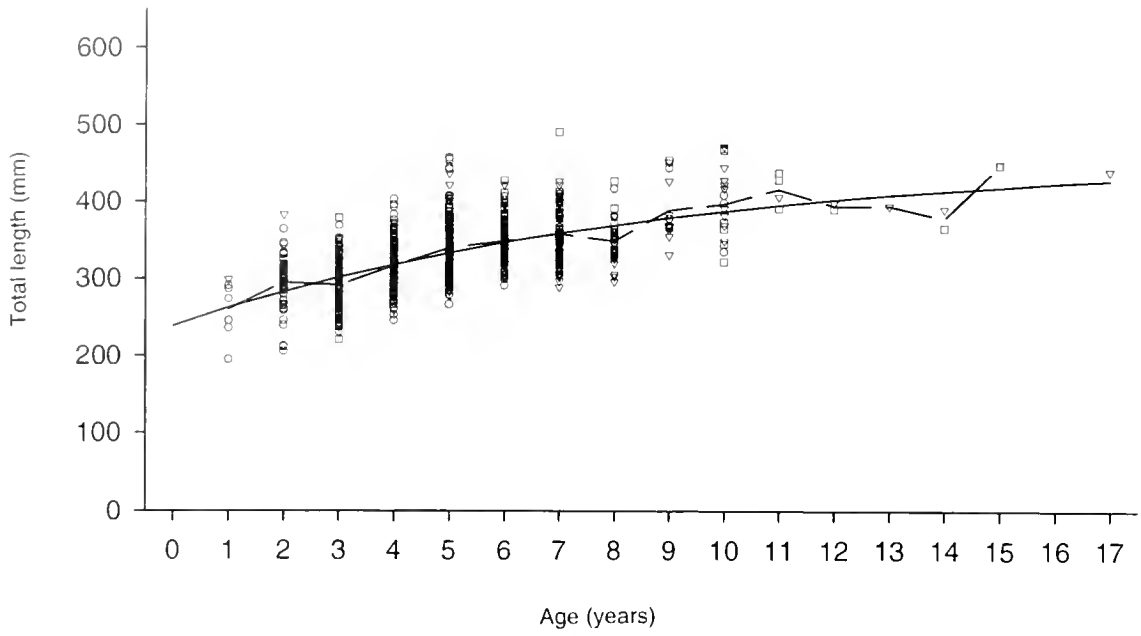

Figure 4

Total length at age, mean length at age (dashed line), and predicted length at age (solid line) of red porgy from the eastern Gulf of Mexico. Circles=females, triangles=males, and squares=unknown sex.

Thompson[1]). These trends may reflect differences between the modal length class (326–350 mm) of fish we sampled from the eastern GOM and earlier collections (349–404 mm[5]) from the Flower Garden Banks off Texas by Nelson (1988). However, because we did not obtain specific depth and gear information for fish we sampled, we cannot discount these factors to explain differences between our samples and Nelson's (1988). Decreases in average and modal lengths for red porgy in the SAB have been associated with increased fishing pressure (Collins and Sedberry, 1991; Harris and McGovern, 1997; Vaughan[5]).

Age, growth, and mortality

Although scales and otoliths have been used to determine the ages of red porgy, which structure is used, as well as how it is prepared, affects ring interpretation. Although we did not use scales to age red porgy, comparisons of ring counts determined from scales and whole otoliths from the same fish have had between 80% and 90% agreement rates (Manooch and Huntsman, 1977; Machias et al., 1998). However, Manooch and Huntsman (1977) cautioned that as age increases, both scales and whole otoliths become more difficult to interpret because the rings at the outer edge become difficult to discern. We used sectioned red porgy otoliths because most studies that have compared aging structures have found that sectioned otoliths provide more reliable estimates of age than either scales or whole otoliths, particularly for older fish (e.g. Beamish and McFarlane, 1983; Collins et al., 1987; Lowerre-Barbieri et al., 1994; Crabtree et al., 1996; Taylor et al.[9]). Sectioning otoliths also increases readability rates; Pajuelo and Lorenzo (1996) and our study were able to assign ages to 81% and 97% of the otoliths, respectively. Whole otoliths and scales used to age red porgy have provided mixed success in assigning ages to fish (54–90%; Manooch and Huntsman, 1977; Nelson, 1988; Vassilopoulou and Papaconstantinou, 1992; Harris and McGovern, 1997; Machias et al., 1998).

Opaque zones in red porgy otoliths appear to be formed annually. From marginal-increment analyses, we found that GOM red porgy form one opaque zone per year in the late spring and summer. Marginal-increment analysis has also been used by others to validate annual zone deposition in aging structures (Manooch and Huntsman, 1977; Nelson, 1988; Pajuelo and Lorenzo, 1996). Additionally, Machias et al. (1998) reported that red porgy from the Mediterranean Sea held in ponds for known periods of time formed annual rings in both scales and otoliths, and Collins et al. (1996) recaptured one oxytetracycline-injected red porgy (released in the SAB) in which the loca-

[5] Reported lengths were transformed from FL to TL by using the equation from Table 2.

[9] Taylor, R. G., J. A. Whittington, H. J. Grier, and R. E. Crabtree. In prep. Age, growth, maturation, and protandric sex reversal in the common snook, *Centropomus undecimalis*, from South Florida waters. Florida Department of Environmental Protection, 100 Eighth Avenue SE, St. Petersburg, FL 33701-5095.

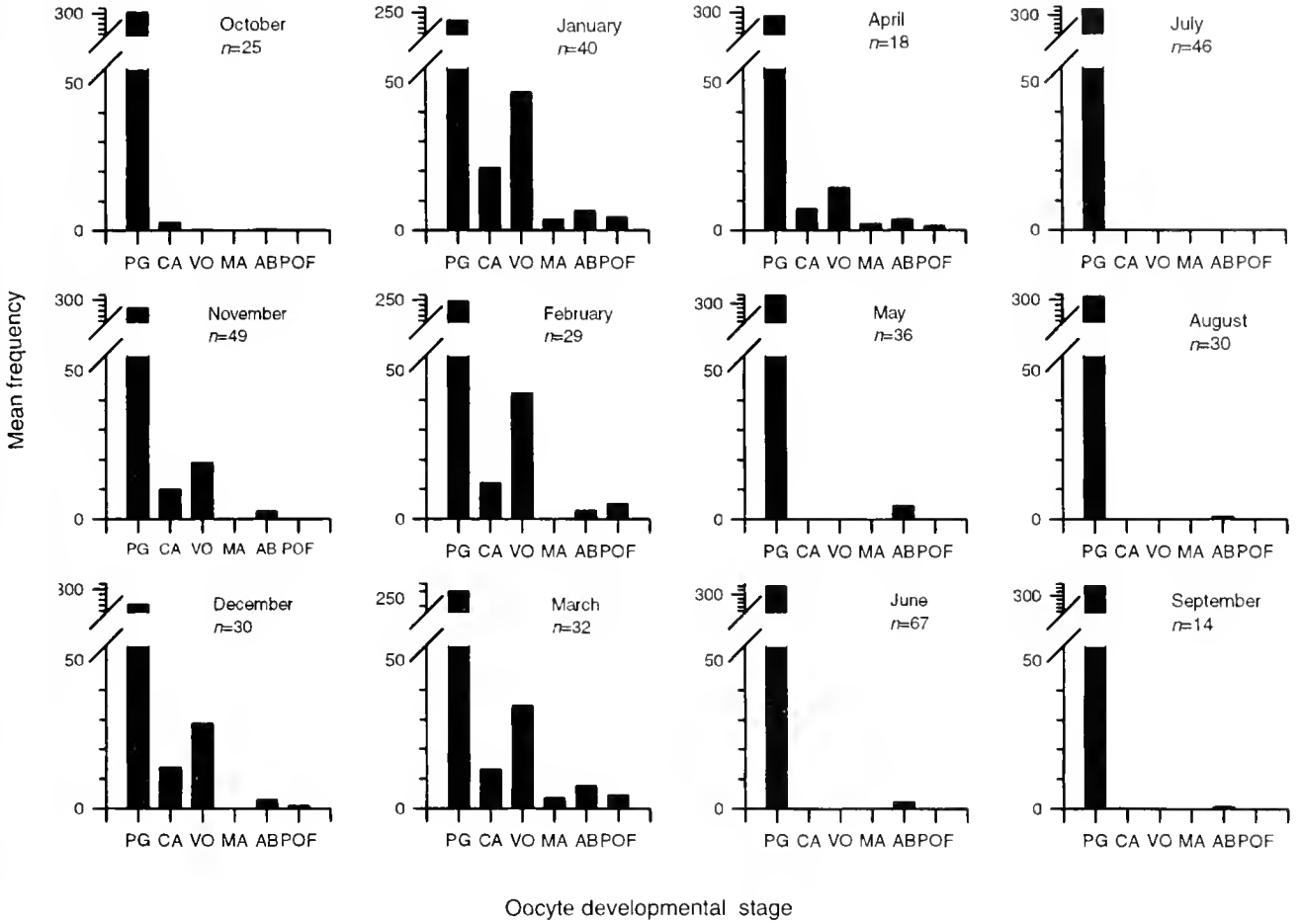

Figure 5

Average frequency of occurrence of oocyte developmental stages by month for red porgy from the eastern Gulf of Mexico. PG = primary growth oocyte, CA = cortical alveolar oocyte, VO = vitellogenic oocyte, MA = mature oocyte, AB = atretic body, and POF = postovulatory follicle.

tion of the oxytetracycline mark was consistent with the annual formation of the opaque zone.

We confirmed that red porgy are moderately long-lived fish (Manooch and Hassler, 1978). The oldest individual we aged was 17 years old, a year younger than the sectioned-otolith-based maximum age of 18 years reported for red porgy in the SAB (Vaughan[5]). Nelson (1988) reported the maximum scale-based age for this species in the GOM was 6 years and suggested that the reason for the lower maximum age than that found in the SAB (15 years by Manooch and Huntsman, 1977) was that older fish had been eliminated through higher rates of mortality. He reported that mortality rates in the western GOM (Z=0.86/yr) were much higher than those in the SAB (Z=0.44/yr; Manooch and Huntsman, 1977). However, this argument is circular because Nelson (1988) estimated mortality from catch curves that had been based on the age structure of the fish he sampled. If his age distribution was truncated owing to sampling or aging bias, then his estimates of mortality would have been higher than the true rate. Nelson's (1988) sample size was small (n=126) and geographically restricted (Flower Garden Banks off Texas) compared with the sample size of Manooch and Huntsman (1977), which was large (n=1777) and from a broad geographic region (SAB).

Our observed and predicted lengths at age were lower than those reported by Nelson (1988) for the Flower Garden off Texas. It is difficult to assess why our observed and predicted lengths at age were lower, but the limited sample size of Nelson (1988) (n=126) may not be representative of the GOM population. Other factors that may contribute to these differences include regional differences in growth within the GOM, depth of capture, hook size, or biases between the aging structures. However, Goodyear and Thompson[1] reported that the depths where red porgy were most commonly captured by GOM fisheries overlapped the depth range in which most of the fish sampled by Nelson (1988) were captured (60–90 m). Hook size

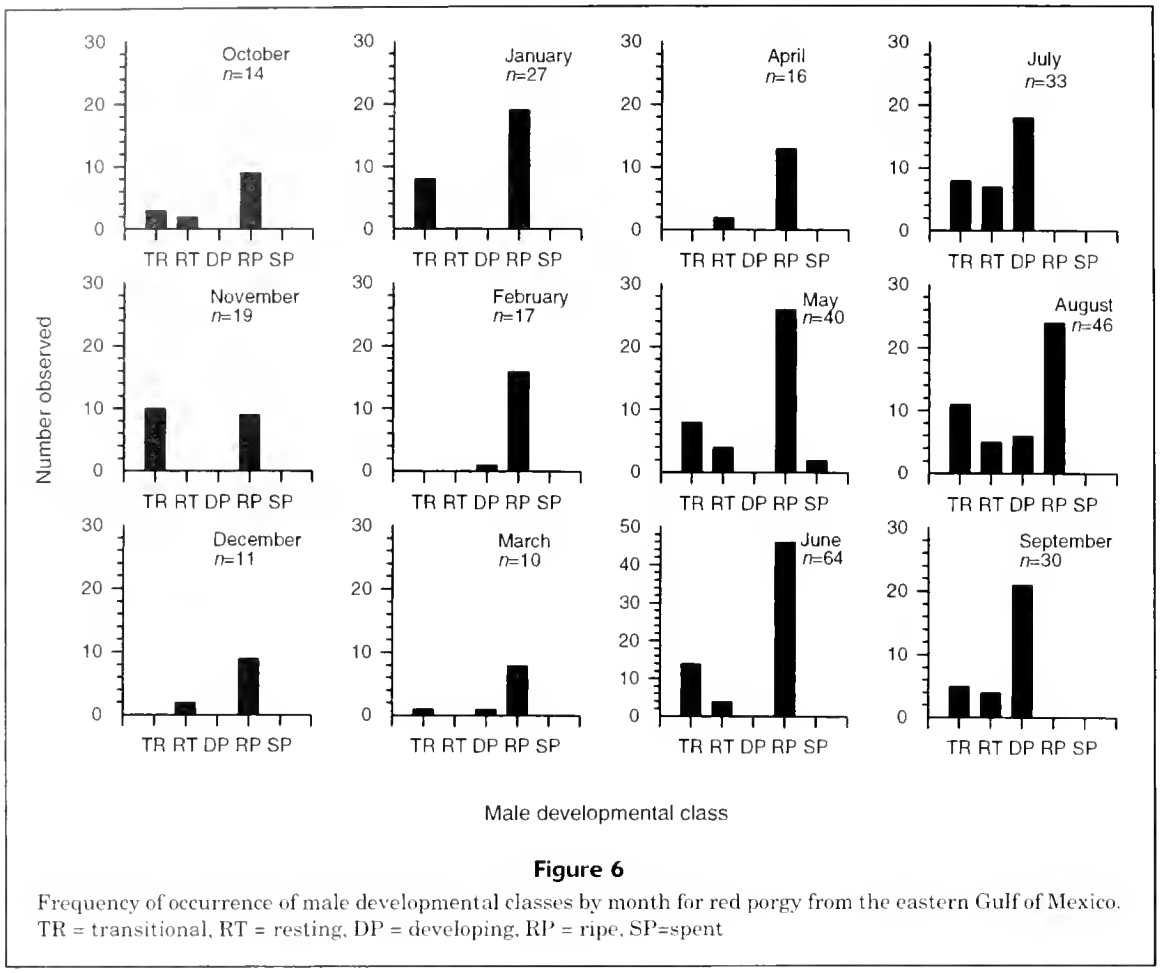

Figure 6

Frequency of occurrence of male developmental classes by month for red porgy from the eastern Gulf of Mexico. TR = transitional, RT = resting, DP = developing, RP = ripe, SP=spent

may have had a limited effect on size differences because the mean lengths at age of fish we sampled that were caught with commercial or recreational gear were not significantly different, and Nelson (1988) reported that the hook sizes did not seem to affect the size distributions of several fish species captured in his study. Finally, biases usually associated with aging structures occur at older ages when rings crowd together at the scale edge and are harder to interpret. Manooch and Huntsman (1977) were able to use scales to age red porgy to 15 years, a much greater age than the maximum age of 6 years reported by Nelson (1988). Therefore, Nelson's estimated ages may accurately describe the ages of the fish he sampled.

Changes in the average length at age between the early 1980s and present may also be the result of size-selective fishing over time, i.e. if larger fish were more vulnerable to capture, then faster-growing fish within an age class would be selectively removed from the population and the result would be a reduced mean size at age for older age classes and an underestimated L_∞ (Ricker, 1969, Pitcher and Hart, 1982). We could not demonstrate size-selective fishing pressure, but there was a shift in the size structure of red porgy stocks in the GOM towards smaller fish (Goodyear and Thompson[1])—a shift that suggests that fishing pressure is affecting the size structure of the stock.

For SAB red porgy stocks, Harris and McGovern (1997) have suggested that size-selective fishing and increases in fishing mortality have caused a decrease in mean lengths at age and L_∞ in SAB red porgy stocks. The average lengths at age 6 years decreased from 451 mm in 1972–74 (Manooch and Huntsman, 1977) to 363 mm[8] in 1991–94 (Harris and McGovern, 1997), and estimated L_∞ decreased from 763 mm and 528 mm[8] for 1972–74 (Manooch and Huntsman, 1977; Harris and McGovern, 1997) to 412 mm[8] for 1991–94 (Harris and McGovern, 1997). Although differences in sampling source (fishery dependent vs. fishery independent) between Manooch and Huntsman (1977) and Harris and McGovern (1997) may have accounted for the observed differences, Harris and McGovern (1997) noted that the same changes occurred from 1979 to 1994 in their fishery-independent samples. Similar trends have been reported for vermilion snapper (*Rhomboplites aurorubens*) in the GOM (Hood and Johnson, 1999) and in the SAB (Zhao et al., 1997), which are a part of the same fishery as red porgy. However, for the SAB, Potts et al. (1998) suggested that differences in gear types may have accounted for differences in length at age reported by Zhao et al. (1997).

Red porgy were fully recruited into the GOM recreational and commercial fisheries by age 4. This is the same

age that red porgy in the Flower Garden Banks were fully recruited to the sampling gear (primarily hook-and-line) used by Nelson (1988). In the SAB, the age of full recruitment decreased from age 5 in 1972–83 to age 4 in 1984–86, probably because of higher exploitation rates (Vaughan et al., 1992). Huntsman et al. (1983) reported that the age of full recruitment to the SAB head boat fishery was 4.1–4.3 years.

Our estimates of Z (0.54–0.87/yr) are within the range of reported estimates for other populations sustaining fishing pressure. Nelson (1988) estimated Z to be 0.86/yr for fish from the Flower Garden Banks off Texas in 1980–82. In the SAB, estimates of Z increased from the early 1970s through the early 1990s: Z = 0.64/yr for SAB populations from 1972 to 1974 (Manooch and Huntsman, 1977) to Z = 1.58/yr for 1991 (Huntsman et al.[10]). Recently, Vaughan[5] estimated Z for the SAB to be between 0.90 to 0.94/yr depending on the input value of natural mortality in his stock assessment model. Vassilopoulou and Papaconstantinou (1992) reported Z = 0.34/yr for a relatively unexploited red porgy stock in the Mediterranean Sea and estimated natural mortality to be 0.28/yr.

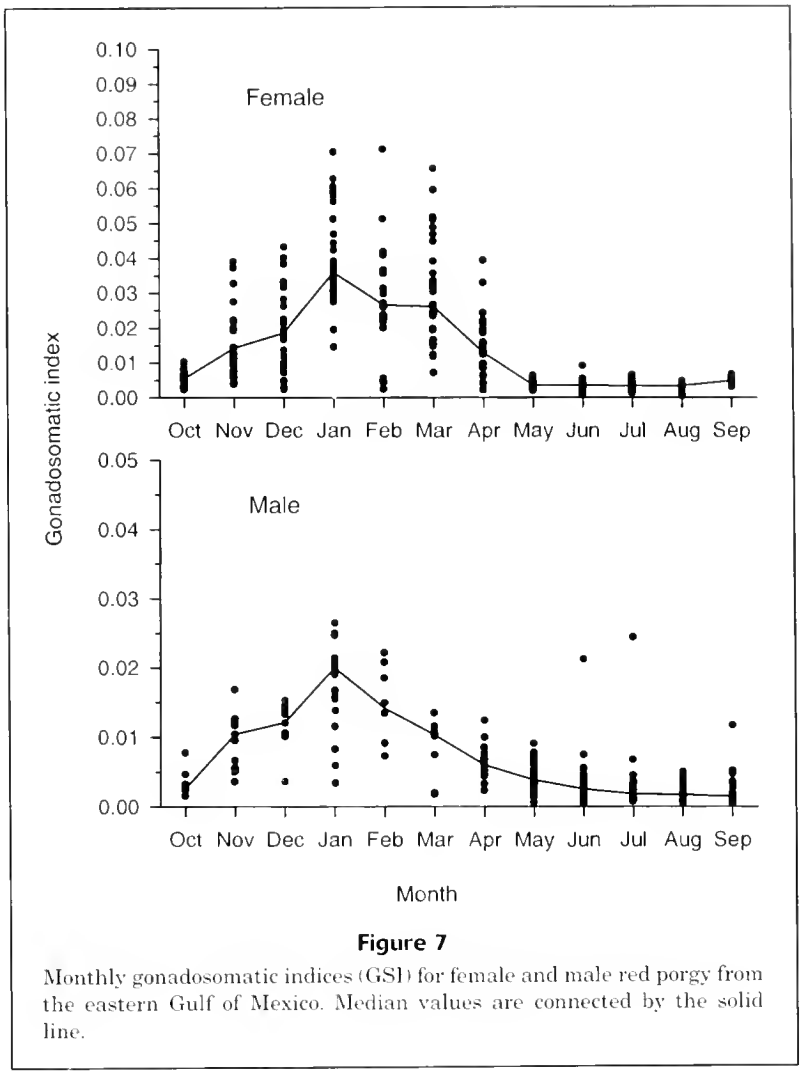

Figure 7

Monthly gonadosomatic indices (GSI) for female and male red porgy from the eastern Gulf of Mexico. Median values are connected by the solid line.

Reproduction

Protogynous hermaphrodites such as red porgy may be more susceptible to overfishing than gonochoristic species if size-selective fishing reduces the number of males available for spawning (Bannerot et al., 1987; Koenig et al., 1996). This trend is not evident for GOM red porgy. Our sex ratio of 1:1.6 had proportionally fewer females than did the 1:2.8 ratio reported by Nelson (1988) for 1980–82. In the SAB, the proportion of females has been increasing in association with fishing pressure. Manooch (1976) estimated that the sex ratio of red porgy in the SAB was 1:2.8 for 1972–74 and that proportionally more males were landed in the fishery than during later years (1:4.9–1:6.5 for 1979–1994; Harris and McGovern, 1997). The sex ratio of another GOM protogynous hermaphroditic reef-fish species, the gag (*Mycteroperca microlepis*), has been affected by overfishing (Koenig et al. 1996) in that there are proportionally fewer male gag in overfished populations than in less fished populations (male-to-female ratio of 1:76.6 for 1991–93 (Koenig et al., 1996) compared with 1:4.9 for 1977–80 [Hood and Schleider, 1992]). Koenig et al. (1996) hypothesized that because males are more aggressive in feeding, they are more likely to be captured by fishermen who target gag aggregations.

Our reported lengths at maturity (most red porgy were mature by 225 mm) were closer to lengths reported for exploited populations (<275 mm; Pajuelo and Lorenzo, 1996; Harris and McGovern, 1997) than for lightly or newly exploited populations (>276 mm; Manooch, 1976; Vassilopoulou and Papaconstantinou, 1992; Harris and McGovern, 1997). Decreases in the size at maturity for red porgy may be associated with increased fishing effort; Harris and McGovern (1997) found 27% of red porgy females were mature between 251 and 275 mm in pooled years 1979–81 compared with 54% in pooled years 1991–94.

Sexual transition occurred at smaller sizes than those reported by Nelson (1988); our estimated length at which half the population is male was 345 mm compared with 404 mm.[8] In the SAB, Harris and McGovern (1997) reported an increasing proportion of males between 351 and 400 mm over time, 12.13% in 1979–81, 32.35% in 1988–90, and 49.33% in 1991–94, which they attributed to size-selective fishing pressure. For most protogynous reef-fish

[10] Huntsman, G. R., D. S. Vaughn, and J. C. Potts. 1993. Trends in population status of the red porgy *Pagrus pagrus* in the Atlantic Ocean of North Carolina and South Carolina, USA, 1971–1992. South Atlantic Fishery Management Council, 1 South Park Circle, Charleston, SC 29422-1997.

species, the removal of males causes females to change sex (Sadovy and Shapiro, 1987). Therefore, the removal of larger fish (males) by fisheries causes smaller and smaller females to change sex and results in an increase in the proportion of smaller-size males.

Based on monthly changes in the percentage of fish in the various maturity classes, the frequencies of different oocyte stages, and GSI, we believe that red porgy spawn in the GOM from January to April. Our findings are consistent with spawning season observations reported for red porgy in the GOM by Nelson (1988), in the SAB by Manooch (1976), in the Canary Islands by Pajuelo and Lorenzo (1996), and in the Mediterranean Sea by Vassilopoulou (1989) and Vassilopoulou and Papaconstantinou (1992).

Acknowledgments

We thank the owners, staff, clients, and especially Capt. Ed Thompson of Hubbard's Marina for their assistance in obtaining samples from recreationally caught fish. We thank the staff of Captain's Finest Seafood, Dick's Seafood, Fishin' Inc., Holiday Seafood, and Nachman's Native Seafood for their assistance in sampling the commercial fishery. We thank Lew Bullock, Eric Eaton, Dave Harshany, Dan Merryman, Heather Patterson, Fred Stengard, and Connie Stevens for their assistance in collecting and processing samples. We thank Barbara Purich and the staff of the Pathology Laboratory, College of Veterinary Medicine, University of Florida, for their assistance in the histological preparation of gonad samples. We thank Bob Dixon for supplying the NMFS Headboat Survey data. We thank Mike Murphy for his assistance in the data analyses of age, growth, and mortality. We thank Susan Lowerre-Barbieri, Roy Crabtree, Judy Leiby, John Merriner, Mike Murphy, Jim Quinn, Ron Taylor, and four anonymous reviewers for their valuable reviews of this paper. We thank Linda Torres for her assistance in the administration of the budget for this study. This study was funded by the U.S. Department of Commerce, National Oceanic and Atmospheric Administration, National Marine Fisheries Service MARFIN program, award number NAS57FF0289.

Literature cited

Bannerot, S. P., W. W. Fox Jr., and J. E. Powers.
1987. Reproductive strategies and the management of snappers and groupers in the Gulf of Mexico and Caribbean. *In* Tropical snappers and groupers: biology and fisheries management (J. J. Polovina and S. Ralston, eds.), p. 561–603. Westview Press, Boulder, CO.

Barans, C. A., and V. J. Henry.
1984. A description of the shelf edge groundfish habitat along the southeastern United States. N.E. Gulf Sci. 7:77–96.

Beamish, R. J., and G. A. McFarlane.
1983. The forgotten requirement for age validation in fisheries biology. Trans. Am. Fish. Soc. 112:735–743.

Ciechomski, J. D., and G. Weiss.
1973. Desove y desarrollo embrionario y larval del besugo, *Pagrus pagrus* (Linne) en el Mar Argentino (Pisces, Sparidae). Physis Secc. A. Oceanos Org. 32:481–487.

Chester, A. J., G. R. Huntsman, P. A. Tester, and C. S. Manooch III.
1984. South Atlantic Bight reef fish communities as represented in hook-and-line catches. Bull. Mar. Sci. 34:267–279.

Collins, M. R., and G. R. Sedberry.
1991. Status of vermilion snapper and red porgy stocks off South Carolina. Trans. Am. Fish. Soc. 120:116–120.

Collins, M. R., S. B. Van Sant, D. J. Schmidt, and G. R. Sedberry.
1996. Age validation, movements, and growth rates of tagged gag (*Mycteroperca microlepis*), black sea bass (*Centropristis striata*), and red porgy (*Pagrus pagrus*). *In* Biology, fisheries and culture of tropical groupers and snappers (F. Arraguin-Sanchez, J. L. Munro, M. C. Balgos, and D. Pauly, eds.), p. 161–165. ICLARM Cong. Proc. 48.

Collins, M. R., C. W. Waltz, W. A. Roumillat, and D. L. Stubbs.
1987. Contribution to the life history and reproductive biology of gag, *Mycteroperca microlepis* (Serranidae), in the south Atlantic Bight. Fish. Bull. 85:648–653.

Crabtree, R. E., C. W. Harnden, D. Snodgrass, and C. Stevens.
1996. Age, growth, and mortality of bonefish, *Albula vulpes*, from the waters of the Florida Keys. Fish. Bull. 94:442–451.

Grier, H. J.
1987. Brown bodies in the gonads of the black sea bass, *Centropristis striatus*. *In* Proc. 3rd Int. Symp. Reprod. Biol. Fish, 199 p. Marine Sciences Research Laboratory, Memorial Univ., Newfoundland, Logy Bay, Newfoundland.

Grimes, C. B., C. S. Manooch III, and G. R. Huntsman.
1982. Reef and rock outcropping fishes of the outer continental shelf of North Carolina and South Carolina, and ecological notes on the red porgy and vermilion snapper. Bull. Mar. Sci. 32:277–289.

Harris, P. J., and J. C. McGovern.
1997. Changes in the life history of red porgy, *Pagrus pagrus*, from the southeastern United States, 1972–1994. Fish. Bull. 95:732–747.

Helland, I. S.
1987. On the interpretation and use of r^2 in regression analysis. Biometrics 43:61–69.

Hood, P. B., and A. K. Johnson.
1999. Age, growth, mortality, and reproduction of vermilion snapper (*Rhomboplites aurorubens*) from the eastern Gulf of Mexico. Fish. Bull. 97:828–841.

Hood, P. B., and R. A. Schlieder.
1992. Age, growth, and reproduction of gag, *Mycteroperca microlepis* (Pisces: Serranidae), in the eastern Gulf of Mexico. Bull. Mar. Sci. 51:337–352.

Humason, G. L.
1972. Animal tissue technique. W. H. Freeman and Co., San Francisco, CA, 641 p.

Huntsman, G. R., C. H. Manooch III, and C. B. Grimes.
1983. Yield per recruit models of some reef fishes of the U.S. South Atlantic Bight. Fish. Bull. 81:679–695.

Hyder, M.
1969. Histological studies on the testis of *Tilapia leucostricta* and other species of the genus *Tilapia* (Pisces: Teleostei). Trans. Am. Microsc. Soc. 88:211–231.

Jandel Corp.
1992. Sigma Stat user's manual. Jandel Corp., San Rafael, CA, unpaginated.

Koenig, C. C., F. C. Coleman, L. A. Collins, Y. Sadovy, and P. L. Colin.
1996. Reproduction in gag, *Mycteroperca microlepis* (Pisces: Serranidae), in the eastern Gulf of Mexico and the consequences of fishing spawning aggregations. *In* Biology,

fisheries and culture of tropical groupers and snappers (F. Arraguin-Sanchez, J. L. Munro, M. C. Balgos, and D. Pauly, eds.), p. 307–322. ICLARM Conf. Proc. 48.

Lowerre-Barbieri, S. K., M. E. Chittenden Jr., and C. M. Jones.
1994. A comparison of validated otolith method to age weakfish, *Cynoscion regalis*, with the traditional scale method. Fish. Bull. 92:555–568.

Machias, A., N. Tsimenides, L. Kokokiris, and P. Divanach.
1998. Ring formation on otoliths and scales of *Pagrus pagrus*: a comparative study. J. Fish Biol. 52:350–361.

Manooch, C. S., III.
1976. Reproductive cycle, fecundity, and sex ratios of the red porgy, *Pagrus pagrus* (Pisces:Sparidae) in North Carolina. Fish. Bull. 74:775–781.

Manooch, C. S., III, and G. R. Huntsman.
1977. Age, growth, and mortality of the red porgy, *Pagrus pagrus* (Pisces:Sparidae) in North Carolina. Trans. Am. Fish. Soc. 106:26–33.

Manooch, C. S., III, and W. W. Hassler.
1978. Synopsis of biological data on the red porgy, *Pagrus pagrus* (Linnaeus). FAO Fisheries Synopsis 116, 19 p.

Moe, M. A., Jr.
1969. Biology of the red grouper *Epinephelus morio* (Valenciennes) from the eastern Gulf of Mexico. Fla. Dep. Nat. Resour. Mar. Res. Lab. Prof. Paper 10, 95 p.

Nelson, R. S.
1988. A study of the life history, ecology, and population dynamics of four sympatric reef predators (*Rhomboplites aurorubens*, Lutjanus *campechanus*, Lutjanidae; *Haemulon melanurum*, Haemulidae; and *Pagrus pagrus*, Sparidae) on the east and west Flower Garden Banks, northwestern Gulf of Mexico. Ph.D. diss., North Carolina State Univ., Raleigh, NC, 197 p.

Optimas Corp.
1996. Optimas 5.0 user's manual. Optimas Corp., Bothell, WA, unpaginated.

Pajuelo, J. G., and J. M. Lorenzo.
1996. Life history of the red porgy *Pagrus pagrus* (Teleostei: Sparidae) off the Canary Islands, central east Atlantic. Fish. Res. 28:163–177.

Pitcher, T. J., and P. J. B. Hart.
1982. Fisheries ecology. AVI Publishing Co., Westport, CT, 414 p.

Potts, J. C., C. S. Manooch III, and D. S. Vaughan.
1998. Age and growth of vermilion snapper from the southeastern United States. Trans. Am.. Fish. Soc. 127:787–795.

Randall, J., and R. Vergara R.
1978. Sparidae. *In* FAO species identification sheets for fishery purposes. Western Central Atlantic (fishing area 31), vol. 3. FAO, Rome.

Ricker, W. E.
1969. Effects of size-selective mortality and sampling bias on estimates of growth, mortality, production, and yield. J. fish. Res. Board Can. 26:479–541.

Sadovy, Y., and D. Y. Shapiro.
1987. Criteria for the diagnosis of hermaphroditism in fishes. Copeia 1987:136–156.

SAS Institute, Inc.
1985. SAS user's guide: statistics. SAS Institute, Inc., Cary, NC, 956 p.

Sedberry, G. R., and R. F. Van Dolah.
1984. Demersal fish assemblages associated with hard bottom habitat in the South Atlantic Bight of the U.S.A. Environ. Biol. Fish. 11:241–258.

Smith, G. B., H. M. Austin, S. A. Bortone, R. W. Hastings, and L. H. Ogren.
1975. Fishes of the Florida Middle Ground with comments on the ecology and zoogeography. Fla. Mar. Res. Publ. 9, 14 p.

Snedecor, G. W., and W. G. Cochran.
1971. Statistical methods. Iowa State Univ. Press, Ames, IA, 593 p.

Sokal, R. R., and F. J. Rohlf.
1981. Biometry. W. H. Freeman and Co., New York, NY, 859 p.

Vassilopoulou, V.
1989. Some biological parameters on the red porgy (*Pagrus pagrus*) in the Kastellorizo area. FAO Fish. Rep. 412: 108–115.

Vassilopoulou, V., and C. Papaconstantinou.
1992. Age, growth, and mortality of the red porgy, *Pagrus pagrus*, in the eastern Mediterranean Sea (Dodecanese, Greece). Vie Milieu 42:51–55.

Vaughan, D. S., G. R. Huntsman, C. S. Manooch III, F. C. Rohde, and G. F. Ulrich.
1992. Population characteristics of the red porgy, *Pagrus pagrus*, stock off the Carolinas. Bull. Mar. Sci. 50:1–20.

Wallace, R. A., and K. Selman.
1981. Cellular and dynamic aspects of oocyte growth in teleosts. Am. Zool. 21:325–343.

West, G.
1990. Methods of assessing ovarian development in fishes: a review. Aust. J. Mar. Freshwater Res. 41:199–222.

Youngs, W. D., and D. S. Robson.
1978. Estimation of population number and mortality rates. *In* Methods for assessment of fish production in fresh waters (T. Bagenal, ed.), p. 137–164. Blackwell Scientific Publications, Oxford, UK.

Zhao, B., J. C. McGovern, and P. J. Harris.
1997. Age, growth, and temporal change in size at age of the vermilion snapper from the South Atlantic Bight. Trans. Am. Fish. Soc. 126:181–193.

Numbers and distribution of beluga whales, *Delphinapterus leucas*, in James Bay, eastern Hudson Bay, and Ungava Bay in Canada during the summer of 1993

Michael C. S. Kingsley

Canadian Department of Fisheries and Oceans
Maurice Lamontagne Institute
850, Route de la mer
Mont-Joli, P.Q. G5H 3Z4
Present address: Pinngortitaleriffik—Greenland Institute of Natural Resources
P.O. Box 570
DK-3900 Nuuk
Greenland

E-mail address: mcsk@natur.gl

Abstract—Aerial surveys to estimate the numbers of beluga whales, *Delphinapterus leucas*, were flown in James Bay, eastern Hudson Bay, and Ungava Bay in Canada in the summer of 1993 on transects systematically spaced 5 or 10 nmi apart. In James Bay and eastern Hudson Bay line-transect methods were used. In Ungava Bay strip transects were used, and off-transect sightings were also recorded. Beluga whales were also counted on coastal flights in eastern Hudson Bay and Ungava Bay. James Bay and eastern Hudson Bay were surveyed in August; Ungava Bay in July and again in August. Watches were kept from land at estuaries in eastern Hudson Bay in 1993 and in Ungava Bay in 1992 and 1993.

The estimates of detectable beluga whales (uncorrected for diving and observer errors) were 3141 (SE=787) in James Bay and 1014 (SE=421) in eastern Hudson Bay. A further 115–148 beluga whales were seen near the coast of eastern Hudson Bay during the coastal survey, but mostly away from traditionally used estuaries. The estimate for James Bay was nearly three times the previous estimate, made in 1985, possibly because ice cover in James Bay was much lower in 1993 than in the 1985 survey. The 1993 estimate for eastern Hudson Bay was close to that for 1985. No beluga whales were seen during aerial transects in Ungava Bay, but they were seen off-transect and on coastal flights, mostly in or near the Whale River estuary in southern Ungava Bay. The largest group sighted and the greatest number seen in any day consisted of 20 individuals, a minimum size for the summer population in Ungava Bay. An upper 90% confidence limit for summer numbers is imprecisely estimated at 150.

Neither the coastal surveys nor the land-based observations in Hudson Bay and Ungava Bay indicated the presence of large, dense herds that might have been inefficiently sampled by transect survey.

Manuscript accepted 28 March 2000
Fish. Bull. 98:736–747 (2000).

James, Hudson and Ungava bays are summering areas for stocks of beluga whales (*Delphinapterus leucas*) (Sergeant and Brodie, 1975; Finley et al., 1982; Smith and Hammill, 1986; Richard et al., 1990). There are several apparently separate summer groups, which include a summer group of ~23,000 individuals in western Hudson Bay, a group of 1500 individuals in the eastern Hudson Bay arc, and a few individuals in Ungava Bay (Smith and Hammill, 1986; Richard et al., 1990). Beluga whales, probably composing other separate groups, also summer in southern Hudson Bay (Richard, 1993) and James Bay (Smith and Hammill, 1986).

A land claim agreement was signed between the Inuit of the central and eastern Canadian Arctic and the Government of Canada in 1990 (Anonymous, 1993). In eastern Hudson Bay, this land agreement defined a marine area around the Belcher Islands (the "Nunavut Settlement Area") for the use of the beneficiaries of that agreement (Figs. 1 and 2). It also defined an area north and east of the settlement area (the "Equal Use and Occupancy Area") to be shared by the Inuit of Nunavut and those of northern Quebec. Other provisions of the agreement, and of the earlier James Bay and Northern Quebec Agreement, assured the aboriginal people of a right to hunt beluga whales in these waters.

The hunting of beluga whales is valued by Inuit in northern Canada as a means of procuring food, as a tradition helping to define their culture, and as a recreation. Maintaining beluga whale hunting, and stocks adequate to support it, are important objectives for the Inuits. Commercial hunting in the 19th century severely reduced numbers of beluga whales on the eastern coast of Hudson Bay and in Ungava Bay and they have not yet recovered (Reeves and Mitchell, 1987a; 1987b; 1989). These stocks were listed as "threatened" and "endangered," respectively, by the Committee on the Status of Endangered Wildlife in Canada (Campbell, 1993), and exploitation still occurs (DFO, 1996; NAMMCO, 1999). A low reproductive rate limits the species's potential for increase (Sergeant, 1981; Kingsley, 1989); therefore careful monitoring and management of stocks are appropriate.

Population management requires periodic evaluations of stock size, as a basis for setting harvest levels and for estimating the effect of harvest on the population trend. Beluga whale stocks are evaluated by aerial survey in their summering areas. The previous, and first, offshore aerial survey of James Bay, eastern Hudson Bay, and Ungava Bay was flown in summer 1985 (Smith and Hammill, 1986), and the development in the early 1990s of a beluga whale management plan for northern Quebec rendered it timely to update information on the population.

This article reports the results of aerial surveys flown in summer 1993. A

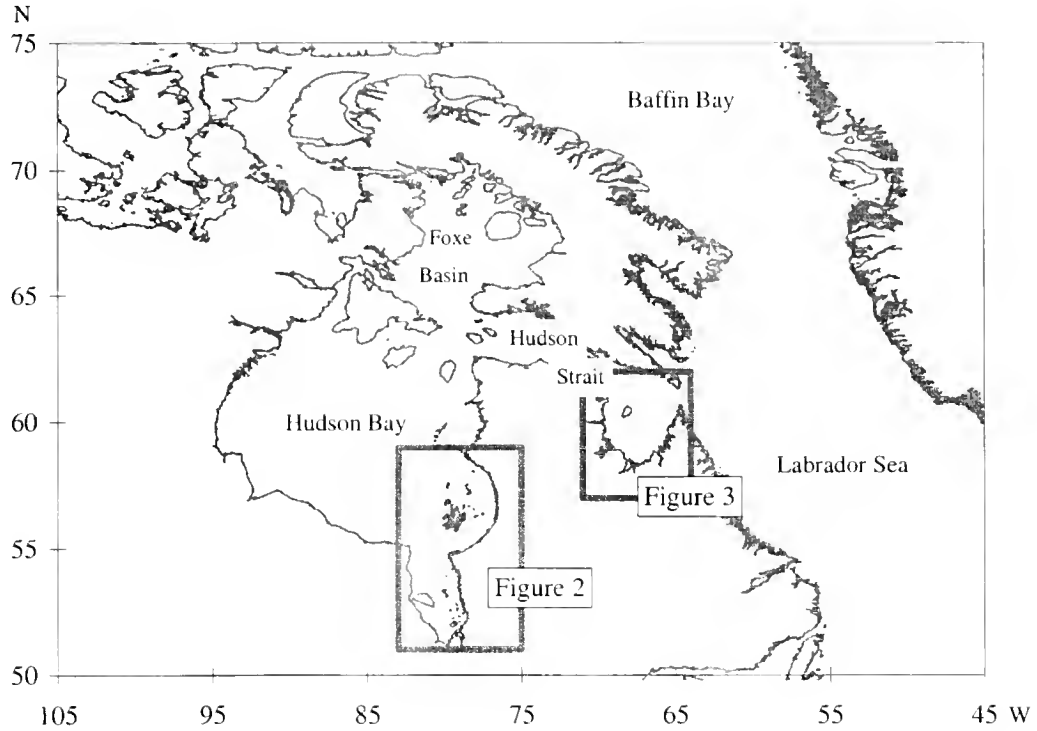

Figure 1

Map of northeastern Canada, showing the locations of the 1993 beluga whale aerial surveys in James Bay, eastern Hudson Bay, and Ungava Bay.

systematic transect survey was flown over offshore areas of James Bay, eastern Hudson Bay, and Ungava Bay (Figs. 1–3). However, summering beluga whales often form dense coastal concentrations, which are inefficiently estimated by sample survey. Therefore, coastal surveys were also flown in eastern Hudson Bay and Ungava Bay to check whether large numbers in concentration areas might have caused serious errors in the results of sample surveys. To the same end, watches were kept over known estuarine concentration areas from vantage points on land in 1992 and 1993.

Methods

Beluga whales concentrate in and around the mouths of rivers in summer, and this habit largely defines accepted stocks (Brown Gladden et al., 1997). Therefore aerial surveys for stock assessment are normally carried out in summer in these areas. The survey area for this study comprised James Bay, the eastern Hudson Bay arc north to 59°N and as far west as 80°20′W, and Ungava Bay. This area was similar to that covered by the previous aerial survey of these stocks in 1985 (Smith and Hammill, 1986). Beluga whales are uncommon in summer along the northern part of the eastern coast of Hudson Bay and the southern coast of Hudson Strait (Finley et al., 1982; Smith and Hammill, 1986); therefore the survey did not include these areas.

The transects in James Bay and eastern Hudson Bay were systematically spaced east–west lines similar to those used in 1985 (Smith and Hammill, 1986) (Fig. 2). They were on exact 10′ lines of latitude (i.e. 18.52 km apart) from the southern end of James Bay at 51°10′N as far as 58°50′N near Inukjuak, and additional lines were interpolated at 5′ (9.26-km) intervals between 55°35′N and 57°35′N, i.e. in the central part of the Hudson Bay arc.

The survey of Ungava Bay was also based on systematic designs (Fig. 3). South of 59°30′N, the initial design had north–south transects on every 15th minute of longitude, a spacing approximately equal to 7.5 minutes of latitude (13.9 km). North of this line the transects lay east–west on every tenth minute of latitude, i.e. 18.52 km apart.

Earlier surveys of Ungava Bay had detected few beluga whales (Finley, 1982; Smith and Hammill, 1986). Inuk hunters had suggested that flying at different times in the summer might produce different results; therefore the Ungava Bay survey was flown twice: in mid-July and in late August. In both surveys, sections of the coastline were followed and surveyed when ferrying to and from transect blocks, so that the coastline, particularly near the logistic base at Kuujjuak, was repeatedly covered.

The transect survey of James Bay and eastern Hudson Bay was flown in a Cessna 337 aircraft, at 1500 feet (457 m) above sea level at about 130 knots, (67 m/s), and navigated by GPS. The aircraft was equipped with flat windows. Observers sat in the two seats behind the pilot. Line-transect survey methods were used, in which all sightings were recorded with their distance from the transect line, and a sighting curve was subsequently calculated to correct for the decreasing detectability of targets with distance.

The angle of view from the horizontal was measured with Suunto inclinometers. Records were made with time-coding tape recorders and were transcribed daily. Ground speeds were calculated from the elapsed time on the transect and sighting positions were interpolated along transects. The state of the sea was assessed and recorded by using the Beaufort Scale of wind force; survey plans included not flying in conditions over Beaufort 4 (i.e. over 10 knots or 5.14 m/s).

The coastline of the eastern Hudson Bay arc was surveyed once, on 21 August, in a flat-windowed "Twin Otter" aircraft flying at 500–1000 ft (152–305 m). The observers, two to seven in number depending on the survey segment, were members of local hunters' and trappers' associations; they sat behind the pilots and recorded observations directly onto sighting maps. The flight line from Kuujjuaraapik followed the mainland coastline northbound to Inukjuak. The southbound leg was flown on the offshore side of the chains of islands close to the coast, and the plane made a detour to survey Richmond Gulf. It flew as far south as the Vauquelin River before returning to end at Kuujjuaraapik (Fig. 2).

The Ungava Bay surveys used strip-transect methods. A "Twin Otter" aircraft was flown at an altitude of 1500 feet (457 m). The transect survey used a systematic design with a strip width of 600 m on each side of the aircraft, but sightings were so few that all were recorded, on- or off-effort and on- or off-transect. Ferry flights to the start of and from the end of each day's transect pattern followed the coastline, detouring to search the largest bays and estuaries. The entire coast was covered in this way, some stretches several times.

Observations made from land at estuaries frequented by beluga whales in summer were a supplementary source of information from which it was possible to assess the probability that large estuarine concentrations had been inefficiently estimated by transect sample survey. Local observers manned camps at the Little Whale River and at the Nastapoca River in eastern Hudson Bay in 1993,[1] and in southern Ungava Bay in 1992[2] and 1993[3] (Fig. 3). From vantage points, the estuary areas were scanned regularly for beluga whales. The estuaries of the Little Whale and Nastapoca rivers are less than 1 km long, and easily covered, but the Whale River estuary in southern Ungava Bay could not be completely covered. The objective was to scan five times a day, at three-hour intervals; but weather sometimes interfered with this schedule. Not only numbers, age class, and behavior of beluga whales were noted, but also boat and air traffic, visibility, wind, weather, and tide.

Line-transect methods were used to analyze the data from James and Hudson Bays. Such methods involved fitting to the sighting data a sighting probability curve $g(x)$, i.e. the probability that an animal group at distance x from the

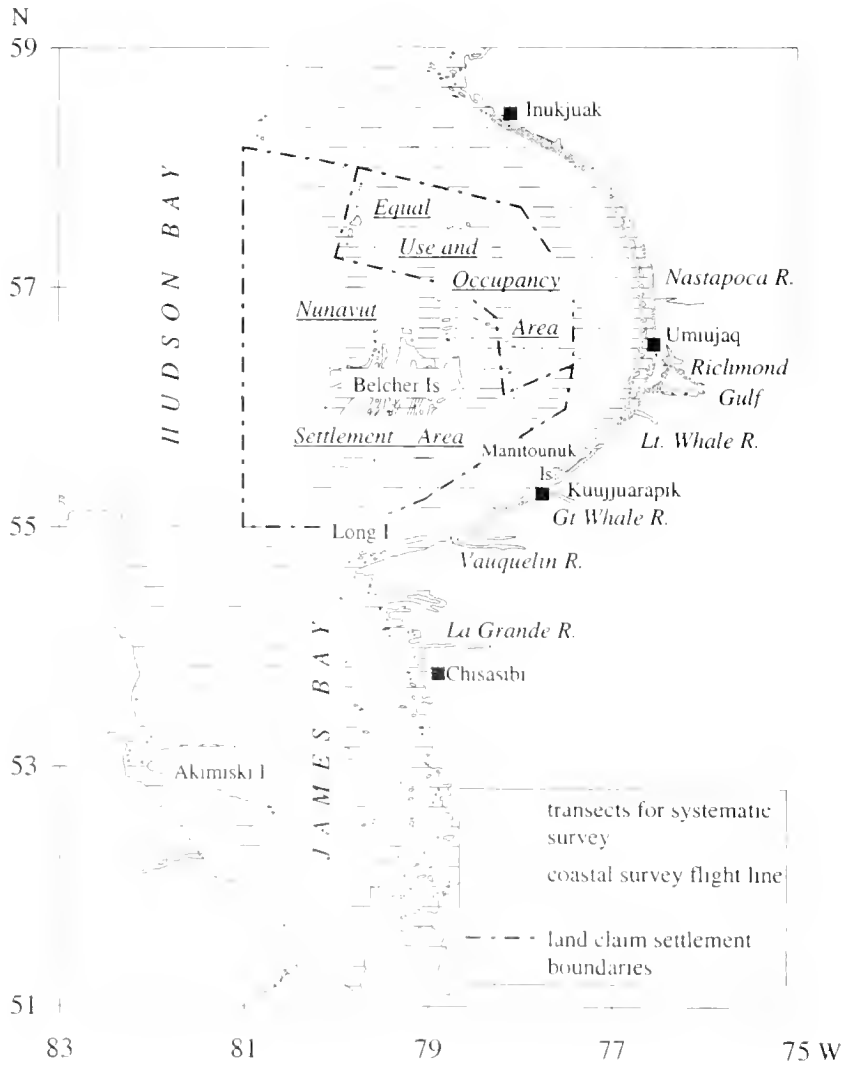

Figure 2

Systematic design for aerial transect survey of beluga whales in James Bay and eastern Hudson Bay, August 1993

[1] Doidge, D. W. 1994. Land-based observation of beluga whales at the Little Whale and Nastapoka rivers, eastern Hudson Bay, summer 1993. Report prepared by Makivik Corp., C.P. 179, Kuujjuaq, P.Q. J0M 1C0 Canada, 30 p.

[2] Makivik Corp. 1993. Land-based observations of belugas in Ungava Bay, summer 1992. Report prepared by Makivik Corp., C.P. 179, Kuujjuaq, P.Q. J0M 1C0 Canada. 7 p.

[3] Doidge, D.W., and A. H. Gordon. 1994. Land-based observations of beluga at Tuututuup Nuvunga, southern Ungava Bay, summer 1993. Report prepared by Makivik Corp., C.P. 179, Kuujjuaq, P.Q. J0M 1C0 Canada, 13 p.

track-line is detected. Commonly, line-transect analysis assumes that 1) $g(0)$ is unity and 2) $g(x)$ is never increasing with x. An associated shape criterion, which improves the behavior of estimates obtained by line-transect survey (Burnham et al., 1980; Buckland, 1985), suggests that the sighting curve should have a "shoulder" or plateau at small x.

Richards' (1959) sigmoidal growth curve, reversed left-to-right, was chosen for its flexibility to fit $g(x)$. The ordinate at the point of inflection was constrained to be less than 0.9. Because of difficulty in seeing straight down from a flat-windowed aircraft, no animals could be seen close to the transect line; therefore, close to the transect line, an increase in $g(x)$ was modeled by an increasing sine^2 function (Fig. 4). It was assumed that $g_{max} = 1$, i.e. that all surface-visible beluga whales situated at the best distance would be detected. Detection bias would occur if this assumption was incorrect.

The data were truncated at 6000 ft (1829 m) from the trackline; beyond this distance, sightings were few, and measured sighting angles and counts of numbers were imprecise. Within this range, the sighting curve was fitted by maximum likelihood to the distribution of distances from the trackline to individual beluga whales, not to the distribution of sighted groups (Hiby and Hammond, 1989). A single sighting curve was fitted, and a single estimate of k was calculated, and for the survey of James Bay and eastern Hudson Bay, all three strata were pooled. It was integrated numerically to calculate the effective strip width.

The transect counts were expanded to an estimate of detectable numbers:

$$\hat{N} = \sum_{s=1}^{S} \hat{N}_s = \sum_{s=1}^{S} kT_s B_s, \qquad [1]$$

where T_s = the transect spacing (km);
B_s = the total count of beluga whales in the s^{th} stratum; and
k = the survey expansion factor (/km) i.e. the reciprocal of the two-sided effective strip width.

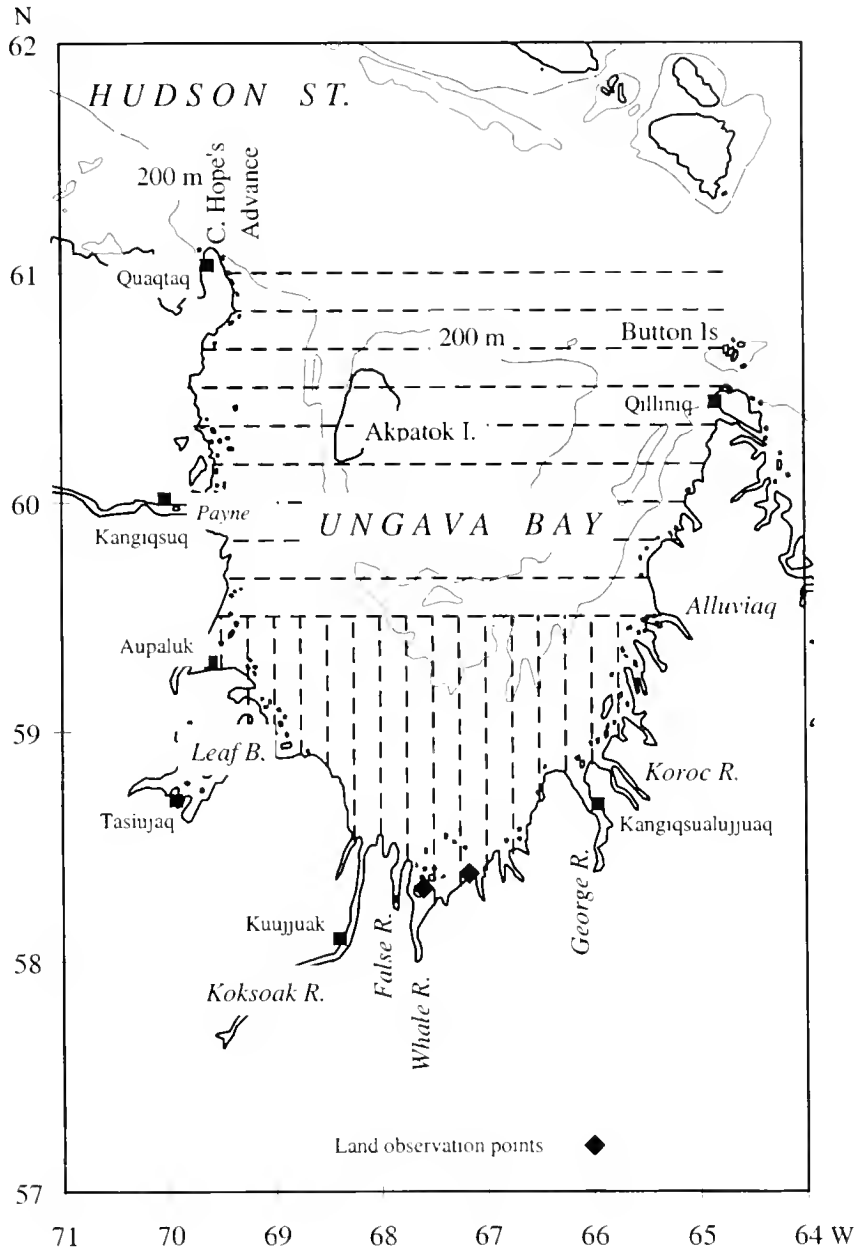

Figure 3

Map of Ungava Bay with the survey design for aerial surveys in July and August 1993.

The uncertainty of N_s was estimated as the sum of V_{s1}, the component from sampling the spatial distribution of beluga whales in the stratum; and V_{s2}, that was due to uncertainty in the estimation of k. V_{s1} was estimated by a serial difference method appropriate to systematic sampling (Cochran, 1977):

$$V_{s1} = kT_s \cdot (kT_s - 1) \cdot \frac{J_s}{J_s - 1} \cdot \frac{\sum_{j=1}^{J-1} (B_j - B_{j+1})^2}{2}, \qquad [2]$$

where B_j beluga whales were sighted on the j^{th} of J_s transects in stratum s.

V_{s2}, the component of sampling error due to uncertainty in the estimation of the effective strip width, was estimated by

$$V_{\hat{N}_2} = \mathrm{var}(k) \cdot (T_c \cdot B_c)^2, \quad [3]$$

The sighting curve was fitted to nonindependent individuals instead of to independently sighted groups, so the standard error of k was estimated by resampling (Hiby and Hammond, 1989). The standard jack-knife method was used (Efron and Tibshirani, 1993), and sightings, presumed independent, were taken as observational units. Maximum-likelihood estimates are not necessarily unbiased in small samples but may be subject to sample-size bias. The effective number of sightings,[4] 57.7, was less than the recommended minimum (Buckland et al., 1993); therefore sample-size bias in the estimate of the survey expansion factor was reduced by using the standard jack-knife bias reduction (Efron and Tibshirani, 1993; Buckland et al., 1993; Kingsley and Reeves, 1998).

Sightings made on stratum-boundary transects where transect spacing changed were given half weight in each stratum.

Few sightings were made on the transect sample survey in Ungava Bay, and none within the designed survey strip. The sightings made outside the transect strip were converted to a population estimate by assuming an effective strip width based on statistics from other line-transect surveys that had used similar platforms. No standard error was calculated, but an upper confidence limit on the number of groups was calculated by assuming independent binomial sighting probabilities and by answering the question "Given that the sampling fraction was f, how many groups could there be for the chance of seeing none or one to be less than p%?"

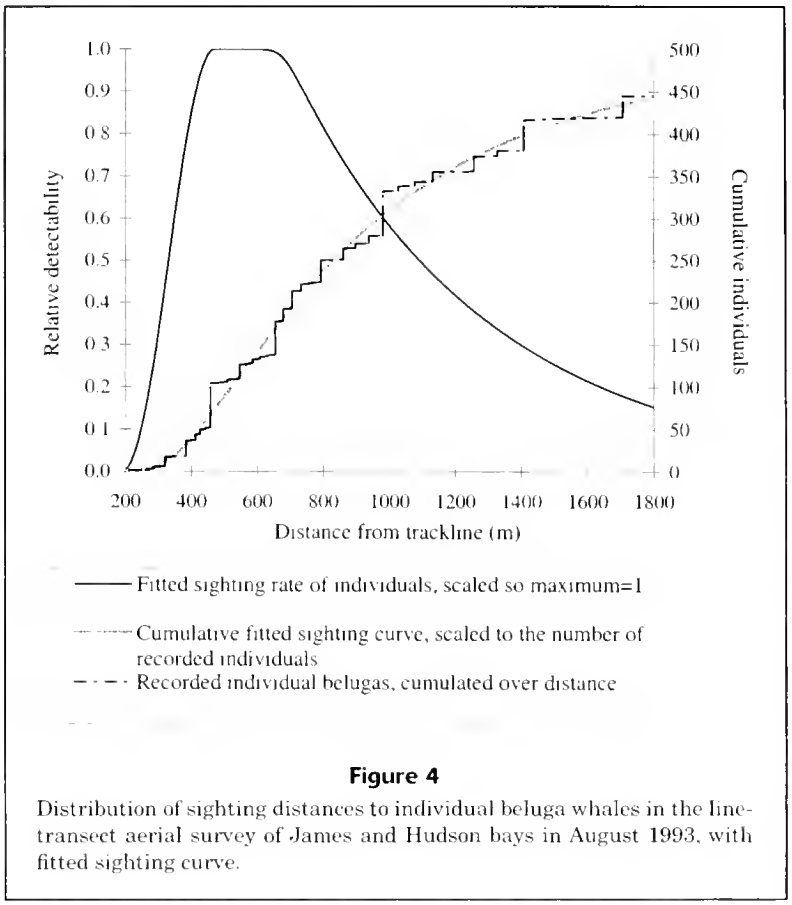

Figure 4

Distribution of sighting distances to individual beluga whales in the line-transect aerial survey of James and Hudson bays in August 1993, with fitted sighting curve.

Results

The survey in James Bay was flown quickly in good conditions from 12 August through 14 August. Winds were light and, apart from occasional fog patches, survey conditions were good. The southern part of eastern Hudson Bay was flown on 15–17 August with light winds and good visibility. Aircraft problems imposed a delay from 18 through 20 August, and on 21 and 24 August there were strong winds. Richmond Gulf was surveyed on 16 August (Fig. 2).

The field of view was limited by the flat windows of the aircraft. No observations were recorded closer than a viewing angle of 65° from the horizontal (at a flying height of 1500 feet, 213 m from the line), and few closer than 55° (320 m) (Fig. 4). Sighting distances were grouped, because the observers tended to round sighting angles. The last-digit frequencies of the recorded angles were analyzed, and it was found that rounding to the nearest 5° was mostly at the expense of the adjacent marks, i.e. those with a remainder of 1° or 4°. Against an expectation of equal frequency of last digits, rounding caused a mean absolute error of 0.42° and was not expected to bias results or to increase uncertainties. Recorded mean group size increased slightly with sighting distance.

The sighting frequency reached its maximum at 467 m (44.2°) and dropped off sharply beyond about 670 m (35°) (Fig. 4). There were few sightings of beluga whales in Hudson Bay; therefore one sighting curve was fitted to the data for all strata. The bias-reduced survey expansion factor was 0.575/km (SE=0.074).

Beluga whales were widely distributed in James Bay (Fig. 5A). There were 123 sightings in 4520 km of transect (27/1000 km), comprising 295 individuals (65/1000 km) (Table 1). Line-transect analysis gave an estimate of 3141 detectable beluga whales for James Bay (Table 2). This number is about three times the estimate obtained by Smith and Hammill (1986). However, their survey was earlier, when a lot of ice still remained in northwest James Bay and may have affected the distribution of these whales. The highest densities in the present survey were in this area. In eastern Hudson Bay (Fig. 5B) there were 63 sightings on 7100 km of transect (9/1000 km) comprising 150 beluga whales (21/1000 km) (Table 2).

[4] Effective number of sightings is defined here as the number of animals seen divided by the contraharmonic mean of group size.

Table 1

Sizes of beluga whale groups sighted on transect survey flights in James Bay, eastern Hudson Bay, and Ungava Bay, during the summer of 1993. CHM = contraharmonic mean, i.e. the size of the group containing the average beluga.

	Sightings	No. of beluga whales	Group size			Effective no. of sightings
			Mean	CHM	SD	
James Bay	123	295	2.40	6.29	3.05	46.9
Hudson Bay	63	150	2.34	10.52	4.40	14.2
Ungava Bay (July survey)	1[1]	4	5.6[2]	13.5[2]	6.93[2]	
Ungava Bay (August survey)	1[1]	19				

[1] These transect-survey sightings were outside the designed survey strip. No sightings were made within the strip.
[2] These statistics are for all 12 sightings in Ungava Bay, including coastal reconnaissance flights, and for both surveys.

Error coefficients of variation (ECV) ranged from 25% for James Bay to 86% for the northern stratum of widely spaced transects in eastern Hudson Bay, where the estimate was based on 10.5 sightings made on 2.5 transects (Table 3). The ECV of the overall estimate was 23%. The use of a common sighting curve reduced the estimated standard errors for individual strata. Uncertainty in k composed only 2% and 20% of the error variances for the two Hudson Bay strata, but 32% of the overall error variance.

On the coastal survey of eastern Hudson Bay, 13 groups of beluga whales were seen, distributed from the northern end of the offshore chain of islands to south of the Great Whale River (Fig. 6). The total number of individuals was 115–148. One large group—70 to 100 individuals—was seen, close to the Manitounuk Islands.[5] A few beluga whales were seen in the Great Whale and Little Whale rivers.

Observers on land at the Little Whale River saw beluga whales on 14 of the 22 observation days. The mean daily maximum count for days on which the whales were seen was 40.4 individuals (range 5–130). At the Nastapoca River, beluga whales were present on 7 of 13 observation days, and the mean daily maximum was 23.3 (1–53). Even on days when they were seen, beluga whales were not continuously present: at the Little Whale River; none were seen on 45% of scans made on days when they were seen at least once, and at the Nastapoca, River, 54% of scans on such days showed no sightings.

The first aerial survey in Ungava Bay was flown on 15–19 July, 1993. It was limited by dense pack ice that remained in the central and northern part of the bay, heavy enough

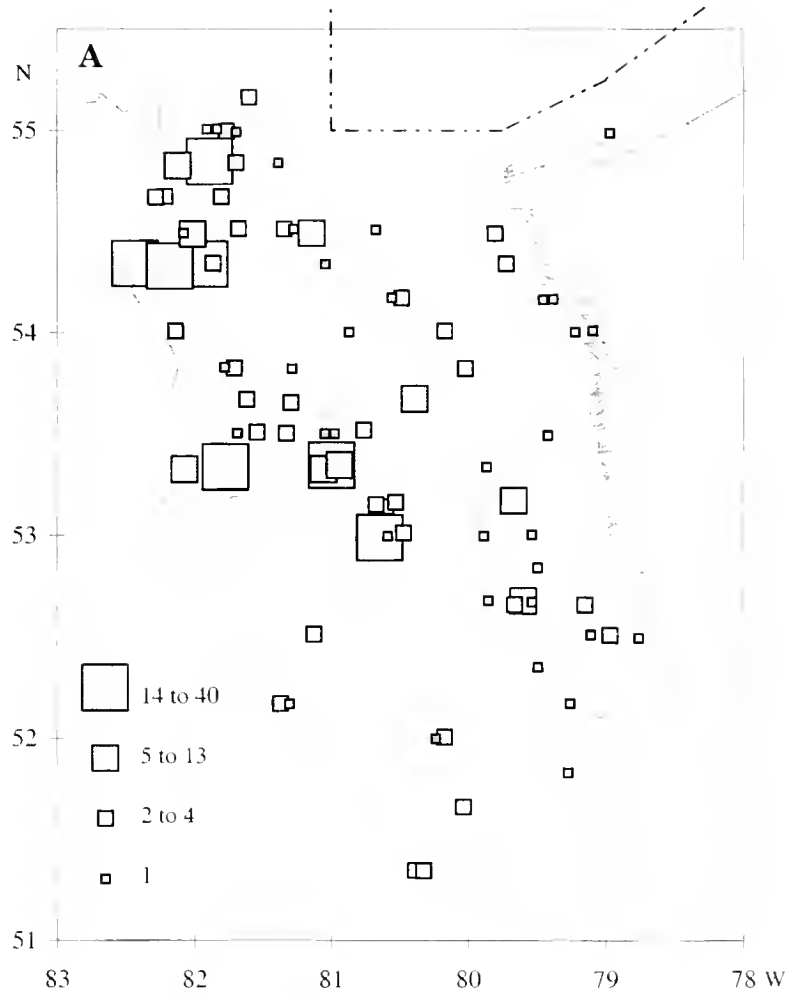

Figure 5

Beluga whale sightings on line-transect aerial survey of (**A**) James Bay and (**B**) eastern Hudson Bay, in August 1993

[5] Doidge, D. W. 1993. Coastal reconnaissance survey for belugas in eastern Hudson Bay, August 21, 1993. Report prepared for the Department of Fisheries and Oceans, 104, rue Dalhousie, Quebec P.Q. G1K 4B8, Canada by Makivik Corp., C.P. 179, Kuujjuaq, P.Q. J0M 1C0 Canada, 8 p.

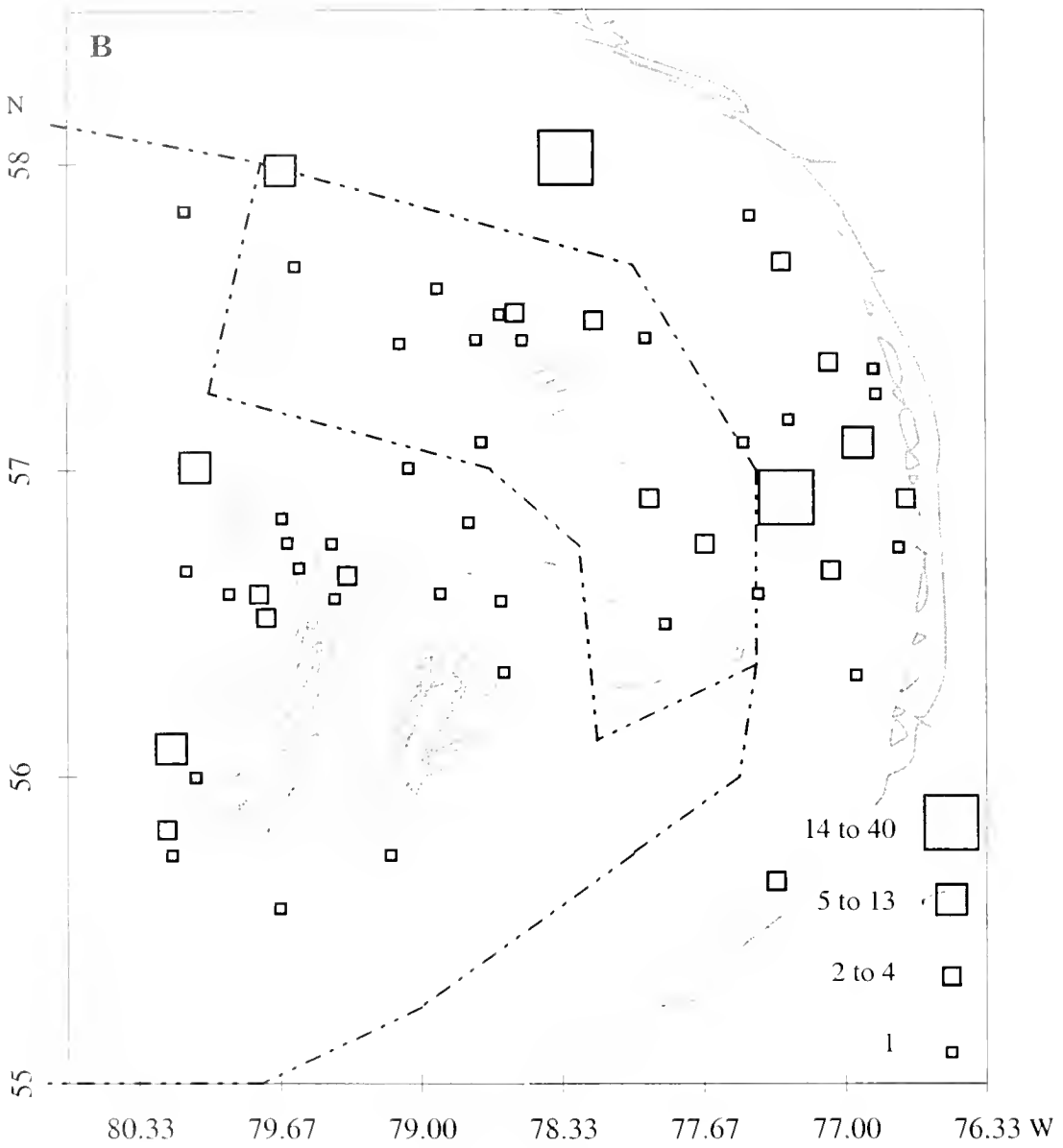

Figure 5 (continued)

to restrict the distribution of beluga whales and to make it difficult to count them. The survey was not extended into this area of heavy ice. North–south transects were flown in southern Ungava Bay, south of the ice. The second survey, 24–29 August, was flown over open water throughout Ungava Bay. However, some planned flight patterns were limited by fog in northeastern Ungava Bay.

In Ungava Bay, beluga whales were seen on four of five flying days in July, with a maximum daily count of 20 individuals in one sighting, and on three of six flying days in August, with 20 individuals in two sightings on the best day (Table 3). In the two surveys together, beluga whales were sighted in the Whale River estuary on six of seven overflights. There were also two sightings in southern Ungava Bay close to the Whale River, and two sightings of small groups in western Ungava Bay. The mean sighting size was 5.6 groups (SE=2.0).

However, no beluga whales were seen within the designed survey strip. From independent binomial sighting probabilities, corresponding upper 90% CLs would be 25.5 groups for the first survey and 34.3 groups for the second (assuming the mean group size of 5.6, equal to 143 and 192 animals). One off-strip sighting was made on a sample survey flight during each survey, but no distance measurements were made. Off-strip effort is considered to have an outer visibility limit similar to that estimated by line transect analysis of the data for James Bay and eastern Hudson Bay, but an inner limiting angle similar to the 72° estimated for a similar platform by Harwood et al. (1996). This would result in a strip width of about

Table 2

Estimates of numbers of beluga whales by stratum and overall, in James Bay, eastern Hudson Bay, and Ungava Bay, during August 1993.

Stratum	Count of beluga	No. of transects	Transect spacing (km)	N_{est}[1]	V_1[2] (10^3)	V_2[3] (10^3)	SE
James Bay (including southern Hudson Bay arc)	295	26.5	18.52	3141	454	165	787
Central Hudson Bay arc: closely spaced transects	109.5	26	9.26	583	25	6	174
Northern Hudson Bay arc: widely spaced transects	40.5	7.5	18.52	431	135	3	372
Central and northern Hudson Bay total	150	33.5	—	1014	160	17	421
Ungava Bay (July survey)	4[4]	15	13.9	38[5]	—	—	—
Ungava Bay (August survey)	19[4]	16	18.52	50[5]	—	—	—

[1] The survey expansion factor k for the line-transect survey in James Bay and eastern Hudson Bay, including the jack-knife bias correction, was 0.575/km with a jack-knife-estimated SE of 0.0742/km. The one-side effective strip width was 870 m.

[2] V_1 is the component of error variance due to the variability in the encounter rate and consequent uncertainty in estimating its mean.

[3] V_2 is the component of error variance due to the uncertainty in estimating the effective strip width.

[4] These sightings were made outside the designed transect strip of the strip-transect survey, and estimates are based on an assumed effective strip width of 1020 m each side; k = 0.49/km (see text).

[5] Population estimates are based on the mean size (5.6) of all groups sighted on reconnaissance and transect flights.

Table 3

Sightings of beluga whales in aerial surveys of Ungava Bay during July and August 1993.

Date	Area covered by flight	No. seen	Where seen	When seen
15 Jul	Transects in southeast Ungava Bay; and the southeast coast from the Kosoak River to the Koroc River			
16 Jul	Transects in southwest Ungava Bay; and the southwest coast from the Whale River to the Leaf River	3 adult	Whale River estuary	between transects
17 Jul	The southern and eastern coasts from the Koksoak River to the Button Islands	20 mixed	Whale River estuary	on coastal flight
18 Jul	The western coast from the Koksoak River to Quaqtaq	2 adult + possibly 1 calf 1 adult	NW Ungava Bay near Leaf Bay	
19 Jul	Transects in southern Ungava Bay between the Leaf River and the George River; also the south coast from the George River to False River	2 adult + cow-calf pair 1 adult; 1 adult + 1 juv. + 1 neonate; 1 adult	SE Ungava Bay Whale River estuary Whale River estuary Whale River estuary	on transect[1] on coastal flight on coastal flight on coastal flight
24 Aug	The western coast, from the Koksoak River to Quaqtaq	10	Whale River mouth	on coastal flight
25 Aug	The southern coast, from the Whale River to the George River	2	Whale River mouth	on coastal flight
26 Aug	Transects in southwest Ungava Bay, and the coasts of Leaf Bay and the Leaf River			
27 Aug	Transects in southeast Ungava Bay, and the southeast coast from Whale River to Alluviaq	19 1	15 km E of Whale River 10 km E of Whale River	on transect[1] on coastal flight
28 Aug	Transects in northwest Ungava Bay, and the coast of Akpatok Island			
29 Aug	Transects in northeast Ungava Bay, and the northeast coast from Alluviaq to the Button Islands			

[1] Sightings made "on transect" were outside the designed transect strip of 600 m each side of the aircraft.

1020 m on each side and survey expansion factors of 6.8 for the first survey and 9 for the second. Resulting estimates would be 6.8 and 9 groups (38 and 50 whales), with approximate 90% upper CLs of 25.0 and 33.8 (119 and 157 whales, if mean group size was 5.6). These estimates and confidence limits were imprecise and did not account for the uncertainty of mean group size or for the known lower bound on numbers.

The large tidal range in southern Ungava Bay creates extensive foreshore flats, and few beluga whales were sighted from the observation points on land. In 1992, 160 scans made over 35 days between 5 Aug. and 30 Sept. showed a total of 24 individuals. In 1993, 145 scans over 29 days in June and July resulted in four sightings totaling 8 individuals; 68 scans over 15 days in August and September resulted in three observations totaling 30 individuals. The largest count in any sighting was 17.

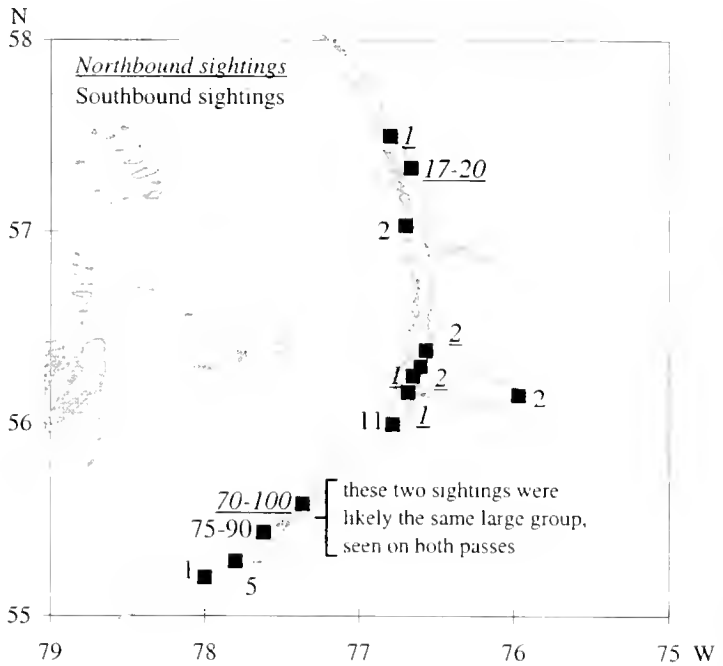

Figure 6

Sightings of beluga whales on coastal aerial survey of eastern Hudson Bay, 21 August 1993.

Discussion

The 1993 estimate of surface-visible beluga whales in James Bay, about 3140, was 2.6 times that of the previous survey (Smith and Hammill, 1986). In that survey, flown in early August, ice cover was still present in northwestern James Bay; most groups were composed of fewer than 5 animals and they were distributed in the southern part of James Bay (Smith and Hammill, 1986, Fig. 1). In the present survey, there was no ice and there were many observations of larger groups. The highest densities were north of Akimiski Island and up the western side of James Bay, where many groups were found in shallow turbid water close to shore (Fig. 5A). The beluga whales may have been distributed differently in the two surveys because of the ice that still remained at survey time in 1985.

It is difficult to ascertain the origin of this population. Significant numbers of beluga whales were once reported wintering in James Bay (Jonkel, 1969) prompting the suggestion that a large part of that population might be resident (Sergeant, 1986). However, a resident population could not increase fast enough to account for the difference between the 1985 estimate and the present one (Eberhardt and Siniff, 1977; Sergeant, 1981; Kingsley, 1989; Doidge, 1990). In 1985 there was significant ice cover in northwest James Bay, and beluga whales moving into James Bay from southwestern Hudson Bay may have been delayed by the ice in 1985, and not in 1993. However, Richard (1993) suggested that the principal southward spring migration route for James Bay beluga whales may be down the east coast of Hudson Bay, in which case ice in northwest James Bay would not have been a barrier. Alternatively, the populations in western and southwestern Hudson Bay (Richard et al., 1990; Richard, 1993) may have been colonizing James Bay. A small fraction of the estimated 23,000 beluga whales of the western Hudson Bay stock would have had a large effect on survey counts if they had been present in James Bay.

The estimated density of beluga whales in eastern Hudson Bay was slightly greater than the 1985 transect-survey estimate (Smith and Hammill, 1986 Table 1). However, for the latter survey, strip transects (with a total width of 2000 m) were used. This distance probably exceeds the range at which beluga whales can be effectively counted in a survey in the Beaufort Sea. With the same platform, target species, and type of aircraft window, Harwood et al. (1996) estimated an effective strip width of about 1300 m. The 1985 strip-transect estimate may have been biased downward in relation to the present survey. In 1985, 200 beluga whales were counted; in 1993, 150 whales were counted on the same transects.

Few beluga whales were seen on the coastal survey of eastern Hudson Bay in 1993. There were no large concentrations in the mouths of rivers, but scattered small groups and probably only one large group. The total was less than 150 individuals. The land-based observations in 1993 also did not record large groups in the estuaries. Therefore, the transect sample survey estimate probably did not have large errors due to inefficient sampling of large estuarine concentrations. In 1985, a total of 481 whales were counted on the eastern Hudson Bay coastal survey, including concentrations in Richmond Gulf and in the estuaries of both the Little Whale and Nastapoca rivers (Smith and Hammill 1986), and land-based observations in 1984 counted as many as 200 individuals in the Nastapoca estuary (on 24 August; Caron and Smith, 1990) compared with the 1993 maximum of 53.

Transect sample survey and nearshore total-count indices apparently corroborate the finding that numbers in

Table 4

Distribution of beluga whale observations and estimated numbers of beluga whales in eastern Hudson Bay between the Nunavik area, the Nunavut Settlement Area, and the Equal Use and Occupancy Area.

	Observations (%)	Mean number per observation	Estimated numbers (%)
Nunavik area	23 (36)	4.2	774 (71)
Nunavut Settlement Area	25 (39)	1.4	211 (19)
Equal Use and Occupancy Area	16 (25)	1.2	111 (10)

eastern Hudson Bay were not larger in 1993 than they had been in 1984–5, but instead were very likely lower.

Sightings of beluga whales in eastern Hudson Bay showed that they were widely distributed in the shallow water between the mainland coast and the Belcher Islands (Fig. 4). Thirty-six percent of sightings were outside the areas defined by the Nunavut Agreement (Table 4), but these were on average the larger groups, and represented 71% of the total numbers. Beluga whales were distributed also around the Belcher Islands, particularly to the north, and as far west as the survey extended. There was no evidence of a discontinuity in the east–west distribution. The survey results were consistent with the hypothesis of a single continuous population distributed from the coast out to the survey limit. However, it is not known for sure whether all the beluga whales in the study area were among those that frequent the estuaries on the eastern Hudson Bay mainland coast, nor whether they would be available to hunters there. It remains possible that the beluga whales using those estuaries are only a fraction of the total numbers counted in the survey area. The question of single or multiple summering stocks in eastern Hudson Bay is important in designing strategies for managing exploitation by residents of the communities on the Belcher Islands and on the eastern Hudson Bay coast; aerial survey results alone can not provide conclusive answers.

The north–south extent of the sightings in eastern Hudson Bay was limited, as in 1985; no beluga whales were seen on the northernmost transects, and there was no continuous distribution extending into areas farther north. There are no large estuaries to attract summering beluga whales to the eastern Hudson Bay coast north of the Nastapoca River, and there are no reports, even anecdotal, of beluga whales spending the summer in those areas. Thus it is unlikely that significant additional numbers would have been detected if this survey had extended farther north.

The estimate of numbers in Ungava Bay was uncertain. In James Bay, beluga whale groups were widely distributed. In Hudson Bay, densities were lower, but sightings were frequent and widely distributed. In Ungava Bay very few beluga whales were seen, indicating a very low density. Population estimates from the transect surveys, based on 0 or 1 sighting per survey, are imprecise, but small, of the same order as the highest daily total counts on survey and reconnaissance flights combined, and consistent with the maximum of about 25 beluga whales in the Mucalic River estuary in summer estimated by Finley et al. (1982). The present survey could have resighted the same small group of about that size, or subgroups of it, on different flights. The largest sighting from land was 17 individuals, on 24 August 1993. Smith and Hammill (1986) surveyed Ungava Bay in 1985, and saw few beluga whales; they were unable to make a population estimate.

Most sightings were made in and near the Whale River estuary, but a few, small, scattered groups were also sighted elsewhere in Ungava Bay (Table 3). Residents of the area see beluga whales in summer, but not in large numbers and not all the time (Brooke[6]; Brooke[7]; Portnoff[8]). Ungava Bay communities capture beluga whales in most years, but often outside the bay and outside the season when they inhabit their summer grounds. Neither survey results nor harvest statistics provided a basis for considering a trend in summering stock size.

Estimates from line-transect survey analysis were conditional on the use of the Richards curve as a sighting curve. Both the hazard-rate curve and the normal curve fitted the data worse. Maximum detection was not obtained until 470 m from the aircraft, owing to its having flat windows. Similar visibility restrictions have been estimated in other surveys. In a line-transect aerial survey of narwhals in Scoresby Sund, in which the survey plane had flat windows, there were poor sighting rates out to a sighting angle of about 40° from the vertical (Larsen et al., 1994) and in an aerial survey of cetaceans in the Gulf of St Lawrence, in which the survey aircraft had shallow bubble windows, maximum detection was not achieved until 35° from the vertical (Kingsley and Reeves 1998). The loss of visibility close to the aircraft militates in favour of lower flying heights if surveys must be carried out in flat-windowed aircraft and raises concerns about detection, if the

[6] Brooke, L. F. No date. A report on the 1994 Nunavik beluga and walrus subsistence harvest study. Unpublished report prepared for the Department of Fisheries and Oceans, 104, rue Dalhousie, Quebec P.Q. G1K 4B8, Canada, 29 p.

[7] Brooke, L. F. No date. A report on the 1995 Nunavik beluga and walrus subsistence harvest study. Unpublished report prepared for the Department of Fisheries and Oceans, 104, rue Dalhousie, Quebec P.Q. G1K 4B8, Canada, 29 p.

[8] Portnoff, M. 1994. The 1993 Nunavik beluga whale and walrus subsistence harvest study. Report prepared for the Department of Fisheries and Oceans, 104, rue Dalhousie, Quebec P.Q. G1K 4B8, Canada by Nunavik Graphics, Montreal, 61 p.

maximum visibility is not reached until so far away from the aircraft. The present results have not been corrected for detection bias, but Harwood et al. (1996) estimated, from paired-observer data, that it would be appropriate to add about 40% to correct for detection bias at the peak of the sighting curve even when using bubble windows.

The sightings curve fitted to the present data set has a shoulder at 670 m, and the width of the maximum-visibility strip, a critical determinant of the precision of the survey, was small. Larsen at al. (1994, Fig. 2) noted a marked drop in visibility of narwhal from the air beyond 823 m. In other studies, visibility of beluga whales dropped off beyond about 600 m from the aircraft (Norton and Harwood 1985), and by 600 m visibility of small cetaceans was less than 40% of maximum (Kingsley and Reeves 1998); both these surveys were flown lower than the 457 m of the present survey.

Estimates were not been corrected for diving beluga whales, but instead were conservative estimates of surface-visible beluga whales. Corrections to counts of beluga whales for diving have been estimated from visual records of their appearance and disappearance (Brodie, 1971; Sergeant, 1973; Fraker, 1980; Gauthier, 1999), by recording surface signals from attached VHF radio transmitters (Frost et al., 1985), and by studying diving behavior with attached pressure recorders (Martin and Smith, 1992; Richard et al., 1997; Heide-Jorgensen et al., 1998; Kingsley, unpubl. data). Early studies (Brodie, 1971; Sergeant, 1973) were restricted to nearshore areas. Correction estimates have ranged from adding 40% (Brodie, 1971) to adding 200% (Sergeant, 1973). A correction for eastern Hudson Bay, deduced from satellite-tag data on five beluga whales tagged in 1993, was about 80%, but there was a wide margin of uncertainty. This value was similar to values estimated for beluga whales summering in other waters of the Canadian Arctic (Martin and Smith, 1992; Richard et al., 1997; Heide-Jorgensen et al., 1998).

Large sampling variability is common in beluga whale surveys, the species being gregarious. Most of the error variance for individual strata in the line-transect survey was due to uncertainty in encounter rate, especially in the northern Hudson Bay stratum, where a few large groups were seen on a few transects. Overall, the error coefficient of variation was 23%, of which about 2/3 was due to uncertainty in encounter rate. The jack-knife bias reduction (Efron, 1982) reduced the estimate of the survey expansion factor by only 1%, from 0.583 /nmi to 0.575 /nmi.

Acknowledgments

This work was financially supported by the Quebec Federal Fisheries Development Plan, an initiative of the Canadian Department of Fisheries and Oceans. I thank the Makivik Corp. for support in the organisation of the Ungava Bay surveys and the coastal survey of Hudson Bay, notably D.W. Doidge, who arranged the aircraft contracts for the Ungava Bay survey and the coastal survey in Hudson Bay, and who also made several comments on the text of the present article. I thank the pilots and the observer teams both from the south and from the local communities. North Shore Air, Air Inuit, and Bradley Air provided charter aircraft, and Air Baffin made fuel available for the transect survey in James and Hudson bays.

Literature cited

Anonymous.
1993. Agreement between the Inuit of the Nunavut Settlement Area and Her Majesty in Right of Canada. Department of Indian and Northern Affairs and the Tungavik Federation of Nunavut, Ottawa, Ontario.

Brodie, P.
1971. A reconsideration of aspects of growth, reproduction, and behaviour of the white whale (*Delphinapterus leucas*) with reference to the Cumberland Sound, Baffin Island, population. J. Fish. Res. Board Can. 28:1309–18.

Brown Gladden, J. G., M. M Ferguson, and J. W. Clayton.
1997. Matriarchal genetic population structure of North American beluga whales *Delphinapterus leucas* (Cetacea: Monodontidae). Molecular Ecology 6:1033–1046.

Buckland, S. T.
1985. Perpendicular distance models for line transect sampling. Biometrics 41:177–195.

Buckland, S. T., D. R. Anderson, K. P. Burnham, and J. L. Laake.
1993. Distance sampling: estimating abundance of biological populations. Chapman and Hall, London, 446 p.

Burnham, K. P., D. R. Anderson, and J. L. Laake.
1980. Estimation of density from line transect sampling of biological populations. Wildlife Monographs 72, 203 p.

Campbell, R. R.
1993. Rare and endangered fishes and marine mammals of Canada: COSEWIC Fish and Marine Mammal Subcommittee Status Reports IX. Can. Field-Nat. 107:395–401.

Caron, L., and T. G. Smith.
1990. Philopatry and site tenacity of belugas, *Delphinapterus leucas*, hunted by the Inuit at the Nastapoka estuary, eastern Hudson Bay. *In* Advances in research on the beluga whale, *Delphinapterus leucas* (T. G. Smith, D. J. St Aubin, and J. R. Geraci, eds.), p. 69–79. Can. Bull. Fish. Aquat. Sci. 224.

Cochran W. G.
1977. Sampling techniques, 3rd ed. Wiley, New York, NY, 428 p.

DFO (Department of Fisheries and Oceans).
1996 Northern Quebec belugas 5 year management plan: 1996–2000. Department of Fisheries and Oceans, Québec, Que. 19 p. + Annexes.

Doidge, D. W.
1990 Age- and stage-based analysis of the population dynamics of beluga whales, *Delphinapterus leucas*, with particular reference to the northern Quebec population. Ph D diss., Dept of Renewable Resources, Macdonald College, McGill University, Ste. Anne de Bellevue, Quebec, 190 p.

Eberhardt, L. L., and D. B. Siniff.
1977. Population dynamics and marine mammal management policies. J. Fish. Res. Board Can. 34:183–190

Efron, B.
1982. The jackknife, the bootstrap and other resampling plans. Conference Board for the Mathematical Sciences and National Science Foundation Regional Conference Series in Applied Mathematics. Society for Industrial and Applied Mathematics, Philadelphia, PA, 92 p.

Efron, B., and R. J. Tibshirani.
1993. An introduction to the bootstrap. Chapman and Hall, New York, NY, 436 p.
Finley, K. J., G. W. Miller, M. Allard, R. A. Davis, and C. R. Evans.
1982. The belugas (*Delphinapterus leucas*) of northern Quebec: distribution, abundance, stock identity, catch history and management. Can. Tech. Rep. Fish. Aquat. Sci. 1123, 57 p.
Fraker, M. A.
1980. Status and harvest of the Mackenzie stock of white whales (*Delphinapterus leucas*). SC/31/SM8. Rep. Int. Whal. Comm. 30:451–458.
Frost, K. J., L. F. Lowry, and R. R. Nelson.
1985. Radiotagging studies of belukha whales (*Delphinapterus leucas*) in Bristol Bay, Alaska. Mar. Mamm. Sci. 1(3):191–202.
Gauthier, I.
1999. La visibilité aérienne des bélugas du Saint-Laurent et les implications pour l'estimation des effectifs. Mémoire de maitrise, Univ. du Québec à Rimouski, 105 p.
Harwood, L. A., S. Innes, P. A. Norton, and M. C. S. Kingsley.
1996. Distribution and abundance of beluga whales in the Mackenzie Estuary, southeast Beaufort Sea and west Amundsen Gulf during late July 1992. Can. J. Fish. Aquat. Sci. 53: 2262–2273.
Heide-Jørgensen, M. P., P. Richard, and A. Rosing-Asvid.
1998. Dive patterns of belugas (*Delphinapterus leucas*) in waters near eastern Devon Island. Arctic 51(1):17–26.
Hiby, A. R., and P. S. Hammond.
1989. Survey techniques for investigating abundance of cetaceans. *In* The comprehensive assessment of whale stocks: the early years (G. P. Donovan, ed.), p. 47–80. Rep. Int. Whal. Comm. Spec. Issue 11.
Jonkel, C. J.
1969. White whales wintering in James Bay. J. Fish. Res. Board Can. 26: 2205–2207.
Kingsley, M. C. S.
1989. Population dynamics of the narwhal *Monodon monoceros*: an initial evaluation (Odontoceti: Monodontidae). J. Zool. (London) 219:201–208.
Kingsley, M. C. S., and R. R. Reeves.
1998. Aerial surveys of cetaceans in the Gulf of St Lawrence in 1995 and 1996. Can. J. Zool. 76:1529–1550.
Larsen, F., M. P. Heide-Jorgensen, A. R. Martin, and E. W. Born.
1994. Line-transect estimation of narwhals (*Monodon monoceros*) in Scoresby Sound and adjacent waters. Meddr Gronland Biosci. 39:87–91.
Martin, A. R., and T. G. Smith.
1992. Deep diving in wild, free-ranging beluga whales, *Delphinapterus leucas*. Can. J. Fish. Aquat. Sci. 49(3):462–466.
NAMMCO (North Atlantic Marine Mammal Commission).
1999. Report of the Scientific Committee working group on the population status of beluga and narwhal in the North Atlantic. North Atlantic Marine Mammal Commission, Tromsø, 57 p.
Norton, P., and L. A. Harwood.
1985. White whale use of the southeastern Beaufort Sea, July–September 1984. Can. Tech. Rep. Fish. Aquat. Sci. 1401, v + 46 p.
Reeves, R. R., and E. D. Mitchell.
1987a. Catch history, former abundance and distribution of white whales in Hudson Strait and Ungava Bay. Naturaliste Can. (Rev. Ecol. Syst.) 114:1–65.
1987b. History of white whale (*Delphinapterus leucas*) exploitation in eastern Hudson Bay and James Bay. Can. Spec. Publ. Fish. Aquat. Sci. 95, 45 p.
1989. Status of white whales, *Delphinapterus leucas*, in Ungava Bay and eastern Hudson Bay. Can. Field-Nat. 103:220–239.
Richard, P. R.
1993. Status of the beluga, *Delphinapterus leucas*, in western and southern Hudson Bay. Can. Field-Nat. 107(4):524–532.
Richard, P. R., A. R. Martin, and J. R. Orr.
1997. Study of summer and fall movements and dive behaviour of Beaufort Sea belugas, using satellite telemetry: 1992–1995. Environ. Studies Res. Funds Rep. 134, 26 p. + appendices.
Richard, P. R., J. R. Orr, and D. G. Barber.
1990. The distribution and abundance of belugas, *Delphinapterus leucas*, in eastern Canadian waters: a review and update. *In* Advances in research on the beluga whale *Delphinapterus leucas* (T. G. Smith, D. J. St Aubin, and J. R. Geraci, eds.), p. 23–28. Can. Bull. Fish. Aquat. Sci. 224.
Richards, F. J.
1959. A flexible growth function for empirical use. J. Exp. Bot. 10:290–300.
Sergeant, D. E.
1973. Biology of white whales (*Delphinapterus leucas*) in western Hudson Bay. J. Fish. Res. Board Can. 30:1065–1090.
1981. On permissible exploitation rates of Monodontidae. Rep. Int. Whal. Comm. 31:583–588.
1986. Sea mammals. *In* Canadian inland seas (I. P. Martini, ed.), p. 327–340. Elsevier Oceanography Series 44, Amsterdam.
Sergeant, D. E., and P. F. Brodie.
1975. Identity, abundance and present status of populations of white whales, *Delphinapterus leucas*, in North America. J. Fish. Res. Board Can. 32:1047–1054.
Smith, T. G., and M. O. Hammill.
1986. Population estimates of the white whale, *Delphinapterus leucas*, in James Bay, eastern Hudson Bay and Ungava Bay. Can. J. Fish. Aquat. Sci. 43:1982–1987.
Stirling, I., W. R. Archibald, and D. P. DeMaster.
1977. Distribution and abundance of seals in the eastern Beaufort Sea. J. Fish. Res. Board Can. 34:976–988.

Age and growth of cutlassfishes, *Trichiurus* spp., from the South China Sea

Kai Yin Kwok
I-Hsun Ni

Department of Biology
Hong Kong University of Science & Technology
Hong Kong SAR, China

E-mail address (for I-H Ni, contact author): bonih@ust.hk

Abstract—Age and growth of two species of cutlassfishes, *Trichiurus* spp. (Trichiuridae), from the South China Sea were examined. Between December 1996 and November 1997, 1495 specimens were collected from coastal waters near Hong Kong. Two species, *Trichiurus lepturus* and *T. nanhaiensis*, were harvested and ages of specimens were estimated by using transverse sections of the sagittal otoliths. Opaque growth rings were verified to have formed annually during February. Lee's phenomenon was not observed for either species, although *T. lepturus* tended to display reverse Lee's phenomenon. Otolith weight was linearly related to age, and accounted for about 72% and 76% of the variation in age (t) for *T. lepturus* and *T. nanhaiensis*, respectively, comparable to the von Bertalanffy growth models in preanal length (PL). For older fish, otolith weight provided a more precise estimate of age than preanal length. Preanal length and age were fitted to the von Bertalanffy growth model by nonlinear regression, resulting in

$$PL\ (\text{mm}) = 589\{1 - e^{[-0.168(t + 2.682)]}\} \quad (T.\ lepturus);$$

$$PL\ (\text{mm}) = 602\{1 - e^{[-0.207(t + 2.044)]}\} \quad (T.\ nanhaiensis).$$

Growth in length of the two species was significantly different (ANCOVA, $F_{2,1245}$=169.69, P<0.001).

Manuscript accepted 24 April 2000
Fish. Bull. 98 748–758 (2000).

The cutlassfish, *Trichiurus lepturus* Linnaeus 1758, occurs throughout tropical and temperate waters of the world, between latitude 60°N and 45°S (Froese and Pauly, 1997). World harvests are approximately 750,000 tonnes annually and China lands about 80% (600,000 tonnes) (Claus, 1995). In terms of weight, cutlassfish is the most important commercial marine fish species in China (Luo, 1991) and has accounted for about 10% to 20% of the total marine fish catch. It is caught in all Chinese seas, the Bo Hai, the Yellow Sea, the East China Sea, and the South China Sea (Jiang et al., 1991), and about 15% of the catch comes from the South China Sea (Fig. 1) (Liu, 1996). Cutlassfish is used as food fish and is caught mainly by bottom trawling (Luo, 1991) and in lower amounts by longline, hand line, gill net, drift net and purse seine (Chen and Liu, 1982).

Age and growth studies and their derived growth parameters are indispensable in determining stock dynamics (Brouard et al., 1984). Numerous age and growth studies of *T. lepturus* have been conducted over the past few decades (Table 1); however, most research has focused on northern populations in the East China Sea, the Yellow Sea, and the Bo Hai. Similar work on populations in the South China Sea has not been available.

Three species of trichiurids occur in the South China Sea, *T. lepturus*, *T. nanhaiensis* (Wang and Xu, 1992, in Wang et al., 1992), and *T. brevis* (Wang and You, 1992, in Wang et al., 1992), whereas only one species, *T. lepturus*, occurs in the waters of China farther north (Wang et al., 1992, 1993, 1994). Populations of *T. lepturus* in the Bo Hai, the Yellow Sea, and the East China Sea suffer from overfishing (Lin, 1985; Du et al., 1988; Ma and Xu, 1989; Luo, 1991; Ye and Rosenberg, 1991; Xu et al., 1994). It is harvested only in the Bo Hai and the Yellow Sea as bycatch in other fisheries (Lin, 1985). The condition of trichiurid stocks in the South China Sea remains unclear.

Numerous methods have been used to age trichiurids. The length-frequency method has proven useful in India (Narasimham, 1976; Chakraborty, 1990) and the Philippines (Ingles and Pauly, 1984). Yet, hard parts such as whole or sectioned otoliths and vertebral centra are most frequently used to age cutlassfish (Table 1). Measuring otolith weight or otolith size may be a cost-effective method for aging some fishes (Barbieri et al., 1994; Ferreira and Russ, 1994; Worthington et al., 1995). Although sectioned otoliths are reliable for aging fish, the method is time consuming and expensive (Beckman et al., 1991).

The aims of our study were 1) to validate age estimates by using transverse sections of sagittal otoliths; 2) to verify Lee's phenomenon; 3) to evaluate the potential of using otolith size and weight to estimate age; 4) to fit the age-length data to the von Bertalanffy growth model; and 5) to provide age-growth information for management of cutlassfish resources from the South China Sea.

Materials and methods

Between December 1996 and November 1997, 960 specimens (preanal length [PL] range:138–468 mm; PL=the tip of the lower jaw with the mouth closed to the middle of anus) of *T. lepturus*, and 535 specimens (PL range:253–551

mm) of *T. nanhaiensis* were obtained from commercial catches in the coastal waters of Hong Kong. Commercial gears included longlines, purse seines and bottom trawls. Fresh specimens were placed on ice, transported to the laboratory, and identified by using the diagnostic key of Wang et al. (1992, 1993): if the frontal bone split laterally, specimens were identified as *T. lepturus*, otherwise *T. nanhaiensis*. Preanal lengths were measured to the nearest mm. Specimens were blotted dry and weighed (whole and gutted) to the nearest 0.01 g. To estimate the relationship between PL and gutted weight (W), the variables were log-transformed to meet the assumptions of normality and homogeneous variance. A linear version of the power function: $W\,(g) = a\,PL^b$ (mm) was fitted to the data.

Distinct growth rings on whole otoliths and vertebral centra were ill-defined. Transverse sections of sagittal otolith yielded "readable" growth rings; the latter were chosen as aging tools. Left and right sagittae were weighed independently to the nearest 0.01 mg after being oven dried at 40°C for 30 min. Otolith length (OL) was measured to the nearest 0.05 mm with calipers. Sagittal otoliths were embedded in resin and sectioned transversely through the nucleus with a low-speed saw. Up to five sections, 0.3 to 0.5 mm thick, were made from each otolith to ensure that at least one passed through the center of the nucleus. Sections were then ground with 1000- and 1200-grit sand paper, mounted on glass slides with clear fingernail polish, and examined with a compound microscope at 40× magnification with transmitted light. The relative age in years was determined by counting the number of opaque growth rings on the dorsal side of the sectioned otoliths (Fig. 2). Thirty-five pairs of sectioned otoliths of both species were processed. No differences in the number of growth rings were found in left and right sections of each pair. Thereafter, the right sagitta was used for age determination.

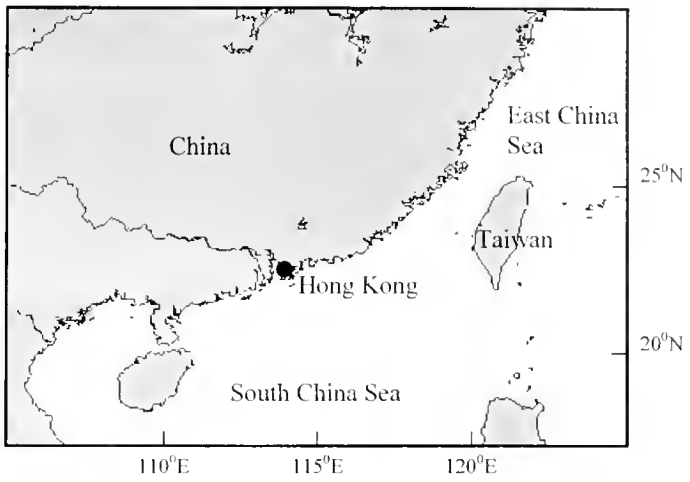

Figure 1
The South China Sea and surrounding area.

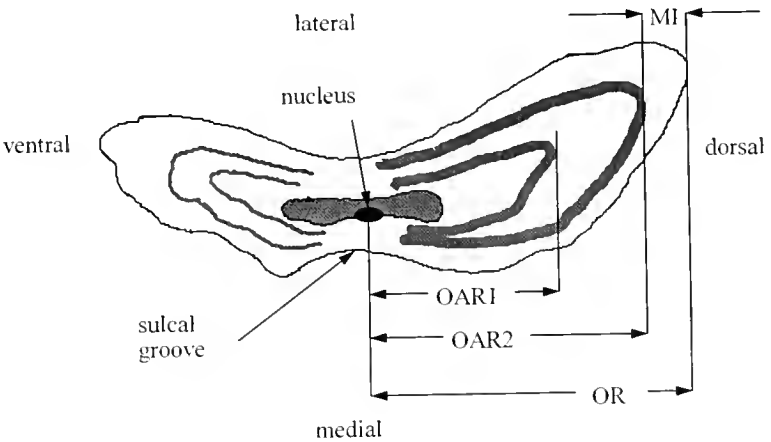

Figure 2
Schematic diagram of a transversely sectioned sagittal otolith of cutlassfishes, *Trichiurus* spp. MI = marginal increment, OAR1 = first otolith annular radius, OAR2 = second otolith annular radius, OR = otolith radius.

Otoliths were read twice (one month apart) in a random order, with no knowledge of fish length or species. Precision was measured by the percentage of agreement between readings (Lowerre-Barbieri et al., 1994). Deviations were counted a third time. Only counts with at least two agreements were used in subsequent analyses. Marginal increment method was used to validate the reading of annuli. Otolith radius (OR), otolith annular radius (OAR), and marginal increment (MI) (Fig. 2) were measured with an ocular micrometer to the nearest 0.025 mm.

The tendency for older fish to reflect smaller back-calculated length at earlier ages than measured length is known as Lee's phenomenon (Smith, 1983), and is related to size-selective mortality (Boehlert et al., 1989). To evaluate this phenomenon, the mean otolith annular radius (MOAR) for each annulus of the same age group was calculated, and the MOAR for each annulus of different age groups was plotted against the age group (Yamaguchi et al., 1990). Thus, we determined if older fish demonstrated slower growth of hard parts at younger ages, i.e. true Lee's phenomenon (Smale and Taylor, 1987). The ANOVA test was used to compare MOARs among different age groups.

Multiple linear-regression models were fitted in a stepwise manner to predict age from otolith weight and length. Variables were log-transformed to meet the assumptions of normality and homogeneous variance. A paired-sample *t*-test showed no significant difference between left and right sagittal otoliths in terms of weight (*T. lepturus*:

Table 1

Summary of age and growth studies of *Trichiurus lepturus*. A = Autumn brood; F = female; L_t = in preanal length; M = male; MI = marginal increment; otolith = sagittal otolith; S = spring brood;

Country	Study area	Study period	Sample size	Sex and brood	Aging and growth methods	Validation method	Growth parameters			Authors
							k(per yr)	L_∞(mm)	t_0(yr)	
China	East China Sea, Yellow Sea & Bo Hai	1954–57	1472		whole otolith, Ford–Walford plot	MI	0.4083	455.7	0.4400	Misu, 1958, 1964
China	East China Sea	1968–69	869		sectioned otolith, Ford–Walford plot	MI	0.1390	766.0	–0.2660	Hamada, 1971
China	East China Sea north	1977–78	3418		sectioned otolith, Ford–Walford plot	MI	0.2928	553.2	–0.6806	Wu et al., 1985a, 1985b
China	Yellow Sea	1964			whole otolith,		0.1100	708.0	–2.8200	Lin and Zhang, 1981
China	Bo Hai	1964			Ford–Walford plot		0.1100	658.0	–2.9100	
China	Yellow Sea & Bo Hai	1962–63	492		whole otolith,	MI	0.4380	501.0	–0.0607	Hong, 1980
Japan	Kii Channel	1972–74	3739		whole otolith, ford–Walford plot	MI	0.2610	568.3	–0.6435	Sakamoto, 1976
Japan	Kumano– Nada	1978–79	213	S	whole otolith,	MI	0.3960	483.0	–0.4350	Suzuki and Kimura,
				A	ford–Walford plot		0.5240	439.0	0.5280	1980
Japan	Suruga Bay	1965	505		whole otolith, ford–Walford plot	MI	0.2886	433.9	–0.4130	Kosaka et al., 1967
Japan	Kagoshima Bay	1993–94	292	F	whole otolith,	MI	0.1670	629.0	–1.7910	El–Haweet and Ozawa,
				M	ford–Walford plot		0.2160	481.0	–1.9750	1996[1]
Japan	Tsushima waters	1967–87	9592	S, F	whole otolith,	MI	0.4090	502.5	–0.4910	Hanabuchi, 1989
				S, M	ford–Walford plot		0.4810	438.7	–0.4580	
				A, F			0.4590	465.1	–0.2200	
				A, M			0.5530	400.7	–0.1960	
China	Taiwan Strait	1962–64	3319		vertebral centrum, Ford–Walford plot	MI	0.2920	477.4	–0.6340	Du et al., 1988
Taiwan	coastal sea (E)	1976–77	154		whole otolith, Ford–Walford plot	MI	0.2710	502.0	–0.2200	Chen and Lee, 1982
Taiwan	coastal sea (SW)	1976–77	341		whole otolith, Ford–Walford plot	MI	0.2890	550.0	–0.7600	Chen and Lee, 1982

[1] Studies used species name *T. japonicus* which was a junior synonym of *T. lepturus* (after Froese and Pauly, 1997).

t=–0.097, df=917, P>0.90; *T. nanhaiensis*: t=–0.762, df=518, P>0.44) and length (*T. lepturus*: t=–0.471, df=916, P>0.45; *T. nanhaiensis*: t=–0.689, df=523, P>0.49). Therefore, average otolith length and weight were used in the analyses. For all the linear regressions mentioned above, analysis of covariance (ANCOVA) was used to compare regressions between sexes and species.

We assigned 1 May and 1 June as the birth dates for *T. lepturus* and *T. nanhaiensis*, respectively (Kwok and Ni, 1999). Relative ages derived from aging were then converted to absolute ages. Von Bertalanffy growth curves were fitted by nonlinear regression on age and preanal length data (SPSS vers. 7.5). The von Bertalanffy growth equation for length is

$$PL_t = PL_\infty \{1 - e^{[-k(t - t_0)]}\},$$

where PL_∞ = the asymptotic length;
k = growth coefficient; and
t_0 = the hypothetical age at zero length.

Plots of residuals from regression models were used to check the assumption of normality. ANCOVA was used to compare log-transformed age-at-length regressions between sexes and species.

Results

The preanal length (mm) and gutted weight (g) regression models were significantly different between sexes (ANCOVA: *T. lepturus*: $F_{2,932}$=4.00, P<0.05; *T. nanhaiensis*: $F_{2,530}$=3.34, P<0.05) and species (ANCOVA: $F_{2,1466}$=83.76, P<0.001). The regression models were

T. lepturus
males:
$W = 1.513 \times 10^{-4}\ PL^{2.571}$ (n=212, r^2=0.9777, P<0.001);
females:
$W = 1.748 \times 10^{-4}\ PL^{2.549}$ (n=724, r^2=0.9761, P<0.001);
sexes combined:
$W = 1.624 \times 10^{-4}\ PL^{2.561}$ (n=936, r^2=0.9771, P<0.001);

T. nanhaiensis
males:
$W = 3.363 \times 10^{-5}\ PL^{2.846}$ (n=282, r^2=0.8506, P<0.001);
females:
$W = 6.553 \times 10^{-5}\ PL^{2.729}$ (n=252, r^2=0.9299, P<0.001);
sexes combined:
$W = 5.672 \times 10^{-5}\ PL^{2.755}$ (n=534, r^2=0.8968, P<0.001).

Sectioned sagittae of both species had an opaque nucleus located above the sulcal groove toward the dorsum. The nucleus was surrounded by a pattern of alternating wide, translucent zones and thin, opaque zones; the latter were considered annuli (Fig. 3). Annuli were distinct on the dorsum of the sections but were usually indecipherable on the ventral side. A total of 757 and 534 otoliths were embedded in resin and sectioned for *T. lepturus* and *T. nanhaiensis*, respectively. Of these, 33 (4.3%) and 9 (1.7%) were unreadable, and the percentage agreement between the two readings for each species was 95.4% and 92.7%, respectively.

The least marginal increment values (Fig. 4) occurred in February for both species, suggesting that one growth ring (annulus) formed each year. Only specimens age 1–4 were included in the analyses because older fish were rare in our collections. The mean otolith annular radius (MOAR) of the first annulus (ANOVA: $F_{5,582}$=3.046, P<0.05) and third annulus (ANOVA: $F_{3,80}$=4.024, P<0.05) of *T. lepturus* were significantly different among different age groups (Fig. 5); MOARs increased slightly with older age groups. However, no particular trend was found with regard to the MOARs of *T. nanhaiensis* (Fig. 5). Lee's phenomenon was not evident for either species, although reverse Lee's phenomenon was possible for *T. lepturus*.

Otolith weight accounted for 68.7% and 68.9% (Table 2) of the variability in age for *T. lepturus* and *T. nanhaiensis*, respectively. A negligible amount of the remaining variability was explained by considering otolith length in addition to otolith weight. The otolith weight-age regression was improved by fitting the untreated variables (otolith weight and age) with simple linear regression models:

T. lepturus:
$OW = 6.3533 + 5.2913Age$ (n=718, r^2=0.7168, P<0.001);
T. nanhaiensis:
$OW = 6.3921 + 3.6850Age$ (n=515, r^2=0.7561, P<0.001).

These regression results suggest a linear relationship between otolith weight and age (Fig. 6). The regression models were significantly different between the two species (ANCOVA: $F_{2,1229}$=224.17, P<0.001). Normal probability and residual plots showed that the regressions complied with the assumptions of normality and homogeneous variance.

Von Bertalanffy growth equations for both species were

T. lepturus
males:
$PL = 755.2\ \{1 - e^{[-0.116(t + 2.737)]}\}$ (n=146, r^2=0.684, P<0.001);
females:
$PL = 601.4\ \{1 - e^{[-0.158(t + 2.850)]}\}$ (n=578, r^2=0.765, P<0.001);
sexes combined:
$PL = 589.1\ \{1 - e^{[-0.168(t + 2.682)]}\}$ (n=724, r^2=0.749, P<0.001);

T. nanhaiensis
males:
$PL = 501.7\ \{1 - e^{[-0.306(t + 1.673)]}\}$ (n=281, r^2=0.682, P<0.001);
females:
$PL = 612.6\ \{1 - e^{[-0.220(t + 1.792)]}\}$ (n=244, r^2=0.726, P<0.001);
sexes combined:
$PL = 602.1\ \{1 - e^{[-0.207(t + 2.044)]}\}$ (n=525, r^2=0.699, P<0.001).

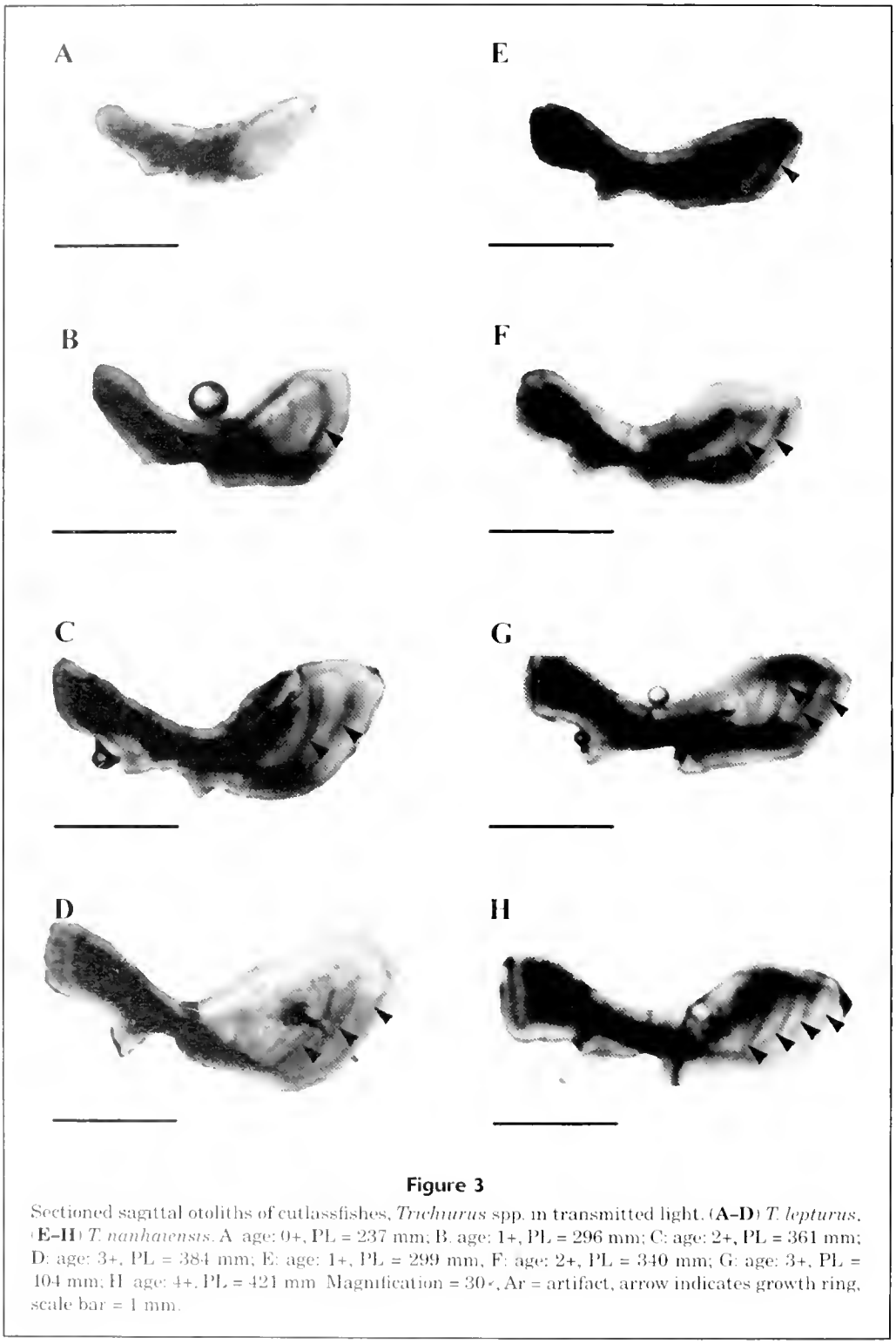

Figure 3

Sectioned sagittal otoliths of cutlassfishes, *Trichiurus* spp. in transmitted light. (**A–D**) *T. lepturus*. (**E–H**) *T. nanhaiensis*. A: age: 0+, PL = 237 mm; B: age: 1+, PL = 296 mm; C: age: 2+, PL = 361 mm; D: age: 3+, PL = 384 mm; E: age: 1+, PL = 299 mm, F: age: 2+, PL = 340 mm; G: age: 3+, PL = 404 mm; H: age: 4+, PL = 421 mm. Magnification = 30×, Ar = artifact, arrow indicates growth ring, scale bar = 1 mm.

Von Bertalanffy growth curves for sexes combined are depicted in Figure 7. No systematic trend was found in the residual plots for all regressions. The t_{max} (age at 95% of asymptotic length) of *T. lepturus* and *T. nanhaiensis* were 15.1 and 12.1 years, respectively. The W_∞ (asymptotic weight: estimated by substituting PL_∞ to the preanal length-weight equations) of *T. lepturus* and *T. nanhaiensis* were 2025 g and 2585 g, respectively. Log-transformed age-at-length regressions were significantly different between sexes (ANCOVA: *T. lepturus*:

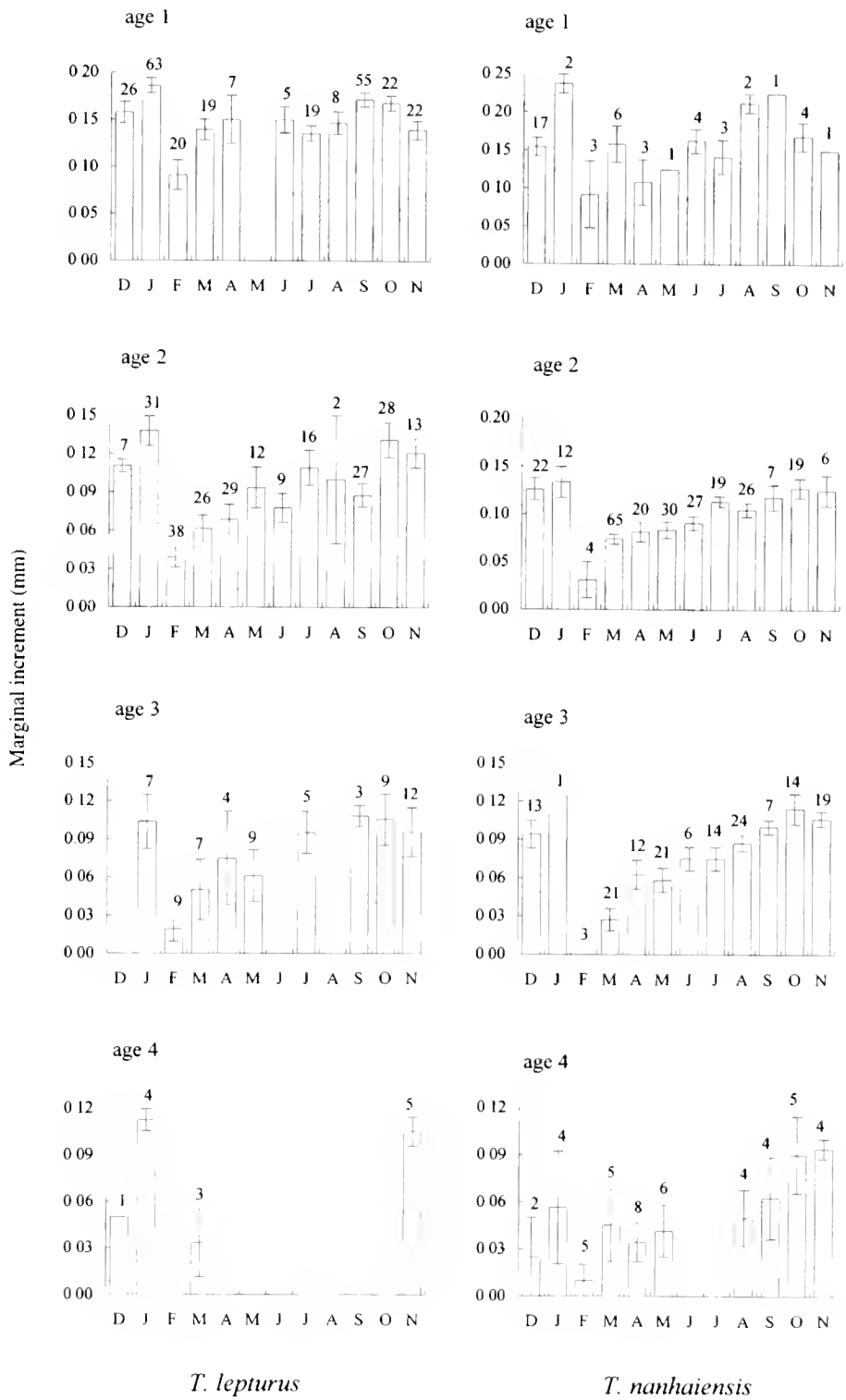

Figure 4

Mean monthly otolith marginal increment for *T. lepturus* (left panel) and *T. nanhaiensis* (right panel). Vertical bars are 1 SE, numbers on the top of vertical bars are sample sizes.

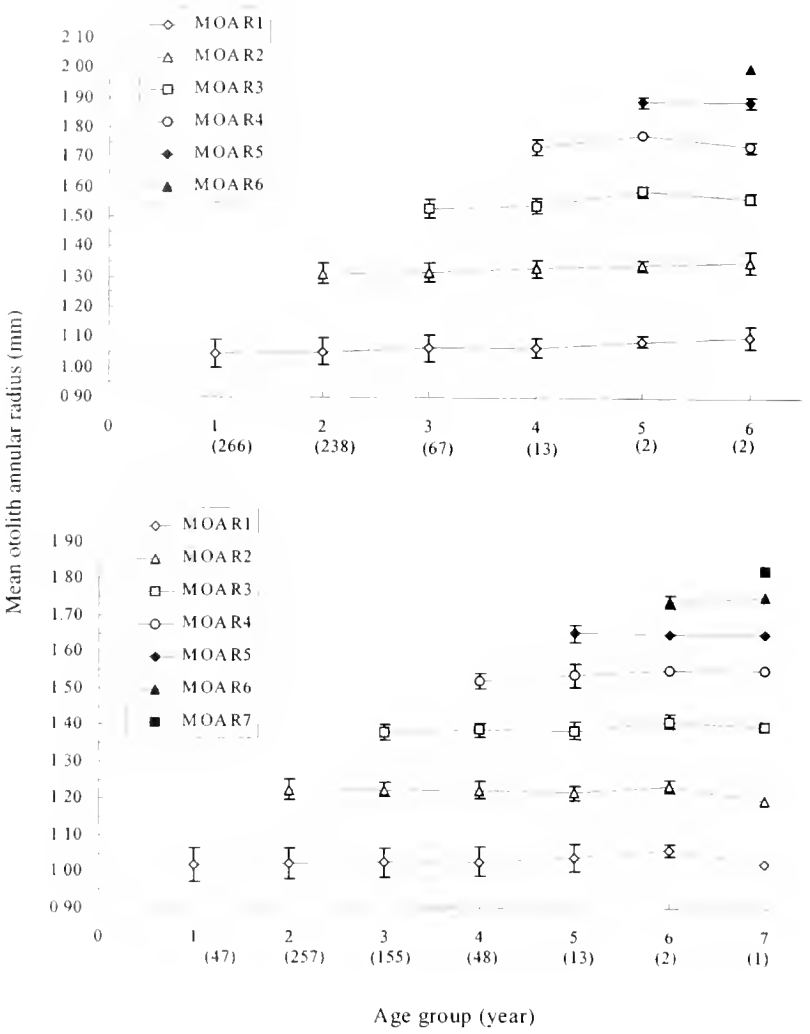

Figure 5

The relationship between mean otolith annular radius (MOAR) and age group for *Trichiurus lepturus* (top panel) and *T. nanhaiensis* (bottom panel). Vertical bars are 1 SE, numbers in parentheses are sample sizes.

$F_{2,720}$=4.39, P<0.05; *T. nanhaiensis*: $F_{2,521}$=23.78, P<0.001) and species (ANCOVA: $F_{2,1245}$=169.69, P<0.001).

Discussion

Our aging study of cutlassfishes from the South China Sea was successful in that we 1) found distinct growth rings on sectional sagittal otolith, 2) had excellent precision in independent ring counts, and 3) used marginal increment analyses to validate our aging method. In general, cutlassfishes from the northern seas of China (Misu, 1958, 1964; Hamada, 1971; Sakamoto, 1976; Hong, 1980; Wu et al., 1985a, Du et al., 1988; Hanabuchi, 1989, El-Haweet and Ozawa, 1996) and the South China Sea (our study) deposit annuli in late winter or early spring, suggesting that ring formation likely occurs in response to reduced water temperatures and is not correlated with peak spawning as indicated in Chen and Lee (1982). Summer is the peak spawning period of *T. lepturus* and *T. nanhaiensis* in the South China Sea (Kwok and Ni, 1999).

El-Haweet and Ozawa (1996) questioned whether Lee's phenomenon existed in a trichiurid population from Japan, having found no indication of Lee's or reverse Lee's phenomenon. We found that *T. lepturus* may exhibit reverse Lee's phenomenon, which suggests that *T. lepturus* are not overfished in the South China Sea or that fishing mortality is not size-selective, or that both situations may apply. Alternatively, fast growing individuals in the *T. lepturus* population may have greater chances of survival and attain older ages.

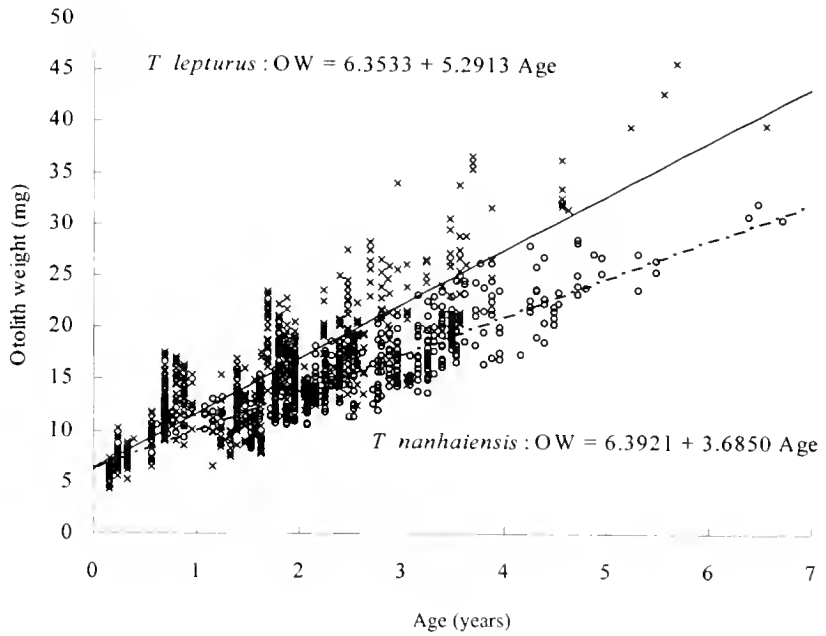

Figure 6

Regression model between otolith weight and age for *Trichiurus* spp. Solid line (regression line) and crosses (raw data): *T. lepturus*. Dotted line (regression line) and circles (raw data): *T. nanhaiensis*.

Table 2

Regression coefficients and statistics on multiple-regression models of age for cutlassfishes, *Trichiurus* spp. Variables were log-transformed for analyses.

Variable	Coefficient	SE	*P*	Partial r^2
T. lepturus (n=718)				
one-variable model (r^2=0.687)				
intercept	−4.404	0.108	<0.0001	
otolith weight	1.629	0.041	<0.0001	0.687
two-variable model (r^2=0.696)				
intercept	−5.922	0.430	<0.0001	
otolith weight	0.966	0.153	<0.0001	0.053
otolith length	2.076	0.461	<0.0001	0.028
T. nanhaiensis (n=515)				
one-variable model (r^2=0.689)				
intercept	−2.692	0.107	<0.0001	
otolith weight	1.305	0.039	<0.0001	0.689
two-variable model (r^2=0.690)				
intercept	−3.068	0.227	<0.0001	
otolith weight	1.123	0.105	<0.0001	0.183
otolith length	0.476	0.255	>0.05	0.007

The linear relation between otolith weight and age (Fig. 6) indicates that cutlassfish otoliths continuously increase in weight with age. The regression models explain 72% and 76% of the variance for *T. lepturus* and *T. nanhaiensis*, respectively, comparable to the von Bertalanffy growth model in preanal length. Thus, otolith weight pro-

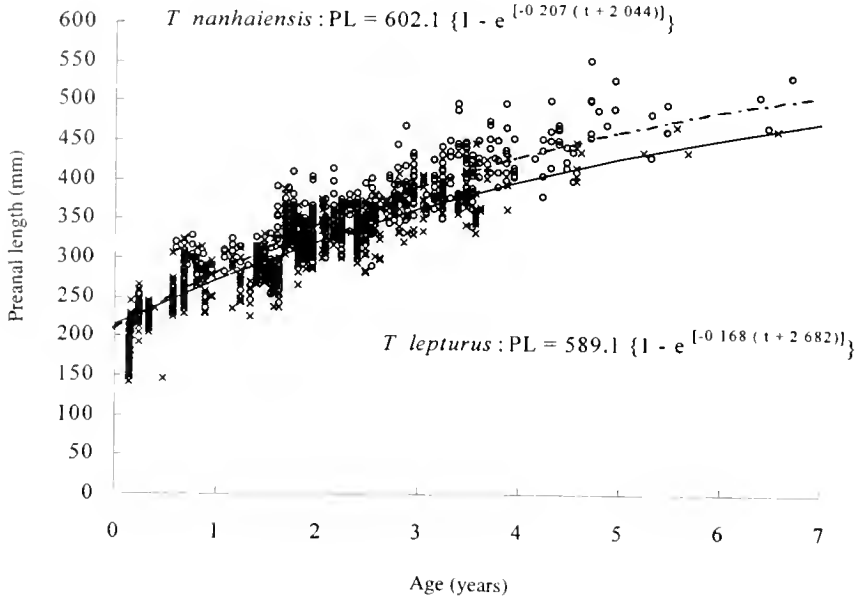

Figure 7

The von Bertalanffy growth curve for *Trichiurus* spp. Solid line (regression line) and crosses (raw data): *T. lepturus*. Dotted line (regression line) and circles (raw data): *T. nanhaiensis*.

vides a more precise estimate of age in older fish. Use of otolith weight to estimate age should be done with caution because these relationships have been shown to be population specific (Worthington et al., 1995).

This study is the first application of nonlinear regression in deriving a von Bertalanffy growth model for the cutlassfish; previously Ford-Walford plots were the most common method. The shortcomings associated with that method include 1) weighing problems due to different sample sizes of each age group; 2) a failure in providing variance-covariance for comparisons; 3) none of the raw data are used (Liu and Yeh, 1991); and 4) a reliance on back-calculated body length, which is usually estimated from the linear regression between hardpart dimension (e.g. otolith radius) and body length. Unfortunately, the growth of otoliths has been shown to be independent of somatic growth (Beckman et al., 1991; Barbieri et al., 1994), i.e. growth of body length ceases with age, while growth of hard parts continue. In comparison, our application of nonlinear regression analysis can avoid all these problems.

Basic growth parameters for these two populations of trichiurids in the South China Sea showed lower growth coefficients and higher asymptotic length, i.e. specimens reached maximum size at a slower pace than other trichiurids from the western Pacific Ocean (Table 1). This finding may be real or may reflect different methods employed for estimating growth.

In our comparison of the two species, *T. nanhaiensis* possessed a higher growth coefficient (k) than *T. lepturus*. Male *T. lepturus* had a lower growth coefficient but attained larger asymptotic size (PL_∞) than did female *T. lepturus*, whereas the opposite held true for *T. nanhaiensis*.

We provide basic growth parameters for use in the study of stock dynamics of trichiurids in the South China Sea. A formal stock assessment should be conducted with special emphasis on establishing an ecologically sustainable cutlassfish fishery in the South China Sea to prevent overfishing, or even fishery collapse, as has occurred in the northern populations of trichiurids.

Acknowledgments

Helpful assistance by Agassi Cheung and Y. K. Tam is much appreciated. We thank V. A. Unkefer for assistance with the writing and three anonymous reviewers for useful comments. Finally, we thank the Biology Department, Hong Kong University of Science and Technology, for providing the necessary funding and facilities.

Literature cited

Barbieri, L. R., M. E. Chittenden Jr., and C. M. Jones.
1994. Age, growth, and mortality of Atlantic croaker, *Micropogonias undulatus*, in the Chesapeake Bay region, with a discussion of apparent geographic changes in population dynamics. Fish. Bull. 92:1–12.

Beckman, D. W., A. L. Stanley, J. H. Render, and C. A. Wilson.
1991 Age and growth-rate estimation of sheepshead *Archosargus probatocephalus* in Louisiana waters using otoliths. Fish. Bull. 89:1–8.

Boehlert, G. W., M. M. Yoklavich, and D. B. Chelton.
1989. Time series of growth in the genus *Sebastes* from the Northeast Pacific Ocean. Fish. Bull. 87:791–806.
Brouard, E., R., Grandperrin, M. Kulbicki, and J. Rivaton.
1984. Note on observation of daily rings on otoliths of deep-water snapper. ICLARM Translation 3, Manila, Philippines, 8 p.
Chakraborty, S. K.
1990. Fishery, age, growth and mortality estimates of *Trichiurus lepturus* Linnaeus from Bombay waters. Indian J. Fish. 37:1–7.
Chen, W., and S. Lee.
1982. Age and growth of the ribbonfishes *Trichiurus* (Perciformes: Trichiuridae) of Taiwan. Bull. Inst. Zool., Academia Sinica 21:9–20.
Chen, Z. C., and J. Q. Liu.
1982. Commercial fishes of South China Sea. Guangdong Science and Technology Press, Guangzhou, China., 266 p. [In Chinese.]
Claus, F.
1995. Multilingual illustrated guide to the world's commercial warmwater fish. Fishing News Book, Cambridge, MA, 215 p.
Du, J. R., F. Z. Li, S. D. Lin, and Q. D. Zhang.
1988. On age and growth of hairtail, *Trichiurus haumela* (Forskål) in western Taiwan Strait. J. Oceanogr. Taiwan Strait 7:339–346. [In Chinese.]
El-Haweet, A. E., and T. Ozawa.
1996. Age, growth of ribbon fish *Trichiurus japanicus* in Kagoshima Bay, Japan. Fish. Sci. 62:529–533.
Ferreira, B. P., and G. R. Russ.
1994. Age validation and estimation of growth rate of the coral trout, *Plectropomus leopardus*. (Lacepede 1802) from Lizard Island, Northern Great Barrier Reef. Fish. Bull. 92:46–57.
Froese, R., and D. Pauly (eds.).
1997. Fishbase—a biological database on fish (software). ICLARM, Manila, Philippines, 256 p.
Hamada, R.
1971. Age and growth of the ribbon fish, *Trichiurus lepturus* based on the transverse section of the otolith. Bull. Seikai Reg. Fish. Res. Lab. 41:53–62. [In Japanese.]
Hanabuchi, S.
1989. Age and growth of cutlassfish, *Trichiurus lepturus* in Tsushima waters. Bull. Seikai Reg. Fish. Lab. 67:37–57. [In Japanese.]
Hong, S.
1980. A study on the age and growth of the hairtail in the Po Hai and Huang Hai. J. Fish. China 4:361–370. [In Chinese.]
Ingles, J., and D. Pauly.
1984. An atlas of the growth, mortality and recruitment of Philippine fishes. Institute of Fisheries Development and Research, College of Fisheries, University of the Philippines in the Visayas, Quezon City, Philippines and International Center for Living Aquatic Resources Management, Manila, Philippines. ICLARM Tech. Rep. 13:114–116.
Jiang, S. F., X. Z. Wang, Y. D. Chen, and X. Q. Zeng (eds.).
1991. Compilation of the statistics of Chinese fishery forty years (1949–1988). Department of Fishery, Ministry of Agriculture, The People's of Republic China. China Ocean Press, Beijin, 256 p. [In Chinese.]
Kosaka, M., M. Ogura, H. Shirai and M. Maeji.
1967. Ecological study on the ribbon fish, *Trichiurus lepturus* LINNÉ, in Suruga Bay. J. College of Mar. Sci. Tech., Tokai Univ. 2:131–146. [In Japanese.]
Kwok, K. Y.
1999. Reproduction of cutlassfishes, *Trichiurus* spp. from South China Sea. Mar. Ecol. Prog. Ser. 176:39–47.
Lin, J. Q.
1985. Hairtails. Agriculture Press, Beijing, 88 p. [In Chinese.]
Lin, J. Q., and M. D. Zhang.
1981. On the characteristic of the growth of the hairtail, *Trichiurus haumela* (Forskål) from the Yellow Sea and Bo-Hai. Mar. Fish. Res. 2:41–56. [In Chinese.]
Liu, C. C., and S. Y. Yeh.
1991. Age determination and growth of red emperor snapper (*Lutjanus sebae*) in the Arafura Sea off North Australia. ACTA Oceanog. Taiwanica 26:36–52.
Liu, S. L. (ed.)
1996. Compilation of the statistics of Chinese fishery (1989–1993). Department of Fishery, Ministry of Agriculture, the People's of Republic China. China Ocean Press, Beijing, 130 p. [In Chinese.]
Lowerre-Barbieri, S. K., M. E. Chittenden Jr, and C. M. Jones.
1994. A comparison of a validated otolith method to age weakfish, *Cynoscion regalis*, with the traditional scale method. Fish. Bull. 92:555–568.
Luo, B.
1991. Cutlassfish. *In* Marine fishery biology (C. Q. Fan, ed.), p. 111–160. Agriculture Press, Beijing. [In Chinese.]
Ma, Y., and J. Xu.
1989. Catch change pattern of hairtail in the East China Sea. Mar. Sci. 5:37–39. [in Chinese with English abstract.]
Misu, H.
1958. Studies on the fisheries biology of the ribbon fish *Trichiurus lepturus* in the East China and Yellow Seas. 1. On the age and the growth. Bull. Seikai Reg. Fish. Res. Lab. 15:1–14. [In Japanese.]
1964. Fisheries biology on the ribbon fish (*Trichiurus lepturus* Linne) in the East China and Yellow Seas. Bull. Seikai Reg. Fish. Lab. 32:1–58. [In Japanese.]
Narasimham, K. A.
1976. Age and growth of ribbonfish *Trichiurus lepturus* Linnaeus. Indian J. Fish. 23:174–182.
Sakamoto, T.
1976. Age and growth of the ribbon fish in the Kii Channel. Bull. Jap. Soc. Sci. Fish. 42:1–11. [In Japanese.]
Smale, M. A., and W. W. Taylor.
1987. Sources of back-calculation error in estimating growth of lake whitefish. *In* The age and growth of fish (R. C. Summerfelt, and G. E. Hall, eds.), p. 189–202. Iowa State Univ. Press, Ames, IA.
Smith, C. L.
1983. Summary of round table discussions on back calculation. U.S. Dep. Commer., NOAA Tech. Rep. NMFS 8:45–47.
SPSS Inc.
1997. SPSS base 7.5 for Windows. SPSS Inc., Chicago, IL. 628 p.
Suzuki, K., and S. Kimura.
1980. Fishery biology of the ribbon Fish, *Trichiurus lepturus*, in Kumano-Nada, central Japan. Faculty Fish. Mie Univ. 7:173–192. [In Japanese.]
Wang, K., L. Liu, F. You, and C. Xu.
1992. Studies on the genetic variation and systematics of the hairtail fishes from South China Sea. Mar. Sci. 2:69–71. [In Chinese.]
Wang, K., P. Zhang, L. Liu, F. You, and C. Xu.
1993. Studies on Trichiuridae from China coastal water. ACTA Oceanol. Sin. 15(2):77–83. [In Chinese.]

Wang, K., P. Zhang, L. Liu, F. You, C. Xu, and J. Wang.
1994. Biochemical assessment of the taxonomic status of Trichiuridae population from China Coastal water. ACTA Oceanol. Sin. 16(1):93–104. [In Chinese.]

Worthington, D. G., P. J. Doherty, and A. J. Fowler.
1995. Variation in the relationship between otolith weight and age: implications for estimation of age of two tropical damselfish (*Pomacentrus moluccensis* and *P. wardi*). Can. J. Fish. Aquat. Sci. 52:232–242.

Wu, H., G. Cheng, and J. Wang.
1985a. A study of the ageing of hairtails, *Trichiurus haumela* (Forskal). Oceanol. Et Limnol. Sinica 16:408–416. [In Chinese.]

Wu, H., G. Cheng, J. Zhou, and J. Wang.
1985b. Study of the growth of the hairtails, *Trichiurus haumela* (Forskal). Oceanol. Et Limnol. Sinica 16:156–167. [In Chinese.]

Xu, H., Z. Liu, Y. Ding, and Y. Xu.
1994. Resource condition and management countermeasure of largehead hairtail in East China Sea. J. Zhejiang Coll. Fish. 13:5–11. [In Chinese.]

Yamaguchi, Y., N. Hirayama, A. Koike, and H. A. Adam.
1990. Age determination and growth of *Oreochromis niloticus* and *Sarotherodon galilaeus* in High Dam Lake, Egypt. Nippon Suisan Gakkaishi (Bull. Jap. Soc. Fish.) 56:437–443.

Ye, Y., and A. A. Rosenberg.
1991. A study of the dynamics and management of the hairtail fishery, *Trichiurus haumela*, in the East China Sea. Aquat. Liv. Res. 4:65–75.

Abstract—When monitoring endangered species, natural resource managers require a recovery benchmark and a statistical procedure to test whether the benchmark has been met. We applied statistical power analysis to devise such a procedure for the endangered Sacramento River winter chinook salmon (*Oncorhynchus tshawytscha*). Winter chinook salmon management currently focuses on population growth rate, and our procedure used a Student's *t*-test to evaluate whether the average population growth rate is significantly lower than the management goal of 0.57 per generation. In the test, the null hypothesis was that the growth rate was not lower than the desired rate. In contrast to the usual hypothesis-testing framework, our procedure did not control for the type-I error rate. Instead, it controlled for the statistical power (the complement of the type-II error rate) and uses the resulting type-I error rate, computed from the sample size and other information, for the test. This procedure is conservative for winter chinook salmon in that, if all assumptions are met, it provides the specified level of assurance of detecting dangerously low population growth rates.

Manuscript accepted 14 March 2000.
Fish. Bull. 98:759–766 (2000).

Monitoring protocol for Sacramento River winter chinook salmon, *Oncorhynchus tshawytscha*: application of statistical power analysis to recovery of an endangered species*

Steven T. Lindley
Michael S. Mohr
Michael H. Prager

Santa Cruz/Tiburon Laboratory
Southwest Fisheries Science Center
National Marine Fisheries Service, NOAA
3150 Paradise Drive
Tiburon, California 94920

E-mail address (for S. T. Lindley): Steve.Lindley@noaa.gov

The Sacramento River winter chinook salmon is listed as an endangered species under the U.S. Endangered Species Act (ESA). The historical spawning grounds of the winter chinook salmon were in upper tributaries of the Sacramento River, including the Upper Sacramento, Pit, and McCloud Rivers (Fig. 1). The completion of Shasta and Keswick Dams in the 1940s blocked access to these spawning grounds, although populations had already declined from historic levels owing to habitat destruction in the upper tributaries (Fisher, 1994). Quantitative winter chinook salmon population size estimates began in 1967 when the Red Bluff Diversion Dam (RBDD), a flashboard dam with three fish ladders, was completed. Since the completion of RBDD, winter chinook salmon spawning runs have declined from over 100,000 adults to a few hundred adults in the 1980s (Fig. 2; Williams and Williams, 1991).

The winter chinook salmon population remains extremely depleted. The California Fish and Game Commission listed the population as a "candidate" species under California's Endangered Species Act in 1988 and declared it endangered under that Act in 1989. The National Marine Fisheries Service (NMFS) declared the species "threatened" under the federal ESA in the same year, and it was declared "endangered" in 1994. NMFS has taken numerous regulatory actions under the ESA to improve winter chinook salmon survival, including changes in the regulations governing California's ocean salmon fisheries.[1]

In 1997, NMFS required that future ocean fishery harvest regulations be designed to achieve at least a 31% increase in the winter chinook salmon average cohort replacement rate over that observed in 1989–93.[2] Because winter chinook salmon females spawn predominantly at age 3 (Fisher, 1994), the cohort replacement rate in year i is, for simplicity, defined as $R_i = N_i/N_{i-3}$, where N_i is the number of adult spawners passing RBDD in year i. For statistical modeling purposes, it is convenient to express this cohort replacement rate on the log scale, $r_i = \log(R_i)$, and refer

* Contribution 103 of the Santa Cruz/Tiburon laboratory, Southwest Fisheries Science Center, National Marine Fisheries Service, NOAA, 3150 Paradise Drive, Tiburon, CA 94920.

[1] Pacific Fishery Management Council. 1998. Review of 1997 ocean salmon fisheries. [Available from Pacific Fishery Management Council, 2130 SW Fifth Avenue, Suite 224, Portland, OR 97201.]

[2] NMFS, 1996. Endangered Species Act-Section 7: Consultation. Biological opinion. The fishery management plan for commercial and recreational salmon fisheries off the coasts of Washington, Oregon, and California of the Pacific Fishery Management Council. National Marine Fisheries Service, Northwest and Southwest Regional Fishery Management Divisions. NMFS, 1997. Reinitiated Section 7: Consultation on the fishery management plan for commercial and recreational salmon fisheries off the coasts of Washington, Oregon, and California as it affects the Sacramento River winter chinook salmon. National Marine Fisheries Service, Northwest and Southwest Regional Fishery Management Divisions.

to r_i simply as the "growth rate" of the cohort returning in year i. Denoting the underlying mean growth rate by ρ, the goal of at least a 31% increase in the average cohort replacement rate over the observed mean of 1.35 for the 1989–1993 period is equivalent to a goal, on the log scale, of $\rho_{goal} \geq \log(1.35 \times 1.31) = 0.57$.

A natural recovery benchmark then is to compare the observed sample mean growth rate $\bar{r}$ in future years to ρ_{goal}. If recovery efforts have the desired effect, and if no increased mortality occurs from other causes, recovery will proceed as desired and $\bar{r}$ will likely exceed ρ_{goal}. However, if $\bar{r} < \rho_{goal}$, recovery may not be proceeding as desired and further conservation measures may need to be implemented. This possibility raises the question of how one should evaluate whether an observed $\bar{r} < \rho_{goal}$ warrants concern.

In our paper, we propose using a one-sample, one-sided t-test to evaluate the statistical significance of a difference between the observed mean growth rate and the target rate. We depart from the usual procedure (Lehmann, 1986), however, by conditioning the test on a specific level of statistical power, rather than on a fixed type-I error rate, in order to provide an adequate detection probability for dangerously low population growth rates. Application of the test requires choosing a particular power level and specifying what constitutes a "dangerously" low population growth rate. Together, these quantities determine the sensitivity of the test for detecting population growth rates below the target, and the likelihood of false positives, i.e. concluding that population growth rate is below the target when it in fact is not. The level of danger posed by a certain growth rate is evaluated by using a population viability model.

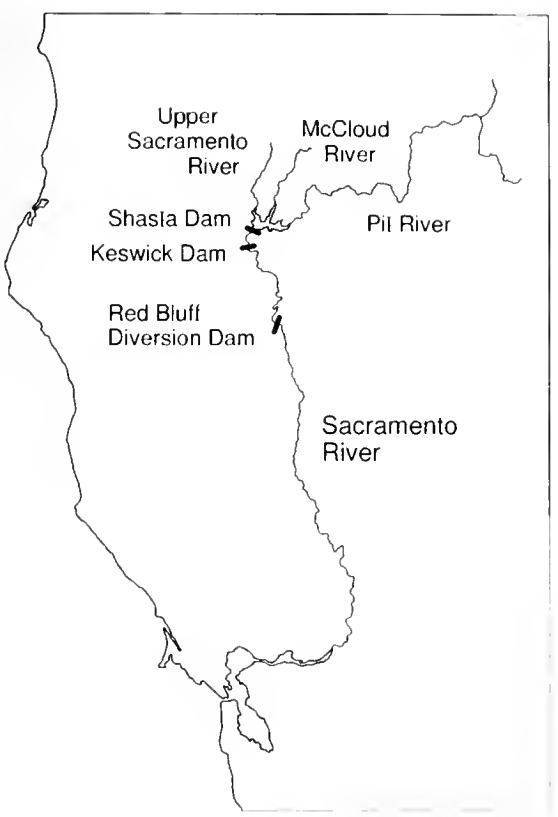

Figure 1

Map of Northern California depicting the Sacramento River, its upper tributaries, and mainstem dams.

Hypothesis testing and statistical power

Evaluating whether or not winter chinook salmon are meeting the recovery goal requires a statistical test because of the variability inherent in $\bar{r}$. We propose that a one-sided t-test be used to decide whether an observed mean population growth rate falls significantly short of the goal—in which case further regulatory action may be necessary. The null hypothesis of the test is that the underlying mean growth rate ρ (estimated by $\bar{r}$) is greater than or equal to ρ_{goal}, and the alternative hypothesis is that ρ is less than ρ_{goal}. That is,

$$H_0: \rho \geq \rho_{goal}$$

$$H_A: \rho < \rho_{goal}$$

with, in this case, $\rho_{goal} = 0.57$. Given a set of $n > 1$ observed r_i values $\{r_1, r_2, \ldots, r_n\}$, with mean $\bar{r}$ and standard deviation s, the test statistic is

$$t = \frac{\bar{r} - \rho_{goal}}{\sigma / \sqrt{n}}, \quad (1)$$

Assuming that the $\{r_i\}$ are independent and identically distributed normal random variables, t has a central t-distribution with $n - 1$ degrees of freedom if $\rho = \rho_{goal}$, and a noncentral t-distribution if $\rho \neq \rho_{goal}$ (Lehmann, 1986). The t-test rejects H_0 in favor of H_A when t is less than some critical value t_c specified *a priori* by the investigator.

A t-test has four possible outcomes, two of which result in correct inference: the test can accept H_0 when it is true, and it can reject H_0 when it is false. The test could also reject H_0 when it is in fact true—a "type-I" error, or it could fail to reject H_0 when it is false—a "type-II" error. The expected rates of type-I and type-II errors are conventionally denoted as α and β, respectively. The probability of correctly rejecting H_0 is known as the power π of the test, and $\pi = 1 - \beta$.

The type-I and type-II error rates are determined by the value of t_c selected for the test. A smaller value of t_c results in a lower type-I error rate α and a higher type-II error rate β. A larger value of t_c has the opposite effects. In all cases, the two error rates change in opposite directions when the value of t_c is changed. Thus, for a given data set of size n, α and β cannot be simultaneously minimized by adjusting t_c.

Given the endangered status of winter chinook salmon, it is clearly necessary to ensure that the statistical test has enough power to detect dangerously low population growth rates. To achieve this goal we propose that the power π of the test be held at a fixed level, rather than the

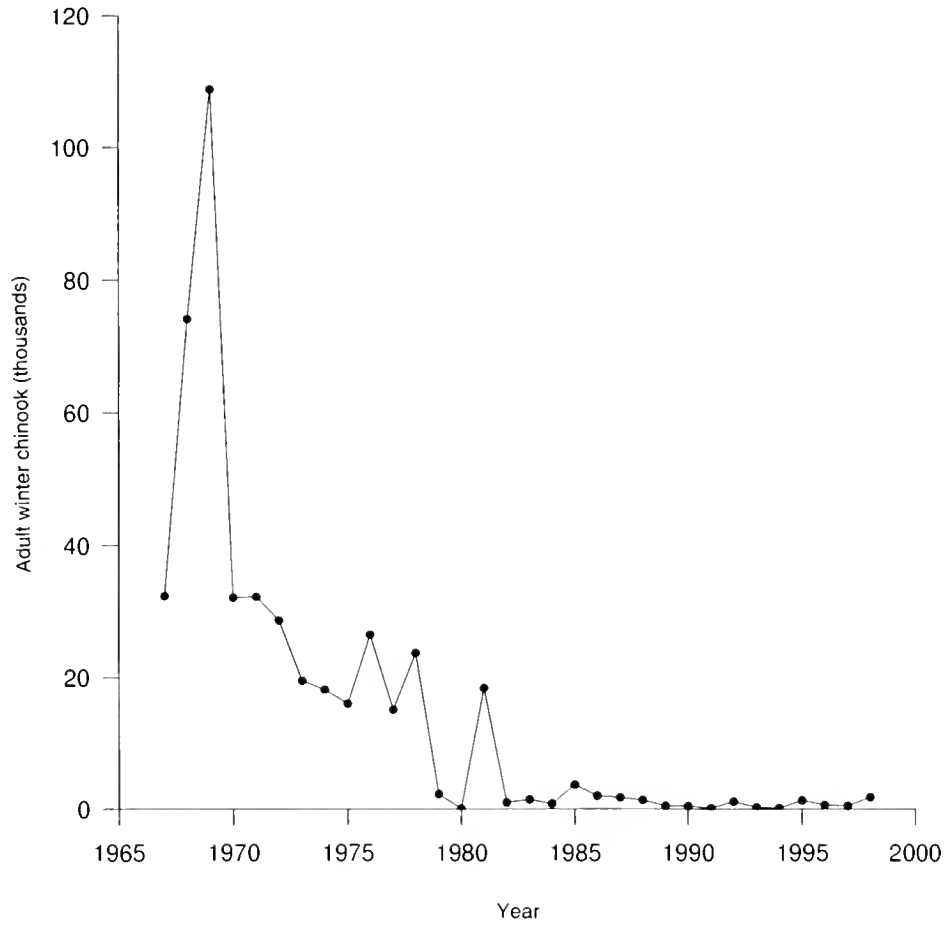

Figure 2
Historical time series of winter chinook salmon adult returns at Red Bluff Diversion Dam.

type-I error rate α. This approach differs from the conventional approach to hypothesis testing in which α is fixed at, say, 0.05, and the resulting power-level is either tolerated, or the sample size n is increased sufficiently to provide an acceptable level of power. Increasing n is not an option in this instance, because in any given year of application the sample size of the $\{r_t\}$ data set will be fixed, and a procedure is required that can be applied in each and every year. In the context of monitoring winter chinook salmon, a failure to reject H_0 may be used to justify "business as usual." By specifying the power π of the test in advance, resource managers will know that if the mean growth rate is falling seriously short of the goal, they will be able to detect this with specified probability π.

Calculation of α given π

In this section, we formulate the relation between π and α. This relation allows one to determine what values of α should be used for the test in order to achieve a specified level of power π.

With the previously stated distributional assumptions, t has a central t-distribution if $\rho = \rho_{goal}$, with cumulative distribution function (cdf) T and inverse cdf T^{-1}. If $\rho \neq \rho_{goal}$, t has a noncentral t-distribution with cdf T_δ, inverse cdf T_δ^{-1}, and noncentrality parameter

$$t = \frac{\bar{r} - \rho_{goal}}{s / \sqrt{n}}. \tag{2}$$

which is the difference between ρ and ρ_{goal} in standard error units (Johnson et al., 1994). Given a particular critical value t_c, the associated type-I error rate and power of the t-test are

$$\alpha = \Pr\{\text{reject } H_0 | H_0 \text{true}\} = T(t_c), \tag{3}$$

$$\pi = \Pr\{\text{reject } H_0 | H_0 \text{false}\} = T_\delta(t_c), \tag{4}$$

α by definition being the largest value of $T_\delta(t_c)$ under H_0, which occurs at $\rho = \rho_{goal}$ where $T_{\delta=0}(t_c) = T(t_c)$. Solving

Equation 4 for t_α and substituting this into Equation 3 gives

$$\alpha = T\left(T_\delta^{-1}(\pi)\right). \quad (5)$$

Equation 5 indicates the type-I error rate, α, associated with the test when conducted at specified power-level π. Note that, π having been specified, α also depends on the magnitude of the underlying difference $\rho - \rho_{goal}$, the variability σ in growth rates, and the sample size n, all through the noncentrality parameter δ.

Relation between α, π, n, and quasi-extinction

Although Equation 5 gives the value of α corresponding to a specified power-level π, the formula itself does not reveal the nature of the relation between α and π, and how this relation is affected by ρ and n. We illustrate these relationships below and consider their consequences in the context of a proposed test for detecting low growth rates in the Sacramento River winter chinook salmon population.

To apply Equation 5, we must specify σ, ρ, and π. We want to know (with probability π) that winter chinook salmon growth is not less than ρ_{goal} by a critical amount. Because the ESA is invoked to prevent extinction, we want to guard against growth rates that could lead to extinction. We used the winter chinook salmon population viability model developed by Botsford and Brittnacher (1998) to identify growth rates corresponding to quasi-extinction probabilities of 0.05, 0.50, and 0.99 over 50 years. Quasi-extinction occurs when a population falls below some threshold level, in this case 200 adults in three consecutive cohorts. We initialized the viability model simulation with winter chinook salmon spawning escapements from the 1989–93 base period, and set σ = 0.552, the observed standard deviation of growth rates during the base period, assuming that this value will continue to hold in the future. The mean growth rates corresponding to the specified quasi-extinction probabilities were found to be about 0.0, –0.14, and –0.40, respectively. We note that if indeed $\rho = \rho_{goal} = 0.57$, quasi-extinction is an extremely unlikely event according to this model.

For each of the three growth rates, δ was computed according to Equation 2, and Equation 5 was then used to determine the type-I error rate α over a range of specified power-levels π and sample sizes n. We calculated Equation 5 by using the Matlab Statistics Toolbox function NCTINV (Jones, 1996). (Fortran and S-PLUS subroutines are also available for the noncentral t-distribution from the Carnegie Mellon University Department of Statistics' StatLib and Oxford University Department of Statistics' FTP archive, respectively. Alternatively, because t_δ is distributed as a ratio of independent random variables, $(Z+\delta)/\sqrt{\chi^2_{n-1}/(n-1)}$, where Z is a standard normal variate and χ^2_{n-1} is a chi-square variate with $n-1$ degrees of freedom, a large number of draws of t_δ could be simulated, and the $100 \cdot \pi$th percentile could be taken as an approximation to $T_\delta^{-1}(\pi)$ in Equation 5.)

Table 1

Type-I error rate (α) necessary to maintain the t-test power-level at π given a fixed number of observations n. Power-level is with respect to detecting a mean growth rate of ρ.

		n			
ρ	π	2	3	4	5
0.0	0.9	0.435	0.326	0.246	0.185
	0.8	0.308	0.216	0.154	0.110
	0.7	0.238	0.157	0.106	0.073
	0.6	0.188	0.117	0.076	0.050
	0.5	0.148	0.087	0.054	0.034
	0.4	0.114	0.063	0.037	0.023
	0.2	0.054	0.027	0.015	0.008
–0.14	0.9	0.334	0.225	0.152	0.102
	0.8	0.243	0.150	0.094	0.059
	0.7	0.190	0.109	0.065	0.039
	0.6	0.151	0.081	0.046	0.027
	0.5	0.120	0.061	0.033	0.018
	0.4	0.092	0.044	0.023	0.012
	0.2	0.044	0.019	0.009	0.004
–0.40	0.9	0.229	0.125	0.068	0.037
	0.8	0.172	0.084	0.042	0.022
	0.7	0.137	0.062	0.029	0.014
	0.6	0.110	0.046	0.021	0.010
	0.5	0.087	0.035	0.015	0.007
	0.4	0.068	0.025	0.010	0.004
	0.2	0.033	0.011	0.004	0.002

The results for $\rho = 0.0$ (Fig. 3) display the general behavior expected: 1) for fixed π, α decreases with n; 2) for fixed n, the higher π is set, the greater α becomes; and 3) for fixed α, power increases with increased sample size. For example, if the power-level were fixed at $\pi = 0.8$ and α set accordingly, a type-I error would be expected about 22% of the time with 3 years of data, 11% of the time with 5 years of data, or 3% of the time with 10 years of data. On the other hand, if the type-I error rate were fixed at $\alpha = 0.05$, there would be roughly an 80% chance of detecting this value of ρ with 7 years of data, but the power of detection would drop to $\pi < 35\%$ with only 3 years of data.

Table 1 lists results for mean growth rates of 0.0, –0.14 and –0.40. Notice that while the type-I error rate required diminishes for a given power-level and sample size as the underlying growth rate declines, use of a fixed $\alpha = 0.05$ even in the most dire case of $\rho = -0.40$ would provide very low power for $n \leq 3$.

Monitoring protocol

A monitoring protocol cannot be designed solely on the basis of statistical considerations—it must be guided by management policy. In this instance, the management policy is to

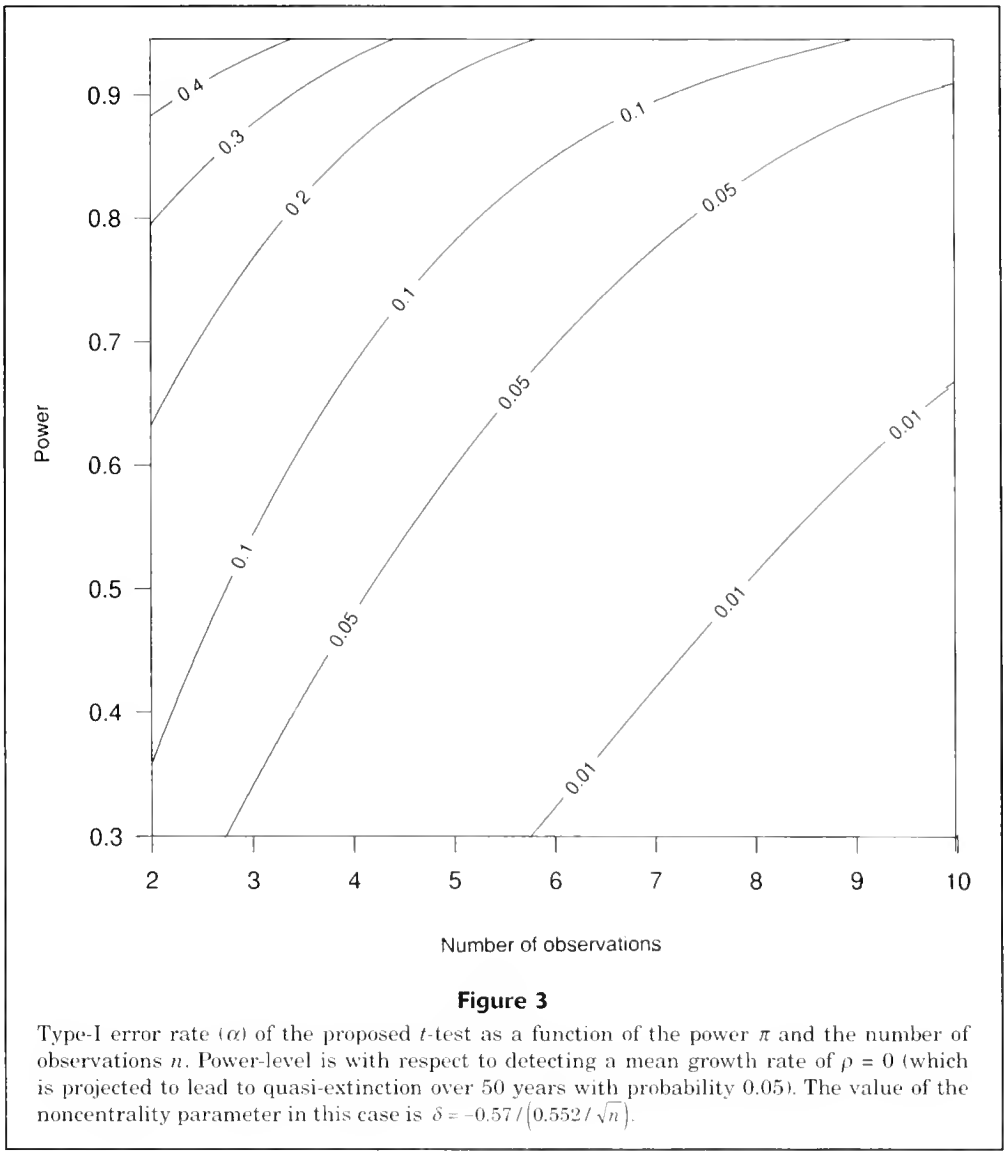

Figure 3

Type-I error rate (α) of the proposed t-test as a function of the power π and the number of observations n. Power-level is with respect to detecting a mean growth rate of $\rho = 0$ (which is projected to lead to quasi-extinction over 50 years with probability 0.05). The value of the noncentrality parameter in this case is $\delta = -0.57/\left(0.552/\sqrt{n}\right)$.

provide an adequate level of protection for winter chinook salmon through timely identification of low growth rates, without incurring too many false positive results.

The suggested protocol, therefore, would be to apply the t-test annually, with a fixed power-level of 80% for detecting a mean population growth rate of $\rho = 0$ (which is projected to lead to quasi-extinction over 50 years with probability 0.05). The choice of π and ρ is somewhat arbitrary, reflecting the perceived costs of type-I and type-II errors, and is discussed in a later section of this paper.

The observed growth rates are defined as $r_t = \log(N_t/N_{t-3})$, and the protocol would commence with the $i = 1997$ and 1998 spawning runs—both runs having benefited from the 1996 shift in ocean harvest regulations designed to reduce fishing mortality on winter chinook salmon.[1] Each year after 1998, the additional observed growth rates would be added to the test data set, until five growth rates are obtained. Beyond the year 2001, the test would be limited to the most recent five growth rates, at which point the α-level will stabilize at 0.11. The protocol's moving five-year data frame will facilitate identification of shifts in winter chinook salmon survival and strengthen the basis for the assumption that the $\{r_t\}$ are identically distributed (discussed below). Survival shifts might be expected in response to naturally arising or management-related changes in the freshwater or marine environment.

To illustrate in concrete terms the proposed monitoring and analysis protocol, we applied it to the historical time series of adult returns $i = 1970,\ldots,1996$, as if the protocol had commenced with the $i = 1970$ and 1971 spawning runs. The calculations and results of this application are presented in Table 2. Throughout the historical time series, $\bar{r}$ failed to reach the target level of 0.57, and this failure would have been declared significant in all years except for 1983–89 and 1996. If the test used a higher π, the number of failures declared significant would be higher. For instance, using $\pi = 0.85$ results in 21 null hypothesis

Table 2

Application of the proposed monitoring protocol to the historical time series of winter chinook salmon adult returns at Red Bluff Diversion Dam. Subscript t denotes year; N = abundance; R = cohort replacement rate; r = log (R) = growth rate; $\bar{r}$ = average growth rate over previous n years; t = t-statistic; π = power of test to detect a mean growth rate of zero; α = type-I error rate of test; t_c = test critical value; H_0 = mean growth rate ≥0.57.

Year(t)	N_t	N_{t-3}	R_t	r_t	$\bar{r}_t$	n_t	t_t	π_t	α_t	$t_{c,t}$	Reject $H_{0,t}$?
1967	32321	—	—	—	—	—	—	—	—	—	—
1968	74115	—	—	—	—	—	—	—	—	—	—
1969	108855	—	—	—	—	—	—	—	—	—	—
1970	32085	32321	0.993	−0.007	—	—	—	—	—	—	—
1971	32225	74115	0.435	−0.833	−0.420	2	−2.399	0.8	0.308	−0.689	yes
1972	28592	108855	0.263	−1.337	−0.726	3	−3.343	0.8	0.216	−0.976	yes
1973	19456	32085	0.606	−0.500	−0.669	4	−4.430	0.8	0.154	−1.225	yes
1974	18109	32225	0.562	−0.576	−0.651	5	−5.613	0.8	0.110	−1.453	yes
1975	15932	28592	0.557	−0.585	−0.766	5	−8.718	0.8	0.110	−1.453	yes
1976	26462	19456	1.360	0.308	−0.538	5	−4.252	0.8	0.110	−1.453	yes
1977	15028	18109	0.830	−0.186	−0.308	5	−5.160	0.8	0.110	−1.453	yes
1978	23669	15932	1.486	0.396	−0.129	5	−3.337	0.8	0.110	−1.453	yes
1979	2251	26462	0.085	−2.464	−0.506	5	−2.068	0.8	0.110	−1.453	yes
1980	84	15028	0.006	−5.187	−1.427	5	−1.859	0.8	0.110	−1.453	yes
1981	18297	23669	0.773	−0.257	−1.540	5	−2.041	0.8	0.110	−1.453	yes
1982	972	2251	0.432	−0.840	−1.671	5	−2.243	0.8	0.110	−1.453	yes
1983	1439	84	17.131	2.841	−1.182	5	−1.327	0.8	0.110	−1.453	no
1984	794	18297	0.043	−3.137	−1.316	5	−1.388	0.8	0.110	−1.453	no
1985	3633	972	3.738	1.318	−0.015	5	−0.579	0.8	0.110	−1.453	no
1986	2013	1439	1.399	0.336	0.104	5	−0.462	0.8	0.110	−1.453	no
1987	1761	794	2.218	0.797	0.431	5	−0.141	0.8	0.110	−1.453	no
1988	1386	3633	0.382	−0.964	−0.330	5	−1.129	0.8	0.110	−1.453	no
1989	480	2013	0.238	−1.434	0.011	5	−1.070	0.8	0.110	−1.453	no
1990	425	1761	0.241	−1.422	−0.537	5	−2.386	0.8	0.110	−1.453	yes
1991	134	1386	0.097	−2.336	−1.072	5	−3.173	0.8	0.110	−1.453	yes
1992	1122	480	2.338	0.849	−1.061	5	−3.096	0.8	0.110	−1.453	yes
1993	267	425	0.628	−0.465	−0.961	5	−2.832	0.8	0.110	−1.453	yes
1994	153	134	1.142	0.133	−0 648	5	−2.165	0.8	0.110	−1.453	yes
1995	1296	1122	1.155	0.144	−0.335	5	−1.670	0.8	0.110	−1.453	yes
1996	612	267	2.292	0.829	0 298	5	−1.101	0.8	0.110	−1.453	no

rejections out of 26 tests, rather than the 18 rejections for π = 0.80. On the other hand, setting α = 0.05 would have rejected H_0 only 14 times.

Discussion

Statistical considerations

Any t-test assumes that the observations are independent and are identically distributed normal random variables. Assuming a normal distribution for r is reasonable, because R (its antilog) has been found to be approximately lognormally distributed (Botsford and Brittnacher, 1998). More generally, observations on fish population sizes or survival rates are often found to be approximately lognormally distributed, as if arising from a series of random multiplicative events (Hennemuth, 1980).

The requirement that the growth rate observations be identically distributed as well (same underlying mean and variance), is not directly verifiable, but this assumption is reasonable given the short time period over which the test is conducted (n=5-year period). Indeed, this was our rationale for limiting the testing protocol to a 5-year time horizon. Although a longer time frame would boost the test's sample size and, for fixed α, increase its power, we believe identity of distribution beyond a 5-year horizon is an untenable assumption. Thus, the proposed protocol limits the test to a 5-year time frame, achieving the necessary power at the expense of a higher type-I error rate.

The issue of independence of observations is more difficult to assess. Winter chinook salmon adults return to

the river for spawning at age 3 or age 4, and although approximately 90% of a brood's spawning adults do so at age 3 (Fisher, 1994), this means that there is imperfect temporal isolation between runs in adjacent years. It is plausible that an environmental factor occurring in a particular spawning year could affect the returns in several future years, creating a lack of independence among observations. Such autocorrelation would decrease the effective sample size. Under this scenario, any test based on the nominal sample size (number of years of data) would have increased levels of both type-I and type-II errors (Lehmann, 1986). Given the relatively low level of information available on this population, this consideration is secondary and can be evaluated more thoroughly as the data base increases. The current time series of $\{r_t\}$ values shows no significant autocorrelation ($P>0.05$), which suggests that a lack of independence is most likely not a serious issue.

Choice of δ and π

In any hypothesis test, one must specify the type-I and type-II error rates. The choice of these rates should reflect the relative costs, as perceived by the investigator, of making these errors (Toft and Shea, 1983). When these costs can be specified in advance, and in comparable terms, one can balance them explicitly through specification of α and π (Mapstone, 1995). However, in the case of our proposed winter chinook salmon monitoring protocol, the cost of making a type-I error is unknown (no specific actions have yet been associated with a rejection of the null hypothesis), whereas type-II errors may be associated with extinction. We believe the appropriate course in this situation is to first identify growth rates that lead to unacceptably high probabilities of extinction, fix the power π of detecting these growth rate levels at a suitably high level, and accept, within reasonable limits, the resulting type-I error rate α. Specifically, for the winter chinook salmon monitoring protocol, we have specified an 80% chance of detecting growth rates that would lead to a ≥5% chance of quasi-extinction in 50 years, and accept the corresponding type-I error rate. We have selected these values because they are consistent with suggestions in the literature (reviewed briefly below); resource managers should carefully consider whether they are appropriate.

Setting δ by way of ρ that leads to an unacceptable predicted extinction risk, as we have done, is natural in the current setting, but just what level of extinction risk should be of concern is debatable. Population viability models have been widely used in conservation biology to quantify extinction risk as a function of population size and the magnitude and variability of population growth rate (Beissinger and Westphal [1998] have provided a recent review). Shaffer (1981), in pioneering work on minimum viable populations, has tentatively suggested that viable populations should have at least a 99% chance of remaining extant for 1000 years, but stated that specific probabilities and time horizons are arbitrary, and other values might be more appropriate. Indeed, other studies have used a variety of criteria: Botsford and Brittnacher (1998) used a 0.10 extinction probability in 50 years to develop criteria for removing winter chinook salmon from the Endangered Species List; Shaffer and Samson (1985) used the criteria of a 0.05 extinction probability over 100 years to identify a minimum viable population size for grizzly bears. We have adopted the 0.05 probability of extinction over 50 years as a moderately conservative criterion.

Specifying the value of π is also somewhat arbitrary. Peterman and M'Gonigal (1992) contend that monitoring programs must have high power ($\pi \geq 0.8$) to detect biologically important effects in order to be reliable. A reliable test should also have a reasonable α value as well as sufficient power. In the proposed winter chinook salmon protocol, the α-level stabilizes at 0.11 after 5 years of data have been collected, and we feel that this behavior represents a reasonable balance between the type-I and type-II error rates.

Power analysis and the precautionary approach

With the decline, collapse, or endangerment of numerous fish populations around the world, the paradigm of precautionary fishery management is receiving increasing attention. The "precautionary approach" to fishery management, as developed by the Food and Agriculture Organization of the United Nations (FAO, 1996), strives to avoid irreversible or slowly reversible damage to fisheries, places priority on conservation of productive capacity, and requires that fishing activities be considered harmful unless proven otherwise. The reauthorization of the U. S. Magnuson-Stevens Fishery Conservation and Management Act (as amended through October 11, 1996) is meant to ensure that "irreversible or long-term adverse effects on fishery resources and the marine environment are avoided."

Peterman and M'Gonigal (1992) have argued that power analysis is a fundamental part of precautionary management, because it provides an estimate of the reliability of the monitoring program. There are four types of power analysis, which correspond to determining one of either n, π, α, or the effect size from the other three (Cohen, 1977). In environmental studies, the determination of n and π are fairly common (e.g. Gerrodette, 1987; Gryska et al., 1997; Urquhart et al., 1998). The determination of α, as we have done here, is least common, in part owing to the "strength of the significance criterion convention, which makes investigators loath to consider "large" values of α" (Cohen, 1977).

Type-II errors in fisheries management are costly because populations and ecosystems can be slow to recover (Dayton, 1998). In endangered species management, the biggest risk is extinction of a species, rather than failure to meet some fiscal or harvest goal, and is truly irreversible. Fixing the type-I error rate at a typical value such as 0.01 or 0.05 would make timely detection of dangerously low growth rates unlikely (Table 1; Peterman, 1990). Thus, we believe that using standard statistical protocols, which control for the type-I error rate and accept the resulting type-II error rate, is not an appropriate method when monitoring endangered species. In such situations, it is more logical, and certainly more precautionary, to set the type-II error rate at an acceptably small value that yields a reasonable type-I error rate.

Acknowledgments

The authors greatly appreciate discussions with L. Holsinger and D. Viele of the National Marine Fisheries Service, Southwest Regional Office. We also wish to thank an anonymous referee for pointing out that the noncentral t-distribution can be straightforwardly simulated if software for the T_{δ}^{-1} function is unavailable. The manuscript was reviewed by D. Viele, L. Goldwasser, and C. Grimes. Any remaining errors are the responsibility of the authors.

Literature cited

Beissinger, S. R., and M. I. Westphal.
1998. On the use of demographic models of population viability analysis in endangered species management. J. Wildl. Manage. 62:821–841.

Botsford, L. W., and J. G. Brittnacher.
1998. Viability of Sacramento River winter-run chinook salmon. Conserv. Biol. 12:65–79.

Cohen, J.
1977. Statistical power analysis for the behavioral sciences. Academic Press, Inc. Orlando, FL, 474 p.

Dayton, P. K.
1998. Reversal of the burden of proof in fisheries management. Science (Washington, D.C.) 279:821–822.

FAO.
1996 Precautionary approach to capture fisheries and species introductions. elaborated by the Technical Consultation on the Precautionary Approach to Capture Fisheries (Including Species Introductions) Lysekil, Sweden, 6–13 June 1995. FAO Technical Guidelines for Responsible Fisheries 2, FAO, Rome, 54 p.

Fisher, F. W.
1994. Past and present status of Central Valley chinook salmon. Conserv. Biol. 8:870–873.

Gerrodette, T.
1987. A power analysis for detecting trends. Ecology 68: 1364–1372.

Gryska, A. D., W. A. Hubert, and K. G. Gerow.
1997. Use of power analysis in developing monitoring protocols for the endangered Kendall Warm Springs dace. N. Am. J. Fish. Manage. 17:1005–1009.

Hennemuth, R. C.
1980. A statistical description of recruitment in eighteen selected fish stocks. J. Northwest Atl. Fish. Sci. 1:101–111.

Johnson, N. L., S. Kotz, and N. Balakrishnan.
1994. Continuous univariate distributions, vol. 2, 2nd ed. John Wiley & Sons, Inc., New York, NY, 719 p.

Jones, B.
1996. Statistics toolbox user's guide. The MathWorks, Inc., Natick, MA, 342 p.

Lehmann, E. L.
1986. Testing statistical hypotheses, 2nd ed. John Wiley & Sons, Inc., New York, NY, 600 p.

Mapstone, B. D.
1995. Scalable decision rules for environmental impact studies: effect size, Type-I, and Type-II errors. Ecol. Appl. 5:401–410.

Peterman, R. M.
1990. Statistical power analysis can improve fisheries research and management. Can. J. Fish. Aquat. Sci. 47:2–15.

Peterman, R. M., and M. M'Gonigal.
1992. Statistical power analysis and the precautionary principle. Mar. Pollut. Bull. 24:1231–1234.

Shaffer, M. L.
1981. Minimum population sizes for species conservation. Bioscience 31:131–134.

Shaffer, M. L., and F. B. Samson.
1985. Population size and extinction: a note on determining critical population size. Am. Nat. 125:144–152.

Toft, C. A. and P. J. Shea.
1983. Detecting community-wide patterns: estimating power strengthens statistical inference. Am. Nat. 122:618–625.

Urquhart, N. S., S. G. Paulsen, and D. P. Larsen.
1998. Monitoring for policy—relevant regional trends over time. Ecol. Appl. 8:246–257.

Williams, J. E., and C. D. Williams.
1991. The Sacramento River winter chinook salmon. Chapter 9 *in* California's salmon and steelhead: the struggle to restore an imperiled resource (A. Lufkin, ed.), p. 105–115. Univ. California Press, Berkeley, CA, 305 p.

Seasonal variation in larval fish assemblages in relation to oceanographic conditions in the Abrolhos Bank region off eastern Brazil

Ricardo H. Nonaka
Yasunobu Matsuura
Kazuko Suzuki

Instituto Oceanográfico da Universidade de São Paulo
Cidade Universitária
Butantã, 05508
São Paulo, Brazil
e-mail: nonaka@usp.br

Abstract—The Abrolhos Bank region off the eastern coast of Brazil, under the influence of the Brazil Current, constitutes a typical tropical coral reef ecosystem that is characterized by a high diversity of tropical fish. Results of three ichthyoplankton surveys conducted in this region during summer, autumn, and winter revealed that there were two dominant fish groups: mesopelagic fish and coral-reef-associated fish. From the 45,614 larvae collected, 83 taxa (77 families and 6 orders) were identified, in which the family Myctophidae was the most abundant accounting for more than 25% of the total catch in the three cruises. Among the Myctophidae, seasonal variation in abundance of *Myctophum affine* was significant; there was an outstanding peak in abundance of this species during the summer surveys. The summer peak in abundance of five other species (*Diaphus* spp., *Lepidophanes guentheri*, *M. nitidulum*, *M. obtusirostre*, and *Hygophum reinhardtii*) was not as pronounced. Larval distribution patterns of these six species showed no remarkable seasonal change, being evenly distributed over the oceanic area. The coral-reef-associated fish larvae were confined to the bank and adjacent waters. The spatiotemporal distribution patterns of these larvae was strongly influenced by hydrographic features and some seasonal variation was observed. Four larval fish assemblages were identified: Abrolhos Bank, neritic, transitional, and oceanic assemblages. The Abrolhos Bank assemblage was characterized by coral-reef-associated fish, mainly Gobiidae, occupying most areas of the bank on the three cruises. The oceanic assemblage was dominated by mesopelagic fish, especially Myctophidae in all seasons and their occurrence was limited to the open ocean. The transitional assemblage was characterized by a mixture of coral-reef-associated fish and mesopelagic fish, with a seasonal change of dominant groups. It occupied mainly the shelf break area. The small pelagic fish (sardine and anchovy) were the dominant group of the neritic assemblage and occupied the coastal region south of the Abrolhos Bank, where the influence of the South Atlantic Central Water was evident.

Manuscript accepted 10 May 2000.
Fish. Bull. 98:767–784 (2000).

The tropical marine ecosystem is characterized by 1) the presence of coral reefs, which support a large variety of fish communities and benthic fauna that are point sources of eggs and larvae and by 2) the open ocean, where mesopelagic fish dominate the fish community. Thus, the larval fish assemblages in tropical marine ecosystems are a result of the spawning activities of these two communities (Ahlstrom, 1971; 1972; Leis and Goldman, 1987; Flores-Coto and Ordonez-Lopez, 1991; Leis, 1993). The formation of larval fish assemblages is mainly influenced by the reproductive cycles of the adult fish populations. The seasonal cycle of fish spawning activities in the tropics is not pronounced because of a low level of variation in environmental conditions (Lowe-McConnell, 1987).

Distribution patterns of fish larvae in any region of the ocean are related to the reproductive activity of the adult population and to topographic and hydrographic features that affect the dispersal of the larvae. A study of the distribution patterns of fish larvae contributes to an understanding of the interrelationships among fish species during their early life stages, as well as an understanding of adult spawning patterns. In addition, information can be obtained on the reproductive strategies adopted by these fish in response to the physical and biological processes of the region. Distribution patterns among ichthyoplankton species arise from the synchronous reproductive activities of different species that are developed during evolutionary adaptation to geographic and oceanographic conditions. This information is important for a rational use of fishery resources and also for an understanding of the ecological status of the component species in a marine ecosystem.

Ichthyoplankton surveys in Brazilian waters are concentrated off southern Brazil (Matsuura and Olivar, 1999); only a small number of sampling cruises have been conducted off the eastern coast (Aboussousan, 1969; Matsuura, 1985).

In our study, temporal and spatial changes in larval fish assemblages in relation to physical processes of the Abrolhos Bank region were examined. Particular emphasis was placed on the seasonal variation of larval fish assemblages of abundant fish taxa. The objective of the present study is to understand the origin and maintenance of these larval fish assemblages and their relation to oceanographic conditions.

Materials and methods

Three survey cruises were conducted along the eastern coast of Brazil. Two cruises of the FINEP Project (FINanciadora de Estudos e Projetos) were made with the RV *Prof. W. Besnard* in June and November–December of 1978. Sixty-four stations between latitudes 17°S and 23°S were sampled with a Nansen bottle containing a reversing thermometer for hydrographic data and with Bongo nets for collecting zooplankton. The third cruise, that of the JOPS II-9 (Joint Oceanographic ProjectS-II,

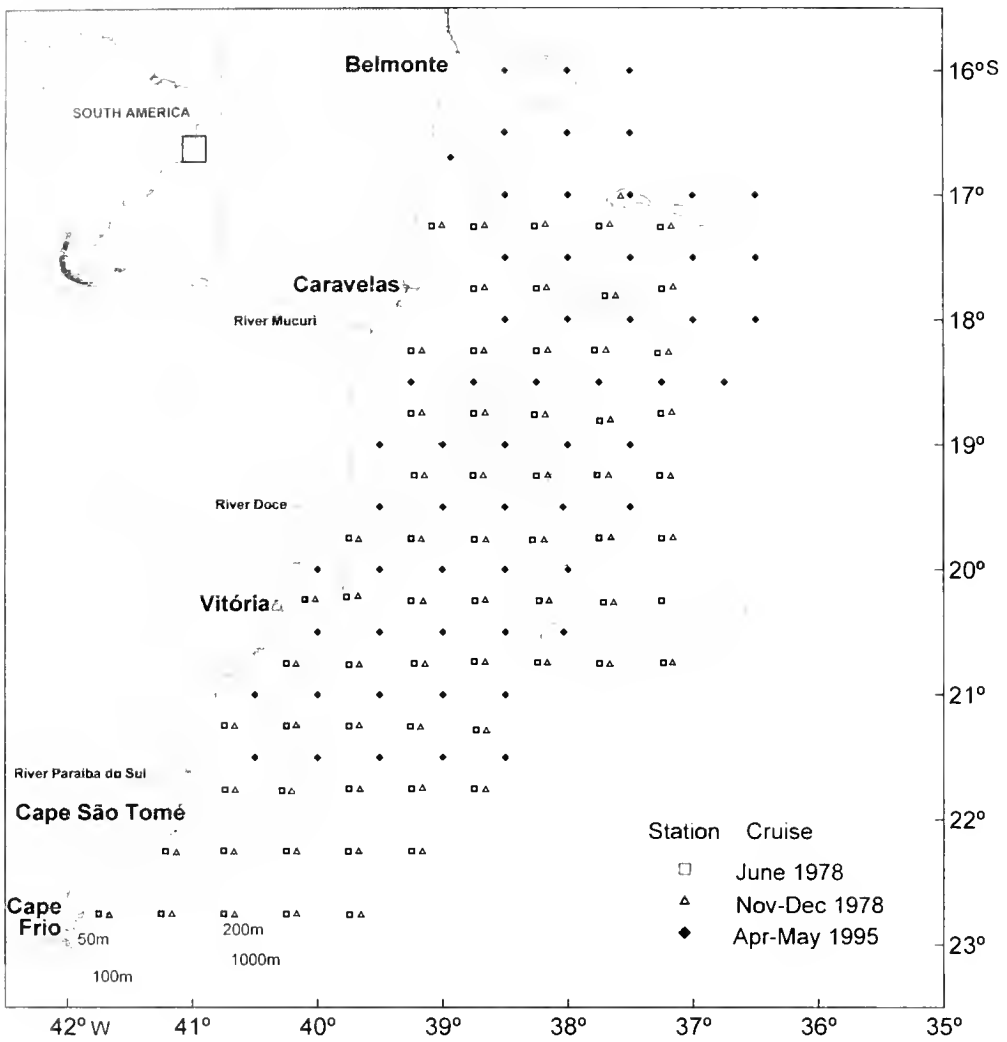

Figure 1

Survey area, sampling stations, and bathymetry off the eastern coast of Brazil.

leg 9), was conducted with the RV *Victor Hensen* in April–May 1995. Fifty-eight stations were sampled between latitudes 16°S and 22°S with a CTD cast for hydrographic data and with Bongo nets for zooplankton (Fig. 1). The interval between stations was 30 nautical miles.

The zooplankton samples were collected by using 60-cm Bongo nets with mesh apertures of 300 µm and 500 µm. The nets were towed obliquely from the surface to a depth of 200 m or down to 5 m above the bottom at shallow stations as the vessel held a 45° wire angle (usually 1.5 knots vessel speed). Winch retrieval rate was 20 m per minute to the surface. In order to increase the water volume filtered, the nets were towed twice down near to the bottom at shallow water (<60 m) stations. The digital flowmeter attached at the center of the net was used to estimate the water volume that was filtered. The plankton samples collected with a 300-µm mesh net were used for both the zooplankton and ichthyoplankton study. Zooplankton volume at each station was measured by using the replacement method (Kramer et al., 1972) and expressed as mL/m^3. The number of fish larvae collected at each station was converted into the number under unit surface area (10 m^2) by using the following equation:

$$Y_i = (10 \times d_i \times x_i) / v_i ,$$

where Y_i = number of standardized larvae under 10 m^2 of sea surface at station i;
x_i = number of larvae taken at station i;
v_i = volume of water filtered (m^3); and
d_i = maximum depth of haul (m).

The total abundance of the larvae of each family was the sum of a standardized number of larvae from all the positive stations. The plankton samples were preserved in a solution of 4% buffered formalin, and the fish eggs and larvae were sorted by using a stereoscopic microscope in the laboratory. Identifications of fish larvae were

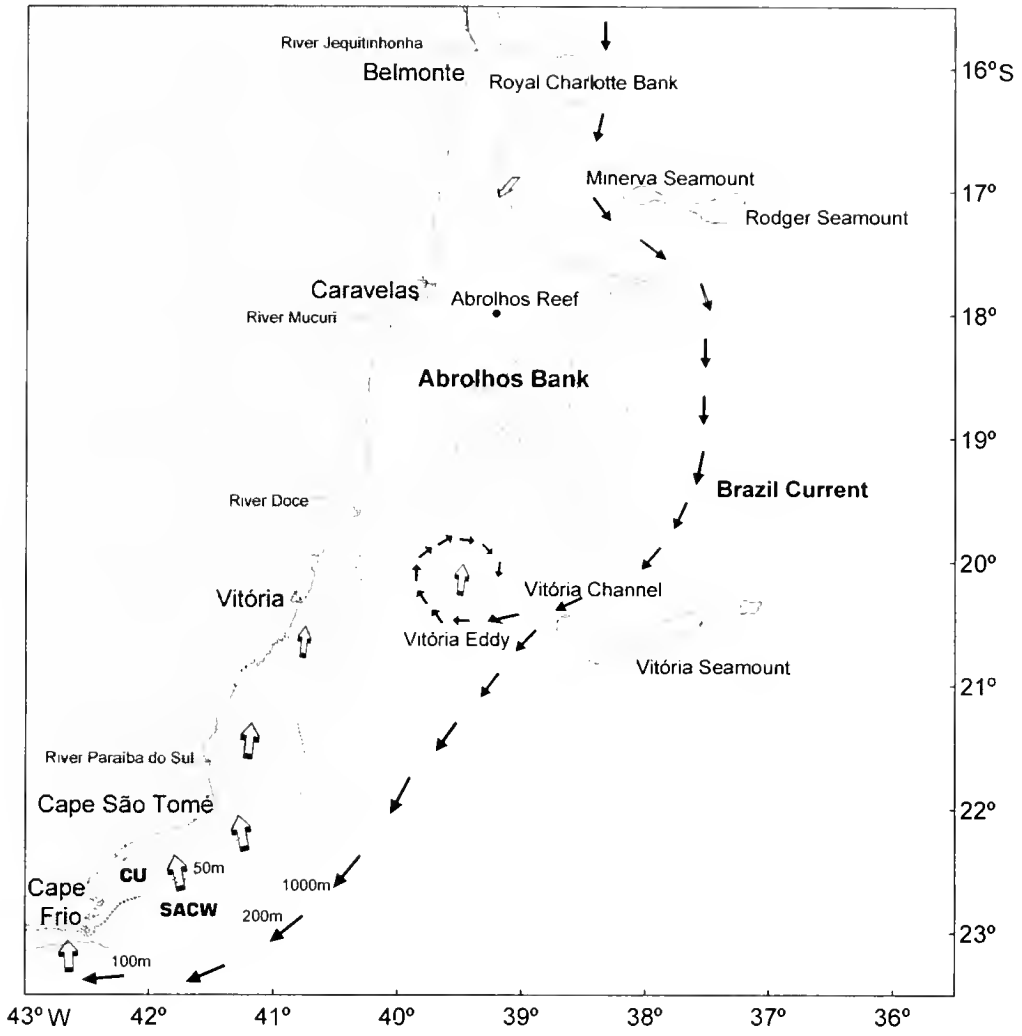

Figure 2

Hydrographic features of the Abrolhos Bank region. The dark arrow shows the main axis of the Brazil Current (BC); the blank arrow the upward movement of the South Atlantic Central Water (SACW), and the shadowed area the coastal upwelling (CU).

based on descriptions in the literature (Fahay, 1983; Leis and Rennis, 1983; Leis and Trnski, 1989; Moser et al., 1984; Moser, 1996; Nafpaktitis et al., 1977; Okiyama, 1988; Olivar, 1988; Olivar and Fortuño, 1991). Larval identification of coral-reef-associated fish is difficult; therefore identification was made only to the family level. The most abundant Myctophidae larvae were identified to species level.

To determine the possible associations among stations, the distribution pattern, and larval abundance, a multivariate analysis of numerical classification was applied by using the two-way indicator species analysis (Hill et al., 1975; Hill, 1979), implemented by the program TWINSPAN. This is a divisive method that classifies stations and families and produces a sorted family by station table, showing the hierarchical classification in binary notation (see "Appendix"). The results of this analysis show the clear ecological preferences of the family groups and are used to identify particular environmental conditions. Only the family groups with an occurrence of more than 10% in each cruise were used in this analysis.

Results

Oceanographic conditions

The continental shelf of the eastern coast of Brazil is generally narrow (ca. 25 km) and is composed of calcareous sediments on the bottom; however, it widens to 230 km offshore at Caravelas (Lat. 18°S), forming the large Abrolhos Bank (AB) to the south (Fig. 2). The depth of shelf break in this region is 100 m with isobathic lines 200 m and 1000 m very close to it. Therefore, we have shown the margin of

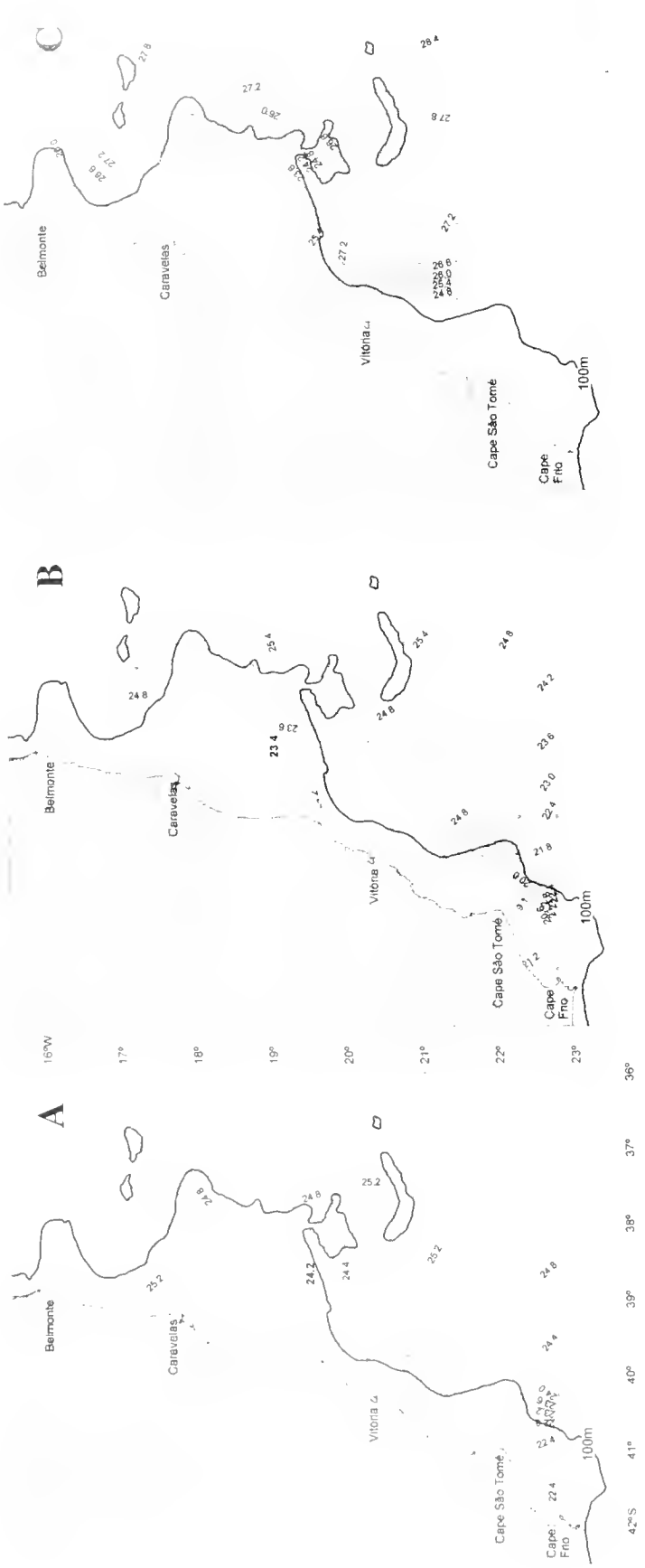

Figure 3

Horizontal distribution of water temperature at 50 m depth for three cruises: winter (**A**); summer (**B**); autumn (**C**) off the eastern coast of Brazil.

continental shelf with the 100-m isobath. This region is characterized by the southward flowing Brazil Current (BC), a typical western boundary current regime (Castro and Miranda, 1998). Because of the topographic impediment of the Abrolhos Bank, the main axis of the Brazil Current flows along the outer edge of the continental slope of the bank and passes through the Vitória Channel formed between the southeastern edge and the Vitória seamount at lat. 20°15′S. It flows southwesterly from this point, approaching the coast near Cape São Tomé (Signorini et al., 1989). Schmid et al. (1995) detected a permanent cyclonic eddy which was formed south of the Abrolhos Bank from the meandering movement of the Brazil Current after passing through the Vitória Channel. Beneath the Brazil Current the South Atlantic Central Water (SACW) occupies the subsurface layer at 120–350 m depth. Prevailing northeast winds induce a coastal upwelling in the region from Cape Frio to Cape São Tomé which is more intense during the austral spring and summer, uplifting the SACW to the surface (Mascarenhas et al., 1971; Silva, 1973; Ikeda et al., 1974).

The horizontal distribution of the water temperature at a depth of 50 m showed a flow pattern similar to that of the Brazil Current on the three cruises, and the thermal front of the SACW of the Cape São Tomé reached the southern rim of the Abrolhos Bank (Fig. 3). The boundary between the Brazil Current and the coastal water was demarcated with a 24.8°C-isotherm line on the three cruises. The temperature gradient between two water masses on the autumn cruise was more pronounced (Fig. 3C). The sea surface temperature at 10 m depth over the Abrolhos Bank ranged from 24.0–25.6°C in winter, and 26.0–26.4°C in summer, to 26.0–28.3°C in autumn. The salinity at 10 m depth ranged from 36.0 to 37.5 psu and showed no seasonal variation.

Zooplankton

The displacement volume of macrozooplankton was low, ranging from 0.07 to1.54 mL/m^3 over the bank and from 0.01 to 0.41 mL/m^3 in the open ocean (Table 1). However, when compared with the displacement volume of macrozooplankton in the north Pacific central gyre, which ranged from 0.05 to 0.10 mL/m^3 (Loeb, 1980), our values in the open ocean were slightly higher.

Table 1

Displacement volume of macrozooplankton (mL/m^3) from three survey cruises in the Abrolhos Bank region.

	Winter		Summer		Autumn	
	Shelf	Open Sea	Shelf	Open Sea	Shelf	Open Sea
No. of stations	26	35	30	34	23	35
Mean volume	0.32	0.09	0.28	0.12	0.26	0.07
Standard deviation	0.219	0.079	0.272	0.047	0.141	0.031
Minimum volume	0.10	0.03	0.07	0.04	0.07	0.01
Maximum volume	1.12	0.41	1.54	0.27	0.69	0.15

Larval fish composition and abundance

A list of the family groups of fish larvae and their abundance is given in Table 2. From the 45,614 larvae collected, 83 taxa (77 families and 6 orders) were identified. The family Myctophidae was the most abundant, accounting for more than 25% of the total catch on the three cruises.

During the winter cruise, 58% of the total larvae taken represented five families in decreasing order of abundance: Myctophidae, Phosichthyidae, Sternoptychidae, Bregmacerotidae, and Serranidae, of which the first four belonged to the mesopelagic fish group.

The total number of larvae collected during the summer cruise was twice as high as that of the other two cruises. Myctophidae represented 27.6% of the total larvae, followed by Scaridae (11.6%), Sternoptychidae (8.2%), Carangidae (4.5%), and Phosichthyidae (4.2%). The following nine families were collected only on the summer cruise: Argentinidae, Clinnidae, Dactyloscopidae, Istiophoridae, Caproidae, Macrorhamphosidae, Malacanthidae, Percophidae and Symphysanodontidae, indicating that these groups spawned only in summer.

During the autumn cruise, the five most abundant families (Myctophidae, Scaridae, Gobiidae, Serranidae, and Phosichthyidae) represented 58.7% of the total larvae taken. Four families (Elopidae, Notosudidae, Scombrolabracidae, and Tripyterigiidae) were collected only in this season, indicating that for these families spawning peaked in autumn.

Seasonal variation in abundance of fish groups

In relation to habitat of adult fish groups, two dominant fish groups were recognized in the survey area: mesopelagic fish and coral-reef-associated fish. Levels of abundance of three families of mesopelagic fish larvae (Myctophidae, Sternoptychidae, and Gonostomatidae) were highest during the summer cruise (Fig. 4). For three other families (Phosichthyidae, Bregmacerotidae, and Paralepididae) levels of abundance were highest for the winter cruise, decreased in summer, and were at a minimum during the autumn cruise. The summer peak in abundance for the myctophid *Myctophum affine* was outstandingly high (Fig. 5). Five other species (*Diaphus* spp., *Lepidophanes guentheri*, *M. nitidulum*, *M. obtusirostre*, and *Hygophum reinhardtii*) were most abundant in summer, but the seasonal differences were not pronounced.

Figure 6 shows a seasonal variation in abundance of the coral-reef-associated fish. Abundance of larval parrotfish (Scaridae) was at a peak in summer, followed by autumn and winter. The same trend was observed in six other families (Labridae, Holocentridae, Balistidae, Pomacanthidae, Acanthuridae, and Pomacentridae). Levels of abundance of larval grouper (Serranidae) were almost the same for three seasons. For the family Gobiidae, a peak in larval abundance was observed during the autumn cruise.

Distribution patterns of fish larvae

Distribution patterns of six species of Myctophidae among each of the cruises are shown in Figure 7. Most of the *Diaphus* spp. larvae were collected at open ocean stations, but also at some coastal stations between Vitória and Cape Frio on the winter and summer cruises. Larvae of *Myctophum affine*, *M. obtusirostre*, *M. nitidulum*, *L. guentheri*, and *H. reinhardtii* were found predominantly at open ocean stations and some at the continental margin, but a considerable number of *Myctophum affine* larvae were also found at coastal stations between Vitória and Cape Frio on the summer cruise (Fig. 7E). The presence of these species along the coast coincided with the presence of the coastal upwelling observed in this area (Fig. 3).

Distribution patterns of the Gobiidae during the summer and autumn cruises were similar, with higher density over the Abrolhos Bank and seamount. Gobiid larvae during the winter cruise were concentrated over the Abrolhos Bank and only a small number of them were collected at open ocean stations south of the bank (Fig. 8). The distribution patterns of the parrotfish larvae (Scaridae) were similar during all three cruises, with higher density at open ocean stations. During the winter cruise the highest densities of grouper larvae (Serranidae) were found around the Vitória Channel, but the Abrolhos Bank stations also showed relatively high density. The stations with the highest densities of grouper larvae during the summer cruise were found along the shelf break and over the seamount. The distribution pattern of grouper larvae during the autumn cruise was different from the former

Table 2

Family groups represented in ichtyoplankton samples collected on the Abrolhos Bank and in adjacent waters off eastern Brazil. Abundance is a sum of a standardized number of larvae from all positive stations and % is a percentage of total abundance.

	Winter Cruise		Summer Cruise		Autumn Cruise	
Taxon	Abundance	%	Abundance	%	Abundance	%
Myctophidae	17911	27.49	31165	27.58	14152	25.44
Scaridae	1224	1.88	13140	11.63	6341	11.40
Sternoptychidae	6042	9.27	9215	8.15	949	1.71
Carangidae	2049	3.14	5103	4.52	544	0.98
Phosichthyidae	6957	10.68	4723	4.18	2380	4.28
Gonostomatidae	414	0.64	4049	3.58	167	0.30
Scombridae	218	0.33	3254	2.88	152	0.27
Engraulidae	1148	1.73	3063	2.71	1075	1.93
Serranidae	3015	4.63	2860	2.53	3704	6.66
Paralepididae	2674	4.10	2527	2.24	672	1.21
Gobiidae	2245	3.45	2280	2.02	6088	10.94
Holocentridae	21	0.03	1976	1.75	54	0.10
Bregmacerotidae	3845	5.90	1657	1.47	1016	1.83
Labridae	114	0.17	1555	1.38	624	1.12
Balistidae	6	0.01	1335	1.18	21	0.04
Pleuronectiformes	625	0.96	1016	0.90	628	1.13
Scorpaenidae	332	0.51	919	0.81	397	0.71
Monacanthidae	94	0.14	857	0.76	353	0.63
Apogonidae	550	0.84	671	0.59	722	1.30
Clupeidae	1248	1.92	660	0.58	483	0.87
Mullidae	1236	1.90	591	0.52	57	0.10
Ophidiiformes	229	0.35	576	0.51	229	0.41
Tetraodontiformes	172	0.26	520	0.46	68	0.12
Pomacentridae	35	0.05	488	0.43	305	0.55
Priacanthidae	0	0	482	0.43	10	0.02
Pomacanthidae	334	0.51	454	0.40	229	0.41
Acanthuridae	44	0.07	424	0.38	127	0.23
Synodontidae	343	0.53	419	0.37	557	1.00
Callionymidae	275	0.42	327	0.29	1872	3.36
Anguilliformes	248	0.38	315	0.28	0	0
Stomiiformes	23	0.03	312	0.28	87	0.16
Triglidae	26	0.04	233	0.21	16	0.03
Gempylidae	110	0.17	210	0.19	84	0.15
Nomeidae	56	0.09	186	0.16	0	0
Lutjanidae	38	0.06	174	0.15	304	0.55
Chaetodontidae	60	0.09	164	0.15	0	0
Cirrhitidae	130	0.20	130	0.12	110	0.20
Exocoetidae	54	0.08	127	0.11	0	0
Syngnathidae	73	0.11	113	0.10	41	0.07
Coryphaenidae	6	0.01	102	0.09	49	0.09
Scopelarchidae	7	0.01	72	0.06	4	0.01
Blenniidae	124	0.19	53	0.05	60	0.11
Chiasmodontidae	42	0.06	50	0.04	75	0.13
Gerreidae	25	0.04	49	0.04	9	0.02
Sphyraenidae	11	0.02	46	0.04	48	0.09

Continued

two and showed an even distribution pattern over the bank and along the shelf break.

The distribution patterns of Clupeidae and Engraulidae were similar; larvae were limited to coastal stations (Fig. 8). The clupeid larvae collected in the coastal region between Vitória and Cape Frio belonged to *Sardinella brasiliensis* and *Harengula jaguana*, and those from the Abrolhos Bank were *Jenkinsia* sp., *Opisthonema* sp., and

Table 2 (continued)

	Winter Cruise		Summer Cruise		Autumn Cruise	
Taxon	Abundance	%	Abundance	%	Abundance	%
Sciaenidae	136	0.21	46	0.04	49	0.09
Fistulariidae	17	0.03	39	0.03	29	0.05
Istiophoridae	0	0	31	0.03	0	0
Lophiiformes	22	0.03	25	0.02	0	0
Percophidae	0	0	22	0.02	0	0
Ostraciidae	0	0	21	0.02	22	0.04
Ogcocephalidae	0	0	20	0.02	6	0.01
Symphysanodontidae	0	0	19	0.02	0	0
Malacanthidae	0	0	18	0.02	0	0
Pomatomidae	11	0.02	18	0.02	2	0
Caproidae	0	0	17	0.02	0	0
Antennariidae	0	0	15	0.01	37	0.07
Carapidae	15	0.02	15	0.01	56	0.10
Echeneidae	0	0	14	0.01	10	0.02
Argentinidae	0	0	13	0.01	0	0
Sparidae	10	0.02	12	0.01	0	0
Trichiuridae	273	0.42	8	0.01	57	0.10
Acropomatidae	153	0.23	6	0.01	400	0.72
Labrisomidae	8	0.01	6	0.01	0	0
Clinnidae	0	0	6	0.005	0	0
Macrorhamphosidae	0	0	4	0.004	0	0
Dactyloscopidae	0	0	4	0.003	0	0
Aulostomidae	9	0.01	3	0.003	99	0.18
Mugilidae	11	0.02	2	0.002	0	0
Opistognathidae	15	0.02	2	0.002	4	0.01
Astronesthidae	7	0.01	0	0	5	0.01
Chlorophthalmidae	33	0.05	0	0	0	0
Elopidae	0	0	0	0	8	0.02
Gadidae	24	0.04	0	0	0	0
Hemiramphidae	12	0.02	0	0	7	0.01
Kyphosidae	6	0.01	0	0	0	0
Melanostomiidae	68	0.10	0	0	15	0.03
Microdesmidae	15	0.02	0	0	10	0.02
Notosudidae	0	0	0	0	31	0.06
Scombrolabracidae	0	0	0	0	4	0.01
Stromateidae	5	0.01	0	0	0	0
Tripyterigiidae	0	0	0	0	4	0.01
Xiphiidae	14	0.02	0	0	6	0.01
Not identified	9856	15.13	13970	12.36	9909	17.81
Total	65154	100.00	112998	100.00	55634	100.00
No. of taxa	65		70		62	

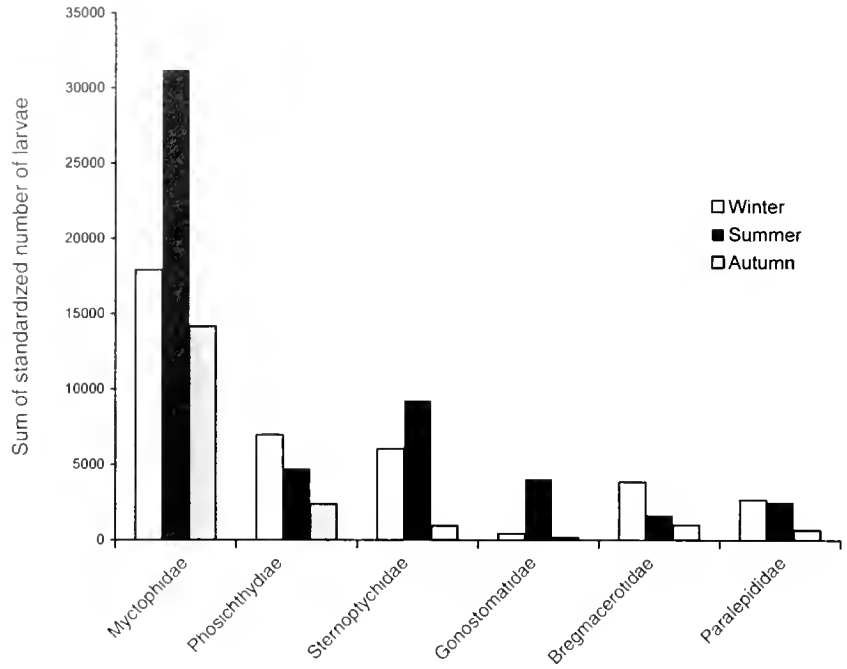

Figure 4

Seasonal variation of larval abundances of mesopelagic fish families in the Abrolhos Bank and adjacent waters.

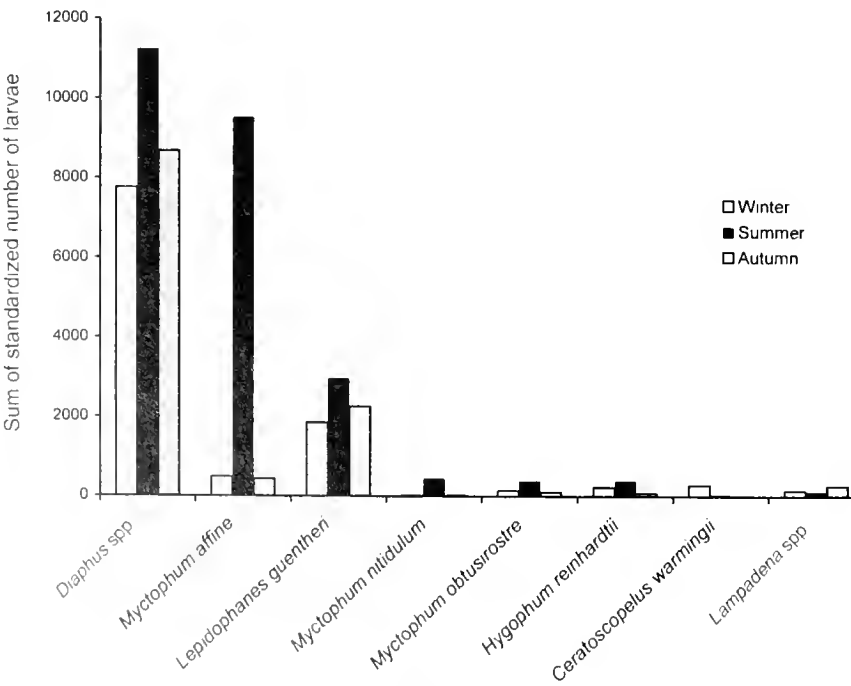

Figure 5

Seasonal variation of larval abundances of lanternfish (Myctophidae) on the Abrolhos Bank and in adjacent waters.

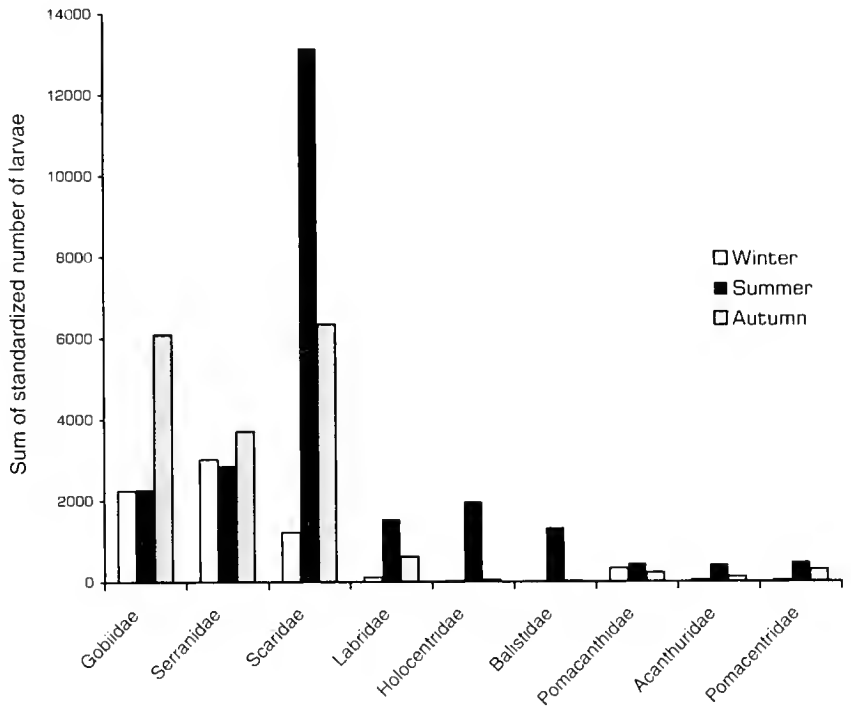

Figure 6

Seasonal variation of larval abundances of coral-reef-associated fish families on the Abrolhos Bank and in adjacent waters

un-identified clupeid larvae. Most of the engraulid larvae collected at coastal stations between Vitória and Cape Frio in winter and autumn were *Engraulis anchoita*, but some larvae found over the AB belonged to *Anchoa* and *Anchovia* that were not identified to species.

Larval fish assemblages

A figure of fish families by station created with the TWINSPAN program is shown in Appendix 1. Clustering the families based on their occurrence and abundance at each station resulted in four major oceanographic groupings: 1) Abrolhos Bank, 2) neritic, 3) transitional, and 4) oceanic.

Abrolhos Bank assemblage The Abrolhos Bank assemblage was situated over the Abrolhos Bank (Fig. 9). During the autumn cruise another subgroup was identified in the coastal region and named "the Abrolhos Bank-coastal assemblage." Taxonomic composition of this assemblage was characterized by the presence of coral-reef-associated fish. The composition was influenced by the seasonal variation of taxa, with the exception of Gobiidae which was the dominant family on all the cruises. The dominant groups of this assemblage were Serranidae, Scaridae, Carangidae, Clupeidae, Apogonidae, Blenniidae, and Labridae.

Neritic assemblage The neritic assemblage was found over the continental shelf between Vitória and Cape Frio. The neritic assemblage was composed of pelagic fish, such as the Clupeidae, Engraulidae, Carangidae, and Bregmacerotidae, as well as the demersal fish Gobiidae and Pleuronectiformes. During the summer cruise the neritic assemblage was limited to the area between Cape São Tomé and Cape Frio, and another subgroup was identified in the northern part between Vitória and Cape São Tomé, named the neritic-north assemblage. This assemblage was characterized by Gobiidae, Engraulidae, and Clupeidae, which accounted for 60% of the total larvae.

Transitional assemblage The transitional assemblage was found mainly along the shelf break area. During the winter cruise the transitional assemblage occurred in two shelf break areas: between Caravelas and Vitória and between Vitória and Cape São Tomé (Fig. 9A). This assemblage was dominated by mesopelagic fish belonging to Myctophidae, Sternoptychidae, Bregmacerotidae, Phosichthyidae, and Paralepididae, but also by the coral-reef-associated fish, such as Serranidae, Carangidae, Mullidae, Pomacanthidae, Apogonidae, and Callionymidae.

The transitional assemblage found during the summer cruise was situated along the outer edge of the Abrolhos Bank, including the oceanic area of the Minerva and Vitória Seamounts (Fig. 9B). Its taxonomic composition was characterized by the great diversity of coral-reef-associated and mesopelagic fish. A transitional-Vitória subassemblage was identified to the south of the Abrol-

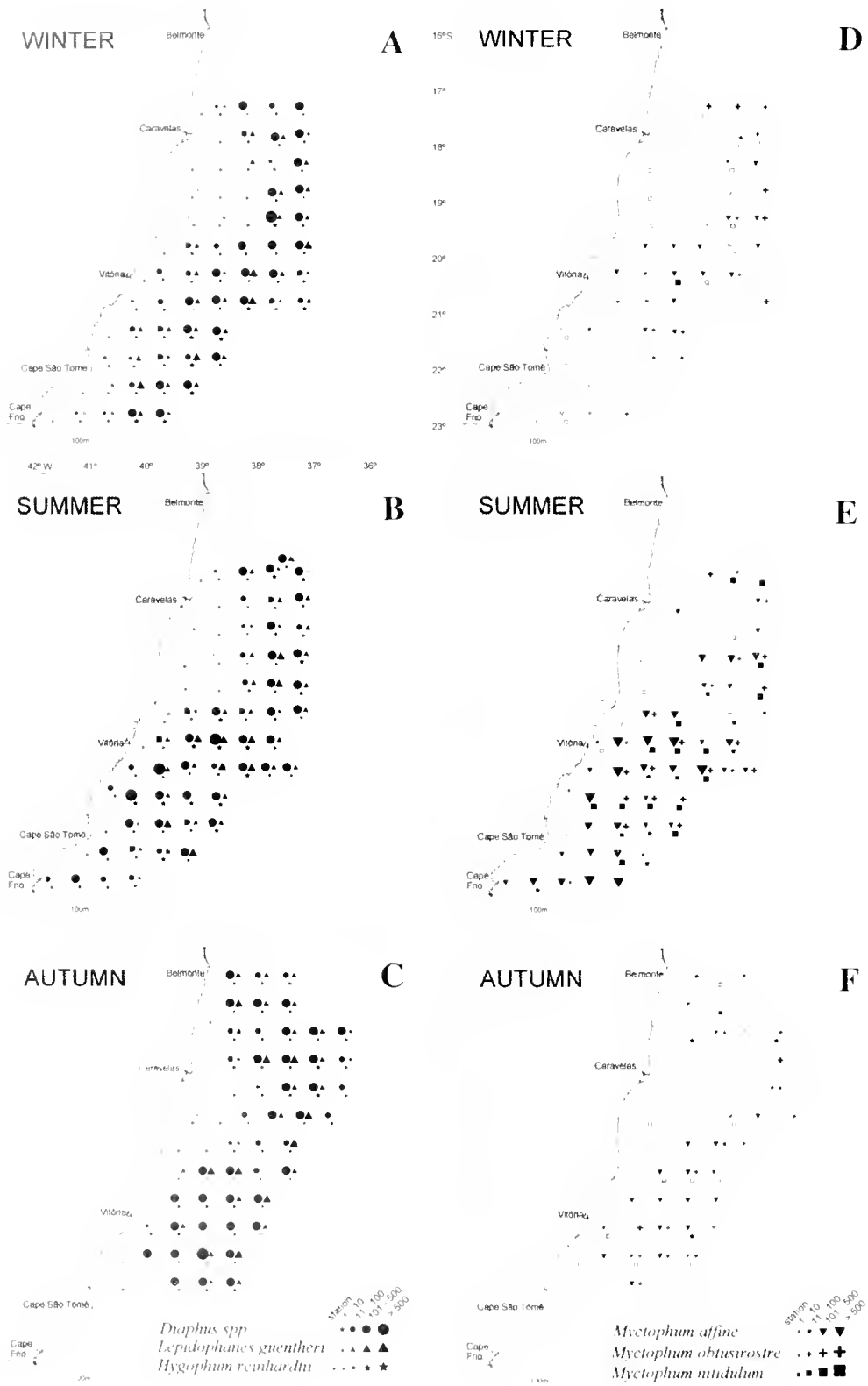

Figure 7

Distribution patterns of lanternfish (Myctophidae) larvae in the Abrolhos Bank region during winter, summer and autumn cruises. (**A–C**) *Lepidophanes guentheri*, *Hygophum reinhardtii*, *Diaphus* spp. (**D–F**) *Myctophum affine*, *M. obtusirostre*, *M. nitidulum*.

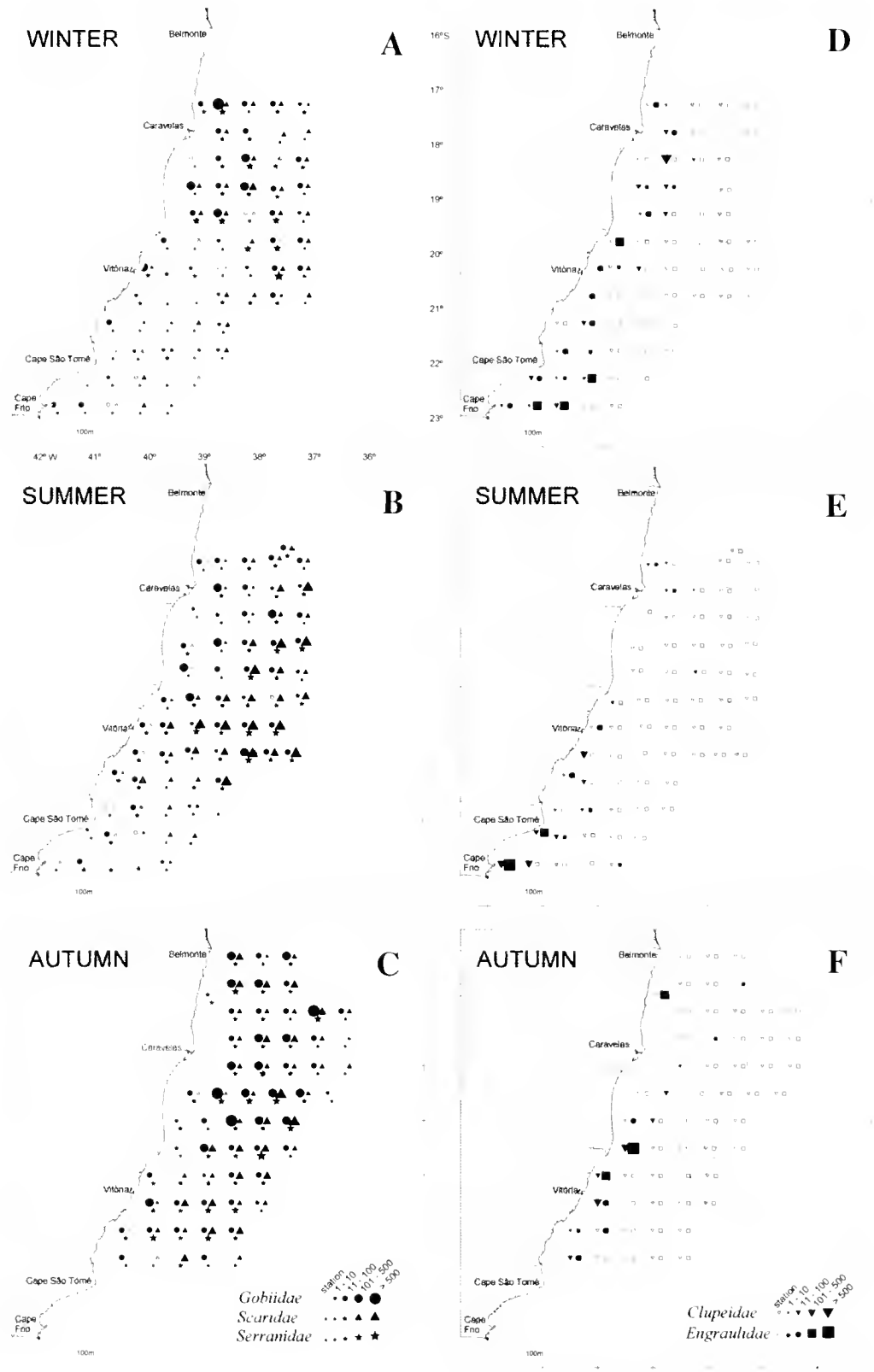

Figure 8

Distribution patterns of coral-reef-associated fish and clupeoid larvae in the Abrolhos Bank region for three cruises: winter (**A, D**), summer (**B, E**) and autumn (**C, F**).

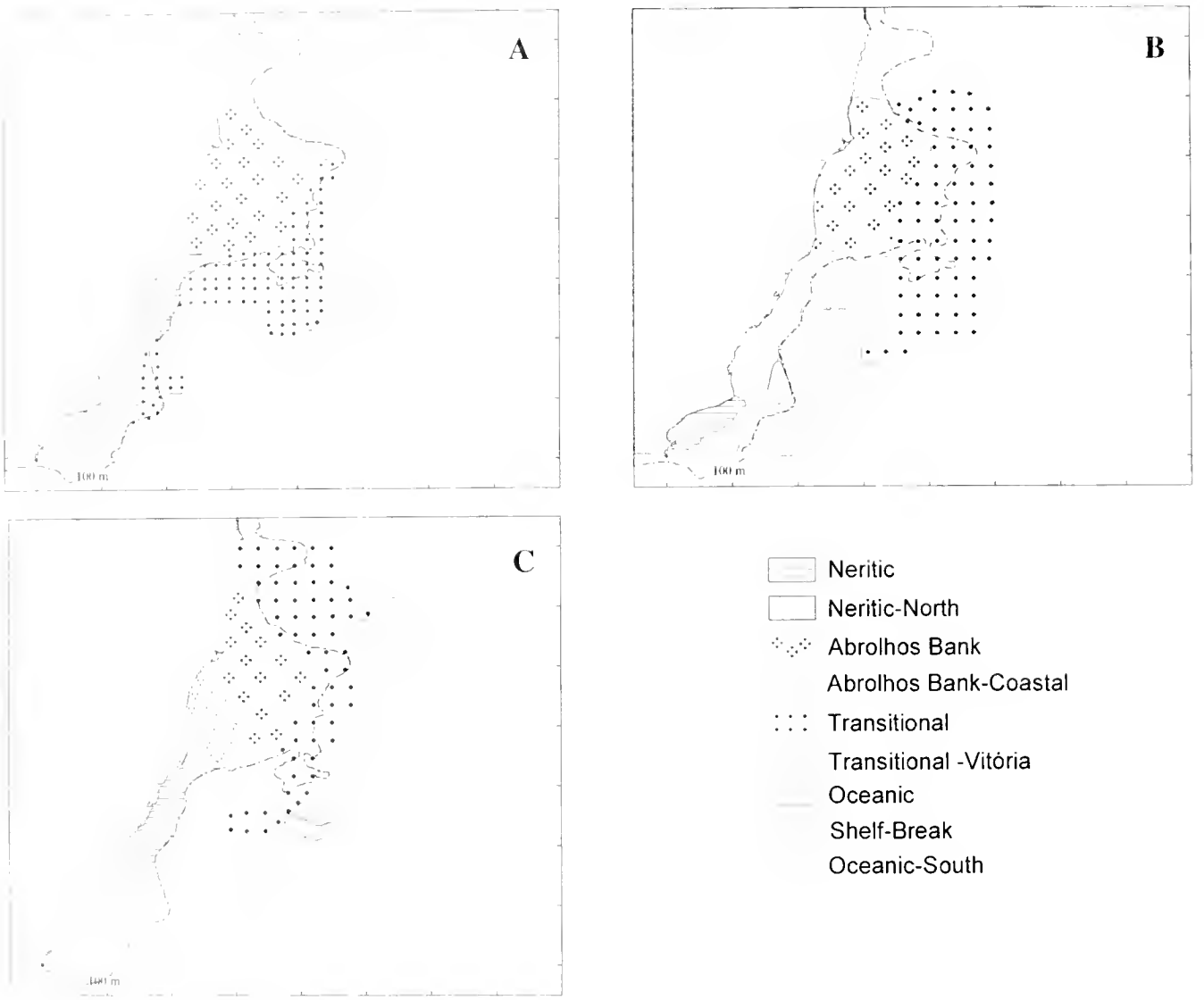

Figure 9

Temporal and spatial distributions of four groups of larval fish assemblages based on the two-way indicator species analysis (TWINSPAN program). (**A**) winter, (**B**) summer and (**C**) autumn.

hos Bank in the oceanic area. The taxonomic composition of this subgroup was similar to that of the transitional assemblage, but mesopelagic fish, such as Myctophidae, Sternoptychidae, and Phosichthyidae dominated.

The transitional assemblage found during the autumn cruise extended along the shelf break area from Royal Charlotte Bank to the Vitoria Seamount (Fig. 9C). Its taxonomic composition was predominantly Myctophidae, Scaridae, Gobiidae, Serranidae, Callionymidae, and Apogonidae.

Oceanic assemblage The oceanic assemblage consisted principally of mesopelagic fish (Myctophidae, Phosichthyidae, Sternoptychidae, Paralepididae, and Gonostomatidae). The oceanic assemblage was found in the entire oceanic area from the Minerva Seamount to Cape Frio during the winter cruise. During the summer cruise the same assemblage was limited to the oceanic area between Vitoria and Cape Frio. The oceanic subassemblage was detected over the outer continental shelf between River Paraiba do Sul and Cape Frio, named the shelf-break subassemblage. This group was represented by a small number of taxa, predominantly Sternoptychidae. During the autumn cruise the oceanic assemblage was located in the oceanic area from the Roger Seamount to Cape São Tome and consisted of Myctophidae. The oceanic subassemblage was identified to the south of the Abrolhos Bank, and consisted predominantly of Myctophidae, Phosichthyidae, Scaridae, and Serranidae.

Discussion

The warm and salty tropical water which covers the entire survey area, is transported southward by the Brazil Current. The cold South Atlantic Central Water occupies the subsurface layer beneath the Brazil Current but owing to the deep thermocline (80–120 m), the nutrient rich SACW does not come up to the euphotic zone in the survey area, with exception of the coastal region of Cape Frio-Cape São Tomé. Consequently this area is known to be oligotrophic with a low concentration of nitrates, chlorophyll-*a* biomass, and primary production (Gaeta et al., 1999). The primary production of the nutrient-depleted surface layer is supported principally by autotrophic and heterotrophic picoplankton which use the recycled nutrients in the water. The heterotrophic dinoflagellates and ciliates are responsible for the transfer of energy produced by picoplankton to the upper trophic levels (Susini-Ribeiro,1999).

There was a time gap between the first two cruises (June and November–December in 1978) and the last one (April–May in 1995); therefore the seasonal variations of hydrographic conditions and larval distribution in this region could have been the result of interannual variation. The El Niño year in the tropical Pacific normally causes a drought in the northeastern Brazil and a flood in the south. Bearing in mind that 1978 and 1995 were not atypical El Niño years, we assumed that the interannual variation in hydrographic conditions between these two periods could be ignored. We had no any other information on the interannual variation in oceanographic conditions in this region.

The fish larvae in the Abrolhos Bank region off the eastern coast of Brazil were produced by a diverse collection of fish species that can be divided into two dominant groups: mesopelagic fish and tropical reef fish. The high diversity of taxa (77 families and 6 orders) is characteristic of the tropical marine ecosystem and similar taxonomic diversity of larval fish is known from the eastern tropical Pacific (Ahlstrom, 1971; 1972) and the Gulf of Mexico (Richards et al., 1993).

The most surprising results were the occurrence of many reef-fish larvae along the shelf break areas. Assuming that the reef fish larvae found along the shelf break area off the Abrolhos Bank are transported southward by the main axis of the Brazil Current, most of them should be trapped in the Vitória eddy after passage through the Vitória Channel. Consequently they can be recruited at the southern margin of the bank. In order to prove this hypothesis, an intensive sampling program, coupled with an application of aging technique for postsettlement juveniles, is necessary in this region.

The dominant taxonomic groups (family) from the three cruises showed a distinct seasonal pattern in abundance. The overall larval abundance of the summer cruise was the highest. Among the Myctophidae, the larval abundance of *Myctophum affine* was highest in summer and insignificant in other seasons. Other species (*Diaphus* spp., *Lepidophanes guentheri, Myctophum nitidulum, M. obtusirostre, Hygophum reinhardtii*) also showed relatively high values in summer. Many dominant species concentrate their spawning activities during the austral summer. Myctophid fish in the temperate and subtropical seas are known to spawn mainly from late winter to summer, coinciding with the seasonal peak of zooplankton production in the area (Clarke, 1973; Doyle et al., 1993). The mean displacement volume of macrozooplankton in the open ocean was 33–50% higher in summer than during winter and autumn, suggesting that many fish species have evolved spawning patterns that are synchronized with zooplankton production in this region.

The composition of dominant myctophid larvae in this region is different from that observed on the other side of the South Atlantic, i.e. the *Lampanyctodes hectoris*, a commercially exploited lanternfish, is the most abundant in the Benguela Current, followed by *Symbolophorus* and *Diaphus* (Ahlstrom et al., 1976; Olivar and Shelton, 1993). Meanwhile, the four abundant genera (*Diaphus, Myctophum, Lepidophanes,* and *Hygophum*) in the eastern tropical Pacific (Ahlstrom, 1971; 1972) were also found in the survey area. Most of the *Maurolicus muelleri* larvae were collected from south of Abrolhos Bank in winter and summer, but their occurrence during the autumn cruise was at a minimum. Because the highest densities of *M. muelleri* larvae were recorded in oceanic waters from south Brazil Bight (23–29°S) (Ribeiro, 1996), those found in the survey area may represent only a northern extention of the southern population.

Multivariate analysis of the dominant taxa in the region suggests the existence of geographically distinct larval fish assemblages that show significant seasonal variation. Observed distribution patterns of dominant groups are the result of synchronous and geographically coherent spawning activities of different groups of adult fish. The Abrolhos Bank assemblage was characterized by coral-reef-associated fish, predominantly Gobiidae, on the three cruises. Small pelagic fish were the dominant group in the neritic assemblage. The transitional assemblage was characterized by a mixture of coral-reef-associated fish and mesopelagic fish and a seasonal change of dominant groups. The oceanic assemblage was dominated by the presence of mesopelagic fish, especially the Myctophidae in all seasons.

The general geographic positions of the four larval fish assemblages showed similar distribution patterns on winter and autumn cruises, but those of the summer cruise were slightly different. The oceanic assemblage, which extended in the offshore area from the Minerva Seamount to Cape São Tome in autumn and winter, was limited to the area between Vitória and Cape Frio during the summer cruise. The offshore area between the Minerva and Vitória Seamounts was occupied by the transitional assemblage in summer. The Abrolhos Bank and neritic assemblages consistently occupied most parts of the continental shelf during the three cruises, but different larval fish assemblages occupied the offshore area south of the Abrolhos Bank. This finding can be interpreted as a result of the seasonal variation of hydrographic conditions in this specific area, such as the formation of the Vitória eddy and the intensity of coastal upwelling.

Acknowledgments

The authors thank Kouichi Kawaguchi of the Ocean Research Institute for critical reading of the manuscript. The FINEP Project was financed by the Financiadora de Estudos e Projetos. The JOPS II Project was financed by the Ministries for Sciences and Technology of Brazil (MCT) and Internationales Büro des BMBF of Germany (project number 03F0144A). Financial support also came from the Fundação de Amparo à Pesquisa do Estado de São Paulo (grant 96/09333-5). The authors received a research fellowship from the Conselho Nacional de Desenvolvimento Cientifico e Tecnológico (RHN: 139340/96-3, YM: 301675/82) during this study.

Literature cited

Aboussoan, A.
1969. Sur une petite collection de larves de Téléostéens récoltée au large du Brésil (Campagne <Calypso> 1962). Vie et Milieu 20(3)A:595–610.

Ahlstrom, E. H.
1971. Kinds and abundance of fish larvae in the eastern tropical Pacific, based on collections made on EASTROPAC I. Fish. Bull. 69(1):3–77.
1972. Kinds and abundance of fish larvae in the eastern tropical Pacific on the second multivessel EASTROPAC survey, and observations on the annual cycle of larval abundance. Fish. Bull. 70(4):1153–1242.

Ahlstrom, E. H., H. G. Moser, and M. J. O'Toole.
1976. Development and distribution of larvae and early juveniles of the commercial lanternfish, *Lampanyctodes hectoris* (Gunther), off the west coast of southern Africa with a discussion of phylogenetic relationship of the genus. Bull. South Calif. Acad. Sci. 75:138–152.

Castro, B. M. and L. B. Miranda.
1998. Physical oceanography of the western Atlantic continental shelf located between 4°N and 34°S coastal segment (4, W). The Sea 11:209–251.

Clarke, T. A.
1973. Some aspects of the ecology of lanternfishes (Myctophidae) in the Pacific Ocean near Hawaii. Fish. Bull. 71(2):401–434.

Doyle, M. J., W. W. Morse, and A. W. Kendall Jr.
1993. A comparison of larval fish assemblages in the temperate zone of the northeast Pacific and northwest Atlantic oceans. Bull. Mar. Sci. 53(2):588–644.

Fahay, M. P.
1983. Guide to the early stages of marine fishes occurring in the western North Atlantic Ocean, Cape Hatteras to the southern Scotian Shelf. J. Northwest Atl. Fish. Sci. 4:1–423.

Flores-Coto, C., and U. Ordonez-Lopez.
1991. Larval distribution and abundance of Myctophidae, Gonostomatidae, and Sternoptychidae from the southern Gulf of Mexico. U.S. Dep. Commer., NOAA Tech. Rep., NMFS 95:55–64.

Gaeta, S. A., J. A. Lorenzzetti, I. B. Miranda, S. M. M. Susini-Ribeiro, M. Pompeu, and C. E. S. Araujo.
1999. The Vitoria eddy and its relation to the phytoplankton biomass and primary productivity during the austral fall of 1995. Arch. Fish. Mar. Res., 47(2/3):253–270.

Hill, M. O.
1979. TWINSPAN-A FORTRAN program for arranging multivariate data in an ordered two-way table by classification of the individuals and attributes. Cornell University, Ithaca, NY, 40 p.

Hill, M. O., R. G. H. Bunce, and M. W. Shaw.
1975. Indicator species analysis, a divisive polythetic method of classification, and its application to a survey of native pinewoods in Scotland. J. Ecol. 63:597–613.

Ikeda, Y., L. B. Miranda, and N. J. Rock.
1974. Observations on stages of upwelling in the region of Cabo Frio (Brazil) as conducted by continuous surface temperature and salinity measurements. Bolm Inst. oceanogr., S Paulo 23:33–46.

Kramer, D., M. J. Kalin, E. G. Stevens, J. R. Thrailkill, and J. R. Zweifel.
1972. Collecting and processing data on fish eggs and larvae in the California Current region. U.S. Dep. Commer., NOAA Tech. Rep., NMFS Circ. (370):1–38.

Leis, J. M.
1993. Larval fish assemblages near Indo-Pacific coral reefs. Bull. Mar. Sci. 53(2):362–392.

Leis, J. M., and B. Goldman.
1987. Composition and distribution of larval fish assemblages in the Great Barrier Reef lagoon, near Lizard Island, Australia. Aust. J. Mar. Freshwater Res. 38:211–223.

Leis, J. M., and D. S. Rennis.
1983. The larvae of Indo-Pacific coral reef fishes. New South Wells Univ. Press, Sydney, 269 p.

Leis, J. M., and T. Trnski.
1989. The larvae of Indo-Pacific shorefishes. Univ. Hawaii Press, Honolulu, HI, 371 p.

Loeb, V. J.
1980. Patterns of spatial and species abundance within the larval fish assemblage of the North Pacific Central Gyre during later summer. Mar. Biol. 60:189–200.

Lowe-McConnell, R. H.
1987. Ecological studies in tropical fish communities. Cambridge Univ. Press, Cambridge, 382 p.

Mascarenhas Jr., A. S., L. B. Miranda, and N. J. Rock.
1971. A study of the oceanographic conditions in the region of Cabo Frio. *In* The fertility of the sea (J. D. Costlow, ed.), p. 285–308. Gordon & Breach, New York, NY.

Matsuura, Y.
1985. Distribution and abundance of skipjack larvae off the coasts of Brazil. Proc. ICCAT Conf. Intern. Skipjack Year Prog., Madrid, p. 285–289.

Matsuura, Y., and M. P. Olivar.
1999. Fish larvae. *In* South Atlantic zooplankton (D. Boltovskoy, ed.), p. 1445–1496. Buckhuys Publ., Leiden.

Moser, H. G. (ed.).
1996. The early stages of fishes in the California Current region. Calif. Coop. Oceanic Fish. Invest., Atlas 33:1–1505.

Moser, H. G., W. J. Richards, D. M. Cohen, M. P. Fahay, A. W. Kendall Jr., and S. L. Richardson, (eds.).
1984. Ontogeny and systematics of fishes. Am. Soc. Ichthyol. Herpetol. Spec. Publ. 1, 760 p.

Nafpaktitis, B. G., R. H. Backus, J. E. Craddock, R. L. Haedrich, B. H. Robison, and C. Karnella.
1977. Fishes of the western North Atlantic. Part 7: Order Inioni (Myctophiformes). Memo. Sears Found. Mar. Res., New Haven, CT, 299 p.

Okiyama, M. (ed.).
1988. An atlas of the early stage fishes in Japan. Tokai Univ. Press, Tokyo, 1154 p.

Olivar, M. P.
1988. Planktonic stages of lanternfishes (Osteichthyes, Myctophidae) in the Benguela upwelling region. Invest. Pesq. 52(3):387–420.

Olivar, M. P., and J. M. Fortuño.
1991. Guide to Ichthyoplankton of the southeast Atlantic (Benguela Current Region). Scientia Marina 55(1):1–383.
Olivar, M. P., and P. A. Shelton.
1993. Larval fish assemblages of the Benguela Current. Bull. Mar. Sci. 53(2):450–474.
Ribeiro, M. R.
1996. Estudos sobre o desenvolvimento larval, abundância e distribuição de ovos e larvas de *Maurolicus muelleri* (Gmelin, 1789) (Teleostei: Sternoptychidae), e possíveis potencialidades ao largo da costa sudeste brasileira, compreendida entre 23°S (Cabo Frio, RJ) e 29°S (Cabo de Santa Marta Grande, SC). Master thesis presented at the Instituto Oceanográfico da Universidade de São Paulo, 160 p.
Richards, W. J., M. F. McGowan, T. Leming, J. T. Lamkin, and S. Kelley.
1993. Larval fish assemblages at the loop current boundary in the Gulf of Mexico. Bull. Mar. Sci. 53(2):475–537.
Schmid, C., H. Schafer, G. Podestá, and W. Zenk.
1995. The Vitoria eddy and its relation to the Brazil Current. J. Phys. Oceanogr. 25:2532–2546.
Signorini, S. R., L. B. Miranda, D. L. Evans, M. R. Stevenson, and H. M. Inostroza.
1989. Corrente do Brasil: estrutura térmica entre 19° e 25° circulação geostrofica. Bolm Inst. Oceanogr., S. Paulo 37(1): 33–49.
Silva, P. C. M.
1973. A ressurgência em Cabo Frio (I). Publ. Inst. Pesquisa Marinha 24:1–31.
Susini-Ribeiro, S. M. M.
1999. Biomass distribution of pico-, nano- and microplankton on the continental shelf of Abrolhos, East Brazil. Arch. Fish. Mar. Res. 47(2/3):271–284.

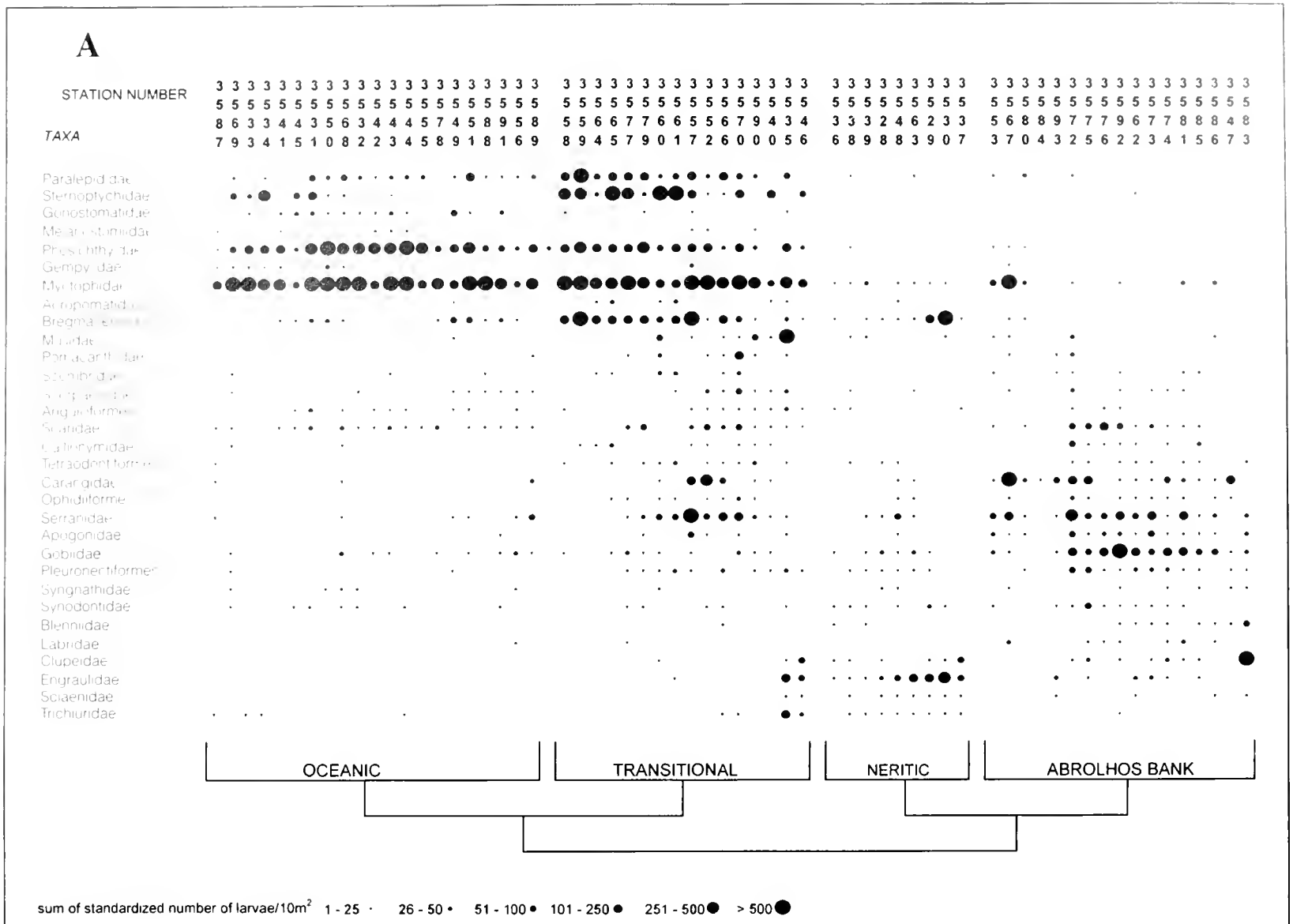

Appendix 1

Figure of stations, with respective families of fish found at these stations, generated by the software program TWINSPAN for the three cruises conducted in the Abrolhos region. Composite clustering of station groups are given along the bottom margin. (**A**) Winter cruise, (**B**) Summer cruise, (**C**) Autumn cruise. TWINSPAN is program CEP-41 in the Cornell Ecology Program series, written by Mark O. Hill.

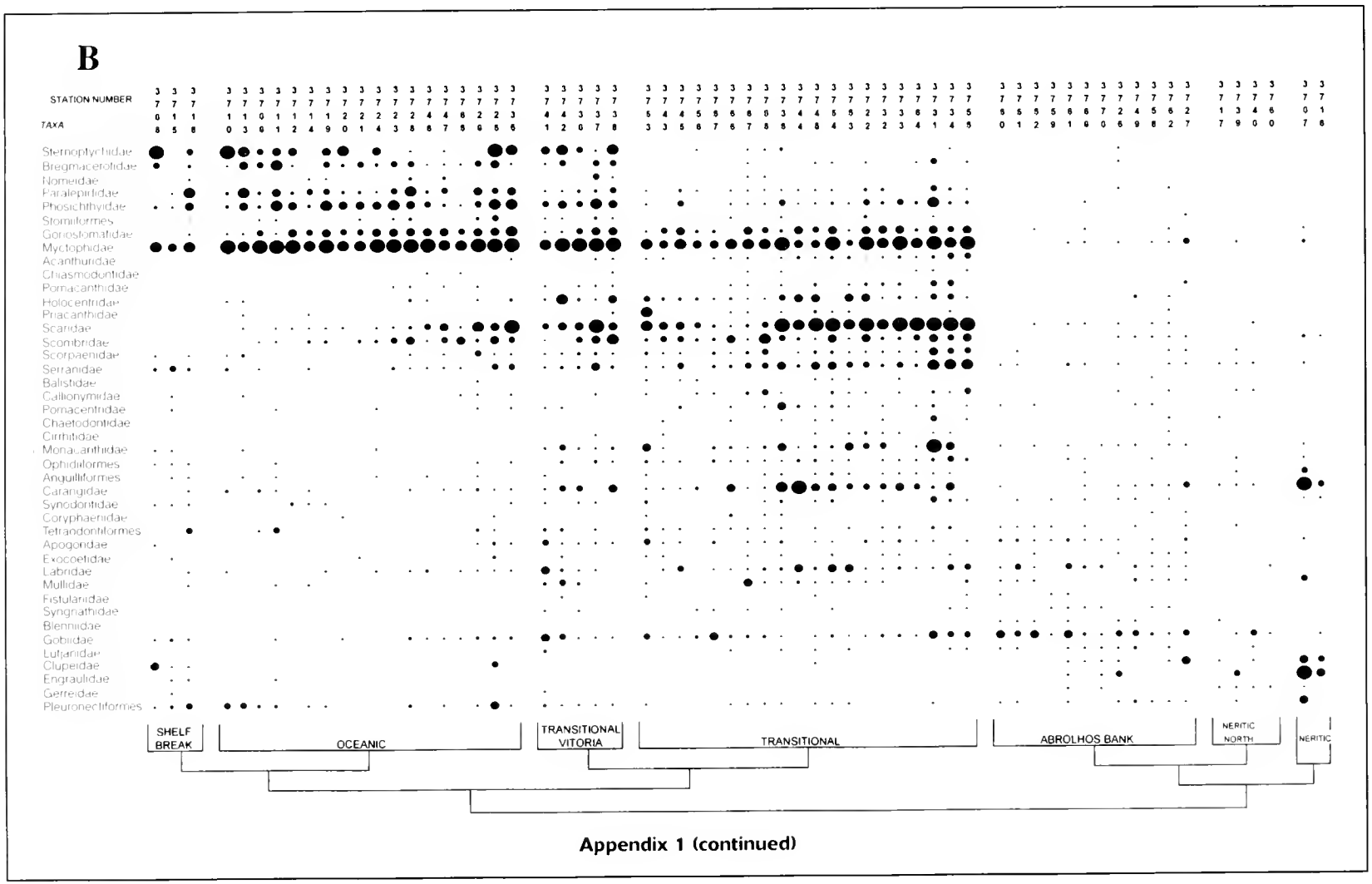

Appendix 1 (continued)

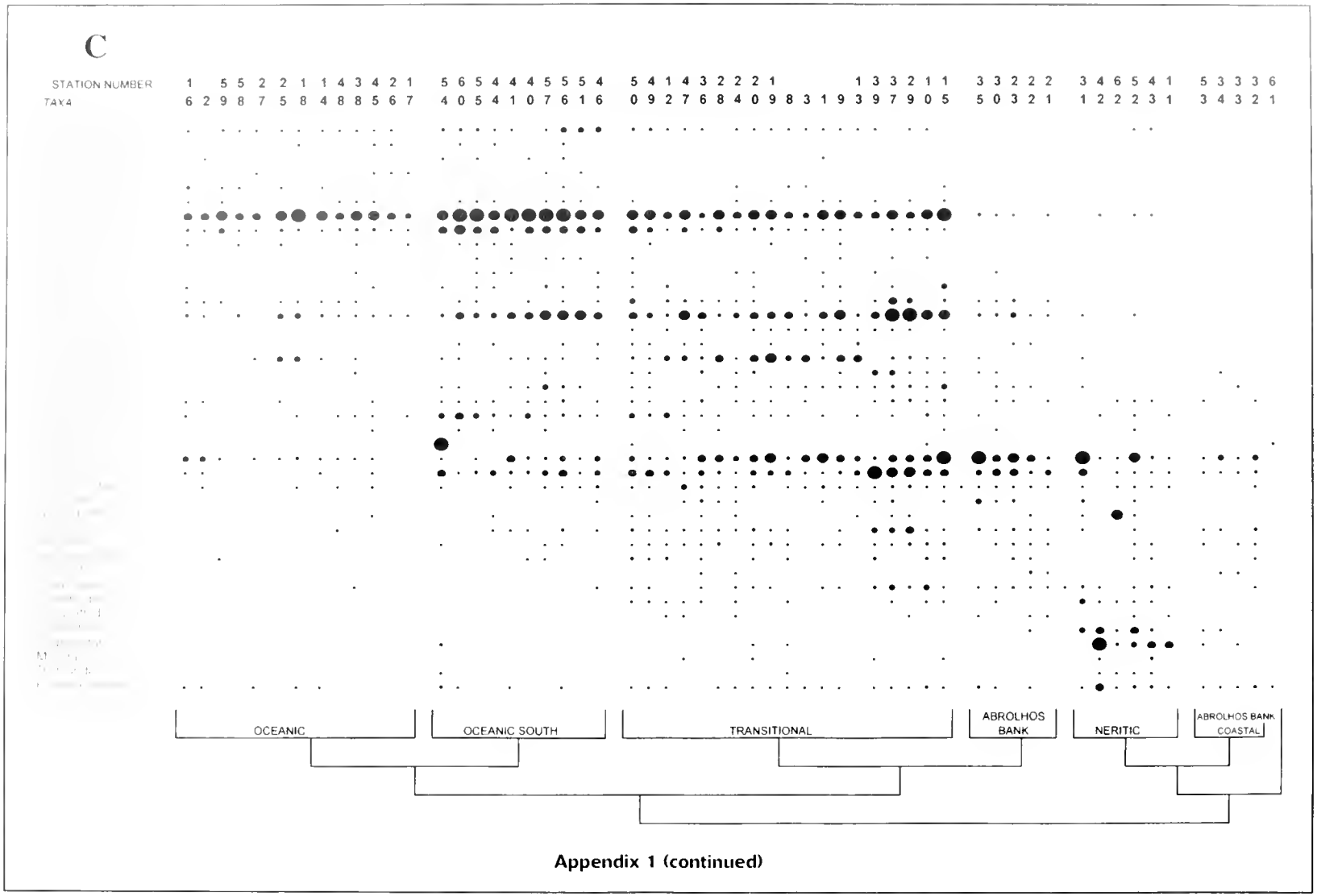

Appendix 1 (continued)

Variation in age compositions and growth rates of *Acanthopagrus butcheri* (Sparidae) among estuaries: some possible contributing factors

Gavin A. Sarre
Ian C. Potter

School of Biological Sciences and Biotechnology
Murdoch University
Western Australia 6150, Australia
E-mail address (for G. A. Sarre): sarre@central.murdoch.edu.au

Abstract—Age compositions and growth rates have been determined for populations of *Acanthopagrus butcheri* in four estuaries and a saline, coastal lake, all of which differ markedly in their morphological, physicochemical, and biotic characteristics. Because the opaque zones in otoliths were shown to form annually, the number of these zones could be used to age individual fish. However, the otoliths of fish that were more than six years old had to be sectioned in order to consistently reveal all opaque zones. The number of annuli on scales did not provide reliable estimates of age. *Acanthopagrus butcheri*, which typically completes its life cycle in estuaries, was represented in each of the five water bodies by fish ≥15 years old and lengths and weights >365 mm and >860 g, respectively. The maximum length and weight of *A. butcheri* recorded in any of the five water bodies were 485 mm and 2196 g, respectively. The values for L_∞ in von Bertalanffy growth equations differed significantly between females and males in three of the four estuarine populations ($P<0.001$ or <0.01), whereas those for both k and t_0 differed significantly between the sexes in only one population and then only at $P < 0.05$. The values for k and L_∞ in the von Bertalanffy growth equations differed significantly among both females and males in the four estuaries at either $P < 0.001$ or $P < 0.05$. These parameters also differed significantly between the males in Lake Clifton and the males in each estuary, except the Swan River Estuary. Growth rates in two of the more northern water bodies were greater than those in the two southern and cooler estuaries. The pattern of growth in the Moore River Estuary, as reflected by changes in length with time, differed from that in the other four water bodies in that it was initially slower and subsequently did not show such a marked tendency to form an asymptote. The slow initial rate of increase in length in the Moore River Estuary may be related to particularly high densities of juvenile *A. butcheri* in nearshore, shallow water, as well as to a relatively lower abundance of appropriate food or very low salinities, or to both of the latter. The percentage contribution made by fish ≥5 years was the lowest by far in the Swan River Estuary, which was subjected to the greatest fishing pressure.

Manuscript accepted 22 March 2000.
Fish. Bull. 98:785–799 (2000).

The black bream, *Acanthopagrus butcheri*, which completes its life cycle within estuaries (Potter and Hyndes, 1999; Sarre and Potter, 1999) is one of the most important recreational and commercial fish species in the estuaries of southern Australia (Lenanton and Potter, 1987; Kailola et al., 1993). The fact that the genetic compositions of the populations of this species in the different estuaries of southwestern Australia vary, suggests that, although some *A. butcheri* are occasionally flushed out of estuaries during those winters when freshwater discharge is particularly heavy, the population in an estuary remains essentially discrete from those in other estuaries (Chaplin et al., 1998; Potter and Hyndes, 1999). The confinement of each population of *A. butcheri* to its natal environment means that, if fishing pressure is sufficiently high in any one estuary, the population in that estuary cannot be replenished naturally by immigration from outside that system. Indeed, there is good evidence that the abundance of this sparid in the Blackwood River Estuary in southwestern Australia declined markedly between the 1970s and 1990s as a result of a combination of commercial and recreational fishing activities (see Valesini et al., 1997; Lenanton et al., 1999; Lenanton[1]; Valesini[2]).

The increasing potential for *A. butcheri* to become overexploited as recreational fishing in estuaries increases means that it is now important to have information on the age compositions of this species in the various estuaries in order to ascertain whether the older age classes are becoming excessively depleted in some of these estuaries. Such data are dependent on accurate estimates of the age of fish. In the past, such estimates for *A. butcheri* have typically been based on the number of annuli on scales (Butcher, 1945; Thomson, 1957; Weng, 1971; Hobday and Moran[3]). However, no attempt was made in any of these studies to use traditional methods to validate that the growth zones (annuli) on that hard structure are formed annually—a procedure now considered essential in aging fish (Beamish and McFarlane, 1983). Although Morison et al. (1998) have recently used the number of opaque zones on otoliths as a criterion of age, their approach to validating that those zones were formed annually was based on the observation that the number of opaque zones on the otoliths of fish in the two cohorts that were the most strongly represented in length-frequency data for four consecutive years increased by one in each successive year.

Recent work on *A. butcheri* in southwestern Australia has focused on populations in four estuaries and a landlocked saline, coastal lake, which vary

[1] Lenanton, R. C. J. 1977. Aspects of the ecology of fish and commercial crustaceans of the Blackwood River Estuary, Western Australia. Report 19, Department of Fisheries and Wildlife, Perth, Western Australia, Australia, 72 p.

[2] Valesini, F. J. 1995. Characteristics of the ichthyofaunas of the Blackwood River Estuary and Flinders Bay. Unpublished honours thesis, Murdoch University, Perth, Western Australia, Australia, 67 p.

[3] Hobday, D., and Moran, M. 1983. Age, growth and fluctuating year class strength of black bream in the Gippsland Lakes, Victoria. Report No. 20. Marine Science Laboratories, Victoria, Australia, 17 p.

markedly in their morphological and physicochemical characteristics and in the composition of their biota (Sarre et al., 2000). Thus, two of these water bodies are permanently open to the sea, while one is intermittently closed, another is normally closed, and one is permanently closed. Furthermore, the regions where *A. butcheri* spawns in these estuaries in the spring and early autumn range in salinity from as low as 3.5–8.0‰ in the intermittently open estuary to over 40‰ in the normally closed estuary and, as a result of their location at different latitudes, they also differ in water temperature (Young et al., 1997; Sarre and Potter, 1999). The differences in the biota of these systems are reflected in marked differences in the dietary composition of *A. butcheri*, with, for example, the overall contribution made by macrophytes to the volume of stomach contents ranging from as low as 8.3% in one population to as high as 56.4% in another (Sarre et al., 2000).

The aims of our study on *A. butcheri* were as follows: 1) to validate that the growth (opaque) zones visible on sectioned otoliths of *A. butcheri* are formed annually; 2) to compare the number of growth (opaque) zones in otoliths prior to and after sectioning in order to determine whether otoliths always have to be sectioned to reveal each of their opaque zones; 3) to ascertain whether the number of annuli on scales corresponds to the number of opaque zones on sectioned otoliths and can thus likewise be used for aging this species; 4) to determine the age composition of *A. butcheri* in the above four estuaries and the saline, coastal lake, in which the fishing pressure on black bream varies from zero to substantial, and thereby ascertain whether there is evidence that heavy exploitation of this species can markedly reduce the proportion of older fish; and 5) to determine the extent to which the growth rates and length at age of *A. butcheri* differ amongst populations in the above five water bodies, which vary markedly in their abiotic and biotic characteristics and amongst which the dietary compositions of *A. butcheri* are significantly different.

Materials and methods

Acanthopagrus butcheri was collected from the permanently open Swan River and intermittently open Moore River estuaries on the lower west coast of Australia (31–32°S) and from the permanently open Nornalup Walpole and normally closed Wellstead estuaries (34–35°S) on the southern coast of Western Australia (see Fig. 1 for locations of these estuaries). *Acanthopagrus butcheri* was also collected from Lake Clifton, a landlocked saline, coastal lake. Because the Department of Conservation and Land Management (CALM) restricted the number of *A. butcheri* that could be collected from this lake to 100, and because 85 of these 100 fish were males, emphasis was placed on the data obtained for this sex in this lacustrine environment.

Fish in estuaries were collected from over sand in nearshore, shallow waters (<1.5 m depth) by using a 11-m seine net with 9-mm mesh in the codend and from offshore, deeper waters (2–5 m depth) by employing composite sunken gill nets containing eight 20 m long × 2 m high panels, each of which had a different mesh size, i.e. 38, 51, 63, 76, 89, 102, 115, or 127 mm. Sampling in the Swan River Estuary commenced in September 1993 and was carried out monthly until April 1995 with seine netting and monthly until February 1995 with gill netting. The same methods were used to sample *A. butcheri* in the Moore River, Nornalup Walpole, and Wellstead estuaries between the spring of 1993 and the summer of 1996–97 (December–January). Sampling in the Swan River, Nornalup Walpole, and Wellstead estuaries was carried out in the saline lower reaches of the tributary rivers, i.e. upper estuary (Fig. 1), which, for most of the year, contain the majority of the *A. butcheri* found in those estuaries (Sarre and Potter, 1999). In contrast, sampling was undertaken throughout the short Moore River Estuary, which does not possess the large central basins that are found in the other three estuaries (Fig. 1). The catches obtained by seine and gill netting in the above four estuaries were supplemented by up to a further 7% by fish obtained with rod and line. A fine mesh seine net, which was 5.5 m long and consisted of 1-mm mesh, was used to collect small *A. butcheri* from extensive beds of the macroalgae *Gracilaria verrucosa* in the downstream and middle regions of the upper Swan River Estuary between December 1998 and March 1999. (See "Results" section for the reason for this additional sampling). The sample of 100 *A. butcheri* collected from Lake Clifton in November 1996 was obtained exclusively by rod and line, in accordance with the conditions laid down by CALM.

Both of the sagittal otoliths were removed from each fish sampled from the four estuaries and Lake Clifton and these otoliths were immersed in methyl salicylate solution. For sectioning, otoliths were mounted and embedded in clear epoxy resin and cut into ca 0.5-mm transverse sections with an Isomet low-speed diamond saw. Sections were ground on sequentially finer grades of carborundum paper (400–1200 grade) and mounted on glass slides with DePX mounting adhesive. Whole otoliths and sectioned otoliths were placed on a black surface and examined microscopically under reflected light.

Measurements were made of the distance between the outer edge of the outermost opaque zone and the periphery of the otolith in the case of the otoliths that were to be used for aging fish in the Swan River Estuary. This distance, i.e. the marginal increment, was then expressed either as a proportion of the distance between the primordium of the otolith and the outer edge of the opaque zone, when only one opaque zone was present, or as a proportion of the distance between the outer edge of the two outermost opaque zones, when two or more opaque zones were present. All measurements were recorded to the nearest 0.05 mm. As with other sparids, a narrow opaque zone is laid down in the otoliths of *A. butcheri* during the cool (winter) period and a wide translucent zone is deposited during the warm (summer) period (Johnson, 1983; Buxton and Clarke, 1991; Francis et al., 1992; Booth and Buxton, 1997).

Otoliths from 239 *A. butcheri*, collected from the Swan River Estuary and covering a wide size range, were used for comparing the number of narrow, opaque zones that could be seen on this hard structure before and after sectioning. The number of opaque zones visible in a subsam-

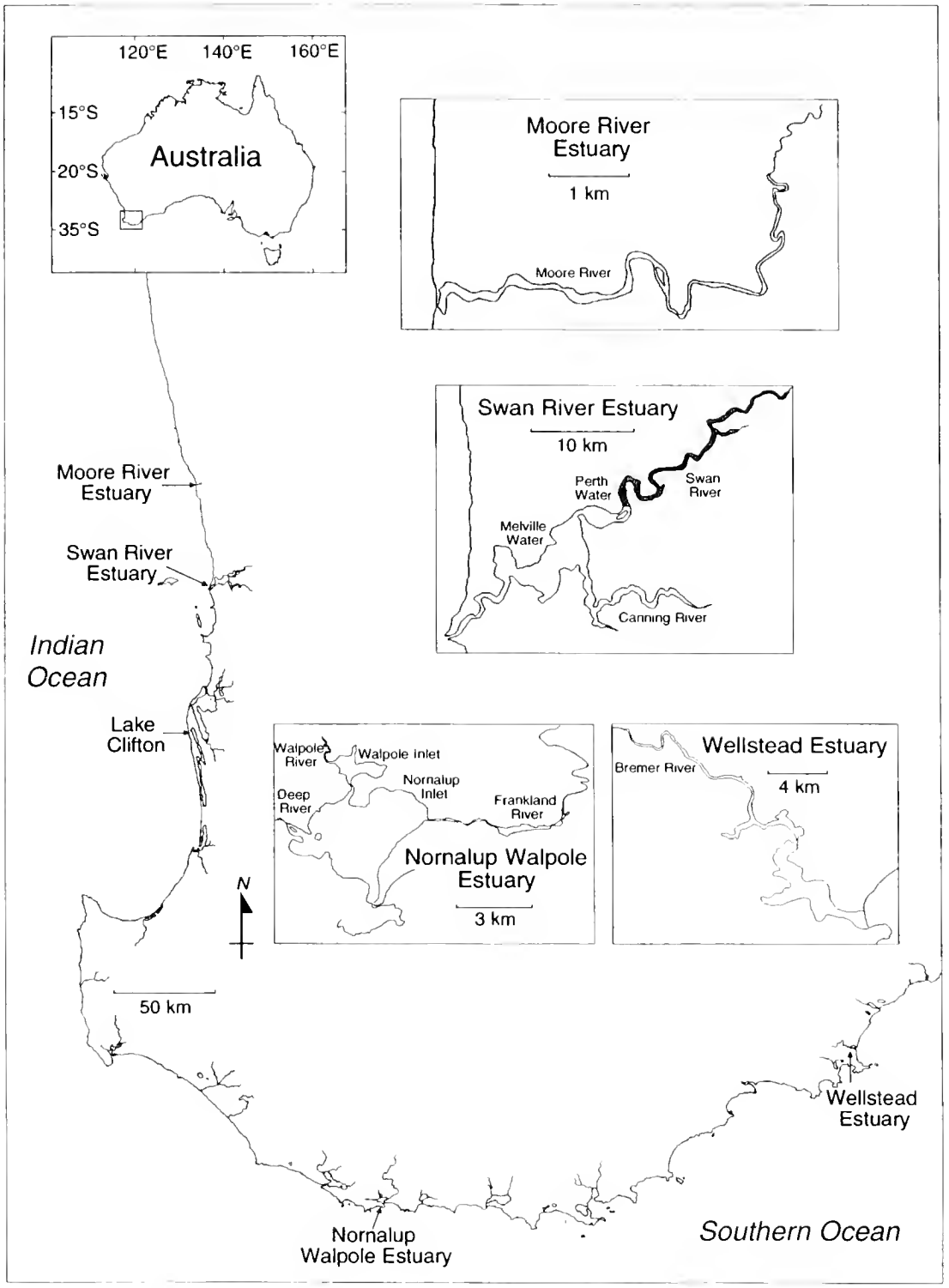

Figure 1

Map showing the location of the four estuaries and Lake Clifton in southwestern Australia from which samples of *Acanthopagrus butcheri* were collected, together with individual maps of each estuary. The shaded area of the Swan River Estuary represents the region sampled in our study.

ple of 126 of the sectioned otoliths were then compared with the numbers of annuli on scales removed from the same fish. The scales used for these comparisons, which were obtained from above the lateral line and directly behind the operculum, were mounted between glass slides and examined microscopically under reflected light.

The number of opaque zones in the whole and sectioned otoliths of a subsample of 162 of the above 239 fish and the number of annuli on the scales of a random subsample of 87 of those fish were also counted by a second reader to determine the level of reproducibility of the counts made of the growth zones on these hard structures by the senior author.

The birth date assigned to *A. butcheri* in each water body corresponds to peak spawning activity, as estimated from the trends exhibited by gonadosomatic indices, stages in gonadal development and pattern of oocyte development (Sarre and Potter, 1999). Von Bertalanffy growth curves were fitted to the individual lengths of female and male fish at their estimated ages at capture by a nonlinear technique (Gallucci and Quinn, 1979) by using a nonlinear subroutine in SPSS (SPSS Inc., 1988). The von Bertalanffy equation is

$$L_t = L_\infty \left[1 - e^{-k(t - t_0)}\right],$$

where L_t = the total length at age t (years);
L_∞ = the mean of the asymptote predicted by the equation;
k = the growth coefficient; and
t_0 = the hypothetical age at which fish would have zero length, if growth followed that predicted by the equation.

The lengths at age of fish whose sex could not be determined under a dissecting microscope were selected at random and placed alternately in the data sets for female and male fish.

Each of the growth parameter estimates for female and male fish in the same estuary and for each sex in the four estuaries were compared by using a likelihood ratio test (see Kimura, 1980). Comparisons were also made between the growth parameters for the males of *A. butcheri* in Lake Clifton, the sex which dominated the catches in that lake, and those of the males of this species in the four estuaries.

The likelihood ratio for the null hypothesis (Kimura, 1980) tests the null hypothesis against the alternative hypothesis where

H_Ω states that the parameters L_∞, k, and t_0 satisfy some set of r linear constraints;

H_ω states that the parameters L_∞, k, and t_0 possibly satisfy no linear constraints.

The maximum likelihood estimates of the error variances $\hat{\sigma}^2_\omega$ and $\hat{\sigma}^2_\Omega(r)$ are given by the sum of squares of residuals from the iteratively reweighted least squares procedure used to fit L_∞, k, and t_0 subject to r linear constraints.

The likelihood ratio test statistic, as described by Cerrato (1990), for two data sets with sample sizes n_1 and n_2 is given by

$$-2\log(\Lambda),$$

where $$\Lambda = \left(\frac{\sigma}{\hat{\sigma}}\right)^{\left(\frac{\sigma}{\hat{\sigma}}\right)}$$

Table 1

The linear constraints and degrees of freedom of each hypothesis, based on Kimura (1980), where $_M$ and $_F$ represent males and females, respectively.

Hypothesis	Linear constraints	Degrees of freedom
H_Ω	none	
$H_{\omega 1}$	$L_{\infty M} = L_{\infty F}$	1
$H_{\omega 2}$	$k_M = k_F$	1
$H_{\omega\beta}$	$t_{0M} = t_{0F}$	1

Under the null hypothesis $-2\log(\Lambda)$ converges to a $\chi^2(r)$ distribution with the degrees of freedom equal to the number of equations required to specify the linear constraints applied to the model (Kimura, 1980). The null hypothesis is rejected at the α level of significance when $-2\log(\Lambda) > \chi^2(r)$.

The types of linear constraints applied to the von Bertalanffy growth equation, the null and alternative hypotheses associated with each constraint and the degrees of freedom of the test statistic are given in Table 1.

Results

Validation of annual deposition of opaque zones in otoliths

The mean monthly marginal increment on sectioned otoliths with one opaque zone declined sharply from 0.57 in September and October 1993 to 0.11 in November 1993, before gradually rising to a maximum of 0.93 in October 1994 (Fig. 2). As in 1993, the mean marginal increment then declined markedly between October and November 1994 and subsequently rose over the ensuing months. The trends exhibited by the mean monthly marginal increment on otoliths with two and three opaque zones were the same as those just described for otoliths with one opaque zone (Fig. 2). Because the number of fish with otoliths displaying four or more opaque zones in the samples for some months was small, the marginal increments for all such otoliths in each month were pooled. Although the trends shown by the mean monthly marginal increments on these otoliths were not quite as "smooth" as those shown by otoliths with one to three opaque zones, they still clearly declined precipitously in November of both 1993 and 1994 and subsequently rose progressively during the ensuing months between early summer and mid-autumn (Fig. 2).

The fact that, irrespective of the number of opaque zones on otoliths, the mean monthly marginal increments on otoliths underwent a pronounced decline and then a progressive rise only once during the year demonstrates that a single opaque zone is formed in otoliths each year. Thus, the number of opaque zones in sectioned otoliths can be used to determine the age of *A. butcheri*.

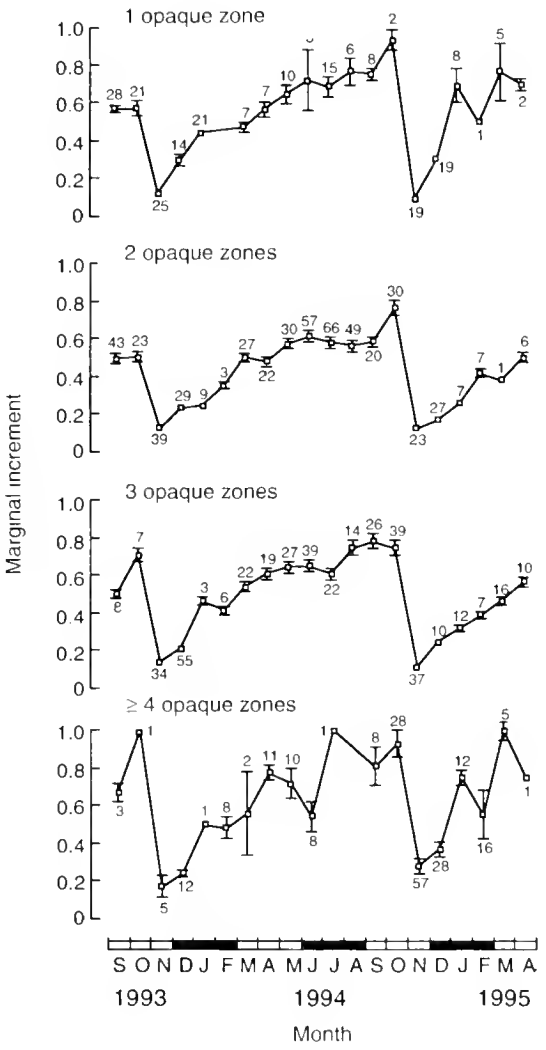

Figure 2

Mean monthly marginal increments ±1SE for sectioned sagittal otoliths of *Acanthopagrus butcheri* in the upper Swan River Estuary. The mean marginal increment is expressed as a proportion of the distance between the primordium and the edge of the opaque zone, when only one such zone was present, and as a proportion of the distance between the outer edges of the two outermost opaque zones, when two or more such zones were present. Sample sizes are given for each month.

Number of growth zones on hard structures

The number of opaque zones detected on a sectioned otolith of *A. butcheri* was always the same as the number observed on the same otolith prior to sectioning, when six or less such zones were visible on the whole otolith (Fig. 3A). However, the use of whole otoliths would have underestimated by one year 15% of seven- and eight-year-old fish, collectively, and, by one or two years, 57% of nine- to 13-year-old fish, collectively. The use of whole otoliths would also have underestimated the age of two 14-year-old fish by three years, two 15-year-old fish by two years, and one 19- and one 21-year-old fish by five years each (Fig. 3A).

The numbers of annuli observed on the scales of *A. butcheri* differed from those recorded in 27, 67, and 40% of the sectioned sagittal otoliths of the same fish, when the otoliths possessed one, two, and three opaque zones, respectively (Fig. 3B). The number of annuli exceeded that of the number of opaque zones in 34% of all cases. The number of annuli on the scales of fish, in which the sectioned otoliths possessed eight to eleven opaque zones, exceeded by one or two the number of opaque zones on those otoliths in 70% of cases (Fig. 3B). On the basis of the number of opaque zones on their sectioned otoliths, one fish that was estimated as 19 and another as 21 years old, displayed seven more annuli on their scales than on their otoliths. Although the number of sectioned otoliths with more than six opaque zones, that were used for comparisons with scales, was only 18, it is still noteworthy that the number of opaque zones on more than half of those otoliths was less than the number of circuli on the scales obtained from the corresponding fish.

The number of opaque zones recorded independently by a second "reader" for sectioned otoliths of *A. butcheri* with 0–3 zones (50 fish), 4–6 zones (50 fish) and 7–10 zones (40 fish), were always the same as those recorded by the senior author for the same otoliths. Furthermore, the second reader recorded the same number of opaque zones on all but two of the 22 sectioned otoliths that the senior author had recorded as having 11 or more opaque zones. Moreover, after reviewing and discussing the two discrepancies, the second reader agreed that he had failed to detect one of the least conspicuous opaque zones near the periphery of the two otoliths for which there were discrepancies, and therefore his counts agreed with the counts made by the senior author. However, the number of annuli counted on the scales by the second reader, that had previously been recorded by the senior author as having 0–3 annuli (50 fish), 4–10 annuli (30 fish), and ≥11 annuli (7 fish), differed in 20%, 43%, and 86% of cases, respectively, which reflects the difficulty in detecting annuli on scales. The differences between counts ranged from one on scales with 0–3 annuli to more than five on scales with ≥11 annuli.

Trends exhibited by length-frequency data for different age classes

The data presented earlier demonstrated that the number of opaque zones on whole otoliths of *A. butcheri* could be used for aging this sparid when there were six or less opaque zones present (Fig. 3A). However, the data in Fig. 3A showed that otoliths had to be sectioned to consistently reveal all of their opaque zones when they displayed seven or more such zones prior to sectioning. Thus, to reduce the margin for producing invalid counts to a minimum, estimates of the age of individual *A. butcheri* were made by using whole otoliths, when five or less opaque zones were present, and by employing sectioned otoliths, when six or more such zones were present.

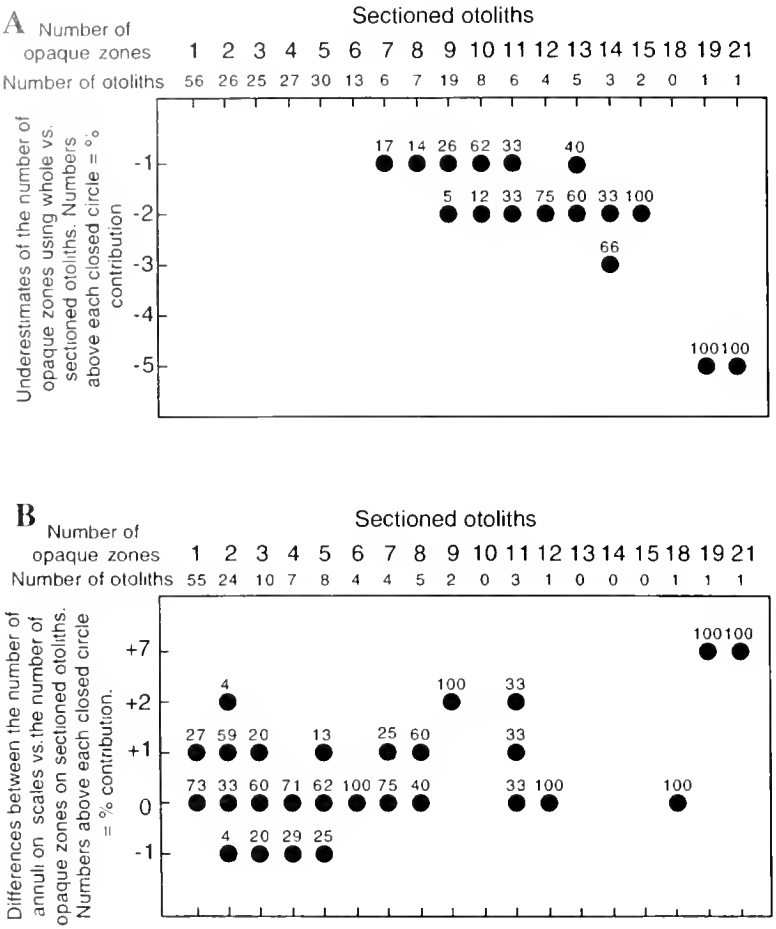

Figure 3

Comparisons between (**A**) the numbers of opaque zones on whole and sectioned otoliths and (**B**) the numbers of annuli on scales and the numbers of opaque zones on sectioned otoliths of *Acanthopagrus butcheri* from the Swan River Estuary.

Although seine netting over sand in nearshore, shallow waters of the upper Swan River Estuary in the summer and early autumn of both 1993–94 and 1994–95 yielded many *A. butcheri* of 50 to 180 mm, it produced only a few smaller individuals of this species. However, sampling of beds of the macroalgae *Gracilaria verrucosa* in the same period in 1998–99 yielded considerable numbers of *A. butcheri* that ranged in length from 16 to 60 mm. Once *A. butcheri* reached lengths of ca. 60 mm, they moved from the beds of *G. verrucosa* to reside over sand. The lengths of these *A. butcheri*, which represented the 0+ recruits resulting from spawning from November to December of 1998 (Sarre and Potter, 1999), and thus represented the 1998 year class, increased from 16–32 mm in December 1998 to 26–63 mm in January 1999 to 44–86 mm in February 1999 and to 36–112 mm in March 1999 (Fig. 4). The mean length ±1SE in the latter month, i.e. 76 mm, did not differ significantly ($P>0.05$) from that of the 0+ age class in March 1994, when a substantial number of these small fish were also caught (Fig. 5).

Because *A. butcheri* spawns predominantly between October and January (spawning peaking in November [Sarre and Potter, 1999]), the cohort of small *A. butcheri* (81–115 mm), that was caught by seine net in the shallow waters of the Swan Estuary in September 1993 and whose otoliths did not possess an opaque zone, was the product of the spawning that took place in the spring to early summer of the previous year, i.e. 1992 (Fig. 5). The lengths of this 1992 year class increased from 81–115 mm in September 1993 to 100–152 mm in November 1993, by which time a single and narrow opaque zone could be discerned on the edge of the otoliths of this year class. Because spawning peaks in November, the members of this cohort were thus now about one year old. By November and December 1994, the lengths of this 1992 year class, now representing early 2+ fish, had increased to 170–220 and 189–224 mm, respectively. The 1993 year class first appeared in seine net catches in March 1994 at lengths of 67–102 mm and was caught until May, when its

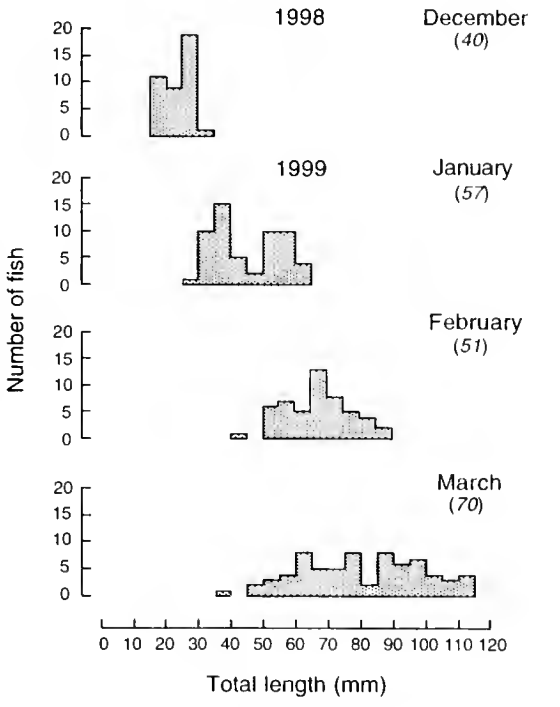

Figure 4

Length-frequency histograms for juvenile *Acanthopagrus butcheri* caught with a 5.5-m seine net (1-mm mesh) in the shallows (<1 m) of the upper Swan River Estuary between December 1998 and March 1999. Numbers in parentheses represent the number of fish measured.

lengths had reached 104–139 mm. When representatives of the 1993 year class reappeared in catches in September 1994, their lengths were still only 96–135 mm, indicating that growth had not occurred during the immediately preceding winter months. The lengths of the 1993 year class subsequently increased to between 136 and 183 mm in January 1995 (Fig. 5). Although the 1994 year class first appeared in March 1995, i.e. in the corresponding month to when the 1993 year class appeared in the previous year, its numbers were small and it was not represented in the following month, i.e. April (Fig. 5).

The 1991 year class was well represented in the majority of months (Fig. 5). The lengths of this strong cohort increased from 163–235 mm in September 1993 to 220–296 mm in September 1994 and to 222–325 mm in November 1994, at which time the fish were entering their fourth year of life. The 1990 year class was a particularly strong cohort (Fig. 5). The lengths of this year class increased from 208–304 mm in September 1993 to 268–349 mm in September 1994 and 259–360 mm at the commencement of their fifth year of life in November. The numbers of fish belonging to earlier year classes, i.e. the 1989, 1988, 1987 year classes, etc., were very low (Fig. 5). Thus, the number of older fish collectively in the Swan River Estuary was also low.

Maximum size and age and von Bertalanffy growth parameters

The spawning activity of *A. butcheri* peaked in early November in the Swan River, Moore River, and Nornalup Walpole estuaries and in early October in the Wellstead Estuary (Sarre and Potter, 1999). The von Bertalanffy growth curves for *A. butcheri* were thus derived by using a birth date of 1 November for the first three estuaries and 1 October for the Wellstead Estuary. Because many fully mature fish were found in Lake Clifton in early November, and this lake was located near the Swan River Estuary, a birth date of 1 November was likewise assigned to the population of *A. butcheri* in that system.

The lowest maximum lengths of female and male *A. butcheri* were 377 and 365 mm, respectively, which were recorded for fish caught in the Wellstead Estuary, whereas the greatest maximum lengths of each sex was 480 mm recorded for a female in the Swan River Estuary and 485 mm recorded fer a male in Lake Clifton (Table 2). The maximum weights of *A. butcheri* in the five systems ranged from a low of 862 g for a female in the Wellstead Estuary to 2196 g for a female in the Swan River Estuary (Table 2). The maximum age of both sexes in each estuary was at least 15 years and the maximum age attained in any system was the 21 years recorded for both a female in the Swan River Estuary and a male in the Nornalup Walpole Estuary (Table 2).

The growth curves of male *A. butcheri* in the Swan River, Nornalup Walpole, and Wellstead estuaries and Lake Clifton followed similar overall trends and thus never crossed one another, and the same was true for the growth curves for females in the above three estuaries (Figs. 6 and 7). The rates of increase in the lengths of both sexes in the Moore River Estuary were initially slower than in each of the above three estuaries, and the rate of increase in the length of males in the Moore River Estuary was also initially less than that of this sex in Lake Clifton. (Note that there were insufficient data for the females in Lake Clifton to make similar comparisons with this sex in this system.) The far slower rate at which length initially increased in the Moore River Estuary is illustrated by the fact that, when male fish were 35–37 months old, i.e. three years in age, their mean length in this estuary was only 151 mm and significantly lower ($P<0.001$) than the 272 mm in the Swan River Estuary, 162 mm in the Nornalup Walpole Estuary, 204 mm in the Wellstead Estuary, and 339 mm in Lake Clifton. Likewise, the mean length of females of *A. butcheri* in the Moore River Estuary at this age was only 144 mm and thus significantly lower than the 285, 161, and 212 mm recorded in the Swan, Nornalup Walpole, and Wellstead estuaries, respectively. It is also noteworthy that the above-mean lengths of males in each of the five systems were significantly different from each other in all cases, except for *A. butcheri* from the Nornalup Walpole and Wellstead estuaries. Corresponding results were obtained for females in the four estuaries. As *A. butcheri* in the Moore River Estuary reached an older age, the growth curves for males and females in this estuary then crossed those for fish from the Nornalup Walpole and Well-

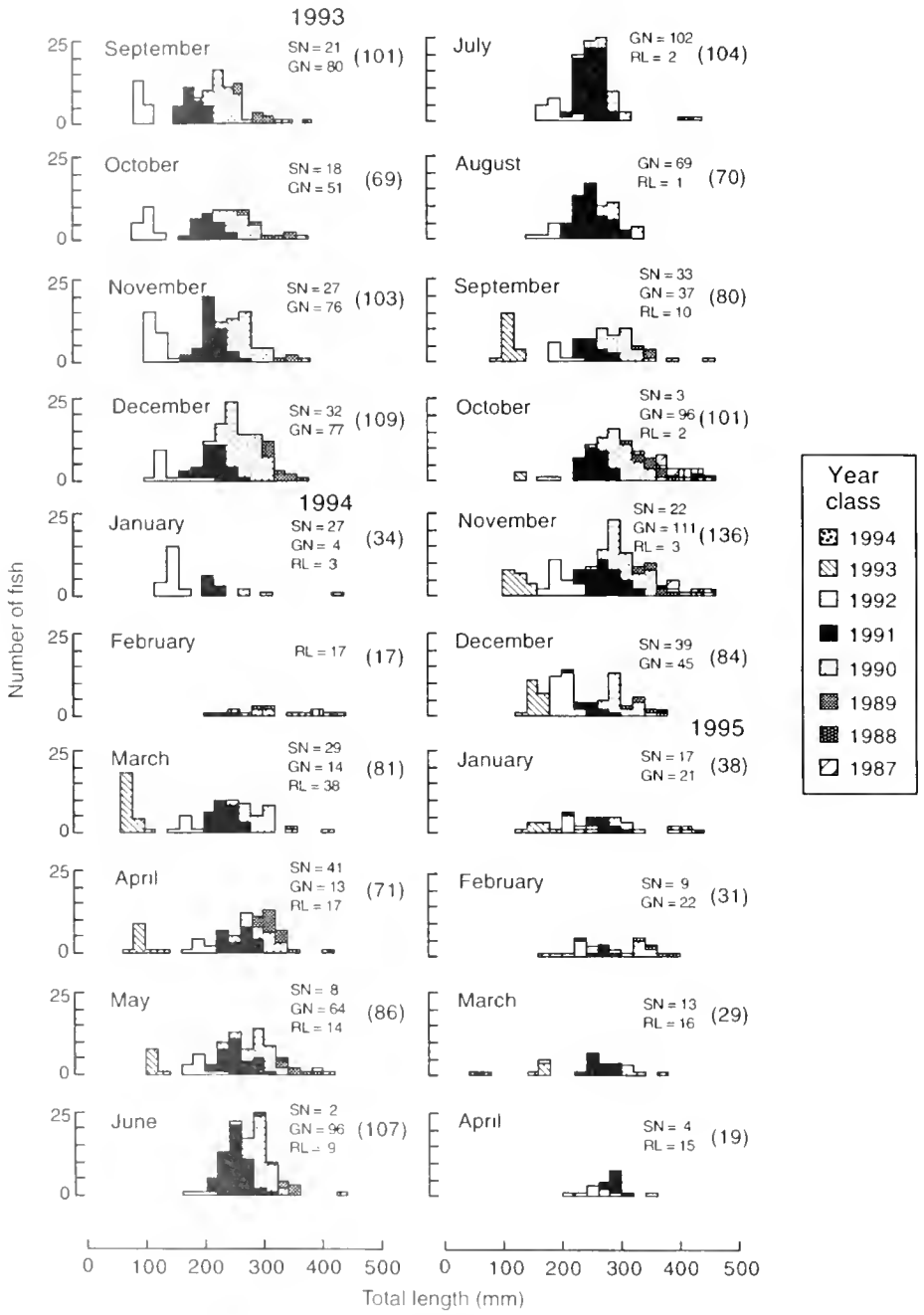

Figure 5

Length-frequency histograms for the different year classes of *Acanthopagrus butcheri*, with data derived from samples of males and females collectively that were caught with seine and gill nets in the upper Swan River Estuary between September 1993 and April 1995. Sample sizes in each month are given for seine netting (SN), gill netting (GN) and rod and line (RL) and in parenthesis for the total sample.

stead estuaries. This feature was reflected in significantly greater asymptotic lengths and lower k values for the Moore River Estuary population than those derived for fish in the latter two estuaries (Table 2, Figs. 6 and 7).

The likelihood ratio test demonstrated that neither the ages at length zero (t_0) nor the growth coefficients (k) in the von Bertalanffy growth equations differed significantly between female and male *A. butcheri* in either the

Table 2

Von Bertalanffy growth parameters and confidence intervals (95%) derived from length-at-age data for female and male *Acanthopagrus butcheri* caught in the Swan River, Moore River, Nornalup Walpole and Wellstead estuaries and for the males in Lake Clifton. n is sample size and L_{max}, W_{max}, and A_{max} are the maximum lengths (mm), weights (g), and ages, respectively. t_0 is the hypothetical age at which fish would have zero length, k is the growth coefficient, L_∞ is the asymptotic length and r^2 is the coefficient of determination.

					von Bertalanffy parameters			
	n	L_{max}	W_{max}	A_{max}	t_0	k	L_∞	r^2
Swan River								
Females	733	480	2196	21	−0.13	0.30	437.8	0.94
95% CL (lower)					−0.17	0.28	426.0	
95% CL (upper)					−0.10	0.31	449.5	
Males	894	475	1780	15	−0.15	0.31	419.3	0.94
95% CL (lower)					−0.19	0.29	10.7	
95% CL (upper)					−0.11	0.32	427.9	
Moore River								
Females	345	403	1192	17	−0.54	0.11	451.6	0.93
95% CL (lower)					−0.68	0.09	416.3	
95% CL (upper)					−0.41	0.12	486.9	
Males	387	394	1162	18	−0.61	0.11	429.2	0.92
95% CL (lower)					−0.76	0.09	395.9	
95% CL (upper)					−0.46	0.12	462.6	
Nornalup Walpole								
Females	346	412	1250	17	−0.60	0.16	367.0	0.91
95% CL (lower)					−0.88	0.14	352.5	
95% CL (upper)					−0.43	0.18	381.6	
Males	265	409	1148	21	−0.31	0.21	323.0	0.90
95% CL (lower)					−0.54	0.19	311.8	
95% CL (upper)					−0.08	0.24	334.6	
Wellstead								
Females	324	377	862	15	−0.17	0.25	377.8	0.91
95% CL (lower)					−0.27	0.23	365.3	
95% CL (upper)					−0.07	0.27	390.3	
Males	331	365	1247	15	−0.18	0.27	344.6	0.92
95% CL (lower)					−0.28	0.25	335.8	
95% CL (upper)					−0.08	0.29	353.4	
Lake Clifton								
Males	85	485	1914	18	−0.46	0.32	441.5	0.96
95% CL (lower)					−0.66	0.28	453.4	
95% CL (upper)					−0.26	0.36	429.6	

Swan River, Moore River or Wellstead estuaries (Table 3). Furthermore, although these two growth parameters did differ significantly between the two sexes in the Nornalup Walpole Estuary, the probability levels in both cases were close to 0.05. However, the asymptotic length (L_∞) for female fish was significantly greater than that of male fish in each estuary except that of the Moore River (Table 3).

The values for k and L_∞ for each sex differed significantly among the populations of *A. butcheri* in the four estuaries and between those of males in each of these estuaries and Lake Clifton ($P<0.001$ or 0.01). Furthermore, the values for t_0 for each sex almost invariably differed significantly ($P<0.001$ or <0.05) among the populations in the four estuaries and between those of males in each of these estuaries and Lake Clifton. Because the three von Bertalanffy parameters for both sexes were each shown almost invariably to differ significantly among the different populations, no attempt was made to test whether there was a common pattern of growth for each sex in each system.

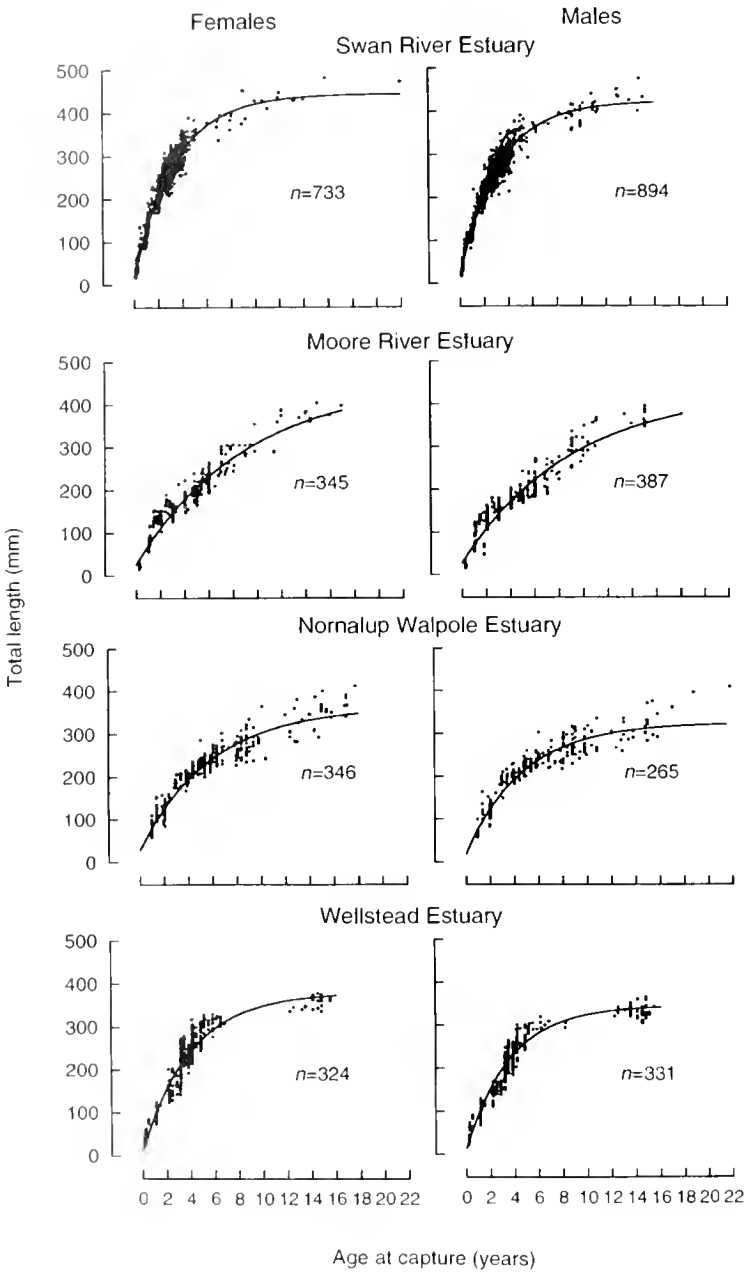

Figure 6

Von Bertalanffy growth curves fitted to length at age data for female and male *Acanthopagrus butcheri* caught in the Swan River, Moore River, Nornalup Walpole and Wellstead estuaries.

The values for k for *A. butcheri* were least in the Moore River Estuary, i.e. 0.11, and greatest in Lake Clifton, i.e. 0.32 (Table 2). The values for L_∞ ranged from a low of 367.0 mm for females and 323.0 mm for males in the Nornalup Walpole Estuary to a high of 451.6 and 441.5 mm for the corresponding sexes in the Moore River Estuary and Lake Clifton, respectively (Table 2). Estimates of t_0 for both sexes of *A. butcheri* in the four estuaries and of the males of *A. butcheri* in Lake Clifton all lay within the relatively narrow range of –0.13 to –0.61 years (Table 2).

Length–weight relationships

The equations relating total length and weight of female and male *A. butcheri* in each estuary and for males in Lake Clifton are presented below, so that, when required, the approxi-

mate weights of fish of a particular length can be estimated. Because analysis of covariance (ANCOVA) showed that neither the slopes nor the y-intercepts in the equations for female and male fish in each estuary differed significantly ($P>0.05$), the equations relating total length and weight for both sexes combined in each estuary are also presented.

Swan River Estuary
- Females: $\log_{10} W = -5.09 + 3.14 \log_{10} L$ ($r^2=0.99, n=865$).
- Males: $\log_{10} W = -5.10 + 3.14 \log_{10} L$ ($r^2=0.99, n=925$).
- Pooled: $\log_{10} W = -5.07 + 3.14 \log_{10} L$ ($r^2=0.99, n=1790$).

Moore River Estuary
- Females: $\log_{10} W = -5.10 + 3.13 \log_{10} L$ ($r^2=0.99, n=250$).
- Males: $\log_{10} W = -5.14 + 3.15 \log_{10} L$ ($r^2=0.99, n=287$).
- Pooled: $\log_{10} W = -5.12 + 3.13 \log_{10} L$ ($r^2=0.99, n=537$).

Nornalup Walpole Estuary
- Females: $\log_{10} W = -4.99 + 3.07 \log_{10} L$ ($r^2=0.99, n=302$).
- Males: $\log_{10} W = -5.03 + 3.09 \log_{10} L$ ($r^2=0.99, n=234$).
- Pooled: $\log_{10} W = -5.00 + 3.08 \log_{10} L$ ($r^2=0.99, n=536$).

Wellstead Estuary
- Females: $\log_{10} W = -4.84 + 3.01 \log_{10} L$ ($r^2=0.99, n=274$).
- Males: $\log_{10} W = -4.89 + 3.03 \log_{10} L$ ($r^2=0.99, n=278$).
- Pooled: $\log_{10} W = -4.85 + 3.02 \log_{10} L$ ($r^2=0.99, n=552$).

Lake Clifton
- Males: $\log_{10} W = -5.12 + 3.14 \log_{10} L$ ($r^2=0.98, n=85$).
- Pooled: $\log_{10} W = -5.10 + 3.13 \log_{10} L$ ($r^2=0.99, n=100$).

Discussion

Validation of the method for aging *Acanthopagrus butcheri*

Our study shows that a growth zone is not laid down in the otoliths of the 0+ age class of *Acanthopagrus butcheri* until winter and that this growth zone does not become clearly delineated until late spring. Because spawning peaks in early November in the Swan Estuary (Sarre and Potter, 1999), the first growth zone becomes delineated as the individuals of this species become one year old. Furthermore, the trends exhibited by the marginal increments on the sectioned otoliths of *A. butcheri* demonstrate that an opaque zone is laid down annually in this hard structure. Our results also demonstrate that the otoliths of *A. butcheri* do not need to be sectioned in order to consistently reveal all of the opaque zones until they had reached a size at which they possessed seven or more such zones. Validation that the opaque zones, which are revealed on the otoliths of *A. butcheri* by sectioning, are formed annually, implies that the estimates of the ages of individual black bream recorded by Morison et al. (1998) using sectioned otoliths are valid for fish caught in the Gippsland Lakes in eastern Australia. However, because the number of annuli on scales frequently differed from the number of opaque zones on sectioned otoliths from the same fish, the number of annuli on scales do not provide a reliable method for aging *A. butcheri*. Thus, those estimates of the age of individual *A. butcheri*, that have been based on the number of annuli on scales (Butcher, 1945; Thomson, 1957; Weng, 1971; Hobday and Moran[3]) are, in many cases, probably invalid.

Table 3

Significance levels for comparisons between the von Bertalanffy growth parameters for female and male *Acanthopagrus butcheri* caught in each of the Swan River, Moore River, Nornalup Walpole, and Wellstead estuaries by using the likelihood ratio test. ***=$P<0.001$, **=$P<0.01$, *=$P<0.05$, NS = Not significant. t_0 is the hypothetical age at which fish would have zero length, k is the growth coefficient, and L_∞ is the asymptotic length.

	von Bertalanffy growth parameter		
Estuary	t_0	k	L_∞
Swan	NS	NS	**
Moore	NS	NS	NS
Nornalup Walpole	*	*	***
Wellstead	NS	NS	***

Differences in age structures amongst populations

Because the majority of *A. butcheri* obtained from the Swan River, Moore River, Nornalup Walpole, and Wellstead estuaries were collected by using the same seine and

gill net sampling regimes, supplemented with a limited amount of angling, any gross differences in the age structure of samples from populations in the different estuaries almost certainly represent real differences. The percentage of *A. butcheri* caught at ≥5 years of age in the Swan River Estuary (5%) was far lower than in either the Moore River Estuary (30%), approximately 100 km farther north on the lower west coast of Australia, or the Nornalup Walpole Estuary (45%) on the south coast of Australia. Note that the estimate for the Swan River Estuary was restricted to data collected during the main sampling period and did not thus include the large samples of small fish that were caught between December 1998 and March 1999. The above differences in the proportion of older fish presumably reflect a greater "mortality" of older fish in the Swan River Estuary than in the other estuaries. It thus appears highly relevant that the population of *A. butcheri* in the Swan River Estuary is exposed to heavy fishing pressure from the recreational sector throughout the year and from commercial fishermen during winter and early spring, whereas the population in the Moore River Estuary is lightly fished and that in the Nornalup Walpole Estuary is not exposed to commercial fishing (Sarre and Potter, 1999).

Although representatives of all age classes up to 15+ were recorded for the populations of *A. butcheri* in each of the above three estuaries, this was not the case with the Wellstead Estuary, which is located 300 km to the east of the Nornalup Walpole Estuary. Thus, in the samples collected from this estuary in 1995 and 1996, the 1989, 1987, 1986, 1985, and 1984 year classes were not represented, and the 1988 year class was represented by only two fish (Fig. 6). This strong implication that, in the Wellstead Estuary, *A. butcheri* either does not spawn or has very limited spawning success in some years parallels the situation recorded for this species in the Gippsland Lakes in eastern Australia (Morison et al., 1998; Hobday and Moran[3]; Coutin et al.[4]). The work of Morison et al. (1998) demonstrated that, in that latter estuary, the commercial catches of *A. butcheri* between 1993 and 1996 were dominated by two year classes and that there had been no strong recruitment of *A. butcheri* since 1989. The absence or weakness of certain year classes in the Gippsland Lakes, and also in the Hopkins River Estuary which is also in eastern Australia, has been attributed to the detrimental influence on spawning success of such unfavourable environmental conditions as heavy freshwater discharge or unsuitable salinities (Newton, 1996; Hobday and Moran[3]). Thus, in the context of the absence of the 1984 year class in samples, it appears relevant that, in the Wellstead Estuary, which has normally remained closed during the last 30 years, there was, as a result of "cyclonic rainfall," an extremely protracted period of heavy freshwater discharge between the early spring of 1984 and the autumn of 1985 (Hodgkin and Clark[5]). This led to a very severe scouring of the substrate and a breaching of the bar at the mouth of this estuary, with the result that this mouth remained open between September 1984 and May 1985. The heavy freshwater discharge that occurred during and immediately after the 1985 spawning season of *A. butcheri* in the Wellstead Estuary would thus almost cer-

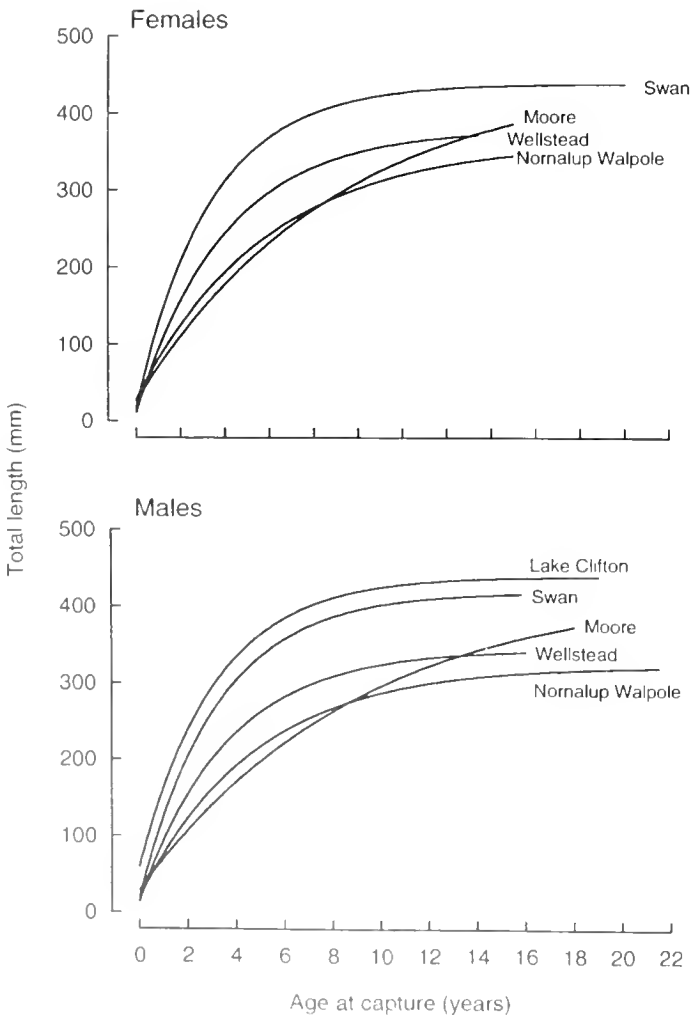

Figure 7

Comparisons between von Bertalanffy growth curves fitted to length-at-age data for female and male *Acanthopagrus butcheri* in the Swan River, Moore River, Nornalup Walpole, and Wellstead estuaries and for males in Lake Clifton in southwestern Australia.

[4] Coutin, P., S. Walker, and A. Morison. 1997. Black bream—1996. Compiled by the Bay & Inlet Fisheries and Stock Assessment Group. Fisheries Victoria Assessment Report 14. Melbourne, Victoria, Australia, 89 p.

[5] Hodgkin, E. P., and R. Clark. 1987. Wellstead Estuary, the estuary of the Bremer River. Estuarine Study Series 1. Environmental Protection Authority, Perth, Western Australia, 22 p.

tainly have flushed out to sea any eggs or larvae of this species that were produced during that period. However, it should also be recognized that freshwater discharge was so strong during that period that even many large *A. butcheri* were flushed out of the estuary, with the result that some of these fish were subsequently caught by anglers along the nearby coast (Spurr[6]). Furthermore, when freshwater discharge is very high, the salinities fall to such low levels that they are unlikely to be conducive to spawning by *A. butcheri* (Haddy and Pankhurst, 2000). Thus, the absence of the 1984 year class in samples may be due to the loss of eggs, larvae, or maturing and mature fish to the ocean in 1984, or to the inhibitory effect of low salinities on spawning, or to a combination of the latter.

The fact that the 1985 year class of *A. butcheri* was also not caught may reflect a low return of large *A. butcheri* to the estuary by the commencement of the spawning period in 1985. The absence of the 1986, 1987, and 1989 year classes and the paucity of the 1988 year class can probably be attributed to the fact that, although freshwater discharge was not as strong as in 1984, it was still sufficient to breach the bar at the estuary mouth during the spawning period in each of those years (Spurr[6]). It would thus also have been likely to result in a loss to the ocean of eggs and larvae produced during the spawning periods in those years or to the emigration of maturing or mature fish, or in both of these effects (Hodgkin and Clark[5]). The view that heavy freshwater flushing or very low salinities, or both, were the main contributors to the lack of spawning success of *A. butcheri* between 1984 and 1989 is consistent with the observation that, when freshwater discharge was not sufficiently strong to breach the estuary mouth, as was the case between 1990 and 1995 (Spurr[6]), there was at least a reasonable recruitment of each of the 1990 to 1995 year classes.

Comparisons between von Bertalanffy growth parameters for females and males

The likelihood ratio test showed that the growth coefficients (k) for female and male fish were significantly different in only one of the four estuaries, i.e. the Nornalup Walpole Estuary, and even then the probability level was close to 0.05, which is consistent with the fact that the values for the 95% confidence intervals for this parameter for the two sexes overlap in each estuary other than the Nornalup Walpole Estuary. The lack of a marked distinction between the growth rates of female and male fish is hardly surprising because *A. butcheri* undergoes a substantial amount of growth before the gonads start to become mature for the first time (Sarre and Potter, 1999). However, the maximum length and asymptotic length (L_∞) were always greater for female than male fish in each of the four estuaries, thereby paralleling the situation with many other fish species in both southwestern Australia (Laurenson et al., 1994; Wise et al., 1994; Hyndes et al., 1996; 1998) and elsewhere (e.g. Kenchington and Augustine, 1987; McPherson, 1992; Crabtree et al., 1995).

[6] Spurr, P. 1995. Local resident and former commercial fisherman. Personal commun. Bremer Bay, Western Australia.

The relatively low values determined for age at length zero for the two sexes in the four estuaries and for males in Lake Clifton, i.e. –0.13 to –0.61 years, reflects in part the good fit of the growth curves to the points for the age at length of the small fish. These low values for t_0 contrast with the –5.21 years for females and –3.70 years for males that were calculated by Morison et al. (1998) for *A. butcheri* in the Gippsland Lakes. Furthermore, the fork lengths at age zero for female and male fish in the Gippsland Lakes were ca. 110 and 100 mm, respectively. Thus, the von Bertalanffy growth equations recorded for *A. butcheri* in the Gippsland Lakes do not provide a good description of the pattern of growth throughout the full size range of fish.

Variations in von Bertalanffy growth parameters among populations

Although the patterns of growth of female and male *A. butcheri* in the Swan River, Wellstead, and Nornalup Walpole estuaries followed the same overall trends, with length increasing rapidly with time initially and then forming asymptotes, the values for k and L_∞ for each sex varied significantly amongst the populations in those estuaries. The initial rate of increase in length in these three estuaries was greatest in the Swan River Estuary and least in the Nornalup Walpole Estuary. Although the value for k for male *A. butcheri* in Lake Clifton differed significantly from that of this sex in the Swan River Estuary, the same was not true for L_∞. However, the value for L_∞ for male *A. butcheri* in Lake Clifton was still similar to that of this sex in the Swan River Estuary. The above comparisons demonstrate that the growth rate in Lake Clifton was similar to that in the Swan River Estuary, which is located only ca. 90 km farther to the north (see also Fig. 1). The von Bertalanffy growth parameters demonstrated that male *A. butcheri* grew more rapidly and attained greater asymptotic lengths in the Swan River Estuary and Lake Clifton than in either the Wellstead or Nornalup Walpole estuaries. The presence of faster growth rates in the Swan River Estuary and Lake Clifton, which are located at latitudes of ca. 32° on the lower west coast of Australia, than in the Nornalup Walpole and Wellstead estuaries, which are situated much farther south at a latitude of ca. 34° on the south coast of Western Australia, may reflect the greater temperatures found in more northern regions.

The pattern of growth of *A. butcheri* in the Moore River Estuary differed from those of this species in each of the other three estuaries and Lake Clifton, in that the increase in length with time was initially slower and the growth curve did not exhibit a marked asymptote. This pattern suggests that some factor or factors were less than optimal for growth during the first few years of life, but that conditions for growth improved later in life. The slow initial rates of increase in length of *A. butcheri* in the Moore River Estuary during early life may be related to the exceptionally high densities of this species in nearshore, shallow waters, the region which constitutes the typical habitat of the juveniles of this species (Sarre, 1999). The far greater density of this species in these waters, than in correspond-

ing waters of the other three estuaries, can be gauged from the fact that, during summer, the densities in such waters sometimes reached 234 fish per 250 m^2 in the Moore River Estuary, whereas they never exceeded 50 fish per 250 m^2 in any of the other three estuaries. Because *A. butcheri* tends to move into offshore and deeper waters as it increases in size, as is the case with several other fish species in southwestern Australian estuaries (Chubb et al., 1981; Chrystal et al., 1985; Potter et al., 1988; Wise et al., 1994), it then becomes more widely dispersed.

Although the high densities of juvenile *A. butcheri* in nearshore, shallow waters of the Moore River Estuary could have contributed to the initially slow rate at which length increased early in life, it also seems possible that the low salinities, i.e. generally <7‰ (Young et al., 1997), and quality of food in this estuary may also have had an inhibiting influence on the rate at which length increased. The view that low salinity has had such an effect is based on a combination of the results of detailed laboratory trials, which demonstrated that *A. butcheri* did not grow as well at 0‰ and 12‰ as at 24‰ (Sarre et al.[7]) and the fact that the upstream regions of other estuaries, where juvenile *A. butcheri* are located between late spring and early autumn when most growth occurs, are characterized by elevated salinities (Potter and Hyndes, 1994; Sarre, 1999). Although low salinities may restrict growth, it is worth noting that growth in the Wellstead Estuary, which was the only estuary to become hypersaline, was greater than in the Nornalup Walpole Estuary, which is likewise located on the south coast of Western Australia. However, as mentioned earlier, growth in the Wellstead Estuary was not as great as in the Swan River Estuary and Lake Clifton farther to the north.

In the context of potential food, it may be relevant that juvenile *A. butcheri* feed to a greater extent on algae in the Moore River Estuary than in other estuaries. As pointed out by Blaber (1974) during his study of another sparid, *Rhabdosargus holubi*, which likewise ingests a large amount of algal material, the volume of digestible material consumed is small. However, as *A. butcheri* increased in size in the Moore River Estuary, it fed to an increasing extent on whole large bivalves (Sarre et al., 2000), a food source that has a particularly high energy content (Whitfield, 1980).

The age compositions recorded in this paper for *A. butcheri* in different water bodies have been combined with data on reproductive biology to determine the lengths and ages at which black bream typically reach maturity in these systems, i.e. the L_{50} and A_{50} (Sarre and Potter, 1999). The resultant data showed that, amongst the estuarine populations, the A_{50} for female *A. butcheri* was lowest in the Swan River Estuary (2.2 years), in which the growth was greatest, and greatest in the Nornalup Walpole Estuary (4.3 years), in which early growth was relatively slow and the asymptotic length the least. The minimum legal length (MLL) for the capture of *A. butcheri* in southwestern Australia, i.e. 250 mm, is attained as early as 2.7 years in the Swan River Estuary and as late as 6.5 and 6.8 years in the Nornalup Walpole and Moore River estuaries. Because the MLL is well above the L_{50} for females and males of *A. butcheri* at first maturity in each system, it allows a substantial number of the members of each population to reach maturity before they are likely to be caught by either recreational or professional fishermen. However, the relatively small contribution made by *A. butcheri* ≥5 years old in the heavily fished Swan River Estuary emphasizes the need to keep the upper part of that estuary closed to commercial fishing and suggests that similar measures may be necessary in other estuaries as they become more heavily fished in the future.

[7] Sarre, G. A., G. J. Partridge, R. C. J. Lenanton, G. I. Jenkins, and I. C. Potter. 1999. Elucidation of the characteristics of inland fresh and saline water bodies that influence growth and survival of black bream. Fisheries Research and Development Corporation. Research Report, Project 97/309. Canberra, ACT, Australia, 68 p.

Acknowledgments

We thank numerous people, particularly D. Mead-Hunter, G. Richard, and D. Tiivel for help in collecting black bream, and N. Hall and M. Platell for helpful comments on the manuscript. Financial support was provided by the Australian Fisheries Research and Development Corporation, Fisheries Western Australia, and Murdoch University. Gratitude is also expressed to two anonymous referees for constructive criticism of our paper.

Literature cited

Beamish, R. J., and G. A. McFarlane.
1983. The forgotten requirements for age validation in fisheries biology. Trans. Am. Fish. Soc. 112:735–743.

Blaber, S. J. M.
1974. Field studies of the diet of *Rhabdosargus holubi* (Pisces: Sparidae). J. Zool. (Lond.) 173:407–417.

Booth, A. J., and C. D. Buxton.
1997. The biology of the panga, *Pterogymnus laniarius* (Teleostei: Sparidae), on the Agulhas Bank, South Africa. Environ. Biol. Fish. 49:207–226.

Butcher, A. D.
1945. The Gippsland Lakes bream fishery. Australian Fisheries Newsletter 4:2–8.

Buxton, C. D., and J. R. Clarke.
1991. The biology of the white musselcracker *Sparodon durbanensis* (Pisces: Sparidae) on the eastern cape coast, South Africa. S. Afr. J. Mar. Sci. 10:285–296.

Cerrato, R. M.
1990. Interpretable statistical tests for growth comparisons using parameters in the von Bertalanffy equation. Can. J. Fish. Aquat. Sci. 47:1416–1426.

Chaplin, J. A., G. A. Baudains, H. S. Gill, R. McCulloch, and I. C. Potter.
1998. Are assemblages of black bream (*Acanthopagrus butcheri*) in different estuaries genetically distinct? Int. J. Salt Lake Res. 6:303–321.

Chrystal, P. J., I. C. Potter, N. R. Loneragan, and C. P. Holt.
1985. Age structure, growth rates, movement patterns and feeding in an estuarine population of the cardinalfish *Apogon rueppellii*. Mar. Biol. 85:185–197.

Chubb, C. F., I. C. Potter, C. J. Grant, R. C. J. Lenanton, and J. Wallace.
1981. The age structure, growth rates and movements of sea mullet, *Mugil cephalus* L., and yellow-eye mullet, *Aldrichetta forsteri* (Valenciennes), in the Swan-Avon River system, Western Australia. Aust. J. Mar. Freshwater Res. 32:605–628.

Crabtree, R. E., E. C. Cyr, and J. M. Dean.
1995. Age and growth of tarpon, *Megalops atlanticus*, from South Florida waters. Fish. Bull. 93:619–628.

Francis, M. P., M. W. Williams, A. C. Pryce, S. Pollard, and S. G. Scott.
1992. Daily increments in otoliths of juvenile snapper, *Pagrus auratus* (Sparidae). Aust. J. Mar. Freshwater Res. 43:1015–1032.

Gallucci, V. F., and T. J. Quinn.
1979. Reparameterizing, fitting and testing a simple growth model. Trans. Am. Fish. Soc. 108:14–25.

Haddy, J. A., and N.W. Pankhurst.
2000. The effects of salinity on reproductive development, plasma steroid levels, fertilisation and egg survival in black bream *Acanthopagrus butcheri*. Aquaculture 188: (1–2):115–131.

Hyndes, G. A., M. E. Platell, I. C. Potter., and R. C. J. Lenanton.
1998. Age composition, growth, reproductive biology and recruitment of King George whiting, *Sillaginodes punctata*, in coastal waters of southwestern Australia. Fish. Bull. 96:258–270.

Hyndes, G. A., I. C. Potter, and S. A. Hesp.
1996. Relationships between the movements, growth, age structures, and reproductive biology of the teleosts *Sillago burrus* and *S. vittata* in temperate marine waters. Mar. Biol. 126:549–558.

Johnson, A. G.
1983. Age and growth of yellowtail snapper from South Florida. Trans. Am. Fish. Soc. 112:173–177.

Kailola, P. J., M. J. Williams, P. C. Stewart, R. E. Reichelt, A. McNee, and C. Grieve.
1993. Australian fisheries resources. Bureau of Resource Sciences, Canberra, 422 p.

Kenchington, T. S., and O. Augustine.
1987. Age and growth of blue grenadier, *Macruronus novaezelandiae* (Hector), in south-eastern Australian waters. Aust. J. Mar. Freshwater Res. 38:625–646.

Kimura, D. K.
1980. Likelihood methods for the von Bertalanffy growth curve. Fish. Bull. 77:765–776.

Laurenson, L. J. B., I. C. Potter, and N. G. Hall.
1994 Comparisons between generalized growth curves for two estuarine populations of the eel tailed catfish *Cnidoglanis macrocephalus*. Fish. Bull. 92:880–889.

Lenanton, R. C. J., S. G. Ayvazian, C. Dibden, G. Jenkins, and G. A. Sarre.
1999. The use of stock enhancement to improve the catch rates of black bream *Acanthopagrus butcheri* (Munro) for Western Australian recreational fishers. *In* Stock enhancement and sea ranching (Bari R. Howell, E. Moksness and T Svasand, eds.), p 219–230. Fishing New Books, London.

Lenanton, R. C. J., and I. C. Potter.
1987. Contribution of estuaries to commercial fisheries in temperate Western Australia and the concept of estuarine dependence. Estuaries 10:28–35.

McPherson, G. R.
1992. Age and growth of the narrow-barred Spanish mackerel (*Scomberomorus commerson* Lacepède, 1800) in north-eastern Queensland waters. Aust. J. Mar. Freshwater. Res. 43:1269–1282.

Morison, A. K., P. C. Coutin, and S. G. Robertson.
1998. Age determination of black bream, *Acanthopagrus butcheri* (Sparidae), from the Gippsland Lakes of south-eastern Australia indicates slow growth and episodic recruitment. Mar. Freshwater Res. 49:491–498.

Newton, G. M.
1996. Estuarine ichthyoplankton ecology in relation to hydrology and zooplankton dynamics in a salt-wedge estuary. Mar. Freshwater Res. 47:99–111.

Potter, I. C., A. J. Cheal, and N. R. Loneragan.
1988. The protracted estuarine phase in the life cycle of the marine pufferfish *Torquigener pleurogramma*. Mar. Biol. 98:317–329.

Potter, I. C., and G. A. Hyndes.
1994 The composition of the fish fauna of a permanently open estuary on the southern coast of Australia, and comparisons with a nearby seasonally closed estuary. Mar. Biol. 121:199–209.
1999. Characteristics of the ichthyofaunas of south-western Australian estuaries, including comparisons with holarctic estuaries and estuaries elsewhere in temperate Australia. Aust. J. Ecol. 24:395–421.

Sarre, G. A.
1999. Age compositions, growth rates, reproductive biology and diets of the black bream *Acanthopagrus butcheri* in four estuaries and a coastal saline lake in south-western Australia. Ph.D. diss., Murdoch University, Western Australia, 184 p.

Sarre, G.A., and I. C. Potter
1999. Comparisons between the reproductive biology of black bream *Acanthopagrus butcheri* (Teleostei : Sparidae) in four estuaries with widely differing characteristics. Int. J. Salt Lake Res. 8:179–210.

Sarre, G.A., M. E. Platell, and I. C. Potter.
2000. Do the dietary compositions of *Acanthopagrus butcheri* (Sparidae) in four estuaries and a coastal lake vary with body size and season and within and amongst these water bodies? J. Fish Biol. 56:103–122.

SPSS Inc.
1988. SPSS-X™ user's guide. SPSS Inc, Chicago, IL, 828 p.

Thomson, J. M.
1957. The size at maturity and spawning times of some Western Australian estuarine fish. Fish. Bull. West. Aust. 8:1–8.

Valesini, F. J., I. C. Potter, M. E. Platell, and G. A. Hyndes.
1997. Comparisons between the shallow water ichthyofaunas of a temperate Australian estuary and an interconnected lagoon and adjacent marine embayment. Mar. Biol. 128:317–328.

Weng, H. T.
1971 The Black Bream, *Acanthopagrus butcheri* (Munro); its life history and its fishery in South Australia. MSc thesis, Univ. Adelaide, South Australia, 144 p.

Whitfield, A. K.
1980. A quantitative study of the trophic relationships within the fish community of the Mhlanga Estuary, South Africa. Estuarine Coastal. Mar. Sci. 10: 417–435.

Wise, B. S., I. C. Potter, and J. H. Wallace.
1994. Growth, movements and diet of the terapontid *Amniataba caudavittata* in an Australian estuary. J. Fish Biol. 45:917–931.

Young, G. C., I. C. Potter, G. A. Hyndes, and S. de Lestang.
1997. The ichthyofauna of an intermittently open estuary: implications of bar breaching and low salinities on faunal composition. Estuarine Coastal Shelf Sci. 45:53–68.

Dispersal and growth of yearling Atlantic sturgeon, *Acipenser oxyrinchus*, released into Chesapeake Bay*

David H. Secor
Edwin J. Niklitschek
Jill T. Stevenson
Troy E. Gunderson
Chesapeake Biological Laboratory
University of Maryland Center of Environmental Science
1 Williams Street
Solomons, Maryland 20688

Steven P. Minkkinen
Brian Richardson
Benjamin Florence
Fisheries Division
Maryland Department of Natural Resources
580 Taylor Avenue B-2
Annapolis, Maryland 21401

Michael Mangold
Jorgen Skjeveland
U S Fish and Wildlife Service, MFRO
177 Admiral Cochrane Drive
Annapolis, Maryland 21401

Anne Henderson-Arzapalo
U S Geological Survey
Leetown Science Center
1700 Leetown Road, Kearneysville, West Virginia 25430

Abstract—Significant fisheries for Chesapeake Bay Atlantic sturgeon, *Acipenser oxyrinchus*, have been absent for nearly a century, and there has been no evidence of recovery in the intervening years. Endangerment of Atlantic sturgeon in the Chesapeake Bay has stimulated interest in aquaculture-based restoration programs. A critical and unknown issue is whether hatchery released fish would encounter habitats that support growth and survival. In July 1996, approximately three thousand Atlantic sturgeon yearlings were released into Nanticoke River (Maryland) and subsequently tracked to evaluate their growth and dispersal. Biotelemetry of 32 individuals showed down-estuary emigration into the Chesapeake mainstem habitat during summer and fall at average ground speeds below 0.5 km/d. During the first year after release, 262 yearlings were captured by commercial fishermen. All yearlings and two-year-old fish were determined to be of hatchery origin (8% capture rate). Yearlings were captured throughout the Chesapeake Bay mainstem and tributaries. Two released sturgeon were captured in the Albemarle Sound System (Chowan River, NC). Juveniles captured during summer and fall experienced ca. 1.5% daily specific growth rate. Diets comprised annelid worms, isopods, amphipods, and mysids. Wide dispersal, high incidence of feeding, and positive growth rates suggested that hatchery-produced juveniles dispersed to areas that supported consumption, growth, and survival. Because the Chesapeake Bay continues to support juvenile habitats, we propose that curtailed or absent spawning stock or spawning habitat, or both, are principal factors that have contributed to lack of Atlantic sturgeon recovery during the twentieth century.

Manuscript accepted 1 June 2000
Fish. Bull. 98:800–810 (2000)

In Chesapeake Bay, Atlantic sturgeon, *Acipenser oxyrinchus*, may be functionally extirpated (Secor[1]; Speir and O'Connell[2]). Although sporadic observations of yearlings and adults have been reported over the last two decades (Colligan et al., 1998), the probability of population extirpation based upon the infrequency of these observations, is high (Grogan and Boreman, 1998). Depletion of Atlantic sturgeon in the Chesapeake Bay followed a period of high exploitation in the late 19th century (Fig. 1), during which overfishing occurred for most Atlantic sturgeon populations (Murawski and Pacheco, 1977; Secor and Waldman, 1999). Also, sedimentation and eutrophication have dramatically affected the Chesapeake Bay's environment during the past century (Officer et al., 1984; Cooper and Brush, 1991), resulting in loss and degradation of spawning and nursery habitats that may have contributed to loss in viability of sturgeon populations.

Contribution 3335 of the University of Maryland Center for Environmental Science, Chesapeake Biological Laboratory, 1 Williams StreetSolomons, Maryland 20688.

[1] Secor, D. H. 1995. Chesapeake Bay Atlantic sturgeon: current status and future recovery. Unpubl. manuscript Chesapeake Biological Laboratory, P.O. Box 38, Solomons, MD 20688-0038, 10 p.

[2] Speir, H., and T. O'Connell. 1996. Status of Atlantic sturgeon in Maryland's Chesapeake Bay. Unpubl. Manuscript MD Dep. Natural Rrsources, Tawes State Office Building, 580 Taylor Avenue, Annapolis, MD 21401, 7 p.

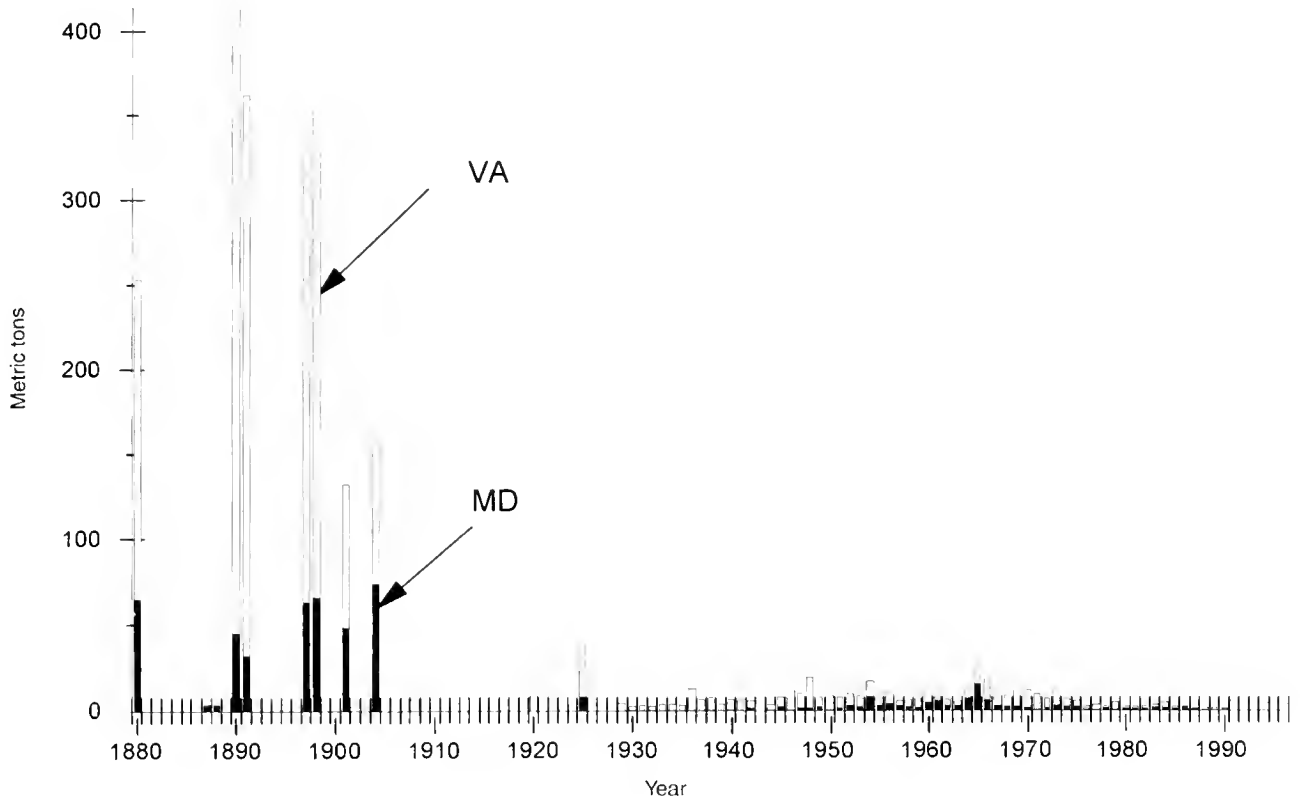

Figure 1

Atlantic sturgeon landings in Chesapeake Bay. Data from Murawski and Pacheco (1977) and Colligan et al. (1998). VA = Virginia; MD = Maryland.

During their first year of life, Atlantic sturgeon remain close to their natal habitats within estuaries (Dovel and Berggren, 1983; Bain, 1997). Following spawning migrations by adults, benthic eggs are deposited on hard, structured surfaces (e.g. cobble) in regions between the salt front and fall-line of large rivers. Historically, Chesapeake Bay Atlantic sturgeon spawned during April–June (Hildebrand and Schroeder, 1927). Young hatch at ca. 4–6 days after spawning, and following a 7–10 d period swimming upriver, adopt a benthic lifestyle (Smith et al., 1980). Young-of-the-year juveniles initiate seasonal migrations within estuaries (Dovel and Berggren, 1983). Emigration from natal estuaries to primarily marine habitats occurs at ages 1 to 5 years, after which subadults wander among coastal and estuarine habitats until maturation, undergoing rapid growth rates (Dovel and Berggren, 1983; Stevenson and Secor, 2000).

Lack of strong evidence of natural recovery has lead state, federal, academic, and nonprofit organizations to consider an aquaculture-based restoration program for Atlantic sturgeon in the Chesapeake Bay. To examine the feasibility of such a program, 3275 hatchery-produced yearlings (Hudson River progeny produced from a single female and four males) were released into the Nanticoke River (Chesapeake Bay) and their subsequent dispersal and growth was monitored over a one-year period. Specifically, we 1) characterized the dispersive behavior of non-native (hatchery-produced) Atlantic sturgeon yearlings through biotelemetry and the capture of sturgeons by fishermen, 2) explored potential relationships between the observed distribution and abiotic environmental factors, and 3) compared growth rate and diet of released juveniles observed in our study to those reported in the literature for naturally produced sturgeon.

Methods

Juvenile Atlantic sturgeon were obtained from the U.S. Fish and Wildlife Service (USFWS), Northeast Fishery Center, Lamar, Pennsylvania. During June 1995, Center personnel collected a large female (2.4 m total length) and three male Atlantic sturgeons from the Hudson River near Hyde Park (river km [rkm] 135). Fish were transported to the Center for artificial spawning and larval rearing. Larvae and early juveniles were reared in fresh water at 17°C and fed *Artemia* nauplii until 30 days after hatching. Juveniles (0.7–2.0 mm diameter) were then fed Biokyowa© fry feed *ad libitum* during their first year of life. A failure of the water heating system at the Center resulted in loss of temperature control, and juveniles >45 days after hatching, were subjected

Table 1

Capture data of coded wire tagged (CWT) and Floy-tagged Atlantic sturgeon, Chesapeake Bay 1996. 95% confidence intervals, based upon a binomial distribution, are given for the proportions of experimental groups in the capture sample. Note that because most fish were captured without T-tags and relatively few fish were sacrificed for CWT information, most of the 262 captures were not identified for release site or size class. Size at stocking could not be evaluated for differences in recapture rate due to small sample size.

Release site or size at stocking	Number released	% total released	Number identified from 262 captures	% group membership in capture sample (±95% CI)
Vienna (rkm 36)	1657	51	61	51 ±9
Sharptown (rkm 50)	1618	49	57	49 ±9
Total	3275		118	
Size class I (6–15 cm TL)	2306	70		
Size class II (22–36 cm TL)	969	30		
Total	3275			

to water temperatures of 10°C. At 6 months of age, ca. 1000 juveniles were transferred to Maryland and reared at 17°C at Maryland Department of Natural Resources (Maryland-DNR) and Potomac Electric Power Company hatchery facilities (Charles County, MD). Owing to differences in rearing temperature between juveniles held in Pennsylvania and Maryland hatcheries, two size classes resulted. At time of stocking, size class I ranged between 6 and 15 cm TL. Size class II ranged between 22 and 36 cm TL.

All stocked sturgeon were injected with an internal coded wire tag (CWT) to identify size class and stocking site. In tank-rearing studies conducted at the MD-DNR hatchery, CWT retention was >95%. Size class II juveniles were also tagged with external Floy T-tags inserted through their dorsal musculature below the fourth dorsal scute. Totals of 2306 and 969 juveniles from size classes I and II, respectively, were released into the Nanticoke River (MD) at river kilometers 36 and 50 on 7 July 1996 (Table 1, Fig. 2). River conditions at stocking sites were 0 and 3.0 ppt salinity, 26° and 27°C, and 4.2 and 7.7 mg/L dissolved oxygen (D.O.) at rkm 36 and 50, respectively. Site conditions varied less than anticipated in the study design, which stipulated release into divergent salinity levels because of high freshwater discharge rates to the Nanticoke River during spring and summer 1996.

Telemetry

To investigate short-term dispersal in the Nanticoke River, 32 juveniles were released at 5 sites over 7 occasions (Table 2) and tracked with Sonotronics™ ultrasonic transmitters. Two size transmitters were used: 28 mm long by 8 mm diameter (2.5 g) and 64 mm long by 16 mm diameter (8 g) for Atlantic sturgeon <45 cm TL (released 7 July–12 August) and >45 cm TL (released 21 October), respectively. Both transmitters had a detection radius of 1 km; life spans were 60 days and 14 months for the small and large transmitters, respectively. Transmitters were attached by using a leather punch to drive 4.5-kg test monofilament through the third and fifth dorsal scutes. Line was affixed to the transistor by using a cyanocrylate glue, looped through the scutes and glued to the other end of the transmitter. A 50-day laboratory experiment on 10 dummy-tagged sturgeon showed 100% retention of transmitters with this method.

Table 2

Date and site of release of Atlantic sturgeon with ultrasonic transmitters, Nanticoke River, 1996.

Date	Release site	Number released	Number relocated	Mean length (cm) at release
8 Jul 96	rkm 36	3	2	39.2
	rkm 50	4	2	37.7
22 Jul 96	rkm 13	4	4	41.4
	rkm 36	4	4	40.9
12 Aug 96	rkm 24	3	2	39.2
	rkm 38	6	4	37.8
21 Oct 96	rkm 24	8	8	52.9
Sum		32	26	

Thirteen biotelemetry surveys were conducted throughout the Nanticoke River from July 1997 to February 1998. Tagged fish were located by using a hydrophone and identified by their coded signals. Position, temperature, salinity, and dissolved oxygen were recorded at each location site. On seven surveys, an otter trawl or 5-cm square gill net, or both, were deployed to capture juveniles that might be in the vicinity of the individual located through telemetry.

Relocation data were used to characterize overall displacement and to evaluate potential correlations with salinity, temperature, and dissolved oxygen conditions. Fish released at river kilometers 36 and 38 were com-

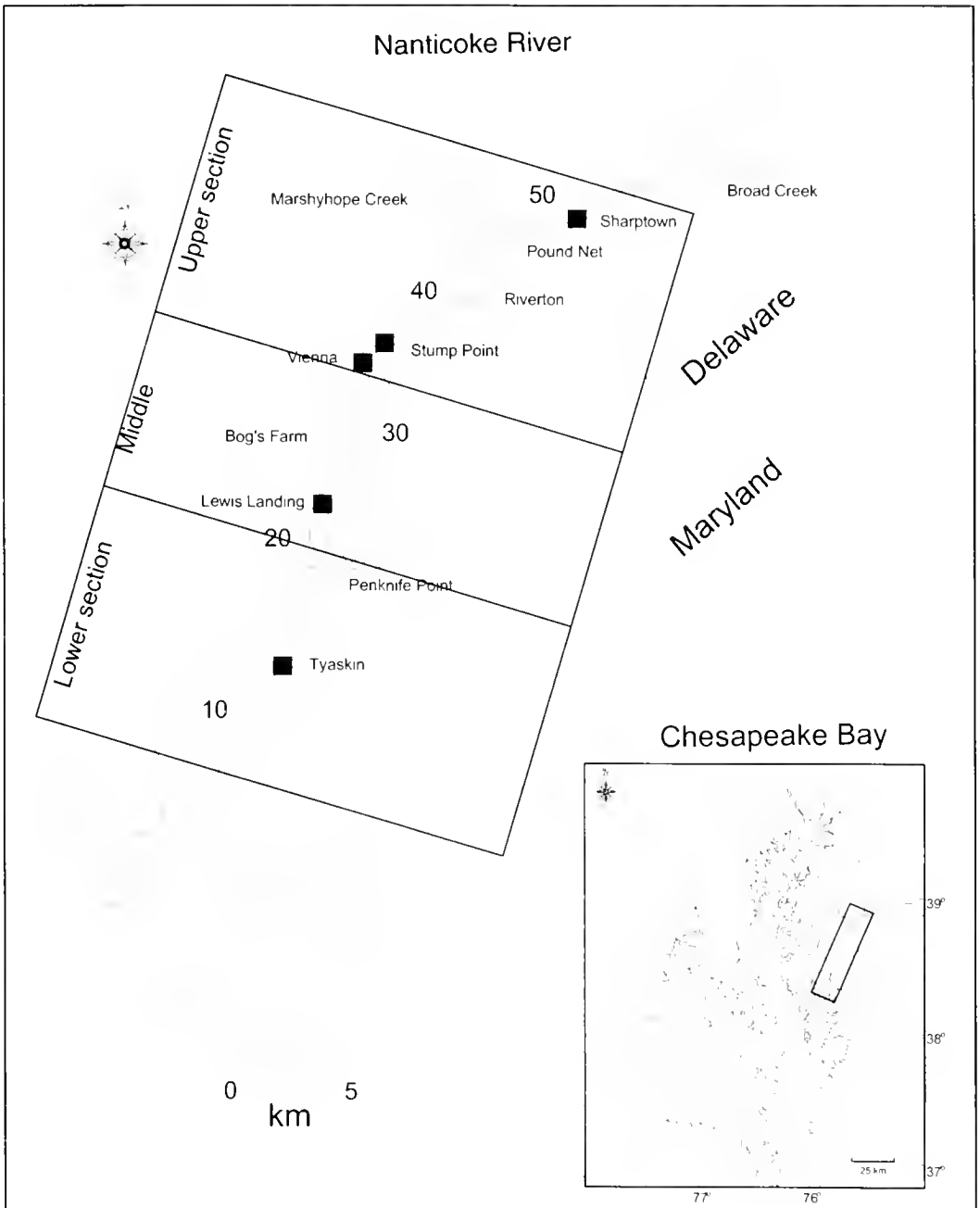

Figure 2

Map of Nanticoke River showing survey region, sites of release of yearling Atlantic sturgeon, and river sections utilized for statistical analysis. On 7 July 1996, >3000 yearlings were released at rkm 36 and 50. Later in summer and fall smaller releases of yearlings fitted with ultrasonic devices (Table 2) were made at rkm 13, 24, 36, and 50.

bined into a single group for statistical analysis. Consistency of mean trajectories and parallelism within and among released fish groups was tested by using multiple regression analysis, after modeling within-individual correlations (repeated measures) through a spatial power covariance model (Littel et al., 1996). Degrees of freedom were adjusted using Satterthwaite's approximation.

On the basis of upon multivariate analysis of available water quality data, the Nanticoke River was divided into three relatively homogeneous sections (Fig. 2): lower river: rkm 8 to 19.9, middle river: rkm 20 to 33.9, and upper river: rkm >34 (Table 3). Discriminate analysis indicated that this classification resulted in consistent differences in temperature, dissolved oxygen, and salinity records across

Table 3

Mean and standard deviations of measured environmental factors in Nanticoke River 8 July 1996–23 October 1996, by river section, see Fig. 2

	River section			
Factor	Lower	Middle	Upper	Overall
River kilometers	8–19.9	20–33.9	34–59	8–59
Temperature (°C)	25.0 ±3.6	24.2 ±4.5	26.1 ±1.6	25.4 ±3.1
Dissolved oxygen (% saturation)	82.9 ±7.5	79.4 ±11.2	81.2 ±11.3	81.2 ±10.4
Salinity (ppt)	5.0 ±1.7	2.3 ±1.1	0.7 ±0.7	2.2 ±2.1
Depth (m)	2.9 ±1.1	5.8 ±2.1	5.8 ±2.5	5.1 ±2.4
Number of observations	32	35	60	125

summer and fall months (Wilk's approximated F, $P<0.001$). The upper river exhibited the highest mean temperature and salinities usually below 1 ppt. The middle section showed intermediate salinity (1–3 ppt), and highly variable temperature and dissolved oxygen conditions. The lower section corresponded to a shallow area with the highest salinity and dissolved oxygen means (Table 3, Fig. 3). Logistic regression analysis was used to explore potential relationships between probability of fish relocation within a river-section and corresponding water quality conditions.

Reward program

Maryland-DNR, in cooperation with USFWS and the Chesapeake Bay Foundation, offered a $25 reward to Chesapeake Bay fishermen for the capture and holding of live juvenile Atlantic sturgeon. The program was initiated in Maryland in July 1996 and extended to Virginia waters after February 1997. Capture data were documented by USFWS agents and measurements and tag information were recorded. In some instances, juveniles were sacrificed for CWT identification (n=22). Twelve of these fish, captured between 24 October 1996 and 8 January 1997, were made available to us for examination of diet (mean TL=56.1 cm ±7.40 SE; mean weight=823 g ±301.6 SE). Prey were classified at the lowest possible taxonomic level and evaluated according to numerical and volumetric contribution to diet.

Captured fish were measured for total length in mm (TL), fork length in mm (FL), and weight in g (W). Because all three measures were not consistently taken, we developed the following regressions to interconvert size measurements:

$$FL = 0.860 + 2.01\ TL \qquad (r^2=0.96,\ n=214) \quad (1)$$

$$\log_e W = -9.25 + 2.52 \log_e TL \qquad (r^2=0.64,\ n=211) \quad (2)$$

Growth was estimated by comparison of size at release (W_0) and size at capture (W_t) according to the formula

$$G_1 = (\ln W_t - \ln W_0)/t, \qquad (3)$$

where t = days after release.

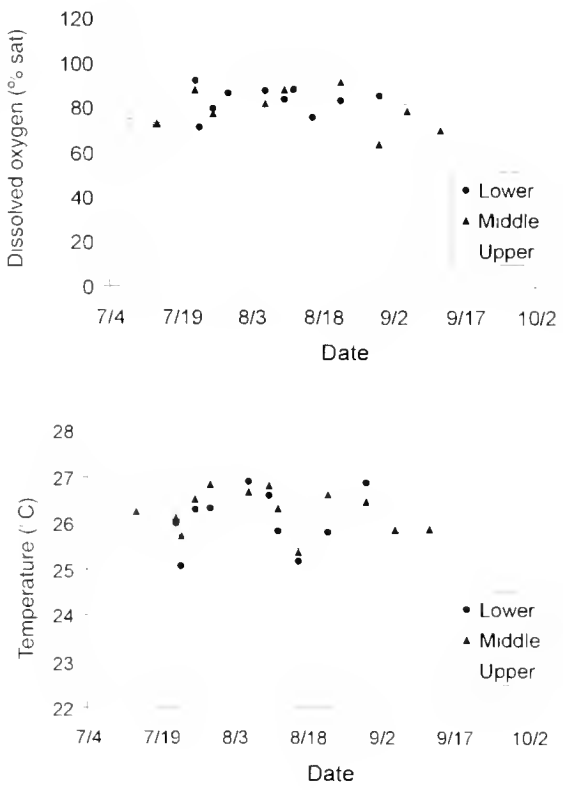

Figure 3

Mean records of (**A**) dissolved oxygen and (**B**) temperature by river section during summer 1996.

Results

Twenty-six fish were relocated during telemetric surveys at least once after release. The mean duration over which fish were tracked (35 days ±37 SD) and the number of relocations (4 relocations ±3.8 SD) were limited, perhaps owing to egress to the lower river and the Chesapeake mainstem (see "Discussion" section). Fish released at the

three most upstream sites (rkm 50, 36, and 24) showed a significant pattern of downriver displacement ($P<0.01$) at average ground speeds of 0.4 ±0.08 SE, 0.11 ±0.04 SE, and 0.08 ±0.02 SE km/day, respectively (Fig. 4). Fish released at rkm 13 did not show a consistent up or downriver movement ($P>0.9$). There were also significant differences in dispersal patterns between fish released at different dates within the same section. For instance, fish released 22 July at rkm 36, and 12 August at rkm 24 did not show a consistent downriver dispersal pattern.

The average probability of relocation tended to be higher in the middle section of the river (0.46 ±0.071 SE) than in the lower and upper sections, where average probabilities of relocation were 0.30 ±0.065 SE and 0.28 ±0.064 SE, respectively. However, such probabilities were not significantly different from each other, as indicated by logistic regression analysis ($P=0.13$). No significant correlations were found between dissolved oxygen, water temperature or salinity, and proportion of total relocations occurring within a given section ($P>0.11$). Although no significant correlation occurred between salinity and distribution of fish relocations, most fish had left freshwater areas (0 to 1 ppt) within one week of being released. More than 90% of later relocations occurred in the range 1 to 7 ppt. All attempts to capture sturgeon where position of fish was triangulated through biotelemetry were unsuccessful. In 25 bottom trawls and five gillnet deployments, only two cultured juveniles were physically captured, one in a gill net on 26 July (24 cm TL) and the other in an otter trawl on 24 October (43 cm TL).

During fall and winter (earliest capture 1 November 1996), fishermen captured juveniles as an incidental catch in the mainstem of the Chesapeake Bay. Location of captures varied seasonally (Fig. 5). During fall and winter months (November–March) most captures occurred in the vicinity of the mouth of the Nanticoke River and north of the Nanticoke River in the mainstem of Chesapeake Bay. As winter progressed, sturgeon captures were concentrated at upper Bay mainstem sites. The distribution of captures tended to spread toward the lower Chesapeake Bay and into tributaries during late winter (March) and spring months, where several sturgeon were captured high up in major tributaries (Patuxent, Potomac, Rappahannock, and James rivers). Much of the shift in captures during spring and summer may have been an artifact of delayed implementation of a reward program in Virginia (initiated February 1997) and seasonal changes in fishing effort (see "Discussion" section). In March 1997, two individuals were captured outside of Chesapeake Bay in the Chowan River (Albemarle-Roanoke estuary, North Carolina).

The majority of juvenile sturgeon (60%) captured by commercial fishermen were ensnared in drift or anchored gill nets set for striped bass, white perch (*Morone americana*), and catfish (*Ictalurus punctatus*, *Ameiurus catus*); 40% of the captures were from pound nets principally set for menhaden (*Brevoortia tyrannus*). Gillnet captures occurred most often between January and early March, with a mean capture length (TL) of 61 cm ±5.6 SE. Poundnet captures were concentrated between April and late June. Mean length for poundnet captures was 66 cm TL ±5.7 SE. Captured yearlings were kept for up to 2 days by fishermen, prior to inspection by USFWS agents, by holding sturgeon in pens and tanks, or by tying them (by the mouth or tail) to fixed structures in the water. Juveniles inspected by agents were all judged to be in good condition and released without apparent harm to the fish.

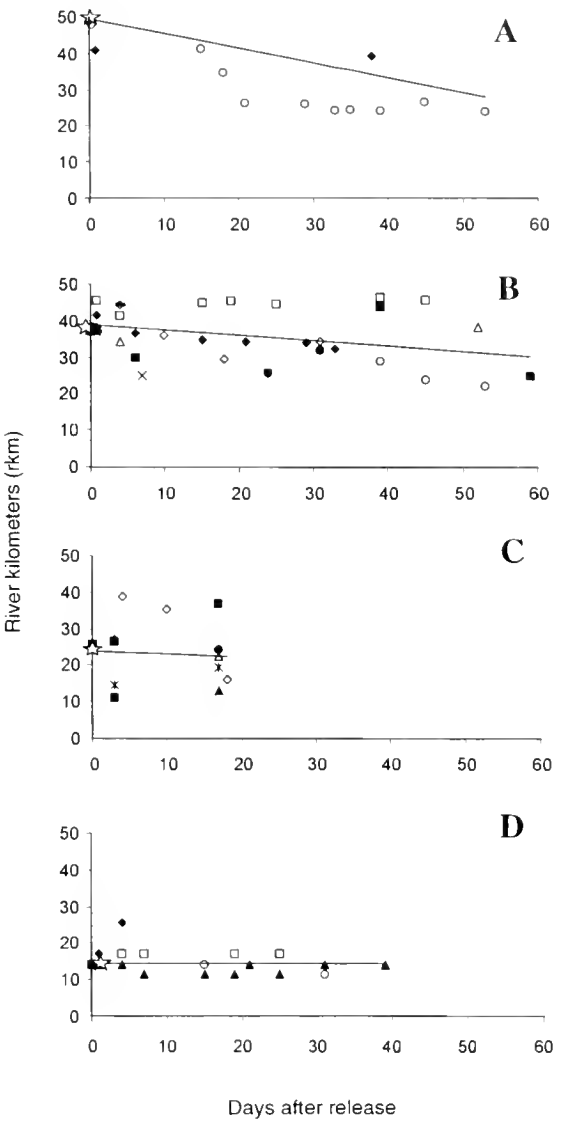

Figure 4

Relocation site (river kilometer) and mean trajectories for fish fitted with ultrasonic devices and released at different locations in the Nanticoke River. (**A**) release site 1 (rkm 50), (**B**) release site 2 (rkm 36–38), (**C**) release site 3 (rkm 24), and (**D**) release site 4 (rkm 13). Star icons indicate release site. Other icons within a graph indicate individual fish. Note that mean trajectories have been corrected for autocorrelation within individuals.

Overall, 8% of stocked juveniles were taken incidentally. Sixteen Floy-tagged juveniles (size class II) were multiple

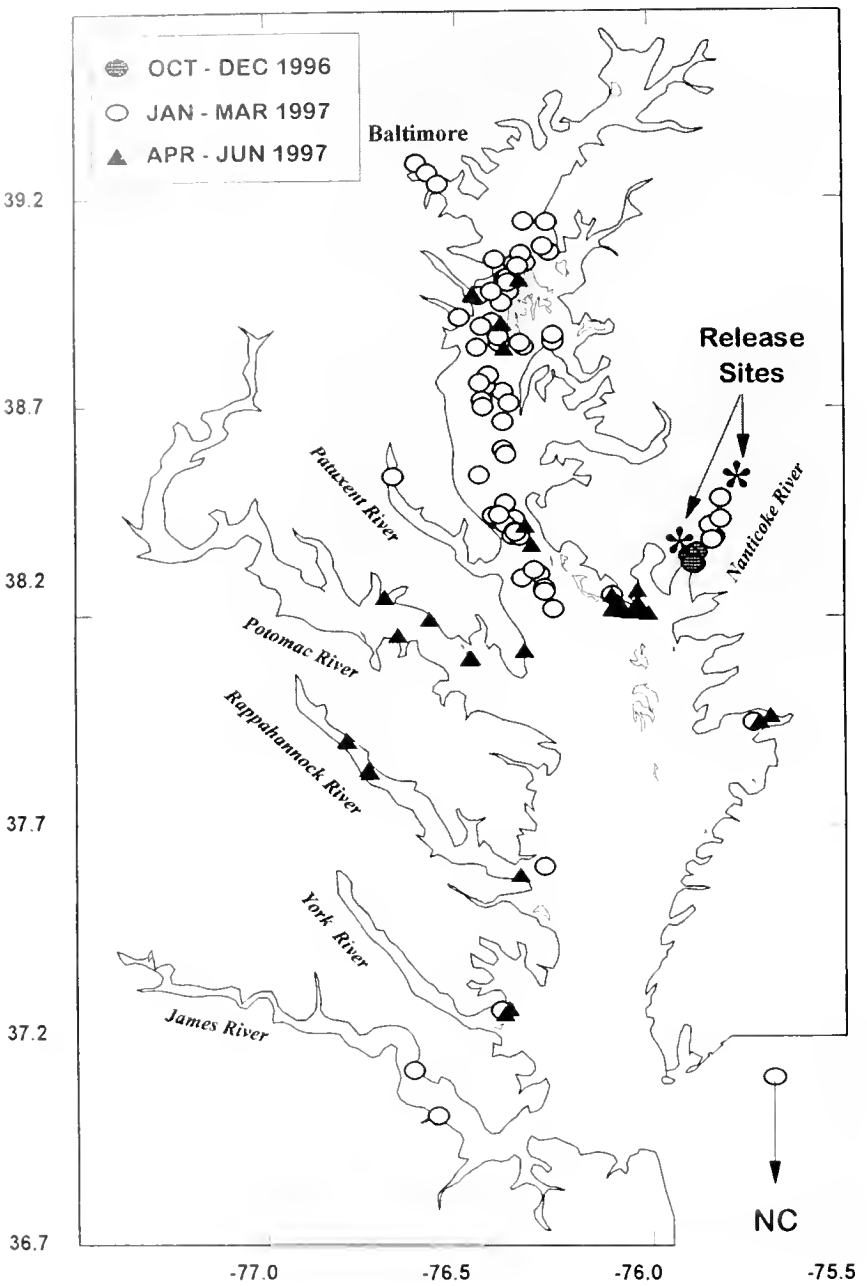

Figure 5

Spatial and temporal distribution of juvenile Atlantic sturgeon captures made by commercial fishermen in Chesapeake Bay

recaptures but no fish were recaptured more than once. Capture rates of juveniles released at either up- or down-river sites were similar and indicated no differential survival between these groups (Table 1). All yearling sturgeon captured by fishermen contained a tag, or evidence of a lost tag. For those that had apparently lost a tag, a subsample of yearlings was determined to be of hatchery origin through analysis of microsatellite nuclear DNA.[1]

Released fish reached an average size of 67.2 cm TL ±3.8 (SE) and an average weight of 1536 g ±69 (SE), after 12 months in the wild (Table 4). Average growth rates, estimated from release to capture sizes, ranged between 0.64 and 1.83%/d. Estimated growth rates from monthly mean lengths and weights showed strong seasonality, with nil or negative growth rates between January and March (Fig. 6). One-third of the juveniles sacrificed for diet information had empty guts. Sand, silt, and detritus accounted for 34% of the combined gut contents. Of the remaining identified diet items, annelid worms were most important by volume

[1] King, T. 1997. Personal commun. Dep. of Interior, Leetown Science Center, 1700 Leetown Road, Kearneysville, WV 25430

Table 4

Mean lengths and weights at ages 1 and 2 for juvenile Atlantic sturgeon observed in current study and reported in the literature.

Age 1 yr		Age 2 yr			
Fork length (cm)	Weight (g)	Fork length (cm)	Weight (g)	Geographical area	Source
20.0		25.0		St. Lawrence River	From Murawski and Pacheco (1977)
36.0		47.0		St. John River	From Murawski and Pacheco (1977)
40.8	500.0	47.7	770.0	Hudson River	Dovel and Berggren (1983)
28.4		43.9		Delaware River	Lazzari et al. (1986)
26.2	103.5	55.5	1535.8	Chesapeake Bay	Our study
57.8		74.4		Winyah Bay	Collins et al. (1996)
35.0		51.0		Suwannee River	From Murawski and Pacheco (1977)

(61%), followed by isopods (*Cyathura polita* and *Cyathura* sp., 23%), amphipods (*Leptocheirus plumulosus* and *Gammarus* sp., 10%), chironomid larvae (1.6%), and mysids (*Neomysis americana*, 1.5%). Occurrence data among yearlings indicated about 50% probability of finding all major food categories—worms, amphipods, and isopods—in feeding fish.

Discussion

Failure to capture a single wild yearling (<70 cm TL; see Peterson et al., 2000, for size criterion) during the course of our study is a strong indication of the Atlantic sturgeon's endangered status in Chesapeake Bay. In the fall of 1997, the floating carcass of a 2.6-m-TL female Atlantic sturgeon was observed in the James River.[4] Also, wild yearlings (<50 cm TL) were observed during 1998 in Virginia tributaries (Musick[5]) suggesting that some reproduction was still occurring in lower Chesapeake Bay. On the other hand, absence of yearling Atlantic sturgeon during Virginia Institute of Marine Science trawl monitoring over the past 15 years led Grogan and Boreman (1998) to predict >95% probability of extirpation in Virginia. Although this prediction has proven false, it still provides strong evidence of extremely depressed reproduction rates.

Results from our study indicated that the Chesapeake Bay can support nursery functions for juvenile Atlantic sturgeon. High capture rates by fishermen suggest high survival of released fish and high vulnerability to the gear types deployed. Wide dispersal and positive growth rates indicate that juveniles dispersed to areas that supported consumption and metabolic needs. Indeed, mean weight increased nearly 20-fold over the first year after release. Sizes at the end of the second year of life (summer 1997) were intermediate between size estimates for 2-year-old juvenile sturgeons from the Hudson River (Dovel and Berggren, 1983) and those from southern populations (Table 4). Thus, hatchery-produced fish had grown at levels that might be expected for juveniles naturally occurring in the Chesapeake Bay.

Although limited by a small sample size, our diet analysis seems consistent with the few published reports on food habits of juvenile Atlantic sturgeon. Aquatic insects, amphipods, isopods, and both polychaete and oligochaete worms are the most common items previously reported for juveniles residing in fresh and brackish waters (Vladykov and Greeley, 1963; Smith, 1985; Moser and Ross, 1995; Haley, 1998). Contrary to Vladykov and Greeley (1963) and Moser and Ross (1995), we found no evidence of juvenile sturgeon predation upon mollusks, which represent the highest biomass of benthic invertebrates in the Chesapeake Bay.

We failed to detect any significant selection among tracked individuals for certain water temperatures or dissolved oxygen conditions. Overall, tracked fish did not encounter severe hypoxia or extremely high temperatures (Table 3, Fig. 4). However, on at least one occasion, other than the day of release, yearlings encountered dissolved oxygen saturations close to 50% (4.3 mg/L, 25.9°C)—a level that might reduce growth and survival rates for this species (Secor and Gunderson, 1998). Preferential use of cooler areas or deep thermal refuges, or both, has been observed in field studies on juvenile Atlantic (Moser and Ross, 1995) and Gulf (Clugston et al., 1995) *A. oxyrinchus desotoi* sturgeons. Such refuges are unavailable in the Nanticoke River, a shallow system (Table 3) with little thermal stratification.

Low rates of use of habitats of salinity below 1 ppt agree with past observations that yearling Atlantic sturgeon principally use brackish water habitats (Dadswell, 1979; Brundage and Meadows, 1982; Smith, 1985; Moser and Ross, 1995; Haley et al., 1996). Observed down-estuary movement is consistent with seasonal movements reported for juvenile Atlantic sturgeon responding to summer peak temperatures in the Hudson River (Dovel and Berggren, 1983). Use of areas below rkm 10 was probably underestimated because river width substantially exceeded the detection range of ultrasonic transmitters and shallow reefs or sills probably obstructed detection.

[4] Spells, A. 1997. Personal commun. USFWS, 11110 Kimages Road, Charles City, VA, 23030.

[5] Musick, J. 1999. Personal commun. Virginia Institute of Marine Science, Gloucester, VA.

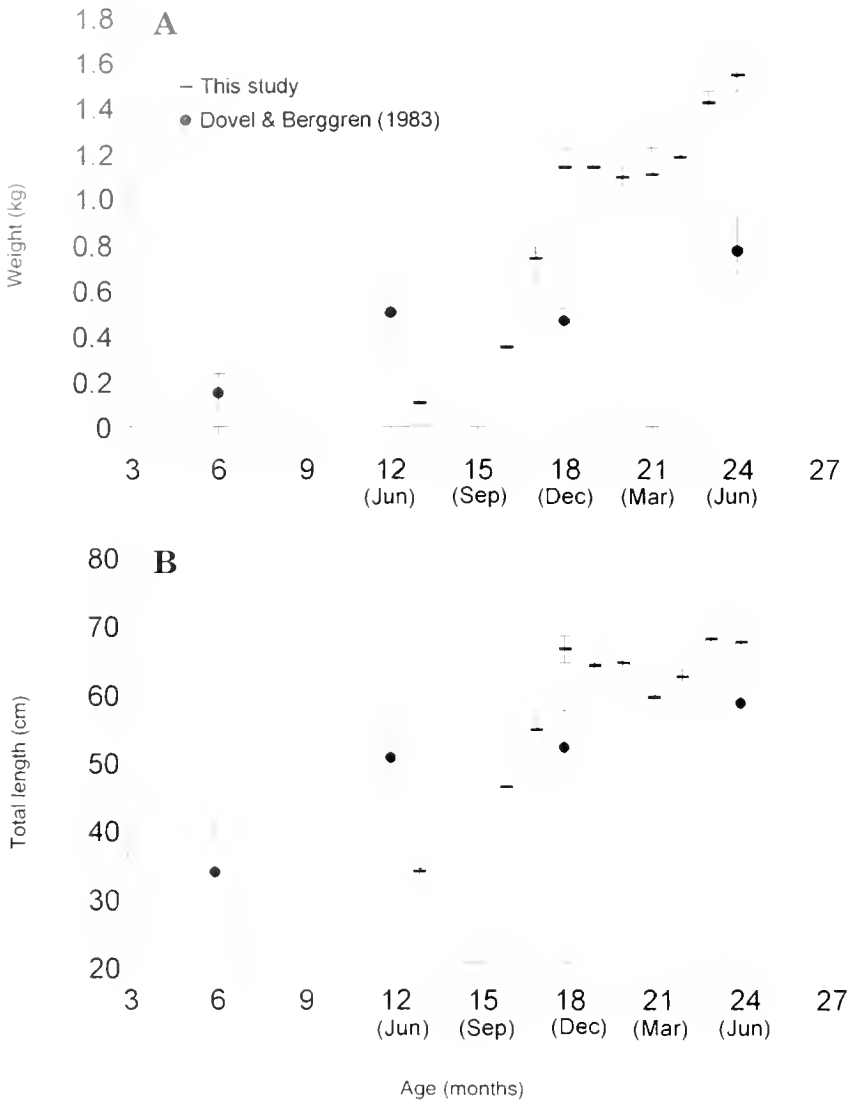

Figure 6

Growth curves as observed from released and captured juvenile Atlantic sturgeon in Chesapeake Bay (**A**) Mean weight at age (month) ±SE. (**B**) Mean length at age (month) ±SE. Values reported by Dovel and Berggren (1983) are included for comparison. Note that Dovel and Berggren's data are averaged for all fish falling within a six-month age interval. Monthly values were fitted with a spline function (dashed line).

Tagging and telemetry studies on North American sturgeons (mostly on subadult and adult fish) tend to show seasonal or reproductive migrations but reduced displacements during intermigratory periods. Estimated home ranges for nonmigrating sturgeon were 0.8 km for landlocked white sturgeon (Haynes et al., 1978), 4 km for Gulf sturgeon (Clugston et al., 1995), and 2–3 km for shortnose sturgeon (Buckley and Kynard, 1985). Nonetheless, extensive wandering behavior was observed in adult shortnose sturgeon by McCleave et al. (1977), i.e. home ranges up to 30 km at average ground speeds around 0.21 body lengths (BL)/s. Moser and Ross (1995) observed gross movements ranging from 0.7 to 1.3 km/d in nonmigratory juvenile Atlantic sturgeon (68–122 cm TL) in Cape Fear River, NC. During seasonal or reproductive migrations, gross movement may increase to 0.8–7 km/d in juvenile (38–79 cm FL) Atlantic sturgeon (Gilbert, 1989), 0.6–6 km/d in Gulf sturgeon (Clugston et al., 1995), and 6.4–36 km/d in shortnose sturgeon (Buckley and Kynard, 1985; Kieffer and Kynard, 1993). We interpret our telemetry observations on initial yearling dispersal as a roving behavior, where fish are oriented toward searching for productive benthic

forage conditions. This is supported by the relatively low rates of dispersal (0–0.4 km/d; 0.1 BL/s), low horizontal gradient observed in abiotic parameters, and a lack of correlation between relocation probability and water quality data. More intensive sampling and benthic resource mapping in Chesapeake Bay could confirm this speculation.

A moderate reward system was highly effective in helping to evaluate the release of hatchery sturgeon. Although we expect more juveniles may have actually been captured than reported, fishermen were keenly interested in the program and very cooperative with USFWS agents in their collection of biological measures. High capture rates of yearling Atlantic sturgeon by fishermen showed that small sturgeons were highly vulnerable to gill and pound nets, as found by Collins et al. (1996). Due consideration needs to be given to incidental catches of juvenile-stage sturgeon in recovery programs.

Seasonal and spatial patterns of captures by fishermen were the result of both seasonal dispersal and distribution of fishing effort in Chesapeake Bay. In winter and early spring months, drift and anchor gill nets were set for striped bass, white perch, and catfish in the upper bay and in tributaries. Later in the spring and summer, pound nets were set for menhaden, croaker (*Micropogonias undulatus*), and spot (*Leiostomus xanthurus*), which tend to occur down-estuary. Therefore, the apparent displacement of captures from the upper to lower Chesapeake Bay may be related to seasonal changes in fishing effort. In addition, Virginia began a reward program in February 1997; therefore captures were less likely to occur prior to that date.

The dispersal of released fish into Chesapeake Bay mainstem by fall 1996 and reported captures in North Carolina by the end of the winter also are consistent with seasonal movement patterns described for Atlantic sturgeon in other systems. Seasonal migration in juvenile Atlantic sturgeon seems primarily regulated by changes in temperature gradients between fresh and brackish waters (Van Den Avyle, 1984). Juveniles tend to use brackish waters close to estuary mouths during the colder months as reported in Hudson River (Dovel and Berggren, 1983; Gilbert, 1989), Delaware River (Brundage and Meadows, 1982; Lazzari et al., 1986), and the Winyah Bay system (Smith et al., 1982). In the Hudson River, juveniles begin moving to saltier waters by July (Dovel and Berggren, 1983), whereas in the Delaware River many fish remain in tidal water until January (Lazzari et al., 1986). A different pattern was observed by Moser and Ross (1995), who noted that juvenile Atlantic sturgeon in the Cape Fear River kept the same center of distribution all year round.

High dispersal rates of released yearlings and absence of schooling behavior were somewhat unexpected. Hatchery-produced striped bass and Pacific salmon (*Oncorhynchus* spp.) juveniles are known to school and remain in restricted regions for weeks and months following release (Nickelson et al., 1986; Hume and Parkinson, 1987; Dorazio et al., 1991; Nagata et al., 1994; Andreasen, 1995). Recent genetic studies indicate strong population structuring within the geographic range of the Atlantic sturgeon (Waldman and Wirgin, 1998), which suggests high fidelity to natal estuaries. Gene flow studies also support consistent homing behavior by the Gulf subspecies (Wirgin et al., 1997). However, the rapid dispersal we observed might suggest that yearlings had insufficient opportunity to imprint to the Nanticoke River and thus might be unlikely to home to it in future spawning migrations. Apart from work on salmonids, little is known on homing behavior in anadromous fishes. In Pacific salmon, the window of imprinting occurs during the premigratory smolt stage (Hasler and Scholz, 1983). Stocking young-of-the-year Atlantic sturgeon in any future hatchery-based restoration program would be prudent because it might increase the duration of exposure to imprinting stimuli.

This study demonstrates that the Nanticoke River and Chesapeake Bay can continue to support nursery roles for Atlantic sturgeon yearlings. Still, several questions remain before we embark on a program of restoration through hatchery-based reintroduction. What are the main factors defining suitable habitat for Atlantic sturgeon juveniles? Would available habitat support historical abundances? Can we obtain sufficient numbers of brood stock from the Hudson River or elsewhere to ward against inbreeding depression? A critical question is whether released juveniles will return and find spawning habitat. Spawning habitats are probably quite degraded from siltation and sedimentation over the past two centuries. Unfortunately, evaluating whether such habitats remain or can be restored will be nearly impossible until an adult biomass can be restored.

Acknowledgments

We are grateful to personnel at the U.S. Fish and Wildlife Service Northeast Fishery Center fort their efforts in producing juvenile sturgeon. E. Zlokovitz and E. Sadler provided assistance in the field and in collection of data. This research was supported by the National Biological Service, Maryland Department of Natural Resources, U.S. Fish and Wildlife Service, and the Chesapeake Bay Foundation.

Literature cited

Andreasen, L. L.
1995. Predation on hatchery-reared striped bass, *Morone saxatilis*, in the Patuxent River, Maryland. M.S. thesis, Univ. Maryland, College Park, MD, 88 p.

Bain, M. B.
1997. Atlantic and shortnose sturgeons of the Hudson river: common and divergent life history attributes. Env. Biol. Fishes 48:347–358.

Brundage, H. M., and R. E. Meadows.
1982. The Atlantic sturgeon, *Acipenser oxyrinchus*, in the Delaware River estuary. Fish. Bull. 80:337–343.

Buckley, J., and B. Kynard.
1985. Yearly movement of shortnose sturgeon in the Connecticut River. Trans. Am. Fish. Soc. 114:813–820.

Clugston, J. P., A. M. Foster, and S. H. Carr.
1995. Gulf sturgeon, *Acipenser oxyrinchus desotoi*, in the Suwannee River, Florida, USA. *In* International Sturgeon Symposium, p. 215–224. VNIRO, Moscow.

Wirgin, I., M. Collins, A. Hecht, M. Hendrix, A. Kahnle, W. Laney, R. St. Pierre, R. Santos, and T. Squiers.
1998. Status review of Atlantic sturgeon (*Acipenser oxyrinchus oxyrinchus*). Atlantic Sturgeon Status Review Team, 124 p.

Collins, M. R., S. G. Rogers, and T. I. J. Smith.
1996. Bycatch of sturgeons along the southern Atlantic coast of the USA. N. Am. J. Fish. Manage. 16:24–29.

Cooper, S. R., and G. S. Brush.
1991. A 2,500-year history of anoxia and eutrophication in the Chesapeake Bay. Estuaries 16:617–626.

Dadswell, M. J.
1979. Biology and population characteristics of the shortnose sturgeon, *Acipenser brevirostrum* Le Seuer 1818 (Osteichthyes: Acipseridae), in the Saint John Estuary, New Brunswick, Canada. Can. J. Zool. 57:2186–2210.

Dorazio, R. M., B. M. Florence, and C. M. Wooley.
1991. Stocking of hatchery-reared striped bass in the Patuxent River, Maryland: survival, relative abundance, and cost-effectiveness. N. Am. J. Fish. Manage. 114:435–442.

Dovel, W. L., and T. J. Berggren.
1983. Atlantic sturgeon of the Hudson Estuary, New York. NY Fish and Game J. 30:140–172.

Gilbert, C. R.
1989. Species profiles: life histories and environmental requirements of coastal fishes and invertebrates (Mid-Atlantic bight)—Atlantic and shortnose sturgeons. U.S. Fish Wildl. Serv. Biol. Rep., 28 p.

Grogan, C. S., and J. Boreman.
1998. Determining the probability that historical populations of fish species are extirpated. N. Am. J. Fish. Manage. 18:522–529.

Haley, N.
1998. A gastric lavage technique for characterizing diets of sturgeons. N. Am. J. Fish. Manage. 18:978–981.

Haley, N., J. Boreman, and M. Bain.
1996. Juvenile sturgeon habitat use in the Hudson River. *In* Final reports of the Tibor T. Polgar Fellowship Program, vol. 1995, p. 1–20. Hudson River Foundation, New York, NY.

Hasler, A. D., and A. T. Scholz.
1983. Olfactory imprinting and homing in Salmon. Investigations into the mechanism of the imprinting process. Springer-Verlag, Berlin, Germany, 134 p.

Haynes, J. M., R. H. Gray, and J. C. Montgomery.
1978. Seasonal movements of white sturgeon (*Acipenser transmontanus*) in the mid-Columbia River. Trans. Am. Fish. Soc. 107:275–280.

Hildebrand, S. F., and W. C. Schroeder.
1927. Fishes of the Chesapeake Bay. U.S. Bureau of Fisheries, Washington, D.C., 388 p.

Hume, J. M., and E. A. Parkinson.
1987. Effect of stocking density on the survival, growth and dispersal of steelhead trout fry (*Salmo gairdneri*). Can. J. Fish. Aquat. Sci. 44:271–281.

Kieffer, M. C., and B. Kynard.
1993. Annual movements of shortnose and Atlantic sturgeon in the Merrimack River, Massachusetts. Trans. Am. Fish. Soc. 122:1088–1103.

Lazzari, M. A., J. C. O'Herron, and R. W. Hastings.
1986. Occurrence of juvenile Atlantic sturgeon, *Acipenser oxyrhinchus* in the upper tidal Delaware River. Estuaries 9:356–361.

Littel, R. C., G. A. Milliken, W. W. Stroup, and R. D. Wolfinger.
1996. SAS system for mixed models. SAS Institute Inc., Cary, NC, 633 p.

McCleave, J. D., S. M. Fried, and A. K. Towt.
1977. Daily movements of shortnose sturgeon, *Acipenser brevirostrum*, in a Maine estuary. Copeia 1977:149–157.

Moser, M. L., and S. W. Ross.
1995. Habitat use and movements of shortnose and Atlantic sturgeons in the lower Cape Fear River, North Carolina. Trans. Am. Fish. Soc. 124:225–234.

Murawski, S. A., and A. L. Pacheco.
1977. Biological and fisheries data on Atlantic sturgeon, *Acipenser oxyrhynchus* (Mitchill). National Marine Fisheries Service, NOAA, Highlands, NJ, 69 p.

Nagata, M., M. Kakajima, and M. Fujihara.
1994. Dispersal of wild and domestic masu salmon fry (*Oncorhynchus masou*) in an artificial channel. J. Fish Biol. 45:99–109.

Nickelson, T. E., M. F. Solazzi, and S. L. Johnson.
1986. Use of hatchery coho salmon (*Oncorhynchus kisutch*) presmolts to rebuild wild populations in Oregon Coastal streams. Can. J. Fish. Aquat. Sci. 43:2443–2449.

Officer, C. B., R. B. Biggs, J. L. Taft, L. E. Cronin, M. A. Tyler, and W. R. Boynton.
1984. Chesapeake Bay anoxia: origin, development, and significance. Science (Wash., D.C). 223:22–27.

Peterson, D.L., M.B. Bain, and N. Haley.
2000. Evidence of declining recruitment of Atlantic sturgeon in the Hudson River. N. Am. J. Fish. Manage. 20:231–238.

Secor, D. H., and T. E. Gunderson.
1998. Effects of hypoxia and temperature on survival, growth, and respiration of juvenile Atlantic sturgeon *Acipenser oxyrynchus*. Fish. Bull. 96:603–613.

Secor, D. H., and J. R. Waldman.
1999. Historical abundance of Delaware Bay Atlantic sturgeon and potential rate of recovery. Am. Fish. Soc. Symp. 23:203–216.

Smith, T. I. J.
1985. The fishery, biology, and management of Atlantic sturgeon, *Acipenser oxyrhynchus*, in North America. Environ. Biol. Fishes 14:61–72.

Smith, T. I. J., E. K. Dingley, and D. E. Marchette.
1980. Induced spawning and culture of Atlantic sturgeon. Progr. Fish-Cult. 42:147–151.

Smith, T. I. J., D. E. Marchette, and R. A. Smiley.
1982. Life history, ecology, management and culture of the Atlantic sturgeon *Acipenser oxyrinxhus oxyrinchus* Mitchill, in South Carolina. South Carolina Wildl. Mar. Resour. Comm. Tech. Rep., 75 p.

Stevenson, J. T., and D. H. Secor.
2000. Age determination and growth of Hudson River Atlantic sturgeon (*Acipenser oxyrinchus*). Fish. Bull. 98:153–166.

Van Den Avyle, M. J.
1984. Species profiles: life histories and environmental requirements of coastal fishes and invertebrates (South Atlantic)—Atlantic sturgeon. U.S. Fish Wildlife Service Biological Report FWS/OBS-82/11.25, Athens, GA, 17 p.

Vladykov, V. D., and J. R. Greeley.
1963. Order Acipenseroidei. Part III *in* Fishes of the western North Atlantic (Y. H. Olsen, ed.), p. 24–60. Memoirs of the Sears Foundation for Marine Research, Yale Univ., vol. 1.

Waldman, J. R. and I. I. Wirgin.
1998. Status and restoration options for Atlantic sturgeon in North America. Cons. Biol. 12:631–638.

Wirgin, I. I., J. E. Stabile, and J. R. Waldman.
1997. Molecular analysis in the conservation of sturgeons and paddlefishes. Env. Biol. Fishes 48:385–398.

Growth rates of juvenile dusky sharks, *Carcharhinus obscurus* (Lesueur, 1818), from southwestern Australia estimated from tag-recapture data

Colin A. Simpfendorfer

Western Australian Marine Research Laboratories
PO Box 20
North Beach
Western Australia 6020, Australia
Present address: Center for Shark Research, Mote Marine Laboratory
1600 Ken Thompson Parkway
Sarasota, Florida, 34236
Email address colins@mote.org

Abstract—Tagged neonate and small juvenile *Carcharhinus obscurus* were released between March 1994 and June 1996 in southwestern Australia. Length and time-at-liberty data from 304 usable recapture data were used to examine growth rates of male, female, oxytetracycline injected, noninjected, and all individuals combined. Recaptures were made up to 4.7 years after release. Four methods of analysis were employed: Gulland and Holt, Fabens, Francis, and length-at-age. Length-at-age analysis was possible because the majority of the animals released had open umbilical scars and so were of known age. The four methods produced varying results. One method was not able to estimate growth parameters, another produced inaccurate estimates of von Bertalanffy growth parameters, and two methods indicated that a linear growth model described growth better than the von Bertalanffy model. Although each produced different results, the three successful methods estimated that the growth rate up to age 5 ranged from 8 cm/year to 11 cm/year. These growth rates agreed closely with those reported for young *C. obscurus*. Length-at-age analysis indicated significant differences in the growth rates between males and females, and between oxytetracycline-injected and noninjected males. Results from the Francis method did not show significant differences between males and females, or injected and noninjected animals. The coefficient of variation of growth variability ranged from 0.24 to 0.40, mean measurement error ranged from 0.0 cm to 0.94 cm, and the standard deviation of measurement error ranged form 2.1 cm to 2.4 cm. The usefulness of each of the methods is discussed—the more detailed methods providing a better understanding of tag-recapture data.

Manuscript accepted 26 June 2000.
Fish. Bull. 98:811–822 (2000).

Tag-recapture data are a useful source of information on the growth of animals. The simplest form of analysis is to estimate an average growth rate, normally for a specific size range, from the period at liberty and the growth increment. This approach has been used in studies examining elasmobranch growth. For example, Thorson and Lacy (1982) estimated the average growth rate of adult sawfish (*Pristis perotteti*), Pratt and Casey (1983) provided average growth rates for shortfin mako sharks (*Isurus oxyrinchus*) in 20-cm size groups, and Casey et al. (1985) provided estimates of growth rates for sandbar sharks (*Carcharhinus plumbeus*) in 20-cm size groups. Although this approach provides information on growth rates that can be compared with those predicted by other techniques, it does not provide estimates of parameters for growth functions (e.g. the von Bertalanffy growth function).

A more useful approach is to fit growth functions to tag-recapture data. A range of techniques have been developed to undertake this type of analysis. Early techniques used relatively simple approaches (e.g. Walford, 1946; Gulland and Holt, 1959; Fabens, 1965) to estimate parameters of the von Bertalanffy growth function. Species of elasmobranchs for which these types of techniques have been used include three species of *Raja* (Holden, 1972), *C. plumbeus* (Wass, 1973; Casey and Natanson, 1992), *Galeorhinus galeus* (Grant et al., 1979), *Squatina californica* (Cailliet et al., 1992) and *Galeocerdo cuvier* (Natanson et al., 1999). With the advent and proliferation of powerful computers, more sophisticated techniques have been developed to deal with tag-recapture data and to allow the fitting of a range of growth functions and the estimation of confidence intervals (Francis, 1988). These growth functions have included both the widely used von Bertalanffy curve, as well as other forms (e.g. Schnute, 1981; Francis, 1995). In addition, functions that allow for the estimation of seasonal growth patterns (e.g. Francis, 1988), growth variability (e.g. Francis, 1988, Wang et al., 1995), and measurement error (e.g. Francis, 1988) have been developed. These more complex functions allow researchers to extract more information from tag-recapture data, as well as identify factors that may be important in determining the growth of individual animals. These types of analysis have not been widely used in elasmobranch studies to date. However, Francis and Francis (1992) and Francis and Mulligan (1998) used the Francis (1988) method for *Mustelus lenticulatus* and *G. galeus*, respectively.

Tagging studies of elasmobranch populations have also been used to validate age data based on vertebrae. Individuals are injected with a marker that is incorporated into calcifying structures so that the number of bands laid down between tagging and recapture can be determined, and the periodicity of band formation validated (Cailliet, 1990). The most commonly used marker in these studies is oxytetracycline (OTC) at dose rates of approximately 25 mg/kg (Gelsleichter et al., 1998). OTC is also a powerful antibiotic with recommended

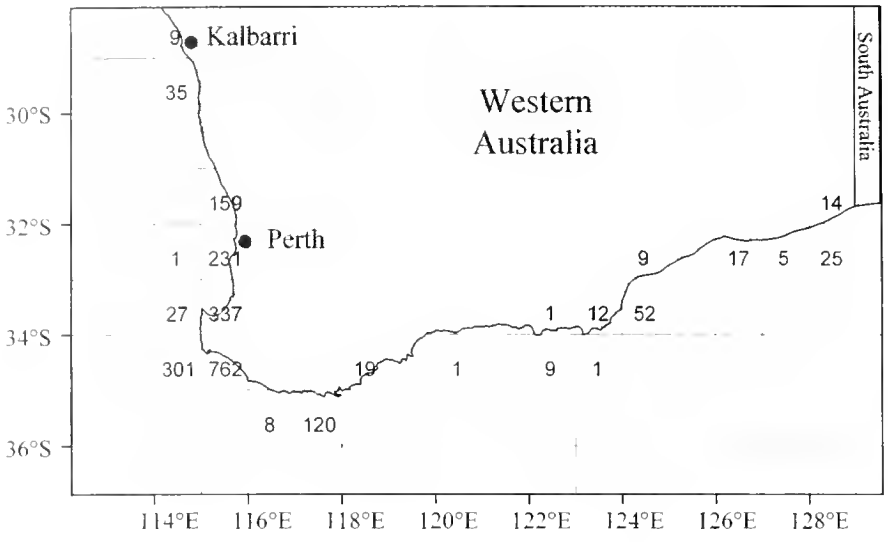

Figure 1

Numbers of juvenile *Carcharhinus obscurus* released in one-degree geographic blocks off southwestern Australia.

...ody, doses of 10mg/kg for elasmobranchs (Stoskopf, 1993). Despite its antibiotic properties it has been demonstrated to have toxic effects on some teleosts (e.g. Marking et al., 1988). Although widely used, the impact of OTC injection on the growth of elasmobranchs has been poorly studied. Tanaka (1990) demonstrated that injection of OTC did not affect the growth of juvenile *Orectolobus japonicus* at normal dosages. Gelsleichter et al. (1998) reported that OTC injection did not affect the growth of nurse sharks (*Ginglymostoma cirratum*), but that it may have some level of hepatotoxicity. In the only reported study of a wild elasmobranchs, Natanson et al. (1999) reported that four *Galeocerdo cuvier* specimens injected with OTC did not have growth rates different from those not injected with OTC.

The dusky shark, *Carcharhinus obscurus*, is a large species of coastal shark that occurs in tropical, subtropical, and temperate oceans world-wide (Compagno, 1984). They are born at 70–100 cm total length (TL), mature at approximately 280 cm TL, and grow to at least 365 cm TL (Last and Stevens, 1994). Natanson et al. (1995) provided estimates of growth parameters for *C. obscurus* from the western North Atlantic, using length-at-age data and length-frequency data. These data indicate that *C. obscurus* is slow growing, reaches maturity at approximately 19–21 years, and possibly lives to 45 years. Natanson and Kohler (1996) estimated growth parameters for *C. obscurus* from the southwest Indian Ocean, using length-at-age data that indicated growth similar to that from the western North Atlantic.

A demersal gillnet fishery in southwestern Australia targets neonate and small juvenile *C. obscurus*, mostly from February to June. The fishery has operated since the 1940s, but significant catches of *C. obscurus* were not taken until the mid 1970s (Simpfendorfer and Donohue, 1998). Increasing fishing effort in the 1980s lead to concerns about the status of this resource and prompted a research project that included a tag and release study to estimate mortality (Simpfendorfer, 1999), movement, and growth parameters for *C. obscurus*. The aims of this paper are 1) to estimate growth rates and growth parameters for *C. obscurus* based on tag-recapture data using four different methods, 2) to investigate differences in growth due to sex or injection with OTC, and 3) to estimate growth variability and measurement error.

Materials and methods

Tagging

Neonate and juvenile *C. obscurus* were caught between March 1994 and June 1996 by commercial demersal gillnet vessels operating in southwestern Australia. These vessels operate in continental shelf waters in depths of 7–100 m. The gill nets are constructed of 16.5-cm and 17.8-cm (stretched) mesh monofilament netting that is 1.5 m to 2.0 m deep. Nets are 3–7 km in length and are set on the sea floor for periods of 7–24 hours.

Individual *C. obscurus* were measured (fork length [FL]: the distance from the tip of the snout to the caudal fork measured as a straight line) to the nearest centimeter, the sex of each fish was determined, and each fish was examined for the presence of an open umbilical scar, and tagged with an individually numbered Jumbo Rototag (Dalton Supplies, Woolgoolga, New South Wales, Australia) in the first dorsal fin. Approximately one in every three animals was injected with OTC (25 mg/kg) to mark the vertebral centra for age validation studies.

A total of 2199 juvenile *C. obscurus* were released from March 1994 to June 1996 between the Western Australian and South Australian border (129°E) and Kalbarri (29°S) (Fig. 1). Tagged sharks ranged in size from 53 cm FL to 108 cm FL but most were 70–81 cm FL (Fig. 2). One thousand seven hundred and thirty (78.7%) had open umbilical scars; 1062 were female, 1100 were male, and 37 were of unknown sex; 879 were injected with OTC and 1320 were not injected. Information on tag-recaptures, including date and location of recapture, and length were reported by commercial fishermen and research observers operating in the demersal gillnet fishery. Fishermen were provided with tape measures and trained to measure fork length in an attempt to improve the accuracy of recapture data.

Analysis

Growth rates of five groups of juvenile *C. obscurus*—males, females, OTC injected, non-OTC-injected, and all recaptures combined—were estimated by using four different

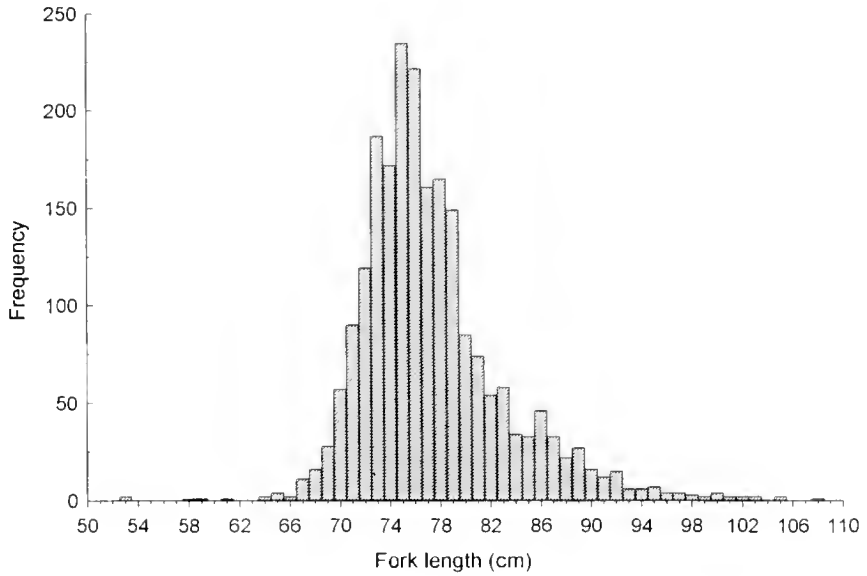

Figure 2

Size at release for 2199 juvenile *Carcharhinus obscurus* tagged off southwestern Australia.

methods. Only recaptures with data that included the date of recapture and accurate length at release and recapture were used in the analyses.

Gulland and Holt (1959) The first method used for estimating growth rates was that of constructing plots of growth rate by average fork length (Gulland and Holt, 1959). The average fork length was calculated as the average of the fork length at release and recapture. Von Bertalanffy growth parameters were estimated by fitting a line through the data. The slope of the line was equal to $-K$, and the intercept with the x-axis was equal to L_∞.

Fabens (1965) The Fabens (1965) method involved fitting the nonlinear function:

$$L_R = L + (L_\infty - L)(1 - e^{-Kd}), \quad (1)$$

where L_R = the length at recapture;
L = the length at release; and
d = the period at liberty.

This function was fitted to the data by using the nonlinear estimation module in STATISTICA (Statsoft, 1998). The value of t_0 was estimated by solving the function for the value of T

$$L_T = L_0 + (L_\infty - L_0)(1 - e^{-KT}), \quad (2)$$

where the value of L_0 = the mean size at birth; and
L_T = 0 cm.

The mean size at birth of *C. obscurus* from southwestern Australia was estimated by fitting a normal probability function to a size-frequency distribution of tagged individuals that had an open umbilical scar (Fig. 3). From these data the mean size at birth was 75.3 cm FL.

Francis (1988) method This method uses a maximum likelihood approach to fitting a growth function that includes estimated growth rates (g_α and g_β) at two selected lengths (α=75 cm FL and β=100 cm FL), the coefficient of variation of growth variability (v), measurement error (assumed to be normally distributed with a mean, m, and standard deviation, s), and outlier probability (p). The estimated growth increment for an individual, i, is given by

$$\Delta L_i = \left[\frac{\beta\ g_\alpha - \alpha \cdot g_\beta}{g_\alpha - g_\beta} - L_i\right]\left[1 - \left(1 + \frac{g_\alpha - g_\beta}{\alpha - \beta}\right)^{\Delta T}\right],$$

where L_i = the length at release; and
ΔT_i = the period at liberty.

Francis (1988) suggested several methods of incorporating growth variability into the model.

The likelihood function is

$$\lambda = \sum_i \log\left[(1-p)\lambda_i + p/R\right],$$

where $\lambda_i = \dfrac{\exp\left[-0.5(\Delta L_i - \mu_i - m)^2/(\sigma_i^2 + s^2)\right]}{\left[2\pi(\sigma_i^2 + s^2)\right]^{0.5}}$;

R = the range of the observed growth increments;

μ_i = the expected value of growth increment of the ith individual; and
σ_i = the standard deviation of the growth variability.

In the present study σ_i was assumed to be proportional to predicted growth increment (i.e. $\sigma_i = v\mu_i$).

The solver function in Microsoft Excel (Microsoft, 1999) was used to maximize the likelihood value of the model. Although the growth model allowed the use of six parameters, the number of parameters used for each of the groups was determined by using the likelihood ratio test (LRT). In its simplest form growth was assumed to be linear ($g_\alpha = g_\beta$) and to include s. The addition of more parameters (nonlinear growth [$g_\alpha \neq g_\beta$], v, m, and p) was significant if the likelihood increased by more than 1.92 per parameter (Francis, 1988). The final model used for each group was the one with the least number of significant parameters.

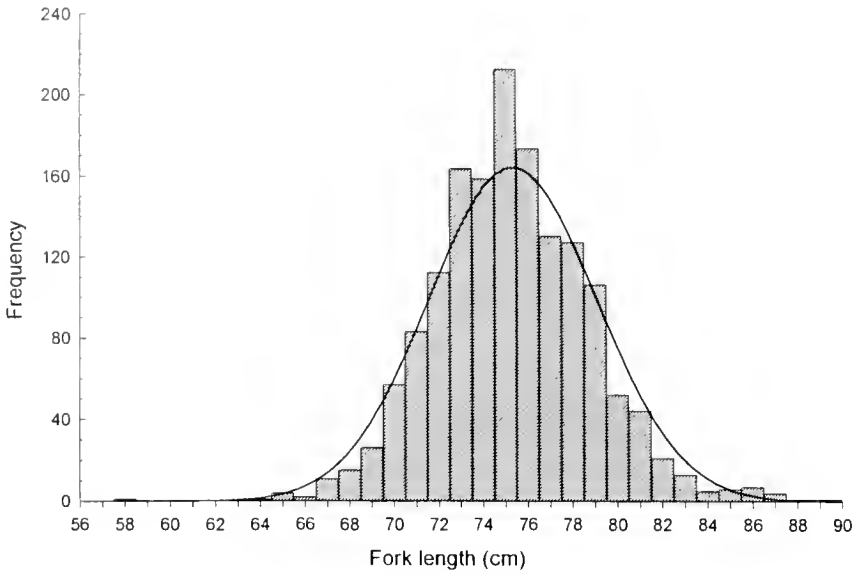

Figure 3

Size-frequency distribution of 1537 neonate *Carcharhinus obscurus* from southwestern Australia with open umbilical scars. The line represents a normal distribution with a mean of 75.3 cm and a standard deviation of 3.75 cm.

Bootstrapping was used to estimate 95% confidence intervals for parameter estimates. New growth increment values were generated by adding randomly selected points from two normal distributions. The first distribution had a mean of the predicted growth increment with a standard deviation equal to $v\mu$ and represented growth and growth variability. The second distribution represented the measurement error and had a mean of m and a standard deviation of s. Five hundred bootstrapped data sets were created by using each method and fitted by using the technique described above. Ninety-five percent confidence intervals were calculated from the 2.5th percentile and the 97.5th percentile of the resulting parameter distributions.

Length-at-age for neonate releases The use of length-at-age data is normally associated with aging studies where the age of an individual shark is estimated from the number of bands on the vertebrae. Because most animals tagged in the current study had open umbilical scars, it was possible to estimate the age of each of the recaptured animals directly from the time at liberty and the rate of healing of the umbilical scar. There is limited information available on the time that it takes for the umbilical scar to close, but most estimates range from 4 to 6 weeks (Bass et al., 1973). If it is assumed that a shark with an open scar was tagged at an age of three weeks (the assumed age at release), the age at recapture is the time at liberty plus three weeks. Preliminary data analysis showed that a linear growth function ($L_t = bL + a$, where b is the growth rate and a is a constant) provided a better fit to the data than a von Bertalanffy function. Thus a linear model was fitted to the length-at-age data. Growth rates (b values) were compared between males and females, and between injected and noninjected animals, using the homogeneity-of-slopes model within the visual general linear model module of STATISTICA. Significant differences in growth rates existed when the interaction term (age × sex or age × injection status) was significant. If there were significant differences in the growth rates for sexes then differences in the growth rates between injected and noninjected animals were assessed separately for males and females, otherwise they were assessed for males and females combined.

Results

A total of 473 recaptures of juvenile *C. obscurus* were reported to September 1998. Recaptured animals were at liberty between 0 and 1716 days (4.7 years); seven were at liberty for more than three years. Tag-recapture data from all individuals with usable data were included in the Francis (1988) method, whereas only those with times at liberty greater than 60 days were used in the other methods of analysis. Individuals at liberty less than 60 days were excluded because many individuals had growth rates that were beyond those considered reasonable because of the short period at liberty (Fig. 4). The size at recapture ranged from 68.5 to 147 cm FL. There were 304 recaptured sharks with usable data, and 274 recaptured sharks with times at liberty greater than 60 days. These recaptured sharks included 153 males (137 at liberty >60 days), 143 females (130 at liberty >60 days), 118 individuals injected

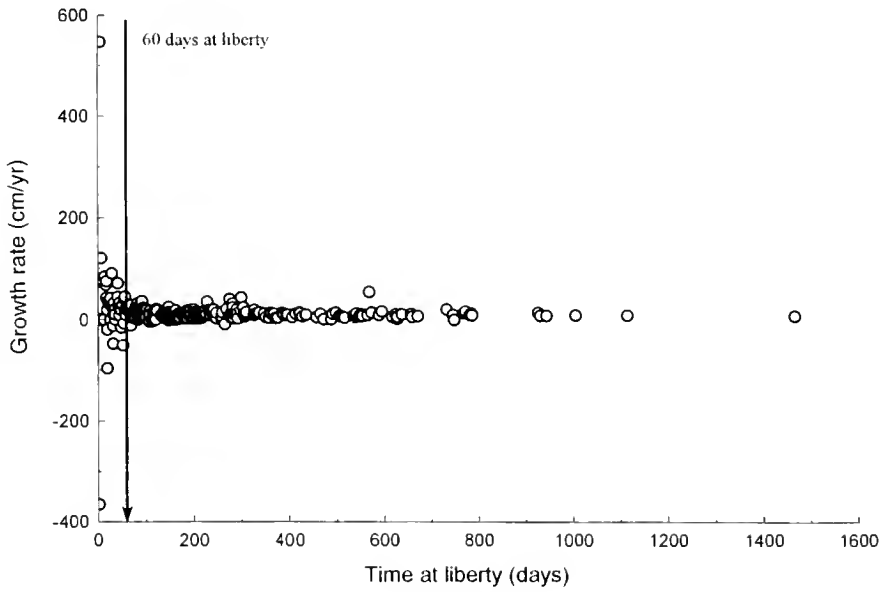

Figure 4

Growth rates of recaptured juvenile *Carcharhinus obscurus* from southwestern Australia as a function of time at liberty. The line indicates 60 days at liberty, the time below which individuals were excluded from analysis.

with OTC (111 at liberty >60 days), and 179 individuals not injected with OTC (160 at liberty >60 days).

Gulland and Holt (1959) method

Linear regressions fitted to the growth rate versus average fork length had positive slopes for all groups examined. As a result estimates of K were negative, and L_∞ was unsolvable. These results indicate that this method was unable to estimate growth parameters for juvenile *C. obscurus*.

Fabens (1965) method

Von Bertalanffy growth parameters estimated by the Fabens (1965) method varied widely (Table 1). All the groups, except the noninjected individuals, produced estimates of K between 0.092/year and 0.187/year, and estimates of L_∞ between 142 cm FL and 194 cm FL. For the noninjected individuals the estimate of K was 0.031/year and L_∞ was 379 cm FL. Values of r^2 for all groups were relatively high, indicating that the von Bertalanffy parameters explained most of the variation in the data.

Francis (1988) method

The likelihood ratio tests for each of the five groups of *C. obscurus* indicated that the appropriate models were relatively simple, containing linear growth (g_α=g_β), v, s, and sometimes m (Table 2). Contamination probability (p) and g_β were not included in the final models for any of the groups. The value of m was assumed to be zero for models in which it was not included.

Table 1

Estimates of von Bertalanffy growth parameters with the Fabens (1965) method for juvenile *Carcharhinus obscurus* from southwestern Australia.

Group	L_∞ (cm)	K (per year)	r^2
All	177	0.111	0.74
Male	195	0.092	0.80
Female	142	0.187	0.67
Injected	156	0.167	0.73
Noninjected	379	0.031	0.72

The Francis (1988) method estimated that the linear growth rate for all juvenile *C. obscurus* was 9.23 cm/year (Table 3). The growth rate of males was 1.1 cm/year higher than that for females, and 2.2 cm/year higher for OTC-injected than for noninjected animals. The 95% confidence intervals (CI), however, indicated that differences in growth rate were not significant between any of the five groups. Estimates of v and s were similar for all groups examined, ranging from 0.24 to 0.40 and from 2.09 cm FL to 2.54 cm FL, respectively. The 95% CIs indicated no significant differences in v or s between groups. The values of m, for models in which it was calculated, ranged from 0.69 cm FL to 0.94 cm FL. There were no significant differences in m between the all, females, and noninjected groups.

Table 2

Likelihood values from the Francis (1988) method for different combinations of parameters. Values in bold indicate the final model used in the analysis for each of the five groups of *Carcharhinus obscurus*. Significance of additional parameters was tested with the likelihood ratio test (see text for details).

Model	All	Male	Female	Injected	Noninjected
g_{75}, s	–807.23	–396.19	–386.90	–305.04	–470.90
g_{75}, v, s	–778.69	**–382.17**	–372.77	**–296.24**	–456.65
g_{75}, v, s, m	**–774.73**	–381.57	**–369.53**	–295.69	**–453.42**
g_{75}, v, s, m, p	–774.73	–381.57	–369.47	–295.69	–452.26
g_{75}, g_{100}, s	–806.76	–395.98	–386.81	–304.90	–497.58
g_{75}, g_{100}, v, s	–778.51	–382.16	–372.62	–295.83	–480.47
g_{75}, g_{100}, v, s, m	–774.69	–381.56	–369.46	–295.52	–476.73
$g_{75}, g_{100}, v, s, m, p$	–774.69	–381.56	–369.39	–295.52	–476.06

Table 3

Growth parameter estimates for five groups of *Carcharhinus obscurus* from southwestern Australia with the Francis (1988) method for the best models determined in Table 2. Numbers in parentheses after estimates are 95% confidence intervals calculated by bootstrapping.

Parameter	All	Male	Female	Injected	Noninjected
g_{75} (cm/year)	9.23	10.24	9.14	10.84	8.69
	(8.24–10.11)	(9.41–11.17)	(7.73–10.49)	(9.68–11.63)	(7.43–10.01)
v	0.34	0.34	0.33	0.24	0.40
	(0.26–0.42)	(0.24–0.43)	(0.21–0.45)	(0.23–0.37)	(0.28–0.52)
s	2.35	2.09	2.54	2.43	2.33
	(2.03–2.63)	(1.69–2.46)	(2.09–2.93)	(1.91–2.74)	(1.94–2.73)
m (cm)	0.69	—	0.94	—	0.83
	(0.22–1.17)		(0.23–1.67)		(0.12–1.49)

As a comparison to estimates of m and s from the Francis (1988) method, differences in the size at release and recapture for animals at liberty less than 30 days were determined. If it is assumed than these animals grew a negligible amount over this period, and the animals were measured perfectly by research staff at release, then the mean and standard deviation of the differences should provide an independent estimate of m and s. The mean difference in size for 38 *C. obscurus* at liberty less than 30 days was 1.17 cm FL, and the standard deviation was 2.09 cm FL (Fig. 5). These values are similar to those estimated from the model for most of the groups.

Length-at-age for neonate releases

A total of 241 released neonates (with open umbilical scars) were recaptured, including 117 males, 120 females, four of unknown sex, 92 OTC-injected animals, and 149 noninjected animals. The linear growth rate based on all neonate recaptures was 9.1 cm/year. The growth rate was higher for males than for females, and higher for injected animals than for noninjected animals (Table 4). Comparison of growth rates with the homogeneity-of-slopes models (Fig. 6, Table 5) indicated that there were significant differences between males and females, and between injected and noninjected males. However, there was no significant difference between injected and noninjected females (Table 5).

Discussion

Shark growth studies have typically used the von Bertalanffy growth function to describe how sharks grow, including previous work on *C. obscurus* (e.g. Natanson et al., 1995; Natanson and Kohler, 1996). However, in the current study the results indicated that a linear growth curve more accurately describes the growth of juvenile *C. obscurus* up to five years of age. Pratt and Casey (1990) suggested that for some slow growing sharks (e.g. *Carcharhinus plumbeus*) a linear growth function might provide a better predictive model than the von Bertalanffy growth function. Although linear growth functions have been rarely used in fish growth studies, Bayliff (1988) reported that this type of function provided the best fit to

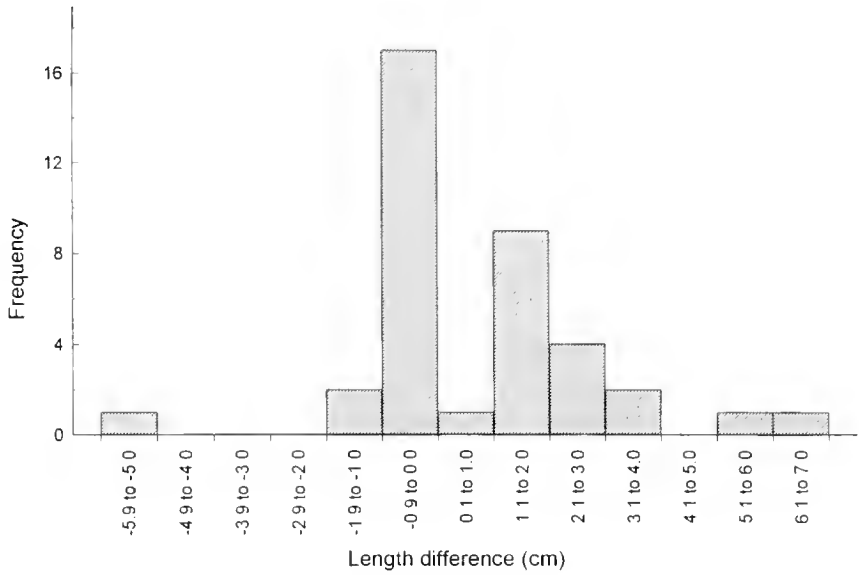

Figure 5

Differences between release and recapture lengths for 38 juvenile *Carcharhinus obscurus* at liberty less than 30 days off southwestern Australia.

growth data from tagged yellowfin tuna (*Thunnus albacares*) up to 100 cm long. Because the current study used only data from individuals up to five years old, which is a short period in relation to the estimated longevity of this species (45 years, Natanson et al., 1995), there was no information in the data on the rate at which the length reaches its asymptote (equivalent to the rate of decrease in the growth rate with increasing age). As a result the von Bertalanffy growth function cannot adequately describe the data. If recapture data were available for individuals from older age classes, it is likely that a decrease in growth rate with increasing age may have been observed and thus a von Bertalanffy growth function (or the Francis (1988) model with $g_\alpha \neq g_\beta$) may have provided the best fit to the data.

The Gulland and Holt (1959) method relies on a decrease in growth rates with increasing age to estimate both L_∞ (x-intercept) and K (slope). Thus, because the tag-recapture data for *C. obscurus* did not contain this information, the method was not able to estimate von Bertalanffy growth parameters. The inability to produce results, while other methods did, illustrates that the Gulland and Holt (1959) method fails in some situations where the periods at liberty are short in relation to the maximum age and where the recaptured individuals cover only a small proportion of the age classes present in the population. The lack of information in the data on the decrease in growth rate with increasing age also caused problems for the estimation of parameters in the Fabens (1965) method. In all cases, except for the noninjected group, this method provided substantially lower values of L_∞ than expected from observations of the maximum length of *C. obscurus* in Western Australian waters (280 cm FL, Simpfendorfer et al., unpubl. data[1]) and from previous growth studies (Natanson et al., 1995; Natanson and Kohler, 1996). Similarly, values of K were substantially higher than literature values (0.034 to 0.062, Natanson et al., 1995; 0.047, Natanson and Kohler, 1996) for each of the groups except the noninjected animals. The von Bertalanffy growth parameters estimated for the noninjected group by the Fabens (1965) method were similar to those estimated by Natanson et al. (1995) and Natanson and Kohler (1996).

Table 4

Linear growth rates (b) of juvenile *Carcharhinus obscurus* based on length-at-age data for neonate releases. Values in parentheses are standard errors of b.

Group	n	b (cm/yr)	r^2
All	241	9.39 (0.38)	0.706
Male	117	10.58 (0.48)	0.787
Female	120	8.46 (0.56)	0.644
Injected	92	10.05 (0.53)	0.773
Noninjected	149	8.54 (0.53)	0.633

[1] Simpfendorfer, C. A., R. McAuley, J. Chidlow, R. Lenanton, and N. Hall. 1999. Biology and stock assessment of Western Australia's commercially important shark species. Unpubl. report. Western Australian Marine Research Laboratories, PO Box 20, North Beach, Western Australia 6020, Australia.

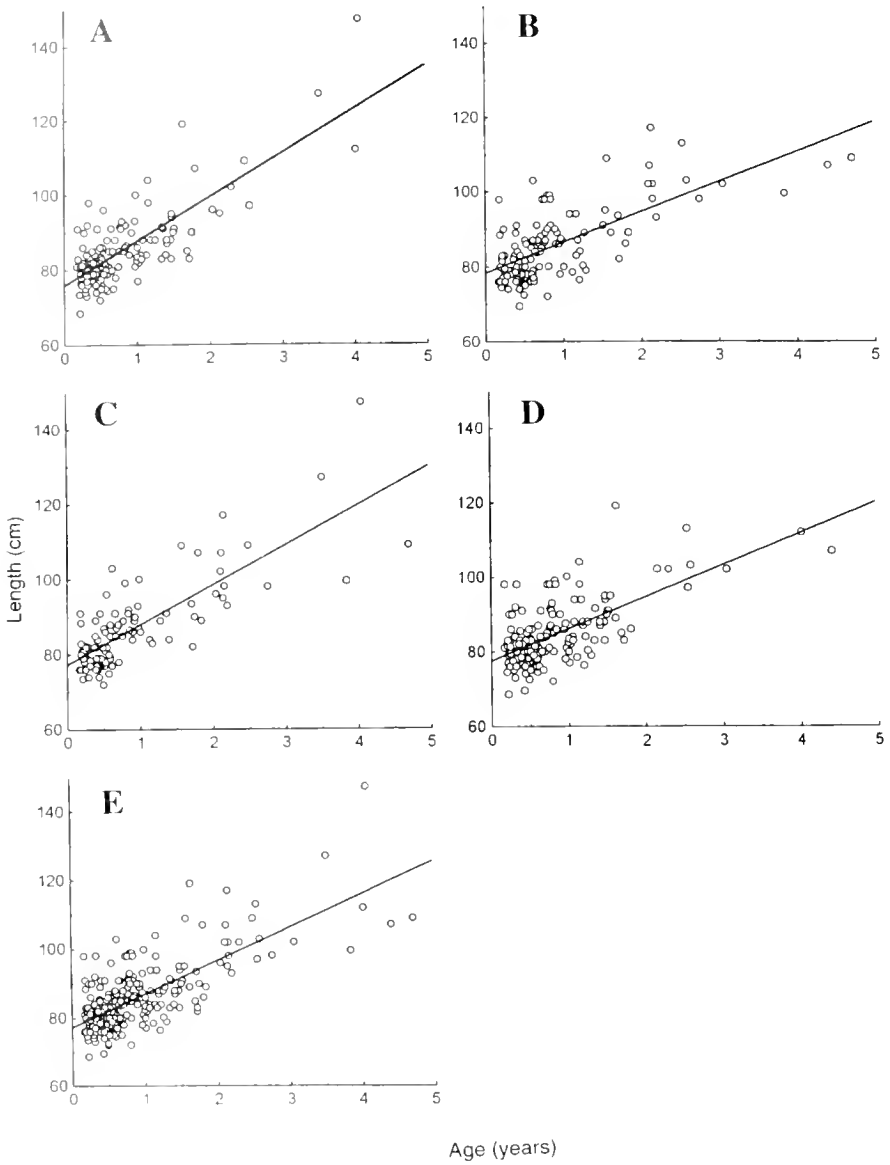

Figure 6

Length-at-age plots for (**A**) male, (**B**) female, (**C**) injected, (**D**) noninjected, and (**E**) all *Carcharhinus obscurus* from southwestern Australia. Lines represent linear growth functions based on parameters given in Table 4.

Despite the difficulties in obtaining von Bertalanffy growth parameters with the Fabens (1965) method, the growth rates from age zero to 5 years were similar to those from the linear growth function from the Francis (1988) and length-at-age methods (Fig. 7). Each of the methods indicates that on average juvenile *C. obscurus* grow 8–11 cm/year. The results from the current study (for all methods) were also similar to those from previous studies for *C. obscurus* in the western North Atlantic and southwestern Indian Ocean by Natanson et al. (1995) and Natanson and Kohler (1996), respectively (Fig. 7). However, the growth rates were lower than those suggested by Branstetter (1990) who used data from Schwartz (1983) to estimate the growth rate of *C. obscurus* pups from the western North Atlantic to be approximately 15 cm/year. At ages greater than five years, the growth rates estimated by the current study corresponded poorly to observed results in other studies. This is a result of the linear growth of the juveniles that does not predict the decrease of growth rates as individuals age. Extrapolation of the results to ages greater than five years is thus invalid and should be avoided

The results of the Francis (1988) method indicate a relatively high level of growth variation in juvenile *C. obscu-*

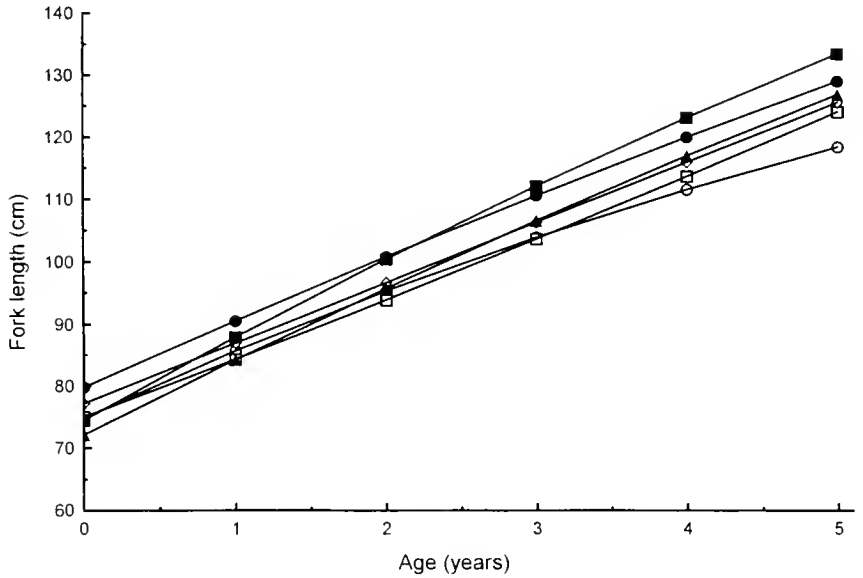

Figure 7

Comparison of growth rates from three methods used in the current study (open symbols: circle = Fabens [1965] method; square = Francis [1988] method; diamond = length-at-age method) and previous research (solid symbols: circle = length-at-age from vertebrae; square = tag-recapture data from Natanson et al. [1995]; triangle = Natanson and Kohler [1996]).

Table 5

Results of homogeneity-of-slopes models in which growth rates between male and female, and injected and noninjected *Carcharhinus obscurus* were compared. ** indicates significant effects. SS = sum of squares.

Comparison	Effect	SS	df	*F*	*P*
Male with female	sex	107.60	1	5.31	0.022**
	age	12997.64	1	641.44	0.000**
	sex × age	161.69	1	7.98	0.005**[1]
Male					
Injected with noninjected	injection status	7.72	1	2.99	0.086
	age	7012.62	1	555.84	0.000**
	injection status × age	224.323	1	17.78	0.000**
Female					
Injected with noninjected	injection status	18.02	1	0.68	0.411
	age	5720.07	1	216.34	0.000**
	injection status × age	0.34	1	0.013	0.910

[1] Because *age* × *sex* interaction is significant, comparisons of injected and noninjected groups must be conducted for males and females separately.

rus. The value of v in the present study (0.24–0.40) was higher than that estimated for *Galeorhinus galeus* (0.06) (Francis and Mulligan, 1998), but lower than for *Mustelus antarcticus* (0.58) (Francis and Francis, 1992). Francis and Mulligan (1998) suggested that their data might not contain enough information to distinguish between measurement error and growth variability. Francis (1997) and Francis et al. (1999) reported similar levels of growth variability for elephantfish (*Callorhinchus milii*) and hapuku (*Polyprion oxygeneios*), respectively. Growth variability therefore appears consistently to be relatively high across a range of elasmobranch, chimaerid, and teleost fishes.

The observed growth variability in juvenile *C. obscurus* may in part have been due to seasonal growth variation, migrations between warmer waters on the west coast of Western Australia, and cooler waters on the south coast. Either of these factors could possibly have produced substantial variation in growth rates. Further research on the influence of temperature on growth of *C. obscurus* would prove useful in isolating the causes of growth variability in this species.

The estimated measurement error parameters from the Francis (1988) method were similar but slightly lower than those from the differences in length for individuals at liberty less than 30 days. The close agreement between these results indicates that the Francis (1988) method provides accurate estimates of measurement error and that the confounding of measurement error and growth variability reported by Francis and Mulligan (1998) was not a problem in the current study. The magnitude of the mean measurement error was small (0–0.94 cm) in relation to the length of the sharks examined (55–140 cm). Previous studies using the Francis (1988) method have indicated that including m in the model does not improve the result, whereas values of s have included 1.2 cm (*C. milii*, Francis, 1997), 1.5 cm (*P. oxygenios*, Francis et al., 1999), 1.6 cm (*Mustelus lenticulatus*, Francis and Francis, 1992) and 7.2 cm (*G. galeus*, Francis and Mulligan, 1998).

The length-at-age analysis indicated that male juvenile *C. obscurus* have significantly higher growth rates than females. This result, however, was not supported by the results from the Francis (1988) method that showed overlap in the 95% confidence intervals derived from bootstrapping. Differences in growth rates do occur between the sexes in sharks, but these differences are most commonly observed at ages close to maturity (approximately 20 years in *C. obscurus*) (e.g. Simpfendorfer, 1993; Simpfendorfer et al., 2000). Thus the lack of significant differences in the growth rate between young male and female *C. obscurus* was not unexpected. The difference in the results between the two methods may be due to the simple linear model fitted to the length-at-age data not being able to account for growth variability and measurement error. This demonstrates the improvement in understanding that the more complex Francis (1988) model can provide over more simplistic approaches.

The results of the length-at-age analysis in the current study indicate that male *C. obscurus* injected with OTC have significantly higher growth rates than noninjected males. However, females showed no significant difference between injection and noninjection with OTC. The parameter estimates from the Francis (1988) model indicated that injected animals grow 2.2 cm/year faster than noninjected animals. However the 95% confidence intervals overlapped slightly (injected, 9.68–11.63; noninjected, 7.43–10.01) indicating that there were no significant differences in growth rates. Although the significance of growth rate differences varied between analysis methods and sexes, suggesting that differences may have been the result of biased data, there is sufficient evidence to warrant further investigation of the effect of OTC injection on juvenile *C. obscurus*. Previous studies of elasmobranchs have not found significant differences in growth rates between injected and noninjected animals (Tanaka, 1990; Gelsleichter et al., 1998; Natanson et al., 1999). However, only one of these studies (Natanson et al., 1999) was carried out on sharks in the wild. This study was based on four OTC-injected *G. cuvier* specimens and no statistical comparison of growth rates between injected and noninjected individuals was undertaken.

If growth differences between OTC-injected and noninjected *C. obscurus* do occur, they may result from the antibiotic properties of OTC. It is likely that injections of OTC would not increase growth rates; rather, the growth of noninjected animals may be lower after tagging. The capture and tagging process is likely to present a significant source of stress for sharks—one that may increase their chances of microbial infection and slow their growth (e.g. Olsen, 1953; Davies and Joubert, 1967; Manire and Gruber, 1991). Animals injected with OTC would be more likely to overcome these infections quickly and thus grow at rates indicative of untagged individuals. If this scenario can be proven, then the faster growth rates predicted by the Francis (1988) method for the injected juvenile *C. obscurus* (10.84 cm/year) are likely to be most representative for this species.

This study indicates that although a range of techniques are available to estimate growth rates and von Bertalanffy growth parameters from tag-recapture data, they can produce variable results. One method, the Gulland and Holt (1959) method, was not able to produce results for juvenile *C. obscurus*. Another, the Fabens (1965) method, produced unrealistic von Bertalanffy growth parameters. Two methods, the Francis (1988) and length-at-age methods, indicated that linear growth functions provided better predictive power for juvenile *C. obscurus* than the nonlinear von Bertalanffy growth function. The use of the Francis (1988) method allowed for a more detailed investigation of the growth of *C. obscurus*, including the investigation of measurement error and growth variability. Estimation of these additional parameters is particularly useful in tag-recapture studies where commercial and recreational fishermen provide the majority of data. Thus, although the more traditional methods are still commonly used for elasmobranchs, researchers should consider the use of more detailed approaches, such as that of Francis (1988), to extract the maximum possible information from their data.

Acknowledgments

Norm Hall provided valuable advice on the implementation of the Francis method. Phil Unsworth, Tony Paust, Justin Chidlow, Adrian Kitchingman, Justin Bellanger, and Rory McAuley provided technical assistance in the field and laboratory. I am grateful to Rod Lenanton for his guidance and support during this project. Malcolm Francis provided valuable comments on the manuscript and data analysis. This project would not have been possible without the commercial gillnet fishermen in southern Western Australia who provided assistance in tagging sharks and who returned many of the tags. This project was funded

by a grant from the Fisheries Research and Development Corporation.

Literature cited

Bass, A. J., J. D. D'Aubrey, and N. Kistnasamy.
1973. Sharks of the east coast of southern Africa. I. The genus *Carcharhinus* (Carcharhinidae). Oceanogr. Res. Inst. (Durban) Invest. Rep. (38), 100 p.

Bayliff, W. H.
1988. Growth of skipjack, *Katsuwonus pelamis*, and yellowfin, *Thunnus albacares*, tunas in the eastern Pacific Ocean, as estimated from tagging data. Bull. I-ATTC (La Jolla) 19(4), 75 p.

Branstetter, S.
1990. Early life-history implications of selected carcharhinoid and lamnoid sharks of the northwest Atlantic. *In* Elasmobranchs as living resources: advances in the biology, ecology, systematics and the status of the fisheries (H. L. Pratt, S. H. Gruber, and T. Taniuchi, eds.), p. 17–28. U.S. Dep. Commer., NOAA Tech. Rep., NMFS 90.

Cailliet, G. M.
1990. Elasmobranch age determination and verification: an updated review. *In* Elasmobranchs as living resources: advances in the biology, ecology, systematics and the status of the fisheries (H. L. Pratt, S. H. Gruber, and T. Taniuchi, eds.), p. 157–165. U.S. Dep. Commer., NOAA Tech. Rep., NMFS 90.

Cailliet, G. M., H. F. Mollet, G .G. Pittenger, D. Bedford, and L. J. Natanson.
1992. Growth and demography of the Pacific angel shark (*Squatina californica*), based upon tag returns off California. Aust. J. Mar. Freshwater Res. 43:1313–1330.

Casey, J. G., and L. G. Natanson.
1992. Revised estimates of age and growth of the sandbar shark (*Carcharhinus plumbeus*). Can. J. Fish. Aquat. Sci. 49:1474–1477.

Casey, J. G., H. L. Pratt, and C. E. Stillwell.
1985. Age and growth of the sandbar shark (*Carcharhinus plumbeus*) from the western North Atlantic. Can. J. Fish. Aquat. Sci. 42:963–975.

Compagno, L. J. V.
1984. FAO species catalogue. Vol. 4: Sharks of the world; annotated and illustrated catalogue of shark species known to date. Part 2: Carcharhiniformes. FAO Fish. Synop. 125:251–655.

Davies, D. H., and L. S. Joubert.
1967. Tag evaluation and shark tagging in South African waters. *In* Sharks, skates and rays (P. W. Gilbert, R. F. Mathewson, and D. P. Rall, eds.), p. 111–140. John Hopkins, Baltimore, MD.

Fabens, A. J.
1965. Properties and fitting of the von Bertalanffy growth curve. Growth 29:265–289.

Francis, M. P.
1997. Spatial and temporal variation in the growth rate of elephantfish (*Callorhincus milii*). N.Z. J. Mar. Freshwater Res. 31:9–24.

Francis, M. P., and R. I. C. C. Francis.
1992. Growth rate estimates of New Zealand rig (*Mustelus lenticulatus*). Aust. J. Mar. Freshwater Res. 43:1157–1176.

Francis, M. P., and K. P. Mulligan.
1998. Age and growth of New Zealand school shark, *Galeorhinus galeus*. N.Z. J. Mar. Freshwater Res. 32:427–440.

Francis, M. P., K. P. Mulligan, N. M. Davies and M. P. Beentjes.
1999. Age and growth estimates for New Zealand hapuku, *Polyprion oxygeneios*. Fish. Bull. 97:227–242.

Francis, R. I. C. C.
1995. An alternative mark-recapture analogue of Schnute's growth model. Fish. Res. 23:95–111.
1988. Maximum likelihood estimation of growth and growth variability from tagging data N.Z. J. Mar. Freshwater Res. 22:42–51.

Gelsleichter, J., E. Cortes, C. A. Manire, R. E. Hueter, and J. A. Musick.
1998. Evaluation of toxicity of oxytetracycline on growth of captive nurse sharks, *Ginglymostoma cirratum*. Fish. Bull. 96:624–627.

Grant, C. J., R. L. Sandland, and A. M. Olsen.
1979. Estimation of growth, mortality and yield per recruit of the Australian school shark, *Galeorhinus australis* (Macleay), from tag recoveries. Aust. J. Mar. Freshwater Res. 30:625–637.

Gulland, J. A., and S. J. Holt.
1959. Estimation of growth parameters for data at unequal time intervals. J. Cons. Int. Explor. Mer 25:47–49.

Holden, M. J.
1972. The growth rates of *Raja brachyura*, *R. clavata* and *R. montagui* as determined from tagging data. J. Cons. Int. Explor. Mer 34:161–168.

Last, P. R. and J. D. Stevens.
1994. Sharks and rays of Australia. CSIRO, Melbourne, 513 p.

Manire, C. A., and S. H. Gruber.
1991. Effect of M-type dart tags on field growth of juvenile lemon sharks. Trans. Am. Fish. Soc. 120:776–780.

Marking, L. L., G. E. Howe, and J. R. Crowther.
1988. Toxicity of erythromycin, oxytetracycline, and tetracycline administered to lake trout in water baths, by injection, or by feeding. Prog. Fish. Cult. 50:197–201.

Microsoft.
1999. Excel. Microsoft, Redmond, WA.

Natanson, L. J., J. G. Casey, and N. E. Kohler.
1995. Age and growth of the dusky shark, *Carcharhinus obscurus*, in the western North Atlantic Ocean. Fish. Bull. 93:116–126.

Natanson, L. J., J. G. Casey, N. E. Kohler, and T. Colket.
1999. Growth of the tiger shark, *Galeocerdo cuvier*, in the western North Atlantic based on tag returns and length frequencies; and a note on the effects of tagging. Fish. Bull. 97:944–953.

Natanson, L. J., and N. E. Kohler.
1996. A preliminary estimate of age and growth of the dusky shark *Carcharhinus obscurus* from the south-west Indian Ocean, with comparisons to the western North Atlantic population. S. Afr. J. Mar. Sci. 17:217–224.

Olsen, A. M.
1953. Tagging of school shark (*Galeorhinus galeus* Macleay) in south-eastern Australian waters. Aust. J. Mar. Freshwater Res. 4:95–104.

Pratt, H. L., and J. G. Casey.
1983. Age and growth of the shortfin mako, *Isurus oxyrinchus*, using four methods. Can. J. Fish. Aquat. Sci. 40:1944–1957.
1990. Shark reproductive strategies as a limiting factor in directed fisheries, with a review of Holden's method of estimating growth-parameters. *In* Elasmobranchs as living resources: advances in the biology, ecology, systematics and the status of the fisheries (H. L. Pratt, S. H. Gruber, and T. Taniuchi, eds.), p. 97–109. U.S. Dep. Commer., NOAA Tech. Rep., NMFS 90.

Schnute, J.
1981. A versatile growth model with statistically stable parameters. Can. J. Fish. Aquat. Sci. 38:1128–1140.

Schwartz, F. J.
1983. Shark ageing methods and age estimation of scalloped hammerhead, *Sphyrna lewini*, and dusky, *Carcharhinus obscurus*, sharks based on vertebral rings. U.S. Dep. Commer., NOAA Tech. Rep., NMFS 8:167–174.

Simpfendorfer, C. A.
1993. Age and growth of the Australian sharpnose shark, *Rhizoprionodon taylori*, from north Queensland, Australia. Environ. Biol. Fish. 36:233–241.
1999. Demographic analysis of the dusky shark fishery in south-western Australia. *In* Life in the slow lane: ecology and conservation of long-lived marine animals (J. A. Musick, ed.), p. 149–160. Am. Fish. Soc. Symp. 23, Bethesda, MD.

Simpfendorfer, C. A., J. Chidlow, R. McAuley, and P. Unsworth.
2000. Age and growth of the whiskery shark, *Furgaleus macki*, from southwestern Australia. Environ. Biol. Fish. 58:335–343.

Simpfendorfer, C. A., and K. Donohue.
1998. Keeping the fish in fish'n'chips: research and management of the Western Australian shark fishery. Mar. Freshwater Res. 49:593–600.

STATSOFT
1998. Statistica Volume I: general conventions and statistics. Statsoft, Tulsa, OK.

Stoskopf, M. K.
1993. Shark pharmacology and toxicology. *In* Fish medicine (M. K. Stoskopf, ed.), p. 809–816. W.B. Saunders, Philadelphia, PA.

Tanaka, S.
1990. Age and growth studies on the calcified structures of newborn sharks in laboratory aquaria using tetracycline. *In* Elasmobranchs as living resources: advances in the biology, ecology, systematics and the status of the fisheries (H. L. Pratt, S. H. Gruber, and T. Taniuchi, eds.), p. 189–202. U.S. Dep. Commer., NOAA Tech. Rep., NMFS 90.

Thorson, T. B., and E. J. Lacy Jr.
1982. Age, growth rate and longevity of *Carcharhinus leucas* estimated from tagging and vertebral rings. Copeia 1982:110–116.

Walford, L. A.
1946. A new graphical method of describing the growth of animals. Biol. Bull. 90:141–147.

Wang, Y., M. R. Thomas, and J. F. Somers.
1995. A maximum likelihood approach for estimating growth from tag-recapture data. Can. J. Fish. Aquat. Sci. 52:252–259.

Wass, R. C.
1973. Size, growth, and reproduction of the sandbar shark, *Carcharhinus milberti*, in Hawaii. Pac. Sci. 27:305–318.

Effects of year and region on the abundance and size of age-0 walleye pollock, *Theragra chalcogramma*, in the western Gulf of Alaska, 1985–1988*

Matthew T. Wilson

Alaska Fisheries Science Center
National Marine Fisheries Service, NOAA
7600 Sand Point Way NE
Seattle, Washington 98115
E-mail address: matt.wilson@noaa.gov

Abstract—Effects of year and region on young-of-the-year (age-0) walleye pollock abundance and size were examined by using bottom and midwater trawl collections made during 1985–88. Samples were collected from shelf and coastal areas in three adjacent regions of the western Gulf of Alaska. The primary focus was to examine regional differences in recruitment prediction and annual differences in fish distribution. Fish density was used to indicate abundance, and length was included as a relevant factor in fish production. Year and region significantly interacted as effects on age-0 density. Recruitment prediction was best in the Kodiak Island region, upstream of the main spawning area, where fish densities were high during 1985 and 1988 in relation to 1986 and 1987. On a large scale, fish were evenly distributed every year, except during 1987 when their density increased strongly from east to west. Age-0 length also varied with year and region. This was apparent after accounting for daily increases in mean length (0.09 cm/d). Fish were comparatively small during 1986, intermediate during 1985, and large during 1987 and 1988. Regional differences in fish length were due to a relative abundance of large-size fish around Kodiak Island where the average size was about 0.75 cm larger than elsewhere. Thus, a relative abundance of large individuals in this region was associated with good recruitment prediction. These results are discussed in terms of their relevance to spatial variation in the production of recruits.

Manuscript accepted 5 April 2000.
Fish. Bull. 98:823–834 (2000).

Young-of-the-year (age-0) fish abundance is used in managing temperate marine resources (Goodyear, 1985; Bailey et al., 1986; Johannessen and Tveite, 1989; Sundby et al., 1989; Galaktionov, 1993; Corten[1]). Estimating the abundance of age-0 fish, however, is complicated by their broad and sometimes variable spatial distributions. This variability, which can obscure shifts in distribution from changes in abundance (Olsen and Soldal, 1989; de LaFontaine et al., 1992; Polacheck et al., 1992; Anderson et al., 1995), may affect survival.

Walleye pollock, *Theragra chalcogramma*, are semidemersal gadids that reside in the North Pacific Ocean (Lynde, 1984; Springer, 1992; Wolotira et al., 1993). The National Oceanic and Atmospheric Administration (NOAA) has sought to understand and predict pollock recruitment better because of the commercial importance and recruitment variability of the species (Kendall and Duker, 1998; Hollowed et al.[2]; Wespestad et al.[3]). Much of the research on pollock recruitment has been done in the western Gulf of Alaska (GOA) as part of NOAA's Fisheries Oceanography Coordinated Investigations (FOCI) program (Schumacher and Kendall, 1991; Kendall et al., 1996).

In the GOA, many pollock spawn during early April in southwestern Shelikof Strait (Picquelle and Megrey, 1993) (Fig. 1). This spawning is believed to be primarily responsible for replenishing the GOA pollock stock (Kendall and Picquelle, 1990; Hollowed et al.[2]). FOCI researchers have devised a transport paradigm for young pollock of Shelikof Strait, in which they move with the prevailing currents from the main spawning area in the Strait to shelf and coastal nurseries farther southwest (Schumacher and Kendall, 1995; Kendall et al., 1996). Although some individuals may be carried beyond the shelf, the oceanic North Pacific is not considered an important pollock nursery area (Smith et al., 1984). This pattern of dispersal, hereafter referred to as the FOCI recruit-pathway paradigm, was demonstrated in 1987 (Hinckley et al., 1991), and it has been simulated by a model of larval transport that incorporates detailed physical and biological information (Hermann et al., 1996a,

* Contribution 0262 of the Fisheries Oceanography Coordinated Investigations, 7600 Sand Point Way, NE, Seattle, WA 98115.

[1] Corten, A. 1986. Application of the results from international young fish surveys in fisheries management in recent years. ICES, Doc. C.M. 1986/G:54, 26 p.

[2] Hollowed, A. B., E. Brown, J. Ianelli, P. Livingston, B. Megrey, and C. Wilson. 1997. Walleye pollock. *In* Stock assessment and fishery evaluation report for the groundfish resources of the Gulf of Alaska, p. 31–119. Prepared by the Gulf of Alaska Groundfish Plan Team, North Pacific Fishery Management Council, P.O. Box 103136, Anchorage, AK 99510.

[3] Wespestad, V. G., J. N. Ianelli, L. Fritz, T. Honkalehto, N. Williamson, and G. Walters. 1997. Bering Sea-Aleutian Islands walleye pollock assessment for 1998. *In* Stock assessment and fishery evaluation report for the groundfish resources of the Bering Sea/Aleutian Islands regions, p. 35–102. Prepared by the Bering Sea/Aleutian Islands Plan Team, North Pacific Fishery Management Council, P.O. Box 103136, Anchorage, AK 99510.

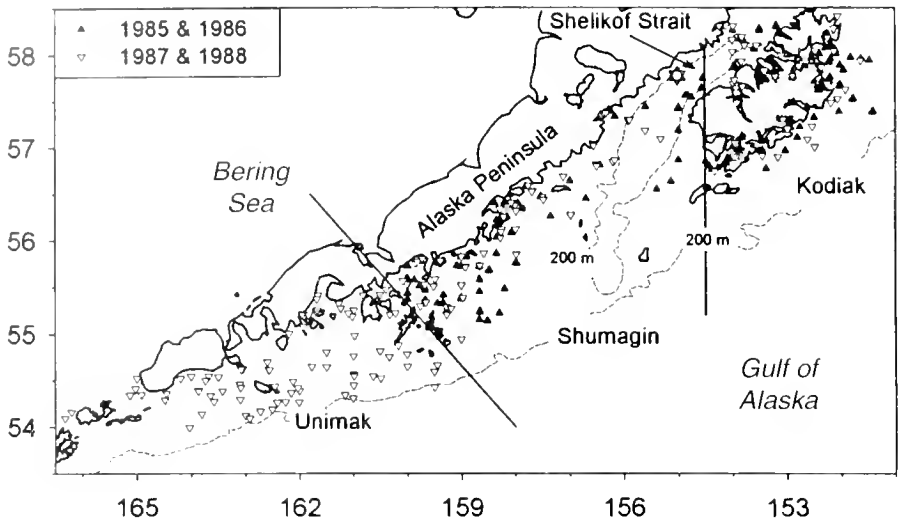

Figure 1

Map of the NMFS exploratory sampling locations for age-0 pollock in the western Gulf of Alaska, August–October, 1985–88. The straight lines delineate the three regions used to group the data geographically. The star (☆), near the head of the arrow pointing to Shelikof Strait, marks the major pollock spawning area.

1996b). Consequently, the shelf area west of Shelikof Strait has received the most attention recently regarding pollock nurseries in the western GOA (Brodeur et al., 1995; Wilson et al., 1996).

Not all observed distributions of age-0 pollock, however, are consistent with the FOCI recruit-pathway paradigm. In 1980–82, some incidental collections of age-0 pollock were made during bottom trawls for shrimp in bays throughout the western GOA. High age-0 densities were found northeast of the main spawning area and led Smith et al. (1984) to conclude that important spawning areas probably exist farther upstream. Small concentrations of pollock eggs, larvae (Kendall and Picquelle, 1990; Dunn et al.[1]), and spawning adults have been found throughout the western GOA (Hirschberger and Smith, 1983; Hollowed et al.[2]; Williamson[3]; Karp[4]; Wilson et al.[5]). This does not, however, preclude the possibility that dispersal of young from Shelikof Strait is more variable than previously thought.

In response to conclusions drawn by Smith et al. (1984), the National Marine Fisheries Service (NMFS) conducted more spatially extensive surveys designed to map age-0 abundance and size (Spring and Bailey[6]). These surveys occurred during 1985–88. The data were included in a compilation of information by Bailey and Spring (1992) primarily to show that year-class strength was set by the age-0 stage. Like Smith et al. (1984), however, Bailey and Spring also found that many juveniles were present in the Kodiak region during some years.

This study presents a re-examination of the 1985–88 survey data. In this study, however, the effects of year and region were evaluated statistically and length was included due to its relevance to recruitment. Among juvenile fish, size often has a positive effect on survival (Sogard, 1997; Hurst and Conover, 1998; Schultz et al., 1998). Emphasis was placed on annual variability within each of three regions owing to interest in developing a recruitment predictor. Emphasis was also placed on within-year regional variability because of the possibility

[1] Dunn, J. R., A. W. Kendall Jr., R. J. Wolotira Jr., J. H. Bowerman Jr., D. B. Dey, A. C. Materese, and J. E. Munk. 1980. Seasonal composition and food web relationships of marine organisms in the nearshore zone—including components of the ichthyoplankton, meroplankton, and holoplankton. Final Report OCSEAP RU551. Northwest and Alaska Fisheries Center, Natl. Mar. Fish. Serv., NOAA, 2725 Montlake Blvd. E., Seattle, WA 98112, 393 p.

[2] Williamson, N. J. 1989. Acoustic-midwater trawl surveys for walleye pollock in the Gulf of Alaska in 1989. *In* Condition of groundfish resources of the Gulf of Alaska in 1989 (T. K. Wilderbuer, ed.), p. 281–311. U.S. Dep. Commer., Alaska Fisheries Science Center, 7600 Sand Point Way NE, Seattle, WA 98115.

[3] Karp, W. A. 1990. Results of echo integration midwater-trawl surveys for walleye pollock in the Gulf of Alaska in 1990. *In* Stock assessment and fishery evaluation report for the 1991 Gulf of Alaska groundfish fishery, Appendix 3, 42 p. Prepared by the Gulf of Alaska Groundfish Plan Team, North Pacific Fishery Management Council, P.O. Box 103136, Anchorage, AK 99510.

[4] Wilson, C., M. Guttormsen, and S. K. de Blois. 1996. Echo integration-trawl survey results for pollock in the Gulf of Alaska during 1996. *In* Stock assessment and fishery evaluation report for the groundfish resources of the Gulf of Alaska, p. 417–443. Prepared by the Gulf of Alaska Groundfish Plan Team, North Pacific Fishery Management Council, P.O. Box 103136, Anchorage, AK 99510.

[5] Spring, S., and K. Bailey. 1991. Distribution and abundance of juvenile pollock from historical shrimp trawl surveys in the western Gulf of Alaska. U.S. Dep. Commer., NOAA Proc. Rep. AFSC 91-18, 66 p.

that the Kodiak region is sometimes a relatively important nursery area despite its position upstream of the main spawning area.

Materials and methods

The data selected for this study comprise the longest time series available from the GOA where the collection method was consistent (Bailey and Spring, 1992; Spring and Bailey[8]). They were collected in late summer (August–October) 1985–88 by the NMFS (Fig. 1, Table 1). The purpose of these surveys was to obtain a coarse picture of the distribution and size of age-0 pollock in the western GOA; These surveys were the first to target age-0 pollock in this area and, as such, were exploratory.

The area surveyed was the continental shelf and bays around Kodiak Island and as far southwest as time allowed (Fig. 1). The Alaska Coastal Current (ACC) flows southwestward through the area but circulation is complicated by sea valleys, islands, and other topographic complexity (Lagerloef, 1983; Reed and Schumacher, 1986; Stabeno et al., 1995). The largest sea valley forms Shelikof Strait and it forms a natural division within the western GOA between eastern and western regions. The Kodiak Island Archipelago is a prominent feature of the eastern region. Smaller islands characterize the western region, which has a relatively broad shelf.

Sampling was accomplished by trawling on echo layers. Echo sign was monitored along predetermined transects. No effort was made to include acoustic data because a preliminary study found no relation between echo sign and age-0 catches (Bailey and Spring, 1992). Samples were collected only during the day, so that the problem of diel vertical fish migration was avoided.

Echo sign believed to be age-0 pollock was sampled by using an 18.6-m high, opening shrimp trawl with steel V-doors (1.5 m × 2.1 m, 568 kg) attached by 18-m bridles. The trawl was made of 3.2-cm stretched-mesh, nylon netting, and a 3-mm mesh liner was inserted into the codend. For bottom samples, a 16.8-m tickler chain was used and the footrope of the net was held above a bottom contact chain by 30-cm chain lengths. For midwater tows, a 363-kg weight was attached to each lower wing to help hold the trawl mouth open, and the chain on the footrope was removed. A netsonde system (BEN-MAR or Furuno) was used to position the trawl vertically at the desired depth. It was not possible to open and close the net at depth. Towing speed and duration averaged about 4.5 km per h and 10–15 min, respectively. At each sampling location, sea surface temperature was measured with a bucket thermometer.

All taxa caught were identified, enumerated, and weighed. At this time of year, age-0 pollock are readily distinguished from older individuals by a clear separation in size (Bailey et al., 1996b; Brodeur and Wilson, 1996a; author's unpubl. data). Fork length was measured to the nearest centimeter. All age-0 pollock were measured except those in large catches, when about 100 randomly selected fish were measured. Length data were missing for five samples, each of which comprised only a few fish.

Table 1

Dates and number of tows made during the 1985–88 NMFS surveys of age-0 pollock in the western Gulf of Alaska. The estimated Gulf-wide abundance for each year class at age-2 from Bailey et al. (1996a) is included as an index of recruitment.

Year	Dates sampled	Number of tows	Recruitment ($\times 10^9$)
1985	21 Aug–10 Sep	113	1.43
1986	3 Sep–9 Oct	95	0.22
1987	12 Aug–20 Sep	118	0.30
1988	18 Aug–10 Sep	80	2.16

The effect of year and region was examined first on age-0 abundance, and then on age-0 length. Finally, year- and region-specific abundance and size estimates were compared with recruitment.

Examination of effects of year and region on age-0 abundance was accomplished in five steps. The first step was to standardize the catch to account for differences in the volume filtered between tows. Volume filtered for each tow was calculated as the trawl mouth area times distance fished. The mouth area was assumed to be 37 m^2 for hauls on the bottom (Wathne, 1977) or 28 m^2 for hauls in midwater (Wilson et al., 1996). No adjustment was made for differences in the depth sampled because most (92%) samples were collected at depths where net dimensions are relatively stable (Wilson et al., 1996). Distance fished was the straight-line distance between two geographic points along which the net was fished at depth. Dividing each age-0 catch by the volume filtered produced fish density (fish per m^3), which was used to indicate abundance. Volume was not converted to sea surface area because of uncertainty about the depth and area represented by each sample. By using density, the assumption of a constant depth and area is explicit, and different values can easily be applied *post-hoc* if an estimate of absolute abundance is desired.

The second step was to adjust for mortality during the 3–5 week survey period. An instantaneous daily mortality rate of 0.014 (Hollowed et al., 1996) was used to adjust each density to the overall median survey date (3 September).

The third step was to account for 22 tows throughout the survey area that were apparently replicates of other tows. Samples were judged to be pseudoreplicates if they were consecutive, were the same type (bottom or midwater), and were within one nautical mile and 50 m depth of each other. The pseudoreplicates were averaged together to give 384 samples from the original 406 trawl hauls.

The fourth step was to group fish densities by geographic area by using the three regions defined by Bailey and Spring (1992). A minor adjustment to this stratification scheme involved moving the delineation between the Unimak and Shumagin regions farther west to better reflect annual differences in sampling effort (Fig. 1). The Unimak Island region was surveyed only during 1987–88. Thus, samples from the area upstream of the main spawn-

ing site were separated from samples collected farther downstream, and the difference in large-scale coverage was accommodated.

Finally, statistical tests were conducted to examine effects of year and region on age-0 density, which was not straightforward owing to the occurrence of many zeros and a few very large values in the catch data. Four different procedures were employed and the results were compared. All statistical tests were accomplished with SYSTAT for Windows (Wilkinson, 1996).

The first procedure was a two-way analysis of variance (ANOVA) of two different transformations of all four years of data. One ANOVA was based on a log-transformation (Sparholt et al., 1991) ($\log_{10}$(density)+0.00001, nonzero catches ranged from 0.00001–0.6 fish per m^3) and the other was based on rank-transformed data (Conover, 1980). Neither transformation, however, removed the spike of zeros in the frequency histogram of densities and thus made the requisite assumption of normality tenuous. To avoid empty cells data from the Unimak region were omitted; they were collected only during 1987–88.

The second procedure was a distribution-free, nonparametric test to again look for effects of year and region (Methven and Bajdik, 1994). Unlike Methven and Bajdik (1994), however, the age-0 data were not paired; therefore the signed rank test was replaced by the Kruskal-Wallis test. Because this is a one-way test, subsets of the data were selected so that the effect of the first factor was examined within a level of the second factor (e.g. year within a region) and *vice-versa* (e.g. region within a year) (Valle et al., 1999). In all, seven tests were run. Significance of the outcome for each test was based on the Bonferroni-corrected alpha level of 0.05.

The third and fourth procedures were conducted primarily as a means to circumvent the zero-catch problem but also because of differences in the information conveyed by zero and nonzero catches (Pennington, 1983; Randa, 1984). Zero catches indicate absence, and nonzero catches indicate presence as well as some measure of abundance.

The third procedure involved chi-square tests to test whether the presence or absence of age-0 pollock was associated with year or region. Annual or regional differences in age-0 frequency of occurrence indicate a change in fish patchiness, or a change in the ability to target them; both may be associated with a change in abundance. It was necessary to conduct one chi-square test for each region to examine annual differences and then for each year to examine regional differences. Thus, Bonferroni corrections were again necessary.

The fourth procedure was a two-way ANOVA test of effects of region and year on nonzero densities. The nonzero densities appeared normally distributed after being $\log_{10}$-transformed. Again, the Unimak data were omitted.

A year-region interaction term was included in the ANOVA tests of the first and fourth procedures. Significance of the interaction term indicates that annual differences vary by region, or that regional differences vary by year. The former identifies regions with high annual variability; whereas the latter implies annual variation in fish distribution. Significance of the interaction term determined which multiple comparison test was used *post hoc*. If it was not significant, a Bonferroni multiple comparison test was used for comparing levels of significant main effects. If it was significant, Fisher's least significant difference (LSD) test was preferred. In SYSTAT, the LSD test does not automatically correct for the number of comparisons being made (Wilkinson, 1996). This correction was desirable because only a subset of all possible pair-wise comparisons was of interest. Only comparisons among regions within year and among years within region were of interest, those involving different years and regions (i.e. 1985 Kodiak versus 1986 Shumagin) were excluded. A Bonferroni correction was then applied to the remaining comparisons to maintain an overall 0.05 alpha level.

Examination of effects of year and region on age-0 length was accomplished by using a two-way analysis of covariance (ANCOVA). An ANCOVA was necessary to account for variation in length due to differences in the collection day-of-year (expressed as the number of days since 1 January). The first ANCOVA was used to examine data collected from the Kodiak and Shumagin regions during all four years. The second ANCOVA was conducted with just the 1987 and 1988 data to compare lengths among all three regions. The covariate was not allowed to interact with the main effects (ie. slope homogeneity was assumed rather than tested) owing to the short duration of collecting in some regions and years in relation to the variation in mean length per haul. As in Anderson et al. (1995), the dependant variable was mean length per haul rather than individual length measurements; this variable simplified the model but allowed no within-haul variability. Mean size was weighted by mortality-adjusted fish density.

The relationship between annual estimates of age-0 density or size and recruitment was examined graphically because there were insufficient degrees of freedom for a global significance test of correlation. Pollock recruitment was indicated by the Gulf-wide abundance of age-2 individuals (Bailey et al., 1996a). No attempt was made to account for autocorrelation in this time series because pollock exhibit low autocorrelation in recruitment (Hollowed et al., 1998).

Results

Overall, 406 trawl samples were collected yielding 384 density estimates (zero and nonzero catches) and 335 estimates of mean length (Table 2). Stations were occupied from west to east, except in 1985 when sampling progressed from east to west and then doubled back to end near northeast Kodiak Island. Sampling around Kodiak Island was mostly over the inner shelf and in bays (Fig. 1). Coverage of the outer shelf was best farther west, between 158° and 164°W longitude. Sample depth varied considerably, and it appears that the daytime vertical position of age-0 pollock was also quite variable (Fig. 2).

Abundance

Results from each of the four statistical procedures consistently indicated that year and region interact in their

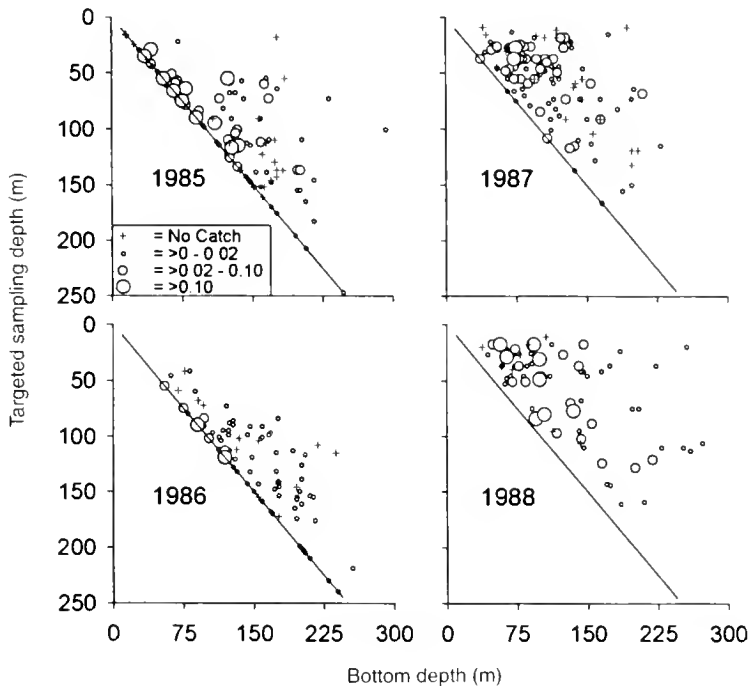

Figure 2

The vertical distribution of age-0 pollock density in the western Gulf of Alaska, August–October, 1985–88. Symbol size indicates the mortality-adjusted number of fish/m^3. The diagonal line indicates bottom depth.

effect on age-0 density. Annual differences were always limited to the Kodiak region where fish densities were high during 1985 and 1988 in relation to 1986 and 1987 (Table 2). Within other regions, annual differences were not significant. As to within-year patterns, regional differences were mostly limited to 1987 when fish density increased strongly from east to west (Fig. 3, Table 2). The distribution in each other year was more even. For brevity, only results from the first statistical procedure are tabulated.

In the first procedure, significant year-region interaction was indicated by each two-way ANOVA of transformed fish densities (Table 3). Fisher's LSD test indicated annual differences only in the Kodiak region (Table 4), where age-0 density was relatively high during 1985 and 1988 (Table 2). The LSD test also indicated regional differences, but only during 1987 or 1988, depending upon transformation (Table 4). When log-transformed, the regional effect was associated with low age-0 densities in the Kodiak region during 1987. When rank-transformed, it was associated with high densities in the same region but during 1988. The Unimak region was excluded from these tests.

In the second procedure, only two of the seven Kruskal-Wallis tests rejected the null hypothesis of equal fish densities. The first indicated an annual effect within the Kodiak region (Kruskal-Wallis test statistic=25.31, $P<<0.0001$). The second indicated a regional effect within 1987, which included the Unimak region (Kruskal-Wallis test statistic=32.24, $P<<0.0001$).

In the third procedure, only one chi-square test outcome was significant (chi-square=15.19, $P=0.0005$). During 1987, the frequency of occurrence around Kodiak Island was low (65%) in relation to occurrences in the Unimak region (98%) (Table 2).

In the fourth procedure, the two-way ANOVA of nonzero densities revealed a significant year-region interaction (df=3,241, $F=4.462$, $P=0.005$). Fisher's LSD test indicated that all differences occurred within the Kodiak region where nonzero density was relatively high during 1985 and 1988 (Table 2).

Length

Overall, 35,530 age-0 pollock were measured. They were collected from 335 trawl hauls and ranged from 3 to 13 cm FL. Significant effects of year and region were detected after accounting for a day-of-year effect (Table 5).

Daily increases in mean length per haul averaged 0.090 cm (Fig. 4), which is within the range of published growth rates for these fish (0.6–1.2 mm/d) (Bailey et al., 1996b). Two samples had unusually low mean length per haul (in 1986 and 1987) and were from bays; these represented few fish and so had little effect on the fitted lines.

Annual differences in length were due to a comparatively small mean size during 1986, a medium size during 1985, and large sizes during 1987 and 1988 (Fig. 4, Table 2). A Bonferroni multiple comparison test indicated that 1985 and

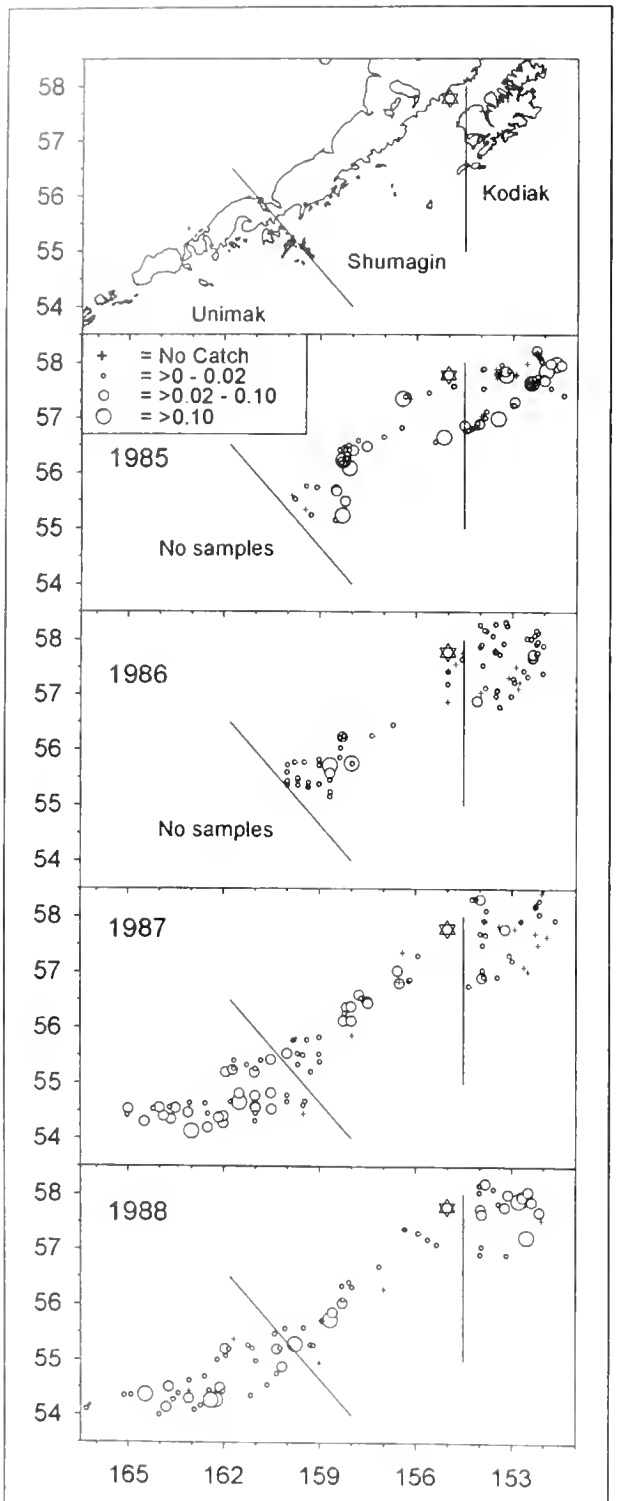

Figure 3

The geographic distribution of age-0 pollock density in the western Gulf of Alaska, August–October, 1985–88. Symbol size indicates the mortality-adjusted number of fish/m^2. The star (☆) marks the major pollock spawning area in Shelikof Strait.

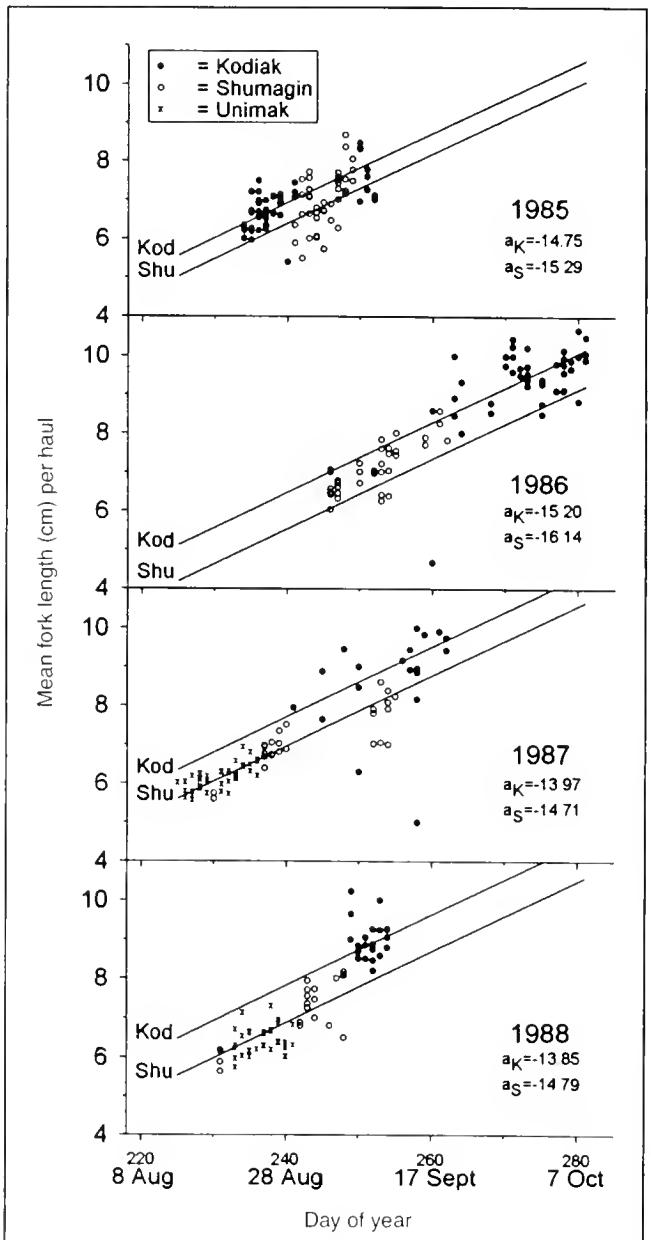

Figure 4

Age-0 pollock mean fork length per haul versus collection date for each year sampled August–October, 1985–88. Symbol type indicates region (see Fig. 1). Lines represent the least-squares linear fit from the ANCOVA of Kodiak and Shumagin data (slope=0.090; intercepts, a_K and a_S, respectively, are given).

1986 were each significantly (P<0.05) different from all other years. The year-region interaction term was marginally not significant (Table 5). A noteworthy correspondence between mean size and water temperature is apparent in Table 2.

Regional differences were due to a relative abundance of large-size fish in the Kodiak region. These fish were on average about 0.5–1.0 cm larger than the fish from elsewhere

Table 2

Catch and sample statistics, by region and year, for age-0 pollock collected in the western Gulf of Alaska during 1985–88. Mean $\log_{10}$, mean fork length (FL), mean sample depth, and mean sea-surface temperature were based on samples where age-0 pollock were caught. As stated in the text, fish density and length were adjusted to the median survey date (3 Sept) to account for differences in collection date. (Freq. occur.=frequency of occurrence).

Year class	Region	Total sample number	Freq. occur. (%)	Mean $\log_{10}$ (fish/m^3)	Mean (fish/m^3)	Median (fish/m^3)	Mean FL (cm)	Mean depth (m)	Mean temp. (°C)
1985	Kodiak	62	77	−2.19	0.0303	0.0038	7.5	101	10.5
	Shumagin	41	90	−2.19	0.0496	0.0073	6.9	88	10.9
1986	Kodiak	52	83	−2.84	0.0060	0.0008	7.0	136	9.3
	Shumagin	40	88	−2.74	0.0147	0.0015	6.1	116	10.8
1987	Kodiak	37	65	−3.06	0.0046	0.0001	8.2	75	11.2
	Shumagin	29	83	−2.32	0.0180	0.0053	7.5	70	11.6
	Unimak	44	98	−1.86	0.0302	0.0264	7.6	40	11.2
1988	Kodiak	20	95	−1.76	0.0544	0.0225	8.4	95	10.8
	Shumagin	23	83	−2.59	0.0242	0.0024	7.4	64	11.7
	Unimak	36	92	−2.12	0.0263	0.0063	7.7	35	11.0

(Table 2). The data from 1985 clearly show how the Kodiak and Shumagin regions contrast in terms of fish size (Fig. 4). Note that the difference in mean size coincides roughly with regional delineation. On closer inspection, it was apparent that large fish tended to concentrate near the northeast- and east-side of Kodiak Island in 1985 and 1988. Thus, size variability appears to also exist on a finer geographic scale. In Figure 4, most mean lengths from the Shumagin region in 1986 are above their respective line because one sample of relatively small fish accounted for almost 30% of the total density. During 1987 and 1988, means from the Unimak region were not different from those in the Shumagin region (Bonferroni, P=0.054) but they were different from the Kodiak group (Bonferroni, P=0.003). This difference was indicated by a second ANCOVA, and a second *post-hoc* multiple comparison test, wherein day (df=1 and 156, F=196, P<0.001) and region (df=2 and 157, F=22, P<0.001) were the only significant effects.

To address a possible association between regional mean size and mean sample depth (Table 2), the ANCOVA of 1985–88 data was rerun with sample depth as a third effect. Sample depth was included as a categorical effect with two levels: 50–100 and 100–150 m. Only 174 mean length estimates were used because the number of estimates at other depths was low or zero in some regions and years. Results were similar to the first run and there was no significant depth effect. Depth was neither significant by itself (df=1 and 157, F=0.118, P=0.731) nor did it interact with other effects (P>0.05). The difference in fish size between the Kodiak and Shumagin regions was therefore not likely due to differences in sampling depths.

Recruitment

Future development of a direct relationship between age-0 abundance and recruitment seems most likely for the Kodiak region (Fig. 5). In this region, linear relationships were evident for the average, log-transformed, nonzero density and for the overall mean density. There was no convincing evidence of a direct linear relationship between mean length and recruitment.

Table 3

Results from two ANOVA tests used to examine year (1985–88) and region (Kodiak versus Shumagin) effects on age-0 pollock density in the western Gulf of Alaska. The first ANOVA was on log-transformed densities and the second was on rank-transformed densities.

Source	df	MS	F	P
ANOVA, log-transformed fish densities				
year	3	9.072	5.3893	0.0013
region	1	0.805	0.4782	0.4898
year × region	3	9.204	5.4679	0.0011
error	296	1.683		
ANOVA, rank-transformed fish densities				
year	3	70809	6.3609	0.0003
region	1	1374	0.1234	0.7256
year × region	3	66291	5.9550	0.0006
error	296	11132		

Discussion

The geographic distribution of age-0 fish integrates the effects of dispersal of young from spawning areas and of spatial differences in mortality; therefore, it helps reveal

Table 4

Probabilities from Fisher's LSD tests, which followed the ANOVA tests summarized in Table 3. The hypothesis that means of transformed age-0 densities are equal was rejected if $P<0.00313$. This reflects a Bonferroni correction of the 0.05 overall alpha level (e.g. 0.05/16). Significantly different pairs of means are indicated by probabilities in bold.

	Comparison by year						Comparison by region
	Kodiak region			Shumagin region			
	1985	1986	1987	1985	1986	1987	Kodiak vs. Shumagin
P-values, log-transformed fish densities							
1985							0.16537
1986	0.11119			0.05592			0.46505
1987	**0.00079**	0.06104		0.31479	0.45564		**0.00307**
1988	0.00716	**0.00018**	**0.00000**	0.10872	0.97748	0.53177	0.00665
P-values, rank-transformed fish densities							
1985							0.21982
1986	0.03708			0.02599			0.49393
1987	**0.00159**	0.21323		0.41495	0.22086		0.00441
1988	**0.00294**	**0.00001**	**0.00000**	0.11894	0.73141	0.45407	**0.00253**

Table 5

ANCOVA results of region, year and day effects on the mean length per haul of age-0 pollock collected from two regions, Kodiak and Shumagin, in the western Gulf of Alaska during August–October, 1985–88. Length was weighted by fish density.

Source	df	MS	*F*	*P*
Year	3	35036	73.907	0.0000
Region	1	37407	78.907	0.0000
Year · Region	3	1211	2.555	0.0560
Day	1	144833	305.518	0.0000
Error	247	474		

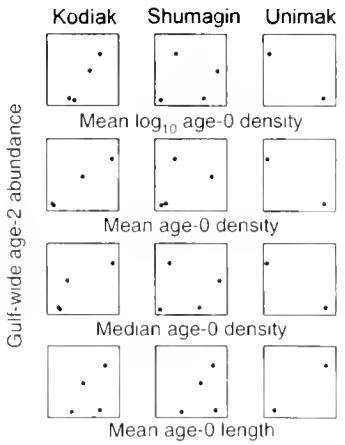

Figure 5

Gulf-wide age-2 pollock abundance (from Table 1) plotted against the regional indices of age-0 abundance and size (from Table 2) for the 1985–88 year classes of pollock in the Gulf of Alaska.

major recruit pathways. In the GOA, the largest aggregation of spawning pollock occurs in Shelikof Strait; and the FOCI recruit-pathway paradigm shows that larvae are carried southwestward from this area (Hinckley et al., 1991; Hermann et al., 1996a, 1996b; Kendall et al., 1996). However, the widespread occurrence of age-0 pollock throughout the areas surveyed, and probably beyond, indicates that the FOCI recruit-pathway paradigm needs to account for more complex dispersal, multiple spawning areas, and possible geographic differences in mortality.

The FOCI recruit-pathway paradigm was expanded to the early juvenile stage by Hinckley et al. (1991) with the inclusion of age-0 distribution data. Their study, however, included only data from 1987. It is now apparent that the age-0 distribution during 1987 was more geographically skewed than in other years during 1985–88. Perhaps this skewed distribution relates to sea surface drift in the greater GOA, which may have been rapid during 1987 (Ingraham et al., 1998), although larval distributions in the Shelikof Strait vicinity seemed normal (Kendall and Picquelle, 1990; Hinckley et al., 1991; Bailey et al., 1996c). Regardless, the 1985 and 1988 age-0 distribution data suggest that the FOCI recruit-pathway paradigm should include the Kodiak Island vicinity as part of the principal nursery for young pollock in the GOA.

Deep countercurrent flows (Reed et al., 1987; Stabeno et al., 1995), eddies (Schumacher and Kendall, 1995), reten-

tion near shore, and possible directed movements by juveniles all complicate "typical" southwestward dispersal of pollock eggs and larvae from Shelikof Strait. For example, the high age-0 densities around Kodiak Island during 1985 may be explained by high larval abundances upstream of the main spawning area (Kendall and Picquelle, 1990), which in turn may reflect northeastward transport of eggs at depth in the countercurrent. On the other hand, the high age-0 densities around Kodiak during 1988 are more difficult to explain. Countercurrent flows have been detected off the Gulf-side of Kodiak Island (Musgrave et al., 1992) but historically this is not an area of high egg or larval abundance. Furthermore, widespread occurrences of high age-0 density suggest that dispersal was both downstream and upstream, or that some fish originated from elsewhere.

The existence of multiple spawning areas further complicates our understanding of pollock recruitment pathways. Sporadic survey effort by the NMFS indicates that spawning occurs at a number of different locations throughout the western GOA between Prince William Sound and Unimak Pass. The percentage of pollock biomass in non-Shelikof spawning areas was 10, 21, 19, 29, and 14% of the total in all areas surveyed in 1989, 1990, 1994–96, respectively (Williamson[5]; Karp[6]; Wilson et al.[7], and references therein). These estimates are conservative because not all known spawning areas were surveyed each year and survey timing may not have coincided with peak spawning. In addition, other surveys of pollock, summarized by Bechtol,[9] indicate that the biomass of prespawning aggregations in Prince William Sound ranged from 28,855 to 114,344 metric tons during 1995, 1997, and 1998. Although these surveys occurred after 1988 and conditions may have changed during the intervening period, it seems likely that at least some age-0 pollock were spawned in areas outside of Shelikof Strait. Estimating relative production, however, is difficult because it is impossible to identify where individual recruits were spawned and because of spatial variations in the processes that remove prerecruits from the GOA. As indicated by studies of other species (Pulliam and Danielson, 1991; Frank, 1992), the relationships among these different spawning groups could be very complex.

The use of age-0 densities in the Kodiak region in forecasting recruitment suggests that "atypical" dispersal of young from Shelikof Strait and production of fish from other spawning areas may be relevant factors in understanding GOA pollock recruitment. Admittedly, this use is based on only a few years of data. However, Smith et al. (1984) reported age-0 densities for the 1980–82 year classes in some bays within the Kodiak region that corresponded with year-class strength estimates. Furthermore, if sampling method is ignored, a time series of mean age-0 density near northeast Kodiak Island is available for the 1980–88 year classes, except 1983, and it corresponds reasonably well with recruitment (Pearson, r=0.74, P=0.04, n=8) (author's unpubl. data). The Shumagin and Unimak regions were comparatively less promising for predicting recruitment, although the relative strength of the 1985 and 1988 year classes was indeed evident among the Shumagin densities. Age-0 fish from both the Kodiak and Shumagin regions may move into Shelikof Strait during winter as indicated by large aggregations of age-1 fish observed there during early spring (McKelvey, 1996). This movement probably involves a relatively constant proportion of the Kodiak and Shumagin age-0 populations because their abundance as age-1 fish in Shelikof Strait continues to be indicative of recruitment (McKelvey, 1996; Guttormsen and Wilson[10]). Farther southwest, in the Unimak region, juveniles may leave the GOA sometime after their first summer. This movement may explain why age-0 densities in the Unimak region during 1987 and 1988 had no relation to recruitment despite a 7-fold variation in subsequent year-class strength.

Given their relevance to recruitment, age-0 pollock around Kodiak Island warrant closer consideration. As previously discussed, some may come from Shelikof Strait. Others may move downstream from spawning areas such as those in or near Prince William Sound and Resurrection Bay (Nelson and Nunnallee, 1985; Muter and Norcross, 1994; Norcross and Frandsen, 1996; Karp[6]). Downstream drift is probable given the distance, currents (Schumacher and Reed, 1980; Stabeno et al., 1995), spawning time (Muter and Norcross, 1994), and estimated age-0 ages.[11] Drift from eastern areas may be relatively important to establishing age-0 populations along the upstream- and Gulf-side of Kodiak Island when the influx of Shelikof fish is low. Retention of young along this part of Kodiak Island may be facilitated by shoreward flows and vortices created by topographical influences on the prevailing current (Lagerlof, 1983; Dunn et al.[4]). Local spawning is another possible source of age-1 pollock as evidenced by adults in prespawning condition in Marmot Bay, which is on northeast Kodiak Island (Karp[6]; Williamson[12]).

The relatively large size of many age-0 fish may reflect favorable conditions in the Kodiak Island vicinity because size is generally regarded as having a positive effect on survival. Walters et al. (1985) first reported a southwest-to-northeast increase in age-0 size; however, a more rigorous

[9] Bechtol, W. R. 1998. Prince William Sound walleye pollock: current assessment and 1999 management recommendations. Regional Information Report No. 2A98-41, 25 p. Alaska Department of Fish and Game, Division of Commercial Fisheries Management and Development, 333 Raspberry Rd., Anchorage, AK 99518.

[10] Guttormsen, M., and C. Wilson. 1998. Echo integration-trawl survey results for walleye pollock in the Gulf of Alaska during 1998. *In* Stock assessment and fishery evaluation report, p. 509–530. Prepared by the Gulf of Alaska Groundfish Plan Team, North Pacific Fishery Management Council, P.O. Box 103136, Anchorage, AK 99510.

[11] Mean age of age-0 pollock in the Kodiak region during 1985–88 ranged from 127 to 143 d. These estimates are based on age-0 length and length-age relationships for the same age-0 populations (Bailey et al., 1996b), to which mortality-adjusted density weights were applied.

[12] Williamson, N. 1999. Personal commun. National Marine Fisheries Service, 7600 Sand Point Way NE, Seattle, WA 98115.

comparison with their study is complicated by differences in gear and survey strategy. One possible explanation for the effect of region on fish size is growth rate variability. Growth rates, estimated from larval and juvenile length-at-age data, were found to increase from southwest to northeast, at least during 1987 (Yoklavich and Bailey, 1990; Brown and Bailey, 1992). Prey quality (Merati and Brodeur, 1996), and physical conditions (Strickland and Sibley, 1989) have also been observed to vary, the supposition being that the Kodiak Island area is a richer nursery habitat than are more southwestern areas. Variation in time of spawning is another possibility; particularly in 1986 and 1988, when regional differences in growth were not evident (Bailey et al., 1996b). It appears, however, that time of spawning throughout the western GOA is fairly synchronous (Picquelle and Megrey, 1993; Muter and Norcross, 1994), except near the Shumagin Islands were it happens about one month earlier (Wilson et al.[7]). Size-related migration and mortality are other possible effects on fish size but evidence is lacking.

Spatial differences in size may translate into spatial differences in mortality. In a review of size-selective mortality among juvenile fishes, Sogard (1997) identified over-winter mortality and predation as major size-selective processes. These mortality vectors may be particularly strong because the first-winter growth of juvenile pollock in the GOA is negligible (Brodeur and Wilson, 1996a), and predation is prevalent (Brodeur and Bailey, 1996). Thus, geographic differences in age-0 size may contribute a spatial component to year-class strength determination. The poor relationship between age-0 size and year-class strength, however, suggests that age-0 size is a minor factor, at least in terms of determining relative recruitment among year classes.

The practice of targeting echo layers was a drawback of these data. This practice has been shown to bias estimates of fish density (Wilson et al., 1996), but its effect on distribution patterns is uncertain. It is possible that the area represented by mean fish density varied with year and region, thereby causing density to be a poor indicator of abundance. Estimates of year- and region-specific density were, however, closely related to the absolute abundance estimates of Bailey and Spring (1992) (Pearson, r=0.78, P=0.008, n=10). On the positive side, the practice of targeting echo sign does reduce the effort needed to collect biological samples (Brodeur and Wilson, 1996b), but this must be carefully weighed against possible adverse effects.

In summary, age-0 pollock appear to have been evenly distributed throughout much of the western GOA during 1985–88, except during 1987 when a strong, east-to-west increase in fish density was observed. The Kodiak region was an important pollock nursery despite its position upstream from what is presumed to be the most important spawning area in the GOA. The Kodiak region was particularly well suited as a recruitment predictor owing, perhaps, to a relative abundance of large-size individuals. Questions emerged about annual variability in the origin and dispersal of young pollock, and regarding the possibility that geographic effects on survival or retention could affect the relative production of GOA recruits among different spawning areas.

Acknowledgments

I thank many people at the Alaska Fisheries Science Center for assistance with this project, in particular Kevin Bailey, Ric Brodeur, Mike Canino, Anne Hollowed, and Art Kendall for commenting on earlier drafts of this manuscript. A great deal of statistical assistance was provided by Kathy Mier and Susan Picquelle. Additional comments by Olav Rune Godø (Institute of Marine Research, Bergen, Norway), the AFSC Publications Unit, Sarah Fisher, and three anonymous reviewers are gratefully acknowledged. Finally, I wish to thank Herb Shippen for overseeing the age-0 surveys, which occurred before my time at the AFSC.

Literature cited

Anderson, J. T., E. L. Dalley, and J. E. Carscadden
1995. Abundance and distribution of pelagic 0-group cod (*Gadus morhua*) in Newfoundland waters: inshore versus offshore. Can. J. Fish. Aquat. Sci. 52:115–125.

Bailey, K. M., R. C. Francis, and K. F. Mais.
1986. Evaluating incidental catches of 0-age Pacific hake to forecast recruitment. CalCOFI Rep. 27:109–112.

Bailey, K. M., R. D. Brodeur, and A. B. Hollowed
1996a. Cohort survival patterns of walleye pollock, *Theragra chalcogramma*, in Shelikof Strait, Alaska: a critical factor analysis. Fish. Oceanogr. 5(suppl. 1):179–188.

Bailey, K. M., A. L. Brown, M. M. Yoklavich, and K. L. Mier.
1996b. Interannual variability in growth of larval and juvenile walleye pollock *Theragra chalcogramma* in the western Gulf of Alaska, 1983–91. Fish. Oceanogr. 5(suppl. 1):137–147.

Bailey, K. M., S. J. Picquelle, and S. M. Spring.
1996c. Mortality of larval walleye pollock *Theragra chalcogramma* in the western Gulf of Alaska, 1988–91. Fish. Oceanogr. 5(suppl. 1):124–136.

Bailey, K. M., and S. M. Spring.
1992. Comparison of larval, age-0 juvenile and age-2 recruit abundance indices of walleye pollock, *Theragra chalcogramma*, in the western Gulf of Alaska. ICES J. Mar. Sci. 49:297–304.

Brodeur, R. D., and K. M. Bailey.
1996. Predation on the early life stages of marine fish: a case study on walleye pollock in the Gulf of Alaska. *In* Survival strategies in early life stages of marine resources (Y. Watanabe, Y. Yamashita, and Y. Oozeki, eds.), p. 245–260. A. A. Balkema, Rotterdam, Netherlands, 367 p.

Brodeur, R. D., M. S. Busby, and M. T. Wilson.
1995. Summer distribution of early life stages of walleye pollock, *Theragra chalcogramma*, and associated species in the western Gulf of Alaska. Fish. Bull. 93:603–618.

Brodeur, R. D., and M. T. Wilson.
1996a. A review of the distribution, ecology, and population dynamics of age-0 walleye pollock in the Gulf of Alaska. Fish. Oceanogr. 5(suppl. 1):148–166.
1996b. Mesoscale acoustic patterns of juvenile walleye pollock (*Theragra chalcogramma*) in the western Gulf of Alaska. Can. J. Fish. Aquat. Sci. 53(9):1951–1963.

Brown, A. L., and K. M. Bailey.
1992. Otolith analysis of juvenile walleye pollock (*Theragra chalcogramma*) from the western Gulf of Alaska. Mar. Biol. 112:23–30.

Conover, W. J.
1980. Practical nonparametric statistics, 2nd ed. John Wiley & Sons, New York, NY, 493 p.

de Lafontaine, Y.
1992. A workshop on juvenile stages: searching for the missing link in fisheries research. *In* Juvenile stages: the missing link in fisheries research (Y. de Lafontaine, T. Lambert, G. R. Lilly, W. D. McKone, and R. J. Miller, eds.), p. 3–11. Can. Tech. Rep. Fish. Aquat. Sci. 1890.

Frank, K. T.
1992. Demographic consequences of age-specific dispersal in marine fish populations. Can. J. Fish. Aquat. Sci., 49:2222–2231.

Galaktionov, G. Z.
1993. Assessment of abundance of 0-age juveniles of the Cape hake, *Merluccius capensis*. J. Ichthyol. 33(8):128–133.

Goodyear, C. P.
1985. Relationship between reported commercial landings and abundance of young striped bass in Cheasapeake Bay, Maryland. Trans. Am. Fish. Soc. 114:92–96.

Hermann, A. J., S. H. Hinckley, B. A. Megrey, and P. J. Stabeno.
1996a. Interannual variability of the early life history of walleye pollock near Shelikof Strait as inferred from a spatially explicit, individual-based model. Fish. Oceanogr. 5(suppl. 1):39–57.

Hermann, A. J., W. C. Rugen, P. J. Stabeno, and N. A. Bond.
1996b. Physical transport of young pollock larvae (*Theragra chalcogramma*) near Shelikof Strait as inferred from a hydrodynamic model. Fish. Oceanogr. 5(suppl. 1):58–70.

Hinckley, S., K. M. Bailey, S. J. Picquelle, J. D. Schumacher, and P. J. Stabeno.
1991. Transport, distribution, and abundance of larval and juvenile walleye pollock (*Theragra chalcogramma*) in the western Gulf of Alaska. Can. J. Fish. Aquat. Sci. 48:91–98.

Hirschberger, W. A., and G. B. Smith.
1983. Spawning of twelve groundfish species in the Alaska and Pacific Coast regions, 1975–81. U.S. Dep. Commer., NOAA Tech. Memo. NMFS F/NWC-44, 50 p.

Hollowed, A. B., K. M. Bailey, and R. D. Brodeur.
1996. Natural mortality estimates of juvenile walleye pollock, *Theragra chalcogramma*, in the Gulf of Alaska. *In* Ecology of juvenile walleye pollock (R. D. Brodeur, P. A. Livingston, T. R. Loughlin, and A. B. Hollowed, eds.), p. 218–219. U.S. Dep. Commer., NOAA Tech. Rep. NMFS 126.

Hollowed, A. B., S. R. Hare, and W. S. Wooster.
1998. Pacific basin climate variability and patterns of northeast Pacific marine fish poduction. *In* Proceedings 'Aha Huliko'a (Biotic impacts of extratropical climate variability in the Pacific), University of Hawaii, January 25–29, 1998 (G. Holloway, P. Muller, and D. Henderson, eds.), p. 89–104. Univ. Hawaii, SOEST Spec. Publ.

Hurst, T. P, and D. O. Conover.
1998. Winter mortality of young-of-the-year Hudson River striped bass (*Morone saxatilis*): size-dependent patterns and effects on recruitment. Can. J. Fish. Aquat. Sci. 55:1122–1130.

Ingraham, W. J., Jr., C. C. Ebbesmeyer, and R. A. Himrichsen.
1998. Imminent climate and circulation shift in northeast Pacific Ocean could have major impact on marine resources. Eos, Trans. Am. Geo. Union. 79(16):197,199, and 201.

Johannessen, T., and S. Tveite.
1989. Influence of various physical environmental factors on 0-group cod recruitment as modelled by partial least-squares regression. Rapp. P.-V. Reun. Cons. Int. Explor. Mer 191:296–302.

Kendall, A. W., Jr., and G. J. Duker.
1998. The development of recruitment fisheries oceanography in the United States. Fish. Oceanogr. 7(2):69–88.

Kendall, A. W., Jr., and S. J. Picquelle.
1990. Egg and larval distributions of walleye pollock *Theragra chalcogramma* in Shelikof Strait, Gulf of Alaska. Fish. Bull. 88:133–154.

Kendall, A. W., Jr., J. D. Schumacher, and S. Kim.
1996. Walleye pollock recruitment in Shelikof Strait: applied fisheries oceanography. Fish. Oceanogr. 5(suppl. 1):4–18.

Lagerloef, G.
1983. Topographically controlled flow around a deep trough transecting the shelf off Kodiak Island, Alaska. J. Phys. Oceanogr. 13:139–146.

Lynde, C. M.
1984. Juvenile and adult walleye pollock of the eastern Bering Sea: literature review and results of ecosystem workshop. *In* Proceedings of the workshop on walleye pollock and its ecosystem in the eastern Bering Sea (D. H. Ito, ed.), p. 43–108. U.S. Dep. Commer., NOAA Tech. Memo. NMFS F/NWC-62.

McKelvey, D. R.
1996. Juvenile walleye pollock, *Theragra chalcogramma*, distribution and abundance in Shelikof Strait—what can we learn from acoustic survey results? *In* Ecology of juvenile walleye pollock (R. D. Brodeur, P. A. Livingston, T. R. Loughlin, and A. B. Hollowed (eds.), p. 25–34. U.S. Dep. Commer., NOAA Tech. Rep. NMFS 126.

Merati, N., and R. Brodeur.
1996. Feeding habits and daily ration of juvenile walleye pollock in the western Gulf of Alaska. *In* Ecology of juvenile walleye pollock (R. D. Brodeur, P. A. Livingston, T. R. Loughlin, and A. B. Hollowed, eds.), p. 65–79. U.S. Dep. Commer., NOAA Tech. Rep. NMFS 126.

Methvan, D. A., and C. Bajdik.
1994 Temporal variation in size and abundance of juvenile Atlantic cod (*Gadus morhua*) at an inshore site off eastern Newfoundland. Can. J. Fish. Aquat. Sci. 51:78–90.

Musgrave, D. L., T. J. Weingartner, and T. C. Royer.
1992. Circulation and hydrography in the northwestern Gulf of Alaska. Deep-Sea Research 39(9):1499–1519.

Muter, F. J., and B. L. Norcross.
1994. Distribution, abundance, and growth of larval walleye pollock, *Theragra chalcogramma*, in an Alaskan fjord. Fish. Bull. 92:579–590.

Nelson, M. O., and E. P. Nunnallee.
1985. Acoustic-midwater trawl surveys of spawning walleye pollock in the Shelikof Strait region, 1980–81 and 1983–84. *In* Condition of groundfish resources of the Gulf of Alaska as assessed in 1984 (R. L. Major, ed.), p. 179–206. U.S. Dep. Commer., NOAA Tech. Memo NMFS F/NWC-80.

Norcross, B. L., and M. Frandsen.
1996. Distribution and abundance of larval fishes in Prince William Sound, Alaska, during 1989 after the *Exxon Valdez* oil spill. Am. Fish. Soc. Symposium 18:463–486.

Olsen, S., and A. Soldal.
1989. Observations on inshore distribution and behaviour of 0-group northeast Arctic cod. Rapp P.-V. Reun. Cons Int. Explor. Mer 191:296–302.

Pennington, M
1983. Efficient estimators of abundance, for fish and plankton surveys. Biometries 39:281–286.

Perquelle, S. J., and B. A. Megrey.
1993. A preliminary spawning biomass estimate of walleye pollock, *Theragra chalcogramma*, in the Shelikof Strait, Alaska, based on the annual egg production method. Bull. Mar. Sci. 53(2):728–749.

Polacheck, T., D. Mountain, D. McMillan, W. Smith, and P. Berrien.
1992. Recruitment of the 1987 year class of Georges Bank haddock (*Melanogrammus aeglefinus*): the influence of unusual larval transport. Can. J. Fish. Aquat. Sci., 49: 484–496.

Pulliam, H. R., and B. J. Danielson.
1991. Sources, sinks, and habitat selection: a landscape perspective on population dynamics. Am. Nat. 137(suppl.): S50–S66.

Randa, K.
1984. Abundance and distribution of 0-group Arcto-Norwegian cod and haddock 1965–1982. *In* The proceedings of the Soviet-Norwegian symposium on reproduction and recruitment of Arctic cod (O. R. Godo, and S. Tilseth, eds.), p. 192–214. Leningrad, U.S.S.R., 26–30 September 1983.

Reed, R. K., and J. D. Schumacher.
1986. Physical oceanography. *In* The Gulf of Alaska: physical and biological resources (D. W. Hood and S. T. Zimmerman (ed.), p. 57–75. Mineral Manage. Serv. Publ. Outer Continental Shelf Study. MMS 86-0095. U.S. Gov. Print. Off., Washington, D.C.

Reed, R. K., J. D. Schumacher, and L. S. Incze.
1987. Circulation in Shelikof Strait, Alaska. J. Phys. Oceanogr. 17:1546–1554.

Schultz, E. T., D. O. Conover, and Amir Ehtisham.
1998. The dead of winter: size-dependent variation and genetic differences in seasonal mortality among Atlantic silverside (Atherinidae: *Menidia menidia*) from different latitudes. Can. J. Fish. Aquat. Sci. 55:1149–1157.

Schumacher, J. D., and A. W. Kendall Jr.
1991. Some interactions between young walleye pollock and their environment in the western Gulf of Alaska. CalCOFI Rep. 32:22–40.
1995. An example of fisheries oceanography: Walleye pollock in Alaskan waters. Rev. Geophys. Suppl.:1153–1163.

Schumacher, J. D., and R. K. Reed.
1980. Coastal flow in the northwest Gulf of Alaska: the Kenai Current. J. Geophys. Res. 6680–6688.

Smith, G. B., G. E. Walters, P. A. Raymore Jr., and W. A. Hirschberger.
1984. Studies of the distribution and abundance of juvenile groundfish in the northwestern Gulf of Alaska, 1980–82: Part I: Three-year comparisons. U.S. Dep. Commer., NOAA Tech. Memo. NMFS F/NWC-59, 100 p.

Sogard, S. M.
1997. Size-selective mortality in the juvenile stage of teleost fishes: a review. Bull. Mar. Sci. 60(3):1129–1157.

Sparholt, H., E. Aro, and J. Modin.
1991. The spatial distribution of cod (*Gadus morhua* L.) in the Baltic Sea. Dana 9:45–56.

Springer, A. M.
1992. A review: walleye pollock in the North Pacific—how much difference do they really make? Fish. Oceanogr. 1(1):80–96.

Stabeno, P. J., R. K. Reed, and J. D. Schumacher.
1995. The Alaska Coastal Current: Continuity of transport and forcing. J. Geophys. Res. 100:2477–2485.

Strickland, R. M., and T. H. Sibley.
1989. Potential effects of water transport on the walleye pollock (*Theragra chalcogramma* Pallas) fishery in the Gulf of Alaska. Rev. Aquat. Sci. 1(2):281–293.

Sundby, S., H. Bjørke, A. V. Soldal, and S. Olsen.
1989. Mortality rates during the early life stages and year-class strength of northeast Arctic cod (*Gadus morhua* L.). Rapp. P.-V. Reun. Cons. int. Explor. Mer 191:296–302.

Valle, C. F., J. W. O'Brien, and K. B. Wiese.
1999. Differential habitat use by California halibut, *Paralichthys californicus*, barred sand bass, *Paralabrax nebulifer*, and other juvenile fishes in Alamitos Bay, California. Fish. Bull. 97:646–660.

Walters, G. E., G. B. Smith, P.A. Raymore Jr., and W. A. Hirschberger.
1985. Studies of the distribution and abundance of juvenile groundfish in the northwest Gulf of Alaska, 1980–82: Part II: Biological characteristics in the extended region. U.S. Dep. Commer., NOAA Tech. Memo. NMFS F/NWC-77, 95 p.

Wathne, F.
1977. Performance of trawls used in resource assessment. Mar. Fish. Rev. 39(6):16–23.

Wilkinson, L.,
1996. SYSTAT 6.0 for Windows: statistics. SPSS Inc., Chicago, IL, 751 p.

Wilson, M. T., R. D. Brodeur, and S. Hinckley.
1996. Distribution of age-0 walleye pollock (*Theragra chalcogramma*) in the western Gulf of Alaska. *In* Ecology of juvenile walleye pollock (R. D. Brodeur, P. A. Livingston, T. R. Loughlin, and A. B. Hollowed, eds.), p. 11–24. U.S. Dep. Commer., NOAA Tech. Rep. NMFS 126.

Wolotira, R. J., Jr., T. M. Sample, S. F. Noel, and C. R. Iten.
1993. Geographic and bathymetric distributions for many commercially important fishes and shellfishes off the West Coast of North America, based on research survey and commercial catch data, 1912–84. U.S. Dep. Commer., NOAA Tech. Memo. NMFS-AFSC-6, 184 p.

Yoklavich, M. M., and K. M. Bailey.
1990. Hatching period, growth and survival of young walleye pollock *Theragra chalcogramma* as determined from otolith analysis. Mar. Ecol. Prog. Ser. 64 13–23.

Use of the original von Bertalanffy growth model to describe the growth of barramundi, *Lates calcarifer* (Bloch)

Yongshun Xiao
SARDI Aquatic Sciences Centre
2 Hamra Avenue
West Beach
Southern Australia 5024, Australia
E-mail address: yongshun.xiao@bigpond.com

Abstract—In the original von Bertalanffy growth equation, the rate of change in body mass of an individual is assumed to result from two opposing biological processes: anabolism and catabolism. Because this differential equation cannot be solved analytically, some of its analytically solvable special cases are commonly used, despite their restrictive assumptions. In this study, I used a generalization of the original von Bertalanffy growth equation and some of its commonly used special cases to estimate parameters from a set of tagging data on times at liberty, lengths at release, and lengths at recapture of a centropomid perch (*Lates calcarifer*) and provide a method for determining the anabolic and catabolic rates of animals in their natural environment. Fitting the original von Bertalanffy growth equation to the tagging data suggests that a 1% increase in body mass of the fish corresponds to a 0.8721% increase in anabolic rate and a 1.0357% increase in catabolic rate. Alternatively, *L. calcarifer* may be interpreted as exhibiting a strong seasonality in growth: it grows fastest in length at the start of autumn, grows less until a full stop in the middle of winter, shrinks until the middle of spring, and then resumes a positive growth for another cycle. Consequently, it is unnecessary to use the analytically solvable special cases of the original von Bertalanffy growth equation in data analysis, unless their assumptions are validated. I also explain why Pauly's index of growth performance is adequate and propose an index of catabolic performance.

Manuscript accepted 15 March 2000.
Fish.Bull. 98:835–841 (2000).

Information on the growth of animals is important for studying their population dynamics, physiology, and biochemistry (Peters, 1983; Calder, 1984; Schmidt-Nielsen, 1984; Reiss, 1989; Xiao, 1998). Many empirical models have been developed to describe the growth of animals macroscopically, including the Gompertz (1825) and logistic growth models (Verhulst, 1838). By contrast, von Bertalanffy (1938) proposed a somewhat mechanistic growth model for body mass $W(a) \geq 0$ of an individual of age a, of the form

$$dW(a)/da = AW(a)^B - CW(a)^D,$$

where A, B, C and D = positive biological constants;
$AW(a)^B$ = the rate of anabolism (building up of body mass) at age a; and
$CW(a)^D$ = the rate of catabolism (breaking down of body mass) at age a.

Thus, in this model, the rate of change in body mass of an individual $dW(a)/da$ at age a is assumed to result from two opposing biological processes (anabolism and catabolism). Although the underlying mechanisms may be too complicated for $dW(a)/da$ to be approximated or even interpreted as such, this differential equation has opened up a line of thought for integrating the macroscopic growth of animals with certain physiological and biochemical processes (Pauly, 1981). Also, it is fairly general, includes almost all previous deterministic growth models as its special cases, and forms a basis for identifying the "right" growth models from amongst all its special cases. Consequently, some work has been done to estimate parameters A, B, C, and D to determine the anabolic and catabolic rates of fish (Ursin, 1967; Pauly, 1981).

However, because the differential equation cannot be solved analytically, its analytically solvable special cases are so commonly used that one simple special case has become known in the fisheries literature as *the* von Bertalanffy growth equation (Xiao, 1996). Nonetheless, assumptions for its various analytically solvable special cases can be very restrictive. Indeed, although assumed to take a value of $^2/_3$ in that simple special case (Pauly, 1981), constant B can take any value from $^2/_5$ to $^5/_7$, because B is often assumed to satisfy $\beta(B-1)+1=0$ and because B in Equation 2 below is known to take any value from $2^1/_2$ to $3^1/_2$. It is also possible that catabolic rate is not proportional to body mass (i.e. $D \neq 1$). In any case, it is best not to make any assumptions about the values of A, B, C, and D.

Like most growth models, the von Bertalanffy (1938) growth equation is age-dependent. Although it can be modified to consider, implicitly, the seasonal growth of animals and the effects of tagging, a general framework was not available for explicitly incorporating time and time-dependent factors (i.e. ambient temperature and food availability) in age-dependent growth models. This prompted Xiao (1999) to derive general age- and time-dependent growth models for animals and to give a comprehensive list of their commonly used special cases. Such models explicitly incorporate age, time, and their de-

pendent factors and are useful for modeling growth at age and time (e.g. from length-at-age data), incremental growth at age and time increment (e.g. data on length increment at age and time increment from tagging studies), the effects of tagging, and, if coupled with a proper age- and time-dependent population dynamics model, the effects on the growth of animals of many population characteristics, such as population size.

Because of experimental constraints, such as difficulties in taking continuous measurements (if measured at all), anabolic and catabolic rates of animals are necessarily measured either by restraining them in the laboratory or in the field. Such restraints can cause stress to animals and hence result in biased measurements. Experimental methods should be developed to estimate the anabolic and catabolic rates of animals in as natural an environment as possible.

In this study, I use an age- and time-dependent von Bertalanffy (1938) growth equation and some of its commonly used special cases for estimating the parameters from a set of tagging data on times at liberty, lengths at release, and lengths at recapture of a centropomid perch, barramundi (*Lates calcarifer*) and provide a method for determining the anabolic and catabolic rates of animals in their natural environment. I also explain why Pauly's (1981) index of growth performance is adequate and propose an index of catabolic performance.

Model

Let $0 \le W(a,t) < \infty$, $-\infty < a_0 \le a < \infty$, $-\infty < t_0 \le t < \infty$, denote the body mass of an individual of age a at time t, with an arbitrary reference age a_0 and an arbitrary reference time t_0. The von Bertalanffy (1938) growth equation can be generalized as

$$\frac{dW(a,t)}{dt} = A(a,t)W(a,t)^B - C(a,t)W(a,t)^D, \qquad (1)$$

where $A(a,t) \ge 0$ and $C(a,t) \ge 0$ = functions of age a and time t; and
B and D = positive biological constants.

For a particular functional form of $A(a,t)$ and $C(a,t)$, Equation 1 can be used for estimating its parameters from data on body masses of animals of different ages at different times, or on two distinct body masses of the same individual at different times. If collected at all, such data are collected mostly for terrestrial and occasionally for aquatic animals. What is most commonly gathered for both terrestrial and aquatic animals is, however, one or more linear dimensions of an individual's body, such as its total length at age, or two distinct measurements at different times. Measurements of linear dimensions of an animal contain useful information on its body mass. Indeed, it is well known that body mass $W(a,t)$ is scaled allometrically to body length $L(a,t)$, i.e.

$$W(a,t) = \alpha L(a,t)^{\beta}, \qquad (2)$$

where α and β = (constant) allometric parameters (Peters, 1983; Calder, 1984; Schmidt-Nielsen, 1984; Reiss, 1989).

Substitution of Equation 2 into Equation 1 yields

$$\frac{dL(a,t)}{dt} = \frac{1}{\beta}\alpha^{B-1}A(a,t)L(a,t)^{\beta(B-1)+1} - \frac{1}{\beta}\alpha^{D-1}C(a,t)L(a,t)^{\beta(D-1)+1}. \qquad (3)$$

Thus, if α and β are known, as is usually assumed, parameters B and D, and those in $A(a,t)$ and $C(a,t)$ can be estimated from data on length-at-age data, or on two distinct lengths of the same individual at different times.

Although too general to be solved even numerically, Equations 1 and 3 are useful in formulating ideas. Now, I consider a special case of Equations 1 and 3 for seasonally varying $A(a,t)$ and $C(a,t)$, such that

$$A(a,t) = \frac{\gamma}{K}\left[K + b\cos\left(\frac{2\pi}{T}(t - t_{\phi})\right)\right] \text{ and}$$

$$C(a,t) = K + b\cos\left(\frac{2\pi}{T}(t - t_{\phi})\right),$$

where γ, $\gamma b/K$, T, and t_{ϕ} are, respectively, the mean, amplitude, period, and time shift for the anabolic process; K, b, T, and t_{ϕ} are, respectively, the mean, amplitude, period, and time shift for the catabolic process. For this special case, Equations 1 and 3 then become, respectively

$$\frac{dW(a,t)}{dt} = \left[K + b\cos\left(\frac{2\pi}{T}(t - t_{\phi})\right)\right] \cdot \left[\frac{\gamma}{K}W(a,t)^B - W(a,t)^D\right] \qquad (4)$$

and

$$\frac{dL(a,t)}{dt} = \frac{1}{\beta}\left[K + b\cos\left(\frac{2\pi}{T}(t - t_{\phi})\right)\right] \cdot \left[\frac{\gamma}{K}\alpha^{B-1}L(a,t)^{\beta(B-1)+1} - \alpha^{D-1}L(a,t)^{\beta(D-1)+1}\right]. \qquad (5)$$

Equations 4 and 5 can be solved numerically but not analytically. For comparison and illustration, I now consider five special cases (four of which are reparameterizations of commonly used growth equations) of Equation 5:

If $b=0$, or if $A(a,t)$ and $C(a,t)$ are constants, Equation 5 becomes

$$\frac{dL(a,t)}{dt} = \frac{1}{\beta}\left(\gamma\alpha^{B-1}L(a,t)^{\beta(B-1)+1} - K\alpha^{D-1}L(a,t)^{\beta(D-1)+1}\right). \qquad (6)$$

If $\beta(B-1)+1=0$ (i.e. $B-1=-1/\beta$) and $\beta(D-1)+1=1$ (i.e. $D=1$), Equation 5 becomes

$$\frac{dL(a,t)}{dt}=\frac{1}{\beta}\left[K+b\cos\left(\frac{2\pi}{T}(t-t_{\phi})\right)\right]\left(\frac{\gamma}{K}\alpha^{1/\beta}-L(a,t)\right), \quad (7)$$

the solution of which as an initial value problem, with $L(a, t)|_{t=t_0} = L(t_0 + a - t, t_0)$ for $a - a_0 \geq t-t_0$ or with $L(a, t)|_{a=a_0} = L(a_0, a_0 + t - a)$ for $a - a_0 < t-t_0$, yields

$$L(a,t)=\begin{cases}\dfrac{\gamma}{K}\alpha^{1/\beta}-\left(\dfrac{\gamma}{K}\alpha^{1/\beta}-L(a_0,t-a+a_0)\right) & \\ \quad\cdot\exp\left(-\dfrac{K}{\beta}(a-a_0)-\dfrac{bT}{\beta\pi}\sin\left(\dfrac{\pi}{T}(a-a_0)\right)\right. & a-a_0<t-t_0\\ \quad\left.\cdot\cos\left(\dfrac{2\pi}{T}\left(t-t_{\phi}-\dfrac{1}{2}(a-a_0)\right)\right)\right) & \\ \dfrac{\gamma}{K}\alpha^{1/\beta}-\left(\dfrac{\gamma}{K}\alpha^{1/\beta}-L(t_0+a-t,t_0)\right)\exp\left(-\dfrac{K}{\beta}(t-t_0)\right. & a-a_0\geq t-t_0\\ \left.-\dfrac{bT}{\beta\pi}\sin\left(\dfrac{\pi}{T}(t-t_0)\right)\cos\left(\dfrac{2\pi}{T}\left(t-t_{\phi}-\dfrac{1}{2}(t-t_0)\right)\right)\right). & \end{cases} \quad (8)$$

Similar age-dependent models have been given, *inter alia*, by Appeldoorn (1987), Pauly et al. (1992), Fontoura and Agostinho (1996), and Xiao (1999). Also, notice that bT (in Appeldoorn (1987) and Pauly et al. (1992), b=C and T=1) is a dimensionless quantity and is useful for interspecific comparison of the strength of seasonal growth oscillations (Pauly, 1984, 1985, 1990).

If $\beta(B-1)+1=0$ (i.e., $B-1=-1/\beta$), $\beta(D-1)+1=1$ (i.e., $D=1$), and b=0, Equation 5 becomes

$$L(a,t)=\begin{cases}\dfrac{\gamma}{K}\alpha^{1/\beta}-\left(\dfrac{\gamma}{K}\alpha^{1/\beta}-L(a_0,t-a+a_0)\right) & \\ \quad\times\exp\left(-\dfrac{K}{\beta}(a-a_0)\right) & a-a_0<t-t_0\\ \dfrac{\gamma}{K}\alpha^{1/\beta}-\left(\dfrac{\gamma}{K}\alpha^{1/\beta}-L(t_0+a-t,t_0)\right) & \\ \quad\times\exp\left(-\dfrac{K}{\beta}(t-t_0)\right), & a-a_0\geq t-t_0\end{cases} \quad (9)$$

a reparameterization of what is commonly called in the fisheries literature the von Bertalanffy (1938) growth equation.

If $\beta(B-1)+1=0$ (i.e., B=1) and $\beta(D-1)+1=2$ (i.e. $D-1=1/\beta$), Equation 5 becomes

$$\frac{dL(a,t)}{dt}=\frac{\gamma}{\beta K}\left[K+b\cos\left(\frac{2\pi}{T}(t-t_{\phi})\right)\right]\times L(a,t)\left(1-\frac{L(a,t)}{\frac{\gamma}{K}\alpha^{-1/\beta}}\right), \quad (10)$$

the solution of which as an initial value problem, with $L(a, t)|_{t=t_0} = L(t_0 + a - t, t_0)$ for $a - a_0 \geq t-t_0$ or with $L(a, t)|_{a=a_0} = L(a_0, a_0 + t - a)$ for $a - a_0 < t-t_0$, yields

$$L(a,t)=\begin{cases}\left[\dfrac{1}{\frac{\gamma}{K}\alpha^{1/\beta}}-\left(\dfrac{1}{\frac{\gamma}{K}\alpha^{1/\beta}}-\dfrac{1}{L(a_0,t-a+a_0)}\right)\right.\\ \quad\times\exp\left(\dfrac{\gamma}{\beta}(a-a_0)-\dfrac{\gamma bT}{\beta K\pi}\sin\left(\dfrac{\pi}{T}(a-a_0)\right)\right.\\ \quad\left.\left.\cdot\cos\left(\dfrac{2\pi}{T}\left(t-t_{\phi}-\dfrac{1}{2}(a-a_0)\right)\right)\right)\right]^{-1} & a-a_0<t-t_0\\ \left[\dfrac{1}{\frac{\gamma}{K}\alpha^{1/\beta}}-\left(\dfrac{1}{\frac{\gamma}{K}\alpha^{1/\beta}}-\dfrac{1}{L(t_0+a-t,t_0)}\right)\right.\\ \quad\times\exp\left(-\dfrac{\gamma}{\beta}(t-t_0)-\dfrac{\gamma bT}{\beta K\pi}\sin\left(\dfrac{\pi}{T}(t-t_0)\right)\right.\\ \quad\left.\left.\cdot\cos\left(\dfrac{2\pi}{T}\left(t-t_{\phi}-\dfrac{1}{2}(t-t_0)\right)\right)\right)\right]^{-1}, & a-a_0\geq t-t_0\end{cases} \quad (11)$$

a reparameterization of the seasonal logistic growth equation (Xiao, 1999).

If $\beta(B-1)+1=1$ (i.e., B=1), $\beta(D-1)+1=2$ (i.e., $D-1=1/\beta$), and b=0, Equation 5 becomes

$$L(a,t)=\begin{cases}\left[\dfrac{1}{\frac{\gamma}{K}\alpha^{1/\beta}}-\left(\dfrac{1}{\frac{\gamma}{K}\alpha^{1/\beta}}-\dfrac{1}{L(a_0,t-a+a_0)}\right)\right.\\ \quad\left.\cdot\exp\left(-\dfrac{\gamma}{\beta}(a-a_0)\right)\right]^{-1} & a-a_0<t-t_0\\ \left[\dfrac{1}{\frac{\gamma}{K}\alpha^{1/\beta}}-\left(\dfrac{1}{\frac{\gamma}{K}\alpha^{1/\beta}}-\dfrac{1}{L(t_0+a-t,t_0)}\right)\right.\\ \quad\left.\cdot\exp\left(-\dfrac{\gamma}{\beta}(t-t_0)\right)\right]^{-1}, & a-a_0\geq t-t_0\end{cases} \quad (12)$$

a reparameterization of the logistic growth equation (Xiao, 1999).

Data and analysis

Equations 8, 9, 11, and 12 are segmented functions (Xiao, 1999); they provide flexibility in analysis of growth data. Thus, by appropriately choosing the value of time t (which is a relative quantity), one can use either segment ($a - a_0 < t-t_0$ or $a - a_0 \geq t-t_0$) for an individual animal or for a group of individuals, or use both segments ($a - a_0 < t-t_0$ and

$a - a_0 < t - t_0$) for a group of individuals. It is, however, more convenient to use only one segment in a single analysis. Indeed, although growth parameters can be estimated by use of either segment of any of Equations 8, 9, 11, and 12, it is easier to use the segment for $a - a_0 < t - t_0$, by letting time t start before the animals whose growth is to be modeled are born, unless time is allowed to take negative values. Use of the other segment, i.e. that for $a - a_0 \geq t - t_0$, gives identical results, but it requires first calculating $L(t_0 + a - t, t_0)$.

The amount of data required to estimate parameters in a growth model is a function of the generality of that model: the more general a model is, the more data it usually requires. Age- and time-dependent growth models generally require knowledge of two ages a_0 and a, time t, and two sizes $L(a_0, t - a + a_0)$ and $L(a,t)$ if $a - a_0 < t - t_0$; or knowledge of two times t_0 and t, age a, and two sizes $L(t_0 + a - t, t_0)$ and $L(a,t)$ if $a - a_0 \geq t - t_0$. However, use of Equations 4, 5, 8, and 11 only requires knowledge of the difference between two ages $a - a_0$, time t, and two sizes $L(a_0, t - a + a_0)$ and $L(a,t)$; or of the difference between two times $t - t_0$, time t, and two sizes $L(t_0 + a - t, t_0)$ and $L(a,t)$. By contrast, use of Equations 9 and 12 only requires knowledge of the difference between two ages, $a - a_0$, and two sizes, $L(a_0, t - a + a_0)$ and $L(a,t)$, or of the difference between two times $t - t_0$, and two sizes $L(t_0 + a - t, t_0)$ and $L(a,t)$.

Interestingly, a reparameterization of Equation 9 has been widely used to model tagging data (Xiao, 1999), where a_0 or t_0 is interpreted as time at release, a or t as time at recapture, $a - a_0$ or $t - t_0$ as time at liberty, $L(a_0, t - a + a_0)$ or $L(t_0 + a - t, t_0)$ as size at release, and $L(a,t)$ as size at recapture. It has also been used extensively to model size-at-age data (obtained, say, by aging animals by reading marks in scales and otoliths) (e.g. Moulton et al., 1992), where a_0 or t_0 is interpreted as age at birth, a or t as age, $L(a_0, t - a + a_0)$ or $L(t_0 + a - t, t_0)$ as size at birth, and $L(a,t)$ as size at age. However, it is rare to know two ages and the corresponding sizes of an animal; what are commonly measured are one age and its corresponding size. Consequently, it is common practice to fit Equation 9 to such size-at-age data to estimate age at birth a_0 or t_0, as well as the growth parameters, thereby implicitly assuming, for all animals concerned, that the size at birth $L(a_0, t - a + a_0)$ or $L(t_0 + a - t, t_0)$ is zero and that the age at birth a_0 or t_0 is the same. Exactly the same argument applies to Equation 12.

The barramundi *L. calcarifer* is a protandrous fish found in estuaries and other coastal areas of the Indo-West Pacific (Griffin, 1987). Between August 1977 and June 1980, 1933 barramundi with a body total length range of about 10–100 cm were captured by a combination of lure fishing, tidal trap, seine and gill net. Fish were measured to the nearest cm, tagged with Floy FT-2 dart tags for fish >35 cm and FD-67 anchor tags for fish <35 cm, and released in rivers flowing into the Van Diemen Gulf and the Gulf of Carpentaria of northern Australia (Davis and Reid, 1982). Of those tagged, 312 of a total length of 23–92 cm with a mean of 60 ±13 (mean ±SE) cm were recaptured, but only 308 were used in the analysis below due to incomplete recapture information. The time at liberty ranged from zero to 932 d, with a mean of 219 ±211 d, and the length increment from –21 to 35 cm, with a mean of 6 ±8 cm. Negative increments in length are often observed in a tagging experiment, because tagged animals can shrink in size immediately after tagging, or because of recording errors at both release and recapture. The estimates of allometric parameters for barramundi, used in the present paper, were those obtained by Reynolds (1978): $\hat{\alpha}=1.06 \times 10^{-5}$ kg $\times$ cm$^{-\hat{\beta}}$ and $\hat{\beta} = 3.02$.

Let a_0 or t_0 denote time at release, a or t time at recapture, $a - a_0$ or $t - t_0$ time at liberty, $L(a_0, t - a + a_0)$ or $L(t_0 + a - t, t_0)$ the length of a fish at release, and $L(a,t)$ its length at recapture. Equation 6 and the segments of Equations 8, 9, 11, and 12 for $a - a_0 < t - t_0$, were fitted to the tagging data, by using the nonlinear least squares method, under the assumptions that T=365.25 d, time started (i.e. time t=0) on 1 January 1960 (see Xiao [1999] for its significance), and errors in $L(a,t)$ follow independent normal distributions, with a mean of $\hat{L}(a,t)$ and a constant variance of σ^2 (Table 1). In these calculations, Equation 6 was numerically solved as an initial value problem with $L(a, t)|_{t = t_0} = L(t_0 + a - t, t_0)$ for $a - a_0 \geq t - t_0$ using the fourth order Runge-Kutta method (Beyer, 1978). A likelihood ratio test suggests that Equation 8 is significantly different from Equation 9 ($F_{2,304}$=48.6892, P<0.0001); and Equation 11 is significantly different from Equation 12 ($F_{2,304}$=45.3460, P<0.0001). Thus, Equations 8 and 11, and their associated estimates of parameters seem adequate for describing the tagging data. Selection among Equations 6, 8, and 11 is difficult because little is known of the underlying mechanisms of the growth process.

Discussion

Fitting of the original von Bertalanffy growth model (Eq. 6) to the tagging data for barramundi suggests that its anabolic rate changes proportionally with the $\hat{B}$=0.8721 power of its body mass and that its catabolic rate changes proportionally ($\hat{D}$=1.03567≈1) with its body mass (i.e. at a 1:1 ratio). Such an estimate of B is 9.0125% higher than that ($\hat{B}$=4/5) obtained for many fish under laboratory conditions (Pauly, 1981). More data are needed to examine the generality of this finding. By contrast, little information is available on the value of D. Nonetheless, it is interesting that the catabolic rate of barramundi increases proportionally with its body mass; a 1% increase in body mass corresponds to about a 1% increase in catabolic rate. Consequently, it is unnecessary to use the analytically solvable special cases of the original von Bertalanffy growth equation in data analysis, unless their assumptions are validated.

Alternatively, like many tropical and subtropical species of fish (Appeldoorn, 1987; Pauly et al., 1992), barramundi may be interpreted as exhibiting a strong seasonal growth. For both models (Eqs. 8 and 11), its growth rate reaches its maximum on 3 or 4 March (i.e. at the start of autumn), slows down to zero on 17 July (i.e. in the middle of winter), reaches its minimum on 2 or 3 September (i.e. at the start of spring), returns to zero on 19 or 20 October (i.e. in the middle of spring), and comes back to its maxi-

mum rate on 3 or 4 March (i.e. at the start of autumn) (Fig. 1). Thus, its length grows fastest on 3 or 4 March (i.e. at the start of autumn), grows less until a full stop on 17 July (i.e. in the middle of winter), shrinks until 19 or 20 October (i.e. in the middle of spring), and resumes a positive growth for another cycle. Thus, barramundi does not grow in length for three months in a year, from 17 July (i.e. in the middle of winter) to 19 or 20 October (i.e. in the middle of spring). However, Equations 8 and 11 have different assumptions and predict different amplitudes of seasonally varying growth rate. Such a strong seasonality in growth rate might be related to seasonal changes in the availability of food and in water temperature.

Similarly, tagging may adversely affect the growth of barramundi perch and bias estimates of parameters in a growth model, where its effects are not taken into proper account. In fact, Xiao (1994) has already interpreted the same set of data in terms of the effects of tagging. However, it is impossible to identify the right model from all possible models, because of the inductive nature of modeling and because of our poor understanding of the underlying mechanisms of growth and how tagging affects growth. In a preliminary analysis, I have constructed a model, and have attempted (but failed) to estimate, simultaneously, both the effects of tagging and seasonally varying growth rates. Such a failure is not surprising because the amount of information in a set of tagging data is limited. Further progress can be made only by better understanding the underlying mechanisms of growth.

This work also puts some of Pauly's (1981) work into perspective. For example, $\alpha^{-1/\beta}\gamma/\mathrm{K}$ and K/β in Equation 9 can be interpreted respectively as the average maximum size and growth rate of a species. As Pauly (1981) proposed, the product $(\alpha^{-1/\beta}\gamma/\mathrm{K})(\mathrm{K}/\beta) = \alpha^{-1/\beta}\gamma/\beta$ is indeed an index of growth performance because it is in direct proportion to the mean anabolic rate. Similarly, $\alpha^{-1/\beta}\gamma/\mathrm{K}$ and γ/β in Equation 12 can be interpreted respectively as the average maximum size and growth rate of a species. The quotient $(\gamma/\beta)/(\alpha^{-1/\beta}\gamma/\mathrm{K}) = \alpha^{1/\beta}\mathrm{K}/\beta$ is an index of catabolic performance, because it is in direct proportion to the mean catabolic rate.

Finally, anabolic and catabolic rates of animals can be estimated from data from a mark-recapture experiment on two distinct lengths of the same individual measured at different times. Thus, the present work has demonstrated a way to estimate anabolic and catabolic rates of animals. Such field-based estimates can be compared with those obtained under laboratory conditions.

Acknowledgments

I wish to thank three anonymous referees for their very constructive and valuable comments on the manuscript, Kate Watt (SARDI Aquatic Sciences Centre) for producing Table 1, and Roland K. Griffin (Northern Territory Department of Primary Industry and Fisheries) and Tim L. O. Davis (CSIRO Division of Fisheries) for supplying *L. calcarifer* data. Roland K. Griffin also provided some references on *L. calcarifer*.

Table 1

Estimates and (in parentheses) standard errors of parameters obtained by fitting Equations 6, 8, 9, 11, and 12 to barramundi tagging data using the least squares method under the assumptions that $T = 365.25$ d, time started (i.e. time $t=0$) in 1 January 1960, and errors in $L(a,t)$ follow independent normal distributions, with a mean of $\hat{L}(a,t)$ and a constant variance of $\hat{\sigma}^2$. $P<0.0001$; $n=308$.

Equation	$\hat{\gamma}$ (kg^{1-B}/d)	$\hat{K}$ (kg^{1-D}/d)	$\hat{b}$ (kg^{1-D}/d)	$\hat{t}_\phi$ (d)	$\hat{B}$	$\hat{D}$	df_1, df_2, F	$\hat{\sigma}^2$	r^2
6	0.00843 (0.00008)	0.00556 (0.00005)	—	—	0.87213 (0.00148)	1.03567 (0.00216)	4,304,15424.6096	22.9793	0.9951
8	0.00474 (0.00052)	0.00184 (0.00034)	0.00265 (0.00054)	62.7197 (6.8279)	—	—	4,304,20333.2966	17.4525	0.9963
9	0.00500 (0.00062)	0.00196 (0.00040)	—	—	—	—	2,306,30966.0441	22.8923	0.9951
11	0.00446 (0.00036)	0.00206 (0.00023)	0.00302 (0.00045)	63.5155 (6.7581)	—	—	4,304,19947.9059	17.7884	0.9962
12	0.00487 (0.00044)	0.00228 (0.00028)	—	—	—	—	2,306,30895.5175	22.9443	0.9951

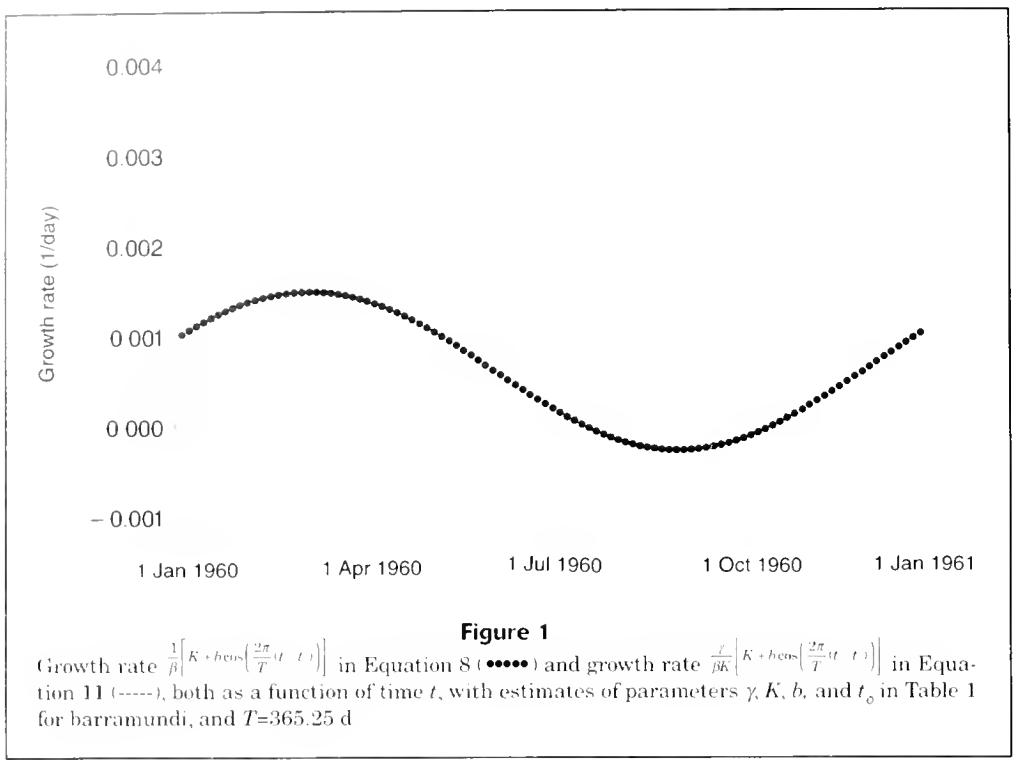

Figure 1

Growth rate $\frac{1}{\beta}\left[K+b\cos\left(\frac{2\pi}{T}(t-t_s)\right)\right]$ in Equation 8 (•••••) and growth rate $\frac{\gamma}{\beta K}\left[K+b\cos\left(\frac{2\pi}{T}(t-t_s)\right)\right]$ in Equation 11 (-----), both as a function of time t, with estimates of parameters γ, K, b, and t_o in Table 1 for barramundi, and T=365.25 d

Literature cited

Appeldoorn, R. S.
1987. Modification of a seasonally oscillating growth function for use with mark-recapture data. J. Cons. Int. l'Explor. Mer 43:194–198.

Beyer, W. H.
1978. CRC handbook of mathematical sciences, 6th ed. CRC Press, Inc., Boca Raton, FL, 860 p.

Calder, W. A.
1984. Size, function, and life history. Harvard Univ. Press, Cambridge, MA. 431 p.

Davis, T. L. O., and D. D. Reid.
1982. Estimates of tag shedding rates for Floy FT-2 dart and FD-67 anchor tags in barramundi, *Lates calcarifer* (Bloch). Aust. J. Mar. Freshwater Res. 33:1113–1117.

Fontoura, N. F., and A. A. Agostinho
1996. Growth with seasonally varying temperatures: an expansion of the von Bertalanffy growth model. J. Fish Biol. 48:569–584.

Gompertz, B.
1825. On the nature of the function expressive of the law of human mortality, and on a new mode of determining the value of life contingencies. Philos. Trans. R. Soc. Lond. 115(1):513–585.

Griffin, R. K.
1987. Life history, distribution, and seasonal migration of barramundi in the Daly River, Northern Territory, Australia. Am. Fish. Soc. Symp. 1:358–363.

Moulton, P. M., T. I. Walker, and S. R. Saddlier
1992. Age and growth studies of gummy shark, *Mustelus antarcticus* Gunther, and school shark, *Galeorhinus galeus* (Linnaeus), from southern-Australian waters. Aust. J. Mar. Freshwater Res. 43:1241–1267.

Pauly, D.
1981. The relationships between gill surface area and growth performance in fish: a generalization of von Bertalanffy's theory of growth. Meeresforschung/Rep. Mar. Res. 28:251–282.
1984. Fish population dynamics in tropical waters: a manual for use with programmable calculators. ICLARM Stud. Rev. 8:40–40.
1985. The population dynamics for short-lived species, with emphasis on squids. NAFO Sci. Counc. Stud. 9:143–154.
1990. Length-converted catch curves and the seasonal growth of fishes. Fishbyte 8:33–38.

Pauly, D., M. Soriano-Bartz, M. J. Moreau, and A. Jarre-Teichmann.
1992. A method accounting for seasonal cessation of growth in fishes. Aust. J. Mar. Freshwater Res. 43:1151–1156.

Peters, R. E.
1983. The ecological implications of body size. Cambridge Univ. Press, Cambridge, 329 p.

Reiss, M. J.
1989. The allometry of growth and reproduction. Cambridge Univ. Press, Cambridge, 182 p.

Reynolds, L. F.
1978. The population dynamics of barramundi *Lates calcarifer* (Pisces: Centropomidae) in Papua New Guinea. MSc thesis, Univ. Papua New Guinea, Port Moresby, 249 p.

Schmidt-Nielsen, K.
1984. Scaling: why is animal size so important? Cambridge Univ. Press, Cambridge, 241 p.

Ursin, E.
1967. A mathematical model of some aspects of fish growth, respiration, and mortality. J. Fish. Res. Board Can. 24:2355–2453.

Verhulst, P. F.
1838. Notice sur la loi que la population pursuit dans son accroissement. Corresp. Math. Phy. 10:113–121.
von Bertalanffy, L.
1938. A quantitative theory of organic growth. Human Biol. 10:181–213.
Xiao, Y.
1994. Growth models with corrections for the retardative effects of tagging. Can. J. Fish. Aquat. Sci. 51:263–267.
1996. How does somatic growth rate affect otolith size in fishes? Can. J. Fish. Aquat. Sci. 53:1675–1682.
1998. What are the units of the parameters in the power function for the length-weight relationship? Fish. Res. 35:247–249.
1999. General age- and time-dependent growth models for animals. Fish. Bull. 97:690–701

The relation between spawning area and biomass of Japanese pilchard, *Sardinops melanostictus*, along the Pacific coast of Japan

Hiromu Zenitani

National Research Institute of Fisheries and Environment of Inland Sea
2-17-5, Maruishi, Ohno-cho Saeki-gun,
Hiroshima, 739-0452 Japan
E-mail address: zenitani@nnf.affrc.go.jp

Sakutaro Yamada

Tokyo University of Fisheries
4-5-7, Konan, Minato-ku,
Tokyo, 108-0075 Japan

Abstract—When stocks are depleted, direct assessments of population levels are not only difficult but may be highly inaccurate. The work reported here was motivated by the need to manage the collapse of the far eastern sardine (*Sardinops melanostictus*) population. Spawning area was chosen as the first indicator of population size because the spatial spread of the stock increases when the spawning population increases. Our objective was to clarify the relation between spawning area and the spawning biomass of this species off the Pacific coast of Japan in order to estimate biomass with the spawning area data.

The pilchard spawning area (A_I) in a given year was calculated by summing the areas of 1° longitude × 1° latitude squares where early developmental stage eggs were present. The optimal relationship between A_I and the spawning biomass (B) was A_I=2.518 $B^{0.1610}$, not a simple linear relationship. One cause of the nonlinear relationship seemed to be that pilchard egg aggregations were distributed over space in a patchy manner.

Finally, we introduced an approximate method for estimating the pilchard spawning biomass by using the inverted equation of the optimal relationship between A_I and B, (B=0.135A_I $^{2.1691}$).

Manuscript accepted 26 June 2000
Fish. Bull. 98:842–848 (2000)

Japanese pilchard, *Sardinops melanostictus* (known as "Japanese pilchard" in Japan) is found off the Pacific coast of Japan and is an important commercial species. The pilchard stock has fluctuated widely over a period of several decades (Kondo et al., 1976). The annual catch in Japan peaked at 1.5 × 10^6 metric tons (t) in the 1930s, but decreased to only 3.0 × 10^4 t in the 1960s. It recovered to 4.6 × 10^6 t in the 1970s and reached the second highest peak for this century in 1988. However, the catch in 1995 fell to one-tenth of that in 1988 (Fig. 1).

When stocks are depleted, direct assessments of population levels are not only difficult but may be highly inaccurate (Hewitt et al.[1]). In such situations, an alternative method of population assessment is to survey egg or larval populations as a means of estimating biomass (e.g. the egg production method; Lasker, 1981). However, the egg production method (EPM) is expensive and time consuming (Mangel and Smith, 1990).

A biological characteristic of the Japanese pilchard is that its distribution range changes in accordance with stock size. During pilchard stock size increases, the distributional range expands widely (Wada and Kashiwai, 1991). In contrast, when stock size is declining, the distributional range may became quite limited (Hiramoto, 1981). The spawning grounds of Japanese pilchard are known to expand with egg abundance increases and contract with abundance declines (Watanabe et al., 1996; Zenitani et al., 1998). In general, as the spawning population increases, the spatial spread of the stock also increases (Rosenzweig, 1981; MacCall, 1988). Therefore, the area of spawning grounds (spawning area) was chosen as the first indicator of pilchard population recovery (Smith, 1973; Smith and Hewitt, 1985).

Our objective was to clarify the relationship between pilchard spawning area and spawning biomass off the Pacific coast of Japan, to estimate biomass with spawning area data. Moreover, to explain why the relationship between pilchard spawning area and spawning biomass formed, we used a model in which a patchy egg distribution was assumed.

Materials and methods

Spawning area and spawning biomass

Intensive egg surveys of coastal pelagic fish have been conducted every year since 1978 by the Fisheries Agency of Japan (Mori et al., 1988; Kikuchi and Konishi, 1990; Ishida and Kikuchi, 1992;

[1] Hewitt, R., A. Bindmann, and N. C. Lo. 1984. Procedures for calculating the egg production estimate of spawning biomass. Administrative Report LJ-84-19, Southwest Fisheries Center, La Jolla, CA 92038-0271

Zenitani et al., 1995). Among these surveys, two governmental institutions, the National Research Institute of Fisheries Science and the Nansei National Fisheries Research Institute, have collaborated on surveys covering the inshore and offshore waters between 128–143°E and 28–36°N since 1978 (Fig. 2). We used data from these surveys covering the waters along the Pacific coast of Japan between 130–142°E and 28–36°N (Fig. 3). In the census, from 149 to 344 ichthyoplankton samples were collected each year by towing two types of conical or cylindrical-conical nets (inside mouth diameter: 45 or 60 cm; mesh aperture: 0.335 mm). Each net was retrieved vertically at 1 m/s from 150 m depth or from the bottom at stations shallower than 150 m.

We calculated two kinds of pilchard spawning area (A_1 and A_2). Pilchard spawning is concentrated into two months, February and March (Watanabe et al., 1996). Therefore, A_1 in any given year was calculated by summing the areas of 1° longitude × 1° latitude squares where early developmental *A*-stage eggs, as categorized by Nakai (1962), were collected during February and March. A_2 was calculated by summing the areas of 1° longitude × 1° latitude squares where eggs of any stage were collected during February and March. The length of time elapsing from fertilization to the end of the *A* stage at the different temperatures, 15.2°, 17.5°, and 20.3°C, are 25, 16, and 10 hours, respectively. The length of time elapsing from fertilization to hatching at the different temperatures, 15.2°, 17.5°, and 20.3°C, are 85, 56, and 34 hours, respectively (Nakai, 1962).

We used the pilchard biomass estimated along the Pacific coast of Japan from 1977 to 1995 by Wada and Jacobson (1998). Biomass estimation was conducted by virtual population analysis (VPA) with the catch-at-age data of the purse-seine fishery. The biomass estimate was for the middle of June, the end of the major spawning season for Japanese pilchard. During the main spawning season, most spawning is done by age-1+ pilchards and a small amount is done by age-1 pilchards (Hiramoto, 1981). The biomass of age-1+ pilchards in year $y-1$ was assumed to be the spawning biomass (B) in year y.

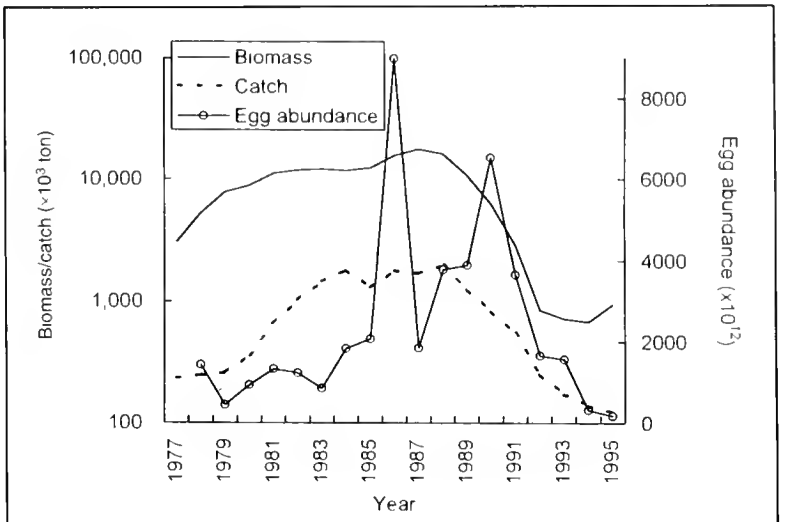

Figure 1

Catch, spawning biomass, and egg abundance of Japanese pilchard along the Pacific coast of Japan from 1978 to 1995 (after Wada and Jacobson, 1998).

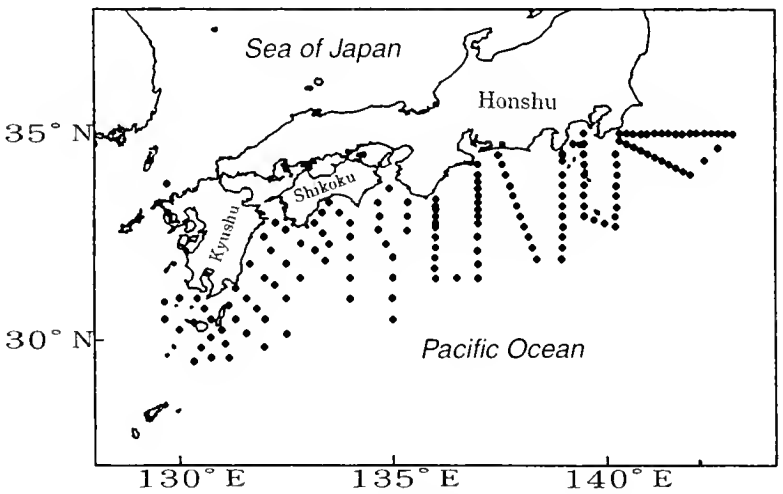

Figure 2

An example of station allocation for the spawning survey of Japanese pilchard in February and March 1994.

Model

To test whether spawning area could be correlated with spawning biomass, statistical analyses were performed. We used five relationships between A (=A_1 or A_2) and B: $A=f(B)$

I $f(B)=u_1B$,
II $f(B)=u_1B+u_2$,
III $f(B)=u_1B^{u2}$,
IV $f(B)=u_1\,exp(u_2B)$, and
V $f(B)=A_s[1-\{u_1/(u_1+u_2B)\}^{u1}]$,

where u_1, u_2 and A_s were parameters.

Relationship V was obtained by a modification of Mangel and Smith's (1990) model. They used the negative binomial model to describe the contagion of pilchard eggs. It is commonly used in ecological modeling (Pielou, 1977; Zweifel and Smith, 1981; Mangel and Smith, 1990; Zenitani et al., 1998). Mangel and Smith (1990) extended the negative binomial model to include the possibility of failure to detect eggs which are present at a station. According to Mangel and Smith (1990),

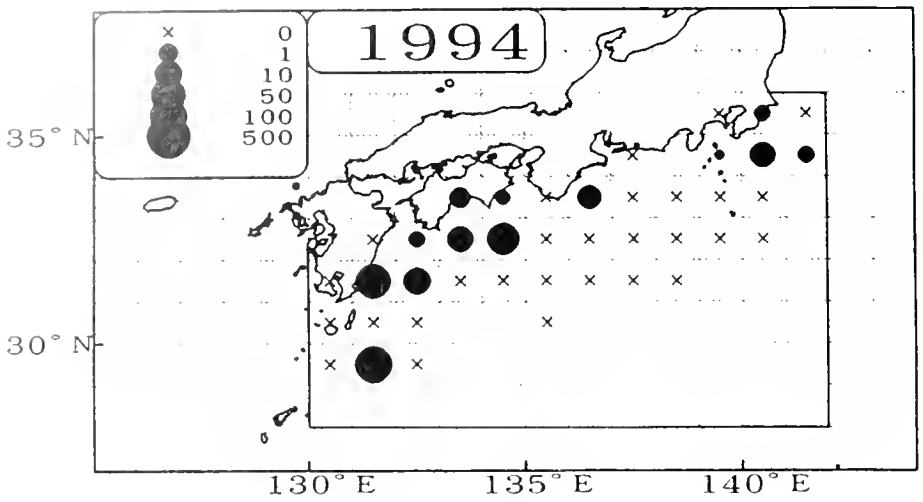

Figure 3

Distribution of pilchard eggs along the Pacific coast of Japan in February and March 1994. Solid circles and crosses show the mean egg density (number of eggs per 0.159 m^2) in 1° × 1° squares. Data in the area surrounded by the bold lines was used for the analysis (after Zenitani et al., 1998).

$$E\{N_p\} = N\alpha p\left[1-\left\{k/(k+m\omega)\right\}^k\right], \quad (1)$$

where N_p and N = number of samples with a positive number of eggs and total number of samples in survey area (A), respectively;

α and ω = sampling efficiency parameters;

p = probability that a observation station is a habitat for spawning stock;

k = the over-dispersion parameter of negative binomial distribution; and

m = mean number of eggs at a habitat area for spawning stock.

To simplify, we assumed that α = 1, p = 1, and ω = 1. Moreover, we assumed that the spawning biomass (B) and total egg abundance (mN) is linearly related, that is $B = \delta mN$, where δ is a constant. Actually, a linear relationship exists between the spawning biomass and egg abundance of the Japanese pilchard (Fig. 4). We assumed that a survey area (A) is equally divided by N stations. Because N_p is a random variable, the observed spawning area $A=A(N_p)=\gamma N_p$ is also a random variable, where γ is a proportional constant ($=A/N$).

From Equation 1, we thus obtain

$$E\{A\} = \gamma E\{N_p\} = A\left[1-\left\{k/(k+\varepsilon B)\right\}^k\right],$$

where $\varepsilon = 1/(N\delta)$.

If $u_1 = k$, $u_2 = \varepsilon$, A = 640 (10 km^2), and $A = E[A]$, we have relationship V between A and B.

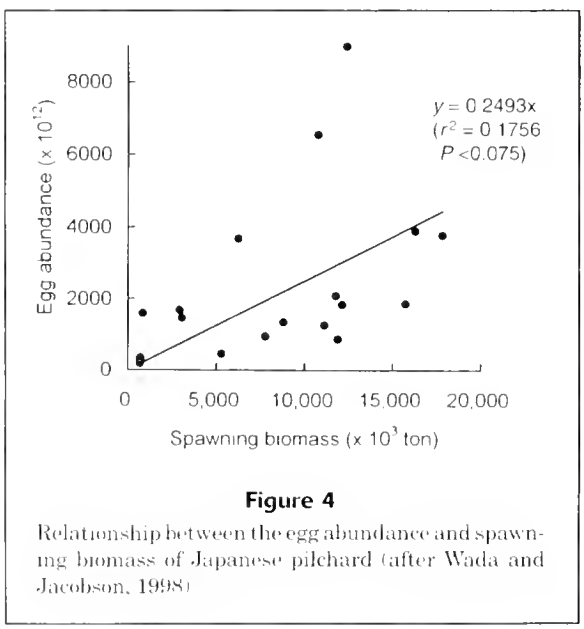

Figure 4

Relationship between the egg abundance and spawning biomass of Japanese pilchard (after Wada and Jacobson, 1998).

Parameters estimation, confidence interval analysis, and selection of the optimal relationship

We assumed that each relationship (I–V) had an error term z; $\ln(A)=\ln(f(B))+\ln(z)$; that z had a log-normal distribution; $\ln(z) \sim N(0,\sigma^2)$; and that $N(0,\sigma^2)$ has a normal distribution of mean zero and variance σ^2. z will take only positive values, so we expected the mean of z, $E[z]=\exp(\sigma^2/2)$, to be larger than 0. In addition, the log-normal distribution has a long tail, which is common with ecological data (Hilborn and Mangel, 1997).

Table 1

Estimated parameter values and 95 % confidence intervals (in parentheses) for each relationship between the spawning area (A_1: 10^3 km^2) and the spawning biomass (B: 10^3metric ton) of Japanese Pilchard along the Pacific Coast of Japan from 1978 to 1995.

Relationship		u_1	u_2	A_s (10^3/km^2)	AIC
I	$A_1=u_1B$	0.02318 (0.023109–0.023240)			41.2
II	$A_1=u_1B+u_2$	0.01204 (0.012012–0.012059)	50.048 (49.9144–50.1824)		11.2
III	$A_1=u_1B^{u2}$	2.518 (2.5157–2.5208)	0.4610 (0.46087–0.46110)		4.2*
IV	$A_1=u_1 exp(u_2B)$	69.604 (69.5169–69.7246)	0.00007941 (0.00079270–0.000079560)		18.0
V	$A_1 = A_s\left[1-\left\{u_1/(u_1+u_2B)\right\}^{u_1}\right]$,	0.1283 (0.12801–0.128509)	0.0001516 (0.00015124–0.00015194)	640	4.3

Asterisk (*) indicates that the relationship is optimal.

Parameter estimation and confidence interval analysis were performed by the following procedure. u_1 and u_2 were estimated by minimizing the sum of squares:

$$\Theta = \sum_y \left(\ln(A_y / \hat{A}_y)\right)^2,$$

where A_y and $\hat{A}_y$ = the observed spawning area in year y and predicted values from relationships I– V, respectively.

The least-squares minimization was performed by the quasi-Newton method in Solver, which is "add in" software for MS-Excel (Microsoft Corp., 1996). The least-squares minimization procedure was stopped if either of the two following conditions were satisfied:

more than 100 iterations were attempted; or

the sum of squared residuals changed by less than 0.01% between iterations.

Confidence intervals of the estimators were calculated through a likelihood ratio test. If $\ln(A_y/\hat{A}_y) \sim N(0,\sigma^2)$, then

U = (u_1, u_2) is a parameter vector,
$\hat{U}$ = $(\hat{u}_1, \hat{u}_2)$ is the estimated parameter vector which minimizes the Θ, and
$\hat{U}_I$ = $(u_1, \hat{u}_2)$ is the parameter vector which minimizes the Θ with respect to a certain value of u.

The confidence interval for a certain parameter u_i was given as the region which satisfied the inequality $2\ln\{L(\hat{U})/L(U)\} \leq x^2(0.95,1)$, where L and $\chi^2(0.95,1)$ were the likelihood and 95% value of the χ^2 distribution with one degree of freedom, respectively. The Akaike information criterion (AIC) was used for selecting an optimal relationship within the set of proposed relationships I–V. The AIC is calculated for candidate models, and the most parsimonious one has the lowest AIC (Akaike, 1973).

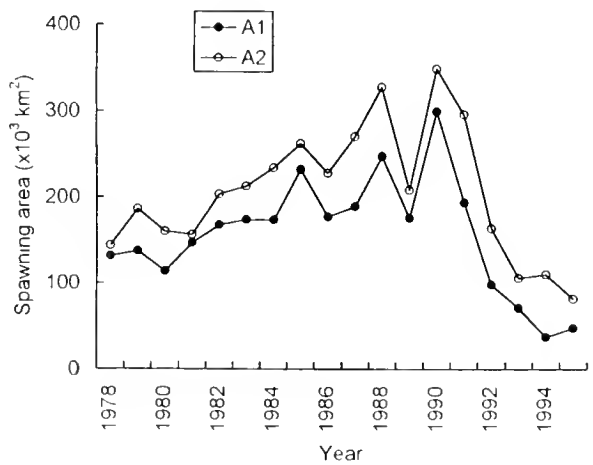

Figure 5

Change in the spawning area of the Japanese pilchard along the Pacific coast of Japan over time. A_1 and A_2 were calculated by summing the areas of 1° longitude × 1° latitude squares where early developmental stage eggs and eggs of any stage occurred, respectively.

Results

The spawning biomass (B) of the Japanese pilchard experienced a remarkable increase in the 1970s, peaked in 1988, and has been declining since the end of the 1980s (Fig. 1; Wada and Jacobson, 1998). A_1 expanded from 114,000 km^2 in 1980 to 299,000 km^2 in 1990, before shrinking to 38,000 km^2 in 1994 (Fig. 5). Estimated parameters, their confidence intervals for each relationship, and AIC are summarized in Table 1. The value of AIC was at a minimum in relationship III and varied considerably compared to the

Table 2

Estimated parameter values and 95% confidence intervals (in parentheses) for each relationship between the spawning area (A_2: 10^3 km^2) and the spawning biomass (B :10^3metric ton) of Japanese pilchard along the Pacific Coast of Japan from 1978 to 1995.

Relationship		u_1	u_2	A_s (10^3/km^2)	AIC
I	$A_2=u_1B$	0.03196 (0.031853–0.032075)			48.7
II	$A_2=u_1B+u_2$	0.01141 (0.011389–0.011438)	102.382 (102.2073–102.5608)		4.7
III	$A_2=u_1B^{u2}$	12.304 (12.2926–12.3154)	0.3156 (0.31546–0.31567)		0.9*
IV	$A_2=u_1 exp(u_2B)$	116.780 (116.5000–116.9103)	0.00005689 (0.00056782–0.000057001)		7.5
V	$A_2 = A\left[1-\left\{u_1/(u_1+u_2B)\right\}^{u_2}\right]$,	0.1176 (0.11737–0.117766)	0.0004710 (0.00046983–0.00047289)	640	3.3

other relationships, except for V. The optimal relationship between A_1 and B was A_1=2.518 $B^{0.4610}$ (Table 1, Fig. 6), although the difference in AIC between relationship III and V was small. Relationship III was statistically significant (r^2=0.833, n=18, P<0.001). A_2 expanded steadily from 144,000 km^2 in 1978 to 327,000 km^2 in 1988 (Fig. 5). The area decreased to 208,000 km^2 in 1989, peaked at 349,000 km^2 in 1990, and then shrank to 82,000 km^2 in 1995. The optimal relationship between A_2 and B was A_2=12.304 $B^{0.3156}$ (Table 2, Fig. 6) and was statistically significant (r^2=0.737, n=18, P<0.001).

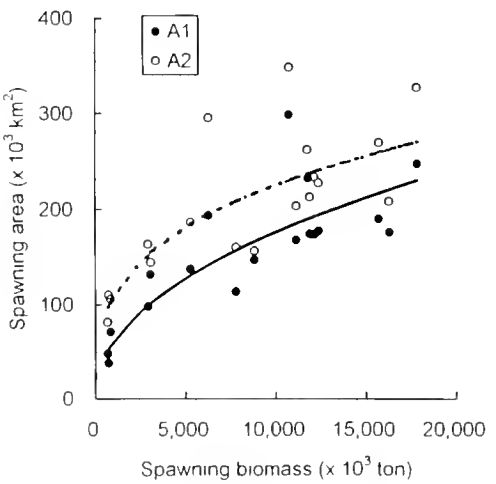

Figure 6

Relationship between the spawning area (A_1 or A_2) and spawning biomass of Japanese pilchard. Closed circles = the spawning area (A_1), open circles = the spawning area (A_2). The solid line indicates the optimal relationship between A_1 and the spawning biomass (B) (A_1=0.2518$B^{0.4610}$). The dotted line indicates the optimal relationship between A_2 and the spawning biomass (A_2=12.304$B^{0.3156}$).

Discussion

The spatial distribution of pilchard eggs may increase over time through transportation by wind-driven currents or the Kuroshio frontal eddy current (Kasai et al., 1992). Because the data for calculating A_2 included the presence of eggs at stages long after spawning had occurred, A_2 was an overestimate of the spawning area. Therefore, A_1 may be a better indicator of the spawning area than A_2. The relationship between A_1 and A_2 was A_1 = 0.8501 A_2 -18.468, and was statistically significant (r^2=0.900, n=18, P<0.001). However, the calculation of A_1 was more expensive and time consuming because egg developmental stages need to be distinguished. Selection of the indicator will depend on our demand for the precision of biomass estimate.

One cause of the nonlinear relationship between the spawning area and spawning biomass seemed to be that pilchard egg aggregations are distributed over space in a patchy manner, in relation of course to the schooling behavior of the adults. Judging from the small difference in AIC between relationship III and V (Table 1) and the similar shapes of III and V (Fig.7), we believed that the model which assumes a patchy egg distribution seemed reasonable.

An estimate of pilchard spawning biomass can be obtained by using the inverted relationship of III (B= $0.135A_1^{2.1691}$). This estimate of spawning biomass might be useful as an abundance index for tuning VPA, such as the adaptive framework described by Gavaris (1988). Frequently, fisheries managers must estimate the biomass of pelagic stocks. Several techniques of abundance estimation may be successfully applied to the pilchard, including the egg production method, acoustic surveys, systematic aerial surveys, or combinations of these (Watanabe, 1983; Hara, 1983; Hara, 1986). Selection or devel-

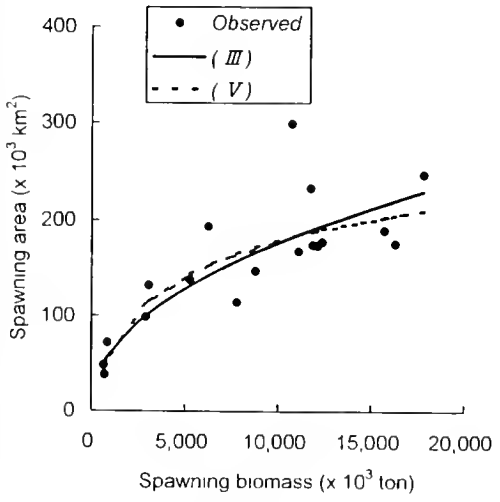

Figure 7

Difference between relationships III and V. Closed circles indicate the observed data. The solid line indicates relationship III (A_1=0.8029$B^{1.8077}$, AIC=4.2). The dotted line indicates relationship V (A_1=640[1 − {0.1283/(0.1283/0.1283 + 0.0001516 B)}$^{0.1283}$], AIC=4.3).

opment of methods will depend on management goals, performance of the resource in recovery, and fishery development. We believe that the method in our study provides a new tool for the estimation of Japanese pilchard biomass when information concerning the fishery is limited.

Acknowledgments

The authors would like to thank T. Wada and M. Ishida, National Research Institute of Fisheries Science, for their assistance with data processing. This work was supported in part by the Bio Cosmos Program of the Ministry of Agriculture, Forestry, and Fisheries.

Literature cited

Akaike, H.
1973. Information theory and an extension of the maximum likelihood principle. *In* International symposium on Information theory (B. N. Petran and F. Csaaki, eds.), p. 267–281. Acadeemiai Kiadi, Budapest.

Gavaris, S.
1988. An adaptive framework for the estimation of population size. Canadian Atl. Fish. Sci. Adv. Comm. (CAFSAC) Res. Doc., 88/29,12 p.

Hara, I.
1983. Estimation of fish density method. Nippon Suisan Gakkaishi. 49:1619–1625.
1986. Stock assessment of Japanese pilchard in the waters off southeast coast of Hokkaido using line transect method. Nippon Suisan Gakkaishi. 52:69–73.

Hilborn, R., and M. Mangel.
1997. The ecological detective. Confronting models with data. Princeton Univ. Press, Princeton, NJ, 315 p.

Hiramoto, K.
1981. Studies on the growth and life-cycle of the Japanese sardine *Sardinops melanosticta* (Temminck et Schlegel) in its Pacific sub-population found in Joban and Boso regions. Bull. Chiba Pref. Fish. Expl. Stn. 39:1–127.

Ishida, M., and H. Kikuchi.
1992. Monthly egg productions of the Japanese sardine, anchovy, and mackerels off the southern coast of Japan by egg censuses: January, 1989 through December, 1990. Nansei National Research Institute and National Research Institute of Fisheries Science, Kochi, Tokyo, p. 1–72. [In Japanese.]

Kasai, A., J. K. Kishi, and T. Sugimoto.
1992. Modeling the transport and survival of Japanese sardine larvae in and around the Kuroshio Current. Fish. Oceanogr. 1:1–10.

Kikuchi, H., and Y. Konishi.
1990. Monthly egg productions of the Japanese sardine, anchovy, and mackerels off the southern coast of Japan by egg censuses: January, 1987 through December, 1988. National Research Institute of Fisheries Science, and Nansei National Research Institute, Tokyo, Kochi, p. 1–72. [In Japanese.]

Kondo, K., Y. Hori, and K. Hiramoto.
1976. Life pattern of the Japanese sardine, *Sardinops melanosticta*, and its practical procedure of marine resources researches of the stock (2nd ed.). *In* Fish. Res. Ser. 30, Jap. Resour. Conserv. Assoc., Tokyo, 68 p. [In Japanese.]

Lasker, R.
1981. Marine fish larvae. Univ. Washington Press, Seattle, WA, 131 p.

MacCall, D.
1988. Dynamic geography of marine fish populations. Univ. Washington Press, Seattle, WA, 153 p.

Mangel, M., and P. E. Smith.
1990. Presence-absence sampling for fisheries management. Can. J. Fish. Aquat. Sci. 47:1875–1887.

Microsoft Corporation.
1996. Microsoft Excel for Windows 95. Microsoft Corp., Singapore, 228 p.

Mori, K., K. Kuroda, and Y. Konishi.
1988. Monthly egg productions of the Japanese sardine, anchovy, and mackerels off the southern coast of Japan by egg censuses: January, 1978 through December, 1986. Tokai Regional Fisheries Research Laboratory, D-12:1–321. [In Japanese.]

Nakai, Z.
1962. Studies relevant to mechanisms underlying the fluctuation in the catch of the Japanese sardine, *Sardinops melanosticta* (T. & S.). Japan. J. Ichthyol. 9:1–115.

Pielou, E. C.
1977. Mathematical ecology. John Wiley and Sons, New York, NY, 385 p.

Rosenzweig, M.
1981. A theory of habitat selection. Ecology. 62:327–335.

Smith, P. E.
1973. The mortality and dispersal of sardine eggs and larvae. Rapp. P.-V. Reun. Cons. Int. Explor. Mer 164:282–292.

Smith, P. E., and R. P. Hewitt.
1985. Sea survey design and analysis for an egg production method of anchovy biomass assessment. U.S. Dep. Commer., NOAA Tech. Rep. NMFS. 36:17–26.

Watanabe, T., and D. Jacobson.
1990. Regime and stock-recruitment relationships in Japanese sardine (*Sardinops melanostictus*), 1951–1995. Can. J. Fish. Aquat. Sci. 55:2455–2463.
Wada, T., and K. Kashiwai.
1991. Changes in growth and feeding ground with fluctuation in stock abundance. *In* Long-term variability of pelagic fish populations and their environments (T. Kawasaki, S. Tanaka, and Y. Toba (eds.), p. 181–190. Pergamon Press, London.
Watanabe, T.
1983. Spawning survey method. *In* Population dynamics of fishery resources (T. Ishii, ed.), p. 2–29. Koseisha-Koseikaku, Tokyo. [In Japanese.]
Watanabe, Y., H. Zenitani, and R. Kimura.
1996. Offshore expansion of spawning of the Japanese sardine, *Sardinops melanostictus*, and its implication for egg and larval survival. Can. J. Fish. Aquat. Sci. 53:55–61.
Zenitani, H., M. Ishida, Y. Konishi, T. Goto, Y. Watanabe, and R. Kimura.
1995. Distribution of eggs and larvae of pelagic fish species around Japan. National Research Institute Fishery Agency Resource Management Research Report A-1:1–368. [In Japanese.]
Zenitani, H., M. Ishida, and S. Yamada.
1998. A relationship between egg abundance and spawning area for fishes under patchy egg distribution. Bull. Jpn. Soc. Fish Oceanogr. 62:97–103. [In Japanese with English abstract.]
Zweifel, J. R., and P. E. Smith.
1981. Estimates of abundance and mortality of larval anchovies (1951–75): application of a new method. Rapp. P.-V. Reun. Cons. Int. Explor. Mer 178:248–259.

Geographic patterns in growth of the giant Pacific sea scallop, *Patinopecten caurinus*

Steve Ignell
Evan Haynes
Auke Bay Laboratory
Alaska Fisheries Science Center
National Marine Fisheries Service, NOAA
11305 Glacier Highway
Juneau, Alaska 99801-8626
E-mail address: Steve.Ignell@noaa.gov

Giant Pacific or weathervane sea scallops, *Patinopecten caurinus*, were first fished commercially in the Gulf of Alaska in 1967, when 3449 kg of unshucked sea scallops (estimated 341 kg of meats) were landed at Kodiak, Alaska (Haynes and Powell, 1968). The discovery of commercially exploitable stocks of giant Pacific sea scallops led to a fishery that expanded rapidly, and landings increased to 856 metric tons (t) of schucked meats by 1969 (ADF&G, 1979). For the next two decades, scallop landings fluctuated greatly (ADF&G, 1987), a result of limited stocks, restrictive regulations, and more lucrative opportunities in other Alaska fisheries (Kaiser, 1986). Since 1990, however, the fishery has changed from a part-time fleet to a dedicated full-time fleet with the influx of larger, more efficient vessels. This change has led to sustained near-record harvests (up to 823 t) and the adoption of new management measures for the fishery (Shirley and Kruse, 1995; NMFS[1]).

Most of the biological literature on giant Pacific scallops relates to fishing exploration (Rathjen and Rivers, 1964; Haynes and Powell, 1968; Ronholt and Hitz, 1968; Haynes and McMullen, 1970; Bourne, 1988), aquaculture (Beattie, 1985; Thompson et al., 1985; Rhee, 1989), or reproductive biology (Hennick, 1970 and 1971; Robinson and Breese, 1984). Age and growth of giant Pacific scallops have been studied in populations off Oregon (Starr and McCrae, 1983), Washington and the Strait of Georgia (Haynes and Hitz, 1971), northern Gulf of Alaska (Kaiser, 1986; Hennick[2]), and the lower Cook Inlet region (Hammarstrom and Merritt, 1985).

A lack of data on biological productivity has affected recent efforts to develop a fishery management plan (FMP) for Alaska giant Pacific scallop stocks (NMFS[1]). It has inhibited the development of yield models and a numeric specification of overfishing (an FMP requirement) and resulted in a simple numeric range given for optimal yield. However, there is a renewed interest in acquiring better information for stock assessments and biological parameters needed to implement an exploitation-rate harvest strategy for the fishery (NMFS[1]).

This note presents results of a comparative growth study of stocks of giant Pacific scallops in the Gulf of Alaska. Samples for this study were collected during the initial explorations for commercial quantities of these scallops in 1968 (Haynes and Powell, 1968); thus these data yield prefishery biological parameters that can provide a baseline to evaluate fishery impacts on the giant Pacific scallop populations in Alaska.

Methods

Giant Pacific scallops were collected at six locations in the Gulf of Alaska from 27 April to 6 June 1968 (Fig. 1). Sampling was done from the chartered FV *Viking Queen* with a standard New Bedford type sea scallop dredge 3.96 m wide (equipped with 10-cm rings). A detailed description of this type of gear is given in Posgay (1957) and Bourne (1964). The locations and depths of sampling were 1) on Albatross Bank at 92–104 m, 2) on Marmot Flats at 73–104 m, 3) in lower Cook Inlet at 108–122 m, 4) off Cape St. Elias at 91–102 m, 5) off Ocean Cape at 82–91 m, and 6) off Lituya Bay at 64–75 m. Areas were selected for their geographic separation and likely abundance of scallops. Giant Pacific scallops were shucked aboard the vessel, and the upper valves were retained for age and growth analyses. At each location, 59–248 scallops were selected (Table 1); the only criterion for selection was that each sample include a wide range of sizes. Because larger (and rarer) scallops were more likely to be chosen, samples were not selected at random. Within a sample, however, the range of sizes at any given age was not great; for the purpose of fitting growth curves, we assumed that each age class was sampled randomly.

Ages were determined by counting clearly visible annuli (growth rings) on the outer surface of the upper valve. The first annulus is formed halfway during the second year of life; scallops spawn in the summer and the annuli are formed in the winter (Haynes and Hitz, 1971). This aging method has been used extensively to study mollusk growth, such as in studies on the North Atlantic sea scallop, *Placopecten magellanicus* (Stevenson, 1934; Stevenson and Dickie, 1954; Merrell et al., 1961), and on the European sea

[1] National Marine Fisheries Service. 1996. Fishery management plan for the scallop fishery off Alaska. Unpubl. document. Natl. Mar. Fish. Serv., P.O. Box 21668, Juneau, AK 99802, 123 p.

[2] Hennick, D. P. 1973. Sea scallop, *Patinopecten caurinus*, investigations in Alaska. Commer. Fish. Res. Develop. Act, project 5-23-R, completion rep. (unpubl.). Alaska Dep. Fish and Game, Juneau, AK 99801, 38 p.

Manuscript accepted 13 March 2000
Fish. Bull. 98:849–853 (2000)

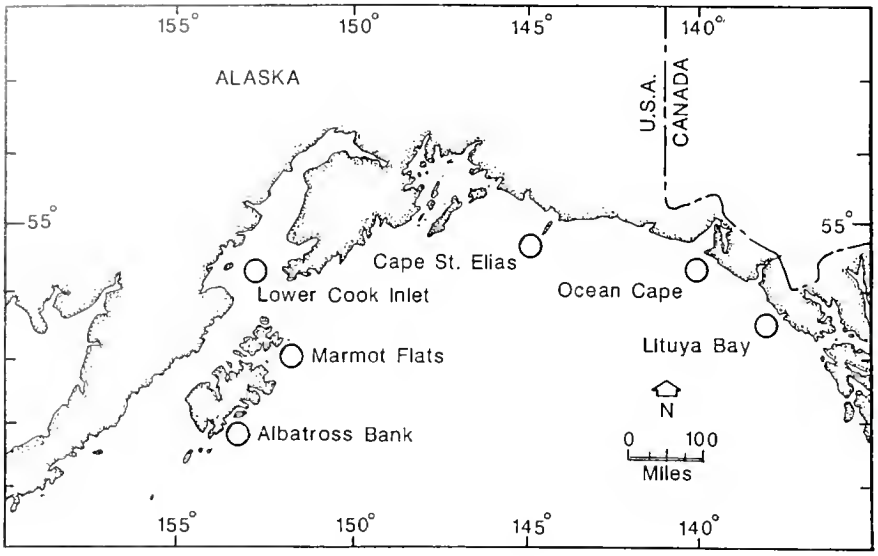

Figure 1

The six areas in the Gulf of Alaska sampled for giant Pacific sea scallops during the *Viking Queen* survey, 1968.

scallop, *Pecten maximus* (Gibson, 1956; Mason, 1957), and shows reasonably good agreement with "true" (isotopically predicted) ages when growth rings are clearly visible (Dare and Deith, 1989). Application of the method to *Patinopecten caurinus* has been verified by Haynes and Hitz (1971).

Terminal shell heights (size of shell to the last annulus; hereafter called "shell heights") were used to fit a growth model for each sample (Table 1). No attempt was made to determine the sex of the scallops because of indications that growth differences between sexes were insignificant.[3] After our sampling, scientists of the ADF&G provided sex and age data for scallops taken in August 1970 northwest of Kodiak Island. The von Bertalanffy growth model was fitted to these data, and growth differences between sexes were tested as described in the following section.

Estimation and fitting of von Bertalanffy curves

Mean shell heights by age were plotted for sea scallops in each sample (Fig. 2). Growth decreased steadily with age, suggesting that sigmoid growth was not present or that the shell heights used were beyond the point of inflection; thus the von Bertalanffy growth model was considered appropriate for our study. In this model, length of the i^{th} individual at age t is

$$l_{it} = l_\infty \left[1 - e^{-k(t-t_0)}\right] + e_i;\ e_i \sim N(0,\sigma^2).$$

Kimura (1980) showed that maximum likelihood estimation for the von Bertalanffy curve is equivalent to finding least-square estimates of model parameters (see also Cerrato, 1990). Least-square estimates for the three parameters were obtained by nonlinear regression methods. Analysis of residuals showed that the von Bertalanffy model provided an adequate fit for all samples. The precision (variance) of parameter estimates varied with age composition of the sample. For example, samples with few young scallops showed relatively large variances for the parameters K and t_0, whereas samples with few old scallops resulted in imprecise estimates of asymptotic length (Table 2). However, the residual mean square error (MSE), denoting variability about fitted growth equations, did not vary widely among samples.

Comparison of growth curves for different areas

No significant difference ($P>0.15$) in growth between sexes was detected in the ADF&G samples, supporting the presurvey decision not to determine the sex of the scallops. Growth of scallops from the six areas was compared by likelihood ratio tests by using two probability models: model 1 specified equality of the von Bertalanffy parameters of each area; model 2 allowed separate parameters for each area (Kimura, 1980). The first model consisted of pooling the data over all areas, yielding one growth equation; the second model allowed separate growth equations for each area. Because there was no *a priori* hypothesis concerning growth differences between the areas, 15 simultaneous tests were performed to evaluate pairwise differences in growth. These tests were equivalent to testing k independent hypotheses at a significance level of α. Applying Bonferonni's inequality (Miller, 1966) to the 15 tests resulted in an experimental-wise significance level $\leq k \times \alpha$. We chose α to equal 0.003, giving an experimental-wise significance level of 0.045. Likelihood ratio tests

[3] ADF&G 1970. Unpubl. observations. Alaska Dept. Fish and Game, Kodiak, AK 99615.

indicated highly significant differences ($P<0.003$) in growth between scallops from each area.

Results and discussion

Sea scallops from the Gulf of Alaska showed a consistent trend in growth geographically: from southeastern Alaska northward and then westward around the perimeter of the Gulf of Alaska, sea scallops tended to be larger. Differences in mean shell height were small at early ages but became more pronounced as the scallops grew older (Fig. 2).

This geographic trend in growth was probably not related to time and depth of sampling. Time of sampling varied little between areas; all areas were sampled within a period of 45 days. Depth of sampling did vary between areas, however, because scallop growth rates are known to vary by water depth, e.g. scallops off Oregon are smaller in deeper waters and have reduced asymptotic lengths (Ronholt and Hitz, 1968; Starr and McCrae, 1983). If this depth-size relationship holds true in Alaska waters, then current estimates of asymptotic size for scallops from the northern areas are biased downwards compared with those from Lituya Bay, where scallops were sampled in shallower waters.

Comparisons of our growth results with two analyses of giant Pacific scallop samples taken after the start of commercial fishing (Kaiser, 1986; Hennick[2]) showed significantly different estimates of asymptotic size. For scallops off Kodiak, values of l_∞ from Hennich's data (182.8 mm) and Kaiser's data (189.8 mm) are larger than our estimate (175.7 mm); for scallops off Yakutat, values of l_∞ from Hennick's data (151.5) and Kaiser's data (143.7 mm) are smaller than our estimate (158.6 mm). Scallop fishing before 1980 occurred entirely in these two areas (Shirley and Kruse, 1995). The reduction in asymptotic size for scallops off Yakutat may indicate an increase in fishing mortality on larger individuals. Both analyses also showed that giant Pacific scallops for a given annular ring are larger from the Kodiak area than from Yakutat, a result that supports our conclusions of geographic growth trends for the giant Pacific sea scallop.

Table 1

Mean shell heights (mm) and standard deviations (SD, in parentheses) and number of giant Pacific sea scallops of given ages sampled from six areas in the Gulf of Alaska. Areas listed are from northwest to southeast.

	Sampling areas											
	Albatross Bank		Marmot Flats		Lower Cook Inlet		Cape St. Elias		Ocean Cape		Lituya Bay	
Age (yr)	Length (SD)	*n*	Length (SD)	*n*	Length (SD)	*n*	Length (SD)	*n*	Length (SD)	*n*	Length (SD)	*n*
1		0		0		0		0		0		0
2		0		0		0		0	51.9 (6.5)	7	37.5 (9.2)	2
3		0		0	70.7 (5.3)	11	77.1 (6.3)	36	76.9 (5.0)	22	69.5 (0.7)	2
4	90.9 (5.8)	47	107.8 (3.3)	4	89.5 (5.5)	19	100.8 (6.4)	21	95.6 (5.7)	117	86.8 (8.3)	62
5	114.2 (4.3)	44	121.2 (3.0)	9	113.1 (6.6)	48	116.6 (6.0)	42	107.1 (5.0)	29	96.9 (7.2)	14
6	134.3 (6.8)	3	137.6 (4.1)	13	127.6 (5.4)	77	135.3 (8.1)	7	117.5 (7.2)	27	110.5 (5.4)	16
7	141.0 (4.5)	21	143.25 (4.8)	8	136.6 (6.0)	58	141.3 (5.2)	4	127.6 (4.5)	11	114.8 (5.6)	33
8	148.8 (3.0)	9	151.6 (2.3)	10	141.3 (6.3)	18	141.0	1	134.5 (7.3)	20	199.7 (6.5)	64
9	157.7 (3.1)	3	156.9 (3.9)	10		0	151.7 (4.5)	3	141.2 (5.9)	9	124.1 (4.2)	9
10	166.0	1	162.5 (0.7)	2		0	152.0	1	144.0 (4.9)	4	129.0 (5.6)	2
11		0	173.0	1		0	153.0	1	155.0	1		0
12		0	166.0 (1.4)	2		0		0		0		0
13		0		0		0	153.0 (0.0)	2		0		0
14		0		0		0	158.5 (4.9)	2		0		0
15		0		0		0	157.0	1		0		0
16		0		0		0		0	156.0	1		0

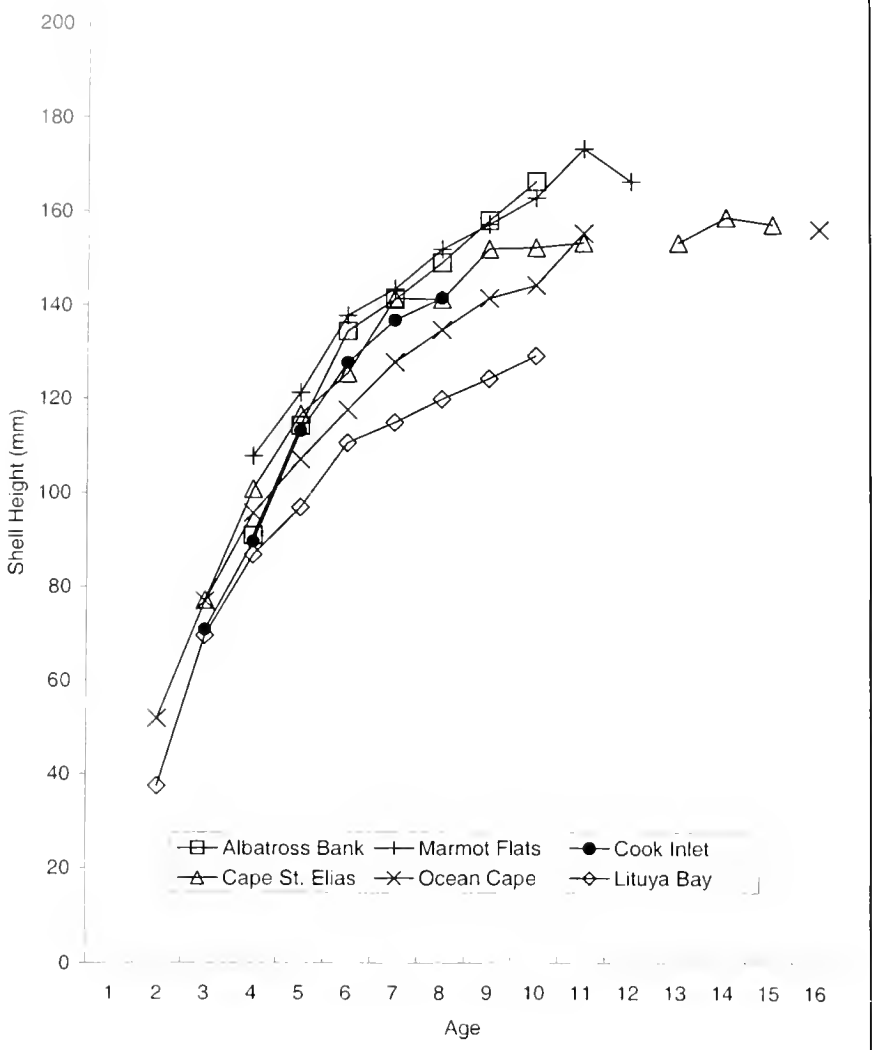

Figure 2

Mean shell heights by age for sea scallops collected in the Gulf of Alaska, 1968.

Table 2

Von Bertalanffy growth parameters (and standard errors) for sea scallops from six Gulf of Alaska areas. Sample areas are given in order from northwest to southeast.

Area	Sample size	Parameter estimates (standard errors)			
		σ^2	L_∞	k	t_0
Albatross Bank	128	23.71	170.1 (4.5)	0.346 (0.035)	1.791 (0.156)
Marmot Flats	59	15.13	175.7 (4.2)	0.265 (0.033)	0.455 (0.387)
Lower Cook Inlet	231	36.88	161.7 (4.1)	0.328 (0.030)	1.353 (0.139)
Cape St. Elias	121	37.64	159.7 (2.8)	0.326 (0.021)	0.974 (0.116)
Ocean Cape	248	34.80	158.6 (3.3)	0.244 (0.017)	0.265 (0.141)
Lituya Bay	204	47.41	130.5 (2.5)	0.367 (0.036)	0.962 (0.207)

Literature cited

ADF&G (Alaska Department of Fish and Game).
1979. 1976 Alaska catch and production—commercial fisheries statistics. Statist. Leafl. 29, Alaska Dep. Fish and Game, Juneau, AK 99801, 47 p.
1987. Alaska 1985 catch and production—commercial fisheries statistics. Statist. Leafl. 8, Alaska Dep. Fish and Game, Juneau, AK 99801, 61 p.

Beattie, J. H.
1985. The weathervane scallop *Patinopecten caurinus* (Gould): a candidate for aquaculture? J. Shellfish Res. 5:49.

Bourne, N.
1964. Scallops and the offshore fishery of the Maritimes. Fish. Res. Board Can., Bull. 145, 60 p.
1988. Scallop resources of British Columbia, Canada. J. Shellfish Res. 7:150.

Cerrato, R. M.
1990. Intrepretable statistical tests for growth comparisons using parameters in the von Bertalanffy equation. Can. J. Fish. Aquat. Sci. 47:1416–1426.

Dare, P. J., and M. R. Deith
1989. Age determination of scallops, *Pecten maximus* (Linaeus, 1758), using stable oxygen isotope analysis, with some implications for fisheries management in British waters. *In* World aquaculture workshops, no. 1 (S. E. Shumway and P. A. Sandifer, eds.) p. 118–133. The World Aquaculture Soc., Baton Rouge, LA.

Gibson, F. A.
1956. Escallops (*Pecten maximus* L.) in Irish waters. Sci. Proc. Dublin Soc. 27:253–270.

Hammarstrom, L. F., and M. F. Merritt.
1985. A survey of Pacific weathervane scallops (*Pecten caurinus*) in Kamishak Bay, Alaska. Alaska Dep. Fish and Game, Div. Commer. Fish., Inform. Leafl. 252, Juneau, AK, 23 p.

Haynes, E. B., and C. R. Hitz.
1971. Age and growth of the giant Pacific sea scallop, *Patinopecten caurinus*, from the Strait of Georgia and outer Washington coast. J. Fish. Res. Board Can. 28:1335–1341.

Haynes, E. B., and J. C. McMullen.
1970. Relation between meat weight and shell height of the giant Pacific sea scallop, *Patinopecten caurinus*, from the Gulf of Alaska. Proc. Natl. Shellfish Assoc. 60:50–53

Haynes, E. B., and G. C. Powell.
1968. A preliminary report on the Alaska sea scallop—fishery exploration, biology and commercial processing. Inform. Leafl. 125, Alaska Dep. Fish and Game, Juneau, AK 99801, 20 p.

Hennick, D. P.
1970. Reproductive cycle, size at maturity, and sexual composition of commercially harvested weathervane scallops (*Patinopecten caurinus*) in Alaska. J. Fish. Res. Board Can. 27:2112–2119.
1971. A hermaphroditic specimen of weathervane scallop, *Patinopecten caurinus*, in Alaska. J. Fish. Res. Board Can. 28:608–609.

Kaiser, R. J.
1986. Characteristics of the Pacific weathervane scallop (*Pecten* [*Patinopecten*] *caurinus*, Gould 1850) fishery in Alaska, 1967–1981. M.S. thesis, Oregon State Univ., Corvallis, OR, 100 p.

Kimura, D. K.
1980. Likelihood methods for the von Bertalanffy growth curve. Fish. Bull. 77:765–777.

Mason, J.
1957. The age and growth of the scallop, *Pecten maximus* (L.), in Manx waters. J. Mar. Biol. Assoc. U.K. 36:473–492.

Merrell, A. S., J. A. Posgay, and F. E. Nichy.
1961. Annual marks on shell and ligament of sea scallop (*Placopecten magellanicus*). Fish. Bull. 65:299–311.

Miller, R.
1966. Simultaneous statistical inference. McGraw-Hill, New York, NY, 271 p.

Posgay, J. A.
1957. Sea scallop boats and gear. U.S. Fish Wildl. Serv., Fish. Leafl. 442, 11 p.

Rathjen, W. F., and J. B. Rivers.
1964. Gulf of Alaska scallop explorations, 1963. Commer. Fish. Rev. 26(3):1–7.

Rhee, Y. W.
1989. Scallop culture in Washington State. J. Shellfish Res. 8:415.

Robinson, A. M., and W. P. Breese.
1984. Spawning cycle of the weathervane scallop *Pecten* (*Patinopecten*) *caurinus* Gould along the Oregon coast. J. Shellfish Res. 4:165–166.

Ronholt, L. L., and C. R. Hitz.
1968. Scallop explorations off Oregon. Commer. Fish. Rev. 30(7):42–49.

Shirley, S. M., and G. H. Kruse.
1995. Development of the fishery for weathervane scallops, *Patinopecten caurinus* (Gould, 1850), in Alaska. J. Shellfish Res. 14(1):71–78.

Starr, R. M., and J. E. McCrae.
1983. Weathervane scallop (*Patinopecten caurinus*) investigations in Oregon, 1981–1983. Oregon Dep. Fish. Wildl. Info. Rep. 83-10, 55 p.

Stevenson, J. A.
1934 The growth rate of Canadian scallops. Fish. Res. Board Can., Progr. Rep. Atl. Biol. Sta. 11:10–11.

Stevenson, J. A., and L. M. Dickie.
1954. Annual growth rings and rate of growth of the giant scallop, *Placopecten magellanicus* (Gmelin), in the Digby area of the Bay of Fundy. J. Fish. Res. Board Can. 11:660–671.

Thompson, D. S., C. Mason, and N. Bourne.
1985. Recent progress in the artificial breeding of four species of scallops. J. Shellfish Res. 51:54–55.

Preliminary examination of the match-mismatch hypothesis and recruitment variability of yellowtail flounder, *Limanda ferruginea*

Donna L. Johnson

James J. Howard Marine Sciences Laboratory at Sandy Hook
Northeast Fisheries Science Center
National Marine Fisheries Service, NOAA
74 Magruder Road
Highlands, New Jersey 07732
E-mail address: Donna.Johnson@noaa.gov

Preliminary examination of the match-mismatch hypothesis and recruitment variability of yellowtail flounder, *Limanda ferruginea*

Donna L. Johnson

James J. Howard Marine Sciences Laboratory at Sandy Hook
Northeast Fisheries Science Center
National Marine Fisheries Service, NOAA
74 Magruder Road
Highlands, New Jersey 07732
E-mail address: Donna.Johnson@noaa.gov

Abstract—The match-mismatch hypothesis was examined for yellowtail flounder (*Limanda ferruginea*) stocks that exist and spawn on Georges Bank (GB) and off Southern New England (SNE) and to observe any correlation between year-class strength and prey abundance. Data from a comprehensive sampling program, the Marine Resources Monitoring, Assessment, and Prediction (MARMAP), structured with broad temporal and geographic coverage, were used for this study. Collections were made during 1977–87 on the U.S. continental shelf from Cape Hatteras to the Gulf of Maine.

Underlying explanations of recruitment variation among fish stocks have been an issue for several decades. An understanding of biological relationships between larval fish and their zooplankton prey is needed for interpreting recruitment success. Recruitment fluctuations often depend upon events occurring during a critical period between spawning and the time of first feeding by larvae (Hjort, 1914). Conditions affecting these early life stages will also determine the number of individuals that survive in a year class. The timing of spawning can enhance the spatial and temporal affinity between larvae and their food resources (Hjort, 1914; Cushing, 1975, 1990; Cushing and Dickson, 1976).

Once resorption of the yolk sac is complete by yolksac larvae, their survival depends entirely upon the amount and accessibility of available food. If sufficient prey is not located after the yolk sac has become exhausted, permanent degeneration of the larva's digestive system will occur (Pitcher and Hart, 1983). Not only are early stage larvae and young juveniles vulnerable because of their dependence on nourishment, they are also susceptible to movement caused by ocean currents (Hjort, 1914, 1926), predation, and starvation (Houde, 1987).

Yellowtail flounder (*Limanda ferruginea*) is an economically important species that experiences marked variation in year-class strength. In the present study, time series data of fish eggs, larvae, and zooplankton were used to determine if a match or mismatch in time and space between yellowtail flounder production and its potential prey existed from Georges Bank and Southern New England 1977 through 1987. Cushing (1975; 1990) hypothesized that links (matches or misses) in time and space among phytoplankton blooms followed by zooplankton and then larval fish lead to year-class variability. A match occurs when there is a close overlap between production curves of fish larvae and their planktonic prey; conversely, a mismatch occurs when there is an extensive temporal difference (Fig. 1) (Cushing, 1975; 1990). A match of peak occurrences would presumably result in a successful year class owing to adequate feeding and growth, and increased chances for survival if other sources of mortality and loss are constrained.

Yellowtail flounder became a key constituent of the U. S. demersal fishery in the early 1930s as a result of stock declines in winter flounder (Royce et al., 1959). There were subsequent drastic reductions in populations and catches during the early 1970s in Southern New England (SNE) and the mid-1970s in Georges Bank (GB). In SNE stocks, landings declined from 3.5 metric tons (t) in 1970 to 1.5 t in 1975. The abundance of New England groundfish declined by 65% from 1977 to 1987 (NEFC, 1991). Three stocks—haddock, redfish, and yellowtail flounder—reached record low levels by the late 1970s.

The present study is the first attempt to examine interannual variability in yellowtail recruitment in the context of the match-mismatch hypothesis. The goal of this study was to test the prediction of the match-mismatch hypothesis for yellowtail flounder stocks that exist and spawn on Georges Bank (GB) and off Southern New England (SNE) and to observe any correlation between year-class strength and prey abundance. Data from a comprehensive sampling program, the Marine Resources Monitoring, Assessment, and Prediction (MARMAP), structured with broad temporal and geographic coverage, were used for this study. Collections were made during 1977–87 on the U.S. continental shelf from Cape Hatteras to the Gulf of Maine.

Materials and methods

A total of 2496 stations from the western North Atlantic were sampled during an eleven-year period from 1977 to 1987. At each station fish eggs, larvae, and zooplankton were collected with a bongo frame (diameter at the mouth of net: 61 cm) (Posgay and Marak, 1980) fitted with 0.333-mm and 0.505-mm mesh nets and a 45 kg depressor. The volume of water filtered by each net was measured by flowmeters suspended in the center of the net mouth. The plankton nets were lowered at a rate of 50 meters per minute, to within 5 meters of the bottom or to a maximum depth of 200 meters, and retrieved at a rate of 20 meters per minute; nets were towed at 1.5 knots at a 45-degree angle. Net contents were preserved in a mixture of 5% formalin and ocean water. Larvae were measured to within 0.1-mm length increments. For complete descriptions of MARMAP sampling procedures see Sibunka and Silverman (1984, 1989).

For each station, catch values were standardized to the number of individuals under 10 m^2 surface area. The delta distribution (Aitchison, 1955) provided unbiased estimates of sample means (Berrien et al., 1981; Pennington, 1983). The abundance and distribution patterns of yellowtail flounder eggs and larvae were monitored and compared with those of *Calanus* and *Pseudocalanus* prey species in the GB and SNE regions from 1977 to 1987.

Although feeding habit studies of yellowtail larvae have not been docu-

Manuscript accepted 8 May 2000
Fish. Bull. 98:854–863 (2000).

mented, *Calanus* sp. and *Pseudocalanus* sp. are both dominant representatives of the zooplankton community of the North Atlantic and are important prey for many spring spawned fish larvae (Cushing, 1982; Runge, 1988). The widespread abundance and distribution of *Calanus* and *Pseudocalanus* favor them to be the most likely prey choice of yellowtail flounder larvae. Collectively, monthly distributions and mean densities of zooplankton for May and June coincide with peak occurrences of yellowtail flounder (Figs. 2 and 3). The Spearman's rank-order correlation analysis was used to measure the association between ichthyoplankton and their zooplankton prey.

An adaptation of the "larval food supply model" (Mertz and Myers, 1994) was used to test the match-mismatch hypothesis, the relationship between spawning variability, and the variability of recruitment. The recruitment estimates were obtained from the Northeast Fisheries Science Center (NEFC, 1991). Two aspects were explored: 1) whether or not a relationship exists between spawning duration and recruitment variability and 2) whether deviations from peak spawning between yellowtail flounder larvae and prey are related to recruitment variability.

The mean and standard deviation of observed abundance versus time was calculated for both yellowtail larvae and their prey for each year and for both subareas. The width and overlap of the abundance curves for predator and prey were analyzed. Selected methods from the Mertz and Myers (1994) study were applied for partial use of this analysis. The following parameters—

t_0 = timing between peaks of larval production and food supply;
Δt_0 = annual differences in (t_0) from its mean value;
δ = one-half width of the production period for larvae; and
σ = one-half width of the production period for zooplankton

—were used to calculate 1) variability in peak timing from the mean for individual species (σ and δ), 2) variability in timing between larval spawning and peak zooplankton production (t_0), and 3) year-to-year variability in peak spawning and production (Δt_0). When t_0 = 0, the match between the peak larvae and production of zooplankton is exact (Mertz and Myers, 1994).

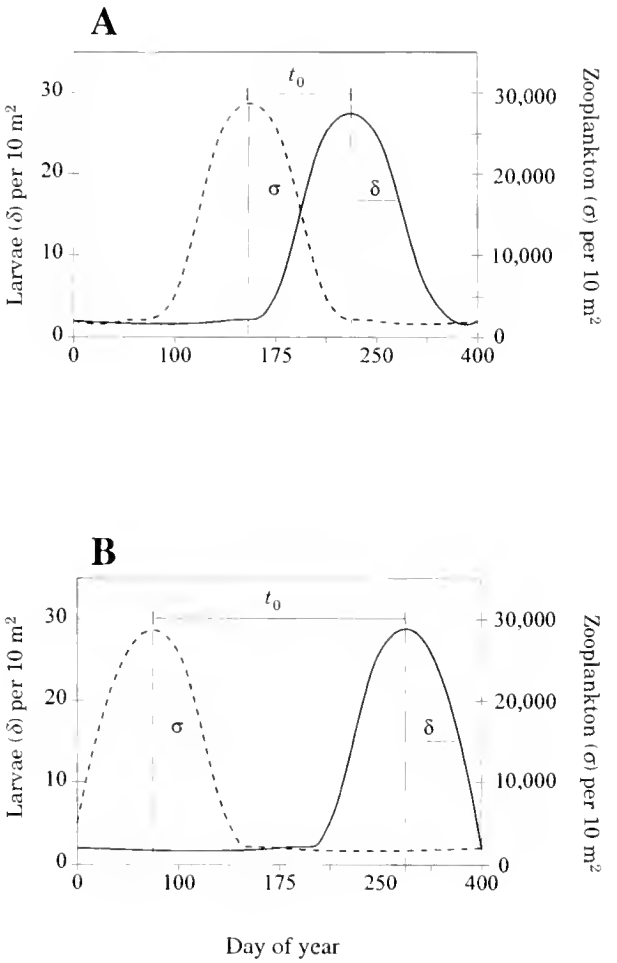

Figure 1

(**A**). A match represented by the overlap of fish larvae and its prey, of the match-mismatch hypothesis. (**B**). A mismatch represented by the lag in time and space between fish larvae and its prey. (δ and σ represent one-half width of the production period of the match-mismatch hypothesis for larvae and zooplankton.) Diagram adapted from Cushing (1990).

Results and conclusions

Variability in timing for individual species

Zooplankton The duration of the *Calanus* sp. peak production (σ) varied from 3.4 to 26.5 days for both subareas. The narrowest distribution occurred during 1984 with 3.4 days, and extremes occurred in 1977 with greater than 12 days for GB and 26.5 days for SNE. The greatest span in peak production for *Pseudocalanus* sp. was 33 days. Smallest duration ranged between 7.8 days (GB) to slightly under 1 day (SNE). The greatest span of time when zooplankton was abundant was 24 days for GB during 1981 and 35 days for SNE during 1982. The low or high zooplankton occurrence was not associated with the strengths or weaknesses of yellowtail recruitment. Both strong (1981) and weak (1982) year classes of yellowtail flounder occurred during times of high variability in peak production of zooplankton.

Ichthyoplankton The difference in timing of peak spawning (Δt_0) from its mean value for yellowtail larvae for both subareas ranged from 1.4 days to approximately 10 days. The largest values of Δt_0 occurred in GB, and again large differences in the timing of spawning did not always reflect years with poor recruitment. Two strong year classes occurred with extreme values of Δt_0: 1977

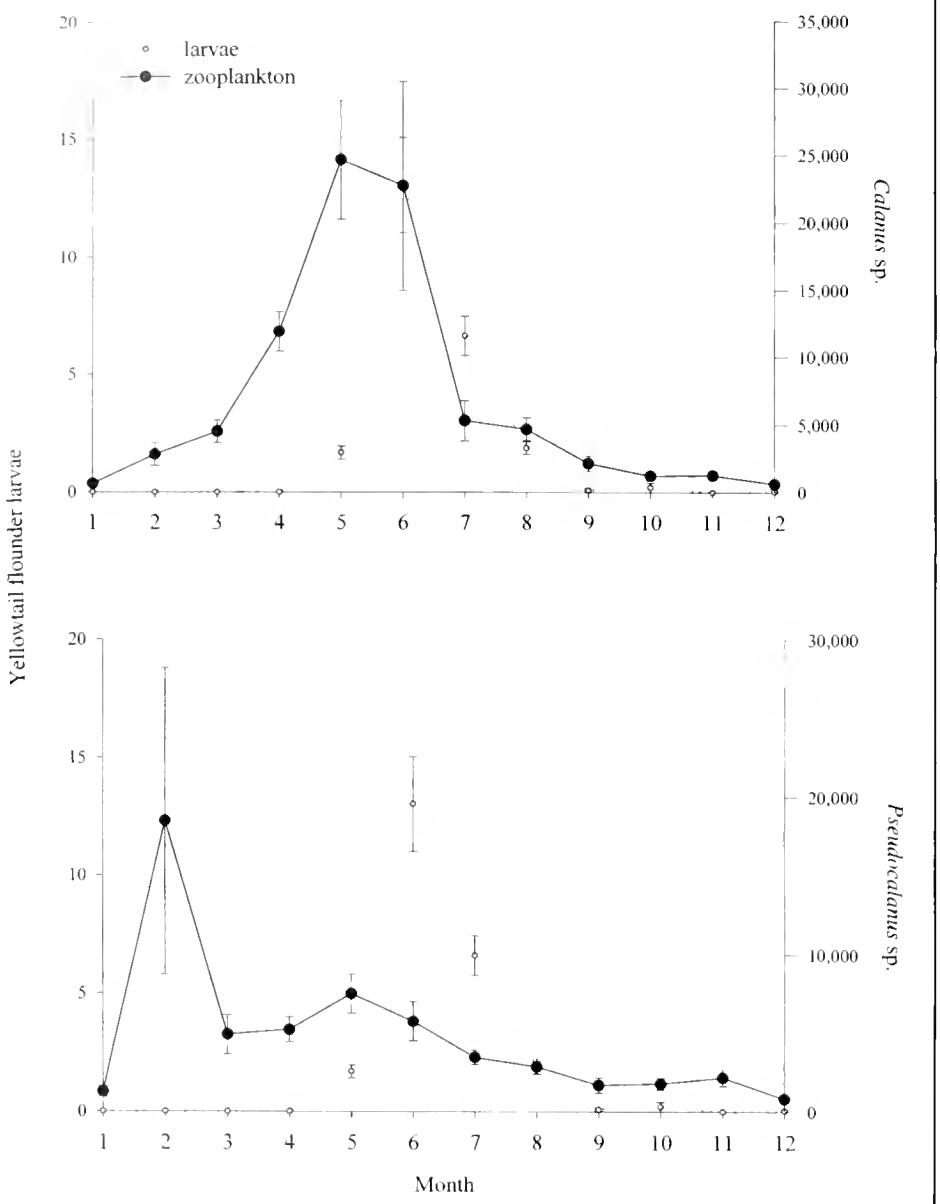

Figure 2

Monthly mean catch per 10 m^2 of *Limanda ferruginea* larvae, *Calanus* sp., and *Pseudocalanus* sp. in Georges Bank for years 1977–87.

with 7 days and 1980 with 3.9 days in GB. In SNE, the weakest year class (1982) possessed the greatest (Δt_0) span with 9.9 days.

Variability in timing between peaks in predator and prey abundance

Examinations of matches and mismatches of larval food and time of yellowtail spawning are shown by the occurrence of width displacements and overlaps from larvae (δ) and its zooplankton prey (σ). The relationship between yellowtail larvae and *Calanus* sp. for SNE display definite matches for years 1980, 1986, and 1987. A slightly larger gap existed between peaks for the year class 1982 (Fig. 4).

During the strong year classes 1980 and 1987, density of yellowtail larvae peaked after that of *Calanus* sp., whereas the reverse occurred in the weaker year classes 1986 and 1982. Similar patterns occurred with the peak spawning and peak production relationships between yellowtail larvae and *Pseudocalanus* sp. The year classes 1982 and

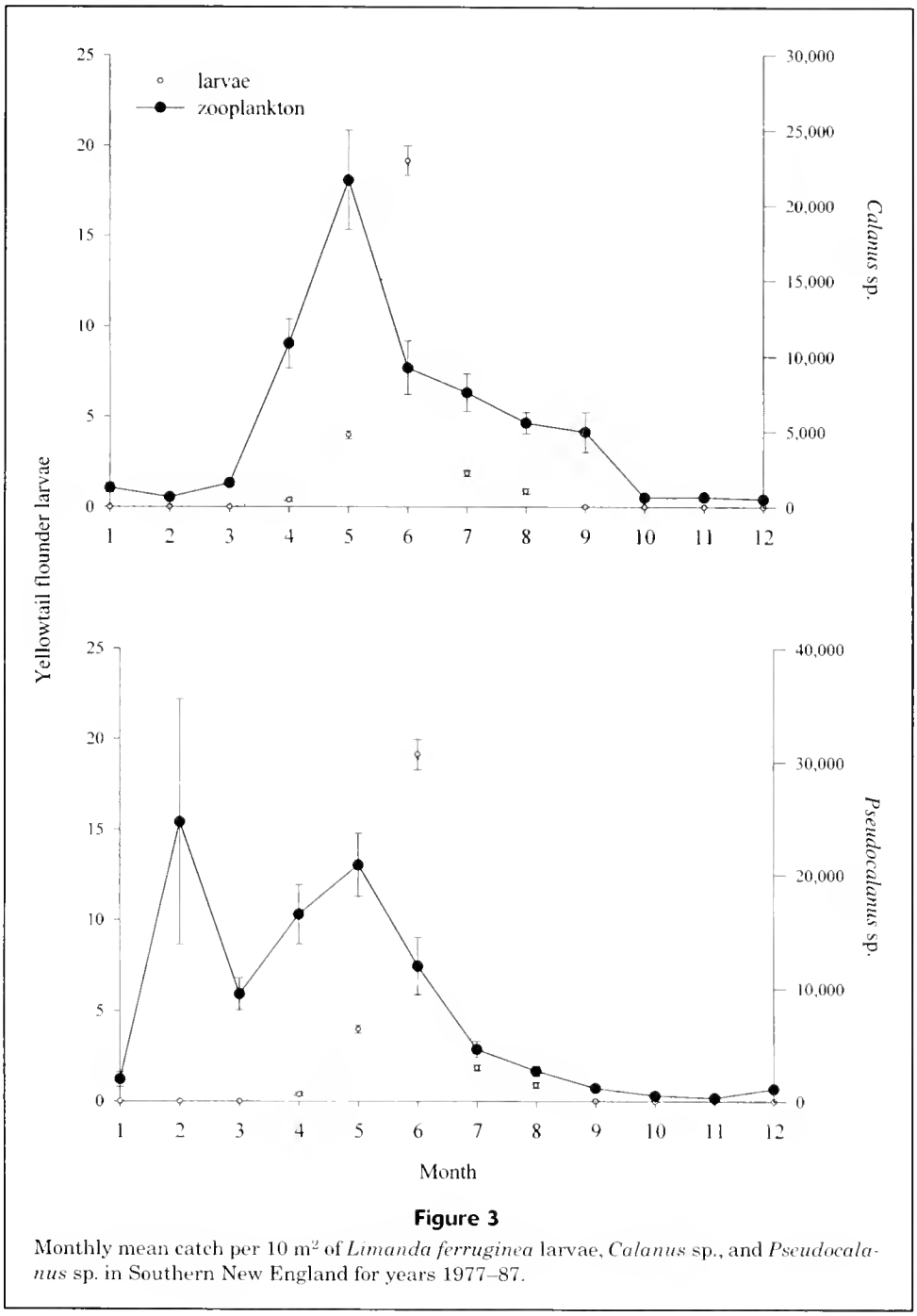

Figure 3

Monthly mean catch per 10 m^2 of *Limanda ferruginea* larvae, *Calanus* sp., and *Pseudocalanus* sp. in Southern New England for years 1977–87.

1987 showed matches in peak spawning and prey production (Fig. 4).

Larger gaps exist between predator and prey in GB for many of the year classes (Fig. 5). There was a temporal gap of almost 56 days between yellowtail flounder and *Calanus* sp. abundance during 1980 and 1982. A slightly smaller mismatch occurred during 1977 at 45 days. The poor year class 1986 had the smallest span in time between predator and prey (16 days) when larvae peaked prior to *Calanus* sp.. For the same year class, 1986, the difference between peaks was slightly greater between larvae and *Pseudocalanus* sp.. There was a smaller mismatch between *Pseudocalanus* sp. and larvae for year class 1982, amounting to 52.6 days (Fig. 5). The stronger year classes, 1977 and 1980, showed more definite matches in spatial timing (<45 days).

To test for a relationship between predator-prey overlap and year-class strength, differences between predator and prey peaks versus year-class strength were plotted for the eleven-year time period (Fig. 6). Two predator and prey combinations (t_0), yellowtail larvae and *Calanus* sp., and

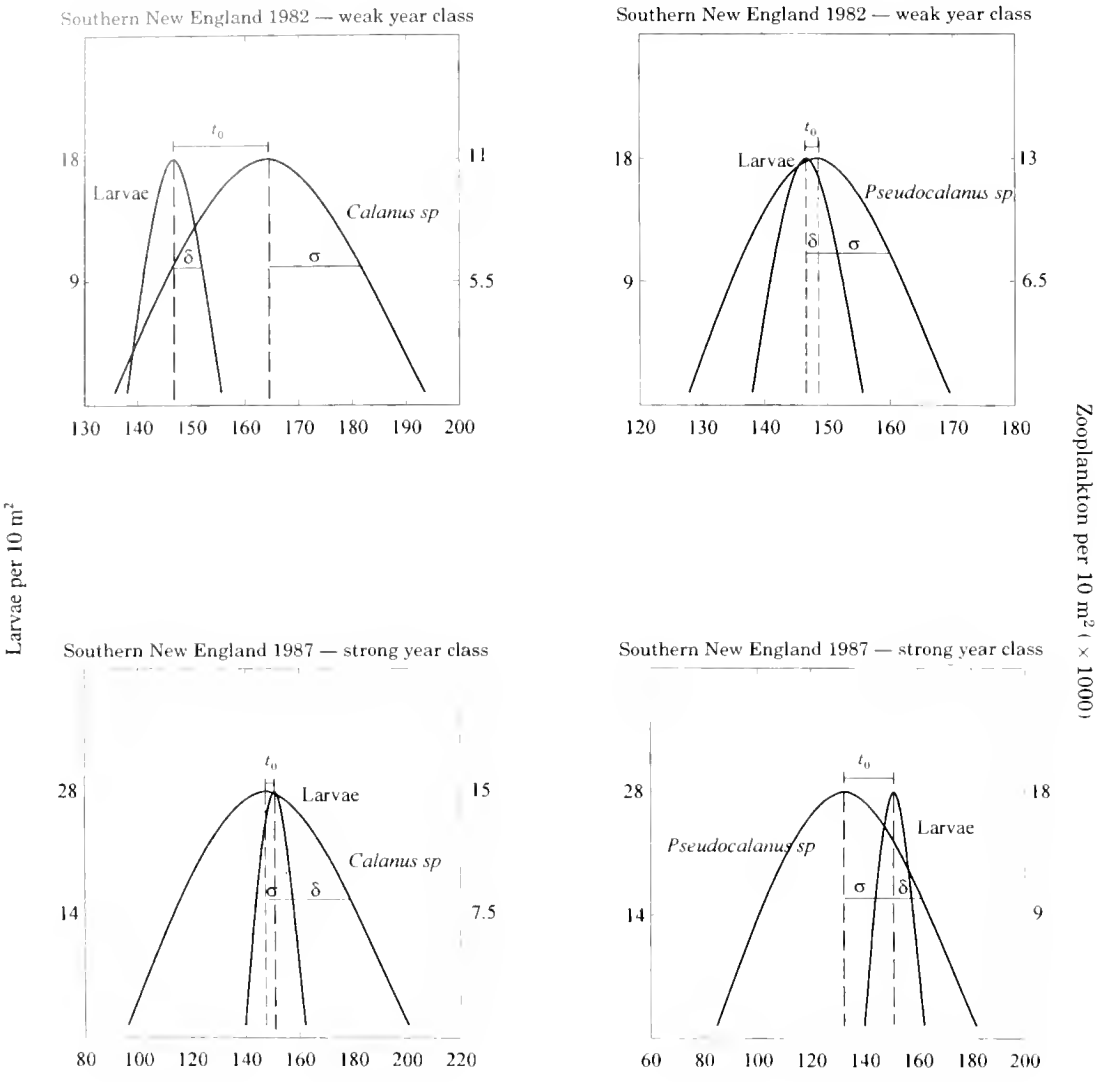

Figure 4

The match or mismatch relationship between yellowtail larvae, *Calanus* sp., and *Pseudocalanus* sp. in Southern New England during the year classes 1982 and 1987.

yellowtail larvae and *Pseudocalanus* sp. were examined for each subarea. In both subareas the strong year classes (1980, 1987 SNE; 1980, 1977 GB) were consistently positioned in ranges of t_0 less than zero. The extreme differences in predator and prey peaks frequently reflected the location of poorer year classes (1982, 1986 for both SNE and GB). Unexpectedly, these year classes normally occurred when predator and prey timing was equal to or greater than zero.

Although not statistically significant, the Spearman's rank-order correlation between predator-prey overlap and larval abundance suggested a possible relationship between recruitment variability and the predator-prey pairs, especially for the combination of larvae and *Calanus* sp. in SNE (Table 1).

Year-to-year variability in peaks of predator and prey abundance

As expected, the greatest anomaly in timing for three of the four predator-prey pairs occurred during the 1982 year class. The large difference in timing between predator and prey was reflected in the contour plot of larvae and zooplankton during 1982 (Fig. 7). There was a mismatch in timing between yellowtail flounder and *Calanus* sp. in GB and between yellowtail flounder and *Pseudocala-*

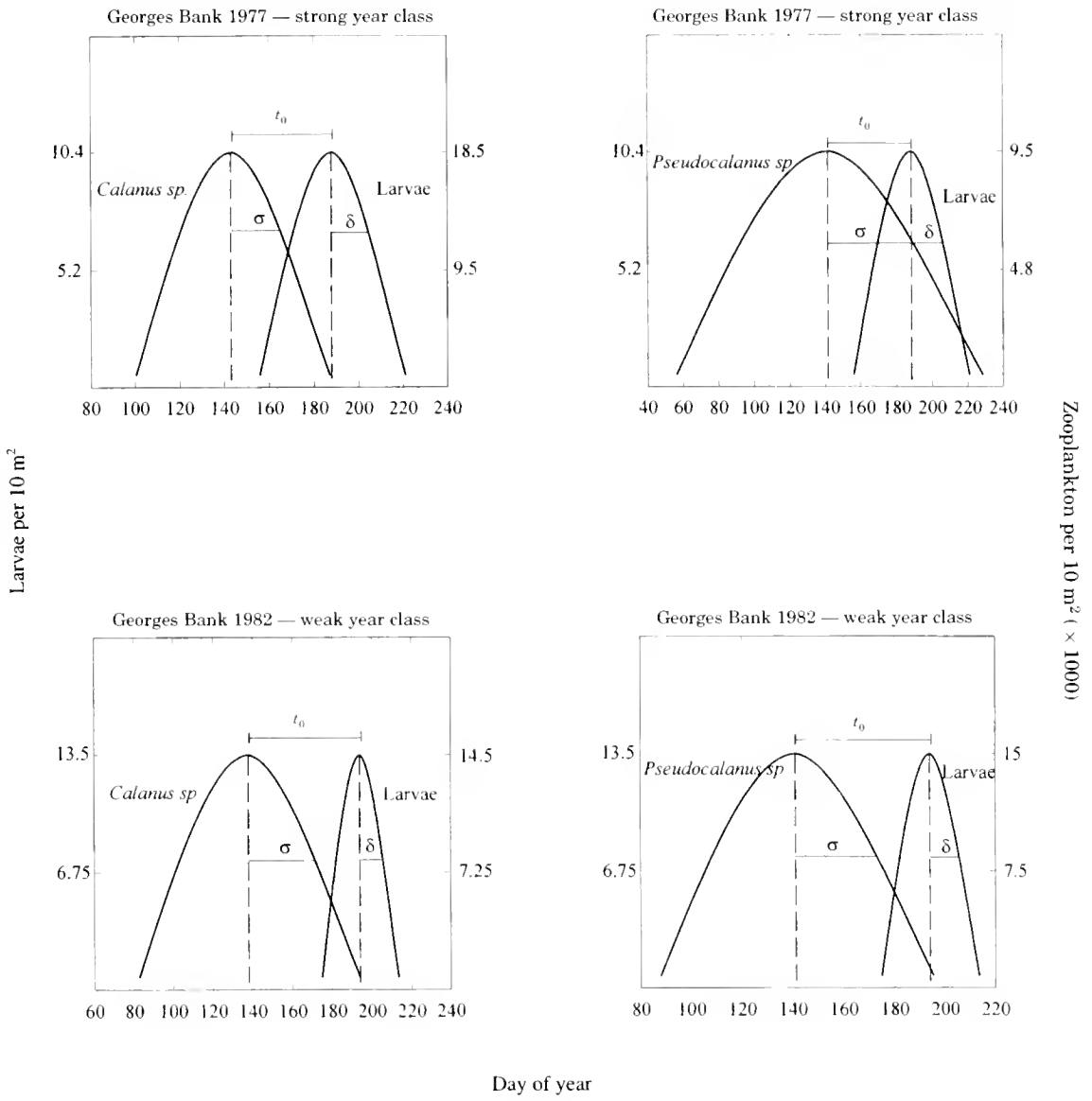

Figure 5

The match or mismatch relationship between yellowtail larvae, *Calanus* sp., and *Pseudocalanus* sp. in Georges Bank during the year classes 1977 and 1982.

nus sp. in SNE. Neither predator-prey pair was synchronous. In GB the yellowtail flounder larvae and *Calanus* sp. did not match in time or space. The zooplankton population appeared strong but the spawning of yellowtail flounder occurred during different times, creating low overlap between the two species. Years with the lowest anomalies in timing were 1984 and 1986 for GB and years 1977, 1980, 1986, and 1987 for SNE.

This study relied on extensive data for yellowtail flounder and zooplankton abundances in SNE and GB to test general predictions of the match-mismatch hypothesis. In general no strong support was found for this hypothesis. High overlap between zooplankton and yellowtail flounder abundances did not necessarily result in strong yellowtail flounder year classes, and some of the strongest year classes occurred when overlap was low.

Annual timing of spawning and production cycles from larvae and zooplankton prey (Table 2) also revealed variations between subareas. The spawning production for yellowtail flounder peaked earlier in the more southern subarea SNE than in GB, for all years excluding 1984. Similar results occurred in the production of *Pseudocalanus* sp., with the majority of first peaks cited in SNE for all years except 1978 and 1982. However, opposite patterns were observed for *Calanus* sp. production. Production cycles peaked first in seven of the eleven years in the

Figure 6

The relationship between peaks in predator-prey combinations and year-class strength for subareas Southern New England and Georges Bank during the years 1977–87.

Table 1

Spearman's rank-order correlation coefficients of predator-prey combinations (t_0) for subareas Southern New England (SNE) and Georges Bank (GB) during the 1977–87 time period

Subarea	Predator-prey combination	r^2	$P>F$
SNE	larvae-*Calanus* sp.	–0.31	0.077
SNE	larvae-*Pseudocalanus* sp.	–0.21	0.160
GB	larvae-*Calanus* sp.	–0.20	0.170
GB	larvae-*Pseudocalanus* sp.	–0.07	0.417

GB subarea; the exceptions were the years 1984 through 1987. The mean differences in peaks for all years was 22.5 for larvae, 26.6 for *Pseudocalanus* sp. and –9.8 for *Calanus* sp.

Although this eleven-year study did reveal some possible relationships between predator and prey, there was no clear demonstration of a match or mismatch for strong or weak year classes. Results from this study were unable to conclude if high or low ratios between predator and prey abundance could determine or even predict the growth and survival of first-feeding larvae and their ultimate year-class success. Questions for future research should include 1) stomach-content analyses of larvae to determine prey, 2) incorporation of abiotic influences, and 3) sampling at a much smaller spatial scale. These additional features would increase the feeding success and growth rate estimation of young yellowtail flounder.

Acknowledgments

This note is dedicated to John B. Pearce in gratitude for his years of service and dedication to the field of fisheries science. He continues to be an inspiration to us all. I would like to thank Peter Berrien and Jay O'Reilly for their knowledge of and assistance in contouring. I would also like to thank Carol Meise for her help and suggestions with the zooplankton data set and especially thank the many people who participated in the MARMAP sampling program: all scientists and crew members aboard the research vessels who worked to collect and process samples during numerous uncertain conditions are gratefully acknowledged. I thank Michael Fogarty, Saran Twombly, William H. Krueger, and Jeremy Collie for their encouragement, review, and helpful suggestions. I also thank Wallace Morse, David Mountain, and John Boreman for insightful technical and policy reviews. Ransom A. Myers and an anonymous reviewer graciously provided helpful comments and suggestions.

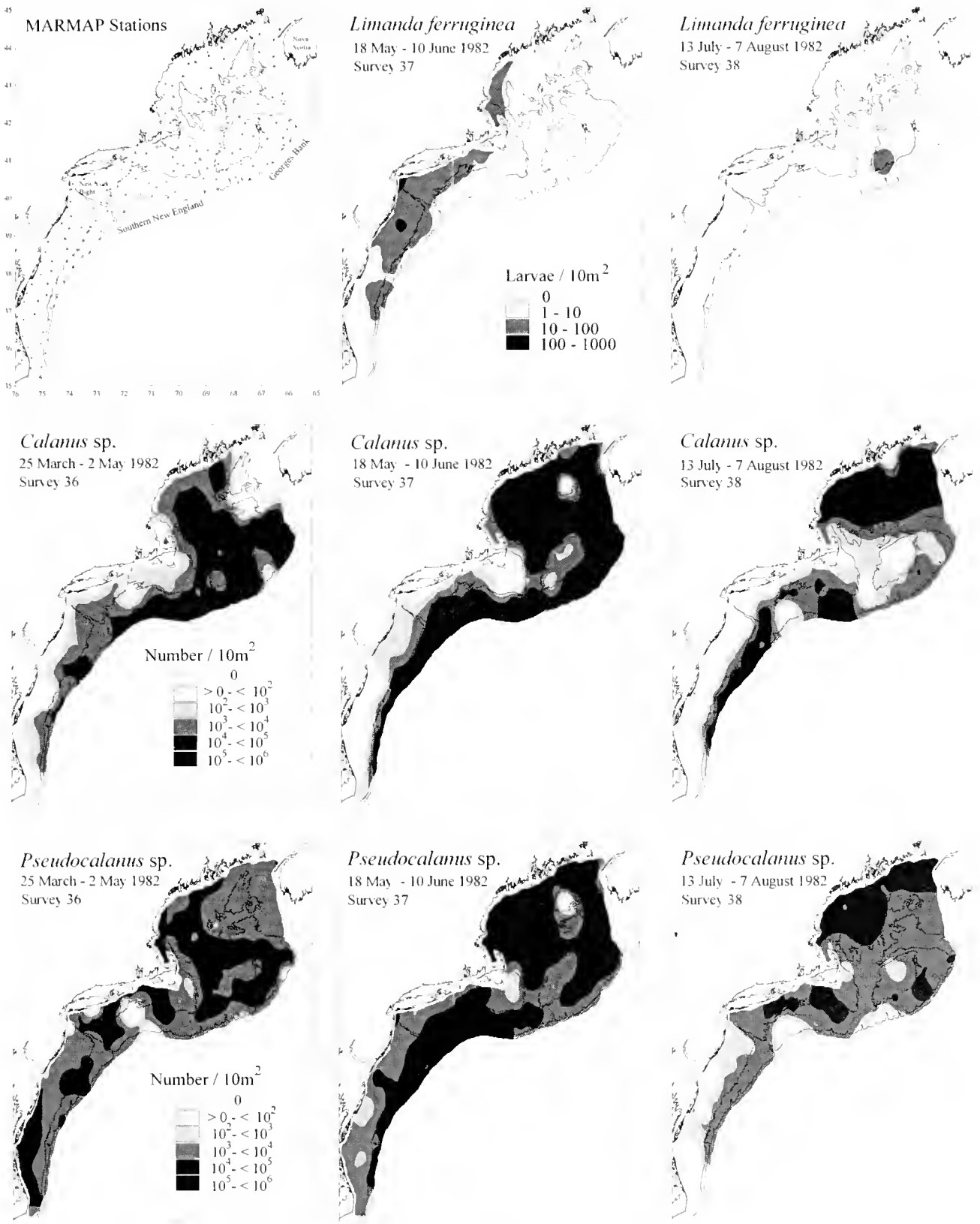

Figure 7

Distribution and abundance of predator *Limanda ferruginea*, and prey *Calanus* sp. and *Pseudocalanus* sp. during the production months of 1982.

Table 2

Mean dates of peak occurrence between spawning and production for yellowtail larvae and zooplankton. C – L = the difference between *Calanus* sp. (C) and larvae (L); and P – L = the difference between *Pseudocalanus* sp. (P) and larvae. (Values in bold were omitted from some parts of the analyses). SNE = Southern New England; GB = Georges Bank.

		Mean numeric date (Julian calendar)			t_0	
Subarea	Year	Yellowtail	*Calanus* sp.	*Pseudocalanus* sp.	C – L	P – L
SNE	1977	142.165	148.283	108.849	6.118	–33.316
	1978	**163.409**	**160.381**	**149.433**	**–3.028**	**–13.976**
	1979	**157.900**	**180.044**	**117.218**	**22.144**	**–40.682**
	1980	165.692	149.971	144.097	–15.721	–21.595
	1981	162.881	145.877	114.694	–17.004	–48.187
	1982	146.877	164.653	148.749	17.776	1.872
	1983	156.263	171.619	123.027	15.356	–33.236
	1984	**167.729**	**158.964**	**115.622**	**–8.765**	**–52.107**
	1985	**145.375**	**151.724**	**136.489**	**6.349**	**–8.886**
	1986	146.906	162.182	160.195	15.276	13.289
	1987	151.111	148.470	133.289	–2.641	–17.822
GB	1977	188.486	143.828	142.521	–44.658	–45.965
	1978	**190.935**	**141.003**	**144.407**	**–49.932**	**–46.528**
	1979	**158.285**	**143.063**	**167.135**	**–15.222**	**8.850**
	1980	198.189	142.306	163.603	–55.883	–34.586
	1981	173.270	125.278	143.250	–47.992	–30.020
	1982	194.324	138.514	141.743	–55.810	–52.581
	1983	**168.289**	**146.770**	**148.058**	**–21.519**	**–20.231**
	1984	162.345	167.399	147.164	5.054	–15.181
	1985	**171.862**	**157.967**	**165.720**	**–13.895**	**–6.142**
	1986	158.822	175.171	201.425	16.349	42.603
	1987	**188.463**	**153.322**	**179.525**	**–35.141**	**–8.938**

Literature cited

Aitchison, J.
1955. On the distribution of a positive random variable having a discrete probability mass at the origin. J. Am. Statis. Assoc. 50:901–908.

Berrien, P. L., N. A. Naplin, and M. Pennington.
1981. Atlantic mackerel, *Scomber scombrus*, egg production and spawning population estimates for 1977 in the Gulf of Maine, Georges Bank, and Middle Atlantic Bight. Rapp. P.-V. Reun. Cons. Int. Explor. Mer 178:278–288.

Cushing, D. H.
1975. Marine ecology and fisheries. Cambridge Univ. Press, Cambridge, England, 278 p.
1982. Climate and fisheries. Academic Press, London, 373 p.
1990. Plankton production and year-class strength in fish populations: an update of the match/mismatch hypothesis. Adv. Mar. Biol. 26:249–293.

Cushing, D. H., and R. R. Dickson.
1976. The biological response in the sea to climatic changes. Adv. Mar. Biol. 14:1–122.

Hjort, J.
1914. Fluctuations in the great fisheries of northern Europe. Rapp. P.-V. Reun. Cons. Int. Explor. Mer 20:1–227.

Hjort, J.
1926. Fluctuations in the year classes of important food fishes. J. Cons. Int. Explor. Mer 1:5–38.

Houde, E.D.
1987. Fish early life dynamics and recruitment variability. Am. Fish. Soc. Symp. 2:17–29.

Mertz, G., and R. A. Myers.
1994. Match/mismatch predictions of spawning durations versus recruitment variability. Fish. Oceanogr. 3:236–245.

NEFC (Northeast Fisheries Center).
1991. Report of the twelfth northeast regional stock assessment workshop (12th SAW), spring 1991. Northeast Fish. Cent. Ref. Doc. 91-03, Northeast Fisheries Center, Natl. Mar. Fish. Serv., NOAA, 187 p.

Pennington, M.
1983. Efficient estimators of abundance, for fish and plankton surveys. Biometrics 39:281–286.

Pitcher, T. J., and P. J. B. Hart.
1983. Fisheries ecology. AVI publishing Co., Westport, CT, 414 p.

Posgay, J. A., and R. R. Marak.
1980. The MARMAP bongo zooplankton samplers. J. Northw. Atl. Fish. Sci. 1:91–99.

Royce, W. F., R. J. Buller, and E. D. Premetz.
1959. Decline of the yellowtail flounder (*Limanda ferruginea*) off New England. Fish. Bull. 59:169–267.

Runge, J. A.
1988. Should we expect a relationship between primary production and fisheries? The role of copepod dynamics as a filter of trophic variability. Hydrobiologia 167/168: 61–71.

Sibunka, J. D., and M. J. Silverman.
1984. MARMAP surveys of the continental shelf from Cape Hatteras, North Carolina, to Cape Sable, Nova Scotia (1977–1983). Atlas 1, summary of operations. U.S. Dep. Commer., NOAA Tech. Memo., NMFS-F/NEC-33, 306 p.
1989. MARMAP surveys of the continental shelf from Cape Hatteras, North Carolina, to Cape Sable, Nova Scotia (1984–1987). Atlas 3, summary of operations. U.S. Dep. Commer., NOAA Tech. Memo., NMFS-F/NEC-68, 197 p.

Onset of association behavior in striped jack, *Pseudocaranx dentex*, in relation to floating objects

Reiji Masuda

Fisheries Research Station
Kyoto University
Nagahama, Maizuru
Kyoto 625-0086, Japan
E-mail address: reiji@kais.kyoto-u.ac.jp

Katsumi Tsukamoto

Ocean Research Institute
University of Tokyo,
1-15-1, Minamidai Nakano
Tokyo 164-8639, Japan

Many marine and freshwater species associate with floating objects (flotsam) during some period of their life history (Senta, 1965; Hunter and Mitchell, 1967; Kingsford, 1993). This association behavior is well known among fishermen, who often choose flotsam-associated schools (Yabe and Mori, 1950; Greenblatt, 1979). Among a wide range of taxa collected in association with flotsam, the Carangidae is one of the most frequently observed groups (Hunter and Mitchell, 1967; Kingsford, 1993; Clarke and Aeby, 1998). The association behavior of carangid fishes has been used by fishermen in Asia. "Payaw" in the Philippines is a flotsam made of bamboo and attracts many species of Carangidae (Ibrahim et al., 1990). Juvenile yellowtail, *Seriola quinqueradiata*, are collected by Japanese fishermen by surrounding drift algae with a small scoop net. These fish are then raised in cages as a net-pen culture (Senta, 1965; Sakakura and Tsukamoto, 1997). Presently, a new sea ranching project is being developed, in which artificially reared juvenile striped jack, *Pseudocaranx dentex*, are released at a floating platform where they naturally aggregate. There they are fed and harvested after growth (Masuda and Tsukamoto, 1998a).

The importance of this association behavior from the perspective of fishery ecology has generated a great deal of field research and experimental work. Hunter and Mitchell (1967) showed that large flotsam attracts more fish than smaller flotsam, and fish associating with flotsam tend to have darker body color, compared with the silvery color of those that are not attracted (Hunter and Mitchell, 1968). Using tag and release techniques, Ibrahim et al. (1990) demonstrated that fish released as far as 180 m from flotsam will swim back to their place of capture, suggesting that these fish can learn the topography of the region surrounding the float. Much ecological research has been conducted with the assumption that floating objects, especially drift algae, are an important habitat for juveniles (reviewed by Kingsford, 1993). Although a considerable amount of field-based work exists, little research has been conducted on the developmental aspects of association behavior in the laboratory.

The ontogenetic changes in association behavior in striped jack, *Pseudocaranx dentex*, were therefore studied with hatchery-raised larvae and juveniles. Possible sensory mechanisms underlying association behavior were examined by comparing four different types of flotsam conditions (transparent flotsam, gray flotsam, shadow flotsam, and no flotsam [control]).

Materials and methods

Two batches of fish were used in our experiments: one hatched on 22 February 1994, the other on 28 March 1994, both at the Komame Branch of the Japan Sea-Farming Association (JASFA). These batches of fish were transferred to the Kamiura Branch of JASFA on the next day. Fish were reared in 150-m^3 concrete tanks on a routine diet of rotifers and *Artemia* nauplii, and formula diet (Masuda and Tsukamoto, 1996). Eight different stages of fish were used in the experiments ranging from 5.5 mm (20 days) to 28 mm (56 days) in mean total length (Table 1). Because large variations in growth occurred in the hatchery, the medium-size fish were selected for each age group, except for the 21-mm fish. The 21-mm fish (54 days) were the smallest group of those hatched on 22 February.

Four different types of flotsam were created in 30-liter polycarbonate tanks with water depths of 25 cm (ca. 26 liters). These were

1 Transparent flotsam: a transparent acrylic pipe (60 mm in outer diameter, 5 mm thickness) cut to 250 mm in length and covered by a transparent circular plate (5 mm thickness) on the bottom. This was filled with water and suspended from the ceiling by fishing line, the height adjusted so that 150 mm of the pipe was in the water (Fig. 1A). The experimental tank was marked into four sections, and the flotsam was located at the center of one randomly chosen section.
2 Gray flotsam: an opaque gray PVC pipe and plate of identical size to that used in type 1 and suspended in the same way (Fig. 1B). This arrangement provided stronger visual stimulus than that provided in type 1.
3 Shadow flotsam: a gray circular opaque PVC plate (60 mm in diameter, 5 mm thickness) was suspended from the ceiling, so that the bottom of the plate was about 5 mm above the water surface. This created a shadow on the water surface, but not on the bottom of the tank (Fig. 1C).
4 No flotsam (control) (Fig. 1D).

Manuscript accepted 27 April 2000.
Fish. Bull. 98:864–869 (2000).

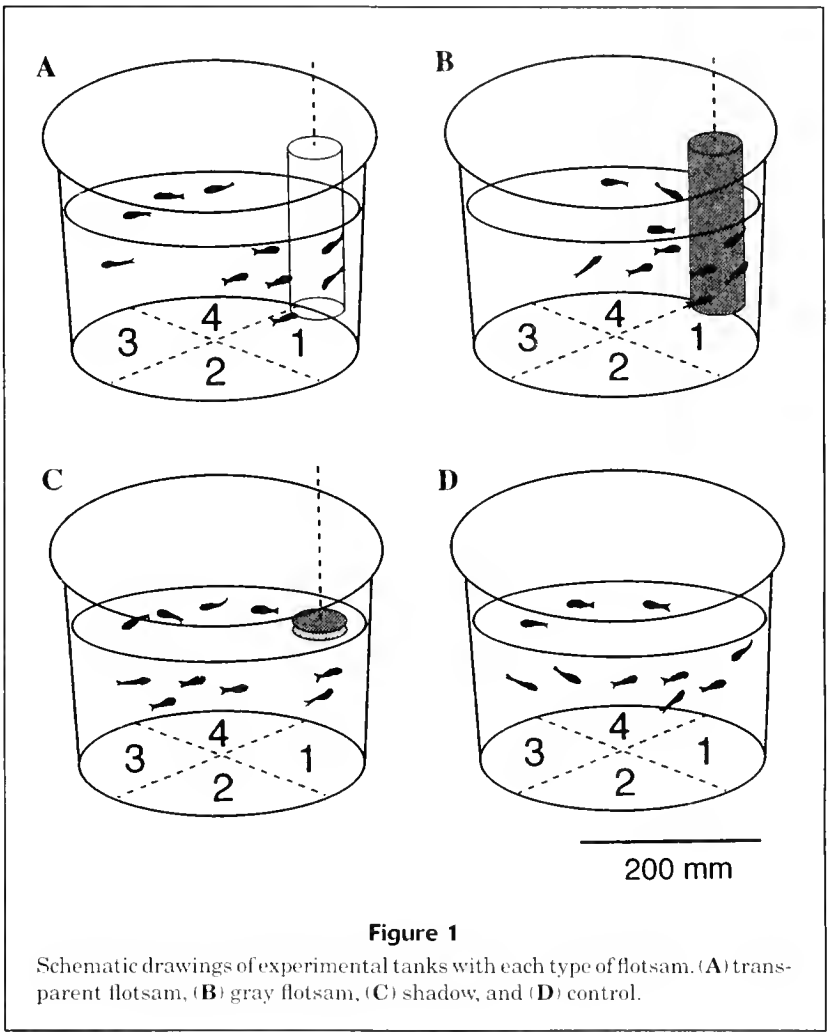

Figure 1

Schematic drawings of experimental tanks with each type of flotsam. (**A**) transparent flotsam, (**B**) gray flotsam, (**C**) shadow, and (**D**) control.

Carangid fish juveniles are commonly seen associated with floating and underwater objects, such as air tubes and vinyl bags, both in hatchery tanks and natural waters (Tachihara et al. 1993). Therefore acrylic and PVC pipes were suitable representative materials for use in examining the developmental changes of association behavior. We observed only horizontal distributions as an index of association behavior because in hatchery tanks, larvae and early juveniles of striped jack usually occur in the upper 30 cm of the water column.

All treatments were triplicated (twelve 30-liter tanks were used in total) and the location of the same type of flotsam was changed among triplicates. Experiments were conducted in an indoor facility and all tanks were placed in a water bath that was strongly aerated. Water temperature in each tank was maintained at hatchery levels (22.5°C). A photoperiod of 8 h light and 16 h dark was provided with 12 halogen illumination lights set above the tanks (light: 08:30–16:30 h). With this lighting, the light intensity at the surface of tanks was 0.01–0.05 lux at 20:00 h, lower than 0.01 lux between 00:00 and 04:00 h, 260–1000 lux at 08:00 h, and 17,000–24,000 lux at 12:00 and 16:00 h.

Table 1

Age, total length (mean ±SD), and hatching batch (+) of *Pseudocaranx dentex* used in the experiment.

		Batch	
Age (days)	TL (mm)	22 Feb	28 Mar 1994
20	5.5 ±0.5		+
27	8.8 ±0.9		+
30	10.3 ±1.1		+
31	11.9 ±2.4	+	
35	14.9 ±1.5		+
36	19.7 ±1.9	+	
54	21.0 ±1.8	+	
56	28.4 ±2.7	+	

At 20:00 h, fish were transferred from the hatchery tank to the 12 experimental tanks and ten fish were introduced into each tank (120 fish in total). Observations were con-

ducted immediately after introduction and once every 4 h over the following 24 h. For 10 mm, 15 mm, 21 mm, and 28 mm fish, observations were also made 36 h after introduction. During each observation period, the number of fish in each section of the tank was counted. At night time (20:00, 00:00 and 04:00 h), infrared illumination aided observation. At each observation, counts were repeated five times for each tank at approximately 5-min intervals. The average number of fish in each section with a flotsam was calculated and then divided by the total number of fish (n=10). This value, defined as the association ratio, would be 1.0 if fish associated strongly to the object and would be 0.25 with random movement or distribution. In the control treatment, the number of fish in the southeast, southwest, or northwest quadrants was counted from the triplicated tanks, respectively. The average value of these three tanks was used as a control. Total lengths of all the fish were measured after the experiment.

Association ratios were compared for each type of flotsam for each time of observation. Because association ratios deviated from normal distribution, we applied arcsine transformation (p'=arcsin $\sqrt{p}$; Zar, 1996). The resultant data showed nearly normal distribution. One-way ANOVA was then applied followed by Scheffé's test as a *post hoc* test (Zar, 1996; Abacus Concepts, Inc., 1992). We considered an association ratio higher than the control (P<0.05, Scheffé's test) to be evidence of association behavior with that flotsam.

Results

In 5.5-mm, 8.8-mm, and 10-mm fish, no association behavior was observed with any types of flotsam, and the average association ratios were always near 0.25 (Fig. 2, A–C). At 12 mm, the first significant association behavior was observed both with transparent and gray objects (Fig. 2D; P<0.05). Association ratios did not differ significantly between these two object types at this stage (P>0.2). At 15 mm, association behavior was not obvious, perhaps because the fish swam around in the tank restlessly in this particular trial, both in test and control groups. At 20 mm, association was again obvious and the association ratio to the gray pipe tended to be higher than that to the transparent pipe (P=0 013 at 20:00 h on the second day, Fig. 2F). Association behavior was especially strong at night, and some individuals almost touched the transparent and gray pipes (Fig. 3). In most cases it took at least 12 h for fish to show an association behavior in the experimental tank, but 21-mm fish showed an association with gray objects immediately after they were introduced to the tank. At 28 mm, an association with transparent and gray pipes was positive, but the association ratio tended to be slightly less than fish at 20 mm and 21 mm. No association behavior with shadows was observed at any life-history stage of the fish.

Association ratios after 12 h and 24 h in the experiment (12:00 h and 20:00 h on the second day) were plotted against the total length of each fish (Fig. 4), showing that striped jack begin association behavior at 12 mm in TL with both transparent and gray objects.

Discussion

Accurate observation of association behavior can suffer from biases attributed to other behavior and taxis. For example, striped jack show strong phototaxis from 3.5 mm TL and rheotaxis from 4.5 mm TL (Masuda and Tsukamoto, 1996). In the present study these potential confounding factors were prevented by illuminating the tanks strongly from above and by using tanks without currents. This procedure was apparently successful because most fish smaller than 10 mm distributed themselves about equally in the experimental tanks (Fig. 2, A–C). Striped jack also exhibit schooling behavior from about 16 mm (Masuda and Tsukamoto, 1998b) which may have contributed to the fluctuating association ratio values with 15-mm or larger fish in the control tanks (Fig. 2, E and F).

Small tank size (30 liters) used in this experiment may have affected the results because the fish may have considered a tank wall as a structure with which to associate. However, fish apparently preferred the pipe to the tank wall and associated closely with it (Fig. 3). Strong aeration outside tanks in the water bath might have minimized their association to the tank wall. The limited swimming ability and shortsightedness of the larvae and juveniles also helped to reduce the effect of the tank wall.

Our results indicate that striped jack first started to show association behavior at 12 mm TL. Hunter and Mitchell (1967) reported six species of carangid fish juveniles associated with flotsam offshore Costa Rica, and their smallest sizes (given as standard lengths) were as follows: *Caranx caballus*: 9 mm; *C. hippos*: 16 mm; *Decapterus sp.*: 17 mm; *Elagatis bipinnulatus*: 11 mm; *Selar crumenophthalmus*: 15 mm; and *Seriola sp.*: 10 mm. From observation of hatchery tanks, Tachihara et al. (1993) reported that artificially reared greater amberjack, *Seriola dumerili*, larger than 11 mm standard length associate with objects. The smallest size of an flotsam-associating individual in natural waters may differ depending on species, area, season, and sampling methods. The smallest size (12 mm in TL) to associate with flotsam in our study was therefore consistent with field and hatchery observations of other carangid species.

We hypothesized that mechanical and visual stimuli may be cues for association behavior. No association with shadow flotsam was observed at any fish stages in our study, suggesting that shade is too weak a stimulus to evoke association behavior. At 12 mm, association behavior was observed to both transparent and gray flotsam, and in fish larger than 20 mm, association to gray flotsam was stronger. This finding suggests that in early juvenile stages, a mechanosensory system, as well as vision, may be involved in association behavior. Striped jack showed stronger association behavior in darkness than in light—a finding that seems to conflict with Gooding and Magnuson (1967) who found that residents of an experimental floating raft accumulate more rapidly by day than by night. In nature striped jack may find flotsam by vision during the daytime and maintain an association with it by a mechanosensory system during night. Floating structures may serve as feeding places, shelters from predation, and

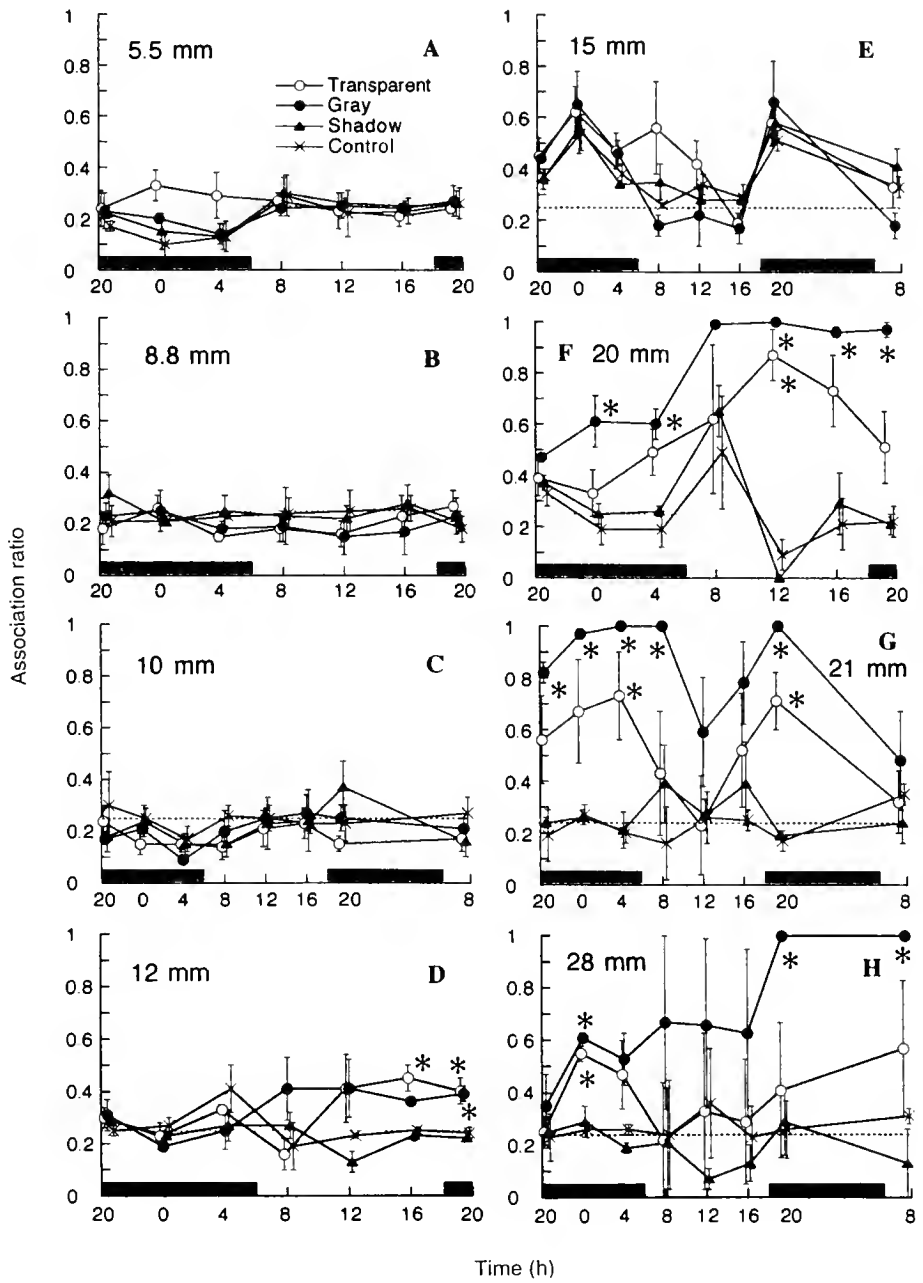

Figure 2

Association ratios for each type of flotsam in each stage. Each plot represents an average (±SE) of three tanks with the same type of flotsam. * shows significant difference between tests and controls ($P<0.05$; Scheffé's test). Expected value of random distribution (=0.25) is represented as a dotted line in each graph. Shaded bar corresponds with dark hours.

cues to migratory orientation (Hunter and Mitchell, 1967; Gooding and Magnuson, 1967; Kingsford, 1993). Flotsam may provide the first cue to finding conspecifics and to forming a school because association behavior may also be related to school formation and maintenance (Masuda and Tsukamoto, 1998b).

In conclusion, the association behavior of striped jack appeared at 12 mm and is probably dependent on a mechanosensory system, as well as vision. Association behavior may also help the development of schools and may provide transportation for migration. Environmental modifications that reduce flotsam, such as the removal of drift

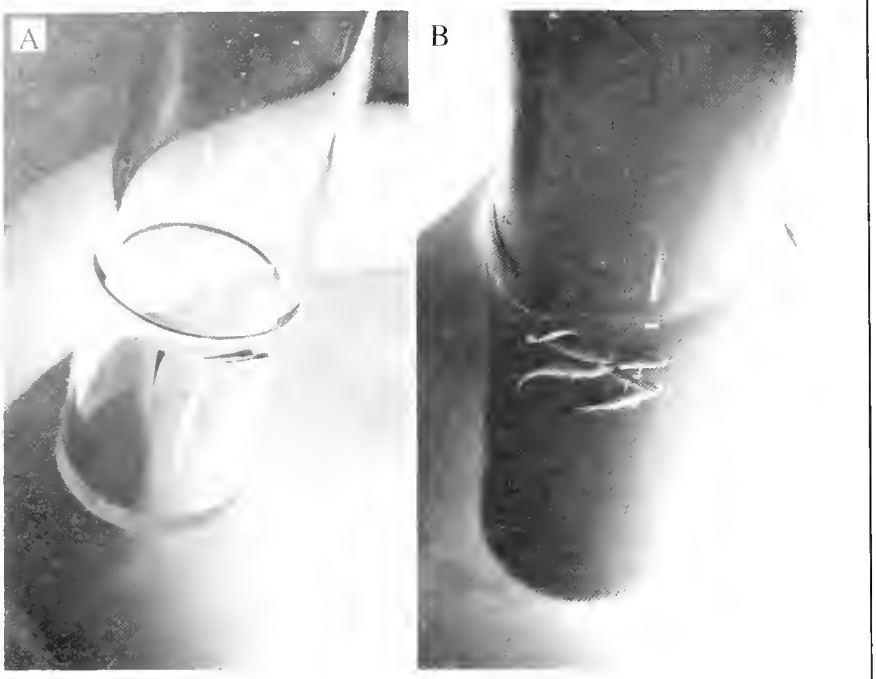

Figure 3

Typical association behavior of striped jack at night observed in 20-mm-TL juveniles: (**A**) transparent flotsam, (**B**) gray flotsam.

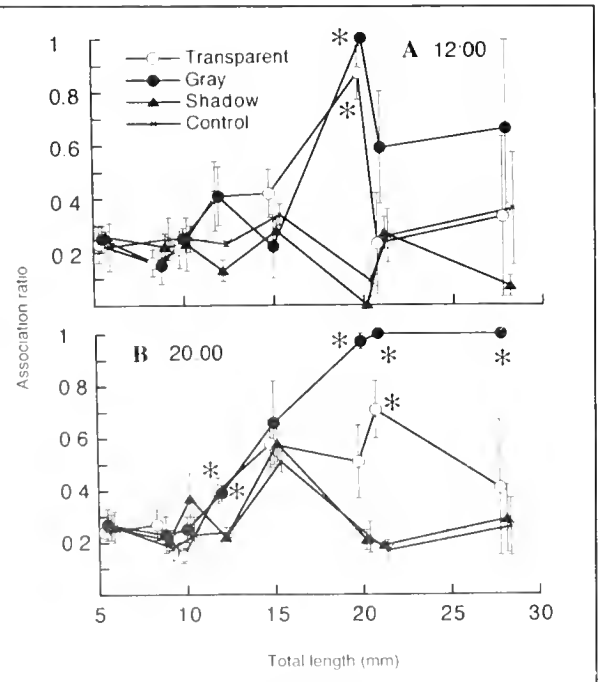

Figure 4

Onset of association behavior in the striped jack. Association ratios at 16 h (**A**) and 24 h (**B**) after starting experiments (12:00 and 20:00) were plotted against total length at each stage. * shows significant difference between tests and controls ($P<0.05$; Scheffe's test).

algae, may influence the recruitment of flotsam-associating species.

Acknowledgments

We would like to thank K. Imaizumi, H. Kuwada, and M. Kanematsu in the Japan Sea-Farming Association for generously providing fish and facilities. We also thank Martin D. J. Sayer of the Dunstaffnage Marine Laboratory and Matthew J. Dunlap of the Oceanic Institute for improving the English text, and three anonymous reviews for constructive comments. This work was partly supported by a grant from Japan Society for the Promotion of Science.

Literature cited

Abacus Concepts, Inc.
1992. Stat View, version 4.51.1. Abacus Concepts, Inc., Berkeley, CA, 464 p.

Clarke, T. A., and G. S. Aeby
1998. The use of small mid-water attraction devices for investigation of the pelagic juveniles of carangid fishes in Kaneohe Bay, Hawaii. Bull. Mar. Sci. 62:947–955.

Gooding, R. M., and J. J. Magnuson.
1967. Ecological significance of a drifting object to pelagic fishes. Pacific Sci. 21:486–497.

Greenblatt, P. R.
1979. Associations of tuna with flotsam in the eastern tropical pacific. Fish. Bull. 77:147–155.

Hunter, J. R., and C. T. Mitchell.
1967. Association of fishes with flotsam in the offshore waters of central America. Fish. Bull. 66:13–29.
1968. Field experiments on the attraction of pelagic fish to floating objects. J. Cons. perm. int. Explor. Mer 31 427–434.
Ibrahim, S., G. Kawamura, and M. A. Ambak.
1990. Effective range of traditional Malaysian FAD as determined by fish-releasing method Fish. Res. 9:299–306.
Kingsford, M. J.
1993. Biotic and abiotic structure in the pelagic environment: importance to small fishes. Bull. Mar. Sci. 53:393–415.
Masuda, R., and K. Tsukamoto.
1996. Morphological development in relation to phototaxis and rheotaxis in the striped jack, *Pseudocaranx dentex*. Mar. Fresh. Behav. Physiol. 2875–90.
1998a. Stock enhancement in Japan: review and perspective Bull. Mar. Sci. 62:337–358.
1998b. The ontogeny of schooling behaviour in the striped jack. J. Fish Biol. 52:483–493.
Sakakura, Y., and K. Tsukamoto.
1997. Age composition in the schools of juvenile yellowtail *Seriola quinqueradiata* associated with drifting seaweeds in the East China Sea. Fish. Sci. 63:37–41.
Senta, T.
1965. Importance of drifting seaweeds in the ecology of fishes. Study Series 13. Japan Fisheries Resource Conservation Association, Tokyo, 55 p. [In Japanese.]
Tachihara, K., R. Ebisu, and Y. Tukashima.
1993. Spawning, eggs, larvae and juveniles of the purplish amberjack *Seriola dumerili*. Nippon Suisan Gakkaishi 59:1479–1488. [In Japanese with English abstract.]
Yabe, H., and T. Mori.
1950. An observation on the habit of bonito, *Katsuwonus vagans*, and yellow fin, *Neothunnus macropterus*, school under the drifting timber on the surface of ocean. Nippon Suisan Gakkaishi 16:35–39. [In Japanese with English abstract.]
Zar, J. H.
1996. Biostatistical analysis, 3rd ed. Prentice Hall, Upper Saddle River, NJ, 662 p.

The occurrence of the provisional Brazilian subspecies of spiny lobster (*Panulirus argus westonii*) in Florida waters*

Shane K. Sarver
Department of Biology
Black Hills State University
Spearfish, South Dakota 57799
E-mail address: ssarver@mystic.bhsu.edu

D. Wilson Freshwater
Center for Marine Science Research
7205 Wrightsville Avenue
Wilmington, North Carolina 28403

Patrick J. Walsh
Division of Marine Biology and Fisheries
Rosenstiel School of Marine and Atmospheric Science
University of Miami
Miami, Florida 33149

The Caribbean spiny lobster, *Panulirus argus*, is distributed from Brazil throughout the Caribbean and the Gulf of Mexico to approximately North Carolina and Bermuda (Holthius, 1991). It supports major commercial fisheries in Florida, the Caribbean and Brazil. Commercially, *P. argus* is especially important to the state of Florida, where the spiny lobster fishery ranks second only to shrimp in terms of economic value. There is also a significant recreational fishery for *P. argus*, particularly in Florida. A number of studies have been initiated to gather information to manage the lobster resource carefully.

Several studies have used genetic techniques to examine population-level patterns of differentiation to delineate reproductively isolated stocks of *P. argus*. Evidence of the stock structure of spiny lobster populations could then be used to implement more effective fishery management plans. These studies have provided somewhat ambiguous results. Using allozymes, Menzies and Kerrigan (1979) and Menzies (1981) provided some evidence for genetic differences among populations, but more recent studies using restriction fragment length polymorphism (RFLP) analysis of mitochondrial DNA have suggested little evidence for genetic differences among Caribbean populations of *P. argus* (Silberman et al., 1994a, 1994b). Analysis of mtDNA RFLPs have revealed suprisingly high levels of diversity among individuals, and several individuals were diverged at levels not usually seen within a species. Because previous studies did not include populations from Brazil, Sarver et al. (1998) compared *P. argus* from Caribbean locations with *P. argus* from Brazil. Using DNA sequence analysis of two mitochondrial genes, Sarver et al. (1998) found high levels of sequence divergence between Caribbean and Brazilian *P. argus*. The levels of nucleotide sequence divergence were greater than that seen between recognized species of *Panulirus*. In addition, there are striking color differences between Caribbean and Brazilian *P. argus*. As a result of these findings Sarver et al. (1998) suggested provisional recognition of two subspecies of *P. argus* (*P. argus argus* in the Caribbean and *P. argus westonii* in Brazil) until a formal taxonomic revision could be done.

The results from these studies, which suggest that *P. argus* in Brazil are genetically and taxonomically distinct from their Caribbean counterparts, have raised questions about the status of the three genetically distinct spiny lobsters reported by Silberman et al. (1994a) in their original survey of mtDNA diversity of Caribbean *P. argus*. This is significant because two of these spiny lobsters found in Silberman et al. (1994a) were caught off the coast of Miami, Florida. Our study uses DNA sequence analysis to identify the three genetically distinct spiny lobsters observed by Silberman et al. (1994a) as the Brazilian form of *P. argus* (provisionally recognized as *P. argus westonii*, in Sarver et al., 1998).

Materials and methods

DNA samples were obtained from the samples examined by Silberman et al. (1994a). Caribbean *Panulirus argus* samples were randomly selected from the samples examined by Silberman et al. (1994a). Samples from Brazil were collected near the Rio Grande do Norte region of Brazil. Tissue samples of *Panulirus argus* from Brazil were frozen prior to DNA isolation. Standard phenol or chloroform DNA extraction techniques were used for DNA isolation (Hillis et al., 1990). A region of the mitochondrial 16S rRNA gene was amplified by the polymerase chain reaction (PCR) by using primers 16Sar and 16Sbr given in Palumbi et al.[1] PCR products were then purified and used as templates for DNA sequencing by using the ΔTaq cycle sequencing kit (U.S. Biochemical Corp., Cleveland, OH). Cycle sequencing reactions were performed by using γ-^{33}P-dATP end-

Contribution 221 of the Center for Marine Science Research, Wilmington, NC 28403.

[1] Palumbi, S. R., A. Martin, S. Romano, W. O. McMillan, L. Stice, and G. Grabowski. 1991. A simple fools guide to PCR, vers. 2.0. Special publication of the University of Hawaii Department of Zoology and Kewalo Marine Laboratory, 46 p. Department of Zoology and Kewalo Marine Laboratory, Univ. Hawaii, Honolulu, HI 96822.

Manuscript accepted 1 June 2000.
Fish. Bull. 98:870–873 (2000).

labeled primers. All sequences were determined in both directions.

Aligned DNA sequence data included 441 sites. Distance and parsimony analyses of the aligned DNA sequences were done with PAUP (Swofford, 1998). Three separate distance calculations were made: uncorrected mean, Jukes-Cantor (Jukes and Cantor, 1969), and Kimura 2-parameter (Kimura, 1980) distances. Neighbor-joining trees (Saitou and Nei, 1987) were generated by using all three distance measures. Parsimony trees were produced by using branch and bound searches. Sites coded as gaps were treated either as missing, or as a fifth character state. The mitochondrial 16S rDNA sequences were aligned by using the SeqPup DNA analysis program (Gilbert[2]). Support for nodes of both parsimony and distance trees was assessed by calculating bootstrap proportion (BP) values (Felsenstein, 1985) from 1000 replicate searches by using the same tree building methods used to produce the trees. *Scyllarides nodifer* (Stimpson) (Decapoda, Scyllaridae) was used as an outgroup for phylogenetic analyses.

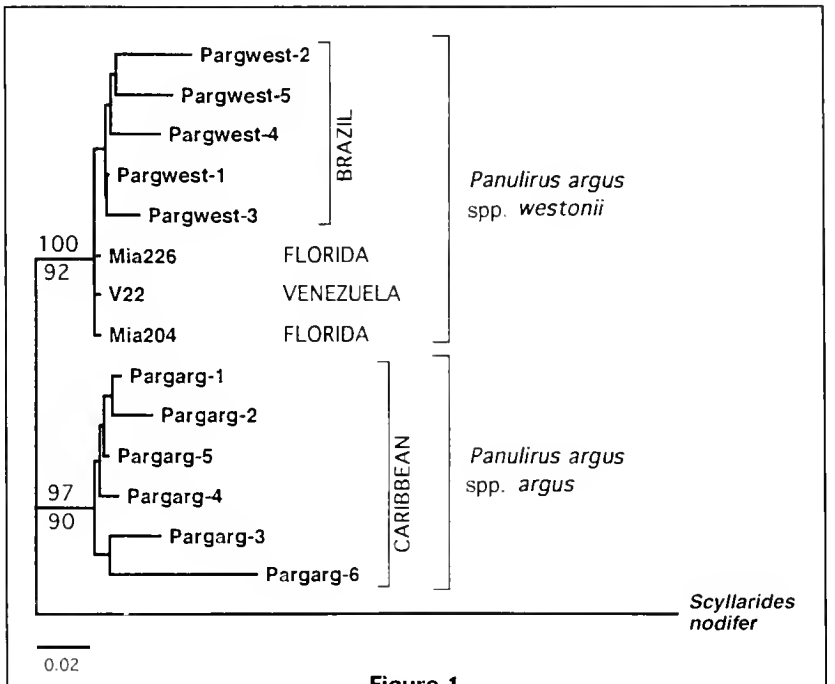

Figure 1

Neighbor joining tree derived from the Kimura two-parameter distances calculated from partial mitochondrial 16S rDNA data for 14 *Panulirus argus* and *Scyllarides nodifer* samples. Bootstrap values calculated from the distance analysis are shown above and bootstrap values calculated from parsimony analysis are shown below strongly supported branches.

Results

The mitochondrial 16S rDNA region analyzed in our study included 441 aligned nucleotide positions. In addition to single base differences, the complete aligned data set included 19 presumptive insertion or deletion mutations (indels) of 1–5 bases in length. The majority of indels involved only one base (13 of 19) and only six were potentially informative.

Regardless of the type of distance calculation, there was little variation in the outcome of the different distance calculations (less than 1%). Results from an analysis with a Kimura 2-parameter model yielded distance values ranging from 5.9% to 15.1% between the Caribbean and Brazilian subspecies of *Panulirus argus* (*P. argus argus* and *P. argus westonii* respectively). For the three genetically distinct Caribbean *P. argus* from Silberman et al. (1994a), sequence divergence estimates indicated closer affinities to Brazilian *P. argus* (2.6%) than to the Caribbean *P. argus* (7.4%).

Phylogenetic analysis of Brazilian, Caribbean and the three divergent Caribbean *P. argus* indicated a tree topology that places the three divergent Caribbean samples of *P. argus* in the Brazilian clade (Fig. 1). This basic tree topology is strongly supported regardless of the method of phylogenetic analysis.

Discussion

Traditionally, *Panulirus argus* has been thought to be distributed from North Carolina in the western Atlantic, throughout the Caribbean to Rio de Janeiro, Brazil. Sarver et al. (1998) presented data that questioned the taxonomic status of *P. argus*. DNA sequence data and morphological differences suggest that populations of *P. argus* from Brazil are genetically distinct from Caribbean populations and that the level of divergence is equivalent to the levels of divergence seen between recognized species of *Panulirus*. As a result they suggested formally recognizing two genetic forms of *P. argus* and have recommended provisional subspecific status: *P. argus argus* (Caribbean) and *P. argus westonii* (Brazil) until a formal taxonomic revision can be done. The occurrence of cryptic species in *Panulirus* is not restricted to *P. argus*. A similar situation exists in *P. longipes*, where there appears to be at least four recognizable forms of uncertain taxonomic status (George, 1972; Sekiguchi, 1991; Chan and Chu, 1996). *Panulirus homarus* has also been broken into three geographic forms that are given the rank of subspecies (Berry, 1974).

We can only speculate on the events that led to this distribution of the two *P. argus* subspecies. During the late Miocene Epoch, a *P. argus* ancestor may have occupied the North Atlantic and as Africa and South America moved apart as a result of continental drift, habitat became available for *P. argus* along the South America coast. These pop-

[2] Gilbert, D. G. 1996. SeqPup biosequence editor and analysis application, vers. 0.6f. Department of Biology, Univ. Indiana, Bloomington, IN 47405.

ulations then could have been isolated as a result of the Andes uplift during the Pliocene Epoch, which altered the pattern of the runoff and changed the course of the major rivers of the Amazon basin. Runoff from the Amazon basin continues to act as a barrier to larval migration and effectively separates Caribbean *P. argus argus* and Brazilian *P. argus westonii*. Levels of nucleotide sequence diversity observed between *P. argus argus* and *P. argus westonii* are compatible with this hypothesis.

Low numbers of the Brazilian form of *P. argus* in the Caribbean may result from rare migration events or the co-occurrence of both forms in the Caribbean. Long-range dispersal of larvae is especially well developed in *P. argus*. The complex life cycle of spiny lobsters is characterized by a protracted larval phase (the phyllosome) which can last from several months to two years and can result in prolonged transport by ocean currents (Sims and Ingle, 1967). Postlarval recruitment for some species of *Panulirus* has been associated with variation in large-scale oceanic processes (Phillips and Pearce, 1997). El niño-like events could alter the current regimes and allow some of the Brazilian forms of *P. argus* to escape into the Caribbean. Episodic recruitment events could also explain the occurrence of *Panulirus laevicauda* in the Caribbean. *Panulirus laevicauda* is abundant in Brazilian waters but is only rarely found in the Caribbean. Evidence for sporadic recruitment of *P. laevicauda* in the Caribbean was reported by Moore (1962), who noted finding a single specimen of *P. laevicauda* near Palm Beach, Florida, during 1949. Later that same year, *P. laevicauda* was reported to be nearly as abundant as *P. argus*, but in the following three years, no *P. laevicauda* were found at this location.

Occurrence of the Brazilian form of *P. argus* in Florida waters raises a number of interesting biological questions. Given the morphological differences and the high degree of genetic differentiation between Caribbean and Brazilian *P. argus*, are they capable of interbreeding? It could be possible that the existence of the Brazilian *P. argus* mtDNA haplotype in the Caribbean could be the consequence of leakage of the Brazilian *P. argus* mtDNA genome across the species boundary as a result of interbreeding. Because most of the research conducted with *P. argus* has been done with Caribbean *P. argus*, do the two forms of *P. argus* differ biologically? George (1997) considers Brazilian and Caribbean *P. argus* to be distinct ecologically and has suggested that *P. argus* is likely a complex of two species. Knowledge of the occurrence of *P. argus argus* in Brazilian waters is lacking. Taxonomic ambiguity surrounding *P. argus* is a concern because of its commercial importance. For example, Florida regulations currently prohibit the transportation or sale of imported *P. argus* during the time of year when the fishery is closed in Florida. If two species become recognized, under the present regulations, *Panulirus* from Brazil could be sold year round in Florida. If there are indeed two species of *P. argus* in Florida waters, as it appears there are, then fishery regulations will need to reflect this reclassification. Currently, fishery regulations apply to *Panulirus argus*, and all subspecies of spiny lobsters are subject to the same rules, but other species are not regulated

Acknowledgments

SKS would like to thank the CMSR Kimon T. Bird Visiting Marine Scientist Program for support during a portion of this study. This work was funded in part by NSF grant DEB-9726170 to DWF.

Literature cited

Berry, P. F.
1974. A revision of the *Panulirus homarus* group of spiny lobsters (Decapoda, Palinuridae). Crustaceana 27:31–42.

Chan, T. Y. and K. H. Chu.
1996. On the different forms of *Panulirus longipes femoristriga* (von Martens, 1872) (Crustacea:Decapoda:Palinuridae) with a description of a new species. J. Natural History 30:367–387.

Felsenstein, J.
1985. Confidence limits on phylogenies: an approach using the bootstrap. Evolution 39:783–791.

George, R. W.
1972. South pacific Islands—rock lobster resources. Document WS/C7959 prepared for the South Pacific Fisheries Development Agency. FAO, Rome.
1997. Tectonic plate movements and the evolution of *Jasus* and *Panulirus* spiny lobsters. N. Z. J. Mar. Freshwater Research 48:1121–1130.

Hillis, D. M., A. Larson, S. K. Davis, and E. A. Zimmer.
1990. Nucleic acids III: sequencing. *In* Molecular systematics (D. M. Hillis and C. Moritz, eds.), p. 318–370. Sinauer Associates, Sunderland, MA.

Holthius, L. B.
1991. FAO species catalogue. Vol. 13: Marine lobsters of the world: an annotated and illustrated catalogue of species of interest to fisheries known to date. FAO Fisheries Synopsis. 125, Rome, Italy, 292 p.

Jukes, T. H., and C. R. Cantor.
1969. Evolution of protein molecules. *In* Mammalian protein metabolism (H. N. Munro, ed.), p. 21–132. Academic Press, New York, NY.

Kimura, M.
1980. A simple method for estimating evolutionary rate of base substitutions through comparative studies of nucleotide sequences. J. Molecular Evolution 16:111–120.

Menzies R. A.
1981. Biochemical population genetics and the spiny lobster larval recruitment problem: an update. Proceedings of the Gulf and Caribbean Fisheries Institute 33:230–243.

Menzies R. A., and J. M. Kerrigan.
1979. Implications of spiny lobster recruitment patterns of the Caribbean —a biochemical genetic approach. Proceedings of the Gulf and Caribbean Fisheries Institute 31:164–178.

Moore, D. R.
1962. Notes on the distribution of the spiny lobster *Panulirus* in Florida and the Gulf of Mexico. Crustaceana 3:318–319.

Phillips, B. F., and A. F. Pearce.
1997. Spiny lobster recruitment of western Australia. Bull. Mar. Sci. 61(1):21–41.

Saitou, N., and M. Nei.
1987. The neighbor-joining method: a new method for reconstructing phylogenetic trees. Molecular Biol. Evol. 4:406–425.

Sarver, S. K., J. D. Silberman, and P. J. Walsh.
1998. Mitochondrial DNA sequence evidence supporting the recognition of two subspecies or species of the Florida spiny lobster *Panulirus argus*. J. Crustacean Biology 18(1): 177–186.

Sekiguchi, H.
1991. Two forms of *Panulirus longipes femoristriga* (Crustacea:Palinuridae) from Ogasawa waters, Japan. Proceedings of the Society of Systematic Zoology. 44:15–25.

Silberman, J. D., S. K. Sarver, and P. J. Walsh.
1994a. Mitochondrial DNA variation and population structure in the spiny lobster *Panulirus argus*. Mar. Biology 120:601–608.

1994b. Mitochondrial DNA variation in seasonal cohorts of spiny lobster (*Panulirus argus*) postlarvae. Molecular Marine Biology and Biotechnology 3(3):165–170.

Sims, H. W., and R. M. Ingle.
1967 Caribbean recruitment of Florida's spiny lobster population. Quarterly Journal of the Florida Academy of Science 29.207–242.

Swofford, D. L.
1998. PAUP: phylogenetic analysis using parsimony (and other methods), vers. 4.01b. Sinaur Associates, Sunderland, MA, 263 p.

On comparison of growth curves: How do we test whether growth rates differ?

You-Gan Wang
CSIRO Mathematical and Information Sciences
P.O. Box 120
Cleveland
Queensland 4163, Australia
Present address: Department of Biostatistics
Harvard School of Public Health
655 Huntington Avenue
Boston, Massachusetts 02115
E-mail address: ygwang@hsph.harvard.edu

David A. Milton
CSIRO Marine Research
P.O. Box 120
Cleveland
Queensland 4163, Australia

Comparisons of growth rates of populations and species are important in fisheries science for a range of reasons that vary with the context of each study. Most studies of fish growth have focused on the practical issues of the most appropriate way of comparing growth rather than on recognizing that there are several methods for making these comparisons and that the conclusions will differ depending on the method chosen.

Francis (1996) discussed the problem of how to compare different growth rates or growth curves. He suggested six plausible ways of making a comparison and suggested that the rate at which the asymptotic size is approached was the most natural method of comparing growth (his method 6). He illustrated the differences between the methods by comparing von Bertalanffy growth equations that are based on fixed growth parameters and that assumed that growth parameters are known and there are no associated uncertainties. However, in practice, the growth parameters are often estimated, and therefore are random variables. Consequently, the corresponding growth curves are also subject to variations.

For comparison with Francis's work, we will assume that growth for a species is adequately described by the von Bertalanffy equation with $t_0 = 0$, as

$$L(t;\beta) = l_\infty (1 - e^{-kt}), \qquad (1)$$

in which $\beta = (k, l_\infty)$ are growth parameters.

Here $l(t)$ is the mean length at age t. If $\hat{\beta}_1$ and $\hat{\beta}_2$ are two estimates of β, how do we test whether the corresponding two growth curves are the same? The traditional way is to compare individual parameters and find out which ones are significantly different. However, the parameter estimates, l_∞ and k, are often strongly correlated (Kirkwood and Somers, 1984; Wang and Thomas, 1995). It may therefore be more appropriate to compare biological reference points (e.g. size at one year of age) rather than growth parameters in the models (Wang and Thomas, 1995). Growth comparisons may, in general, be classified into two types: within species and between species. In practice, the following comparisons may be of interest:

1 Comparison of the growth rates for the same species, say E, in which two sets of growth parameter estimates, $\hat{\beta}_1$ and $\hat{\beta}_2$, are obtained from different time periods, different areas or sexes.

2 Comparison of growth rates for two different species to see which one grows faster.

As mentioned earlier, Francis (1996) considered six methods for comparing growth. For the within-species comparison, it seems all six methods are valid. However, these methods compare different characteristics of growth and therefore may reach different conclusions. For example, if we obtain $\hat{\beta}_1 = (0.5,50)$ from area A and $\hat{\beta}_2 = (0.4,60)$ from area B, we would conclude that species E does not grow as large in area A as in area B and that the k value (rate at which the asymptotic length is approached) in area A is larger than that in area B.

For between-species comparisons, we agree with Francis (1996) that his method 6 (k value comparison) is probably the most appropriate, especially in the context of comparing growth between, for example, herring and orange roughy. However, in some cases, comparing absolute growth rates at age or length between species could be of practical interest.

For example, if you are interested in choosing one of two species of fish or crustacean to farm and these two species look alike and have the same commercial value, it is more economical to farm the faster-growing species to shorten the time taken to reach market size. In Australia, the tiger prawn *P. esculentus* has a larger k value than the very similar *P. semisulcatus* (Somers and Kirkwood 1991), but *P. semisulcatus* has the potential of reaching a commercial size sooner (Fig. 1). Therefore, we would conclude that *P. semisulcatus* grows faster than *P. esculentus* in this context, and a comparison based only on k values may be misleading.

Therefore, in this note we will extend Francis's theoretical study by developing procedures for establishing statistical hypotheses for the six methods and suggest test statistics for comparing growth curves. We will demonstrate the differences in conclusions that can occur among the methods with data on

Manuscript accepted 1 July 2000.
Fish. Bull. 98:874–880 (2000).

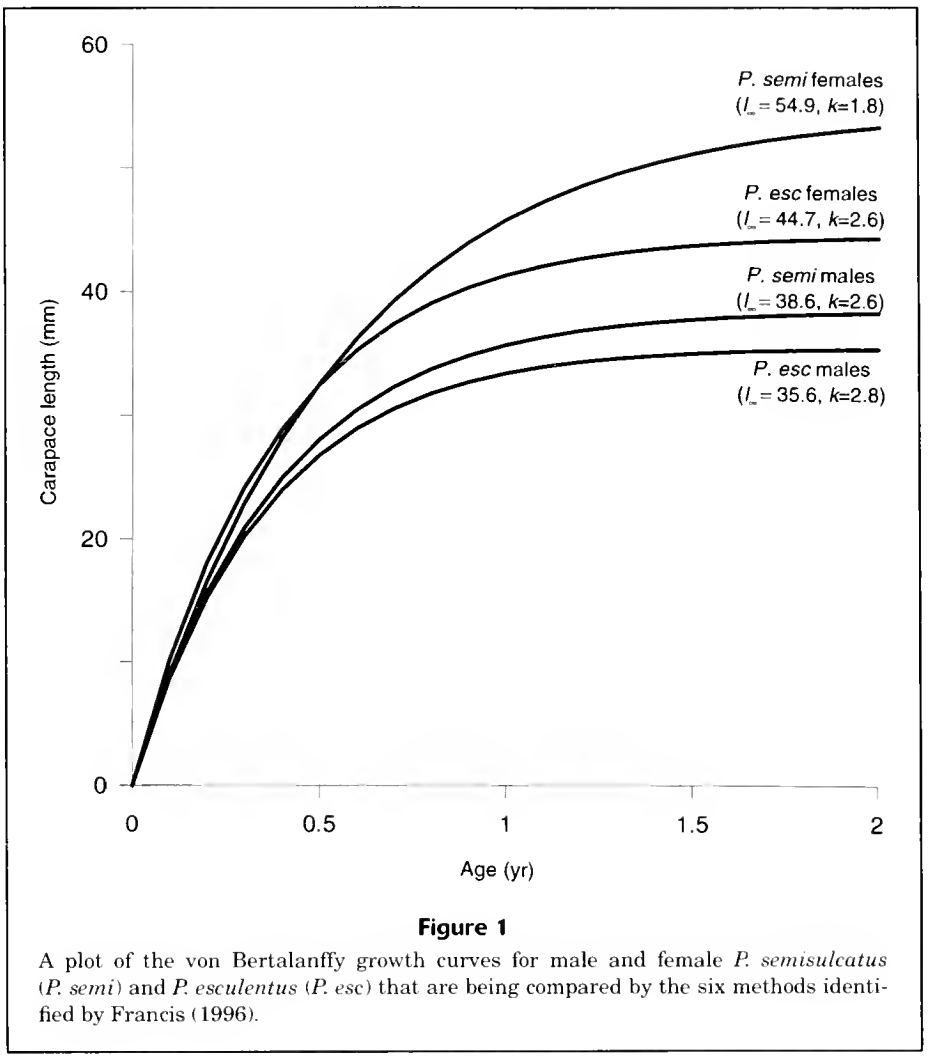

Figure 1

A plot of the von Bertalanffy growth curves for male and female *P. semisulcatus* (*P. semi*) and *P. esculentus* (*P. esc*) that are being compared by the six methods identified by Francis (1996).

growth rates of two species of tiger prawn (shrimp) from northern Australia.

Methods

Overall hypothesis tests on two sets of parameters

Suppose we are interested in testing the hypothesis that the underlying growth curves corresponding to the two sets of parameter estimates $\hat{\beta}_1 = (k_1, l_{\infty 1})$ and $\hat{\beta}_2 = (k_2, l_{\infty 2})$ are the same. According to the large-sample theory, it is quite reasonable in most cases to assume that $\hat{\beta}_1$ and $\hat{\beta}_2$ are normally distributed. To be general, we will allow $\hat{\beta}_1$ to be correlated with $\hat{\beta}_2$. In notation,

$$\begin{pmatrix} \hat{\beta}_1 \\ \hat{\beta}_2 \end{pmatrix} \approx N\left(\begin{pmatrix} \beta_1 \\ \beta_2 \end{pmatrix}, \begin{pmatrix} \Sigma_1 & \Sigma_{12} \\ \Sigma_{12} & \Sigma_2 \end{pmatrix} \right) \quad (1)$$

Note that if $\hat{\beta}_1$ and $\hat{\beta}_2$ are estimated from different data sets, they may be assumed to be independent, because both $\hat{\beta}_1$ and $\hat{\beta}_2$ are estimates and $\hat{\beta}_1 - \hat{\beta}_2$ is approximately multivariate normal. To test whether the two growth patterns determined by $\hat{\beta}_1$ and $\hat{\beta}_2$ are the same or not, we can use the generalised T^2-statistic (Anderson, 1971):

$$T^2 = (\hat{\beta}_1 - \hat{\beta}_2)' V^{-1} (\hat{\beta}_1 - \hat{\beta}_2), \quad (2)$$

in which V = the covariance of $\hat{\beta}_1 - \hat{\beta}_2$.

The distribution of the T^2-statistic is approximately chi-squared with 2 degrees of freedom, χ^2_2. If the significance level is α, the corresponding critical value is $\chi^2_2(\alpha)$.

In many cases, we are interested in the slope of the growth curve (growth rate) rather than the curve itself. For example, we may be interested in comparing the growth rate during a particular age interval. Owing to natural mortality or fishing mortality, the period outside of this age range may be of no practical interest. In this case, it is may be more appropriate to consider the growth patterns over a specified age or length range rather than the whole range, which would put more emphasis (weight) on the asymptotic length in the comparison.

Tests to compare two growth equations Let g be a growth function of (k, l_∞) that we are interested in comparing. Table 1 lists the six g functions corresponding to the six methods identified by Francis (1996). For a given function g, we will test $g(\beta_1) = g(\beta_2)$ versus $g(\beta_1) \neq g(\beta_2)$ or $g(\beta_1) > g(\beta_2)$, depending on the context. Standard normal tests may be used for a specified g function. The test will rely on the properties of $D=g(\hat{\beta}_1) - g(\hat{\beta}_2)$. Let $E(D)$ and $V(D)$ be the corresponding expectation and variance of D when β is the true parameter. Under the null hypothesis, $g(\beta_1) = g(\beta_2)$, and using standard Taylor series expansion, we can work out analytic expressions of $E(D)$ and $V(D)$. Some pooled estimates of β may be required to input to $E(D)$ and $V(D)$ to obtain approximate values of $E(D)$ and $V(D)$. We can obtain $E(D)$ from $Eg(\hat{\beta}_1) - Eg(\hat{\beta}_2)$ and

$$E\left(g(\hat{\beta})\right) = g(\beta) + \frac{1}{2}\left(f_{11}\sigma_{11}^2 + 2f_{12}\sigma_{12} + f_{22}\sigma_{22}^2\right), \tag{3}$$

in which f values are from the second derivative of g with respect to β (Table 1) and

$$\begin{pmatrix} \sigma_{11}^2 & \sigma_{12} \\ \sigma_{12} & \sigma_{22}^2 \end{pmatrix} = V(\hat{\beta}). \tag{4}$$

The variance of D can be obtained from

$$V(D) = X_1^T \Sigma_1 X_1 + X_2^T \Sigma_2 X_2 - 2X_1^T \Sigma_{12} X_2, \tag{5}$$

in which X_i = the gradient or first derivative of g_i (Table 1); and

Σ's = the components of the covariance defined earlier.

Note that the last term disappears if $\hat{\beta}_1$ and $\hat{\beta}_2$ are independent of each other. There are a few possible ways to obtain the approximate significance level, P. However, the most widely used method assumes D is normally distributed. Then we can use the z-test, which is based on the normal approximation for large sample sizes. For a one-sided test $g(\beta_1) = g(\beta_2)$ vs. $g(\beta_1) > g(\beta_2)$

$$P \approx 1 - \Phi\left(\frac{\hat{D}}{\sqrt{V(\hat{D})}} = \Phi\left(\frac{-\hat{D}}{\sqrt{V(\hat{D})}}\right)\right), \tag{6}$$

where Φ = the standard normal distribution function.

For a two-sided test, we have

$$P \approx 2\Phi\left(\frac{-\left|\hat{D}\right|}{\sqrt{V(\hat{D})}}\right). \tag{7}$$

If we are interested in the growth for a range of ages (t_{min}, t_{max}), or the sizes (l_{min}, l_{max}), we may consider the in-

Table 1

The six growth models $g(\beta)$ that correspond to methods of comparing mean growth of two species or populations in Francis (1996) and their first $X = \frac{dg}{d\beta}$ and second $F = \frac{d^2g}{d\beta}$ derivatives assuming $\beta \sim (\beta_0, \Sigma)$.

Method	$g(\beta)$	X	F
1 Comparison of lengths at each age	$g = l_\infty(1 - e^{-kt})$	$\begin{pmatrix} l_\infty t e^{-kt} \\ 1 - e^{-kt} \end{pmatrix}$	$\begin{pmatrix} -l_\infty t^2 e^{-kt} & t e^{-kt} \\ t e^{-kt} & 0 \end{pmatrix}$
2 Comparison of absolute growth rates at each age	$g = l_\infty k e^{-kt}$	$\begin{pmatrix} l_\infty e^{-kt}(1-kt) \\ k e^{-kt} \end{pmatrix}$	$\begin{pmatrix} -(2-kt)t l_\infty e^{-kt} & (1-kt)e^{-kt} \\ (1-kt)e^{-kt} & 0 \end{pmatrix}$
3 Comparison of absolute growth rates at each length	$g = (l_\infty - l)k$	$\begin{pmatrix} l_\infty - l \\ k \end{pmatrix}$	$\begin{pmatrix} 0 & 1 \\ 1 & 0 \end{pmatrix}$
4 Comparison of relative growth rates at each age	$g = \frac{k e^{-kt}}{1 - e^{-kt}}$	$\begin{pmatrix} \frac{1 - e^{-kt} - kt}{(1-e^{-kt})^2} e^{-kt} \\ 0 \end{pmatrix}$	$\begin{pmatrix} \frac{kt^2(1+e^{-kt})e^{-kt}}{(1-e^{-kt})^2} & \frac{2te^{-kt}}{(1-e^{-kt})^2} \\ 0 & 0 \end{pmatrix}$
5 Comparison of relative growth rates at each length	$g = \frac{(l_\infty - l)k}{l}$	$\begin{pmatrix} \frac{l_\infty}{l} - 1 \\ \frac{k}{l} \end{pmatrix}$	$\begin{pmatrix} 0 & \frac{1}{l} \\ \frac{1}{l} & 0 \end{pmatrix}$
6 Comparison of rates at which the asymptotic size is approached	$g = k$	$\begin{pmatrix} 1 \\ 0 \end{pmatrix}$	$\begin{pmatrix} 0 & 0 \\ 0 & 0 \end{pmatrix}$

tegrated squared difference over the specified range. For example, if $g_1 = \lambda_1 e^{-k_1 t}$ and $g_2 = \lambda_2 e^{-k_2 t}$, in which $\lambda_1 = k_2 l_{\infty 1}$ and $\lambda_2 = k_2 l_{\infty 2}$, we will rely on

$$D = \int_{t_0}^{t_{\infty}} (g_1(t) - g_2(t))dt.$$

The corresponding expectation and variance can also be approximated by the delta method.

We then apply each method to comparisons of the growth of males and females of two species of tiger prawn caught during tagging studies in northern Australia (Somers and Kirkwood 1991). We will consider two scenarios: 1) growth at age 0.5 yr (for methods 1, 2, and 4) or growth at length 30 mm (for methods 3 and 5); 2) growth at age one yr (for methods1, 2, and 4) or growth at length 35 mm (for methods 3 and 5). In order to verify that our test assumption that D was normally distributed, we obtained frequency plots for the bootstrapped estimates of the growth parameters.

Results

We first bootstrapped the parameter estimates for each group to assess whether our assumption that the parameters were normally distributed was valid. The plot for male *P. semisulcatus* showed that there was little evidence of skewness in our estimates (Fig. 2). Plots for other groups are similar and not shown here. The t tests proposed in this paper, although based on normal distributions, are well known to be robust to violation to normality (which is why they are also known as "robust" test in statistics). On the other hand, the proposed tests rely only on mean and covariance estimates and the covariance matrix is often obtained from asymptotic distribution (normal) of the estimates in nonlinear regression.

We tested for the overall significance of each comparison before proceeding with testing the six methods. All were highly significant ($P<<0.00001$) and T^2 statistics ranged from 43.2 for the comparison of *P. semisulcatus* females versus *P. esculentus* females to 385.7 for *P. esculentus* males versus *P. semisulcatus* females. Given that the overall growth curves differed among species, then it is reasonable to then look further at the growth rates yielded by the different methods.

The growth models for the six methods of comparing growth and their first and second derivatives differed between methods (Table 1). The growth parameters used in the comparison show apparent differences in the size of both l_∞ and k among the species and sexes (Wang, 1998). These differences in the absolute value of each parameter translate into quite large differences in the shape of the growth curves (Fig. 1). The effect is most striking for *Penaeus semisulcatus*, but does growth differ? Is it affected if we choose a particular length or age?

The results of tests from the six methods are shown in Table 2. The difference in lengths between P. *esculentus* and P. *semisulcatus* at the age of 0.5 yr is not significant for either males or females (in method 1 in Table 2), but the difference becomes very significant at age 1 yr. This result is consistent with the plot in Figure 1. However, the conclusion is reversed when comparing growth rate (method 2 in Table 2) instead of length. The relative growth rates at either age (0.5 yr or 1 yr) for *P. esculentus* do not differ significantly between males and females (method 4), whereas the rates at length 30 mm or 35 mm differ significantly. This is also biologically plausible because the growth rate at length 35 mm is very close to zero for *P. esculentus* males (the asymptotic size is only 35.6 mm) and there is a substantial growth to be gained for females (the asymptotical size is 44.7 mm). For method 6, the comparion is independent of specified length or age (two scenarios give the same results).

In prawn farms, *P. esculentus* and *P. semisulcatus* are harvested after 6 or 12 months, depending on the circumstances, such as the farmer's need to increase the number of generations within the growing season at higher latitudes. Tests comparing the growth of each sex of each species (Table 3) show that the significance of the results varies with the hypothesis being tested. For example, the comparison of length-at-age (method 1) of *Penaeus semisulcatus* and *P. esculentus* and females was not significant ($P<0.87$) at both six months of age (Table 3). However, when the absolute growth rates of the two species were compared (method 2), they were highly significantly different ($P<0.001$). Other tests, such as comparisons of the growth of male and female *P. semisulcatus*, were highly significant for all methods ($P<0.001$). As Francis (1996) pointed out, the results from all comparisons with methods 3 and 5 produce similar results and methods 4 and 6 give very similar results but in the opposite direction.

Table 2

The von Bertalanffy growth parameter estimates of *Penaeus esculentus* and *P. semisulcatus* from the Gulf of Carpentaria, northern Australia, used in growth comparisons between sexes of each species and between the two species for the same sex. The unbiased estimates were obtained by the equation of Wang (1998) and based on tagged prawn data from Somers and Kirkwood (1991).

Species	Sex	n	$l_\infty \pm$ SE (mm)	$k \pm$ SE (per yr)	Cov (l_∞, k)
P. esculentus	M	333	35.6 ± 0.3	2.8 ± 0.2	−0.0565
	F	224	44.7 ± 1.2	2.6 ± 0.3	−0.395
P. semisulcatus	M	159	38.6 ± 0.5	2.6 ± 0.2	−0.0886
	F	204	54.9 ± 1.7	1.8 ± 0.2	−0.2788

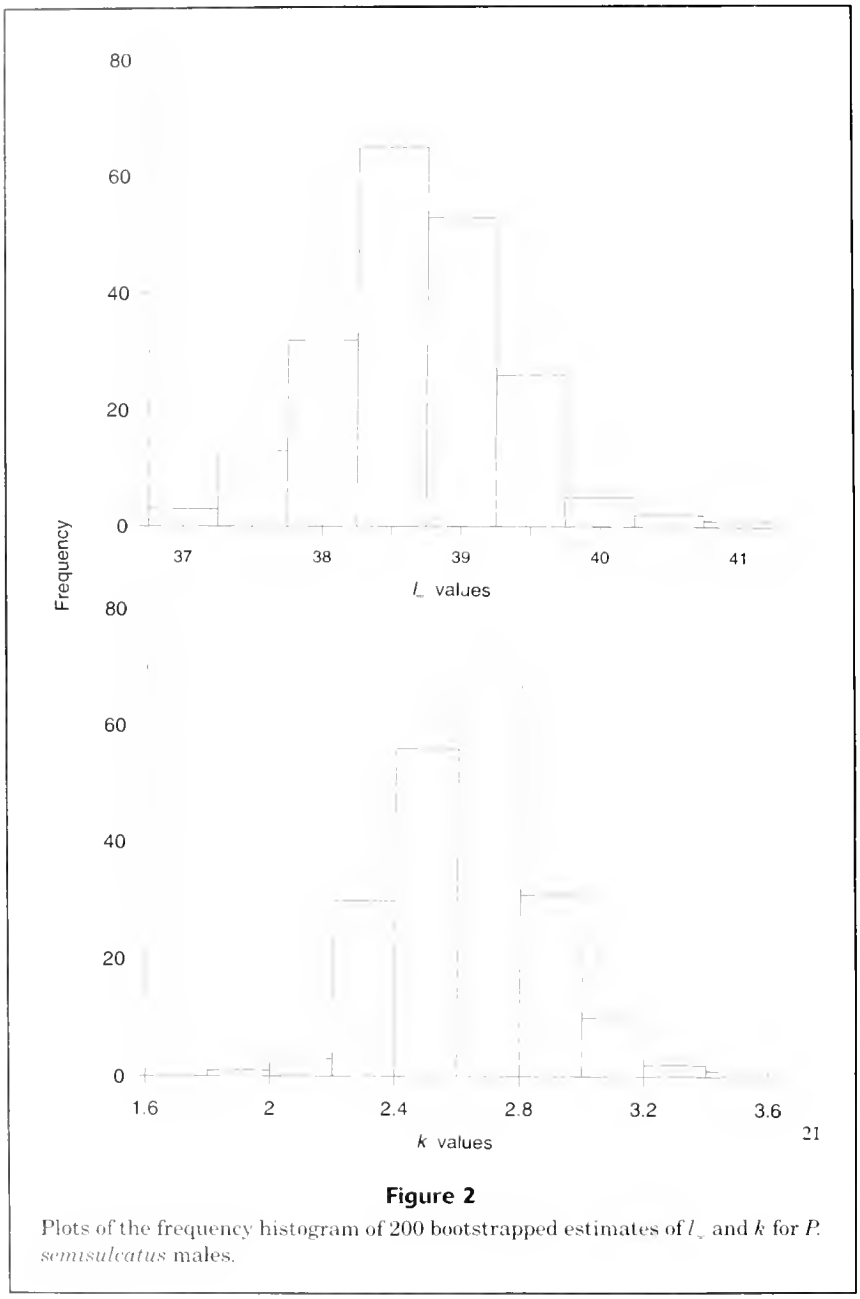

Figure 2

Plots of the frequency histogram of 200 bootstrapped estimates of L_∞ and k for *P. semisulcatus* males.

Our tests, in which the two tiger prawn species were compared, show that the significance of the results varies with the hypothesis. In our example, we have tried to choose lengths and ages that were approximately comparable. The results of the six tests for any particular interspecific or intraspecific hypothesis under either scenario are not directly comparable because methods 1, 2, and 4 compare growth rate at age (6 month or 1 yr) and the other methods compare growth rate in relation to length (30 mm or 35 mm). This distinction is more important for the interspecific comparisons because growth rate, rather than sexes, is more likely to vary between species for most phyla.

Discussion

Tests to compare growth by comparing length-at-age (method 1) show that there were no significant differences in the size of each sex of the two species, but there were highly significant differences in size between the sexes of each species. This finding differs from the interpretation if k-values were compared (method 6). In the situation where a farmer is deciding which species reaches a minimum marketable size earlier, we think that method 1 would be the most logical to use. However, if the farmer were trying to decide the potential benefit or tradeoff of

Table 3

Results of tests to compare within-species and between-species differences in the growth of males (M) and females (F) of two commercial penaeid prawns, *Penaeus esculentus* (*P.e*) and *P. semisulcatus* (*P.s*), from the Gulf of Carpentaria, northern Australia. The unbiased estimates from tagged prawns were obtained by the equation of Wang (1998). $D = g(\hat{\beta}_1) - g(\hat{\beta}_2)$, V = the corresponding variance. Comparisons were made against the alternate hypothesis $g(\beta_1) \leq g(\beta_2)$ under two scenarios: 1) at age (t) = 0.5 yr for methods 1, 2, and 4 or at length (l) = 30 mm for methods 3 and 5; 2) at age (t) = 1 yr for methods 1, 2, and 4 or length (l) = 35 mm for methods 3 and 5. P_1 and P_2 are the P-values under scenarios 1 and 2.

			Scenario 1 (l=30 mm or t=0.5 yr)			Scenario 2 (l=35 mm or t=1.0 yr)		
Method	Comparison	Type of comparison	D	V	p_1	D	V	p_2
1 Comparison of lengths at each age	*P.s* M vs. *P.s* F	within-species	–4.0	1.2	0.001	–9.7	0.4	0.001
	P.e M vs. *P.e* F	within–species	5.6	1.5	0.001	7.9	0.3	0.001
	P.e M vs. *P.s* M	between-species	1.3	1.0	0.18	2.4	0.3	0.001
	P.e F vs. *P.s* F	between-species	–0.26	1.7	0.87	4.2	0.4	0.001
2 Comparison of absolute growth rates at each age	*P.s* M vs. *P.s* F	within-species	–12.7	1.2	0.001	–9.2	2.0	0.001
	P.e M vs. *P.e* F	within-species	7.2	2.2	0.001	2.7	2.2	0.23
	P.e M vs. *P.s* M	between-species	2.8	1.3	0.03	1.4	1.3	0.29
	P.e F vs. *P.s* F	between-species	8.3	2.2	0.001	7.9	2.7	0.003
3 Comparison of absolute growth rates at each length	*P.s* M vs. *P.s* F	within-species	–21.4	1.6	0.001	–25.6	0.94	0.000
	P.e M vs. *P.e* F	within-species	22.3	2.3	0.001	23.4	1.08	0.000
	P.e M vs. *P.s* M	between-species	6.9	0.8	0.001	7.9	0.94	0.000
	P.s F vs. *P.e* F	between-species	5.9	2.7	0.03	10.03	1.09	0.000
4 Comparison of relative growth rates at each age	*P.s* M vs. *P.s* F	within-species	–0.27	0.08	0.001	–0.16	0.05	0.001
	P.e M vs. *P.e* F	within-species	0.06	0.11	0.59	0.03	0.06	0.60
	P.e M vs. *P.s* M	between-species	0.06	0.08	0.49	0.03	0.04	0.49
	P.s F vs. *P.e* F	between-species	0.27	0.12	0.03	0.15	0.06	0.02
5 Comparison of relative growth rates at each length	*P.s* M vs. *P.s* F	within-species	–0.71	0.05	0.001	–0.73	0.03	0.000
	P.e M vs. *P.e* F	within-species	0.74	0.08	0.001	0.67	0.03	0.000
	P.e M vs. *P.s* M	between-species	0.23	0.03	0.001	0.22	0.03	0.000
	P.s F vs. *P.e* F	between-species	0.20	0.09	0.03	0.29	0.03	0.000
6 Comparison of rates at which the asymptotic size is approached	*P.s* M vs. *P.s* F	within-species	0.84	0.26	0.001	0.84	0.26	0.001
	P.e M vs. *P.e* F	within-species	–0.22	0.4	0.58	–0.22	0.4	0.58
	P.e M vs. *P.s* M	between-species	–0.20	0.28	0.49	–0.20	0.28	0.49
	P.s F vs. *P.e* F	between-species	–0.82	0.39	0.03	–0.82	0.39	0.03

leaving the prawns in the ponds for longer, then one of the methods that test for relative changes in growth rate (method 4 or 5) would probably be more appropriate.

The difference in parameter estimates, and hence growth rates, may have important implications when researchers are trying to compare growth between species or between regions. Francis (1988) argued that length-at-age data do not contain precise information on the expected growth rate of fish of a given length. He concluded that length-at-age data and tagging data contain different information on growth; therefore the parameters estimated from them had different meanings and were not directly comparable.

Our proposed tests for different methods, including the overall test, aim to incorporate all the parameters and the overall uncertainties and correlations between each other. Further research can be carried out to study the robustness of the proposed test and to apply it to other growth models. The method suggested for constructing tests to compare growth rates could be easily modified to apply to other types of growth equation besides the von Bertalanffy equation.

Acknowledgments

We thank David Die, Chris Francis, and Vivienne Mawson for constructive comments on an earlier draft of our manuscript. We are also grateful to four reviewers for insightful comments that led to a much improved version.

Literature cited

Anderson, T. W.
1971. An introduction to multivariate statistical analysis. John Wiley & Sons, New York, NY, 284 p.

Francis, R. I. C. C.
1988. Are growth parameters estimated from tagging and age-length data comparable? Can. J. Fish. Aquat. Sci. 45:936–942.
1996. Do herring grow faster than orange roughy? Fish. Bull. 94:783–786.

Kirkwood, G. P., and I. F. Somers.
1984. Growth of the two species of tiger prawn, *Penaeus esculentus* and *Penaeus semisulcatus*, in the western Gulf of Carpentaria. Aust. J. Mar. Freshwater Res. 35:703–712.

Somers, I. F., and G. P. Kirkwood.
1991. Population ecology of the grooved tiger prawn, *Penaeus semisulcatus*, in the north-western Gulf of Carpentaria, Australia: growth, movement, age structure and infestation by the bopyrid parasite *Epipenaeon ingens*. Aust. J. Mar. Freshwater Res. 42:349–467.

Wang, Y.-G.
1998. An improved Fabens method for estimation of growth parameters in the von Bertalanffy model with individual asymptotes. Can. J. Fish. Aquat. Sci. 55:397–400.

Wang, Y. -G., and M. R. Thomas.
1995. Accounting for the individual variability in the von Bertalanffy growth model. Can. J. Fish. Aquat. Sci. 52: 1368–1375.

Occurrence of Pacific sardine, *Sardinops sagax*, off southeastern Alaska

Bruce L. Wing
James M. Murphy
Thomas L. Rutecki

Auke Bay Laboratory
Alaska Fisheries Science Center
11305 Glacier Highway
Juneau, Alaska 99801-8626
E-mail address (for B. Wing): Bruce.Wing@noaa.gov

Pacific sardines, *Sardinops sagax* (Jenyns, 1842), are an important forage and commercial species off central and southern California. From the late 1920s through the early 1940s, sardines were a major resource of the oil and meal fisheries of British Columbia, Washington, and Oregon (Hart, 1973). In 1931, sardines were unusually abundant on southern and central British Columbia fishing grounds and more numerous than usual in northern British Columbia (Shultz et al., 1932). In the early 1940s, however, yield of these fisheries declined radically and the species range was restricted to waters off central and southern California. After the decline, Pacific sardines were rarely reported north of the California–Oregon border (Reid, 1960; Mearns, 1988). Since 1992, Pacific sardines have again been observed off southern and central British Columbia (Hargreaves et al., 1994; McFarlane and Beamish, 1999).

Although the occurrence and changes in abundance of Pacific sardines in British Columbia waters are well documented, the presence of this species off Alaska is poorly documented. Schultz et al. (1932) reported Pacific sardines from Alaska on the basis of 24 adult specimens collected 8 August 1931 from the Cape Ommaney herring fishery (Clark, 1936; 1947). No additional specimen was documented from Alaska until 1992, when larval Pacific sardines were collected southwest of the Shumagin Islands, southwestern Alaska (Busby et al[1]).

Specimen collection

Eight adult sardines were captured in a surface trawl at 57°31′N, 136°34′W, 28 km west of Khaz Point, northern southeastern Alaska, on 20 August 1998. The fish were captured during a National Marine Fisheries Service research cruise to compare rope trawl and gill-net sampling methods for juvenile sablefish, *Anoplopoma fimbria*, and juvenile salmon, *Oncorhynchus* spp., in coastal Alaska. We used a Nordic 264-rope trawl (24-m horizontal opening, 30-m vertical opening) equipped with 3-m foam-filled doors and extra trawl floats to hold it at the surface.

Two additional specimens from Garnet Point (54°43′N, 130°41′W), near Nakat Bay, southern southeastern Alaska, were taken in a commercial salmon gill net on 1 September 1998. Fishermen reported that sardines were common but not numerous in eastern Dixon Entrance near Nakat Bay through August and early September 1998.

Both collections were frozen before being transported to the Auke Bay Laboratory, where lengths and weights of thawed fish were recorded. The fish were fixed in 4% formaldehyde, transferred to isopropyl alcohol, and then dissected to determine sex, maturity, and stomach contents. The fish were then deposited in the Auke Bay Laboratory reference collections.

Results

The 10 Pacific sardines averaged 233.3 ±11.30 mm standard length and 183 ±38.02 g wet weight (Table 1). On the basis of scale annuli, the collections were divided equally between 7- and 8-year-old fish. They were equally divided between males and females, and all gonads were in the resting stage. The fish had been feeding and had mesenteric fat deposits. Identifiable foods consisted of diatoms and euphausiids (*Euphausia pacifica* and *Thysanoessa* spp.) at Garnet Point and euphausiids (*E. pacifica* and *Thysanoessa* spp.) and small calanoid copepods (*Acartia* spp. and *Pseudocalanus* spp.) at Khaz Point.

Discussion

The occurrence of adult Pacific sardines in Alaska coastal waters is probably due to a northward extension of their summer feeding migration. Pacific sardines have a complex migration and spawning cycle, moving northward from California spawning areas during summer. The largest, oldest fish reach central Vancouver Island or farther north (Hart 1973). Historically, few Pacific sardines have overwintered in southern British Columbia (Schultz et al., 1932; Hart, 1943; Hargreaves et al., 1994), but during February–April 1998, juvenile sardines were observed off the western coast of Vancouver (McFarlane and Beamish, 1999). Sardines overwintering in British Columbia could migrate north into Alaska waters the following summer. In summer 1931, sardines were observed at many northern British Columbia locations near the Alaska border and were common in the fall and winter

[1] Busby, M. S., W. W. Watson, and W. Shaw. 2000. Identification of larval and juvenile Pacific herring (*Clupea pallasi*) and Pacific sardine (*Sardinops sagax*) and their distribution in waters off British Columbia and in the Gulf of Alaska. *In* prep. [Available from M. S. Busby, RACE, Alaska Fisheries Science Center, 7600 Sand Point Way NE, Bin 15700, Seattle WA 98115-0070.]

Manuscript accepted 26 June 2000.
Fish. Bull. 98:881–883 (2000).

Table 1

Biological data for Pacific sardines, *Sardinops sagax*, collected in Alaska, during summer 1998.

Standard length (mm)	Wet weight (g)	Age (yr)	Sex	Maturation stage	Food
Collection no. AB 98-39, Garnet Point, 54°43′N, 140°41′W, 1 Sep 1998, 2 specimens					
233	153	7	M	resting	diatoms
235	155	7	M	resting	diatoms and euphausiids
Collection no. AB 98-44, Khaz Point, 57°31′N, 136°34′W, 20 Aug 1998, 8 specimens					
225	155	7	M	resting	euphausiids and copepods
225	157	8	M	resting	trace of zooplankton
230	204	8	F	resting	trace of zooplankton
215	156	7	F	resting	trace of zooplankton
255	254	8	F	resting	euphausiids and copepods
240	207	8	F	resting	trace of zooplankton
230	157	7	F	resting	trace of zooplankton
245	232	8	M	resting	euphausiids and copepods

herring fisheries of southern British Columbia (Shultz et al., 1932).

Both years in which Pacific sardines were observed in southeastern Alaska were exceptionally warm and at the end of strong El Niño periods. The occurrence of sardines in Alaska reported in our study followed the exceptionally strong 1997–98 El Niño and is similar to the 1931 occurrence of Pacific sardines in Alaska, which followed the 1930–31 El Niño. Increased water temperature associated with El Niño events typically results in northward range extensions and anomalous distributions of fishes (Radovich, 1961; Schoener and Fluharty, 1985; Mearns, 1988). Although not specifically associated with sardines, several fishes were recorded north of their normal ranges during the 1930–31 (Walford, 1931; Mearns, 1988), 1982–83, and 1997–98 El Niños (Table 2). Included in 1997–98 records is an unconfirmed report of coho salmon, *Oncorhynchus kisutch*, feeding on northern anchovy, *Engraulis mordax*, near Yakutat, Alaska. Northern anchovy previously have not been reported north of the Queen Charlotte Islands, British Columbia. Interannual variations of El Niños and their effects on the distribution of marine organisms are difficult to assess because adequate time series data are lacking (Schoener and Fluharty, 1985), especially for Alaska coastal waters before 1960. In addition, not all unusual occurrences associated with El Niños are range extensions. More frequently, these occurrences are the result of anomalous strayings beyond normal ranges or are the result of changes in abundance or shifts in habitats (Table 2).

Although water temperature is a factor determining sardine distribution (Radovich, 1961), other factors may determine abundance and whether a range extension persists. Most Pacific sardine spawning occurs off southern California at 15–18°C temperatures (at a lower threshold limit

Table 2

Inter-El Niño comparison of unusual northern occurrences of marine fishes in Alaska coastal waters. Occurrences were coded according to Schoener and Fluharty (1985). E = range extension, H = habitat anomaly, A = range anomaly, C = change in abundance (+ or −). Sources: 1930–31 (Shultz et al., 1932); 1957–58 (Radovich, 1961); 1982–83 (Karinen et al., 1985; Pearcy and Schoener, 1987); 1991–94 (Wing, unpublished files); 1997–98 (Wing, unpubl. files).

Species	1930–31	1957–58	1982–83	1991–94	1997–98
Sardinops sagax	E				E
Alosa sapidissima			A	A	
Engraulis mordax					E
Cololabis saira			A		A
Sarda chiliensis		E	A		
Scomber japonicus				C+	C+
Thunnus alalunga		C+	C+		C+
Thunnus thynnus		E			
Seriola lalandi					E
Trachurus symmetricus				C+	C+
Merluccius productus					C+
Sphyraena argentea		A	A		A
Mola mola			A	A	A
Brama japonica			A	C+	C+
Atractoscion nobilis		E			
Balistes polylepis			E		
Prionace glauca			A/C+		C+
Carcharodon carcharias			A		A

of 13°C) (Ahlstrom, 1954). Laboratory studies have shown high mortalities and abnormal development at temperatures below 14°C (Lasker, 1964). There is some spawning off northern Oregon (Clark, 1938; Ahlstrom, 1948; Bentley et al., 1996). No spawning has been documented off British Columbia, although mature females with loose eggs have been reported from British Columbia (Walford and Mosher, 1941; Hart, 1943, 1973). Water temperatures off the northern British Columbia and southeastern Alaska coasts are sufficiently high for successful spawning and development of eggs and larvae in July and August. The progeny may not survive, however, to maturity if subsequent foraging, predation, and overwintering conditions are severe. If spawning does occur off British Columbia, it may be only a temporary extension of the spawning range and may not create long-lasting populations. In Alaska, such a temporary range extension was observed in the early 1980s for the California market squid, *Loligo opalescens*, whose range expanded northward for several years before contracting southward again (Wing and Mercer, 1990).

Literature cited

Ahlstrom, E. H.
1948. A record of pilchard eggs and larvae collected during surveys made in 1939 and to 1941. U.S. Fish. Wildlf. Serv. Spec. Sci. Rep. 54, 82 p.
1954. Distribution and abundance of egg and larval populations of the Pacific sardine. Fish. Bull. 56:82–140.

Bentley, P. J., R. L. Emmett, N. C. H. Lo, and G. Moser.
1996. Egg production of Pacific sardine (*Sardinops sagax*) off Oregon in 1994. CalCOFI Rep. 37:193–200.

Clark, F. N.
1936. Variations in the number of vertebrae of the sardine, *Sardinops caerulea* (Girard). Copeia 1936 (3):147–150.
1938. Small sardines taken off Oregon. Calif. Fish Game 24(1):71.
1947. Analysis of populations of the Pacific sardine on the basis of vertebral counts. Calif. Fish Game Bull. 65, 26 p.

Hargreaves, N. B., D. M. Ware, and G. A. McFarlane.
1994. Return of Pacific sardine (*Sardinops sagax*) to the British Columbia coast in 1992. Can J. Fish. Aquat. Sci. 51:460–463.

Hart, J. L.
1943. The pilchard *Sardinops caerulea* (Girard) on Canadian fishing grounds with special reference to an unusual abundance of young fish. Trans. R. Soc. Can., ser. 3, 37(5): 55–73.
1973. Pacific fishes of Canada. Fish. Res. Board Can. Bull. 180, 740 p.

Karinen, J. F., B. L. Wing, and R. R. Straty.
1985. Records and sightings of fish and invertebrates in the eastern Gulf of Alaska and oceanic phenomena related to the 1983 El Niño event. *In* El Niño north: Niño effects in the eastern subarctic Pacific Ocean (W. S. Wooster and D. L. Fluharty, eds.), p. 253–267. Washington Sea Grant Program, WSG-WO 85-3, Univ. Washington, Seattle, WA.

Lasker, R.
1964. An experimental study of the effect of temperature on the incubation time, development, and growth of Pacific sardine embryos and larvae. Copeia 1964:399–405.

McFarlane, G. A., and R. J. Beamish.
1999. Sardines return to British Columbia waters. *In* Proceedings of the 1998 Science Board Symposium on the impacts of the 1997/98 El Niño event on the North Pacific ocean and its marginal seas (H. J. Freeland, W. T. Peterson, and A. Tyler, eds.), p. 77–82. PICES Sci. Rep. 10, Institute of Ocean Sciences, Sidney, British Columbia.

Mearns, A. J.
1988. The "Odd Fish": Unusual occurrences of marine life as indicators of changing ocean conditions. *In* Marine organisms as indicators (D. F. Soule and G. S. Kleppel, eds.), p. 137–176. Springer-Verlag, New York, NY.

Pearcy, W. G., and A. Schoener.
1987. Changes in the marine biota coincident with the 1982–1983 El Niño in the northeastern subarctic Pacific Ocean. J. Geophys. Res. 92(C13):14,417–14,428.

Radovich, J.
1961. Relationships of some marine organisms of the northeast Pacific to water temperatures, particularly during 1957 through 1959. Calif. Fish Game Bull. 112, 62 p.

Reid, C. F.
1960. Note on four specimens of the Pacific sardine taken in August 1957 off British Columbia and Oregon. Calif. Fish Game 46:195–198.

Schoener, A., and D. L. Fluharty.
1985. Biological anomalies off Washington in 1982–83 and other major Niño periods. *In* El Niño north: Niño effects in the eastern subarctic Pacific Ocean (W. S. Wooster and D. L. Fluharty, eds.), p. 211–225. Washington Sea Grant Program, WSG-WO 85-3, Univ. Washington, Seattle, WA.

Schultz, L. P., J. L. Hart, and F. J. Gunderson.
1932. New records of marine west coast fishes. Copeia 1932 (2):65–68.

Walford, L. A.
1931. Northward occurrence of southern fish off San Pedro in 1931. Calif. Fish Game 17:401–405.

Walford, L. A., and K. Mosher.
1941. Extension of pilchard spawning to north Pacific waters indicated. Pacific Fisherman 39(3):47.

Wing, B. L., and R. W. Mercer.
1990. Temporary northern range extension of the squid *Loligo opalescens* in Southeast Alaska. Veliger 33:238–240.

Announcement

The editorial staff of *Fishery Bulletin* would like to thank the following referees for their time and efforts in providing reviews of the manuscripts published in 1999–2000. Their contributions have helped ensure the publication of quality science.

Dr. Dean W. Ahrenholz
Dr. M. James Allen
Dr. Robert Allman
Dr. John S. Anderson
Dr. Richard S. Appeldoorn
Dr. P.L. Appelton
Dr. Dean W Arhrenholz
Dr. Freddy Arocha
Dr. Francisco Arreguin-Sanchez
Dr. Whitlow W.L. Au
Dr. Jerald S. Ault
Ms. Amy Ball
Dr. Terry D. Beacham
Dr. Daniel W. Beckman
Dr. Jim Beets
Dr. Gavin Begg
Dr. James R. Bence
Dr. Kurt Benirschke
Dr. Paul Bentzen
Dr. J.A.H. Benzie
Dr. Keith A. Bigelow
Dr. James A. Bohnsack
Dr. Brian W. Bowen
Dr. Steven Branstetter
Dr. Matt K Broadhurst
Dr. Edward B. Brothers
Dr. J.A. Brown
Dr. Jeffrey A Buckel
Mr. Britt W. Bumguardner
Dr. John L. Butler
Dr. Deqin Cai
Dr. Mark H. Carr
Dr. Gonzalo C. Castillo
Dr. Jose I. Castro
Dr. D. Chapman
Dr. Kenneth K Chew
Dr. Seinen Chow
Dr. Malcolm R. Clark
Dr. Thomas A. Clarke
Dr. L.D. Coen
Dr. Pat L. Colin
Dr. Jeremy S. Collie
Mr. L. Alan Collins
Dr. Mark R Collins
Dr. Robert L. Colura
Dr. M. Comeau
Dr. Justin G. Cooke
Dr. P.D. Cowley
Dr. J. Cramer
Dr Maurice K. Crawford
Dr. Maria M. Criales
Dr. Paul K. Dayton
Dr Douglas A. DeVries
Dr David Die
Dr. James G. Ditty
Dr. Andrew E. Dizon
Dr. Martin W. Dorn
Dr. Miriam J. Doyle
Dr. Brett R. Dumbauld
Dr. Anne-Marie Ecklund
Dr. Elizabeth F. Edwards
Dr. A. El-Haweet
Dr. J.R. Ellis
Mr. Rober L. Emmett
Dr. Sheryan P. Epperly
Mr. Ronald J. Essig
Dr. Mary Fabrizio
Dr. Michael P. Fahay
Ms. Virginia Fay
Dr. James D. Felley
Dr. Beatrice Padovani Ferriera
Dr. Paul C. Fieldler
Dr. Joseph P. Fisher
Dr. Gary R. Fitzhugh
Dr. Michael J. Fogarty
Dr. Malcolm P. Francis
Dr. R.I.C.C. Francis
Dr. Ken Gerow
Dr. Carter Gilbert
Dr. V. Guillory
Dr. Donald R. Gunderson
Dr. M G Hamann
Dr. Bill Hamlet
Dr. Patrick J. Harris
Dr. James T. Harvey
Dr. Emma Hatfield
Dr. Selina S. Heppell
Dr. Roger P. Hewitt
Dr Rod Hobbs
Dr. Edward D. Houde
Dr. Glenn A. Hydnes
Dr. J. Jeffery Isely
Dr. Walter C. Jaap
Dr. Larry D Jacobson
Dr. B Johnson
Dr. D Jory
Dr. Michael J Kaiser
Ms. Paula Keener-Chavis
Dr. Trevor J Kenchington
Dr. Arthur W. Kendall Jr.
Dr Daniel K Kimura
Dr. Michael J Kingsford
Dr James E. Kirkley
Dr Elin Kjorsvik
Dr Pierre A. Kliebor
Dr Robert G. Kope
Dr A. Koronkiewicz
Dr. S. Kraul
Dr Thomas E. Ladig
Lt Cdr. John T Lamkin
Mr. C.H. Leblanc
Dr. Christopher M. Legault
Dr. Ben H. Letcher
Dr. C.C. Levings
Dr. Juna Lin
Ms. Patricia A. Livingston
Dr. Jordi Lleonart
Dr. Daniel Lluch-Belda
Dr. Nancy C.H. Lo
Dr. A. Lombarte
Dr. Milton S. Love
Dr. Lloyd F. Lowry
Dr. Brian Luckhurst
Dr. Molly E. Lutcavage
Dr. Pamely M. Mace
Dr. Gary L. Maillet
Dr. K.D. Malloy
Dr. Marc Mangel
Dr. Charles S. Manooch, III
Dr. Agnaldo Silva Martins
Dr. Enric Massuti
Dr. C.P. Matthews
Dr. Tim McClanahan
Dr. Russell B. Millar
Dr. Greg Mitchell
Dr. Mary L. Moser
Dr. Peter B. Moyle
Dr. Robert G. Muller
Dr. Keith D. Mullin
Dr. Hiroyuki Munehara
Dr. M.G. Munekiyo
Dr. Ransom A. Myers
Prof. Gunner Naevdal
Dr. Brian S. Nakashima
Dr. James Nance
Dr. Lisa J. Natanson
Dr. Russell S. Nelson
Dr. Brenda L. Norcross
Dr. Loretta O'Brien
Dr. Ron K. O'Dor
Dr. M.P. Olivar
Dr. John Olney
Dr. Jeff Olsen
Dr. Jose M. Orensanz
Dr J.R. Ovenden
Dr. Hazel A. Oxenford
Dr. Debra Palka
Dr. Daniel Pauly
Dr. M.G. Pawson
Dr. William G. Pearcy
Dr. Jerome J. Pella
Dr. Michael A. Perez
Dr. Randall M Peterman
Dr. Bruce F. Phillips
Dr. Michael H Prager
Dr. Harold L. Pratt Jr.
Dr. Andre E. Punt
Dr. Otto Putz
Dr. Terrance Quinn II
Dr. Richard L. Radtke
Dr. Stephen Ralston
Dr. Robert W Rangeley
Dr. Richard C. Raynie
Dr. Slobodan Regner
Dr. R. Anne Richards
Dr. William J Richards

dr. Linda R. Richardson
Dr. T.A. Rien
Dr. Roger E. Robbins
Dr. Donna R. Rogers
Dr. Craig S. Rose
Dr. Aaron Rosenfield
Dr. Michael R. Ross
Dr. A.A. Rowden
Dr. David J. Rugh
Dr. Bernard Sainte-Marie
Dr. R.A. Santos
Dr. Thomas Sawyer
Dr. Kurt M. Schaefer
Dr. Daniel R. Scoles
Dr. James E. Seeb
Dr. Lisa W. Seeb
Dr. Richard F. Shaw
Dr. R.G.J. Shelton
Dr. Jonathan M. Shenker
Dr. Michiyo Shima
Dr. Colin Simfendorfer
Dr. David W. Sims
Dr. Malacolm J. Smale
Mr. Joseph W. Smith
Dr. Susan M. Sogard
Dr. David A. Somerton
Dr. Harley Speir
Dr. Cluney Stagg
Dr. Frank W. Steimle
Dr. John S. Stephens Jr.
Dr. E. Don Stevens
Dr. J.D. Stevens
Dr. David M. Taylor
Dr. Mark Terceiro
Dr. James P. Thomas
Dr. Grant G. Thompson
Dr. T. Tokai
Dr. A.M. Tokranov
Dr. B. Jack Turnock
Mr. James H. Uchiyama
Dr. Yuju Uozumi
Dr. Douglas S. Vaughan
Dr. Michael Vecchione
Mr. David A. Ventresca
Dr. Roger Villanueva
Dr. I.H. Von Herbing
Dr. Paul R. Wade
Dr. Robert D. Ward
Dr. Stanley M. Warlen
Dr. Alex C. Wertheimer
Dr. Vidar G. Wespestad
Dr. Austin B. Williams
Dr. Austin B. Williams
Dr. Charles A. Wilson III
Dr. George H. Winters
Dr. Sabine Petra Wintner
Dr. B.S. Wise
Dr. Peter R. Witthames
Dr. Ian K. Workman
Dr. Bernd Wursig
Dr. Yimen Ye
Dr. Mary M. Yoklavich

Fishery Bulletin Index

Volume 98 (1–4), 2000

List of titles

98(3)

98(4)

Fishery Bulletin Index

Volume 98 (1–4), 2000

List of authors

Fishery Bulletin index

Volume 98 (1–4), 2000

List of subjects

This statement is required by the Act of August 12, 1970, Section 3685, Title 39, U.S. Code, showing ownership, management, and circulation of the *Fishery Bulletin*, publication number 366-370, and was filed on 28 September, 2000. The *Bulletin* is published quarterly (four issues annually) with an annual subscription price of $50.00 (sold by the Superintendent of Documents, U.S. Government Printing Office, Washington, DC 20402). The complete mailing address of the office of publication is NMFS Scientific Publications Office, NOAA, 7600 Sand Point Way NE, BIN C15700, Seattle, WA 98115. The complete mailing address of the headquarters of the publishing agency is National Marine Fisheries Service, NOAA, Department of Commerce, 1335 East-West Highway, Silver Spring, MD 20910. The name of the publisher is Willis Hobart and the managing editor is Sharyn Matriotti; their mailing address is: NMFS Scientific Publications Office, 7600 Sand Point Way NE, BIN 15700, Seattle, WA 98115. The owner is the U.S. Department of Commerce, 14th St. N.W., Washington, DC 20230; there are no bondholders, mortgages, or other security holders. The purpose, function, and nonprofit status of the organization (agency) and the exempt status for Federal income tax purposes has not changed during the preceding 12 months. The extent and nature of circulation is as follows: total number of copies (A) (average number of copies of each issue during the preceding 12 months) was 1958 and the actual number of copies of the single issue published nearest to the filing dates was 1958. Paid circulation (B) is handled by the U.S. Government Printing Office, Washington, DC 20402, and the total number printed for their sales (mail subscriptions and individual sales) was 525 for both the average number of copies each issue during the preceding 12 months and the actual number of copies of the single issue published nearest to the filing date. Free distribution (D) by mail; samples, complimentary and other free copies (average number of copies each issue during the preceding 12 months) was 0 and the actual number of copies of the single issue published nearest to the filing date was 0. Free distribution outside the mail (E) by carriers or other means was 0 for both average number of copies and actual number of copies. Total free distribution (F) was 0 for both average number of copies and actual number of copies of the single issue published nearest the filing date. The total distribution (G: sum of C and G) (average number of copies each issue during the preceding 12 months) was 1958 and the actual number of copies of the single issue published nearest to the filing date was 1958. There were no copies not distributed or returned from news agents (H). The total (I: sum of G and H) is equal to the net press run figures shown in Item A: 1958 and 1958 copies, respectively. I certify that the statements made by me above are correct and complete. (Signed) Willis Hobart, Publisher

Fishery Bulletin

Guide for Contributors

Content

Articles published in *Fishery Bulletin* describe original research in fishery marine science, engineering and economics, and the environmental and ecological sciences, including modeling. Articles may range from relatively short to extensive.

Notes are reports of 5 to 10 pages without an abstract and describing methods or results not supported by a large body of data.

Although all contributions are subject to peer review, responsibility for the contents of papers rests upon the authors and not upon the editor or the publisher. It is therefore important that the contents of the manuscript are carefully considered by the authors.

Submission of an article is understood to imply that the article is original and is not being considered for publication elsewhere. Manuscripts should be written in English. Authors whose native language is not English are strongly advised to have their manuscripts checked by English-speaking colleagues prior to submission.

Preparation

Title page should include authors' full names and mailing addresses, the corresponding author's telephone, FAX number, and e-mail address, and a list of key words to describe the contents of the manuscript.

Abstract should not exceed one double-spaced typed page. It should state the main scope of the research but emphasize its conclusions and relevant findings. Because abstracts are circulated by abstracting agencies, it is important that they represent the research clearly and concisely.

Text must be typed double-spaced throughout. A brief introduction should portray the broad significance of the paper; the remainder of the paper should be divided into the following sections: Materials and methods, Results, Discussion (or Conclusions), and Acknowledgments. Headings within each section must be short, reflect a logical sequence, and follow the rules of multiple subdivision (i.e. there can be no subdivision without at least two items). The entire text should be intelligible to interdisciplinary readers; therefore, all acronyms, abbreviations, and technical terms should be spelled out the first time they are mentioned. The scientific names of species must be written out the first time they are mentioned; subsequent mention of scientific names may be abbreviated. Follow Scientific Style and Format: the CBE Manual for Authors, Editors, and Publishers (6th ed.), for editorial style, and the most current issue of the American Fisheries Society's Common and Scientific Names of Fishes from the United States and Canada, for fish nomenclature. Dates should be written as follows: 11 November 1991. Measurements should be expressed in metric units, e.g. metric tons as t; if other units of measurement are used, please make this fact explicit to the reader. The numeral one (1) should be typed as a one, not as a lower-case el (l). Use of appendices is discouraged.

Text footnotes should be numbered with Arabic numerals and inserted at the bottom of text. Footnote all personal communications, unpublished data, and unpublished manuscripts with full address of the communicator or author, or, as in the case of unpublished data, where the data are on file. Authors are advised to avoid references to nonstandard (gray) literature, such as internal, project, processed, or administrative reports. Where these references are used, please include whether they are available from NTIS (National Technical Information Service) or from some other public depository.

Literature cited comprises published works and those accepted for publication in peer reviewed literature (in press). Follow the name and year system for citation format. In the text, cite as follows: Smith and Jones (1977) or (Smith and Jones, 1977). If there is a sequence of citations, list alphabetically by author(s): Smith, 1987; Smith and Jones, 1985; Smith and Peterson, 1986. Abbreviations of serials should conform to abbreviations given in Serial Sources for the BIOSIS Previews Database. Authors are responsible for the accuracy and completeness of all citations.

Tables should not be excessive in size and must be cited in numerical order in the text. Headings within tables should be short but ample enough to allow the table to be intelligible on its own. All unusual symbols must be explained in the table legend. Other incidental comments may be footnoted with italic numerals. Use the asterisk only to indicate probability in statistical data. Zeros should precede all decimal points for values less than one.

Figures must be cited in numerical order in the text. The senior author's last name and the figure number should be written on the back of each one. Hand-drawn illustrations should be submitted as originals and not as photocopies. Submit photographs as glossy prints or slides with good contrast, otherwise we cannot guarantee a good final printed copy. Graphs should be submitted as laser-printed copies, not as photocopies. Label all figures with Helvetica typeface and capitalize the first letter of the first word in axis labels. Italicize species name and variables in equations. Use zeros before all decimal points. Use uppercase Times Roman bold typeface to label the parts of a figure, e.g. A, B, C, etc. Each figure legend should explain all symbols and abbreviations in the figure and should be double-spaced and placed at the end of the manuscript.

Copyright law Government publications are not copyrighted; they fall within the public domain. If an author reproduces any part of a government publication in his work, reference to source is appreciated.

Submission

Send printed copies (original and three copies without staples) to the Scientific Editor:

Dr. John V. Merriner
Southeast Fisheries Science Center
National Marine Fisheries Service
101 Pivers Island Road
Beaufort, NC 28516

Once the manuscript has been accepted for publication, you will be asked to submit an electronic copy of your manuscript to the Managing Editor. The electronic copy should be submitted in WordPerfect or Microsoft Word text format and placed on a 3.5-inch disk that is double-sided, double or high density, and that is compatible with either DOS or Macintosh systems.

A copy of page proofs will be sent to the author for final approval prior to publication.

Reprints (copies of published articles and notes) are available free of charge to the senior author (50 copies) and to his or her laboratory (50 copies). Additional copies may be purchased in lots of 100 when the author receives page proofs.